



Euratom
European Commission

**Nuclear fission safety
programme
1992-94**

Radiation protection research action

Final report

Volume 3

EUR 16769 DE/EN/FR

**Comisión Europea
Europa-Kommissionen
Europäische Kommission
Ευρωπαϊκή Επιτροπή
European Commission
Commission européenne
Commissione europea
Europese Commissie
Comissão Europeia**

Euratom

Programa
SEGURIDADDE LA FISIÓN NUCLEAR
Plan de «Investigación en materia de protección contra las radiaciones»

Program
SIKKERHED I FORBINDELSE MED KERNESPALTING
Programmet »Forskning vedrørende Strålingsbeskyttelse«

Programm
SICHERHEIT BEI DER KERNSPALTUNG
Aktion „Strahlenschutzforschung“

Πρόγραμμα
ΑΣΦΑΛΕΙΑ ΣΤΗΝ ΠΥΡΗΝΙΚΗ ΣΧΑΣΗ
Δράση «Έρευνα στον τομέα της Ακτινοσταυίας»

NUCLEAR FISSION SAFETY
programme
Action 'Radiation protection research'

Programme
« SÛRETÉ DE LA FISSION NUCLÉAIRE »
Action «Recherche en radioprotection»

Programma
SICUREZZA DELLA FISSIONE NUCLEARE
Azione «Ricerca sulla radioprotezione»

Programma
VEILIGHEID VAN KERNSPLIJTING
Actie „Onderzoek Stralingsbescherming“

Programa
SEGURANÇA DA CISÃO NUCLEAR
Acção «Investigação no domino da protecção contra radiações»

1992-1994

Final report

Volume 3

HINWEIS

Weder die Europäische Kommission noch Personen, die im Namen dieser Kommission handeln, sind für die etwaige Verwendung der nachstehenden Informationen verantwortlich.

LEGAL NOTICE

Neither the European Commission nor any person acting on behalf of the Commission is responsible for the use which might be made of the following information.

AVERTISSEMENT

Ni la Commission européenne ni aucune personne agissant au nom de la Commission n'est responsable de l'usage qui pourrait être fait des informations ci-après.

Zahlreiche weitere Informationen zur Europäischen Union sind verfügbar über Internet, Server Europa (<http://europa.eu.int>).

A great deal of additional information on the European Union is available on the Internet. It can be accessed through the Europa server (<http://europa.eu.int>)

De nombreuses autres informations sur l'Union européenne sont disponibles sur Internet via le serveur Europa (<http://europa.eu.int>).

Bibliographische Daten befinden sich am Ende der Veröffentlichung.

Cataloguing data can be found at the end of this publication.

Une fiche bibliographique figure à la fin de l'ouvrage.

Luxembourg: Office des publications officielles des Communautés européennes, 1997

ISBN 92-827-7985-8

© Europäische Gemeinschaften, 1997
Nachdruck mit Quellenangabe gestattet.

© European Communities, 1997
Reproduction is authorized provided the source is acknowledged.

© Communautés européennes, 1997
Reproduction autorisée, moyennant mention de la source

INHALTSVERZEICHNIS

TABLE OF CONTENTS

TABLE DES MATIERES

VOLUME 1	Page
I. Einleitung/Introduction	1
II. Mitglieder und Experten 1993-95 Beratender Verwaltungs und Koordinierungsausschuss "Strahlenschutz" Members and Experts 1993-95 Management and Coordination Advisory Committee "Radiation Protection" Membres et Experts 1993-95 Comité Consultatif en matière de Gestion et de Coordination "Radioprotection"	9
III. Forschungstätigkeit Strahlenschutz Research in Radiation Protection Recherche en Radioprotection	13
 A EXPOSITION DES MENSCHEN DURCH STRAHLEN UND RADIOACTIVITÄT HUMAN EXPOSURE TO RADIATION AND RADIOACTIVITY EXPOSITION DE L'HOMME AUX RAYONNEMENTS ET À LA RADIOACTIVITÉ	15
A1 Measurement of radiation dose and its interpretation.	
A1A ICRU	
FI3P-CT920054-A1A	17
Radiation quantities units and measurement techniques for radiation protection.	
1 Allisy	BIPM
A1B EURADOS	
FI3P-CT920001-A1B	25
Collaboration on radiation dosimetry for radiation protection applications (EURADOS).	
1 Dietze	EURADOS
2 Golnik	IAE-RPD
A11 Development and implementation of standards and procedures linked to the concepts of dose equivalent quantities for both external and internal exposure.	
FI3P-CT920040-A11	55
Accident dosimetry in populated areas: the use of solid-state dosimetry techniques with ceramics and other natural materials.	
1 Bailiff	Univ. Durham
2 Goeksu	GSF
3 Stoneham	Univ. Oxford
4 Bøtter-Jensen	Lab. Risø
5 Nolte	Univ. München - Technische
6 Hütt	EAAS.IG (PECO contract)
7 Lippmaa	ICPB

FI3P-CT920064h-A11	123
The measurement of the spectral and angular distribution of external radiations in the workplace and implications for personal dosimetry.		
1	Clark	NRPB
2	Spencer	UKAEA
3	Gualdrini	ENEA
4	Chartier	CEA - FAR
A12	Radiation measurement and instrumentation for individual and area dosimetry.	
FI3P-CT920002-A12	161
Realistic neutron calibration fields and related dosimetric quantities.		
1	Klein	PTB
2	Thomas	NPL
3	Chartier	CEA - FAR
4	Schraube	GSF
5	Kralik	CSAS.IRD
6	Osmera	NRIRR
7	Grecescu	IRA
FI3P-CT920018-A12	219
The measurement of environmental radiation doses and dose rates.		
1	Bøtter-Jensen	Lab. Risø
2	Lauterbach	PTB
3	Delgado Martínez	CIEMAT
4	Pernicka	CSAS.IRD
5	Waligorski	INP. Krakow
6	Osvay	II. Budapest
FI3P-CT920026-A12	283
Detection and dosimetry of neutrons and charged particles at aviation altitudes in the earth's atmosphere.		
1	McAulay	Univ. Dublin
2	Tommasino	ENEA
3	Schraube	GSF
4	O'Sullivan	DIAS
5	Grillmaier	Univ. Saarlandes
6	Hoefert	CERN
7	Spurný	CSAS.IRD
FI3P-CT920032-A12	339
Dosimetry of beta and low-energy photon radiations.		
1	Christensen	Lab. Risø
2	Chartier	CEA - FAR
3	Francis	NRPB
4	Herbaut	CEA - Grenoble
5	Spencer	UKAEA
6	Gasiot	Univ. Montpellier II
7	Scharmann	Univ. Giessen
8	Charles	Nuclear Electric
9	Olko	INP
10	Uchrin	MTA

FI3P-CT920039-A12 435
 Development of instruments and methods for radiation protection dosimetry with the variance-covariance method.

- | | | |
|---|----------|--|
| 1 | Kellerer | Univ. München |
| 2 | Lindborg | Inst. Nat. of Radiation Protection |
| 3 | Jessen | Univ. Århus - Hospital |
| 4 | Scendró | Microvacuum Ltd. Budapest (<i>PECO contract</i>) |

FI3P-CT920045-A12 467
 The use of microdosimetric methods for determination of dose equivalent quantities and of basic data for dosimetry.

- | | | |
|---|------------|--------------------------------|
| 1 | Séгур | ADPA |
| 2 | Brede | PTB |
| 3 | Zoetelief | TNO - Delft |
| 4 | Schmitz | KFA |
| 5 | Grillmaier | Univ. Saarlandes |
| 6 | Bordy | IPSN - CEA - FAR |
| 7 | Morstin | CITEC (<i>PECO contract</i>) |
| 8 | Sabol | TECH.UNIV.CZ |

FI3P-CT930072-A12 533
 Individual electronic neutron dosimeter.

- | | | |
|---|--------------------|----------------------------|
| 1 | Vareille | Univ. Limoges |
| 2 | Zamani-Valassiadou | Univ. Thessaloniki |
| 3 | Barthe | CEA - FAR |
| 4 | Fernández Moreno | Univ. Barcelona - Autónoma |
| 5 | Curzio | Univ. Pisa |
| 6 | Charvat | IRD |
| 7 | Moiseev | IFIN |

A14 Assessment of internal exposure.

FI3P-CT920048-A14 605
 Assessment of internal dose from plutonium and other radionuclides using stable isotope tracer techniques in man.

- | | | |
|---|----------|----------------------|
| 1 | Roth | GSF |
| 2 | Molho | Univ. Milano |
| 3 | Taylor | Univ. Wales, Cardiff |
| 4 | McAughey | UKAEA |

FI3P-CT920060-A14 651
 Radionuclide dosimetry.

- | | | |
|---|---------------|----------------------|
| 1 | Nosske | BFS |
| 2 | Kendall | NRPB |
| 3 | Taylor | Univ. Wales, Cardiff |
| 4 | van Rotterdam | TNO - Delft |
| 5 | Andrási | KFKI |
| 6 | Toader | IHPH |

FI3P-CT920064a-A14 *703
 Inhalation and ingestion of radionuclides.

1	Bailey	NRPB
2	Stahlhofen	GSF
3	Roy	CEA - FAR
4	Patrick	MRC
5	Stradling	NRPB
6	Iranzo	CIEMAT
7	Popplewell	NRPB
8	Strong	UKAEA
9	Jonhston	Inst. Occupational Medicine
10	Koblinger	HAS.RIAE
11	Gradón	ICH-MAW
12	Salowsky	UMP

A2 Transfer and behaviour of radionuclides in the environment.

A2A IUR

FI3P-CT920003-A2A 795
 Promotion of formation, knowledge and exchange of information in radioecology.

1	Cigna	UIR
---	-------	-----

A21 Environmental behaviour of radionuclides in situations meriting particular attention for long-term behaviour or post-accident conditions.

FI3P-CT920029-A21 813
 Towards a functional model of radionuclide transport in freshwaters.

1	Hilton	NERC
2	Ortins	Direcção-Geral do Ambiente
3	Cremers	Univ. Leuven (KUL)
4	Foulquier	CEA - FAR
6	Sansone	ENEA
7	Blust	Univ. Antwerpen
8	Fernández	Univ. Málaga
10	Comans	ECN
	Forset	NINA

FI3P-CT920046-A21 905
 Mechanisms governing the behaviour and transport of transuranics (analogues) and other radionuclides in marine ecosystems.

1	Mitchell	Univ. Dublin - College
2	Gascó	CIEMAT
3	Guéguéniat	CEA - Cherbourg
4	Papucci	ENEA
5	Woodhead	MAFF
6	Holm	Univ. Lund
7	Sánchez-Cabeza	Univ. Barcelona - Autónoma
8	Dahlgaard	Lab. Risø
9	Salbu	Univ. Norway - Agricultural

A22 Natural radioactivity in the environment and its pathways to man.

FI3P-CT920035-A22 991
Pathways of radionuclides emitted by non nuclear industries.

1	Lembrechts	RIVM
2	Germain	CEA - FAR
3	Travesi Jiménez	CIEMAT
4	Ortins	Direcção-Geral do Ambiente
5	García-León	Univ. Sevilla
6	McGarry	RPII
7	Ortins	Direcção-Geral do Ambiente
8	Dahlgaard	Lab. Risø
9	Heaton	Univ. Aberdeen
10	Zagyvai	TUBUD.INT

FI3P-CT930075-A22 1059
Investigation on exposure to natural radionuclides in selected areas affected by U-processing.

1	Belot	CEA - FAR
2	Röhnsch	BFS
3	Massmeyer	GRS

A23 Influence of speciation, chemical modification, changes in physico-chemical properties and biological conversion.

FI3P-CT920010-A23 1085
The bio-availability of long-lived radionuclides in relation to their physico-chemical form in soil systems.

1	Lembrechts	RIVM
2	Wilkins	NRPB
3	Cremers	Univ. Leuven (KUL)
4	Merckx	Univ. Leuven (KUL)
5	Staunton	INRA - Montpellier
6	Berthelin	CNRS
7	Mocanu	ROIAP
8	Szabó	NRIRR (<i>PECO contract</i>)

FI3P-CT920022-A23 1169
Investigations and modelling of the dynamics of environmental HT/HTO/OBT levels resulting from tritium releases.

1	Bunnenberg	ZSR
2	Belot	CEA - FAR
3	Kim	Univ. München - Technische
4	Dertinger	KfK
5	Eikenberg	Inst. Paul Scherrer
6	Uchrin	HAS.II
7	Paunescu	IFIN

A24 The behaviour of accidentally released radionuclides, evaluation of the reliability of transfer parameters and experimental studies.

FI3P-CT920006-A24 1237
Transfer of radionuclides in animal production systems.

- | | | |
|---|----------------|----------------------------------|
| 1 | Howard | ITE |
| 2 | Assimakopoulos | Univ. Ioannina |
| 3 | Crout | Univ. Nottingham |
| 4 | Mayes | Inst. MacAulay Land Use Research |
| 5 | Voigt | GSF |
| 6 | Vandecasteele | CEN/SCK Mol |
| 7 | Zelenka | UAB.FAGR |
| 8 | Hove | Univ. Norway - Agricultural |
| 9 | Hinton | Inst. Paul Scherrer |

A25 The role of retention and release of radionuclides in natural ecosystems and in marginal agricultural areas.

FI3P-CT920016-A25 1327
Deposition of radionuclides on tree canopies and their subsequent fate in forest ecosystems - Further studies.

- | | | |
|---|---------|----------------------------|
| 1 | Minski | IMPCOL |
| 2 | Rauret | Fundació "Bosch i Gimpera" |
| 3 | Ronneau | Univ. Louvain (UCL) - LLN |

FI3P-CT920050-A25 1359
Cycling of cesium 137 and strontium 90 in natural ecosystems.

- | | | |
|----|--------------------|-------------------------------------|
| 1 | Wirth | BFS |
| 2 | Moberg | Inst. Nat. of Radiation Protection |
| 3 | Bergman | Swedish Defense Research Establish. |
| 4 | Palo | Univ. Agricultural Sci. of Sweden |
| 5 | Impens | Faculté Sciences Agronom. Gembloux |
| 6 | Belli | ENEA |
| 7 | Feoli | CETA |
| 8 | Nimis | Univ. Trieste |
| 9 | Antonopoulos-Domis | Univ. Thessaloniki |
| 10 | Pietrzak-Flis | CLRP Warsaw |

FI3P-CT920058-A25 1481
Radiation doses and pathways to man from semi-natural ecosystems.

- | | | |
|---|------------|---------------------------------------|
| 1 | McGarry | RPII |
| 2 | Horrill | NERC |
| 3 | Nielsen | Lab. Risø |
| 4 | Johanson | Univ. Umeå - Agr.Sci. - Dep. Forestry |
| 5 | Veresoglou | Univ. Thessaloniki |

A26 Development of countermeasures to reduce the contamination in the environment and to impede its transfer to man.

FI3P-CT920013a-A26 1533
Studies of methods for the rehabilitation of soils and surfaces after a nuclear accident (RESSAC).

- | | | |
|---|---------------|------------------------------------|
| 1 | Foulquier | CEA - Cadarache |
| 2 | Sandalls | UKAEA |
| 3 | Vandecasteele | CEN/SCK Brussels |
| 4 | Vallejo | Fundació "Bosch i Gimpera" |
| 5 | Förstel | KFA |
| 6 | Gutierrez | CIEMAT |
| 7 | Arapis | Univ. Athens |
| 8 | Kirchmann | Faculté Sciences Agronom. Gembloux |

FI3P-CT920049-A26 1617
Transfer of accidentally released radionuclides in agricultural systems.

- | | | |
|---|--------|----------------------------|
| 1 | Cancio | CIEMAT |
| 2 | Real | IPSN |
| 3 | Rauret | Fundació "Bosch i Gimpera" |

FI3P-CT930071-A26 1647
Influence of the food-processing techniques on the level of radionuclides in foodstuffs.

- | | | |
|---|-----------|---------------|
| 1 | Colle | CEA - FAR |
| 2 | Nicholson | UKAEA |
| 3 | Grandison | Univ. Reading |

VOLUME 2

**B FOLGEN DER STRAHLENEXPOSITION DES MENSCHEN; IHRE
ABSCHÄTZUNG, VERHÜNTUNG UND BEHANDLUNG
CONSEQUENCES OF RADIATION EXPOSURE TO MAN; THEIR
ASSESSMENT, PREVENTION AND TREATMENT
CONSEQUENCES POUR L'HOMME DE L'EXPOSITION AUX
RAYONNEMENTS; EVALUATION, PREVENTION ET TRAITEMENT 1685**

B1 Stochastic effects of radiation.

B1A EULEP

FI3P-CT920030-B1A 1687
Co-operative research on late somatic effects of ionizing radiation in the mammalian organism.

- | | | |
|---|--------|-------|
| 1 | Maisin | EULEP |
|---|--------|-------|

B11 Interpretation of low dose and low dose rate effects with the help of microdosimetry.

FI3P-CT920027-B11 *1705
Biophysical models for the effectiveness of different radiations.

- | | | |
|---|-------------|------------------|
| 1 | Paretzke | GSF |
| 2 | Goodhead | MRC |
| 3 | Terrissol | ADPA |
| 4 | Leenhouts | RIVM |
| 5 | Von Sonntag | Inst. Max-Planck |
| 6 | Smith | Univ. London |
| 7 | O'Neill | MRC |

FI3P-CT920041-B11 1769
Specification of radiation quality at nanometre level.

- | | | |
|---|----------|--------------------------|
| 1 | Colautti | INFN - Legnaro |
| 2 | Watt | Univ. St. Andrews |
| 3 | Harder | Univ. Göttingen |
| 4 | Leuthold | GSF |
| 5 | Izzo | Univ. Roma - Tor Vergata |
| 6 | Kraft | GSI |
| 7 | Pszona | SINS.PL |

B12 Repair and modification of genetic damage and individual radiosensitivity.

FI3P-CT920007-B12 1823
Molecular basis of radiosensitivity.

- | | | |
|---|------------------|---------------------------|
| 1 | Lohman | Univ. Leiden |
| 2 | Bridges | MRC |
| 3 | Bootsma | Univ. Rotterdam - Erasmus |
| 4 | Moustacchi | CIR |
| 5 | Thacker | MRC |
| 6 | Backendorf | Univ. Leiden |
| 7 | Eckardt-Schupp | GSF |
| 8 | Szumiel | ICHTJ |
| 9 | Szymczyk-Wasiluk | WMS |

FI3P-CT930080-B12 1889
Radiation induced mitotic aneuploidy.

- | | | |
|---|----------------|-----------------------|
| 1 | Parry | Univ. Wales, Cardiff |
| 2 | Tanzarella | CNR |
| 3 | Kirsch Volders | Univ. Bruxelles (VUB) |

B13 Cellular, molecular and animal studies to determine the risk of stochastic somatic effects of radiation with respect to low dose, low dose rate and radiation quality.

FI3P-CT920011-B13 1923
Cytogenetic and molecular mechanisms of radiation myeloid leukaemogenesis in the mouse.

- | | | |
|---|----------|------|
| 1 | Janowski | VITO |
| 2 | Cox | NRPB |
| 3 | Huiskamp | ECN |

FI3P-CT920017-B13 1937
Studies on radiation induced chromosomal aberrations.

- | | | |
|---|-----------|----------------------------|
| 1 | Natarajan | Univ. Leiden |
| 3 | Ortins | Direcção-Geral do Ambiente |
| 4 | Bryant | Univ. St. Andrews |
| 5 | Pantelias | NCSR "Demokritos" |
| 6 | Benova | NCRRP |

FI3P-CT920028-B13 1979
Radiation-induced processes in mammalian cells: principles of response modification and involvement in carcinogenesis.

- | | | |
|---|---------------|-------------------|
| 1 | Van der Eb | Univ. Leiden |
| 2 | Sarasin | CNRS |
| 3 | Devoret | CNRS |
| 4 | Rommelaere | DKFZ |
| 5 | Bertazzoni | CNR |
| 6 | Thomou-Politi | NCSR "Demokritos" |
| 7 | Herrlich | KfK |
| 8 | Simons | Univ. Leiden |
| 9 | Russev | BAS |

FI3P-CT920031-B13 2039
Studies on radiation-induced chromosome aberrations in mammalian cells. 2) Applied aspects.

- | | | |
|---|------------------|--------------------------|
| 1 | Olivieri | Univ. Roma "La Sapienza" |
| 2 | Cortés-Benavides | Univ. Sevilla |
| 4 | Palitti | Univ. Viterbo |
| 5 | Savage | MRC |
| 6 | Kalina | Univ. Safarikis |

FI3P-CT920042-B13 2071
Carcinogenic effects of low radiation doses and underlying mechanisms.

- | | | |
|---|------------|--------------|
| 1 | Davelaar | Univ. Leiden |
| 2 | Coppola | ENEA |
| 3 | Bentvelzen | TNO - Delft |
| 4 | Masse | CEA - Paris |
| 5 | Chmelevsky | GSF |
| 6 | Zurcher | TNO - Delft |

FI3P-CT920043-B13 2107
Measurement of oncogenic transformation of mammalian cells in-vitro by low doses of ionising radiation.

- | | | |
|---|------------------|------------------|
| 1 | Mill | Nuclear Electric |
| 2 | Frankenberg | Univ. Göttingen |
| 3 | Roberts | UKAEA |
| 4 | Tallone Lombardi | Univ. Milano |
| 5 | Kellerer | Univ. München |
| 6 | Saran | ENEA |

FI3P-CT920053-B13	2165
Molecular and cellular effectiveness of charged particles (light and heavy ions) and neutrons.		
1	Cherubini	INFN - Legnaro
2	Michael	Hosp. Mount Vernon
3	Goodhead	MRC
4	Belli	ISS
5	Sideris	NCSR "Demokritos"
6	Kiefer	Univ. Giessen
7	Reist	Inst. Paul Scherrer
FI3P-CT920063-B13	2231
New technologies in the automated detection of radiation-induced cytometric effects.		
1	Aten	Univ. Amsterdam
2	Nüsse	GSF
3	Bauchinger	GSF
5	Green	MRC
FI3P-CT920064i-B13	2275
The induction of chromosomal changes in human lymphocytes by accelerated charged particles.		
1	Edwards	NRPB
2	Natarajan	Univ. Leiden
3	Bimbot	CNRS
4	Dutrillaux	CIR
5	Kraft	GSI
FI3P-CT930067-B13	2317
Development and investigation of systems for the quantification of radiation induced carcinogenesis in humans.		
1	Mothersill	Inst. of Technology - Dublin
2	Riches	Univ. St. Andrews
5	Luccioni	CEA - Paris
6	Martin	CEA - IPSN
7	Arrand	Univ. Brunel
8	Franek	IMG-DFC
FI3P-CT930081-B13	2365
Development and validation of an image analysis system for automated detection of micronuclei in cytokinesis-blocked lymphocytes. A tool for biological dosimetry in individuals or populations occupationally or accidentally exposed to ionizing radiation.		
1	Tates	Univ. Leiden
2	Thierens	Univ. Gent
3	De Ridder	Univ. Gent

B14 Assessment of genetic risks in man.

FI3P-CT920005-B14 2389
Radiation-induced genetic effects in mammals and the estimation of genetic risks in man: a concerted approach using theoretical, epidemiological, cytogenetic, biochemical and molecular methods.

- 1 Sankaranarayanan Univ. Leiden
- 2 Tease MRC
- 3 Jacquet CEN/SCK Mol
- 4 Streffer Univ. Essen
- 5 Czeizel WHO

FI3P-CT920055-B14 2433
Genetic risks associated with exposure to ionizing radiation.

- 1 Favor GSF
- 2 Van Buul Univ. Leiden
- 3 Cattanach MRC
- 4 de Rooij Univ. Utrecht
- 5 Miró Ametller Univ. Barcelona - Autònoma
- 6 Eeken Univ. Leiden
- 7 Hulten EBHA

B15 Action of radionuclides on target cells in relation to radionuclide metabolism and studies on biological models for radionuclide-induced cancer.

FI3P-CT920021-B15 2487
Dose assessment early cellular and late carcinogenic effects of exposure to radon and its progeny.

- 1 Fritsch CEA - Paris
- 2 Collier UKAEA

FI3P-CT920051-B15 2513
Induction of osteosarcoma and leukaemia by bone-seeking alpha-emitting radionuclides.

- 1 Höfler GSF
- 2 Harrison NRPB
- 3 Wright MRC
- 4 Erfle GSF
- 5 Skou Pedersen Univ. Århus
- 6 Höfler Univ. München - Technische

B2 Non-stochastic Effects of Radiation.

B21 Radiation syndromes and their treatment after exposure of large parts of the body.

FI3P-CT920008-B21 2545
Research on the management of accidentally radiation exposed persons.

- 1 Fliedner Univ. Ulm
- 2 Wagemaker Univ. Rotterdam - Erasmus
- 3 Covelli ENEA
- 4 Jammet CIR

FI3P-CT930069-B21	2605
Radiation effects and their treatment on the connective and vascular tissues in various organs.		
1	Magdelenat	CIR
2	Van der Kogel	Univ. Nijmegen
B22	Irradiation and committed exposure from incorporated radionuclides.	
FI3P-CT920064b-B22	2617
Reduction of risk of late effects from incorporated radionuclides.		
1	Stradling	NRPB
2	Volf	KfK
3	Poncy	CEA - Bruyères-le-Châtel
4	Archimbaud	CEA - Pierrelatte
5	Burgada	ADFAC
6	Rencova	CHZ
B23	Radiation syndromes and their treatment after local exposure to skin and subcutaneous tissues.	
FI3P-CT920059-B23	2661
Radiation effects and their treatment after local exposure of skin and sub-cutaneous tissues.		
1	Masse	CEA - FAR
2	Hopewell	Univ. Oxford
3	Coggle	Hosp. St. Bartholomew
4	Di Carlo	IFO
B24	Radiation damage to lens, thyroid and other tissues of relevance in radiation protection.	
FI3P-CT930076-B24	2719
Thyroid and its proximate tissues radiation dosimetry; stochastic and deterministic biological effects in humans and model systems.		
1	Lamy	Univ. Bruxelles (ULB)
2	Malone	Hosp. Federated Dublin Voluntarys
3	Smyth	Univ. Dublin - College
4	Williams	Univ. Cambridge
B3	Radiation effects on the developing organism.	
B31	Damage to the central nervous system and hematopoiesis.	
FI3P-CT920015-B31	2763
Effects of protracted exposures to low doses of radiations during the prenatal development of the central nervous system.		
1	Reyners	CEN/SCK Brussels
2	Coffigny	CEA - Bruyères-le-Châtel
3	Ferrer	Hosp. Principes de España
4	Saunders	NRPB
5	Janeczko	Univ. Jagiellonian

B33 Transfer of radionuclides in utero.

FI3P-CT920064c-B33 2805

Dosimetry and effects of parental, fetal and neonatal exposure to incorporated radionuclides and external radiation.

- | | | |
|---|----------------|----------------------------|
| 1 | Harrison | NRPB |
| 2 | Henshaw | Univ. Bristol |
| 3 | Van den Heuvel | VITO |
| 4 | Lord | Inst. Paterson |
| 5 | Visser | TNO - Delft |
| 6 | Tejero | Univ. Madrid - Complutense |
| 7 | Bueren | CIEMAT |
| 8 | Archimbaud | CEA - Bruyères-le-Châtel |

VOLUME 3

**C RISKEN DER STRAHLENEXPOSITION UND IHRE BEWÄLTIGUNG
RISKS AND MANAGEMENT OF RADIATION PROTECTION
RISQUES ET GESTION DE L'EXPOSITION AUX RAYONNEMENTS 2877**

C1 Assessment of human exposure and risks.

C12 Exposure to natural radioactivity and evaluation of parameters influencing these risks.

FI3P-CT920025-C12 2879

Retrospective assessment of radon exposure from long-lived decay products.

- | | | |
|---|------------|------------------------------------|
| 1 | Vanmarcke | CEN/SCK Mol |
| 2 | McLaughlin | Univ. Dublin - College |
| 3 | Falk | Inst. Nat. of Radiation Protection |
| 4 | Poffijn | Univ. Gent |
| 5 | Fehér | HAS,RIAE (<i>PECO contract</i>) |
| 6 | Samuelsson | Univ. Lund |

FI3P-CT920034-C12 2921

Characteristics of airborne radon and thoron decay products.

- | | | |
|----|---------------|------------------------------------|
| 1 | Porstendörfer | Univ. Göttingen |
| 2 | Poffijn | Univ. Gent |
| 3 | Vanmarcke | CEN/SCK Brussels |
| 4 | Akselsson | Univ. Lund |
| 5 | Falk | Inst. Nat. of Radiation Protection |
| 6 | Tymen | Univ. Brest |
| 7 | Ortega | Univ. Catalunya - Politècnica |
| 8 | Lebecka | CMI |
| 9 | Kobal | IJS |
| 11 | Schuler | Inst. Paul Scherrer |

FI3P-CT920061-C12 3019
 Study of the different techniques to mitigate high radon concentrations level disclosed in dwelling.

- | | | |
|---|-----------------|----------------------------------|
| 1 | Sabroux | CEA - IPSN |
| 2 | Torri | ENEA |
| 3 | Ortins | Direcção-Geral do Ambiente |
| 4 | Quindós Poncela | Univ. Cantabria |
| 5 | Kritidis | NCSR "Demokritos" |
| 6 | Proukakis | Univ. Athens (Not yet submitted) |

FI3P-CT920064d-C12 3069
 Radon sources models and countermeasures.

- | | | |
|---|-----------|------------------------------------|
| 1 | Miles | NRPB |
| 2 | De Meijer | Univ. Groningen |
| 3 | Andersen | Lab. Risø |
| 4 | Wouters | CSTC-WTCB |
| 5 | Ball | NERC |
| 6 | De Meijer | Univ. Groningen |
| 7 | Hubbard | Inst. Nat. of Radiation Protection |
| 8 | Balek | BIJO |
| 9 | Cosma | NPL.RO |

FI3P-CT930074-C12 3159
 Evaluation of the combined helium/radon in soil gas mapping methodology as an indicator of areas in which elevated indoor radon concentrations may be found.

- | | | |
|---|---------------|---------------------------|
| 1 | Madden | RPII |
| 2 | O'Connor | Geological Survey (Irish) |
| 3 | Van den Boom | ENMOTEC GmbH |
| 4 | Porstendörfer | Univ. Göttingen |

C13 Comparative assessment of exposure and risks.

FI3P-CT920019-C13 3219
 Comparative assessment and management of radiological and non-radiological risks associated with energy systems.

- | | | |
|---|--------------|-----------------|
| 1 | Dreicer | CEPN |
| 2 | Friedrich | Univ. Stuttgart |
| 3 | Uijt de Haag | RIVM |

FI3P-CT920064e-C13 3249
 Studies related to the expression of the detriment associated with radiation exposure.

- | | | |
|---|-----------|------|
| 1 | Muirhead | NRPB |
| 2 | Schneider | CEPN |

C14 Epidemiological studies in human populations.

FI3P-CT920047-C14 3271

Investigation of late effects in humans after artificial irradiation (Thorotrast-patients)
- Follow-up study.

- | | | |
|---|------------------|---------------------------------------|
| 1 | van Kaick | DKFZ |
| 2 | Priest | UKAEA |
| 3 | Wallin | KBFOC |
| 4 | dos Santos Silva | School Hygie.and Tropic.Med. - London |
| 5 | Malveiro | Inst. Higiene e Medicina Tropical |

FI3P-CT920056-C14 3303

The risk assessment of indoor radon exposure.

- | | | |
|---|-------------|-----------------------|
| 1 | Poffijn | Univ. Gent |
| 2 | Tirmarche | CEA - FAR |
| 3 | Kreienbrock | Univ. Wuppertal |
| 4 | Kayser | Dir. Santé Luxembourg |
| 5 | Darby | ICRF |
| 6 | Miles | NRPB |
| 7 | Kunz | NIPHE.CRH |
| 8 | Kunz | CHZ |
| 9 | Cosma | NPL.RO |

FI3P-CT920062-C14 3341

European childhood leukaemia/lymphoma incidence study.

- | | | |
|---|------------|------|
| 1 | Parkin | IARC |
| 2 | Gurevicius | LOC |
| 3 | Rahu | ECR |
| 4 | Tulbure | IISP |

FI3P-CT920064f-C14 3351

Epidemiological studies and tables.

- | | | |
|----|-------------|----------------------|
| 1 | Muirhead | NRPB |
| 2 | Kellerer | Univ. München |
| 3 | Chmelevsky | GSF |
| 4 | Oberhausen | Univ. Saarlandes |
| 5 | Holm | Inst. Karolinska |
| 6 | Becciolini | Univ. Firenze |
| 7 | Richardson | INSERM |
| 8 | Hill | Inst. Gustave Roussy |
| 9 | de Vathaire | INSERM |
| 10 | Wick | GSF |
| 11 | Spiess | Univ. München |
| 12 | Kellerer | Univ. München |
| 13 | Muirhead | NRPB |
| 14 | Kellerer | GSF |
| 15 | Kolb | Univ. München |
| 16 | Socie | Hosp. St. Louis |

FI3P-CT930065-C14 3473
Risk estimates of lung cancer from the follow-up of uranium miners.

- | | | |
|---|------------|-----------|
| 1 | Chmelevsky | GSF |
| 2 | Tirmarche | CEA - FAR |
| 3 | Muirhead | NRPB |
| 4 | Darby | ICRF |
| 5 | Kunz | NIPHE.CRH |

FI3P-CT930066-C14 3529
International collaborative study of cancer risk among nuclear industry workers.

- | | | |
|---|----------|-------|
| 1 | Cardis | IARC |
| 2 | Sztanyik | NRIRR |
| 3 | Cesnek | SEP |

C2 Optimisation and management of radiation protection.

C2A ICRP

FI3P-CT920004-C2A 3547
Development of fundamental data for radiological protection.

- | | | |
|---|-------|------|
| 1 | Smith | ICRP |
|---|-------|------|

C21 Optimisation of radiological protection.

FI3P-CT920033-C21 3555
Alara in installations.

- | | | |
|---|----------|-------------|
| 1 | Lefaire | CEPN |
| 2 | Zeevaert | CEN/SCK Mol |
| 3 | Pfeffer | GRS |
| 4 | Wrixon | NRPB |

C22 Reduction of patient exposure in medical diagnostic radiology.

FI3P-CT920014-C22 3597
Digital Medical Imaging: Optimization of the dose for the examination.

- | | | |
|---|-----------|------------------------------------|
| 1 | Malone | Hosp. Federated Dublin Voluntaries |
| 2 | Faulkner | Hosp. Newcastle |
| 3 | Busch | Univ. Heidelberg |
| 4 | Jankowski | IOM |
| 5 | Shehu | Inst. Onkologijise |

FI3P-CT920020-C22 3653
Quality assurance parameters and image quality criteria in computed tomography.

- | | | |
|---|-----------|----------------------------|
| 1 | Jessen | Univ. Århus - Hospital |
| 2 | Ortins | Direcção-Geral do Ambiente |
| 3 | Schneider | Univ. München |
| 4 | Moores | IRS Ltd. |

FI3P-CT920024-C22	3691
Diagnosis related dose: an investigation on patient risk and image quality in european hospitals.		
1	Van Loon	Univ. Bruxelles (VUB)
2	Thijssen	Univ. Nijmegen
3	Milu	IHPH
4	Karlinger	SUM

FI3P-CT920037-C22	3723
Optimisation of image quality and reduction of patient exposure in medical diagnostic radiology.		
1	Maccia	CAATS
2	Moores	IRS Ltd.
4	Dance	Hosp. Royal Marsden
5	Padovani	Unitá Sanitaria Locale - Udine
6	Vañó Carruana	Univ. Madrid - Complutense
FI3P-CT920052-C22	3759
Patient dose from radiopharmaceuticals.		
1	Smith	Hosp. Great Ormand Street
3	Petoussi	GSF
4	Evans	Univ. London
FI3P-CT920064g-C22	3797
Medical dose assessment and evaluation of risk.		
1	Wall	NRPB
2	Drexler	GSF
3	Fitzgerald	Hosp. St. Georges
4	Zoetelief	TNO - Delft
FI3P-CT930070-C22	3839
Evaluation of dose and risk due to interventional radiology techniques.		
1	Schmidt	Klinikum Nürnberg
2	Maccia	CAATS
3	Padovani	Unitá Sanitaria Locale - Udine
4	Vañó Carruana	Univ. Madrid - Complutense
5	Neofotistou	Hosp. General Athens
C23	Management of radiological protection in normal and accident situations.	
FI3P-CT920013b-C23	3873
Evaluation and management of post-accident situations. Project 1: Database and decision-aiding techniques.		
1	Després	CEA - FAR
2	Alonso	Univ. Madrid Politéc, Fundación Gral.
3	French	Univ. Leeds
4	Vanderpooten	Univ. Paris IX

FI3P-CT930068-C23	3913
	Assessment and management of post accidental situations. Radiation detriment, risk perception and risk communication.	
1	Brenot	CEA - FAR
2	Joussen	IFS
3	Sjoberg	CFR
C24	Probabilistic risk assessment and real-time models for assessing the consequences of accidental releases and for evaluating effectiveness and feasibility of countermeasures.	
FI3P-CT920023-C24	3943
	CEC/USNRC joint project on uncertainty analysis of probabilistic accident consequence codes.	
1	Goossens	Univ. Delft
2	Haywood	NRPB
3	Ehrhardt	KfK
4	Boardman	UKAEA
5	Roelofsen	ECN
6	Hofer	GRS
FI3P-CT920036-C24	3973
	Development of a comprehensive decision support system for nuclear emergencies in Europe following an accidental release to atmosphere.	
1	Ehrhardt	KfK
2	Gland	EDF
3	Müller	GSF
4	French	Univ. Leeds
5	Sohier	CEN/SCK Mol
6	Haywood	NRPB
7	Bleasdale	Nuclear Electric
8	Zelanzy	IEA, CCC
9	Kanyar	OSSKI
10	Zelasny	Cyfronet
11	Mateescu	IFIN
12	Stubna	NPPRI
FI3P-CT920038-C24	4109
	Deposition of artificial radionuclides, their subsequent relocation in the environment and implications for radiation exposure.	
1	Tschiersch	GSF
2	Roed	Lab. Risø
3	Brown	NRPB
4	Goddard	IMPCOL
5	Roed	Lab. Risø
6	Rybacek	CSAS,IRD
7	Jansta	Inst. Radioecology
8	Zomoori	KFKI

FI3P-CT920044-C24 4225
 Coordination of atmospheric dispersion activities for the real-time decision support system under development at KFK.

- | | | |
|---|------------------|-----------------------------------|
| 1 | Mikkelsen | Lab. Risø |
| 2 | ApSimon | IMPCOL |
| 4 | Desiato | ENEA |
| 5 | Rasmussen | DMI |
| 6 | Thytkier-Nielsen | Lab. Risø |
| 7 | Bartzis | NCSR "Demokritos" |
| 8 | Massmeyer | GRS |
| 9 | Deme | HAS.RIAE (<i>PECO contract</i>) |

FI3P-CT920057-C24 4291
 Methodology for evaluating the radiological consequences of radioactive effluent released in accidents - the MARIA project.

- | | | |
|---|---------------|---------------------------------------|
| 1 | Jones | NRPB |
| 2 | Ehrhardt | KfK |
| 3 | Alonso | Univ. Madrid Politéc. Fundación Gral. |
| 4 | Van der Steen | KEMA N.V. |
| 5 | Iordanov | BAS |
| 6 | Koblinger | AEKI |

FI3P-CT930073-C24 4357
 Analysis and modelling of the migration of radionuclides deposited in catchment basins of fresh water systems.

- | | | |
|---|---------------|--------------|
| 1 | Monte | ENEA |
| 2 | Van der Steen | KEMA N.V. |
| 3 | Boardman | UKAEA |
| 4 | Kozhoukharov | BAS |
| 5 | Bergström | Studivisk AB |

FI3P-CT930077-C24 4411
 Multifractal analysis and simulation of Chernobyl radioactive fall-out in Europe.

- | | | |
|---|-----------|-------------|
| 1 | Ratti | Univ. Pavia |
| 2 | Schertzer | CNRM |

IV. Koordinierungstätigkeit
 Coordination activities
 Activités de coordination 4435

V. - ERPET -
 Europäische Aus-und Fortbildung auf dem Gebiet des Strahlenschutzes
 European Radiation Protection Education and Training
 Enseignement et formation européens en Radioprotection 4477

VI.	Auswahl einiger auf Veranlassung der Kommission erschienener Veröffentlichungen Selection of publications issued on the initiative of the Commission Choix des publications éditées à l'initiative de la Commission	4495
VII.	Liste des Acronyme und Abkürzungen List of acronyms and abbreviations Liste des acronymes et des abréviations	4541
VIII.	Verzeichnis der Forschungsgruppenleiter List of research group leaders Index des chefs de groupes de recherche	4545

III C

RISIKEN DER STRAHLENEXPOSITION UND IHRE BEWÄLTIGUNG

RISKS AND MANAGEMENT OF RADIATION PROTECTION

RISQUES ET GESTION DE L'EXPOSITION AUX RAYONNEMENTS



Final Report 1992-1995

Contract: F13PCT920025 Duration 1.9.92 to 30.6.95

Sector: C12

Title: Retrospective assessment of radon exposure from long-lived decay products.

- | | | |
|----|------------|------------------------------------|
| 1) | Vanmarcke | CEN/SCK Mol |
| 2) | McLaughlin | Univ. Dublin - College, UCD |
| 3) | Falk | SSI Stockholm (SSI contract) |
| 4) | Poffijn | Univ. Gent |
| 5) | Fehér | HAS.RIAE (PECO contract) |
| 6) | Samuelsson | Lund University, LU (SSI contract) |

I. Summary of Project Global Objectives and Achievements

The main objectives of the RARE (Retrospective Assessment of Radon Exposure) project are to study the chain of processes in the indoor environment which leads from airborne radon to trapped long-lived radon daughters (LRnDs) and to reveal those exposure conditions in which the trapped activity concentration is a useful estimate of the lung cancer risk caused by radon exposure.

Based on the experience gained from the first phase of the RARE project (CEC Contract No. B17-CT90-0013) the project period 1992-95 has resulted in necessary and important developments for practical application of RARE methods. Major advancements in background discriminating track-etch devices for specific measurement of implanted ^{210}Po have been made and together with progresses in the volume-trap approach, large-area alpha spectrometry, and chemical analyses of surface activities, there now exist a whole range of RARE techniques that can be applied for instance in radon epidemiology investigations. The development of reliable ^{210}Po track-etch devices is of special significance, making large-scale and non-destructive *in situ* investigations of implanted ^{210}Po feasible. The volume trap technique developed and investigated by Mol is also of great importance as the surface trap problem of plate-out variabilities is avoided.

The task of using the track-etch techniques for autoradiographic measurement of implanted ^{210}Po has been approached from several different angles. Three different track-etch materials have been investigated using commercial available CR-39, LR115, and Makrofol. The two latter materials must be supplied with attenuation foils in order to be sensitive to the 5.3 MeV alpha particle from ^{210}Po . In order to obtain reasonable specificity and sensitivity for implanted ^{210}Po in glass surfaces it is necessary to correct for alpha background. The bulk alpha activity of glass materials can vary substantially but is dominated by energy degraded low-energy alpha particles. SSI has investigated three different background subtraction techniques, the Front/Back, Absorption foil, and the CR-39/LR115 difference methods. The Front/Back method works well but requires that the backside of the glass sample is accessible to measurement and that it has not been exposed to the indoor atmosphere, a fact that exclude this method from being generally applicable. An absorption foil of thickness 1.8 mg/cm² between the glass surface and the CR-39 reduces the ^{210}Po tracks by 20% and the background tracks by 50%, but according to SSI this absorption method has certain drawbacks apart from being less specific. Handling thin foils in practice is awkward and it is also difficult to avoid additional background tracks. As a consequence SSI has abandoned the absorption method in favour of the CR39-LR115 difference

method.

The alpha energy acceptance window for Kodak LR115 is below the alpha energy of ^{210}Po (5.3 MeV). Autoradiography with CR-39 and LR115 track-etch detectors side by side means that CR-39 measures ^{210}Po + background, while the LR115 film only responds to the alpha background. The use of two different detector materials is laborious but yields excellent results. Tested on well known ^{210}Po surface activities on glass panes of different background intensities the CR-39/LR115 difference method gave a standard deviation of less than 1 Bq m^{-2} in the ^{210}Po determination. One restriction in the applicability of LR115 films is that exposure to UV light (sunlight) is deleterious, as pointed out and shown experimentally by Gent.

Another technique for specific ^{210}Po measurement with track-etch detectors is based on the fact that the area of the track opening in the CR-39 surface is related to the alpha particle energy. By a careful standardization of all exposure and etching conditions it is shown by UCD that an operational energy resolution of 0.5 MeV can be achieved. By mounting two discs of CR-39 on perspex frame a device for a simultaneous measurement of ^{210}Po , airborne radon gas, and plate-out has been developed by UCD. The ^{210}Po and radon gas sensitivity quoted by UCD is $71 \text{ tracks cm}^{-2} \text{ per kBq h m}^{-2}$ and $1.66 \text{ tracks cm}^{-2} \text{ per kBq h m}^{-3}$ respectively. By comparison, SSI reports for their CR-39 device a ^{210}Po sensitivities of $80 \text{ tracks cm}^{-2} \text{ per kBq h m}^{-2}$, while the Makrofol detector used by the Gent group is less sensitive, $22 \pm 0.6 \text{ tracks cm}^{-2} \text{ per kBq h m}^{-2}$.

Radiochemical separation methods to extract and measure ^{210}Bi from glass surfaces have been utilized by HASRIAE. A comparison of radiochemistry and CR-39 autoradiographic methods on the same sample showed consistent and well correlated ($r^2 = 0.93$) results. Though destructive to the sample, the radiochemistry method applied to surface traps is an important complement to surface alpha spectrometry. By radiochemistry ^{210}Pb can be analyzed more directly and the demand on sample surface flatness can be relaxed.

Radiochemical methods are necessary when utilizing LRnD trapped in porous materials (i.e. volume traps). Mol has calibrated polyester samples in a radon room and by correcting for the sample density the linear increase of ^{210}Pb volume activity a_v of the porous material follows the equation $a_v = 0.0481 \pm 0.0009 \text{ mBq cm}^{-3} / (\text{kBq m}^{-3} \text{ y})$. Using 100 cm^3 of polyester material the detection limit at 30% uncertainty is estimated to 100 Bq m^{-3} over 20 years. The first *in situ* exercises involving volume traps were performed by the Mol group during the contract period.

Pulse ionization chambers (PIC) have been used by Gent and LU for large-area alpha spectrometry. By improving the shielding characteristics of the chamber the energy resolution of the LU detector is now below 40 keV (FWHM) for several hours measurement on 20 cm diameter glass samples. The versatility of the PIC detector as a laboratory instrument has been demonstrated by LU. The ^{210}Po areal distribution on glass samples from radon houses has been measured by scanning the surface with a collimated (circular or slit) detector. By this scanning technique the fall off in implanted activity in the glass very close to the surrounding frame was revealed. PIC detectors have been very useful to the program as reference alpha spectrometers of large-area glass sheet ^{210}Po sources.

Many field measurements using the different RARE techniques mentioned above have been designed and tested. The evaluation of the obtained results is not straightforward, especially in the case where the exposure age and history of the samples investigated are not well defined.

LU has followed four framed glass samples in a high level radon dwelling occupied by an elderly couple. During a period of 3.5 years radon was measured by track-etch detectors (from SSI) attached to each sample, and each time the radon detectors were exchanged a measurement of the implanted ^{210}Po activity was taken by the PIC detector. The results stress the importance of exposure geometry. The growth of implanted ^{210}Pb was very consistent at all four locations, despite large seasonal variations in radon concentration, but the ^{210}Pb growth rate on the two objects placed deliberately at recessed positions was low by 45 and 65%, respectively, compared

to the two frames openly exposed on a wall. When also the existing glass objects in the house were analysed an exposure period up to about 45 years was covered. For such a long time span it is always difficult to estimate the true radon exposure, but even so there is a clear tendency that the oldest samples contains lower activity of implanted ^{210}Pb than expected. The observation that the ratio of implanted ^{210}Pb to integrated Rn decreases faster with exposure time than theoretically predicted, is also made by HASRIAE, investigating dwellings in Hungary, and by UCD using their ^{210}Po track-etch devices in 41 houses in Belgium, Germany, Ireland and Sweden. Further investigations are needed in order to establish the reason why the effective half life of implanted ^{210}Pb in glass objects appears to be less than 22 years.

RARE techniques utilizing LRnD activities left behind in dwellings are a true low-radioactivity task and involves many complexities and it is strongly recommended that RARE methods are applied with care. Since small track-etch devices for ^{210}Po measurements are available, many-sample-per-house investigations can now be performed within a reasonable budget. Such a multi-approach, with both surface and volume traps is recommendable in order to increase the accuracy in the assessment of risks connected to radon exposure. It should be noted that with a limited budget there exists no alternative methods to the RARE techniques that can quantify radon exposure in retrospect and that can be applied on a large-scale basis.

Head of project 1: Dr. Vanmarcke

II. Objectives for the reporting period

Investigation of volume-traps as long-term radon monitors by analysing the α -activity of ^{210}Po deposited inside the material :

- 1 Selection of appropriate material.
- 2 Determination of the conversion factor between the α -activity and the radon exposure
- 3 Investigation of the influence of specific material properties

Performance of in-situ measurements.

III. Progress achieved including publications

In order to retrospectively radon exposures in dwellings it has been proposed to measure the ^{210}Po -activity implanted in glass-surfaces [1,2]. Since this signal depends on the plate-out of the short-lived radon decay products it is strongly influenced by the attachment rate to aerosol particles and the fluctuations in plate-out rate due to local turbulences, the precision of this method is at best about a factor of 2 [3,4]. Therefore, SCK•CEN started measuring the ^{210}Po -activity of the decay products deposited in volume traps, e.g. spongy materials used for mattresses. Since these materials have a long diffusion length for radon, but are inaccessible for its decay products, the signal should be better related to the radon exposure.

Experimental conditions and analysis

Recently produced polyester material has been exposed to radon-laden air. The exposures correspond to radon concentrations between 390 Bq/m^3 and 3.9 kBq/m^3 over a 20 years period. After a waiting period of about 138 d in a radon-free environment ($< 20 \text{ Bq/m}^3$) to let ^{210}Po approaching radioactive equilibrium, samples of about 100 cm^3 were cutted from the inside and treated chemically to separate ^{210}Po . The efficiency of the separation procedure was determined individually by adding a radioactive tracer material (^{208}Po). For details it is referred to

refs. [5,6,7]. At the end of the procedure the polonium autodeposited on a silver-plate, which finally was analysed by means of α -spectrometry.

Polyester samples with four different densities have been investigated. In Fig. 1 the measured specific sample activity a_s (mBq/g) is shown as a function of the radon exposure. Measurements on unexposed samples for background determination are included. Different symbols refer to different sample densities ρ_s . All data show a perfectly linear dependence on the radon exposure. The calibration factor, i.e. the slope, decreases with increasing sample density ρ_s . This effect is due to the decreasing ratio of the air volume to the polyester volume. The relative uncertainty on the calibration factors are of the order of 2 %.

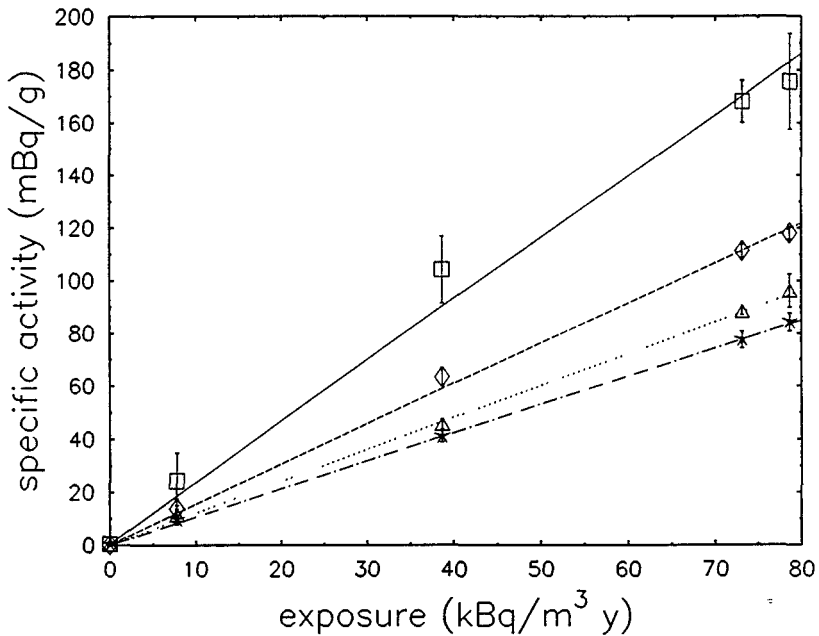


Fig. 1: Specific sample activity a_s as a function of the radon exposure. Different symbols refer to different sample densities. The lines indicate the respective linear regression fit to the experimental data.

Discussion

Our results indicate that this technique is more accurate by at least one order of magnitude compared to other common methods based on the measurement of ^{210}Po implanted in glass surfaces. In case of polyester materials the detection limit for a measuring period of about 108 h is estimated to about $2 \text{ kBq/m}^3 \text{ y}$ at 30 % uncertainty. This corresponds to an average radon concentration of 100 Bq/m^3 over 20 years.

In a next step the data have further been reduced by multiplying them by the corresponding sample density ρ_s . The resulting volume activity a_V expressed in mBq/cm^3 should be independent of ρ_s . Furthermore, assuming the diffusion length for radon much larger than the dimension of the material, the conversion factor $a_{V(1)}$ can be directly derived from the number of deposited ^{210}Pb -atoms per unit exposure ($\text{kBq/m}^3 \text{ y}$)

$$a_{V(1)} = 0.0455 \text{ mBq/cm}^3 / (\text{kBq/m}^3 \text{ y}) \quad (1)$$

In order to compare this value with the experimental data a correction factor k_f for the effective free air volume inside the sample material has to be applied to the data, which is defined by

$$k_f = (\rho_m - \rho_s) / (\rho_m - \rho_l), \quad (2)$$

where ρ_m and ρ_l are the density of the material (polyester $\rho_m = 1.05 \text{ g/cm}^3$) and air ($\rho_l = 0.00125 \text{ g/cm}^3$), respectively. Thus, the volume activity a_V is calculated by

$$a_V = \rho_s a_s / k_f \quad (3)$$

In the present case an average value $\bar{k}_f = 0.969$ has been applied to the data. In Fig. 2 the volume activity a_V (symbols) is shown as a function of the radon exposure together with the corresponding linear regression fit (full line). The fitted slope, i.e. the conversion factor,

$$a_{V(1)} = 0.0481 \pm 0.0009 \text{ mBq/m}^3 / (\text{kBq/m}^3 \text{ y}), \quad (4)$$

which is in very good agreement with the expected value from eq. (1). Therefore, considering the volume activity a_V of a sample this new retrospective radon monitor is not only very accurate as well as very sensitive, but applicable to all types of volume-trap materials.

First in-situ monitoring

Up to now two different samples could be acquired from dwellings with different radon histories. First, mattress filling material (wool) from a house with actually very low radon concentrations was analysed. The sample density $\rho_{s,1}$ during exposure could be estimated to 0.0285 g/cm^3 ($\pm 13\%$). From five measurements of about 5 d an average volume activity of about $(5.5 \pm 1.9) \mu\text{Bq/cm}^3$ was obtained corresponding to a radon exposure of only $0.2 \text{ kBq/m}^3 \text{ y}$ ($\pm 35\%|_{\text{stat}} \pm 13\%|_{\text{sys}}$). The data are shown in Fig. 3 (•). Considering an exposure period of 25 y, this result demonstrates the high sensitivity of this monitoring method.

The second sample was a wrapped table-cloth, which is entirely not a volume trap. However, it was stocked in a cupboard 10~cm above the floor during about 38 y and radon could have been diffused through the inner layers. Due to the inhomogeneity the sample density $\rho_{s,2}$ during exposure could only be estimated with an uncertainty of more than 20% to 0.28 g/cm^3 . The data in Fig. 3 (▲) roughly divide into two groups, which might be attributed to surface effects from different layers of the table-cloth. The average volume activity was determined to $(3.72 \pm 0.43) \text{ mBq/cm}^3$, which corresponds to an annual average radon concentration of $(1.5 \pm 0.2|_{\text{stat}} \pm 0.3|_{\text{sys}}) \text{ kBq/m}^3$. The reported average radon concentration obtained by CR-39 track-etch detectors during two succeeding years was $(3.2 \pm 1.5) \text{ kBq/m}^3$ [8]. However, the

reported annual average concentrations differ by more than a factor of 6. Taking this into account the agreement is remarkable and shows the flexibility of the presented retrospective radon monitor with respect to the investigated sample material

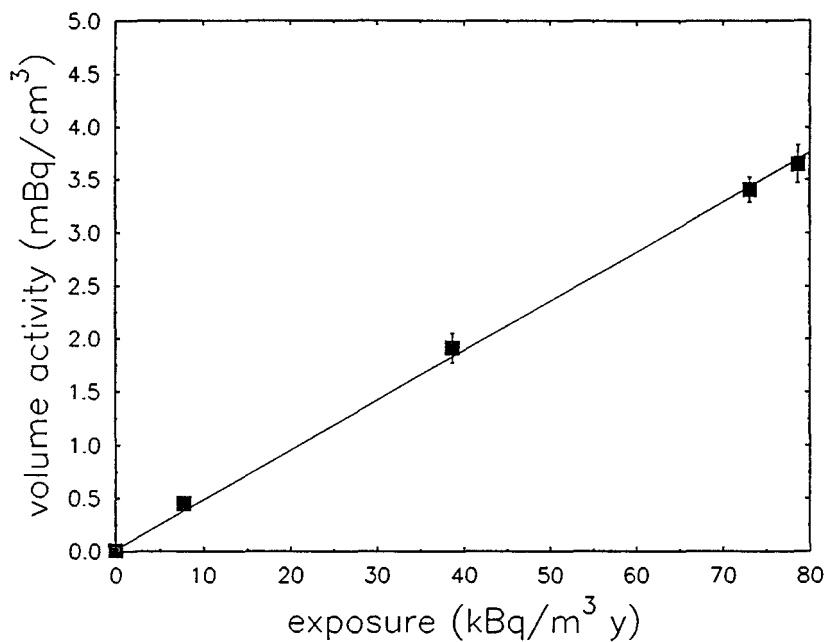


Fig 2 : Volume activity a_V as a function of the radon exposure The full line indicates the linear regression fit to the experimental data.

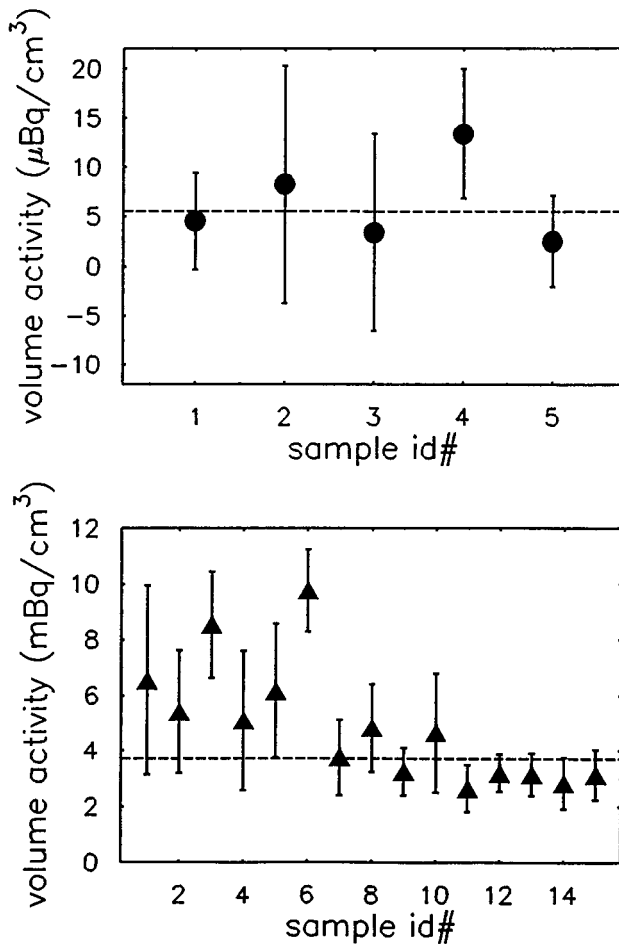


Fig 3 : Results from two in-situ monitoring exercises; (1) Mattress filling material (•) . the data indicate radon exposures close to the detection limit. (2) wrapped table cloth (▲) : not entirely a volume-trap material, fluctuations are due to inhomogeneities of the sample material (see text).

References

- [1] Lively R S and E P. Ney, *Surface radioactivity resulting from the deposition of ^{222}Rn daughter products*, Health Phys. 52 (1987) 411
- [2] Samuelsson C , *Retrospective determination of radon in houses*, Nature 334 (1988) 338
- [3] Cornelis J , C Landsheere, A. van Trier, H. Vanmarcke and A. Poffijn, *Experiments on glass-absorbed Polonium-210*, Appl. Radiat. Isot. Vol 43, No 1/2 (1992) 127
- [4] Samuelsson C , L Johansson and M Wolff, *^{210}Po as a tracer for radon in dwellings*, Rad Prot Dos Vol 45 (1992) 73
- [5] Oberstedt S and H Vanmarcke, *Volume Traps - A New Retrospective Radon Monitor*, SCK•CEN Internal Report BLG 666, and Health Phys , in press
- [6] Benoit G and H F Hemond, *Improved Methods for the measurement of ^{210}Po , ^{210}Pb and ^{226}Ra or Biogeochemistry of lead-210 and polonium-210 in fresh waters and sediments*, NTIS report PB88-227467 (1988) 30
- [7] Narita H., K Harada, W C Burnett, S Tsunogai and W. J Mc Cabe, *Determination of ^{210}Pb , ^{210}Bi and ^{210}Po in natural waters and other materials by electrochemical separation*, Talanta Vol 36 (1989) 925
- [8] Tóth E , private communication (1995)

Contributions to International Conferences and Journals

Recent Investigations on Indoor Radon at SCK•CEN Mol

- ✦ S. Oberstedt and H. Vanmarcke, Euregional Symposium on Radon in our EUREGIO Nov. 4-6, 1993, Liège (Belgium) and Annales de l'Association belge de Radioprotection, Vol 19, 1-2 (1994) 255

Radon in the Indoor Environment

S Oberstedt, H. Vanmarcke, SCK•CEN scientific report (1993) 114

Retrospective Assessment of Radon Exposure in Dwellings by Investigating Spongy Materials

S. Oberstedt and H. Vanmarcke, Verhandlungen der DPG Frühjahrstagung Hamburg, März 1994

Personal Radon Dosemeter

S Oberstedt and H. Vanmarcke, SCK•CEN Internal Report BLG 649, March 1994

Volume Traps - A New Retrospective Radon Monitor

S Oberstedt, H Vanmarcke, SCK•CEN Internal Report BLG 666, November 1994, and Health Phys , in press

Radon in the Indoor Environment

S. Oberstedt, H. Vanmarcke, SCK•CEN scientific report (1994), in press

Volume Traps as Retrospective Radon Monitors

S. Oberstedt and H. Vanmarcke, Verhandlungen der DPG Frühjahrstagung Berlin, März 1995

Radon in the Indoor Environment (A Status Report)

S. Oberstedt, Scientific Programme Report (1 02.93-31.01.95), SCK•CEN Internal Report BLG 679, March 1995

Retrospective Radon Monitoring in Spongy Materials

S. Oberstedt, H. Vanmarcke, Sixth International Symposium on the Natural Radiation Environment June 5-9, 1995, Montreal (Canada), Book of Abstracts, p. 175

Riskassessment via Retrospective Radon Monitoring

S. Oberstedt, H. Vanmarcke, International Conference on Healthy Buildings in Mild Climate (healthy buildings '95), September 11-14, 1995, Milano (Italy)

Head of project 2: Dr. McLaughlin

II. Objectives for the reporting period

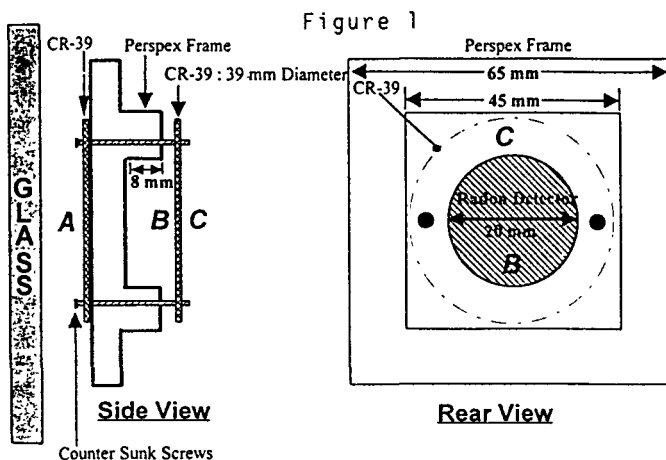
The main objective for the reporting period was to develop and field test practical passive alpha track detector methods suitable for large scale in-situ measurements of recoil implanted Polonium-210 in glass surfaces in dwellings. A principal aim of this work was to develop these alpha track techniques to be of assistance to radon epidemiological studies of the general population by improving retrospective radon exposure estimates. In addition, using room models, these techniques could be used to determine whether a significant difference exists between present and past radon levels in dwellings.

III. Progress achieved including publications

Detector Development.

A new detector configuration for use in dwellings was developed together with a protocol for its use. A number of different configurations were constructed and tested for field suitability. The final design chosen is shown in Figure 1. Two discs of the alpha track plastic CR-39 are mounted on a perspex frame. When the detector frame is attached using a strong adhesive tape to a glass surface as shown in Figure 1 surface A of one CR-39 disc is in direct contact with the glass. It records alpha activity from both Po-210 on the glass surface and also from the intrinsic bulk alpha activity of the glass. By means of alpha track geometry analysis, as described later, those tracks due to Po-210 may be identified. Surface B of the second CR-39 disc faces into an 8 mm deep air cavity thus forming a small radon diffusion chamber. Surface B is thus used to obtain the contemporary radon gas concentration in a room of a dwelling during the exposure period. Surface C which faces into the room air behaves as an open face detector and records alpha particles from airborne activity and from plateout shortlived radon progeny activity. As

the central part of Surface C is covered with an adhesive paper disc alpha tracks are only recorded on the annulus around this disc. If the adhesive disc were not used optical effects due to the high track density on surface C would make it difficult to achieve accurate alpha track counting on surface B.



A : Surface A : ^{210}Po in Glass Signal

B : Surface B : ^{222}Rn Signal

C : Surface C : ^{214}Po Plateout Signal

This detector configuration is, in principle, capable of giving quantitative information on the following:

- (a) The recoil implanted Polonium-210 surface activity on the glass (from the analysis of alpha tracks on surface A).
- (b) The contemporary concentration of Radon-222 in the dwelling air (by means of surface B track density)
- (c) The contemporary equilibrium surface activity of Polonium-214 by means of surface C used as a surrogate for the glass surface.

The sensitivities, to their respective sources, of surfaces A and B were as follows :

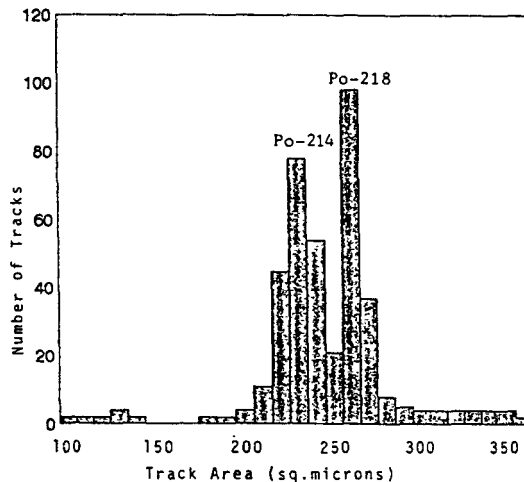
Surface A (for Po-210): $0.198 (+/- 0.0184) \text{ tracks} \cdot \text{m}^{-2} \cdot \text{Bq}^{-1} \cdot \text{m}^2 \cdot \text{sec}^{-1}$
 This sensitivity was determined on the basis of pulse ionisation chamber measurements of Po-210 on glass surfaces carried out by contract partners at Lund and at Gent Universities.

Surface B (for Rn-222): $1.66 \text{ tracks} \cdot \text{cm}^{-2} \cdot \text{kBq}^{-1} \cdot \text{m}^3 \cdot \text{hr}^{-1}$
 This sensitivity was determined by intercalibration against standard closed radon detectors and by the use of radon gas standards from the National Physical Laboratory (UK).

As the alpha track density on surface C is a complex function of of airborne activity and plateout conditions each detector must be individually analysed for the Po-214 activity measurement.

The principal methods used to identify alpha tracks from individual emitters such as Po-214 or Po-210 was based on the analysis of track geometrical characteristics. Two such approaches were used. In the Dublin laboratory by means of Americium-241 sources and electrostatically collected shortlived radon progeny an image analysis system (Quantimet Q520) was used to establish the relationship between alpha track area (the area of the track intersection opening at the CR-39 surface) and alpha track energy. Track area is determined on the basis of the product of major and minor axis. An example of this for an electrostatically collected Po-218/Po-214 is shown in Figure 2. It should be noted, in keeping with CR-39 track formation characteristics for the etching conditions used, that the higher energy and longer range Po-214 alphas produces track areas at the surface which are smaller than those for the lower energy alphas from Po-218.

Figure 2



It was found that an operational alpha energy resolution of about 0.5 MeV could be achieved. As track formation in CR-39 changes with the age of the plastic an improvement on this energy resolution for field measurements cannot be realistically expected. In a second approach to alpha energy identification a number of detectors already processed and analysed in Dublin were sent to the TASL laboratories at Bristol University for analysis. The TASL/Bristol method of analysis measures a number of separate geometrical features of each track at different depths in the CR-39 and uses them in iterative equations that describe track formation. A number of self calibrating relationships between the track parameters are applied that allow adjustment to be made for such phenomena as plastic ageing. A comparison carried out between the Dublin and Bristol methods of analyses showed that

the mean values for Po-210 levels on glass agreed within 3.5 %.

Field Work

In order to minimise background effects and other potential contributors to measurement error a strict protocol was formulated for field trials of the detectors. This protocol covered detector transport, placement in dwellings and the recovery phase. Its main features are as now described.

Control detectors were used in all cases. Detectors were at all times, except during exposures, kept in heatsealed radon proof bags. Before attaching a detector to a glass surface the surface was cleaned using alcohol. Following cleaning the portion of the glass surface to be measured was covered with a sheet of thin cardboard (a plateout shield) for a period of at least an hour if possible. This plateout shield fulfilled two objectives. Firstly it allowed recently deposited shortlived radon progeny activity on the glass to decay to acceptable levels. This might otherwise contribute significantly to the track density on surface A of the detector when exposed to the glass. Secondly the plateout shield prevented the fresh buildup of plateout activity on the glass during the period of its use. In order to minimise background effects the detector was removed from its heat sealed radon proof bag and immediately mounted on the glass following the removal of the plateout shield. After the period of exposure, which ranged from some days to a number of weeks the detector was removed and immediately sealed in a radon proof bag together with a background control detector for dispatch to the laboratory. Where possible such heat sealing took place in a low radon environment (i.e. outdoor air) to avoid the inclusion of high radon content dwelling air with the detector.

As part of the protocol a detailed questionnaire was prepared and used in field measurements. This contained questions relating to dwelling occupants and information on the dwelling and its use which were considered relevant to interpretation of the detector data. The most important parameter that was sought was the age of the glass chosen for measurement. Where possible a photograph of each detector mounted on the glass and its surroundings was taken. This together with information on room surface to volume ratios, ventilation patterns and aerosol conditions were needed to apply modified Jacobi room models in the interpretation of detector data. As aerosol or ventilation measurements cannot for practical/economic reasons be part of large scale field measurements only approximate assessments of these parameters can be made from answers to questions relating to smoking, cooking and ventilation habits of the occupants.

In the main phase of the work field measurements were successfully carried out in a total of 41 houses in a number of countries : Belgium, German, Ireland and Sweden. In the case of the German exposures these were in houses chosen with the assistance of BfS (Berlin) in a former uranium mining district in the east of Germany. In the last three months of the contract period

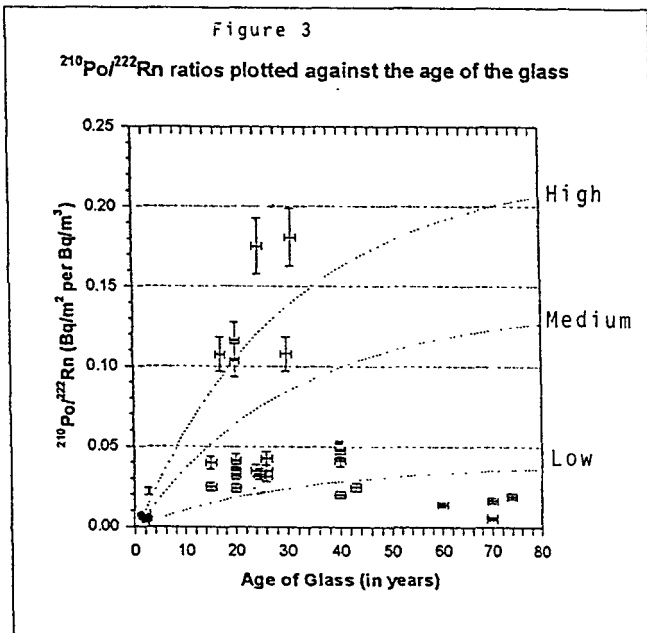
detectors of a modified form were placed, in collaboration with BfS, in a further 15 houses in this area. At the time of writing these latter detectors are still been analysed.

The field exposure conditions for the detectors were quite varied. The ages of the glasses chosen for Po-210 measurements ranges from about 1.3 to 75 years and included window glasses, mirrors, furniture glass and picture frame glass. The contemporary radon levels in these houses ranged from about 20 to 20000 Bq/m³.

The results of most of these field tests are presented in Figure 3 where the ratio of the measured Po-210 surface activity on the glass to the contemporary Radon-222 concentration is plotted against the age of the glass. Included in Figure 3 are three curves labelled High, Medium and Low. The High and Low curves represent the boundaries, using a modified Jacobi room model procedure, of the likely extremes of plateout conditions in most normal dwellings and the Medium curve represents typical likely conditions. The table below gives the values of relevant parameters used to generate these curves.

Plateout regime	Ventilation rate (hr ⁻¹)	Room surface to volume ratio (m ⁻¹)	Attachment rate const. (hr ⁻¹)
Low	1.5	2	500
Medium	0.55	3	50
High	0.2	4	5

Plateout/deposition velocities of radon decay products used here are : 5 m.hr⁻¹ (unattached) and 0.05 m.hr⁻¹. (attached)



Many of the experimental points lie well within the envelope bounded by the High and Low curves. The data points for seven houses with glasses of age less than three years are clustered together and because of measurement uncertainties at low Po-210 levels it is difficult to decide if they lie within the acceptable plateout boundary curves. Of some interest to retrospective radon exposure assessment are a number of points obtained from houses in the former uranium town of Schneeberg. A group of points in Figure 3 for glasses of age between 60 and 75 years from these houses all lie below the Low plateout curve. This indicates that for a substantial period in the past it is likely the radon levels in these houses were much lower than at present. This is not an unreasonable hypothesis as mining galleries lie directly under many of these houses and since the cessation of mining ventilation has been reduced or eliminated with a consequential increase in house radon levels compared to those during the past period of mining. The ongoing analysis of the most recent exposures to glasses in another uranium mining town in the east of Germany will in part be used to address this hypothesis.

The field tests have demonstrated that the use of passive alpha track detectors for the assessment of radon exposure in the past based on Po-210 measurements on glass surfaces is a viable technique. It is a technique that can easily be integrated in future radon epidemiological studies of the general population.

Publications

Mc Laughlin, J.P. and Fitzgerald, B. "A new technique to measure the activities of short-lived radon progeny deposited on surfaces." Radiation Protection Dosimetry, Vol 45, 115, 1992.

Mc Laughlin, J.P. "Radon in the Context of Indoor Air", Annalen van de Belgische Stralingbescherming Vol 19, Nos 1-2, 1994.

Mc Laughlin, J.P. and Fitzgerald, B "Models for determining the response of passive alpha particle detectors to radon and its progeny in cylindrical detecting volumes." Radiation Protection Dosimetry, Vol 50, 241, 1994.

Fitzgerald, B. and Mc Laughlin, J.P. " The measurement and assessment of Polonium-210 surface activity on glasses in dwellings." Natural Radiation Environment VI International Symposium, Montreal Canada, June 5-9 1995.

Head of project 3: Dr. Falk

II. Objectives for the reporting period

To develop a field method for the measurement of ^{210}Po implanted in indoor glass surfaces, using autoradiographic alpha-track methods.

To test and compare the developed methods on glass panes with well known ^{210}Po surface activity, with special consideration to variation in background activity.

To study the feasibility to use a combination of CR-39 and Kodak LR-115 detectors for measurement of ^{210}Po and background on glass panes during laboratory and field conditions.

Adoption of the technique to field measurement.

III. Progress achieved including publications

Autoradiographic alpha-track methods for the measurement of ^{210}Po implanted in glass surfaces have been investigated with the aim to find a simple and reliable method for field use.

There are several sources of error associated with estimation of past radon concentration from measurements of implanted ^{210}Pb in indoor surfaces. The "plate-out" of ^{222}Rn decay products on surfaces is dependent on many factors as aerosol concentration, air movements etc. and may result in non-uniform surface activity distribution as well as different activity levels for same radon exposure. These aspects have been studied by colleagues in the RARE- group.

One limiting factor when using autoradiographic alpha-track methods for the measurement of ^{210}Po implanted in glass surfaces is the alpha particles emitted from background activity in the glass and the different activity levels found among glass panes. The energy spectrum of the alpha-particles emanating from the background source differs however from the ^{210}Po surface source.

An alpha-spectrum taken with a large area pulse-ionisation chamber (Cooperation with University of Lund, Samuelsson) from a glass surface show a continuous energy spectrum from the alpha activity in the bulk material and on top of it a narrow energy peak from the surface implanted ^{210}Po activity. This fact can be used to discriminate the background from the signal.

The CR-39 detector, with simple number of tracks counting technique, we use for ordinary radon detectors (Mellander et al., 1992) is also used for the measurement of the surface implanted ^{210}Po activity

Another technique, where the track dimensions are used to analyse the energy of the alpha-particle detected, was investigated by others in the "RARE-group".

Three different methods have been tested and evaluated

In the first method, which is the simplest, is the CR-39 detector surface attached directly against the glass surface to be investigated. The track density is in this case the sum of the ^{210}Po alphas and the alphas from the glass itself. When the backside of the glass has not been exposed to indoor atmosphere, e.g. a glass pane covering a photo, an additional CR-39 detector can be attached to the backside for a specific background measurement.

The second method tested is based on an absorption technique. With this technique, two CR-39 detectors were used. One detector is directly attached against the glass surface. The other detector has an absorber placed between the glass surface and the CR-39 detector. The absorber chosen is a mylar foil coated with a thin layer of aluminium and with a total thickness of 1.8 mg/cm^2 . The thickness of the absorber was chosen so that most of the alpha particles emitted from the surface will penetrate the absorber and leave tracks, while alpha particles emitted from activity within the glass to a lesser extent will be recorded, due to absorption both in glass and in the absorber. Both detectors are placed side by side on the same glass surface.

In the third method, two different detector materials are used, CR-39 and KODAK LR-115 cellulose-nitrate film. The KODAK LR-115 is sensitive to alpha particles with energies in the range 1.2 - 4.8 MeV while the CR-39 is sensitive for alpha-particles up to much higher energies. As the alpha particles from ^{210}Po have an energy of 5.3 MeV, they will not be detected by the LR-115 while a part of the background alphas will be detected. By using the LR-115 and CR-39 side by side on glass panes the background of the glass is measured by the LR-115 and the background and signal by the CR-39 detector.

Sensitivity and background levels

Earlier measurements show that the intrinsic background alpha-activity of the glass is an important limiting factor for the measurement of low levels of ^{210}Po surface activity. Autoradiographic exposure of several glass panes with known ^{210}Po surface activity has been performed and analysed. These glass panes have been measured with a well calibrated large pulse ionisation chamber at Lund University (L. Johansson, B. Roos and C. Samuelsson. Alpha-Particle Spectrometry of Large-Area Samples using an Open-Flow Pulse Ionization Chamber, Appl. Radiat. Isot. 43(1/2) 119-125 (1992).) The back side of the glass panes all have an insignificant surface activity of ^{210}Po .

For all three methods investigated it is necessary to ensure that the **background** alpha activity surface distribution is uniform. The back side of several glass panes were covered with CR-39 detectors and exposed. No significant unevenness could be found. Figure 1 is an example of results obtained from this study.

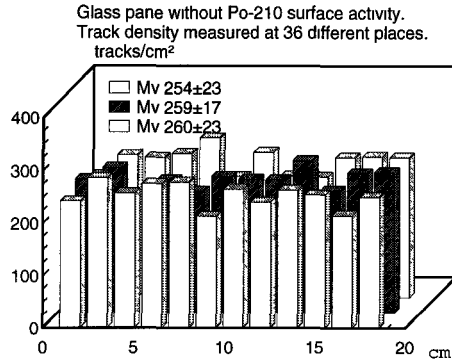


Fig.1 Measured uniformity of background alpha-activity

Simplest technique

To establish the relation between the surface activity of ²¹⁰Po and the net track density for the CR-39 detector a number of glass panes with known surface activity of ²¹⁰Po were autoradiographically exposed during 100 days. Both the front side and the back side of the panes were monitored.

Figures 2 and 3 shows the relation between the ²¹⁰Po surface activity and the track density for seven different glass panes. The results of repeated exposures are also shown in the figures.

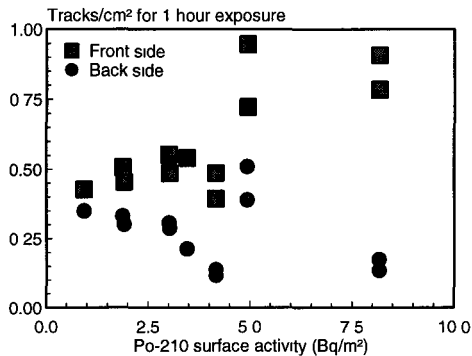


Fig 2. The relation between the ²¹⁰Po surface activity and the track density for CR-39 detectors placed both on front side and back side of glass panes .Most of the samples were measured twice..

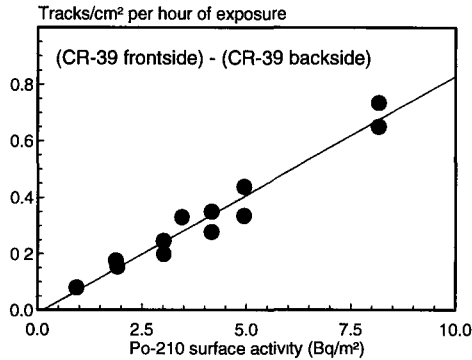


Fig 3. Net track surface density as function of surface activity

The sensitivity as tracks·cm⁻² (per hour the detectors have been in contact with the active surface) / Bq·m⁻² (²¹⁰Po surface activity) is shown in Figure 4 as a function of the ²¹⁰Po surface activity. The sensitivity is found to be the same within a standard error of about 5% when the backside of the glass is used as background

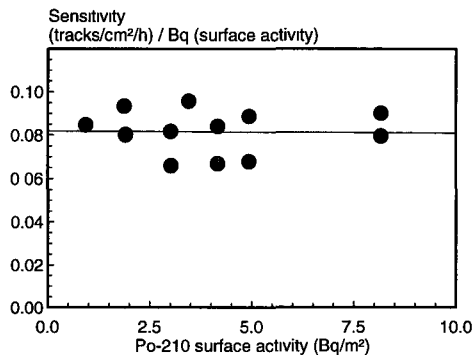


Fig 4. Sensitivity for CR-39 to surface activity of ²¹⁰Po.

The detector efficiency for ²¹⁰Po alphas is 28 %. As can be seen in Fig 2, the background track density shows a substantial variation between different glass panes. This variation of the background activity is found to be so large that only higher radon levels with exposure times over 15-20 years could be measured with acceptable accuracy. The method is however useful if one can measure the unexposed backside of the glass pane with another detector simultaneously.

Absorber technique

The use of two CR-39 detectors in parallel on the same side where one has an absorber between glass surface and detector surface enable a rough estimation of the background activity for each separate pane. The 1.8 mg/cm² absorber is found to reduce the ²¹⁰Po tracks with 20 % and the background tracks with 50 %. There are however a couple of drawbacks

with the absorption method. When handling the detectors with absorber foil between the glass pane and the detector, additional background tracks could not be avoided. This uncertainty combined with the fact that the signal is reduced and the difference between two fairly similar numbers gives an unnecessary high uncertainty at low surface activity. Nevertheless it is found that the sensitivity of the CR-39 absorption technique can be satisfactory if the glasses are exposed to normal or higher levels of radon in houses for more than 15 years.

The (CR-LR) difference technique

The use of the two different detector materials is more laborious as it involves establishment of two different routines for handling and etching the detectors. More care has to be taken when using the LR-115 material as it is much more sensitive to impurities and temperature gradients during the etching with NaOH compared to CR-39.

The evaluation of this method is done by exposures of LR-115 and CR-39 in parallel on seven different glass panes with known ^{210}Po surface activity. Both the "active-" and the "back-" side of the glass panes were exposed to the two sets of detectors for 81 days. To assess the internal background from the detectors a number of detector sets was "exposed" to an inactive surface (blank measurement) of Plexiglas during the same period. The results of these measurements are presented in Fig 5 and 6. Figure 5 shows the results obtained from measurement with LR 115 on seven glass panes both on front side with known ^{210}Po activity and on the back side. Repeated measurements are also shown in the figure.

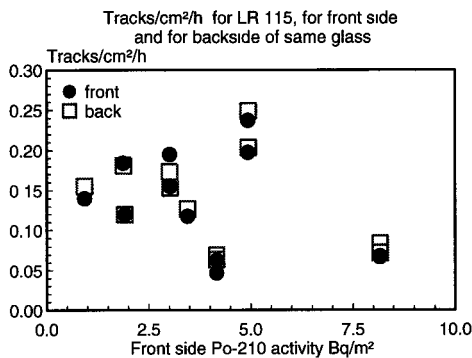


Fig 5. Tracks/cm²/h on LR115 for frontside and for back side of same glass
Front side has known ^{210}Po activity, backside no ^{210}Po activity.

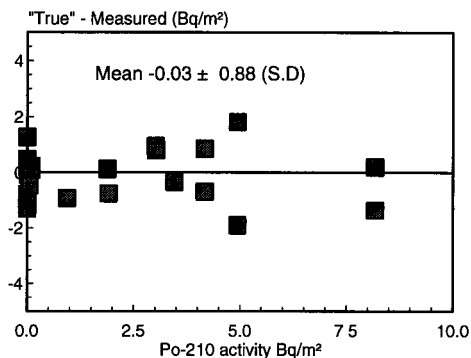


Fig 6. Deviation between given and measured ^{210}Po surface activity on glass panes using (CR-LR) difference technique

Measurements with CR-39 and LR-115 side by side on the backside of the glass panes gave the relation between the background sensitivity for the two different detector materials. By knowing the ^{210}Po surface activity and the time the detector had been in contact with surfaces the following relation was obtained.

$$^{210}\text{Po surface activity (Bq}\cdot\text{m}^{-2}) = (\text{CR}_n - 1.97 \cdot \text{LR}_n) / 0.081$$

where CR_n and LR_n is the net tracks/cm² per hour of exposure of the detectors to the glass panes. An exposure to an inactive surface of Plexiglas is used to assess the intrinsic background of the two detector materials.

Applying this relation to repeated measurements of these panes both on front side and back side show that the (CR-LR) difference method gave correct value with a standard deviation of less than 1 Bq·m⁻², see Fig 6. This result can be compared with results from a single measurement with one CR-39 detector giving deviation from the correct value between 1.8 and 6.1 Bq·m⁻². The conclusion from these measurements using the (CR-LR) difference method is that there is no need to separately measure the background of the glass pane, which under field conditions generally often is impossible.

Field studies and conclusions.

To investigate how the method performs during field conditions, 20 sets of "(CR-LR) detectors" and radon detectors were distributed to 10 colleagues at our institute.. After 81 days of exposure the glass detectors as well as radon detectors were evaluated. With the experiences gained from this field study an additional set of 21 dwellings were monitored in the same way for about 3 month. These dwellings in middle of Sweden were a part of a selection of detached houses investigated for other reasons. All these dwellings had been monitored for radon previously.

Fig 7 show the relation between measured surface activity of ^{210}Po on glass panes and estimated radon exposure.

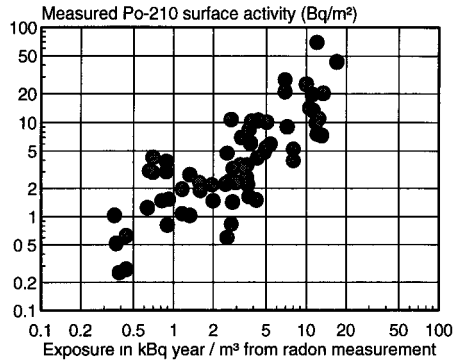


Fig 7. Measured relation between surface activity of ^{210}Po on glass panes and estimated radon exposure of the glass panes. The measured values are normalised to an exposure time of 20 years.

Radon exposure is estimated by using available radon concentration data and the time each separate surface items had been exposed. For most cases a mean value of earlier and actual radon data is used. As a complete radon history of the dwellings is not obtainable large uncertainties are attributed to the exposure data. To have comparable data the surface activity of ^{210}Po is normalised to 20 years exposure in the figure. The normalisation, where the build-up and decay of ^{210}Pb and ^{210}Po is taken into account, is done with the assumption that the radon concentration and the plate-out rate had been the same over the years. From these field studies it is obvious that the ^{210}Po surface activity is correlated to the past radon history. It can also be seen in the figure that there are quite large differences in estimated radon exposure for the same measured ^{210}Po surface activity. This difference include, beside the uncertainty in radon exposure estimation, also the different plate-out rates for the actual surface, which depend on aerosol concentration, air movements, ventilation rate etc. Despite these and possible other uncertainties, it is demonstrated that the measurement of long-lived radon progeny on hard surfaces can be used to estimate the past radon history for the subject and is thus a complementary and alternative technique for assessing the radon exposure in radon epidemiological studies. Another advantage of the method is that a *single* measurement of personal belonging, as e.g. a mirror, or a alarm clock, will act as a personal radon exposure meter even if the person has changed dwelling several times. The method also gives the possibility to assess radon data from dwellings that no longer exist.

Publications:

H. Mellander and A. Enflo. The alpha track method used in the Swedish radon epidemiological study. Rad. Prot. Dosim. 45, 1/4 pp 65-71 1992.

R. Falk, H. Mellander L. Nyblom and I. Östergren. Retrospective Assessment of Radon Exposure by Measurements of ^{210}Po Embedded in Surfaces Using an Alpha Track Detector Technique. Presented at NRE-VI, June 5-9, 1995, Montreal, Canada. Submitted for publication in Environmental International, 1995.

Head of project 4 : Dr. A. Poffijn

II. Objectives for the reporting period

- Jacobi Room Model calculations to investigate the influence of the different indoor parameters with respect to the implanted ^{210}Po activity.
- Development of a secondary reference ionization chamber for calibration of passive retrospective detectors.
- Development of a simple and easy to use passive retrospective detector for later use in epidemiological studies.

III. Progress achieved including publications

For a given radon concentration, the total amount of implanted ^{210}Po is determined by different parameters. This can be described by the Jacobi Room Model (Jacobi, 1972; Raabe, 1969). The most important parameters are the ventilation rate (l_v), the attach rate to aerosols (X) and the deposition rates on surfaces (l_{du} and l_{da}). These parameters are mainly determined by local conditions in the dwelling such as aerosol concentration and distribution, ventilation patterns, ... In order to estimate the influence of the different parameters on the total implanted ^{210}Po activity, computer simulations have been performed on the basis of the Jacobi Room Model. These simulations show that, for a given radon concentration, the influence of the ventilation rate on the implanted ^{210}Po activity is negligible. The attach rate and thus the aerosol conditions of the dwelling however have a big influence. This can result in a difference of a factor 2 depending on smoking or non-smoking conditions. The influence of the deposition rate is less important as this parameter is relatively constant for different dwellings (Vanmarcke, 1986).

Theoretical calculations on the behavior of radon progenies in glass have been conducted (Cornelis, 1993). These calculations are necessary to obtain an answer on questions like how far the implanted layer of radon progenies extends into the glass and to what extent dust and grease deposited on the glass surface may influence the full implantation of the radon progenies. The most fundamental reason for these calculations however is to know the escape probability of the implanted ^{210}Pb recoil nuclei towards the surface of the glass. This value is needed as a parameter in the Jacobi Room Model that gives a relation between the radon levels in air and the ^{210}Po activity implanted in glass.

^{214}Pb and ^{210}Pb distributions have been evaluated, starting from a thin ^{218}Po or ^{214}Po source deposited on a flat surface. For this purpose, we applied a procedure based on the theory of low energy heavy ion ranges in amorphous media. During our experiment, we encountered ^{214}Pb ions with recoil energies of 112 keV and ^{210}Pb ions with recoil energies of 146 keV. Using these parameters together with parameters for the average composition of glass, depth distributions for ^{214}Pb and ^{210}Pb can be calculated (fig 1). These calculations show that the implanted layer thickness for both nuclei is not bigger than 55 nm.

The α decay of ^{214}Po coming from implanted ^{214}Pb modifies this implanted distribution because of the recoil energy the daughter nucleus gets. This results in deeper implantation on the one hand and loss due to ejection out of the glass on the other hand. This escape probability follows from the calculations and is 29.8 %. The resulting distribution is also given in fig 1. In reality, the ^{210}Po distribution will always be a mixture of both ^{210}Pb curves. The portion of each line depends on the air activity properties and especially on the attachment rate to aerosols.

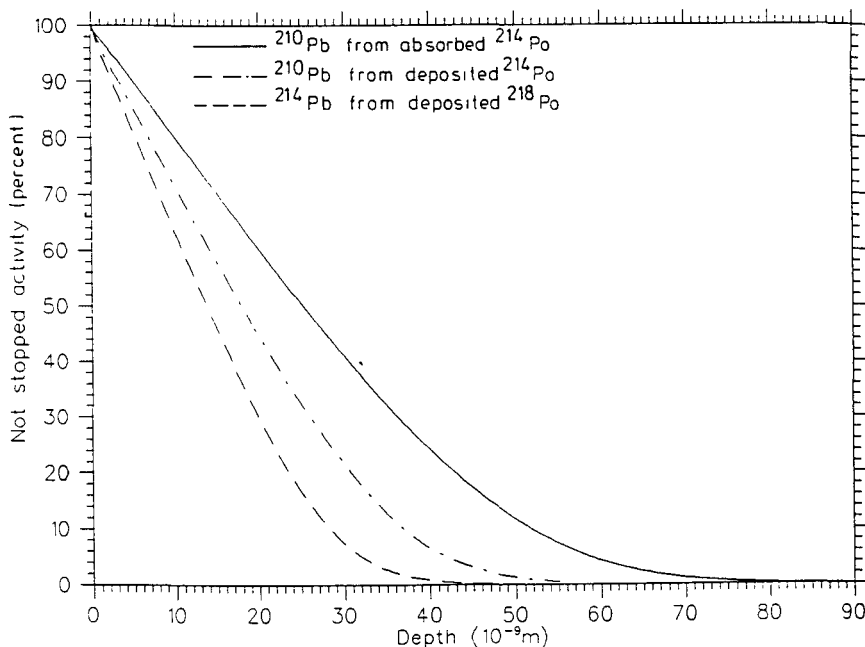


Fig. 1: The penetration depth distribution of ^{214}Pb and ^{210}Pb nuclei in glass. Deposited ^{218}Po produces the dashed distribution of ^{214}Pb , which turns, by the α -decay of ^{214}Po , into the distribution of ^{210}Pb . Deposited ^{210}Po produces the dot and dash distribution of ^{210}Pb .

A pulse ionization chamber of the open flow type was constructed as a secondary standard for calibrating active glass sheets (Meesen, 1992). This chamber is of the same design as our partner from Lund University. The active measuring surface is 380 cm². The obtained α energy resolution is 100 keV. A typical spectrum from a glass sheet is given in fig 2.

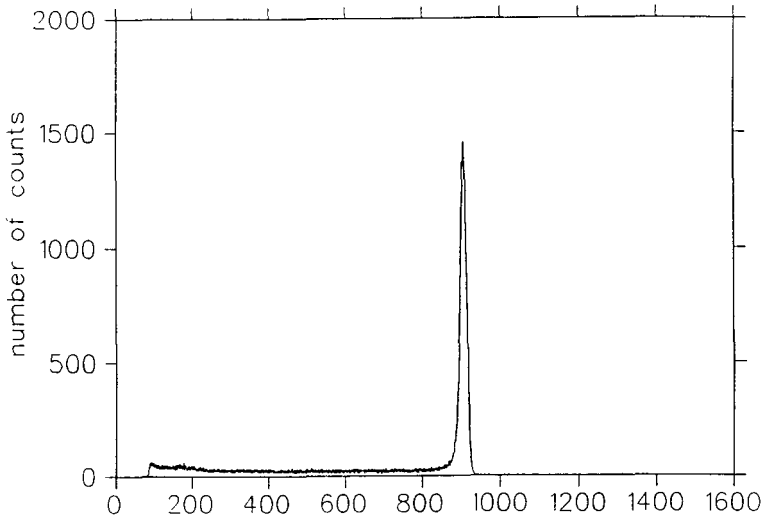


Fig. 2 : α spectrum of implanted ^{210}Po in glass. Measured by a pulse ionisation chamber.

For large scale measurements of the implanted ^{210}Po activity, different passive detectors have been developed by the different partners in the project. The detector developed in Gent (Meesen, 1993) is based on polycarbonate Makrofol foils with a diameter of 47 mm (frequently used in radon detectors based on diffusion chambers). In our standard etching conditions, the foils have an optimum sensitivity for α particles with energies between 0.3 - 2.0 MeV (Vanmarcke, 1986). Because of this energy window, it was necessary to lower the energy of the α particles emitted by ^{210}Po (5.31 MeV). For this purpose, a 23 μm layer of Mylar is placed between the glass plate and the detector material. The choice of this thickness has been confirmed by Monte Carlo simulations of α particles emitted from a simulated ^{210}Po layer in glass. The combination of Makrofol detector and Mylar is mounted on the glass by means of an adhesive tape, large enough to hold the detector firmly to the glass for a long period. This total setup is called the " ^{210}Po detector".

In order to calibrate the ^{210}Po detector, a large flat reference source with high implanted ^{210}Po activity was needed. This source was prepared by constructing a box of glass with dimensions 50 x 50 x 2 cm (Meesen, 1992). This box was flushed with radon gas in a closed circuit during 105 days. This resulted in an average implanted ^{210}Po activity (after ingrowth) of 2000 Bq/m² with a variation of 15 % over the surface of the glass.

The ^{210}Po detector was calibrated by exposing different series of detectors on one spot of the glass plate. The activity on the calibration spot as measured by a calibrated surface barrier detector was $2160 \pm 90 \text{ Bq/m}^2$. The response curve is shown in fig 3. The slope of the linear fit gives a response factor of $22.0 \pm 0.6 \text{ (tracks/cm}^2\text{)/(h kBq/m}^2\text{)}$.

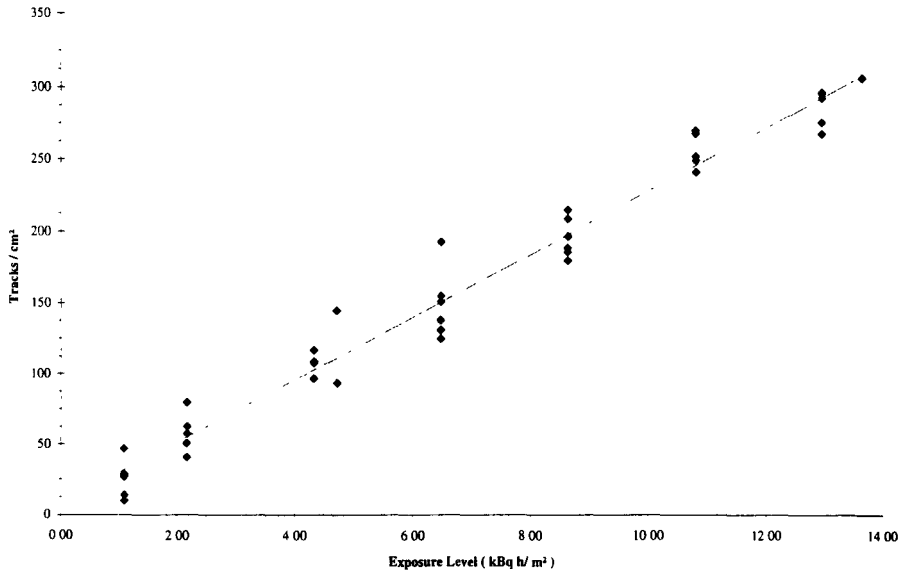


Fig. 3 : Response curve for retrospective ^{210}Po detector.

Tests have shown that long time storage of Makrofol detectors can increase the number of background tracks on the foils (Meesen, 1995). Because of the low surface activities to measure, a low background is desirable. To reduce the number of background tracks, the foils are heated to a temperature of 100 °C during 48 hours before α irradiation. This procedure reduces the number of background tracks from 36 ± 5 (tracks/cm²) to 7 ± 4 (tracks/cm²). The sensitivity is reduced by 10 %. The long term stability of this heat treatment is good.

During their exposure in dwellings, the passive ^{210}Po detectors can also be exposed to direct ultra violet light from the sun. The influence of this part of the light spectrum has been investigated. These tests consisted of illuminating different kind of passive detectors with ultra violet light during 2 and days before and after mono energetic α exposure. These 7 days simulate direct sunlight during 4 to 6 months, depending on the season and the country. The results give an indication that Makrofol shows little or no effect from UV illumination. CR-39 gave less tracks after UV exposure and showed an increase in bulk etch rate. The LR-115 gave poor results. Even after an exposure of only 2 days, the red color of the film disappeared completely after etching. These results show that exposure sites facing direct sunlight have to be avoided.

Considering our current calibration, the ^{210}Po detector can measure 1 Bq/m² of implanted ^{210}Po activity with an accuracy of 16 % (1σ) in 6 months. This corresponds with 50 Bq/m³ radon during 10 years of exposure (calculated by means of the Jacobi Room Model with appropriate parameters). Preparations for using the detector on a large scale in the framework of a national survey are being made. As the radon measurements itself last for 6 months, the lower sensitivity of Makrofol compared to CR-39 and LR-115 gives no big problems.

References.

Vanmarcke, H. (1986). De bijdrage van het woonmilieu tot de blootstelling aan straling afkomstig van nucliden uit de natuurlijke ^{238}U reeks. In : *Ph.D. Dissertation*.

IV. Publications

Meesen, G. (1992). Studie en ontwikkeling van een referentiepulsonisatiekamer voor retrospectieve radonbepalingen. In : *Licentiaat Thesis*.

Cornelis, J., H. Vanmarcke, C. Landsheere, A. Poffijn (1993). Modeling radon progeny absorbed in glass. *Health Physics*, 65, 414-417.

Meesen, G., J. Uyttenhove, A. Poffijn, K. Van Laere, J. Buysse (1993). Passive detector for measurement of the implanted ^{210}Po activity in glass. In : *Nuclear Science Symposium 1993, Conference records, Part1*. 236-239.

Meesen, G., J. Uyttenhove, A. Poffijn, K. Van Laere, J. Buysse (1994). Passive detector for measurement of the implanted ^{210}Po activity in glass. *Annales de l'Association belge de Radioprotection*, 19, n° 1-2, 275-282.

Meesen, G., A. Poffijn (1994). Use of retrospective radon measurements for risk assessment. *Annales de l'Association belge de Radioprotection*, 19, n° 4, 573-577.

Meesen, G., A. Poffijn, J. Uyttenhove, J. Buysse (1995). Study of a passive detector for retrospective radon measurements. *Radiation Measurements*, 25, n° 1-4, 591-594.

II. Objectives for the reporting period (15.9.1993 till 30.6.1995)

1. Development of a method for a long-term integrating radon concentration measurement to monitor the experimental irradiation to be performed for testing the retrospective methods. Calibration were performed at NRPB, Harwell, UK and at the EML, New York, U.S.A.
2. Development of radiochemical and SSNTD methods to measure the concentration of ^{210}Bi and ^{210}Po in glass, and comparison of two methods.
3. Taking into consideration the effects of dirtiness during the exposure and cleaning of the glass surface.
4. Investigation of samples from Mátraderecske and other areas of interest in Hungary.

III. Progress achieved including publications

1. Long-term integrating radon concentration measurement in air

For the purpose the same system as developed at NRPB (U.K.) was introduced. The dosimeter is a small and robust diffusion chamber which excludes radon progeny and detritus whilst allowing access of radon gas, this subsequently decays and the emitted alpha particles are detected by an SSNTD of CR-39 type. The evaluation is performed by an image analyzer. The system was first calibrated on the 1991 intercomparison at the NRPB and then at the EML (New York) in 1993. This resulted in a licence enabling us to perform measurements in dwellings and work places with official consequences. We participated on the next intercomparison in Harwell in 1995, too. The preliminary results reported ensures us that our measurements fall into the acceptable range of the nominal radon concentrations.

2. Development of methods for estimation of ^{210}Pb surface concentration in glass

2.1. Radiochemical method for estimation of ^{210}Bi surface concentration

The radiochemical method for detecting the beta particles emitted by the ^{210}Bi , consists of the following steps.

- Preparation: the glass sheet (typically 360 cm^2) is cleaned with CCl_4 .
- Etching: the glass sheet is immersed at room temperature in a 250 ml solution of 0.33 mole HNO_3 + 0.18 mole HF and 75 mg Bi + 10 mg Pb carriers (the ^{210}Pb contamination of the carriers is less than 0.2 mBq/sample). The etching velocity is calculated from the Si content of the solution and values between 0.04

and 0.05 $\mu\text{m}/\text{min}$ are accepted. The etching time is adjusted (4-5 min) to achieve a removed layer of 0.2 μm .

- Separation of the Bi and determination of ^{210}Bi activity: after treating the flouride solution with boric acid and alkalifying, the Bi carrier is filtered as $\text{Bi}(\text{OH})_3$ but the Pb carrier remains in the solution. After washing, the precipitation is dissolved by 2 mole hot HNO_3 , after alkalifying the solution with NaOH , the Bi carrier is reduced by formaldehyde. The chemical yield is about 100%. The precipitate is deposited on a tray of 50 mm in diameter and after drying it is covered with aluminium foil of 1.5 mg/cm^2 . The separation of ^{210}Bi from ^{210}Pb mother element is tested by half life measurement. The beta activity of the ^{210}Bi is measured by a Berthold LB770 flow beta counter. The typical background is 0.6 cpm, the counting time is 20 hours, the minimum detectable level is 0.2 Bq/m^2 (~7 mBq/sample) with 95% confidence.

- Calibration: the procedure detailed above is repeated with ^{210}Pb standard solution of 2 Bq activity. The averaged efficiency is 0.38 ± 0.04 .

2.2. SSNTD autoradiography method for measurement of ^{210}Po surface concentration

- Track detector materials: Two types of SSNTDs were chosen: Kodak Pathé LR115 and CR-39 called TASKTRAK from TASL, Bristol, UK. Properties found: LR115 sensitivity to alpha particles falls in the energy range of 1.6-4.7 MeV. Therefore, a Mylar filter of 1.1 mg/cm^2 should be applied to extend the sensitivity for higher energy particles as ^{210}Po and ^{241}Am alphas. The detection efficiency versus removed layer thickness was determined for both normal and etched through tracks. Critical angle was found to be 38° for over etched tracks (Fig. 1). A thin ^{241}Am alpha source of 5.5 MeV was used. The alpha energy was degraded by Mylar foil of 1.1 mg/cm^2 (1, 2 or 3 layers). The open markers represent the normal tracks (dark spot on a red background) while the filled-up markers indicate the etched through tracks (green spots on black background). The solid and the dashed lines represent measurements using two different parameter set-up for the image analyzer i.e. solid line: when shape factor of 1-1.4 was used, dashed line: no shape factor was used. The removed layer was measured by a thickness measuring device called TESATRONIC DIGITAL (manufactured by TESA GmbH, Swiss). The error bars represent 3σ .

The same investigations were carried out for the CR-39 detector using a thin ^{241}Am alpha source. For the critical angle a value of 62° was found.

- Considerations for track analysis and calibration: Since the ^{210}Pb and its decay products are embedded within the upper glass layer of 0.04 μm thick, the energy of the ^{210}Po α particles emerging from the glass and entering the track detector remains around 5.3 MeV. The etchable range in the plastic detectors is about 30 μm . For calibration an ^{241}Am source is applicable with α energy of 5.5 MeV.

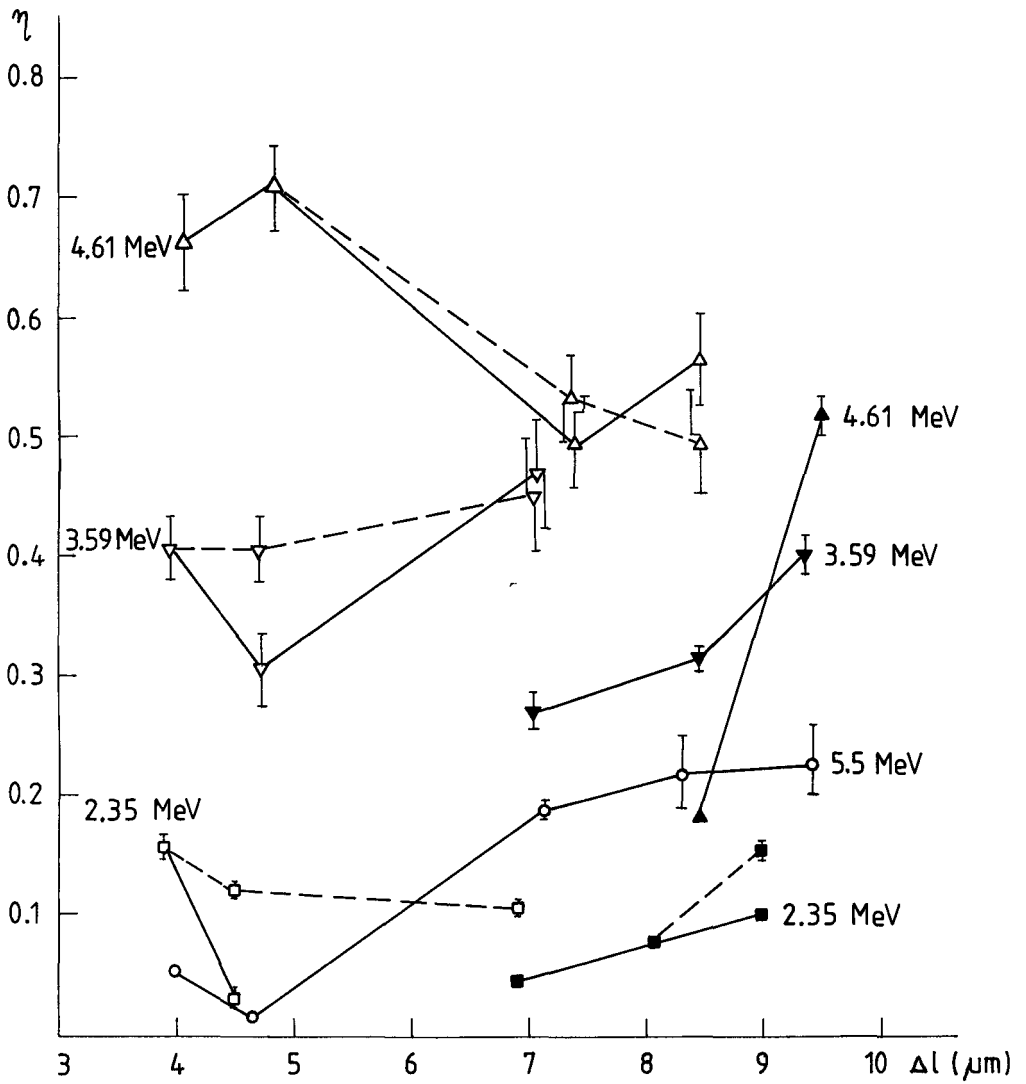


Fig. 1 Alpha particle detection efficiency for LR115 type detector versus the removed layer thickness.

In the case of the detector LR115 a 9.4 μm thick layer should be removed to be able to count the over etched tracks with the possible maximum efficiency of 38%. (Track etch rate is 4.1 $\mu\text{m}/\text{h}$, bulk etch rate is 2.54 $\mu\text{m}/\text{h}$). The parameters of the image analyser should be adjusted in such a way that it detects only green spots on black background with a shape factor between 1 and 1.4 if a green light filter is in use. Once the proper adjustment is performed all the other tracks are considered as background ones and automatically discriminated.

For CR-39 a layer of about 10 μm should be etched off to achieve an efficiency of 80%. If this is done so, then the tracks are etched down to the end of their etchable range resulting in conical tracks with sharp peak. Such kinds of tracks appear under the microscope as very dark spots with a good contrast and the shape factor is in between 1 and 1.5 (Track etch rate is 2.65 $\mu\text{m}/\text{h}$, while the bulk etch rate is 1.77 $\mu\text{m}/\text{h}$).

- Condition of exposures:

The glass surfaces were cleaned with CCl_4 before mounting the track detectors. The detectors were preetched for two hours to allow the development of background tracks that then were counted. Detectors were fixed to the glass surface by a chemically neutral wax applied on the edges. The exposure took place in a desiccator filled up with "old Nitrogen gas" to ensure a Radon free environment during the exposure time.

The background surface activity concentration was found to be 1.7 Bq/m^2 . From the measured track density the surface activity concentration was calculated in the following way.

It was assumed that within the critical angle (θ_c) the detection efficiencies (η) are 38% and 80% for LR115 and CR-39 detectors, respectively. This means that two correction factors had to be applied to calculate correctly the total alpha activity (A_s) within the upper 0.04 μm thick layer of the glass.

$$A_s = \frac{360}{2 \cdot \theta_c} \cdot \frac{T}{\eta \cdot t} \text{ Bq} / \text{m}^2;$$

where T is the measured track density in m^{-2} after subtracting the background and t is the exposure time in sec.

2.3. Comparison of two methods

In each case the surface activity concentration was measured by the radiochemical (RC) and the SSNTD methods. We made 3-7 parallel measurement by the two methods on each glass sample. The empirical standard deviations varied between 10 and 25% for both methods. The result of comparison of two methods is given Fig. 2. The radiochemical and SSNTD methods agreed well within the empirical standard deviations.

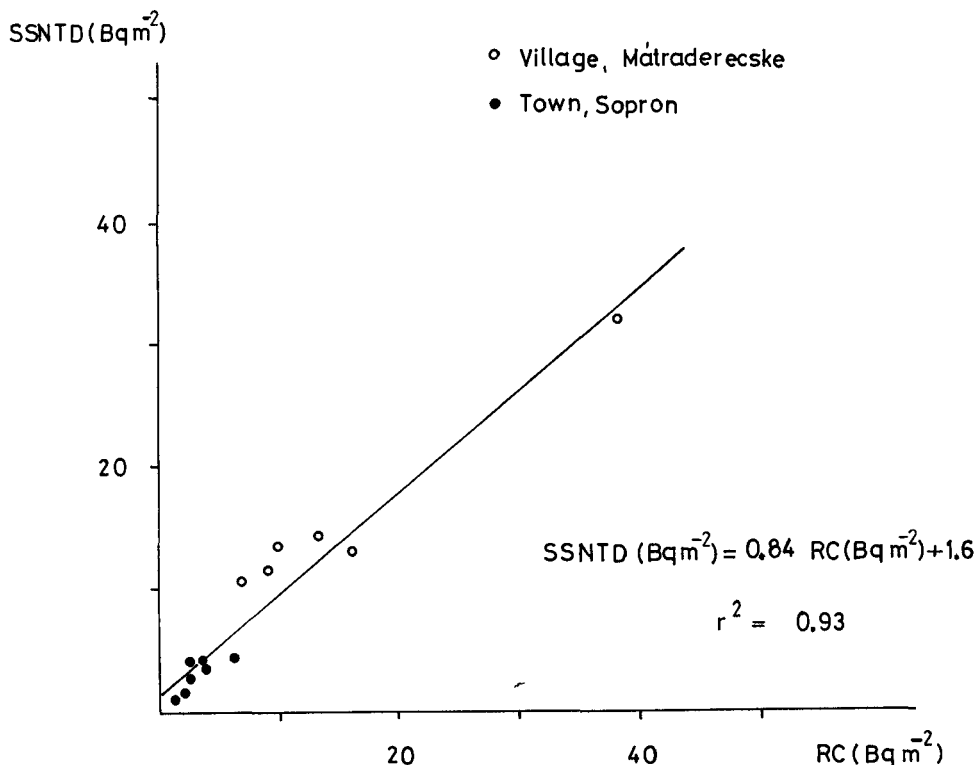


Fig. 2 Intercomparison of RC and SSNTD methods

3. Studies on glass surfaces

3.1. Some investigations on old glass surfaces

A second 0.2 μm layer of glass was etched from its exposed side following the first radiochemical procedure to look at the remained ^{210}Bi in the glass. The surface activity of ^{210}Bi ranged from 0.7 to 1.2 Bq/m^2 in this depth. It corresponds to the 1.7 Bq/m^2 background of fresh glass sheets.

The exposed side of glass was covered with paraffin to etch its overleaf and measure ^{210}Bi in it. The average surface activity of ^{210}Bi was found to be 1.0 ± 0.2 Bq/m^2 on overleaves of some old glass sheets, therefore we have not used any coating layer on glass for etching later.

The surface of glass samples, that were from the same old glass sheet, were covered with different kinds of dirtiness in several smaller or larger spots. A part of spots could be removed with mild wipe of CCl_4 but not all. We wanted to know how much of ^{210}Bi was in dirtiness and how much of it was implanted in the glass.

- The glass surface was rubbed off 10 times with fresh soaked glass fibre filter type GF/A (Whatman) in CCl_4 . The pieces of GF/A were collected and left them in cc. HNO_3 with Bi carrier in it to steep off Bi for 20 hours. ^{210}Bi was prepared from HNO_3 solution and measured, the glass sample was processed as usual. This method could remove different parts of all ^{210}Bi (in dirtiness and glass together) between 12% and 58%.

- Some glass samples were immersed into 0.5 mole HNO_3 solution with Bi and Pb carriers in it to soak off ^{210}Bi from their surfaces for 20 hours. ^{210}Bi was prepared from HNO_3 solution and the glass sample was processed as usual. The removable parts of all ^{210}Bi (in dirtiness and glass together) ranged between 7% and 22% this way.

3.2. Investigation on influence of dirtiness

Fresh glass sheet was cut into pieces to measure them directly in a Berthold LB770 flow alpha and beta counter. After cleaning, the glass samples were measured for alpha and beta background. Samples were coated with vaseline in 4 steps of thickness from $2 \cdot 10^{-4}$ mg/cm² some of them rested uncoated. Samples were exposed in a cave for 60 days and radon concentration was measured there in air with SSNTD all the time.

After the exposure when the ^{210}Bi had obtained the equilibrium with ^{210}Pb on samples they were measured without any cleaning. Vaseline was washed off with benzine and samples were measured again. The expected result was that the surface activity on the samples would be different in wide range but it was not. In spite of different thickness of covering vaseline layers the rested activities on the samples did not differ from each other significantly neither for alpha nor for beta. Only 10% parts of activities could be removed this way. This experience is unexpected and we have no reasonable explanation to it. It needs to investigate these phenomenon in details in the future.

4. Investigation of glass samples from Mátraderecske (a village) and Sopron (a town)

The results are presented in Table 1.

In Fig. 3 we present the measurements in a different way. The ratio of the ^{210}Bi concentration and the time integral of the radon concentration measured in air versus the glass exposure time is given. It can be observed that the values measured in the village compared to values measured in a given town more or less follow the same curve. This means that the local geological conditions do not influence the surface activity caused by the unit time integral of the radon concentration in air.

There may be several reasons why the ratio decreases with exposure time; Samuelsson in Sweden obtained similar results, i.e. the radon concentration or the plate-out rate were less in the past and/or the randomly performed cleaning

Location	Average Radon* Concentration kBq m ⁻³	Exposure Time of Glass year	Surface Activity** Bq m ⁻²
Village V1	3.7	16	38
V2	0.98	34	8.9
V3	0.89	42	6.6
V4	1.6	38	16
V5	1.1	20	13
Town T1	0.23	30	4.1
T2	0.27	8	3.6
T3	0.56	15	6.2
T4	0.19	12	2.8
T5	0.17	15	2.1
T6	0.15	11	1.5
T7	0.26	55	2.4

Overall error * 24%
** 17%

Table 1 Meassured Average Radon Concentration Exposure and Glass Surface Activity

and the gradual deposition of dirt, as well as the corrosion of the glass surface all may cause the same effect. Taking our own result into consideration we may exclude the drastic change in the radon concentration during the long exposure time of the glass since in both places i.e. village and town and also in Sweden, the shape of the curve is similar. Further investigations are necessary to establish the determining reason for the decrease of the ratio function.

Bearing in mind all the uncertainties of the measurements it is concluded that the radon concentrations in the places from where the glass samples were collected have not changed during the exposure time by more than a factor of two.

By means of the radiochemical method about 10 glass samples can be investigated daily; the only disadvantage of the method is that it is destructive, measurements cannot be repeated on the same surface.

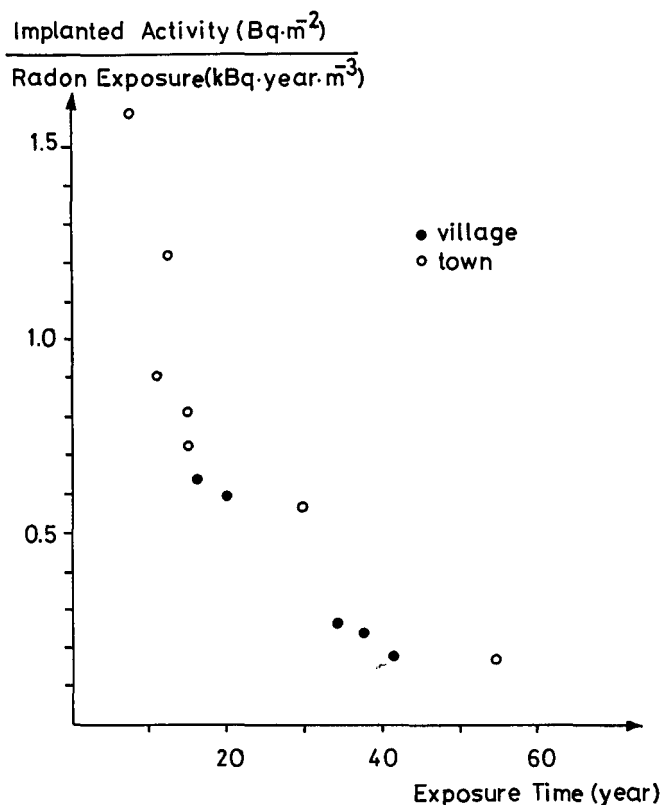


Fig. 3 Measured Ratio of Glass Surface ^{210}Bi Activity Concentration and ^{222}Rn Concentration Time Integral vs. Exposure Time

Relevant publications related to this research

- I.Fehér, M. Lőrinc, J. Pálfalvi, Retrospective Assessment of Radon Exposure, (Oral presentation) 19th Workshop on Radiation Protection, 3-5 May, 1994, Balatonkenese, Hungary
- I. Fehér, M. Lőrinc, J. Pálfalvi, Retrospective Estimation on of Time Integral of Radon Concentration, Proc. of the Second Symposium of the Croatian Radiation Protection Association, 1994, Zagreb, p. 285-288.
- J. Pálfalvi, I. Fehér, M. Lőrinc, Studies on Retrospective Assessment of Radon Exposure, Rad. Meas. 25. 585-586 (1995)
- I. Fehér, M. Lőrinc, J. Pálfalvi, New Method for Measurement of ^{210}Bi on Glass Sheet to Estimate Retrospective Radon Exposure, 11th Solid State Dosimetry Conference, Budapest, July 1995 (poster presentation) Rad. Prot. Dos. (under publication).

Head of project 6: Dr. Samuelsson

II. Objectives for the reporting period

To improve the design and the performance of pulse ionization chambers (PIC) as reference detectors for alpha spectrometry (^{210}Po) of large area samples from dwellings. To support partners with large-area alpha reference sources and with reference ^{210}Po measurements. To investigate the durability of and local variations of implanted ^{210}Pb activity during authentic living conditions. To investigate the surface homogeneity of ^{210}Pb activity on glass samples taken from dwellings. To evaluate the time behaviour of implanted activity in dwellings.

III. Progress achieved including publications

A new pulse ionization chamber has been built with technical assistance from the Technical University of Denmark (Dr. Niels Jonassen). The major modification compare to the older generation chambers is a modular design, facilitating construction, decontamination, and electrode exchange of the chamber.

The new detector is as before of the open-flow type suitable for non-destructive alpha spectrometry of semi-infinite glass samples. By a system of aluminium collimators the area investigated can be reduced from the area corresponding the the maximum diameter of 26 cm (530 cm²). The sensitivity and energy resolution of the PIC detector as a function of collimator area/diameter is given in Figure 1 and 2 respectively. One and the same glass sample, taken from a radon dwelling, and with a homogeneous surface distribution of implanted Po-activity has been used. As seen from the figures, the outermost ring of the sample in the uncollimated geometry does not contribute significantly to the alpha count rate, instead the energy resolution is deteriorated due to oblique alpha particle emission. In normal use the PIC detector used in Figure 1 and 2 is always collimated down to a diameter of 20 cm, which give optimum sensitivity and a resolution better than 40 keV (FWHM).

Four new framed glass samples (28 cm x 35 cm) were hanged in a high level radon dwelling in December 1990 and have until July 1994 on a regular basis been taken to

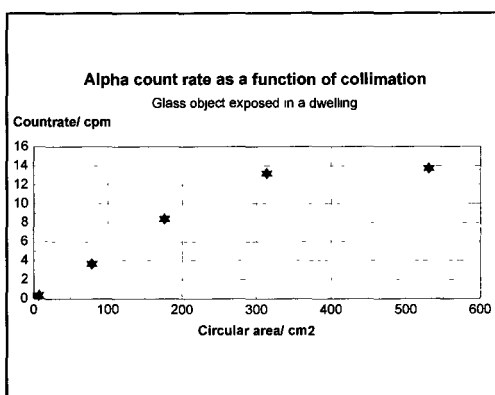


Figure 1. Sensitivity of the PIC as a function of area of collimation. The sample area outside $\phi = 20$ cm (314 cm²) contributes very little to the countrate in the full energy peak.

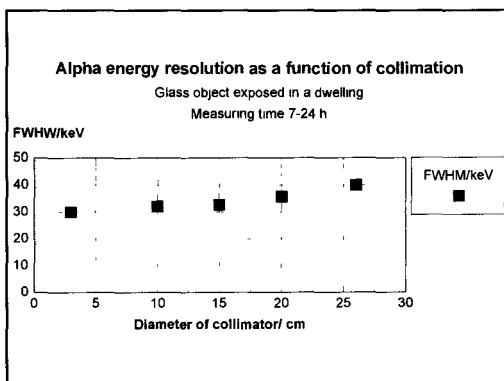


Figure 2. PIC energy resolution corresponding to Figure 1.

the laboratory for analysis of the implanted LRnD activity and exchange of two radon track etch detectors (supplied by partner 3, R. Falk, SSI) attached to each frame. Two of the frames (OP1 and OP1) have been openly exposed in the bedroom hanging on the wall, while the two other frames have been deliberately exposed in recessed positions. Object B2 stands close to the ceiling on top of a bookshelf in the livingroom, leaning against the wall behind the bookshelf. A low vase has part of the time been positioned in front of frame B2 (Figure 3). Frame B1 hangs on a wall in the dining area beneath a close staircase. The radon concentration results exhibit large variations (Figure 4), mainly due to seasonal variations. The dining area values (frame B1) are consistently lower than at the other three positions.

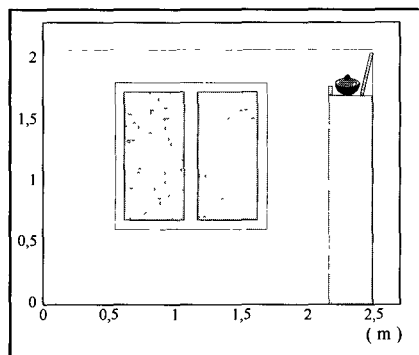


Figure 3 Exposure geometry, object B2.

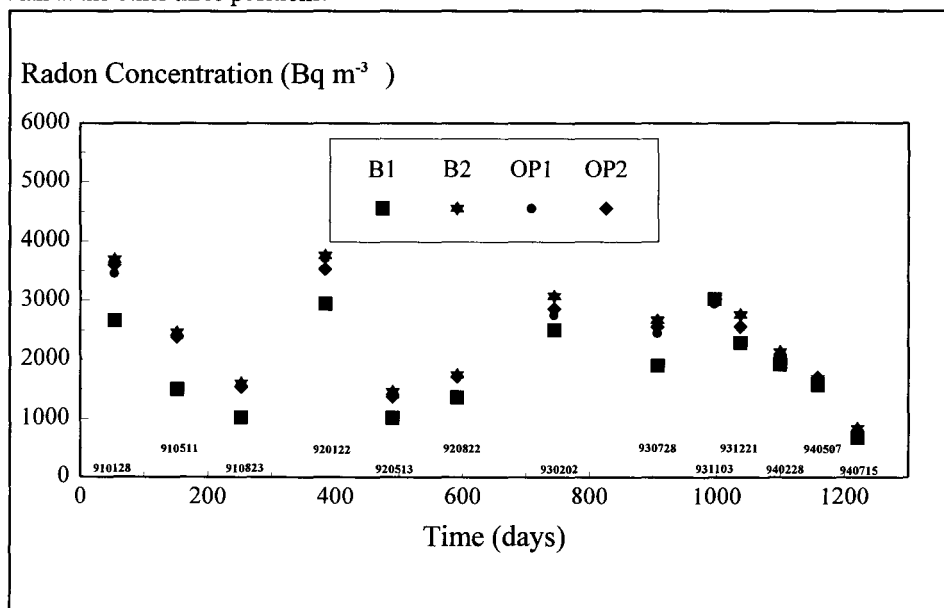


Figure 4. Radon concentration as measured by track-etch detectors at each sample position. The date at the end of each exposure period is given (yy/mm/dd).

The measured growth of ^{210}Po has been converted to implanted ^{210}Pb activity under the assumption that the radon concentration and plate-out conditions have been constant in each time period between measurements. The implanted ^{210}Pb activity is plotted against the radon exposure, as accumulated by the radon track-etch detectors, in Figure 5. Considering the large variations in radon concentration, the ^{210}Pb growth rates are smooth, indicating the mean deposition velocity of radon decay products is approximately constant at each frame position throughout the observation period (3.5 y). On the other hand, in the blocked view positions the relative plate-out rate is low by 45% (B2 above bookshelf) and 65% (B1 under the staircase) respectively. The results of Figure 5 stress clearly the importance of exposure geometry. Only glass objects

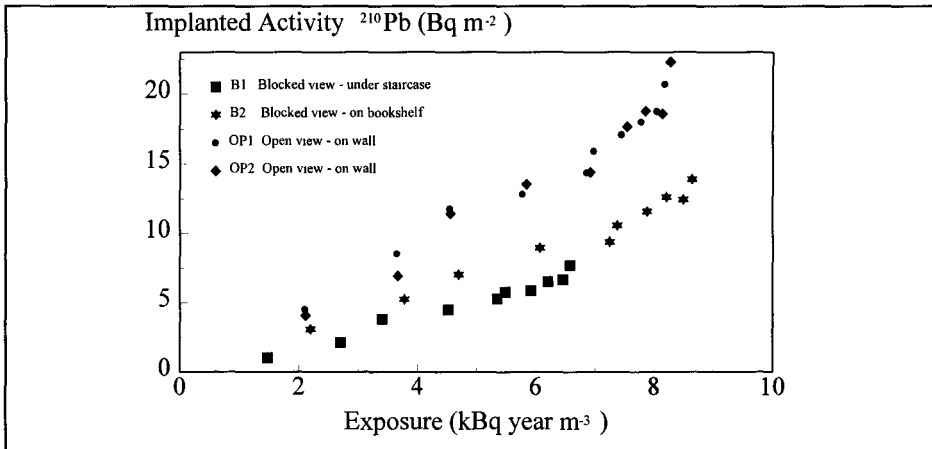


Figure 5. The implanted ²¹⁰Pb activity, as calculated from ²¹⁰Po measurements on the four framed glass sheets. The exposure time equals 3.5 years.

exposed during similar conditions can be compared with each other without the introduction of correction factors. It should be noted that none of the four frames in Figure 5 resides close to radiators or ventilation openings.

For the same dwelling as above the ratio of implanted ²¹⁰Pb to the estimated radon exposure for existing glass sheets is plotted against exposure time in Figure 6. The shape of the theoretical ratio, corresponding to constant radon concentration and constant plate-out and implantation rates, and the results from Figure 5 are included for comparison. The older samples of Figure 6 exhibit a consistently lower ²¹⁰Pb/radon ratio than expected from the open-view (OP1&2) exposure results of Figure 5. This low ratio may reflect a half life of implanted ²¹⁰Pb in glass less than 22 years or merely recessed exposure positions or lower radon concentrations or lower plate-out rates of the past. The number of family members as well as smoking habits have changed over the years and it is not possible at the moment to determine the major reason for the time behaviour in Figure 6.

The small implantation depth favours high-resolution alpha spectroscopy but raises questions of durability and interference from dirt on the surface. All our experience from glass measurements supports the hypothesis that the removal of implanted LRnD is only caused by radioactive decay. Normal glass-cleaning procedures will not influence or remove the implanted activity. The results illustrated in Figure 5 support

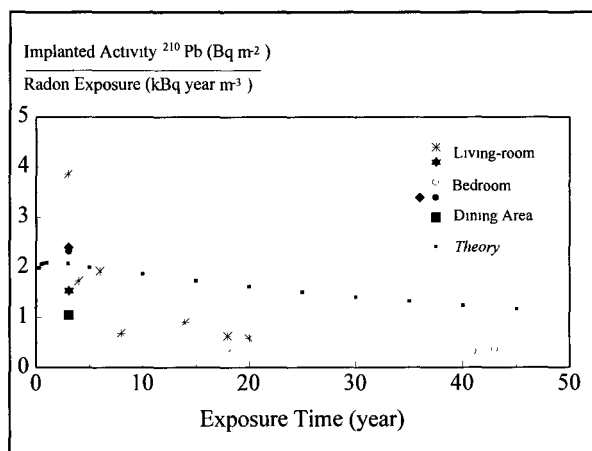


Figure 6. The implanted ²¹⁰Pb activity calculated from pulse ionization chamber measurement of ²¹⁰Po on existing glass sheets and on the four samples of Figure 5.

this conclusion. The glass sheets of Figure 5 have been thoroughly washed in our laboratory 3-4 times a year, prior to each measurement, a procedure that apparently does not effect the implantation process.

It is easy to show experimentally that it takes a destructive cleaning method to remove the implanted $^{210}\text{Pb}/^{210}\text{Po}$ activity from glass sheets. Cleaning repeatedly with a household detergent and lukewarm water seems not to tear off any activity (Figure 7), but the implanted activity is apparently removed if glass surface is treated with abrasive agents (Figure 8). It should be remembered however, that implant integrity may be impaired during long-term exposure to water condensing conditions, due to surface corrosion of glass.

Due to regular cleaning, the interference from dust and grease is of little significance for the samples in Figure 5, but we can not exclude the possibility that in other indoor environments surface contaminants may have a deleterious effect on the implantation process. Systematic studies on how household contaminants on surfaces interfere with the implantation process are lacking. Our results from a pilot study of household glass sheets exposed in a walk-in radon chamber indicate that a significant fraction of implantation can take place in the surface dust [1]. The removable fraction of ^{210}Po after exposure was 32 and 49% for clean and dusty samples, respectively, but the spread in the individual results of the 20 samples was large. The results from the pilot study in reference [1] support the hypothesis that indoor surface contaminants can significantly reduce the implantation rate of LRnD into the glass matrix, though the reduction is much less than expected from pure range/mass-load calculations, due to the very uneven surface distribution of the dust.

The PIC detector of Figure 5 is used with an opening diameter of 20 cm and do not reveal the detailed (say, on a centimeter scale) surface distribution of implanted activity. When utilizing track-etch devices or

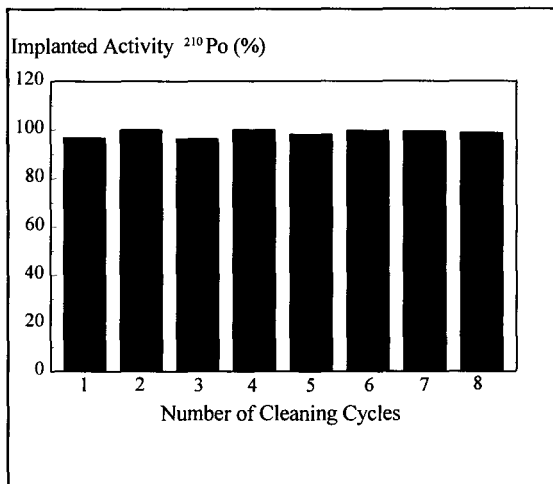


Figure 7. Cleaning glass sheets with lukewarm water and a household detergent does not remove the implanted activity.

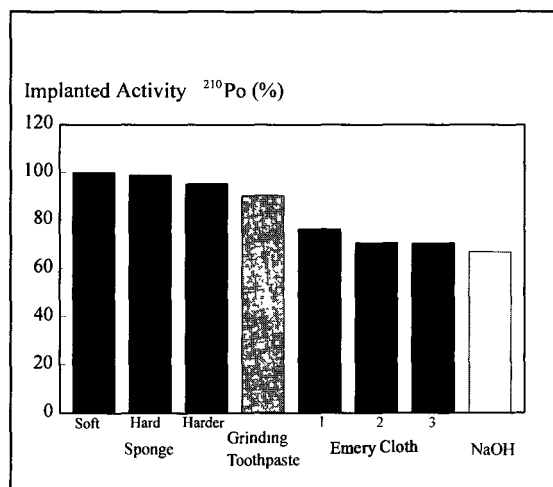


Figure 8. The implanted activity after consecutive (left to right) abrasive treatments of a glass sheet.

other small-area detectors on glass surfaces inhomogeneities in the surface distribution of ^{210}Po may influence the measured result. It is therefore of interest to make a more detail investigation of the areal distribution of implanted ^{210}Pb in household objects used for RARE purposes. The framed glass sheets in Figure 5 have therefore been scanned with the PIC detector collimated to either a slit or a circular opening of area 7 cm^2 . The results reveal an even distribution of ^{210}Pb for all objects exposed openly on the wall. Only very close to the wooden frame surrounding the glass sheet is the implanted activity reduced, being zero on the part of the glass covered by the frame. The lower activity concentration close to the wooden frame (cf. Figure 9a) reflects presumably an interrupted boundary layer as the wooden frame extends above the surface of the glass sheet. A slightly more uneven distribution can be found on glass sheets in recessed positions, as illustrated in Figure 9 b-d, presumably due to uneven airflow patterns. From the scan of object B2 (cf. Figure 3 and 9 b-d) it is apparent that the low vase in front casts a "shadow", i.e. diminishing the implanted activity in the lower part of the object. The conclusion from our scanning experiments is that in the centre part of glass sheets inhomogeneities in the ^{210}Pb areal distribution are of minor importance and do not normally prohibit the use of small-area detectors, e.g. ion implanted Si-detectors. Small detectors will however, give raise to sensitivity problems due to the low surface concentration of implanted activity.

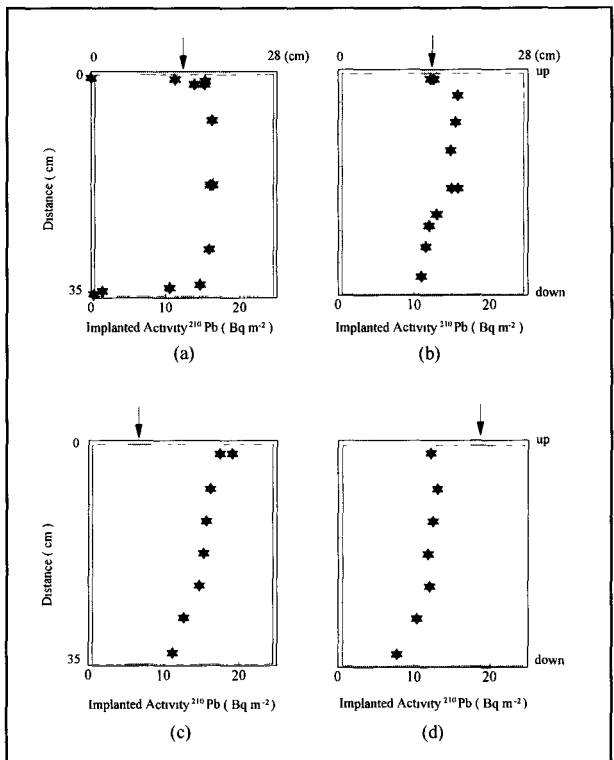


Figure 9. Results from scanning the sample OP2 with a slit ($5.3 \times 138\text{ mm}^2$) collimator (a) and sample B2 with a circular ($\phi = 30\text{ mm}$) collimator in the middle (b), to the left (c), and to the right (d). The exposure geometry of B2 is given in Figure 3.

The results in Figure 5 are obtained during authentic living conditions and a good control of the radon exposure conditions, cleaning procedures etc. This well controlled situation is not met when collecting samples from dwellings for assessment of radon exposure in retrospect. But RARE methods can be put to test in the existing dwelling stock provided we compare similar exposure geometries and know the time of exposure. A test of the time behaviour of the implanted activity is illustrated in Figure 10 in which four existant glass frames from two houses have been analysed for total surface and implanted ^{210}Po activity at two different occasions. There is about 4 years between the two measurements and a very important observation is that the

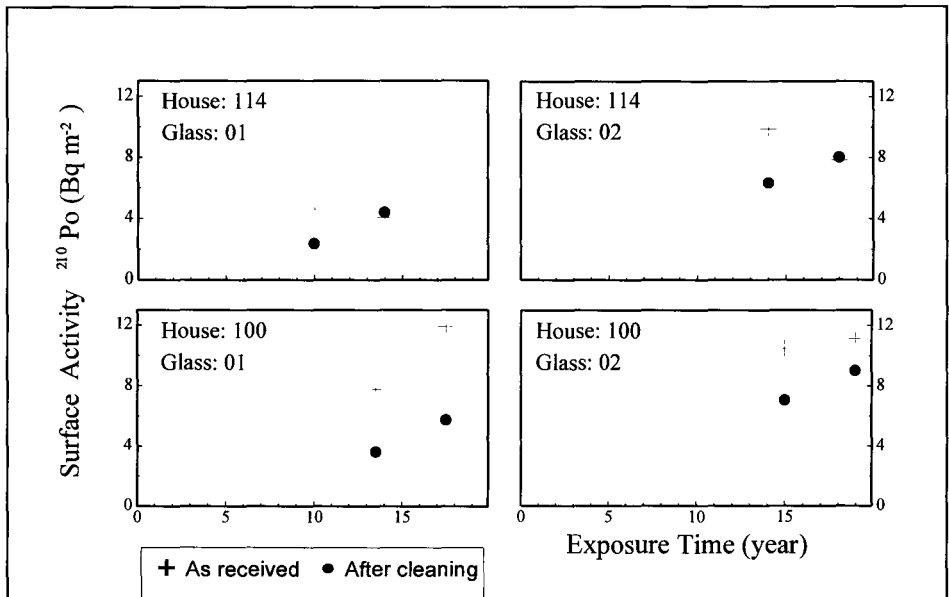


Figure 10. Four individual glass samples from two different dwellings analysed at two different occasions four years apart.

growth of the implanted activity seems to follow the same trend as during the first 10-15 years, irrespective of eventual differences in cleaning habits. On some objects, the removable LRnD activity exceeds 50%. This does not necessarily prove that a significant implantation of alpha recoils takes place in the surface contaminant itself, rather than in the solid glass. One reason for this is that the dust landing on the glass surface may be of different age and therefore of different LRnD concentration. This idea is speculative, but as some of the samples are positioned beneath an open staircase, significant resuspension and fallout of old dust is not out of the question.

It is obvious from the results presented above that several factors can interfere with the implantation process, but through a careful choice of samples and a preferably a multi-sample-per-dwelling approach, the correlation between radon exposure and implanted activity is expected to be good within a factor of two.

Publications

- [1] L Johansson., M. Wolff and C. Samuelsson. "The influence of Dust on ²¹⁰Po Signal in Retrospective Radon Measurements" Rad. Prot. Dosim. **56** 1-4, p141-143, 1994.

C. Samuelsson and L. Johansson "Long-Lived Radon Decay Products as a Long-Term Radon Exposure Indicator" Rad. Prot. Dosim. **56** 1-4, p123-126, 1994.

**Final Report
1992 - 1994**

Contract: FI3PCT920034 Duration: 1.9.92 to 30.6.95

Sector: C12

Title: Characteristics of airborne radon and thoron decay products.

1)	Porstendörfer	Univ. Göttingen
2)	Poffijn	Univ. Gent
3)	Vanmarcke	CEN/SCK Brussels
4)	Akselsson	Univ. Lund
5)	Falk	SSI Stockholm
6)	Tymen	Univ. Brest
7)	Ortega	Univ. Catalunya - Politecnica Barcelona
8)	Lebecka	CMI, Katowice
9)	Kobal	IJS, Ljubljana
10)	Cuculeanu	NIMH, Bucarest
11)	Schuler	PSI, Villigen

I. Summary of Project Global Objectives and Achievements

GLOBAL OBJECTIVES

Besides the airborne activity concentrations, the size characteristics of the unattached and attached decay products and the quantity of unattached activity are important parameters in all models for dose calculations. The information on the size characteristics are also essential for understanding and describing the behaviour of the airborne activity in indoor and outdoor environments. For example, the retrospective assessment of indoor exposure to radon (^{210}Pb in smooth surfaces) needs information of the variation and size dependence of the airborne activities.

Values for the size distribution of the unattached and aerosol-attached activity in the domestic environment and the magnitude of the unattached activity are quite limited and consequently uncertain. The information available in the literature shows that it is necessary to determine aerosol and room conditions (such as aerosol particle concentrations, ventilation, type of aerosol and vapour sources, humidity) during measurements. For the correct determination of the real variation of these parameters under normal living conditions more efforts have to be done to reduce uncertainties concerning activity measurements, to calibrate and improve size fractionating instruments, to compare different data evaluation methods, and to simulate the behaviour of airborne activities by model calculations.

The improvement and development of experimental techniques, controlled chamber studies and intercomparison measurements were important topics of this project. Other important points of emphasis were to determine aerosol size characteristics, activity concentrations of radon, thoron and their short-lived decay products (fp, F) in the domestic environment and to determine or simulate deposited activities in the human lung. Finally, by the group of Göttingen a new dose model based on the actual lung deposition values (recommended by ICRP66) was developed to assess the influence of biological and aerosol parameters on the lung dose.

Within the framework of PECO92 and PECO93 collaboration with groups of the Eastern part of Europe (Romania, Poland, Slovenia) were supported by the CEC during some periods of this project.

Groups of the non-CEC-countries Sweden (Lund, Stockholm) and Switzerland (PSI) continued or started their co-operation in this radiation protection project.

GLOBAL ACHIEVEMENTS

Dose calculations based on the actual lung deposition values demonstrate the importance of the size of the unattached activities (clusters) and of the aerosol-associated activities of the nuclei and coarse modes. Key results of calculations with the new developed lung dose model of the group of Göttingen are summarised in figure 1.

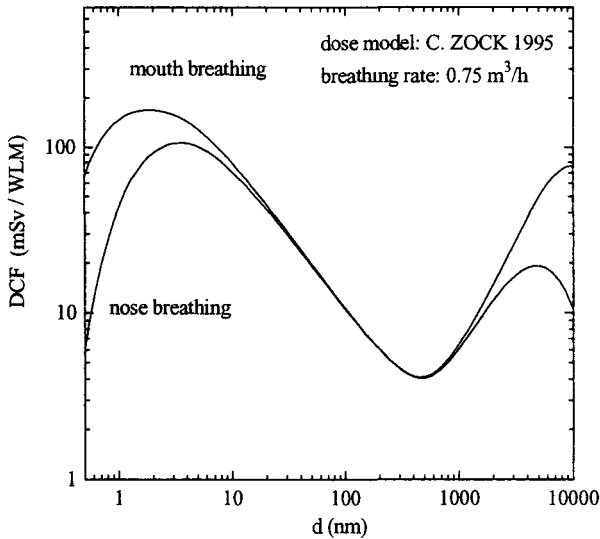


Figure 1: Dose conversion factors (DCF) as a function of particle diameter d of inhaled radon progeny. Calculations based on a dose model developed by C. Zock, 1995.

Size *distributions of the unattached radon decay products* were measured by the group of Göttingen in homes and at working places in several rooms with elevated activity concentrations at different atmospheric conditions. In general, it can be concluded from these measurements that the distributions of the ultrafine fraction is narrow in size ($\sigma_g < 1.4$) with median diameters ranging between 0.5 - 1.4 nm corresponding to Stokes-Einstein diffusion coefficients D of 0.02 - 0.20 cm^2/s . There are indications of three different modes with diameters around 0.53 nm, 0.82 nm and 1.3 nm. These modes probably corresponds to the neutral and charged states of the clusters and uncompleted hydrated clusters. In rooms with an aged aerosol the cluster size of ^{214}Pb is larger (1.4 nm) compared to ^{218}Po (0.8 nm). This latter finding is supported by measurements of the groups of SSI, Stockholm and PSI, Switzerland using aerosol-filtered air.

Controlled chamber experiments of the groups of PSI and Göttingen show no effect of cluster growth by variation of SO_2 between 0 - 0.5 ppm (environmental level) and relative humidity between 5-80%.

The groups of Brest and Stockholm developed and calibrated diffusion detectors in combination with the track-etch technique for integrated measurements of the sizes of the unattached radon progeny. Successful test measurements were performed at environmental levels with sampling

times of 5 days.

The group of Barcelona set-up an automated system based on a single-screen technique for continuous measurements of the integral amount of the unattached and of the aerosol-attached radon progeny. Continuous measurements and monitoring of pressure and temperature were performed during several weeks in four houses in the catalonia area in Spain. During these measurement campaigns different kind of passive integrated detectors were tested.

The Belgian group of Gent tested during an intercomparison campaign in Sweden a commercial available monitor (Fa. Streil) for continuous measurements of f_p and F during a 3 months period.

After calibration and modification of the so-called Bronchial dosimeter first experimental experience were made at laboratory conditions by the group of Mol to simulate lung deposition mainly of the unattached activities.

By the groups of Brest and Göttingen measurements of **the size distributions of the aerosol-associated activities** in homes were performed with impactors and techniques based on electrostatic classification. Both groups confirm former results that the distributions of the different radon progeny a similar. The Brest group also found sometimes a significant activity fraction in the coarse mode size range of some microns. This findings support results of intercomparison measurements organised by the group of Göttingen. Participants of this campaign were the US-DOE (USA) and ARL(Australia). Essential progress is necessary to clarify if this activity in the coarse mode range is real or a misinterpretation of the ultrafine radon progeny. Furthermore the Brest and Göttingen groups spent special effort in testing data evaluation methods concerning size analysis of aerosol measurements.

The Lund group of Sweden designed and calibrated a multi-orifice impactor and showed that this impactor can be used to measure sizes down to 35 nm.

In an improved radon chamber in Lund the hygroscopic growth of different kind of indoor household aerosol was investigated.

The group of Barcelona constructed and developed a **walk-in radon chamber** with controlled and monitored atmospheric conditions. The PSI group improved model calculations for describing the behaviour (attachment, plate-out) in a radon chamber. In the radon chamber of SSI, Stockholm an experimental technique for studying the deposition of radon progeny in humans was modified and tested.

The SSI of Sweden continued their survey program for **thoron and thoron decay products**. From the current results can be estimated that the averaged dose equivalent of Thoron of 0.1 mSv/y is negligible compared to 2 mSv/y corresponding to the radon exposure in Sweden.

National radiation protection programmes concerning radon exposure of groups of Bucarest (RO), Ljubljana (SL) and Katowice (PL) were **temporary supported by the CEC**. The Bucarest group developed a theoretical model to derive exact solutions of turbulent diffusion for the unattached and attached radon decay products and a model for calculating the concentration profiles in the outdoor atmosphere.

The Slovenian group completed a nationwide radon survey in kindergartens and schools with detailed decay product measurements in different geological and climatological regions. Others projects dealt with measurements in caves for speleotherapy and a plate-out monitor for dosimetry of radon decay products.

The group of Poland is responsible for monitoring of radon decay products in underground coal mines. During this project instruments for measurements of the unattached fraction of radon progeny were built based on the single-screen technique used by the group of Göttingen. Intercomparison measurements and training courses of polish specialists were performed with the group of Göttingen and other groups in Europe and USA.

Head of project 1: Dr. Porstendörfer

II. Objectives for the reporting period

Special parts of the radon related radiation protection programmes of the IL were involved in the CEC supported project:

- Controlled chamber experiments to study the influence of trace gases and humidity on cluster growth and neutralisation processes of the unattached activities of ^{218}Po .
- Measurements of size distributions of the aerosol-attached activities and of the unattached activities at different atmospheric and under representative living and working conditions. It is of special interest to investigate differences of the cluster sizes (or diffusion coefficients) of the different decay products ^{218}Po , ^{214}Pb and ^{214}Bi .
- Intercomparison measurements with groups of USA and Australia will be continued.
- A new dose model will be developed to estimate the variation of the dose using experimental derived aerosol parameters.

III. Progress achieved including publications

CHAMBER STUDIES

In a cylindrical radon chamber (length: 1 m, volume: 0.036 m^3) neutralisation rates, front to total ratios (ftr) and cluster sizes of ^{218}Po were measured at elevated radon gas concentrations for aerosol-free room air at different air humidities:

a) For determination of the ftr-values as a function of the penetration P the ^{218}Po activities were sampled on 6 single-screens with different mesh numbers and on a membrane filter for two different flow velocities. The total screen-deposited activities and the activity on the membrane filter were measured via ^{214}Bi by γ -spectroscopy and the activities on the screen surface by α -spectroscopy via ^{214}Po .

Figure 1 shows the results of the ftr-measurements. Because of the dependence on the deposition of the clusters around the screen-wire the ftr is a function of screen-penetration. The measured values are valid for small distances ($< 5 \text{ mm}$) between screen and alpha-detector. For this case, with only consideration of alpha particle losses in the source-wire a theoretical ftr-value of 0.59 can be calculated using classical deposition equations. However, these deposition equations are only valid for constant number concentrations of the clusters before and behind the screens, that means for a high penetration. The measurements were also performed for vanishing penetration values which yield increased ftr-values up to 0.8. This value is not theoretically predictable because for this case there exist no theoretical description of the deposition around the wires.

b) The deposition by diffusion on the screens was used to determine the size (or diffusion coefficients D) of ^{218}Po -clusters at the end of the chamber. The activity on the top-side of five screens were measured with a surface barrier detector. Diffusion equivalent activity median diameters of 0.68 nm were evaluated for all relative humidities RH ranging between 2 - 70%, corresponding to $D = 0.11 \text{ cm}^2/\text{s}$. Former chamber studies of Porstendörfer and Hopke indicate a reduction of about 1/3 of the diffusion coefficient of charged clusters compared to neutral one assuming the same cluster size. In the present study it was found that 29% of the ^{218}Po clusters were positively charged at RH=2% and only 12% at RH=70%. If the real cluster size is assumed as the same for all humidities and assuming the same charge states, it will be expected that the median diffusion coefficient will only be reduced by 5% from RH=70% to RH=2%. Theoretical studies of cluster growth predicts that the real equilibrium cluster size

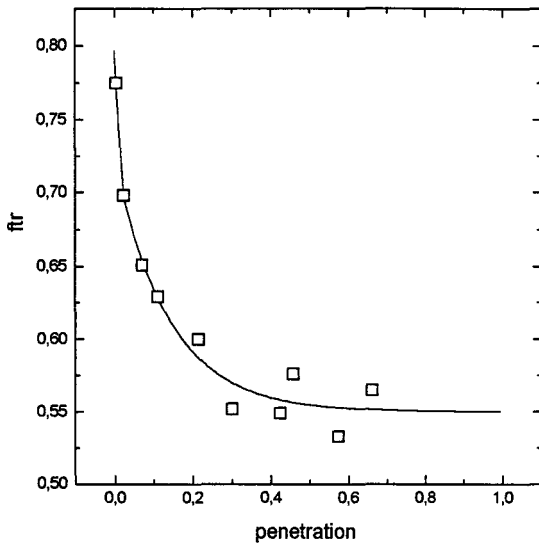


Figure 1: Front to total ratio f_{tr} of single screens as a function of the penetration value P . The measured values can be approximated for $P < 0.023$ by $f_{tr} = -4.278 \cdot P + 0.796$ and for $P > 0.023$ by $f_{tr} = 0.55 + 0.1745 \cdot \exp(-7.17 \cdot P)$.

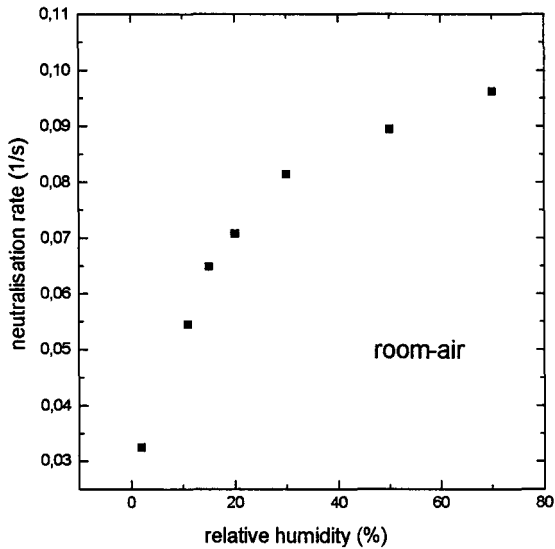


Figure 2: Neutralisation rate of ^{218}Po clusters as a function of the relative humidity RH.

of ^{218}Po -water clusters decrease with decreasing humidities. These two effects will have an opposite influence on the diffusion coefficient and may compensate themselves.

c) The rate of neutralisation of ^{218}Po was determined by separating the charged clusters from the total number of clusters in a cylindrical condenser. In Figure 2 the dependence of the neutralisation on the air humidity is shown. The measurement indicates that the neutralisation depends strongly on the humidity at low values and reaches saturation at higher humidities. The increase of the neutralisation rate for increasing humidity is caused by the higher concentration of hydroxyl radicals from the radiolysis. These hydroxyl radicals may act as electron scavengers. The neutralisation of ^{218}Po occurs by means of OH^\cdot . It is plausible that a saturation will be reached when the whole alpha energy is used for water radiolysis.

SIZE DISTRIBUTION MEASUREMENTS

aerosol-attached activities

For the measurement of activity - weighted size distributions in the nucleus mode size range with diameters between 10 - 100 nm experimental methods based on the analysis of the electric mobility of aerosol particles have the best size resolution, compared to impactors and diffusion techniques. To improve the sensitivity of this technique for radioactive aerosol particles and for modelling radioactive and inactive size distributions, an electrostatic classifier in connection with a condensation nuclei counter (CNC) and a unit for alpha-spectroscopy was built up and tested. For this device a computer program was written and hardware modifications were done to perform automatic and continuous measurements. From the particle losses inside the classifier, the charging probability of the aerosol particles and the response function of the CNC it can be estimated that the detection limit for size analysis of number size distributions is about 4-5 nm and 250 nm, respectively.

The activity of ^{218}Po - associated particles can be measured continuously after electrostatic classification by alpha spectroscopy using a surface barrier detector. Sufficient counting statistics also for particle sizes of about (10 - 20) nm can be achieved in atmospheres with elevated radon gas concentrations of 2000 - 3000 Bq/m^3 corresponding to concentrations of ^{218}Po of 1000 - 2000 Bq/m^3 .

In addition to the method of electrostatic classification an optical system (LAS X) for size analysis in the diameter range between 200 - 7000 nm was tested and a computer program was written to support automatic measurements.

In a low ventilated room without any additional aerosol sources (aged aerosol: $Z = 6000 - 9000$ particles/ cm^3) at radon gas concentrations of 7000 Bq/m^3 the different experimental techniques (classifier and impactor) were compared. In Fig. 3 the measured averaged activity size distributions of ^{218}Po are shown. The advantage of the size analysis with the electrical mobility analyser is the excellent size resolution. However, due to the low air flow rate of the classifier (< 10 l/min), due to the registration of only single charged particles (unipolar equilibrium) with this unit of activity measurement (α -spectroscopy) a complete activity size spectrum can only be measured during 8 hours. From Fig. 3 it can be seen that both size distributions are in good agreement. The maximums of the accumulation mode ranged between 200 - 300 nm and agree with former impactor measurements.

From the above described indoor measurements with the on-line- α -impactor the size distributions of the different short-lived decay products ^{218}Po , ^{214}Pb and ^{214}Bi can be evaluated. The averaged parameters of the lognormally approximated main mode (accumulation mode) and the extreme values of the single measurements are summarised in table 1. The average median diameter of the primary decay product ^{218}Po (AMAD=234 nm) is slightly smaller than those of ^{214}Pb and ^{214}Bi (AMAD=251-253 nm). This effect can be the result of detachment processes due to the recoil during the α -decay of ^{218}Po and of re-attachment processes to an aerosol particle.

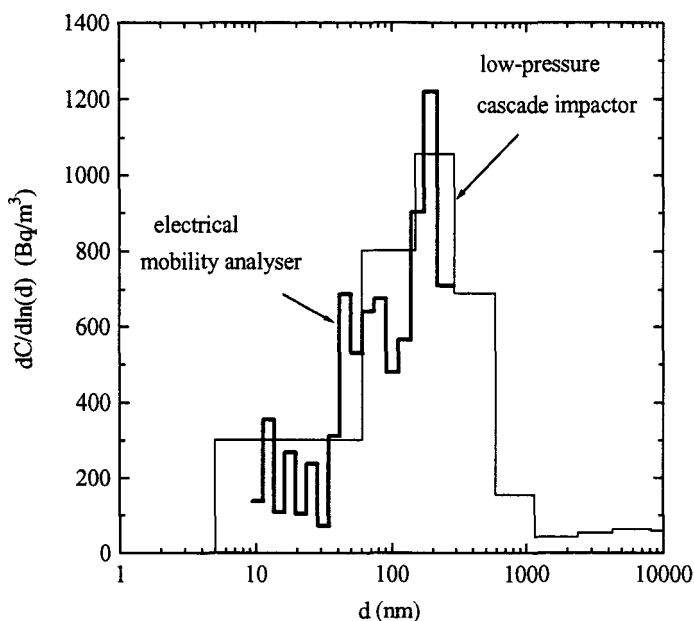


Figure 3: Averaged size distributions of ^{218}Po measured with an on-line- α -impactor and an electrical mobility analyser in connection with a detector unit for α -spectroscopy. These measurement were performed in a low ventilated room with an aged aerosol.

Table 1: Mean parameters of the lognormally approximated accumulation mode of the aerosol-attached short-lived radon decay products. These measurements were performed with the on-line- α -impactor in a low ventilated room with an aged aerosol. Extreme values of the single measurements are listed in parenthesis.

Nuclide	AMAD [nm]	σ_g	fraction [%]
^{218}Po	234 [197 - 357]	2.2 [1.9 - 2.5]	76 [63 - 79]
^{214}Pb	253 [210 - 352]	2.1 [2.0 - 2.3]	74 [61 - 80]
^{214}Bi	251 [204 - 343]	2.0 [1.8 - 2.3]	75 [59 - 83]

"Unattached" activities

The size distribution of the uncombined short-lived radon decay products in the diameter range 0.5-10 nm ("unattached" fraction) was measured taking six parallel air samples, five with screen diffusion batteries and one without as an absolute sample. To avoid entrance losses all sampling units were operated open faced. The activity concentrations of the different radon decay products were determined from the analysis of the decay curve by alpha spectroscopy and the size

distributions were evaluated from the penetration values using the expectation maximisation (EM) method.

Measurements were performed in homes and at two working places in rooms with elevated radon gas concentrations c_0 at different atmospheric conditions. In table 2 the mean values of c_0 , the aerosol particle concentration Z , the equilibrium factor F , and the unattached fraction f_p , of the different rooms are summarised.

Table 2: Mean values of the radon gas concentration c_0 , the aerosol particle concentration Z , the equilibrium factor F , the unattached fraction f_p and room description. In these rooms also the size distributions of the unattached short-lived radon decay products were measured (see table 3). H: home; W: working place.

room H/W	room description	atmosphere	no. of runs	Z [cm ⁻³]	C ₀ [Bq/m ³]	F	f _p
1 H1	cellar room	aged aerosol	18	3100	1510	0.25	0.191
		during air clean.	8	550	807	0.05	0.727
2 H2	cellar room (butanol vapours ¹)	aged aerosol	8	9600	7682	0.35	0.123
		burning candle	3	> 10 ⁵	8193	0.45	0.059
3 W1	water purif. unit laboratory	Z varying	4	11200	10600	0.54	0.062
4 W1	water purif. unit cellar room	Z varying	3	14000	29346	0.44	0.071
5 W1	water purif. unit filter room	Z varying	4	12800	22810	0.25	0.093
6 W1	water purif. unit water storage	Z varying	4	32700	489500	0.25	0.032
7 W2	asthma therapy mine	natural filtered air	5	< 200	8260	0.09	0.912

In table 3 preliminary results of the size analysis are compared (mean values). In general, it can be concluded from these measurements that most distributions of the uncombined fraction are narrow in size ($\sigma_g < 1.4$) with maximum diameters smaller than 5 nm. The mean median diameters ranged between 0.5 - 1.4 nm corresponding to the Stokes-Einstein diffusion coefficients D of 0.02 - 0.20 cm²/s.

Regarding all measurements there are indications of three different modes with median diameters around 0.53 nm ($D = 0.17$ cm²/s), 0.82 nm ($D = 0.08$ cm²/s) and 1.3 nm ($D = 0.03$ cm²/s). It is speculative to identify the first mode with pure or uncomplete hydrated ions and the others with charged and neutral clusters, because electrostatic interaction of charged aerosol particles or clusters with polar gas molecules yield lower diffusion coefficients compared to neutral species.

It is surprising that in room 1 with the most stable aerosol conditions a larger fraction of ²¹⁴Pb clusters may be charged compared to those of ²¹⁸Po. It further seems that atmospheres with vapours and other compounds of a burning candle (room 2) reduced neutralisation rates resulting in higher charged fractions of ²¹⁸Po, now similar to the values of ²¹⁴Pb. Higher amount of water vapours in the air (rooms 4-7) and butanol vapours (room 2) may increase neutralisation rates and yield similar diffusion coefficients of ²¹⁸Po and ²¹⁴Pb which corresponds to neutral clusters.

In two cases (rooms 1 and 7) the diffusion coefficient of the decay products ^{214}Bi was determined and yield values corresponding to neutral or pure ions. This result raise the question if neutral cluster may evaporate with time?

Further measurements including studies concerning the charged and neutral status of the ultrafine clusters are necessary to explain the differences between the size and diffusion coefficients summarised in table 3.

Table 3: Mean parameters of lognormally approximated size distributions of the short-lived radon decay products and the corresponding mean diffusion coefficients. Measurements were performed in homes (H) and at several working places (W) at different atmospheric conditions. Data evaluation method: EM-method.

room H/W	no. of runs	atmosphere	Nuclide	d_1 [nm]	σ_{g1}	f_1	d_2 [nm]	σ_{g2}	f_2	D [cm ² /s]
1 H1	18	aged aerosol RH=60%, T=20°C	^{218}Po	0.85	1.10	0.62	-	-	-	0.070
			^{214}Pb	1.37	1.09	0.11	-	-	-	0.027
	8	during air clean. RH=50%, T=20°C	^{218}Po	0.61	1.20	0.31	0.79	1.11	0.58	0.104
			^{214}Pb	1.10	1.07	0.44	-	-	-	0.042
			^{214}Bi	0.57	1.06	0.18				0.157
2 H2	8	aged aerosol + butanol vapours RH=50%, T=20°C	^{218}Po	0.52	1.07	0.10	0.61	1.28	0.33	0.149
			^{214}Pb	0.51	1.05	0.05	0.76	1.20	0.03	0.153
	3	burning candle + butanol vapours RH=50%, T=20°C	^{218}Po	1.36	1.09	0.19	-	-	-	0.028
			^{214}Pb	1.21	1.06	0.04	-	-	-	0.035
3 W1	4	varying aerosol concentration RH=60%, T=20°C	^{218}Po	0.61	1.22	0.11	0.83	1.12	0.25	0.095
			^{214}Pb	0.52	1.03	0.02	1.33	1.08	0.02	0.111
4 W1	3	varying aerosol concentration RH=90%, T=8°C	^{218}Po	0.51	1.07	0.13	0.87	1.13	0.20	0.117
			^{214}Pb	?	?	?	?	?	?	?
5 W1	4	varying aerosol concentration RH=100%, T=8°C	^{218}Po	0.53	1.17	0.07	0.85	1.12	0.24	0.097
			^{214}Pb	?	?	?	?	?	?	?
6 W1	4	varying aerosol concentration RH=100%, T=8°C	^{218}Po	0.52	1.03	0.11	0.83	1.34	0.01	0.184
			^{214}Pb	0.75	1.06	0.03	-	-	-	0.090
7 W2	5	natural filtered air RH=100%, T=8°C	^{218}Po	0.57	1.44	0.97	-	-	-	0.156
			^{214}Pb	0.89	1.02	0.89	-	-	-	0.064
			^{214}Bi	0.53	1.06	0.56	0.95	1.15	0.11	0.160

INTERCOMPARISON MEASUREMENTS

Side-by-side measurements were performed during October 2-4, 1991 in Northern Bavaria (Germany) in a house with elevated radon gas concentration by the following participants: EML of the US-DOE, New York, USA; ARL of the Department of Community and Health, Yallambie, Australia and the IL of the University, Göttingen, Germany.

One important objective of this intercomparison was to clarify if the methods for size analysis of these three laboratories yield equivalent results with regard to finally derived dose conversion factors. Although the results of the determined activity size distributions of the single measurements are sometimes considerable different, the averaged size distributions (three days) are in agreement on the main points.

In table 4 the averaged size distributions of ^{218}Po in the diameter range < 10 nm are compared. Although the median diameters of this size distributions agree only within a factor of two ($d_1 = 0.54-1.2$ nm; $D = 0.036-0.17$ cm^2/sec), the influence of these differences on the calculated average effective dose can be neglected (difference $< 30\%$). However, the difference of total amount of the "unattached" ^{218}Po (34-54%) is significant. The data evaluation sometimes yielded bimodal ^{218}Po distributions, with the additional mode in the size range 4-5 nm. This finding is important for future studies to understand the behaviour of radioactive aerosols or clusters in the environment; but the current dose models (1,2) show only minor influence on the calculated dose conversion factors using unimodal or bimodal distributions of the "unattached" activities.

In table 5 the results of the complete size distribution of the PAEC, measured by different screen diffusion techniques of ARL and EML are summarised. The weighted effective HE-DCF_s of the daily-averaged measurement differ less than 30%. The sizes of the aerosol-attached activities of the accumulation mode ($\text{AMD} = 192-297$) are quite different.

Activity size distributions of ^{214}Pb performed with different kind of low-pressure impactors of EML and IL are summarised in table 6. The difference of the median diameters of the accumulation mode ($\text{AMAD} = 238-332$) is surprising. However, both methods clearly show that a significant amount of ^{214}Pb is associated with aerosol particles in the diameter range 10-100 nm and sometimes in the diameter range of the coarse mode (~ 2000 nm). This findings are very important for correct dose calculations. The data of table 6 show the problem of accurate particle size measurements in the diameter range 10-100 nm.

From the results of these intercomparison can be concluded that there is agreement on the main points, but some disagreements on details of peak location and shape. However, most of this disagreements do not affect dose calculations very much. But these joint measurement clearly showed that accurate measurement of activity size distribution in the diameter range 10-100 nm, especially the range below the cut-size of the last impactor stage, is a difficult task that has not been fully solved as yet. The amount of short-lived radon decay products in this nuclei size range will have a major influence on the calculated dose. Furthermore this study show that it is necessary to have a closer look to the coarse mode size range with diameters of some microns. Additional measurements are necessary to clarify if the measured activity in this size range is real or if it is an artefact of the method or a misinterpretation of smaller particles.

During June 12-15, 1995 the US-DOE organised an international intercomparison measurement campaign for radon progeny size distributions at the environmental monitoring laboratory (EML), New York. In a radon chamber different experimental techniques (diffusion batteries, impactors) were compared under controlled aerosol conditions. Participants of this intercomparison measurements were EML, US-DOE (USA), AEA Technology (Great Britain), Australian Radiation Laboratory (Australia), US Bureau of Mines (USA), Clarkson University (USA), and the IL of the University Göttingen (Germany). A detailed data evaluation of all measurements is in progress. At the end of this year the results will be published as a DOE report.

Table 4: Activity size distributions of unattached ^{218}Po : average results of measurements performed during three days in a moderate ventilated room ($v < 0.5 \text{ h}^{-1}$). Average aerosol particle concentrations of $Z = 4450 \text{ cm}^{-3}$ (range: 2400-8000 cm^{-3}). The corresponding effective dose conversion factors HE-DCF(mSv/WLM) were derived from ICRP Task Group Model LUDEP, Version May 1993 (1,2).

Group/no. of measur.	method	d_1 [nm]	σ_1	f_1 [%]	d_2 [nm]	σ_2	f_2 [%]	HE- DCF [mSv/WLM]
IL Göttingen 7	Simplex, unimod. EM, unimodal	1.05	1.62	54	3.16	2.59	17	34.4
		0.84	1.76	52				30.6
	Simplex, bimodal EM, bimodal	0.84	1.01	41				3.88
ARL Yallambie 8	EM Twomey	0.59	1.15	20	2.80	1.20	20	27.3
		0.54	1.11	19	2.09	1.40	43	45.5
EML New York, 5	EM	1.19	1.20	34				22.3

Table 5: PAEC size distributions measured with screen diffusion techniques from EML and from ARL.

Date	group	"unattached" activities			accumulation mode		
		AMD (nm)	σ_g	fraction (%)	AMD (nm)	σ_g	fraction (%)
2 Oct. 1991	EML	1.2	1.4	18	173	2.5	82
	ARL	0.85	1.2	13	303	2.6	87
3 Oct. 1991	EML	1.25	1.3	11	222	2.0	89
	ARL	1.12	2.0	15	248	2.3	85
4 Oct. 1991	EML	1.1	1.3	14	180	2.2	86
		0.59	1.4	18	333	2.5	67
	ARL	4.5	1.5	15			

Table 6: Size distributions of aerosol-attached ^{214}Pb activities measured with a low-pressure cascade impactor (BERNER) and screens in series (IL, Göttingen) and a MOUDI impactor (EML, New York).

Date	group	Nuclei mode			Accumulation mode			Coarse Mode		
		AMAD (nm)	σ_g	fraction (%)	AMAD (nm)	σ_g	fraction (%)	AMAD (nm)	σ_g	fraction (%)
2 Oct. 1991	IL	27	2.1	32	367	1.6	44	~2000	?	24
	EML	< 50	?	18	235	1.9	70	1690	1.4	13
3 Oct. 1991	IL	51	< 1.2	25	353	2.1	74	~2000	?	1
	EML	< 50	?	19	248	1.9	75	1790	1.4	6
4 Oct. 1991	IL	48	< 1.2	26	255	2.3	66	~2000	?	8
	EML	< 50	?	35	225	2.0	61	1830	1.4	4
average	IL	44	< 1.2	27	332	2.0	65	~2000	?	9
	EML	< 50	?	22	238	1.9	70	1760	1.4	8

DOSE CALCULATIONS

Inhalation of short-lived radon decay products (^{218}Po , ^{214}Pb , ^{214}Bi / ^{214}Po) produces the largest amount of natural radiation exposure. The International Commission on Radiological Protection recommends a value of the effective dose per unit exposure of short-lived radon decay products by using an epidemiological approach. The dose conversion factor for the public is 3.9 mSv/WLM while the dosimetric convention for persons at working places is 5.1 mSv/WLM⁽³⁾. This procedure is unsatisfactory in terms of radiation protection because dose model calculations prove that the dosimetric impact of inhaled short-lived radon decay products may be underestimated by using an epidemiological approach⁽⁴⁾.

The purpose of this dose studies was to assess the influence of biological and aerosol parameters on human lung dose with regard to a comparison with the corresponding recommended dose values of the International Commission on Radiological Protection (ICRP)⁽³⁾. The dose conversion factor which gives the relationship between effective dose equivalent and potential alpha energy concentration of inhaled short-lived radon decay products was calculated with a dosimetric approach. The calculations base on a lung dose model with a structure that is related to the recommended ICRP dose model⁽⁵⁾. Because of the short half-lives of the investigated nuclides modifications of the model were necessary especially concerning particle deposition in the respiratory tract and the mathematical description of assumed nuclide pathways.

Main emphasis was focused on biological and aerosol parameter variability like variation of breathing rate and breathing mode, clearance velocities, critical cells for the induction of lung cancer, particle size and dispersion of the activity size distributions. Dose calculations with this improved model shows that the dosimetric approach leads to a dose conversion convention which is a factor of more than two times higher than the recommended epidemiological values of the ICRP. The dosimetric results yield both for indoor and mine aerosol conditions dose conversion factors in the range of 10 mSv/WLM to 15 mSv/WLM depending on breathing mode.

The uncertainty of biological or aerosol parameters cannot explain the discrepancy of the epidemiological and dosimetric approach. Clearance mechanisms are of minor importance for the dosimetry of short-lived decay products due to the short half-lives of these nuclides. A significant dose reduction as consequence of nuclide transfer to blood is only expected for transfer rates in the order of the half-lives of the investigated nuclides. Experimental results give no indication for this assumption⁽⁶⁾. In contrast to the above mentioned parameters the deposition pattern in the respiratory tract and the choice of critical cell types in the epithelium are more dose relevant. The deposition model of Rudolf et. al.⁽⁷⁾ which serves as a standard in the presented study takes into account the results of all relevant deposition studies in the past twenty years. The algebraic formulation of these experimental results seems to be a reliable data base.

The assumption that secretory cells alone are the critical cells for the induction of lung cancer lead to an increase of dose conversion factors. In addition there are other indications that the calculated values form the lower limit of the dosimetric approach. The recommended apportionment factors of 0.333/0.333/0.333 for the bronchial, bronchiolar and alveolar region should be replaced by a weighting procedure with higher dose contribution of the bronchial region⁽⁸⁾. This would increase total lung dose especially for high concentrations of unattached activity as well as a higher breathing rate of 1.7 m³/h which is recommended by the ICRP Task Group for "heavy working conditions"⁽³⁾.

Within the framework of the dosimetric approach a possible source of uncertainty may be the alpha radiation weighting factor ($w_r = 20$)⁽⁹⁾. The discrepancy of the dosimetric and epidemiological approach may be interpreted in that way that the alpha radiation weighting factor is overestimated as already proposed by Birchall and James⁽⁴⁾. But it has to keep in mind that a reassessment of the alpha radiation weighting factor would also influence the dosimetry of all alpha emitting nuclides but not only the dosimetry of radon decay products.

References

- [1] James, A.C., Gehr, P., Masse, R., Cuddihy, R.G. Cross, F.T., Birchall, J.S. Durham, J.S. and Briant, J.K. *Dosimetry model for bronchial and extrathoracic tissues of the respiratory tract*. Radiation Protect. Dosim. 37, 221-230(1991).
- [2] James, A.C. Private Communication, May 1993
- [3] International Commission on Radiological Protection. *Protection against Radon-222 at Home and at Work*, ICRP Publication 65, Ann. ICRP 23 (2) (Oxford: Pergamon Press) (1994).
- [4] Birchall, A. and James, A.C. *Uncertainty Analysis of the Effective Dose per Unit Exposure from Radon Progeny and Implications for ICRP Risk-Weighting Factors* Radiation Protection Dosimetry 53, 133-140 (1994).
- [5] International Commission on Radiological Protection. *Human Respiratory Tract Model for Radiological Protection*. ICRP Publication 66, Ann. ICRP 24 (1/4) (Oxford Pergamon Press) (1994).
- [6] Greenhalgh, J.R., Birchall, A., James, A.C., Smith, H. and Hodgson, A. *Differential Retention of Pb-212 Ions and Insoluble Particles in Nasal Mucosa of the Rat*. Phys. Med. Biol. 27 (6), 837-851 (1982).
- [7] Rudolf, G., Köbrich, R. and Stahlhofen, W. *Modelling and Algebraic Formulation of Regional Aerosol Deposition in Man*. J. Aerosol Sci. 21 (Suppl. 1), 403-406 (1990).
- [8] Askin, F.B. and Kaufman, D.G. *Histomorphology of Human Lung Cancer Carcinogenesis: a Comprehensive Study*, Cancer of the respiratory tract: predisposing factors, Raven Press, 8, 17-21 (1985).
- [9] Schwartz, J.L., Rotmensch, J., Atcher, R.W., Jostes, R.F., Cross, F.T., Hui, T.E., Chen, D., Carpenter, S., Evans, H.H., Menci, J., Bakale, G. and Rao, P.S. *Interlaboratory Comparison of Different Alpha-Particle and Radon Sources: Cell Survival and Relative Biological Effectiveness*. Health Physics 62 (5), 458-461 (1992).

PUBLICATIONS

A. Reineking, G. Butterweck, J. Porstendörfer, J.C. Strong, H. Vanmarcke, R. Van Dingenen

"Intercomparison of methods for investigating the physical characteristics of radon decay products in the indoor environment", Radiat. Prot. Dosim. 45, 41-46, 1992

G. Butterweck, J. Porstendörfer, A. Reineking, J. Kesten

"Unattached fraction and the aerosol size distribution of the radon progeny in a natural cave and mine atmospheres", Radiat. Prot. Dosim. 45, 167-170, 1992.

J. Porstendörfer, A. Reineking

"Indoor behaviour and characteristics of radon progeny", Radiat. Prot. Dosim. 45, 303-311, 1992

A. Reineking, G. Butterweck, J. Kesten, J. Porstendörfer

"Thoron gas concentration and aerosol characteristics of thoron decay products", Radiat. Prot. Dosim. 45, 353-356, 1992

A. Reineking, G. Butterweck, J. Kesten, O. Malolepsy, B. Kopka, H.-J. Heymel, E. Speer, J. Porstendörfer

"A monitor for continuous and simultaneous measurement of environmental thoron and radon gas"
Proceedings of thoron/thoron progeny intercomparison, (Editor J. Bigu), Elliot Lake, Canada, November 2-6, 1992

P.K. Hopke, R. Strydom, M. Ramamurthi, E.O. Knutson, K.W. Tu, P. Scofield, R.F. Holub, Y.S. Cheng, Y.F. Su, W. Winkelmayr, J.C. Strong, S. Solomon, A. Reineking
"The Measurements of Activity-Weighted Size Distributions of Radon Progeny: Methods and Laboratory Intercomparison Studies", Health Physics 63, 560 - 570, 1992

J. Kesten, G. Butterweck, J. Porstendörfer, A. Reineking, H.-J. Heymel
"An Online α -impactor for Short-Lived Radon Daughters", Aerosol Science and Technology 18, 156-164, 1993

A. Reineking, J. Kesten, G. Butterweck, J. Porstendörfer, E.A. Knutson, A.C. George, S.B. Solomon
"Size distributions of unattached and aerosol-attached short-lived radon decay products:some results of intercomparison measurements", Radiat. Prot. Dosim. 56, 113-118, 1994

A. Reineking, J. Porstendörfer, G. Butterweck
"Size distribution of "unattached" short-lived radon decay products in dwellings.
Journal of Aerosol Science 25, S67-S68, 1994

C. Zock, J. Porstendörfer, A. Reineking
"Measurements of indoor number size distributions and activity distributions of ^{218}Po "
Journal of Aerosol Science 25, S251-S252, 1994

J. Porstendörfer, C. Zock, A. Reineking
"Comparison of the aerosol number size distribution with the activity size distribution of the radon daughters aerosol."
in: INDOOR AIR: An integrated approach. pp 145-148. Proceedings of an International workshop, Gold Coast Australia, 27 November - 1 December 1994. (Eds.: L. Morawska, N.D. Bofinger, M. Maroni), Elsevier Science, Oxford, UK, 1995

Head of project 2: Dr. Poffijn

II. Objectives for the reporting period

- Laboratory and field measurements of radon and radon daughter concentrations in collaboration with the SCK/CEN “Bronchial Dosimeter”.
- Tests with new on-line radon and radon daughter measuring devices.

III. Progress achieved including publications

The aerosol equipment of our group (TSI 3020) has participated in an inter-comparison exercise done by Rita Van Dingenen at ISPRA (Italy). This exercise consisted of two parts : laboratory tests under controlled conditions where the accuracy of the equipment in the different modes was tested and field measurements during the “Hudson Cruise”, a transatlantic measuring campaign to collect data on general pollution of the air. The results of this exercise exposed some problems with the equipment. These problems were solved by repairing the equipment or changing the software.

Simultaneous measurements with the “Bronchial Dosimeter” from the SCK/CEN and with the radon daughter measuring system from the UGent have been performed in a couple of dwellings. Results of one of the measurements are shown in fig. 1. This graph shows the equilibrium factor as measured by the SCK/CEN and the UGent. Both results are in good agreement with each other. Due to problems with the aerosol equipment, no useful data was available for this part of the exercise.

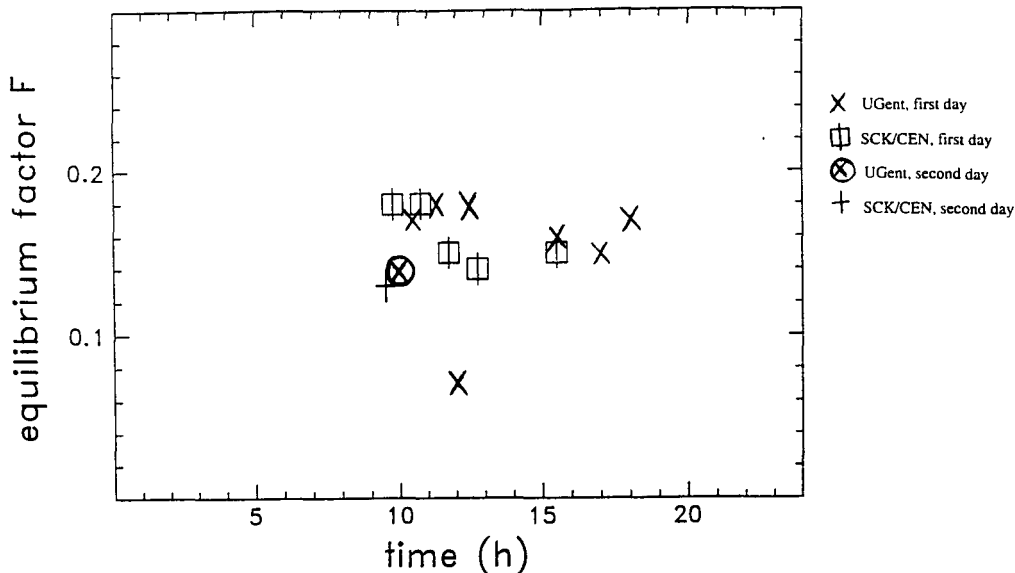


Fig 1 : Equilibrium factor in a Belgium dwelling, measured by SCK/CEN and UGent.

Laboratory tests with a new type of on-line radon daughter measuring devices have been conducted. These tests were done in close collaboration with Dr. Thomas Streil from Sarad GmbH. This measuring device (type EQF3000) consists of a sampling head with filter and a radon measuring chamber. After air sampling, the activity on the filter and in the radon measuring chamber is measured. This results in values for the radon concentration and the equilibrium factor every 2 hour. Different measurements in high and medium radon concentrations have been performed. Fig 2 shows results from measurements in our radon chamber. The equilibrium factor changes drastically under the influence of changing aerosol conditions. Fig 3 shows results from a measurement in a cellar from our laboratory. The values of the radon concentration and of the equilibrium factor were in good agreement with our own measurements.

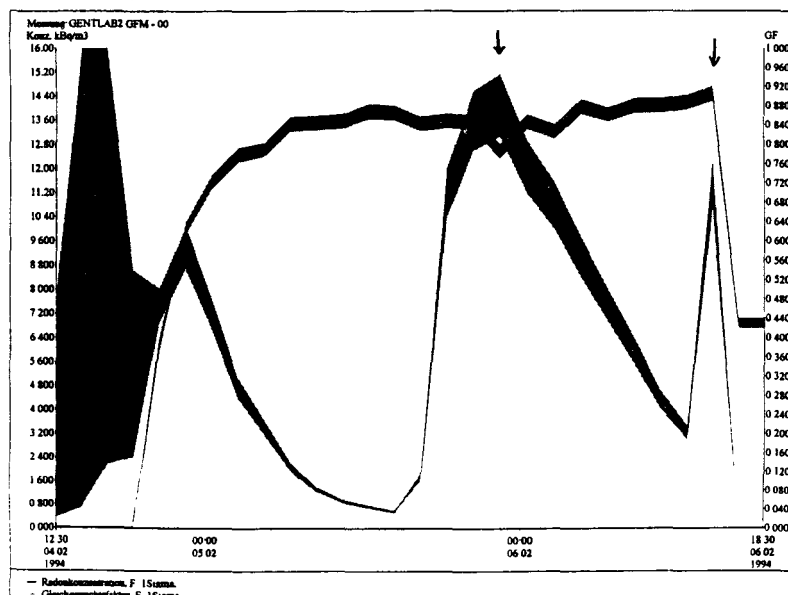


Fig 2 : Radon and equilibrium factor measurements in the radon exposure facility of UGent. The peaks in equilibrium represent drastic changes in aerosol concentration.

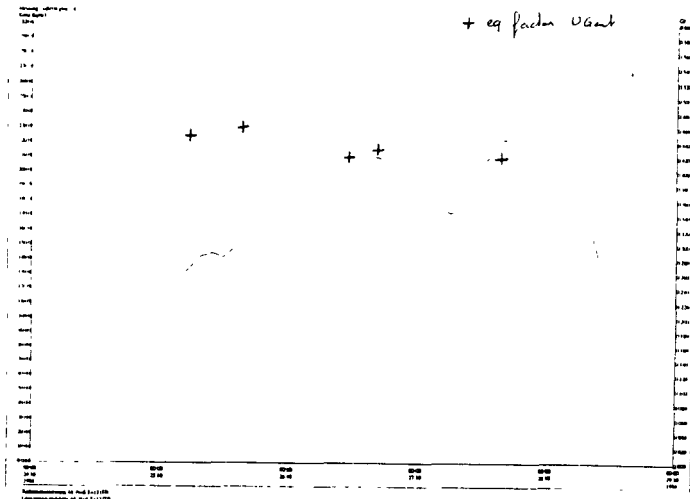


Fig 3 : Radon and equilibrium factor measurements in a cellar.

The EQF3000 device was tested for long term measurements in the framework of the CEC Radon intercomparison campaign that was held during spring 1995. This campaign consisted of 2 parts : laboratory exposures in the radon chamber from the NRPB and house exposures in three dwellings in Sweden, Luxembourg and Italy for a period of 2-3 months. The radon chamber exposures were performed under controlled radon and aerosol conditions. For the house exposures the local responsible scientists monitored different parameters of the dwelling. The result of one of the EQF3000 measurements is shown in fig 4.

First analysis of the laboratory and house results show that the EQF3000 devices performed satisfactory. Detailed analysis of these results is expected in the coming months (autumn 1995).

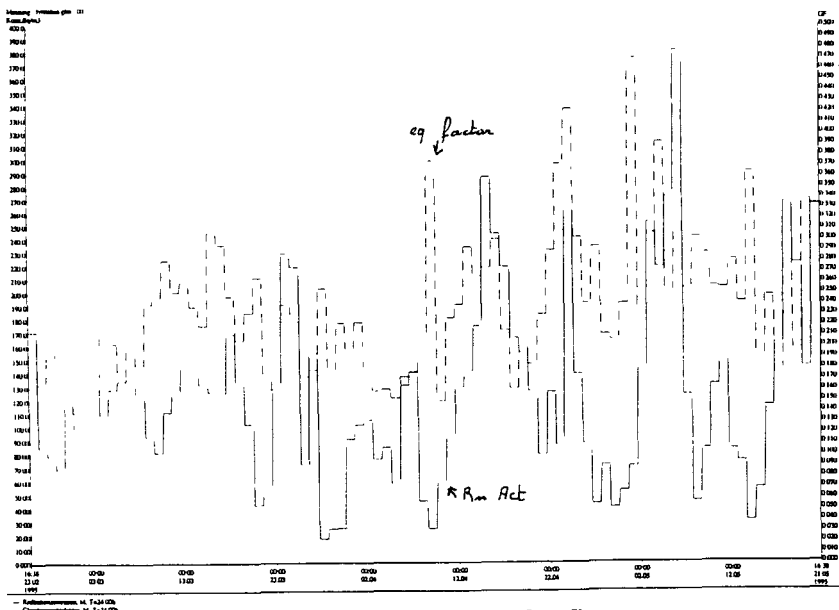


Fig 4 : Radon and equilibrium factor measurements in a dwelling in Sweden during 3 months.

Head of project 3: Dr. Vanmarcke

II. Objectives for the reporting period

Design and built-up of a measurement system to assess directly the deposition characteristics of the short-level radon decay-products in the respiratory tract.

Investigations on possible differences in the plate-out rate between the different unattached radon daughters.

III. Progress achieved including publications

The airborne decay products of radon deposit in the respiratory tract leading to a radiation dose to the lung. In the indoor environment this deposition strongly depends on the attachment rate of the freshly formed decay products to aerosol-particles and on the plate-out rate to indoor surfaces. Since it is known that the unattached fraction of the decay products is a major contributor to the radiation dose, several attempts have been made to measure the activity size distribution of the unattached fraction. These measurements on the basis of wire-screen methods were only partially successful, because there are intrinsic problems to separate the unattached fraction completely from the rest of the activity size distribution [1].

Therefore, it has been suggested to simulate the deposition characteristics of the short-lived radon daughters in the nasal and bronchial regions and measure the deposited activity directly. According to the theoretical concept of such a measurement system [2] a so-called bronchial dosimeter has been built at the Belgian Nuclear Research Center, SCK•CEN.

Concept of the bronchial dosimeter and efficiency determination

Basically, it is assumed that the deposition characteristics of the nasal cavity and the bronchial tree may be simulated by different numbers of screens [3,4] Their respective sizes and numbers are determined by comparing models of the respiratory tract with results from the screen penetration theory. For an average nasal inspiration flow rate of 30 l/min, a 400 mesh screen operated at a face velocity of about 12 cm/s provides a rather good approximation to the nasal absorption characteristics [5]. Adding up four such screens provides a good approximation to the bronchial tree [6,7].

The bronchial dosimeter consists basically of two different units. The first unit is the sampling section, which is used to collect the airborne radon decay products. This part of the dosimeter consists of three different sampling channels:

1. The sampling head of the first channel consists of an open-faced polycarbonate membrane filter with a pore size of 0.4 μm , which collects the total airborne activity
2. In the second head the filter is covered by a 400 mesh screen in order to collect the activity penetrating the nasal cavity. The activity deposited in the nasal cavity is then given by the difference between the activity collected on filter (1) and filter (2).
3. The filter of the third sampling head is covered by five 400 mesh screens to collect the difference between the airborne activity and what deposits in the nasal cavity plus bronchial tree. From the difference between the activity collected on filters (2) and (3) the activity absorbed in the bronchial tree is obtained.

The sampling section of the bronchial dosimeter is shown in Fig.1 For further details it is referred to ref. [8].

The second unit of the bronchial dosimeter is the alpha-spectrometer section which consists of three separate α -detectors. After sampling the filters remain mounted on their sampling heads in order to keep the counting geometry reproducible. The sampling heads are put into the vacuum chambers, where the filter activities due to the α -decay of ^{218}Po and ^{214}Po are measured. From the peak areas obtained in two subsequent measurements the decay product concentrations of ^{218}Po , ^{214}Pb , and ^{214}Bi (^{214}Po) collected on the filters can be calculated.

The efficiency of the bronchial dosimeter is determined by the efficiency of one sampling channel and the intercomparison of all three channels. The efficiency of one sampling channel is determined by measuring the α -activity from ^{218}Po and ^{214}Po and the γ -activity following the β -decay of ^{214}Bi .

During the efficiency determination the sampling section of the bronchial dosimeter was placed in a chamber with a volume of about 6 m^3 . The radon activity concentration c_{Rn} varied between 26 kBq/m^3 and 10 kBq/m^3 . The sampling time was 10 min. After sampling the filters were transferred to the vacuum chambers within 1 min. The α -activity of all sampling heads were measured for 5 min and then for 15 min. Afterwards, the sampling head of channel (1) was transferred to a germanium detector. The γ -activity of filter (1) and the α -activities of filter (2) and (3) were measured for 30 min. From the area under the γ -peak at $E_\gamma = 609.3 \text{ keV}$, the photon branching ratio and the γ -detection efficiency the expected number of α -particles $N_\alpha^{(e)}$ from ^{214}Po is determined. The detection efficiency for α -particles ϵ_α of this

sampling channel is then the ratio between the number of α -particles extrapolated from the α -measurements, $N_{\alpha}^{(m)}$, and $N_{\alpha}^{(e)}$

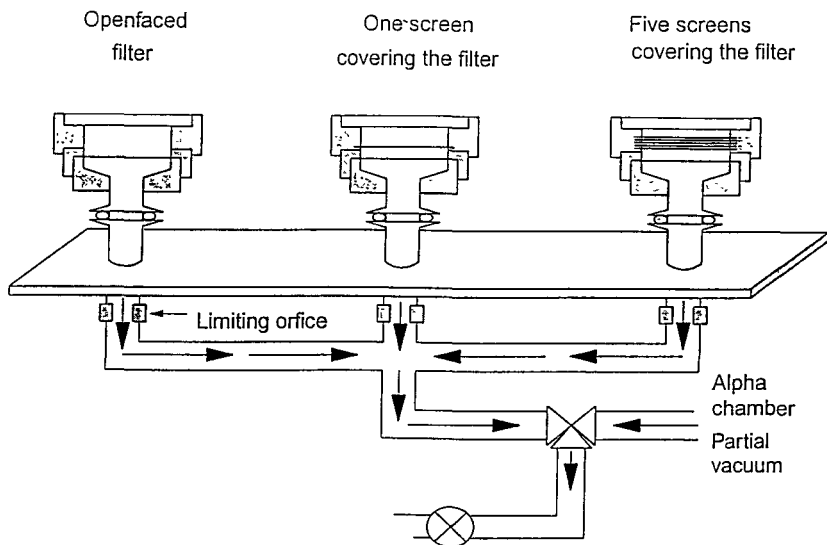


Fig. 1: Sampling section of the bronchial dosimeter. The open diameter of one sampling channel is 4 cm. The flow rate at standard atmospheric conditions is 9.1 l/min leading to a face velocity of 12 cm/s.

The efficiency of sampling channel (1), $\epsilon_{\alpha,1}$, obtained from six measurements is indicated in Fig. 2 together with the respective data. From these data the efficiency of the other two sampling channels, $\epsilon_{\alpha,2}$ and $\epsilon_{\alpha,3}$, were determined by intercomparing the equilibrium equivalent radon concentrations (EEC). The results are also given in Fig. 2. Their relative uncertainty on the mean value is less than 1.1 % at one standard deviation.

3. First experimental experience

Under laboratory conditions test measurements with the complete system were performed. In the beginning the radon concentration was about 4.5 kBq/m³ and drops to about 1.5 kBq/m³ at the end of the test period. The sampling period was 5, 6 or 7 min. The filter activities were measured during two periods for 10 min and 35 min, respectively.

From the open-faced filter of sampling channel (1) the EEC in air was obtained. Division of an EEC-value by its corresponding radon activity concentration c_{Rn} gives the equilibrium factor F, which gives a characterization of the aerosol-concentration present (see e.g. ref. [9]).

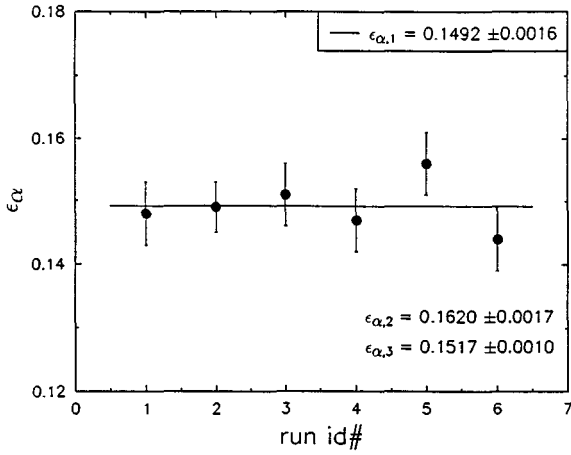


Fig. 2: Efficiency of sampling channel (1) obtained at a distance of 0.7 cm from the detector. The full line indicates the weighted average of the data.

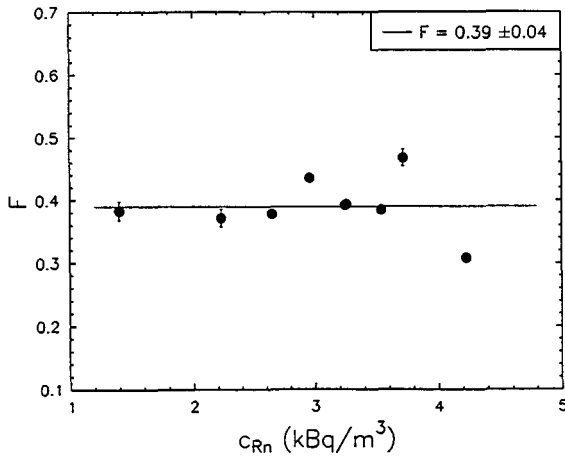


Fig. 3: Equilibrium factor F as a function of the radon concentration c_{Rn} . The average value for F = 0.39 with a relative standard deviation less than 11 %.

In Fig. 3 F is shown as a function of c_{Rn} . The average equilibrium factor throughout the test measurements was 0.39 with a relative uncertainty less than 11 % at one standard deviation, which indicates rather stable atmospheric conditions during the measurement campaign. The obtained fractional deposition of the short-lived decay products in the nasal cavity (f_n) as well as in the bronchial tree (f_b) is shown as a function of F in Fig. 4 for each nuclei separately. Although the data show some fluctuations, it is still valid to define average fractional depositions for the different decay products. Average values \bar{f}_n and \bar{f}_b taken from the data of ten measurements are summarized in Tab. 1.

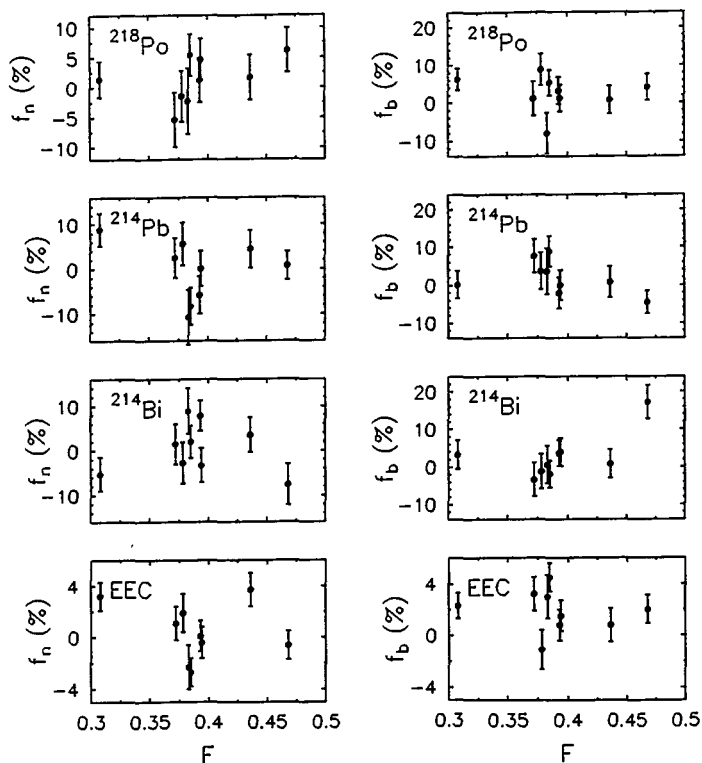


Fig. 4: Fractional deposition of the short-lived radon decay products ^{218}Po , ^{214}Pb , ^{214}Bi and the equivalent equivalent radon concentration (EEC) as a function of the equilibrium factor F . The left part shows the fraction of decay products deposited in the nasal cavity (f_n), and the right part shows the fractional deposition in the bronchial tree (f_b).

Table 1: Average fractional deposition of the short-lived radon decay products in the nasal cavity \bar{f}_n and the bronchial tree \bar{f}_b . The values are averaged over nine measurements with equilibrium factors $F = 0.39 \pm 0.04$

Average fractional deposition	^{218}Po 10^{-2}	^{214}Pb 10^{-2}	^{214}Bi 10^{-2}	EEC 10^{-2}
Nasal cavity \bar{f}_n	1.3 ± 1.3	-0.3 ± 2.2	0.5 ± 1.9	0.4 ± 0.7
Bronchial tree \bar{f}_b	4.4 ± 1.0	1.1 ± 1.6	2.5 ± 2.0	1.9 ± 0.5

4. Conclusion

According to the conceptual design of a multiple wire screen sampler in ref. [2] a bronchial dosimeter has been built. First test measurements were performed under laboratory conditions. It turned out, that the bronchial dosimeter is a suitable facility to individually assess deposition characteristics of the different short-lived radon decay products in the nasal cavity as well as in the bronchial tree. However, the interpretation of the data strongly depend on the underlying model of the respiratory tract, which influences the choice of the mesh size as well as the number of screens used for the sampling heads. For instance, according to recent model calculations [11] the nasal absorption might be better simulated by a screen with a 100 mesh grid.

References

- [1] Ramamurthi, M. and P. H. Hopke, Health Physics 56 (1989) 189
- [2] Hopke P. H., M. Ramamurthi and E. O. Knudson, Health Physics 58 (1990) 291
- [3] Cheng Y. S. and H. C. Yeh, J. Aerosol Sci. 11 (1980) 313
- [4] Cheng Y. S., J. A. Keating and G. M. Kanapilly, J. Aerosol Sci. 11 (1980) 549
- [5] Cheng Y. S., Y. Yamamda, H. C. Yeh and D. L. Swift, J. Aerosol Sci. 19 (1988) 741
- [6] James A. C., Radon and its Decay Products (edited by P. K. Hopke) ACS Symposium Series 331 (1987), 400
- [7] James A. C., Radon and its Decay Products in Indoor Air (edited by W. W. Nazaroff and A. V. Nero) Wiley-Interscience (1988) 259
- [8] Oberstedt S. and H. Vanmarcke, Rad. Prot. Dosim. 59 (1995) 285
- [9] Porstendörfer J., Fifth International Symposium on the Natural Radiation Environment (tutorial sessions), edited by the Commission of the European Communities, EUR 14411 EN (1993) 69
- [10] Wilkening M., Studies in Environmental Science 40 (Radon in the Environment), Elsevier (1990) 126
- [11] George A. C. and E. O. Knudson, Radiat. Prot. Dosim. 45 (1992) 689

Contributions to International Conferences and Journals

Calibration of a Polycarbonate Track-etch Detector

H. Vanmarcke, A. Toye, S. Oberstedt, Posterpresentation at the First International Workshop on Indoor Radon Remedial Action 27.06 - 2.07.1993, Rimini (Italy), and Rad. Prot. Dosim Vol. 56, 1-4 (1994) 239

Recent Investigations on Indoor Radon at SCK•CEN Mol

S. Oberstedt and H. Vanmarcke, Euregional Symposium on Radon in our EUREGIO Nov. 4-6, 1993, Liège (Belgium) and Annales de l'Association belge de Radioprotection, Vol. 19, 1-2 (1994) 255

Radon in the Indoor Environment

S. Oberstedt, H. Vanmarcke, SCK•CEN scientific report (1993) 114

The Bronchial Dosemeter

S. Oberstedt, H. Vanmarcke, SCK•CEN Internal Report BLG 667, November 1994, and Rad. Prot. Dosim. 59 (1995) 285

Lack of Consistency in the ICRP Approach on Protection Against ^{222}Rn at Home and at Work

H. Vanmarcke, Health Phys. 67 (1994) 668

Radon in the Indoor Environment

S. Oberstedt, H. Vanmarcke, SCK•CEN scientific report (1994), in press

Radon in the Indoor Environment (A Status Report)

S. Oberstedt, Scientific Programme Report (1 02.93-31.01 95), SCK•CEN Internal Report BLG 679, March 1995

National Intercalibration Exercise on Polycarbonate Track-etch Detectors

S. Oberstedt and H. Vanmarcke, SCK•CEN Internal Report BLG 683, May 1995

Manageability, the Clue to the ICRP Radon Approach

H. Vanmarcke, P. Govaerts and S. Oberstedt, Sixth International Symposium on the Natural Radiation Environment June 5-9, 1995, Montreal (Canada), Book of Abstracts, p. 265, and Environment International, in press

A Radon Exhalation Monitor

S. Oberstedt and H. Vanmarcke, SCK•CEN Internal Report BLG 684, July 1995, and sent for publication

Assessment of radon-daughter deposition in the respiratory tract

S. Oberstedt, H. Vanmarcke, International Symposium on Radiation Protection in Neighbouring Countries, September 4-7, 1995, Portoroz (Slovenia)

New techniques for radon progeny monitoring

S. Oberstedt, Invited Lecture at Institute Laue-Langevin, Grenoble (France), 23.06.95

Head of project 4: Prof. Akselsson

II. Objectives for the reporting period

The objectives were to design and construct an improved radon exposure chamber for studying radon / aerosol interaction, to further develop and characterise a multi - orifice impactor for radon progeny size measurements, to investigate the hygroscopic growth of indoor aerosols using the Tandem DMA technique.

III. Progress achieved including publications

The new improved radon environmental chamber has been finished during the reporting period. It has proved to be a very useful tool for conducting radon/radon progeny experiments during well controlled conditions. The radon chamber is described in detail in a separate report (publication 1).

The characterisation of the multi-orifice impactor with 50 μm nozzles has been completed during the reporting period. The results show that steep collection efficiency curves with cut-off diameter as low as 35 nm can be achieved with a plate porosity of 1 % (figure 1). This means that the impactor can be used to measure the size distribution of radon progeny activity in the, from a dosimetric view, important size range below 0.1 μm . The extensive study of the performance of the impactor shows however, that the so-called cross-flow limits the maximum air flow rate through the impactor as well as the diameter of the nozzle cluster. In the next phase of this study, we will investigate how this limitation affects the sampling in dwellings with low or moderate radon concentrations. A full technical description of the impactor can be found in resulting publication 2.

The multi-jet impactor will be used in the new radon progeny sampler which is currently being designed and constructed in our laboratory. The sampler uses track-etch technique and will be used as an integrating dose-meter in dwellings.

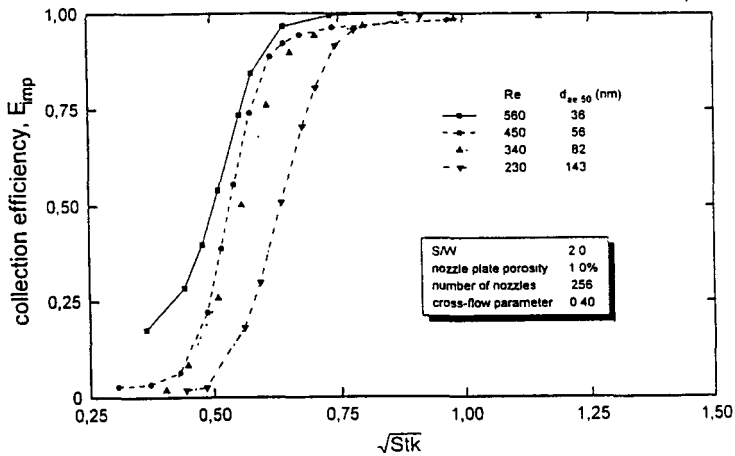


Figure 1. Collection characteristics of the multi-orifice impactor.

Within the aerosol group of Lund University a system for measuring hygroscopic growth of particles has been developed. This system uses a so-called Tandem Differential Mobility Analyzer (TDMA), where the first DMA separates the particles into discrete size bins. After the aerosol has been humidified, the resulting size distribution is analysed with the second DMA. A schematic picture of the TDMA is shown in figure 2. The issue of particle growth during humid conditions is extremely important for accurate dose calculations, since the dose per inhaled unit of radon progeny activity is depending strongly on size distribution of the progeny. In so-called lung models, typically no growth or a twofold growth is assumed, but little data is available.

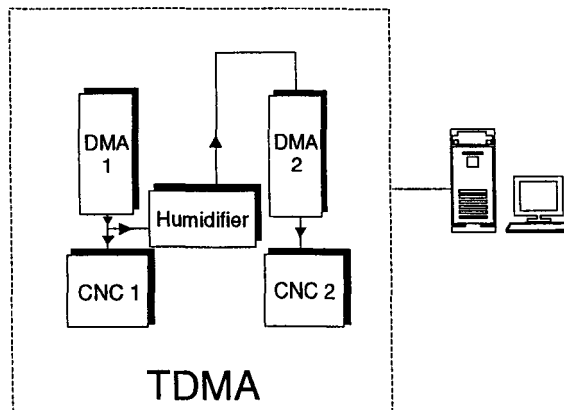


Figure 2. Schematic view of the TDMA system. CNC=Condensation Nucleus Counter, DMA=Differential Mobility Analyzer

We have used the TDMA system in our radon chamber, for analysing common indoor aerosols, such as cigarette smoke, dust, and particles produced by cooking. During our experiments, the relative humidity in the TDMA was 90-93 %, which is a bit low to really mimic the human respiratory tract, but the humidity can be increased if the system is slightly modified. The preliminary results from this study can be found in resulting publication 3. One example of the results is shown in figure 3. In short, the study shows that the TDMA is a powerful tool for studying hygroscopic growth of particles. More studies have to be carried out at a higher relative humidity before anything conclusive can be said about the behaviour of "household" aerosols in the human airways.

In the future we want to systematically study each possible source of particles in the domestic environment, in order to determine the strength of the source and the growth of the particles in the TDMA. This study will initially be performed in our radon chamber, but it is our intention to conduct experiments in a real dwelling.

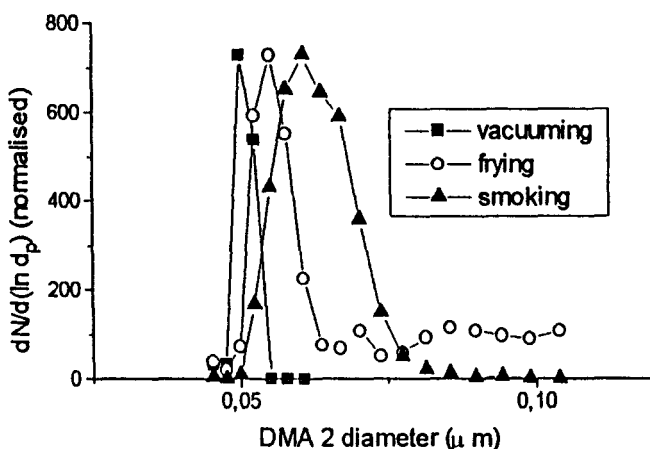


Figure 3. The measured particle size distributions after humidification. The diameter of the particles before humidification was 50 nm.

A study has also been performed to investigate possible discrepancies between radon progeny concentration close to the human body and in free air, respectively. The results from this study, which is described in resulting publication 4, showed that the possible depletion of particles and radon progeny close to the human body surface is negligible in most cases. Sampling far from the body is therefore representative also for determining radon progeny concentration and unattached fraction in the breathing zone.

Resulting Publications

1. Eklund, P. "The Walk-In Radon Exposure Chamber at the Department of Working Environment, Lund Institute of Technology" Dept. of Working Environment Report ISRN LUTMDN/TMAT--7001--SE (1995)

2. Gudmundsson, A. Bohgard, M. and Hansson, H.C. "Characteristics of Multi-Nozzle Impactors with 50 μm Laser-Drilled Holes" J. Aerosol. Sci. 26:915-931 (1995)
3. Eklund, P. Berg, O. and Swietlicki, E. "Characteristics of Aerosols from some Typical Domestic Sources" Proc. of the Symposium of the Nordic Society for Aerosol Research (NOSA), Lund, Sweden, 1994 (1994)
4. Eklund, P. and Bohgard, M. "Aerosol Properties and Unattached Fraction of Radon Daughters Close to the Human Face" Rad. Prot. Dosim. Vol. 56, Nos. 1-4, 133-135 (1994)
5. Eklund, P. "Design and Operation of a Walk-in Radon Environmental Chamber" Licentiate thesis, Dept. of Working Environment, Lund Institute of Technology (1995)

Head of project 5: Dr. Falk

II. Objectives for the reporting period

Modification of the experimental technique for the continuation of deposition studies on radon progeny in humans.

Size determination of the unattached fraction of the three radon daughters using wire screen technique.

To develop and investigate the properties of a simple field device for the measurement of size distribution of "unattached" radon progeny in dwellings.

Measurements of ^{220}Rn and ^{222}Rn progeny indoors in some Swedish dwellings and if possible determine the ^{220}Rn progeny unattached fraction.

II. Progress achieved including publications

Human studies

The experimental study to determine the fraction of inhaled radon daughters deposited in the human air ways has been carried out with a combination of two different techniques. The total amount of radon daughter deposited during the exposure was determined by measurement of the radon daughter concentration in inhaled and exhaled air. The sites of deposited radon daughters were immediately after the end of the exposure assessed by external γ -measurements of the subject in a low level whole-body laboratory.

The experiments carried out during previous reported period was focused on the different deposition pattern between the "unattached" fraction and the radon daughters carried by an aged aerosol. The experiences acquire from these studies show difficulties to have control of necessary parameters when the exposure was performed with high unattached fraction. Plate-out on clothes and body surfaces added to the difficulties.

A new design of the arrangements for the collection of exhaled radon progeny has been developed and will be used in the continuation of the study. In principle the exhaled air is sucked through a filter placed at very short distance from the exhalation mouthpiece. In order obtain a breathing condition as natural as possible a pressure gauge attached to the mouthpiece controls the speed of the air-pump sucking the exhaled air through the filter. By these arrangements no breathing force is needed independent of breathing rate. See fig 1.

The external γ -measurements of subjects for the regional deposition determination of the inhaled radon progeny is difficult to arrive at using collimated detector systems due to limited activity available and also due to relative high γ -energies emitted. The approach used with multi-detectors placed close to the body surface over chest and head seems to be a feasible technique. For future studies 5 large NaI(Tl) detectors (\varnothing 125 mm x 100 mm) will be used. Two over the head, one over the upper airways and two over the lungs. Higher sensitivity, better reproducibility and possibility to clearance studies is expected from this new set up.

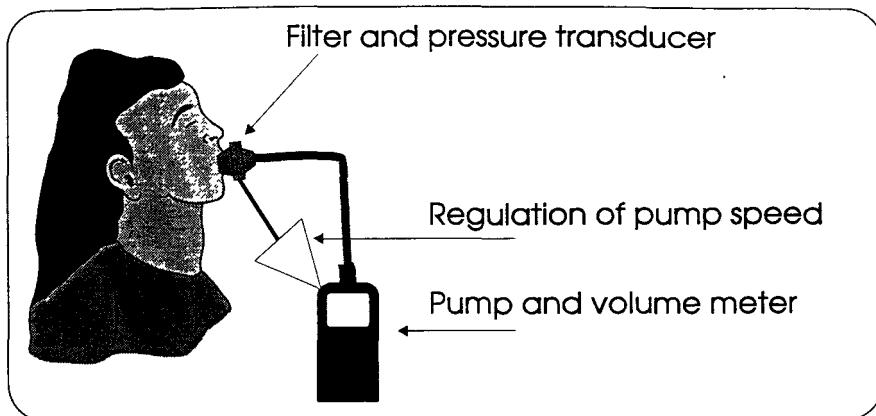


Fig 1. New design of apparatus for collection of exhaled radon progeny.

Size distribution studies of "unattached fraction"

The determination of the size for the unattached fraction of airborne radon progeny has been performed in a test-chamber inside a walk-in radon-room. The aerosol concentration in the room was lowered to less than 1000 particles/cm³. With an additional filter for the test-chamber the aerosol concentration during the study was typical less than 200p/cm³ giving practically no attached radon progeny in the test atmosphere.

Using different flow-rates and different mesh sizes for the wire screens, the collection efficiency of the unattached daughters could experimentally be determined. Knowing the characteristics dimensions of the screen and the flow-rate used, the aerodynamic size of the unattached fraction could be calculated by use of the screen-type diffusion battery theory. A significant difference in size of the unattached ²¹⁸Po and ²¹⁴Bi was found. No data for the "unattached" ²¹⁴Po could be obtained due to large counting statistical errors. The "unattached" ²¹⁸Po cluster is about 0.8 nm diameter while the ²¹⁸Bi cluster is somewhat larger or about 1.2 nm. As can be seen in fig 2 the results are in agreement for the three different mesh sizes used. The error bars represent the SD from repeated experiments with different flow-rates, ranging from 4 - 24 litres/min. The result obtained is a confirmation of findings from other groups when "unattached" radon progeny is studied in fairly clean laboratory air.

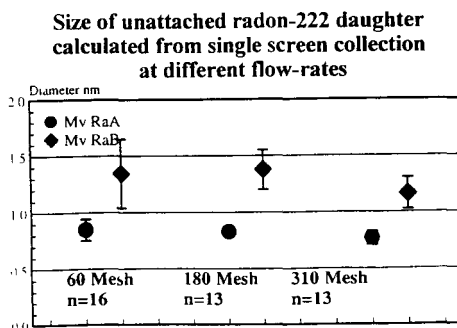
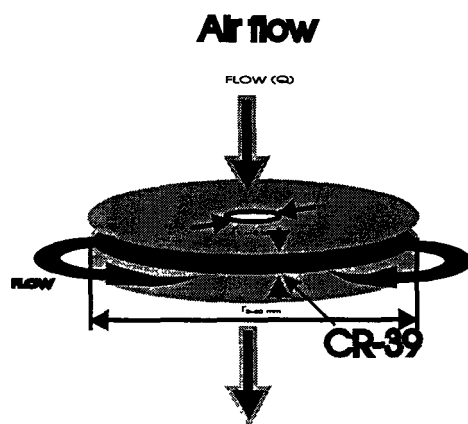


Fig 2. Measured size of unattached radon progeny

Reports on enlargements of the unattached clusters in atmospheres with SO₂ and other pollutants is found in the literature. An increased size of the unattached fraction in indoor air will have a substantial effect on the dose to the bronchial cells. A simple field device for measurement of the size distribution of radon progeny indoors in the nm size as a mean over a longer period has been the goal for the designed diffusion sampler.

The device is a circular parallel plate diffusion chamber using CR-39 as one of the plates. The diffusion sampler consist of two flat circular metal plates with an inlet and outlet in the centre. Between the two metal plates is a circular disk of CR-39 arranged so that the air sucked through the central opening of the circular metal disk passes between the flat inner metal surface of the disk and the CR-39 film (the diffusion chamber). At the edge of the CR-39 film the air passes through a filter to remove the progeny that has not plated out on the disk or the CR-39 film.

The progeny free air is then passed between the other side of the CR-39 and the other metal disk from the edges inwards. The alphas giving tracks on this side origin from the radon-gas. This track density is the *background to the front side, since both sides will be exposed to the same radon concentration*. The flow rate in the parallel plate diffusion chamber will be higher in the centre region and lower at the edges. *With the present design the flow-rate will slow down a factor of 10 towards the edges. Thus a longitudinal deposition compression will occur so that a larger span of aerosol sizes can be deposited on the relatively short distance of the CR-39 surface.*



The total number of tracks at different radius of the CR-39 film is a measure of the deposited amount of radon progeny at that radius. The distribution of tracks versus radius will then be dependent on the size distribution of the aerosols carrying the radon progeny.

The deposition pattern for different monodisperse aerosols has been calculated from the penetration formula given by Bowen, B.D., S. Levine and N. Epstein: [Fine Particle deposition in laminar flow through parallel-plate and cylindrical channels in J. Colloid Interface Sci. 54:375-90, (1976)]

$$P = 0.9104e^{-2.827\mu} + 0.0531e^{-32.147\mu} + 0.01528e^{-93.475\mu} + 0.00681e^{-186.805\mu}$$

for $\mu > 0.05$

$$P = 1 - 1.526\mu^{2/3} + 0.15\mu + 0.00342\mu^{4/3}$$

for $\mu \leq 0.05$

$$\mu = \frac{8\pi D(r_2^2 - r_1^2)}{3QH}$$

The field diffusion sampler for size distribution measurement of radon progeny in the nm range at environmental levels of radon has successfully been tested. A few results is presented below. The results from measurements with filtered laboratory air with ^{222}Rn is shown in fig 3. The unattached ^{218}Po seems to be close to 1 nm (aerodynamic diameter) according to the theoretical calculation. In fig 4 where ^{220}Rn is used as source the unattached ^{220}Rn -progeny is also close to 1 nm in diameter. Fig 5 show the result from a 5 days sampling indoors in a house in the suburb of Stockholm. The size of the unattached fraction seems to be larger, about 1.2 nm.

Fig 3 ^{222}Rn in clean air Flow rate 1.20 l/min

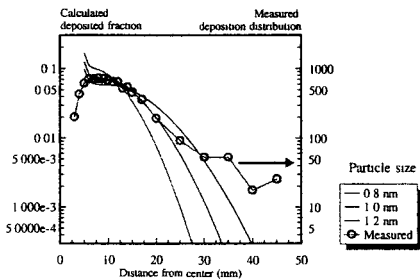


Fig 4 ^{220}Rn in clean air Flow rate 1.14 l/min

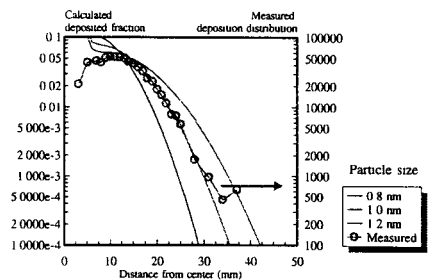
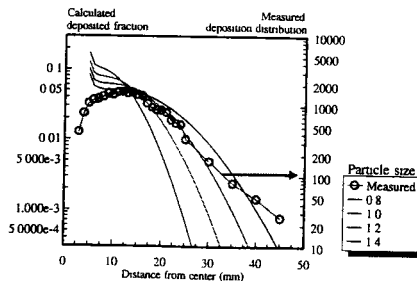


Fig 5. 150 Bq/m³ of ^{222}Rn indoor air for 5 days



^{220}Rn (thoron) studies

Measurements of thoron has been performed in some 90 buildings during 1992 and 1993, as a part of two different investigations. The measurements were performed in order to form a basis for assessing the risk for high thoron levels indoors in Sweden.

Measurement of ^{220}Rn progeny has been undertaken in 61 dwellings at 13 different places. Most buildings were situated in areas with elevated natural thorium concentrations. The radon (^{222}Rn) progeny concentration was measured at the same time.. The measurements were performed at two locations in each dwelling, living-room or bedroom and basement lounge or other room in the basement. Typical values of EET in dwelling was found in the range 0.1 to 0.4 Bq/m³ with maximum value of 16 Bq/m³. The unattached fraction was measured to be in the range 0.003-0.03 Bq/m³ with a maximum value of 0.8 Bq/m³ EET (61 nJ/m³). The EET values found from measurements in the basements are typically 0.3 - 1.5 Bq/m³ with a maximum value of 12 Bq/m³. The unattached fraction was measured to be in the range 0.01 - 0.05 Bq/m³ with a maximum value of 6.3 Bq/m³. A few measurements of the ^{220}Rn gas were performed in the basement and showed typically values between 10 and 80 Bq/m³ with a maximum value of 430 Bq/m³.

Measurement of ^{220}Rn has been performed in a part of a random selected group of dwellings in Sweden. The preliminary results from 31 dwellings show a mean-value of 13 Bq/m³, a median of 4 Bq/m³. A single high value of 150 Bq/m³ was also found. All the ^{220}Rn results reported here are one day mean-values.

The estimated population mean for thoron progeny in Swedish homes is 0.5 Bq/m³ or (38 nJ/ m³). This would give an approximate annual effective dose to the average Swede of 0.1 mSv. The corresponding mean annual effective dose from radon progeny is about 2 mSv in Sweden.

The mean thoron gas concentration in Swedish dwellings can be estimated to be 10 to 15 Bq/m³ and contribute less than 0.01 mSv to the annual effective dose.

REFERENCES

- R Falk, H Möre, L Nyblom and I Östergren. Regional deposition of radon decay products in human airways. *Radiat. Prot. Dosimetry*. Vol 45, No 1/4, 685-687, 1992.
- L. Mjönes, R. Falk, H. Mellander and L Nyblom. Measurements of Thoron and Thoron Progeny Indoors in Sweden. *Radiat. Prot. Dosimetry*. Vol 45, No 1/4, 349-352, 1992.
- Falk, R., Möre, H. and Nyblom, L. Measuring techniques for environmental levels of radon-220 in air using flow-through Lucas cell and multiple time analysis of recorded pulse events. *Appl. Radiat. Isot.* Vol 43, No 1/2, pp 111-118, 1992.
- R Falk, H Möre and L Nyblom . Measurements of ^{220}Rn in air using a flow-through Lucas cell and multiple time analysis of recorded pulse events. *Radiat. Prot. Dosimetry*. Vol 45, No 1/4, 111-113, 1992.
- R. Falk, H. Mellander and I. Östergren. A field diffusion sampler for sizing the radon progeny aerosols in indoor air. Poster at the NRE-VI, June 5-9, 1995, Montreal, Canada
- H. Möre, R. Falk and L. Nyblom. A Calibration Chamber for ^{220}Rn . Submitted to the NRE-VI, June 5-9, 1995, Montreal, Canada
- Falk, R., Hagberg N., Mjönes Ld., Möre H., Nyblom L. and Swedjemark G. A. Standards, calibration and quality assurance of ^{222}Rn measurements in Sweden. *Nuclear Instruments and Methods in Physics Research A* 339, 254-263, 1994.
- Mjönes, L., Falk, R., Mellander, H., Nilsson I, and Nyblom, L. Thoron and Thoron Progeny in Buildings in Sweden Submitted to the NRE-VI, June 5-9, 1995, Montreal, Canada

Head of project 6: Prof. Tymen

II. Objectives of the reporting report.

The main objective of the 1992-1995 contract period was centred on two major programs:

I- To improve the α -activity counting procedure of radon daughters collected by the SDI 2000 sampling device and consequently to determine more accurately the size distribution of radon daughters in indoor environments. This achievement was based on i) the modification of the diffusional part of the SDI 2000, ii) the implementation of a new α -activity counting unit, iii) the use of data inversion methods to reconstruct the size distribution of individual radon decay product.

II- To perform a method devoted to the measurement of Rn-daughters unattached fraction, integrated over a large sampling time and based on the use of an alpha track detector as support of free radon daughters collected in an annular diffusion channel.

This research work was also carried out in collaboration with the "Laboratoire de Physique et Métrologie des Aérosols" (LPMA) of the Commissariat à l'Energie Atomique (Dr. BOULAUD).

III. Progress achieved including publications.

First program

I) METHODOLOGY

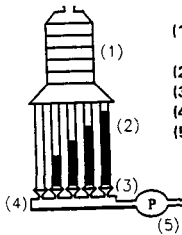
1.1 Experimental device

Ambient radon daughters were sampled by using the modified SDI2000 equipment (diffusional and inertial spectrometer) designed at the Institut de Protection et de Sureté Nucléaire of the Commissariat à l'Energie Atomique. The instrument has been already used in previous experiments carried out in houses, but, the results obtained did not give satisfaction mainly because too much time was consumed in handling samples.

As illustrated in fig.1 the present system combines four stages of the 8-stage Andersen MKII impactor with 5-channel granular bed diffusion battery. This diffusional system comprises four tubes containing 1-5 mm glass beds under various depths, the fifth being used as an open channel. Cut-off diameters of granular beds are given in table 1. Flow-rate through the system was controlled by critical orifice. A special attention was paid to redesign the filterholders in order to make the sample handling easier and consequently to reduce the time to be waited before counting.

Our methodology requires nine units of alpha counting to study the alpha decaying of radon daughters after sampling. A special effort was made to the counting procedure carried out through nine-surface barrier alpha detectors. Four of them, 50 mm in diameter (Camberra CAM 2000) were devoted to the impactor plates and the five others, 25 mm in diameter (Camberra CAM 450) were used for the five filters

placed downstream the diffusion granular beds. Suitable filterholders were made to get a short transfer time between the end of sampling and the start of counting phase. This last one is based on



- (1) cascade impactor
- (2) ANDERSEN MK II granular beds
- (3) downstream filters
- (4) critical orifice
- (5) pump

Stage	Cut-off Diameters (nm)
F5 (open channel)	/
F4	12
F3	30
F2	70
F1	170
D4	315
D3	620
D2	1750
D1	4500

Fig.1 Schematic representation of the SDI2000

Table 1 Cut-off diameters of the SDI2000 stages

the use of the *Time Evolved Least Square* (TELS) method which determines in real-time the number of atoms radon daughters present on each sample during the counting procedure. The basis of calculation is to fit the experimental total counts to the theoretical ones by using a least square method: the number of atoms of each radon daughter present in the sample is used as the fit parameters (Hartley 1989). It is then an extent of traditional methods using several fixed counting time intervals as in Thomas' method (Thomas, 1972) for which it is not easy to choose those corresponding to the best optimization.

To sum up, the principle of the TELS calculation method consists in approximating the total alpha count C_α expressed in the following form:

$$C_\alpha = \sum_{i=1}^n H(t - t_i)$$

where $H(t-t_i) = 1$ if $t > t_i$ and 0 if $t < t_i$, t_i being defined as the arrival time of each alpha particle up to a time t' , by the function:

$$F(t) = \alpha_A(1 - e^{-\lambda_A t}) + \alpha_B(1 - e^{-\lambda_B t}) + \alpha_C(1 - e^{-\lambda_C t})$$

$\alpha_A, \alpha_B, \alpha_C$, are function of RnD concentrations and have to minimize the following integral:

$$I = \int_0^{t'} [C_\alpha(t) - F(t)]^2 dt$$

This data processing program has been specially written for PC to be easily used. The duration of experiment (sampling and counting) is totally controlled by the computer from the start to the end.

1.2 Data evaluation

Once the activity concentration of individual radon nuclides was measured on each plate and filter, the problem was to reconstruct the size distribution of Po^{218} , Pb^{214} and Bi^{214} from data. This was made through the non-linear inversion method like Twomey algorithm or Extreme Value Estimation (EVE) method. Due to the fact that nanometric size radon daughters are collected by diffusion at the inlet of the SDI 2001

sampler and the first impactor plate (not counted), the applicable size range varies from about 8 nm to 10000 nm.

The data processing from Twomey and EVE algorithm is based on the resolution of the following equation:

$$F_i = \sum_{j=1}^M K(i, d_{p_j}) f(d_{p_j}) + \varepsilon'_i$$

where F_i are experimental results (concentration of individual radon daughter on each impactor plate and filter), $K(i, d_{p_j})$ is the kernel matrix of the SDI 2001, $f(d_{p_j})$ is the size distribution of each radon daughter, M is the number of size classes used in the reconstruction process, ε'_i is the error term.

The unknown function in EVE method is represented by a superposition of smooth basis curves e.g. log-normals (Aalto et al., 1990). The original feature of this deconvolution algorithm lies in the restitution of a central solution among all possible and acceptable ones both with one minimum and maximum solution depending on known confidence levels. The method is innovative because errors on measurements are taken into account in the previous term ε'_i and have to be input both with measured data. A general study of simulation has been carried out in the purpose of testing the ability of the method to reconstitute spectra of given shapes (Droal, 1995).

II. RESULTS

Radon daughter size measurements were performed using the above instrumentation in an experimental house where relatively high radon concentrations were frequently observed.

Successive experiments were conducted for a 15-min sampling period followed by a 1-min handling time to arrange the samples in the nine-channel alpha counting unit. Activity data were then processed in real-time according to the Time Evolved Least Square method and size distributions determined as previously indicated.

An example of such reconstructed distributions is given in Fig. 2. It can be noted that for the three radon radionuclides the Activity Median Aerodynamic Diameter was approximatively the same as reported in other published results (Kesten et al. 1993). The presence of radon products in the coarse particle mode found in this particular example can be explained by a large amount of particles generated by works carried out in the room during this set of experiments.

Fig.2 also illustrates the comparison between EVE algorithm and Twomey inversion method. The different results obtained confirm that the modified SDI is capable of restituting the individual radon daughter activity size in the 5-10 000 nm range. A rather good agreement in the presence of significative modes of the distributions, with sometimes a slight deviation in the AMAD, is generally observed. Otherwise, it appears that the Twomey method presents oscillations in some cases. Uncertainties at the tails of the size, relevant to inversion techniques, constitute another problem. This is particularly critical with the Twomey algorithm even when, in the case of EVE, the restitution of a smoothed central solution between a minimal and maximal solution with the higher confidence level allows to substantiate the reconstructed curves. Nevertheless it will be necessary later to improve inversion techniques.

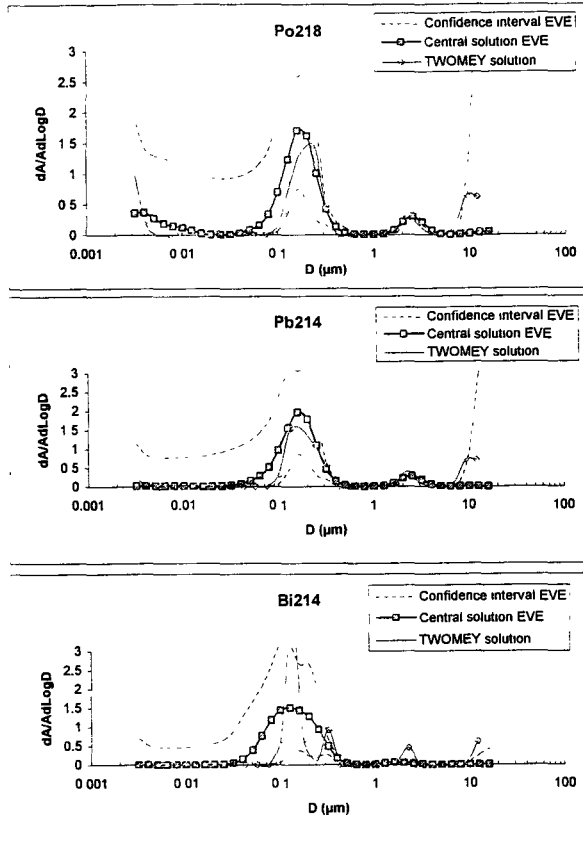


Fig.2 Example of attached activity size distribution of RnD.

Second program

1) Methodology.

The use of an alpha track detector to study the unattached component of radon daughters has not been addressed up to now. The choice of an annular channel as diffusion sampler was supported by the need to design and make a compact instrument in which the detector could be inserted and removed easily.

The sampler (figure 3) consists in two coaxial cylinders forming an annular diffusion channel of 30 cm in length, 2.5 mm in distance between the two axial cylinders. The inner one was designed to receive a LR115 Kodak film wound on all its surface, itself covered by a 13 μm thick Mylar foil in order to register (record?) ultrafine Po²¹⁸ only. The sampling flow-rate was determined by fixing the cut-off size at 4 nm

The energetic detection range of the LR115 film ranging approximatively from 1.5 Mev to 4.5 Mev, it was necessary to use a 13 μm thick Mylar foil, placed upon the detector to reduce the ²¹⁸Po alpha particle energy. In this configuration ²¹⁴Po α emission

is not detectable. However, as α emitters from ^{218}Po and ^{222}Rn have energies of the same magnitude, the ability for radon gas to produce tracks during the air transit, had to be evaluated. As seen in fig. 3, unattached ^{218}Po collected on the two internal surfaces can produce tracks on the film detector.

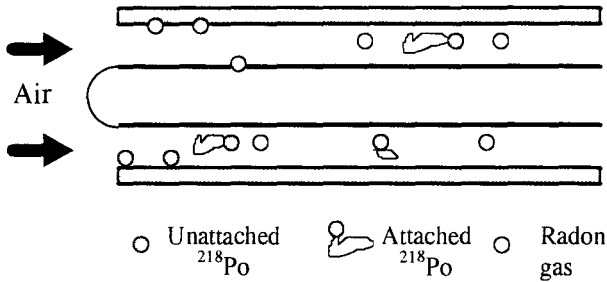


Fig.3 Schematic diagram of the annular diffusion channel

Lots of preliminar experiments were initially conducted in a radon chamber of 0.3m^3 in order to examine the behavior of radon gas on track density. Fig. 4 shows a fairly good agreement between the number of alpha tracks due to radon, effectively counted and their estimated number.

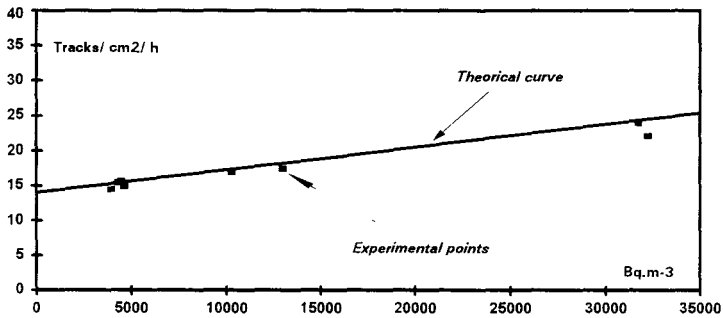


fig. 4 Influence of Radon gas on track density

According to our estimations and taking into account the various correction factors involved, the influence of radon gas on the track density can be estimated at about 10% over a month exposure in a 200Bq m^{-3} radon concentration and assuming that 20% of the ^{218}Po is in an unattached form.

In parallel with this experimental work, we have also studied the penetration performances for unattached fraction through the classical theory of diffusion but applied to an annular space of internal and external radius R_1 and R_2 . Solution of the classical diffusion equation applied to an annular channel of length L and with a mean velocity \bar{U} yields to express the efficiency E of collection according to the diffusion coefficient D of particles (C_0 and \bar{C} being respectively the mean particle concentration at inlet and outlet of the tube) as the following analytic form:

$$(1) \quad E = 1 - \frac{\bar{C}}{C_0} = 1 - \sum_{n=1}^{\infty} K_n e^{-2\alpha_n^2 \Delta}$$

$$\text{with } (2) \quad \Delta = \frac{DL}{4\bar{U}(R_2 - R_1)^2}$$

Eigenvalues α_n and coefficients K_n are obtained with boundary conditions $C(R_1, x) = C(R_2, x) = 0$ (x in $]0, L[$).

For a wide range of ratios R_1/R_2 (from about 0.25 to 1), the annular diffusion channel was shown to have almost the same collection efficiency as the flat rectangular channel which can be considered as one of the best devices available to measure the particle size distribution of submicron aerosols (Kerouanton et al.1995). Besides, for a similar efficiency, the annular channel does not present the boundary problems encountered when using the rectangular channel and can provide a useful cylindrical geometry appreciated in many practical applications and more particularly in the ultrafine radon decay products.

2) Experimental procedure to study unattached ^{218}Po .

The experimental set-up consists in a 350 liters closed vessel connected to the annular diffusion channel, equipped with the detector film. Samplings took place on 2-hour period. Radon gas was produced from a 1 mCi ^{226}Ra source. The air circulates continuously in closed circuit in order to maintain constant the Radon concentration. During the experiments, ^{222}Rn and its daughters activity concentration was measured respectively by a dual filter technique and by a classical filter-screen method.

After sampling the detector was removed for etching in a soda bath (10% NaOH, 60°C) for 140min. The film was then cut in 2.5 cm width strips and track density was counted by means of a spark counting technique.

In our experimental conditions, Radon was mixed with filtered air to get a proportion of unattached fraction greater than 90% of the total Polonium concentration and the equilibrium factor was about 40% to 60%.

3) Experimental results.

The most recent experimental results obtained show that the annular channel equipped with an alpha track film detector is able to record efficiently ^{218}Po tracks due to unattached fraction. The mean experimental track density is 20% upper than the theoretical estimation. At the present state of study it is difficult to clarify this observation but it can be thought that the track density takes into account uncertainties such as the residual thickness of the film after etching or the track counting efficiency of the spark counter. Although the ability of this last one to distinguish the true holes separately from the etched pits is not clearly assessed, we can however say that the concordance between the theory and the experiment is rather good.

Another original application of this method consists in the determination of ^{218}Po nanometric particle size distribution from inversion of track density data recorded on the

detector film. This study was undertaken by using the Extreme Value Estimation (EVE algorithm) mentioned previously. It has been then performed a special kernel matrix from the set of virtual diffusion annular channels of 2.5 cm length corresponding to different analysed film strips. The size distribution of nanometer-sized ^{218}Po was then reconstructed as shown in Fig.5. In our experimental conditions (mixture of filtered laboratory air and radon in closed atmosphere at 55-60 % RH) the activity diameter of unattached ^{218}Po would be of 0.75 nm (0.65-0.8 nm), which is comparable to the results obtained by Reineking et al.(1993) and of Rammamurthi et al. (1993). Additional experiments will be carried out soon to study the ^{214}Pb nanometric particle size distribution with a different Mylar foil thickness.

Other experiments in different ambient conditions in the experimental chamber are now planned for a complete evaluation of the annular diffusion channel behaviour before tests in dwelling atmospheres.

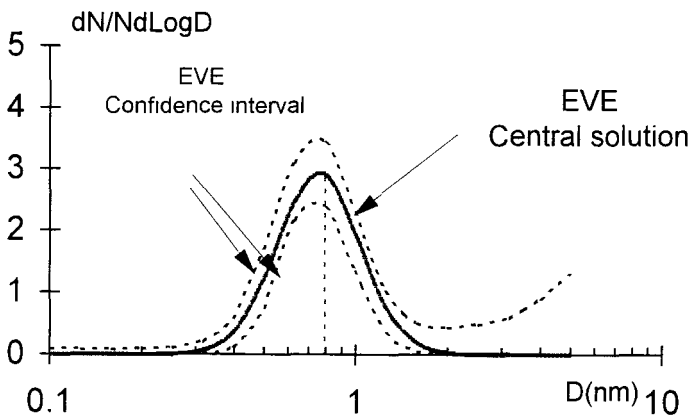


Fig 5 Size distribution of unattached ^{218}Po .

References

- Aalto P., Tapper U., Paatero P. and Raunemaa T.(1990) Deconvolution of particle size distributions by means of Extreme Value Estimation Method, *J. Aerosol Science*, 21, S1, S159-S162
- Droal C., (1995) Aérosols et microorganismes- Techniques de prélèvements et d'analyses des spectres dimensionnels- applications au milieu de l'élevage porcin. *PhD University of Brest*.
- Hartley B.M., Hartley M.I., (1989) "A new method for the determination of the activity of short half-life descendants of radon" *J. of Radio Prot.*, 9, 3, 165-177.
- Kerouanton D., Tymen G., Boulaud : " Diffusion of small particles in an annular diffusion channel". in progress of correction after reviewing for publication in *J.of Aerosol Science*.
- Kesten J., Butterweeck J., Porstendörfer J., Reineking A., Heymel H.J. (1993) " An online α -impactor for short-lived radon daughters", *Aerosol Science and Technology*, 18, 156-164.

Ramamuthi M., Strydom R., Hopke P.K., Holub R.F., (1993), " Nanometer and ultrafine aerosols from radon radiolysis", *J.of Aerosol Science*, 24,3,393-407.

Reineking A.,Kesten J., Butterweck G., Porstendörfer J., Knutson E.E., Geöge A.C., Solomon S.B. (1993) " Size distribution of unattached and aerosol-attached short-lived radon decay products: some results of intercomparison measurements" *First international workshop on indoor radon remedial action*, Rimini, Italy, June27-July 32,

Thomas J.W. (1992, "Measurement of radon daughters in air" *Health Physics*, 23, 9, 783.

Publications.

- 1 - **M.C. ROBE, A. RANNOU, G. TYMEN, J. LE BRONEC.**
"Radon diagnosis based on investigation of radon sources and radon entry in houses". *Radiation Protection Dosimetry*, Vol. 45, n° 1-4, 1992, pp. 319-322.
- 2 - **G. TYMEN, M.C. ROBE, A. RANNOU.**
"Measurements of Aerosol and Radon Daughter size distributions in five radon houses". *Radiation Protection Dosimetry*, Vol. 45, n° 1-4, 1992, pp. 391-393.
- 3.- **A.M.GOURONNEC, M.C.ROBE, N.MONTASSIER, D.BOULAUD, G.TYMEN, A.RENOUX.** "Modelling of the behavior of radon and its decay products in dwellings and experimental validation of the model". *Indoor air congress 1993, Helsinski.*
- 4 - **G.TYMEN**
"Airborne radon daughter particle". *J. of Aerosol Science*, vol.25, ppS67-S68
- 5 - **D. KEROUANTON, G. TYMEN, D. BOULAUD.**
"Use of an annular diffusion channel for a time integrated measurement of the unattached fraction of radon-222 progeny". *J. of Aerosol Science*, vol.25, ppS249-S250
- 6 - **A.M. GOURONNEC, F. GOUTELARD, G. TYMEN, N. MONTASSIER, D. BOULAUD, A. RENOUX.**
"Radon and radon decay product behaviour in a house: comparison between modelling and measurements". *J. of Aerosol Science*, vol.25, ppS73-S74
- 7- **D.KEROUANTON, G.TYMEN, D. BOULAUD:**" Diffusion of small particles in an annular diffusion channel". in progress of correction after reviewing for publication in *J.of Aerosol Science*.
- 8- **A.M. GOURONNEC, F.GOUTELARD, N.MONTASSIER, D.BOULAUD, A.RENOUX, G.TYMEN:** " Comportement du radon et de ses descendants dans une enceinte d'habitation: comparaison modèle - expérience ". Proposed for publication in *Radioprotection*.

- 9- **TYMEN G., GOURONNEC A.M., MONTASSIER N.**, " Anew instrument to measure individual size distribution of radon daughters", *International Symposium on the Natural Radiation Environment*, June 5-9, 1995, Montréal, Québec, Canada.
- 10- **TYMEN G., KEROUANTON D., BOULAUD D.**, "Time integrated measurement of unattached fraction of Radon-222 daughters by using alpha track detectot in an annular diffusion channel", *International Symposium on the Natural Radiation Environment*, June 5-9, 1995, Montréal, Québec, Canada

Head of project 7: Dr. Ortega

II. Objectives for the reporting period

- Consolidate a research group in the "Universitat Politècnica de Catalunya" linked to the Göttingen University radon group of Dr. Porstendörfer and Dr. Reinenking.
- Improve radon detection systems: passive-integrated and continuous devices, and continuous radon daughters detection systems: equilibrium factor and unattached fraction.
- Performance of a set of "in situ" measurements in 50 dwellings representative of the habitat of the region of Catalonia (Spain), and selection of some of them to carry out continuous measurements.
- Determination of the temporal evolution of the radon concentration, equilibrium factor and unattached fraction in the dwellings selected in the previous objective. This will be complemented with the aerosol size distribution, which is dependent upon funds from the Spanish research authorities.

III. Progress achieved including publications

1. Development of the radon research group

The training plan in the radon area began in a previous period of collaboration in an EC programme with the stay of two researchers (Dr. X Dies and Dr M. Novell) at the radon group of Göttingen University (Dr. Porstendörfer). In the reporting period the aim of the training plan was to improve knowledge in the area of aerosol measurement techniques and systems to calibrate radon and radon daughters devices. In this context a researcher (A. Vargas) has continued with visits to other groups: one week at Göttingen, one week at the radon group of the Swedish Radiation Protection Institute (Dr. R. Falk) and two weeks at the aerosol group of Lund University (Dr. M. Bohgard).

Because of the different tasks that the radon-group of the "Universitat Politècnica de Catalunya" are carrying out, the group comprises a project director, a head of the radon laboratory, a laboratory worker, a person responsible for "in situ" continuous measurements, a person responsible for "in situ" integrated measurements, a PhD student and a final-year student.

2. Improving radon detection systems

Passive-integrated system

During this period a passive detection system was set up and checked. The passive detector contains 90g of active charcoal kept in a canister with a layer of 50g of desiccant (silica gel). The desiccant acts as a diffusion barrier and minimises the effect of relative humidity and also reduces the effect of short-term temporal variations in the environmental Rn concentrations.

The amount of radon adsorbed in the canister is measured after being exposed to indoor air for a few days (3-4 days), by counting the gamma rays using a 3"x3" NaI(Tl) scintillation counter

The canisters' system was calibrated at the NRPB in Chilton UK. A set of canisters were exposed to a constant Rn concentration for different exposure times for two different relative humidity values and it has been seen that for this humidity range the dependence on the calibration factor for an exposure time ranging from 3 to 4 days is not significant compared with the calibration uncertainty (Fig.1).

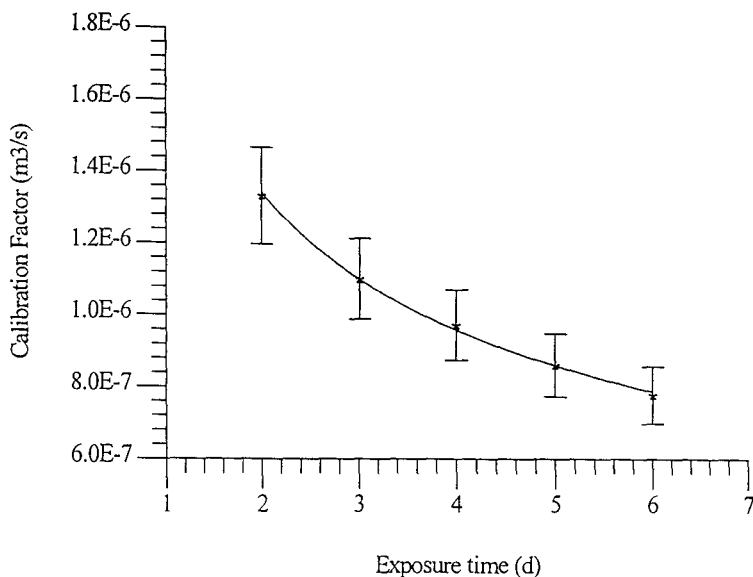


Fig.1. Calibration factor for a relative humidity of 50%

In order to check the passive detection system, a preliminary survey campaign over 15 dwellings in the city of Barcelona was carried out. Two systems of passive dosimeters were used: canisters and track-etched detectors of two types, one open type which uses LR-115 typeII strippable and one closed type that uses Makrofol ED

An intercomparison between those three types of passive detectors and an active device was carried out in a closed area in the INTE building. The results are shown in figure 2.

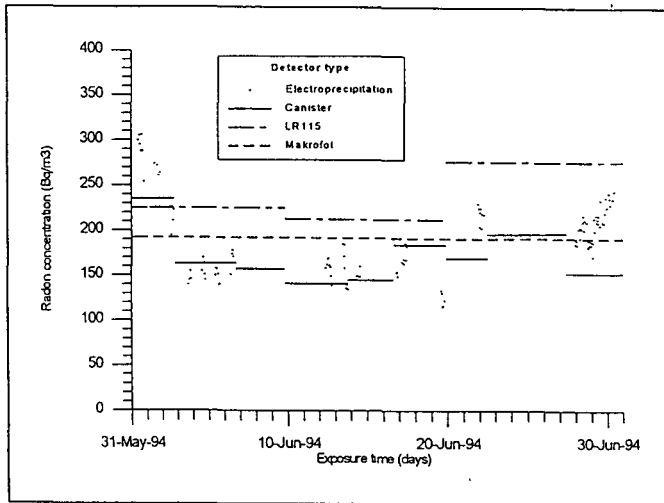


Fig.2. Radon concentration obtained with several passive detectors and an active device.

Continuous system

In relation to the continuous measurement the following systems have been set up

1. Radon gas concentration is measured by electroprecipitation of positively charged ^{218}Po ion in an electric field (17 kV, spherical glass chamber, volume 5 l) in a surface barrier detector. This radon gas monitor was manufactured and calibrated by the radon group of Göttingen
2. Radon progeny is measured continuously by a compact sampler unit based on alpha spectroscopy with one sampling counting period and another postsampling period for each cycle. The sampled air is drawn through a 5 mm slit between a surface barrier silicon alpha detector and a 1.2 μm pore diameter filter. The radiation on the filter is counted by the detector and a portable PC-based spectroscopy system is used to acquire and analyse the data.
3. To determine the unattached fraction, a sampler detector unit similar to the one mentioned above was used. A 2x280 mesh wire screen was placed at the entrance of the sampled air through the slit. The air velocity through the screen is calculated to obtain a 50 % collection efficiency with a cut-off diameter of 4 nm.
4. *Automation of the system* The equipment mentioned above is controlled by a portable PC which switches the multichannel buffer and the pumping station on and off, measures the mass flow rate and measures the meteorological parameters through a PC data acquisition board. The portable PC performs the data evaluation and the storage of the data in files. Moreover, the results

of radiological and meteorological parameters could be represented in "on line" graphs during the measurement period that was established as up to three days because of the possibility of clogging up the filter

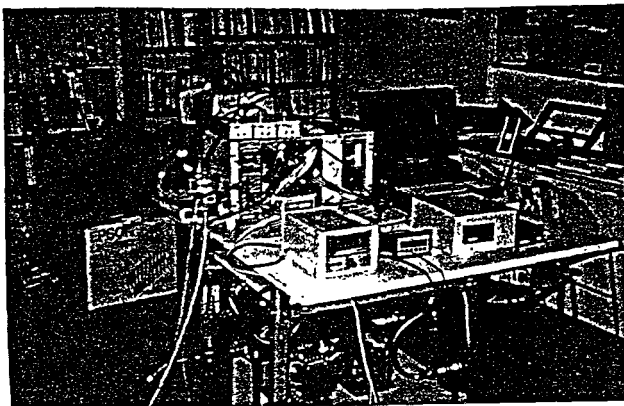


Fig. 3. Photograph of the radon continuous measurement system and aerosol size distribution equipment.

5 *Optimisation of the measurement* conditions in order to achieve greater accuracy A computer programm has been developed that simulates the temporal variation of the radon daughters activity in the membrane filters during the continuous measurements Figure 4 shows the temporal evolution of the alpha particle detected of ^{218}Po and ^{214}Po , the time cycling was 20 min for sampling counting period, 20 min for waiting period and 20 min for postsampling waiting period and the radon daughters concentration in the air was 110 Bq/m^3 of ^{218}Po , 70 Bq/m^3 of ^{214}Pb and 60 Bq/m^3 of ^{214}Bi . These concentrations were obtained in a real situation and the number of detections were compared with the simulated ones

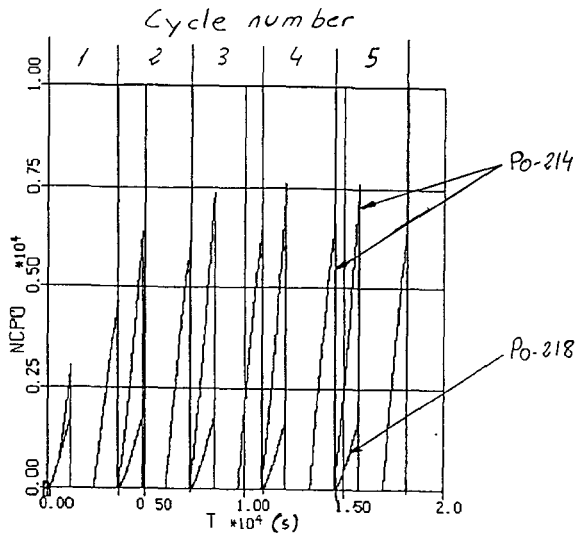


Fig 4. Simulation of the temporal evolution of the alpha particle detected of ^{218}Po and ^{214}Po

6. Error propagation technique has been used to find the associated error in the radon and radon daughters concentrations.

7. Purchasing and setting up the equipment for measuring the aerosol size distribution in the submicrometer range. The equipment is the Scanning Mobility Particle Sizer (SMPS 3934) of the TSI company (5 nm to 1000 nm) The equipment was obtained with the sponsorship of CICYT Spanish office

Passive integrated measurements

A campaign has been carried out with passive detectors in about 50 dwellings in Catalonia and 2 or 3 sites in each dwelling. Three types of passive detectors have been used. Each type of dosimeter was exposed over different periods of time: 3-4 months for the Makrofol, 10 days for the LR-115, and 3-4 days for the canisters. This campaign was performed first from November 1993 to March 1994 and afterwards from November 1994 to March 1995. The geometric mean of radon concentration was 30 Bq/m^3 and 28 Bq/m^3 respectively for the two periods. The results for the canisters of the first period of the campaign are shown in figure 5. At the present time a complete analysis of the results is being done.

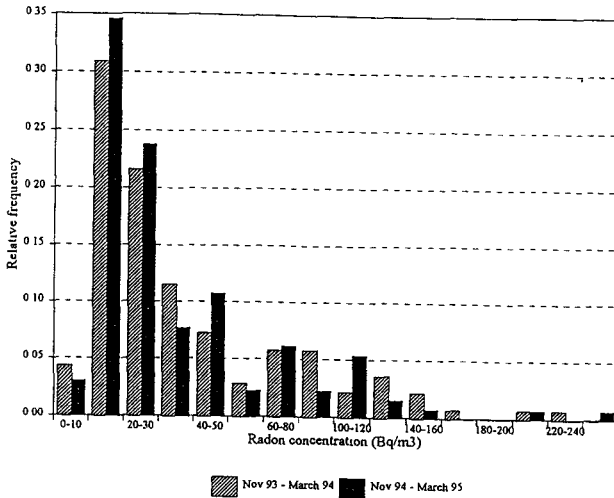


Fig.5. Results of the radon concentration in Catalonia

Participation during the first five months of 1995 in the CEC Radon Intercomparison of passive detectors. Preliminary results showed a deviation of less than 15 % between our canisters and the reference value of the NRPB.

Continuous Measurements

The sites that were selected to carry out the continuous measurements are placed in different locations of Catalonia as shown in figure 6

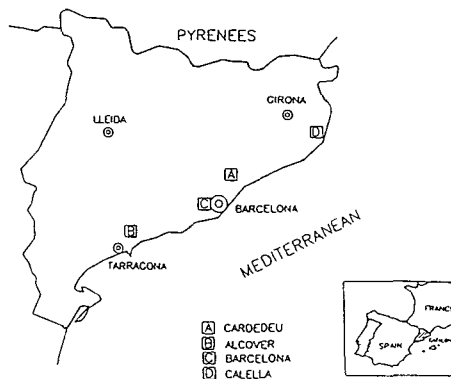


Fig. 6. Situation of Catalonia in the Mediterranean area of Europe. Location of the four sites on the coast of Catalonia.

The main characteristics of the four sites are:

- A.- A detached house in the village of Cardedeu 30 km to the north of Barcelona. Height above sea level: 195 m. Material: brick.
- B.- An old farmhouse in the country near the village of Alcover with three floors, situated in the coastal mountain range in the province of Tarragona, 25 km from the city. Height above sea level: 575 m. Material: stone.
- C.- A big building of 200 m² and 14 m height situated in Barcelona. It is the containment of a decommissioned training Reactor of the Universitat Politècnica de Catalunya. Height above sea level: 120 m. Material: 35 cm concrete.
- D.- A three-floor house in Calella de Palafrugell on the north coast of Catalonia 30 km from the city of Girona. Situation: on a little hill 100 m above sea level. Material: brick.

Due to the large variation in radon concentration found in dwelling D (from 10 Bq/m³ to more than 3000 Bq/m³), measurements were carried out for longer than in the other places. In figure 7 the radon and radon progeny concentrations, equilibrium factor, attached fraction, outdoor temperature and barometric pressure over almost 11 days are shown.

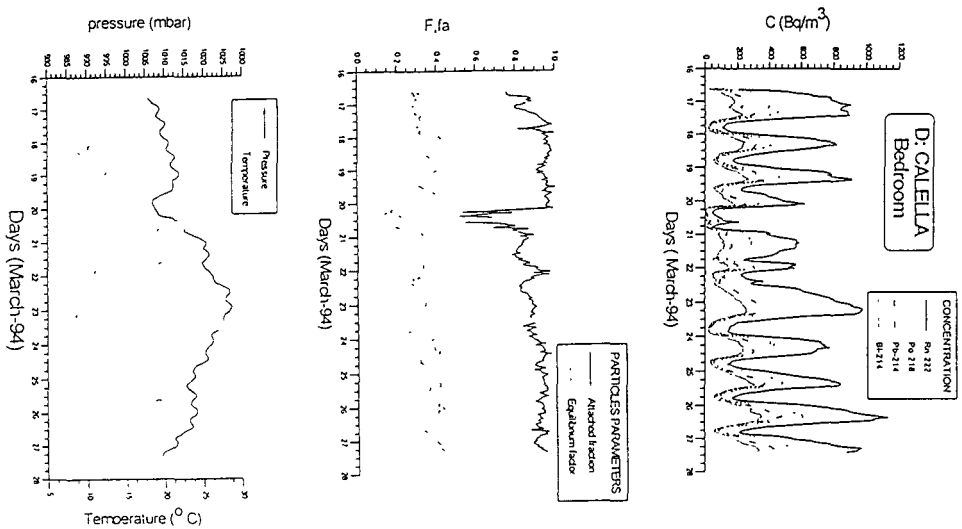


Fig. 7. Results of temporal measurements in the main bedroom of the first floor in Calella over a period of almost 11 days. Radon and radon progeny concentrations, equilibrium factor, attached fraction, outdoor temperature and barometric pressure are shown.

The results in table 1 summarise the average, the maximum and the minimum values in the four sites

Site	C_{Rn} (Bq/m ³)	F	f_p	Z (part/cm ³)
A	200 (100-500)	0.15 (0.12-0.22)	0.2 (0.12-0.42)	1.6 10 ³
B	400 (100-1000)	0.04 (0.02-0.1)	0.3 (0.1-0.7)	6 10 ³ (4 10 ³ -10 ⁴)
C	200 (100-300)	0.55 (0.45-0.65)	0.02 (0-0.1)	7.3 10 ³
D	450 (30-3000)	0.35 (0.13-0.45)	0.1 (0-0.5)	2.5 10 ³ (1.3 10 ³ -4.7 10 ³)

Table 1. Summary of measurement results at the four sites in Catalonia.

The experiments performed in the four sites in the region of Catalonia, characteristic of a Mediterranean zone with extensive geographical and climatic differences, have shown several radon exhalation mechanisms existing in the different sites studied. As a result, it has been established that if the advection form of radon entrance is predominant, the exhalation rates vary widely depending on temperature changes and also on the wind direction and intensity.

In the case of the house with three floors, radon concentrations that vary from 10 Bq/m³ to more than 3500 Bq/m³ were measured on the first floor in the area adjacent to the bathroom over a period of a few hours. Moreover, the observed daily variations in the radon concentrations corresponded to daily temperature oscillations. The mechanism of exhalation was advection through the drainpipes. The equilibrium factor ranged from 0.13 to 0.45 and the unattached fraction registered levels between 0 to 0.5. The thoron concentration reached levels up to 50 Bq/m³ (approximately a factor of 1/100 to radon concentration). Radon concentration was normally higher on the first floor, the first and the second floor radon concentrations fitted the time variation well, while the concentration on the ground level floor registered lower levels and the variation did not coincide with the others floors.

The particle size distribution was different at each site and considerable changes were observed in Calella related mainly to the wind intensity.

3. Other Progress achieved in this period

In order to check and improve equipment to measure the radon and the radon daughters, the influence of aerosol and climatic parameters in the measurements and in the behaviour of the radon daughters a radon laboratory with a walk-radon-chamber (20 m³) has been developed.

The main characteristics of the radon-chamber, that will be working at the end of 1995, are.

The physical layout

The radon calibration chamber is 2.91 x 2.91 x 2.30 m (20 m³) with a separate anteroom (1.94 x 0.97 x 2 m) leading into the main room. The walls are made of 2 mm thick stainless steel sheets that will be welded so that they are air tight. In two of the four walls there are access ports, through which samples can be taken without entering the exposure room, electrical connections, data collection, ventilation and air conditioning and glass window to view the inside. The access ports are also made of 50 x 50 cm sheets of stainless steel or glass that are joined to the chamber with a system of screws.

Radon generation system

The radon source will be a 2000 kBq (54 μ Ci) solid radium source housed in a shielded container (commercial source). The air flow through it and the exhalation is 252 Bq/min independent of the flow rate. The outflow of the source is fed into a tube extending around the perimeter of the exposure room or part of the outflow could be sent into the atmosphere before entering the chamber in order to control the activity inside. The radon concentration in the chamber will be controlled up to 70000 Bq/m³ without air ventilation. The air ventilation will be used to clean the room and to simulate a standard room in a house. So the radon concentration in the chamber will be controlled over the range of 100 Bq/m³ to 2000 Bq/m³ with a ventilation rate of 0.3 h⁻¹ to 6 h⁻¹

Environmental conditioning system

The conditioning system contains a commercial refrigeration unit with electrical heating in the outflow to control the temperature and to decrease the relative humidity. The unit is located outside the chamber and the rectangular ducts are connected to the chamber forming a closed loop. To increase the relative humidity a steam generator located in the chamber is used. Sensors for monitoring temperature and humidity will be located in the exposure room and will be collected with a data acquisition system and controlled with PC software. The temperature and humidity in the chamber will be controlled over the range of 10 to 45 °C and 40 to 100 %.

Continuous monitoring of the radon and radon daughters concentration

The radon and the radon daughters concentrations in the chamber will be monitored continuously with the same system as the one described in point 2. So the continuous system monitors the equilibrium factor and the attached fraction.

Aerosol control

The particle concentration will be monitored with an electrostatic classifier. A system of filters (HEPA) in the ventilation ducts cleans the inflow air and with a particle generator it is possible to control the concentration and the dimension of the particles. The dimension of the particles will be controlled from 0.005 to 1 μ m and the concentration from 1 to 10⁷ part/cm³.

4. Publications

[1] M.Novell, X.Ortega, L.Batet. "Puesta apunto de un sistema pasivo de determinación de concentraciones de radón. Aplicación a una campaña de medidas en Cataluña". 5º Congreso de la Sociedad Española de Protección Radiológica, 26-29 April 1994.

[2] X.Ortega, C.Baixeras, M.Novell, L.Font, A. Vargas. "Study of the variation of Rn indoor concentration with several passive detectors and an active detection system". Accepted in "The Science of the Total Environment".

[3] X.Dies, X.Ortega, A. Vargas. "Determinación de concentración de gas radón y descendientes y del grado de adherencia a los aerosoles atmosféricos". 5º Congreso de la Sociedad Española de Protección Radiológica, 26-29 April 1994.

[4] X. Ortega, A.Vargas. "Characteristics and temporal variation of airborne radon decay progeny in the indoor environment in Catalonia (Spain)" Accepted in "The Science of the Total Environment".

[5] X.Ortega, A.Vargas. "Development of a chamber to test and calibrate radon and radon progeny detection systems" To publish in XXI Reunión Anual dela Sociedad Nuclear Española Octubre 1995.

Head of project 8: Dr. Jolanta Lebecka

II. Objectives for the reporting period

- Analysis and report on the present state of monitoring of radon daughters in underground coal mines in Poland and of radiation hazard in coal mines; outlining main scientific and technical problems,
- Performing intercomparison measurements with other groups,
- Completing instrumentation for measurements of unattached fraction of radon progeny,
- Training of Polish specialists in measurements of unattached fraction of radon daughters,
- Choice of investigation sites for measurements of unattached fraction and particle size distribution of radon progeny in underground coal mines; preliminary measurements of concentrations of radon and radon daughters,
- Measurements of unattached fraction of radon daughters in chosen mine workings - planned in the nearest future.

III. Progress achieved

- A report on radiation hazard in Polish coal mines, including methods of monitoring and main problems arising was presented at the Contractors Meeting in Switzerland in October 1994.
- We have participated in intercomparison measurements of radon and potential alpha energy concentration. In 1995 we participated in intercomparison exercise organised by IAEA, EPA and BOM in Twilight Mine, Colorado USA. We have also performed bilateral intercomparison with various partners, including Georg August Universität, Göttingen.
- We are planning to complete instrumentation for sampling and measurements of unattached fraction of radon daughters.
- Our specialist Krystian Skubacz visited Georg August Universität in Göttingen, where during two days he had got a short training in measurements of unattached fraction and particle size distribution of radon daughters. Another colleague Stanisław Chałupnik participated as an observer in the Sixth IRPM Intercomparison Test and Workshop, organised by UNDO in New York in June 1995.
- We have chosen two mines for testing instrumentation and measurements of unattached radon daughters and particle size distribution. We plan to take the measurements of radon and radon daughters and to prepare maps.
- We plan to take common preliminary measurements of unattached fraction of radon daughters in these mines and prepare future particle size distribution measurements, it means together with our colleagues from Georg August Universität, Göttingen.
- We have elaborated the computer programme enabling a solution of problems connected with the radioactive isotopes from specified series as well as the measurements of short lived products of radon and thoron by liquid scintillation method and alpha spectroscopy method.

IV. Detailed description of work

Introduction

The aim of this work is to get more information on the characteristics of airborne radon daughter products occurring in underground coal mines. Radon progeny is the most significant source of radiation exposure of miners not only in uranium mines but in mines of other minerals as well. In spite of this, monitoring of radon daughters in non uranium mines is not very common to be a routine practice in most countries. Even much less is known about the particle size distribution and about the unattached fraction. In Polish coal mines concentrations of radon daughters in air have been measured on regular basis since 1989. Therefore the radiation exposure of miners is rather well recognised compared with other countries. However, the unattached fraction and the particle size distribution has not been measured so far. Moreover, according to the dosimetric models, the unattached fraction contributes much more to the dose than it would result from its activity participation. Additionally, there are serious discrepancies between results of measurements of radon daughter concentration obtained by different methods of measurements and by different teams. One of the possible explanations was, that this could be caused by the unattached fraction. On the other hand, a rather well developed system of monitoring of radiation hazard in Polish coal mines gives an good opportunity to study the characteristic of airborne radon daughters in coal mine atmospheres. Particularly this work is aimed to measure the unattached fraction and in some extend the particle size distribution of radon daughters and to explain the discrepancies in results of measurements obtained by different methods (active device with TLD chips, and passive bare track etch detectors).

Legal regulations-system of monitoring

Monitoring of radiation hazard in Polish mines has been obligatory since 1989. Between 1975 and 1989 measurements of radon and radon daughters in air as well as gamma dose rates and radioactivity of waste rocks and water were performed within scientific research programmes or occasionally on request of mine managers. Since 1989 monitoring has become a routine and has been done on permanent basis. Following measurements are request by law:

- concentration of potential energy of short living radon daughters at specified work places,
- concentration of radium isotopes in water in specified sampling points,
- concentration of natural radionuclides in deposits from settling ponds, water galleries, gutters and so on (only when radium-bearing are present in the mine),
- gamma dose rates or personal gamma doses (at workplaces where radioactive deposits precipitated out of radium-bearing waters are present)

We have described the present system of monitoring of radiation hazard in Polish coal mines on the International Conference of Safety in Mines Research Institutes in Pretoria (Lebecka and Skowronek. 1993). In 1994 a new Act on Geology and Mining was forced by The Polish Parliament (Geological and Mining Law. 1994). According to this Act new regulations are issued. These regulations include also monitoring and control of radiation hazard. According to Decree of Ministry of Industry and Trade (1995) the effective dose equivalent should not exceed 100 mSv during five successive years, whereas during one year should not exceed 50 mSv. For radon progeny the inspection level is $0.8 \mu\text{J}/\text{m}^3$ and the intervention level is equal to $2.0 \mu\text{J}/\text{m}^3$. The measurements should be taken in the following places:

- regional air streams,
- longwall outlets,
- endgates
- others (water galleries and water pump stations where radioactive deposits are present, etc.).

Depending on the PAEC level the required frequency of measurements is from once per three months ($PAEC \leq 0.8 \mu J/m^3$), through once a month ($0.8 < PAEC \leq 2.0 \mu J/m^3$) up to three times a month ($PAEC > 2.0 \mu J/m^3$). These frequencies of measurements comply with those of respirable dust concentration measurements, therefore both measurements are usually taken simultaneously by the same man and the same instrument. This convenience is essential for the total cost of monitoring and simplicity of organisation.

Techniques of measurements

Measurements of radon daughters concentration and gamma doses samples are performed by TLD technique, radium isotopes in water samples are determined by liquid scintillation technique and concentration of natural radionuclides in sediments, waste rocks and so on are measured by gamma spectroscopy (Lebecka et al, 1993. Lebecka et al, 1988).

Fixed point measurements

Measurements of potential alpha energy concentration of short living radon daughters are performed by means of typical gravimetric dust samplers "Barbara 3A" used in Polish hard coal mines, provided with an additional part called ALFA-31 sampling probe (Fig.1). The instrument and the results of tests trials have been published elsewhere (Lebecka et al, 1984). Here we only give the principle of operation and basic technical data. Dust sampler "Barbara 3A" pumps $0.3 \text{ m}^3/\text{h}$ of air through a membrane filter onto which dust as well as attached fraction of radon daughters are deposited. Above filter in a distance of about 1.5 mm three heads containing $\text{CaSO}_4:\text{Dy}$ TLD chips are placed. Each head contains two TLD chips separated by an aluminium disk. The upper chips are used for background subtraction. One shift (6 hours) sampling is usually done. After sampling the dust concentration is derived from weight of the filter and potential alpha energy concentration is determined after reading out of TLD chips in TL laboratory. The results include not only radon daughters but thoron daughters as well. The dust sampler is provided by a microcyclone in order to separate the respirable dust particles. This inlet cuts off unattached fraction of radon daughters as well, which has been proved by laboratory tests (Lebecka et al, 1993). The instruments allow measurement of short living radon-daughters concentration from about $0.05 \mu J/m^3$. Dust samplers "Barbara 3A" have been widely used since 1989 in all 66 Polish collieries. About 7000 measurements of potential alpha energy concentration were done. Most of these measurements are performed by the way of regular measurements of dust concentration. Similar solution has been recommended to EC as result of a research project done by British Coal (Page, 1989).

Calibration is done in the radon chamber of the Central Mining Institute. The chamber is a steel box of 7.5 m^3 volume. Following radon sources are used:

As a source of aerosols we usually use an inhalator producing water aerosols with diameters of $3 \mu\text{m}$ (AMD). Calibration of instruments for radon daughters measurements is done by simultaneous measurements by an instrument to be calibrated and by the absolute method developed in our laboratory (Chałupnik et al, 1985). This method consists in collecting of radon daughters on a membrane filter, immersing the filter in a scintillation vial filed by toluene cocktail and measuring the total alpha and beta activity in three time intervals according to timing proposed by Thomas (Thomas, 1972). In the liquid scintillation cocktail the counting

efficiency of alpha and beta activity is close to 100% therefore we can assume, that this method is an absolute one. Using number of counts obtained in three different time intervals after sampling, the potential alpha energy concentration as well as concentration of radon daughters products can be calculated.

Measurements of individual exposure of miners

Measurements of individual doses are obligatory when the annual dose is likely to exceed 15 mSv. According to results of our fixed point measurements, such cases are rare. Personal dosimetry is performed by The Institute of Occupational Medicine, Łódź, Poland. Bare track detectors of the type LR-115 have been used (Domański et al, 1975). Tracks are

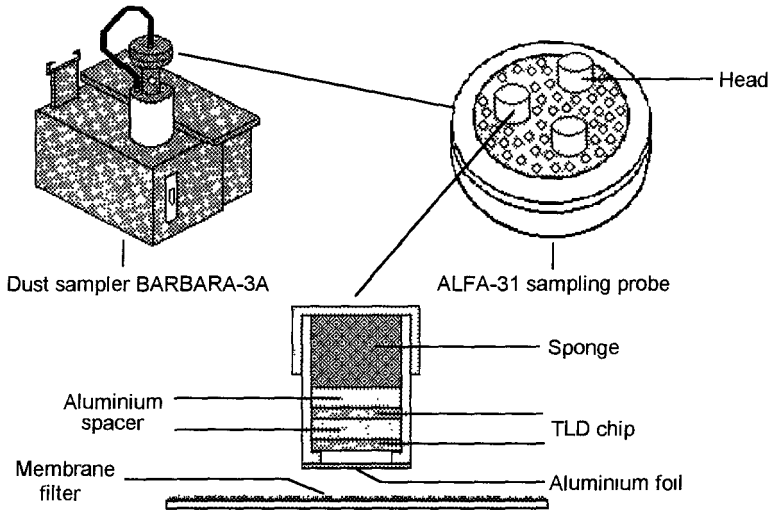


Fig. 1. Dust sampler „BARBARA 3A” with ALFA-31 sampling probe

formed by alpha particles emitted by radon and radon daughters. This method can lead to very large errors when equilibrium factor F is below 0.15. There are big discrepancies between doses estimated from fixed point measurements made by ALFA-31 sampling probes and personal bare LR-115 dosimeters. LR-115 give results higher by one or even two orders of magnitude (Skowronek et al, 1993). Results of doses estimated from fixed point measurements by means of ALFA-31 sampling probes were compared with the results obtained by means of French active personal dosimeters (readout was done by COGEMA-Limoges). Although the differences exceeded the error of measurements, but they were much smaller than discrepancies between active ALFA-31 and passive LR-115 (Skowronek et al, 1993). Since the problem seems to be very serious, we would like to investigate all the possible factors, which may affect results obtained by ALFA-31 sampling probes. For this reason we would like to investigate the unattached fraction and the particle size distribution of radon daughters in coal mine atmospheres.

Radiation hazard caused by radon progeny in Polish hard coal mines

In Poland there are 66 underground hard coal mines. Measurements of PAEC in places listed above have been performed as routine since 1989. Every year a report on the state of radiation hazard in mines is prepared by our institute. In 1994 7110 measurements of PAEC were done. The inspection level $0.8 \mu\text{J}/\text{m}^3$ was exceeded in 434 cases in 18 mines, while the inspection level $2.0 \mu\text{J}/\text{m}^3$ was exceeded only in 92 cases in 7 mines.

Instruments for measurements of unattached fraction of radon progeny (completed within this project)

Since our laboratory was not equipped with instrumentation for measurement of unattached radon daughters or particle size distribution we had to complete a necessary equipment. Because of limited funds and time we have decided to complete instruments for unattached fraction, while the particle size distribution in Polish mines will be measured with the aid of Georg August Universität, Göttingen. We have decided to resolve the problem of measurement of the unattached fraction basing on a method proposed by A. Reineking and J. Porstendörfer (Health Physics, vol. 58). In this method an air is sucked from one side directly onto a filter, and from the other side by a diffusive screen. According to A. Reineking and J. Porstendörfer a 50% cut-off diameter should be placed in a range of 4 to 6 nm. In order to achieve this value there is necessary to select carefully the air flow and the effective diameter for each screen.

A scheme of the whole air sampling system is presented in the Fig.2.

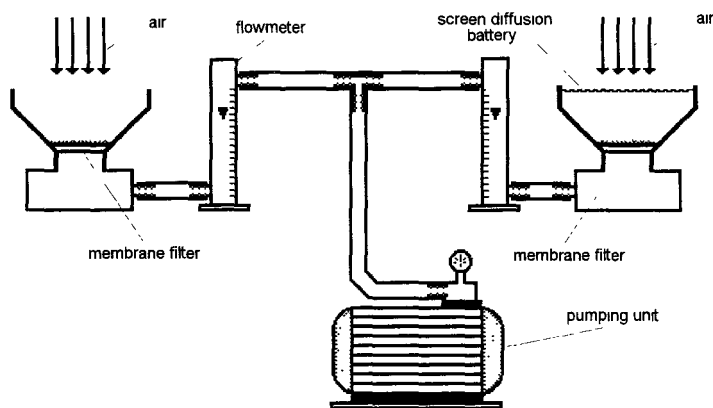


Fig.2. Measurement system during air sampling

Basing on the experimental data pointing out the fact, that the unattached fraction of bismuth can be neglected, we can accomplish an estimation of the unattached fraction of short-living radon decay products by comparison of radon daughters activity collected on two filters (with and without a screen). At least two spectrometric measurements of alpha activity collected on filters must be performed in different time intervals. A scheme of the measurement set is presented in Fig.3. The sampling system has been designed and constructed in our institute using the instructions obtained in Georg August Universität, Göttingen.

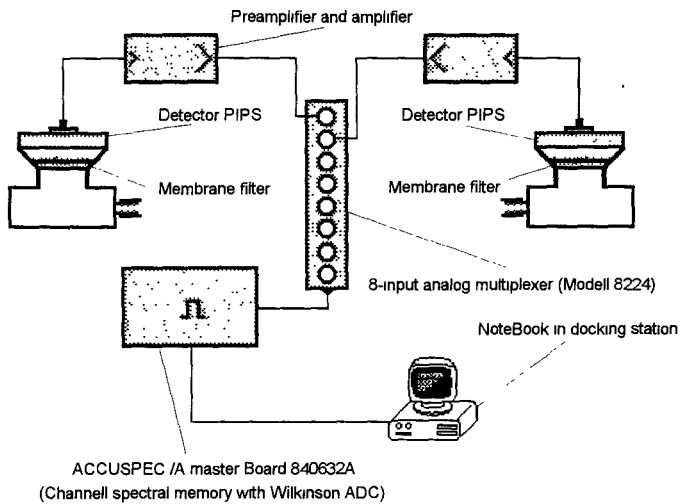


Fig. 3. Counting system

The measuring system was completed mostly of elements bought at CANBERA (USA). This system (Fig .3) includes:

- filters,
- two PIPS detectors,
- preamplifiers and amplifiers,
- multiplexer,
- a chart of multichannel analyser,
- a notebook .

For this system we have developed a computer programme designed ,among other things, for processing of results of measurements, calculations of the unattached fraction and for data storage (Appendix 1). This programme will be very useful for all kinds of natural radioisotope measurements in coal mines and their natural environment.

Intercomparison measurements

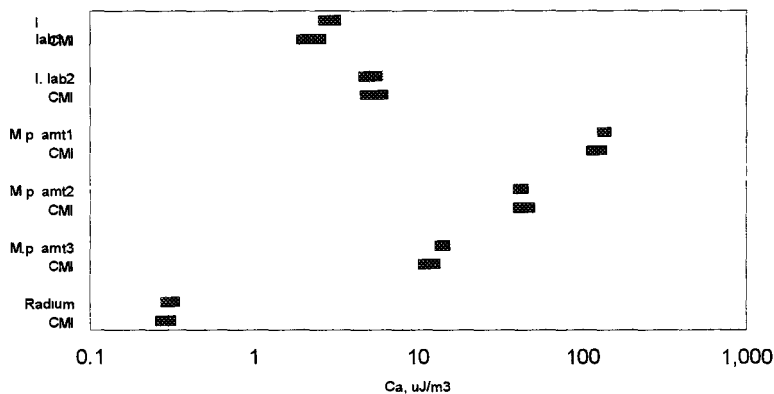
We have participated in several interlaboratory tests to prove the calibration method. Results of this tests are shown in Fig.4. Generally our results were in good agreement with other teams. One exercise, performed with dr Reineking from Georg August Universität, Göttingen was especially valuable, because dr Reineking measured also the unattached fraction of radon daughters (table 1). The results obtained show clearly, that using our dust sampler with ALFA-31 sampling probe and microcyclone was cut off the unattached fraction of radon daughters. In 1994 we also participated in the intercomparison exercise organised by the US Environmental Protection Agency (The provisional report was made by EPA). Our results of measurements of radon concentration by means of charcoal canisters were in rather good agreement with the target value (6.8% lower), while our results of measurements of potential alpha energy concentration were 26% lower than the target value. This result caused that we started a careful and detailed check up of our whole calibration procedure. During this step by step check up we have found, that we loose some

Table 1. Comparative measurements in Universität, Göttingen.

Measurement conditions	Universität, Göttingen / Central Mining Institute
without additional aerosol source, particle concentration in air: 9600 cm ⁻³	2.02±0.31 (with microcyclone)
	1.35±0.21 (without microcyclone)
with additional aerosol source, particle concentration in air: 330 000 cm ⁻³	0.82±0.12 (with microcyclone)
	0.81±0.12 (without microcyclone)

Note The air in Central Mining Institute equipment flowed through the microcyclone or directly onto the filter.

counts in our reference measurement due to high count rate and limited time resolution in our spectrometer. This caused a systematic error of about 15 %. We have decided that after correction for this error our results can be accepted.



I lab - University of Göttingen, M p amt - Materialprüfungsamt
Dortmund, Radium - Radiumforschung Institute, University of
Vienna

Fig.4. Results of comparative measurements of radon daughters

Selection of investigation sites

We have chosen for the investigation of unattached fraction and size particle distribution two underground coal mines. One is a small experimental mine (Experimental Mine Barbara - EMB) used solely for research of ventilation particularly explosions in underground mines and prevention measures. In this mine galleries are drilled on two levels 30m and 46m below the ground level. We have chosen this mine for our experiments, because there are good possibilities of changing ventilation and dust concentration and because there are facilities enabling using various instrumentation and equipment. We also intend to use this mine in the nearest future as place for national intercalibration and intercomparison measurements. We have done measurements of radon and potential alpha energy concentration in the EMB mine workings with natural ventilation only and with operating principal ventilation as well. The results are shown in Fig.5,6,7,8. The concentrations of radon and daughter products are high

enough to assure a good accuracy of measurements. The maximum value of PAEC was $9.1 \mu\text{J}/\text{m}^3$. Radon concentration in air reached a maximum value $3735 \text{ Bq}/\text{m}^3$.

The second mine chosen for the experiment is an active large hard coal mine, where coal is extracted at the depth up to 700 m below the ground level. We have chosen this mine out of 66 active coal mines located in the Upper Silesia because of following reasons:

- there are high concentrations of radon and daughter products (PAEC up to $10 \mu\text{J}/\text{m}^3$),
- there is no serious methane hazard therefore there is easier to get approval for the usage of electrical equipment,
- we have done there a very detailed study of radon and radon daughters in air in different conditions (mining, ventilation) therefore we can expect to find places with lower and higher concentration of unattached fraction,
- there is a possibility to take measurements in mine workings where different systems of exploitation have been applied.

In this mine were done 791 measurements from June 1994 to May 1995. The maximum value was $6.35 \mu\text{J}/\text{m}^3$ ($0.01 \mu\text{J}/\text{m}^3$ - $6.35 \mu\text{J}/\text{m}^3$ and medium value $0.82 \mu\text{J}/\text{m}^3$).

V. References

Chałupnik S., K.Skubacz, J.Lebecka. 1985. A method of absolute measurement radon-daughter concentration in air. Proceedings of the Third International Conference on Low Radioactivity's, Bratislava 1985. Physics and Applications, Vol.13,pp.289-291.

Decree of the Ministry of Industry and Trade. 1995. Act of April 14, 1995. Polish Legislation Journal No. 67. Warsaw, June 19, 1995 (Polish only).

Domański T., Chruścielewski W., Liniecki J. 1975. Evaluation of radon and its daughter products concentration in the air using track foils. Nukleonika 20, p.589-600, Warszawa, 1975.

Geological and Mining Law. 1994. Act of February 4, 1994. Polish Legislation Journal no.27, Warsaw, Marth 1, 1994 (Polish only).

Lebecka J., I.Tomza, K.Skubacz, T.Niewiadomski, E.Ryba. 1984. Monitoring of radon daughters in coal mine atmospheres. Proceedings of the Third International Mine Ventilation Congress. Harrogate, 1984: pp.121-126, (Eds Howes M.J. and Jones M.J., London 1984).

Lebecka J., J.Skowronek, I.Tomza, B.Michalik, S.Chałupnik, K.Skubacz. 1988. A termoluminescent monitor of low radon-daughter concentration in air. Journal of Applied Radiation and Isotopes, Vol.39, No.9, 1988.

Lebecka J., Skowronek J. 1993. Monitoring and Control of Radiation Exposure in Polish Coal Mines. Proceedings of 25th International Conference of Safety in Mines Research Institute, Pretoria 13-17 September 1993.

Lebecka J., Skubacz K., Chałupnik S., Michalik B. 1993. Methods of Monitoring of Radiation Exposure Used in Polish Coal Mines. Nukleonika 38 no.4, p. 137-154, Warszawa, 1993.

Page D. 1989. Report on Radon Decay Products Monitoring in Coal Mines. Commission of the European Communities. Directorate General XVIIB-Energy, 1989.

Skowronek J., Skubacz S., Chałupnik S., Kajdasz R., Nalepa S. 1993. Comparison of Environmental and Personal Control of Short-Lived Radon Decay Products in Hard Coal Mines. Nukleonika 38, no.4, p. 121-136, Warszawa 1993.

Thomas J.W. 1972. Measurement of radon daughters in air. Health Physics, vol.23, p. 783, 1972.

The computer programme serves to resolve two groups of tasks. The first one enables a solution of problems connected with the radioactive decay law in relation to the groups of radioactive isotopes from specified series and chosen by the user. Particularly these tasks are as follows:

- number of isotopes,
- activity of isotopes,
- integral of activity,
- sum of isotope numbers,
- sum of isotope activities,
- integral of sum of isotope activities.

The second group of tasks makes it possible to resolve problems connected with the measurements of short living products of radon and thoron basing on the following methods:

- Liquid Scintillation Method,
- Alpha Spectroscopy Method.

By the liquid scintillation method it can be calculated the coefficients of equations for the optional parameters such as an air flow through filter, detection and filtration yield and radiation as well as the activities based on the actual measurement data for the actually selected measurement set. This part of computer programme is helpful not only for the liquid scintillation method but also for the others, in which an filter activation measurement is performed in the different time intervals to make the calculation of the activity (or potential alpha energy concentration) of the short living products of radon and thorone.

By the alpha spectroscopy method it can be made the proper calculations for the presented above method of determination of the unattached fraction elaborated by A. Reineking and J. Porstendorfer. In this case , the suitable calculations can be performed after introducing measurements parameters for an open face filter and shielded filter such as time and rate of pumped air, time intervals in which the alpha radiation detection emitted by isotopes is performed, as well as the detection yields and counting obtained in the suitable time intervals. The calculation can be made in units chosen by an user. The results obtained together with an information about the measurements place and time of its performance can be stored on a disc file. This part of programme has been checked basing on the data obtained in Georg August Universität , Göttingen (Isotopenlabor) during training of our colleague .

"Barbara" Experimental Mine - level 30 m, ventilation on

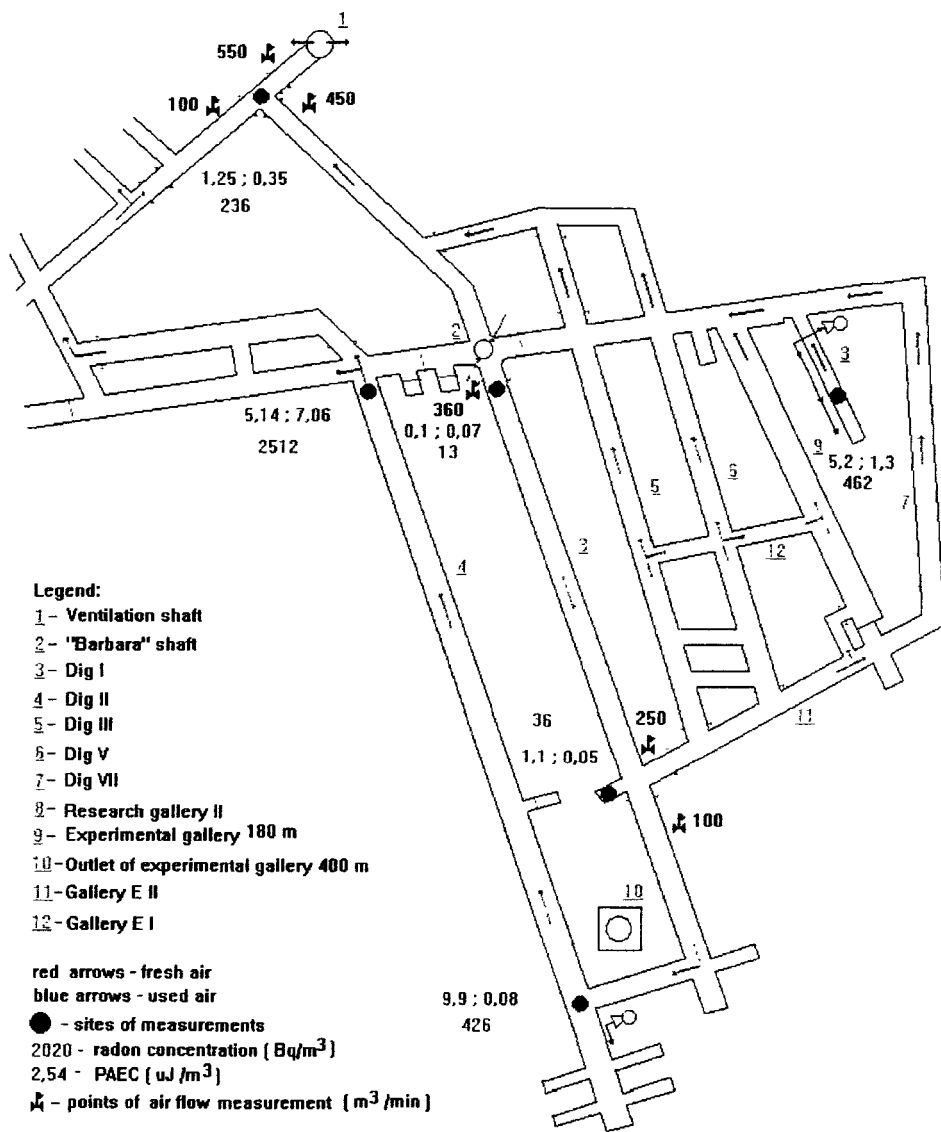


Fig. 5. The results of measurements of radon and its short lived daughters concentration in an air of the „Barbara” Experimental Mine.

"Barbara" Experimental Mine - level 30 m, ventilation off

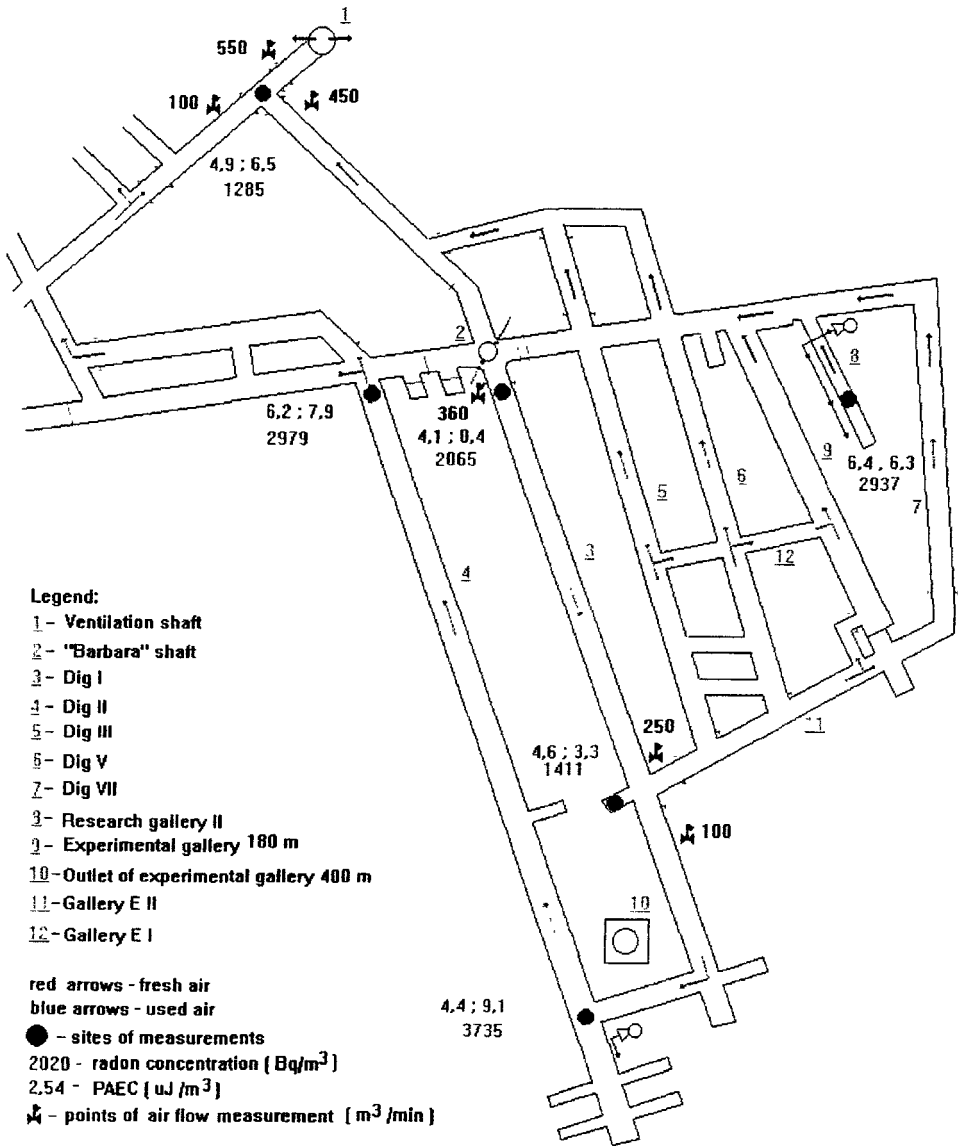


Fig. 6. The results of measurements of radon and its short lived daughters concentration in an air of the „Barbara” Experimental Mine.

"Barbara" Experimental Mine - level 46 m, ventilation on

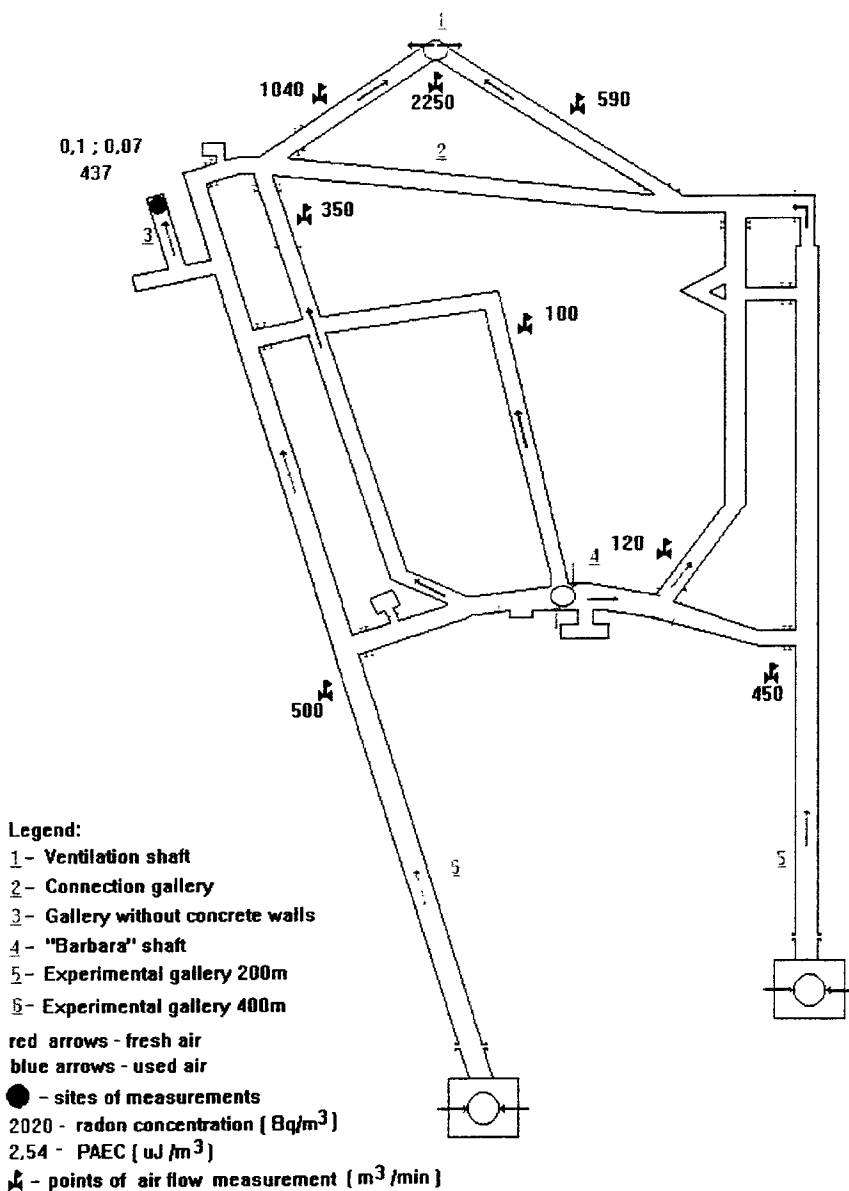


Fig. 7. The results of measurements of radon and its short lived daughters concentration in an air of the „Barbara” Experimental Mine.

"Barbara" Experimental Mine - level 46 m, ventilation on

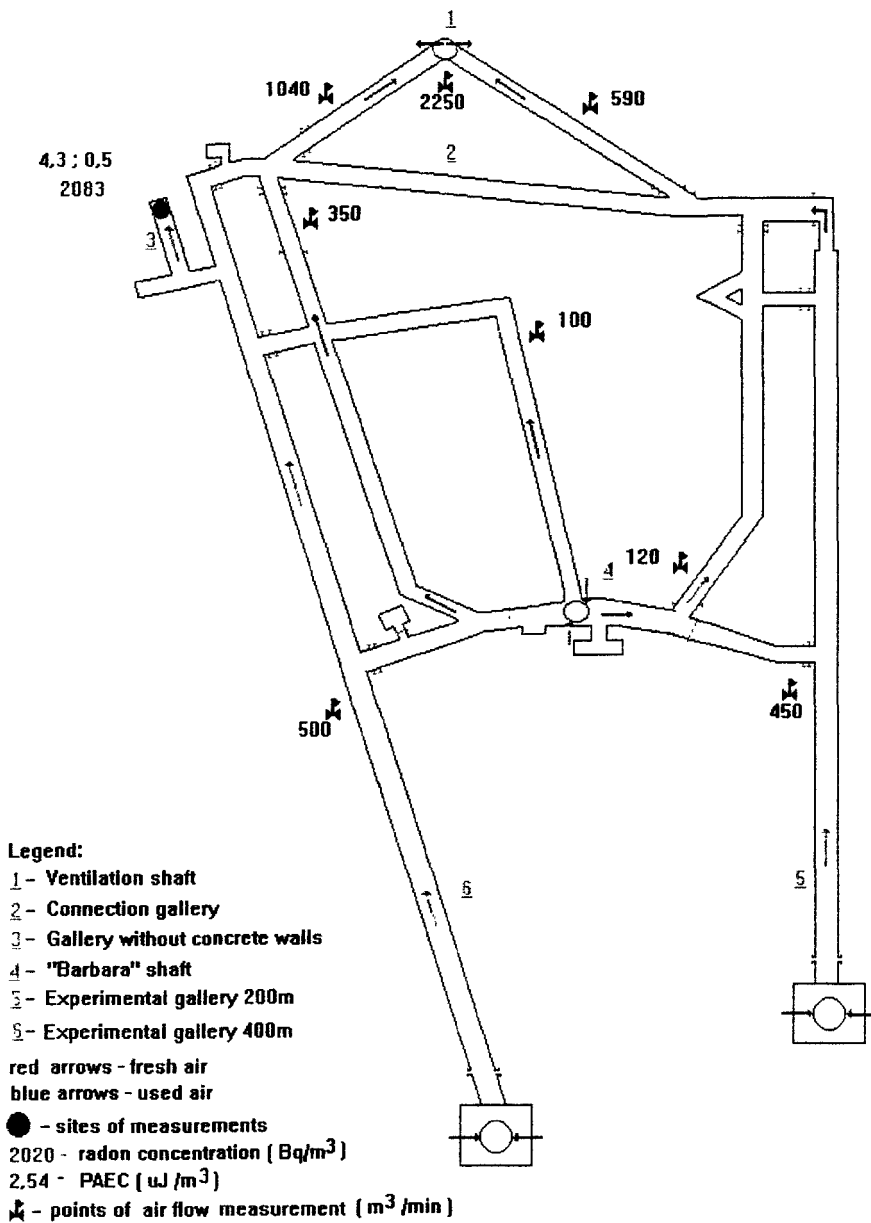


Fig. 8. The results of measurements of radon and its short lived daughters concentration in an air of the „Barbara” Experimental Mine.

Head of project 9: Dr. Kobal

II. Objectives for the reporting period

During the period between June 1994 and June 1995 groups of the "J. Stefan" Institute of Ljubljana, Slovenia were included in the current radon project within the framework of PECO93. Projects of three subgroups were supported.

Subgroup 1 (Dr. Janja Vaupotic, Department of Physics and Environmental Chemistry):

- Completion of nationwide survey of Radon in kindergartens and schools
- Radon mitigation in kindergartens with the highest radon levels.
- Detailed measurements in different geological and climatological regions to understand the behaviour of radon in indoor air.
- Calculations of doses obtained by children and staff in the kindergarten, outdoors and in their homes.

Subgroup 2 (Peter Jovanovic, Institute of Occupational Safety)

- Radon measurements in karst caves in Slovenia used for speleotherapy

Subgroup 3 (Prof. Rado Ilic, Department of Reactor Physics)

- Adsorption of radon and radon daughters on solid surfaces and applications of these phenomena for characterisation of materials in radon dosimetry.

III. Progress achieved including publications

Subgroup 1:

Introduction

In Slovenia, a nation wide indoor radon programme started a few years ago. Within this programme instantaneous indoor radon concentrations were determined in all the 730 kindergartens (1) and 890 schools under so called closed conditions and a 3-month concentration averages were obtained in 1000 randomly selected dwellings using the track etch technique. Two kindergartens with the highest radon levels (2,3) were mitigated (4). In addition the fractal analysis of the kindergarten and school data was applied (5) and contributed to a better understanding of radon behaviour in the indoor air.

The aim of the study included into the EU project was to perform additional measurements in order to obtain all the data necessary for dose calculations. The work was carried out within a doctor dissertation (6). For this purpose four kindergartens were selected in different geological and climatological regions and for a year and a half, the concentration of radon and radon decay products, and the equilibrium factor in air were measured using complementary methods. On the basis of these results the advantages and disadvantages of different techniques could be critically appraised and the relationships among the concentration values obtained by different methods and

different averages evaluated. The measurements were carried out not only in the kindergartens themselves, but also outdoors and in several homes of the children and kindergarten staff.

The next step was calculation of the doses obtained by children and staff in the kindergarten, outdoors and in their homes. Our interest was not only the dose itself, but also the various dose contributions and the parameters influencing them. For dose calculation, dose conversion factors were either taken from the literature (7) or calculated by applying a computer program package for dose modelling (8). In the calculations, different physical activities and the size distribution of air particles was taken into consideration. Using the experience from these four selected kindergartens, a dose estimate was made for all the 730 Slovene kindergartens.

Results

For our study four kindergartens (vrtec) with elevated indoor radon concentrations were selected: two in Ljubljana (vrtec 3 and 4), one in the Alpine region (vrtec 2), and one in the Karst (vrtec 1) region. In each place a few rooms with the highest radon level were selected for measurements. In teach room, track etch detectors were exposed for 3 or 6 months over 15 months to measure radon concentration averages and equilibrium factors according to Planini (9). In addition, in each yearly season radon and radon decay products concentrations were followed by continuous instruments AlphaGuard, WLM-30, and Scintrex System-30. All the measurements carried out and their time schedule are summarized in Table (Tabela) 6 of Ref. 6. In addition to kindergartens, measurements were also carried out in some flats (stan.) where children or kindergarten personnel live. The results of 3- and 6-month radon concentration averages and average equilibrium factors (9) as obtained by track etch detectors are summarized in Table (Tabela) 7 and 8, respectively, in Ref. 6 (zima=winter, pomlad=spring, poletje=summer, jesen=autumn). The 3-month values for kindergarten (vrtec) 1 and 2 are also shown graphically on Figure (Slika) 14 and 15, respectively. A typical run of indoor radon concentration is presented by the situation in the kindergarten (vrtec) 2 (Alpine region) in Figure (Slika) 22 in Ref. 6. Using data taken from AlphaGuard, EDA-30 and Scintrex System-30, radon or radon decay products concentration averages were calculated for different time periods, as follows: (a) the total time of measurement (for instance 18 days, p18d) what might be close to the value obtained by track etch detector (p3m), (b) the working time only, for instance between 6 and 16 hours (p6-16). It is obvious from Figures (Slika) 25-29 in Ref. 6 that the p6-16 average is usually much lower than the p3m average. That means that the dose calculated on the basis of track etch data, what is a general practice, is usually higher than the concentration to which the persons are really exposed during the stay indoor. Thus using track etch data for dose estimate we are on the safe side from the radiation protection point of view.

Doses received by a child (otrok) and a nurse (vzgojiteljica) in a kindergarten (vrtec) were calculated applying ICRP-50 methodology, DCF-ICRP-50 (10), and using dose conversion factors either obtained from literature, DCF-James (7) or calculated by using Hofmann's computer program package, DCF-izra'cunani (8). As expected, ICRP gave the lowest doses, as seen on Figure (Slika) 52a, b, c. Even though in these four kindergartens the indoor radon concentrations were elevated, the main contribution to the dose (as seen from Figure (Slika) 60) originates from radon in dwellings (doma), the kindergarten (vrtec) contribution is up to 20%, while the outdoor (zunaj) radon contributes only a few percents. On the basis of the instantaneous indoor radon concentrations (1) as presented on Figure (Slika) 62 of Ref. 6, the yearly effective doses were estimated for children in all the 730 kindergartens in Slovenia applying the ICRP-50 (10) and UNSCAR (11) methodology. The results are presented in a log-normal diagram in Figure (Slika) 63 in Ref. 6.

In the beginning, this EU project was planned for three years and within it also particle size distribution and unattached fraction measurements were foreseen. Because the project was cancelled after the first year, we were not able to carry out these measurements.

References

1. J. Vaupotič, M. Križman, J. Planinić, J. Pezdič, K. Adamič, P. Stegnar, I. Kobal, Systematic indoor radon and gamma measurements in kindergartens and play schools in Slovenia, *Health Phys.*, **66**, 550-556, 1994.
2. J. Vaupotič, P. Stegnar, I. Kobal, Thorough investigation of indoor radon in a kindergarten with elevated levels, *Proc. 2nd Symp. Croatian Radiation Protection Association, Zagreb, Croatia, 1994*, pp 309- 313.
3. J. Vaupotič, M. Križman, J. Pezdič, P. Stegnar, I. Kobal, Examples of high indoor radon concentrations in kindergartens and play schools in Slovenia, *Regional IRPA Conference, Obergurgl, Austria, 1993*, pp. 418-421.
4. J. Vaupotič, M. Križman, J. Planinić, I. Kobal, Radon level reduction into two kindergartens in Slovenia, *Health Phys.* **66**, 568-572, 1994.
5. G. Salvadori, S. P. Ratti, G. Belli, I. Kobal, J. Vaupotič, The spatial distribution of ^{222}Rn "indoor" in Slovenia as a stochastic multi-fractal process. *Regional IRPA Conference, Portorož, Slovenia, 1995*, PP25
6. J. Vaupotič, Indoor radon and decay products concentration and dose modelling, Ph. D. Thesis, University of Ljubljana, Slovenia, 1995 (in Slovene, only abstract in English).
7. A. C. James, Lung dosimetry, Part 3, Chapter 7 in *Radon and its decay products in indoor air*, Ed. A. R. Robkin, D. R. Stadler, University of Washington Press, Seattle, 1987, pp. 76-90.
8. W. Hofmann, Institute of Physics and Biophysics. University of Salzburg, Salzburg, Austria. Computer program package for dose modelling.
9. J. Planinić, Z. Faj, The equilibrium factor F between radon and its daughters, *Nucl. Instrum. Meth.* A278. 550- 552, 1990.
10. International Commission for Radiological Protection (ICRP), Lung cancer risk from indoor exposures to radon daughters. A report of a Task Group. *Publication 50*, 1987.
11. United Nations scientific Committee on the effects of atomic Radiation (UNSCEAR), Sources and effects of ionizing radiation. *Publication E.88.IX.7*. 1988.

Subgroup 2

1. Introduction

As Slovenia is intending to establish in some of the karst caves a speleotherapy (1), the dose of patients and medical staff has to be investigated. A karst cave near the town Sežana has been investigated with respect to radon and its daughter concentrations, temperature, humidity, concentrations of ions (positive and negative) and concentrations of microbes in the air. The fact of measuring so many cave parameters can be used in analyzing the aerosol characteristics of radon daughters, thus yielding valuable information for the dose assessment in natural caves.

Speleotherapy is a special kind of climatotherapy and is being used as an additional treatment for curing bronchial and asthmatic diseases of children and adults (2,3) in last 40 years in many countries (Czech Rep., Hungary, Italy, Germany, Russia...).

The cave microclimate is a special system built up from several individual parameters with biological activity of their own, but the general effect on the human organism is due to a collective influence of all these factors. The most important elements of cave microclimate (4,5) are low temperature (8 °C - 14 °C), high relative humidity (93 -99 %), high concentrations of aerosols (Ca, Mg, ...), radioactivity (radon) and ionization (high concentrations of negative ions in air). The water with Ca and Mg hydrocarbonates is dropping in the cave steadily forming a fine spray in the air. The water droplets are ionized mainly with negative polarity what is a natural consequence of the origin (water-fall effect). Due to the decay of radon there are alpha particles and ionized daughter products in the air (6). All these components react together and produce different ionizing or natural aerosols.

Evident improvements of some vital lung functions are mainly due to a high relative humidity in caves, a high concentration of natural aerosols, high concentration of negative ions, which purportedly affect mucociliary clearance and thereby bronchial dose (7,8). Lately much attention has also been paid to the influence of the concentration of negative ions and radon concentrations on the health of patients (9). Theoretical considerations of the interaction of alpha particles with cellular targets suggest that hormesis may be interpreted as a biopositive reaction of a small number of cells in an organ to alpha exposure (10,11). By measuring climate parameters and the amount of the ionising radiation present in some caves the ones suitable for the speleotherapy were determined.

2. Methods

In the period from Sep 1991 to Jul 1992 several caves in our karst region (near Sežana), both accessible and inaccessible for tourists, were chosen for measurements. These are: Škocjan cave, Divaška cave, Dimnice, the cave near Sežana hospital, Medvejek cave, Lipiška cave, Malenca cave, Koščak cave, Pliskavica cave and Tavčar cave.

In the first step we were just looking at the caves, to have more information about the atmospheric parameters, important for the speleotherapy. Then we decided to make monthly measurements in the cave near hospital, where the speleotherapy is going on and in Vilenica cave, which will be next cave used for the speleotherapeutic treatment. These measurements were made in the period from March 1994 to July 1995.

Measurements of radon and radon daughter concentrations were performed by the RGA-40 radon gas monitor and WLM-30 working level monitor from Scintrex, Canada. Temperature, relative humidity and air velocity in caves were measured by standard digital instruments. Concentrations of gases were measured by the Dröger pipes. The dose rate of gamma radiation was measured by NaI scintillation detector (PRM-7, Eberline, USA). The instrument was calibrated and its precision is estimated to under 10 %. Ion concentrations were measured by ionometer Schomadt, Germany. The accuracy of the instrument is not good, so that we would only to find the range of concentrations and not the exact values.

3. Results

Results from the measurements in the cave near Sežana hospital and in Vilenica cave mentioned above are presented in Tables 1,2 and in Figures 1,2. Concentrations in caves are like in other caves in our country (12,13). During the winter season than in summer. The reason for that is changing of air flow in winter and summer because of different temperature gradient (14,15).

3.1 *The cave near Sežana Hospital*

It is an artificially built cave with a 40 m long and 5 m wide central part. The relative humidity is over 90 % throughout all year , the temperature varies between 10° C in winter and 13° C in summer. The air velocity is less then 0.05 m/s, air flow is 5-10 m³/min, ventilation rate lies between 0.5-1/h. Gamma dose rate is 40 nGy/h, CO₂ concentration varies between 0.05 vol % and 0.2 vol % and the concentrations of ozone, sulphur dioxide, nitrate, fluorides and carbon monoxide were not detected. Monthly averaged radon concentrations vary between 50 Bq/m³ and 2000 Bq/m³ (Table 1). Monthly radon concentrations at different measuring points in the cave are presented in Fig. 1. Radon concentrations in summer were much higher than in winter season. The radon daughter equivalent concentrations were during the measuring period in the range from 30 Bq/m³ to 1000 Bq/m³. The equilibrium factor varies between 0.1 and 0.75 and it is higher in winter than in summer. The concentrations of positive and negative ions were in the range from 100 ions/cm³ and 3000 ions/cm³ .

3.2 *The Vilenica cave*

The cave Vilenica is natural cave about 1300 m long and 180 m deep. One third of the cave is open for the visitors. We didn't detect any ozone, sulphur dioxide, nitrate, fluorides and carbon monoxide only carbon dioxide CO₂, its concentrations were in range from 0.1 vol % to 0.3 vol % (Table 2). Temperature and relative humidity were constant, 10 °C and 98 %, respectively. Positive and negative ion concentrations vary between 2000 ion /cm³ and 10000 ion/cm³. In July the concentrations of both were higher and it was evident difference between (about 10% higher concentration of positively charged ions) Monthly averaged radon concentrations were between 250 Bq/m³ and 2350 Bq/m³, higher in summer season (Table 2). Monthly radon concentrations on different locations are presented in Fig. 2. Equilibrium factor varies between 0.1 and 0.5, higher values in winter than in summer.

4. Dose estimation

In the period of three weeks patients and medical personal are located in the cave four hours per day. Between these therapy they have special activities (walking, sleeping...). Our dose calculations based on three different models, ICRP 50, Jacobi-Eisfeld and James-Birchall (16,17). We didn't measure AMAD and unattached fraction of radon daughter, so we take into account values from Postojna cave (3), $f_p = 0.05$ and 0.1 and $AMAD = 0.2 \mu m$. Annual effective doses for medical staff are in the range from $15 mSv$ to $25 mSv$. Effective doses for patients for the period of one therapy are in the range from $50 \mu Sv$ to $200 \mu Sv$.

5. Conclusions and future

Annual doses due to inhalation of radon and radon daughters ranging from $0.1 mSv$ for patients to several tens mSv for medical staff. We will investigate the influence of aerosol characteristics to the lung tissue of the patients.

During the winter season than in summer. The reason for that is changing of air flow in winter and summer because of different temperature gradient (14,15). As we have seen, equilibrium factor in winter time is always 2 to 3 times higher then in the summer time. For better understanding of the difference between seasons we will measure and pressure in the cave in outside from the cave.

In future we will made measurements of the aerosol size distribution and concentration of unattached radon daughters in one cave (the cave near hospital in Sežana), because the measurements can help us by the understanding of longterm effects of the therapy.

6. References

1. Jovanovič, P., Debevec, A., Naracsik, P. Entwicklungsmöglichkeiten der Speläotherapie im klassischen Karst der Republik Slowenien; 10. Int. Symp. für Speläotherapie, Bad Bleiberg (1992), Verband Österreichischer Höhlenforscher, Wien 1994.
2. Spannagel, H. Zschr. angew. Bäder-Klimahk. 7.6.684, 1960.
3. Kirchknopf, M. Arch. Physik. Ther. 17.6.423, 1965.
4. Horvath, T. Our actual knowledge and ideas about speleotherapy, Wissenschaftliche Beihefte zur Zeitschrift Die Höhle Nr. 43, Wien 1992.
5. Cauer, H. Chemisch-physikalische Untersuchungen der Klimaverhältnisse in der Kluterhöhle, Archiv für Physikalische Therapie, 6. Jahrgang, Heft 1, Scholtz, Berlin, 1954.
6. Raabe, O. G. (1969). Concerning the interaction that occur between radon decay products and aerosol, Health Phys., 17.
7. Benneth, W. D., Chapman, W. F., Lay, J.C. and Gerity, T. R. (1993), Pulmonary clearance of inhaled particles 24 to 48 hours post deposition: Effects of beta adrenergic stimulation, J. Aerosol Med., 6, 53-62.
8. Foster, W. M., Langenback, E. G. and Bergofsky, E. H. (1982). Lung mucosiliary function in man: Interdependance of bronchial and tracheal mucus transport velocities with lung clearance in bronchial asthma and healthy subjects. In: Inhaled Particles V, Proc. of an Int. Symp. org. by the British Occupational Hygiene Society, Cardiff, 8-12. Sept. 1980. Ann. Occup. Hyg. 26,227-244.
9. Deetjen, P. Zum Stand der Radon-Therapie 1991, Rep. of the Inst. Gastein - Tauernreg. (Austria), 1, 1-6, 1991.
10. Hofmann, W. Gibt es biopositive Effecte bei der Radontherapie, Z. Phys. Med. Baln. Med. Klim. (Sonderheft 2) 19 (1990);
11. Luckey, T. D. Radiation Hormesis. CRC, Boca Raton, Florida, 1991
12. Jovanovič, P., Kanduč, M., and Kuhar, B. (1992). Dose estimates to Rn-222 Concentrations in Postojna cave. Rad Prot Dos 45, 191-192.
13. Kobal, I., Smodiš, B., and Škofljanec, M. (1986). Radon-222 air concentrations

- in the Slovenian karst caves of Yugoslavia. Health Phys. 50, 830 - 834.
14. Yarborough, K. A. Alpha radiation in natural cave, Int. Conf. Radiation hazards in mining, control, measurement and medical aspects, Colorado (USA), Oct 4-9, 1981, American Institute of Mining, NY 1981.
 15. Wilkening, M. H. and Watkins, D. E. Air exchange and ^{222}Rn concentrations in the Carsbad caverns (1976), Health Phys., Vol 31, pp. 139- 145
 16. ICRP 50. Lung Cancer Risk from Indoor Exposures to Radon Daughter, Pergamon, 1986.
 17. NEA. Dosimetry aspects of exposure to radon and thoron daughter products, OECD, Paris, 1993.

Table 1. Measurements of radon concentrations and some other physico-chemical parameters in the cave near hospital in Sežana

Period Mar 94- Jun 95	Average radon concentration		Daughter conc. Bq / m ³	Relative humidity %	Temp deg C	Ion concentration		CO ₂ conc	Equilib. factor F
	Bq / m ³	Bq / m ³				positive ion / cm ³	negative ion / cm ³		
Mar	300	+ - 30	224	95	12	500	500	0.1	0.75
Apr	500	+ - 40	286	95	12	600	500	0.08	0.57
May	1150	+ - 80	1050	95	13	1400	1500	0.07	0.91
Jun	2000	+ - 150	429	90	13	3000	3000	0.1	0.21
Jul	1900	+ - 150	400	90	14	2000	2000	0.1	0.21
Aug	1800	+ - 150	888	88	14	3000	2500	0.1	0.49
Sep	1950	+ - 150	950	85	14	2400	2400	0.1	0.49
Oct	1500	+ - 100	600	90	14	500	450	0.05	0.40
Nov	50	+ - 20	32	90	13	300	300	0.05	0.65
Dec	70	+ - 30	33	95	12	150	150	0.05	0.47
Jan	60	+ - 40	24	95	11	100	100	0.05	0.40
Feb	70	+ - 40	53	95	10	200	300	0.05	0.75
Mar	50	+ - 30	31	95	11	200	200	0.1	0.62
Apr	300	+ - 50	185	95	12	2200	2200	0.06	0.62
May	1400	+ - 80	341	90	13	2000	2000	0.1	0.24
Jun	1550	+ - 100	153	90	14	2100	2100	0.2	0.10

Table 2. Measurements of radon concentrations and some other physico-chemical parameters in the Vilenica cave

Period Jan 95- Jul.95	Average radon concentration		Daughter conc. Bq / m3	Relative humidity %	Temp deg C	Ion concentration		CO2 conc	Equilib. factor F
	Bq / m3	Bq / m3				positive ion / cm3	negative ion / cm3		
Jan	250	+ - 40	112	98	10	3200	3200	0.05	0.45
Feb	500	+ - 50	218	98	10	3600	3500	0.05	0.44
Mar	450	+ - 50	225	98	10	4000	4000	0.1	0.50
Apr	1300	+ - 100	204	99	10	2200	2200	0.1	0.16
May	1900	+ - 150	148	99	10	2000	2000	0.15	0.08
Jun	2000	+ - 200	160	98	10	4000	3900	0.2	0.08
Jul	2350	+ - 250	311	98	10	10000	9000	0.3	0.13

Fig 1. Radon concentrations in the cave near the Hospital in the period Mar - Jun 1995

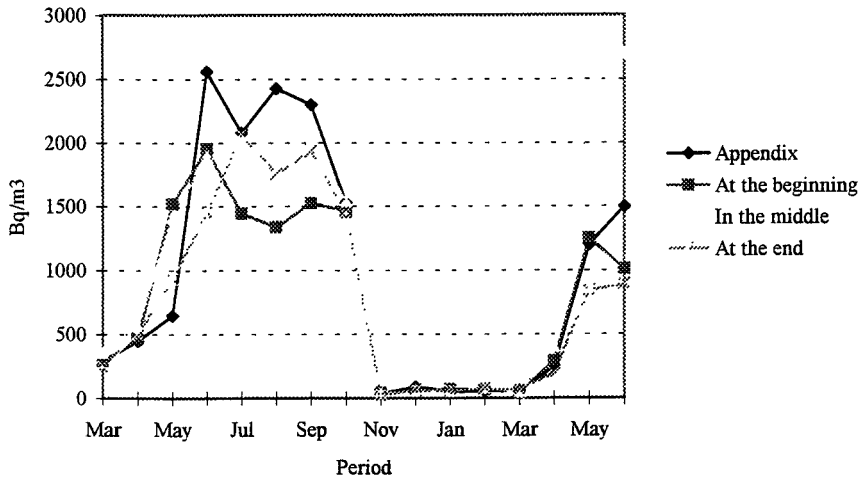
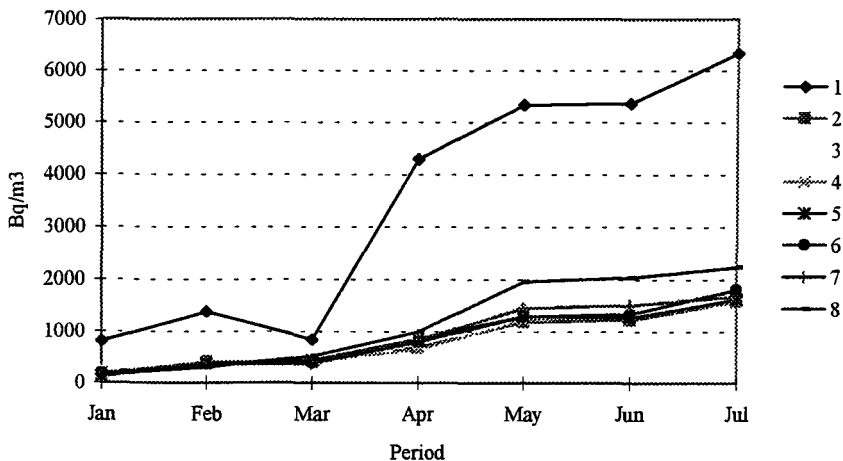


Fig 2. Radon concentrations in the Vilenica cave in the period Jan - Jul 1995 .



- Legend:
- | | |
|----------------------|-----------------------------------|
| 1 Dancing hall | 5 Above the Fairy hall |
| 2 Red hall | 6 Before the Fairy hall |
| 3 Under the Red hall | 7 Fairy hall |
| 4 Near the water | 8 On the bottom of the Fairy hall |

Subgroup 3

Introduction

The objective for the project was investigation of adsorption of radon and radon daughters on solid surfaces and application of these phenomena for the characterization of materials and radon dosimetry.

Results

Ability of activated charcoal to collect radon from a large volume of air has been employed in active radon monitoring devices for a long time. In contrast to this, we developed a passive radon dosimeter [1] which utilizes an active charcoal in combination with a solid state nuclear track detector. A 5 mm thick layer of charcoal is contained in an air-tight dosimeter which is opened for the time of radon collection. Filter at one side of charcoal layer allows radon to penetrate inside the charcoal. On the other side of the charcoal is a 10 μ m thick Al foil which is thin enough to allow alpha particles emitted by Rn and Po to reach CR-39 detector placed under the foil. Sensitivity and response of this dosimeter were calculated by an analytical model which describes adsorption of radon on the surface of charcoal layer and its diffusion inside the charcoal. A diffusion equation was solved for one-dimensional geometry similar to the dosimeter set-up. Results were compared with those obtained in an experiment and they were found to be in agreement. In comparison to ordinary passive radon dosimeters the newly developed dosimeter shows approximately six times higher sensitivity. For short times of exposure, response of this dosimeter can be as much as two orders of magnitude higher than those of standard etched track dosimeters. Radon exposures as low as Bq/m³ can be measured in an exposure time of 3 h.

Another method of radon detection, based on collection of radon progeny on the surface of etched track detector, was proposed [2]. Radon penetrates through a filter made of 10 μm thick polypropylene into a collection chamber made of Al. At the bottom of the chamber there is an electrode at an electrostatic potential of 5 kV against the chamber shield. A CR-39 detector, placed above the electrode, collects charged radon progeny on its surface. This method assumes ability to distinguish tracks from Po-218 and Po-214 and find pairs of tracks which come from the same parent nuclei. If the total number of tracks and the number of track pairs is known, it turns out that the total radon concentration in the air can be calculated even without knowing exact registration efficiencies for individual isotopes of Po because they practically cancel out in a large range of possible values. Further development of this method requires solution for many experimental difficulties.

Interaction of radon with solid surfaces was investigated by a method we named radonography [3]. In an experiment a specimen made of different plastic materials and aluminium was exposed in a radon atmosphere for few days. After that it was placed on a CR-39 detectors for few hours to allow for a decay of radon progeny adsorbed on the surface. Another detector was used then to register alpha particles emitted by Rn and its progeny in an exposure of few days. After etching both detectors were evaluated by an automatic image analysis system TRACOS, developed at J. Stefan Institute. Position of every individual track was stored for a later display. On the first detector, which registered radon daughters only, there was no variation in local track density. However, on the second detector every material had clearly different track density due to different adsorption and diffusion coefficients for radon. A technique, developed for this purpose, shows good spatial resolution and can be combined with measurement of other track parameters such as track size and shape.

References

1. Sutej, T. Sensitivity of a Combined Charcoal and Etched Track Technique for Rn-222, Rad. Prot. Dos. 56 (1994) 255-258.
2. Yu. G. Teterev, S. P. Tretyakova, A. N. Golovchenko, R. Ili and J. Skvarc, Determination of the Absolute Radon Concentration in Air Using an Electrostatic Method and CR-39 Detector, Radiat. Meas. 25 (1995) 645-646.
3. Skvarc, J., Ilic, R., Radonography, Nucl. Instr. Meth. B88 (1994) 430-434.

Head of project 10: Dr. Cuculeanu

II. Objectives for the reporting period

A. Development of a theoretical model aiming at the deriving of the exact solutions of the diffusion equation for the attached-to- and unattached-to-aerosol $^{222}\text{Rn}/^{220}\text{Rn}$ daughters using the Green's function method;

B. Investigation of the model accuracy by comparison of the predicted results with corresponding experimental data;

C. Radiological impact assessment by making use of the dose factor formalism and model output;

D. Development of a computer code (PC version) for calculating the concentration profiles of the attached and unattached $^{222}\text{Rn}/^{220}\text{Rn}$ daughters, the equilibrium factor (F), the unattached fraction (f_p), and the potential alpha energy concentration ($PAEC$).

III. Progress achieved including publications

A. Development of a theoretical model aiming at the deriving of the exact solutions of the diffusion equation for the attached-to- and unattached-to-aerosol $^{222}\text{Rn}/^{220}\text{Rn}$ daughters using the Green's function method

Diffusion equation of radon/thoron and their decay products

The differential equation governing the average rate of change in concentration of the i -th radionuclide $c_i(z)$ in the $^{222}\text{Rn}/^{220}\text{Rn}$ decay chains may be written as:

$$\frac{\partial c_i}{\partial t} = -\nabla F_i + \lambda_{i-1}c_{i-1} - (\lambda_i + \Lambda_i)c_i + v_{di} \frac{\partial c_i}{\partial z} \quad (1)$$

where t is the time, z is the altitude, F_i is the turbulent flux vector, λ_i is the decay constant, Λ_i is the removal rate by washout and rainout and v_{di} is the sedimentation velocity. The sedimentation velocity is taken as positive in the downward negative z -direction.

The physical assumptions underlying equation (1) are:

- the concentration field is horizontally homogenous;
- the mean vertical wind is zero;
- the daughter sources are the parent isotopes in the atmosphere;
- the sinks are radioactive decay, washout and rainout.

The model categorizes daughters in attached-to- and unattached-to-aerosol (*two group daughters model*). Supposing that the meteorological conditions do not change in time, and the turbulent flux is proportional to the concentration gradient along z -axis ('K-theory' hypothesis), i. e., $F_i = -K_z (\partial c_i / \partial z)$, where K_z is the turbulent diffusion coefficient, the steady-state diffusion equation is obtained from equation (1):

$$L c_0(z) = 0 \quad (2)$$

for radon/thoron, and:

$$L c_{1f} = -\lambda_0 c_0 \quad (3)$$

$$L c_{1a} = -\alpha c_{1f} \quad (4)$$

$$L c_{2f} = -\lambda_1 R c_{1a} - \lambda_1 c_{1f} \quad (5)$$

$$L c_{2a} = -\alpha c_{2f} - (1-R) \lambda_1 c_{1a} \quad (6)$$

$$L c_{3f} = -\lambda_2 c_{2f} \quad (7)$$

$$L c_{3a} = -\lambda_2 c_{2a} - \alpha c_{3a} \quad (8)$$

for the first three daughters, where: c_{if} is the concentration of the unattached i daughter, c_{ia} is the concentration of the attached i daughter, α is the attachment rate, and R is the recoil detachment probability. The operator L has the expression:

$$L \equiv \frac{d}{dz} \left(K_z \frac{d}{dz} \right) + v_{di} \frac{d}{dz} - \sigma \quad (9)$$

where: $\sigma = \lambda_0$ for $^{222}\text{Rn}/^{220}\text{Rn}$ ($\Lambda_0 = 0$), $\sigma = \lambda_i + \Lambda_i + \alpha$ ($i \geq 1$) for unattached (free) daughters, and $\sigma = \lambda_i + \Lambda_i$ ($i \geq 1$) for attached daughters. The associated boundary conditions are:

$$\lim_{z \rightarrow 0} K_z \frac{dc_0}{dz} = -E \quad (10)$$

$$\lim_{z \rightarrow \infty} c_i(z) = 0, \quad i \geq 0 \quad (11)$$

$$\lim_{z \rightarrow 0} c_i(z) = 0, \quad i \geq 1 \quad (12)$$

where E is the $^{222}\text{Rn}/^{220}\text{Rn}$ exhalation.

The steady-state diffusion equation predicts realistic radon/daughter profiles when constant atmospheric mixing persists for several hours (at least 4 hours – Cohen *et al.*, 1972). In order to compare the concentrations generated by the time-independent model with the experimental data, Beck and Gogolak (1979) performed their measurements after 6 - 9 hours of nearly constant stability. The scale analysis shows (Cohen *et al.*, 1972) that during neutral and weakly stable conditions the time-dependent term becomes small compared to the flux divergence. The error caused by neglect of time variation may be as small as 1%. However, under very stable stratification the time dependence becomes proportional to the vertical transfer and the steady-state approximation is less valid.

Eddy diffusivity profiles

K_z for the atmosphere. In order to characterize the intensity of the vertical mixing in the atmosphere, a K_z expressed by a linear law of z (Ikebe, 1970; Roffman, 1972) is being used: $K_z = a + bz$, where a is the molecular diffusion at the ground level, and b quantifies the turbulence intensity and may be defined as the turbulent diffusion coefficient at a unit altitude. Two types of K_z profiles are currently

used (Ikebe, 1970):

- case 1:

$$K_z = a + bz, \quad 0 \leq z < \infty \quad (13)$$

- case 2:

$$K_z = \begin{cases} a + bz, & 0 \leq z < H \\ a + bH, & H \leq z < \infty \end{cases} \quad (14)$$

The corresponding values of b for Jacobi and André's profiles (Jacobi and André, 1963) are displayed in table 1, and for Draxler's profiles (Draxler, 1979) in table 2. The value of a is $0.54 \times 10^{-3} m^2 s^{-1}$.

Table 1. Parameters for the eddy-diffusivity profiles (Jacobi and André, 1963)

Turbulence	b (m/s)	K_z profile
IWN	0.001	case 1 or case 2, $H = 2000$
WNN	0.01	case 1 or case 2, $H = 2000$
NNN	0.1	case 2, $H = 200$ m
SSN	1.	case 2, $H = 100$ m

Table 2. Parameters for the eddy-diffusivity profiles (Draxler, 1979)

Stability class	b (m/s)	K_z profile
A, very unstable	1.61	case 2, $H = 100$ m
B, moderately	1.01	case 2, $H = 100$ m
C, slightly unstable	0.67	case 2, $H = 100$ m
D, neutral	0.15	case 2, $H = 100$ m
E, slightly stable	0.05	case 2, $H = 100$ m
F, moderately stable	0.015	case 2, $H = 100$ m

K_z for vegetation. Although the nature of transport in vegetation is not fully understood, it is possible to develop models that generate realistic canopy microclimates (Monteith and Unsworth, 1990). In order to derive fluxes in canopies, most biosphere models assume that transport is one-dimensional, and that fluxes and quantities (momentum, mass, heat) are related by 'K-theory' with K_z an increasing function of z between the soil surface and the top of the canopy. The use of 'K-theory' within the canopy may be physically unrealistic because of possible large changes in the gradient of quantity over distances that are smaller than the eddy sizes that determine K_z , but because it yields reasonable results this method is used until suitable second-order closure models can be applied.

In order to apply the 'K-theory' within vegetation, an eddy diffusion coefficient with linear dependence on z , K_{zv} , has been introduced. Thus, the atmosphere consists of two layers: the first one near the ground surface, characterized by the height h and the turbulent diffusion coefficient K_{zv} , and the second one lying between $z=h$ and $z=\infty$, with the turbulent diffusion coefficient K_{za} . According to this model we may write:

- for vegetation:

$$K_{zv} = a_1 + b_1 z, \quad 0 \leq z < h \quad (15)$$

- for air above vegetation:

$$K_{za} = a_2 + b_2(z-h), \quad h \leq z < \infty \quad (16)$$

where: a_1 is the molecular diffusion coefficient, a_2 is calculated from the continuity condition of the diffusion coefficient at $z=h$: $K_{zv}(z)|_h = K_{za}(z)|_h$, and b_2 takes the values of b for the atmosphere in accordance with the intensity of the vertical mixing. As to the choice of h , for a dense and homogeneous vegetation (like grass, wheat, etc.), it seems to be appropriate to take it equal to the plant height. For somewhat less dense and less uniform canopies like forests, this model is questionable because the horizontal and vertical non-homogeneities cannot be described by a one-dimensional diffusion equation.

In view of the experimental indication (Butterweck, 1991) that the eddy diffusion coefficient within vegetation is 20 times lower than just above the canopy, we took $b_1 \equiv b_2 / 20$.

Analytical approach. Green's function method

The numerical modelling of radon and daughter diffusion in the atmosphere encounters practical difficulties due to the fact that convergence of the numerical schemes is, in certain cases, dependent on the type of K_z , the mesh step and the height at which the vanishing condition for concentration is met (Cuculeanu, 1994). Sometimes the error introduced by the numerical schemes could result in a completely spurious solution. The analytical solving has the advantage of providing a unique solution for the diffusion equation.

The daughter diffusion process is governed by the equations (3) – (8), which may be put in the form:

$$Lc_{f,a} = u_{f,a} \quad (17)$$

According to the Green's function theory (Greenberg, 1971; Cuculeanu and Popa, 1993) the concentration profile for the i -th decay product may be expressed as:

$$c_{f,a}(z) = \int_0^{\infty} u_{f,a}(\xi) G_{f,a}(\xi, z) d\xi \quad (18)$$

where the Green's function $G_i(\xi, z)$ satisfies the boundary value problem:

$$L^* G_i(\xi, z) = \delta(\xi - z) \quad (19)$$

$$G_i(0, z) = 0 \quad (20)$$

$$G_i(\infty, z) = 0 \quad (21)$$

where $\delta(\xi - z)$ stands for the Dirac's function and L^* for the adjoint operator of L . In order to obtain the Green's function for the two layers, the continuity of radon flux is assumed at $z=h$. The radon concentration is supposed to be known (Ikebe, 1970).

B. Investigation of the model accuracy by comparison of the predicted results with corresponding experimental data

Using a computer program based on the above model (see section D), calculations have been performed for an exhalation rate $E = 10^4$ atoms $m^{-2} s^{-1}$ for both radon and thoron, an attachment rate $\alpha = 0.02 s^{-1}$ and a recoil detachment probability of 0.5 (Schery *et al.*, 1992). The chosen attachment rate is based on an average aerosol concentration of 10,000 particles per cubic cm and an attachment rate coefficient of $2 \times 10^{-6} cm^3 s^{-1}$. In fig. 1 the model calculated thoron profile for a grass cover and NNN atmospheric state is compared with experimental values (Porstendörfer, 1994). The same data for radon in the case of a wheat canopy and SSN are displayed in fig. 2 (Butterweck, 1991). Because the exhalation rate was unknown, the computed values have been normalized to the experimental data within vegetation in order that the comparison be possible. A rather good agreement between predicted

values and experimental data may be noticed against the bare soil case. This proves that the model can reasonably simulate the radon/thoron diffusion process near the Earth's surface for a soil covered with vegetation.

In what follows results concerning the vertical activity distributions of radon/thoron daughters, the equilibrium factor as well as the unattached fraction will be discussed. Supposing that all the decay products are attached to aerosol particles, the model prediction for ^{222}Rn and ^{218}Po activity concentrations for *IWN* turbulence type, with and without vegetation cover is displayed in figure 3. Figure 4 shows the vertical profiles of thoron and its progeny for *NNN* and 1-metre high vegetation canopy in the case of the two group daughters. As it was expected, the model predicts a marked increase of the activity concentration within vegetation for both radon/thoron and daughters. This is due to the fact that within the layer associated to the canopy the diffusion and transport processes are slowed down, hence the accumulation of radon/thoron and its daughters is enhanced. The mean increase of the radon specific activity inside vegetation against the bare soil is slightly dependent on the atmospheric turbulence intensity. In the case of radon daughters this increase is more pronounced under inversion conditions. As far as thoron is concerned, this relative increase is about one order of magnitude in the case *NNN*, while during the inversion is less significant (≈ 1.5 times). This shows that the thoron concentration near the Earth's surface ($z < 20$ cm) is less influenced by the presence of the vegetation canopy for very weak atmospheric diffusion. As expected, the model has predicted an activity concentration level of free ^{216}Po much greater than that of attached ^{216}Po . This is explained by the fact that due to its very short half-life (0.15 s), ^{216}Po more probably decays than attaches to an aerosol particle. The calculations show that the vegetation has a more pronounced effect on the unattached daughters.

The equilibrium factor was calculated for $h \in [1 \text{ cm}, 1 \text{ m}]$ and $z \in [1 \text{ cm}, 10 \text{ m}]$. The corresponding results for radon, *IWN* atmospheric turbulence are presented in a 3D-diagram in fig. 5. An interesting finding is the prediction of an equilibrium factor above vegetation greater than that for the case of bare soil (no vegetation) at the same heights. In this model the vegetation behaves as a medium which slows down the turbulent diffusion, thus enhancing daughter accumulation. At the same time the F values within vegetation are generally less than those for bare soil at the same heights. The decrease of F is specific to a decrease of the mixing intensity at lower heights.

The unattached fraction as a function of h and z for radon daughters, *IWN* case is illustrated in fig. 6. Irrespective of the atmospheric turbulence type, the model predicts a decrease of f_p in the atmospheric layer above the vegetation as compared to the bare soil values at the same heights. The gradient of variation is more pronounced for the weak mixing categories (*IWN*, *WNN*). Within vegetation, for *IWN*, *WNN* and *NNN*, as a result of the increase of parent-nuclei concentration, the unattached fraction has greater values than those when vegetation is absent. The strong turbulence levels the f_p profile in the atmosphere (the gradient average value between 1 cm and 20 m is about $0.036\% \text{ m}^{-1}$). The predicted f_p values at $z = 1 \text{ m}$ in the presence of vegetation of 1 cm , 5 cm , 20 cm , 50 cm thickness do not exceed $\approx 2.6\text{--}3.0\%$, depending on *NNN* or *SSN* diffusivity profiles (generally specific to day time). This seems to be in agreement with the mean measured unattached fraction value of 0.02 for the outdoor atmosphere of Göttingen at 1 m above ground, day time (Reineking and Porstendörfer, 1990). Also, the measured values of F seem to prove that the presence of vegetation determines an increase of F , the values measured during the seasons with vegetation being greater than the values for winter (Reineking and Porstendörfer, 1990).

In figures 7 and 8 the measured F and f_p values are compared with the model predicted ones. Figure 7 shows F as a function of height for *D* turbulence type, while figure 8 set out f_p as a function of height for *F* turbulence category and different attachment rates. It can be seen (fig. 8) that values closer to the experimental data can be obtained for an attachment rate of $\alpha = 0.01 \text{ s}^{-1}$. As far as F is concerned, for the bare soil the deviation between the experimental and predicted values ranges within 60% , while for the vegetation covered soil it decreases significantly (30%). As it can be noted, the vegetation determines a decrease of the F and f_p gradient.

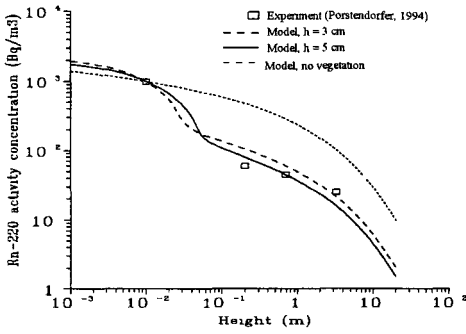


Fig 1 Thoron profile, grass canopy, normal turbulence (NNN)

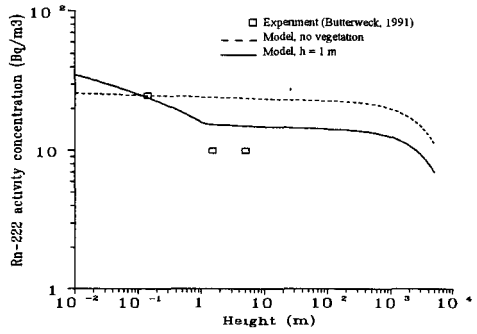


Fig. 2 Radon profile, wheat canopy, strong turbulence (SSN)

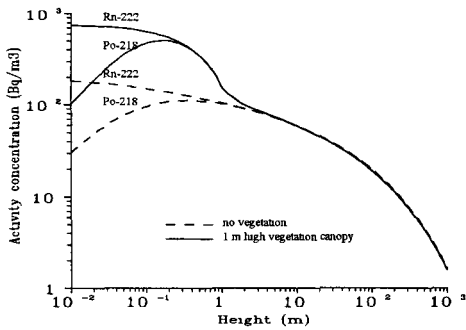


Fig. 3. Vertical profiles of Rn-222 and Po-218 (one group), inversion (IWN)

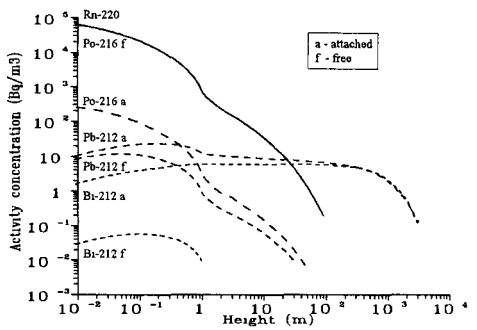


Fig 4 Vertical profiles of thoron and its progeny (two groups), normal turbulence (NNN), 1 m high vegetation canopy

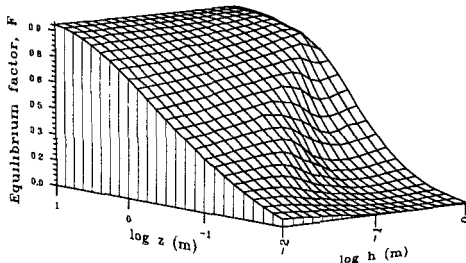


Fig 5 Equilibrium factor for Rn-222, inversion (IWN)

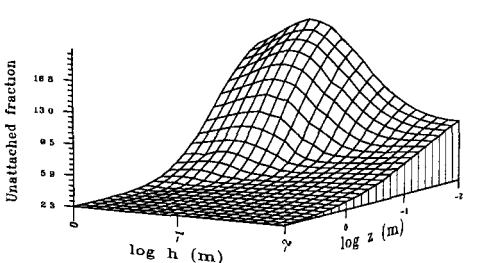


Fig. 6 Unattached fraction (%) for Rn-222, inversion (IWN)

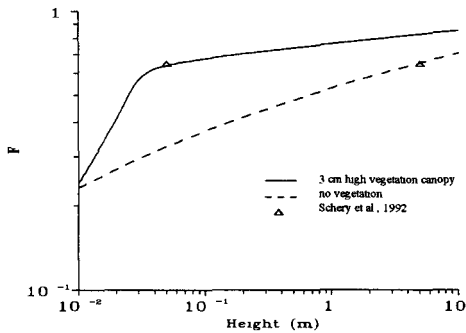


Fig. 7. Equilibrium factor for Rn-222, neutral conditions (D)

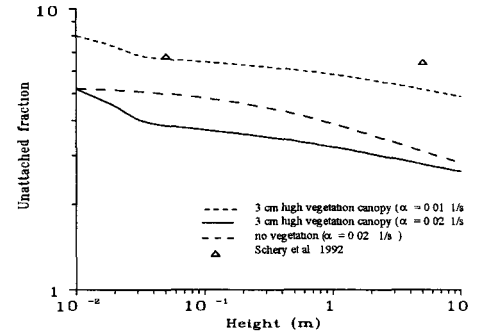


Fig 8 Unattached fraction (%) for Rn-222, moderately stable conditions (F)

C. Radiological impact assessment by making use of the dose factor formalism and model output

Because of their different physical properties, radon isotope gases and their decay products have to be considered separately when estimating the dose (Porstendörfer, 1994). Inhaled radon and thoron, being noble gases, are constantly present in the air volume of the lungs at the concentration in air and are partly dissolved in soft tissues. The effective dose equivalent rate can be calculated from the equation:

$$H_{e,Rn(Th)}[\text{nSv h}^{-1}] = f \cdot c_0[\text{Bq m}^{-3}] \quad (22)$$

where $f = 0.18$ for radon and $f = 0.1$ for thoron and c_0 is the activity concentration.

The inhaled radon and thoron daughters have a biological half-life of a few hours in the human lung as retention studies indicate. This means that the main fraction of the potential alpha energy of radon daughters deposited in the lung is absorbed in this organ; the dose to other tissues delivers a negligible contribution to the effective dose.

Table 3. Annual dose and dose rates to the general public (adults) by inhalation of outdoor radon and their short-lived daughters under different mixing conditions

Turbulence	SSN	NNN	WNN	IWN
F	0.51	0.53	0.53	0.76
$c_0[\text{Bq m}^{-3}]$	1.51	4.01	14.65	98.05
$\dot{H}_T[\text{nSv h}^{-1}]$	55.11	151.70	554.54	5321.59
$\dot{H}_A[\text{nSv h}^{-1}]$	25.43	68.18	248.86	2389.20
$\dot{H}_e[\text{nSv h}^{-1}]$	4.54	13.07	47.73	458.52
$\dot{H}_{e,Rn}[\text{nSv h}^{-1}]$	0.272	0.722	2.637	17.73
$H_T[\text{mSv}]$	0.097	0.267	0.976	9.366
$H_A[\text{mSv}]$	0.043	0.120	0.438	4.205
$H_e[\text{mSv}]$	0.008	0.023	0.084	0.807
$H_{e,Rn}[\text{mSv}]$	0.0005	0.0013	0.0046	0.0311

In order to calculate the annual dose to the general public (adults) by inhalation of the outdoor radon daughters we assumed a mean outdoor residence of 1760 hours per year. Using the dose conversion factors given by the Jacobi-Eisfeld model (Porstendörfer, 1994) the following relations were employed:

$$H_T[\text{mSv}] = f_T \cdot E_p[\text{WLM}] \quad (23)$$

$$H_A[\text{mSv}] = f_A \cdot E_p[\text{WLM}] \quad (24)$$

$$H_e[\text{mSv}] = f_e \cdot E_p[\text{WLM}] \quad (25)$$

where H_T , H_A are the annual doses for the tracheo-bronchial region and alveolar region respectively, H_e is the annual effective dose equivalent, and f_T , f_A , f_e are the corresponding dose factors. E_p is the annual exposure and has the expression:

$$E_p[\text{WLM}] = 2.85 \cdot 10^{-3} \cdot F \cdot c_0[\text{Bq m}^{-3}] \quad (26)$$

In this last equation F is the equilibrium factor and c_0 is the activity concentration of radon.

Calculations were done for the four turbulence classes of Jacobi and André for radon supposing that all daughters attach to aerosol particles and there is no vegetation cover. The results are presented in table 3. As it can be seen, the dose values of the radon gas are small in comparison to its progeny. The dose equivalent of radon daughters in the tracheo-bronchial region is about two times higher than in the alveolar region. For different mixing conditions the dose equivalent can vary over as much as two orders of magnitude.

D. Development of a computer code (PC version) for calculating the concentration profiles of the attached and unattached $^{222}\text{Rn}/^{220}\text{Rn}$ daughters, the equilibrium factor (F), the unattached fraction (f_p), and the potential alpha energy concentration (PAEC)

A computer code based on the above theoretical model was written in *Microsoft FORTRAN* and *C*. Its flow diagram is presented in figure 9. The main program (function "main") initializes the computations by reading the configuration file `radon.cfg` (see description below) and prompting the user for a particular run (radon or thoron, which stability category to use, whether to take into account or not aerosol attachment and/or sedimentation, the height of the vegetation canopy). The computation of the vertical concentration profile of the parent gas is done in function "parent". The vertical profiles of the progeny are worked out in function "daughter": the Green's function is firstly determined, then the Romberg's integration scheme (Press *et al.*, 1992) is applied in equation 18 (function "Romberg"). In order to save computing time, beginning with the second daughter the parent concentration used in the integration routine is estimated by cubic spline interpolation through the points previously computed (function "spline"). If a proper set of height points is chosen (in the configuration file `radon.cfg`) the error in the concentration values can be made very low (e. g., about 1% for 65 points spread over 10 km in the z -direction). The modified Bessel functions of fractional order used in function "parent" and for determining the Green's function are calculated by using series expansions.

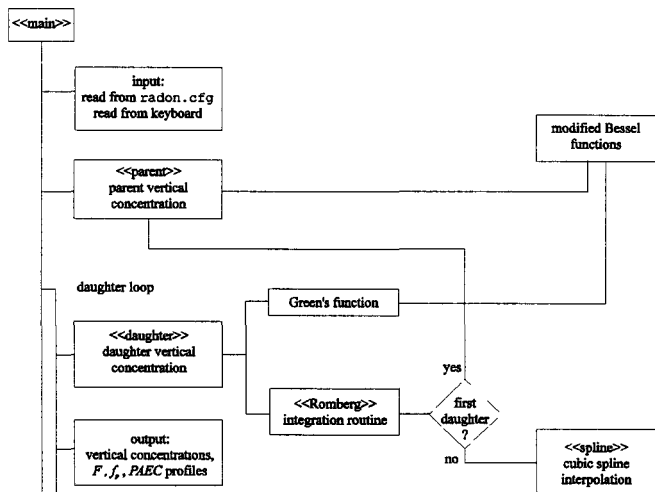


Fig 9. Flow diagram for the computer code

The configuration file `radon.cfg` is a text file and can be modified using any ASCII text editor. This is a printout of the file with the default values:

```

1.e-5    » EPS, fractional accuracy desired (in Romberg)
0.5      » R, recoil detachment probability (adim.)
0.01     » alp, aerosol attachment rate (1/s)
10000.   » Ea, exhalation rate (atom/m2/s)
1.5d-5   » a1, molecular diffusion coefficient (m2/s)
-1.d-3   » vf, sedim. velocity for unattached daughters (m/s)
-1.d-2   » va, sedim. velocity for aerosol-attached daughters (m/s)
1.d-5    » least significant activity concentration (Bq/m3)
1.d-7    » h for bare soil (no vegetation) (m)
0.03     » h for grass (m)
1.       » h for wheat (m)
2.       » h for forest (m)
0.       » the following lines initialize the height array (m)
1.d-4
1.d-3
2.d-3
3.d-3
.....   (and so forth)
1.d4

```

The output files of the code have the filename extension .DAT and contain:

- the radon/daughter vertical activity distributions, $c(z)$ (each radionuclide is assigned a separate file with its chemical symbol as a filename; tag A appended to the filename means attached, tag F – free);
- the equilibrium factor (filename EQ-F-RN.DAT/EQ-F-TN.DAT):

$$F_{Rn} = c_{eq,Rn}/c_0 = (0.105 \times c_1 + 0.516 \times c_2 + 0.379 \times c_3)/c_0,$$

$$F_{Tn} = c_{eq,Tn}/c_0 = (0.913 \times c_2 + 0.083 \times c_3)/c_0$$

(where c_{eq} is the equilibrium equivalent concentration);

- the potential alpha energy concentration, PAEC (filename PAEC-RN.DAT/PAEC-TN.DAT):

$$PAEC_{Rn}[WL] = c_{eq,Rn} [Bq\ m^{-3}] / 3700,$$

$$PAEC_{Tn}[WL] = c_{eq,Tn} [Bq\ m^{-3}] / 275;$$

- the unattached fraction (filename FP-RN.DAT/FP-TN.DAT):

$$f_p = c^f_{eq} / c_{eq}.$$

The record structure of the output files consists of two fields separated by blanks. The first field contains the height z (in m) and the second field contains the corresponding activity concentration (in Bq per cubic m), the equilibrium factor, the potential alpha energy concentration (in WL, working level), or the unattached fraction (in %).

Test case. In table 4 we are partly presenting the output of the computer code for radon, *NNN* turbulence (Jacobi and André's classes), aerosol attachment, no sedimentation, and wheat canopy. The configuration file assumes the default values.

A copy of the code is provided with this report on a 3½" floppy disk.

Table 4. Output for test case

z (m)	²²² Rn (Bq/m ³)	²¹⁸ Po free (Bq/m ³)	²¹⁸ Po attached (Bq/m ³)	F	f_p (%)
	RN-222.DAT	PO-218-F.DAT	PO-218-A.DAT	EQ-F-RN.DAT	FP-RN.DAT
0.01	23	1.27	1.17	0.0416	16.4
0.1	14.3	2.27	2.66	0.154	13.3
1	4.76	1.25	2.79	0.649	6.03
10	3.67	1.01	2.57	0.851	4.99
100	3.18	0.872	2.3	0.954	4.51

Publications

- Cuculeanu, V. and A. Lupu, 1994. Influence of vegetation on radon diffusion in the atmosphere. *Studii de Meteorologie*, 1.
- Cuculeanu, V. and C. Popa, 1994. Analytical calculation of the vertical activity distribution of radon daughters in the ambient air. *Radiat. Prot. Dosim.*, 56: 197-198.
- Cuculeanu, V. and A. Lupu, 1995. Effects of vegetation-induced turbulence on radon diffusion in the atmosphere. Sixth International Symposium on the Natural Radiation Environment, Montreal, June 5-9, 1995. (to be published in *Environ. Internat.*)
- Cuculeanu, V. and A. Lupu, 1995. Fractal dimensions of the outdoor radon/thoron time series. Sixth International Symposium on the Natural Radiation Environment, Montreal, June 5-9, 1995. (to be published in *Environ. Internat.*)

References

- Beck, H. L. and C. V. Gogolak, 1979. Time-dependent calculation of the vertical distribution of Rn^{222} and its decay products in the atmosphere. *J. Geophys. Res.*, 84: 3139-3148.
- Brunet, Y., J. J. Finnigan and M. R. Raupach, 1994. A wind tunnel study of air flow in waving wheat: single-point velocity statistics. *Boundary Layer Meteor.*, 70: 95-132.
- Butterweck, G., 1991. Natürliche Radionuklide als Tracer zur Messung des turbulenten Austausches und der trockenen Deposition in der Umwelt, Ph. D. Thesis, University of Göttingen, 116pp.
- Cohen, L. D., S. Barr, R. Krablin and H. Newstein, 1972. Steady-state vertical turbulent diffusion of radon. *J. Geophys. Res.*, 77: 2654-2668.
- Cuculeanu, V., 1994. Numerical modelling of radon and thoron diffusion in the atmosphere. *Romanian J. Meteor.*, 1: 21-26.
- Cuculeanu, V. and C. Popa, 1994. Analytical calculation of the vertical activity distribution of radon daughters in the ambient air. *Radiat. Prot. Dosim.*, 56: 197-198.
- Draxler, R. R., 1979. Estimating vertical diffusion from routine meteorological tower measurements. *Atmos. Environ.*, 13: 1559-1546.
- Greenberg, M. D., 1971. *Application of Green's Functions in Science and Engineering*. Prentice-Hall, 141 pp.
- Ikebe, Y., 1970. Variation of radon and thoron concentrations in relation to the wind speed. *J. Meteor. Soc. Japan*, 48: 461-467.
- Jacobi, W. and K. André, 1963. The vertical distribution of Radon 222, Radon 220 and their decay products in the atmosphere. *J. Geophys. Res.*, 68: 3799-3814.
- Monteith, J. L. and M. H. Unsworth, 1990. *Principles of Environmental Physics*. Edward Arnold, 291pp.
- Oltchev, A., G. Gravenhorst, J. Constantin, J. Löffler and O. Riese, 1994. Momentum transfer on a spruce forest: model and experimental results. European Conference on the Global Energy and Water Cycle, 18-22 July, 1994, The Royal Society, United Kingdom.
- Porstendörfer, J., 1994. Properties and behaviour of radon and thoron and their decay products in the air. *J. Aerosol Sci.*, 25: 219-263.
- Press, W. H., B. P. Flannery, S. A. Teukolsky and W. T. Vetterling, 1992. *Numerical Recipes in FORTRAN: the art of scientific computing*. Cambridge University Press, 963pp.
- Reineking, A. and J. Porstendörfer, 1990. "Unattached" fraction of short-lived Rn decay products in indoor and outdoor environments: an improved single-screen method and results. *Health Phys.*, 58: 715-727.
- Roffman, A., 1972. Short-lived daughter ions of Radon 222 in relation to some atmospheric processes. *J. Geophys. Res.*, 30: 5883-5899.
- Schery, S. D., R. Wang, K. Eack and S. Whittlestone, 1992. New models for radon progeny near the Earth's surface. *Radiat. Prot. Dosim.*, 45: 343-347.

Head of project 11: Dr. Ch. Schuler

II. Objectives for the reporting period

After the decay of radon, the ^{218}Po ion is neutralised due to small ion recombination, electron transfer and electron scavenging. The neutral atom is then incorporated into ultrafine clusters produced by radiolytical processes from trace gases like H_2O and SO_2 .

This process is important for the understanding of the measurements of size distributions of the unattached fraction of the radon progeny. As many of the influencing parameters under realistic living conditions are not controllable, the behaviour of radon and thoron decay products has to be studied in radon chambers under controlled conditions.

Experiments in the PSI radon chamber (10 m^3 volume) were focused on the interaction of unattached radon decay products with trace gases (SO_2 , H_2O) and artificial/natural aerosols. The aim of this investigation was to better understand the cluster formation of ^{218}Po as influenced by trace gases and to measure the attachment rate of this nuclide to aerosols as a function of trace gas concentration and aerosol size distribution.

III. Progress achieved including publications

1. PSI Radon chamber

The PSI radon chamber consists of a stainless steel chamber with 10.2 m^3 volume and an airlock with 1.6 m^3 volume (Fig. 1). The air is circulated through the chamber by means of a rectangular air duct, in which ventilator, humidifier and heater are incorporated. Radon and trace gases are either injected into the output of the ventilation duct or into a ring pipe at the bottom of the radon chamber. The radon activity concentration is controlled by a feedback system consisting of a continuous radon monitor of the flow-through ionisation chamber type which is coupled on-line to a personal computer. In a similar way, the SO_2 concentration in the radon chamber is controlled, using a 100 ppm SO_2 supply.

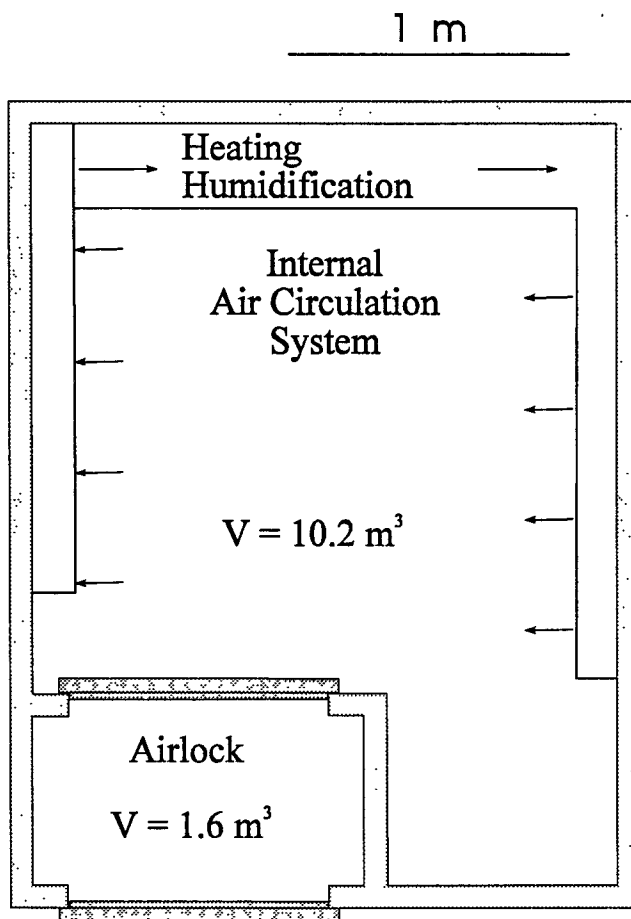


Fig. 1: Schematic diagram of the PSI radon chamber

2. Modelling the radon chamber atmosphere

The model calculations were brought about by results of Vanmarcke et al. (1991) and Reineking (1993), who found that in ambient indoor air with aged aerosol, differences in the size distribution of the unattached fraction between ^{218}Po and ^{214}Pb , ^{214}Bi can occur. The diffusion constant of the first radon decay product, ^{218}Po , has been reported to be about a factor of two larger than the diffusion constant of the following decay products ^{214}Pb and ^{214}Bi . This will result in a larger attachment and deposition rate of ^{218}Po .

The measurements showed that ^{218}Po has the greatest mobility, corresponding to an activity median diameter (AMD) of about 1 nm. The size of the ^{214}Pb cluster is determined both by the decay of unattached ^{218}Po and recoiling ions from the aerosol attached ^{218}Po , resulting in a bimodal structure of the size distribution with median diameters of 1 nm and 4 nm. The size of the small amount of $^{214}\text{Bi}/^{214}\text{Po}$ clusters in the atmosphere is reported to be at an AMD of 4 nm. The size of the aerosol-attached radon progeny for an aged aerosol is identical for these nuclides. Differences have been found for non-steady-state aerosol conditions, especially, when aerosol sources are turned on or off (Kesten et al., 1993). Therefore all parameters in the PSI chamber model concerning size dependent

behaviour of the radon daughters, i. e. attachment rates and deposition rates, have been considered as being different for each radon decay product.

The influence of measurements on the chamber conditions was also included into the PSI radon chamber model. The recycling of gaseous components of the chamber air back into the radon chamber can be achieved, whereas for most of the measurements (e. g. radon progeny, aerosol concentration, sulphur dioxide, size distributions, radon) the particulate phase in the chamber air is removed. For this reason a sink term for the radon decay products has been introduced.

The analytical solution of the differential equations is presented in Butterweck and Schuler (1995).

The performance of the computer code developed from the analytical solutions of the equations has been tested with a set of data published by Knutson (1988), yielding good agreement between both calculations (Butterweck and Schuler, 1995).

Different modes of operation of a radon chamber have been calculated with the PSI radon chamber model (Butterweck and Schuler, 1995).

Measurements in a radon chamber mostly consist of filtering of the chamber air, while recycling the gaseous components back into the chamber. The effect of such a measurement is demonstrated in Fig. 2. The unattached fraction f_p is increased by up to three percent during the aerosol sampling. After filtering, normal conditions are reached with the half-lives of the radon progeny. The equilibrium factor between the radon decay products and the radon concentration, F , is decreased by up to three percent during this time. The amount of air sampled was 400 l, about 3.9 percent of the total chamber volume. For larger sampling flows or smaller chamber volumes the effect will be more drastic.

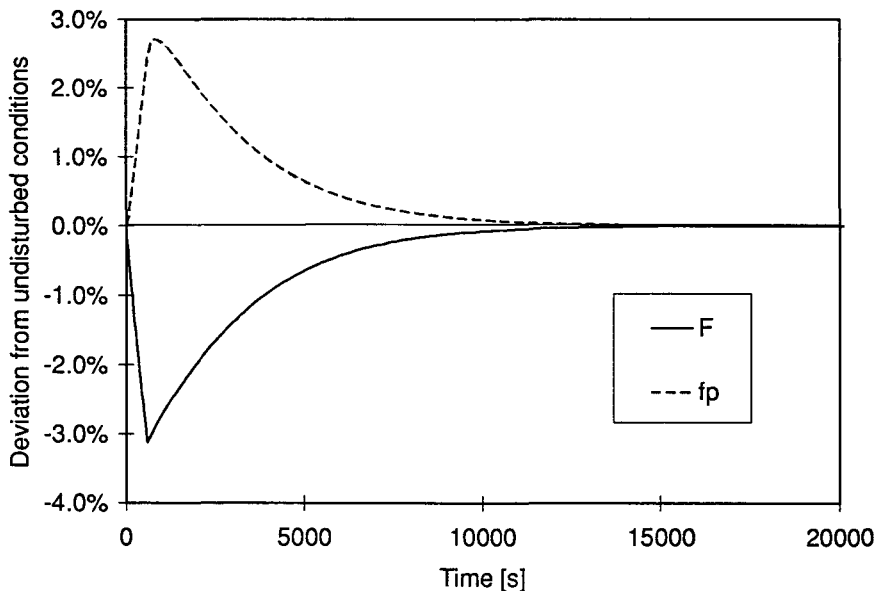


Fig. 2: Response of the equilibrium factor F and the unattached fraction f_p in the chamber atmosphere to a measurement consisting of 10 minutes of air filtering with a flow rate of 40 l min^{-1} . A constant radon concentration was sustained with a neglectable source flow. Parameters for all radon daughters: Attachment rate 40 h^{-1} , deposition rate unattached 10 h^{-1} , attached 0.1 h^{-1} , chamber surface to volume ratio 3 m^{-1} , detachment probability of recoiling ^{214}Pb from aerosol 0.83, from wall 0.1.

The PSI radon chamber model allows calculations concerning the influence of different diffusion constants between the radon progeny on observable quantities in the radon chamber atmosphere. As the diffusion constant influences both attachment and deposition of the unattached activity, the coupling has to be considered. As a first approximation the attachment rate is assumed to be four times larger than the deposition rate. The attachment rates of ^{214}Pb and ^{214}Bi were assumed to be at constant 40 h^{-1} .

The amount of unattached ^{218}Po is decreasing with an increasing attachment rate of ^{218}Po . Accordingly, the attached activity concentration of ^{218}Po displays a reverse behaviour. The attached concentration of ^{214}Pb and ^{214}Bi is slightly decreasing due to the enhanced deposition of the unattached ^{218}Po . The equilibrium factor between radon progeny concentrations and radon gas concentration, F , remains approximately the same, whereas the unattached fraction of the radon progeny, f_p , is reduced to 60 percent of its original value, if the attachment and deposition rate of unattached ^{218}Po increases 2.5 fold (Fig. 3).

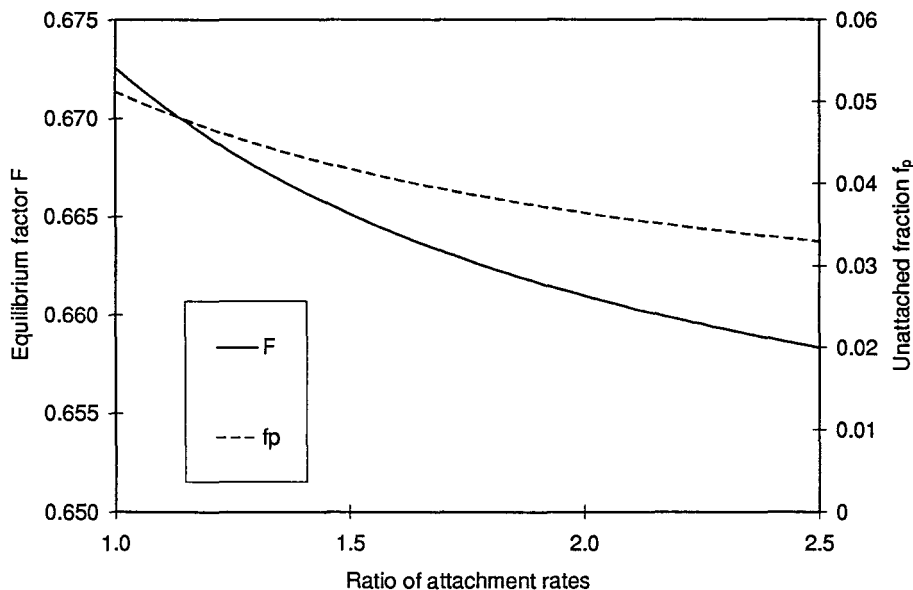


Fig. 3: Dependence of the equilibrium factor F and the unattached fraction f_p of the radon progeny on the ratio between the attachment rates of ^{218}Po and ^{214}Pb (^{214}Bi).

3. Measurement of attachment rate of radon progeny

One of the main parameters for the behaviour of the airborne decay products, the attachment rate X , was measured directly with the Epiphaniometer, an instrument developed at PSI (Baltensperger et al., 1988). The air to be monitored is pumped into a 2 l volume, where decay products from a dry actinium source are attached to the aerosol particles in the sample airflow during 2 min residence time. To remove unattached activity, the air passes a capillary tube and the remaining aerosol attached fraction is deposited on a filter (Fig. 4). The alpha emissions of the actinon decay product ^{211}Bi on the filter are measured with a surface barrier detector. The count rate of ^{211}Bi , the Epiphaniometer signal, is proportional to the attachment rate of the aerosol particles in the sample air. Summed up, the Epiphaniometer works as a small radon chamber, where the aerosol attached activity is analysed. The calibration has been performed with monodisperse aerosols and using a

modified form of the PSI radon chamber model (Butterweck and Schuler, 1995, Rogak et al., 1991). The source strength is high enough to prevent unwanted noise coming from the deposition of aerosol bound radon progeny. The direct measurement of the attachment rate has the advantage, that operation of a mobility analyser in combination with a condensation nuclei counter is not necessary for routine purposes.

Fig. 5 shows the reduction of aerosol particles in the radon chamber due to plate-out and the internal air circulation system. Steady state conditions are reached, when the production of particles and the removal is in equilibrium. The final value is governed mostly by the air humidity. The attachment rate increases linearly with the relative humidity in the chamber air. As all experiments were performed at the same air temperature of 20°C, this is also valid for the absolute humidity.

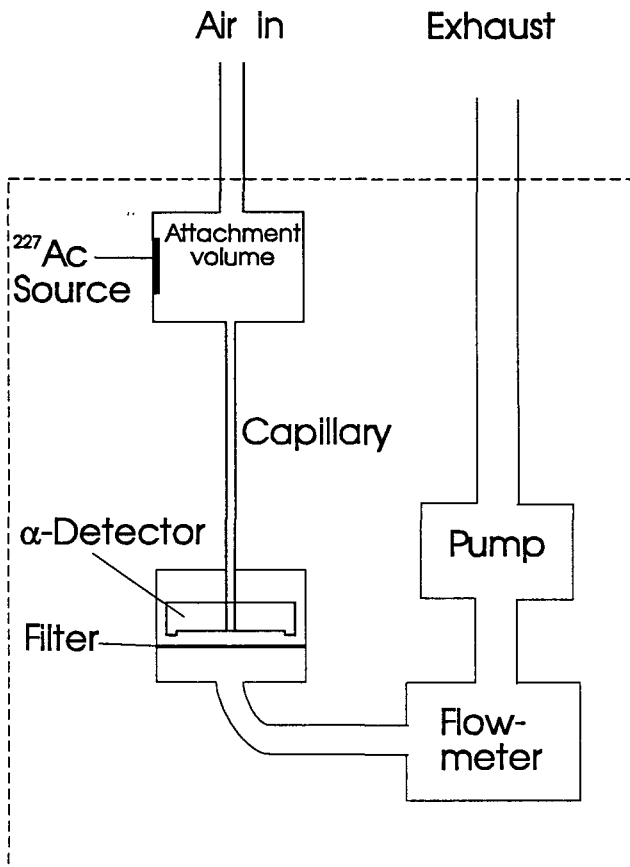


Fig. 4: Schematic diagram of the Epiphaniometer

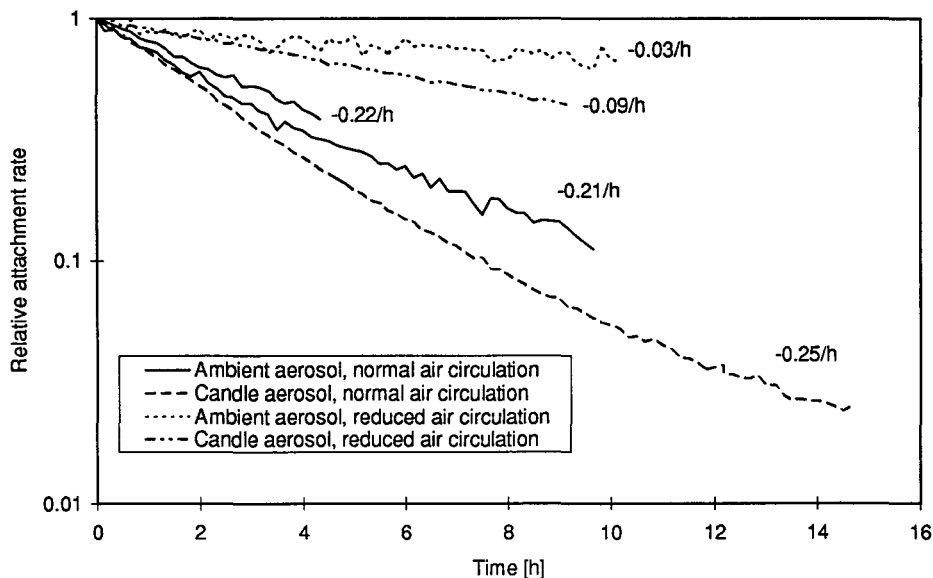


Fig 5: Reduction of the attachment rate in the PSI radon chamber due to deposition and air circulation. The normal air circulation is obtained with the internal chamber air circulation system, the reduced air circulation is performed with two small ventilators installed in the chamber. The attachment rates are normalised to the value at $t=0$, which are 4.1 h^{-1} and 7.9 h^{-1} for the ambient aerosol with normal air circulation and 1.1 h^{-1} with reduced air circulation. The values at $t=0$ are 76.7 h^{-1} for candle aerosol with normal air circulation and 66.1 h^{-1} with reduced air circulation.

4. Measurement of size fractionated radon progeny activity concentration

4.1 Gross-alpha counting

For the measurement of the size distribution of the unattached fraction of the short-lived radon progeny scintillation counting instruments were used in the beginning of the project. They consist of a photomultiplier with attached electronics, which allows counting of the scintillations and performance of complex sampling routines. The airborne radon progeny is sampled on a membrane filter (thickness $9 \mu\text{m}$), supported on a thin grid though which the air sample is pumped. Below the grid a ZnS-scintillator is mounted, shielded from light passing through the filter with a mylar foil, which registers the emitted alpha particles after they have passed the filter. The possibility of an open-faced air sampling is thus given with counting of the deposited activity during and after air sampling.

The activity concentration of radon progeny deposited on the filter was measured by gross alpha counting in several time intervals during and after sampling. For the results presented, the unattached fraction was determined using a single screen with a lower 50% cut-off of 4.8 nm . Additionally, a second single screen with a lower 50% cut-off of 1.3 nm was used to separate clusters with significantly larger diameters than the single ions of the radon progeny. The air was sampled at a flow rate of 4 l min^{-1} , controlled by mass flow controllers during a sampling interval of 10 min. The

total cycle time was three hours, separated into 5 minute intervals. The concentrations were calculated with an iterative process by minimising the deviation between modelled counts for given concentrations of all three radon decay products and the measured counts.

As only a small part of the airborne activity is deposited on the wire screens, the relative deviation of the instruments has to be very small. Experience from the group of Göttingen University showed, that the deviation between the calculated activity concentrations during a simultaneous sampling with several heads without a wire screen at the entrance of the sampling head should not exceed one percent. Since this accuracy range was not reached with the gross alpha counting equipment, it was only used for the determination of the unattached fraction and for the size fractionated sampling at very low attachment rates.

4.2 Spectroscopic counting

Due to the above mentioned restrictions of the gross-alpha counting, new instrumentation was implemented to measure the size distribution with alpha-spectroscopic discrimination between the alpha particles emitted from ^{218}Po and ^{214}Po . This method has been used in the determination of the size distribution of the unattached fraction with great success by the group of the University of Göttingen. The principle of measuring the alpha-particles through the filter, which has been used by the gross-alpha counting method, was implemented in the construction of the sampling heads. The alpha particles passing through the filter suffer a significant, statistically distributed energy loss. By using the supporting grid of the filter as a collimator for the alpha particles, the energy resolution for the spectroscopic counting is still sufficient to distinguish between alpha particles emitted from ^{218}Po and ^{214}Po . The flow rate through the screens is controlled by a personal computer, yielding the possibility to change automatically the penetration characteristics of the wire screens without the necessity to enter the radon chamber. During stable conditions in the radon chamber, the flow rate can be changed for each sampling cycle for increasing the number of different penetrations with a limited number of sampling heads. The efficiency for the detection of an alpha particle emitted from the filter (4π steradian) is about 20% with the use of 2000 mm^2 passivated ion implanted surface barrier detectors. The maximum flow rate through the filter can be up to 20 l/min.

4.3 Data Evaluation

The measurement of radon progeny in ambient air is performed by collecting the unattached and aerosol bound activity on a filter.

For the different counting techniques and the different sampling and counting protocols, a variety of evaluation methods has evolved, optimising the calculation of the radon progeny concentrations. The calculations are highly specialised to special sampling and counting protocols as they include the analytical solution of the dependence of concentrations on the measured counts. Analytical calculations determine the concentrations stepwise, as the preceding radon decay product has to be taken as an input parameter for the further calculations. Thus measuring errors are influencing the calculated concentrations of the radon progeny with a bias, often leading to mathematically correct solutions, which are physically not reasonable, e.g. negative concentrations of the last of the short-lived radon decay products, ^{214}Bi .

A simple three dimensional interpolation is used to make a more generalised approach to this problem. It is easy to adopt to different sampling protocols and counting techniques. The mathematical approach is straightforward and easy to comprehend without more than basic mathematical training. The disadvantage of this method lies in the slow convergence, compared to more refined mathematical approaches. But with the high performance of modern personal computers, results are obtained in acceptable periods.

The concentrations are estimated using an iteration process by comparing the measured counts with modelled counts and optimising the deviation to the measured result. A simple and straightforward approach for this iteration can be achieved with a three dimensional linear interpolation in the case of unknown activity concentrations of radon progeny. For most other problems, for example the calculation of the deposition velocity of unattached and attached progeny, only a two-dimensional iteration is needed.

Basis of the iteration is a cube in the relative concentration room. It is moved or shrunk, depending on the results obtained on 27 points on its edges and walls (Publication in preparation).

4.4 Results

The measurements with gross alpha counting were performed with low attachment rates and only with determination of two size classes. The lower 50% cut-off diameters of two single screens were chosen to be 1.3 nm and 4.8 nm. The latter gives the separation between the attached and unattached fraction, whereas the difference of activity deposited on the screens gives an indication how much of the unattached activity is associated with ultrafine clusters larger than the usually used 1 nm. It was found that 22% of ^{218}Po were in the size range between 1.3 and 4.8 nm, whereas 44% of ^{214}Bi was found in this size range. The remainder was found below the lower cut-off diameter of 1.3 nm. The results were obtained at low attachment rates between 0.5 to 5 per hour. An influence of humidity on this result was not observed between 20% and 80% RH (experiments performed at 20 °C). Neither was an influence of the concentration of the trace gas SO_2 observed at environmental levels between 0 and 0.5 ppm.

For the comparison of chamber conditions at low and high attachment rates, the alpha spectrometric method was used. With the four sampling heads available the fraction above 1 nm could be separated into two parts. The results of the gross-alpha measurements were confirmed under conditions with low attachment rates (0.2 h^{-1} - 0.9 h^{-1}). 98% of ^{218}Po were found in the size range between 0.8 and 2.3 nm, whereas only 77% of ^{214}Pb and 68% of ^{214}Bi , respectively, were found in this size range. The remainder, 2% of ^{218}Po , 23% of ^{214}Pb and 32% of ^{214}Bi were found in the size range between 2.3 and 5.4 nm.

Conditions with larger attachment rates (28 h^{-1} - 170 h^{-1}) were achieved with a burning candle. Under these conditions screens with lower cut-offs of 1.3 nm, 3.6 nm and 8.6 nm were used. 39% of the ^{218}Po was found in the size range between 1.3 nm and 3.6 nm, whereas 22% of ^{214}Pb was found in this size range. 61% of ^{218}Po and 78% of ^{214}Pb were larger than 3.6 nm.

The following conclusions can be drawn from these results:

1. At environmental concentrations of water vapour and SO_2 , there is no detectable influence of these two trace gases on the size of the ultrafine cluster mode of the short-lived radon progeny.
2. Under conditions with low attachment rates, ^{218}Po clusters show a smaller diameter than the next nuclides in the decay scheme.
3. Under conditions with large attachment rates, produced with a burning candle, the size of the clusters is shifted to larger diameters and the differences between the primary radon decay product, ^{218}Po , to the nuclides following in the decay series are reduced. A possible explanation for the increase of the size of ^{218}Po could be the interaction of the radon progeny with organic vapours produced by the burning candle.

5. References

- Baltensperger, U., H.W. Gaeggeler, and D.T. Jost (1988) The Epiphaniometer, a New Device for Continuous Aerosol Monitoring, *J. Aerosol Sci.* 19(7), 931 - 934
- Butterweck, G. and Ch. Schuler (1995) The PSI Radon Chamber Model, PSI Report 95-02, ISSN 1019-0643
- Kesten, J., G. Butterweck, J. Porstendörfer, A. Reineking and H.-J. Heymel (1993) An Online Alpha-Impactor for Shortlived Radon Daughters, *Aerosol Sci. Technol.* 18: 156 - 164
- Knutson, E.O. (1988) Modeling Indoor Concentrations of Radon's Decay Products, In: *Radon and its Decay Products in Indoor Air*, W. W. Nazaroff and A. V. Nero jr. eds., 161 - 202
- Reineking, A. (1993) Unpublished results
- Rogak, S.N., U. Baltensperger and R. C. Flagan (1991) Measurement of Mass Transfer to Agglomerate Aerosols, *Aerosol Sci. Technol.* 14, 447 - 458
- Vanmarcke, H., C. Landsheere, R. Van-Dingenen, and A. Poffijn (1991) Influence of Turbulence on the Deposition Rate Constant of the Unattached Radon Decay Products, *Aerosol. Sci. Technol.* 14, 257 - 265

6. Publications

- Reineking, A., E. A. Knutson, A. C. George, S. B. Solomon, J. Kesten, G. Butterweck und J. Porstendörfer (1994) Size Distribution of Unattached and Aerosol Attached Short-Lived Radon Decay Products: Some Results of Intercomparison Measurements, *Radiat. Prot. Dosim.* 56 No. 1-4, 113-118
- Butterweck, G. and Ch. Schuler (1995) The PSI Radon Chamber Model, PSI Report 95-02, ISSN 1019-0643
- Butterweck, G. and Ch. Schuler (1996) An Extended Radon Chamber Model, to be published in *Env. Int.*

Final Report 1992-1995

Contract: FI3P-CT920061 Duration 1/09/92 to 30/06/95

Sector: C12

Title: Study of the different techniques to mitigate high radon concentration levels disclosed in dwellings.

1)	Sabroux	CEA-IPSN
2)	Torri	ANPA
3)	Ortins de Bettencourt	DGA-DPSR
4)	Quindós Poncela	Univ. Cantabria
5)	Kritidis	NCSR "Demokritos"
6)	Proukakis	Univ. Athens

I. Summary of Project Global Objectives and Achievements

The six Participants to this Project represent five European countries that have not yet promulgated any recommendation, regulation or enforcement of an action level for indoor radon. Thus, no large statistical data base concerning the efficiency ("after/before" ratios) of various mitigation methods in actual houses are readily available from these countries.

On the other hand, a wealth of data have been gathered so far on the radioactivity of soils, soil emanation characteristics and high radon-prone areas during the Indoor Radon National Surveys of France, Italy, Portugal, Spain and Greece — some of these surveys still being under completion, however (e.g., France).

In many instances, it has been found that high radium concentrations in soils and/or unusual soil characteristics (e.g., high permeability) were not the exclusive explanations for abnormal indoor radon : building materials, indeed, may also contribute substantially to the high levels of indoor radon disclosed in some dwelling houses.

The general objective of the Project was thus to design, investigate and validate the most appropriate mitigation techniques taking into account the particular features of the housing stock in each of the Participants' country. Researches had to be carried out both in the laboratory and in the so called "laboratory houses" — either actual houses (under the householder good will), or specially designed laboratory rooms. This objective encompasses also the laboratory study of building and decorative materials, either as a source of indoor radon, or as a radon barrier.

Typically, both the radium content and the exhalation rate of representative samples of raw materials or structural modules have been measured, yielding an evaluation of the emanation factor (Portugal, Spain, Greece). The ability of various readily available covering materials to lower this emanation factor has also been thoroughly investigated (France, Portugal, Spain). Both regimes of radon transport, namely diffusion and viscous flow, have been investigated, yielding experimental values of the diffusion and permeability coefficients.

Most Participants have implemented research in actual houses or laboratory rooms for investigating on:

- the soil and crawl-space ventilation (Italy);
- the radon barriers such as slabs, coverings and floorings (France);
- the contribution of decorative materials to indoor radon (Portugal).

At last, mitigation experiments at scale 1:1, either in test rooms (Portugal), "radon chambers" (Spain) or in actual houses (France, Italy and Portugal) are going on, that encompass most of the state-of-the-art radon mitigation strategies, with sub-slab ventilation, when available, ranking among the most efficient techniques.

Integration of each Participant's contribution to the global Project was greatly enhanced by the two Radon Contractors Coordination Meetings held at Göttingen, Germany (September 6-8, 1993) and at Villigen, Switzerland (October 12-14, 1994).

International Symposia — e.g., *Indoor Radon Remedial Action* (Rimini, Italy, June 27-July 2, 1993), *Indoor Air*, (Helsinki, Finland, July 4-8, 1993) and *Natural Radiation Environment* (Montreal, Canada, June 5-9, 1995) — partly or totally devoted to indoor radon, allowed also fruitful comparisons of experiences.

Inter-comparison exercises — *Gamma Spectrometry of Soils and Building Materials*, in the framework of this Project, or *Soil Gas Radon and Radon Exhalation from Soil* (New-York, June 12-15, 1995) — provided also a good opportunity to gauge the relative performances of each laboratory in the basic field of metrology. However, this Project, that generated researches some of which are ongoing, would deserve a final Assessment Meeting — attended by all Participants — that is still to be organized.

Head of Project 1: Dr. J.C. Sabroux and M.C. Robé

II. Objectives for the reporting period

1°) To develop and validate an experimental device for testing, in the laboratory, the efficiency of various coatings, coverings, floorings and sealants as potential radon barriers (with results expressed in terms of radon diffusion and permeability coefficients). The device should be derived from the experimental setup already designed for testing polymer membranes; its use should be extended to the study of special additives liable to enhance the efficiency of concrete slabs as a radon barrier.

2°) To implement the most relevant radon mitigation techniques in a dwelling house selected for its high indoor radon concentrations, and thoroughly monitored beforehand. The radon reduction strategy will incorporate some of the materials tested in the laboratory, and recognized for their high radon mitigation potential.

3°) After implementing the radon reduction scheme in the said house, to resume, for an equivalent amount of time, the comprehensive radon monitoring already carried out before any mitigation attempt. The overall investigation is aimed to yield the fortnightly average efficiency of the mitigation approach selected.

The research summarized hereafter is part of the IPSN commitment — a) to increase its knowledge on the sources and on the migration mechanisms of radon and radon progeny, and — b) to strengthen its expertise in radon metrology. The completion of this Project, and experience assembled henceforth, entitles IPSN to put forward, on request, validated and affordable technical means that anyone, on his own free will, may select and implement to lower his exposition to indoor radon at home.

III. Progress achieved including publications

1°) Laboratory study of potential radon barriers.—

It was shown experimentally that the presence of cracks in a concrete slab increases substantially the rate of radon escape, by creating preferential passages of very high permeability. In order to cut down these leakages, and thus to close radon escape routes, various paints could be applied on the concrete slab for improving its efficiency as a radon barrier.

A specially designed experimental device based on the measurement of the radon concentration in two air-tight compartments separated by the sample, allowed to measure accurately the transport properties of radon across a thin layer of dry paint. Depending on their composition (solvents, binders, pigments and additives), paints differ widely in performance, expressed by their radon diffusion coefficient.

SABROUX

It can be derived from Table I that epoxy paints may greatly decrease the radon emanation of a wall or floor surface.

TABLE I
Diffusion coefficient of radon in some paints

PAINT	DENSITY	THICKNESS (mm)	COMPOSITION (%)			DIFFUSION COEFF. (10^{-8} cm ² .s ⁻¹)
			Solvent	Dry extract		
				binder	pigment	
Epoxy + Polyurethane	1.3	0.360	2	80	18	72
Glycerophthalic	1.16	0.176	66	81	19	1.35
Acrylic-1	1.09	0.115	55	51	49	0.95
Acrylic-2	1.10	0.122	53	42	58	1.45
Alkyde urethane	1.15	0.141	34	51	49	1
Polyurethane	1.06	0.143	36	47	52	0.18
Epoxy-1	1.85	0.352	12	33	67	0.35
Epoxy-2	1.35	0.384	10	66	34	0.005
Epoxy-3	1.1	0.339	10	100	0	0.005

After this study on several commercially available paints — that complemented our comparable investigations on polymer membranes¹, concluded at the beginning of this Project — a similar laboratory apparatus was designed for studying, under controlled environmental conditions, the diffusion and permeation of radon through samples of concrete. Samples of mortar for wall roughcasting were also studied.

The versatility of the experimental setup allowed to measure the diffusion and permeability coefficients of a great number of samples with different cement/water, cement/sand and cement/aggregates (if any) ratios. The effectiveness of several fillers and additives was also investigated. The best additive selected (Pozolite™) is originally designed to facilitate the pouring of concrete (more fluidity with less water).

By choosing appropriate ratios of constituents, and relevant fillers and additives, the diffusion coefficient can be kept below 10^{-5} cm².s⁻¹, for both concrete and mortar. On the other hand, the lowest permeability turned out to be 3×10^{-18} m² and 4×10^{-15} m² for concrete and mortar, respectively.

1. This study of polymers clearly sanctioned the polyester Mylar™ membrane as the most efficient radon diffusion barrier.

2°) Radon baseline and mitigation in a high-radon house.—

A — RADON BASELINE. The building selected for the "before/after" study of radon mitigation is the City Hall of a 3,000-inhabitant rural district of Brittany, a conspicuously granitic region of France, but not a distinct uranium-ore province. The choice of this particular public building — identified, during our 1983 regional survey, as a "high radon house" — did not mean that our research should be limited to the study of radon risk mitigation in the work-place². Due to its comparatively lower occupancy factor, especially at night, such a building is obviously simpler to use as a "laboratory house", without any disturbance of its inhabitants' private life, than any other dwelling. Moreover, in a City Hall, the living habits of the occupants are clearly directed by the office hours, with sharp contrasts in building occupancy between week-days and week-ends, or holidays. At last, no real-estate property issues could interfere with our research needs³.

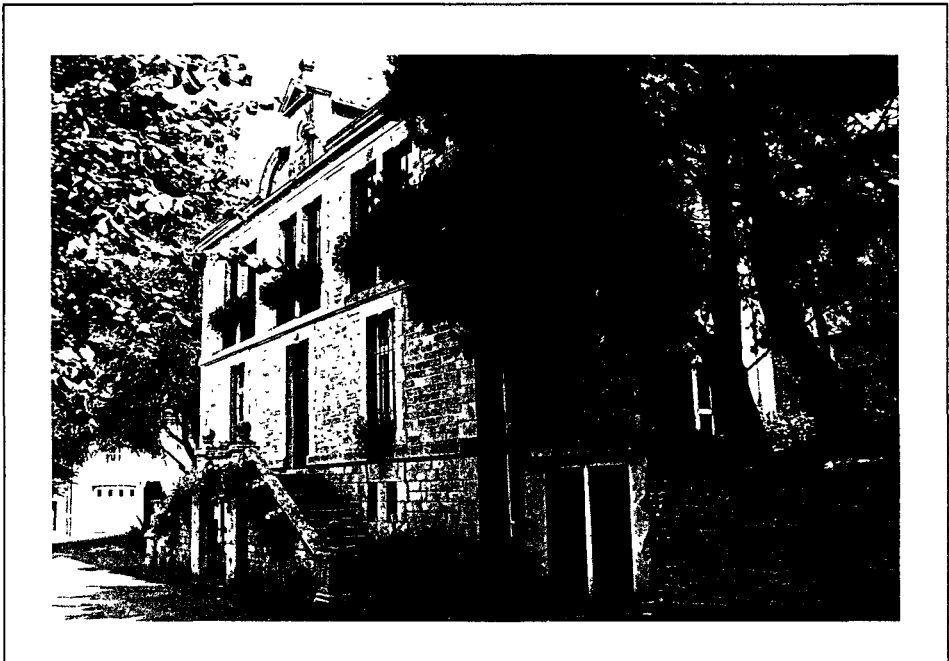


Figure 1 — A typical public building in Brittany, France.

2. Consequently, we considered the generally accepted 400 Bq.m^{-3} action level for ^{222}Rn in existing dwellings as the challenge for our remedial action. From this value, we derived a potential alpha energy concentration (PAEC) upper limit of 880 nJ.m^{-3} , with the conventional values of equilibrium (0.4) and occupancy factors.

3. Throughout our two-year investigation, we congratulated ourselves on the choice we made of this particular building, and we are particularly indebted to the elected representatives and clerks of this City Hall for their good will to make our research work easier.

SABROUX

The building chosen is a granite freestone four-story house (including the attic and the half-buried basement), built in 1910. Part of the basement is taken up by a boiler room, with a hard-packed ground (dirt floor, except for a small concrete slab holding the boiler for central-heating in winter). The oil-fired boiler, when in operation, induces a powerful periodical (ca. 3 min every 15 min) stack effect, that helped to identify unambiguously the soil gas as the main radon source with a flux density (exhalation) ranging between $100 \text{ mBq}\cdot\text{m}^{-2}\cdot\text{s}^{-1}$ and $500 \text{ mBq}\cdot\text{m}^{-2}\cdot\text{s}^{-1}$ (up to thirty times the worldwide continental average).

From the basement, the radon is drawn into the house along pathways (e.g., the stairs) that were experimentally traced using simultaneously CO_2 , He and SF_6 , during a comprehensive test carried out under various ventilation regimes (e.g., in winter, the ventilation rate in the boiler room ranges between 0.2 h^{-1} and 0.5 h^{-1}). This experiment clearly substantiated the basement dirt floor as the prominent radon source, maybe still strengthened by the backfill emanating through the south wall of the boiler room, and the soil emanating through the floor of the room contiguous to the boiler room (Room I in Fig. 2).

Radon levels averaging $7,000 \text{ Bq}\cdot\text{m}^{-3}$ and $600 \text{ Bq}\cdot\text{m}^{-3}$ were measured in the boiler room and office rooms (rooms I to V in Fig. 2), respectively, with peak values higher than $20,000 \text{ Bq}\cdot\text{m}^{-3}$ in the former and $3,000 \text{ Bq}\cdot\text{m}^{-3}$ in the latter. It was shown that the ^{220}Rn (thoron) contribution to this volumic activity was not significant. The γ background ranges from $200 \text{ nGy}\cdot\text{h}^{-1}$ (boiler room) down to $140 \text{ nGy}\cdot\text{h}^{-1}$ (office rooms upstairs), whereas it is $120 \text{ nGy}\cdot\text{h}^{-1}$ outdoors (60 m a.s.l.).

Measurements routinely carried out in the building included (Fig. 2):

- radon indoors and outdoors, by means of ionization chambers, passive dosimeters (solid-state nuclear track detectors and electrets) and silicon detectors;
- PAEC by means of α site-dosimeters;
- airborne-dust bulk concentration (collection on weighted filters);
- emanation from the dirt floor of the boiler room (main radon source);
- indoor and outdoor temperature, differential pressure.

Our fully-fledged "radon test house" provided the unique opportunity to refine the procedures of radon (both spot and integrated) measurements, and to inter-compare the monitoring methods on the long run: e.g., a diffusion ionization chamber (GENITRON *Alphaguard*TM) and a solid-state silicon α detector in a diffusion chamber (ALGADE *Barasol*TM), or the SSNTDs (KODALPHATM) and the electrets (E-PERM[®] RADELEC). This house was even used to validate, for the first time, our numerical model *PRADDO* (based on Jacobi's model), which describes the evolution of radon and its progeny in a multi-chamber system as a function of the ventilation rate and of the aerosol concentration and size distribution.

Finally, we took advantage of the thirteen-month extension of the Project (from 31/05/94 till 30/06/95) to carry on with this set of measurements for almost one year — before any mitigation measure. The diurnal and seasonal effects on indoor radon concentrations were thus satisfactorily determined. Moreover, exceptional climatic events, such as windstorms (December 1994) or a secular flood (January 1995), allowed to calibrate the response of indoor radon to meteorological disturbances.

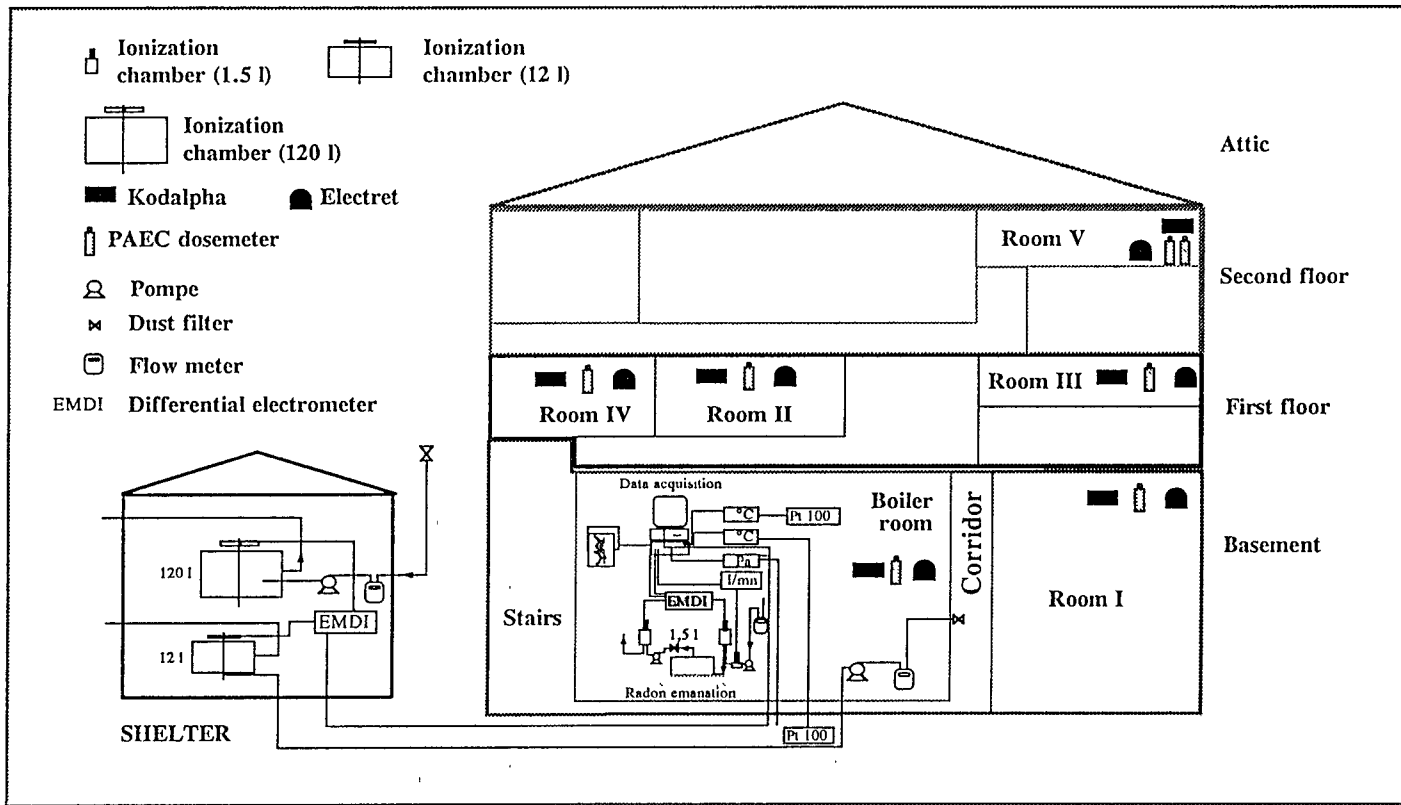


Figure 2 — The comprehensive experimental setup in the test house. The use of a shelter outside the building was made necessary to accommodate the most bulky equipment and the ambient radon monitors, which could not cope with the high radon background of the building. As of March 1995, most of the instruments were electronically connected to our Laboratory in Saclay, Paris region, *via* a modem.

B — MITIGATION. The mitigation strategy, which was first implemented in early November 1994, is centered on sub-slab ventilation. This stems from the comprehensive study of radon entry and distribution in the house, as described above, and from theoretical knowledge and assessment of the various techniques available so far for radon mitigation⁴.

The floor plan of the house at the basement level is given in Figure 3, as well as vertical cross sections. We placed on top of the dirt floor (boiler room) a double-barrier made up of a polyester Mylar™ membrane 100 μm thick, a ca. 10 cm layer of gravel (quarried locally) and a concrete slab (poured with the additive previously selected). Three pits (or sumps) were put in the gravel layer in order to ventilate it efficiently. Without ventilation, radon volumic activity in the sumps under the concrete slab rose up to 90,000 Bq.m⁻³. The pits were connected to the outdoors by a 10 cm diameter PVC pipe network (Fig. 4a and 4b). The whole system was implemented by small local building contractors: the extra outlay generated by the special "anti-radon" design of the works was kept remarkably low.

The ventilation system was extended below the already existing concrete slab of the corridor (between boiler room and room I) and into the backfill, through the south wall of the boiler room (Fig. 3). A thorough characterization of the sub-slab pressure field showed that the de-pressurization was very efficient as far as pit C3, and still enhanced after carefully sealing the holes and cracks in the new concrete slab. Nevertheless, the de-pressurization remained almost unnoticeable under the slab of room I.

The fan chosen is a 32 W axial rotor yielding 185 m³.h⁻¹ at 0 Pa (maximum flow-rate), or -155 Pa at 0 m³.h⁻¹ (maximum de-pressurization). The speed of the fan (electrical power input) is regulated by an electronic potentiometer. Once installed and activated at different speeds, the fan generates a depression that is directly related to the flow-rate (Table I). Note that when ΔP = 0 Pa ("fan power off"), the flow rate is reversed by natural draught due the fact that air pressure is always lower in the building than outside.

TABLE I
Relation between the depression and the flow-rate of the ventilation system,
at different fan speed

Depression (Pa)	-91	-90	-85	-80	-75	-70	-65	-60	-55	-50
Flow-rate (m ³ .h ⁻¹)	144	140	137	133	127	120	113	109	106	103
Depression (Pa)	-45	-40	-35	-30	-25	-20	-15	-10	-5	0
Flow-rate (m ³ .h ⁻¹)	92	86	82	72	65	55	48	34	21	-3

Depression zero means "fan power off".

4. At this stage of the study, the expertise of the *Groupe Informatique et Systèmes Energétiques* with the *Ecole Nationale des Ponts & Chaussées* proved determining.

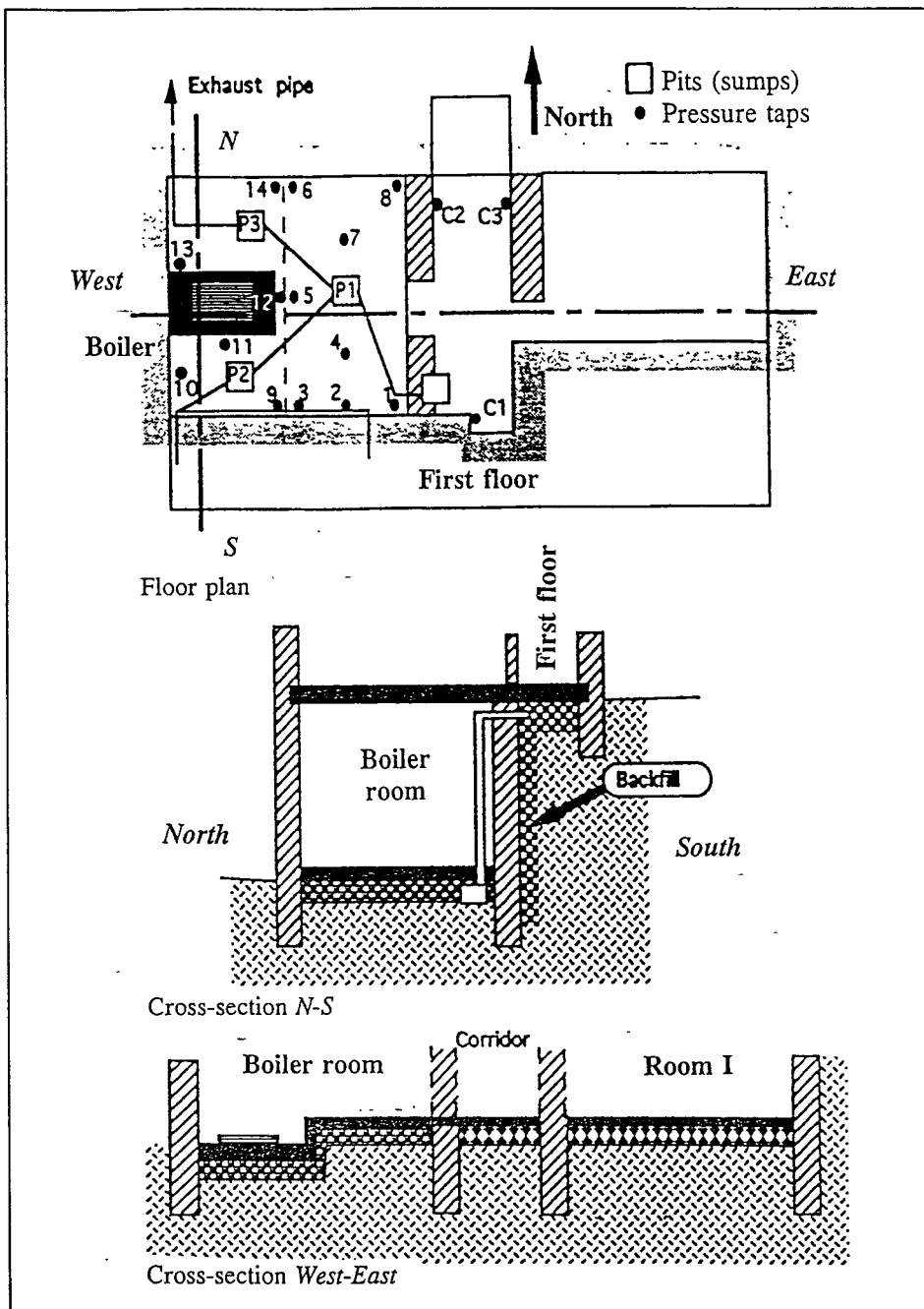


Figure 3 — Floor plan view with sumps and pressure taps locations (at top), and vertical cross sections of the basement of the high radon test house.



Figure 4a — Installation of the ventilation network with a sump on the Mylar™ membrane.

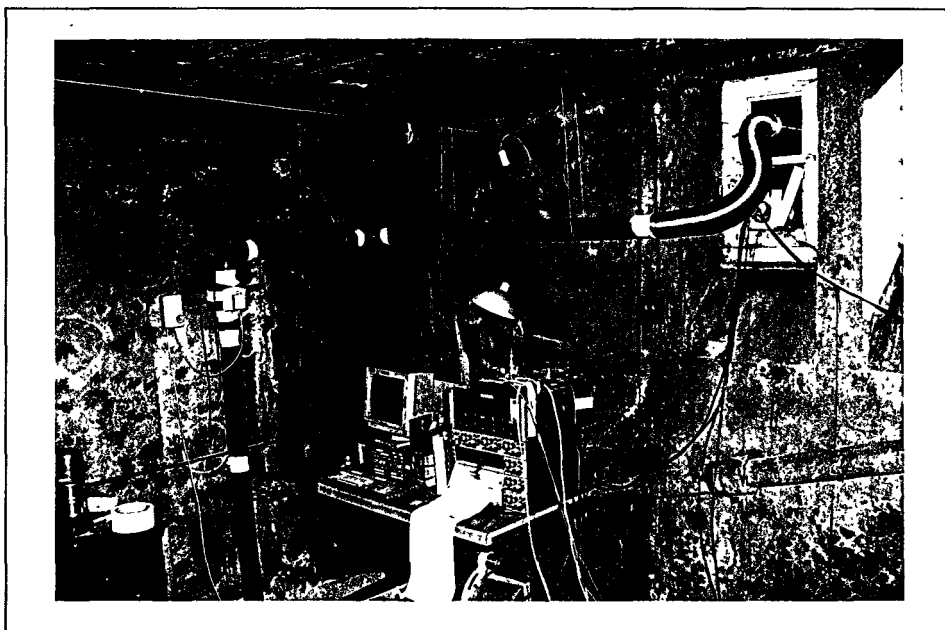


Figure 4b — The fan and the exhaust pipe of the ventilation system, with part of the continuous monitoring setup.

3°) Efficiency of radon mitigation.—

The efficiency of the double-barrier has been dramatically demonstrated since the very beginning of operation of the ventilation system, although the differential pressure in the ventilated room was lowered only by one pascal or so (Fig. 5). On the long run, the efficiency of the mitigation system can be recognized in Figures 6 and 7.

Moreover, it was demonstrated that the system was still fully efficient at one third of its maximum operating de-pressurization. Therefore, we can conclude that a 10 W fan could be sufficient, that would lower the running costs accordingly. At 5 % of the maximum de-pressurization, the radon volumic activity in the boiler room is not higher than $1,000 \text{ Bq.m}^{-3}$, *i.e.*, almost a tenth of its value without remedial action: this exemplifies the feasibility of using a passive double-barrier sub-slab ventilation system powered only by the natural stack effect of the building.

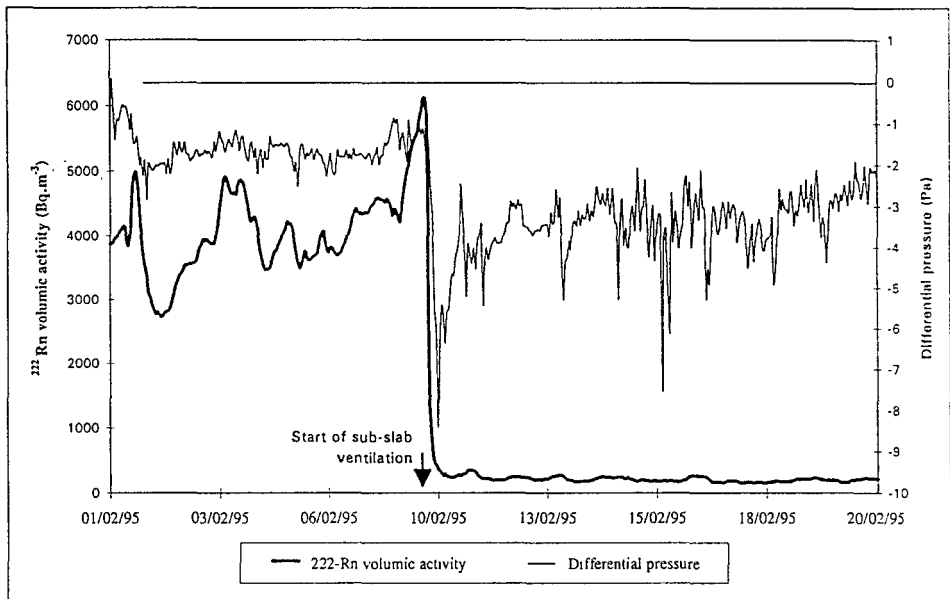


Figure 5 — This time series compares the radon volumic activity in the boiler room without forced ventilation (*ca.* $4,000 \text{ Bq.m}^{-3}$) and at full fan speed (below 400 Bq.m^{-3}). In the basement of our test house, the radon is tunable at a fingertip, only by acting on ventilation fan speed.

Besides the huge data base established throughout this three-year experiment — which deserves further processing and comprehensive interpretation — the results obtained, in terms of radon reduction in the test house, clearly exceeded our expectations. They could readily be applied to many other dwellings built on a similar design, very common in the granitic provinces, which are the most radon-prone areas in France.

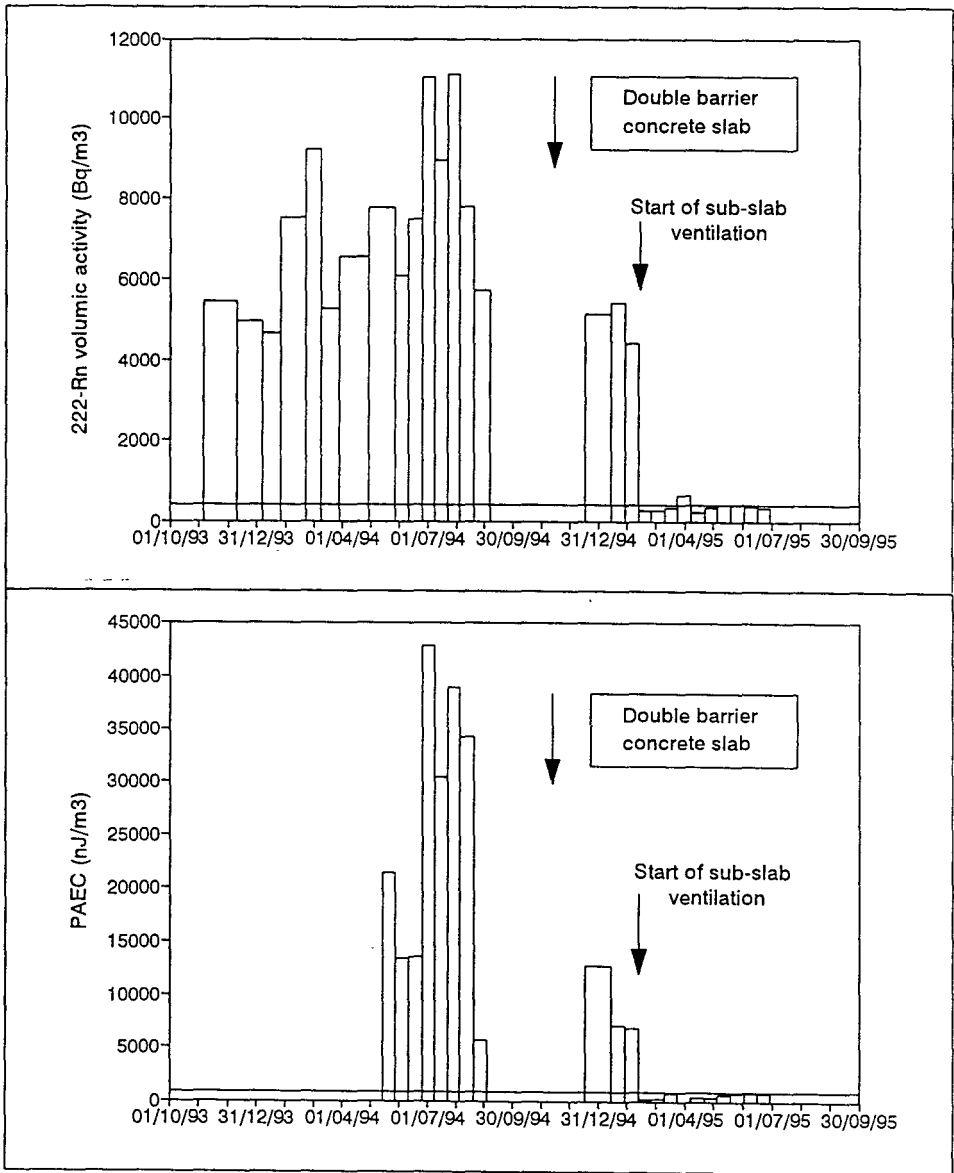


Figure 6 — Integrated radon volumic activity (measured by means of Solid-State Nuclear Track Detectors SSNTDs KODALPHA™) and Potential Alpha Energy Concentration PAEC (measured by α site-dosimeters ALGADE) before and after the alleviative action in the boiler room (basement) of a high radon house of Brittany, France. The horizontal line is the 400 $\text{Bq}\cdot\text{m}^{-3}$ action level for radon, and the derived 880 $\text{nJ}\cdot\text{m}^{-3}$ limit for PAEC (see text). The slight rise of radon during the fortnight period centered on 01/04/95 is due to ventilation tests (ventilation fan at variable speeds). Zero values mean no data.

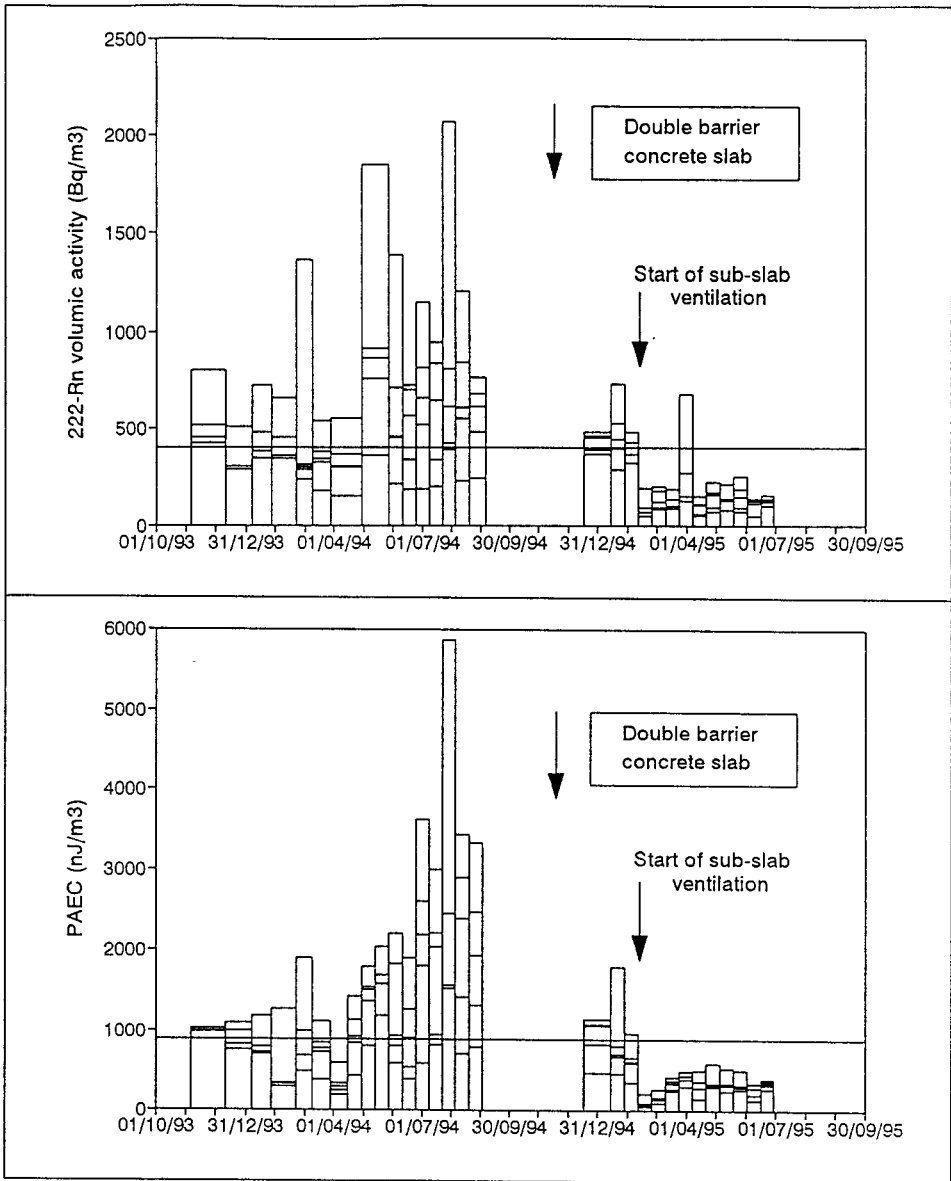


Figure 7 — Integrated radon volumetric activity (measured by means of Solid-State Nuclear Track Detectors SSNTDs KODALPHA™) and Potential Alpha Energy Concentration PAEC (measured by α site-dosimeters ALGADE) before and after the alleviative action in five office rooms of a high radon house of Brittany, France (five bars — one for each room — superimposed, not stacked, for each time period). The horizontal line is the 400 $\text{Bq}\cdot\text{m}^{-3}$ action level for radon, and the derived 880 $\text{nJ}\cdot\text{m}^{-3}$ limit for PAEC (see text). The significant rise of radon (in at least one room) during the fortnight period centered on 01/04/95 is due to ventilation tests (ventilation fan at variable speeds). Zero values mean no data.

PUBLICATIONS

- Goutelard, F., Lecoq, E., Pelleter, X. and Robé, M.C., 1993. Techniques for reducing radon concentration in dwellings: an experimental study of the efficiency of confinement barriers. *Sixth International Conference on Indoor Air Quality and Climate*, Helsinki, Finland, 4-8 July.
- Goutelard, F., Beneito, A., Pelleter, X. and Robé, M.C., 1993. Techniques for reducing radon concentration in dwellings: permeability of paints. *First International Workshop on Indoor Radon Remedial Action*, Rimini, Italy, 27 June - 2 July.
- Pelleter, X., 1993. Etude de l'utilisation des peintures en tant que barrière radon. *Internal Report*, SERAC, Centre d'Etudes de Saclay, France, 46 pp.
- Goutelard, F., 1994. Mesures du radon et de ses descendants dans la Mairie d'E. (Morbihan): dispositif expérimental et résultats des mesures (novembre 1993 - juin 1994). *Internal Report*. SERAC, Centre d'Etudes de Saclay, France, 64 pp.
- Lantoine, M., 1994. Techniques de réduction du radon dans l'habitat: étude bibliographique. *Internal Report*, SERAC, Centre d'Etudes de Saclay, France, 35 pp.
- Tarlay, V., 1994. Etude de l'utilisation des bétons en tant que barrière au radon. *Internal Report*, SERAC, Centre d'Etudes de Saclay, France, 35 pp. + ann.
- Bonnefous, Y., 1994. Conseils techniques pour la mise en place d'une technique de réduction de la concentration en radon à la Mairie d'E. (Morbihan). *Rapport de mission*, GISE-ENPC, Noisy le Grand, France, 22 pp.
- Bonnefous, Y.C., Richon, P., Arnautou, J.C. and Sabroux, J.C., 1995. Sub-slab ventilation system: installation and follow-up in a high radon house in Brittany, France. *NRE VI, Sixth International Symposium on the Natural Radiation Environment*, Montreal, Canada, 5-9 June.
- Arnautou, J.C., 1995. Saisie et analyse des données numériques relatives à une expérience de réduction des concentrations en radon dans un bâtiment. *Internal Report*, SERAC, Centre d'Etudes de Saclay, France, 26 pp. + ann.
- Bonnefous, Y.C., Richon, P., Arnautou, J.C. and Sabroux, J.C., 1995. Réhabilitation d'une habitation à forte concentration en radon par un système de ventilation du sol à double barrière. *GEVRA, Congrès du Groupement des Experts en Ventilation et Renouvellement d'Air*, Sophia-Antipolis, France, 25-26 octobre.
- Gouronnec, A.M., Goutelard, F., Montassier, N., Boulaud, D., Renoux, A. and Tymen, G., *in prep.* Comportement du radon et de ses descendants dans une enceinte d'habitation: comparaison modèle-expérience. *Radioprot.*
- Gouronnec, A.M., Goutelard, F., Montassier, N., Boulaud, D., Renoux, A. and Tymen, G., *in press.* Behavior of radon and its daughters in a house basement: model-experiment comparison. *Aerosol Sci. Technol.*

Head of Project 2: Dr. G. Torri

II. Objectives for the reporting period

The objective of the Project was to test different remedial actions in houses where high radon concentrations were found.

In spite of the fact that a wide experience has been gathered so far in several countries, the different building practices from one country to another make it necessary to evaluate the most appropriate actions for the Italian/Mediterranean typology of houses.

The elongated geographical setting of Italy from North to South, and its strikingly distinctive geological formations are responsible of very different radon emanations from the soil and building materials. Moreover, the dissimilar climate and social situations yield a wide range of building typology and life habits of the occupants.

The main objective of the Project was to study the performance of the most appropriate remedial action — selected from the literature — on houses which represent the most "at risk" for radon entry and, at the same time, are very widespread in the typology of Italian houses.

Cost evaluation of the different actions is also an important objective of the Project. This factor has to be considered in the general strategy aimed at setting reference levels for the protection of the general public.

III. Progress achieved including publications

From the results of the Italian Survey on Indoor Radon, two areas have been selected in which houses with high indoor radon have been found: Friuli-Venezia-Giulia in the north, and Lazio in the center of Italy.

Within these areas, four houses were selected — two for each area — which can be considered "at risk", and which share similar architectural characteristics:

- single family house;
- presence of a crawl-space;
- living area distributed on a single flat (Friuli), or on two flats (Lazio);

The main differences between the two houses in Friuli and the two houses in Lazio are the following:

- crawl-space of different heights, *ca.* 40 cm filled with gravel in Friuli houses, and 100 to 150 cm without any filling in the Lazio houses. The difference generates a dissimilar distribution of the differential pressure between the house, the soil and the crawl space;

TORRI

- the geology of the areas are very different, since in Friuli the soil shows a high permeability with a relatively low content of uranium and radium, whereas in the selected area of Lazio (tuff and pozzuolana), the soil has a high content of uranium and radium, but a low permeability;
- all the houses have been built using local building materials which, in the Lazio region, are characterized by their high uranium and radium content;
- the absence of openings (air bricks) for the ventilation of the crawl-space in the Friuli houses, and the presence of two openings (\varnothing 10 cm) in the Lazio houses.

After selection of the houses, all the most efficient remedial actions were thoroughly investigated for a possible application. Among these, three main actions have been selected as the most appropriate:

- depressurization of the soil beneath the house with a sump;
- depressurization of the crawl-space;
- increased (fan-assisted ventilation of the crawl-space).

A unique experimental setup has been designed for all the houses, as shown in Fig. 1.

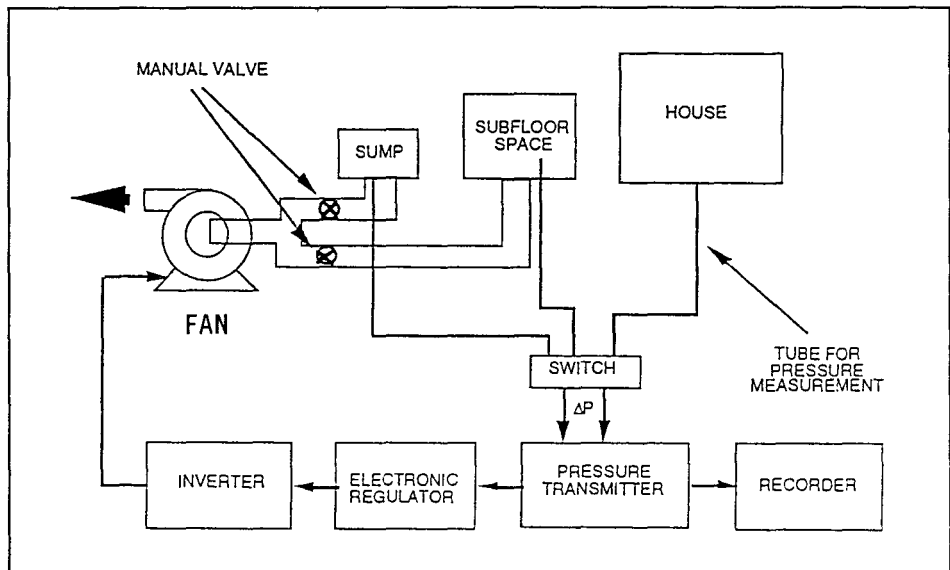


Figure 1 — Block diagram of the experimental setup for testing remedial actions.

It consists in the introduction of ventilation tubes into the crawl-space, and in the installation of a sump under, or close to, the house. The crawl-space and the sump are connected *via* manual valves to a 250 W fan. The power of the fan can be automatically regulated for maintaining a constant differential pressure (ΔP) between the house and the soil or the crawl-space (Fig. 1). Finally, it can operate in both directions, by pushing or sucking air. A total of three openings (\varnothing 10 cm air bricks) were made to increase the ventilation of the crawl-space, but with the possibility to be closed.

Such a configuration allows the testing of different actions, using the same fan:

- depressurization of the soil (or sump);
- depressurization of the crawl-space;
- pressurization of the soil (or sump);
- pressurization of the crawl-space;
- ventilation of the crawl-space by pushing air;
- ventilation of the crawl space by sucking air.

All these actions can be made at different power of the fan, by regulating the rpm of the synchronous motor, producing various ΔP or air flow-rates.

To allow the collection of the experimental data, the test of a single remedial action lasted approximately two weeks. This period is normally followed by a period of the same duration without any remedial action in the house. The efficiency of the action was then evaluated according to a reduction factor RF, *i.e.*, the ratio of the radon concentration with and without the remedial action in operation.

The measurement strategy has been the continuous detection of indoor radon, using a PYLON AB5 counting system; plus passive diffusion scintillation cells located in the bedroom of each house. Limited to the Lazio houses, continuous measurements have also been made in the crawl-space. Solid State Nuclear Track Detectors (SSNTD) were also used in other rooms, and in the crawl space.

The experimental tests started in winter and ended in summer, same year. The radon concentration in summer was lower than in winter. The difference can well affect the RF, since the winter/summer variation of radon concentration, without remedial action, are much larger than these variations when remedial action is implemented (much lower mean radon level).

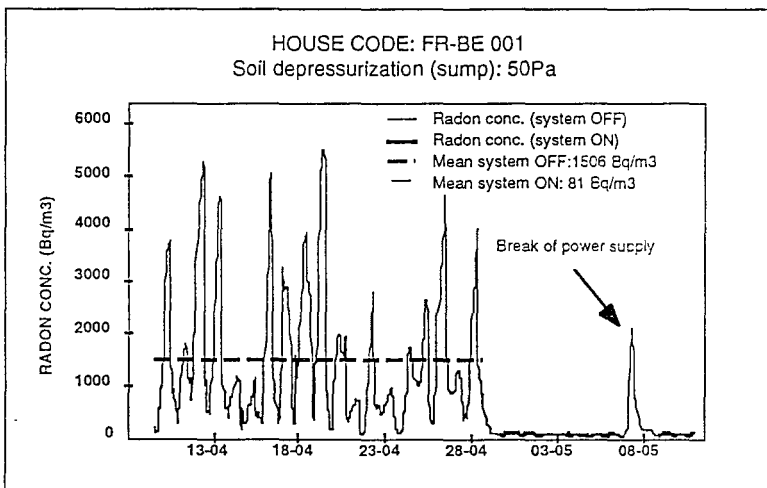


Figure 2 — Example of application of a remedial action.

From these results, we can draw a first conclusion: the response of indoor radon to the remedial action is very fast (*i.e.*, of the order of a few hours). This is an important finding, that permits a rapid evaluation of a given remedial action potential. In other words, there is no need to wait for months in order to evaluate the effectiveness of a particular remedial action.

A second result is the confirmation of the higher values of radon concentrations at night (Rn_n), as compared with daily concentrations (Rn_d). The mean ratio Rn_n/Rn_d amounts to 1.7 ("night" spans arbitrarily from 7:30 *pm* to 7:30 *am*). This should be taken into account when dose/concentration factors are evaluated: as a matter of fact, occupants spend most of their time at home during the night, when radon concentrations are comparatively higher.

The particular remedial actions tested during the Project were:

- depressurization of the sump at three different ΔP (10, 50 and 100 Pa);
- ventilation by suction of the crawl space at three different speeds of the 250 W fan (30, 40 and 50 Hz);
- depressurization of the crawl-space (with closed openings).

1° Soil (sump) depressurization.—

The sump depressurization adopted for the Friuli houses (FR) gives in general a very good reduction in the radon concentration, while in the Lazio houses (LA), it does not seem to reduce significantly the radon entry. This is probably due to the presence, in the Lazio houses, of the large void volume of the crawl-space, without any concrete slab or flooring on the soil, while in the Friuli houses, the void volume of the crawl-space is much smaller, due to the presence of the gravel filling. This distinct setting causes a different distribution of the soil pressure: even if a sump low pressure can be obtained in both cases, in large void crawl-spaces, with no soil covering, the low soil pressure does not affect the total surface of the house. The different permeability of the soil can also play a very important role, causing an odd pressure distribution.

TABLE I
Reduction factors obtained with the depressurization of the soil for the four houses

Differential pressure ΔP	House FR-BE 001	House FR-PA 002	House LA-PO 003	House LA-PE 004
10 Pa	3 (284)	2 (344)	1 (235)	1 (248)
50 Pa	11 (81)	14 (14)	2 (253)	2 (217)
100 Pa	39* (23)	20 (28)	1 (151)	—

The radon concentrations are displayed in brackets.

* For this test, the maximum ΔP was 75 Pa instead of 100 Pa.

For the Friuli houses, the efficiency of soil depressurization depends on the under-pressure that can be obtained in the sump. A differential pressure of 50 Pa seems sufficient to reduce the radon concentration at satisfactory low levels. These values are obtained with a reduced speed of the fan. Therefore, the use of a 70-100 W fan should be sufficient to reach the required ΔP .

2°) Crawl-space depressurization.—

The crawl-space depressurization was obtained by sucking air with the ventilation openings in the closed position.

TABLE II
Reduction factors, for the four houses, at different speeds of the 250 W fan

FAN SPEED	<i>House FR-BE</i> 001	<i>House FR-PA</i> 002	<i>House LA-PO</i> 003	<i>House LA-PE</i> 004
30 Hz	20 (17)	—	—	—
40 Hz	19 (18)	4 (22)	—	—
50 Hz	24 (20)	13 (21)	1 (284)	2 (229)

The radon concentrations are displayed in brackets.

This action was successful in the Friuli houses, while in the Lazio houses, no effects were observed. The reasons for this behavior are the same as in the case of soil depressurization. Yet, for the latter houses, a reduction factor of 4 was observed in the crawl-space.

3°) Crawl space ventilation.—

The crawl-space ventilation was obtained with the fan at maximum speed (50 Hz) sucking air with the openings in the open position.

TABLE III
Reduction factors for the four houses, at full fan speed (50 Hz)

<i>House FR-BE</i> 001	<i>House FR-PA</i> 002	<i>House LA-PO</i> 003	<i>House LA-PE</i> 004
20 (24)	12 (26)	2 (217)	1 (158)

The radon concentrations are displayed in brackets.

Again in the Friuli houses, the reduced void of the crawl-space is the main factor conditioning the efficiency of the ventilation.

The poor efficiency of all actions in the Lazio houses is probably due to the large void of the crawl-space. Further tests should be made after covering the soil of the crawl space area by concrete (expensive solution) or by sheets of thick polyethylene.

In conclusion, during completion of the Project, the main objective achieved has been the understanding of some important parameters that influence the entry of radon into the selected types of houses — types which are very common in Italy, and which can be considered "at risk", due to the building practices. Further investigations should be made to evaluate the possible actions in houses with other typologies.

PUBLICATIONS

Torri, G. *et al.*, 1994. Azioni di rimedio in edifici con elevata concentrazione di radon. *ARIA 94, Atti del Convegno Nazionale*, Monteporzio Catone, Italy, 26-28 October: 107-113.

Head of Project 3: Dr. A. Ortins de Bettencourt

II. Objectives for the reporting period

The analysis of the results concerning the Indoor Radon National Survey carried out in Portugal permitted to identify some regions with high indoor radon concentrations. These areas are mainly situated over granitic geological structures, and the highest indoor radon values were found in a granitic and uranium mining region.

On the other hand, it is known that some materials originating from industrial processes, like fly-ash and phosphogypsum, have been used as building materials and, as they contain high concentrations of natural radionuclides, contribute to increase the indoor radon levels.

So, in the framework of the above mentioned Contract, the Departamento de Protecção e Segurança Radiológica (DPSR), Portugal, proposed a research program including the following activities.

1°) A — To analyze and to describe in detail the special characteristics of the dwellings from regions where high indoor radon concentrations were found: climatic aspects, predominant living habits of the population at stake, and occupancy factors should also be described.
B — To perform radon exhalation rate measurements from ground and walls, using classic methods, in order to identify the main radon source term.

2°) To perform laboratory radon migration experiments testing some usual building materials, to be used as a barrier to radon transport from the soil under the house.

3°) A — To verify the influence of phosphogypsum, used as wall coating in an experimental room built specially for this purpose, in the increase of indoor radon concentrations.
B — To study some kinds of wall paints as mitigation procedures, and to test their respective effectiveness.

4°) To implement remedial actions in real situations, in order to decrease the indoor radon concentrations, and to verify its effectiveness.

III. Progress achieved including publications

1°) Radon measurements in real dwellings.—

The granitic region in the center of the country, where we found the highest indoor radon values, is situated 400 km apart from Lisbon, and has a predominant continental weather.

The most of its population is rural, having a farming occupation, whereas some people work also in local industries. In general, the people spend a lot of time outside.

ORTINS

The dwellings are mainly built with local building materials (stone and sand). Three dwellings were previously selected, and indoor radon as well as radon daughters measurements had been performed during some months. Nevertheless, for applying future mitigation procedures, only one of them was considered available enough. It is a workplace of masonry type, built around 1950, with external granite ornaments. It consists in a ground and first floor, and it has a kind of a crawl-space, with opposite open holes. Every room has window and door, and the floor is a wood suspended timber floor. An available room situated at the ground floor was made available for our study.

Long term measurements were performed in this selected dwelling, in order to know the indoor and outdoor radon, and the radon daughters concentrations.

Concerning the indoor radon measurements, integrated and spot samples measurements were performed (Table I), with the door and windows closed. For the integrated measurements, passive alpha track detectors (LR-115 KODAK films) were exposed during a 2- to 3-month period. After chemical etching, the films were counted in a spark counter.

For evaluation of radon and radon daughters spot measurements, air sampling at 1.5 m above the floor were performed. A portable equipment (RDA-200 from PYLON) was employed; for the radon daughters calculation, the Thomas Method was used.

TABLE I
Radon and radon daughters measurement in a dwelling of Portugal
(before remedial action)

	<i>Average</i>	<i>Range</i>
Integrated indoor radon (Bq.m ⁻³)	1,940	1,363—2,928
Spot indoor radon (Bq.m ⁻³)	4,748	231—12,723
PAEC (nJ.m ⁻³)	140	50—360

Several spot outdoor radon and radon daughters measurements were also carried out around the house throughout the year, and under different meteorological conditions. The respective values ranged from 16 Bq.m⁻³ to 426 Bq.m⁻³.

In order to identify the main indoor radon source term, some exhalation measurements from the walls and the wooden suspended floor were performed. For these measurements, some special devices were employed, and well tighten on the surfaces to be investigated. Air samples were transferred from these devices to Lucas cells, and further counted in an alpha counting equipment. Exhalation rates from 1.1 mBq.m⁻².s⁻¹ to 19.2 mBq.m⁻².s⁻¹, and from 0.5 mBq.m⁻².s⁻¹ to 22.8 mBq.m⁻².s⁻¹ were found for floor and walls, respectively.

Radon exhalation measurements from soil adjacent to the dwelling were also carried out. The radon flux determination was based on an accumulation method. Nuclear track detector films were exposed in special devices with *ca.* 10 liters volume, and having an open end

placed on soil, 60 cm deep, during 24 hours. This duration was experimentally determined, in order to avoid a build up to a level where the radon concentration would be comparatively reduced by back-diffusion towards the area under measurement. The individual values obtained ranged from $72 \text{ mBq.m}^{-2}.\text{s}^{-1}$ to $336 \text{ mBq.m}^{-2}.\text{s}^{-1}$.

In the neighborhood of the house, several soil samples were collected in a layer up to 10 cm and analyzed by gamma spectrometry, in a Ge(Li) detector. An average ^{226}Ra specific activity of $723 \pm 13 \text{ Bq.kg}^{-1}$ was obtained.

An overall analysis of all the results obtained shows that indoor radon is significantly higher than outdoor values. Considering that the mean exhalation rate of a standard soil is $20 \text{ mBq.m}^{-2}.\text{s}^{-1}$, the radon exhalation from the soil adjacent to the house investigated is higher. Indeed, these soils have in their composition a significant amount of waste rock materials originating from the nearby uranium mining activities, and the indoor radon source is likely mainly due to the soil beneath the house. Nevertheless, the radon exhalation rates from the walls are not negligible, and have also probably a significant contribution.

2°) Radon measurements in an experimental room.—

The use of phosphogypsum as a substitute for natural gypsum may constitute an additional source of indoor radon. In Portugal there are big piles of phosphogypsum, originating from phosphate industries, that can eventually be employed as building material: therefore, we studied the influence of this by-product on the indoor radon concentrations.

An experimental room was built, close to our Department, using common building materials. This experimental room has a window, a door, an area of about 12 m^2 and a volume of 28 m^3 : it is representative of a typical bedroom.

Several integrated radon measurements were carried out in the room, using passive alpha track detectors (LR-115 KODAK films). The values obtained ranged from 45 Bq.m^{-3} to 67 Bq.m^{-3} , with a mean of $50 \pm 9 \text{ Bq.m}^{-3}$.

The walls of the room were covered with phosphogypsum leading to a ^{226}Ra surfacic activity of $2,405 \text{ Bq.m}^{-2}$, as a final stucco-work, on a total area of about 24 m^2 (subtracting, from the wall area, the window and door areas).

Integrated indoor radon measurements were repeated, and the values obtained ranged from 250 Bq.m^{-3} to 326 Bq.m^{-3} , with a mean of $297 \pm 30 \text{ Bq.m}^{-3}$.

After the application of phosphogypsum, it is noticed that the radon concentration in the room is more than six times higher than the initial values.

3°) Experimental tests on coating materials.—

The high indoor radon levels are specially due to radon gas originating from the soil beneath the houses. Sometimes, the use of some building materials having a high natural radionuclides

concentration may also contribute significantly to these levels. Thus, some experimental tests on coating materials were developed in order to study their respective effectiveness in a radon mitigation procedure.

To study the diffusion properties and the permeability of different flooring materials to be used as a barrier to radon transport from the soil to the house, several laboratory experiments were performed. A special cylindrical container was designed, consisting in a closed symmetrical two-compartment structure: one compartment contains a radon source (^{226}Ra -contaminated soil), the other compartment being upside-down and separated from the first by the radon barrier — the building material to be studied.

From the radon concentrations measured in air samples collected from the two separated compartments, it is possible to determine the effectiveness of the material as a barrier to the radon transport.

Different materials were tested:

- a concrete block 3 cm thick;
- two different materials, normally used for floor covering, namely a vinyl flooring of $3,300 \text{ g.m}^{-2}$ and a double coating material — "MOFIBE" (polyethylene and aluminum) of $2,500 \text{ g.m}^{-2}$ — and a black plastic membrane of 48 g.m^{-2} .

Four sets of experiments were carried out in order to evaluate the effectiveness as a radon barrier of each floor covering. The material was placed between the two symmetric compartments tightly fitted to each other. This assemblage was maintained during a few weeks. Subsequently, air sampling was performed from each compartment into a Lucas scintillation flask, and the corresponding activity measured in an alpha counting equipment.

Figure 1 summarizes the radon reduction values obtained with the different materials studied and used as potential diffusion barrier for radon gas. The vinyl flooring and the "MOFIBE" yield a significant radon reduction, potentially useful in a radon mitigation procedure.

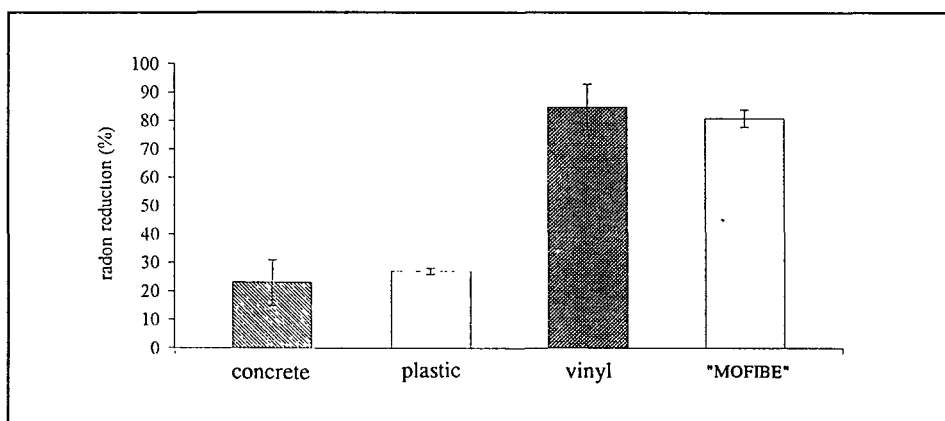


Figure 1 — Efficiency of different coating materials used as a radon barrier.

In order to study the radon mitigation after the implementation of phosphogypsum covering, three types of wall coatings were selected for applying in the experimental room: a wallpaper of 140 g.m⁻², a simple whitewash paint using water as a solvent, and an epoxy paint — chosen for its very low radon diffusion coefficient.

Before the applying of each of the coating materials tested, the indoor radon levels were restored by covering the walls with another layer of phosphogypsum.

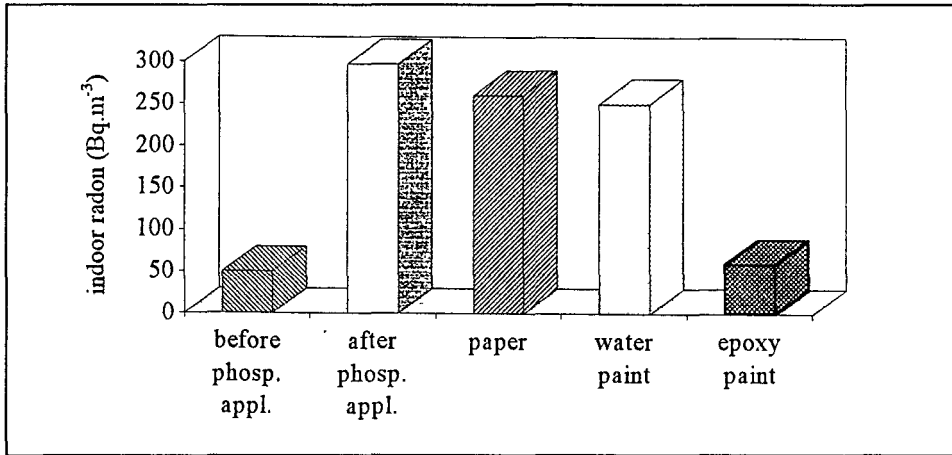


Figure 2 — Averages of indoor radon results in the experimental room.

Integrated indoor radon measurements were carried out after the applying of each covering material. The results obtained are displayed in Figure 2, for the three materials studied, and compared with the radon concentrations in the room with and without phosphogypsum. The epoxy paint achieves a reduction of ca. 100% of indoor radon, that is almost lowered down to its pre-phosphogypsum level.

4°) Remedial actions in the real house. —

Since the dwelling studied has a suspended timber floor, its high indoor radon level proved difficult to remedy. A natural ventilation being the simplest and cheapest way to mitigate the indoor radon, it was tested in priority. Several spot radon and radon daughters measurements were carried out in different natural conditions. The results obtained are displayed in Figures 3 and 4.

From these results, it can be seen that the radon concentrations can decrease down to a factor ten, only with natural ventilation.

According with the results obtained in the laboratory experiments, an heavy vinyl flooring of 3,300 g.m⁻² was selected to cover the floor of the dwelling, and an elastic sealant was implemented to seal the floor-to-wall gaps. Integrated and spot radon measurements were again carried out with the door and windows closed.

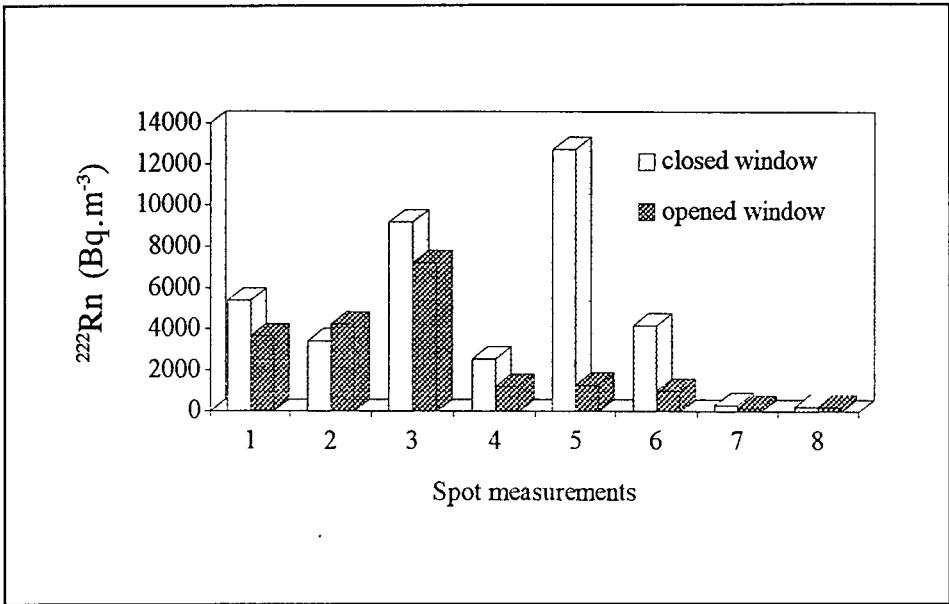


Figure 3 — Influence of natural ventilation (1 to 3 hours) on indoor radon.

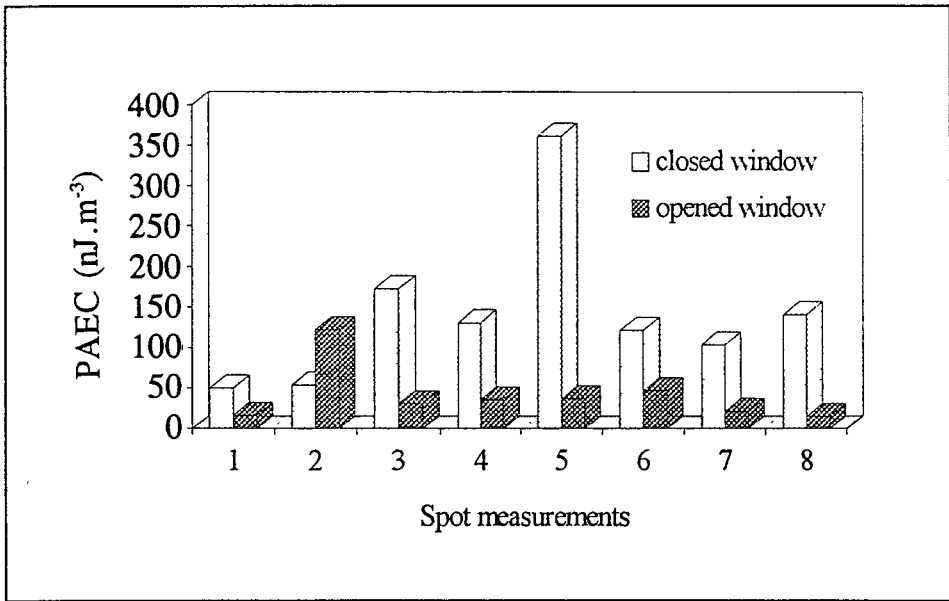


Figure 4 — Influence of natural ventilation (1 to 3 hours) on indoor radon daughters.

TABLE II
Radon and radon daughters measurements in a dwelling of Portugal
(after remedial action, see text)

	<i>Average</i>	<i>Range</i>
Integrated indoor radon (Bq.m ⁻³)	1,460	1,302—1,820
Spot indoor radon (Bq.m ⁻³)	625	363—1,316
PAEC (nJ.m ⁻³)	32	13—60

Concerning the integrated indoor radon averages, a reduction of about 25% was obtained. For the radon daughters levels, a reduction of about 80% was achieved (Table II).

5°) Conclusions.—

Considering the different mitigation procedures implemented in the real dwelling, a significant influence of natural ventilation on radon levels was clearly observed. Nevertheless, as the dwelling is situated in a region of comparatively cold weather, this type of remedial action is not adequate.

The sole material selected for covering the suspended timber floor and for acting as a barrier to radon transport from the soil to the house appears, in practice, not effective enough to reduce the indoor radon concentrations in this dwelling. However, the radon exhalation from the walls also contribute to the high indoor radon levels measured in this particular and other dwellings in Portugal: according to our experimental tests, the covering of the walls with a resin paint could be a significant contribution to a better mitigation of the high indoor radon concentrations.

PUBLICATIONS

Faísca, M.C. and Teixeira, M.M.R., 1992. Determinação da energia potencial alfa dos descendentes do radão. *8a Conferência Nacional de Física*, Vila Real, September.

Crispim, J.A., Teixeira, M.M.R. and Faísca, M.C., 1993. Alguns dados sobre os teores de radão no ar das grutas turísticas do centro de Portugal. *ALGAR, Bol. Soc. Portuguesa Espeleologia*, 4.

Faísca, M.C., Alves, J.G., Teixeira, M.M.R., Crispim, J.A. and Vaz Carreiro, J., 1994. Doses de radiação natural em grutas. *Proc., V Congresso da Sociedade Espanhola de Protecção Radiológica e las Jornadas Hispano-Lusas de Protecção Radiológica*, Santiago de Compostela, 309-315.

Faísca, M.C., 1994. Exposição da população ao radão. *Ias Jornadas da Sociedade Portuguesa de Protecção contra radiações*, Lisboa, March.

Faísca, M.C. and Teixeira, M.M.R., 1994. Resistência através de barreiras ao transportede radão. *9a Conferência Nacional de Física*, Covilhã, Portugal, 19-23 September.

Faísca, M.C., Reis, M., Teixeira, M.M.R. and Brogueira, A., 1995. Radon exhalation from Urgeiriça uranium tailings. *International Symposium on Environmental Impact of Radioactive Releases*, Vienna, May.

Faísca, M.C. and Teixeira, M.M.R., 1995. Study of different reduction techniques to mitigate high indoor radon levels. *International Health Building Conference*, Milão, September.

Head of Project 4: Dr. L.S. Quindós Poncela

II. Objectives for the reporting period

Within the framework of the Project, the objectives to be developed by our research Group are basically related to the contribution of building materials as a source of radon, in order to study for them effective remedial actions that contribute to the decrease of radon in houses where the building materials have an important incidence. These objectives could be summarized as follows:

- 1°) identification, classification and measurement of radioactivity in building materials of common use in Spain, with special emphasis on cements under control by the Spanish Authorities, and on granites;
- 2°) development of protocols for the measurement, in porous materials, of physical parameters such as radium content, radon emanation factor, exhalation rates, diffusion coefficients, porosity and permeability. In this task, specific inter-comparison exercises for the measurement of these parameters, especially among the participants to the EC contracts under the Radiation Protection Program, are absolutely necessary for a good evaluation not only of the contribution of building materials, but also of soils, as sources of indoor radon;
- 3°) evaluation, in a test structure, of the contribution of granite — the main building material employed in an area of Spain identified as having a high indoor radon level — to the total indoor radon measured in houses, and study of the conditions under which permeability of concrete and granite may be responsible for the presence of high radon levels in houses;
- 4°) laboratory study of the efficiency of some caulking compounds and mitigation techniques in the reduction of radon levels in homes;
- 5°) development of *in situ* measurements in selected houses to evaluate the relevance and availability of the laboratory measurements described above.

III. Progress achieved including publications

1°) Identification, classification and measurement of radioactivity in building materials of common use in Spain, with special emphasis on cements under control by the Spanish Authorities, and on granites.—

Granite has generally a higher radium content than "normal" soils. The presence of granite affects not only the external gamma dose to the population, but also the indoor radon levels. This holds when granite is used as a building material, and/or when the house is built on granitic soils. During the National Survey in Spain, we found that the highest figures for houses with high levels of indoor radon were concentrated in the granitic areas.

QUINDOS

These high levels were measured not only in houses with direct contact with the soil, but also in the upper stories of the building. At that time, we tested the hypothesis according to which the granite used in these buildings is an important source of indoor radon. The first objective mentioned above is the initial step of the research that we were carrying out in order to validate this hypothesis.

Granite has a double function in the Spanish building trade: it is used, first, as an ornamental covering for walls and floors and, second, as a primary building material in some parts of the country. The characteristics of granite from Spain and from abroad are not controlled by Spanish law: there is only an inventory drawn up by the producers showing a high proportion of imported granite for use as an ornament.

A total of 110 granite samples, representing 98% of those used in Spain, were collected: their radioactivity content was analyzed, with special emphasis to the radium content of the samples. The results are shown in Figure 1, which represents, within different intervals of radium concentration, the percentage found.

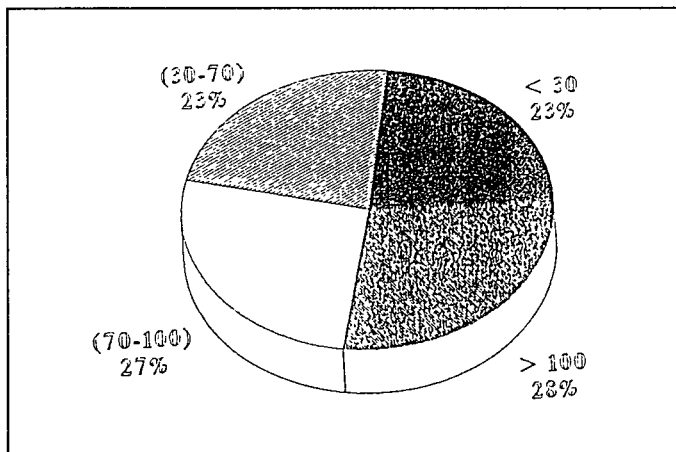


Figure 1 — Concentration of ²²⁶Ra in Spanish granite.

As we can see, about 28% have values above 100 Bq.kg⁻¹: we should point out here that a high proportion of the granites with these high radium concentration levels comes from the communities where the high indoor radon levels mentioned above were measured. Moreover, the granite from these communities is used mainly as a primary building material.

Besides granite, there are two reasons for studying also cements. First, it is a component of concrete, the main building material in our country, and the principal subject of our studies. Moreover, it is the only component of concrete that is under control of the Spanish authorities, whereas the aggregates used in concrete are not subject to regulation. The second reason is that more and more cement is being imported to Spain, and that the authorities are being forced by pressure from the cement companies to enforce stronger quality controls. Then, although a control of the radioactivity of cements has not been considered so far, it may become so in the near future.

A total of 120 cement samples collected from different producers are covering about 95% of the Spanish cements, and a small proportion of imported cements. Figure 2 shows the values found for the radium content and indicates that only 7% of the Spanish cements studied have values over the reference value of 100 Bq.kg^{-1} . On the other hand, all of the ten imported cement samples available for study are over this value.

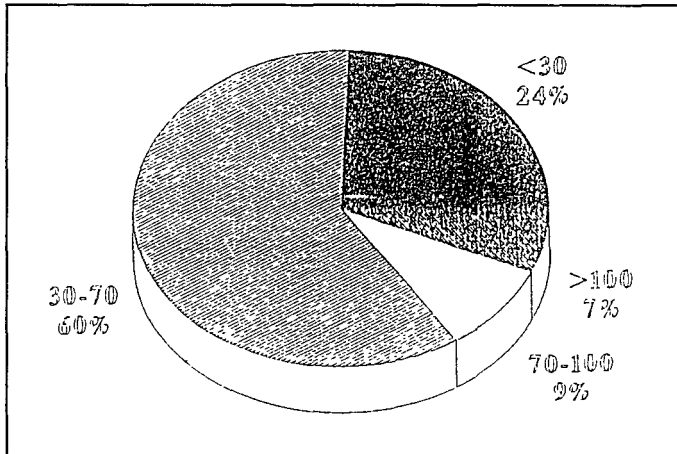


Figure 2 — Concentration of ^{226}Ra in Spanish cements.

As we have already mentioned, and as far as radon is concerned, our interest is in concrete. The composition of concrete is extremely variable. For this reason, more than 300 aggregate samples were collected throughout the country. As a result, average values for radium content are available for these aggregates, for each autonomous community, together with those for the most commonly used cements. These data have allowed us to be prepared for a very representative study on samples or raw materials used for making up concrete throughout the country. In conclusion, we can consider that this objective has been covered satisfactorily; the results achieved will be used for the development of the next objectives.

These results show also that, in general, the capability of the participating laboratories in developing good measurements by gamma spectrometry is high. However, as we concluded after the first inter-comparison, the development of such exercises, that could allow the participants to identify the conditions causing potential problems in their measurements, are absolutely necessary to ensure a good quality control of the results.

The emanation factor requires extremely accurate evaluation. To measure this parameter, we have developed the technique that we presented at the International Meeting in Rimini (1993), and that has been published later in *Radiation Protection Dosimetry*, under the title: "A technique for the measurement of the exhalation rate of ^{222}Rn from small samples of porous materials". It basically requires to place the sample to be analyzed in a scintillation cell, and to observe the increase of its radon concentration. From this, the value of the emanation factor is deduced, and compared with that obtained from the steady state reached after three weeks of equilibration.

From the measurements made so far, we can state that the technique proposed minimizes some disadvantages usually present in the experimental procedures based on the accumulation method, such as the time required for the measurement of the parameter studied, and the problems related to possible pressure changes in the accumulation volume. Also, minimum exhalation rates and emanation factors measurable are lowered by the technique, yielding values as low as 0.005 for the emanation factor, and of 0.36 Bq.h⁻¹ for the total exhalation rate.

The method has been applied in our laboratory to study the dependance of the emanation factor on humidity for a set of soils as well as for granites and concrete. A specific inter-comparison for a sand sample was developed with KVI (The Netherlands). A good agreement was found between the results of both laboratories. Nevertheless, more exercises are absolutely necessary in order to prepare a common protocol in this field.

The cements analyzed, with radium concentrations higher than 100 Bq.kg⁻¹, yielded emanation factors within the range 0.6% to 5%. Similar values were found for the granites studied, while for these samples, atypical values of 20% were measured for a couple of samples used as building materials in some places of the country.

In our Laboratory, the measurement of the diffusion coefficient was made initially by continuous measurement of the radon concentration in two containers, following the approach described some years ago by several authors. The said approach eliminates the need to collect a sample that can alter normal conditions of diffusion in the sample. Nevertheless, while the first results were in good agreement with experimental data available, the main problem encountered was related with the extremely low thickness of the sample used, that involves losses of air through the valves, and made the technique only valid for soil samples.

For this reason, a new method has been developed in our Laboratory for the measurement of diffusion coefficient in granite and concrete. It basically involves the knowledge of the exhalation rate from two samples of different thickness, placed in an accumulator. The value for the diffusion coefficient, or diffusion length, is derived from the theoretical formulas that control the exhalation process.

At this moment, typical diffusion lengths between 1 and 10 cm were evaluated for the granite samples studied, with increase of this range up to 20 cm for the concrete sample analyzed. However, more experience in this field is necessary, in order to characterize correctly this parameter for the building materials.

Finally, the measurements of porosity and permeability of porous samples are also ready to be applied for any samples (e.g., cements, concretes and granites). For this, a plan has been established with the Department of Materials at the University of Cantabria, in order to refine a highly sensitive technique for the laboratory measurement of these parameters. For the cements, the porosity ranges from 40% to 60%, while for granites, it is always below 2%. Regarding the permeability, typical values are 10⁻¹³ m² and 10⁻¹⁷ m², for cements and granites, respectively.

QUINDOS

2°) Development of protocols for the measurement, in porous materials, of physical parameters such as radium content, radon emanation factor, exhalation rates, diffusion coefficients, porosity and permeability.—

Concerning the radium content in samples, thirteen laboratories, almost all of them involved in the Radiation Protection Research Action have agreed on the proposal to perform radium measurements on two samples in a Marinelli beaker, or by using their own geometry, in order to evaluate the radium content of the samples. Results from each laboratory were analyzed and discussed by the participants. As a summary of the work, a paper entitled "Results of the Second Inter-comparison of gamma spectrometry measurements of the radioactivity in soils and building materials" has been published. As an overview of the results, Table I shows the laboratories the results of which are between the percentiles 25% and 75% (*IN*), or out of this range (*OUT*), thus giving a general view of the inter-comparison, which is the only common protocol available so far in this field.

TABLE I
Radioactivity measurements performed by 13 European laboratories,
the results of which are within the percentiles 25—75% (*IN*) or outside this range (*OUT*)

LABORATORY CODE	E1	E2	E3	E4	E5	E6	E7	E8	E9	E10	E11	E12	E13
²²⁶ Ra phosphate (all lines)	<i>OUT</i>	<i>OUT</i>	<i>OUT</i>	—	<i>OUT</i>	<i>IN</i>	<i>OUT</i>	<i>IN</i>	<i>IN</i>	<i>IN</i>	<i>IN</i>	<i>IN</i>	<i>IN</i>
²²⁶ Ra sand (all lines)	<i>IN</i>	<i>IN</i>	<i>OUT</i>	—	<i>OUT</i>	<i>IN</i>	<i>OUT</i>	<i>IN</i>	<i>OUT</i>	<i>OUT</i>	<i>IN</i>	<i>IN</i>	<i>OUT</i>
²²⁶ Ra phosphate (609.32 keV line)	<i>IN</i>	<i>OUT</i>	<i>OUT</i>	—	<i>IN</i>	<i>IN</i>	<i>OUT</i>	<i>OUT</i>	<i>IN</i>	<i>IN</i>	<i>IN</i>	<i>IN</i>	<i>IN</i>
²²⁶ Ra sand (609.32 keV line)	<i>IN</i>	<i>IN</i>	<i>IN</i>	—	<i>IN</i>	<i>IN</i>	<i>OUT</i>	<i>IN</i>	<i>OUT</i>	<i>OUT</i>	<i>IN</i>	<i>OUT</i>	—
²²⁶ Ra phosphate (1,764.51 keV line)	<i>OUT</i>	<i>OUT</i>	<i>IN</i>	—	<i>OUT</i>	<i>IN</i>	<i>IN</i>	<i>OUT</i>	<i>IN</i>	<i>IN</i>	<i>IN</i>	—	<i>IN</i>
²²⁶ Ra sand (1,764.51 keV line)	<i>IN</i>	<i>IN</i>	<i>OUT</i>	—	<i>OUT</i>	<i>IN</i>	<i>OUT</i>	<i>IN</i>	<i>IN</i>	<i>OUT</i>	<i>IN</i>	—	—
²²⁸ Ac phosphate (all lines)	<i>IN</i>	<i>OUT</i>	<i>IN</i>	<i>IN</i>	<i>IN</i>	<i>OUT</i>	<i>OUT</i>	<i>IN</i>	—	—	<i>IN</i>	<i>OUT</i>	<i>IN</i>
²²⁸ Ac sand (all lines)	<i>IN</i>	<i>IN</i>	<i>IN</i>	<i>OUT</i>	<i>OUT</i>	<i>IN</i>	<i>OUT</i>	<i>IN</i>	<i>IN</i>	—	<i>OUT</i>	<i>OUT</i>	<i>OUT</i>
²²⁸ Th phosphate (all lines)	<i>OUT</i>	<i>IN</i>	<i>IN</i>	<i>IN</i>	<i>IN</i>	<i>OUT</i>	<i>OUT</i>	<i>IN</i>	<i>IN</i>	<i>OUT</i>	<i>IN</i>	<i>IN</i>	<i>OUT</i>
²²⁸ Th sand (all lines)	<i>OUT</i>	<i>IN</i>	<i>IN</i>	<i>IN</i>	<i>OUT</i>	<i>IN</i>	<i>OUT</i>	<i>IN</i>	<i>IN</i>	<i>IN</i>	<i>IN</i>	<i>IN</i>	<i>OUT</i>
⁴⁰ K phosphate (1,460.75 keV line)	<i>IN</i>	<i>OUT</i>	<i>IN</i>	<i>OUT</i>	<i>OUT</i>	<i>IN</i>	<i>OUT</i>	<i>IN</i>	<i>OUT</i>	<i>IN</i>	<i>OUT</i>	<i>IN</i>	<i>IN</i>
⁴⁰ K sand (1,460.75 keV line)	<i>IN</i>	<i>OUT</i>	<i>OUT</i>	<i>IN</i>	<i>IN</i>	<i>IN</i>	<i>OUT</i>	<i>IN</i>	<i>OUT</i>	<i>OUT</i>	<i>IN</i>	<i>OUT</i>	<i>IN</i>

As a summary of this objective, it is on this point — the characterization of materials from the measurement of their most important parameters — that we have concentrated most of our efforts. It has become quite clear that, while we are in a good position for the evaluation of all of them, inter-comparisons are necessary to refine the techniques used: they must be included in the research programs in this field.

3°) Evaluation, in a test structure, of the contribution of granite — the main building material employed in an area of Spain identified as having a high indoor radon level — to the total indoor radon measured in houses, and study of the conditions under which permeability of concrete and granite may be responsible for the presence of high radon levels in houses.—

For the laboratory evaluation of the contribution of granite to indoor radon, we have designed a test structure shown in Figure 3. It consists of a platform on which we can build small "houses" made up of concrete, granite, or any other material. It will allow us, by means of its lower chamber, to simulate the presence or not of a source of radon gas to the platform. By continuous monitoring of parameters such as radon levels, differences in temperature and pressure, and the possibility to change them at will, we have studied the contribution of building materials to indoor radon by diffusion and convection mechanisms.

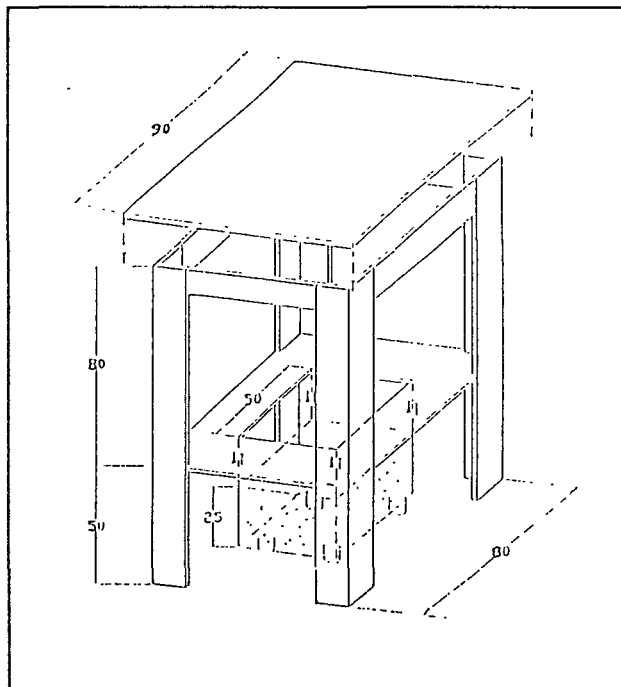


Figure 3 — The test "house": effective volume 1.875 m^3 , volume of chamber with radon source 0.040 m^3 , and effective exhalation area 1.5 m^2 .

QUINDOS

For different granite and concrete samples, commonly used as building materials in some regions of the country, the exhalation rate has been measured from the equilibrium radon concentration inside the house. Values in the range from $0.01 \text{ mBq}\cdot\text{m}^{-2}\cdot\text{s}^{-1}$ to $5.6 \text{ mBq}\cdot\text{m}^{-2}\cdot\text{s}^{-1}$ were measured, the lower values corresponding to the concrete samples which produce a low contribution of this material to indoor radon. Nevertheless, from the higher value — corresponding to a granite sample — we can now evaluate that the building material contribution to the total indoor radon in a typical Spanish house made of granite is $40 \text{ Bq}\cdot\text{m}^{-3}$ for a ventilation rate of 1 h^{-1} , or $400 \text{ Bq}\cdot\text{m}^{-3}$ for a ventilation rate reduced to 0.1 h^{-1} (with, in both cases, a S/V ratio of 2 m^{-1} for the house).

Of course, when we take into account the soil source placed under the test house, the radon levels are increased, thus reaching higher concentrations as a function of higher differential pressure. This effect was studied globally, because the contribution of soil as a source of indoor radon was outside the objectives of this Project. Then, by using the test structure, it is possible to simulate in the laboratory any condition in order to know the contribution of any building material. However, by using the test structure, we have checked so far the comparatively weak incidence of the convective radon transport through the concrete and granite samples. This is, in fact, related to the low values measured for the permeability of both materials.

4°) Laboratory study of the efficiency of some caulking compounds and mitigation techniques in the reduction of radon levels in homes.—

There are different types of protective and preventive techniques to reduce indoor radon levels in new and old buildings as well, based mainly on improved ventilation systems. Nevertheless, when the building materials become as important a source of radon, the covering of the walls could be a good method to reduce their contribution to indoor radon. For the study of this effect, mitigation tests have been developed in our Laboratory. Several covering materials were tested, including epoxy, polyurethane and acrylic paints commonly used for the decoration of walls and ceilings.

The set of paints was applied to small test walls ($24\times 24\times 2 \text{ cm}$) and enclosed in an air-tight container ($24\times 24\times 50 \text{ cm}$). Prior to the exhalation measurements, the test walls were conditioned with respect to temperature and relative humidity (20°C , $60\% \text{RH}$) during at least four weeks. The free exhalation rate of each individual test sample was determined before and after application of the radon sealant. After the radon concentration in the container has reached a steady state concentration, a sample of air is taken by using a scintillation cell which is counted three hours later. The retaining action of the sealant is expressed by a reduction factor, R , which is defined as the quotient of the exhalation rate per unit surface of the coated test wall over its original (uncoated) value. Based on the mean variation coefficient of the analytical method, a significant reductive effect is obtained if R is less than 0.85 (Student's t test: p less than 0.01).

For the set of 10 different acrylate dispersion paints, no reduction in the exhalation rate could be demonstrated in any of the investigated sealants. Nevertheless, for the set of 15 different epoxy and polyurethane paints, the reduction was significant. Depending on the

type of coating and the number of layers applied, a reduction factor of about 0.1 can be obtained. An average value of the reduction factor of 0.4 was evaluated for the epoxy paints studied. Moreover, in our study, this value was still higher (0.6) for the same thickness of the polyurethane coatings tested. For these values, for the granite tested with the higher exhalation rate, the use of these paints reduce the contribution of this building material to indoor radon by a factor of two, thus providing a relatively inexpensive method for controlling the radon emissions from walls and floors in existing homes.

However, it should be borne in mind that any cracks that may develop later in the paint will generate leaks that negate a large portion of its sealing effectiveness; in such a way that we are now focussing our research in this field, specially when we take into account the radon coming from the soil.

5°) Development of *in situ* measurements in selected houses to evaluate the relevance and availability of the laboratory measurements described above.—

The availability, for research purposes, of houses built in granite is very scarce. For this reason, few measurements are available for analysis at the present time. The only experience was made in a house located in a granitic area, where the radium content in the soil surrounding the house is on average 100 Bq.kg^{-1} , and the exhalation derived from the measurement of 10 points around the house — by using the accumulation method with an activated charcoal technique — is $140 \text{ Bq.m}^{-2}.\text{h}^{-1}$. The *in situ* measurement of the exhalation rate from the walls, by placing an accumulator in the walls, yielded a value of $20 \text{ Bq.m}^{-2}.\text{h}^{-1}$. From these values, a ratio $S/V = 1.5 \text{ m}^{-1}$ and a ventilation rate of 0.5 h^{-1} measured by using carbon dioxide as a tracer gas, the contribution of granite to indoor radon could be assumed as 60 Bq.m^{-3} . Nevertheless, the average indoor radon during the three-day measurement period was as high as 500 Bq.m^{-3} .

Two more experiences in the same houses had been carried out during different periods of the year, yielding practically the same results, that we can summarize as a mean contribution for the granite to indoor radon of 12%, less than the 30% reported in the literature. This, of course, is related to the important contribution of the soil as the main source of indoor radon in the houses of these areas. It also emphasizes the interest to develop this kind of measurements in buildings which are relatively isolated from the soil, e.g., multi-floor buildings. Efforts in this way are now in progress with the local authorities, in order to find an appropriate building, in an adequate area of the country, available for research.

PUBLICATIONS

Soto, J., Fernández, P.L. and Quindós, L.S., 1992. Geología y niveles de radon in viviendas españolas. *Revis. Española Física*, 6/1: 35-37.

Soto, J., Delgado, M.T., Fernández, P.L., Gómez, J. and Quindós, L.S., 1992. Niveles de radiactividad en balnearios de Galicia. *Revis. Mapfre Medicina*. 3/3: 211-214.

- Soto, J., Fernández, P.L., Gómez, J., Quindós, L.S. and Delgado, M.T., 1992. Radon en el agua en una region de alto nivel de radiacion natural. *Bol. Soc. Española Hidrol. Medica*, VII/2: 85-88.
- Soto, J., Diaz-Caneja, N., Fernández, P.L., Gutierrez, I. and Quindós, L.S., 1992. Potabilidad del agua en una region de alto nivel de radiacion natural. *Revis. Sanidad Higiene Publ.*, 66/3-4: 197-201.
- Quindós, L.S., Fernández, P.L., Ródenas, C. and Soto, J., 1992. Estimate of external gamma exposure outdoors in Spain. *Radiat. Prot. Dosim.*, 45/1-4: 527-529.
- Quindós, L.S., Fernández, P.L. and Soto, J., 1993. Exposure to natural sources of radiation in Spain. *Nucl. Tracks Radiat. Measur.*, 21/2: 295-298.
- Quindós, L.S., Fernández, P.L. and Soto, J., 1993. A technique for the measurement of the exhalation rate of ^{222}Rn from small samples of porous materials. *First International Workshop on Indoor Radon Remedial Actions*, Rimini, Italy, June.
- Quindós, L.S., Fernández, P.L., Soto, J., Ródenas, C. and Gómez, J., 1993. Natural radioactivity of cements and granites in Spain. *Symposium on Radon in Dwellings, Schools and Workplaces*, Liège, Belgium, November.
- Quindós, L.S., Fernández, P.L. and Soto, J., 1993. Dosis de radiacion debidas al radon in España. *Radioproteccion*, 2: 5-10.
- Quindós, L.S., Fernández, P.L., Soto, J., Ródenas, C. and Gómez, J., 1994. Natural radioactivity in Spanish soils. *Health Phys.*, 66/2: 194-200.
- Quindós, L.S., Fernández, P.L. and Soto, J., 1994. A method for the measurement of the emanation factor for ^{222}Rn in small samples of porous materials. *Radiat. Prot. Dosim.*, 56/1-4: 171-173.
- Quindós, L.S., Fernández, P.L. and Soto, J., 1994. Radioactividad natural y radon. *Bol. SEFM*, 3.
- Quindós, L.S., Fernández, P.L., Soto, J., Ródenas, C., Gómez, J. and Arteché, J., 1994. Natural radioactivity of cements and granites in Spain. *Ann. Assoc. Belge Radioprot.*, 19/1: 289-298.
- Soto, J., Fernández, P.L., Quindós, L.S. and Gómez, J., 1995. Radioactivity in Spanish spas. *Sci. Total Environ.*, 162: 187-192.
- Quindós, L.S., Fernández, P.L. and Soto, J., 1995. Study of areas of Spain with high indoor radon. *Radiat. Measur.*, 34/2: 207-210.
- Quindós, L.S., Fernández, P.L., Soto, J., Gómez, J. and Olást, M., 1995. Results of the Second Inter-comparison of gamma spectrometry measurements of radioactivity in soils and building materials. *Ed. Univ. Cantabria*.

Head of Project 5: Dr. P. Kritidis

II. Objectives for the reporting period

The main objectives of Project 5 were as follows:

- 1°) the establishment of methodologies and measuring devices for laboratory and *in situ* determination of the exhalation rate of radon from solid sources. This includes laboratory systems for the determination of the exhalation rate from sample materials of volume up to 1 dm³, and *in situ* systems for nearly non-destructive measurements of the specific radon exhalation rate (in mBq.m⁻².s⁻¹) from building surfaces (floors and walls);
- 2°) the use of the methods developed together with high-resolution gamma spectrometry for a limited survey of the building materials used in the Athens region, in order to characterize these materials as indoor radon sources, and to identify the cases where some specific countermeasures should (and could) be applied;
- 3°) the development of methodology and measuring devices for the determination of the effectiveness of various covering materials (building, decorative) as moderators of radon exhalation;
- 4°) the development of reliable model(s) for estimating the contribution of the building material sources to the indoor radon concentrations. This should provide an experimentally provable relation between the source parameters measured, and the average indoor radon concentrations, under various conditions (e.g., various air exchange rates).

III. Progress achieved including publications

1°) Determination of radon exhalation rates.—

Several laboratory systems for the determination of radon exhalation rates have been constructed and tested with various sampling and measuring parameters (volume of the sampling chamber, sampling and measuring duration). The results have been compared with theoretical relations derived for each case by the use of analytical expressions for the radon build-up in the system, and Monte-Carlo calculations for the counting efficiency of the measuring chamber (cylindrical Lucas cell chamber), where the different decay of radon and its progeny in the chamber has been taken into account.

The influence of reverse entry of radon into the sample was evaluated by comparison of the time dependance of the signals from the thin radon standard (with negligible reverse entry) and those from the material measured.

KRITIDIS

Two variants of sampling chambers, with volumes of 1.2 l and 5.3 l, have been tested more extensively. In each case, two sampling/measuring schemes have been applied. In the first scheme, the accumulation time is relatively short, the air is circulating continuously, and the counting is continuous as well. In the second, the accumulation period is longer and, consequently, both circulation and counting follow time intervals. The low limits of detection (3σ of the background) of some variants of these methods are given in Table I.

TABLE I
Parameters of the methods for the determination of the radon exhalation rate

Accumulation		Circulation		Counting		LLD (Bq.h ⁻¹)
<i>volume</i> (l)	<i>duration</i> (h)	<i>from</i> (h:min)	<i>to</i> (h:min)	<i>from</i> (h)	<i>to</i> (h)	
1.2	20	20:00	20:10	23	24	2×10^{-3}
1.2	70	70:00	70:10	73	74	9×10^{-4}
1.2	8	00:00	08:00	0	8	5×10^{-3}
5.3	20	20:00	20:10	23	24	1.2×10^{-2}

It is clear that the method relying on the smaller sampling volume leads to a lower detection limit, but is potentially more affected by the reverse entry process. According to our comparisons between theoretical results and experimental data, the short time continuous accumulation/counting variant (No. 3 in the Table above) provides a good compromise between LLD and accuracy (lower impact of the reverse entry process).

Details of the methods have been published and presented in a number of National and International Conferences.

2°) Survey of building materials used in the wider Athens region.—

Survey of bricks and concretes used in the wider Athens region (Attiki, where nearly 40% of the Greek population live) have been accomplished. The measurements include the determination of:

- specific activity of natural radionuclides (Bq.kg⁻¹);
- radium-equivalent specific activity (Bq.kg⁻¹);
- specific exhalation rate of ²²²Rn (Bq.kg⁻¹.h⁻¹);
- radon emanation coefficient (%).

The results of the surveys have been published, and also presented in a number of National and International Conferences (Ref. 3 to 6). Tables II to IV display the summarized results, compared with those from different Greek regions, as reported by our Group and other Greek laboratories.

It can be noted that the Athens region concretes are characterized by lower ^{226}Ra and ^{232}Th , as compared with the concretes from other regions of the country. The average emanation coefficient of radon in Athens concretes falls well within the range of values reported for other countries.

TABLE II
Natural radionuclides content and exhalation rate of ^{222}Rn in bricks from Attiki and other regions of Greece

		Specific activities (Bq.kg ⁻¹)			Specific exhalation rate (Bq.kg ⁻¹ .h ⁻¹)	Emanation coefficient (%)
		^{226}Ra	^{232}Th	^{40}K	^{222}Rn	^{222}Rn
This study	<i>range</i>	25—83	35—65	540—1,060	0.0013—0.035	0.5—12.4
	<i>average</i>	36	51	730	0.008	2.8
	<i>s.d.</i>	12	8.9	160	0.009	3.2
Epirus	<i>range</i>	48—93	41—42	550—860		
	<i>average</i>					
	<i>s.d.</i>					
Thessaloniki	<i>range</i>	31—80	19—32	580—970		

TABLE III
Natural radionuclides content and exhalation rate of ^{222}Rn in concretes from Attiki and other regions of Greece

		Specific activities (Bq.kg ⁻¹)			Specific exhalation rate (Bq.kg ⁻¹ .h ⁻¹)	Emanation coefficient (%)
		^{226}Ra	^{232}Th	^{40}K	^{222}Rn	^{222}Rn
This study	<i>range</i>	7—41	1.2—4.7	57—96	0.004—0.024	5—25
	<i>average</i>	14	3.2	70	0.012	13
	<i>s.d.</i>	7.7	0.8	10	0.004	4.6
Epirus	<i>range</i>	22—85	3—6	23—96		
	<i>average</i>	39	4	37		
	<i>s.d.</i>	17	1	20		
Thessaloniki	<i>range</i>	23—72	4—11	153—330		

TABLE IV
Radium-equivalent specific activity of the Attiki building material

	Radium-equivalent specific activity (Bq.kg ⁻¹)	
	brick	concrete
<i>range</i>	127—254	15—53
<i>average</i>	166	24
<i>s.d.</i>	31	9

3°) Methodology and measuring devices for the determination of the effectiveness of various covering materials as moderators of radon exhalation.—

A measuring device using a large emanation chamber (20 l) has been developed, calibrated and currently used for the determination of the exhalation rate of radon from brick and concrete samples (15×20×30 cm), without cover and covered with various layers of painting materials. The first results have been reported in 1995. The basic part of the work will exceed the duration of the current Project.

4°) Development of models for estimating the contribution of building materials as a source of indoor radon.—

A theoretical model for calculation of the specific radon exhalation from a wall made of a material with known radon specific exhalation rate and emanation coefficient is under development. Some preliminary results have been already reported in 1995, but basic part of the work will exceed the duration of this Project.

PUBLICATIONS

Savidou, A., Raptis, C. and Kritidis, P., 1993. A study of Greek building materials as indoor radon sources. *Proc., 4th Panhellenic Symposium on Nuclear Physics*, Ioannina, 1-2 October: 180.

Kritidis, P., Savidou, A. and Raptis, C., 1993. The indoor radon problem. *Proc., 3th National Congress of Environmental Science and Technology*, Molyvos, 6-9 September: 419.

Savidou, A., Raptis, C. and Kritidis, P., 1995. A study of the radiological state of Greek building materials and a related risk assessment. *Proc., 6th Panhellenic Symposium on Nuclear Physics*, TEI of Piraeus, 16-27 May.

KRITIDIS

- Savidou, A., Raptis, C. and Kritidis, P., 1995. The Attiki building materials as sources of natural ionizing radiations. *Proc., 4th National Congress of Environmental Science and Technology*, Molyvos, 4-7 September: 557.
- Raptis, C., Savidou, A. and Kritidis, P., 1995. A theoretical study of indoor radon concentrations. *Proc., 4th National Congress of Environmental Science and Technology*, Molyvos, 4-7 September: 550.
- Savidou, A., Kritidis, P., Raptis, C. and Michaleas, S., 1995. The effects of typical wall covers on radon exhalation from building materials surface. *8th International Symposium on Environmental Pollution and its Impact on Life in the Mediterranean Region*, Rhodes, 8-12 October.
- Savidou, A., Raptis, C. and Kritidis, P., 1995. Natural radioactivity and radon exhalation from building materials used in Attica region, Greece. *Radiat. Prot. Dosim.*, 59: 309-312.
- Savidou, A., Raptis, C. and Kritidis, P., *in press*. A study of natural radionuclides and radon emanation in bricks used in the Attica region, Greece. *J. Environ. Radioact.*

KRITIDIS

Head of project 6 : Prof.Proukakis

II. Objectives for the whole project period.

The main objective of this project is the *"Investigation on the Existence of a Relation between ^{226}Ra Content of Building Materials and Radon Exhalation Rates"*. The principal steps to be undertaken for this investigation have been identified as it follows:

- Radon exhalation rate measurements of prototype structural modules (concrete slabs, brick and cement-brick walls) frequently used in greek dwellings by α -spectroscopy.
- ^{226}Ra content measurements of specimens of the building materials to be used to construct the above modules, using γ -spectroscopy.
- Investigation about the existence of a correlation between the radioactivity of these modules, due to their ^{226}Ra content, and the ^{222}Rn exhalation rate.
- Parametric study of the above correlation at various discrete steps, during the construction of the modules to be examined.
- Study of the effect of various types of paints and ceramic wall tiles on the mitigation of the exhalation rate of structural modules.
- Study of the effect of the aging of the structural modules on the exhalation rate.

All these steps were undertaken and relevant research was successfully conducted, with the exception of the last one. In this latter case it was almost impossible to proceed due to the extremely short time elapsed since the preparation of the specimens.

III. Progress achieved including publications.

The project was started on May 1993 and the following activities and results may be reported:

- Sampling of building materials (cement, bricks, sand, gravel, marble powder, lime, gypsum and pumice stone) produced by industries located at various sites of the country.
- Pulverisation of the samples down to less than $90\mu\text{m}$, and preparation of specimens for γ -radioactivity measurements using high-resolution Ge detectors.
- Analysis of the samples appearing in Table 1 for natural radioactivity (^{226}Ra , ^{232}Th & ^{40}K).
- Design and manufacturing of a $1200\times 1200\times 700$ mm ($\sim 1\text{m}^3$) steel container to conduct the radon exhalation measurements. Fitting of measuring and control instrumentation to this container. Software development for the monitoring and control of the container environmental parameters (temperature, pressure changes, humidity, aerosol concentration).
- Alpha spectrographic set-up calibration for radon daughter analysis using a PIPS solid state detector and on-line software tools.
- Gamma spectrographic set-up calibration for radon daughter analysis.
- Radon exhalation measurements of raw materials (cement, bricks) and structural modules (concrete slab, brick wall).
- Radon exhalation measurements of structural modules after being conditioned with plaster and painted with epoxy resins.

A detailed presentation of the progress achieved can be summarised as it follows:

NATURAL RADIOACTIVITY CONTENT

Sampling and Experimental Procedure

Specimens of cement originating from the three main greek cement industries, clay bricks fabricated by five big furnaces, which use raw material mined at five different sites around the country, and also other materials of -presumably- minor radiological importance, were collected for the purpose of this investigation. The specimens -if necessary- were dried under ambient temperature and pulverised to less than 90 μm . Finally, their water content was determined. Each one of the specimens was then used to fill two plastic 0.282 lt plastic cylindrical boxes, about 72 mm in diameter and 70 mm high. The boxes were hermetically sealed and covered with a film of epoxy resin to limit - as far as possible - escape of radon. Thus, in each case duplicate specimens were further analysed.

The concentrations of ^{226}Ra , ^{232}Th and ^{40}K in the specimens were determined by high-resolution γ -spectroscopy. Detailed information concerning both the hardware and software configuration of the γ -spectroscopy set-ups used can be found in Simopoulos and Angelopoulos (1987). In order to allow for equilibrium of ^{226}Ra and ^{232}Th with their decay products, all specimens were analysed at least three weeks after the boxes were sealed. The counting times were about 1.5×10^5 s.

The ^{226}Ra concentrations have been derived from the weighted mean of the activities of two photopeaks of ^{214}Pb (295.2, 352.0 keV) and of three photopeaks of ^{214}Bi (609.3, 1120.3, 1764.5 keV). In the case of ^{232}Th , two photopeaks of ^{228}Ac (338.4, 911.1 keV) and the photopeaks of ^{212}Pb (238.6 keV) and ^{208}Tl (583.1 keV) were used in the same way. Finally, the concentration of ^{40}K was obtained from the single photopeak of this isotope at 1460.8 keV.

Results

Table 1 summarizes the range (min-max) of the ^{226}Ra , ^{232}Th and ^{40}K concentrations in the building materials analysed. The total uncertainty associated with these results, calculated from the systematic and random error of the measurements, ranges within 5-10% of the reported values.

Table 1 : Specific activity (Bq/kg) of natural radionuclides in greek building materials

Material	Sample size	Range (Min - Max)			^{226}Ra Worldwide range (Min-Max)
		^{226}Ra	^{232}Th	^{40}K	
Cement	52	29 - 147	13 - 30	172 - 331	6 - 196
White cement	10	14 - 26	7 - 13	5 - 67	
Clay bricks	5	28 - 48	37 - 56	727 - 895	4 - 200
Sea sand	6	7 - 13	8 - 16	145 - 302	
Sand	9	1 - 4	- 3	1 - 37	1 - 113
Marble powder	8			- 25	
Mosaic	7	1 - 3	1 - 3	- 23	15 - 55
Gypsum	6	6 - 17	- 10	5 - 40	4 - 330
Pumice stone	4	50 - 874	54 - 60	1048 - 1160	
Quicklime	2	9 - 32			8 - 20
Perlite	1	46	56	1048	
Wall tiles	1	58	46	409	63 - 91

The same Table 1 summarizes worldwide data compiled from Eichholz *et al.* (1980), Keller (1979), Porstendoerfer (1993), Sciocchetti *et al.* (1983), Strandén E. (1988) and UNSCEAR(1982). It is apparent, from this Table, that the natural radioactivity content of the various greek building materials examined is very low. Only a few specimens of cement and clay bricks present a rather high ^{226}Ra concentration up to 147 and 48 Bq/kg respectively. However, these values are well within the range of similar materials used in other countries.

RADON EXHALATION MEASUREMENTS

Exhalation Container

The exhalation rate of the building materials with relatively high radium content appearing in Table 1 was assessed using a specially designed steel clad 1m^3 air-tight container as introduced by Jonassen and MacLaughlin (1980); the volume of the sample material, which could also be a structural module such as a test wall or slab, should not exceed 10% of the total volume of the container, following the suggestions by Poffijn *et al.* (1984) and Samuelsson (1987). The following important environmental parameters, which affect an exhalation experiment, are monitored in the container through analogue-to-digital converters interfaced to the bus of a PC: pressure changes, using a ± 50 mbar differential pressure transducer, temperature and relative humidity. An aerosol generating system is also used to produce particles.

Three methods are employed for determining the radon concentration in the container environment. Two of these methods are based on grab sampling of a small portion (15-20%) of the container gas through filters. The filters are then analysed using:

- α -spectroscopic analysis of the radon daughters ^{218}Po and ^{214}Po using a PIPS detector set-up.
- γ -spectroscopic analysis of the radon daughters ^{214}Pb and ^{214}Bi using a Ge detector set-up as introduced by Simopoulos and Angelopoulos (1990).

A third method, introduced by Simopoulos and Angelopoulos (1990), was applied in order

to conduct *in-situ* radon progeny measurements inside the container, using an ^{241}Am doped 2x2" NaJ detector, which records the area under the 609 keV photopeak of ^{214}Bi .

For the calibration of the container a Pylon 2000A - NIST cross-certified source of a nominal ^{226}Ra activity of 102.8 kBq was used. According to the systematic results already obtained in an aerosol free environment, within the range of radon concentration 0.1-30 kBqm⁻³, temperature 19-21 °C and relative humidity 30-40%, the efficiency of the facility, in terms of the fraction of radon progeny collected on the filter, is determined to 0.10 with an rms error about 15%. Furthermore, preliminary results show that the efficiency is increased by up to 4 times in the case of an aerosol saturated environment.

Exhalation Rate Results

A least squares fitting to the radon growth curve data of the examined materials was used to calculate their radon exhalation rate (Figure 1); for this purpose each one of the specimens was enclosed in the container for a period of about 20 days. The estimated effective decay constants (Stranden, 1988) did not significantly differ from the decay constant of ^{222}Rn ; the total uncertainty associated with these calculations was about 25%. According to the results obtained the cement specimens with ^{226}Ra concentrations in the range 100-140 Bq/kg present exhalation rates between 15-20 $\mu\text{Bqkg}^{-1}\text{s}^{-1}$. Pulverised to less than 90 μm brick specimens with ^{226}Ra concentrations in the range of Table 1 present exhalation rates between 3-10 $\mu\text{Bqkg}^{-1}\text{s}^{-1}$.

Furthermore, two typical greek structural modules, a clay brick wall and a concrete slab (both 10 cm thick), of an exhaling area of 1m², constructed from raw materials in Table 1 with the highest ^{226}Ra concentrations, were also tested. The exhalation rate of the wall, with calculated value of ^{226}Ra content equal to 40 Bq/kg, was 2 mBqm⁻²s⁻¹ while that of the slab with ^{226}Ra content equal to 26 Bq/kg, was 3 mBqm⁻²s⁻¹. The total weight of the brick wall was 64 kg and that of the concrete slab was 140 kg.

The above values did not statistically significantly change when the specimens were covered with a 2 cm thick cement aggregate plaster (^{226}Ra content of this aggregate: ~23 Bq/kg). The plastering added approximately 35 kg to the weight of the specimens. The exhalation rate of these plastered specimens was further experimentally measured after painting them with an emulsion paint. Again, no significant change was observed. However, when the plastered slab was painted with an epoxy resin (Sikkens Metakote colourless varnish), its exhalation rate was reduced by 3 times.

CONCLUSIONS

Despite the relatively high ^{226}Ra concentrations of Greek cements (29-147 Bq/kg) and bricks (28-48 Bq/kg) the radon exhalation rates of concrete slab and brick wall specimens using the above materials is very reasonable (2-3 mBqm⁻²s⁻¹). The above exhalation rates are not affected by plaster or emulsion paints; however, they are reduced by three times if the specimens are painted with an epoxy resin. Despite an obvious increasing trend, no correlation between the ^{226}Ra concentration and the radon exhalation rate can be justified from the results obtained. A final conclusion drawn from the above results is that a typical Greek room (4x4x3.5m) constructed using materials with the above exhalation rates, and an air-exchange rate of 0.5h⁻¹ the maximum radon concentration is assessed equal to 34 Bqm⁻³

(Stranden, 1988), which is much lower than the 150 Bq m^{-3} recommended action level.

REFERENCES

- Eichholz, G.G., F.J. Clarke and B. Kahn (1980). In: *Natural Radiation Environment III* (T.F. Gessel and W.M. Lawder, eds.), Vol. II, pp. 1331-1336. U.S.DOE Symposium Series 51, Springfield VA.
- Jonassen, N. and J.P. MacLaughlin (1980). In: *Natural Radiation Environment III* (T.F. Gessel and W.M. Lawder, eds.), Vol. II, pp. 1211-1224. U.S.DOE Symposium Series 51, Springfield VA.
- Keller, G. (1979). In: *Seminar on the Radiological Burden of Man from Natural Radioactivity in the Countries of the European Communities*, pp. 193-208. CEC, Paris.
- Poffijn, A., R. Bourgoignie, R. Marijns, J. Uyttenhove, A. Jansens and R. Jacobs (1984). Laboratory Measurements of Radon Exhalation and Diffusion. *Radiation Protection Dosimetry*, 7, 77-79.
- Porstendoerfer, J. (1993). In: *Fifth International Symposium on the Natural Radiation Environment. Report EUR14441 EN*, pp. 69-150. DG XIII, CEC, Luxembourg.
- Samuelsson, C. (1987). A Critical Assessment of Radon-222 Exhalation Measurements Using the Closed-Can Method. *ACS Symposium series*, 331, 203-218.
- Sciocchetti, G., F. Scacco, P.G. Baldassini, L. Monte and R. Sarao (1983). Indoor Measurements of Airborne Natural Radioactivity in Italy. *Radiation Protection Dosimetry*, 7(1-4), 347-351.
- Simopoulos, S.E. and M.G. Angelopoulos (1987). Natural Radioactivity Releases from Lignite Power Plants in Greece. *J. Environ. Radioactivity*, 5, 379-389.
- Simopoulos, S.E. and M.G. Angelopoulos (1990). Spectroscopic Determination of the ^{222}Rn and ^{220}Rn Content of Air. In: *First Panhellenic Conference on Radiation Protection*, pp. 89-90, Athens.
- Stranden, E. (1988). In: *Radon and its Decay Products in Indoor Air* (W.W. Nazaroff and A.V. Nero Jr. eds.), Chap. 3, pp. 113-130. J.Wiley & Sons Inc., New York.
- UNSCEAR, United Nations Scientific Committee on the Effects of Atomic Radiation (1982). In: *Ionizing Radiation: Sources and Biological Effects*, Annex C, pp. 107-140, UN, New York.

Publications.

Katsanevakis S., N.P. Petropoulos, E.P. Hinis, S.E. Simopoulos, A. Louiz and C. Proukakis (1995). Natural Radioactivity Content of Greek Cigarettes and the effect of their Smoke to the Indoor Air Radon Daughters Concentration. In: *Natural Radiation Environment VI, International Symposium*, Montreal (accepted for presentation).

Louizi, A., C. Proukakis, N.P. Petropoulos, S.E. Simopoulos and D.J. Leonidou (1994). Mini Radon House: A Prototype Container for the Measurement of Radon Exhalation from Building Materials and Structural Modules. In: *1st Mediterranean Congress on Radiation Protection*, Athens.

Louizi, A., C. Proukakis, N.P. Petropoulos, M.J. Anagnostakis, S.E. Simopoulos and M.G. Angelopoulos (1994). Measurements of Natural Radioactivity in Greek Building Materials. In: *1st Mediterranean Congress on Radiation Protection*, Athens.

Louizi, A., C. Proukakis, N.P. Petropoulos and S.E. Simopoulos (1995). Natural Radioactivity Content and Radon Exhalation Rates of Greek Building Materials. In: *Indoor Air, An Integrated Approach, International Workshop*, pp. 131-134, Brisbane.

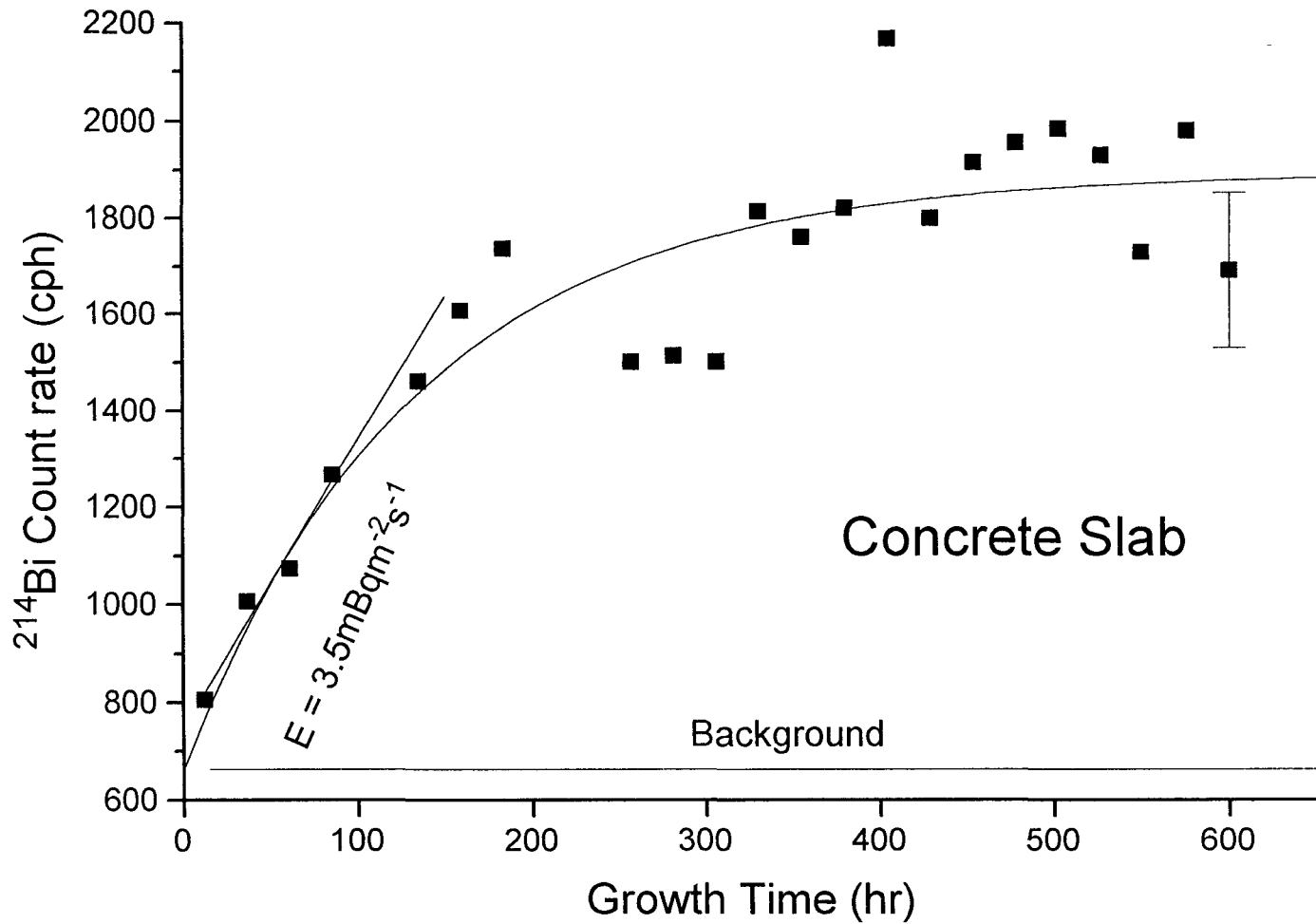
Louizi, A., C. Proukakis, N.P. Petropoulos, E.P. Hinis and S.E. Simopoulos (1994). Radon Exhalation Rates of Greek Building Materials and Structures. In: *IAEA International Conference on "Radiation and Society: Comprehending Radiation Risks"*, Paris (to be published in the proceedings of the conference).

Simopoulos, S.E., E.P. Hinis, M.J. Anagnostakis, N.P. Petropoulos, A. Louizi and C. Proukakis (1995). Radon Exhalation Rates from Greek Fly Ash and Cement. In: *Natural Radioactivity in Human Environment, Scientific Meeting*, Centre for Solid Fuels Technology and Applications, Kozani, Greece (in press).

Participation in the following intercomparison/intercalibration exercises:

1. Intercomparison of gamma spectrometry measurements of natural radioactivity in soils. CEC-RPP - Luis S.Quindos Poncela University of Cantabria.
2. NPL, Environmental Radioactivity Intercomparison 1993, NPL Report RSA (Ext)49, April 1994.
3. NPL, 2nd Euromet Intercomparison of ^{222}Rn Measurement Systems, 1994.

Figure 1



Final Report 1992 - 1995

Contract: F13P-CT920064d Duration: 1.7.92 to 30.6.95 Sector: C12

Title: Radon sources models and countemeasures.

1)	Miles	NRPB
2)	De Meijer	Univ. Groningen
3)	Andersen	Lab. Risø
4)	Wouters	CSTC/WTCB (BBRI)
5)	Ball	NERC
6)	De Meijer	Univ. Groningen
7)	Hubbard	SSI
8)	Balek	BIJO
9)	Cosma	NPL.RO

I. Summary of Project Global Objectives and Achievements

Global objectives

The objective of the project is to enable people to avoid excessive exposure to radon decay products by improving the understanding of the sources of radon, how it moves through the ground and materials and into buildings, and the measures to counteract ingress. This has been achieved by developing techniques to map the probability of high radon levels occurring indoors, by the use of models and experiments on the movement of radon in the ground, building materials, sub-floor spaces and buildings, and by developing and testing preventive and remedial measures.

Global achievements

Techniques for mapping radon-prone areas

NRPB, NERC and NPL.RO have studied this subject. NERC chose field study areas to combine a high density of house measurements with geological features typical of Europe. The main controls on radon generation from bedrock were found to be permeability, uranium content and mineralogy. The major rock types giving rise to problems in houses were granites (high uranium content and fracture permeability), limestones (high permeability and dispersed uranium), sandstones (fracture and granular permeability) and shales (if the uranium content is high).

NERC and NRPB collaborated on a new technique for analysing the data. NRPB data on radon levels in houses were passed to NERC and grouped by geological unit. This showed, for example, that one geological formation produced high levels of radon with about 24% of the houses exceeding 200 Bq m⁻³ in one area, but only about 8% on the same formation in an adjacent area. Superficial deposits can also have large effects on the radon in houses, changing the proportion of houses affected by up to a factor of 15. Taking these factors into account, lognormal modelling of house data grouped by geological unit was able to provide radon potential maps which are more detailed than grid square maps and more accurate in estimating numbers of homes affected than mapping based only on geology.

NRPB examined house radon data grouped by 5 km grid squares. The data showed that lognormal modelling of the distribution of radon levels could accurately estimate the fraction of homes above a radon threshold even where data was sparse. A new weighted smoothing technique was developed to provide improved estimates of GM in squares with few results.

For mapping using house radon data, it was shown that it is essential that the measurements be carried out using an appropriate selection of homes, location of detectors, duration of measurements, and accuracy of results over a wide range of concentrations. Results need to be corrected to take account of outdoor radon levels, bias in selection of homes, and season of measurement. This data can then be used with lognormal modelling to produce accurate maps by grouping data either by grid square or by geological unit.

NPLRO carried out radon flux measurements with a view to trace out possible high radon areas in Romania. The method used is the adsorption of radon on active charcoal. In the Cerna Valley the daytime flux values are a little higher than the night values and fall into the 17-240 mBq/m².s range, the higher values being in the proximity of some faults in the sedimentary rocks which cover the granite and the geothermal deposit of this zone. The re-measurement of the radon flux in Cluj-Napoca city in February and May 1995 confirmed the values determined previously.

High indoor radon values were found for Baita Plai (646 Bq m⁻³), Baita Sat (325 Bq m⁻³) in the mining region of Stei and relatively high values were also found for the town of Oradea (115 Bq m⁻³) and smaller values for Cluj-Napoca city (76 Bq m⁻³). These values represent the arithmetic mean of 30- 35 dwellings, in each dwelling being measured twice a year in the cold and warm season in bedrooms, living-rooms and kitchens using the Kusnetz method. Etched track measurements in Cluj-Napoca and Herculane Spa gave results in the range 100-200 Bq m⁻³.

Movement of radon in the ground, into buildings and within buildings

KVI, CSTC/WTCB (BBRI), Risø and SSI contributed in this area of work. KVI used a laboratory facility that consists of a cylindrical vessel (height and diameter 2 m) with measuring probes that allow measurement of pore-water content, air permeability of the soil and radon concentrations at various depths. This was used to study both diffusive and advective radon transport in situations simulating crawl spaces of different heights, with and without forced ventilation and with and without a ground water level in the sand.

Starting from well known initial conditions the complexity of the situation was increased step by step. After each step a series of measurements is carried out and the results are compared with calculations. It was observed that a sharp rise in emanation factor occurred as the pore moisture content was increased to only 2.5%. For higher moisture contents, the emanation factor decreases slightly and increases again for moisture contents higher than 15%.

The data obtained with dry sand were compared with results of calculations using one set of input parameters. Results of experiments with diffusive transport only or with depressurisation of the perforated box were compared with one-dimensional analytical model calculations, whereas results of experiments with time-varying pressurisation of the perforated box were compared with two-dimensional numerical model calculations. Both analytical and numerical analysis showed good agreement with experimental results, showing a maximum deviation between model and experiment of less than 10%. KVI conclude that the radon transport models have been validated for dry sand.

Risø used a simple 2.6 m x 2.6 m test structure located on a clayey-till field site to evaluate how well numerical modelling and soil characterization techniques describe radon transport through soils and entry into houses under field conditions. Over a three-year period, radon concentrations have been measured in more than 40 probes located in the ground under and around the structure. The numerical model tested in this work is an implementation of a set of physical equations generally considered to govern soil-gas and radon transport. The key elements are the Darcy-flow approximation of soil-gas transport plus combined diffusion and advection of radon. The main assumption concerns the application of the homogeneous-soil approximation - i.e. the approximation that field soil can be simulated as a homogeneous porous medium having certain effective parameters.

The results of the study demonstrate that under field conditions model estimates of soil-gas entry rates may be off by as much as one order of magnitude. Since the uncertainties of the modelling (e.g. the geometrical description of the structure and the mathematical accuracy of the model) and the experimental results are relatively small, the cause of the discrepancy seems to be that the measured permeability is different from the value that actually controls soil-gas entry into the structure. This could be due to cracks and fractures in the soil dominating the flow of soil gas here, as opposed to the dry sand described earlier or the SSI house on permeable ground described below.

In collaboration with the KVI and SSI, Risø compared modelling results with data from real houses of the crawl-space type. In the case of the KVI house, the model was used to identify advective entry into the crawl space and to assess the mitigative impact of sealing the crawl space with polyethylene foil in combination with pressurizing or depressurizing the crawl space. The investigation of the SSI house had two objectives: to provide additional verification of the numerical model, and to help deduce the relative importance of diffusive and advective entry of radon.

In collaboration with SSI, BBRI developed a simplified model to simulate radon infiltration from the subfloor of the SSI test house. The results were compared with measurements performed by SSI. The model yielded a source strength in good agreement with the measured value. It was concluded that the use of a finite difference code which had already proved to be well suited for the design and the evaluation of soil depressurisation remedial actions was also able to estimate the gas flow rate from the soil into a crawlspace under natural ventilation conditions.

SSI concentrated its research effort on the detailed understanding of radon dynamics in one occupied house. This house and the underlying ground have been monitored in detail during the project, resulting in a large time series data set. This study has resulted in: 1) showing that measurements made over a short time span can be used to characterise the behaviour of a house over a longer time period, enabling more efficient design of mitigation systems and better predictions of the yearly average radon indoors, and 2) new understanding on the variation of radon in soil with time and the dependence of radon on the dynamics of nearby buildings and weather parameters.

Statistical analysis of the large data set has shown that outdoor temperature is the strongest indicator of the indoor radon in this house. It was decided to investigate whether the temperature can be used to estimate longer term behaviour of the indoor radon. Regression was performed between radon indoors and outdoor temperature obtained from a local weather station after testing and eliminating other parameters. The regression fit was used to predict the radon variation and average values over 2 years, excluding the summer data. This data agrees within 10% with the measured averaged radon concentration.

Knowledge of variation in soil gas radon is needed to interpret soil gas measurements made at one time. Strong correlations of soil radon with barometric pressure and outdoor temperature occur at the research house site. The maximum soil gas concentrations occur during the summer months and the minimum occur during the winter, with the summer and winter levels differing by a factor of between two and three, depending on location. Changes in the 24-hour averaged indoor radon concentration correlate well with the changes in the soil radon. This procedure could be generalised to find a protocol for determining the dominant parameters governing radon entry for suitable houses to assist in designing effective mitigation systems.

The indoor radon is also well correlated with the soil gas radon concentration. These observations are consistent with the following scenario. The natural-draught ventilation system of the house causes pressure differences between the house and the soil which increase with increasing temperature difference between the indoors and the outdoors. This increases airflows into the house from both the outdoor air and the soil gas air, ventilating the permeable soil and decreasing soil radon in the winter. The simple yet useful result of these observations is that in this soil and in this house, temperature alone can be used as an indicator of the radon concentration.

Production and transport of radon in building materials

KVI and Bijo contributed in this area. In its second project, KVI studied production and transport of radon in building materials. A set-up was constructed that consists of a stainless steel box closed off with a sealed lid. Inside the box a concrete sample was placed on a steel inner rim, dividing the set-up into two compartments: in the lower compartment a radon source may be placed, the upper compartment is used to detect the transported radon. The sample itself is sealed by treating the side surfaces with an epoxy. The sample is sealed to the inner walls of the set-up by the use of an inflatable tube inside a U-profile. For radon concentration measurements two Lucas cell monitors are used.

In all experiments without a radon source, the equilibrium concentration in both compartments was approximately equal. It was realized that this result could only be explained if the flow did not take place through the sample but along the sample. It was found that the sample is at least a factor 1000 less permeable than ordered. Due to this, leakage due to imperfect sealing became magnified in importance. Furthermore it was found that analysis could be strongly improved if the ventilation rates of the upper and lower compartment are experimentally known. An additional difficulty is the fact that the ingrowth of radon may lead to so-called "back-diffusion", so that one does not measure the free-production rate any more.

It was decided to redesign the set-up, based on the first set-up but with all flow rates controlled and measured and the humidity around the sample controlled. A constant pressure difference is obtained by applying controlled nitrogen flows through the two compartments using flow controllers. Radon release rates are measured by leading the nitrogen flow to a radon trap consisting of a vial filled with cooled activated charcoal.

The results of radon exhalation measurements show that the method gives reproducible results even for quite different adsorption times. Measurements of the emanation rate from the original concrete sample correspond well with the value obtained with the first design of the instrument. However, effects were observed that imply that a very small change in absolute pressure (0.3%) can considerably influence the measured exhalation rate (in our case 7%). It is concluded that radon transparency measurements are far from trivial and may be extremely sensitive to small leaks and other effects. With the improved instrument radon exhalation rates as low as $0.025 \text{ Bq m}^{-2} \text{ h}^{-1}$ can be measured within 10% statistical uncertainty.

Bijo studied the influence of humidity and temperature on radon release from soils, rocks, building materials. A physical model for radon and thoron release from porous materials was designed. In the model, recoil and diffusion mechanisms, dissolution of radium and radon in water present in pores, and adsorption of radon on dry and wet surfaces of porous materials at constant temperature were considered. A new mathematical description of the processes causing the transport of radium and radon and thoron was proposed for the steady state conditions.

The influence of humidity and porosity on radon exhalations was modelled. The results show that the exhalation ED of radon strongly depends on the porosity. At low relative humidity values the dependence of ED on humidity has an increasing trend. However, at higher relative humidity values the character of this dependence is different, exhibiting a maximum, after which the ED values decrease with increasing porosity. This can be explained by the role of the water filled in open pores at the higher humidity values.

The differences in the transport behaviour of radon and thoron are due to the different half-lives of the radon isotopes, as well as to the subsequent recoil processes. Thoron was used to investigate dynamic changes taking place in the solid matrices and porous systems. The results obtained from the thoron measurements can be used for the description of the changes influencing the release of radon from the materials under dynamic conditions.

The measurement of thoron release rate from the sample of bentonite clay was carried out during heating at the rate of 1K/min up to 150°C, then cooling. During cooling, the bentonite clay heated up to 150°C was investigated with air of different humidities. Differences in the curves were observed: higher values of E were measured in the case when humid air was used instead of dry air. The results show that the increase of the thoron release rate E was observed at temperatures lower than 50°C in the case when the sample was overflowed with the humid air. This observation can be explained by the condensation of water in micropores, which lead to the lower indirect recoil effect by stopping the recoiled atoms of radium and thoron in the water condensed.

Remedial measures

CSTC/WTCB (BBRI) and NRPB studied remedial measures. BBRI investigated three dwellings to achieve a better understanding of radon transport and to define the parameters to be measured to allow the choice of appropriate remedial actions. One dwelling had two cellars, with radon levels up to 4,500 Bq/m³ in the occupied rooms and 10,000 Bq/m³ in the cellars. The building is not very airtight and therefore has quite high ventilation rates. The flow of air between cellars and living rooms was evaluated using tracer gases. The analysis shows that both cellars behave as important source rooms. Reducing the radon concentrations to low levels by ventilation would result in huge ventilation rates. Therefore, soil depressurisation technique was finally chosen. A sump was placed in the cellar beneath the living room only. Despite a very weak pressure field extension to other parts of the building, the radon concentration dropped to less than 100 Bq/m³ in the occupied rooms.

In a second building, a subslab natural ventilation system had already been installed but had not reduced the radon concentrations. The pipes already installed were used to install and evaluate the active sub soil depressurisation technique, in spite of difficult conditions: very bad airtightness of the slab, clayey soil, installed suction pipes placed at an unfavourable position. The pressure difference between the soil and the house measured far from the suction pipes indicated that the pressure field extension was weak. In spite of that, the remedial action was a success. This type of remedial action also proved to be very efficient in reducing the radon concentrations in another dwelling. An important conclusion about the soil depressurisation technique may be drawn: in contrast to what is sometimes said, it is not always necessary to create great pressure differences between the soil and the interior of the building at each point.

To investigate remedial measures, NRPB carried out simple radon measurements before and after remediation in a large number of homes which had remedial measures installed. To ensure the collection of high quality data, householders were offered a free measurement of radon provided they completed a questionnaire about the measures installed. The results for 1119 such homes show that a range of techniques is effective in reducing radon levels in homes. The most commonly used remedial action is underfloor depressurisation (sump). This is by far the most effective remedial techniques, causing reductions in radon levels by up to a factor of 100 or more. Disappointing results occur occasionally with all methods, but failures are rarer for sumps than other techniques.

Properties with high radon levels and suspended timber floors were more problematic to remediate than those with concrete floors. Increased natural ventilation of the underfloor void is very weather dependent, relying on wind direction and speed to maintain a rapid turnover of the void air. In general the reduction factors obtained for increased natural ventilation are quite low, but could be significantly increased by the use of a fan.

In order to determine how durable various techniques were, 56 homes with successful remediation were enrolled in a further study in which the radon levels are remeasured every year. It is apparent from the data that effectiveness can be maintained in most cases. Underfloor sumps, as well as being the most effective remedial measure were also very reliable. In the 30 sumps investigated there was either no significant change in radon level or a further decrease.

Head of project 1: J C H Miles

II. Objectives for the reporting period:

The objectives of the project were:

(1) to compile and analyse a large database on the effectiveness of different types of radon remedial measures installed in homes to determine the most appropriate measures for different types of construction and different radon levels. To identify house types for which existing remedial measures are insufficiently effective or reliable and to improve techniques for reducing radon levels for these houses. To study the durability of remedial measures in homes by making annual measurements of radon levels in a sample of homes with remedial measures installed.

(3) to use the large numbers of measurements of radon in UK homes to develop and test techniques for mapping radon-prone areas accurately and economically, by mapping results both by grid square and by geology using lognormal modelling. To test the effectiveness of the techniques in areas where data may be sparse and geology variable.

III. Progress achieved including publications:

Radon remedial measures

Background

Radon remedial measures in houses with high radon levels are an extremely cost-effective way of reducing the radiation exposure of members of the public. Nevertheless, it is important to ensure that when such measures are installed, they are as inexpensive, effective and durable as possible. There have been various detailed studies of remedial measures in individual buildings. In these cases the remedial measures have generally been installed under scientific supervision, and often in houses which have unusual problems. Because of the small numbers of houses and the circumstances under which the measures have been installed, it is not clear how effective such measures would be when installed without supervision in a range of normal houses.

In this project, NRPB has taken a different approach: to carry out simple radon measurements before and after remediation in a large number of homes which had remedial measures installed by commercial firms or by the householder, usually at the expense of the householder. To ensure the collection of high quality data, householders were offered a free post-remediation measurement of radon provided they completed a questionnaire about the measures installed. Analysis of the data collected allows a much better understanding of what measures are appropriate for different building types and radon levels, what measures produce the greatest reduction in radon levels, their reliability and durability.

Data collection and analysis

NRPB has made measurements of radon in 230 000 homes in the UK, using passive radon detectors exposed for three or more months. Of these some 20 000 are above the UK Action Level of 200 Bq m^{-3} , and the householders have been advised to reduce the radon

concentrations. Surveys have suggested that more than 2000 householders have taken the advice and remediated. Approximately 1450 of them have taken part in this study, and have been sent passive detectors to remeasure radon levels in their homes after installing radon remedial measures.

Results from 1119 such homes are available and are shown in Table 1, divided up into bands depending on the radon concentration before remediation. These results are discussed in more detail by Cliff et al (1992, 1994) and by Naismith (1994). The reduction factor in the table is the ratio of seasonally-adjusted radon concentrations before and after remedial action. The arithmetic mean (AM) and the geometric mean (GM) are both given, although the AM can be distorted by very high values, and hence be misleading. The GM is therefore is a better indication of expected reduction.

Table 1: Radon reduction factors for different radon remedial actions in existing homes.

METHOD	ORIGINAL RADON CONCENTRATION											
	200-749 Bq m ³			750-1500 Bq m ³			>1500 Bq M ³					
	N	Reduction factor			N	Reduction factor			N	Reduction factor		
	AM	GM	Max		AM	GM	Max		AM	GM	Max	
Positive ventilation	103	2.8	2.0	25	21	5.8	3.9	24	0	-	-	-
Additional natural ventilation	100	2.5	1.8	25	11	5.6	3.9	17	0	-	-	-
Additional natural ventilation of underfloor void	119	2.6	1.8	23	7	1.7	1.5	3.1	1	-	-	10
Mechanical ventilation of underfloor void	42	6.4	2.9	58	5	1.7	1.5	3.0	2	20	6.0	39
Sealing only	73	2.2	1.5	32	7	1.8	1.7	2.6	3	2.7	2.0	6
Membrane covering floor	23	1.9	1.7	7	2	2.3	2.3	2.4	1	-	-	6
Sump	280	14	7.4	136	87	25	13	163	19	27	14	100
Sump with other method(s)	75	10	3.9	112	18	15	8.0	67	6	11	6.7	26
Combination of methods, no sump	98	2.7	2.0	17	15	4.2	2.8	22	1	-	-	13

The Table shows that a range of techniques is effective in reducing radon levels in homes. The most commonly used remedial action is the underfloor depressurisation (sump) system. The results show that this is by far the most effective of all radon remedial techniques, giving rise to reductions in radon levels by up to a factor of 100. Disappointing results can occur on occasion with all methods, but such occurrences are rarer for sump systems than other techniques.

Because the installation of a sump system is often seen as disruptive by the householder, one major contractor is installing mini-sumps, for which all the installation work is carried out outside the building. An opening is made in the foundation wall below floor level, and a cavity excavated in the hardcore beneath the floor. The extract pipe is taken up the outside wall and the fan installed under the eaves. The measurement results suggest that the mini-sump is less effective than a sump placed more centrally under the floor, but is usually sufficiently effective. Houses with wooden floors can also be successfully remediated using this technique if the underfloor void has a layer of concrete covering the ground.

In general sump systems have fans to reduce pressure under the floor, but in some cases 'passive stack' systems have been installed by householders, in which warm air rising up a pipe is relied on to reduce the pressure. This is sometimes effective, but in general the reduction factors achieved by this technique are low. However, if a passive stack is ineffective, it is relatively easy to fit a fan to it.

Positive ventilation systems, in which a fan blows filtered loft air into the living space, have been installed in a number of houses. This system has sometimes been described as 'positive pressurisation', but this term is misleading as the fans used are not powerful enough to pressurise the building. It appears that they are effective mainly because they reduce the underpressure in buildings and so reduce the inflow of soil air. They require a fairly draughtproof house to have this effect. The results show that such systems can be effective in houses with solid or suspended floors, but reduction factors are mostly lower than those of sump systems. Where the initial radon level exceeded 750 Bq m^{-3} these systems were generally unsuccessful in reducing the radon levels to below 200 Bq m^{-3} .

Properties with high radon levels and suspended timber floors were more problematic to remediate than those with concrete floors. There are only two viable radon reduction methods that can be used in this case. The first is increased natural ventilation of the underfloor void. This method is very weather dependent, relying on wind direction and speed to maintain a rapid turnover of the void air. The position of the property (whether exposed or shielded from the wind) also affects how successful this method is. In general the reduction factors obtained for increased natural ventilation are quite low.

Because of the problems experienced with this type of construction, some properties were investigated in more detail. In one case it was found that the radon level increased by two orders of magnitude when the wind was in one narrowly defined direction. The effectiveness of underfloor ventilation can be substantially increased by installing a fan to provide a constant flow of air under the building. In most cases the fan is used to extract air from the void, but in some cases, when this has been unsuccessful, it has been found that blowing air into the void is effective. If air is blown into the void, care has to be taken to ensure that any water services running in the void are well insulated to prevent freezing, and floors may feel cold in winter.

Sealing of floors without other remedial measures was used by some householders, but with limited success. The technique is also very time-consuming and labour intensive, and therefore expensive if carried out by a contractor.

Durability of remedial measures

In order to keep radon exposures low and contain costs it is important that remedial actions remain effective for many years after installation. In order to determine how durable various techniques were, 56 homes with successful remediation were enrolled in a further study. In this study the radon levels in each property are remeasured every winter using passive radon detectors. The results are shown in Table 2.

Table 2. Durability of radon remedial measures up to 3 years after installation.

Method	Durability											
	1st Year				2nd Year				3rd Year			
	N	AM	GM	Range	N	AM	GM	Range	N	AM	GM	Range
Positive ventilation	7	0.83	0.92	0.4-1.4	5	1.16	1.23	0.9-2.6	5	0.70	0.71	0.55 - 0.93
Additional natural ventilation of underfloor void	9	0.85	0.97	0.5-2.8	4	0.81	1.12	0.3-2.2	3	0.56	0.69	0.29 - 1.10
Mechanical ventilation of underfloor void	6	0.81	0.86	0.5-1.3	5	0.65	0.72	0.4-1.2	3	0.67	1.36	0.41 - 1.11
Sealing only	3	1.05	1.15	0.6-1.6	3	0.85	0.86	0.7-1.1	3	0.85	0.93	0.52 - 1.27
Membrane covering floor	1	1.10			1	0.70			1	0.68		
Sump	30	0.75	0.88	0.2-2.4	14	0.83	0.91	0.5-2.5	13	0.72	0.81	0.36 - 1.82

The durability of each method is expressed as a ratio of each annual radon level to the radon level immediately following remedial action has been calculated. A value of less than one means the radon concentration has decreased further, and values of more than one imply an increase since the first post-remediation measurement. Small increases are not important: a value of 1.5 may signify that a house which was reduced to 50 Bq m⁻³ has increased to 75 Bq m⁻³. There are 56, 32 and 29 results available for 1993, 1994 and 1995 respectively. It is apparent from the data that effectiveness can be maintained in most cases. Underfloor sumps, as well as being the most effective remedial measure (as shown in Table 1), were also very reliable. In the 30 cases investigated there was no significant change in radon level or a further decrease.

The most serious failure of a remedial action was that of a property with mechanical ventilation of the void under a suspended floor, in which the radon concentration returned to its initial level of more than 1000 Bq m⁻³. On investigation it was found that the inlet to the fan had been blocked. In another case where the remeasured radon level went above the Action Level, this was attributed to varying weather patterns. All other cases where the ratio is greater than unity, the radon levels after remedial action remained below the UK Action Level of 200 Bq m⁻³.

Mapping radon-prone areas

Background

In order to identify homes with high radon levels as efficiently as possible, it is necessary to have accurate numerical information on radon-prone areas. Maps based on purely geological indicators are generally qualitative and sometimes contain significant errors. Maps based on radon measurement in homes are definitive if sufficient results are available. Often there are small numbers of measurements, making it difficult to map the fraction of the housing stock which exceeds the reference level.

To map radon prone areas using house radon data, a decision must be made about the smallest mappable unit. Too small an area results in uncertainty in the estimates of the magnitude of the radon problem because it contains too few results, but too large an area results in too coarse a map. For this work, it was decided to investigate whether grid squares as small as 5 km by 5 km could be used, despite the sparseness of the data. To test this, it is helpful to have a large database of results. This allows hypotheses about the data to be tested, and allows trial mapping by selecting a small subset of the data, mapping using the techniques developed, and comparing with the full data set.

It has been observed that the distribution of radon concentrations in homes is approximately lognormally distributed. If this is true over the whole range of radon levels, one can estimate the parameters of the distribution from the data and calculate what fraction of the distribution exceeds any threshold. A database of 62,555 radon results in southwest England was used to test whether the data within 5 km grid squares was consistent with lognormal distributions and to develop techniques for estimating the fraction of homes exceeding a radon reference level in each grid square, even where data are sparse.

Lognormality of data

Standard statistical tests (chi-square and Kolmogorov-Smirnoff) to determine whether the distributions of radon levels in homes within each grid square were lognormal gave conflicting results, so an alternative and more appropriate test was carried out. The geometric mean (GM) and geometric standard deviation (GSD) were calculated for each distribution and used to calculate the expected fraction of homes above the 200 Bq m⁻³. This was compared directly with the measured fraction above the level. The obvious way to calculate the GMs and GSDs is to take logarithms of all results for a grid square and use standard formulae to calculate mean and standard deviation. However, even if the underlying distribution of radon levels in homes is lognormal, there are two factors which distort the observed distribution and lead to erroneous estimates of GM and GSD. These are the contribution of outdoor radon to indoor levels and random uncertainties in radon measurements. Both of these are analysed by Miles (1993); the effect of the first factor is summarised below.

The data shows that the UK national distribution of radon levels is not well represented by a lognormal but that if the outdoor radon concentration (4 Bq m⁻³) is subtracted from the results, the distribution of net radon concentrations conforms to a lognormal between 3 and 300 Bq m⁻³. This is because the radon concentration in any home can be represented by the equation:

$$R_i = R_o + \text{source} \times A \times B \times C \times \dots$$

where R_i and R_o are radon concentrations indoors and outdoors, 'source' is a term depending on the concentration of radon in the ground and A, B, C,... are terms depending on factors such as permeability of the ground, number and size of entry routes, underpressure in the building and ventilation of the building. The model assumes that these terms are largely independent and are multiplicative apart from the contribution from outdoor radon. The equation can be rewritten as:

$$\ln(R_i - R_o) = \ln(\text{source}) + \ln(A) + \ln(B) + \ln(C) + \dots$$

If there are sufficiently many independent terms, each randomly distributed, the distribution of $\ln(R_i - R_o)$ between homes should be normal, as was found to be the case. In estimating the parameters of the lognormal distribution it is therefore important to subtract outdoor radon first.

The 62,555 radon results had outdoor radon subtracted, were corrected for seasonal variation and selection bias, and were grouped by 5 km grid square of measurement. The fraction of the results in each grid square exceeding 200 Bq m⁻³ was determined directly from the data and compared with the fraction estimated using the techniques described above. Figure 1 shows the ratio of the measured fraction above 200 Bq m⁻³ to the estimated fraction as a function of the estimated fraction for all squares with 100 or more results, 25 or more of them above 200 Bq m⁻³, with uncertainties (one standard deviation). It is clear that the lognormal model, used in this way, is a very good estimator of the fraction of the housing stock above a threshold over a wide range of values.

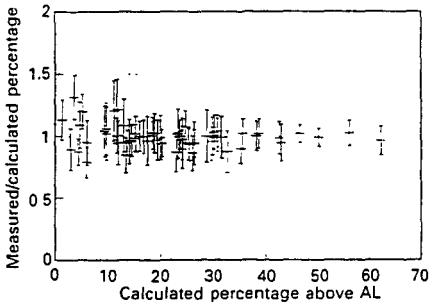


Figure 1 Ratio of measured to calculated percentage of homes above the Action Level using medians and GSDs from the sort technique

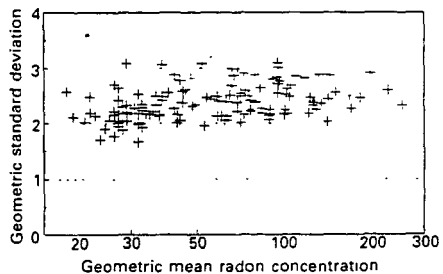


Figure 2 Geometric standard deviation as a function of geometric mean for 137 5 km grid squares with 100 or more results

If the lognormal model is to be used in practice for radon mapping, it is necessary to estimate the GM and GSD for grid squares in which few data are available. Figure 2 shows the estimated GSDs as a function of GM in all squares with 100 or more results. Although the GMs of the distributions vary from 18 Bq m⁻³ to 250 Bq m⁻³, it is clear that the variation with GM is small: only a suggestion of slightly lower GSD with low GM is apparent. This implies that the same GSD may be used for all squares within this area. Surveys tend to produce large numbers of results in some areas even if the data are sparse in other areas, so the mean GSD determined from a few squares with many results may be used for all.

Again the best test of the technique is its accuracy in predicting the fraction of the housing stock above a reference level. Figure 3 shows the result of using the mean GSD in all

squares and comparing the estimated fraction of homes above 200 Bq m^{-3} with the measured fraction. Comparison with Figure 1 shows that this procedure has increased the uncertainty in the estimates at low levels, but does not seem to have biased them. This great simplification seems to work remarkably well.

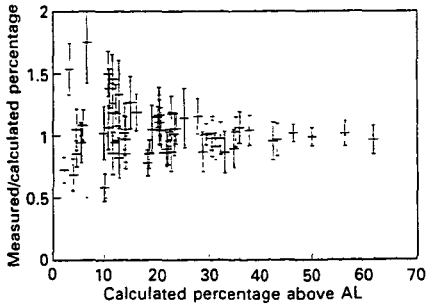


Figure 3 Ratio of measured to calculated percentage of homes above the Action Level using medians from the sort technique and GSD = 2.4

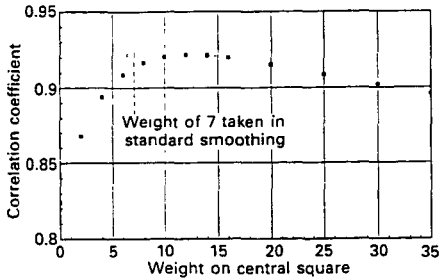


Figure 4 Variation in correlation coefficient between estimated GM (from smoothed GM of 5 results) and GM of 100 or more results as a function of the weighting on the central square in the smoothing function

Smoothing between grid squares

In order to estimate the GM where few data are available a different strategy must be applied. The GM varies greatly between squares (this is the reason for mapping) so it is not possible to use the mean of the GMs in different squares. However, there is considerable uncertainty in the estimate of GM for a square if only a few results are available, and it is desirable to reduce this uncertainty. If the GMs in adjacent squares are correlated, it may be possible to improve the estimate of GM by smoothing between squares. To derive the smoothed estimate for a grid square a weighted mean was taken of the values for the square and the eight surrounding squares. A weight of 7 was applied to the central square, weights of 3 to vertically or horizontally adjacent squares, and weights of 2 to diagonally adjacent squares.

To discover whether this procedure improved the estimate of the GM in cases where the data were sparse, a subset of the data was used. For each grid square 5 of the available results were selected at random, and the GMs estimated. The correlation coefficient between these GMs and the GMs of all data for the corresponding grid squares was calculated. Then the GMs derived from 5 results were smoothed and the correlation coefficient calculated again.

This procedure was repeated with different weights on the central square and the results plotted in Figure 4. This shows that smoothing GMs where results are sparse does indeed improve the correlation with the GMs from the full data set. The graph suggests that for optimum smoothing of these data the weight on the central square should be 12 rather than 7. The optimum weight depends on the number of observations and the spatial variation of the radon potential in the soil. The optimisation procedure described above was repeated for different numbers of measurements. Figures 5 and 6 show the results of the optimisation.

Figure 5. Optimum weights for the central square when smoothing estimated geometric means based on limited numbers of results.

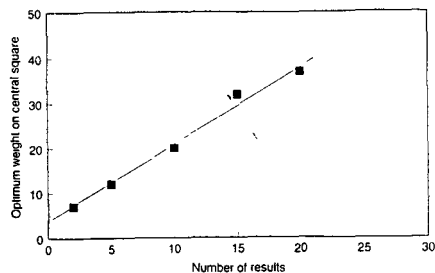
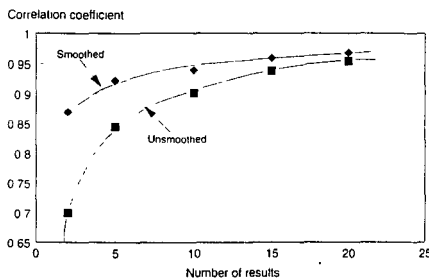


Figure 6. Correlation coefficient between grid square geometric means based on a limited number of results per grid square and geometric means based on the full data set, the means based on limited results either being unsmoothed or smoothed using the function shown in Figure 5



A study was made of the effects the sizes of areas used when applying lognormal modelling of the distribution of radon levels to estimate the proportion of homes above a threshold. It has been shown earlier that this technique is accurate in predicting the proportion of homes above a threshold in 5 km grid squares if appropriate techniques are used to estimate the parameters of the distribution. A difficulty arises when larger areas are taken, such as 10 km grid squares or administrative areas. With larger areas there is a much greater probability that they will overlap two geologies with different geometric means (GMs). The geometrical standard deviations (GSDs) of such distributions have been shown earlier to be very similar despite wide differences in GM.

A modelling study was carried out using artificially generated lognormal distributions to examine the effects of pooling different distributions, as happens in effect when 10 km grid squares are considered instead of 5 km squares. If two distributions with the same GSDs and GMs are combined, the pooled distribution has of course the same parameters as the original distributions and there is no difficulty in applying the lognormal modelling technique. If the two distributions have the same GSD but different GMs, the pooled distribution will have a GM intermediate between the two original distributions, but a larger GSD.

The question then arises of whether the measured parameters of the pooled distribution can be used to estimate the fraction of the housing stock above a threshold, or whether a different combination of parameters (such as the pooled GM with the original GSDs) should be used. Tests using artificial distributions showed that pooling distributions with GMs of 20 and 120, both with GSD 2.5, gave a distribution with GM 50 and GSD 3.6. Using these parameters directly to estimate the fraction of homes above 200 Bq m⁻³ gives a result of 14%, very close to the value of 15% derived from the two separate distributions before pooling. This result therefore shows that the lognormal model is very robust, and can accommodate cases where widely differing populations are combined, provided the parameters of the distribution can be estimated accurately.

Use of house radon data with geological boundaries

It is shown above that measurements of radon levels in homes analysed by grid square can be used to provide accurate estimates of the proportion of homes above a reference level, but cannot provide high resolution. Geological parameters, including the properties of individual rock types, can provide detailed maps, but without assistance from results of

measurements in homes cannot provide accurate estimates of radon potential. An alternative mapping technique is to group house radon measurements by geological unit. Where enough results of house measurements are available, this has the potential to provide maps which are both detailed and accurate. Where there are too few houses to provide good data, the technique can be extended using measurements of radon in soil gas under carefully controlled conditions.

For this exercise, house radon data from the areas of two adjacent British Geological Survey (BGS) sheets were used (Northampton and Wellingborough), with a total of 36,570 radon results. The exposed bedrock in this area is entirely from the Jurassic Period, ranging from Lower Liassic mudstones through to the Oxford Clay. The maps used for the geological classification show superficial cover only where it is more than 1 metre thick. The thickness and composition of rock types in geological formations in this area vary significantly across the maps. The locations of the houses were identified from the postcode. The grid reference of a house can be obtained with an uncertainty of about a few hundred metres or less in towns, but the uncertainty may be 1 km or more elsewhere.

Each set of house radon results for a particular combination of geology and superficial cover was analysed separately. The mean UK outdoor radon concentration (4 Bq m^{-3}) was subtracted from each result and the GM and GSD of each set were calculated. These parameters were used to estimate the fraction of homes above 200 Bq m^{-3} on the assumption that the distribution was lognormal. The estimated fraction could then be compared with the actual fraction found above the threshold in each data set. Table 1 shows the results for rock types which appear on both the Northampton and Wellingborough sheets, in areas without superficial cover. The measured percentage of homes above 200 Bq m^{-3} is in all cases close to the percentage estimated using the lognormal model, showing that the data conforms well to this model. The results also show the large variation in the percentage of homes above 200 Bq m^{-3} between different rocks, from 0.5% to > 20%.

The GMs for particular rock types vary by up to a factor of 2.2 between the two geological survey sheets. There are no differences in housing type or age of housing between the two sheets that could account for this difference, which is therefore attributed to lateral variation in the geological formations. This demonstrates that conclusions about radon potential over individual geological formations cannot necessarily be extrapolated to adjacent areas. This is likely to be particularly true of areas with a high proportion of shelf facies sedimentary rocks.

The GSDs for the different rock types vary from 2.3 to 3.0, compared with a range of 2.6 to 4.7 found when the data is grouped by 5 km grid squares instead of by geology. The smaller GSDs found when data is grouped by geology suggest that the data sets are more homogeneous when grouped in this way. The smallest GSDs were found for rock types where the GM varied by less than a factor of two between the two geological sheets. This suggests that much of the remaining variation between radon levels in homes when the data is grouped by geology is caused by the lateral variation in the geological formations. Analysis of the geographical variation in radon potential between houses on the same lithology may therefore produce even more detailed and accurate estimates of the fraction of homes exceeding a reference level.

Conclusions

1. The distributions of radon levels in 5 km grid squares are consistent with the lognormal distribution, and this model can be used to produce accurate maps on the basis of sparse data.
2. It is essential that the measurements be carried out using an appropriate selection of homes, location of detectors, duration of measurements, and accuracy of results over a wide range of concentrations.
3. Results need to be corrected to take account of outdoor radon levels, bias in selection of homes, and season of measurement.
4. In areas where there are too few results to allow GSD to be estimated directly, the mean GSD from squares with enough results may be used.
5. Smoothing GM values with those in adjacent squares improves the accuracy of the estimated GM in squares with few results.
6. Lognormal modelling of house data grouped by geological unit gives accurate and detailed maps of radon-prone areas.
7. When mapping by geological unit, lateral variations within units and superficial cover must be taken into account.

Publications

Cliff, K. D., Green, B. M. R. and Lomas, P. R. Domestic radon remedies. *Radiation Protection Dosimetry*, **45**, 599-601 (1992)

Cliff, K. D., Naismith, SP, Scivyer, C, and Stephen, R. The efficacy and durability of radon remedial measures. Presented at the First International Workshop on Indoor Radon Remedial Action, Rimini, Italy, June 1993.

S Naismith, 1994. Efficacy of radon remedial measures. *Radiological Protection Bulletin* 152, 10-13. NRPB Chilton.

Kendall, GM, Miles, JCH, Cliff, KD Green, BMR, Muirhead, CR, Dixon, DW, Lomas, PR, and Goodridge, SM, 1994. Exposure to radon in UK dwellings. NRPB-R272.

Miles, JCH, 1994. Mapping the proportion of the housing stock exceeding a radon reference level. *Radiation Protection Dosimetry* 56, 207-210.

Cliff, KD, Miles, JCH, and Naismith, SP, 1994. False positive and false negative radon measurement results due to uncertainties in seasonal correction factors. *Radiation Protection Dosimetry* 56, 291-292.

Green, BMR, Kendall, GM and Miles, JCH, 1995. Domestic exposure to radon in the UK. *Radiological Protection Bulletin* 161, 7-11.

Miles, JCH, Green, BMR and Lomas, PR, 1993. Radon affected areas: Scotland, Radon affected areas: Northern Ireland. *Documents of the NRPB*, 4,6 1-15.

Pinel, J, Fearn, T, Darby, SC and Miles, JCH, 1995. Seasonal correction factors for indoor radon measurements in the United Kingdom. *Radiation Protection Dosimetry* 58, 127-132.

Miles, JCH, and Ball, TK, 1995. Mapping radon-prone areas using house radon data and geological boundaries. Presented at the Sixth International Symposium on the Natural Radiation Environment, Montreal, 1995 June 5-9

Head of project 2: Prof. Dr. R.J. de Meijer.

2 Objectives for the reporting period

The objective of the project is to obtain better understanding of transport of radon in soil and in particular transport from soil to crawl space. This objective will be met by studying under well defined and controlled conditions both transport of radon in soil and radon exhalation by soil as a function of a number of physical quantities. For this, a laboratory facility was built that consists of a large cylindrical vessel with radially inserted measuring probes that allow measurement of pore-water content, air permeability of the soil and radon concentrations in the soil gas at various depths under the soil surface.

More specifically the objectives for the reporting period were to study both diffusive and (time-dependent) advective radon transport in situations simulating crawl spaces of different heights, with and without forced ventilation and with and without a ground water level set in the sand column underlying the crawl space.

3 Progress achieved including publications

3.1 Introduction

To allow validation of radon transport models, a laboratory facility was built, see Fig. 1. In short, this facility consists of a cylindrical (height and diameter 2 m; bottom slightly curved for strength) stainless steel vessel presently filled with sand. The vessel can be closed by lowering a lid into a water-filled ring surrounding the upper part of the vessel. This lid is adjustable in height and the space between the lid and the sand can be considered to simulate a crawl space. At several heights, probes are inserted radially to measure, near the axis of the vessel, the radon concentration in the soil gas. For the study of advective radon transport, a perforated circular box (diameter 162 cm, height 3 cm) was placed at a distance of 163 cm below the sand surface. By (de)-pressurizing this box an air flow may be induced through the sand column on top. This facility allows investigation of radon transport processes under well defined and controlled conditions and consequently it enables validation of radon transport models.

Starting from a well known initial condition (simple geometry and soil type, no ground water and no lid on the vessel) the complexity of the situation is increased step by step. After each step a series of measurements is carried out and the results are compared with transport model calculations. Only when the models satisfactorily describe the measured radon concentrations, the complexity is increased. In case of larger deviations between models and measurements, the models are adjusted or extended.

Measurements with the vessel were carried out on diffusive and advective radon transport for a situation without and with a crawl space of several different volumes. In addition, the influence of time-dependent advective transport was investigated as well as the effect of forced crawl-space ventilation on the radon concentration. Finally, measurements were performed with a water level set at different heights.

Large unsurmountable discrepancies between models and measurements were not encountered for experiments with dry sand. However, relatively large differences, up to 80% relative deviation, were observed between experiment and model when a water level is set in the sand column.

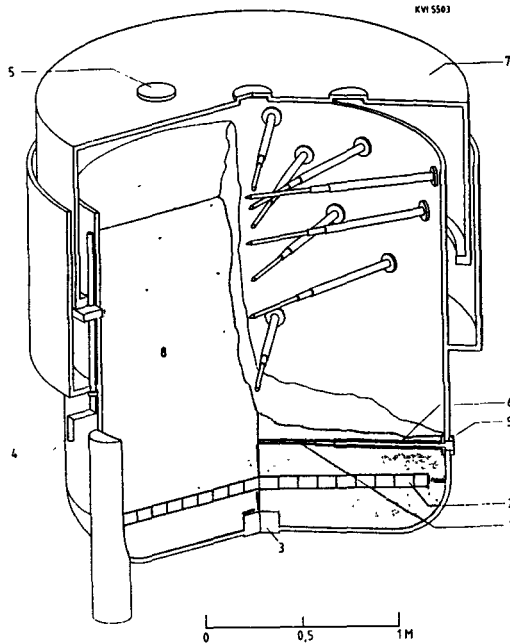


Figure 1: Schematic drawing of the vessel. 1) probe; 2) perforated circular box; 3) water inlet/outlet; 4) adjustment point for height of the lid; 5) flange; 6) sleeve; 7) lid; 8) soil.

3.2 Theory

In this section the time dependent equation describing radon transport in porous materials is stated, which is used in the modelling. In the derivation it is assumed that the partitioning of radon between the gas phase, liquid phase and radon adsorbed on the solid phase of the pore space is permanently in equilibrium. Further, it is assumed that transport of radon in the liquid phase over a distance larger than the grain size is negligible. This assumption is only valid when soil is only partly moisturised and most transport takes place in the gas phase. Consequently, the equation is not valid for soils having a high pore-water content. For these soils, the (spatial) distribution of gas and liquid phases in the pores and probably also the kinetics of the phase partitioning must be taken into account in the derivation of time-dependent equations for radon transport.

If adsorption of radon to the sand grains and mechanical dispersion are negligible and that the sand may be considered as a partly moisturised porous medium, the diffusive and advective transport of radon through the sand is governed by,

$$\beta \frac{\partial C}{\partial t} = \nabla \cdot (\epsilon \tau D_a \nabla C) + \frac{k}{\mu} \nabla P \cdot \nabla C - \beta \lambda C + \eta \rho \lambda C_{Ra} \quad (1)$$

where

- β = partition corrected porosity: $\epsilon_a + L\epsilon_w$
- ϵ_a = air-filled porosity
- L = Ostwald coefficient (=0.26 at 20 °C)
- ϵ_w = water-filled porosity
- C = pore-air radon concentration (Bq m⁻³)
- t = time (t)
- ϵ = porosity
- τ = tortuosity
- D_a = diffusion coefficient of radon in air (m² s⁻¹)
- k = intrinsic permeability (m²)
- μ = dynamic viscosity of air (= 1.83 · 10⁻⁵ Pa s)
- P = pressure (Pa)
- λ = radon decay constant (= 2.1 · 10⁻⁶ s⁻¹)
- η = radon emanation factor
- ρ = bulk dry density (kg m⁻³)
- C_{Ra} = radium content (Bq kg⁻¹)

3.3 Model calculations for dry sand

Using the method of Laplace transformation the one-dimensional (1D) counterpart of Eq. 1 with the advective term omitted was solved with boundary conditions that reflect the situation of the vessel with lid (crawl-space situation). The boundary conditions are that the bottom of the vessel is impermeable for radon diffusion and that the radon concentration at the surface of the sand changes due to exhalation from the sand, due to decay and due to leakage out of the crawl space (described by a leakage parameter). Eq. 1 was also solved with boundary conditions that reflect the situation of the vessel without the lid. For this situation we assume that the radon concentration at the surface of the sand is zero. In both cases, initially, the radon concentration in the sand is assumed to be zero.

Also the one-dimensional stationary counterpart of Eq. 1 was solved with boundary conditions that reflect the situation of the vessel without lid and de-pressurisation of the perforated box (downward air flow). In this case the boundary conditions are that the bottom of the vessel is impermeable for radon transport, that the radon concentration at the surface of the sand is zero and that the diffusive flux of radon concentration into the perforated box is in equilibrium with radon decay. The pressure field is calculated using Darcy's law. In the one-dimensional case it takes the simple form that in the area between the perforated box and the surface of the sand column the gradient of the pressure is constant.

Finally, two numerical models, one- and two-dimensional, have been constructed to calculate the radon concentration in an inhomogeneous porous medium as a function of space and time in a situation with time-independent boundary conditions for the pressure field and from a given initial condition for the radon-concentration field. In these models it is assumed that air flows (advection) are described by Darcy's law and are stationary and that the situation is isothermal, i.e. temperature effects are not taken into account. First, the pressure field is calculated using the control volume method. Secondly, the calculated pressure field is used as input in the time-dependent radon-transport equation. Similar to the pressure field, the radon-concentration field is calculated for each time step using the control volume method.

3.4 Parameters of the sand

All parameters of the sand, occurring in the radon transport equation, have been determined with independent experiments. Table I lists the values of these parameters, which were used in all model calculations in this report.

Table I: Parameters of the sand.

Grain size	0.25 - 0.50 mm
Porosity	0.340 ± 0.010
Bulk dry density	$(1.74 \pm 0.05) \cdot 10^3 \text{ kg m}^{-3}$
Permeability	$(5.45 \pm 0.13) \cdot 10^{-11} \text{ m}^2$
Radium content	$3.68 \pm 0.13 \text{ Bq kg}^{-1}$
Tortuosity	0.640 ± 0.010

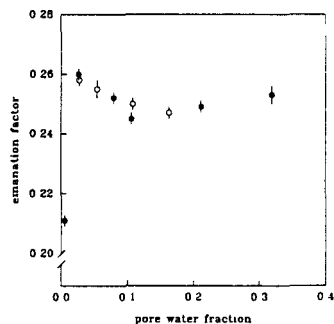


Figure 2: Emanation factor as function of pore water content

It is well known that the radon emanation factor (the fraction of radon atoms that escape from a mineral grain) may be very sensitive to the moisture content of the porous medium. Therefore, a study was started of the effect of moisture on the emanation factor of the sand. The two identical instruments used to measure the emanation factors, consisted of a closed cylinder (diameter 20 cm, height 30 cm) of which the lower half was filled with a dry sand sample of about 8 kg. After a period of four weeks the radon concentration inside the cylinder has virtually reached its equilibrium value and air from the void space above the sand was sampled using a piston. The radon concentration of the air sample was measured with the same equipment as used in the vessel experiments. This procedure was carried out with a range of moisture contents which were obtained by simply pouring known amounts of water on top of the sand sample.

It was observed that a sharp rise in emanation factor occurred as the pore moisture content was increased to only 2.5%. For higher moisture contents, the emanation factor decreases slightly and increases again for moisture contents higher than 15%. The measured emanation factor as function of the pore water fraction is presented in Fig. 2. The mechanisms by which moisture affects the radon emanation factor is only partly understood. Qualitatively it can be stated that in a dry porous medium a reasonable fraction of the radon atoms that escape from a grain due to recoil bury themselves in another grain. Since the recoil range in water is much smaller than in air, addition of water to the pore space inhibits this mechanism by which the emanation factor is increased. The behaviour that is observed for moisture contents larger than 3% is not understood and has not been reported earlier in literature.

An extra difficulty was introduced by this dependency of the radon emanation factor to the moisture content. At the start of the experiments the sand was dried by inducing an air flow of 50 L min^{-1} through the column for more than a week. This procedure, however, might not have left the sand completely dry. In addition, during the experiments with the lid installed, the relative humidity in the crawl space was approximately 100% and this might have moisturised the sand. Therefore, the exact moisture content is not known and might even vary with height. To allow analytical modelling of radon transport, a constant emanation factor is mandatory. Which value of the emanation factor to use is dependent on the moisture

content of the sand. The latter was determined by measuring the mass loss after drying of a sand sample from the vessel. This resulted in a value of 1% for the moisture saturation. When assuming that the emanation factor is directly proportional to the moisture content in the region for moisture contents smaller than 2.5%, a value of approximately 0.22 is obtained for the emanation factor.

Results of measurements of the homogeneity of the sand column showed that deviations from the ideal case, at which the sand column is perfectly homogeneous, are less than 15%.

3.5 Results and discussion

3.5.1 Experiments with diffusive transport

Results of measurements with diffusive radon transport only, are presented together with results of analytical model calculations. These experiments concern radon ingrowth in the situation without a crawl space, ingrowth of radon with a crawl space and the equilibrium state with different values of the crawl-space ventilation rate.

At the start of the experiments with ingrowth of radon concentration, the sand column was flushed by inducing a flow of radon-free air (50 L min^{-1}) through the perforated box. Thereafter, radon concentrations at all nine probes were measured as a function of time after stopping the flow. The measured radon concentrations C (Bq m^{-3}) as function of height z (m) in the vessel and time for the experiment without a crawl space are presented in Fig. 3 (left). The results of the measurements with a 92 cm crawl space are presented in the same figure (right). For clearness, only a few of the measured radon profiles are shown in this figure. The solid lines are results of analytical calculations. In comparing the experimental and calculational data, a good correspondence is observed.

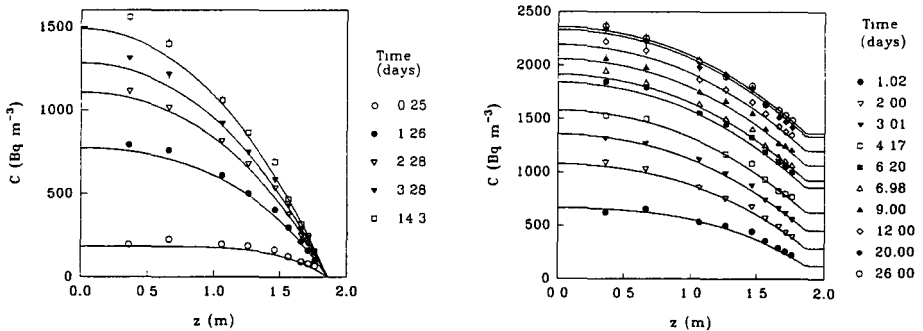


Figure 3: Results of experiments with diffusive transport.

The experiment with different ventilation rates of a 50 cm crawl space concerned measurements of the equilibrium radon concentration as function of height (z). A controlled flow of radon-free air was continuously forced into the crawl space through an opening at one side of the lid, while at the other side a small diameter outlet tube of several meters length was connected to allow crawl-space air to escape. These measurements were carried out with a crawl space ventilation rate of 2.65, 5.3, 10.6, 21, 46 and $94 \cdot 10^{-6} \text{ s}^{-1}$. Fig. 4 shows the measured equilibrium radon-concentration profiles (left) and measured radon concentration

C_{cs} in the crawl space as function of the ventilation rate (right) with results of analytical calculations.

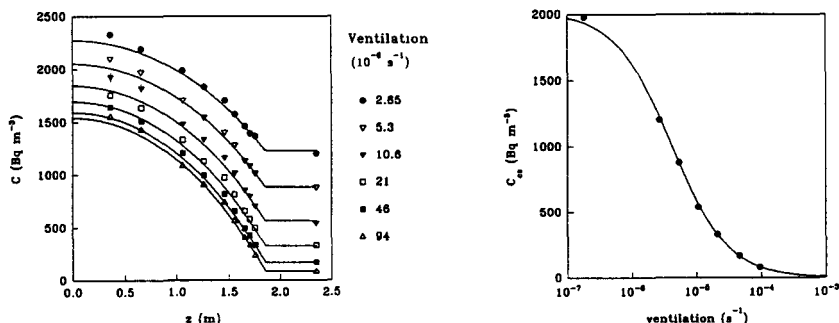


Figure 4: Results of experiment with different crawl-space ventilation rates.

Also this experiment shows a satisfying agreement between model and measurement. It is observed that even a very small ventilation rate of once a day ($\approx 1.2 \cdot 10^{-5} \text{ s}^{-1}$) reduces the crawl space concentration by a factor five with respect to the situation without ventilation (for the vessel geometry). However, this reduction factor decreases sharply with increasing initial ventilation rate. For practical purposes this implies that knowledge of the natural ventilation is necessary to calculate the effect of forced ventilation. It is also seen that mitigation of a crawl space by forced ventilation will be more difficult for cases with a 'normal' natural ventilation rate.

3.5.2 Experiments with diffusive and steady advective transport

Results of measurements with diffusive and steady advective radon transport in equilibrium are presented together with results of analytical (downward air flow, experiment without a crawl space) and two-dimensional numerical model calculations (upward air flow, experiment with a 50 cm crawl space).

In the experiment with de-pressurisation of the perforated box (downward air flow) and without a crawl space, steady-state radon-concentration profiles were measured with air flows of 0.1, 0.2, 0.4 and 0.8 $L \text{ min}^{-1}$. The results of this experiment together with the results of analytical modelling are shown in Fig. 5 (left).

In the experiment with pressurisation of the perforated box (upward air flow) and with a 50 cm crawl space, steady state radon-concentration profiles were measured with air flows of 0.1, 0.2, 0.4, 0.8 and approximately 2.2 and 4.8 $L \text{ min}^{-1}$. When the perforated box is pressurised, the situation can no longer be described by an 1D-model. This can most easily be appreciated by inspection of the radon concentration inside the box when air with zero radon concentration is forced through the box at the centre of its bottom plate. The concentration at this position will be zero but increases in the radial direction due to influx of radon through the surfaces of the box. This implies that in the model also the radial coordinate has to be taken into account (2D-modelling). The results of this experiment are presented in Fig. 5 (right), together with results of calculations with the numerical 2D-model (solid lines in this figure). A good correspondence between experiment and model is observed.

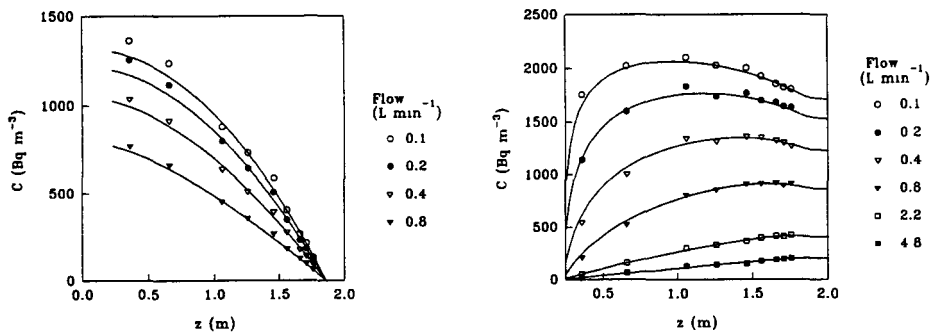


Figure 5: Results of experiments with diffusive and steady advective transport.

3.5.3 Experiments with diffusive and time-dependent advective transport

In reality, pressure differences are seldomly constant but change with time. To allow validation of modelling of time dependent advective transport, several experiments were carried out with a pulsed air flow through the sand column. An upward air flow was induced in the column for a certain time interval, whereafter this air flow was turned off for an equal time interval. The sum of these two intervals is the period of the pulsed air-flow experiment. Experiments were carried out with two different air flows and three different periods. Radon concentration in the 50 cm crawl space and the radon concentration at 60 cm below the sand surface were measured as function of time. In Fig. 6 (left) the radon concentration C_{cs} in the crawl space is shown as function of time for the experiment with an upward air flow of 0.4 L min^{-1} through the sand column. In the same figure (right) the radon concentration C_p at 60 cm below the sand surface is shown as function of time for the same experiment. Solid lines in this figure are results of the numerical 2D-model. Again, a good correspondence is observed.

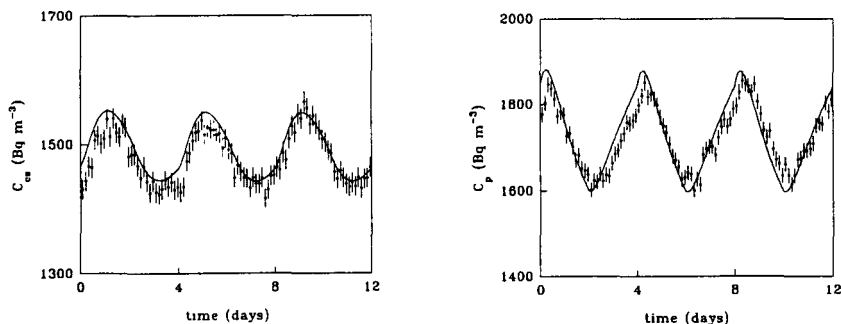


Figure 6: Results of experiment with diffusive and time-dependent advective transport.

Also from results of the other experiments with a different period and/or air flow, it is observed that the concentrations calculated with the 2D-model agree well with the measured

concentrations considering amplitude, phase and absolute value. The best agreement concerns the amplitude. The absolute value deviate somewhat for the crawl space data, with the measured concentrations being fractionally lower than calculated. On the other hand, the phase of the signal differs slightly for the radon concentration at 60 cm below the sand surface.

The small difference in absolute value may be due the uncertainty in the measuring efficiency of the equipment used in these experiments. The phase shift for the radon concentration at 60 cm below the sand surface varies from experiment to experiment, but seems to be more pronounced for the measurements with the higher air flow. The measured concentrations lag the calculated concentrations by at least several hours. The time lag is longer during the intervals with the air flow turned off than in the cycle with advective transport. A plausible explanation for this phenomenon may be that air taken out of the pore volume at 60 cm depth, is being returned at a depth of 80 cm. Diffusive supply of radon at those depths is possibly slower than advective supply, resulting in a larger time lag when the air flow is turned off.

3.5.4 Experiments with a ground water level

Finally, experiments were performed with a ground water level set at several different heights in the radon vessel. This was accomplished by supply of water into the vessel through an opening at the centre of the bottom. The water level was consecutively set at 160, 120, 80, 40 and 0 cm below the sand surface (rising water table). At each level, equilibrium pore-air radon concentrations at the position of probes located above the water level were measured. These experiments were carried with a 50 cm crawl space, ventilated with an air flow of 0.25 L min^{-1} . After the experiment with a completely saturated sand column (water level 0 cm below sand surface), the experiments were repeated with the water level sequentially set at 40, 80, 120 and 160 cm below the sand surface (falling water table).

Introduction of water to the pore space of the sand largely increases the complexity of the radon transport process because several input parameters in the radon transport equation (Eq. 1) are influenced by the presence of water. This includes the partition corrected porosity β , the emanation factor η and the bulk diffusion coefficient D (since only cases with diffusive transport have been studied the advective term can be ignored). For some parameters the precise dependency is not well known. As a consequence, the modelling is hampered by these uncertainties. Moreover, since the moisture content varies with height in the vessel, these parameters dependent also on the height. Therefore, the one-dimensional numerical model was used to analyse the experimental data.

For modelling, the moisture content of the sand as function of the suction pressure (water retention curve) was determined using both directions of change of the water suction pressure (hysteresis effects are present). For the bulk diffusion coefficient of radon as function of the pore water fraction of the sand a correlation function was used developed by Rogers and Nielson (Health Physics 61, 225-230, 1991). This correlation function only approximates the diffusion coefficient because each type of soil exhibits a different behaviour, based on differences in porosity, tortuosity, pore size distribution etc. Finally, the functional dependency of the emanation factor on the pore water fraction, discussed previously, was introduced in the model calculations.

The experimental results are presented in Fig. 7 (left). This graph shows the equilibrium pore air radon concentration as function of the z -coordinate for the different levels of the water table. Identical shapes of the markers indicate that these two profiles were measured with the same water level. The open markers designate that the water level was attained by

addition of water through an opening at the bottom of the vessel containing dry sand initially (rising water table) whereas the closed markers indicate that the water level was established by removal of excess water, also through an opening at the bottom of the vessel (and with initially saturated sand). The height of the water level in the vessel for the several profiles is shown by dashed lines with perpendicularly a short solid line that indicates this height.

The difference in radon concentration for equal water levels is remarkable, with typical differences in the order of 5-20%. This result is probably due to hysteresis of the water retention of the sand. It is also concluded that the radon concentration in the crawl space decreases with increasing water level.

The results of model calculations are presented in Fig. 7 for a rising water table (right top) and a falling water table (right bottom). It is observed that all calculated concentrations are higher than measured, with increasing relative deviations at higher water tables. For the profile measured with a water table at 40 cm below the sand surface, the calculated concentrations are almost a factor two higher than measured (rising water table). However, the shape of the measured and calculated curves are very similar, only showing a shift in magnitude. This shift is partly caused by the higher emanation factor at higher pore water fractions (Fig. 2), assumed in the modelling. On the other hand, this shift is the result of Henry's Law. In tracing the cause of the discrepancies, these two aspects must be studied more thoroughly. Also, during sampling, physical phenomena occur that may affect the result of the measurements. Relatively large advective flows are induced in the sand which may influence the radon partitioning between the water and air phase. This partitioning may also be influenced by the sudden pressure drop during sampling. For modelling purposes, it is recommended to investigate these effects. Finally, also the numerical model itself (for moisturised sand) should be thoroughly tested and checked in order to assure that the results of the model calculations are correct.

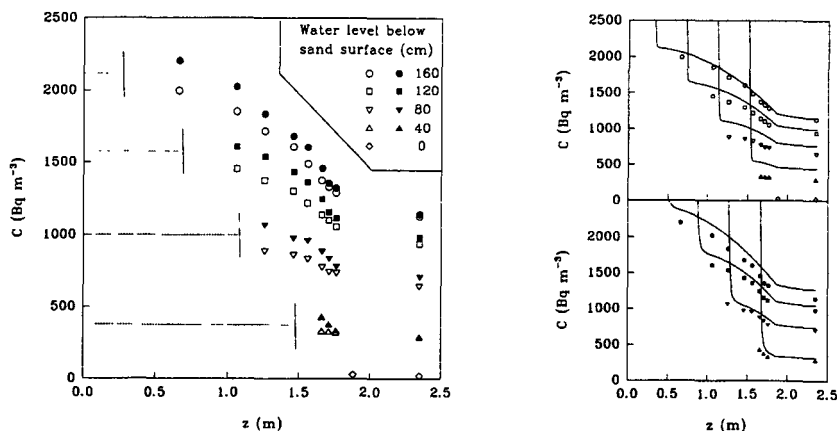


Figure 7: Results of experiment with different water tables in the sand column.

3.6 Conclusions

The data obtained with dry sand were compared with results of calculations using one set of input parameters. Results of experiments with diffusive transport only or with depressurisation

of the perforated box were compared with one-dimensional analytical model calculations, whereas results of experiments with (time-dependent) pressurisation of the perforated box (upward air flow in the sand column) were compared with two-dimensional numerical model calculations. Both the analytical and numerical analysis showed a good correspondence with experimental results, showing a maximum deviation between model and experiment of less than 10%. For these reasons, we may conclude that the radon transport models have been validated for dry sand.

In addition, experiments were carried out with several different ground water levels set in the vessel. With respect to all previous experiments the complexity was only increased by introducing one extra parameter: the pore water fraction of the sand. However, addition of water to sand leads to a much more complex situation with respect to radon transport. Not only two phase transport must be considered, but also several other parameters in the radon transport equation are influenced by the presence of pore water. These are the emanation factor, the bulk diffusion coefficient and the partition-corrected porosity. The correspondence between model and experiment is poor (80% relative deviation) for the experiments with a high water level but better (10% relative deviation) for the experiments with a low water level. At present, we do not have sufficient knowledge about the processes involved to accurately model radon transport in moisturised porous materials. More research should be initiated to solve the discrepancies between experiment and model.

In conclusion, a validated two-dimensional radon transport model for dry sand has become available. On the contrary, the models fail to predict radon concentrations in moisturised sand (max. 80% deviation).

3.7 Publications

van der Spoel, W.H., *Modelling of radon transport in the KVI radon vessel*. KVI internal report R57, 1993.

van der Graaf, E.R., Witteman, G.A.A., van der Spoel, W.H., Andersen, C.E., de Meijer, R.J., *Measurements on and modelling of diffusive and advective radon transport in soil*. Radiat. Prot. Dosim., 56, 167-170, 1994.

van der Graaf, E.R., Witteman, G.A.A., van der Spoel, de Meijer, R.J., *Radon transport in soil: Measurements on and modelling of diffusive and advective transport in a homogeneous column of sand*. Annales de l'Association Belge de Radioprotection, 91, 335-350, 1994.

de Meijer, R.J., van der Graaf, E.R., *Naar een radon-arm binnenhuismilieu*. Bouwfysica, 5, 22-24, 1994.

van der Spoel, W.H., van der Graaf, E.R., de Meijer, R.J., *Measurements on, and modelling of diffusive and advective radon transport in a homogeneous column of sand*. Indoor Air, an integrated approach, Elsevier, 119-122, 1995.

de Meijer, R.J., van der Graaf, E.R., *A research programme towards construction of low-radon houses*. Indoor Air, an integrated approach, Elsevier, 367-370, 1995.

Head of project 3: Claus E. Andersen

II. Objectives of the reporting period

The objectives of the reporting period were: (i) to finish the experimental investigations, the site characterization and the modelling of the radon test structure, and to compare the results of the experimental investigations with the results of the numerical modelling based on measured soil parameters, and (ii) to compare modelling results with data from real houses.

III. Progress achieved including publications

Introduction and project summary

The primary purpose of this study has been to evaluate how well numerical modelling and soil characterization techniques describe radon transport through soils and entry into houses under field conditions.

Numerical or analytical models of radon transport have two applications. Firstly, such models provide a quantitative and physical description of the problem in question. It is from this theoretical basis that field measurements are interpreted and understood. Likewise, mathematical models are essential tools when field observations or technology relating to the entry of other soil-gas pollutants such as landfill gas or volatile organic compounds are transferred to the radon problem - or vice versa. Secondly, mathematical models are used to identify critical building and soil related features controlling radon entry, and to help in the design of optimal radon-mitigation systems or improved building practices.

The experimental basis of the model evaluation is a simple 2.6 m x 2.6 m test structure located on a clayey-till field site at Risø National Laboratory. Over a three-year period, radon concentrations have been measured in more than 40 probes located in the ground under and around the structure. In total, more than 2000 scintillation-cell radon measurements have been taken. The data have been divided into 7 groups corresponding to forced flows of soil gas into - or out of - the structure at flow rates equal to approx. ± 20 , ± 10 , ± 5 , and 0 litres per minute.

The idea of using a test structure for that type of work - as opposed to a real house - was that the research could be focused on the soil-related part of the problem while keeping the influence of house occupants, ventilation, and unknown building characteristics at a minimum. The decision to conduct experiments under a range of forced-flow conditions was made because it focuses on the ability of the model to describe combined advective and diffusive transport, and because these situations resemble radon-mitigation systems based on sub-slab depressurization and pressurization.

The numerical model tested in this work is a specific implementation of a set of physical equations generally considered to govern soil-gas and radon transport. The key elements are the Darcy-flow approximation of soil-gas transport plus combined diffusion and advection of radon. The main assumption concerns the application of the homogeneous-soil approximation - i.e. the approximation that field soil can be simulated as a homogeneous porous medium having certain effective parameters.

Input parameters to the model are: gas permeability, radon diffusivity, radon-generation rate, soil porosity, and soil-moisture content. For a given pressurization of the structure, the model calculates steady-state pressure, flow and radon-concentration fields in the soil. The main

output from the model is: (i) field values at locations corresponding to those of the soil probes and (ii) integrated entry rates of soil gas and radon into the structure.

The main finding of this study is that under field conditions, model estimates of soil-gas and radon entry rates may be off by as much as one order of magnitude: The model underestimates the soil-gas entry rate and overestimates the radon concentration associated with this enhanced flow. The critical element in the model assessments is the measurement of gas permeability.

As a side effect of the investigation, it was observed that the soil-gas entry rate correlates directly with the depth of the water table. At winter time, when the water table is at a shallow depth, the soil-gas entry rate for a given depressurization is a factor of 2 to 10 lower than during the summer. This phenomenon may also play a role for real houses, and it may therefore influence the temporal variation of indoor radon levels.

In collaboration with the KVI and SSI (project no. 2 and 7, respectively) Risø has compared modelling results with data from real houses of the crawl-space type. In the case of the KVI house, the model was used to identify advective entry into the crawl space and to assess the mitigative impact of sealing the crawl space with polyethylene foil in combination with pressurizing or depressurizing the crawl space. The investigation of the SSI house had two objectives: to provide additional verification of the numerical model, and to help deduce the relative importance of diffusive and advective entry of radon. A publication of this is under preparation.

Test-structure design

The test structure is located on a clayey-till field site. The soil is fairly heterogeneous with observed layers of sand and pockets of gravel. The structure is quadratic with a side length of 2.6 m. The footing extends approx. 0.8 m below the soil surface. The concrete wall and the slab provide an airtight interface to the soil.

A 40 litres cylindrical measuring chamber is bolted to a steel plate that has been poured into the centre of the slab. Radon and soil gas enter the measuring chamber through a 9.5 cm cylindrical hole in the plate. The top of the test structure is closed off with two PVC membranes placed on a base of wood and an aluminium hatch. Thus, the measuring chamber is confined in a mini-basement as shown in Figure 1. In terms of air flows, the measuring chamber is fully isolated from the mini-basement. A layer of highly permeable gravel is located below the slab.

Experimental results: Soil gas

The so-called inverse flow resistance (i.e. the soil-gas entry rate into the structure per pascal depressurization) is measured as follows: The mass-flow controller is set to give a certain flow rate of air. In exhaust mode, this forces an identical flow of air from the soil through the 9.5 cm hole into the cylinder. In supply mode, the flow is reversed and the cylinder is pressurized. Combined measurements of soil-gas flow and differential pressure between the cylinder and the outdoors are obtained for a series of flow settings. The relationship between flow rate and pressure difference is linear, and the slope defines the inverse flow resistance.

All paired measurements of the inverse flow resistance and water-table depth are plotted in Figure 2. As can be seen, the two variables are strongly correlated: the inverse flow resistance

increases monotonically with the depth to the water table from less than $0.1 \text{ L min}^{-1} \text{ Pa}^{-1}$ at 1 m to $0.4 \text{ L min}^{-1} \text{ Pa}^{-1}$ at 1.9 m. The correlation seems to hold true even when the water table is at 1.6 m or deeper: a weighted linear-regression analysis gives a slope which is significantly different from zero at the 5 %-level ($p=0.036$, $N=8$).

Experimental results: Radon

The radon experiments reported in the following have been conducted - primarily - during the summers of 1993, 1994, and 1995 in accordance with the following procedure: Firstly, the mass-flow controller is set to give a certain flow rate. After one to three weeks the soil is assumed to be in equilibrium - i.e. the radon-concentration field in the soil now reflects the new flow condition. At this point, radon measurements begin. Scintillation cells are used for grab sampling of soil-gas radon in the 40 probes located in the ground under and around the test structure. Typically, the measuring campaign goes on for 4 weeks, but in one case it lasted only 2 weeks whereas in another case it lasted 9 weeks. The probes are two-and-two located symmetrically around the test structure. The reported measurements of radon concentrations are observed means found from measurements in two (or four) paired probes over the period of the measuring campaign. The observed standard deviations are used as measures of the uncertainty of the reported radon concentrations and therefore reflect (i) probe-to-probe (i.e. spacial) variation, (ii) temporal variation during the campaign caused by natural changes of the weather and soil conditions, and (iii) imprecision linked to the sampling technique and the radiometric measurements.

The entry rate of soil-gas radon into the structure is estimated as the product of the measured soil-gas entry rate and the measured radon concentration in the sub-slab gravel layer. The measured radon-entry rates are listed in Table 2.

Soil parameters

In situ gas permeabilities were measured in the ground under and around the test structure with a conventional single-probe technique. The values range over four orders of magnitudes with maximum values at $11 \times 10^{-12} \text{ m}^2$, and geometrical mean and standard deviation equal to $7 \times 10^{-13} \text{ m}^2$ and 7.8, respectively. Soil porosity (0.3) and moisture content (10.5 % by mass) was measured using 17 intact soil samples collected June 20-22, 1994 at depths from 0.2 to 3 m. Radon diffusivity and radon-generation rate was estimated based on the radon concentrations measured under diffusive conditions in probes 2 m or more from the structure. An analytical one-dimensional diffusion model was fitted to the data, and a series of combinations of radon diffusivity and generation rate were found to be consistent with the data. These include diffusion lengths in the range 0.6 to 1.05 m and maximum radon concentrations in the range 78 to 116 kBq m^{-3} .

Numerical model

The numerical model RnMod2d was developed at Risø in the previous CEC project. It is a two-dimensional steady-state finite-difference model based on the control-volume approach. The model solves the partial-differential equations for transport of (i) soil gas: Darcy's law and mass continuity and (ii) radon: combined diffusive and advective transport, radon generation, decay, phase partition, and mass continuity. In the simulations presented in this report, the soil is assumed to be homogeneous, and the computational plane extends vertically from the soil surface to the water table (in most cases 1.8 m) and horizontally 15 m from the centre of the structure. The plane is divided into 4704 control volumes of varying sizes.

Two sets of model calculations are performed: One for soil gas and one for radon. In the soil-gas case, the permeability of the ground is the only input parameter. In the radon case, the results of the soil-gas calculations are imported to account for advective transport, and therefore the radon calculation also depends on the selected gas permeability. In addition, the following parameters are needed: soil porosity, water content, radon-generation rate and diffusivity.

In the radon case, the following simple procedure is used to transfer the estimated uncertainty relating to radon diffusivity and generation rate to an uncertainty of modelling results: All calculations are performed four times; one time for each of the following four combinations of radon-diffusion length and maximum radon concentration: (0.6 m, 105 kBq m⁻³), (1.05 m, 105 kBq m⁻³), (0.77 m, 78 kBq m⁻³), and (0.77 m, 116 kBq m⁻³). For all of the considered output elements - such as the radon concentration at a given probe location - the mean value of these four calculations is used as the final result, and the observed standard deviation is used as an estimate of its uncertainty.

Model versus measurements: Soil-gas entry rates

The four cases when the permeability and the inverse flow resistance (i.e. the soil-gas entry rate per pascal depressurization) have been measured almost simultaneously are listed in Table 1. The model predictions are based on the assumption that the soil is homogeneous with a permeability equal to the highest of the measured values at the time of the flow-resistance determination. The model predictions therefore ought to overestimate the inverse flow resistance. However, as seen from the table, the measured values are factors of 2 to 3 higher than predicted by the model.

The effective permeability of the ground - i.e. the permeability that inserted into the model gives the same flow resistance as found experimentally - amounts to $2.4 \times 10^{-11} \text{ m}^2$. This value is used in all of the following radon calculations.

Model versus measurements: Radon-entry rates

Table 2 shows predicted and measured radon-entry rates into the structure for flow rates in the range from 0 to 20 L min⁻¹. At 0 L min⁻¹ (pure diffusion) the predicted value is in perfect agreement with the measurement, but when the flow is imposed, the predicted values are consistently larger than the measured ones. The discrepancy increases with the flow rate, starting from being insignificant at 5.5 L min⁻¹ (considering the estimated uncertainties) to being highly significant at 20 L min⁻¹.

Model versus measurements: Radon-concentration fields

The predicted and measured radon concentrations as function of the entry rate of soil gas into the structure are shown for four selected locations in the ground in Figure 3. There is a very good agreement between the predicted and the measured radon-concentration curves. In particular, the model gives good predictions of the slope and symmetry (or asymmetry) of the curves. The absolute values are, however, in some cases significantly different from the measured ones.

Discussion and conclusions

During summertime conditions the inverse flow resistance is approx. 0.3 to 0.4 L min⁻¹ Pa⁻¹ which is only slightly less than the values 0.4 to 0.5 L min⁻¹ Pa⁻¹ found in a previous experiment using another structure located 14 m away from this one (our previous CEC

project). This is a striking result since the measured single-probe permeabilities within each of the two field sites vary over four orders of magnitude. Given the similarity between the two structures, it indicates that the type of clayey till present at the site has a certain characteristic (gross) permeability, and that entry into houses located on that type of soil will be determined by that permeability.

The correlation between water-table depth and inverse flow resistance shows that the soil-gas flow depends on the condition of the soil and that the flow is not merely supplied e.g. through leaks along the building shell. Hence, the enhanced soil-gas entry rate is a feature of the soil and not the building.

As for the old test structure, the predicted soil-gas entry rates are much lower than the measured values. If we base the model calculations on the geometrical mean of all measured permeabilities at the site, the discrepancy is a factor of 30. Even if the soil is assigned the highest of the measured permeabilities, the model is still off by a factor of two to three. Similar discrepancies between modelled and measured soil-gas entry rates have been reported by Garbesi et al. at the Lawrence Berkeley Laboratory in the USA.

Since the uncertainty relating to the modelling (e.g. the geometrical description of the structure and the mathematical accuracy of the model) and the experimental part of the work is relatively small, the cause of the discrepancy seems to be that the measured permeability - used as input to the model - is different from the value that actually controls soil-gas entry into the structure. This could be because the soil is simply too heterogeneous or anisotropic to be characterized appropriately with a single-probe permeability technique of the type used in this study. In fact, the permeability measurements indicate that the spacial variation is very large: four orders of magnitude for the 13 different locations below and around the structure. Garbesi et al. have previously identified the conventional single-probe permeability measurement technique as an important source of a similar discrepancy between predicted and observed soil-gas entry rates into a well-defined basement structure.

If the soil-gas flow predominantly follows cracks and macro pores in the soil, the permeability becomes scale-dependent such that the permeability measured at the 10-cm scale (with a single-probe technique) is much lower than the value controlling the flow into the house (i.e. the permeability at the scale of several metres). Since it has recently been established that clayey tills are often cracked (and may transport various types of pesticides and other pollutants fairly easily from the soil surface to ground-water reservoirs) it is not unlikely that such structural effects are also present at the site used in this investigation and that this therefore may be the main cause for the observed discrepancy between the predicted and the measured soil-gas entry rates.

To this end, it is interesting that the model predictions of the amount of radon associated with the enhanced soil-gas flow is higher than the measured values since this is qualitatively what is to be expected if the enhanced soil-gas entry rate is provided by cracks or other high-flow paths as speculated above: A flow of soil-gas confined to high-flow paths can transport less of the radon generated in the soil matrix compared to the situation where the same flow is distributed over the matrix in a more homogeneous fashion. This is so because radon needs to diffuse to the high-flow paths to be moved by the gas flow whereas this is not the case when the flow is distributed more uniformly over the full soil matrix.

The overestimation of the radon-entry rate could, however, also be caused by soil anisotropy or if the permeability decreases with the depth. In these cases, less radon will enter the structure from the deeper layers than predicted using the homogeneous-soil approximation, and since these layers tend to have higher radon concentration than those at the top, the model will overestimate the radon-entry rate.

The above discussion therefore leads to the following conceptual model: (i) The effective (or gross) permeability of the building site controls the soil-gas entry rate into the house. (ii) The spacial distribution of this permeability (e.g. layer by layer) controls from where radon is supplied. (iii) The division of the effective permeability into matrix permeability and fracture permeability controls the availability of radon from those regions where the flow goes (i.e. the effectiveness with which the flow can move radon generated in the soil matrix).

This study demonstrates that - under field conditions - model estimates of soil-gas and radon entry rates may be off by as much as one order of magnitude, and that the critical element in the model assessments is the measurement of gas permeability. For the application of numerical models to predict entry into real houses, the following three observations are relevant:

(i) Model predictions of soil-gas and radon entry into houses located on less heterogeneous soils than clayey till - where the permeability is easier to measure - are likely to give much better results than those presented in this study.

(ii) The observed discrepancy between predicted and measured radon-entry rates is statistically insignificant for flows below 6 L min^{-1} ($0.4 \text{ m}^3 \text{ h}^{-1}$) which correspond to what is considered to be a typical soil-gas entry rate into a house depressurized only by natural means. If scaled to a real house - assuming the flow is proportional to the area of the slab - this limit corresponds to a flow as high as $7 \text{ m}^3 \text{ h}^{-1}$.

(iii) The two discrepancies (the underestimation of soil-gas entry rate and the overestimation of the associated radon concentration) will tend to cancel each other and give a better prediction of radon-entry rate than showed in this study where the radon simulations were based on the correct entry rates of soil gas (not those incorrectly predicted by the model).

In conclusion, the good agreement between predicted and measured radon-concentration fields in the soil below and around the structure shows that the model itself is well founded. It is the assessment of gas permeability of the soil that is the critical parameter when predicting - not only - the amount of soil gas that enters a house, but also from where it comes and how effectively it can transport the available radon.

Publications

Andersen, C.E.; Koopmans, M.; Berger, H.; de Meijer, R.J.: The effect of a foil on the floor of a crawl space in relation to radon entry. In: Proceedings of the international workshop Indoor air - An integrated approach, Gold Coast Australia, 27 November - 1 December 1994.

Andersen, C.E.; Koopmans, M.; de Meijer, R.J.: Identification of advective entry of soil-gas radon into a crawl space covered with sheets of polyethylene foil. **DRAFT** dated December 16, 1994. Report R-58. Kernfysisch Versneller Instituut, the Netherlands (pp. 134).

Andersen, C.E.; Søgaard-Hansen, J.; Damkjær, A.; Majborn, B.: Modellering og måling af radons indtrængning i bygninger - analoger til indtrængning af andre gasser. (In Danish). IN: Vurdering af inde- og udeklima på grunde forurenede med flygtige organiske kemikalier. ATV møde, København (DK), 4. November 1993 (ATV-komiteen vedrørende grundvandsforurening, Institut for Geologi og Geoteknik, Lyngby, 1993) p. 133-150.

Andersen, C.E.; Søgaard-Hansen, J.; Damkjær, A.; Majborn, B.: Enhanced soil-gas entry into a radon test structure located on clayey till. Submitted to the Sixth International Symposium on the Natural Radiation Environment, Montreal, June 5-9, 1995.

Andersen, C.E.; Søgaard-Hansen, J.; Majborn, B.: Soil-gas and radon entry into a simple test structure: Comparison of experimental and modelling results. Radiation Protection Dosimetry, vol. 56, Nos. 1-4, 151-155, 1994.

van der Graff, E.R.; Witteman, G.A.A.; van der Spool, W.H.; Andersen, C.E.; de Meijer, R.J.: Measurements on, and modelling of diffusive and advective radon transport in soil. Radiation Protection Dosimetry, vol. 56, Nos. 1-4, 167-170, 1994.

Table 1: Comparison of predicted and measured soil-gas entry rates. The model predictions are based on the maximum permeability observed at the site at the date of the entry-rate determination.

Date	Maximum observed permeability	Soil-gas entry rate per pascal depressurization (Inverse flow resistance)		
		Model prediction	Measurement	Model-measurement ratio
-	$\times 10^{-12} \text{ m}^2$	$\text{L min}^{-1} \text{ Pa}^{-1}$	$\text{L min}^{-1} \text{ Pa}^{-1}$	-
Oct. 8, 1992	5	0.088	0.28±0.01	0.31
Aug. 4, 1994	11	0.19	0.42±0.01	0.45
Aug. 11, 1994	10	0.17	0.41±0.17	0.41
May 1, 1995	6	0.10	0.30±0.10	0.33

Table 2: Comparison of predicted and measured radon-entry rates. Uncertainties relating to the model predictions come from the uncertainty of the input parameters to the model. An effective permeability equal to $2.4 \times 10^{-11} \text{ m}^2$ is used in all of the calculations. This is the soil-permeability "as seen from the structure".

Soil-gas flow into the structure	Radon-entry rate into the structure		
	Model prediction	Measurement	Model-measurement ratio
L min^{-1}	Bq s^{-1}	Bq s^{-1}	-
0 (diffusion)	$(4 \pm 1) \times 10^{-3}$	$(4 \pm 1) \times 10^{-3}$	1.0±0.4
5.5	2.5±0.4	1.8±0.6	1.4±0.5
10	3.5±0.6	1.1±0.2	3.2±0.8
20	4.7±0.8	1.3±0.2	3.6±0.8

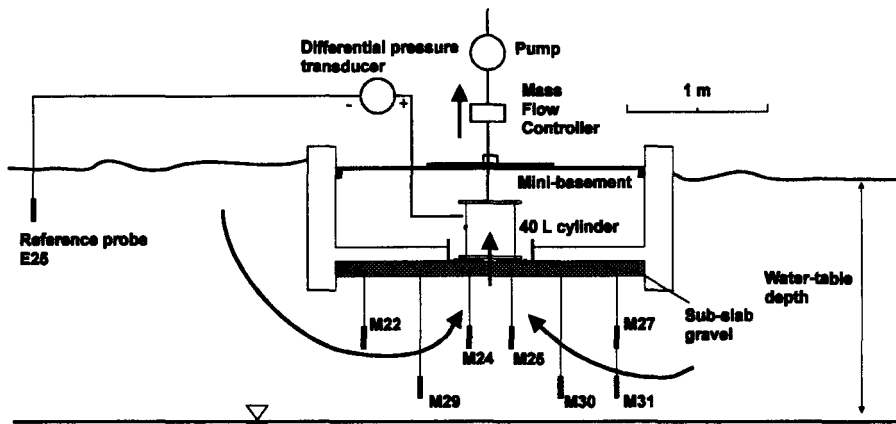


Figure 1: Cross-sectional view of the test structure. Some of the probes located below the structure (labelled M22 to M31) are also shown.

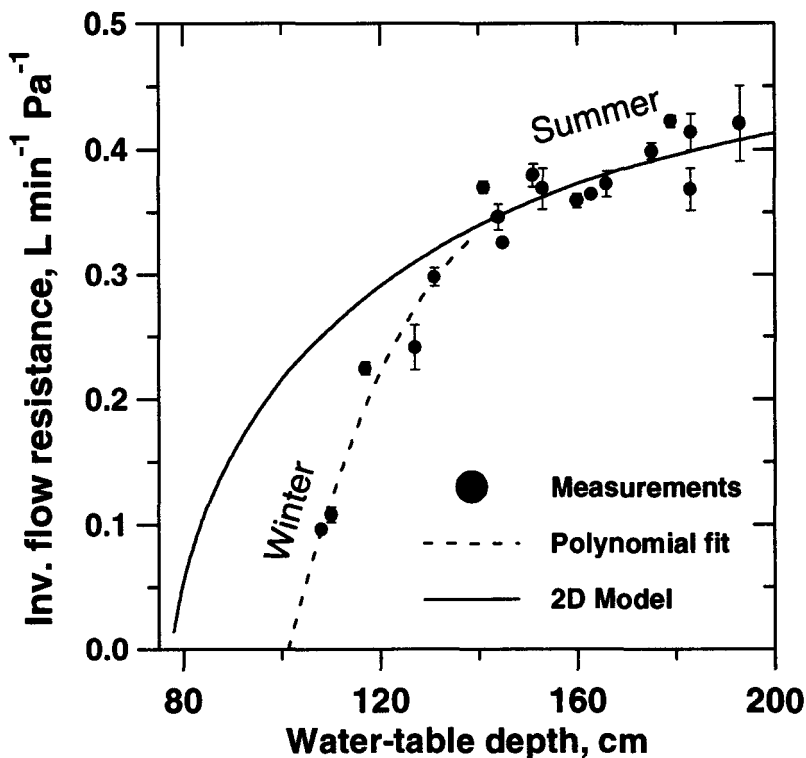


Figure 2: Inv. flow resistance (i.e. the soil-gas entry rate per Pa depressurization) versus water-table depth. The model calculation is for homogeneous soil with a permeability of $2.4 \times 10^{-11} \text{ m}^2$.

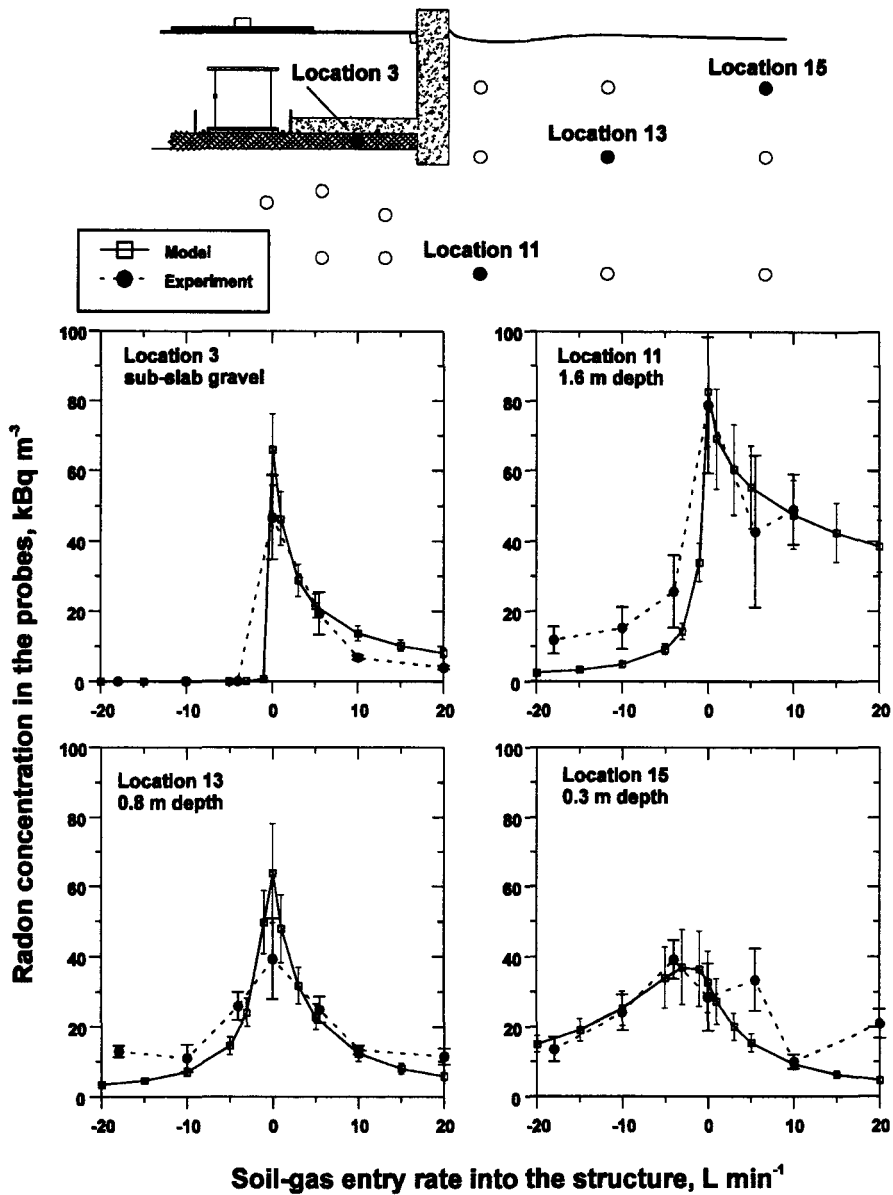


Figure 3: Comparison of model calculations (\square) and measurements (\bullet) of radon concentrations in four probes. Negative entry rates occur when the structure is pressurized (air is forced from the structure into the soil).

Head of project 4: P. Wouters

II. Objectives of the reporting period

The general objective of the BBRI contribution to the project was to study, from theoretical and experimental viewpoints, the role of ventilation and air flow patterns in the context of radon, with a particular attention paid to radon reduction techniques.

Air flows play a role at two levels in the radon context, on the one hand, the radon transport in the ground (soil gas movement) and, on the other hand, the air movements in the building (interzonal air flow). Both aspects were studied which involves model calculations and in-situ experiments, some of them in collaboration with other participants to the project.

III. Progress achieved including publications

III.1 In situ studies: selection and evaluation of mitigation techniques for radon reduction in dwellings

A large part of the project was devoted to in-situ studies. Three Belgian dwellings were investigated one located in Court-St-Etienne, one located in Olen and the last one in Visé.

The objective of these experimental studies was to define and evaluate remedial techniques and to achieve a better understanding of the radon transport. These three studies deal, among others, with the questions about the choice of the parameters to be measured in order to define appropriate remedial actions. Indeed, parameters related to the characteristics of buildings, to their use and to the occupant behaviour, as well as the characteristics of the soil, play a role of first importance and strongly complicate the problem. This complexity is at the root of the difficulties which arise when defining and applying suitable corrective measures, and justifies that research activities are developed on the topic.

The Visé dwelling has been the subject of several investigations, including a study of the inside air movements with tracer gas techniques. This comprehensive study provides a good example illustrating the scientific approach followed for tackling radon problems in dwellings with the most appropriate technique and will be therefore presented with some details in this final report. Both other case studies are more succinctly reported.

a) A case study in Visé

The building

Figure 1 shows a sketch of the ground floor of the Visé dwelling. It consists of two old buildings: a house dating from the beginning of the 19th century and an annex built in 1938. The annex is mainly composed of the kitchen and of the play-room. The ground floor rooms are built either on basements either on the soil. Figure 1 allows to see that the basements only cover 30 % of the total ground floor area. Each basement has a vent. The first floor consists of two bedrooms, a bathroom and a hall. The second floor corresponds to the attic used as a lumber room. When visiting the dwelling, it can be quickly noticed that the building is poorly airtight and presents visible airtightness defects among others on window-frames, particularly at the first floor, and at the roof level.

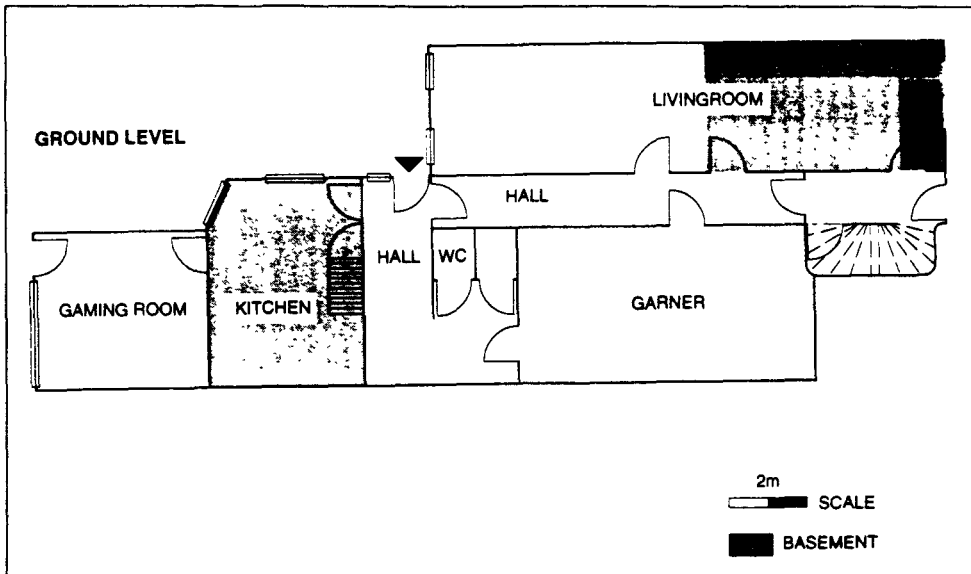


Figure 1 - The Visé dwelling - Sketch of the ground floor

Radon concentrations

Radon concentrations up to 4500 Bq/m^3 were measured in the occupied rooms of this dwelling while concentrations of 10000 Bq/m^3 were found in the cellars. It is interesting to mention that the measurements performed in the closest neighbouring dwellings revealed radon concentrations between 50 and 150 Bq/m^3 which is below usual action levels and, in comparison with the studied dwelling, very low

Evaluation of some building characteristics

It has been recognised that determining the characteristics of the building is an essential step to define, with the highest probability of success, appropriate corrective measures. In practice, it is important to choose the minimal number of parameters sufficient to manage with success the choice of the most appropriate corrective measure. With this respect, it seems to us that the parameters connected to the airtightness of the building (airtightness of the envelope but also of certain rooms in particular) are among the most important ones. Indeed, airtightness seems to play an important part in relation with the different corrective techniques of which main principles can be found in the literature (I, II and III) sealing of entry routes, techniques based on ventilation and techniques aimed to reverse the radon driving pressure difference.

The important findings resulting from the measurements and inspections performed can be summarised as follows:

- The cellars probably play an important role since there is no ground covering and many entry routes exist between them and the rest of the building
- Nothing allows however to state that these cellars are the only radon entry paths in the building since radon can also enter directly in the other rooms in contact with the soil.
- The building is not very airtight and therefore is submitted to quite high ventilation rates
- As well the airtightness of the cellars is very poor but it seems possible to highly improve it at low cost

- The dwelling being located along the river Meuse, it is possible to find river gravel when digging the soil

Choice of an appropriate mitigation technique

Since a lot of entry routes were detected between the basements and the rest of the building, a first logical action is to reduce them as much as possible. In view of the very high radon concentrations measured, it is clear that this first step is certainly not sufficient but it will nevertheless help to diminish the radon ingress into the dwelling and therefore increase the efficiency of other possible techniques.

Active remedial techniques are generally categorised in two groups: the ones which are based on the building ventilation and the ones based on the reduction of the radon entry rate from the soil. As the evaluation of building characteristics showed that the airtightness of the building and of the different rooms was poor, the building is already well naturally ventilated. Considering the high radon concentrations measured, reducing them to an acceptable level would result in huge ventilation rates. Therefore, the techniques based on building ventilation were not retained.

In order to reduce the radon gas entry from the soil, one must inverse the pressure gradient which can be achieved either by increasing the pressure in the rooms in contact with the soil (room pressurisation technique) or by decreasing the pressure in the soil (soil depressurisation technique). The pressurisation technique can only be applied in rooms which are quite airtight. Otherwise, the air flow rates needed to increase sufficiently the room pressure would be too high. Therefore, this technique could only be applied in the two basements. Indeed, the entry paths getting indoors and outdoors were well localised and the airtightness of these rooms could be sufficiently improved. However, this technique will only have a favourable influence on the radon concentrations measured in the rest of the dwelling if the two basements are the only rooms through which radon enters. In the opposite case, all the other lower rooms through which this gas could enter will also have to be pressurised. This seems difficult in the prevailing case considering the bad airtightness of the building and the type of rooms which are to be processed.

Soil depressurisation technique was finally chosen. This technique allows in principle to prevent radon ingress through entry paths situated in all the lower rooms and this without that it is necessary to modify the airtightness characteristics of the building envelope. Moreover, some gravels could be found since the dwelling is located near the river "Meuse" which could increase the soil permeability hence the probability of success.

Evaluation of the chosen corrective technique

A sump was realised in the cellar beneath the living room, near the left lower corner of this basement so as to obtain the more central position with respect to the whole dwelling.

The pressure field extension was estimated by looking at the pressure difference between the soil and the other cellar: only a few tenths of Pascal were measured.

Despite the very weak pressure field extension, the radon concentration measurements performed to evaluate the efficiency of the remedial technique provided values lower than 100 Bq/m³ in the occupied rooms.

It can therefore be concluded that the selected method proves to be efficient in spite of a weak pressure field extension, and in spite of the absence of an airtight covering on the soil of the basement where the suction point is located. In opposition to what is sometimes stated, it seems not always necessary to create high pressure differences between the soil and the interior of the building at each point. A depressurisation of the soil of some tenths of Pa in points distant from the suction point, showing that there is an effect linked to the suction, seems to be

largely sufficient This conclusion confirms some findings concerning the effectiveness, in difficult situations, of the soil depressurisation technique applied in the UK (IV).

Radon entry and transport inside the dwelling

The above conclusion concerning the effectiveness of the soil depressurisation in difficult situation would have to be reconsidered if the soil of the cellar beneath the kitchen was presumed not to act as a radon source for the dwelling

Tracer gas measurements were performed to make a final evaluation of the SSD technique implemented in the dwelling and to validate the use of tracer gas for studying radon transport

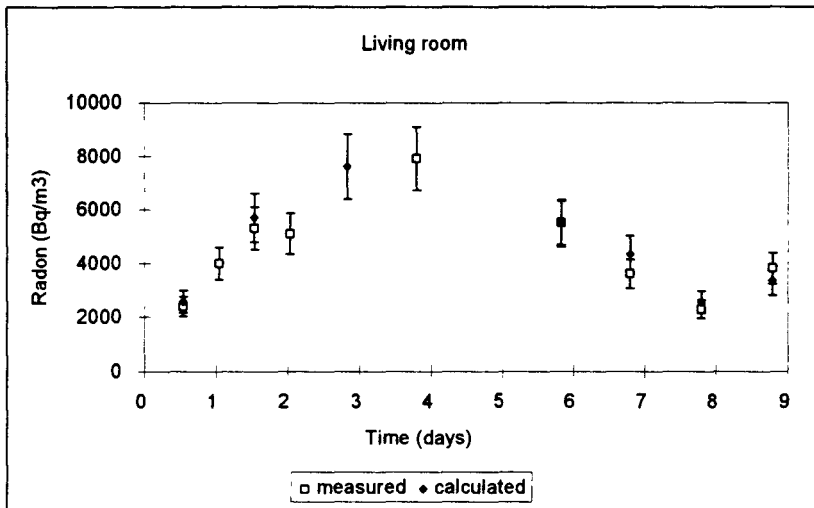


Figure 2 - Predicted and measured radon concentrations in the living-room

Two tracer gases were used simultaneously N_2O was injected in the cellar situated beneath the living-room, while SF_6 was injected in the cellar beneath the kitchen. The injection was adjusted in function of time, in order to maintain a constant concentration in each of these cellars. The concentrations of each one of these two gases were measured in the cellars and in each room, in function of time

From the tracer concentrations in one specific cellar and one specific room, one can calculate a "pollution index" which represents the amount of air in the room which comes from the cellar. Both pollution indexes (for both cellars) were evaluated in the seven rooms. Knowing the radon concentrations in both cellars, one can predict the radon concentrations in these seven rooms. However, this calculation makes the implicit assumption that all the radon found in the rooms comes from the cellars. If it was not the case, no agreement would be found between predicted and measured values. Figure 2 shows the predicted and measured concentrations in the living-room. As it can be seen, the agreement between both concentrations is quite good.

On the one hand, the overall analysis shows that the two cellars behave as important source rooms, the building can be divided in two parts, each of them dominated by one source room, there is no other major source room in the dwelling.

On the other hand, the tracer gas measurement performed confirmed that the SSD technique was successful in reducing the radon concentration in the occupied rooms in spite of the weak pressure field extension.

A detailed description of this study can be found in [10].

b) A case study in Court-St-Etienne

The Court-St-Etienne dwelling is another building with high radon concentrations (several thousands Bq/m³ in occupied rooms)

Before contacting BBRI, the inhabitants had installed a subslab natural ventilation system but without achieving a reduction of the radon concentrations. The pipes installed by the occupants were used to install and evaluate the active sub soil depressurisation technique, in spite of the existing difficult conditions: very bad airtightness of the slab, clayey soil, installed suction pipes placed at an unfavourable position. The pressure difference between the soil and the house measured far from the suction pipes indicated that the pressure field extension was weak. In spite of that, the radon concentration measurements proved the remedial action was a success.

A detailed description of this study can be found in [4].

c) A case study in Olen

The Olen dwelling is a building in which radon concentrations of several Bq/m³ were measured. An investigation carried out by the CEN-Mol (team of H. Vanmarcke) showed that the soil situated under the veranda would be the main radon source. After visual inspection, a soil depressurisation technique was chosen owing to the characteristics (among others the airtightness) of the veranda. This remedial action proved to be very efficient in reducing the radon concentrations in the dwelling. More information can be found in [6].

d) Conclusions

The lessons that can be drawn from these in-situ studies concern the results of the measurements of the radon concentrations, the procedure followed to define the adequate corrective measures, the soil depressurisation technique itself, and, finally, the use of tracer gas for evaluating radon transport in dwellings.

Regarding the radon concentrations, an interesting result is the difference between the values measured in the Visé dwelling and the neighbouring dwellings. This confirms that it may be misleading to generalise conclusions based on the study of a very limited sample of dwellings.

Regarding the procedure which led to the choice of the soil depressurisation technique, it is important to point out that the investigations made allowed to choose, at the first attempt, the right method to apply (at least for the Visé and the Court-St-Etienne dwellings). It is tempting hence to state that these success shows in a certain way that the parameters related to airtightness are of the highest importance to determine the appropriate corrective techniques.

An important conclusion related to the soil depressurisation technique is also to be drawn from this studies: it seems that in contrast to what is sometimes said, it is not always required to create great pressure differences between the soil and the interior of the building at each point. A depressurisation of the soil of some tenths of Pa, showing that there is an effect linked to the suction, seems to be largely sufficient in points distant from the suction point. It must also be added that this technique proved efficient without being necessary to put an airtight covering (concrete or plastic sheet) on the soil of the basement where the suction point was located. This also goes against some principles concerning this method.

Finally, tracer gas techniques proved to be very efficient in assessing radon transport within dwelling.

III.2 Soil gas movement modelling

The radon gas movement in the soil depends on various phenomena advection, diffusion, decay, emanation, etc. The complete study of the problem leads to transport equations which involves a lot of material characteristics (material porosity, diffusion coefficient, permeability, ...) These can vary in the space and should, for the sake of exactness, be known at each point of the studied system. Fortunately, the characteristics of the same layer of material (concrete, clay, sand...) take generally similar values at every point. But, all the same, one has to know the geometric configuration of the layers forming the system and the properties of each of them. We believe that such models are very important to understand the radon transport within the soil but are too complex to be used in the definition of mitigation techniques in the field (for cost and time consumption reasons)

However, simplifications can be made which makes it possible to use soil gas modelling more widely, especially in the framework of mitigation techniques. Commonly used simplifications consist in neglecting other transport phenomena than the advection and assuming laminar air flows in the soil (V). A linear relation is then found between the pressure gradient and the soil gas velocity, the so-called Darcy's law, taking account of only one material characteristic, the permeability. The assumptions made are perhaps quite severe but more complex models would require material characteristics which are in most cases not available. It should be noted that even permeability values are difficult to estimate in practice and that only order of magnitude can generally be given. In particular, Bell P. and Cripps A. pointed out that the permeability could vary with the flow path length (VI).

Since Darcy's law is linear, the finite difference codes which solve any kind of linear flow models can be used. The code TRISCO (VII) was used within the framework of this project. This approach appears to be well suited for the design and the evaluation of soil depressurisation remedial actions (V). It should be noted that in the case of soil depressurisation techniques, the assumption consisting in neglecting diffusion transport is certainly valid since the advection is forced by the fan. However, air velocities being high, Darcy's law must be used with care. In the case of natural convection, it is not clear whether diffusion can be neglected or not but the low velocities encountered are more likely to follow Darcy's law.

a) A user friendly simulation tool intended for architects

The use of most of the finite differences or finite elements programs is not evident for non-specialists, and this as well with respect to the understanding of the software as with respect to the collection of the input data and the interpretation of the results.

Therefore, the Belgian firm Physibel developed in 1992 a software package allowing to develop a so-called 'atlas of thermal bridges': KOBRA (VIII). The software in combination with a useful atlas of building details should allow architects, building contractors, engineers, to evaluate in a very simple way the importance of certain thermal bridges as well as the impact of certain modifications.

The development of such atlas is a huge task. Therefore, BBRI brought organisation of 7 countries together for developing a European atlas. This project at present receives support from the EC-DGXII SAVE program.

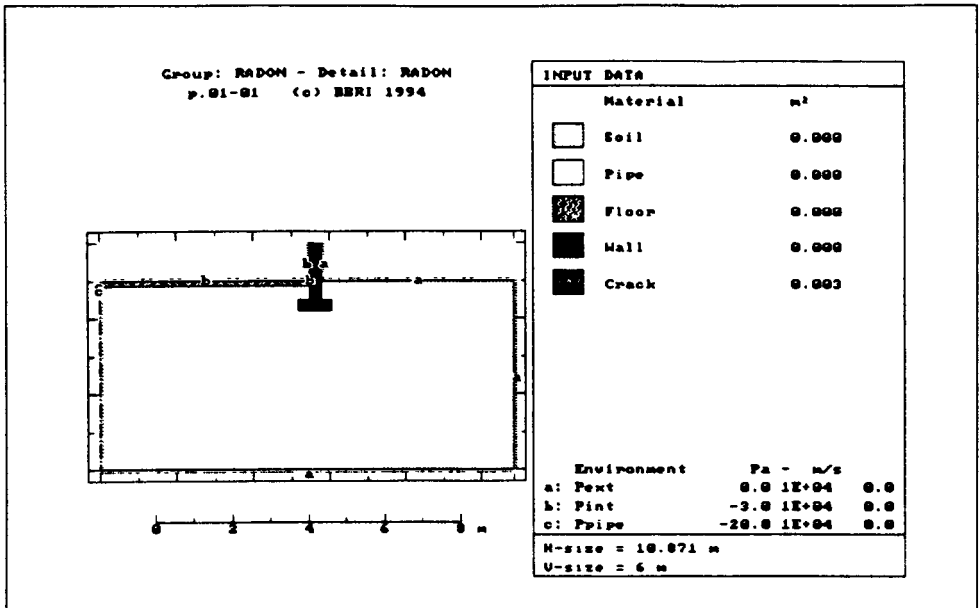


Figure 3 - Evaluation report of the KOBRA software

Given the similarity between heat flow by conduction and laminar air flow processes in the ground, the concept could be used for the problem of radon transport in the ground. The final product would be a collection of construction details frequently encountered in the framework of radon problems. The end user could easily adapt all parameters (size of different elements, permeability, pressure at boundaries, ...) and get immediate results.

Some construction details relevant for the evaluation of soil depressurisation techniques were introduced in the software. Figure 3 gives an example of evaluation report that can be obtained.

The current version of KOBRA handles only 2 dimensional details which could be a serious limitation in the case of soil gas modelling. It is however intended to enlarge the thermal bridge atlas to 3 dimensional details which are more relevant for the evaluation of radon transport in the ground, especially for the modelling of sub slab depressurisation mitigation technique.

b) Soil gas modelling in the SSI test house

In collaboration with SSI, a model was developed to simulate radon infiltration from the subfloor of one test house of which the ground composition is quite well known. Figure 4 shows a 3D view of the model.

The objective of the modelling exercise was to calculate the amount of air flowing from the soil into the crawl space. Knowing the radon concentration in the soil, it is then possible to determine the radon flow rate into the dwelling. The obtained results are compared with the measurements performed by SSI (Hubbard L., project 7).

Let us note that, in this case, the convection is natural which means that diffusion plays perhaps a not negligible role in the transport but is not taken into account by the model.

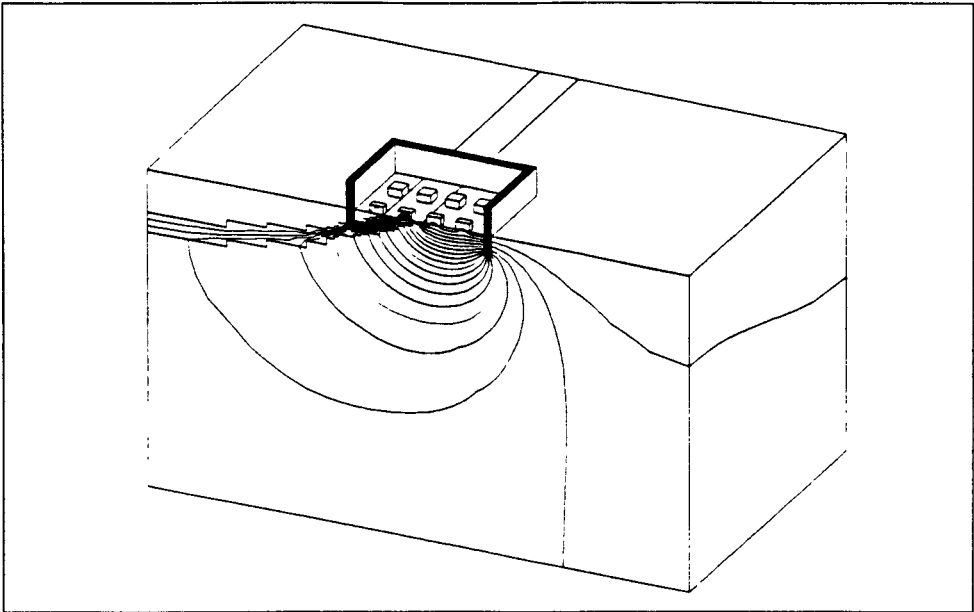


Figure 4 - Soil gas modelling in the SSI test house - 3D view of the foundation model

Figure 4 shows also the isobars in the soil calculated by the model. The calculated total flow resistance between the crawlspace and the outside is equal to $2.0 \cdot 10^4 \text{ Pa.s/m}^3$

SSI has measured an average (15 days) source strength to the crawlspace of about 4.1 Bq/s using passive tracer gas technique in combination with radon concentration measurements

On the same measurement period, the average radon concentration in the soil under the house was about 34000 Bq/m^3 and the pressure difference between the crawlspace and the outside was about 2.8 Pa . Using those values with the soil model yields a source strength of 4.7 Bq/s to the crawlspace which is in very good agreement with the measured value when thinking of the numerous assumptions made

It can be concluded that the use of a finite difference code which had already proved to be well suited for the design and the evaluation of soil depressurisation remedial actions (V), was also able to estimate the gas flow rate from the soil into a crawlspace under natural ventilation conditions

Besides, two other simulations were performed with altered values of permeability so as to evaluate their impacts on the gas flow rate. The results showed that the permeability of the clay layer had a little impact on the calculation: a variation of 2 orders of magnitude entails a variation of only 5% on the calculated gas flow rate. On the contrary, variations of the permeability of more permeable layers (sand in this case) have almost a proportional effect which means that the uncertainties on the soil permeabilities in practice have a strong impact on the simulation results

This study is described in detail in [11]

c) State-of-the-art document

A part of the work during this working period was dedicated to the synthesis of what is achievable with the available modelling tools and how to collect the necessary input data. This

results in a document ("Air flow related modelling aspects in the context of radon problems in dwellings an overview of the state-of-the-art") intended for non-specialist person involved in the radon research. At the present stage, a working draft version is available.

III.3 Publications

1. Cohilis, P., Wouters, P., Voordecker, P., Radon reduction in buildings the case of two Belgian schools, presented at the International Conference on Building Design, Technology & Occupant Well-Being in Temperate Climates, Brussels, Belgium, 1993
2. Poffijn, P., Eggermont, G., Hallez, S., Cohilis, P., Radon in Belgium: Mapping and mitigation in the affected area of Visé, presented at the First International Workshop on Indoor Radon Remedial Action, Rimini, Italy, 1993.
3. Cohilis, P., Poffijn, A., Voordecker, P., Meesen, G., Wouters, P., Radon reduction in buildings selection and evaluation of a mitigation techniques. A case study in Visé (Belgium), presented at the Euroregional Symposium on Radon, Liège, Belgium, 1993
4. Cohilis, P., Tondeur, F., Voordecker, P., Wouters, P., Radon reduction in buildings evaluation of SSD technique in a dwelling in Court-St-Etienne (Belgium), CSTC-WTCB, internal report, 1993
5. Cohilis, P., Wouters, P., Short description of the contribution of the Belgian Building Research Institute (WTCB/CSTC) to the "Radon Sources, Models and Countermeasures", presented at the 2nd Radon Contractor's meeting, Göttingen, 1993
6. Cohilis, P., Que faire lorsque l'on découvre l'existence du radon dans une construction?, presented at the conference "Le radon dans notre région" in Liège, Belgium, 1993
7. Cohilis, P., Proposition d'une technique corrective pour diminuer les concentrations de radon dans une habitation de Olen, CSTC-WTCB, Internal report, 1993
8. Cohilis, P., Poffijn, A., L'Heureux, D., Wouters, P., Voordecker, P., Bossicard, R., Meesen, G., A case study in Visé tracer gas measurements and final evaluation of the soil depressurisation technique, BBRI and the State University of Ghent, 1994.
9. Ducarme, D., Wouters, P., Martin, S., Air flow related modelling aspects in the context of radon problems in dwellings an overview of the state of the art, CSTC-WTCB, Internal report, 1995
10. Cohilis, P., Poffijn, A., L'Heureux, D., Wouters, P., Voordecker, P., Bossicard, R., Meesen, G., Ducarme, D., Selection and Evaluation of a Mitigation Technique for Radon Reduction in Dwellings, submitted for publication in Health Physics, 1995.
11. Ducarme, D., Martin, S., Soil gas modelling in the SSI test house n° 902, CSTC-WTCB, Internal report, 1995

III.4 References

- I. Belgian Building Research Institute (BBRI - CSTC - WTCB, Belgium), Le radon dans les habitations, 1991.
- II. Department of the Environment (DE, UK). The householders' guide to Radon, second edition, 1990.
- III. Environmental Protection Agency (EPA, USA) Radon Reduction Techniques for Detached Houses (Technical Guidance), second edition, 1988

- IV Miles, J. National Radiological Protection Board (NRPB, UK), private communication, 1992
- V Cohilis, P , Wouters, P , L'Heureux, D , Use of finite difference code for the prediction of the ability of subfloor ventilation strategies in order to reduce indoor air radon concentrations, Radiation Protection Dosimetry, Vol 45 N°1/4 pp 575-579, 1992
- VI Bell, P., Cripps, A., Using pressure extension tests to improve radon protection of UK housing, proceedings of the 15th AIVC Conference, Vol. 2, pp. 204-213, 1994
- VII Physibel, TRISCO. computer program to calculate three-dimensional steady-state heat transfer in objects described in a beam shaped grid using the energy balance technique, 1994
- VIII. Physibel, KOBRA. computer program to query an atlas of building details on their thermal behaviour (two-dimensional steady state), 1995

Head of project 5: Dr TK Ball

II. Objectives for the reporting period

The aims and objectives of the project were: to develop radon potential mapping techniques, to investigate the roles that existing geological and geochemical data sets; new measurements of soil and bed-rock radioelement concentrations; and in particular the determination of soil gas radon levels, might have to the efficient recognition of zones of high radon values in houses. As well as understanding the factors influencing the generation of radon from the ground the relationship with house levels was to be determined. Field areas were chosen to combine a high density of house measurements with geological features typical of an European context. The areas were underlain by a variety of rock types and in glaciated and non-glaciated regions. The glaciated areas are characterised by being both glacially eroded, with relatively minor areas of glacial deposition and also representative of major areas of glacial deposition. Such work is complementary to studies in the more heavily glaciated regions of Sweden, and would typify the situation in many European countries which were at or near the limit of glaciation, mostly to the area south of the Baltic Sea.

Geochemical data were collected in Spring-Autumn 1992 for Somerset and Spring/Autumn 1993 for Derbyshire, where large house data set were available for comparison. Field work was undertaken in late Spring 1994 in Scotland and Northern England.

III. Progress achieved during the Reporting Period

SOMERSET

Somerset adjoins the designated radon affected counties of Cornwall and Devon, and a large NRPB housing data set was available. Rock types ranging from various limestones through calcareous shales to clays, and relatively unconsolidated sandstones to competent sandstones and shales, were available for testing. The rocks are characterised by a small range of uranium concentrations but a wide spread of bed-rock permeabilities. This contrasts with Derbyshire and Northamptonshire where the uranium concentrations were more widespread. Somerset was south of the limit of ice during the Pleistocene and retains many of the erosional features which predated this period. Head, formed under periglacial conditions, mantles much of the area, but is absent or sparse on limestone terrains. It is an unstratified or poorly stratified accumulation of rock fragments of local origin, mantling high ground but often transported by solifluction onto valley slopes and bottoms. Another common overburden is valley terrace deposits. These line river valleys at a higher level than the current flood plain. Since the area has an extensive coast-line there are also thick deposits of estuarine alluvium in low lying coastal areas, and which extend inland. Estuarine alluvium is clay dominated and relatively impermeable. There are also thick deposits of peat underlying large areas of low ground. Overlying the Cretaceous Chalk there is commonly a residual overburden deposit: Clay-with-Flints. This is of varying age but is characteristically much more uraniumiferous than the parent chalk.

The field work took place during September 1992. Soil gas surveys and geological data have been compared with the NRPB house data set. By considering the permeabilities and the radon in soil gas values a reasonable relationship exists with the percentage of houses above the action level. This relationship enables the geochemical data to aid the identification of areas of high radon potential where house data are absent or sparse, and to advise on the construction of contours for maps based upon house data.

Considerations of the aquifer characteristics of the bed-rock give an indication of the permeability to fluids passing through the bed-rock and hence give an indication of the likely transport of ground gas. There are many aquifers, both exploited and potential, in the area and

consideration, in any modelling exercise, must be given to the characteristics of these. The properties may be summarised:

Granular aquifers. Primary porosity, fairly homogenous, isotropic, Darcy's Law applies, flow is slow and laminar.

Fractured rock aquifers. Secondary permeability along joints, bedding planes and faults. Less homogenous and isotropic but depends on scale. Darcy's law sometimes applies, flow may be turbulent.

Karst aquifers. Ternary permeability by solutional enlargement of fractures. Inhomogeneous, anisotropic, Darcy's law does not apply. Flow is irregular and almost always turbulent.

Generally the aquifers are separated from each other by aquicludes. The main aquicludes are clay bearing formations, although some sandstones have properties which similarly prevent the rapid flow of fluids.

The main granular aquifers are the sandstones such as the Upper Lias Sand Formations. Fractured rock aquifers are typified by the harder sandstones such as those in the Coal Measures or some of the least karstified limestones.

Karstic Aquifers are represented by the major limestone units. The Carboniferous Limestones in particular have extensive cave systems, whilst many of the other limestones show evidence for small scale karstic and epi-karstic development.

It is clear that there are some rocks which show characteristics common to several aquifer types. The Lower Cretaceous Chalk deposit, for example, is a highly porous rock but the necks of the pore spaces are so small that there is little transfer of fluids between the pores. Because of the slow flow of water in this regime the main migration route for radon in the bulk of the rock is by diffusion, but the distances in water are relatively small, being limited to about 10 cms. There is thus little transport of radon in the granular regime. The Chalk is however an excellent aquifer because it is mainly a fractured rock aquifer. The radon content of the groundwater therefore reflects the radon emanating from the walls of the fractures. The fracturing is irregular and tends to occur in zones. Some of these fractures are enlarged by karstic processes. Radon in overburden gases reflects this inhomogeneity, with a wide spread of values reflecting the variable nature of the fracturing.

Some of the geological formations are typified by mixed rock types. For example the Lower Lias ranges in composition from a relatively pure limestone near the northern limit through to dominantly clay with sparse interbedded limestone in the south of the county. An element of judgement is thus necessary in assigning a radon potential to areas underlain by this rock type.

Where there are sufficient houses (>80) house radon distribution values for geological formations in general approximate to the lognormal rule and identify unimodal populations. There is a good relationship between the actual percentage of houses above the Action Level and the percentage expected from the distribution data. Two of the formations show bimodality. The Yeovil Sand Formation (in the Upper Lias) for example, can be divided into two lognormally distributed populations with means of 25 Bq/m³, accounting for 90% of the data, whilst the remainder has a mean of 125 Bq/m³. The only other formation with strong evidence for bimodality is the Morte Slates within the Devonian. The data for this formation, can be resolved into two components; the upper 5% having a mean of 370 Bq/m³, with over 99% of this sub-population being above the action level, whilst the remainder has a mean value of 40 Bq/m³ and with 0.5% expected to be above the action level.

A comparison between the geological assessment of the individual rock types with the actual data obtained from the housing survey is given in Table 1. Because the individual housing data are confidential it is only possible to assign a rock type to the data in general terms, and houses are not included in such a data set if the positioning is ambiguous. A small inbuilt bias is thus introduced since houses positioned near the junctions between rock formations are thus under-represented. The classes used relate to: High, where 10% or more of houses are above the Action Level. Moderate, where 1%-10% are above the action level. Low+ where it is judged that the potential is low but there may be isolated high values. Low,

where <1% are affected. Agreement is generally good despite the small populations available for certain rock types. The greatest disagreement is with the Cornbrash, which is a clay rich ferruginous limestone. Moderate levels of radon were observed in related soils and the nature of the rock type indicates moderate permeability. However the housing data indicates that less than 1% is affected.

DERBYSHIRE

The county of Derbyshire has contrasting uranium levels in the bed-rock and also contrasting permeabilities. The logistics of extending out from the well surveyed Chapel en le Frith area, mapped in the first round, to include similar lithologies in neighbouring areas and hence to develop procedures for covering larger areas more efficiently, were studied. A simplified geological map for Derbyshire and adjoining areas is given in Figure 3. The oldest rocks are the heavily karstified Carboniferous Limestones with included basic igneous rocks. These generally have low uranium levels (commonly 1-2ppm) but the uranium bearing minerals are often widely disseminated or are in low density components of the rocks. The specific surface area of the uranium bearing phases is often large and radon can be generated from the mineral host with great efficiency. Some of the marginal limestones are uranium enriched.

The limestones are overlain by Namurian rocks the basal members of which are highly radioactive black shales. The main part of the succession however comprises a sequence of thick shales and sandstones with average uranium concentrations. These are overlain in turn by the Coal Measures (= Westphalian): a cyclothem sequence of sandstones, shales, seat-earths and coals. In places, especially in the Lower Coal Measures, the sandstone units are thick and abundant. Highly radioactive "Marine Bands" occur sparsely within the Namurian and Westphalian Strata.

The rocks were folded uplifted and eroded prior to the deposition of Permo-Triassic rocks. In the east the first representative of these periods is the Magnesian Limestone. Elsewhere the lower beds belong to the Sherwood Sandstone Group (= Bunter Sandstones) overlain by marls of the Mercia Mudstone Group (= Keuper).

The whole region was glaciated during the Pleistocene. Since the area is largely upland the main part underwent glacial erosion, with deposition on the lower ground, which is mostly underlain by the Permo-Triassic rocks. In the high ground glacial deposits are mostly valley confined fluvio-glacial, comprising sands, gravels and terrace deposits..

Limestones are the most important radon generators in the region. The Permian Limestone, which is karstified but to a smaller extent than those in the Carboniferous, shows lower levels of radon emanation, which is also reflected in houses. On the basis of the geochemical sampling, predictions were made for radon characteristics of the rock types and then these indications were compared with the house data. The clay rich rocks in the south of the area were predicted to have little radon potential and this remains so. However there are small area sub-environments which have a higher potential.

The sandstones in the Namurian and Westphalian are fractured rock aquifers and despite having low levels of uranium, much of this is disseminated in the cement surrounding the individual sand-grains. They are consistent moderate generators of radon.

Radon from the shales of the Namurian and Westphalian conforms with their uranium concentrations. The highest levels occur over shales (Edale Shales) in the lowermost part of the Namurian and over marine incursion horizons higher in the Namurian and the Westphalian.

The whole area was glaciated with erosion in the high ground but with glacial and fluvio-glacial deposition in the low lying areas.

Radon in houses is related to the geological features. Most of the geological units show a strong unimodal lognormal distribution of the data. There are exceptions, e.g. where the houses overlie unconsolidated overburden, the data either fits very poorly to a lognormal distribution or fits better to a normal distribution.

The geological map of Derbyshire and the surrounding area has been recast to show the potential for radon to be produced in the areas underlain by the individual rock units (Figure 3).

a). Boulder Clay

In Derbyshire the main glacial deposit is Boulder Clay, a form of ground moraine produced by the comminution of rock. It is usually a stiff tenacious clay containing sub-angular blocks of various sizes. It forms a mantle of centimetres to several metres thickness. The deposit is usually locally derived although it may contain large erratic blocks from a distance of several kilometres.

The nature of the deposit is one of low permeability. It would be expected that this deposit would reduce the flow of ground gas and provide an effective restraint on radon entering buildings. The average ratio (Houses affected on Bed-rock / Boulder Clay) is 14.6 but the range is 2.5 to 25. The largest ratios are for the sandstones and gritstones, the lowest for the shales where the permeability difference is smaller. Only two limestone units have sufficient houses also underlain by Boulder Clay for statistically valid comparisons.

However there are rare and isolated occurrences where the presence of Boulder Clay enhances the radon problem. Boulder Clay over some of the Sherwood Sandstone units appears to generate high levels of radon. This is shown in houses in Derbyshire, and from soil gas and total radon emanation studies in the adjoining area to the west of Derbyshire.

b). Head.

The effect of Head in increasing the radon flux from the ground was noted for the Somerset area which was south of the glacial front. In that region Head is likely to have formed over a long period in response to separate events during the whole of the Pleistocene. Because the whole of Derbyshire was glaciated, Head is likely to be much younger and consequently less mature than in Somerset.

Where Head is found on sandstones and grits the effect is to enhance the radon levels in both houses and in soil gas. The presence of Head over the shales reduces the effect of the shales in general, although local geomorphology has a profound effect.

In upland areas downhill movement of Head means that the Head found on certain horizons reflects the properties of the rocks further uphill rather than the rocks on which the Head is presently found. For example the highly uraniferous Edale Shales has Head derived from the much less uraniferous overlying Mam Tor beds which are mixed sandstones and shales, and this is reflected in the radon levels in the soils and in houses, and so on.

In Somerset the land forms were such that Head developed upon the Mercia Mudstone remained on this rock unit, the resulting higher permeability caused an increase in the radon component of soil gas and was also reflected in houses. We have only 4 examples of houses on Head on the Mercia Mudstone in Derbyshire and of these, two are above the Action Level.

Generally speaking therefore Head as a deposit underlies a high proportion of affected houses and although the affect clearly varies with bed-rock type and provenance its presence is certainly cause for concern.

c). Alluvium.

Alluvium varies in grain size but in the Derbyshire area is generally coarse, from sand size, upwards. Alluvium has been shown to emanate moderate to high levels of radon, because of its high permeability, and this is reflected in high radon in house measurements.

GLACIAL DEPOSITS IN SCOTLAND AND NORTHERN ENGLAND.

The following specific glacial features were investigated:

a). Eskers occur when river channels are formed beneath the ice of a valley glacier or ice-sheet. The beds of the rivers are filled or partly filled with sand and/or gravel. When the ice disappears the gravel remains to form a ridge which can extend for several kilometres. Usually it forms a pronounced feature above the surrounding more subdued glacial deposits. In the heavily glaciated areas of Scandinavia the eskers may be several tens of metres high and high levels of radon are often found in buildings constructed on the eskers. Mostly the

affected eskers in Sweden are composed of granitic debris which has high radon emanation characteristics.

The purpose of the current investigation was to examine some eskers in Southern Scotland and in Northern England. The geology is complex in both areas but the rock types making up the eskers are different to those which provide high levels of radon in Sweden.

Generally we can conclude that eskers in Britain seem to generate low to moderate amounts of radon but, because of the high permeability, it is expected that some houses built over eskers would be affected by radon ingress. However eskers in Britain are relatively unpopular sites to live on, often with steep slopes and insecure foundations to buildings, so that the proportion of dwellings as part of the overall housing stock is low.

b). Terminal Moraines are formed at the fronts of valley glaciers or ice sheets. They usually have a high proportion of coarse material with high permeability as a consequence. They are arcuate usually and frequently form when there is a temporary standstill during glacial recession.

c). Ground moraine. Fragments of rock which find their way into the bottom of glaciers by falling down crevasses, together with other fragments plucked from the floor of the valley, are dragged beneath the ice to form ground moraine.

The high likely permeability indicates a potential for high radon emanation. However the amount of radon is dependent upon the composition of the morainic material. In terminal moraines or where the morainic debris is particularly thick the included material controls the amount of radon generated. Very high levels of radon emanate from uranium specialised granite debris whilst there is a reduced amount obtained from less uraniumiferous rock-types.

d). Boulder Clay is a form of ground moraine. It obscures much of the solid geology of Eastern, Central and Northern England and most of Lowland Scotland.

Generally Boulder Clay reduces the effect of radon from the underlying bed-rock. It usually has a high clay content and consequently the dominant effect seems to be that it forms a relatively impermeable blanket over the bed-rock. There are some circumstances where it may be envisaged that the effects may be to increase the level of mobile radon where there is an especially permeable substrate. High radon emanation measurements from soil samples as well as elevated radon values in dwellings occur where there is a combination of Boulder Clay over the Sherwood Sandstone Group (a highly permeable granular aquifer). If the Boulder Clay contains debris from uraniumiferous shales then the presence of a limestone substrate may increase the radon values in soils.

The Peterhead Granite in Scotland is covered by till, some of which is from the sea (noted as Coastal Drift) and some from Inland (Inland Drift). The Inland Drift, which has a higher proportion of material derived from the granite, emanates significantly higher levels of radon.

PARTS OF NORTHAMPTONSHIRE

A very extensive house data set became available for parts of Northamptonshire. The county is close to the southern limit of the ice sheets during the late Pleistocene. This house data set has been analysed with particular regard to the relationship between the bedrock and overburden geology. The house data were analysed in relation to geological features. Two adjoining geological survey sheets (Northampton and Wellingborough, Figure 1) have been examined. Large numbers of house surveys for radon were available for these sheets.

The Northampton Sand Formation (worked in places for iron ore) produces the highest levels of radon with about 24% of the houses exceeding the Action Level in the Wellingborough area, but this reduces to about 8% on the Northampton Sheet. This difference is concluded to be due to the presence of the so-called "Variable Beds" which forms the upper portion of the Northampton Sand Formation in the Northampton area but are largely missing from the Wellingborough area. The Variable Beds are well indurated with low radon generation and transmission properties.

In an area with low dips and interbedded hard and soft rocks the hard rocks underlie larger areas than would be expected from their thicknesses alone. Because of the better load bearing

characteristics, the harder rocks also have more buildings on them than the softer rocks. The Jurassic rocks in the area are of Shelf Facies and show considerable lateral facies variation. This is exemplified by great changes in thickness over short distances and variation in the rock types encountered in each geological formation. Limestones with their high permeability are potent emanators of radon into the gas phase despite their generally low levels of uranium. However thickness is also a factor, there must be enough gas phase present to be drawn into buildings and then generate a problem. Thin limestone units enclosed in clay-rich rocks therefore present less of a problem than thick limestone units. One unit (the Blisworth Limestone) is thicker in the Wellingborough area than in Northampton and the proportion of affected houses is higher (4.5% against 1.2%).

Clay rich rocks in the area are not free from radon problems with the exception of the Oxford Clay. The other major units all have house data-sets with more than one percent of the houses affected.

Generally Boulder Clay in the Northampton area, just as elsewhere, reduces the effect of the radon emanating from the underlying bed-rock. The reduction is greatest for the Blisworth Limestone (1.2%>AL, Boulder Clay on Blisworth Limestone <0.01%) and in this case the data set is sufficiently large that, in terms of the legislative classification, the boulder clay areas could be treated differently to the un-glaciated areas.

The same argument may be applied to the Middle Lias Silts and Clays (3.79%>AL, compared with 0.9%>AL for the Boulder Clay covered areas). The other rock types either have too few houses over the Boulder Clay covered areas or show such a small difference to the "bare" rock as not to require a different classification.

CONCLUSIONS

The main controls on radon generation from bedrock are permeability, uranium content and mineralogy and these conclusions are substantiated for the main part of the investigations. The major bedrock types giving rise to problems in houses in the UK may be classified in descending order as granites, limestones, sandstones shales. The granites mostly because of their high uranium content and fracture permeability; the limestones because of their high permeability and widely dispersed uranium distribution; the sandstones because of their fracture and granular permeability. The shales only produce high radon where the uranium content is high.

In general terms the ground moraine producing the Boulder Clay deposits reflects the immediately underlying bed-rock. This is not altogether surprising since much of the morainic debris would be locally derived.

Superficial deposits should not be treated as an unit. It would be misleading to include, for example, all of the Boulder Clay in one data-set. One should always relate the superficial deposits to the bed-rock.

Detailed subdivision of certain areas and geological formations means that the geological map may be used with considerable confidence for predicting radon risk even in the absence of site investigations. However because of lateral facies variation in areas of shelf facies rocks conclusions drawn for one area should be used with caution when extrapolated to adjoining areas. What results apply to one geological map sheet may not apply to others, and even contiguous areas show very marked differences in the proportions of affected houses over apparently the same rock type.

Publications

T.K.Ball, Cameron D.G. and Colman T.B 1992, Aspects of Radon Potential Mapping in Britain. Proceedings of the Fifth International Symposium on the Natural Radiation Environment. Radiation Protection Dosimetry. vol. 25. 211-214.

T.K.Ball and J.C.H. Miles 1993. Geological/geochemical factors affecting the radon concentrations in homes in Cornwall and Devon. Environmental Geochemistry and Health. vol. 15. 27-36

T.K.Ball. Radon Mapping Techniques. Paper read to the Society for Environmental Geochemistry and Health in May 1994, and published in Abstract.

Miles, JCH, and Ball, TK, 1995. Mapping radon-prone areas using house radon data and geological boundaries. Presented at the Sixth International Symposium on the Natural Radiation Environment, Montreal, 1995 June 5-9

Table 1. Relationship between actual and predicted house data.

Lithology	Radon Minimum	Radon Maximum	Number	% > A.L.	Predicted % Lognormal	Predicted Geological	Mean	Geo-mean
Peat	10	44	7	0.00	0.13	Low	22	18
Head on Mercia Mudstone	10	120	15	0.00	2.00	Moderate	46	36
Head	10	500	258	2.72	3.00	Moderate	63	45
Burtle Beds	10.68	135	13	0.00	0.90	Low	37	29
Blown Sand	10	89	20	0.00	0.01	Low	19	16
Alluvial Cone	59.14	88	13	0.00	0.01	Low	41	37
Marine/Estuarine Alluvium	10	85	59	0.00	0.01	Low	24	20
Valley Gravels	11.5	389	115	2.61	2.00	Moderate	45	32
Alluvium	10.07	468	80	2.50	1.70	Moderate	51	36
Clay w. Flints	15.39	224	20	5.00	6.00	Moderate	91	61.11
Upper Greensand	10	342	63	12.70	9.00	High	83	57
Oxford Clay and Kellaways Beds	10	87	32	0.00	0.15	Low	26	21
Cornbrash	10	93	37	0.00	0.40	Moderate	32	26
Forest Marble	10	168	99	0.00	0.15	Low	28	21
Fullers Earth & FE rock	10	242	35	2.86	1.60	Low +	41	29
Inferior Oolite	10	357	61	11.48	13.00	High	110	63
Bdry. Dolomitic Conglom.	66.45	353	4	75.00	50.00	High	242	204
& Inferior Oolite								
Yeovil Sands	10	263	174	1.72	0.60	Moderate	38.42	28.9
Midford Sands	10	566	17	23.53	26.00	High	154	81
Junction Beds	10	88	29	0.00	0.15	Low	41	35
Pennard Sands	10	152	187	0.00	0.10	Low	28	23
Middle Lias	10	136	28	0.00	0.25	Low +	37	31
L/M Lias Silts/Marls	11.11	101	17	0.00	0.30	Low	38	32
Lower Lias(Blue Lias)	10	1163	1122	6.24	6.00	Moderate	74	47
Littoral Facies	17.7	867	49	28.57	31.00	High	181	127
White/Blue Lias	11.2	238	9	22.00	18.00	High	220	51
Rheanian inc. Penarth	10	285	42	7.14	4.00	Moderate	64	47
Blue Anchor Formation	10	62	16	0.00	0.02	Low	30	25
New Red Marls	10	337	371	0.81	0.30	Low	31	29
New Red Sst	10	343	83	2.41	1.00	Low +	43	32
Dolomitic Conglomerate	10	1007	46	2.30	6.00	High	74	47
Permo-Triassic Breccia	18.87	101	9	0.00	1.60	Moderate	33	25
Conglomerate								
Lower Coal Series	10	67	12	0.00	0.05	Low	21	18
Hotwells Lst	119.63	303	4	25.00	44.00	High	184	171
Bampton Lst Group	39.21	86	11	0.00	1.70	Moderate	59	52
Clifton Down limestone	10	232	14	14.00	11.00	High	80	56
Black Rock Lst	24.31	1291	22	22.73	28.00	High	192	101
Lower Limestone Shale	10	307.4	8	12.50	10.00	High	74	45
Doddyscombe Beds	10.1	625	8	37.50	31.00	High	200	100
Pilton Beds	22.36	165	8	0.00	4.00	Moderate	59	41
Baggy Beds	18.33	298	13	7.69	8.00	Moderate	78	55
Pickwell Down Beds	10	558	43	4.65	13.00	Moderate	100	61
Morte Slates	19.34	505	59	6.78	6.50	Moderate	83	61.2
Kentsbury Slates	32.21	129	6	0.00	6.00	Moderate	83	74
Brendon Hill Beds	36.89	264	6	33.33	30.00	High	150	117
Leighland Beds	10	274	20	10.00	12.00	Moderate	82	55
Avil Group & Cutcombe slates	10	306	27	7.00	6.00	Moderate	66	47
Hangman Grit	10	127	12	0.00	1.50	Moderate	34	30
Lower / Middle Devonian	52.06	120	5	0.00	5.00	Moderate	83	79

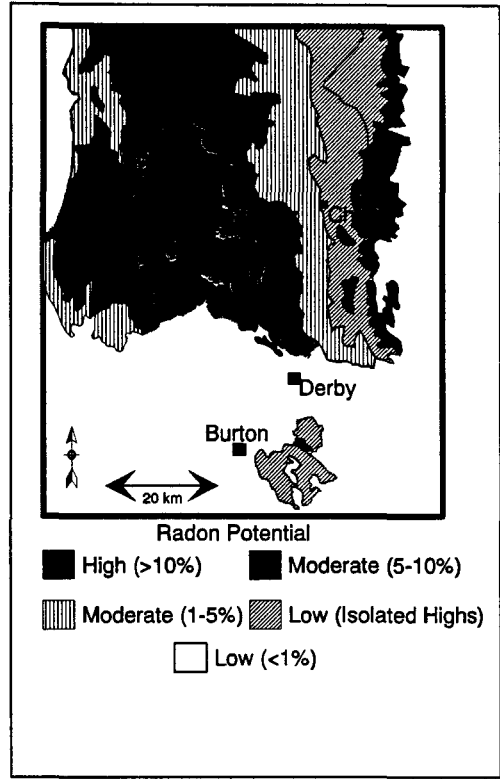
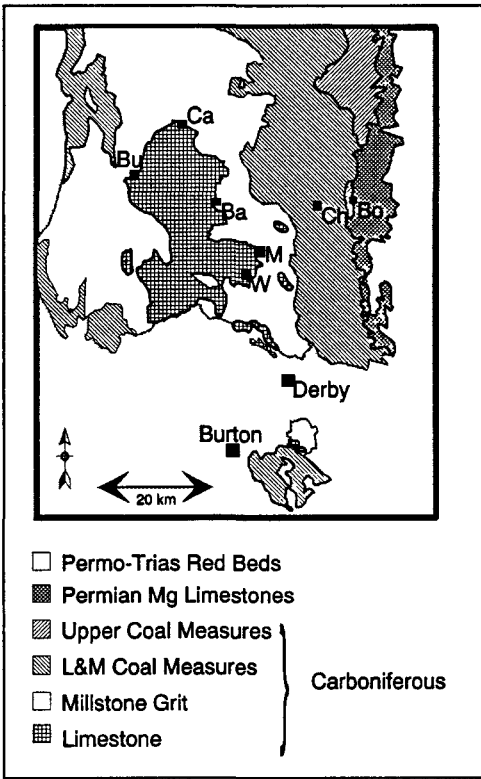


FIGURE 3

RELATIONSHIP BETWEEN THE GEOLOGICAL SUCCESSION AND HOUSE DATA

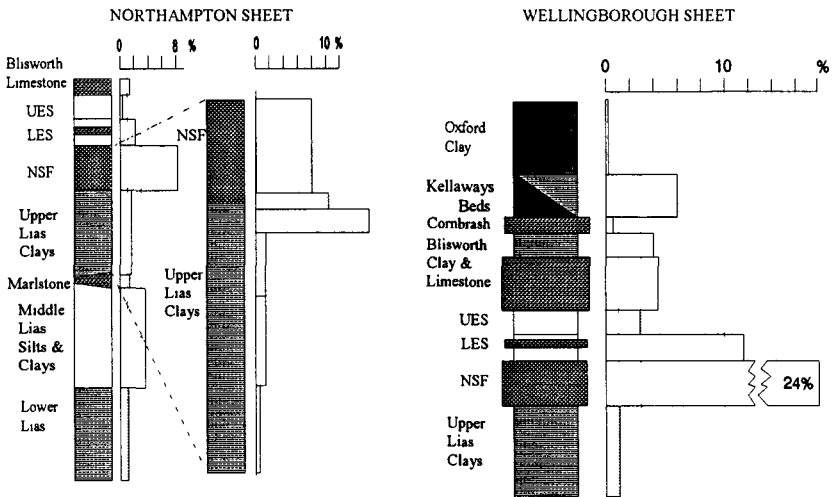


FIGURE 4

Head of project 6: Prof. Dr. R.J. de Meijer.

2 Objectives for the reporting period

The role of building materials with respect to the indoor radon concentration is twofold namely, building materials produce radon and thus are a source and building materials may act as a barrier for radon. The objective of this project is to obtain better understanding of the processes that are responsible for the production and transport in building materials. This will contribute to the development of both efficient reduction measures for radon entry from the soil and low-radon producing building materials.

This objective will be met by the construction of an instrument to measure 1-dimensional radon transport through building materials. With this instrument measurements will be performed on radon production and transport from and through various building materials. The results of these measurements will be compared with 1-dimensional radon transport models.

3 Progress achieved including publications

3.1 Introduction

Building materials play an important role in the magnitude of the indoor radon concentration. This role is twofold: building materials produce radon and as such are a source, and they are a barrier for radon. Basically four processes contribute to the amount of radon released from a surface,

- 1) diffusion of radon produced (internally) by the material;
- 2) diffusion of externally produced radon through the material;
- 3) advection of radon produced (internally) by the material and
- 4) advection of externally produced radon through the material.

In this case, externally produced radon designates radon that originates from the soil or from other building materials. For a certain building material the relative importance of the above-mentioned processes is determined by its characteristic parameters and by ambient conditions such as,

- 1) air pressure difference over the surfaces of the material, this will determine the magnitude of radon release by advection;
- 2) radon concentration difference over the surfaces of the material, this will determine the magnitude of radon release by diffusion;
- 3) moisture content of the material, this will both effect diffusive and advective radon release;
- 4) temperature of the material, this may effect the moisture content and thus indirectly radon release.

To unravel the relative importance of diffusive and advective radon release systematic measurements of the radon release rate for samples with different parameters and under different and controlled ambient conditions are needed.

In this final report we present results of experiments on radon release, from a sample of concrete using a first design of an experimental set-up. During these experi-

ments some experimental difficulties with the set-up were encountered and we decided to redesign the experimental set-up. First results with this improved set-up are also presented.

3.2 First design of the instrument

The first design of the experimental set-up was based on the following considerations:

- 1) As the measurements are compared with 1-dimensional models radon transport has to take place along a straight path. This implies that the sample should be as homogeneous as possible, meaning that variations in composition ought to be minimized and cracks should be avoided. Moreover edge effects should be reduced as much as possible.
- 2) Measurements have to be continued until equilibrium in the radon concentration is reached since the model calculations are made for steady-state conditions.
- 3) To unravel the relative importance of the contributions of diffusive and advective transport, experiments have to be carried out under a number of combinations of concentration and pressure differences.
- 4) Advection should be restricted to flow of air through the sample; no air should flow via the sealing along the edges of the sample.
- 5) Pressure differences over the sample ought to be constant, also during long-run experiments of several weeks.

Based on these considerations a set-up was constructed that consists of a stainless steel box closed off with a sealed lid (Fig. 1). The outer dimensions are $0.662 \times 0.462 \times 0.314 \text{ m}^3$. Inside the set-up a concrete sample (see Table 1 for sample characteristics) was placed on a steel inner rim. The sample dimensions are $0.6 \times 0.4 \times 0.1 \text{ m}^3$. These sizes are such that an optimum is reached between the reduction of edge effects and the ease to handle the sample. The sample divides the set-up in two compartments: in the lower compartment a radon source may be placed, the upper compartment is used to detect the transported radon. The sample itself is sealed by treating the side surfaces with an epoxy (Araldite). The sample is sealed to the inner walls of the set-up by the use of an inflatable tube inside a U-profile.

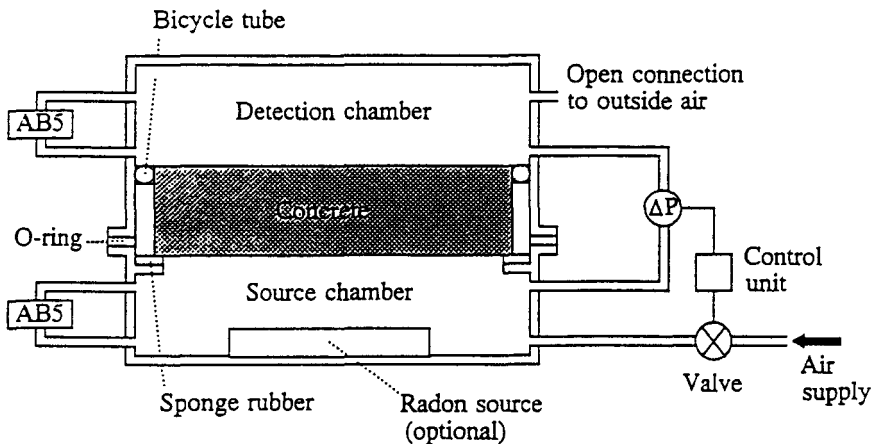


Figure 1: First design of experimental set-up

In the walls of the set-up ten multi-functional connectors are mounted, to be used for pressure and radon concentration measurements, air supply and air outlet. For radon concentration measurements two quasi-continuous, Lucas cell based monitors (PYLON AB5) are used. The monitors are programmed such that the air circulated via a filter for one hour and registered the α -counts for three subsequent one hour intervals. An algorithm was developed to calculate radon concentrations from the count rate with a correction for outplated progeny on the walls of the Lucas cell.

Table 1: Characteristics of concrete sample

intrin. perm. (specified)	$1.3 \cdot 10^{-14} \text{ m}^2$
intrin. perm. (measured)	$< 1.9 \cdot 10^{-17} \text{ m}^2$
eff. diff. coeff. (measured)	$6.6 \cdot 10^{-9} \text{ m}^2 \text{ s}^{-1}$
porosity	0.146
density	2260 kg m^{-3}
radium content	13.9 Bq kg^{-1}

The pressure difference over the sample is regulated by an electronically steered valve. With this valve pressure differences can be kept constant within $\pm 1 \text{ Pa}$ at 0 Pa and $\pm 15 \text{ Pa}$ at 1000 Pa . In the lid of the set-up one of the multi-functional connectors serves as a narrow "free flow" outlet to ambient air. For the anticipated value of the permeability the flow of air through the sample should be large enough for the system to be stable even under rapidly falling barometric pressures.

3.3 Experiments with concrete sample

Eight experiments were carried out without a radon source in the lower compartment (Table 2; #1-8), and with pressure differences over the concrete sample of 0 Pa (2x), 100 Pa , 300 Pa , 600 Pa and 1000 Pa (3x). Two experiments were done with a radon source in the lower compartment (Table 2; #9-10), one with a pressure difference of 0 Pa and one with 1000 Pa .

3.4 Discussion of results with first experimental design

It was found that in all experiments without a radon source the equilibrium concentration in both compartments was approximately equal. During the experiments it was realized that this result could only be explained qualitatively from the model if the observed flow did not take place through the sample but along the sample due to limitations in the sealing capacity of the inner tube. From a number of experiments in which we followed the pressure drop in time, with the pressure control system off, we found an upper limit of $1.9 \cdot 10^{-17} \text{ m}^2$ for the intrinsic permeability. This implies that our sample is at least a factor 1000 less permeable than ordered (value specified to the manufacturer was $1.3 \cdot 10^{-14} \text{ m}^2$). Due to this extreme small permeability of the sample, leakage due to imperfect sealing became magnified in importance. Therefore, we were not able to sensitively test the 1-dimensional radon transport code. We have tried to simulate the data with optimized parameters for the leak along the sample. In some cases reasonable agreement was obtained, in others it was not possible to reproduce the measured values. Furthermore it

was found that analysis could be strongly improved if the ventilation rates of the upper and lower compartment are experimentally known. An additional difficulty, realised during this phase of the project, is the fact that in the original set-up the ingrowth of radon may lead to so-called "back-diffusion", so that one does not measure the free-production rate anymore. The latter rate is the quantity relevant to indoor radon concentrations.

Confronted with these difficulties we decided to redesign the set-up. Design criteria for this improved set-up were that all flow rates should be controlled and measured and the humidity around the sample should be controlled. The latter criterion was added because the analysis of the data suggested that drying of the sample (and thus of its radon release properties) may have occurred during the experiments due to the use of dry gas flows.

Table 2: Equilibrium radon concentrations in source (s) and detection (d) compartment

#	T(days)	$\Delta P(\text{Pa})$	Source	$C_s(\text{Bq m}^{-3})$	$C_d(\text{Bq m}^{-3})$
1	21	0	-	1760 (70)	4860 (70)
2	10	1000	-	2800 (40)	3440 (50)
3	11	1000	-	2200 (40)	2930 (30)
4	7	600	-	2540 (30)	3180 (50)
5	7	300	-	3040 (40)	3490 (60)
6	14	100	-	3780 (50)	3970 (60)
7	22	0	-	4320 (40)	4140 (60)
8	14	1000	-	1780 (40)	3310 (60)
9	34	0	+	114000 (3000)	9660 (160)
10	23	1000	+	34200 (1800)	9300 (200)

3.5 Improved design of the instrument

The improved instrument is based on the first set-up. The instrument consists of the same stainless steel box with sealed lid. Inside the box a sample ($0.6 \times 0.4 \times 0.1 \text{ m}^3$; BM in Fig. 2) can be placed on a steel inner rim.

A pressure difference over the sample is set by applying controlled nitrogen flows through the detection and source compartment using two flow controllers (FC in Fig. 2) for each compartment. In this way a constant pressure difference is obtained that is not sensitive for variations in barometric pressure. The magnitude of the pressure difference can be regulated by adjusting the magnitude of the air flow rates. A differential pressure transducer (dP in Fig. 2) is used to measure the pressure difference between the two compartments. Test experiments showed that the pressure difference could be controlled within 1% provided temperature fluctuations are less than 1 K. By either placing a radon source in the source compartment or leading the nitrogen flow via a radon source through the source compartment a radon concentration difference can be set between the two compartments. The concentration in the source compartment will be measured by using

standard scintillation cell methods. The radon concentration in the source compartment can be varied by either adjusting the nitrogen flow or by using radon sources of different strength. To prevent changes in the conditioned moisture content of the sample during experiments the humidity of the nitrogen flows is controlled by humidifiers (H in Fig. 2). Temperature fluctuations will be prevented by placing the instrument in a temperature controlled room. The temperature and relative humidity of the ingoing flows are measured with combined temperature and humidity sensors (TRH in Fig. 2).

Radon release rates are measured by leading the nitrogen flow from the detection compartment through a pre-dryer (D1 in Fig. 2) consisting of a large column of silicagel and a water trap (D2 in Fig. 2) consisting of a tube cooled to liquid nitrogen temperature. Thereafter the flow is led through a radon trap. This trap consists of a vial filled with activated charcoal (ACC in Fig. 2). To enhance adsorption this vial is also cooled to liquid nitrogen temperature. The radon activity on the activated charcoal is measured with gamma-ray spectrometry. From the measured activity the radon release rate can be calculated by dividing this activity by the adsorption time and the surface area of the sample.

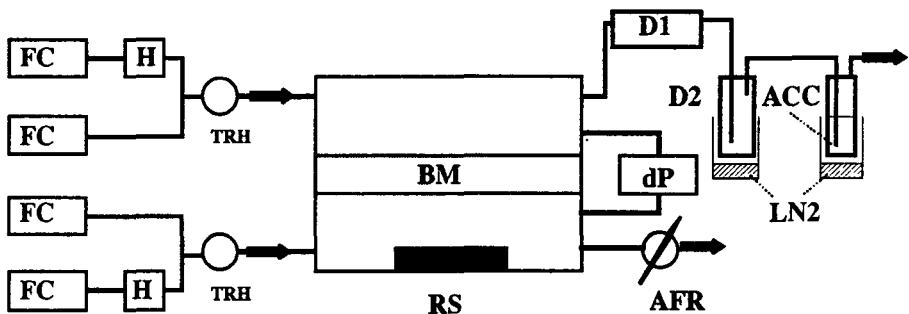


Figure 2: Schematic drawing of the improved instrument to measure radon release rates from building materials. FC: air flow controller; H: humidifier; TRH: temperature and relative humidity sensor; BM: building material; dP: differential pressure transducer; D1: silicagel dryer; D2: water trap; LN2: liquid nitrogen; ACC: activated charcoal; AFR: adjustable flow resistance; RS: radon source (optional).

3.6 Measurement of adsorbed radon activity by gamma-ray spectroscopy

To measure the radon activity adsorbed on the charcoal adsorber the KVI low-background planar gamma-ray detector is used. In principle, the adsorbed activity of the gamma-ray emitting decay products ^{214}Pb and ^{214}Bi could be used for such a measurement. However, the sensitivity of the measurement can be enlarged by a factor of 10 by using the total

count rate in the energy window from 0 to 700 KeV. In figure 3 a spectrum taken with the gamma-ray detector is shown for 17.1 gr ACC (the amount needed to fill the standard calibrated KVI pill-box geometry; used in all experiments) with 38 Bq adsorbed radon (top). This spectrum shows both the 295, 351 and 609 KeV gamma-rays from ^{214}Pb and the 609 KeV gamma-ray from ^{214}Bi . At the low energy part of the spectrum lines are detected from X-ray fluorescence (e.g. $\text{K}_{\alpha 1}$ and $\text{K}_{\alpha 2}$) of the lead shielding of the detector. This fluorescence is induced by gamma-rays from the sample exciting the lead atoms of the shielding and thus are also a measure for the activity on the ACC. Figure 3 (bottom) shows a background spectrum taken with 17.1 gr ACC without radon activity; the total count rate due to background in the energy interval from 0 to 700 KeV was found to be 0.5942 ± 0.0012 cps.

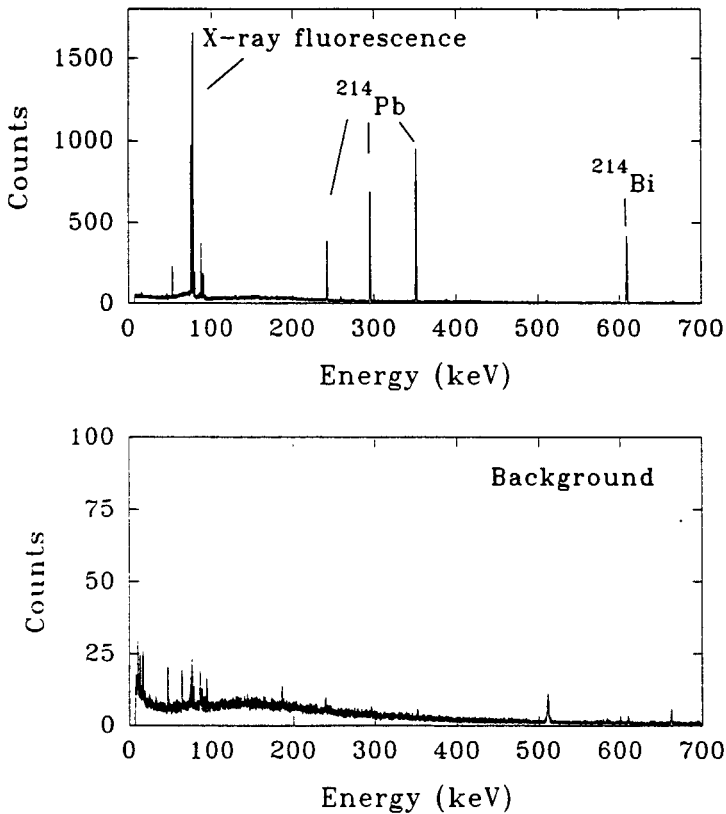


Figure 3: Spectra taken with the KVI low-background planar gamma-ray detector. Top: 17.1 gr ACC with 38 Bq radon activity; Bottom: 17.1 gr ACC without radon. Live time of both spectra is 10 hour.

To relate the total count rate in the energy window of 0-700 KeV to the radon activity on the charcoal we prepared calibrated radon release sources. Three sources were made by using different quantities (Table 3) of sand originating from the former Wismut mining operation. This sand has a high radium and low thorium content. As the radon release may

depend on moisture content and temperature the sources were equilibrated with air of 20°C and 50% RH by placing each source in a 5L stainless steel cylindrical (leaktight) can and inducing (overnight) an air flow of 1L min⁻¹ of moisturised radon-free air (using a humidifier). After equilibration the air in- and outlets of the cans were closed and after about 24 hour air samples were drawn from the cans and the radon concentrations of these samples were analysed with calibrated Lucas cells. The radon release rate of the sources was then calculated from these concentrations (Table 3).

Table 3: Radon release rates of sources used for calibration

Source	Mass (gr)	Radon release rate (Bq h ⁻¹)
RS1	518.9 ± 0.1	6.28 ± 0.09
RS2	270.6 ± 0.1	3.20 ± 0.04
RS3	28.0 ± 0.1	0.332 ± 0.007

Using the RS1 calibration source test experiments were performed to assess if undesired absorption of radon in the silicagel dryer and in the water trap occurs. In these experiments the RS1 source was placed in the upper compartment that was sealed from the lower compartment with a leaktight stainless steel plate. A flow of nitrogen was led through the set-up in which two Pylon AB5 monitors were inserted. One monitor was placed directly after the outlet of the box; the other was placed directly after the water trap. Comparing the count rates from both monitors, corrected for the relative efficiencies of the monitors and Lucas cells and averaged over a measuring period of several days, we found that the relative difference of the count rates was not significant and less than 2%. From this we conclude that if any radon is lost in the drying procedure this amount is negligible.

To assess if all radon in the nitrogen flow is adsorbed on the activated charcoal we performed a test experiment with the RS1 source and with about two times the standard amount of 17.1 gr activated charcoal. After an adsorption period of several hours the charcoal was removed and split in two equal fractions; one taken from the upflow side of the adsorber and one taken from the downflow side. Both fractions were analysed with the planar germanium detector. Only on the upflow fraction activity was found which shows that no radon leaves the adsorber.

With the calibrated sources 14 calibration experiments were performed. In these experiments the upper compartment was also sealed from the lower compartment with a leaktight stainless steel plate. In each experiment one of the calibrated sources was placed in the upper compartment through which a flow of nitrogen (20°C; 50% RH) was led. In all experiments a flow rate of approximately 0.7 L min⁻¹ was used and radon was adsorbed on 17.1 gr of activated charcoal. As the volume of the upper compartment is approximately 40L this resulted in a ventilation rate of about 1 h⁻¹. Different adsorption times were used to obtain a range of radon activities on the ACC adsorber. The results of these calibration experiments showed a completely linear relation between the nett count rate in the gamma-energy window from 0-700 KeV and the adsorbed radon activity as calculated from the release rates of the sources (Figure 4). These adsorbed activities were corrected for radioactivity decay during the time interval between adsorption and gamma-ray measurement.

A linear relation $n \text{ (cps)} = c A_{Rn} \text{ (Bq)}$ was fitted to the calibration data. This resulted in a calibration constant $c = 0.0870 \pm 0.0007 \text{ (cps Bq}^{-1}\text{)}$. This is an order of magnitude higher than if only the count rates in the ^{214}Pb and ^{214}Bi photo peaks are used ($0.007 \text{ cps Bq}^{-1}$).

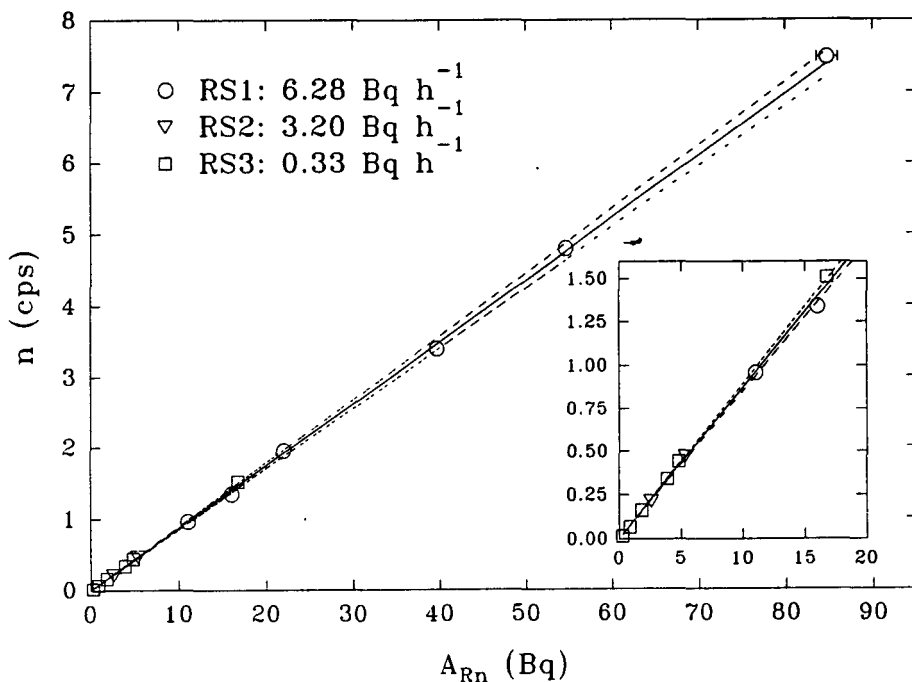


Figure 4: Results of experiments with calibrated sources RS1 (6 experiments); RS2 (2 experiments) and RS3 (6 experiments). Plotted is the nett count rate n (cps) in the energy window 0-700 KeV against the adsorbed radon activity A_{Rn} as calculated from the adsorption time and the radon release rate of the source. Solid line represents linear fit to data. Dashed lines represent 95% confidence lines.

3.7 Experimental results with improved instrument

Three measurements were made of the radon exhalation rate from a rectangular block of phosfogypsum containing approximately 480 Bq kg^{-1} and with dimensions $7 \times 13 \times 24.5 \text{ cm}^3$. The sample was placed in the upper compartment on the leaktight steel plate and equilibrated at 20°C and 50% RH. The results (Table 4) show that the method gives reproducible results even for quite different adsorption times.

Similar measurements were made with the concrete sample previously used with the first set-up. The sample was placed between the upper and lower compartment and both compartments were connected and flushed simultaneously with nitrogen (20°C ;

50% RH). The flow out of both compartments was led through the charcoal adsorber, meaning that radon exhaling both from the upper and lower surface of the sample was collected. The results (table 4) show that the measured exhalation rates correspond well with the value obtained with the first design of the instrument. However, a slight decrease of the measured exhalation rate with increasing adsorption time is observed. This may be related to the small increase of the absolute pressure in the instrument after the start of a measurement, caused by the flow resistance of the activated charcoal bed. The absolute pressure raised with 1 mbar h⁻¹ during the first two hours and with 0.1 mbar h⁻¹ in the following hours. To assess whether this small increase of absolute pressure influences the exhalation rate of the concrete, numerical one-dimensional model calculations were performed in which the governing equation for small pressure perturbations in porous media was linked to the equation for radon transport. In these calculations an intrinsic permeability of 1.0·10⁻¹⁷ m² for the concrete slab was used. The results are presented between brackets in table 4, with a reference exhalation rate for the first experiment. A similar dependence of the mean exhalation rate on the adsorption time is observed. We may conclude that a very small change in absolute pressure (0.3%) can considerably influence the measured exhalation rate (in our case 7%). Therefore, in exhalation rate determinations it is recommended to keep the absolute pressure variations within 100 Pa in addition to maintaining the pressure difference over the material constant within 1%-2%.

Table 4: Results of experiments with phosphogypsum and concrete samples. Results of model calculations for concrete are presented between brackets.

Sample	exp. number	adsorption time (min)	exhalation rate (Bq m ² h ⁻¹)
phosphogypsum	1	270	12.39 ± 0.15
	2	485	12.06 ± 0.12
	3	1040	12.65 ± 0.13
concrete	result with first design		5.1 ± 0.5
	1	52	4.93 ± 0.10 (4.93)
	2	122	4.88 ± 0.07 (4.83)
	3	355	4.59 ± 0.04 (4.60)
	4	1016	4.57 ± 0.04 (4.63)

3.8 Conclusions

It is concluded from the experience with the first design that radon transparency measurements are far from trivial and may be extremely sensitive to small leaks in the set-up. Contrary to the general belief we recommend rather high vacuum criteria for the experimental set-up and measurements of flows entering and leaving the set-up. Sealing of the sample becomes extremely important for low permeable samples. Measurements of the tightness of the sealant are of importance although not straightforward.

The experiments with the improved design have shown with this instrument radon exhalation rates can be measured with good reproducibility. In order to unravel the relative importance of diffusive and advective radon release, pressure conditions inside the instru-

ment should be extremely stable. With the improved instrument radon exhalation rates as low as $0.025 \text{ Bq m}^{-2} \text{ h}^{-1}$ can be measured under controlled ambient conditions, within 10% statistical uncertainty using adsorption and counting times of 12 hours.

3.9 Publications

Koopmans, M., de Meijer, R.J. *Radon doorlaatbaarheid van bouwmaterialen*. KVI internal report R46, 1993.

Koopmans, M., de Meijer, R.J. *Radon transparency of building materials*. Paper presented at the "First international workshop on indoor radon remedial action", 1993, Rimini, Italy, KVI internal report R47, 1993.

de Meijer, R.J., van der Graaf, E.R., *A research programme towards construction of low-radon houses*. Radiat. Prot. Dosim., 56, 189-192, 1994.

Head of project 7: Dr. Lynn Marie Hubbard

The research reported here was never funded by the European Commission, because of a very late signature of the Association Agreement between the Commission and Sweden. However, we proceeded under the assumption that it would have been. In the end, the funding came directly from Sweden.

II. Objectives for the reporting period.

The objective for this project has been to obtain enough information from the detailed study of house dynamics to gain expertise in knowing how to simplify models for making predictions on radon behavior indoors, which leads to a better estimate of exposure and to the design of efficient and adequate mitigation. Specific objectives for obtaining this goal have been: 1) to study the time dynamics at one house in detail to obtain a data base useful for testing models and predictions (a benchmark house), 2) to determine the effect of seasonal weather versus house parameters on the soil radon concentration and its variation with time, 3) to create a usable data base containing all the time series data collected at the SSI research house, (labeled 902).

III. Progress achieved including publications.

A large research effort has been concentrated on understanding SSI research house (902). It provides a good example of a well-behaved house regarding its physical interaction with the environment, in particular, the dependency of airflows on temperature changes and wind, and the resulting radon entry. The house is occupied, has a dirt-floor crawlspace, is built of wood upon a granite wall foundation, has electrical radiators for heating, and sits on sandy soil (with a clay underlayer under a portion of the house foundation) on the edge of an esker. The house has been described in publication 1.

It is extremely important to understand that the value in studies of detailed dynamics in one or a few houses lies not in understanding a particular house in detail, but in being able to use the data to confirm more general models on the physics of radon entry and dispersion. Every house is of course unique, special. But every house's interaction with the environment is driven by the same physics.

The process of radon entry into buildings from a source in the soil occurs because of convective flow or diffusion. These processes are always dependent on the same parameters. What varies between each house is what value the different parameters assume; the makeup of that set of parameters is unique to each spot. A correct description of the physics allows one to assume any value of the parameters and predict the radon behaviour indoors at that spot. Simplifying assumptions allow an easier or quicker way to make predictions. The whole point of modeling a physical system is to obtain enough understanding of a physical process to know the extent or range of each parameter governing the system, to understand how the system reacts for all combinations of the parameter range, and which simplifying assumptions are appropriate.

In addition to the work reported below, we have collaborated with D. Ducarme from CSTC-WTCB, contractor 4, and Claus Andersen from RISOE, contractor 3. These collaborations have involved model calculations of the flow of soil gas into the crawlspace structure of our research house. They discuss the collaboration in their sections. This

information is useful as input into an indoor airflow model which can account for radon movement indoors. We have obtained the public domain indoor airflow model COMIS for use in the radon flow modeling.

III.1. Studies on Temporal Variations of Radon in Swedish Single-Family Houses.

The goal of the study described in this section has been to test a procedure for using temporal variations of indoor radon and other parameters measured over a short time period to predict longer time-averaged indoor radon. Results of the procedure presented here show agreement to within 10% between actual measured indoor radon over a long time period and predicted concentrations from shorter time measurements.

The current practice in characterizing the severity of radon contamination in a house is to use the yearly averaged radon concentration. The most commonly used method today for obtaining the yearly average is simply to assume that a short-termed averaged radon concentration measured in the heating season gives a good estimate of a yearly average. For example, in Sweden an average radon gas concentration obtained from a minimum of a two-month measuring time during the heating season is used as representative of the yearly averaged radon concentration. Many other countries use a similar procedure and sometimes a shorter time period. Errors that result from this procedure of estimating the yearly average can lead to incorrectly applied or unnecessary mitigation, or no mitigation when it is needed.

III.1.a Results

Figure 1 shows the daily, bimonthly, and yearly averaged indoor radon concentrations measured over a 3.5 year period. The daily 24-hour averages vary considerably around each yearly average. Each point along the black curve, labeled bimonthly, represents a two month average with the two-month period starting on that day. Although the variation is less than with the daily averages, there is still considerable spread around the yearly average. The annual average is overestimated by around 20% on the average during the summer and during the winter months it is underestimated considerably. During winter 1993-1994 the underestimation is by more than 50%.

The graph also shows a variation from year to year in the annual average, most marked between 1991 and 1992, leading one to ponder the meaning of an annual average. If 200 Bq/m³ radon gas is a recommended action limit then in 1991 a full year measurement of indoor radon would have led to implementation of mitigation, unlike 1992 and 1993. The average indoor radon concentration for the entire time-span is 182 Bq/m³.

Figure 2 shows the radon indoors and the outdoor temperature as daily averages. Although correlations of the indoor radon with the outdoor temperature, over different time scales, are not as strong as those between the soil radon concentration and the outdoor temperature (publication 6, and the discussion in section III.2), outdoor temperature is a strong indicator of the indoor radon due to the dominant effect of stack pressures in causing airflows in this house. The mechanisms by which temperature affects radon flows are discussed in publication 1. Figure 2 is meant as a tool for visualizing the strong relationship between temperature and indoor radon. Statistical analysis of the large data set has shown that temperature is the strongest indicator of the indoor radon in this house.

Given this information, it is worthwhile to investigate whether the temperature can be used to map longer term behavior of the indoor radon. The time period between January 1 and April 30, 1992 has been investigated for accuracy in longer term prediction of the radon concentration using regressions of radon against outdoor temperature and/or wind speed for both single-day, hourly averaged time series and 7-day, daily-averaged time series. Shown in Figure 3 are the results of a prediction based on a regression from a single 24-hour period, February 11, 1992. This 24-hour period was representative of the days between Jan. 1 and April 30; it was neither the best nor the worst.

The regression was performed only between radon indoors and outdoor temperature obtained from a local official weather station (SMHI, Sveriges meteorologiska och hydrologiska institut, 1995), after testing and eliminating other parameters. The weather station temperature data was used to demonstrate the feasibility of using local weather data instead of data collected on the site. The intercept for this regression is 93 Bq/m³ and the coefficient is 32. The r² correlation coefficient is 0.52, which is a value representative of the fits, and not the best or worst value. No time lag was introduced for this fit.

The predicted time series gives reasonable agreement with the measured data, as seen in Figure 3. But what is more impressive is the agreement of the average values over this 4-month period. The average value for the 4-month period predicted from a regression over 24 hours during this 4-month period differs from the measured average value by less than 10 Bq/m³, out of a measured average of 145 Bq/m³.

Figure 4 shows the data from using the same regression fit to predict the radon time series and average values over a 2 year period, excluding the summer data. Again the agreement is quite acceptable, with the averages differing by around 5%. The third average value plotted in the figure as a dotted line is calculated from using an average of 30 years of daily outdoor temperature data over an entire year, obtained from a weather station located about 15 km from the house (SMHI, 1995). This data also agrees well, within 10%, with the measured averaged radon concentration. The 30-year averaged temperature data was used to demonstrate that past time averaged temperature data can be used to compute the radon averages. That is, one does not need future temperature data to predict an average value for the current year. This agreement is quite encouraging. This is an important point in confirming the usefulness of this technique.

III.1.b Conclusions.

The data demonstrates a strong dependence of the indoor radon concentration on the outdoor temperature in a single well-studied house. The temperature dominates as a predictor for the radon, due to the strong effect of the stack pressures. A long time-averaged radon concentration can easily be modelled with a simple regression technique. One remaining question is what is the shortest time scale that we can measure the dynamics and obtain enough information to make longer term predictions with reasonable accuracy, and what is the requirement on the dynamic conditions during the regression time period.

III.2 Time-Variation of the Soil Gas Radon Concentration Under and Near a Swedish House.

Although there have been several studies documenting the measurement and modeling of the time variation of radon in indoor air, there have been only a few studies of the time variation of radon in the soil gas in the earth under or near an occupied house.

Knowledge on how much soil gas radon varies is needed for understanding the reliability and usefulness of soil gas measurements made at one point in time, and determining which measurements are appropriate for soil radon risk classification. Another use for this knowledge is in understanding how the radon source strength available to the indoor air varies with time, for use in model calculations aimed at estimating the long-term exposure to radon in indoor air.

Since the spring of 1993 the soil radon gas concentration has also been measured as a time series at SSI research house (902). The soil data has been collected at a depth of one meter in three locations under and near the house. This section discusses the degree to which the house versus the weather interacts with and influences the soil gas radon concentration, and how much the influence of these two factors on the soil gas radon content varies with season and location. Strong correlations with barometric pressure and outdoor temperature occur. The maximum soil gas concentrations occur during the summer months and the minimum concentrations occur during the winter, with the summer and winter levels differing by a factor of between two and three, depending on location. Changes in the 24-hour averaged indoor radon concentration correlate well with the changes in the soil radon. The degree to which soil gas radon content may be used as an indicator of indoor radon contamination is discussed.

III.2.a Measurements

Three soil radon detectors based on digital counters which count alpha-decays from radon gas have been constructed, calibrated and installed in the earth. The modified detectors are calibrated in the radon room at SSI approximately every 6 months. The results from those calibrations show that the detectors are stable under different ambient conditions, i.e., low temperature (down to 0 C), and high humidity. Two of the counters are located one meter from the perimeter of the house centered on two different sides, north and east. The third counter is buried one meter deep directly under the center of the house. In those three locations continuous time series of data have been recorded during long time periods starting from May, 1993. Measurements in a fourth location, half way up to the top of the esker, 15m from the nearest house, were started in the late winter of 1995, using the counter which had previously been located on the east perimeter. This measuring point will give soil radon concentrations not affected by the house. Details on construction and operation of these detectors can be found in publication 6.

Hourly averaged radon in the soil gas at three different locations under and around the research house are recorded on the data logger. The other parameters which are recorded at the same time are measurements of radon in different indoor zones, pressure differentials across the building shell, temperatures in the soil and air, barometric pressure, and wind speed and direction. With continuous radon measurements in these locations, we observe changes in the soil gas radon concentrations due to the effects of the weather versus the effect of the house on the soil. These time-series measurements are used to study correlations between the soil gas radon concentrations and house versus weather

dynamics.

III.2.b Observations and Discussion

The house affects the soil through the stack induced pressure gradient between the house and the soil, and through pressure differences due to the wind. The soil directly under the house remains dry during all seasons, so that the flow properties of the soil, e.g., the permeability, which change with changing water content, remain constant under the house. Beyond the perimeter of the house this is not true. How much these differences affect the time variations, or dynamics, of the soil gas radon content is one useful observation of these measurements. The degree to which these dynamics change with seasons is another.

Figure 5 displays data from one week in the summer of 1993 when the house was unoccupied and the windows and doors were left closed, so that the indoor radon behaved according to the physical mechanisms driven by the environment, i.e., there was no airing of the house by the occupants. The wind was insignificant throughout this week. The left scale measures the indoor radon in Bq/mn and the barometric pressure on a scale to magnify the variations recorded in mbar. The maximum daily averaged barometric pressure for this time period was 1020 mbar and the minimum was 999 mbar. The barometric pressure scale is magnified in order to visualize the correlation in its behavior and the other parameters. The right scale measures the soil gas radon one meter beyond the north side of the house and 1 meter deep in the soil.

There are 24 hourly averaged points plotted each day with a continuous line for the two radon concentrations. In addition, a 24-hour average of each parameter is plotted as a little box at the center of each daily period. The ticks marking each day are at midnight, hour 24:00. This data display two different time scales of physical processes. The first is the hourly variation of the indoor radon concentration so typical of a non-windy period, with the variation in the indoor radon concentration driven by the indoor-outdoor temperature difference. The second time scale is a 24-hour averaged, daily scale. The radon concentration in the soil does not show the same type of hourly pattern as the indoor radon but instead shows a variation anti-correlated with the barometric pressure: increased barometric pressure, and decreased soil radon.

Although the indoor radon has an hourly temperature dependent pattern, the daily 24-hour averaged values are very well correlated with the soil radon, which is also the source to the indoors. The indoor radon has an hourly temperature dependent pattern which is modulated by the more slowly varying radon source in the soil. This correlation is most marked during non-windy periods.

Figure 6 shows the seasonally averaged values of the soil radon content at the three locations under and next to the house, measured between May, 1993 and August, 1994. The measurements show a variation between the locations which, as described above, are only meters apart. The probe on the north side of the house was higher than the other two locations during both summer periods. What is most markedly displayed by the figure is the strong seasonal variation in all three locations with winter time radon values being lowest.

The strongly seasonally dependent pattern in the soil radon concentrations is well

correlated with the outdoor temperature, shown in Figure 7 as daily averages of the two time series. The correlation is strongest in the fall, winter, and spring seasons with r values over most week-long periods between 0.8 and a little over 0.9. The r values fall off to around 0.2 - 0.5 during the warmer summer periods. A 1-day time lag for the soil radon concentration response to the outdoor temperature is found to be optimum for the daily averaged time series.

The house sits on sandy soil with a thin clay layer under part of the house about 1 m deep. Most of the available soil is high in permeability, consistent with sand with permeabilities measured between 10-9 and 10-11. The time series data gives a clear strong correlation between the pressure difference between the crawlspace and the living level of the house and the outdoor temperature, as expected because the house has a natural draught ventilation system. The indoor radon is also well correlated with the soil gas radon concentration, especially when analyzed as a daily-averaged time series. The observations described above are consistent with the following scenario.

The natural-draught ventilation system of the house causes pressure differences between the house and the soil which increase with increasing temperature difference between the indoors and the outdoors. The increased pressure differences cause increased airflows into the house from both the outdoor air and the soil gas air. That is a well known phenomenon. In this house, which sits on highly permeable soil, the increased airflows and resulting ventilation of the house during colder temperatures also ventilates the soil resulting in the seasonal variations shown in figures 6 and 7: decreased soil radon in the winter.

If this is the mechanism explaining the strong dependence of the soil radon on the temperature, then there should be less correlation between the soil radon and the outdoor temperature in the summer compared to the winter. This is because the ventilation effect of the soil would be less with the smaller indoor-outdoor temperature differences in the summer. In fact, as mentioned above, r^2 coefficients from linear regressions between soil radon and outdoor temperature are considerably greater in the winter than in the summer.

An alternate mechanism for the observed pattern would be a stack effect occurring in the esker itself. The research house sits at the bottom of a classic Swedish esker. The esker itself rises about 40 m above the house. During weather colder than about 8 C, which is approximately the temperature inside the esker, the highly permeable esker material would transport air up from the bottom out the top, resulting in a depletion of radon in the soil at the bottom of the esker. The opposite would happen during warmer weather.

Although the pressure field from the house should dominate in the measurements made near or under the house, it could be that a combination of these two mechanisms is occurring. Other mechanisms related to temperature seem less likely, such as temperature induced humidity or water content changes in the soil which would lead to different fractions of dissolved versus gas phase radon. Because the response time of changes in the soil gas radon to changes in temperature is so short, a ventilation effect is most likely.

A discussion on how much the wind affects the soil radon content can be found in publication 6.

Figure 8 shows daily-averaged measured and predicted radon in the soil under the house. The prediction is based on a simple linear regression of radon as a function of temperature over March and April months. The regression was optimized to a 1-day lag of the radon behind the temperature, with an r^2 value of 0.91. The regression constants were then used to calculate a full years soil radon concentration. It is shown in the figure as the -predicted- curve. It follows the measured curve remarkably well. The agreement between the measured and predicted yearly averaged values differs by just over 1000 Bq/m³, which is only a 2% error. The yearly curve was also predicted using the same regression constants but outdoor temperature data obtained from the local weather station. The temperature data is the average of 30 years of daily-averaged temperatures. The curve itself is quite smooth; all the short-time daily variations seen in figure 8 are smoothed away. But the annual average was again within 1000 Bq/m³ of the measured value, a nice agreement.

III.2.c Conclusions

The simple yet useful result of these observations is that in this soil, temperature alone can be used as an indicator of the radon concentration.

Publications.

1. Hubbard, L.M., Hagberg, N., Enflo, A., Temperature effect on radon dynamics in two Swedish dwellings, *Radiation Protection Dosimetry* 45, No. 1/4, 381-386, 1992.
2. Hubbard, L.M., Swedjemark, G.A., Challenges in comparing radon data sets from the same Swedish houses: 1955-1990, *Indoor Air* 3, 361-368, 1993.
3. Swedjemark, G.A., Hubbard, L.M., Boman, C.A., Radon in the same Swedish dwellings in 1976 and in 1990, *Radiation Protection Dosimetry* 56, No.1/4, 315-318, 1994.
4. Hubbard, L.M., Time-variation of radon in the soil gas near a Swedish house, proceedings of the Second International Workshop on the Geological Aspects of Radon Risk Mapping, September 20-22, Prague, Czech Republic, 1994.
5. Hubbard, L.M., Mellander, H., Swedjemark, G.A., Studies on temporal variations of radon in Swedish single-family houses, accepted for publication in the proceedings of NRE VI in *Environment International*, 1995.
6. Hubbard, L.M., Hagberg, N., Time-variation of the soil gas radon concentration under and near a Swedish house, accepted for publication in the proceedings of NRE VI in *Environment International*, 1995.

Daily, bimonthly, and yearly averaged indoor radon.

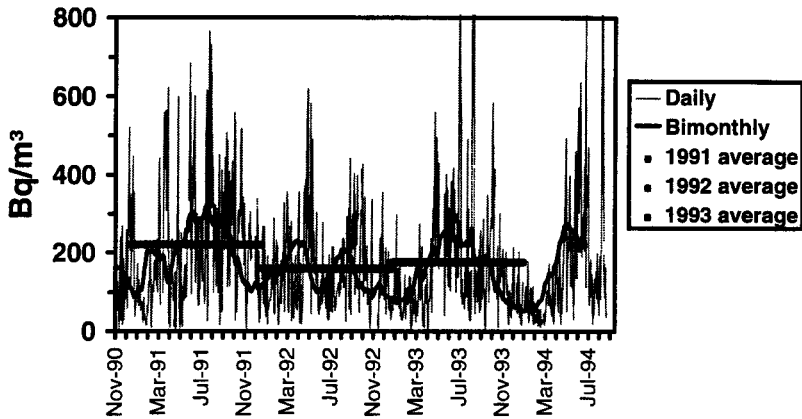


Figure 1. Average indoor radon for the whole data set = 182 Bq/m³.
 Swedish Radiation Protection Institute

Radon indoors and outdoor temperature, daily averages during a 2.5 month period.

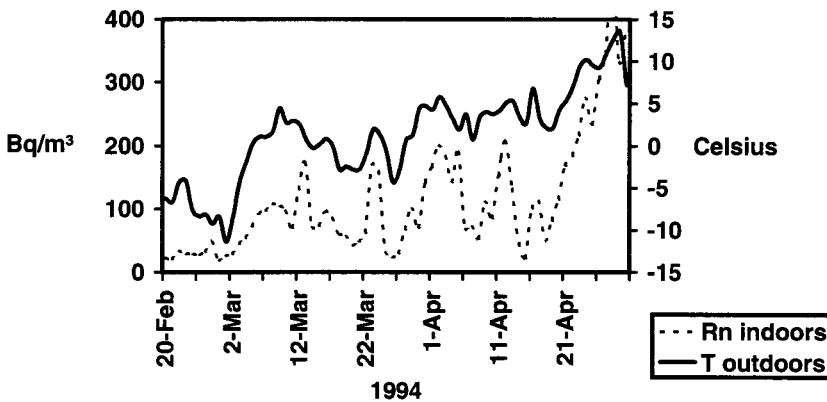


Figure 2.
 Swedish Radiation Protection Institute

Radon indoors measured and predicted.

The prediction is based on a regression from a single 24-hour period on February 11, 1992.

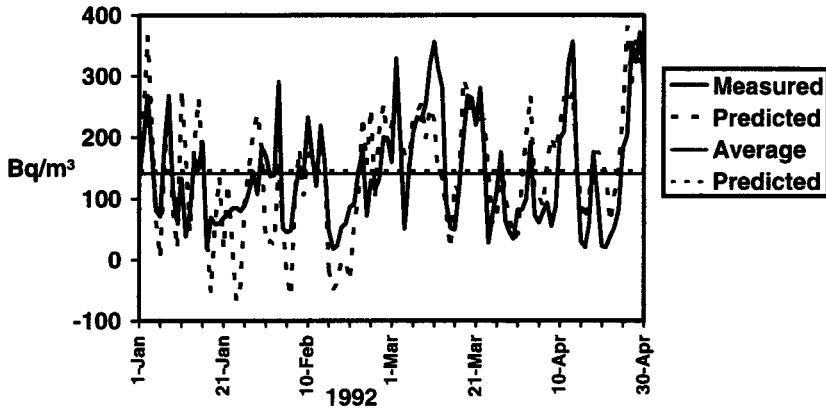


Figure 3. Regression performed between indoor radon measured over a 24-hour period and outdoor temperature obtained from a weather station. *Swedish Radiation Protection Institute*

Measured and predicted indoor radon during the heating season over two years.

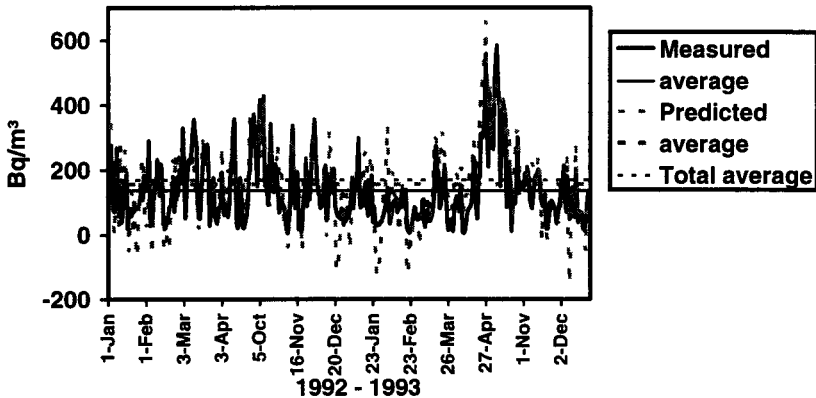


Figure 4. Prediction based on a regression between indoor radon measured over a single 24-hour period and outdoor temperature obtained from a local weather station, same as in figure 3.

Swedish Radiation Protection Institute

Rn indoors, in the soil, and barometric pressure, non-windy days. Hourly and daily averages shown.

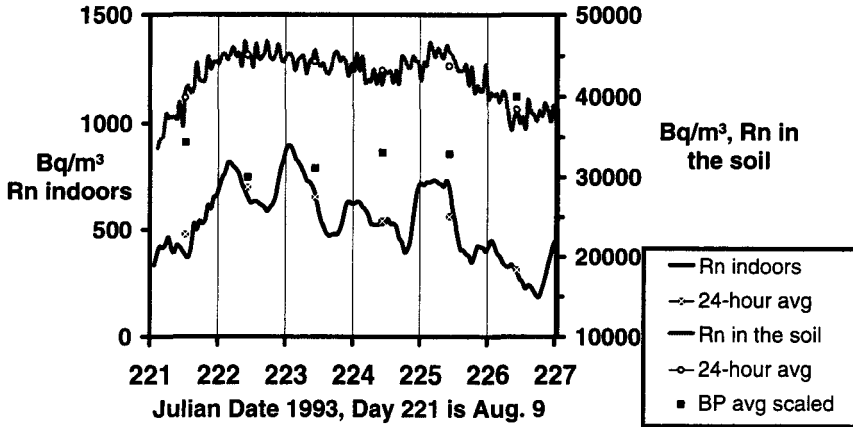


Figure 5.
Swedish Radiation Protection Institute

Seasonal averages of radon in the soil gas in three locations, 1 meter deep. The three locations are directly under the house, 1 meter beyond the north wall, and 1 meter beyond the east wall.

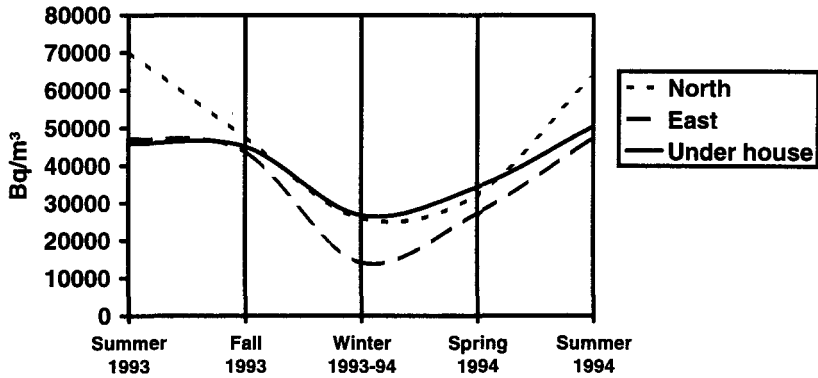


Figure 6.
Swedish Radiation Protection Institute

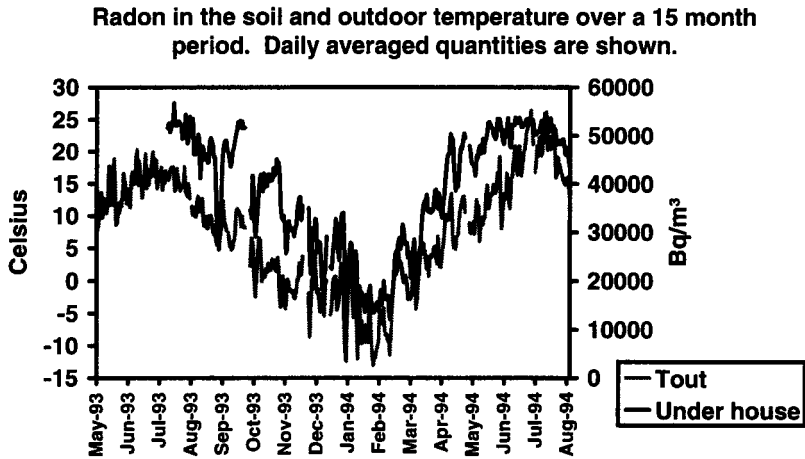


Figure 7.
Swedish Radiation Protection Institute

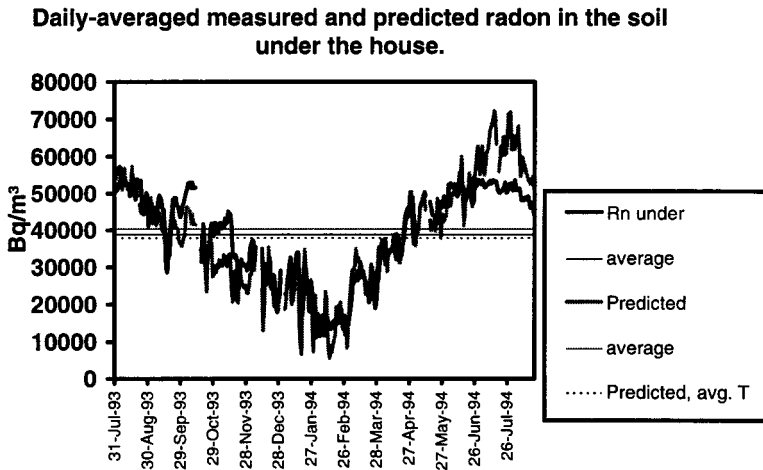


Figure 8. Shown with the daily-averaged measured and predicted radon are the averaged values over the entire measuring period based on the measurements, the prediction, and the prediction using daily outdoor temperatures resulting from a 30-year average of daily temperatures.
Swedish Radiation Protection Institute

Head of project 8: Dr. V. Balek

II. Objectives for the reporting period.

The improvement of understanding the influence of humidity and temperature on radon release from soils, rocks, building materials and the prediction capability for radon/thoron release from soils and building materials.

III. Progress achieved including publications.

1. A physical model for radon and thoron release from porous materials was designed. The recoil and diffusion mechanisms, the dissolution of radium and radon in water present in pores, the adsorption of radon on dry and wet surfaces of porous materials at the constant temperature were considered in the model. During the development of the model the critical analysis of the relevant literature sources was done.

A new mathematical description of the processes participating in the transport of radium and radon and thoron was proposed for the steady state conditions (the processes of the subsequent recoil of Ra-224 and Rn-220 were considered).

2. Mathematical modelling of the influence of humidity and porosity of the materials on radon and thoron exhalations from porous materials was carried out.

The theory proposed by Rogers and Nielson [1] for radon generation and transport in porous materials was used for the mathematical modelling of the influence of humidity and porosity on radon exhalations. The results of the mathematical modelling are demonstrated in Figure 1. As is shown in Figure 1, the exhalation ED of radon strongly depends on the porosity. At low relative humidity values (see curves 1,2 and 3, Figure 1) the dependence of ED on humidity has an increasing trend. However, at higher relative humidity values (see curves 4-7, Figure 1) the character of this dependence is different, exhibiting a maximum, after which the ED values decrease with increasing porosity. This can be explained by the role of the water filled in open pores at the higher humidity values.

In Figure 2 we have demonstrated that at a given porosity $E = 0.4$ the radon exhalation decreases with increasing humidity of the gas surrounding the porous sample. In the mathematical modelling different values of the radium solubility constant were considered. In the case of the low dissolution of radium from the surface into pores filled by water the nearly linear dependence between ED and relative humidity values was found.

3. The differences in the behaviour of radon Rn-222 and thoron Rn-220 in their transport in porous solids were outlined. The differences are due to the different half lives, of the radon isotopes, as well as to the subsequent recoil processes which take place in the sample labelled by Th-228 and Ra-224 (and Ra-226), respectively. It was pointed out that the application of thoron in the revealing and investigation of dynamic changes taking place in the solid matrices as well as in the porous systems is more advantageous in comparison to radon application. In its turn, the results obtained from the thoron measurements can be used for the description of the changes influencing the release of radon from the materials under dynamic conditions (i.e. heating and cooling of samples).

4. The following samples of soils, building materials and isolation materials were selected for investigation in this project :

- bentonite clay
- sandy soil
- concrete block
- pieces of wood
- polystyrol
- cotton

The selection of materials was made with respect to different porosity and water content of the materials. The viewpoint of practical application of the results was also considered : the samples represent the components of soils (bentonite clay, sandy soil), building materials (concrete) as well as insulation materials (wood, pieces of polystyrol and cotton). The selected materials represent both hydrophilic and hydrophobic surfaces.

5. The labelling of the samples of the materials by Th-228 and Ra-224 was made by the surface adsorption of the water solution containing the above radionuclides. The samples have been stored before the experimental measurement of thoron release for at least I month to allow the radioactive equilibrium between Th-228 and Ra-224 is attained.

6. The measurement of thoron release rate from the sample of bentonite clay was carried out using the equipment described by Balek [2]. The measurement was performed every minute in the conditions of constant temperature as well as during heating at the rate of 1K/min. The temperature interval used for the heating was -10°C to +150°C.

After the sample heating, its cooling to room temperature was carried out at the rate of 1K/min. Several heating runs in humid air (100 % R.H. obtained by passing the air flow through the water container at 25°C) and dry air (obtained by passing the air flow through concentrated sulphuric acid) overflowing the sample were carried out. The air flow was used to transport the released thoron from the sample into the detection chamber [2].

The results of the experimental measurements of the thoron release rate from bentonite clay sample are represented in Figure 3.

The heating of bentonite clay was carried out in the wide temperature interval (from -10°C to $+150^{\circ}\text{C}$) with the aim to observe effects of different processes on radon exhalation from the clay, namely the desorption of water from different types of pores. The sample heating was performed at the conditions of different humidities of the flowing air in order to simulate environmental conditions.

The cooling of the clay sample, previously heated to 150°C , was performed with the aim to investigate the effect of humidity of the surrounding air on the radon exhalation from the bentonite clay, from which the internal water in the pores was released.

We have observed that during the heating of bentonite clay remarkable changes in the thoron exhalation take place, which can be ascribed to the changes in the water content in pores, as well as to the changes in the pore volume.

At the temperatures of 67 and 84°C the heating at the rate of $1\text{K}/\text{min}$. was interrupted for 20-30 minutes in order to investigate the behaviour of the sample at isothermal conditions of 67 and 84°C . The time dependencies of the thoron release measured at these temperatures differ, as is shown in Figure 4.

The differences reflect different behaviour of the sample at these temperatures, caused by different water content in the pores and possibly by a decrease of pore volume.

During cooling, the bentonite clay heated up to 150°C was investigated, the air of different humidities overflowed the sample measured. The differences in the curves (Figure 5) were observed : higher values of E were measured in the case when the sample was overflowed with humid air in comparison with dry air. As is shown in Figure 5, curve I the increase of the thoron release rate E was observed at the temperatures lower than 50°C in the case when the sample was overflowed with the humid air. This observation can be explained by the condensation of water in micropores, which lead to the lower indirect recoil effect by stopping the recoiled atoms of radium and thoron in the water condensed.

WORKING PLAN FOR THE NEXT PERIOD :

1. Design of the improved mathematical model for radon/thoron release as influenced by the humidity and porosity changes during heating and cooling of the samples.
2. Mathematical modelling of the influence of humidity and porosity during sample heating and cooling using the improved model developed for the dynamic (non-steady state) conditions.
3. Experimental measurements of thoron release from various samples of building materials and isolation materials (sandy soil, concrete block, piece of wood, polystyrol and

cotton) during heating and cooling at varying humidity condition.

4. comparison of theoretical curves (obtained by mathematical modelling) and experimental curves (obtained by measurement) of thoron release from the materials.

5. Mathematical description of the differences in the release of radon and thoron from porous materials at varying humidity and porosity.

6. Recommendations for the practical use of the project results, especially with respect to the prediction of radon exhalation capacities of various porous materials under different temperature and humidity.

7. Preparation of the project final report.

REFERENCES

1. V.C. Rogers, K.K.Nielson, Health Physics 60 (1991) 801-815

2. V.Balek, J.Tolgyessy : Emanation Thermal Analysis and other radiometric emanation methods (Vol.XII C of the Wilson and Wilson's Comprehensive Analytical Chemistry, Elsevier Publ. Co 1984, 304 pp

FIGURES

Fig 1.: The dependence of radon exhalation from porous solid on the total porosity values at various fraction of water saturation of pores.

The fraction of water saturation of pores m equal :

$m = 0.1$ (curve 1), 0.2 (curve 2), 0.3 (curve 3), 0.4 (curve 4),
 0.9 (curve 5), 0.6 (curve 6), 0.7 (curve 7) .

In the modelling the following parameters were considered :

thickness of the plate -like porous sample = 1 cm , radon surface adsorption coefficient equals to zero , radium dissolution constant in solid -to-pore liquid equals to 100 , radon equilibrium distribution coefficient equals to 0.25, radon diffusion coefficient in air equals to $0.11 \text{ cm}^2/\text{s}$, local coefficient of radon emanation into the pore air phase.

Fig .2.:The dependence of radon exhalation from porous solid on the fraction of water saturation of pores at various values of the radium dissolution constant .

The radium dissolution constants in solid-to-pore liquid equal :

$K = 1.5$ (curve 1), 2 (curve 2), 4 (curve 3), 6 (curve 4), 8 (curve 5),
 10 (curve 6), 20 (curve 7) .

In the modelling the same parameters as in Fig.1 were considered, the considered value of total porosity was 0.4.

Fig. 3.:Results of the experimental measurements of thoron release rate from bentonite clay sample heated at the heating rate $1\text{K}/\text{min}$ in humid air (curve 1) and in dry air (curve 2) .

Fig.4.:Results of the experimental measurements of thoron release rate from bentonite clay sample isothermally heated at 67 C (curve 1) and 84 C (curve 2) in dry air .

Fig 5.:Results of the experimental measurements of thoron release rate from bentonite clay sample heated to 150 C obtained during the sample cooling to room temperature at the rate $1\text{K}/\text{min}$ in humid air flow (curve 1) and in dry air flow (curve 2) .

Figure 1

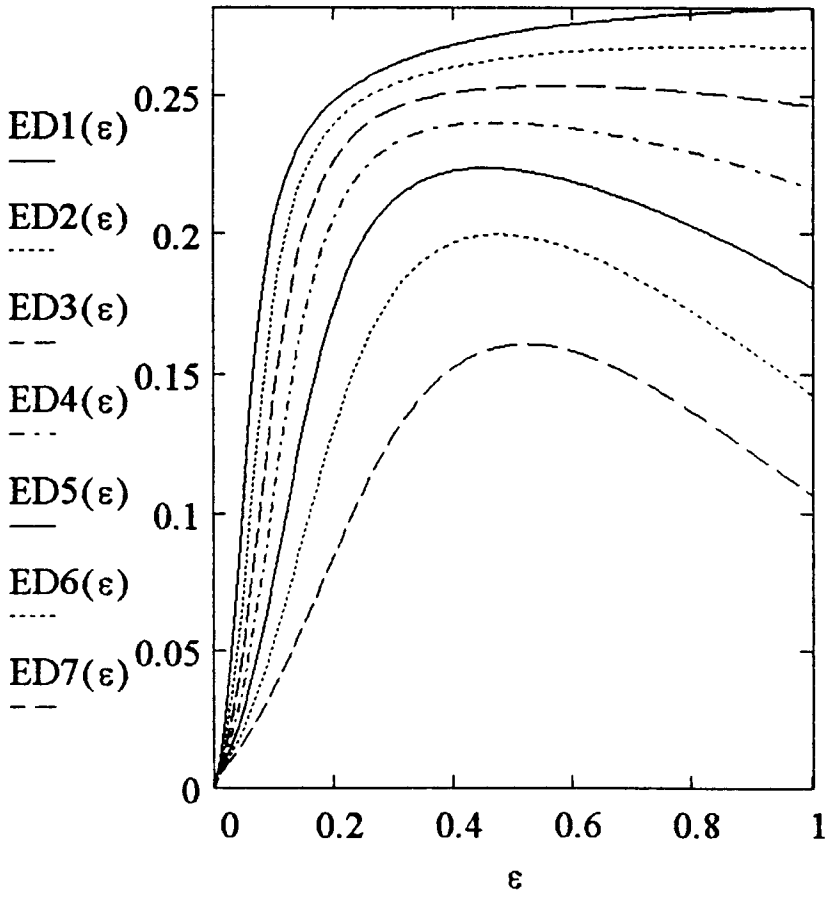


Figure 2

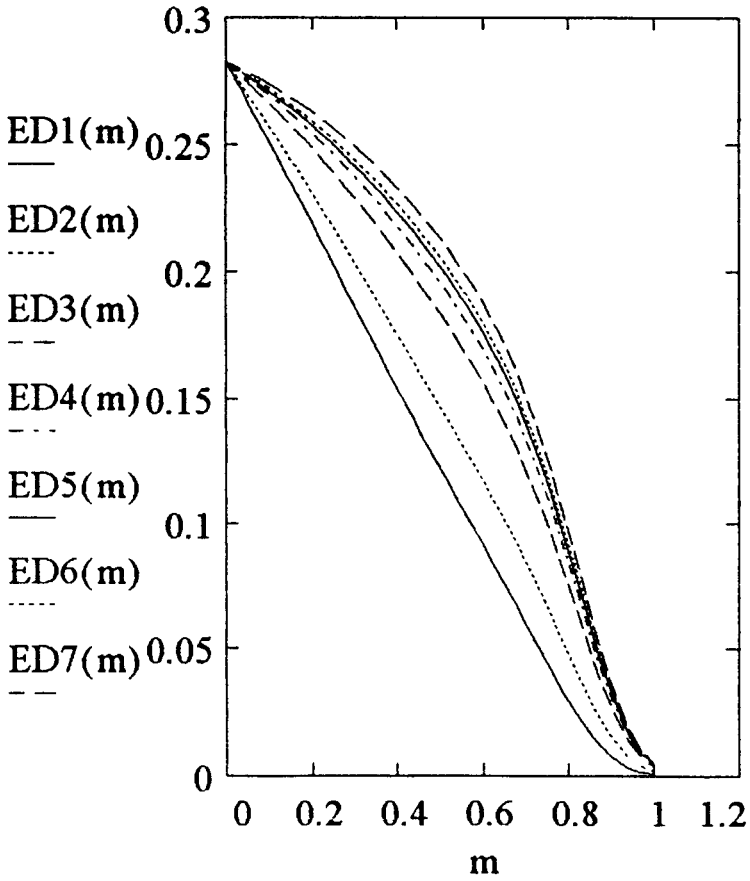


Figure 3

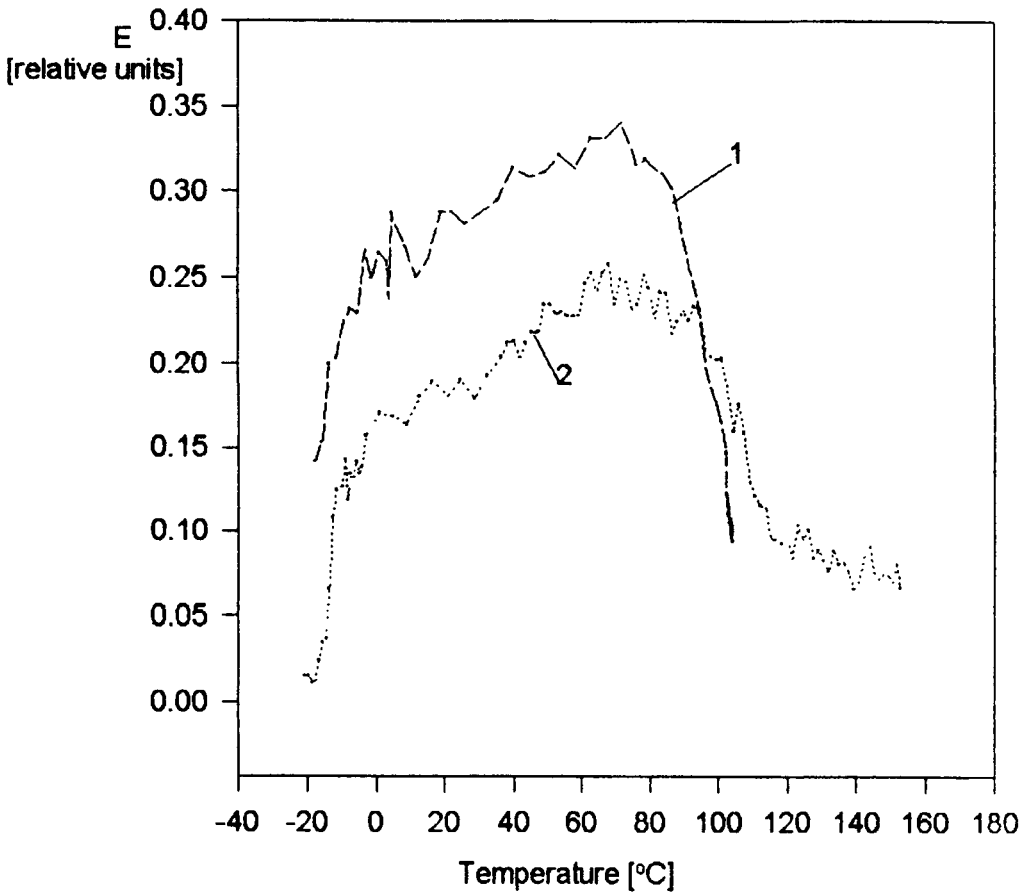


Figure 4

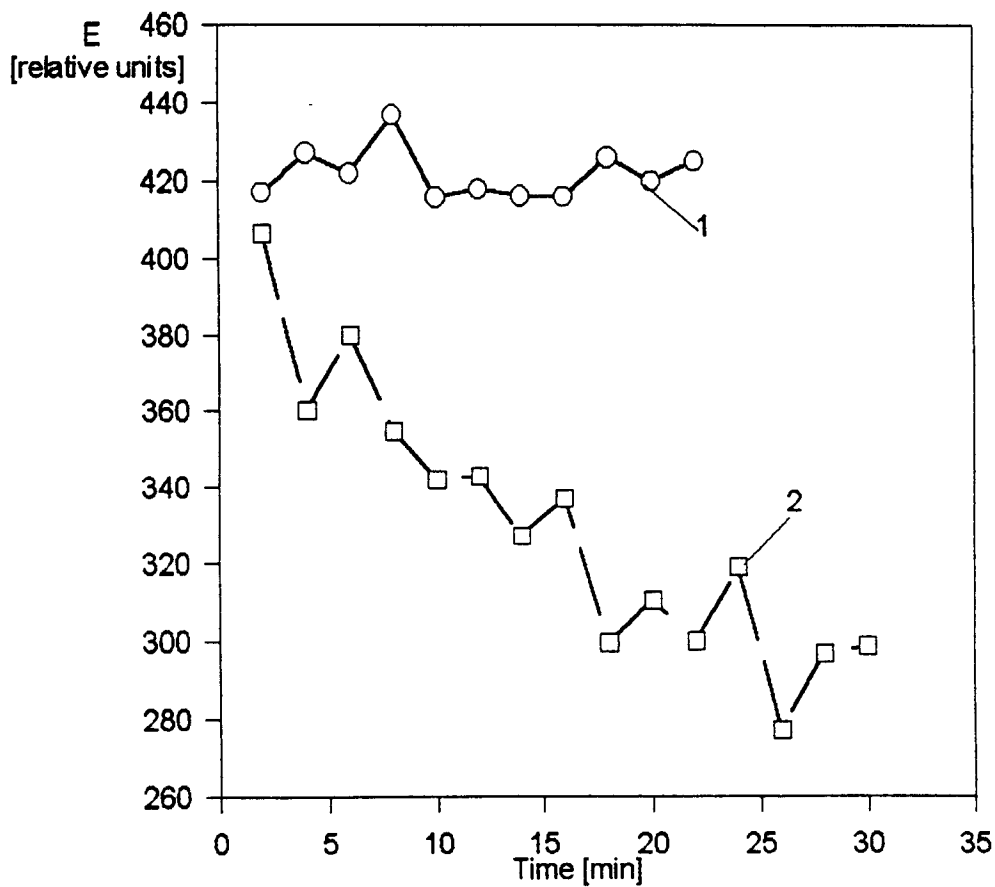
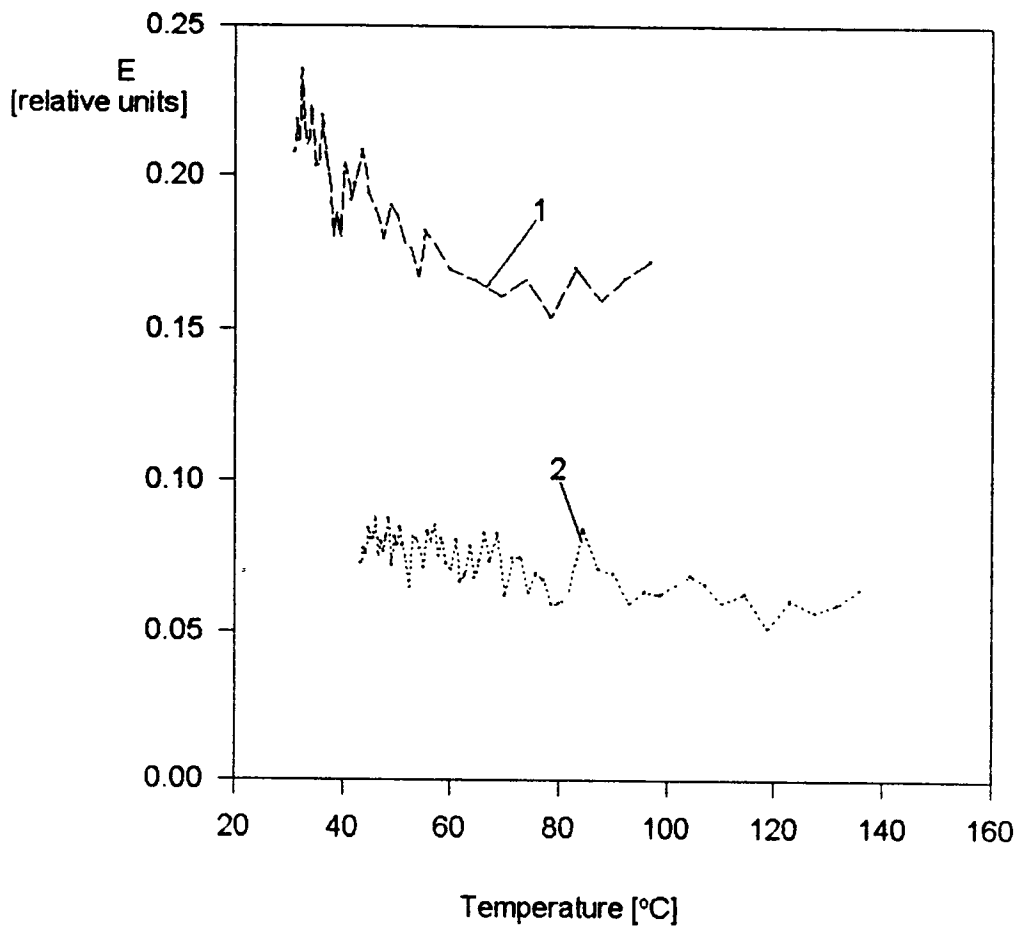


Figure 5



Head of project 9: Dr. C Cosma

II. Objectives for the reporting period.

- 1) To improve the radon flux measuring method by adsorption on activated coal and confrontation with other laboratories. To re- measure the radon flux in already supposed "high radon areas" (Cerna Valley, Cluj-Napoca, Stei region).
- 2) Correlation between radon flux, meteorological parameters and indoor radon concentration.
- 3) Measurements of indoor radon by Kusnetz method and promoting indoor radon integrating measurements in relevant areas.
- 4) Getting accustomed to theoretical models of radon mitigation (in soil, under buildings, penetration into dwellings, ventilation).

III. Progress achieved including publications.

Background

Although research on radon in geothermal waters in Romania has been done since 1908 intensive and steady progress in this field has been found only in the last 2-3 years. The research regarding the radioactivity of mineral and geothermal waters in Romania between 1925-1975 are summarized in: "Selected Works" (by G.Athanasiu) Romanian Academic Press, Bucuresti, 1977 and "Radioactive Waters and Gases in Romania" (by A.Szabo) Ed. Dacia, Cluj-Napoca, 1978.

Since the 1970s research was also concerned with radon in mines and in uranium mines in Romania but the measurements were kept secret, still, some of them were published after 1990. Between 1980-1990 two Ph.D.Theses were worked out (M.Zoran and C.Cosma), on outdoor radon and radon content in geothermal gases and waters.

There also are certain unpublished data concerning indoor radon and the radioactive content of building materials, data belonging to the Hygienic Public Health Institutes network (Bucureti, Cluj, Timisoara, Iasi).

As regard indoor radon all the measurements are short period measurements (Kusnetz method or method of filtered samples).

The National Institute of Meteorology and Hydrology, Bucharest deals with such matters as well (S.Sonoc, I.Dovlete, V.Cuculean, I.Oswath).

Only beginning with 1994 the method of indoor radon integrating measurements was used (Karlsruhe detectors).

The author of the present report (C.Cosma) made measurements of radon in gases emanated from minerals and geothermal waters sources and measurements of the soil radon flux (between 1980- 1987). The results obtained were published in the Ph.D.theses. After Chernobyl period and especially after 1990 I started again doing measurements of the soil radon exhalation and since 1993 (with my acceptance in a PECO program collaboration) I have been developing these concerns and on the other hand, I made measurements on indoor radon in particular areas in Romania, using integrating methods as well.

Progress

The method used for radon flux measurement is that proposed by Megumi and Mamuro (J.Geophys.Res. 77,3052,1972) namely the adsorption on active charcoal of the radon flux from a determined area (0.25m²) and a given period (2-12 hours). The adsorbed radon in a quantity of 220g of charcoal is measured by gamma spectrometry in Marinelli vessels using NaI(Tl) scintillation detectors.

For the calibration of the device during the first measurements we used the radon extracted from water with a known radon content. In the second phase we used a RaCl₂ Romanian standard solution (STANDARD 12.051 AIR).

The method was checked by measuring the same sample both in our laboratory and in the Nuclear Physics Laboratory from Gent University using a calibrated Ge detector, a Canberra gamma spectrometer and a SAMPO 90 program for spectra processing. The difference between the results obtained is in the range of experimental errors (8%).

This was the method used to remeasure the radon flux in Cerna Valley (Herculane Spa area, for 7 places) in March 1995. The daytime values are a little higher than the night-values and fall into the 17-240mBq/m².s range, the higher values being associated to the proximity of some faults in the sedimentary rocks which cover the granite and the geothermal deposit of this zone. The results obtained in March 95 are in good agreement with previous measurements (Oct.90, Nov.94). These results together with measurements of radioisotope content of soil (U,Ra,Th,K) and other measurements of radon content in gases emanated from geothermal sources were presented at NRE VI Symposium, June 5-9, Montreal and will be published in [1].

The re-measurement of the radon flux in Cluj-Napoca city in February and May 1995 provided the values determined previously, respectively in the range 10-20 mBq/m².s. In October 95 determinations will be made for the radon flux in the Stei region (Uranium mine) and especially in the waste dump area. In Cluj- Napoca city, during March-April 95 there were made simultaneous measurements for the radon flux from soil (10-15 m distance from the building) and indoor radon at groundfloor level by Kusnetz method in

16 places. The measurements show a close connection between the values of the radon flux and the indoor radon concentrations. The results were also displayed at NRE VI Symposium (Montreal) and are to be published in [2].

During the period 14 March-15 April 95 at the meteorological station of the Cluj-Napoca airport the radon flux was measured daily in association with the wind speed, soil temperature, air humidity and temperature and also atmospheric pressure.

The graphic representation of the radon flux and the parameters mentioned above shows an intricate dependence but with a visible influence of pressure and temperature of soil.

To study the influence of the atmospheric pressure alone we worked out an experiment consisting in simultaneous measurement on two identical radon collectors, one of them allowing pressure variation using a water column.

The experiment is being made and the results will be presented in the final report.

Concerning the indoor radon in relevant areas (Cerna Valley, Cluj-Napoca and Stei region) the results obtained up to the present will be presented more detailed in the December report. High values were found for Baita Plai (646 Bq/m³), Baita Sat (325 Bq/m³) in the mining region of Stei and relative high values were also found for the town of Oradea (115 Bq/m³) and smaller values for Cluj-Napoca city (76 Bq/m³). These values represent the arithmetic mean of 30- 35 dwellings, in each dwelling being measured twice a year in the cold and warm season in bedrooms, living-rooms and kitchens using the Kusnetz's method.

In Cerna Valley (Herculane Spa) and in Cluj-Napoca there also were made measurements with Kalsruhe integrating detectors, the results being as follows: 98 Bq/m³ during the warm season and 198 Bq/m³ during the cold season for Herculane Spa and 156 Bq/m³ during the cold season for Cluj-Napoca (representing the arithmetic mean for 20 dwellings situated at groundfloor).

In one of the quarters of Oradea city in which geothermal water with high Ra content is used for house-keeping needs, a higher value of the indoor radon (120 Bq/m³) could be noticed as compared to the rest of the city (90 Bq/m³) [Kusnetz method]. The interpretation of these results can be found in [3].

In parallel with these measurements we are concerned with theoretical aspects of radon mitigation in soil, on which we presented a paper at the Symposium on Radiation Protection in Neighboring Countries in Central Europe, Portoroz, Slovenia, September 4-8 1995.

Objectives for the next reporting period:

1. Radon flux measurements and radon soil content determination with a view to trace out possible high radon areas in Romania.
2. Measurements on indoor radon in some presumptive high radon areas using our method (Kusnetz) also the first integrated measurements. To design our own method for indoor radon measurement with track detectors.
3. Development of theoretical models for radon mitigation (soil migration, radon entry to house, ventilation).

Publications

- [1] C.Cosma, A.Poffign, D.Ristoiu, G.Meesen "Radon in Various Environmental Samples in Herculane Spa (Cerna Valley) Romania" presented at NRE VI, Montreal, June 5- 9, 96 to be published in Environment International.
- [2] C.Cosma, S.Ramboiu, D.Ristoiu, O.Cozar, V.Znamirovski, L.D, F Eban, I.Chereji "Some Aspects of Radon Radioactivity in Romania" presented at NRE VI Conference, Montreal, June 5-9, 1995 to be published in Environment International.
- [3] C.Cosma, I.Pop, S.Ramboiu, T.Jurcut, D.Ristoiu "Radioactive Aspects of Use of Geothermal Waters in Oradea" Proc.of World Geothermal Congress, 21-26 May, 1995, Florence, Italy, vol.4, pg.2791-2795.
- [4] D.Ristoiu, C.Cosma, T.Ristoiu, J.Miles "Radon mitigation in soils" presented at Radiation Protection Symposium in Neighboring Countries in Central Europe, Portoroz, Slovenia, sept. 4-8, 1995.

Final Report

Contract : F13P-CT030074 Duration 1.1.93 to 30.6.95 Sector C12

Title: Evaluation of the combined Helium/Radon in Soil Gas mapping methodology as an indicator of areas in which elevated indoor radon concentrations may be found.

1. Madden RPII
2. O'Connor Geological Survey (Irish)
3. Van den Boom ENMOTEC GmbH
4. Porstendorfer Univ. Gottingen

1. Summary of Project Global Objectives and Achievements

Introduction

Radon mapping methodologies based on established soil-gas sampling techniques are being developed in several EU and non-EU countries. The ability of these mapping procedures to successfully identify areas with elevated indoor radon concentrations has not so far been critically assessed. National agencies with responsibility for radiological protection of the general population in many countries worldwide are developing strategies, based on indoor radon mapping, to limit the radiological risk to the population at large. If radon in soil-gas mapping techniques are to be of assistance to national authorities then critical assessments of these techniques including their predictive capacity need to be carried out.

Global Objectives

The primary objectives of the project were to

- i) assess the effectiveness of the Helium/Radon in soil-gas mapping methodology as an indicator of areas in which elevated indoor radon concentrations may be found
- ii) improve our understanding of the geological factors which control the generation, migration and ingress of radon into buildings
- iii) investigate the variations in radon exhalation from the ground and ingress into buildings due to changing meteorological conditions

Global Achievements

A survey area of some 25 km² was chosen, centred on the town of Claremorris, Co. Mayo, western Ireland (see Figure 1). This area was selected because it is underlain by well-bedded, crystalline, Lower Carboniferous limestone, and because no information existed on the domestic indoor radon concentrations. It therefore, provided an ideal testing ground in which to evaluate and assess the predictive capacity of the combined He/Rn in soil-gas mapping technique in identifying high radon potential areas. Preparatory work for the project was carried out by RPII in Spring 1993 through a

publicity campaign involving local media and public meetings. A vacant house with elevated indoor radon levels was secured for the project team at Milltown, Co. Galway some 15 km SE of the Claremorris survey area (see Figure 1). An integrated field campaign by the project team was undertaken in May 1993 and May 1994.

Indoor radon gas measurements were carried out by RPII and over 1200 radon dosimeters were issued to householders during the course of the project. Local detailed geophysical surveys were carried out by University College Galway (under subcontract to RPII) at the test house site in Milltown, and at Eskerlevalla (Area 1) and Mount St. Michael Primary School (Area 3) in support of the indoor radon and soil-gas radon surveys (see Figure 1). A geochemical analysis of a suite of soil/rock samples taken from the survey areas was completed by RPII using high resolution gamma spectroscopy.

A reconnaissance or low-density sampling survey of soil-gas radon and helium concentrations was carried out by Enmotec together with detailed soil-gas surveys (high-density sampling) in three selected sub-areas, Eskerlevalla (Area 1), Lugatemple (Area 2) and Mount St. Michael Primary School (Area 3) in Claremorris (see Figure 1), and at the test house site in Milltown, Co. Galway. A total of 526 soil-gas samples were analysed by Enmotec for Rn-222 with 179 samples analysed for helium by the US Geological Survey.

Reconnaissance mapping of the bedrock geology and glacial geology was completed by GSI for both the Claremorris and Milltown survey areas. All extant geological data in GSI files was compiled and provided to the project team together with topographic base maps for the survey areas.

At the test house in Milltown, Co. Galway a detailed programme of continuous monitoring of soil-gas radon concentration at 1 m depth; radon concentration at 50 cm depth beneath the floor slab; indoor radon concentration at several locations within the house; pressure differences between indoor air, subslab air and outdoor air, and temperature differences between indoor and outdoor air was carried out by Gottingen during the two week field campaign in May 1993. Gottingen also constructed, calibrated and field tested a special soil probe for continuous measurement of the vertical radon gas profile in soil down to a depth of 3.5 m. The field testing of the probe took place in Germany during 1995.

Correlation of Soil-Gas Radon and Indoor Radon Spatial Distributions

In the low-density sampling regional survey soil-gas radon concentrations ranged from 350 Bq m⁻³ up to 393000 Bq m⁻³ with an arithmetic mean value of 83000 Bq m⁻³ and a median value of 71000 Bq m⁻³. From a statistical analysis of the data a threshold value of 70000 Bq m⁻³ was considered appropriate for designating high radon potential zones within the survey area. It was also concluded, however, that a threshold value in excess of 100000 Bq m⁻³ could not be ruled out. A high radon potential zone was taken to be one in which 50% or greater of houses within the zone had radon concentrations in excess of the national Reference Level of 200 Bq m⁻³.

A statistical analysis of the indoor radon data incorporating 2 x 2 contingency tables which compared the high/low radon potential zones in terms of monitored indoor radon levels supported the threshold value of 100000 Bq m⁻³. At this threshold value 41% of houses within the designated high radon potential zone had radon concentrations in excess of 200 Bq m⁻³, as against 33% of houses when the 70000 Bq m⁻³ threshold value was considered. This statistical analysis was taken a stage further to determine the optimum soil-gas radon threshold value which could discriminate between high/low radon potential zones on the premiss that a high radon potential zone is defined as one in which 10% or greater of houses within the zone have elevated indoor radon levels. This classification of high radon potential zones is currently in use in Ireland. Using this criterion the threshold value which maintained the best sensitivity and specificity and which kept the number of false negatives (i.e. high

radon houses in the low radon potential zone) to a minimum was 40000 Bq m⁻³. Ninety-eight percent of all monitored high radon houses in the survey area fell within the designated high radon potential zone. Two percent of houses within the low radon potential zone had elevated indoor radon levels. The discrimination between zones was also good at 40000 Bq m⁻³ with a house in the high radon potential zone having a risk c. 17 times greater than one in the low radon potential zone of having an indoor radon concentration in excess of 200 Bq m⁻³.

Analysis of the detailed surveys especially the Lugatemple (Area 2) survey gave broadly consistent results with a threshold value of 55000 - 60000 Bq m⁻³. Six out of 8 identified high radon houses fell within the designated high radon potential zone. Notwithstanding the limited data set the results of this particular study suggest that high-density sampling may provide an effective technique for correctly identifying the radon potential of individual house sites, but further work is needed on this aspect of radon potential mapping.

Correlation of Geology with Soil-Gas Radon and Helium Concentrations

The predominant patterns in the spatial distribution of soil-gas radon are elongate zones trending NE-SW with a subsidiary trend WNW-ESE also evident. These trends are broadly coincident with the mapped joint directions in the limestone bedrock, in particular, the 47°E shear joint direction and the 117°E tension joint direction. Anomalous helium concentrations also reveal lineaments that parallel the principal joint directions mapped in the field, and support the view that the soil-gas radon patterns appear to be structurally controlled by bedrock features such as fractures and joints. These features together with the evidence in the near surface limestone sequence of partial karstification due to percolating groundwater most likely provide the main lateral and vertical pathways or natural plumbing system for the upward migration of radon to the surface.

The radon source in the area is considered to be the thick (> 1 km) Lower Carboniferous limestone sequence which underlies the entire area. At last two near surface limestone beds have elevated Ra-226 concentrations, and in the central part of the survey area, thin soils locally developed from in-situ weathering of the limestone show elevated Ra-226 concentrations > 100 Bq kg⁻¹. The conclusion is that both the limestones and their derived soils are the primary source of soil-gas radon in the area.

Meteorological Influences on Soil-Gas Radon Transport and Ingress into Buildings

The series of measurements performed at the test house in Milltown, Co. Galway confirmed the dependence of the indoor radon concentration on the pressure difference between subslab and indoor air. This pressure gradient was mainly governed by the wind pressure applied to the house. The variation of indoor radon could be reproduced during the measuring campaign by a source factor, calculated from the product of the pressure gradient between subslab and indoor air and the subslab radon concentration, supporting the view of convective entry of soil air into the house as a major radon entry mechanism.

The compartmentalised structure beneath the subslab which was highlighted by the Ground Probing Radar (GPR) survey of the interior of the house helped explain the temporal variation in subslab radon concentration when compared to the soil-gas radon variations at 1 m depth. It also helped explain the large transport resistance evident between subslab air and outdoor air.

An experiment with a small fan blowing attic air into the ground floor yielded a substantial decrease in indoor radon concentration. A 1 Pa reduction in the pressure difference between subslab and indoor air caused a thirteenfold reduction in the average ground floor radon concentration. The significance of this as a potential radon remedial technique in Irish houses warrants further investigation.

The construction, calibration and field testing of a special soil probe for continuous measurement of the vertical radon profile in soil was also undertaken by Gottingen. Preliminary field measurements have been obtained but additional measurements need to be done to interpret their results. Experiments are planned for the future to study the influence of meteorological parameters on radon gas concentrations in the soil using the above soil probe.

Geophysical Investigations

Geophysical investigations were carried out in an attempt to map any sub-surface structural features in the vicinity of houses with elevated indoor radon levels. Combinations of techniques incorporating Ground Probing Radar (GPR), EM-VLF-R, EM-VLF, Wenner Resistivity Profiling and Total field Magnetics were employed during the course of the work. The overriding conclusion from the battery of geophysical investigations is of a mainly weathered bedrock close to, or at the surface with karstification and solution features prominent in the surveyed areas.

At the test house in Milltown the indoor GPR survey successfully identified footings beneath the subslab structure which it is believed affect both the subslab radon concentration and the movement of subslab air to outdoor air. The main findings of the outdoor GPR survey is that the limestone surface is jointed and large solution features may be present. The house apparently straddles an E-W trending ridge of shallow bedrock which may be related to the observed 102°E tension joints in the area. This ridge may be giving rise to strains in the foundation slab which are evident from cracks in the exterior and interior walls of the house, thus providing a pathway for ingress of radon into the house.

As Eskerlevala (Area 1), the geophysical investigations indicated ridges of shallow competent bedrock, possibly related to a predominant jointing pattern in the area, with zones of increased weathering or karstification enveloping the ridges. The inference is that houses built on the competent limestone ridges, unlike those in the transition zone, will have no large scale jointing in the vicinity of the house foundations to provide a pathway for bringing radon gas close to the house foundations.

The geophysical surveys conducted at Mount St. Michael Primary School (Area 3) highlighted the fact that the bedrock surface is not uniform, and hence the thickness of overburden varies greatly both within and outside the school perimeter fence. This variation brings jointed bedrock close to the surface in the vicinity of the school, and also allows for thick accumulation of clay in other areas within the school perimeter fence. Some of the accumulations of clay lie within depressions in the bedrock surface which, according to local information, may have been extensively excavated and back filled with permeable hardcore during construction of the school foundations. This situation may provide a highly permeable zone both in contact with the jointed limestone bedrock and the foundations of the school, again providing an ideal pathway for radon ingress into the school building.

Seasonal Variability of Indoor Radon Concentration in Domestic Dwellings

Significant variability is evident in the limited data set. Radon measurements carried out during the Autumn-Winter period may overestimate the long-term average radon concentration by as much as 20%. Similar measurements carried out during the Spring-Summer period may underestimate the long term average value by as much as 20% - 40%.

Conclusions

1. The Claremorris survey area is one of high soil-gas radon concentrations and elevated indoor radon concentrations.
2. Regional He/Rn in soil-gas mapping has identified high radon potential zones within the

studied area on the basis of the $>70000 \text{ Bq m}^3$ or $>100000 \text{ Bq m}^3$ soil-gas radon concentration threshold value.

3. Independent indoor radon mapping has confirmed that c. 40% of houses within the designated high radon potential zone ($>100000 \text{ Bq m}^3$) have elevated indoor radon concentrations.
4. Detailed He/Rn in soil-gas mapping may provide an effective technique for correctly identifying the radon potential of individual house sites.
5. Soil-gas radon patterns in the studied area appear to be structurally controlled by bedrock features such as fractures and joints. Supporting evidence for this also comes from the helium in soil-gas mapping and the geophysical site investigations.
6. The indoor radon concentration in the test house can be correlated to the pressure difference between subslab and indoor air. This indicates that convective flow of subslab air into the house is the dominant radon ingress mechanism. In the climatic conditions, pertaining to the west of Ireland this pressure difference is mainly governed by windspeed.

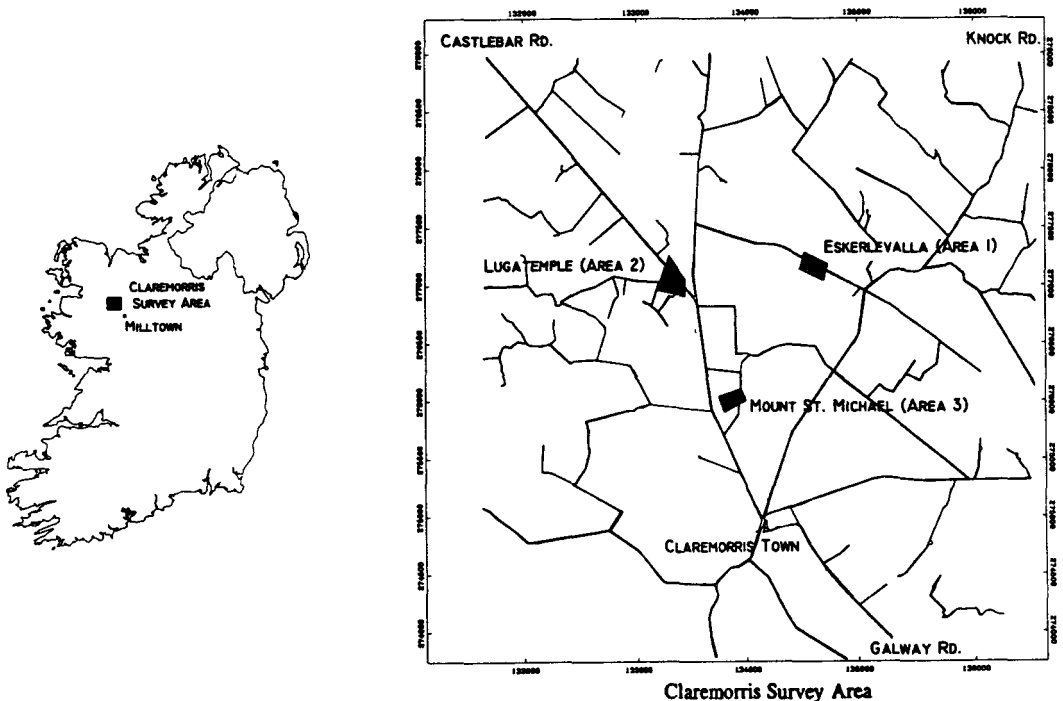


Figure 1: Geographical Location of Claremorris Survey Area and Milltown.

Head of Project 1: Dr. Madden

II. Objectives for the reporting period

The primary objectives of the Radiological Protection Institute of Ireland (RPII) in this project were:

- (i) Determine the geographical distribution of indoor radon concentrations in the survey area of Claremorris, Co. Mayo, western of Ireland.
- (ii) Evaluate the degree of correlation between the observed spatial patterns of soil-gas Rn/He concentrations and indoor radon concentrations.
- (iii) Assess the predictive capacity of the combined Rn/He mapping technique in identifying areas in which elevated indoor radon concentrations may be found.

III. Progress achieved including publications

Introduction

The chosen field study area is approximately 25 km² in extent, centred on the town of Claremorris, Co. Mayo, western Ireland (see Figure 1). The area has a population of c. 2500 with an average housing density of approximately 29 houses per km². The local housing stock is comprised of bungalows and one - and two- storey farm houses, all of which are of slab-on-grade construction. At the onset of the project no information existed on the local domestic indoor radon levels. In 1989 RPII identified a school within the present survey area with radon concentrations in excess of 1000 Bq m⁻³ in several classrooms. The entire survey area is underlain by well-bedded, crystalline, Lower Carboniferous limestone.

Indoor radon gas measurements were carried out by RPII to map the spatial or geographical distribution of indoor radon concentrations in the survey area, and to assess the seasonal variability in indoor radon levels in a preselected sample of dwellings. Over 1200 passive radon dosimeters were issued during the course of the project. Geophysical site investigations were carried out by University College Galway (under subcontract to RPII) at Eskerlevalla (Area 1) and Mount St. Michael Primary School (Area 3) in Claremorris (see Figure 1), and at the test house site in Milltown, Co. Galway. These investigations assisted in characterising surface conditions at the various sites by mapping any sub-surface structural features in the vicinity of buildings. These features if present may have some control on the ingress of radon into the buildings. High resolution gamma spectroscopic analysis of a representative suite of soil/rock samples from the survey area was carried out by RPII to determine their Ra-226 content.

Indoor Radon Gas Measurements

In Spring 1993 the residents in 718 houses in the Claremorris District Electoral Division (field survey area) were contacted by RPII regarding participation in the project. The residents in 250 dwellings agreed to take part, and indoor radon gas measurements were completed in 204 houses. The house locations of all participating householders were plotted on 1:2500 scale O.S. maps, digitised and converted to Irish National Grid Co-ordinates, and integrated with all other spatial geodata using GPS (Global Positioning Systems) and computer-based mapping software. The spatial distribution of monitored houses is shown in Figure 2. Thirty-one houses geographically distributed throughout the survey area were also selected for detailed investigation of the seasonal variability in indoor radon levels. The selected dwellings comprised 19 bungalows and 12 two-storey houses.

In all houses time integrated radon gas concentrations were measured using the standard RPII domestic radon dosimeter. This is a passive, closed, alpha track-etch radon detector with Cr-39 plastic as the detecting medium. On return the Cr-39 plastics were chemically etched and counted by an image analysis system. The standard etching conditions used were 10N Sodium Hydroxide (NaOH) at 70°C for eight hours. The dosimeters were calibrated in the RPII Radon Calibration Chamber, and by participation in a recent series of intercomparisons carried out by the EU.

The adopted protocol for mapping the geographical distribution of indoor radon concentrations was two dosimeters per house; one in the principal living area and the other in the principal bedroom for an exposure period of at least six months. A whole-house average radon gas concentration was determined and adjusted to an annual concentration using standard in-house correction factors.

In order to assess the seasonal variability in indoor radon levels the adopted protocol was 24 radon dosimeters per house; one group of 12 was located in the principal living area and the other group in the principal bedroom. Each group of 12 dosimeters was placed inside a single, open plastic bag, which was positioned at one location within each monitored room. At one month intervals the householders retrieved a single dosimeter from each group and returned them to RPII for processing.

Results

The frequency distribution of regional indoor radon gas concentrations is shown in Figure 3 and approximates to a log-normal distribution. Indoor radon gas levels range from 20 Bq m⁻³ up to c. 1950 Bq m⁻³ with an arithmetic mean value of 189 Bq m⁻³. Twenty-five percent of monitored houses have radon concentrations in excess of the national Reference Level of 200 Bq m⁻³. In Ireland, at present, 10 km x 10 km grid square areas are classified as high radon potential areas if greater than 10% of houses are predicted to have indoor radon levels in excess of 200 Bq m⁻³. Using this criterion the entire survey area would be classified as a high radon potential area.

The assessment of the seasonal variability in indoor radon levels proved to be problematic due to difficulties encountered in retrieving dosimeters from participating householders at the relevant time intervals. As a consequence of these logistical problems the data for only five houses are suitable for presentation and analysis. The five houses comprise four bungalows and one two-storey house and the results are presented in Table 1.

The data for each house were time weighted to give average radon concentrations for the seasons Autumn, Winter, Spring and Summer where appropriate, and then normalised relative to the long-term average radon concentration in the house. From Table 1 it is evident that there is significant seasonal variability both within and between house types. The limited data suggest that radon measurements carried out during the Autumn-Winter period in the bedroom and living areas of bungalows will tend to overestimate the long-term average radon concentrations at these locations. Similar measurements carried out in the Spring-Autumn period will tend to underestimate the long-term average radon concentrations.

Correlation of Indoor Radon and Soil-Gas Radon Spatial Distributions

To assess the degree of correlation between the spatial distributions of soil-gas radon concentrations and indoor radon levels a computer generated contour map of the regional soil-gas radon data was produced (see Figure 4) for comparison with the indoor radon data. The regional soil-gas data were gridded at 125 m grid cell size (c. half the spacing interval of 250 m) using a log-linear gridding which takes account of the fact that the data are irregularly spaced and tending towards log-normality.

Geographical areas were classified as high/low radon potential zones using the soil-gas radon contours as threshold values. Within these zones monitored houses were classified as high/low radon houses relative to the national Reference Level of 200 Bq m^{-3} and grouped accordingly. The degree of correlation between the spatial data sets, and the predictive capacity of the mapping technique to identify high radon potential areas was assessed using 2×2 contingency tables which compare high/low radon potential zones in terms of monitored indoor radon levels (see Table 2). In this analysis sensitivity is defined as the number of high radon houses correctly identified in the high radon potential zone as a percentage of the total number of high radon houses found in the whole survey area. Specificity is likewise defined as the number of low radon houses correctly identified in the low radon potential zone as a percentage of the total number of low radon houses found in the whole survey area. A similar analysis was performed on the detailed soil-gas radon data from the Lugatemple survey (Area 2). In this case the soil-gas data were gridded at 10 m grid cell size, again using a log-linear gridding routine (see Figure 5 and Table 3). Plots of sensitivity against 1 - specificity for all chosen threshold values of soil-gas radon are presented in Figure 6.

Enmotec conclude from their analysis and interpretation of the regional data sets that soil-gas radon concentrations in excess of 70000 Bq m^{-3} are anomalous, and that a threshold value of 70000 Bq m^{-3} may be appropriate for the survey area. They also suggest however that a threshold value in excess of 100000 Bq m^{-3} cannot be ruled out. In their interpretation a high radon potential area is defined as one in which 50% or greater of the houses within the zone exceed the national Reference level of 200 Bq m^{-3} . Using this criterion for designating high radon potential zones our analysis of the soil-gas radon and indoor radon data sets would tend to favour the threshold value of 100000 Bq m^{-3} . At this threshold value 41% of houses within the designated high radon potential zone have radon concentration in excess of 200 Bq m^{-3} (see Table 2). From our perspective as a radiological protection institute, RPII has defined high radon potential zones as zones in which greater than 10% of houses are predicted to exceed 200 Bq m^{-3} . Using this criterion the 100000 Bq m^{-3} threshold value is not the optimum discriminatory threshold since 22% of houses in the presumed low radon potential zone still have radon concentrations in excess of 200 Bq m^{-3} (see Table 2).

For the combined mapping technique to be of benefit under the RPII criterion for designating high/low radon potential areas it is important that the majority of high radon houses within the survey area occur within the high radon potential zone, and that the minimum number of high radon houses lie within the low radon potential zone. In our analysis of the data this means that the sensitivity and specificity should be as high as possible, and the number of false negatives i.e. high radon houses in the low radon potential zone should be as small as possible.

The threshold value which maintains the best sensitivity and specificity, and keeps the number of false negatives to a minimum is 40000 Bq m^{-3} (see Figure 6a). Fifty-one out of 52 identified high radon houses in the survey area lie within the high radon potential zone constrained by the 40000 Bq m^{-3} soil-gas radon contour. This constitutes 98% of all identified high radon houses and 35% of all monitored houses within the high radon potential zone (see Table 2). The high radon potential zone covers c. 75% of the field study area. The low radon potential zone contains c. 25% of all measured houses and encompasses c. 25% of the total survey area. Two percent of houses within this zone have concentrations in excess of 200 Bq m^{-3} , which is an acceptable percentage of false negatives. The discrimination between zones is also quite good at the 40000 Bq m^{-3} threshold value as indicated by the relative risk figure of 17.5 (see Table 2). This indicates that a house in the high radon potential zone has a risk c. 17 times greater than one in the low radon potential zone of having an indoor radon concentration in excess of 200 Bq m^{-3} .

Our analysis of the Lugatemple data suggests an optimum threshold value of 60000 Bq m^{-3} (see Figure 6b and Table 3). This is consistent with the 55000 Bq m^{-3} threshold value suggested by Enmotec. However with such small numbers of houses in the Lugatemple area the misclassification of a single high radon house into the low radon potential zone can seriously distort the statistics.

Notwithstanding this, 6 out of 8 identified high radon houses lie within the designated high radon potential zone (see Table 3).

Geophysical Investigations

Detailed geophysical site investigations were carried out in three specific areas of high indoor radon concentrations and/or elevated soil-gas radon concentrations. These surveys were carried out to assist in characterising the surface conditions by mapping any sub-surface features in the vicinity of houses with elevated indoor radon levels. These structural features being assumed to have some control on the ingress of radon into the houses. Geophysical surveys were carried out at Eskerlevalla (Area 1) and Mount St. Michael Primary School (Area 3) in Claremorris, and at the test house site in Milltown. Combinations of techniques including Ground Probing Radar (GPR), EM-VLF-R, EM-VLF, Wenner Resistivity Profiling and Total Field Magnetism were employed during these surveys.

Eskerlevalla Survey (Area 1)

An EM-VLF-R survey was carried out in the area surrounding 3 houses. The survey used wall and field boundaries to help locate measurement positions and the station spacing was generally 25 m. A contour map of the resistivity values is shown in Figure 7. The houses under investigation are situated on, or near, shallow, high resistivity (> 1200 Ohm-metres) bedrock which also corresponds to a local topographic high. The overall pattern of the resistivity contours is interpreted as being due to shallowly buried ridges of competent limestone bedrock generally trending NNE-SSW, but with a WNN-ESE trend also apparent. These ridges could be related to a predominant jointing pattern in the area with lower resistivity (< 700 Ohm-metres) zones enveloping the ridges, and indicating zones of karstification or weathering. The two houses with elevated indoor radon concentrations (House A and House B) are situated on top of a ridge of competent limestone (House A), and in a transition zone or edge between a ridge and a weathered zone (House B). The third house (House C) with low indoor radon also lies on a block of competent, shallowly buried limestone.

In this area there is no clear correlation between the local geology and the incidence of elevated indoor radon levels. It could be argued that House B with elevated indoor radon levels is built on jointed, weathered, limestone consistent with the transition zone, and that this provides a pathway for radon to be brought near to the house foundations. In the case of the low radon house, House C, which lies on competent limestone bedrock the argument would be that no large scale jointing exists in the vicinity of the house foundations. House A, the high radon house situated on competent limestone is not readily explainable since it is difficult to argue that large scale jointing is responsible for the radon ingress in this case. Jointing may exist in the vicinity of this house which has not been detected by the survey at a station spacing of 25 m, but it is also likely that differences in house type and construction may ultimately be the controlling factor in deciding the final indoor radon concentration in these specific houses.

Mount St. Michael Primary School (Area 3)

A series of geophysical traverses were carried out in the immediate vicinity of the school building, and in the grounds surrounding the school (see Figure 8a). The near-school surveys were carried out to map the depth to bedrock, and those outside the school perimeter were sited to map any structural trends.

To the west of the school resistivity traverses and vertical electric soundings indicate bedrock generally lies within 2-3 m of the surface with outcrop close to the surface to the NW and SW of the school premises. A zone of increased overburden thickness is apparent from GPR and resistivity surveys in the vicinity of the western edge of the school playground. To the east of the school premises bedrock lies close to the surface with outcrop evident in the eastern approach. EM-VLF-R

and resistivity traverses to the north and south of the school perimeter fence indicate a zone of low resistivity. If the data can be correlated across the intervening buildings and playground, than a N - S zone of low resistivity (< 1000 Ohm-metres) can be defined (see Figure 8b). To the east of this zone lies high resistivity (> 1000 Ohm-metres) bedrock, close to or at the surface, and to the west possibly lie a number of zones of alternating high and low resistivity.

The central low resistivity zone is approximately 60 m in length and can be further divided with lower resistivity (< 500 Ohm-metres) to the north. If the correlation of the data across the school premises is correct, the implication is that there is a zone of increased weathering crossing the school and deepening to the north. With regard to this N-S zone of increased weathering the area to the north may relate to a solution feature containing a thick, low resistivity clay sequence. To the south the zone may relate to weathering or karstification associated with joints and/or a channel-like feature.

The main inference from the geophysical surveys is that the bedrock surface is not uniform and hence the thickness of overburden varies greatly both within and outside the school perimeter fence. This variation brings jointed bedrock close to the surface in the vicinity of the school, and also allows for thick accumulations of clay in other areas within the perimeter fence. Some of these accumulations of clay lie within depressions in the bedrock surface which may have been excavated and back-filled with hardcore during construction of the school foundations. This situation may provide a permeable zone both in contact with the jointed limestone bedrock and the foundations of the school which would be an ideal pathway for radon ingress into the school.

Enmotec have identified high soil-gas radon concentrations to the NE, NW, W and SW of the school premises which correlate with the generally shallow bedrock in these areas. Low soil-gas radon concentrations to the north of the school premises correlate with the solution-like feature where thickening clay cover may be acting as a radon seal over the bedrock. High soil-gas radon concentrations to the south of the school premises correlate with the shallowing channel or solution-like feature as it grades into weathered bedrock.

Milltown Test Home Site

GPR surveys were carried out both inside and outside the test house. A series of GPR profiles were run along corridors and across rooms inside the house. The outdoor survey concentrated largely on the front and eastern side of the house. Some survey lines were also carried out at the rear of the house (see Figure 9a).

The relevant findings of the indoor survey relate to the house construction where it was found that the exterior walls and dividing walls were constructed on footings which give rise to a compartmentalised structure beneath the floor slab. This compartmentalised subslab structure is believed by Gottingen to be the cause of the massive transport resistance evident between the subslab air and the open atmosphere (see Gottingen section of this report).

The objective of the outdoor GPR survey was to determine the depth to bedrock and hence the thickness of the fill material on which the house is built. The interface between the soil/fill material and the underlying limestone bedrock is clearly seen on most radar sections and this has been compiled and presented as a depth to bedrock map in Figure 9b. The main findings of the survey are that the limestone surface is jointed and the character of the radar records indicate that there may be large solution features present. The soil/fill thickness is thinnest in the immediate vicinity of the house (0.5 - 1 m) but thickens to 3.0 m at the boundary wall to the south of the house. A similar thickening of soil/fill is apparent at the rear of the house, to the north. The result is that the house foundation apparently straddles an E-W trending ridge of shallow bedrock. This ridge may be giving

rise to strains in the foundation slab which are evident from cracks seen in the outer walls, footpaths and inner walls of the house. These cracks or their source may be providing pathways for radon ingress into the house.

A series of resistivity surveys in a field across the road from the house i.e. to the south indicate very shallow bedrock. Since this field is topographically about 2 m lower than the foundation slab of the test house, the implication is that the E-W trending bedrock ridge may form part of a larger system of E-W features such as weathered joints and/or minor faults. This E-W trending feature is broadly coincident with the observed 102°E direction for tension joints in the area.

Ra-226 in Soil and Rock Samples

Representative samples of soil and bedrock were recovered from the Claremorris and Milltown areas for Ra-226 analysis by high resolution gamma spectroscopy. In the Claremorris survey area 26 soil samples from 5-30 cm depth were collected, together with an additional 14 soil samples from the primary school site in Area 3. At the test house site in Milltown 4 soil samples were collected in the immediate vicinity of the house. Eleven rock samples were collected from disused quarries in the survey areas.

Ra-226 activity concentrations in all samples were determined using the 186 keV line. U-238 was determined from the 63 keV and 93 keV lines of Th-234 assuming secular equilibrium between U-238 and Th-234. The U-235 interference at 186 keV was calculated, assuming a U-238 to U-235 ratio of 22.3:1. Detection efficiencies were determined using a soil sample, similar in composition to the soils determined, spiked with a certified radionuclide reference solution.

Results

The Ra-226 activity concentrations of soil samples recovered from the Claremorris and Milltown areas are summarised in Table 4. In the Claremorris area Ra-226 activity concentrations range from 20 Bq kg⁻¹ up to 214 Bq kg⁻¹ with a mean value of 76 Bq kg⁻¹. This compares with the average value of radium in soil found in the national soil survey of 46 Bq kg⁻¹, and the interval 35-65 Bq kg⁻¹ assigned to the 10 km x 10 km national grid square encompassing Claremorris. At the site level Ra-226 activity concentrations in the Mount St. Michael Primary School (Area 3) range from 42 Bq kg⁻¹ up to 95 Bq kg⁻¹ with a mean value of 56 Bq kg⁻¹, and in the test house site at Milltown activity concentrations range from 31 Bq kg⁻¹ up to 160 Bq m⁻³ with a mean value of 102 Bq kg⁻¹.

Ra-226 activity concentrations greater than 100 Bq kg⁻¹ have generally been taken to represent potentially hazardous activity concentrations, and concentrations in excess of 100 Bq kg⁻¹ have been found both in Claremorris and Milltown. In particular in Claremorris, elevated Ra-226 activity concentrations form a spatially coherent group to the east/south east of Mount St. Michael Primary School (Area 3) (see GSI section of this report).

Rock samples from both Claremorris and Milltown have Ra-226 activity concentrations in the range <20 Bq kg⁻¹ up to 98 Bq kg⁻¹. The majority of samples are low apart from two which came from two quarries close to Claremorris town. These two samples have activity concentrations of 80 Bq kg⁻¹ and 98 Bq kg⁻¹ and are elevated relative to the rest of the samples, which do not exceed 38 Bq kg⁻¹. Samples of chert and shale taken from between the limestone beds in Claremorris all show low Ra-226 activity concentrations <20 Bq kg⁻¹, whereas in Milltown a shale parting from between limestone beds has 84 Bq kg⁻¹. A detailed discussion of the Ra-226 activity concentration in soils and rocks collected from both Claremorris and Milltown, and their significance as a potential radon source is left to the GSI section of this report.

Publications

Porstendorfer, J., Butterweck, G., Madden, J. and Reineking, A. 1993. Influence of meteorological parameters on the transport of radon from soil air into indoor and outdoor air. First International Workshop on Indoor Radon Remedial Action, Rimini, Italy June 27th - July 2nd, 1993

Madden, J.S., van den Boom, G., O'Connor, P.J., McGarry, A.T. and Reimer, G.M. 1995. Evaluation of the combined helium/radon in soil-gas mapping methodology as an indicator of areas in which elevated indoor radon concentrations may be found. Natural Radiation Environment VI, Montreal, June 1995 (Abstract).

Ort, M., Reimer, G.M., van den Boom, G., O'Connor, P.J. and Madden, J.S. 1995. Radon distribution and control in the limestone terrain of western Ireland. Natural Radiation Environment VI, Montreal, June 1995 (Abstract).

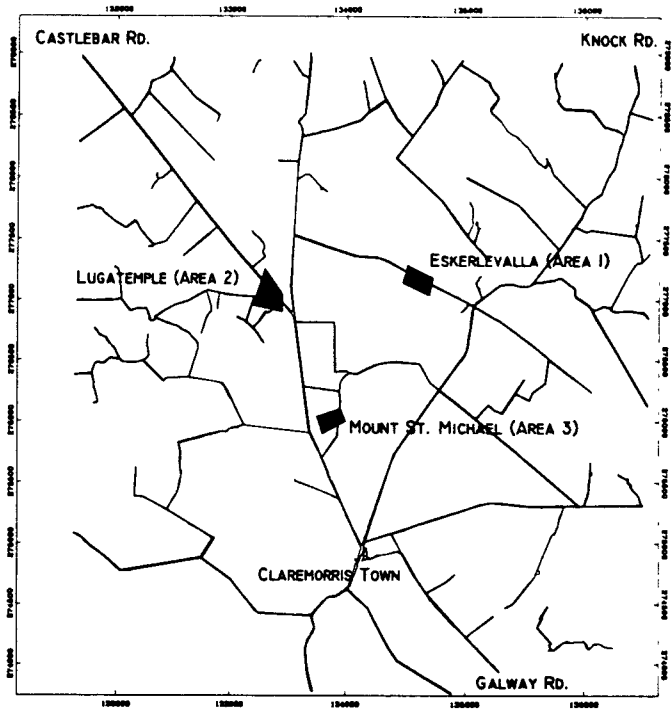


Figure 1: Claremorris Survey Area

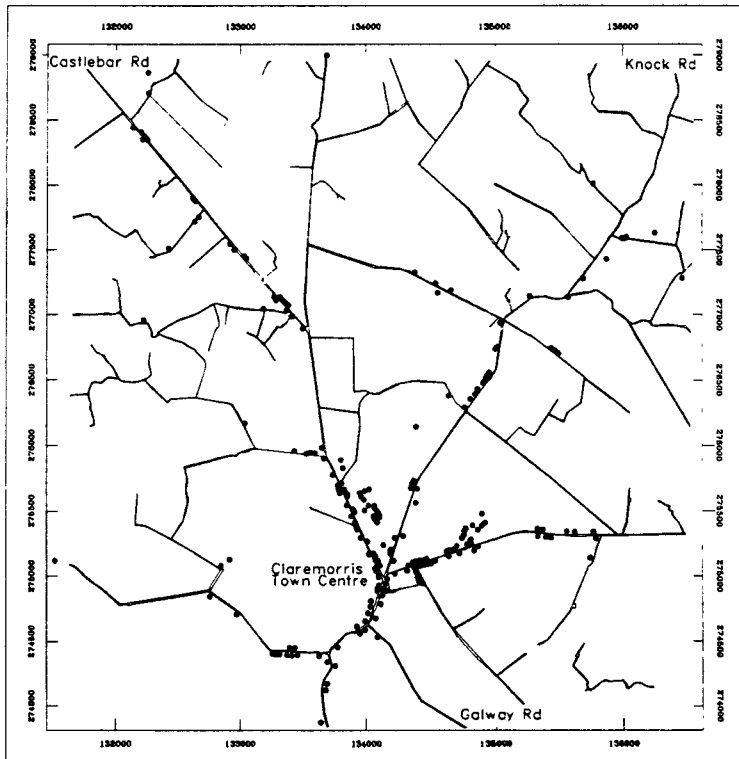


Figure 2: Spatial Distribution of Monitored Houses

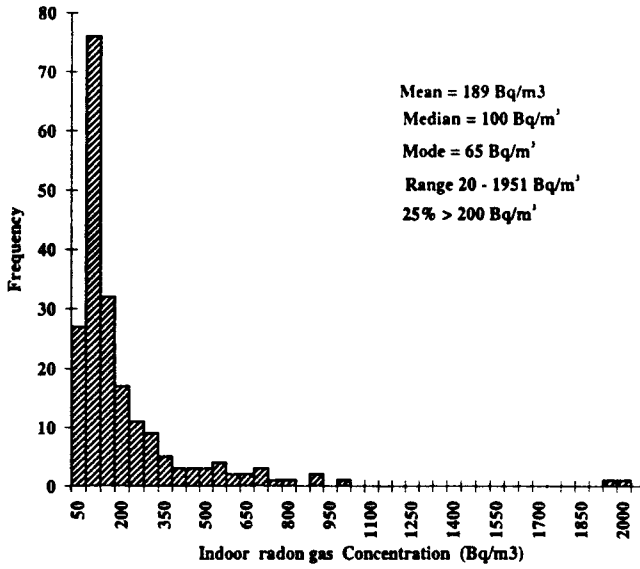


Figure 3: Frequency Distribution of Indoor Radon Gas Concentrations

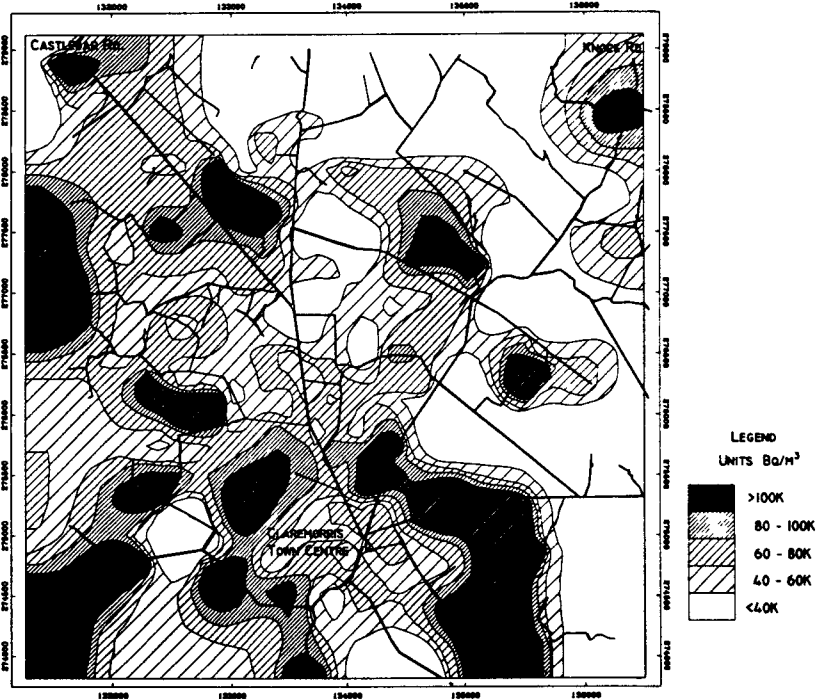


Figure 4: Contour Map of Claremorris Soil-gas Radon Concentrations

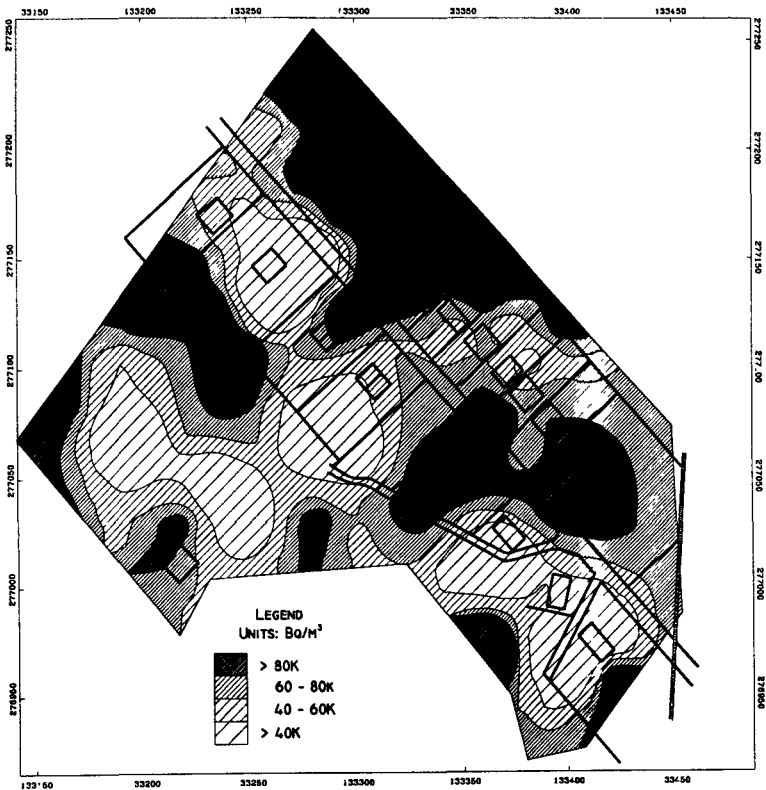


Figure 5: Contour Map of Lugateemple Soil-gas Radon Concentrations

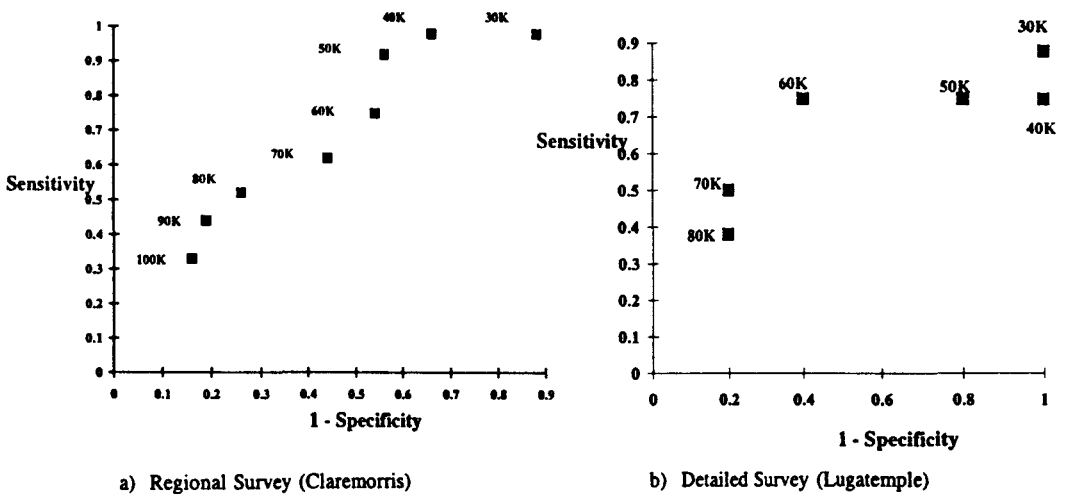


Figure 6: Plots of Sensitivity v 1-Specificity

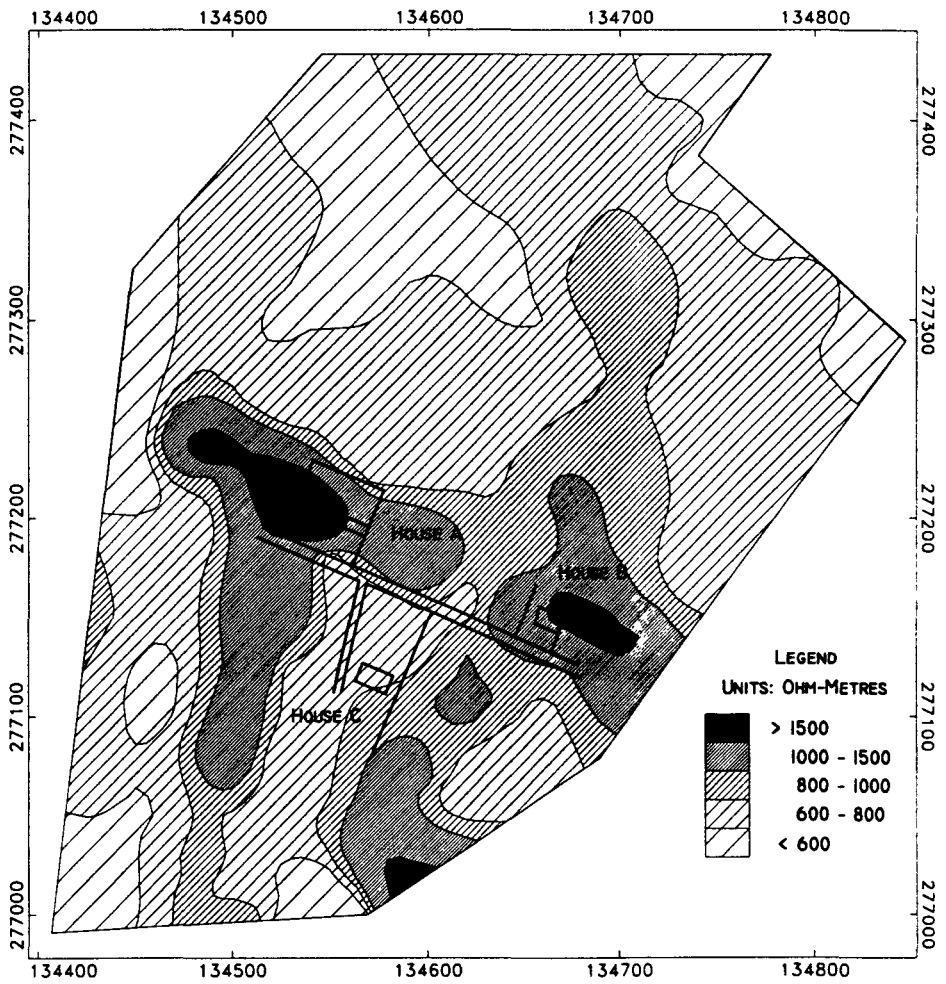


Figure 7: Contour Map of EM-VLF-R Resistivity Values

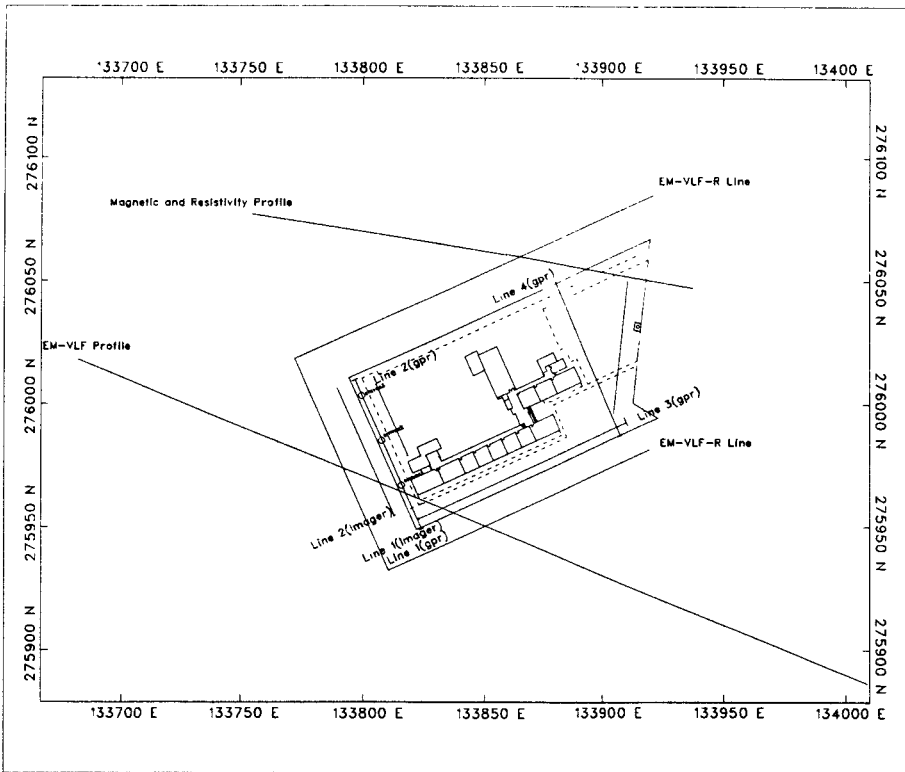


Figure 8a: Schematic diagramme of Mount St. Michael Primary School and siting of Geophysical Traverses.

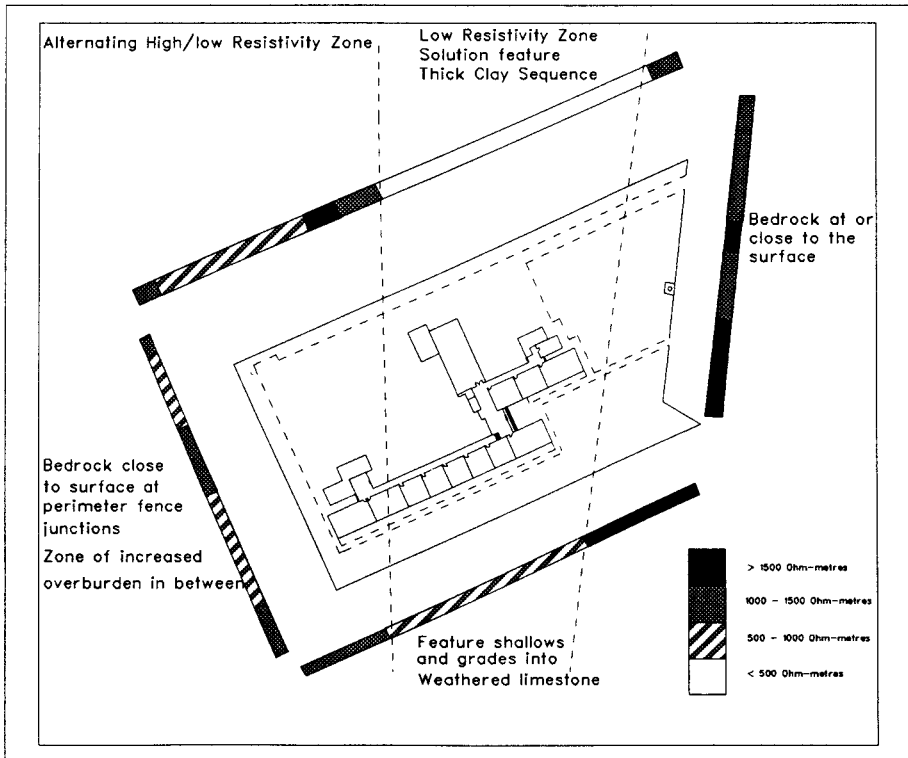


Figure 8b: Interpretation of Geophysical Surveys at Mount St. Michael Primary School (Area 3)

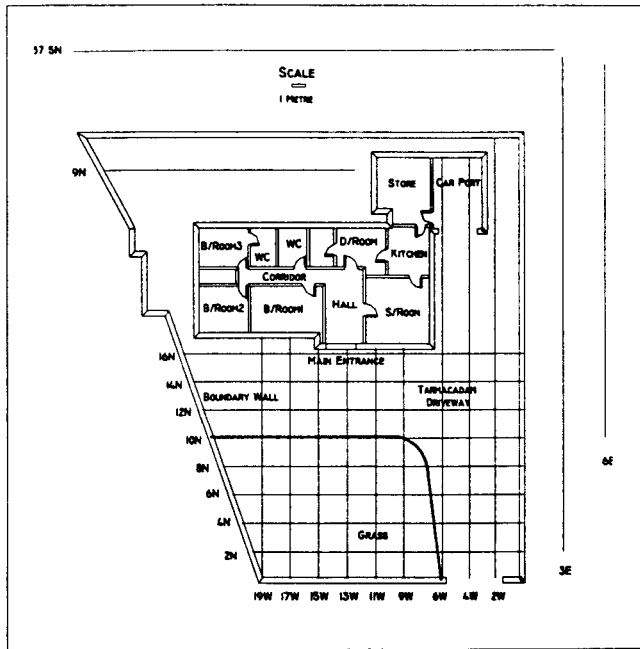


Figure 9a: Schematic diagramme of Milltown Test House and siting of GPR Survey Lines

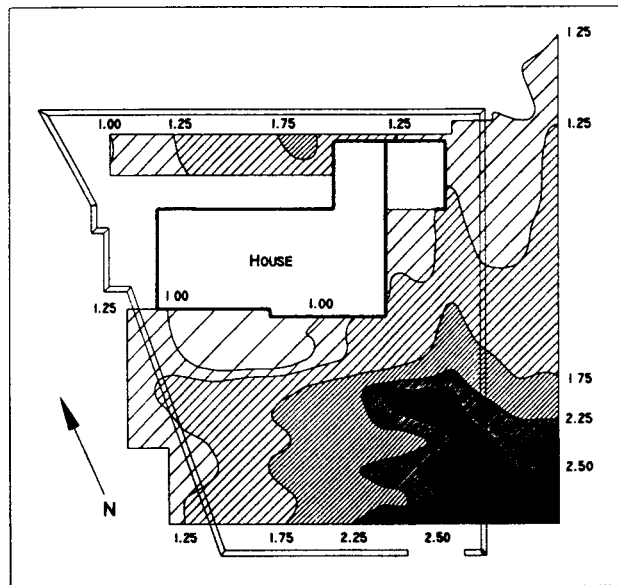


Figure 9b: Interpretation of GPR Survey at Milltown Test House (depth to bedrock contour map in metres)

Season	House Type											
	Bungalow		Bungalow		Bungalow		Bungalow		Average		Two-Storey	
	Bed	Liv	Bed	Liv	Bed	Liv	Bed	Liv	Bed	Liv	Bed	Liv
Autumn	1.09	1.06	1.25	1.61	1.21	0.58	0.92	0.42	1.12	0.92	1.60	1.10
Winter	1.25	0.95	1.70	1.13	0.91	1.31	1.07	1.17	1.30	1.14	0.52	1.25
Spring	1.21	1.07	0.66	0.59	-	-	-	-	0.66	0.83	1.10	0.6
Summer	0.92	0.92	0.39	0.67	-	-	-	-	0.57	0.80	0.70	1.10

Table 1: Seasonal variability in Indoor Radon concentrations

Zone	Specificity (34%)		Sensitivity (98%)		
	Number of Houses < 200 Bq m ⁻³		Number of Houses > 200 Bq m ⁻³		
< 40000 Bq m ⁻³	50	(98%)	1	(2%)	51
> 40000 Bq m ⁻³	96	(65%)	51	(35%)	147
	146		52		198

Relative Risk = 17.5

Zone	Specificity (56%)		Sensitivity (62%)		
	Number of Houses < 200 Bq m ⁻³		Number of Houses > 200 Bq m ⁻³		
< 70000 Bq m ⁻³	82	(80%)	20	(20%)	102
> 70000 Bq m ⁻³	64	(67%)	32	(33%)	96
	146		52		198

Relative Risk = 1.7

Zone	Specificity (84%)		Sensitivity (33%)		
	Number of Houses < 200 Bq m ⁻³		Number of Houses > 200 Bq m ⁻³		
< 100000 Bq m ⁻³	122	(78%)	35	(22%)	157
> 100000 Bq m ⁻³	24	(59%)	17	(41%)	41
	146		52		198

Relative Risk = 1.9

Table 2: Two x Two Contingency Tables (Regional Data)

Zone	Specificity (0%)		Sensitivity (75%)		
	Number of Houses < 200 Bq m ⁻³		Number of Houses > 200 Bq m ⁻³		
<40000 Bq m ⁻³	-	-	2	(100%)	2
>40000 Bq m ⁻³	5	(45%)	6	(55%)	11
	5		8		13

Relative Risk = 0.6

Zone	Specificity (60%)		Sensitivity (75%)		
	Number of Houses < 200 Bq m ⁻³		Number of Houses > 200 Bq m ⁻³		
<60000 Bq m ⁻³	3	(60%)	2	(40%)	5
>60000 Bq m ⁻³	2	(25%)	6	(75%)	8
	5		8		13

Relative Risk = 1.9

Zone	Specificity (80%)		Sensitivity (38%)		
	Number of Houses < 200 Bq m ⁻³		Number of Houses > 200 Bq m ⁻³		
<80000 Bq m ⁻³	4	(44%)	5	(56%)	9
>80000 Bq m ⁻³	1	(25%)	3	(75%)	4
	5		8		13

Relative Risk = 1.3

Table 3: Two x Two Contingency Table (Lugatemple Data)

Statistic	Ra-226 (Bq kg ⁻¹) in Soils		
	Claremorris Area N = 24	Mount St. Michael (Area 3) N = 14	Milltown N = 4
Mean	76	56	102
S. Dev	51	16	65
Minimum	20	42	31
Maximum	214	95	160

Table 4: Ra-226 activity concentration in soils

FINAL REPORT

CONTRACT: F13P-CT93-0074
Period: 1st January 1993 to 30 June 1995 (30 months)

I. Head of Project 2: Dr. Patrick J. O'Connor

II. OBJECTIVES FOR THE REPORTING PERIOD

- (a) Provision of topographic maps (1:10,560 and 1:2,500 scale) of survey areas to partners RPII and Enmotec.
- (b) Assistance in the planning and execution of field surveys by project team in May 1993 and May 1994.
- (c) Compilation of extant geological data from GSI files for the Claremorris and Milltown study areas.
- (d) Reconnaissance mapping of the bedrock geology and glacial geology of both study areas.
- (e) Collection of a suite of representative rock and soil samples for both survey areas (with RPII) for ^{226}Ra analysis and evaluation of abundance data.
- (f) Evaluation of the degree of spatial correlation between geology, soil ^{226}Ra and soil gas ^{222}Rn .

III. PROGRESS ACHIEVED INCLUDING PUBLICATIONS

Compilation of all extant geological information in GSI files on 1:10,560 topographic basemaps for both study areas was completed. Data sources for this compilation included the relevant 19th century GSI geological maps (1:10,560 and 1:63,360 scales), recent geological data from the GSI Mineral Exploration Open File Records, data derived from 1:30,000 scale aerial photos and results from reconnaissance field mapping in May 1993 and May 1994.

Geology of Study Areas

(a) Claremorris Area, Co. Mayo

The town of Claremorris, Co. Mayo is situated on the eastern margin of an extensive undulating lowland which is predominantly above 60m O.D. elevation (Fig. 1). To the west and southwest of the town, flatlands (<60m O.D.) extend as far as Lough Mask and Lough Corrib, some 30km distant. In general, surface rivers drain the landscape from NE to SW, with tributaries extending NW-SE along intervening depressions. The surface drainage pattern can be correlated with bedrock structures (see below).

Immediately SW of the town, Mayfield Lough and Clare Lough occupy an elongate NW-SE depression in which basin peat is well developed. Further to the SW the land rises to over 100m along a NW-SE bedrock ridge with a shallow glacial drift (till)

cover. To the N, NE and E of the town the land rises gradually to form an undulating lowland of 60 -100m elevation in which is developed a number of peat-filled depressions, generally elongated NW-SE. The glacial till covering of this undulating lowland is for the most part thinly developed (usually < 1m depth). The till itself is poorly sorted and is composed predominantly of limestone cobbles. The soils developed on the till are shallow brown earths and rendzinas with subordinate grey brown podzolics and basin peat (National Soil Survey Map, 1980).

Some 2km NE of Claremorris a series of sub-parallel and somewhat sinuous esker ridges is developed. At numerous localities, the esker ridges have been exploited for their sand and gravel content and extraction is continuing to mar the landscape. The ridges are often discontinuous and stand up to 5m high above the surrounding blanket of glacial till. In cross-section, the eskers show alternating graded bands of coarser and finer well-rounded limestone gravels. In their upper portion, finer sand lenses are often developed suggesting more distal development from the local ice-front and/or the action of waning depositional currents. The disposition of esker ridges, indicative of melt-water channels developed broadly perpendicular to the ice front, suggests that the local ice front extended from NW to SE across the area and retreated northeastwards.

Outcrop in the area is extremely sparse. Observations are confined mostly to a few disused quarry localities (Fig 2) immediately NW of the town (Localities 7 and 9) and 2.5km SSW of the town (Locality 8). On the basis of lithologies observed in the drift, the entire area is underlain by Lower Carboniferous limestones. The quarry localities collectively provide a vertical stratigraphic sequence of approximately 50m (assuming no faulting has occurred between localities). At all three quarry localities massive, well-bedded crystalline limestones are developed. Bedding dips gently at 3° - 5° to the SW or SSW and bed thickness varies from 0.1 to 1.5m, averaging 0.6m. Minor chert bands (up to 5cm in thickness) are developed at Locs. 7 and 9 while thin shaly partings between limestone beds are seen at Locality 9. The limestones vary in colour from grey through blue-grey to black in vertical sequence. They contain a well-developed macrofauna of crinoids (comminuted), solitary corals (zaphrentids), colonial corals (syringopora) and productid brachiopods. They would appear to have been deposited in a low-energy shallow shelf environment.

There are a number of vertical joint directions developed in the limestones, with those trending 27°E, 47°E, 117° and 157° best developed and exploited during quarrying activities. Joint spacing ranges from 0.1 to 1m, averaging 0.6m. (Fig. 2).

Dissolution, due to groundwater movement, is most obvious along the limestone bedding planes directly above the shaly partings. The bedding surfaces are coated in secondary calcareous tufa (travertine) deposited by circulating groundwaters (e.g. Loc. 7). The uppermost limestone beds directly beneath the glacial till show more advanced karstification.

Total gamma activities measured at all sites were constant and low (20 - 30 cps). Slightly higher gamma readings of c.50cps were observed at shaly partings in the

limestone sequence.

(b) Claremount Primary School Site

The school site (Fig. 2) lies 300m NW of the nearest limestone outcrop in the disused quarry (Loc. 7) in Clare Townland and is almost certainly underlain by the same gently dipping lithologies. The glacial overburden is likely to be shallow (generally < 1m depth).

Two principal vertical or near-vertical joint sets have been measured in the limestones exposed in the quarry (Fig. 2, Loc. 7).

- (a) Orthogonal sets of tension joints developed parallel to bedding dip and strike directions (27°E and 117°E). Those trending 117°E are well-spaced (approx. 2m apart), open and continuous master-joints while those trending 27°E are closer-spaced (5-20cm apart) tight fractures.
- (b) Non-orthogonal sets of shear joints developed along 47°E and 157°E directions. The 47°E joint set are open-spaced (approx 1m apart) and the 157°E set are close-spaced (5-20cm apart) tight fractures.

In terms of permeability, therefore, the 117°E and 47°E fracture directions are likely to represent the most important vertical pathways developed in the limestone bedrock and to constitute the primary "plumbing system" for the lateral and upward transmission of radon.

(c) Milltown Area, Co. Galway

The village of Milltown, Co. Galway is situated on the river Clare (Fig. 3). The surrounding countryside is generally flat and low-lying (<50m O.D.) and slopes gently to the southwest. The glacial drift cover is thin (generally < 1m thick) and the drift is composed of limestone debris. The limestone cobbles are angular to subangular in shape and suggest short transport distances prior to deposition. The matrix of the drift is gravelly, with some clay component, and appears quite permeable. In topographic depressions, the drift is overlain by thin peat and such areas are often swampy in wet weather.

Outcrop in the area is sparse and mainly confined to sections along the river Clare. The Milltown area is generally underlain by thinly-bedded to well-bedded impure or muddy bioclastic limestones of Lower Carboniferous age (Fig 1). The limestones contain an abundant macrofauna of productids, brachiopods, solitary corals (e.g. zaphrentids) and fenestellids. Stratigraphically, the limestone sequence at Milltown underlies the sequence exposed around Claremorris.

The limestone beds are generally 0.1 - 0.5m thick with thin (<0.2m) shaly partings. Total-count gamma readings of 35-45 cps on limestone and 45-55 cps on shaly partings are typical.

The limestone beds are folded/warped and dips up to 30° - 40° are present locally. The gentle folding of the limestone bedrock reflects proximity to a major NE-SW fault zone to the east of Milltown (Fig 1).

(d) Milltown Test House Site (Loc. 3)

The test house lies c.700m NE of the centre of Milltown village on the main Claremorris road (Fig. 3). The site is level and at 52m elevation O.D. The ground to the south of the test house slopes gently southwards towards the river Clare. A number of springs rise in this area suggesting that the main groundwater flow is from north to south across the area towards the river.

The drift cover at the test house site is very shallow and generally < 1m deep. Bedrock outcrops by the roadside, 100m SE of the test house. The bedrock is a blue-grey fossiliferous limestone, thinly-bedded with shaly partings. The bedding planes are gently warped/folded on an axis trending 142°E; bedding dips at 10° - 20° to the SW. Two joint sets are developed:-

- (a) tension joints trending 8°W and 102°E
- (b) shear joints trending 47° and 117°

Joint spacings are generally 0.2 - 0.6m.

The 117°E trending joints are parallel to the long axis of the test house (Fig 3).

Radium Content of Rocks and Soils

(a) Sampling

Representative samples of bedrock and soils were recovered from the Claremorris and Milltown areas for ²²⁶Ra analysis (see RPII Reports). Outcrop in both areas is extremely sparse and 11 rock samples were collected from disused quarry exposures. In the Claremorris area, 26 shallow soil samples were collected, together with 14 soil samples from the school site at Claremount. At the test house site near Milltown, 4 soil samples were collected in the immediate vicinity of the house.

(b) Radium Content of Rocks

The content of ²²⁶Ra in rock samples from the Claremorris and Milltown areas is presented in Table 1. The samples are arranged in approximate stratigraphic order in the table, with the oldest sample at the bottom and the youngest at the top.

In the Claremorris area, underlain by limestone, six samples of this rock type from quarries SW and N of the town show a range of ²²⁶Ra contents of < 20 Bq/kg- 98 Bq/kg. A single limestone sample from each of the quarries (930526, 930541) shows elevated ²²⁶Ra contents (98 and 80 Bq/kg respectively). Individual samples of chert (930523) and shale (930543) have low ²²⁶Ra contents.

Table 1. Contents of ^{226}Ra in Rock Samples from Claremorris (Co. Mayo) and Milltown (Co. Galway), Ireland.

Sample	Grid Reference	Locality	Rock Type	^{226}Ra (Bq/kg)
930526	13270 27288	Madden's Quarry (disused), Brookhill Townland, 2.5km SW of Claremorris	Dark bioclastic limestone (Lower Carboniferous)	98
930542	13270 27288	Madden's Quarry (as above)	Blue-grey bioclastic Limestone (Lower Carboniferous)	≤ 20
930543	13270 27288	Madden' Quarry (as above)	Black Shale parting (Lower Carboniferous)	≤ 20
930522	13384 27568	Quarry (disused), Clare Townland, 1km N. of Claremorris	Blue-grey bioclastic Limestone (Lower Carboniferous)	31
930541	13384 27568	Quarry (disused) as above	Blue-grey bioclastic Limestone (Lower Carboniferous)	80
930523	13384 27568	Quarry (disused) as above	Black Chert band (Lower Carboniferous)	20
930527	13356 27549	Quarry (disused), Clare Townland, adjacent railway line 1km NW of Claremorris	Grey bioclastic Limestone (Lower Carboniferous)	≤ 20
930520	14103 26361	Quarry (disused), Lack Townland, 1km NE of Milltown, Co. Galway	Black bioclastic Limestone (Lower Carboniferous)	38
930521	14103 26361	Quarry (disused), as above	Black Shale parting (Lower Carboniferous)	84
930528	14016 26327	Roadside outcrop, Milltown Townland, 0.7km NE of Milltown, Co. Galway	Blue-grey Limestone (Lower Carboniferous)	32
930540	15570 26990	Outcrop, Slieve Dart inlier, 5km SE of Cloonfad, Co. Galway	Brecciated Felsite (Lower Devonian)	≤ 20

Table 2 Contents of ²²⁶Ra in Soils from Claremorris (Co. Mayo) and Milltown (Co. Galway), Ireland.

Claremorris Regional Soil Survey

Sample Number	²²⁶Ra (Bq/kg)
SS1	214
SS2	157
SS3	107
SS4	118
SS5	95
SS6	44
SS7	146
SS8	93
SS9	118
SS10	128
SS11	25
SS12	86
SS13	42
SS14	36
SS15	≤ 20
SS16	-
SS17	49
SS18	-
SS19	23
SS20	29
SS21	37
SS22	52
SS23	47
SS24	49
SS25	63
SS26	40

Statistics

N=24 **Mean** 75.75

Geometric Mean 61.5

Median 50.5

Standard Deviation 50.6

Table 2 (Continued)

**Claremount Primary School, Claremorris
(Detailed Soil Survey)**

Sample No.	²²⁶ Ra (Bq/kg)
MSC1	42
MSC2	62
MSC3	95
MSC4	44
MSC5	69
MSC6	46
MSC7	61
MSC8	77
MSC9	48
MSC10	54
MSC11	42
MSC12	43
MSC13	48
MSC14	51

STATISTICS

N=14

Mean 55.9

Median 49.5

Milltown Test House Site

Sample No.	²²⁶ Ra (Bq/kg)
MT1	154
MT2	62
MT3	160
MT4	31

In the neighbourhood of Milltown, limestone samples have intermediate ^{226}Ra contents of 32 - 38 Bq/kg, but a shale parting between limestone beds (930521) has an elevated ^{226}Ra content of 84 Bq/kg.

Thus, in terms of ^{222}Rn potential, certain limestone beds in the Claremorris area and shale partings at Milltown are likely candidates.

(c) Radium Content of Soils

The ^{226}Ra contents of 24 soil samples from the Regional Claremorris Survey range from < 20 Bq/kg to 214 Bq/kg (Table 2). The mean ^{226}Ra content is 75.8 Bq/kg which is 50% higher than the national average for Irish soils of 46 Bq/kg (McAulay & Marsh, 1992).

Nine sites with elevated soil ^{222}Ra (Range 93 - 214 Bq/kg) form a spatially coherent group centred about 1.5km north of Claremorris town centre and to the SE of the Primary school (Fig. 4). The highest soil ^{226}Ra value of 214 Bq/kg is close to the disused quarry in Clare Townland (Locality 7) where a sampled limestone bed contains 80 Bq/kg of ^{226}Ra . The soils in this area are very thin (< 30cm) and may have been derived, largely, through insitu weathering of the limestone substrate with consequent ^{226}Ra enrichment.

At the Primary school site in Claremount townland 14 soil samples showed a range of ^{226}Ra contents of 42 - 95 Bq/kg; the median value was 49.5 Bq/kg, similar to the regional median of 50.5 Bq/kg (Table 2). The highest soil ^{226}Ra values of 77 Bq/kg and 95 Bq/kg occur near the SE boundary of the site (Fig. 5) and are coincident with a zone of elevated soil gas ^{222}Rn values (Enmotec, Fig. 12). The possibility that some of the soils at the school site are imported (rather than indigenous) cannot be excluded.

Only 4 soil samples were collected in the immediate vicinity of the test house near Milltown, Co. Galway. The ^{226}Ra contents range from 31 to 160 Bq/kg (Table 2). The highest ^{226}Ra values of 154 Bq/kg (MT1) and 160 Bq/kg (MT 3) are located on the western side of the site.

Correlation of Geology with soil gas ^{222}Rn and ^4He concentrations

Soil gas ^{222}Rn and ^4He data for the Claremorris area are presented by Enmotec. ^{222}Rn soil gas values range up to 393,000 Bq/m³ (median 71,000 Bq/m³) and are high throughout the Claremorris area. Enmotec define breaks in the distribution of ^{222}Rn values at 70,000 Bq/m³ and 100,000 Bq/m³ and they define 4 classes for contouring purposes: 0-50 KBq/m³, 50-70 KBq/m³, 70-100 KBq/m³ and > 100KBq/m³ (Enmotec, Fig. 6). When the spatial pattern of regional soil gas ^{222}Rn is considered in conjunction with observed geological structures and soil ^{226}Ra contents the following observations can be made:

- * There is a strong spatial coincidence between the soil ^{222}Ra anomaly (1.5 km north of Claremorris town centre) and high soil gas ^{222}Rn (> 80KBq/m³) at this

the high soil gas ^{222}Rn concentrations observed. The soils in this area are thin (0.1m - 0.3m) and may be largely residual in nature being derived from in situ weathering of the underlying karstic limestone. At least one limestone bed exposed in a nearby quarry has a ^{226}Ra content of 80Bq/kg and weathering of such material could provide a residual soil with an elevated ^{226}Ra content.

- * The predominant pattern in the regional distribution of soil gas ^{222}Rn in Fig. 6 (Enmotec) is one of elongate zones ($> 100\text{KBq/m}^3$) which trend NE-SW broadly coincident with the 47°E direction observed for spaced shear joints in the limestone bedrock (Fig. 2). The distribution of anomalous soil gas ^4He concentrations is interpreted by Enmotec to define 'lineaments' trending $25-45^\circ\text{E}$ (Enmotec, Fig. 5), some of which in the western part of the study area may be related to the 47°E shear joint direction and others of which in the eastern part of the area may relate to the 27°E tension joint direction. It is not possible to make a clearer directional distinction on the basis of the anomalous ^4He values plotted on Fig. 5 (Enmotec).
- * A subsidiary trend WNW-ESE in soil gas ^{222}Rn anomalies is also evident in Fig. 6 (Enmotec), broadly coincident with the 117°E direction of major, open, spaced tension joints observed in bedrock (Fig. 2). Enmotec also define a suite of anomalous ^4He lineaments striking $115 - 125^\circ\text{E}$ (Enmotec Fig. 5) which probably reflects the 117°E major joint direction (Fig. 2).

Radon Sources and Pathways

The radon source in the Claremorris area is ubiquitous and geographically widespread. The immediate source is the thick ($> 1\text{ km}$) Lower Carboniferous limestone sequence which underlies the entire area. At least two separate near surface limestone beds (in an exposed vertical sequence of c.50m) have elevated ^{226}Ra contents. Thin soils, locally developed by in situ weathering of the limestone, show elevated ^{226}Ra contents of 100-200 Bq/kg. It is concluded that both the limestones and their derived soils are the primary source of soil gas ^{222}Rn in the area.

Radon pathways are largely controlled by permeability (O'Connor et al. 1992; 1993). The limestone sequence near surface shows partial karstification due to dissolution by percolating groundwater. Both tension and shear joint systems are well developed in the bedded sequence and these structures provide the main lateral and vertical pathways or "plumbing system" for the upward transmission of radon to the surface. The overlying soils are generally permeable and offer little resistance to upward radon migration.

Soil gas ^{222}Rn patterns appears to be controlled by bedrock structure (fracture, joint directions) and locally by elevated soil ^{226}Ra concentrations. Alignment of anomalous ^4He soil gas values also support the view that soil gas ^{222}Rn patterns are structurally controlled.

PUBLICATIONS

O'Connor, P.J. 1993. Correlating geology with Radon pockets. U.S. DOE Radon Research Notes, August, p. 8-10.

O'Connor, P.J., V. Gallagher, V., Madden, J.S., van den Boom, G., McLaughlin, J.P., McAulay, I.R., Barton, K.J., Duffy, J.T., Müller, R., Grimley, S., Marsh, D., Mackin, G., MacNiocaill, C. 1993, Assessment of the geological factors influencing the occurrence of radon hazard areas in a karstic region. Geological Survey of Ireland Report Series RS 93/2, 204pp.

O'Connor, P.J. 1994. Radon risk mapping. The Irish Scientist, January, p.14.

O'Connor, P.J. 1994. Radon risk mapping. 4th Irish Environmental Researchers' colloquium, University College Galway, January 1994, p. 15 (Abstracts volume).

O'Connor, P.J. Pyne, J.F., McLaughlin, J.P. and Madden, J.S. 1994. Radon exhalative properties, radioelement content and rare earth element composition of Namurian Phosphorite deposits, Co. Clare. Geological Survey of Ireland Report Series RS 94/3, 29pp.

O'Connor, P.J. 1994. Radon risk assessment in karstic limestone terrain. 12th SEGH European Meeting on Contaminated Land, British Geological Survey (Keyworth, U.K.), April 1994.

Madden, J.S., van den Boom, G. **O'Connor, P.J.** McGarry, A.T., Reimer, G.M., 1995 (in press): Evaluation of the combined helium/radon in soil-gas mapping methodology as an indicator of areas in which elevated indoor radon concentrations may be found. Natural Radiation Environment VI Montreal, June 1995 (abstract).

Ort Matthias, Reimer, G.M., van den Boom, G., **O'Connor, P.J.** and Madden, J.S., 1995 (in press): Radon distribution and control in the limestone terrain of western Ireland. Natural Radiation Environment VI, Montreal, June 1995, (abstract).

Madden, J.S., Van den Boom, G., **O'Connor, P.J.**, McGarry, A.T. and Reimer, G.M. 1995. Radon/helium in soil gas mapping as an indicator of high risk radon areas and high radon or "hot" houses. 5th Environmental Researchers Colloquium, January 1995, University College, Cork.

O'Connor, P.J. 1995. The correlation of geology with indoor radon. GSI 150th Anniversary Environmental Geology Symposium, Dublin, October 1995.

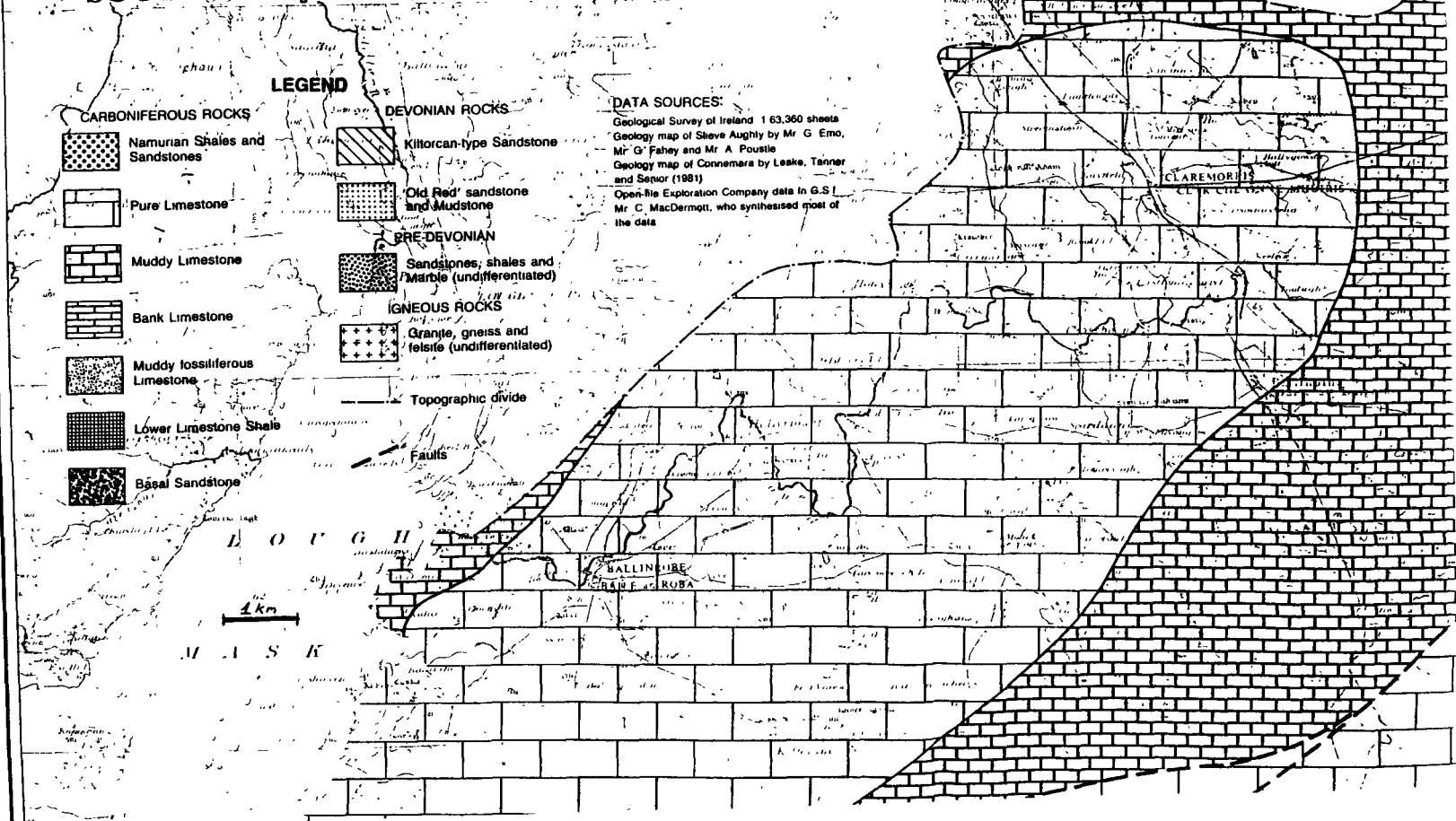
GSI REPORT

APPENDIX

Figures 1 - 5


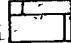

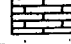





BEDROCK GEOLOGY OF MID-GALWAY, SOUTH MAYO AND NORTH CLARE



LEGEND


CARBONIFEROUS ROCKS

-  Namurian Shales and Sandstones
-  Pure Limestone
-  Muddy Limestone
-  Bank Limestone
-  Muddy fossiliferous Limestone
-  Lower Limestone Shale
-  Basal Sandstone

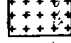
DEVONIAN ROCKS

-  Kiltorcan-type Sandstone
-  Old Red sandstone and Mudstone

PRE-DEVONIAN

-  Sandstones, shales and Marble (undifferentiated)

IGNEOUS ROCKS

-  Granite, gneiss and felsite (undifferentiated)

 Topographic divide

 Faults

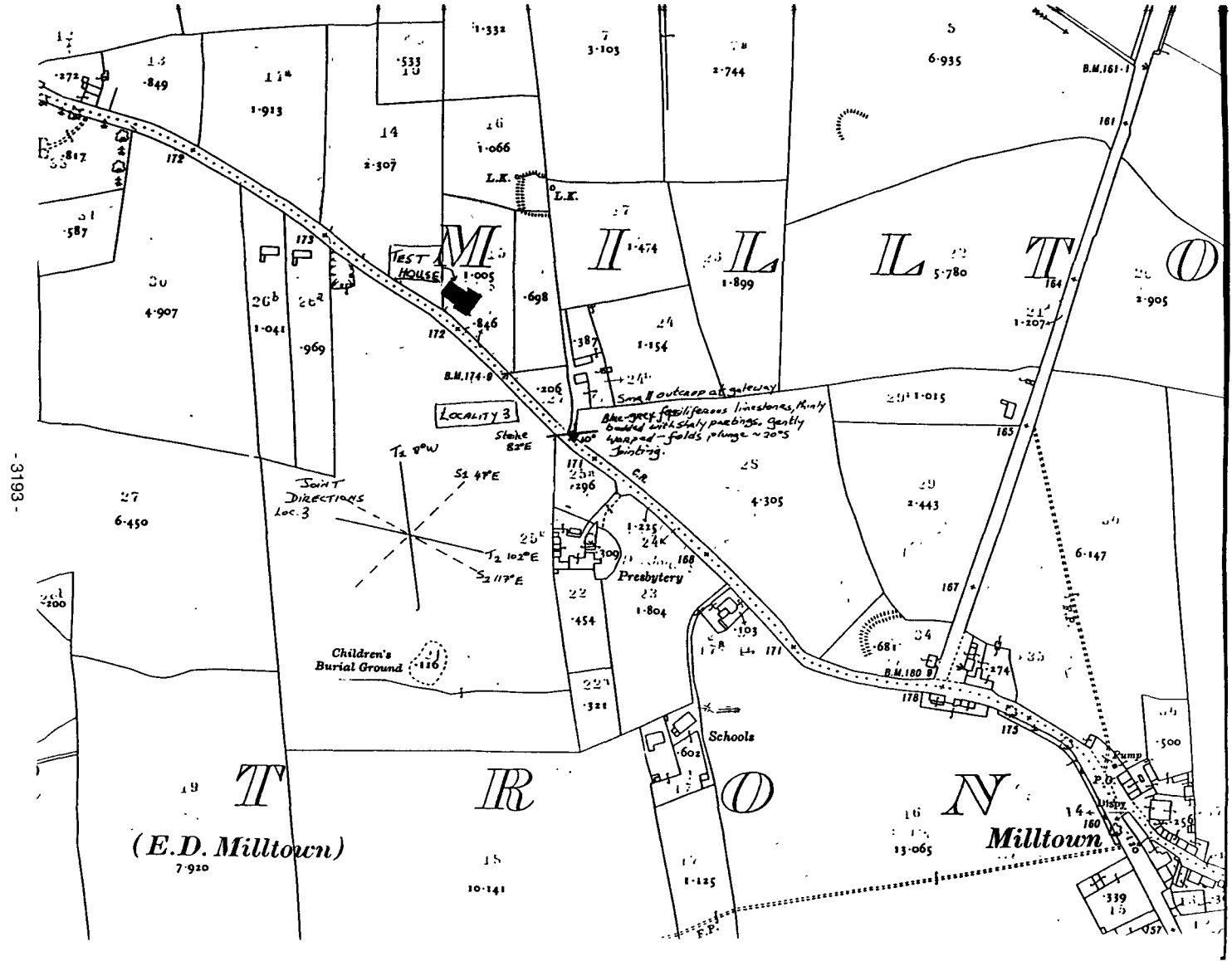
DATA SOURCES:

Geological Survey of Ireland 1 63,360 sheets
 Geology map of Slieve Aughty by Mr G. Emo,
 Mr G. Fahey and Mr A. Poustie
 Geology map of Connemara by Leske, Tanner
 and Senior (1981)
 Open File Exploration Company data in G.S.I.
 Mr C. MacDermott, who synthesised most of
 the data

1 km

Fig 1

50m



- 3193 -

Fig 3

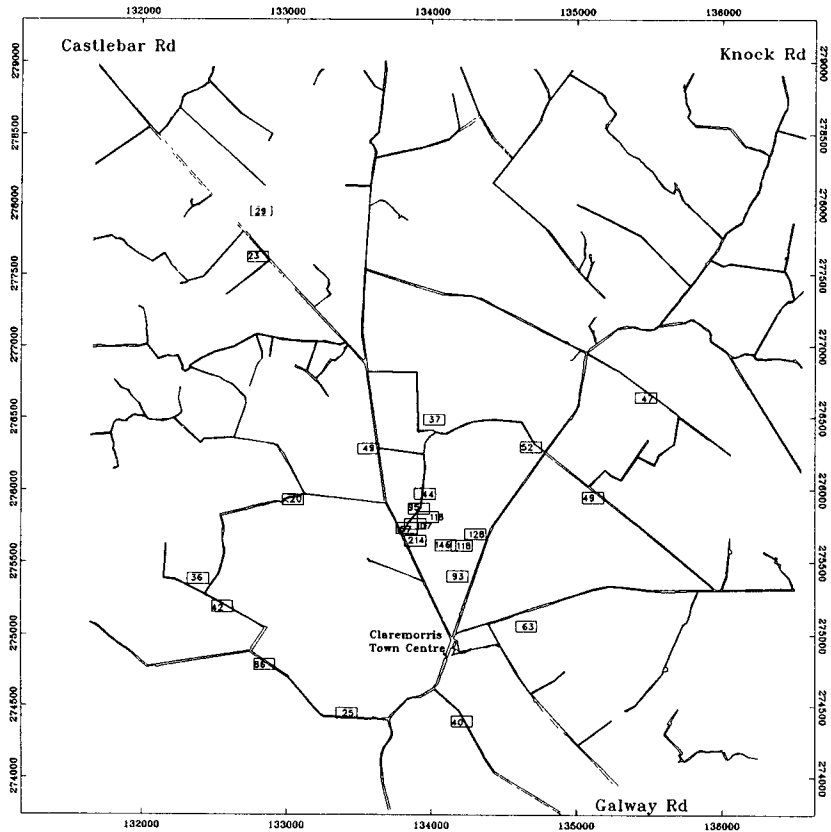


Fig. 4 Ra-226 Activity Conc. in Soils (Regional Survey)

Head of Project 3: Dr. van den Boom

II. OBJECTIVES FOR THE REPORTING PERIOD

- Evaluation of the combined helium/radon in soil-gas mapping methodology as an indicator of areas in which elevated indoor radon concentrations may be found.
- Identification of the major parameters controlling the radon distribution in this geographic area and evaluation of the use of soil-gas radon concentrations as an assessment technique to identify areas of different radon potential or to estimate a portion of an area that may be classified as providing elevated radon potential.
- Testing the utility of low-density and high-density sampling strategies and defining both the capability and the limitations of a single method technique for developing radon potential estimations for an area.
- Estimation of high soil-gas radon potential areas based on comparison with measured indoor radon concentrations
- Application of helium measurements for defining migration channels for mobile terrestrial gases.

IV. PROGRESS ACHIEVED INCLUDING PUBLICATIONS

Radon and helium mapping were conducted in western Ireland as a part of a cooperative study involving the European Union, the U.S. Department of Energy and the U.S. Geological Survey. The Radiological Protection Institute of Ireland and the Geological Survey of Ireland conducted radon indoor analyses and geological studies. ENMOTEC GmbH collected and analyzed soil-gas samples for radon, and the U.S. Geological Survey conducted the helium analyses. The regional survey of 230 soil-gas radon concentrations in a karst region of western Ireland was used to estimate radon potential for an area of approximately 110 km². In many areas of the world thorough complimentary data bases, such as wide-area gamma-ray spectrometer surveys, soil characterization, and even detailed geologic mapping as well as decent geographic maps, are lacking and would be prohibitively expensive to acquire. Therefore, techniques that estimate the regional indoor-radon potential in the absence of previously mentioned detailed information are needed. Also, in view of the finite resource that some governments can devote to the issue of radon and public health, these techniques need to be affordable.

Technical Background

The radon concentration in any soil or rock is dependent upon the concentration of its progenitor radium. Weathering (climate), mineralogy (composition and form), and natural distribution of forces (local tectonic stresses) control the physical and chemical distribution of radium and help establish the emanation and transport pathways for radon. Geologic information allows estimations of the radon potential from particular rock types or soils (Akerblom, 1987; Reimer & Gundersen, 1989; Kunz, 1988; Gates & Gundersen, 1989; Sutherland, 1991; Ball & others, 1991).

Climate is a strong factor controlling soil development and properties as well as the chemical distribution of elements throughout the various soil horizons (Asher-Bolinder & others, 1990). Using rock classification as a general guide, higher Rn concentrations might be expected from rocks that typically have higher uranium and thorium concentrations, such as granites. Conversely, low radon concentrations might be expected from rocks such as basalts and limestones which typically have lower uranium and thorium concentrations.

However, in the course of making indoor measurements in Ireland, homes that had been built on limestone having thin soil cover were found with elevated radon concentrations. Although this might seem enigmatic, a detailed study of the radon distribution in a limestone terrain in Ireland indicates that there are very sound geologic reasons, such as dissolution enhanced permeability, that explain the findings (O'Connor et al, 1993).

In a moist climate as this, concentration of radium in the formation of residual soils could also be a major factor. A comprehensive technique for estimating radon potential has been recently developed by Schumann (1993). That successful approach utilized input parameters of five different data sources:

- Aeroradiometric data
- Soil classification
- Lithological data
- Indoor radon screening measurements (less than 90 days duration)
- General house construction technique that is, whether the house has a basement, crawl space, or was constructed on a ground-contact slab.

Soil-gas radon concentrations were not considered as a primary factor because extensive data bases are not available. However, the analyses are relatively inexpensive compared to geologic mapping and airborne radiation mapping at the similar scales.

Soil-gas Sampling and Analytical Techniques

Soil-gas samples were collected using a method described in detail by Reimer (1990) and in former progress report of this project. Therefore, only a short description of the method is given here. In order to collect a soil-gas sample, a hollow steel probe was hammered into the ground by use of a slide hammer fitted over the shaft of the probe. The probe is then fitted with a septum device that makes an air-tight seal around the upper opening of the hollow probe. The tip of the probe was set at a depth of 1 m and, after purging air from the probe, a sample of soil-gas was collected with a hypodermic syringe. The gas sample was transferred from the syringe into a phosphor-coated scintillation cell for the radon analysis and another sample from the syringe was transferred to a stainless steel container for subsequent helium analysis. Radon concentrations were calculated at the field site based upon previous primary calibration of the alpha scintillometer and individual scintillation cells.

Study Area

Soil-gas radon and helium measurements were conducted in the vicinity of Claremorris, County Mayo, Ireland. In this part of western Ireland, the only geologic information available was bedrock information, surficial morphology (based on a geographic map updated 1916), and structural jointing analysis (O'Connor et al, 1993). The 110 km² study area is underlain by a single limestone formation. The only topographic coverage is from a map published in the last century and updated 1916 by the Geological Survey of Ireland. No soil description or gamma-ray measurements are available. A detailed description of the geology of the study area is given by the Geological Survey of Ireland. The soil-gas surveys were conducted in May of 1993 and 1994. The overall study area is rectangular in shape and approximately 11 km by 10 km. The sample spacing was 200 to 300 m for the reconnaissance survey. 231 samples were collected (Figure 1). The sampling was not random because the samples were primarily collected near pathways and roads (within the right of way but away from the disturbance of road construction). Within that constraint, and the limits imposed by the occurrence of local bogs, the sampling density was about 1 sample per 0.5 km². In addition to the low-density sampling program a detailed high-density sampling soil gas study had been carried out in three selected areas where radon indoor data were available.

Results

Statistical Parameters and Frequency Distribution of Radon and Helium in Soil-gas

During the entire field campaign 525 radon soil gas samples were collected and analyzed. Table 1 shows the statistical parameters. A comparison between the different study areas shows that area 1 has the highest geo-metric mean value for soil-gas radon of 84 600 Bq/m³. The other two areas show 58 200 Bq/m³ (area 2) and 61 800 Bq/m³ as geometric mean. The definition and distribution of high risk and low risk radon areas depend on the frequency distribution of radon, the number of populations, and the threshold value which marks the beginning of anomalous radon concentrations. According to the histogram shown in figure 3 the frequency distribution of radon shows several populations. The first one may be considered as normal and reaches from the lowest value to 50 000 Bq/m³. This population is mainly distributed in the eastern portion of the area investigated. A second population from 50 000 to 70 000 Bq/m³ covers a large portion of the western part of the study area, where most of the faults or deep reaching joints are present. Both populations are still considered as background populations and might represent different soils or glacial covers. All samples with radon concentrations greater than 70 000 Bq/m³ are classified anomalous. This group can be subdivided in two populations: 70 000 to 100 000 Bq/m³ and > 100 000 Bq/m³. The existence of a second anomalous population is also clearly shown on figure 4, where a probability plot marks a distinct break at approximately 100 000 Bq/m³.

Variable	Area 1 Radon	Area 2 Radon	Area 3 Radon	
Sample size		88	104	82
Average	104000	Bq/m ³	70000	Bq/m ³
Median	100000	-	71000	67000
Mode	38000	-	70000	68000
Geometr. Mean	86000	-	88000	62000
Variance	2.73	-	9.72	2.37
Std. Deviation	52000	-	31000	49000
Minimum	1900	-	2000	3000
Maximum	237000	-	141000	246000
Range	236000	-	139000	243000
<hr/>				
	Claremorris Area		Claremorris + Area 1-3	
Sample size		231		628
Average	82000	Bq/m ³	83000	Bq/m ³
Median		71000		78000
Mode		62000		62000
Geometr. Mean		60000		64000
Variance	3.2	-	2.7	-
Std. Deviation		57000		52000
Minimum	350	-	350	-
Maximum		393000		393000
Range		393000		393000

Table 1 : Statistical parameters for radon concentration in soil air samples in the area of Claremorris (reconnaissance) and areas 1 - 3 (detail).

The two thresholds of 70 000 Bq/m³ and 100 000 Bq/m³ seem to be high, but all other statistical parameters give the impression that the radon distribution in the Claremorris area generally is very high and that the entire region seems to be a high-risk area for radon. It is not clear from the frequency distribution of radon in the collected soil-gas samples where the threshold for the anomalous radon concentrations occurs. Geometric mean, median and average radon concentrations lie between 60 000 and 82 000 Bq/m³ and it seems difficult to understand that these three parameters define the threshold of the radon anomaly in the Claremorris region. On the other hand a threshold of 100 000 Bq/m³ seems to be very high. But the situation in this geographic part of Ireland is very specific and such a high threshold for radon can not be ruled out. The histogram in figure 2 shows the helium frequency distribution. The occurrence of a second population is obvious. Here the threshold which defines the beginning of the anomalous population lies between 5 300 and 5 350 ppb.

Reconnaissance Survey (Low Density Sampling) Area Claremorris

Regional Distribution of Helium in Soil-gas

The regional distribution of soil-gas helium is shown in figure 5. Helium concentrations in the area reveal alignments that parallel the joint system and are interpreted as being an indication of zones that suggest transport of gases from greater depth. It reflects a degree of openness that is not homogeneously distributed throughout the Claremorris region. One direction which coincides to a certain degree with the 27 ° vertical tension joint system measured by the Geological Survey of Ireland strikes 25 ° to 35 °. This direction of anomalous helium gas samples is crossed by a second group of lineaments striking approximately 115 ° to 125 ° which also runs more or less parallel to the second direction of tension joints with 117° striking.

Regional distribution of Radon in Soil-gas

Reconnaissance soil-gas radon concentrations in the study area averaged about 80 000 Bq/m³ with a median value of approximately 70 000 Bq/m³ and a geometric mean of 60 000 Bq/m³. By comparison, the average soil-gas concentration range world wide is 20 000 to 60 000 Bq/m³. Radon soil-gas concentrations greater than 70 000 Bq/m³ can be considered anomalous, because they have the greatest potential of causing elevated indoor radon concentrations (Gundersen et al, 1988). The current threshold of indoor radon adopted by the European Community is 250 Bq/m³, above which simple mitigation techniques, such as sealing foundation cracks and other obvious entry points, are recommended. For indoor concentrations above 600 Bq/m³, more stronger mitigation procedures, such as sub-foundation suction are recommended (Becker, 1994). Four contour intervalls are plotted in figure 6. The two high contours indicate the upper half of radon distribution, which corresponds to those samples with greater 70 000 Bq/m³.

This contour was chosen because it represents the soil-gas radon concentrations above which the soil-gas radon is likely to contribute to indoor concentrations that exceed the lower indoor radon threshold adopted by the European Community. For world-wide measurements of soil-gas radon this selection is equivalent to the 60 000 Bq/m³ threshold earlier described as having a high probability, that is, involving more than half the homes in an area, of contributing to indoor concentrations that exceed the lower indoor radon threshold adopted by the U.S. Environmental Protection Agency (148 Bq/m³). The highest contour on figure 6 identifies concentrations in the upper quintile of the distribution, that is, those above 100 000 Bq/m³. At this value the probability plot (figure 4) and percentiles distribution (figure 7) show a discontinuity which points out that this value represents a special threshold and indicates a high probability that the indoor radon concentration will exceed the upper threshold limit (600 Bq/m³) adopted by the European Community. Figure 6 should not be regarded as a radon potential map. Rather, it is a display of an estimated distribution of soil-gas radon concentrations derived solely from the soil-gas radon measurements. It is used to determine the utility of soil-gas radon measurements in defining radon potential areas at this scale of sample collection. The ultimate comparison is to determine if a derived estimation of radon potential has a significant correlation with measured indoor concentrations. Two general methods are employed to use the soil-gas radon concentrations for this evaluation. The first evaluation approach used the mapped distribution of radon and compared them with indoor radon concentrations. The second evaluation approach used the proportion of samples with concentrations exceeding the high radon probability threshold. In this second case, some concern should be reserved because neither the indoor measurements nor the soil-gas samples were randomly distributed. In the study area, 160 homes had indoor radon concentrations measured by long-term alpha-track detectors (1-year duration). Only 26 of 160 measured homes exceeded 250 Bq/m³ and 9 exceeded 600 Bq/m³. That is, only about 16 % exceeded the lower limit threshold. Of this total of 26 homes, 11 were in an area that would be classified as low radon potential by the reconnaissance contour distribution, and 15 were in areas that would be classified as having high radon potential. The difference is not significant because of the small sample size. In addition, it must be noted that home construction and lifestyle have a large part in controlling the indoor radon concentrations. It should also be observed that soil-gas radon concentrations vary daily and seasonally and are influenced greatly by meteorologic conditions. For the first evaluation, using the mapped distribution of all soil-gas samples collected in the reconnaissance study, about 50 % of the area has soil-gas radon concentrations above 70 000 Bq/m³. This is not an artefact of sample spacing as can be seen by the distribution of sample points in figure 6. In the second approach, using the total sample population, also every second sample has radon concentrations that exceed 70 000 Bq/m³. The difference between house-measured radon and soil-gas mapped radon distribution is striking. The reconnaissance survey indicates a classification of high-radon potential would be applied to about half the mapped area, a factor of 3 greater than suggested by the actual home measurements (16 %). Comparison to the number of soil-gas samples with concentrations indicative of high radon potential (> 70 000 Bq/m³) indicates a factor of 3 greater estimation, too. These comparisons indicate that the reconnaissance soil-gas survey tends to overestimate by up to 200 %, regardless which comparison is used, the area that might be classified as having high radon potential. If one considers only those samples anomalous which have radon concentrations > 100 000 Bq/m³, as indicated by the radon probability plot and the percentile curve, only 57 samples out of 231 show this high radon concentration, that means that 25 % instead of 50% are classified anomalous by the soil-gas method which comes close to the 16 % of high indoor radon concentrations. This compares with observations for the entire United States where a radon potential map using 5 input parameters for classification, described earlier (Schuman, 1993), estimated that about 30 % of the land has the potential for exceeding the threshold level. However, a random survey in the U.S. using alpha track detectors (U.S.EPA, 1992) provided an estimate that only 6 % of the homes exceeded the threshold of high radon classification (148 Bq/m³). In addition, the study in Ireland indicates that by itself, a soil-gas survey by this low-density scale of sampling is not adequate to accurately define specific geographic boundaries of radon potential zones.

Detailed Survey (High Density Sampling)

Based on the results of indoor radon measurements carried out by RPII, Dublin, three small areas were chosen where soil-gas samples were collected every 10, 25 m and 50 m, respectively. The location of these areas are shown on figure 1.

Area 1 (Eskerlavalla)

Area 1 of high density sampling covers an area of 150 by 275 meters. It is situated approximately 5 km north of the center of Claremorris and 3 km east of the Limerick and Sligo Railway Branch. During the course of the regional radon survey (low density) three samples were collected within the limits of this area. Two of those samples showed radon concentrations higher than 70 000 Bq/m³, exactly 119 000 and 87 000 Bq/m³ and the third one had 54 000 Bq/m³.

The high density sampling was conducted with 10 - 25 m spacings. It included sampling around three houses that had indoor radon concentrations of 648, 558, and 121 Bq/m³ (see figure 11). The EU has defined the threshold concentration for simple radon mitigation in houses as 250 Bq/m³. The percentile distribution of radon from area 1 shown in figure 8 indicates that more than 75 % of the data exceed the threshold of 70 kBq/m³. That means that only 25 % of the study area is not considered as a high risk area for radon (based on a soil-gas threshold). The house with the highest indoor radon concentration of 648 Bq/m³ is located in an area with soil-gas radon concentrations between 50 000 and 70 000 Bq/m³. This medium high radon level is represented by a very small area, surrounded by anomalous radon samples. The influence of the adjacent high radon area must be considerable. The 558 Bequerel house is situated in an area with 100 000 - 150 000 Bq/m³ soil-gas radon. The surrounding of the house with the lowest indoor radon concentration is similar to that with the highest Rn value. But the low radon neighbourhood is represented by a larger area and the house touches the anomalous area only with the south western corner of the building. Therefore a lower radon concentration was expected. However, it is not known if there are also differences in house construction and home use of the inhabitants. Only three homes were measured for indoor radon concentrations. Two of these houses showed radon levels higher than the 250 - Bequerel - level. The third house had only 121 Bq/m³. Approximately 80 % of the surveyed area showed soil-gas radon concentrations of > 70 000 Bq/m³. A correct classification in this case is not possible because of the small number of houses measured.

Area 2 (Lugatemple)

AREA 2 is located 6 km NW of the center of Claremorris, on the road to Balla and just to the west of the Limerick-Sligo railway branch. The area surveyed is 800 x 650 m (see figure 12). Only one sample was collected in this area during the regional survey. This sample indicated a low radon concentration of 30 000 Bq/m³. Twelve houses were measured indoor with the following results:

House # 1 : 516 Bq/m ³ (high)	House # 6 : 116 Bq/m ³ (low)
House # 2 : 521 " (high)	House # 7 : 44 " (low)
House # 3 : 449 " (high)	House # 8 : 66 " (low)
House # 4 : 160 " (low)	House # 9 : 160 " (low)
House # 5 : 338 " (high)	House # 10 : 1951 " (high)
	House # 11 : 1921 " (high)
	House # 12 : 601 " (high)

Eight houses (66%) show high indoor radon concentrations and 4 (33%) are below the level of 250 Bq/m³. The map shows that two houses, house # 8 with 66 Bq/m³ and house # 12 with 601 Bq/m³ would be misclassified on the basis of a soil-gas radon potential map. Figure 9 shows the percentiles of the outdoor radon concentrations in soil-air from area 2. The 65 % percentile which corresponds with the 66 % portion of high houses in this area has a radon concentration of 85 000 Bq/m³. The 33 % of low houses may be compared with the 35 % percentile which is 55 000 Bq/m³. This 35-percentile is shown as a contour-line in on the radon distribution map of area 2. Two houses are wrongly classified : house # 8 lies in a radon area above 55 000 Bq/m³ and house # 12 is located in an area with low radon concentration. Thirty-five helium samples were collected in this area and 23 were greater than 5400 ppb. However, the low density sampling for helium does not permit an evaluation of structural control, although, as in area 1, many of the high helium samples are located on alignments striking around 35°.

Area 3 (Mount St. Clare)

The study within AREA 3 was concentrated at the Claremount Primary Convent School. This area is 160 x 230 m (see figure 13). The indoor radon concentration in some rooms of the school was 1600 Bq/m³. Ninety two soil-gas samples were collected for radon

analysis on nine perimeter traverses around the school building. Radon concentrations with values greater than 100 000 Bq/m³ were found in the western part of the area and south of the school building. Also in the northeastern corner of the study area samples with high radon concentrations were found. These anomalous and very high radon areas are accompanied by areas with radon concentrations greater than 70 000 Bq/m³ which are also anomalous. Besides 20 soil-gas samples for helium analyses were collected in area 3. None of those samples exceeded 5400 ppb and only three samples had helium concentrations greater than 5300 ppb. Those three samples were aligned in the 27 ° joint direction. The overall absence of high helium concentrations is attributed to the fact that the tension joint system is considered to be very shallow in this area; while it provides pathways for radon localisation and transport, it does not permit transport of helium from deeper sources. The correlation between soil-gas radon and indoor radon in the school building is discussed by J. Madden from RPII, Dublin.

Conclusion

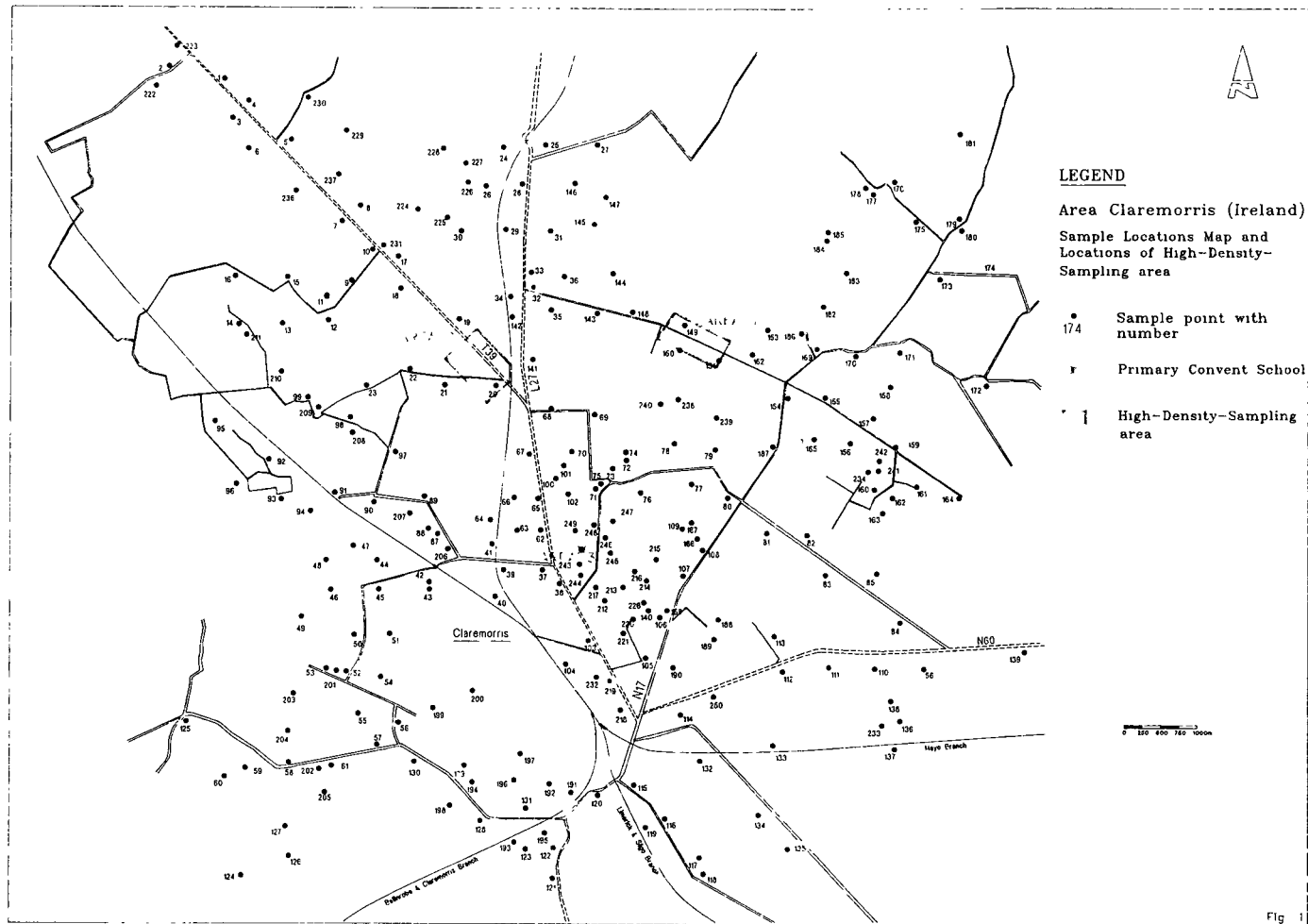
The study in the area of Claremorris, Ireland demonstrates the utility of soil-gas mapping and defines both the capabilities and the limitations of such a single method technique for developing radon potential estimations for an area. Soil-gas radon mapping provides a crude but helpful estimate of the radon potential of an area. Low-density sampling cannot define specific geographic areas of radon potential but can help estimate the magnitude of the classification for the entire studied area. The estimate of high-radon potential areas is generally higher than that confirmed by measured indoor concentrations, perhaps being several hundred percent higher. But in the absence of complementary data, such as decent topographic and geological maps, hydrological data, results of gamma measurements and similar basic data, the relatively inexpensive radon survey can help local officials determine the extent of the problem, and plan resources, priorities, information distribution, and building codes accordingly. On the other hand high-density sampling programs showed very good correspondence with the indoor radon results. Although the numbers are few, the study suggests that a higher density sampling has a better chance of more precisely identifying radon potential for specific zones. This is also reflected in a study in the United States where high density soil-gas sampling and analysis for radon was shown to correctly identify the radon potential of individual home sites (Reimer & Gundersen, 1989).

Publications

Madden, J.S., van den Boom, G., O'Connor, P.J., McGarry, A.T., Reimer, G.M., 1995 (in press): Evaluation of the combined helium/radon in soil-gas mapping methodology as an indicator of areas in which elevated indoor radon concentrations may be found. - Natural Radiation Environment VI Montreal, June 1995 (abstract).

O'Connor, P.J., Gallagher, V., Madden, J.S., van den Boom, G., McLaughlin, J.P., McAuly, I.P., Barton, K.J., Duf I.T., Müller, R., Grimley, S., Maersh, D., Mackin, G., MacNiocail, C., 1993 Assessment of the geological factors influencing the occurrence of radon hazard areas in a karstic region. - Geological Survey of Ireland, Report Series RS93/2, Dublin, 172 p.

Ort, Matthias, Reimer, G.M., van den Boom, G., O'Connor, P.J. and Madden, J.S., 1995 (in press): Radon distribution and control in the limestone terrain of western Ireland. - Natural Radiation Environment VI, Montreal, June 1995, (abstract).



FREQUENCY HISTOGRAM HELIUM
AREA CLAREMORRIS

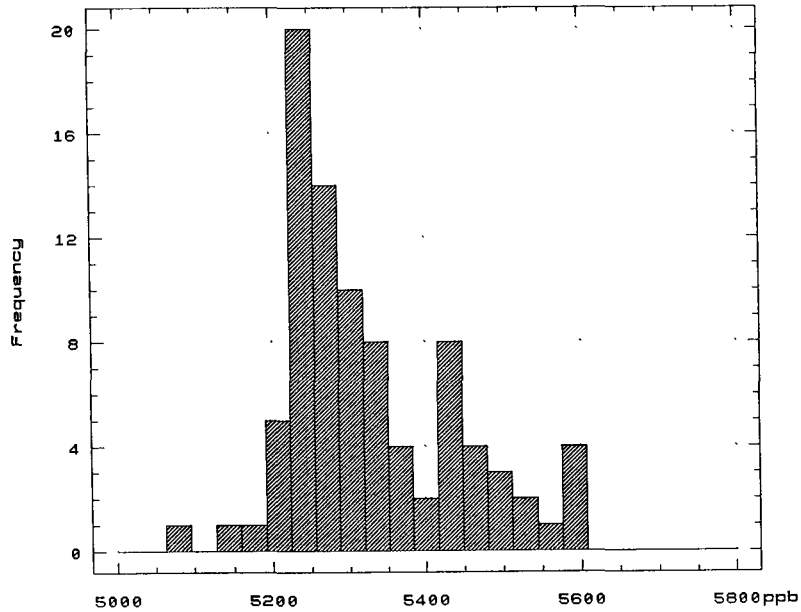


FIGURE 2 : HELIUM FREQUENCY DISTRIBUTION
AREA CLAREMORRIS, IRELAND

HAUFIGKEITS-HISTOGRAMM

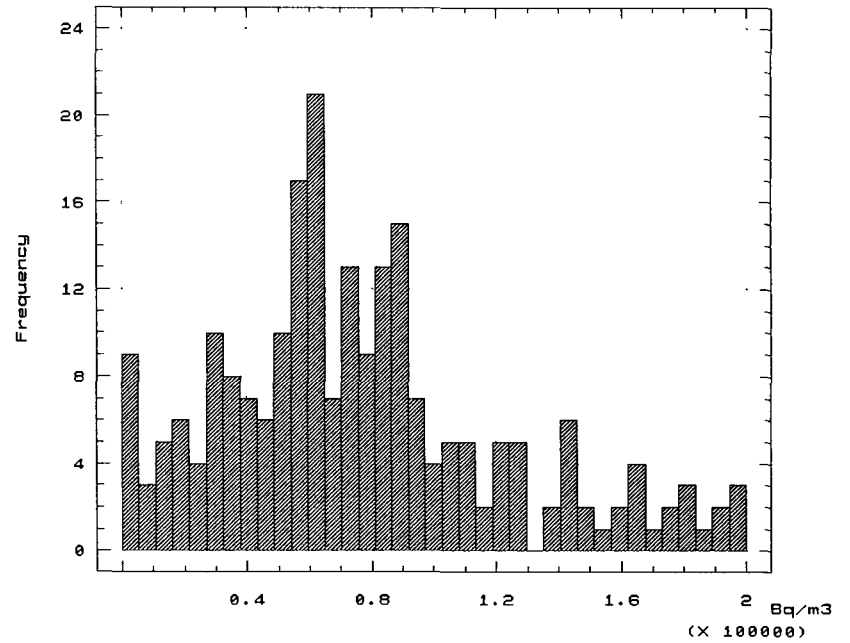


FIGURE 3: RADON FREQUENCY DISTRIBUTION
AREA CLAREMORRIS, IRELAND

PROBABILITY PLOT RADON
AREA CLAREMORRIS

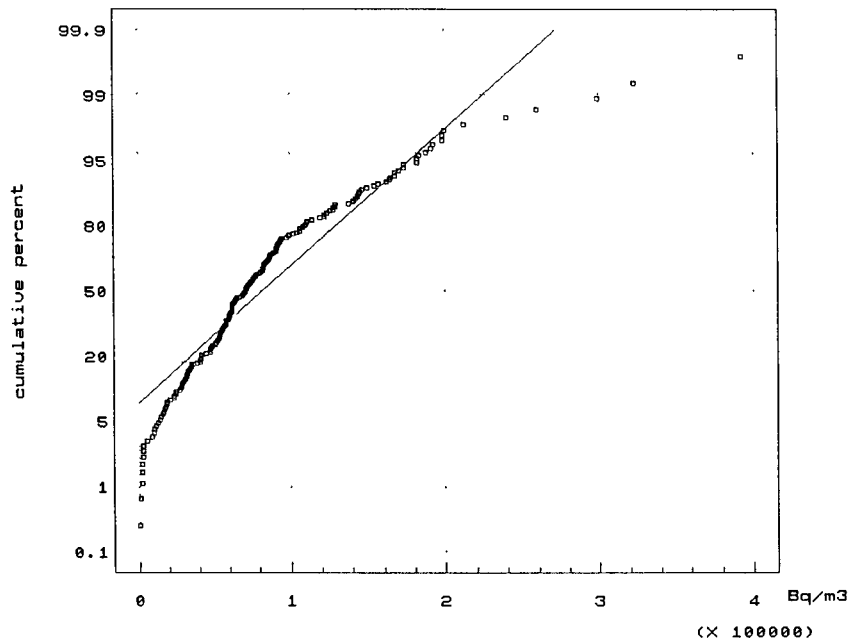


FIGURE 4: RADON PROBABILITY PLOT
AREA CLAREMORRIS, IRELAND

PERCENTILE DISTRIBUTION
AREA CLAREMORRIS

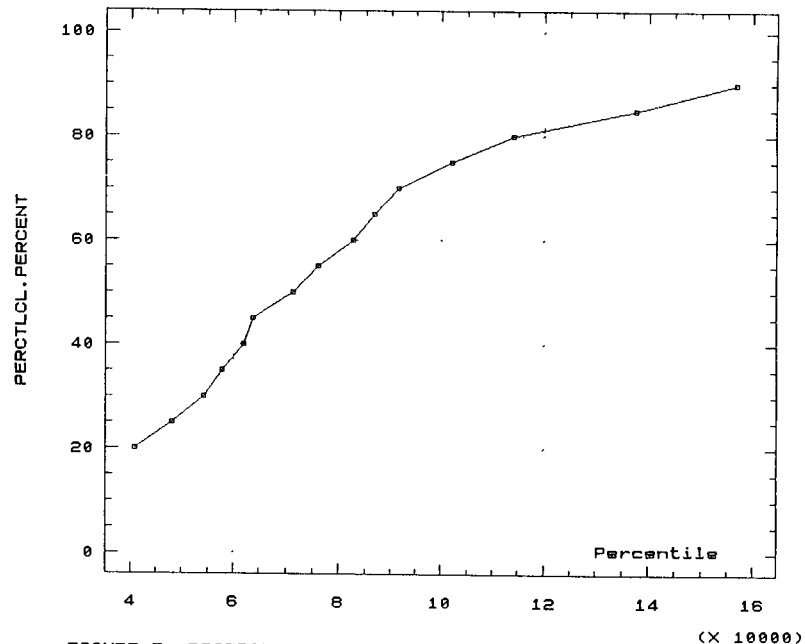
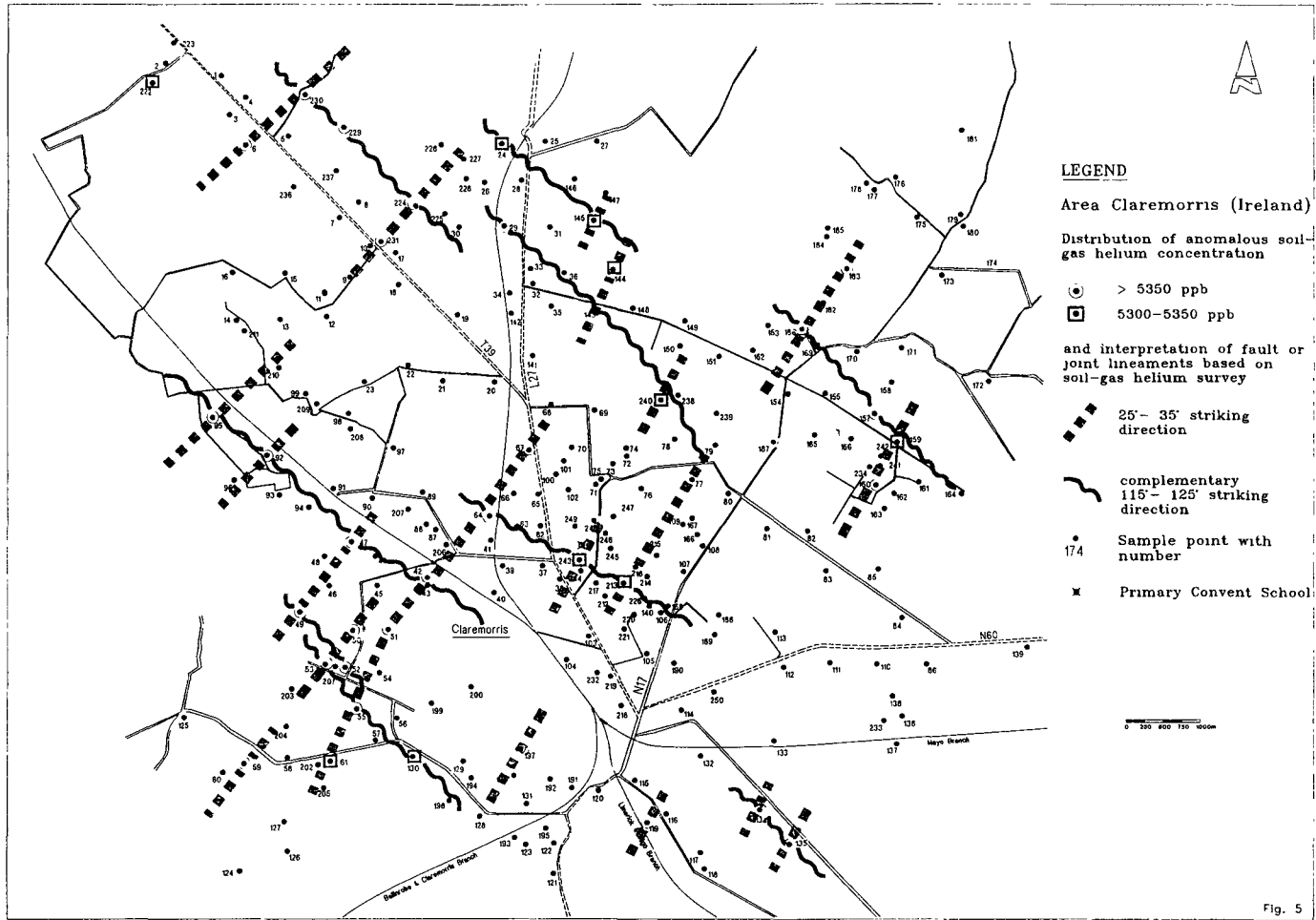
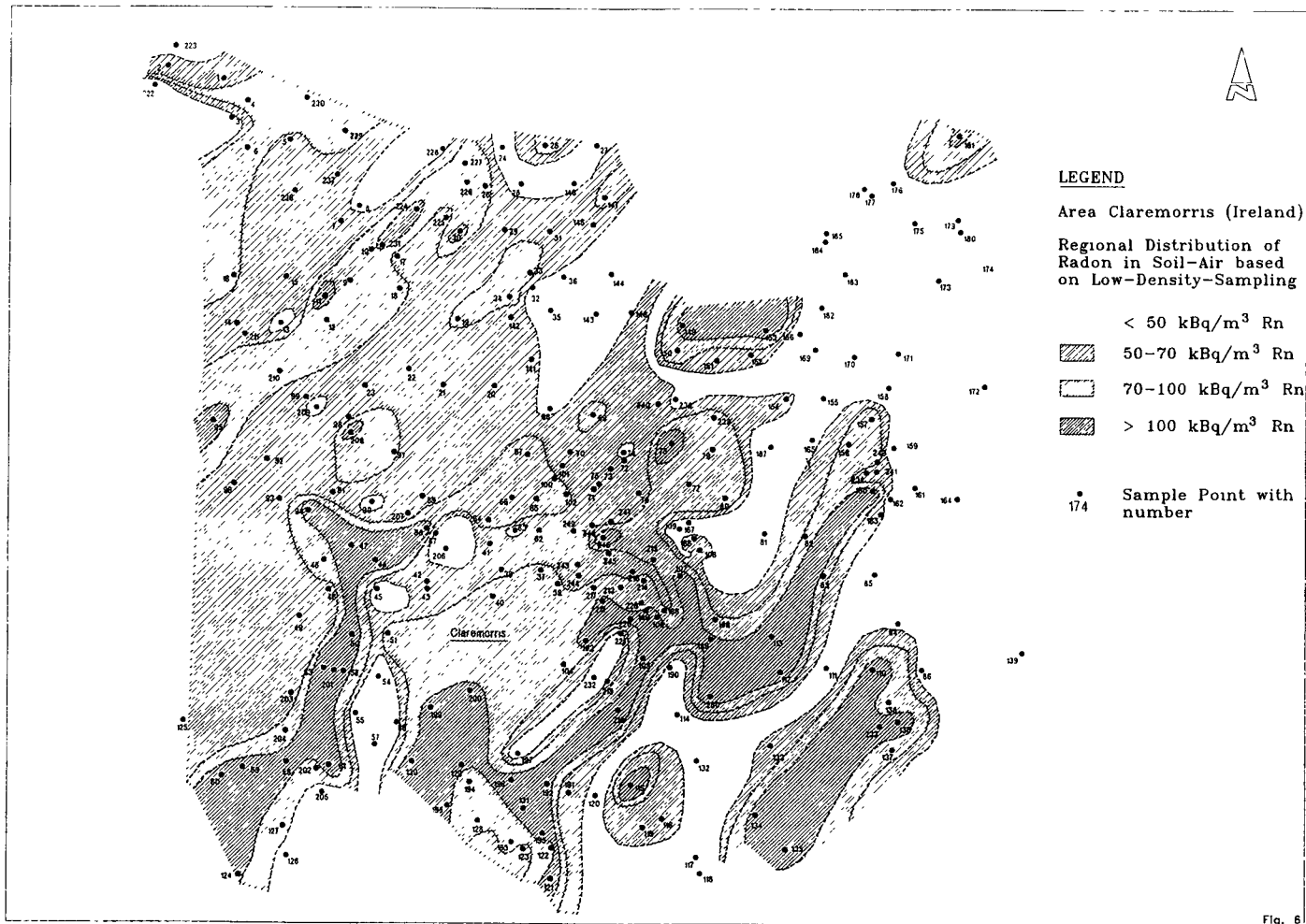


FIGURE 7: DISTRIBUTION OF RADON PERCENTILES
AREA CLAREMORRIS





PERCENTILE DISTRIBUTION
AREA 1

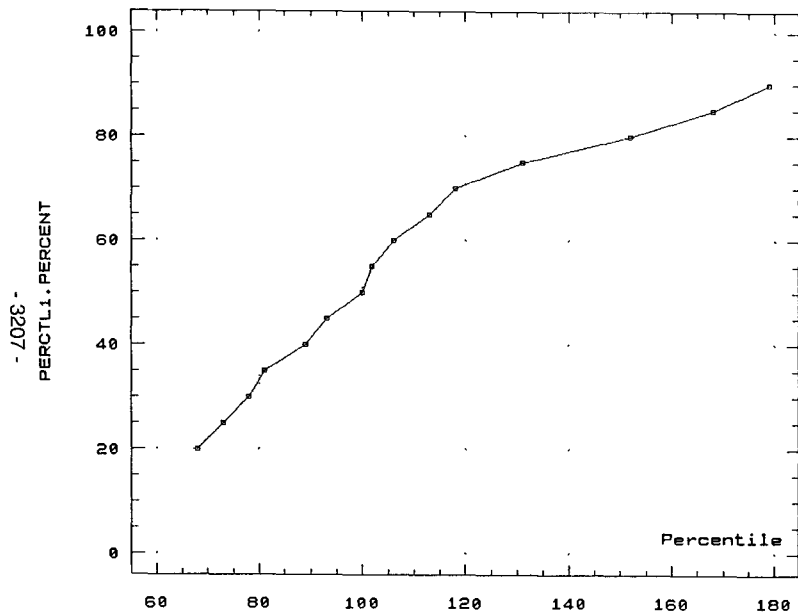


FIGURE 8: DISTRIBUTION OF RADON PERCENTILES

AREA 1 (ESKERLAVALLA), IRELAND

PERCENTILE DISTRIBUTION
AREA 2

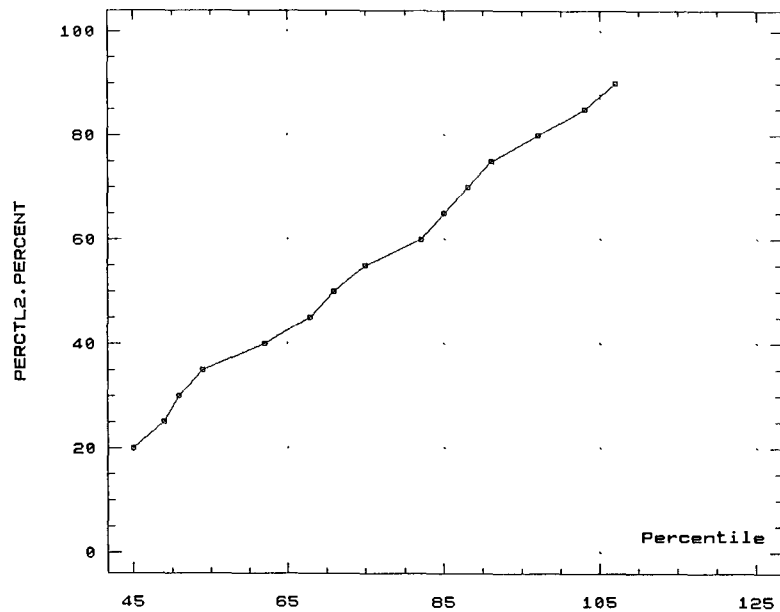
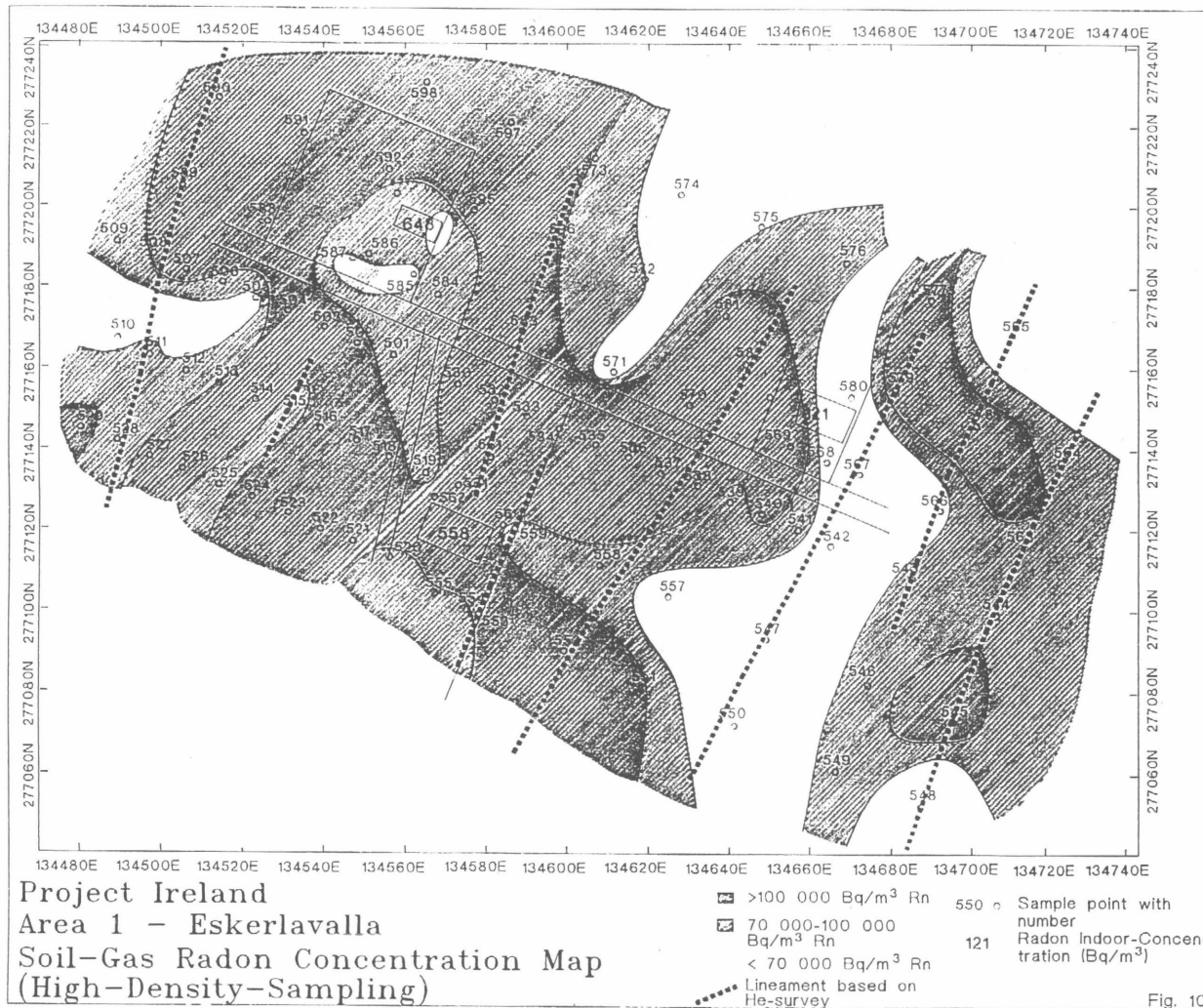
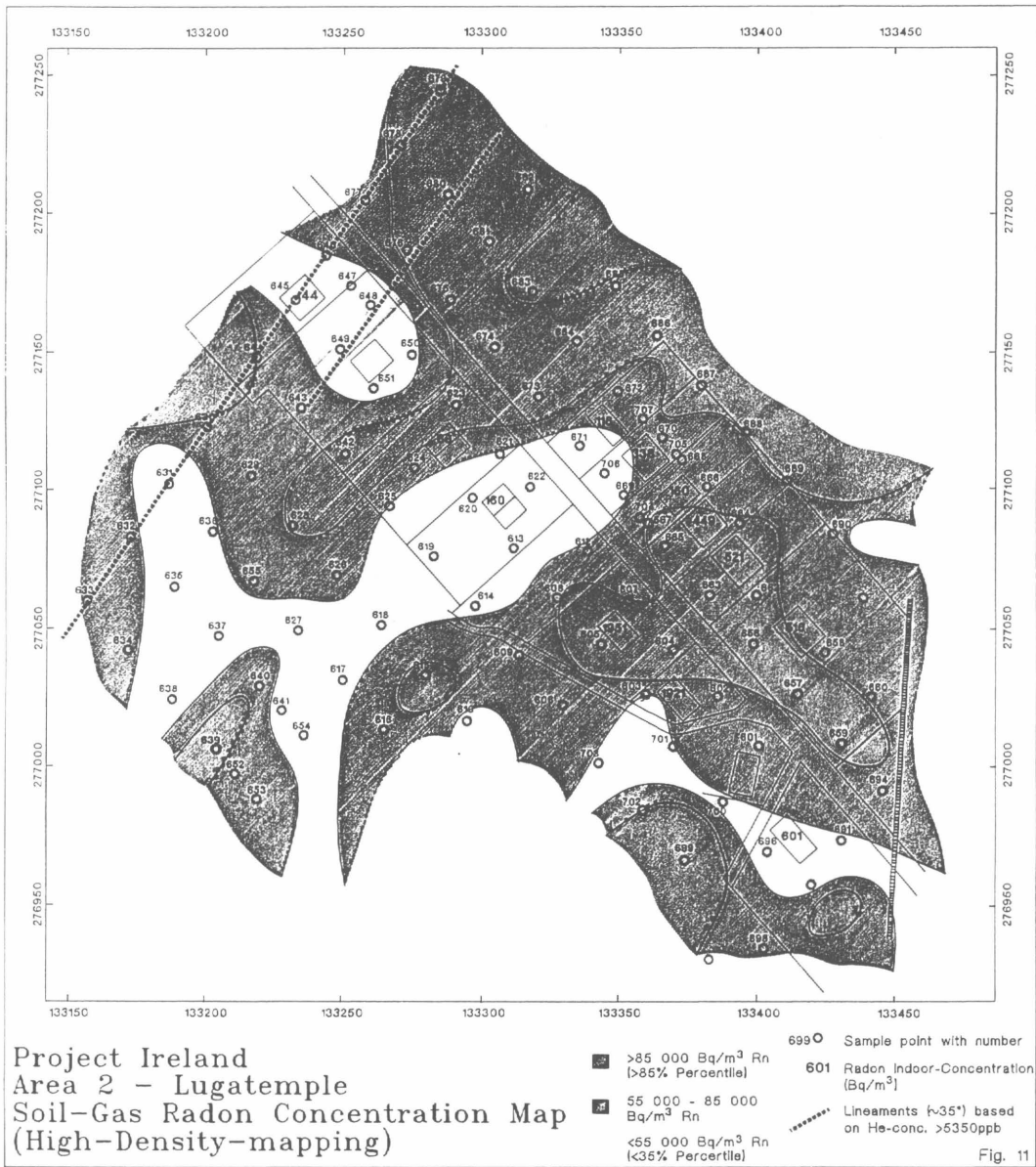








FIGURE 9: DISTRIBUTION OF RADON PERCENTILES

AREA 2 (LUGATEMPLE), IRELAND





Project Ireland
 Area 2 - Lugatemple
 Soil-Gas Radon Concentration Map
 (High-Density-mapping)

-  >85 000 Bq/m³ Rn (>85% Percentile)
-  55 000 - 85 000 Bq/m³ Rn
-  <55 000 Bq/m³ Rn (<35% Percentile)
-  699 Sample point with number
-  601 Radon Indoor-Concentration (Bq/m³)
-  Lineaments (~35°) based on He-conc. >5350ppb

Head of project 4: Dr. Porstendörfer

II. Objectives for the reporting period

Measurement campaign in Ireland:

During the reporting period a measuring campaign of all in the project included groups in Ireland was planned, where the IL should take the part looking upon the change of radon concentration in soil and indoor air due to meteorological conditions. Followig continuously monitoring was planned:

- soil radon concentration in 1 m depth (sampling depth of the Enmotec group)
- radon concentration beneath the slab of a uninhabited measuring house
- indoor radon in several parts of the house
- pressure differences between indoor air, subslab and outdoor air
- temperature differences between indoor and outdoor air was planned.

Vertical radon profile in the soil:

A soil probe and the corresponding radon/thoron monitors were constructed for continuous measurement of the vertical radon profile in the soil air:

- construction of a probe for simultaneous and continuous measurement of radon and thoron in different depths between soil surface and 5 m depth.
- building and calibration of specially designed radon chambers for the measurement of soil radon and thoron activities (method: electroprecipitation).
- first test measurements with the new probe and radon chambers in the vicinity of Göttingen.

III. Progress achieved including publications

Measurement campaign in Ireland:

During the measuring campaign in Milltown (Ireland) radon concentrations in the ground floor (all rooms open), attic, 50 cm below the slab, outdoors and in the soil (1 m depth) and additional the temperatures in the ground floor, in the attic and outdoors. The pressure differences between outdoor atmosphere, attic and subslab soil to the indoor air were measured. Additional meteorological data, like wind speed, atmospheric pressure, soil temperatures and rain intensity were supplied by the Meteorological Service of Ireland (Claremorris station, 10 km from Milltown). The measurements were performed during a joint measurement together with the Radiation Protection Institute of Ireland and ENMOTEC Company, Germany during the time between May 10th and May 20th 1993. The house was built 20 years ago in a plane region. The subslab zone is divided by footings into compartments of the size of the overlying rooms.

The radon and thoron activity concentration were measured continuously with the method of electroprecipitation of freshly in a decay volume produced daughter products on a surface barrier detector and alpha-spectroscopy. For room air measurements a 5 l chamber was used with a detection limit of 6 Bq/m³ for radon and 12 Bq/m³ for thoron (1 hour counting interval, 1 s statistical uncertainty). The soil air measurements were carried out with a chamber volume of 0.27 l and detection limits of 60 Bq/m³ and 150 Bq/m³ for radon and thoron respectively.

The probe for the soil radon measurements consists of a steel pipe (diameter 1 cm) containing two stainless steel tubes of 1 mm inner diameter, sealed against the hull pipe (see Fig. 7). The sample air was sucked through one tube with a flow rate of 10 l/h, passed the detector and was pumped through the second tube back into the soil, thus minimising the influence of the measurement on the soil radon concentration. For soil measurements the probe was driven into the soil, using the whole length of the hull pipe as sealing against entry of outdoor air. For the measurement of subslab radon the probe was sealed in the drill hole with a standard silicon sealing compound.

Pressure differences were measured with a micromanometer (MKS Baratron) with a resolution of 0.01 Pa and air temperatures were measured with thermistors (resolution 0.1 °C). Ventilation rates were computed from the decrease of artificially elevated CO₂ concentrations.

A dependence of the indoor radon concentration of the pressure gradient was confirmed with measurements performed at Milltown (Ireland). The variation of the indoor radon could be reproduced by a source factor, calculated from pressure gradient between subslab and indoor air and subslab radon concentration, during the whole measuring campaign, confirming that the pressure difference between indoor and subslab air governs the radon entry by convective flow from subslab air into the building (Fig. 1). The pressure difference between subslab air and ground floor is varying according to the pressure difference between outdoor air and ground floor (Fig. 2), aside from a reduction of amplitude by a factor of about 9, which indicates a massive transport resistance between the subslab air and the open atmosphere, probably due to the compartment structure of the subslab region.

Considering the subslab radon concentration in comparison to the soil radon concentration in 1 m depth, a smoothing of the temporal change can be observed (Fig. 3), which is also due to the compartment structure of the subslab section.

During the measuring period in Milltown (Ireland) the pressure difference between outdoor and indoor air and also between subslab and indoor air was mainly governed by the wind pressure applied to the house (Fig. 4). As the house was not heated during the measuring campaign, the influence of the temperature difference between indoor and outdoor air on the pressure difference (stack effect) had to be weak and could not be separated from the dominating dependence of the pressure gradient on wind speed.

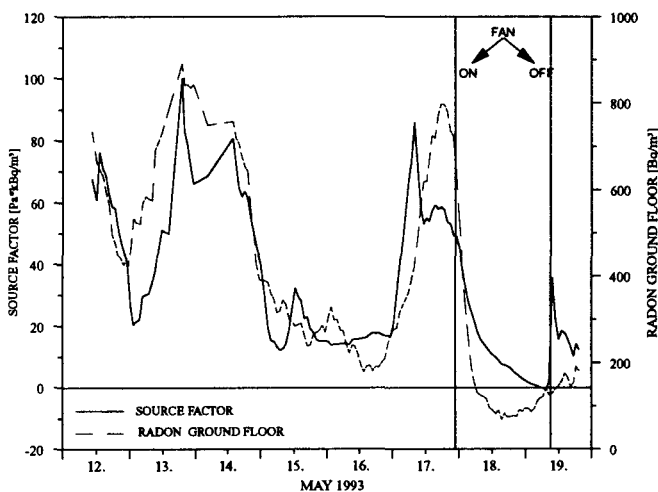


Fig. 1: Comparison of the indoor radon concentration to a source factor (product of pressure difference indoor - subslab and the subslab radon concentration).

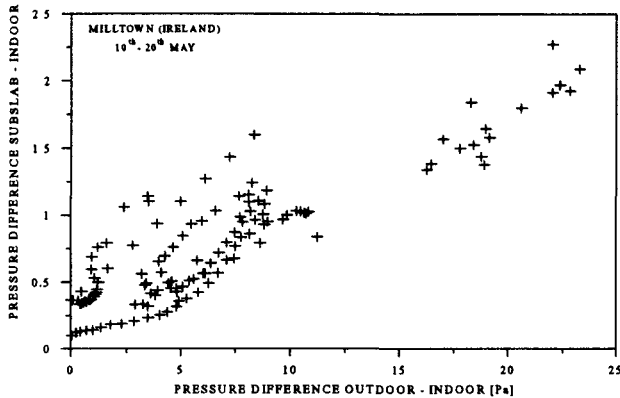


Fig. 2: Dependence of the pressure difference between subslab region and ground floor on the pressure difference between outdoor air and ground floor.

As the radon entry into the building is governed by the pressure difference between subslab and indoor air an experiment was performed to reduce radon entry by an artificial overpressuring of the house with a small fan blowing air from the attic into the ground floor. The experiment started at May 17th and ended 19th (for the influence on source term and radon concentration see Fig. 1). The distribution of the ratio of pressure difference between subslab and indoor air to the wind speed was shifted to lower values. If the pressure difference between subslab region and indoor air is considered roughly proportional to the wind speed, the ratio between pressure difference and wind speed describes the radon entry largely independent on wind speed and as it is the dominating influence parameter on weather conditions. Under normal conditions the average value was 0.31 Pa s/m (range 0.08 - 2.72 Pa s/m) and with fan blowing attic air into the ground floor 0.04 Pa s/m (range 0 - 0.16 Pa s/m). If the radon concentration in the ground floor is considered proportional to the pressure difference (Fig. 1), the reduction of the average radon concentration in the ground floor due to the effect of the fan would be about a factor of 13. The ventilation rate with operating fan ($V = 0.31 \text{ h}^{-1}$) was only slightly increased compared to the normal conditions ($V = 0.24 \text{ h}^{-1}$) and its effect on radon reduction was neglected.

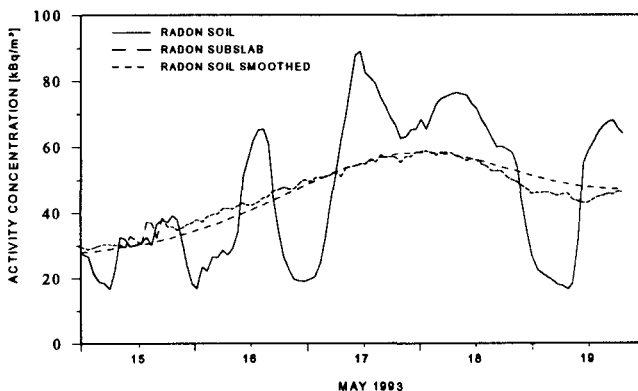


Fig. 3: Comparison of subslab radon concentration to values obtained by smoothing of the undisturbed soil concentration.

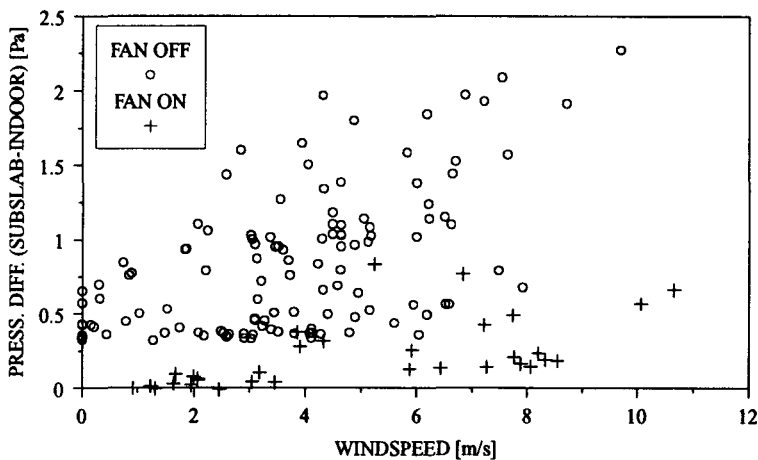


Fig. 4. Dependence of the pressure gradient between outdoor and indoor air on the wind speed under normal conditions and with a fan blowing attic air into the ground floor.

Vertical radon profile in the soil:

A soil probe and the corresponding radon/thoron monitors were constructed for continuous measurements of the vertical radon profile in the soil. After calibration of the radon/thoron monitors first test measurements were performed.

Radon/Thoron monitors: It is planned to measure simultaneous the radon activity concentration in soil in four depths down to about five meters. For continuous measurements four identical radon/thoron monitors were built depending on the method of electroprecipitation of the charged radon and thoron decay products on surface barrier detectors. Since the radon gas concentrations in the soil are in the order of several kBq a small decay volume V of 250 cm^3 (cylindrical form) was used. These monitors were carefully calibrated in the laboratory by varying the high voltage U (for electroprecipitation), the air flow rate v and the air humidity. Best operating conditions were found for $U = 6 \text{ kV}$ and $v = 40 \text{ l/h}$. The absolute counting efficiencies for radon gas measurements using dried air ($\text{RH} = 6\%$) and normal room air ($\text{RH} = 40 - 70\%$) are summarised for all monitors in table 1.

Monitor	ϵ ($10^{-5} \text{ cps}/(\text{Bq m}^{-3})$)	
	RH = 6%	RH = 40 - 70%
1	4.57	4.53
2	4.20	4.12
3	5.50	5.19
4	5.50	5.27

Table 1: Absolute counting efficiency ϵ ($\text{cps}/\text{Bq}/\text{m}^3$) for radon gas measurements of all radon/thoron monitors: $V = 250 \text{ cm}^3$, $U = 6 \text{ kV}$, $v = 40 \text{ l/h}$. Comparison of dried air ($\text{RH} = 6\%$) and normal room air ($\text{RH} = 40 - 70\%$).

Soil probe: The probe was constructed for simultaneous measurements at four different depths at 0.5, 1.5, 2.5 and 3.5 m. The complete probe is a module system consisting of four different parts which can be connected. Each part consists of a steel pipe (diameter 60 mm) containing two tubes of 1 mm inner diameter, sealed against the hull pipe. The sample air is sucked through one tube, passed the radon/thoron monitor and is pumped back through the second tube into the soil. To avoid an air flow between the different components of the pipe and the outdoor air each unit is sealed in the drill hole above and under the air entry/exhaust port by packers. These packers consist of inner tubes which can be inflated (see Figure 5).

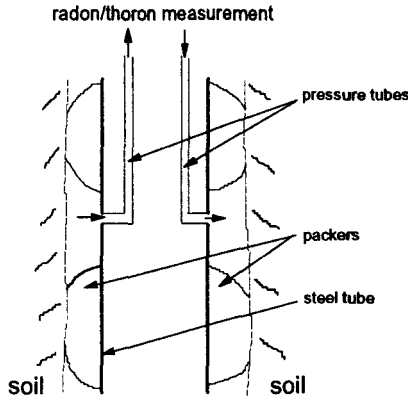


Figure 5: Schematic diagram of the soil probe (SP) at one depth with inflated packers.

The soil air is pumped through pressure tubes into the radon monitors. Previously it is dried with CaCl_2 to keep the soil air humidity constant, because the efficiencies of the monitors depend on the humidity of the soil air. The monitors and the measuring electronics are installed in an air conditioned caravan to prevent diurnal temperature variations, which might have an influence on the measurement.

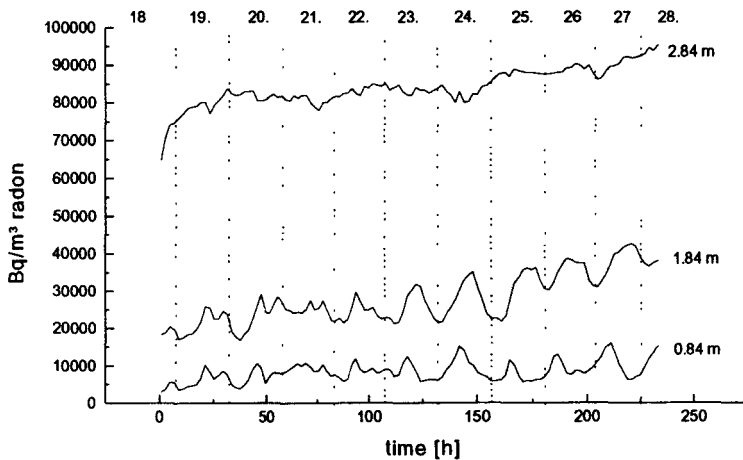


Figure 6: Variation of radon gas concentrations in soil air at depths 0.84, 1.84 and 2.84 m.

The measurement was done from Aug. 18th until Aug. 28th 1995. The probe was tested for several days in a drill hole at three depths. During this period there have been relative stable weather conditions without big air pressure changes or periods with strong rainfall. The results in Figure 6 show the radon gas concentration in three depths. With increasing depth the radon gas concentration increases from 8 kBq/m³ at 0.84 m to 80 kBq/m³ at 2.84 m. For the first 100 h there are relative stable radon gas concentrations in all three depths without any significant variations. After this time there are periodic diurnal variations in radon gas concentration at depths of 0.84 m and 1.84 m. The maximum of the radon gas concentration is always in the afternoon and has an amplitude of 5-10 kBq/m³. At 2.84 m there is no significant periodic variation observable, but the radon gas concentration increases slightly from 80 to 90 kBq/m³.

Another measurement with the soil probe was done from Sept. 5th until Sept. 11th 1995. Simultaneously the radon gas concentration at 0.84 m was measured with a stick soil probe (see Fig. 7). The soil is less disturbed by the stick soil probe because it needs no drill hole. So this measurement was a test for the soil probe.

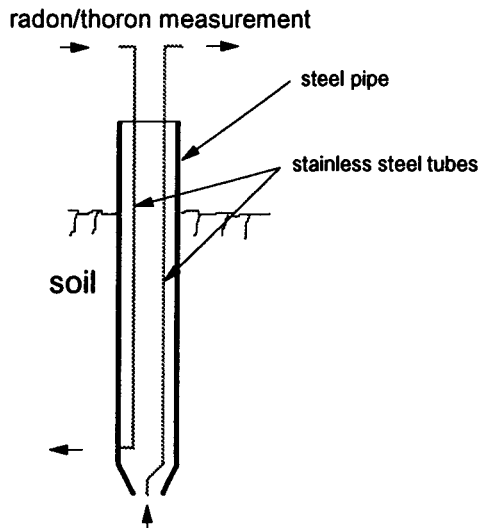


Fig. 7: Schematic diagram of the stick soil probe (STSP).

The measuring results of the soil probe at 0.84 m show a good agreement with the measuring results of the stick soil probe at 0.84 m (see Fig. 8). From 5th until 7th there have been stable weather conditions. At 0.84 m there are strong diurnal variations between 10 and 20 kBq/m³. At 1.84 m there are also diurnal variations, but they are smoothed in comparison to 0.84 m. Simultaneously the air pressure was measured. There was a relative strong increase of air pressure at 8th and 9th from 732 Torr to 744 Torr. During this time the radon gas concentration decreased at 0.84 m significantly but it increased at 1.84 m. This is a reference to pressure driven advection of soil air.

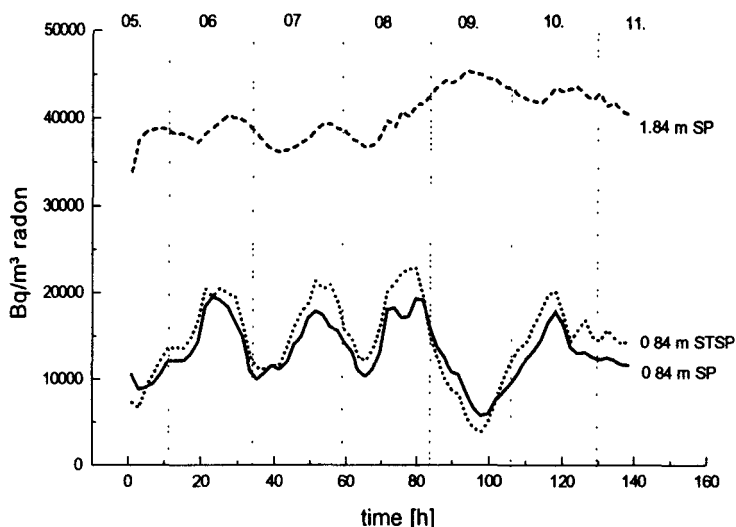


Fig.8: Variation of radon gas concentration in soil air at depths 0.84 and 1.84 m with soil probe (SP) and for comparison at 0.84 m with stick soil probe (STSP).

Further measurements have to be done to interpretate the results. Especially the drill hole should be in a homogeneous soil to separate the meteorological influences on the radon gas concentration from the effect of inhomogenities in soil (different exhalation and uranium content of the soil). The diurnal variations could be a reference to temperature induced convection of the soil air. Experiments will be continued to study the influence of meteorological parameters on radon gas concentration in the soil using above described and tested gas probe.

List of publications.

A. Reineking, G. Butterweck, J. Kesten, O. Malolepsy, B. Kopka, H.-J. Heymel, E. Speer, J. Porstendörfer

"A monitor for continuous and simultaneous measurement of environmental thoron and radon gas", Proceedings of thoron/thoron progeny intercomparison, (Editor J. Bigu), Elliot Lake, Canada, November 2-6, 1992

J. Porstendörfer, G. Butterweck, J. Madden, A. Reineking

"Influence of meteorological parameters on the transport of radon from soil air into indoor and outdoor air", first international workshop on indoor radon remedial action, Rimini, Italy, June 27 - July 2, 1993

J. Porstendörfer, G. Butterweck, A. Reineking

"Der Einfluß meteorologischer Größen auf die Radonkonzentration in der Raumluft" Umweltradioaktivität, Radioökologie, Strahlenwirkung. 25. Jahrestagung Fachverband für Strahlenschutz, Binz auf Rügen, Germany, September 28-30, 1993
Tagungsband (Herausgeber: M. Winter, A. Wicke), pp125-130

J. Porstendörfer, G. Butterweck, A. Reineking

"Daily Variation of the Radon Concentration Indoors and Outdoors and the Influence of Meteorological Parameters", *Health Physics* 67, 283-287, 1994

A. Reineking, O. Malolepsy, G. Butterweck, J. Porstendörfer

"Einfluß der Luftfeuchte auf die Ansprechwahrscheinlichkeit eines Radon / Thoron Monitors für kontinuierliche Messungen" *Strahlenschutz: Physik und Meßtechnik*. 26. Jahrestagung des Fachverbands für Strahlenschutz e.V., Karlsruhe, Germany, 24.-26. Mai 1994. Tagungsband (Herausgeber: W. Koelzer, R. Maushart), pp 757-762, 1994

Comparative Assessment and Management of Radiological and Non-Radiological Risks Associated with Energy Systems

Final Report: July 1992 - June 1995

- 1) M. Dreicer CEPN
- 2) R. Freidrich IER
- 3) U. de Haag RIVM

I. Summary of project: global objectives and achievements

Background

Decisions on the choice of methods of generating electricity are made by public and privately-owned utilities within the context of controls, regulations and national energy policies. A decision framework, presented by the Nuclear Energy Agency of the OECD in a report on the Broad Economic Impact of Nuclear Energy, indicates that the current position is continually influenced by the changing information related to the environment and the overall national economy. This is a dynamic process, but in general, these factors have been taken into account in setting energy policy and investments. The weights of these factors vary over time and differ from country to country.

Recently there has been more concern that these types of decisions are based, in some part, on subjective judgements and trade-offs and that the extent of some of the social impacts, or external costs are not well understood. With the increased awareness of the importance of environmental protection, it became increasingly necessary to focus on the link between energy production and the environment. Further work has been carried out during the last decade to broaden the base of knowledge on the public health and environmental impacts that result from the production of electricity. The initial aim of energy comparison studies was to rank the various electricity production systems. It is now recognised that this was merely an academic exercise, with a limited impact in decision-making.

Objectives

The important objective of providing the data needed to make informed choices has been an on-going effort in various international and national projects. The need to develop more coherent, comprehensive and equitable approaches for the comparison and management of health and environmental impacts of energy systems is obvious.

The global objectives of this project was to improve the methodology for the comparison of radiological and non-radiological risks associated with energy systems, particularly the coal and nuclear fuel cycles. Within the context of this work, the risks considered were in the health and environmental domains. Some of the complications facing these types of comparative assessments are:

- The differing scales of time and space that the impacts can potentially span create difficulties in making direct comparisons.
- The populations that are exposed to the risks may be different - occupational risks may be considered differently than public risks.
- The integration of low probability but high consequence events is difficult, especially when the issues of risk aversion are considered.

Within this project a methodology of comparative risk analysis has been developed for multi-criteria utility techniques using a commercially available software system. On this basis, a comparison between the nuclear and coal fuel cycles in France and Germany has been performed. Furthermore, applicable risk indicators for human health and the environment have been developed and the problem of the range of uncertainty associated with the risk estimates has been addressed.

Framework for risk assessment

The framework set for the assessment of the risks of electricity production has very serious implications for the application of the final results. The choice of stages of the fuel cycle, processes, technology, sites, units for normalisation, methodologies for assessment and key impact indicators play an important role.

The classical dimensions used in comparative studies have been taken into consideration: public and occupational populations, normal operations and accidental situations, human health impacts and gross environmental impacts. The fuel cycles have been divided into the logical stages of: fuel extraction, fuel preparation and conversion, fuel fabrication (in the nuclear fuel cycle), electricity generation (including the construction and decommissioning of the plant), material transport, waste processing and final waste disposal.

The early studies reported mainly fatalities as the key risk indicators because it presented a simplified indicator of a serious risk in units of a common denominator. However, during the intervening years, many more health and environmental indicators have been identified due to expanding assessment capabilities and changes in societal attitudes. By using a willingness-to-pay approach for the quantification of the risks, some of the factors concerning occupational risk versus public risk, time dimension, risk aversion, may be taken into account. However this assumes that the willingness-to-pay valuation at the basic indicator level takes into account the potential different weightings that might be considered at higher levels of the risk hierarchy (e.g. local impacts vs. regional impacts).

The most important choices for the assessment of the nuclear fuel cycle concern the definition of time and space boundaries. Due to the long half-life of some of the radionuclides low-level doses will exist very far into the future. These low-level doses can add up to larger number when spread across many people and many years (assuming constant conditions). The validity of this type of modelling has been widely discussed. On one hand, there is a need to evaluate all the possible impacts if a complete assessment of the fuel cycle is to be made. On the other hand, the uncertainty of the models increases and the level of doses, that are estimated, fall into the range where there is no clear evidence of resulting radiological health effects.

The analysis of the assessment framework for the coal fuel cycle clearly points out the need to cover a distance of up to several hundreds of kilometres in order to capture a major fraction of the expected impacts. Furthermore, because of the lack of exposure-effect relationship, the assessments for the coal fuel cycle is mainly focused on local and acute effects. For this fuel cycle, the risks mainly concerns occupational effects for the medium term associated with exposures in underground mining.

Environmental

The assessment of environmental impacts is more difficult since the impacts of many pollutants are not well understood. In order to adequately compare the environmental impacts between fuel cycles, two paths may be taken:

- convert indicators into units that can be consistently applied. The monetary valuation of impacts and damages can be used in this way.
- multi-dimensional analysis can be used to compare different measures of impacts and damages. By applying a method, such as multi-attribute analysis, the complexity of various indicators, different probabilities of occurrence, and the different time and space dimensions can be tackled.

Presently the monetary valuation of the damages is utilised. For example, the loss of utility or the cost of the loss of the utility resulting from the damage has been used as an indicator of the impacts.

Quantification of impacts

The objective of the first phase of this project was to develop a risk assessment framework that could be used in later phases to conduct comparative assessments between different energy fuel cycles and provide the information needed in the decision-making process.

The experience gained in this first phase showed that further work was required in the development of a comparative assessment methodology. Fine-tuning was required for the development of consistent indicators, and furthermore the development of a multi-dimensional method for comparing the wide variation of risks resulting from the production of energy from different fuel cycles.

A multi-criteria analysis on the health impacts of the nuclear and coal fuel cycles has been conducted, based on the results that have been published by CEPN and IER within the ExterneE project. The first step of this analysis was based on the physical indicators derived from the ExterneE project. As far as no common denominator exists between the various impacts considered in the study (i.e. health versus

environment; fatal versus non fatal effects...), the application of the multi-attribute analysis implies to rank all of them. Thus, it clearly appeared that, for this approach, the weighting process was too complicated and did not provide enough information to the decision maker. The second step of the analysis was based on the monetary valuation of the various health and environmental indicators adopted in the ExternE project. Starting from this valuation, a framework for the multi-attribute analysis has been developed in order to take into account the social attitude towards the risk such as: local versus global impact; normal versus accidental risk; radiological versus non-radiological; risk for present generation versus future generation...

Towards an elicitation of preferences within the decision-making process

In general, the main impacts that can be expected from the different fuel cycles have been considered in the various studies. Nevertheless, some of them are not yet quantified (i.e. the environmental impacts and the evaluation of the consequences of major accidents) and furthermore, the various dimensions of the risk are not necessary tackled when the valuation is based on the willingness to pay approach. In fact, the monetary values derived from this approach generally reflect preferences which are specific to the context considered in each study. For example, the value of life may vary according to the economic level of the country, the type of risk considered (i.e. risk associated with normal exposure or severe accident,...), the category of people exposed (i.e. public, workers, children,...) and the same kind of criticisms should be made for environmental indicators which are really dependent of the utility associated with the environment at a specific time and a specific location. These remarks point out the need for a global approach reflecting the "trade-off" of the society as far as the risk is concerned in order to allow the comparison of health and environmental impacts of the different fuel cycles. For this purpose, the multi-attribute analysis may consider the preferences between present and future generations, the risk aversion towards accidental situations, the regional and global impacts characterised by very low individual risk but concern a large population, the importance of environmental impacts... Beyond the development of the health and environmental indicators and the framework for the multi-attribute analysis, further developments are needed to elicit the preferences of the decision-makers regarding the various dimensions of the risks.

Head of project 1: M. Dreicer

II. Objectives of the reporting period

The aim of this project was to compile all the risk data available for use in the multi-criteria utility analysis and to define a model including the relative criteria to be evaluated, and to evaluate the relative importance of the criteria (weighting). A sensitivity analysis has been carried out to investigate the robustness of the decision to changes in scores and weights.

As part of the EC/DGXII-US project on the External Costs of Energy Fuel Cycles, CEPN has developed a risk assessment methodology for all stages of the nuclear fuel cycle. The impact pathway analysis approach that has been used includes the estimation of risk for different health or environmental indicators and, in the final step, to value the impacts. The data collected have been used in the evaluation of the comparative analysis methodology developed for this project.

III. Progress achieved including publications

Background

With the rising demand for energy and increased awareness of the importance of environmental protection, it has become necessary to focus on the health and environmental impacts of energy systems. To make choices between systems is difficult. The indicators of risk for each fuel cycle can vary in type, magnitude and time scale. The public perception of acceptability varies greatly between different technologies for production of energy. By designing a consistent framework for the environmental and health risks associated with all fuel cycles and developing techniques for the comparison of complex and varied indicators, it is hoped that a link can be made between risk assessment and decision-making.

The differing scales of time and space that the impacts can potentially span, create difficulties in making direct comparisons. For example, the impacts from radioactive waste disposal are not likely to be seen for tens of thousands of years and will be generally local effects. The emission of greenhouse gases from fossil fuel cycles may have potential global impacts in the not too distant future.

Occupational and public risks are generally considered differently and have different levels of importance in the decision making process. The integration of low probability of occurrence but high consequence events is also a difficult task, especially when the issues of the public's aversion to large impacts (no matter how low the probability) is considered.

The risks resulting from the production of energy can be classified into environment and human health impacts. Past work has shown that the risks must be considered in terms of a time and space matrix. The time categories of short, medium and long can be designated depending on the impact being considered. In the case of nuclear power, the short-term can be considered to be 1 year, the medium-term would be an average person lifetime and long-term would stretch into future generations. The context of space can be generally divided into local, regional and global. For the different populations (worker, public) and situations (normal, accidental) the impacts would fall into different categories of the time-space matrix.

Within the context of the comparison of energy systems, there has been a lot of work on the definition and quantification of common risk indicators that allow for direct comparison between the fuel cycles being considered. For the purpose of testing the feasibility of using Multi-Attribute Utility Analysis (MAUA) to conduct a comparative analysis between coal and nuclear fuel cycles, it was only possible, in a first step, to consider the indicators for impacts to human health. The second step started directly with the monetary valuation of the health and environmental indicators and was mainly devoted to the delineation of the framework allowing to take into account the social attitude towards the risk within the decision-making process for energy policy.

Multi-attribute utility analysis principle

The underlying principle behind a multi-attribute utility analysis is that a complex problem can be divided into a number of smaller decisions. The dimensions and attributes underlying each decision can be taken into account. The results of the smaller decisions are re-assembled to provide an overall decision on the larger picture. The attributes are defined as the factors that the decision-makers find relevant to the problem to be considered. MAUA provides a structure and process to

be used by the decision-makers in considering these decisions. During this process, criteria are developed and structured according to priorities. Weights are assigned to the criteria and indicators are developed so that each criteria can be scored in a qualitative or quantitative way. One of the largest difficulties in using this methodology is the determination of the appropriate weights for the criteria. It is expected that these are influenced greatly by the background and interests of the group making the decisions.

MAUA for the comparison of nuclear and coal fuel cycles

The CEPN has conducted a multi-attribute utility analysis on the health impacts of the nuclear and coal fuel cycle, based on the results that have been published by CEPN and IER within the framework of the ExternE project of the European Commission. Because the comparison of two options was too simplistic, two other "options" were created by including additional information on the minimum risk for each fuel cycle. Thus, the multi-attribute utility analysis has been performed with four options: 'nuclear', 'coal', 'minimum coal' and 'minimum nuclear'.

The criteria that have been selected reflect the different risk dimensions that exist, according to the situation (normal or accidental), the group of population exposed (public or workers), the time and space definition of the impact (local, regional global and short, medium and long term) and finally the severity of the health impacts (mortality or morbidity). Figure 1 illustrates the criteria and the risk indicators considered for the two fuel cycles in the first part of the study and includes the simple assumptions for the corresponding weights that were assigned. It must be stressed that the weights were simply apportioned between the criteria and are not intended to represent reality as far as the main objective of this first analysis was to demonstrate the advantages and limitations of using MAUA.

A sensitivity analysis has been conducted by giving different values to the criteria. In general, the variation of the weighting factors concerning the type of populations exposed or the time distribution of the effects leads to an important change in the final score of the different scenarios, as well as the use of a public risk aversion coefficient.

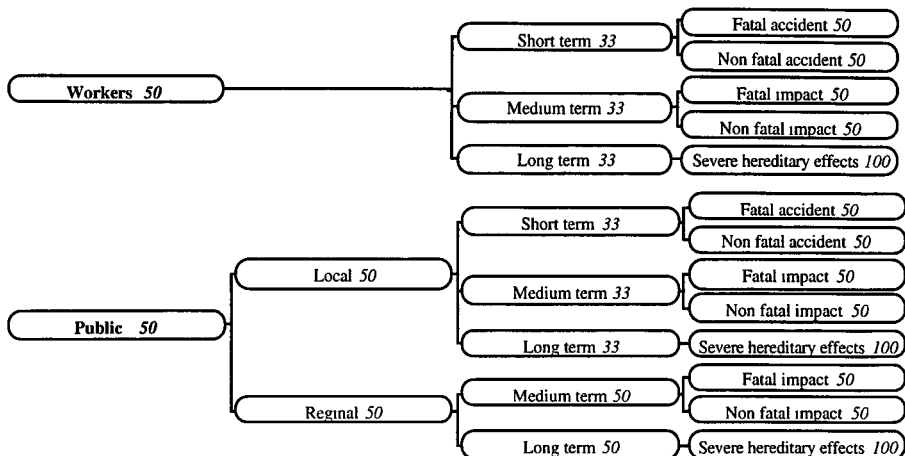


Figure 1. Weights assigned to the criteria used in the feasibility study

For the four options designated (coal, nuclear, minimum coal, and minimum nuclear) it was not possible to directly compare the impact of a severe nuclear accident with the coal fuel cycle because an equivalent analysis does not exist for the coal fuel cycle. To integrate the impacts of a severe nuclear accident into the study, the results were weighted and added to the normal operation impacts for the nuclear options. It was decided that the public's aversion to risk would be used in weighting the impacts of an accident. Risk aversion has been estimated to increase the impacts by an exponential factor of 1.2 to 2 for nuclear issues. For the feasibility study, a constant value of 1.2 was applied to the impacts from a severe nuclear accident and the impacts were added to the normal operation impacts.

In choosing a utility function for scoring the estimated risks (impacts) of the fuel cycle options, a different consideration for risk aversion was also required. It was considered that the populations' aversion to risk increases with the increasing magnitude of risk, regardless of the origin of the risk. With this in mind, an evolving risk aversion utility function was chosen. If the risk aversion factor is noted as a , then the shape of the utility function is defined by $0 < a(\text{minimum risk}) < 1$ and $a(\text{maximum risk}) > 1$. This is illustrated in the [Figure 2](#) below.

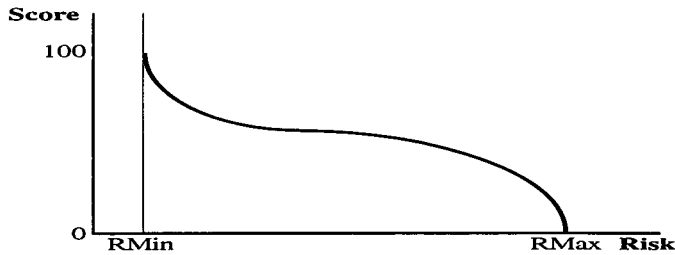
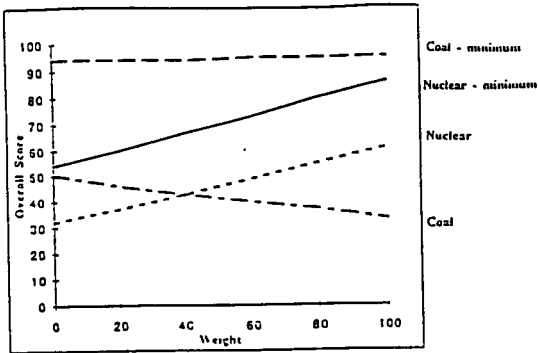
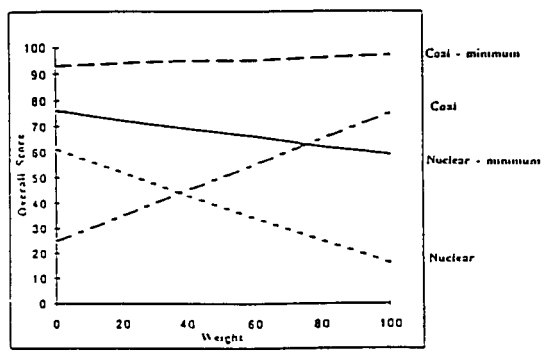


Figure 2 . Utility function for an increasing aversion to risk

Using the data collected, a test case was run to compare the 4 options assuming a utility function as illustrated above. This was then used to test the sensitivity of the system to the variation of the weights assigned to the criteria (Figure 1). Figures 3 illustrates some of the overall scoring results for the 4 options, given the simplistic assumptions that were taken. Figure 3a presents the variation of the score according to the weights assigned to the worker and public impacts. If they are equally weighted (both 50%), the ranking of the options is minimum coal, minimum nuclear, nuclear and coal (from best to worst). If the weight is increased on the impacts of workers and therefore the weight of the impacts on the public is decreased, the order of the ranking does not change significantly, even though the utility of coal decreases. If the weight of worker impacts is decreased, the ranking between coal and nuclear change. Figure 3b illustrates the sensitivity of varying the weight given to the long-term health effects of workers in comparison to the weight given to the short- and medium-term effects. In this case, increasing the weight slightly changes the ranks of coal and nuclear.



(a) workers/public



(b) workers:
long-term/low, medium-term

Figure 3. Sensitivity analysis of weights assigned to criteria

The sensitivity of the resulting ranking of the 4 options to the risk aversion factor, for the impacts of a severe nuclear accident, was tested by varying the aversion factor, over the 1.2 to 2 range, while keeping rest of weighting factors unchanged. Figure 4 illustrates how important the choice of values for this factor can have in the final outcome of the ranking.

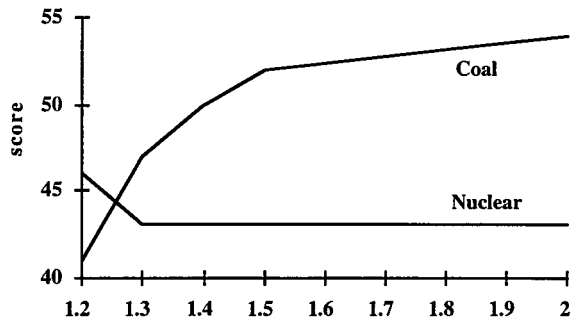


Figure 4. Impact of risk aversion factor on the score of the Coal and Nuclear Fuel Cycles

From these results, it can be seen that the first difficulty of performing a MAUA concerns the aggregation of the impact indicator. For this first analysis, only health impacts were considered allowing to combine them and pointing out the influence of the weights for the main dimensions of the risk.

MAUA and willingness to pay approach

Because of the major difficulties which emerged during the first analysis for the aggregation of the indicators, the second step of the project explored the possibility to develop a methodology for the comparative analysis of fuel cycles using MAUA, on the basis of the monetary valuation of the impacts. Therefore, the second stage of the study was to determine the weight of the different criteria based on the costs of the impacts calculated with the willingness-to-pay method (WTP). Indeed, it is assumed that with the WTP approach, a certain weight is already included in the costs and the main advantage is to allow direct comparisons of the various indicators avoiding to ask the decision-makers to rank the large list of indicators without any information concerning their relative importance. On this basis, several sensitivity analyses were performed in order to take into account the sensitivity of the total external cost of the impacts to the weight assigned to the some of the dimensions of the risk: i.e. public versus workers, local versus regional, normal versus accidental, “classical risk” versus radiological effects. Figures 5a and 5b present, respectively for the nuclear fuel cycle and the coal fuel cycle, the variation of these categories of

costs in the total external cost when one death for a member of the public is weighted higher than one death for a worker. On these curves, R reflects the contribution of the radiological risks in the total external cost, L the contribution of the local impacts, N the contribution of the normal situations, T the contribution of the occupational impacts. Figure 6 presents the same analysis when the accidental situation is weighted differently than the normal situation. In that case, only the external cost associated with the nuclear fuel cycle is affected.

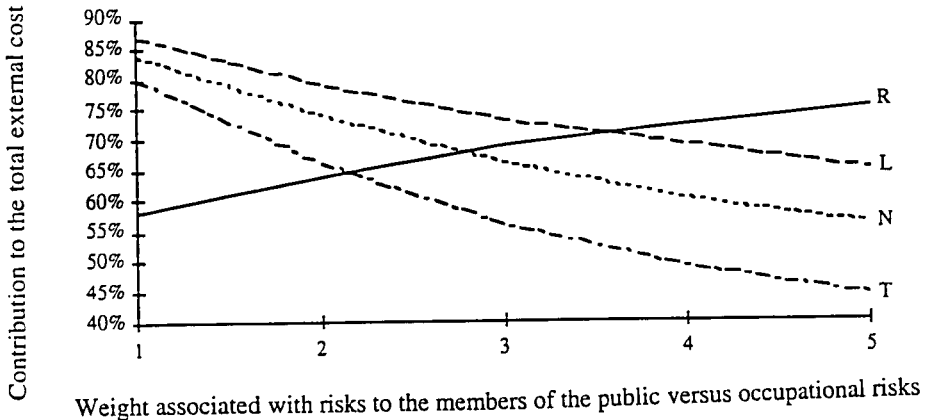


Figure 5a. Contribution of each category of risk in the total external cost for the nuclear fuel cycle according to the weight associated with the impacts to the members of the public

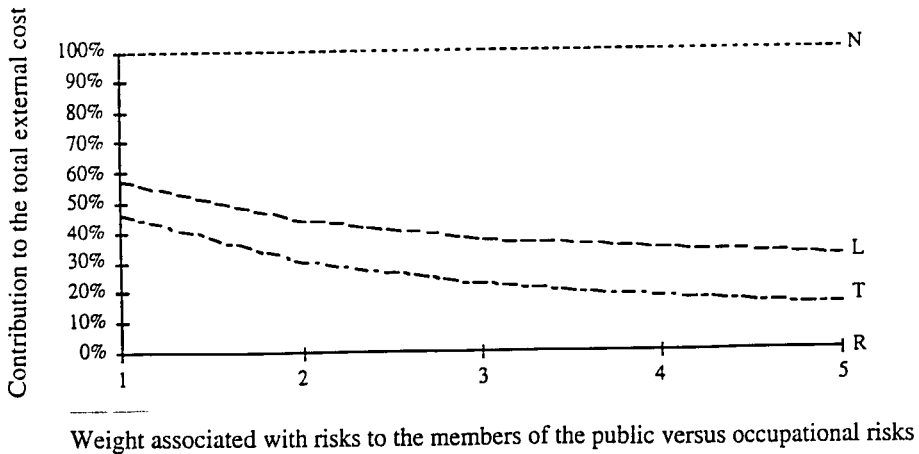


Figure 5b. Contribution of each category of risk in the total external cost for the coal fuel cycle according to the weight associated with the impacts to the members of the public

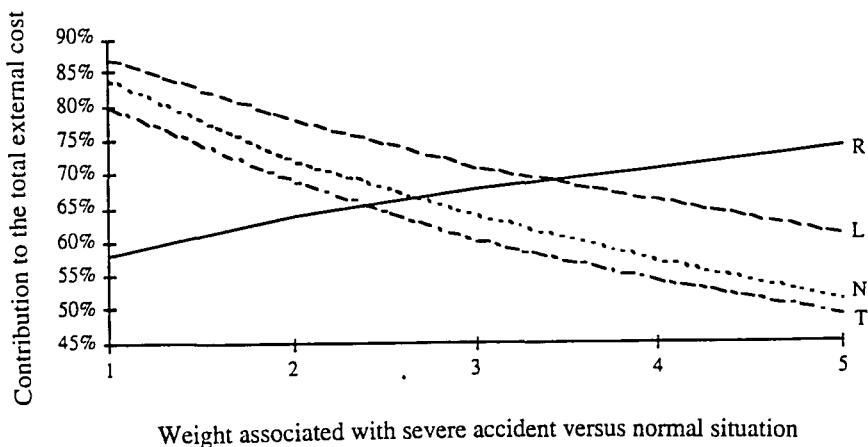


Figure 6. Contribution of each category of risk in the total external cost for the nuclear fuel cycle according to the weight associated with the severe accident

Need for the elicitation of decision-makers preferences

From these analyses, the general framework allowing a comparative assessment of the health and environmental impacts for nuclear and coal fuel cycles has been delineated, but do not provides precise results that can be used to rank the energy systems. Indeed, the results of this multi-criteria analysis are very limited: the environmental effects have to be further developed, a lot of arbitrary choices have been done, particularly with the use a certain value for the risk aversion, the utility functions or the weighting factors....

These analyses point out the need for a global approach reflecting the “trade-off” of the society as far as the risk is concerned. For this purpose, the multi-attribute analysis should be a useful tool allowing to deal with the preferences between present and future generations, the risk aversion towards accidental situations, the regional and global impacts characterised by very low individual risk but concern a large population, the importance of environmental impacts... This study demonstrates the need for further developments to elicit the preferences of the decision-makers regarding the various dimensions of the risks. These preferences will be very specific to the population concerned with the ranking of the options. The advantage of using MAUA, is that it is possible to work interactively with the software and the people that are making the choices.

PUBLICATIONS

Dreicer, M., Kuentzmann, P., Schneider, T., Krewitt, W., 1994 "The use of multi-attribute analysis for comparing the health and environmental impacts of different fuel cycles - a feasibility study for the comparison between coal and nuclear fuel cycles", Proceedings of PSAM II, San Diego, USA.

Kuentzmann, P., 1993 "Analyse multicritères pour la comparaison des risques sanitaires et environnementaux associés aux filières nucléaire et charbon", CEPN-Report.

Kuentzmann, P., Dreicer, M., 1995 "Analyse multicritères et consentement à payer : comparaison des filières charbon et nucléaire", CEPN-Report.

Head of project 2: Dr. Friedrich

II. Objectives for the reporting period

Based on the work carried out under a previous contract, the development of a conceptual framework supporting risk assessment and risk comparison had to be completed, focussing on the quantification of health risks from airborne pollutants from the coal fuel cycle. A set of appropriate air quality and dose-effect models had to be identified and implemented. Health effects resulting from the operation of a reference coal fired power station were to be estimated and provided as an input to the comparison of risks from the coal and the nuclear fuel cycle based on the concept of Multi-Attribute-Utility Analysis. The approach of Multi-Attribute-Utility Analysis and the concept of External Costs had to be evaluated on a theoretical level with regard to their use for risk comparison.

III. Progress achieved including publications

1. Development of a consistent framework for risk assessment - the issue of system boundaries

The geographical range of analysis

Analysing health and environmental impacts from air pollution, there are no clear guidelines that suggest appropriate system boundaries for impact assessment in terms of geographical distance from the source of pollutants. The analysis of impacts is often restricted to a distance of up to several tens of kilometers from the source, assuming that the main portion of impacts would occur within this area. Using linear dose-response functions, a simple conservation of matter argument leads to the conclusion that the range of analysis needs to cover a distance of up to several hundreds of kilometers in order to capture a major fraction of the expected impacts.

System boundaries with regard to the technical process steps considered

A consistent definition of system boundaries with regard to up- and downstream process steps linked to the energy system is required for comparison of different energy systems. A new concept of combining micro and macro analysis techniques was proposed to quantify occupational health risks. While process analysis traditionally used in risk assessment studies

provides process specific results with a high accuracy, the data requirement is prohibitive for a full life cycle analysis, so that Input-Output Analysis as a macro analysis tool might be used to analyse up- and downstream process steps. Results indicate that risks from up- and downstream process steps due to electricity production in a coal fired power plant amount to 10 - 20% of the risks from activities on the first order process chain (i.e. coal mining, coal transport, power plant operation, waste disposal).

2. Public Health Effects

The incremental air pollution attributable to power generation is a mixture of pollutants mainly emitted from the power station and those formed subsequently as the emissions interact with the external environment. The air pollutants considered are particulates, SO₂, NO_x, ozone and aerosols. Ambient air concentrations of primary pollutants on a local scale were assessed using a Gaussian plume model. The Windrose Trajectory Model (WTM) that has been developed at IER based on the Harwell Trajectory Model was used to estimate the concentration and deposition of acid species on a regional range. Health impacts from increased levels of airborne pollutants were calculated using a set of exposure-response functions recently compiled by the EU ExternE Project (Joule Programme) based on a comprehensive literature review. While direct impacts from SO₂ and NO_x are assumed to be negligible, health effects are dominated by secondary particulates (sulfate and nitrate aerosols) subsequently formed from gaseous SO₂ and NO_x emissions. For the implementation of the impact assessment procedure, the computer system ECOSENSE has been developed at IER. ECOSENSE is an integrated tool for environmental impact assessment, combining an extensive database on European-wide meteorological and receptor specific data with a set of air quality and dose-effect models.

Mass balance studies reveal that coal combustion in power plants produces a selective partitioning of trace elements between various exit streams which is based on a volatilization/condensation mechanism. Both the FGD-plant and the electrostatic dust precipitator are considerable sinks for trace elements, so that elements of major health concern like lead, cadmium and arsenic were not detectable in the flue gas after FGD in mass balance studies carried out in German power plants.

Based on the methodological approach described above, health risks from power plant operation have been quantified, resulting in a wide range of different health impacts, including e.g. 2.9 additional deaths, 11 350 restricted activity days or 179 490 symptom days per TWh within the European population.

3. Occupational Health Risks

As the comparative risk assessment should focus on the marginal (i.e. the additional) risk which is induced by adding one specific unit of a technology to the existing system, the concept of net-risk has been introduced, taking into account only the difference between the risks of average industrial activities and the specific activity related to the fuel cycle of concern. The concept of net risk has major implications on the comparison of impacts between different fuel cycles, in particular if work intensive technologies like e.g. photovoltaic are considered.

Occupational health impacts were assessed by evaluating occupational health statistics. In the case of diseases occurring after a long time latency period like e.g. lung cancer from exposure to radon in underground mining or coal workers' pneumoconiosis (black lung), dose-effect models were used to estimate impacts from today's exposure conditions. The occupational risks from the German coal fuel cycle are mainly dominated by fatal accidents in underground mining activities.

4. Framework for Risk evaluation and Risk Comparison

The time and space dimensions of risk

The so called "Time and Space Matrix" has been established to consistently present risks on the different time and space dimensions. In the absence of reliable exposure-effect relationships for chronic mortality, the present analysis mainly focuses on the quantification of acute health impacts. However, there is strong evidence that health effects from chronic exposure might result in a considerable contribution to the overall risks. Occupational health risks are restricted to the local range and are clearly dominated by acute effects. A small amount of medium term risks result from occupational diseases with a long latency period like coal worker's pneumoconiosis or lung cancer from exposure to radon in underground mining.

Integration of health risk indicators into the Multi-Criteria Analysis framework

Based on monetary values derived for a set of health impacts in the EU ExternE-Project (JOULE Programme), a preliminary weighing scheme was set up to facilitate the use of the available health indicators in the Multi-Criteria Analysis framework. Current results show that a further aggregation is necessary in order to provide an operational weighing scheme.

From a comparison of cost-benefit analysis and multi-attribute utility analysis on a theoretical level it was concluded, that - in the case of using individuals' preferences as a basis for risk evaluation - cost-benefit analysis seems to be the more consequent and consistent approach. However, since in the field of environmental risk assessment we are far away from being able to transfer all the environmental consequences correctly to monetary values, there is a need to consider monetary cost-benefit analysis and non-monetary multi-criteria approaches as complementary rather than competitive approaches.

Publications

Krewitt, W., Mayerhofer, P., Friedrich, R., Greßmann, A., Dreicer, M.: *External Costs as an Indicator for Comparative Risk Assessment of Different Energy Systems - a Case Study for Comparing the Nuclear and the Coal Fuel Cycle*, in: An International Conference Devoted to the Advancement of System-based Methods for the Design and Operation of Technical Systems and Processes, Proceedings of the PSAM-II, Vol. II, San Diego, USA, March 20-25, 1994, pp. 067/13-18

Dreicer, M., Kuentzmann, P., Schneider, T., Krewitt, W.: *The Use of Multi-Attribute Analysis for Comparing the Health and Environmental Impacts of Different Fuel Cycles - A Feasibility Study for the Comparison between the Coal and Nuclear Fuel Cycles*, in: An International Conference Devoted to the Advancement of System-based Methods for the Design and Operation of Technical Systems and Processes, Proceedings of the PSAM-II, Vol. II, San Diego, USA, March 20-25, 1994, pp. 067/19-24

W. Krewitt, Hurley, F., Trukenmüller, A., Friedrich, R.: *Health Risk Assessment from Fossil Electricity Generation*. Paper presented at the annual meeting of the Society for Risk Analysis "Risk Analysis and Management in a Global Economy", Ludwigsburg, May 21-24, 1995

Krewitt, W., Friedrich, R.: *Health Risks of Energy Systems*. Proceedings of the International Symposium on Electricity, Health and the Environment, Vienna, 16-19 October 1995, to be published.

Head of project 3: Dr. Uijt de Haag

2 Objectives for the reporting period

In the project, energy fuel cycles are to be compared in a Multi Attribute Utility Analysis (MAUA). Therefore, criteria have to be developed to weigh their (environmental) impacts. The main objective for the reporting period was to develop a set of environmental indicators, which could be used as criteria in a MAUA.

Furthermore, it is recognised that the uncertainties associated with the calculation of the various impacts is important to the weighing of the impacts. Hence the second objective was to perform a global analysis of the uncertainty associated with the risk assessment.

In brief, the two distinct objectives for the reporting period are: (1) the development of a set of environmental indicators and (2) a global investigation of main sources of uncertainty.

3 Progress achieved including publications

3.1 Requirements on environmental indicators

In a Multi Attribute Utility Analysis (MAUA) of energy fuel cycles, the impacts of different energy fuel cycles have to be compared. Therefore a set of criteria to weigh the environmental impacts has to be developed: the environmental indicators.

Environmental indicators describe the impacts of the fuel cycles on the environment and can be defined in every step in the calculation of the risk (see Figure 1). Different kinds of indicators were studied, varying from stress or pressure indicators, which are related to the emissions of the energy systems, to state or effect indicators describing the quality of the environment and the quality and quantity of the resources.

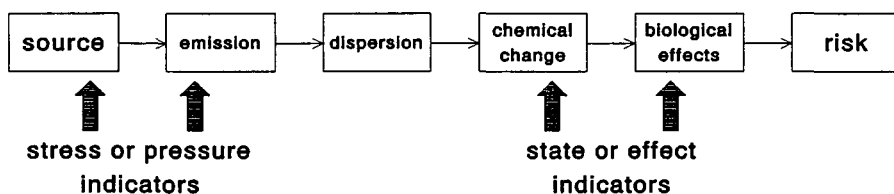


Figure 1 The different steps in a risk assessment and the various environmental indicators.

When defining indicators for the comparison of the environmental impacts of different energy fuel cycles in a MAUA, it is necessary to examine the demands imposed on the set of indicators by the user and by the intended application. It is assumed in this study that the user is a policy-decision maker, who wants to make a comparison between a number of different options for electricity generation. Keeping this in mind, the following demands are distinguished:

- **Limited number - highly aggregated**

When comparing energy fuel cycles in a MAUA a limited number of criteria should be used, otherwise the decision support system is blurred with detail. The indicators

should therefore be as aggregated as possible. It is not useful to distinguish too many end-points and environmental effects. It is therefore suggested to combine similar environmental effects into environmental issues, and to use one single indicator for each environmental issue. In this way approximately ten environmental indicators are necessary to describe the environmental impacts. A number of relevant environmental issues are given in Table 1 (based on e.g. [RIVM94]).

Table 1 Environmental issues for use in the aggregation of environmental indicators.

Changes in climate (greenhouse effect)
Depletion of the ozone layer
Eutrophication of waters and soils
Acidification of waters and soils
Photochemical oxidants/ground-level ozone
Contamination with (organic) toxic substances
Contamination with radionuclides
Contamination with heavy metals
Use of renewable natural resources biomass, fish, wood, water, ...
Use of finite natural resources metals, minerals, fossil fuels, ..
Exploitation of land for construction and infrastructure
Soil degradation desertification, erosion, dehydration

- **Sensitivity to environmental impacts**
For the comparison of the energy fuel cycles in a MAUA, the indicator must be sensitive to the environmental impacts and must reflect changes in the environment due to the emissions from an energy fuel cycle.
- **Availability of data**
To calculate the value of an indicator, it is important that all data are available with the required spatial and temporal resolution. Extrapolation or interpolation of data with different resolution introduces additional uncertainties.
- **Related to the cause - effect chain**
The indicator for the environmental impact must be clearly related to the emissions of the energy fuel cycle. For instance, if the relationship between an observed environmental effect and the emission of the fuel cycle is not well established, it is more useful to define an indicator in the beginning of the chain, i.e. a pressure indicator or a chemical state indicator.

- **Easy to interpret, direct appeal, international consensus**

The indicator must be easy to interpret: complex biological and chemical indicators lack a direct appeal. An indicator which has a direct relationship with environmental policy planning is preferred.

Based on these demands, the advantages and disadvantages of various kinds of environmental impact indicators are determined. Sustainable development, being a starting point in the Dutch national environmental policy planning, is used as keyword in the development of the environmental indicators. It appeared that non-location specific environmental impacts are described with pressure indicators, whereas for location-specific environmental effects indicators based on no-effect levels and critical loads are proposed.

In this report some examples of environmental impact indicators for application in a MAUA are presented. The issues 'use of finite natural resources' and 'climate change' are used to illustrate the non-location specific indicators. The issues 'acidification', 'radionuclides' and 'heavy metals' demonstrate the way location-specific indicators are defined. To show the computability of the indicators, worked-out calculations are given for the reference plant located on a hypothetical site in the middle of the Netherlands.

3.2 Examples of environmental indicators

3.2.1 Use of finite natural resources

Non-renewable energy sources, such as combustion of fossil fuel and nuclear fission, make use of a finite supply of resources. The use of finite resources reduces their availability in the future. Scarcity leads gradually to the exploration of lower grade ores, at the expense of secondary energy resources and land area.

The availability of uranium and coal is not a local affair, and does not depend on the location of the power plant. Therefore it is best to describe the environmental impacts by a pressure indicator, based on the ratio between the amount of required material and the total amount of available material. Measures of the available amount are either the reserves (stocks with proven occurrence, exploitable at current market prices with present-day technology) or the resources (stocks likely to be present, exploitable at a specified price level with technology likely to become available). For the example of uranium, the reserves would include all the uranium present in high grade ores (defined as uranium contents more than 0.05%) and exploitable at a price level of less than the current market price. For the example of uranium, the resources would comprise the estimated amount, which is likely to be present and exploitable at a cost price lower than (for example) \$260/kg U. Also the uranium in sea water, present in a concentration of 3 mg per cubic meter and presumably exploitable at exploitation costs of \$500-\$800 per kg U, might possibly be included in the resources.

The definitions indicate that it is hard to define conclusively the amount of material available: both reserves and resources are not measures of the occurrence of a material only, but include the efforts of the industry and the operation of the economic market. Still, an indicator based on the ratio between the amount of required material per unit electricity produced and the reserves gives insight in the expenditure of the finite amount of material.

3.2.2 Global warming

The 'greenhouse' gases play an important role in the radiation balance of the Earth as they absorb and re-emit part of the outgoing infra-red thermal radiation of the Earth's surface. Consequently, the Earth loses less heat to space by radiation than it would in the absence of the greenhouse gases.

The most important greenhouse gases are water vapour, carbon dioxide, methane, ozone, nitrous oxide and chlorofluorocarbons (CFCs). Their concentration, with the exception of that of water vapour, is influenced by human activities and have been increasing since pre-industrial times. The increase is likely to affect the radiation balance of the Earth and consequently the climate.

An important source for the emission of carbon dioxide to the atmosphere is the combustion of fossil fuels, whereas coal mining may lead to the release of methane. In the nuclear fuel cycle, the emission of greenhouse gases occurs due to e.g. construction and transportation. However, these contributions are small in comparison with the emissions related to mining and combustion of coal.

The prediction of the climate change and the environmental impacts, especially on a regional scale, has a large uncertainty, due to combined uncertainties in the various long-term emission scenarios and in the understanding of the processes and feedback mechanisms in the climate. However, to determine the environmental effects of the emission of greenhouse gases, all possible direct and indirect effects have to be quantified on a regional scale. Due to the large uncertainty it is not possible to quantify the environmental impacts of the emissions of a single power plant. Therefore a state or effect indicator is not applicable. Furthermore, the impacts do not depend on the location of the power plant. It is therefore proposed to use a pressure indicator. The pressure indicator describes the emission of greenhouse gases in kg per year or kg per kWh, weighed with the ability of the gas to contribute to the climate change, the Global Warming Potential (GWP). The value of this indicator has no direct relation with environmental effects. However, policy plans and international agreements are stated in terms of reductions of greenhouse gas emissions [RIVM94]. The value of the indicator related to the total emission shows directly the contribution of the fuel cycle to the total emission and to the reduction required.

3.2.3 Acidification and eutrophication

Major contributors to the soil acidification and eutrophication process are the inputs of sulphur dioxide and nitrogen dioxide produced by the burning of fossil fuels. Since nitrogen deposition contributes to both the acidification and the eutrophication process both effects have to be examined in one.

A main disadvantage of a pressure indicator for acidification and eutrophication is that the impacts of nitrogen and sulphur deposition depend on site specific soil properties, type of ecosystem and climate. By using a chemical state or effect indicator this location specific information can be taken into account. Therefore, it is recommended to assess the impacts of acidification based on the critical load concept, being a widely used and generally accepted environmental indicator. The critical load concept is an approach for estimating the quantity of pollutants that can be absorbed by sensitive ecosystems on a sustainable basis. A critical load provides a value for the maximum allowable load of one or more pollutants at which risk of damage or ecological changes to the most sensitive part of an ecosystem is negligible.

To demonstrate the calculation process example calculations are performed for a reference coal fired power plant and for two locations in the Netherlands (Figures 2 and 3).

SO_x and NO_x depositions resulting from the releases by the reference power plant used in the coal fuel cycle are calculated with the OPS dispersion model, a modified Gaussian plume model. Emissions are based on the emissions of the reference plant at Lauffen. About 0.8 g/kWh_{el} SO₂ and 0.8 g/kWh_{el} NO_x are emitted by the reference power plant.

Critical load data on an ecosystem scale are not available yet. However, critical load maps for NO_x and critical deposition maps for SO_x, calculated by the Dutch NFC, are available on a 10 x 10 km² grid [SC93; CCE93]. In Figure 4 and 5 the ratio of the total deposition of SO_x respectively NO_x and the critical load for SO_x respectively NO_x are presented.

An indicator for acidification expressed as a single number is now calculated as the ratio between the total amount of acidifying deposition and the critical load, summed over the grid:

$$\text{Ind}_{\text{CL}} = \sum_i \frac{\text{deposition}_i}{\text{critical load}_i} \times \text{area}_i$$

where:

- Ind_{CL} = the value of the indicator [km²] for acidification and eutrophication
- deposition_i = the deposition of acid equivalents per unit area per year [Aeq.km².a⁻¹]
- critical load_i = the critical load of grid cell *i* [Aeq.km².a⁻¹]
- area_i = the area of grid cell *i* [km²]

It can be concluded that in each grid cell the deposition of SO_x and NO_x is at least a factor 100 less than the critical depositions for SO_x and the critical loads for NO_x respectively. The indicator for SO_x is calculated at 2.1·10⁻³ km².MW⁻¹ and the indicator for NO_x is calculated at 1.2·10⁻⁴ km².MW⁻¹ for the reference plant situated in the middle of the Netherlands. This shows that the contribution of coal combustion to acidification is dominated by the SO_x emissions.

A possible modification of this indicator would be the inclusion of the current level of acidifying deposition emitted by industry, traffic and agriculture.

3.2.4 Contamination with radionuclides

When assessing the risk of the emission of radionuclides, the calculation of the impact is usually restricted to the damage to human health. The detrimental effects to the environment are neglected, following the principle that the standard of environmental control protecting humans to the degree currently thought desirable will ensure that other species are not put at risk.

The regular emissions of radionuclides in the energy fuel cycles is usually in inhabited regions and the resulting radiation dose to humans is in general below the standards set. Nevertheless, radionuclides accumulate in the environment, which may lead to a decreased utility value for future generations. Therefore it is important to quantify the contamination of the environment and to develop an indicator to determine the impact on the environment associated with the releases within the energy fuel cycles.

The indicator for the environmental impacts of radionuclides should be comparable to the indicator for e.g. heavy metals and acidifying compounds. It is proposed to use an

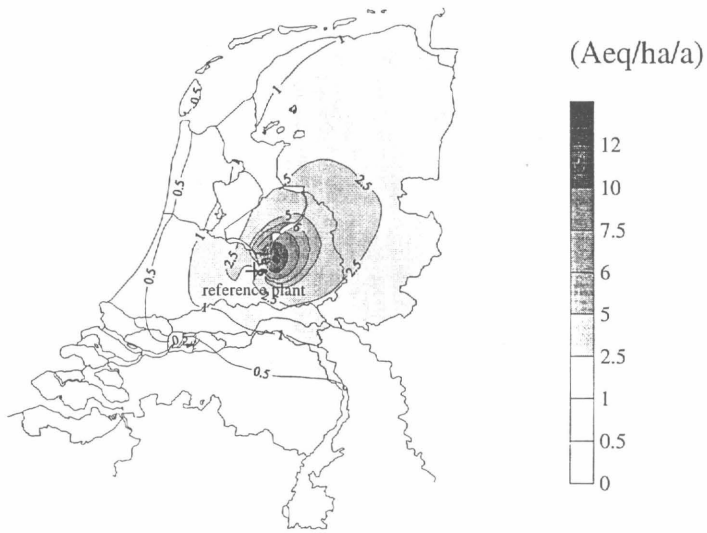


Figure 2 Total deposition of SO_x ($\text{Aeq}\cdot\text{ha}^{-1}\cdot\text{a}^{-1}$) emitted by a coal fuel reference plant located at the centre of the Netherlands.

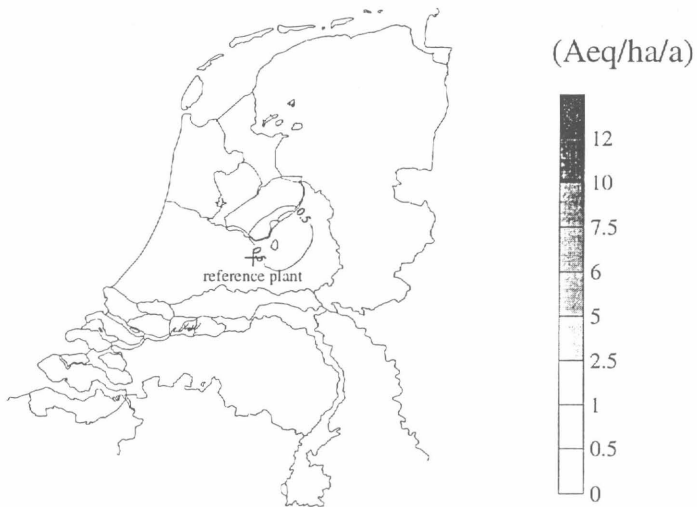


Figure 3 Total deposition of NO_x ($\text{Aeq}\cdot\text{ha}^{-1}\cdot\text{a}^{-1}$) emitted by a coal fuel reference plant located at the centre of the Netherlands.

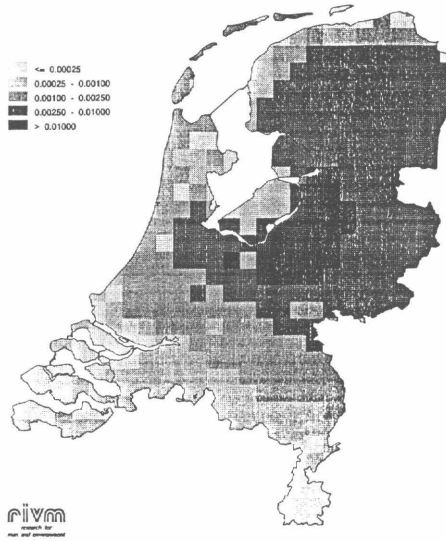


Figure 4 Ratio between the total SO_x deposition and the critical load for SO_x for the reference power plant in the middle of the Netherlands.

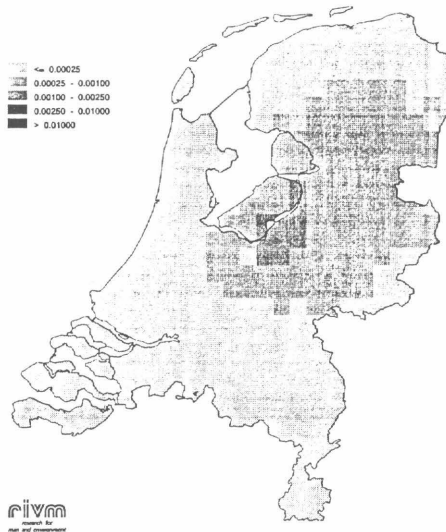


Figure 5 Ratio between the total NO_x deposition and the critical load for NO_x for the reference power plant in the middle of the Netherlands.

environmental impact indicator for radionuclides based on the ratio between the dose to (concentration in) the environment and the no-effect level (concentration). In the indicator presented the only location specific information is the ecosystem used, e.g. terrestrial or aquatic. However, a location-specific background radiation is present, which could be included in the indicator.

With respect to protection of ecosystems, dose limits are set for populations rather than for individuals. This means that occasionally individual members of non-human species might be harmed, but not to the extent of endangering whole populations or creating imbalance between species. It is suggested to set the no-effect level for terrestrial animal populations, terrestrial plant populations and the maximally exposed individuals in the aquatic environment at 1 mGy.d^{-1} , 10 mGy.d^{-1} respectively 10 mGy.d^{-1} in case of chronic irradiation, based on the review of effects of ionizing radiation on plants and animals [IAEA92]. With respect to acute exposure, a dose limit of 0.1 Gy appears to be a sensible level for populations or communities of terrestrial plants or animals [IAEA92].

To demonstrate the calculation process, an example calculation is performed for an imaginary reprocessing plant located in the centre of the Netherlands (Figures 6 and 7). The radiation dose to biota are calculated using a simple chain model based on transfer factors. The assessment end-points used are cattle, sheep, soil organisms, grass and plants, as data for these biota were available. How far these assessment end-points represent a natural ecosystems is subject of further study.

The maximum dose for ^{129}I to grass, plants, cattle, sheep and soil organisms is $1.1 \cdot 10^{-10}$, $2.9 \cdot 10^{-10}$, $3.4 \cdot 10^{-10}$, $4.2 \cdot 10^{-11}$ and $1.1 \cdot 10^{-15} [\text{Gy.a}^{-1}]$ respectively. This is well below the no-effect level of 0.37 Gy.a^{-1} . Summing the ratio between the dose and the no-effect level over all grid cells results in an indicator value comparable to the indicator for acidification. The value of the indicator for ^{129}I is calculated at $1.3 \cdot 10^{-7} \text{ km}^2 \cdot \text{MW}^{-1}$ for plants and $1.7 \cdot 10^{-6} \text{ km}^2 \cdot \text{MW}^{-1}$ for cattle.

The results show that the regular emission of radionuclides to air within the nuclear fuel cycle and during normal operation does not have significant effects on the environment. In case of a major nuclear accident calculations indicate that no-effect levels may be exceeded in an area close to the reference plant.

3.2.5 Heavy metals

The release of heavy metals as a result of electricity generation may lead to undesirably high concentrations in soil, surface waters and drinking waters. No generally accepted indicators which describe the impacts of heavy metals on soil and soil water were found. Several countries have standards for the maximum concentration of heavy metals in agricultural products or legislation with respect to the cleanup of polluted soils. However, these standards are based on different starting points and objectives, and are therefore not directly applicable to the comparison of energy fuel cycles.

If the assessment of impacts of heavy metals is based on an environmental stress indicator like e.g. emission equivalents, being the total emission within the fuel cycle, the calculation is very straightforward compared to other options. The main disadvantage of this type of indicator is that site-specific elements are neglected and the relation to environmental damage is not obvious. Therefore, we selected an indicator which is based

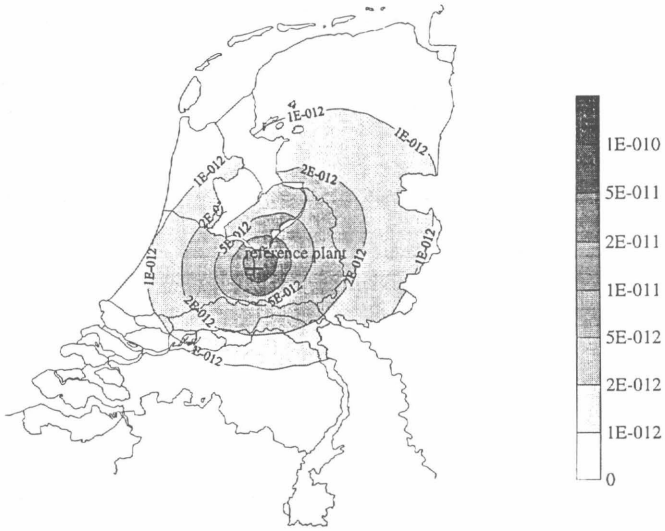


Figure 6 Ratio between the total dose on cattle for ^{129}I and its no-effect level.

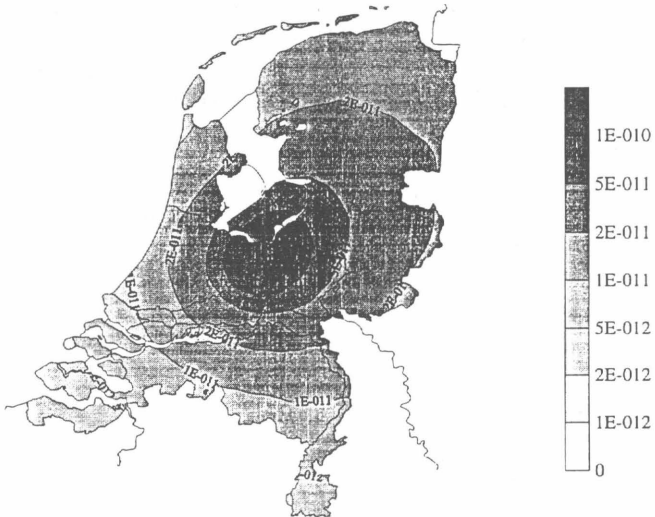


Figure 7 Ratio between the total dose on plants for ^{238}U and its no-effect level.

on the no-effect concentration of each single heavy metal.

Negative effects of heavy metals on plants, animals or humans are assumed not to occur below a threshold value, the no-effect level (NEL). For each ecosystem a different NEL can be defined, and the concentration of heavy metals in soil or surface waters due to emissions within the fuel cycles can be compared with the NEL. In this way, site specific information is incorporated.

The calculation of the indicator for acidification resembles that of the indicator for heavy metals and radionuclides. All indicators are based on no-effect concentrations and have the same units, which will make comparison more easy.

3.3 Uncertainty

The inclusion of the uncertainty is important in the decision-making process. An activity may appear to obey the regulation standard when expressed as a single number, and a permit might be granted. However, when the uncertainty in the result is considered, there can be a possibility that the regulation standard is exceeded. The potential of exceeding the standard might be considered to be too great, and a permit may be denied. This potential becomes clear only when uncertainty is taken into account.

Uncertainty is also of importance in the ranking of alternatives, especially if the weighing function between alternatives is a non-linear function. The utility function in a Multi Attribute Utility Analysis may value the upper part of a distribution much higher than the lower part of a distribution to account for risk aversion factors. The order of the scores of two alternatives on a criterium may therefore be interchanged if uncertainties are taken into account.

It is therefore clear that uncertainties play an important role in the comparison of energy fuel cycles. However, up to now the investigation on uncertainty has been limited. Only a small sensitivity analysis is performed, focusing on the importance of the location of the reference plant on the indicator value for acidification. It appeared that shifting the location of the reference plant from the centre of the Netherlands to the West coast resulted in a decrease of the indicator value with only 10%. It is concluded that the uncertainty in the models is therefore much larger than the variation due to the location. However, a complete uncertainty analysis remains to be done.

3.4 Conclusions

A number of environmental indicators for application in a Multi-Criteria Analysis as a decision support system for policy decision makers have been investigated. For environmental problems with an impact that is not location specific, like the depletion of natural resources and the emission of greenhouse gases, it is proposed to use a pressure indicator. If the environmental impacts are location specific, like acidification and eutrophication and pollution with heavy metals and radionuclides, it is proposed to use an indicator based on no-effect levels.

It is demonstrated that the values of the indicators can be readily calculated from the data available. However, the usefulness of the set of indicators in a MAUA still has to be demonstrated.

3.5 References

- [CCE93] *Calculation and Mapping of Critical Loads in Europe*, CCE Status Report 1993, Coordination Center for Effects, RIVM report no. 259101003, 1993.
- [IAEA82] IAEA Safety Series 57. *Generic models and parameters for assessing the environmental transfer of radionuclides from routine releases*. IAEA, Vienna, 1982.
- [IAEA92] IAEA Technical Reports Series No. 332. *Effects of Ionizing Radiation on Plants and Animals at Levels Implied by Current Radiation Protection Standards*. Vienna, 1992.
- [RIVM94] *National Environmental Outlook 3, 1993 - 2015*. RIVM, 1994.
- [SC93] C. van de Salm, J.C.H. Voogd and W. de Vries. *SMB - a Simple Mass Balance model to calculate critical loads. Model description and user manual*. Staring Centrum, Agricultural Research Department, Technical Document 11, Wageningen, 1993.

PUBLICATIONS:

H. Jeeninga and P.A.M. Uijt de Haag. *Environmental Impact Indicators for application in a Multi Criteria Analysis*. Technical Committee Meeting on Development and Use of Environmental Impact Indicators for Comparative Risk Assessment of Different Energy Sources. IAEA Headquarters, Vienna, 3 - 6 May 1994.

EC Contract FI3P-CT920064e (Sector C13)

Studies Related to the Expression of the Detriment associated with Radiation Exposure

Final Report : July 1992 - June 1995

- 1) Muirhead NRPB
- 2) Schneider CEPN

I. Summary of Project Global Objectives and Achievements

Background and Aims

Following the publication of data on cancer risks among the Japanese atomic bomb survivors based on the DS86 dosimetry, several health effects models utilising various risk projection assumptions have been developed; for example, by the United Nations Scientific Committee on the Effects of Atomic Radiation (UNSCEAR), the International Commission on Radiological Protection (ICRP), the US Committee on the Biological Effects of Ionising Radiation (BEIR V) and NRPB. However, comparisons of radiation detriment using these models are not straightforward.

The main aim of this contract was to develop ASQRAD (Assessment System for the Quantification of Radiation Detriment), a PC-based code which provides a common framework for studying the detriment associated with radiation exposure. The code, which runs under Windows, includes the main health effects models and allows risks to different populations, including age and sex-specific groups to be investigated. It permits a review of the effects of the modelling assumptions and clarification of the important factors contained within calculations of detriment (ie. concerning the risks of fatal and non-fatal cancers and of hereditary effects). Consequently, ASQRAD has a role *inter alia* in :

- (a) decision-making, because it focuses attention on the sensitivity of estimates to the assumptions applied;
- (b) general training, since it is easy to use and comprehensive;
- (c) investigating the effect on risks of new control regimes and/or dose reduction strategies.

The sensitivity of risk calculations to the models and assumptions adopted was also examined in detail in the case of breast cancer. This analysis showed that estimates of lifetime risk

and of years of life lost can vary considerably according to *inter alia* the models used to project risks over time and across populations.

Scope and Content of ASQRAD

i) The models

The range of somatic effects models available within the program consists of the multiplicative and additive models proposed by UNSCEAR in its 1988 report and the US BEIR V Committee, as well as the models proposed by researchers at the Radiation Effects Research Foundation (RERF) and at NRPB. The model detailed in ICRP Publication 60 to quantify the hereditary effects of radiation exposure is also included within ASQRAD.

ii) The data

ASQRAD contains various sets of data, eg, demographic data, morbidity rates and fertility rates within its database facility. These tables of data, which are specific to various countries, cannot be edited or changed. However, the powerful database facility enables the user to copy any of the data provided to create duplicate tables within ASQRAD and then to edit them as desired using a spreadsheet facility. This set-up prevents the original data from becoming accidentally corrupted. The user is also able to enter new data as desired. The same format is used for the entry and editing of all types of data in ASQRAD.

iii) The types of calculation available

ASQRAD is able to perform four main types of detriment calculation, based on different combinations of individual or population exposure and somatic or hereditary effects. Each of these types of calculation has various options, which are detailed in the following table:

Calculations available	Exposure type	Exposure Duration	Age at exposure (acute exposure only)
Individual Somatic	Whole Body or Organ Specific	Acute or Extended	Single or Multiple
Population Somatic	Whole Body or Organ Specific	Acute	n/a
Individual Hereditary	Whole body	Acute or Extended	Single or Multiple
Population Hereditary	Whole body	Acute	n/a

iv) The measures of detriment

ASQRAD provides various measures of detriment depending on the type of calculation being performed.

For somatic effects the measures of detriment provided are the number of fatal cancers, the total cancer incidence and the predicted loss of life expectancy. In addition to these, a number of intermediate measures that are derived during the process of obtaining the main measures are made available to the user.

For hereditary effects the measures of detriment provided are the weighted probability of an effect and the predicted years of life lost due to hereditary effects in all subsequent generations. The distribution of these effects over the first, second, third and subsequent generations is provided for two categories of hereditary effect: mutational and chromosomal effects combined; and multifactorial effects. The measures of detriment are also provided aggregated over the two classes of effect and over all generations.

v) Types of output

ASQRAD is able to display and output measures of detriment, either as a spreadsheet or in graphical form.

The spreadsheet output takes the same form as that used to enter or edit data within ASQRAD. The only difference is that the results cannot be modified. They can, however, be transferred into a file of a suitable form for entering into commonly available spreadsheet packages. Alternatively, the measures of detriment can be output to a printer via the Windows print manager.

The graphical output can take two forms depending on the measure being displayed, namely bar charts or point/line plots. The graphical facility within ASQRAD is very flexible. It allows the user to define many of the parameters of the plot, eg. the titles of the axes, the range of the axes, the colours used in the plot and many more. Again the required graphical presentation can be output to a printer, or to a graphics file in bitmap format.

vi) User Manual

Documentation for users is available both as a manual and via an on-line help facility. This material describes not only how to run ASQRAD, but also gives some background to the models.

Peer Review

A panel of experts was assembled in 1994 to review a preliminary version of the software. The reviewers provided a range of helpful suggestions on improvements to the system, as well

as its scope. In particular, they suggested that the first version of ASQRAD should be aimed at those requiring a tool for decision making, risk communication and training, but that later versions should improve its capabilities as a research tool. Future work is planned to address the later objective.

Training Course

On behalf of the European Commission, NRPB and CEPN organised a successful ERPET training course on ASQRAD in June 1995. The course provided background to the relevant health effects models, described the scope of ASQRAD, and illustrated its application through demonstrations and syndicate exercises involving 'hands-on' experience.

Summary

ASQRAD is a flexible tool for displaying the various components of radiation detriment. By incorporating several health effects models, it enables the sensitivity of assumptions made in these models to be investigated. It also allows a wide range of exposure scenarios to be studied and for the user to specify various characteristics of the baseline population, such as its age distribution and cancer rates. The first version of ASQRAD is due to be released around the end of 1995.

Participating organisation: NRPB

Head of project 1: Dr C R Muirhead

II. Objectives for the Reporting Period:

To provide support and guidance in the development of the ASQRAD package. Specifically, to prepare the user manual, and to advise and assist with the health effects models, the collation of data and quality assurance procedures.

To participate in organising a peer review of the software.

To organise an ERPET-supported training course on ASQRAD.

III. Progress achieved including publications:

General

During the contract period a series of meetings were held at NRPB and CEPN involving researchers from the two institutes. Both these meetings and numerous other contacts served to oversee the general progress of the project and to address various specific issues. As well as overall project coordination, NRPB advised CEPN on the structure and content of ASQRAD, eg, the format of the screens and the text therein. Various issues relating to the health effects models utilised in the system were also addressed.

NRPB was primarily responsible for preparing the user manual for the software, together with the text for the on-line help facility. This material describes not only how to run ASQRAD, but also gives some background to the models utilised. NRPB staff assembled some of the data contained in the package, eg, some of the baseline cancer rates. They also checked output from various test versions of the software as part of the quality assurance procedures.

Peer Review

In order to obtain external advice on satisfactory software performance and software improvement, a peer review panel was assembled in 1994.

After distributing a preliminary version of the software and associated documentation to the panel, a meeting was held in Paris on 7-8 November 1994 to receive the panel's comments and suggestions for modifications. A list of those attending this meeting and of other persons who provided comments is attached.

Points made by the panel included:

- (I) the first version of ASQRAD should be aimed at those requiring a tool for decision making, risk

communication and training, whilst future developments should improve its potential as a research tool;

- (ii) the presentation of results could be made less complicated through the use of a summary table;
- (iii) distinction should be made in calculations of somatic effects between exposure of one organ alone and exposure of a range of organs, to account for competing causes of death;
- (iv) the hereditary effects calculations should not be extensive, owing to the paucity of reliable data;
- (v) ASQRAD should output the various components of detriment and the documentation should explain how they might be combined into the ICRP detriment, whilst pointing out that the ICRP measure is dependent on various assumptions;
- (vi) the main body of the user manual should cover the working of the program, whereas technical details should be placed in an appendix;
- (vii) future versions of the software should cover more flexible model definitions and enhanced facilities for sensitivity analysis.

The comments of the peer review panel were highly useful and will be implemented in the software that will be released.

Training Course

On behalf of the European Commission, NRPB organised an ERPET (European Radiation Protection Education and Training) course on ASQRAD in conjunction with CEPN. This course was held at the NRPB Training centre at Chilton from 5 to 7 June 1995. The aims were to provide background to the relevant health effects models, to describe the scope of ASQRAD, and to illustrate its application through demonstrations and syndicate exercises involving 'hands-on' experience. A copy of the programme is attached; the lectures, demonstrations and exercises were led by NRPB and CEPN staff.

In the light of the peer review panel's recommendations, the course was aimed primarily at practitioners in radiological protection who are interested in detriment. There were 19 delegates who came from throughout Europe plus one from the USA (see attached list). Overall they were very satisfied with the course, which virtually all thought would be useful in their professional activities. The comments of the delegates were also helpful in identifying potential enhancements to the software which could be implemented either in the first release (eg, the inclusion of models given in the 1994 UNSCEAR report) or in a later version (eg, the calculation of 'probability of causation' in relation to radiation exposure and the occurrence of cancer).

Publication

Schneider, T; Delaigue, S; Degrange, J P; Haylock, R G E; Muirhead, C R and Robb, J. Applying ASQRAD to demonstrate the sensitivity of radiation detriment to the assumption adopted. IN Proceedings of the 17th IRPA Regional Congress on Radiological Protection (Portsmouth, 6-10 June 1994) pp 225-228.

Annex : Members of the review panel present at the meeting in Paris

Professor M. Vaeth
Department of Biostatistics
University of Aarhus
Nørrebrogade 44, Building 2C
DK-8000 ÅRHUS C
Denmark

Professor B. Lindell
Swedish Radiation Protection Institute
Box 60204
S-10401 STOCKHOLM
Sweden

Other participants at the peer review meeting

Dr T Schneider - CEPN
Dr D Chmelevsky - CEPN
Mr J P Degrange - CEPN
Ms. S Delaigue - CEPN
Dr C R Muirhead - NRPB
Mr R Haylock - NRPB

Comments about the package were also received from :

Dr G N Kelly
Radiation Protection Research Action
European Commission, DG XII/F/6
Rue de la Loi 200 (ARTS 3/53)
B-1049 BRUSSELS
Belgium

Mr M J Crick
Radiation Safety Section
Division of Nuclear Safety
International Atomic Energy Agency
Wagramerstrasse 5
P.O. Box 100
A-1400 VIENNA
Austria

EUROPEAN COMMISSION

ERPET

European Radiation Protection Education and Training

Training Course on

ASQRAD

Software for Studying
the Detriment Associated
with Radiation Exposure

**NRPB CHILTON
UK**

5 – 7 June 1995

National Radiological Protection Board
(NRPB)

Centre d'étude sur l'Évaluation de la
Protection dans le domaine Nucléaire
(CEPN)



National Radiological Protection Board, Training Section, Chilton, Didcot, Oxon, OX11 0RQ
Telephone: (01235) 831800 ext. 2312/2701 · Fax: (01235) 833891

ASQRAD COURSE 5 - 7 June 1995

Delegate List

Mr G Amat	Home Office
Dr W Atkinson	AEA Technology
Mr LM Bevington	Health & Safety Executive
Mr K Binks	Westlakes Research Institute
Dr A Brachner	Inst. for Radiation Hygiene- Germany
Dr M Charles	University of Birmingham
Miss J Denvir	AWE Aldermaston
Dr HA Grogan	USA
Dr F Hardeman	SCK/CEN - Belgium
Dr W Heidenreich	GSF/ISS - Germany
Dr JA Heslop	Tracerco, ICI C & P Ltd
Mrs M Montero	CIEMAT, Spain
Mr A Preece	Home Office
Mr DE Preece	Walsgrave Hospitals NHS Trust
Dr R Ramos De La Plaza	Nuclear Safety Council of Spain
Mr AE Riddell	Westlakes Research Institute
Mme M-A Telle	CEA/IPSN
Dr FR Verdun	Dept. Sante Communautaire - Switzerland
Dr R Wakeford	British Nuclear Fuels Plc

ASQRAD Training Course
NRPB, Chilton, 5-7 June 1995

Programme

Monday 5 June

09.00	Welcome	C. Sharp
09.15	Aims of the course	C.R. Muirhead
09.25	The value of software for studying radiation detriment	T. Schneider
09.50	Coffee	

Health Effects Models

10.10	Source data on late effects of ionising radiation	C.R. Muirhead
10.40	Factors affecting radiation-induced cancer risks	M.P. Little
11.15	Sensitivity of risk estimates to model assumptions	C.R. Muirhead
11.35	Discussion on uncertainties in risk estimates	
12.00	Lunch	

Description of ASQRAD

13.00	Organisation of software	T. Schneider
13.20	Description of somatic effects calculations	D. Chmelevsky
13.50	Demonstration of software - Installation - Overview - Data input - Basic somatic effects calculations - Output	R. Haylock
14.50	Tea	

Somatic Effects

- 15.10 Syndicate exercise (1)
 - Basic somatic effects calculations
- 16.30 Close

Tuesday 6 June

- 09.00 Discussion of exercise (1)
- 09.30 Demonstration
 - Creation of new databases
 - Advanced somatic effects calculations
 - Output
- 10.10 Coffee
- 10.30 Syndicate exercise (2)
 - Advanced somatic effects calculations
- 12.00 Lunch
- 13.00 Syndicate exercise (2) (continued)
- 13.20 Discussion of exercise (2)

**R. Haylock/
J.-P. Degrange**

Hereditary Effects

- 13.50 Description of hereditary effects calculations
- 14.10 Demonstration
 - Data input
 - Hereditary effects calculations
 - Output
- 14.40 Tea
- 15.00 Syndicate exercise (3)
 - Hereditary effects
- 16.00 Discussion of exercise (3)
- 16.30 Close
- 19.30
(for 20.00) Course Dinner (at Shillingford Bridge Hotel)

**D. Chmelevsky
J.-P. Degrange**

Wednesday 7 June

09.00	Comparison with other software	C.R. Muirhead/ D.A. Jackson
09.30	Coffee	
09.50	Syndicate exercise (4) - Comparison of results based on different modelling assumptions	
11.10	Discussion of exercise (4)	
11.30	Future developments of ASQRAD	C.R. Muirhead/ T. Schneider
11.50	Concluding discussion and course review	
12.25	Closing remarks	
12.30	Close (lunch)	

Participating organisation : CEPN

Head of project 2: Dr. T. SCHNEIDER

II. Objectives for the reporting period

Following the earlier EC contract on the evaluation of detriment which defined the scope of the ASQRAD software and in which a first version of the program was prepared, the following objectives have been assigned to CEPN for this reporting period:

- Review of health effects models and collation of demographic data;
- Improvement of the system coding; and
- Development of new software facilities within the Windows environment.

Furthermore, according to the advancement of the software during this contract period, a peer review has been organised as well as a training course of ASQRAD.

III. Progress achieved including publications

III.1. Review of health effects models

A key but controversial area of work is how risk coefficients should be transferred across populations. In this perspective, the work achieved during this contract period was devoted to the mathematical description of the various assumptions adopted for the calculation of lifetime risk for both somatic and hereditary effects. Furthermore, based on the available dose-effect relationships concerning radiation-induced breast cancer, a sensitivity analysis has been performed which points out some considerations on the transfer of coefficients across populations.

This sensitivity analysis has been performed in order to demonstrate the importance of the various assumptions adopted, such as the risk coefficients applied and the choice of a reference population. In this particular example, several sets of risk coefficients were used: those of Shimizu et al. (1988) on mortality amongst the A-bomb survivors; and those from the follow-up of patients in North America with medical exposures (e.g.. Canadian women treated by fluoroscopy from Miller et al. 1989). Both these studies define exposure-risk relationships in terms of additive risk (excess cases per 10^4 person-year Gray (PY.Gy)), and relative risk (percentage of excess cases per gray) as illustrated in Table 1.

Table 1. Epidemiological studies on breast cancer after irradiation

Reference	Study	Follow-up period (mean)	Exposed population (deaths from breast cancer)	Age at irradiation	Relative risk (Gy) ⁻¹	Excess risk (10 ⁴ PY Gy) ⁻¹
SHIMIZU (1990)	Hiroshima/Nagasaki	1950-85	45,557 (155)	0-9	2.90	0.32
				10-19	3.34	2.23
				20-29	2.21	1.21
				30-39	2.26	1.54
				40+	1.11	0.18
MILLER (1989)	Canadian tuberculosis patients	1950-80 (24 years)	8,371 (163)	10-14	4.46	6.06
				15-24	1.77	3.05
				25-34	1.25	1.72
				35+	1.10	1.23

The sensitivity analysis has been performed using demographic data from three populations: Japan (1988), England and Wales (1985), and France (1989). The death rates for all causes are similar for these countries. However, Japanese breast cancer death rates are much lower than those of France and of England and Wales. Table 2 presents the results of the ASQRAD calculations according to these three populations, using the multiplicative model published by Shimizu for an exposure at 10 years of age. The large differences observed in this Table are directly related to the baseline death rates for breast cancer.

Table 2. Number of lifetime excess deaths from breast cancer per 100,000 women individually exposed to 10 mSv - acute irradiation (Shimizu - multiplicative model)

Age at exposure	Japan	England and Wales	France
10	18.5	101.5	73.9

Table 3 presents the lifetime excess deaths from breast cancer for the French population derived using the multiplicative and additive models published by Shimizu and Miller. The multiplicative model from Miller leads to higher estimates than those of Shimizu for young ages at exposure. The risks are similar for women exposed at 50 years of age, and the difference is greatest for women exposed between 20 and 40 years old. The additive model published by Miller leads to higher estimates than those of Shimizu for all ages at exposure. These results reflect the different baseline breast cancer death rates for the reference populations in these two epidemiological studies.

Table 3. Number of lifetime excess deaths from breast cancer per 100,000 women individually exposed to 10 mSv acute irradiation (France 1989)

Age at exposure	Shimizu	Miller
Multiplicative model		
10	73.9	109.3
50	2.6	2.4
Additive model		
10	13.3	36.1
50	0.38	2.6

The loss of life expectancy indicator allows one to take into account the variation of breast radiation sensitivity according to age. Assuming an individual acute exposure at 10 mSv, the loss of life expectancy (number of days per person exposed) derived from Miller's multiplicative model applied to the French population leads to: 6.3 and 0.09 days for exposures at 10 and 50 years of age respectively. It should be noted, that the main occurrence of radiation-induced breast cancer is between ages 60 and 90 years. Thus, the loss of life expectancy given that a death occurs is 16 (10.6) years for an exposure at 10 (50) years of age.

This analysis illustrates the importance of cautious interpretation of data in light of the uncertainties that remain. In this context, ASQRAD is a powerful tool that allows the sensitivity of different measures of detriment to demographic parameters and modelling assumptions to be examined, both numerically and graphically. This analysis also demonstrates the role in research and decision-making that computer tools such as ASQRAD can have through their ability to accommodate and manipulate all the relevant information in a user-friendly format.

III.2. Software development

Further to the definition of the fundamental calculations as well as indicators of detriment, the main achievement of this contract concerns the development of the user interface of ASQRAD to ensure that the code is as friendly to the user as possible. For this purpose, the software has been designed with a menu-driven system including a help facility within the Windows environment. The main menu of ASQRAD distinguishes two functions: the database management system and the calculations of somatic and hereditary effects.

The database

All of the data within ASQRAD are controlled by a database system that is incorporated into the program. Within this facility, data are grouped together in the form of tables. The user may examine each table, create new tables of data with a format of his or her own choosing, edit tables and output the data in various form. Space is also provided within each table for the inclusion of references to the origin of its data.

The first set of tables concerns the demographic characteristics of the various populations: the size of the population; death rates for all causes; death rates for various cancers; morbidity data (specified in terms of lethality fraction or incidence rates for the various cancers); and fertility rates.

The second set of tables provides the definitions of the models. These tables fall into two distinct groups. The first group contains those tables that define the basic model coefficients and the reference information on its publication and characteristics (multiplicative versus additive; age groups considered; death causes...). ASQRAD contains the somatic effects models proposed by the four scientific organisations (UNSCEAR: United Nations Scientific Committee on the Effects of Atomic Radiation; BEIR: Biological Effects of Ionising Radiation; RERF: Radiation Effects Research Foundation, NRPB: National Radiological Protection Board), as well as health effects models published from different studies, especially from medical irradiation (e.g. paper from Miller et al.). The user may also introduce new published models by creating new tables that specifying their characteristics. Accessing the somatic basic models database reveals box no. 1.

The second group of tables defines how the basic somatic effects model are to be used in a calculation. Again these tables fall into two types. Those that define 'Whole body exposure' calculations and those that define "Organ exposure" calculations.

The first type of models allows the calculation of radiological detriment for whole body exposure and concerns the models published by national or international organisations (UNSCEAR, BEIR, RERF, NRPB). The second type of models concerns the dose effect relationships for each organ and allows the user to combine different models and in studying a restricted list of organs. Thus, ASQRAD proposes a selection module which specifies, for each cause of death, the available models (see box no. 2).

For hereditary effects, ASQRAD contains the table of the coefficients of the ICRP 60 model. This model is characterised by the following parameters: spontaneous prevalence; doubling dose; mutational component; excess incidence in the first generation; excess incidence at equilibrium; intergenerational transmission factor; and severity weighting factor.

Somatic effects calculations

These risk coefficients are used within ASQRAD to calculate detriment to either populations or individuals and from either whole body or organ specific exposure. The user has to specify the scenario of exposure: i.e. whole body or organ exposure; acute or extended exposure; sex; the level of dose (and the duration of the exposure if necessary) and the age at exposure. It is also possible to introduce different ages at exposure and/or different doses. Furthermore, the user has to select the demographic data and the somatic models for the calculations. Box no. 3 details the selection menu for the calculations.

The primary measures of detriment are the expected number of excess deaths, the associated loss of life expectancy, and the risk of excess non-fatal cancers. These results are summarised together with the assumptions adopted for the calculations (see box no. 4) and then access to more detailed results is allowed via tables and graphs. Detriment calculations are also performed for hereditary effects.

Although ASQRAD does not calculate a single measure of detriment, it provides the elements for such a calculation. The main objectives of the computer code to illustrate of risk calculations for training purposes and to calculate of risk estimates for policy makers. The scope of the code may be enlarged in the next future to allow users to introduce their own risk models. This might make ASQRAD into a research tool for comparison of models.

Publications:

S. DELAIGUE, T. SCHNEIDER, J.P. DEGRANGE :
Evaluation des risques associés au cancer du sein après irradiation.
Rapport CEPN No222, Mars 1994.

T. SCHNEIDER, S. DELAIGUE, J.P. DEGRANGE, R.G.E. HAYLOCK, C.R. MUIRHEAD,
J. ROBB:
Applying ASQRAD to demonstrate the sensitivity of radiation detriment to the assumptions
adopted.
In: Proceedings of the 17th Congress, IRPA Regional Congress on Radiological
Protection, 6th-10th June 1994, Portsmouth, UK, pp. 225-228.

T. SCHNEIDER, D. HUBERT, J.P. DEGRANGE, M. BERTIN:
Use of risk projection models for the comparison of mortality from radiation-induced breast
cancer in various populations.
Health Physics, April 1995, Vol. 68, No 4, pp. 452-459.

D. CHMELEVSKY, S. DELAIGUE:
Calculations of hereditary effects in ASQRAD.
CEPN-NTE/95/11, June 1995.

D. CHMELEVSKY, S. DELAIGUE:
Calculations of somatic effects in ASQRAD.
CEPN-NTE/95/12, June 1995.

T. SCHNEIDER:
The value of software for studying radiation detriment.
CEPN-NTE/95/13, June 1995.

D. CHMELEVSKY, S. DELAIGUE, J.P. DEGRANGE, T. SCHNEIDER:
ASQRAD: A computer code to estimate the stochastic risks of radiation exposure. In:
International Conference on Radiological Protection and Medicine,
Montpellier, France 28-30 June 1995.

Box no 1, Basic models for somatic calculations

ASQRAD * Data-Base * List of Tables	
Basic models for somatic calculations	
Tables	UNSCEAR - 1988 x
Summary	
Title	UNSCEAR - 1988 x
Author	ASQRAD : UNSCEAR 1988
Comment	United Nations Scientific Committee on the Effects of Atomic Radiation : Sources, Effects and Risks of Ionizing Radiations 1988 Table 54, p. 522 ; DS86 subcohort
Definitions	
Cube:	Type : Multiplicative [/Gy]
Sheet:	Sex : Standard
Row:	Ages groups : Model with only one age group
Column:	Death causes.../ Organs : UNSCEAR
Status	
Status	System
Last update	11/04/95

Exit

Help

New

Duplicate

Delete

Visualization

Summary

Convert

Values

Box no 2, Somatic model selection

ASQRAD * Somatic model selection (Organs exposure)

File ?

UNSCEAR 1988+ System

Available death causes		Selected death causes	Associated models	Type
All cancers	+	Oesophagus cancer	UNSCEAR - 1988 +	+
Bone cancer		Stomach cancer	UNSCEAR - 1988 +	+
Digestive tract cancers		Colon cancer	UNSCEAR - 1988 +	+
Liver cancer		Lung cancer	UNSCEAR - 1988 +	+
Other cancers (BEIR)		Breast cancer	UNSCEAR - 1988 +	+
Residual cancers (RERF)		Ovary cancer	UNSCEAR - 1988 +	+
Respiratory cancer		Bladder cancer	UNSCEAR - 1988 +	+
Skin cancer		Mult.myeloma	UNSCEAR - 1988 +	+
Thyroid cancer		Leukemia	UNSCEAR - 1988 +	+
		All cancers except leuk	UNSCEAR - 1988 +	+

Available models

Model =>

<= Model

Death c. =>

<= Death c.

Exit Summary

Box no 3, Somatic effects - calculation selection

ASGRAD - Somatic effects for individual exposure

Data-Base 2

Exposure

Whole body

Organ

Simultaneous

Distinct

Acute

Extended

Demography UNITED KINGDOM - 1988

Mortality ICRP60 - 1990

Exp.periods DEFAULT

Sex

Male

Female

DBREF DEFAULT - 1

Age

Single

Multiple

Models UNSCEAR 1988+
(Organ)

Dose

Single

Multiple

Age(years) 0

Dose(sievert) 0

Calculation Exit

Box no 4, Somatic effects - summary of results

ASORAD

Somatic effects for population exposure (Whole body)

Exit

Demography	UNITED KINGDOM - 19	D D R E F	DEFAULT- 1
Morbidity	ICRP60 - 1990	Whole body	UNSCEAR 1988 x
Exp. periods	DEFAULT		

Help

Details

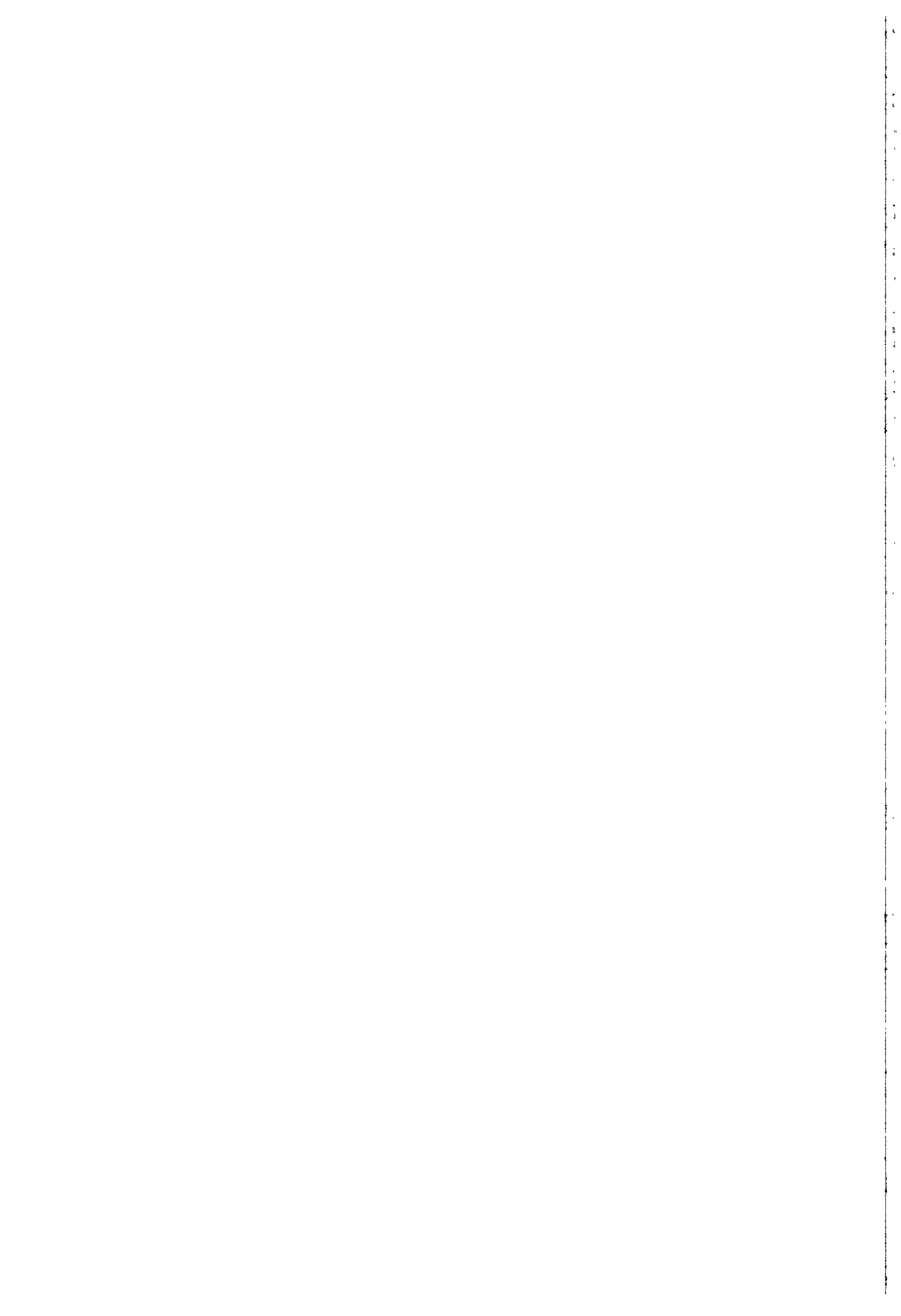
Exposure: Simult. Acute Sex: Both Ages: All Duration: No Dose:

Excess number of fatal cancers (per 100000):

Sex	Leukemia	All cancers except leuk	Total
Male	1.550E3	7.857E3	9.407E3
Female	1.225E3	6.242E3	7.468E3
Both	1.385E3	7.035E3	8.420E3

Excess incidence of cancers (per 100000):

Sex	Leukemia	All cancers except leuk	Total



**Final Report
1992-1994**

Contract: FI3P-CT920047 Duration: 1.9.92 to 30.6.95 Sector: C14

**Title: Investigation of late effects in humans after artificial irradiation
(Thorotrast-patients)**

1)	van Kaick	DKFZ
2)	Priest	UKAEA
3)	Wallin	KBFOC
4)	dos Santos Silva	School Hygie. and Tropic. Med. - London
5)	Malveiro	Inst. Higiene e Medicina Tropical

I. Summary of Project Global Objectives and Achievements

Global objectives:

- to calculate high LET risk estimates for ThO₂ depositing organs: liver, spleen, bone marrow and marrow free bone
- to calculate high LET risk estimates for the non-depositing organs: adrenal glands, testes, pancreas, kidneys, prostate, urinary bladder
- to recalculate the tissue dose rate of the depositing and non-depositing organs
- to assess the spatial and temporal distribution of Thorotrast in the yellow and red bone marrow
- to assess the dose rate to the target cells of the bronchial mucosa
- to strengthen the statistical results by evaluating a larger number of exposed persons
- to assess the frequency and pattern of mutations in the p53 tumor suppressor gene
- to offer preventive medical care to the exposed persons

Global achievements:

Within the framework of clinical examinations of the **German group** liver cancers at an early stage could be detected by using modern imaging methods. The tumors were surgically removed. Analysis of 82 Thorotrast patients with liver lesions revealed a dependency on the size of the tumor and the time of survival.

High concentrations of thorium dioxide were found by X-ray and computed tomography (CT) in the spleen, the abdominal lymph nodes and paravascular deposits. Neoplastic diseases in these areas of high exposure, however, were extremely rare.

Preliminary results of ophthalmological examinations could not prove radiation induced cataracts in Thorotrast patients.

Liver cancer continues to be the leading cause of death among Thorotrast patients, whereas leukemias were not registered during the reporting period. Excess rates of Thorotrast induced neoplastic diseases stabilized with the exception of the carcinoma of the esophagus.

Several approaches were performed to optimize the dosimetric calculations. Translocation of Thorotrast particles in two patients after liver transplantation proved to be very low. This was confirmed and analysed in an animal experiment with rats.

CT evaluation of liver and spleen volume revealed substantial shrinkage of the organs which changed the former calculations of Thorotrast distribution and concentration in the body.

Comparing the data of whole body counting and of hospital records we found relevant discrepancies. It became apparent that some patients did not receive the total documented volume of Thorotrast.

The dose to the so-called non-storing organs (adrenal glands, testes, pancreas, etc.) was calculated with respect to the mean cellular dose.

Animal studies on the pathogenesis of Thorotrast induced liver and lung tumors were performed. The results show that in the liver the carcinogenic property of Thorotrast can be exclusively attributed to radiation without any foreign body effect. In the lung, however, the additional treatment of Thorotrast injected rats with quartz had a pronounced tumor promoting effect.

The activities of the **British group** were concentrated on distribution and biokinetics of Thorotrast particles and the local dose in the red and yellow bone marrow. Concentration of thorium in the bone marrow of selected human and monkey bones were measured (2 body donations and 4 monkeys). Thorium concentrations were also measured in German and Japanese bone marrow samples. The level of thorium in these samples are in general agreement with those levels measured in the USTUR case bones and monkey bones with relatively small differences at different red marrow sites. The level of injected Thorotrast had no effect on its final distribution. Within the red bone marrow there were two components of distribution: diffuse and locally concentrated deposits. The important conclusion of this study is that the ICRP quality factor for α -emitters with respect to leukemia seems to be too high.

The data of the **Danish study** were evaluated and published in eight very good papers. Taking into account that the number of the Danish Thorotrast patients, who died more than three years after injection of Thorotrast, are about one third of the German Thorotrast group the figures of primary liver cancer and leukemia are closely related. An excess rate of malignant mesotheliomas was also registered in both studies. Another important result of the Danish group was the fact that children of Thorotrast patients had no elevated risk for cancer.

The study sponsored by the EC dealt with the examination of the existence of a specific pattern of mutations in the tumor suppressor gene p53 in Thorotrast induced tumors. Paraffin embedded, formalin fixed archival tissues of 36 liver cancers in Thorotrast patients were analysed. The message of this study was that the rate of p53 point mutations in liver and lung tumors and in malignant mesotheliomas seems to be lower than in tumors with other etiology.

The **Portugese Thorotrast** study was reactivated. The total number of studied subjects was markedly enlarged using information on 'place of birth' to ascertain the vital status of those patients who were identified from hospital records but who, in the past, could not be traced by other means. Computer programs for data entry and validation were developed and two new standardized data extraction forms were created: an administrative and a clinical one. The past records of 87 patients, who died from primary liver cancer until 1977, were reviewed. The analysis of the complete study will be concluded in 1996.

Head of Project 1: Prof. Dr. G. van Kaick

II. Objectives for the reporting period

The scientific work of the clinical and epidemiological study is an extension of the program which was set up by the coordinating committee. Research activities include:

- Clinical, biochemical and radiological examinations of the Thorotrast and control patients
- Biophysical examinations to calculate the tissue dose based on the thoriumdioxide (ThO₂) deposits and their radioactive daughter products
- Identification of causes of death of Thorotrast patients and members of the control group
- Consideration of new dosimetric results
- Estimation of the dose to the non-depositing organs
- Ophthalmologic examinations to evaluate the cataract response in Thorotrast patients caused by the daughter product ²²⁴Ra

III. Progress achieved including publications

Clinical examinations

Examinations of outpatients during the reporting period

During the reporting period 185 outpatient examinations of Thorotrast patients and 162 examinations of control persons were performed. Remarkable results of the clinical diagnoses are: 15 primary liver cancers, 7 recurrences of liver cancer, and 1 extrahepatic bile duct carcinoma in the Thorotrast group, whereas no liver or extrahepatic bile duct cancer was seen in the controls. In all cases oncological treatment was initiated if possible.

Liver Cancer: Detection and Treatment

The results of liver cancer detection and treatment were evaluated during the time period 1979 to 1993. 1069 examinations were performed in Thorotrast patients, 1052 in the controls. The patients were invited to our institute for follow-ups in intervals of 2 years including physical examination, laboratory tests and imaging methods. In 82 Thorotrast patients liver lesions suspected to be malignant could be detected, but none in the controls. In all patients the diagnosis was confirmed by biopsy, operation or clinical follow-up. At the time of examination patients with liver tumors had clinically no symptoms. Pathohistological examination revealed 36 cholangiocarcinomas, 14 hepatocellular carcinomas, and 8 haemangiosarcomas. In 24 patients the tumor was specified as „carcinoma of the liver“. Liver cirrhosis was associated in 21% of the patients with liver cancer. Table I demonstrates the survival of Thorotrast patients suffering from liver cancer, type of therapy, and size of tumor. The mean life expectancy in patients with liver cancer is 9 years less compared to the controls and five years less in comparison to deceased Thorotrast patients without liver cancer. The 1-, 3-, and 5-year survival rates in our patients are 66%, 28%, and 6% respectively. 75% of the resected tumors were cholangiocarcinomas. According to the medical literature the prognosis for these tumors is worse compared to hepatocellular carcinomas due to early intra- and extra-hepatic spreading. Compared to non-Thorotrast induced liver tumors in Japanese studies, with a 5-year

survival rate of 28%, the survival of Thorotrast patients with resectable liver tumors is shorter. Therefore it remains an open question whether Thorotrast induced liver tumors are biologically more aggressive than malignant liver tumors of different etiology. Thorotrast induced secondary neoplasms of the liver may be responsible for the very low 5-years survival rate (Lührs et al., 1995).

Table I: 50% survival (Kaplan-Meier estimates) of Thorotrast patients with liver cancer: Comparison of curative resection, no therapy and tumor size

Therapy	Diameter of tumor (cm)	Number of patients	Time period diagnosis-death (mo)
Resection	<3.4	16	30
Resection	>3.4 <6.5	12	15
Resection	>6.5	4	6
No therapy	<6.5	13	10
No therapy	>6.5	15	3

Abdominal lymph nodes and spleen

The regional lymph nodes of liver and spleen can be visualized by X-ray plain films of the upper abdomen and by CT. On CT scans of 22 Thorotrast patients about 1300 lymph nodes could be detected (mean 63 ± 24 per patient; CT-density >500 HU). The number of Thorotrast storing lymph nodes in the affected anatomical regions were: pancreas head and liver hilus 15 (mean value); pancreas body and pancreas tail and hilus of the spleen: 22; paraaortic, paracaval, and paracoeliac lymph nodes: 15. No tumor arising from the abdominal Thorotrast storing lymph nodes was detected up to now (Görich et al., 1994).

During the last 10 years CT examinations of the spleen were performed in all Thorotrast patients of the follow-up study. We detected only 6 patients with a focal hypodense lesion which proved to be an infarction in one case and haematoma in another case. The follow-up of the other 4 patients proved no change of the lesion over a period of more than two years. These lesions measured 2.5×2.5 cm. During a CT and ultrasound examination one patient was detected with a mesothelioma surrounding the spleen. This tumor could be caused by Thorotrast deposits in the spleen, as the α -particles can reach the adjacent layer of peritoneal cells.

Paravascular deposits

Paravascular injection of Thorotrast caused a lifelong deposit of thorium dioxide (ThO_2) particles surrounding vessels, nerves, and connective tissue structures. In 899 examined German Thorotrast patients 245 paravascular deposits were found by X-ray plain films in the area of injection (A. carotis: 157; A.A. brachialis, axillaris, subclavia: 33; A.A. femoralis,

poplitea: 55). First clinical symptoms manifested 19 years after injection on average depending on the region of injection and the extension of the deposit. Important late effects were: paralysis of nerves, occlusion and stenosis of veins, and more rarely also arteries, compression of esophagus, trachea, ureter, and chronic painful inflammation. 6 patients died from non-neoplastic direct late effects of the paravascular deposits and only 1 patient 30 years later from a metastasizing sarcoma growing at the edge of a paravascular Thorotrast granuloma (Liebermann et al., 1995).

Ophthalmologic examinations

Thorotrast patients are also chronically exposed to ^{224}Ra , which can cause radiation-induced cataracts. In Thorotrast patients a cumulative rate of 2 - 4% cataracts should be expected after an exposure time of more than 30 years. Up to now ophthalmologic examinations were performed on 19 Thorotrast and 16 control patients. To date no significant difference concerning lense opacities between both groups were observed. Especially no posterior subcapsular lense opacification as reported to be typical for radiation induced cataracts, could be detected (Hornik et al., 1994).

Causes of death of deceased patients during the reporting period

Causes of death were clarified in 53 Thorotrast and 75 control patients who died during the reporting period (Table II). More than 50% of the Thorotrast patients died of primary liver cancer. No case of leukemia but one case each of plasmacytoma in both groups were registered. Esophagus carcinoma in 3 controls decreased the former excess rate. Thus the T/C value changed from 2.1 to 1.4 (Table V).

Table II: Causes of death in Thorotrast and Control Patients* during the Reporting Period (1.1.1992-30.6 1995)

Diagnoses	Thorotrast n=53	Controls n= 75
Liver cancer	28	0
Extrahepatic bile duct carcinoma	2	0
Gallbladder carcinoma	0	1
Unknown primary tumor	4	0
Lung carcinoma	1	3
Esophagus carcinoma	0	3
Pancreas carcinoma	0	1
Larynx carcinoma	0	1
Colon carcinoma	0	2
Stomach carcinoma	1	0
Malignant brain tumor	0	1
Rectum carcinoma	0	1
Kidney carcinoma	0	2
Prostate carcinoma	1	4
Breast carcinoma	0	2
Plasmacytoma	1	1
Liver cirrhosis	5	0
Haemorrhage leading to death due to paravascular deposit of Thorotrast	1	0
Myocardial infarction	6	33
Mesenteric infarction	0	1
Pneumonia	1	4
Urosepsis	1	0
Perforated stomach ulcer	0	1
Apoplectic stroke	0	11
Pulmonary embolism	0	1
Sepsis	0	1
Contusio cerebri	0	1
Unknown causes	1	0

* in 21 additional deceased patients the search for the cause of death is not yet completed.

Epidemiological results

The German Thorotrast study comprises 2326 Thorotrast patients (1718 m; 608 f) who were injected intravascularly with the X-ray contrast medium Thorotrast and 1890 contemporary matched patients in the control group (1407 m; 483 f). At the end of June 1995 70 Thorotrast patients and 286 persons of the control group are still living. Excluded from the figures of deceased patients are those patients who died within the first 3 years after injection of Thorotrast or the admission to the hospital respectively. This should be considered when comparing our results with the Danish Thorotrast study which includes patients who died within the first 3 years after angiography with Thorotrast (Table III).

Table III: German Thorotrast Study - Evaluated Patients (Status 30.06.95)

Patients' Status	Thorotrast	Control
Patients examined	899	662
deceased	829	376
living	70	286
Patients not examined	1427	1228
Total	2326	1890

The final fate of the Thorotrast patients is the most important parameter for the calculation of Thorotrast late effects. A summary of the most important diseases leading to death is given in Tables IV and V. Table IV presents diseases with a clear excess rate ($T/C > 1,5$) and Table V diseases without apparent excess rate ($T/C < 1,5$).

Table IV: German Thorotrast Study - Diseases with High or Probable Excess Rate

(Status 30.06.1995)

Causes of Death	Thorotrast (T)		Control (C)		T/C
	n=2256 from 2326		n=1603 from 1890		
Liver cancer **	439*	[+5] (19.45%)	2	(0.12%)	162.0
Extrahepatic bile duct ca.	24	[+3] (1.19%)	3	(0.19%)	6.2
Gall-bladder carcinoma	12	[+1] (0.57%)	4	(0.24%)	2.3
Liver cirrhosis	191	[+177] (16.34%)	47	[+2] (3.09%)	5.3
Pancreas carcinoma	18	(0.79%)	6	(0,37%)	2.1
Mal. Mesothelioma					
Peritoneal	4	[+1] (0.22%)	0		-
Pleural	5	[+1] (0.26%)	0		-
Larynx carcinoma	6	[+1] (0.31%)	2	[+1] (0.18%)	1.7
Non lymphatic leukemia	37	[+3] (1.77%)	5	(0.31%)	5.7
Myelodysplastic syndrome	30	(1.32%)	4	[+2] (0.37%)	3.5
Plasmacytoma	8	[+2] (0.44%)	2	(0.12%)	3.6
Non Hodgkin lymphoma	14	[+2] (0.71%)	3	(0.18%)	3.9
Bone sarcoma	4	[+1] (0.22%)	1	(0.06%)	3.6

[] Additional cases with another disease leading to death

* 5 patients with combined carcinoma and sarcoma

() Inclusive additional cases related to n

T/C Frequency of the disease in the Thorotrast group (expressed as percentage) divided by the frequency of the control group.

** After a new revision of the pathohistological descriptions in 6/95 12 cases of liver cancer were re-classified: 7 cholangiocarcinomas were changed to extrahepatic bile duct carcinomas and in 5 cases the diagnosis „ liver cancer“ was cancelled due to misclassification.

Table V: German Thorotrast Study - Diseases Without Apparent Excess Rate * (Status 30.6.1995)

Causes of death	Thorotrast n=2256 of 2326		Control n=1603 of 1890		T/C
Chronic lymphat.leukemia	3	(0,13%)	3	(0,18%)	0.7
Acute lymphat.leukemia	1	(0.04%)	0		
Hodgkin' s disease	2	(0.08%)	2	(0.12%)	0.6
Lung carcinoma	51 [+2]	(2.35%)	51	(3.18%)	0.7
Esophagus carcinoma	7 [+1]	(0.35%)	4	(0.24%)	1.4
Kidney carcinoma	8 [+5]	(0.57%)	8	(0.49%)	1.1
Urinary bladder ca.	5 [+4]	(0.39%)	6 [+1]	(0.43%)	0.9
Adrenal carcinoma	1	(0.04%)	1	(0.06%)	0.6
Stomach carcinoma	30 [+3]	(1.46%)	46	(2.86%)	0.5
Colon carcinoma	10 [+4]	(0.62%)	20	(1.24%)	0.5
Rectal carcinoma	9 [+1]	(0.44%)	14 [+1]	(0.93%)	0.4
Prostate carcinoma	19 [+1]	(0.88%)	17	(1.06%)	0.8
Breast carcinoma	10	(0.44%)	19	(1.18%)	0.3
Ovary carcinoma	5	(0.22%)	4	(0.24%)	0.9
Brain tumor	19	(0.84%)	12	(0.74%)	1.1

[] Additional cases with another disease leading to death

() Inclusive additional cases related to n

* T/C < 1,5

The increase in frequency of primary liver cancer in the Thorotrast group continues. Cholangiocarcinoma was the most frequent pathohistologic tumor diagnosis. About 30% of the liver tumor patients also suffered from liver cirrhosis compared to 10% liver cirrhosis frequency in Thorotrast patients without the development of liver cancer. As previously reported, there is a correlation between the dose rate in the liver and the cumulative rate of primary malignant liver tumors (Fig. 1).

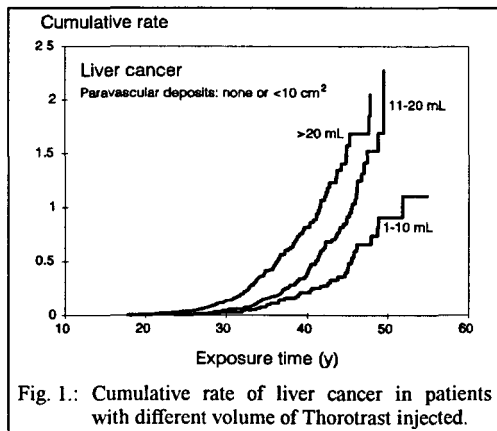
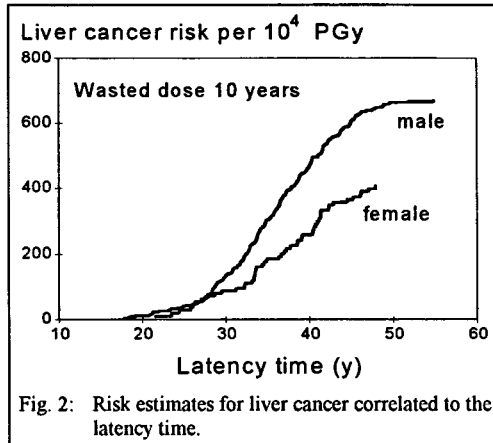


Fig. 1.: Cumulative rate of liver cancer in patients with different volume of Thorotrast injected.

This also holds true for liver cirrhosis. Age at injection did not influence the frequency of liver tumor development. The male/female ratio of hepatic carcinoma patients in the general population is approximately 2/1. This sex associated difference was also maintained in the German population with Thorotrast induced liver tumors about 1.6/1 (Fig. 2).

The most recent data in our study show a further increase in the risk estimate for men of approximately 680 and for women of 400 liver cancers/ 10^4 person Gy.

An unexpected observation, which was supported by the Danish data, was the excess rate of gall bladder carcinomas including carcinomas of the extra-hepatic bile ducts. A small excess rate of pancreatic carcinomas was also noted. Whether these regions - bile ducts and pancreas - were exposed to radiation by the Thorotrast deposits or by daughter products of ^{232}Th needs to be clarified by calculation of the probable accumulated dose.



Whether these regions - bile ducts and pancreas - were exposed to radiation by the Thorotrast deposits or by daughter products of ^{232}Th needs to be clarified by calculation of the probable accumulated dose.

Acute non-lymphocytic leukemias are predominant (T/C 5,7) followed by plasmacytoma (T/C 3,6) (Table V). Patients developed leukemias for up to 45 years after Thorotrast injection. It is noteworthy that no additional leukemias were diagnosed in the last years. The German and the Danish studies failed to identify a relationship between the bone marrow dose rate, the age of injection, and the incidence of leukemia.

As in the Japanese study no excess rate of lung carcinoma was observed, although ^{220}Rn causes chronic irradiation of the respiratory epithelium of the bronchi (Table V).

A Thorotrast volume-dependent lifespan reduction, independent of the Thorotrast induced malignant diseases became apparent in the German and the Japanese population in recent years.

Dosimetry

Translocation of Thorotrast in the Body

To learn more about the extent to which translocation of ThO_2 occurs in the body after deposition in the reticuloendothelial system, the liver of rats injected with Thorotrast was extirpated and replaced by a Thorotrast-free donor liver. Measurements of the ^{232}Th content of the donor liver at different times after implantation and the histological examination demonstrated an increased uptake of ^{232}Th with time. Within 231 days about 3% of the total body burden of ^{232}Th was translocated into the implanted organ. The additional removal of the spleen resulted in a significantly lower transport of ^{232}Th into the implanted liver.

The results of this study including the data from two human Thorotrast carriers suggest that there is a permanent translocation of a mobile fraction of ThO_2 in the body of an organism injected with Thorotrast.

The consequences for dosimetric consideration can be summarized as follows: compared with ^{220}Rn activity in the blood of Thorotrast patients from 40 to 400 mBq/ml, the small activity concentration of ^{232}Th (<0,1 mBq/ml) contributes very little to the exposure of the organs to radiation of the blood. However, in the extra-vascular space, release by migrating macrophages may cause a regional aggregation of ^{232}Th particles resulting in a high local radiation dose (Spiethoff et al., 1994).

Volume measurements of liver and spleen by CT

Computerized tomography was used for volume measurements of liver and spleen in 52 cases of Thorotrast patients. The mean actual organ weight as calculated by CT was 1393 g (range 1031 - 2161 g) for the liver and 62 g (range 10 - 188 g) for the spleen. The ideal organ weight depending on body surface area was calculated for each patient and compared with the actual organ weight. The differences reveal a shrinkage of the organs. The actual organ weight was in the mean 260 g below the ideal value for the liver and 43 g below the ideal weight of the spleen. The distribution of thorium was recalculated for the evaluated organ rates: liver 66.7%, spleen 16.5% of the intravascularly applied thorium. At a Thorotrast volume of 17.4 ml (mean volume of the examined group) the dose rates for liver and spleen are 24.44 cGy/y and 68.5 cGy/y. This means a difference of 32.9% for the liver and 22.6% for the spleen compared to the results of usual dose rate calculations for a constant standard liver and spleen weight (1700 g, 150 g) (Bast et al., 1995).

Whole body counting and data of hospital records

The most common approach in estimating the incorporated Thorotrast is to use the data of the hospital records. It is also possible to estimate the incorporated quantity of Thorotrast in the living patients using a whole body counter. Both procedures were compared in the German patients whenever hospital records included the appropriate information. However, patients with large paravascular deposits were excluded from this evaluation. The documented volumes clearly suggest that most patients received 24 ml respectively 12 ml. The determination of incorporated Thorotrast using the whole body counter indicated that certain patients had not received the total documented volume (Fig. 3).

Paravascular Thorotrast deposits increase the uncertainty of dosimetric calculations even more. Patients with very large paravascular deposits (X-ray projected area larger than 10^2 cm) should be excluded from the evaluation when using whole body counting values (van Kaick et al., 1995).

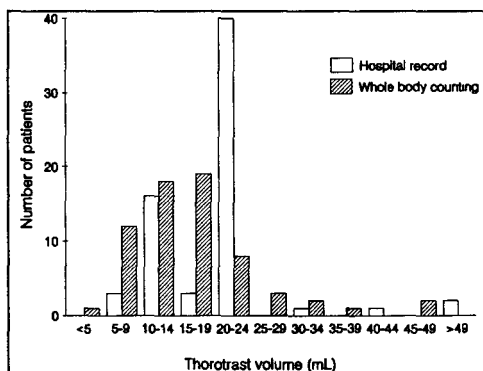


Fig. 3: Thorotrast volume in the hospital records (1 injection) or calculated by whole body counting.

Mean and median values: Hospital record:
20.6 / 24.0 mL

Whole body counting: 17.0 / 15.4 mL

Dose to non-storing organs of Thorotrast patients

The mean cellular dose (i.e. dose to tissue within the maximum range of α -particles) for so-called non-storing organs was calculated for a male Thorotrast patient injected with 20 ml of Thorotrast. Size and local distribution of Thorotrast conglomerates within these organs were measured using an image analysing system. The dose values in these tissue regions are: adrenal gland - 17 mGy/y; testes - 2,9 mGy/y; pancreas - 3,0 mGy/y; kidney - 1,0 mGy/y; prostate - 0,99 mGy/y; and urinary bladder - 0,82 mGy/y (Dalheimer et al., 1995).

Dose to the lungs

The lung tissue of Thorotrast patients is continuously exposed due to exhalation of ^{220}Rn and daughters dissolved in the blood and Thorotrast conglomerates deposited in the lung tissue. The total cumulative dose to basal cells both, due to ^{220}Rn exhalation and ^{220}Rn dissolved in the blood, amounts to 64 cGy in the lobar bronchi and 306 cGy in the segmental bronchi using the minimum thickness of the epithelium 40 years after Thorotrast administration (Hornik et al 1995).

Animal studies on the pathogenesis of Thorotrast-induced liver and lung tumors

Neutron irradiation of the liver

The liver of rats was irradiated with high LET radiation (fractionated fast neutrons to simulate the chronic alpha-irradiation of Thorotrast) after application of a non-radioactive colloid (Zirconium dioxide) in the liver. By clearly separating radiation and non-radiation effects the aim was a real conclusive answer to the question of a possible foreign body involvement in the liver tumor induction by Thorotrast. One year after beginning irradiation, the first liver tumor was detected. At the end of the life-span study, the incidence of irradiated animals with liver tumors was about 40 %. In the animals treated additionally with ZrO_2 the incidence of liver tumors was nearly equal indicating that the lifelong-deposited Zr O_2 colloid had no tumor promoting effect. The same observation was made in the ZrO_2 only treated group which had the same liver tumor incidence of about 5% as the untreated control group. Compared to earlier animal studies treated with Thorotrast, the same histological types of liver tumors were found. In conjunction with earlier studies the results now permit a definitive statement about the liver tumor inducing property of Thorotrast: it is the permanent alpha-particle irradiation of ^{232}Th and its decay products which is responsible for tumor development. Other effects of the colloid can be neglected (Spiethoff et al., 1992). The examination of preneoplastic changes of the irradiated liver by means of enzyme histochemical and morphometric methods revealed focal lesions similar to those identified in chemical and viral carcinogenesis. A further result was the observation that the homogeneous neutron irradiation induced more precancerous lesions than the non homogeneous α -radiation of Thorotrast (Ober et al., 1994).

Combined exposure to quartz and Thorotrast

In all epidemiological studies on late effects of Thorotrast no excess rate of lung tumors became obvious despite permanent alpha-exposure of the lungs of Thorotrast patients from the exhalation of ^{220}Rn . This is in clear contrast to lung cancer risk estimates derived from uranium miners exposed to ^{222}Rn . Mining hazards are not only restricted to increased ^{222}Rn levels.

The carcinogenic influences of other damaging agents as mineral dust containing toxic elements must be considered as well. Therefore we exposed in a long-term animal study 360 rats to different levels of quartz (6 mg/m^3 and 30 mg/m^3) prior to the injection of enriched Thorotrast. One year after exposure the first lung tumor was found in a combined treated animal. The lung tumor incidence at the end of the study was more than 40% in all quartz exposed groups. The additional Thorotrast treatment led to a marked shortening of latency times and to a higher total incidence in the group exposed to the higher quartz concentration. The results demonstrate a strong interaction of quartz and Thorotrast on tumor development. In contrast to the neutron experiment the results of this study prove that the carcinogenic effects of radiation in the lung can be strongly influenced by other agents (Spiethoff et al., 1992).

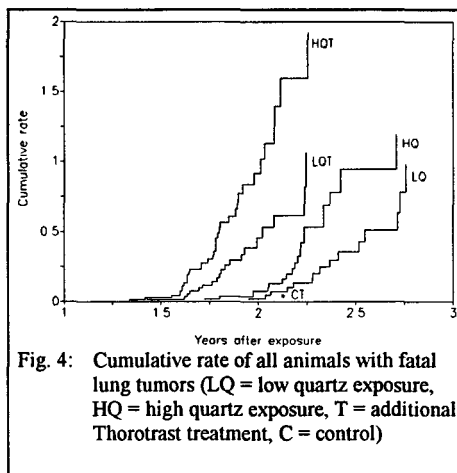


Fig. 4: Cumulative rate of all animals with fatal lung tumors (LQ = low quartz exposure, HQ = high quartz exposure, T = additional Thorotrast treatment, C = control)

References

Bast, Th.

Volumetrische und densitometrische CT-Untersuchungen der Oberbauchorgane bei Thorotrastpatienten. Inaugural Dissertation, 1994. Faculty of Medicine, Ruprecht-Karls-Universität, Heidelberg.

Bast, Th., Zuna, I., Layer, G., van Kaick, G.

CT-measurements of Liver and Spleen in Thorotrast Patients and Their Influence to Dose Rate Calculations, 1995. In: Health Effects of Internally Deposited Radionuclides: Emphasis on Radium and Thorium (Eds. G. van Kaick, A. Karaoglou & A.M. Kellerer), 235, World Scientific Publ. Co., Singapore, New Jersey, London, Hong Kong.

Dalheimer, A.R., Spiethoff, A., Kaul, A.

Calculation of Dose to Non-Storing Organs of Thorotrast Patients. 1995. In: Health Effects of Internally Deposited Radionuclides: Emphasis on Radium and Thorium (Eds. G. van Kaick, A. Karaoglou & A.M. Kellerer), 39, World Scientific Publ. Co., Singapore, New Jersey, London, Hong Kong.

Görich, J., Liebermann, D., Lührs, H., Beyer-Enke, S.A., and van Kaick, G.

Regional lymph nodes of liver and spleen: topographic evaluation based on CT examinations of Thorotrast patients. 1994. Eur. Radiol. 4, 302-306.

Hornik, S., Rohrschneider, K., Wenkster, A., and Kaul, A.
Cataracts in Thorotrast Patients - Risk Calculation and First Results of Ophthalmologic Examinations. 1994. In: Programme and Book of Abstracts, Intern. Seminar „Health Effects of Internally Deposited Radionuclides: Emphasis on Radium and Thorium“, 18-21 Apr. 1994, Deutsches Krebsforschungszentrum, Heidelberg.

Hornik, S. and Kaul, A.

The calculated α -Dose and Lung Cancer Risk in Thorotrast Patients, 1995. In: Health Effects of Internally Deposited Radionuclides: Emphasis on Radium and Thorium (Eds. G. van Kaick, A. Karaoglou & A.M. Kellerer), 43, World Scientific Publ. Co., Singapore, New Jersey, London, Hong Kong.

van Kaick, G., Wesch, H., Luehrs, H., Liebermann, D., Kaul, A.

Epidemiological Results and Dosimetric Calculations - An Update of the German Thorotrast Study, 1995. In: Health Effects of Internally Deposited Radionuclides: Emphasis on Radium and Thorium (Eds. G. van Kaick, A. Karaoglou & A.M. Kellerer), 171, World Scientific Publ. Co., Singapore, New Jersey, London, Hong Kong.

Krezdorn, P.F.

Neoplasien der Leber bei Patienten der Deutschen Thorotraststudie, 1991. Inaugural Dissertation, Faculty of Medicine, Ruprecht-Karls-Universität, Heidelberg.

Liebermann, D., Luehrs, H., van Kaick, G.

Late Effects by Paravascular Thorotrast Deposits, 1995. In: Health Effects of Internally Deposited Radionuclides: Emphasis on Radium and Thorium (Eds. G. van Kaick, A. Karaoglou & A.M. Kellerer), 271, World Scientific Publ. Co., Singapore, New Jersey, London, Hong Kong.

Luehrs, H., Liebermann, D., Wesch, H., van Kaick, G.

Therapeutic Results of Thorotrast Patients with Primary Liver Cancer, 1995. In: Health Effects of Internally Deposited Radionuclides: Emphasis on Radium and Thorium (Eds. G. van Kaick, A. Karaoglou & A.M. Kellerer), 267, World Scientific Publ. Co., Singapore, New Jersey, London, Hong Kong.

Ober, S., Zerban, H., Spiethoff, A., Wegener K., Schwarz M., Bannasch P.

Preneoplastic foci of altered hepatocytes induced in rats by irradiation with α -particles of Thorotrast and neutrons, 1994. Cancer letters 83:81-88.

Spiethoff, A., Wesch, H., Wegener, K., Klimisch, H.J.

The combined and separate action of neutron radiation and zirconium dioxide on the liver of rats, 1992. Health Physics 63:111-118.

Spiethoff, A., Wesch, H., Wegener, K., Klimisch, H.J.

The effects of Thorotrast and quartz on the induction of lung tumors in rats, 1992. Health Physics 63:101-110.

Spiethoff, A., Wesch, H., Wegener, K., Hanisch, E., Kaul, A.

Translocation of Thorotrast in the Body, 1994. Radiation Research 138, 409-414.

Head of Project 2: Dr. N. Priest

II. Objectives for the reporting period.

The programme of research at AEA Technology, Harwell, was designed to examine the validity of the use of risk estimates for leukaemia based on the well documented incidence of leukaemia in groups of former patients that had been injected with Thorotrast for radiography. The programme aimed to answer the following questions:

- Is Thorotrast significantly deposited in the yellow bone marrow, which is not a designated target tissue for leukaemia?
- Is Thorotrast deposited evenly throughout the bone marrow at the level of individual bones?
- Are all target cells for leukaemia (i.e., is all the bone marrow) irradiated / potentially irradiated by Thorotrast?
- Does Thorotrast change its distribution with time producing temporal changes in the distribution of dose?
- To what extent does Thorotrast irradiate target cells for lymphatic leukaemia?

III. Progress achieved including publications.

Introduction

Thorotrast is a colloidal suspension of thorium dioxide which was injected into patients as a radiographic contrast agent until about 1955. Thorotrast is persistent in tissues with little evident solubilisation and loss from the body by excretion. Therefore, being radioactive (due to the presence of long-lived ^{232}Th and its decay daughters) Thorotrast chronically irradiates the tissues in which it is deposited - namely those comprising the reticulo-endothelial system, principally the liver, spleen, lymph nodes and bone marrow. Subsequently, many patients, perhaps as many as 50% of those injected, have developed radiation induced disease. The most common diseases are liver cancer, liver cirrhosis and leukaemia. It follows that if a secure dosimetry is established then risk estimates for these diseases may be determined which are based on the observed incidence of disease in humans exposed to chronic alpha-irradiation rather than to acute, low LET whole body irradiation - i.e. the Japanese bomb survivors. This is important because the validity of the latter for establishing the risk of diseases such as leukaemia following intakes of bone-seeking high LET alpha-emitters, such as plutonium, is far from clear. Indeed, in the case of leukaemia the actual numbers of radiation induced tumours in human populations exposed to alpha-emitting isotopes is 10 to 20 times lower than would be predicted based upon estimates calculated using low LET risk estimates.

In the case of the bone marrow establishing a secure dosimetry was particularly challenging for a number of main reasons:

- the fraction of Thorotrast that deposits in the red bone marrow was unknown with any degree of precision;
- the concentration of Thorotrast within the red bone marrow at different skeletal sites was unclear;
- within the red bone marrow, at any given skeletal site, the uniformity of the Thorotrast pattern of deposition was unknown;
- temporal changes in the distribution of Thorotrast had not been established.

The AEA Technology studies were designed to address each of these areas and to a large extent have succeeded in securing a basic understanding of the dosimetry of Thorotrast. For ease of description the progress achieved is best described in sections with the following headings:

- Fraction of Thorotrast Deposited in the Red Bone Marrow
- Thorotrast Concentrations at Different Skeletal Sites
- Effect of Local Accumulations of Thorotrast at the Microscopic Level
- Temporal Changes in the Distribution of Thorotrast
- Conclusions
- Publications

The Fraction of Thorotrast Deposited in the Red Bone Marrow.

Earlier publications of the German Thorotrast group have suggested that about 8% of the injected quantity of Thorotrast is deposited in the red bone marrow (see Table 3). This fraction was calculated by the extrapolation of results calculated for relatively small bone marrow samples collected at autopsy. More recently, the results of analysis of complete tissues removed from the cadaver of a whole body donation to the United States Uranium Registry have suggested a much larger figure of about 25%. Given that the results from the whole-body were based on the measurement of complete tissues their accuracy is assured. It follows that if such a large fraction were typical then current estimates of the dose received by the red bone marrow and hence the risk estimates derived for this tissue, would be wrong by a factor of about 2. This problem has been addressed in collaboration with colleagues in the United States, Germany and Japan. Firstly, a second whole body donation has been received by the USUR - a German émigré to the USA whose details are included in the German study cohort. Complete tissues have been examined at Los Alamos and Harwell. The fraction of total systemic Thorotrast in the red bone marrow has been determined by Los Alamos and AEA Technology, and in addition AEA Technology has measured the uniformity of the Thorotrast concentration in the marrow of different bones. Secondly, samples of bone marrow and liver have been obtained from the Japanese Cancer Institute, Tokyo. These have been analysed by neutron activation at the German Cancer Centre - Heidelberg and by X-ray fluorescence (XRF) at Harwell. The results of this study are complete, were described at the CEC Heidelberg meeting and have been published. The results confirm that the fraction of Thorotrast deposited in the red bone marrow is currently underestimated by a factor of at least 2. Moreover, the study showed that the disease processes including bone marrow diseases produced no changes in the measured fraction. It was concluded, therefore, that the risk estimates for leukaemia as previously determined by the Danish Thorotrast study group should be divided by a factor of 2, as their calculations assumed 8% deposition of the contrast medium in the red bone marrow, giving an overall risk of about 100 leukaemia's per 10^4 persons per Gy - this is approximately equal to the low LET risk estimate for this disease.

Note: Since the preparation of the last report additional information has been provided by two large, life-span mouse studies with regard to the RBE of alpha-particles (from Cm-244; $T_{1/2} = 143$ d), with respect to lung cancer, liver cancer and leukaemia, compared with low LET radiations (from Ca-45; $T_{1/2} = 143$ d). For these the radionuclides were administered, either by inhalation or injection, as labelled fused clay particles which when deposited in tissues (lung, liver, bone marrow) and resulted in the same temporal and spatial distribution of radiation dose within the organ. Consideration of the life-span toxicity data collected to date, for all of the above cancer types, suggests low RBE values, not inconsistent with the human, Thorotrast, data.

Thorotrast Concentration at Different Skeletal Sites.

Notwithstanding the above it has been suggested that risk estimates for leukaemia, based on epidemiological studies of Thorotrast patient groups are unrealistically low because of Thorotrast accumulation at a few sites resulting in local cell sterilisation effects and wasted dose due to self absorption within areas of high contrast medium accumulation. Studies have been undertaken at Harwell to measure the uniformity of the concentration of the Thorotrast deposit at up to 30 skeletal sites. Studies have been undertaken using tissues collected from both body donations to the USTUR and from monkeys injected with the contrast agent. The monkey samples were measured because no human data is available for measuring distribution at shorter times after injection. Tissues samples for analysis were embedded in resin and the blocks produced cut with a microtome to produce a flat face. The concentration of thorium in the tissues was then measured using XRF. All human and monkey tissues have now been analysed. For both man and monkey the results show rather uniform red bone marrow concentrations - irrespective of the skeletal site - but the yellow fatty bone marrow contained little Thorotrast (see Table 1).

TABLE 1.
Concentration of Thorium in the Bone Marrow of Selected Human and Monkey Bones.

Bone	Projected Thorium Content $\mu\text{g cm}^{-2}$		
	USTUR Case 1	USTUR Case 2	Monkey (mean of 4 results)
<i>Red Bone Marrow Sites</i>			
Rib	201	113	105
Sternum	243	232	186
Lumbar Vertebrae	240	135	227
Thoracic Vertebrae	265	126	175
Cervical Vertebrae	192	114	35*
<i>Yellow Bone Marrow Sites</i>			
Mandible	<5	5	67*
Humerus	<5	21	70*
Distal Femur	<5	2	45*
Patella	<5	1	6

* Samples contained red and yellow marrow components

In addition to the above additional bone marrow samples received from German patients and Japanese patients have been analysed by XRF. The levels of thorium measured are in general agreement with those measured in the USTUR case bones and monkey bones with relatively small, and radiologically insignificant, differences being found between the concentration of thorium in the bone marrow at different marrow sites of the same type (Table 2). This is especially true given that many of those differences found may be explained by the different amounts of Thorotrast injected into these patients. An analysis of the amounts of Thorotrast

injected into the individual patients for whom bone samples were analysed suggests that the level of injected Thorotrast has not affected its final distribution.

Overall, no evidence has been found which would suggest that risk estimates should be modified to take account of irregularities in the distribution of Thorotrast within the red bone marrow at the tissue level.

TABLE 2
Thorium Concentrations Measured in German and Japanese Bone Marrow Samples.

Case # / Marrow Type	Source	Projected Thorium Content $\mu\text{g cm}^{-2}$	Number Samples n
Case 1 / Cellular Marrow	G	89	4
Case 1 / Fatty Marrow	G	2.3	2
Case 2 / Mixed Marrow	G	51	2
Case 2 / Fatty Marrow	G	2.6	2
Case 3 / Mixed Marrow	G	82	3
Case 3 / Fatty Marrow	G	1.3	1
Case 4 / Mixed Marrow	G	39	2
Case 5 / Mixed Marrow	G	80	3
Case 5 / Fatty Marrow	G	6.8	1
All Mixed Samples	J	46	10
All Fatty Samples	J	5.8	7

Effect of Local Accumulations of Thorotrast at the Microscopic Level.

Within the red bone marrow the Thorotrast deposit is characterised by two components of its distribution. Some Thorotrast is deposited throughout the bone marrow tissue forming a diffuse deposit and some is locally concentrated within "hot spots". As for irregularities at the tissue level such local variations in Thorotrast concentration could result in sub-optimal irradiation of the sensitive target cells for leukaemia within the red bone marrow. This could occur if alpha-particles originating from the "hot spots" were either self-absorbed within local colloid deposits or were intensely irradiating a small volume of, perhaps fibrotic, tissue with little or no residual leukaemogenic potential. Moreover, it is possible that if the diffuse deposit is sufficiently sparse then some target cells may remain unirradiated. Studies at Harwell were designed to address this potential dosimetric problem. Autoradiographs have been prepared from 5 μm tissue sections of the red bone marrow using CR39 plastic slides as alpha-detectors. Using these the distribution of alpha-particle emitter within the tissue section can be assessed. The results have shown that at early times after injection, in monkey marrow, all regions of the red bone marrow are uniformly irradiated, but at later times (3 - 4 years post injection) some local accumulations were present. The situation in the human bones, collected at very much later times after injection is more complicated as the distribution of alpha-tracks, by these times is clearly non-uniform. For example, the autoradiographs examined to date clearly show much more thorium close to bone surfaces. Nevertheless, even in these cases no red bone marrow areas could be identified that were unambiguously unirradiated by fixed alpha-sources. In addition, *in vivo* tissues will be irradiated by radon arising from the Thorotrast, much of which may be expected to concentrate in fat deposits throughout the bone marrow. Overall, the dis-

tribution studies suggest that Thorotrast-based risk estimates may be particularly good at predicting the risk of leukaemia following plutonium exposure given the association of this element with bone surfaces and macrophages close to bone surfaces.

An alternative approach to the analysis of the above problem was also attempted in that the distribution of thorium in the tissue sections, as a function of distance from bone surfaces was determined using either Particle Induced X-Ray Emission Spectrometry (PIXE) or Synchrotron X-Ray Fluorescence (sXRF). The latter study was undertaken in association with the University of Warwick and employed a focused beam of synchrotron radiation produced on the Daresbury Laboratory Synchrotron. It generated a plot of thorium content within tissue in scan lines across the bone marrow. The tissues studied using this technique included bone marrow samples removed from both humans and monkeys. Measurements using this technique were completed, but it was not possible to deconvolute the data generated. Accordingly, this approach has been abandoned.

Temporal Changes in the Distribution of Thorotrast.

All of the human tissue available for examination from the USA, Germany and Japan was removed from patients that had died at long intervals after Thorotrast injection. However, the latency period for leukaemia is relatively short (about 5 years). Consequently, if Thorotrast becomes redistributed with time within the red bone marrow the pattern of dose defined on the basis of the examination of human post-mortem tissues may be inappropriate when considering the causation of early leukaemia's. For this reason four cynomolgus monkeys were injected with Thorotrast, two by an intra-venous route and two by an intra-arterial route. Two of the animals were sacrificed at one week after injection and two after several years. The distribution of thorium in the red bone marrow has been determined as for the analysis of the human tissues using a variety of techniques including Secondary Ion Mass Spectrometry (SIMS), scanning electron microscopy with elemental analysis, light microscopy and XRF. In addition, tissues have been sent for thorium determinations using neutron activation at the Heidelberg German cancer centre reactor. The results have shown that the cynomolgous monkey is a relatively good model for man with similar levels of Thorotrast deposition in the liver and bone marrow, but with lower levels of deposition in the spleen (Tables 1 and 3). No indication of time-related changes in organ distribution were found.

As described above the results have also shown that the bone marrow "hot spots" seen in the human tissues are absent at early times after injection in the monkey and even at several years post-injection are poorly defined. At these early times Thorotrast within the red bone marrow is evenly distributed. It likely that a similar period is required for the establishment of "hot spots" in man and that no dosimetry corrections would be necessary for calculating the risk of early leukaemia's. Also, given that leukaemia incidence in man seems to be adequately represented by a linear function with time, no new results have been produced which would suggest other than that the later formation of areas of high Thorotrast accumulation has little effect on leukaemia risk.

TABLE 3
Comparison of the Gross Distribution of Thorotrast in Monkeys and Man

Tissue	Man		Monkey	
	USTUR Case 1	<i>Kaul et al., 84</i>	142	144
Liver	44%	59%	52%	77%
Spleen	13%	29%	5%	4%
Red Bone Marrow	32%	9%	43%	19%

Conclusions

Two important issues have been raised in objection to the use of Thorotrast-derived risk estimates; the first being that it is claimed that the distribution of the Thorotrast is likely to be inappropriate with very high concentrations in some sites, and with low concentrations in others, which would result in some high local α -doses and overall decreased toxicity. However, the present studies have shown that no such non-uniformity exists at the tissue, whole organ level. Nevertheless, at the microscopic level the studies have also shown that Thorotrast is not evenly distributed at later times after injection. The examination of Thorotrast contaminated bone marrow from injected patients, examined in association with the United States Transuranium and Uranium Registry shows the presence of "hot areas" of α -activity, in addition to a diffuse deposit. These are often found in the bone marrow close to bone surfaces. Whilst such Thorotrast clusters will inevitably result in a decreased dose to bone marrow target cells which are distributed more widely it is important to point out that in the special case of risk estimates for plutonium this distribution may strengthen the case for the use of Thorotrast-derived risk estimates, rather than weaken it, as the resultant distribution of Thorotrast is very similar to the distribution of plutonium in bone marrow macrophages at sites of high bone turnover. It follows that it is difficult to make a good case against the use of Thorotrast-derived risk estimates using distribution type arguments.

The second objection raised to the use Thorotrast-based risk estimates is based on the historical failure of any of the epidemiological studies of Thorotrast patients to demonstrate a dose-effect relationship for leukaemia. It has been argued that in the absence of such a relationship any risk estimates derived are valueless. However, this argument is no longer tenable given the results of the latest studies of our Danish collaborators, designed specifically to look at the risk of leukaemia, which show a good dose-response relationship between α -irradiation of the bone marrow by Thorotrast and leukaemia. The risk estimate of 100 cases / 10^4 persons / Gy given above was based on the results of this group, but modified to account for a higher than assumed fractional deposition of Thorotrast in the red bone marrow.

In conclusion it would seem, therefore, that the ICRP quality factor (dose modifying factor) for α -emitters, with respect to leukaemia, is too high. This being the inescapable conclusion of the radium and Thorotrast studies and that a dose modifying factor of unity would be more appropriate. The adoption of such lower risk estimates would go a long way to explaining why we see so few leukaemia's in the radium dial painters and in the Thorotrast exposed people.

Publications

N.D. Priest, J.A.H. Humphreys, Y. Ishikawa and R. Kathren (1995) The distribution of Thorotrast in the bone marrow: A study using human and monkey tissues, 69-74. In: G. van Kaick, A. Karaoglou and A.M. Kellerer (eds.) Health effects of internally deposited radionuclides: Emphasis on Radium and Thorium. World Scientific Publishing Co., Singapore-New Jersey-London-Hong Kong.

J.A.H. Humphreys, N.D. Priest, Ishikawa, K.M.S. Townsend, and J.F. McInroy (1995) Studies of the distribution of Thorotrast in bone, 75-79. In: G. van Kaick, A. Karaoglou and A.M. Kellerer (eds.) Health effects of internally deposited radionuclides: Emphasis on Radium and Thorium. World Scientific Publishing Co., Singapore-New Jersey-London-Hong Kong.

Y. Ishikawa, J.A.H. Humphreys, N.D. Priest, T. Mori, and Y. Kato (1995) Thorium deposition in the bone marrow of Thorotrast patients, 81-85. In: G. van Kaick, A. Karaoglou and A.M. Kellerer (eds.) Health effects of internally deposited radionuclides: Emphasis on Radium and Thorium. World Scientific Publishing Co., Singapore-New Jersey-London-Hong Kong.

Head of project 3: Dr. Wallin

II. Objectives for the reporting period

The Danish Thorotrast study was reactivated in 1989. A cohort of approximately 1000 neurosurgical patients, who received injections with Thorotrast in the period 1935-47 was re-established. The objectives have been to study the cancer incidence and mortality standardized against the general population. The incidence of liver cancer, leukemia, mesothelioma and lung cancer have been studied in some detail. Mortality and cancer incidence of the patients children have been investigated. It has been examined whether there in tumors is a specific pattern of mutations in the tumor suppressor gene p53 which can be related to the cancer induction by Thorotrast. This study may provide evidence as to whether specific p53 point mutations are relevant in α -particle carcinogenesis.

III. Progress achieved including publications

The patients who received injections with Thorotrast were found to have an increased risk for liver cancer and leukemia, but also a general cancer susceptibility (1). Likewise, mortality rates were elevated for all causes of death (2). Seven mesotheliomas were identified in the cohort compared to the expected 0.6 cases, and the risk seemed to related to amount Thorotrast injected (7). A possible association between Thorotrast and small cell lung cancer was suggested (7). Children of patients injected with Thorotrast had no elevated risk for cancer (4).

In hepatocellular carcinomas supposedly induced by aflatoxin exposure often contain a specific point mutation in codon 249, and in lung cancers of miners with heavy radon-exposure another specific point mutation in codon 249 suggestive of an α -particle-specific mutation has been shown. The people injected with the x-ray contrast medium Thorotrast in the past experience an enormous risk of liver tumors and virtually all of these are supposedly induced by α -particles from the decay of ^{232}Th .

Paraffin-embedded, formalin-fixed archival tissues from 18 hepatocellular carcinomas, 9 cholangiocarcinomas, and 9 hepatic angiosarcomas from Thorotrast-exposed patients were collected (8). The tissues were analyzed for p53 protein expression by immunohistochemical staining using the monoclonal antibody DO-7, and for mutations of exon 5-8 by polymerase chain reaction and constant denaturant gel electrophoresis. G->T transversions of the third base of codon 249 of the p53 gene were specifically screened for by restriction enzymes. No high score for p53 protein expression (i.e. positive staining of >20% of examined cells) was observed; lower scores were seen in 5/18 (28%) hepatocellular carcinomas, 1/9 (11%) cholangiocarcinomas, and 0/8 (0%) hepatic angiosarcomas. Only one p53 mutation, a heterozygous T->G transversion of the first base of codon 176, occurred in a hepatocellular carcinoma (8).

Paraffin blocks of tissues of seven lung carcinomas and five malignant mesotheliomas were analyzed for p53 mutations. Only one mutation, in an adenocarcinoma, was detected (7).

The rate of p53 point mutations in liver, and lung tumors and in mesotheliomas (7,8) seems to be lower than in tumors with other etiology. However, this may be consistent with that α -particle carcinogenesis may involve inactivation of p53 by large deletions of the gene, but seems not to be similar to a proposed specificity of point mutations of codon 249 in cancer supposedly induced by α -particles from radon progeny (7).

Publications

1. Anderson, M., and Storm, H., Cancer incidence among Danish Thorotrast-exposed patients, J. Natl. Cancer Inst. 84, 1318-1325, 1992.
2. Anderson, M., Juel, K., and Storm, H.H., Pattern of mortality among Danish Thorotrast patients, J. Clin. Epidemiol. 46, 637-644, 1993.
3. Anderson, M., Carstensen, B., and Visfeldt, J., Leukemia and other related hematological disorders among Danish patients exposed to Thorotrast, Radiation Res. 134, 224-233, 1993.
4. Anderson, M., Juel, K., Ishikawa, Y., and Storm, H.H., Effects of preconceptional irradiation on the mortality and cancer incidence of patients given injections of Thorotrast, J. Natl Cancer Inst. 86, 1866-1870, 1994
5. Anderson, M., Vyberg, M., Visfeldt, J., Carstensen, B., and Storm, H., Primary liver cancer among Danish patients exposed to Thorotrast, Radiation Res. 137, 262-273, 1994.
6. Anderson, M., Carstensen, B., and Storm, H., Mortality and cancer incidence after cerebral arteriography with or without Thorotrast, Radiation Res. 142, 305-320, 1995.
7. Anderson, M., Wallin, H. Jönsson, M., Nielsen, L.L., Visfeldt, J., Vyberg, M., Bennet, W.P., DeBenedetti, V.M.G., Travis, L.B., and Storm, H., Lung carcinoma and malignant mesothelioma in

patients exposed to Thorotrast: Incidence, histology and p53 status, Int. J. Cancer In press.

8. Anderson, M., Jönsson, M., Nielsen, L.L., Vyberg, M., Visfeldt, J., Storm, H.H., and Wallin, H., Mutations in the tumor suppressor gene p53 in human liver cancer induced by alpha-particles, Cancer Epidemiol. Biomarker and Prev., In press.

Head of project 4: Md. dos Santos Silva

II. Objectives for the reporting period

- * To coordinate the reactivation of the Portuguese cohort study in collaboration with our colleagues at the Instituto de Higiene e Medicina Tropical (Lisbon).
- * To develop suitable computer programs for data entry, management of field work and preliminary analyses.
- * To analyse data from all primary liver cancer cases that occurred up to 1977 (when the previous follow-up of the cohort stopped), to present the results from this analysis in the International Seminar held in Heidelberg and to submit a manuscript for publication in its Proceedings.
- * To keep close contacts with the investigators in Lisbon, to collaborate in the planning of the field work and to monitor the implementation of the various methods to be used for tracing the study subjects.
- * To monitor the progress of the data collection throughout the period.
- * To carry out the analyses.

III. Progress achieved including publications

The Portuguese Thorotrast study started later than the other European Thorotrast studies included in the present contract. The contract between the European Commission and the London School of Hygiene and Tropical Medicine was signed only in December 1993.

The aim of this project is to re-activate and enlarge the Portuguese cohort of Thorotrast-exposed patients in order to obtain more accurate estimates of the health risks from internally deposited alpha-particle emitters.

This cohort, the second largest cohort of its type in the world, comprises 2,436 patients who received high doses of Thorotrast for diagnostic purposes during 1930-52 and a similar number of controls who were administered nonradioactive contrast agents matched by sex, age and underlying diagnosis. Until 1977, 1,244 Thorotrast patients and a similar number of controls were traced but no follow-up has been conducted since then. In addition to further follow-up beyond 1977 of the cohort of 1,244 previously traced cases and their controls, we are enlarging the cohort

substantially by using a new method to trace the other thousand Thorotrast patients and a similar number of controls who were identified from hospital records but who, in the past, could not be traced by other means and therefore had not been followed up at all.

We have maintained close contacts with our colleagues in the Instituto de Higiene e Medicina Tropical (Lisbon) throughout the study to design the methods to be used to trace the study subjects and organise how they should be implemented. We also planned together the methods of data collection, coding and computerisation.

Data collected during the previous follow-up were available on cards but not in computerised form. Computer programs for data entry and validation were developed by us in collaboration with our colleagues in Lisbon. To facilitate data coding for computer entry, two new standardised data extraction forms were also created: an 'administrative' and a 'clinical' one. The 'administrative' data extraction form was completed for each member of the cohort. It contained all the available identifiable data (full name, sex, date and place of birth, hospital from which the patient was identified, last known address and telephone, etc) which could help to trace the study subject. An appropriate computer program was developed for computerisation of these administrative data for the entire cohort. This database assisted us in the planning of the field work and in the daily management of the study.

A standardized 'clinical' data sheet was also developed for extraction of all the clinical information assembled in the previous follow-up. This information is now being up-dated with the information collected in the present study. We also developed an appropriate computer program for computerisation, validation and preliminary analyses of these clinical data.

Data from all primary liver cancer cases that occurred up to 1977 (when the previous follow-up stopped) were reviewed in collaboration with our Portuguese colleagues. This review provided a good opportunity to assess the format and content of the 'clinical' data sheet and computer programmes for data entry and analyses, to introduce the necessary changes and to establish standardised criteria for data coding. The data from these liver cancer cases were analysed jointly by us and our colleagues in Lisbon. A poster with the main results was presented at the International Seminar on the health effects of internally deposited radionuclides, held in Heidelberg. A paper was also submitted and accepted for publication in the Proceedings of this Seminar ¹.

Appropriate computer programs have been developed and statistical methods refined to carry out the analyses of the data. Analyses will be carried out to calculate site-specific risks for cancer and other causes of mortality in relation to alpha-radiation exposure. Person-years analyses will be used to calculate the mortality risks in the

Thorotrast-exposed cohort using two different approaches. Firstly, the mortality of the Thorotrast-exposed patients will be compared with that of the general population of Portugal; the 'expected' numbers of deaths in the Thorotrast-exposed cohort will be calculated by multiplying the number of person-years at risk by the corresponding national death rates for Portugal. Secondly, the mortality in the Thorotrast patients will be compared with that in the non-Thorotrast control group. We have obtained from the World Health Organisation magnetic tapes with number of deaths for different causes of death and the necessary population data to carry out the first of these two analysis. These data have been downloaded and converted into an appropriate format suitable to our statistical analysis, and sex- and age-specific national rates for different causes of death (according to the International Classification of Diseases) have been calculated.

Following our small preliminary analyses, risks will be analysed in relation to amount of Thorotrast given to the patient, route of administration, time since administration and age at the time of injection, sex and attained age. Radiobiological models will be used to estimate cumulative absorbed radiation dose for each site allowing for differences according to route of administration. Analyses will be adjusted for potential confounders (i.e. alcohol and smoking habits) for which information is available for all individuals who were clinically examined and followed up.

We plan to conclude the analyses in 1996. We will then submit a final report to the European Commission with the main results from this study.

PUBLICATIONS

1. dos Santos Silva I, Malveiro F, Portugal R, Swerdlow AJ, Cayolla da Motta L (in press). Mortality from primary liver cancers in the Portuguese Thorotrast cohort study. In: *Proceedings of the International Seminar on Health Effects of Internally Deposited Radionuclides. Emphasis on Radium and Thorium*. 18-21 April 1994. Heidelberg, Germany. World Scientific Publishing Co., Singapore.

Head of project 5: Dra. Malveiro

II. Objectives for the reporting period

- * To reactivate the Portuguese cohort study in collaboration with our colleagues in London.
- * To help to develop 'administrative' and 'clinical' data extraction forms in order to be able to collect in a standardised way all the relevant data, to establish criteria for data coding, and to develop suitable computer programs for management of the field work, data entry and validation, and preliminary analyses.
- * To ascertain the fate of the study individuals by contacting local vital statistics registrars and, if necessary, the patients (or their families), certifying physicians and other doctors, hospitals and other health centres.
- * To complete a 'clinical' data sheet for each member of the cohort using the information assembled in the past follow-up, up-dated with the information collected in the present study and to code all the data for computer entry.
- * To computerize the clinical information, to validate the data, and to participate in the statistical analysis.

III. Progress achieved including publications

The Portuguese Thorotrast study started later than the other European Thorotrast studies included in the present contract. The contract between the European Commission and the Instituto de Higiene e Medicina Tropical (Lisbon) was signed only in December 1993.

The aim of the Portuguese Thorotrast study is to re-activate and enlarge the Portuguese cohort of Thorotrast-exposed patients in order to obtain more accurate estimates of the health risks from internally deposited alpha-particle emitters. This cohort, the second largest cohort of its type in the world, comprises 2,436 patients who received high doses of Thorotrast for diagnostic purposes during 1930-52 and 2,086 controls who were administered nonradioactive contrast agents matched by sex, age and underlying diagnosis. Until 1977, 1,244 Thorotrast patients and a similar number of controls were traced but no follow-up has been conducted since then.

We organised in close collaboration with the London School of Hygiene and Tropical Medicine, the re-activation of the follow-up of the Portuguese study, implementing the different approaches to be used to trace the study subjects, and to obtain information from death certificates and anatomo-pathological reports. We are also responsible for coding and computerizing the data for the entire cohort.

In addition to further follow-up beyond 1977 of the cohort of 1,244 previously traced cases and their controls, the cohort was substantially enlarged by using a new method based on information on 'place of birth' of the study individuals to trace the other thousand Thorotrast patients and a similar number of controls who were identified from hospital records but who, in the past, could not be traced by other means.

In Portugal, there is no national system by which individuals can be traced and only local vital statistics registrars, of which there are hundreds throughout the country, hold the necessary identifiable data to be able to ascertain the fate of any particular individual. It is, however, a legal requirement for the registrar of the place of death of an individual (or the Portuguese consulate, if the death occurs outside the country) to notify the death of that person to the registrar of his/her place of birth before permission is given for a body to be buried. Information on 'place of birth' was collected for most of the study individuals and, therefore, it was possible to ascertain their vital status by contacting the birth registrar of his/her place of birth. This method proved to be very efficient as long as the available information on the subjects' names, date of birth and place of birth was correct. The register of the place of birth will contain information on the vital status of the subject and, if the death occurred outside their catchment area, and on the vital statistics register which holds the death certificate.

In order to plan the field work, a standardised 'administrative' data sheet was developed in collaboration with our colleagues at the London School. This data sheet was completed by us for each of the 4,520 members of the cohort by using all the information collected in the past follow-up, which could help us to trace the patients. All the identifiable data of the patient (full name, sex, date and place of birth, hospital/department from which the patient was initially identified, last known address and telephone number, and GPs/hospitals/health centres that may be useful to contact) were extracted from the study cards used in the previous follow-up into this new standardised 'administrative form'.

The information on 'place of birth' (or place of death if known) was then coded to the appropriate local vital statistics registrar. This task was more complicated and time-consuming than we had predicted since the organisation of these vital statistics registrars suffered several re-organizations since 1870 (the earliest year of birth of the study subjects), with successive changes in their catchment areas, formation of

new registrars and abolishment of others. Therefore, we compiled from various governmental publications all the necessary information on the administrative changes that occurred since 1870, and established through direct contact with the current registrars which ones currently held the old registry books. This information allowed us to construct an algorithm with which we identified the relevant registrar(s) who needed to be approached for each member of the cohort.

A computer program was developed in collaboration with our colleagues in London to allow computerization of the data from this 'administrative form. We were responsible for entering the data for the entire cohort into this database. This database was essential in the planning of the field study and in the daily management of the study. During the field work, we tried to cover each geographical area of the country at a time, trying to minimize as much as possible repeated journeys to distant places. Lists with all individuals to be traced in geographically proximate registers were produced from the computer database to assist on this. Since the vital statistics registrars do not allow us to make copies of the death certificates (or of any other relevant material), a new data form was created to facilitate extraction of the data from death certificates.

For study individuals for whom information on place of birth was missing or not available in enough detail, or who were born outside Portugal (e.g., in the ex-Portuguese colonies), or for whom the above approach failed to give any definite information, we tried other methods. The past addresses (and telephone numbers) of patients traced in the previous follow up were available and were used to make direct contact with the patient, or surviving relative, or current inhabitants of the houses. If the study individual was not known to the people currently living in that address, the vital statistics registrar and health authorities of the area of last known residence were contacted to inquire about his/her fate, date last known alive, and health authority to which his/her medical records were transferred. Using these various methods we have had good success in achieving the follow up needed.

The clinical data collected in the previous follow-up were again available on cards but not in computerised form. A 'clinical' data sheet and an appropriate computer program for data entry were developed in collaboration with our colleagues at the London School of Hygiene and Tropical Medicine. All the relevant clinical data were extracted from the study cards used in the previous follow-up, coded and computerized. This database is now being updated with the information obtained from the present follow-up. Causes of death were coded according to the appropriate Revision of the International Classification of Diseases.

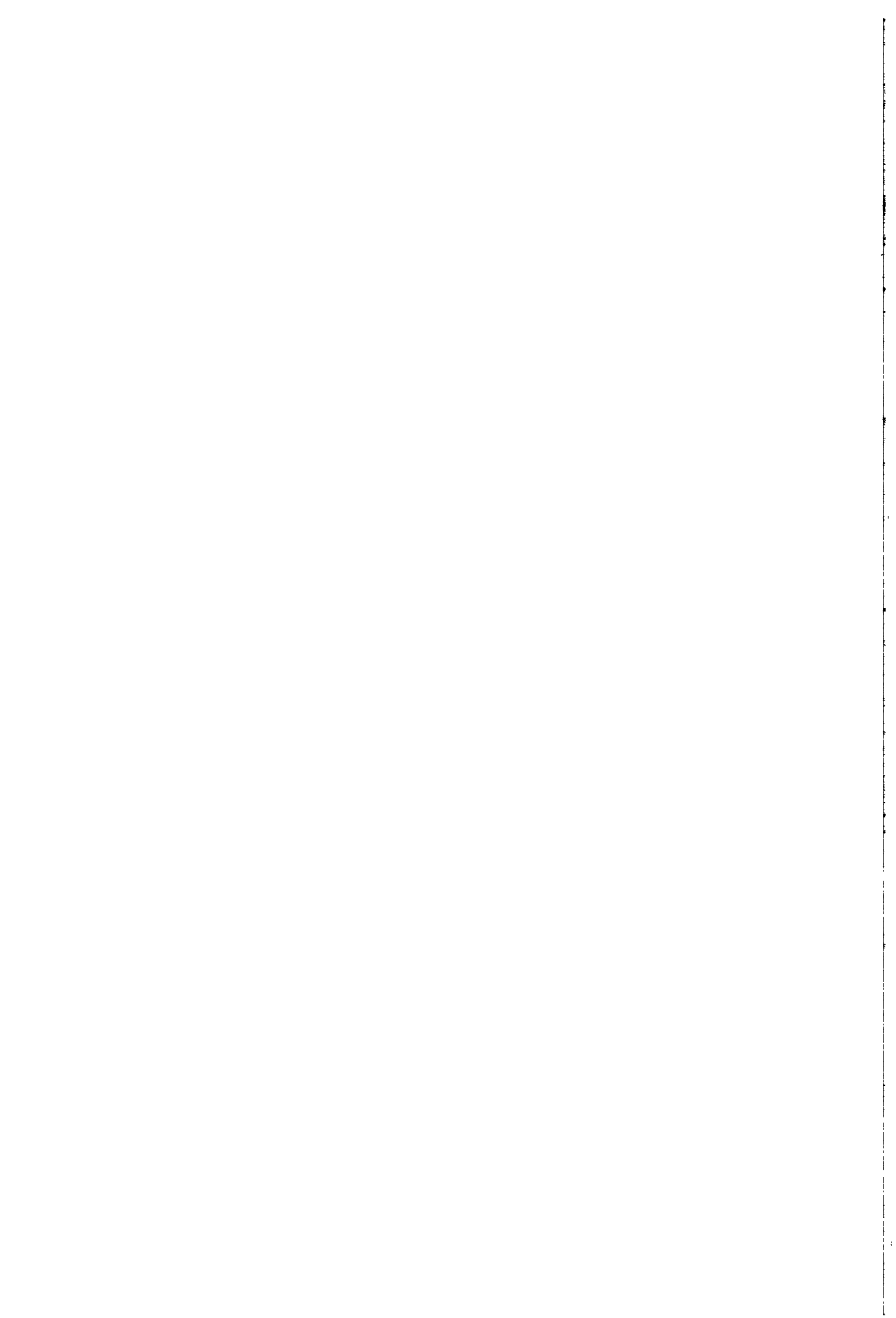
We have also reviewed all the past records of the 87 patients who died from primary liver cancer up to 1977 (when the previous follow-up stopped). This review provided a good opportunity to assess the format and content of the 'clinical' data sheet and computer program for data entry and preliminary analyses, to introduce the necessary

changes and to establish standardized criteria for data coding. The data from these liver cancer cases were analysed in collaboration with colleagues in the London School, and a poster with the main results was presented at the International Seminar on the health effects of internally deposited radionuclides, held in Heidelberg in April 1994. These results were also published in the Proceedings of this Seminar ¹.

We plan to finish the field work in the next few months. A report with the main results will then be sent to the European Commission.

PUBLICATIONS

dos Santos Silva I, Malveiro F, Portugal R, Swerdlow AJ, Cayolla da Motta L (1995). Mortality from primary liver cancers in the Portuguese Thorotrast cohort study. In: *Proceedings of the International Seminar on Health Effects of Internally Deposited Radionuclides. Emphasis on Radium and Thorium*. 18-21 April 1994. Heidelberg, Germany. World Scientific Publishing Co., Singapore.



Final Report

1992 - 1994

Contract : FI3PCT920056

Duration : 1.9.92 to 30.6.95

Sector : C14

Title : The risk assessment of indoor radon exposure.

1)	Poffijn	Univ. Gent
2)	Tirmarche	CEA/IPSN
3)	Kreienbrock	Univ. Wuppertal
4)	Kayser	Dir. Santé Luxembourg
5)	Darby	ICRF
6)	Miles	NRPB
7)	Kunz	NIPHE.CRH
8)	Kunz	CHZ
9)	Cosma	NPL.RO

I. Summary of Project Global Objectives and Achievements

Up to 1993 the project consisted of three major studies about the health risk of indoor radon exposure :

- Radon and lung cancer in the Ardennes-Eiffel region.
- Radon dans les habitations de Brittany-Vendée et du Massif Central et risque de cancer du poumon.
- Investigation on the relationship between lung cancer and radon in houses (UK).

In 1993 3 PECO projects, 2 in the Czech Republic and 1 in Romania, were joined to the group. (see later)

The ultimate objective is the quantification of the risk of indoor radon exposure by means of multi-centre studies with participants in France (Centre d'Energie Atomique), Germany (University of Wuppertal), Luxemburg (Division de la Radio-protection), the United Kingdom (Imperial Cancer Research Fund and National Radiation Protection Board) and Belgium (University of Gent) .

The Ardennes-Eiffel study is aimed to arrive at complete data of some 1200 cases and 2400 hospital controls. At present interviews have been completed for some 1000 cases and 1400 controls. Some details are summarised in Table 1. In the analysis of the complete set of data, a more refined categorisation of smoking will be used. It should be pointed out also that the final exposure distribution for the controls may be different from the one given in Table 1, as previous houses will also be included. Corrections will be made on the measurement results to incorporate seasonal effects.

Table 1 : Present status Ardennes-Eiffel study

	Cas (M+F)		Cont (M+F)		
NUMBER of INTERVIEWS	971		1370		
SMOKING HABITS					
Ever Smoker	94%		67%		
Never Smoker	6%		33%		
AGE DISTRIBUTION					
40-49	11%		f		
			r		
			e		
			q		
			u		
			e		
50-59	24%		n		
			c		
			y		
			m		
60-69	49%		a		
			t		
			c		
			h		
			e		
70-74	16%		d		
RN PRESENT HOME (Bq/m ³)					
	<50	50-99	100-199	200-399	≥ 400
Controls	48%	33%	14%	4%	1%
Population study area	47%	36%	13%	3%	1%

In the radon health study organised in Brittany-Vendée by CEA/IPSN, in close collaboration with the University of Brest and INSERM, 270 lung cancer cases matched each with 2 controls have been registered. The set-up is in complete conformity with that of the Ardennes-Eiffel study. For the moment the study has also been initiated in other parts (Limousin, Auvergne, Languedoc-Roussillon) of France. In the almost completed epidemiological study organised in Cornwall-Devon by ICRF and NRPB, with a protocol very similar to that of the previously mentioned studies, complete information has been obtained for a total of 965 confirmed cases of lung cancer and for about 1400 (hospital as well as community) controls .

Meetings of the members of the group have been organised about every 6 month, in order to finalise the common approach and schedule the plans for the future. It was agreed that case and control enrolment should last up to mid 1995. Measurements in current homes will be completed by the end of 1995. Measurements in past homes will be intensified and are planned to be completed by September 1996.

As different types (open and closed) of radon detectors are used by the radon laboratories of the involved countries, quality control tests in the radon chamber at the university of Gent, as well as side-by-side inter-comparisons in real house conditions were organised at regular intervals. The University Gent did act as co-ordinator for these tests.

In a first experiment 5 different type of detectors were exposed under controlled laboratory conditions, followed immediately by a field test under comparable exposure conditions ($660 \text{ kBq/m}^3\cdot\text{h}$). One type of detector was out of range as compared to the others and was therefore excluded for further use in the study.

In a second experiment, the 4 remaining types of detectors were installed in 5 houses with exposure levels within the range encountered frequently in the study area. Five detectors of each type were exposed in every house for respectively 3 and 6 months. For reasons of multiple control of all influencing effects, an analysis of variance scheme (ANOVA) was conducted . No significant differences were observed between the different types of closed detectors and a small difference of about 15% was observed between the means of open and closed detectors.

The radon levels in all participating houses are rather low. In order to study the validity of the observations over a wide range of exposure levels, the exercise has been extended to some houses within the $200\text{-}500 \text{ Bq/m}^3$ exposure range. From the observations made it became clear that, in a pooling on a larger scale, much attention will also have to be paid to the (differences in) response of the different types of radon detectors under epidemiological field conditions. Therefore such a large-scale inter-comparison exercise for epidemiology, was set-up in December 1993. Currently all available results are being analysed.

In all of the studies it is impossible to perform radon measurements in some of the former residences. For assessing missing past exposures, the usefulness of geological information in combination with the details obtained during the interview as to the construction of the dwellings, and/or the information obtained from the measurements of implanted Po-210 activity is being studied. After all, appropriate past exposure determination is a key issue for correct risk estimation.

From the present status of the studies it can be foreseen that by the end of 1996 complete information for the originally planned number of cases and controls will be attained. It is expected that only limited number of data will be available for relatively high exposure levels. In order to obtain a precise estimate about the risk of indoor radon over a wide range of exposure levels, it will be necessary to perform a pooled analysis of different studies. Care needs to be taken as to the compatibility of the data to be pooled. In this field, the experience gained by the Ardennes-Eiffel study group in co-ordinating and pooling of epidemiological data will be of great use.

In view of carrying out a pooled analysis on a large European scale, a feasibility study was carried out by the British Centre. Following a successful meeting with the principal investigators of ongoing and completed studies in Europe, organised in Oxford in December 1992, a proposal to carry out a pooled analysis of European studies has been submitted to the CEC.

In the course of 1993 three PECO projects were joined to the the original radon risk assessment group :

- two studies are conducted by The National Institute of Public Health of the Czech Republic in the Pluton area of Central Bohemia. A cohort study was set up in this area. From the 3193 deaths registered up to the end of 1994, 194 were identified as being due to lung cancer. One year measurements with open detectors have been performed in about 2480 dwellings of the area. As part of these studies measurements of Po-210 implanted in glass , as indicator of past exposures, have been initiated. A separate part of the work is related to the direct measurement of Pb-210 in the skull of people exposed for a long time to high radon levels.
- the third project is a pilot epidemiological study in the districts of Bihor and Cluj in Romania, set up by researchers from the Physics Department of the University of Cluj-Napoca. In this study the same protocol as in the Ardennes-Eiffel region is being applied. One of the secondary aims of the Romanian study is to carry-out the first systematic radon survey in the north-west part of Romania.

Head of project 1 : Dr. Poffijn

II. Objectives for the reporting period

The major objectives for the reporting period were :

- to interview cases and controls in the different departments of all 5 participating hospitals;
- to perform radon measurements in the current and past homes of the patients;
- to set-up a general system for optimising contact with the inhabitants of past houses;
- to test the data filter on a basic set of house-data delivered by the different collaborating institutes in the different participating countries;
- to draw conclusions out of the field and laboratory inter-comparison exercise organised within the Ardennes-Eifel group;
- to integrate the Peco-partners in the ongoing work of the Ardennes-Eifel group.

III. Progress achieved including publications

A total of 807 patients has been contacted in the 5 hospital centres. In the major hospital (Mont Godinne) the recruitment of patients has come to its end. About 9% was excluded based upon the selection criteria of the common protocol and 6% refused to collaborate.

Installation of long term radon measurement devices , both in the living-room and major bedroom of the current houses of the patients recruited during the reporting period is almost completed (90%) . The assessment of past exposure has been one of the priorities for the last year of the reporting period. To avoid all mistakes the complete list of addresses is being checked for every patient. This information is officially asked for at the respective municipality services, as the (direct) consultation of population registers for scientific purposes is very restricted. Installation of detectors in previous houses is in good progress, although much more time consuming than for current homes. To minimise time-loss, a network of local contact persons has been set-up.

The construction of the data filter is being finalised. For all members of the Ardennes-Eifel study, one or more sets of data has already been tested.

All medical data of cases recruited up to the end of 1994 have been reviewed by a medical doctor, engaged especially for this purpose.

In close collaboration with the involved teams in the different countries and with the responsables of NRPB, quality control and performance tests for the different types of detectors used in the study by the different radon laboratories, were organised both in field and laboratory conditions. The influence of different factors and effects was studied. In general the results for the different laboratories and types of detectors are not statistically

different. In a (very limited) number of cases some of the results of one type of detector did differ very much from the others.

The cause(s) and the influence as well as the consequences for the common epidemiological study will be studied in detail in the coming months together with the other members of the group.

The estimation of missing and past radon values will be one of the principal challenges for the next period. The study on the usefulness of geological information, combined with building characteristics for assessing missing radon, as well as on the value of Po-210 as tracer for past radon exposures has been initiated. The fact that after all only radon exposures of the past are relevant for lung cancer risk experienced today, opens perspectives for such a retrospective technique.

In preparation of a future (potential) pooling on an European scale, the radon research group of the University of Gent participated in and co-ordinated the inter-comparison exercise for epidemiology, that started in December 1993. Except from one institute, all data are completed. When the still missing data will be available, the overall analysis will start immediately.

Publications :

A. Poffijn, M. Tirmarche, L. Kreienbrock, P. Kayser, S. Darby : Radon and Lung Cancer : Protocol and procedures of the multi-center studies in the Ardennes-Eiffel region, Brittany and the Massif Central Region. Radiation Protection Dosimetry, vol 45, 1-4, p. 651-656, 1992.

L. Kreienbrock, A. Poffijn, M. Tirmarche, P. Kayser, S. Darby, H.-E. Wichmann : Radon and lung cancer in the Ardennes-Eiffel region - Concepts, experiences and current progress of an international epidemiological study. In : Medizinische Informatik, Biometrie und Epidemiologie 76, p. 19-23; Medizin Verlag München 1993.

A. Poffijn : Results of a pilot study on radon and lung cancer in the Belgian Ardennes. Book of abstracts Fifth International Conference of the International Society for Environmental Epidemiology, p. 32; Stockholm, Sweden, August 15-18, 1993.

L. Kreienbrock, A. Poffijn, M. Feider, M. Tirmarche, S. Darby : Intercomparison of α -track detectors for epidemiological purposes (to appear).

A. Poffijn, M. Feider, L. Kreienbrock, M. Tirmarche : Recent figures of case-control recruitment in the international Ardennes-Eiffel study on radon and lung cancer. (to appear in Environment International)

A. Poffijn : Indoor Radon in Belgium and Lung Cancer (to appear in Archives belges de Santé Publique)

A. Poffijn : Résultats de l'étude pilote sur le rôle du radon dans le risque de cancer bronchique en Ardennes, Annals of the Belgian Society for Radiation Protection Vol 19 No 1-2, 1994.

A. Poffijn : Europe : Ardennes - Eifel, Radon Research Notes, issue 16, summer 1995.

Head of project 2: Dr. Timarche

II. Objectives for the reporting period (1992-1995)

Estimating the risk of lung cancer related to low chronic exposure of radon in houses was the main aim of this project. In order to calculate the attributable risk for public health, a second objective was the test of interaction between radon and tobacco exposure. Estimating this relatively low risk in comparison to the large risk linked to tobacco, made it necessary to include a high number of cases.

Our efforts were to create an organisation of this study in France, in all points comparable to studies conducted in other European countries at the same calendar period. The purpose of this international collaboration has been the possibility of a joint analysis able to study a large number of lung cancer cases and controls, which increases the statistical power in comparison to isolated individual studies and makes it possible to take in account in this analysis factors that may interact on the dose-response relationship between radon decay exposure, cumulated during the last 30 years, and lung cancer risk. The approach adopted by all the partners, included in this European study is the case-control approach. The protocol and questionnaire of the common study has been elaborated by the scientific responsible of the different countries involved in this collaboration. During the period here mentioned, the study has been progressively organised in the major granite regions of France.

Parallel to this organisation involving interviewers in hospitals and persons in charge of dosimeter placement in the different houses, we have also validated, on an international basis, the various approaches used in epidemiological studies for estimation of individual radon exposure. Estimation of the variation of the measured results, linked to the technics used (laboratory and device) in each country, made it necessary to create an intercomparison of the different devices, used in standard conditions in the homes of the different participating countries.

III. Progress achieved including publications

The criteria of inclusion in the case-control study in France are as follows:

- less than 75 years old;
- resident at least 25 years during the last 35 years in a precise region; the region is defined in function of local conditions:

In the Ardennes region, the region of inclusion is limited to the northern part of this "département", the southern part being of different geological subsoil and consequently less interesting for our study.

In the region of Brittany-Vendée, second region included in our study, 6 "départements" are accepted in the including criteria.

In the region of Limousin, 3 "départements" are included

In the region of Auvergne 4 "départements" are accepted

In the last region included, Languedoc-Roussillon, 6 "départements" are defined.

(Fig.1).

The difference in the size of the regions included is mainly explained by geological criteria, giving us the opportunity of having a large variety of individual radon exposures: in other words, including larger regions but only with low radon exposures, can't increase the power of this study.

The **cases** included are histologically verified primary lung cancer patients of one of the hospitals included in this study; each case is individually matched with 2 controls. These **controls** are hospitalised controls, individually matched by age (± 5 years), sex, and the reason for their present hospitalisation must not be a disease directly linked to tobacco consumption; these diseases are defined in a list including mainly cardio-vascular diseases, chronic bronchitis or emphysema, gastric ulcer, cancers like those of the mouth and lips, larynx or pharynx, pancreas, kidney or bladder. The reason of this exclusion criteria is argued by the expectation of a correct representation of the different groups of smokers (non-smokers, ex-smokers and present smokers) in the control group, in order to be able to test an interaction of radon with tobacco, for different degrees of smoking.

Interviewing of cases and controls is realised in hospital environment, cases being interviewed as soon as possible; the delay between diagnosis and interviewing must not exceed 6 months.

Interviewers hired for this study have been trained for this specific interviewing and meet on an annual basis for exchange of experience. As the study has been extended progressively over the different regions involved, the experience of our interviewers in Brittany and Ardennes has been of great interest for those having begun later. In some regional hospitals, like Cholet, in Vendée, the number of interviews was on a low rate, the number of included cases being very low; and the low income linked to this activity didn't motivate the interviewer. Consequently, our efforts are mainly concentrated on large university hospitals; in each region one pneumologist is considered as a local coordinator of the organisation of the study.

Parallel to this "hospital" organisation, several persons have been hired in order

- 1) to validate the different addresses mentioned for the various houses occupied by each of the interviewed patients,
- 2) to be in contact with the present inhabitants of these houses and to make acceptable the placement of dosimeters in these houses: 2 per home, one in the sleeping room, one in the room mentioned by the patient as the main room occupied during the day; the duration of exposure of these devices is 6 months. The dosimeters used in France are "Kodalpha" detectors, an open alpha track detector. Development of the films is realised by the society Dosirad, results being sent directly to our

institute or to our correspondent for dosimetric survey in Brest: Pr Tymen of the laboratory of aerosols and natural radioactivity of the University of Sciences of Brest; he is also acting as a consultant for radon decay exposure measurements

For practical reasons, the study in France started first in the **Ardennes departement**, in close connection with the international Ardennes-Eiffel study. Recruitment of cases and controls is realised in 2 hospitals; a total of 3 persons are involved in this study, co-ordinated by the society: Ardennes Epidemiologie. The first year being considered as a test of feasibility, the duration of inclusion of patients is presently for 3 years; in a total, the duration of inclusion will be 4 years, the number of expected cases matched with controls being about 120-150.

In the others parts of France, the study began in Bretagne-Vendée, under the supervision of the University of Sciences. The main interviewer in the hospitals is a female person, with a masters in geology, who had stopped working for familial reasons, our interviewers being paid in function of the number of questionnaires realised by month, she considered this job as a half time job compatible with family life. She is now, after 2.5 years of interviewing, considered as our main interviewer, involved in training of those hired in a later period. End of interviewing in this region, as in most of the other regions included, will be end of 1996.

The role of the interviewers is of great importance in our study. Once the doctors have agreed to participate, they are more or less involved in the local organisation of the interviewing of their patients. In most hospitals, as time passes, the contribution of doctors is declining and the role of an interviewer, accepted as part of the clinical team, is of major importance.

A total of 600 cases matched with their controls is expected in France.

The **actual point** of the French study has been presented recently, in February 1995, in a meeting of DOE-CEC in Baltimore, completed by a recent publication of the point of the European Ardennes-Eiffel study in a meeting in Montreal in June 1995 (International Symposium on the Natural Radiation Environment, NRE VI). At the end of June 1995, 80 cancers and 190 controls have been interviewed in the Ardennes region. In the other parts of France 270 cancers matched each with 2 controls have been registered.

In conclusion, we need at least an extension of 18 months of our study in the hospitals to be able to recruit a satisfactory number of cases, able to estimate the risk linked to radon. As the measurement of radon is always delayed by at least 6 months (duration of exposure of the film) after interviewing, we expect finishing exposure measurements during 1997.

Descriptive analysis on this on-going study has not been undertaken on a large scale, some points have been tested, in order to have an idea of the characteristics of a subgroup.

Fig.2 indicates the distribution of cumulative frequency on the data collected in Brittany up to February 1995: median of radon decay concentration measured: 68 Bq per m³

In the Ardennes-Eiffel study, distribution of age has been verified:

<u>age:</u>	<u>for cases</u>	<u>for controls:</u>
< 50 years old:	5.7 %	7.2%
51-60	28.6 %	28.2%
61-70	51,4 %	54.1%
>70	14 3 %	10.5%

Another variable that is followed on a regular basis is the distribution of cases and controls in function of residence in cities or in rural regions; indeed, in University Hospitals, cancer patients may be recruited from a larger region than controls, whose diagnosis may be broken legs, rhumatitis or other relatively common diseases, that are more often treated in local regional hospitals. Or it would be an error to compare cases coming from cities and rural regions, to controls coming mainly from houses of the city close to the hospital; indeed it is well-known that living in cities, mainly in flats decreases significantly individual domestic exposure.

Parallel to this study an intercomparison of the devices used in standard conditions in labs and in houses has been conducted. In houses, the exposure was 3, 6 12 months; the houses used presented radon concentrations on various levels. The results will be analysed and published in a near future by the Ardennes-Eifel group.

In conclusion, we consider this study as one of the first in France, using an individual approach with the aim of estimating, on a large scale, cumulative domestic exposure over 30 years parallel to other carcinogenic components. The acceptance of this approach by the public and patients was globally positive, even if a large number of them were ignoring the existence of this radioactive gas.

ANNEXE: Recent publications in the field of radon epidemiology :

Tirmarche M., Raphalen A., Allin F., Chameaud J., Bredon P. Mortality of a Cohort of French Uranium Miners Exposed to Relatively Low Radon Concentrations. Br. J. Cancer 1993 ; 67 : 1090-1097.

Tirmarche M., Rannou A., Mollie A., Sauvé A. Epidemiological Study of Regional Cancer Mortality in France and Natural Radioation. Rad. Prot. Dosimetry (1988), 24 1 ; 479-482.

Tirmarche M. Indoor Exposure to Radon. In Prevention of Respiratory Diseases, Ed: Macel Decker, Inc. New York (1993), 195-207.

Tirmarche M. Exposition au radon et risque de Cancer. Radioprotection, (1994), 29, 101-114.

Poffijn A., Tirmarche M., Kreienbrock L., Kayser P., Darby S. Radon and Lung Cancer : Procedures of the multicentre Studies in the Ardennes-Eifel region, Brittany and the Massif Central region. Radiation Protection Dosimetry, (1992), 45 : 1, 651-656.

Lubin JH., Boice JD., Edling C., Hornung RW., Howe J., Kunz E., Kusiak RA., Morrison HI., Radford ED., Samet JM., Tirmarche M., Woodward A., Xiang YS., Pierce D., Radon and lung cancer risk : A joint analysis of 11 underground miner studies. National Institutes of Health ,NIH Publication N° 94-3644.

Darby S., Whitley E., Howe G., Hutchings S., Kusiak RA,; Lubin JH., Morriso, HI,; Tirmarche M., Tomasek L., Radford ED,; RoscoeRJ,; Samet JH., Xiang YS., Radon and lung cancer in underground miners. A collaborative analysis of 11 studies. in press JNCI 1995.



FIG. 1

Radon lung cancer case-control study

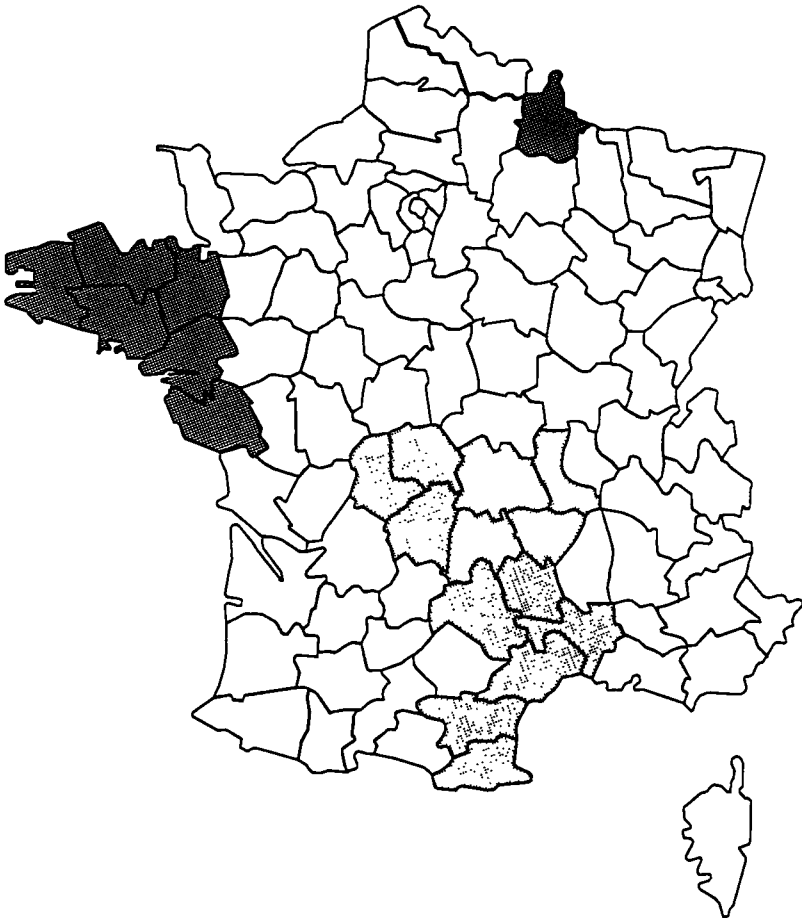
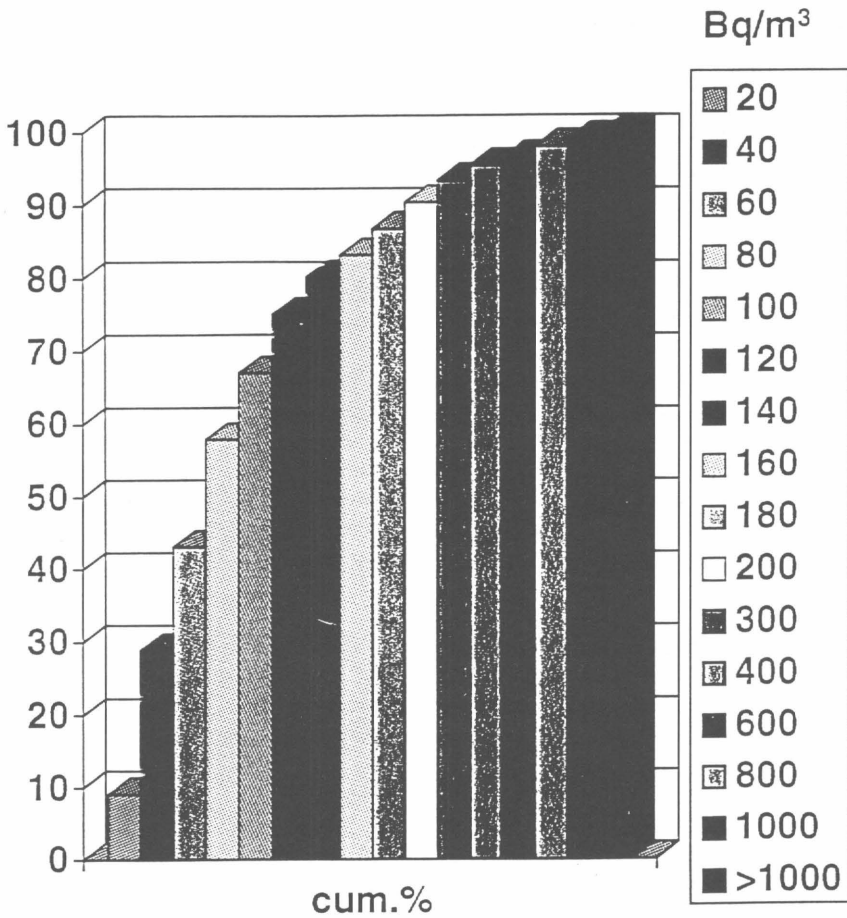


FIG. 2

domestic radon concentrations in Brittany: median: 68 Bq /m³



The Ardennes-Eifel Lung Cancer and Radon Study Scientific Report 1990 - 1995

Head of project 3: PD Dr. Lothar Krcienbrock,
University of Wuppertal, Germany (1990-1994)
GSF Research Center for Environment and Health Neuherberg, Germany (since 1994)

II. Objectives for the reporting period

The Ardennes-Eifel Lung Cancer and Radon Study was prepared in 1989 by A. Poffijn, Rijksuniversiteit Gent, Belgium, P. Kayser and M. Feider, Direction de la Sante Luxembourg, Luxembourg, M. Tirmarche, Commissariat a l'Energie Atomique, Fontenay-Aux-Roses, France, S.C. Darby, Imperial Cancer Research Fund Oxford, United Kingdom and L. Krcienbrock, University of Wuppertal, Germany (now GSF-Research Center for Environment and Health, Neuherberg, Germany) to deal with an European study on the role of indoor radon on the etiology of lung cancer.

The University of Wuppertal / GSF Neuherberg was acting as the German participant of the study.

The University of Wuppertal / GSF Neuherberg was acting as the German participant of the study. The German team was responsible for the personnel involved in the study in his subregion(s), interviewing of cases and controls and the Rn-measurements in dwellings. Furthermore the team from Wuppertal / Neuherberg should analyze common datasets which are created in close collaboration with the coordinator in Gent and the team of Oxford. In addition pooling exercises and m-intercomparisons should be analyzed.

III. Progress achieved including publications

The study was conducted as a case-control study. In a preparatory phase in 1990/91, the details of a common protocol were compiled, describing the minimum criteria that every participating country should meet. In a second step a common coding schedule has been compiled, according to which every country will send, the national data, as a standardised ASCII-file to the coordinating center in Gent. Here a data filter was applied in order to transfer all data in an appropriate form to the statistical analysis center Wuppertal / Neuherberg (for details see [1]).

As more than one type of detector was being used and those are being evaluated in laboratories in several different countries, regular quality control exercises were of great interest. For this reasons four intercomparison exercises were conducted in the reporting period.

The study was designed with a preparation phase, an interview recruitment period four years and additional two years of Rn-analysis (within all houses) and statistical analysis. The time schedule was as follows:

- 1990: - study begin

- 1990 / 91: - common protocol
 - individual questionnaires on a common core
 - pilot

- 1991: - beginning of interviews
 - beginning of rn-measurements in participants homes
 - beginning of common core coding schedule
 - first rn-intercomparison

- 1992 - 1995: - interviews
 - rn-measurements in participants homes
 - beginning of rn-measurements in former homes
 - finishing the common core coding shedule
 - rn-intercomparisons

In the reporting period 628 cases (511 men, 117 women) and 635 community controls (510 men, 125 women) were interviewed. Around 300 hospital controls are interviewed at the end of the reporting period. As documented in other studies on lung cancer within Germany only 2 % of the male and 22 % of the female cases were never-smokers. In the control population these figures are 25 % for the males and 65 % for the females. An attributable occupational exposure (mainly from mining and metal industries) may be possible for around 10 % of the cases.

In preparing a common data base the team of Wuppertal prepared first datasets for testing the data filter at the coordination center in Gent.

For all participants Rn-measurements with charcoal- and with α -track-detectors both in the living room and in the bedroom of the participants homes were conducted. The arithmetic mean concentration in the participants homes is around 50 Bq/m³ α -track and around 65 Bq/m³ for charcoal, where cases' average is slightly higher than controls', which reflect the situation in the general population of the study area.

To conduct an exposure assessment for each subject (case or control) included in the study, attempts were made to measure the Rn-concentration in each home in the study area where the subject has lived for more than one year during the last 35 years. The recruitment of former dwellings was started in the reporting period (but not yet finished).

Because the laboratory and detector facilities used in the study are different in the participating countries a series of different intercomparisons under laboratory and under real home conditions were made. The team of Wuppertal / Neuherberg was acting as the German coordination center for the ongoing intercomparison exercise and was conducting a statistical analysis using analysis of variance models to find rules for possible adjustment. The results of this intercomparisons were discussed and a final draft for publication was prepared [3]. Overall closed detectors and open detectors differ in terms of a multiple correction factor which is influenced by means of equilibrium. The magnitude of this correction is less than the variability of Rn-measurement in general. Therefore Rn-measurements of differnt laboratories could be used for the pooled risk assessment of Rn in homes.

The following paper was prepared in the reporting period:

- [1] Poffijn, A., Tirmarche, M., Kreienbrock, L., Kayser, P., Darby, S.C.: Radon and lung cancer: Protocol and procedures of the multicenter studies in the Ardennes-Eifel region, Brittany and the Massiv Central Region. Radiation Protection Dosimetry 45, 1/4 supplement, 1992, p. 651-656
- [2] Kreienbrock, L., Poffijn, A., Tirmarche, M., Kayser, P., Darby, S.C.: Radon and lung cancer in the Ardennes and Eifel region - Concepts, experiences and current progress of an international epidemiologic study. In: Michaelis, J., Hommel, G., Wellek, S. / Ed. Europäische Perspektiven der Medizinischen Informatik, Biometrie und Epidemiologie. Medizinische Informatik, Biometrie und Epidemiologie 76. Medizin Verlag, München, 1993, p. 19-23
- [3] Kreienbrock, L., Poffijn, A., Tirmarche, M., Feider, M., Darby, S.C.: Intercomparison of passive radon-detectors under field conditions in epidemiological studies. in preparation

Wuppertal / Neuherberg, 26. Oktober 1995

(Lothar Kreienbrock)

Objectives for the reporting period:

Dans le cadre de l'étude épidémiologique des Ardennes-Eifel portant sur les effets du radon sur le cancer des poumons, le Luxembourg avait pour mission d'organiser et d'exécuter cette étude sur son territoire national. Suivant les critères établis dans un protocole commun par les quatre pays participants, il s'agissait d'organiser notamment : le recrutement de patients touchés d'un cancer des poumons, le recrutement des témoins hospitaliers par le biais de certains départements médicaux de différents hôpitaux; le recrutement des témoins issus de la population générale choisis de façon aléatoire à partir des annuaires téléphoniques; l'exécution des interrogatoires des personnes participant à l'étude par une enquêtrice expérimentée; la vérification au niveau des critères d'inclusion, notamment de ceux des Cas; la vérification de la qualité des enquêtes en écartant toutes sources d'imprécision et d'erreur; la distribution et la collecte des détecteurs de radon dans les maisons occupées par les personnes participant à l'étude ainsi que dans les maisons habitées antérieurement par ces participants; la détermination de la teneur en radon dans ces habitations.

Une des préoccupations devrait être la détermination des valeurs de radon manquantes des habitations occupées antérieurement par les personnes participant à l'étude. Il s'agit d'établir une procédure commune qui permettrait de procéder à une estimation de la teneur en radon dans les habitations et qui, pour différentes raisons, ne sont plus accessibles.

Une estimation des données manquantes sur le radon pourrait se faire à partir de données géologiques, des caractéristiques du sol (perméabilité, teneur en radon, teneur en radium) et des caractéristiques architecturales. Il s'agit d'établir un lien entre ces paramètres physiques et la teneur en radon dans les habitations situées sur des géologies spécifiques.

Une attention particulière devrait être adressée à l'assurance de la qualité des mesures du radon avec des détecteurs à traces nucléaires.

II. Progress achieved including publications.

En étroite collaboration avec le Registre Morphologique des Tumeurs du Luxembourg et certains pneumologues, des patients touchés d'un cancer primaire des poumons ont été recrutés. De 1992 jusqu'en juin 1995, 197 cas ont été choisis par le Registre Morphologique et qui du point de vue diagnostic auraient pu participer à l'étude. 11 Cas ont été écartés parce qu'ils ne remplissaient pas tous les critères d'inclusion. 10 patients ont refusé tout de suite leur collaboration, pour 36 patients l'état de santé s'est dégradé rapidement de façon qu'un interrogatoire s'est avéré impossible. 45 patients n'étaient pas disponibles pour différentes raisons (collaboration avec le médecin traitant faisait défaut, patient immigré, parti pour des soins à l'étranger etc). Dans 17 cas, une enquête n'était plus possible, bien que ces patients avaient donné a priori leur assentiment. Finalement, 78 Cas ont participé à l'enquête épidémiologique.

191 témoins hospitaliers remplissant les conditions d'inclusion ont été choisis par les services de chirurgie générale, d'orthopédie et de radiologie.

Environ 200 personnes ont été recrutées dans la population générale comme témoins. Ce recrutement a été organisé en étroite collaboration avec les corps de sapeurs-pompiers régionaux, qui ont contacté les personnes choisies de façon aléatoire à partir de l'annuaire téléphonique dans diverses régions du pays. Cette façon de contacter les participants à l'étude s'est avérée très efficace. Actuellement, 57 de ces témoins issus de la population générale ont été inclus à l'étude.

Les mesures du radon dans les habitations occupées par les personnes faisant partie de l'étude sont presque terminées.

L'organisation des mesures du radon dans les maisons habitées antérieurement par les personnes participant à l'étude s'est avérée particulièrement laborieuse. Les indications fournies par les participants lors des interrogatoires sont souvent inexactes et incomplètes. Il y a lieu de vérifier, en collaboration avec les autorités locales, toutes les adresses des habitations antérieures et de les regrouper suivant les régions avant de contacter les propriétaires actuels. Bien que ces travaux soient en cours, elles sont loin d'être terminés.

Afin d'essayer d'établir un lien entre les caractéristiques du sol et la teneur en radon dans les habitations, des mesures portant sur la perméabilité du sol, sa teneur en gaz radon et en radium ont été entamées, ceci en collaboration étroite avec le Département de Physique du Centre Universitaire de Luxembourg. En quelques dizaines d'emplacements, situés dans des régions à risque à radon élevé et moyen, la corrélation entre ces caractéristiques et la teneur en radon à l'intérieur des habitations est étudiée. Bien que ces travaux ne soient pas encore terminés, les résultats actuellement disponibles ne permettent pas d'établir une corrélation simple, qui permettrait une estimation appropriée et fiable de ces valeurs manquantes.

Pour assurer la qualité des mesures du radon, le Luxembourg a participé de 1992 à 1995 à environ 12 programmes d'intercomparaison nationaux ou internationaux.

Head of project 5: Dr Darby

II. Objectives for the reporting period

The overall project is a case-control study of exposure to radon in the home in South West England and lung cancer. The main objectives for this contract were: to complete the interviewing of cases of suspected lung cancer and hospital and community controls; to review the final diagnoses of all hospital patients; to make long term measurements of the radon concentrations in as many as possible of the current houses of both cases and controls; to commence a programme of measurement of radon levels in the past houses of cases and controls; to commence the computerisation of the data and preparations for analysis; and to commence work on appropriate statistical methods for the analysis of the study. Additional objectives were to test the recent suggestion that a specific mutation in the p53 gene may be a marker for radon-induced lung cancer and to start preparations for a pooled analysis of European studies of indoor radon and lung cancer.

III. Progress achieved including publications

1. Interviewing of cases of suspected lung cancer and controls

Interviewing of cases of suspected lung cancer and hospital and community controls is now complete in all five study centres (see Table 1). A total of 1419 suspected cases, 1424 hospital controls and 1493 community controls who were long term residents of the counties of Devon or Cornwall were interviewed. The refusal rate was low in all three groups.

2. Review of final diagnosis of all hospital patients

The hospital notes of all cases of lung cancer who were interviewed were reviewed after the patient's discharge from hospital. For 965 patients the final diagnosis was lung cancer. For 659 (68.3%) of these the diagnosis was confirmed by histology, and for a further 110 (11.4%) it was confirmed by cytology. In addition the notes of all hospital controls were reviewed after the patients discharge. For only 36 did the final diagnosis a disease strongly related to smoking, thus rendering the patient ineligible for inclusion in the study.

3. Radon measurements in current houses

The programme of measuring radon levels in the current houses of cases and controls is now virtually complete, and a total of 4,057 measurements in current houses have been obtained, with only 5 outstanding.

4. Radon measurements in past houses

The programme of radon measurements in past houses is now substantially complete. Measurements are available for a total of 4,552 homes, and work is in progress to obtain approximately 500 more measurements.

5. Computerisation and Data Cleaning

The computerisation of the data is now virtually complete, and process of "cleaning" and checking the data is well underway.

6. Development of appropriate statistical methodology

Work developing appropriate methods to take into account seasonal variations in domestic radon concentrations is completed and published. Additional work is underway to develop appropriate statistical methods for the analysis of the study. This includes methods for estimating the radon exposure in a home where it has not been possible to obtain a measurement and methods to take into account the specific structure of the uncertainties involved in estimating the radon exposures of cases and controls.

7. Study of mutation in the p53 gene

Following suggestions that an AGG to ATG transversion of codon 249 of the p53 gene occurs in a high proportion of radon-induced lung cancers, a laboratory study was carried out in which pathological specimens of lung cancer cases with high domestic radon concentrations were screened for this specific mutation. None was found, suggesting either that few if any of these cases were radon-induced or that this mutation is not, in fact, a marker for radon-induced lung cancer. This work is now completed and published.

8. Preparations for a pooled analysis of European studies of indoor radon and lung cancer

Following a successful meeting of European investigators of indoor radon and lung cancer, a proposal to carry out a pooled analysis of European studies of lung cancer and residential radon during the next contract period has been submitted to the CEC.

9. Publications

Gunby, J.A., Darby, S.C., Miles, J.C.H., Green, B.M.R., Cox, D.R., (1993) Factors affecting indoor radon concentrations in the UK. *Health Physics*, **64**, 2-12.

Kreienbrock, L., Poffijn, A., Tirmarche, M., Kayser, P., Darby, S., Wichmann, H.E. (1993). Radon and lung cancer in the ardennes and Eifel region-concepts and experiences of an international epidemiological study. In: *Europäische Perspektiven der Medizinische Informatik, Biometrie und Epidemiologie*. (Edited by J. Michaelis, G. Hommel, S. Wellek). *Medizinische Informatik, Biometrie und Epidemiologie*, **76**, pp. 19-23. München: MMV Medizin Verlag.

Poffijn, A., Tirmarche, M., Kreienbrock, L., Kayser, P., Darby, S. (1993). Radon and lung cancer: Protocol and procedures of the multicentre studies in the Ardennes-Eifel region, Brittany and the Massif Central region. *Radiation Protection Dosimetry*, **45**, 651-656.

Peto, J., Darby, S.C. (1994). Radon risk reassessed. *Nature*, **368**, 97-98.

Darby, S.C., Samet, J. (1994). Radon. In: 'Epidemiology of Lung Cancer' (edited by Samet J), pp. 219-243. Marcel Dekker, Inc., New York.

Lo, Y.M.D., Darby, S., Noakes, L., Whitley, E., Silcocks, P.B.S., Fleming, K.A., Bell, J.I. (1995). Screening for codon 249 p53 mutation in lung cancer associated with domestic radon exposure. *Lancet*, 345, 60.

Pinel, J., Fearn, T., Darby, S.C., Miles, J.C.H. (1995) Seasonal correction factors for indoor radon measurements in the United Kingdom. *Radiation Protection Dosimetry*, 58, 127-132.

Table 1 Numbers of patients with suspected lung cancer, patients with other diseases suitable for comparison purposes and community controls identified in Devon and Cornwall

CASES OF SUSPECTED LUNG CANCER

Full interview	Short residence	Patient refused	Medical staff refused	Patient died before interview	Total
1419	1171	69	266	31	2956

HOSPITAL CONTROLS

Full interview	Short residence	Patient refused	Medical staff refused	Total
1424	869	34	64	2391

COMMUNITY CONTROLS

Full interview	Short residence	Subject too ill	Subject refused	GP refused	Ineligible	Total
1493	1112	43	271	160	2113	5190

Head of project 6: Mr Miles

II. Objectives for the reporting period

The objective for the reporting period is to obtain the best estimate of the past radon exposure of both cases and controls recruited into a case control study of the effect of radon in houses. The study has been undertaken jointly by The National Radiological Protection Board (NRPB) and the Imperial Cancer Research Fund (ICRF).

The responsibility for radon measurements lies with NRPB and the ideal is to measure radon levels in all the dwellings inhabited by the study subjects in the last 35 years. In practice, a small percentage of the dwellings have been demolished or extensively altered; others are untraceable or the current occupants unwilling to allow measurements to be made. A realistic objective is to complete measurements in at least 80% of the identified dwellings where cases or controls have lived in the past 35 years.

NRPB also provides a secretariat for the steering group for the study and administers the external funding.

III. Progress achieved including publications

Radon concentrations have been measured in the present and past homes of subjects (cases and controls) using etched track radon detectors. For measurements in current addresses, NRPB provided detectors to ICRF interviewers, who placed them in the homes. Addresses of past homes were provided to NRPB, which wrote directly to the present occupants to obtain agreement for radon measurements to take place.

The addresses were subject to a critical review to identify those dwellings with results available from previous surveys which were removed from the following process. Letters were sent by NRPB requesting the cooperation of the present householders and the subsequent survey was undertaken by post. In cases of refusal, no reply after three letters, or other query, details were reviewed jointly with ICRF for further action. This could be a personal visit by a local interviewer, expansion or correction of address data followed by recycling through the contact programme or deferment to the end of the programme. This follow up programme was labour intensive, but necessary if measurements were to be undertaken in a high percentage of past dwellings. Exposed detectors from past and present homes of cases and controls were returned to NRPB for processing and assessment.

The same measurement protocol was used for both present and past addresses. The standardised protocol employed two passive detectors, one in the main living room and one in a bedroom in regular use, over a six-month measurement period. An annual average for the whole house was calculated using typical occupancy patterns (45% of time at home spent in the living room, 55% in the bedroom). The results were then corrected for seasonal variations using correction factors from the UK national survey of radon levels in homes and adjusting for known seasonal variations in radon levels indoors. NRPB reported the results to ICRF as estimated average annual mean radon concentration.

A total of some 12,000 addresses, including both current and past homes, has been identified by ICRF staff during interviews with study subjects. Measurements have been completed and results obtained for over 8,700 of these dwellings. Measurements are currently in progress in a further 450 homes and results are available from other measurement programmes undertaken by NRPB for another 750 of the identified addresses. Results are therefore available for over 78% of the identified addresses and underway in almost another 4%.

Table 1. Measurements in past dwellings of cases and controls.

Parameter	Before May 1994		After May 1994		Totals	
	Number	Per cent	Number	Per cent	Number	Per cent
Number of addresses	6699	100%	627	100%	7326	100%
Agreed from letter	3491	52%	268	43%	3759	51%
Agreed from visit	1264	19%	38	6%	1302	18%
In other programmes	564	8%	56	9%	620	8%
Total positives	5319	79%	362	58%	5681	78%
Results available	4698	70%	84	13%	4782	65%

The proportion of measurements completed in past dwellings of cases and controls is shown in Table 1. The results from households contacted before May 1994 show that it should be possible to obtain results in about 80% of homes. The process is not complete for homes

contacted after May 1994, but it is expected that a similar success rate will be obtained in these homes.

Results summarised in Table 2 are available for a total of 8181 dwellings. Detectors are installed in a further 900 or so dwellings. In addition, results are available for over 600 dwellings from other radon measurement programmes.

Table 2. Results of radon measurements in current and past dwellings

Parameter	Current dwellings	Past dwellings	Totals
Number of results	4117	4162	8181
Mean value (Bq m ⁻³)	59	48	54
Number above 200 Bq m ⁻³	202	133	335

Publications

Gunby, JA, Darby, SC, Miles, JCH, Green, BMR, and Cox, DR, 1993. Factors affecting indoor radon concentrations in the United Kingdom. *Health Physics* 64, 2-12.

Kendall, G M, Miles, J C H, Cliff, K D, Green, BMR, Muirhead, C R, Dixon, D W, Lomas, P R and Goodridge, S M. Exposure to radon in UK dwellings. NRPB-R272 (London, HMSO) 1994.

Green, B M R and Lomas, P R. Logic and logistics of large radon surveys. *Rad. Protect. Dosim.*, 56, p299 (1994).

Lomas, P R and Green, B M R. Causes and consequences of variations of radon levels in dwellings. *Rad. Protect. Dosim.*, 56, p323 (1994).

Miles, J C H. Mapping and proportion of the housing stock exceeding a radon reference level. *Rad. Protect. Dosim.*, 56, p299 (1994).

NATIONAL INSTITUTE of PUBLIC HEALTH
CENTRE of RADIATION HYGIENE

Šrobárova 48, Praha 10, 10000 Czech Republic
Telephone: 422 67311239 Telefax: 422 67311410

Scientific report
on a CEC contract ERBCIPDCT925078
" The risk assessment of indoor radon exposure : The Czech Pluton area"

Head of the project: Dr. Emil Kunz
Time interval: 1.9.1993- 30. 6. 1995

1. Summary

A cohort study of lung cancer incidence among inhabitants of a rural area in Central Bohemia exhibiting high levels of indoor radon concentrations has been developed. Indoor radon progeny concentrations were measured during the whole year in all residencies of the members of the cohort indicating variable levels of indoor exposure, substantially higher than the average in the country. Data on building changes in the residencies during the time of residence were also gathered, so that individual cumulative exposure to radon progeny can be calculated by a special model relating radon concentrations to radon ingress rate from the soil and ventilating conditions and developed for this purpose.

A study which aims at assessing the possibility of using measurements of Pb^{210} in glass surfaces for determining or verifying the cumulative exposure to radon transformation products has been started. To the very aim, a special pilot study for identifying equipment and methods for in vivo determining Pb^{210} in human skulls as a method of improving the assessment of cumulative exposure to radon progeny was performed.

Data on vital status of each cohort member, residences during different time periods, smoking habits, occupational and other exposures have been collected through interviews of residents or relatives at home during which also data on constructional changes of buildings have been gained. Information on vital conditions and causes of death is being collected and/or verified in the Central Population Registry and in the health documentation of medical institutions. Up to now By the end of 1994, 3 193 deaths have been registered in the cohort. In 3 043 cases (95.3 % of deaths) was the cause of death identified. There were 149 cases of lung cancer (4.7 % of all deaths) in the cohort of about 11 900 persons, who lived in the area for at least 3 years, at least one year between 1960 and 1989.

The preliminary analysis of partial data indicates that even in the situation of generally lower general and specific mortality in the cohort, the dependence of lung cancer risk on exposure to radon transformation products cannot be excluded.

A study of possibility of direct measurement of Pb^{210} in the skull of humans as a method of parallel assessment of cumulative exposure to radon progeny using a planar HP Ge detector and spectrometry chain was performed together with methodical studies of spectrometric and radiochemical determination of this nuclide

in samples of foodstuffs and water indicating the necessary equipment and methods which would be needed for this methodical approach.

The objectives of the given period of this long-term cohort study have been achieved: the cohort was established, the collection of data on the members of the cohort was started and majority of basic data on vital status and exposure to the important factors was already collected and verified.

Further effort will be aimed at finishing collection and verification of data on the cohort members, especially those who moved from the area, assessing their individual cumulative exposure and analysing the findings by appropriate statistical methods. A nested-in case control study will be performed, enabling comparison or pooling data with similar studies.

2. Introduction.

Epidemiological studies on miners, as well as experimental studies on animals, demonstrated that exposure to radon and its daughter products has a carcinogenic effect. Analyses of results of these studies, among which an important place is held by the studies on Czech uranium miners, yielded a measure of this risk and elucidated the role of some other factors, as a basis for an adequate protection of the miners.

Radon, a gaseous daughter of Ra^{226} present in soil and ores, is ubiquitous and thus a source of constant exposure not only of miners, but of all human beings. The exposure to Rn 222 and its daughter products in dwellings represents the largest population exposure to ionising radiation. The indoor radon concentration can vary significantly in different buildings and exceed even those observed now in uranium mines. There are differences in exposure conditions between working underground and living in dwellings, such as in duration of exposure, weight distribution of the activity of the daughter products, fraction of free ions, presence of other aerosols and influence of other noxae. This, together also with differences in important characteristics of these two population groups, make it highly advisable, with regard also to the large costs of the necessary very extent population protection measures, to look for risk estimates assessed on the basis of analysis of data directly characterising health impact of indoor radon exposure. However, up to now only few studies found higher radon exposure of persons died due to lung cancer than of those died for other reasons. The study of the lung cancer incidence in a population group under conditions of high, but variable indoor radon concentrations, is therefore considered as highly topical.

In 1991 the team, headed then by the late Dr. Ševc, started an epidemiological study of lung cancer incidence in inhabitants of a specific area in Central Bohemia exposed to different and prevailing high levels of radon in dwellings. Above approximately the centre of a large area of granitoids, carrying a geological term the Central-Bohemian Pluton, there is a locality mostly agricultural with considerable geological disturbances, called "Devil's burden". The houses situated on the lines of such breaks exhibit high levels of radon-222 and its daughter products, while in the adjacent houses outside the lines of disturbances the concentrations of radon are often manifold lower. The area has been delimited on the basis of a pilot study (see table 1) and geological data. A pilot study indicated also the existence of two groups of dwellings with different mean concentrations, probably connected with different relations to geological breaks both substantially higher than the indicated mean value for the country. The area is agricultural with only small migration of inhabitants. Generally, the conditions for

performing an epidemiological study of lung cancer incidence in relation to exposure to radon daughter products in the area are favourable .

3. Description of the actual stage of the study.

The study, which started in 1991, is a long-term prospective (nonparallel) cohort study of lung cancer and possibly other causes of death in inhabitants of the area, who resided there at least three years and at least one of them between 1.1.1960 and 31.12.1989). People with previous occupational underground experience were not entered into the cohort.

Data on vital status of each cohort member, residences during different time periods, smoking habits, occupational and other exposures were gathered through interviews of residents or relatives at home on the basis of a prepared questionnaire. Data on constructional changes of buildings were also collected.

Information on vital conditions and causes of death was collected and/or verified at local authorities, in the Central Population Registry, in health documentation of the corresponding district hospitals or oncological facilities and departments of pathologic anatomy (with regard to histological characteristics of the tumour).

Measurements of radon daughter products by integral dosimeters (open track etched detectors with Kodak film LR 115) has been performed in about 2480 dwellings of the specified area. One dosimeter was displayed in each of two most used rooms of the dwelling for the period of one year, after this period the dosimeters were collected and the tracks counted and the radon progeny concentration evaluated in the laboratory of dosimetry of the Institute of Industrial Hygiene in Uranium Mining .A study of measurements of Pb^{210} on the surfaces of glass as a possible method of estimating the past exposure to radon was started.

A separate part of the work was the pilot study of direct measurement of Pb^{210} in the skull of people exposed for the long time to high levels of indoor radon by a team of the spectrometric laboratory. Planar HP Ge detector together with spectrometry chain was purchased for this study. Experiments were aimed at the minimalization of the detection limits of different measurement arrangements. For this purpose, the maximal efficiency and minimal background have to be reached. The background (without presence of phantom) was studied with different detectors and different shieldings. Semiconductor HP Ge detectors of different types (p-type, n-type with beryllium window, planar detector with beryllium window) were used in whole body counter shielded with old steel, in the shielding from steel of a special contemporary production and in the lead shielding for semiconductor detectors. Also, combination of these shieldings with additional shielding from copper, tungsten and old steel bricks was used.

3. Results of the study.

One-year lasting measurements (N=3734) in practically all dwellings in the area displayed the following distribution of the equivalent equilibrium concentration of radon (EEC), compared to the results of a 1991 pilot study¹ :

Table 1. Distribution of the equivalent equilibrium concentration of radon (EEC) in dwellings.

EEC Rn Bq/m ³	Petrovice ¹ %	all the area N=3734 %
10-199	22	45
200-499	30	40,8
500-999	32	11,9
1000+	16	2,3

The geometrical mean of the EEC is 204 Bq.m⁻³; the arithmetical mean 344 Bq.m⁻³. (The estimated average EEC in dwellings in the country is 40- 80 Bq.m⁻³). The maximum value found was 11 000 Bq.m⁻³.

A preliminary analysis confirmed also existence of two groups of dwellings with different radon levels, both substantially higher than the indicated average country value.

By the end of 1994, 3 193 deaths have been registered in the cohort of about 11 900 persons. In 3 043 cases (95.3 % of deaths) was the cause of death identified. There were 149 cases of lung cancer (4.7 % of all deaths).

The following table 2 displays the distribution of death causes and the ratio of observed to expected cases (on the basis of national data) among already collected death cases in the cohort.

Table 2. Cause specific mortality by 1990

Died	Total	Ca lung	O/E ¹	Ca other	O/E	violence	O/E	other causes	O/E	un ident
M	1 482	125	1,04	203	0,8	83	0,57	960	0,9	111
F	1 145	10	0,66	194	0,76	33	0,49	806	0,82	102
M+F	2 627	135		397		116		1 766		213

The next table 3 displays values of EEC in detailed administrative division of the area.

The differences in the ratios of observed to expected lung cancer cases (uncompleted yet data) among the communities indicate that even in the situation of generally lower general and specific mortality the dependence of lung cancer mortality on exposure to radon progeny cannot be excluded.

Table 3. Summary of radon measurements and mortality by communities .

Community	number of measur.	Aver. EEC Bq/m ³	max. value Bq/m ³	died men women	O/E	died lung cancer	O/E
Petrovice	572	463	11 160	305 239	0.95 0.91	16 4	0.67 1.37
Hrazany	203	351	1 730	79 57	1.00 0.94	8 0	1.29 0.00
Kovářov	784	330	3 550	138 89	0.87 0.66	15 0	1.24 0.00
Kostelec/Vlt.	526	322	2 640	121 98	0.99 0.74	16 4	1.63 2.59
Záhořany	332	261	1 470	104 77	0.87 0.86	8 0	0.86 0.00
Hřejkovice	264	237	860	108 96	0.96 0.89	8 0	0.92 0.00
Chyšky	479	225	1 260	278 211	0.94 0.87	29 2	0.88 0.08
Dmýštica	167	208	910	103 69	1.05 1.03	8 0	1.08 0.00
Zhoř	162	205	1 030	80 67	0.91 1.02	3 0	0.46 0.00
Kučer	239	164	920	166 142	0.86 0.88	14 0	0.97 0.00

The most important lesson from the experimental work on determining Pb^{210} in human skull was that in measuring with the planar HP Ge detector the main source of Pb^{210} contributing to the peak of Pb^{210} was with highest probability the beryllium window of the detector. To reduce the minimum detectable activity, it is therefore necessary to reconstruct the detector and procure second detector with a guaranteed low background in the area of 46 keV peak. Simultaneously with the research of the background of the different detectors, a calibration of the detector for the skull measurements was performed. The aim of these calibration measurements was the choice of optimal geometry for the in vivo skull measurements. Calibration were performed with the real human skull with small planar Pb^{210} source, scanned on both surfaces of the skull. Variations in the thickness of the different skulls and variations in its composition were taken into account by the use of more different skull tops. Also, angular dependence for the planar detector was measured using radionuclides with the X and gamma ray energy range from 14 keV.

For the calculation of the expected activity of Pb^{210} in the bones originated from inhaled radon, also the direct intake of Pb^{210} from inhalation and ingestion has to be known. Pilot studies in this direction were performed and the content of Pb^{210} was measured in air and in drinking and mineral table water. Also, some older results of radiochemical separation of Pb^{210} in drinking waters were reviewed.

The adequacy of the Pb^{210} gamma spectrometry was repeatedly proved in international intercomparison exercises organised by IAEA

4. Further work within the study

The epidemiological study is still being continued. In 1996 a cumulative individual exposure assessment will be made on the basis of radon measurements or assessments for all dwellings the respondents lived in, the information about the time spent there and estimation of previous exposure levels by a model accounting for constructional changes in buildings.

Although the majority of deaths in the cohort has already been registered further cases will be identified a.o among those respondents who moved out from the area. Data on individual cumulative exposure and lung cancer incidence will then be analysed by appropriate statistical methods, taking account of the factors which can influence the lung cancer incidence such as age, gender, smoking habits, exposure to another noxae in occupation etc. For the analysis, regional and national data on age and gender specific lung cancer mortality as well as an internal control group approach will be used.

A nested-in case-control study will proceed. The exposure to residential radon will be verified and compared between all those who died of lung cancer and 2 to 3 controls, consisting of inhabitants matched by gender, time of birth and for dead controls also by time of death. Personal data and exposure to other with interviews by a standardised form and by visits to medical and administrative institutions. Statistical analysis expected to be performed in 1996 -67 by methods specific for this type of studies will take into account the modifying factors and different reliability of exposure assessment in different time periods.

7.7. 1995



Dr. Emil Kunz, Head of the project

NATIONAL INSTITUTE of PUBLIC HEALTH

CENTRE of RADIATION HYGIENE

Šrobárova 48, Praha 10, 10042 Czech Republic

Telephone: 422 67311448 Telefax :422 67311410

CEC project ERBCIPDCT930411

Interim report

on the epidemiological study of inhabitants of the Middle- Bohemian Pluton area exposed to high concentrations of radon and products of its transformation

Description of the study and its objectives:

Under the co-ordination by the Centre of Radiation Hygiene of the National Institute of Public Health in Prague an epidemiological study has been started of lung cancer incidence in inhabitants of a specific locality in the middle of a larger area of granitoids, carrying geological term Middle-Bohemian Pluton. The locality, mostly agricultural, exhibits considerable geological disturbances (breaks) and the inhabitants are exposed to different, prevailingly high levels of radon in dwellings. The houses situated on the lines of disturbances exhibit very high levels of radon-222 and its daughter products, while in the adjacent houses outside the lines of the breaks the concentrations of radon are often manifold lower, still being higher than average for the country.

The study is a long-term prospective (non-parallel) cohort study of lung cancer and possibly other causes of death in inhabitants of the area, who resided there at least three years and at least one of them between 1.1.1960 and 31.12.1989, no miner has been included (the number of cohort members is 11 870).

Data on vital statuses of each cohort member, residences during different time periods, smoking habits, occupational and other exposures were gathered through interviews of residents or relatives at home during which also data on constructional changes of buildings were collected. Information on vital conditions and causes of death was collected and/or verified in the Central Population Register, in health documentation of the corresponding district hospital or oncological facility and their pathologico-anatomical department (with regard to histological characteristics of the tumour).

The cumulative exposure of each respondent is being assessed on the basis of measurements in dwellings, time spent there and estimation of previous exposure levels by a model accounting for constructional changes in buildings.

One year lasting measurements of radon daughter products by integral dosimeters (Kodak film LR 115) were performed in 2480 dwellings of the specified area.

A model relating radon concentrations to radon ingress rate from the soil and ventilating conditions has been introduced and was with positive results tested in this and the Joachimstal area, permitting to estimate the influence of performed building changes on the consequent residential radon concentration. A study of possibilities in improvement of cumulative exposure assessment by determination of Pb-210 in glass objects in the dwellings and by measuring Pb-210 in persons with parallel determination of Pb-210 intakes is being started.

Results obtained before the end of the contract.

Table 1. summarises the performed measurements and compares them with the results of a pilot study in Petrovice in 1990-91 which gave the stimulus for the epidemiological study.

Table 1. Distribution of the equivalent equilibrium concentration of radon (EEC) in dwellings.

EEC Rn Bq/m ³	Petrovice %	all the area N=3734 %
10-199	22	45
200-499	30	40,8
500-999	32	11,9
1000+	16	2,3

Mean =300,4 Bq.m⁻³. Geometrical mean = 203,6 Bq.m⁻³ (95% C.I.:197,1; 210,4); maximal value found was 11 kBq.m⁻³. (The country mean EEC estimate in dwellings is 40-80 Bq.m⁻³)

An analysis confirmed the existence of two groups of dwellings with G.M 380 and 190 Bq.m⁻³

By the end of 1994, 3 193 deaths have been registered in the cohort In 3 043 cases (95.3 % of deaths) was the cause of death identified. There were 149 cases of lung cancer (4.7 % of all deaths).

Table 2. displays the distribution of death causes by 1990 and the ratio of observed to expected cases (on the basis of national data) among collected death cases in the cohort, the lower than one ratio for all groups of death causes, with the exception of lung cancer deaths in man, reflects the non- industrial character of the region.

Table 2. Cause specific mortality by 1990

Died	Total	Ca lung	O/E ¹	Ca other	O/E	violence	O/E	other causes	O/E	un ident
M	1 482	125	1,04	203	0,8	83	0,57	960	0,9	111
F	1 145	10	0,66	194	0,76	33	0,49	806	0,82	102
M+F	2 627	135		397		116		1 766		213

¹O/E Observed/ expected

The differences in the ratio of observed to expected (on the basis of national rates) lung cancer cases among the communities given in table 3. indicate that even in the situation of generally lower than the population general and specific mortality, the dependence of lung cancer mortality on exposure to radon transformation products cannot be excluded.

Table 3.
Summary of radon measurements and mortality by communities .

Community	number of measur.	Aver. EEC Bq/m3	max. value Bq/m3	died men women	O/E	died lung cancer	O/E
Petrovice	572	463	11 160	305	0.95	16	0.67
				239	0.91	4	1.37
Hrazany	203	351	1 730	79	1.00	8	1.29
				57	0.94	0	0.00
Kovářov	784	330	3 550	138	0.87	15	1.24
				89	0.66	0	0.00
Kostelec/Vlt.	526	322	2 640	121	0.99	16	1.63
				98	0.74	4	2.59
Záhořany	332	261	1 470	104	0.87	8	0.86
				77	0.86	0	0.00
Hřejkovice	264	237	860	108	0.96	8	0.92
				96	0.89	0	0.00
Chyšky	479	225	1 260	278	0.94	29	0.88
				211	0.87	2	0.08
Dmýštica	167	208	910	103	1.05	8	1.08
				69	1.03	0	0.00
Zhoř	162	205	1 030	80	0.91	3	0.46
				67	1.02	0	0.00
Kučeř	239	164	92	166	0.86	14	0.97
				142	0.88	0	0.00

The epidemiological study is still being continued. In 1996 a cumulative individual exposure assessment will be made on the basis of radon measurements or assessments for all dwellings the respondents lived in, the information about the time spent there and estimation of previous exposure levels by a model accounting for constructional changes in buildings.

Although the majority of deaths in the cohort has already been registered further cases will be identified a.o. among those respondents who moved out from the area. Data on individual cumulative exposure and lung cancer incidence will then be analysed by appropriate statistical methods, taking account of the factors which can influence the lung cancer incidence such as age, gender, smoking habits, exposure to another noxae in occupation etc. For the analysis, regional and national data on age and gender specific lung cancer mortality as well as an internal control group approach will be used.

A nested-in case-control study will proceed. The exposure to residential radon will be verified and compared between all those who died of lung cancer and 2 to 3 controls, consisting of inhabitants matched by gender, time of birth and for dead controls also by time of death. Personal data and exposure to other with

interviews by a standardised form and by visits to medical and administrative institutions. Statistical analysis expected to be performed in 1996-67 by methods specific for this type of studies will take into account the modifying factors and different reliability of exposure assessment in different time periods.

29.9.95


Dr. Emil Kunz, Head of the project

From: C.Cosma
University Babes-Bolyai
Faculty of Physics
Cluj-Napoca, Romania
Fax: 40-64-191906
Date: 18.08.95
Total Page Number: 3

To: Andre Poffijn
Radon Research Group
Proeftuinstraat 86
Gent BELGIUM
Fax: 32-9-2646699

Re: ERBCIPD-CT93-0411

TITLE:

THE RISK ASSESSMENT OF INDOOR RADON EXPOSURE:
A PILOT STUDY IN ROMANIA

HEAD OF PROJECT: C.COSMA

I.OBJECTIVES AND CONTENTS

1) To carry out the first indoor radon measurements in Romania, using integrating detection method for establishing certain Romanian areas as areas with high radon potential.

2) To put into evidence the season variations of the indoor radon concentrations in Romania for a better evaluation of long-term exposure to radon.

3) Organizing and starting a 2-year pilot study in Romania (1st March 1995-1st March 1997; the districts of Bihor and Cluj) following the pattern of epidemiological study Ardennes-Eifel.

This study should involve 140 cases and 280 controls, in other words a minimum of 420 integrating radon measurement. The financing of this study will be provided by the PECO subcontract (existing) for the period 1st March 1995-1st March 1996 and on the basis of an internal contract (expected) for the following period.

The subobjectives of this study are:

- to obtain preliminary maps of indoor radon in the two districts mentioned;
- to evaluate the lung cancer death rate within the age groups according to sex and other considerations (smokers, no-smokers);
- to process the obtained data by means of the questionnaires and the radon measurements used in the Ardennes-Eifel pattern-study;

4) To design an original method (in our own laboratory) for indoor radon measurement with track detectors.

II.OBJECTIVES FOR REPORTING PERIOD (30.06.94-31.12.95)

- indoor radon measurement in Herculane-Pecinisca area, where previous measurements showed high radon concentration in geothermal waters and also rather high values of the soil radon flux.
- the pursuit of winter-summer variations of the indoors radon concentrations in this zone
- preliminary measurements of the indoor radon in the cities Cluj and Oradea and in other important towns in the two districts (Dej, Huedin, Turda, Stei, Salonta, Alesd)
- organizing of the epidemiological study: to design and print the questionnaires; to select and organize the group involved in this study; to estimate the lung cancer death rate in Cluj and Bihor districts on the basis of the medical reference material
- to instal detectors and measure by the end of the year (dec.1995) of indoor radon for 60-70 cases and 100-140 controls. Detectors for 30 cases and 50 controls were placed up to now (sept.1) after having selected the cases and the controls.
- to make the first experiments in connection with the exposure and etching of Kodak LR 115 and AZOMURES films in our laboratory.

III.PROGRESS ACHIEVED INCLUDING PUBLICATIONS

1) It was measured in Herculane-Spa including Pecinisca village the indoor radon concentrations for 15 dwellings in summer and winter period (7 big buildings as hotels, schools block of flats and 8 are houses). The Karlsruhe type detectors were placed at the ground floor during a three month period. The arithmetic mean value for the winter period (198 Bq/m^3) is two time greater then the corresponding value for the summer period (98 Bq/m^3).

While only 20% of indoor radon values for the summer period are greater than 200 Bq/m^3 , in the winter period more than 40% of these concentrations exceeded this value.

These results and other data in connection with radon contents of various environmental samples from Herculane Spa were presented at the Sixth International Symposium on the Natural Radiation Environment; June 5-9, 1995 Montreal, Canada and will be published in Environment International(1996).

Radon in various environmental factors in Herculane SPA, Cernea Valley (Romania); C.Cosma, A.Poffijn, D.Ristoiu, G.Messen.

2) In Cluj Napoca for winter period using 3 month integrating measurements were measured the radon indoors for 20 dwellings (at ground floor). The mean value is 156 Bq/m^3 . Non integrating measurements of indoor radon also were made here by Kusnetz method for 30 dwellings in summer and winter period (not selected ground floor) and the mean value was 76 Bq/m^3 .

Relative high radon content was found for a block of flats ($1,2 \text{ kBq/m}^3$ for cave and 105 Bq/m^3 for fifth floor).

In Oradea town (Bihor district-225.000 inhabitants) was measured the indoor radon

by Kusnetz method for 35 dwellings (unselected) and a mean value for summer-winter period of 115 Bq/m³ was found. The mean values for four measurements in winter period at ground floor using integrating three month determination was 124 Bq/m³ in this town.

The results obtained by Kusnetz method in Oradea town were published together with other data in connection with radon and radium in geothermal water used for house-keeping necessities in:

Proceedings of World Geothermal Congress Florence, Italy, 18-31 May 1995, Vol 4 pg 2791-2795

Environmental radioactive aspects of the use of the geothermal waters in Oradea (Romania)

C.Cosma, I.Pop, S.Ramboiu, T.Jurcut, D.Ristoiu.

3) The epidemiological study carries on:

Up to now: - the questionnaires were translated and printed

- 80 Karlsruhe detector were placed (case and controls)

4) In Bihor district on the basis of a medical study concerning the lung cancer a reference material is in preparation. This will be presented at Symposium on Radiation Protection in neighboring countries in Central Europe-1995, Portoroz, Slovenia, September 4-8:

Preliminary study on the rate of bronchopulmonary cancer in Bihor department (Romania) for the estimation of radon risk exposure;

T. Vaida, V. Pacurar, Fl. Maghiar, C. Cosma, D.Ristoiu, S. Ramboiu, A. Poffijn.

5) Romanian publications

- Radon as risk factor in lung cancer disease; C. Cosma, T. Vaida, C. Zamora; Simpozionul de Oncologie, 2-3 iunie 1994, Oradea; Abstract Volume, pg 14.(in Romanian).

- Radon contribution at natural radiation exposure; C. Cosma, D. Ristoiu, T. Vaida, C. Zamora; Analele Universitatii Oradea, 4, 45-53 (1994) (in Romanian)

This letter will be send by post together with the Cost Statement and other information.

Thank you for your accept on Medical Physics Conference.

Yours sincerely,

C.Cosma



Final Report

1992 - 1994

Contract: FI3PCT920062 Duration: 1.9.92 to 30.6.95 Sector: C14

Title: European childhood leukaemia/lymphoma incidence study

- 1) Parkin IARC
- 2) Gurevicius LOC
- 3) Rahu ECR
- 4) Tulbure IISP
- 5) Plesko

I Summary of Project Global Objectives and Achievements

The overall objective is to investigate the incidence of childhood leukaemia in Europe since 1980, and to determine whether any of the changes in incidence which are observed are related to exposure to radiation from the accident at the nuclear power plant at Chernobyl in April 1986. The study follows the recommendations of the CEC Task Group (Report EUR 12551 EN), in choosing as indicator health effect childhood leukaemia (in the age group 0-14), and in using existing registration schemes which meet adequate quality standards rather than establishing special ad hoc data collection systems.

The study began in 1988. Those cancer registries throughout Europe which were considered capable of providing accurate and consistent data on incident cases of childhood leukaemia (and, if possible, also on lymphomas) were invited to participate. Eventually, by the end of the contract period, 36 cancer registries in 23 countries were providing data (Table A1).

Each collaborating centre follows a common protocol (IARC Internal Report 89/002 rev 1 : attached as Annex B). The protocol demands that they provide, each year, data on all recorded cases of childhood leukaemia and lymphoma. These data are provided in the form of an updated file, each line comprising the following minimal information on each registered case number, date of birth, sex, date of diagnosis, place of residence, basis of diagnosis, and histological diagnosis. In addition, each centre provides annual estimates of the childhood population, in the maximum detail (age/sex grouping, and place of residence) as possible. Collation of the data from the different centres is carried out at IARC. The case data are transformed into a standard format for analysis, including

recoding of cancer diagnoses to standard ICD-O codes using the "CONVERT" programs(Ferlay, 1994). All data sets are submitted to a standard set of controls to check for internal inconsistencies-eg in age vs date of birth. Impossible or unlikely combinations of values for recorded cases are returned to the registry for checking.

The estimate excess radiation exposure to the populations of the areas under study , for the first and subsequent years post-accident are provided by UNSCEAR. Although national data on radiation levels, and estimated personal exposures are produced in most of the participating countries, the methods used are not comparable, so that the greater detail available is of no value in the analysis of international datasets.

By the end of the contract period(30/6/95), the protocol required participants to have completed data submission to December 1992, and the majority of centres had done so - see Table A1. All received data sets had been verified for internal consistency, as described above. The case and population at risk data are used to calculate incidence rates (by diagnosis, age group, sex, geographic subunit). The coherence of the estimated incidence with expected values is checked. Other controls on data quality include calculation of percentage of cases histologically verified, or registered as "Death Certificate Only" cases. Trends in these various estimators over time are an important indicator of the value of the data in a comparative study.

Analysis involves firstly the classical presentation of incidence rates, by sex, age group, and geographic area. The diagnostic groups examined comprise :Leukaemia(all), Acute lymphocytic leukaemia, Acute Non-lymphocytic leukaemia, Non-Hodgkin lymphoma. In order to investigate the relationship between changes in incidence, and exposure to Chernobyl-related radiation, a different approach was used . This involves allocation of all cases of leukaemia/lymphoma, and the entire population at risk, an estimated cumulative dose of "excess"radiation. This is calculated based on birthdate, and place of residence. The methodology is described in the latest report of the study, attached as ANNEX A.

Annual Reports of the results of the study have been prepared and circulated to all participants, and to the CEC. The 1993 report, describing the background to the study, the methodology, and presenting background incidence of leukaemia, was published in the scientific literature(Parkin et al 1993). The 1995 report (Annex A) has been submitted for publication. It presents full results up to the end of 1991. At that time, although there was an evident small increase in incidence in childhood leukaemia on a Europe-wide basis, the patterns of increase , by age and place of residence, suggest that the radiation from Chernobyl is not an important factor. The results therefore confirm that the leukaemogenic effects of ionising radiation cannot be much larger than those estimated from the "Lifespan Study" of Japanese A-bomb survivors, as they would have to have been to yield a demonstrable effect.

Head of project 1 : Dr. Parkin

II Objectives for the Reporting Period

The objectives were :

1. To expand the number of participants to include all centers in those european countries which had received substantial exposure to radiation as a result of the accident(notably in central and eastern Europe) and which were capable of providing data of sufficient quality to meet the criteria of the study protocol.
2. To complete data collection from all participants for the period 1980 - 1992, including estimates of the childhood population at risk
3. To complete quality control procedures on these data sets, and with the corrected material, to produce annual analyses of trends in incidence of leukaemias and lymphomas in Europe, linking observed trends to the exposure to radiation from the accident.
4. To publish the results of the study in the scientific literature, as well as in technical reports to the EU
5. To review progress, operational problems, and to agree future plans for the main study, and ancillary projects, with the study collaborators.

III Progress achieved including publications

1. A meeting of all study participants was held in September, 1993, to review progress and future plans. The feasibility of using the ECLIS database for other related epidemiological studies was discussed .
2. Support for participants in central and eastern Europe was obtained through the ECP-7 funding mechanisms (Belarus, Bulgaria, Russian Federation) , and via the PECO programme(Estonia, Lithuania, Romania, Slovakia).
3. Consultant visits were made to Belarus, Russia, and Romania, to review the case finding methods used by these participants, and to discuss methodology.
4. Data on childhood leukaemia in Greece(1980-1990) was supplied, and examined. Because of uncertainties about completeness over the 11 year period, a

decision on their inclusion into the ECLIS database was deferred until a consultant visit could be arranged.

5. The protocol `required submission of data for the period 1980-1992 during the contract period. The status of data reception at 30/6/95 is shown in Table A1. These data have been subject to the quality control procedures summarised in I.

6. Analysis of the main results of the study takes place annually. The objective is to publish these results in the scientific literature. The following publications have been made/submitted during the study period:

PARKIN DM, CARDIS E, MASUYER EM & 34 OTHERS(1993) Childhood leukaemia following the Chernobyl accident:the European Childhood Leukaemia-Lymphoma Incidence study(ECLIS) . Europ. J. Cancer, **29A**, 87-95

PARKIN DM, CLAYTON D, MASUYER E, & 43 OTHERS(1994)Childhood leukaemia in Europe post-Chernobyl:Four and a half year follow up. Environmental Research- submitted

PARKIN DM, CLAYTON D, BLACK RJ & 42 OTHERS(1995)Childhood leukaemia in Europe after chernobyl:Five year follow-up. Radiation Research submitted.

EUROPEAN CHILDHOOD LEUKAEMIAS/LYMPHOMAS INCIDENCE STUDY

Data received on 14/06/95

Registry	Period	Cases
Austria	1980-93	Leukaemia/Lymphoma
Belarus, Brest Region	1980-92	Leukaemia/Lymphoma
Gomel Region	1980-92	Leukaemia/Lymphoma
Grodno Region	1980-92	Leukaemia/Lymphoma
Minsk Region	1980-92	Leukaemia/Lymphoma
Mogilev Region	1980-92	Leukaemia/Lymphoma
Vitebsk Region	1980-92	Leukaemia/Lymphoma
Bulgaria	1980-92	Leukaemia/Lymphoma
Czech Republic	1980-91	Leukaemia/Lymphoma
Denmark	1980-91	Leukaemia/N.H.L.
Estonia	1980-91	Leukaemia/Lymphoma
Finland	1980-91	Leukaemia/Lymphoma
France, Bas-Rhin	1980-89	Leukaemia/Lymphoma
Dijon	1980-92	Leukaemia/Lymphoma
Doubs	1980-92	Leukaemia/Lymphoma
Isere	1980-90	Leukaemia/Lymphoma
Lorraine	1983-92	Leukaemia/Lymphoma
PACA & Corsica	1984-91	Leukaemia/Lymphoma
ex-German Dem. Rep.	1980-93	Leukaemia/N.H.L.
ex-Germany, Fed. Rep.	1980-93	Leukaemia/Lymphoma
Hungary	1980-91	Leukaemia (Lymphoma: 1980-89)
Italy, Piedmont	1980-91	Leukaemia
Varese	1980-87	Leukaemia/Lymphoma
Latvia	1980-92	Leukaemia
Lithuania	1980-92	Leukaemia/Lymphoma
Netherlands	1980-90	Leukaemia
Norway	1980-90	Leukaemia/Lymphoma
Poland	1980-92	Leukaemia/Lymphoma
Russia, Moscow	1980-92	Leukaemia/Lymphoma
St-Petersburg	1980-90	Leukaemia
Slovakia	1980-90	Leukaemia/Lymphoma
Slovenia	1980-92	Leukaemia/Lymphoma
Sweden	1980-91	Leukaemia/Lymphoma
Switzerland, Basel	1980-92	Leukaemia/Lymphoma
Geneva	1980-93	Leukaemia/Lymphoma
Neuchatel	1980-92	Leukaemia/Lymphoma
Saint-Gallen	1980-91	Leukaemia/Lymphoma
Vaud	1980-92	Leukaemia/Lymphoma
Zurich	1980-91	Leukaemia/Lymphoma
UK, England & Wales	1980-90	Leukaemia/Lymphoma
UK, Scotland	1980-92	Leukaemia/Lymphoma

**Head of Project I: European Childhood Leukaemia/Lymphoma Incidence Study (ECLIS)-
Dr R. Kriauciunas, Lithuanian Oncology Center, Vilnius, Lithuania**

II Objectives of the Reporting Period

The objectives were:

1. To complete data collection and entry from the registry area, undertake the routine procedures (checking for duplicates, inaccuracies), and to submit to the study center at IARC an updated file, comprising cases of leukaemia and lymphoma age less than 15 at the time of diagnosis, in accordance with the study protocol (IARC Internal Report 89/002 Rev.1). Submission date is 31 December of each year for the year ending 24 months previously. At the same time, estimates of the population of the study area are provided, by sex and single year of age, for the same years.
2. To review and comment upon reports of the study prior to their submission for publication.
3. To review progress, operational problems, and to agree future plans for the main study, and ancillary projects, with the study collaborators.

III. Progress achieved including publications

1. Data submission

The registry joined the ECLIS study in 1989. Data submissions were made in accordance with the study protocol. The most recent case data supplied were for the period 1980-1992. Population data are supplied by sex, single year of age.

2. Meetings

Representatives from the registry participated in the most recent review meeting.

3. Publications

The following publications have been made/submitted during the study period:

Parkin, D.M. & 36 others (1993) Childhood leukaemia following the Chernobyl accident: the European Childhood Leukaemia-Lymphoma Incidence Study (ECLIS). Eur. J. Cancer, 29A, 87-95

Parkin, D.M., Clayton, D., Masuyer, E. and 43 others. Childhood leukaemia in Europe post-Chernobyl; Four and a half year follow-up. Environmental Research 1994 (submitted).

Parkin, D.M., Clayton, D., Black, R.J. and 42 others. Childhood leukaemia in Europe after Chernobyl; Five year follow-up. Radiation Research 1995 (submitted).

Head of Project I: European Childhood Leukaemia/Lymphoma Incidence Study (ECLIS)-
Dr M Rahu, Estonian Institute of Experimental & Clinical Research,
Tallinn, Estonia

II Objectives of the Reporting Period

The objectives were:

1. To complete data collection and entry from the Estonian Cancer Registry area, undertake the routine procedures (checking for duplicates, inaccuracies), and to submit to the study center at IARC an updated file, comprising cases of leukaemia and lymphoma age less than 15 at the time of diagnosis, in accordance with the study protocol (IARC Internal Report 89/002 Rev.1). Submission date is December of each year for the year ending 24 months previously. At the same time, estimates of the population of the study area are provided, by sex and single year of age, for the same years.
2. To review and comment upon reports of the study prior to their submission for publication.
3. To review progress, operational problems, and to agree future plans for the main study, and ancillary projects, with the study collaborators.

III. Progress achieved including publications

1. Data submission

The registry joined the ECLIS study in 1987. Data submissions were made in accordance with the study protocol. The most recent data supplied were for the period 1980-1992. Population data are supplied by sex, single year of age, and by sex and age-group (0, 1-4, 5-9, 10-14) for Estonia.

2. Meetings

Representatives from the registry did not participate in the most recent review meeting since the registry had not become a full participant in the study at that time.

3. Publications

The following publications have been made/submitted during the study period:

Parkin, D.M. & 36 others (1993) Childhood leukaemia following the Chernobyl accident: the European Childhood Leukaemia-Lymphoma Incidence Study (ECLIS). *Eur. J. Cancer*, 29A, 87-95

Parkin, D.M., Clayton, D., Masuyer, E. and 43 others. Childhood leukaemia in Europe post-Chernobyl; Four and a half year follow-up. *Environmental Research* 1994 (submitted).

Parkin, D.M., Clayton, D., Black, R.J. and 42 others. Childhood leukaemia in Europe after Chernobyl; Five year follow-up. *Radiation Research* 1995 (submitted).

Head of Project I: European Childhood Leukaemia/Lymphoma Incidence Study (ECLIS)
Dr Rodica Tulbure, Institute of Hygiene, Public Health, Health Services
and Management, Bucharest, Romania

II Objectives for the Reporting Period

The objective was:

Data collection from all possible sources for the Bucharest area, checking for duplicates and inaccuracies, and submitting to the study centre at IARC an updated file, comprising cases of leukaemia and lymphoma age less than 15 at the time of diagnosis, in accordance with the study protocol (IARC Internal Report 89/002 Rev.1). Submission dates were 31 December 1994 for the period 1980-1991, and 30 June 1995 for the period 1991-1993. At the same time, estimates of the population of the study area (Bucharest) were provided, by sex, and single year of age, for the same years.

III Progress Achieved

Data submission:

The Institute joined the ECLIS study in 1994. Since in Romania there is no reliable cancer registry, the information on cases of childhood leukaemia and lymphoma were collected from all possible sources and include:

- all hospitals in the Bucharest area where children with these diseases may be diagnosed or treated;
- all laboratories of haematology and pathology which could be responsible for these diagnoses;
- death certificates, mentioning leukaemia or lymphoma in the 'cause of death' section for children aged 0-14.

Data submissions were made in accordance with the study protocol, modified as stated in the Collaborative Research Agreement No. DEP/94/06 RC/94/03072. The most recent case data supplied were for the period 1992-1993. Population data are supplied by sex and single year of age for Bucharest.

Observations

Data collection as described above was a laborious process; all records for the period 1980-1993 (hospital admissions, laboratories of haematology and pathology and death certificates) are kept on paper and could only be found in the archives; in some cases (specified as such in the files submitted to the IARC), the record of the first hospital admission could not be found, the incidence date could only be estimated based on data recorded in the medical history from a later admission (for treatment).

We are planning to have a meeting with the physicians, cancer specialists, to discuss the problems we encountered, and to ensure their collaboration for a reliable cancer registry.

Head of Project I: European Childhood Leukaemia/Lymphoma Incidence Study (ECLIS)

Dr Ivan Plesko, Head, National Cancer Registry of Slovakia and Dept. of Epidemiology, Cancer Research Institute of the Slovak Academy of Sciences, Bratislava, Slovakia

II Objectives for the Reporting Period

1. To complete data collection and entry from the registry area, undertake the routine procedures (checking for duplicates, inaccuracies), and submit to the study center at IARC in Lyon an updated file, comprising cases of leukaemia and lymphoma age less than 15 years at the time of diagnosis, in accordance with the study protocol (IARC Internal Report 89/002 Rev.1). Submission date is 31 December of each year for the year ending 24 months previously. At the same time, estimates of the population of the study areas are provided, by sex and single year of age, for the same years.
2. To review and comment upon reports of the study prior to their submission for publication.
3. To review progress, operational problems, and to agree future plans for the main study, and ancillary projects, with the study collaborators.
4. To provide the services of a staff member at the Department of Epidemiology, Cancer Research Institute of the SAS in Bratislava (Dr Eva Kramarova, Ph.D.) to assist in the analysis of the ECLIS data base.

III. Progress achieved including publications

1. Data submission

The National Cancer Registry of Slovakia joined the ECLIS study in 1987. Data submissions were made in accordance with the study protocol. The first data covered the period 1980-1985 (before accident in Chernobyl), the further data were supplied each year for the period 1986-1997. All the data were reportedly checked in the registry, for nearly all cases microscopic results were obtained from local (district) pathologist, in some cases from autopsy reports (necropsy results). The whole work was positively influenced by the existing network of Out-Patients Clinics of Clinical Oncology existing in every district of Slovakia since 1976, headed by the physician, specialised in clinical oncology as well as by the simultaneous utilisation of ICD-9 codes for topography (4 digits) and morphology (5 digits) and code for grading (1 digit) in our registry. All cases of childhood tumours were reexamined and recoded using both classifications in the largest possible extent. Some inaccurate or missing data were completed by mail, phone or personal visits of the registry staff in the given districts, particularly in the recent years, after dramatic political changes in our country, having negative influence on the financial situation of the registry and worsening of notification. The registry remained without any financial support during two years (1992 and 1993). The situation is but stabilized now, the registry achieved in March 1995 the status of the independent institution in the Ministry of Health and health services and institutions in Slovakia) but insufficient for its whole function. The most difficult problem was the completion of the data of childhood leukaemia and lymphoma for the critical years 1989, 1990 and 1991. The data for 1992 are completed also and the data for 1993 will be finalised in some months. The data for the years 1994 and 1995 are now assured.

The data from Slovakia were regularly completed by the cases with delayed notification or found in autopsy reports. Comments to the collected data were prepared regularly or when required by IARC.

The problem will be the introduction of ICD-0 in Slovakia from 1.1.1993. We do want to send the data to IARC using ICD-0 1.ed. Population data were also supplied by sex and single year of age for the national population and by sex and age-group (0, 1-4, 5-9, 10-14) for each of 38 districts of Slovakia. There will be another problem with expected changes in geographic division of Slovakia in future years; the division of the territory into 4 counties and 38 districts should be changed into 10-14 regions.

The patients in the registry are well identified by name, date and place of birth and permanent address (town or village, street and number) so we are able to send to IARC the data respecting the old territories division of Slovakia and in this way the good continuity of the study. There are no problems until now with the submission of data on population structure in districts at least until the end of 1997.

2. Provision and assistance

Under the terms of Collaborative Research Agreement DE/94/07 the services of Dr Eva Kramarova, Ph.D. were provided for the period 1.11.1994-30.4.1996 in order to assist in the exploitation of the database established by the ECLIS Collaborators.

3. Meetings

Representatives of the National Cancer Registry of Slovakia participated in all meetings including the most recent ones.

4. Publications

The following publications have been made/submitted during the study period:

Parkin, D.M. & 36 others (1993) Childhood leukaemia following the Chernobyl accident: the European Childhood Leukaemia-Lymphoma Incidence Study (ECLIS). *Eur. J. Cancer*, 29A, 87-95

Parkin, D.M., Clayton, D., Masuyer, E. and 43 others. Childhood leukaemia in Europe post-Chernobyl; Four and a half year follow-up. *Environmental Research* 1994 (submitted).

Parkin, D.M., Clayton, D., Black, R.J. and 42 others. Childhood leukaemia in Europe after Chernobyl; Five year follow-up. *Radiation Research* 1995 (submitted).

EC Contract FI3P-CT920064f (Sector C14)

Epidemiological studies and tables

Final Report: July 1992 - June 1995

1)	Muirhead	NRPB
2)	Kellerer	Univ. München
3)	Chmelevsky	GSF (now at CEPN)
4)	Oberhausen	Univ. Saarland
5)	Holm	Karolinska Institute
6)	Becciolini	Univ. Firenze
7)	Richardson	INSERM-U.170
8)	Hill	Inst. Gustave Roussy
9)	de Vathaire	INSERM-U.351
10)	Wick	GSF
11)	Spiess	Univ. München
12)	Kellerer	Univ. München
13)	Muirhead	NRPB
14)	Kellerer	GSF
15)	Kolb	Univ. München
16)	Socié	Hôpital Saint-Louis

Summary of Project Global Objectives and Achievements

The global objectives of the project were as follows:

- (i) To conduct epidemiological studies and obtain information on radiation-induced cancer risks based on the following medically-irradiated cohorts:
 - (a) persons irradiated in childhood for skin haemangioma;
 - (b) patients injected with Ra-224;
 - (c) persons given radiotherapy for a first cancer, either in childhood or in adulthood, and followed to determine second cancer incidence;
 - (d) patients with exposures to I-131 or I-123;
 - (e) bone marrow transplantation patients.

- (ii) To develop models for radiation-induced cancer risks, based on the analysis of data on populations exposed to high doses such as the Japanese atomic bomb survivors, and to examine associated methodological issues. To construct 'probability of causation' (radioepidemiological) tables that are specific to European countries. To review information on cancer risks in relation to pre-conception and *in utero* irradiation.

- (iii) To analyse the geographical distribution of cancer in relation to natural radiation, socio-demographic variables and proximity to nuclear installations, and to address methodological issues associated with geographical studies.
- (iv) To continue and extend a study of occupational radiation exposure and mortality, namely the UK National Registry for Radiation Workers.

Further details of the progress by individual participants are described in their contributions to this report. The global achievements were as follows.

Medically Irradiated Populations

Cancer risks among over 14,000 patients irradiated in infancy for skin haemangioma between 1920 and 1959 have been studied at the Karolinska Institute (Sweden). Doses to various organs were estimated, in order to permit dose-response analyses. Seventeen thyroid cancers were observed in the cohort, whose mean thyroid dose was 0.26 Gy, and there was an increasing trend in risk with dose (excess relative risk 4.92 Gy^{-1} , 95% CI 1.26-10.2). There were also indications of a positive dose-response relationship for breast cancer, particularly in the period more than 50 years following exposure. Cataract examinations have been performed for about 500 patients, with a view to examining the effect of irradiation. In addition, discussions to plan collaborative studies have been held with researchers in Gothenburg and in Villejuif (France) who are responsible for other cohorts of haemangioma patients.

At the University of Munich (Germany), the follow-up of 900 patients injected with Ra-224 after World War II mainly for the treatment of tuberculosis and ankylosing spondylitis has been extended to 1995. A total of 26 breast cancers have been observed compared with 7 expected. Estimates of the dose to the breast from Ra-224 have been made, but analyses indicate that these doses could explain only a small part of the excess risk. However, repeated x-ray fluoroscopy during the treatment may well be of relevance, and attempts are being made to quantify the associated doses. A control group of just under 200 patients not treated with Ra-224 has also been set up and followed, but has not shown a significant breast cancer excess. A histopathological review of the bone cancers in the irradiated cohort, performed at GSF, suggests different patterns of induction for osteosarcoma and fibrohistiocytic sarcoma. Measurements of lens opacities have been made by the University of Munich, both for Ra-224 patients and other groups, such as workers at Mayak in the Southern Urals and bone marrow transplant patients (see below). Improvements in quantifying lens opacities have been achieved through the development of computer algorithms.

Follow-up also continued at GSF (Germany) of a later cohort of about 1500 ankylosing spondylitis patients treated with Ra-224. Seven cases of myeloid leukaemia have been observed in this group, compared with 1.6 expected from regional rates ($p=0.001$). In contrast, there were 3 myeloid leukaemias in a non-irradiated control group, compared with 2.1 expected. Furthermore, unlike the earlier Ra-224 cohort, no excess of breast cancer has been observed in the irradiated group.

Based on just over 1,000 patients in France and the UK given radiotherapy (but not chemotherapy) for a first cancer in childhood, INSERM-U.351 (France) has analysed the second cancer risk in relation to time since exposure. A total of 26 solid cancers were observed, compared with 5.6 expected and, with up to about 30 years of follow-up, there was a statistically significant decrease over time in the relative risk of solid cancers overall. This result is in agreement with results from some other studies of irradiation in childhood. However, the data currently available have limited statistical power to address the possibility of different time trends for different cancers.

The incidence of second cancers following treatment for a first cancer in adulthood has been studied at the University of Florence and other treatment centres in central Italy. Among over 5,000 patients treated in Florence for breast cancer, there was a raised risk of leukaemia associated with radiotherapy (relative risk 8.1, 90% CI 1.4-48, based on 7 cases) which appeared to be concentrated in the five years following irradiation. However, there did not appear to be an association between radiotherapy and the risk of contralateral breast cancer. Follow-up was also conducted of 465 breast cancer patients treated in Pisa. While no leukaemias were observed in this cohort, the level of follow-up is not as high as that in Florence. Clinical records for 713 patients treated in Florence for thyroid cancer have been studied. Second cancers were observed among 23 of these patients, while it may be of interest to note that 46 patients had received external irradiation to the head and neck region prior to the first cancer.

Studies of thyroid cancer following medical exposures to iodine have been conducted at the University of Saarland (Germany). Among over 11,000 patients given I-131, 31 cases of thyroid cancer have been identified, compared with about 9-10 expected from regional rates. While there is some indication of differences in thyroid cancer rates according to the level of activity of I-131 administered, these rates also vary according to the condition which was under investigation or treatment (eg. goitre). There is consequently the possibility that these results are confounded with each other. Another cohort of about 10,000 patients who, since 1977, have been given iodine-123 rather than iodine-131 has been constructed. Checks have been made to ensure that members of the I-123 cohort had not also been given I-131, since the doses from the former procedure are much lower than those from the latter. Follow-up of this cohort is currently being conducted via registration offices, following which checks will be made against thyroid cancers listed in the Saarland Cancer Registry.

Data on new malignancies among bone marrow transplantation patients have been assembled at the University of Munich (Germany) from almost 50 European centres. A total of 41 cancers have been observed among 982 patients given whole body irradiation, compared 7 cancers among 229 non-irradiated patients. Significantly raised risks were seen for cancers of the oesophagus, cervix, and skin (other than melanoma), as well as oral cancers. Analyses performed at GSF (Germany) indicate that the second cancer risk increases with increasing time since treatment. Fifty-five centres have agreed to participate in a tumour banking study organised by Hôpital Saint-Louis (France) and some samples have been frozen; a retrospective study of malignant melanoma is planned.

Risk Modelling

Research into the development and application of mechanistic models to cancer data

has been performed at NRPB (UK). Parallel analyses, performed in collaboration with the US National Cancer Institute, have shown that the Armitage-Doll multi-stage model does not provide a good fit for breast cancer and leukaemia, based on mortality data for the Japanese atomic bomb survivors and incidence data for women with medical exposures. A generalisation of both this model and the two-mutation model of Moolgavkar, Venzon and Knudson (MVK) has been derived and its properties studied. Fits of this generalised model to data on baseline leukaemia rates in England and Wales, conducted in conjunction with the Childhood Cancer Research Group (University of Oxford), indicate that rates for both acute and chronic lymphatic leukaemia can both be adequately described by a two-stage model, although the latter can also be described by a model with three stages.

Tables of probability of causation for member states of the European Union are at an advanced stage of preparation and, in the case of Germany, are in the course of publication. This work has been performed at CEPN (France), in collaboration with the University of Munich. These tables are based mainly on BEIR V models derived from mortality data for the Japanese atomic bomb survivors. However, separate models have been derived using incidence data on the A-bomb survivors for those cancers with high cure rates, eg, breast, thyroid and skin. In the case of radon exposure, a model for lung cancer based on that derived by the BEIR IV Committee has been used. Extensive use has been made of diagrams that show how the probability of causation (PC) and other measures vary with age at exposure and attained age. Uncertainties in PC-values associated with factors such as the transport of risks across populations have also been addressed.

A computer algorithm has been developed at the University of Munich to simplify the fitting of risk models to data on populations with protracted exposures. The algorithm reduces greatly requirements for storage and computing time, so enabling a wider range of models to be fitted. A paper describing analyses of uranium miner data using this algorithm is in the course of preparation. Joint publications with Russian researchers on analyses of data on lung cancer among workers at the Mayak plant are also in progress.

Risks of childhood leukaemia risks in relation to paternal preconception irradiation (PPI) were analysed at NRPB based on data on the offspring of Sellafield workers and other groups of radiation workers, as well as the A-bomb survivors. Apart from the Seascale-born children of Sellafield workers, all of the other data were consistent in showing no association with PPI. In the case of the offspring of the A-bomb survivors, this conclusion held even after allowing for the possibility that some early leukaemia deaths might have been mis-diagnosed. A review was prepared of studies of cancer following irradiation *in utero* from prenatal x-rays. A particular source of uncertainty in risk estimates concerns cancer risks in adulthood. It was concluded that this topic can best be examined by using data for the A-bomb survivors, rather than attempting to follow those who received prenatal x-rays.

Geographical Studies

Researchers at Institut Gustave Roussy (France) have extended their study of mortality around French nuclear installations. The new study covers 13 installations in operation before 1985, compared with six sites analysed previously, and the follow-up has been extended up to 1989. Overall, leukaemia rates among young persons living near these installations were lower than national values (SMR 80, 95% CI 62-101). There was no evidence of increasing

rates with greater proximity to the sites, nor of differences between reprocessing and other installations. Study of other cancers among persons aged less than 65 years showed that rates near installations were close to or smaller than national values. Leukaemia mortality was also examined for young persons living in French towns with a recent and large increase in population. In contrast to L. Kinlen's findings in Great Britain, there was no indication of an association between leukaemia risk and the rate of population increase.

Analyses have been conducted of the geographical variation in childhood leukaemia incidence in Great Britain in relation to natural radiation levels and socio-economic status. INSERM-U.170 (France), in collaboration with NRPB (UK) and the Childhood Cancer Research Group (CCRG) (University of Oxford), analysed these data using both a standard Poisson regression approach and a more recently-developed approach that allows for extra-Poisson variation. The latter method indicated that such variation was present both in the form of clusters across districts and in the form of general heterogeneity in district-specific leukaemia rates. After allowing for these factors, there was no significant association between childhood leukaemia and average levels of gamma radiation or indoor radon levels. In contrast, leukaemia rates were significantly higher in districts of higher socio-economic status. Similar conclusions were reached in an analysis by NRPB, conducted in conjunction with CCRG, using additional data on indoor radon levels in Great Britain collected through offers of measurements in radon-affected areas, as well as other localised surveys.

Methodological work relating to the analysis of geographical studies has been performed. INSERM-U.170 quantified the biases arising in correlation studies from the joint effect of risk factors and studied a method of correcting for this. NRPB examined the properties of methods for detecting 'over-dispersion' (excess variation) in geographically-defined disease rates. Although the application of the latter methods to data for three metropolitan regions in the USA did not indicate clustering of childhood leukaemia in small areas, these data did show significantly higher leukaemia rates in areas of high population density.

Radiation Workers

Work has progressed at NRPB towards the second analysis of the UK National Registry for Radiation Workers (NRRW). Extra groups of workers have been enrolled into this study and data on follow-up to the end of 1992 are being collected. In contrast to the first analysis, which was based on a cohort of about 95,000 workers with a follow-up summing to 1.2 million person-years, the second analysis is likely to be based over 120,000 workers with over 2 million person-years. Consequently, this analysis should provide substantially more information on cancer risks following chronic low dose exposure. Further analysis of data from the first follow-up showed that chronic myeloid leukaemia was the leukaemia sub-type having the most significant trend in risk with dose; this subtype has also been linked strongly to radiation in high dose studies.

Heads of Project 1: Dr C R Muirhead
Dr M P Little (NRPB)

Objectives for the Reporting Period:

To model radiation-induced cancer risks using data on the Japanese atomic bomb survivors and on groups exposed for medical reasons.

To examine the fit of mechanistic models to these data and to develop refinements of such models. To compare leukaemia risks among the offspring of various groups of radiation workers and among the offspring of the Japanese atomic bomb survivors.

To review information on cancer risks associated with *in utero* exposure to prenatal x-rays.

To analyse the geographical distribution of childhood leukaemia in relation to both natural radiation and socio-economic status throughout Great Britain, and in relation to socio-demographic variables in metropolitan regions in the USA.

To study the properties of statistical methods for detecting 'over-dispersion' (excess variation) in geographically-defined disease rates and to apply them to data on childhood leukaemia in parts of the USA.

Progress achieved:

Modelling of Radiation-induced Cancer Risks

(a) Mechanistic Models

The Radiation Effects Research Foundation (RERF) and other groups (Shimizu et al., *Radiat. Res.* 121:120-41 1990; BEIR V 1990) have fitted a variety of purely descriptive empirical models to various cancer sites in the Japanese atomic bomb survivor Life Span Study (LSS) 11 cancer mortality data. Because of the missing first five years of follow-up in the Japanese data and the indications from other data (Little, 1993a) that leukaemia risk might be significantly increased in the period up to five years after exposure, a combined analysis has also been carried out at NRPB of the Japanese leukaemia data with the leukaemia mortality data from the UK ankylosing spondylitis patients (Little, 1993a). The resulting models, together with other models fitted to the Japanese solid cancer data have been used to assess population cancer risks for UK and Japanese populations (Little, 1993a).

A striking feature of both solid cancer and leukaemia risks in a variety of exposed groups is the decrease of excess relative risk with increasing age at exposure (Little, 1993a). For leukaemia it is well known that the excess relative risk reduces with increasing time after exposure (Little, 1993a). There is also some evidence that for solid cancer the relative risk eventually decreases with increasing time after exposure for those exposed in childhood (Little, 1993a). In order to explain these and other observations more biologically based models have also been fitted to a variety of exposed datasets (Little et al., 1992, Little, 1993a, 1993c, Little et al., 1994a). In particular, Armitage-Doll type multistage models have been fitted to the Japanese atomic bomb survivor LSS 11 mortality data. The Armitage-Doll model assumes that each susceptible stem cell undergoes a succession of mutations in a probabilistic manner. When the cell has acquired a specific number of mutations in a specified order it becomes malignant, at which point there is assumed to be rapid progression of the single malignant cell to a clinically detectable malignancy. The model with three stages - the first of which is radiation

affected - is found to provide an adequate qualitative description of solid cancer incidence, while a model with three stages - the first two of which are radiation affected - gives a reasonable qualitative description of leukaemia (Little et al., 1992, Little, 1993a, 1993c, Little et al., 1994a). In particular, the pronounced variation of relative risk with age and time that is seen, for both solid cancers and leukaemia, is predicted by the optimal models (Little et al., 1992, Little, 1993a, 1993c, Little et al., 1994a) (see Figure 1). For leukaemia there can be no more than about 3 stages (Little et al., 1994a), although for solid cancer less information is available as to the number of stages. It is a feature of the Armitage-Doll model, and other multistage models of carcinogenesis, that if radiation acts at more than one stage then inverse dose-rate effects may arise as a result of interactions between the effects of a protracted dose at the various radiation-affected stages. However, it has been shown that population cancer risk in general displays fairly slight dependence on administered dose in the range 0.001 to 1.0 Sv and on the length of the time period over which the dose is administered in the range one year to 100 years (Little et al., 1992, Little, 1993a, 1993c, Little et al., 1994a) (see Table 1). Dose-rate effects resulting from the protraction of a radiation exposure over many years acting on (the same) cells at various stages of a multi-step process of carcinogenesis are therefore expected to be slight. Dose-rate effects which have been observed in epidemiological studies and cellular radiobiology may thus find their explanation in other phenomena such as short-term intracellular repair.

The application of mechanistic models to describe patterns of cancer induction by ionising radiation also involved a parallel analysis of the Japanese leukaemia mortality data in conjunction with data released by the US National Cancer Institute on the IRSCC (cervical cancer) leukaemia case-control study. A paper describing this work is in press (Little et al., 1995d). The main conclusion of this analysis is that the classical multistage model does not provide a good description of radiation-induced leukaemia. As a result of these indications of lack of fit of the Armitage-Doll model, a generalisation of this model and also of the two-mutation model of Moolgavkar, Venzon and Knudson has been developed and a paper describing the mathematical behaviour of the model is in press (Little, 1996). Comparison of the mathematical predictions of this model with what is known about the time course of radiation-induced cancer leads to the conclusion that while the two-mutation model of Moolgavkar et al. might provide a good description of excess leukaemia incidence following exposure to radiation, it would appear not to be able to describe the temporal pattern of excess risk seen for solid cancers (Little, 1996). Childhood leukaemia data supplied by the Childhood Cancer Research Group (University of Oxford) has been used in conjunction with OPCS adult leukaemia incidence data to fit this generalised two-mutation model. The analysis indicates that acute lymphatic leukaemia and chronic lymphatic leukaemia can be adequately described by a two-stage model, although chronic lymphatic leukaemia can also be adequately described by a three stage model (Little et al., 1995c).

(b) Preconception Irradiation

Following the 1990 study of Gardner et al. (BMJ 300:423-9 1990), which suggested a possible association between childhood leukaemia and paternal preconception radiation exposure, analyses have been conducted of the trends with dose in this and other datasets to test the compatibility of the risks in the offspring of the various exposed groups (Little, 1992, 1993b, Little et al., 1994b, 1994c). The statistically most powerful of these other datasets is the (F₁) offspring of the Japanese atomic bomb survivors. The relative risk coefficients for leukaemia, as a function of paternal and maternal gonadal pre-conception dose, in the offspring of the Japanese survivors and in children of the Sellafield workforce have been compared, and statistically significant differences have been found (Little, 1992). The statistical significance of these differences is equally marked if the analysis is restricted to those born before the end of 1950 in the Japanese cohort; therefore it is

Figure 1

Predicted Excess Relative Risk at 1 Sv for the Optimal Armitage-Doll Models Fitted to the Japanese Bomb Survivors for Solid Cancers (with 3 Stages, the First of Which is Radiation-Affected) and for Leukaemia (with 3 Stages, the First and Second of Which are Radiation-Affected)) (From Little, 1993a, 1993c)

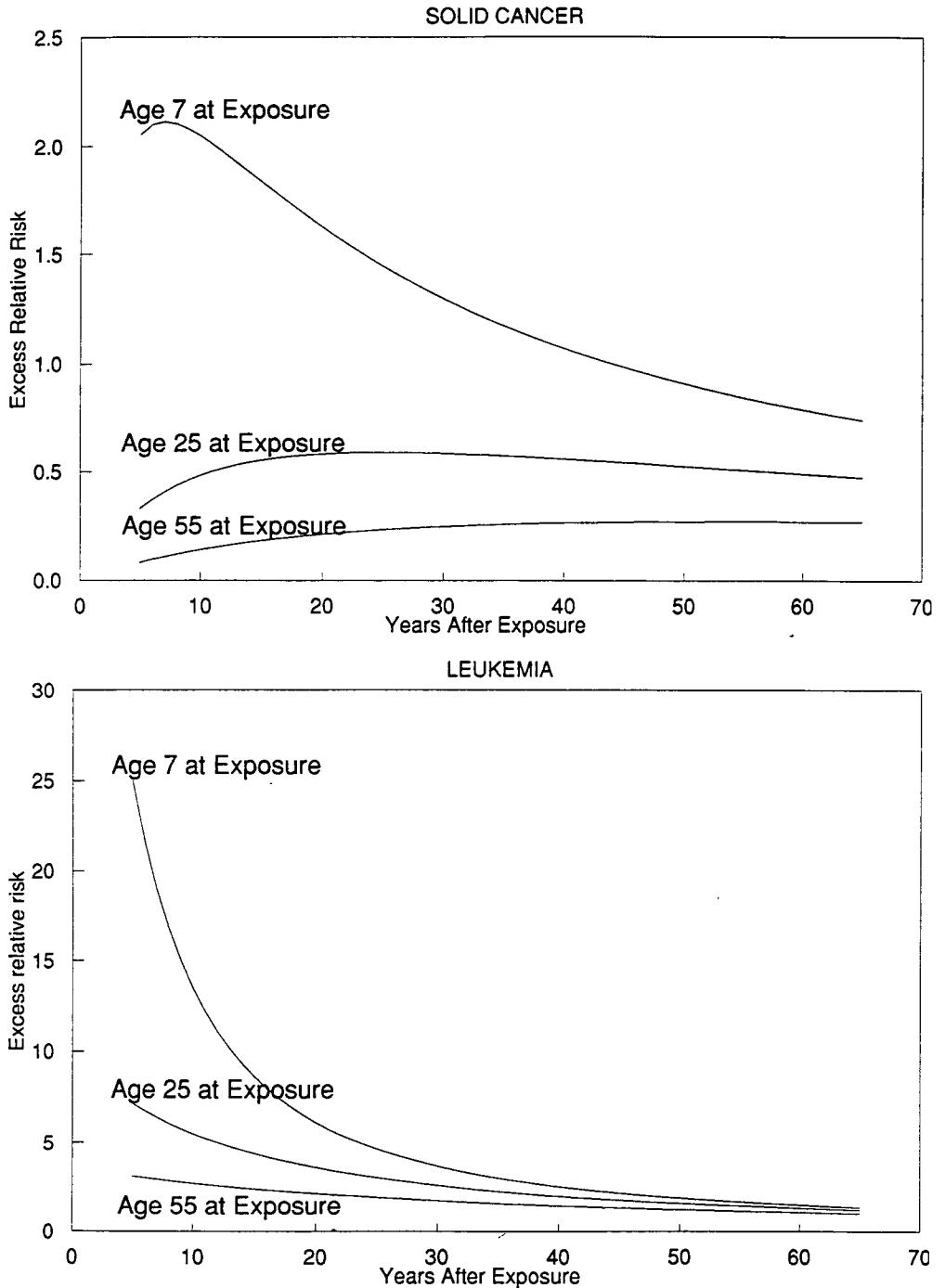


Table 1

Population Cancer Risks as a Function of Dose and Period over which Dose is Administered using the Armitage-Doll Model with various Total Numbers of Stages (k) and Radiation-Affected Stages (j,i) Fitted to the Japanese LSS 11 Data (From Little et al., 1994a)

Dose Period (Years)	1	100	1	100
Dose (Sv)	1.0	1.0	0.001	0.001
<u>1987 England and Wales Population*</u>				
Non-Leukaemia k=3,j=1	7.8 x 10 ^{-2b}	8.3 x 10 ⁻²	8.7 x 10 ⁻²	8.7 x 10 ⁻²
Leukaemia k=2,j=1	9.6 x 10 ⁻²	10.2 x 10 ⁻²	10.6 x 10 ⁻²	10.6 x 10 ⁻²
	1.37	1.43	1.46	1.46
Non-Leukaemia k=3,j=1	7.6 x 10 ⁻²	7.9 x 10 ⁻²	8.1 x 10 ⁻²	8.1 x 10 ⁻²
Leukaemia k=3,j=1	9.3 x 10 ⁻²	9.6 x 10 ⁻²	9.9 x 10 ⁻²	9.9 x 10 ⁻²
	1.38	1.33	1.33	1.33
Non-Leukaemia k=6,j=5,i=2	7.4 x 10 ⁻²	7.8 x 10 ⁻²	7.7 x 10 ⁻²	7.7 x 10 ⁻²
Leukaemia k=3,j=2,i=1	9.0 x 10 ⁻²	9.5 x 10 ⁻²	9.4 x 10 ⁻²	9.4 x 10 ⁻²
	1.35	1.32	1.28	1.28
<u>1983 Japanese Population*</u>				
Non-Leukaemia k=3,j=1	6.3 x 10 ⁻²	6.6 x 10 ⁻²	6.9 x 10 ⁻²	6.9 x 10 ⁻²
Leukaemia k=2,j=1	7.6 x 10 ⁻²	7.9 x 10 ⁻²	8.2 x 10 ⁻²	8.2 x 10 ⁻²
	0.92	0.94	0.94	0.94
Non-Leukaemia k=3,j=1	6.2 x 10 ⁻²	6.3 x 10 ⁻²	6.5 x 10 ⁻²	6.5 x 10 ⁻²
Leukaemia k=3,j=2,i=1	7.4 x 10 ⁻²	7.5 x 10 ⁻²	7.7 x 10 ⁻²	7.7 x 10 ⁻²
	0.99	0.85	0.83	0.83
Non-Leukaemia k=6,j=5,i=2	6.0 x 10 ⁻²	6.2 x 10 ⁻²	6.1 x 10 ⁻²	6.1 x 10 ⁻²
Leukaemia k=3,j=2,i=1	7.2 x 10 ⁻²	7.3 x 10 ⁻²	7.3 x 10 ⁻²	7.3 x 10 ⁻²
	0.95	0.83	0.78	0.78

* Calculated for a population in equilibrium having the mortality rates of the 1987 England and Wales and 1983 Japanese populations (truncated at the age of 120 years)

^b The first figure in each group is excess cancer deaths Sv⁻¹; the second figure is radiation-induced cancer deaths Sv⁻¹; the third figure is years of life lost Sv⁻¹

unlikely that the differences between the pre-conception irradiation leukaemia risks in the Japanese and Sellafield datasets are a result of the different distributions of parental ages at exposure in the two groups, or of the different lengths of time between exposure of spermatogonia and conception. The statistical discrepancies between the two datasets are found to be robust to possible dosimetric uncertainties in the Sellafield group.

Analysis has also been conducted of various categories of non-cancer mortality in the Japanese F₁ dataset (Little, 1992). Only for three of the eight categories of non-cancer mortality analysed is there any evidence of a significant positive dose-response, namely: "respiratory diseases"; "digestive diseases"; and "all other diseases". For each of these disease categories the trend is largely confined to those born in one or other of the cities (for the first and third of these diseases it is Hiroshima, for the second Nagasaki). Furthermore, in the case of "respiratory diseases", the trend is not apparent among those born within 5 years of the bombings. Hence these findings probably do not represent the effect of pre-conception radiation, but are more likely the result of some unknown confounding (perhaps socioeconomic) factor, or chance. There is therefore little evidence that leukaemia deaths in the F₁ cohort might have been "missed" in the early years after the bombings as a result of deaths from non-malignant disease, which has been suggested as a possible explanation for the discrepant results for leukaemia relative risk.

Comparisons have also been conducted of leukaemia risks in the offspring of various groups of radiation workers apart from the Sellafield workforce. In particular, an analysis of the leukaemia risks in the offspring of the Ontario (McLaughlin et al. AECB INFO-0424) and the Scottish radiation workforces (Kinlen et al. BMJ 306:1153-8 1993) with those in the Japanese and Sellafield F₁ datasets has been published (Little, 1993b). The pre-conception exposure leukaemia risks in the Japanese data are consistent with those in the Canadian and Scottish studies, but there are indications at borderline levels of statistical significance (two-sided P = 0.1) of incompatibility between the risks in the Scottish and Canadian datasets and those in the West Cumbrian data. The appearance of the HSE report (1993) highlighted the discrepancy between the leukaemia pre-conception exposure risks in those offspring of the Sellafield workforce born in Seascale and those born elsewhere in west Cumbria. Further comparisons of the risks in the Seascale-born and non-Seascale-born children has underlined the significantly higher leukaemia risks seen in the Seascale-born children compared with those in all the other datasets (offspring of the Sellafield workforce born elsewhere in west Cumbria and the Ontario and Scottish workforces and offspring of the Japanese bomb survivors) (Little et al., 1994b). The risks in all the non-Seascale-born children are entirely compatible (Little et al, 1994b) (see Table 2). The Japanese F₁ dataset has also been subject to further analyses of the risks of leukaemia, lymphoma and various other malignancies, as well as certain categories of non-cancer mortality (blood-related diseases, deaths due to infectious diseases, deaths due to unknown causes) (Little et al. 1994c). Any trends found might have been of interest both in themselves and as possible indications of "missing" cases of leukaemia. However, no strong evidence was found for there being any such effects (Little et al., 1994c). A review paper has been published that summarises the current radiobiological and epidemiological evidence on whether or not leukaemia might be induced by paternal pre-conception irradiation (Little et al., 1995a).

(c) In Utero Irradiation

A review of epidemiological studies of childhood cancer following irradiation *in utero* from prenatal x-rays was prepared and presented at the 11th American Statistical Association Conference on Radiation and Health (Muirhead, to appear). Particular attention was paid to the role of potential confounders, such as a reason for the x-ray examination, and to variations in risk with, for example, time since exposure and calendar period.

Table 2

Relative risks of leukaemia as a result of 100 mSv total paternal pre-conception dose for the offspring of the Sellafield workforce born in Seascale and elsewhere in West Cumbria and for the offspring of the Japanese bomb Survivors and the Scottish and Ontario workforces (with 95% confidence intervals) (from Little et al, 1994b)

Dataset	Factor for West Cumbrian Rates	Relative Risk Model	
		Linear ^b	Exponential ^c
Offspring of Sellafield Workers Born in Seascale	$\lambda = 1$ λ free	36.0 (14.3, 73.0) +∞ (3.96, +∞)	13.3 (6.94, 21.3) 6.31 (2.11, 23.5)
Offspring of Sellafield Workers Born Elsewhere in West Cumbria	$\lambda = 1$ λ free	1.27 (0.51, 3.36) 0.73 (0.47, 2.08)	1.22 (0.36, 2.51) 0.66 (0.14, 1.82)
Offspring of Sellafield Workers Total	$\lambda = 1$ λ free	3.72 (1.81, 6.66) 1.93 (0.83, 6.02)	2.55 (1.48, 3.85) 1.70 (0.81, 3.28)
Japanese Conjoint Parental Dose		1.01 (<0.99, 1.19)	1.00 (0.90, 1.07)
Japanese Paternal Gonadal Dose		<0.98 (<0.98, 1.10)	0.76 (<0.31, 1.03)
Ontario Workforce		0.63 (< 0.27, 3.40)	0.75 (0.07, 3.31)
Scottish Workforce		<0.51 (<0.51, 2.95)	0.83 (0.19, 2.33)
Ontario & Scottish Workforces		0.55 (<0.51, 2.15)	0.80 (0.25, 1.93)
Total Non-Seascale (Japanese Conjoint Parental Dose)	$\lambda = 1$ λ free	1.01 (<0.99, 1.18) 1.00 (<0.99, 1.16)	1.00 (0.90, 1.07) 1.00 (0.90, 1.07)
Total Non-Seascale (Japanese Paternal Dose)	$\lambda = 1$ λ free	<0.98 (<0.98, 1.10) <0.98 (<0.98, 1.08)	0.83 (0.49, 1.04) 0.75 (0.41, 1.02)

^a The factor of proportionality between baseline rates in the HSE West Cumbrian dataset and national rates is taken to be either 1 or is left free to be determined by the fit to the data.

^b Relative risk varies as a linear function of dose.

^c Relative risk varies as an exponential function of dose.

Based on findings from the Oxford Survey of Childhood Cancers, the risk of the incidence of all cancers up to age 15 years was estimated as $6.10^{-2} \text{ Sv}^{-1}$ (Muirhead *et al.*, 1993). This estimate is subject to uncertainties in the doses received more than 40 years ago, although Mole had arrived at a similar estimate based on independent dose data.

Another source of uncertainty concerns the risks of cancer in adulthood following *in utero* irradiation. Prenatal x-ray exposures would be predicted to yield an excess relative risk of adult cancer of only a few percent and so not be detectable epidemiologically (Muirhead, *to appear*). Study of those exposed *in utero* as a consequence of the atomic bombings of Hiroshima and Nagasaki should therefore provide the best means of estimating cancer risks in adulthood. Indeed a recent publication by Yoshimoto *et al.* (Lancet, **344**, 345-6 (1994)) indicates that, like those exposed in childhood to A-bomb radiation, the relative risk of solid tumours in the Japanese *in utero* cohort is decreasing with increasing time since exposure.

Geographical Distribution of Childhood Cancer

(i) Testing for Over-Dispersion in Childhood Leukaemia Rates

Tests of the statistical significance of the level of disease incidence in a specified geographical locality, such as around a nuclear installation, are usually based around the hypothesis that the observed number of cases is distributed as Poisson about the expected number of cases (as calculated on the basis of rates elsewhere). However, this procedure would not be appropriate if the underlying distribution were not Poisson. Consequently study of the pattern of disease incidence in small areas separate from those of prior interest is important.

It is still not entirely clear whether childhood leukaemia has a 'natural' tendency to cluster. In part this may be due to lack of statistical power inherent in the methods available for analysing such data. To address this topic, the International Agency for Research on Cancer conducted a comparison of some methods for detecting localised clustering of disease (Alexander and Boyle, IARC, *in press*). One of the methods utilised in this comparison was a test for over-dispersion (excess variation) relative to the Poisson distribution originally described by Pothoff and Whittinghill (Biometrika, **53**, 167-190 (1966)) and subsequently amended by NRPB staff under the previous CEC contract B16.347.UK (H) for use in the context of disease clustering (Muirhead and Butland, *in press*). Under the current EC contract, further study has been made of the properties of this method, including determining those forms of over-dispersion that the method is best placed to detect.

Simulations and theoretical results indicate that the Pothoff-Whittinghill test is more powerful than the simple chi-squared test to detect over-dispersion generally, particularly if the distribution of area-specific population sizes is skew towards low values. The Pothoff-Whittinghill test is more powerful than that based on a statistic defined by Breslow (Appl. Statist., **33**, 38-44 (1984)) to detect over-dispersion such that the variance of the number of cases per area is proportional to (but greater than) the mean number of cases. This advantage is pronounced if the total number of areas is large and the distribution of area-specific population sizes is skew towards low values. However, the Breslow test is generally more powerful than the Pothoff-Whittinghill test if the excess variance of the number of cases per area is proportional to the square of the mean number of cases.

These methods have been applied to data on childhood leukaemia in certain parts of the United States. These data were collected through the US National Cancer Institute's SEER (Surveillance, Epidemiology and

End Results) programme. An analysis in Connecticut showed evidence of over-dispersion in rates of childhood leukaemia and non-Hodgkin's lymphoma (NHL) among counties not containing nuclear installations, based on the Pothoff-Whittinghill test. However, this result appeared to be influenced largely by low rates in just one county. After allowing for this heterogeneity in the baseline distribution, there was a marked increase in the p-value for significance tests in the two counties containing nuclear installations. A difficulty with interpreting this type of analysis is that US counties can be fairly large. Another analysis using data for much smaller areas, namely census tracts, was conducted and is described in the following section. In this instance, there was no evidence of over-dispersion in childhood leukaemia and NHL rates.

A summary of this work (Muirhead, 1994) was presented at an EC-supported Workshop on 'Childhood Cancer Clusters and Radiation', held at Westlakes Research Institute (UK).

(ii) Childhood Leukaemia and Socio-Demographic Factors in the USA

An analysis was performed to investigate whether childhood leukaemia and non-Hodgkin's lymphoma (NHL) clusters geographically or correlates with socio-demographic factors, based on small-area data from the United States (Muirhead, 1995). These data were provided by the US National Cancer Institute. Owing to restrictions on the availability of small area census data, the analysis was confined to metropolitan regions centred on San Francisco-Oakland, Detroit and Atlanta. During 1978-82, 346 cases of leukaemia and NHL were registered in these regions among 1.3 million white children aged under 15 years. Data were available on the number of cases and the child population size for each of about 2,000 census tracts that make up these regions.

The Pothoff-Whittinghill and Breslow statistical tests referred to earlier did not suggest any general tendency for leukaemia and NHL to cluster within the above areas. Furthermore, there was no indication of trends in incidence rates with either median family income or median adult education for the census tracts (see Table 3). However, the incidence of leukaemia and NHL in census tracts with high population density (based either on the white or total population) was about 40% higher than that in tracts with low population density (Table 3). The trend in risk with increasing population density was statistically significant ($p < 0.05$).

The interpretation of the population density result is unclear. Whilst the possibility that it represents a chance finding cannot be excluded, it is notable that the same trend was seen in each of the three regions studied. The result might appear also not to be in line with findings from Britain indicating higher childhood leukaemia risks in rural than in urban areas (Draper *et al.*, OPCS, 1991). However, the analysis described above was restricted to metropolitan areas in the United States. Since the association, if real, is likely to reflect not population density *per se* but perhaps some facet of 'population mixing' related to Kinlen's and Greaves's hypotheses on this topic, the difference between the British and US findings might have resulted from different types of population movement. Further research is desirable to examine whether the findings in the USA can be replicated, either there or in Europe, and whether any association can be explained by individuals' exposure to infections in early life.

(iii) Childhood Leukaemia and Natural Radiation in Great Britain

NRPB and the Childhood Cancer Research Group (CCRG) (University of Oxford) have collaborated with INSERM-U.170 (France) in an analysis of the geographical distribution of childhood leukaemia incidence

Table 3

Incidence of leukaemia and NHL among white children aged 0-14 years during 1978-82 for three US Metropolitan regions - correlation with 1980 census variables for census tracts (from Muirhead, 1995)

	White Population Density				p-value for trend^a
	Low	Medium	High		
Observed cases	61	144	141		
Relative Risk (95% CI)	1	1.34 (0.99, 1.82)	1.44 (1.06, 1.95)		0.03
	Total Population Density				p-value for trend^a
	Low	Medium	High		
Observed cases	98	206	42		
Relative Risk (95% CI)	1	1.21 (0.98, 1.58)	1.42 (0.98, 2.04)		0.04
	Median Annual White Family Income (\$k)				p-value for trend^a
	<15	15-	25-	30+	
Observed cases	37	127	105	77	
Relative Risk (95% CI)	1	1.05 (0.72, 1.53)	1.02 (0.70, 1.50)	0.85 (0.57, 1.30)	0.8
	Median White Education^c				p-value for trend^a
	<12y	High School graduate	Some college	College graduate	
Observed cases	39	214	73	20	
Relative Risk (95% CI)	1	0.98 (0.70, 1.39)	0.85 (0.54, 1.37)	1.27 (0.64, 2.49)	0.7

Notes:

- (^a) Two-sided test.
- (^b) Risk relative to the lowest census variable category.
- (^c) Defined for persons aged 25+ yrs.

and NHL in Great Britain in relation to natural radiation levels and socio-economic status. This analysis, which used recently-developed statistical methods to model spatial variations, is described in detail in the report for project 7. No evidence was found of a positive association between the incidence of childhood leukaemia/NHL and levels of indoor or outdoor gamma radiation, and there was no consistent evidence of any association with indoor radon levels (Richardson *et al.*, 1995).

NRPB has also collaborated with CCRG in a childhood leukaemia/NHL analysis that utilises more extensive radon measurements made in parts of Great Britain. These data were collected through offers of free radon measurements in those living in radon-affected areas and through other localised surveys. This information should assist in provide a better description of average radon levels in districts, ie. the areas for which childhood leukaemia data are available. The effect of a 'socio-economic score' (SES), representing areas of high socio-economic status, was also investigated.

Table 4 summarises the main results of this analysis. Without adjustment for SES, the leukaemia data for districts show no significant correlations with either the updated radon data or gamma levels, whereas over larger areas (counties) there are indications of a positive correlation with radon and a negative correlation with indoor gamma. This is in accord with the earlier analysis of Muirhead *et al* (Lancet, 337, 503-4 (1991)). However, there is a statistically significant correlation between childhood leukaemia and areas of high SES. Once adjustment is made for SES, there are no indications of correlations with radon or gamma, either at the district or county level. This suggests that socio-economic variables had confounded the earlier county-based results, as Muirhead *et al* had speculated. Subsidiary analyses give broadly similar results. The conclusions based on the updated radon data are also in general agreement with those from the analysis of Richardson *et al* (see above) that utilised earlier radon data. The results based on the updated data are now being prepared for publication.

Table 4 Regression coefficients from fits of natural radiation measures and socio-economic score (SES) to incidence rates for leukaemia and NHL, ages 0-14 years, 1969-83.

Regression coefficients relate to the annual number of cases per 10⁶ per unit change in variable (standard error in parentheses).

	Adjustment for SES	District-level data, adjusted for county	County-level data
SES	N/A	193.31 (106.07)	283.05 (71.23)
Indoor radon (Bq m ⁻³)	Unadj.	-2.17 (10.96)	13.62 (8.10)
	Adj.	-8.24 (11.25)	1.62 (9.41)
Indoor gamma (nGy h ⁻¹)	Unadj.	6.02 (5.05)	-10.65 (5.58)
	Adj.	6.82 (5.08)	-4.67 (6.08)
Outdoor gamma (nGy h ⁻¹)	Unadj.	0.55 (7.77)	-3.84 (10.98)
	Adj.	1.95 (7.78)	3.84 (11.41)

Publications

Little, M P, Hawkins, M M, Charles, M W and Hildreth, N G, 1992. Fitting the Armitage-Doll model to radiation-exposed cohorts and implications for population cancer risks, *Radiat. Res.*, **132**, 207-221.

Little, M P, 1992. The risks of leukaemia and non-cancer mortality in the offspring of the Japanese bomb survivors and a comparison of leukaemia risks with those in the offspring of the Sellafield workforce. *J. Radiol. Prot.*, **12**, 203-218; **13**, 295.

Little, M P, 1993a. Risks of radiation-induced cancer at high doses and dose rates, *J. Radiol. Prot.* **13**, 3-25.

Little, M P, 1993b. A comparison of the risks of childhood leukaemia in the offspring of the Japanese bomb survivors and those of the Sellafield workforce with those in the offspring of the Ontario and Scottish workforces. *J. Radiol. Prot.* **13**, 161-175.

Little, M P, 1993c. Correction to the paper "Risks of radiation-induced cancer at high doses and dose rates". *J. Radiol. Prot.*, **13**, 287-292.

Muirhead, C R, Cox, R, Stather, J W, MacGibbon, B H, Edwards, A A and Haylock, R G E, 1993. Estimates of late radiation risks to the UK population. *Doc. NRPB*, **4**, no. 4, 15-157 (1993).

Little, M P, Hawkins, M M, Charles, M W and Hildreth, N G, 1994a. Corrections to the paper "Fitting the Armitage-Doll model to radiation-exposed cohorts and implications for population cancer risks" (letter to the editor). *Radiat. Res.*, **137**, 124-128.

Little, M P and Charles, M W, 1994. Cancer risk modelling using multistage models fitted to the Japanese bomb survivors. In: *Molecular mechanisms in radiation mutagenesis and carcinogenesis* (K.H. Chadwick, R. Cox, H.P. Leenhouts and J. Thacker eds.), pp.305-310. European Commission, Luxembourg.

Little, M P, Wakeford, R, and Charles, M W, 1994b. A comparison of the risks of leukaemia in the offspring of the Sellafield workforce born in Seascale and those born elsewhere in west Cumbria with the risks in the offspring of the Ontario and Scottish workforces and the Japanese bomb survivors. *J. Radiol. Prot.*, **14**, 187-201.

Little, M P, Wakeford, R. and Charles, M W, 1994c. An analysis of leukaemia, lymphoma and other malignancies together with certain categories of non-cancer mortality in the first generation offspring (F_1) of the Japanese bomb survivors. *J. Radiol. Prot.*, **14**, 203-218.

Muirhead, C R, 1994. Analyses of childhood leukaemia clustering. Abstract from the International Workshop on Childhood Cancer Clusters and Ionising Radiation, Westlakes Research Institute, West Cumbria, UK. 4-7 October 1993. *Leukaemia*, **8**, 2015-6 (1994).

Little, M P, Charles, M W and Wakeford, R, 1995a. A review of the risks of leukaemia in relation to parental pre-conception exposure to radiation, *Health Phys.* **68**, 299-310.

Little, M P and Muirhead, C R, 1995. Mechanistic models of carcinogenesis, *Radiol. Prot. Bull.* **164**, 10-19.

Little, M P, Wakeford, R, and Charles, M W, 1995b. Paternal irradiation and childhood leukaemia (letter to the editor), *Br. Med. J.* **310**, 1198.

Little, M P, Muirhead, C R and Stiller, C A, 1995c. Modelling lymphocytic leukaemia incidence in England and Wales using generalisations of the two-mutation model of carcinogenesis of Moolgavkar, Venzon and Knudson. *Statist. Med.* (in press)

Little, M P, Muirhead, C R, Boice, J D and Kleinerman, R A, 1995d. Using multistage models to describe radiation-induced leukaemia. *J. Radiol. Prot.* (in press)

Little, M P, 1995. Generalisations of the two-mutation and classical multi-stage models of carcinogenesis fitted to the Japanese atomic bomb survivor data. Submitted to *J. Radiol. Prot.*

Muirhead, C R, 1995. Childhood leukaemia in metropolitan regions in the United States: a possible relation to population density? *Cancer Causes and Control*, 6, 383-388.

Richardson, S, Monfort, C, Green, M, Draper, G and Muirhead, C, 1995. Spatial variation of natural radiation and childhood leukaemia incidence in Great Britain. *Statistics in Medicine* (in press).

Little, M P, 1996. Are two mutations sufficient to cause cancer? Some generalizations of the two-mutation model of carcinogenesis of Moolgavkar, Venzon, and Knudson, and of the multi-stage model of Armitage and Doll. *Biometrics* (in press).

Muirhead, C R, to appear. Prenatal x-rays and cancer. Summary of presentation at the 11th American Statistical Association on Radiation and Health (Nantucket, USA, 26 June - 1 July 1994). *Risk Analysis*.

CEC / NRPB Association Agreement

F13P-CT92-0064

NRPB 13306 (2)

Final Report for the Period July 1, 1992 to June 30, 1995

Project 2:	Modelling of Radiation Risks and Construction of Radioepidemiological Tables
Participating Organization:	Ludwig-Maximilians-Universität München Strahlenbiologisches Institut
Scientific Head of Project:	Prof. Dr. A.M. Kellerer

Objectives for Reporting Period:

Quantitative risk estimates of stochastic radiation effects, and especially carcinogenesis, have become increasingly important for the setting of limits in radiation protection. The estimates are obtained by the modelling of dose, age, and time dependencies of excess cancer rates in large cohorts of exposed persons. One objective of the project in this reporting period has been the development of better methods of comparison of models and their application to the compilation of tables of probabilities of causation. A second major objective has been the extension of the numerical methods of maximum likelihood calculations with models that depend explicitly on the temporal distribution of exposures. To overcome numerical difficulties and to avoid the need for approximations in the analysis of late effects due to long term exposures, a new analytical procedure has been developed. It permits explicit regression analyses with greatly reduced storage and computing time requirements and, thereby, widens considerably the range of models that can be treated.

Progress Achieved During Reporting Period:

The work on risk modelling was focused on the attempts to attain improved estimates of the risk of radiation induced cancer and its dependence on radiation quality, the magnitude and the temporal distribution of exposure, the age at exposure, and the time since exposure. There are three basic aspects of the effort:

- Dosimetric information and health data assessments for a number of exposed cohorts.
- Fitting of different risk models to the data and comparison with regard to their dose and age dependencies and their risk projections in time.
- Improvement of numerical regression techniques, specifically to make them applicable to continuous exposures.

The main progress in these three areas was:

- Jointly with Russian colleagues, a synopsis has been prepared of dosimetry, health data and preliminary analyses in connection with the radioactive contaminations of the Techa river and the exposures of large groups of the population, as well as the high radiation exposures of thousands of workers at the plutonium generating facilities of Mayak. This synopsis has appeared as a special issue of *The Science of the Total Environment* (Elsevier): Radiation in the Southern Urals (W. Burkart and A.M. Kellerer, Eds.).

In 1995, a co-operation with the Public Health Ministry of the Russian Federation, Biophysics Institute Branch N1, Ozersk, has been established to investigate lung cancer data of 4,279 workers in the radiochemical plant Mayak who were exposed chronically to radiation, both externally, and internally from incorporation of plutonium. Joint publications with Dr. V.F. Khokhryakov and his colleagues are in preparation.

The epidemiological data on the patients treated with Ra-224 were extended in collaboration with projects NRPB 13306 (11) and NRPB 13306 (10). This included efforts to revise the Ra-224 dosimetry.

In cooperation with project NRPB 13306 (15) further data on secondary tumors in whole body and partial body irradiated patients were collected.

The work on the lung cancer data of uranium miners of the Soviet-German WISMUT AG is still in the preliminary phase. The workers compensation boards have settled a contract with the German government to prepare a basic data set including 60 000 miners; these data will, within the next years, begin to be available for analysis.

- The development of radioepidemiological tables for the probability of causation has, in cooperation with the Institute of Radiation Protection of the GSF, been concluded. The resulting document consists of a practical part with probability of causation diagrams for routine use, and a theoretical part that details various models, compares them, and analyses the remaining uncertainties. The study is largely based on earlier efforts of the NIH, the BEIR IV, and the BEIR V committees, but it provides a more coherent set of relative risk models for those types of tumors that are of major interest. The work is, at this point, restricted to sparsely ionizing radiation and to radon.

The study on the probabilities of causation makes extensive use of contour diagrams, the so-called a-e-diagrams, that represent excess relative risk, excess absolute risk, or probabilities of causation in their dependence on age attained and age at exposure. These diagrams are a major departure from the format of earlier studies, they facilitate the comparison of models, and they have, specifically, been used to assess the difference between the different models utilised for radon exposures (Chmelevsky et al., Health Phys.). As an example Figures 1 and 2 compare the excess relative rate at 100 WLM for the BEIR IV model and the model presented by Jacobi et al.(1992) for Western data.

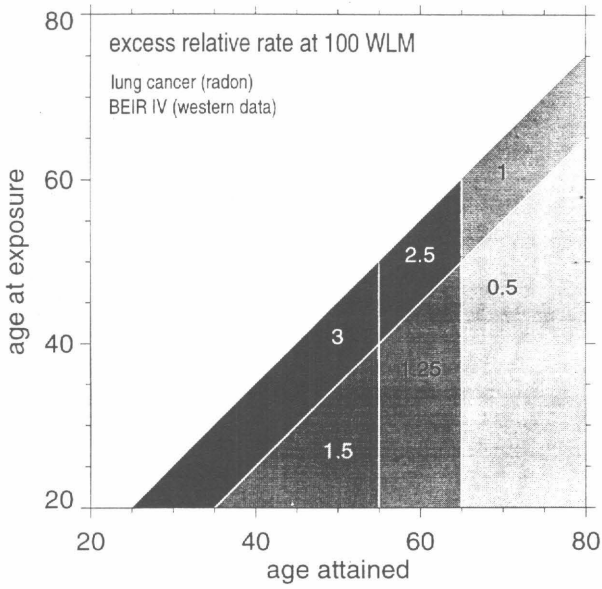


FIG 1: Regions in the age-attained vs. age-at-exposure plane, of constant excess relative rate after a single exposure to 100 WLM, according to the preferred model of the BEIR IV Committee.

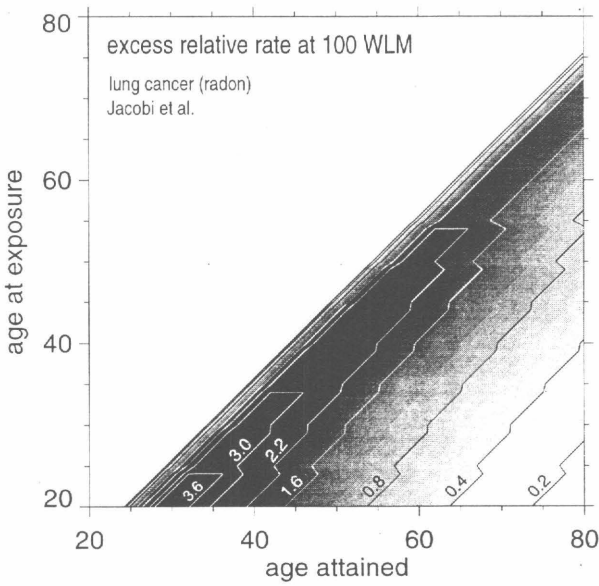


FIG 2: Lines (in the age-attained vs. age-at-exposure plane) of constant excess relative rate after a single exposure of 100 WLM, according to the model developed by Jacobi et al. (1992).

- In the past, risk modelling has been performed in terms of Poisson regression to the grouped data from large data sets, such as atomic bomb survivors or uranium miners. The major tool is the software package EPICURE with the programme for Poisson regression AMFIT. Poisson regression is a suitable method for many applications. For continuous exposure, however, it is of limited applicability. In the past, approximations of uncertain validity had to be used to model aspects, such as the distribution of latent times. We have developed an algorithm that is applicable also to continuous exposures and that avoids the grouping of data and achieves, thereby, better numerical stability (Kellerer et al, 1995).

The new hybrid algorithm is to be used, when the data for the WISMUT miners are available, it will also be utilized in the analysis of the data of workers in the radiochemical plant Mayak, as soon as the collection of the data has been completed. In preliminary studies it has been applied in the analysis of the lung cancer data of the Colorado uranium miners. As an example Fig. 3 shows maximum likelihood estimates of latent period distribution, $h(t)$ (with $t=a-e$), in a relative risk model:

$$r(a, e, C) = r_0(a) \cdot (1 + c \cdot e^{-\gamma a} \cdot \int h(a-e) \cdot C(e) de)$$

a : age attained e : age at exposure $C(e)$: exposure rate at age e .

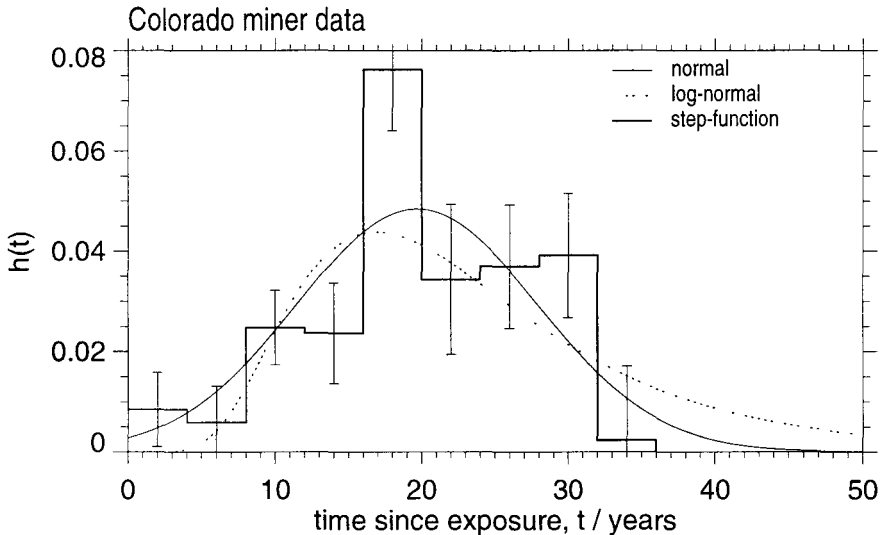


FIG 3: Estimates obtained with the hybrid likelihood algorithm for the function $h(t)$ in the analysis of lung cancer data of the Colorado uranium miners.

The solutions are given in terms of a normal distribution, a log normal distribution, and a step function with more narrow step widths than can be accommodated by earlier methods. Somewhat in contrast to current assumptions of a distribution that is markedly skewed to the right, the distribution $h(t)$ appears nearly symmetrical, and this emphasizes the need for further analyses of the latent periods of radiation induced cancers.

A cruder step function for the latent time distribution $h(t)$ can be employed by AMFIT, but even then the new algorithm is advantageous, because it avoids the influence of the grouping of data in rough cells of dose and age. Fig. 4 gives as an example the different results that are obtained in terms of AMFIT and the exact calculations. The differences are substantial and show the advantage of using an algorithm that utilizes the exact data.

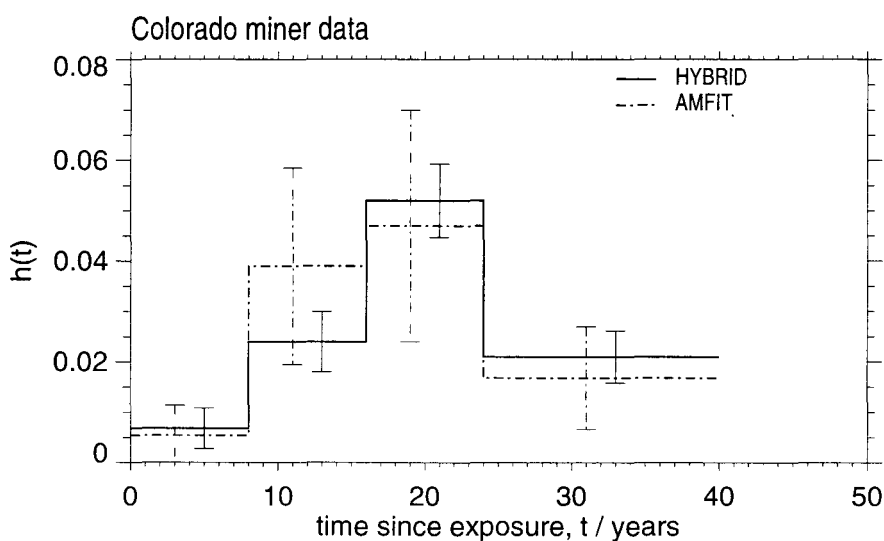


FIG 4: Estimates of $h(t)$ in terms of a step function with broader windows, as they need to be used with the Poisson regression (AMFIT). The difference of the results is due to the grouping of data in the Poisson regression; the hybrid algorithm utilizes the exact data.

Initial steps have been taken to extend the new hybrid likelihood algorithm to nonparametric modelling with non-linear constraints. The first practical applications of this approach have been related to the analysis of cancer data in long term exposed cohorts, specifically in uranium miners (publication in preparation).

List of Publications:

Kellerer AM, Kreisheimer M, Chmelevsky D, Barclay D: A hybrid likelihood algorithm for risk modelling. *Rad. Environ. Biophys.* 34/1, 13-20 (1995)

Kellerer AM: Risk projections in time. *Chinese J. Rad. Med. Prot.* 13/6, 398-403 (1993)

Kellerer AM, Chen J.: A comparison of models for risk assessment. *Asia Congress of Radiation Protection* (1993)

Kellerer AM, Barclay D: Age dependences in the modelling of radiation carcinogenesis. *Radiat. Prot. Dosim.* 41/2-4 273-281 (1992)

Chmelevsky D, Barclay D, Kellerer A.M, Tomasek L, Kunz E, Placek V: Probability of causation for lung cancer after exposure to radon daughters - a comparison of models and of data. *Health Phys.* 67, 15-23 (1994)

Kellerer AM: Kernenergie in Europa und ihre radiologischen Folgen. *Atomwirtschaft, Atomtechnik* 7, 513-516 (1993)

Chmelevsky D, Nekolla E, Barclay D: Strahlenepidemiologische Tabellen - Die Berechnung von Verursachungswahrscheinlichkeiten bösartiger Neubildungen nach vorausgegangener Strahlenexposition - Monographie, ISS und ISB, GSF und LMU München, 1994

Burkart W, Kellerer AM, Eds.: Radiation Exposure in the Southern Urals. *The Science of the Total Environment*, Vol. 142/1.2 Special Issue, Elsevier, Ireland, 1994

Project 3: Radioepidemiological tables for use in the countries of the European Community.

Participating organisation: CEPN

Head of project: Dr.D.Chmelevsky

Objectives for the reporting period

Tables of probability of causation are mainly intended for occupational exposures, i.e. for low exposures in adult age. In such situations it is only for cases of leukaemias that the probability of causation may reach significant values. For all other malignancies the doses would have to be in ranges not allowed under the present regulations in radiation protection. However, high probabilities of causation cannot be excluded in accidental situations or in relation to earlier exposures.

In the tables that are being prepared, relative risk models are used for all locations including leukaemias. For solid cancers the models are, with few modifications, those of the BEIR V Committee. Separate tables are derived for cancers with low lethality. For these sites the risk estimates are drawn from the extensive study of cancer incidence among the Japanese atomic bomb survivors. Tables are provided for cancers of the respiratory tract following exposures to radon and its daughter products; the model used is derived from the preferred model of the BEIR IV Committee.

This work has been performed in collaboration with the Institute of Radiation Biology at the University of Munich.

Progress achieved

Background information

Models

Tables applicable to a German population have recently been prepared following a request by the federal government. The models used were all relative risk models, in agreement with the analysis of the BEIR V Committee. They were based on the last update of the Japanese follow-up and on the preferred models of the BEIR V Committee. One result of the Japanese follow-up was that the simple relative risk model fits the data for solid cancers better than an absolute risk model. The analysis of the BEIR V Committee has shown further that a relative risk model that includes a time modifier fits the leukaemia data as well as an absolute risk model. Relative risk models simplify markedly the establishment of radioepidemiological tables, since age and sex-dependent spontaneous rates of cancer are not required. It seems presently reasonable to base radioepidemiological data on relative risk models, since these models fit adequately the existing epidemiological data.

The dose dependency

A linear-quadratic dose-effect relation is used to calculate the probability of causation (PC) values for leukaemia. This type of malignancy is the only one in the Japanese cohort for which a non-linearity is apparent. It seemed therefore justified to use the relation indicated by the observations. For all other solid cancers the risk modelling was done with linear relations. At low doses the PC-values are too high, according to the ICRP recommendations, if they are obtained without the inclusion of a DDREF (dose and dose rate effectiveness factor). This is not very critical for solid tumours since probabilities of causation can be significant only at high doses (or in the case of exposure at young ages). In most situations the tables will have the purpose of showing that radiation is unlikely to have caused the cancer being considered.

The transfer of radiation risks across populations

The comparison performed by ICRP of procedures to transport radiation risk across populations has shown that while the hypothesis chosen to transport risks does not substantially influence overall lifetime risk estimates, significant differences result when locations, age at exposure or sexes are considered separately. It is worth noting that the two equally acceptable transport procedures, i.e. the transport of an absolute excess to calculate a relative risk in a western country and the transport of a relative excess, have differing consequences for the extrapolated lifetime risk and the PC-values. These inconsistencies are important for cancer types with particularly marked differences in baseline rates between the Japanese and western populations.

In the tables presently prepared, relative excess risks are transported from the Japanese to the European population. This hypothesis would be most critical for stomach cancers, since under the other alternative hypothesis higher risks would be inferred for Europeans. Stomach cancer is, however, not considered separately but together with other cancers of the digestive tract. In this way, differences between risks obtained with different transfer methods are not as great.

The different models for solid cancers following gamma irradiation

The models of the BEIR V Committee have been used with slight modifications for most locations. For breast, non-melanoma skin and thyroid cancers, it seemed important to base the radioepidemiological tables on the results of the incidence study in Hiroshima and Nagasaki, since these locations show significant differences between incidence and mortality. For lung cancer, smoking habits have been taken into account in the quantification of risk. A sub-multiplicative interaction between radiation and smoking has been postulated as well as equality of the background risks between males and females for an equal level of smoking. Tables will be included for extended exposures in the case of radon inhalation.

The tables in preparation

The radioepidemiological tables that are being prepared are based on currently accepted assumptions and models. They should be applicable to any European population, since they are based on generalised relative risk models. They should not be considered as a definitive

product, owing to the fact that radiation risk estimates have changed in the past and are expected to change again with the accumulation of epidemiological evidence and possibly with advances in molecular biology.

Uncertainties on the PC-values are roughly assessed by a comparison of values obtained under different, but equally acceptable, models or assumptions.

Related publication:

Chmelevsky D., Nekolla E., and Barclay D.: Strahlenepidemiologische Tabellen, die Berechnung von Verursachungswahrscheinlichkeiten nach vorausgegangener Strahlenexposition. Veröffentlichungen der Strahlenschutzkommission, in print.

**Project 4: Epidemiological Studies of Thyroid Cancer following Medical Exposures to
Radioactive Iodine**

Participating Organisation: University of Saarland
 Department of Nuclear Medicine

Head of Project: Professor Dr. Dr. E. Oberhausen

Objectives for the Reporting Period

After completing the comparison between the patients treated with I-131 and those persons registered with thyroid cancer in the Cancer Registry of the Saarland, we have carried out some statistical calculations using the results of this comparison.

All patients of the Department of Nuclear Medicine who were treated with I-123 up to the 31 October 1993 are being registered in a second database. Checks of medical documents provide information about the diagnosis and any earlier treatments with I-131 for these patients.

Progress achieved during Reporting Period

Study of patients who were treated with I-131

Based on the vital status and place of residence of our former patients we have divided them into 4 groups (Table 1).

Table 1

Information about Vital-Status and Residence				
Group	Vital-Status	Date of Death	Residence	Number
A	unknown	unknown	unknown	1291
B	deceased	known	-	1438
C	deceased	unknown	-	153
D	living	-	Saarland	8893

Then we calculated risk years as follows:

For every person we determined the age at the time of first examination. We then considered the period between the year of first examination and the year 1990, ie. the latest year for which the Cancer Registry published incidence data. For each year we added one in that age group related to the age of the person. This procedure was followed for the members of group D. For the members of group B the last year of the study period was the year of death.

For the members of groups A and C we calculated the risk years in two ways:

First, we assumed that they were all still living in the Saarland at the end of 1990. For this we calculated risk years based on the time period from date of first examination to the year 1990 (as for members of the group D). This type of calculation gives a maximum number of risk years.

Second, we assumed that they died or left the Saarland directly after the last date of examination in our Department. So we calculated the risk years between the year of first examination and the year of last examination. This type of calculation gives a minimal number of risk years.

The sum of the products of the number of age- and sex-specific risk years with the age- and sex-specific incidence rates for the population of the Saarland gives the expectation values (Table 2).

Table 2

Expectation values for Thyroid Carcinoma in the patient cohort		
	Men min / max	Women min / max
Expectation value		
- Latency Period: 0 y	1.05 / 1.20	7.75 / 8.85
- Latency Period: 5 y	0.78 / 0.91	5.69 / 6.58
- Latency Period: 10 y	0.50 / 0.59	3.43 / 4.02

Table 3 shows the number of our former patients treated with I-131 who are registered in the Cancer Registry of the Saarland:

Table 3

Observed values according to latency period		
	Men	Women
registered until 1990 (incl.)	8	23
Latency period > 5 years	6	19
Latency period > 10 years	4	14

The next two Tables show the Standardized Incidence Ratio (SIR) and the 95% confidence interval for the minimal (Table 4) and maximum (Table 5) number of risk years, according to the length of the latency period.

Table 4

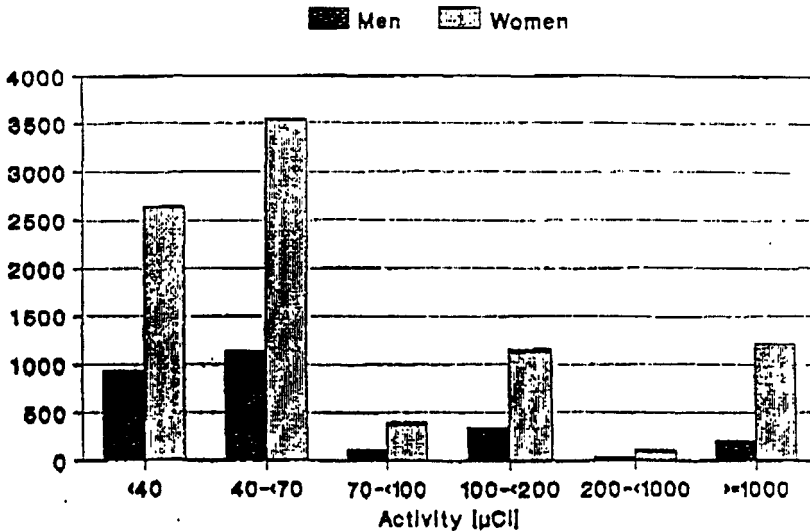
Standardized Incidence Ratio with 95% confidence interval using the minimal number of risk years		
Latency period (years)	Men	Women
0	7.62 [3.28 ; 15.01]	2.97 [1.88 ; 4.45]
5	7.69 [2.80 ; 16.74]	3.34 [2.01 ; 5.21]
10	8.00 [2.15 ; 19.30]	4.08 [2.23 ; 6.85]

Table 5

Standardized Incidence Ratio with 95% confidence interval using the maximum number of risk years		
Latency period (years)	Men	Women
0	6.67 [2.87 ; 13.14]	2.60 [1.65 ; 3.90]
5	6.59 [2.40 ; 14.35]	2.89 [1.74 ; 4.51]
10	6.78 [1.83 ; 17.36]	3.48 [1.90 ; 5.84]

Another possible division of our patient cohort is on the basis of the activity applied. Figure 1 shows that the majority of our patients were treated with less than 70 μCi (2.6 MBq). The last group (greater than or equal to 1mCi (37 MBq) consists of patients given therapy.

Figure 1 **Distribution of the patient collective related to the activity**



Tables 6 and 7 show the SIR with the 95% confidence interval and the cumulative expectation and observed values without consideration of any latency period, according to the activity applied for the number of minimal (Table 6) and maximum (Table 7) risk years.

Table 6

Standardized Incidence Ratio with 95% confidence interval for cumulative values without latency period using minimal risk years		
Activity (μCi)	Men	Women
<40	3.08 [0.08 ; 15.88]	0.94 [0.11 ; 3.39]
<70	5.18 [1.40 ; 13.30]	2.77 [1.51 ; 4.64]
<100	5.00 [1.35 ; 12.80]	2.75 [1.55 ; 4.56]
<200	7.57 [2.95 ; 15.13]	3.53 [2.80 ; 5.05]
<1000	7.14 [2.86 ; 14.72]	3.25 [2.04 ; 4.93]
all	7.62 [3.28 ; 15.01]	2.97 [1.68 ; 4.45]

Table 7

Standardized Incidence Ratio with 95% confidence interval for cumulative values without latency period using maximum risk years		
Activity (μCi)	Men	Women
<40	2.56 [0.06 ; 14.28]	0.79 [0.09 ; 2.36]
<70	4.85 [1.26 ; 11.91]	2.39 [1.31 ; 4.01]
<100	4.35 [1.17 ; 11.18]	2.38 [1.33 ; 3.98]
<200	6.42 [2.57 ; 13.23]	2.89 [1.81 ; 4.35]
<1000	6.31 [2.52 ; 12.99]	2.84 [1.78 ; 4.29]
all	6.72 [2.89 ; 13.25]	2.60 [1.65 ; 3.90]

Furthermore we can divide our study population according to the diagnosis at the time of first examination. Table 8 shows the distribution of diagnoses, divided between those patients who were treated for diagnostic purposes and those who were treated for therapeutic purposes.

Table 8

Distribution of the Diagnosis		
Diagnose	Diagnostic	Therapy
Normal function	17	0
Goitre	60	22
Thyroiditis	1	0
Autonomous Adenoma	13	57
Hyperthyroidism	4	21
Hypothyroidism	5	0

Tables 9 and 10 show the SIR and the 95% confidence interval for each diagnosis based on the number of minimal (Table 9) and maximum (Table 10) risk years.

Table 9

Standardized Incidence Ratio with 95% confidence interval for the number of minimal risk years		
Diagnosis	Men	Women
Normal function	12,5 [2,55 ; 36,53]	0,79 [0,02 ; 4,39]
Goitre	1,79 [0,05 ; 9,95]	3,85 [2,24 ; 8,16]
Thyroiditis	0	10,00 [0,25 ; 66,69]
Autonomous Adenomas	27,27 [5,55 ; 79,70]	1,87 [0,22 ; 8,75]
Hyperthyroidism	0	0
Hypothyroidism	11,11 [0,28 ; 61,65]	5,71 [0,69 ; 20,64]

Table 10

Standardized Incidence Ratio with 95% confidence interval for the number of maximum risk years		
Diagnosis	Men	Women
Normal function	9,55 [1,87 ; 28,28]	0,65 [0,02 ; 6,76]
Goitre	1,56 [0,04 ; 8,70]	2,35 [1,85 ; 5,37]
Thyroiditis	0	9,09 [0,23 ; 50,83]
Autonomous Adenomas	25,00 [5,09 ; 73,06]	1,68 [0,20 ; 8,07]
Hyperthyroidism	0	0
Hypothyroidism	10,00 [0,25 ; 66,69]	5,28 [0,83 ; 19,01]

Study of patients who were treated with I-123

For comparison with our study group of persons who were treated with the radionuclide I-131, we have created a second group which contains all these patients of our Department who were treated with the radionuclide I-123 after 1977.

Since 1977 the thyroid gland-examinations in our department of nuclear medicine in the university hospital Homburg/Saar are done with iodine-123 instead of iodine-131 which was used before in the diagnosis and until now for the therapy. Because of different characteristics the organ dose caused by one examination with the same activity injected will be lower by a factor of 100 if you take iodine 123.

We have looked for how often people examined only with iodine-123 and not with iodine-131 suffers from thyroid gland-cancer. Furthermore will compare these patients with the other patients of our department who were examined until 1977 with iodine-131.

We only took such patients into the study who fulfilled some criterions.

First it is necessary that the place of residence at time of first examination is in the Saarland. This is necessary because all patients will similar to the iodine-131-patients be compared with the Saarländischen Krebsregister (the cancer registration in the Saarland where every resident of our land who suffers from any kind of cancer is registered). The second condition was that no patient ever received a therapy with radionuclides, especially iodine-131. Furthermore it goes with saying that no patient in this study can be examined with free and unbounded iodine-131. At last it is not allowed that the thyroid gland-specific diagnosis is thyroid gland-cancer at time of first examination.

Many of our patients are not only examined with iodine-123 concerning the thyroid gland but they were also examined with technetium-99m for bone-scintigraphy for example.

Estimations concerning the organ dose for the thyroid gland showed that the dose caused by other examinations in nuclear medicine compared with the organ dose caused by free iodine-123 is in most cases as low that it can be neglected. The organ dose of the bone produced by ohne bone-scintigraphy with 555 MBq technetium-99m for example is nearly seven times lower than the organ dose in the thyroid gland produced by 10 MBq iodine-123; so in the thyroid it will be nearing zero. We didn't took such patients into the study who undergone an examination with high organ dose for the thyroid gland like for example the brain-SPECT with technetium-99m-HMPAO with a organ dose of 46 mSv for the thyroid gland. In the case of iodine-131-hippuran to determine the global kidney function there is nearly no organ dose to the thyroid gland because

there is nearly no free iodine-131 and nearly all iodine-131-hippuran injected will be cleared by the kidneys in some minutes because of the high tubular function.

The organ dose of the thyroid gland is not only depending on the activity injected, it also depends on the functional state and the size of the thyroid gland. In case of hyperthyroidism the organ dose caused by the same amount of activity in the same volume of the gland is 2,4- fold the organ dose in normal functioning glands. (all numbers taken from EMRICH's Testbook of nuclear medicine).

The process of taking patients into the current study is not finished until today, so it is not possible to say something definite about the size and the composition of the collective. Therefore the state of things is given until the effective day 30.06.95.

Taking all criterions of admission and exclusion into consideration the collective comprises including the 30.06.95 9945 patients, among these 7076 women corresponding to 71% and 2869 men corresponding to 29% of the patient-collective.

We divided the patients separated by their sex into 5-years-age groups. Decisive for this classification was the exact age at time of the first examination with iodine-123 in our department. The classification followed continuous steps up to the last group of patients older than 85 years at time of first examination. Most of the patients were while time of the first thyroid gland-examination between fifteen and seventy years, only a little number for men and women was younger than ten or older than 85 years.

The period of observation is beginning with the exchange of the thyroid examination-nuclide in our department from iodine-131 to iodine-123. This change took place in the second half of 1977 when iodine-123 replaced iodine-131.

The period of observation of each single patient begins with the first thyroid-examination with iodine-123 in our department. A change of the period of observation can be caused by the comparison with the residents' registration offices in the Saarland.

Fig.2 and 3 show the age distribution of the patients

With about 77% the far greatest part of the patients got only one application of iodine-123 for a thyroid-examination in our department. The part of patients undergoing at most two examinations with iodine-123 until now is about 91,5%. Less than 1% of our patients was examined more than five times. The injected activity per examination was between 7,4 and 10 MBq. The number of examinations with iodine-123 was in one case twelve and in one case ten otherwise maximally seven.

Beside the totally injected activity the organ dose to the thyroid depends from the thyroid gland-diagnosis and its size.

So we'll observe the patients separated by their diagnosis. We'll take the same code of diagnosis like it was used to subdivide the iodine-131-exposed patients. At the moment we do a square of patients-addresses with the residents' registration offices which is necessary before comparing our collective with the Saarländische Krebsregister.

Figure 2

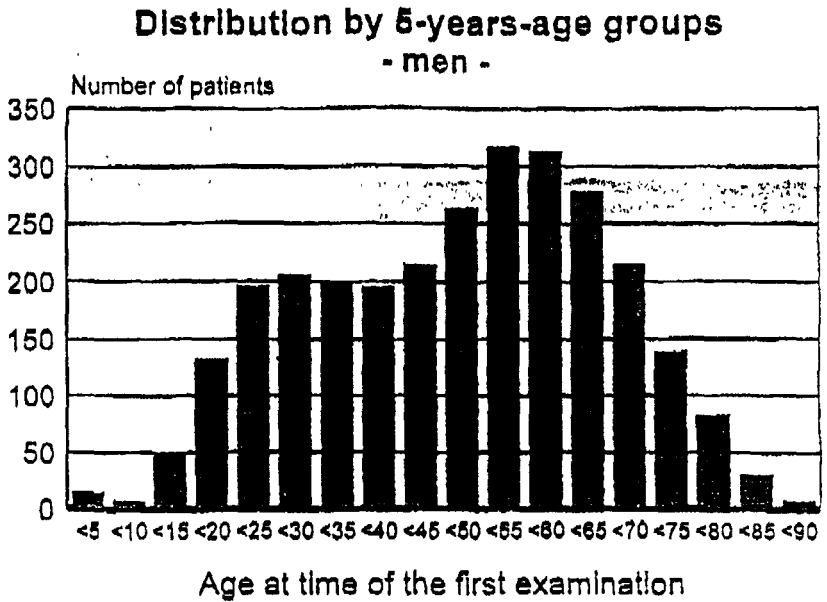
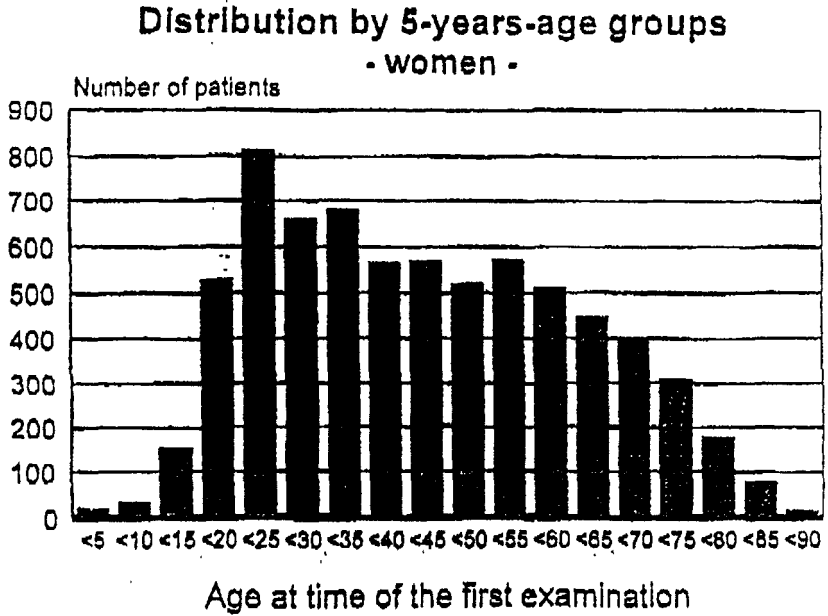


Figure 3



Publication

F.Fehringer, E. Oberhausen
Morbiditätsrisiko für Schilddrüsen-Karzinome nach Behandlung
mit I-131
in M. Winter, A. Wicke
Umweltradioaktivität, Radioökologie, Strahlenwirkungen Band
II, Seite 939
Verlag TÜV Rheinland 1993

Project 5: Cancer Incidence and Mortality After Radio-therapy for Skin Haemangioma in Childhood.

Name of Participating Organisation: Karolinska Institute, S-104 01 Stockholm, Sweden

Head of Project: Lars-Erik Holm, M.D., Ph.D., Radiumhemmet, Karolinska hospital, S-104 01 Stockholm, and National Institute of Public Health, P.O. Box 27848, S-115 93 Stockholm, Sweden, Tel. No. -46 8783 3566, Fax. No. -46 8783 3545

Objectives for the reporting period.

To study the incidence of solid tumours and leukaemia as well as leukaemia mortality in a cohort of infants exposed to ionizing radiation for skin haemangioma, to study dose-response relationships, to calculate life-time excess cancer risks, and to set up a study of the risk of cataract in the same population to study the risk of cataract in relation to lenticular dose.

Progress for the reporting period.

The dosimetry of the treatment techniques has been described in a paper (1).

Cancer incidence has been studied by record-linkage with the Swedish Cancer Register for the period 1958-1986. During this period, a total of 300 cancers were diagnosed in the 14,351 Swedish infants irradiated for skin haemangioma between 1920 and 1959. The standardised incidence ratio (SIR) was 1.11 (95% CI 0.99-1.24) based on age-, sex-, and year-specific cancer incidence data obtained from the registry. Most sites did not show any increased number of cancers, and no increased risk of leukaemias was observed. The median age of the population at the end of follow-up was only 38 years, and most subjects have thus not yet reached ages when cancers become prevalent (2).

The risk of thyroid cancer has been studied and presented in a separate article (3). A total of seventeen thyroid cancers were observed and the SIR was 2.28 (95% CI 1.33-3.65). The excess relative risk (ERR) persisted at least 40 years after exposure, and the mean absorbed thyroid dose was 0.26 Gy. A positive dose-response relationship could be observed. No differences in risk estimates between the sexes were found. The ERR per Gy was 4.92 (95% CI 1.26-10.2).

Seventy-five breast cancers were observed among the females in the cohort and SIR was 1.24 (95% CI 0.98-1.54). The ERR increased with increasing time after exposure with no signs of levelling off and for 50 years after exposure or more the fitted ERR at 1 Gy was 2.25 (95% CI 0.59-5.6). The mean absorbed dose was 0.39 Gy and a statistically significant linear dose-response relationship was observed (4).

In a separate study we have analyzed the risk of leukaemia (5). These analyses were based on mortality data, since most of the leukaemias appeared before 1958 when the Swedish Cancer Registry was established.

In May 1995, Ms Marie Lundell successfully defended her thesis entitled "Carcinogenic Effects of Low Dose Irradiation in Early Childhood. A Dosimetric and Epidemiologic Study" (6). The thesis was entirely based on studies of the haemangioma cohort.

Cataract

A study was set up to analyze the risk of cataract following radiotherapy for skin haemangioma. We have now completed the clinical examination of the eyes of nearly 450 patients treated with 226-Ra in the head region and of 100 patients not receiving radiotherapy: The clinical eye examination has been carried out at the Department of Ophthalmology at Karolinska Hospital. Each subject has also completed a questionnaire regarding previous and current health status, medications and treatments. The US Lens Opacities Classification Systems III has been used for characterizing the type and quantifying the degree of cataract. The radiation dose to the lenses is currently being estimated, and dose-response relationships will be analyzed thereafter.

National collaboration

A first joint planning meeting between the Stockholm group and the Gothenburg group (with a similar cohort of infants irradiated for skin haemangioma) took place in October 1993, with the purpose of sharing experience and discussing possibilities of pooling the data for future analyses. Since then the two groups have met once to twice a year, and the Stockholm group has actively supported and encouraged the Gothenburg group to begin analysing cancer risks in their cohort by sharing data and experiences.

International collaboration

We have had discussions with Professor Kellerer in Munich regarding the planned collaboration with the purpose to compare the German and the Swedish methods for diagnosing and quantifying cataract, as well as to compare risks for cataracts in the two populations. However, since we have not yet presented any data on cataract incidence, no steps have as yet been taken regarding this collaboration. As soon as we have more detailed data we intend to continue the discussions with the German group.

We have also established contact with the research group at Institut Gustave-Roussy, in Villejuif, France. This group also has a cohort of children irradiated for skin haemangioma, and we have discussed how the results from studying the three haemangioma cohorts can be analysed jointly.

Publications

1. Estimates of absorbed dose in different organs in children treated with radium for skin hemangiomas. *Radiat Res* 140:327-333,1994.
2. Lundell M, Holm L-E. Risk of solid tumors after irradiation in infancy. *Acta Oncol* in press, 1995.
3. Lundell M, Hakulinen T, Holm L-E. Thyroid cancer after radiotherapy for skin hemangioma in infancy. *Radiat Res* 140:334-339,1994.
4. Lundell M, Mattsson A, Hakulinen T, Holm L-E Breast cancer after radiotherapy for skin hemangioma in infancy. Submitted for publication.
5. Lundell M, Holm L-E. Risk of leukemia after irradiation in infancy for skin hemangioma. Submitted for publication.
6. Lundell M. Carcinogenic effects of low dose irradiation in early childhood. A dosimetric and epidemiologic study. Thesis. Karolinska Institute, Stockholm, 1995.

Project 6

Head of the Project:

Prof. Aldo Becciolini

Coworkers:

A. Biggeri, P. Pacini, M. Balzi, V. Giachè, A. Castagnoli,
D. De Maria (MO), M. Laddaga (PI)

II. Objectives for the Reporting Period:

The aim of the study was to evaluate the incidence of second primary tumours in patients treated with ionizing radiations for cancer in different sites. The study deals with the analysis of clinical records and of the continuous follow up, chiefly concerning: a) patients affected by breast cancer and treated in Florence with radiotherapy or chemotherapy and/or hormonotherapy from 1965 to 1993; b) breast cancer treated with ionizing radiations in the Institute of Radiobiology, University of Pisa; c) analysis of clinical records collected by the Radiotherapy Centre of the University of Modena; d) patients affected by thyroid carcinoma and treated with ^{131}I after surgery from 1976 to 1994; e) geographical clustering study of epidemiological approach to spatial analysis of rare diseases including cancers.

III. Progress achieved including publications

BREAST CANCER

In Florence data on 5249 patients of breast cancers submitted to radio- or chemo- and/or hormonotherapy have been collected from 1965 to December 1993. Mean and median age were 54.7 y and 54 y respectively (range 23-86 y). Of these patients 51.3% received adjuvant radiotherapy and for 74.0% of these the exposed volume was the breast only, compared with breast and lymphatic drainage in 26.0% (17.5% mammary chain and supraclavicular nodes and in 8.5% even the chest wall was irradiated). The radiation sources were a telecobalt unit (dose rate 0.80-1.20 Gy/min) or linear accelerator. A treatment schedule of 2 Gy/day, 5 days/week, for a total dose 44-60 Gy was used. As concerns the dosimetry for contralateral breast and for the nearest bone marrow sites some determinations were taken into account by measures of a) "in vivo" dosimetry with TLD; b) diffuse dose by using water phantom; c) doses calculated with CT size treatment planning, that assures an accuracy of $\pm 3\%$. In the last years different irradiation techniques with linear

accelerator, 6 MVX rays, were used: a) two tangential fields; b) 2 tangential fields plus a direct irradiation with electron beam of 12 MeV. The values, calculated on 80 treated patients showed that in the first case a 12% of total dose was absorbed 3 cm distant from the irradiated volume which decreases progressively to 2.4% at 12 cm. In the second case the absorbed dose was 3.8% of the total at 3 cm and 1.4% at 12 cm. The need for a precise dosimetry of the treatment planning, to establish a relationship dose/incidence of the second tumour, led us to a collaborative study with the Institute Gustave Roussy, Villejuif, France. The aim is to obtain a more precise determination of the dose absorbed in different sites of the policy for breast cancer changed in time: before 1977 radical mastectomy and radiotherapy and from 1980 conservative surgery and radiotherapy were the more frequent treatment.

Adjuvant chemotherapy, usually CMF, was given in 15.2% and hormonotherapy in 24.4% of cases. When the second tumour appeared within the first year after treatment it was considered synchronous and excluded from the study.

Bilateral synchronous cancer was observed in 1.54% (81) of patients. A total of 300 second metachronous tumours were observed. Among these 174 (3.37%) were contralateral breast cancers whereas 126 (2.44%) were tumours of other sides. The mean and median follow up were respectively 7.4 and 6.0 y. The mean and the median time at whom the second primary cancer was observed were 5.75 and 4.55 y respectively. The results are reported in Table 1.

The more frequent sites of metachronous cancer were breast (174 cases of which 73 were in the irradiated group) while other sites account for 126 cases, 61 of which were in the irradiated group.

In this last group the more frequent were colorectal, stomach, endometrial, ovary cancers whereas those of kidney, lung, skin, melanoma and others were less frequent. Moreover 8 leukemias (7 in the irradiated group and one in the non irradiated group) and 3 non Hodgking lymphoma were observed. The incidence of second primary tumours was compared with expected values obtained from the Tuscany Cancer Registry (1985-1987).

The results of the incidence of a second tumour in patients treated by radiotherapy, chemotherapy or hormonotherapy are reported separately in Table 2-4. Poisson regression analysis for all malignancies according to type of therapy, time of follow up (Tfu), age and period before and after 1980 with the estimated Rate Ratios and 90% confidence intervals is reported in Table 5.

The interval analysis confirmed a slight excess of subsequent malignancies in the radiation treated sub-cohort, as previously reported in Table 2 using external standard

rates. In particular the risk appeared to concentrate in the time span between 10 and 15 years after radiotherapy. No definite conclusion could be achieved due to the small size of the cohort (14979 person years) which reflects wide confidence intervals.

No excess risk, associated with radiation therapy emerged for contralateral breast cancer in contrast with the results based on external standard rates. This could be therefore explained by a selection of the cohort on risk factors for breast cancer. A separate analysis by means of Poisson regression has been replicated for leukemia (204-210 ICD) (Table 6). The high risk reported using external standard rates has been confirmed. The risk appeared to concentrate in the period immediately following the radiation therapy (5 years). No excess risk was evident associated to chemotherapy.

PISA

Up to now 465 cases are eligible for the study. The schedule of dose administration is similar to that of the Florence group (2 Gy/day, 5 days/week, 48 Gy total dose).

Mean and median age at time of diagnosis of this group were 56 and 57 respectively and the mean and median follow up were 6.5 and 5 y. The comparison with the data collected in Florence showed that only about 20% of the treated cases are actively surveilled by the Radiotherapy Centre compared with 70-80% of cases in follow up in Florence. This fact could explain the differences in the incidence of second primary tumour observed between the two cohorts.

The mean and median time at whom the second primary cancer was detected were 8.5 and 7.5 y respectively.

All patients in Pisa received radiotherapy: 307 radiotherapy only, 28 plus chemotherapy, 84 plus hormonotherapy and 46 plus hormone and chemotherapy. a total of 71 second primary cancers was observed in this group: 4 of whom were contralateral breast cancers (1 in HT and 3 in HT+ChT groups). Colorectal (5 cases), uterus (7), ovary (4) were the other most frequent tumours. The global SIR was 2.91 and 7.9 for breast. In this cohort no cases with leukemia were observed. The results are reported in Table 11.

The results of the analysis of the data in the Radiotherapy Centre of the University of Modena have been previously reported.

THYROID CANCER

The study deals with the analysis of the clinical records, collected from 1965 to 1994, of 713 patients, 645 of which treated with ¹³¹I for thyroid carcinoma. At present only

preliminary data are available. The mean age of patients was 44.3 y with a mean time of 11 month between surgery and ^{131}I therapy. Mean and median follow up were 9.5 and 5 y respectively (range 1.0-35 y). In 65.3% of cases only one treatment was given, two treatments in 20.1%, three in 7.6%, four in 3.6%, five in 2.5% and six in 0.9% of cases. When the treatments were repeated the mean time between the doses ranged from 2.3 to 2.9 y.

A second primary tumour was observed in 23 patients. Four of them were leukemia, one preleukemic syndrome and one lymphoma. Two leukemias occurred in patients treated only once with activities ranging from 50 to 100 mCi of ^{131}I ; in the other cases the treatment was repeated two or more times. Other second primary tumours were colon (4), breast (2), bladder (2) and other less frequent carcinomas. The median time of the appearance of the second cancer was 9.3 y (range 0.5-23.1 y).

The analysis of the clinical records showed that 46 out 713 (6.45%) patients were previously exposed to external beams of ionizing radiations for benign pathologies chiefly (87%) in the head and neck region. The median time for the appearance of the thyroid carcinoma was 27.2 y (range 6.1-59.1 y).

Geographical clustering

A part of the research has been recently devoted to an epidemiological approach to the spatial analysis of rare diseases, including tumours, by the estimation of biological parameters. A method based on Monte Carlo simulations has been proposed to evaluate the dimension of the clustering process, the total numbers of clusters and the proportion of cases attributable to clustering. Some preliminary data have been submitted for publication (Statistical Ecology).

	LEUKAEMIA	METACHRONOUS BREAST CANCER	OTHER CANCERS	ALL CANCERS	N° PTS
RT BREAST	3	34	32	87	1966
RT BREAST+SUPRACLAV.	3	30	23	61	464
RT BREAST+SUPRACLAV+CHEST WALL	1	9	6	16	230
NO RT	1	101	65	217	2659
TOTAL	6	174	126	381	6249

table 1

Table 2: Florence Breast Cancer Cohort. 1965-1994

Radiation-Treated Sub-Cohort (excl. first year of follow-up)				
ICD-9	Observed	Expected	SIR RTT 85-87	95% CI
14-	0	1.2409	0.00	0.0-3.0
15-	19	28.8745	0.66	0.4-1.0
16-	3	5.0843	0.59	0.1-1.7
17-	1	8.3602	0.12	0.0-0.7
174	73	27.9234	2.61	2.0-3.3
18-	16	19.1595	0.84	0.5-1.4
19-	1	4.6805	0.21	0.0-1.2
20-	10	5.7938	1.73	0.8-3.2
204-10	7	1.7440	4.01	1.6-8.3
all mlg	123	101.1392	1.22	1.0-1.5

Table 3: Florence Breast Cancer Cohort. 1965-1994

Chemotherapy-Treated Sub-Cohort (excl. first year of follow-up)				
ICD-9	Observed	Expected	SIR RTT 85-87	95% CI
14-	0	0.2785	0.00	0.0-13.2
15-	3	5.2785	0.57	0.1- 1.7
16-	0	1.0209	0.00	0.0- 3.6
17-	1	1.8388	0.54	0.0- 3.0
174	22	7.2195	3.05	1.9- 4.6
18-	2	4.2454	0.47	0.1- 1.7
19-	0	1.0917	0.00	0.0- 3.4
20-	0	1.1782	0.00	0.0- 3.1
all mlg	28	22.1936	1.26	0.8- 1.8

Table 4: Florence Breast Cancer Cohort. 1965-1994

Hormonotherapy-Treated Sub-Cohort (excl. first year of follow-up)				
ICD-9	Observed	Expected	SIR RTT 85-87	95% CI
14-	0	0.6273	0.00	0.0-5.8
15-	12	17.6730	0.68	0.4-1.2
16-	0	2.6395	0.00	0.0-1.4
17-	0	4.4412	0.00	0.0-0.8
174	19	11.8379	1.61	1.0-2.5
18-	7	9.0725	0.77	0.3-1.6
19-	0	2.2718	0.00	0.0-1.6
20-	1	3.1227	0.32	0.0-1.8
all mlg	39	51.8188	0.75	0.5-1.0

Table 5: Florence Breast Cancer Cohort. 1965-1994. Poisson regression: estimated Rate Ratios and 90% Confidence Intervals.

Internal comparisons: All Malignancies			
Term	Rate Ratio	90% CI	
Chemo= yes	.6700	.4987	.9001
Hormo= yes	.7617	.5982	.9697
Tfu= 5-9	.7492	.5714	.9823
Tfu= 10-14	.6723	.4548	.9939
Tfu= ≥ 15 yrs	1.257	.7049	2.241
Rt=yes for tfu= < 5	.8176	.6544	1.022
Rt=yes for tfu= 5-9	1.147	.8010	1.641
Rt=yes for tfu= 10-14	1.421	.8270	2.443
Rt=yes for tfu= ≥ 15 yrs	1.062	.5199	2.168

Table 6: Florence Breast Cancer Cohort. 1965-1994. Poisson regression: estimated Rate Ratios and 90% Confidence Intervals.

Internal comparisons: Leukemia			
Term	Rate Ratio	90% CI	
Rt= yes	8.099	1.374	47.740
Age= 50-59	0.427	0.100	1.815
Age= ≥ 60 yrs	0.311	0.069	1.405
Period= ≥ 1980	0.342	0.096	1.222

Table 7: Pisa Breast Cancer Cohort. 1967-1993

Radiation-Treated Cohort (excl. first year of follow-up)				
ICD-9	Observed	Expected	SIR RTT 85-87	95% CI
14-	0	0.2	-	0.0-14.6
15-	6	6.5	0.9	0.3-2.0
16-	2	1.0	2.0	0.2-7.1
17-	0	1.7	-	0.0-2.2
174	39	5.0	7.9	5.6-10.8
18-	11	3.6	3.0	1.5-5.4
19-	1	0.9	1.1	0.0-6.2
20-	0	1.2	-	0.0-3.1
all mlg	59	20.3	2.9	2.2-3.8

PUBLICATIONS

C.R. MUIRHEAD, A.M. KELLERER, D. CHMELEVSKY, E. OBERHAUSEN, L.E. HOLM, A. BECCIOLINI

Statistical studies of radiation risks

Radiation Protection Programme, EUR 13387, 229-233, 1991

A. BECCIOLINI, S. PORCIANI, A. LANINI, L. CIONINI, R. SANTONI

Urinary polyamines in patients with advanced or recurrent cervical cancer during and after radiotherapy

Acta Cicol. 31, 327-331, 1992

B. DUBRAY, T. GIRINSKY, H.D. THAMER, A. BECCIOLINI, S. PORCIANI, C. HENNEQUIN, G. SOCIE', M. BONNAY, J.M. COSSET

Post irradiation hyperamylasemia as a biological dosimeter

Radiother. Oncol. 24, 21-26, 1992

A. BECCIOLINI, M. BALZI, S. PORCIANI

Biological and biochemical parameters for the characterization of radiation damage

in: "Topics on Biomedical Physics", L. Andreucci, A. Schenone Eds., World Scientific, Singapore, London, 204-212, 1992

A. BECCIOLINI, M. BALZI, S. PORCIANI

Effetto delle radiazioni ionizzanti sui tessuti e meccanismi di induzione del danno

Atti XVIII Congr. Naz. AIRB, Idelson, Napoli, 107-125, 1993

A. BECCIOLINI, S. PORCIANI, A. LANINI

Polyamines

In "Up dating on tumor markers in tissue and in biological fluids: basic aspects and clinical applications" A. Ballesta, G.C. Torre, E. Bombardieri, M. Gion, R. Molina Eds., Minerva

Medica, Torino, 413-434, 1993

A. BECCIOLINI, S. PORCIANI, A. LANINI, M. TOMMASI, P. OLMI, A. CHIAVACCI

Prognostic significance of Tissue Polypeptide Antigen (TPA) in the head and neck carcinoma

Acta Oncologica 32, 295-299, 1993

A. BECCIOLINI, M. BALZI, S. PORCIANI

Attualita' e prospettive della ricerca radiobiologica in radioterapia

Atti Convegno AIRB, Accademia Lincei, "L'evoluzione scientifica della Radiobiologia in Italia", Idelson, Napoli, 37-70, 1993

C. LAGAZZO, A. BIGGERI

An epidemiological approach to the spatial analysis of rare disease: estimation of biological parameters

Proc. Int. Workshop "Statistical and Spatial Processes: Theory and Application" IRMA-CNR, Bari 1993

A. BECCIOLINI

Epidemiological studies of radiation risks (NRPB association)
Progress Report, 1990-91, EUR 14927, 1993, pag 1253 - 1254

A. BECCIOLINI, S. PORCIANI, A. LANINI, A. BENUCCI, A. CASTAGNOLI,
A. PUPI

Serum amylase and tissue polypeptide antigen as biochemical
indicators of salivary gland injury during iodine 131 therapy
Eur. J. Nucl. Med. 21, 1121-1125, 1994

C.R. MUIRHEAD, A.M. KELLERER, D. CHMELEVSKY, E. OBERHAUSEN, A.
BECCIOLINI, S. RICHARDSON, C. HILL, F. DE VATHAIRE, R.R. WICK, H.
SPIESS, G.M. KENDALL

Epidemiological studies in human population

Report EUR 15238, 517-536, 1994

A. BIGGERI, M. MARCHI

Case control design for the detection of space clusters of
disease

Environmetrics 6, 1995

C. CISLAGHI, A. BIGGERI et al.

Dirty or biased disease mapping in geographical epidemiology

Statistics in Medicine, in press

A. BECCIOLINI, P. PACINI, A. BIGGERI, V. GIACHE' et al.

Incidence of a second primary tumour in patients treated for
breast cancer

in preparation

Head of project 7 : Dr. S. RICHARDSON

Project : *Statistical methods, biases and interpretation of geographical correlation studies with application in analysing the geographical association of cancer and radiation exposure*

II - Objectives for the reporting period

This project, which is centered on geographical studies, has a dual aim :

- a detailed study of some specific sources of bias in geographical studies, regrouped under the generic name : *ecological bias* . In particular we have :
 - quantified the biases resulting from ignoring *joint variations* of risk factors in each geographical unit ;
 - proposed a method for correcting this source of bias and investigate its performance using a flexible simulation model ;
- an analysis of the geographical distribution of childhood leukemia in Great Britain in relation to indoor radon concentrations and natural gamma radiation levels (in collaboration with C. Muirhead, NRPB and G. Draper, CCRG). Childhood leukemia incidence data was analysed at a fine geographical scale over 3 consecutive 5-year periods (on average 5 cases/unit/5-year period). To take into account the small area variability and the geographical structure, the analysis was performed in two complementary ways using :
 - Poisson regressions with the inclusion of a spatial component,
 - a hierarchical Bayesian model.

III - Progress achieved including publications

A - Ecological bias

An inherent source of bias in geographical studies (and in general, in studies at group level) lies with the *between group* confounding which results from the difficulty in adequately controlling *joint effect* of risk factors at a geographical level.

Recently, attention has been turned towards including data on confounders with the aim of reducing between-group confounding. This raises the issue of what level of information (mean, variance, joint distribution.....) are required on both exposure and confounders in order to reduce the ecological bias.

We considered the following situation. Let X and Y be 2 dichotomous risk factors with marginal prevalence x and y in an area, R_X (R_Y), the rate ratio for *sole* exposure to X (resp. to Y) and R_{XY} the rate ratio for *joint* exposure to X and Y with corresponding joint prevalence z.

The rate in this area is given by :

$$I(x,y,z) = I_0 \{1+x (R_X - 1) + y(R_Y - 1) + z(1 - R_X -R_Y+R_{XY})\} \quad (1)$$

where I_0 is the baseline rate for the unexposed.

In general joint exposure prevalence z is not known for each area and it is standard practise to carry out a multiple regression involving solely x and y :

$$I(x,y) = I_0 \{1 + x (R_X - 1) + y (R_Y - 1)\} \quad (2).$$

Note that regression (2) assumes that $R_{XY} = R_X + R_Y - 1$, i.e. that the joint effect of X and Y is additive, which is not a common risk model for joint effect ; usually a multiplicative risk model $R_{XY} = R_X R_Y$ is preferred.

Instead of using regression (2), progress can be made if one is prepared to approximate z by the product xy. This corresponds to assume that the distributions of X and Y *within each group* are approximately independent, and leads to introduce a cross product term xy in regression (1), which becomes :

$$I(x,y) = I_0 \{1 + x (R_X - 1) + y (R_Y - 1) + xy (1 - R_X -R_Y+R_{XY})\} \quad (3).$$

Hence, when only the marginal prevalences x and y are known, one is faced with the choice of using regressions (2) or (3).

A simulation model was set up to assess the consequences of using inappropriately equations (2) or (3) ; in particular with respect to :

- misspecification of the regression model with respect to the underlying Relative Risk model,
- use of xy as a joint prevalence even when the exposures are not independent within each unit.

Simulation set up

We considered 50 geographical units with marginal prevalences x_i and y_i , $i = 1, \dots, 50$, for the 2 risk factors. The geographical association between X and Y *across* the 50 units is characterised by a parameter δ . The within-unit association between X and Y is specified by an odds ratio ψ (the same for all units). Independence between the risk factors X and Y within-unit is thus equivalent to $\psi = 1$. The joint effect of the risk factors followed either an additive risk model or a multiplicative risk model.

Two cases were considered for simulating the incidence rate in each area.

a) Gaussian case

The incidence rate for each unit was generated by using equation (1) plus a normally distributed random error term. The ratio of within-unit variance to the between-units variance can be controlled by the variance of the random error term. This incidence model is not appropriate for small units or rare disease where Poisson-like fluctuations are observed.

b) Poisson case

The observed number of cases O_i in each area is generated following a Poisson with mean $I_i(x_i, y_i, z_i)$ given by equation (3). The baseline incidence is set to $I_0=10$.

Each set up (a) and (b) was simulated 100 times.

Results

a) Gaussian case

Estimation of the coefficients in regressions (2) or (3) was obtained using multiple regression techniques. From these coefficients the corresponding values of R_X and R_Y were deduced. First the case of independent risk factors within unit ($z=xy$) was investigated (Table 1). When the regression model corresponds to the underlying risk models (diagonal elements in Table 1), estimation of the relative risks is correct. Misspecification is assessed on the off-diagonal elements of Table 1. The results are clearly asymmetric : when the risk model is multiplicative, using the regression model (2) leads to *overestimation* of the RR, whereas when the risk model is additive, using the regression model (3) still produces good estimates with only slightly increased variances.

These results were confirmed for different values of the geographical association δ , and for other values of R_X and R_Y .

Table 1 : Gaussian case - True relative risks : $R_X = R_Y = 2$, $z = xy$ ($\psi = 1$), $\delta = 0.5$

Regression models	Risk model	
	Additive	Multiplicative
$b_0 + b_1x + b_2y$ (2)	$\bar{R}_X = 2.01$ (0.02)	$\bar{R}_X = 2.97$ (0.05)
	$\bar{R}_Y = 2.01$ (0.02)	$\bar{R}_Y = 2.97$ (0.05)
$b_0 + b_1x + b_2y + b_3xy$ (3)	$\bar{R}_X = 1.99$ (0.04)	$\bar{R}_X = 1.98$ (0.04)
	$\bar{R}_Y = 1.99$ (0.04)	$\bar{R}_Y = 1.98$ (0.07)

[within-unit s.d./between-unit s.d. = 1/4]. In this table and the following are given, the mean estimate of R_X (respectively R_Y) over the 100 simulations and in bracket the half-width of the associated 95% confidence interval.

When the within-unit fluctuations is increased and becomes of the same order as the geographical variance, regression with equation (3) in the case of the multiplicative model leads to relative risks estimates which are somewhat biased downwards, but the degree of bias is less severe than that encountered if regression model (2) is used.

Finally the performance of ecological regressions given by equation (3) was assessed when the true joint exposure prevalence z is different from xy (or equivalently when $\psi \neq 1$) (Table 2). As in Table 1, regression equation (2) in the case of a multiplicative risk model leads to an *overestimation* of the RR. We note a good performance of regression equation (3) for moderate within-unit association between the risk factors ($2 \leq \psi \leq 3$). When the within-unit association between the risk factors is strong ($\psi=4$), regression equation (3) leads to slight overestimation with increased standard error.

Table 2 : Gaussian case - True relative risks : $R_X = R_Y = 2, \delta = 0.5$

Regression models	Multiplicative risk model		
	$\psi = 2$	$\psi = 3$	$\psi = 4$
$b_0 + b_1x + b_2y$ (2)	$\bar{R}_X = 2.90$ (0.04)	$\bar{R}_X = 3.11$ (0.05)	$\bar{R}_X = 3.54$ (0.08)
	$\bar{R}_Y = 2.85$ (0.04)	$\bar{R}_Y = 3.12$ (0.06)	$\bar{R}_Y = 3.55$ (0.08)
$b_0 + b_1x + b_2y + b_3xy$ (3)	$\bar{R}_X = 2.09$ (0.07)	$\bar{R}_X = 2.04$ (0.11)	$\bar{R}_X = 2.32$ (0.15)
	$\bar{R}_Y = 2.05$ (0.07)	$\bar{R}_Y = 2.05$ (0.11)	$\bar{R}_Y = 2.30$ (0.15)

[within-unit s.d./between-unit s.d. = 1/4]

The good performance of regression equation (3) when $1 \leq \psi \leq 3$ was checked for different values of the geographical association δ and for other values of R_X and R_Y . As previously, we found that in this multivariate normal setting, a key factor for a correct estimation of the relative risks using equation (3), is that the between-unit variance should be large with respect to the within-unit variance.

b) Poisson case

Maximum likelihood estimation of the coefficients in regressions (2) or (3) was obtained by an iterative Newton-Raphson method.

Results are reported for the same simulation set ups than in the Gaussian case. Table 3 evaluates the biases when $\psi \neq 1$. The conclusion derived from Table 3 are similar to those derived from Table 1. Regression (3) leads to good estimates of the true relative risks for both the additive and the multiplicative risk models, whereas the estimates arising from regression (2) are substantially biased in the multiplicative case. In comparison to Table 1, one can see that, as expected, the variances of the RR estimates are larger. When the value of the base-line incidence rate I_0 is halved to equal 5, the results deteriorate and regression (3) overestimates the relative risks.

Finally the case where $\psi \neq 1$ was investigated (Table 4). One can see that a small bias remains in the estimates of the relative risks when using regression (3). Note that the bias arising from using regression (2) is more important. When the base-line incidence is increased from 10 to 30, the results are improved and the estimates given by regression (3) are very close to the true relative risks, even when there is strong within-unit correlation between X and Y ($\psi = 4$).

Conclusion

To summarize the results of this extensive study, reported in detail in [1], we would recommend the inclusion of a cross-product term in the geographical regression when the two risk factors are dichotomous. As discussed in [2], appropriate extension of this proposition to the continuous case needs to be investigated in detail. Preliminary results in a case involving a mixture of discrete and continuous risk factors and a non linear dose-response model are given in [3].

Table 3 : Poisson case - $I_0 = 10$, $\delta = 0.5$ True relative risks : $R_X = R_Y = 2$, $z = xy$ ($\psi = 1$),

Regression models	Risk model	
	Additive	Multiplicative
$b_0 + b_1x + b_2y$ (2)	$\bar{R}_X = 2.00$ (0.04)	$\bar{R}_X = 2.88$ (0.08)
	$\bar{R}_Y = 2.02$ (0.04)	$\bar{R}_Y = 2.94$ (0.08)
$b_0 + b_1x + b_2y + b_3xy$ (3)	$\bar{R}_X = 2.09$ (0.12)	$\bar{R}_X = 2.00$ (0.11)
	$\bar{R}_Y = 2.12$ (0.12)	$\bar{R}_Y = 2.04$ (0.11)

Table 4 : Poisson case - $I_0 = 10$, $\delta = 0.5$ True relative risks : $R_X = R_Y = 2$, $z = xy$

Regression models	Multiplicative risk model		
	$\psi = 2$	$\psi = 3$	$\psi = 4$
$b_0 + b_1x + b_2y$ (2)	$\bar{R}_X = 2.87$ (0.07)	$\bar{R}_X = 3.26$ (0.13)	$\bar{R}_X = 3.46$ (0.18)
	$\bar{R}_Y = 2.88$ (0.07)	$\bar{R}_Y = 3.22$ (0.12)	$\bar{R}_Y = 3.39$ (0.16)
$b_0 + b_1x + b_2y + b_3xy$ (3)	$\bar{R}_X = 2.24$ (0.12)	$\bar{R}_X = 1.88$ (0.10)	$\bar{R}_X = 1.74$ (0.07)
	$\bar{R}_Y = 2.24$ (0.12)	$\bar{R}_Y = 1.87$ (0.11)	$\bar{R}_Y = 1.72$ (0.07)

B - Geographical distribution of childhood leukemia in Great-Britain

We completed the analysis of the geographical variation of childhood leukaemia incidence in Great Britain over a 15 year period in relation to natural radiation (gamma and radon). Potential geographical confounding by socio-economic factors was also investigated. Data at the level of the 459 district level local authorities in England, Wales and regional districts in Scotland were analysed in two complementary ways : firstly, by Poisson regressions with the inclusion of environmental covariates and a smooth spatial structure ; secondly, by a hierarchical Bayesian model in which extra-Poisson variability is explicitly modelled in terms of spatial (clustering) and non-spatial (unstructured heterogeneity) components. These results will be published in [4].

Data

• 6691 cases of leukaemia diagnosed between 1969 and 1983, which are further sub-classified as lymphocytic and unspecified leukaemias (LL) (80.2 %) and acute non-lymphocytic leukaemia (ANLL) (16.5 %)

- Mean indoor radon concentrations, indoor and outdoor gamma dose rates estimated from a national survey carried out by the National Radiological Protection Board. In this survey, the number of measurement per district varied according to population geographical spread. These measures were combined using arithmetic means for gamma dose rates and a geometric mean for indoor radon concentration as the distribution was skewed and approximately lognormal.
- Socio-economic variables (period 71-81) : % of active male, % of cars per households, % owner occupied homes, from which a socioeconomic indicator was calculated for each area. A geographical data file at the scale of 459 county districts in England and Wales was set up including :
 - the geographical coordinates for each county chosen as the latitude and the longitude of a main town in the county
 - a nearest neighbourhood structure for each county represented by a matrix $W = (W_{ij})$ where $W_{ij} = 1$ when areas i and j are contiguous.

This will allow to take into account spatial trends as well as to introduce a potential local clustering effect in the analyses

Statistical methods

For each area (indexed by i), we denote by O_i the observed number of cases (known), E_i the expected number of cases (age adjusted), and by θ_i the relative risk (unknown). Since the observed numbers of events are small, we make the hypothesis that the number of cases follows a Poisson distribution : $O_i \sim \text{Poisson}(E_i \theta_i)$

To study the influence of covariates Z_i ($px1$), we have used two approaches.

1 - Poisson regressions

We consider that O_i are independent Poisson variables, with mean $E [O_i | \beta, E_i]$ satisfying :

$$\log E [O_i | \beta, E_i] = \log E_i + \beta' Z_i$$

with β : a ($px1$) vector of regression coefficients.

To take into account an overall smooth spatial structure of the incidence data, a linear function of the coordinates of each area can be introduced :

$$\log E [O_i | \beta, \gamma, E_i] = \log E_i + \beta' Z_i + \gamma' T_i$$

where $T_i = (\text{lat}_i, \text{long}_i)$ characterises a linear spatial trend.

Poisson regressions were fitted using the *glm* procedure of S-PLUS. Statistical significance was assessed using analysis of deviance with an asymptotic chi-square distribution for the deviance difference. The indication of statistical significance has to be treated with caution as some of the observed number of cases are very small and there is some evidence of overdispersion.

It is clear that it is a paramount importance to model properly the spatial structure and that the choice of model will influence the regression coefficients β . For geographical studies at a larger scale where within-unit Poisson variations become negligible, appropriate spatial regression models have been discussed in a related paper [5].

2 - Hierarchical Bayesian model

Poisson fluctuation is modelled at a first level and a log linear mixed model for θ_i is specified at a second level, with area-specific random effects further decomposed into a component that models unstructured heterogeneity and a spatially structured component modelling local clustering.

The hierarchical model is thus formulated as :

1st level - local variability (within area) :

$$O_i \sim \text{Poisson}(E_i \theta_i)$$

2nd level - structure between areas: log linear mixed model

$$\log \theta_i = \mu + u_i + v_i + \beta' Z_i$$

where, Z_i are the covariates and u_i and v_i are random effects representing respectively unstructured heterogeneity and spatial clustering. Note that u_i and v_i can be included separately or jointly and that the constraint: $\sum u_i = \sum v_i = 0$ is used for identifiability.

The following distributional forms are adopted for the two random effects :

Heterogeneity :

$$[u_i | u_j, j \neq i] \sim N(\bar{u}_i, (\lambda_u)^{-1}) \text{ where } \bar{u}_i = \sum_{j \neq i} u_j / N-1$$

Clustering :

$$[v_i | v_j, j \neq i] \sim N(\bar{v}_i, (n_i \lambda_v)^{-1}) \text{ where } \bar{v}_i = \sum_{j \neq i} W_{ij} v_j / n_i$$

and n_i is the number of neighbours of area i .

The parameters λ_u and λ_v control the amount of variability in u_i and v_i respectively and consequently the variability of the relative risks.

In order to carry out a full Bayesian analysis, hyperprior distributions are specified for μ , β , λ_u and λ_v . The estimation of this hierarchical model calls upon stochastic simulation techniques. It was developed in a Bayesian framework by D. Clayton and is implemented in the software BEAM (Bayesian Ecological Analysis Method). A sample of values of u_i , v_i , λ_u , λ_v , μ and β is produced which can be considered (after an initial warming up period) as values for the joint posterior distribution of the parameters conditional on the data. Analysis of this sample produces both point and interval estimates.

A summary of the variability of the random effects, allowing the assessment of their relative contribution to the overall variability of the θ_i , is given by :

$$SD_u = \left(\frac{\sum u_i^2}{n-1} \right)^{1/2} \text{ and } SD_v = \left(\frac{\sum v_i^2}{n-1} \right)^{1/2}$$

RESULTS

a) *Univariate and multivariate Poisson regressions* were carried out systematically for the 3 time periods : 69-73, 74-78 and 79-83, with leukemia cases considered all together or further subclassified as lymphocytic and unspecified leukaemias (LL) (80.2 %) and acute non-lymphocytic leukaemia (ANLL) (16.5 %).

- From the univariate analyses, no overall coherent pattern of association between radiation exposure and leukaemia incidence emerges (Table 5).

- There is weak evidence of a positive association with radon in the middle period related solely to LL, but not for the other two periods, nor for ANLL.

- A significant negative association between all leukaemias, and in particular ANLL, and indoor gamma radiation is also found for the third period but not for the earlier periods.

- There is no evidence of association of leukaemia incidence with outdoor gamma radiation.

• Next multivariate analyses were carried out (see Table 6).

- In the period 74-78, we see that the contribution of radon to LL and overall leukemias incidence is still significant after adjustment on the socio-economic score and the linear spatial trend (which both contribute significantly). In view of these results, multivariate models were also estimated separately for the three age groups. The regression coefficients are overall of the same order of magnitude for the three age groups but the association with radon appears stronger for the 5-9 years old and becomes borderline significant for LL. Note that the small number of cases confers low power to the analyses per age group.

- In the period 79-83, the negative links found with indoor gamma radiation are partially explained by the socio-economic score or a simple spatial structure (results not shown).

Table 5 : Poisson regressions of childhood leukaemias incidence rates : Change in deviance with inclusion (separately) of radon, indoor gamma, outdoor gamma, socio-economic score and spatial trend

DIAGNOSIS	PERIOD	RADON	INDOOR	OUTDOOR	SOCIO-	SPATIAL
		(1df)	GAMMA	GAMMA	ECONOMIC	TREND
		(1 df)	(1 df)	(1 df)	SCORE	(2 df)
		N = 402	N = 391	N = 394	(1 df)	N = 459
All leukaemias	1969 - 73	0.05	0.01	0.56	12.08 (+)	4.75
	1974 - 78	3.49	0.09	0.01	5.32 (+)	2.32
	1979 - 83	0.28	4.79 (-)	2.20	2.97	4.39
Lymphocytic and unspecified leukaemias	1969 - 73	0.73	0.10	1.47	6.75 (+)	2.08
	1974 - 78	4.19 (+)	0.09	0.00	6.31 (+)	2.42
	1979 - 83	0.98	2.31	0.69	2.94	1.39
Acute non-lymphocytic leukaemias	1969 - 73	2.03	0.61	2.51	1.83	4.21
	1974 - 78	0.02	0.25	0.35	0.60	0.94
	1979 - 83	0.97	4.35 (-)	2.93	1.28	6.39

Using the chi-squared approximation to the distribution of scaled deviance in this table. the critical values at the 5 % significance level are 3.84 for 1 degree of freedom and 5.99 for 2 degrees of freedom.

Change in deviance significant at the 5 % level are in bold, accompanied by the sign in bracket of the regression coefficient (for univariate regressors).

b) Bayesian log linear mixed hierarchical model

As shown by the deviances of the Poisson regressions, there is evidence of over-dispersion. The analysis of the structure of leukaemia incidence in the three periods was pursued in the framework of the Bayesian log linear mixed hierarchical model described in the methods.

At first the log-linear mixed model was fitted separately for the three periods without the inclusion of any covariates. The "shrinkage" effect of considering a hierarchical model for the θ_i 's rather than estimating them directly by the corresponding SMR's is illustrated in Figure 1. Some extreme SMR's corresponding to areas with very few cases and a small population are shrunk towards as the Bayesian estimate takes account of local neighbouring values of θ_i and of their overall distribution.

- Characteristics of the heterogeneity (SD_U) and the clustering components (SD_V) for the three periods are given in Table 7. A coherent picture emerges. Both the clustering and the heterogeneity components contribute significantly to the overall variability and there is a stability of their relative contribution over the three periods. Furthermore the clustering component appears in each period to be larger than the heterogeneity component. This is true for the incidence of all leukaemias as well as that of LL.

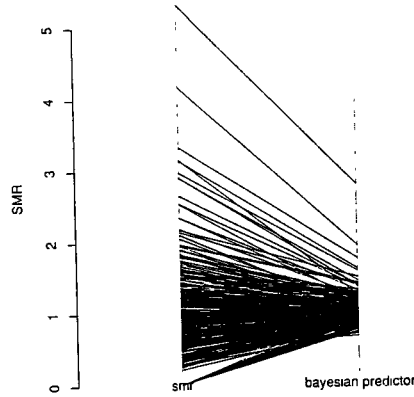
Table 6 : Poisson regressions of childhood leukaemias incidence rates by period : Regression coefficients (s.d.) and t values for radon, socio-economic score, latitude and longitude.

DIAGNOSIS	PERIOD	AGE GROUP (years)	RADON		SOCIO-ECO		LATITUDE		LONGITUDE		DEVIANCE
			Coeff.	t	Coeff.	t	Coeff.	t	Coeff.	t	
<i>All leukaemias</i>	1969 - 73	0 - 14	- 0.0021 (0.0018)	- 0.95	0.0275 (0.0091)	3.00	- 0.0121 (0.0177)	- 0.68	0.0098 (0.0177)	0.55	459.0 (397)
	1974 - 78	0 - 4	0.0026 (0.0022)	1.20	0.0254 (0.0130)	1.98	0.0515 (0.0248)	2.07	- 0.0145 (0.0259)	- 1.60	472.5 (397)
		5 - 9	0.0037 (0.0024)	1.57	- 0.0155 (0.0161)	0.96	0.0580 (0.0331)	- 1.75	- 0.0102 (0.0324)	0.31	462.6 (397)
		10 - 14	0.0035 (0.0035)	0.99	0.0039 (0.0189)	0.21	0.0946 (0.0375)	2.52	- 0.1079 (0.0404)	- 2.67	404.7 (397)
		0 - 14	0.0033 (0.0015)	2.26	0.0108 (0.0089)	1.21	0.0300 (0.0176)	1.71	- 0.0460 (0.0181)	- 2.54	458.0 (397)
	1979 - 83	0 - 14	- 0.00004 (0.0018)	- 0.02	0.0083 (0.0097)	0.86	- 0.0246 (0.0189)	- 1.31	- 0.0036 (0.0191)	- 0.19	429.7 (397)
<i>Lymphocytic and unspecified leukaemias</i>	1969 - 73	0 - 14	- 0.0031 (0.0022)	- 1.40	0.0249 (0.0102)	2.44	- 0.0007 (0.0199)	- 0.03	- 0.0059 (0.0200)	- 0.29	476.6 (397)
	1974 - 78	0 - 4	0.0033 (0.0023)	1.47	0.0311 (0.0141)	2.19	0.0474 (0.0271)	1.75	- 0.0477 (0.0280)	- 1.70	469.9 (397)
		5 - 9	0.0043 (0.0025)	1.75	- 0.0182 (0.0178)	- 1.02	- 0.0625 (0.0366)	- 1.70	- 0.0006 (0.0358)	- 0.01	438.0 (397)
		10 - 14	0.0009 (0.0053)	0.17	0.0099 (0.0238)	0.42	0.1040 (0.0471)	2.20	- 0.1437 (0.0511)	- 2.81	389.3 (397)
		0 - 14	0.0037 (0.0016)	2.30	0.0146 (0.0100)	1.45	0.0252 (0.0198)	- 1.27	- 0.0489 (0.0203)	- 2.41	483.6 (397)
	1979 - 83	0 - 14	0.0009 (0.0018)	0.51	0.0148 (0.0107)	1.38	- 0.0063 (0.0206)	- 0.30	- 0.0004 (0.0210)	- 0.02	455.7 (397)

coefficients statistically significant at the 5% level are in bold.

Figure 1

Comparing the dispersion of SMR and bayesian estimates



- Cross-period correlations were calculated for these components for the two pairs of consecutive time periods (Table 8). For all leukaemias and LL, the cross-period correlations are very low for the heterogeneity component, reflecting that this component of over-Poisson dispersion has no spatial stability over time. On the other hand for LL, the local values of the clustering component show a certain amount of stability over time, indicating that the same districts keep high (or low) values of the clustering component over time.

- Covariates, i.e. radon levels and the socio-economic score, were introduced in the log linear mixed model (Table 9). For the socio-economic score, there is a close similarity between the values of the regression coefficient estimates for the Poisson regressions or the log linear mixed model. In contrast, the significant positive associations between radon levels and leukaemia incidence (all leukaemias and LL) which had been found in the period 74-78 are no longer present.

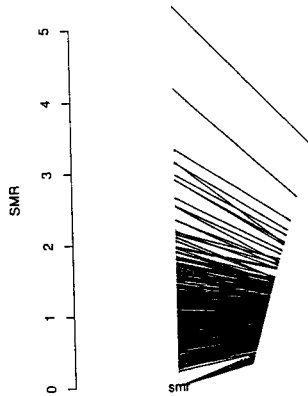
Table 7 : Bayesian hierarchical model : estimation of the relative contribution of the heterogeneity and clustering components to the overall variability of the relative risks. Posterior means with posterior standard deviations in bracket.

Period	All leukaemias				Lymphocytic and unspecified leukaemias			
	Heterogeneity SD_u		Clustering SD_v		Heterogeneity SD_u		Clustering SD_v	
	without covariates	with covariates*	without covariates	with covariates*	without covariates	with covariates*	without covariates	with covariates*
69-73	0.033 (0.014)	0.032 (0.011)	0.055 (0.019)	0.041 (0.016)	0.035 (0.017)	0.034 (0.015)	0.042 (0.018)	0.034 (0.011)
74-78	0.035 (0.021)	0.037 (0.024)	0.054 (0.035)	0.035 (0.014)	0.033 (0.013)	0.043 (0.034)	0.059 (0.037)	0.043 (0.021)
79-83	0.034 (0.013)	0.033 (0.012)	0.041 (0.015)	0.039 (0.016)	0.033 (0.015)	0.035 (0.015)	0.037 (0.015)	0.037 (0.014)

* covariates : radon level and socio-economic score

Figure 1

Comparing the dispersion of SMR and bayes



- Cross-period correlations were calculated for these components for the two pairs of consecutive time periods (Table 8). For all leukaemias and LL, the cross-period correlations are very low for the heterogeneity component, reflecting that this component of over-Poisson dispersion has no spatial stability over time. On the other hand for LL, the local values of the clustering component show a certain amount of stability over time, indicating that the same districts keep high (or low) values of the clustering component over time.

- Covariates, i.e. radon levels and the socio-economic score, were introduced in the log linear mixed model (Table 9). For the socio-economic score, there is a close similarity between the values of the regression coefficient estimates for the Poisson regressions or the log linear mixed model. In contrast, the significant positive associations between radon levels and leukaemia incidence (all leukaemias and LL) which had been found in the period 74-78 are no longer present.

Table 7 : Bayesian hierarchical model : estimation of the relative contribution of the heterogeneity and clustering components to the overall variability of the relative risks. Posterior means with posterior standard deviations in bracket.

Period	All leukaemias				Lymphocytic and unspecified leukaemias			
	Heterogeneity SD_u		Clustering SD_v		Heterogeneity SD_u		Clustering SD_v	
	without covariates	with covariates*	without covariates	with covariates*	without covariates	with covariates*	without covariates	with covariates*
69-73	0.033 (0.014)	0.032 (0.011)	0.055 (0.019)	0.041 (0.016)	0.035 (0.017)	0.034 (0.015)	0.042 (0.018)	0.034 (0.011)
74-78	0.035 (0.021)	0.037 (0.024)	0.054 (0.035)	0.035 (0.014)	0.033 (0.013)	0.043 (0.034)	0.059 (0.037)	0.043 (0.021)
79-83	0.034 (0.013)	0.033 (0.012)	0.041 (0.015)	0.039 (0.016)	0.033 (0.015)	0.035 (0.015)	0.037 (0.015)	0.037 (0.014)

* covariates : radon level and socio-economic score

Table 8 : Geographical correlations between successive periods of the estimated random effects corresponding to the heterogeneity or the clustering components.

Periods	All leukaemias		Lymphocytic and unspecified leukaemias	
	Heterogeneity	Clustering	Heterogeneity	Clustering
	without covariates	without covariates	without covariates	without covariates
69-73 / 74-78	0.077	0.004	0.103	0.479
74-78 / 79-83	0.084	0.386	0.024	0.668

Table 9 : Bayesian hierarchical model : estimation of the regression coefficients in the log linear mixed model. Posterior means with posterior standard deviations (in bracket) and their ratio.

Period	All leukaemias				Lymphocytic and unspecified leukaemias			
	Radon		Socio-economic score		Radon		Socio-economic score	
69-73	- 0.0026 (0.0020)	1.30	0.0288 (0.0086)	3.35	- 0.0043 (0.0022)	1.95	0.0268 (0.0094)	2.85
74-78	0.0019 (0.0014)	1.36	0.0120 (0.0084)	1.33	0.0022 (0.0017)	1.29	0.0182 (0.0094)	1.94
79-83	- 0.0001 (0.0017)	0.06	0.0120 (0.0090)	1.33	- 0.0008 (0.0017)	0.47	(0.0149)	1.51 (0.0099)

Conclusion

We deduce a strong indication that a main part of the variability of childhood leukemia accounted for by a local neighbourhood "clustering" structure. This structure is furthermore relatively stable over the 15 year period for the lymphocytic leukaemias which make up the majority of observed cases.

Thus there is some evidence that local risk factors, relatively stable over time, are influencing the spatial structure of leukaemia incidence. These local risk factors might correspond to a complex combination of environmental and socio-demographic local characteristics and it would be interesting to be able to extend this analysis after 1983 to investigate the persistence of this local structure.

We found no evidence of a positive association of childhood leukaemia incidence with outdoor or indoor gamma radiation levels.

There is no consistent evidence of any association with radon levels. Indeed, in the Poisson regressions, a significant positive association was only observed for one 5-year period, a result which is not compatible with a stable environmental effect. Moreover, this positive association became clearly non-significant when over-dispersion relative to the Poisson distribution was taken into account.

Publications

- [1] V. Lasserre, C. Guihenneuc, S. Richardson.
Biais des études de corrélations écologiques.
Technical Report - University of Paris V 1994; 219-234.
- [2] S. Richardson
Vote of thanks for the paper by Plummer and Clayton.
J R Stat Soc [B] 1995; in press.

- [3] V. Lasserre, C. Guihenneuc, S. Richardson.
Ecologic studies - biases, misconceptions, and counterexamples".
Letter to appear in the American Journal of Epidemiology, 1995.
- [4] S. Richardson, C. Monfort, M. Green, G. Draper, C. Muirhead.
Spatial variation of natural radiation and childhood leukaemia incidence in the Great-Britain.
To appear in Statistics in Medicine (1995).
- [5] S. Richardson, C. Guihenneuc, V. Lasserre.
Spatial linear models with autocorrelated error structure.
The Statistician, 41, 53 9-557 (1992).

Project 8

Participating organisation: Institut Gustave Roussy

Head of project: Catherine Hill

Objectives for the reporting period

- a) To extend the leukaemia mortality study around nuclear sites to all 13 installations operating before 1985, including all deaths occurring between 1968 and 1989 in the population aged 0 to 24.
- b) To study mortality for the main cancer sites potentially related to radiation (lung, bone, brain, thyroid, Hodgkin's disease, other lymphomas, multiple myeloma and leukaemia) and for all cancers around the thirteen installations operating before 1985, in the population aged 0 to 64. To produce detailed tables for each cancer site by age, sex, distance from installation and by nuclear site.
- c) To study leukaemia mortality among children living in French towns with a recent and large increase in population.

Progress achieved during the reporting period

a) We studied the main nuclear sites operating in 1985. During the period under study, a total of 4,132,000 person-years of observation were accumulated in the population aged 0-24 residing in the 503 exposed communes. The observed number of leukaemia deaths was 69, which was slightly less than the 86.15 deaths expected according to national mortality statistics: SMR = 80 (95% confidence interval: 62-101, $p=0.07$).

Table 1 gives the number of leukaemia deaths by sex, age, type of installation and distance from the nuclear site. Two of the 13 SMR's are significantly lower than expected; after correction for multiple testing, there is no effect of sex and age, no difference between reprocessing plants and reactors, and no linear trend with an increasing distance from the installation.

Table 1 : Number of person-years, observed (O) and expected (E) number of leukaemia deaths, and standardised mortality ratios (SMR) by sex, age, type of installation and distance from nuclear installations

Characteristics		Person-years in		Number of leukaemia deaths		SMR % (95%CI)	
		thousands	Observed	Expected			
Sex	Male	2,129	36	51.30	70*	(49- 97)	
	Female	2,003	33	34.85	95	(65-133)	
Age (years)	0-4	816	12	16.95	71	(37-124)	
	5-9	862	15	22.16	68	(38-112)	
	10-14	871	12	17.17	70	(36-122)	
	15-19	859	17	16.96	100	(58-160)	
	20-24	724	13	12.91	101	(54-172)	
Installation	Reprocessing	1,284	21	28.66	73	(45-112)	
	Others	2,848	48	57.49	83	(62-111)	
Distance (km)	<5	460	7	9.63	73	(29-150)	
	5-9,9	1,469	26	31.05	84	(55-123)	
	10-12,9	802	8	16.20	49 ^b	(21- 97)	
	13-15,9	1,401	28	29.27	96	(64-138)	
Total		4,132	69	86.15	80	(62-101)	

SMR = standardised mortality ratio (SMR(%)=100(O/E))

95%CI = 95% confidence interval

^a p=0.03 (two-sided test)

^b p=0.04 (two-sided test)

b) We studied mortality for lung, bone, breast, brain, thyroid cancers, Hodgkin's disease, other lymphomas, myelomas, leukaemias, and all cancer sites, around the 13 installations operating before 1985, in the population aged 0 to 64. Nine million person-years of observation were accumulated, and Table 2 gives the observed and expected numbers of death for each cause. The observed numbers were close to the expected numbers for all sites studied except for breast for which the observed mortality was lower than expected.

Table 2: Observed and expected number of deaths, and standardised mortality ratios (SMR)

Cancer site	Number of deaths		SMR %	(95%CI)
	Observed	Expected		
Lung	1,312	1,287.9	102	(99-108)
Bone	90	75.6	119	(96-146)
Breast	573	640.8	89	(82-97)*
Brain	212	213.2	99	(86-114)
Thyroid	17	25.3	67	(39-107)
Hodgkin's disease	59	59.4	99	(76-128)
Other lymphomas	157	144.2	109	(93-127)
Myelomas	45	57.2	79	(57-105)
Leukaemia	269	302.7	89	(79-100)
All sites	7,467	7,330.7	102	(100-104)

Number of person-years : 8,970,000

* p=0.007

A paper summarising these results and an INSERM report containing detailed tables are in the course of publication.

c) We studied the population under age 25 residing in the 43 French communes in which a large and rapid population increase had occurred between 1968 and 1990. The observed number of leukaemia deaths was 101, slightly less than the 112.0 expected based on national mortality statistics: SMR = 90 (95% confidence interval: 73-110).

Table 3 gives the number of leukaemia deaths by sex, age, size of the population increase between two consecutive censuses, location of commune ("Ile de France" region versus others) and period. Period "0" is defined as the period when the first increase of more than 100% was observed (1968-1975 for 31 communes, 1975-1982 for 10 communes and 1982-1989 for 2 communes), period "1" directly follows period "0" (1975-1982 for 31 communes and 1982-1989 for 10 communes) and period "2" directly follows period "1" (1982-1989 for 31 communes). The observed number of leukaemia deaths was 101, which was slightly less than the 112.0 deaths expected according to national mortality statistics: SMR = 90 (95% confidence interval: 73-110). There was no difference in the risk of leukaemia mortality according to sex, age, size of the population increase, "Ile de France" region versus others, or period.

Table 3 : Number of person-years, observed and expected number of leukaemia deaths, and standardised mortality ratios (SMR) by sex, age, region, period and size of population increase

Characteristics		Person-years in thousands	Number of leukaemia deaths		SMR % (95% CI)
			Observed	Expected	
Sex	Male	2,660	62	65.4	95 (73 - 122)
	Female	2,611	39	46.6	84 (60 - 114)
Age	0-4	1,195	17	25.4	67 (39 - 107)
	5-9	1,185	42	31.4	134 (96 - 181)
	10-14	1,075	12	21.5	56* (29 - 98)
	15-19	932	14	18.2	77 (42 - 129)
	20-24	884	16	15.5	103 (59 - 168)
Population increase between two censuses	100%	3,479	57	69.3	82 (62 - 107)
	101%-200%	1,255	30	29.3	102 (69 - 146)
	201%-300%	176	4	4.5	89 (24 - 228)
	301%-400%	88	2	2.2	90 (10 - 328)
	>400%	273	8	6.7	120 (51 - 235)
Region	Ile de France	2,849	66	59.4	112 (86 - 141)
	Others	2,422	35	52.6	67*(46 - 93)
Period	0	1,159	30	30.2	99 (67 - 142)
	1	2,012	38	44.5	85 (60 - 117)
	2	2,100	33	37.3	88 (61 - 124)
Total		5,271	101	112.0	90 (73 - 110)

Publications :

Hill C, Laplanche A. La mortalité entre 0 et 24 ans autour d'installations nucléaires françaises. Paris: INSERM 1992. 54 pages.

Hill C, Laplanche A. Mortality under age 25 around six French nuclear sites. Proceedings of the 8-th congress of the International Radioprotection Association. Montreal 1992;1 : 541-544.

Hill C, Laplanche A. Overall mortality and cancer mortality around French nuclear sites. In : Beral V, Roman E, Bobrow M. Childhood cancer and nuclear installations. London: Br Med J 1993: 436-438.

Hattchouel JM. Etude de la mortalité par leucémies autour des installations nucléaires françaises mises en service avant 1985, chez les sujets âgés de moins de 25 ans. Mémoire pour le Diplôme d'Etudes Approfondies de Santé Publique. Université Paris-Sud 1993. 47 pages.

Hubert D, Hill C. Etude des populations habitant près des installations nucléaires. Radioprotection 1994; 29: 89-100.

Hill C. Frequency of cancer near French nuclear sites and in French new towns. Leukemia 1994;8: 2012-2013 (abstract).

Laplanche A, de Vathaire F. Leukaemia mortality in French communes (administrative units) with a large and rapid population increase. Br J Cancer 1994; 69: 110-113.

Hattchouel JM, Laplanche A, Hill C. Leukaemia mortality around French nuclear sites. Br J Cancer 1995; 71: 651-653.

Hattchouel JM, Laplanche A, Hill C. Cancer mortality around French nuclear sites. Annals of epidemiology 1995 in press.

Hattchouel JM, Laplanche A, Hill C. Mortalité par cancer entre 0 et 64 ans, autour d'installations nucléaires françaises. Paris: INSERM in press.

1) PROPOSAL TITLE AND NUMBER :

Proposal 9 : Second cancers incidence after a first cancer in childhood.

2) PARTICIPATING ORGANISATION AND SCIENTIFIC HEAD OF PROJECT

Head of project : Florent de VATHAIRE
INSTITUT NATIONAL DE LA SANTE ET DE LA RECHERCHE MEDICALE
UNITE 351

3) OBJECTIVES FOR REPORTING PERIOD

The objective of the project was to monitor a cohort study about second cancers incidence among patients treated for cancer during childhood. It was planned to include about 5000 patients in order to observe about 200 second cancers.

In this study, particular attention was focussed on the dosimetry : for each irradiated patients, the doses of radiations were estimated to about 150 pts of the body. This was done using a software specially developed for this study.

4) PROGRESS ACHIEVED DURING CONTRACT PERIOD

At the beginning of the contract, 2423 children were yet included. From July 1992 to July 1993, 1183 new children were included., additional 505 children have been included from July 1993 to July 1994, and another 456 children have been included from July 1994 to July 1995. Hence, a total of 2144 children were included during the contract period, leading to a total of 4567 children in the study.

The estimation of doses delivered by machines using photon have been finished during end of 1994. At the opposite, the estimation of doses delivered by curietherapy and by machines using electrons has to be finished. We hope finish this estimation during the year 1995.

We finished the analysis of the temporal pattern of the excess of risk of second cancer in the cohort. Since July 1995, we are analysing the dose-response relationship for bone sarcomas and thyroid cancer.

5) RESULTS

The following table details the number of patients and the period of diagnosis in each participating center.

Table I : General characteristics of the the 4567 children from the cohort, according to the center of treatment.

Center treatment	Nb patients	% of females	mean date of diagnosis (min-max)	mean age at diagnosis in months (min-max)
Institut Gustave Roussy, Villejuif	2696	45 %	1974 (1942-1993)	72 (0 - 203)
Great Ormond Street Hospital, London	653	45 %	1973 (1942-1991)	58 (0 - 203)
Institut Curie, Paris	360	44 %	1980 (1973-1984)	63 (0 - 199)
St Bartholomew's Hospital, London	298	41 %	1970 (1947-1985)	88 (0 - 178)
Royal Marsden Hospital, London	267	44 %	1973 (1953-1985)	98 (0 - 180)
Centre Claudius Regaud, Toulouse	187	41 %	1978 (1965-1985)	86 (0 - 193)
Institut Jean Godinot, Reims	87	40 %	1980 (1974-1986)	97 (0 - 191)
Centre Antoine Lacassagne, Nice	19	47 %	1974 (1968-1979)	89 (4 - 185)
Whole cohort	4567	45 %	1975 (1942-1993)	6 (0-16)

The table II shows the state of the dose estimation at June 30 1995.

Table II - State of dosimetry estimation at June 30 1995.

Center of treatment	Radiotherapy	Disponible dosimetry	No available dosimetry (june 1995)	
		Photons	Curietherapy or impossible	Electrons
Institut Gustave Roussy	1972	1495	240	237
Great Ormond Street	331	274	45	12
Institut Curie	224	128	38	58
St Bartholomew's	214	214	28	9
Royal Marsden	230	191	29	10
Centre Claudius Regaud	166	152	5	9
Institut Jean Godinot	65	44	8	13
Centre Antoine Lacassagne	19	15	3	1
Whole cohorte	3258	2513	399	346

Among the 4567 children treated in 8 centres in France and in Great Britain was studied, we excluded from the analysis of the temporal risk patten 3110 patients who had received chemotherapy. Of the 1457 remaining patients, 402 were not included because they were treated by surgery alone.

The remaining 1055 patients were included in the analysis of the temporal pattern of risk of solid cancer. Twenty six solid cancers occurred among these patients, as compared to 5,6 cases expected, thus the mean ERR was 3.6 (90%CI:2.2-5.4). Table III shows the number of PY at risk, the expected

and observed numbers of solid SMN, the observed and excess incidence and the relative risk of solid SMN, by 5-year period of follow-up.

Table III - Solid second malignant neoplasms occurrence according to time since irradiation.

Years after irradiation	PY	Solid SMN		Annual Incidence / 100.000 persons		Relative risk (90%CI)
		Observed	Expected	Total	Excess	(O/E)
2-4	3038	0	0,26	0	-9	0
5-9	4575	3	0,53	66	54	5.7 (1.5-14.6)
10-14	3644	4	0,70	110	91	5.7 (1.9-13.1)
15-19	2676	7	0,87	262	229	8.1 (3.8-15.1)
20-24	1882	5	0,98	266	214	5.1 (2.0-10.7)
25-29	1196	4	1.02	334	249	3.9 (1.3-9.0)
≥ 30	843	3	1.29	360	203	2.3 (0.6-6.0)
Total	17855	26	5.64	146	114	4,6 (3.2-6.4)

Table IV shows that both excess of annual incidence of relative risk of solid second malignant neoplasms decreased with age at time of irradiation.

Table IV - Solid second malignant neoplasm occurrence according to age at irradiation.

Age at irradiation (years)	Nb patients	Mean follow-up	PY	Solid SMN		Annual incidence / 100.000 persons		Relative risk (IC90%)
				Observed	Expected	Total	Excess	
0-4	449	20	8384	15	1,74	179	158	8.6 (5.3-13.3)
5-9	272	18	4431	6	1,40	135	104	4.3 (1.9-8.5)
10-16	334	17	5039	5	2,51	99	49	2.0 (0.8-4.2)

PY: person-years at risk.

SMN : second malignant neoplasm.

When taking into account age at time of irradiation, sex, and country of treatment together, a decrease of the ERR of solid SMN with time after irradiation was shown : $\alpha_0 = -2.8$ (sd=1.2), $\chi^2 = 89.64 - 84.46 = 5.18$, df=1, p=0.002). We did not find a significant modification of the ERR decrease rate with age at time of irradiation ($\chi^2 = 84.46 - 82.39 = 2.07$, df=2, p=0.4).

When taking into account the mean dose received to the 3 main sites of SMN (i.e., thyroid, brain and breast) and modelling the ERR per Gy of cancer of any one of these 3 sites, the results remained similar : $\alpha_0 = -2.1$ (sd=1.4), $\chi^2 = 2.2$, p=0.1.

This result did not depend of the assumption that the background rate in the cohort was equal to the rate in the general population : when introducing an additional coefficient for a spontaneous higher risk in the cohort (due to genetic susceptibility, by example), in both models 4 and 5, results remained similar : $\alpha_0 = -2.3$ (sd=1.7), $\chi^2 = 2.0$, p=0.15.

Our results confirms that the ERR of solid cancers decreases after irradiation in childhood, as shown

by Mark Little of the NRPB using a pool of 3 cohorts, and also recently confirmed using the atomic bomb survivors. According to the type of analysis, we found an ERR decrease rate ranging from $t^{-2.0}$ to $t^{-3.8}$, compatible with that published by Little (from $t^{-2.0}$ to $t^{-3.2}$), where t represents the time after the peak of incidence. It is important to note that this result concerns the overall risk of solid cancer, and care needs to be taken in extrapolating to specific sites of radio-induced cancers.

Although we concur with Mark Little that the ERR of thyroid, breast, and brain cancer, as a group, decreases, other studies did not show such results : none of the other published studies showed a significant decrease of the ERR of either thyroid cancer or breast cancer with time since exposure. In contrast, the decrease of ERR of brain and nervous system tumors with time since exposure has previously been reported .

6) LIST OF ANY PUBLICATIONS

- Aubert B, Mertz L Cintrat L, **de Vathaire F**. Programme d'évaluation dosimétrique interactif (PEDIgray) dans le cas d'administration de radionucléides. *Radioprotection*, 1994, 29:177-184.
- **de Vathaire F**. Cancers du sein et leucémies après irradiation. *Radioprotection*, 1994, 29:59-65.
- **de Vathaire F**, Shamsaldin A., Grimaud E, et al. Solid malignant neoplasms after childhood irradiation : decrease of the relative risk with time after irradiation. *Comptes Rendus de l'Académie des Sciences de Paris*. 1995 ; 318:483-490.
- Schlumberger M, **de Vathaire F**, Cecarrelli C, et al. Exposure to radio-iodine did not exclude pregnancy in thyroid cancers patients. *The Journal of Nuclear Medicine*. In press.
- Challeton C, Du Villard J.A, Caillou B, **de Vathaire F**, et al. Pattern of Ras and Gsp oncogene mutations in radiation-associated human thyroid tumour. *Oncogene*, In press.
- **de Vathaire F**, Schlumberger M, Delisle MJ, et al. Leukemias and cancers following ^{131}I administration for a thyroid cancer. Submitted for publication.
- Grimaud E, Shamsaldin A, Lamon A, et al.. Evaluation expérimentale des estimations par DOSEG de doses absorbées pour des plan des plans de traitements type. *XXXIIIème Congrès de la Société Française des Physiciens d'Hôpital*, Marseille, France 2-4 juin 1994.
- Benoit MB, Tournade MF, Jean R, et al. Effect on pulmonary function in adult irradiated on whole lung in childhood for lung metastasis of Wilms tumours treated between 1960 and 1973. *SIOP XXVI Meeting (Paris 20-24 september 1994) abstracts - Medical and Pediatric Oncology*; 33, 3:250.
- Oberlin O, Raquin MA, Karmar A, et al. Influence of the first cancer type on the incidence of second malignant neoplasm (SMN) after cancer in childhood. An european cohort study of 4111 children with solid tumor. *SIOP XXVI Meeting (Paris 20-24 september 1994) abstracts - Medical and Pediatric Oncology*; 33, 3:240.
- Schlumberger M, Delisle MJ, Théobald S, et al. Cancer in children born of patients with epithelial thyroid carcinoma : no influence of radio-iodine treatment. *SIOP XXVI Meeting (Paris 20-24 september 1994) abstracts - Medical and Pediatric Oncology*; 33, 3:178.
- Aubier F, Oberlin O, **de Vathaire F**, et al. Influence of chemotherapy on male fertility : A study of 175 with solid tumor treated at the Institut Gustave Roussy between 1963 and 1988. *SIOP XXVI Meeting (Paris 20-24 september 1994) abstracts - Medical and Pediatric Oncology*; 33, 3:177.
- Bessa E, Orinel R, Vassal G, et al. Secondary bone and soft tissue sarcomas versus mechanism of action of different drugs associated with radiotherapy : a european cohort study of 4111 children. *SIOP XXVI Meeting (Paris 20-24 september 1994) abstracts - Medical and Pediatric Oncology*; 33, 3:175.

Project 10: Late effects in ^{224}Ra treated ankylosing spondylitis patients

Participating organisation: GSF - Forschungszentrum für Umwelt und Gesundheit Neuherberg,
Institut für Strahlenbiologie

Head of Project: Dr. R. R. Wick

Final Report 1992 - 1994

II. Objectives for the reporting period

The objectives for the reporting period included: Contact and follow-up of patients of the exposure group and the control group; registration of causes of death; comparison of the results from the exposure and control groups with respect to the risk of late effects in bone, haematopoietic tissue, and other organs known of supposed from Project 11 to be related to the $^{224}\text{Radium}$ treatment.

III. Progress achieved including publications

In the years between 1946 and 1950 about 2000 people, many of them children and juveniles, were treated for various diseases in a German hospital with repeated intravenous injections of „Peteosthor“, an aqueous mixture of ^{224}Ra with traces of eosin and colloidal platinum. Positive therapeutic effects, however, were reported only for ankylosing spondylitis, whereas, beginning in the early 1950's objections to the treatment of tuberculosis were raised - the primary one being that ^{224}Ra deposited in the growing skeleton of the children and juveniles would cause severe damage.

The method of treating ankylosing spondylitis with lower doses of ^{224}Ra and omitting the completely ineffective platinum and eosin spread from the Orthopaedic University Hospital at Münster, where it was first used on a large scale, to other institutions too. After an enormous increase of different bone lesions having become manifest, the most severe being the induction of 56 bone sarcomas among the 900 patients mostly treated as children and juveniles and now followed in Project 11, a new study was started at the GSF (this project) with the objective of evaluating the late effects risk for bone tumours and other lesions especially in the critical region just below the lowest dose of 0.9 Gy associated with a bone sarcoma in the earlier study of Project 11.

Study Population

The study includes most patients treated in West Germany for ankylosing spondylitis with minor amounts of Radium-224, and not yet followed in Project 11. By end of June 1995, the study consists of more than 1500 ankylosing spondylitis patients from 9 hospitals (Table 1). The majority of the patients, most of them treated in the years 1948-75, received one series of 10 weekly injections of about 1 MBq of ^{224}Ra each. This was the usual dosage for the treatment of ankylosing spondylitis performed until very recently and leads to a cumulative α -dose of 0.56 Gy to the marrow-free skeleton of a 70 kg man.

In addition there exists a control group of ankylosing spondylitis patients with roughly the same age distribution and who have not been treated with radioactive drugs or X-rays. This group has been assembled to provide comparative information on causes of death and lesions possibly related to the basic disease itself or to its

treatment with drugs. Patients for this control group have been drawn mainly from a hospital known to refuse ^{224}Ra treatment on principle.

Table 1: *Follow-up status and exposure parameters of the ankylosing spondylitis patients*

	Exposure Group	Control Group
Total number of patients	1577	1462
Treated with X-rays additionally	106	126
Remaining patients	1471	1336
Deceased patients	636	744
Cause of death certified	624	691
Cases still pending	12	53
Mean injected amount of ^{224}Ra (Mbc/kg)	0.17	-
Mean α -dose to the skeleton (Gy)	0.67	-
Mean injection period (weeks)	10.4	-
Mean follow-up time (years)	20.6	21.0

Personal and treatment data for the patients of the exposure and the control group have been drawn from the hospital records. Information on the current status of patients is gained from re-examinations at different times after treatment and from questionnaires sent periodically to the patients. Causes of death were determined preferentially from hospital records and death certificates. For a great number of patients also histologically confirmed diagnoses were available. The underlying causes of death were classified and registered according to the 7th revision of the *International Classification of Diseases* (ICD) and to the *Klinischer Diagnoseschlüssel* (KDS).

Results

Up till now, 636 patients in the exposure group and 744 control patients have died. Causes of death have been ascertained in 624 patients of the exposure group and of 691 control patients. The remaining cases are still pending.

Table 2 shows the tumours of bone/bone marrow and haematopoietic tissue observed so far. In the exposure group, four cases of malignant primary bone tumours (according to the *Histological Typing of Bone Tumours* of the WHO) have been observed: one fibrosarcoma of bone, one malignant fibrous histiocytoma, one reticulum cell sarcoma (malignant lymphoma) of bone, and one medullary plasmocytoma (myeloma), originally observed in the bone marrow of sternum and pelvis. In the control group only one case of skeletal tumour, also a plasmocytoma, has been observed.

Diseases of the haematopoietic tissue among living and dead patients included: leukaemias (12 in the exposure group vs. 7 in the control group) as well as one case of osteomyelosclerosis in the exposure group.

Table 3 shows the types of tumours occurring in our patient groups compared to the cases expected from the three regional tumour registries of the FRG, namely the registry of the Saarland, of Hamburg and of the former GDR. The expected cases shown there are the ranges resulting from calculations from these three registries

Table 2: *Tumours of bone/bone marrow and haematopoietic tissue after treatment with ²²⁴Radium*

	Exposure Group	Control Group
Deceased patients, cause of death certified	624	691
Total tumours	149 (30*)	158 (20)
<i>TUMOURS OF BONE AND BONE MARROW</i>	5 (1)	2
Exostosis (osteochondroma)	1 (1)	1
Malignant tumours of bone and bone marrow	4	1
Fibrosarcoma	1	0
Malignant fibrous histiocytoma	1	0
Reticulum cell sarcoma	1	0
Medullary plasmocytoma	1	1
<i>MYELOPROLIFERATIVE DISEASES</i>	8 (1)	3
Myeloid leukaemia	7	3
Chronic myeloid leukaemia	4	1
Acute myeloid leukaemia	3	2
Osteomyelosclerosis	1 (1)	0
<i>LYMPHATIC LEUKAEMIA</i>	4	2
<i>LEUKAEMIA OF UNKNOWN TYPE</i>	1	1

* living

Table 3: *Observed malignant tumours in the exposure and control group and cases obs/exp*

	Exposure Group		Control Group	
	obs.	exp.	obs.	exp.
<i>TOTAL NUMBER OF TUMOURS</i>	149	126 - 153	158	158 - 192
Stomach	17	16.4 - 20.0	15	16.4 - 19.5
Liver	1	2.7 - 3.9	7	3.5 - 4.9
Urinary system	10	8.8 - 11.3	10	10.9 - 14.2
Female breast	1	2.5 - 4.0	1	2.1 - 3.4
Non-Hodgkin-Lymphoma	2	0.9 - 1.8	1	1.0 - 2.3
Hodgkin's disease	1	0.8 - 1.1	0	0.8 - 1.1
Skeleton	4	0.7 - 2.7	1	0.8 - 3.0
Leukaemia	12	2.6 - 2.9	7	3.4 - 3.6
Myeloid leukaemia	7	1.4 - 1.6	3	1.6 - 2.1
Chronic myeloid leukaemia	4	0.8	1	0.8
Acute myeloid leukaemia	3	0.7	2	0.8
Lymphatic leukaemia	4	1.3 - 1.4	2	1.4 - 1.6
Leukaemia of unknown type	1		2	

as there is no Federal cancer registry of the whole FRG. In the table we restricted our interest to those diseases that are known or implied from the study of Project 11, the higher dose group, to be associated with a former administration of ^{224}Ra . There is, in contrast to the high dose group, no significant difference between observed and expected cases for cancers of stomach, liver, urinary system, or the female breast neither for the exposure nor for the control group. Furthermore, additionally to the four cases of malignant tumours in the skeletal region that already have been reported earlier, we observed 12 cases of leukaemia in the exposure group. As shown in Figure 1, this increase in total leukaemias (12 cases obs. vs. 2.6 - 2.9 cases exp., $p < 0.001$) is highly significant for the exposure group, compared to a standard population, and borderline significant also for the controls (7 cases of leukaemia vs. 3.4 - 3.6 exp., $p = 0.07$). Subclassification of the leukaemias, however, shows a clear preference for the chronic myeloid leukaemia (CML) in the exposure group (4 cases obs. vs. 0.8 cases exp., $p = 0.009$), whereas in the control group the observed cases of CML are within the range of expectancy.

Table 4: *Chronic myeloid leukaemias in the exposure group*

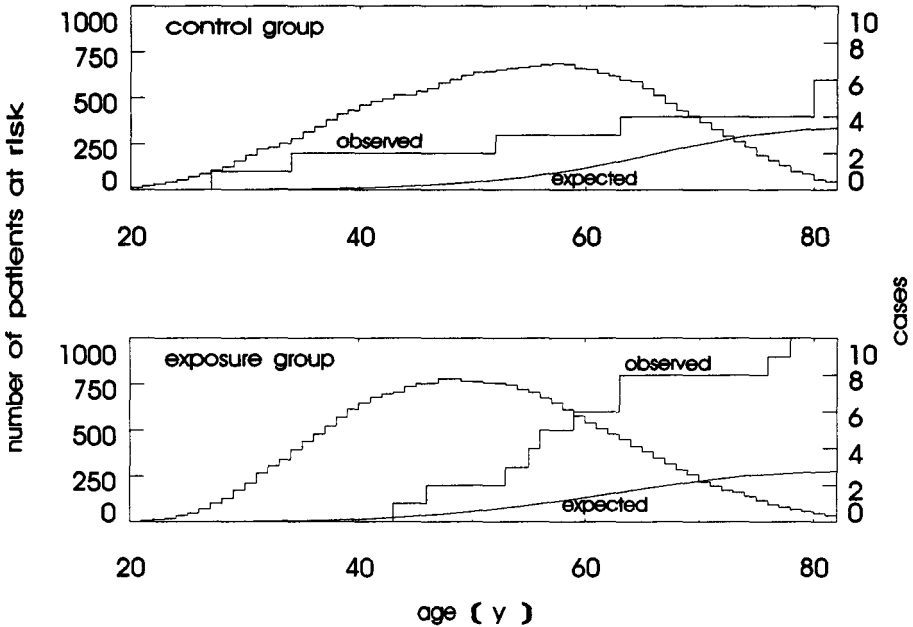
pat. No.	91	371	7004	7227
diagnosis	CML	CML	CML	CML
start of treatment (mo.yr)	10.49	08.52	1956 [?] /10.62	1950
treatment period (weeks)	9 ?	10	12 [?] /4	10
ThX ¹ , Peteosthor ²	2	1	1	2
body weight (kg)	55	75	69	o. A.
total amount of ^{224}Ra (μCi)	812	260	336 [?] /114	536
skeletal dose (rad)	207	49	68 [?] /23	107
date of birth (mo.yr)	01.00	04.97	01.30	10.00
date of diagnosis/death	09.55/12.58	[?] /04.56	1976/07.80	[?] /03.77
age of death	59	59	50	77
latency (years)	6	< 4	14/30 [?]	< 27

Whereas bone sarcomas were the major late effect seen in patients injected before 1948, it is concluded, according to similar results from animal experiments, that patients having been injected more recently are at greater risk from chronic myeloid leukaemia than from bone sarcoma in a region of administered ^{224}Ra below that which was used in the treatment of the patients of Project 11. Myeloproliferative diseases, mostly acute or chronic myeloid leukaemias, have also been reported following Thorotrast application. Risk assessments including these observations at very low dose burdens of only 1.7 mGy/week, but with burden times of more than 30 years suggest that not only the *total dose* but also the *dose rate* may play an important role in the induction of malignancies in man.

In animals, rather low dose rates of bone-seeking α -emitters have been demonstrated by different authors to induce leukaemias. Results with varying amounts of ^{224}Ra indicate that animals given amounts of ^{224}Ra less than those found to cause osteosarcomas may be at risk instead from myeloid leukaemia. The induction of

myeloid leukaemia in mice has been demonstrated down to dose rates of only a few mGy/day, not only for ^{224}Ra , but also for ^{239}Pu , an α -emitter that, like ^{224}Ra , deposits preferentially on the bone surface.

Figure 1: Cases of total leukaemias obs/exp vs. number of patients at risk



Histopathological review of the bone sarcomas

Our knowledge of the pathology of ^{224}Ra induced bone tumours is based on autopsy protocols, histopathology or hospital reports, mostly recorded between 1950 and 1970. Over the last two decades the wide variation and heterogeneity seen in the histopathology of bone tumours, causing many diagnostic problems, generated much discussions among pathologists.

Bone tumours may arise from any of the elements inherent to bone, including diverse marrow cells as well as vascular and neural components. Some schemes for the classification of these tumours have been based on histogenic concepts. Furthermore osteoblasts, chondroblasts and skeletal fibroblasts are not immutable species of cells, but can readily undergo metaplastic transformation to another phenotype in pathological states. The WHO scheme of classification is based on histological criteria, particularly the type of differentiation shown by the tumours cells and the nature of any intercellular material they produce. The revised 1993 WHO-classification describes 14 additional new entities of malignant bone tumours, including fibrohistiocytic neoplasia, which was non-existent in the first 1972 WHO-classification. Therefore we must anticipate that radiation-induced bone sarcomas will reflect this wide spectrum of differentiation, and will not just be limited to osteosarcomas and

osteogenic sarcomas; the latter designation very frequently encountered within the reports of radium cases.

This review is based on those 41 of the bone tumours cases of Project 11 for which histopathological diagnoses are available. Within that group osteosarcoma was the most common histologic type, accounting for 44% of the cases. Fibrosarcomas and fibrohistiocytic sarcomas (originally diagnosed as spindle cell-, giant cell-, or pleomorphic-sarcomas) accounted for an additional 37%. The remainder were chondrosarcomas and bone marrow tumours.

The most frequently occurring bone tumour types, osteosarcoma and fibrohistiocytic bone sarcoma, have been selected for this study. We compared these two histologic variants according to basic disease, sex, age at exposure, latency period, skeletal dose, injection period, and skeletal distribution. Whilst the small sample size precludes statistical analysis we observed several trends. There is an indication that the ratio of fibrohistiocytic bone sarcomas is higher in ankylosing spondylitis and female patients and in patients older than 18 yr at the time of first exposure. In addition there is a trend of fibrohistiocytic sarcoma occurrence with shorter latency periods, lower skeletal doses (less than 2 Gy) and injection periods less than 3 months (Tables 5 and 6).

Table 5: *Distribution of basic disease, sex, age at first exposure and latency period in patients with osteosarcoma and fibrohistiocytic bone sarcoma*

	Osteosarcoma (n = 18)	Fibrohistiocytic bone sarcoma (n = 15)
Tuberculosis	89%	67%
Ankylosing spondylitis	11%	33%
<hr/>		
Males	72%	53%
Females	28%	47%
<hr/>		
<u>Age at first exposure:</u> 3 - 18 yr	72%	47%
18 - 56 yr	28%	53%
<hr/>		
<u>Latency period:</u> 4 - 20 yr	83%	93%
20 - 38 yr	17%	7%

Table 6: *Comparison of skeletal dose and injection period in patients developing osteosarcoma and fibrohistiocytic bone sarcoma*

	Osteosarcoma (n = 18)	Fibrohistiocytic bone sarcoma (n = 12)
<u>Skeletal dose:</u> Less than 2 Gy	6%	25%
More than 2 Gy	94%	75%
<hr/>		
<u>Injection period:</u> Less than 3 mo	6%	33%
More than 3 mo	94%	67%

The two most common histologic types of radiation-induced bone tumours are bone-producing osteosarcoma and non-bone-producing fibrohistiocytic sarcoma. This has already been shown after therapeutic external irradiation and has been confirmed after internal irradiation with ^{224}Ra now.

Therefore, it is not unreasonable to believe that radiation may induce two different types of bone sarcoma. This may be either by transformation of different precursor cell types or by modulation of tumour progression resulting in different lines of differentiation. Potential factors which may be involved are genetic instability, epigenetic modulation or selection by microenvironment or host factors. A better understanding of the mechanisms of induction of various types of bone tumours induced by radiation may be very valuable for carcinogenic risk assessment.

Publications

R. R. Wick, W. Gössner: History and current uses of ^{224}Ra in ankylosing spondylitis and other diseases. *Environm. Intern.* **19**, 467 - 473 (1993)

R. R. Wick, D. Chmelevsky, W. Gössner: Mortality from chronic myeloid leukaemia and other diseases in Ra-224 treated ankylosing spondylitis patients. European Society for Radiation Biology, 24th Annual Meeting, Erfurt (Germany), October 4 - 8, 1992, Book of Abstracts, p. 153

R. R. Wick, D. Chmelevsky, W. Gössner: Leukämierisiko nach intravenöser ^{224}Ra -Behandlung - Ergebnisse einer Langzeitstudie an Bechterew-Patienten. In: *Umweltradioaktivität, Radioökologie, Strahlenwirkungen, 25. Jahrestagung des Fachverbandes für Strahlenschutz e. V.* (Eds. M. Winter, A. Wicke), Bd. II, Köln: TÜV Rheinland, S. 909 - 914 (1993)

R. R. Wick, D. Chmelevsky, W. Gössner: Current status of the follow-up of Radium-224 treated ankylosing spondylitis patients. In: *Health Effects of Internally Deposited Radionuclides: Emphasis on Radium and Thorium* (Eds.: G. van Kaick, A. Karaoglou, A. M. Kellerer), Singapore: World Scientific, p. 165 - 169 (1995)

W. Gössner, R. R. Wick, H. Spiess: Histopathological review of Radium-224 induced bone sarcomas. In: *Health Effects of Internally Deposited Radionuclides: Emphasis on Radium and Thorium* (Eds.: G. van Kaick, A. Karaoglou, A. M. Kellerer), Singapore: World Scientific, p. 255 - 259 (1995)

Project 11: Late Effects in Ra-224 Treated Juvenile and Adult Patients

Participating Organisation: Kinderpoliklinik der Ludwigs-Maximilians-Universität München

Head of Project: Prof Dr. H. Spiess

II. Objectives of the project:

To continue the life-time follow-up of the registered cohort of patients treated with intravenous injections of Ra-224.

To confirm the retrieved anamnestic data by contacting medical institutions and family doctors. To determine causes of death.

To identify increased incidence rates of malignant and benigne diseases among the Ra-224 patients.

To establish a contemporal comparison group of patients not treated with Ra-224.

In cooperation with project no.12 of this contract:

To judge the relationship between radiation exposure and elevated incidences by analyzing their dependance on dose, time and age.

To visit Ra-224 patients and check for cataracts using the mobile Scheimpflug-camera system.

III. Progress achieved including publications

The study population comprises 900 patients who received repeated injections of Ra-224 shortly after World War II for the treatment of tuberculosis, ankylosing spondylitis and for a few other non-cancerous diseases. Follow-up of the first patients started in 1946 and has been continued periodically till today.

During the reporting period, two updates were carried out in 1992 and 1995 by mailing standard questionnaires to all patients who had responded previously. After the latest survey, 26,9% (242 indiv.) of the starting collective are alive and in contact with the study. The overall loss to follow-up remains smaller than 5%. Table 1 gives a summary of the present cohort's observation status

Table 1. Observation status of the Ra-224 patients (as of July 31,1995)

age at first injection	≤ 20 years		> 20 years		Σ
	218		682		
	107 ♀	111 ♂	173 ♀	509 ♂	900
alive	51	55	48	88	242
pending*	4	7	3	9	23
loss to follow-up	7	5	5	21	38
deceased	45	44	117	391	597

* last contact at penultimate survey 1992

Table 2 shows an overview of the number of malignancies which were observed in the Ra-224 patients. Expectation values computed from the age distribution of person years at risk and the age specific incidence rates from the Saarland Tumor Registry are given in Table 3.

Over the last years the progressive occurrence of mammary carcinomas has become a remarkable finding of the Ra-224 study. Due to four additionally reported and confirmed breast cancers in the recent follow-up, the total number of observed cases has increased to 26 vs. 7 expected cases. Each of these newly detected carcinomas developed in females treated before the age of 21 and the resulting excess in this subgroup (n=107) is even more marked: 15 obs. vs. 1.5 exp., $p < 0.001$.

The *Extended Dosimetry for Studies with Ra-224 Patients*⁵ has been used to calculate doses to the breast tissue of the female patients ranging from 3 to 447 mGy. As detailed in project no. 12, a dose dependence of the excess breast cancer risk can be shown, if the analysis includes an additional age at exposure dependence.

The number of observed kidney cancers has risen to 9 cases (vs. 3.4 exp.). It is an interesting fact that six of these cancers occurred in individuals treated for tuberculosis. Almost 45% of the Ra-224 patients suffered originally from ankylosing spondylitis, a disease which requires in general a long-time analgetic treatment. Chronic use of painkilling substances like phenacetine is known to induce renal failure and possibly nephrocarcinomas. Nevertheless, not only kidney malignancies but also severe chronic renal failure occurred more frequently in the subgroup of tuberculosis patients.

A histopathological review⁴ based on the revised WHO classification of bone tumors made it necessary to reclassify four former cases of osteosarcomas, which are now included in the total number of six soft tissue malignancies.

The striking late effect of 54 bone sarcomas appeared very early in a wave shaped distribution with a maximum only a few years after the injections and no additional cases were reported since 1988.

Comparison group

A contemporal comparison group of tuberculosis patients not treated with Ra-224 has been set up on the basis of 290 old files, which were still available at a clinic specialized in TB-treatment in Wangen, State of Baden Württemberg. Table 4 indicates the status of this group. 40 years after dismissal, we were able to get actual health status information in 174 cases.

Among 90 females, four mammary carcinomas have occurred (vs 2.2 exp., not sign.). Therefore, the substantially enhanced incidence of mammary tumors is specific for the group of Ra-224 patients.

However, it is somewhat problematical, that the distribution of different types of tuberculosis varies between the comparison group and the Ra-224 cohort. While 75% of the patients in Wangen turned out to be treated for lung TB, only 17% of the Ra-224 tuberculosis patients showed this type. Instead, 59% of the latter were diagnosed to have bone TB. Consequently, a considerable difference in the frequency of chest x-rays and fluoroscopies can be expected. In order to determine number and methods of diagnostic x-ray procedures, the old files from Wangen were transferred to Munich and have been reviewed. In cooperation with Prof. Stieve, GSF, these data are now used for quantification of the resulting x-ray doses to the breast tissue. This work has not been completed yet, since we had to face time consuming difficulties to get the permission for transferring the medical records to our clinic.

Table 2. Summary of malignant diseases observed in the group of Radium-224 patients (as of July 31, 1995)

Age at First Injection	≤ 20 ys. (218 pat.)		>20 ys. (682 pat.)		total (900 pat.)	
	♀	♂	♀	♂	♀	♂
	107	111	173	509	280	620
Skeletal Diseases:						
Malignant Bone Tumors	18	18	4	15	22	33
Bone Sarcomas (ICD*170)	18	18	4	14**	22	32
Malignant Chordom (ICD 170)	-	-	-	1	-	1
Soft Tissue Diseases:						
Tumors of Organs & Soft Tissue	26	10	42	73	68	83
Mamma (female) (ICD 174)	15	-	11	-	26	-
Mamma (male) (ICD 175)	-	-	-	1	-	1
Lung (ICD 162)	1	1	1	14	2	15
Connective / Soft Tissue (ICD 171)	2	-	2	2	4	2
Skin (ICD 172, 173)	2	1	2	3	4	4
Thyroid Gland (ICD 193)	1	-	-	1	1	1
Brain (ICD 191)	-	-	-	1	-	1
Nervous Syst., unknown local. (ICD 192)	1	-	-	-	1	-
Uro-Genital Region	3	3	12	24	15	27
Prostate (ICD 185)	-	1	-	13	-	14
Bladder (ICD 188)	-	-	1	7	1	7
Kidney (ICD 189)	2	2	1	4	3	6
Uterus (ICD 179, 180, 182)	1	-	6	-	7	-
Ovar (ICD 183)	1	-	3	-	4	-
Gen. Region, not specified (ICD 184)	-	-	1	-	1	-
Intestinal Region	-	5	14	27	14	32
Stomach (ICD 151)	-	1	6	8	6	9
Liver (ICD 155)	-	3	1	3	1	6
Colon (ICD 153)	-	-	1	7	1	7
Rectum (ICD 154)	-	1	2	3	2	4
Pancreas (ICD 157)	-	-	3	2	3	2
Gallbladder (ICD 156)	-	-	-	1	-	1
Esophagus (ICD 150)	-	-	-	1	-	1
Small Intestine (ICD 152, 159)	-	-	1	2	1	2
Other Malignant Diseases (total):						
	1	2	4	6	5	8
Leukemia (ICD 204-208)	1	-	2	3	3	3
Plasmocytoma (ICD 203)	-	1	-	1	-	2
Morbus Hodgkin (ICD 201)	-	-	-	1	-	1
Malign. Neoplasm, unknown loc. (ICD 199)	-	1	2	1	2	2

* International Classification of Diseases, 9th Revision

** observed in 13 individuals, 1 patient showed 2 primary bone sarcomas

Table 3. Ra-224 cohort: Observed / expected cases and rate ratios for a number of solid cancers, for cancers of soft tissue and for leukemias.
In comparison with table 2, two gastric tumors, one tumor of the uterus and one unspecified tumor of the genital region were excluded under the assumption of a minimal latency period of 5 years for solid cancers.

Tumor	observed	expected*	Rate Ratio	p-value
Bladder	8	6.3	1.27	not sign.
Colon	8	9.1	0.88	not sign.
Connective Tissue	6	1.2	5	< 0.01
Kidney	9	3.2	2.8	< 0.01
Leukemia	6	2.7	2.2	= 0.06
Liver	7	1.9	3.7	< 0.01
Lung	17	29.6	0.57	< 0.01
Mamma (female)	26	7	3.71	< 0.001
Ovary	4	1.3	3.08	< 0.05
Pancreas	5	3.4	1.47	not sign.
Prostate	14	9.6	1.46	not sign.
Rectum	6	8.4	0.71	not sign.
Stomach	13	11.3	1.15	not sign.
Uterus	6	3.8	1.58	not sign.

*calculated on the basis of the age specific incidences reported by the Saarland Tumor Registry

Table 4. Status of the comparison group (as of July 31,1995)

patients	♀	♂	Σ
alive*	76	72	148
deceased**	14	12	26
	90	84	174

* in contact with study

** causes of death identified

Scheimpflug examinations

The part of our project dealing with cataracts is based on the 218 juvenile Ra-224 patients in order to avoid confusion with age-related cataracts. During the reporting period a total of 61 Ra-224 patients and 20 members of the comparison group have been visited to examine their eye lenses with the Scheimpflug camera. For results see procect 12.

Publications

1. E. Nekolla, D. Chmelevsky, A.M. Kellerer, H. Spiess: Malignancies in Patients Treated with Ra-224*.
2. K. Papke, A. M. Kellerer, D. Korber, E. Nekolla, T. Roedler -Vogelsang, H.Spiess: Mammary Carcinomas in Patients treated with Ra-224*.
3. H. Spiess : The Ra-224 Study: the Past, Present and Future*.
4. W. Gössner: Histopathological Review of Radium-Induced Bone Sarcomas*.
5. K. Henrichs, D. Nosske, L. Bogner, T. Roedler-Vogelsang: Extended Dosimetry for Studies with Ra-224 Patients. *.
6. J.P. Scharff, E. Nekolla, P. Egner, H. Roos, A. Wegener, A.M. Kellerer, H. Spiess, F.H. Stefani: Findings in Human Lenses 40 Years After Injection of Ra-224, *Ophthalmic Research* 26(Suppl.1). 73-78 (1994).
7. P.Egner, H. Roos, A.M. Kellerer: Entwicklung eines elektronischen Systems zur Erfassung von Linsentrübungen mittels der Scheimpflugtechnik, *Medizinische Physik*, Hrsg. J. Erb, Erlangen 1993.

* Health Effects Of Internally Deposited Radionuclides: Emphasis on Radium and Thorium; Eds.: G. van Kaick, A.Karaoglou & A.M Kellerer, World Scientific, Brussels 1995.

Poster

P. Egner, H. Roos, A. M. Kellerer: Development of an Electronic Scheimpflug System for Cataract Studies among the Radium-224 Patients, presented at the Int. Symposium in Heidelberg "*Health Effects Of Internally Deposited Radionuclides*", 1994.

H Spiess, A M Kellerer, E Nekolla, K. Papke: Excess Malignancies and their Appearance Times after Ra-224 Injections in Men, presented at the "*XVI International Cancer Congress*", New Dehli, 30 Oct.- 5 Nov 1994.

CEC / NRPB Association Agreement

F13P-CT92-0064
NRPB 13306 (12)

Final Report for the Period July 1, 1992 to June 30, 1995

Project 12: Epidemiology of Radiation
Carcinogenesis and Cataract
Studies.

Participating Organisation: Ludwig - Maximilians -
Universität München
Strahlenbiologisches Institut

Scientific Head of Project: Prof. Dr. A.M. Kellerer

Studies of Ra-224 Induced Malignancies:

As detailed in the report of project 13306(11), the follow-up of the Ra-224 patients (n = 900) has been considerably extended during the project period. Questionnaires were sent out at tri-annual intervals. The last update was in 1995, when questionnaires were sent to the 304 persons treated with Ra-224 and still alive at the time of their last follow-up. Special attention has been given in the later phases of the project to the statistical evaluation of nonskeletal malignancies.

The striking enhancement of malignant bone tumors is now paralleled by excess incidences of organ and soft tissue malignancies. In this group of evaluated tumors, 155 cases were observed versus 135 expected cases. The expected numbers of cases were computed from the age distribution of person years at risk and the age specific incidence rates from the Saarland Cancer Registry of the years 1968 to 1988. A subdivision of the entire collective into subgroups of patients of different sex, age at first injection, and original disease, makes it clear that the tumor occurrence is substantially enhanced especially among the patients treated as juveniles and in the group of female Ra-224 patients (fig.1). This observation is predominantly due to a striking excess of mammary tumors. The trend of enhanced breast cancer rates has increased in the last follow-up due to the occurrence of four additional cases. The low number of lung cancers may explain the fact that the group of patients treated as adults, especially the males, shows conspicuously low total rates compared to an average population.

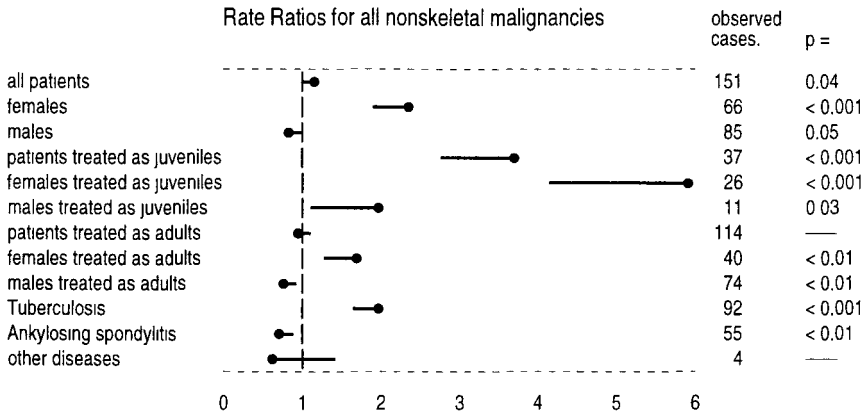


Fig.1: Rate ratios (i.e. quotients of the observed and the expected number of tumors, under the assumption of a minimum latency period of five years) for all nonskeletal malignancies after the Ra-224 treatment in the entire patient group and the respective subgroups, and their 95% single tailed confidence intervals.

Figure 2 gives the rate ratios for malignant tumors of soft tissue, for leukemias, and for a number of (numerically relevant) nonskeletal solid malignancies.

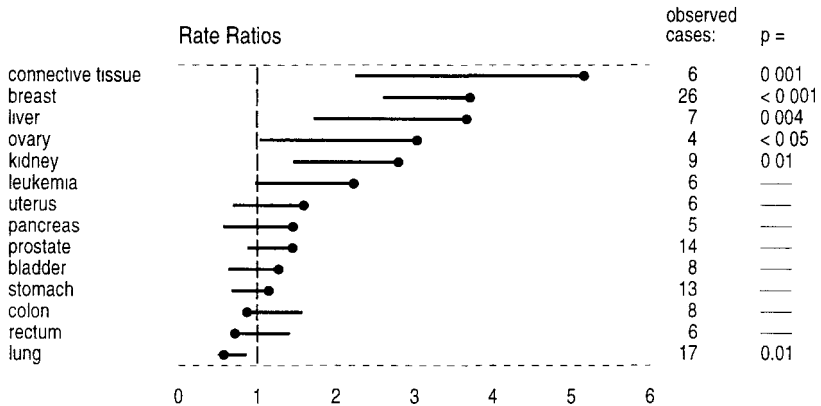


Fig.2: Rate ratios for a number of solid cancers, for cancers of soft tissue and for leukemias, and their 95% single tailed confidence intervals.

Soft tissue malignancies have occurred in 6 patients, while 1.2 cases were expected. In this group, 3 tumors classified as 'bone sarcomas' in earlier publications are now included.

Liver carcinomas have developed in 7 patients vs. 1.9 expected. However, these cancers are taken to be associated with pre-existing liver disease. Therefore, the enhanced liver cancer rate may be due to the fact that many of the Ra-224 patients had some form of hepatitis during the time of their treatment.

Mammary carcinomas have occurred in 26 patients vs. 7 cases expected. For females treated as juveniles the incidence is 10 times higher than expected (15 vs. 1.5). Figure 3 gives the

cumulative hazard functions for the entire female group, fig.4 the cumulative hazard functions for females treated as juveniles. The comparison to the population rate would show similar excesses, if the Danish Cancer Registry data were used, rather than those of the Saarland.

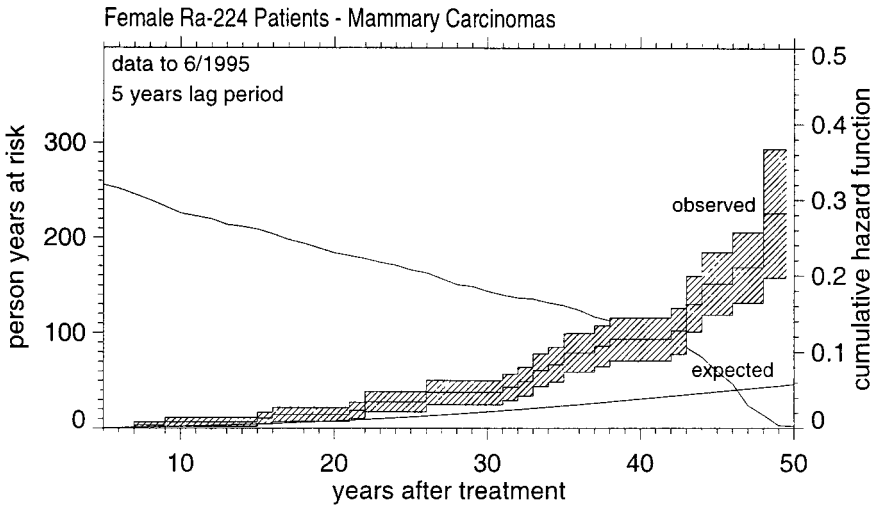


Fig.3: The grey shaded area gives the number of female patients under observation as a function of time since treatment (person years at risk). The step function with the hatched range of standard errors represents the observed cumulative rate of mammary carcinomas, the lower curve gives the cumulative rate that would be expected according to data of the Saarland Cancer Registry.

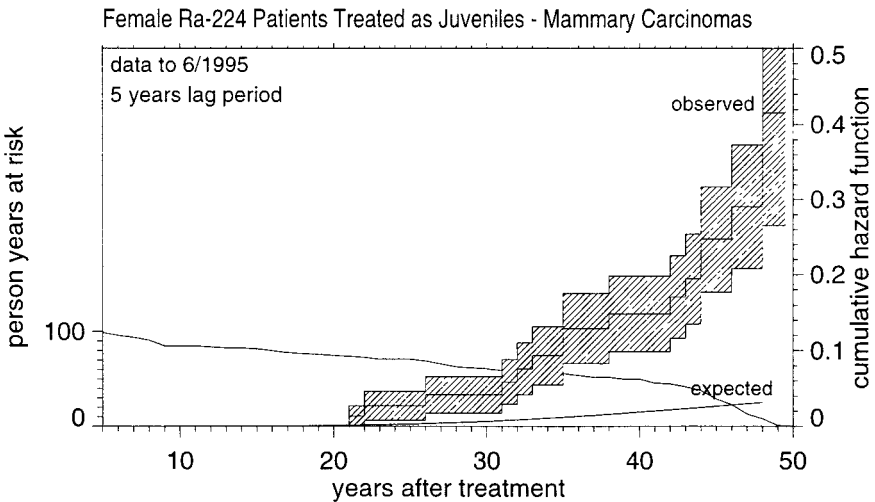


Fig.4: Number of female patients under observation (person years at risk), and the cumulative tumor rates of the observed and the expected mammary carcinomas as functions of time since treatment (as in fig.3).

New dosimetric models have been developed during the project that provide dose estimates for the breast tissue: The calculated breast doses of the female patients range from 3 to 447 mGy. There is no significant indication of higher doses among the cases. Likewise, first calculations with the software package EPICURE (AMFIT) do not show a recognisable correlation of the mammary carcinomas with dose. However, a dose dependence of the excess breast cancer risk results, if the analysis includes an additional age at exposure dependence that increases up to ages of 11 and decreases from then on. The best fit has been obtained with an additional factor for the baseline risk, indicating a 1.7 times enhanced breast cancer rate for the Ra-224 cohort. This indicates that part of excess may not be due to Ra-224 exposure. Efforts were, therefore, made to quantify diagnostic x-ray doses to the breast tissue, but an initial estimation indicates that these doses are too low to explain a marked excess. Nevertheless, repeated x-ray fluoroscopy during the Ra-224 treatment might have contributed to the increased baseline rate. In view of the importance of these observations, a comparison group of tuberculosis patients not treated with Ra-224 has been formed, and, up to now, no significant breast cancer excess was found in this group.

Kidney cancers have been observed in 9 patients (vs. 3.4). One may argue that an increase of kidney cancer could be due to the use of pain-killing drugs among the ankylosing spondylitis patients. However, 6 cases (vs. 1.3) occurred in the subgroup of tuberculosis patients. Figure 5 gives the cumulated kidney tumor rates.

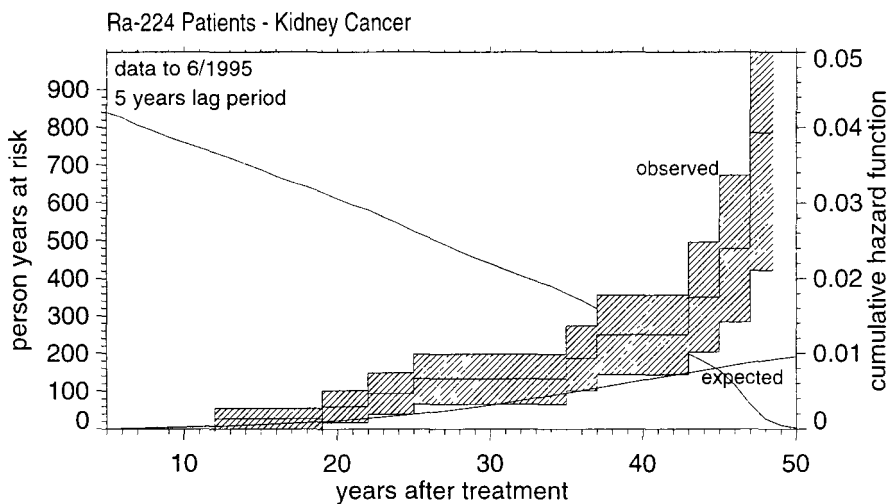


Fig.5: Number of patients under observation (person years at risk), and the cumulated tumor rates of the observed and the expected kidney cancers as functions of time since treatment (as in fig.3).

Different models have been fitted to the kidney cancer data using AMFIT. The best fit has been obtained with a relative risk model and functions depending on dose (linear), time since exposure (exponentially decreasing), age at exposure (exponentially decreasing); an additional indicator function for sex accounted for the lower spontaneous risk in females.

Studies of Radiation Induced Lens Opacifications:

Objectives of the Study, Methods, and Instrumentation:

Opacification of the lens of the eye is an important late effect of exposure to ionizing radiation, and it is of special relevance to radiation protection, because recent investigations indicate that the induction of cataracts is in some aspects a stochastic effect. Several cohorts of radiation exposed persons have been examined qualitatively for cataracts in the past. However, it has been difficult to quantify the results and, in particular, to assess quantitatively slight opacifications or the evolution of lens opacifications. Such investigations require Scheimpflug photography which is considerably more complex than the conventional slit lamp investigations.

In contrast to the usual slit-lamp technique, it is possible with the Scheimpflug photography to obtain sharp images of plain sections through the lens of the eye. The Scheimpflug instrumentation, developed within the project, is based on a rotating slit lamp (*Topcon sl-45b*). Our system has been improved by substituting the conventional camera with an electronic camera and an electronic image storing system. The image of the ocular lens is recorded by a CCD-camera (*Sony*). The output signals are continuously digitized by an image processing board (*Leutron*) which is installed in the computer. The image is permanently visible on a video monitor, and it is used for the adjustment of the slit lamp. The adjustment is, in this way, achieved more easily, more quickly, and with higher precision and reproducibility than with the conventional cameras. After proper setting is achieved, a flashlight is released, and a bright image with high contrast is frozen on the monitor screen and is stored in the computer. The data are written on write-once optical discs for permanent storing. Parameters of the image, such as the flashlight intensity or the orientation of the slit lamp, are determined and stored automatically.

In contrast to the conventional technique, the quality of the image can be judged immediately, and additional images can be taken when necessary. Quantitative information is thus available within seconds. If the images are taken in the conventional photographic way, quantitative evaluations have to await the lengthy and less fail-safe procedures of film development and film densitometry.

The system has been fitted into a mini-van to facilitate a program of repeated ophthalmic investigations with the Scheimpflug camera without the necessity that patients visit an ophthalmic clinic. The examination of patients at home is often more convenient and cost effective.

Analysis of Images:

In fig.6 the Scheimpflug image of the lens of a 34 year old person is shown. This lens does not exhibit obvious abnormal opacities, however, substructures of the lens are visible due to their different light scattering. Light areas indicate reduced scattering of light and the dark areas an increase of opacity. A scan of the opacity along the broken line is given in fig.7. In this scan, apart from the corneal peak at the right boarder of the image, 14 anatomical structures can be identified. Such scans of the opacity are immediately available after the image has been taken.

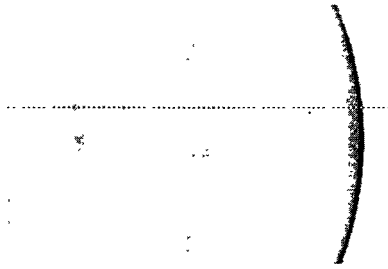


Fig.6: Scheimpflug image of the lens of a 34 year old person. The anatomical structure of the lens is clearly recognizable.

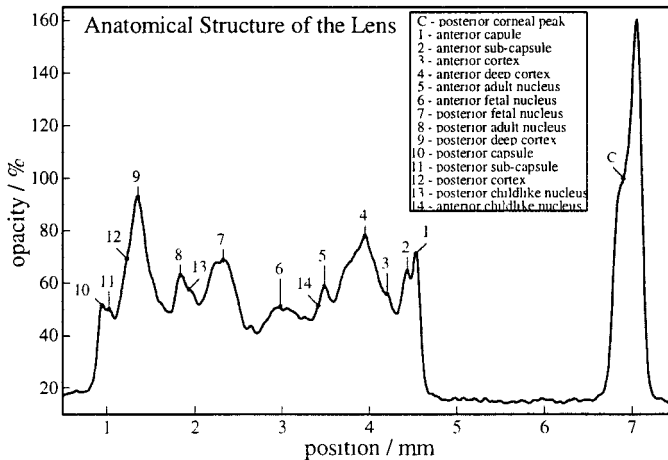


Fig.7: Scan of the opacity along the broken line, as indicated in fig.6. Several anatomical structures are identified and their corresponding names are given in the inserted box.

Evaluations of lens opacities and geometric parameters of the anterior eye from Scheimpflug images suffer from constraints which are inherent to the technique. In the conventional Scheimpflug technique sharp images are achieved, but image distortions have to be tolerated. However, image distortions do not merely change distances, but influence also the measured local intensities. In addition to this, the imaging lenses do not accept the same fraction of the light scattered from different positions in the eye lens, which is a second source of intensity distortions in Scheimpflug images. With the digital image processing it has become possible to overcome most of these constraints. Within the project it has been possible to analyse the distortions inherent to the Scheimpflug technique, and computer algorithms have been developed and applied successfully, in order to eliminate the influence of such distortions on the images.

In epidemiological studies of radiation induced lens opacities not all the details are relevant that are visible in fig.7. Therefore, mean values of the opacities are determined for 5 areas, which correspond in their horizontal dimension to the main anatomical structures of the lens (anterior capsule, anterior cortex, nucleus, posterior cortex, posterior capsule, whole lens). This division is adapted to the 'LOCS II + LOCS III' and 'New Grading System for Cataracts' which are commonly used for the classification of cataracts. In fig.8 these areas are numbered I-V. The mean value for the small box, located outside the lens, is used for reference.

The image shown in this figure is the same as in fig.6, but has been subjected to digital image processing for enhanced visibility of small structures. It is no problem to determine the outer borders of the lens automatically, but it is difficult to determine the borders between substructures. The locations of the vertical lines which separate the areas I to V were, therefore, determined by visual inspection of the images.

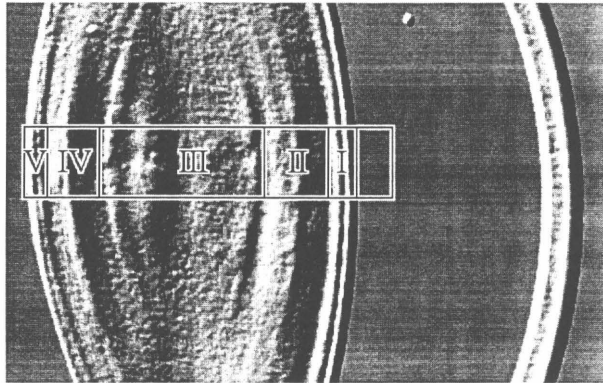


Fig.8: Division of the lens of the eye into the main anatomical structures. The indicated areas are used to determine mean opacity values.

To evaluate many images automatically a simple scaling is utilised relative to the lens thickness. To test the validity of this procedure images of the right eye of 139 men, were taken and analysed for their geometry (age distribution see fig.12). The positions of 8 clearly recognisable structures, indicated in the insertion of fig.9, were determined and scaled with the lens thickness. The distributions of positions are given in fig.9; and the mean values are indicated by vertical lines. Obviously the positions

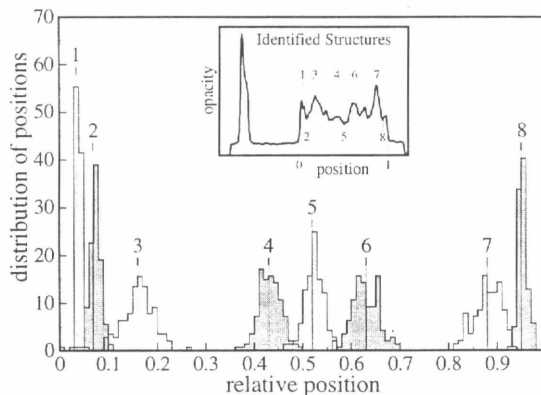


Fig.9: The distribution of positions of 8 clearly recognisable structures (see the inserted graph) which are scaled by the thickness of the lens. The mean value of the position of each structure is marked with the corresponding number.

vary considerably. However, the mean opacities within the areas I-V do not depend critically on the position of the border lines. Fig.10 compares opacities of the nucleus that are manually

and automatically determined. The graph indicates that rough evaluations can be performed automatically. The reason for a small systematic deviation will have to be examined.

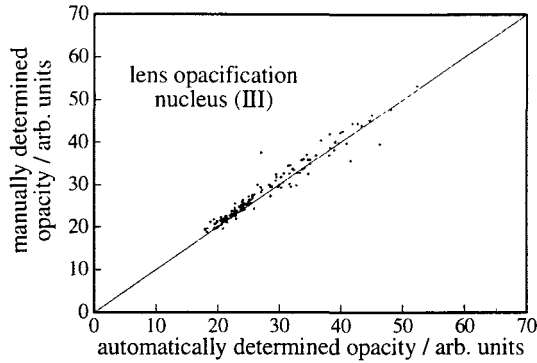


Fig.10: Comparison of manually and automatically determined opacity of the nucleus of the lens. The evaluation is based on Scheimpflug images of the control group.

Scaling of Opacities:

To eliminate the influence of fluctuations of illumination intensities, correct scaling of the observed opacity profiles is essential. The use of two different reference values for this purpose has been examined, the inner corneal opacity signal and the determination of the flash light intensity with a photoelectric cell. The inner corneal signal provides an inherent standard for an eye, it has the advantage of being unaffected by the reflection of light at the outer corneal surface. The measurement of light intensity can be performed with higher accuracy.

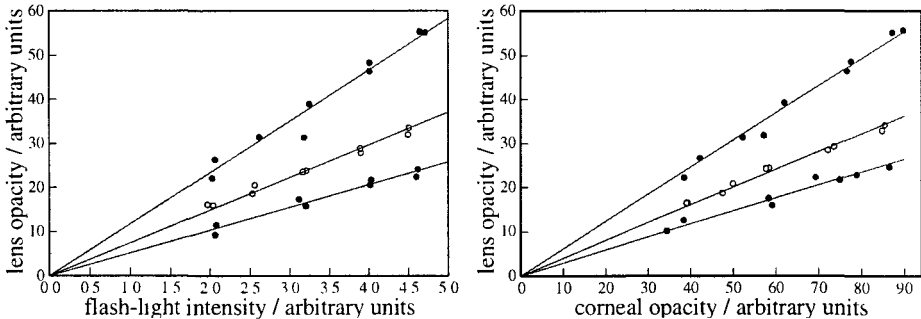


Fig.11: Lens opacity in its dependence on the flash-light intensity (left panel).
 Lens opacity in its dependence on the corneal opacity signal (right panel).

Fig.11 gives the mean values of the opacity profile for 3 persons of different age versus the flash light intensity (left panel) and versus the corneal opacity (right panel). In both cases variations of the light intensity were increased by using filters. The figure shows that the corneal opacity and the light intensity are both suitable reference values for scaling.

Long-Term Stability

Long-term follow-up studies of lens opacification require reproducible and quantitative results, especially in repeated examinations. To check the overall stability of the instrument a sphere made from opaque glass is used as a 'reference eye'. In each series of examinations an image of the glass sphere is taken and the opacities of this image are used as reference values.

Epidemiological Studies of Radiation Induced Lens Opacities

The technique has been applied to 4 cohorts: Control group; Ra-224 patients; Southern Ural group; Bone marrow transplant patients.

Control Group:

A cohort of 139 male military personnel was examined initially to test the instrumentation and to develop the methods for image processing and image evaluation. One advantage of this group is that the Scheimpflug analyses can be part of the regular, annual health check up and that they will be available for several years for repeated examinations. Another advantage is the reliable documentation of their health status during the past. The age span covers about 40 years, from age 17 to 57 (see fig.12). While this cohort is not representative for the total population, it can be the starting point of a permanent control group for lens opacities.

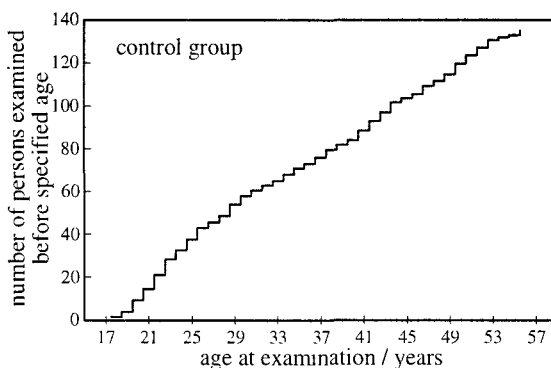


Fig.12: Number of persons examined up to specified age.

In fig.13 the age dependence of lens opacities is shown for the whole lens and for substructures. From each proband 5 images, at different orientations of the camera, were taken of each eye. There were no significant differences between the right and the left eyes, so the data were averaged. The small points in fig.13 therefore represent averaged opacities for individual persons. The linear regressions of these data are given as solid lines to increase the readability of the graphs. The rectangular points represent the opacity averages of persons within an age at examination interval of 4 years; the error bars are standard errors.

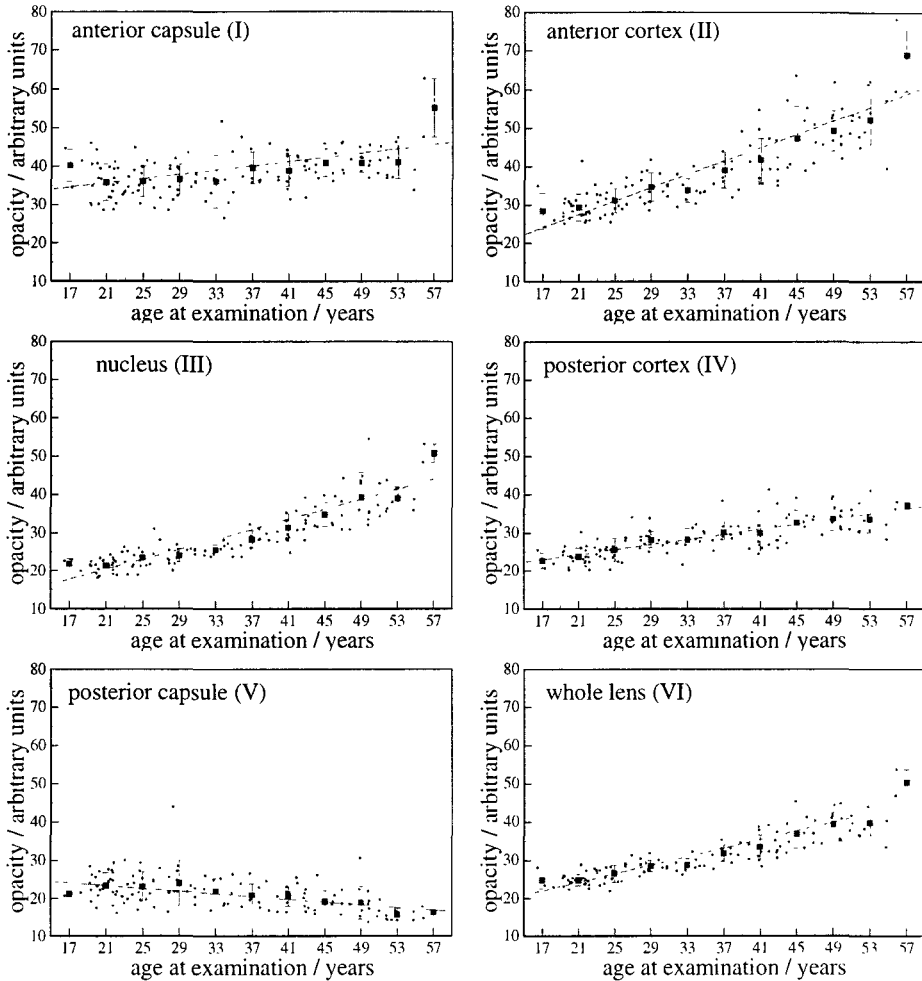


Fig.13: Mean opacity in the control group of the whole lens and of substructures versus age at examination.

Increasing opacity with increasing age, is found for all substructures, except the posterior capsule. The reversal trend for the posterior capsule may be a technical artefact, and that needs to be examined further.

Radium-224 Patients:

64 Ra-224 treated patients, have undergone Scheimpflug analysis. At an earlier stage of the study conventional Scheimpflug-photography was applied. The data derived with this system have been published (see ref.6).

With the digital system 17 female and 12 male patients were examined. The examinations and the evaluations of the images were performed in the same way as the control group. In fig.14 the opacity is given vs. age at examination. The closed dots indicate the average opacity for an individual patient. For comparison the data of the control group are inserted; the comparison is limited by the lack of older persons in the control group.

The data of the Ra-224 patients show more variation than those of the control group. The most significant increase of opacity, compared to the control group, is observed within the posterior cortex (area IV).

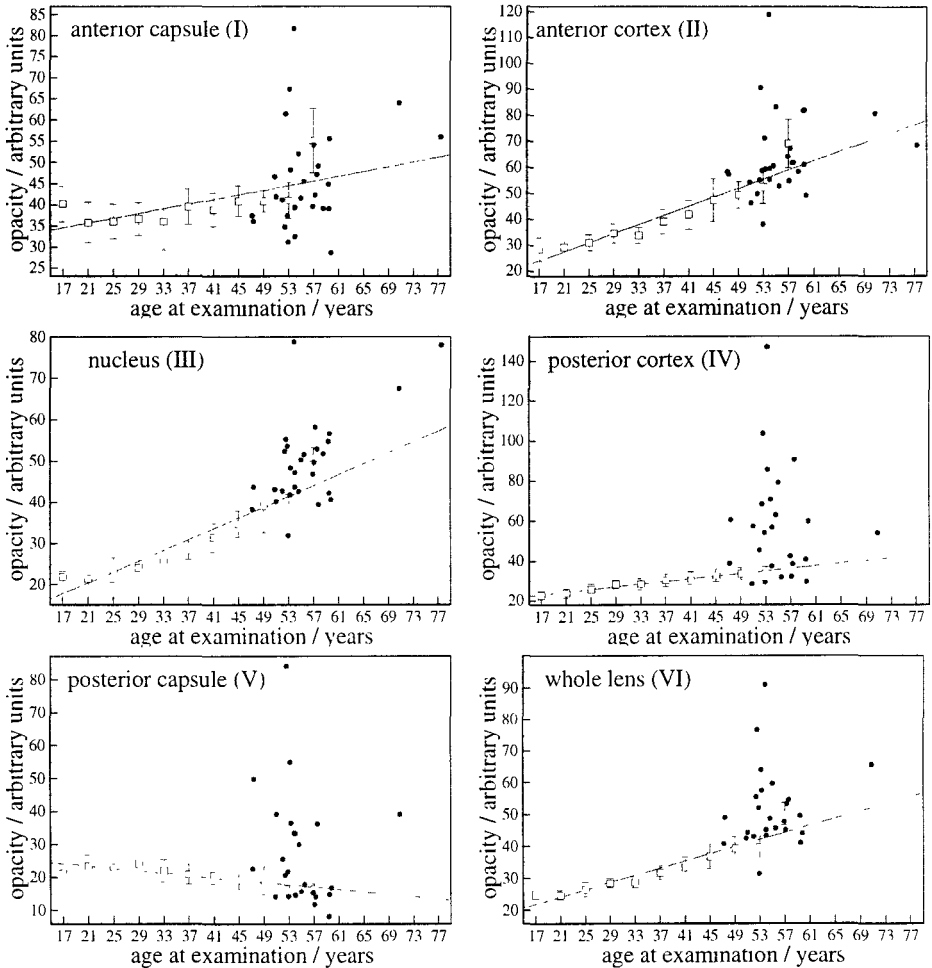


Fig.14: Mean opacity of the whole lens and of substructures versus age at examination. All panels refer to the cohort of Ra-224 patients.

Southern Ural Group:

In spring 1995, in a mission to Mayak, 96 persons, who had been exposed to radioactivity through the Mayak nuclear facilities, were examined for lens opacifications. In this pilot study mydriatica which are usually applied could not be used, and due to the insufficient dilatation of the pupil the evaluation of opacities had to be restricted to the anterior capsule. In a subgroup of 46 persons, the opacity of the central part of the whole lens could be determined. Again the evaluation was performed in the same way as in the control group. In fig.15 the results are compared to those of the control group. The open points refer to the control group, the closed to the Southern Ural group. All points represent the averages of persons for 4 year interval of

age at examination. Although there is an indication of increased opacities in the anterior capsule no definite conclusions are possible, until the control group is extended to higher ages.

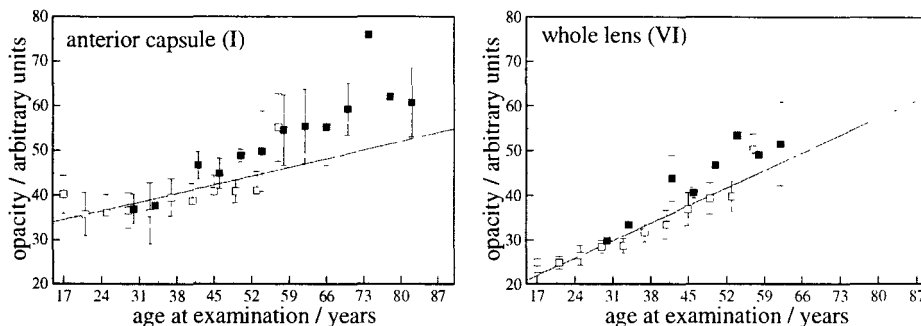


Fig.15: Mean opacity of the anterior capsule and of the entire lens versus age at examination. Panels refer to the Southern Ural group.

Bone Marrow Transplant Patients:

The lens opacities of 120 patients who have received a bone marrow transplantation have been determined. Half of these patients have been subjected to whole body irradiations in preparation of the transplantation. The analysis of these data is under way.

Conclusions:

Within this project the Scheimpflug technique has been developed to a quantitative tool for examination of the anterior eye. More than 4000 images have been taken and analysed with the digital system. The system permits high reproducibility and accuracy. With the technique it has become possible to observe and quantify even small increases of opacity in the ocular lens, obviating the need for rough classifications as in the conventional slit lamp examinations.

References

1. P.Egner H.Roos A.M.Kellerer, Entwicklung eines elektronischen Systems zur Erfassung von Linsentrübungen mittels der Scheimpflugtechnik, in Medizinische Physik, Hrsg J.Erb, Erlangen 1993
2. P.Egner. H.Roos, A.M.Kellerer, Development of an Electronic Scheimpflug System for Cataract Studies among the Ra-224 Patients, in *
3. P.Egner, H.Roos, A.M.Kellerer, Applicability and Technical Features of an Electronic Scheimpflug System for Cataract Studies. (to be published in Ophthalmic Research)
4. E.Nekolla, D.Chmelevsky, A.M.Kellerer and H.Spiess, Malignancies in Patients Treated with Ra-224, in *
5. K.Papke, A.M.Kellerer, D.Korber, E.Nekolla, T.Roedler-Vogelsang and H.Spiess, Mammary Carcinomas in Patients Treated with Ra-224, in *
6. J-P.Scharff, E.Nekolla, P.Egner, H.Roos, A.Wegener, A.M.Kellerer, H.Spiess, F.H.Stefani: Findings in Human Lenses 40 Years After Injection of Ra-224; Ophthal Res. 26 (Suppl.1), 73-78 (1994).

* Health Effects of Internally Deposited Radionuclides: Emphasis on Radium and Thorium. Eds. G.van Kaick. A.Karaoglu & A.M.Kellerer, World Scientific, Brussels 1995

Project 13: UK NATIONAL REGISTRY FOR RADIATION WORKERS (NRRW)

Participating organisation: NRPB

Heads of project 13: Dr C R Muirhead
Dr G M Kendall Dr M P Little

II. Objectives for the reporting period

To conduct further analyses of data from the first follow-up of the UK's National Registry for Radiation Workers (NRRW), including assessments of the robustness of the results from the main analysis published previously.

To expand the cohort and extend the follow-up for the second NRRW analysis.

III. Progress achieved including publications

Further Analysis of Data from First Follow-up

A further analysis of data from the first follow-up of the NRRW has been published (Little *et al.*, 1993). The main analysis of these data had shown a statistically significant trend in the risk of leukaemia (excluding chronic lymphatic leukaemia (CLL)) with external dose, and weaker evidence of a trend with dose in the risk of all cancers (Kendall *et al.*, Br. Med. J., 304, 220-225 (1992)). The purpose of the latest analysis was to assess the robustness of the findings in the main analysis to various assumptions on latent period and sub-stratifications, as well as to determine the leukaemia subtypes in which the trend with radiation dose might be most concentrated.

Table 1 shows the trends with dose for various leukaemia subtypes. It can be seen that chronic myeloid leukaemia is the leukaemia subtype with the most significant trend with dose, as well as the largest relative risk coefficient. This subtype has also been linked strongly to radiation in various high dose studies (UNSCEAR,1994), such as those of the Japanese atomic bomb survivors and of UK ankylosing spondylitis patients. In contrast, there is no evidence of an increasing trend with dose in the risk of chronic lymphatic leukaemia (CLL) (Table 1). Again this is in accord with the findings from high dose studies which suggest that CLL may not be radiation-inducible (UNSCEAR,1994).

Table 1

Significance of the trend with dose for leukaemia and lymphoma mortality by subtype
 (from Little *et al.*, 1993)

	Deaths [†]	Excess relative risk Sv ⁻¹ (+90% CI)	Significance level‡
<i>Leukaemias</i>			
Acute myeloid	24	1.24 (-1.23, 8.55)	0.27
Acute lymphatic	5	1.16 (< -1.93, 89.19)	0.38
All acute leukaemias	35	2.12 (-0.56, 8.63)	0.13
All acute + unspecified	38	1.62 (-0.91, 8.02)	0.20
Chronic myeloid	9	121.4 (7.66, 733.7)	0.01
Chronic myeloid + unspecified	12	136.9 (0.33, 860.7)	0.05
Chronic lymphatic	12	<-1.93 (<-1.93, 7.22)	0.78
All chronic leukaemias	21	4.10 (-0.72, 31.02)	0.14
All chronic + unspecified	24	2.68 (-1.11, 31.03)	0.22
Unspecified leukaemias	3	<-1.93 (< -1.93, -)§	0.58
All leukaemia (ex CLL)	47	4.28 (0.40, 13.58)	0.03
All leukaemias	59	2.29 (-0.32, 8.37)	0.10
<i>Hodgkin's disease and non-Hodgkin's lymphoma (NHL)</i>			
Hodgkin's disease	13	< -1.96 (<-1.96, 1.19)	0.95
Non-Hodgkin's lymphoma (NHL)	38	-1.21 (<-1.96, 3.00)	0.69
Hodgkin's disease + NHL	51	-1.92 (<-1.96, 1.15)	0.87

† Deaths in informative strata.

‡ One-sided test for trend based on score statistic.

§ Upper confidence limit did not converge.

The sensitivity analyses demonstrated that the significance and magnitude of the trend with dose for leukaemia (excluding CLL) is robust to the choice of lag periods of five years or less; see Table 2. Again this result is consistent with the pattern of the raised leukaemia risk seen in the Japanese atomic bomb survivors and various other irradiated groups. Assumptions about missing or below threshold doses in the NRRW were found to have little influence on the analyses by dose for leukaemia or other cancers. Taken together, these results strengthen the likelihood that the leukaemia excess observed in the first NRRW analysis is genuinely radiation-induced.

Table 2

Influence of lag period on the test for trend with dose in mortality from leukaemia (excluding CLL) (from Little *et al.*, 1993)

Lag (years)	Deaths†	Excess RR Sv ⁻¹ (+ 90% CI)	Significance‡
Leukaemias excluding chronic lymphatic leukaemia			
0	48	4.33 (0.39, 13.28)	p = 0.03
2	47	4.28 (0.40, 13.58)	p = 0.03
5	40	2.96 (-0.22, 10.19)	p = 0.07
10	35	2.68 (-0.74, 11.99)	p = 0.13
15	24	2.89 (-1.19, 13.97)	p = 0.17
20	18	3.27 (<-2.06, 20.20)	p = 0.22

† Deaths in informative strata.

‡ One-sided test for trend based on score statistic.

Database for the Second NRRW Analysis

The first analysis of the NRRW was based on a cohort of about 95,000 workers, followed up to the end of 1988 in most instances. Work has been performed both to expand this cohort and to extend the period of follow-up to the end of 1992, in order to increase the statistical power of the study.

(i) Expanding the Cohort

Data have been collated for extra groups of workers who were not included in the first NRRW analysis. This covers workers at Amersham International and Scottish Nuclear, as well as past workers at Nuclear Electric. In addition, new workers at organisations already participating in the NRRW have been included through the processing of annual data provided by these organisations. Checks are made on these personal and dose data via audits of samples of records held at the relevant sites.

Table 3 contrasts some of the key features of the cohorts for the first and second NRRW analyses. The latter cohort is likely to contain at least 25,000 more workers than the first. This enlargement also affects the collective dose through the inclusion of past workers who received doses many years ago, at levels higher than those received commonly under present conditions. Thus the collective dose for the second analysis is likely to be at least 500 man Sv higher than that for the first analysis.

Table 3
Comparison of cohorts for the first and second NRRW analyses

Follow up	NRRW	
	1st analysis end 1988	2nd analysis end 1992
Collective dose, man sievert	3,198	> 3,700
Person years	1.2 10 ⁶	>2 10 ⁶
Number of deaths	6,660	> 13,000
Number of individuals	95,217	> 120,000

(ii) Extending the Follow-up

The principal sources of follow-up information are the National Health Service Central Registers (NHSCRs), located at Southport (for England and Wales) and Edinburgh (for Scotland). The NHSCRs provide data on mortality and emigrations. Cancer registrations are also supplied, although it is likely that the second analysis will, like the first, be based on mortality. Checks on follow-up are conducted using other data sources, such as information held by the Records Branch of the Department of Social Security. Overall, the quality of the follow-up data is thought to be high.

Table 3 presents some statistics for the first and second follow-ups. Although the additional period of follow-up is only four years for some workers, this period is longer for certain groups of workers followed only to the late 1970s or early 1980s in the first analysis. Furthermore, the extended cohort contains new groups of workers, as well as some workers with an earlier NRRW start date following the identification of a cohort at an earlier time in the past (eg. at Nuclear Electric). As a consequence, the second analysis should involve almost twice the number of person-years as that in the first analysis. Furthermore, the number of deaths should have increased from about 6,600 to over 12,000.

(iii) Statistical Power

As indicated by Table 3, the second NRRW analysis will have much higher statistical power than the first, by virtue of the enlarged cohort and collective dose and of the longer follow-up. Preliminary calculations suggest that the confidence intervals for the estimates of risk per unit dose should be smaller by at least 30% in the case of all cancers combined and 20% in the case of leukaemia (excluding CLL). Thus the second NRRW analysis should provide substantially more information on cancer risks following chronic low dose exposure.

Publications

Little. M P, Kendall. G M. Muirhead. C R, MacGibbon. B H. Haylock, R G E. Thomas, J M and Goodill, A A. Further analysis. incorporating assessment of the robustness of risks of cancer mortality in the National Registry for Radiation Workers. *J. Radiol. Prot.*, **13**, 95-108, 295 (1993).

Little. M P, Kendall, G M and Muirhead. C R. Letter to the editor. *J. Radiol. Prot.*, **14**, 279-280 (1994).

Kendall. G M and Muirhead. C R. An investigation in the United Kingdom of the risks of occupational exposure to radiation. *Kerntechnik*. **58**. 216-219 (1993).

Kendall. G M. Muirhead. C R and MacGibbon. B H. Leukaemia risks: fact or fiction? *Nucl. Eng. Intl.*, **37**, 42-44 (1992).

Kendall. G M. Muirhead. C R and MacGibbon. B H. The UK's National Registry for Radiation Workers: first results. *Nucl. Eng. Intl.. Dosimetry and Radiation Protection*, 2-3 (1993).

Muirhead, C R, Kendall, G M and Little. M P. Mortality and occupational radiation exposure: First analysis of the UK National Registry for Radiation Workers. Submitted to Radiological Safety in Ukraine.

Muirhead, C R. Kendall. G M and MacGibbon. B H. Mortality and occupational radiation exposure: First analysis of the UK National Registry for Radiation Workers. IN *Low Dose Irradiation and Biological Defence Mechanisms* (eds. T. Sugahara et al). 95-98. Amsterdam, Elsevier Science Publishers BV (1992).

Muirhead. C R. Kendall. G M and MacGibbon, B H. Analysis of mortality based on the UK National Registry for Radiation Workers. *Radiat. Res.*, **133**. 124-126 (1993).

CEC / NRPB Association Agreement

**F13P-CT92-0064
NRPB 13306 (14)**

Final Report for the Period July 1, 1992 to June 30, 1995

Project 14: Statistical Analysis of the
Follow-Up Data and Risk Modelling

Participating Organization: GSF, Forschungszentrum für
Umwelt und Gesundheit, Neuherberg
Institut für Strahlenbiologie

Scientific Head of Project: Prof. Dr. A.M. Kellerer

Objectives for Reporting Period:

This contract of very limited size had the function to co-ordinate the study of secondary tumors in patients treated with total body and partial body irradiation prior to bone marrow transplantation. It ensured that the data were collected and updated in a form suitable for their utilisation in radiation risk modelling.

The project is closely connected with projects NRPB 13306 (15) and NRPB 13306 (16).

Progress Achieved During Reporting Period:

The follow-up has been successfully continued and extended. The analyses are now based on the observation of 1211 patients (transplanted prior to 1990) from almost 50 European Bone Marrow Transplant Centers.

A subgroup of 982 patients has received total or partial body irradiations. In this group 41 secondary malignancies were found (4.2% of this group), while in the subgroup of 229 non-irradiated patients, 7 tumors occurred (3.1% of this group). Compared to the expected numbers of tumors computed using the age distribution of person years at risk and the age specific incidence rates from the Saarland Cancer Registry and the Danish Cancer Registry, there are highly significant excesses in the entire patient group as well as in both, the irradiated and the non-irradiated subgroups. Significant excesses are also seen in the subgroups of patients treated for acute lymphoblastic leukemia, acute myeloid leukemia and severe aplastic anaemia (Fig.1). The analyses have derived hazard functions that indicate a substantial excess of the tumor rates in their dependence on time since transplantation (Fig.2).

Rate Ratios for all post treatment malignancies

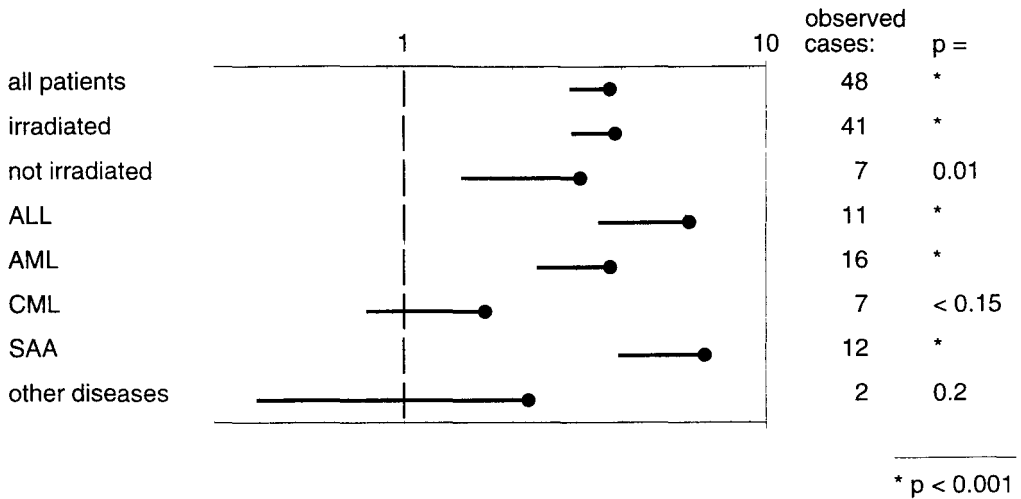


Fig.1: Rate ratios for all malignancies observed after the treatment in the entire patient group and the respective subgroups, and their 95% single tailed confidence intervals.

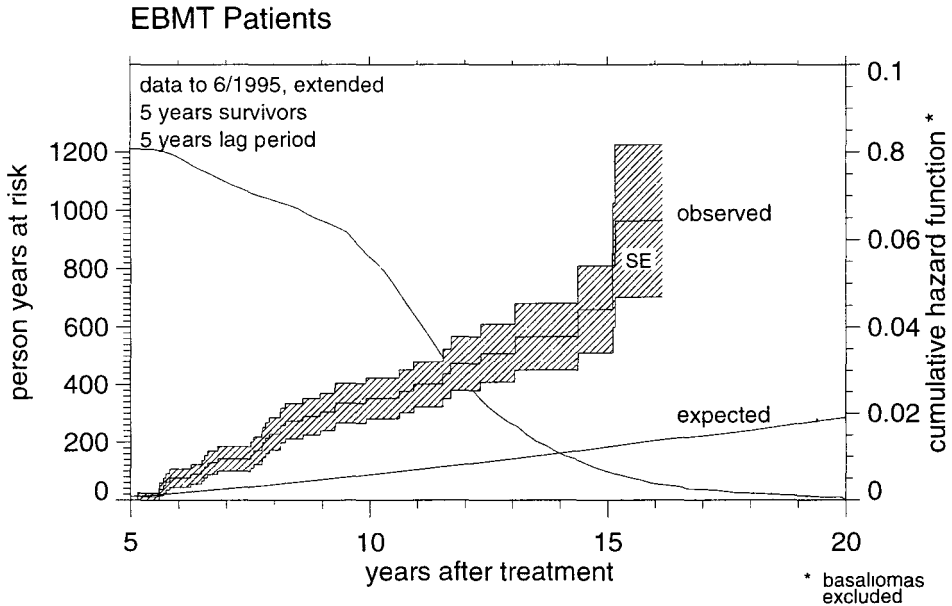


Fig.2: The grey shaded area gives the number of patients under observation as a function of time since treatment (person years at risk). The step function with the hatched range of standard errors represents the cumulative tumor rate of the observed, the lower curve of the expected tumors (7 basaliomas are excluded, since they are more likely to be observed in the group of transplant patients than in the general population).

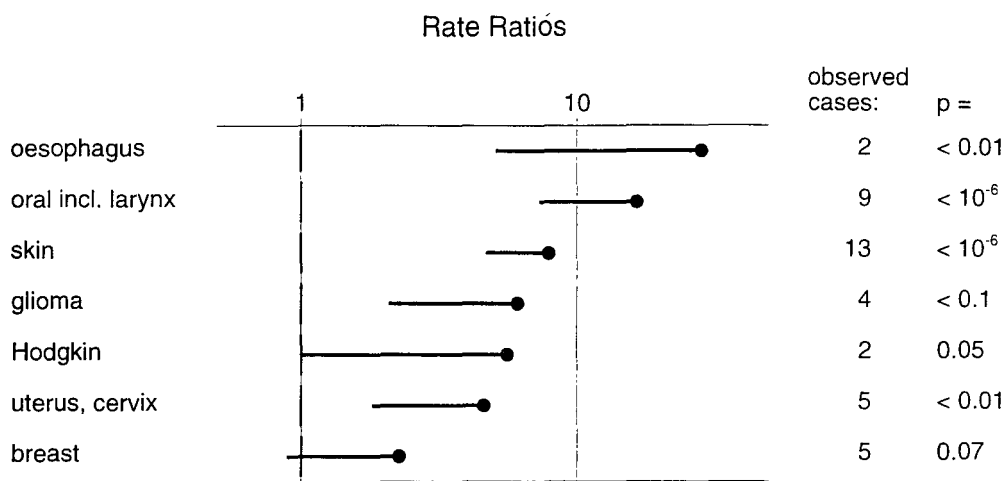


Fig.3: Rate ratios for a number of tumor sites or groups of tumor sites and their 95% single tailed confidence intervals.

Project NRPB 13306 (15) has been supported by extended numerical work and graphics. In a linkage to Project NRPB 13306 (12), the induction of lens opacifications, a deterministic effect with certain stochastic features, has been determined in 120 patients of this group who have been treated at the bone marrow transplant center in Munich.

Project 15: Data bank on Radiation Late Effects after Bone Marrow Transplantation: Coordination of the Follow-up and Collection of Data

Participating Organisation: Ludwig-Maximilians-Universität München, Medizinische Klinik III

Head of Project: Professor Dr. H.J. Kolb

RISK OF NEW MALIGNANCIES IN BONE MARROW TRANSPLANT PATIENTS SURVIVING MORE THAN 5 YEARS.

H.J.Kolb, T.Duell, G.Socié, M.T. Van Lint, E. Carreras, A.Tichelli, P.Ljungman, N.Jacobsen, J.F. Apperley, B.Hertenstein, M.Weiss, E.Nekolla, A.Juergens, and A.H.Goldstone on behalf of the Working Party Late Effects of the European Group for Blood and Marrow Transplantation (EBMT), and the European Late Effect Project Group.

Medizinische Klinik III, Universität München, and GSF - Forschungszentrum für Umwelt und Gesundheit, München, Germany (H J Kolb, Professor, T Duell. MD, E Nekolla, PhD, A Juergens. MD), **Ospedale San Martino, Genova, Italy** (M T Van Lint), **Hopital St. Louis, Paris, France** (G Socié, MD), **Hospital Clinic Barcelona** (E Carreras, MD), **Kantonsspital Basel, Dept. Haematology, Switzerland** (A Tichelli), **Dept. of Medicine, Huddinge Hospital, Huddinge, Sweden** (P Ljungman), **Rigshospitalet Copenhagen Denmark** (N Jacobsen), **Hammersmith Hospital, Royal Postgraduate School of Medicine, London, U K** (J F Apperley) **Med. Klinik III, Universität Ulm** (B Hertenstein), **Institut für Arbeitsmedizin, Universität Ulm, Germany** (M Weiss), **University College Hospital London, UK** (A.Goldstone).

Summary

Marrow transplant patients are at an increased risk of a new malignancy. The extent of this problem and the risk factors have not been assessed in a larger group of long term survivors. We did a retrospective multicenter study in Europe to assess the risk and to identify risk factors in patients surviving more than 5 years.

Detailed reports were collected from 46 European centers on 1159 patients. The median time after transplant was 9 years (range: 5 - 19.5 yr.). New malignancies were observed in 47 patients, the actuarial incidence was 4% ($\pm 0.7\%$ SE) at 10 yr and 12.5% ($\pm 3\%$ SE) at 15 yr. The rate was 3.8 fold of that in an age-matched control population ($p < 0.000001$). Most frequent were squamous cell neoplasias in skin, oral cavity, esophagus and larynx of 23 of 48 patients (48%). Risk factors were age of the donor above 30 yr ($p = 0.0002$) and the occurrence of chronic graft-versus-host disease ($p = 0.008$). In patients with chronic graft-versus-host disease treatment with cyclosporin A, thalidomide, and methotrexate increased the risk significantly ($p = 0.005$, $p = 0.01$ and $p = 0.05$ respectively).

The results indicate that chronic graft-versus-host disease and chronic immunosuppressive treatment are the most important risk factors for the development of new malignancies in marrow transplant patients.

Introduction

Marrow transplantation improves survival of patients with leukaemia, lymphoma and severe aplastic anemia {}, and an increasing number of patients survive more than 10 years. One of the anticipated late effects is the development of new malignancies as a result of radiation. The role of cytotoxic chemotherapy and the predisposition of the patient treated for a malignant primary disease is less well known {}. Immune deficiency is a condition associated with an increased risk of neoplasms {}. After transplantation reconstitution of the immune system requires several months as determined by normalization of lymphocyte counts, immunoglobulins and a variety of in vitro tests {Witherspoon}. Immunoblastic lymphomas associated with reactivation of Epstein Barr Virus infection is not rare in severely immunosuppressed patients {}. The use of antilymphocyte antibodies may be a risk factor for these lymphomas {}.

We limited our study to patients surviving more than 5 years after transplantation, because we were interested in the role of ionizing radiation in the development of new malignancies after marrow transplantation. Radiation induced neoplasms rarely occur in the first 5 years. Moreover other transplant-related complications with a potential impact on the development of secondary neoplasms have occurred at that time and may be evaluated. We have studied 1159 patients that were transplanted in 46 European centers cooperating in the European Group for Blood and Marrow Transplantation. The aim of this study was the assessment of the risk of new malignancies in long term survivors of marrow transplantation and the identification of risk factors of new malignancies. In particular we were interested whether conditioning treatment with radiation would increase the risk significantly.

Methods

In Europe marrow transplant programs were started in the early seventies in several University hospitals. The indication for marrow transplantation changed with time, prior to 1976 the main indication was severe aplastic anaemia, and after 1980 the main indication was leukaemia. In 1977 the European cooperative group for bone marrow transplantation (EBMT) was founded. A central registry of all cooperating centres was instituted at the University of Leiden with basic information on disease related and transplant-related variables including the form of radiation, radiation dose, dose rate, fractionation and treatment times. We limited our study to patients surviving more than 5 years for two reasons. First, mortality due to transplant-related complications other than new malignancies and recurrence of the original disease is high in the first years. Second, major complications other than new malignancies may have occurred at that time and their influence on the development of new malignancies can be tested independently.

Data collection

The EBMT registry provided basic data on transplants performed prior to 1986 and the transplant centres. Transplant centres were asked to correct and supplement this information. The information included age and sex of the patient and his/her donor, diagnosis and status of the disease at the time of transplant, histocompatibility with the donor in the categories monozygotic twin, HLA-identical family member, HLA-mismatched family member and autologous transplants, conditioning treatment including radiation, radiation source, radiation field, radiation dose, dose rate, fractionation schedule, days with radiation and the form of chemotherapy, methods of prevention of graft-versus-host disease (GVHD), the occurrence of acute GVHD graded in a 0 to 4 scale and chronic GVHD in a 0 - 2 scale, agents used for treatment of GVHD, the date of tumor detection and last follow up, the histology report of the tumor, the ICD number, information on recurrence and treatment of the original disease, clinical performance status at the time of last follow up, cause of morbidity or death, information on work and school activities (Table 1). Reports were solicited from all European centers that performed marrow transplantation before December 31, 1985. 1211 reports were collected from 46 centers in 13 countries. Questions included age and sex of the patients and their donors, histocompatibility, diagnosis and stage of their disease, date of transplantation, survival status, conditioning treatment including radiation, treatment for prophylaxis of GVHD, stage of acute and chronic GVHD, treatment of GVHD, date of diagnosis and type of new malignancy, status of original disease, Karnofsky index of clinical performance, work or school attendance, and cause of morbidity or death. Radiation as preparative treatment was classified as single dose or fractionated total body radiation and partial body radiation including total lymphoid and thoraco-abdominal radiation. The radiation source, dose, acute dose rate, number of fractions, number of days with radiation, and dose to the lungs were scored as radiation parameters.

Statistical Analysis

A Kaplan-Meier survival analysis was performed to estimate the risk of new malignancies with time after transplantation (770). The date of onset of new malignancy was the date on which the clinical diagnosis was first suspected. For comparison the risk of neoplasia was calculated for an example of the general population, matched for age and sex. Data were provided by the Danish Cancer Registry on the annual incidence of all malignant cancer sites including cancer of the skin () and the Cancer Registry of the Saarland/Germany (). The expected number of cases (E) in the cohort was calculated using their age, sex and length of follow-up and the incidence rates compared with the incidence in the transplant cohort (O). Significance was assessed under the null hypothesis that O is equal with E in a Poisson distribution. A standardized ratio (O/E) was also calculated.

Analysis of potential risk factors was performed with the time to diagnosis of new malignancy in a log rank test for univariate analysis. Multivariate regression analysis was performed with the Cox model for

proportional hazards. Analyses were performed using NCCS statistical package (Dr.J.L.Hintze,Kaysville, Utah, USA).

Results

Survival

86 patients died more than 5 years after transplantation, 41 patients with recurrence of the original disease. The risk of death was 9% at 10 years and 14% at 15 years after transplantation. 10 patients died with secondary malignancies, 4 with brain tumors, 4 with squamous cell carcinoma of the oral cavity, larynx and esophagus, and one with secondary leukaemia and neurofibrosarcoma respectively. Other causes of death were chronic GVHD with infections, transfusion-induced AIDS, and accidents. The median time of observation is 108 months, the longest time 235 months.

Tumors

New malignancies were diagnosed in 47 patients, the most frequent tumors were carcinomas of the skin, basal cell and spinal cell carcinomas, tumors of the oral cavity, carcinomas of the uterus including carcinoma in situ of the cervix, breast cancer and brain tumors (Fig. 1). The actuarial risk of a new malignancy is 4 % ($\pm 0.7\%$ SE) at 10 years and 12% ($\pm 3\%$ SE) at 15 years. The overall incidence of malignant tumors is significantly increased above that of age and sex matched population (Fig. 2). The increase is more than 10-fold for skin cancer and cancer of the oral cavity and esophagus, not significantly increased for breast cancer (Fig.3).

Risk Factor Analysis

In univariate analysis the age of the donor, the development of chronic GVHD and its treatment with cyclosporin A, thalidomide, azathioprin and methotrexate were significant risk factors for new malignancies (Table 1). In multivariate analysis only age of the donor above 30 yr. and chronic GVHD remained significant after entering donor age and chronic GVHD in a stepwise fashion (Table 2). Treatment of chronic GVHD with cyclosporin A and thalidomide increased the risk of new malignancies most significantly.

Discussion

The treatment of acute and chronic leukaemia has improved over the past decades. A minority of adult patients and the majority of children may even be cured by chemotherapy. For patients with CML and the majority of patients with acute leukaemia marrow transplantation is the treatment of choice that provides a chance of cure, if a suitable donor is available. However the long term outcome of this intensive form of treatment may be overshadowed by serious late effects. One of the most serious late effects is the development of a new malignancy in a patient cured of a primary malignancy or other haematological and immunological disorder.

The use of radiation for conditioning treatment is advantageous for several reasons. Tissue doses of radiation can be calculated with reasonable accuracy as compared to chemotherapy. Radiation is active even in leukaemia resistant to chemotherapy. It is highly immunosuppressive and provides space for the transplanted stem cells by its toxicity on stem cells of the host. However the use of radiation has been a major concern for most transplant physicians because of its well known late effects including carcinogenesis. Nevertheless the role of radiation as carcinogenic factor in marrow transplantation can only be seen in the context with many other risk factors involved.

In previous studies of single centres {Witherspoon} a larger proportion of patients tended to develop high grade lymphoma, but these malignancies occurred early after transplantation and most were associated with Epstein Barr virus infection. Risk factors for these lymphomas were the use of immunosuppressive antibodies for prevention and treatment of acute GVHD. A multicenter study of malignancies in patients with severe aplastic anaemia found an increased risk of leukaemia in patients treated by immunosuppression only and an increased risk of solid tumors in patients transplanted with the use of radiation for conditioning {Socié}. The possibility of severe aplastic anaemia being a preleukaemic condition had been raised by a previous report on long term follow up of patients treated with immunosuppression in a single centre {Tichelli}.

In chemotherapy studies of childhood acute leukaemia and Hodgkin's disease a definite risk of secondary malignancy has been shown in several reports {A.Meadows}. AML was most frequent as malignancy secondary to treatment of a primary malignancy {Petersen-Bjergaard, Pui, Tucker, Meadows}. The use of alkylating agents {Petersen-Bjergaard} and intensive treatment protocols with epipodophyllotoxins {Pui} were risk factors in these patients. The incidence of solid tumors was higher in patients treated with radiotherapy, in particular brain tumors in preschool children treated with cranial irradiation for prevention of leukaemic meningiosis {Neglia}. In patients with Hodgkin's disease solid tumors tend to occur in the radiation field {Tucker}. However the radiation doses used for treatment of lymphomas and prophylaxis of leukaemic meningiosis is higher than those used for total body radiation.

Another group for comparing risk factors of carcinogenesis are patients after organ transplantation. These patients are not treated regularly with radiation, but they are on chronic immunosuppressive treatment. The majority of tumors seen in these patients are skin cancers and lymphomas {Penn}. An increased incidence of skin cancers were first observed in kidney transplant recipients in Australia {Sheil}, but a recent report from northern England confirms this finding in another geographic region {London}. Significant risk factors in that cohort of patients were age of the patient and length of time on dialysis. As the spectrum of tumors in marrow transplant patients is similar to that in kidney transplant patients it was suspected that chronic immunosuppression is the major risk factor. Indeed we could show that chronic GVHD and its treatment is the major risk factor in marrow transplant patients. The age of the donor is similar to the age of the recipient, since the majority of patients were transplanted from HLA-identical sibling donors. The most significant difference was seen in comparing age groups below and above 30 years. Immunization by pregnancies and other ways may have an additional influence on the occurrence of new malignancies, since it increases the risk of GVHD. Finally the sites of many new malignancies are the target sites of chronic GVHD, i.e. skin, mouth, esophagus. Obviously chronic GVHD is a cocarcinogenic factor that may be separated from its treatment. The role of immunosuppressive treatment of chronic GVHD varies with the agents used. Cyclosporin A and thalidomide seem to have a greater role

than methylprednisolone and azathioprin. However information on immunosuppressive agents used is limited.

The results of this evaluation indicate an increased risk of new malignancies in marrow transplant patients. Fortunately many of these tumors are limited to the skin and can be cured by careful observation and excision. As the major risk factor is chronic GVHD new attempts should be made to improve the treatment of chronic GVHD or better prevent acute GVHD which is the most frequent precondition for chronic GVHD.

Supported in part by European Late Effect Project Group (EULEP), and CEC Contract FI3P-CT920064f - Epidemiological studies and tables

The following centers have contributed reports (No.of patients):

Antwerpen (5); Barcelona (95); Basel (69); Besancon (14); Bologna (16); Brussels St.Luc (25); Copenhagen (60); Cremona (1); Creteil (37); Essen (19); Genova (157); Grenoble (10); Heidelberg (2); Helsinki Adult (18); Helsinki Ped. (22); Huddinge (65); Inn sbruck (2); Kiel Ped. (3); Leiden Ped. (23); Leiden Adults (17); Leuven (14); London Univ.College (31); London Charing Cross (11); London Hammersmith (51); London Royal Free (35); Lyon (4); Marseille (14); Milano ISM (1); Munich (103); Nancy (2); Nantes (19); Nijmegen (19); NIH-Budapest (1); Paris St. Louis (114); Pavia (2); Pesaro (18); Rome La Sapienza (10); Rotterdam (6); Santander (14); St.Etienne (2); Tuebingen (8); Turku (9); Ulm Ped. (5); Ulm Adults (34); Vienna (7); Zuerich (4).

Table 1

NEW MALIGNANCIES AFTER BONE MARROW TRANSPLANTATION
EBMT - Late Effect Working Party 8/95
 Univariate Analysis

Variable tested	No.of patients transplanted	No.of pats. with malignancy	log rank test (time until tumor detection)
Sex male	658	28	n.s.
female	501	19	
Age < 10 yr.	171	6	n.s.
- 20 yr.	351	11	
- 30 yr.	326	13	
- 40 yr.	222	10	
> 40 yr.	89	7	
Donor Sex male	461	15	n.s.
female	378	18	
Donor Age <= 30 yr.	936	30	p = 0.0006
> 30 yr.	223	17	
HLA allogeneic	1074	47	n.s.
syngeneic/autologous	85	0	
Diagnosis AML/MDS ¹	361	16	n.s.
ALL ²	255	11	
CML ³	254	6	
SAA ⁴	215	12	
other ⁵	76	2	
Conditioning Chemoth.only ⁶	193	7	n.s.
Radiation + chemo	951	40	
Single dose TBI ⁷	533	23	
Fract. TBI	322	11	
TLI / TAI ⁸	96	6	

GVH-Prophylaxis				
MTX ⁹	270	16	n.s.	
CSA ¹⁰	446	22		
CSA-MTX	117	2		
ATG/T-depl. ¹¹	87	1		
GVHD				
acute > I	915	31		
acute < II	244	16	n.s.	
chronic = 0	558	16		
limited	292	15		
extended	169	12	p = 0.03	
Treatment of cGVHD				
methylprednisolone	717	32	n.s.	
CSA ¹⁰	115	12	p < 0.0001	
azathioprin	52	6	p = 0.0068	
thalidomide	15	4	p < 0.0001	
ATG ¹¹	7	1	n.s.	
cyclophosphamide	4	0	n.s.	
MTX ⁹	7	2	p = 0.009	
no. of agents	0	705	20	p < 0.0001
	1	172	9	
	>1	125	11	

n s = not significant, 1 AML = acute myeloid leukaemia, MDS = myelodysplastic syndrome, 2 acute lymphoblastic leukaemia, 3 = chronic myelogenous leukaemia, 4 = severe aplastic anaemia; 5 = other diagnoses including solid tumors (N= 32), lymphoma (N=35), and inborn errors of metabolism (N=9), 6 including single drugs busulfan, melphalan, nitrosourea, cytosin-arabinoside, VP-16, daunorubicin, 7 TBI = total body irradiation, 8 TLI = total lymphoid irradiation including mantle field and inverted Y, TAI = thoraco-abdominal irradiation including the trunk, 9 = methotrexate; 10 = cyclosporin A, 11 = antithymocyte globulin, depletion of T-cells from the marrow prior to transplantation

Table 2

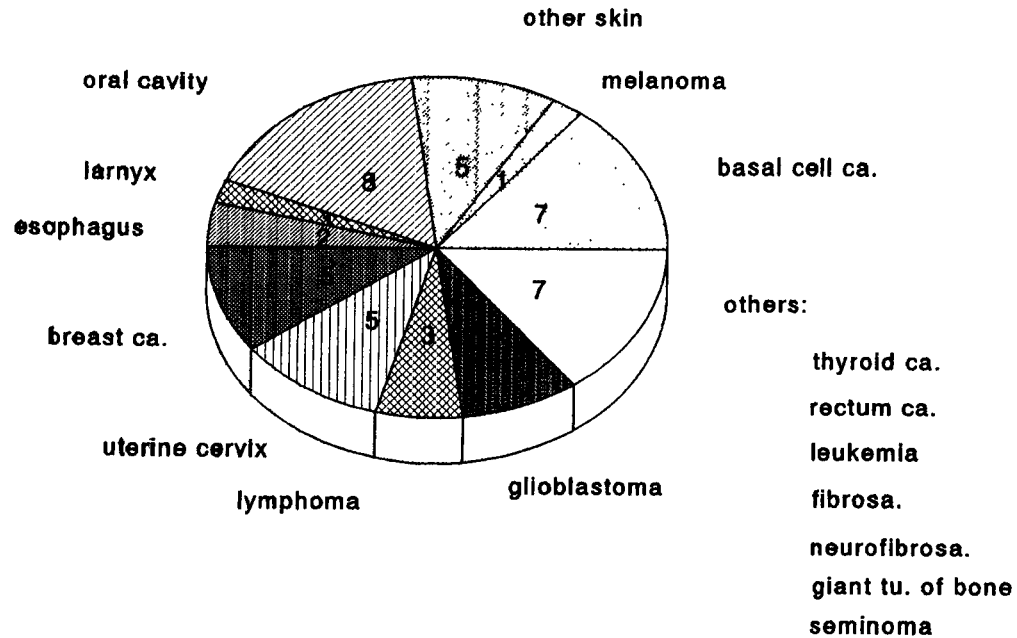
NEW MALIGNANCIES AFTER BONE MARROW TRANSPLANTATION
EBMT - Late Effect Working Party 8/95
 Multivariate Analysis in Cox Proportional Hazards Model

Covariate	p-value at entry	multivariate p-value	relative risk (95% confid.limits)
Whole Group			
Donor Age Group	0.0001	0.0002	3.2 (2.9 - 3.5)
cGVHD	0.0071	0.008	1.7 (1.5 -1.8)
Pat. Age Group	0.0025	0.388	
aGVHD	0.0112	0.227	
Radiation	0.1376	0.17	
HLA	0.5528	0.621	
Treatment in pats with cGVHD only			
Cyclosporin A	0.0002	0.005	3.5 (3.0 - 3.9)
Methotrexate	0.0098	0.05	4.4 (3.6 - 5.2)
Thalidomide	0.0002	0.01	4.3 (3.7 - 4.8)
Azathioprin	0.1263	0.84	
No. of treatments	0.0011	0.7	

NEW MALIGNANCY AFTER BMT

EBMT - 1995

Fig. 1



EBMT Patients

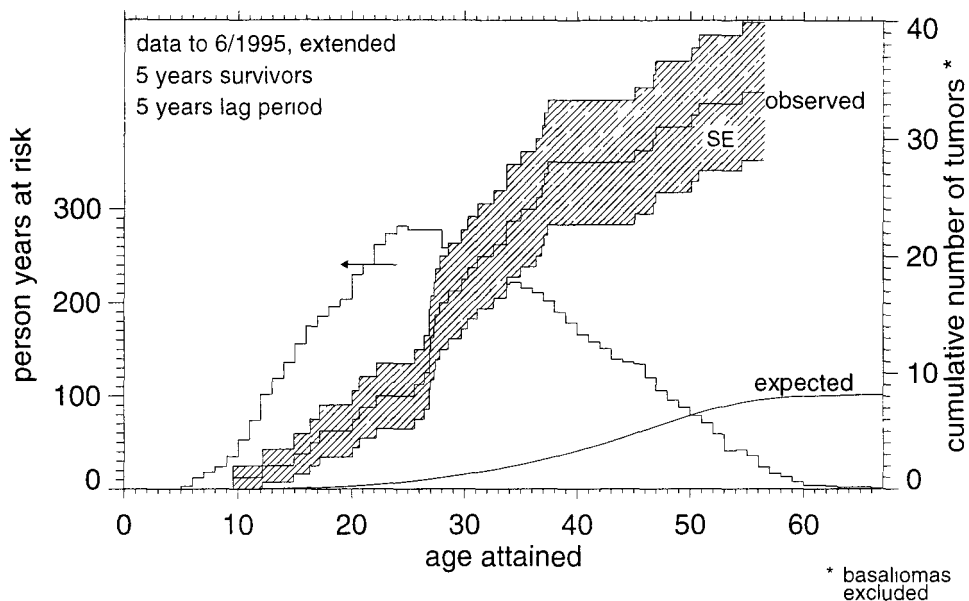


Fig.2: The grey shaded area gives the number of patients whose period under observation includes the specified age (person years at risk). The step function with the hatched range of standard errors represents the observed cumulative number of tumors (basaliomas excluded) as a function of attained age; the lower curve indicates the expected number of tumors.

Health And Functional Status of Long Term Survivors of Bone Marrow Transplantation - A Study of the Late Effects Working Party of the European Group for Blood and Marrow Transplantation.

Thomas Duell¹, MD; Maria Teresa van Lint², MD, PhD; Per Ljungman³, MD, PhD; André Tichelli⁴, MD, PhD; Gerard Socié⁵, MD, PhD; Jane F. Apperley⁶, MD, PhD; Melanie Weiss⁷, MD; Amon Cohen⁸, MD, PhD; Elke Nekolla⁹, PhD; and Hans-Jochem Kolb¹, MD, PhD for the EBMT Working Party on Late Effects and EULEP Study Group on Late Effects.

1 Medizinische Klinik III, Universität München, and GSF - Forschungszentrum für Umwelt und Gesundheit, München, Germany; 2 Ospedale San Martino, Genova, Italy; 3 Dept of Medicine, Huddinge Hospital, Huddinge, Sweden; 4 Dept. Haematology, Kantonsspital Basel, Basel, Switzerland; 5 Hopital St. Louis, Paris, France; 6 Hammersmith Hospital, Royal Postgraduate School of Medicine, London, United Kingdom; 7 Institut fuer Klinische Physiologie und Sozialmedizin, University of Ulm, Ulm, Germany; 8 Dept. Pediatrics, Istituto Giannina Gaslini, Genova, Italy; 9 Institut fuer Strahlenkunde, University of Munich, München, Germany.

Short title. Long term survivors after marrow transplantation

Supported in part by European Late Effect Project Group (EULEP), and CEC Contract FI3P-CT920064f - Epidemiological studies and tables

Correspondence to:
Prof. Dr. Hans-Jochem Kolb
Med Klinik III - Knochenmarktransplantation
Klinikum Großhadern - Universität München
Marchioninstr. 15
81377 MÜNCHEN Germany

Tel: 0049 89 7095 3039; Fax: 0049 89 7095 8824

No. of words: 3000.

Objective: Evaluation of long term effects of marrow transplantation on the health and life style of patients surviving more than 5 years after their transplant.

Design: Retrospective multicenter study.

Patients: Data were collected on 860 recipients of marrow transplants (528 adults, 332 children) from 48 European centers. Patients were transplanted before December 1985 and had survived at least 5 years. The median observation time was 8.4 years (range 5 - 19 years). The patients received allogeneic, syngeneic or autologous marrow for a variety of indications, but the main diagnoses were acute and chronic leukemia and severe aplastic anemia.

Measurements and Main Results: Actuarial mortality of this group was 8 % at 10 years and 14 % percent at 15 years. The leading causes of death were disease recurrence, chronic graft-versus-host disease (cGVHD) with complicating infections and lung diseases, secondary malignancies and acquired immunodeficiency syndrome (AIDS). In multivariate analysis, disease recurrence, secondary malignancy and advanced stage of disease at the time of transplant were significantly associated with an increased risk of late mortality. 93.6 % of patients had a normal Karnofsky score (90 - 100%) and 89% of patients were at work or school full-time. The causes of reduced performance status included chronic GVHD, AIDS, secondary malignancy, organ dysfunction and neurological and/or psychological problems. For patients without recurrent disease chronic GVHD was the most important risk factor for reduced clinical performance and incomplete social reintegration. Other risk factors on multivariate analysis included female sex, older age at transplant and the development of secondary malignancy.

Conclusions: More than 5 years after bone marrow transplantation most patients are in good health (94%) and at work and school full-time (89%). Recurrence of the disease, secondary malignancy, chronic GVHD and its sequel remain problems for a minority of patients.

TUMOR BANKING AFTER BONE MARROW TRANSPLANTATION.

CEC Contract N° FI3P-CT8920064f

FINAL REPORT

G. Socié, MD, PhD : Service de Greffe de Moëlle et Unité de Recherche sur la Biologie des Cellules Souches, Hôpital Saint Louis, 1 Avenue Claude Vellefaux 75475, Paris Cedex 10, France.

PROJECT 16. TUMOR BANKING : A PROSPECTIVE EBMT-LATE EFFECTS WORKING PARTY CLINICO-BIOLOGICAL STUDY OF MALIGNANT DISEASE OCCURRING AFTER BONE MARROW TRANSPLANTATION.

II. Objectives for Reporting Period.

1.) To collect ***prospectively*** pathological material from all new cases of secondary solid tumours occurring after BMT and to provide guidelines for tumor samples collection and reporting new cases to the member of the EBMT*-late effect working party for patients developing such secondary malignancies after bone marrow transplantation.

2.) To make ***retrospective analyses*** from archival tissues on pre-defined pathological tumor types (e.g. Malignant Melanomas, for example).

These objectives has to be achieved in bringing together a panel of expert pathologists and physicians who cared transplanted patients.

*(EBMT denotes : European group for bone Marrow Transplantation).

III. Progress achieved during Reporting Period.

Among the late effects that have been described after allogeneic bone marrow transplantation malignant diseases are of particular clinical concern as increasing numbers of patients survive the early phase after transplantation and remain free of their original disease. We first reviewed on behalf of the Late Effect Working Party of the European Group for Bone Marrow Transplantation (EBMT) the problem of malignant diseases after allogeneic bone marrow transplantation (BMT) and we urged physicians who care for long-term successfully grafted patients to report systematically such rare complications in order that risk factors may be assessed in multi-institutional registries [ref 1]. An EBMT retrospective study which addressed this problem of risk factors has been recently completed and allowed an assessment of risk factors for late malignancies among two cohorts of patients : the first one included patients transplanted before December 1980 and the second patients transplanted in 1984. The results of this study have been presented in part at the 1994 annual meeting of the EBMT. However, in this *Study* we would like to stress the importance of continuing to report such rare malignant events to registries. Since we are far from a thorough knowledge of all potent, interactive factors that lead to malignancies after BMT, refined risk-factor analyses for these complications (and consequent prevention or early detection) still need more patients with long follow-up. At the international level, under the auspices of the *National Institute of Health* of the United States, a survey on malignant diseases occurring after BMT is also ongoing, and will include patients reported to the *International Bone Marrow Transplant Registry* (IBMTR) and patients treated at the *Fred Hutchinson Cancer Research Center* in Seattle.

Two ongoing prospective studies of the Late Effect Working EBMT illustrate this need for patient reporting. These two studies aim to compare the risk of malignant complication in patients who underwent BMT after an irradiation-based conditioning with those who received chemotherapy only as the conditioning regimen. These two preparative regimens have been compared

prospectively in a randomized fashion mainly in two diseases, ie. chronic myelogenous leukemia (CML) and acute myelogenous leukemia (AML). Therefore, a close follow-up of these two patient populations will be able, in the forthcoming years, to delineate the exact role of whole body irradiation as compared to Busulfan (a radiomimetic drug), almost certainly by meta-analyses of cancer risk in a single disease (CML and AML).

To date, secondary malignancies have almost exclusively been reported following allogeneic BMT. However, we draw attention in an *Editorial* to the fact that patients undergoing autologous BMT (ABMT), or peripheral blood stem cells transplant, are also likely to encounter these complications. The reasons for this inference are, at least two-fold. Firstly, the high doses of drugs and radiation currently used within the conditioning regimen are basically the same in ABMT and in allogeneic transplants, and both (chemotherapy drugs and radiation) are strong mutagenic agents. Secondly, for some of the main diseases for which ABMT is performed [lymphoma (NHL and Hodgkin's disease), breast cancer and solid tumours in childhood] an increased risk of malignant complications is already documented in patients treated with otherwise conventional chemotherapy. Thus, for at least these two reasons it is highly likely that there will be reports on secondary malignancies after ABMT. In fact, recent reports have shown an increased incidence of myelodysplastic syndromes and acute leukaemia in patients with lymphoma who underwent ABMT. We thus infer that reports of secondary solid tumours will, unfortunately, occur once more patients with more follow-up have been recruited. Therefore, the main question in ABMT, as in allogeneic BMT, is: Is there an increased malignancy-risk due to the transplant procedure itself and/or are transplant-related "secondary" malignancies subsequent to an acquired or inherited predisposition in individuals to develop malignant diseases ? Only the prospective follow-up of all patients who have undergone bone marrow or

peripheral blood stem cell transplants, be autologous or allogeneic will allow to answer this question.

There is compelling evidence that cancer arises via a multistep process. Age, as a risk factor among BMT recipients, is a well known factor in "de novo" cancer where it has been taken as evidence for the requirement for multiple molecular events before the solid tumour emerges (or is diagnosed). Molecular analysis of human cancers commonly shows multiple genetic lesions in a single cancer including chromosomal translocations, gene amplification, point mutations. In several cases the mutational activation of an oncogene and the loss of a growth suppressor gene have been found in the same cancer cell population. These multiple genomic lesions have led to the concept of cooperation between oncogenes and/or the association of activated oncogenes with loss of tumour suppressor genes. As part of a multistep carcinogenesis cancers arise and/or spread in the body (metastasise) because of the failure of the immune system to control malignant cells. Solid tumours occurring after BMT might be of unique interest in study of the interrelationship between molecular oncogenesis and regulation through the immune system because, generally speaking, solid tumours remain of host origin and the immune system of donor origin. However, most of our knowledge about these interrelationships remains in its infancy and we will probably learn a lot about this process in view of the rapidly growing discoveries in all aspects of molecular oncogenesis. Thus, it will be of major importance, not only to report to registries such rare events, but also to systematically freeze a part of the tumor to allow systematic molecular analysis of any secondary solid tumour type within the near future. In this regard, it is of great interest to note that, most recently, a report has been published that demonstrated a link between EBV and a rare form of solid tumour (smooth-muscle tumours) in recipients of organ transplants. In this prospective study of the EBMT late Effect Working Party Study we aim to collect, and systematically freeze samples from all new malignancies occurring

after BMT (either allogeneic or ABMT) to allow such biological studies to be performed.

To reach the aims of this study we made the followings.

1. Guidelines for tumour collection and clinical data sheets have been circulating to all EBMT centers (*see appendix 1*), and 55 centers over all Europe have given their formal agreement to this study (*see appendix 2* ; one haematologist and one pathologist per center). Furthermore, since some center thought that this study was restricted only to patients who underwent allogeneic bone marrow transplantation, we wrote an Editorial to the Journal *Bone Marrow Transplantation* (paper in press, October, 1995) to provide again the clinicians with the main background arguments that show that patients who had underwent an autologous bone marrow transplantation are also at risk for developing malignancies post-transplant.

2. All EBMT-Working parties of the EBMT agreed for providing data and help for pathological material collection and a number of expert pathologists have given their agreement to participate to this project.

3. Nowadays clinical data concerning ten patients who developed a secondary solid tumors have been prospectively collected and tumor samples have been kept by respective centers for future biological studies.

4. The first clinico-biological retrospective study on malignant melanoma occurring after transplantation is planned.

Publications.

- Malignancies occurring after treatment of aplastic anemia: a survey conducted by the severe aplastic anemia working party of the European group for Bone Marrow Transplantation. **Socié G**, Heny-Amar M, Bacigalupo A, Hows J, Tichelli A, Ljungman P, Mc Cann SR, Frickhofen N, Van't Veer-Korthof E, Gluckman E. *N. Engl. J. Med.*, 329, 1152-1157, 1993.

- Late effects III - Long term results and secondary malignancies. **Socié G**, Kolb H.J. *Bone Marrow Transplant.* 12 (Suppl 4), s115-s116, 1993.

- Secondary solid malignant tumors occurring after bone marrow transplantation for severe aplastic anemia given thoraco-abdominal irradiation. Cytophosphamide regimen : dosimetric aspects. **Socié G**, Devergie A, Bridier A, Girinsky T, Nguyen J, Pierga JY, Cosset JM, Gluckman E. *Radiother. Oncol.* 30, 55-58, 1994.

- Malignant disease after allogeneic bone marrow transplantation: the case for assessment of risk factors. **Socié G**, Kolb HJ, Ljungman P. *Br J Haematol* 80, 427-430 1992.

- Malignant diseases after allogeneic bone marrow transplantation : an updated overview. **Socié G**, Henry-Amar M, Devergie A, Esperou-Bourdeau H, Ribaud P, Traineau R & Gluckman E. *Nouv. Rev. Fr. Hematol.*, 36(suppl1), S75-S77, 1994

- Secondary malignancies after bone marrow transplantation : the case for tumor banking. **Socié G**, Kolb HJ: *Bone Marrow Transplant.*, *in press*.

Appendix 1

GUIDELINES FOR TUMOUR BANKING.

1.) This work should be done in **close cooperation with single centers' pathologists.**

2.) When a secondary solid tumor is suspected, Pathologists and Surgeons should be awoken of the rarity of the case in order to obtain a **large** biopsy and 20 ml of peripheral blood have to be frozen to allow chimerism study (to allow genotypic comparison between donor and recipient).

Whenever possible half of the biopsy had to be retain for classical pathological study and the other half had to be immediatly frozen in liquid nitrogen and then stored at - 80°C. Tissue sampling must be done as soon as possible after excision of the specimen. The samples may be snap frozen without without cryoprotection at - 80°C for subsequent use in procedures requiring the extraction of genomic DNA, mRNA, or protein. To preserve tissue architecture and cytologic features for immunohistochemistry and *in-situ* hybridization, the tissue should be frozen at - 80°C or colder with a cryoprotectant such as OCT [*Diag. Mol. Pathol.*, 1, 73-79]. Long-term storage of the frozen tissue is recommended at -140°C in a locked liquid nitrogen freezer. Tissue sampled and stored under these conditions can be used successfully in a wide variety of molecular techniques.

3.) : Summary of

a - main clinical parameters dealing with Patient s' Transplant Course (copy of MED-A and MED-B forms or other institutional forms)

b - Cancer course, Pathological Type, and Risk Factor (s)

CLINICAL SUMMARY should be sent to :

G. SOCIE, MD, PhD, Laboratoire de Biologie des cellules Souches,
Hôpital Saint Louis, 1 Avenue Claude Vellefaux, 75475, Paris CEDEX 10, FRANCE.

Phone 33.1.42.98.24, Fax 33.1 42.49.26.99.

FROZEN MATERIAL IS KEPT IN EACH INSTITUTION UNTIL ANALYSIS

IN PROSPECTIVE MULTIISTITUTIONAL STUDIES.

Appendix 2

List of participating Centers

Belgium	Brussels	Pr A Ferrant
Croatia	Zagreb	Pr B Labar
England	Bristol	Pr J Hows
England	London	Pr EC Gordon-Smith
England	London	Pr G Prentice
England	London	Pr J Goldman
England	Newatle upon Tyre	Pr JJ Proctor
England	Southampton	Dr JW Sweetenam
France	Besançon	Pr JY Cahn
France	Bordeaux	Pr J Reiffers
France	Marseille	Pr D Blaise, Dr L Xerri
France	Paris	Dr JM Zucker
France	Paris	Pr E Gluckman, Dr G Socié
France	Paris	Pr NC Gorin
France	St Etienne	Pr F Freycon
France	Tours	Pr P Colombat
Germany	Heidelberg	Dr R Haas
Germany	Munchen	Pr HJ Kolb
Germany	Nuernberg	Dr H Wandt
Germany	Stuttgart	Dr S Koscenliak
Greece	Athens	Dr S Graphakos
Greece	Athens	Pr A Efremidis
Greece	Athens	Pr N Harhalatis
Greece	Thessaloniki	Pr A Fassas
Ireland	Belfast	Dr C Morris
Israel	Jerusalem	Pr A Nagler
Italy	Bolzano	Pr P Coser
Italy	Firenze	Pr A Bosi
Italy	Milano	Pr C Uderzo
Italy	Milano	Pr G Lambertenghi

Italy	Roma	Pr De Rosa
Italy	Roma	Pr W Arcese
Italy	Turino	Pr R Miniero
Norway	Oslo	Pr c Albrechtsen
Poland	Wroclaw	Pr A Lange
Portugal	Lisboa	Pr M Abecasis
Scotland	Edimburgh	Dr AC Parker
Slovakia	Bratislava	Pr M Mistrik
Slovakia	Praha	Dr P Kobyla
South Africa	Cape town	Pr P Jacobs
Spain	Barcelona	Pr A Granema Batista
Spain	Barcelona	Pr JJ Ortega
Spain	Barcelona	Pr M Martin
Spain	Madrid	Pr M Rubio
Sweden	Huddinge	Pr P Ljungman
Sweden	Lund	Pr A Bekassy
The Netherland	Nijmegen	Pr T de Witte
The Netherland	Utrecht	Pr L Veronck
Wales	Gwynedd	Dr H Parry

**Final Report
1992 - 1994**

Contract: FI3PCT930065 Duration: 1.1.93 to 30.6.95

Sector: C14

Title: Risk estimates of lung cancer from the follow-up of uranium miners.

1)	Chmelevsky	GSF
2)	Tirmarche	CEA - FAR
3)	Muirhead	NRPB
4)	Darby	ICRF
5)	Kunz	NIPHE.CRH

I. Summary of Project Global Objectives and Achievements

Objectives: The overall objective of this contract was the improvement of the risk estimates for radon inhalation, obtained from uranium miners studies. Within this frame more specific objectives were:

1. Comparison and development of models. The type of models considered are relative risk models with modifiers, and mechanistic models (clonal expansion models).
2. Improvement of already existing data sets. The data sets considered are the French miners, the Czech miners, and the Colorado Plateau miners, as made available by the "Freedom of information act" of the US.
3. Analysis of actual data available to our project.

In the first years of the project, GSF and ICRF were working with the Czech data. CEN-FAR was improving and analysing the French data, and NRPB was applying mechanistic models to the Colorado Plateau data. Later NIPH became a PECO partner of the project. They maintain the Czech data set and clearly they were to improve and analyse it. As a consequence of this strengthening of our manpower concerning this data set (and Dr. Chmelevsky leaving GSF for Paris), the GSF activities shifted towards mechanistic modelling, which was expected to require additional work.

Achievements: The French and the Czech data sets were continuously improved and updated. The French data set now comprises 1785 miners followed up to 1985, a larger data set with about 6000 miners is in preparation. This data set has low dose rates in average. The Czech cohort S has 4320 miners with 708 cases, followed up to 1990. The newer cohorts L and N have 72 cases in the data set. The data sets are also included in an analysis of pooled data of 11 studies.

Both the French and the Czech data set show an increased rate of lung cancer in the Uranium miners. In the Czech cohort S, the relative risk is about 5; it is increased particularly in the period 4-14 years after exposure (ICRF). Also strongly increased in this cohort, but presumably not linked to Radon exposure are homicide and mental disorder.

Obtained coefficients for excess relative risk per Sievert reach from 0.35% for the French data set (CEN-FAR) to 0.71% for the Czech cohort S (NIPH) and up to 1.36%

(0.52 to 3.44 at 95% confidence level) (ICRF) for the Czech cohort S when considering only miners aged 55+ years with exposures 5-14 years prior to observation. (The analysis of pooled data from 11 studies gives 0.49%.) The variation of the risk coefficients can be explained partly by statistical fluctuations, partly they are due to different composition of the subgroups with different risk. It is clear that a single number is a too crude measure for risk: it is necessary to consider risk as function of various confounders.

The risk function favored by the Czech data weighs cumulative exposures in different years since exposure (groups of 5-14, 15-24, and 25-34 years are considered) and has a weak dependence on the age at median exposure. The risk function has a strong dependence on time since exposure, and shows an inverse dose-rate effect. A detailed analysis of the data gave, that the inverse dose-rate effect is especially pronounced for high dose rates over 4 WL, which cause fewer lung tumor cases than extended exposures with the same cumulative dose. In the French data set, no effect of the period of exposure, and thus no inverse dose rate effect was found. This may be due to poor statistics, or due to the relatively low dose rates in this cohort.

An alternative model for analysing miners data is the clonal expansion model in its various forms. A complete set of parameters for such a model was derived by fitting it to the Colorado plateau miners (NRPB), for which individual smoking information is available. Some features of the best fitting version are:

- Radon dose enters linear-quadratic.
- Radon and smoking act more than multiplicative (this is surprising; other analyses find less than multiplicative, but more than additive).
- The risk decreases, after the radon exposure returns to the baseline.
- Radon dominates the initiation, smoking the promotion, interaction of the two is in cell kinetics.

GSF participated up to 1994 in the analysis of the Czech data, see the report of 1994. Later it was decided to move to mechanistic modelling. It was found, that the two existing analyses of an animal experiment of F.T. Cross et. al. with rats exposed to radon gave very different biological parameters; the same is true for different analyses of the Colorado plateau miners data, and the British doctors data for smoking only. The models in use can give comparable quality of fit to existing data by widely different parameter values. It was concluded, that a better understanding of the models is necessary: it must be clarified, which parameters (or parameter combinations) can be determined from existing data. and which not. Part of this work overlaps with the project "biophysical modelling" and is described there. A preliminary result is, that smoking affects mostly the second mutation rate. This finding is consistent with the results of NRPB.

Radon could also increase other cancer types than lung tumor. In the French data set, the cancer of the larynx was investigated, and no significant increase was found (CEN-FAR). In the Czech data set, there was no significant increase of other cancers. This agrees with the analysis of pooled data of 11 studies, where a significant increase was only found for stomach, liver, and leukemia in the first 10 years after exposure, but none of these could be related significantly to the cumulative exposure to radon (ICRF). Consequently, the protection standards for radon should continue to be based on considerations of the lung cancer risk alone.

Head of project 1: Dr. Chmelevsky

II. Objectives for the reporting period

Analysis of the Czech data set of uranium miners with various models used for the atomic bomb survivor data with the software package EPICURE.

Later, due to the inclusion of the Czech PECO partner, and the moving of Dr. Chmelevsky to Paris, the emphasis was shifted to mechanistic modelling: Use of the clonal expansion model to analyse data of rats exposed to radon, and to data of humans exposed to radon and smoking.

III. Progress achieved including publications

1 Overview

The work on the Czech data set is summarized in [9] and in [10].

Later we studied the clonal expansion models for modelling Radon induced lung cancer in rats, and in men. These models go back to Armitage and Doll [1], and later Moolkavkar, Venzon, and Knudson [2, 3]. Their aim is a quantitative description of tumor development in biological terms like cell growth, cell death, and mutation rates. So they connect molecular biology and epidemiology

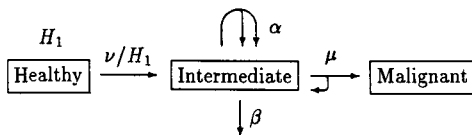


Figure 1: Scheme of the MVK model

In these models it is assumed (see Fig. 1) that

1. Healthy stem cells mutate with an exposure dependent probability to intermediate cells. The number of healthy cells is determined by regulating mechanisms of the body and constant for adult organisms.
2. The intermediate cells have their own growth dynamics, (clonal expansion) which also depends on the exposure.
3. With another exposure dependent probability the intermediate cells convert to malignant cells.
4. The malignant cells become observable after deterministic growth. The incidence rate of tumors is used to determine the parameters as far as possible.

Depending on how the clonal expansion is dealt with mathematically, there are two versions of the model in use:

- The “epidemiological approximation” models the net growth rate of the intermediate cells deterministically. After an initial period it gives an exponential growth of hazard with age [1, 2].
- The “exact formulation” derived by modelling stochastically the birth-death process of the intermediate cells. In this case the exponential growth eventually levels off to a constant hazard [4]. We use the term MVK model only for this version.

	0	320	640	1280	2500	5000	10000
50	1 ± 1	6 ± 1	26 ± 3	53 ± 7	68 ± 10	78 ± 10	
500	0 ± 1	7 ± 1	5 ± 1	15 ± 5	28 ± 6	38 ± 7	57 ± 7

Table 1: Tumor probability in percent for dose rates in WLM/w and total dose in WLM

In Section 2 we investigate two papers on an experiment of F. Cross with rats exposed to radon. The two analysis by Moolgavkar et. al. and by Leenhouts and Chadwick use very different mathematical techniques, and very different assumptions about the dose dependence of the relevant parameters. In Section 3 we discuss the applications of the clonal expansion models to lung cancer incidence of miners. exposed to radon and to tobacco smoke.

2 Radon induced lung cancer in rats

In the experiment of F Cross at the Pacific North-West Laboratories about 1800 SPF Wistar rats were exposed to air enriched with radon, radon-daughters, and uranium dust. The exposure started from the 14 week for 18 hours daily, 5 days a week. The rate varied from 0 to 500 WLM per week, the duration lasted up to about 100 weeks, with a total dose between 0 and 10000 WLM. The rats were examined histologically after death or sacrifice. Some of the observed tumor rates are given in Table 1.

2.1 Moolgavkar et. al.

We describe model A in [5]. The various steps of the model are in more detail:

1. The number of stem cells is not known, but constant; the model only requires the product of this number with the first mutation rate, i.e. the number $\nu(d)$ of newly originating intermediate cells per time unit, here a week. The authors give this as function of the dose in WLM/w as

$$\nu(d) = 0.1015 * (1 + d)^{0.8113}. \quad (1)$$

2. The intermediate cells undergo a birth-death process. The cell division rate ($\alpha = 10.00$ per week) is taken from in vitro experiments, and is assumed to be independent of radiation. The death rate is a fitted quantity. The difference is

$$\gamma(d) = \alpha - \beta(d) = 0.07259 + 0.02018 * \ln(1 + d) \quad (2)$$

and is less than 2% of the division rate for our values of d . This fine-tuning is not explained.

3. The second mutation rate has a different dependency from radiation,

$$\mu(d) = 3.379 * 10^{-6} * (1 + d)^{0.115}. \quad (3)$$

4. The time between appearance of a malignant cell and the observation of the tumor is assumed to be constant (in the calculations it is zero). Each malignant cell leads to a tumor.

Due to the high birth and death rates of the intermediate cells it is necessary to work with stochastic modelling. The functional form of the dose dependence of the parameters is assumed, the numbers are the result of fitting the incidence rates. We have found exact, albeit clumsy exact formulas for the hazard function in the described exposure pattern; they confirm the plotted hazard function of the paper. We have not yet tried to find a fit of the data ourselves, as we obtained the original data from F Cross only very recently.

2.2 Leenhouts and Chadwick

The steps described above are modelled in the following way:

1. The number of stem cells in the adult rat lung is assumed to be 160000, for the first 8 months of life a linear growth is modelled. The two mutation rates are described equally, as

$$\mu(D) = (9.6 * 10^{-6} + 3.4 * 10^{-6} D) * e^{-2.8 * 10^{-3} D}. \quad (4)$$

	Moolgavkar et. al.	Leenhouts et. al.
$\nu(0)$	0.1015	0.384
$\nu(50)$	2.465	15.9
$\nu(500)$	15.73	1.10
α	10.00	$\gamma(d)$
$\gamma(0)$	0.07259	0.0135
$\gamma(50)$	0.1519	-0.0868
$\gamma(500)$	0.198	-0.989
$\mu(0)$	$3.379 * 10^{-6}$	$2.4 * 10^{-6}$
$\mu(50)$	$5.311 * 10^{-6}$	$9.94 * 10^{-5}$
$\mu(500)$	$6.91 * 10^{-6}$	$6.9 * 10^{-6}$

Table 2. Comparison of the parameters

2. The intermediate cells grow with a rate

$$\gamma(D) = 0.054 - 2.0 * 10^{-3}D, \quad (5)$$

3. and mutate to a malignant cell with rate $\mu(D)$.

4. Between three and six months later each malignant cell develops into a observable tumor (lag time and expression time).

Here D is the dose per month, i.e. $D = 4 * d$. The expectation value of the number of intermediate and malignant cells is calculated with a step size of 1 month. We replaced this by differential equations, which can be solved explicitly; unfortunately our solutions do not agree with the values given in the paper; we guess that the step size is too large for the modelled dynamics.

2.3 Comparison of the parameters

Although the two variants of the clonal expansion model are quite different, we can compare the mutation rates and the growth rates at the radiation doses used in the experiment, see Table 2. We recalculate the rates given per month (cell cycle) in [6] linearly in rates per week. $\nu(d)$ is the rate at which intermediate cells originate, α is the cell division rate, $\gamma(d)$ the growth rate ($\alpha - \beta$) per week of the intermediate cells, $\mu(d)$ the second mutation rate per week and cell. d is the radiation dose rate; we consider only the spontaneous rate $d = 0$, $d = 50$ WLM/w and $d = 500$ WLM/w. The radiation dependence of the mutation rates and the growth rates is very different in the two approaches, both in the assumed functional dependence, and in the fitted parameters in Table 2

We conclude

- The observed lung tumor rates can well be described with the clonal expansion model
- The functional dependence of the biological parameters mutation rates and growth-death parameters on dose rate is controversial. They are in principle accessible to direct measurement independent of tumor incidence rates.
- The incidence data can give some of the parameters but great care should be taken; very different parameter sets may give acceptable fits, without an easy way to decide between them.

3 Lung cancer risk of uranium miners

Cigarette smoking is known to be a strong carcinogen for lung cancer. If one wants to make a mechanistic model for the radon risk of miners, it is unavoidable to also model the smoking habits of the miners. Of the larger epidemiological studies, until now only the Colorado plateau miners seem to contain useful information on smoking. Moolgavkar et. al. [7] have given a very interesting analysis of these data using the MVK-model. The paper does not give explicit hazard functions, but describes the model used and gives the parameters. In order to calculate hazards, we have developed fast algorithms to calculate the hazard functions explicitly, or numerically for stepwise constant parameters.

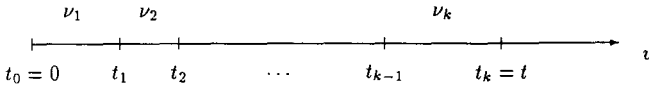


Figure 2: The parameters of the MVK-model are assumed to be stepwise constant

3.1 The MVK-model with stepwise constant parameters

We assume, that the biological parameters ν, α, β, μ of the MVK-model are stepwise constant, so that e.g.

$$\nu(u) = \nu_i \text{ in the interval } t_{i-1} < u < t_i, \quad (6)$$

holds, with (see Fig. 2)

$$0 = t_0 < t_1 < \dots < t_k = t. \quad (7)$$

The Riccati-equation for $y(u, t)$ has the stepwise defined solution (s. [4, Eq.13])

$$y(u, t) = \frac{B_i(y(t_i, t) - A_i)e^{\alpha_i B_i(u-t_i)} + A_i(B_i - y(t_i, t))e^{\alpha_i A_i(u-t_i)}}{(y(t_i, t) - A_i)e^{\alpha_i B_i(u-t_i)} + (B_i - y(t_i, t))e^{\alpha_i A_i(u-t_i)}} \quad (8)$$

in the interval $t_{i-1} \leq u \leq t_i$, with the initial conditions $y(t_i, t) = 1$. The initial conditions $y(t_i, t)$ can be calculated iteratively from $y(t_{i+1}, t)$ with this equation. The functions $y(u, t)$ and $\frac{\partial}{\partial t} y(u, t)$ are continuous in u .

The survival function can be obtained by integration; this integral can be decomposed into subintegrals

$$\ln \psi(t) = \int_0^t (y(u, t) - 1)\nu(u)du = \sum_{i=1}^k \int_{t_{i-1}}^{t_i} (y(u, t) - 1)\nu(u)du. \quad (9)$$

Moolgavkar et al. stress, that these integrals can be solved explicitly for constant parameters, but they calculate them numerically. Here we give explicit expressions. Crucial for a simple result is the observation, that in each interval $t_{i-1} \leq u \leq t_i$,

$$y(u, t) = \frac{\partial f_i(u, t)}{\alpha_i f_i(u, t)} = \frac{\partial}{\alpha_i \partial u} \ln f_i(u, t), \text{ with} \quad (10)$$

$$f_i(u, t) = (y(t_i, t) - A_i)e^{\alpha_i B_i(u-t_i)} + (B_i - y(t_i, t))e^{\alpha_i A_i(u-t_i)}. \quad (11)$$

The k functions f_i are only defined up to a factor which does not depend on u . With our choice, the value at the upper end of the interval is especially simple,

$$f_i(t_i, t) = B_i - A_i \quad (12)$$

Another choice would be, to choose the f_i in such a way that they can be glued together to a continuous function $f(u, t)$.

With this form of $y(u, t)$ the integrals in Eq (9) can be trivially solved,

$$\ln \psi(t) = \sum_{i=1}^k \frac{\nu_i}{\alpha_i} \left(\ln \frac{B_i - A_i}{f_i(t_{i-1}, t)} - \alpha_i(t_i - t_{i-1}) \right). \quad (13)$$

The hazard becomes

$$\begin{aligned} h(t) &= -\frac{\partial}{\partial t} \ln \psi(t) \\ &= \sum_{i=1}^k \frac{\nu_i \frac{\partial}{\partial t} f_i(t_{i-1}, t)}{\alpha_i f_i(t_{i-1}, t)} + \nu_k. \end{aligned} \quad (14)$$

The last summand stems from $\alpha_k t_k$ due to $t_k = t$ in Eq. (13). So we also need $\frac{\partial}{\partial t} f_i(t_{i-1}, t)$ and for this we need $\frac{\partial}{\partial t} y(t_{i-1}, t)$. At first we find by taking the derivative of Eq. (8) using the initial condition $\frac{\partial}{\partial t} y(t_k, t) = 0$ the iteration formula

$$\frac{\partial}{\partial t} y(t_{i-1}, t) = \frac{(B_i - A_i)^2 e^{\alpha_i(A_i+B_i)(t_{i-1}-t_i)}}{(f_i(t_{i-1}, t))^2} \begin{cases} -\alpha_k(1 - A_k)(B_k - 1) & (i = k) \\ \frac{\partial}{\partial t} y(t_i, t) & (i < k) \end{cases}. \quad (15)$$

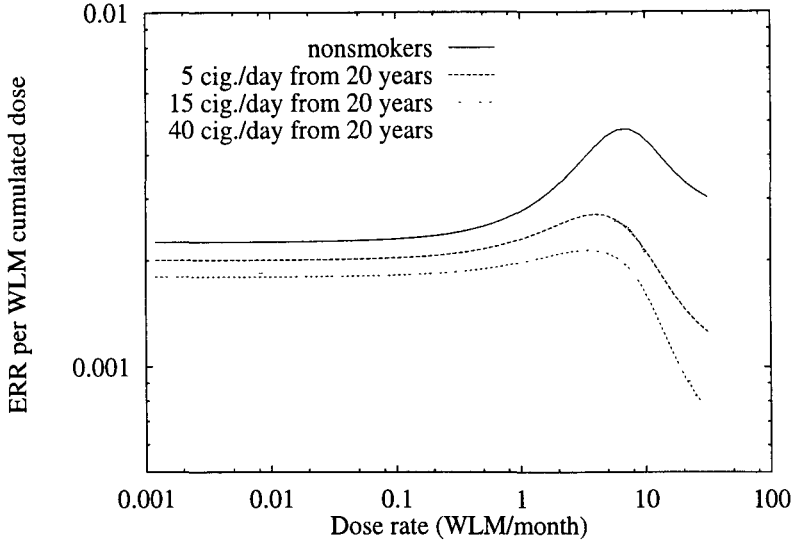


Figure 3: The excess relative risk of miners at age 60 years which smoke from age 20 years, and are exposed two radon from age 30 to 50 years in the model of Moolgavkar et.al.

Then we get

$$\frac{\partial}{\partial t} f_i(t_{i-1}, t) = \left(e^{\alpha_i B_i(t_{i-1}-t_i)} - e^{\alpha_i A_i(t_{i-1}-t_i)} \right) \begin{cases} \alpha_k A_k B_k & (i = k) \\ \frac{\partial}{\partial t} y(t_i, t) & (i < k) \end{cases} \quad (16)$$

All expressions given here are exact. Inserting iteratively gives exact, but clumsy expressions. If one is only interested in numbers for say the hazard, then it is more efficient to do the iterations numerically.

Using this formalism, we calculated the hazard predicted by the parameters of Moolgavkar et al. for various interesting exposure schemes. As an example we give the excess relative risk of miners at age 60 years as a function of dose rate exposed to radon from age 30 to 50 years, and to tobacco smoke from age 20, see Fig 3. The corresponding relative risk of smokers and nonsmokers is plotted in Fig 4. It can be seen that the model is able to describe quite complicated dependencies on the two noxes.

3.2 Smoking

The work of Moolgavkar et.al. discussed above uses in addition to the Colorado plateau miners the British Doctors study for smoking hazard only. In an earlier paper [8] these data were analysed using the 'epidemiological approximation' of the clonal expansion model. The great differences in the obtained parameters between these two analysis by (partly) the same people shows, that one problem of the technique is that very different parameter sets can give equally good fits to incidence data. If we not only want to get a hazard function which fits the data, but want to extract parameters which can be determined independently, then we have to investigate, what we can really learn about these parameters from the incidence data. By making use of the exact solutions Eq. (16) given above we found for the spontaneous hazard that only three quantities of the four biological parameters ν, α, β, μ can be determined [12], namely

$$X_m = \mu\nu, \quad \gamma = \alpha - \beta - \mu, \quad q = \frac{\mu}{1-A}, \quad (17)$$

with

$$A = \frac{b - \sqrt{b^2 - 4\alpha\beta}}{2\alpha}, \quad b = \alpha + \beta + \mu. \quad (18)$$

In Fig 5 the action of these parameters can be seen. γ determines the slope of the logarithm of hazard during the period of exponential growth, X_m shifts the hazard vertically, and X_m/q is the hazard in the limit of high age.

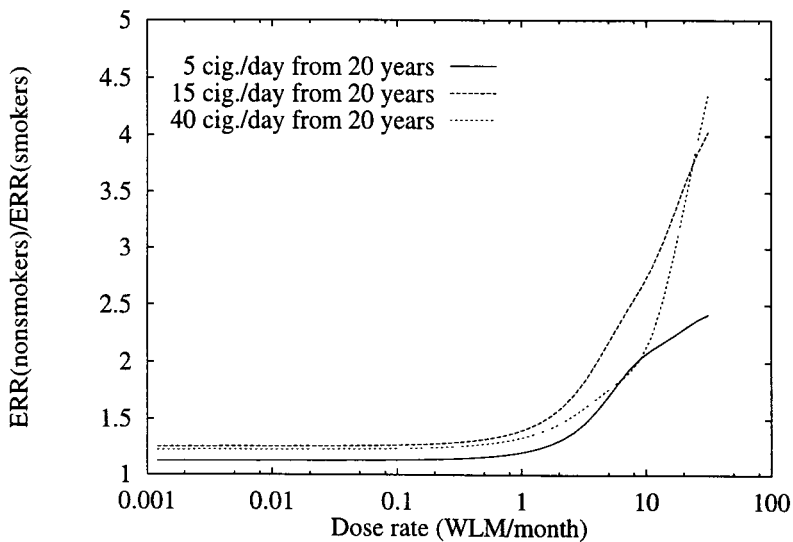


Figure 4: The relative risk of nonsmoking to smoking miners at age 60 years

μ	ν	α	β	$\alpha - \beta$	β/α
10^{-4}	0.03	0.130	0.000	0.130	0.000
10^{-5}	0.30	1.301	1.171	0.130	0.900
10^{-6}	3.00	13.01	12.88	0.130	0.990

(19)

Table 3: Some sets of values for the biological parameters, which all give the hazard function plotted in figure 5.

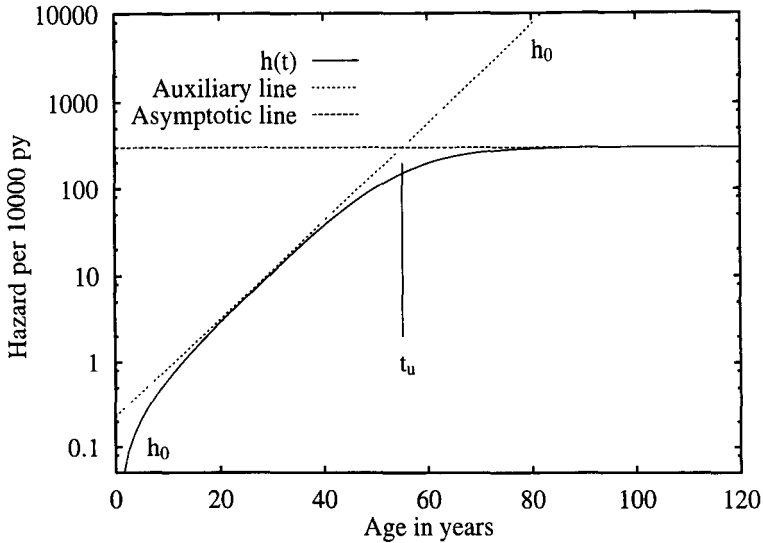


Figure 5: The role of the constant parameters in incidence curves ($X_m = 3 \cdot 10^{-6} [a^{-2}]$, $\gamma = 0.13 [a^{-1}]$, $q = 10^{-4} [a^{-1}]$). The auxiliary line has the equation $\exp(\ln(X_m/\gamma) + \gamma t)$, the asymptotic horizontal line is at hazard X_m/q .

The same hazard function can be obtained with very different biological parameters [11], as given in Table 3.

The four biological parameters can only be calculated, if one of them can be estimated from other sources of information. For example the number of susceptible cells might be estimated and the two mutation rates assumed to be equal.

For the more complicated situation of the stepwise constant parameters we do not yet have complete results of this kind. A partial result in this direction concerns the mutation rates affected by smoking. If any one of them, or both are enhanced, then the hazard of smokers is increased. If only the second one is enhanced, then the hazard of exsmokers should asymptotically go down again to the hazard of nonsmokers, while this is not the case if the first mutation rate is increased. According to Prof Doll (private communication) the hazard is going down. Contrary to this, Moolgavkar et.al. find that the second mutation rate is not affected by smoking. An inclusion of exsmokers in the analysis (for which data are not yet available in the British doctors study) might change this picture.

References

- [1] P. Armitage and R. Doll. The two-stage theory of carcinogenesis in relation to the age distribution of human cancers. *Brit. Journ. Cancer*, 11:161-169, 1957.
- [2] S. H. Moolgavkar and Jr. A. G. Knudson. Mutation and cancer: A model for human carcinogenesis. *Journal of the National Academy of Sciences (USA)*, 66:1037-1052, 1981.
- [3] S. H. Moolgavkar, A. Dewanji, and D. J. Venzon. A stochastic two-stage model for cancer risk assessment. I. the hazard function and the probability of tumor. *Risk Analysis*, 8:383-392, 1988.
- [4] S. H. Moolgavkar. Cancer models. In K. H. Chadwick, G. Moschini, and M. N. Varma. editors, *Biophysical Modelling of Radiation Effects*, pages 239-252. Adam Hilger, Bristol, 1992.
- [5] S. H. Moolgavkar, F. T. Cross, G. Luebeck, and G. E. Dagle. A two-mutation model for radon-induced lung tumors in rats. *Radiation Research*, 121:28-37, 1990.
- [6] H. P. Leenhouts and K. H. Chadwick. A two-mutation model of radiation carcinogenesis application to lung tumours in rodents and implications for risk evaluation. *J. Radiol. Prot.*, 14:115-130, 1994.

- [7] S. H. Moolgavkar, G. Luebeck, D. Krewski, and J. M. Zielinski. Radon, cigarette smoke, and lung cancer: A re-analysis of the colorado plateau uranium miner's data. *Epidemiology*, 4:204-217, 1993.
- [8] S. H. Moolgavkar, A. Dewanji, and G. Luebeck. Cigarette smoking and lung cancer: Reanalysis of the British doctor's data. *Journ. Nation. Cancer Institute*, 81:415-420, 1989.

Publications

- [9] J. Servc, L. Tomasek, E. Kunz, V. Placek, D. Chmelevsky, D. Barclay, and A.M. Kellerer. A survey of the czechoslovak follow-up of lung cancer mortality in uranium miners. *Health Physics*, 64:335-369, 1993.
- [10] A.M. Kellerer, D. Chmelevsky, M. Kreisheimer, and D. Barclay. A hybrid likelihood algorithm for risk modelling - 1. the formalism -. *Submitted*.
- [11] W. F. Heidenreich. On the parameters of the MVK model. *Submitted to Radiation and Environmental Biophysics*.
- [12] W. F. Heidenreich, P. Jacob, and H.G. Paretzke. Solutions of the clonal expansion model and their application to the tumor incidence of the atomic bomb survivors. *In preparation*.

Head of project 2: Dr. Tirmarche

II. Objectives for the reporting period

French uranium miners have been exposed to relatively low annual exposures of radon decay products, in comparison to most of the other cohorts of miners recently published. Their individual survey of radon exposure, of external gamma exposure and of uranium dust exposure has been registered on a monthly or weekly basis, since 1956. For the first 10 years, following the opening of the mines (1946-1955), a retrospective estimation of individual exposure in function of the working conditions and the enrichment of ore in each mining site has been realized by a committee of experts, including previous miners.

Their low annual exposure rate and in time registration of the three components of their radioactive exposure gave us the opportunity to conduct a cohort study in order to evaluate the risk of cancer mortality linked to this low chronic exposure. Our first aim was an estimation of the lung cancer mortality linked to cumulative radon exposure. It has been achieved by the publication of this study in 1993 in the British Journal of Cancer. The different causes of mortality have been described in comparison to the national reference population and a linear dose-response relationship has been described for lung cancer mortality in relation to cumulative radon exposure. The slope, or excess relative risk per unit of exposure is 0.35% per WLM (WLM, Working Level Month, is an international unit of radon decay exposure : 1 WLM corresponds to 170 working hours in an atmosphere with a concentration of 1 WL of radon decay products ; 1 WL = 100 picoCuries per liter).

These results have to be discussed in front of those of other cohorts, having experienced higher cumulative radon exposures, by taking in account the different methodologies used for the description of this dose-response relationship.

III. Progress achieved including publications

A : French uranium miners cohort study

Reconstruction on computerized files of the individual yearly exposure to radon, gamma and uranium ore dust with an historic approach since 1946 has been undertaken in our institute ; the main efforts during the first years have focused on storage and reconstruction of the dosimetry of the first ten years following the opening of the mines (1946-1955). Since 1956, individual registration of exposure is existing on paper documents, and since 1967, the same annual information exists on computerized files stored on magnetic tapes.

As epidemiologists, we were preferentially interested in those miners having attained age groups, able to express lung cancer mortality and we selected for a first analysis those miners having experienced relatively high radon exposure. The two criteria of inclusion for this first cohort study were : -more than two years of underground mining,
-first radon exposure before 1972.

The endpoint of the present survey of this cohort being end of december 1985, these miners have experienced at least 13 years of follow-up, the maximum, 40 years being for those having entered in 1946. The statistical power calculated for the 1785 miners of this first cohort was high (99%), the assumption being a doubling of the risk of lung cancer mortality in comparison to the national reference population.

Descriptive analysis :

Description of the retrospective approach used for validation of the individual radon exposure has been described in detail in the BJC publication (in annexe, reference : (1993), 67, 1090-1097). The description of the different causes of death by cancer demonstrated an excess of lung and of larynx cancer in comparison to the national reference population. The methodology used was an indirect standardization. The results linked to brain cancer mortality are discussed in function of the reference data used from the national statistics. Causes of death other than cancer are also described ; they confirm the excess of violent deaths observed in all the cohorts of miners ; they give also an indirect indication of the habits of live, mainly when focusing on the causes of death linked to tobacco or alcohol consumption. It has to be noticed that the SMR (standardized mortality ratio) of the causes of death other than cancer is close to one : $SMR = 0.98$, that the SMRs for deaths of the circulatory system or the digestive system (including alcoholism and cirrhosis) are both less than 1, indicating that this population has probably a tobacco and alcohol consumption less different from the national population than expected.

Dose-response relationship :

The second part of this study is testing the potential positive trend that may exist between a precise cause of death and the occupational exposure, in our opinion the only approach able to demonstrate that a specific component of this occupational environment is involved in a carcinogenic process. The hypothesis tested is the influence of cumulative radon decay products on lung cancer and on larynx cancer mortality. The different groups of cumulative exposure used are : < 10 WLM, 10-50 WLM, 50-150 WLM, 150-300 WLM, > 300 WLM. A miner may contribute person-years to several exposure groups, depending how he cumulated the radon exposure during his working period. It has to be mentioned that the French uranium miners of this cohort have a mean duration of underground working of 14.5 years. The calculation of this dose-response relationship has taken in account a lag time of 5 years.

We demonstrate a significant positive trend for lung cancer mortality ($p=0.03$, one tailed test), but no trend for larynx cancer mortality. A Poisson regression modelling was applied to the same data, computed by GLIM software, using a generalized linear model with Poisson errors and an identity link function ; the linear model has been used in most of the analyses of cohorts of uranium miners. It is based on the following assumptions : the effect linked to radon exposure is proportional to "natural" background mortality of the considered population (constant relative risk model), and the relative risk increases linearly with dose.

Applied to SMR of lung cancer as a function of the cumulated radon exposure, the following relationship is obtained : $SMR = 1.68 + 0.0058 D$, D being expressed in WLM, the standard error of this excess coefficient being 0.004. An approximation of the excess relative risk can be obtained by the ratio : slope/intercept ; here 0,35%. An analysis of deviance, applied to the same data demonstrated no influence on this dose-response relationship, when taking in account the period of exposure (before or since 1956).

In conclusion, we consider that this first cohort confirms the risk of lung cancer mortality linked to radon exposure ; larynx cancer mortality, in excess in this cohort, is not increasing with increasing exposure to radon decay products. In comparison to most of the other cohort studies of uranium miners, the estimated excess risk per unit of exposure, based on Poisson regression modelling, is relatively low, but within the range of the estimations of international committees : ICRP 50 (1987), Beir IV report, (1988).

B : International collaboration

Since 1993, the data of our cohort have been participating in two international joint analyses, the first has been initiated by the NCI (National Institute of Cancer) in Bethesda (USA), the second by the University of Oxford (England). The first collaboration was collecting data of eleven cohorts of miners with individual radon exposure, in order to precise different factors, able to influence the dose-response relationship of lung cancer mortality, the second is studying the risk of mortality from cancers other than lung cancer in relation to radon exposure.

The methodologies used were different : in the first study, individual data per miner and per year were sent in the same format by all of the "contributors" and the same modelling of the dose-response relationship was applied, using the AMFIT software and an internal analysis approach. In the second approach, each participant sent the data in form of tables with the expected and observed numbers of deaths by cancers of the different types and the results were expressed by SMR. In this last study, the number of cancer sites being high, some of the excesses observed may be due by chance ; there was no evidence of an increasing risk of a specific cancer in relation to increasing cumulated radon exposure. Consequently this study does not support the hypothesis that rose from some geographic correlation studies, of an increase of cancers other than lung cancer related to domestic radon

exposure. The detailed results of this collaborative analysis have been published in the Journal of the National Cancer Institute, Vol 87, 5, march 1, 1995, 378-384.

The joint analysis, directed by NCI, has been presented during an NIH monography (NIH publication N°94-3644), presenting in detail the estimation of the excess relative risk per WLM and the form of the dose-response relationship of each of the individual studies and of the combined data.

It has to be mentioned that this large number of lung cancer deaths (n : 2736, 2620 in exposed and 116 in non-exposed miners, observed on a total of 67846 miners, followed on average for 17.2 years) makes it possible to introduce in this study the analysis of futher factors, that may influence the linear dose-response relationship : variation of the excess relative risk coefficient with attained age, with duration of exposure, rate of exposure, age at first exposure, time since an exposure occurs and time since exposure stopped. Joint effects of smoking and radon exposure could be tested on a subgroup of 6 cohorts having smoking data available, but for some of them, this information was quite sparse, limited to : smoker: yes, no. In several cohorts, concomittant exposure to other carcinogenic substances, present in the mines, or prior to entry in the uranium mines could also be taken in account.

The risk regression model used for modelling the radon decay exposure was based on relative risk models. It is assumed that the lung cancer mortality rate r is depending on the cumulated exposure (in WLM) w , a vector of covariates x , describing the background disease rate ; a vector of covariates z , may influence the exposure-response relationship. In this analysis, components of x are variables for age group and cohort and for other mine exposure. As in the BEIR IV report, the cumulated WLM exposure was divided into time since exposure windows ; for each year of age, the cumulated exposure (minus the 5 year lag time) is expressed as follows :

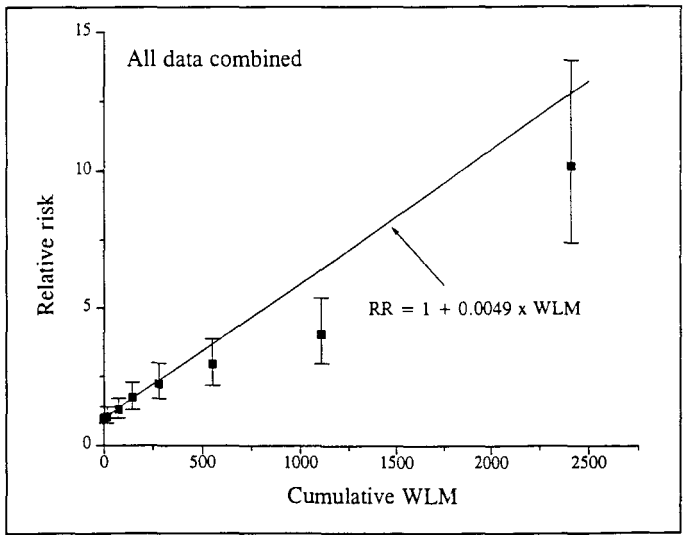
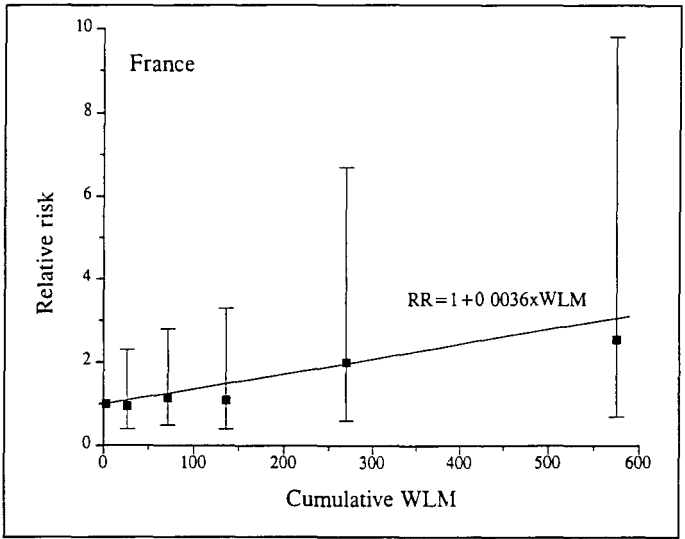
$$W = W_{5-14} + W_{15-24} + W_{25-34} + W_{35}$$

where w_{5-14} is the cumulated exposure received 5 to 14 years prior to the specific age, etc..

The two following figures indicate the results of the French cohort and of the combined analysis. The observed slope is 0.36 % per WLM for the French cohort, close to the combined analysis giving a slope of 0.49 %. This result is also close to what has been concluded from our previous analysis, based on external, national reference rates.

The excess relative risk is not influenced by age at first exposure, but is decreasing with attained age, with time since exposure and with time after cessation of exposure.

Over a large range of cumulative exposure, higher lung cancer risks were observed with lower rates of exposure. The French study, in spite of low chronic exposure protracted over long periods of exposure, was the only study, unable to demonstrate this inverse dose-rate effect. The number of lung cancer deaths in this cohort may be too low for a clear answer linked to the dose-rate effect, but



if the inverse dose-rate effect is true, even at very low annual exposure, we should have expected the French data to demonstrate a high excess relative risk per unit of exposure.

The influence of the dose-rate effect is crucial for extrapolation to low dose effects, as well in occupational situations or for domestic exposures.

Consequently, for the next years, our efforts will be in constructing a large cohort of about 6000 miners, regrouping all those that have worked in uranium mining environment ; this cohort will be typical for low annual exposures to radon decay products and will be more powerful than the first study for the evaluation of a risk of lung cancer linked to low exposures.

C : Risk of cancer linked to external gamma exposure in mines

An approach for the evaluation of the part of risk of lung cancer, that may be linked to external irradiation in the mines has also been undertaken. As individual gamma exposure was registered for each miner since 1955, we decided to limit the cohort to those miners having entered the mines between 1956 and 1972 ; a total of 992 miners were included. A descriptive analysis has been achieved, presenting the correlation of these two components on an annual or cumulative basis and testing the influence of gamma exposure, in presence of radon exposure, on the mortality of lung cancer. The results indicate that each type of exposure, considered on an annual basis, shows a weak correlation ($r = 0.37$), in comparison to the matrix of correlation tested for cumulative individual exposure : $r = 0.88$.

Using a Poisson regression approach, the estimated slope : excess risk per unit of radon exposure is at 0.9% per WLM ; this slope doesn't increase significantly with increasing groups of cumulated gamma exposure, but the power of this study was too low to expect identification of a potential effect of the external radiation. This study was realized during preparation of a Ph. D. in epidemiology by a medical student. It will be submitted for publication in Health Physics. This approach of the evaluation of a cancer risk, linked to gamma exposure will be continued on the French cohort, not only for testing a modifying factor on the dose-response relationship between radon and lung cancer, but also in order to identify a potential effect of leukemia risk, some of these miners reaching gamma exposures in the same range than nuclear workers. In this study the mean cumulative exposure is 112 mGy, with a maximum at 470 mGy and a median at 77 mGy.

Recent publications :

Tirmarche M., Raphalen A., Allin F., Chameaud F., Bredon P.

Mortality of a cohort of french uranium miners exposed to relatively low radon concentrations

British Journal of Cancer ,1993, 67, 1090-1097

Tirmarche M., Rannou A., Mollie A., Sauvé A.

Epidemiological study of regional cancer mortality in France and natural radiation
Radiation Protection Dosimetry, 1988, 24, 1, 479-482

Tirmarche M.

Indoor exposure to radon

Prevention of Respiratory Diseases, Ed. Marcel Decker, Inc, New York, 1993, 195-207

Tirmarche M.

Exposition au radon et risque de cancer

Radioprotection, 1994, 29, 101-114

Poffijn A, Tirmarche M., Kreienbrock L., Kayser P., Darby S.

Radon and lung cancer : procedures of the multicentre studies in the Ardennes-Eiffel region, Brittany
and the Massif Central region

Radiation Protection Dosimetry, 1992, 45, 1, 651-656

Lubin JH., Boice JD., Edling C., Homung RW., Howe J., Kunz E., Kusiak RA., Morrison HI.,
Radford ED., Samet JM., Tirmarche M., Woodward A., Xiang YS., Pierce D.

Radon and lung cancer risk : a joint analysis of 11 underground miner studies

National Institute of Health, NIH Publication n°94-3644, 1994

Darby S., Whitley E., Howe G., Hutchings S., Kusiak RA., Lubin JH., Morriso HI., Tirmarche M.,
Tomasek L., Radford ED., Roscoe RJ., Samet JH., Xiang YS.

Radon and lung cancer in underground miners. A collaborative analysis of 11 studies

Journal of the National Cancer Institute, 1995, 87, 5, March 1, 378-384

Report for the Period 1992-1995

Project 3

Participating Organisation: National Radiological Protection Board (UK)

Heads of Project: Dr. C.R. Muirhead
Dr. M.P. Little

Objectives for the Reporting Period

To conduct analyses of the effects of radon exposure and smoking on the risk of lung cancer mortality among Colorado Plateau uranium miners, using both empirical and mechanistic models.

Progress achieved during the Reporting Period.

Work was performed to examine a number of issues associated with the evaluation of lung cancer risk among miners exposed occupationally to radon. These issues include:

- (i) the temporal pattern of risk, which affects estimates of the lifetime risk;
- (ii) the joint effect of radon and smoking, which affects estimates of risk among smokers and non-smokers separately;
- (iii) the possibility of exposure rate effect, which may affect extrapolations of risk from a mining to an indoor environment.

Examination was also made of some methodological issues associated with the analysis of miner data, related to the fact that exposures are received over a prolonged period of time rather than instantaneously.

The above topics were studied using data on just under 3,350 uranium miners who worked on the Colorado Plateau in the USA. These data, which were reported upon by Hornung and Meinhardt (Health Phys., 52, 417-30 (1987)), were obtained from the US National Institute for Occupational Safety and Health. Up until the end of 1982, 258 of these miners had died of lung cancer. An advantage of these data over those for some other groups of radon-exposed miners is that information on smoking habits is available.

After some consideration, it was decided to analyse these data using a nested case-control approach. For each lung cancer case, up to 15 controls were randomly selected according to the following criteria:

- * control was alive in the year of the case's death
- * control was born within one/two years of the case

The actual selection procedure was as follows. Initially attempts were made to match the birth year of the controls to within one year of the cases. If there were 15 or more controls available to match with the case, then 15 were randomly selected. If there were fewer than 15, the criteria

were loosened and possible controls were identified amongst those born within two years of the case. Fifteen controls were then randomly selected from them. If there were still fewer than 15 available, the reduced number of controls was used rather than loosening the criteria further. Two cases had only 9 and 10 controls for matching.

This case-control approach has the following advantages:

- (i) It allows data on chronic exposures to be handled in a fairly simple fashion, in contrast to Poisson regression which requires a complex partition of the person-years at risk.
- (ii) By utilising data for a subset of miners rather than for all those at risk at the time of each lung cancer death (as in the case of Cox regression), it ensures a large reduction in computational requirements at the expense of a minimal loss of statistical power.

Empirical Modelling

The empirical based modelling paralleled that performed by Thomas *et al* (Health Phys., 66, 257-62 (1994)) in studying dose and dose rate effects for radon and smoking. In particular, the radon-induced excess relative risk (ERR) at attained age A was modelled as:

$$ERR = \beta X^d \quad (1) \quad \text{where} \quad X = \int_0^{A-5} [r(t)]^g dt \quad (2)$$

and where β is the scaling parameter for the excess relative risk, d is the power of total "dose" X in the ERR, g is the power of radon exposure rate $r(t)$ at age t , and a five-year latency period is assumed. If the parameter g in equation (2) is set to 1, then X represents the cumulative exposure. In this instance, varying the value of d in equation (1) allows examination of whether the data are consistent with a linear function of cumulative exposure ($d=1$) or with the slope of the exposure-risk relationship either increasing ($d>1$) or decreasing ($d<1$) with increasing cumulative exposure. Alternatively, by setting d to 1, varying g allows examination of whether, for a given cumulative exposure, the risk is higher ($g<1$) or lower ($g>1$) with decreasing exposure rate. A third class of models, such that g is set equal to $1/d$, was also considered. In this case, the relative risk increases in proportion to cumulative exposure for a given pattern of exposure, but can vary according to whether the exposures are received over a short or a long period. Analogous models were fitted to describe the effects of smoking. The models were fitted using the PECAN program within EPICURE (Preston *et al*, Hirosoft, Seattle, 1993).

For radon, fitting the above model with g set to 1 to the data for all the Colorado Plateau miners yielded a maximum likelihood estimate of d close to 0.8 and provided some evidence of a decreasing exposure-risk relationship at high cumulative exposures. However, since it is thought that some of the highest exposures are over-estimates, the BEIR IV Committee in its analysis of these data restricted attention to those miners with cumulative exposures less than 2000 WLM. For g set to 1, the data are consistent with $d=1$, corresponding to a linear trend in risk with cumulative exposure. However, allowing g to vary with d set to either 1 or $1/g$ yields an estimate of g which is close to 0.7 and which is statistically significantly different from 1. This suggests that, for a given cumulative exposure, the risk is higher if received at a lower exposure rate. The original analysis of these data by Hornung and Meinhardt (1987) had also suggested that such an effect may be present.

For smoking, the data showed little variation with smoking rate in the risk for a given cumulative consumption. However, there was evidence of a decrease in trend in risk with cumulative consumption at high cumulative values (d was estimated as 0.7).

Mechanistic Modelling

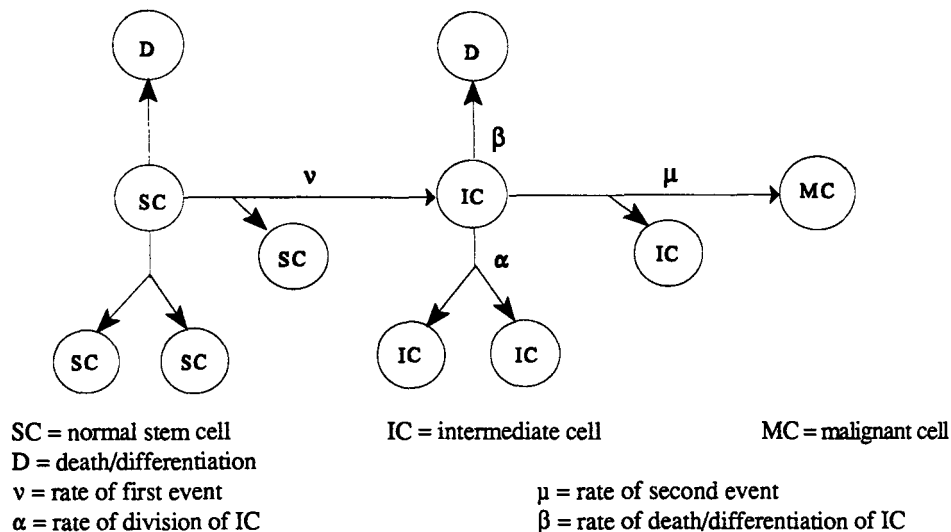
Background

The same nested case-control data were used in order to fit the two-stage model of carcinogenesis first introduced by Moolgavkar and colleagues (Moolgavkar and Venzon, *Math. Biosciences*, **47**, 55-77 (1979); Moolgavkar and Knudson, *J. Natl. Canc. Inst.*, **66**, 1037-1052, (1981)). The carcinogenic process is postulated to be the result of two events, the change of a normal cell to an intermediate cell and the subsequent change of the intermediate cell to a malignant cell. These two events are broadly viewed as mutations occurring at some baseline rate which can be altered by exposure to radon and smoking. The two-stage model also incorporates a component that takes into account the birth/death process of the intermediate cells and this component, usually referred to as the intermediate cell kinetics, can also be affected by exposure to radon and smoking. Figure 1 provides a pictorial description of the two-stage model.

A detailed exposure history of both radon and smoking was constructed for the lung cancer cases and controls. This was done by taking exposure rates for radon and for smoking to vary over time as step functions, with cutpoints based on dates at which either a given cumulative exposure (in the case of radon) or a given exposure rate (in the case of smoking) was reached. The approximate solution of the two-stage model for carcinogenesis was then adapted to incorporate these detailed exposure histories into the model and a hazard function derived for lung cancer mortality. The number of normal cells was considered to be constant over time and, as with the empirical modelling described earlier, a five year latency period was assumed.

A FORTRAN program was written to calculate the hazard functions for cases and controls and to maximise the associated conditional likelihood.

Figure 1 Two-stage model for carcinogenesis



The covariates relating to the radon and smoking rates were introduced into the model via v , μ , and $(\alpha-\beta)$, (see Figure 1). v_i and $(\alpha-\beta)_i$ are functions of the radon and smoking rates $d_{r,i}$ and $d_{s,i}$ respectively which are taken to be constant throughout the i^{th} interval of an exposure history. However, μ is a function of the last relevant exposure rates prior to the case's death, these rates

being denoted by d_r and d_s without the subscript i .

A basic form of the model including both radon and smoking was considered and is given below:

$$\begin{aligned} v_i &= 1 + a_r d_n + a_s d_s \\ \mu &= 1 + b_r d_r + b_s d_s \\ (\alpha-\beta)_i &= c_0 + c_{r1} d_n + c_{s1} d_s \end{aligned}$$

This model and all subsequent models have not included baseline parameters, a_0 and b_0 , for the first and second mutation rates because the form of the **relative hazard** is such that a_0 and b_0 will cancel out. The parameters $a_r, a_s, b_r,$ and b_s then represent ratios of the change in a mutation rate, per unit change in exposure rate, relative to that at a zero exposure rate. By not having to consider a_0 and b_0 , the number of parameters that need to be estimated from the data will also be reduced.

The need for quadratic or interaction terms was also assessed. There was a significant quadratic term only for the effect of radon on the cell kinetics (i.e. $\alpha-\beta$). The cell kinetics component of the model also contained the only interaction term which achieved statistical significance.

The most parsimonious model

It was found that the most parsimonious model (i.e. fitting the data with the fewest parameters) was that given below:

$$\begin{aligned} v_i &= 1 + a_r d_n + a_s d_s \\ \mu &= 1 \\ (\alpha-\beta)_i &= c_0 + c_{r1} d_n + c_{r2} d_n^2 + c_{s1} d_s + c_{rs} d_n d_s \end{aligned}$$

Table 1 shows the significance of each of the terms in the best fitting model adjusted for all the other terms. This then provides the results from which inferences can be made concerning the effects of radon and smoking on each of the components of the two-stage model.

Table 1 Testing the parameters in the best fitting model

Test	Change in -2lnL	Change in d.f.	Significance
$a_r=0$	41.23	1	$p << 0.001$
$a_s=0$	16.00	1	$p < 0.001$
$c_{rs}=0$	9.01	1	$p = 0.003$
$c_{r2}=0$	4.93	1	$p = 0.03$
$c_{r1}=0$ †	1.31	1	$p = 0.25$
$c_{s1}=0$ ††	4.70	1	$p = 0.03$

† This is based on comparing a model including a_r, a_s, c_0, c_{r1} and c_{s1} with the same model but without c_{r1}

†† This is based on comparing a model including $a_r, a_s, c_0, c_{r1}, c_{r2}$ and c_{rs} with the same model but without c_{s1} .

Table 2 gives the parameter estimates based on the best fitting model.

Table 2 Parameter estimates for the best fitting model

Parameter	a_1	a_2	c_0	c_{x1}	c_{x2}	c_{s1}	c_{sx}
Estimate	1.28E+8	5.37E+6	-2.46E-4	2.15E-5	-1.02E-4	-2.44E-5	5.23E-4

The smoking and radon effects on the first mutation rate (ν) are both highly significant. Neither radon nor smoking was found to have a significant effect on the second mutation rate (μ). The cell kinetics component of the model (α - β) is affected by both radon and smoking; the linear effect of smoking was significant and there was no evidence of a quadratic effect, whereas the reverse was true for radon. A very significant interaction was found between radon and smoking, but only for the cell kinetics with no evidence of an interaction at the first stage.

Predictions from the best fitting model

The parameter estimates from the best fitting model, given in Table 2, can be used to predict the relative hazards for two miners of the same age but with different exposure histories.

There was no miner in the dataset who neither smoked nor received zero occupational radon exposure. Making comparisons relative to a zero radon exposed non-smoker would, therefore, result in unstable estimates of the relative hazard. Instead, an average radon rate (0.4 WLM/day) and average smoking rate (0.9 packs/day) was used as the baseline for calculating relative hazards. These values were the medians of the average exposure rates found for the controls in the case-control dataset.

Table 3 shows the estimated relative hazard at age 60 resulting from different scenarios of either increasing only the radon or smoking rate, relative to that of a miner with average exposure, or increasing both radon and smoking. Table 3 shows that as the radon rate is increased the relative hazard increases in a linear quadratic fashion. The same effect is also seen when the smoking rate is increased, although here the departure from linearity is not as great. Increasing both the radon and smoking simultaneously has more than a multiplicative effect on the relative hazard.

Table 3 Relative hazard at age 60 for different scenarios of single and joint increased exposure to radon and smoking.

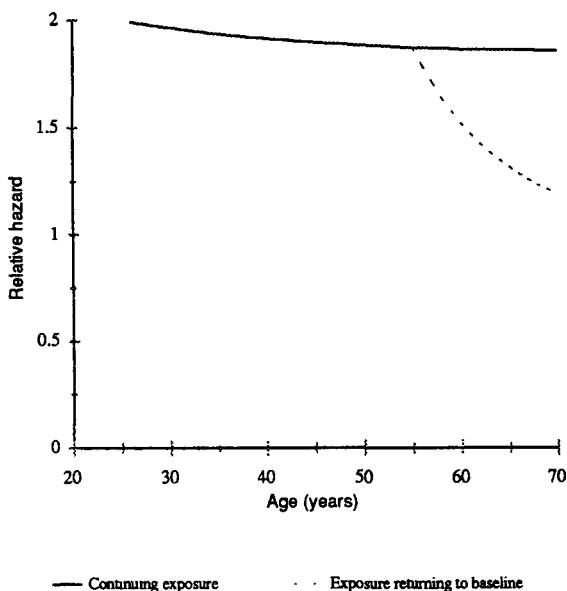
Exposure to smoking is between 15 and 55 years of age and exposure to radon is between 30 and 40 years of age. Note that the exposure to radon is totally contained within the smoking exposure period.

		smoking rate (packs/day)		
		0.9	1.35	1.8
radon rate (WLM/day)	0.4	1.0	1.2	1.5
	0.8	2.1	3.0	4.4
	1.6	5.6	12.5	32.1

Figure 2 shows the relative hazard with age for both a doubling of the radon rate and a doubling of the smoking rate. Assuming that the effect of radon or smoking does not depend on age, a constant relative hazard would be expected with increasing age. Based on a continuing exposure to radon, there is only a slight decrease in the relative hazard as the age of a miner increases. However, the relative hazard decreases substantially a few years after the radon exposure returns to the baseline.

Figure 2 Relative hazard of radon rate with age. The effect of returning to the baseline rate.

Relative hazard for a miner exposed to 0.8 WLM/day and smoking 0.9 packs/day relative to a miner exposed to 0.4 WLM/day smoking 0.9 packs/day. Miners exposed to both smoking and radon from age 20 to 65. The dotted line indicates the effect of returning to 0.4 WLM/day at age 50.



The relative hazard of smoking rate with age and the effect of returning smoking to the baseline rate showed a very similar pattern to that given in Figure 2.

Figure 3 demonstrates the effect of including a term relating to an interaction between radon and smoking for the cell kinetics component of the two-stage model. The figure shows the relative hazard, at age 70, of a given radon rate in two groups, non-smokers and average smokers. Note that both persons being compared are either non-smokers or average smokers. The relative hazard is then calculated for a miner with a radon rate between 0.4 and 0.8 WLM/day relative to a miner with a baseline radon rate of 0.4 WLM/day. For non-smokers the relative hazard increases in a linear fashion as the radon rate increases but for average smokers, the relative hazard rapidly increases with increasing radon rate in a non-linear fashion. If no interaction term is included in the model, the form of the relative hazard for an average smoker is almost identical to that of a non-smoker.

Figure 3 Relative hazard of radon rate in smokers and non-smokers. Model with interaction term.

Relative hazard for a miner exposed to a radon rate of between 0.4 and 0.8 WLM/day and not smoking/smoking, both exposures starting from 20 years old. Baseline radon rate is 0.4 WLM/day.

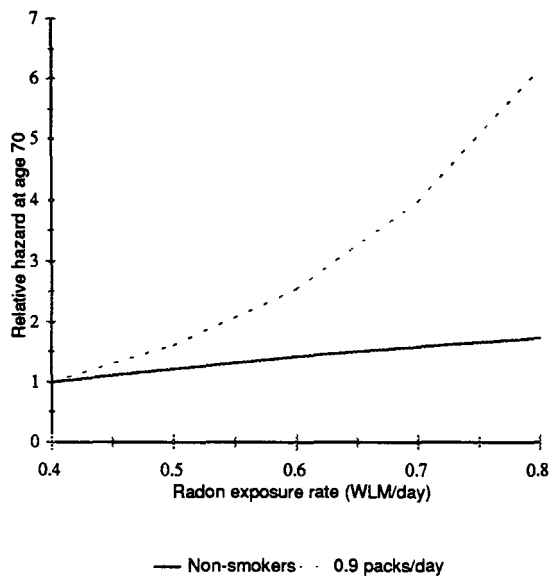
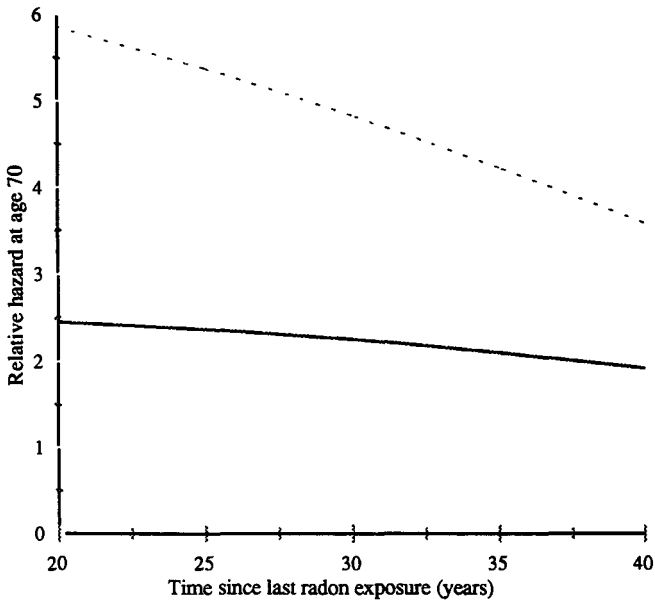


Figure 4 shows the relative hazard, at age 70, for a miner exposed to twice the average radon rate and investigates the effect of time since the last radon exposure. The solid line shows that, for a fixed smoking history, the relative hazard is slightly higher if the radon exposure was more recent. The dotted line demonstrates the compounding effect of the miner also smoking at twice the average rate as well as being exposed to twice the average radon rate. If the miner was last exposed to radon 40 years ago and still hasn't died from lung cancer, then he is much less likely to die at age 70 than a miner whose last exposure was only 20 years ago.

Figure 4 Time since last radon exposure.

Relative hazard at age 70 for a miner exposed to 0.8 WLM/day for 10 years relative to a miner exposed at the baseline rate of 0.4 WLM/day also for 10 years. Smoking took place between the ages of 20 and 50. The solid line relates to both miners smoking at the average rate of 0.9 packs/day whereas the dotted line gives the relative hazard for a miner smoking 1.8 packs/day relative to a miner on 0.9 packs/day.

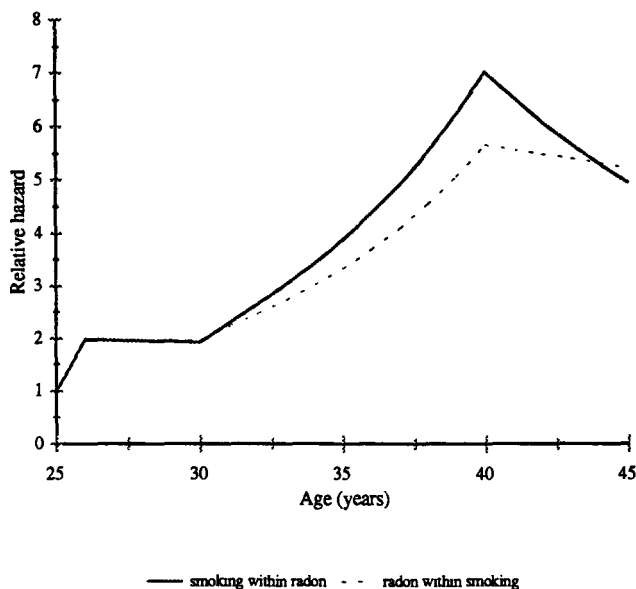


The importance of the order in which the two exposures are received was found to depend on whether or not the exposures overlap. When the exposures do not overlap there is very little difference between the relative hazard when a radon exposure follows a smoking exposure and the relative hazard when the same smoking exposure follows the radon exposure. Figure 5 demonstrates the effect of the order in which the radon and smoking exposures take place when one exposure is contained within the other. The relative hazard at age 70 for the two scenarios gives a value of 5.0 for a miner starting and stopping smoking whilst being exposed to radon, whereas starting and stopping exposure to radon whilst being a smoker gives a slightly higher relative hazard of 5.2. However, Figure 5 shows a higher relative hazard for the scenario in which smoking is contained within the radon exposure during the period between age 30 and 40 which is when both exposures are having an effect, allowing for the five year latency period.

After age 40, five years after one of the exposures ceases, the relative hazard decreases much more rapidly when the smoking ceases and radon exposure continues than when radon ceases and smoking continues. This would suggest that the interaction between radon and smoking is driven more by the smoking than by the radon exposure. This is largely due to the fact that smoking was found to have more of an effect on the cell kinetics of the intermediate cells than radon.

Figure 5 The effect of ordering the radon and smoking exposures. One exposure contained in the other.

Relative hazard, for a given age, in a miner exposed to twice the average radon rate of 0.4 WLM/day and smoking twice the average smoking rate of 0.9 packs/day. The two lines represent two different scenarios. The solid line postulates the miners are exposed to radon between age 20 and 40 and smoke from 25 to 35, whereas the dotted line is the reverse, with smoking from 20 to 40 and exposure to radon from 25 to 35.



The best-fitting model also predicts that a miner has a greater hazard of lung cancer death if the exposure is protracted over a long time and therefore at a lower rate, than a miner with the same total exposure but exposed for a shorter period of time at a greater rate. Therefore, long low radon rates are relatively more hazardous than short high rates. Such an exposure rate effect is in agreement with the findings based on empirical models.

Conclusions

The evidence from this research into mechanistic models is that radon plays a greater role in initiation of the carcinogenic process in the lung than does smoking, whereas there is evidence that smoking has a greater role in promotion than radon. Evidence was also found for an interaction between radon and smoking, but acting only on the cell kinetics of the intermediate cells. Under the best-fitting mechanistic model, smoking not only increases the level of the radon-induced risk, but also modifies the effect of factors such as time since last radon exposure. Further work to examine the implications of models such as this is planned.

Head of project 4: Dr. Darby

Risk Estimates of lung cancer from the follow-up of uranium miners.

Laboratory: Imperial Cancer Research Fund Cancer Epidemiology Unit

This project, was carried out in conjunction with Dr Emil Kunz and Dr Ladislav Tomášek, of the Institute of Public Health, Prague.

Introduction

The outcome of the project has been summarised in six publications in the open literature. The scheme of this report is that, following an overall description of the project, each one of the publications is summarised in detail.

Overall Description of the Project

The project was set up to carry out further work on the major cohort of uranium miners in West Bohemia, started by the late Josef Sevc. Publication 1 describes the extension of the follow-up of the cohort by five years, and the use and importance of multiple methods of follow-up in establishing correctly the vital status of all cohort members at the end of the follow-up period. It also presents a broad analysis of mortality from all causes and from specific causes. Publication 2 concentrates on lung cancer and presents a detailed quantitative analysis of patterns of radon-

related lung cancer risk in this population. Also described is the revision of the estimates of exposure that was carried out in conjunction with Dr Tomášek. There have been a number of recent publications from different groups on the suited of West Bohemian miners, leading to somewhat different estimates of lung cancer risks. These are reviewed in publication 3, and the differences between them discussed and explained.

A detailed analysis of mortality from cancers other than lung cancer is presented in publication 4. This revealed an association between radon exposures and cancers of the gallbladder and multiple myeloma. In order to ascertain whether the association was generally present in radon exposed miners, data from other cohorts was sought, firstly in Swedish iron miners, described in publication 5, and then in a collaborative analysis of data from 11 studies. This analysis, which is described in publication 6 and includes all the major cohorts of underground miners exposed to radon gas established that men who are exposed to high concentrations of radon gas at work do not experience a material risk of mortality from cancers other than lung cancer. It was therefore concluded that protection standards for radon should continue to be based on consideration of the lung cancer risk alone.

Publication 1

Mortality in uranium miners in West Bohemia: a long term cohort study. L Tomášek, AJ Swerdlow, SC Darby, V Pláček, E Kunz. Occupational and Environmental Medicine, **51**, 308-315 (1994).

A cohort of 4320 uranium miners in West Bohemia who started work at the mines during 1948 to 1959 and worked there for at least four years were followed up to the end of 1990 to determine cause specific mortality risks in relation to exposures in the mines. The miners had experienced high radon exposures, on average 219 working level months during their uranium mining careers, for which detailed measurements were available. They had also been exposed to high arsenic levels in one of the two major mines, and to dust. New follow up methods, not previously used for occupational cohorts in Czechoslovakia, were utilised. By the end of follow up 2415 (56%) of the cohort were known to have died. Overall mortality was significantly raised compared with that in the general population (relative risk (RR) = 1.56, 95% confidence interval (95% CI) 1.50-1.63), with significantly raised risks of lung cancer (RR = 5.08, 95% CI 4.71-5.47), accidents (RR = 1.59, 95% CI 1.34-1.87), homicide (RR = 5.57, 95% CI 2.66-10.21), mental disorders (RR = 5.18, 95% CI 2.83-8.70), cirrhosis (RR = 1.51, 95% CI 1.16-1.94), and non-rheumatic circulatory diseases (RR = 1.16, 95% CI 1.08-1.25). The relative risk of lung cancer was greatest four to 14 years after entry to the mines. Relative risks for homicide and accidents were raised up to 25 years from entry but not after this. Substantial significantly raised risks at 15 to 24 years after entry occurred for cirrhosis, non-rheumatic circulatory diseases, and pneumonia and other respiratory infections. Sizeable significantly raised risks at 25 and more years after entry, but not earlier, were present for mental disorders, tuberculosis, and non-malignant non-infectious respiratory conditions. No specific causes showed risks significantly related to age at entry to mining. Risk of lung cancer was significantly positively related to radon exposure, estimated arsenic exposure, and duration of work in the mines, but no other cause was significantly

positively related to these variables. The raised risk of lung cancer in uranium miners, which is well established, is related aetiologically to radon exposure, and in the present cohort it may also in part have been due to exposure to arsenic. The raised risks of accidents, tuberculosis, and non-infectious respiratory diseases have also been seen in other uranium mining cohorts, and are likely to reflect the dangerous and dusty working conditions and the confined spaces in which work occurred. The cirrhosis and homicide deaths probably relate to the lifestyle associated with mining. The raised risk of circulatory diseases does not seem to be related to radon or arsenic exposure; its causes are unclear. The use of multiple follow up methods was found to be critical to correct ascertainment of mortality in the cohort.

Publication 2

Patterns of lung cancer mortality among uranium miners in West Bohemia with varying rates of exposure to radon and its progeny. L Tomášek, SC Darby, T Fearn, AJ Swerdlow, V Pláček, E Kunz. *Radiation Research*, **137**, 251-261 (1994).

Lung cancer mortality in a cohort of 4320 miners first employed during 1948-1959 at the Jáchymov and Horní Slavkov uranium mines in West Bohemia and followed until 1 January 1991 has been studied to gain a greater understanding of the consequences of exposure to radon and its progeny. Among men whose exposure rates never exceeded 10 working levels, excess relative risks per unit exposure were greater in younger men, and exposures received in the periods 15-24, 25-34

and 35+ years previously were found to have 47, 24 and 0% of the effect of exposures 5-14 years previously. Within this low-exposure-rate group excess relative risk increased linearly with time-weighted cumulative exposure and did not depend on exposure rate or duration of exposure. For men who spent less than 20% of their employment at the Jáchymov mine the excess relative risk per working level month was 1.36% (95% confidence interval 0.52-3.54) in the baseline category (age group 55+ and exposure received 5-14 years previously). For men who spent more than 20% of their employment at Jáchymov, the corresponding excess relative risk per working level month was higher by a factor of 1.80 (95% confidence interval 1.27-2.97). The difference may be due to the fact that men who spent more than 20% of their employment at Jáchymov were exposed to the much higher levels of arsenic in the dust at the Jáchymov mine than at other mines. When men with exposure rates above 10 working levels were included in the analysis, patterns of risk were complex and depended on both exposure rate and duration of exposure in addition to the factors mentioned above. If these findings are confirmed elsewhere, calculation of risk estimates for extrapolation to modern occupational or environmental exposures should be based on miners with exposure rates below about 10 working levels. Further investigation is desirable of the influence of dusts containing arsenic on lung cancer risk in miners exposed to radon.

Publication 3

Recent results from the study of West Bohemian uranium miners exposed to radon and its progeny. L Tomášek, SC Darby. Environmental Health Perspectives, **103**, Supplement 2, 55-57 (1995).

A brief description is given of the study of West Bohemian uranium miners, and recent and ongoing efforts to improve the quality of the data are summarized. Three recent analyses of the data from the cohort have led to rather different estimates of the excess relative risk of mortality from lung cancer per working-level month. The reasons for these different estimates are described, and it is concluded that estimates of lung cancer risk are strongly influenced by the quality of the exposure estimates, especially by the omission of some exposures accumulated during employment at other uranium mines, following the closure of most of the shafts at the original two mines. The most recent analysis has shown that, in common with other cohorts of radon-exposed miners, the excess relative risk of lung cancer per working-level month is modified by age and time since exposure. An inverse effect of exposure rate was also demonstrated, but it affected only men at very high concentrations and appears to be related to the time pattern of exposure. In addition, the risk was found to differ between the two main mines, possibly due to the influence of arsenic in the dust of the mines.

Publication 4

Radon exposure and cancers other than lung cancer among uranium miners in West Bohemia. L Tomášek, SC Darby, AJ Swerdlow, V Pláček, E Kunz. *Lancet*, **341**, 919-923 (1993).

Recent observations have suggested that radon in the ambient air may cause cancers at sites other than the lung, but the evidence is indirect. We have studied

site-specific cancer mortality in 4320 uranium miners in West Bohemia who have been followed-up for an average of 25 years, and in whom a four-fold radon-related excess of lung cancer has already been established.

For all cancers other than lung cancer the number of deaths observed was slightly greater than that expected from national rates, but the increase was not significant statistically (ratio of observed to expected deaths [O/E]=1.11, 95% confidence interval [CI]=0.98-1.24) and mortality did not increase with duration of employment underground or with cumulative exposure to radon. Non-lung cancer mortality was significantly raised among men who started mining work aged under 25 but the increase was not related to cumulative radon exposure. When twenty-eight individual sites and types of cancer were examined, significantly increased risks were found for cancers of the liver (O/E=1.67) and gallbladder and extrahepatic bile ducts (O/E=2.26). For liver cancer, mortality did not increase with duration of employment underground or with cumulative radon exposure. For cancer of the gallbladder and extrahepatic bile ducts, mortality did not increase with duration of employment, but increased with cumulative exposure to radon. Mortality from multiple myeloma, although not significantly increased overall (O/E=1.08), increased with cumulative exposure to radon. Mortality from leukaemia was not increased overall (O/E=0.91) and was not related to cumulative radon exposure, but did increase with increasing duration of employment in the mines.

There is no evidence in these miners that a radon-rich atmosphere increases the risk of any cancer other than lung cancer. Possible exceptions are cancer of the

gallbladder and extrahepatic bile ducts and multiple myeloma but further study is needed before it can be concluded that the associations found are causal.

Publication 5

Radon exposure and cancers other than lung cancer in Swedish iron miners. SC Darby, EP Radford, E Whitley. Environmental Health Perspectives, 103, Supplement 2, 45-47 (1995).

Data are presented on the risks of cancers other than lung cancer in a cohort of iron miners from northern Sweden occupationally exposed to elevated levels of the radioactive gas radon. Compared with rates for the four northernmost counties of Sweden, mortality was increased for all cancers other than lung cancer (ratio of observed to expected deaths 1.21, 95% confidence interval 1.03-1.41), stomach cancer (ratio of observed to expected deaths 1.45, 95% confidence interval 1.04-1.98), and rectal cancer (ratio of observed to expected deaths 1.94, 95% confidence interval 1.03-3.31). Despite these overall increases, mortality was not significantly associated with cumulative exposure to radon, either for all cancers other than lung cancer or for any site of cancer other than lung cancer individually. However, the data from this cohort on its own have limited power; and for several sites of cancer the data in this study would be consistent with a radon-related increase. Further study of cancers other than lung cancer in populations exposed to radon is required.

Publication 6

Radon and cancers other than lung cancer in underground miners: a collaborative analysis of 11 studies. SC Darby, E Whitley, GR Howe, SJ Hutchings, RA Kusiak, JH Lubin, HI Morrison, M Tirmarche, L Tomášek, EP Radford, RJ Roscoe, JM Samet, YS Xiang. *Journal of the National Cancer Institute*, **87**, 378-384 (1995).

Background: Exposure to the radioactive gas radon and its progeny has recently been linked to a variety of cancers other than lung cancer in geographical correlation studies of domestic radon exposure and in individual cohorts of occupationally exposed miners. *Purpose:* This study therefore aimed to characterize further the risks for cancers other than lung cancer from atmospheric radon. *Methods:* Mortality from non-lung cancer was examined in a collaborative analysis using data from 11 cohorts of underground miners in which radon-related excesses of lung cancer had been established. The study included 64,209 men who were employed in the mines for 6.4 years on average, received average cumulative exposures of 155 working level months (WLM), and were followed on average for 16.9 years. *Results:* For all non-lung cancers combined, mortality was close to that expected from mortality rates in the areas surrounding the mines (ratio of observed to expected deaths (O/E):1.01, 95% confidence interval (CI): 0.95-1.07, based on 1179 deaths), and mortality did not increase with increasing cumulative exposure. Among 28 individual cancer categories, mortality was significantly increased for cancers of the stomach (O/E:1.33, 95% CI:1.16-1.52) and liver (O/E:1.73, 95% CI: 1.29-2.28), and significantly decreased for cancers of the tongue and mouth (O/E: 0.52, 95% CI: 0.26-0.93), pharynx (O/E: 0.35, 95% CI: 0.16-0.66), and colon (O/E: 0.77, 95% CI: 0.63-0.95). For leukemia, mortality was increased in the period less than 10 years since starting work (O/E=1.93,

95% CI: 1.19-2.95) but not subsequently. For none of these diseases was mortality significantly related to cumulative exposure. Among the remaining individual categories of non-lung cancer, mortality was related to cumulative exposure only for cancer of the pancreas (excess relative risk per WLM=0.07%, 95% CI: 0.01-0.12) and, in the period less than 10 years since start of employment, for other and unspecified cancers (excess relative risk per WLM=0.22%, 95% CI: 0.08-0.37). *Conclusions:* The increases of stomach cancer, liver cancer and leukemia are unlikely to be caused by radon as they are unrelated to cumulative exposure. The association between cumulative exposure and pancreatic cancer seems likely to be a chance finding, while the association between cumulative exposure and other and unspecified cancers was caused by deaths certified as due to carcinomatosis which are likely to have been lung cancers. This study therefore provides considerable evidence that high concentrations of radon in air do not cause a material risk of mortality from cancers other than lung cancer. *Implications:* Protection standards for radon should continue to be based on consideration of the lung cancer risk alone.

Head of project 5: Dr. Kunz

Studies of underground miners of uranium and other substances are at present the principal source of information on the effects of exposure to radon and its progeny. One of the largest such studies is that of uranium miners in West Bohemia. This study, sometimes referred to as the S cohort, was set up in 1970 by the late Josef Ševc. About ten years later, two further cohorts were delineated by him. One of uranium miners (N) who worked under improved conditions mostly in the Příbram mines, and the second one of burnt clay miners (L) located in the Rakovník district. A brief description of the cohorts is given below (Tab.1).

Tab.1 Czech miners studies by 1990

Study	Since	Size	Cases	O/E	Died	WLM	Dur
S	1952	4320	708	5.06	56 %	228	8
L	1960	915	42	1.73	32 %	24	14
N	1969	5628	30	1.57	6 %	6	6

M e t h o d s

Cohort definition

The study population of the S cohort was established by means of a search of the employment records at the Jáchymov and Horní Slavkov mines. A man was included in the cohort if he commenced underground work in the period 1948-59, the work lasted at least four years, and details of his employment history were available. A total of 4320 men satisfied these criteria and were included in the study. The cohort comprised workers from all over the former Czechoslovakia, and after the closure of the mines, many of the men moved away from the locality. Therefore the national

rather than local mortality data for calculation of expected numbers were used. Annual national death rates by five year age group for 1953-90 were obtained from the WHO and Czechoslovak Federal Statistical Office, and these were bridge coded to the same (9th) revision as for the miners' data. Estimates of the national death rates by single year of age were made by interpolation.

Tab.2: S cohort - status by 1990

Died	2433	56.3%
Emigrated	314	7.3%
Lost	24	0.6%
Alive	1549	35.8%
Total	4320	100.0%

Follow-up

During the decade up to 1990, follow-up of the cohort mainly relied on the national population registry at the Ministry of the Interior. However, mortality analyses from causes other than lung cancer or violence by calendar period (realised in 1991) suggested that a substantial number of deaths had been missed, partly because of errors in the personal data of the cohort members and partly because of imperfections in the population registry. Therefore, a series of additional checks were conducted: in the files of the Czech and Slovak Pensions Offices, by local enquiries, and by direct correspondence (Tomášek et al, 1994b). These additional efforts resulted in an increase of more than 10% in the numbers of men known to have died or emigrated. The additional checks conducted on men apparently alive in the Ministry's files substantially altered the findings for recent follow-up, for instance the all cause mortality for 1981-85 and 1986-90 rose from 1.11 and 0.86

respectively before these checks to 1.40 and 1.43 after them.

The newly found deaths were not biased by cause compared with those already known, implying that if there are any deaths still missing, they are unlikely to be biased by cause. Mortality (O/E) from main three causes (Tab.3) suggests the present follow-up by the end of 1990 is correct. There were 29 deaths in the study with cause unknown, mainly because the place of death within Czechoslovakia was unknown and therefore the death certificate could not be located. These deaths imply that the true cause specific mortality, if cause were known for all deaths, would be about 1% greater than those shown.

Tab.3: S cohort - mortality by calendar period

Period	Lung Cancer	Violent Deaths	Other Causes	All Causes
52-60	5.60	2.13	0.87	1.49
61-65	9.43	1.42	1.06	1.81
66-70	9.89	1.87	1.11	1.97
71-75	5.95	1.12	1.22	1.65
76-80	4.15	1.58	1.26	1.58
81-85	3.88	1.19	1.12	1.40
86-90	2.71	1.24	1.28	1.43
Total	5.06	1.53	1.17	1.58

Exposure estimation

An exceptional feature of the S study is the large number of measurements of radon concentrations made in each mine-shaft of the Czechoslovak uranium mines in almost every year, including the early period (mean number of measurements per year and shaft was 223 in the period 1949-60). When the cohort was set up, manual calculations were carried out combining these data with the men's

employment details to estimate each man's annual exposure to radon progeny in terms of working levels. A recent review of these exposure estimates revealed that there were errors in these manual estimates (Tomášek et al, 1994a). In addition, some men also worked at other Czechoslovak uranium mines and, for some of the men (about 10%), involved exposures at these mines had not previously been taken into account. Therefore, in early 1993, a major revision of the exposure estimates was carried out, see (Tomášek et al, 1994a) for further details.

Statistical methods and modelling

Generally, person-years at risk were calculated for each man, starting at four years after entering underground employment at the mines and ending at the earliest of date of death, emigration, 85th birthday, loss to follow-up, or 1 January 1991. In order to evaluate the risk, person-years and their associated observed and expected deaths were cross-classified by attained age, age-at-first-exposure, time-since-exposure (TSE), cumulated exposure in windows created by TSE and exposure rate. Time dependent quantities were classified according to their current values at each moment of follow-up, but exposure experience within the last 5 years was ignored (lagging). All these quantities were represented in cells by person-year weighted means.

Poisson regression models for excess relative risk (ERR) were fitted by maximum likelihood method using the AMFIT module of the Epicure software (Preston et al, 1992). In the fitted models, it was assumed that the number of deaths observed in each cell had mean in the form

$$E k(a) (1 + ERR(w,x)),$$

where E is the number expected from national rates, ERR is

excess relative risk, w and x denote exposure history and modifying variable, and $k(a)$ is an intercept term that allows the mortality rate for 'unexposed' cohort to differ from that in the general population. Significance levels were assessed by residual deviance.

Confidence interval (CI, usually 95%) for relative risk (O/E) were based on the Poisson distribution of the observed numbers. The statistical significance (denoted by *) represents one-sided test of hypothesis $O/E=1$ against alternative $O/E>1$ at the 5% significance level.

Results and discussion

Mortality

The increased mortality (O/E=1.58) in the cohort is largely affected by mortality from lung cancer. Nevertheless the mortality from violence and accidents is also increased, namely in the first part of follow-up, whereas the mortality from other causes increases after 20 years since first exposure (Tab.4).

Tab.4: S cohort - time and cause specific mortality

Time since 1st exposure	Lung cancer	Violent deaths	Other causes
4- 4.9	2.56	3.54 *	0.26
5- 9.9	5.54 *	1.41 *	0.86
10-14.9	9.28 *	1.58 *	1.10
15-19.9	8.34 *	1.87 *	1.09
20-24.9	6.06 *	1.18	1.34 *
25-29.9	4.49 *	1.39	1.17 *
30-34.9	3.36 *	1.39	1.17 *
35-	2.72 *	1.13	1.23 *

The same time pattern in all the three cohorts combined is observed in some groups of diseases associated with tobacco consumption (Tab.5).

Tab.5: Time and cause specific mortality (all cohorts)

Cause	Time since 1st exposure			
	0-9	10-19	20-29	30-
Respiratory diseases	0.35	1.07	1.42*	1.27*
Circulatory diseases	0.86	1.10	1.24*	1.12*
Cancers excl lung	0.81	0.93	1.15	1.28*

When the S cohort was identified in 1970, the original mines had already closed and so information on the smoking habits in the cohorts could be recorded only in the two new

cohorts (L,N). The proportion of smokers in the two combined studies is 76% , a survey (conducted in the 1970s) in general population estimated 66% smokers. As the increase in mortality from cancers other than lung cancer is not likely to be associated with radon exposure (Darby et al, 1995), the data about smoking habits in cohorts N and L together with mortality patterns (Tab.5) indicate that the smoking in the S cohort might be different from the general population.

Risk estimates

During the years 1993-94, three somewhat different overall risk estimates have been reported for this study. Firstly, in an analysis of data based on follow-up of the cohort to 1985, but excluding the recent improvements in the quality of the follow-up and revisions to the exposure estimates, a simple model in which the excess relative risk (ERR) increased linearly with cumulative exposure lagged by 5 years led to an estimated ERR per WLM of 0.0169 (Ševc et al,1993). Secondly, data including follow-up to 1990, but before the additional revisions, were made available for a joint analysis of 11 underground miners studies (Lubin et al,1994). In this analysis, an apparently similar model led to an estimated ERR/WLM of 0.0034 for the Czech data. Finally, in an analysis carried out after the follow-up had been improved and the exposures revised, a linear model led to an estimated ERR/WLM of 0.0064 (Tomášek et al,1994a).

The reasons for this wide range of risk estimates are partly methodological and partly due to differences in the data. The principal cause of the high estimate given for the analysis of data up to the end of 1985 (Ševc et al,1993) is that it was assumed that, in the absence of exposure to radon, the age- and calendar year-specific mortality rates from lung cancer for the men in the cohort would have been

identical to those for men in Czechoslovakia as a whole. For example, if a similar assumption is made for the data used in the most recent analysis (Tomášek et al,1994), the estimated ERR/WLM is 0.0189 , not very different from that obtained for the earlier data set, but if two additional parameters (K,k) are included in the model, ie.

$$RR = K \exp(k(a-60)) (1 + b w) ,$$

allowing for age-dependent departures in the baseline lung cancer rate from the national values, the estimated risk coefficient drops by a factor of three to the value of 0.0064 given in (Tomášek et al,1994a) and referred to above. In contrast, the difference between the risk estimate of 0.0034 reported in the joint analysis (Lubin et al,1994), and the more recent value of 0.0064 (Tomášek et al,1994a) was primarily due to the changes and improvements in the data that have become available during 1992-3, and investigations show that the revision of the exposure estimates had a larger influence than the improvement of the follow-up. The recent data, which include further additional later exposures, lead to a slightly higher risk estimate (Tab.6).

Tab.6: Linear ERR model (model 1)

	Estimate	95% CI	
Intercept	1.899	1.395	2.586
k	-.0631	-.0719	-.0543
ERR/WLM	.0071	.0044	.0116

Factors influencing risk coefficients

Factors known to influence the excess relative risk per unit exposure were analyzed in details. Similarly as in the BEIR IV report (1988), the strong effect of time-since-exposure windows was found (Tab.7).

Tab.7: Time-since-exposure windows (model 2)

	Estimate	95% CI		
Intercept	1.854	1.348	2.551	chi-sq(3)=84.61
k	-.0460	-.0552	-.0368	
ERR/WLM	.0163	.0105	.0255	
TSE:				
5-14	1			
15-24	0.531	0.354	0.708	
25-34	0.173	0.055	0.291	
35-	0.132	-0.061	0.325	

In addition, the effect of exposure rate was analyzed. The cumulative lagged exposures in the four TSE windows were further divided into three categories (windows) according to their relevant radon daughter concentrations (WL) in the underground atmosphere (0-1.9, 2-3.9, 4+).

Tab.8: Effect of exposure rate (model 3)

	Estimate	95% CI		
Intercept	0.822	0.349	1.934	chi-sq(2)=27.83
k	-.0466	-.0559	-.0373	
ERR/WLM	.0559	.0215	.1454	
TSE:				
5-14	1			
15-24	0.483	0.346	0.619	
25-34	0.313	0.197	0.426	
35-	0.019	-0.225	0.263	
Exp.rate:				
0-1.9	1			
2-3.9	1.100	0.670	1.529	
4-	0.277	0.120	0.433	

It was found that there is almost no difference in the first two categories as for the risk coefficients, but the effect of exposures from concentrations over 4WL was significantly different from lower ones. (Tab.8).

Effect of age

The strong modifying effect of attained age that was found in almost all miner studies (Lubin, 1994) was investigated here in details. Three age related variables were constructed:

- (1) attained age,
- (2) age at first exposure,
- (3) age when median exposure was reached.

Tab.9: Effect of age

	Attained age (model 4.1)	Age at-1st-exp (model 4.2)	Age at-med-exp (model 4.3)
	Estim chi-sq	Estim chi-sq	Estim chi-sq
Intercept	1.023	1.411	1.405
k	.0115	-.0200	-.0102
ERR/WLM	.0439	.0540	.0785
TSE:			
5-14	1	1	1
15-24	0.473	0.292	0.248
25-34	0.286	0.117	0.092
35-	0.028	-0.019	-0.038
Exp.rate			
0-3.9	1	1	1
4-	0.286	0.310	0.250
Age	-.0717 5.99	-.0357 2.63	-.0491 5.26
Deviance	4708.82	4712.18	4709.55

The effect of age was modelled in the following way:

$$RR = K(a) (1 + f(w) \exp(g (a_x - a_0))),$$

where $K(a)$ is the age dependent intercept, $f(w)$ is TSE and exposure rate weighted effective exposure, and the a_x in the exponential term is one of the above three age variables. The constant a_0 relates the other parameters to value 60 for attained age and to value 30 for other two age variables.

From the deviances (Tab.9), it can be seen that models 4.1 and 4.3 are very similar, 4.1 being slightly better. But when both age variables (1 and 3) are included in a model for comparison, the effect of age-at-median exposure is stronger.

The effect of exposure duration (together with exposure rate) was analysed as well, and it was found significant. But when time since last exposure was included in the model, the effect of duration disappeared. From the methodological point of view, the effect of a variable (duration and/or time since last exposure, which depend on survival) seems be questionable. The duration effect should be analyzed in the way suggested by Fox (1976), ie. separating overlapping categories of duration and time since last exposure. Therefore, the recommended model is 4.3. In addition, this model reduces the value of the intercept within the whole age range to a realistic value of about 1.4, i.e. in the absence of exposure to radon, the estimated mortality from lung cancer in the cohort is 1.4 times higher than in the general population. In that case the ERR/WLM coefficient related to simple non-weighted cumulative exposure is estimated by a value of 0.0125.

The issue of the time pattern of exposure rate, originally observed by Ševc (1988), was also analyzed

(Tomášek, Darby, 1993). The effect was found similar for the present data, ie. high exposure rates occurring after several years of underground employment cause relatively lower subsequent risk per unit exposure.

Histology

The extensive number of lung cancer cases observed in the S cohort made possible analyses from the point of view of histologic types. The earlier publications (Horáček et al, 1977) found an increased mortality, particularly for the epidermoid and small cell types. It was also found that time pattern of exposure rates had different influence in the risk models for the two main histological types (Ševc et al, 1988).

Tab.10: Histologic types of lung cancer in the S cohort

Type	Cases	%
Epidermoid	173	24.4
Small cells	185	26.1
Adenocarcinoma	31	4.4
Other	29	4.1
Non-differenciated	40	5.6
No material	46	6.5
Yet unknown	204	28.8
Total	708	100.0

In order to verify Ševc's histological observations, further efforts are being made to classify the lung cancer cases by histological types. The process of ascertaining histological information has not yet been completed (Tab.10), but preliminary results based on 458 known cases confirm differences between epidermoid and small cell types (Tabs 11 and 12).

Tab.11: Age and histologic type specific mortality

Age	Epidermoid		Small cell	
	O	O/E	O	O/E
-44	7	10.64	24	35.02
45-54	39	7.20	71	11.97
55-64	81	5.39	65	4.27
65-84	46	3.79	25	2.65
Total	173	5.13	185	5.86

Tab.12: Time and histologic type specific mortality

Time since 1st exposure	Epidermoid		Small cell	
	O	O/E	O	O/E
0 - 4.9	0	.00	0	.00
5 - 9.9	1	1.07	5	5.16
10 - 14.9	15	6.79	33	14.87
15 - 19.9	28	8.25	48	14.47
20 - 24.9	37	8.11	29	6.64
25 - 29.9	36	5.22	31	4.75
30 - 34.9	42	4.54	24	2.82
35 -	14	2.21	15	2.69
Total	173	5.13	185	5.86

The type specific mortality is different both from the point of view of age and time since exposure. The younger age categories are more affected by the small cell type, but the effect of exposure is shorter than for the epidermoid type of lung cancer.

Results from the L and N study

Two younger cohorts (L and N) of miners exposed to radon, prevailingly below the annual limits, were followed until the end of 1990. By 1990, the mean attained age was

55 (L) and 44 (N), compared to age 65 in the S study. Because of age, the observed numbers of deaths are very low (Tab.13).

Tab.13: L and N cohorts status by 1990

	L Study		N Study	
Died	297	32.5%	357	6.4%
Emigrated	0	0.0%	35	0.6%
Lost	0	0.0%	39	0.7%
Alive	618	67.5%	5197	92.3%
Total	915	100.0%	5628	100.0%

Nevertheless the mortality from lung cancer in both cohorts is significantly raised already after 15 years since first exposure (Tab.14). The decreasing trend in mortality from violence is similar to that in the S cohort (Tab.4), and the mortality from other causes is in line with the healthy worker effect.

Tab.14: Time and cause specific mortality (L and N cohorts)

Time since 1st exp.	Lung cancer		Violent deaths		Other causes	
	L	N	L	N	L	N
0- 4	1.63	0.00	1.79	2.68 *	0.30	0.29
5- 9	1.33	0.79	0.70	1.92 *	0.78	0.76
10-14	1.50	1.58	1.09	1.22	0.86	0.85
15-19	1.59	1.78 *	1.87	0.89	0.89	0.71
20-24	3.03 *	2.52	0.25	0.89	0.89	1.22
25-29	0.69		0.97		1.22	
30-	1.80 *		1.61		1.05	
Total	1.73 *	1.57 *	1.18	1.67 *	0.97	0.76

A total of 72 lung cancer cases were observed in the combined study. The number does not allow to analyze the effect of radon exposure to lung cancer risk in such details as in the S study, where time since exposure covers more

than 35 years and age range involves practically all categories. The internal estimate of the intercept cannot be made use of in these analyses. Therefore the risk was related just to the general male Czech population, with a unit intercept. The risk coefficient per unit exposure for the combined (L+N) studies (Tab.15) was found not very different from the S study, where the same intercept approach was used for purpose of comparison.

Tab.15: Linear ERR model

	ERR/WLM	95%CI	
L+N study	.0232	.0083	.0380
S study	.0186	.0168	.0202

The TSE approach could be utilized here only in two time since exposure windows (5-14,15+ years). The estimated risk coefficients in both periods are very similar for both L+N and S studies (Tab.16).

Tab.16: TSE model

	TSE	ERR/WLM	95%CI	
L+N study	5-14	.0501	.0029	.0973
	15+	.0139	-.0059	.0336
S study	5-14	.0483	.0418	.0548
	15+	.0116	.0099	.0133

S u m m a r y

Lung cancer risk from radon was analysed in three cohorts of uranium (N=4320+5628) and burnt clay (N=915) miners. The follow-up of miners was extended up to 1990. Most of the cases (708) have been observed in the oldest (S) cohort followed since 1952. The other two cohorts, 18 years younger in average, with substantially lower exposures contributed 72 cases. Therefore the main analyses of risk from radon were based on the S cohort.

The data of the S cohort were subjected to checks both as for the exposures of the miners and the completeness of follow-up. The present mortality analyses from other causes suggest the follow-up is correct. In addition, the general patterns of mortality from violent deaths and diseases other than lung cancer show similar features in all the three cohorts, i.e. decreasing trend with time since first exposure in the first case, and increasing trend in the second one, confirming thus the healthy worker effect in the first 20 years. The raised mortality was observed in later periods in respiratory and circulatory diseases and also in cancers other than lung cancer, suggesting that smoking habits among miners might be more frequent than in the general population.

The estimates of lung cancer risk were based on relative linear models, where cumulative exposure were lagged by 5 years. The linear effect of cumulative exposure was substantially modified by time since exposure, exposure rate, and age at exposure. In all fitted models, the approach of the so called age dependent intercept was used, allowing for departure in the baseline lung cancer rate from the national values.

The final model estimated the relative risk (RR) in the following way:

$$RR(a) = 1 + 0.079 (w_{5-14} + 0.25 w_{15-24} + 0.09 w_{25-34}) \cdot \exp (-0.049(a_e - 30)) ,$$

where w_{5-14} , w_{15-24} , and w_{25-34} are exposures (WLM) received 5-14, 15-24, and 25-34 years previously, a_e age when median of exposure was reached. The above model holds for exposure rates below 4WL. Exposures from higher concentrations have to be multiplied by a reduction factor of 0.25 .

The intercept corresponding to the above model was practically independent on attained age. In other words in the absence of exposure to radon, the estimated mortality from lung cancer in the cohort is about 1.4 times higher than in the general population.

References

Fox AJ, Collier PF. Low mortality rates in industrial cohort studies due to selection for work and survival in the industry. *Brit J Prev Soc Med* 30:225-230 (1976).

Horáček J, Plaček V, Ševc J. Histologic types of bronchogenic cancer in relation to different conditions of radiation exposure. *Cancer* 40:832-835 (1977).

National Research Council, Committee on Biological Effects of Ionizing Radiation. Health risk of radon and other internally deposited alpha-emitters (BEIR IV). National Academy Press, Washington DC, 1988.

Ševc J, Kunz E, Tomášek L, Plaček V, Horáček J. Cancer in man after exposure to Rn daughters. *Health Phys* 54:27-46 (1988).

Tomášek L, Darby S, Swerdlow A, Kunz E. Epidemiological study of uranium miners in Western Bohemia. *Proc. Int. Workshop on Health Effects of Inhaled Radionuclides: Implications for radiation protection in mining*, Jabiru NT, Australia, Sept 1992.

Preston DL, Lubin JH, Pierce DA. *Epicure*. Hirosoft, Seattle, WA, 1992.

Ševc J, Tomášek L, Kunz E, Plaček V, Chmelevsky D, Barclay D, Kellerer AM. A survey of the Czechoslovak follow-up of lung cancer mortality in uranium miners. *Health Phys* 64:355-369 (1993).

Tomášek L, Darby SC, Swerdlow AJ, Plaček V, Kunz E. Radon exposure and cancers other than lung cancer among uranium miners in West Bohemia. *Lancet* 341:919-923 (1993).

Tomášek L, Darby SD. Recent results from the study of West Bohemian uranium miners exposed to radon and its progeny. *Environ Hlth Persp*, Vol 103, Suppl 2:55-57, 1995 (presented Aug 1993).

Tomášek L, Darby SC, Fearn T, Swerdlow AJ, Plaček V, Kunz E: Pattern of lung cancer mortality among uranium miners in West Bohemia with varying rates of exposure to radon and its progeny. *Radiat Res* 137:251-261 (1994a).

Tomášek L, Swerdlow AJ, Darby SC, Plaček V, Kunz E. Mortality in uranium miners in West Bohemia: a long term cohort study. *Occup Environ Med* 51:308-315 (1994b).

Lubin JH, Boice JD, Hornung RW, Edling C, Howe GR, Kunz E, Kusiak RA, Morrison HI, Radford EP, Samet JM, Tirmarche M, Woodward A, Xiang TS, Pierce DA. Radon and lung cancer risk: a joint analysis of 11 underground miners studies. Natl Inst Hlth, NIH Publ 94-3644, (1994).

Darby SC, Whitley E, Howe GR, Hutchings SJ, Kusiak RA, Lubin JH, Morrison HI, Tirmarche M, Tomášek L, Radford EP, Roscoe RJ, Samet JM, Yao SX. Radon and cancers other than lung cancer in underground miners: a collaborative analysis of 11 studies. JNCI, Vol 87:378-384 (1995).



**Final Report
1992-1994**

Contract: F13PCT930066 Duration: 1.1.93 to 30.6.95 Sector: C14
Title: International collaborative study of cancer risk among nuclear industry workers.

- | | | |
|----|----------|-------|
| 1) | Cardis | IARC |
| 2) | Sztanyik | NRIRR |
| 3) | Cesnek | SEP |

1. Summary of Project Global Objectives and Achievements

Global objectives

The overall objective of the project is to evaluate directly the effects of low dose chronic exposure to low LET ionizing radiation on risk of all forms of cancer and particular types of cancer defined a priori. The specific objective is to provide actual data on cancer risk following low dose protracted exposures for comparison with risk estimates derived from high dose/high dose-rate studies. This will provide a direct test of the adequacy of the current extrapolation models used for risk assessment and for setting of radiation protection standards and may assist in the construction of improved risk assessment models (1). The approach chosen was to set up and carry out an international retrospective cohort study of cancer risk among radiation workers in the nuclear industry, using a detailed common core protocol (2). This study is expected to be completed in 1999.

During the contract period (1 January 1993 to 30 June 1995) the objectives were:

- to set up an international collaborative study of cancer risk among nuclear industry workers from 12 countries (eight from Europe, including seven states which are members of the European Union) and to co-ordinate data collection and validation in these countries;
- to evaluate the feasibility of carrying out similar studies in Hungary and the Slovak Republic, and if feasible, to prepare detailed procedures documents and initiate studies of the cancer mortality of nuclear workers in these countries on the basis of the Protocol of the International Collaborative Study of Cancer Risk among Radiation Workers in the Nuclear Industry.

Funding under the current contract was received for support of the central coordination of the study by the International Agency for Research on Cancer (IARC) and extension of the study and conduct of feasibility studies in Hungary and the Slovak Republic.

Achievements

During the reporting period, the International Collaborative Study on Cancer Risk among Radiation Workers in the Nuclear Industry was set up in the following 12 countries: Australia, Belgium, Canada, Finland, France, Germany, Japan, Spain, Sweden, Switzerland, the UK and the USA. In addition, the feasibility of extending the study to Hungary and the Slovak Republic was established. In the USA, the study was extended to two new cohorts, that of Portsmouth Naval Shipyard employees and that of Idaho National Engineering Laboratory workers.

A common core protocol is in use in all countries to ensure comparability of study design and analyses. The document outlining the detailed procedures for setting up the study and for data collection was prepared and distributed. Throughout the reporting period, IARC staff carried out site visits to participating countries, as needed, to review difficulties encountered in setting up the cohorts, collecting basic employment and dosimetric data and carrying out long-term mortality follow-up, and providing assistance to National Study Group members with problems of data collection and analysis. After two years, a revised and expanded version of the Procedures Document was prepared by IARC to reflect changes in data collection approaches which had taken place at the national level because of the logistic or legal difficulties encountered.

In addition, protocols for studies aimed at assessing and ensuring the comparability – across countries and over time – of occupational external dose estimates and of cause of death coding have been prepared by IARC and are being implemented in participating countries.

A critical review of existing software for management and analysis of the combined data set has been carried out at IARC, and the database is being redesigned for greater flexibility and speed of data retrieval and analysis. Approaches for routine validations and basic analyses are being developed and compared. Simple, portable software for trend test analyses is being written and will be sent to collaborators.

At the national level, progress has been dependent on logistic, legal and financial problems. Permission from appropriate authorities for collecting the information required for the purpose of the International Collaborative Study have been obtained from all countries. In some countries, obtention of the required authorisations has considerably delayed the beginning of the study.

Construction of cohorts has been completed in all countries except Spain. The collection, computerisation and validation of entry data has started in all 12 countries. Mortality follow-up has also started in most countries. Follow-up for mortality is near complete and analyses are starting in Finland, Japan, Sweden and the UK. Follow-up for cancer incidence has been completed in Finland and Sweden.

In Hungary and the Slovak Republic, the feasibility study was successful. Results of additional pilot studies are awaited before the detailed procedures documents are finalised. Construction of the cohorts has been carried out and the progress of these studies is expected to be rapid.

Head of Project 1: Dr. Cardis

II. Objectives for the reporting period

During the contract period (1 January 1993 to 30 June 1995) the objectives were:

- to set up an international collaborative study of cancer risk among nuclear industry workers from 12 countries (eight from Europe, including seven states which are members of the European Union) and co-ordinate data collection and validation in these countries; this includes providing assistance to National Study Group members, as needed, with problems of data collection and analysis;
- to investigate the feasibility of extending the study to additional countries: Hungary, India and the Slovak Republic and to additional cohorts in the United States of America;
- to develop procedures for validation and quality assurance to be implemented at the national and international levels; in particular to set-up studies of the comparability of dose and outcome data;
- to modify and/or design software for database management and analysis of the combined data set in order to resolve logistic difficulties caused by the size of the database and complex analyses.

III. Progress achieved including publications

Progress of the International Collaborative Study

The International Collaborative Study of Cancer Risk among Radiation Workers in the Nuclear Industry was set up in all twelve participating countries: Australia, Belgium, Canada, Finland, France, Germany, Japan, Spain, Sweden, Switzerland, the UK and the USA, between 1 January 1993 and 31 July 1994. The cohorts included in each country are listed in Annex 1. A Procedures Document (3), outlining detailed procedures for setting up the cohorts and for data collection was prepared by IARC staff in collaboration with the members of the International Study Group (see list in Annex 2) and distributed to all study participants in 1993. This document complements the Protocol of the International Study (4).

Throughout the reporting period, IARC staff carried out site visits to participating countries, as needed, to review difficulties encountered in setting up the cohorts, collecting basic employment and dosimetric data and carrying out long-term mortality follow-up, and providing assistance to National Study Group members with problems of data collection and analysis. In the second half of 1994 and early 1995, IARC staff revised and expanded the detailed Procedures Document (5) to reflect changes in data collection approaches which had taken place at the national level because of the logistic or legal difficulties encountered. These changes were discussed in detail at a meeting of the International Study Group which took place in December 1994. Procedures for validation and quality assurance were included in the revised Procedures Document.

Permission from appropriate authorities for collecting the information required for the purpose of the International Collaborative Study have been obtained from all countries. In some countries, obtention of the required authorisations has considerably delayed the beginning of the study; in Switzerland, in particular, a specific directive had to be issued at the governmental level.

Construction of cohorts has been completed in all countries except Spain. The study population consists of all workers who have been monitored for external ionizing radiation exposure, through the use of personal dosimeters, at some time during their employment in a

public or private facility of the nuclear industry in a participating country, and for whom dose records are kept. In some countries, cohorts of contract workers are also included if it is possible to follow them up and to reconstruct their work and exposure history in a complete and systematic fashion.

The collection, computerisation and validation of entry data has started in all 12 countries. Mortality follow-up has also started in most countries, and follow-up for cancer incidence has been completed in Finland and Sweden.

At the national level, progress has been dependent on logistic, legal and financial problems. Specific details of the progress of the study are given, on a country by country basis, below:

Australia

After a slow beginning, most of the logistic problems of the Australian study have been resolved and the study is progressing well. Ethical committee approvals have been obtained from the appropriate authorities. The cohort of Lucas Heights workers has been constructed. A database has been designed to re-enter detailed dosimetric data from paper records. A database for combining the dosimetry data with personnel, medical, morbidity and mortality data is in the final stages of development. Data entry is starting.

Belgium

Construction of a cohort of 4700 workers from the 3 facilities in the Mol-Dessel region (SCK, Belgoprocess and Belgonucléaire) is complete. Collection of dosimetric data (external radiation only) is complete. Mortality data up to the end of 1992 has been collected for SCK workers. Legal difficulties were encountered for the follow-up of workers from Belgoprocess and Belgonucléaire because of changes in the legislation concerning protection of privacy. It is expected that an exception to the law will be passed shortly allowing access to the National Population Registry for scientific purposes. Alternative sources are currently being used for vital status ascertainment. A personal letter has been sent to all past and current employees of the study facilities requesting permission to access personal information from medical files and population registries for the purpose of this study. A smoking survey has been set up among current workers.

Negotiations to extend the study to the power plants and to the "Institut des Radioéléments" are underway. Additional funding is being sought for this.

Canada

The original cohort file of the National Dose Registry has been updated to include workers monitored up to 1992. This file is now being checked for discrepancies in the identifying information from any merged records. When this is complete, the file will be linked to the radiation dose records. Validation of the dosimetric data will be carried out by comparing recorded dose for a sample of records with the dosimetric records of individual facilities.

Authorisations have been received for linkage of the data to the National Mortality Database. Funding for this linkage is being sought.

Finland

The cohort of 13 000 Finnish workers has been identified and all entry data abstracted. Follow-up for vital status and cancer incidence has been carried out. Follow-up of the 1 000

Finns working in Swedish nuclear installations is underway. Analyses of data will begin shortly.

France

CEA

The construction of a cohort of over 40 000 civilian CEA workers employed between 1950 and 1992 has been constructed. The linkage of data from personnel and dosimetry records up to 1985 is underway. Dosimetry records since 1985 are being entered. Dosimetric archives for the division of military applications of Marcoule, La Hague and other subsidiaries are being computerised.

Authorisation to use the Répertoire National des Personnes Physiques (National population registry) for vital status ascertainment is awaited; if it is not received, vital status will be ascertained through the Town Hall of birth.

The historical review of dosimetric and monitoring practices for the study of errors in dosimetry is complete. A study of potential exposures to selected work-place carcinogens is underway.

EDF

The cohort of 21 000 radiation workers at EDF has been constructed. Identification and dosimetric data are being collected and, where necessary, computerised. Exposure data prior to 1968 need to be reconstructed. A file allowing reconstruction of employment history has been obtained from personnel records. It also contains information about education level and vital status. The procedure to obtain medical cause of death information is being developed.

A job/exposure matrix allows the reconstruction of occupational exposure to approximately 30 workplace carcinogens used at EDF currently or in the past. Data on cigarette and alcohol consumption will be available for workers who volunteered to participate in an on-going cohort survey. A survey of smoking prevalence among workers in activity will also be carried out.

Contract workers

A study of radiation workers employed in nine large contracting companies is planned. Negotiations are underway and funding is being sought for the reconstruction of employment and exposure histories of these workers.

Germany

After a slow beginning, work is progressing well: an agreement has been reached to obtain annual dose from all plants. 16 000 abstract forms are now available. A cohort of approximately 6 000 workers from nuclear power stations has been constructed. The remainder are from contracting companies and it is not yet clear which of these can be included in the study. Funding is being sought in order to ensure the continuation of the study - in particular to permit the computerisation of dosimetric data from the plants. Twelve percent of the workers have left employment and 5% are no longer radiation workers.

Hungary

See report of project 2, attached.

Japan

The study in Japan is well advanced. A stratified random sample of 50 000 workers was taken from the registry on all radiation workers in the nuclear industry and information on notified address was obtained from nuclear facilities. All dosimetric data have been abstracted. Letters were mailed to local public offices to determine vital status of the study subjects. For deceased workers thus identified, national vital status tapes were consulted to determine underlying cause of death. The method of linkage appears to be satisfactory thus far. Statistical analyses of the data are underway.

Slovak Republic

See report of project 2, attached.

Spain

The beginning of the Spanish study has been very slow. Formal co-operation of the electricity industry has now been secured through the physicians of all nuclear power plants and the persons responsible for dosimetry records. The final draft of the national study protocol is being discussed with Nuclear Safety Council which supports the study and should provide funds for it.

Sweden

The cohort of 22 581 Swedish workers has been identified and all entry data abstracted. Follow-up for vital status and cancer incidence has been carried out. Follow-up of the Swedes working in Finnish nuclear installations is underway. Analyses of data will begin shortly.

Switzerland

The beginning of the study was delayed because of a new data protection law. A special directive was, however, passed on 1 April 1994 giving the study co-ordinators legal right to access the data requested in the study protocol. Since then the study has progressed well.

The cohort of workers in the five power production facilities in Switzerland has been constructed. Data collection on the site of the two oldest power plants has been completed. Dosimetric data as well as additional identifiers necessary for follow-up have been obtained from the dosimetric services and personnel departments of the power plant and transferred into an ACCESS database set up for the study. The data were complete and well documented.

Mortality follow-up is currently underway in parallel with the collection of data from the other study facilities and the completion of dosimetric history for workers from all study facilities who left employment before 1990, year of the creation of the National Dose Registry.

UK

The cohort has been increased from approximately 95 000 workers in published analyses (6) to over 120 000 by including workers employed by Amersham International and Scottish Nuclear, as well as past workers employed by Nuclear Electric and more recent workers for participating organisations. Annual updates of dosimetry and employment details for persons in the National Registry for Radiation Workers (NRRW) continue to be received from participating organisations and processed. Audits of data held by participating organisations have started.

Follow-up information is received mainly from the National Health Service Central Registers (NHSCRs). However, it is planned to conduct a vital status check of the Department of Social Security later this year. Analyses will start shortly.

USA

Portsmouth Naval Shipyard

The extension of an earlier study is underway. The study population covers approximately 25 000 shipyard workers, 7 000 of whom had been involved in nuclear work, primarily with external exposures from cobalt 60. The vital status follow-up of the cohort is complete. Cause of death ascertainment is continuing.

Idaho National Engineering Laboratory

The cohort has been constructed and the database is in preparation. NIOSH personnel are on location characterising exposures to radiation and chemical compounds and are inventorying existing record systems. No attempt has yet been made to ascertain vital status, but this activity is planned to start shortly.

Other studies

No update of the follow-up of cohorts included in the previous combined analyses or of other DOE cohorts which will be included in the International Collaborative Study of Cancer Risk among Radiation Workers in the Nuclear Industry (Mound, Savannah River, Los Alamos National Laboratory) has yet been carried out.

Extension of the study

Hungary and the Slovak Republic

The feasibility of carrying out a study of cancer risk among nuclear industry workers in Hungary and the Slovak Republic, using the common core Protocol of the International Collaborative Study, has been evaluated. This has entailed a thorough review of existing sources of data and of their completeness. Pilot studies have been carried out to evaluate the feasibility of ascertaining cause of death from population registries and of linking data from different sources (personnel records, dosimetric records, records of the national dose registry in Hungary, population registries, etc. ...). In both countries, the feasibility of the study has been established (see enclosed reports of projects 2 and 3). A detailed protocol and document of procedures for each study is in preparation in collaboration with IARC staff. The construction of the cohorts has been completed. Results of a pilot study in Hungary to assess possible inconsistencies in the data contained in the dosimetric databases of the power plant and of the National Personal Dosimetry Service are awaited.

USA

It has been agreed that the USA component of the study will include, in addition to the studies included in the previous combined analyses (i.e. Hanford, Oak Ridge National Laboratory and Rocky Flats), the studies of Los Alamos National Laboratory, Mound and Savannah River if they meet all study criteria. In addition, two new cohort studies have been started, as described above, and are part of the International Collaborative Study of Cancer Risk among Radiation Workers in the Nuclear Industry: Idaho National Engineering Laboratory and Portsmouth Naval Shipyard.

India

Following initial contacts, the protocol and questionnaire for the feasibility study were sent to Bhaba Atomic Research Centre (BARC) in Bombay in order to obtain additional

information about the size of the Indian nuclear workforce, the detail of dosimetric and employment history data kept and possible approaches for carrying out mortality follow-up. Despite several letters sent in following years, the questionnaire was never returned although additional contacts confirmed an interest in participating in the study. IARC staff visited BARC in November 1994. Discussions revealed that no clear decision has been made about the participation in such a study. There was general support for the study and a willingness to join. An official decision to participate is awaiting negotiations within the Department of Atomic Energy.

Quality and comparability assurance

An aspect of particular importance in the conduct of the International Collaborative Study of Cancer Risk among Radiation Workers in the Nuclear Industry, before carrying out the combined analyses of data from different facilities and countries, is to ensure the comparability of data collected. A common core protocol is in use in all countries to ensure comparability of study design and analyses. In addition, studies aimed at assessing and ensuring the comparability – across countries and over time – of occupational external dose estimates and of cause of death coding will be carried out within the project.

Although radiation exposure in the nuclear industry has been assessed more precisely than exposure to most other occupational carcinogens, the accuracy of individual dose estimates varies with time and place. A Dosimetry SubCommittee has been formed to evaluate the comparability of recorded doses in the international study and a study of errors in dosimetry has been set-up. A draft protocol for this study was prepared by IARC staff in collaboration with members of the SubCommittee; it was discussed at a meeting of the SubCommittee in June 1993, circulated to persons responsible for radiation protection and dosimetry in the participating countries for comments, finalised at a meeting in June 1994 and circulated to the participants for testing of the approaches. This test revealed some difficulties and some aspects which needed clarification and the protocol was discussed again and revised at the meeting of the full Study Group in December 1994. It is included in the revised Procedures Document (5). Collection of the data requested has started in most countries. Flexible instructions for the abstraction of detailed dosimetric information have also been provided.

The comparability of mortality data is also a fundamental requirement in international mortality studies. IARC staff prepared a draft protocol for a study of the comparability of coding of cause of death from death certificates across study cohorts, with a view to identifying systematic biases (if any) and assessing their impact on the radiation risk estimates. This draft was discussed at the meeting of the Epidemiology SubCommittee in June 1994, circulated to participants and finalised at the meeting of the International Study Group. The protocol for this study is also included in the Procedures Document (5).

Definition of comparable categorisations of important study variables across countries were derived. A tentative categorisation of the socio-economic status variable was achieved; it is also included in the Procedures Document (5). It will need to be reviewed once abstraction of data from employment records is more complete in some countries: the completeness and comparability of information in historical records is presently unclear.

Management and analysis of data

A critical review of existing software for management and analysis of the combined data set has been carried out, on the basis of the experience gained in previous international combined analyses (1), with a view to solving the important logistic difficulties posed by the size of the database and the complexity of the analyses to be carried out. The SIR database is

being redesigned for greater flexibility and speed of data retrieval and analysis. Approaches for routine validations and basic analyses (within the database management package or in FORTRAN, C or SAS) are being developed and compared. Simple, portable software for trend test analyses is being written and will be sent to collaborators.

Publications

As this study is still in the data collection and validation phase, no results have been published. The procedures document has been published as an IARC Internal Report (3,5). Related publications have appeared during the contract period; they were however of a general nature (7,8) or concerned the results of previous combined analyses of data on cancer risk among nuclear industry workers (1,9,10), not supported by the current contract.

Head of Project 2: Dr. Sztanyik

II. Objectives for the reporting period

To carry out a detailed study in order to assess the feasibility of carrying out a study of cancer risk among nuclear industry workers in the Hungary. If such a study proved feasible, to prepare a detailed procedures document in collaboration with IARC and begin implementation of the study - construction of the study cohort, collection of entry data - in accordance to the common core protocol of the International Collaborative Study of Cancer Risk among Radiation Workers in the Nuclear Industry.

III. Progress achieved including publications

The feasibility of carrying out a study according to the Protocol of the International Collaborative Study of Cancer Risk among Radiation Workers in the Nuclear Industry has been demonstrated. Problems encountered were discussed during a site visit of IARC staff to Budapest with scientists from the nuclear power plant at Paks, the Central Office of Statistics and the NRIRR. A pilot study is underway to assess the uncertainties and possible inconsistencies in the data contained in the dosimetric databases of the power plant and of the National Personal Dosimetry Services. A comparison of data from personnel and radiation files is also being carried out on a random sample of the workers. On the basis of these results, the primary approach for mortality follow-up will be decided and the detailed procedures document will be finalised in collaboration with IARC staff.

A database of all workers having left the nuclear power plant (approximately 2 100 persons) has been prepared and sent to the National Office for Population Registry to obtain information on vital status and a current address.

Head of Project 3: Dr. Cesnek

II. Objectives for the reporting period

To carry out a detailed study in order to assess the feasibility of carrying out a study of cancer risk among nuclear industry workers in the Slovak Republic. If such a study proved feasible, to prepare a detailed procedures document in collaboration with IARC and begin implementation of the study - construction of the study cohort, collection of entry data - in accordance to the common core protocol of the International Collaborative Study of Cancer Risk among Radiation Workers in the Nuclear Industry.

III. Progress achieved including publications

The feasibility of carrying out a study according to the Protocol of the International Collaborative Study of Cancer Risk among Radiation Workers in the Nuclear Industry has been demonstrated. In particular, a pilot study of a random sample of 460 workers was carried out to test the feasibility and completeness of linkage to sources of vital status data. The results of the pilot study are being analyzed and a complete report will be prepared by the end of November 1995. On the basis of these results, the primary approach for mortality follow-up will be decided and the detailed procedures document will be finalised in collaboration with IARC staff.

The study cohort, which consists of 2 498 former or current employees of the nuclear power plant Jaslovski Bohunice, has been constructed. The database for the study is being constructed on the basis of the employer's database. Collection of entry data has started.

Bibliography

1. E. Cardis, E.S. Gilbert, L. Carpenter et al., Effects of low doses and low dose-rates of external ionizing radiation: Cancer mortality among nuclear industry workers in three countries.. *Radiation Research* **142**, 117-132 (1995).
2. E. Cardis, J. Esteve and B.K. Armstrong, Meeting Recommends International Study of Nuclear Industry Workers. *Health Phys.* **63**, 465-466 (1992).
3. E. Cardis and I. Kato, *International Collaborative Study of Cancer Risk among Nuclear Industry Workers, III -Procedures document*. IARC Internal Reports 93/003, International Agency for Research on Cancer, Lyon (1993).
4. E. Cardis and J. Esteve, *International Collaborative Study of Cancer Risk Among Nuclear Industry Workers, I-Protocol*. IARC Internal Report 92/001, International Agency for Research on Cancer, Lyon (1992).
5. E. Cardis, A. Mylvaganam and I. Kato, *International Collaborative Study of Cancer Risk among Nuclear Industry Workers, III -Procedures document, rev. I*. IARC Internal Reports 95/001, International Agency for Research on Cancer, Lyon (1995).
6. G.M. Kendall, C.R. Muirhead, B.H. MacGibbon et al., Mortality and occupational exposure to radiation: first analysis of the National Registry for Radiation Workers. *Br. Med. J.* **304**, 220-225 (1992).
7. M. Goldberg and E. Cardis, Epidemiologie et rayonnements ionisants: quelques aspects methodologiques. *Radioprotection* **29**, 11-43 (1994).
8. I. Kato and E. Cardis, A review on cohort studies of nuclear workers. *Radioprotection* **29**, 79-87 (1994).
9. IARC Study Group on cancer risk among nuclear industry workers, Direct estimates of cancer mortality due to low doses of ionizing radiation: an international study. *Lancet* **344**, 1039-1043 (1994).
10. E. Cardis, E.S. Gilbert, L. Carpenter et al., *Report of the combined analyses of cancer mortality among nuclear industry workers in three countries*. IARC Technical Report 25, International Agency for Research on Cancer (IARC), Lyon (1994).

Annex 1

International Collaborative Study of Cancer Risk among Radiation Workers in the Nuclear Industry

List of cohorts included

1. Australia: Employees of the Australian Nuclear Science and Technology Organisation (ANSTO) (1958-1991)¹.
2. Belgium: Nuclear Research Center (SCK/CEN) (1953-1992), Belgonucléaire (nuclear fuel production) (1957-1992), Belgoprocess (nuclear waste treatment) (1985-1992).
3. Canada: National Dose Registry (NDR) (1944-1991), restricted to workers in the nuclear industry, specifically employees of the fuel cycle facility: Eldorado resources; the nuclear research facility: AECL-Nuclear Research; the power generating facilities operated by Ontario Hydro (- to be confirmed - Douglas Point, Rolphton, Pickering A/B, Bruce A/B, Darlington, Bruce Heavy Water Plant), Hydro Québec (Gentilly 1, Gentilly 2) and New Brunswick Electric (Point Lepreau); and contracting companies: to be determined.
4. Finland: National Dose Registry (NDR) (1962-1991), restricted to monitored workers in the nuclear industry, specifically employees of the nuclear research facility: Fir 1; of the power generation facilities: Loviisa 1, Olkiluoto 1, Loviisa 2 and Olkiluoto 2; and of contracting companies.
5. France: Employees of the fuel cycle facility (COGEMA-Compagnie Générale des Matières Nucléaires (1976-1991); the nuclear research facilities (CEA-Commissariat à l'Energie atomique) (1946-1991), CEA-DAM (Division des applications militaires) (1954-1991); the power generating company (Electricité de France - Division de la Protection Thermique (EDF-DPT) (1961-1991) and selected contracting companies: (to be specified).
6. Germany: Berufsgenossenschaft registry (1968-1991), including employees of the fuel cycle facility: Siemens; the power generation facilities: KWO Obrigheim, KKS Stade, KWW Wurgassen, KWB A Biblis, KWB B Biblis, GKN-1 Neckar, KKR Brunsbittel, KKI-1 Isar, KKU Unterweser, KKP-1 Philippsburg, KKG Grafenrheinfeld, KKK Krummel, KRB B Gundremmingen, KWG Grohnde, KRB C Gundremmingen, KKP-2 Philippsburg, KBR Brokdorf, KKI-2 Isar, KKE Emsland, GKN-2 Neckar and Greifswald; and selected contracting companies: to be specified.
7. Hungary: Workers of nuclear power plant (NPP) Paks.
8. Japan: Radiation Dose Registration Center for Workers (RADREC) (1957-1991), including employees and contractors of the power generation facilities: Tokai, Tsuruga 1, Mihama 1, Fukushima Dai-ichi 1, Mihama 2, Fukushima Dai-ichi 2, Takahama 1, Shimane 1, Takahama 2, Genkai 1, Fukushima Dai-ichi 3,

¹ study period is in parentheses

Hamaoka 1, Mihama 3, Ikata 1, Tokai dai-ni, Fukushima Dai-ichi 4, Fukushima Dai-ichi 5, Hamaoka 2, Fukushima Dai-ichi 6, Ohi 1, Ohi 2, Fugen, Genkai 2, Ikata 2, Fukushima Dai-ni 1, Onagawa 1, Fukushima Dai-ni 2, Sendai 1, Sendai 2, Fukushima Dai-ni 3, Kashiwazaki-Kariwa 1, Takahama 3, Takahama 4, Tsuruga 2, Fukushima Dai-ni 4, Hamaoka 3, Tomari 1, Shimane 2, Kashiwazaki-Kariwa 2, Kashiwazaki-Kariwa 5 and Tomari 2.

9. Slovak Republic: Employees of the nuclear power plant Jaslovské Bohunice (1972-1993).
10. Spain: Employees of the nuclear waste storage facility Enresa (1985-1992) and the power generation facilities José Cabrera (1968-1992), Santa Maria de Garoña (1971-1992), Vandellos I (1972-1992), Almaraz I (1981-1992), Asco I (1983-1992), Almaraz II (1983-1992), Cofrentes (1984-1992), Asco II (1985-1992), Vandellos II (1987-1992), Trillo I (1988-1992).
11. Sweden: Centralized Dose Register (CDR) (1954-1991) covering employees of the fuel cycle facility: ABB atom; the nuclear research facility: Atomenergi AB (Studsvick); the power generation facilities: Oskarshamm 1, Oskarshamm 2, Ringhals 2, Barseback, Ringhals 1, Forsmark, Ringhals 3 and Ringhals 4; and the contracting companies: (list to be provided).
12. Switzerland: National Dose Registry (since 1989) and employees of the power production facilities Beznal I and II (1969/71-1993), Mühleberg (1972-1993), Gösgen (1979-1993), Leibstadt (1984-1993).
13. UK: National Registry for Radiation Workers (NRRW) (1943-current). This includes employees and ex-employees of British Nuclear Fuels plc, AEA Technology, Nuclear Electric plc, Scottish Nuclear Ltd, Amersham International, the Science and Engineering Research Council, the Ministry of Defence, contracting companies to these organisations and a number of smaller independent organisations (to be specified).
14. USA: Portsmouth Naval Shipyard, Idaho National Engineering Laboratories, Hanford, Rocky Flats, Oak Ridge National Laboratory, Mound, Savannah River, Los Alamos National Laboratory.

Annex 2

International Collaborative Study of Cancer Risk among Radiation Workers in the Nuclear Industry

List of study group members

Dr Patrick Ashmore
National Dose Registry
Occupational Radiation Hazards Division
775 Brookfield Road
Ottawa, Ontario K1A 1C1
Canada

Dr Anssi Auvinen
Finnish Center for Radiation & Nuclear
Safety
P.O.Box 14
00881 Helsinki
Finland

Mr Francis Bermann
c/o Mr le Conseiller Médical du CEA
31-33 rue de la Fédération
75752 Paris Cedex 15
France

Dr Juan Bernar Solano
Asociación de Medicina y Seguridad
en el Trabajo de UNESA
para la Industria Eléctrica
c/Francisco Gervás
28020 Madrid
Spain

Mr Alain Biau
Département de Radiophysique
Office de Protection contre
les Rayonnements Ionisants
B.P. 35
78110 Le Vesinet
France

Dr Maria Blettner
Institut für Epidemiologie und Biometrie
Deutsches Krebsforschungszentrum
Im Neuenheimer Feld 280
69009 Heidelberg 1
Germany

Dr Lucy Carpenter
Department of Public Health
and Primary Care
Gibson Building
The Radcliffe Infirmary
Oxford OX2 6HE
United Kingdom

Mr George Cowper
4 Cartier Circle
Deep River, Ontario K0J1P0
Canada

Dr Pascal Deboodt
SCK/CEN
Boeretang 200
2400 Mol
Belgium

Dr Asunción Diez Sacristán
Consejo de Seguridad Nuclear
Justo Dorado 11
28040 Madrid
Spain

Dr Monica Eklöf
Statens Vattenfallsverk Forsmark
742 00 Osthämmar
Sweden

Dr Hilde Engels
SCK-CEN
Medical Department
Boeretang 200
2400 Mol
Belgium

Dr Jack Fix
Pacific Northwest Laboratories
Battelle
P.O. Box 999
Richland, WA 99352
USA

Dr Ethel S. Gilbert
Pacific Northwest Laboratories
Battelle
P.O. Box 999
Richland, WA 99352
USA

Dr Lois M. Green
Health Services Department
Health and Safety Division
Ontario Hydro
700 University Avenue
Toronto, Ontario M5G 1X6
Canada

Dr E. Gubéran
Médecin inspecteur du travail
Rue Ferdinand-Hodler 23
1207 Genève
Switzerland

Dr Gabriel Gulis
Institute of Hygiene and Epidemiology
Limbova 6
917 00 Trnava
Slovak Republic

Dr Celia Hacker
Australian Nuclear Science
Technology Organisation
Health and Safety
PMB 1
Menai, NSW 2234
Australia

Dr Matti Hakama
Department of Public Health
University of Tampere
33101 Tampere
Finland

Dr Catherine Hill
Institut Gustave-Roussy
39, rue Camille Desmoulins
94508 Villejuif Cedex
France

Dr Karol Holan
Slovenske elektrárne a.s.
Hranicná 12
82736 Bratislava
Slovak Republic

Dr Yutaka Hosoda
Institute of Radiation Epidemiology
Radiation Effects Association
Kanda Kajicho 3-6-7
Chiyodaku Tokyo 101
Japan

Dr Geoffrey Howe
School of Public Health
Columbia University
600 West 168th Street
New York, N.Y. 10032
USA

Dr John Kaldor
National Centre in HIV Epidemiology
and Clinical Research
376 Victoria Street
Sydney, NSW 2010
Australia

Dr Gerry Kendall
National Radiological Protection Board
Chilton, Didcot, Oxon OX 11 0RQ
United Kingdom

Dr Andor Kerekes
"Frédéric Joliot-Curie" National
Research Institute for Radiobiology
and Radiohygiene
P.O.Box 101
H - 1221 Budapest
Hungary

Dr Hans Malcker
Midsweden Research and Development
Center
Sundsvall Hospital
85186 Sundsvall
Sweden

Mr Tony Mazzocchi
OCAW International Union
c/o CSRL
P.O.Box 19367
Washington, DC 20036
USA

Dr Mirjana Moser
Bundesamt für Gesundheitswesen
und Strahlenschutz
Bollwerk 27
3001 Bern
Switzerland

Dr Colin R. Muirhead
National Radiological Protection Board
Chilton, Didcot, Oxon OX11 0RQ
United Kingdom

Mr William Murray
Department of Health &
Human Services - NIOSH
4676 Columbia Parkway
Mail Stop R-44
Cincinnati OH 45226-1988
USA

Mr Robert Rinsky
Department of Health &
Human Services - NIOSH
4676 Columbia Parkway
Mail Stop R-44
Cincinnati OH 45226-1988
USA

Professor Tapio Rytomaa
Finnish Centre for Radiation
and Nuclear Safety
P.O.Box 14
00881 Helsinki
Finland

Mr Len Salmon
8, Upton Close
Abingdon, Oxon OX14 2AL
United Kingdom

Dr Günter Seitz
Berufsgenossenschaft Feinmechanik
und Elektrotechnik
Gustav-Heinemann-Ufer 130
5000 Köln 51
Germany

Dr Istvan Turai
"Frédéric Joliot-Curie" National
Research Institute for Radiobiology
and Radiohygiene
P.O.Box 101
H - 1221 Budapest
Hungary

Prof. Takesumi Yoshimura
Institute of Industrial Ecological
Sciences
University of Occupational and
Environmental Health Japan
1-1 Iseigaoka Yahatanishiku
Kitakyushu 807
Japan

IARC: Dr E. Cardis
Dr B.K. Armstrong
Dr I. Kato
Dr A. Mylvaganam
Ms C. Lavé
Ms H. Renard

Annex 3

International Collaborative Study of Cancer Risk among Radiation Workers in the Nuclear Industry

List of meetings of the Study Group and SubCommittees

- Spring 1993: meeting of the Epidemiology and Dosimetry SubCommittees to discuss and expand draft Procedures Document and discuss study of errors in dosimetry;
- Spring 1994: meeting of the Epidemiology SubCommittee to review problems, progress of data collection and modify procedures as needed;
- Spring 1994: meeting of the Dosimetry SubCommittee to finalise the protocol of the retrospective dosimetry study and review problems with collection of dosimetric data;
- Fall 1994: meeting of full Study Group to discuss progress and problems.

**Final Report
1992 - 1994**

Contract: FI3PCT920004 Duration: 1.9.92 to 30.6.95

Sector: C2A

Title: Development of fundamental data for radiological protection.

1) Smith ICRP

I. Summary of Project Global Objectives and Achievements

The primary aim of radiological protection is to provide an appropriate standard of protection of man without unduly limiting the beneficial practices giving rise to radiation exposure. To achieve this end, it is necessary to quantify the detriment associated with exposure and to develop general policies for protection of populations and individuals exposed to external penetrating radiations and incorporated radionuclides.

Such protection policies are published in the form of recommendations of the International Commission on Radiological Protection (hereafter, the Commission). The Commission is aided by four standing scientific committees and ad hoc task groups, who meet at appropriate intervals to allow interchange of information, thereby coalescing the opinions and experience of about one hundred eminent scientists who have established reputations in the fields of radiation protection, radiobiology, radiation physics and medical radiology. This form of international cooperation which provides a consensus on radiological protection policy is intended to meet the guidelines of a multi-disciplinary and trans-national effort. In the past it has provided guidelines for the Commission of the European Community to prepare and update its directives on health protection within the community and as a basis for rationalisation of the Community programme on the development of nuclear energy.

The most recent conceptual framework of radiological protection published in 1990 (*ICRP Publication 60*) depends on a system of protection which requires justifying a practice, optimising the protection using source-related dose constraints to individuals, and overriding dose or risk limits. The objectives of the committees and task groups in aiding the Commission are:-

- To assess the risk and severity of deterministic effects and the induction rates of stochastic effects. Current considerations are the physical characteristic of different radiations and tissues, the molecular changes caused by the interaction of radiation with cells and genetic susceptibility to induced stochastic effects.
- To develop values of secondary standards, based on the Commission's recommended basic dose limits. This involves the derivation of limits for intakes of radionuclides that lead to *in situ* tissue and organ irradiation and the derivation of maximum fluences for external irradiation.
- To provide advice on radiation protection in medicine. Matters requiring attention include protection of the patient in radiodiagnosis and nuclear medicine and optimising protection of medical workers exposed to ionising radiations in the environment of radiology and radiotherapy departments and wards.
- To provide advice on the practical applications of the Commission's system of radiological protection of workers in the nuclear industry and members of the public who may be exposed as a consequence of releases of radioactivity into the environment from nuclear sites.

Head of project 1: Dr. Smith

II. Objectives for the reporting period

Adoption of the basic recommendations necessitated a revision of several important concepts in their application. These are described in Section III in a series of reports published during the contractual period. They include providing dose coefficients from intakes of radionuclides; defining the relationship between radiological protection quantities recommended by ICRP and the operational quantities recommended by ICRU; and the principles for intervention for protecting the public in a radiological emergency.

III. Progress achieved including publications

One report (*ICRP Publication 63*) discusses the principles for intervention for protecting the public in a radiological emergency. It provides guidance on the protective actions necessary to avert exposures via various pathways and on techniques to derive generically optimised intervention levels. This report updates and extends earlier advice (*ICRP Publication 40*) and includes quantitative guidance on intervention levels. This guidance covers the introduction of such protective actions over very short times, their introduction and continuation following periodic review over protracted timescales and intervention over larger areas of contamination.

A second report (*ICRP Publication 64*) outlines a conceptual framework for protection from potential exposures, that is exposures that, while not certain to occur, can be anticipated as a result of introducing or modifying a practice, and to which a probability of occurrence can be assigned. The report provides a unified set of principles combining radiological protection and nuclear safety. It gives numerical values for constraints on annual probabilities of sequences of events leading to detrimental health effects.

A third report (*ICRP Publication 65*) discusses protection against radon-222 at home and at work. It summarises the extent of current knowledge about the health effects of inhaled radon and its progeny and makes recommendations for the control of exposure to radon-222 in both dwellings and workplaces. It aims to give guidance to national advisory and regulatory agencies and to practitioners of radiological protection concerned with radon in dwellings and workplaces. On the basis of a nominal fatality and detriment coefficient of 8×10^{-5} per (mJ h m^{-3}) and dose conversion conventions expressed as effective dose per unit exposure, of 1.1 and 1.4 mSv per (mJ h m^{-3}) at home and at work respectively, the action level ranges recommended in dwellings and workplaces are 200-600 and 500-1500 Bq m^{-3} respectively. These values correspond to an annual effective dose of 3 - 10 mSv for both members of the public and workers. The occupational limit of exposure recommended is 14 mJ h m^{-3} per year averaged over 5 years, with a maximum of 35 mJ h m^{-3} in a single year. In historical units, these values correspond to 4 WLM per year averaged over 5 years, with a maximum of 10 WLM in a single year.

A fourth report (*ICRP Publication 66*) describes in detail how to calculate radiation doses to the respiratory tract resulting from intakes of airborne radionuclides. This respiratory tract model which supersedes the previous model introduced in 1966, was motivated by the availability of increased knowledge of the anatomy and physiology of the respiratory tract, of the deposition and clearance characteristics of inhaled particulate and the effects of inhaled radioactive substances. The model considers the competitive processes of translocation of inhaled material to blood and the mechanical clearance of particles from the airways. It provides most of the flexibility needed to calculate doses to the respiratory tract for a wide range of exposure conditions and for specific individuals. The model allows calculations of doses for members of the public in addition to workers; is useful for predictive and assessment purposes as well as for deriving limits on intakes; accounts for the influence of smoking, air pollutants, and respiratory tract diseases; provides for estimates of respiratory tract tissue doses from bioassay data; and is equally applicable to radioactive gases as well as to particles.

In 1987, a task group was established with the objective of evaluating dose per unit intake for members of the public using age-dependent physical models and appropriate biokinetic information. The first report (*ICRP Publication 56*) provided dose coefficients to members of the public from intakes by ingestion of radioisotopes of eleven elements this report has been supplemented (*ICRP Publication 67*) with information on dose coefficients from intakes by ingestion of radioisotopes of a further thirteen elements. This report gives parameters for the tissue distribution and retention of these elements with data on urinary and faecal excretion. New biokinetics models for strontium, plutonium, americium and neptunium are also included.

In order to permit immediate application of the 1990 basic recommendations, revised values of the Annual Limits on Intake based on the methodology and biokinetic data used in *ICRP Publication 30*, but which incorporated the new dose limits and tissue weighting factors from *ICRP Publication 60* were issued as *ICRP Publication 61*. Since this publication, a revised kinetic and dosimetric model of the human respiratory tract has been published. A consequent report (*ICRP Publication 68*) gives values of dose coefficients for workers using this new respiratory tract model. It provides doses per unit intake values for aerosols of 1 μm and 5 μm AMAD and revised biokinetic models for some elements. The report summarises

the new respiratory tract model in a convenient form and lists the sources of data which differ from those adopted previously in *ICRP Publication 30* and *ICRP Publication 61*. The report also includes a treatment of gases and vapours which is not addressed in *ICRP Publication 61*. A number of radionuclides discussed in the report decay to isotopes of other elements which are themselves radioactive, but which behave differently to the parent radionuclide once they enter the body. With this in mind, doses were calculated for the parent and its decay products separately in the case of the elements lead, radium, tellurium, thorium and uranium.

A seventh (*ICRP Publication 69*) covers the development of age-dependent physical and biokinetic models and the selection of parameter values to calculate dose per unit intake for members of the public for the isotopes of iron, selenium, antimony, thorium and uranium. The generic biokinetic models used in *ICRP Publication 67* for the actinides have been applied to thorium and uranium respectively. This is the third of a series of reports of this Task Group on doses to members of the public.

In order to progress the work of the Task Group on Reference Man, the Commission had previously agreed that there would not be a single report as there had been in *ICRP Publication 23* but rather, that separate reports would be issued on specific aspects as the work was completed. The first is on the skeleton and has been adopted by the Commission to appear as *ICRP Publication 70*. Increased emphasis has been given to the normal biological variability among humans and to information on children. This extensive review of the current state of knowledge of the skeleton will be of widespread use, not only in the radiation protection community, but generally in medical and other fields. The reference skeleton is intended to represent Western man, although selected data for non-Western man has been included, where appropriate. The next two reports of this Task Group are planned to cover the basic anatomical and physiological data required for dose calculations and the gastrointestinal tract.

A draft report of the joint Task Group with ICRU on "*Dose-related Quantities for Radiological Protection against External Radiation*" is now under consideration for adoption. The key question to be addressed is whether the operational quantities recommended by ICRU, and using the new Q-LET relationship in *ICRP Publication 60*, represent adequately the Commission's protection quantities, principally effective dose. The issue will be discussed by both Commissions in September and it is to be anticipated that a report will be published thereafter.

Publications

ICRP Publication 30, Limits for the Intake of Radionuclides by Workers, Part 1. *Annals of the ICRP* 2 (3/4), 1979.

ICRP Publication 40, Protection of the Public in the Event of Major Radiation Accidents: Principles for Planning. *Annals of the ICRP* 14 (2) 1984.

ICRP Publication 60, 1990 Recommendations of the International Commission on Radiological Protection. *Annals of the ICRP* 21 (1-3), 1991.

ICRP Publication 61, Annual Limits on Intake of Radionuclides by Workers Based on the 1990 Recommendations. *Annals of the ICRP* 21 (4), 1991.

ICRP Publication 63, Principles for Intervention for Protection of the Public in a Radiological Emergency. *Annals of the ICRP* 22 (4), 1991.

ICRP Publication 64, Protection from Potential Exposure: A Conceptual Framework. *Annals of the ICRP* 23 (1) 1993.

ICRP Publication 65, Protection against Radon at Home and at Work. *Annals of the ICRP* 23 (2) 1993.

ICRP Publication 56 Part 2, Age Dependent Doses to Members of the Public from Intake of Radionuclides. *Annals of the ICRP* 23 (3/4) 1993 (in press).

ICRP Publication 66, Human Respiratory Tract Model for Radiological Protection. *Annals of the ICRP* 24 (1-3) 1994.

ICRP Publication 67, Age-Dependent Doses to Members of the Public from Intake of Radionuclides: Part 2, *Annals of the ICRP* 23 (2-3) 1993.

ICRP Publication 68, Dose Coefficients for Intakes of Radionuclides by Workers: A Replacement of ICRP Publication 61. *Annals of the ICRP* 24 (4) 1994, [in press].

Summary of the current ICRP principles for Protection of the Patient in Nuclear Medicine. To appear as a supplement in the *Annals of the ICRP* 24 (4) 1994, [in press].

ICRP Publication 69, Age Dependent Doses to Members of the Public from Intake of Radionuclides: Part 3. Ingestion Dose Coefficients

ICRP Publication 70, Basic Anatomical and Physiological Data for Use in Radiological Protection. Part 1. Skeleton

ICRP Publication 71, Dose-Related Quantities for Radiological Protection Against External Radiation. A joint report with ICRU (1995/96).

Financial report for the period 1/9/92 - 30/6/95

Details of the breakdown of costs as discussed in the original proposal are as follows:

Labour (Scientific Secretary and Administrative Assistant)

54,706 ECU, representing 35.5 % of the total cost of 218,822 ECU

Travel for members attending meetings

96,312 ECU, representing 62.5 % of the total cost of 385,250 ECU

Consumables (office stationery etc.)

3,082 ECU, representing 2% of the total cost of 12,328 ECU.

Details of travel

Travel funds used from the CEC contract for those European members of ICRP claiming expenses to attend meetings within the period 01/09/92 to 30/06/95. Those claiming expenses include:

H P Jammet

J H Hendry

L E Holm

K Sankaranarayanan

I A Likhtarev

D M Taylor

W Jaschke

G J Köteles

S Mattsson

P Ortiz

H Ringertz

P J Roberts

J G B Russell

C Zuur

R Hock

C J Huyskens

F Luyckx

K Ulbak

J Valentin

COMMITTEE 1 MEETINGS

Bournemouth, UK 20 - 24 September 1993

Committee 1 Task Group meetings on Genetic Predisposition to Cancer

Hungerford, UK 27 - 29 June 1993

COMMITTEE 2 MEETINGS

Bournemouth, UK 20 - 24 September 1993

Cadarache, France 30 May - 3 June 1994

Committee 2 Task Group meeting on Age-Dependent Doses to Members of the Public
from Intakes of Radionuclides

Berlin, Germany 25 - 28 April 1993

Committee 2 Task Group meetings on Age-Dependent Doses from Internal Dosimetry
Chilton, UK 25 - 29 April 1994

Committee 2 Task Group meetings on Dose Calculations
Chilton, UK 24 - 28 January 1994

Committee 2 Task Group meetings on Data for Use in Radiation Protection Against
External Radiation

Neuherberg, Germany 10 - 14 May 1993

Chilton, UK 28 November - 2 December 1994

Munich, Germany 27 - 31 March 1995

COMMITTEE 3 MEETINGS

Bournemouth, UK 20 - 24 September 1993

Vienna, Austria 25 - 29 April 1994

Committee 3 Task Group meetings on Radiological Protection and Safety in Medicine
The Hague, The Netherlands 15 - 16 December 1993 and 6 - 8 October 1994

Committee 3 Task Group meetings on Radiation Doses to Patients from
Radiopharmaceuticals

Malmo, Sweden 18 - 20 June 1993 and 10 - 11 April 1994

COMMITTEE 4 MEETINGS

Bournemouth, UK 20 - 24 September 1993

Stockholm, Sweden 18 - 22 April 1994

Committee 4 Task Group meetings on Principles for Protection of the Public against
Chronic Exposure Situations

Chilton, UK 12 - 16 December 1994

Paris, France 24 - 28 April 1995

Committee 4 Task Group meetings on General Principles for the Radiation Protection
of Workers

Eindhoven, The Netherlands 12 - 14 January 1994

Paris, France September 1994 and 24 - 28 April 1995

Committee 4 Task Group meetings on Protection from Potential Exposures:
Application to selected radiation sources

Offenbach-am-Main, Germany 31 January - 4 February 1994

Stockholm, Sweden 1 - 5 May 1995



**Final Report
1992 - 1994**

Contract: F13PCT920033 Duration: 1.9.92 to 30.6.95 Sector: C21

Title: ALARA in Installations.

- | | | |
|----|----------|------------|
| 1) | Lefaire | CEPN |
| 2) | Zeevaert | CENSCK Mol |
| 3) | Pfeffer | GRS |
| 4) | Wrixon | NRPB |

I. Summary of Project Global Objectives and Achievements

I.1 Introduction

The ALARA principle (all exposures shall be kept As Low A reasonably Achievable) is an explicit requirement of the E.C. Directives laying down the basic safety standards for radiological protection. It has been progressively incorporated into most European national regulations where in most cases it appears as a top level general requirement or objective.

ALARA and National regulations in Europe

Countries	Date and reference text	Wording of optimisation
Belgium	Royal Decree, 25/04/1987	
Ireland	Statutory Instruments 43, 1991	
Luxembourg	Grand-ducal Regulation, 29/10/1990	"...as low as reasonably possible"
Netherlands	Decree, 10/09/1986	
Spain	Royal Decree 53/1992, 24/01/1992	
Denmark	Regulation 383, 1986	"as low as reasonably achievable"
United Kingdom	Regulations 1985	"restrict so far as reasonably practicable"
Greece	Decree, 19/07/1991	"as low as reasonably achievable technological feasibilities, results of cost-benefit analysis and in general every other social and economic factor being taken into account"
France	Decree, 20/06/1966 modified 1988 (general principles of radiation protection) Decree, 02/10/1986 modified 1988 and Decree, 28/04/1975 modified 1988 (occupational radiation protection)	"...as low as possible" "...as low as reasonably possible"
Italy	President Decree, 13/02/1964, never revised	"...to reduce workers exposures, taking into account good current practice"

I.2 Global objectives during the period 1992-1995

The first CEC joint project in ALARA (1986-1989), involving NRPB (UK) and CEPN (France), focused mainly on fundamental concepts (detriment, man sievert value ...) and ALARA methodology (the so called ALARA Procedure, ALARA Audit, Predictive ALARA Planning and decision aiding techniques...). The end product was the CEC book « ALARA: From theory towards practice ».

The second CEC / NRPB CEPN contract (1990-1991) began with the development of structured ALARA Programmes at the operational stage of Nuclear Installations, covering management commitment, appropriate organisational structures and the motivation, awareness and training of staff. This contract saw the definition of softwares and databases to facilitate the actual implementation of the ALARA methodology .

The joint project (1992-1995) was the final step of the whole programme started in 1986, ALARA being now, not only part of all regulations, but also more and more part of the actual practices. This step aimed mainly at completing the previous work in:

- taking into consideration the impact of ICRP 60 recommendations on ALARA theoretical background (dose and risk constraints, equity and alpha value, potential exposures, complex situations, risk management and social values...) as well as on their integration into radiation protection programmes.
- covering larger areas of research for the setting up of ALARA Programmes : at the design and decommissioning stages of installations ; through « management of work » during normal operations; allowing to take into account radiation protection optimisation for Nuclear Safety decisions ; within the non nuclear industrial sector...
- developing a new generation of ALARA tools such as decision aiding softwares and feed back data bases to allow a wide dissemination of the ALARA practice.

Four teams (SCK-CEN MOL, CEPN, GRS, NRPB) from four CEC member states (Belgium, France, Germany, United Kingdom) have been selected for this joint project.

I.3. Achievements

I.3.1 Dissemination of the ALARA methodology

As expected the ALARA methodology has been tested in, and applied to, several areas where specific methodological problems had to be solved.

ALARA and decommissioning

This problem was the core of the work programme of SCK-CEN MOL. Decommissioning appeared rapidly as a quite complex situation with four decision levels : - the global strategy level with decision to be taken on the scale and timing of the different consecutive phases of the decommissioning; - the decommissioning methodology where choices are to be made between various dismantling techniques and between protection options; - the dismantling operation level that raises the problems of both skin dose and internal contamination ; - the level of waste management with a total amount of wastes generated as important as during the total operational life of the installation.

As a first approach to optimisation, technical, radiological, economical and social attributes have been considered as a function of the time. The evolution of these major attributes have been graphically depicted for a reactor of the BR3 type (PWR at SCK.CEN). Although the optimisation of the decommissioning strategy can be considered from the radiological point

of view, it is obvious that cost benefit analysis use is not worthwhile, as many other factors are of major importance, particularly the economical ones.

ALARA and internal exposure

Already raised through the previous thema, the application of ALARA to internal exposure appeared to be an important subject to be discussed « per se », as over the years most optimisation studies have tended to focus on situations involving relatively predictable doses from external exposure. Both NRPB and CEPN teams gave particular focus of work on that topic during the contract. The first team approached the problem through a discussion of how the ALARA Procedure might be implemented; the second team focused on problems dealing with the probabilistic component of occurrence of most internal exposure cases. Some of the more important points discussed were that:

- a good knowledge of work pattern associated with exposure routes, probabilities of exposure, and level of exposure appears to be a prerequisite to optimisation implementation.
- in many cases inhalation is likely to be the dominant internal exposure route and the adaptability of personal air sampling to provide task specific data makes it the monitoring technique that is most likely to provide a useful input to ALARA studies.
- even if there is a general consensus that individuals are more reluctant to receive internal exposure than external exposure, there is no evidence for valuing internal exposure differently to external one, as far as the reference monetary value of the man sievert is concerned.

ALARA and Work Management

During last decades much has been done to reduce doses through management of sources and dose rates. There was then a need to identify, and to quantify, the various factors influencing the level of exposed workload, in order to develop a « model » aiming at quantifying the effectiveness of protection actions, both from dosimetric and economic point of views. GRS and CEPN participated to that work during this contract.

GRS mainly focused on inspections and tests frequencies, planning and preparation in Nuclear Power Plants through a very detailed survey of the activities and doses of one plant. It has showed that it is reasonable and practicable to harmonise and concentrate tests inspection and maintenance on systems and components, avoiding then redundancies in preparative work, and increasing cost efficiency of dose reduction options.

CEPN identified various factors having direct or indirect impacts on the productive exposed time, such as working conditions (individual and collective protections, noise, light, thermal conditions etc...), "Human factors" (qualification of workers, radiation protection education, experience level, ...), work organisation (scheduling of tasks, preparation of working areas...). A detailed survey was carried out in five French nuclear power plants and was augmented by a literature review. It allowed to quantify the impact of some working conditions factors. In order to complement the survey, a specific study has been performed to quantify the impact of various types of protective suits used in French nuclear installations according to the type of work to be done. A study of outage organisation in 4 different nuclear power plants from various countries has then been performed. It allowed to highlight some "good practices" favouring the implementation of ALARA programmes.

ALARA courses and workshops

There has been a strong interaction between the work of this project and the series of CEC sponsored courses on Optimisation of Radiation Protection for which CEPN and NRPB have provided the joint scientific coordinators. These courses have been a means of increasing the

awareness of the radiological protection community to work management approaches and to their effectiveness. They have also provided an important input to the work on optimisation and internal exposure. During the contract, courses were held at Vattenfall Nuclear Power Plant, Ringhals (Sweden), KfK, Karlsruhe (Germany), and Madrid (Spain).

During the early part of the contract a major feature of the work was the input to the Fourth European Scientific Seminar on Optimisation, Luxembourg 1993. A number of other presentations were made during the contract to further disseminate these ideas. It is perhaps of note that the last of these presentations at the 3rd International Workshop on the Implementation of ALARA, at BNL Brookhaven USA, effectively reviewed the 'state of the art' of optimisation in Europe.

I.3.2. A new generation of ALARA tools

In order to facilitate an even more wide dissemination of the ALARA culture and practice it appeared necessary to develop specific tools, such as feed back data bases or decision aiding software.

Ionising Radiation incident Database (IRID)

A key element in preventing accidents and being able to mitigate their consequences is the ability to learn rapidly from previous mistakes. In most countries there is no system to deal with that problem in the non nuclear sector, despite the widespread use of ionising radiation in the industry. Therefore, during this contract, NRPB has developed the structure and operational methods of an accident data base: IRID. The database has been designed to cover radiological accidents in industry, medical research and teaching. It operates on a personal computer using dBase V software.

DECOM Database

A serious problem pointed out through the analysis of ALARA and decommissioning was the lack of data for various important radiological protection factors. Therefore during this contract SCK.CEN has developed the structure of a specific database including doses, costs and wastes for dismantling operations. This database has been developed using MS-ACCESS (version 2). Fields were first determined and data input, based on the BR3 dismantling operations. The possibility of importing data from other databases has then been investigated. With the help of GRS, the selection and appending of data from the CEC DB-COST database, was carried out readily.

OPTI-RP software

Earlier in the project it was identified that there was a need for the development of user friendly software that would facilitate non specialists using decision aiding techniques. The development of this software, called OPTI-RP, has been performed by CEPN, in collaboration with NRPB, during that step of the project. It has been developed using Access® under Windows®. The software is available in French and English languages. A French users guide is to be provided by the end of November 1996. Three decision aiding techniques are included in the software: Cost-Benefit Analysis, Differential Cost-Benefit Analysis and Reasonable Cost Analysis.

I.3.3 Conceptual and theoretical improvements

Within the framework of the CEC Research Programme on Optimisation of Radiation Protection, two workshops were organised by CEPN at Cernay (France) in June 1993 and at Mons (Belgium) in June 1994. The aim of these workshops was to discuss with a group of European economists how some recent methodological developments and models in the

field of economics, insurance and risk theory could be the bases for integrating social and ethical issues within radiological risk management.

A model for the monetary valuation of the unit of the collective exposure depending upon the individual level of exposure was finalised, taking into consideration not only the collective exposure to ionising radiation but also its dispersion in the population. The second subject was related to the time dimension and the use of classical discounting procedures when dealing with radiological protection and health care investments. Demonstration was also made that the financial interest rate is not the only factor to drive the integration of time in case of "non marketable goods" such as radiological protection investments.

Other topics were discussed like - the individual perception of low probability effects, - equity issues and risk transfers in radiological risk management, - the 'willingness to pay' approach, - the methodological problems raised by catastrophic events and far future radiological exposures. They pointed out perspectives on the methodological developments on the integration of social and ethical issues within radiological risk management.

I.4 Future challenges

On the one hand as far as ALARA and normal operation of installations is concerned, much has been done during the three periods of this joint project and one may say that ALARA is now an applied European concept belonging less and less to the research field. What appears now important is to consolidate the programme in its practical applications and to further disseminate the ALARA concept, culture and tools in broader fields. This should be done through the next EC ALARA courses, and mainly through a European ALARA Network allowing: - to promote the wider and more uniform use of optimisation techniques in the various sectors of use in Europe, - to provide focuses and mechanisms for the exchange and dissemination of information from practical experience and, - to provide feedback to users and the commission's work programme on practical difficulties and identification of further conceptual and methodological developments.

On the other hand the research on concepts and tools allowing an implementation of ALARA in complex situations is far from being achieved.

The question of perception of low probabilities events by individuals, using preference revelation methods should be developed.

When facing risk transfer situations, further developments, could be devoted to the key factors explaining the differentiation between the exposed populations, taking into account equity and economic considerations (i.e. aversion towards the dispersion of risk, confidence of the public, differentiation between public and workers,...).

Finally, the problem of 'intergenerational' radiological risk transfers (for example in the case of the treatment and storage of nuclear wastes) need to be addressed as a specific case of risk transfer because the use of discounting methods when facing very long horizons does not seem to be satisfactory. This problem could be explored in the light of the optimal allocation of social resources taking into account the welfare of all future generations.

Head of project 1: Dr. Lefauve

II. Objectives for the reporting period

The CEPN objectives in this contract were:

- to discuss concepts and methods for the integration of social and ethical values in the radiological risk assessment ; the main topic of this work being to discuss a model aiming at providing a reference monetary value system for the man-sievert ensuring an equitable implementation of ALARA .
- to determine and develop specific concepts, procedures and tools allowing to better apply the ALARA Principle to the management of the duration of exposure and the number of exposed workers, i.e. to focus on a generic approach of ALARA and Work Management.
- to provide those in charge of performing ALARA studies with an «ALARA» decision aiding tool, i.e a very user friendly software package for performing cost benefit and reasonable cost analysis, taking into account the new ICRP 60 framework and the developments in valuating the man sievert.
- to disseminate the main results of the joint project through general publications, specific E.C courses and seminars [5, 7, 12, 14, 16].

III. Progress achieved including publications

III.1. Theoretical improvements

Within the framework of the CEC Research Programme on Optimisation of Radiation Protection, a first workshop was organised in Cernay (France) in June 1993. The aim of this workshop was to discuss with a group of European economists how some recent methodological developments and models in the field of economics, insurance and risk theory could be the bases for integrating social and ethical issues within radiological risk management.

Several subjects were discussed. The first one concerned the concept of aversion to the dispersion of exposure as the International Commission on Radiological Protection (ICRP) stressed the need to take into consideration not only the collective exposure to ionising radiation but also its dispersion in the population when radiological investments are performed and analysed. This concept was discussed in its relation with the monetary valuation of the unit of collective exposure that is to be used in cost benefit analyses. The interdependence of the various key parameters included in this monetary valuation and especially the role of the coefficient characterising the degree of aversion to the dispersion of risks were pointed out. The following model for the monetary valuation of the unit of the collective exposure depending upon the individual level of exposure was finalised [1].

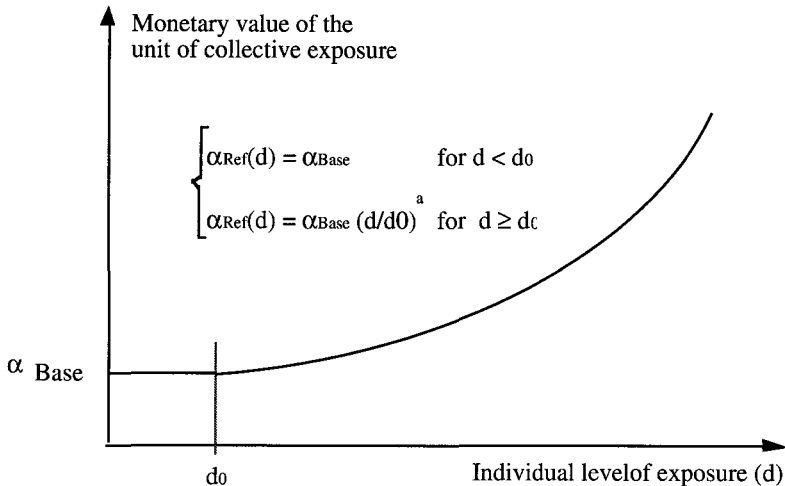
$$\begin{array}{l} \alpha_{\text{Ref}}(d) = \alpha_{\text{Base}} \quad \text{for } d < d_0 \\ \alpha_{\text{Ref}}(d) = \alpha_{\text{Base}} (d/d_0)^a \quad \text{for } d \geq d_0 \end{array}$$

where:

$\alpha_{\text{Ref}}(d)$: reference monetary value of the unit of collective dose for the annual level of individual exposure d
 d : annual level of individual exposure

- α_{Base} : basic monetary value of a unit collective exposure
- d_0 : upper level of individual exposure for which $\alpha_{Ref}(d) = \alpha_{Base}$
- a : coefficient characterising the degree of aversion to the dispersion of risks
($a = 0$ for $d < d_0$; $a \neq 0$ for $d \geq d_0$)

This model is illustrated in the following figure where the ordinate is the monetary value of the unit of collective exposure, and on the abscissa is the individual level of exposure, generally in term of annual dose.



A model for the monetary valuation of the radiological detriment

The second subject was related to the time dimension and the use of classical discounting procedures when dealing with radiological protection and health care investments. The topic was discussed with regards to the economic theory which demonstrates that the financial interest rate is not the only factor to drive the integration of time in case of "non marketable goods" such as radiological protection investments [2, 3].

Finally, the group discussed the methodological problems raised by catastrophic events and far future radiological exposures. Starting from the technical evaluations of consequences due to nuclear accident and high level waste disposal, social and economic issues were pointed out. The questions of low probability events and very long term effects were discussed and it appeared that there was a need for further investigations in this field.

As a result of the seminar, a first series of papers was prepared. A second workshop was then organised in June 1994 at the Catholic University of Mons (Belgium) to go deeper into specific subjects. Three main topics were discussed :

The first one dealt with the individual perception of low probability effects. Some recent researches in the economic modelling of individual behaviours when dealing with low probability events were presented as well as the results of an experimental study in the field of radiation exposure.

The second topic was devoted to equity issues in radiological risk management. Some preliminary reflections on risk transfers were presented, focused on transfers between public and workers exposures and its consequences on the monetary valuation of the unit of collective exposures.

Finally, a specific attention was also given to the 'willingness to pay' approach developed by economists to reveal individual and social preferences concerning health and safety investments [10].

These two workshops have been summarised in a global report [20]. They pointed out perspectives on the methodological developments on the integration of social and ethical issues within radiological risk management. In particular, it appears necessary to integrate within the optimisation procedures considerations related to potential exposures, those related to the risk transfers between different exposed populations, as well as those to be expected in the far future.

Concerning potential exposure, it has appeared necessary to identify and to describe the various exposure situations. Above this description, the development of the methodologies for implementing optimisation in the case of potential exposures could be focused on:

- the analysis of the perception of low probabilities by individuals, using preference revelation methods;
- the integration of experimentation results in terms of low probability perception as well as risk aversion within prevention policies and optimisation process in radiation protection.

When facing risk transfer situations, further developments, especially from an economic point of view, could be devoted to the definition of the key factors explaining the differentiation between the exposed populations, taking into account equity and economic considerations (i.e. aversion towards the dispersion of risk [19], confidence of the public, differentiation between public and workers,...). Additionally, the use of contingent valuation approaches to reveal preferences of each category of exposed population towards risk dispersion could be explored. Finally, the problem of 'intergenerational' radiological risk transfers (for example in the case of the treatment and storage of nuclear wastes) need to be addressed as a specific case of risk transfer because the use of discounting methods when facing very long horizons does not seem to be satisfactory since discounting reduces costs exponentially and makes the welfare of future generations less important than the welfare of current generations. This problem could be explored in the light of the optimal allocation of social resources taking into account the welfare of all future generations.

III.2. ALARA and potential exposures

Up to now, the optimisation of radiation protection has been mainly applied to external exposure during normal operations of plants. Exposures due to incidents as well as contamination, were more or less excluded of the ALARA scheme. It is then necessary to develop specific methods dealing both with the reduction of probability of occurrences (prevention), and level of the damage (mitigation). Such a work began during the reporting period and it already led to a presentation at a BNL meeting (US) in May 1994 [13]. A first conclusion proposes that the same alpha value system might be used for both internal and external exposures, taking into account the actual level of risk and the aversion towards risk dispersion.

III.3. ALARA and Work Management

During last decades much has been done to reduce doses through management of sources and dose rates. The goal of the research concerning ALARA and work management was to identify, and to quantify, the various factors influencing the level of exposed workload, in order to develop a « model » aiming at quantifying the effectiveness of protection actions,

both from dosimetric and economic point of views. This work has been implemented with an active support of Electricité de France and Framatome.

While analysing the total exposed time resulting from any maintenance operation, it appears that it can be split into two main parts: the "productive" and the "non-productive" time. The productive exposed time can be defined as the time which is technically necessary in order to complete the task, given the state of the technology and the set of working conditions. The non-productive exposed time usually results of mishaps due to bad training of workers, malfunctioning of tools etc....

Various factors having direct or indirect impacts on the productive exposed time have been identified. They can be grouped together into three main categories:

a) Working conditions

- Individual and collective protections
- Noise, light, thermal conditions etc....
- Dimension of the working area
- Ambient dose rate
- Adaptation of tools

b) "Human factors"

- Qualification of workers
 - Radiation protection education
 - Specific speciality related training
 - Specific task related training
- Experience level
 - Individual experience
 - Transfer of experience between teams
- Motivation of actors
 - Individual motivation
 - Management commitment

c) Work organisation

- Scheduling of tasks
- Preparation of working areas
- Preparation of equipments
- Level of information of the workers

A modification of one or several working conditions' factors will have a direct impact on the productivity of workers and then influence directly the productive exposed time. The factors characterising the operators will modify the productive exposed time and mainly the non productive one which is usually due to a bad knowledge of working areas and tasks to be performed. The general work organisation will particularly affect the non productive exposed time.

In order to quantify the impact of these factors, a detailed survey was carried out in five French nuclear power plants, focusing on three types of operations: primary valves maintenance, decontamination of reactor cavity and specialised maintenance operations on the steam generator. This survey was augmented by a literature review on the influence of "hostile" environment on working conditions. It allowed to quantify the impact of some working conditions factors [4,6]. In order to complement the survey, a specific study has been performed in order to quantify the impact of various types of protective suits used in French nuclear installations according to the type of work to be done [8].

The following tables presents a summary of both literature and survey results.

Impact of working conditions on the exposed time

Working conditions	Impact on exposed time
Light	+ 20 % if lighting of working areas is insufficient.
Audio links	+20% in case of absence of audio link for jobs where workers are distant one from another
Working space : Not very congested area	+ 20 % in comparison with a situation with open area
Working space : Highly congested area	+ 40 % in comparison with a situation with open area

Impact of protective suits on exposed time (as a supplementary time percentage compared to reference cotton clothing)

	Type of work 1	Type of work 2	Type of work 3
	<ul style="list-style-type: none"> - permanent concentration - precise work - heavy effort - duration < 2 mn - very restricted workspace - uncomfortable posture <p>(ex. Installation of maintenance 'spider' in steam generator channel head)</p>	<ul style="list-style-type: none"> - permanent concentration - precise work - heavy/light effort - duration < 10 mn - restricted workspace - uncomfortable posture <p>(ex. remove, place and adjust of 2 limit switches on a '2 inch' valve)</p>	<ul style="list-style-type: none"> - non permanent concentration - no precise work - heavy effort - duration < 10 mn - not much workspace - comfortable posture <p>(ex. unscrew, remove and screw of 12 nuts on a '12 inch' valve)</p>
Non ventilated cotton clothing			
2. Cotton coverall + mask	34 % (±17)	34 % (±14)	19 % (± 14)
Non ventilated impervious clothing (PVC or Tyvek)			
3. Non ventilated Chadoc + ventilated mask	34 % (± 19)	65 % (±20)	21 % (± 13)
4. Impervious clothing + mask	29 % (± 8)	46 % (± 18)	25 % (±13)
5. Impervious clothing + ventilated hood	28 % (±12)	27 % (±16)	22 % (±10)
Air fed pressurised clothing (PVC)			
6. Air fed pressurised Mururoa®	30 % (± 11)	37 % (± 25)	8 % (± 4)
7. Air fed pressurised Chadoc + ventilated mask	51 % (±12)	57 % (± 25)	16 % (±14)
8. Shrunken air fed pressurised Mururoa®	21 % (±12)	-	-

The direct impact of general organisation is more difficult to quantify. Nevertheless, some studies on causes of mishaps occurring during outage maintenance jobs in French nuclear power plants shown that up to 30 % of mishaps/dose can be attributed to organisation problems (planning, scheduling...). A study of outage organisation in 4 different nuclear power plant from various countries has then been performed. It allowed to highlight some "good practices" favouring the implementation of ALARA programmes [9, 11]. The main conclusion can be summarised in 6 points :

- Integration of radiation protection criterion in the overall outage process, from planning stage to feed back experience.
- Management commitment.
- Effective coordination and collaboration of all sections concerned by the outage.
- Important decision making power of health physicists.
- Feed back data bases for jobs, doses, dose rates...
- Motivation and commitment of all actors towards ALARA principles.

All these factors have been included in a model aiming at quantifying the effectiveness of protection actions, both from dosimetric and economic point of views. In addition to the theoretical part, a practical example has been elaborated using actual data coming from feed back experience data bases. This example allowed to show how a good management of exposed jobs can help to reduce the level of exposure as well as operating costs.

Finally this research played a very active role in favouring exchanges on the topic at an international level. This occurred, not only within the CEC joint project, but also through international seminars (Westinghouse REM seminar in 1993 [4]; Brookhaven ALARA Seminar in 1994 [15]), journals [17, 18], and particularly through an NEA ISOE Expert Group on the Impact of Work Management on Occupational Exposure. The later was created in 1994 to provide a document presenting "Good Practices in Work Management" (to be published in 1996).

III.4. Development of an ALARA tool: the OPTI-RP software

Earlier in the project it was identified that there were a need for the development of user friendly software that would facilitate non specialists using decision aiding techniques. The development of this software, called OPTI-RP, has been performed during that step of the project.

The software OPTI-RP is finalised in its version 1.0. It has been developed using Access® under Windows®. The software is available in French and English languages. A French users guide is to be provided by the end of November 1996 [21].

Three decisions aiding techniques are included in the software : Cost-Benefit Analysis, Differential Cost-Benefit Analysis and Reasonable Cost Analysis.

The selection of optimal options is made using a system of reference monetary values of the man-sievert (system of alpha values). This system allows to obtain the monetary value of the collective dose associated with the protection options, in order to compare it with their financial protection cost. The software gives the possibility to take into account several monetary values of the man-sievert depending upon the level of individual dose. The user can either creates its own system of monetary values of the man-sievert, or use the library of systems input in the software.

The radiation protection options are characterised by two factors:

- The collective dose which can be distributed among the individual dose ranges corresponding to the selected system of alpha values.

- The financial protection cost which can be defined as a total cost, an annualised cost or a discounted cost. For the two last options, it is possible to enter an investment cost, an annual operating cost, an interest rate and the life time of the investment. The annualised cost, or the discounted cost is then calculated by the software.

The elaboration of the software has been conducted by CEPN in cooperation with NRPB. Demonstrations and tests were implemented during successive European ALARA Courses. The software has therefore taken into account feed back, not only from the other members of the project, but also from many potential users.

III.5. Publications

- [1] LEFAURE C., LOCHARD J., SCHNEIDER T., SCHIEBER C. - **Proposition pour un système de valeurs monétaires de référence de l'homme-sievert**, CEPN-R-193, Février 1993.
- [2] SCHIEBER C., SCHNEIDER T., EECKHOUDT L. - **Valeurs monétaires de l'homme-sievert et prise en compte du temps**, CEPN-R-214, Mars 1993.
- [3] SCHNEIDER T. - **La prise en compte du temps et de la dimension probabiliste du risque : le cas de la filière nucléaire**, In : Gestion du risque et systèmes énergétiques, Actes de la Journée du Centre Universitaire d'Etude des Problèmes de l'Énergie 1992, Université de Genève, 13 Octobre 1992, Publication CUEPE N° 52, Avril 1993, pp. 20-34.
- [4] SCHIEBER C. - **ALARA and Work Management**, In : Radiation Exposure Management Seminar (REM), Pittsburgh, USA, 12-15 September 1993, 14 p.
- [5] CROFT J.R., LEFAURE C., EGNER K., and SCHNUER K. - **Role of Optimization in the Management of Workers Exposure**, In: Radiation Protection Optimization: Achievements and Opportunities, Fourth European Scientific Seminar, Luxembourg, 20-22 April 1993, CEC Report, 1994, EUR 15234 EN, pp. 21-72.
- [6] SCHIEBER C. - **Optimisation de la radioprotection et organisation du travail**, CEPN-R-227, Septembre 1994.
- [7] LOCHARD J et al. - **L'optimisation de la radioprotection des travailleurs**, CEPN-R-233, Novembre 1994.
- [8] SCHIEBER C. - **Equipements de protection individuelle en milieu nucléaire : impact**, CEPN-R-226, Septembre 1994.
- [9] MARGERIE H., SCHIEBER C., LEFAURE C. - **Optimisation of Radiation Protection and Organisation of Unit Outages at the Clinton, Koeberg, Philippsburg and Ringhals Nuclear Power Plants**, CEPN-R-223, September 1994.
- [10] LEBLANC G., SCHIEBER C., SCHNEIDER T. - **Détermination de la valeur monétaire de l'homme-sievert par la méthode du consentement à payer : étude de faisabilité**, CEPN-R-221, Novembre 1994.

- [11] MARGERIE H., SCHIEBER C., LEFAURE C., CHARRIERE J.L. - **ALARA and the Organisation of Outages in Nuclear Power Plants : An International Perspective**, In : IRPA Regional Congress on Radiological Protection, Portsmouth, England, 6-10 June 1994, pp. 443-446.
- [12] LEFAURE C., CROFT J.R., PFEFFER W., ZEEVAERT T. - **ALARA in European Installations**, In: Third International Workshop on Implementation of ALARA at Nuclear Power Plants, Brookhaven National Laboratory, Upton, New York, 8-11 May 1994, part 4-3, 12p.
- [13] CROUAIL P., GUIMARAES L. - **The Optimisation of Occupational Potential Exposures**, In: Third International Workshop on Implementation of ALARA at Nuclear Power Plants, Brookhaven National Laboratory, Upton, New York, 8-11 May 1994, part 6-11, 8p.
- [14] LOCHARD J. - **Optimisation of Radiological Protection and the Design of Nuclear Facilities**, In: Intakes of Radionuclides, Proceedings of a Workshop held in Bath, England, 13-17 September 1993, Radiation Protection Dosimetry, Vol.53, N° 1-4, 1994, pp.43-48.
- [15] SCHIEBER C., PERIN M., SAUMON P. - **ALARA and Work Management**, In: Third International Workshop on Implementation of ALARA at Nuclear Power Plants, Brookhaven National Laboratory, Upton, New York, 8-11 May 1994, part 6-8, 8p.
- [16] HOCK R., HOEGBERG L., KELLY G.N., LOCHARD J., REYNES L., TAYLOR R.H. - **Optimization in Complex Situations**, In: Radiation Protection Optimization: Achievements and Opportunities, Fourth European Scientific Seminar, Luxembourg, 20-22 April 1993, CEC Report, 1994, EUR 15234 EN, pp. 241-264.
- [17] VIKTORSSON C., SCHIEBER C. - **Occupational Dose Reduction at Nuclear Installations through Work Management and ALARA**, Radioprotection, 30, 3, 1995, pp. 391-400.
- [18] VIKTORSSON C., SCHIEBER C. - **How ALARA can increase Worker Efficiency**, Nuclear Engineering International, February 1995, pp.34-35.
- [19] EECKHOUDT L., GOLLIER C., SCHNEIDER T. - **Risk Aversion, Prudence and Temperance: A Unified Approach**, Economics Letters, 48, 1995, pp. 331-336.
- [20] LOCHARD J., SCHIEBER C., SCHNEIDER T. - **Ethical and Social Values in Radiological Risk Management**, CEPN-R-239, (to be published late 1995).
- [21] FROSSARD M., SCHIEBER C., **Le logiciel OPTI-RP : présentation et guide d'utilisation** (to be published as a European Report in 1996).

Head of project 2: Dr. Zeevaert

II. Objectives for the reporting period

The work programme of SCK•CEN in this project concerned the integration of the ALARA principle in the decommissioning stage. The main objectives of the programme were:

- to draw up an inventory of trade-offs (decisions) typical for decommissioning, with respect to radiological optimization
- to examine the optimization of the decommissioning strategy:
 - to identify important attributes (radiological protection factors), and
 - to quantify the attributes as a function of time
- to establish the structure of a database, enabling to collect information from decommissioning experiences in the past
- to demonstrate the application of decision-aiding software (multi-criteria analysis) available.

III. Progress achieved including publications

- 0 It became rapidly apparent that it was not possible to cover all objectives mentioned above in a satisfactory way within a two and a half years' period. Consequently most of the effort was drawn to the establishment of a database structure, considering the lack of data of various important radiological protection factors which seriously hampers the optimization of decommissioning operations. The other objectives were treated in a more concise manner.
- 1 Concerning trade-offs (decisions) specific for decommissioning with respect to radiological optimization, an inventory has been drawn up in a contribution to the 14th European Seminar on Radiation Protection Optimization in Luxembourg [1]. Typical trade-offs were identified at several levels:
 - at the level of the global strategy:
 - decisions on the scale and timing of the consecutive phases of the decommissioning are to be taken, considering economical, technical and radiological arguments as a function of time
 - at the level of the decommissioning methodology:
 - choices are to be made between various dismantling techniques and between protection options, for example:
 - the use of a telemetric monitoring system or local survey
 - a contamination confinement philosophy or periodical clean-up of dispersed contamination
 - the application of quick cutting techniques generating a lot of volatile secondary waste (e.g. plasma torch-burning) or slow mechanical sawing generating less, large-sized scraps

- at the level of the dismantling operations:
the specificity of dismantling activities is related to the fact that besides external gamma dose, which is mostly the major radiological attribute of maintenance activities, also skin dose, internal contamination and in particular waste generation are important and can dominate decision making
- at the level of waste management:
the importance of waste management with respect to decommissioning is illustrated by the fact that the decommissioning of an installation may generate as much radioactive waste as what has been generated during the total operational life of the installation.

2 As a first approach to the optimization of the decommissioning strategy, technical, radiological, economical and social attributes have been considered as a function of the point of time of dismantling [2]. Some of the attributes are in favour of an early dismantling, others are to the detriment of it:

In favour of an early dismantling are (among others):
 the economical costs of survey and maintenance
 the dose to workers during survey and maintenance
 the degradation of the infrastructure
 the erosion of know-how of the personnel
 the degradation of barriers to human intrusion
 the removal of unrest of the population.

To the detriment of an early dismantling are (among others):
 the economical cost of dismantling and the capitalization of the monetary provisions for it
 the doses to workers during dismantling
 the social preference for costs to be paid and doses to be incurred far in the future.

The evolution of the major attributes as a function of time (between the stopping of a reactor and the dismantling) are graphically depicted for a reactor of the type of BR3 (PWR at SCK•CEN) in Fig. 1 [3].

Although the optimization of the decommissioning strategy can be considered as a radiological optimization exercise, it is obvious that economical arguments will mostly control the decisions.

- 3 A serious problem when carrying out a radiological optimization of decommissioning activities is the lack of data for various important radiological protection factors. The appropriate means to overcome this problem in the future is the establishment of a database in which relevant data from dismantling operations executed, are collected. Prior to the elaboration of a structure for such a database, the important radiological protection factors for which data are needed, were identified. They included:
- Collective doses
 - Distribution of individual doses
 - Economical costs: labour costs
investment costs
consumable costs

- Waste production: quantities (masses - volumes)
activities - concentrations
physical forms

The factors with respect to the waste production may also be converted into:
waste costs (for treatment, transport, disposal) and
waste doses (to operators and population).

An illustration of how these factors fit into a hierarchy of attributes, in a multi-attribute type of analysis, is shown in Fig. 2.

Elements determining radiological protection factors and for which quantitative information from a data bank is most useful, are:

- duration of work for dismantling tasks, applying specific techniques;
- costs of equipment;
- quantities and physical forms of wastes produced (in particular: secondary waste).

Since the values of these factors do not only depend on the operation or task considered but also on the conditions under which the operation has to be executed, the data have to be fully specified in terms of conditions they are related to. If possible, normalised values (with relation to reference units) should be specified in order to facilitate derivation of values for other conditions. Deterministic values for these factors are not primordial, uncertainty ranges (pdf when available) are very useful with a view on the testing of the robustness of the solution.

Concerning the structure of the database, major requirements were put ahead with a view to the application in a multi-criteria analysis.

They include:

simplicity

transparency

easy access to all data

a logical relational structure, enabling the data to be stored at only one place in the database.

In order to meet these requirements, the database has been developed in MS-ACCESS (version 2.0), a relational database system under Windows. The data are grouped in several tables in a logical way. The tables are interrelated in such a way that duplication of data is avoided. Each record of a table is unambiguously identified by a unique combination of so-called primary key values (identification fields). Links (or joins) between the tables are created by using the same primary keys in tables that are to be related.

Following tables were determined (see also Table 1):

- the table *Tasks*, containing specifications of the tasks performed and the techniques applied. It is linked with the table *Objects* through the identification number of the objects (Object ID);
- the table *Objects*, containing information concerning the objects on which, and the workplaces where the tasks are performed. It is linked with the table *Installation* through the identification number of the installations (Installation ID);
- the table *Installation*, identifying the installation (type, name, address) where tasks are performed or to which the object belongs;
- the table *Labour/Dose*, storing the labour times (per qualification group of workers) and the doses of the individual workers having executed the tasks. Distinction is made

between variable labour times and doses on one hand and fixed labour times and doses on the other hand, referring to labour times and doses that are either proportional to the work volume or independent on it. This table is linked with the table **Tasks** through the identification number of the task (Task ID) and with the table **Personnel** through the identification number of the individual workers or group of workers (Individual ID);

- the table **Personnel**, identifying the individual workers or group of workers and linked with the table **Qualification** through the identification number of the qualification of the workers (Qualification ID);
- the table **Qualification**, specifying the qualification and wages (unit costs) of the workers;
- the table **Suppl_Coll_Dose**, collecting doses respectively labour times which could not be assigned to a specific individual worker respectively group of individual workers with the same qualification, and that are to be taken into account for calculating collective doses and total labour times. For that purpose the doses and labour times in this table are to be associated with arbitrary individual workers. This table is linked with the table **Tasks** through the identification number of the task (Task ID) and with the table **Personnel** through the identification number of the individual workers or group of workers (Individual ID);
- the tables **Equipment**, **Consumables**, and **Wastes**, containing characteristics and unit costs of equipment, consumables and waste types (secondary or tertiary);
- the tables **Equipm_in_Tasks**, **Cons_in_Tasks** and **Waste_in_Tasks**, containing the amount of equipment, consumables and waste types used or produced in each task. The tables are linked with the tables **Equipment**, **Consumables** and **Waste** through the identification number of the equipment (Equipment ID), the consumables (Consumable ID) and waste types (Waste ID) and with the table **Task** through the identification number of the task (Task ID).

In a first approach, fields were determined and data introduced, based on dismantling operations carried out at BR3 (SCK•CEN). A list of tables and fields determined in that way is shown in Table 1. In a second phase the possibility of importing data from other databases has been investigated. An inquiry has been made concerning existing international databases on decommissioning/dismantling in Europe. Two programmes, developing such databases, were identified: the OECD/NEA co-operative programme on decommissioning, and the EC Decommissioning Programme (Working Group C of DG XII).

The type of information and data present in the databases of the OECD/NEA programme were not relevant or suited for radiological optimization purposes as intended in this project. Furthermore their contents is confidential and non-members of the programme normally do not have access to them. Consequently they were not considered further.

In the programme of Working Group C of DGXII (EC) two databases have been established, DB-COST and DB-TOOLS, from which the first one (concerning costs and radiation exposure) appeared to be very valuable for our purposes. This database has been developed and implemented by NIS (Hanau, Germany) assisted by CEA (Marcoule, France) and BNFL (Sellafield, UK). It is a very comprehensive database, containing much more information than what is really needed for radiological optimization purposes. However valuable information including specific values on costs, wastes ... related to

reference values is present. DB-COST is developed in the relational ORACLE database management system. In order to import data from DB-COST into our database (called DECOM), the former has been converted into a MS-ACCESS version (by the service of Mr. W. Pfeffer - GRS) and the fields with data or information relevant for our purposes were selected and appended to fields in DECOM.

Precedingly some adaptations of both MS-ACCESS databases (DB-COST and DECOM) had to be carried out.

- The formats of the corresponding fields in both databases were to be brought into concordance.
- Some additional fields had to be created in both databases in order to adapt data from DB-COST to conditions and units in DECOM and vice versa.
- The records in the identification fields had to be adapted.

The selection and appending of data from DB-COST to DECOM was carried out quite readily through the application of "append queries".

As a result the final version of database (structure) DECOM was realized as shown in Table 2. The fields where data or information could be added from DB-COST, are indicated with an asterisk.

More information about the database structure is given in [4].

- 4 As an application of decision-aiding software for multi-criteria analysis, the three cutting techniques used for the dismantling of the thermal shield of the BR3 reactor at SCK•CEN (mechanical sawing, electro-erosion and plasma-arc torch cutting) have been compared, on the basis of data collected in DECOM, and using the VISA (Visual Interactive Sensitivity Analysis) software developed by Dr. V. Belton and SPV Software Products. The attributes derived from the database DECOM comprised:

- collective doses
- individual dose distributions
- labour costs
- investment costs (infrastructure)
- consumable costs
- waste costs.

For the sake of comparability, the values were normalized (per m² of surface area cut) since the techniques were applied to different parts of the operation. The surface area to be considered for the fixed doses and costs is the whole cutting surface area of the thermal shield, for the variable doses and costs it is the surface area cut with the technique considered. The normalised attribute values were calculated per technique through the use of "crosstab-queries" (MS-ACCESS) and introduced into VISA. In VISA, the - preference - values of the attributes for each technique and weighting factors for each attribute can be varied and the results are directly graphically displayed. Mechanical sawing was shown to be the optimal technique (among the mentioned ones) for cutting the thermal shield of BR3, for a wide range of weighting factors for the various attributes.

5 Publications

- [1] P. Govaerts, Th. Zeevaert
Integration of the ALARA principle in decommissioning activities.
Presented at the Fourth European Seminar on Radiation Protection Optimisation, Luxembourg, 20-22 April 1993.

- [2] P. Govaerts, Th. Zeevaert
Le déclassement et les principes de base de la radioprotection.
Presented at the "Journées de la SFRP: Optimisation de la radioprotection des travailleurs dans les domaines électronucléaire, industriel et médical", La Rochelle (F), 20-21 septembre 1994.

- [3] Th. Zeevaert, P. Govaerts
De ontmanteling van de BR3-reactor, een opportuniteit voor ALARA-toepassing en onderzoek.
Annalen van de Belgische Vereniging voor Stralingsbescherming 18, 1: 61-78 (1993).

- [4] Th. Zeevaert, B. Van de Walle
A database structure for radiological optimization analysis of decommissioning operations.
SCK-Report BLG-686 (1995).

- [5] C. Lefaire, J. Croft, W. Pfeffer, Th. Zeevaert
ALARA in European Nuclear Installations.
Presented at the 3rd International Workshop on Implementation of ALARA at the Nuclear Power Plants, Hauppauge, New York, 8-11 May 1994.

- [6] P. Govaerts, Th. Zeevaert
ALARA in decommissioning.
in: CEC Training Course on Optimisation of Radiological Protection in the Design and Operation of Nuclear Facilities, Karlsruhe KfK, 7-11 November 1994.

Table 1: Tables and Fields of the database DECOM (first version)

Tasks	Labour/Dose	Equipment
Task ID	Task ID	Equipment ID
Task Type	Individual ID	Equipment Name
Technique Type	Fixed Dose	Kerf width
Technique Specification	Variable Dose	Cutting step
Object ID	Fixed Labour time	Execution speed
Job Period	Variable Labour time	Equipment Cost
Reference Surface Area		
Number of elementary tasks		Equipm_in_Tasks
Task Description		Task ID
		Equipment ID
		Number of equipment
Objects	Suppl_Coll_Dose	
Object ID	Task ID	
Object Name	Fixed Coll. Dose	
Installation ID	Variable Coll. Dose	
Ambient Dose Rate	Fixed Labour time	Consumables
Air Contamination	Variable Labour time	Consumable ID
Object Type	Individual ID	Consumable Name
Activity Type		Composition
Activity Concentration		Application
Material Type		Diameter Cons
Object shape/form	Personnel	Thickness Cons
Object mass	Individual ID	Length/Height Cons
Object volume	Qualification ID	Volume Cons
Object thickness	(Firm)	Unit Cons Cost
Object diameter	(Name)	
Object height/length		Cons_in_Tasks
	Qualifications	Task ID
	Qualification ID	Consumable ID
	Qualification Description	Amount Cons
	Qualification Unit Cost	
Installation		Waste
Installation ID		Waste ID
Installation Type		Waste Type
Installation Name		Package Form
Installation Part		Unit Waste Cost
Institution Name		
City		
Country		
		Waste_in_Tasks
		Task ID
		Consumable ID
		Waste ID
		Amount Waste
		Material Collected
		Activity

Table 2: Tables and Fields of the database DECOM (final version)

Tasks	Labour/Dose	Equipment
Task ID*	Task ID	Equipment ID*
Task Type*	Individual ID	Equipment Name*
Technique Type*	Fixed Dose	Kerf width
Technique Specification*	Variable Dose	Cutting step
Object ID	Fixed Labour Time	Execution speed
Job Period	Variable Labour Time	Equipment Cost*
Refvalki*(1)		Totalnac*(1)
Reference Value*		
Refeunit*(1)		
Number of elementary tasks		Equipm in_Tasks
Task Description*		Task ID*
		Equipment ID*
		Number of equipment*
Objects	Suppl_Coll_Dose	Consumables
Object ID	Task ID*	Consumable ID*
Object Name	Fixed Coll. Dose*	Consumable Name*
Installation ID	Variable Coll. Dose	Composition
Ambient Dose Rate	Fixed Labour Time*	Application
Air Contamination	Variable Labour Time	Diameter Cons
Object Type	Individual ID*	Thickness Cons
Activity Type		Length/Height Cons
Activity Concentration		Volume Cons
Material Type	Personnel	Unit Cons Cost*
Object shape/form	Individual ID*	Tconsnac*(1)
Object mass	Qualification ID*	
Object volume	Persnumb*(1)	
Object thickness	(Firm)	
Object diameter	(Name)	
Object height/length		
	Qualifications	Cons in Tasks
	Qualification ID*	Task ID*
	Qualification Description*	Consumable ID*
	Qualification Unit Cost	Amount Cons*
Installation		Waste
Installation ID		Waste ID*
Installation Type		Waste Type*
Installation Name*		Package Form*
Installation Part		Caskvolu*(1)
Institution Name		Unit Waste Cost*
City		Currency*(1)
Country*		
		Waste in Tasks
		Task ID*
		Consumable ID*
		Waste ID*
		Amount Waste*
		Swamount*(1)
		Swamunit*(1)
		Material Collected
		Activity

(1) Fields imported from DB-COST.

* Fields in which data or information were appended from DB-COST.

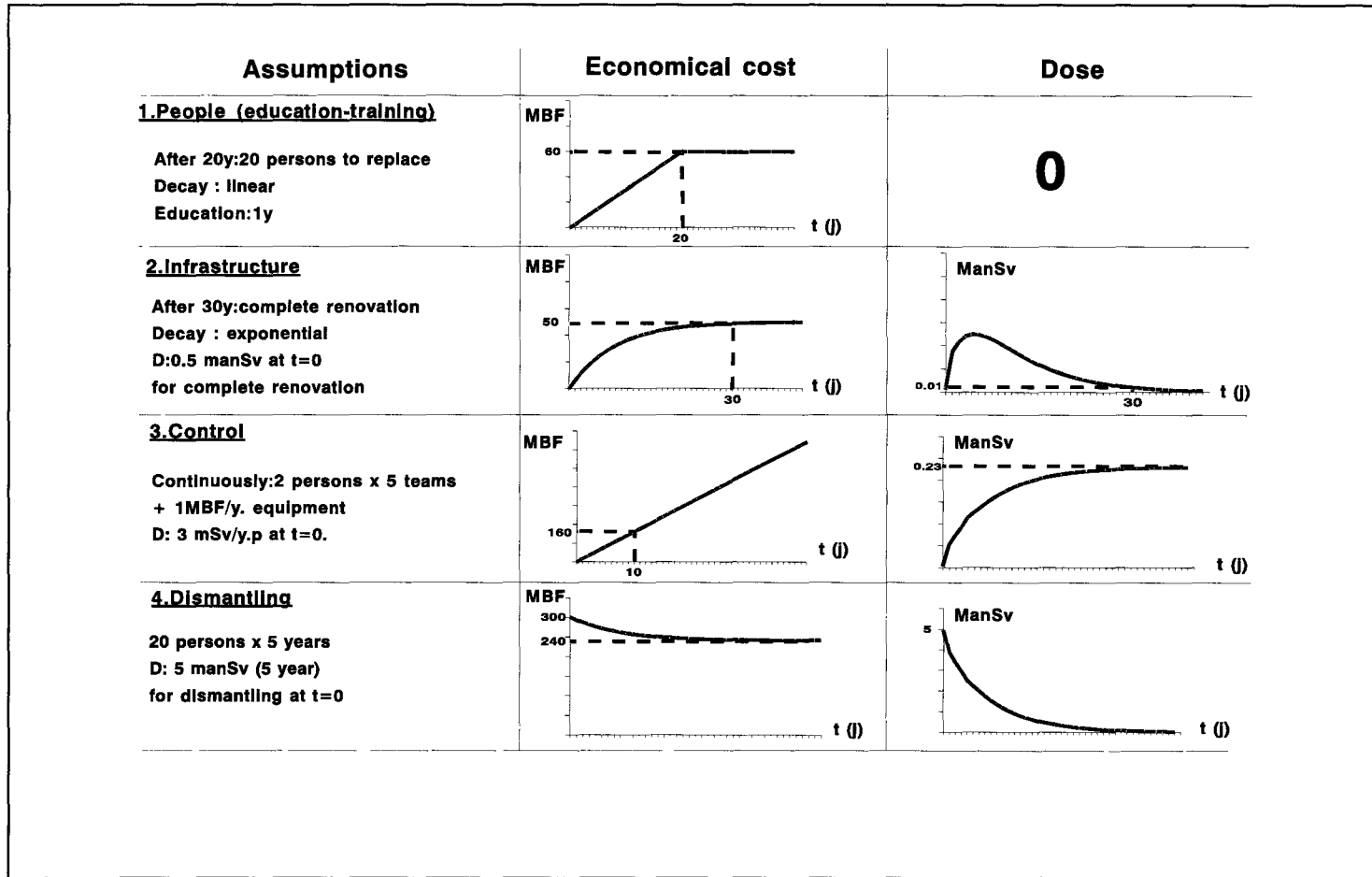


Figure 1: Evolution of attributes with time

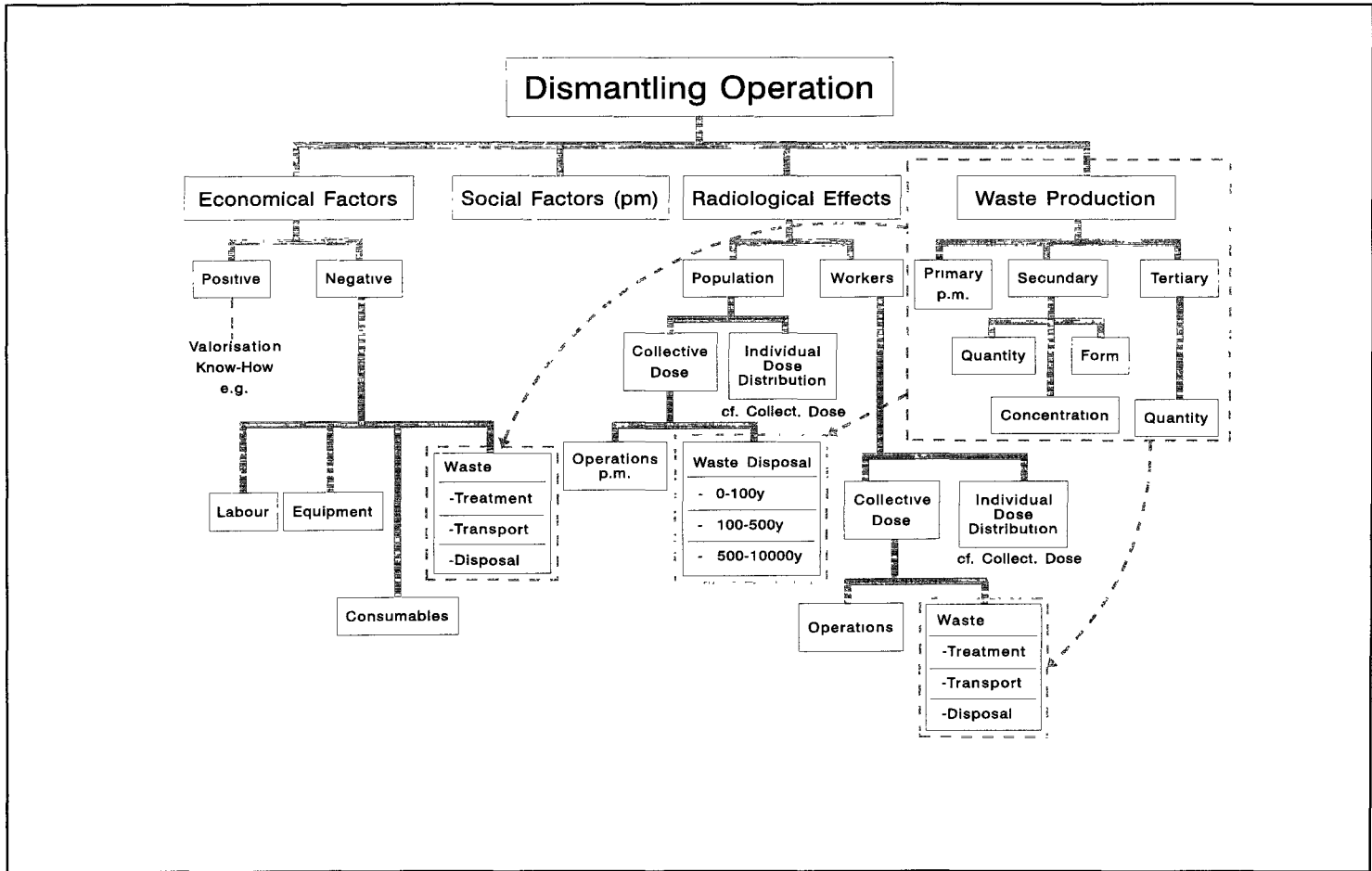


Figure 2: Hierarchy of attributes

Head of Project 3: Dr. Pfeffer

II Objectives for the reporting period

In the reporting period the evaluation of the data was carried on and finished. Additional data available from the plant for 1993 and 1994 were integrated into the work. Areas for special consideration in this phase were selected tests at the steam generator as eddy current tests, tube sheet flushing and visual inspections of flanges, and tests and inspections at the emergency core cooling system and the volume control system in selected rooms of the containment. For these tests and inspections potential areas of optimisation were investigated and documented. The results of the investigations were summarised in a main report. Though a detailed quantification of the potential was not possible due to the limitations of the data, areas of potential improvements could be identified. For the steam generators a reduction of the tests under consideration due to increasing reliability and operational experience can be identified. E.g. tube sheet flushing performed once a year in the early years of operation has not been performed in the last years; the frequency of eddy current tests was reduced from about once a year to once every two to three years. Regarding visual inspections consideration of optimisation was recommended. For the evaluation of the other two systems under consideration potential for optimisation was identified in the harmonisation of tests at the components and to a certain extent on the focussing of tests in a room. An example for this practice could be worked out for one room showing a high potential for reduction of the collective dose by taking advantage of sophisticated decontamination techniques for all jobs, which would not be cost effective for single jobs in this room.

III Progress achieved

Optimisation of Radiation Protection in Inspection and Tests in a German Nuclear Power Plant

1. Introduction

1.1 Goals of the Study

Main goal of the study was to identify possibilities to optimise radiation protection in inspection and tests in outages of NPP and to derive hints and recommendations to reduce the collective exposures in the plants if possible. In this area not only radiation protection aspects of the tasks have to be considered but also safety aspects of the plant which e.g. will govern test frequencies and the amount of testing to be performed. In this area also the influence of different organisations as the operator, the authorities and technical surveillance organisations are involved and their influence should be regarded. Due to the theoretical approach of the study the work especially had to focus on tasks performed more frequent in the outages as recurrent testing and more frequent routine inspections and maintenance to get a better basis and comparable data for the evaluation.

It is to be stressed that the study does not intend to check the quality of radiation protection awareness in a plant or to check the number of tests performed with respect to the tests prescribed. The only intention is to identify any potential available for optimisation of radiation

protection in this special field so to extend and to support the general activities and the discussion on radiation protection optimisation already under way in Germany. The evaluation may cover

- areas already practised by the utility to forward the good and recommendable practice and to show the possibility of optimisation in this areas or
- those areas that might show additional potential of optimisation and should be considered in further planning.

1.2 Basic Considerations Governing the Study

As mentioned in the previous chapter the study was intended to be carried out on data available from the radiation protection documentation of the plants and had to focus on more frequent tasks carried out in the plants. Principally the tasks performed in the plant range from plant walk-throughs of personnel to inspections, recurrent testing, and maintenance on large components during the outages. It would have been desirable to tackle all these areas of tasks, but obviously radiation protection data and files in the plants in detail are only available for more important tasks. For this reason the work focused on important tasks in the outage considering especially recurrent testing and activities carried out more often during the lifetime of the plant. In this way also test frequencies and test intervals could be considered.

1.3 Nuclear power plant chosen for the evaluation

As it was intended to identify major contributors to the collective dose and also to evaluate dose contributions from specific activities (e.g. preparatory work) performed in the tasks under consideration, the doses received by the personnel in the tasks had to be significant and measurable. A comparison of the collective exposures of German PWRs showed potential candidates for the survey. Contacts with plants taken into consideration for the study resulted in a co-operation with the nuclear power plant GKN-I, the unit 1 of the "Gemeinschaftskernkraftwerk Neckarwestheim".

1.4 Restrictions and Boundary Conditions of the Study to be Mentioned.

In the study also recurrent tests which only may be performed once in several years were to be considered. It might have been very interesting and probably would have resulted in a more detailed insight into single jobs, if jobs would have been accompanied by one of the authors of the study when these jobs are performed. But there are several reasons which did not allow this practice. So to evaluate these tasks and tests, the respective files and dose records of the tasks had to be used to get information on the dose contribution. This evaluation was combined with discussions with the personnel in the plant to integrate also practical aspects not available from the files. Resulting from this practice the degree of details contained in the files and in the dose records as well as the dosimetric system used in the plant to a certain degree had an influence on the evaluation in the study. This influence could be reduced and compensated for by the good co-operation and the detailed discussion with the specialists in GKN to a large extent.

1.5 Basic Steps of the Study

First considerations how this study should be performed and which topics should be considered were carried out on an early and on a quite theoretical basis and - as turned out later - were too optimistic about the degree of details that could be derived from the data. In a discussion with the specialists in the plant the scope of work was brought to a more applicable basis and a first set of

data was transferred to GRS for further evaluation. These data mainly covered dose files for tasks performed on

- the primary circuit and its components and
- the emergency core cooling/residual heat removal system (TH-system) and the volume control system (TA-system) of the plant,

as these systems show a large number of tests and cause a large contribution to the collective exposure of the personnel due to larger amount of work and often higher dose rate fields.

For easier handling these data were transferred into a data bank for further evaluation. On the basis of these data in a next step of the evaluation the scope of the study was even more reduced to focus further work on a limited number of tasks and a limited number of work areas which, however, were expected to give a good basis for the study and after the detailed analyses of these areas would give answers to the questions under consideration in this study.

From this detailed analysis general conclusions regarding the optimisation potential could be derived. For most of the areas under consideration it was, however, not possible to give quantitative numbers regarding dose savings for potential improvements as will be discussed later.

1.6 Acknowledgements

The authors would like to express their thanks to everybody who has contributed to this study in co-operation and discussions, especially

- to the specialists of Neckarwestheim nuclear power plant for the agreement to co-operate, for the submission of data, for the excellent co-operation during the transfer of data and for very helpful discussions during the meetings in GKN,
- to the colleagues in the co-operation within the EU-contract on optimisation of radiation protection for supportive discussions and for understanding and accepting some formal problems during the contract, and last not least
- to the EU for funding this project.

2. Summary of Information about GKN-I Nuclear Power Plant

The NPP GKN-I "Gemeinschaftskernkraftwerk Neckarwestheim, Block 1" is one of the early pressurised water reactors built in Germany. It's a 3-loop PWR, built by Kraftwerk-Union (KWU) with a gross production of 840 MW_{el}. The first criticality of GKN-I was in 1976, and the plant was commissioned in 1976. The design of GKN-I - except for the number of steam generators - is quite similar to Biblis nuclear power plant. Since 1988 a Convoy-plant (GKN-2) is in operation at the same site at Neckarwestheim.

Since the early years of operation in GKN big efforts were taken to reduce the exposure of the personnel. The awareness of the management and the personnel in GKN regarding the importance of radiation protection aspects resulted in a reduction of the exposure either by improving the radiation condition in the plant or by improving the work conditions for the personnel due to experience feedback from operation and backfitting actions. E.g. in several steps material containing Cobalt was replaced to the extent possible, seals of the main coolant

pumps were replaced to remove Antimony from the primary coolant, modifications were performed on the main coolant pumps to ease tests of the shaft, insulation of loops and components was replaced by improved systems which were quicker to mount or dismount, and provisions for automatic tests of welding were installed. Additionally experience from work carried out was fed back into operation by work planning.

These efforts resulted in a quite low exposure level for GNK-I considering this unit being one of the older plants in Germany.

Starting from a non optimised design regarding the construction material in the early plant from a radiation protection view the efforts in the plant obviously have resulted in a very good improvement of the situation and to a reduction of collective exposures in the recent years. The results of the study are documented in a GRS-report in more detail. This report also presents data regarding the radiation protection performance and the effects of the improvements.

3. Selection of Systems of the Plant for Further Consideration

As discussed earlier it is not possible in the frame of the contract to analyse all activities in the plant. Special areas had to be identified which were considered to be a good bases for the evaluation. To identify these areas all important systems were checked in a first evaluation with respect to

- the collective exposure received by the personnel during their work on these systems. High contributions to total collective dose e.g. result from TA (volume control)-, TH (emergency core cooling and residual heat removal)-, TR (liquid waste management) -system and from the systems in the primary circuit as YA (primary loops), YB (steam generator), YC (pressure vessel), and YD (main coolant pumps).
- the amount of inspections and recurrent tests performed in the systems and at the components and considering especially areas in which tests might be necessary in high dose rate fields due to the plant conditions. Here the number of tests as well as the test cycles at the components had to be considered.

As a result of the discussion of the preliminary results in GKN further work in the study focused on two main areas:

- evaluation of the work at the steam generator, as this field (due to the larger number of three steam generators) offered the advantage of detailed data giving information on several larger inspections and tests in which tasks contributing (e.g. work on insulation, preparative activities,..) could be identified and evaluated and
- evaluation of the maintenance, tests and inspections in the TA- and TH-system, which offer information
 - on many tasks on the systems and components,
 - with activities in high dose rate areas and
 - with work to be performed on several components in one room, which may also be an aspect of harmonisation.

4. Basic Theoretical Considerations

Points to be considered from a first very general and basic approach of radiation protection philosophy might be:

- Planning and performing inspections, maintenance and recurrent tests should, if possible, aim at a reduction / minimisation of tests considering, however, the safety requirements of the plant.
- Planning should assure that preparative activities are carried out only once and should be utilised for as many tasks in that work place as possible; especially
 - double work should be avoided
 - resources (e.g. scaffolding, shielding) should be used for as many tasks as possible
 - protective actions (shielding, decontamination) should be available for several activities at the same place.

The utilisation and applicability of these basic ideas of radiation protection for optimisation should be checked in the study basing on the data available. Probably there will be the possibility to point out good practices where these ideas already have been implemented to some extent; it's the goal of the study to identify further areas of applicability of these considerations giving rise to further potential for optimisation.

It is to be expected, however, that in practice some or even many features will be interfering with this general intention of optimisation. These features should be identified, discussed and possibly reduced or even eliminated.

5. Analyses Regarding the Steam Generator

5.1 Steps of Work Performed in the Study

Documents and files available from the utility regarding tests and inspections performed at the three steam generators at GKN-I in the outages from 1984 to 1992 were analysed regarding

- the types of tests and inspections performed in the outages. In this field
 - non destructive tests at the steam generator,
 - internal inspection of the secondary side of the steam generator,
 - eddy-current tests of the steam generator tubes,
 - flushing of the steam generator tube sheet, and
 - visual inspectionswere considered.
- the frequency of the tests and inspections performed in the outages and the frequencies of tests prescribed by the authority in the test manual (Prüfhandbuch),
- the splitting of tests and inspections into tasks to be performed during the test and contributing to the exposure of the personnel, as e.g. work on insulation, opening of flanges, test, cleaning, decontamination, and other activities

- basic data which may be supportive for the analyses of the data and for the discussion of the background, e.g. dose rates measured at the steam generator or in the steam generator compartment.

The first screening of the data showed that it would be interesting to focus on three main activities for further evaluation:

- eddy-current-tests of the steam generator tubes,
- flushing of the tube sheet of the steam generator, and
- visual inspection on flanges, especially considering work on the insulation of the steam generator at the flanges of man holes and hand holes.

Chapter 7 gives a summary of the results regarding the evaluation of the steam generator tests under consideration. The detailed results of the evaluation can not be presented in this summary paper but will be documented in a GRS-Report.

6. Analyses Regarding the TA- and TH-system

6.1 Steps of Work Performed in the Study

Due to the large number of data for the TA-system (Volume Control System) and the TH-system (Emergency Core Cooling and Residual Heat Removal System) all data from the radiation protection files from 1984 to 1994 giving

- the number of the radiation work permit (Strahlenschutzschein),
- a short description of the job,
- the systems or components worked at, and
- the collective dose of the job

were transferred into a data base for further evaluation to ease the evaluation and to be able to analyse the data with respect to special combinations of conditions. To get information on test intervals the test manual of the plant giving the test frequencies and the tests to be performed on the components was implemented into this data bank too to identify the test intervals of the components under consideration. Additionally more detailed data on special jobs and data on dose rates in special areas of the plant were handed out by the plant for further evaluation and to support the identification of effects and benefits.

6.2 First Evaluation and Screening of Data

Due to the large amount of data interesting areas for further evaluation had to be identified in a first screening. Topics under consideration were:

- Evaluation of test frequencies as prescribed by the documentation and frequencies of work on components in practice, compared to the prescribed numbers.
- Evaluation of the tests performed in rooms on specific components considering the possibility to concentrate work in a room and to make use of resources in the room for the work in this room.
- Evaluation of concentrations of a larger number of tests in a single room perhaps also calling for combining tests as discussed in chapter 4 as a theoretical approach for optimisation.

Similarly to the practice in the study on the steam generator the screening activities resulted in focusing on special areas of work, which will be presented in more detail in the next chapters to present important examples of the findings. There are, however, some differences compared to the data available for the steam generators, which should be pointed out:

- The number of components, rooms, tests, and the number of jobs is much larger than for the steam generator.
- The number of jobs with similar work is much smaller and there are hardly any steps of work to be identified in the databases which are easily comparable and might allow to derive quantitative results. Even having the same description they normally either differ by the amount of work performed or by the kind of the component.

So as will be obvious in the evaluation it was only possible to derive general, not quantitative recommendations.

It has to be stressed here, that this problem did not result from any lack of co-operation of the specialists in the utility but to a certain extent was caused by the data base used in the study and here by limits of dose-accounting system - which certainly never had been designed to answer this special kind of question - and by the limited time of the contract, which did not allow to go too far into time-consuming detailed studies of further detailed material probably answering some quantitative questions.

It also has to be mentioned here that some modifications of the dose accounting system from 1994 give some additional information e.g. on dose contributions of preparative work and other background information. This could only be used for some examples in the study, but would give a more improved basis for further evaluations by the utility and could improve experience feed back.

In the frame of these systems the following topics were analysed in more detail:

- test intervals in selected rooms
- work on components in selected rooms
- work on the REKU heat exchanger as a special example of concentration of work on several components in a room with high dose rate fields.

As discussed in chapter 5 only a summary of the findings can be given in this paper and persons interested are referred to the specific report.

7. Summary of the Findings of the Study

7.1 Boundary Conditions and Restrictions of the Study

Though it first was intended during the planning phase of the study to derive quantitative results regarding the optimisation potential in the areas under consideration, during the work it became obvious that this goal could not be reached to the extent intended. Only in some special cases trends or quantitative results for the potential of reduction could be shown, as e.g. for the optimisation performed at the REKU-heat exchanger. It once again has to be stressed that this drawback does not result from any lack of co-operation of the specialists in GKN. On the contrary everything was done by them to support the work in this study, but as already discussed earlier the very broad data base available did not give direct answers to quantitative questions of this kind (as it was not designed for the special purposes of this study) and the time for further

evaluation on the bases of basic documentation was not available in the frame of the study. Due to the improvement of the dose accounting system in 1994 more data were available on details for this year, but the data set for 1994 was not sufficient for a reasonable quantitative evaluation as only a limited number of components was affected in this year.

The data and the evaluation in this study only represent the situation in one of the German power plants. Possibly the practice is not the same in all plants and the findings in the study may not be valid for all plants.

In spite of these constraints we think that the data evaluated gave several hints regarding potential for improvements and optimisation of radiation protection, which may be valid and applicable in general and can be transferred to other plants. To a certain extent practices already are applied in the plant under consideration which may be taken from the examples and from the good radiation protection performance of the plant

The potential for improvements derived will be summarised in this chapter. Due to the work performed and due to the data screened during the work we think that the general ideas derived are transferable to all other systems in the plant, and to other plants for improvement and should be taken as an impetus for considerations on optimisation in the future.

We once again want to point out that the call for harmonisation and in case for flexibility in the inspection intervals does not mean a reduction without consideration of safety or reliability aspects of the plant. But we think that a harmonisation of radiation protection aspects and of plant safety would be an important approach in the future.

7.2 Steam Generator

Regarding tests and inspections on the steam generators in the early years many tests were performed due to problems with steam generators and due to the need to gain experience and knowledge in the operation to reduce steam generator tube corrosion. This resulted in a test frequency and a cleaning (tube flushing) of about once a year for each steam generator.

Tests were performed not only due to the prescribed test cycles but to get information on the status of the tubes to be able to prevent steam generator tube leaks and to assure safe and reliable operation. The same held for visual inspections of the steam generator and for cleaning / flushing of the tube sheet to reduce or to prevent corrosion. Possibly radiation protection aspects in some of this cases were not necessarily balanced to the need of the tests.

With increase of experience and increase of the performance of the steam generators tests could be reduced to intervals more in line with the test intervals prescribed. So eddy current tests have test intervals of two to three years compared to prescribed intervals of four years. Activities as flushing of the tube sheet also could be reduced.

Consideration now could concentrate on activities prescribed to reduce occupational exposures e.g. by avoiding dose intensive preparative work. As an example the amount of tubes tested in the eddy current tests of the steam generator may be taken. Due to the high doses necessary for opening, closing and cleaning of flanges it would be preferable to perform a "complete" test for a steam generator in the cycle prescribed than to perform a limited test with the need to have a second test in between or to consider prolongation of test frequencies on the basis of positive test results and experience as far as safety aspects are not interfered with.

Another example of consideration may be precautionary measures causing doses to the personnel. Here work on insulation may be quoted as far as removal of insulation for precautionary visual inspection for leak tightness is concerned. In this case it might be an aspect

of optimisation to leave the insulation in place or even to improve the facilities for the identification of leaks during start up by technical means.

7.3 TA- and TH-System

Test and inspection or maintenance frequencies as prescribed differ depending on the components and on the type of work to be performed. Quite often different tests to be performed on the same components have slightly different intervals which may afford similar work to be performed in both cases calling for harmonisation. Comparison of the intervals in practice with intervals prescribed shows that work is performed more often than prescribed on several components under consideration in this study and that test are performed with different test cycles on parts of a component with the test cycles not being "in line" to perform the tests on this component at the same time. So e.g. prescribed tests intervals of 4, 5, 6 or 8 years can be found for different tests of the parts of the same component, and for some components work and tests is carried out more often. There may be many reasons contributing to this practice. As already discussed preventive checks may be performed to get additional information about the status of the component to avoid failure in operation, there may be indication in operation or there may be events in other plants calling for additional checks. Demand of the authority in some cases may increase the number of tests and reduce the real intervals between tests scheduled. Its not possible to analyse the reasons of each tests or activity from the data available, but the occurrence of these activities is taken as a hint and trigger for further consideration of harmonisation and concentration of tests, especially for tests at the same component with slightly different intervals .

Regarding concentration of activities in a compartment the data on the TA- and TH-system did not give general results in the evaluation regarding the possibility to concentrate work in a room to one outage. On the other hand concentration may not always be possible. E.g. there may be arguments against concentration as tests in redundancies which may call for specific time schedules in different outages for safety reasons. But anyway concentration can be an excellent tool for optimisation and reduction of exposure in an outage as has been shown by the utility in an example in 1992 in the maintenance of all components in the room of the REKU-heat exchanger, as in this case benefit may be taken for all tasks from efforts of dose reduction, which might not have been applied otherwise as the efforts perhaps would have been not cost effective for short work. Intensive decontamination of the components with high dose rate resulted in a reduction of the dose rate of about a factor of ten in one room and also could reduce the collective dose for jobs in this room. The range of this reduction varies from about two to about one hundred depending on the job.

7.4 Conclusion

Summarising the findings on the systems and component under consideration it seems to be desirable, reasonable and practicable to harmonise and to concentrate tests, inspection and maintenance on systems and components. This will help to reduce doses and perhaps also a part of cost by

- avoiding a certain part of work as e.g. preparative work for the test (scaffolding, insulation,...) or also work to be performed in the test as mounting or dismantling drives or measuring the performance of components or aligning switches...)
- taking benefits from dose reduction measures which perhaps would not be implemented to the same degree for a short work.

To do so it will be important to check the respective intervals and to apply a certain flexibility to the extent necessary and to the extent possible. But certainly all activities to optimise work or to reduce doses will have to be performed considering the safety aspects and the safe operation of the plant.

As it was not possible and due to the complexity of the complete problem not reasonable to derive general quantitative procedures for harmonisation, an important tool to perform optimisation and to implement intentions as discussed in this report will be work management in the plant integrating all groups in the plant as technical division (mechanical and electrical) and the radiation protection division into a close co-operation working closely together. Additionally to co-operation further practices may be important especially for the harmonisation and concentration of activities e.g. in a compartment or at a component:

- Starting planning of outages in a long-term process very early considering even longer intervals in planning than the interval to the next outage and working out tests and inspection necessary and important,
- reviewing the need of tests and work performed for tasks to be scheduled by the utility on the basis of experience, safety and reliability.

Considering most of these aspects also other parties are closely involved in this process of harmonisation and co-operation due to the large number of tests, inspection and maintenance formally prescribed for safety equipment due to rules issued by the supervisory authorities and due to conventional rules valid e.g. for pressure vessels. Here authorities and technical surveillance organisations are addressed and should contribute by thoroughly considering and reviewing

- the need and the time schedule of new tests in case triggered by findings in other plants,
- the need of tests triggered in former years which still have to be performed and may perhaps no longer be necessary
- the flexibility of test intervals.

So as a very general but also very important finding work management and especially communication and close co-operation of all organisations is considered to be the most important contribution to optimisation of radiation protection of nuclear power plants assuring not only dose reduction but also safe operation of the plants.

7.5 Publications

Pfeffer, W., L.Ackermann, H.Marx

Optimisation of Radiation Protection in Inspection and Tests in a German Nuclear Power Plant
GRS-Report,

To be published

Head of Project 4: Dr. Wrixon

II. Objectives for the reporting period

1. To further develop the integration of ALARA Tools into a Work Management approach to Optimisation; with particular attention given to situations involving internal exposures.
2. To develop methodologies for the derivation of dose constraints and to identify how they can be practically implemented into radiation protection programmes.
3. To develop an accident and incident database for the non-nuclear sector.

III. Progress achieved including publications

1. Integration of ALARA tools into a Work Management approach to Optimisation

1.1 Consolidation and dissemination

This contract saw the continuation of a programme of work from previous contracts to develop approaches to, and the practical implementation of, the optimisation principle. Structured approaches such as the ALARA Procedure, ALARA Audits and Predictive ALARA Planning had previously been developed. However, the principal focus of the preceding contract had been to integrate these 'ALARA Tools' into a work management ethos, covering management commitment, appropriate organisational structures and the motivation, awareness and training of staff. The culmination of this work was the CEC Book, ALARA: From theory towards practice⁽¹⁾.

One objective of the present contract was to consolidate the work management approach by providing practical examples demonstrating the benefits and to disseminate this work. During the early part of the contract a major feature of the work of NRPB and its partners^(2,3,4) was the input to the Fourth European Scientific Seminar on Optimisation, Luxembourg 1993. A number of other presentations^(5,6,7) were made during the contract to further disseminate these ideas. It

is perhaps of note that the last of these presentations at the 3rd International Workshop on the Implementation of ALARA, at BNL Brookhaven USA, effectively reviewed the 'state of the art' of optimisation in Europe.

There has been a strong interaction between the work of this project and the series of CEC sponsored courses on Optimisation of Radiation Protection for which NRPB and CEPN have provided the joint scientific coordinators. These courses have been another means of increasing the awareness of the radiological protection community to work management approaches and to their effectiveness. They have also provided an important input to the project in terms of identifying successes and problem areas in the practical implementation of optimisation. Indeed the work in section 1.4 stemmed largely from this feedback. During the contract, courses were held at Vattenfall Nuclear Power Plant, Ringhals, Sweden and KfK, Karlsruhe Germany. A further course in Madrid, Spain will be held in 1995.

1.2 Development of a Structure Operational Protection and Safety Programme

The CEC Book, ALARA : From theory towards practice⁽¹⁾ introduced the concept of using analytical trees to depict an operational radiation protection programme. Such programmes were then available as a tool to assist in ALARA reviews. Since that time the concept of reviews has been extended and a major update has been completed of an operational protection and safety programme, appropriate to the uses of ionising radiations in industry, medicine, research and teaching. Furthermore, the presentation of the analytical trees has been significantly improved by the use of a modern computer programme. This work was completed during the latter part of the contract period and will be published by NRPB.

1.3 Development of OPTI-RP Software

Early in the project it was identified that there was a need for the development of user friendly software that would facilitate non specialists using decision-aiding techniques. To this end CEPN and NRPB have collaborated in the development of OPTI-RP, a software that allows the user to carry out cost effectiveness and cost benefit analysis techniques. This uses 'ACCESS' running under 'Windows', can accommodate both single and sets of alpha values, temporal distributions of costs and a significant number of protections options. The software, in both French and English, will be available by the end of 1995.

1.4 Optimisation and Internal Exposures

Over the years most optimisation studies have tended to focus on situations involving relatively predictable doses stemming from external exposure. A particular focus of work during the contract has been to review situations where internal exposures are involved and to identify how structured approaches might be more effectively used. A report⁽⁸⁾ has been produced, which discusses how the ALARA Procedure might be implemented for internal exposures and identifies the problems involved. Some of the more important points are:

- (i) It is essential to establish the base case, ie define the work pattern and the associated levels of routine and potential exposure arising from both the external and internal exposure routes. This is a necessary precursor to identifying and evaluating protection options.

- (ii) Internal dose data is typically inferior to external dose data and the implementation of a suitable monitoring programme may be necessary before ALARA can be effectively addressed. In many cases inhalation is likely to be the dominant internal exposure route and the adaptability of personal air sampling to provide task specific data makes it the monitoring technique that is most likely to provide a useful input to ALARA studies.
- (iii) Decision aiding techniques such as cost benefit analysis have a role but do not by themselves determine what is ALARA. The usefulness of these techniques may be limited by the significant uncertainties associated with internal dosimetry and the evaluation of potential exposures. An increasingly popular view in these circumstances is to regard optimisation as essentially a qualitative process whereby ALARA can be achieved by a series of judgements as to whether or not a range of available options should be implemented. Such judgements must necessarily be able to evaluate the options and the possible interactions with the various exposure routes. This underlines the need to address points (i) and (ii) above.
- (iv) The presence of contamination in the workplace gives rise to a financial burden, not just for current operational costs but also for future years, through to, and including, decommissioning costs. These may be significantly greater than the potential savings in internal exposure detriment. Thus protection options that reduce contamination may provide both a net financial and radiological benefit.
- (v) There appears to be a general consensus that individuals are more reluctant to receive internal exposures than external exposures⁽⁹⁾. This works against the ALARA principle in that effort to reduce internal exposure can result in larger increases in external exposure. It is concluded that it is a perceptual problem and that there is no basis for valuing internal exposure differently to external exposure. Further, there is a need for managements to address this problem by better informing the workforce. It has been noted that the availability of personal monitoring data for intakes, significantly helps in this process.

The last contract period saw the publication of an NRPB memorandum describing proposals for the categorisation and designation of working areas in which unsealed radioactive materials are used⁽¹⁰⁾. This identified the fact that no previous definitive publication on the subject could be found and consequently the new proposals tackled the problem from first principles. A follow up study within the present contract has examined how the proposals compare with the concept of the optimisation of protection. The proposals imply that an organisation wishing to use increased amounts of unsealed radioactive materials should upgrade the facilities to the category of area appropriate to the new quantities. This requires expenditure in order to control doses to the workers. The new study looks at a comparison between the costs of upgrading facilities with the increase in the detriment value of the doses that would be incurred if the work were to go ahead without upgrading. It is concluded that stricter operational controls may be more cost effective than upgrading, if the desired increase in quantities used is not too great or if the increased usage is for only a fixed period of time. It is usually more cost-effective to pay the cost of upgrading if a tenfold, or greater, increase in usage is required. The work was again completed towards the end of the contract period and will be published by NRPB.

2. Dose Constraints

The 1990 Recommendations of ICRP (Publication 60) introduced a new element to the optimisation principle by stating "This procedure should be constrained by restrictions on the doses to individuals (dose constraints), so as to limit the inequity likely to result from the inherent economic and social judgements". The concept of dose constraints and their practical implementation has been the subject of extensive debate in the subsequent years. In 1993, the NRPB fulfilled its UK statutory function of advising on ICRP's recommendation and endorsed the principles and concepts, including the concept of dose constraints⁽¹¹⁾. This was accompanied by guidance⁽¹²⁾ on the recommendations which *inter alia* addressed the use of dose constraints for occupational, public and medical exposure. For occupational exposure it was recommended that:

- (i) dose constraints should be defined for the purpose of providing an upper bound on the optimisation process and used in a prospective sense;
- (ii) they are not dose limits and parallel investigation levels should be established for use in a retrospective sense; and
- (iii) doses above the investigation level should be investigated by management to determine whether they were as low as reasonably achievable and whether any changes need to be made to the operating arrangements.

These and other aspects of dose constraints were further developed during the period and addressed in several publications^(2,3,5,6). One aspect in particular that has been addressed within the project has been the process of choosing values for dose constraints⁽¹³⁾.

ICRP noted that information on doses likely to be incurred in well managed operations can be used to establish dose constraints for a type of occupation, such as work in x-ray diagnostic departments, the routine operation of nuclear power plants or their inspection and maintenance. The NRPB considers that the process by which dose constraints should be quantified should include the assessment of levels of individual dose presently achieved from particular tasks or operations, identification of any subgroups of workers receiving the higher doses and clarification of the driving forces behind these doses. The underlying theme of the analysis should be to determine the distribution of individual doses that is 'reasonably achievable' in the particular circumstances, with a view to setting the dose constraints in the region of the upper end of the distribution. This raises practical questions regarding the dose information required; how to define the group of workers to whom a dose constraint applies, and should the values be chosen at a national level or by managements? Work was carried out to review the data available in the UK and how it could be best used.

In the UK the Health and Safety Executive (HSE) compile an annual summary of doses, recorded for classified persons in the Central Index of Dose Information (CIDI)⁽¹⁴⁾. These doses are sorted by the occupational category reported by the employers. Thirty-one categories exist and are all general in nature eg application and servicing of machines producing ionising radiations, transport work, medical applications - radiographers, industrial radiography using permanent installations etc. The dose distribution for each category is given as the number of individuals in a dose bandwidth eg 0.0, 0.1-1.0, 1.1-5.0, 5.1-10.0, 10.1-15.0, 15.1-20.0, 20.1-30.0, 30.1-50.0 and >50.0 mSv. It was found that the data as currently available did not

provide the necessary sensitivity to choose dose constraints that would have relevance for the majority of workers. Whilst re-evaluation of raw data might slightly improve this situation, a number of other problems arise from this aggregation of data. These relate to the applicability and validity of the occupational categories to groups of workers and the validity of data in the upper parts of the dose distribution.

To investigate these matters further, NRPB carried out a study, covering 1990 to 1994, of doses greater than 10 mSv in a year which had been recorded for employees or organisations for which the NRPB acted as RPA (Radiological Protection Adviser). As RPA the NRPB was in a position to review in detail documents relating to the circumstances of the exposure.

The study revealed that out of 177 such cases, 33 related to situations where the legally recorded doses were probably not received, with in many cases the likely doses being zero. This over reporting was a function of the burden of proof required to remove a suspect dose from the dose records and the fact that there was little incentive for the employer to expend significant effort if the dose was less than the dose limit. Importantly the study also identified that of the 177 cases, 64 were assessed as being related to the wrong work category. Most of the 177 cases related to industrial radiography where there are two work categories, "using permanent installations" and "on site or works of engineering construction". In many cases employees were involved in both work categories and had been categorised in the former because this constituted the largest element of work, but the real doses and spurious doses (eg dropped badges) were mainly coming from site radiology work. It was concluded that the present CIDI categories could disguise within a category a wide range of job descriptions each with its own annual or task dose implications.

Many of the problems outlined above could be successfully addressed if there was a requirement for dose constraints to be set by local managements, with them defining the groupings of tasks or employees. This would still be open to regulatory review and would be another mechanism to get managements to recognise their responsibilities and address doses in a prospective approach.

To provide an example of how this might be done in practice the NRPB has set dose constraints for its own staff^(5,13). Had this been based on the national CIDI data, one category "radiation protection" might have been used, which would not have been representative of the work undertaken by NRPB staff. The values actually set by NRPB's management were able to take into account differences between laboratory based staff, those involved in consultancy work at other organisations and those involved in radon work. This permitted the setting of an integrated package of dose constraints and associated investigation levels.

Overall it has been concluded that the setting of dose constraints by local management is the preferred approach.

3. Ionising Radiation Incident Database (IRID)

A key element in preventing accidents and being able to mitigate their consequences when they do occur, is the ability to learn from our mistakes in a speedy and efficient manner. In the nuclear industry there are a number of systems designed for this purpose. However this is not the case in the non-nuclear sector, despite the widespread use of ionising radiation in the industry,

medicine, research and teaching. The need for databases to cover this was identified at the 4th European Seminar on Optimisation⁽³⁾ and indeed was emphasised in the discussions of the session on the 'Application of the Optimisation Principle to Worker Exposure".

Therefore an objective of the contract was the development of the structure and operational methods of an accident database. The initial outline in 1993 consisted of a data element dictionary covering 43 fields with some examples culled from NRPB's experience of investigating radiological accidents. As a result of this CEC sponsored initiative NRPB and the Health and Safety Executive (HSE) have now entered into a partnership to develop and operate the Ionising Radiation Incident Database (IRID) for the UK⁽¹⁵⁾. Its objectives are:

- (a) to act as a national focus for incidents, primarily in the non-nuclear sector;
- (b) through appropriate publications to provide feedback and guidance to users of ionising radiations on preventing or limiting the consequences of radiation incidents; and
- (c) to provide regulatory bodies and others with advisory responsibilities with analyses of accident data that help in assessing resource allocation.

It is designed to cover radiological accidents in industry, medical research and teaching. It will not cover nuclear incidents, transport accidents or accidents only involving patient exposure, as there are separate provisions for these. However it would include radiological incidents that occur on a nuclear site eg in industrial radiography. Importantly it will also cover 'near misses' ie significant failures in the radiation protection system that fortuitously did not result in significant doses. There are often useful lessons to be learned from this category of incident, which currently goes unreported.

The database has been designed to operate on a personal computer using dBaseV software. The number of fields has been reduced to 22, to both simplify the database and strike the correct balance between making it user friendly and providing sufficient data to categorise incidents. The fields are:

1 Case number	12 Category of use
2 HSE Area	13 Isotope(s) involved
3 Incident Date	14 Activity
4 Accident Level	15 Kilovoltage of radiation generator
5 Type of accident	16 Cause of incident
6 Number exposed: occupational	17 Availability and effectiveness of contingency plans
7 Number exposed: public	18 RPA: appointed, involved in investigation
8 Whole body dose(s)	19 RPS: appointed, suitable involvement in investigation
9 Extremity dose(s)	20 Follow up action (eg improvements)
10 Internal organ dose(s)	21 Date of entry in database
11 Occupation of worker	22 Description: text field

Fields 1 to 21 have been designed to permit useful analyses of the database and to allow searching of the database for cases which fit a number of templates eg. incidents over a specified period of time involving a category of use and resulting in doses in excess of any specified dose. Field 22 is a text field that will contain formatted descriptions of the incident, ie the cause, the consequences, follow up actions and lessons to be learned. These descriptions will be used in publications to provide feedback to the users.

It was clear from the beginning of the project that confidentiality of information would be a major issue and that to maximise the contributions to the database, confidentiality would have to be guaranteed. The fields and the format of the text descriptions of the accident have therefore been designed to maintain this confidentiality. Only the originator of the information will know the names of the organisations and persons involved.

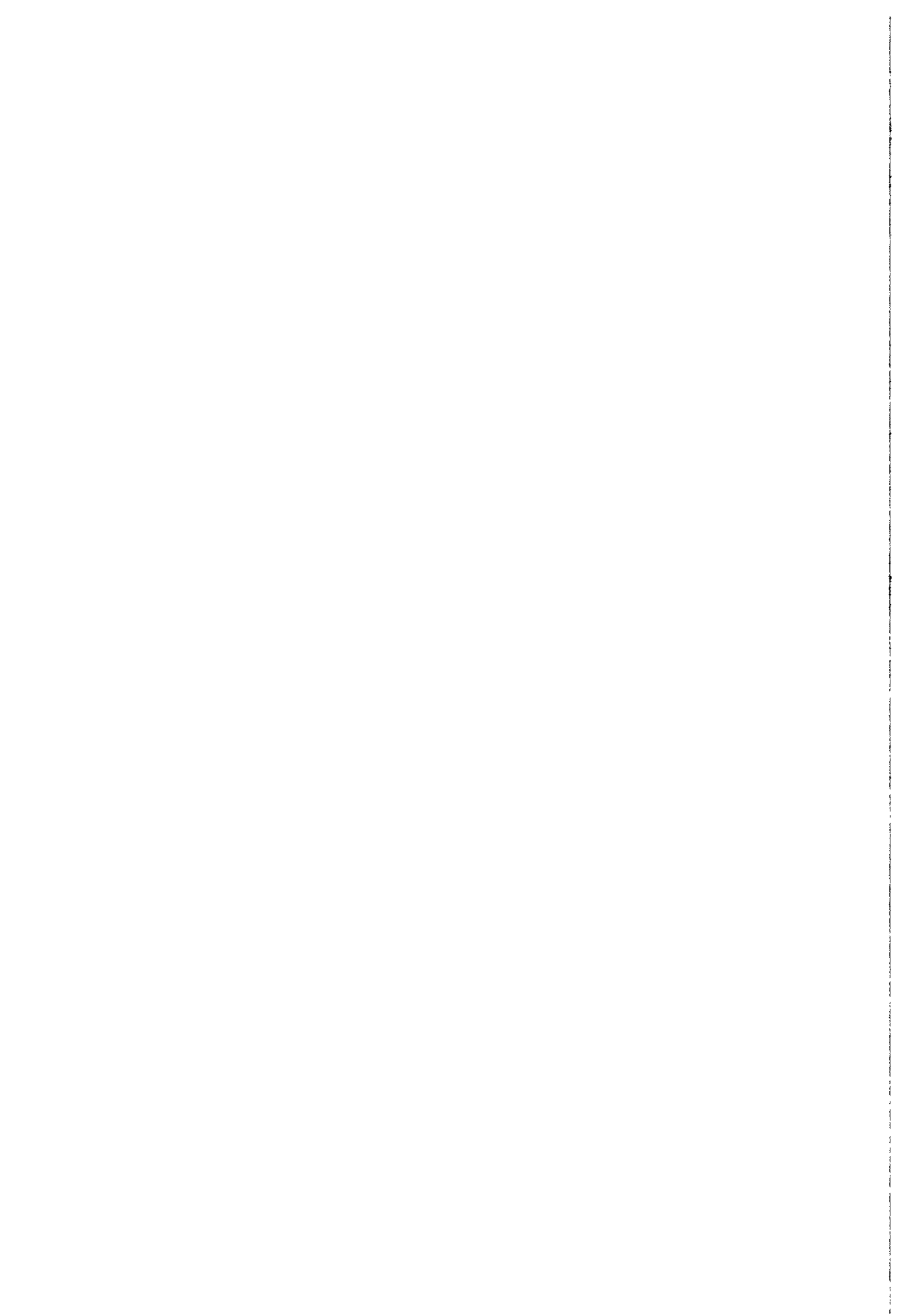
A report detailing the technical specifications, data element dictionary and method of operation will be published at the beginning of 1996⁽¹⁵⁾. At the same time the first of a periodic review of accidents and incidents will be published. In the main, this will be a compilation of the text descriptions from field 22, with for the more important incidents, artwork in the form of diagrams or drawings of accident scenes to improve communication of the message.

In the first instance the incidents included in IRID will come from the files of NRPB and HSE, but in time this will be expanded to encourage input from other sources. Consideration is also being given to the importing and exporting of data from and to other national and international databases.

References

- 1 Stokell P J, Croft J R, Lochard J and Lombard J. ALARA - From theory towards practice. Luxembourg, CEC EUR 13976 EN (1991).
- 2 Croft J R, Lefaire C, Egner K, Schnuer K. Role of Optimisation in the management of worker exposure. Proceedings of the Fourth European Scientific Seminar: Radiation Protection Optimisation 'Achievements and Opportunities' 20-22 April 1993, CEC EUR 15234 EN.
- 3 Croft J R. Optimisation of radiation protection in the non-nuclear sector. Ibid.
- 4 Govaerts P, Zeevaert T. Integration of the ALARA principle in decommissioning activities. Ibid.
- 5 Wrixon A D. Current NRPB recommendations on optimisation of protection of workers. JRP, Vol 14, No 3, 219 (1994).
- 6 Wrixon A D, Croft J R. Gestation du risque radiologique dans les secteurs industriel et medical au Royaume-Uni. Journees SFRP 'Optimisation de la radioprotection des travailleurs dans les domaines electronucleaire, industriel et medical, 20-21 Septembre 1994, La Rochelle.
- 7 Lefaire C, Croft J R, Pfeffer W, Zeevaert T. ALARA in European Nuclear Installations. Proceedings of 3rd International Workshop on the Implementation of ALARA at Nuclear Power Plants, 8-11 May 1994, BNL Brookhaven.
- 8 Shaw P V, Hudson A P. The implementation of ALARA in relation to internal occupational exposures. Tech Memo IOD (4)95, NRPB.

- 9 Coates R. Optimisation problems in processing radioactive substances. Proceedings of the Fourth European Scientific Seminar: Radiation Protection Optimisation 'Achievements and Opportunities' 20-22 April 1993, CEC EUR 15234 EN.
- 10 Hudson A P, Shaw J. Categorisation and designation of working areas in which unsealed radioactive materials are used. Chilton, NRPB-M443 (1993).
- 11 NRPB. Board statement on the 1990 Recommendations of ICRP. Doc NRPB Vol 4, No 1, 1993.
- 12 NRPB. Occupational, public and medical exposures. Doc NRPB Vol 4, No 2, 1993.
- 13 Lloyd S, Croft J R. Dose Constraints in occupational exposure. Tech Memo IOD(5)95, NRPB.
- 14 HSE. Occupational exposure to ionising radiation 1986-1991: Analysis of doses reported to the Health and Safety Executive's Central Index of Dose Information, HMSO 1993.
- 15 Thomas G O, Williams M K, Croft J R. IRID: Specifications for the Ionising Radiations Incident Database (to be published by NRPB/HSE 1996).



Final Report
1992-1994

Contract: FI3P-CT920014 **Duration:** 1.9.92 to 30.6.95 **Sector:** C22

Title: Digital Medical Imaging: Optimization of the dose for the examination.

- 1) Malone Hosp. Federated Dublin Voluntarys
- 2) Faulkner Hosp. Newcastle
- 3) Busch Univ. Hiedelberg
- 4) Jankowski IOM
- 5) Shehu Inst. Onkologjise

I. Summary of Project Global Objectives and Achievements

During the previous three years considerable progress has been achieved towards the overall project objectives. This progress is represented by the significant contribution of work by both individual groups and collaborative efforts to the greater body of published literature to areas of image quality assessment, patient and staff dosimetry, radiation protection, dose optimization and Digital Subtraction Angiography (DSA). At this point, several of the work initiatives have been carried to their successful completion stages, with conclusions and recommendations in the aforementioned fields that should be taken on board by the wider scientific community. However, some areas of endeavour tackled by the contract groups have not yet reached fruition, and would require further collaborative research with a broader group of workers in order to derive useful and conclusive scientific and clinical endpoints.

Much of the work has focused on image intensifier radiography, where comparisons were made between digital and analogue systems which were paralleled with developing Quality Assurance protocols (since existing QA protocols are restrictive in terms of technique factors and dose rates) and optimization studies utilizing specialised custom built test objects and phantoms. Such a comparison of imaging methods and systems was completed for chest

and abdomen examinations. It was also found from a large fluoroscopic dosimetry survey using dose area product meters that newer digital screening units offered superior dosimetric possibilities than their older conventional counterparts, with such facilities as variable frame rates, real time image processing (particularly temporal averaging) and last frame digital hold.

Optimization studies, with a particular emphasis on DSA, have been ongoing throughout the contract period. Several approaches to this end have been taken by the various working groups, such as from the perspectives of image quality, dosimetry and clinical simulation with the aid of vascular phantoms with varying degrees of stenosis. It yet remains, however, to form a unified approach to the question of optimization for DSA examinations, and this issue will inevitably require further collaborative work. It has also been identified that technology alone will not create optimal pathways, and that the education of radiologists will play a pivotal role in the optimization of DSA doses, as indeed patient doses arising from other radiological examinations and procedures.

Other areas of interest which been investigated are the present status of multiformat cameras and viewing conditions. Protocols have been developed for the performance of quality assurance measurements for these important aspects of the digital imaging chain, as they are often neglected or not considered as an integral part of presently established QA programmes. This work has highlighted the fact multiformat imagers and viewing conditions are components requiring optimization and rigorous quality assurance.

There has been considerable interaction and communication between Western groups and the PECO partners over the past two years, in terms of expert meetings and collaborative work. This alliance has proved to be mutually beneficial in terms of scientific insights and support. Comparisons of methodologies, practices and dosimetry has enlightened all involved, and has facilitated much original and necessary work. The final report on the PECO component of the project was deferred from June 1995 for some time to allow completion of the work involved. In the past year there has also been significant interaction and involvement with other radiological research groups within the EC with a view to future scientific and clinical collaboration. It was apparent that from these groups a comprehensive proposal within the new programme addressing unresolved problems arising from the new now widespread applications of new digital technology could be developed.

Head of project 1: Prof. J.F. Malone

II. Objectives for the reporting period

- * To initiate a survey of MTF measurements from different imaging modalities, and combine these with already existing Wiener spectra measurements to yield DQE measurements for various systems.
- * To continue existing organ dosimetry in GI examinations in GI examinations studying the impact of AEC, operator and IRCP 60 on patient dose.
- * To expand the image noise - Image Intensifier Entrance Exposure model to incorporate other image quality indices such as MTF , DQE etc.
- * To rigorously assess the image quality of film based imaging using Wiener spectra and MTF indices and a high resolution film digitizer.

III. Progress achieve including publications

Image Quality Studies

Image Quality assessment techniques have played an active research role in this departments work. It would seem that most image quality assurance is performed using subjective approaches such as resolution test patterns (e.g. Huttner phantom) and contrast detail detectability phantoms (e.g. Leeds TO10). However, since the thrust of this work is optimization, the sensitivity and reproducibility of these methods may be called into question, and may lead to inappropriate or incorrect conclusions. It is for this reason that much effort focused on the development of more robust second order objective techniques (such as Modulation Transfer Functions [MTF] and Wiener spectra). Present and future work will be directed towards the unification of these approaches using a comprehensive mathematical model which should incorporate such objective measures with the psychophysical aspects of the human visual process, which, in essence, will provide a necessary subjective/objective

bridge yielding open ended endpoints to rigorously assess and model image quality.

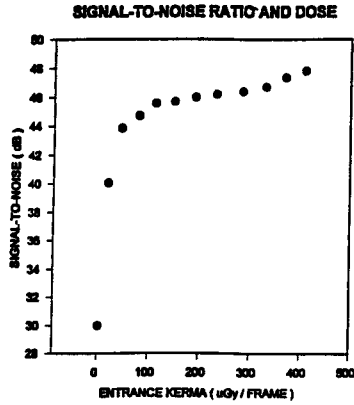
Objective Image Quality Indices / Optimization

During the course of this work a comprehensive study and comparison of Wiener spectra and Signal-to-Noise Ratio (SNR) measurements from various imaging modalities including conventional fluoroscopy, Digital Subtraction Angiography, Digital Cardiac Imaging, ultrasound, and nuclear medicine has been completed. The results of this survey highlight the utility, flexibility and ubiquity of such indices, and also serves to demonstrate their dose sensitivity, thus indicating their viability in any technical optimization regime. Some of the original survey work has now been augmented by a series of MTF measurements. Many MTF methods have been explored; however, it was established that the use of an edge should be the method of choice with image intensifier systems. It was further established that the alignment of the edge had a minimal effect on the resulting spectrum, which increases the ease to which this method may be applied.

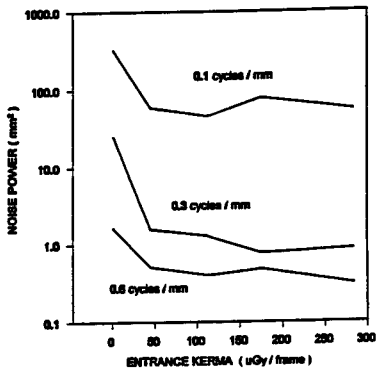
Collaborative work with the Newcastle group has been conducted to study the relationship between subjective and objective approaches to image quality assessment, and to model the interdependence of noise power spectra and contrast detail detectability using custom built test objects specifically designed by the Newcastle group for this purpose. However, this joint work has not yet reached maturity, and will be the subject of future collaborative efforts.

A technical optimization / dose evaluation of a Digital Subtraction Angiography (DSA) system was also performed, the results of which were presented at the European Congress of Radiology, Vienna. This study outlines an approach for the use of SNR, Wiener spectra and MTF in an optimization exercise to a first approximation. It was found for the system in question, that the aforementioned indices reached plateau at ~ 50 μGy / frame (as measured at the image receptor), an exposure level that is lower than some clinical set-ups, thereby suggesting a net dose saving (in some instances a dose reduction of $\sim 30\%$). However, this optimization is technical in nature, and must be coupled with a subjective / clinical optimization effort, which is presently under way.

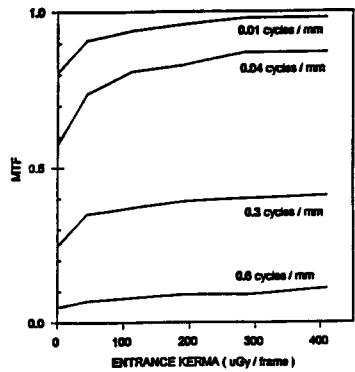
A smaller optimization study using the same indices was conducted in nuclear medicine, where technical and clinical optimization approaches were juxtaposed. An interesting conclusion of this study was the fact that MTF optimization seemed to correlate more closely to clinically optimal endpoints. Further work needs to be carried out in order



NOISE POWER AS A FUNCTION OF ENTRANCE KERMA



MTF AS A FUNCTION OF ENTRANCE KERMA



Optimization curves for a DSA system using Signal-to-Noise Ratios, Modulation Transfer Functions and Wiener Spectra. These Curves indicate an optimum operating point at ~50 uGy / frame.

to assess the full scope and validity of this conclusion when applied to photoelectric systems.

Approaches to use Detective Quantum Efficiency (DQE) estimates calculated from MTF and Wiener spectra measurements are under consideration and could prove to be of greater value in optimization studies than our present protocols.

Dosimetry

The Gastro Intestinal (GI) examination work that was initiated two years ago is still active. The results of this work has shown significant differences in dose estimates between IRCP 26 and IRCP 60. More recent work in this field using framegrabbed images with Dose Area Product (DAP) and screening times superimposed was downloaded to a VCR for analysis by a panel of radiologists. This is a novel technique which was used to estimate the Effective Dose to patients undergoing small bowel examinations. A patient Effective Dose of ~3 mSv was estimated for this examination.

Other work in this field investigated the effect of mA on DAP measurements during Barium Enema examinations. It was found that by setting the mA to the minimum level available to the system, there was no adverse effects on image quality with significant dose saving. Effective Doses have yet to be estimated for this examination.

Image Digitisation / Workstations

The image quality of radiographic and CT images which have been digitised using a high resolution film digitiser been assessed independently by a panel of radiologists and physicists. It was found that there was little advantage in using matrix sizes in excess of 2k x 2k, however it was necessary to use 12 bit resolution except in the case of multiformat camera images where 8 bit resolution was adequate. It was also found that 2k x 2k x 12 bit was an optimal operating point if the resulting digitised image was to be transported via a network to another centre, as higher order configurations constitute a greater data load which significantly effects transfer times. However, since this particular digitisation system is still in its developmental stages, we have been as yet unable to evaluate its full image processing potential, which could yield other optimal set-ups, depending on the nature of the images being transmitted.

Automatic Exposure Control

During the latter years of this contract, substantial effort has been directed at the design and philosophy of Automatic Exposure Control (AEC). It has been found that the ALARA principle (which should be the underlying philosophy of AEC) was not strictly adhered to in the design of AEC systems, with relatively large doses present where they were not considered justified. Studies which have investigated the impact of patient thickness on image receptor entrance kerma, image SNR, film densities (for spot imaging, 100 mm imaging cine as well as radiographic film), and subjective evaluations of the resulting image quality. It was found that although some of these parameters varied widely, these variations were not necessarily reflected in subjective assessments using limiting resolution and contrast detail detectability measurements. It was also discovered that different manufacturers exploit different methods to achieve AEC, which creates considerable confusion among end users, who may not derive the full benefits of AEC as a result. This finding demonstrates a need for standardisation in AEC design, and also adequate training for personnel in the use of AEC.

Recent efforts by this group into the study of AEC have concentrated on the functional aspects of AEC. The objective of this work has been to understand the engineering principles employed in AEC systems, with a view to building a general framework from which the specific functional behaviour of a given system may be modeled and predicted in a way that is not currently available.

Multiformat Imaging

For many expensive high technology digital imaging systems, the final hard copy (which is often used for a clinical diagnosis) is produced on a multiformat camera, or more recently a laser imager. This fact should place stringent criteria on the Quality Assurance (QA) and quality control of these devices, which are often neglected in presently established QA programmes. In the absence of any standard QA protocols for these devices, a basic QA approach was developed to study the contrast rendition and resolution properties of these systems using software generated software test patterns. It was found that these devices exhibited large variations in image quality, and in some cases poor contrast was noted. It was also found that QA was severely hindered or could not be performed on many format cameras, due to the non-accessibility of vital optical components. It was clear from this work that the QA issue of multiformat cameras is one that needs to be addressed in terms of standardised

design and QA measurement methods.

Viewing Conditions

As part of any radiological imaging chain, the final stage is that of human interpretation. Thus, this stage should be assessed as an integral part of a systematic optimization process. For this reason, a survey of viewing boxes was conducted and compared with the criteria laid down by the EC working document. It was found that none of the viewing boxes surveyed fulfilled all of the EC criteria, and 70% of them did not meet any of the criteria. In addition to surveying the viewing boxes, a protocol was developed for assessing their condition, which can be readily applied. It can be recommended from this work that hospitals should consider this equipment to be included as part of their routine QA programmes.

Dose Modelling

A simple theoretical model of the effect of image intensifier entrance exposure on the resulting image SNR and contrast has been explored, and is still being developed. This model seeks to investigate and understand the utilisation of such relatively high doses for subtraction imaging methods such as DSA (sometimes these doses are orders of magnitude higher than those used for unsubtracted imaging) are really necessary. The developed model will also be used to theoretically optimize exposures for DSA, which are presently arrived at in a fashion not subject to objective critical review. Thus, this optimization approach, which is of a rational nature, should provide optimal solutions which are independent of the solutions derived empirically.

Mobile Radiological Equipment

Mobile radiological equipment is finding greater application in latter years, in particular the use of mobile C-arms in vascular and orthopedic surgery. Since this equipment is often offsite from the main radiological facility, it can be overlooked in terms of routine quality assurance. On this basis it was decided to conduct separate surveys (for mobile radiographic and fluoroscopic image intensifier systems) as to the condition of this equipment. Since there were no standard QA protocols available, an approach was developed which incorporated

electrical and mechanical safety in addition to the traditional radiation safety and image quality assessment that is applied to stationary radiological imaging systems. During the course of these surveys it was found that little attention has been previously addressed to the QA of mobile systems, and significant performance variations with respect to image quality were observed. Furthermore, this work identified a lack of 'write off' criteria for these devices; this problem of 'write off' criteria is one that is shared by stationary radiological equipment.

PECO Partners

There has been considerable interaction and communication between members of this group and the PECO partners, in the form of expert meetings and scientific support. Members of this group and the Newcastle group have conducted a survey of the radiological facilities in Albania. Basic QA was performed on a number of selected radiological systems using Western materials and methods. It was found that none of the systems examined met the criteria required in Western countries. Most radiological equipment was very old (average age ~35 years), and in some cases equipment manufactured in the 1920's found routine clinical application. Mechanical timers and mains operated hand-held switches are the norm, as is poor beam filtration and limitation. Direct fluoroscopy with dark adaption is still widely practised. It was also noted that this country seriously lacked technical expertise to repair old and install newer equipment.

Publications

- 1) **Radiation Protection Problems with Dental Radiographic Equipment.**
Cooney P., Gavin G., Rajan J. and Malone J.F.
Radiation Protection Dosimetry, Vol. 57, Nos. 1-4, pp 339-342 (1995).

- 2) **Survey of Image Viewing conditions for X-ray Film.**
Cooney P., Davis C., Chua J.B.Y., van der Putten W and Malone J.F.
Radiation Protection Dosimetry, Vol. 57, Nos. 1-4, pp 305-308 (1995).

- 3) **Automatic Exposure Control in Fluoroscopic Imaging.**
Cooney P. Marsh D.M. and Malone J.F.
Radiation Protection Dosimetry, Vol. 57, Nos. 1-4, pp 269-272 (1995).
- 4) **An Assessment of the Variations in Image Quality with Multiformat Cameras.**
Marsh D.M., Cooney P. and Malone J.F.
Radiation Protection Dosimetry, Vol. 57, Nos. 1-4, pp 277-280 (1995).
- 5) **Measurement of Wiener Spectra in Digital Systems.**
Marsh D.M., Cooney P., McMahon B.P. and Malone J.F.
Radiation Protection Dosimetry, Vol. 57, Nos. 1-4, pp 273-276 (1995).
- 6) **Quality Assurance Programme Applied to Mobile X-ray Equipment.**
Tuohy B., Cooney P., Tuohy G., Moran B. and Malone J.F.
Radiation Protection Dosimetry, Vol. 57, Nos. 1-4, pp 241-244 (1995).
- 7) **A Practical Approach to Implementation of a QA Programme for Radiology at Constancy Check Level.** Moran B., Upton J., Cooney P. and Malone J.F.
Radiation Protection Dosimetry, Vol. 57, Nos. 1-4, pp 263-267 (1995).
- 8) **Optimization of Radiographic AEC System Performance.**
Upton J., Moran B. and Malone J.F.
Radiation Protection Dosimetry, Vol. 57, Nos. 1-4, pp 237-240 (1995).
- 9) **A Review of the Background to the Decision to Write-Off Fluoroscopic Equipment in 15 Instances and the Impact of Patient Dose and Image Quality in Practice.**
Malone J.F., Busch H.P. and Faulkner K.
Radiation Protection Dosimetry, Vol. 57, Nos. 1-4, pp 249-252 (1995).
- 10) **Image Quality Criteria Applied to Digital Radiography.**
Busch H.P., Faulkner K., Malone J.F.
Radiation Protection Dosimetry, Vol. 57, Nos. 1-4, pp 139-140 (1995).

- 11) **Daylight Film/Processor/Loader Systems - Aspects of Performance and Distribution.**
Upton J., Moran B., Duggan M., Malone J.F.
Radiation Protection Dosimetry, Vol. 57, Nos. 1-4, pp 343-346 (1995).
- 12) **An Initial Report on the Investigation of High Patient Dose for the Lumbar-Sacral Projection in the Lumbar Spine Examination.**
Moran B., Upton J., Rafferty M., Boyle G. and Malone J.F.
Radiation Protection Dosimetry, Vol. 57, Nos. 1-4, pp 423-427 (1995).
- 13) **Automatic and Preprogrammed Exposure (APEX) Selection in Fluoroscopy through Indirect Control: an Update on the Concept of AEC.** Malone J.F., Marsh D.M. and Cooney P. British Institute of Radiology Meeting ' Radiation Protection in Interventional Radiology', 6th December 1993, London.
- 14) **An Investigation into the Radiation Dose Associated with Different Imaging Systems for Chest Radiology.** Marshall N.W., Faulkner K., Busch H.P., Marsh D.M and Pfennig H. British Journal of Radiology, 1994:67(796), 353-359.
- 15) **A comparison of Radiation Doses in Examinations of the Abdomen Using Different Imaging Techniques.** Marshall N.W., Faulkner K., Busch H.P., Marsh D.M and Pfennig H. British Journal of Radiology, 1994:67,478-484.
- 16) **A Comparison of Two Methods for Estimating Effective Dose in Abdominal Radiology.** Marshall N.W., Faulkner K., Busch H.P., Marsh D.M and Pfennig H. Radiation Protection Dosimetry, Vol. 57, Nos. 1-4, pp 367-369 (1995).
- 17) **Implications of IRCP-60 in GIT Fluoroscopy.**
Quinn A., Wallis F., Molloy M., Upton J. and Malone J.F. Presented at the Proceedings of the 52nd Annual Congress of the British Institute of Radiology, Harrogate, 23-25 May 1994.

- 18) Review and Analysis of Radiation Incidents.**
Malone J.F. Presented at CEC/Hellenic Dental Association Meeting, Athens and Thessalonica.
- 19) Electrical and Mechanical Safety of Dental Radiological Equipment.**
Malone J.F. Presented at CEC/Hellenic Dental Association Meeting, Athens and Thessalonica.
- 20) Assessment of Organs in the Field of View during Fluoroscopic Studies of the GI Tract.** Quinn A., Wallis F., Molloy M., Upton J. and Malone.
Presented at 'Data Analysis in Quality Control and Radiation Protection of the Patient in Diagnostic Radiology and Nuclear Medicine', CEC Workshop, Grado, Italy, September 1993.
- 21) Quality Assurance Programme Applied to Mobile C-Arm Fluoroscopy Systems.**
Tuohy B., Marsh D.M., O'Reilly G., Dowling A., Cooney P. and Malone J.F.
Presented at the European Congress of Radiology, Vienna, March 1995. (In press).
- 22) The Dose Optimization of a DSA System.**
Marsh D.M., Cooney P., McMahon B.P., Sheahan N. and Malone J.F.
Presented at the European Congress of Radiology, Vienna, March 1995.
- 23) Review and Analysis of an Incident with Dental Radiological Equipment.**
Malone J.F. and Hone C.
In "Radiation Incidents in Hospitals". Ed: K. Faulkner et al. British Institute of Radiology, London (in press).
- 24) Standards for Interventional Radiology Equipment.**
Malone J.F.
Categorical Course Syllabus. Radiological Society of North America (in press).

Head of project 2: Dr. Faulkner

II. Objectives for the reporting period

I. Initiate a Regional quality assurance survey on fluoroscopy and digital imaging systems to establish norms for the above measurements.

II. Optimise staff protection in fluoroscopy and digital imaging. Initiate a Monte Carlo study to deduce the scattered radiation dose to the foetus of occupationally exposed workers. Verify the model.

III. Develop a method of assessing patient entrance dose-rate and air-kerma rate at the image receptor input surface for fluoroscopy and digital imaging systems.

IV. Commence a large scale Regional intercomparison of imaging performance of fluoroscopy and digital imaging systems, integrate with theoretical model of imaging performance.

V. Investigate the effects of real time image processing options available on image intensifier systems, with particular emphasis on mobiles used in operating theatres.

III Progress achieved including publications

The use of contrast detail test objects to monitor subjective indices of performance such as contrast detail detectability and other methods to determine quantitative indices, are widely accepted approaches to the assessment of image intensifier television systems. However, these approaches have their limitations, as measurements can only be performed at certain combinations of technique factors and dose-rates. Standard performance data is only available for a limited number of field sizes. It was therefore decided to review current test procedures, refine the methodology and propose a modified test protocol. An internal quality assurance test protocol has been written. Measurements, using this protocol, have been performed on 80 different fluoroscopy units. The results of this survey are currently being analysed. It is intended to publish the quality assurance protocol and normative data in due course. Initial comparisons of the results with a theoretical model of contrast detail behaviour indicate good agreement.

Threshold contrast detail test objects have been a valuable tool for the non-invasive assessment of the imaging performance of X-ray image intensifier - TV systems. Image intensifier systems have evolved over the years to the stage that existing procedures for contrast detail testing may no longer be applicable. Two situations where difficulty can occur are when the image intensifier input diameter is significantly different from the 34cm field diameter normally used for comparative measurements, and when the intensifier TV system is permanently coupled to a digital image processing unit for real time weighted frame averaging and last image hold during fluoroscopy.

Random noise fluctuations in fluoroscopy arising from both X-ray photon and electronic noise are reduced by temporal averaging. Digital real-time weighted frame averaging is method of applying a controlled amount of persistence to the image to reduce the noise in static and slow moving images. A numerical model of the frame averaging process, which include the effects of the observer and the analogue components of the system has been developed and experimentally verified. Experimental threshold contrast detail measurements have shown that both the real time digital frame averaging and analogue persistence of the image intensifier - TV system combine to affect the overall imaging performance. The conclusions of the survey is that persistence measurements will be required either to set dose-rates consistent with the existing performance standard or to match up to a more flexible standard.

A large scale survey of patient dose levels in fluoroscopy has been initiated. Patient doses are monitored according to the national patient dosimetry protocol. The main objectives of this survey is twofold; first to provide baseline dose data for a range of examination and second to compare departments. Dose-area product meters linked to laptop computers have been installed on over 20 fluoroscopy rooms. Data is collated at a central database which now holds patient dose records for over 30,000 adult and 2,000 paediatric examinations. Analysis of the survey results has indicated that doses to patients having barium studies on digital equipment are significantly less than those examined a conventional fluoroscopy units.

Radiation protection legislation in many member states and other countries make reference to limiting values for patient entrance surface dose-rate. However, no universally accepted measurement protocol exists, nor have many survey been reported. Consequently, an internal quality assurance measurement protocol has been developed to assess patient entrance surface and image intensifier input dose rates. The former measurement is performed in the presence of scattered radiation using Perspex blocks and the later using copper to simulate the attenuation of the patient. It is suggested that image intensifier input dose-rates are measured in minimum scatter conditions. Quality assurance measurements using these protocols have been performed on 80 fluoroscopy units, of which 35 had digital imaging capability. The measurement protocols and results of the survey will be disseminated through the usual academic channels. Recommendation for normal values will be promulgated.

A main source of uncertainty in patient dosimetry data is the influence of patient size. Allowance in the analysis of patient dosimetry data may be made on the basis of equivalent diameter. This approach has been extended by the development of a prospective correction method. The prospective method is based on the use of a simple phantom to deduced size correction factors. A validation study was performed which indicated that the suggested derived correction factors were in good agreement with those determined retrospectively from patient dose survey data. The chief advantage of using size correction factor is that it allows all patients to be included in the analysis.

An investigation into the optimisation of personal shielding for fluoroscopy examinations was undertaken. Scattered x-ray distributions from an anthropomorphic phantom were used to irradiate a Rando phantom. This phantom had been loaded with Lithium fluoride thermoluminescent dosimeters at positions corresponding to radiosensitive organs. The variation of effective dose with the use of lead aprons of different thickness was studied as well as the impact of the use of a thyroid shield and lead acrylic face mask. It was deduced from the results of these experiments that increasing lead apron thickness above 0.35mm had only a marginal effect in reducing effective dose. By contrast wearing a thyroid shield or a lead acrylic face mask always reduced the effective dose to a greater degree than changing from a 0.35mm to 0.5mm lead apron. It was concluded that in general, it is always better to shield more organs than to increase the shielding of a few. These recommendations have been published at a CEC meeting.

In general radiation doses to staff in diagnostic radiology are usually a small fraction of the average dose to a typical member of the population from all sources. The introduction of interventional radiology procedures involving extended fluoroscopy times has led to higher staff doses. This group of individuals may be monitored using a combination of two or more dosimeters. Whilst one dosimeter reading may yield a reasonable estimate of effective dose, a suitable combination of dosimeter readings should achieve improved accuracy in personal monitoring in diagnostic radiology. Improved dosimetry for this group of individuals is important as in some instances their dose could approach a dose-limit. Mathematical analysis of the results of a previous investigation into the relationship between effective dose and dosimeter reading has been performed. This approach involves the use of a minimum error function analysis. It is possible to combine above apron and below apron dosimeter readings to provide an estimate of effective dose to within 30%.

The development of a Monte Carlo model, based on the EGS4 code, for the simulation of the irradiation of the foetus to pregnant staff in diagnostic radiology has commenced. An initial, simplified mathematical model of a pregnant woman has been developed. Modelling of the interaction of various diagnostic x-ray spectra with the abdomen of a pregnant woman has commenced. Complementing this study has been an experimental investigation to determine x-ray spectra produced when X-rays are scattered by an anthropomorphic phantom.

Software for the derivation of the Noise power spectrum of image intensifier television systems is currently being developed. This approach uses a frame grabber linked to a lap top computer. Some refinement of the algorithm is requested prior to use on x-ray equipment.

PUBLICATIONS

C-L Chapple, K Faulkner, REJ Lee, EW Hunter. Results of a survey of doses to paediatric patients undergoing common radiological examinations. 1993 Yearbook of Diagnostic Radiology. 557-559 (CV Mosby yearbook inc, Chicago, USA).

K Faulkner, NW Marshall. The relationship of effective dose to personnel and monitor reading for simulated fluoroscopic irradiation conditions. Health Physics. 1993;64(5);502-508.

AR Lecomber, K Faulkner. Dose reduction in panoramic radiography. International Journal of Dentomaxillofacial Radiology. 1993;22;69-73.

NW Marshall, K Faulkner. Normalised organ dose data measured as a function of field size for abdominal examinations. Physics in Medicine and Biology 1993;38;1131-1136.

KJ Robson, CJ Kotre, K Faulkner. Contrast and signal to noise ratio in radiographic images. Radiology 1993;188(3);878-879.

CL Chapple, K Faulkner, E Hunter, REJ Lee. Radiation doses to paediatric patients undergoing less common radiological procedures involving fluoroscopy. British Journal of Radiology 1993;66;823-827.

AR Lecomber, K Faulkner. Organ absorbed doses in intra-oral dental radiography. British Journal of Radiology 1993;66;1035-1041.

NW Marshall, K Faulkner, HP Busch. A quantitative test object for optimisation studies in image intensifier-TV and digital imaging systems. Radiation Protection Dosimetry 1993;49;269-271.

K Faulkner, NW Marshall. Personal monitoring of pregnant staff in diagnostic radiology. Journal of Radiation Protection 1993;13(4);259-265.

NW Marshall, K Faulkner, HP Busch, D Marsh, H Pfennig. An investigation into the radiation dose associated with different imaging systems for chest radiology. *British Journal of Radiology* 1994;67(796);353-359.

CL Chapple, K Faulkner, E Hunter. Energy imparted to neonates during X-ray examinations in a special care baby unit. *British Journal of Radiology* 1994;67(796);366-370.

NW Marshall, K Faulkner, HP Busch, D Marsh, H Pfennig. A comparison of radiation doses in examinations of the abdomen using different imaging techniques. *British Journal of Radiology* 1994;67;478-484.

CL Chapple, K Faulkner, E Hunter, REJ Lee. The selection of age groupings for the results of radiation dose surveys in paediatric radiology. *British Journal of Radiology* 1994;67;513.

AR Lecomber, K Faulkner. Organ absorbed doses in intra-oral dental radiography. *British Journal of Radiology*. 1994;67;744.

CL Chapple, K Faulkner, NW Marshall, DJ Rawlings. The implications of ICRP 60 on the monitoring of pregnant hospital staff. *Radiation Protection Dosimetry* 1994 54(3/4) 299-302.

NW Marshall, K Faulkner, HP Busch, KJ Lehmann. A theoretical model of the contrast detail behaviour of digital imaging systems. *Physics in Medicine and Biology* 1994 39 2289-2303.

K Faulkner, D Teunen Eds. Radiation protection in interventional radiology. *British Institute of Radiology* 1995 ISBN 0 905 749 34 0. iii+52p.

NW Marshall, K Faulkner. Optimisation of personnel shielding in interventional radiology. in K Faulkner, D Teunen Eds. Radiation protection in interventional radiology. *British Institute of Radiology* 1995 ISBN 0 905 749 34 0. 29-33.

K Faulkner. Summary and conclusions of the meeting on radiation protection in interventional radiology. in K Faulkner, D Teunen Eds. Radiation protection in interventional radiology. *British Institute of Radiology* 1995 ISBN 0 905 749 34 0. 51-52.

NW Marshall, K Faulkner, HP Busch, DM Marsh H Pfennig. A comparison of two methods for estimating effective dose in abdominal radiology. *Radiation Protection Dosimetry* 1995 57(1-4) 367-369.

CJ Kotre, NW Marshall, K Faulkner. Contrast detail testing techniques for modern X-ray image intensifier systems. *Radiation Protection Dosimetry* 1995 57(1-4) 245-247.

HP Busch, K Faulkner, JF Malone. Image quality criteria applied to digital radiography. *Radiation Protection Dosimetry* 1995 57(1-4) 139-140.

JF Malone, HP Busch, K Faulkner. Writing off old fluoroscopy equipment- impact of patient dose and image quality in practice. *Radiation Protection Dosimetry* 1995 57(1-4) 249-252.

K Faulkner, C-L Chapple. 1995. Automated quality assurance and patient dosimetry in diagnostic radiology. in *Die Messung des Dosis-Flächen-Produktes zur Ermittlung der Strahlenexposition des Patienten in der Röntgendiagnostik* (H Hoffmann Verlag GmbH, Germany). 186-193. ISBN 3-87344-095-4.

K Faulkner, NW Marshall. 1995. The correlation of air-Kerma area product with staff dose in fluoroscopy. in Die Messung des Dosis-Flächen-Produktes zur Ermittlung der Strahlenexposition des Patienten in der Röntgendiagnostik (H Hoffmann Verlag GmbH, Germany). 203-210. ISBN 3-87344-095-4.

CL Chapple, K Faulkner, E Hunter, REJ Lee. Radiation doses to paediatric patients undergoing less common radiological procedures involving fluoroscopy. 1995 Yearbook of Diagnostic Radiology (CV Mosby yearbook inc, Chicago, USA).

NW Marshall, J Noble, K Faulkner. 1995 Radiation doses to patients and staff from neuroradiology. British Journal of Radiology 68 495-501.

K Faulkner, AP Jones, A Walker. 1995 Safety in diagnostic radiology. Institute of Physical Sciences in Medicine Report 72.

K Faulkner, 1995 Quality assurance in diagnostic radiology. in Safety in diagnostic radiology. eds K Faulkner, AP Jones, A Walker. Institute of Physical Sciences in Medicine 64-71.

K Faulkner. 1995 Organisation of radiation protection in the United Kingdom. In Safety control in diagnostic radiology. Proceedings of a one day meeting. (National Institute of Health, Korea) 3-5.

NW Marshall, K Faulkner. 1995 Optimisation of personal shielding in interventional radiology. In Safety control in diagnostic radiology. Proceedings of a one day meeting. (National Institute of Health, Korea) 7-12.

NW Marshall, K Faulkner, HP Busch, DM Marsh, H Pfenning. 1995 A comparison of radiation doses in examination of the abdomen using different radiological imaging techniques. In Safety control in diagnostic radiology. Proceedings of a one day meeting. (National Institute of Health, Korea) 13-18.

NW Marshall, K Faulkner, HP Busch, KJ Lehmann. 1995 The contrast detail behaviour of a photostimulable storage phosphor based computed radiography system. In Safety control in diagnostic radiology. Proceedings of a one day meeting. (National Institute of Health, Korea) 19-33.

NW Marshall, K Faulkner, HP Busch, DM Marsh, H Pfenning. 1995 An investigation into the radiation dose associated with different imaging systems for chest radiology. In Safety control in diagnostic radiology. Proceedings of a one day meeting. (National Institute of Health, Korea) 35-41.

NW Marshall, K Faulkner, P Clarke. 1995 An investigation into the effect of protective devices on the dose to radiosensitive organs in the head and neck. In Safety control in diagnostic radiology. Proceedings of a one day meeting. (National Institute of Health, Korea) 42-45.

DA Broadhead, C-L Chapple, K Faulkner. (in press) The impact of digital imaging on patient doses during barium studies. British Journal of Radiology.

C-L Chapple, DA Broadhead, K Faulkner. (in press) A phantom based method for deriving typical patient doses from measurements of dose-area product on populations of patients. British Journal of Radiology.

RM Harrison, K Faulkner, ML Davies, CL Chapple, KJ Robson, DA Broadhead. (in press) Patient dosimetry in diagnostic radiology - some considerations in an NHS region. Journal of Radiation Protection

CONFERENCE PRESENTATIONS AND INVITED SEMINARS

NW Marshall, K Faulkner, HP Busch. A set of quantitative test objects for optimisation in fluoroscopy and digital imaging systems. Commission of the European Communities Workshop, 15th-17th June 1992, Wurzburg.

K Faulkner. Introduction to radiation physics. Commission of European Communities Meeting: Optimisation and radiation protection for radiological imaging in dentistry, 26th-27th November 1992, Amsterdam.

K Faulkner. Dose reduction and optimisation in dental radiology. Commission of the European Communities Meeting; Optimisation and radiation protection for radiological imaging in dentistry, 26th-27th November 1992, Amsterdam.

C-L Chapple, K Faulkner, E Hunter. Radiation risk to neonates in a special care baby unit. Radiology and Oncology 93, 17th-19th May 1993, Glasgow.

C-L Chapple, K Faulkner, D Lauckner. Computer tomography dosimetry audit in the Northern Region. Radiology and Oncology 93, 17th-19th May 1993, Glasgow.

NW Marshall, K Faulkner, HP Busch, KJ Lehmann. Contrast -detail performance of various X-ray digital imaging systems. Institute of Physical Sciences in Medicine Meeting. The assessment of X-ray digital imaging systems. 29th June 1993, Birmingham.

NW Marshall, K Faulkner, HP Busch, DM Marsh H Pfennig. A comparison of two methods for estimating effective dose in abdominal radiology. Commission of the European Communities Workshop 'Data analysis in quality control and radiation protection of the patient in diagnostic radiology and nuclear medicine'. 29th September- 1st October 1993. Grado, Italy.

CJ Kotre, NW Marshall, K Faulkner. Contrast detail testing techniques for modern X-ray image intensifier systems. Commission of the European Communities Workshop 'Data analysis in quality control and radiation protection of the patient in diagnostic radiology and nuclear medicine'. 29th September- 1st October 1993. Grado, Italy.

C-L Chapple, K Faulkner. Automated patient dosimetry in diagnostic radiology departments. Commission of the European Communities Workshop 'Data analysis in quality control and radiation protection of the patient in diagnostic radiology and nuclear medicine'. 29th September- 1st October 1993. Grado, Italy.

C-L Chapple, K Faulkner, D Lauckner. Computed tomography dose audit. Commission of the European Communities Workshop 'Data analysis in quality control and radiation protection of the patient in diagnostic radiology and nuclear medicine'. 29th September- 1st October 1993. Grado, Italy.

HP Busch, K Faulkner, JF Malone. Image quality criteria applied to digital radiography. Commission of the European Communities Workshop 'Data analysis in quality control and radiation protection of the patient in diagnostic radiology and nuclear medicine'. 29th September- 1st October 1993. Grado, Italy.

JF Malone, HP Busch, K Faulkner. Writing off old fluoroscopy equipment- impact of patient dose and image quality in practice. Commission of the European Communities Workshop 'Data analysis in quality control and radiation protection of the patient in diagnostic radiology and nuclear medicine'. 29th September- 1st October 1993. Grado, Italy.

NW Marshall, K Faulkner. Optimisation of personnel shielding in interventional radiology. British Institute of Radiology Meeting 'Radiation protection in interventional radiology' 6th December, 1993, London.

K Faulkner. Quality control of X-ray tubes and generators. International Organisation of Medical Physicists/ South African Association of Medical Physicists Workshop 'Quality control in diagnostic radiology' Mount Amanzi, Transvaal, South Africa. 14th March, 1994

K Faulkner. Practical aspects of tube and generator quality assurance. International Organisation of Medical Physicists/ South African Association of Medical Physicists Workshop 'Quality control in diagnostic radiology' Ga Rankawa, Bophuthatswana, South Africa. 14th March, 1994.

K Faulkner. Specification and acceptance testing of diagnostic radiology equipment. International Organisation of Medical Physicists/ South African Association of Medical Physicists Workshop 'Quality control in diagnostic radiology' Mount Amanzi, Transvaal, South Africa. 15th March, 1994

K Faulkner. Quality control of Tomographic Equipment International Organisation of Medical Physicists/ South African Association of Medical Physicists Workshop 'Quality control in diagnostic radiology' Mount Amanzi, Transvaal, South Africa. 15th March, 1994.

K Faulkner. Practical aspects of quality assurance of computed tomography scanners and conventional tomographic equipment. International Organisation of Medical Physicists/ South African Association of Medical Physicists Workshop 'Quality control in diagnostic radiology' Ga Rankawa, Bopustwana, South Africa. 15th March, 1994.

K Faulkner. Optimisation of digital imaging systems. South African Association of Medical Physicists Annual Conference. Mount Amanzi, Transvaal, South Africa. 16th March, 1994.

K Faulkner, NW Marshall. Optimisation of personnel shielding in diagnostic radiology. South African Association of Medical Physicists Annual conference. Mount Amanzi, Transvaal, South Africa. 17th March, 1994.

K Faulkner. Automated quality assurance and patient dosimetry, Groote Schoor Hospital, Cape Town, South Africa. 21st March, 1994.

K Faulkner. Subjective assessment of imaging performance, Groote Schoor Hospital, Cape Town, South Africa. 21st March, 1994.

K Faulkner, C-L Chapple. Radiation doses in paediatric radiology, Tygerberg Hospital, Cape Town, South Africa. 22nd March, 1994.

K Faulkner. Subjective assessment of imaging performance, University of the Orange Free State, South Africa. 23rd March, 1994.

K Faulkner. Automated quality assurance and patient dosimetry, University of the Orange Free State, South Africa. 24th March, 1994.

K Faulkner, NW Marshall. Optimisation of personnel shielding in diagnostic radiology , University of the Orange Free State, South Africa. 24th March, 1994.

RM Harrison, K Faulkner. Patient dosimetry - some practical considerations in an NHS Region. Radiology and Oncology 94, Harrogate, 23rd-25th May 1994. Abstract in British Journal of Radiology 67 Congress supplement 96.

AR Lecomber, K Faulkner. Effective dose calculations in dental radiology. Radiology and Oncology 94, Harrogate, 23rd-25th May 1994. Abstract in British Journal of Radiology 67 Congress supplement 8.

K Faulkner. New procedures and technologies for diagnostic radiology. World Congress on Medical Physics and Biomedical Engineering. Rio de Janeiro, Brasil. 21st-26th August 1994. Abstract in conference proceedings.

K Faulkner, HV James, C-L Chapple. Monitoring occupationally exposed individuals in brachytherapy. World Congress on Medical Physics and Biomedical Engineering. Rio de Janeiro, Brasil. 21st-26th August 1994. Abstract in conference proceedings.

K Faulkner, NW Marshall, HP Busch, DM Marsh, H Pfenning. Patient doses in digital radiology - a comparison of techniques. World Congress on Medical Physics and Biomedical Engineering. Rio de Janeiro, Brasil. 21st-26th August 1994. Abstract in conference proceedings.

K Faulkner. Personal monitoring in brachytherapy. University of Caracas, Venezuela. 29th August 1994.

C-L Chapple, DA Broadhead, K Faulkner. Radiation dose audit in the Northern Region. Institute of Physical Sciences in Medicine Meeting, Quality assurance and patient dose measurements in diagnostic radiology, Royal Marsden Hospital, London. 19th October 1994.

K Faulkner. Patient and staff doses in fluoroscopy and digital radiology. Irish Association of Physicists in Medicine. Trinity College, Dublin, Ireland. 11th November 1994.

K Faulkner. The nurse and interventional radiology and special procedures. Radiation protection for nurses, St James' Hospital, Dublin, Ireland. 12th November 1994.

K Faulkner and JF Malone. Dosimetry. Clinical optimisation and radiation protection in digital radiology. Commission of the European Communities/European Association of Radiology Meeting, Trier, Germany. 22nd-25th February 1995.

JF Malone and K Faulkner. Image quality and dose. Clinical optimisation and radiation protection in digital radiology. Commission of the European Communities/European Association of Radiology Meeting, Trier, Germany. 22nd-25th February 1995.

K Faulkner. Assessment of radiation risks to staff in radiology. British Institute of Radiology Meeting, Risks in diagnostic radiology. BIR, London. 29th March 1995.

DA Broadhead, C-L Chapple and K Faulkner. Performance testing of the Harshaw 6600 extremity system for patient dosimetry. Roentgen centenary congress, Birmingham. Conference abstract book 492-493

DA Broadhead, C-L Chapple and K Faulkner. Comparison of dose-area product from digital and non-digital systems during barium studies. Roentgen centenary congress, Birmingham. Conference abstract book 497

K Faulkner, HV James and K Faulkner. Assessment of radiation dose to staff in brachytherapy. Roentgen centenary congress, Birmingham.

K Faulkner. Organisation of radiation protection in the United Kingdom. Safety Control in Diagnostic Radiology. National Institute of Health, Seoul, Korea. 29th June 1995

K Faulkner. The contrast detail behaviour of a photostimulable storage phosphor base computed radiography system. Safety Control in Diagnostic Radiology. National Institute of Health, Seoul, Korea. 29th June 1995

K Faulkner. Radiation dose associated with different imaging systems for chest and abdomen radiology. Safety Control in Diagnostic Radiology. National Institute of Health, Seoul, Korea. 29th June 1995

K Faulkner. Optimisation of personnel shielding in diagnostic radiology. Safety Control in Diagnostic Radiology. National Institute of Health, Seoul, Korea. 29th June 1995

K Faulkner. Patient dose measurement methods. British Institute of Radiology Meeting, Dose descriptors and their measurement in diagnostic radiology and nuclear medicine. BIR London. 23rd October 1995.

Head of project 3: Prof.Dr.Busch

II. Objectives for the reporting period

1. Identification of suitable and unsuitable clinical indications for new digital imaging methods
2. Preselectable dose values to fulfil the requirements of necessary image quality
3. Comparative dose measurements for digital and analog imaging methods
4. Evaluation of new protocols for constancy tests
5. Comparison of five different analog and digital imaging methods for chest examinations
6. Influence of newest DSA-techniques("Rotation Angiography", "DSA-Stepping Angiography")
7. Evaluation of the influence of dose on image quality for DSA
8. What is the lowest dose for DSA? Strategy and Results

III. Progress achieved

1. Identification of suitable and unsuitable clinical indications for new digital imaging methods

Digital image intensifier radiography can be used in a broad spectrum of examinations. It is particularly suitable for all examinations, which are performed in a fluoroscopic examination unit. Images can be immediately evaluated on monitors. The result is a decrease in examination time. The combination of different modalities like tomography, projection radiography and DSA in one examination can offer advantages. Double and mono contrast studies of the GI-tract as well as phlebography, cholecystography, pyelography, myelography, hysterosalpingography and arthrography are the most frequent examinations performed by digital image intensifier radiography(1,7,8).

Postprocessing capabilities include window adjustment of greyscale values, contrast, edge enhancement and magnification. Image postprocessing rarely gives an increase in diagnostic information, but in some instances poorly exposed areas are easier to evaluate. Edge enhancement, window adjustment and image magnification, however, can improve the quality of image demonstration.

It is possible to vary dose used over a broad range of values depending on the clinical problem. Acquisition parameters were defined for three groups of examinations according to the required diagnostic quality(1):

group 1: high image quality
group 2: limited image quality
group 3: low image quality (with maximum of dose reduction)

The most frequent examinations of group 1 are double contrast studies of the GI-tract. Group 2 consists of various mono contrast studies like cholecystography, phlebography, etc. Pelvimetry, some pediatric problems such as cystourethrography and control of catheter position belong to group 3. The decrease of dose compared to film-screen radiography (speed 200) is 60% in group 1, 85% in group 2 and 95% in group 3.

Digital image intensifier radiography was tested in different clinical studies. The demonstration of gastric mucosal pattern is a suitable criterion of high image quality. Image quality of the GI-tract is equivalent or (using small image intensifier diameter) sometimes superior to film screen radiography. Because the matrix size (1024X1024) is independent of the image intensifier diameter in the system used high resolution is only possible using a small image intensifier field. Therefore digital image intensifier radiography is less suited for examinations required high spatial resolution in a large area, e.g. chest and skeletal imaging.

Storage phosphor radiography has been applied to the whole spectrum of projection radiography instead of conventional film/screen images. Most frequent indication is imaging under difficult exposure conditions (e.g. without phototimer). Radiographic examinations in the intensive care unit are an advantageous application of storage phosphor technique. By the large dynamic range and the optimized assignment of grey values to the image information the number of faulty exposures has been significantly decreased.

For conventional thoracic imaging at the wall stand advantages of storage phosphor radiography are not as obvious as for bedside images taken without a phototimer. Some clinical studies demonstrated that image quality of storage phosphor radiography was graded slightly higher for the mediastinal field and the thoracic wall. Bone imaging studies proved that storage phosphor radiography gave equivalent information compared to film/screen radiography. For difficult exposure conditions image quality of storage phosphor radiography was graded higher. The broad range of dose selection can be used to lower the dose for specific diagnostic questions significantly(e.g. fracture control after plaster bandage). In these cases the increase of noise doesn't limitate the necessary information. In some cases postprocessing methods rendered additional diagnostic information in the area of soft tissue(3,7). In Trier we have now started work with the newest generation of storage phosphor systems (AGFA: ADC70). The new software ("MUSICA") seems to be an especially promising step forward.

2. Preselectable dose values to fulfil the requirements of necessary image quality

Due to the wide dynamic range available it is possible to vary the dose for digital Image Intensifier Radiography for each type of examination according to the required image quality. To define the possible decrease of dose compared to film-screen radiography (speed 200) the dependance of spatial resolution and contrast detectability upon dose was evaluated. We used a Polytron 1000 which was connected to a Siregraph D and an Optilux 57. Acquisition parameters were fixed for different types of examination and tested by imaging anthropomorphic phantoms as well as patients (n=114). Our results demonstrate that dose can be reduced by 60% for double contrast studies. Although Digital Image Intensifier Radiography is less suited for chest and skeletal imaging, a 14cm image intensifier can be used for imaging small lesions. If poor image quality is acceptable (e.g. pelvimetry, sometimes in paediatrics) a maximum reduction of 95% is possible (1).

3. Comparative dose measurements for digital and analog imaging methods

Investigations into radiation dose associated with different imaging systems for chest radiology were performed together with the Regional Medical Physics Department in Newcastle and the Department of Medical Physics and Bioengineering in Dublin. Typical doses were assessed using anthropomorphic phantoms for posterior-anterior and lateral projections of the chest. The risk related quantities were then calculated from these organ doses. Typical radiation doses associated with the use of conventional film/screen system, 100 mm technique, large field image intensifier radiography, computed radiography and a scanning slit system (AMBER) were compared. The results are described in a publication of Marshall, Faulkner, Busch, Marsh and Pfenning (16). Another publication of these authors (14) described a comparison of radiation dose in examination of the abdomen using different radiological imaging techniques. This study compared typical radiation doses for abdominal examinations using a conventional film/screen method, a 100mm camera combination and a phosphor storage computed radiography system. A comparison of the imaging techniques on the basis of effective dose indicated that significant dose reduction may be expected when the abdomen is imaged by digital imaging systems.

4. Evaluation of new protocols for constancy tests

In Mannheim test phantoms have been used for evaluation of performance characteristics and for quality assurance measurements. Different methods were developed for digital image intensifier radiography, but they can be transferred to digital storage phosphor radiography. The aim of our test phantom measurements was the development of effective test procedures for performance characteristics and quality control, which are easy to handle with limited additional equipment, not time consuming and representative for clinical imaging. In Mannheim digital image intensifier radiography quality control measurements have been performed on a weekly basis. The test procedure includes single shot and DSA mode and was applied on a Polytron-System (Siemens),. Parameters for quality control measurements were dose, noise, signal/noise, grey value, dynamic range and detectability of structures (simulated vessels) after image subtraction. One advantage of quality control measurements in digital radiography units is the option of evaluating the parameters in digital form. As yet, no commercially available digital system has implemented this possibility for quality control in routine use. Additional parameters, which can be obtained automatically by pixel values include density and dynamic range, noise and signal/noise ratio. A prerequisite for high image quality is the high performance of the complete imaging chain, including documentation and film processing. In addition to the measurements described, quality of documentation and film processing must be controlled by digital test images. A detailed description of the recommended quality control procedures for digital image intensifier radiographie is in the paper "Test phantoms in Digital Radiography"(12).

5. Comparison of five different analog and digital imaging methods for chest examinations

In recent years new analogue and digital techniques have become available for chest imaging. This study compares conventional film/screen, asymmetric film/screen (InSight), equalization (AMBER), storage phosphor and digital image intensifier techniques by phantom exposures and patient examinations. The quality of chest images of 43 patients was classified by seven observers in four different hospitals. Arising from the results of phantom measurements and previous studies, digital image intensifier radiography was excluded because of its low image quality. The AMBER system had the best image quality. Images of the storage phosphor system were of good quality in both mediastinal and peripheral fields of the chest. Compared to conventional film/Screen, the assymmetric film/screen (InSight) was graded higher in the mediastinal field, but lower in the peripheral field. A combination of storage phosphor radiography and the AMBER-system didn't show further improvements of the image quality(3,10).

6. Influence of newest DSA-techniques

In the last year new DSA features became available. Rotational angiography and digital stepping angiography seems to be useful and potentially most promising diagnostic tools. In Trier we have used these new techniques since May 1994. Parameters to grade the clinical value of these features are the diagnostic value, and with respect to side effects the dose required and the volume of contrast medium used. Rotational angiography is useful especially for neuroradiological problems. By rotation imaging with a velocity of 30 degrees/second an aneurysm for instance can be imaged in different projections of 90 degrees within 3 seconds. But with an image frequency of 6 images/second the total number of images is high. Therefore a main subject of our study is to decrease the dose/image as much as possible. Imaging techniques in a stepping mode with or without subtraction can decrease the volume of contrast medium. We are now studying the possibility of lowering the dose in comparison to standard DSA sequences. A publication on our clinical experience with these new techniques is in preparation.

7. Evaluation of the influence of dose on image quality for DSA

For DSA the question has to be answered: What is the optimal dose for a diagnostic problem? Up to a certain point an increase of dose is related to an increase of image quality. Higher dose values are unnecessary in relation to image quality criteria. At first this point has to be determined by phantom measurements and by analysis of image quality. A future question may be: can we make different classes of diagnostic problems in angiography, which are connected to different levels of image quality and dose? For digital projection radiography this problem is solved (1,7,8), but for DSA up to now there is not enough experience with different dose levels. In Trier we are now investigating the relation between dose and image quality for DSA in different exposure modes. Parameters for evaluation are spatial resolution, contrast detectability and signal to noise ratio. The following figures demonstrate some examples of these measurements. By these results we can calculate the influence of different exposure parameters like dose, matrix size, voltage and diameter of the entrance field on the image quality.

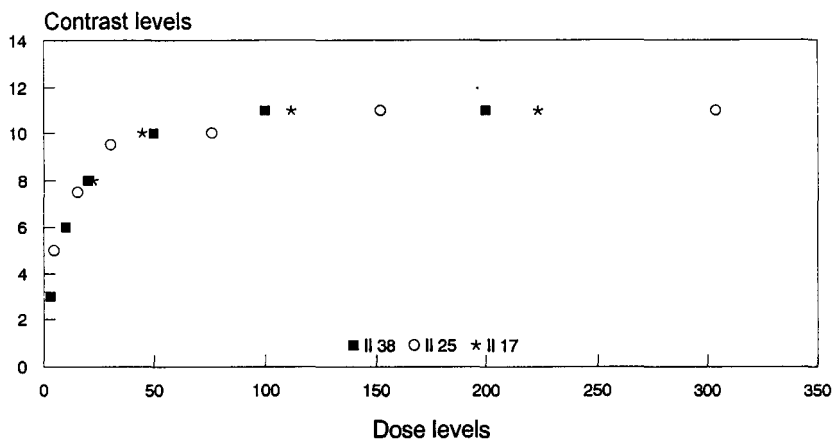


Fig1: Contrast detectability and dose level for image intensifier fields of 38, 25, 17cm diameter for DSA

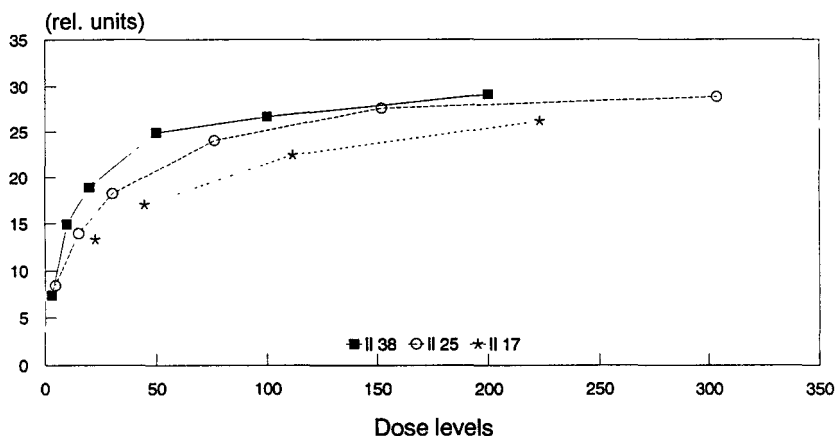


Fig2: Signal/noise and dose levels for image intensifier fields of 38, 25, 17cm diameter for DSA

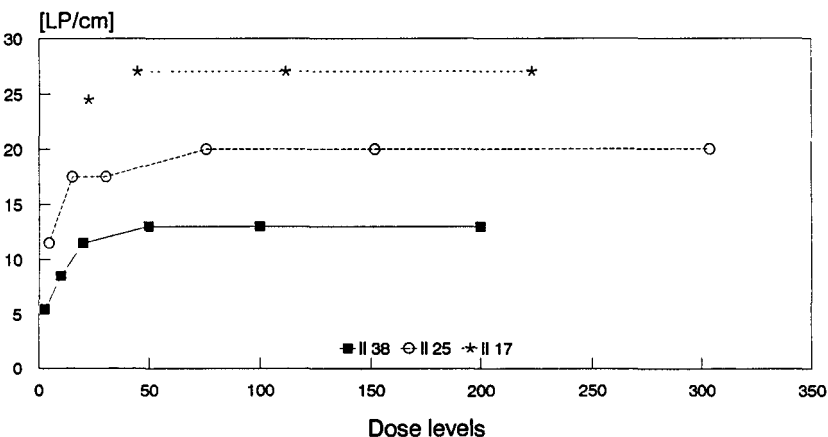


Fig.3: Spatial resolution and dose for image intensifier fields of 38, 25, 17 cm diameter for DSA

8. What is the lowest dose for DSA ? Strategy and results

The starting point for the determination of the optimal dose value are the described phantom measurements for dose and image quality. By these measurements we can calculate the point of highest image quality and necessary dose value. With these dose selections we are now getting clinical experience for different examinations. In routine use especially for interventional procedures it seems very important to select a dose value as low as possible, because the numbers of images is very high. A publication on our first results is in preparation. The results will be presented first on the meeting "Digital Imaging" (Organisator: Prof.Dr.F.E.Stieve, Prof.Dr.Th.Schmidt - Seon Nov. 1995).

Publications:

1. K.J.Lehmann, H.P.Busch, M.Georgi:
Digitale Bildverstärkerradiographie -
Welche Aufnahmedosis für welche Fragestellung?
Akt.Radiol. 2(1992), 111-115
2. H.P.Busch, J.Hartmann, M.C.Freund, K.J.Lehmann,, M.Georgi,
K.Richter:
Thoraxaufnahmen mit dem AMBER-System.
Fortschr.Röntgenstr. 156,3(1992), 241-246
3. H.P.Busch, K.J.Lehmann, P.Drescher, M.Georgi:
New Chest Imaging Techniques - A comparison of five analog
and digital methods
European Radiology 2(1992) 335-341
5. K.Falkner, H.P.Busch, P.Cooney, J.F.Malone, N.M.Marshall,
D.J.Rawlings:
An international intercomparison of dose area product meters.
Radiation Protection Dosimetry(1992), vol.43 no 1/4, 131-134
6. H.P.Busch, K.J.Lehmann, M.C.Freund, M.Georgi:
Digitale Projektionsradiographie - Teil 2: Klinische
Anwendungsmöglichkeiten
Röntgenpraxis 45(1992), 35-43
7. H.P.Busch, M.Georgi(Eds.):
Digital Radiography
Clinical Experiences
with Digital Image Intensifier and Storage Phosphor
Radiography
Blackwell Wissenschaft, Berlin 1992
8. M.Georgi, H.P.Busch:
Digitale Radiographie in der Gastrointestinalen Diagnostik
In: R.W.Günther, H.P.Gockel: Jahrbuch der Radiologie 1992,
Biermann Verlag 1993, 27 - 35

9. H.P.Busch, M.Georgi:
Digital Radiography: Quality assurance and radiation protection
Radiologia diagnostica (1993)
10. K.J.Lehmann, H.P.Busch, P.Drescher, R.Loose, M.Georgi:
Neue Bildgebende Methoden in der Thoraxdiagnostik -
Eine Studie zur Evaluation von Speicherfolienradiographie,
Schlitztechnik, asymmetrischer und konventioneller Film
- Folientechnik
Akt.Radiol. 3(1993) 14 - 19
- 11.H.P.Busch, M.Georgi:
Neue analoge und digitale Bildaufnahmeverfahren zur
Thoraxdiagnostik.
Prinzip - klinische Wertigkeit - Wirtschaftlichkeit
Akt.Radiol. 3(1993) 6 - 13
12. H.P.Busch, S.May, R.Wörtche, K.J.Lehmann:
Test Phantoms in Digital Radiography
Radiation Protection Dosimetry
Vol 49,Nos1/3(1993), 261-264
13. K.J.Lehmann, H.P.Busch, M.Georgi:
Digital fluoroscopic radiology: evaluation of clinical impact
European Journal of Radiology 17(1993) 3 - 7
14. N.W.Marshall, K.Faulkner, H.P.Busch, D.M.Marsh, H.Pfenning
A comparison of radiation dose in examination of the
abdomen using different radiological imaging techniques
The British Journal of Radiology 67(1994) 478-484
15. N.W.Marshall, K.Faulkner, H.P.Busch, K.J.Lehmann:
The contrast-detail behaviour of a photostimulable phosphor
based computed radiography system
Phys. Med.Biol 39(1994) 2289-2303
16. N.W.Marshall, K.Faulkner, H.P.Busch, D.M.Marsh, H.Pfenning
An investigation into the radiation dose associated with
different imaging systems for chest radiology.
The British Journal of Radiology 67(1994), 353 -359
17. H.P.Busch, K.Faulkner, J.F.Malone
Image Quality Criteria applied to digital radiography
Radiation Protection Dosimetry
Vol 57(1995), Nos 1 -4, 139 - 140
18. H.P.Busch
Digital Radiography: Comparison of Different Methods
for Imaging of the Thorax and the Gastrointestinal Tracts
Journal of Digital Imaging, Vol8(1995), 1 - 5
19. R.Wörtche
Konstanzprüfung an einer Röntgenanlage zur
Digitalen - Subtraktions - Angiographie (DSA)
Dissertation an der Ruprecht Karls Universität Heidelberg
1995

S.K.Mai
Qualitätskontrolle in der Digitalen
Bildverstärker-Radiographie
Dissertation an der Ruprecht Karls Universität Heidelberg
1995

Head of project 4: Prof. J. Jankowski

1. Objectives for the reporting period

Exposure conditions used in X-Ray diagnostics in Poland have been analyzed, taking into consideration type of X-Ray units. A special attention was paid for fluoroscopic procedures and interventional radiology. Entrance air kerma for patients was measured together with recognising of doses to staff. Effective doses to patients were evaluated basing on the results of theoretical computations of absorbed organ doses. This is presented for three fluoroscopic procedures and two types of angiography. Together with these the results of dose measurements for workers are referred, as well those obtained in routine dosimetry as from special measurements made for the staff dealing with interventional radiology.

III: Progress achieved including publications

I. DOSES TO PATIENTS IN DIAGNOSTICS AND INTERVENTIONAL RADIOLOGY

In Poland, X-ray diagnostics provide the highest contribution to annual per caput dose to the population.

Data concerning the frequency of X-ray examinations were collected in the last national survey (1986), which indicated that 21.4 million of examinations were performed per year. (This corresponds to 570 examinations per 1000 population.) [5]. The most significant contribution to this number comes from common (basic) examinations.

Exposure conditions

Doses to patients are extremely dependent on technical exposure parameters chosen for examination performance.

Data concerning these parameters have been collected in Poland from 70 X-ray departments (in 13 districts) and concern all types of examinations. (The necessary information was registered in X-ray laboratories by qualified sanitary officers.) Analysis of the results for 15 the most frequently performed examinations allows to see a great differentiation: entrance air kerma differs more than two orders of magnitude from one X-ray unit to another, for the same procedure and for patient from the same age group.

The data cover also fluoroscopies, in the case of which an average, typical time of exposure was registered together with the anode current value.

To investigate the problem of exposure conditions in the more detailed way, the entrance air kerma during L-S spine radiography (AP) of standard adult patient was additionally controlled for about 200 X-ray units (from 14 districts) in Poland. For that purpose exposure parameters were also chosen by the staff of departments, and entrance air kerma were measured using thermoluminescent dosimeters (TLD). The dosimeters had been calibrated using NOMEX (PTW Frieberg) and RMI Multi-Function Meter (240 A). The readings of entrance air kerma given by NOMEX were compared with indications of RMI Meter expressed as Relative Film Exposure (RFE). Apart from this the kVp readings of the both meters were compared. (The remaining components of RMI Kit are also used to elaborate quality control measurement procedure for Polish diagnostic X-ray departments.)

The sample of results concerning exposure conditions is the distribution of entrance air kerma during L-S spine radiography measured for adult patients, which is shown in Fig.1 .

Doses to patients

Absorbed organ doses have been evaluated theoretically for six age groups, i.e. 0, 1, 5, 10, 15 years and adults. The computations were performed using Staniszevska computer code for Monte Carlo simulation. Reference patients were represented by mathematical human phantoms, being the modified versions of those of Cristy . A description of the computation method and the results have already been published . The absorbed doses were obtained for 19 soft organs, the skeleton as whole and for the four separate parts of it. Effective doses were calculated according to ICRP recommendations given in Publ.No.60 [8].

The technical exposure parameters presently used during X-ray examinations in Poland were used as input data for dose computations.

A. Fluoroscopies

Doses to patients were computed for three types of fluoroscopic examinations: chest , stomach and LLI (Barium enema). For each type of examinations three classes of exposure conditions were distinguished, named as LOW, AVER and HIGH, for which dose calculations were performed separately. The classification of exposure conditions were based on entrance air kerma distribution, which describes values found for the analysed examination. (The distributions of kerma were prepared on the basis of collected data about presently used exposure conditions; these distributions were found to be of a log-normal form.)

The values of particular parameters in each of the classes (i.e. LOW, AVER, HIGH) were calculated as an arithmetical mean of the appropriate values taken from records included in the given class. Parameters of AVER class were calculated from this group of original data records (for the analysed examination) for which air kerma did not differ from median of distribution more than \pm one standard deviation on a logarithmic scale. Consequently, parameters of LOW class were constructed basing on the left end of kerma distributin, and HIGH class parameters from the right tail of this distribution.

The results of computations are given in Tables 1(I), 2(I), 3(I); they include the absorbed organ dose and effective dose values which can be obtained by a standard adult patient during whole examination (i.e. fluoroscopy only for chest, fluoroscopy and radiographies for stomach and LLD).

The dose values included in Tables 1(I)-3(I) correspond with the exposures performed using conventional X-ray units (i.e. generators with 6-12 simplifiers, very rarely -constant potential); X-ray units with digital recording are not used for "common" examinations.

B. Interventional radiology

The term "interventional radiology" covers all radiological activity carried out using "invasive" techniques such as catheterization, dilatation, embolization, etc.. These practices include angiographic procedures, stone subtraction and radiological control during or after surgery.

Although these procedures do not contribute significantly to the total number of X-ray examinations performed annually in Poland (below 1% of 21.4 million) they should receive particular attention as they can result in high dose to patient and to staff as well. Special procedures are applied to all anatomical regions and can include very complicated radiological protocols, with possibility of a long use of fluoroscopy. Specific character and aim of these procedures are the reason for great variation in dose, values of which are strongly dependent on: - technical exposure parameters necessary for given X-ray system to produce good quality image, - experience and manual perfection of medical team performing the examination, and - anatomical constitution of patient (i.e. pathology in vessel system).

The data from literature indicate that entrance skin dose for individual patient approaches 1 Gy, and the greatest values are associated with the imaging of the heart. Together, the values of effective dose equivalents corresponding with these high entrance skin doses are not so extremely high and have not been reported higher than 50 mSv.

One of the interventional radiology procedures that are carried out in Poland most frequently are angiographies (with possibility of additional vessel therapy).

The study was performed in three hospitals, using devices made by Siemens: two of these were Polydors (with pulsed generators), and the third - the oldest one - was Angiotron CMP (with constant potential, conventional generator).

Doses to patients were investigated in two stages: - entrance surface doses were measured and - absorbed and effective doses were computed.

Entrance surface doses were measured using thermoluminescence (abv. TL) dosimeters which were placed directly on the patient skin (inside of plexiglass cassettes), on the three levels corresponding with the following constant anatomical points: jugular incisure of sternum (on the front and back surfaces), enciform (xiphoid) process (on the front, the back and both lateral surfaces) and upper edge of pubis (on the front, the back and both lateral surfaces).

Air kerma values caused by the given projection type were evaluated as linear combination of entrance doses registered in the points of measurement exposed in the considered projection. As these points were situated on three levels, this evaluation has been made for each level separately. The values corresponding to the level of the highest kerma were treated as representative ones for the examination.

Absorbed doses to patients were also computed using Monte Carlo simulation programme (Staniszewska code). For each projection type and for each beam quality (kVp and total filtration) the series of coefficients which meant the absorbed organ doses per unit of entrance air kerma were computed. Final results understood as absorbed organ doses and effective doses to individual patients were obtained by multiplying the adequate series of coefficients by the individual (measured) value of entrance air kerma.

Detailed analyses of doses were performed for six patients: five undergoing coronarography and one subjected to renal arteries catheterization. The coronarographies were carried out using Polydoros units, and for renal examination Angiotron CMP was used. The obtained results are presented in Table 4(D) and Table 5(D).

Effective doses to patients subjected to coronarography are rather low: 0.20 - 0.73 mSv; the effective dose to patient during renal arteries catheterization is higher - 2.29 mSv. It ought to be highlighted that all these values are significantly lower than those resulting from typical fluoroscopic procedures carried out in Poland; the same refers to common X-ray examinations. The comparison of effective dose values for adult patient is given in Table 6(D).

This difference -very beneficial for patients- is result of modern technical solutions in X-ray equipment being in use for interventional practices: constant potential or pulsed generators and digital recording systems permit to decrease real time of fluoroscopic exposure.

II. DOSES FOR WORKERS

Nofer Institute of Occupational Medicine (NIOM), Radiation Dosimetry Department has been conducting dosimetric survey for all people occupationally exposed to X-rays in Poland since 1966. Presently population under control is about 26,000. The structure of this population is shown in Fig.1(II) and Fig.2(II).

The system of individual dosimetry is based on centrally held computer data bases of occupationally exposed persons and their doses in each workplaces. It allows to accumulate annual doses received by each person in different X-ray departments and it helps to identify a place where dose limit has been exceeded. If the registered dose in a given department exceeds 0.1 of the annual limit, then the appropriate Regional Sanitary and Epidemiologic Station is informed; they directly control the working conditions in such a department, elucidate the reasons for excessive dose value and recommend measures to prevent such excess in the future.

Regarding to Polish law it is obligatory that each person occupationally exposed to X-rays is under dosimetric control of our Institute.

X-ray dosimetry in Poland uses films for dose assessment. There are several advantages of they:

- wide measurement range,
- possibility to determine direction and energy of radiation,
- possibility to differentiate between acute and fractional irradiation.
- possibility to check condition of irradiation, that is presence or absence of filter images,
- dosimetric films are documents and allow to repeat the dose readings,
- film system is cheaper than thermoluminescent and others.

For the routine measurements as dosimeters we use badges consisting cassette and dosimetric X-ray films both made in Poland. The cassette contains a set of copper filters (0.05, 0.05, 1.5 mm), one lead filter and a steel rod for direction and energy dependence. The badges are worn on the upper left side of the chest of worker and dosimetric films are changed every two months periods. The films are sent back to NIOM for dose assessment. Detail density analysis are done, taking into account direction and energy dependence. Finally dose are calculating using Dresel method [6]. All dose measurements are calibrating to effective dose measured in mSv. The results are sent to X-ray departments and recorded in central data base.

In 1994 measurements were performed for more than 26,000 workers employed in about 2600 X-ray departments. The population is still growing (about one hundred of new persons every year), but the structure of monitored persons is quite stable. Fig. 1(II) and Fig.2(II) shows the percentage of individuals according to the type of institutions and professions. Health care workers constitute about 80% of the total monitored population. The biggest group of occupationally exposed people are radiographers - about 60%, whereas physicians constitute only 20% of the total population subjected to control.

The detail results of dose measurements in last year are presented in Table 1(II). The table shows doses from specified ranges for each group of workers. Annual dose for 98% of people under control is below 1 mSv. A similar percentage applies to all categories of workers except those undertaking operational radiology. Of these - 93.12% received doses below 1 mSv per year. This information, however, does not provide enough details concerning the insight into the peculiarities of exposure. For that, the additional dosimetric measurements using thermoluminescent (abv. TL) method were done for group of workers engaged in interventional radiology. For that purpose group of 20 hospitals were selected and the following groups of interventions were chosen: cardiological interventions, urological interventions, biliary routes and orthopaedic surgery. TL dosimeters were placed in special plastic apron. Aprons with dosimeters were worn by operating physician, assisting physician and nurses during interventions. Exposure on the body surface were a measured value, which were afterwards recalculated to effective dose. Measurements were performed during 228 operations. The values of the estimated annual effective doses are presented in the Fig.3(II), Fig.4(II) and Fig.5(II).

In all hospitals the operating physician was the one who received the highest doses. This is understandable because the operating physician was -as a rule- positioned next to an X-ray tube. The remaining participants stayed further away from the source of radiation.

Similar results were obtained from the next measurements of entrance air kerma, which had been performed for operating teams during coronarography and renal arteries catheterization. Doses to staff were also measured using TL dosimeters placed into plastic cassettes: one cassette was placed under the lead apron, the second on this apron and two additional dosimeters were placed on the fingers of both hand. The values of measured doses were higher than zero (per one examination) only for the operating physician; these was found for the dosimeters placed on the lead apron and on the fingers. For the both analysed examinations doses on the lead apron (level of the jugular incisure of sternum on the front surface) do not exceed 0.01 mGy. The doses registered in

finger dosimeters were as follows: 0.02 mGy per one coronarography (Polydoros units), and 0.30 mGy during renal catheterization (Angiotron CMP unit).

To summarize, the individual values of effective doses for workers in interventional radiology range from 0.1 mSv to about 45 mSv per year. The highest values are achieved in enunereous cases; it is mainly resulted from an uncorrect technique of operation or poor technical state of X-ray unit (old machines, mainly). Such situations are recommended to quick change.

In majority of cases, at the current workload, the value does not exceed 5 mSv per year.

Hence, if the annual limit of 20 mSv recommended for workers by the ICRP [8] would be introduced to Polish regulations, it do not affect actual situation significantly.

III. TRAINING

The following video-films (by IAEA) were translated for presentation during courses organised by Institute of Occupational Medicine for radiation protection officers from diagnostic X-ray departments, post-graduate courses for radiologists, post-graduate courses for physicians working in occupational medicine and post-graduate courses for workers of Sanitary Epidemiological Stations- Radiation Prtection Department:

- 1) Principles of Radiation Protection,
- 2) Protection from Ionizing Radiation,
- 3) Radiation: Types and Effects,
- 4) Radiation: Origins and Control,
- 5) Dosimetry,
- 6) Quality Assurance in Radiology,
- 7) Dose Minimization in Diagnostic Radiology,
- 8) Safety first,
- 9) International Chernobyl Project,
- 10) Documentary of Chernobyl Accident,
- 11) Treatment of Radiation induced Skin Injuries,
- 12) Chernobyl Medical Aspects.

Fig. 1) Distribution of entrance air kerma measured during L-S spine radiography of standard adult patients. (The data for 201 X-ray units in Poland).

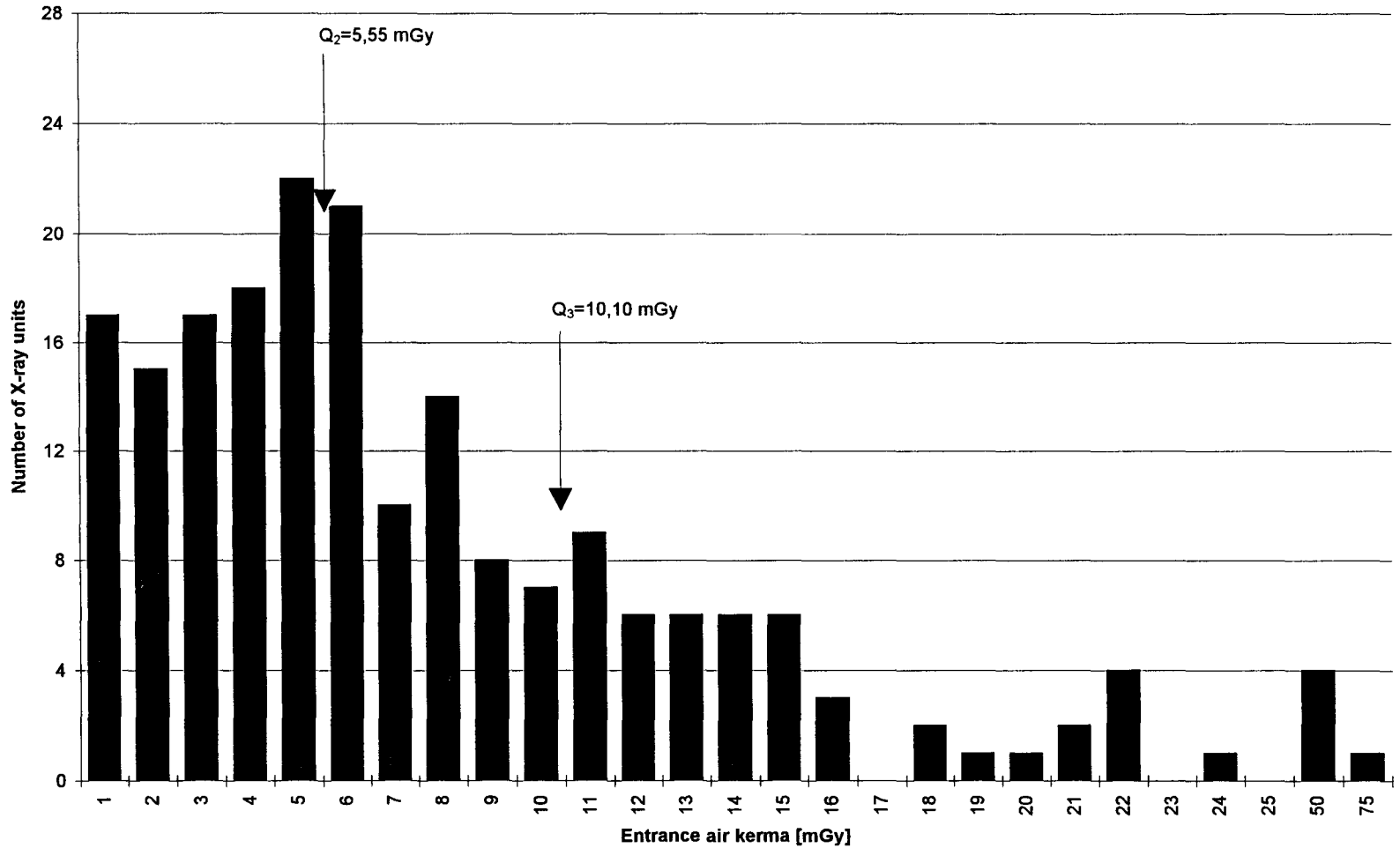


Table 1(D). Doses to standard adult patient during lung fluoroscopy.

Projection: AP

Technical parameters:	Type of exposure conditions		
	LOW	AVER	HIGH
U (kV)	60	70	90
TF (mm Al)	4.2	3.2	2.0
I*t (mAs)	100	210	240
SSD (cm)	40	50	30
Beam size (cm*cm)	36.0x43.0	36.0x43.0	36.0x43.0
Organ doses (mGy):			
- RBM	0.75	1.89	7.90
- lungs	12.62	33.67	136.11
- breast	13.09	25.11	122.36
- SI	0.99	0.02	0.02
- LI	0.90	0.01	0.01
- stomach wall	0.10	0.20	0.61
- liver	0.06	0.25	1.03
- spleen	0.07	0.00	0.49
- pancreas	0.00	0.32	0.30
- thyroid	23.39	65.63	230.32
- u.bladder wall	0.00	0.00	0.00
- bone cells	0.94	2.22	9.60
- ovaries	0.00	0.00	0.00
- testes	0.00	0.00	0.00
- brain	0.06	0.36	1.70
- heart	4.93	13.99	52.53
- kidneys	0.03	0.00	0.61
- uterus	0.00	0.00	0.00
- leg muscles	0.00	0.00	0.01
- other soft parts	3.82	8.14	36.51
Effective dose (mSv):	3.89	10.06	39.63

Table 2(D). Doses to standard adult patient during stomach examination.

Projection: PA

Technical parameters:	Type of exposure conditions		
	LOW	AVER	HIGH
Fluoroscopy			
U [kV]	75	90	90
TF [mm Al]	2.5	2.0	5.0
I*t [mA-s]	180	180	540
SSD [cm]	45	45	45
Beam size [cm*cm]	24.9x28.0	24.9x28.0	24.9x28.0
Radiographies:			
U [kV]	80	90	110
TF [mm Al]	4.6	2.0	3.2
I*t [mAs]	60	80	18
SSD [cm]	45	45	30
Beam size [cm*cm]	(I)18.0x24.0 (II)24.0x24.0	24.9x28.0	(I)18.0x24.0 (II)24.9x28.0
Number of exposures:4*I+1*II		4	4*I+4*II
Organ doses [mGy]:			
- RBM	1.88	3.30	7.21
- lungs	0.22	0.43	0.73
- breast	0.00	0.12	0.00
- SI	12.51	21.68	45.34
- LI	6.37	11.20	23.56
- stomach wall	8.17	9.44	25.85
- liver	0.06	0.24	0.39
- spleen	26.17	34.12	70.09
- pancreas	5.89	10.13	23.27
- thyroid	0.00	0.00	0.00
- u.bladder wall	0.40	0.06	2.20
- bone cells	2.22	4.75	7.61
- ovaries	2.33	2.31	14.68
- testes	0.01	0.01	0.12
- brain	0.00	0.00	0.00
- heart	0.03	0.06	0.04
- kidneys	68.52	100.51	169.02
- uterus	1.92	3.62	10.58
- leg muscles	0.00	0.00	0.00
- other soft parts	9.03	16.25	23.59
Effective dose [mSv]:	3.51	5.64	11.62

Table 3(D). Doses to standard adult patient during colon contrast enema.

Projection: AP

Technical parameters:	Type of exposure conditions		
	LOW	AVER	HIGH *
Fluoroscopy			
U (kV)	80	90	90
TF (mm Al)	4.6	3.3	2.0
I*t (mAs)	125	55	50
SSD (cm)	40	40	30
Beam size (cm*cm)	36.0x43.0	35.0x35.0	38.0x36.0
Radiographies:			
U (kV)	80	90	90
TF (mm Al)	4.6	3.3	2.0
I*t (mAs)	100	120	170
SSD (cm)	90	90	30
Beam size (cm*cm)	36.0x43.0	35.0x35.0	30.0x36.0

Number of exposures: fluoroscopy + 3*

Organ doses (mGy):

- RBM	1.48	0.54	5.18
- lungs	4.89	1.19	10.72
- breast	1.06	0.19	1.01
- SI	16.11	13.84	102.29
- LI	7.77	6.59	50.95
- stomach wall	54.52	41.39	319.08
- liver	44.91	29.34	230.07
- spleen	11.29	10.30	41.06
- pancreas	21.29	15.50	105.56
- thyroid	0.00	0.00	0.00
- u.bladder wall	0.58	0.35	6.37
- bone cells	1.66	0.63	6.30
- ovaries	1.67	1.17	22.87
- testes	0.03	0.21	1.32
- brain	0.00	0.00	0.00
- heart	1.93	0.68	5.82
- kidneys	7.65	6.33	37.43
- uterus	1.16	0.57	16.61
- leg muscles	0.02	0.00	0.31
- other soft parts	12.05	8.35	80.51
Effective dose (mSv):	11.18	8.08	64.01

* Except of HIGH exposure conditions when additional right lateral projection (during radiography) is performed, with beam size of 19.8 x 36.0 cm*cm.

Table 4(D). Doses to patients during coronarography

Hospital I: Siemens Polydoros (max. dose-rate per pulse: 80 $\mu\text{R/s}$)

Patient	Proj.	Beam quality (kVp+TF)	EAK [mGy]	$\frac{\text{DEF}}{\text{EAK}} \left[\frac{\text{mSv}}{\text{mGy}} \right]$	DEF [mSv]
I	PA	75kV+2.5mmAl	31.48	0.0164±0.0005	0.52±0.02
	RPO	110kV+3.2mmAl	11.78	0.0099±0.0005	0.12±0.01
	LPO	110kV+3.2mmAl	11.45	0.0075±0.0006	0.09±0.01
	Σ		54.71		0.73±0.01
II	PA	75kV+2.5mmAl	12.08	0.0164±0.0005	0.20±0.01
	RPO	110kV+3.2mmAl	17.70	0.0099±0.00005	0.18±0.01
	LPO	110kV+3.2mmAl	7.27	0.0075±0.0006	0.06±<0.01
	Σ		37.05		0.43±0.01
Average for hospital I:			45.88		0.58

Hospital II: Siemens Polydoros (max. dose-rate per pulse 40 $\mu\text{R/s}$)

I	PA	60kV+3.5mmAl	3.63	0.0170±0.0006	0.06±0.002
	RPO	70kV+3.2mmAl	2.05	0.0092±0.0005	0.02±0.001
	LPO	70kV+3.2mmAl	13.46	0.0072±0.0005	0.10±0.007
	LLAT	80kV+6.0mmAl(*)	3.84	0.0129±0.0004	0.05±0.002
	Σ		22.98		0.23±0.007
II	PA	80kV+2.7mmAl	5.20	0.0246±0.0007	0.13±0.004
	RPO	110kV+3.2mmAl	3.07	0.0099±0.0005	0.03±0.002
	LPO	110kV+3.2mmAl	4.02	0.0075±0.0006	0.03±0.003
	LLAT	80kV+6.0mmAl(*)	0.91	0.0129±0.0004	0.01±<0.001
	Σ		13.20		0.20±0.005

Table 4(I) -contd. (coronarography)

Hospital II: Siemens Polydoros (max. dose-rate per pulse: 40 μ R/s)

Patient	Proj.	Beam quality (kVp+TF)	EAK [mGy]	$\frac{\text{DEF}}{\text{EAK}} \left[\frac{\text{mSv}}{\text{mGy}} \right]$	DEF [mSv]
III	PA	60kV+3.5mmAl	15.74	0.0170 \pm 0.0006	0.27 \pm 0.010
	RPO	90kV+3.3mmAl	6.66	0.0102 \pm 0.0005	0.07 \pm 0.003
	LPO	90kV+3.3mmAl	9.90	0.0075 \pm 0.0004	0.07 \pm 0.004
	LLAT	80kV+6.0mmAl(*)	1.16	0.0129 \pm 0.0004	0.01 \pm <0.001
Σ			33.46		0.42 \pm 0.01
Average for hospital II:			23.21		0.28

Table 5(I). Doses to patient during renal arteries catheterization

Patient	Proj.	Beam quality (kVp+TF)	EAK [mGy]	$\frac{\text{DEF}}{\text{EAK}} \left[\frac{\text{mSv}}{\text{mGy}} \right]$	DEF [mSv]
I	PA	120kV+3.5mmAl	18.90	0.0217 \pm 0.0017	0.41 \pm 0.032
	RPO	120kV+3.5mmAl	94.70	0.0129 \pm 0.0008	1.23 \pm 0.080
	LPO	120kV+3.5mmAl	59.30	0.0110 \pm 0.0005	0.65 \pm 0.029
Σ			172.90		2.29 \pm 0.091

EAK - entrance air kerma (mGy);

DEF - effective dose (mSv);

Σ indicates the sum of doses per whole examination.

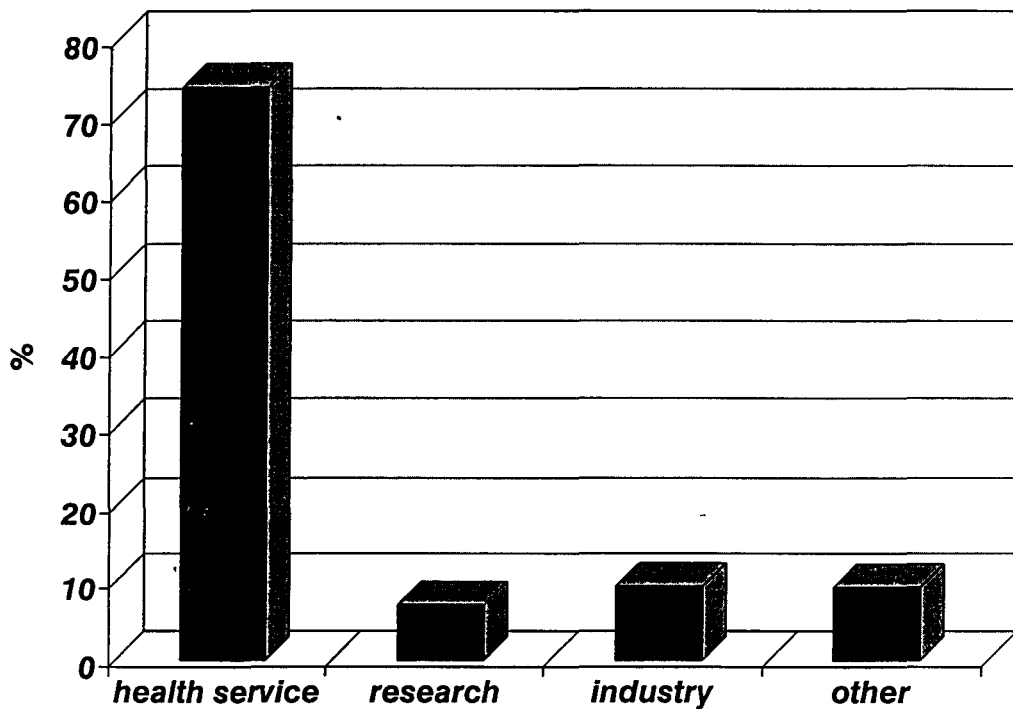
(*) added filtration (0.1 mm Cu + 3.6 mm Al) is activated in LLAT projection, when the X-tube is in a free air (not under the table);

Table 6(I). Effective doses to adult patient in the angiographic procedures analysed here versus other X-ray examinations (5). (*)

Examination	Effective dose [mSv]
Coronarography (mean for 5 patients)	0.40
Renal arteriography	2.30
Barium meal	7.7
Barium enema	30.3
Chest fluoroscopy	17.8
Thor.spine radiography	6.2
L-S spine radiography	4.4
Abdomen radiography	1.2
Chest radiography (PA)	0.1

(*) The effective doses for the other examinations are given as the weighted mean values, with taking into consideration the frequency of using the three types of exposure conditions (i.e. LOW, AVER, HIGH).

Distribution of persons occupationally exposed to X-rays in different workplaces



. Fig 1 (ii)

DISTRIBUTION OF DOSES RECEIVED BY PEOPLE OCCUPATIONALLY EXPOSED TO X-RAYS in 1994

Type of institution	Number of persons	Percentage of persons received annual dose equivalent in a specified ranges [mSv]						
		below 1	1-2	2-5	5-10	10-20	20-50	ab. 50
Health care	20600.00	97.97	1.04	0.66	0.17	0.08	0.04	0.05
- operating theaters	2903.00	98.69	0.31	0.24	0.17	0.10	0.17	0.31
-interventional radiology	770.00	93.12	2.34	2.86	1.43	0.13	0.13	0.00
Industry	1899.00	99.68	0.26	0.05	0.00	0.00	0.00	0.00
Research inst.	901.00	99.89	0.11	0.00	0.00	0.00	0.00	0.00
Medical schools	1742.00	99.71	0.11	0.17	0.00	0.00	0.00	0.00
Sanitary Epidemiological Stations	152.00	99.34	0.66	0.00	0.00	0.00	0.00	0.00
X-ray unit repairshops	507.00	97.24	1.78	0.99	0.00	0.00	0.00	0.00
Veterinary medicine	104.00	99.04	0.96	0.00	0.00	0.00	0.00	0.00
Others	167.00	100.00	0.00	0.00	0.00	0.00	0.00	0.00
Total	26072.00	98.29	0.90	0.55	0.13	0.06	0.03	0.04

Table 1(ii)

Annual effective dose equivalent urological interventions

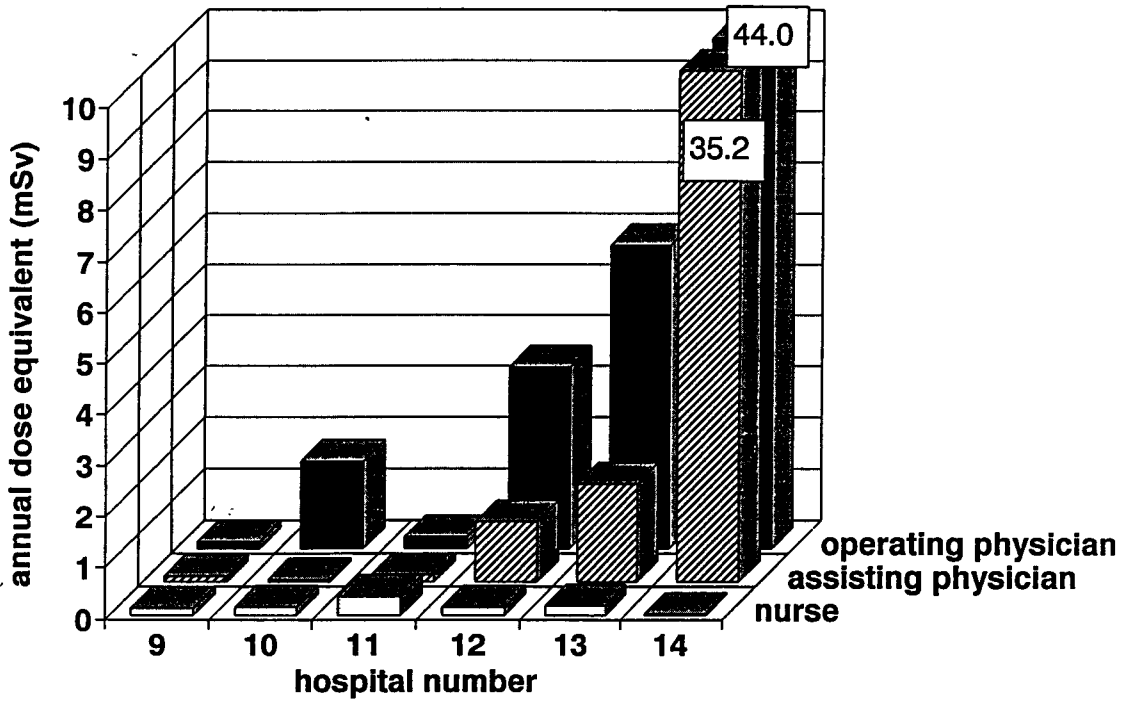


Fig. 3 (II)

Annual effective dose equivalent cardiological interventions

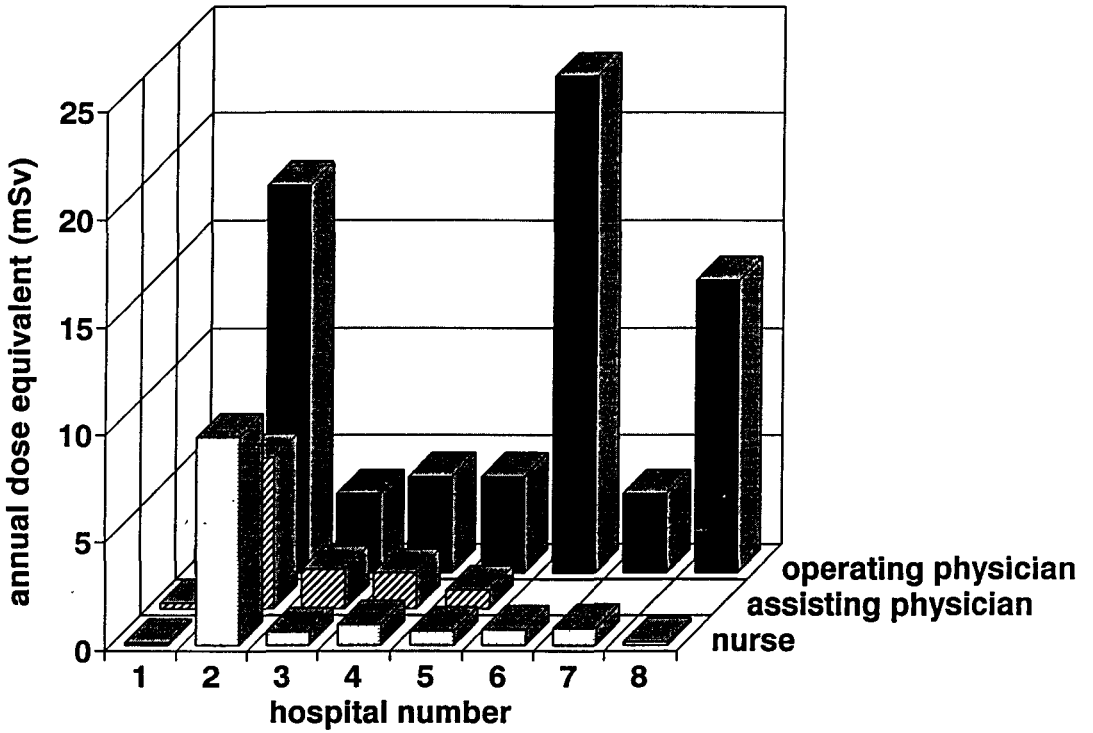


Fig. 4(II)

Annual effective dose equivalent biliary routes and orthopaedic surgery

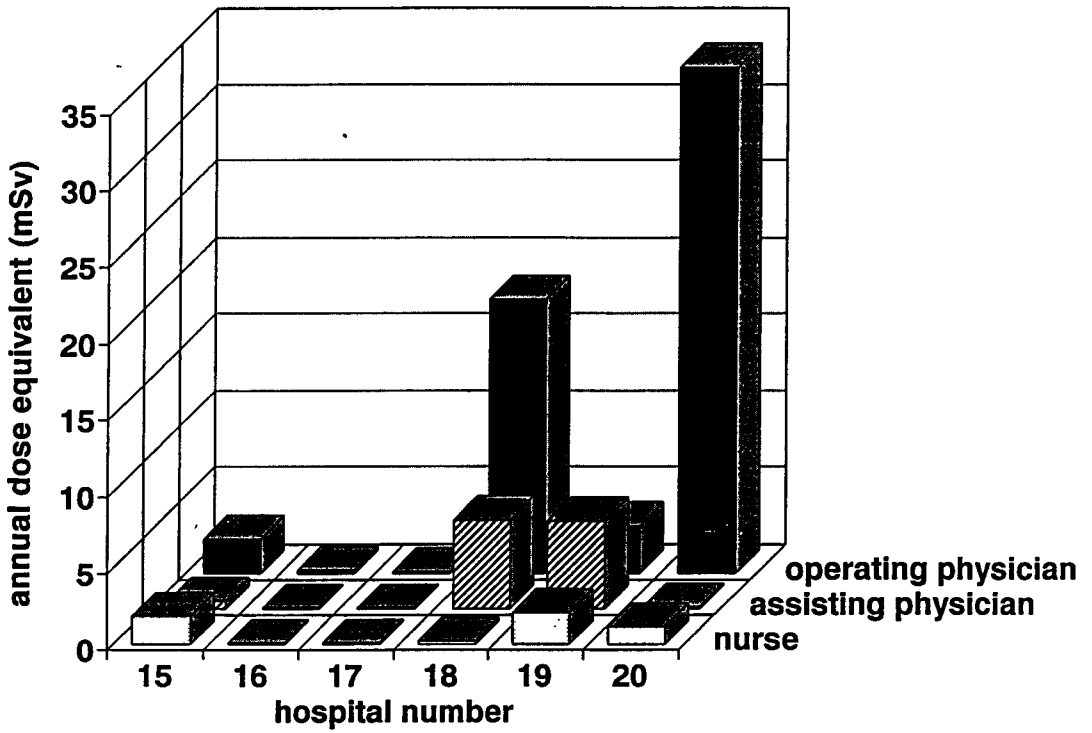


Fig. 5 (ii)

PUBLICATIONS:

1. Jankowski J., Lapiński K.: Estimation of doses received by interventional radiology workers in Poland. Proceedings of the meeting "Radiation Protection in Interventional Radiology" organised by Radiation Protection Committee of BIR and EC (1993) in London; BIR, London 1995, p.45-50;
2. Staniszevska M.A., Jankowski J.: Exposure to patients in diagnostic X-ray examinations in Poland. Proceedings of International Conference on "Radiation Protection and Medicine"; Montpellier - France, 28-30 June 1995;
3. Staniszevska M.A., Jankowski J.: Exposure to patients in interventional radiology. (as above)
4. Jankowski J., Lapiński K.: Thirty years of the assessment of occupational exposure to X-rays in Poland. (as above)
5. Jankowski J., Staniszevska M.A., Pednarek A., Błaszczyk M.: A comparison of patient doses in lumbar spine radiography from various X-ray units in Poland. Polish Journal of Medical Physics & Engineering. (in print);
6. Staniszevska M.A.: Doses in X-ray examinations: results of Monte Carlo simulation in comparison with experimental values for the X-ray units with different types of generators. (as above);
7. Jankowski J., Staniszevska M.A.: Interventional radiology doses to patients during angiography. (as above).

Head of project 5: Prof. Shehu

I. Objectives for the reporting period.

- * To summarise work done to date, including that performed by myself on the practice of fluoroscopy and radiography in Albania.
- * To compare and contrast this data with available data from Western countries.
- * To perform studies in dosimetry, examination frequency, and quality assurance with other members of the team, using methodologies that are consistent with theirs.
- * To perform staff and patient dosimetry for the most common examinations which are fluoroscopy of the chest and skeletal radiography.

II. Progress achieved including publications

Work was initially started with measurement data, statistical data and other dosimetric approaches performed by me over a 20 year period (1974-1994). The first report was prepared and presented at the partner's meeting in Dublin (August 1994). The main content of this report was: a) The distribution map of radiological equipment in Albania. Statistics show that the quantity of equipment in Albania is high (500 units or ~1 unit per 6000 inhabitants) but its quality is low in comparison to other European countries. The equipment is 30% Russian production (produced before 1961), 25% Chinese production (produced between 1962 and 1978), 5% are of Italian production (produced before the second World War), 10% are Albanian production (a hybridisation of Russian and Chinese technology with East European X-ray tubes), 15% are of East European production (Hungarian, Czechoslovakian etc.) and 15% were produced in West European countries. The average equipment age is greater than 35 years. About 75% of the equipment has oblique anodes, and 40% does not have proper collimation.

Linked with the above mentioned studies, before joining this project, the following work was carried out for most of the used equipment: 1) asymmetry of beam in cathode -

anode direction, 2) measurements of the penumbra and its spatial distribution around the primary beam, 3) distribution of scattered secondary and primary radiation and the preparation of dose distribution maps, 4) advice on radiation shielding (especially for equipment without light beam diaphragms and collimation), 5) the compilation of guide tables (as a result of our measurements) for the technique factors (kV, mAs, distance), for the most frequently used equipment, to standardise and optimize exposures etc.

The frequencies for the most common examinations are: chest fluoroscopies - 307 / 1000 inhabitants / year, GI tract Barium fluoroscopies 35 / 1000 inhabitants / year, and skeletal radiography 130 / 1000 inhabitants / year. Using measurements and statistics the Gonad Significant Dose was estimated for these examinations.

Skin doses and half value layer measurements were made for the most common examinations on the most used equipment, in addition to X-ray beam size measurements using film exposures.

Following my first report on the Albanian radiological situation, it was decided by the partners to a) conduct a deeper study of examination frequencies, b) measure skin doses in most common examinations, c) give special interest to paediatrics and reproductive groups for dosimetry studies, d) conduct QA measurements of beam homogeneity and beam limitation.

The second report was prepared and presented at the partners meeting in London (December). During the period June - December ~5% of equipment was replaced, plus an additional 5% was replaced due to donations. The situation is fast improving for dental equipment due to new (and used) private installations. The frequency of chest fluoroscopies has been seen to decrease by ~10% following new legislation and a newly formed organisation responsible for radiation protection in Albania (that is the High Commission of Radiation Protection). This has occurred as a direct result of my work in this field.

During this short period a dosimetry survey was conducted for staff and patients using TLDs. The conclusions are 1) staff doses are under 50 mRem / week which is due to good protection measures and a small number of examinations per worker as well as a reduced working day (5-6 hours / day or ~30 hours / week). The patient doses are, of course, generally high due to old equipment (mostly without image intensifiers), poor maintenance and poor

knowledge of patient protection. Since there are only two part time physicists involved in diagnostic radiology, and limited equipment, I have engaged some dosimetrists from other sectors to make measurements (QA and dosimetry) on ~25 systems, as well as to overlook examinations in order to improve patient protection. There is still much to do in the field of optimization and radiation protection, but this will be helped a lot by the new organization of radiation protection in Albania. Into this new model (following the model in Ireland and some other countries) I, as a member of the High Commission of Radiation Protection, together with some colleagues have prepared new legislation which will provide for more medical physicists in Albania. Since medicine is being gradually privatised, the necessity of this legislation is becoming more urgent, to eliminate old equipment step by step, and to allow the import of viable equipment only. Even exposures are often not standard, due to a diversity of film type and equipment age. Our work was valuable, especially for chest fluoroscopies and exposures to children. The doses reported by me are comparable to those estimated by other colleagues. In this field there is still much future work to be done, especially in country hospitals and with very old equipment not yet eliminated.

My work in 1995 until now (after the December meeting) consists mostly of more indepth studies of patient dosimetry and QA measurements. During this period I have used ~400 TLDs for different fluoroscopic and radiological examinations, for both patients and staff doses. Of these ~250 have been measured in Newcastle, and the others will be measured in due course. These initial measurements have shown the same staff doses as before. Some of these dose measurements were made with parallel measurements using ionization chambers; so for the personal dosimetry of staff we have estimated doses of less than 50 mRem / week. With the new legislation, and with the help of the IAEA, which will provide an independent TLD system this year, we would be able to perform staff dosimetry for all Albania.

I have used TLDs to measure X-ray beam homogeneity for both old and new equipment. The new equipment (10 years old) with light beam diaphragms has good correlation between light and X-ray fields and good distribution within the field limits. For old equipment (greater than 35 years old) the homogeneity was not good, even though the clinical radiographs were good. The QA during this period was realised with the help of David Marsh and Nick Marshall, who helped survey about 20 units (~10 in Tirana). The most frequently used units were chosen. This collaborative work gives a good overview of the radiological situation in Albania, and this work will be continued by me independently in the

future, as we will receive some test equipment from the IAEA.

Conclusions

This project coincides with the 'period of transition' in Albania, and with the partners co-operation has given the following achievements:

- 1) The actual diagnostic radiological situation in Albania is now known and reported to the EC.
- 2) Modern elements of QA have been introduced, where no QA existed previously.
- 3) There have been improvements to both patient and staff dosimetry in terms of methodology and measurements with the use of TLDs.
- 4) A new framework for legislation has been drafted, which accommodates the new radiological situation in Albania (i.e. private, semi-private and state radiological services)
- 5) The way has been opened (with the help of the IAEA who will provide test equipment and a TLD system) for the continuation of QA and dosimetry in Albania.

Publications

- 1) 'The localisation of cervix utery throughout AP and LL radiographs', Balconic Conference of Medical Physics , Ismir,Turkey, September 1993. (Abstract).
- 2) 'The paragonal of heard doses received during chest irradiations with and without filtration', European Congress of Medical Physics, Tenerife, Spain, September 1993. (Abstract).
- 3) 'The penumbra in Ro-therapeutic and Ro-diagnostic machines with slanting anode', Leuvan, Belgium, ESTRO meeting, Gardone Riveria, Italy, July 1995. (Abstract).
- 4) 'Patient and background irradiation measured with TLDs', Balconic conference on Radiology, Athens, Greece, June 1996. (Abstract).

**Final Report
1992 - 1994**

Contract: FI3PCT920020

Duration: 1.9.92 to 30.6.95

Sector: C22

Title: Quality assurance parameters and image quality criteria in computed tomography

- | | | |
|----|-----------|---|
| 1) | Jessen | Univ. Århus - Hospital |
| 2) | Ortins | Direcção-Geral do Ambiente |
| 3) | Schneider | Univ. München |
| 4) | Moore | Integrated Radiological Services Ltd., Liverpool (from 1.6.94 to 30.6.95) |

1. Summary of Project Global Objectives and Achievements

Since the introduction of Computed Tomography (CT) into clinical practice in 1972 there has been a steady increasing use of CT and recent developments in technology does this high dose modality even more attractive. CT has become a major source of exposure to diagnostic X-rays for the population. Although CT accounts for less than 5% of all X-ray examinations, it contributes as much as 20% of the collective dose from diagnostic radiology in some countries of the European Union. In many clinical situations, in order to achieve a correct diagnosis based on CT examinations of the patient, it can be necessary to use high values of mAs and thin slices, thus increasing the dose to the patient. Special concern is related to the use of computed tomography in paediatric radiology where recent Informations emphasize that in children there is an additional hazard of detrimental radiation effects.

CT has improved the possible low contrast detectability considerably and although the contribution from non-useful scattered X-rays, which is a problem in conventional tomographic techniques, is reduced in CT, the complexity of the technology and the variability of scanner settings may in comparison to conventional radiology result in image quality reduction and dose increase. Therefore, there is a need to establish quality criteria for CT which will contribute to the possible reduction of patient exposure, while providing the required clinical information in its optimum form. The quality criteria concept, as developed for conventional X-ray examinations of adult and paediatric patients by the European Commission's research actions, has proven to be an efficient means of optimising the use of ionising radiation in medical imaging procedures. The purpose of such quality criteria for CT should therefore be to provide an operational framework for radiation protection initiatives, which links the desired image quality of a CT examination to the technical parameters necessary to produce this quality at reasonable patient doses.

The criteria of image quality in CT are basically of two different types: anatomical and physical image quality criteria. The anatomical image quality criteria include the clinical requirements which must be fulfilled when specific questions should be answered. The anatomical criteria for image quality can be defined by visualization or reproduction of

pure anatomical components. Evaluation of quality based on anatomical components takes into account both the anatomical structure typical of the organ concerned, the difference in density caused by the particular tissue, and differences in density which are essential for the detection of discrete pathological changes.

The physical image quality criteria are measurable by objective means. It is mandatory for all departments carrying out CT to employ a suitable quality assurance programme to maintain performance at optimal levels by quality control of the equipment. Routine tests are specified for physical image quality parameters such as picture element noise, spatial resolution, linearity, homogeneity and stability of the CT numbers, slice width and dose.

The International Commission on Radiological Protection introduced in the 1990 recommendations (ICRP60) the concept of dose constraints with the main implication in diagnostic radiology being that of dose constraints for the patient. This new concept should not be mistaken for the principle of dose limits which is not applicable for medical use of ionising radiation, but contribute towards the introduction of reference dose levels applying to typical practices for an X-ray department and allow comparison of examination techniques at different hospitals.

This coordinated project has primarily been dealing with five subject areas having the objectives described and the achievements obtained are given in detail by each contractors report.

Basic research of general image quality parameters in CT

An evaluation of the methods for dosimetric measurements of CT-scanners has been performed together with assessments of uncertainties of dose values and detailed analyses of transverse dose profiles. The reference doses must be based on well-defined dose descriptors. Proposals are given for reference doses based either on Computed Tomography Dosimetric Index (CTDI) measured free-in-air at the centre of rotation or on Multi Slice Average Dose (MSAD) values measured in standard phantoms as such descriptors.

Image Quality Criteria for adults CT

Tests of image quality criteria and their implementation for cerebrum, mediastinum and retroperitoneum have been performed together with further developments of existing criteria formulated by organisations and individuals in order to create a list of quality criteria that have the greatest impact on dose defined both for the medical image/information and for the equipment performance. There has been a cooperation with the European Study Group in producing a document on "Quality Criteria for Computed Tomography" for adults. Evaluation of standard protocols for newly installed CT units by assessments of doses and image quality parameters has been performed. For nearly equal score of image quality for specific examinations variations with a factor of six in doses to the patient are found.

Image Quality Criteria for paediatric CT. Optimisation studies for brain and lung paediatric CT examinations and their contribution to the establishment of image quality criteria has been performed based on field studies in Portugal together with a dosimetric survey on paediatric CT in Southern Germany. It is demonstrated, that clinical information was kept even for lower doses than recommended by the scanner manufacturer. Preliminary tests of the effect of mAs decrease and its influence on image quality in chest and abdominal CT of young patients has been performed.

General developments of Quality Criteria for adult and paediatric patients. The existing CEC Quality Criteria for Radiographic Images has been assessed in terms of the relevant relationships between image quality, radiographic factors and patient dose and a complete restructuring of the original Document from 1990 has been performed.

Conventional radiography and fluoroscopy in paediatric and adult examinations. A framework whereby the dose delivered to a patient can be directly related to the radiographic factors employed has been assessed and recommended to be implemented. The wide field European study on the 5 year old child, use so-called "TLD-3" study has been extended to a study of also a 10 year old child. Evaluations have resulted in a reformulating some of the image criteria in order to make them more precise. It has been concluded that adherence to the guidelines for good radiographic technique leads to a significant reduction in dose without less of image quality.

Head of project 1: Dr. K.A. Jessen

II. Objectives for the reporting period.

- Evaluation of standard protocols with comparison of anatomical image quality criteria and doses assessed for each type of examination.
- Testing and developments of image quality criteria in cooperation with the European Study group in "Quality Criteria for Computed Tomography".
- Establishing a firm and consistent base for reference doses for Computed Tomography exposures.
- Coordination of the project as a whole.

III. Progress achieved including publications.

The influence of the scanning parameters on patient dose and image quality is a basic problem in the radiation protection in CT examinations.

In order to obtain an adequate image quality and to ensure optimal radiation protection in computed tomography, it is necessary to have a precise medical information to select the examination technique specifically according to the information which is wished to obtain, and to minimize the radiation exposure to sensitive organs and tissues.

The image quality in CT primarily depends on the technical parameters, which can be divided in those related to the dose consisting of kV, mAs settings, slice thickness, number of slices and couch increment, and parameters related to the processing of images such as FOV, reconstructions matrix size, reconstructions algorithms, window settings.

All these technical parameters should be selected so the dose is as low as consistent with required image quality.

The work has been concentrated on evaluation of standard protocols in seven departments for seven newly installed CT units in Denmark and comparison with the image quality criteria formulated by assessments of dose and image parameters measured in phantoms. The study include also implementation into general clinical environment of facilities for a direct dose calculation for a specific examination based on accepted dosimetric methodologies. In total 2380 examinations have been registered. Three examinations: cerebrum, mediastinum and retroperitoneum have been selected for a pilot study to define the guidelines in determining the reference doses and quality criteria in CT, and with it to evaluate the limits of dose reduction, which still allow a diagnostic sufficient image quality.

Physical image quality parameters

Linearity, homogeneity, stability, spatial resolution and noise. The measurements of correlation between CT numbers and electron density relative to water have been performed with RMI (model 465) electron density phantom. The 33 cm diameter phantom has twenty 2.5 cm diameter holes into which are inserted: 6 rods made of commercially available plastic, 11 rods simulating different tissues with known elemental composition and electron densities and 3 rods made of solid water, the same material as the phantom. The rods have been placed in identical position in the phantom for all measurements.

Typical relationship between electron density relative to water and CT numbers of

materials in the Electron Density CT Phantom can be described by two straight lines one for soft tissue and one for bone tissue. The lines can be defined by two parameters slope and point on the line. The CT number for water has been chosen as the reference point in this comparison for both lines. The representation of such lines is given in Table 1 for soft and bone tissue.

Table 1. Representation of the mean relationship in bone and soft tissue between electron density relative to water and CT number.

Scanner identification	Bone Tissue		Soft Tissue	
	CT water value [HU]	Slope of curve ($\cdot 10^{-3}$)	CT water value [HU]	Slope of curve ($\cdot 10^{-3}$)
1. Siemens Somatom Plus S	-115,9	0,519	-8,6	1,039
2. Siemens Somatom Plus S	-110,4	0,520	-4,6	1,047
3. Siemens Somatom HiQ	-128,4	0,518	-7,2	1,039
4. Picker PQ 2000	- 90,2	0,573	-3,8	1,086
5. Philips Tomoscan SR	-128,4	0,547	-20,7	1,156
6. Philips Tomoscan LX	-134,1	0,523	-20,9	1,101
7. Philips Tomoscan LX	-142,2	0,511	-23,5	1,085

The measurements of spatial resolution (R) and noise (S) have been performed with an RMI (model 461 A) combined Head/Body quality assurance phantom. Spatial resolution have been determined as a Full-Width-Half-Maximum of the point spread function of a 0.3 mm wire in air.

Noise have been measured as the normalized standard deviation of an array of CT values at the centre of a single scan of an uniform RMI phantom.

Results of measurements and calculations of R and S together with 'Figure of Merit' Q ($Q = [1000 / R^3 \cdot D \cdot T \cdot S^2]^{1/2}$) are shown in Table 2.

Table 2. Physical image quality parameters.

Scanner identification	Scanner- settings		Dose	Noise	Spatial resolution	Figure of Merit
	KV	Slice T	D	S	R	Q
	kV	mm	mGy	%	mm	$\text{mm}^{-2} \cdot \text{Gy}^{-1/2}$
1	120	10	39,4	1,29	1,32	0,81
2	137	8	40,7	1,60	1,20	0,83
3	133	10	78,6	1,02	1,66	0,52
4	130	10	69,2	1,17	1,20	0,78
5	120	10	63,5	0,68	1,78	0,78
6	120	10	45,0	1,17	1,31	0,85
7	120	10	46,3	1,49	1,8	0,41

Dose descriptors. Two main components of describing the exposures from CT can be identified based on the following definitions:

- The Computed Tomography Dosimetry Index (CTDI) related to the radiation field delivered from the CT scanner in a specific point, normally at the centre of rotation, measured free-in-air.
- The Multiple Slice Average Dose (MSAD) related to the absorbed dose to a standard body phantom in a multi slice exposure measured at the center and 1 cm below the surface of the phantom.

Fiftyone dose profiles have been measured with Thermoluminescent Dosimeters (TLD). The CTDI and real slice thickness (FWHM) has been calculated from the dose profile measured at the centre of rotation $CTDI_C$, and 10 cm of axis $CTDI_{10\text{ cm}}$. All TL dosimeters have been calibrated in a ^{60}Co radiation field before and after measurements. A correction factor of 0.8 for the quality difference has been used. Results of TLD measurements are shown in Table 3 and Table 4.

Table 3. Real and nominal slice thickness.

CT scanner identification	Nominal slice thickness, mm							
	1.0	1.5	2.0	3.0	4.0	5.0	8.0	10.0
1	1.0	---	2.0	3.2	---	5.1	---	9.8
2	1.9	---	2.4	---	4.4	---	8.0	9.8
3	---	---	1.9	---	---	4.9	7.6	9.4
4	---	1.7	---	3.0	3.9	4.8	8.2	9.6
5	---	1.6	---	3.0	---	5.0	---	9.9
6	---	1.7	---	3.0	---	5.1	---	9.8
7	---	1.4	---	2.8	---	4.7	---	9.7

The MSAD values have been measured with a Capintec PC-4P pencil shaped ionisation chamber at the centre ($MSAD_C$) and 1 cm below the surface ($MSAD_S$) of a perspex (PMMA) phantoms with diameters of 16 cm, 22 cm and 32 cm for a single slice exposure. Employing the principle of volume averaging the exposure measurement obtained is equivalent to the exposure at the midpoint of series of contiguous slices equivalent to the active length of the chamber (~ 10 cm). The $MSAD_{AV,H}$ is defined by:

$$MSAD_{AV,H} = \frac{1}{2} MSAD_C + \frac{3}{2} MSAD_S$$

where H is for head and neck examinations (phantom diameter of 16 cm) and $MSAD_{AV,B}$ for body examinations a similar equation apply (phantom diameter of 32 cm).

The $CTDI_C$, $CTDI_{10\text{ cm}}$ and $MSAD_{AV}$ values are given in Table 4.

The $CTDI_{IEC}$ and Multi-slice doses have been also measured for different condition of radiation.

Table 4. Dose descriptor values in mGy/mAs for 10 mm slices.

CT System	MSAD _{AV,H}	MSAD _{AV,22}	MSAD _{AV,B}	CTDI _c	CTDI _{10 CM}
	mGy/mAs	mGy/mAs	mGy/mAs	mGy/mAs	mGy/mAs
Somatom Plus S, 120 kV	0.110	0.092	0.062	0.128	0.113
Somatom Plus S, 137 kV	0.141	0.120	0.082	0.169	---
Somatom HiQ, 133 kV	0.161	0.140	0.093	0.199	0.164
Picker PQ 2000, 130 kV	0.287	0.194	0.150	0.323	0.133
Tomoscan SR, 120 kV	0.152	0.124	0.079	0.204	0.145
Tomoscan LX, 120 kV	0.160	0.120	0.082	0.200	0.141

Reference dose.

Significant differences in radiological practice between hospitals have previously been observed for conventional X-ray examinations. Reductions of these wide variations in patient exposure have been encouraged by the introduction of quality criteria for diagnostic images, which include reference dose levels.

The reference doses for CT can be based on either CTDI or MSAD dose descriptors. The CTDI and MSAD are easy to measure and therefore practicable as the dosimetric base for defining reference doses.

By using CTDI values and existing catalogues (NRPB-R250 report) giving organ doses, the effective doses, can be calculated for examinations performed by 27 common models of CT scanners.

The effective dose for cerebrum mediastinum and retroperitoneum examinations, for the seven CT scanners mentioned before were calculated.

Unfortunately the NRPB -250 does not include conversion factors for Somatom Plus S, Somatom HiQ, Picker PQ 2000 and Tomoscan SR scanners, therefore we have for Somatom Plus S and Somatom HiQ, used Monte Carlo set 3, and for Picker PQ 2000 Monte Carlo set 5 and for Tomoscan SR Monte Carlo set 18.

For the examinations, which consist of more than one series of slices (for example examinations with and without contrast medium), the organ doses for each series have been summed to obtain results for complete examinations.

It was not possible to calculate all organ doses necessary for estimation of effective dose. The absorbed dose in oesophagus was estimated to be equal to the absorbed dose in lungs. The mean values of the absorbed dose to eleven organs were used as an estimate of the absorbed dose to the remainder. The results of effective dose calculations are shown in Table 5 for cerebrum, in Table 6 for mediastinum and in Table 7 for retroperitoneum.

For MSAD a value called Dose Length Product (DLP) is proposed as a reference dose defined by:

$$DLP = MSAD_{AV} \cdot T \cdot N \cdot C \quad [mGy \cdot cm]$$

where T is the slice thickness, N is the number of slices and C is the exposure settings.

The DLP is the CT equivalent of the dose-area-product (DAP) for conventional radiography and can be considered as an expression for the total energy imparted

to the patient. The DLP values have been calculated for cerebrum, mediastinum and retroperitoneum and are also shown in Table 5, Table 6 and Table 7.

Table 5. DLP values and effective doses for different protocols for examinations of the cerebrum.

CT scanner identification	KV	C	T	<N>	DLP	Effective dose
	kV	mAs	cm	mean	mGy · cm	mSv
1. Somatom Plus S	120	420	1.0	13.2	610	1.2
2. Somatom Plus S	120	500	0.8	33.6*	1478	2.9
3. Somatom HiQ	133	700	0.5	9.5	1271	3.2
	+ 133	+ 475	+ 1.0	+ 8.8		
4. Picker PQ 200	130	300	1.0	21.7	1868	2.2
7. Tomoscan LX	120	580	0.3	9.0	1053	1.5
	+ 120	+ 435	+ 1.0	+ 11.3		

Table 6. DLP values and effective doses for different protocols for examinations of the mediastinum.

CT scanner identification	KV	C	T	<N>	DLP	Effective dose
	kV	mAs	cm	mean	mGy · cm	mSv
1. Somatom Plus S	120	420	1.0	20.7	539	8.8
2. Somatom Plus S	137	275	0.8	30.4	548	7.7
4. Picker PQ 2000	130	300	1.0	59.0*	2655	26.5
5. Tomoscan SR	120	250	1.0	28.5	563	7.3
6. Tomoscan LX	120	332.5	1.0	47.7*	1301	18.1
7. Tomoscan LX	120	332.5	1.0	26.1	712	10.6

Table 7. DLP values and effective doses for different protocols for examinations of the retroperitoneum.

CT scanner identification	KV	C	T	<N>	DLP	Effective dose
	kV	mAs	cm	mean	mGy · cm	mSv
1. Somatom Plus S	120	420	1.0	37.3	971	12.1
2. Somatom Plus S	137	420	0.4	39.1	571	8.6
3. Somatom HiQ	133	240	1.0	34.7	775	13.8
4. Picker PQ 2000	130	315	0.5	59.3*	1308	12.8
5. Tomoscan SR	120	250	1.0	28.0	553	8.0
6. Tomoscan LX	120	380	1.0	34.3	1069	14.7
7. Tomoscan LX	120	380	1.0	33.6	1047	18.4

* with and without contrast.

It seems to be possible to find a factor for a conversion of the DLP values to effective dose. For five general examinations: head, neck, chest abdomen and pelvis ratios between the DLP and effective dose are given in Table 8. This ratio is independent of number of slices and exposure settings.

Table 8. F factor = DLP / effective dose.

CT system	Head	Neck	Chest	Abdomen	Pelvis
Somatom Plus S, 120 kV	446	189	56	64	50
Somatom HiQ, 133 kV	419	178	54	62	48
Picker PQ 2000, 130 Kv	782	332	97	110	86
Tomoscan SR, 120 kV	456	193	59	67	52
Tomoscan LX, 120 kV	437	185	58	66	52
Mean F ± 1 S.D.	440 ± 14	186 ± 6	57 ± 2	65 ± 2	51 ± 2

The mean values of F factors was calculated excluding F factors for Picker PQ 2000 scanner.

'Anatomical or diagnostic' image quality criteria.

Image quality criteria can be measured by well established physical tests mentioned before, but these do not take patient related parameters into account. It is therefore necessary to have a method for measuring the 'anatomical or diagnostic' quality. There are no objectives diagnostic quality criteria used, but it is possible to define a set of anatomical image criteria which must be fulfilled for optimal diagnostic quality.

We have elaborated a set of criteria for the cerebrum, mediastinum and retroperitoneum.

All the examinations of the three types from the survey period have been evaluated by four experts trained in CT. The image quality of a total 93 cerebrum, 113 mediastinum and 68 retroperitoneum examinations have been evaluated. A score yes or no has been given for fulfillment of the individual criteria for each examination.

For perfect image quality all criteria should be fulfilled, but this will for a given equipment and examination protocol not always be the case irrespective the dose used because the image quality as mentioned is influenced by many factors such as movement artefacts. If the criteria are fulfilled in an acceptable amount of patients the image quality for the examination can be deemed acceptable.

For the cerebrum the following criteria were used: reproduction of: total cerebrum from foramen magnum to vertex, the osseous skull base and total teca cranium. Sharp reproduction of: line between grey and white substance, basal ganglia, ventricles and cerebrospinal fluid (spaces around cerebellum, brain stem,

mesencephalon and cerebrum).

For the mediastinum the criteria were: sharp reproduction of the pleuro-mediastinal border, the anterior mediastinum, the thoracic aorta, the trachea and main bronchia, the paratracheal tissue, the carina and lymph node area, the diaphragm and costophrenic angles. Besides reproduction of oesophagus and paravertebral space and lymph nodes lesser than 15 mm.

For the retroperitoneal space the criteria were: sharp reproduction of the perivascular retroperitoneal space, where sharp reproduction means that the anatomical details is clearly defined. Sharp reproduction of the aorta, the bifurcation and its rami, the inferior cava vein and its tributaries. Besides reproduction of lymph nodes lesser than 15 mm, where reproduction means that the anatomical details is visible, but not necessary clearly defined.

On the basis of quality criteria the quality factor QC has been defined⁽⁵⁾.

The values of QC factor for cerebrum, mediastinum and retroperitoneum are given in Table 9.

Table 9. The values of QC factor in %.

CT system	Cerebrum	Mediastinum	Retroperitoneum
1. Somatom Plus S	51.8	72.7	82.2
2. Somatom Plus S	44.5	39.2	47.8
3. Somatom HiQ	50.9	---	50.0
4. Picker PQ 2000	51.6	47.8	77.5
5. Tomoscan SR	---	55.6	62.5
6. Tomoscan LX	---	33.8	43.8
7. Tomoscan LX	53.3	51.1	72.5

The QC factor as a function of DLP are shown in Figure 1 for cerebrum, Figure 2 for mediastinum and Figure 3 for retroperitoneum.

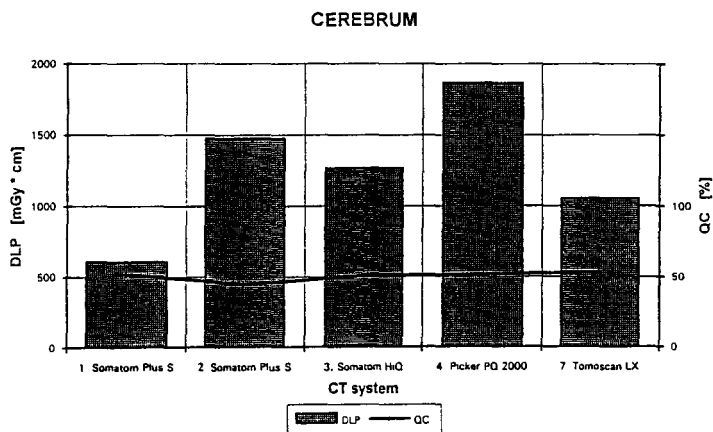


Figure 1. QC factor as a function of DLP. Cerebrum.

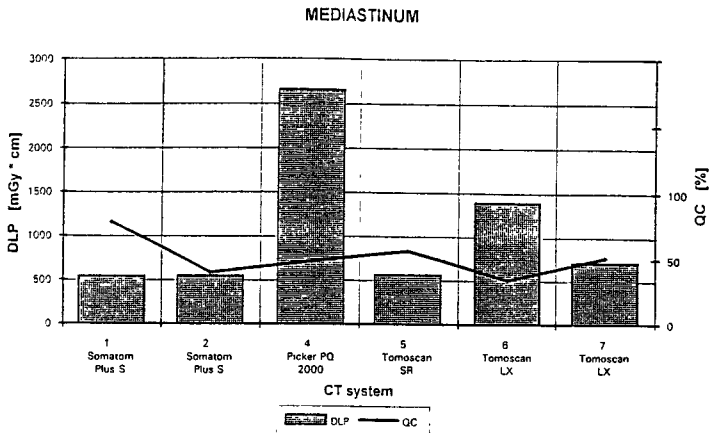


Figure 2. QC factor as a function of DLP. Mediastinum.

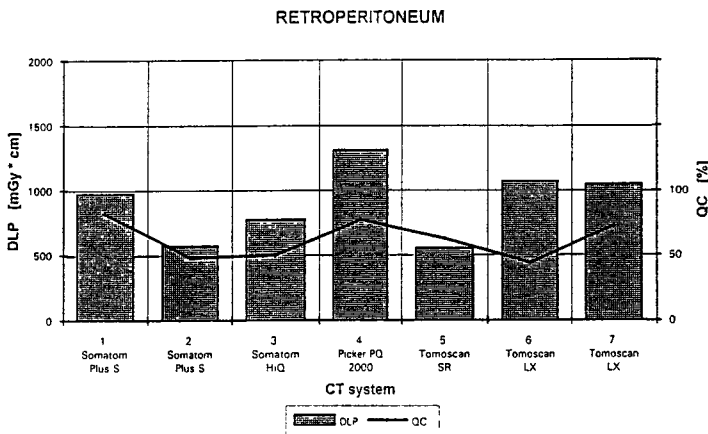


Figure 3. QC factor as a function of DLP. Retroperitoneum.

Conclusion.

Physical image quality parameters. The Q varied between 0.41 to 0.85 mm⁻² · Gy⁻¹ from scanner to scanner.

The measured FWHM of the dose profiles for nearly all scanners, especially for thin slices, does not coincide with the nominal slice thickness T, CTDI values are systematically under or over estimated.

A good agreement is obtained for the MSAD, CTDI_{IEC}, and Multi-slice dose descriptors for the scanner system investigated and a significant deviation to the CTDI descriptor measured free-in-air is observed. Even higher discrepancies have been registered for systems with shaped filters.

Reference dose. The total dose for a complete CT examination is determined by the

irradiated volume of the patient (number and width of slices imaged), the couch increment between slices, the use of contrast medium for additional slices and the exposure settings. Therefore the reference dose for a full examination have to incorporate the exposure settings, number of slice, the slice thickness exposure settings. The reference dose should also be simple to measure, applicable to all current and new types of scanner, and should primarily provide an indication of overall patient exposure for complete examinations.

The average number of slices for cerebrum examination ranged from 13.2 to 33.6, for mediastinum from 20.7 to 59 and for retroperitoneum from 28.0 to 53.6.

Effective dose. The variation in basic dose data and the scan protocols between scanners leads to effective dose differences of factor 3 for cerebrum, factor 4 for mediastinum and factor 2 retroperitoneum examinations.

The value of effective dose for cerebrum examinations ranged from 1.2 to 3.2 mSv, for the mediastinum from 7.7 to 26.6 mSv and for retroperitoneum from 8.0 to 18.4 mSv .

The wide variation in doses between different departments were partly related to the type of scanner and the mAs settings, but the number of slices seems more important.

DLP. As Table 5 shows there is a good agreement between values of effective dose and DLP. The differences between effective dose and DLP are generally acceptable. some of the discrepancies can be explained by measurement uncertainties for CTDI and MSAD, and in calculation of the effective dose for the CT scanners not included in the NRPB-R250 report.

The DLP as opposed to effective dose is a directly measurable quantity. It is easy to measure and calculate, is applicable to all scanners and examinations, and it is possible to calculate the effective dose from DLP.

Image quality. For cerebrum and mediastinum examination there seems to be correlation between the quality assessed and the dose (Figure 1 and Figure 2). For retroperitoneum (Figure 3) there seems to be a slight correlation between dose and the mean score of image quality, but there is still a great variation in dose. The variations are caused both by the scanner settings (mAs) and by examinations procedures (number of slices). Many departments follow the protocol given by the manufacture.

It is recommended to analyse and optimise the image quality and dose for each examination protocol to assure a dose as low as consistent with required image quality.

At attempts of dose reductions it is important that the examinations procedure must be optimal with regard to the mAs value and more important by reduction number of slice for each examination protocol.

Diagnostic image quality criteria can be used to evaluate that the image quality is adequate when one will change the examination parameters.

In Table 10 proposed values of reference levels for the three examinations are given as the 3rd quartile of all doses registered based on DLP .

Table 10. Reference dose levels for cerebrum, mediastinum and retroperitoneum.

		CEREBRUM	MEDIASTINUM	RETROPERITONEUM
Number of examinations		451	68	106
DLP [mGy · cm]	minimum	231	221	326
	mean ± 1 S.D.	1208 ± 493	1006 ± 1018	856 ± 400
	maximum	4605	4860	2066
	third quartile	1363	946	1154

It is recommended to analyse and optimise the image quality and dose for each examinations protocol.

Publications:

1. K.A.Jessen, J.J.Christensen, J.Jørgensen, J.Petersen and E.W.Sørensen, *Determination of collective effective dose equivalent due to computed tomography in Denmark in 1989*. Radiat. Prot. Dosim., 43, 37-40 (1992).
2. K.A.Jessen, J.J.Christensen, J.Jørgensen, J.Petersen and E.W.Sørensen, *Dosimetric Investigation in Computed Tomography*. Radiat. Prot. Dosim., 43, 233-236 (1992).
3. K.A.Jessen, P.Franklin, J.Hansen, L.C. Jensen and J.J.Christensen, *Quality Control in Quantitative Computed Tomography for Treatment Planning*. Proc. Medical Physics 93 & IX Congreso Nacional de Fisica Medica. Tenerife. September 93, 183-186 (1993).
4. K.A.Jessen, P.Franklin, L.C.Jensen and J.J.Christensen, *Phantom Measurements for Quality Control in Quantitative Computed Tomography*. Radiat. Prot. Dosim., 49, 237-240 (1993).
5. J.Hansen, L.C.Jensen, K.A.Jessen and A.G.Jurik, *Assessments of doses and image quality for some newly installed CT units in Denmark*. Internal Report, 1995.
6. J.Albrechtsen, J.Hansen, L.C. Jensen, K.A.Jessen and A.G.Jurik, *Quality Control and Image Quality Criteria in Computed Tomography*. Radiat. Prot. Dosim., 57, 125-127 (1995).
7. A.F. Carvalho, A.D. Oliveira, A.G. Alves, J.V.Carreiro, L.C.Jensen and K.A.Jessen, *Quality Control in Computed Tomography performed in Portugal and Denmark*. Radiat. Prot. Dosim., 57, 333-337 (1995).
8. A.G.Jurik, K.A.Jessen and J.Hansen, *Image Quality and Dose in Computed Tomography*. To be published elsewhere.
9. K.A.Jessen, J.Hansen and A.G.Jurik, *Dose descriptors for implementation of referece doses in Computed Tomography*. To be published elsewhere.

Head of project 2: Dr. Ortins de Bettencourt

II. Objectives for the reporting period

1. Research on the dose evaluation in Computed Tomography.
2. Constancy of technical parameters and radiation doses of CT scanners.
3. Optimisation studies for brain and lungs paediatric CT examinations and its contribution to the establishment of image quality criteria.

III. Progress achieved, including publications

1 Research on the dose evaluation in Computed Tomography.

The accuracy of doses measured in CT can be affected by definition of dose descriptors, scanner technical specifications and their constancy, reproducibility of radiation output, experimental set-up to carry out the measurements and their relations with dimension and position of patient body (or phantom) into the radiation beam

In this work we used dosimetric and mathematical methods to analyse the *transverse dose profile* and the *radial dose profile*. The former is a function developed to fit the TLD readings of transverse section of a slice. The latter is an investigation using mathematical methods (analytical and Monte Carlo simulation) to relate the dose at the centre of a cylindrical phantom with that at any other point up to the surface.

1.1 Transverse dose profile analysis in CT

Previous published works^(1,2) developed a function to describe the *dose profile*. Here we rename *dose profile* as *transverse dose profile* to distinguish from the *radial dose profile* presented in the next section. Extended work was carried out in the multiple slices dose profile⁽³⁾. The profile function allows a thorough characterisation of the radiation beam providing parameters such as: symmetry or asymmetry, left and right penumbrae, full width at half maximum (FWHM) and plateau lengths that we cannot easily obtain by other methods (figure 1.1)

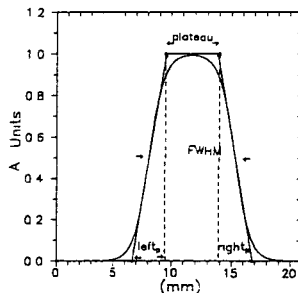


Figure 1.1 - Parameters used to characterise the dose profile.

We use a set of 20 TLD chips stacked together along a line perpendicular to the tomogram to measure the dose free-in-air. These data give a discrete information about a continuous curve named transverse dose profile. Using the profile function to fit the TLD readings of the dose profile in a single slice we observed that for nearly all scanners, the FWHM and the nominal slice thickness do not coincide. Therefore we defined a new dose descriptor (CTDI₁) using the

FWHM instead of the nominal slice thickness, used in the conventional CTDI, obtaining a more realistic dose descriptor (figure 1.2)

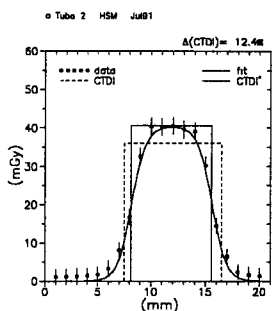


Figure 1.2 - Dose profile and comparison between CTDI and CTDI*.

In two of the four scanners studied the CTDI present a deviation of 33% higher and 22% lower than compared with a CTDI calculated using the actual slice thickness instead of the nominal value

Furthermore we defined a *plateau dose* and shown that is nearly coincident with our new definition of the CTDI (using the FWHM), which means that the dose in CT examinations may be described by either the CTDI* or the *plateau dose*.

Several *transverse dose profiles* may be added to obtain a multiple sliced profile⁽³⁾. In this work the multiple slice profile was used to study the displacement of the treatment table. In some cases we observed a superposition of the slices leading to a local increase in the absorbed dose (figure 1.3).

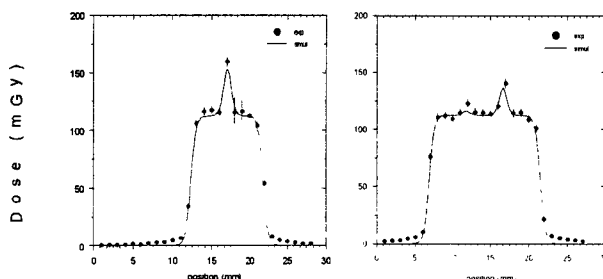


Figure 1.3 - Two slices of 5 mm with displacement of 5 mm and three slices of 5 mm with displacement of 5 mm

1.2 Radial dose profile

As we state above we want to relate the dose at the centre of a cylindrical phantom with that at any other point up to the surface. The study of the radial dose profile was performed through two approaches: analytical and numerical models.

One application of this work is that we need to make measures in phantom, only in the centre of it, avoiding expending more time with any other measures with the phantom. As we know the CT installations are usually very busy with patient examinations.

Analytical model

Figure 1.1 represents the geometry adopted.

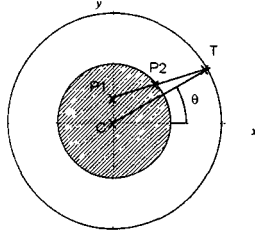


Figure 1.1 - Irradiation geometry in Computed Tomography.

The phantom is a perspex cylinder placed in the rotation axis of the x ray tube. The shaded circle in figure 1.1 represents a section of the phantom and T represents the x ray tube that rotates in the circle of radius \overline{CT} . We want to obtain the ratio of the doses at P_1 and C.

To develop a simple model we make some assumptions like the neglecting of the secondary radiation and the air attenuation from the x ray tube to the phantom and used the inverse square law and the exponential attenuation in the material. The beam is considered monoenergetic and may be a parallel or a fan beam.

Using the above assumptions we developed an analytical model for the calculation of the ratio between the radial and the central detectors and named RC .

The conditions of calculation were: the phantom radius, R_{ph} , are 8 cm, the distance \overline{CT} is 78.5 cm obtained from the Siemens Somatom DRH literature. For the photon energy we used 70 keV that is near to the mean energy of a spectrum of 125 kV with 2.5 mmAl + 0.4 mmCu for the Siemens Somatom. We calculate the RC for integer values of $r = \overline{CP_1}$ from 1 to 8 cm.

Figure 1.2 presents the results

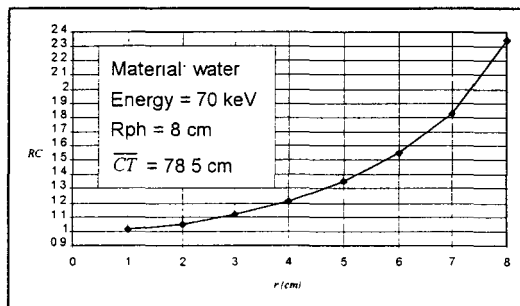


Figure 1.2 - The ratio RC for a 70 keV beam

Numerical model.

We developed a Monte Carlo code to apply in Computed Tomography with the same intent as in the previous section. With this method we investigated the scattered and secondary radiation. The implemented code considers the three fundamental interactions of photon with matter: photoelectric effect, coherent scattering corrected with the form factor and incoherent scattering corrected with the incoherent-scattering function.

We assumed the phantom to be of water. We take his composition in account for the calculation of the form factors, the incoherent-scattering functions and the total linear attenuation coefficient.

We used a 486DX, 66 MHz computer working for two days for each test of the code (30000 histories). Several running tests were performed. The time to simulate one CT slice was four days (60000 histories). We implemented the code in Microsoft® Visual Basic for Application with the Excel spreadsheet.

For the application to computed tomography we need to consider that the geometry is now rotational, instead of the classical linear geometry in diagnostic radiology and further we have a fan x ray beam. We take that in to account in developing some new codes for that geometry of irradiation

The Monte Carlo code was running in the same conditions as in the previous section: a water phantom with 8 cm of radius. The photon energy used was 70 keV to compare with the analytical model and the 125 kV spectrum of the Siemens Somatom. We used four detectors, one at the centre of the phantom and the others at the radial positions of 2, 4 and 6 cm. The radius of the detectors was 2 cm We obtain the RC values presented in the next table

Table 1.1 - Results of the Monte Carlo simulations.

energy	RC	mean	2 × stand. dev. sample
70 keV	1	1.34	0.02
	2	2.97	0.04
	3	5.28	0.06
125 kV spectrum	1	1.25	0.02
	2	2.77	0.06
	3	5.07	0.10

Discussion

With the analytical model of section 1.1 we make calculation for several photon energies and the results together with the Monte Carlo results are in figure 1.3 where we may compare him.

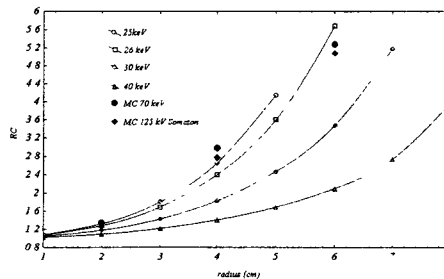


Figure 1.3 - Radial dose profile for analytical and Monte Carlo models

We see that the results for the monoenergetic beam of 70 keV and for the 125 kV spectrum are of the same order. The analytical model reaches to very different results, which we expected, due to the neglect of the scattered and secondary radiation.

Conclusion

1 In the Monte Carlo simulation both radial dose profiles of 70 keV and 125 kV photon beams are similar, allowing that we may substitute a spectrum with their mean energy when analysing radial dose profiles.

2. It is of interest to have an analytical model to facilitate the calculations in routine verifications of CT installations. As we can see the results of Monte Carlo simulation are reproduced in the analytical model for a very low photon energy, of the order of 25 keV This is expected, because we neglected the scattered and the secondary radiation, but it will be interesting to develop further this model, in future works, to correct the primary analytical model with some scattered factor

2. Constancy of technical parameters and radiation doses of CT scanners

Constancy tests have been carried out in Portugal, where 4 CT systems were followed for 10 months, while in Danmark similar tests were carried out in two scanners during 4 months. Results of these two sets of tests were published together in a report(4)

The purpose of this investigation was monitor relevant image and dose parameters before and after monthly service with the aim of evaluating the necessity of additional Quality Control (QC) tests to be carried out by the user's operator to ensure the quality and to point out changes, if any, in scanner performance due to service and maintenance.

In the portuguese monitoring a standard RMI-463 phantom was used to measure accuracy of slice thickness, spatial resolution, low contrast detectability, linearity of CT numbers and noise. Image noise was evaluated as the standard deviation of CT numbers in "solid water" in a ROI at the centre of the RMI phantom in a single scan. Dose measurements were determined with LiF dosimeters (TLD100).

Results presented in Table 2.1 were obtained assuming that the base line value for each scanner would be the average for each parameter studied.

Table 2.1 Results of the portuguese series of tests

	Siemens-Somaton HiQ		Siemens-Somaton 2N		Philips-Tomoscan 350		GE-CT 9800 Quick	
	mean deviation (%)	max. absolute deviation (%)	mean deviation (%)	max absolute deviation (%)	mean deviation (%)	max. absolute deviation (%)	mean deviation (%)	max absolute deviation (%)
noise	3.8	12.9	3.8	12.9	-6.7	13.3	-13.8	19.5
spatial resolution low contrast	-6.7	20.0	0.0	0.0	0.0	0.0	0.0	0.0
CT number stability	0.1	0.3	0.1	0.2	-0.4	0.6	-0.5	3.2
CTDI	3.9	5.9	-2.9	9.3	-4.6	6.0	-1.7	2.5

It is shown that the maximum absolute deviation from the average dose in CTDI is 5.9% over a period of 10 months. However, noise measurements exceeded the IEC maximum acceptable deviation (IEC 1223-2-6 draft)

The main conclusion was that the constancy of scanners performance is very high and that monthly service practised by most manufacturers seems sufficient and that extra Quality Control tests would not improve performance. A daily check of the noise level should be recommended and a registration of this parameter should be done.

3 Optimisation studies for brain and lungs paediatric CT examinations and its contribution to the establishment of image quality criteria

3.1 Proper milliampere-second settings for paediatric CT brain examination

In fifty paediatric CT brain examinations two additional images were obtained in a chosen plane to determine the optimum milliampere-second settings in the sense of lower radiation dose to produce images containing the required diagnostic information.

This study was performed in the Radiology Department of a Lisbon university hospital using a Philips Tomoscan 350, with the following technical factors: 120 kV; scan time of 4.8 s, 120 mAs with 6 mm slice thickness (TH); 180 mAs with 9 mm TH; 360 mAs with 9 mm TH, 480 mAs with 6 mm TH.

The paediatric study group for brain CT examination was composed by 50 patients (25 male, 25 female) with the following age distribution. 12 in the age group of 0 - 1 years; 24 with ages between >1 - 5 years; 8 with ages between >5 - 10 years and 6 with ages >10 - 15 years. Brain CT examinations were performed following hospital procedures and medical judgement on clinical information available from each patient. However different technical parameters were used taking into account mainly patient ages, as is shown on Table 3.1.

Table 3.1 - Frequency of technical parameters used to perform brain CT examinations distributed by patient age group

age group(years)	120 mAs	180 mAs	360 mAs	480 mAs
0 - 1	92 %	8 %	---	---
>1 -5	5 %	65 %	30 %	---
>5-10	---	10 %	70 %	20 %
>10-15	---	25 %	50 %	25 %

After CT examination has been concluded an image in the central brain region was chosen by the radiologist participating in this study and two additional scans were performed in the same plane. The three images were reconstructed with the same algorithm and registered with identical window levels and width appropriate for brain details

Whole experimental images (1 from the examination and 2 additional) from each patient included in the study group were stored and later whole images from the study group were independently reviewed and assessed by two radiologists in two steps:

- a) Image medical quality - characteristic image
- b) Images with reading -diagnostic information

Image medical quality was assessed through the application of an evaluation criteria and score. Evaluation criteria included the following items: ventricular system (limits, plexus choroideus); parenchyma (differentiation of white/grey matter; internal capsule, thalamus, morphology of cortex furrows), vascular structures (morphology; identification), lesion(dimension; limits; aspects); limits of subdural-epidural space; artefacts (beam hardening; others). Results of this evaluation are summarised in Table 3.2

Table 3.2 - Normalised scoring of image medical quality

mAs settings used in CT examination	scoring per milliampere-second settings			
	120 mAs	180 mAs	360 mAs	480 mAs
120 mAs	308	423	231	38
180 mAs	128	410	308	154
360 mAs	170	254	373	203

Images with reading - or images keeping the required diagnostic information-were evaluated as 93 to 95% of whole images (examination+additional images) However a more detailed information can be seen on Table 3.3

Table 3.3 - Percentage of images with reading, distributed by milliampere-second settings

mAs settings used in CT examination	images with reading			
	120 mAs	180 mAs	360 mAs	480 mAs
120 mAs	100 %	100 %	100 %	100 %
180 mAs	75 %	100 %	100 %	100 %
360 mAs	80 %	80 %	100 %	100 %

We can assume for this study on paediatric CT brain examinations the following conclusions:

i) Technical parameters for the examination were chosen taking into account mainly the brain size (or age) and in few cases with changes decided thinking over clinical or pathological indications

ii) The better medical image quality was observed, in general, in the image included in the CT examination

iii) The majority of experimental images kept the diagnostic information, even those produced with a very large reduction of radiation dose. Therefore the majority of examinations should be carried out with reduced dose.

In this study was not possible investigate what types of pathology would require higher doses if any relation exist at all.

3.2 Analysis of organ doses dependence from technical factors

Organ doses were evaluated for paediatric CT brain and lung examinations in two study groups. Calculations were carried out using conversion factors published by GSF(Bericht 30/93) to paediatric CT examinations and NRPB(SR250) for adults CT examinations. The organ doses dependence from body size, milliamperere-second settings and scanners radiation output were analysed for brain and lung CT examinations.

3.2.1 Organ doses of CT brain examinations

Data collected from CT brain examinations performed in the study group characterised in paragraph 3.1 was taken as the source of data used in the organ doses calculations.

Data from patients with ages fitting phantom "ages" of GSF and NRPB phantoms was selected to calculate "organ conversion factors" ($\Sigma f(organ, z)$) and these values were used to extrapolate conversion factors for other "ages" or body sizes. Extrapolation was done following two approaches: GSF and NRPB anatomical landmarks were fitted to the standard body height and sizes used as reference to the portuguese population; length of body scanned covered the standard length of the brain to every age.

Results of conversion factors for a "baby", "child" and an "adult" are shown on Table 3.4. to calculate some organs doses and effective dose.

Table 3.4 - Conversion factors to calculate some organ doses and effective dose from CT brain examination (120 kV / 2.5 Al+ 0.25 Cu) assuming scan length equal to brain length

	conversion factors to calculate					effective dose
	organ doses		bone surf.	skin (w.b)	thyroid	
	brain	b marrow				
baby (8 weeks old)	0.88	0.25	1.04	0.14	0.06	0.07
child (6 years old)	0.73	0.09	0.46	0.07	0.02	0.04
adult	0.56	0.03	0.14	0.03	0.02	0.02

From the data of our study group it can be assumed as the most frequent medical practice to carry out brain CT examination in a Philips Tomoscan 350 the following technical parameters:

baby CT - 120 kV; 120 mAs, 16 slices of 6 mm; CTDI(free-in-air) 19.4 mGy
 child CT - 120 kV, 180 mAs; 12 slices of 9 mm; CTDI(free-in-air) 31.5 mGy
 adult CT - 120 kV; 360 mAs, 16 slices of 9 mm; CTDI(free-in-air) 63.0 mGy

These technical parameters led to the dose values shown on Table 3.5, where effective dose was calculated applying tissue weighting factors proposed in ICRP60.

Table 3.5 - Organ doses and effective doses for CT brain examinations, assuming that at every age the length of scan and brain are equal.

	organ doses (mGy)				effective dose (mSv)	
	brain	b. marrow	bone surf	skin (w.b)	thyroid	
baby (120 mAs)	17.1	4.9	20.2	2.7	1.2	1.3
child (180 mAs)	23.0	2.8	14.5	2.2	0.6	1.3
adult (360 mAs)	35.3	1.9	8.8	1.9	1.3	1.3

Weighted doses estimated to the study group characterized in paragraph 3.1 and CT examinations performed with technical parameters described in Table 3.1 are presented in Table 3.6

Table 3.6 - Doses estimated to the brain CT study group. Doses were weighted with the frequency of milliampere-second settings used in each age group

age group (year)	Effective dose * (mSv)
0 - 1	1.4
>1 - 5	2.0
>5 - 10	2.2
>10 - 15	1.5

* single organ scan (no contrast)

In conclusion it was shown that in CT brain examination the use of milliampere-second settings appropriate to the head size - lower mAs to smaller head - can produce an effective dose approximately equal to all head sizes. However, in medical practice the CT brain examination of a group of patients originate effective doses a bit higher due to radiologist option for higher milliampere-second settings required for a few pathologic cases

3.2.2 Organ doses of CT lungs examination

A CT lungs study group of 30 patients was the source of data used to carry out an evaluation of organ doses their variation with body size. CT examinations were performed in a Philips Tomoscan LX with the following technical parameters: 120 kV, 175 mA, 1.9 s, slice thickness 10 mm (few cases 5 mm). The study group is characterized on Table 3.7

Table 3.7 - Study group constitution and average no. of scans (slices) per examination

age group (year)	no of patients	no. of scans
>1 - 5	1	14
>5 - 10	10	18
>10 - 15	5	22
>15	14	25

Data from patients with ages fitting phantom "ages of GSF and NRPB phantoms was selected to calculate "conversion factors and these values were used to extrapolate conversion factors to other ages (different body sizes) Extrapolation was done following the methodology described in paragraph 3.2.1 for brain CT examination.

In Table 3 8 are presented results of conversion factors for some of the most significant organ and for the calculation of effective dose It was assumed that radiation quality of Tomoscan LX would be similar to radiation quality used in GSF catalogue of organ dose conversion factors(Bericht-30/93).

Table 3.8 - Conversion factors to calculate some organ doses and effective dose from CT lungs examination (120 kV / radiation quality not corrected for Tomoscan LX) assuming scan length equal to lungs length

	conversion factors to calculate					effective dose
	organ doses (most significant)				breast	
	lungs	b. marrow	bone surf.	skin (w.b.)		
baby (8 weeks old)	0.92	0.18	0.77	0.14	0.94	0.37
child (6 years old)	0.74	0.10	0.39	0.07	0.85	0.29
adult	0.50	0.11	0.32	0.03	0.57	0.15

In the CT lungs study group quite all scans were carried out with 332.5 mAs and most frequently (90 %) with slices of 10 mm The CTDI (free-in-air) evaluated for the scanner used in the study was 66.5 mGy. In Table 3 9 are presented most significant organ doses and effective dose for the three body sizes - baby, child and adult - used as reference in this report

Table 3.9 - Organ doses and effective doses for CT lungs examinations, assuming that at every age the length of scan and lungs are equal.

	organ doses (mGy)				effective dose (mSv)	
	lungs	b. marrow	bone surf.	skin (w.b.)	breasts	
baby	61.2	12.0	51.2	9.3	62.5	24.6
child	49.2	6.7	25.9	4.7	56.5	19.3
adult	33.3	7.3	21.3	2.0	37.9	10.0

Effective doses were calculated for patients in our study group and average values for each age group are presented on Table 3 10 Calculation of effective dose was done applying tissue weighting factors proposed by ICRP60

Table 3 10 - Doses estimated to the lungs CT study group.

age group (year)	Effective dose * (mSv)
>1 - 5	21.2
>5 - 10	17.2
>10 - 15	14.0
>15	11.6

* single organ scan (no contrast)

The investigation on lungs CT shows that the use in paediatric patients of milliampere-second settings recommended for adults would be responsible for high organ and effective doses. In our study group younger (>1 - 5 years) received doses nearly two times higher than the older (>15 years)

3 2 3 Organs and effective doses dependence on scanners models

Scanners radiation output is largely dependent on scanners technology, manufacturer and model. A survey of doses measurements and technical parameters was carried out in different hospitals. The data was applied to simulate CT examinations of a child in four different scanners and calculate the effective doses and some organ doses. Results of this simulation are presented on Table 3.11.

Table 3.11 - Organ and effective doses of a child (6 years old) submitted to simulated CT brain examination. CTDI and technical parameters collected in four radiology departments.

hospital dose	scanner	CTDI (mGy) for		
		brain examination	brain dose (mGy)	effective (mSv)
A	(1)	31.5	23.0	1.3
B	(2)	76.0	55.5	3.0
C	(3)	111.5	81.4	4.5
D	(4)	60.3	44.0	2.4

(1) Philips-Tomoscan 350, (2) Philips-Tomoscan LX, (3) General Electric Sytec 3000, (4) Shimadzu- SCT 5000TX

As is shown in Table 3.10 patient doses are dependent in large extent on scanners radiation output. The establishment of guidance levels for paediatric examinations shall take into account those differences in radiation output.

Summary of conclusions:

- a) CTDI measured free-in-air it is not the most convenient dose descriptor due to lack of accuracy resulting on the use in its definition the nominal slice thickness which did not coincide usually with width of dose profile. However, we have developed a method to correct the calculation of CTDI, replacing the value of nominal slice thickness by FWHM (full width half maximum)
- b) Technical parameters to be used in paediatric CT examinations shall be appropriated to the patient body size. Milliampere-second settings for adults when applied in children originate high radiation doses,
- c) In the majority of routine paediatric brain examinations image could be obtained with reduced exposure. It is suspected that in few clinical cases and pathologies would be necessary use technical parameters recommended by manufacturers.
- d) The establishment of guidance levels for paediatric CT examinations should take into account the dramatic differences in scanners radiation output what requires a new approach to the problem

Publications

- (1) - Oliveira, A.D., Alves, J.G., Carvalho, A.F., Carreiro, J.V., *Dose profile and dose index analysis in computed tomography*, Radiat. Protect. Dosimetry, 57, 1-4, 387-391, 1995
- (2) - Oliveira, A.D., Alves, J.G., Carvalho, A.F., Carreiro, J.V., *Estudo de um feixe de raios X em tomografia axial computadorizada*, Presented at the 8th Conf. Nacional de Física, Vila Real, 1992
- (3) - Alves, J.G., Oliveira, A.D., Carvalho, A.F., Carreiro, J.V., *Estudo do perfil de dose em tomogramas múltiplos*, Presented at the "Primeras Jornadas Hispano-Lusas de Protección Radiológica", Santiago de Compostela, 1994.
- (4) - Carvalho, A.F., Oliveira, A.D., Alves, J., Carreiro, J.V., Jensen, L.C., and Jessen, K.A., *Quality Control in Computed Tomography performed in Portugal and Denmark*, Radiat. Protect. Dosimetry, 57, 1-4, 333-337, 1995

Head of project 3: Dr. Schneider

II. Objectives for the reporting period

1. Dosimetric surveys in children's hospitals in Europe

- 1.1. Europe-wide dosimetric surveys in 5 and 10 years old children for frequent X-ray examinations
- 1.2. Data analysis of equipment, radiographic technique and image quality
- 1.3. Analysis of the field size of chest x-ray
- 1.4. Reevaluation and reformulation of image criteria of the 'Working Document'

2. Dosimetric pilot study of computed tomography (CT) on infants and children in Southern Germany

- 2.1. Evaluation of measured doses (thermoluminescence dosimetry 'free in air') for different equipment settings
- 2.2. Analysis on the equipment and radiographic technique
- 2.3. Development of 'Quality Criteria on Computed Tomography in Paediatrics'

III. Progress achieved including publications

ad 1.1.

Based on the experience gained from the dosimetric studies of X-ray examinations in infants within the member states of the European Union, two further surveys including entrance surface dose (ESD) measurements with Ca_2F -thermoluminescence-dosimeters (TLDs) for the 5 and 10 years old child were performed **Tab.1**. These surveys were extended to other organs (urinary tract in the 5 years old, spine in the 10 years old child) and to lateral projections of the skull and chest (a total of 11 examinations). The lateral projections were not studied in the earlier surveys. Attempts were made to include more children's clinics from all of Europe in this survey and thereby gain a more comprehensive overview of radiographic technique and ESD. This survey provided again the opportunity to test the "Quality Criteria" of the Working Document on radiographs of older children and other X-ray-examinations.

Tab. 1 lists the number of x-ray examinations studied for all four surveys in children's hospitals covering the period from 1989 to 1995. Different organs were chosen for the various age groups based on frequency and clinical importance.

	Infant (TLD I)	Infant (TLD II)	5 years (TLD III)	10 years (TLD IV)	Total
Chest ap 1000 g (mobile)	72	61	---	---	133
Chest pa/ap	77	57	104	113	251
Chest ap (mobile)	42	79	51	36	208
Chest lateral	---	---	80	78	158
Abdomen ap	53	---	68	67	188
IV-Urography	---	---	28	---	28
Pelvis	56	---	61	61	178
Skull ap/pa	66	---	73	61	200
Skull lateral	---	---	74	66	140
Thoracic Spine ap	---	---	---	45	45
Thoracic Spine lat	---	---	---	44	44
Lumbar Spine ap	---	---	---	57	57
Full spine (infants) / Lumbar Spine lat. (10 yrs)	44	---	---	60	104

Tab.1 Number of examinations in four dosimetric surveys on frequent X-ray examinations in paediatrics

ad 1.2.

Dose measurements were prepared, collected and analysed by the same three centres of the previous surveys: NRPB for UK, Ireland, Iceland and Scandinavia; USLN N^o7 for the Mediterranean area; and GSF for central Europe. The organisation and further analysis of the questionnaires on X-ray equipment, radiographic technique and film-reading was carried out in Munich Children's Clinic as the coordination centre.

Wide variations in ESD were also found in the last two surveys which were hardly less than those found in the first two surveys. Dose range varies for the different organs and is generally higher for younger patients. The minimum to maximum ratio from about 1:20 to 1:70 and decreases with age **Tab.2**.

Entrance Surface Dose median min - max ratio(min:max)	Infant (TLD I)	Infant (TLD II)	5 years (TLD III)	10 years (TLD IV)
Chest ap 1000 g (mobile)	45 11 - 386 1:35	87 31 - 395 1:13	---	---
Chest pa/ap	75 21 - 979 1:47	76 8 - 1373 1:171	64 19 - 1347 1:71	71 17 - 1157 1:68
Chest ap (mobile)	90 34 - 718 1:21	39 9 - 236 1:26	67 29 - 481 1:17	91 29 - 760 1:26
Chest lateral	---	---	141 37 - 666 1:18	153 39 - 1976 1:51
Abdomen ap	440 77 - 3210 1:42	---	518 56 - 2679 1:48	729 148 - 3981 1:27
IV-Urography	---	---	552 136 - 3600 1:26	---
Pelvis	260 18 - 1369 1:76	---	460 86 - 2785 1:32	812 89 - 4167 1:47
Skull ap/pa	930 152 - 4514 1:30	---	1006 242 - 5186 1:21	1036 130 - 5210 1:40
Skull lateral	---	---	713 138 - 3720 1:27	577 113 - 3767 1:33
Thoracic Spine ap	---	---	---	887 204 - 4312 1:21
Thoracic Spine lat	---	---	---	1629 303 - 6660 1:22
Lumbar Spine ap	---	---	---	1146 131 - 5685 1:43
Full Spine (infants) / Lumbar Spine lat (10yrs)	867 107 - 4351 1:41	---	---	2427 249 - 23465 1:94

Tab.2 Variation of entrance surface dose (ESD in μGy) in European children's hospitals: median, minimum/maximum values and corresponding ratio on frequent X-ray examinations in paediatric patients.

Dose histograms showed a relatively homogenous left skewed curve for all chest exams (stationary, mobile, lateral views) In addition, the dose distribution for the chest pa/ap was about the same for all three age groups (Fig.1). Two thirds of the ESD values are below 100 μ Gy. For the other organs ESDs were generally higher and more inhomogenously distributed This suggests that infants are subjected to considerably higher ESD relative to their size as compared with older children.

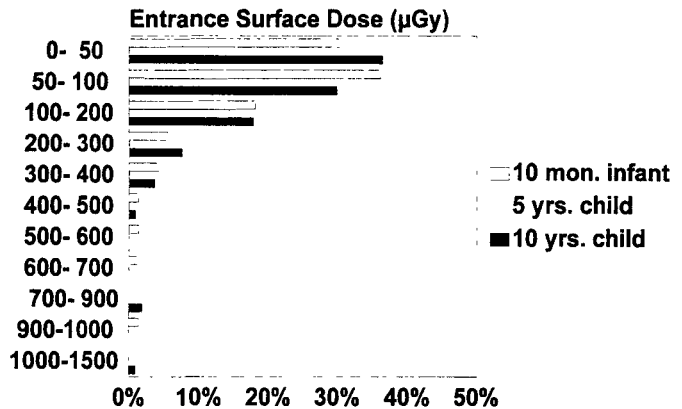


Fig.1 Chest pa/ap: Comparison of dose distribution for 3 survey age groups

There is a close relationship between ESD and radiographic technique, as was shown previously (Schneider et al. 1993). Tab.3 summarizes the breakdown of clinics fulfilling the Quality Criteria for good radiographic technique listed in the Working Document (only six criteria directly affecting dose were included in this analysis) for the survey of the five year old child. Only a few clinics fulfilled all of the criteria, the greater majority only 3 or 4 criteria. As in the infant study, it was also shown in these surveys of older children that the ESD can be significantly reduced when the “criteria for good radiographic technique” listed in the Working Document of the CEC are fulfilled.

	zero criteria		one criteria		two criteria		three criteria		four criteria		five criteria		six criteria	
	n	μ Gv	n	μ Gv	n	μ Gv	n	μ Gv	n	μ Gv	n	μ Gv	n	μ Gv
Chest pa/ap	--	--	--	--	8	143	13	193	40	80	18	54	6	25
Chest ap (mobile)	--	--	--	--	--	--	9	131	19	88	13	88	--	--
Chest lateral	--	--	1	120	3	273	14	246	30	214	17	103	4	53
Abdomen ap	--	--	--	--	2	386	10	1171	25	769	9	470	5	270
Pelvis	--	--	1	1085	9	1307	24	533	11	851	5	302	--	--
Skull ap/pa	--	--	--	--	2	1422	7	1558	24	1637	19	881	4	654
Skull lateral	--	--	--	--	1	435	10	1149	26	865	19	771	6	464

Tab.3 Frequency (n) of fulfillment of the criteria in good radiographic technique in the 5 years old child. The corresponding mean ESD values (μ Gy) are given.

Good radiographic technique is specifically defined for every X-ray examination in the Working Document. Among the most important are: kVp setting, use of a grid, additional filtration and high speed film-screen combinations (400-600). There is no need for anti-scatter grid, for chest X-rays of children under 8 years. Use of grid for these examinations is significantly associated with higher ESD (Fig.2). 25% of the hospitals use a grid for chest-X-ray of infants and nearly one half of the hospitals do this unnecessarily in the 5 years old.

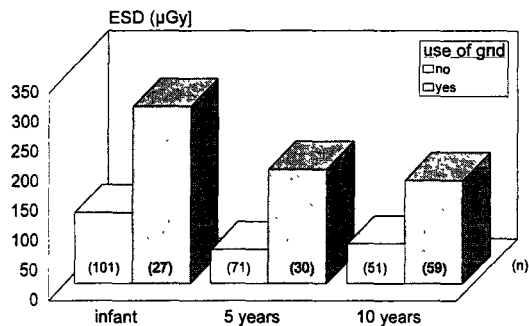


Fig.2 Chest pa/ap: Mean ESD for grid use; comparison of 3 survey age groups

In older children (10 yrs) a grid is necessary for the chest exams especially when a high kVp technique is used. These findings clearly demonstrates that the grid must be easily removable in order to save dose in children.

Another important technical parameter is correct kVp setting. Significant deviation of recommended kVp was seen in the infant study. In the last two surveys the set voltages were considerably different from the recommended values of the Working Document. Curiously, we found very low voltage settings for the pelvis. Only 15 to 25% of the clinics set kVp correctly between 70 and 80 kVp.

Most hospitals used kVp-values between 60 to 70 kVp. 40% of the departments used even lower settings for the pelvis of the 5 years old child. Settings of relatively high kVp, in the range between 70 and 80 is very important because the speed of rare earth screens is kVp-dependent and reaches the maximum at this range.

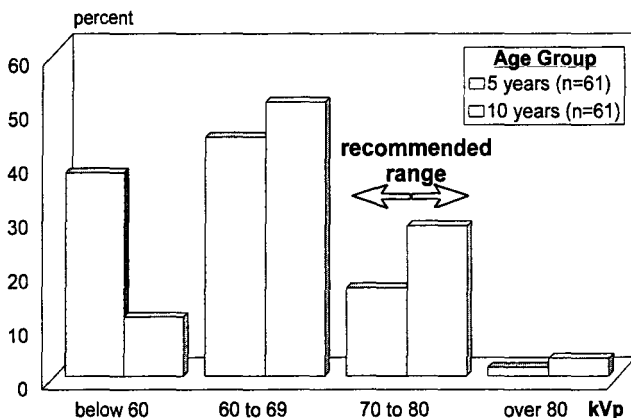


Fig.3 Pelvis ap: Distribution of kilovoltage settings. Comparison in two survey age groups. Recommended kVp-range indicated.

The rating of image quality of the original films from both studies in older children again showed that image quality is not negatively affected when radiographic criteria are fulfilled and ESD reduced. Each participating clinic received a feedback letter with their individual results (e.g. dose and image quality) in comparison total survey sample; this information could help to initiate optimisation measures, where necessary.

The most important aspect for dose reduction is the use of rare earth screens with a speed class >400. Using the example of skull X-rays of the 5 years old patient, one can see that practically only speed classes of this type were used for examinations with ESD below 700 μGy (Fig.4). The examinations with higher dose had a speed class of mostly 200, some even less. Two departments had higher ESD despite the use of high speed screens (>600).

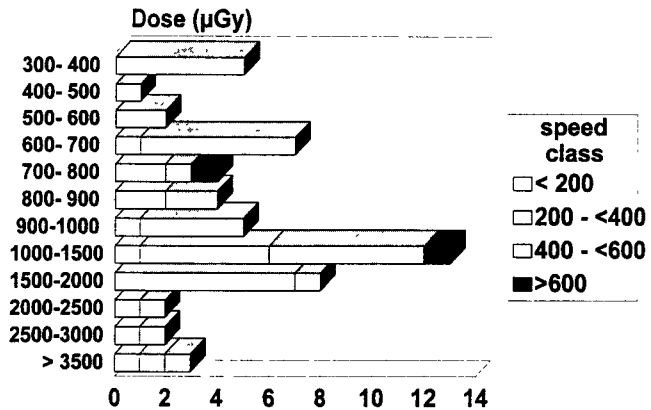


Fig.4 Skull ap/pa: ESD distribution and speed class in the 5 years old child.

There are still examinations with relatively high dose in spite of the use of high speed classes; this is somewhat due to low-voltage settings because rare earth screens have a lower amplification in the low kVp-range.

ad 1.3.

Besides beam quality and entrance surface dose, field size is also an important and easily measured parameter for patient exposure. Measurements of field size were made for the most frequent x-ray examination, chest pa/ap. A high percentage of these measurements could not be made because the field borders were outside of the exposed film edges. When the field size was measurable, the actual field area was compared to an "ideal" field size (as defined by the preamble of the Working Document). In prematures and infants only 10% were in the optimal range, 80% were above and 15 - 20% of measurable chest films had an extreme field between 200 and 300% of the ideal field. Similarly, up to 75% percentual field increase could be measured in the 5 years old child. Field size evaluation in the last survey of the 10 years old is in progress.

ad 1.4.

Based on the film reading experience, it was possible to revise the criteria of the "Working Document"; in some cases, elements were added, and in others rephrasing for more precision was made. Analysis of field size showed that the field borders have to be more exactly defined for an optimal collimation and patient positioning, especially for chest x-rays. This varies for the distinctive anatomy for different ages. In addition, the image quality criteria were extended to specific image details (e.g. visualisation of the hilar vessels in the lateral projection of the chest). Dose limits for the 5 and 10 years old child still have to be defined. The concepts of the optimal ("achievable") and tolerable ("reference") dose, as was implemented for infants, can also be used here.

ad 2.1.

The pilot dosimetric study in Bavaria in 43 clinics and private practises was completed and feedback letters were sent to all participants. Depending on the kVp settings and mAs, dose variation (measured with TLD free in the axis) varied between 23 and 150 mGy per slice for head examinations and 14.2 and 101.5 mGy for abdominal exams. A wide variation in dose was found in the same department or private practise for different examinations. Often the settings of the manufacturer were used with no or inadequate adaption to specific paediatric pathology. The study was not extended to the spiral CT technique.

ad 2.2.

Because CT is a high dose examination and there still are indications for this examination even in paediatric patients: Further dosimetric examinations were performed and correlated with the equipment settings and the image quality reached **Tab.5 and 6** (Dr A.E. Horwitz).

Dose	20.85 mGy	15.3 mGy	7.65 mGy
Voltage	140 kVp	120 kVp	120 kVp
Current	110 mAs	110 mAs	55 mAs
Slice thickness	1 mm	1 mm	1 mm
Image quality	sufficient	sufficient	sufficient

Tab.5 Chest: Dose free in air, equipment settings and image quality

Dose reduction is possible for lung CT-examinations. In one case reduction from 20.8 mGy to 7.65 mGy was achieved with no significant loss of image quality. However, this approach was not successful in abdominal CT. Similar dose reduction in abdominal examination would lead to considerable loss of diagnostic information, even with good opacification of the bowel and a good intravenous contrast. The overall results in the second studies showed,

that some decline in image quality (mottle) occurs and can be accepted. More studies on this topic are needed.

Dose	20.9 mGy	7.5 mGy	3.73 mGy
Voltage	120 kVp	90 kVp	90 kVp
Current	150 mAs	110 mAs	55 mAs
Slice thickness	6.5 mm	5 mm	5 mm
Image quality	sufficient	sufficient	insufficient
Tab.6 Abdomen: Dose free in air, equipment settings and image quality			

The analysis of the questionnaires and correlation with dose measurements showed:

- there are no standards for CT-technique for examinations of children,
- the variation in patient dose for comparable equipment in different departments is large,
- patient dose is basically determined by the CT company and the user trying to achieve high (optimal) image quality,
- the dose per slice is not dependent on equipment age.

ad.2.3

Quality criteria on computed tomography were developed as a draft document. It describes special problems in paediatrics. The paper should be revised and must include spiral CT technique as an important new modality of special importance for paediatric patients.

References

Drexler G, Schneider K.

Dose assessment in paediatric radiology.

Eur. Radiol. Suppl. 3:232 (1993).

Fichtner C, Schneider K, Freidhof C, Endemann B, Horwitz AE, Kohn MM, Fendel H.

Critical analysis of field size in chest x-rays of infants — a EC-wide survey in children's clinics.

Eur. Radiol. Suppl. 3:389 (1993).

Horwitz AE, Schneider K

Die besondere Bedeutung des Strahlenschutzes in der Kinderradiologie: Derzeitiger Stand und neuere Entwicklungen

Radiologe Suppl.1, 35:129 (1995).

Horwitz AE, Schneider K, Kohn MM, Freidhof C, Endemann B, Ernst G, Scheurer C, Panzer W, Menzel ML

Patient dose in paediatric computed tomographic examinations. Results from a pilot field study in Bavaria.

Pediatr. Radiol. 24:447 (1994).

Schneider K, Fendel H, Bakowski C, Stein E, Kohn MM, Kellner M, Schweighofer K, Cartagena G, Padovani R, Panzer W, Scheurer C, Wall B.

Results of a dosimetric study in the European Community on frequent x-ray examinations in infants.

Radiation Protection Dosimetry 43:31-36, (1992).

Schneider K, Kohn MM, Bakowski C, Stein E, Freidhof C, Horwitz AE, Padovani R, Wall B, Panzer W, Fendel H.

Impact of radiographic imaging criteria on dose and image quality in infants in an EC-wide survey.

Radiation Protection Dosimetry 49:73-77 (1993)

Schneider K, Fichtner C, Horwitz AE, Kohn MM, Endemann B

Analysis of field size in chest radiographs of premature babies and older infants

Pediatr. Radiol. 24:465 (1994).

Schneider K, Kohn MM, Endemann B, Ernst G, Panzer W, Padovani R, Wall B.

Variation in radiation dose and image quality of common X-rays of the five years old child - A European wide survey in children's clinics. Eur Radiol. Suppl. 5:192 (1995).

Schneider K

Qualitätssicherung in der Kinderradiologie

Radiologe Suppl.1, 35:129 (1995).

Schneider K

Evolution of Quality Assurance in Paediatric Radiology. Radiation Protection Dosimetry 57:119-125 (1995)

Head of project 4: Dr. B.M. Moores

II. Objectives for the reporting period

1. To co-ordinate the development of Quality Criteria for paediatric radiology with the development of existing criteria for the adult.
2. To assess the framework of existing criteria in terms of the relevant relationships between image quality, radiographic factors and patient dose.
3. To assess effective routine patient dose assessment strategies for both paediatric and adult examinations, both radiographic and fluoroscopic techniques.

III. Progress achieved including publications

A project to develop strong links between the development of Quality Criteria for both the adult and paediatric patients was established within the framework of contract F13P-CT92-0020 for the duration of the supplementary agreement 01.06.1994 to 30.06.1995 and the work undertaken in this project is presented here.

In 1991 a European wide trial was undertaken of the CEC Quality Criteria for Radiographic Images. Three types of radiographic examinations of the adult patient were included; chest, lumbar spine and breast. A preliminary analysis and evaluation of the results of the Trial was produced by CAATS in April 1993 and a CEC Working Party was set up in February 1994 in order to undertake further detailed analysis of these results. One of the main aims of this analysis was to highlight possible deficiencies in the Quality Criteria which could be corrected in the light of new findings.

Detailed analysis of this data was undertaken throughout the latter part of 1994 and results presented in three parts

- Radiographic technique
- Patient dose
- Image quality

A study of the relevant published literature was also undertaken in order to develop a more comprehensive scientific framework and basis for the Quality Criteria Document.

In the light of the results of this study a Working Party was set up in June 1995 in order to revise the existing Quality Criteria Document for the adult patient. This revision took place in the period June to September 1995 and involved a complete restructuring of the Document.

The Quality Criteria of radiographic images of the original six examinations of the adult patient were themselves modified in the light of the detailed analysis of the 1991 Trial data and other published findings. A second section was included which provided a detailed review of the results of the two previous European wide trials of the Criteria which had already been performed. The purpose of this section was to provide a detailed scientific background to the Quality Criteria for the reader. Finally a section was included which provided advice and guidance on

implementation of the Criteria as an audit process. Included in this section were data sheets which had been developed during the trials of the Quality Criteria. In particular data sheets which had been developed by the expert panel of radiologists involved in assessing the radiographic images for the 1991 Trial were included. The revised document is now available for publication at the end of 1995.

In order to ensure effective co-ordination of the development of the Quality Criteria for both the adult and paediatric patients operational links were established with the Paediatric Group operating under contract F13P-CT92-0020. A review of the situation in paediatric radiography indicated two important differences between it and the adult domain.

- The paediatric patient covers a wide range of anatomical variations due to natural growth.
- Doses are generally much lower for paediatric examinations than for adult patients and dosimetric techniques need careful consideration.

Notwithstanding any differences between the adult and paediatric situations it was decided that it was desirable and possible for the Quality Criteria Documents for both adult and paediatric patients to be complimentary and presented in the same overall format. Consequently a redraft of the paediatric document is underway utilising the experience gained in development of the adult document. A Working Party has been established to revise and update the paediatric document as well as review the present situation. This involved a detailed analysis of all trials and auxiliary scientific studies. These results are being incorporated into the revised version.

A supporting study undertaken as part of the present contract has involved the assessment of routine patient dose measurements for both paediatric and adult x-ray examinations. In particular to try and establish a framework whereby the dose delivered to a patient can be directly related to the radiographic factors employed. The study involved comparing dose measurement undertaken by:-

- Thermoluminescent dosimeters employing Lithium Fluoride
- Calibrating the x-ray generator and calculating the entrance surface dose from the radiographic exposure factors

Two examinations were studied, AP abdomen and PA chest. Although undertaken on adult patients the study was relevant to the paediatric situation since entrance surface doses for chest examinations are in many cases very small, analogous to the situation which exists for paediatric examinations. The study involved over 100 abdominal and 500 chest x-ray examinations.

Excellent agreement was observed between the TLD and calculated entrance surface dose values measured for the abdomen. This is indicated in Figure 1. And Table 2. However, for the chest examinations this was not the case as shown in Table 1. The reason for this discrepancy most probably lies in the fact that the

entrance surface dose values for the chest x-ray examinations is relatively low and therefore close to the limits of the sensitivity of the TLD material.

This is indicated more clearly in Table 3. which compares the calculated entrance surface dose values in the study with other UK studies. The lowest measured values were 20 μGy which corresponds roughly to the threshold dose level for lithium Fluoride dosimeters which have been annealed completely.

Another comparative dosimetry exercise was undertaken at Alder Hey Children's Hospital as part of a locally funded project. In this study three dosimetric techniques were compared in paediatric cardiac catheterisation procedures. The three methods were:

- Dose-area product meter
- Thermo-luminescent dosimeter (TLD)
- Calculated entrance surface dose from calibrated radiographic factors

In this study also the TLD measurements were often erroneous due to the small x-ray field sizes employed and the fact that the dosimeter was not always located in the x-ray field. Excellent correlation was observed between the dose-area product measurements and calculated values when taking reasonable account of the x-ray field sizes employed [McDonald (1993)].

The following conclusions may be drawn from work undertaken:-

- The structure and format of Quality Criteria for Paediatric Radiography should be similar to those developed for the adult patient.
- In order to reduce, as much as possible, effects due to anatomical variations created by the maturing paediatric patients a clear framework for categorising this type of patients e.g. height, weight, age etc needs to be developed.
- Accurate dosimetric techniques, which permit the assessment of entrance surface dose for each individual paediatric patient need to be implemented

REFERENCES

Harrison R.M., Clayton C.B., Day M.J., Owen M.B. and York M.F. 1983. A Survey of radiation doses to patients in five common examination. *British Journal of Radiology*. 56, 383-395.

McDonald E.A. 1993. The assessment of suitability of radiation dosimetry method in paediatric cardiac catheterisation. MSc Thesis, University of Liverpool.

Shrimpton P.C., Wall B.F., Jones D.G., Fisher E.S., Hiller M.C., Kendall G.M., Harrison R.M. 1986. A national survey of doses of patients undergoing a selection of routine x-ray examination in English hospitals. NRPB Report 200.

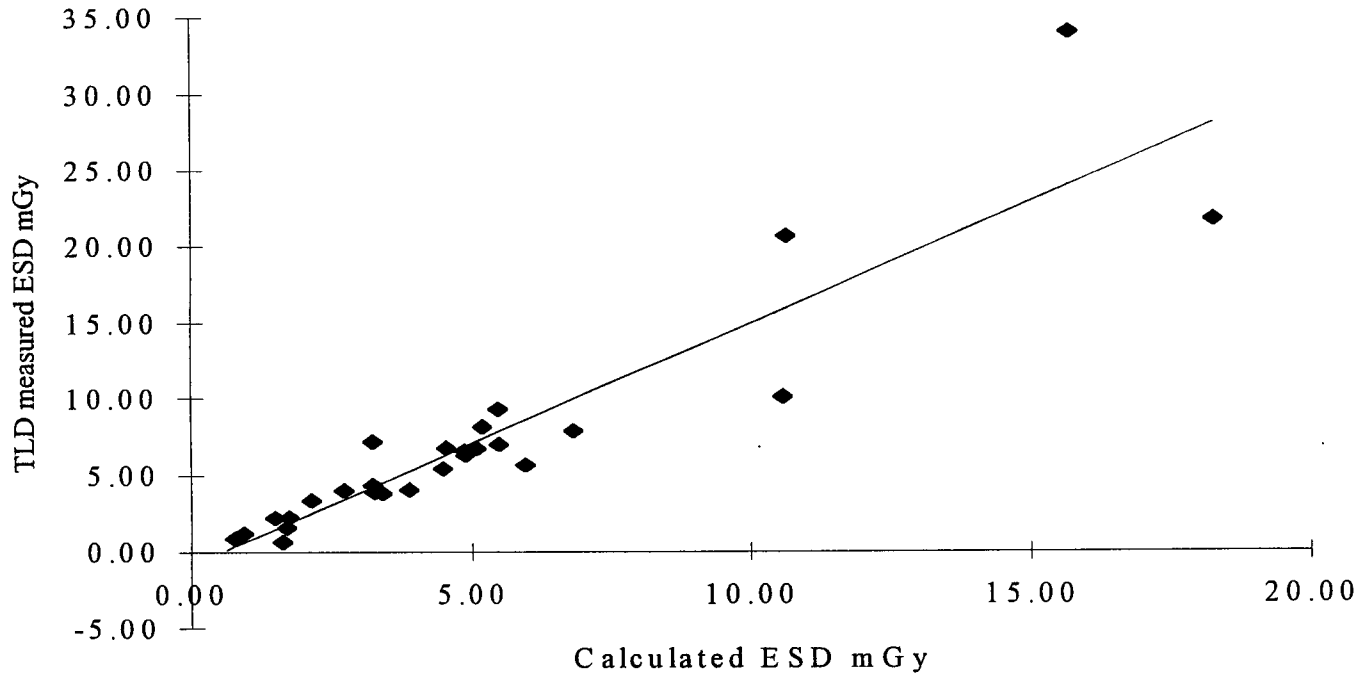


Figure 1: XY scatter plot TLD vs Calculation - AP abdomen exam

Table 1: Correlation coefficient TLD vs Calculation - PA chest

Correlation Coefficient	0.13
Standard error	0.08
Intercept	0.11
Gradient	0.18

Table 2: Correlation coefficient TLD vs Calculation - AP abdomen

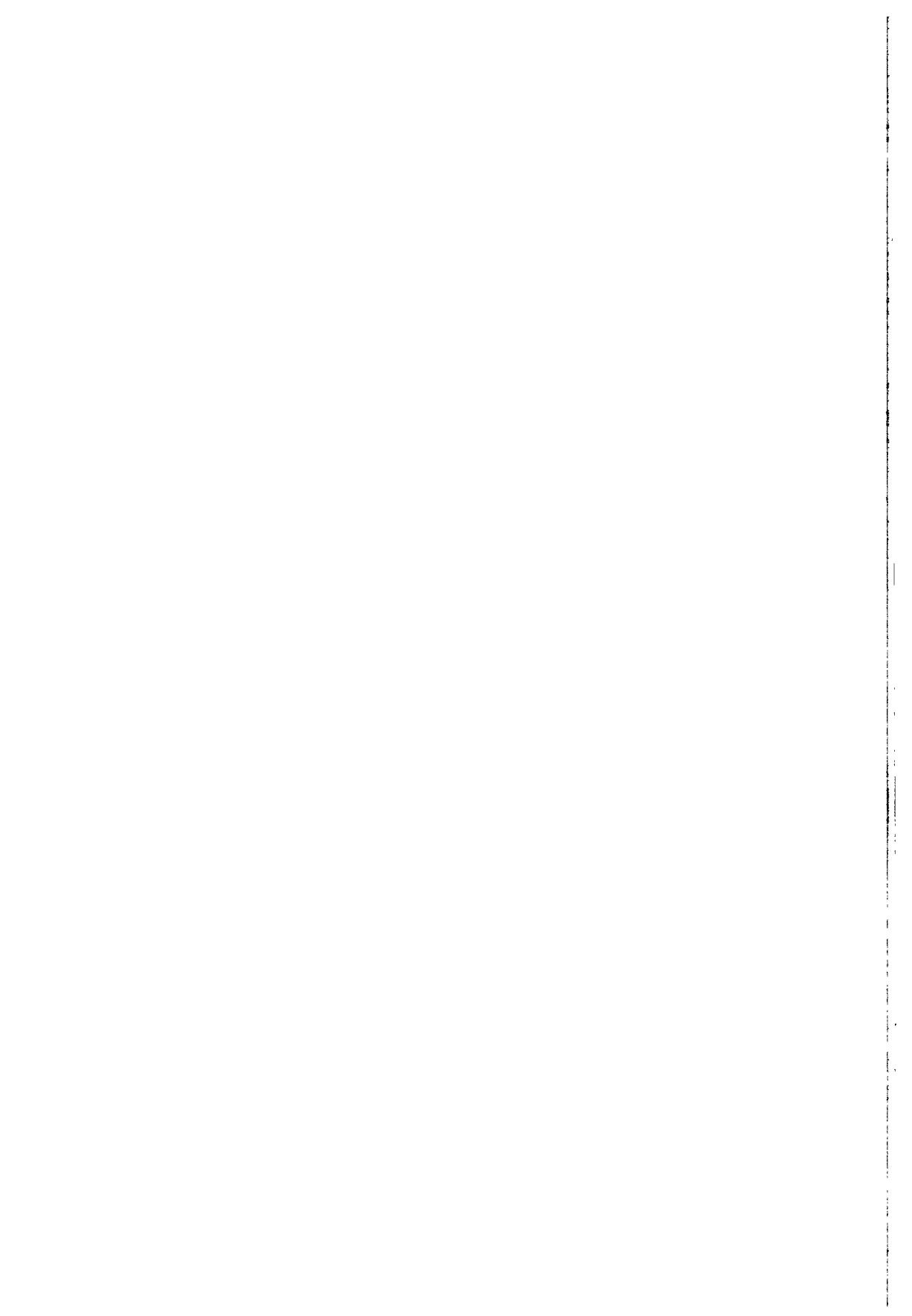
Correlation Coefficient	0.91
Standard error	3.01
Intercept	-0.82
Gradient	1.57

Table 3: Comparison of calculated entrance surface dose (mGy) between this study and other workers. - PA chest

Statistic	This study	Shrimpton et al	Harrison et al
Mean	0.10	0.23	0.22
Standard Deviation	0.05	0.18	N.A.
3rd Quartile	0.12	0.26	
Minimum	0.02	0.03	0.10
Maximum	0.68	1.43	0.39
Range Factor	34	47.7	4

Table 4: Comparison of calculated entrance surface dose (mGy) between this study and other workers. - AP abdomen

Statistic	This study	Shrimpton et al
Mean	3.80	8.43
Standard Deviation	2.81	6.08
3rd Quartile	4.78	10.78
Minimum	0.27	0.71
Maximum	18.3	62.41
Range Factor	67.7	87.9



**Final Report
1992 - 1994**

Contract: F13PCT920024

Duration: 1.9.92 to 30.6.95

Sector C22

Title: Diagnosis related dose: an investigation on patient risk and image quality in European hospitals.

- | | |
|--------------|----------------------|
| 1) Van Loon | Univ. Brussels (VUB) |
| 2) Thijssen | Univ. Nijmegen |
| 3) Milu | IHPH |
| 4) Karlinger | SUM |

I. Summary of Project Global Objectives and Achievements

Objectives

The main sources of low dose radiation to the European population are the medical diagnostic examinations in radiology and nuclear medicine. The amount of radiation given before a certain diagnosis is made, depends on factors of medical, technical and/or organisational character.

- In the medical sector there is the justification of an examination and the protocol leading to a diagnosis. Little work has been done so far on the influence of these items on the dose.
- In the technical sector numerous variables are identified and much effort is involved to study the effects of quality assurance and to establish guidelines for the improvement of image quality and the reduction of patient dose.
- In the organisational sector a series of intrinsic and logistic factors - e.g. factors that are linked to the differences in the organisation of the health services- can influence an optimum cost/benefit relation.

The goal of the project was to relate the doses and therefore the risk to those three factors in order to establish an optimised diagnosis in different European hospitals. The method used was the concept of diagnostic groups (DGs): a DG is the set of examinations and procedures that has led to one and the same diagnosis. The pilot study "Diagnosis Related Dose" ¹ showed that a DG can be established and clearly described- at least for some diagnoses - and that the elements determining the dose can be retrieved.

To compare the risk to the patient of different pathways leading to a given diagnosis the "effective dose" as defined by the ICRP ² was chosen as the common factor. The quality of the radiological image and therefore the diagnostic power of the examination strongly depends on the dose. The quality of the image was, therefore, taken into account in the comparison.

The research work consisted of the following parts:

- Collection of information on examinations and procedures used to set the diagnoses "Lumbar Hernia Discalis" and "Renal Cell Carcinoma" by the contractors and the three subcontractors in Madrid, Paris and Udine.
- Collection of the same data in two centres for a third diagnosis in the paediatric field, "Vesico-Ureteral Reflux".
- Measurement of entrance doses, image quality and additional relevant parameters of all radiological equipment involved in two DGs, Renal Cell Carcinoma and Lumbar Hernia Discalis.
- Processing of the data on examination types, patient dose and image quality. The influence of the type of examinations, the equipment used and the examination parameters set, on the total dose to the patient and the quality of the images was examined,
- Evaluation of the dosimetric and image quality results by all participating centres. Special attention was given to medical, technical and social aspects that could lead to the differences in diagnostic pathways and patient doses.

Method

Patient data collection:

Relevant data were collected for three DGs: Renal Cell Carcinoma (7 centres), Lumbar Hernia Discalis (7 centres) and Vesico Ureteral Reflux (2 centres).

The procedure of data collection was identical for all DGs. For each DG up to 40 files per centre

¹ CEC, DGXII, Radiation Protection Programme, Programme 1990-91, Sector C22 Contract B17-054.

² ICRP (1991), '1990 Recommendations of the International Commission on Radiological Protection', ICRP publication 60, Pergamon Press.

Renal Cell Carcinoma (Detection by imaging procedures using ionising radiation, resulting in surgical treatment of a RCC)	Lumbar Hernia Discalis Detection by imaging procedures using ionising radiation and resulting in surgical treatment.	Vesico Ureteral Reflux Detection and grading by imaging procedures using radiation and resulting in either medical or surgical treatment.
<u>Golden Standard:</u> Surgical and histological proof.	Hernia Discalis proved by operation. (Operation protocol).	Radiological proof and precise grading according to the International System of Radiographic Grading of Vesico Ureteral Reflux.
<u>Exit point:</u> Surgical treatment of Renal Cell Carcinoma.	Surgical treatment of the hernia.	Decision of either medical (for lower grades) or surgical (for higher grades) treatment.
<u>Entry point:</u> First radiological examination following initial complaints or first examination demonstrating RCC as incidental finding. The first examination must be performed between January 1. 1988 and December 31. 1992.	First radiological examination following the complaints of e.g. lower back pain (LBP) or sciatalgy. In case of chronic LBP we take into account examinations of up to one year before surgery. The first examination must be performed between January 1. 1988 and December 31. 1992.	First imaging examination following first proven urinary tract infection in boys and recurrent infection or infection due to an unusual bacterial agent in girls. The first examination must be performed between February 1. 1994 and February 1. 1995. The patient must be younger than 6 years.
<u>Criteria of exclusion:</u> Radiological examination not available or incomplete for review.	Radiological examination not available or incomplete for review. We will also exclude patients who already had surgery for a hernia discalis.	Radiological examination not available or incomplete for review.
<u>Examinations to be retrieved for dosimetric study:</u> All techniques involving ionising radiation (Conventional Radiography, CT, Angiography, Nuclear Medicine), MRI and Ultrasound. Examinations performed in another centre or private practice will be included with technical factors in the participating centre.		
<u>Data collection:</u> Collection of relevant information on a data sheet.		
<ul style="list-style-type: none"> -patient identification -chronological enumeration of all the radiological examinations as stated above -technical data (physics) -exposure data including beam direction, Field Of View (FOV), Film-Focus Distance (FFD), kV and number of films exposed. 		

Table 1 Selection Criteria for the three Diagnostic Groups

of patients matching the criteria of table 1 were collected by a medical doctor. In some countries different hospitals supplied data for the different DGs.

For every patient file a chronological list of all examinations performed during the diagnostic process was established: those where ionising radiation was involved as well as other diagnostic tools such as MR and Ultrasound.

For every DG the examinations involving ionising radiation (Radiography, Angiography, CT and Nuclear Medicine) that are performed on at least 10% of the patients information about exposures and equipment properties was collected. The exact parameters used to examine the specific patient were seldom available at a department. A 'standard examination', consisting of the examination room, number of exposures, film size etc. was either available or was obtained by interviewing the technologists who perform the specific examination routinely. The technical specifications for every system used for the examinations were collected. A database system was established by the Brussels team, to allow processing of the patient and, in a later stage, dosimetric data.

Dose and Image Quality Evaluation:

A protocol for dosimetric measurements was defined by the teams in Nijmegen and Brussels. To be independent of patient geometry, dose measurements were performed on a flat perspex-aluminium phantom for conventional radiological examinations. The Nijmegen team developed the set of test objects for the most important radiographic views. For CT the CTDI was measured free in air in the centre of the gantry

The measurements were performed with TLD LiF-100 chips. The calibration and read-out was done in Nijmegen. The team in Brussels calculated the effective dose for every examination type

in all centres using the information of the dose measurements and tables with organ doses from the NRPB³. To correct the absorbed doses for the energy spectrum of the beam used, high voltage and beam filtration for all the equipment involved in the different departments were measured by the teams of Brussels and Nijmegen. By combining the effective dose per examination with the number of examinations per patient the mean total effective dose per patient for the whole diagnostic path can be calculated.

When measuring dose, the image quality of the system was determined at standardized conditions. For radiography equipment a Contrast Detail test object is used which allows the introduction of the Image Quality Figure⁴ for a quantification of the image quality for conventional radiological techniques. For CT examinations the noise in the image was used as the figure for the image quality. The Nijmegen team developed a system to select for every radiological technique the system with the optimal dose-image quality relation. This information and the results of additional experiments facilitate the separation of the influences of technical specifications of the equipment and of parameters set at the console on patient dose and image quality.

Results

During the data collection large discrepancies were observed between local protocols and the daily routine at a department.

Comparison of the patient data shows that there are important differences in the diagnostic strategies between the different centres for all three diagnoses. The number of examinations per patient, the choice of examination type and the way the examinations are performed vary between the centres. These differences are most striking for the DG Renal Cell Carcinoma. Between 2 and 16 examinations per patient are observed, while the mean number of examinations per patient varies from 3.5 to 7.4 between the centres for this DG.

For the DG Lumbar Hernia Discalis the mean number of patients differs from 3.3 till 5.5 and from 3.1 to 7.1 for the DG Vesico Ureteral Reflux.

It is noted that at some centres a protocol is used to set a diagnosis. This leads to a restricted number of examination types. Other centres use a very broad range of examinations. The DG Renal Cell carcinoma contains from 7 to 24 examination types for the different centres. For the DGs Lumbar Hernia Discalis and Vesico-Ureteral Reflux these numbers go from 7 to 13 and from 3 to 9 respectively.

The parameters used to perform a specific examination differ between the centres. Differences are observed in the number of films, the number of CT slices, the kVp, the use of the Automatic Exposure Control and in the technical specifications of the equipment. All these differences influence the total effective dose to the patient for the examination and the quality of the images. Differences in effective dose per examination from a factor of 2 (Myelography) up to 10 (Angiography) or even 40 (Chest) are noted.

The variation between the centres in the frequency of examinations per patient and in the effective doses per examination lead to differences in the mean effective dose per patient used to set a diagnosis. For the Renal Cell Carcinoma this dose differs by a factor of 4, for the Lumbar Hernia Discalis a factor of 6.

When the mean effective dose per patient per centre is calculated using dose data from 'reference equipment' (i.e. the dose per examination is only influenced by the medical practice; number of films/slices, fluoroscopy time) the relative differences between the centres are more or less the same as with the local equipment.

No correlation is found between the results of this study and the quality indicators for 'good radiological practice' as described in the CFC document⁵.

Evaluation Results

The results of the DRD-project were internally discussed by the medical and technical staff in the participating centres. A final evaluation was organized with representatives of 6 of the 7 centres. Reactions were given on the results by all participants.

³ Jones DG, Wall BF (1985), 'Organ doses from medical X-ray examinations calculated using Monte Carlo techniques', NRPB report 186 and personal communication.

And: Jones DG, Shrimpton PC (1991), 'Normalised organ doses for X-ray computed tomography calculated using Monte Carlo techniques' NRPB software SR250.

⁴ Thijssen MAO et al. . 'A definition of Image Quality', British Institute of Radiology, Report 20, p29-34 (1989), London.

⁵ CEC (1990), 'CEC quality criteria for diagnostic radiographic images and patient exposure trial', report EUR 12952.

- *Differences in numbers and types of examinations between the countries.*
All agree that the availability of equipment is one main reason for differences in types of examinations. But also the history, organisation and culture of the department are mentioned. And the experience of radiologists and radiographers with certain types of examinations lead to a preferential choice for these types. There are also differences in protocols used by radiologists and referring physicians. Some radiologists find the differences relatively small.
- *Justification of examinations.*
One centre is convinced that it is rare for an examination not to give extra information. Sometimes an examination is performed by a radiologist, doubting the value of the result. The examination is still performed when the frequency is low and when the radiologist has confidence in the referring physician. Justification in general depends strongly on the relation between the radiologist and the referring specialist.
Due to time limitations sometimes examinations are performed before having evaluated the results of the previous ones.
In one centre some routine examinations, like pre-operative chest X-ray, have been skipped after discussion with the specialists.
- *Differences in number of films, CT-slices, Fluoroscopy time etc.*
The position of the examination in the protocol determines the exact composition of the examination (e.g. the number of CT slices, the slice thickness or number of films).
The experience of the radiologist and his attitude towards radiation protection strongly influence the number of films and especially the time of fluoroscopy.
The number of films is often fixed in a local protocol and this number depends in some countries on reimbursement regulations.
- *The use of a pre-set protocol.*
A very rigid protocol is not recommended by the participants. A protocol with a branching structure is proposed. Depending on the results of former examinations extra examinations are performed. It is recognised that such a structure is more time consuming and not easily applicable in daily practice in most of the hospitals.
- *The influence of "external" parameters on the dose.*
The organisation of the department often obliges referring physicians to ask for several examinations in one time. These examinations are performed without waiting for the results of former ones. The relation between radiologist and referring specialist is very important in this. When the radiologist is involved in the discussion about the most appropriate diagnostic strategy, optimisation of the patient dose is possible. When the specialist defines the strategy himself, the influence of the radiologist can be very restricted.
Availability and location of equipment determines the steps in the decision tree. When non-ionising techniques can be used without loss of essential information, a choice is possible.
In some countries some examinations are only reimbursed when a prescribed number of films is used, or e.g. for CT, when a contrast medium is used. In some countries the radiologist is only reimbursed for examinations that are officially requested by the referring physician. The amount of reimbursement is then independent of the examination time, number of films, etc.
- *The choice of the examination type and the way in which the examinations are carried out seem to have a large influence on the total dose to the patient.*
Possibilities to decrease the patient dose.
The above mentioned accomplishment of diagnostic protocols can be a good procedure. The staff responsible for certain types of equipment must be highly experienced with the type of system. The presence and direct supervision of the radiologist, with experience in topics of radiological protection and the permanency of well trained radiographers- with specific training in radiological protection- in the same workplace is advisable.
Periodic patient dose surveys, reporting the results to the radiology department staff, and comparing them with local, national and international reference values are valuable.
In one centre it is recommended to exchange myelography by MRI. Attention has to be given to the number of films in the protocol.
It is generally recognised that the diagnostic protocol is insufficiently questioned internally in most hospitals. Multidisciplinary reflection on that field must be encouraged.

Conclusions and Recommendations

- The method of DGs and the dosimetric system developed has proved to be a powerful tool to compare the radiological practice in different centres.
- It has been possible to study the influence of the choice of the radiological techniques, the quality of the radiological equipment, and the examination parameters on the effective dose to the patient.
- Important differences are detected in the radiological strategies used to set the three diagnoses; Renal Cell Carcinoma, Lumbar Hernia Discalis and Vesico Ureteral Reflux in Children in the co-operating centres. These differences are detected in the field of the choice of the examination type, the number of examinations performed, the way the examinations are performed and the technical specifications of the equipment.
- The above mentioned differences have all an important influence on the total effective dose to the patient. The mean dose per patient differs up to a factor of 6 between the centres for one diagnosis.
- The availability of equipment is one main reason for differences in the choice of examination types. Modern diagnostic techniques can, in some situations, reduce the dose considerable. e.g. MRI can replace Myelography.
- As the main reasons for differences in the total dose to the patient from a diagnostic path we clearly observed the choice of the examination types and the way these examinations are performed (number of slices, fluoroscopy time etc.).
- In the chain of examinations of a diagnostic process one complex radiological examination (Angiography, Myelography or CT) can contribute for up to 80% of the total effective dose to the patient. Attention should, therefore, be given to the optimisation, Quality Control and use of these types of examinations.
- 'External parameters' as reimbursement regulations have an important influence on the total dose to the patient. An obligated minimal number of films can lead to a doubling of the dose to the patient. The reported practices showed that these regulations often intervene with complex examination types (CT abdomen, Myelography, IVU) and have, therefore, a severe effect on the dose to the patient.
- It is generally recognised by the representatives in the co-operating centres that the diagnostic protocols are insufficiently questioned internally in most hospitals. However, due to the magnitude and complexity of the task pertaining to the conclusions mentioned above, a multidisciplinary discussion on diagnosis related techniques is necessary. Efforts should be made to increase the awareness of radiologists towards the dosimetric impact of the examinations they perform on their patients. It is recommended that at all discussions on radiological techniques (e.g. at ECR) a discussion and evaluation of the dosimetric consequences is included.
- Confronting radiologists with the way their confrères work could be one way of changing their attitude towards radiological protection.
- It would be advisable to implement software in new equipment that gives, at every image, information about the dose for the patient for the whole examination, i.e. dose not only for that image, but for all films or CT-slices and fluoroscopy used. When information about patient examinations is recorded it should contain information about all films, CT slices etc., not only those that are finally used for the diagnosis.

Head of project 1: Prof. Van Loon

II. Objectives for the reporting period

- Development of protocols for the collection of patient information and the measurement of dose and additional technical parameters of the equipment. Assistance to the measurements of physical parameters and patient dose in the subcontractors' institutes for the DGs Renal Cell Carcinoma and Lumbar Hernia Discalis, to warrant a coherent evaluation of dose, risk and image quality.
- Description, test, and collection of data in at least two centres for one extra DG, Vesico Ureteral Reflux in children.
- Calculation of absorbed dose from skin-dose for different radiological techniques used. If possible, assessment of radiation risk per examination and per patient.
- Development of a database to analyse the data on patient dose and examination techniques.
- Comparison of the results on patient dose and radiological techniques with the "CEC quality criteria for diagnostic radiographic images"¹.
- Inventory, comparison and interpretation of the variations observed in the examinations and procedures of DGs in the participating centres.
- Evaluation of the method.

III. Progress achieved.

Methods

1. *Development of protocols.*

A first protocol was developed to collect in an unambiguous way information on patients, examinations and equipment in the different co-operating centres.

After thorough discussion it was decided to collect the information on patients retrospective. A prospective study would require too much time and work (follow up of patients).

A second protocol defined the procedures to collect information on beam quality, patient dose and the image quality of the equipment used.

- 1.1. In a first stage, information was collected by the staff of the co-operating centres about the examination types used to establish one of the diagnoses under consideration. For this purpose a set of data forms was prepared. A test-run of these forms was first made in the centres of Nijmegen and Brussels. Afterwards these forms were sent to the other contractors and subcontractors accompanied by a document explaining the procedure of the data collection.

For each DG, information that matched the criteria for the DG (see table 1 of part I) from patient files was selected. This selection is made by a medical doctor. The statistics required a total of files from 40 patients per DG per centre. If more files were available the most recent ones were chosen.

For every patient file selected, a data sheet was completed. Required data: a patient reference, the diagnostic group, date of birth, sex., initial complaints (if available) and the 'diagnostic path': i.e. a chronological list of all examinations where ionising radiation was involved as well as MR and Ultrasound, performed during the diagnostic process. Date, examination type, and remarks (if any) are given for every examination.

From all examinations mentioned, except Ultrasound and MR, information about exposure modalities and equipment properties are collected. This information was used for dose calculation purposes. To limit the amount of work, only those examination types involving ionising radiation (Radiography, Angiography, CT and Nuclear Medicine) that were performed to at least 10% of the patients in one DG were considered. MR and Ultrasound are mentioned to register alternative examination protocols. The examination information consists of the number of films, slices or frames, film sizes and field position used during the examination.

Finally for all equipment used, technical specifications were collected.

- 1.2. In co-operation with the team in Nijmegen a protocol was defined to measure patient dose and quality of the radiological images. This protocol defined clearly for three radiological techniques (conventional radiology, Angiography, and Computed Radiology) the different parameters to be collected.

- For all radiography equipment the tube voltage was tested for all relevant values used for the

¹ CEC (1990), 'CEC quality criteria for diagnostic radiographic images and patient exposure trial', report EUR 12952.

examinations selected. This information is used to correct the calculations of the absorbed doses to the patient. For the same purpose the Half Value Layer was determined at all radiographic equipment. Also the tube voltage set at the console was determined giving an effective tube voltage of 125 kVp for chest radiography or 75 kVp for other examinations. This information is used for the assessment of the image quality. The measurements were performed with an RTI® Digi-X Plus kilovoltage Detector.

- Whenever possible the sensitometric curve of the film and the processor used were determined.
- For all exposure modalities used on all equipment dose measurements were performed. For conventional radiography and angiography equipment the patient entrance skin dose was measured on flat Perspex-Aluminium test objects with TLD LiF-100 chips. The composition of the test-object depended on the radiological projection under investigation. The development of these test objects and the different compositions are described by the team of Nijmegen.

For CT equipment the CTDI was measured free in air in the centre of the gantry using 15 or 30 TLD chips in a thin tube as described by the NRPB ². The measurements were performed for all slice thicknesses used in clinical routine.

- Image quality measurements were performed under standardized conditions at all equipment. This part of the work was co-ordinated by the team of Nijmegen and is reported by them.

The measurements were performed in all centres by the teams of Brussels and Nijmegen together to warrant a consistent collection of the data.

1.3. Selection criteria were defined for patient files for a third diagnosis in paediatrics, Vesico Ureteral Reflux. These criteria can be found in table 1 of part I of this report. In two centres information from patient files was collected for this DG. No dosimetry measurements have been performed.

2. Calculation of risk for the patient per examination

The effective dose as defined by the ICRP, in report Nr. 60 ³, was chosen as the quantity to evaluate the impact of ionising radiation from the different diagnostic strategies. This quantity can be assessed for all different techniques used; conventional radiology, CT and Nuclear Medicine, and the results can be cumulated for comparison of the total risk to the patient. To calculate the effective doses for all examinations involved in the different diagnostic paths, organ doses were derived for all projections and all parameter settings used in the co-operating institutes. This was done using the entrance surface dose and CTDI data and the data sets calculated by the NRPB for conventional ⁴ and CT radiology ².

The input parameters for the calculation of the organ doses for conventional radiological techniques were: the radiological projection, the tube voltage and the tube filtration as measured on the equipment, and the entrance surface dose including backscatter as measured on the test object. The NRPB data-set contains data for all organs contributing to the effective dose as defined by the ICRP.

In some cases the beam geometry used in one of the centres did not coincide with the one used by the NRPB. Three projections used in the participating centres were not available in the data set: the Lumbar Spine PA, the Lumbar Sacral Joint AP and the Lumbar Sacral Joint PA projection. For the Lumbar Sacral Joint projections the Lumbar Spine data PA were used. To estimate the organ doses for a Lumbar Spine PA projection instead of AP, a correction was made based on the results from the AP and PA views for abdomen and kidneys.

Input parameters for organ dose calculations for CT examinations were: scanner type, nominal slice thickness, number of slices, table increment, position of the central slice at the patient, mAs and the normalised CTDI in the centre of the gantry, free-in-air. The NRPB tables supply data for most of the organs necessary to calculate the effective dose. The mean body dose was taken as the dose to the muscles. For 3 of the 11 scanners, installed at the participating centres, no NRPB data were available. In those cases the effective dose was taken as the mean of the effective doses calculated from the data of the scanners used in the other centres.

3. Development of a Database

To handle and process the information derived from patient files, equipment specifications, and data from dose and quality control measurements, a database was developed based on the Claris®

² Jones DG and Shrimpton PC (1991), 'Normalised organ doses for X-ray Computed Tomography calculated using Monte Carlo techniques', NRPB software **SR250**.

³ ICRP (1991), '1990 Recommendations of the International Commission on Radiological Protection', ICRP publication **60**, Pergamon Press.

⁴ Jones DG and Wall BF (1985), 'Organ doses for medical X-ray examinations calculated using Monte Carlo techniques', NRPB report **R186** and personal communication.

Filemaker Pro programme. The structure of the database consisted of three files; one with the different diagnostic paths from patient files, a second with information on examination modalities in the different centres, including the effective dose per exposure and information on the image quality. The third file contains technical information on the equipment.

The information in the different files is linked by codes, depending on the centre, diagnostic group, radiological technique (radiology, Angiography, CT or Nuclear Medicine), and examination type. Information can be derived from the system about the number of examinations per patient, the examination types used, the effective dose per examination in the different centres and the effective dose per diagnostic path for the different patients. In figure 1 the structure of the data collection process and the database is drawn.

4. Comparison of results with the CEC quality criteria.

The CEC document defines 'criteria for good radiological practice' for a number of examination types. Table 1 lists these criteria for the examination types for which data are available from the underlying project.

The criteria for the focus and grid parameters that are set by the CEC are not included in the comparison; it was not possible to retrieve the information for the majority of the equipment involved in the study. All the equipment, however, is equipped with a grid. For AEC-cells, only the fact that the AEC is used, or not used, is taken into account. Finally the AP or PA projection compared with the projection defined by the CEC is introduced as a criterion.

Examination	Chest PA	chest LAT	lumbar spine AP	lumbar spine LAT	lumbar spine LSJ	pelvis AP	Urinary tract AP
Filtration (mm Al)	>3.0	>3.0	>3.0	>3.0	>3.0	>3.0	>3.0
speed class film/screen	200-400	200-400	400	400-800	400-800	400	400-800
focus film distance	140-200	140-200	100-150	100-150	100-150	100-150	100-150
Tube voltage (kVp)	100-150	100-150	70-90	90-100	90-110	70-90	70-90
AEC	lat	lat	central	central	*	*	*
entr. skin dose (mGy)	0.3	1.5	10	30	40	10	10
projection	PA		AP			AP	AP

Table 1: Criteria for good radiological practice

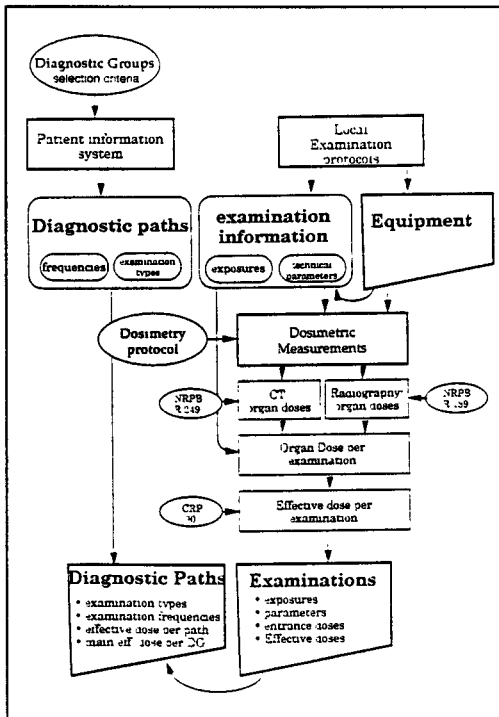


Figure 1: A schematic representation of the data collection and database files

For all the relevant examinations in the different centres the correlation was examined between the fulfilment of these criteria and the effective dose to the patient. It was also investigated whether the CEC criteria can be used to predict the global quality of the radiological practice of a department.

Results

1. Distribution of examination types

Table 2 shows the mean number of examinations per diagnostic path in the centres for the three DGs. In this table the examinations that are performed on less than 20% of the patients, in all centres, are included in the category 'rest'.

2. Intra-country variation of diagnostic paths.

Data were collected from patient files in three hospitals in one city for two DGs. These hospitals were numbered 1 to 3. These data are presented in table 3.

3. Number of films, CT slices and fluoroscopy time.

Table 4 gives for all examination types, the number of films, CT slices and fluoroscopy time for the DGs Lumbar Hernia Discalis and Renal Cell Carcinoma.

4. *Effective dose per examination.*

Using the information about entrance dose, tube voltage, beam quality, the CTDI (for CT equipment), and the examination modalities mentioned in table 4, the effective dose per examination was calculated. The results are listed for the six centres for both DGs in table 5.

5. *Effective dose per diagnostic path*

Combining the number of examinations with the effective dose of the examinations in a centre, the total effective dose for a diagnostic path can be calculated. Results of the calculations are presented in figure 2. Mean values and upper and lower limits, are given.

6. *Comparison radiological technique with the CEC criteria*

For the examination types listed in table 4 the parameters are compared with the criteria of the CEC. Table 6 shows the entrance skin doses for different examination types and for different centres. The data followed by an asterisk exceed the CEC limits.

Table 7 lists for the projections mentioned by the CEC the percentage of selected parameters in the different centres that meet the CEC criteria. The dose is not taken into account here. The effective dose for the projection is noted in the same table. The effective dose is taken here because this value is influenced by all the parameters mentioned by the CEC as important for the quality of the examination.

centre	A	B	C	D	E	F	G
<i>Nr. Patient files</i>	34	23	40	34	41	28	40
CT Lumbar Spine	1.06	0.83	1.25	0.44	1.32	0.46	
Chest	1.03	1.00	0.95	0.09	1.02	0.71	1.15
Lumbar Spine	1.50	1.04	1.03	1.06	0.46	1.11	1.60
Myelography	0.18			1.03	0.24	0.43	0.80
Pelvis	0.26	0.17	0.88	0.68	0.12	0.11	0.10
Discography	0.03		0.80		0.02		
CT pre discography		0.22	0.68				
MRI	0.41	0.22	0.05	0.03	0.29	0.04	
Ultrasound				0.32	0.02		
Rest	0.15	0.04			0.15	0.21	0.30
Total	4.6	3.5	5.6	3.6	3.7	3.1	4.0
minimal exams/patient	3	2	2	2	1	1	2
maximum exams/patient	8	5	8	5	8	7	10

2a)

centre	A	B	C	D	E	F	G
<i>Nr. Patient files</i>	39	29	37	37	30	25	40
Chest	1.08	1.00	1.11	1.35	1.67	1.68	0.93
CT abdomen	1.03	1.00	1.14	0.68	0.87	0.48	0.83
IVU	0.59	0.68	0.38	0.46	0.63	1.28	1.25
Bone scan	0.08	0.03	0.57	0.41	0.63	0.08	0.10
Abdomen	0.18	0.68	0.11	0.14	0.23	0.04	1.28
CT chest	0.13			0.03	0.13		
Angiography	0.46	0.34	0.11	0.62	0.13	0.28	
Chest tomography				0.73		0.04	0.03
Ribs						0.20	
Ultrasound	0.87	0.79	1.00	0.97	1.67	2.16	1.25
Rest	0.33		0.11	0.19	0.77	1.16	0.33
Total	4.7	4.6	4.5	5.6	6.7	7.4	5.9
minimal exams/patient	3	3	2	2	3	3	4
maximum exams/patient	9	6	7	11	16	16	6

2b)

Centre	E	F
<i>Nr. of Patient files</i>	31	28
chest		0,6
IVU		0,5
retrograde cystography	1,0	1,3
nuclear medicine	1,1	1,4
ultrasound	1,0	3,1
rest		0,21
Total	3,1	7,1

2c)

Table 2: Mean, total, minimum and maximum number of examinations per diagnostic path for a) Lumbar Hernia Discalis, b) Renal Cell Carcinoma, c) Vesico Ureteral Reflux in Children.

Centre	1	2	3
<i>Nr Patient files</i>	33	40	23
Chest	1.00	1.05	1.00
CT lumbar spine	0.94	1.05	0.83
Lumbar Spine	0.88	1.08	1.04
Myelography	0.16		
Pelvis	0.16		0.17
CT discography			0.22
Dorsal Spine			0.04
MRI	0.42	0.25	0.22
Total	3.55	3.50	3.52

a)

Table 3: Mean number of examinations per diagnostic path in three hospitals in one city. a) for Lumbar Hernia Discalis, b) for Renal Cell Carcinoma

Centre	1	2	3
<i>Nr. Patient files</i>	29	40	29
Chest	1.24	1.23	1.00
Abdomen	0.24	0.53	0.69
Angiography	0.28	0.50	0.34
Bone Scan	0.79	0.03	0.03
Liver Spleen scan	0.17		
CT abdomen	0.90	0.98	1.00
IVU	0.62	1.10	0.69
Ultrasound	0.86	0.75	0.79
Total	5.10	5.10	4.55

b)

Centre	A	B	C	D	E	F	G
chest	2	2	2	2	2	1	1
lumbar spine	3	2	3	2	5	3	2
pelvis	1	1	1	1	1		
Myelography	15			16	12	7	2
<i>fluoroscopy time (s)</i>	330			120	750	180	180
discography			15				
<i>fluoroscopy time (s)</i>			250				
CT lumbar spine	20	16	12	13	24	20	
CT (pre) discography		1	1				

4a)

Centre	A	B	C	D	E	F	G
chest	2	2	2	2	2	1	2
IVU	8	6	8	6	10	3	4
abdomen	1	1			1	1	1
chest tomography				19			
angiography	20	26	15	30	30	8	
<i>fluoroscopy time (s)</i>	480	160	60	120	90	240	
CT abdomen	42	20	40	24	24	53	40
CT chest	40				15		

4b)

Table 4: Number of films, CT slices and fluoroscopy time per examination for a) Lumbar Hernia Discalis, b) Renal Cell Carcinoma.

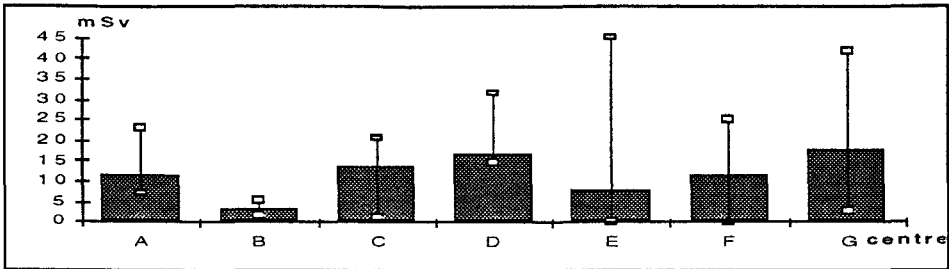
Centre	A	B	C	D	E	F	G
chest	0.38	0.32	0.03	0.04	0.16	0.01	0.32
lumbar spine	3.15	1.26	2.64	0.88	1.61	1.87	2.50
pelvis	0.92	1.46	1.20	0.33	0.43		
Myelography	11.8			13.9	20.0	21.2	17.0
discography			10.1				
CT lumbar spine	3.64	1.62	1.39	2.84	1.61	1.26	
CT (pre) discography		0.10	0.07				

5a)

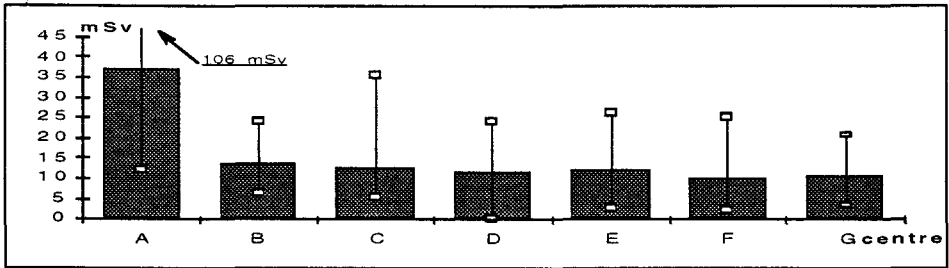
Centre	A	B	C	D	E	F	G
chest	0.18	0.32	0.12	0.04	0.16	0.07	0.29
IVU	12.2	2.94	4.47	3.04	2.47	2.19	4.28
abdomen	1.89	0.51	0.71	0.21	0.35	0.73	3.45
chest tomography				0.39			
angiography	31.4	13.9	13.9	3.43	6.57	7.87	
CT abdomen	11.9	6.15	5.29	7.59	5.62	6.91	3.20
CT chest					6.8		
bone scan	4.90		4.90	5.95	4.77	4.3	

5b)

Table 5: Effective dose per examination in mSv for a) Lumbar Hernia Discalis, b) Renal Cell Carcinoma.



2a)



2b)

Figure 2: Effective doses (mean, minimum and maximum values) per diagnostic path for a) Lumbar Hernia Discalis, b) Renal Cell Carcinoma.

centre		A	B	C	D	E	F	G
chest	PA	0.40 *	0.45 *	0.25	0.09	0.54 *	0.04	2.0 *
	LAT	3.2 *	3.2 *	1.2	0.32	1.4	-	-
lumbar spine	AP	9.6	9.2	9.1	5.5	7.7	9.7	11.7 *
	LAT	15.9	26.4	18.0	14.3	10.7	22.2	30.9 *
pelvis	LSJ	18.0	-	10.6	-	6.30	15.3	-
	AP	7.2	11.8 *	10.5 *	2.3	3.1	-	-

6a)

centre		A	B	C	D	E	F	G
chest	PA	0.32 *	0.45 *	0.44 *	0.09	0.54 *	0.07	1.5 *
	LAT	1.3	3.2	1.2	0.32	1.4	-	1.8 *
Urinary tract (abdomen)	AP	15.8 *	4.8	6.3	1.9	3.1	7.0	7.7

6b)

Table 6: Entrance skin doses in mGy for 3 examination types in 7 centres for a) Lumbar Hernia Discalis, b) Renal Cell Carcinoma. Values followed by an asterisk (*) exceed the limits of the CEC quality criteria

centre		A	B	C	D	E	F	G
chest	PA	67 -0.09	100 -0.06	67 -0.03	100 -0.01	100 -0.06	80 -0.01	40 -0.30
	LAT	100 -0.29	100 -0.26	-	100 -0.03	100 -0.10	-	-
lumbar spine	AP	67 -1.07	33 -0.80	83 -1.14	100 -0.55	67 -0.51	40 -0.83	80 -1.50
	LAT	50 -1.81	33 -0.46	67 -0.36	83 -0.33	50 -0.22	60 -0.47	80 -1.00
	LSJ	50 -0.27	-	50 -1.14	-	50 -0.37	-	-
pelvis	AP	67 -0.92	50 -1.46	67 -1.70	100 -0.33	83 -0.43	-	-
mean		67	63	67	97	75	60	67

7a)

centre		A	B	C	D	E	F	G
chest	PA	83 -0.08	100 -0.06	67 -0.03	100 -0.01	100 -0.06	80 -0.07	40 -0.27
	LAT	100 -0.10	100 -0.26	67 -0.08	100 -0.03	100 -0.10	-	60 -0.02
Urinary tract (abdomen)	AP	83 -1.89	83 -0.51	83 -0.71	100 -0.21	83 -0.34	40 -0.73	80 -1.15
mean		87	94	72	100	94	67	60

7b)

Table 7: Percentage of examination parameters that meet the CEC criteria of good radiological technique and effective dose for one exposure (in mSv) for Lumbar Hernia Discalis (a) and Renal Cell Carcinoma (b).

Discussion

1. Frequency and type of examinations

Analysis of the results in table 2, the examinations per diagnostic path, shows that there are important differences in the diagnostic strategies between the different centres for all three diagnoses. Variations are observed in the choice of the examinations as well as in the number of examinations used to state a certain diagnosis.

For the DGs Lumbar Hernia Discalis and Renal Cell Carcinoma the variation in the mean number of examinations per diagnostic path is about 20%. There are also large differences observed in the number of examinations in individual diagnostic paths. These variations are especially large for the DG Renal Cell Carcinoma. The number of examinations per patient varies between 2 and 16. These variations are smaller for the Lumbar Hernia Discalis.

For the DG Lumbar Hernia Discalis a high frequency of myelography in two centres, a low frequency of chest examinations in one centre and the use of discography another are observed.

A relative high number of 'rest' examinations is noted at the DG Renal Cell Carcinoma, especial at centres E and F. For this DG there is clearly no agreement on the use of the bone scan technique. For the DG Vesico Ureteral Reflux in children the differences between the two centres are large. It is clearly shown that in one centre a very well defined protocol is used when examining children with a urine infection. A very limited number of examination types is used. The other centre (F) uses a wide range of examination types. This is stressed by the relative high frequency of 'rest' examinations (21%).

2. Intra-country variations.

Although there are differences in frequency and type of examinations between the centres from one and the same city (table 3), these variations are much smaller than those between the centres in different countries (table 2). This indicates that, despite personal preferences, nation depended factors influence diagnostic strategies.

3. Examination parameters: number of films, CT slices and fluoroscopy time.

Centre E uses much more films than the other centres for a lumbar spine as well as an IVU examination. It showed up that in this country for these examinations a minimal number of films was required for reimbursement.

The same centre used also extremely long fluoroscopy times for a myelography examination. This is probable caused by the fact that this examination was performed only seldom. This argument is stressed by the fact that centre D, where myelography was done still in routine at the time of the data collection, uses the shortest fluoroscopy time for this examination.

Centre A uses markedly long fluoroscopy times at angiography examinations.

It is noted that for CT the number of slices varies up to a factor of 2.7 for the same examination.

4. Effective dose per examination.

In centre B effective dose data were available from another study for some of the examination types presently studied. These data were obtained from dose measurements on patients. In table 8 a comparison is made between the effective dose data from both studies. It can be seen that the test object data are all well within the variation we observe in data obtained from patient measurements.

Examination	measured on patients	measured on test objects
Chest	0.08 - 0.40	0.32
Lumbar Spine	0.18 - 5.01	1.26
Pelvis	0.32 - 7.40	1.46
Abdomen	0.18 - 5.01	0.51
IVU	0.98 - 14.6	2.94

Table 8: Effective dose per examination measured on patients or on test objects (DRD) minimum - maximum or mean values in mSv.

Table 5 shows that the effective dose for the patient from one and the same examination can vary considerable between different centres. The largest variation is observed for a chest examination. The minimum and maximum value differ by a factor of 38! Smaller, but more important differences are observed for myelography (a factor of 2), IVU (5) or angiography examinations (10). In the case of the angiography, the highest dose is clearly due to the high fluoroscopy time. For the IVU and myelography the high doses are not directly linked to the number of films or time of fluoroscopy .

5. Total dose per diagnostic path.

For the DG Lumbar Hernia Discalis the variation in mean effective dose per diagnostic path is 43%. For the DG Renal Cell Carcinoma this variation is 62%, but this variation is mainly due to the high value of centre A. The variation between the other centres is only 11%.

It is remarkably that for the DG Renal Cell Carcinoma, the high variation in examination types between the centres is not reflected in the effective dose.

The centres with the highest doses for the DG Lumbar Hernia Discalis have a relative high frequency of myelography in their diagnostic path. Centre C with the third highest dose uses discography in 80% of the patients.

The high effective doses for angiography, CT abdomen and IVU are responsible for the extreme high effective dose for the DG Renal Cell Carcinoma in centre A. The high frequencies for 'rest' or chest examinations in other centres have little influence on the total effective dose.

6. Comparison with CEC criteria for 'good radiological practise'.

Comparison of the entrance doses of the equipment in the co-operating centres with the dose criteria of the CEC guidelines shows that 2 out of 7 centres comply for all projections with the criteria and 31% of the entrance doses exceeds the CEC criteria.

No clear relation is found between the effective dose to the patient and the compliance to the criteria. It would be expected that a better score for the criteria lowers the dose to the patient. For some projections a slight trend can be noticed proving this relation. Data of other projections however show just the opposite. Figure 3 shows the results for the Lumbar Spine AP projection and for the Abdomen AP projection.

Also no relation can be found between the mean score to the different projections and the mean total effective dose for a DG. The results for the two DGs are shown in figure 3.

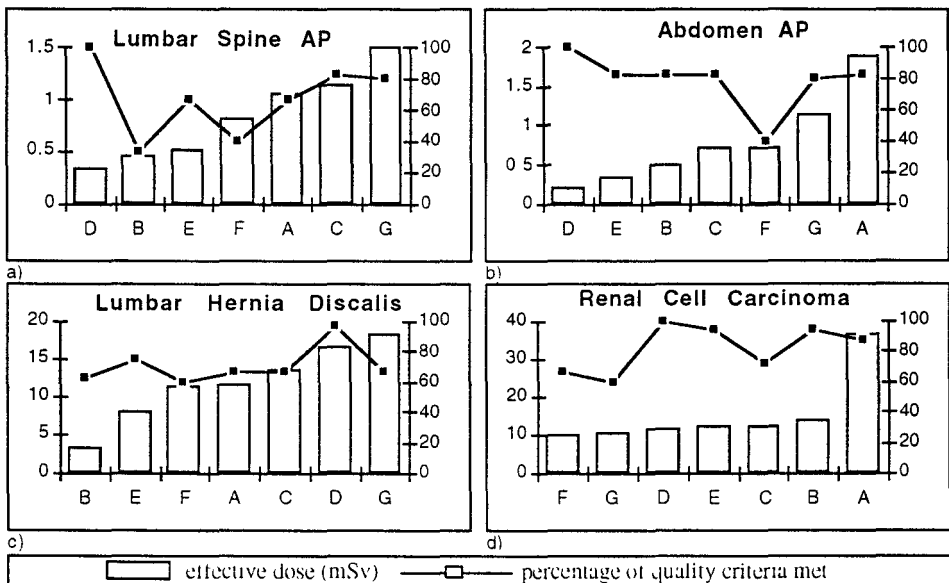


Figure 3: effective dose in mSv and percentage of parameters that meet the criteria of the CEC. a) for a Lumbar spine AP projection, b) for an Abdomen AP projection and the total effective dose for a mean diagnostic path and the main percentage of the criteria met for the DGs Lumbar Hernia Discalis (c) and Renal Cell Carcinoma (d).

Conclusions

- The method of DGs and the dosimetric system used in the study allows a comparison of the radiological practice in different centres, with respect to the dose to the patient.
- It has been possible to study the influence of the radiological techniques, the quality of the radiological equipment, and the examination parameters on the effective dose to the patient.
- Important differences are detected in the radiological strategies used to set the three diagnoses; Renal Cell Carcinoma, Lumbar Hernia Discalis and Vesico Ureteral Reflux in Children in the co-operating centres. Differences are detected in the choice of the examination type and the

number of examinations performed. The use of a diagnostic protocol can be observed in one centre..

- Important differences are found in the way the examinations are performed and the technical specifications of the equipment in co-operating centres for the DGs Lumbar Hernia Discalis and Renal Cell Carcinoma.
- The above mentioned differences have all an important influence on the total effective dose to the patient. The mean dose per patient differs up to a factor of 6 between the centres for one diagnosis.
- As the main reasons for differences in the total dose to the patient from a diagnostic path we clearly observed the choice of the examination types and the way these examinations are performed (number of slices, fluoroscopy time etc.). The technical quality of the equipment, contributes to a smaller extent.
- In the chain of examinations of a diagnostic process one complex radiological examination (Angiography, Myelography or CT) can contribute for up to 80% of the total effective dose to the patient. Attention should, therefore, be given to the optimisation and use of these types of examinations.
- 'External parameters' as reimbursement regulations have an important influence on the total dose to the patient. An obligated minimal number of films can lead to a doubling of the dose to the patient. The reported practices showed that these regulations often intervene with complex examination types (CT abdomen, Myelography, IVU) and have, therefore, a severe effect on the dose to the patient.
- The 'Examples of Radiographic Technique' as described in the 'Quality Criteria for Diagnostic Radiographic Images' of the CEC proved to have no clear relation with the effective dose to the patient. The defined criteria can not be used as indicators for the total effective dose to the patient for a diagnostic process. This may not be surprising since the criteria are only defined for relatively simple radiographic techniques and as is observed above the main risk to the patient comes from the complex radiographic techniques.

Remark

- The reasons for differences in the diagnostic strategies (medical, organisational, availability of equipment) were discussed with staff members of the participating centres. The results of this discussion are reported in Part I

Head of project 2: Dr. Thijssen

II. Objectives for the reporting period

1. Field measurements of dose and image quality in the participating centers.
2. The Development of Test Objects corresponding to different parts of the human body.
3. Dosimetry: methods and TLD-reading.
4. The quantification of Image Quality in terms of the Image Quality Figure (IQF).
5. Comparison of the dose-image-quality-relation in the different hospitals
6. Study on the influence of the external parameters to dose and image quality.
7. Discussion and assessment of role of physical and medical/organisational factors.

III. Progress achieved

introduction

1. In cooperation with the team of Brussels measurements were performed in the participating hospitals. After the patient data were received from the institutions, the relevant examinations were performed on test-objects, determining the entrance dose and the Image Quality obtained, using the local X-ray system. Also technical information about the X-ray systems was gathered.

For a correct performance and evaluation of the local measurements, additional investigations were made as described in the following sections.

methods

2. In order to standardize the dose measurements, test objects were developed for different parts of the human body. Since simplicity and reproducibility are of importance, the test objects were chosen to be made of plexiglass and aluminum for the soft tissue and bone respectively. To find the right combination of the two materials, corresponding to abdomen, lumbar spine, pelvis and chest of a patient of medium size and about 70 kg, clinical data about kVp, mAs and thickness were collected in the hospital of Nijmegen. By assessment by the radiographers, patients were divided into 3 classes of size and weight: 1 thin, 2 average, and 3 fat. After gathering this information the average mAs of the second group of patients was calculated.

As the equivalent for the soft tissue 19 cm of plexiglass was chosen. The correct thickness for the aluminum was retrieved by adding aluminum to the plexiglass until the same mAs setting was required as the average mAs of the group of patients of average size and thickness. Since this was done for different types of examinations, a correct equivalent of the different parts of the human body could be retrieved in the form of plexiglass and aluminum.

examination	plexiglass (cm)	aluminum (mm)
chest PA	12	0
chest lat	19	0
pelvis AP	19	2
lumbar spine AP	19	8
abdomen AP	19	8

table 1. The test objects that were used in this study

3. To measure the entrance dose, thermo-luminescence dosimeters (TLD-100, LiF) were used. In this study the goal was to measure the skin entrance dose, i.e. the radiation that is absorbed in the outermost layer of the tissue. Primary radiation as well as backscatter are included. For angiography and all techniques of plain radiography, TLDs were put on top of the test objects, or under the test objects, between table and plexiglass if the tube was located under the table. For measurement the TLD-crystals were put in the same thin holder made of plexiglass as was used during calibration. Each holder contains three crystals. For calibration the TLDs were irradiated free in air and at the same time the exposure was measured with a calibrated ionisation chamber. From this procedure for every TLD the exact calibration factor was known. To convert the measured dose from R to mGy a conversion factor of 9.3 was used. I.e. an exposure of 1.0 R causes an absorbed dose in soft human tissue of 9.3 mGy.

For CT dosimetry the CTDI (Computed Tomography Dose Index) was determined. The CTDI is an index used by the NRPB in their report R248 to represent the free-in-air single dose of a CT equipment. For a dose measurement of the CT equipment a set of TLDs were stacked inside a hollow, cylindrical perspex capsule. This capsule was positioned along the axis of rotation of the scanner. After a single slice exposure an axial dose profile was found in the form of a Gaussian curve. The CTDI is defined as:

$$CTDI = \frac{\int D(z) dz}{w}$$

formula 1

where D is the dose and w the nominal width of the slice.

Because a stack of n TLDs can not give a continuous curve, this expression must be approximated by:

$$CTDI = \frac{\sum_{i=1}^{i=n} (D_i t)}{w}$$

formula 2

where D_i is the dose to the ith TLD and t is the thickness of one TLD.

Since all the TLD reading was performed in Nijmegen, it was not possible to do the reading immediately after the irradiation. For this reason the influence of spontaneous decay of a set of irradiated TLDs was checked as a function of time. Because of the short time between irradiation and reading (less than a week), no correction appeared to be necessary.

4. The dose that is required to make an image should always be seen in relation to the image quality that is established. There is a close relation between dose and image quality. When images are made with a very low dose of radiation, the image quality might be very poor and there could rise problems with finding the right diagnosis. In other words a good image quality can be a justification for a higher dose.

For this reason in this study aside from dosimetry, image quality was an important issue. To determine the image quality in plain film radiography, with all X-ray systems an image was made of a Contrast Detail Phantom. In fact this Contrast Detail Phantom was part of the flat test objects that correspond to the different parts of the human body; it was placed in the midplane of the test object. The Contrast Detail Phantom is a 1 cm plate of plexiglass with holes of various diameters and depths drilled in it. The plate is divided into 225 squares (15 x 15). In one direction the diameter of the holes decreases from 8.0 to 0.3 mm. In the orthogonal direction the depth of the holes decreases from 8.0 to 0.3 mm. In the resulting image the holes are visible as discs on a homogeneous background. Because of the small diameter and depth of some of the holes, only a part of the discs will be visible, depending on the quality of the entire imaging system.

To approximate the way radiologists evaluate X-ray images, a psycho-physical element is incorporated in the quantification of the image quality; in each square of the phantom a second identical hole is drilled in one of the four corners. The observer not only must indicate whether he has seen a disc, but also in which corner. From the observers results an Image Quality Figure (IQF) can be calculated by adding up the products of the contrasts (C_i) and Details (D_i) for all just visible contrasts in the phantom. In formula:

$$IQF = \sum_i C_i \cdot D_i$$

formula 3

To determine the image quality of CT systems, a cylindrical test object filled with water was used. Additionally there was a thin metallic wire in the phantom. After imaging a slice of 5 mm of the phantom, the image quality could be determined. The standard deviation of the Hounsfield Units in the water region was used as a measure for the noise. This standard deviation was measured in the center of the image in a sufficiently large region of interest, so that the SD did not change anymore by further increase. The width at half maximum of the point spread function of imaged metallic wire was used as a measure for the resolution in the CT image.

For both diagnoses the total patient dose during the diagnostic pathway was calculated. Dose differences during the diagnostic procedure are caused by factors of medical/organisational or physical character. To retrieve the impact of the medical/organisational factors and factors of physical character separately, the physical factors were eliminated by calculating the patient dose, assuming that all examinations in the hospital were performed on the same reference system. For all types of examinations: angiography, myelography, chest X-ray, other plain radiography and CT, that system was chosen as a reference system that produces a rather good image quality, using a rather low dose.

To express the impact of the physical differences of the systems to the total patient dose, calculations were made assuming that all hospitals used one and the same diagnostic protocol, but still performing the examinations using their own X-ray systems. As the reference protocol we chose the one with the smallest number of examinations and the smallest number of images per examination.

results

5. Because of the way it is defined, the IQF decreases when the image quality is improved. It can be shown that there is a clear relation to be expected between image quality (IQF) and the applied dose:

$$IQF \sim \frac{k}{\sqrt{D}}$$

formula 4

Where k is a constant and D the dose.

When values of dose and the resulting IQFs from one and the same equipment would be plotted in a graph it would give a smooth curve obeying formula 4. Nevertheless similar measurements on dose and image quality from various systems show, when plotted, more or less a cloud of points. This is because the quality of all aspects of the procedure of establishing an image differ from one X-ray equipment to another. A subdivision was made in different types of X-ray equipment: equipment for angiography, myelography, chest X-ray, other plain radiography and CT. For each type of equipment dose and image quality, measured under standard conditions are plotted in graphs (Fig 1,2,3,4) For each type we find a large variation in dose as well as in image quality. The relation as was expected by formula 4 is not found. Because images are made under standard conditions, the only reason can be a wide variation in the quality of the equipment in the different hospitals. For angiography no quantification of the image quality is available.

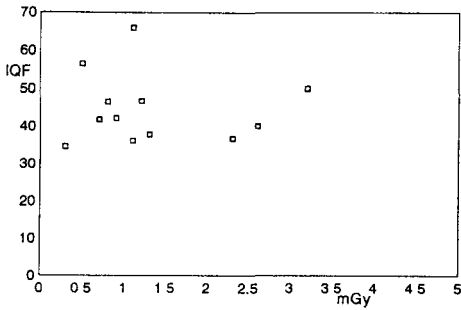
angiography

hospital	dose (mGy)
A	5.7
B	6.8
C	13.1
D	2.7
E	5.2
F	15.9

table 2. The entrance dose for angiography systems under standard conditions.

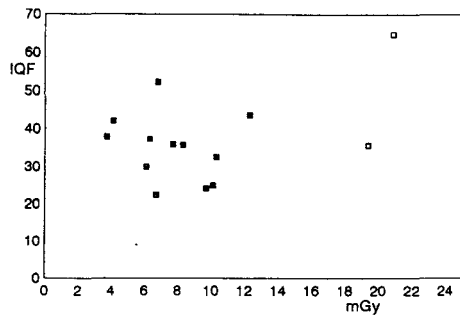
dose image quality relation

chest X-ray



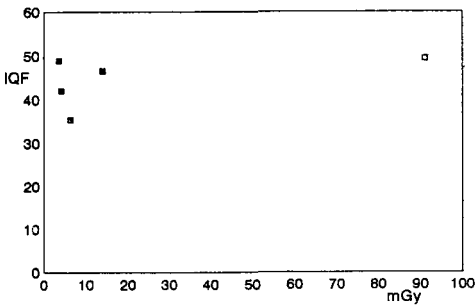
dose image quality relation

plain radiography



dose image quality relation

systems for myelography



dose image quality relation

CT

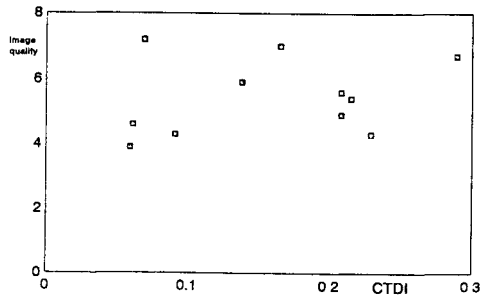


Fig. 1,2,3,4. The relation between dose and image quality for four types of examinations. Each dot represents an X-ray system in one of the participating hospitals. The image quality here defined for the CT systems is determined by a figure for noise and a figure for the resolution. The lower the value of the figure, the better the image quality. Also the IQF decreases when the image quality improves.

6. There is a large number of factors that can influence the dose and the image quality. Among them the intrinsic parameters of an X-ray equipment. I.e. the parameters that can not be changed easily, e.g. the quality of the tube, the transparency of the table and the quality of development procedure.

On the other hand there is a number of parameters that have to be chosen by the radiographer and/or radiologist and that do affect dose and image quality as well:

- kVp
- focal spot size
- focus film distance
- extra filtration
- mean optical density
- film screen combination

The latter could be seen as a parameter that is somewhere in between an intrinsic and a free to choose parameter; only when more than one combination is available, the radiographer can make a choice.

To find out to what extent these parameters have an influence, additional measurements on dose and image quality were performed. By varying just one of the parameters, their individual contribution to the dose and image quality was determined.

The results in table 3 show that there is a clear decrease in the absorbed dose for higher kVp. A lot of low energy radiation is absorbed in the patient, not contributing to the establishment of the image.

Rising the kVp from 60 to 70 kVp or higher, shows a decrease of image quality because of loss of low contrast.

kVp	dose (mGy)	IQF
60	700	31
70	275	40
77	219	38
81	162	41

table 3. Influence of kVp on dose and image quality.

foc spot size	dose (mGy)	IQF
large	219	38
small	223	36

table 4. The influence of the focal spot size on dose and image quality.

No differences in dose and hardly any differences in image quality are measured between images performed with a small or a large focal spot (table 4).

film foc dist(cm)	dose (mGy)	IQF
90	302	42
100	241	44
110	219	38
120	221	45

table 5. The influence of the film focus distance on dose and image quality.

mm Al	dose (mGy)	IQF
0	219	38
1	227	40
2	200	39
3	175	42
4	168	44
6	170	48

table 6. The influence of added filtration on dose and image quality.

The variation of the film focus distance (table 5) shows an increase of the dose when the distance decreases. No clear relation to the image quality was found.

The focus of the grid may cause an additional effect. However the image quality is optimal for the film focus distance routinely used.

When extra filtration is added to the tube a decrease of the absorbed dose is found. The inherent filtration by the housing of the tube determines the effectiveness of the added filtration. Low energy radiation is absorbed by the aluminum. This results in a decrease of the low contrast. The latter is the reason for the decreasing image quality, found in table 6.

Table 7 shows that the image quality will improve when the radiologist chooses a higher optical density. It is obvious that therefor a higher dose to the patient is unavoidable.

opt dens	IQF
0.90	54
1.19	38
1.40	34
1.75	28

table 7. The influence of the optical density on image quality.

Much attention should be payed to the choice of the film screen combination. Investigation of 10 commercially available film screen combinations by the team of Nijmegen showed a wide variation of the required dose and several aspects of the image quality. The required dose for an optical density of 1.0 + base + fog as well as the resulting image quality in IQF and resolution in line pairs per mm was determined for 60 kVp and 90 kVp. Tables 8a and b show the results:

60 kVp

film screen combination	dose mGy	base+fog	resolution lp/mm	Image qual. IQF
1	2.4	0.17	4.9	25
2	3.4	0.22	5.0	25
3	3.0	0.22	5.0	27
4	2.0	0.17	5.0	28
5	2.3	0.23	5.0	26
6	2.0	0.22	6.0	25
7	3.5	0.17	4.9	24
8	2.2	0.17	4.6	24
9	2.7	0.23	4.6	27
10	2.0	0.23	4.3	28

table 8a. The results of a test of 10 different film screen combinations, for 60 kVp.

90 kVp

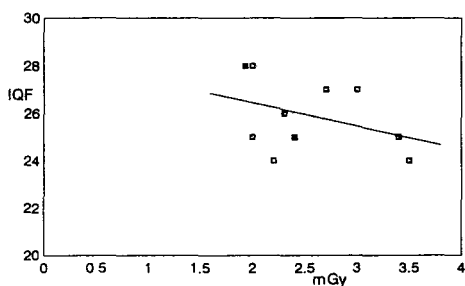
film screen combination	dose mGy	base + fog	resolution lp/mm	Image qual. IQF
1	0.7	0.17	4.2	37
2	1.3	0.22	4.5	31
3	0.9	0.22	4.5	34
4	0.8	0.18	4.5	37
5	0.7	0.23	4.3	39
6	0.8	0.22	5.3	35
7	1.0	0.17	4.6	35
8	0.6	0.17	3.6	38
9	1.0	0.23	4.1	36
10	0.7	0.23	4.0	33

table 8b. The results of a test of 10 different film screen combinations, for 90 kVp.

When the results of dose and IQF are plotted in a graph (Fig. 5 and 6), for both energies 60 and 90 kVp a tendency becomes obvious that the image quality improves when a larger dose of radiation was applied to establish the image. Nevertheless it is clear that some combinations can produce a better image with the same or lower dose than other. So also the choice of the film screen combination appears to be one of the parameters that influence dose and image quality.

Dose-Image Quality relation

10 film screen combinations
60 kVp



Dose-Image Quality relation

10 film screen combinations
90 kVp

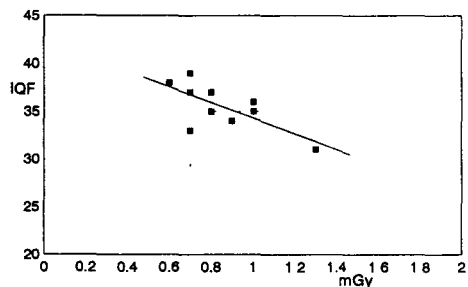


Fig. 5 and 6

discussion

7. The results on total dose in the different pathways in the different hospitals show a wide variation for both diagnoses. The reasons for these differences can be divided into two groups: factors with a physical origin (quality of the equipment) and factors of medical/organisational character (choice of examinations and the number of images, slices and

time of fluoroscopy). In section 5 we already found that there was a clear difference in the imaging qualities of the different equipment.

To express to what extent these physical factors are responsible for the dose differences in the hospitals and to what extent the dose differences are caused by medical and organisational factors, new calculations were made. To retrieve the impact of the medical/organisational factors, all other factors should be eliminated. New calculations on total patient dose are made, based on fictitious examinations in all participating hospitals using one and the same equipment for each type of examination. Separately for angiography, myelography, chest X-ray, other plain radiography and CT, one system was chosen as the one on which in each hospital all examinations were performed fictitiously with local protocols and numbers of images. We have chosen a system that produced a rather good image quality, using a rather low dose. This means we chose a system corresponding to a dot somewhere in the lower left corner of the graphs of Fig. 1,2,3,4 respectively. For angiography the system with the lowest dose was chosen. Then again the dose in the total diagnostic pathway was calculated. Fig. 7 and 8 show the results. The dark bars show the results of the local equipments in combination with the local protocol. The light bars show the fictitious doses as described before. Variations that are found in Fig. 7 a and b are caused by medical and organisational factors only. We see that there is a change in the total patient dose in the different hospitals, but the extend of variation is almost unchanged.

real/fictitious total patient dose performed on local/reference X-ray systems
Renal Cell Carcinoma **real/fictitious total patient dose performed on local/reference X-ray systems**
Lumber Hernia Discalis

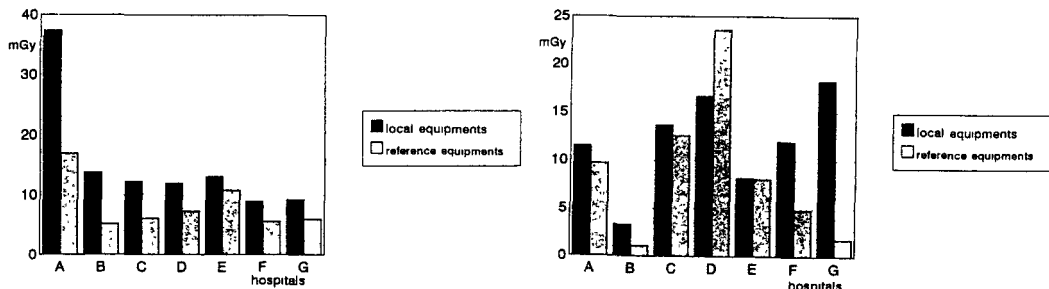


Fig. 7 a. For both diagnosis the total patient dose per hospital as measured with the local X-ray systems using the local protocol. b. The total patient dose per hospital fictitiously calculated, with the local diagnostic protocol but using reference X-ray systems for each type of examination.

To find out the contribution of the physics (quality of the X-ray imaging systems) to the total patient dose, we now choose one diagnostic pathway, i.e. one set of diagnostic examinations that must lead to a diagnosis.

Then we calculated the dose again assuming that in each hospital patients were examined, performing exactly the same set of examinations and numbers of images etc., but using their local X-ray systems. These results are shown in Fig. 8 a and b. Variations in dose

real/fictitious total patient dose real/fictitious total patient dose
 local/reference diagnostic pathway local/reference diagnostic pathway
 Renal Cell Carcinoma Lumbar Hernia Discalis

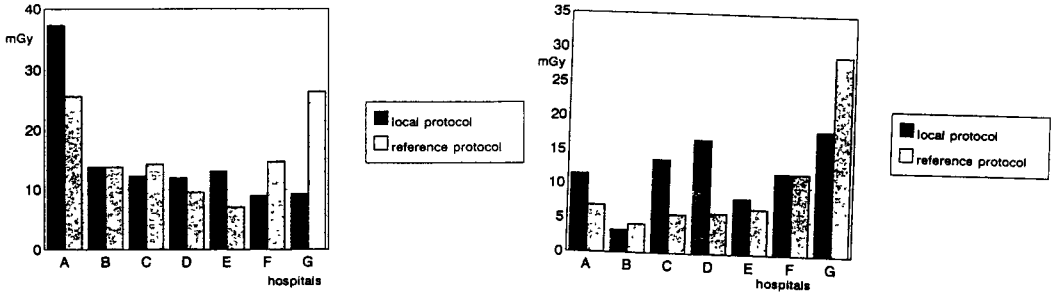


Fig. 8 a. For both diagnosis the total patient dose per hospital as measured with the local X-ray systems using the local protocol. b. The total patient dose per hospital fictitiously calculated, with the local X-ray systems but using a reference diagnostic protocol.

represented by the light bars are caused by physical parameters only. Again there is a shift in the results but the extend of the dose variation is almost unchanged. So we can conclude that both the physical and the medical/organisational factors have an important influence on the total patient dose in a diagnostic pathway. Dose reduction can be realised by paying attention to the physical quality of the X-ray systems, but to the same extend by evaluating the medical protocol, including the number of images, used in the hospitals.

References

M.A.O. Thijssen et al. (1989), A Defenition of Image Quality, British Institute of Radiology, Report 20, p. 29-34, London.

M.A.O. Thijssen, 1993 Assessment and Control of the Image Quality in Diagnostic Radiology. (in Dutch), Thesis University of Nijmegen, The Netherlands.

P.C. Shrimpton et al., Survey of CT Practice in the UK, NRPB-R248, 249

FINAL REPORT

I. PECO - Subcontract ROMANIA - Milu ERBCIPD CT930427

Head of project 3 : Dr.C.Milu

Institute of Hygiene, Public Health, Health Services and Management

Str.Dr.Leonte No.1-3

R - 76256 Bucharest 35

ROMANIA

Period covered : March 30, 1994 - June 30, 1995

II. Specific objectives for the reporting period

- Collection of patient data as described for the Diagnosis Related Dose (DRD) project, for two diagnostic groups(D.G's):Renal Cell Carcinoma(RCC) and Lumbar Hernia Discalis(LHD).

- Carry out dosimetric measurements for most frequent examinations using the protocol developed in Brussels and Nijmegen.

- Intercomparison between dosimetric results from TLD measurements and the DRD methodology.

III. Global achievements

The statistics performed on the information about all relevant examinations from 40 adult patients per D.G. allowed to establish that the mean number of total examinations per patient was 5.98 for DG - RCC and 3.95 for DG - LHD. The most frequent examinations were : IVU (1.20), kidneys rg.(1.25), CT abdomen (0.83) and Ultra-Sound (1.25) for RCC and lumbar spine rg. (1.60) and myelography (0.80) for LHD. In both DGs the chest rg. is present, as a routine examination : 0.93 (RCC) and 1.15 (LHD).

The calculated mean effective doses per patient using DRD methodology was 9.3 mSv for RCC and 18.3 mSv for LHD, in comparison with 12.7 mSv and resp.11.1 mSv from our previous determinations performed directly on patients using TLDs. The main explanations of the discrepancies were done by our previous under-estimation of myelography dose for LHD and an extra-estimation for CT patient dose for RCC.

RESULTS OBTAINED

1. Number of examinations

The statistics data on number of examinations per diagnostic group are presented in table 1

Table 1

	Diagnostic group	
	Lumbar Hernia Discalis	Renal Cell Carcinoma
Number of patients	40	40
Total number of examinations	158	239
Total number of examinations per patient	3.95	5.98

Mean number of examinations per patient per type of examination

Chest rg.	1.15	0.93
Lumbar spine	1.60	
Myelography	0.80	
Pelvis	0.10	
CT abdomen		0.83
IVU		1.25
Abdomen rg.		1.28
Bone scan		0.10
Tomo chest		0.03
Ultra Sound		1.25
Other	0.30	0.31

2. Number of films, slices or fluoroscopy time per examination

The collected data are presented in table 2.

Table 2

	Lumbar Hernia Discalis	Renal Cell Carcinoma
Chest	1	2
Lumbar spine	2	
Myelo fluoro (min)	2 3.0	
IVU		4
Abdomen		1
CT abdomen		40

3. Doses per film, slice, fluoroscopy time and mean effective dose per patient (mSv)
The results obtained using DRD methodology are given in table 3.

Table 3

		Lumbar Hernia Discalis	Renal Cell Carcinoma
Chest	PA	2.0	1.5
	LAT		1.8
Lumbar spine	AP	11.7	
	LAT	30.9	
Myelography	AP	37.9	
	LAT	146.7	
	fluoro	16.0	
IVU abdomen bladder	AP		7.7
	AP		3.3
CT abdomen			
	CTDI		0.059
	CTDI mAs		13.6
MEAN EFFECTIVE DOSE PER PATIENT		18.3	9.3

4. Comparison of methods

Several direct patient dose measurements (TLD) were performed by us before 1994 using TLDs. The effective dose was calculated using NRPB method, as in DRD study (DRD), starting from measured entrance dose. In our previous determinations, the surface patient dose (directly measured) was used. The differences of doses per examination (TLD, DRD) shown in table 4, are done by difference in positioning and in the irradiation parameters : in our former case : as used during patient radiological examination, in DRD study : mean reported parameters by operators.

Table 4

	Lumbar Hernia Discalis		Renal Cell Carcinoma	
	TLD	DRD	TLD	DRD
Mean effective dose per patient	11.3	18.3	12.7	9.3
Chest	0.23	0.37	0.25	0.3
Lumbar spine	1.93	4.00		
Pelvis	0.27	0.27		
Myelography	10.12	13.59		
IVU			3.53	4.6
Abdomen rg.			1.40	1.5
CT abdomen			6.90	2.6

As regards the discrepancy between mean effective dose per patient and per diagnostic group, in our previous determination there is an under-estimation of patient dose for myelography for LHD and an over-estimation for CT abdomen in the RCC diagnostic group

Practical possibilities for patient dose reduction:

1. In chest PA radiography, the surface patient doses are 3 to 5 times higher than the guidance level (0.4 mGy), due by the use of low kV values. The application of an appropriate technique (high kV) could reduce the dose. Similar situation is in mielography.
2. The increase of the speed of film/screen combination can further reduce the dose.
3. The processing of the films is done manually, with an important retake rate.
4. The investigations were done in two big and well organised hospitals from Bucharest ("Fundeni" and "Hospital nr. 9"). The choice of the examination type and the way in which the examinations are carried out (especially by using a pre-set protocol) seem to have more influence on the total dose to the patient, than equipment parameters.
5. The circulation of diagnostic information can be improved too, by implementation of computerised system, reducing the unuseful repetition of radiological examinations.

Head of project 4: Prof. Dr. Med. K. Karlinger

II. Objectives for the reporting period

- Collection of patient data as described in the documents for Diagnosis Related Dose prepared by the Brussels and Nijmegen teams.
- As MD., contribute to the search for and elaboration of further DG descriptions
- Collection of data in Budapest for the two extra DG, Vesical Ureteral Reflux in children and Aortic Aneurism

III. Progress achieved.

Methods

Development of protocols.

In co-operation with radiologists of Belgium and physicists of the other participating centres, two extra DG's, suitable for evaluation by the DRD procedure were established: Vesical Ureteral Reflux and Aortic Aneurism.

Methodology for Ureteral Vesical Reflux is given in the main part of this report.

Radiological Diagnosis of Aortic Aneurism (AA).

Detection by imaging procedures using ionising radiation and resulting in surgical treatment. The surgical treatment is programmed. The emergency cases are not included in this study.

Golden standard:

AA proved by operation (Operation Protocol)

Exit point:

Surgical treatment of the AA.

Entry point:

Radiological examinations performed before the treatment. We take into account all examinations up to one year before surgery. The first examination must be performed between January 1, 1988 and December 31, 1993.

Criteria of exclusion:

We only accept patients who can account for all their radiological examinations, even if some of them were taken in other hospitals.

Examinations to be reviewed for dosimetric study:

All techniques involving ionising radiation (conventional radiography, CT, angio and arteriography, nuclear medicine), and MR and Ultrasound (B or Doppler).

Examinations performed in another centre or private practice will be included as if they were performed in the participating centre.

Data collection:

Relevant information will be collected on a data sheet.

- patient identification
- chronological enumeration of all radiological examinations as above
- technical data (physics)
- exposure data, including beam direction, field of view, film-focus distance, tube kV and number of films exposed.

Results.

The four studies were executed basing upon the collected final documentation of each single patient. These documentations are in the archives of the clinic/hospital or collected separately for caring purpose at the special department of the given institute. Somewhere the radiological documentation are separately collected and the X ray pictures are kept in the radiological departments where those are available. (e.g. Paediatric Clinic)

Other places even the X ray pictures were collected together with all documentation, in their case-history-dossier were available relatively easily. (e.g. ORFI-hospital)

There were problematic documentations where only the perioperative periode was well documented but the diagnostic process itself was documented incompletely. (e.g. Vessel and Heart Surgery)

The Nuclear Medicine was done in most of the cases at the department of Radiological Clinic so if the complete data were not available (however mostly they did) on the spot, the documentations were completed on the basis of the document of these department. Those cases where the place of former investigations were known either at one of the University Clinics or in a Hospital of the Capital, by re-following the path, the documentations were studied and the data were collected even from there for completing our material.

After having the collected data every single item was re-checked according to the golden Standard, entry and exit point and consider the exclusion criteria. The unsuitable cases were rejected and the most appropriate ones were prepared for the further work-up.

The patient Examinations Overview and the Examination Sheets were filled out according to the project-rules in chronological order.

1. *Renal Cell Carcinoma*

It was the first task to be done.

It was completed at the Urological Clinic of Semmelweis Medical University which is the main centre to operate this disease. There were collected 124 cases, operated during the given period, but some of them had incomplete documentation, because they were investigated before operation other places and the given data were not enough for our purposes. All the histological diagnoses were searched and matched to every single patients to be sure of renal cell carcinoma but not a removed kidney because of some else tumour.

In cases where patients were investigated in an other place their route was re-followed and the x-ray data were gained form the place of former investigations.

After rechecking the whole pool 27 proper cases were selected, those who completely filled the requirements of this project.

2. *Lumbar Hernia Discalis*

Data pool was the Hospital ORFI (which is the National Institute of Rheumatology and Physiotherapy where this type of patients are completely investigated until the diagnosis and operated on the spine, thereafter cared till their complete re convalescence at the same hospital. Therefore they could be followed relatively easily from the first symptoms until operation. The steps are fulfilled different stations of this huge Insitution but it has only two main Radiological departments.

To collect the proper patients for the LHD there were checked all the reports and documents of the pool of operated patients could be find according to the given period.

In the first circle data of 46 patients was estimated to be fit for our purpose. Fortunately at this Hospital not only the approximate data of the X ray exams, but even the majority of the X ray copies were found in almost all package of every single patients.

All of these 46 patients data were collected and then 24 of them were selected for the project.

3. *Vesico Ureteral Reflux*

The first Paediatric Clinic of the Semmelweis Medical University is the main place for these little patients for operating, caring and following.

They have two main pools among these patients:

- in the first one are the younger children who are diagnosed almost immediately after birth (sometimes even before and after ensured only)

- in the second one are the small, only some year old children who are sometimes followed and

investigated several times before deciding to be operated.

Because the very strict cautela of this project the patient selection was very circumspect according to the entry and exit points, the patients age and sex and the grade of VUR.

The places of investigations were favourable because the patient pool was very centralised.

35 of the children seemed to be suitable for our purposes and after rechecking there were found complete 29.

Even the dose of used isotopes was found either in the documentation of every single patients or in the personal documentation in the department of nuclear medicine of Radiological Clinic.

4. *Aortic Aneurism*

The Vessel and Heart Surgical Clinic and National Institute is the place where the overwhelming majority of AA-s are operated.

The only problem is that they are coming there mostly after having been investigated and diagnosed. Therefore the investigation data are very scattered and discordant.

A lot of them were diagnosed with US and/or CT on other places and were operated at the Clinic basically on these data. After having been operated the pictures were send back with the patients to their original place to be cared further.

Because of this reason the detailed data of investigations were estimated according to the proper protocols.

There were find more or less fit 65 cases and were selected 58 from them (There were 50 cases operated because of Abdominal Aortic Aneurysm signed with AAA and 8 Aorta Thoracalis Aneurysm signed with ATA and one case having both AAA-ATA)

Final Report
1992 - 1994

Contract: FI3PCT920037

Duration: 1.9.92 to 30.6.95

Sector: C22

Title: Optimisation of image quality and reduction of patient exposure in medical diagnostic radiology.

1)	Maccia	CAATS
2)	Moores	IRS Ltd.
4)	Dance	Hosp. Royal Marsden
5)	Padovani	Unitá Sanitaria Locale - Udine
6)	Vañó Carruana	Univ. Madrid - Complutense

I. Summary of Project Global Objectives and Achievements

The overall observations emerged from the work carried out during the reporting period are :

- the scientific work concerning the design of an Expert System prototype for Quality Control in mammography successfully attained the objectives of the program (project n° 1, 4, 5 and 6). The benefits of such a novel approach were highlighted and compared to the current practices. Although the amount of knowledge encoded in the prototype is not sufficient to cover the whole range of real situations, a strong progress has been made in the automatic interpretation of equipment malfunctions and in the optimisation of technical parameters to be used to comply with the ALARA principle in patient radiation protection.
- the laboratories (project n° 4 and University of Linköping) involved in theoretical aspects of computing codes and mathematical simulation made significant progresses in extending their computer program to include the effects of patient inhomogeneities. Within this context, an important methodological work was carried out in order to select the most available and flexible approach to be used. The adopted solution was writing a voxel phantom computer program which enable advantage to be taken of any developments in models without major rewriting of already existing programs. This objective was completely achieved through a good cooperation of the involved laboratories.
- different studies were performed to investigate the quantitative and qualitative assessment of clinical image quality in radiology by applying the image criteria approach as suggested in the CEC Criteria Document (project n° 1, 2, 4 and 6). Results obtained were used to updating the knowledge in this field and to improve the existing CEC working document.

- an assessment of image quality from mammographic phantom images was made in view of complementing clinical image evaluation (project n° 4) (use of a computer algorithm to locate phantom features of varying contrast and size on digitized mammographic films).

Head of project 1 : Dr. Maccia

II. Objectives for the reporting period

The principal objectives for the reporting period were (1) to continue to provide relevant information to Udine laboratory in Italy concerning real equipment faults demonstrated by mammographic quality control checks. (2) to finish analysing data collected during the CEC Trial and contribute to the preparation of the final version of the CEC Document on Quality Criteria for Diagnostic Radiographic Images.

III. Progress achieved including publications

Part 1 : Expert system for Quality Control in mammography (QUACKS).

According to the work programme established together with Udine laboratory, a collection of data relating to technical malfunctions of processors was performed in order to help testing the QUACKS prototype.

A retrospective study was therefore carried out on real processor malfunctions which had involved both significant and minor trouble-shooting in the course of a routine quality control programme. A selection of twenty two different malfunctions was done for the purpose of this phase of work.

This includes problems such as increased or decreased processing temperature, timing of processing, exhausted developer, contaminated developer, developer dilution, auto-mixer failure, exhausted fixer, inadequate replenishment rate (too low), film washing, crossover assemblies and rack assemblies not correctly reinstalled, etc.

The Knowledge Acquisition Forms (KAF) provided by Udine laboratory were then used to fulfill the required technical information related to different film processing systems considered.

This interesting exercise enabled us to achieve four different objectives :

- to identify the type of QC test and related parameters which could allow the observed malfunction to be discovered (i.e. QC test: film sensitometry ; related parameter: loss of contrast index ; observed malfunction: processing time too short).
- to establish possible relationships between the observed malfunction and the corresponding image quality change or, in other words, the sensitivity of the

phantom used (the Leeds TOR MAX mammographic phantom did show relevant image parameter variations only in the case of significant malfunctions);

- to learn about the diagnostic path followed by the operating staff to actually deduce a given malfunction ;
- to compare the actual interpretations of the malfunction made by staff in charge of running the QC programme with those provided by the expert system prototype.

Finally, the fulfilled KAF were sent to Udine laboratory which used them to extend the knowledge database of QUACKS and test the robustness of the developed system.

Part 2 : Image Quality criteria.

The work carried out in this field was mainly devoted to:

- finishing the analysis of data collected during the second CEC Trial on Quality Criteria for Diagnostic Radiographic Images as requested by the other laboratories participating to the preparation of the final version of the Criteria Document .
- undertaking a complete revision of the CEC draft report issued in April 1993.

According to the workplan established in February 1994 and to the final meeting held in Bruxelles mid 1995 it was decided to consider the full report on the evaluation of the 1991 Trial under three headings : part (1) radiographic techniques and their practices in the European Union ; part (2) radiographic techniques and dose to the patient ; part (3) radiographic techniques and image quality in the European Union.

In the preparation of the final version of the Criteria Document the following tasks were carried out :

- verification of data illustrating « example of good radiographic technique » (consistency with the data gathered during the 1991 CEC trial);
- harmonisation of image criteria presentation ;
- improvement of questionnaires to be used to check the fulfilment of the image criteria
- update of scoring tables

Concerning the complete revision of the draft report issued in April 1993 a particular effort has been made in reminding historical process of the image criteria evaluation performed within the CEC radiation protection programme (first and second European trial initiatives) ; describing methodological aspects related to the image criteria ; clarifying interpretation of the results and, finally, showing the applicability of the image criteria concept as a tool for the optimisation of the image quality and radiation protection of the patient.

References

C. Maccia, M. Ariche-Cohen, C. Severo, X. Nadeau. The 1991 Trial on Quality Criteria for radiographic images CEC draft report XII/221/93.

C. Maccia, R. Renaud, S. Castellano, P. Schaffer, R. Whal, P. Haehnel, G. Dale, B. Gairard. Quality control in mammography : an initiative in France. *The British Journal of radiology*, 67, 371-383 (1994).

M. Ariche-Cohen. Validation et utilisation d'un système de critères de qualité d'image pour l'examen du rachis lombaire - Thèse pour le doctorat en Médecine (1994).

C. Maccia, X. Nadeau, R. Renaud, S. Castellano, P. Schaffer, R. Wahl, P. Haehnel, G. Dale and B. Gairard. Quality Control in Mammography : the pilot campaign of breast screening in the Bas Rhin region. *Radiation Protection Dosimetry - Quality Control and Radiation Protection of the Patient in Diagnostic Radiology and Nuclear Medicine*. Vol. 57, Nos. 1-4. 323-328, (1995) ISBN 1 870965 37X.

C. Maccia, M. Ariche-Cohen, X. Nadeau, C. Severo. The 1991 CEC Trial on Quality Criteria for Diagnostic Radiographic Images. *Radiation Protection Dosimetry - Quality Control and Radiation Protection of the Patient in Diagnostic Radiology and Nuclear Medicine*. Vol. 57, Nos. 1-4. 111-117, (1995) ISBN 1 870965 37X.

G. Contento, R. Padovani, V. Roberto, C. Della Giusta, C. Maccia. A Knowledge-Based System for Quality Control in Diagnostic Radiology. *European Radiology*, Suppl. to Vol. 5, 404. (1195).

G. Contento, R. Padovani, O. Varin, S. Castellano, C. Maccia, M. Chevalier del Rio, J.M. Fernandez Soto, P. Moran, E. Vano, V. Roberto. The use of Test Phantoms in Knowledge-Based Systems for diagnosing malfunctions of the radiological equipment. *Radiation Protection Dosimetry*, 49, 153-156 (1993).

Head of project 2: Dr. Moores

II. Objectives for the reporting period

1. To assess the results of the first two European trials of the CEC Working Document on Quality Criteria for Diagnostic Radiographic Images.
2. To continue to evaluate factors which effect image quality measurements obtained from the test phantoms in mammography with special consideration to the work presented at the Würzburg Workshop.
3. To develop a framework for incorporating test phantom measurements within the Quality Criteria.

III. Progress achieved during publications

This report covers the period 01.06.1993 to 31.05.1994 under Contract No. F13P-CT92-0037. The period 01.06.1994 to 30.06.1995 is covered under Contract No. F13P-CT92-0020 and has been reported separately.

A working party was established in February 1994 to analyse in detail the results of the European trials of the Quality Criteria Document of the Commission which had been undertaken in 1991. Detailed analysis of these results continued throughout 1994 and revision of the Criteria Document has been undertaken in mid 1995. A completed revised Document will be available by the end of 1995.

Detailed analysis of the factors which can affect image quality measurements obtained from test phantoms in mammography was undertaken. The aim of this work was to assess the viability of implementing computer aided data management systems. Results indicate that even when detailed Quality Control programmes are initiated, wide variations in image quality as assessed from test phantom images can result due to the large number of factors which can affect overall image quality. The need for the routine application of effective data management systems is paramount in order to ensure the large amount and varied data generated by such programmes can be usefully employed.

A computer based data management system was installed in April 1990 and has now been running for 5 years. The data collected and managed by the system is in accordance with the UK National Protocol guidelines for quality control in breast screening which is compatible with the European Protocol for the Quality Control of the Technical Aspects of Mammography Screening. This study has highlighted a number of important considerations:-

- Wide variations in image quality parameters are observed in routine mammographic quality control programmes. No clear guidelines exist concerning tolerances and limiting values for such image quality measures nor is there a clear understanding of their effect on overall clinical diagnosis. Our results were also supported by results obtained in two studies undertaken as part of the UK Breast Screening Programme [Young et al (1992, 1995)].

- To be fully effective computer based data management must be user friendly in that untrained staff should be able to input data accurately and efficiently. Data verification against known pre-determined tolerances is important as well as the facility to present results in an easily understood format for audit purposes.
- Computer based quality control support systems must be flexible and compatible with rapid ongoing developments in both hardware and software platforms. In particular, multi-user, multi-tasking systems are being employed increasingly in departments of radiology and quality control computer based systems must be compatible with this environment.

There is a general lack of ability, to relate objective physical measures of image quality derived from test phantom images to assessments of image quality of clinical images. Therefore, a framework for incorporating test phantom measurements within the Commission of European Communities Quality Criteria concept has been developed. It is hoped that this concept will be further developed within the Fourth Framework Research Programme.

REFERENCES

Young K.C., Ramsdale M.L. and Horton P.W. 1992. Review of Mammography Equipment and its Performance NHS Breast Screening Programme Publication No. 24, Sheffield, England

Young K.C., Ramsdale M.L. and Rust A. 1995 Mammographic Dose and Image Quality in the UK. Breast Screening Programme. NHS Breast Screening Programme Publication No. 35, Sheffield, England

IV Publications

The role of Phantoms in Standardisation of the Radiological Process. B.M. Moores Radiation Protection Dosimetry - Test Phantoms and Optimisation in Diagnostic Radiology and Nuclear Medicine. VOL 49, Nos. 1-3, 19-26 (1993) ISBN 1 870965 26.4.

Test phantoms for conventional tomography. B.M. Moores and F.E. Stieve. Radiation Protection Dosimetry. Test Phantoms and Optimisation in Diagnostic Radiology and Nuclear Medicine. VOL 49, Nos. 1-3, 219-222, (1993) ISBN 1 870965 26.4.

CEC Quality Criteria for Diagnostic Radiographic Images - Basic Concepts. B.M. Moores. Radiation Protection Dosimetry - Quality Control and Radiation Protection of the Patient in Diagnostic Radiology and Nuclear Medicine. VOL. 57, Nos. 1-4. 105-110, (1995) ISBN 1 870965 37X

Computer Applications in Radiation Protection. P.R. Cole and B.M. Moores. Radiation Protection Dosimetry - Quality Control and Radiation Protection of the Patient in Diagnostic Radiology and Nuclear Medicine. VOL 57, Nos. 1-4, 203-206, (1995)

Diagnostic Radiology: Better Images - Lower Doses, Compromise or Correlation? A European Strategy with Historical Overview. H. Schibilla and B.M. Moores. In "100 years of Radiology" Proceedings of the Belgian Roentgen Centenary Congress. 241-248, (1995) ISBN 90-8025751-6.

Head Of Project 4: Dr D R Dance

II. Objectives for the reporting period

The objectives were (1) to continue with the publication of our work on grid optimisation using a block phantom model; (2) to modify our Monte Carlo program by including the front face of the screen-film cassette and to study the influence of the cassette front material on image quality / patient dose; (3) to select a method for the inclusion of patient inhomogeneities within the model; (4) to acquire voxel phantoms simulating infant, child and adult patients; (5) to plan the efficient computation of the collision density estimator used by the program; (6) to modify and test the computer program; (7) to use the modified program to study the variation of scatter over the image plane and to optimise grid design; (8) to quantify image quality from clinical and phantom mammographic images; (9) to collect mammographic quality control data for the QUACKS database; (10) to make Monte Carlo calculations for breast dosimetry.

III. Progress achieved including publications

Introduction and organisational details

This first aspect of this project has been concerned with the development and application of a computer program which models the use of anti-scatter grids in diagnostic radiology. This program was developed under a previous CEC contract, and its realism and use has been extended here. An important part of our work program has been the addition of an inhomogeneous patient phantom and the front face of the radiographic cassette to the model. Modelling of the image receptor has been considerably extended and improved. It is our intention that the program be used to study the influence of scatter in diagnostic radiology, taking due account of patient inhomogeneities, and to optimise grid design. The work has been done jointly with the Department of Radiation Physics, University Hospital Linköping. The addition of patient inhomogeneities and cassette front has been done in London and the improvement of the receptor in Linköping, but close contact has been maintained throughout to ensure agreement in methodology at all stages. The majority of the programming and application work on the phantom in London was done by a PhD student. This student was appointed in March 1993, after the signed contract was received. She was not able, however, to begin work until the start of the Academic Year, October 1993. The consequence is a delay in the progression of the project, and although good progress has been made, the original objectives have not *yet* been fully achieved. However, it is pointed out that it is our intention to complete this work by making a study of scatter and a revised optimisation of grid design. A supplementary report will be prepared in due course.

To compensate for the delayed start to the development of our computer based model of the radiological imaging system, we have extended the work that we had planned on the quantitative assessment of image quality. The initial intention of this work was to make a pilot study of the quantitative assessment of image quality from clinical images taking into account the requirements of the CRC quality criteria document. A study was made of paired mammographic images taken with different screen-film combinations and assessments of resolution, noise and contrast were based on the appearance of the clinical images. To complement and extend this study, a computer based method of assessing test phantom images

for mammography has also been devised and tested, with most encouraging results. This is important because test phantoms are routinely used throughout Europe for mammographic quality control.

We have helped our colleagues in Udine, by obtaining data on equipment faults from the United Kingdom Breast Screening Programme, and other European colleagues by calculating data for the European protocol on dosimetry in mammography.

To facilitate the collaboration between our institution and our Swedish collaborators, annual meetings have been held in each Institution and close contact has made by fax, telephone and e-mail. The PhD student has spent 6 weeks working in Sweden learning about modelling the image receptor within the program, and attending a course on Monte Carlo methods. We are pleased to note that the work on this joint collaborative project and the previous CEC funded project with the University of Linköping has led to the Swedish PhD student being awarded the "Hanns-Langendorff-Preis 1994" by the Vereinigung Deutscher Strahlenschutzärzte.

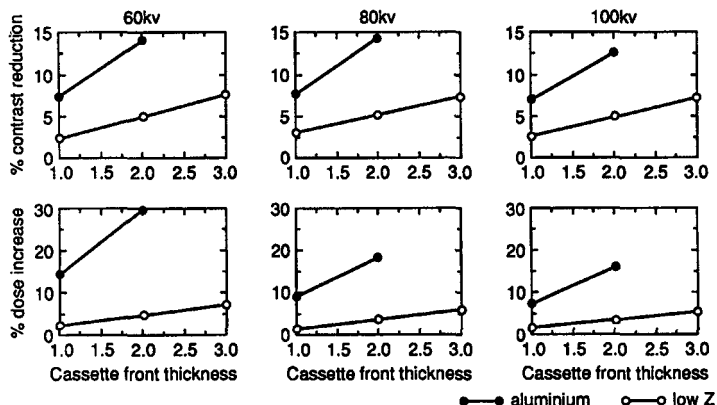
The slab model computer program and its applications

Our computer program used to model the anti-scatter grid, with the patient being simulated by a slab phantom, is based on the collision density estimator. This provides a means of calculating quantities of interest with high precision at points within the image plane. The program has been used to calculate grid performance measures for a wide range of imaging situations, and has led to several publications. During the present reporting period, papers on the advantages of low atomic number materials for grid covers and grid interspaces, and on the performance of a range of commercially available grids have been revised and are now published [1,2]. Papers have also been written and published on the optimisation of grid design for situations with small, medium and large scattering volumes [3], and on our methodology and the checks which have been made on the program [4]. A further paper on the optimisation of grid design in digital radiology has been written and published [5]. This paper includes an important experimental validation of our methodology. This involved calculation and measurement of the signal-to-noise ratio for imaging an iodine test detail with an image intensifier. The work was done by a member of the Swedish group in collaboration with staff at STUK in Helsinki and with ourselves. Papers on the program and its applications were presented at the CEC meeting on Data analysis in quality control and radiation protection of the patient in diagnostic radiology and nuclear medicine [6,7]. An invited paper on grid selection has been given at the British Institute of Radiology meeting on *Image quality in the selection of equipment* [8]. Papers have also been given at the Svenska Läkaresällskapets Handligar in Stockholm [9] and the 1995 European Congress of Radiology [10].

In the original version of the computer program, the image receptor was placed immediately after the anti-scatter grid with no intervening material apart from the lower cover to the grid. This was felt to be an appropriate model for our initial work. Now that the detail of the model is increased, the front face of the cassette has been added to the model.

It has been stated in the literature that it is good practice to use cassettes with a low atomic number entry face in order to save patient dose. Work in Sweden, however, (Leitz, private communication) has suggested that better image quality may be achieved by using a cassette with an aluminium entry face. Possible reasons for this include the generation of scatter within the low atomic number front face of the cassette, and the higher attenuation aluminium offers to the scattered radiation transmitted by the grid. We have therefore used the revised program to investigate the effect of the choice of material for the cassette front on both

radiation dose and image contrast. Four plain film radiographic examinations (PA adult chest, AP and lateral adult lumbar spine and AP paediatric pelvis) were studied. In each case cassette front thicknesses in the range 0-2 mm aluminium and 0-3 mm carbon fibre were investigated. The figure shows for the paediatric pelvis examination the dependence on tube potential of the dose increase and contrast reduction associated with various cassette fronts.



At 60 kV replacing 1 mm of aluminium with 1 or 2 mm of carbon fibre gives dose savings of 12% and 10% and contrast improvements of 5% and 2.5% respectively. Similar results were obtained for the other examinations studied, with the advantages decreasing with increasing tube potential.

The results confirm the advantage of using a low Z cassette front which can both reduce dose and improve contrast. They provide important quantification of this advantage which was not previously available. Such data must form part of any cost benefit justification for the purchase of dose saving X-ray equipment. This work was presented at the 1995 European Congress of Radiology [11] and is being prepared for publication.

The voxel model computer program and its applications

Our Monte Carlo program which models the patient as a homogeneous slab of tissue has provided a number of very useful results. The program does, however, have a number of important limitations. These include the facts that the amount of scatter recorded in the image will vary across the image plane due to patient inhomogeneities and that no account has been taken of the dynamic range of the image receptor. In addition, system optimisation is based on minimising the energy imparted to the patient slab, rather than effective dose or organ dose. It was therefore decided to make a major extension of the program to include the effects of patient inhomogeneities.

Studies were made of the methodologies available for incorporating patient inhomogeneities into the program. Three types of inhomogeneous phantom have been described in the literature. The first describes the human body and the organs which it contains in terms of combinations of simple geometrical volumes defined in a closed form by the mathematical equations of their surfaces. Geometrical models are available for both children and adults and, for example, are used by the group at NRPB in Chilton. The second type of phantom describes the patient in terms of a series of voxels of known composition and size. Voxel data is avail-

able for children from the group at GSF in Neuherberg [19]. The third type of phantom treats the patient as a series of slices, with the intersection of each organ with the slice being treated as a cylinder defined by a series of boundary points. Phantoms of this type are being used, for example, by the group at STUK in Helsinki. Contact was made with the above three groups with a view to using the best available data for our purposes. It was clear from these contacts that phantom development for radiation dosimetry is still being actively pursued. In view of this we thought there were advantages in developing code which can use data obtained from any of the above models. It was therefore decided to develop a voxel based model. This approach had the important advantage that it could use input data from any of the above sources (for example, the geometrical model could be interpreted as its voxel based equivalent). We have therefore retained maximum flexibility which will enable advantage to be taken of any developments in models without major rewriting of the program.

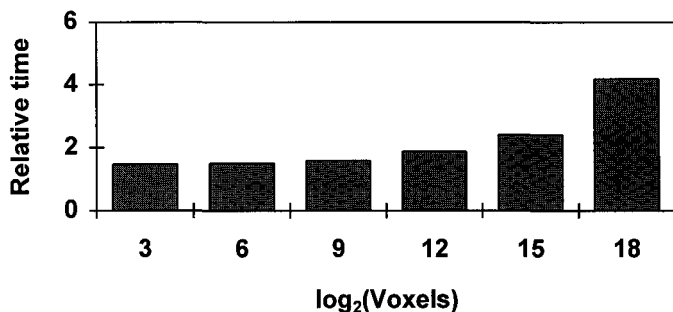
Three voxel based mathematical phantoms were acquired which simulate an 8 week old baby, a 7 year old child and an adult male. We do not think that anyone has yet constructed an adult female voxel phantom. The baby and child phantoms were obtained from GSF [19], who have also provided code for reading the data files. In these models the voxels are 8 mm in height and 1.54 mm in width and depth. Seven different tissues are simulated. Both compact bone and bone marrow are modelled with the bone marrow of the baby being denser than that of the child because it consists only of active (red) marrow. Good contact has been established with GSF to facilitate the use of these phantoms. The adult phantom was obtained from Yale University School of Medicine [20]. It represents a male patient of weight 70.5 kg and height 1.78 m. The voxels are 10 mm and 5 mm in the body and head regions respectively and 4 mm in the other two directions. Contact has also been established with the group at Yale.

The Monte Carlo program makes use of a variance reduction technique known as the collision density estimator. This is necessary in order to calculate with high precision the amount of scatter reaching small areas in the image plane. An important consequence of the use of this estimator is that it is necessary to calculate the full radiological path lengths between photon interaction points in the phantom and the points of interest in the image plane. This calculation is not necessary for analogue Monte Carlo calculations of organ dose and is very computationally intensive. It was anticipated therefore that a major obstacle to the use of the computer program for extended investigations would be the computation time required. An efficient computation strategy was therefore devised making use of the method of Coleman [21] to select interaction points and the method of Siddon [22] to determine the radiological path lengths required for the computation of the collision density estimator.

The writing of the voxel phantom computer program has now been completed. The figure shows how the computation time varies with the number of voxels in the phantom. The computation times are normalised to the equivalent time taken using the slab phantom. For fewer than about 1000 voxels, the computation time is dominated by processes other than the computation of the radiological path length. As the number of voxels increases, the computation of the radiological path length becomes dominant and the computation time doubles with every eight fold increase in the number of voxels. The figure demonstrates that the time overhead for computation with voxel phantoms is not unacceptable and indeed it is within the power of the computers which are available to us.

An important part of the development of any computer program is validation. This program has been validated in two ways. Firstly, the existing slab phantom was voxelised and the results compared with the original runs. Secondly calculations of the doses to the various or-

gans within one of the phantoms have been compared with the results obtained at GSF. For the this purpose care was taken to use the same X-ray spectra. Good agreement was obtained for both checks. This also provides a validation of the work at GSF. Work is now in progress to quantify the variation of scatter over the image plane, and to study the effect on the dynamic range of the image and the optimisation of grid design.



Work-in-progress papers on the work with the voxel phantom had been given at CIEMAT [12] and at the recent NRPB workshop [13]. An invited teach-in review, which includes this work, will be given at the 1996 Annual Congress of the British Institute of Radiology.

Receptor modelling

The work by our collaborators in Linköping on modelling receptor resolution and noise has been both experimental and theoretical. The aim of the work is develop and validate theoretical models, which can in due course be used for system optimisation. We have participated in the direction and planning of this work and discussion of the results obtained. An important initial step that we made was a literature survey of the factors which control and limit the performance of screen-film systems and of the barium fluoro-halide imaging plates used for computed radiography. This survey has been summarised and published in [14,15].

As a separate report of the work in Linköping is not being provided, an outline of this work is included here. As a starting point it was considered important to explore the limits of the previous model which only considers low spatial frequencies i.e. large-area details. Simultaneous measurements of the signal-to-noise ratio, SNR, and mean absorbed dose, D, in an acrylic phantom were therefore performed with a Philips image intensifier for disc-details of 1-10 mm diameter, using methods developed by Tapiovaara. In many X-ray imaging systems image quality, as expressed by the square of the SNR, depends linearly on the absorbed dose in the patient for a wide range of doses, if the conditions of the examination are left unchanged. It is then possible to optimise the imaging system by finding the imaging conditions where the patient dose is utilised in the most efficient way, i.e. SNR^2 / D is minimised. The measurements were compared to Monte Carlo simulations as the size of the test detail was reduced. The results show [16] that the model accurately predicted the value of SNR^2 within the measurement accuracy for details with a diameter larger than 3 mm, when corrections for non-quantum noise (video noise 1-7% of total noise) and certain statistical factors were made. The good agreement has encouraged the use of the model for the evaluation of image

quality in fluoroscopy by studying the effects of changes in tube potential, added filter, grid design, receptor protective layer and receptor thickness [16].

The modelling of fluorescent screens has also been studied, specially the effects on unsharpness of the diffusion of light photons and the absorption of characteristic K-photons. The light photon diffusion in the fluorescent screen was included in the model by adopting an expression developed by Swank. This model enables the calculation of the contribution from different layers of the screen to the total light reaching the optical detector (film) as well as to the modulation transfer function, MTF. It further allows calculation of the additional noise, due to unequal light outputs from equal X-ray absorption in the receptor. Including the crossover of light from one film emulsion to the other is important for some screen-film systems and preliminary methods have been developed to take this into account. The energy and spatial frequency dependence of signal and noise due to absorbed K-photons was included by simulating the line spread functions of such photons in the receptor using Monte Carlo techniques.

Assessment of image quality from clinical mammograms

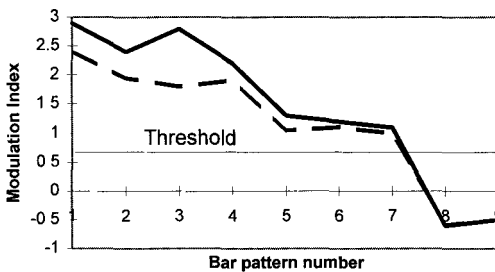
A pilot study has been performed to investigate the quantitative assessment of clinical image quality in radiology. The mammographic examination was selected for the study because of our experience of quality control [17] and the computer analysis of images for this examination. For mammography the CEC quality criteria document [23] requires visually sharp images with good imaging performance of round details and of micro-calcifications. In this initial study we developed measures of contrast, noise and unsharpness. These three quantities are of particular relevance to the detection of the above mammographic features. Measures of image quality should take into account the variation of slope of the film characteristic over the image. This slope is small in regions of high and low density leading to inadequate contrast, increased noise and loss of image information. Our measures of contrast and noise provide information about performance over the full range of densities in the image. The contrast measure was based on weighted averages of the local slope of the film characteristic and the noise measure on averages of the local noise determined using an analysis technique developed in our group (as part of a different research program) [24]. Six pairs of mammograms were digitised at 50 micron resolution using our Joyce-Loebl scanning microdensitometer. Each pair comprised two images taken in the medio-lateral oblique projection of the same breast using different screen-film combinations. The images were available because of a change in screen-film combinations and correspond to different visits to the Hospital. Each image was segmented into background, adipose tissue, breast parenchyma and pectoral muscle using neural network software have developed previously (as part of a different research project) [25]. The breast parenchyma is the region where the breast cancer is usually detected. The measures of contrast and noise were applied separately to the adipose and parenchymal regions. In each case and for each region there were differences between images taken with the two screen-film combinations. The differences were statistically significant and were consistent with visual assessment of the films. The methods developed for assessing unsharpness were based on measuring the edge profiles of breast structures. These measures did not show significant differences between the different screen-film combinations. It is concluded that our measures of noise and contrast may be of some value and further investigation is justified.

Assessment of image quality from phantom images

The need for test objects that can provide an objective measure of image quality pertinent to clinical problems is well documented, and we have complemented our clinical study with a study of the use of computers to read mammographic test phantom images. Recent studies, in which the performance of routinely used test objects is compared, demonstrate that these are not as sensitive to known changes in the imaging system as would be desired. Most test objects rely on the identification by an observer of a number of elements in well defined positions (such as occur in the Leeds TOR (MAX) test object). It is inevitable that, despite explicit instructions for viewing the image, each observer will apply his or her own decision criteria, and the resulting inter-observer variations may be greater than the fluctuations in image quality that the QC programme is seeking to detect. We have tried to develop a set of objective measures of image quality which can be automatically extracted from the image.

A set of 25 films was digitised using our high resolution scanning microdensitometer. The films were selected retrospectively from two years' quality control test films as examples of a) continuous system operation, b) changes in system operation, such as introduction of new film-screen combinations, and c) different imaging systems.

The image of the test object contain features which are assessed to extract measures of the quality of the imaging system. These include horizontal and vertical high resolution gratings, a low contrast test grating, circular details of varying contrast and size. We have developed a computer algorithm to locate some of these features in the digitised image, so that the film may be scored automatically. Our results show that the computer scores for each test detail can reliably reproduce the average scores of 5 human observers, and that the variability of the computer scoring system is less than that of the human observers. This is an important advantage which we believe should be exploited for national comparisons of imaging performance. It should be noted however, that we did not attempt to automatically locate the smallest details (0.25 mm) details in the phantom. This was a more difficult task for which there was insufficient time.



The scoring system that we have developed is based on calculated values of various parameters exceeding a pre-defined threshold. This mimics the scoring process of the human observer. It may not, however, offer the best discrimination possible between systems, and we believe that integral rather than point measures may be more valid. The figure illustrates this by demonstrating a modulation index

measured for the set of low contrast test gratings and for two different films. Both films achieve the same score as their curves cross at the threshold value, but one film will offer higher modulation than the other when the threshold is exceeded. We recommend therefore that alternative methods of scoring test phantom images be investigated.

This work was presented at the 1995 UK Röntgen Centenary Congress [18] and is being prepared for publication.

Survey of fault indications from mammographic quality control

We have helped our colleagues in Udine to extend their data base of mammographic equipment faults demonstrated by mammographic quality control. This data is needed as part of the development and testing of their "QUACKS" expert system. Following discussion with the United Kingdom National Centre for the Physics of Mammography, and with the group at Udine, 69 faults from 42 centres were identified as being of interest. The nature of the faults is listed in the table. Contact was established with 40 centres covering 66 faults. Copies of the "Knowledge Acquisition Forms" developed at Udine were sent with an explanatory letter and a copy of a completed form for guidance. Replies for a total of 32

Nature of faults	No of faults
automatic exposure control	25
compression or Bucky assembly	7
"suspicious exposures"	4
loss of image quality	1
film processing	32

faults were received and forward to Udine. We analysed the quality of the responses, and identified particular problems related to how well the fault was initially documented or remembered. Feedback from correspondents indicated the difficulty in conducting this exercise is retrospect.

Comparison of breast dose measurement protocols

We undertook as part of this contract to make Monte Carlo calculations using our model of the mammographic imaging system where this would provide useful information for other contractors.

The Commission of the European Communities has been paying special attention to the mammographic examination because of its importance in the screen detection of breast cancer. One of the initiatives being supported is the production of a European Protocol for Dosimetry in Mammography. This protocol presents standardised approaches which may be used throughout Europe. There are, however, many different national protocols in use and it is important to be able to relate breast doses measured using these different protocols. We have modified and used our computer program [26] to simulate the different protocols and to provide factors which may be used to convert between them. The calculations were based on the assumption that in each case the same amount on energy is absorbed per unit incident area of a gadolinium oxysulphide mammographic screen and allowance was made for the presence of a mammographic anti-scatter grid. The calculations were made for five radiation qualities, and four thicknesses of Perspex. Similar calculations were made by H Zoetelief in Holland, and good agreement was obtained. The resulting table in the European protocol [27] gives conversion factors which facilitate comparison with the IPSM, NRPA/SSI, AAPM, NCS, SEFM/SEPR and GIM protocols.

References: (a) Publications and presentations

1. Sandborg M, Dance D R, Alm Carlsson G and Persliden J 1993 Selection of anti-scatter grids for different imaging tasks: the advantage of low atomic number cover and inter-space material. *Brit. J. Radiol.* **66** 1151-1163

2. Sandborg M, Dance D R, Alm Carlsson G and Persliden J 1993 Monte Carlo study of grid performance in diagnostic radiology: factors which affect the selection of tube potential and grid ratio. *Brit. J Radiol.* 66 1164-1176
3. Sandborg M, Dance D R, Alm Carlsson G and Persliden J 1994 Monte Carlo study of grid performance in diagnostic radiology: task dependent optimisation for screen-film imaging. *Brit. J. Radiol.* *Brit. J Radiol.* 67 76-85
4. Sandborg M, Dance D R, Alm Carlsson G and Persliden J 1994 A Monte Carlo program for the simulation of image quality and absorbed dose in diagnostic radiology. *Computer Methods and Programs in Biomedicine* 42(3) 167-180
5. Sandborg M, Dance D R, Alm Carlsson G, Persliden J and Tapiovaara M J 1994 Monte Carlo study of grid performance in diagnostic radiology: task dependent optimisation for digital imaging. *Phys. Med. Biol.* 39 1659-1676
6. Dance D R, Sandborg M, Alm Carlsson G and Persliden J 1995 Optimisation of the design of anti-scatter grids by computer modelling. CEC Workshop on Data analysis in quality control and radiation protection of the patient in diagnostic radiology and nuclear medicine, Grado, Italy, October 1993. *Rad. Prot. Dosim.* 57 207-210
7. Sandborg M, Dance D R, Alm Carlsson G and Persliden J 1995 Results from an optimisation of grid design in diagnostic radiology. CEC Workshop on Data analysis in quality control and radiation protection of the patient in diagnostic radiology and nuclear medicine, Grado, Italy, October 1993. *Rad. Prot. Dosim.* 57 211-215
8. Sandborg M, Dance D R, Alm Carlsson G and Persliden J 1993 Selection of anti-scatter grids for different imaging tasks. Invited paper presented at British Institute of Radiology meeting on Image quality in the selection of equipment, London, 2 February 1993.
9. Sandborg M, Dance D R, Alm Carlsson G and Persliden J 1992 Optimal val av raster för röntgendiagnostik (Abstract). *Svenska Läkaresällskapets Handlingar, Hygiea*, 101 258
10. Sandborg M, Dance D R, Alm Carlsson G and Persliden J 1995 A Monte Carlo study of grid performance in diagnostic radiology: task dependent optimisation for digital imaging Scientific Programme and Abstracts, 9th European Congress of Radiology, Vienna, March 1995 p70
11. Lester S A, Dance D R, Sandborg M , Alm Carlsson G and Persliden J 1995 Calculation of radiographic cassette performance: the advantage of low atomic number cassette fronts. Scientific Programme and Abstracts, 9th European Congress of Radiology, Vienna, March 1995 p398
12. Dance D R and Alm Carlsson G 1994 Optimisation of the design of anti-scatter grids by computer modelling. Invited lecture. Seminar on the optimisation of image quality and the reduction of patient dose in diagnostic radiology. CIEMAT and The Medical School, Complutense University, Madrid, December 1994
13. Dance D R, Lester S A, Sandborg M , Alm Carlsson G and Persliden 1995 Simulation of X-ray imaging systems using a Monte Carlo computer program. NRPB workshop on voxel phantoms, July 1995.
14. Dance D R 1994 Radiographic films and screens. In *Medical radiation detectors: fundamental and applied aspects*. Proceedings of First Mayneord-Phillips Summer School, Oxford, July 1993. Ed N Kember (Institute of Physics, New York) pp57-73
15. Dance D R 1994 Storage phosphor plates and Xerox receptors. In *Medical radiation detectors: fundamental and applied aspects*. Proceedings of First Mayneord-Phillips Summer School, Oxford, July 1993. Ed N Kember (Institute of Physics, New York) pp75-87
16. Tapiovaara M J and Sandborg M 1995 Optimisation of fluoroscopy. Comparison of measurements and Monte Carlo calculations. *Phys. Med. Biol.* 40 589-607 (work by Linköping and STUK only)

17. Castellano I A, Dance D R, Davis R, Evans S H, Jones C H and Parsons C A 1995 Quality assurance and patient dosimetry in mammography: a retrospective. CEC Workshop on Data analysis in quality control and radiation protection of the patient in diagnostic radiology and nuclear medicine, Grado, Italy, October 1993. *Rad. Prot. Dosim.* 57 159-162
18. Smith A D, Dance D R and Castellano I A 1995 Objective assessment of image quality in mammography: a feasibility study. Programme and Abstracts Book, Röntgen Centenary Congress, Birmingham, June 1995, p248

References: (b) Other papers cited in text

19. Zankl M, Veit R, Williams G, Schneider K, Fendl H, Petoussi N and Drexler G 1988. The construction of computer tomographic phantoms and their application in diagnostic radiology and radiation protection. *Radiat. Environ. Biophys.* 27 153-164
20. Zubal I G, Harrell C R, Smith E O, Z, Gindi G and Hoffer P B 1994 Computerised three-dimensional segmented human anatomy. *Med. Phys.* 21 299-302
21. Coleman W A 1968 Mathematical verification of a certain Monte Carlo sampling technique. *Nucl. Science Eng.* 32 76-81
22. Siddon R 1985 Fast calculation of the exact radiological path for a three dimensional CT array. *Med. Phys.* 12 252-255
23. Moores B M, Wall B F, Eriskat H and Schibilla H (Editors) 1989 Quality criteria for diagnostic radiographic images. BIR Report 20 271-278
24. Parker J 1995 Ph D thesis (in preparation)
25. Suckling J, Dance D R, Moscovic E, Lewis D J and Blacker S G 1995 Segmentation of mammograms using self-organising neural networks. *Medical Physics* 22 145-152.
26. Dance D R 1990 Monte Carlo calculation of conversion factors for the estimation of mean glandular breast dose. *Phys. Med. Biol.* 35 1211-1219
27. Zoetelief Z, Fitzgerald M, Leitz W and Säbel M 1995 European protocol on dosimetry in mammography (draft).

Head of project 5: Dr. Padovani

II. Objectives for the reporting period

The revision and improvement of the prototype of a knowledge based system for quality control in mammography along the following lines:

- modelisation of the problem solving process according to a well established methodology,
- use of the logbook data in the inferential process to exploit redundancy for supporting conclusions and to increase the system ability to make differential diagnoses of the malfunctions of the radiological system;
- generalisation of the inference machine to support diagnoses based on data collected with phantoms other than the Leeds Tor[Max];
- experimental simulations of malfunctions of the radiological system and their effects on phantom test images;
- development of a protocol for the knowledge acquisition process.

III. Progress achieved including publications

Modelisation of the problem solving process

Conceptual modelling is a major step in the development of Knowledge Based Systems (KBS). We carried out the conceptual analysis referring to the KADS methodology and identified two basic levels: domain and tasks.

At the domain level, object structures have been identified and organised in hierarchies of semantic networks, with usual relations as arc labels. e.g., Has, Part-of for part/whole and Is-a for set membership and inclusion relations. Malfunctions and symptoms are also organised in networks. Details concerning the conceptual model of domain objects, concepts and relations have been reported elsewhere [2,3,4,5].

Quality Control tasks have been structured into three levels of abstraction associated to planning, generic actions and specific actions respectively. *Planning* is the ability of animals and humans to select the most appropriate set of actions to achieve a specified goal: we call plan a set of such actions; a plan includes high-level tasks, called *phases*. Examples of plans are verifying the equipment conformity with purchase specifications at acceptance testing; optimising the equipment performance; executing routine tests; consulting the log-book.

Examples of phases include activities as: input of data, plausibility/consistency checks fo input data, comparison with baseline, diagnose of malfunctions. Phases are chosen so as to maintain a wide general scope, independent of the type of test under consideration.

Each phase is formed by sub-tasks, the *generic actions*, which are not directly involved in planning, but still result in a set of more specific activities. The relations between generic actions represent the logical or chronological connections between the parts of a QC procedure. Generic actions are usually test-dependent. *Specific actions* are decisions/physical operations to be taken on the environment. Some of them are inferences, i.e. operations to be taken as consequences of some premises.

One example will help to clarify the conceptual model and show the type of knowledge and tasks underlying the expertise in QC. The example refers to the use of a test object for assessing image quality in mammography. Various test objects have been devised to measure routine imaging performance of mammographic units. Test objects usually include physical details for measuring the low-contrast sensitivity and the high-contrast spatial resolution, thus having the advantage to provide an immediate evaluation of image quality. Once a variation of performance is detected, the significance of this change should be investigated. However, it

may not be easily understood what is the cause of the imaging deficiency, because a lot of individual relevant parameters concur to form the image. For example, a loss of low-contrast sensitivity could be determined by one or more factors, including film processing conditions, film storage conditions, kVp calibration, tube filtration, increase in the scattering component of radiation.

Additional information is therefore needed to individuate likely causes of changes. Two are the sources of information:

- i) the results of previous QC tests performed to assess individual relevant parameters; they can be retrieved from the log-book;
- ii) further tests, specially devised to discern possible causes of the problem

A schematic tree of procedures and sub-tasks at the generic action level is represented in Figure 1.

Table I. Examples of tasks at all the conceptual levels: phases, generic and specific actions.

PLAN: Phantom Test Execution and Diagnosis				
PHASE	Generic Action	Specific Action		
		<i>Findings</i>		<i>Associations</i>
ANALYSE	Comparison with baseline	For every observable of the phantom image: there is no significant difference from baseline values		The equipment works properly
	Comparison with baseline	For every observable of the phantom image: there is a significant difference from baseline values		The equipment may not work properly The phantom test may have been executed incorrectly
DIAGNOSE	Heuristic Classification	Overall film density increases High-Contrast Resolution and Low-Contrast Sensitivity are unchanged mAs readout is outside the limiting value Film processor works properly	AND AND AND	Possible failure of the Automatic Exposure Control
	Heuristic Classification	Overall film density increases High-Contrast Resolution and Low-Contrast Sensitivity are unchanged mAs readout is within the limiting value Film processor works properly	AND AND AND	Possible variation of film batch speed Incorrect exposure geometry Wrong cassette
	Heuristic Classification	Overall film density is unchanged Low-Contrast Sensitivity is decreased The decrease is sudden Film processor works properly	AND AND AND	kVp miscalibration Incorrect test execution Bad viewing conditions Imperfect screen-film contact
	Diagnosis Refinement	Cause under investigation is AEC failure		Check the AEC reproducibility results in the log-book. Perform a repeatability measurement.
	Diagnosis Refinement	Cause under investigation is AEC failure AEC repeatability measurements are outside 10% of the mean	AND	Confirm the malfunction AEC failure

PHANTOM TEST (FILM PROCESSOR WORKS PROPERLY)

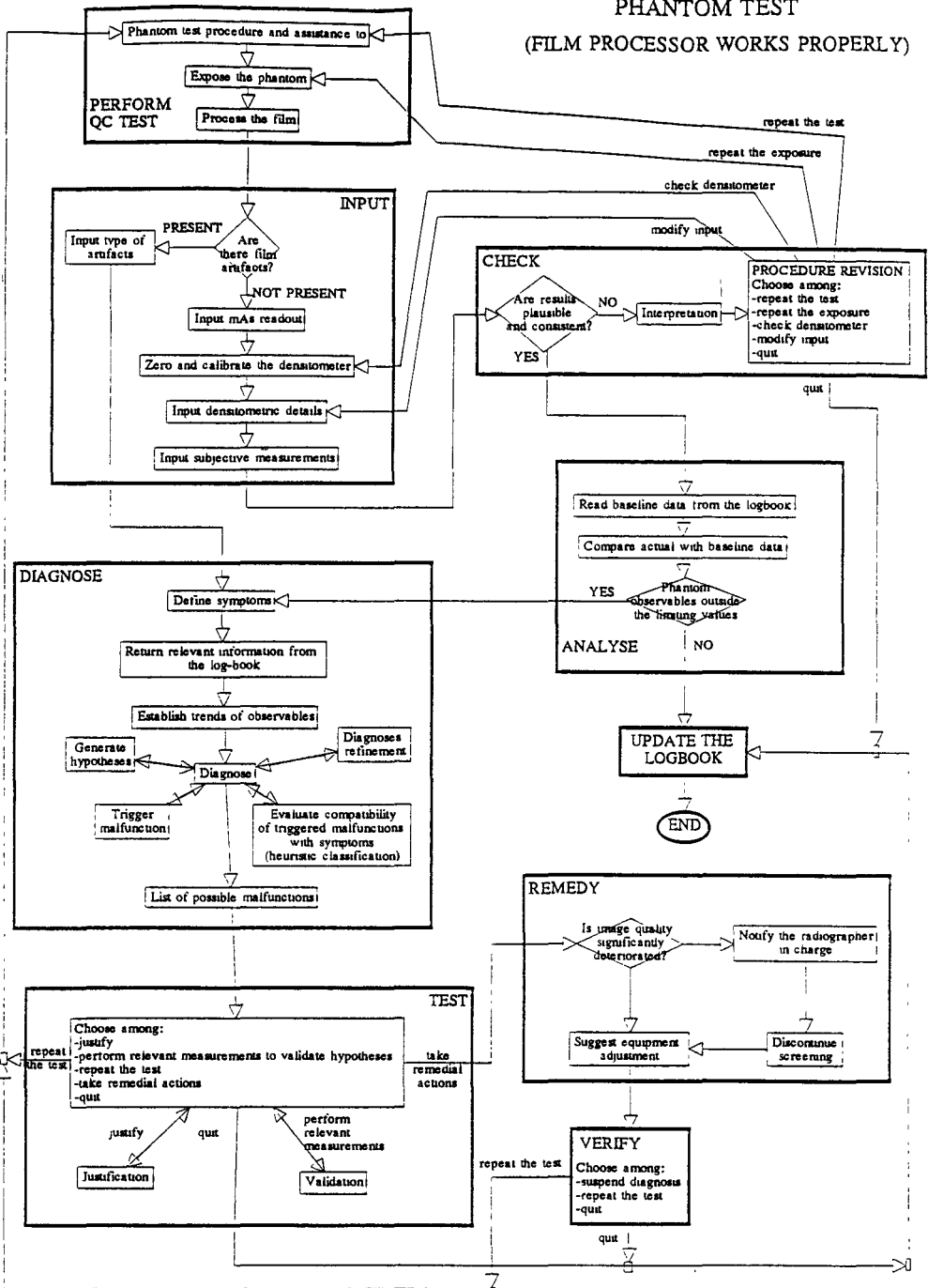


Figure 1. The test to assess image quality with a performance phantom in mammography. Phases are expanded to show the underlying generic actions. The complexity of the plan justifies the introduction of several levels of action descriptions.

It is supposed that, immediately before the phantom test, a sensitometric test has been performed so as to ascertain a proper behaviour of the film processing system. Each node necessitates further development and explicit description in terms of the observables of the phantom, which typically include base+fog, background, high and low-contrast resolution, low-contrast sensitivity, small-detail visibility. Expansions may be conveniently done at the specific action level (Table I).

The logbook.

The diagnostic system acquires greater power by accessing the information stored in the logbook (a database) to allow comparisons, discover trends, detect abnormal functions even before control limits are reached.

Inter alia, the log-book includes the following information: results of test procedures, reference information and histories of previously debugged problems.

Since results of tests must be evaluated immediately by comparison at least with baseline performance and limiting values, the log-book must contain some reference information concerning:

1. *General reference standards* of performance for equipment with the same specifications. They serve to ascertain compliance with minimum levels of performance usually achievable with that kind of equipment.
2. *Departmental standards*. Uniformity of performance at departmental level is also of great value and variations between equipments (e.g., the difference in radiation output from the various generators for a given mA and kVp) should be determined against average departmental standards.
3. *Baselines*. They define the current level of performance of the equipment by means of the results of QC tests performed soon after the most recent optimisation phase.
4. *Tolerances*. Maximum errors (precision) of measurements tolerated in QC tests.
5. *Limiting values*. Maximum allowable variations of the test results from the baseline.

As for the representation of reference information, it seems convenient to define standards and baselines as instances of the frame TEST [3,4] thus allowing straightforward comparison with the results of tests. Tolerances may be represented as instances of the object TEST-TOOL since they depend on the type of measuring device. Eventually, limiting values themselves are to be represented as objects of type TEST. A case histories library will help every accessor to the log-book to find out analogies and similarities with previously-solved problems encountered with the same equipment.

Adaptability to different environments and instruments.

The architecture of the KBS is so devised that local aspects of organisation (e.g. maintenance surveys), idiosyncracies of the radiological equipment (e.g., ascertained and not remediable defects that can produce known effects), and methods and instruments of QC procedures can be accounted for into the system. As a general strategy adopted in the architecture, is the system that must adapt itself to the local context and not viceversa. First, the user is free to maintain his own QC protocol. He/she only has to teach the system what his/her protocol is: type and frequency of tests, instruments used. This is made in a configuration phase preliminary to the effective use of the system. For instance, the prototype uses the Leeds TOR[MAX] performance phantom, but the system is ready to accept every other phantom existent or of future implementation. Another structure that helps to take account of practical situations are the *evaluation rules*. They make feasible to modify the possibility values (the credibility) of the different interpretations of equipment problems

Knowledge Acquisition.

A crucial step in the development of a knowledge-based system is the knowledge acquisition. To standardise the collection of information from different experts a number of *Knowledge Acquisition Forms* has been designed with the following objectives:

- define type and frequencies of the malfunctions of the radiological equipment (including the film processor);
- identify the measurements (QC tests) that in practice discover the malfunction,
- establish relationships (also empirical and qualitative) between the malfunction and its effects on the image quality;
- learn how different experts find out the type of malfunction from the observations (*the diagnostic path*). The diagnostic path includes interventions, inspections and measurements following the initial event and taken to diagnose the cause of the malfunction.

The forms help the expert to identify and communicate the relevant information in a manner suitable for the knowledge representation. Besides details concerning the equipment and the QC programme, important data useful for the knowledge base of the system are: the description of the malfunction, including the final diagnosis; the event that discovered the malfunction and, where available, any further information that can help to identify the state of the equipment (e.g. trends of some observable measured during the QC programme); how the malfunction was diagnosed starting from the initial event. The forms have been distributed to the partners of the present contract and some retrospective data collected

Tests and Performances

The first attempt to evaluate the KBS was informal, simply to show that a few practical cases could be handled by the prototype system. Informal test cases were run through the developing system, the system's performance was observed and feedback was sought from the expert collaborators and potential end-users. This iterative process was protracted until the actual stage of system development was attained, where the knowledge base and the reasoning process seem sound and consistent. In the next stage, a systematic evaluation of performance was attempted by feeding the system with real data (a phantom image and a sensitometric strip) obtained in a study designed for the evaluation of the sensitivity of the Leeds TOR[*MAX*] mammographic phantom [6]. In this study, several malfunctions affecting the X-ray unit performance were simulated in a controlled environment by purposely varying the kilovoltage, the density control of the Automatic Exposure Control (AEC), the phantom position and the filter type.

Forty-two tests were run and the results, conveniently lumped in 8 groups, are shown in Table II.

These performance tests made it possible to reach the following conclusions:

- The system is sufficiently not sensitive to small fluctuations in the performance of both AEC and film processor, and intra-batch changes in film sensitivity. Ten cases of no fault (baseline conditions) were properly processed by the system, though exhibiting significant differences between them (Table II, Test Group 1).
- As a consequence of the low sensitivity of the used phantom [2], the system is unable to detect early manifestations of malfunctions of the mammographic equipment (Table II, Test Groups 2,3).
- Where the effects of malfunctions on the phantom image are relevant, the system is able to make sound hypotheses and properly discriminate among the different types of malfunctions (Table II, Test Groups 4,5)

Table II. Tests of the prototype based on simulations of malfunctions of the X-ray unit, performed on a mammographic unit in a controlled environment. The input data are the sensitometric strip and the observables of the Leeds TOR[**MAX**] phantom, including film densities, contrast and resolution. The reliability of a hypothesis expresses the degree of consistency of the input data with the symptoms typically disclosed by the malfunction.

Test Group	Number of cases	Simulated malfunction	Diagnosis (number of cases)	Average Reliability
1	10	No malfunction (Baseline)	No malfunction (10)	--
			No malfunction (6)	
2	10	Density Control: one step variation	Variation of film batch speed (4)	0.60
			Densitometer out of control (1)	0.27
3	10	Kilovoltage: 1 kVp variation	No malfunction (9)	--
			Lack of kVp reproducibility (1)	0.1
4	4	Kilovoltage: 3 kVp variation	Lack of correspondence between actual and indicated kVp (4)	0.76
			Lack of kVp reproducibility (4)	0.32
			Lack of output reproducibility (4)	0.67
5	4	Density Control: 2 steps variation	Lack of AEC reproducibility (4)	0.51
			Failure of the AEC (4)	0.20
			Variation of film batch speed (4)	0.10
			Failure of the AEC (2)	0.58
6	2	Different Filter: 0.75 mm Al	Lack of output reproducibility (2)	0.43
			Lack of AEC reproducibility (2)	0.29
			Lack of correspondence between actual and indicated kVp (1)	0.90
7	1	Kilovoltage: 3 kVp variation. Density Control: one step variation	Lack of kVp reproducibility (1)	0.40
			Erroneous film-to-film distance (1)	0.31
			Phantom not exactly positioned (1)	0.80
8	1	Kilovoltage: 3 kVp variation Phantom position shifted	Lack of output reproducibility (1)	0.77
			Lack of AEC reproducibility (1)	0.77
			Failure of the AEC (1)	0.74

Three other groups (6,7,8) of simulated cases were investigated to probe the responses of the system to situations not yet fully implemented in the KBS. Obviously, the system cannot be expected to provide the correct diagnosis when the malfunction is not encoded in the

malfunction database. However, we were interested in the degradation of the system performances, i.e. how the system responses are related to the correct ones. For example, at the time of testing a change in the filter type was not included in the malfunction database. One case (Table II, Test Group 6) was run and the system suggested a problem of output or AEC, thus privileging in its interpretation the effect of the absorption more than the hardening of the X-ray beam. Other tests (Table II, Test Groups 7,8) were concerned with two simultaneous malfunctions to underpin the intrinsic robustness of the system: the latter reacts by evidencing the more striking malfunction (Test Group 7), or both when sufficiently independent effects are observed (Test Group 8).

Conclusions and perspectives

A conceptual analysis has been performed on typical QC activities: we individuated relevant objects, concepts, actions, plans, all occurring in the work of a domain expert. The resulting documents were used as the main source of information to design a KBS aimed at assisting a human operator in QC tests on a mammographic equipment.

A prototype of the KBS has been realised to assess, on practical grounds, the validity and limitations of the proposed approach.

We highlight the benefits of the novel approach proposed as compared to the current practices. In routine QC of a mammographic equipment, a well accepted and widely used protocol prescribes the daily execution of a sensitometric strip and a performance phantom test by a radiographer. Data acquisition requires the measurements of optical densities and the subjective evaluations of the visibility of a number of different details embedded in the phantom. These procedures remain substantially unaffected in the novel approach when a manual input of data is performed.

In case of significant variations from the baseline conditions, the non-expert is faced to unresolvable problems: stops of the radiological activity and calls to the service engineer are the most likely consequences. This is the situation where the KBS mostly shows its potential benefits: the diagnostic module is able to support the unexperienced user with friendly hypotheses on the possible causes of the malfunction; new tests or repetition of the executed tests may be suggested to refine the diagnosis; when possible, remedial actions can be proposed to help the user to recover the equipment working conditions. In an alternative scenario, the QC expert himself can freely use the features of the KBS as a decision-aid tool.

Moreover, peculiar benefits of the AI approach include the availability of an integrated and consistent set of databases where all the relevant knowledge is encoded. Consultation and updating of this information is feasible with little effort by the user. In this framework, room is given even to site-specific practices ranging from test-tools, measuring instruments and radiological equipment to procedures and protocols. For all these features, a KBS might be used as a powerful tool for training, since students are allowed to design and carry out simulations and novel experiments, learn from mistakes and suffer the results born from insufficient data.

At present, the amount of knowledge encoded in the system prototype is not sufficient to cover the whole range of practical situations. The system should undergo several developments while preserving its basic architecture. In particular, the databases of objects, malfunctions, symptoms and plans should be extended. The diagnosis mechanism should be developed by including contextual (dependent on active hypotheses) information that guides the user in the acquisition of additional data to refine the diagnosis. Hypertext and related techniques could be designed to enrich the user-system dialogue.

List of Publications

- [1] CONTENTO G., PADOVANI R., CASTELLANO S., MACCIA C., 1991. An Expert System for Quality Control for X-Ray Diagnostic Imaging Equipment. *Medical & Biological Engineering & Computing*, Suppl. to Vol 29, 203.
- [2] CONTENTO G., PADOVANI R., VARIN O., CASTELLANO S., MACCIA C., CHEVALIER DEL RIO M., FERNANDEZ SOTO J.M., MORAN PENCO P, VAÑO CARRUANA E. & ROBERTO V., 1993. The Use of Test Phantoms in Knowledge-Based Systems for Diagnosing Malfunctions of the Radiological Equipment. *Radiation Protection Dosimetry*, 49, 153-156.
- [3] CONTENTO G., PADOVANI R., ROBERTO V. , VARIN O. & DELLA GIUSTA C., 1995. Knowledge-Based Approach to Quality Control in Diagnostic Radiology. *Radiation Protection Dosimetry*, 57, 185-189
- [4] PADOVANI R., CONTENTO G. CEC Radiation Protection programme, Annual Report 1993
- [5] PADOVANI R., CONTENTO G. CEC Radiation Protection programme, Annual Report 1994.
- [6] MORAN P., CHEVALIER M, CONTENTO G., VAÑO E. , 1993. Evaluation of the Sensitivity of the Leeds TOR(MAX) Mammographic Phantom. *Radiation Protection Dosimetry*, 49, 163-166
- [7] CONTENTO G., PADOVANI R, ROBERTO V. , VARIN O. & DELLA GIUSTA C., 1994. Introducing artificial intelligence technology into QA in diagnostic radiology. *Proc. 11th ISQua Int. Conf., Venice, May 24-28 1994.*
- [8] CONTENTO G , PADOVANI R., ROBERTO V. , DELLA GIUSTA C., MACCIA C. ,1995. A Knowledge-Based System for Quality Control in Diagnostic Radiology. *European Radiology*, Suppl. to Vol. 5, 404.

Head of project 6: Prof. Vañó Carruana

II. Objectives for the reporting period.

a. Conventional radiology.

* Application of image quality criteria by using different test objects and phantoms.

* Evaluation of image quality according to the anatomical image criteria proposed by the EC expert group and comparison with the results obtained with test objects and phantoms. Application to rejected images and proposal of modifications.

* Application of basic quality control procedures (estimates of patient doses and image quality) in order to verify the efficiency of the optimization processes.

* Evaluation of strategies for dose reductions and improvements on image quality by using different film-screen combinations.

b. Mammography.

* Obtention of data from several rooms of diagnostic radiology in order to contribute to the evaluation of the expert system prototype for quality control and analysis of the optimization processes.

c. Paediatric radiology

* Estimation of doses associated with the paediatric X-ray exposures.

III. Progress achieved including publications.

III.a. Conventional radiology.

a.1. Test objects and phantoms.

Requirements that should meet the test objects and phantoms used to evaluate image quality in conventional diagnostic radiology have been analyzed. The following conclusions have been found: 1) They should be easily employed both on the table and on a wall stand; 2) The beam attenuation and scattering properties of the human tissue should be simulated in order to ensure that entrance doses be similar to those of a standard patient; 3) The points where the background optical density must be measured should be clearly identified; 4) Simple test pattern of line pairs (both for high and low contrasts) which could be arranged at an angle of less than 45° to the strips of the grid and allow detection values between 0.5 to 5.0 lp/mm should be included; 5) They should also contain copper meshes to evaluate appropriate film-screen contact areas; 6) Some marks should be present in order to check the alignment of the light field edges with the X-ray field; 7) Some details with different sizes and absorptions, comparable to those normally found in patient radiographs, enabling the detection of changes in the actual kV should be included; 8) A calibrated step wedge should be included; 9) They should contain a lead strip that allows a further sensitometric exposure on the same film; 9) The test images viewing conditions should be clearly defined; 10) Criteria for scoring the obtained image should be attached indicating the expected and recommended values for certain techniques and film-screen combinations and, 11) The possibility of designing mobile objects, in order to avoid the capacity of the observer to learn and remember their position, would be eventually valuable.

Using the TOR(CDR) test by the Leeds University in different placements between appropriate attenuators (similar to the ANSI basic phantom), a new test object that allows the simulation of real examinations (those contained in the CEC, XII/173/90 document on Image Quality Criteria in Diagnostic Radiology) has been designed. The results obtained with this phantom have been used and compared with those of TOR(CDR) and those using Wellhofer test (designed according to the DIN standard), in more than 12 X-ray rooms.

The sensitivity of the new designed phantom has been also analyzed, both for spatial resolution and for low and high contrast thresholds, and for different kV and optical densities.

a.2. Anatomical image quality criteria.

The image quality criteria proposed in the CE XII/173/90 report are being to be routinely applied to the clinical images obtained in several rooms. In addition, the image quality in these rooms is evaluated by means of physical test objects. The sensitivity and effectiveness of each of the criteria is being studied by statistically analysing if the images that accomplish them are suitable or not for diagnosis. The most effective criteria will be used in analysing the image quality level routinely obtained in order to propose corrective actions when it will be necessary.

The image quality criteria have been applied to 1500 chest images (valid for diagnostic) obtained in two rooms of the San Carlos University Hospital. The rejected images (and the rejection causes) have been also collected in order to apply the image quality criteria. Those images rejected that fulfilled the quality criteria were retained for making an additional evaluation by a radiologist board.

Figure 1 shows frequencies of not-fulfilled criteria in a sample of 691 acceptable for diagnosis and 82 rejected chest PA examinations. One important conclusion derived from figures 1 is the high fulfillment of all accepted films for all criteria, except PA.3. The fact that PA.3 "medial border of the scapulae outside the lung fields", is not met in 40% of the examinations analysed by our group,

independently of being acceptable or not for diagnosis, implies a lack of relevance of this criterion.

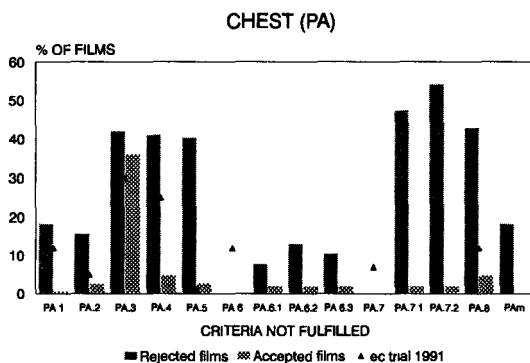


Figure 1

Some approaches to replace appreciation of blackening criteria by anatomic visualization criteria were formulated by our group. With this purpose "the lower dorsal spine should be no more than faintly appreciable" has been introduced and analysed. It is assumed

that too light images will not clearly achieve this criterion and too dark images will usually produce a visually reproduction of the dorsal spine.

Another criterion proposed and analysed by the group of Madrid is LAM: "the posterior costal arcs should appear superimposed". This criterion tries to define the strict "laterality" in chest lateral projections in the same way that PA.2: "symmetrical reproduction of the thorax" describes the exact projection (not rotated thorax) in PA chest projection. The tolerance of this lack of "laterality" should be defined, since there are a high percentage of accepted films that do not fulfill it (about 25%).

Figure 2 (for chest PA) describes the statistical distributions in which the unfulfilled criteria appear. Notice that 40% of the accepted PA films have all criteria achieved (zero anomalies), 35% in the EU trial. The percentage rises to more than 60% for lateral projection. These facts could be easily interpreted fitting histograms to some statistical distribution. Accepted films fit with high correlation to binomial distributions with a probability of 10% of not fulfilling one criterion. The area (percentage of image criteria met by films) and the peak (with for 10% of probability is close to zero and represents the number of films fulfilling all criteria) in binomial distributions are, for a limited number of events, highly dependent on this number. A similar discussion arises from the distributions of not-fulfilled criteria in rejected films. Now data can be fitted to binomial distributions with a probability of 36% of non-fulfilment of a certain criterion. The most important conclusion, however, is that there is no binomial distribution that correlates exactly with experimental data. The reason for this could be that now events are not fully independent, in other words, in rejected films the probability of not achieving a certain criterion depends on the accomplishment of other criteria. To reinforce that idea the probability that a certain not-fulfilled criterion is followed by non fulfilment of another was also analysed. Conclusions of that study were, for example that, whenever PA.8 is not fulfilled ("visualisation of the retrocardiac lung and mediastinum") PA.6.1 is also not fulfilled ("visually sharp reproduction of the trachea and proximal bronchi") and so on.

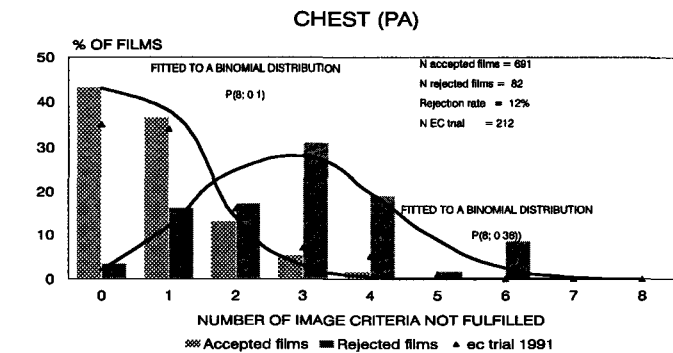


Figure 2

Accepted films fit with high correlation to binomial distributions with a probability of 10% of not fulfilling one criterion. The area (percentage of image criteria met by films) and the peak (with for 10% of probability is close to zero and represents the number of films fulfilling all criteria) in binomial distributions are, for a limited number of events, highly dependent on this number. A similar discussion arises from the distributions of not-fulfilled criteria in rejected films. Now data can be fitted to binomial distributions with a probability of 36% of non-fulfilment of a certain criterion. The most important conclusion, however, is that there is no binomial distribution that correlates exactly with experimental data. The reason for this could be that now events are not fully independent, in other words, in rejected films the probability of not achieving a certain criterion depends on the accomplishment of other criteria. To reinforce that idea the probability that a certain not-fulfilled criterion is followed by non fulfilment of another was also analysed. Conclusions of that study were, for example that, whenever PA.8 is not fulfilled ("visualisation of the retrocardiac lung and mediastinum") PA.6.1 is also not fulfilled ("visually sharp reproduction of the trachea and proximal bronchi") and so on.

Table I for chest PA summarize the authors' contributions to define anatomical criteria in a more precise way. Six criteria (marked as *PAm.x* in table I) are formulated for chest PA and seven for lateral chest examinations

Table I

PROPOSED BY EU EXPERTS, Paris-1992.	PROPOSED BY AUTHORS, Madrid, 1994.
PA.1 Performed at deep inspiration (as assessed by the position of the ribs above the diaphragm either 6 anteriorly or 10 posteriorly) and with suspended respiration.	<i>PAm.1</i> Reproduction of the costal arcs either 6 anteriorly or 10 posteriorly. (PERFORMED AT DEEP INSPIRATION).
PA.2 Symmetrical reproduction of the thorax.	<i>PAm.2</i> The spinal apophysis of the dorsal vertebrae must be equidistant from the inner borders of the clavicles. (NOT ROTATED THORAX).
PA.3 Medial border of the scapulae outside the lung fields.	NOT RELEVANT FOR IQ
PA.4 Reproduction of the whole rib cage above the diaphragm.	<i>PAm.3</i> Reproduction from the 7th cervical vertebra to the bottom of both costophrenic sinus (REPRODUCTION OF THE WHOLE THORACIC CAVITY)
PA.5 Reproduction of the vascular pattern in the whole lung, particularly the peripheral vessels.	<i>PAm.4</i> Visually sharp reproduction of the peripheral vessels and both hemidiaphragms (PERFORMED WITH SUSPENDED RESPIRATION)
PA.6.1 Visually sharp reproduction of the trachea and proximal bronchi.	INCLUDED IN PA 8
PA.6.2 Visually sharp reproduction of the borders of the heart	<i>PAm.5</i> Visually sharp reproduction of the borders of the cardiac silhouette*
PA.6.3 Visually sharp reproduction of the aorta	INCLUDED IN PA.6.2
PA.7.1 Visually sharp reproduction of the diaphragm.	INCLUDED IN <i>PAm.5</i>
PA.7.2 Visually sharp reproduction of costophrenic angles.	INCLUDED IN <i>PAm.4</i>
PA.8 Visualisation of the retrocardiac lung and mediastinum	<i>PAm.6</i> Visualisation of the lung vessels through the cardiac silhouette.
PA.9 Blackening (Optimal, too light, too dark)	INCORRECT BLACKENING SHOULD AFFECT OTHER IQ CRITERIA as <i>PAm.4</i> ** and <i>PAm.7</i> The lower dorsal spine should be no more than faintly appreciable and visualisation of the intervertebral spaces***

* RELEVANT CRITERION FOR IQ IN PA CHEST EXAMINATIONS** NOT FULFILLED FOR TOO DARK BLACKENING *** NOT FULFILLED FOR TOO LIGHT BLACKENING

The criteria numbered *m1* to *m4* mainly evaluate the correct position of the patient and his/her collaboration in performing the chest examinations (a complete image of the thorax is required, the patient should not be rotated with respect to the selected projection and the image should be taken at deep inspiration with suspended respiration). The rest of the criteria (including number *m4*) are related to the technique and the quality control of the X-ray equipment and the image system. This last group of criteria allows for the evaluation of blackening (*PAm.4* and *PAm.7*) and criteria could be simulated by phantoms with test objects (with pattern bars and contrast objects). To validate this second category of criteria, simultaneous evaluations with the phantom selected by our group were performed. Results were completely coincident; phantom images highly scored by physicists coincide in time with clinical images fulfilling anatomic criteria *PAm.4* to *PAm.7*.

a.3. Optimization processes.

It has been carried out estimations of patient dose reductions as a consequence of a pilot quality control programme in thorax radiology rooms, achieving entrance dose reductions up to 60% by correcting some anomalies due to the generator. In traumatology rooms, values of lumbar spine and hip and pelvis doses were reduced up to 35% by adding filtration and adjusting radiographic techniques.

One of the most important achieved optimization has been carried out in a centre, which participated in the 1991 CEC trial and in which, in spite of being X-ray equipment and processors in excellent order, lumbar spine entrance patient doses were the highest of the european trial. The optimization, in this case, consisted in modifying the techniques applied by radiographers (basically increasing kV and distance) and using one darkness step below the normal, in the automatic exposure. Thus, dose values were reduced under the reference ones.

The evolution of annual effective equivalent doses in different examinations has been analyzed for one of the hospitals participating in the quality control pilot programme since 1987. In this way, a global indicator of the achieved benefit after the application of the mentioned programme has been obtained.

a.4. Influence of the film-screen combinations.

Due to the strong dependence that the image receptors have on doses and image quality, we have analysed most of the new film/screen combinations used in conventional radiology and paediatrics in our area. The evaluation has been made by a type ANSI phantom and the TOR(CDR) test from the Leeds University. Images of the two phantoms were obtained by selecting the clinical technical factors used in abdomen examinations. The parameters analysed were entrance dose, thresholds for the visibility of low and high contrast objects and high contrast resolution. The results show that the image quality can be optimized with low dose values by combining some specific films with the suitable screens. More than 20 screen-film systems were analysed. The use of the CEC Image criteria together with phantom images was also used for a thorax asymmetric screen-film system.

III.b. Mammography.

Our group has offered a wide experimental measurement database in mammography using the Leeds TOR(MAX) object, to contribute to the knowledge base of the expert system on quality control, which is being developed in Udine. A number of images obtained in different conditions (kV, optical density, etc.) have been performed and analyzed in order to simulate possible anomalies of mammographic equipment. It has been necessary to carry out a previous study of the sensitivity of the Leeds phantom to detect anomalous working of mammographic equipment.

In mammography, the image quality controls have been carried out using the TOR(MAX) phantom by the Leeds University, for different screen-film

combinations. A comparison of these dose values with the obtained image qualities and the equipment conditions has been made. It has been analyzed by groups: mamographic units of hospitals, outpatient centres, private centres and those dedicated specifically to screening programmes. Measured entrance air kerma values have ranged from 2.9 mGy (in outpatient centres) to 6.4 mGy (in screening units), while the obtained image qualities, assigning a global score using the test details, vary from 33 (in outpatient centres) to 42 (in screening units).

Breast doses and image quality produced by seventeen X-ray units in the area of Madrid were evaluated during the period 89-91. The study pointed out that the main factors which dramatically affected the breast dose and image quality were the use of inadequate radiographic factors, the lack of accuracy of the kV, inadequate image receptors and malfunctions of both automatic exposure control (AEC) or processors giving too low optical density values. Also, approximately half of the units belonged to the first generations of dedicated mamographic units (old units) and, in consequence, their features (broad focus, short source-image distance, without grid) limited the image quality. The results derived from this first study were reported to each facility and several actions recommended in order to overcome the detected faults. The impact of these actions on breast dose and image quality was one of the aims of a second study carried out during the period 92-93. The variations in image quality have been analyzed and compared with the mean air kerma values obtained in both periods. Thus, the benefit of the action can be derived from the image quality/breast dose relationship. In addition, the relative importance of each recommended action has been analyzed by estimating variations in collective equivalent breast doses per year (CEBD).

The results point out that the important changes occurred were more motivated by the data reported to the facilities corresponding to the dose values and image quality than by the less cost recommendations. The actions at the different facilities have improved noticeably the quality of mammography in Madrid area.

The actions have generally represented important methods to reduce the dose values since their contribution to the CEBD savings outweighed the substantial increase in the number of examinations made in the area of Madrid. During the period 92-93, the facilities considered in this study contributed to the CEBD with 122 person Sv/year (approx. 60% lower than the one estimated for the period 89-91). The effectiveness of all actions becomes more evident from the CEBD value which would be obtained in the case of the actions would not had taken place. In this case, the CEBD value, which would be approximately 394 person Sv/year and the total CEBD saving related to all actions was 272 person Sv/year.

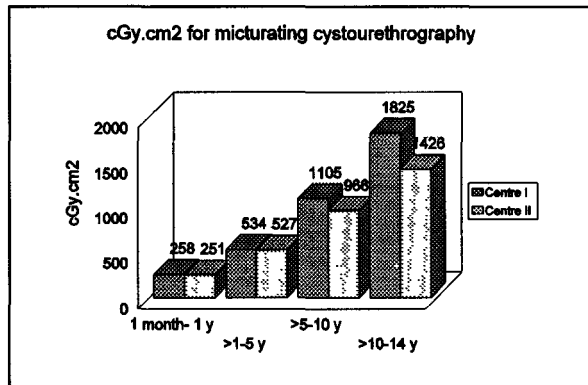
Table II shows the three actions that were considered as the main causes of the variations in image quality and breast doses and the mean values of the high contrast resolution, score and air kerma in both periods. The score were obtained by counting the number of the visible details in the TOR[**MAX**] phantom images with the exception of the high contrast resolution and subtracting the number of details which were always clearly seen in all phantom films.

Table II

ACTION	Period	X-ray unit replacement	Image receptor replacement	Quality Control
CASES		5	8	5
Mean High Contrast Resolution \pm S (lp/mm) (Range)	1989-91	7.6 \pm 3.4 (6 - 14.3)	11.9 \pm 3.1 (7.8 - 18.3)	11.6 \pm 2.6 (7.1 - 13.4)
	1992-93	14.9 \pm 1.5 (12.5 - 16.6)	12.8 \pm 3.4 (7.1 - 16.6)	12.4 \pm 3.1 (7.1 - 14.6)
Mean Score \pm S (Range)	1989-91	11.1 \pm 4.4 (6 - 18.3)	13.8 \pm 4.4 (8.0 - 21.0)	14.4 \pm 5.0 (8.5 - 22.0)
	1992-93	18.0 \pm 6.0 (8.0 - 21.5)	15.2 \pm 5.9 (3.0 - 20.7)	17.8 \pm 3.0 (13.3 - 21.7)
Air Kerma Mean Values \pm S (mGy) (Range)	1989-91	5.3 \pm 3.9 (1.0 - 10.4)	12.6 \pm 14.4 (3.1 - 46.1)	5.8 \pm 3.0 (3.2 - 10.4)
	1992-93	8.7 \pm 5.8 (5.5 - 8.9)	4.8 \pm 2.7 (0.9 - 8.4)	3.4 \pm 0.7 (2.4 - 4.1)

III.c. Paediatric radiology

The optimization has been applied to chest, abdomen and mictional cystoureterography. The use of high speed systems (800, when it is possible due to the image characteristics to be viewed), to withdraw the

**Figure 3**

bucky, strict collimation, interrupted use of fluoroscopy and correct use of the automatic exposure have allowed dose reductions up to a factor 3. Patient doses have been also estimated in rooms devoted to conventional complex paediatric examinations. In the case of the micturating cystourethrography examination, we have measured the dose-area product in patient samples of two centres and the results were grouped according to the four typical age ranges (see Figure 3). We have found differences up to 26% between the mean values of cGy.cm² obtained for the same age group in the two rooms. On the other hand, several optimization processes have been proposed and their effectiveness has been evaluated by estimating the dose reductions achieved with them. It has been found that some

of these procedures may reduce the dose values up to 80%.

Several simple paediatric examinations have also been monitored in order to update the local reference dose values for each age group. Table III show the values of the mean patient entrance dose values (mGy), the third quartile and the sample size for each age group by examination and projection.

Table III

Examination	Proj.	Age group (years)			
		0.0 - 1.0	1.1 - 5.0	5.1 - 10.0	10.1 - 14.0
Chest	PA	0.161±0.066 0.189 (5)	0.174±0.1 04 0.162 (19)	0.185±0.131 0.195 (13)	0.181±0.111 0.324 (8)
	LAT	0.260±0.092 0.325 (2)	0.260±0.0 71 0.325 (6)	0.184±0.043 0.195 (6)	0.672±0.830 0.795 (7)
Head	AP	0.780±0.198 0.963 (3)	1.837±1.5 38 1.863 (5)	2.296±0.865 2.296 (6)	2.889±0.439 3.199 (2)
	LAT	1.058±0.482 1.444 (3)	1.184±0.6 68 1.178 (8)	1.737±0.657 2.298 (13)	3.246±0.066 3.292 (2)
Pelvis	AP	0.401±0.203 0.447 (17)	1.134±0.4 32 1.457 (4)	1.909±2.155 4.994 (4)	-

Publications:

- Contento, G.; Padovani, R.; Varin, O.; Castellano, S.; Maccia, C.; Chevalier, M.; Fernández, J.M.; Morán, P.; Vañó, E. and V. Roberto. The use of test phantoms in knowledge based systems for diagnosing malfunctions of the radiological equipment. Radiation Protection Dosimetry, Vol. 49, No. 1/3, 153-156 (1993).

- Chevalier, M.; Morán, P.; Vañó, E. Impact of several recommended actions for improving the image quality in mammography. Radiation Protection Dosimetry, vol 57, No. 1/4, 155-158 (1995).

- Fernández, J.M. and Guibelalde, E. Physical Evaluation of recent KODAK films for mammography. The British Journal of Radiology, 66, 828-832 (1993).

- González, L.; Vañó, E.; Ruíz, M.J. Radiation doses to paediatric patients undergoing micturation cystourethrography examinations and their potential reduction by RP optimization. The British Journal of Radiology, 68, 291-295 (1995).

- Guibelalde, E.; Fernández, J.M.; Vañó, E.; Llorca, A.; Ruíz, M.J. Image quality and patient dose for different screen-film combinations. The British Journal of Radiology, 67, 166-173 (1994).

- Guibelalde E. and Vañó, E. Design criteria for the evaluation of phantoms employed in conventional radiography. *Rad. Protect. Dosim.* Vol. 49, No. 1/3, pp 39-46 (1993).
- Guibelalde, E. Morillo, A. Fernández, J.M, Vaño, E. Use of the European image quality criteria for screen-film comparison: application to asymmetric systems. Accepted in the *BJR*.
- Llorca, A.L.; Guibelalde, E.; Fernández, J.M.; Vañó, E. Estudio comparativo de películas para radiología convencional (Comparative study of films for conventional radiology). *Radiología*, 35(1), 35-42, (1993) (in Spanish).
- Llorca, A.L.; Guibelalde, E.; Vañó, E.; Ruiz, M.J. Analysis of image quality parameters using a combination of an ANSI type phantom and the Leeds TOR(CDR) test in simulations of simple examinations. *Rad. Protect. Dosim.* Vol. 49, No. 1/3, 47-49 (1993)
- Llorca, A.L.; Guibelalde, E.; Ruiz, M.J.; Vaño, E. Control de calidad de la imagen en grafía utilizando maniqués: El test TOR(CDR) de la Universidad de Leeds (Image Quality Control in radiography using phantoms: the TOR(CDR) test) *Radiología*, Vol 37, 33-36 (1995) (in Spanish)..
- Morán, P.; Chevalier, M.; Contento, G. and Vañó, E. Evaluation of the sensitivity of the Leeds TOR(MAX) Mammographic Phantom. *Rad. Protect. Dosim.* Vol. 49, No. 1/3, 163-166 (1993).
- Morán, P.; Chevalier, M.; Vañó, E. Comparative study of dose values and image quality in mammography in the area of Madrid. *The British Journal of Radiology*, 67, 556-563 (1994).
- Morán, P.; Chevalier, M.; Vañó, E. Recommended actions for reduction of breast doses in the area of Madrid: An evaluation. *Radiation Protection Dosimetry*, vol 57, No. 1/4, 429-432 (1995).
- Ruiz, M.J.; Llorca, A.L.; González, L.; Vañó, E. y Martínez, A. Radiodiagnóstico pediátrico: reducción de dosis de radiación a pacientes. (Paediatric Diagnostic Radiology: patient dose reductions) *Radiología*, 35(3), 169-172, (1993) (in Spanish).
- Ruiz, M.J.; Llorca, A.L. y Vañó, E. Reducción de dosis de radiación a los pacientes. Casos prácticos. (Patient dose reductions: practical cases) *Radiología*, 35(4), 297-298 (1993) (in Spanish)..
- Vañó, E.; Velasco, A.; Morán, P.; González, L. and Alvarez Pedrosa, C. Evolution of diagnostic radiology in a big hospital during a five year period and the derived collective dose. *The British Journal of Radiology*, 66, 892-898 (1993).
- Vaño, E; Gonzalez, L.; Guibelalde, E.; Fernandez, J.M; Calzado, A.; Ruiz, M.J. Some results from a diagnostic radiology optimization programme in the Madrid area. *Radiation Protection Dosimetry*, vol 57, No 1/4, 289-292 (1995).
- Vaño, E.; Guibelalde, E.; Morillo, A.; Alvarez-Pedrosa, C.S.; Fernández, J.M. Evaluation of the European image quality criteria for chest examination. Accepted in the *BJR*.



Final Report
1992 - 1995

Contract: F13PCT920052 Duration: 1.9.92 to 30.6.95

Sector: C22

Title: Patient dose from radiopharmaceuticals

- | | | |
|----|----------|--------------|
| 1) | Smith | MRC |
| 3) | Petoussi | GSF |
| 4) | Evans | Univ. London |

I. Summary of Project Global Objectives and Achievements

Nuclear Medicine, involving the application of radiopharmaceuticals to aid diagnosis, treatment and research, has a well established role in clinical patient care. Over the past 30 years there have been extensive developments in radiopharmaceuticals, with new products coming into use while others have become obsolete. Radiation dose estimates are needed for assessment of the risk to patients associated with the use of radiopharmaceuticals both for comparison with the possible benefit of an investigation and to help in giving adequate information to the patient. They provide information for regulatory authorities who make recommendations on acceptable amounts of administered radiopharmaceutical activity and also provide guidance to ethical committees making decisions on research projects involving the administration of radiopharmaceuticals to volunteers, who receive no individual benefit.

Internal radiation dosimetry requires a knowledge of both biological and physical parameters and it is necessary to consider the ways in which this can be maximised in order to make progress towards more reliable dose estimates. Thus, in parallel with the search for more extensive biokinetic data from patients undergoing radiopharmaceutical investigations, there has been concerted effort to optimise those physical factors needed to convert organ tracer residence times (the biological end-point) to organ radiation doses. The overall task is vast, requiring the retrospective assessment of the existing armoury of clinically useful radiopharmaceuticals as well as keeping pace with the dosimetry of new ones.

The contract project has embraced the investigation of a number of the techniques involved in internal radiopharmaceutical dosimetry, from the initial injection of the patient to the final estimate of effective dose. Thus, the general objective of the contract work has been to subscribe to the core knowledge of radiopharmaceutical dosimetry, and this has been achieved by two principal aims:-

- 1) To perform detailed studies of biodistribution of certain radiopharmaceuticals, either by the use of direct nuclear medicine methods or kinetic modelling, to allow accurate determination of the biological data required for radiation dose calculation.
- 2) To examine methods of data acquisition and analysis to identify influential sources of error and to improve the accuracy of the physical parameters crucial for dose estimation.

In recent years, legal requirements of national regulatory authorities governing the administration of radioactive substances to patients have emphasised the need for making comprehensive dose estimates. Dose estimates were formerly based on limited biokinetic data, an unsatisfactory state of affairs which prompted the International Commission on Radiological

Protection (ICRP) to appeal for the collection of the particular information needed for dose calculations and that this should be made available in the open literature. In recent years there has been a marked response and an increasing number of dosimetry orientated studies are appearing in the scientific literature. These have shown a trend to greater sophistication and accuracy in techniques of biodistribution and data analysis. This is exemplified in work undertaken in this contract (**Smith - MRC**) by the description of a biodistribution study designed to provide dosimetry information on a relatively new substance of proven clinical value (^{111}In - antimyosin antibody). This investigation has incorporated refinements, such as the use of the attenuation-corrected geometric mean technique for estimation of organ uptake, which are nowadays expected in reliable dosimetry studies.

At the present time, the vast majority of dosimetry data has resulted from clinical studies on adults. Attention now has to be given to expanding the spectrum of subject age and size. A serious gap in our knowledge of the application of radiopharmaceutical dosimetry is highlighted by the small amount of available biokinetic data in children. In view of the possibly greater radiation risk to children there is a compelling need for more paediatric dosimetry information, both for established and new radiopharmaceuticals. It has often been necessary to estimate paediatric doses on the basis of adult biokinetic data, possibly leading to seriously inaccurate dosimetry. The influence of paediatric biokinetics on dose estimates needs to be addressed and, to this end, the present contract has involved a study of the dosimetry of $^{99\text{m}}\text{Tc}$ - DMSA in children over a wide age range (**Evans - Univ. London**). This substance is typical of many for which there was formerly no alternative to the use of adult biokinetic data to predict doses to children.

In addition, internal dosimetry has to embrace the full spectrum of available radiopharmaceuticals, especially to include the short-lived positron-emitting tracers. Until recently, very little dosimetry had been performed on PET substances, mainly because of the practical difficulties of carrying out biodistribution studies using tracers with half-lives of only a few minutes. This deficiency has led to the development of modelling techniques, combining both measured data and known physiological parameters, as a substitute for conventional methods. The description of such a model for estimation of the dosimetry of ^{15}O -water is included in this contract (**Smith - MRC**).

With respect to the physical aspects of internal dosimetry, one of the most crucial requirements is to establish values of so-called inter-organ absorbed fractions, which specify, with appropriate limits on accuracy, the fraction of the penetrating energy emitted by radioactivity in a given organ which is absorbed in itself and in other organs. This is the pivotal information which allows the calculation of summed energy absorption in organs, and hence dose, from the amounts of radiopharmaceutical taken up in different organs as measured in biodistribution studies or estimated from models. This information has to account for the wide range of body size and relative organ geometry ranging from the newborn child to the mature adult. This was formerly done by devising an adult phantom in which organs and body parts were described by three-dimensional mathematical relationships, while phantoms for children were simply scaled-down versions of the adult phantom (Oak Ridge National Laboratory). Monte Carlo methods for electron and gamma ray transport codes were used in conjunction with these phantoms to derive the organ absorbed fractions from the known physical output data of the radionuclide of interest. Recently, more sophisticated mathematical models (Cristy phantoms) have come into use, and are especially improved for children since they incorporate the changes which take place during physical maturity. At the present time most available dosimetry is based on the Cristy phantoms. Notwithstanding this fact, there remain several disadvantages with the general use of mathematical phantoms. In view of the small number of

phantoms (newborn, 1y, 5y, 10y, 15y, adult) they provide limited scope for a continuous range of age and body dimensions. Consequently, accurate biokinetic data, painstakingly acquired in planned biodistribution studies, may be compromised to a greater or lesser extent because of the inability to match the patient rigorously to a particular mathematical phantom for the conversion of biokinetic information to dose estimates. This is a problem which may not be fully appreciated when biological data are used with dose-calculation software, with the result that greater weight may be attached to the accuracy of the dosimetry than is warranted. The problem may be particularly acute in paediatric studies due to the rapid developmental changes which occur. In the paediatric studies which constitute part of this contract, attempts have been made to compensate for the stepwise nature of the phantom database by performing interpolation between phantoms according to the weight of the measured child in relation to the phantom weights (**Evans - Univ. London**).

Furthermore, whilst the mathematical models were designed to match the physical characteristics of reference man, woman and children, they do not necessarily represent closely the patient under study, in relation to geometrical distribution and shape of organs and to the general body form. Ideally, it would be possible to model a phantom specific for the subject under investigation to use with the biological data measured directly on the subject. This situation is unattainable in practice on a wide scale but, in theory, it becomes a possibility on a limited scale through the recent development of CT phantoms. This innovation, in which three dimensional images of the patient's body and organs are constructed with high resolution by CT scanning techniques, represents a significant advance towards more realistic representation of the human body. Previously devised for the dosimetry of external radiation, the investigation of the application of CT phantoms to internal dosimetry is still in its infancy. However, an important part of the work of this contract has been to examine CT phantoms for this very purpose (**Petoussi - GSF**). Specific absorbed fractions have been calculated for a wide range of organs and, using biodistribution data from ICRP 53 or those supplied by another contractor in this project, organ and effective doses have been estimated. These data have been compared with values based on the MIRD type phantoms. Of particular importance are the results for bone and bone-marrow. These tissues are modelled by the CT technique in a fundamentally different way to that employed using MIRD phantoms, providing for a more scientific basis of skeletal dosimetry. It must be emphasised that, at the present time, the CT phantoms are limited in number and differences would be expected to exist, reflecting differences in stature between the human bodies used for derivation of CT phantoms and representative mathematical phantoms based on average body dimensions. However, this work has revealed that, in some circumstances, larger than expected differences are apparent, and further research is needed to establish the reasons for these observations.

Summary of aims and achievements of individual contractors

Project 1: Smith - MRC

One of the aims was to carry out biodistribution/dosimetry studies on new radiopharmaceuticals. The protocol of a collaborative study with the Cardiology Department at Northwick Park Hospital, in which ^{111}In antimyosin was assessed for investigation of idiopathic inflammatory myopathy, provided this opportunity. Extensive whole-body and localised imaging over a period of 72h, as well as serial blood sampling and urinalysis, provided the basis of high-grade biodistribution studies. Application of attenuation correction and the geometric-mean conjugate counting method increased the accuracy and reliability of organ uptake measurements. The observed biokinetic data, when used with MIRDOSE dose-calculation software based on MIRD phantoms, yielded organ and effective dose values. These

were found to be dependent to a significant extent on the background subtraction method employed, but the best estimate of effective dose was 12.4 mSv for the usual amount of administered activity (74MBq). Since there was no evidence of uptake in skeletal muscle sites in the patients with idiopathic inflammatory myopathy, it is concluded that this dose estimate is appropriate for normal subjects. This work has been submitted for publication and will represent the first appearance of ^{111}In antimyosin in the open literature.

A further aim has been to produce dosimetry data for water labelled with short-lived (2.04 min) ^{15}O , used extensively in research studies. This work was carried out in collaboration with the MRC Cyclotron Unit at Hammersmith Hospital. Previous dose estimates based on uniform water distribution models were suspected of underestimating dosimetry. The present work has underlined the value and potential scope of biokinetic modelling techniques as alternatives to conventional imaging methods which are difficult to apply for very short-lived radionuclides. The proposed model is based only on accurate measurements of administered activity and its concentration in arterial blood, together with literature values of organ blood flows and water distribution space. One advantage of the model, therefore, is that residence times can be determined for every organ for which these parameters exist, and this provides a much wider diversity of source organs than is possible with imaging methods. The main conclusion from this work is that the effective dose of $1\ 2\mu\text{Sv}\cdot\text{MBq}^{-1}$ ^{15}O -water is 2 to 3 times greater than the value derived using uniform distribution models and is, therefore, much more restrictive in research studies than was previously thought. Results from other centres using similar models, and also conventional biodistribution methods, have shown good agreement with the results of the current work.

Previous work on the dosimetry of a novel myocardial perfusion imaging agent ($^{99\text{m}}\text{Tc}$ P53; Amersham International) highlighted the difficulty of estimating low values of organ uptake in biodistribution studies. The heart uptake of this substance was only about 2%. In the present project this has been measured using two different methods in patients after exercise and at rest, using either P53 or MIBI, an established radiopharmaceutical with similar properties. An attenuation-corrected planar technique was compared with SPECT. The results emphasised the large influence of background subtraction method in such low uptake levels where differences of 100% were shown to be possible. A calculated background subtraction, based on lateral images gave closest agreement with SPECT. There was no significant difference between exercise and rest heart uptake, which was estimated to be 1.8%, but further research is required to establish the most appropriate background subtraction method.

Project 3: Petoussi - GSF

The aim was to determine organ absorbed fractions for internal dose calculations by using voxel phantoms of a baby, child and adult. Furthermore, differences to the respective data obtained with MIRD-type phantoms were to be quantified and documented. In view of the high resolution of CT imaging and the fact that this procedure is performed on human bodies, the development of CT phantoms provides a more realistic basis for dose calculation than the currently used anthropomorphic mathematical phantoms. This follows from the ability of the CT procedure not only to localise organ voxels accurately in 3-dimensional space but to use the attenuation information inherent in each voxel to permit estimation of tissue density. This is of particular importance with regard to the skeleton, where separation of hard bone and marrow, and estimation of the relative proportions of these tissues in a given voxel, are possible. Since these proportions vary with age in a complex way and in different skeletal regions, particular emphasis was given to the distribution of bone marrow in the construction of these CT phantoms for children. The CT phantoms thus exhibit marked improvements on the MIRD type phantoms, in which all skeletal components are homogeneously distributed in

the skeleton and there is no geometrical representation of the trabecular bone filled with marrow. The GSF CT phantoms for a baby and child have been used to derive a wide range of specific absorbed fractions for source and target organ combinations. In addition, biokinetic data from either ICRP Publication 53 or supplied by another contractor (Smith - MRC) has allowed dose estimates both for established and new radiopharmaceuticals. In comparison with data from MIRL type phantoms, these results have illustrated some larger than expected differences. For example, results for the CT phantom of the 7 year old child were more compatible with the MIRL phantom age range of 10 to 15 years and it is now important to establish the reasons for these apparent discrepancies. However, the most noteworthy differences have resulted from the improved estimation of bone and bone marrow dosimetry, which is one of the major contributions to emerge from the contract work on CT voxel phantoms.

For adult dosimetry, an adult CT voxel phantom stemming from Yale University was used. This phantom was found to be unsuitable for dose calculations, demonstrating that such voxel phantoms should be segmented with greater detail than is achieved with commercial software available in hospitals. The calculations will be repeated with the GSF adult phantom to be released at the end of 1995.

Project 4: Evans - Univ. London

The aim was to carry out paediatric biodistribution and dosimetry studies of ^{99m}Tc DMSA in a wide age range of children with normal or abnormal renal function. Although this renal radiopharmaceutical has been established in nuclear medicine methodology for many years, the lack of biokinetic data in children, in common with most other radiopharmaceuticals, has meant that paediatric dose estimates have previously had to be based on adult biokinetic data, without any indication of the validity of this substitution. The present study, involving serial biodistribution imaging and measurement of excreted radioactivity, represents one of the few attempts to acquire comprehensive reliable biokinetic data in children. Successful studies have been achieved in children aged from 5 weeks to 15 years. It should be emphasised that practical investigations of this kind are extremely difficult to conduct, especially in the younger children, and one of the achievements has been to bring this project to a successful conclusion. The high scientific content of the data has allowed estimation of renal uptakes, and uptake and elimination rates in normal and abnormal states, as well as uptake in, and elimination from, other organs and tissues including the metaphyseal growth complexes. In addition, the data have allowed the investigation of age-dependency on these various parameters. Although dosimetry has been based on MIRL phantoms, a novel method of linear interpolation between phantoms, based on the weights of the children under study, was introduced in an attempt to reduce the potential for large errors when trying to match a child to one of a limited series of discrete phantoms. Differences in dose estimates of almost 70% were observed between these methods in this series of children. In normal children, the effective dose was 1mSv per administered activity, when the latter was scaled on body surface area rather than body weight. Little evidence of age dependency of the biokinetics of this radiopharmaceutical was observed and, therefore, a single biokinetic model was proposed for estimation of paediatric dosimetry of ^{99m}Tc DMSA independent of age below 15 years. Scaling the amount of administered activity according to body surface area was shown to give good uniformity of effective dose over the age range investigated. Thus, this study has provided the scientific basis for a policy of radiopharmaceutical scheduling, which is an important criterion for optimisation of radiation dose and image quality in nuclear medicine procedures.

Head of project 1: Dr. Smith.

II. Objectives for the reporting period

1. To perform biodistribution studies in patients administered with ^{111}In - antimyosin antibody for investigation of idiopathic inflammatory myopathy and to use these data to estimate organ equivalent doses and the effective dose for this relatively new radiopharmaceutical.
2. To develop a kinetic model, based on the continuous measurement of arterial blood concentration of ^{15}O , to establish the radiation dosimetry of intravenously administered ^{15}O -labelled water. Additionally, to compare this dosimetry with that from modelling techniques reported by other centres; and to compare dosimetry from models with that resulting from direct PET measurement.
3. To investigate the accuracy of the measurement of radiopharmaceutical content of an organ with low uptake, by reference to the estimation of heart uptake of $^{99\text{m}}\text{Tc}$ myocardial perfusion imaging agents by two different techniques, paying particular attention to the effects of different background subtraction methods.

III. Progress achieved including publications

1. Biodistribution and radiation dosimetry of ^{111}In antimyosin antibody

Introduction

Antimyosin antibody ('Myoscint' - Centecor) has been available for a number of years for the study of myocardial infarction. Following its successful use for this purpose, it has been suggested that ^{111}In antimyosin might have a useful role in the assessment of skeletal muscle disease. In the present study, 12 patients with idiopathic inflammatory myopathies (IIM) who were referred for immunoscintigraphy and two control patients without muscle disease were investigated for 72h after administration of ^{111}In -antimyosin. The aim of the study was to assess the possible value of the labelled antibody for investigating the extent of both myocardial and skeletal muscle involvement in this disease. In addition, the study protocol provided the means to acquire the type of biodistribution data essential for radiation dosimetry, which is the main topic of the study reviewed in this report. To the best of our knowledge, the dosimetry of this substance is not available in the open literature.

Methods

Following the injection of 2mCi (74 MBq) of ^{111}In antimyosin, patients were monitored by whole-body scanning using an IGE 400AT gamma-camera fitted with a medium energy collimator. Scans were made at 5min, 30min (in only 5 patients), 2, 7, 24, 48 and 72h post-injection. Overlapping, longitudinal split-field scans were obtained with the patient both supine and prone to allow the determination of conjugate whole-body and organ counts. Additional planar images were obtained over the heart and specific muscle sites at 24 and 48h. Complete collections of urine were made in the intervals 0-2, 2-4, 4-7, 7-24, 24-48 and 48-72h and the total urinary activity in each time interval was measured using a calibrated bulk-sample detector. No faecal collections were made because there was no evidence of the presence of activity in the gastrointestinal tract throughout these studies. Blood samples were withdrawn at the same times as the scans and aliquots of whole-blood and plasma were counted against diluted standards of the administered activity in an LKB Compugamma automatic sample counter. Anterior and posterior whole-body images were analysed by regions-of-interest (ROI) to provide estimates of serial total-body and source organ geometric mean counts. Source organs were heart, lungs, spleen, liver, kidneys, urinary bladder and bone-marrow. Organ ROIs were corrected for blood background, tissue attenuation and radioactive decay and then referred to phantom calibration data to establish the absolute activity content of the source organs. Attenuation correction was based on a transmission scanning technique. Residence times for whole-body (less bladder activity) and source organs were obtained by integration of mathematical equations fitted to retention data, and these were used with a dose-calculation program MIRDOSE 2 (Oak Ridge Associated Universities, USA) to give dose estimates to 25 target organs, from which the effective dose (ED) was calculated.

Results

^{111}In antimyosin was retained for a long time in the blood pool and images up to 2 h were characterised by activity in the vascular tree. About 60% of administered activity left the blood with a half-time of about 2 h and 40% with a half-time of 27 h, the activity being confined to the plasma space. Excretion of the radioactive label occurred almost entirely via the renal system; after 72 h, the average amount excreted in urine was $32.1(\pm 9.1)\%$. Organs showing major uptake were liver (10% at 24 h), kidneys (6.4% at 7 h), and bone-marrow (12% after 24 h) with smaller amounts in heart, lungs and spleen. Highest organ concentration, however, was found in kidneys. In addition, there was uptake in facial tissues (1.2%) and in male genitalia (0.5%).

Analysis of the images by experienced observers revealed no evidence of myocarditis in any of the patients investigated or of ^{111}In antimyosin uptake at localised muscle sites. The ratio of thigh counts to blood activity showed an increasing trend with time in all patients suggesting that some generalised tissue uptake occurred: but this was also observed in two control patients without muscle disease, suggesting that this uptake is not specific to idiopathic inflammatory myopathy. In view of these clinical findings, the biodistribution data of all 14 subjects were considered as a single group for dosimetry purposes and it is assumed that the dosimetry would apply for normal subjects. As stated in a previous periodic report, the organ dose estimates were dependent to a greater or lesser extent on the adopted method of background subtraction. A thigh background correction gave values intermediate between those obtained by subtraction of the system background only and of an average value of background in tissue adjacent to the margin of the organ in question. It is concluded that the thigh correction, though arbitrary, probably results in a more accurate assessment of organ content. Accordingly, Table 1 shows the estimated organ equivalent doses ($\text{mGy}\cdot\text{MBq}^{-1}$) and the effective dose ($\text{mSv}\cdot\text{MBq}^{-1}$) and the values for the standard amount of administered activity (74 MBq) estimated by using this correction method.

Table 1 Organ equivalent doses and the effective dose for ^{111}In antimyosin

organ	mGy·MBq ⁻¹	mGy·74MBq ⁻¹	organ	mGy·MBq ⁻¹	mGy·74MBq ⁻¹
adrenals	0.21	15.2	muscle	0.073	5.4
brain	0.045	3.3	ovaries	0.090	6.6
breast	0.058	4.3	pancreas	0.19	13.8
gall bl. wall	0.22	16.1	red marrow	0.31	23.1
GI tract:			bone surfaces	0.17	12.7
LLI	0.083	6.2	skin	0.042	3.1
SI	0.11	7.8	spleen	0.49	36.6
Stomach	0.11	8.2	testes	0.045	3.3
ULI	0.11	8.1	thymus	0.088	6.5
heart wall	0.23	17.3	thyroid	0.055	4.1
kidney	0.96	70.8	bladder wall	0.14	10.4
liver	0.52	38.5	uterus	0.090	6.5
lungs	0.17	12.7	total body	0.098	7.2
effective dose	0.17	12.4			

Discussion

This study confirmed the absence of myocarditis in the patients with IIM and no evidence was seen of localised uptake at various skeletal muscle sites, including those regions known to be affected by their IIM. The highest mean absorbed dose (9.6×10^{-1} mGy·MBq⁻¹) was calculated for kidneys with doses to liver (5.2×10^{-1} mGy·MBq⁻¹) and spleen (4.9×10^{-1} mGy·MBq⁻¹) substantially higher than doses to other organs. The effective dose was 0.17 mSv·MBq⁻¹. These results are in good agreement with those of Bushe et al. (private communication - Centecor Inc.) when their data are corrected for the effects of the presence of $^{114\text{m}}\text{In}$, a contaminant of the ^{111}In used to produce the labelled antimyosin. These authors also estimated that the highest mean dose was received by the kidneys (9.5×10^{-1} mGy·MBq⁻¹ of ^{111}In) and their data suggest an effective dose of 0.17 mSv·MBq⁻¹ of ^{111}In . Their original estimations were based on an $^{114\text{m}}\text{In}$ content of 0.16%, being the maximal proportion at the time of expiry of the ^{111}In . This contamination level contributed on average 14.1% of the combined dose to organs from both isotopes. The ^{111}In used in our studies was supplied by Amersham International and was stated to contain < 0.08% of $^{114\text{m}}\text{In}$ on the reference date. All our injections were made on or prior to the reference date and it can be concluded that the average increase in the doses to our patients as a result of $^{114\text{m}}\text{In}$ contamination would not have exceeded 7% of the dose from ^{111}In alone. It is, however, important that the additional dose resulting from $^{114\text{m}}\text{In}$ is estimated and taken into account when assessing the radiation dosimetry of ^{111}In antimyosin.

Conclusions

The present studies failed to demonstrate evidence of localised uptake of ^{111}In antimyosin either in the myocardium or in focal skeletal muscle sites in patients with IIM. For a typical administered activity of 74 MBq ^{111}In , the highest mean organ absorbed dose is estimated to be 71mGy to kidneys, and the effective dose 12.4mSv from ^{111}In alone. The choice of background correction method for quantifying organ uptake has significant bearing on dose estimates, but our results are in good agreement with those of other investigators.

2. PET dosimetry studies: a kinetic model for the radiation dosimetry of intravenously administered ^{15}O -water. (In collaboration with the MRC Cyclotron Unit, Hammersmith Hospital)

Introduction

Although there have been some recent attempts to make dose estimates by conventional means such as the measurement of organ uptakes by PET scanning, there are considerable practical problems due to the very short half-life of ^{15}O (2.04 min). In the circumstances, the use of kinetic modelling may offer a more accurate and versatile alternative. Previous periodic reports have described the kinetic model we have developed to establish the dosimetry of ^{15}O -water in man.

Methods

The model was based on studies in 21 patients and depends on the accurate measurement of both the amount of ^{15}O -water activity infused or injected, usually via a forearm vein, and the time-course of arterial blood concentration of ^{15}O (arterial input function), usually sampled from the other arm. The required data for dosimetry purposes, residence time of ^{15}O in organs, are derived by convolution of the arterial input function with the organ transit time function. The latter is derived from the blood flow rate (F) to the organ and the water distribution volume (Vd) in the organ, together with the radionuclide decay function. The parameters F and Vd were obtained from literature data and it was thus possible to calculate residence times from the model for 20 different organs. The residence times were used with MIRDOSE 2 software (Oak Ridge Associated Universities, USA) specially written for the estimation of organ radiation doses from internally administered radioactive substances, by application of the principles of the Medical Internal Radiation Dose Committee of America (MIRD). In this analysis, special calculations were made for certain organs, especially those with walls such as GI tract and bladder, where residence times could be calculated but which were not designated as source organs in MIRDOSE 2.

Results

The results of dose estimates for 21 subjects showed that highest doses (2-3 $\mu\text{Gy}\cdot\text{MBq}^{-1}$) were received by heart wall, kidneys and liver and the estimated effective dose was 1.16 (± 0.15) $\mu\text{Sv}\cdot\text{MBq}^{-1}$, which is more than double that predicted by a uniform distribution model. Since the last periodic report, results from other PET centres, using similar models for the dosimetry of ^{15}O -water, have become available and it is therefore possible to make inter-centre comparisons. In Table 2 the estimated doses are presented for up to 24 different organs obtained by modelling methods at four different centres (¹⁻⁴). The mean values of organ doses together with standard deviations are also shown. There was good agreement by modelling methods at four different centres on the estimated value of effective dose, 1.1 (± 0.09) $\mu\text{Sv}\cdot\text{MBq}^{-1}$ and, with one or two exceptions, there was reasonable agreement for most of the individual organ doses. For further comparison, the results of some dose estimates obtained by PET scanning methods to determine uptake in selected organs (Berridge *et al.*^{5,6}) are also presented. It can be seen that for many of the major organs (brain, heart wall, kidneys, liver, lungs, marrow, pancreas, ovaries, spleen and testes) the agreement with mean values predicted by models was reasonable. The main difference appears to be in dose estimates to the GI tract, where values by direct methods were only about half those predicted by models. However, in the former method, this may be the result of including the GI tract in the remaining tissues, whereas models can specify the actual dose to GI tract walls. In view of the relatively large tissue weighting factor of 0.24 assigned to the sum of doses to stomach and colon, the

effective dose estimated by direct PET measurements is lower ($0.71 \mu\text{Sv}\cdot\text{MBq}^{-1}$) than the models predict.

Table 2 Values of organ doses and effective doses ($\mu\text{Gy}\cdot\text{MBq}^{-1}$) for bolus injection of ^{15}O - water from five different centres.

Organ	¹ Eichling* <i>et al</i>	² Herscovich* <i>et al</i>	³ Smith <i>et al</i>	⁴ Brihaye <i>et al</i>	Mean (¹⁻⁴) (sd)	^{5,6} Berridge* <i>et al</i>
adrenals	1.8	1.3	1.4	-	1.5 (0.26)	-
bone surface	0.22	0.51	0.50	1.1	0.59 (0.38)	-
brain	1.6	1.3	1.5	0.71	1.3 (0.41)	1.2
breast	0.72	0.30	0.40	1.2	0.51 (0.43)	-
GB wall	-	0.46	0.44	1.2	0.70 (0.43)	-
GI tract:						
stomach wall	1.6	1.1	1.3	1.2	1.3 (0.25)	0.76
SI wall	1.8	1.1	1.9	1.1	1.5 (0.43)	0.62
ULI wall	1.8	1.1	1.7	1.3	1.5 (0.30)	0.62
LLI wall	1.6	1.1	1.6	1.5	1.5 (0.25)	0.62
heart wall	1.6	2.2	2.5	0.67	1.8 (0.81)	2.4
kidney	1.6	1.9	2.2	0.95	1.7 (0.54)	1.4
liver	1.7	1.5	2.0	0.75	1.5 (0.51)	1.4
lungs	2.2	1.9	1.9	0.57	1.6 (0.73)	0.92
red marrow	0.24	0.89	0.97	1.5	0.89 (0.51)	0.68
muscle	0.30	0.27	0.32	0.15	0.26 (0.08)	0.22
ovaries	0.31	0.35	0.32	1.2	0.54 (0.43)	0.41
pancreas	1.2	1.6	1.6	1.2	1.4 (0.23)	1.2
skin	0.17	0.26	0.57	1.1	0.51 (0.41)	-
spleen	1.6	1.6	1.8	1.2	1.6 (0.26)	1.5
testes	0.19	0.68	0.83	1.1	0.70 (0.38)	0.38
thymus	-	0.35	1.3	-	0.84 (0.68)	-
thyroid	1.4	1.7	1.9	1.1	1.5 (0.35)	-
bladder wall	1.5	0.30	0.23	1.2	0.81 (0.62)	0.38
uterus	0.16	0.35	0.27	1.2	0.49 (0.46)	0.76
effective dose	1.1	0.97	1.2	1.1	1.1 (0.09)	0.71

* values supplied by S. Schwarz (*Personal communication*)

¹ Eichling JO, Bergman SR, Schwarz SW and Siegel BA. Equivalent dose estimates in adults for intravenously administered O-15-water (*Unpublished data*)

² Herscovich P, Carson RE, Stabin M and Stubbs JB. A new kinetic approach to estimate the radiation dosimetry of flow-based radiotracers. *J Nucl Med* 1993, 34: 155P

³ Smith T, Tong C, Lammertsma AA, Butler KR, Schnorr L, Watson JDG, Ramsay S, Clark JC and Jones T. Dosimetry of intravenously administered oxygen-15 labelled water in man: a model based on experimental human data from 21 subjects. *Eur J Nucl Med* 1994, 21:1126-1134

⁴ Brihaye C, Depresseux J-C and Comar D. Radiation dosimetry for bolus administration of oxygen -15-water. *J Nucl Med* 1995, 36: 651-656

⁵ Berridge MS, Adler LP and Rao PS Radiation absorbed dose for O-15-butanol and O-15-water estimated by positron emission tomography. *J Nucl Med* 1991, 32 1043

⁶ Berridge MS (S. Schwarz - Personal communication)

Discussion and Conclusions

With one or two exceptions, there is good agreement on individual organ doses and the effective dose predicted by modelling techniques at four different centres. The mean effective dose by these methods is $1.1 (\pm 0.09) \mu\text{Sv}\cdot\text{MBq}^{-1}$. Estimates of organ doses by practical techniques (Berridge *et al.*) agree reasonably well with the models for most organs but may be artificially low for segments of the GI tract wall, with the result that the effective dose is predicted to be lower. In the circumstances, the effective dose estimated from models is recommended for purposes of planning research studies with ¹⁵O-water. It is more than double the value ($0.45 \mu\text{Sv}\cdot\text{MBq}^{-1}$) derived from oversimplistic uniform distribution water models. It can be seen (Table 2) that the present study tends to lead to higher dose estimates for certain organs and for the effective dose than values from other centres using modelling techniques: this may be the result of a more detailed appraisal of dose estimates in the walls of hollow organs.

3. Accuracy of estimating the radiopharmaceutical content of organs with low uptake: measurement of heart uptake using two different myocardial perfusion imaging agents.

Introduction

This study was undertaken to examine some of the factors which limit the accuracy of measurement of organ uptake values in patients given radiopharmaceuticals for clinical diagnosis. Whereas various methods now exist for improving the overall accuracy of such measurements, the question of appropriate background subtraction assumes major importance in assessing low uptake organs. This limitation on accurate measurement has been examined in the estimation of heart uptake of ^{99m}Tc - labelled myocardial perfusion imaging agents, which is only about 2%. Two different agents were investigated by two different techniques in patients both at peak exercise and at rest.

Methods

Studies were carried out on outpatients attending Northwick Park Hospital for diagnostic cardiac studies, including cardioscintigraphy, following the injection of one of two different ^{99m}Tc-labelled myocardial perfusion imaging agents: MIBI ('Cardiolite' - Du Pont) and P53 ('tetrofosmin' - Amersham International). The patients were investigated on two separate occasions within 7 days, firstly after exercise on a treadmill to peak exercise and secondly at rest. The same imaging agent was used on both occasions. The measurements made for the purposes of the present study were additional to the diagnostic procedures and were obtained using a different gamma-camera (400AT, IGE). Twelve patients (9 male, 3 female) given MIBI and 17 patients (16 male and 1 female) given P53 were measured by planar scintigraphy, after exercise and at rest, using the geometric mean attenuation-corrected method to quantitate uptake in the myocardium. In 8 patients from each of these groups, SPECT was also performed on both occasions to compare the estimates of myocardial uptake with those obtained by planar scintigraphy.

Planar scintigraphy and attenuation correction

Planar scintigraphy was performed on average 105 minutes after the injection, as soon as possible after diagnostic scintigraphy had been completed elsewhere. On the first occasion, after exercise, anterior, posterior and left lateral images of the chest were taken and the thickness of the chest at the position of the heart was measured with the patient lying supine on the couch. On the second occasion, with the patient at rest, only the anterior and posterior images were repeated. However, on this occasion and before the injection, a transmission scan was performed using a ^{99m}Tc -filled flood phantom beneath the supine patient's chest. A planar image was also obtained after removing the patient, without moving the camera, transmission source or couch. A ROI was drawn around the myocardium in the anterior image obtained with MIBI or P53 and, after reversal, the same ROI was fitted to the posterior image. After background correction, the geometric mean of anterior and posterior ROI counts was calculated. The same ROI was also transferred to the transmission images with and without the patient to obtain an attenuation factor which was related to an equivalent thickness of water by reference to a relationship previously obtained using a water phantom in conjunction with the transmission source. From calibration curves of counting efficiency (geometric mean counts- $\text{MBq}^{-1}\cdot\text{sec}^{-1}$) versus water thickness observed for different sized ^{99m}Tc sources in a water phantom, the activity content of the myocardium was derived (% of administered activity). Three different background values were used to correct the counts from the myocardial ROIs:- A) the mean of at least 6 values obtained with a small rectangular ROI positioned adjacent to the myocardial margin; B) the system background (no patient); and C) a calculated background. The latter accounted for the effects of tissue overlying and underlying the heart and was determined from the thickness of these regions as measured from the left lateral scans, and assuming uniform distribution of activity in background tissue.

SPECT

SPECT imaging of the heart (360° ; 64×10 sec views) was performed before the planar scintigraphy, on average 96 minutes after the injection. Reconstructed slices were obtained using a Ramp-Hanning filter and three different values of attenuation coefficient, 0; 0.07 (the default value of the system); and 0.12 pixel^{-1} . Thresholds of 40%, 41% and 42% of the maximum pixel count were used, respectively, to obtain the pixel and count content of the reconstructed myocardial images. These thresholds were optimum values obtained from calibration studies with ^{99m}Tc sources of differing volume in a water phantom and measured using the same technique. For each of the three attenuation correction methods, relationships were derived between the average voxel (cubic pixel) count rate and activity concentration, and used to determine the absolute activity content of the heart from which the % of administered activity in the heart was calculated. The latter values were then compared with those estimated by planar scintigraphy.

Results

1. Myocardial uptake

i) Planar scintigraphy with attenuation correction

These results are shown in Table 3 for the two myocardial perfusion imaging agents and the three different methods of correcting for background activity.

ii) SPECT

These results are given in Table 4 for the two myocardial perfusion agents using three different linear attenuation coefficients ($\mu \text{ pixel}^{-1}$) for image reconstruction.

Table 3 Myocardial uptake of two ^{99m}Tc -labelled myocardial perfusion imaging agents estimated by planar scintigraphy with attenuation correction and using three methods of background correction, after exercise and at rest.

agent	mean % of administered activity in myocardium (sd)					
	exercise			rest		
	Bgd A	Bgd B	Bgd C	Bgd A	Bgd B	Bgd C
MIBI (n = 12)	1.50 (0.40)	3.0 (0.82)	1.94 (0.52)	1.42 (0.35)	2.92 (0.71)	1.86 (0.44)
MIBI (n = 8)*	1.37 (0.33)	2.67 (0.52)	1.74 (0.36)	1.29 (0.28)	2.65 (0.48)	1.69 (0.30)
P53 (n = 17)	1.25 (0.24)	2.65 (0.51)	1.71 (0.33)	1.28 (0.25)	2.71 (0.53)	1.74 (0.34)
P53 (n = 8)*	1.17 (0.14)	2.61 (0.39)	1.60 (0.18)	1.22 (0.21)	2.71 (0.46)	1.66 (0.27)

* Patients also studied by SPECT

Bgd A, B, C : see text

Table 4 Uptake by the heart (% of administered activity) of the two agents measured by SPECT using three different attenuation coefficients ($\mu \text{ pixel}^{-1}$).

agent	mean % of administered activity in myocardium (sd)					
	exercise			rest		
	$\mu = 0$	$\mu = 0.07$	$\mu = 0.12$	$\mu = 0$	$\mu = 0.07$	$\mu = 0.12$
MIBI (n = 8)	1.56 (0.35)	1.94 (0.42)	2.08 (0.46)	1.59 (0.34)	1.94 (0.28)	2.15 (0.26)
P53 (n = 8)	1.23 (0.24)	1.63 (0.25)	1.81 (0.25)	1.30 (0.25)	1.59 (0.20)	1.84 (0.25)

2. Differences between heart uptakes after exercise and at rest.

These results are given in Table 5 as the mean (± 1 sd) values for the exercise uptake minus the rest uptake (% of administered activity). The significance of the differences was tested by paired 't' - test.

3. Differences between planar and SPECT imaging

Differences have been calculated between heart uptake values measured by planar imaging, using the calculated background subtraction method (C), and those measured by SPECT imaging, using three different values for the attenuation coefficient ($\mu \text{ pixel}^{-1}$). The results are shown in Table 6, expressed as the mean of planar minus SPECT values (± 1 sd) together with the p value estimated using the paired 't'-test. Values are given for both myocardial perfusion imaging agents both at exercise and at rest.

Table 5 Differences between heart uptakes (exercise minus rest (\pm 1sd)) for the two agents and two different techniques.

type of measurement	condition	exercise minus rest mean (% adm. activity)	number of studies	p value
planar				
MIBI	bgd A	+ 0.088 (0.144)	12	> 0.05
	"	+ 0.078 (0.173)	8	> 0.2
	bgd B	+ 0.084 (0.167)	12	> 0.1
	"	+ 0.025 (0.131)	8	> 0.6
	bgd C	+ 0.081 (0.143)	12	> 0.05
	"	+ 0.05 (0.157)	8	> 0.3
P53	bgd A	- 0.03 (0.133)	17	> 0.3
	"	- 0.044 (0.159)	8	> 0.4
	bgd B	- 0.066 (0.233)	17	> 0.2
	"	- 0.104 (0.168)	8	> 0.1
	bgd C	- 0.039 (0.162)	17	> 0.3
	"	- 0.063 (0.166)	8	> 0.3
SPECT				
MIBI	$\mu = 0$	- 0.031 (0.227)	8	> 0.7
	$\mu = 0.07$	- 0.004 (0.239)	8	> 0.9
	$\mu = 0.12$	- 0.068 (0.238)	8	> 0.4
P53	$\mu = 0$	- 0.072 (0.192)	8	> 0.3
	$\mu = 0.07$	+ 0.037 (0.314)	8	> 0.7
	$\mu = 0.12$	- 0.033 (0.319)	8	> 0.7

Table 6 Differences in heart uptake: Planar (calculated background) minus SPECT

		$\mu = 0$	$\mu = 0.07$	$\mu = 0.12$
MIBI	exercise	+ 0.181 (0.31) (p > 0.1)	- 0.196 (0.343) (p > 0.1)	- 0.345 (0.337) (p < 0.05)
	rest	+ 0.10 (0.29) (p > 0.3)	- 0.25 (0.209) (p < 0.02)	- 0.463 (0.266) (p < 0.005)
P53	exercise	+ 0.371 (0.361) (p < 0.05)	- 0.029 (0.356) (p > 0.8)	- 0.211 (0.352) (p > 0.1)
	rest	+ 0.362 (0.373) (p < 0.05)	+ 0.071 (0.381) (p > 0.6)	- 0.181 (0.429) (p > 0.2)

Discussion and Conclusions

The above results show that the heart uptake of two relatively new ^{99m}Tc labelled myocardial perfusion imaging agents (MIBI and P53) is only in the order of 1-3% of administered activity. In such situations, the accuracy of the estimated organ uptake is critically dependent on the choice of background subtraction used to determine net organ counts. Since this is a prerequisite prior to the application of well established methods of improving accuracy, such as the geometric mean technique and attenuation correction, it is possibly the most limiting factor on the accuracy of estimating low organ uptakes. For example, the subtraction of only the system background leads to uptake estimates double those obtained using background levels from tissues adjacent to the heart. Intuitively, it would seem that these two methods set upper and lower bounds to the estimate and that the correct value lies between the two. The calculated background method, therefore, appears to provide a more scientifically based alternative since it attempts to allow for count rate contributions from tissue over and underlying the heart. However, even the latter method is only an approximation of the true background and it is clear that the uncertainty of background correction can have a profound effect on the accuracy of low uptake estimation.

The additional estimations of heart uptake by the SPECT method in general support the use of the calculated background subtraction method, particularly when the default value for μ of 0.07 pixel^{-1} , equivalent to 0.11 cm^{-1} , is used for image reconstruction. This value is an acceptable broad beam attenuation coefficient for ^{99m}Tc gamma radiation in soft tissue. However, since neither of these imaging techniques, planar or SPECT, can be considered to be a 'gold standard', the true estimate of myocardial uptake cannot be determined by these methods.

Of clinical interest is the fact that there was no significant difference between myocardial uptakes after exercise or at rest. There was an apparent tendency for MIBI uptake to be slightly greater after exercise. However, P53 showed slightly higher uptake at rest and the results of SPECT measurements generally support this tendency using either agent.

Publications

Smith T, Tong C, Lammertsma A, Butler KR, Schnorr L, Watson J, Ramsay S, Clark JC and Jones T (1993). A kinetic model for the radiation dosimetry of intravenously administered H_2^{15}O . *Nucl. Med. Comm.*, 14, 300, (abstr).

Smith T, Tong C, Lammertsma A, Butler KR, Schnorr L, Watson J, Ramsay S, Clark JC and Jones T (1994). Dosimetry of intravenously administered ^{15}O -labelled water in man: a model based on experimental human data from 21 subjects. *Eur. J. Nucl. Med.*, 21, 1126-1134.

Smith T, Senior R, Raval U, Bruckner FE, Dasgupta B and Lahiri A (1995). Investigation of the use of Indium-111 antimyosin in patients with idiopathic inflammatory myopathies: clinical studies, biodistribution and radiation dosimetry. Submitted to *J. Nucl. Med.*

Head of project 3: Dr. Petoussi

II. Objectives for the reporting period

The first aim of this project was to obtain estimates of the specific absorbed fractions (SAF) and specific absorbed energies (SEE) by using voxel phantoms (CHILD, BABY and adult) together with Monte Carlo codes. On the basis of these SAF values and by using software specially developed for this purpose, calculations of organ doses per incorporated activity were performed. Particular consideration was given to:

- the differences between SAFs and consequently organ doses obtained with the MIRD type phantoms and the voxel phantoms
- some new radiopharmaceuticals not included in the ICRP Publication 53 (Radiation Dose to Patient from Radiopharmaceuticals); the relevant biokinetic data were provided by the contract partners

Extensive tables of doses to ca. 24 organs and effective doses due to the most common radiopharmaceuticals were obtained to complement the data of ICRP 53. These data can be used in particular to assess individual patient doses, if individual biokinetic data are provided.

III. Progress achieved including publications

Introduction

Similar studies have been performed until now with the help of MIRD anthropomorphic phantoms (adult and paediatric) (1,2) which are mathematical phantoms describing the geometry of the body and its organs by simple equations. Besides obtaining new dose data for a baby, a child and an adult, one of the main objectives of this study was to investigate to what extent the model, MIRD or voxel, influences the resulting dose equivalents. Also, the degree of improved accuracy of the current data should be examined, in view of doses delivered to individual nuclear medicine patients.

Before beginning this project, the voxel phantoms, which are still under development at the GSF, have been used at our research group for simulation of external exposures only. Integration of internal emitters into the computer program provided an extension of their application.

Method and Results

The phantoms used

For this study, three voxel phantoms were used: a phantom of a 8 week old baby (BABY), of a 7-year old child (CHILD), and of an adult (Yale Man). The former two were constructed at the GSF, whereas the Yale Man was constructed at Yale University, USA.

Table 1 shows some characteristic data of these phantoms.

Table 1: Some characteristic data of the voxel phantoms used for this study

	BABY	CHILD	Yale Man
Age	8 weeks	7 years	adult
Height (cm)	57	115	118 (178)*
Width (cm)	21.8	33.1	40.0
Depth (cm)	12.2	17.6	28.0
Weight (kg)	4.2	21.7	65.2 (70.2)*
Slice width (mm)	4	8	10 or 5
Pixel side length (mm)	0.85	1.54	4
Voxel size (mm ³)	2.9	19.0	64.0
Number of slices	141	144	129
Matrix size	256x256	256x256	128x128
Constructed at	GSF	GSF	Yale Univ.

*The Yale phantom is a phantom from the top of the head to the mid thigh i.e the phantom does not include the whole of the legs. The height and the weight of the patient are shown in parentheses.

The voxel phantoms were constructed from computed tomographic data of human subjects obtained with a very fine CT. In this way, a greater degree of realism can be achieved with a voxel-type phantom than with a mathematical MIRD type phantom concerning the shape and location of the organs and the derivation of red bone marrow. For the BABY and CHILD, the red bone marrow was assessed in each single skeletal voxel directly from the CT data; seven different media were simulated according to their elemental composition: bone, bone marrow, soft tissue, skin, lung tissue, muscle tissue and air. Detailed description of the BABY and CHILD as well as the GSF method of constructing voxel phantoms can be found elsewhere /3, 4/.

The Yale phantom has been recently released and is intended by its constructors to be used for dose calculations for internal and external radiation sources in the field of health physics and therapy /5/. It was for the first time used by our group for dosimetric calculations and in order to discuss the results, some details on its construction and characteristics are given below: an adult male patient was chosen whose external dimensions were similar to the dimensions of the MIRD phantom. The patient was suspected to have diffuse melanoma but had no advanced signs of disease during the time of the scans. The CT slices were segmented manually and 36 organs and tissues were defined.

To assess the validity of the Yale phantom, the masses of some of its organs were estimated, by counting the voxels belonging to the respective organs and multiplying by the voxel volumes and the organ densities. Table 2 shows some organ masses together with the respective masses of the Reference man of ICRP 23 /6/.

Table 2: Masses in g of tissues and organs of the Yale adult voxel phantom and the Reference Man from ICRP 23

Tissue	Yale phantom	Reference man
Bladder	211	45
Bone marrow*	1391	1500
Colon	1328	370
Liver	1967	1800
Lung	1038	1000
Skeleton*	7336	10000
Stomach	345	150
Testes	116	35
Thyroid	7	20
Adrenals	4	14
Brain	1230	1400
Kidneys	512	310
Pancreas	53	100
Small intestine	1777	640
Spleen	374	180
Gall bladder	22	10
Heart	628	570 incl. blood
Skeletal muscle*	24080	28000
Oesophagus	43	40
Prostate	29	16
Eye lens	1.6	0.4

*The Yale phantom is a phantom from the top of the head to the mid thigh.

As it can be seen, there are large differences for some organs, particularly for those with a "wall" like bladder, colon, stomach, small intestine where it was obviously difficult to recognise their external contours and distinguish between the organ and its contents. Furthermore, small organs like thyroid, adrenals, gall bladder, eye lens, present difficulties at segmentation because of their small size. The masses of liver and lungs, two organs easily recognizable in the CT pictures show a good agreement.

Calculations of SAF and absorbed doses

The Monte Carlo calculations were performed on an intel ipsc/2 hypercube parallel computer, achieving a statistical accuracy which lies generally below 5 %. The monoenergetic photons simulated were in the energy range 0.02-3.00 MeV (see Table 3 for a detailed list of energies). SAF were obtained for 24 source organs and over 100 target organs. Uniform distribution in each source region was assumed and mean values were used for energy absorption in target organs. As an example of the data obtained, Table 3 gives the SAF values of the CHILD in kg^{-1} for thyroid as the source organ and for the most

Table 3: Specific absorbed fractions of photon energy in 1/kg, for a 7 year old child (21.7 kg)

Source organ: KIDNEYS										
Energy (MeV)										
Target organ	0.020	0.030	0.040	0.050	0.060	0.070	0.080	0.090	0.100	0.150
Adrenals	2.1E-01	2.5E-01	2.0E-01	1.6E-01	1.4E-01	1.2E-01	1.1E-01	1.0E-01	9.6E-02	8.9E-02
Bladder wall	6.3E-05	2.4E-03	6.1E-03	7.9E-03	8.4E-03	8.6E-03	8.5E-03	8.2E-03	8.2E-03	7.9E-03
Bone	1.0E-02	3.2E-02	3.9E-02	3.6E-02	3.1E-02	2.7E-02	2.3E-02	2.1E-02	1.8E-02	1.3E-02
Brain	0.0E+00	1.4E-06	1.8E-05	5.1E-05	8.4E-05	1.1E-04	1.3E-04	1.5E-04	1.6E-04	2.2E-04
Breast	1.3E-05	1.7E-03	4.9E-03	6.5E-03	6.8E-03	6.9E-03	6.8E-03	6.7E-03	6.7E-03	6.7E-03
Colon wall	9.0E-02	1.4E-01	1.3E-01	1.1E-01	8.9E-02	7.9E-02	7.2E-02	6.7E-02	6.4E-02	5.8E-02
Kidneys	3.2E+00	1.7E+00	9.4E-01	6.3E-01	4.8E-01	4.1E-01	3.7E-01	3.5E-01	3.4E-01	3.3E-01
Liver	5.2E-02	8.3E-02	7.9E-02	6.8E-02	5.9E-02	5.3E-02	4.9E-02	4.6E-02	4.4E-02	4.0E-02
Lungs	3.5E-04	4.7E-03	8.8E-03	1.0E-02	1.0E-02	1.0E-02	1.0E-02	9.7E-03	9.5E-03	9.0E-03
Muscle	2.0E-02	2.3E-02	2.0E-02	1.7E-02	1.5E-02	1.4E-02	1.3E-02	1.3E-02	1.2E-02	1.2E-02
Oesophagus	4.7E-04	5.5E-03	9.8E-03	1.2E-02	1.2E-02	1.2E-02	1.1E-02	1.1E-02	1.0E-02	9.7E-03
Ovaries	7.9E-03	3.6E-02	4.8E-02	4.7E-02	4.4E-02	4.0E-02	3.8E-02	3.6E-02	3.4E-02	3.1E-02
Pancreas	1.2E-01	2.0E-01	1.8E-01	1.5E-01	1.2E-01	1.1E-01	9.8E-02	9.1E-02	8.7E-02	7.9E-02
Red marrow	1.7E-03	7.2E-03	9.9E-03	1.1E-02	1.1E-02	1.1E-02	1.1E-02	1.1E-02	1.1E-02	1.1E-02
Skin	1.7E-03	5.4E-03	6.4E-03	6.2E-03	5.8E-03	5.5E-03	5.3E-03	5.2E-03	5.1E-03	5.2E-03
Small intest	2.4E-02	5.6E-02	6.0E-02	5.5E-02	4.9E-02	4.4E-02	4.1E-02	3.8E-02	3.7E-02	3.3E-02
Spleen	1.0E-01	1.4E-01	1.2E-01	9.4E-02	7.8E-02	6.8E-02	6.2E-02	5.8E-02	5.6E-02	5.2E-02
Stomach wall	5.9E-03	3.7E-02	5.0E-02	4.8E-02	4.4E-02	4.0E-02	3.7E-02	3.5E-02	3.3E-02	3.0E-02
Testes	0.0E+00	1.1E-04	6.0E-04	7.7E-04	1.1E-03	1.4E-03	1.2E-03	1.3E-03	1.4E-03	1.5E-03
Thymus	5.6E-06	7.4E-04	2.5E-03	3.8E-03	4.5E-03	4.6E-03	4.6E-03	4.6E-03	4.6E-03	4.4E-03
Thyroid	0.0E+00	1.4E-04	8.2E-04	1.5E-03	1.8E-03	1.9E-03	2.0E-03	2.2E-03	2.1E-03	2.1E-03
ULI wall	1.1E-01	1.8E-01	1.6E-01	1.3E-01	1.1E-01	9.8E-02	8.9E-02	8.3E-02	7.9E-02	7.1E-02
Uterus	4.8E-04	9.1E-03	1.8E-02	2.0E-02	2.1E-02	2.0E-02	1.9E-02	1.8E-02	1.8E-02	1.7E-02

Target organ	0.200	0.300	0.400	0.500	0.700	1.000	1.500	2.000	3.000	3.000
Adrenals	8.8E-02	8.7E-02	8.6E-02	8.6E-02	8.1E-02	7.9E-02	7.1E-02	6.5E-02	5.7E-02	5.7E-02
Bladder wall	7.8E-03	7.7E-03	7.8E-03	8.0E-03	7.8E-03	7.6E-03	7.2E-03	6.9E-03	6.7E-03	6.7E-03
Bone	1.1E-02	9.6E-03	9.1E-03	8.8E-03	8.4E-03	8.1E-03	7.5E-03	7.0E-03	6.3E-03	6.3E-03
Brain	2.5E-04	3.2E-04	3.7E-04	4.3E-04	4.9E-04	5.7E-04	6.3E-04	6.6E-04	6.8E-04	6.8E-04
Breast	6.9E-03	7.0E-03	7.2E-03	7.5E-03	7.5E-03	7.5E-03	7.1E-03	6.9E-03	6.1E-03	6.1E-03
Colon wall	5.7E-02	5.6E-02	5.5E-02	5.5E-02	5.2E-02	5.0E-02	4.6E-02	4.2E-02	3.8E-02	3.8E-02
Kidneys	3.4E-01	3.6E-01	3.6E-01	3.6E-01	3.5E-01	3.3E-01	3.0E-01	2.8E-01	2.5E-01	2.5E-01
Liver	3.9E-02	3.9E-02	3.8E-02	3.8E-02	3.6E-02	3.5E-02	3.2E-02	3.0E-02	2.6E-02	2.6E-02
Lungs	8.9E-03	9.0E-03	9.0E-03	9.0E-03	8.8E-03	8.7E-03	8.0E-03	7.7E-03	7.0E-03	7.0E-03
Muscle	1.2E-02	1.2E-02	1.2E-02	1.2E-02	1.2E-02	1.2E-02	1.1E-02	1.0E-02	9.1E-03	9.1E-03
Oesophagus	9.5E-03	9.4E-03	9.7E-03	9.6E-03	9.4E-03	8.7E-03	8.4E-03	7.6E-03	7.2E-03	7.2E-03
Ovaries	3.1E-02	3.0E-02	2.9E-02	2.9E-02	2.7E-02	2.5E-02	2.4E-02	2.1E-02	1.9E-02	1.9E-02
Pancreas	7.7E-02	7.6E-02	7.4E-02	7.3E-02	7.0E-02	6.6E-02	6.1E-02	5.6E-02	5.0E-02	5.0E-02
Red marrow	1.0E-02	1.0E-02	1.0E-02	1.0E-02	1.0E-02	9.6E-03	9.0E-03	8.4E-03	7.6E-03	7.6E-03
Skin	5.3E-03	5.6E-03	5.8E-03	5.9E-03	5.9E-03	5.8E-03	5.5E-03	5.3E-03	4.8E-03	4.8E-03
Small intest	3.2E-02	3.2E-02	3.1E-02	3.1E-02	3.0E-02	2.8E-02	2.6E-02	2.4E-02	2.2E-02	2.2E-02
Spleen	5.1E-02	5.1E-02	5.0E-02	5.0E-02	4.9E-02	4.6E-02	4.2E-02	3.9E-02	3.5E-02	3.5E-02
Stomach wall	2.9E-02	2.8E-02	2.8E-02	2.7E-02	2.6E-02	2.5E-02	2.3E-02	2.1E-02	1.9E-02	1.9E-02
Testes	1.7E-03	1.7E-03	2.2E-03	2.0E-03	2.4E-03	2.5E-03	2.6E-03	2.2E-03	2.2E-03	2.2E-03
Thymus	4.6E-03	4.5E-03	4.6E-03	4.7E-03	4.7E-03	4.6E-03	4.6E-03	4.3E-03	3.8E-03	3.8E-03
Thyroid	2.3E-03	2.2E-03	2.6E-03	2.4E-03	2.5E-03	2.6E-03	2.6E-03	2.6E-03	2.4E-03	2.4E-03
ULI wall	7.0E-02	6.8E-02	6.8E-02	6.7E-02	6.4E-02	6.1E-02	5.6E-02	5.1E-02	4.6E-02	4.6E-02
Uterus	1.6E-02	1.6E-02	1.6E-02	1.5E-02	1.5E-02	1.4E-02	1.3E-02	1.3E-02	1.1E-02	1.1E-02

important target tissues. Extensive tables of SAFs for the BABY and CHILD can be found elsewhere /7/.

In order to calculate the absorbed doses in target organs from the administration of unit activity of a radioactive substance, new software had to be developed. This computational tool uses data on specific absorbed fractions of energy in a target organ from the relevant source organs; biokinetic data of the substance administered and nuclear transformation data. It is relatively easy to use and can cope with any radionuclide internally administered, provided the above data are available. For electrons, alpha particles and recoil nuclei, the radiation is assumed to be absorbed entirely in the source organ. The nuclear decay data for the emitted gamma rays, the beta spectra and the discrete Auger and conversion electrons were taken from BRENK /8/; these data are identical to the data of ICRP 38 /9/ on nuclear transformations. The beta spectra were calculated according to Dillman /10/. For beta dosimetry, the full beta spectra are used (not average energies for beta transitions). The data for the alphas were taken from the ICRP 38.

Table 4 gives the dose equivalents per unit activity incorporated for $^{99}\text{Tc}^m$ pertechnetate, ^{123}I iodide and ^{131}I iodide for several target tissues of the BABY. The biokinetic data were taken from the ICRP publication 53 /2/ on the dosimetry of radiopharmaceuticals. As an example of new radiopharmaceuticals, Table 5 gives dose equivalents per unit administered activity of ^{111}In antimyosin and ^{15}O water, for CHILD. The biokinetic data of the last two substances were recently acquired from our contract partners at Medical Research Council, London (Dr. T. Smith).

Table 4: Dose equivalents per unit activity administered (Sv.Bq⁻¹) for ⁹⁹Tc^m pertechnetate, ¹²³I iodide and ¹³¹I iodide for the BABY voxel phantom

Tissue	⁹⁹ Tc ^m without blocking the thyroid	¹²³ I thyroid uptake 25%	¹³¹ I thyroid uptake 25%
ADRENALS	2.46e-11	5.71e-11	2.83e-10
BLADDER	2.41e-10	9.33e-10	7.72e-09
BONE	2.09e-11	8.16e-11	6.41e-10
BRAIN	5.12e-11	1.53e-11	3.08e-10
BREAST	1.40e-11	5.78e-11	1.15e-09
COLON	2.04e-09	9.37e-11	2.77e-10
KIDNEYS	4.45e-11	1.03e-10	6.10e-10
LIVER	2.16e-11	5.42e-11	3.24e-10
LUNGS	1.59e-11	6.12e-11	1.02e-09
MUSCLE	1.92e-11	5.74e-11	7.16e-10
OESOPHAGUS	2.02e-11	1.09e-10	2.18e-09
OVARIES	6.97e-11	1.68e-10	4.26e-10
PANCREAS	4.21e-11	1.29e-10	4.23e-10
RED BONE MARROW	1.50e-11	3.89e-11	6.41e-10
SKIN	1.14e-11	3.05e-11	3.54e-10
SMALL INTESTINE	8.30e-11	7.04e-10	6.14e-09
SPLEEN	2.68e-11	8.00e-11	3.68e-10
STOMACH	8.06e-10	5.55e-09	5.46e-08
TESTES	2.10e-11	4.39e-11	1.36e-10
THYMUS	1.72e-11	1.97e-10	4.74e-09
THYROID	2.91e-10	4.04e-08	4.43-06
UTERUS	7.61e-11	2.24e-10	5.43e-10

Table 5: Dose equivalents per unit activity administered (Sv.Bq⁻¹) for ¹¹¹In antimyosin and ¹⁵O water for the 7 year old child (voxel phantom)

Tissue	¹¹¹ In Antimyosin	¹⁵ O Water
ADRENALS	4.79e-10	5.32e-12
BLADDER	2.47e-10	4.69e-13
LARGE INTESTINE	2.81e-10	6.92e-13
SMALL INTESTINE	1.91e-10	2.48e-12
KIDNEYS	1.29e-09	3.68e-12
LIVER	1.04e-09	5.15e-12
LUNGS	4.95e-10	1.15e-11
OVARIES	2.16e-10	4.59e-13
PANCREAS	4.04e-10	4.77e-12
SPLEEN	5.43e-10	2.38e-12
STOMACH	2.74e-10	4.41e-12
TESTES	1.12e-10	1.52e-11
THYMUS	2.16e-10	1.49e-12
THYROID	1.61e-10	7.75e-12
UTERUS	2.01e-10	3.48e-13
SKELETON	2.23e-10	3.57e-12
SKIN	9.66e-11	1.27e-12
RED BONE MARROW	3.63e-10	9.92e-13

Comparison of data obtained with the voxel and MIRD-type phantoms

The BABY and CHILD phantoms

Table 6 gives SAF values for the 7 year old child (21.7 kg), together with the SAF values of a 5 year old child (19 kg) and a 10 year old child (32 kg) from the data of Cristy and Eckerman, for the kidneys as source organ. It can be seen that different modelling does result in different organ doses, particularly for lower energies and organs distant to the source organ; therefore it would be justified to use the more realistic voxel phantoms instead of the mathematical phantoms.

The dose equivalents obtained for the BABY and CHILD can be compared with the values given in ICRP publication 53, based on the Cristy MIRD-type phantoms (Oak Ridge National Laboratories). These were obtained with the mathematical phantoms of 1 year, 5 year, 10 year, 15 year old and an adult. As an example, table 7 gives the dose equivalents per unit activity incorporated for ⁹⁹Tc^m pertechnetate, ¹²³I iodide for the CHILD and the 5 year old MIRD phantom. Generally, it was found that the discrepancies of the SAF's are smoothed when one considers the dose equivalents from radionuclides, where the electrons are playing the dominant part: the doses of the 7 year old voxel phantom are lying mostly between the doses of the MIRD-5 and MIRD-10 year old, as

Table 6: Specific Absorbed Fractions (SAF) of photon energy in 1/kg, for a 5 year old child (19 kg)*, a 7 year old child (21.7 kg)** and a 10 year old child (32 kg)*

		Source Organ : KIDNEYS								
Target	Organ	Energy [MeV]								
		0.030			0.100			1.000		
		5 yr	7 yr	10 yr	5 yr	7 yr	10 yr	5 yr	7 yr	10 yr
ADRENALS		2.7E-01	2.5E-01	1.6E-01	1.1E-01	9.6E-02	7.5E-02	9.9E-02	7.9E-02	6.7E-02
BRAIN		6.1E-07	1.4E-06	5.7E-08	1.1E-04	1.6E-04	5.3E-05	4.4E-04	5.7E-04	1.9E-04
KIDNEYS		2.1E+00	1.7E+00	1.5E+00	4.5E-01	3.4E-01	3.5E-01	4.8E-01	3.3E-01	3.5E-01
LIVER		6.2E-02	8.3E-02	3.9E-02	3.7E-02	4.4E-02	2.7E-02	3.2E-02	3.5E-02	2.2E-02
LUNGS		1.1E-02	4.7E-03	5.3E-03	1.2E-02	9.5E-03	7.9E-03	1.1E-02	8.7E-03	7.1E-03
OVARIES		5.2E-03	3.6E-02	2.3E-03	1.6E-02	3.4E-02	8.8E-03	1.2E-02	2.5E-02	7.5E-03
PANCREAS		1.1E-01	2.0E-01	6.2E-02	6.3E-02	8.7E-02	4.7E-02	5.1E-02	6.6E-02	3.4E-02
THYROID		4.3E-05	1.4E-04	5.1E-06	1.7E-03	2.1E-03	6.2E-04	1.9E-03	2.6E-03	8.4E-04
SKELETON		7.1E-02	3.2E-02	3.7E-02	2.9E-02	1.8E-02	1.9E-02	1.2E-02	8.1E-03	7.3E-03
RED BONE MARROW		1.9E-02	7.2E-03	1.2E-02	1.8E-02	1.1E-02	1.4E-02	1.6E-02	9.6E-03	1.2E-02

* Data of Cristy and Eckerman, ORNL, obtained using MIRD type mathematical phantoms (2).

** Data obtained from the present study, using a voxel phantom.

expected. Similarly, the doses of the voxel BABY are generally higher than the doses of the MIRDO-1 year old. However, deviations were observed particularly when one considers the SAF's for monoenergetic photons, the lower energies, small organs, or the organs mostly removed from the source organ. Differences were also observed for the bone marrow. Here, one has to consider the differences of the modelling of this tissue: the bone of the mathematical MIRDO phantoms is modelled as a homogeneous mixture of bone marrow and hard bone whereas, in the voxel phantoms, the bone is an inhomogeneous mixture and the bone marrow in each part of the skeleton is determined with high linear resolution from the original grey values of the CT scan. Differences in modelling exist also for the gastrointestinal tract.

Table 7: Comparison of organ dose equivalents per unit activity administered ($\text{Sv}\cdot\text{Bq}^{-1}$) for $^{99}\text{Tc}^m$ pertechnetate and ^{123}I iodide for the 7-year child voxel phantom and the 5-year MIRDO phantom

Tissue	$^{99}\text{Tc}^m$ pertechnetate without blocking the thyroid		^{123}I iodide thyroid uptake 25%	
	CHILD	MIRDO (5y)	CHILD	MIRDO (5y)
ADRENALS	1.1e-11	1.1e-11	2.1e-11	2.1e-11
BLADDER	2.5e-11	5.1e-11	8.9e-11	1.9e-10
LARGE INTESTINE	1.5e-10	2.7e-10	3.0e-11	3.8e-11
SMALL INTESTINE	2.9e-11	5.2e-11	8.0e-11	1.4e-10
KIDNEYS	1.5e-11	1.3e-11	2.3e-11	2.7e-11
LIVER	8.8e-12	1.3e-11	1.4e-11	2.1e-11
LUNGS	4.9e-12	7.9e-12	2.0e-11	2.0e-11
OVARIES	1.7e-11	2.7e-11	3.6e-11	3.8 e-11
PANCREAS	1.7e-11	1.6e-11	3.5e-11	3.6e-11
SPLEEN	8.9e-12	1.2e-11	1.7e-11	2.5e-11
STOMACH	7.2e-11	8.1e-11	4.2e-10	2.0e-10
THYROID	8.2e-11	1.2e-10	1.1e-08	1.6e-08
UTERUS	1.6e-11	2.4e-11	4.4e-11	4.7e-11
SKELETON	6.4e-12	1.0e-11	1.8e-11	2.3e-11
RED BONE MARROW	4.7e-12	1.3e-11	1.1e-11	2.6e-11

The Yale adult phantom

In general, the specific absorbed fractions of the Yale phantom were systematically higher than those obtained with the MIRDO type adult phantom, approximately up to a factor of 2 but sometimes even higher. If one considers the situation of a source organ being on the same time a target organ, the SAFs show a good agreement when the masses agree, for example for the liver, lungs and kidneys. When large differences on the masses are observed, the SAFs depend on the organ mass, i.e. the SAFs for a given organ decrease as organ size increases. Similarly, the dose equivalents per unit activity for radionuclides

were found to be mostly higher for the Yale phantom by a factor up to 2 or sometimes more.

The above deviations could be attributed to the different nature of the mathematical phantoms, i.e. one is a voxel phantom and the other a mathematical one, and to the effect introduced by the "realistic" simulation of the location and shape of the organs. However, the large differences of some of the organ masses of the Yale phantom and the adult reference man as shown in table 2, indicate either an enormous deviation of this individual patient's anatomy from the average or an inaccuracy of the segmentation process. As the differences are larger for either small or hollow organs, the pixel size length of 4 mm might be too large for a proper segmentation of these fine structures.

It is planned to repeat these calculations with the GSF adult voxel phantom. The latter was unfortunately not released on time to be used for this project as initially planned. It is believed that testing the Yale adult voxel phantom contributed to the field of numerical dosimetry using human voxel phantoms.

Conclusions

In conclusion, the availability of the voxel phantoms CHILD and BABY to be used for estimation of dose equivalents due to internal emitters was demonstrated. Variations of the SAFs and organ doses per unit activity obtained with voxel and MIRD-type phantoms methods were observed. The suitability of the Yale adult phantom has still to be investigated.

References

1. Cristy, M. and Eckerman, K.F. 1987. Specific absorbed fractions of energy at various ages from internal photon sources. Oak Ridge National Laboratory Rep. ORNL/TM-8381:Vol. 1 -7.
2. International Commission on Radiological Protection. 1987. ICRP Publication 53. Radiation dose to patients from radiopharmaceuticals. Pergamon Press, Oxford.
3. Zankl, M., Veit, R., Petoussi, Mannweiler, E., Wittmann, A. and Drexler, G. 1994. Realistic Computerized human phantoms. *Adv. Space Res.* Vol. 14 (10), pp. (10)423-(10)431.
4. Zankl, M., Petoussi-Henss, N., Wittmann, A. 1995. The GSF voxel phantoms and their application in radiology and radiation protection. In: *Proceedings of a Workshop on Voxel Phantom Development*, NRPB Chilton, U.K., 6-7 July 1995, NRPB Report, (in press).
5. Zubal, I. G., Harell, C.R., Smith, E.O., Rattner, Z., Gindi, G. R. and Hoffer, P.B. 1994. Computerized three-dimensional segmented human anatomy. *Med. Phys* 21 (2), pp229-302.

6. International Commission on Radiological Protection. 1975. ICRP Publication 23. The Reference Man: Anatomical, physiological and metabolic characteristics. Pergamon Press, Oxford.
7. Petoussi, N., Zankl, M. and Henrichs, K. (in preparation). Tomographic Anthropomorphic Models. Part III: Specific absorbed fractions of energy for a baby and a child from internal photon sources. GSF-Bericht, Neuherberg.
8. Brenk, H. D.: Dosisfaktoren für ca. 800 Radionuklide zur Berechnung der externen Strahlenexposition durch Photonen-und Elektronenstrahlung. 1983. Brenk Systemplanung, Aachen.
9. International Commission on Radiological Protection: Radionuclide transformations: Energy and Intensity of emissions. 1983. ICRP Publication 38, Annals of the ICRP 11-13. Pergamon Press, Oxford.
10. Dillman, M. J. : EDISTER - A computer program to obtain a nuclear decay data base for radiation dosimetry. 1980. Oak Ridge National Laboratory, Report ORNLTM-6689.

List of publications

Moores, B.M., Petoussi, N., Schibilla, H., Teunen, D. (Eds.) (1993): Test Phantoms and Optimisation in Diagnostic Radiology and Nuclear Medicine. Radiat. Prot. Dosim. 49 (1/3).

Zankl, M., Veit, R., Petoussi, Mannweiler, E., Wittmann, A. and Drexler, G. 1994. Realistic Computerized human phantoms. Adv. Space Res. Vol. **14** (10), pp. (10)423-(10)431.

Zankl, M. Petoussi-Henss, N., Wittmann, A. 1995. The GSF voxel phantoms and their application in radiology and radiation protection. In: Proceedings of a Workshop on Voxel Phantom Development, NRPB Chilton, U.K., 6-7 July 1995, NRPB Report, (in press).

Petoussi, N., Zankl, M. and Henrichs, K. (in preparation). Tomographic Anthropomorphic Models. Part III: Specific absorbed fractions of energy for a baby and a child from internal photon sources. GSF-Bericht, Neuherberg.

Head of project 4: Mr. K. Evans.

II. Objectives for the reporting period

^{99m}Tc-dimercaptosuccinic acid (^{99m}Tc-DMSA) is used in routine paediatric nuclear medicine for the diagnosis of kidney disorders. Although the biokinetics of this radiopharmaceutical are well documented in adults, there is little quantitative information in children. The object of this study therefore, is to obtain biokinetic data from children of differing age and degree of renal dysfunction after the administration of ^{99m}Tc-DMSA in order to look for evidence of age-dependency and to examine the effects of renal pathology. The data will then be used to make radiation dose estimates for each child using five paediatric anthropomorphic phantoms and the Medical Internal Radiation Dose (MIRD) Committee formulary for dosimetry. In view of the inability to match perfectly the size of each child to a discrete phantom, a method of interpolation between dose estimates derived from two adjacent phantoms will be investigated as a more accurate method of dosimetry in children.

A further objective is to compare the uniformity of radiation dose values resulting from scaling the adult administered activity of 100MBq by body surface area, with the uniformity resulting from an administered activity schedule based on body weight.

Finally, it is planned to set up criteria for the reproducibility of the clinical interpretation of the ^{99m}Tc-DMSA scans and to construct a classification so that a clinical museum could be developed.

III. Progress achieved including publications

The time-course of biodistribution and dosimetry after administration of ^{99m}Tc-DMSA in 24 children (15 normals and 9 abnormal) aged from 5 weeks to 14.8 years undergoing routine diagnostic imaging at Great Ormond Street Hospital NHS Trust, have been investigated.

METHODS

Patients were imaged with a gamma camera up to 30h after injection of an amount of ^{99m}Tc-DMSA calculated by scaling the adult activity of 100MBq according to relative body surface area. An attenuation-corrected conjugate counting technique was used to estimate the absolute activities in six organs and tissues (kidneys, liver, spleen, bladder contents, knees and whole body). After correcting for radioactive decay, these were expressed as biological retention data relative to the amount of administered activity. The observed uptake of ^{99m}Tc-DMSA in knees has been assumed to concentrate in the metaphyses of the long bones. The rates of renal uptake and elimination, and the urinary excretion of the DMSA were also measured

Dedicated in-house software was generated to obtain time-activity plots and residence times of the activity in the source organs. Residence time in kidneys was estimated by separate integration of the uptake phase and clearance phase of the kidney retention curves. Residence times in other organs and tissues were estimated by integration of their effective retention curves. During the period of study, there was no observable diminution of the measured uptake in knees and consequently this was assumed to be retained with an elimination half-time which was large in relation to the radioactive half-life. Residence time in whole-body was calculated from measured retention data after subtraction of the activity in bladder contents at each measured time. The residence time in remaining body was obtained by subtracting the sum of residence times in kidneys, liver and spleen from the whole-body residence time

The MIRDOSE 2 dose calculation program was used to derive estimates of radiation doses in 25 target organs following input of the residence time values in the six source organs. Residence time of bladder contents was automatically calculated by the MIRDOSE 2 program after inputting values of the retention parameters (magnitude and half-times of components) derived from equations of observed whole-body retention after subtraction of bladder activity, together with the appropriate bladder voiding period for a given child. The doses to the metaphyseal growth complexes in the knees were obtained separately by calculation of the S-value for self-dose in this tissue.

In four patients who had unilateral renal uptake, the dose to the functioning kidney was assumed to be twice the value yielded by the MIRDOSE 2 program for a pair of normally functioning kidneys. This allowed for the fact that all the kidney residence time in such cases, is associated with a single kidney. In two patients with a large disproportionality in renal uptake, proportional corrections were made. The higher estimate was used for dosimetry purposes.

From values of equivalent dose to the 25 target organs, the effective dose (E) and the effective dose equivalent (He) were calculated for each patient using the relevant tissue weighting factors. In order to reduce errors in these dose estimates arising from mismatch of a given patient to one of the five paediatric anthropomorphic MIRD phantoms, calculations of the equivalent doses to the target organs were repeated using an interpolation method based on body weight. The MIRDOSE 2 program was used to determine equivalent organ doses to each child using two adjacent phantoms whose differential weight range included the weight of the child. A computer program was written to perform linear interpolation between organ doses calculated using the two phantoms. This provided more accurate estimates than those from either of the single phantoms unless of course, the child's weight matched exactly to the phantom. E and He were then recalculated using the interpolated equivalent organ doses.

RESULTS

Biokinetics

In 15 normal patients aged from 7 weeks to 14.8 years, the maximal global renal uptake of ^{99m}Tc -DMSA was $42.4 \pm 5.4\%$ of the administered activity. One patient with a single kidney, had a unilateral uptake of 44%, but in the other 14 patients, there was no significant difference between maximal uptake values for the individual kidneys. The maximal global renal uptake of the normal patients of less than 1 year of age (6 patients) was $41.8 \pm 6.4\%$ and for those over 1 year (9 patients) was $42.9 \pm 4.9\%$ and were not significantly different. Similarly, there was no significant age dependency in individual kidney uptakes.

In 9 patients with renal pathology, the mean global kidney uptake was $15.8 \pm 8.2\%$. This is, understandably, significantly lower than that of the normal group

The kidney biological retention data were described as the sum of exponential uptake and elimination components (λ_u and λ_e) and the rate constants of these two components were used to compare renal kinetics in the different patient groups. In the 15 normal subjects, the mean values of λ_u for left and right kidneys were $0.68 \pm 0.13\text{h}^{-1}$ and $0.72 \pm 0.14\text{h}^{-1}$ respectively and a paired "t" test showed no significant difference, consequently they were taken as a single group giving a mean λ_u value of $0.70 \pm 0.14\text{h}^{-1}$. Thus the mean uptake half time in normals was almost exactly 1 hour which agrees with the accepted adult value. Again there was no evidence of age dependency of the renal uptake rate.

Taking all abnormal patients as a single group, the mean uptake rates by left and right kidneys were $0.63 \pm 0.31\text{h}^{-1}$ and $0.56 \pm 0.16\text{h}^{-1}$ respectively and were not significantly different on a paired "t" test. The mean value of combined left and right uptake rates, excluding one patient with very low kidney uptake was $0.65 \pm 0.16\text{h}^{-1}$ and was not significantly different from that of the normal group. There was no significant difference in the kidney biological elimination rates in the normal and abnormal groups, the mean λ_e value being $0.009 \pm 0.006\text{h}^{-1}$ and $0.0108 \pm 0.0086\text{h}^{-1}$ respectively.

In normal patients the mean cumulative activity in urine was $10.4 \pm 4.1\%$ at 6 hours and $18.0 \pm 4.4\%$ at 24 hours. For the abnormal patients, the mean cumulative activity was $20.0 \pm 9.4\%$ at 6 hours and $32.4 \pm 11.1\%$ at 24 hours and these values were significantly higher than the normal group. When normal and abnormal patients were considered as a single group, there was a significant negative correlation between kidney global uptake and both the 6h and 24h cumulative urinary excretion. This result shows that when renal uptake is reduced, some of the excess $^{99\text{m}}\text{Tc-DMSA}$ is cleared to urine.

The mean uptake of $^{99\text{m}}\text{Tc-DMSA}$ in liver and spleen in 15 children with normal renal function was $4.6 \pm 2.0\%$ and $1.9 \pm 1.0\%$ respectively. Significant correlation was found only between liver uptake and 24h urine activity ($r = -0.66$; $p < 0.02$). In abnormal renal function, the mean values of liver uptake ($4.9 \pm 1.7\%$) and spleen uptake ($2.0 \pm 1.0\%$) were not significantly different from normal values.

Combined uptake in knees of 15 children with normal renal function was $1.40 \pm 0.99\%$ with a range of 0.4 to 4.1% of administered activity. In 6 children younger than one year, the mean uptake was significantly lower than in 9 children older than one year. There was no significant difference in mean knee uptake in 9 abnormal children from that of the normal group.

This biodistribution and biokinetic study demonstrated that there was little evidence of age dependency apart from reduced urinary excretion and knee uptake in children with normal renal function and younger than one year. Generally speaking, the biokinetics in normal children could be approximated by those observed in normal adults lending support to the use of adult biokinetic data to predict paediatric radiation dose estimates from this radiopharmaceutical. As expected, in pathological cases of renal disease, the major observed difference compared with normal biokinetics was a reduction in global kidney uptake, together with a non-commensurate increase in urinary excretion of the radiopharmaceutical.

Dosimetry

In 15 children with normal renal function, the residence times in kidneys, liver, spleen, bladder and remaining body were $3.01 \pm 0.41\text{h}$, $0.35 \pm 0.16\text{h}$, $0.13 \pm 0.08\text{h}$, $0.18 \pm 0.09\text{h}$ and $4.08 \pm 0.49\text{h}$ respectively. There was no significant correlation between kidney, liver or spleen residence times and age or weight. There were, however, significant correlations between remaining body residence time (τ_{rb}) and both age and weight. The regression equations were:-

$$\tau_{\text{rb}} (\text{h}) = 4.43 - 0.014 \times \text{weight (kg)} \quad (r = -0.73; p < 0.005).$$

$$\tau_{\text{rb}} (\text{h}) = 4.45 - 0.065 \times \text{age (y)} \quad (r = -0.74; p < 0.005).$$

As reported earlier, children younger than 1 year excrete a significantly lower proportion of the administered activity in urine than children older than 1 year. This would lead to an increase in remaining body residence time in children under 1 year.

In 9 children with renal pathology, the mean residence times in kidneys, liver, spleen, bladder and remaining body were $1.07 \pm 0.60\text{h}$, $0.39 \pm 0.15\text{h}$, $0.10 \pm 0.07\text{h}$, $0.23 \pm 0.12\text{h}$ and $5.39 \pm 0.83\text{h}$ respectively.

Radiation dose estimates obtained both by reference to discrete paediatric phantoms by age and by interpolation between phantoms by weight are given in Tables 1 and 2 for children with normal renal function and for those with renal pathology respectively. In three cases where children were reasonably closely matched to one or other of the discrete phantoms (within 1kg), there was little difference in effective dose from the two methods of dose estimation ($< 7\%$). In the remaining 21 children, larger differences of up to $+67\%$ were observed. The largest increase occurred in a child (No. 13) aged 8 months whose weight was almost exactly mid-way between those of the neonate and 1y phantoms. On the other hand, the largest decrease (-38%) occurred in an 11 year old child (No. 10) for whom the 10y phantom was used but whose weight of 65kg approached that of the adult phantom. In 14 normal patients, excluding one with unilateral compensatory hypertrophy, the mean value of E was 0.99 ± 0.29 mSv using discrete phantoms and 1.0 ± 0.11 mSv using the interpolated method. The standard deviation was reduced considerably by application of the interpolated method. With either method, the values of effective dose equivalent (He), 1.8 ± 0.6 and 1.8 ± 0.2 mSv respectively, were almost double the values of E, reflecting the changes in tissue weighting factors between ICRP 60 and ICRP 26 particularly for kidneys, which receive the highest dose (18.6 ± 3.0 mSv), representing 0.47 ± 0.08 mSv to the effective dose of 1.0 mSv.

In children with renal pathology, the mean values of E were 0.89 ± 0.22 mSv using discrete phantoms and 0.79 ± 0.16 mSv using the interpolated method. The values of He were again greater than E, but by a smaller factor than in normals because of lower values of kidney uptake and dose. The values of E from the interpolated method were significantly higher in children with normal renal function than in children with renal pathology showing that, in the latter group, the effects of reduced kidney uptake and faster elimination of radioactivity, which tend to reduce the E value, outweigh the effects of raised urinary bladder cumulated activity, which tend to increase it.

At this hospital, the amount of administered $^{99\text{m}}\text{Tc}$ -DMSA is calculated according to a schedule based on the body surface area of a child, relative to that of the adult value of 1.73m^2 , and an adult administered activity of 100 MBq. Figure 1 curve(A) shows the relationship between effective dose, calculated by the interpolated method, and body weight which results from the use of this schedule in 14 children with normal bilateral renal function. Although the effective dose is reasonably constant over the range of body weight, there is a significant negative correlation ($r = -0.74$, $p = 0.005$) and the regression equation is given by:-

$$\text{effective dose (mSv)} = 1.1 - 0.0035 \times \text{weight (kg)}$$

Figure 1 curve (B) shows the relationship between E and body weight that would have resulted if a body weight scaling factor had been used to calculate the administered activity. In this case, the effective dose decreases significantly with decreasing weight. This raised the question as to whether the reduced activities administered to children below about 40 kg, although leading to progressively lower effective doses, would result in unsatisfactory clinical images. Furthermore, if this schedule had been used in the present study, 5 normal children weighing less than 7 kg would have required the minimum administered activity of 10 MBq, resulting in a return to larger values of E for these children as indicated in Fig 1, curve (B).

The results have shown little age-dependency of biokinetic parameters in children aged 5

weeks to 14.8 years, suggesting that biokinetic models based on adult studies may be directly applicable to paediatric dosimetry. This finding lends support, for this radiopharmaceutical at least, for the validity of the principle adopted in ICRP publication 53 where doses were estimated for children of four different ages using biokinetic data gleaned largely from studies on adults. Not surprisingly, our data differed slightly in detail from the ICRP 53 model since they were based on an ad hoc study and no similarly detailed body of information was available when ICRP 53 was compiled. Our value of 0.45 (Table 3) for the fractional distribution (F_s) of kidneys was lower than that used in ICRP 53 (0.5) and thereafter shows distinct elimination from the kidneys with a mean half-time of 3.2 days. This leads to a value of 0.424, our observed mean maximal kidney uptake, at the observed mean time-to-maximum of 6.8h. The renal uptake half-time, however, was identical in the two models (1h). The overall effect was to give a lower value for kidney residence time (3.1h) compared with that of the ICRP 53 model (3.7h). The mean values for uptake in liver (0.046) and spleen (0.019) also differed from the ICRP 53 values of 0.1 and 0.01 respectively. One of the main differences was in the value of residence time in remaining body, where our value of 3.9 ± 0.5 h was substantially higher than that derived from the ICRP 53 model (2.6h) and arises mainly because of a larger whole body residence time and smaller kidney residence time. The consequence of this was to imply larger doses to those organs not specified in the model as source organs.

From the results of the present study, a biokinetic model, applicable for dosimetry in children of all ages with normal renal function, has been presented in the format of ICRP 53 (Table 3). When applied to the group of 14 normal children (excluding one with unilateral kidney function), the model predicted a mean effective dose of 1.0 ± 0.10 mSv using the described method of interpolating organ doses between phantoms, compared with the actual mean value of 1.0 ± 0.11 mSv. The mean paired difference was 0.003 ± 0.061 mSv ($p > 0.7$). The model gives a mean value of 1.8 ± 0.20 mSv for He, compared with the actual value of 1.8 ± 0.22 mSv.

A clinical classification of ^{99m}Tc -DMSA scans in paediatrics was also developed. This included both the indications for the study as well as the results of the examination. It was presented to the Paediatric Task Group of the European Association of Nuclear Medicine in Dusseldorf 1994. A pathological classification of ^{99m}Tc -DMSA scans has been set up at this institution (Table 4). Over 500 children who underwent ^{99m}Tc -DMSA scans have been reviewed, two hundred and fifty eight of these cases have been placed in the museum. All these cases have full clinical and pathological correlation documentation.

PUBLICATIONS

1. Evans K, Lythgoe MF, Anderson PJ et al. The biokinetic behaviour of ^{99m}Tc -DMSA in children. *J Nucl Med* (in press).
2. Smith T, Evans K, Lythgoe MF et al. Radiation dosimetry of ^{99m}Tc -DMSA in children. *J Nucl Med* (in press).
3. Gordon I et al. Can ^{99m}Tc -MAG3 replace ^{99m}Tc -DMSA in the exclusion of a focal renal defect? *J Nucl Med*, 1992; 33, 2090-2093.

Table 1

Dosimetry of [^{99m}Tc] DMSA in 15 Children with Normal Renal Function

PATIENT	3	5	4	24	13	9	12	22	1	16	21	10	2	18	11	
Age	7w	4m	5m	6m	8m	11.5m	1.3y	4.1y	6.1y	8.2y	10.2y	11.0y	12.8y	13.0y	14.8y	
Weight (kg)	4.2	6.6	4	4.1	6.5	7.6	8	15	16.5	20	35	65	41	56	80	
Max % kidney uptake (L/R)	19.5/19.9	23.0/19.1	19.4/19.6	22.4/26.0	15.8/16.5	23.5/25.9	19.5/18.6	20.7/21.9	0/44	18.6/22.1	17.0/20.2	22.9/24.2	27.0/22.4	18.8/18.6	24.2/25.2	
Administered activity (MBq)	14	20	14	14	19	22	23	38	42	46	70	98	77	92	100	
RESIDENCE TIMES (h)																
Kidneys	2.9	2.91	2.79	3.37	2.18	3.56	2.64	2.97	3.1	3.02	2.66	3.26	3.58	2.63	3.64	
Liver	0.1	0.53	0.57	0.511	0.103	0.4	0.23	0.361	0.31	0.17	0.441	0.44	0.177	0.509	0.38	
Spleen	0.11	0.071	0.11	0.121	0.076	0.2	0.05	0.141	0.03	0.129	0.206	0.27	0.04	0.259	0.21	
Bladder	0.133	0.045	0.228	0.027	0.189	0.052	0.194	0.173	0.169	0.339	0.235	0.247	0.188	0.347	0.201	
Remaining body	5.07	4.61	4.24	4.44	4.68	3.77	4.19	3.97	4.14	3.62	3.99	3.42	4.1	3.4	3.54	
DISCRETE PHANTOM METHOD																
Paediatric phantom used	Neonate	Neonate	Neonate	Neonate	1 y	1 y	1 y	5 y	5 y	10 y	10 y	10 y	15 y	15 y	15 y	
Organ dose (mSv MBq⁻¹)																
Kidneys	1.5E+00	1.5E+00	1.5E+00	1.8E+00	4.5E-01	7.4E-01	5.5E-01	3.5E-01	7.3E-01	2.5E-01	2.2E-01	2.7E-01	2.1E-01	1.6E-01	2.2E-01	
Liver	4.6E-02	9.6E-02	9.9E-02	9.7E-02	2.0E-02	4.1E-02	2.8E-02	2.2E-02	2.1E-02	1.2E-02	1.7E-02	1.8E-02	8.6E-03	1.2E-02	1.2E-02	
Bone surface	6.7E-02	6.4E-02	6.1E-02	6.6E-02	2.8E-02	3.0E-02	2.8E-02	1.5E-02	1.6E-02	9.8E-03	1.0E-02	1.0E-02	7.4E-03	6.4E-03	7.1E-03	
Spleen	2.1E-01	1.6E-01	2.1E-01	2.3E-01	6.6E-02	1.4E-01	5.7E-02	6.1E-02	3.2E-02	3.9E-02	5.2E-02	6.5E-02	1.7E-02	4.0E-02	3.7E-02	
UB wall	9.6E-02	5.1E-02	1.4E-01	4.2E-02	5.3E-02	2.4E-02	5.3E-02	2.6E-02	2.6E-02	3.0E-02	2.2E-02	2.3E-02	1.3E-02	2.1E-02	1.4E-02	
Gonads	3.4E-02	3.0E-02	4.8E-02	2.9E-02	1.4E-02	2.1E-02	1.3E-02	1.2E-02	1.2E-02	7.6E-03	4.5E-03	4.0E-03	2.9E-03	4.8E-03	4.9E-03	
E (mSv)	1.1E+00	1.6E+00	1.2E+00	1.2E+00	5.7E-01	8.4E-01	7.4E-01	7.9E-01	1.3E+00	6.7E-01	9.3E-01	1.4E+00	7.9E-01	8.9E-01	1.1E+00	
H _e (mSv)	2.0E+00	2.8E+00	2.1E+00	2.3E+00	9.4E-01	1.6E+00	1.3E+00	1.4E+00	2.4E+00	1.2E+00	1.7E+00	2.7E+00	1.5E+00	1.6E+00	2.1E+00	
INTERPOLATED PHANTOM METHOD:																
Organ dose (mSv.MBq⁻¹)																
Kidneys	1.4E+00	1.1E+00	1.4E+00	1.6E+00	8.1E-01	1.1E+00	7.8E-01	4.7E-01	8.8E-01	3.5E-01	2.1E-01	1.8E-01	2.7E-01	1.6E-01	1.8E-01	
Liver	4.3E-02	7.1E-02	9.4E-02	9.1E-02	3.1E-02	5.5E-02	3.6E-02	2.8E-02	2.4E-02	1.6E-02	1.6E-02	1.1E-02	1.1E-02	1.3E-02	9.3E-03	
Bone surface	6.3E-02	4.8E-02	5.8E-02	6.3E-02	4.4E-02	4.1E-02	3.6E-02	2.1E-02	1.9E-02	1.4E-02	9.8E-03	6.0E-03	9.7E-03	6.5E-03	5.7E-03	
Spleen	1.9E-01	1.2E-01	1.9E-01	2.2E-01	1.1E-01	2.1E-01	7.6E-02	8.0E-02	3.7E-02	5.6E-02	4.9E-02	3.6E-02	2.3E-02	4.1E-02	2.8E-02	
UB wall	9.0E-02	3.7E-02	1.3E-01	4.0E-02	8.7E-02	3.3E-02	7.2E-02	3.6E-02	3.2E-02	3.1E-02	2.2E-02	1.5E-02	1.6E-02	2.4E-02	1.0E-02	
Gonads	3.2E-02	2.2E-02	4.5E-02	2.7E-02	2.4E-02	2.9E-02	1.8E-02	1.6E-02	1.5E-02	1.1E-02	4.3E-03	2.3E-03	3.8E-03	5.1E-03	3.8E-03	
E (mSv)	1.1E+00	1.1E+00	1.1E+00	1.1E+00	9.5E-01	1.2E+00	1.0E+00	1.0E+00	1.5E+00	9.2E-01	9.0E-01	8.8E-01	1.0E+00	9.3E-01	8.9E-01	
H _e (mSv)	1.9E+00	2.0E+00	2.0E+00	2.1E+00	1.6E+00	2.4E+00	1.7E+00	1.8E+00	2.9E+00	1.6E+00	1.6E+00	1.7E+00	1.8E+00	1.7E+00	1.7E+00	

TABLE 2

Dosimetry of [^{99m}Tc] DMSA in 9 Children with Renal Pathology

PATIENT	20	19	15	6	7	23	8	14	17
Age	5 w	3 5 m	2.3y	2 7y	5.1y	5.2y	7y	11.2y	12 4y
Weight (kg)	2 2	4 3	15	16.2	21.4	18	32	34	38
Max % kidney uptake (L/R)	1.7/4.5	6.7/9 0	0/9.1	0/5.1	13.1/12.1	0/28.1	2.9/18.0	11.3/8.0	5.7/7.0
Administered activity(MBq)	10	15	38	41	49	44	65	68	73
RESIDENCE TIMES (h)									
Kidneys	0 425	1.12	0.57	0.36	1 8	1 97	1.4	1.35	0 662
Liver	0.447	0.502	0.58	0.291	0.171	0.399	0.229	0.29	0.561
Spleen	0 142	0.029	0 043	0.131	0.034	0.03	0.168	0 21	0.137
Bladder	0.167	0.189	0.239	0 351	0.227	0 26	0.129	0.473	0.071
Remaining body	6.17	5 47	5.53	4.94	4.92	4.4	5 85	4 38	6.87

DISCRETE PHANTOM METHOD:

Paediatric phantom used	Neonate	Neonate	1 y	1 y	5 y	5 y	5 y	10 y	10 y
Organ dose (mSv.MBq ⁻¹)									
Kidneys	3.5E-01	6.0E-01	2 5E-01	1 7E-01	2.2E-01	4.7E-01	2 9E-01	1.1E-01	6.0E-02
Liver	7.3E-02	8.2E-02	4 1E-02	2 4E-02	1 4E-02	2 1E-02	1 5E-02	1 1E-02	1.7E-02
Bone surface	6.2E-02	6.0E-02	2 8E-02	2 4E-02	1 5E-02	1.5E-02	1 7E-02	9.4E-03	1.3E-02
Spleen	2.1E-01	7 6E-02	3 7E-02	7.6E-02	2.5E-02	2 5E-02	6.1E-02	4.7E-02	3.2E-02
UB wall	1.1E-01	1.2E-01	6 4E-02	8 5E-02	3 3E-02	3.6E-02	2 3E-02	4.0E-02	1.2E-02
Gonads	3.9E-02	4 9E-02	1 7E-02	1.6E-02	8.3E-03	7 8E-03	1 4E-02	5 6E-03	6.3E-03
E (mSv)	5.4E-01	9 5E-01	1.1E+00	8 8E-01	8 0E-01	1.0E+00	1.3E+00	7 6E-01	7 4E-01
H _e (mSv)	7.0E-01	1.3E+00	1 4E+00	1.4E+00	1.2E+00	1.8E+00	2.2E+00	1 2E+00	9 5E-01

INTERPOLATED PHANTOM METHOD:

Organ dose (mSv.MBq ⁻¹)									
Kidneys	3 5E-01	5.5E-01	1.9E-01	1 2E-01	2.0E-01	5.1E-01	2.1E-01	1.1E-01	5 6E-02
Liver	7 3E-02	7.6E-02	3.1E-02	1 7E-02	1.3E-02	2 2E-02	1 1E-02	1 1E-02	1 6E-02
Bone surface	6 2E-02	5 6E-02	2 0E-02	1.7E-02	1.4E-02	1 6E-02	1 2E-02	9.2E-03	1 2E-02
Spleen	2.1E-01	7.0E-02	2 8E-02	5 3E-02	2.4E-02	2 7E-02	4 0E-02	4.5E-02	3 0E-02
UB wall	1.1E-01	1.1E-01	4.8E-02	5 8E-02	3.3E-02	3 9E-02	2 1E-02	3 9E-02	1 2E-02
Gonads	3.9E-02	4.5E-02	1 2E-02	1 1E-02	7.8E-03	8 5E-03	8 9E-03	5.4E-03	5.8E-03
E (mSv)	5.4E-01	8 7E-01	7 9E-01	7 1E-01	7.6E-01	1.1E+00	9.1E-01	7.4E-01	6.8E-01
H _e (mSv)	7.0E-01	1 2E+00	1.1E+00	9 6E-01	1 2E+00	1 9E+00	1 5E+00	1.2E+00	8.8E-01

TABLE 3

Biokinetic Model for Dosimetry of [^{99m}Tc] DMSA in Children
with Normal Renal Function

ORGAN	F _s	T	a	τ
Total body (excluding bladder contents)	1.0	50min 4.9d	0.11 0.89	7.47h
Kidneys	0.45	1h 3.2d	-1.0 1.0	3.07h
Liver	0.046	1.6d	1.0	20.8min
Spleen	0.019	17h	1.0	7.2min
Remaining body				3.93h
Urinary bladder contents (2h void)				9.4min
(3h void)				14.5min
(3.5h void)				17.0min

F_s = fractional distribution

T = biological half time of retention components

a = fractional retention component (-ve sign indicates uptake)

τ = residence time

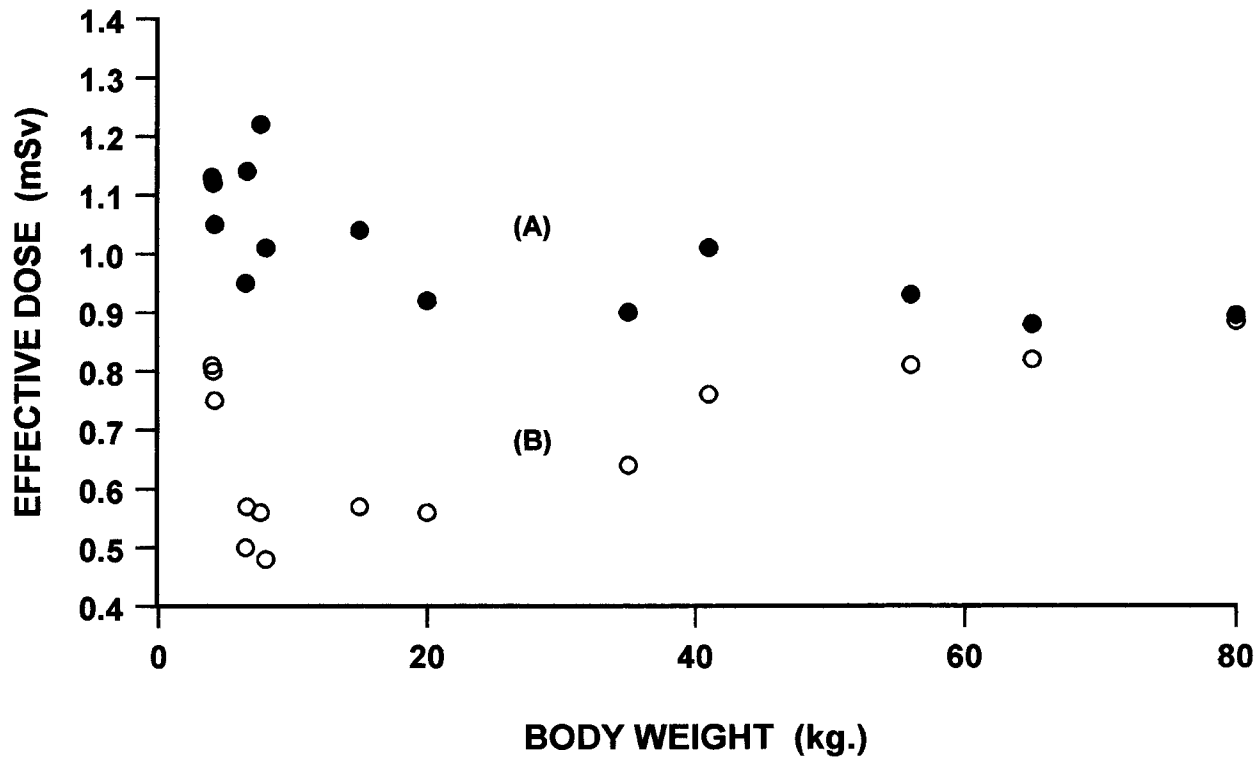
Table 4

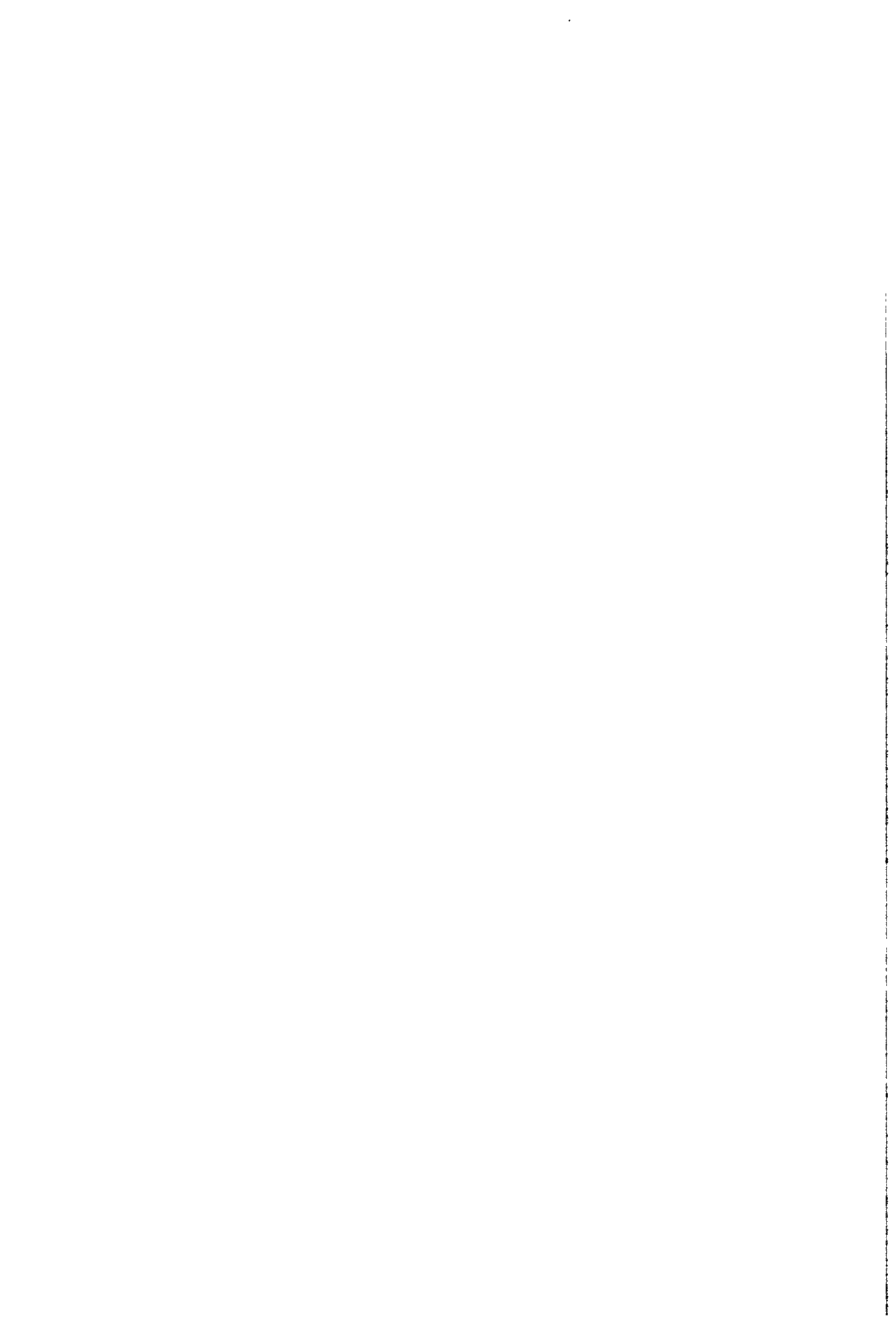
Classification of DMSA

1.	Duplex	<ul style="list-style-type: none"> 1.1 Upper Moiety Path <ul style="list-style-type: none"> 1.1.1 Dysplasia 1.1.2 Obstruction 1.1.3 VUR 1.1.4 Other 1.1.5 Ectopic non dilated 1.1.9 Normal function 1.2 Lower Moiety <ul style="list-style-type: none"> 1.2.1 VUR 1.2.2 Obstruction 1.2.3 Other 1.2.4 Dysplasia 1.2.9 Normal function 	<ul style="list-style-type: none"> 4.1.4 Ureterocoel - simplex 4.1.5 VUR - duplex 4.1.6 VUR - simplex 4.1.7 Duplex - no obstruction 4.2 Bladder pathology 4.3 Megaureter 4.4 Focal renal damage 4.5 Calculi 4.6 Diversion 4.7 Prune Belly Syndrome
2.	UTI :	<ul style="list-style-type: none"> 2.1 No VUR <ul style="list-style-type: none"> 2.1.1 Focal defect - normal function 2.1.2 Focal defect - abnormal function 2.1.3 Global decrease (no focal defect) 2.1.4 Focal defect - preserved outline 2.1.5 Deterioration 2.1.6 Improvement 2.1.7 Abnormal other 2.1.8 Dysplasia 2.2 Plus VUR <ul style="list-style-type: none"> 2.2.1 Focal defect - normal function 2.2.2 Focal defect - abnormal function 2.2.3 Global decrease 2.2.4 Focal defect - preserved outline 2.2.5 Deterioration 2.2.6 Improvement 2.2.7 Abnormal other 2.2.8 Dysplasia 2.3 Plus Hydronephrosis only <ul style="list-style-type: none"> 2.3.1 PUJ 2.3.2 VUJ 2.3.3 PUV 2.3.4 Bladder abnorm 2.3.5 Megacalycosis 	<ul style="list-style-type: none"> 5. Miscellaneous <ul style="list-style-type: none"> 5.1 Hypertension <ul style="list-style-type: none"> 5.1.1 Renovascular 5.1.2 Damaged kidney query cause 5.1.3 With Hydronephrosis 5.1.4 With Reflux 5.2 Trauma <ul style="list-style-type: none"> 5.2.1 Iatrogenic 5.2.2 Focal defect 5.2.3 Radiotherapy 5.3 Metabolic disease <ul style="list-style-type: none"> 5.3.1 Tubular abnormalities 5.3.2 Renal Tubular acidosis 5.4 Vasculitis <ul style="list-style-type: none"> 5.4.1 Renal vein thrombosis 5.5 Calculi 6 Mass <ul style="list-style-type: none"> 6.1 Cyst 6.2 Tumour <ul style="list-style-type: none"> 6.2.1 Benign 6.2.2 Malignant 7. Renal failure <ul style="list-style-type: none"> 7.1 Acute 7.2 Chronic 7.3 Calculi 8 Abnormal position <ul style="list-style-type: none"> 8.1 Pelvic 8.2 Crossed Fused Ectopia 8.3 Horseshoe 8.4 Single kidney 8.5 Malrotated 8.6 Ectopic single system 9. Technical variants <ul style="list-style-type: none"> 9.1 Normal 9.2 Variant of normal <ul style="list-style-type: none"> 9.2.1 Normal duplex 9.3 Normal with VUR
3.	VUR	<ul style="list-style-type: none"> 3.1 No UTI <ul style="list-style-type: none"> 3.1.1 Focal defect - normal function 3.1.2 Focal defect - abnormal function 3.1.3 Global decrease 3.1.4 Abnormal other 	
4.	Hydronephrosis	<ul style="list-style-type: none"> 4.1 Antenatal diagnosis <ul style="list-style-type: none"> 4.1.1 PUJ 4.1.2 Megaureter 4.1.3 Ureterocoel - duplex 	

Fig.1 Relationship between effective dose and body weight in normal children.

Administered activity scaled on body surface area (curve A) or body weight (curve B)





**Final Report
1992 - 1994**

Contract:F13PCT920064g **Duration:** 1.7.92 to 30.6.95

Sector: C22

Title: Medical dose assessment and evaluation of risk.

- | | | |
|----|------------|------------------------------|
| 1) | Wall | NRPB |
| 2) | Drexler | GSF |
| 3) | Fitzgerald | St George's Hospital, London |
| 4) | Zoetelief | TNO - Delft |

I. Summary of Project Global Objectives and Achievements

Objectives

The contract combined a number of projects concerned with radiation dosimetry and quality assurance in diagnostic radiology aimed at improving methods for assessing radiation doses and risks to patients and reducing them without compromising the diagnostic value of the examinations. Particular attention was to be paid to meeting these objectives in the important areas, from a radiation protection standpoint, of paediatric radiology and mammography.

The main objective for three of the partners (NRPB, GSF and TNO) was to use Monte Carlo radiation transport codes and appropriate phantoms to calculate conversion coefficients relating organ doses to measurable dose quantities for patients undergoing x-ray examinations. The provision of these coefficients and comparisons of results obtained using different Monte Carlo codes, different phantoms and different exposure conditions, all help to improve the ease and accuracy with which doses to patients from x-ray examinations can be estimated and to develop a common basis for patient dosimetry and risk evaluation within the European Community. TNO were to concentrate on a detailed study of mammography in view of the relatively high sensitivity of the breast to radiation and the increasing use of mammography in breast cancer screening programmes in Europe. NRPB and GSF were to develop computational dosimetry techniques for simulating a wide range of x-ray examinations using phantoms representing the whole body and to pay particular attention to paediatric radiology in view of the potentially higher risks to children from x-ray exposure compared to adults. As a supplementary project, NRPB were to investigate the effect of age at exposure on the lifetime risk of radiation detriment in an attempt to quantify the degree of the increased risk to children from typical x-ray examinations.

This concern about radiation protection for children undergoing x-ray examination provides the link with the other projects in the contract. St George's Hospital were to carry out a thorough investigation of paediatric radiology practices at four London hospitals, including assessments of image quality, patient dose and radiographic technique. Some of this information would assist NRPB in simulating appropriate exposure conditions in their computational dosimetry calculations. St George's would seek to implement a Quality Management System meeting the requirements of EN 29000 (now BS EN ISO 9002) at one

of the specialist paediatric radiology departments and they would develop guidelines on best practice for common paediatric examinations which would be made available to a CEC study group developing quality criteria for paediatric radiology. Links with this study group would also be maintained by NRPB and GSF in providing dosimetry support for European trials of their quality criteria.

Two other CEC study groups have been developing similar sets of quality criteria for common radiographic examinations on adults and for CT examinations on adults. Both NRPB and GSF were to participate in the work of these groups throughout this contract period.

Achievements

Monte Carlo organ dose calculations

Development of these techniques with whole body phantoms able to simulate a wide range of diagnostic x-ray examinations has proceeded in parallel at NRPB and GSF. The two groups have generally adopted the same principles and methods but there are inevitable differences in details related to the particular ways in which their computer codes have been developed over the years and in the intended use of the results.

For x-ray examinations on adults, NRPB has published both hardcopy reports and software packages providing organ doses and effective dose normalised to either entrance surface dose or dose-area product and covering 68 individual radiographic projections and a number of complete examinations. Entrance surface dose and dose-area product measurements are being increasingly undertaken in the UK as part of x-ray department quality assurance programmes and these extensive sets of normalised doses are intended to increase the value of the measurements by making them more directly relatable to radiation risk. The errors involved in a pragmatic approach, suggested by NRPB, of using a single conversion coefficient to cover a particular type of x-ray examination without accounting for details of the technique, were studied by both NRPB and GSF.

For the above calculations NRPB used a mathematical phantom to represent an average (hermaphrodite) adult patient. GSF also used their existing adult mathematical phantoms ADAM and EVA for detailed organ dose calculations for three types of complex fluoroscopic examination. Much of their effort over the contract period, however, has been devoted to the construction of an adult voxel phantom based on a whole body computed tomography (CT) scan of a 38 year old male. Construction of the adult voxel phantom was just completed by the end of the contract period and there was no opportunity to compare results of organ dose calculations with this new phantom and the earlier mathematical phantoms. However, GSF have used their existing voxel phantoms of a baby and a 7 year old child for some valuable organ dose calculations in paediatric CT. These follow the same approach adopted in earlier CT dose calculations for adult patients by both GSF and NRPB, where coefficients relating organ doses to the free-in-air dose on the axis of the CT scanner are calculated for any 1 cm thick CT slice across the body. Organ doses for a complete CT examination are derived by summing the coefficients from the appropriate selection of slices and GSF have produced a user-friendly PC program to do this.

NRPB have concentrated on conventional paediatric x-ray examinations but have

covered a wider range of patient sizes. They have calculated organ dose conversion coefficients for about 20 common radiographic projections on five mathematical phantoms representing newborn, 1, 5, 10, and 15 year old patients. As for the adult patient calculations, the results will be made available on computer disc in an NRPB software report. It was possible to compare results obtained using the GSF baby and child voxel phantoms with those obtained with the NRPB mathematical paediatric phantoms. For the comparison additional calculations were made for four conventional radiographic examinations where exposure conditions and phantom sizes were matched as closely as possible. Whereas the coefficients for most organs and examinations agreed to within a few percent, there were a few organs where differences in their size, shape and position in the two phantoms led to differences of more than a factor of two in the coefficients. Such comparisons provide useful information for decisions concerning the required anatomical realism of dosimetric phantoms for use in diagnostic radiology.

Mammography

TNO have used Monte Carlo calculations to estimate coefficients (referred to as g values in this context) for converting air kerma free-in-air to average glandular tissue dose in the breast for mammography. These calculations use a simplified mathematical model of the breast consisting of a central region surrounded by a superficial layer, both of variable thickness and composition. Estimates of g as a function of the half value layer (HVL) of the x-ray beam have been published by various authors and TNO have studied the influence of the different photon interaction data and spectra used in the calculations, the composition and thicknesses of the regions of the phantom, the presence of a compression plate and the use of new anode/filter combinations in mammography. Parameters of most influence were found to be the phantom thickness and the tissue composition assumed for the various layers in the phantom. Measurements of breast thickness and composition on women during actual mammography and observation of the radiographic factors and tube outputs employed, enabled TNO to assess the uncertainties in estimates of average glandular tissue dose when a typical breast composition is assumed. The observed variation of breast composition (and hence of g) with age, enabled TNO to predict whether average breast doses delivered by modern mammography equipment to women in relevant age bands would meet draft European guidelines. This work has been invaluable for the preparation of a European Protocol on Dosimetry in Mammography by another CEC study group in which TNO is actively involved.

TNO has also taken advantage of the mammography x-ray qualities available at the secondary standard calibration laboratory at St George's Hospital (a unique facility at such laboratories) to intercompare the calibration of standard mammography dosimeters and kVp meters from the Netherlands and the UK.

Paediatric radiology

St George's Hospital completed studies of the frequency of paediatric x-ray examinations at a sample of London hospitals and collected information on the radiographic procedures adopted during the most common types of examination. This information was passed on to NRPB so that they could select the most appropriate examinations and exposure conditions to model in their Monte Carlo calculations. The St George's group collected a

wealth of information on referral criteria, radiographic and examination technique, image quality (assessed both by physical measurement and clinical diagnostic value) and patient dose. Guidelines on best practice for 16 paediatric x-ray examinations have been developed from this information, which will be made available to a CEC study group developing quality criteria for paediatric radiology. Progress in the implementation of an EN 29000 Quality Management System in the x-ray department of a children's hospital was temporarily delayed by the relocation of the department to a specialised paediatric unit within a larger general hospital. However, the detailed procedure guidelines which had been prepared as an essential part of the Quality Manual prior to the move, proved invaluable for staff training in the new enlarged department.

NRPB's study of the effect of age at exposure on the lifetime risk of radiation detriment led to the broad conclusion that children exposed to typical x-ray examinations are at about twice the risk per unit effective dose than the general population and that patients over 70 years old are at less than one fifth of the risk. This lends support to the decision to pay particular attention to paediatric radiology.

Other projects concerned with the optimisation of paediatric radiology included the supply and readout of dosimeters by GSF and NRPB for European trials of a quality criteria document for paediatric radiology being developed by a CEC study group. NRPB and GSF also participated in two other CEC study groups developing similar sets of quality criteria for common radiographic examinations on adults and for CT examinations on adults. NRPB have drafted sections dealing with patient dosimetry and the derivation of reference doses for the guideline documents being prepared by both of these groups.

Head of Project 1: Mr. Wall

II. Objectives for the reporting period

1. To extend the calculation of organ doses from x-ray examinations using Monte Carlo techniques and mathematical phantoms to cover more organs and a wider range of examinations for both adult and paediatric patients.
2. To evaluate the radiation risks from medical x-rays with particular attention to the effect of age at exposure.
3. To provide dosimetry and technical advisory support for European trials of draft CEC working documents on "Quality Criteria for Diagnostic Radiographic Images" in both adult and paediatric radiology.

III. Progress achieved including publications

1. Monte Carlo organ dose calculations

Adult patients

A Monte Carlo radiation transport code developed at NRPB is used to calculate the energy deposited in geometrically defined volumes representing various organs within a mathematical phantom designed to model an hermaphrodite adult patient. The mathematical phantom is based on the MIRD-5 phantom developed at the Oak Ridge National Laboratory, USA, originally by Snyder and latterly by Cristy. For the new set of Monte Carlo organ dose calculations described below, the phantom was further modified by the addition of an oesophagus so that all of the 23 organs (including the remainder organs) specified by ICRP in the new quantity "effective dose" were modelled in the phantom.

Organ dose calculations were performed for a much extended range of x-ray examinations by simulating the exposure conditions for 68 different radiographic projections. As well as covering routine radiographic examinations of the head, chest, abdomen, spine and pelvis, these projections include those listed in Table 1 which are used during complex examinations involving fluoroscopy, such as barium studies of the gastro-intestinal tract and cardiac catheterisation.

An NRPB Software Report (NRPB-SR262) was published containing files of coefficients for converting entrance surface dose and dose-area product measurements into organ doses for a typical adult patient for the 68 different radiographic projections. For each projection there is a choice of 40 diagnostic x-ray spectra defined in terms of the tube voltage and the total beam filtration and ranging from 50 - 120 kVp, in 10 kV steps, each with 5 values of beam filtration ranging from 2 to 5 mmAl. A user-friendly software package (XDOSE) is also available from the National Radiation Laboratory, New Zealand, which manipulates these data files to provide organ doses for any x-ray examination specified by the user.

Table 1: Projections applicable to specific examinations

EXAMINATION	PROJECTIONS
Barium swallow	Throat L.LAT, R.LAT. Oesophagus RAO, LAO, LPO.
Barium meal	Stomach AP, PA, RAO, LPO, LAO, L.LAT. Upper stomach AP, PA. Duodenum AP, PA, RAO, LPO.
Barium follow-through	Small intestine AP, PA.
Barium enema	Colon AP, PA (identical to Pelvis AP, PA). Colon RAO, LPO, LAO. Rectum AP, PA, LPO, RAO, L.LAT, R.LAT. L. Flexure LAO. R. Flexure RAO.
Cardiac catheterisation	Heart AP, PA, LAO, RAO, L.LAT, R.LAT.

RAO = Right Anterior Oblique
 LAO = Left Anterior Oblique
 RPO = Right Posterior Oblique
 LPO = Left Posterior Oblique

Effective doses are also calculated in this software package and a separate complementary report (NRPB-R262) was published containing only the effective dose conversion coefficients for the 68 individual radiographic projections. Values for each of the 40 individual x-ray spectra are given in the report as well as a generalised value for use when the x-ray spectrum is not known, with an indication of the likely maximum error. These coefficients are useful for estimating effective doses from x-ray examinations when measured values of entrance surface dose or dose-area product are available for each projection.

More often, dose-area product measurements are made for complete examinations, comprising many radiographs and possibly fluoroscopy, as an indication of the total exposure of the patient. Studies were therefore made of the variation in the relationship between the total dose-area product and the effective dose for different types of x-ray examination. For the more simple radiographic examinations, sufficient data were available from previous surveys to study the extent of the variations for each type of examination and to derive a representative value of the effective dose per total dose-area product and an estimate of the likely maximum error. For barium meal and barium enema examinations a detailed study at local hospitals was necessary to determine the influence of the wide variations in examination technique adopted by different radiologists. Despite wide differences in the number of films and the amount of fluoroscopy used, the coefficients for converting dose-area product to effective dose remained remarkably constant for each type of examination (eg. for all barium enemas). This indicates that the dose is distributed in much the same way between the most exposed organs no matter how a particular type of examination is conducted. An implication of this result is that only one coefficient may be necessary for each type of examination to obtain a sufficiently reliable estimate of the effective dose from a dose-area product measurement. The coefficients selected for this purpose together with an estimate of the

potential maximum error are shown in Table 2. This level of potential error is probably inconsequential if the results are to be used for risk estimation purposes where other sources of uncertainty are likely to be greater. If more accurate estimates of organ doses or effective dose are required for a complete x-ray examination, each individual projection should be treated separately, but this requires far more detailed dose measurements.

Table 2: Conversion coefficients to give effective dose from dose-area product for complete examinations

Examination	Conversion coefficient (mSv/Gycm ²)	Potential Max. error (%)
Skull	0.028	46
Chest	0.1	50
Thoracic spine	0.19	53
Lumbar spine	0.21	33
Abdomen	0.26	42
Pelvis	0.29	34
Barium meal	0.2	25
Barium enema	0.28	17
IVU	0.18	17

Paediatric patients

Organ dose conversion coefficients for common paediatric x-ray examinations have been calculated by simulating about 20 different radiographic projections on five mathematical phantoms representing newborn and 1, 5, 10 and 15 year old patients. The phantoms were again based on those developed by Cristy with an oesophagus added to each one to make up the complement of organs required to estimate effective dose. Information on the frequency of x-ray examinations conducted on children at a sample of London hospitals was obtained in the St George's hospital project and was used to select the examinations and projections to include in the Monte Carlo calculations. Radiographic examinations of the head, cervical spine, chest, abdomen, lumbar spine, pelvis and urinary bladder were chosen. Information on the size and position of the x-ray fields commonly used on patients of these ages was obtained from copies of typical radiographs collected by the St Georges's Hospital group, from paediatric radiology textbooks and from the literature. Coefficients relating organ doses and effective dose to both entrance surface dose and dose-area product have been calculated for appropriate projections on each of the paediatric phantoms. Results are available for the same 40 x-ray spectra included in the above adult patient calculations plus some additional spectra involving 0.1 and 0.2 mm of copper filtration as are recommended for paediatric x-ray examinations in the CEC working document on Quality Criteria for Diagnostic Radiographic Images in Paediatrics. An NRPB software report (corresponding to NRPB-SR262 for adult patients) containing datafiles listing all the organ dose conversion coefficients on a computer disc is in preparation together with a printed report (corresponding to NRPB-R262 for adult patients) containing only the effective dose conversion coefficients. Meanwhile, the organ dose datafiles on computer disc have been supplied to St George's Hospital for use with the extensive paediatric patient dose measurements which they have collected during the course of their project for this contract.

Comparisons have been made with similar calculations by GSF using their voxel phantoms of a baby and a 7 year old child. AP projections of the head, chest, abdomen and pelvis were simulated on the two voxel phantoms and on the newborn and 5 year old mathematical phantoms. The voxel sizes in the GSF phantoms were adjusted so that their AP thicknesses matched those of the corresponding mathematical phantom in the centre of the beam as closely as possible. The same irradiation parameters (kV, filtration, field size, position of field centre and focus to film distance) were used in the two sets of calculations. However, despite trying to match the exposure conditions as closely as possible, the differences in the position, shape and size of the organs within the corresponding voxel and mathematical phantoms are still sufficient to lead to significant differences in some of the organ dose conversion coefficients, sometimes exceeding a factor of two. Most of the large differences occur for organs close to the edge of the field which are irradiated to markedly different extents in the two phantoms. The few large differences in the conversion coefficients that are evident for organs well within the beam, can mostly be explained by differences in the depths of the organs below the entrance skin surface in the two phantoms. Thus differences between the results of the two sets of calculations which cannot be explained by anatomical differences in the two phantoms rarely exceed about 15%. This provides some valuable reassurance regarding the consistency of the two Monte Carlo codes but emphasises the critical impact of small differences in patient or phantom size and anatomy on organ doses.

2. Evaluation of radiation risks

The 1990 recommendations of the ICRP, together with the latest epidemiological data and radiation risk models, have been studied to evaluate the risks to patients from x-ray examinations. The new ICRP concept of aggregated detriment and the corresponding definition of effective dose have been considered, with regard to their possible application to medical exposures. In particular the influence of age at exposure on risk coefficients and on the definition of effective dose has been assessed, to devise a simple system to account for these factors when estimating radiation detriment to patients particularly when they are either geriatric or paediatric.

Age and sex specific risk coefficients for radiation-induced health effects and risk projection models derived from the latest epidemiological data have been used by NRPB together with UK life tables and baseline cancer rates to estimate the late radiation risks for the UK population. Non-fatal cancers and severe hereditary effects have been incorporated with appropriate weighting factors to provide age and sex specific coefficients for the lifetime risk of aggregated detriment for the different radiosensitive organs. Summing the risks for all organs provides the total lifetime risk of aggregated detriment which shows little difference between the two sexes but a marked fall with age at exposure, due to the reduced opportunity for the expression of genetic effects and delayed cancers later in life.

However, the contribution of each organ to the total aggregated detriment varies markedly with age at exposure so that the overall trend in risk of aggregated detriment as a function of age depends on which organs are receiving the bulk of the radiation dose. For diagnostic x-ray exposures this obviously depends on the type examination being considered. Figure 1 shows age-specific estimates of aggregated detriment (averaged for males and females because the values are so similar) for six types of routine x-ray examination. The

values are expressed as a ratio, relative to the value obtained by averaging the risks over all age groups, which is essentially the procedure adopted in the concept of effective dose.

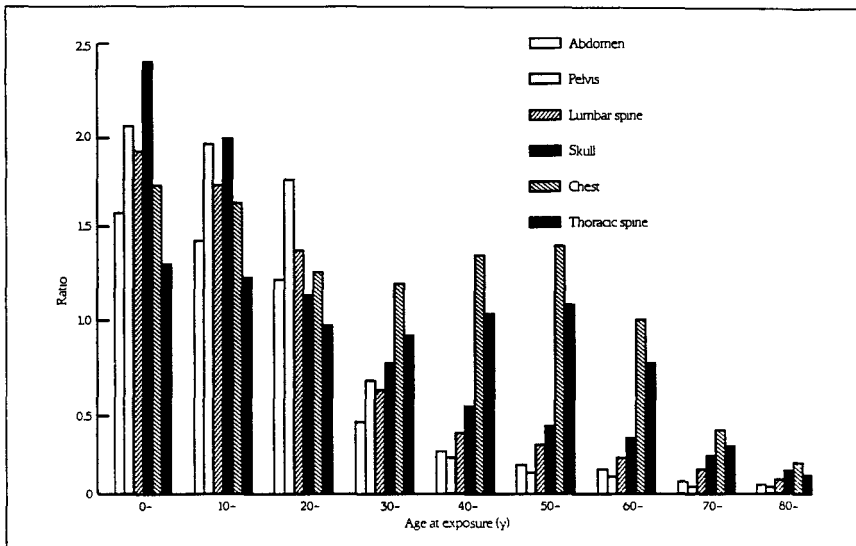


Figure 1: Age-specific estimates of aggregated detriment for six types of x-ray examination

There is still a general tendency for the ratios to fall as the age at exposure increases but with considerable differences between some examinations. However, no examination differs by more than about a factor of two from the average value for the six examinations for each age band, so it is suggested that the average values as shown in Figure 2 could form

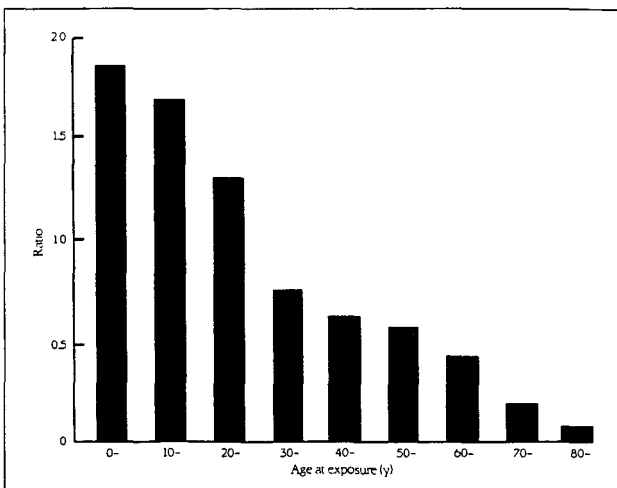


Figure 2: Typical age-specific detriment ratios for x-ray examinations

the basis of a set of age related modifying factors for applying to the effective dose to estimate a more realistic lifetime risk of aggregated detriment per unit effective dose for patients of different ages.

In view of the large uncertainties in this analysis, a further averaging of the ratios over just three broad age bands was considered appropriate by NRPB in advising that when the effective dose is used for assessing the detriment from diagnostic medical exposures, it should be recognised that it will underestimate the detriment from paediatric exposure by about a factor of two and overestimate that from geriatric exposure by at least a factor of five.

3. Support for CEC Quality Criteria Working Documents

Paediatric Patient Working Document

Two European-wide trials of the CEC working document on Quality Criteria for Diagnostic Radiographic Images in Paediatrics have been organised by the Children's Hospital of the University of Munich, during the contract period. NRPB together with GSF (partner 2 in this contract) and the Unita Sanitaria Locale, Udine, Italy, provided and processed thermoluminescent dosimeters (TLDs) used to measure the entrance surface doses to patients of specified age from common radiographic procedures. The first trial concentrated on 7 radiographic projections commonly performed on 5 year old children and the second trial on 11 radiographic projections commonly performed on 10 year old children. NRPB provided TLDs for 25 British, Irish and Scandinavian hospitals taking part in the trials. Despite the fact that each hospital was asked to include only one patient in the trial for each type of radiograph, there were a number of hospitals which were unable to make a complete return.

A summary of the doses measured by NRPB are given in the tables below. The median values and the wide ranges show a close similarity to those measured by GSF on other hospitals taking part in the same trials which are also tabulated in the following progress report from GSF.

Table 3: Entrance surface doses (μGy) from examinations on 5 year old children

Examination	n	Median	1st Quartile	3rd Quartile	Range
Abdomen AP (1 film)	17	556	457	1038	81 - 2427
Pelvis AP	15	537	266	788	86 - 1514
Skull AP/PA	23	799	376	1260	15 - 2687
Skull LAT	7	484	300	656	82 - 847
Chest AP/PA (mobile)	9	63	55	86	30 - 262
Chest LAT	13	132	112	186	3 - 425
Chest AP/PA	21	55	40	86	2 - 347

n = no. of examinations

Table 4: Entrance surface doses (μGy) from 7 examinations on 10 year old children

Examination	n	Median	1st Quartile	2nd Quartile	Range
Chest PA	22	51	32	64	1 - 88
Chest LAT	13	122	101	159	59 - 1006
Chest PA/AP (mobile)	9	88	69	119	29 - 188
Skull AP	8	911	606	1088	367 - 1429
Skull LAT	13	491	438	600	267 - 1268
Abdomen AP/PA	15	656	462	1206	325 - 1860
Pelvis AP	16	568	424	802	200 - 1494
Lumbar spine AP	17	959	737	1395	366 - 2321
Lumbar spine LAT	18	2432	1021	3084	474 - 6939
Thoracic spine AP	11	688	453	931	204 - 1232
Thoracic spine LAT	10	1547	1028	1684	534 - 3134

n = no. of examinations

Adult Patient Working Document

A European-wide trial of the CEC working document on Quality Criteria for Diagnostic Radiographic Images for adult patients took place in 1991. A report on the trial results was prepared by Maccia and colleagues from CAATS, Paris, in 1993 and detailed comments on this report were provided by NRPB and by other members of the original CEC study group which developed the working document. A further more restricted study group on Quality Criteria Development met in early 1994 to produce a revised version of the 1991 trial report and NRPB prepared an analysis of the relationship between radiographic technique and patient dose as revealed by the trial results. This analysis, which proved to be rather inconclusive because of the confounding influence of the many technique variables which can affect the dose, will form part of a full report on the evaluation of the 1991 trial to be published by the CEC. Meanwhile a summary of it has been prepared for inclusion in a revised and final version of the working document to be called *European Guidelines on Quality Criteria for Diagnostic Radiographic Images*. Also, the appendix on radiation dose to the patient has been revised and a new chapter outlining suitable procedures for implementing the Quality Criteria in an x-ray department and auditing their impact on practice has been written.

NRPB is also participating in another CEC study group on Quality Criteria for Computed Tomography. Having circulated a discussion paper on the important subject of defining and deriving suitable reference doses for CT examinations, draft recommendations are being prepared.

Publications

Hart, D, Jones, D G and Wall, B F, 1993. Estimation of effective dose in diagnostic radiology from entrance surface dose and dose-area product measurements. NRPB-R262 (HMSO, London)

Hart, D, Jones, D G and Wall, B F, 1994. Normalised organ doses for medical x-ray examinations calculated using Monte Carlo techniques. NRPB-SR262 (NRPB, Chilton)

Hart, D and Wall, B F, 1994. Estimation of effective dose from dose-area product measurements for barium meals and barium enemas. Br. J. Radiol. 67, 485-489

Hart, D, 1994. Effective dose to patients from x-ray examinations. NRPB Radn. Prot. Bull. No. 155.

Hart, D, Jones, D G and Wall, B F. Coefficients for estimating effective doses from paediatric x-ray examinations. NRPB-R***, To be published.

Hart, D, Jones, D G and Wall, B F. Normalised organ doses for paediatric x-ray examinations. NRPB-SR***. To be published.

Wall, B F, 1992. Risk assessment for the medical use of ionising radiation. Annales de l'Association Belge de Radioprotection, Vol 17, no. 2-3. p. 89.

Wall, B F, 1993. Risks of Imaging. Proc. R. Coll. Physicians Edinb. vol. 23, 164-169.

Shrimpton, P C, Wall, B F, Croft, J R and Webb, G A M, 1993. Medical Exposure. Guidance on the 1990 Recommendations of the ICRP. Docs. of the NRPB, 4, 2 (London, HMSO)

Schneider, K, Kohn, M, Bakowski, C, Stein, E, Freidhof, C, Horwitz, A E, Padovani, R, Wall, B, Panzer, W and Fendel, H, 1993. Impact of radiographic imaging criteria on dose and image quality in infants in an EC-wide survey. Radiat. Prot. Dosim., 49, 73-76.

P C Shrimpton, 1992. Protection of the Patient in X-ray Computed Tomography. Doc. NRPB, 3, 4 (London, HMSO).

Shrimpton, P C and Wall, B F, 1992. Assessment of patient dose from computed tomography. Radiation Protection Dosimetry, Vol. 43. No. 1/4, pp 205- 208.

Shrimpton, P C and Jones, D G, 1993. Normalised organ doses for x-ray computed tomography calculated using Monte Carlo techniques and a mathematical anthropomorphic phantom. Radiat. Prot. Dosim. 49, 241-243.

Shrimpton, P C and Wall, B F, 1993. CT - an increasingly important slice of the medical exposure of patients. Br. J. Radiol. 66, 1067-1068.

Shrimpton, P C and Wall, B F, 1995. The increasing importance of x-ray computed tomography as a source of medical exposure. Radiat. Prot. Dosim. 57, 413-415.

Head of project 2: G. Drexler

II. Objectives for the reporting period

- Continuation of construction of voxel models using computed tomographic data of real patients. This work aimed also to the development of an automatized segmentation technique.
- Extension of the calculations of medical organ doses using existing and new phantoms together with Monte Carlo codes for
 - CT examinations of children (in cooperation with the Children's Hospital of the University of Munich)
 - Assessment of the impact on patient doses of the radiographic techniques recommended in the CEC Working Document on „Quality Criteria for Diagnostic Images in Paediatrics“.
 - Extension of the already elaborated set of scaling factors for the determination of organ doses for children of all sizes to more types of examinations.
- Dose measurements and field studies in routine x-ray diagnostic procedures to support coordinated CEC projects and initiatives. Special emphasis should be given to paediatric examinations, including CT (in cooperation with the Children's Hospital of the University of Munich)
- Support to the revision of the CEC Working Document on „Quality Criteria for Diagnostic Radiographic Images“ as a consequence of the results of the 1991 CEC trial.

III. Progress achieved including publications

Phantoms.

Construction of an adult voxel phantom.

An adult voxel phantom was constructed based on data from a whole body CT examination of a 38 year old male patient, consisting of 220 contiguous slices of 8 mm thickness. The size of the volume elements (voxels) is 35 mm³. This phantom offers an improved description of the patient (skeleton, head, red bone marrow, separation of adipose and muscle tissue) and extends the earlier constructed set of voxel phantoms (BABY and CHILD); it will be used to substantiate or revise the numerous results achieved by means of geometrical MIRD type phantoms and to calculate organ doses to phantoms of varying size to study the impact of phantom size on the determination of organ doses.

Using newly developed algorithms and avoiding manual interference, so far the segmentation of the following objects was performed: patient couch, outer contour of the phantom, all bones of the skeleton separately, red bone marrow, soft tissue organs of head, neck thorax and part of the abdomen. The segmentation of the phantom will be finished in 1995.

It was necessary to segment the phantom in the frame of a research program, because available routine segmentation programs now exist only for restricted body regions consisting of high contrast objects (bones, contrast media filled vessels etc.) and do not result in the necessary detail.

Calculations of organ dose conversion factors.

Organ doses conversion factors for paediatric CT-examinations.

With CT-examinations there is a large variability in length and site of the scanned body region. Hence there is little use in determining organ doses for standard examinations. On the other hand it is out of scope to provide data for all exposure parameters which might occur. To overcome this difficulty for the voxel phantoms BABY and CHILD organ dose conversion factors were calculated resulting from any 1 cm CT-slice across the whole body. This was done for two radiation qualities (80 kV, 2.2 mm Al+0.2 mm Cu and 125 kV, 2.2 mm Al+0.2 mm Cu) and scanning angles of 180° and 360°. The determination of organ dose then follows the simple formula:

$$D_{organ} = D_e \times f_{c,organ}$$

with D_e the dose free in air on the axis of rotation (available from measurements or from the literature) and

$$f_{c,organ} = \sum_{z_l}^{z_u} f_{c,z,organ}$$

with z_l the lower and z_u the upper boundary of the scanned body region.

For CHILD the consequences of eccentric (6 cm) positioning of the patient were examined: differences from the situation when the phantom was centrally positioned, were detectable but small compared with those resulting from other discrepancies between a real and the simulated situation.

For CHILD also the influence of asymmetric (25 cm+10 cm in focus to axis distance instead of 25 cm+25 cm) fan beams was investigated: such beams lead to markedly lower doses in parts of the phantom outside the inner 10 cm field. For red bone marrow in the clavicles and the scapulae the doses are reduced to 9%-10%, for the red marrow in the arm bones the reduction amounts to 24%.

PC program for organ doses conversion factors for CT examinations.

To facilitate the determination of organ doses from CT-examinations, the results of the above calculations of organ dose conversion factors from single 1 cm-slices from the phantoms CHILD and BABY and earlier results from the phantoms ADAM and EVA were incorporated into a PC program, available for distribution now on diskette. The program provides a comfortable user interface and the user has just to select the respective phantom and to enter the lower (z_l) and upper (z_u) boundary of the scanned body region (along anatomical landmarks available from published GSF-reports on the above results) to achieve conversion factors for the calculation of doses (D_{organ}) to 33 organs, resulting from CT-examinations with any thinkable length and site. Table 1 shows an example for organ dose conversion factors $f_{c,organ}$ from a pelvic CT examination of adult patients, ranging from the bottom of the trunk (0 cm) to lumbar vertebra 5 (25.0 cm).

Table 1: Organ dose conversion factors on monitor screen or printout for a pelvic CT-examination of adult patients.

Examination type: Pelvis, contiguous slices						
Scanned body height: .0 cm - 25.0 cm						
	Conversion factors for					
	Male phantom ADAM			Female phantom EVA		
	137 kV	125 kV	80 kV	137 kV	125 kV	80 kV
Adrenals	.011	.009	.005	.016	.017	.007
Bladder	.633	.619	.491	.665	.653	.519
Brain	.000	.000	.000	.000	.000	.000
Breast	---	---	---	.002	.002	.001
Colon (a+t)	.427	.416	.309	.533	.519	.395
Colon (d+s)	.529	.518	.380	.572	.560	.416
Eye lenses	.000	.000	.000	.000	.000	.000
Kidneys	.048	.045	.027	.072	.069	.046
Liver	.027	.026	.016	.042	.041	.027
Lungs	.002	.001	.000	.003	.003	.001
Ovaries	---	---	---	.590	.593	.422
Pancreas	.023	.022	.010	.034	.031	.018
RM arm bones	.000	.000	.000	.000	.000	.000
RM clavicles	.000	.000	.000	.000	.000	.000
RM cranium	.000	.000	.000	.000	.000	.000
RM fac.skel.	.000	.000	.000	.000	.000	.000
RM leg bones	.034	.033	.017	.032	.032	.017
RM pelvis	.551	.540	.365	.583	.579	.390
RM ribs	.002	.002	.001	.004	.003	.001
RM scapulae	.000	.000	.000	.000	.000	.000
RM cerv.sp.	.000	.000	.000	.000	.000	.000
RM thor.sp.	.002	.002	.000	.003	.003	.001
RM lumb.sp.	.126	.124	.073	.185	.185	.113
Red marrow	.214	.209	.140	.231	.230	.153
Skeleton	.224	.225	.194	.241	.246	.211
Skin (wh.b.)	.147	.140	.133	.155	.151	.141
Small int.	.461	.450	.327	.549	.541	.401
Spleen	.021	.020	.010	.033	.032	.019
Stomach	.040	.037	.024	.060	.056	.039
Testes	.126	.122	.091	---	---	---
Thymus	.000	.000	.000	.000	.000	.000
Thyroid	.000	.000	.000	.000	.000	.000
Uterus	---	---	---	.585	.578	.418

Improvement of organ dose calculations using the MIRD-type phantoms ADAM and EVA.

One weakness of the calculation of absolute organ doses, using ADAM and EVA was corrected: in former calculations the entrance surface dose and exit surface dose was treated as the average dose across an area of the surface of the phantom which is projected to an imaginary area of 10 cm × 10 cm perpendicular to the central beam in the source to surface distance. In case of the lateral examinations of thoracic and lumbar spine with the central beam outside the axis of the phantoms, this caused a certain underestimation of the conversion factor for entrance surface dose and a similar overestimation of the conversion factor for exit surface dose, but did not affect the conversion factors for all other organs. For absolute calculations of organ doses based on image receptor doses, however this caused a severe underestimation, because in these calculations the ratio between exit and entrance dose is used. Redefinition of the imaginary area with regard to size and inclination now results in realistic values for surface and organ doses.

Organ dose conversion factors for complex fluoroscopic examinations.

An increasing number of invasive procedures, diagnostic and also therapeutic and involving the use of devices under fluoroscopic guidance, are becoming more and more medical practise. These procedures involve heavy load X-ray tubes and generators and are characterised by long examination times. They may provide significant advantage over former methods but there are numerous reports on severe radiation induced skin burns to patients. Consequently they are of interest for organ dose calculations.

Using the adult phantoms ADAM and EVA and certain reference procedures provided by clinical partners, each of these procedures being made up of several single projections varying in tube voltage, field position and field size and direction of beam incidence, organ dose conversion factors were calculated for:

Cardiac catheterisation:

Following the specifications of the Hospital of the Technical University, Eindhoven, organ dose calculations were performed for a reference procedure consisting of 69 single projections in the fluoroscopic part and 23 in the cinematographic part. The organ dose conversion coefficients (organ dose / entrance dose free in air) which were primarily evaluated by the Monte Carlo calculations were multiplied with typical values of entrance doses as measured at the hospital and summed up to result in actual organ doses for the reference procedure.

Furthermore, organ dose conversion coefficients were calculated for a set of 11 typical projections used for fluoroscopic and cineangiographic examinations of the coronary arteries, provided by the Center for Devices and Radiological Health, Food and Drug Administration, Rockville. These projections are based on a study of 230 examinations conducted at the Institut de Cardiologie de Montreal. The organ dose conversion coefficients are to appear in a handbook of selected tissue doses allowing both a detailed assessment of the doses resulting from a specific examination (following a view-by-view analysis of the examination) and a quick but less accurate estimation of nominal organ doses for a complete examination without detailed specifications for the particular views.

Aorta-iliac-femoral arteriogram and carotid arteriogram:

This study was conducted in collaboration with hospitals in Saint Louis and Alton. The interventional procedures on 10 patients (5 aorta-iliac-femoral arteriograms and 5 carotid arteriograms) were analysed in detail regarding the single projections applied during these examinations. The number of single projections per examination ranged from 26 to 63. The organ dose conversion coefficients were multiplied with values of entrance doses free in air measured for each view and summed up to result in organ doses for each single examination.

Peripheral arteriography:

Input data for the Monte Carlo calculations were derived from real-time measurements from an automated data acquisition system applied in about 450 procedures of arteriography of the lower limbs performed at the University Hospital, Maastricht. The calculations were performed for 39 single diagnostic projections during fluoroscopy, radiography and digital subtraction angiography. The examination types were Seldinger catheterisation for arteriography of both legs, percutaneous needle puncture for arteriography of one leg and intravenous digital subtraction arteriography of both legs. Again, the organ dose conversion coefficients are

multiplied with measured entrance dose values and summed up to result in absolute doses for an entire examination.

For part of the fields to be applied in the above studies, it was necessary to modify the Monte Carlo code to achieve an improved modelling of the actual situation: circular beam shapes had to be introduced in addition to the rectangular ones, and a patient couch was included into the simulation as a scattering and attenuating object. For the simulation of the peripheral arteriography of the lower limbs, the leg model had to be changed: for the examinations of both legs, the legs had to lie flat on the patient support in a closed position; for the examination of only one leg, they had to be separated.

In view of the importance of the discussion on organ doses resulting from fluoroscopic procedures, the opportunities for cooperation with clinical partners were made use of and, therefore, these studies were performed in addition to the programme proposed initially for the reporting period. As a consequence, the studies on organ doses from conventional radiology of paediatric patients (impact of the CEC Quality Criteria Document and variation of the doses with patient size) were postponed for the moment and will be completed after the end of this contract.

Comparison of organ dose conversion factors for voxel phantoms CHILD and BABY and the respective paediatric MIRDO type phantoms.

The comparison was performed for a series of paediatric X-ray examinations together with the NRPB. Irradiation conditions were chosen to fit as closely as possible. For most examinations and organs the dose conversion factors agreed within a few percent, but there were also examinations where discrepancies of a factor two and more were observed as shown in table 2. Differences of that magnitude were not only found for organs close to the field edge (where they might be expected), but also for organs located fully in the beam, indicating a strong impact of the phantom anatomy on calculated organ doses.

As long as organ doses are only used in context with the risk of stochastic radiation effects, differences up to a factor of 2 between organ doses from the same irradiation of a MIRDO type phantom and a voxel phantom (as observed in paediatric radiology, where both types of phantoms do already exist) might be of minor consequences; however this is not acceptable in optimisation strategies (e.g. in X-ray diagnosis) when dose to patient, among other parameters, becomes a decisive criterion in the process of optimisation. Further effort is necessary to explain the differences and produce a unique set of organ dose conversion factors.

Table 2: Comparison of organ dose conversion factors for the voxel phantom CHILD and the 5-year MIRL phantom. Examination: Abdomen a.p.

Tube voltage: 70 kV Field size: 25 cm × 39 cm
 Filtration: 3.5 mm Al Focus to film distance: 110 cm

Organ dose per entrance dose (mGy/mGy)

Tissue	CHILD	MIRD (5 y)
Adrenals	0.33	0.16
Bladder	0.86	0.73
Upper large intestines	0.77	0.57
Lower large intestines	0.58	0.38
Small intestines	0.96	0.48
Kidneys	0.30	0.14
Liver	0.60	0.58
Lungs	0.21	0.29
Ovaries	0.58	0.40
Pancreas	0.53	0.37
Spleen	0.45	0.25
Stomach	1.04	0.73
Thyroid	0.01	0.01
Uterus	0.66	0.49
Skeleton	0.32	0.24
Red bone marrow	0.07	0.08

Relation between Effective Dose and Dose-Area-Product (DAP).

Recent publications indicated that a simple, empirical relation could exist between effective dose to the patient and DAP. This gave rise to the hope that only a very small number of conversion factors would enable a reliable estimation of effective dose from measured values of DAP; no detailed knowledge of the examination parameters (e.g. field size and position, radiation quality, direction of incidence) would be required but a coarse knowledge of tube voltage and direction of the beam would be adequate. This appeared to be an enormous advantage, especially for fluoroscopic examinations, where dose estimations are extremely difficult due to not recorded variations of the irradiation parameters during the course of the examination. Effective doses were calculated for radiographic and fluoroscopic examinations of thorax and abdomen.

Besides the question, whether effective dose can be considered as a reasonable dose descriptor for patients, our own study showed, that not only the organ dose conversion factors depend strongly on the above irradiation parameters but also those of effective dose. For examinations in the thorax region, differences of a factor 2 were found for effective doses related to the same DAP value. This discrepancy is strong enough to demonstrate that more or less exact knowledge and consideration of the irradiation parameters is also indispensable for the determination of effective dose from the dose area product.

Dose measurements on patients

Measurements of entrance skin doses in paediatric radiology were carried out together with the National Radiological Protection Board (NRPB), Didcot, UK, the Unita Sanitaria Locale, Udine, Italy and the Children's Hospital of the University of Munich. They aimed to extend the basis for quality criteria, recommendations for good radiographic technique and reference dose values to the age groups of 5 and 10 years, and to CT-examinations (tables 3, 4, 5).

Individually calibrated TL dosimeters were sent to a great number of European paediatric X-ray departments participating in the field studies, to be exposed during the most common X-ray examinations on the entrance side of patients of standard size and returned for evaluation.

Table 3: Entrance surface doses (μGy) from 8 examinations of 5 year old children.

Examination	#	Median	1. Quartile	3. Quartile	Range
Abdomen a.p. / IVP*	36	523	283	878	126 - 1740
Abdomen a.p. / IVP**	16	1445	1003	2329	462 - 3812
Pelvis a.p.	26	387	245	924	103 - 2785
Skull a.p. / p.a.	37	997	726	1369	284 - 4626
Skull lat.	37	703	435	1076	195 - 2358
Chest a.p. / p.a. (mobile)	29	74	65	94	34 - 481
Chest lat. (station.)	41	131	86	233	37 - 662
Chest a.p. / p.a. (station.)	55	63	41	112	19 - 438

#: Number of examinations

*: IVP one film

**: IVP all films

Table 4: Entrance surface doses (μGy) from 11 examinations of 10 year old children.

Examination	#	Median	1. Quartile	3. Quartile	Range
Chest p.a. stationary unit	53	71	36	123	21 - 1156
Chest lat. stationary unit	50	128	86	346	39 - 1976
Chest p.a./a.p. mobile unit	29	92	50	119	18 - 947
Skull a.p.	34	1212	725	1948	142 - 4704
Skull lat.	34	569	367	1037	63 - 3827
Abdomen a.p./p.a.	33	544	363	811	148 - 3981
Pelvis a.p.	24	754	430	1611	89 - 4167
Lumbar spine a.p.	24	1014	550	1474	131 - 5685
Lumbar spine lat.	26	1991	992	4244	249 - 23465
Thoracic spine a.p.	19	783	354	2724	182 - 4312
Thoracic spine lat.	19	1183	500	1765	303 - 2493

#: Number of examinations

Table 5: Doses (mGy) free in air on the axis of rotation from 4 CT-examinations of 1 year old children from 20 facilities.

Examination	Median	1. Quartile	3. Quartile	Range
Skull	39	24	44.7	13.9 - 74.2
Thorax	33.1	29.4	59.9	13.0 - 95.5
Abdomen	31.7	20.3	52	15.2 - 94.7
Spine	53.8	37.9	73.4	11.5 - 132

The most surprising result were the free in air dose values from table 5: calculation of organ doses using these values reveals, that they are (with one exception: red bone marrow) significantly higher than for adults (table 6). This is strongly inconsistent with the experience in conventional radiology, where doses to babies are by orders of magnitude smaller than those to adults. This problem has to be clarified and will become a central point for the next EU research programme.

Table 6: Comparison of median organ doses (mGy) for two CT-examinations of infants (BABY) and adults (EVA).

Examination: Thorax Abdomen

Organ	BABY	EVA	Organ	BABY	EVA
Breast	33	26	Kidneys	29	25
Lungs	34	25	Colon	35	21
Rbm*	9	6	Ovaries	41	22
Thymus	35	24	Rbm*	4	10
Thyroid	34	4			

Rbm*: Red bone marrow

CEC Working Document

A series of comments and proposals was forwarded to the working group for the revision of the CEC Working Document on Quality Criteria for Diagnostic Radiographic Images. Furthermore, comments and proposals were also contributed to the working group for the CEC Working Document on Quality Criteria for Computed Tomographic Examinations. These referred to the choice of the most suitable dose descriptors to figure reference doses for CT examinations which should not be exceeded in practice.

List of publications

Panzer, W., Petoussi, N.: Diagnostic X-ray spectra behind phantoms and antiscatter grids. Radiat. Prot. Dosim. 43, 151-154 (1992)

Petoussi, N., Zankl, M., Panzer, W., Drexler, G., Nette, P.: Photon spectra in standard dosimetric or imaging phantoms calculated with Monte Carlo methods. *Radiat. Prot. Dosim.* 43, 147-149 (1992)

Schneider, K., Fendel, H., Bakowski, C., Stein E., Kohn, M., Kellner, M., Schweighofer, K., Cartagena G., Padovani, R., Panzer, W., Scheurer, C., Wall, B.: Results of a dosimetry study in the European Community on frequent X-ray examinations in infants. *Radiat. Prot. Dosim.* 43, 31-36 (1992)

Stieve, F.-E., Zankl, M., Nahrstedt, U., Kühnel, A., Schult, S.: Entrance dose measurements on patients and their relation to organ doses. *Radiat. Prot. Dosim.* 43, 161-163 (1992)

Veit, R., Zankl, M.: Influence of patient size on organ doses in diagnostic radiology. *Radiat. Prot. Dosim.* 43, 241-243 (1992)

Zankl, M., Panzer W., Drexler, G.: The calculation of organ doses from computed tomography examinations. *Radiat. Prot. Dosim.* 43, 237-239 (1992)

Zankl, M. (Co-Author): Phantoms and computational models in therapy, diagnosis and protection. International Commission on Radiation Units and Measurements: ICRU Report 48 (1992)

Drexler, G.: Das Konzept der Effektiven Dosis in der Röntgendiagnostik. In: *Strahlenschutz in Forschung und Praxis*, Band 34: Strahlenexposition bei neuen diagnostischen Verfahren (Hrsg.: F. Holeczke et al.). Stuttgart: Gustav Fischer Verlag, 1-14 (1993)

Drexler, G., Panzer, W., Petoussi, N., Zankl, M.: Effective dose - how effective for patients? *Radiat. Environ. Biophys.* 32, 209-219 (1993)

Drexler, G., Panzer, W., Stieve, F.-E., Widenmann, L., Zankl, M.: Die Bestimmung von Organdosen in der Röntgendiagnostik. Berlin: H. Hoffmann Verlag (1993)

Moore, B.M., Petoussi, N., Schibilla, H., Teunen, D. (Eds.): Test Phantoms and Optimisation in Diagnostic Radiology and Nuclear Medicine. *Radiat. Prot. Dosim.* 49 (1/3) (1993)

Panzer, W., Zankl, M.: Die Strahlenexposition des Patienten bei computertomographischen Untersuchungen. *Röntgenpraxis* 46, 15-18 (1993)

Schneider, K., Kohn, M.M., Bakowski, C., Stein, E., Freidhof, C., Horwitz, A.E., Padovani, R., Wall, B.F., Panzer, W., Fendel, H.: Impact of radiographic imaging criteria on dose and image quality in infants in an EC-wide survey. *Radiat. Prot. Dosim.* 49 (1/3), 73-76 (1993)

Veit, R., Zankl, M.: Variation of organ doses in paediatric radiology due to patient diameter, calculated with phantoms of varying voxel size. *Radiat. Prot. Dosim.* 49 (1/3), 353-356 (1993)

Zankl, M.: Computational models employed for dose assessment in diagnostic radiology. *Radiat. Prot. Dosim.* 49 (1/3), 339-344 (1993)

Zankl, M., Panzer, W., Drexler, G.: Tomographic anthropomorphic models. Part II: Organ doses from computed tomographic examinations in paediatric radiology. *GSF-Bericht* 30/93 (1993)

Panzer, W.: Grundlagen und Begriffe der Dosimetrie. In: Strahlenschutzkurs für Ärzte (Hrsg.: F.-E. Stieve). Berlin: H. Hoffmann Verlag, 91-112 (1994)

Zankl, M., Veit, R., Petoussi, N., Mannweiler, E., Wittmann, A., Drexler, G.: Realistic computerized human phantoms. Adv. Space Res. 14, (10)423-(10)431 (1994)

Drexler, G.: Diskussion. Die Messung des Dosisflächenproduktes in der diagnostischen Radiologie als Methode zur Ermittlung der Strahlenexposition (Ergebnisse, Erfahrungen, Verbesserungsvorschläge und Empfehlungen zum Strahlenschutz). Bericht über ein Expertentreffen (Hrsg.: W. Löster et al.). Berlin: H. Hoffmann Verlag, 248-257 (1995)

Drexler, G., Panzer, W.: Dosimetrische Kenngrößen, Methodik der Dosisermittlung, Anwendbarkeit und Grenzen des Konzepts der Effektivdosis. In: Strahlenexposition in der medizinischen Diagnostik. Veröffentlichungen der Strahlenschutzkommission, Band 30 (Hrsg.: Bundesministerium für Umwelt, Naturschutz und Reaktorsicherheit). Stuttgart, Jena, New York: Gustav Fischer Verlag, 29-47 (1995)

Panzer, W., Zankl, M.: Beziehung zwischen Dosisflächenprodukt und Einfalldosis, Oberflächendosis, Organdosen, absorbierte Energie (Integraldosis) und Effektivdosis. Die Messung des Dosisflächenproduktes in der diagnostischen Radiologie als Methode zur Ermittlung der Strahlenexposition (Ergebnisse, Erfahrungen, Verbesserungsvorschläge und Empfehlungen zum Strahlenschutz). Bericht über ein Expertentreffen (Hrsg.: W. Löster et al.). Berlin: H. Hoffmann Verlag, 38-48 (1995)

Petoussi-Henß, N., Panzer, W., Zankl, M., Drexler, G.: Dose-area product and body doses. Radiat. Prot. Dosim. 57 (1-4), 363-366 (1995)

Zankl, M., Panzer, W., Petoussi-Henß, N., Drexler, G.: Organ doses for children from computed tomographic examinations. Radiat. Prot. Dosim. 57 (1-4), 393-396 (1995)

Hidajat, N., Vogl, T., Biamino, G., Michel, L., Wust, P., Panzer, W., Zankl, M., Felix, R.: Strahlenexposition in der interventionellen Radiologie am Beispiel der Chemoembolisation des hepatozellulären Karzinomes und der Laserangioplastie der Beckenarterien. Fortschr. Röntgenstr. (submitted)

Pohlman, M.E., Zankl, M.: Dose estimates in interventional procedures. Radiology (submitted)

Zankl, M., Petoussi-Henß, N., Wittmann, A.: The GSF voxel phantoms and their application in radiology and radiation protection. In: Proceedings of a Workshop on Voxel Phantom Development, Chilton, UK, 6.-7.7.1995, NRPB Report (in press)

Head of project 3: Mr. M. Fitzgerald

II. Objectives for the reporting period

1. To determine the frequency of paediatric examinations and the referral criteria adopted at two dedicated children's hospitals (C1,C2) and four general hospitals (G1-4).
2. To compare the differences in paediatric radiographic and radiological practice at the above centres.
3. To carry out a patient dose survey at the above centres in order to obtain baseline data.
4. To assess the physical and clinical image quality of films.
5. To implement a quality management system meeting EN 29000 (now BS EN ISO 9002¹) at one of the children's hospitals and to assess the impact both on image quality and patient dose.
6. To establish guidelines on best practice in paediatric radiology.

III. Progress achieved including publications

This was a multidisciplinary project involving a number of interconnecting studies which are summarised in the following sections.

1. Frequency of examinations

Data on the frequency of x-ray examinations was collected retrospectively from each hospital for the periods May 1992 and January 1993, ie one winter month and one summer to allow for any possible epidemics which might have effected referrals. Each examination was sub-divided into 5 age groups used throughout the project, but no differentiation was made between males and females. Table 1 shows the examinations which were selected for further study. CT was outside the scope of the project.

Table 1: Selected common examinations

Examination	Examination
Chest AP/PA and lateral.	Lateral cephalometry.
Abdomen AP.	Wrist PA and lateral.
Skull AP/PA and lateral.	Ankle AP and lateral.
Hips AP and lateral	Knee AP and lateral (tunnel and sky line)
Whole spine AP.	Barium meal
Lumbar spine AP and lateral.	Barium enema.
Sinuses OM and lateral post nasal space.	Micturating cystourethrogram (MCU)
Orthopantomogram (OPG).	Intravenous urogram(IVU).

The chest is the commonest referral up to 5y. In hospitals where dental x-rays are included they become the the most frequent referral for children between the ages of 10-15y. Extremities particularly of the upper limb become more frequent in the 5-10y and the 10-15y age ranges. Referrals for skull x-rays are much higher in the 1-5y age range in the two general hospitals than one of the childrens's hospitals (C1).

2. Referral criteria

The radiologist at each of the participating departments was asked to provide referral criteria for the examinations listed above. Referral criteria at both of the children's hospitals were far more detailed than those at the general hospitals reflecting the experience of the specialised paediatric radiologists and the larger throughput of patients with a variety of paediatric conditions at these hospitals. Some radiographs were taken at C2 outside their referral criteria due to the absence of a radiologist at some sessions. It is considered that a radiologist constantly reviewing referrals is the optimum but this was not practical at C2 during the time of the project. Referral criteria at the general hospitals were mostly in line with the guidelines of the Royal College of Radiologists² but less routine examinations would have to be tailored for the patient by the radiologist involved. This sometimes led to more investigations being performed for some conditions at the general hospitals.

3. Radiographic Technique

The purpose was to record those factors which would most influence radiation dose and identify the best practice that would give the optimum combination of image quality and patient dose. The radiographic techniques of all examinations were documented at one of the children's hospitals (C1) in line with the requirements of the quality management system. At the remaining hospitals, two radiographers were interviewed and the radiographic techniques were documented for the 16 examinations listed above.

Experienced paediatric radiographers at the specialist centres had consistent and standardised practices aimed at producing radiographs of technically very high quality. However, this quality sometimes exceeded what was required for diagnosis. All departments used radiation protection techniques but C1 had detailed protocols for its use and used specific window shielding for the hip. Differences in radiographic technique have been analysed and it is evident that the dose reductions obtained from the absence of a grid and utilisation of a faster film-screen combination far outweigh such factors as improved coning, better positioning and optimum film density.

4. Radiological Technique

In each department the radiologist with most overall responsibility for paediatric examinations was asked to provide relevant information regarding radiological procedures.

At the specialist hospitals, the radiologists gave detailed accounts of appropriate screening procedures in a variety of conditions reflecting the increased experience at these hospitals. Imaging was also performed on more complex cases, whereas the routine imaging at the general hospitals was for more common conditions.

All hospitals were aware that the use of a grid should be avoided in young patients but this did not routinely occur in the general hospitals as the screening units were also used for adult patients or had an immovable grid. At G2 the grid was only routinely removed for babies.

The specialist hospitals used a 100mm camera routinely for all screening and only used large format films where indicated. This is only possible with over-couch x-ray

tubes. C1 used 100mm film for IVU's with large format film for individual cases. C1 also recommended that a minimum focus film distance should be used and coning/positioning should be by use of the light beam diaphragm rather than screening the patient into position. At C1 lead protection was used to shield areas adjacent to the x-ray beam and magnification techniques were also kept to a minimum. These recommendations could also be adhered to at the general hospitals and it is advisable that all screening units at general hospitals should have an easily removable grid, otherwise they are unlikely to be removed between adult and paediatric screening lists.

General hospitals tended to use more large format films for barium examinations and IVU's. This may represent some lack of confidence because of the fewer patients examined. One general hospital had no video playback equipment and 100mm at the rate of two per second films were used for MCU's. All paediatric fluoroscopic equipment should have facilities for video playback and a 100mm camera. The views taken were similar in all hospitals although the specialist hospitals tended to take fewer spot radiographs and the general hospitals were more likely to tailor examinations to individual clinical problems. A detailed analysis of the differences in referral criteria, radiographic and radiological practice and their influence on image quality and dose is given in Cook et al³.

5. Dosimetry

A dosimetric survey of all the examinations listed in Table 1 (except OPG and lateral cephalometry) was carried out between 1993 and 1995 at the two children's hospitals and four general hospitals. The survey involved the calculation and measurement of nearly 3000 doses. Entrance surface doses (ESD) were calculated from exposure factors for radiographic procedures and dose area products (DAP) were recorded for both radiographic and fluoroscopic procedures. The doses were in good agreement with the literature, but for some procedures were found to be significantly lower than those reported from other European countries. The main dose influencing factors for radiographic procedures were found to be the speed of the film/screen system and the use of an anti-scatter grid. For the main head/trunk examinations, the specialist centres often delivered higher doses to the younger children as a result of their widespread use of an anti-scatter grid. In fluoroscopy however, where the main dose influencing factors were seen to be the use of an anti-scatter grid and the dose rate dependence of the image intensifier, the children's hospitals consistently delivered significantly lower doses.

Both ESDs and DAPs were found to increase with patient age for the main head / trunk examinations, although in some cases (e.g., AP/PA chest) this relationship was weak. The dependence of dose on age necessitates the subdivision of the paediatric sample into a number of age categories. In order to allow meaningful inter-survey comparison of doses it is suggested that all authors use the same age groupings.

A sample of the results is given in the Tables below. Table 2 shows, for four routine head / trunk radiographic examinations (chest AP/PA, abdomen AP, hip AP, skull AP), the average exposure factors, ESDs and DAPs recorded at two children's hospitals (C1, C2) and two general hospitals (G1, G2). Table 3 shows average exposure factors and DAPs for two routine fluoroscopic procedures (barium meal, micturating cystourethrography) recorded at two children's hospitals (C1, C2) and two general hospitals (G3, G4). Fuller details are given in Kyriou et al⁴.

Table 2: Sample of results for radiographic examinations

1m-12m AP/PA CHEST							
	kVp	mAs	FFD (cm)	grid used	film/screen speed	mean ESD (mGy)	mean DAP (cGycm ²)
C1	67	3.8	178	N	200	0.06	1.9
C2	57	3.3	158	N	375	0.04	1.1
G1	57	3.5	167	N	400	0.05	2.9
G2	61	3.9	116	N	400	0.13	2.5

1y-5y AP/PA CHEST							
	kVp	mAs	FFD (cm)	grid used	film/screen speed	mean ESD (mGy)	mean DAP (cGycm ²)
C1	69	4	180	N	200	0.07	2.2
C2	58	3.4	155	N	375	0.05	2.1
G1	58	3.9	176	N	400	0.06	2.5
G2	67	4.5	159	N	400	0.11	3.6

5y-10y AP/PA CHEST							
	kVp	mAs	FFD (cm)	grid used	film/screen speed	mean ESD (mGy)	mean DAP (cGycm ²)
C1	70	4	180	N	200	0.07	3.4
C2	59	3.4	153	N	375	0.06	2.8
G1	61	3.6	182	N	400	0.05	3.7
G2	69	4.6	181	N	400	0.08	4.7

10y-15y AP/PA CHEST							
	kVp	mAs	FFD (cm)	grid used	film/screen speed	mean ESD (mGy)	mean DAP (cGycm ²)
C1	71	4	180	N	200	0.07	5.1
C2	62	3.6	155	N	375	0.07	4.7
G1	66	4.1	181	N	400	0.07	6.2
G2	82	4.9	181	N	400	0.1	6.8

1m-12m AP ABDOMEN							
	kVp	mAs	FFD (cm)	grid used	film/screen speed	mean ESD (mGy)	mean DAP (cGycm ²)
C1	-	-	-	-	-	-	-
C2	63	6	114	Y	375	0.25	6.9
G1	53	3.8	110	N	400	0.11	2.5
G2	-	-	-	-	-	-	-

1y-5y AP ABDOMEN							
	kVp	mAs	FFD (cm)	grid used	film/screen speed	mean ESD (mGy)	mean DAP (cGycm ²)
C1	64	11.1	101	Y	200	0.66	14.8
C2	65	7.5	115	Y	375	0.33	11.9
G1	55	4	100	N	400	0.17	4.6
G2	65	23	100	Y	400	1.69	35

5y-10y AP ABDOMEN							
	kVp	mAs	FFD (cm)	grid used	film/screen speed	mean ESD (mGy)	mean DAP (cGycm ²)
C1	68	13	102	Y	200	0.91	50.3
C2	69	8.7	114	Y	375	0.54	23.3
G1	57	5.1	100	N	400	0.24	9.3
G2	60	10	100	N	400	0.64	18.7

10y-15y AP ABDOMEN							
	kVp	mAs	FFD (cm)	grid used	film/screen speed	mean ESD (mGy)	mean DAP (cGycm ²)
C1	70	14.3	98	Y	200	1.28	53.2
C2	73	10.6	115	Y	375	0.77	42.1
G1	61	12.6	100	Y/N	400	0.94	30.5
G2	74	20	100	Y	400	2.2	52

1m-12m AP HIP							
	kVp	mAs	FFD (cm)	grid used	film/screen speed	mean ESD (mGy)	mean DAP (cGycm ²)
C1	56	2.3	99	N	200	0.08	1.9
C2	62	5.8	115	Y	375	0.23	3.6
G1	53	3.7	100	N	400	0.13	1.5
G2	57	4.4	98	N	400	0.17	4.4

1y-5y AP HIP							
	kVp	mAs	FFD (cm)	grid used	film/screen speed	mean ESD (mGy)	mean DAP (cGycm ²)
C1	63	7.6	100	Y	200	0.44	6.3
C2	64	6.5	113	Y	375	0.31	7.1
G1	56	3.6	100	N	400	0.15	3.3
G2	56	4.7	100	N	400	0.17	3.6

5y-10y AP HIP							
	kVp	mAs	FFD (cm)	grid used	film/screen speed	mean ESD (mGy)	mean DAP (cGycm ²)
C1	62	14.5	100	Y	200	0.91	16.2
C2	68	7.1	114	Y	375	0.41	12
G1	59	3.3	100	N	400	0.17	6
G2	66	5	100	N	400	0.29	15.5

10y-15y AP							
	kVp	mAs	FFD (cm)	grid used	film/screen speed	mean ESD (mGy)	mean DAP (cGycm ²)
C1	71	14.6	104	Y	200	1.18	35.8
C2	72	10.7	114	Y	375	0.77	34.4
G1	59	21.5	100	Y/N	400	1.5	56.5
G2	-	-	-	-	-	-	-

1m-12m AP SKULL							
	kVp	mAs	FFD (cm)	grid used	film/screen speed	mean ESD (mGy)	mean DAP (cGycm ²)
C1	64	11.4	109	Y	200	0.54	14.8
C2	70	8	115	Y	375	0.42	10.6
G1	57	4.7	100	N	400	0.2	5.2
G2	60	4	100	N	400	0.16	4.5

1y-5y AP SKULL							
	kVp	mAs	FFD (cm)	grid used	film/screen speed	mean ESD (mGy)	mean DAP (cGycm ²)
C1	71	15.1	101	Y	200	1.12	39.4
C2	70	9.1	112	Y	375	0.54	14.25
G1	60	9.4	100	N	400	0.53	12.1
G2	-	-	-	-	-	-	-

5y-10y AP SKULL							
	kVp	mAs	FFD (cm)	grid used	film/screen speed	mean ESD (mGy)	mean DAP (cGycm ²)
C1	73	17.3	101	Y	200	1.32	44.5
C2	77	11.3	115	Y	375	0.86	22.7
G1	61	19.3	100	Y/N	400	1.3	21.5
G2	-	-	-	-	-	-	-

10y-15y AP SKULL							
	kVp	mAs	FFD (cm)	grid used	film/screen speed	mean ESD (mGy)	mean DAP (cGycm ²)
C1	75	17.5	100	Y	200	1.44	45.8
C2	79	12.5	115	Y	375	1.1	-
G1	66	28	100	Y	400	2.1	55.5
G2	-	-	-	-	-	-	-

Table 3: Sample of results for fluoroscopic examinations

1m-12m BARIUM MEAL					
	kVp	screen time	grid used	no of (100mm)	mean DAP (cGycm ²)
C1	81	169	N	7.3	69
C2	60	160	N	6.4	81
G3	62	156	Y	6	147
G4	66	48	N	7.9	105

1y-5y BARIUM MEAL					
	kVp	screen time (s)	grid used	no of films (100mm)	mean DAP (cGycm ²)
C1	65	198	N	8.5	136
C2	60	162	N	6.3	109
G3	65	132	Y	5	292
G4	66	42	N	7.4	87

5y-10y BARIUM MEAL					
	kVp	screen time	grid used	no of (100mm)	mean DAP (cGycm ²)
C1	68	174	N	9.3	191
C2	61	144	N	6.4	134
G3	80	198	Y	8.7	388
G4	65	0.8	N	6.3	217

10y-15y BARIUM MEAL					
	kVp	screen time (s)	grid used	no of films (100mm)	mean DAP (cGycm ²)
C1	78	288	N	9.9	313
C2	64	210	N	7.5	276
G3	70	156	Y	12	409
G4	82	49.2	N	12.7	454

1m-12m MCU					
	kVp	screen time	grid used	no. of (100mm)	mean DAP (cGycm ²)
C1	82	66	N	5.1	40
C2	60	84	N	3.9	28
G3	62	66	Y	4.5	51.7
G4	66	60	N	5.7	221

1y-5y MCU					
	kVp	screen time (s)	grid used	no of films (100mm)	mean DAP (cGycm ²)
C1	65	198	N	8.5	136
C2	61	162	N	6.3	109
G3	70	2.2	Y	5	292
G4	67	0.7	N	42	87

5y-10y MCU					
	kVp	screen time	grid used	no of (100mm)	mean DAP (cGycm ²)
C1	70	78	N	6.5	87
C2	66	222	N	3.5	72
G3	-	-	-	-	-
G4	-	-	-	-	-

10y-15y MCU					
	kVp	screen time (s)	grid used	no of films (100mm)	mean DAP (cGycm ²)
C1	70	48	N	7	178
C2	63	222	N	11	287
G3	-	-	-	-	-
G4	75	54	N	10	596

6. Physical Image Quality Analysis

A study into the scope for patient dose reduction in children undergoing diagnostic X-ray procedures was undertaken with a view to implementing a lower dose technique at a specialist children's hospital. The relationship between entrance surface dose (ESD) and image quality was assessed and the chosen technique combined low dose with a suitable level of image quality for the imaging of a one year old chest. A contrast detail phantom (Thijssen et al⁵) was used to relate image quality to ESD.

Three variables were identified as having a significant influence on patient dose, namely, kV/mAs combination, total tube filtration and film/screen speed. A series of films was taken of the phantom combining the three variables to produce films of equal density but varying ESD at the phantom surface. A unique image quality figure (IQF) was produced for each film based on the scoring of the films by a panel of paediatric radiologists. The IQFs and ESDs for each film were compared to those for a control film based on the exposure factors then in use at the children's hospital for the imaging of a one year old chest. The films are ranked by IQF and ESD in Table 4 below. An ESD rank of 1 indicates the lowest dose film and an IQF rank of 1 indicates the highest quality of images. Therefore a low ESD rank and a low IQF rank are desired.

Significant reductions in ESD were achieved (mainly due to the use of faster film/screens). However, the largest reductions were accompanied by significant detriment to image quality. A compromise technique (film no. 10) was selected by the radiologists, employing a 400 speed film/screen combination (double the original

Table 4: Summary of assessment of physical image quality

film no	kV	total filtration mm	film/screen speed	%ESD saving vs control	IQF rank	ESD rank
1*	65	2.5Al	200	0%	1	18
2	65	2.5Al+0.05Nb	200	28%	5	16
3	65	1Al+0.1Er	200	40%	7	14
4	75	2.5Al	200	18%	11	17
5	75	2.5Al+0.05Nb	200	39%	15	15
6	75	1Al+0.1Er	200	47%	9	13
7	65	2.5Al	400	48%	2	12
8	65	2.5Al+0.05Nb	400	62%	10	10
9	65	1Al+0.1Er	400	70%	3	7
10**	75	2.5Al	400	56%	12	11
11	75	2.5Al+0.05Nb	400	67%	7	8
12	75	1Al+0.1Er	400	73%	13	5
13	65	2.5Al	800	64%	4	9
14	65	2.5Al+0.05Nb	800	76%	17	4
15	65	1Al+0.1Er	800	80%	16	2
16	75	2.5Al	800	71%	6	6
17	75	2.5Al+0.05Nb	800	79%	14	3
18	75	1Al+0.1Er	800	79%	18	1

* control film using original factors

** chosen technique employing faster film/screen and higher kV.

speed) and a peak tube potential of 75kV (10kV higher). The estimated ESD saving compared to the original (control) technique is 56%. The faster 800 speed film/screens performed well in some cases, but the radiologists were dissatisfied with the more grainy images. The ranking system used should be regarded only as a simple method of ordering and not as a linear system of classification. In fact the difference in IQF between the middle ranked films is small and likely to be due to random error. Although the radiographic technique was optimised for a one year old chest, use of the faster film/screens was implemented for all head/trunk work and the radiologists were satisfied with the quality of the images taken on real patients. Fuller details are given in Kyriou et al⁶.

7. Radiological Image Quality Analysis

Two paediatric radiologists from C1 assessed all films at C1 over a two year period with regard to image quality and these were compared with dose measurements. Image quality forms were produced which were based on expanded CEC criteria of image quality⁷. Five areas were assessed:

- i) The request form.
- ii) Film labelling and recording of exposure factors.
- iii) Radiographic technique including film density, coning, processing artefacts and position of gonad or lead protection.
- iv) Image criteria.
- v) Use of lead protection outside the field and requirements for repeats or copies.

The same two paediatric radiologists also assessed a sample of 240 films from the other specialist hospital and two general hospitals. The films were selected from patients on whom the corresponding doses had been measured. The quality of

imaging at the two specialist centres accurately reflected current practice in those departments whereas the quality of radiographs in the general hospital tended to reflect their best practice when compared with assessments of other radiographs in the patients' x-ray folders for which doses had not been measured. No attempt was made to assess the accuracy of the diagnostic reports.

At the two specialist centres all paediatric films were filed separately and were readily retrievable, whereas at one general hospital 15% of films were untraceable and the request forms were not kept routinely in the film packets. This could result in unnecessary repeat films being taken. At the specialist centres all x-ray packets had accompanying request forms and exposures were written on all radiographs or request forms. At the general hospitals very few had exposures recorded and this resulted in some patients having follow-up films of different densities but no cases of undiagnostic films as a result of this were noted.

The main problem with technique at the general hospitals was coning and restraining or positioning the patient. At the general hospitals larger films with wide cones, often exposing other areas of the body were included in the field. There were also significantly more films where the holders' hands or fingers were on the film compared to the specialist centres. This is of particular concern when a member of staff has to hold the patients. However, despite the problems with wide coning and positioning and some films being of suboptimal density, the general hospitals still invariably produced films where it was possible to provide a diagnosis.

An attempt was made to obtain reject analysis at each hospital. Unfortunately one hospital did not perform reject analysis and at the other two hospitals separate paediatric reject analysis was not obtained. It was noted that the criteria for rejecting films may vary between hospitals and this aspect is also to be investigated as part of image quality assessment.

In summary, image quality was of a very high standard at the specialist hospitals with excellent filing, record keeping and documentation of exposure. The radiographs at the general hospitals were still mostly diagnostic but reflected the lack of time or experience of radiographers in restraining and positioning young children. The general hospitals also tended to have fewer simple restraining apparatus available to them.

8. Implementation of a Quality Management System

The X-ray Department at C1 set out to implement a quality management system meeting the requirements of BS EN ISO 9002¹ and to measure the improvement this had on image quality and patient dose. One of the requirements of the standard is that the service processes are identified and documented. The process of conducting a radiological examination may be considered to begin with the receipt of the x-ray request form and to end with the issue of a radiological report. A quality manual⁸ has been compiled, organised into four levels. Level 1 sets out the quality management policies in relation to the requirements of the Standard, level 2 contains quality management procedures, level 3 documents the work instructions for all the components of the radiological process and level 4 contains forms and records.

Reflecting the prior interests of the radiologists, the specialist department already had written guidelines and instructions relevant to most of the day-to-day work of the

department. However, the application of the standard provided a clearer organisational framework which brought more consistency to the work of the department and allowed improved assessments of dose and quality. It was illuminating to find that a wide range of practice actually existed in what was originally a small dedicated unit.

Written guidelines on all aspects of routine procedures have been documented and a booklet has been produced "Making the best of a Paediatric Imaging Department" which has eased the work of requesting clinicians and reception staff.

Due to the closure of the original paediatric hospital and its transfer to a specialised unit in a general hospital, there were delays and difficulties in implementing the quality system. However, the move has resulted in the necessity for more staff training within the department and the procedure manuals have proved invaluable for this. The current situation of a specialised paediatric unit within a larger general hospital with rotating staff reflects the trend in the UK away from dedicated children's hospitals with many long-standing staff.

Aiming towards the implementation of a quality system has increased the awareness and improved the morale of the staff. There is now more of an organised team approach with each member aware of their responsibilities towards achieving the main objectives of the department.

9. Dose Reduction at a Children's Hospital

A number of techniques have been implemented at C1 with the specific aim of reducing the dose to the patient.

The film/screen combination speed was doubled from 200 to 400 for all head/trunk work as a result of the study of physical image quality analysis described above. The theoretical ESD reductions of 50% were observed in many cases although the range was 0% - 60%. This stage of the dosimetry is still in progress. No decline in the diagnostic quality of the images has been observed.

Anti-scatter grids are no longer routinely used on the younger patients for various head/trunk procedures. The use of an anti-scatter grid corresponds to an increase in ESD by a factor of between two and three.

A very fast 800 speed film/screen combination is now used for all follow-up spine X-rays of patients with scoliosis. Although the films are noticeably grainy, they are of sufficient quality for the purpose and result in minimal dose to the patient.

A Polaroid camera has been attached to the video for hard copy imaging in fluoroscopy. This takes the place of a 100mm camera attached to the image intensifier. The Polaroid camera requires no extra dose as images are taken automatically from the video. The impact of this method on patient dose is currently under assessment.

Other "common sense" measures to keep patient dose to a minimum are practised at the department, such as use of gonad protection when necessary, tight coning, use of the light beam to position patients for screening procedures (only possible with an overcouch screening tube), clear and accurate marking and filing of all X-ray films, the writing of clear and strict referral criteria etc. Furthermore, protocols and

procedures describing all examinations have been written and issued to all radiographic staff in an attempt to standardise practice throughout the department.

The dosimetric effect of all the new techniques listed above is under continuous monitoring as part of the implementation of a quality system. Dose area product meters have been fitted onto both radiographic and fluoroscopic X-ray tubes and exposure factors are being recorded for all examinations.

10. Guidelines on Best Practice in Paediatric Radiology

From the foregoing studies, guidelines on best practice have been derived for the sixteen examinations considered⁹. For each examination, guidance is given on the referral criteria, image criteria, radiographic or radiological technique and the expected dose range. Guidance on technique covers equipment characteristics, positioning and radiation protection.

11. References

1. BS EN ISO 9002, 1994. Quality systems - Specification for Production, Installation and Servicing. (London HMSO).
2. RCR, 1995. Making the Best Use of a Department of Clinical Radiology. Guidelines for Doctors. (London, Royal College of Radiologists).
5. Thijsson MAO, Thijsson HOM, Merx JL, Lindeijer JM, and Bijkerk, KR, 1989. A definition of image quality: the image quality figure. In: Optimisation of Image Quality and Patient Exposure in Diagnostic Radiology. Proceedings of a Workshop edited by Moores et al. BIR Report 20. (London, British Institute of Radiology.)
7. CEC Radiation Protection Programme/ European Society of Paediatric Radiology, 1992. Quality criteria for diagnostic radiographic images in paediatrics. CEC Draft Working Document XII/307/91.

12. Publications

3. Cook JV, Pablot S, Pettett A, Kyriou JC and Fitzgerald M, 1995. Influence of technique on image quality and dose in paediatric radiology: a comparison between specialist and non-specialist centres. To be submitted to Clinical Radiology.
4. Kyriou J C, Fitzgerald M, Pettett A, Cook JV and Pablot SM, 1995. A comparison of doses between specialist non-specialist centres in the diagnostic x-ray imaging of children. Submitted to the British Journal of Radiology.
6. Kyriou JC, Cook JV, Pablot SM, Fitzgerald M and Pettett A, 1995. Relating patient dose to image quality in the imaging of children - the scope for dose reduction. Poster presented at the Roentgen Centenary Congress, Birmingham, June 12-16.
8. Queen Mary's Hospital for Children. Diagnostic Imaging Department, 1995. Quality manual. (Internal document).
9. Queen Mary's Hospital for Children. Diagnostic Imaging Department, 1995. Guidelines on Best Practice in Paediatric Radiology for sixteen Selected X-ray Examinations.

Head of project 4: Dr. J. Zoetelief

II. Objectives for the reporting period

National standards laboratories do only provide calibration facilities at near mammography qualities but not for routine use. At St. George's Hospital a calibration facility for mammography has been established which employs real mammography units and is therefore unique. A dosimetry intercomparison between TNO and St. George's Hospital will be valuable to obtain insight in absolute dosimetry for mammography.

Air kerma to average glandular dose (AGD) conversion factors (g-values) are published by various authors as a function of half value layer (HVL) for simple breast phantoms. Calculations by different authors differ in radiation transport codes and photon interaction data used, photon spectra, composition and thickness of superficial layer of simulated breasts and are not performed with the tissue compositions recommended by the ICRU. The influence of these parameters on AGD will be studied.

Up to now, calculations of g-values are performed for Mo anode and Mo filter mammography units. Modern mammography units employ a larger variety of anode/filter combinations. Values of g will be calculated for different breast thicknesses and compositions using the new filter combinations. The data on g-values will be used in a joint study of the University of Erlangen/Nürnberg, Siemens and TNO, involving patients examined with different anode/filter combinations depending on breast thickness.

Progress achieved including publications

Dosimetry intercomparison between St. George's Hospital and TNO

The dosimetry intercomparison between St. George's Hospital and TNO at real mammography qualities was carried out in May, 1994 at the mammography calibration facility at St. George's Hospital. In addition, the readings from the TNO digital kVp meter (Radiation Measurements Incorporated, Middleton, Wisconsin, USA, model 232) were compared to the results obtained from St. George's Dynalyser.

The TNO dosimetry system consisted of a 0.6 cm³ thimble graphite Farmer type ionization chamber (Nuclear Enterprises, Reading, UK, type 2571) connected to an electrometer (Keithley, Cleveland, Ohio, USA, model 617). The chamber was operated at a collecting potential of 250 V. For various tube voltages supplied by the Polydoros 80 generator to a Pantix Molybdenum anode tube and employing 0.030 mm Mo + 1 mm Be filter, the TNO system was compared to St. George's 6 cm³ mammo secondary standard chamber. The results are shown in Table 1.

Table 1: Calibration factors (factors by which the readings must be multiplied to give the corrected readings) for the TNO dosimetry system at different mammography qualities.

<i>focal distance</i> (m)	<i>*total filt./</i> <i>waveform</i>	<i>set kV</i>	<i>HVL (mm Al)</i>	<i>calibration</i> <i>factor</i>	<i>** # e in %</i>
1.0	B/MF	25	0.36	1.01	2.7
1.0	B/MF	28	0.39	1.00	2.8
1.0	B/MF	30	0.41	1.00	2.7
1.0	B/MF	32	0.43	1.00	2.8
1.0	B/MF	35	0.44	1.00	2.7

* B/MF refers to Mo anode and 0.03 mm Mo + 1 mm Be filtration/medium frequency high voltage generator.

** # e refers to relative accuracy; the precision of the measurements was about 0.1 per cent.

It is concluded from the table that the differences between TNO and St. George's Hospital are one per cent at maximum i.e. not significantly different. The results of the comparison of the TNO kVp meter to St. George's Dynalyser are shown in Table 2.

Table 2: Deviations of TNO kVp meter (positive values indicate a too low reading of the TNO RMI-232) from St. George's Hospital's results obtained with a Dynalyser. The RMI kVp filter was read out at constant potential (CP) and three phase (3Ø) settings.

<i>focal distance</i> (m)	<i>*total filtration/ waveform</i>	<i>kV</i>	<i>C.P. mean deviation</i> (kV)	<i>3Ø mean deviation</i> (kV)	<i>** e in %</i>
0,5	B/MF	25	1.1	0.3	3.3
0.5	B/MF	28	0.3	-0.7	3.0
0.5	B/MF	30	0.2	-0.9	2.9
0.5	B/MF	32	0.4	-0.8	2.8
0.5	B/MF	35	0.6	-0.8	2.7
0.5	C/MF	25	0.6	-0.2	3.3
0.5	C/MF	28	0.7	-0.3	3.0
0.5	C/MF	30	0.9	-0.2	2.9
0.5	C/MF	32	1.2	0.1	2.8
0.5	C/MF	35	1.8	0.5	2.7

* BMF: refers to Mo anode and 0.03 mm + 1 mm Be filtration/medium frequency generator.
C/MF: refers to W anode and 0.5 mm Al + 1 mm Be filtration/medium frequency generator.
** e refers to relative accuracy; the precision of the measurements was about 0.1 kV.

For a medium frequency generated high voltage the measurements of the RMI kVp meter at constant potential (CP) are assumed to be too low and at three phase (3Ø) are most likely too high. The average values of CP and 3Ø readings are probably the best estimate for medium frequency generated tube voltage. When this mean value is taken maximum differences of 0.7, 0.7 and 1.2 kV occur at 25 kV Mo/Mo, 32 kV and 35 kV W/Al, respectively. Only the value at 35 kV W/Al exceeds the stated accuracy.

Study on the influence of various parameters on calculation of kerma to AGD conversion factors (g)

The influence on the calculation of g-values (and AGD) was studied of various parameters including density and composition of glandular and adipose tissue; thickness and composition of the superficial layer of the breast phantoms; presence and absence of a compression plate; influence of breast thickness; cross section data used for the calculations; and spectral data used.

Mathematical standard breast models were employed consisting of a central region with a mixture of 50 per cent glandular tissue and 50 per cent adipose tissue of varying thickness surrounded by a superficial layer of adipose tissue of 0.5 cm thickness. The total phantom thickness was varied from 2.0 to 8.0 cm, since this is approximately the range of breast thicknesses met in practice. Calculations were made at a fixed focus-to-backscatter plate distance of 60.0 cm. The backscatter plate consisted of 2.0 cm of PMMA. For some calculations the superficial layer of 0.5 cm of adipose tissue was replaced by 0.4 cm of glandular tissue, since this is also used to represent skin and underlying adipose tissue by some investigators.

The density and the elemental compositions of glandular tissue and adipose tissue were determined by Hammerstein et al. (1979) for five samples of fresh mastectomy specimens. Data of Woodard and White (1986) refer to glands embedded in, but separated from a large mass of hormonally controlled adipose tissue and are the means of seven specimens from postmenopausal women. According to White (private communication, 1991) the two sources of data on

glandular tissue composition are essentially the same. As the specimens considered contained both "normal" and "abnormal" tissue, Woodard and White attempted to select only "normal" tissue. Therefore, the ICRU (1989) recommended the average value of Woodard and White as reference composition for glandular tissue. It should be noted, however, that the composition of Hammerstein et al. is usually employed for dosimetry.

The results of calculations for 5.0 and 6.0 cm thick "standard" breasts are presented in Table 3 for calculations with photon spectra of Birch et al., 1992.

For 6 cm thick breasts, g-values show maximum differences of 13 per cent at an HVL of 0.30 mm Al with those of other investigators i.e. Dance, 1990. The maximum difference is reduced to 8 per cent at an HVL of 0.40 mm Al and refers to values of Wu et al., 1991. These differences concern the situation where all investigators use elemental compositions of Hammerstein et al.

Table 3: Conversion factors, g, for 5 and 6 cm thick "standard" breasts with tissue compositions according to Hammerstein et al. and ICRU-44

HVL (mm Al)	elemental composition of Hammerstein et al.		elemental composition of ICRU-44	
	5 cm thickness	6 cm thickness	5 cm thickness	6 cm thickness
0.30	0.154	0.124	0.135	0.108
0.35	0.182	0.147	0.159	0.128
0.40	0.212	0.173	0.186	0.151

It is clear from Table 3 that the differences due to elemental compositions of Hammerstein et al. compared to ICRU-44 are considerable i.e. about 14 to 15 per cent.

The influence of the composition and thickness of the superficial layer representing skin and underlying adipose tissue is dependent on the source used for elemental composition of breast composing tissues. The use of data from Hammerstein et al. result in a difference of 17 per cent between g-values for phantoms with superficial layers of 0.4 cm glandular tissue and 0.5 cm adipose tissue. Using data from ICRU-44 this difference is reduced to about 7 per cent. The elemental composition of adipose and glandular tissues requires further investigation.

Conversion factors, g, were calculated (using MCNP and XCOM as database for cross-sections) in the presence and absence of a 3 mm thick polymethylmetacrylate compression plate. In the half value layer (HVL) range of 0.30 to 0.40 mm Al, the present calculations yield 4.5 ± 1.5 per cent lower g-values in presence of the compression plate at the same HVL of X rays incident on the phantom. This is in agreement with values reported by other investigators.

The influence of breast thickness on g was calculated in the presence of the compression plate for two spectra. The g-values decrease when the breast thickness is changed from 2 cm to 8 cm by factors of 4.0 (HVL: 0.37 mm Al) and 3.8 (HVL: 0.42 mm Al). This variation is in agreement with values reported by Dance (1990), but larger than those reported by other investigators.

Calculations were also made with different cross-section data, for 5.5 cm thick phantoms and two spectra. The values of g obtained with MCPLIB (usually used in MCNP) were 10 per cent higher than those using XCOM (Berger and Hubbell, 1987). This difference is due to a renormalization of the photo-effect cross-sections.

Values of g are calculated for various photon spectra in presence and absence of the compression plate. At fixed HVL, the spectral influence on g-values can cause differences up to about 7 per cent (see Figure 1), all data referring to Mo/Mo anode/filter combinations. A summary of the influence of the variations in various parameters on g-values is given in Table 4.

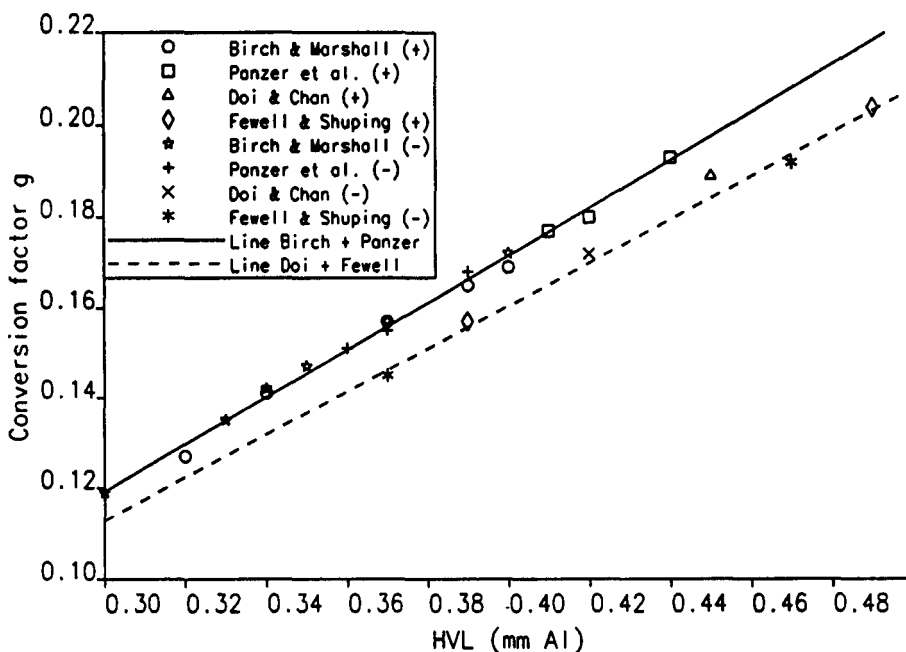


Figure 1: Conversion factor g as a function of HVL employing photon spectra from various authors in the presence and absence of a 3 mm thick PMMA compression plate. The values refer to a 5.5 cm thick breast phantom (superficial layer: 0.5 cm adipose tissue) and ICRU report 44 tissue compositions.

Table 4: Summary of the influence of variations in various parameters on g -values.

parameter	estimated relative difference in g -value (per cent)
Monte Carlo technique	< 1
Cross-section data	10 (MCPLIB versus XCOM)
Backscatter material	< 1
Compression plate	4 (no plate versus 3 mm PMMA)
Tissue composition	15 (ICRU-44 versus Hammerstein et al.)
Superficial breast phantom layer	7-17 (4 mm gland versus 5 mm adipose)
Source of spectrum at same HVL	7 (see Figure 1)
Breast thickness	400 (thickness at about 0.40 mm HVL range 2 to 8 cm)

Conversion factors g for mammography units with anode/filter combination other than Mo/Mo
 Until recently, almost exclusively Mo/Mo anode/filter combinations were used for mammography. Modern mammography units, however, employ a variety of K-edge filters (e.g. Mo, Pd, Rh) combined with Mo, W and Rh anodes with the aim of adapting the spectrum to breast thickness and composition. Values of g , however, are generally restricted to Mo/Mo anode/filter combinations. The variation in HVL of units with the new anode/filter combinations is considerably larger than that of Mo/Mo units in approximately the same range of tube voltages (Table 5). Therefore, values of g are calculated for different breast thicknesses and compositions based on spectral information provided by Siemens for their new anode/filter

combinations.

Table 5: Typical half-value layers (HVL) in mm Al for mammography units with different anode/filter combinations operated at various tube voltages (maximum variation ± 0.03 mm Al) (Jansen and Zoetelief, 1994)

Anode and filter materials	Tube voltage (kV)	HVL (mm Al)	
		without compression plate	with compression plate (3 mm PMMA)
Mo + 30 μ m Mo	25	0.28	0.34
	28	0.32	0.37
	30	0.34	0.38
	31	0.35	0.39
	34	0.36	0.40
Mo + 25 μ m Rh	22	0.30	0.34
	25	0.36	0.40
	28	0.40	0.44
	34	0.41	0.46
W + 60 μ m Mo	22	0.33	0.37
	25	0.35	0.39
	28	0.37	0.41
	30	0.38	0.42
W + 50 μ m Rh	22	0.41	0.43
	25	0.48	0.51
	28	0.51	0.54
	30	0.53	0.56
W + 40 μ m Pd	22	0.36	0.40
	25	0.44	0.48
	28	0.48	0.53
	30	0.50	0.55
Rh + 25 μ m Rh	23	0.31	0.36
	25	0.34	0.40
	28	0.39	0.45
	30	0.42	0.48

The spectra used are measured by Dr. J. Dierker Siemens AG (1994), for an anode angle of 16° without additional filtration (inherent filtration 1 mm Be) using a high purity planar Ge-detector based spectrometer in energy increments of 0.1 keV. The measured spectra are corrected for detector efficiency and Ge-escape. All spectra are measured at the tube voltages indicated except the Mo and W-anode cases at 28 kV, which are interpolated from unfiltered spectra at 25 and 30 kV. The influences of K-edge filters on the spectra are calculated, using mass attenuation coefficients published by Storm and Israel (1970). The spectra and breast thicknesses for which the conversion factors are calculated are those employed in a study performed at the Klinik für Frauenheilkunde der Universität, Erlangen/Nürnberg. The anode filter combinations, compressed breast thicknesses and tube voltages used are shown in Table 6.

The breast phantoms used for the calculations consist of halved cylinders (cut in half along the cylinder central axis) with a radius of 8 cm. A 5 mm superficial layer representing skin and

underlying adipose tissue consisting of adipose tissue surrounds the central region of the breast phantom. The central region consists of either 100% adipose tissue or 50%/50% (by mass) adipose/glandular tissue (termed mix) or 100% glandular tissue. Tissue compositions are according to Hammerstein et al. (1979). The thickness of the breast phantom is variable and ranges from 2 cm to 9 cm (including skin). The source is positioned at a distance of 60 cm from the exit plane of the phantom. A 3 mm thick PMMA compression plate is positioned on top of the phantom. Backscatter materials are not employed for the calculations. The photon fluence to dose function used for glandular tissue are according to the tissue compositions of Hammerstein et al. (1979).

Table 6: Factor g (mGy/mGy) for conversion of air kerma free-in-air at the entrance position of the breast into AGD, for various breast thicknesses (50% adipose/50% gland), anode/filter combinations and tube voltages. The first HVL is calculated for the spectra behind a 3 mm thick PMMA compression plate. The relative standard deviation is less than 1% for each conversion factor.

Anode mat.	filter th. μm	tube mat.	tube volt. kV	first HVL mm Al	breast thickness (mm):							
					20	30	40	50	60	70	80	90
Mo	25	Rh	28	0.44				0.216	0.178	0.151	0.130	
Mo	25	Rh	30	0.46					0.186	0.158	0.136	0.120
Mo	25	Rh	32	0.47					0.192	0.163	0.141	0.124
Mo	30	Mo	25	0.35	0.407	0.284	0.213	0.168				
Mo	30	Mo	28	0.39		0.313	0.237	0.187	0.154	0.130		
Mo	30	Mo	30	0.40				0.198	0.163	0.137	0.118	
Mo	30	Mo	32	0.42					0.170	0.143	0.124	0.109
Rh	25	Rh	28	0.45				0.229	0.190	0.161	0.140	
Rh	25	Rh	30	0.48					0.205	0.175	0.152	0.134
Rh	25	Rh	32	0.51					0.218	0.186	0.162	0.142
W	50	Rh	28	0.54				0.267	0.222	0.189	0.164	
W	50	Rh	30	0.56				0.278	0.232	0.198	0.172	
W	50	Rh	32	0.58					0.237	0.202	0.176	0.155
W	50	Rh	34	0.60					0.246	0.210	0.183	0.162
W	60	Mo	25	0.39	0.444	0.314	0.236	0.186				
W	60	Mo	28	0.41		0.325	0.246	0.195	0.160	0.135		
W	60	Mo	30	0.42				0.206	0.170	0.144	0.124	

The conversion factors, g , calculated for various breast thicknesses, anode filter combinations and tube voltages are shown in Table 6. The statistical uncertainties due to the calculations are less than 1 per cent. The calculations have been performed for 100 per cent adipose, 100 per cent gland and 50%/50% adipose/gland breast compositions. In the table only the latter data were shown. The other results are published elsewhere (Jansen et al., 1994). The conversion factor g increases as the adipose content of the breast becomes higher. In practice the adipose to glandular tissue ratio varies continuously and interpolations have to be applied to obtain the appropriate g value. By deriving g for the mix phantom from the pure adipose and glandular tissue values, an optimal interpolation technique is selected. Three interpolation functions have been investigated namely linear, reciprocal and logarithmic. The maximum deviations between interpolated and calculated values are 5, 1 and 2 per cent for the three methods, respectively, and the average deviations 3.8, 0.8 and 1.5 per cent, respectively. The preferred interpolation function is the reciprocal one.

For fixed breast composition and thickness, in general, the conversion factor g increases with increasing HVL. This relationship is nearly linear, although significant differences for the various anode filter combinations and tube voltages occur. Especially for the Rh/Rh combination the conversion factor is significantly higher than those for the other anode filter combina-

tions at the same HVL (Figure 2).

For fixed HVL (obtained for various anode filter combinations and tube voltages) and stated breast composition, the conversion factor g decreases with increasing breast thickness. The change in conversion factor with thickness is greater for small compressed breast thicknesses and becomes smaller for larger thicknesses. Also the ratio of the conversion factor for 100 per cent adipose and 100 per cent gland is dependent on breast thickness being approximately 1.25 for 20 mm, 1.4 for 30 mm, about 1.5 for 40 and 50 mm and 1.55 for thicker breasts.

When accurate absorbed dose values are required, conversion factors have to be obtained from Table 6 either directly, or by interpolation from neighbouring conversion factors. For radiation protection often less accuracy is sufficient and approximations might be practical. The following function of the conversion factor g as a function of HVL (mm Al) and compressed breast thickness, d (mm), might be useful:

$$g(d, \text{HVL}) = \left(1 + \frac{g_1}{d}\right) \cdot \left(g_2 + g_3 \cdot \text{HVL}\right) \quad \text{for} \quad \begin{cases} d \leq 50 \text{ mm} \ \& \ 0.35 \leq \text{HVL} \leq 0.41 \text{ mm Al} \\ d \geq 50 \text{ mm} \ \& \ 0.40 \leq \text{HVL} \leq 0.60 \text{ mm Al} \end{cases} \quad (1)$$

Table 7: Parameters g_1 , g_2 and g_3 as derived from least squares fitting of the conversion factor as a function of breast thickness, d , and first HVL. The parameters are given for both the 100 per cent adipose and 100 per cent glandular breast composition. Values of g for intermediate breast compositions can be interpolated using equation (2).

<i>breast composition</i>	g_1 (mm)	g_2	g_3 (mm Al) ⁻¹
100% adipose	359	0.000207	0.0728
100% glandular	-825	0.00136	-0.0292

Parameters g_1 , g_2 and g_3 are given in Table 7 for 100 per cent adipose and 100 per cent glandular tissue breasts. The maximum relative differences between the use of the function and the calculated conversion factors are 7.9 per cent and 5.3 per cent for 100 per cent adipose and 100 per cent glandular tissue breast compositions, respectively. The average relative differences being less than 0.3 per cent having relative standard deviations of 3.4 per cent and 2.4 per cent, respectively. For the 100 per cent adipose tissue breasts, larger deviations with the conversion factor function are found for 20 and 90 mm thick breasts. For the 100 per cent glandular tissue breasts, the conversion factor function results only for one situation in a difference in excess of 5 per cent. The conversion factor for 100 per cent glandular composition using the Rh/Rh anode filter combination is between 3.3 per cent and 4.8 per cent higher than expected from the function. For the 100 per cent adipose composition is this effect not so evident as the calculated conversion factors range from 1.9 per cent lower to 5.6 per cent higher than expected by the function.

As stated before, for various breast compositions, the conversion factor can be derived from reciprocal interpolation:

$$g_{\text{mix}} = \frac{1}{\left(\frac{w_{\text{adipose}}}{g_{\text{adipose}}} + \frac{w_{\text{gland}}}{g_{\text{gland}}}\right)} \quad (2)$$

Where w denotes the fraction by mass of the composition in the mix and the following relation holds:

$$w_{\text{adipose}} + w_{\text{gland}} = 1 \quad (3)$$

Using the conversion factor functions for 100 per cent adipose and 100 per cent glandular breast compositions and applying reciprocal interpolation to derive g for a 50%/50% mix breast the largest deviation with the calculated values is 5.6 % compared to the detailed calculations, the average deviation is less than 1 per cent and the relative standard deviation is 2.3 per cent. The backscatter factor (BSF) is calculated with a relative standard deviation of less than 1 per cent for all conditions in Table 6. The BSF is on average 1 per cent higher for the 100 per cent adipose tissue when compared to the 100 per cent glandular tissue. The influence of breast thickness on the BSF is small, i.e., less than 1 per cent. The BSF increases with increasing HVL. Calculated BSF can be approximated with less than 1 per cent deviation by the function:

$$\text{BSF}(w, \text{HVL}) = 1.025 + (0.180 \cdot w_{\text{adipose}} + 0.148 \cdot w_{\text{gland}}) \cdot \text{HVL} \quad (4)$$

Where the symbols are the same as stated before.

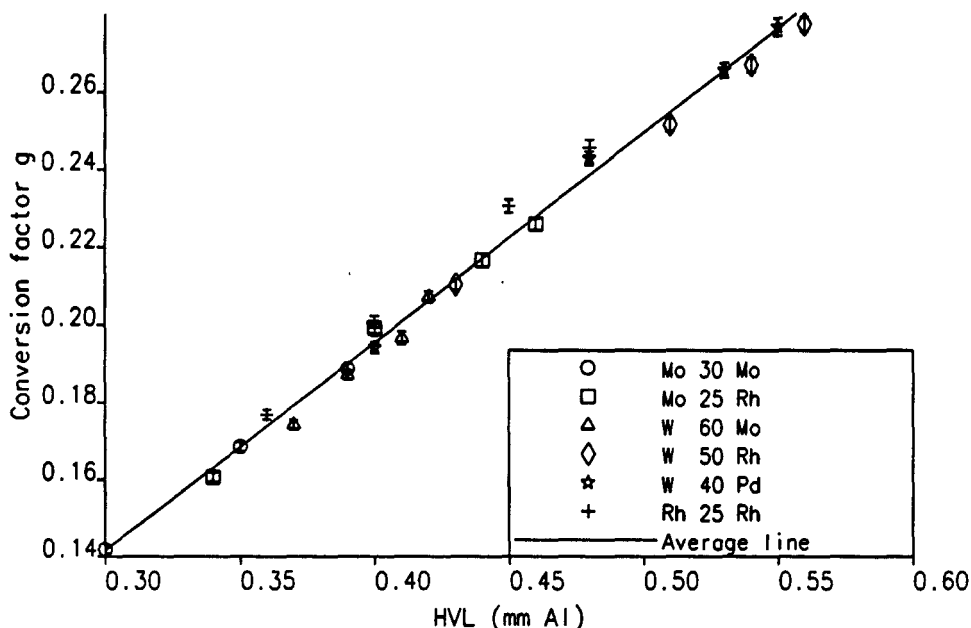


Figure 2: Calculated conversion factors g for the 50 mm thick standard breast (central region: 50% adipose/50% glandular tissue and superficial layer: 0.5 cm adipose tissue) using spectra of Dierker (1994) for various anode/filter combinations.

AGD of patients examined at modern mammography units employing different anode/filter combinations

In a joint effort of the University of Erlangen/Nürnberg, Siemens and TNO, compressed breast thickness, breast composition, tube output and tube loading have been determined during actual mammography. In addition, breast thickness and composition were determined as a function of age.

It is concluded from these studies (Klein et al., in preparation) that reasonable glandular dose (AGD) values can be obtained using average breast composition of 50 per cent adipose/50 per

cent glandular tissue composition allowing an uncertainty of less than 10 per cent for the total group of women undergoing mammography. However, for individuals variations up to 25 per cent can occur between breast composition adapted to the fraction of glandular tissue and average (50% adipose/50% gland) conversion factors. The requirements by various European actions can be met in practice. The dependence on age observed in the present studies shows that younger women i.e. of ages below 30 years have a factor of two higher AGD than women in excess of about 75 years. For ages of 40 to about 70 years the average radiation doses can be well below 2 mGy and at maximum below 2.5 mGy. The dose levels are directly influenced by the optical density to the radiographs, the levels of which are presently a subject of discussion.

References

- Berger, M.J. and Hubbell, J.H. XCOM: photon cross-sections on a personal computer. National Bureau of Standards, Gaithersburg, MD, USA, version 1.2 (1987).
- Birch, R. and Marshall, M. Program to calculate photon spectra; spectra were kindly provided by Dr. D.R. Dance, pers. comm. (1992).
- Dance, D.R. Monte Carlo calculation of conversion factors for the estimation of mean glandular breast dose. *Phys. Med. Biol.* 35, 1211-1219 (1990).
- Dierker J., Siemens AG. Personal Communication (1994).
- Doi, K. and Chan, H.-P., Evaluation of absorbed dose in mammography: Monte Carlo simulation studies. *Radiology* 135, 199-208 (1980).
- Fewell, T.R. and Shuping, R.E., Handbook of mammographic X-ray spectra. HEW Publication FDA-79-8071, Rockville, MD, USA (1979).
- Hammerstein, G.R., Miller, D.W., White, D.R., Masterson, M.E., Woodard, H.Q. and Laughlin, J.S. Absorbed radiation dose in mammography. *Radiology* 130, 485-491 (1979).
- ICRU. Physical aspects of irradiation. Report 10b. NBS Handbook 85. (NBS, Gaithersburg MD, USA) (1964).
- ICRU. Tissue substitutes in radiation dosimetry and measurement, Report 44 (Bethesda, MD, USA: ICRU) (1989).
- MCPLIB. Cross-section data of the MCNP code based on refs. Hubbell et al. and Everett and Cashwell.
- NCRP. Mammography: A user's guide, Report 85 (Bethesda, MD, USA: NCRP Publications) (1986).
- Panzer, W., Drexler, G., Widenmann, L. and Platz, L. Spectra and exposure values in mammography. *GSF-Bericht S 518* (1978).
- Storm and Israel. Photon Cross Sections from 1 keV to 100 MeV for Elements Z=1 to 100. *Nucl. Data Tables A7*, 565 (1970).
- Woodard, H.Q. and White, D.R. The composition of body tissues. *Brit. J. Radiol.* 59, 1209-1218, (1986).
- Wu, X., Barnes, G.T. and Tucker, D.M. Spectral dependence of glandular tissue dose in screen-film mammography. *Radiology* 179, 143-148 (1991).

Publications

- Zoetelief, J., Jansen, J.T.M., De Wit, N.J.P. Determination of image quality in relation to absorbed dose in mammography. *Radiat. Prot. Dosim.* 49, 157-161, (1993).
- Zoetelief, J., Aalbers, A.H.L., Beentjes, L.B., Broerse, J.J., Julius, H.W., Zuur, C. Dosimetric aspects of mammography. Report 6 of the Netherlands Commission on Radiation Dosimetry. (1993).
- Jansen, J.Th.M., Dierker, J., Zoetelief, J. Calculation of air kerma to mean glandular dose conversion factors for mammography units employing various target-filter combinations. In: B. Schaeken, J. Vanregemorter (eds.). *Proc- Xth Annual Symposium, Belgian Association of Hospital Physicists* (1994).

- Zoetelief, J. and Jansen, J.Th.M. Calculation of air kerma to average glandular tissue dose conversion factors for mammography. *Radiat. Prot. Dosim.* vol. 57, 397-400, (1995).
- Klein, R., Achinger, H., Dierker, J., Jansen, J.T.M., Joite-Barfuss, S., Säbel, M., Schulz-Wendtland, R., Zoetelief, J. Determination of average glandular dose from modern mammography units. In preparation.



Final Report
1992 - 1994

Contract: F13PCT930070

Duration: 1.1.93 to 30.6.95

Sector: C22

Title. Evaluation of dose and risk due to interventional radiology techniques

- | | | |
|----|---------------|--------------------------------|
| 1) | Schmidt | Klinikum Nuernberg . |
| 2) | Maccia | CAATS |
| 3) | Padovani | Unitá Sanitaria Locale - Udine |
| 4) | Vanó Carruana | Univ. Madrid - Complutense |
| 5) | Neofotistou | Hosp. General Athens |

1. Summary of Project Gobar Objectives and Achievements

About 30 years ago, angiographic diagnostic procedures were used for the first time to perform therapies within the radiology. Today "interventional radiology (IR)" is an essential part of the minimally invasive methodologies within radiology, worldwide. Some interventional procedures have shown two-digit growth rates per year

The aim of the 5 European groups participating in the research study was to assess the radiation exposure to both the patients and the personnel in association with interventional procedures. This was done to estimate the significance of such exposure for every person involved and with regard to its proportion of the total volume of radiation exposure in the framework of medical procedures, and to identify factors which will be essential for radiation protection purposes. Because of the different situations in the various countries with regard to the organization of radiology, the current regulations, the standards of the equipment used and the quality assurance, the different working groups mostly focused on special fields of interventional radiology

Today, interventional radiology is mainly used in

- Angiology
- Cardiology
- Neurology
- Gastroenterology
- Urology
- Pulmonary Medicine
- Orthopedy
- Pediatry
- Biopsies and Drainages and the
Application of Cytostatic Agents.

The frequency of performance of specific interventional procedures was determined for the different countries, and exemplary dose measurements on patients and personnel were performed for different techniques. On the basis of the data obtained and the measured values risk-relevant dose rates can be provided with regard to their potential for stochastic effects to the patients. The deterministic effects - especially to the skin - as a result of interventional procedures (mainly in cardiology) have attracted great attention. For this

reason not only the dose area product of different procedures, but also the entrance surface dose had to be determined for the definition of risk-relevant doses.

For an effective radiation protection for the patients, special requirements have to be met at interventional units. As shown in the different reports, the most important aspects are properly functioning equipments, complemented by dosimetry on both the patients and the physicians and personnel involved in the use of the equipment, as well as good training and further education of the physicians. These demands include above all improvements of the equipment such as additional filtration or indication of the dose rate or the cumulative dose. It is recommended to establish reference dose rates for each of the different interventional procedures. The reports of the different countries for interventions performed in the various medical disciplines such as cardiology, neuroradiology or angiology show comparable dose values. The members of our working group feel that the further education and training of the personnel involved in interventional radiology procedures is of high importance.

The sometimes relatively high dose rates per intervention that were reported by the different participants in the project underline the demand for optimum radiation protection at all units where interventions are performed. Another demand is the control of the doses to the personnel involved in these procedures, at regular time intervals. From the measured values a maximum dose value can be set for the physicians and the personnel performing or assisting in interventional procedures requiring high doses, to avoid an exceeding of these limits.

The final report of this research project enables a relatively detailed insight into the problems of radiation protection during interventional procedures. It also presents valuable proposals for improvement of the radiation protection in interventional radiology.

Head of project: 1: Prof. Dr. Theodor Schmidt
(Staff member of the research team: Dr. Michael Wucherer)

II. Objectives for the reporting period

Interventional radiology has received worldwide attention for being associated with dose-expansive examinations within the past years.

Contrary to diagnostic radiology, in interventional radiology besides the stochastic effects potential deterministic effects as a result of radiation exposure have to be considered. The purpose of the study was therefore to determine in detail risk-relevant factors for the interventional procedures performed in Germany and to show up tendencies, where at both the mean values, the variations and the proportion of the dose-related factors respectively, are of interest. The aim of the study was to show the necessity for and possibilities of an optimization of the radiation protection to patients and personnel.

III. Progress achieved including publications

Introduction

Interventional radiology is part of the invasive methods as used in diagnostic radiology. The aim of radiological procedures is not only the diagnosis, but moreover the therapy of diseases.

When introducing a new methodology, the benefits and risks of the procedure have to be balanced; this also applies to interventional radiology. As since its employment it has been a well-known fact that IR procedures go along with high radiation exposure due to long fluoroscopic times, it was obligatory to perform investigations on dose-relevant values.

Methodology

The survey of the statistical distribution of number and type of interventional procedures within radiology was done in co-operation with the "Arbeitsgemeinschaft Interventionelle Radiology" (Working Group on Interventional Radiology) within the German Radiological Society. For this research project the following was evaluated on the basis of 50,000 interventions:

- the type of intervention
- the location of the lesion
- age and sex of the patients
- the imaging system used
- the fluoroscopic time and
- the number of images.

Corresponding data for cardiologic interventions were established with the assistance of the German Society of Cardiology

Furthermore, specific data for the different interventions, such as the patients age and characteristics and dose-relevant parameters were collected in 14 large German hospitals

Typical dose parameters were determined by measurements on phantoms at the interventional units.

Recommended dose values for the patient are the dose-area product (DAP) and the entrance surface dose (ESD). These dose values were established using a DAP meter system developed by company PTW which disposes of two ionization chambers, at a DSA and a conventional fluoroscopic unit each. For determination of the DAP, the focus-skin distances were individually measured for every patient.

Parallel to the dose measurements on about 100 patients undergoing the same procedure, the ESD at the head, the hands, the feet and at the body trunk of the physician - outside the protective clothing - were measured. For these dose measurements on the personnel TLD 200 rods were used, which had been specifically calibrated in diagnostic radiation qualities.

Results

As the investigations within the framework of this study have shown, the number of interventional procedures has been clearly increasing within the past 10 years. In 1994, about 180,000 interventions were performed in Germany (see Figures 1 and 2) This corresponds to about 2,000 interventions per million of the population per year. Nearly half of the interventions were performed in cardiology. Due to political-professional and traditional reasons, interventions on the heart are nearly exclusively performed by cardiologists. For this reason, the findings from cardiology are mentioned separately from the other interventions.

More than 90% of all interventions in cardiology (pace-makers were not considered) are percutaneous transluminal coronary angioplasties (PTCA). The share of the different interventional radiological techniques is demonstrated in Figure 3. About 55% of all interventions in radiology are angioplasties. Other important techniques are embolizations, biopsies and drainages. Especially in pain therapy and for biopsies and drainages systems providing cross-sectional images are employed. Mainly computed tomography (CT) units are used for this purpose, but also ultrasound (US) and magnetic resonance imaging (MRI)

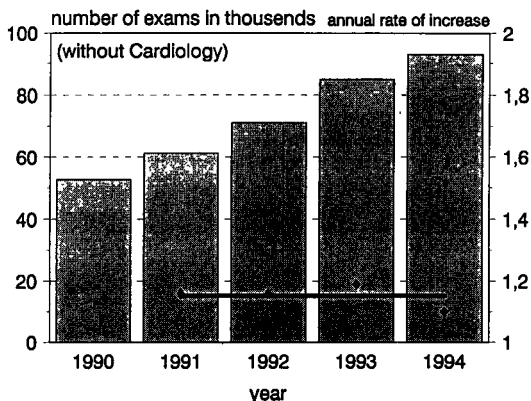


Figure 1: Interventional Radiology in Germany, 1990-1994

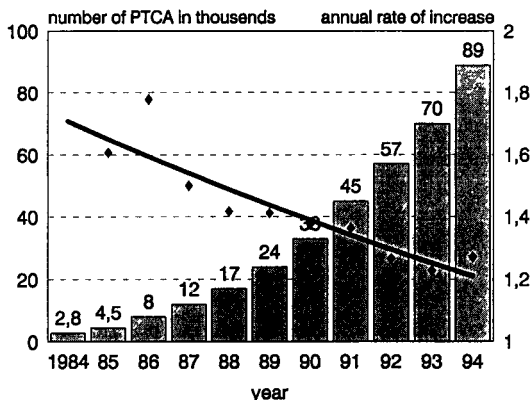


Figure 2: Interventional Cardiology in Germany 1984-1994

have gained in importance during the last years.

During pain therapy (in tumour patients) under CT-control normally 3 to 6 scans per imaging series are acquired. This series of scans can be repeated up to 10 times until such an intervention is finished.

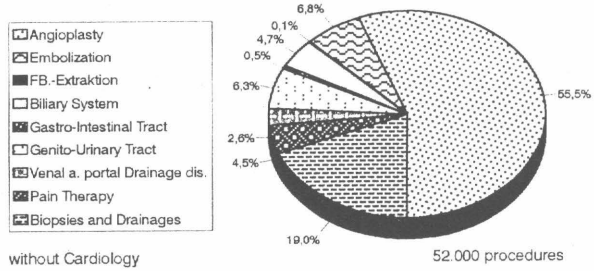


Figure 3: Types of interventional radiology

Nearly 70% of all radiologic interventions and far more than 90% of all cardiologic interventions are performed using fluoroscopy.

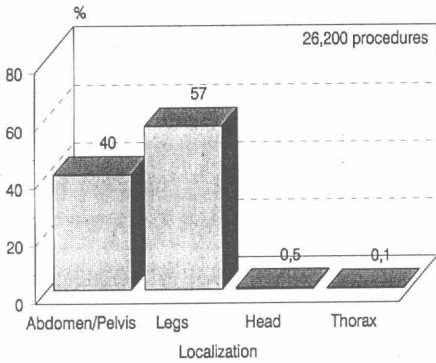


Figure 4: Lokalization of angioplasties

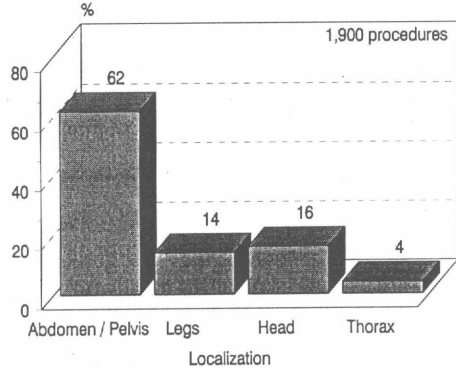


Figure 5: Lokalization of embolizations

Figures 4 and 5 show the locations in which angioplasties and embolizations are performed. About 40% of all percutaneous transluminal angioplasties (PTA) fell on the share of the abdomen and the pelvis. Most PTAs, however, are performed in the legs, whereby in limb-threatening situations an amputation can often be avoided. More than 60% of all embolizations are carried out in the region of the pelvis or the abdomen. In addition to the data regarding number and distribution of the interventional procedures, also risk-relevant data of the patients were collected. As can be seen from Figure 6, at least 60% of all patients in interventional radiology are men. The corresponding figure for cardiologic interventions is 70%. The share of women receiving angioplasties has, however, increased to 38% in the year 1994, compared to 32% in 1990. When comparing the age of patients in interventional radiology to those of

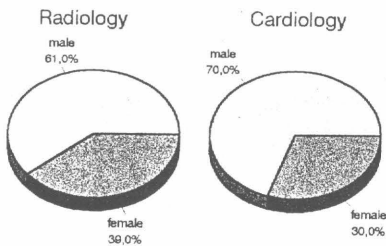


Figure 6: Sex distribution in interventional radiology and cardiology

cardiology, it becomes evident that in IR about 55% of the patients are older than 60 years of age, whereas in PTCA 55% are under 60 years of age (see Figure 7). Within the past 5 years

the percentage of patients aged over 60 who underwent interventional procedures increased from 53% in 1990 to 65% in 1994. This indicates to the growing experience and practice of the radiologists performing IR procedures, most probably going along with a decrease of the risk of complications associated with these procedures.

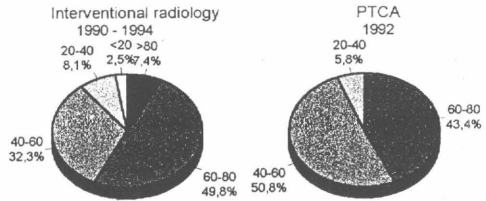


Figure 7: Age distribution in interventional radiology and cardiology

Figure 8 shows the comparison of the age distribution within the German population with those persons who received an angioplasty.

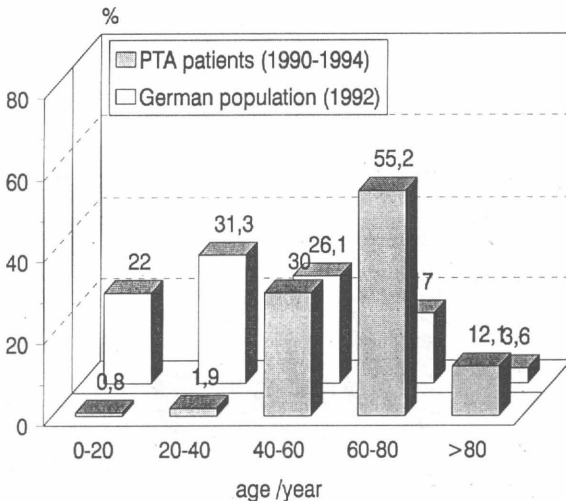


Figure 8: Age distribution of angioplasty patients and of the German population

By using the age-related risk-coefficients for fatal cancer according to ICRP 60 Annex C, the attributable life-time probability of death was converted for the different age groups, as a mean value from both sexes (Figure 9). The mean value for the German population corresponds to the risk coefficient of 5% per Sv as given in the ICRP (fatal cancer, multiplicative model). In relation to 5% per Sv for the average of the population relative risk coefficients were calculated for the different patient groups according to age, as shown in Figure 10. For comparison purposes, Figure 10 also contains the relative value for the working population (4% per Sv).

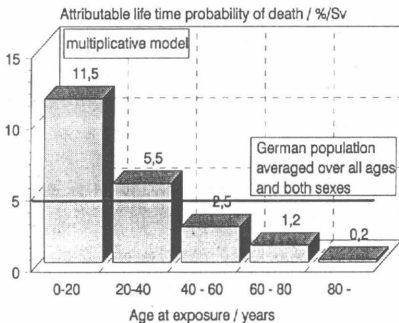


Figure 9: Attributable life time probability of death (ICRP 60, Annex C)

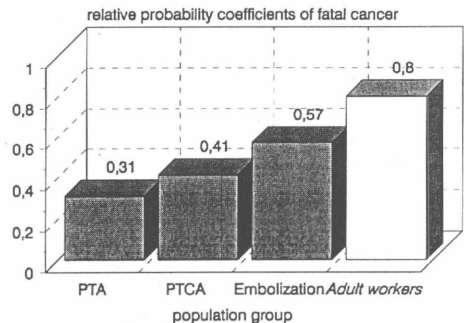


Figure 10: Ratio of the attributable life time probability of death to the ICRP 60 population average (5%)

For imaging during interventional procedures digital subtraction angiography (DSA) is increasingly being utilized. During the years 1990 to 1994 the share of DSA used in angioplasties increased from 51% to 77%, and from 59% to 84% in embolizations.

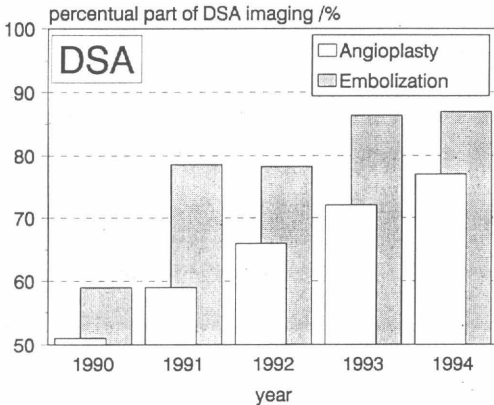


Figure 11: Development of IR in Germany
Imaging of angioplasty and embolization (1990-1994)

times and number of frames were evaluated. Digital imaging was used in all cases. With regard to the radiation exposure, 5 images correspond to 1 minute of fluoroscopy as a rule (see Figure 12). Under consideration of these facts, the coordinates for fluoroscopic time and number of frames are shown dose-weighted.

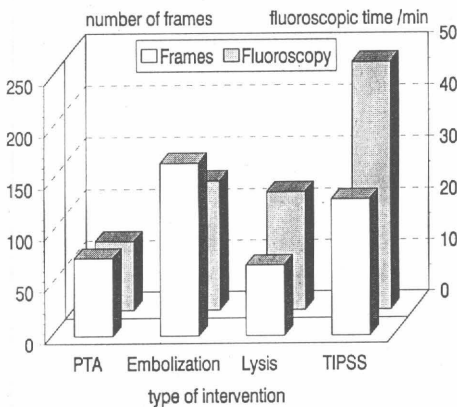


Figure 12: Mean values of number of frames and fluoroscopic time per interventional procedure

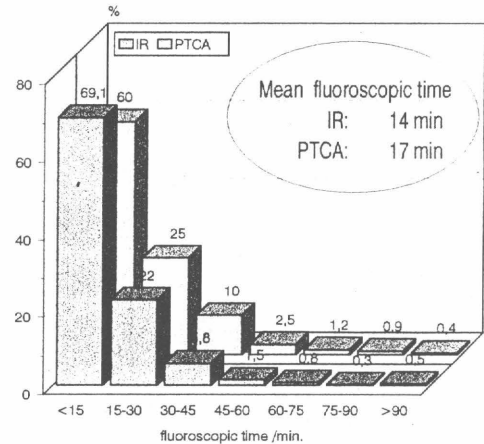


Figure 13: Distribution of fluoroscopic time of interventions in radiology and cardiology

Figure 13 demonstrates the fluoroscopic times of PTA and PTCA. The mean value for PTA is 14 minutes, compared to 17 minutes in PTCA. The higher mean fluoroscopic time in PTCA demonstrates the higher share of measures with long fluoroscopic times. Having a look at the development of the mean fluoroscopic time within the past 5 years, it becomes obvious, that it has increased from 13 minutes in 1990 to 15 minutes in 1994. Also the share of interventional procedures in radiology requiring fluoroscopic times of over 30 minutes, but

In the biliary system and in the genito-urinary tract CT and ultrasound are being employed in 1 to 3% of all cases. In contrast to the biliary system, where the share of DSA rose from 14% (1990) to 45% (1994) it did not exceed 10% in the genito-urinary tract. Figure 11 demonstrates the development of imaging during angioplasty and embolizations within the past 5 years. In biopsies and drainages the proportion of CT (40%) and ultrasound (30%) is relatively high. Over two third of all PTCAs are currently performed with DSA equipment. Especially in cardiology and neuro-radiology, 2-plane systems are preferred in new installations. On the example of 4 types of intervention performed in 14 large German hospitals the mean fluoroscopic

less than 60 minutes increased from 6 to 9% during the years 1990 to 1994. Procedures with fluoroscopic times exceeding 60 minutes increased from some 1.2% to 2% during the same time period. About 0.5% of all interventional procedures involve fluoroscopic times exceeding 90 minutes. Table 1 shows the distribution of all the fluoroscopically-guided interventional techniques. These values may help in estimating the magnitude of deterministic effects to the skin.

Table 1: Development of the distribution of fluoroscopic time of IR and the mean value of fluoroscopic time.

year	number of patients			mean fluoro time
	total	30'<t<60'	t>60'	
1990	4,781	6.4%	1.4%	13.1 min
1991	6,118	6.1%	1.1%	12.4 min
1992	7,348	7.1%	1.8%	14.1 min
1993	8,331	8.3%	1.7%	14.3 min
1994*	4,061	8.8%	2.1%	15.0 min

The mean fluoroscopic times of the interventional techniques in question have to be determined on the basis of data from 16 large German hospitals frequently performing these techniques. Figure 14 shows the corresponding mean fluoroscopic times of angioplasties performed in 1994. Median and mean values are nearly equal at 14 minutes. The quotient from maximum to minimum fluoroscopic time is about 3. When further differentiating angioplasties into those performed in the legs and the pelvis/the abdomen it turns out that both the median third quartile and the maximum value for legs is higher than that of the pelvic and abdominal area. Opposing the mean fluoroscopic time from 16 hospitals in the years 1991 to 1994 inclusively, it reveals that the 3rd quartile has increased from 16.9 minutes to 18.1 minutes, and also the variations between maximum and minimum fluoroscopic time has risen from 2.6 to 3.3. Figure 15 shows the distribution for embolizations, for comparison. As can be seen, both the third quartile and the maximum value are distinctly higher than for angioplasties. The ratio of maximum to minimum fluoroscopic time in embolizations is 6. On the basis of these data and by application of the mean dose-area product per minute dose reference values can be given.

* data incomplete 0.5% of all patients t>90 min

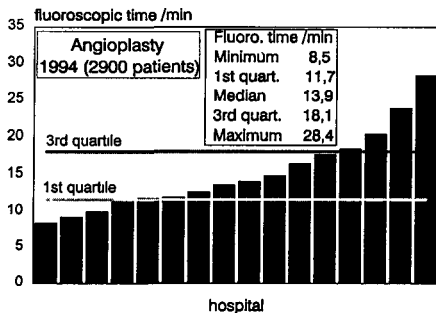


Figure 14: Distribution of mean fluoroscopic time of angioplasty at 16 German hospitals

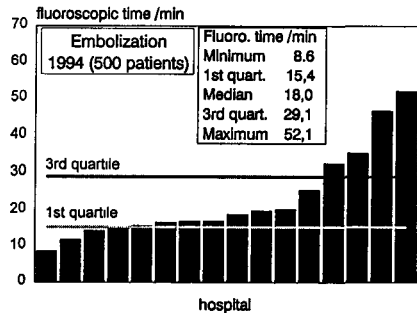


Figure 15: Distribution of mean fluoroscopic time of embolization at 16 German hospitals

Besides the important variations of the mean fluoroscopic time, for instance for angioplasties performed in different hospitals, also the x-ray units shown significant deviations of their dose characteristics. The dose rate at the image intensifier entrance at equal image intensifier diameters and equal modes of operations (PTA in the pelvis) shows a variation in the range of a factor of 4 for two groups each of devices from different manufacturers. Also in measure-

ments on phantoms, the DAP varies by a factor of more than 3 for comparable image intensifier diameters and examination modes.

Dose measurements on patients:

DAP and ESD in PTA are shown in Figure 16 and Table 2, comparing DSA equipments to conventional x-ray units. The data were obtained from measurements on about 100 patients. While the mean fluoroscopic time does only slightly differ for both devices the mean DAP and the ESD are clearly higher for the DSA units. A comparison of this results with the literature published in the past years proves, that the mean values of our results are representative. The DAP in PTAs is influenced by two factors, i.e., the fluoroscopic time and the number of frames (see Figure 12). The significant variations of both the DAP and the ESD depending on the fluoroscopic duration can be attributed to several causes. The mean dose rate at the patient's skin surface was about 15 mGy per minute during the fluoroscopy mode. However, in the course of the intervention the dose rate was switched several times from high dose rate to normal dose rate modes of operation. A precise analysis of the data proved that in the DSA mode the image intensifier format was more significantly varied. The number of images increased in average with the fluoroscopic time. A significant correlation between high ESD and the number of frames was not found. Last but not least it has to be pointed out, that different physicians were operating the two units. The physicians emphasized their opinion, that the radiation exposure to the patient were lower at the DSA equipment, compared to the conventional equipment.

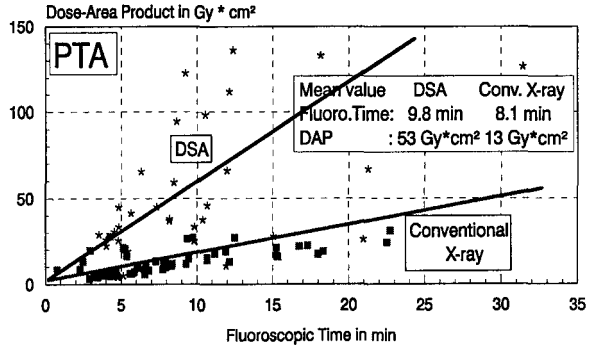


Figure 16: Dose-Area-Product in dependence on fluoroscopic time of PTA procedures performed at DSA and conventional x-ray units

Table 2: Patient exposure values of PTA performed at DSA and conventional x-ray unit (100 patients)

PTA	Fluoro. time min		DAP Gy*cm ²		ESD mGy	
	DSA	conv.	DSA	conv.	DSA	conv.
Mean	10	8	53	13	400	200
DSA/conv.	1.2		4.4		2	
Min	4	1	5	3	30	50
Max	35	25	140	30	1500	500
SD	6	5	40	7	400	100

the average patient as a basis, the result is 5×10^{-4} . The risk of PTA in the leg is lower by a factor of 10.

- The contribution of interventional radiology to the total of radiation exposure to the German population due to the data obtained is estimated at 50 μ Sv currently (2.5%).
- The permitted maximum dose rates to the personnel are limited by the doses set for the hands and the eyes. While in other radiological methods these values are unlikely to be achieved, this cannot be excluded for the interventional radiological techniques.

The investigations performed have demonstrated the need for action in this field. An optimization will include improvements of the equipment and better training of the personnel and physicians performing the and assisting at interventional procedures. As to technical improvements of the equipment, the following has to be discussed:

- optimum beam filtration
- last image hold
- increase of the kV (optimization!)
- pulsed fluoroscopy (optimization of the pulse sequences)
- visual indication of the integral DAP
- display of the high level mode of operation and limitation of the same
- estimation of the ESD for fluoroscopic times exceeding a given limit
- optimization of the protective shields for the personnel.

All these technical measures can, however, not replace appropriate education and training of the physicians, enabling them to make use of the possibilities for dose reduction as provided by the different equipment. A prerequisite for these interventions is, of course, that physicians properly select the indications. An important task for the near future must be to make the persons involved in interventional techniques aware of the high doses occurring in the course of these interventions. Dose reference values may be a help on this way.

Of course, it should not be forgotten, that interventional procedures in radiology are an alternative to operations which in general are associated with considerably higher risk. Interventional radiology is capable of improving the quality of life of many patients, by means of comparably little invasive methods.

Publications

Maccia C., E. Neofotistou, R. Padovani, E. Vano, M. Wucherer, Patient doses in interventional radiology, BIR-CEC meeting, London, December 1993.

Schmidt Th., M. Wucherer, E. Zeitler, Überblick über die Strahlenexposition bei interventionellen Maßnahmen in der Röntgendiagnostik, Tagungsband 25. Wissenschaftliche Tagung der Deutschen Gesellschaft für Medizinische Physik e.V., Erfurt 1994, S. 250-251

Schmidt Th., M. Wucherer, Patient and staff dose measurements of DSA, Tagungsband 26. Wissenschaftliche Tagung der Deutschen Gesellschaft für Medizinische Physik e.V., Würzburg 1995, S. 140-141

Schmidt Th., M. Wucherer, E. Zeitler, Radiation exposure related factors in the different techniques of interventional radiology, Tagungsband 26. Wissenschaftliche Tagung der Deutschen Gesellschaft für Medizinische Physik e.V., Würzburg 1995, S. 138-139

Dose measurements on the personnel:

The dose measurements on the personnel which were carried out parallel to those on the patients are shown in Table 3. The values measured at the head, the fingers, the body and the feet vary significantly in dependence on the fluoroscopic time. A better correlation can be achieved by dependence on DAP. The mean values measured on the personnel working at conventional or DSA equipments differ in a similar way as the mean values of the DAP. In relation to the dose limits for personnel according to ICRP 60 the head and the hands are the most exposed parts of the body in PTA procedures. At both working places no additional protection shields were installed between patient and physician.

Table 3: Exposure values of the physicians, who performed PTA at DSA and conventional x-ray unit

PTA	Body* / μ Gy		Head / μ Gy		Finger / μ Gy		Foot / μ Gy	
	DSA	conv.	DSA	conv.	DSA	conv.	DSA	conv.
Mean	90 (3)	20(0.7)	70	25	220	50	180	70
DSA/conv	4.5		2.8		4.4		2.6	
Min	10(0.4)	5(0.2)	3	4	20	5	10	6
Max	380(13)	110(4)	300	150	1600	320	1600	390
SD	90	24	70	33	320	85	310	90

Discussion and Conclusion

The justification of an interventional measure is strictly associated with the likelihood of success of this treatment. The analysis of benefit versus risks has to consider mainly the risk of complications of such an intervention, compared to that of alternative surgical treatments and to potential risks, if the disease remains untreated. The risk of radiation exposure is in general very low and not decisive in such cases.

The potential of complications as a result of an interventional procedure depends partly also from the demands to the quality of images acquired for monitoring of the procedure. With regard to this, an optimization from the radiologist's view means, that the image quality is as good as necessary, and that the radiation exposure to patient and personnel is as low as feasible.

Also to the interventional therapeutic measures the principle for radiation protection as formulated by the ICRP in 1970 applies: "As Low As Reasonably Achievable".

The investigations performed and the results permit for the following conclusions:

- The mean entrance surface doses justify the EU's interest in interventional radiological procedures
- In about 0.5% to 1% of all interventions fluoroscopic times of over 90 minutes were observed. Considering the corresponding doses, deterministic injuries to the skin can be expected.
- From the mean identified DAP of 100 Gy x cm² per intervention an effective dose of about 30 mSv (for example in the pelvic region) can be anticipated. These values were calculated on the basis of the conversion factors according to NRPB report 262. On this example, and using the average risk coefficient of 1.5% per Sv for PTAs in the pelvis of

Head of project 2 : Dr. Maccia

II. Objectives of the reporting period

- a) to continue to collect patient dose data related to cardiac interventional radiology procedures (PTCA and coronography) ;
- b) to contribute to the establishment of reference values representative of the radiological risk of the patient.

III. Progress report achieved including publications

According to the preliminary results of the phase I of the study carried out on a small sample of patients undergoing cardiac IR procedures (10 adult and 10 children) and in agreement with the conclusions commonly drawn by the other laboratories participating to the project, a more appropriate dosimetric methodology was used to better estimate the dose received by patient during the such procedures.

This consists in performing two different types of measurements simultaneously for the same patient during the whole procedure : the dose-area-product (DAP) and the surface dose in the most irradiated area of the body.

In such a way, DAP measurement results may be used as an indicator of the patient stochastic risk level while the surface dose may provide an estimate of possible deterministic effects.

For each cardiac IR procedure, the DAP was measured using a calibrated transmission ion chamber (Diamentor) installed as close as possible to the x-ray tube housing while the surface dose was measured using four TLDs placed over, under and on both sides of the perimeter of the most irradiated patient volume. For comparison purposes the sum of the four dose values obtained was used as surface dose indicator (SI).

Three university hospitals were involved in this phase of the study and 120 cardiac IR procedures (79 coronography and 41 PTCA) were monitored according to this methodology.

Additional information was also collected concerning the protective devices used by medical (cardiologists) and paramedical (radiographers) staff during a cardiac IR procedure.

The overall results of the study confirmed the general trends already observed in the first phase:

- a) the diamentor readings markedly varied among the considered patients ;
- b) cardiologists's preferred techniques were significantly different depending on the patient pathology and interfered with the fluoroscopy screening time and cine frame rates employed.

The Table 1 details the results obtained for the two examination categories considered.

Type of procedures	Sample size	Diamentor readings cGy.cm ²	Mean value cGy.cm ²	Median value cGy.cm ²	3rd quartile value cGy.cm ²
PTCA	41	1889 - 32643	9179	7309	13307
Coronography	79	1559 - 56778	7429	5779	8438

Table 1 : Statistical data on cardiac interventional radiology procedures.

Unfortunately, complete information about the level of radiological risk cannot be univocally deduced from DAP values since it depends on the body area irradiated.

In cardiac IR procedures, which involve several different beam projections, the surface dose indicator (SI) allows a reasonably precise determination of the patient surface dose if the TLD are suitably positioned. An intercomparison of the individual TLD readings (anteriorly or posteriorly positioned) may indeed provide a valuable information which can be used for optimising the adopted medical protocols.

An example of the individual assessed SI values related to 79 coronography patients examined in three hospitals is illustrated in the Figure 1. As it can be seen, only a small number of procedures lead to very high dose levels to the patient. Such a result highlights the need for the establishment of a reference dose value above which deeper investigations should be performed.

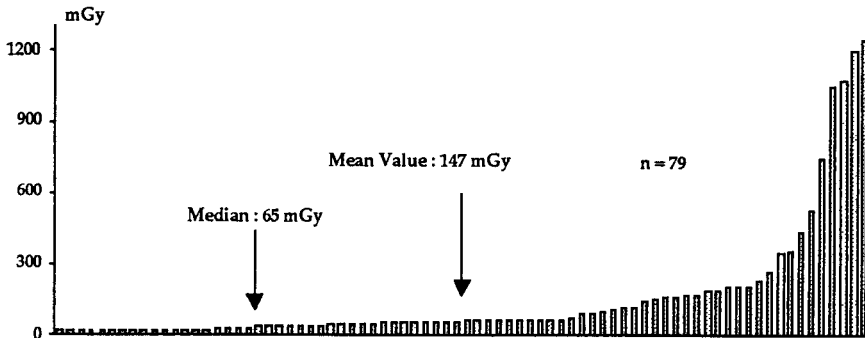


Figure 1 : Individual surface dose indicator (SI) for coronography.

Publications :

Head of project 3: Dr. Padovani

II. Objectives for the reporting period

Interventional Radiology (IR) represents one of the most recent applications of modern imaging technology in radiology and in many cases it substitutes surgical intervention. The aim of the project is to evaluate type and frequency of neuroradiological interventional and invasive procedures performed in Italy and relative patient and staff doses.

III. Progress achieved including publications

Introduction

In neuroradiology, important diagnostic procedure is diagnostic arteriography which is an established, safe and accurate method of evaluating vascular disease. However, diagnostic arteriography is an invasive procedure with a small but definite risk of complications and in some cases high dose levels for patient and staff are reported. Due to the varying skill levels and training of physicians performing arteriographic procedures, the potential exists for variation in success rates, complication rates, diagnostic study quality and patient and staff doses. A diagnostic arteriogram is defined as the result of percutaneous passage of a catheter or needle into an artery under fluoroscopic guidance, followed by injection of contrast material and imaging of vascular distribution in question using serial film or digital imaging systems. Interventional Radiology (IR) is part of invasive methods of diagnostic radiology. The aim of such radiological procedures is not only diagnosis but moreover therapy of diseases. Invasive neuroradiology includes also diagnostic and therapeutic procedures of the spinal column.

An European group started in 1993 the evaluation of practice and doses in all types of interventional radiology. Common methods have been adopted in order to collect comparable data in the participating European countries. In Italy a collaboration with the Neuroradiological Italian Society and Bracco society has been established.

Methodology

The evaluation of type and number of interventional procedures performed in neuroradiology departments in Italy was made adopting a questionnaire developed in collaboration with Italian Association of Neuroradiology and in accordance with the other participants to the project. The questionnaire includes two parts:

A) A part to be filled for each procedure with information on patient, patient pathology and invasive: angiography, biopsy, mielography or interventional: embolisation, chemotherapy, angioplasty, nucleolysis procedure performed. For each patient the following data have been collected:

1. region of the body interested by fluoroscopy and radiography
2. catheters, contrast media and accessories used

3. technical radiological parameters adopted: number of films, film sizes, number of sequences, no. of exposures/sequence, fluoroscopy time, mean kV and mA and total time of the procedure
4. type of x-ray equipment used
5. number and qualification of staff involved.

B) A second part more general concerns the activity of the department. Data on the number and type of procedures performed in the last years, type and characteristics of x-ray equipment installed and number and qualification of the personnel.

A dosimetric procedure for the evaluation of patient and staff doses during the procedure was also developed in collaboration with the other partners in the project:

A) Staff dose is evaluated measuring the dose received by each operator for each procedure using two thermoluminescent dosimeters (TLD): one fixed over the apron at collar level and the other on the most exposed hand. In this report the results are reported in terms of surface doses.

B) Patient dose evaluation. Due to the variability of direction, position and field size of the beams and the intense use of fluoroscopy during the procedure, Dose Area Product (DAP) is the dosimetric quantity suitable for patient dose evaluation and chosen for the purpose of the study. From information on part of the body irradiated and direction of beams, organ doses can be derived per each procedure using appropriate conversion factors derived from MC simulations on mathematical anthropomorphic phantoms. TL dosimeters are also used in some procedures for surface dose evaluation of the most irradiated patient volume.

The reliability of the transmission ion chambers used for DAP measurements and the TLD system have been periodically checked to assure the precision of results obtained. Transmission chamber calibration was performed at each installation, while TLD system checks and calibration at each annealing procedure. The dosimetric system was also tested in the Neuroradiological department of Udine hospital for the evaluation of patient dose from Chemonucleolysis and Nucleoaspiration interventional procedures. Testes and breast dose were evaluated for 15 patients with TLD measurements while other organ doses were derived from DAP measurements.

Quality control measurements have been also included in the study with the purpose to evaluate the performance level of the radiological equipment used in the procedures.

Results

The frequency study has been performed collecting information on 4611 procedures in 12 Italian neuroradiological departments for a period of 18 months (from June 1993 to December 1994). Table 1 presents the number of procedures evaluated, the relative frequencies and the mean patient age and weight. Owing to the low frequency of some procedures, the patient data were useful in the dosimetric survey for a correct patient dose evaluation.

Table 1. Neuroradiological procedures performed in 12 Italian neuroradiological departments. Characteristics of procedures collected from June 93 to December 94. Data reported are mean values and SD (in brackets).

<i>Procedure</i>	<i>N.</i>	<i>%</i>	<i>Patient age</i>	<i>Patient weight (kg)</i>
Angiography (art)	3092	67.0	52.3 (16.5)	68.7 (13.9)
Angiography (ven.)	307	6.6	69.9 (8.1)	71.9 (12.0)
Biopsy	24	0.5	53.7 (15.3)	65.0 (12.9)
Embolisation	318	6.9	42.9 (17.7)	65.9 (14.8)
Chemotherapy	272	5.9	52.2 (12.3)	73.5 (11.1)
Angioplasty (Dilation)	61	1.3	62.0 (11.5)	71.3 (10.3)
Thrombolysis	10	0.2	61.0 (18.8)	70.5 (8.3)
Discography, nucleotomy	324	7.0	42.1 (12.9)	71.7 (12.5)
Mielography	81	1.8	52.0 (15.5)	71.3 (13.2)
Saccoradiculography	101	2.2	51.1 (13.8)	74.6 (14.2)
Cisternography	21	0.5	49.4 (17.8)	69.4 (15.7)
total n.	4611	100	53.5	70.3

Table 2 reports mean values, SD (in brackets) and median of relevant radiological parameters adopted in the sample of invasive neuroradiological procedures. Data show that high number of DSA sequences and long fluoroscopy time is necessary in some invasive (mielography) and interventional procedures (embolisation, angioplasty and thrombolysis).

Table 2. Mean values, SD (in brackets) and median of relevant radiological parameters adopted in the sample of invasive neuroradiological procedures.

<i>Procedure</i>	<i>No. of DSA sequences</i>		<i>Fluoroscopy time (min)</i>	
Angiography (art.)	8.4 (5.1)	8	10.5 (9.2)	8.0
Angiography (ven.)	6.5 (1.6)	6	4.8 (3.0)	4.0
Embolisation	16.7 (9.6)	14	44.7 (28.1)	40.0
Chemotherapy	4.0 (2.7)	3	6.1 (8.7)	5.0
Angioplasty (Dilation)	7.1 (4.3)	6	18.0 (11.4)	15.0
Thrombolysis	7.0 (3.7)	7	25.9 (27.3)	15.0
Discography, nucleotomy	2.5 (1.4)	2	5.8 (5.4)	5.0
Mielography	10.0 (8.0)	8	2.6 (3.8)	2.0
Saccoradiculography	6.2 (1.9)	6	2.6 (2.3)	2.0
Cisterography	3.5 (2.1)	3	1.2 (1.4)	0.7

In the dosimetric survey, measurements on 207 invasive procedures in 4 neuroradiological departments have been performed and table 3 presents the Dose Area Product (DAP) values measured. For low frequency procedures the values reported have to be considered only as a first crude estimation of patient exposure. The distribution of individual DAP values for angiographic procedures is shown in figure 1; the distribution does not exhibit a normal shape for the fact that data came from different departments and the large distribution of values can be explained by differences in performance of x-ray equipment, training of specialists and technical and methodological parameters used.

Table 3. Mean, SD (in brackets) and median values of patient dose expressed as Dose Area Product (DAP) measured in 207 neuroradiological invasive procedures.

Procedure	No	Dose Area Product (Gy.cm ²)		
		Mean (SD)	Median	Maximum value
Angiography art.	117	116.3 (125.6)	80.7	1043
Angiography ven.	9	62.1 (23.6)	53.8	109
Embolisation	26	248.5 (213.4)	178.0	942
Chemotherapy	33	18.9 (12.4)	17.1	57
Angioplasty	9	71.8 (41.0)	68.0	129
Discography	13	41.6 (27.8)	27.8	109

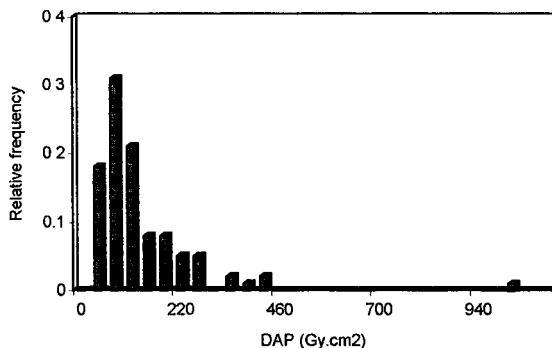


Figure 1. Distribution of individual DAP values for angiographic procedures performed in 4 neuroradiological departments.

Table 4 reports the mean dose per patient evaluated for the radiologist. The radiologist is the most exposed specialist in neuroradiological invasive and interventional procedures. In particular nucleotomy, interesting the patient spinal column, represents the more irradiating procedure. The same set of values have been obtained for nurses and radiographers, for these specialists mean doses evaluated are generally lower of a factor from 3 to 10.

Table 4. Mean, SD (in brackets) and maximum dose values to the body and the most exposed hand of radiologists, (body dose is called the surface dose measured over the apron at the level of the neck) measured on a sample of neuroradiological procedures.

Procedure	Radiologist dose				
	No.	Body (mGy)	Body max. value (mGy)	Hand (mGy)	Hand max. value (mGy)
Angiography art.	105	0.070 (0.049)	0.221	0.081 (0.073)	0.515
Angiography ven.	5	0.031 (0.060)	0.058	0.015 (0.015)	0.036
Embolisation	12	0.120 (0.109)	0.402	0.232 (0.287)	1.150
Chemotherapy	32	0.056 (0.036)	0.166	0.072 (0.042)	0.172
Angioplasty (Dilation)	9	0.088 (0.035)	0.145	0.147 (0.126)	0.377
Discography, nucleotomy	15	0.308 (0.209)	1.189	0.370 (0.306)	1.044

Discussion

The study has evidenced that invasive and interventional neuroradiology procedure are techniques that can imply high exposure level for the patient and the staff. Analysis of data have not evidenced clear correlation between patient dose, staff doses, and performance of x-ray equipment. More complex dependencies, including methods for the procedure, protecting equipment used, individual pathologies or diagnostic requests and training of specialists, have to be investigated.

In particular, some unresolved questions have to be better studied and defined in the future:

- a) more extensive studies are necessary for a better patient and staff evaluation, mainly in low frequency procedures;
- b) dosimetric quantities more appropriate for risk (stochastic and non-stochastic) evaluation in IR have to be better defined;
- c) the concept of reference dose values have to be introduced;
- d) characteristics of optimal equipments and protective devices for invasive procedures have to be defined with the purpose to improve image quality and reduce patient and staff doses;

Finally, quality assurance and training programmes for specialists involved in invasive and interventional radiology have also to be defined and implemented for an effective improvement of the practice and for patients and staff protection reducing unnecessary doses.

Publications

1. C. Maccia, R. Padovani, et al., Patient doses in interventional radiology, CEC-BIR Workshop: Radiation Protection in Interventional Radiology, London, Dec. 1993
2. R. Padovani et al., Dose al paziente e agli operatori nelle procedure invasive di neuroradiologia: risultati preliminari, Congr. naz. di neuroradiologia, Oct. 1993, Taormina (Italy)
3. R. Padovani, Patient and staff doses in invasive and interventional neuroradiological procedures, Course on RP and QA, CIEMAT, Madrid, 1994
4. R. Padovani, G. Contento, M. Floreani, Patient and staff doses in invasive and interventional neuroradiological procedures, 9th European Congr. of Radiology, March 1995, Vienna (Austria)
5. R. Padovani, New trends in patient protection, Int. Conference on Radiation Protection and Medicine, June 1995, Montpellier (France)
6. A. Fadone, M. Floreani, R. Padovani, Dose al paziente ed agli operatori nelle procedure neuroradiologiche interventzionali ed invasive, XI Congr. Nazionale TSRM, Sept 1995, Pescara (Italy)
7. R. Padovani, New Italian legislation and initiatives for the quality assurance in diagnostic radiology, September 1995, Salamanca (Spain)
8. R. Padovani, G. Contento, M. Floreani, A. Fadone, Dose al paziente e agli operatori nelle procedure invasive ed interventzionali di neuroradiologia in Italia, XXIX Congresso della Associazione Italiana di Radioprotezione, Sept 1995, Trieste (Italy)

Head of project 4: Prof. Vañó Carruana

II. Objectives for the reporting period.

* Establishing contacts with Spanish professional Interventional Radiology (IR) societies, organization and evaluation of two national Radiation Protection (RP) trials jointly organized with these societies.

* Evaluation of occupational doses in some IR rooms and for specific IR procedures.

* Analysis of patient dose data (dose-area product) as a function of the examination type, x-ray equipment used, etc, for optimization purposes and in order to establish future European comparisons.

* Proposal of a methodology to evaluate radiological patient risk in centres where a dose-area product meter is not available, using thermoluminescent dosimeters and the surface dose indicator.

III. Progress achieved.

National Trials on Radiation Protection in Interventional Radiology.

Formal contacts have been established with the Spanish Society of Vascular and Interventional Radiology (SERVEI) and with the Section of Hemodynamics of the Spanish Society of Cardiology, asking for its collaboration in the project. Two national surveys have been carried out dealing with certain aspects of Radiological Protection on Interventional Radiology (IR).

Spanish Society of Vascular and Interventional Radiology.

The main results from the surveys performed between the SERVEI fellows were as follows:

1) Nearly 30% of the SERVEI members (38 professionals) have answered the questionnaires. Some 4900 data have been collected and processed aiming to know the current status of the installations and the current opinion of the IR specialists.

2) A handicap in RP knowledge is recognised in above one third of the questionnaires, with respect to the level considered suitable to practice the specialty.

3) Concerning the modernity of the IR facilities used by the answerers, a trend to the renewal of old equipment is clearly observed: in 56% of the cases, the age of the x-ray equipment is less than five years. However, there is still a 22% of equipment over fifteen years old.

4) Referring to the x-ray tube position, 33% of the rooms keep overcouch systems, what is

consistent with the equipment older than fifteen years.

5) With respect to the image system, 26% of the facilities lack in digital acquisition capabilities.

6) Concerning the opinion of the specialists on risk prevention, solely 70% consider that the installations are updated. A number of installations about 20 to 30% in which workers feel that the radiation risk is greater than desirable and over the half of the answers consider necessary to build in more protective elements in equipment design.

7) In that refers to the question about detailed knowledge of all the operation capabilities of their respective equipment, a 60% of the answers believe necessary a more complete information on using possibilities.

8) In relation to elements for external protection available in installations, in 40% of the cases are felt not sufficient. Concerning dosimetry, 22% of the answers consider it unsuitable. Dosimetric control of arm/shoulder is only performed in 18% of the cases and in 69% of the cases for hand dosimetry. It is possible to find in 8% of the installations some workers without personal dosimeter.

9) About important irradiation incidents, they have arisen in 6% of the installations.

10) From the 38 answers, 37 feel that endeavours to improve the RP should be reinforced, likewise to advance in the knowledge of the values of doses imparted to the patients.

This is one of the main results of the survey. In fact, the belief of the IR specialists in respect of RP is to improve the knowledge about risks assumed by themselves and by patients with the aim of improve the use of the protective goods available and to develop patient protection strategies.

11) About interventional rate per specialist, the majority of them (86%) perform between 2 and 5 interventions a day. Assuming an averaged value of 4 interventions a day for the members of the SERVEI and 200 days of work in the year, 130 specialists must perform some 104000 studies annually in Spain (there not including those carried out by other professionals not members of the SERVEI)

12) Thought the half of the specialists which answered the questionnaires have more than two years of experience, the percent with an experience between 2 and 5 years is high, that means an important number of new radiologists is joining the specialty and every effort developed in training programmes is going to have a quick outcome in good RP practice.

13) About the subject of RP training, 75% consider that continuous training for the installation staff would be helpful. A percent between 18 and 31% think that there are workers without sufficient training in RP.

14) Almost all the installations have maintenance contracts, though nearly 40% of them do not have quality control programmes implemented and the results of maintenance actions usually are not known.

As a result from the study, the SERVEI is pondering the following actions:

* To encourage continuous training RP programmes for IR specialists and to review the current RP training programmes which run during the residence period.

* To demand the renewal of equipment more than 15 years old and overcouch x-ray tube, and to promote the inclusion of protection and dose control devices in the facilities.

* To improve the information level to make the IR specialists aware of the potential risks of their installations and of the need of using protective means.

* To ask the manufacturers after capabilities and operation performance of their IR equipment.

* To analyze the causes of accidental irradiations and to publish them in restricted reports or in the scientific literature.

* To encourage collaboration with the RP units, to ask for hand and arm/lens dosimetric control when suitable, and lend attention to the dosimetric results.

* To encourage cooperation in patient dose evaluation programmes and in national and European trials. To encourage and facilitate the quality control of equipment, to lend attention to the results obtained and to carry out a follow up of the correcting measures proposed.

Section of Hemodynamics of the Spanish Society of Cardiology.

In the case of this Society, the survey pamphlets were distributed in the sessions of the 1994 National Congress of the Hemodynamics Section. A total of 41 filled questionnaires were received, which comprised opinions from 61 facilities. In this case, some 6100 data have been collected.

Answers of a given specialist related to several rooms (where he works) have been treated separately, as individual questionnaires from different professionals.

Results are fairly similar to those above commented, albeit some differences appear in the following items:

1) 51% of the answers (against 30% of the specialists which are radiologists) consider RP knowledge not sufficient to exercise the specialty.

2) In 25% of the cases, available elements for external protection are considered not sufficient (versus 40% in the other survey). Dosimetric control is also felt unsuitable in 30% of the cases (against 22% between radiologist specialists).

3) Answers of installations reporting cases of some workers which do not use lead apron (10%); articulated shielding (26%), though it is available; leaded glasses or lens protectors (67%), or protective gloves (74%).

4) Reported average values of interventions daily carried out are one intervention (21%); between 2 and 5 (75%) and 2 specialists perform over 5 interventions a day.

5) 72% of the answers refer to professionals with over 10 years of experience, 13% between 5 and 10 years and 15% between 2 and 5 years.

6) Almost all the answers show the opinion that, from the RP view, it would be convenient to know the dose ranges presumably imparted to patients and those received by the specialists themselves.

Training activities in Radiation Protection.

Four pilot training courses about RP on IR were organized for medical specialists and for nursery and auxiliary staff on December 1993 and 1994, following the list of teaching objectives of the EC VALUE programme, and implementing a list of new specific objectives for the interventional radiology practice.

Also an invited refreshing course about Protection in IR has been imparted at the 9th European Congress of Radiology, Vienna (Austria), March 5-10, 1995.

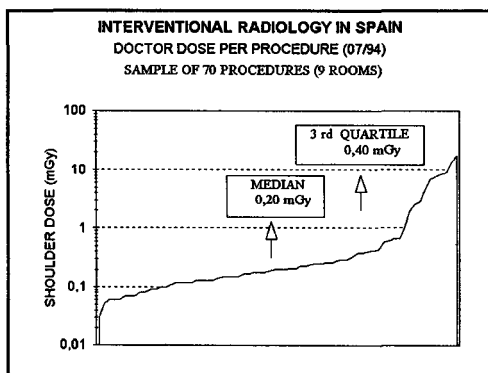
Occupational doses.

About 100 individual evaluations of the dose received by staff per examination have been carried out (placing between two and twenty dosimeters for each evaluation), therefore about 1000 measurements of occupational doses have been analysed.

Due to the wide variety of intervention types, equipment, room designs, different IR specialists and different number of centres to be potentially evaluated in a pilot programme, two different types of procedures have been implemented, having both of them worked out satisfactorily. Within an extended procedure, ten pairs of TL crystals were used, placing them at different positions on the specialist who performed the intervention (arm, forearm, left hand, right hand, neck, the forehead, left goggle arm, right goggle arm, shoulder and one for control). Protective means used by personnel were registered (lead goggles, mobile screen, lead gloves, etc). Alternatively, a simplified procedure was used where the staff was only controlled by shoulder and hand dosimeters.

As a matter of fact, the risk level is extremely variable and depends on multiple parameters (examination type, equipment characteristics, protective devices used, patient peculiarities, number of monthly interventions, specialists' experience, previous training on radiological protection, etc), for that reason, it is difficult to foresee the dose level received by this staff.

It is also proved that the main factors to reduce risk are the training and knowledge of the specialists on RP and the systematic use of protective devices as mobile screens and lead gloves. In centres with old equipment and high working loads the dose limits could be easily surpassed in case of



do not systematically use protective devices.

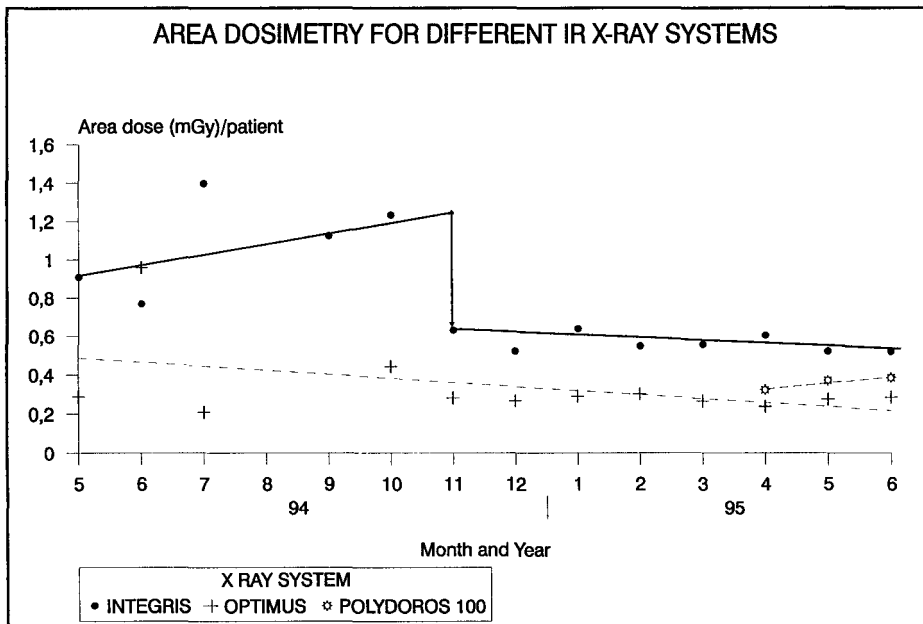
The figure above shows a plot of the measured dose values in the shoulder of the specialist in a sample from 9 different IR rooms.

A summary of results from a centre is presented in the next table.

OCCUPATIONAL RISK IN HEMODYNAMICS. MEASURED DOSES ON SHOULDER			
WITHOUT PROTECTIVE MOBILE SCREEN		WITH PROTECTIVE MOBILE SCREEN, USED DURING 80% OF THE INTERVENTION TIME	
MONTHLY VALUES BETWEEN 20 - 100 mSv	2 mSv PER PROCEDURE (RANGE 1-5)	MONTHLY VALUES BETWEEN 1 - 40 mSv	0,3 mSv PER PROCEDURE (RANGE 0,1-0,5)

In the interventional cardiology rooms from one of the centres where the evaluation has been specially complete, occupational dose values which can be considered typical of hemodynamics rooms are registered. Shoulder measured doses (over the leaded apron) for specialists with the highest workload (50-100 monthly procedures) range between 0.2 and 0.3 mSv per intervention. The determination comes from daily individual dosimetric controls, using calibrated TLD chips. In this circumstance, shoulder doses ranging between 15-30 mSv/month are usual, that makes essential the use of leaded glasses and articulated shieldings.

Using a Philips Integris 3000 equipment, dose on shoulder in a given room keeps reasonably close to 0.05% of the patient entrance dose (in this equipment, a transmission ion chamber continuously stores the dose-area product).



By using electronic personal dosimeters (Siemens-NRPB, model EPD1) merged on the C arm of the x-ray equipment, comparative studies have been also made about environmental radiation levels in different IR systems, as a function of the workload. The above figure shows the results obtained with a Siemens Polydoros 100, basically used for interventional vascular radiology, and two Philips, Optimus and an Integris 3000. Plots present the averaged area dose value per patient and procedure (registered by the dosimeter merged to the C arm, at some 70 cm from the centre of the scatterer volume and at some 30° measured from the horizontal plan, to downwards). The Philips Integris 3000 system shows higher values due to the use of copper filters in the beam (up to 0.4 mm in thickness) to reduce patient doses. The sharp decrease in the trend shown in this equipment corresponds to a maintenance intervention in which filter configuration was changed.

Patient dosimetry.

A pilot programme for patient dose evaluation in Interventional Radiology has been started in Spain. The difficulty of obtaining large samples for some studies, together with the problem of limited human and material resources, has made it necessary to form groups including different types of interventions, despite the negative effects this has on comparisons. The Medical Physics Group (MPG) of the Complutense University tries to achieve a consensus in working meetings with the IR Societies involved, to group the different types of interventions with regard to patient dosimetry, and to indicate what might be the most representative examinations for a programme that will make comparisons at the national and European level.

The practice of Interventional Cardiology (IC) in Spain is well known through the Spanish Society of Interventional Cardiology (SECI) annual reports. In 1993, IC was practised in 65 centres with 81 rooms, carrying out a total of 50,000 diagnostic procedures (617 per room and year); of these, 75% were coronary angiographies. This figure represents 1.28 diagnostic procedures per 1000 inhabitants per year. The total number of therapeutic coronary procedures during 1993 was 8687 (15% of the procedures carried out in cardiac catheterization rooms) and, of these, 88% are percutaneous transluminal coronary angioplasties (PTCA) (in Spain about 200 PTCAs per million population are carried out per year). About 17% more IC procedures were accomplished in 1993 than in 1992.

Figures for non-cardiac IR are less well known because it is performed in many rooms devoted to conventional radiology, even by professionals not members of the SERVEI.

The DAP was measured using a transmission ion chamber. As well, the surface dose of the most irradiated patient volume was measured with thermoluminescence (TL) LiF Harshaw TLD-100 crystals. In centres that showed interest in participating in the programme but had no transmission chamber available, only the latter method was used.

The surface dose was measured using four dosimeters placed over, under and on both sides of the perimeter of the most irradiated patient volume during the intervention. The sum of the four values obtained was used as a surface dose indicator (SDI) for comparison purposes.

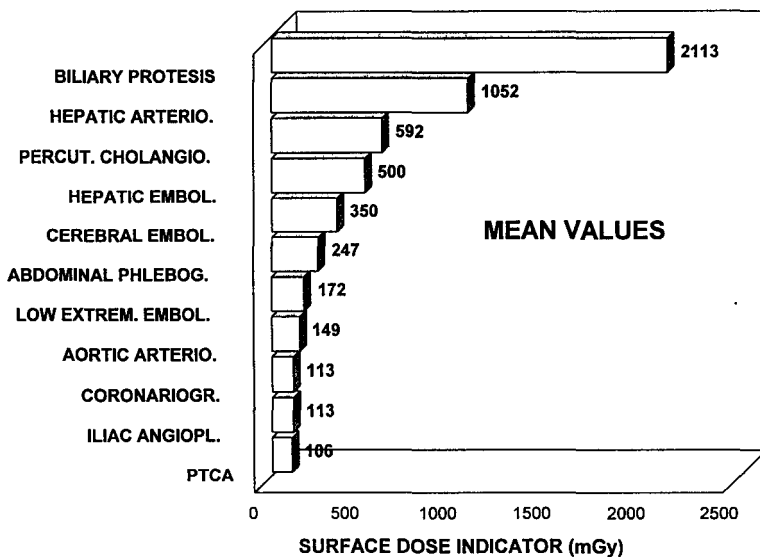
Some 1000 patient dosimetric evaluations have been carried out, using transmission chambers and TL dosimeters. The following table presents the DAP values found for some cardiac and non cardiac procedures, for which large enough samples are available to give statistical

meaning. The results come from five university hospitals (one of them contributing the largest share of the available data), three private and two non-university public centres. All of them have provided data on at least ten patients (in cardiology, in non-cardiac IR, or in both specialties).

PROCEDURE	SAMPLE SIZE	RANGE cGy.cm ²	MEAN VALUE cGy.cm ²	MEDIAN cGy.cm ²	3rd QUARTILE cGy.cm ²
PMV (1)	6	3375-16200	9642	9638	11928
PTCA (2)	45	1275-34535	8750	6675	12226
CORONARIOGRAPHY	288	1160-48233	6651	4575	6928
LOW EXTREM. ARTER.	40	1484-23193	6663	5175	8789
BILIAR DRAINAGE	10	2964-16262	6887	5334	8452
RENAL ARTER.	14	3172-18592	9292	8272	11768
UPPER EXTR. FISTUL.	15	127-2921	871	767	1108
LOW EXTREM. PHLEB.	35	59-4145	294	170	224
CEREBRAL ARTER.	13	1631-13578	6816	7309	8278

- (1) Percutaneous Mitral Valvuloplasty.
 (2) Percutaneous Transluminal Coronary Angioplasty.

The following figure shows examples of SDI mean values measured in some typical interventions.



Estimators such as the surface dose or the DAP, which are easily measured in patient procedures, may constitute a plausible approach to predict or correlate with radiological risk and to serve as an indicative value in optimization programmes. The DAP is an easily available estimate, but full information about the level of radiological risk cannot be deduced directly from its value, since it depends on the body area irradiated. In the case of IR, given the complicated procedures (which can include changes in magnification, focus-skin and focus-intensifier distances, beam orientation, very variable in C-arm systems, and others, during the intervention), it is very difficult to correlate DAP with skin dose.

In interventions with highly localized irradiation (coronary procedures, renal arteriographies, trans jugular intra hepatic porto systemic shunts (TIPS), hepatic embolizations and others) the earlier defined SDI must allow a reasonably precise determination of the patient surface dose, if the dosimeters are suitably positioned. For procedures involving several different beam incidence directions it will be usually possible to distinguish them by comparing the readings of each chip with those of the adjacent ones, that constitutes valuable information for optimization programmes, especially in the analysis of intervention protocols.

PUBLICATIONS

Ruiz, M.J.; Fernández, J.M.; Vañó, E.; Macaya, C. and Bañuelos, C. Cardiac catheterism: dosimetry to a pregnant patient during a percutaneous mitral valvuloplasty procedure. Radiation protection (in Spanish), *Mapfre Medicina*, Vol. 3, pp. 19-24, 1992.

Vañó, E. Trial on Radiation Protection aspects in Interventional Radiology (In Spanish), *Radioprotección*, Num. 1, pp 57-59, 1994.

Vañó, E.; Guibelalde, E.; Fernández-Soto, J.M.; Gallego, J.J. and Hernández-Lezana, A. A preliminary study on radiation protection aspects in interventional vascular radiology (in Spanish), *Radioprotección*. Num. 2, pp 12-20, 1994.

Maccia, C.; Neofotistou, E.; Padovani, R.; Vañó, E. and Wucherer, M., Patient doses in Interventional Radiology. In *Radiation Protection in Interventional Radiology*, pp 39-44. Proceedings of a BIR- CEC meeting held on 6 December 1993. British Institute of Radiology, 1995.

Vañó, E.; Fernández, J.M.; Delgado, V. and González, L. Evaluation of tungsten and lead surgical gloves for radiation protection, *Health Physics*, 68(6), pp. 855-858, 1995.

Vañó, E.; Gallego, J.J.; Fernández, J.M. and Hernández-Lezana, A. Radiation Protection in radiology procedures for haemodialysis accesses interventions (in Spanish). To be published in *Radiología*.

Vañó, E.; González, L.; Fernández, J.M. and Guibelalde, E. Patient dose values in Interventional Radiology, *The British Journal of Radiology* (in press) 1995.

SCIENTIFIC MEETINGS

Vañó, E.; Gallego, J.J.; Fernández, J.M. and Hernández-Lezana, A. Radiation protection in diagnostic and interventional procedures in haemodialysis accesses (In Spanish), IV National Congress on Vascular and Interventional Radiology, Marbella (Málaga), September 1995.

Jiménez, A.; Fernández, J.M.; Guibelalde, E. and Vañó, E. Corrections to registered dose-area product values for their use as risk indicator in diagnostic and interventional radiology (In Spanish), X National Congress of Medical Physics, Salamanca, September 1995.

Vañó, E.; Lezana, A.; González, L.; Fernández, J.M.; Guibelalde, E. and Gallego, J.J. Protection in Interventional Radiology, Invited Refresher Course, 9th European Congress of Radiology, Vienna (Austria), March 1995.

Vañó, E. Practical and regulation aspects on radiation protection in Hemodynamics (In Spanish), Invited lecture, V Annual Meeting of the Hemodynamics and Interventional Cardiology Section, Benalmádena (Málaga), May 1994.

Vañó, E.; Fernández, J.M.; Guibelalde, E.; González, L.; Gallego, J.J. and Hernández, A. First results from a pilot programme of dosimetry in interventional radiology (In Spanish), XXII Congress of the Spanish Society of Medical Radiology, Santiago de Compostela, September 1994.

Maccia, C.; Neofotistou, E.; Padovani, R.; Vañó, E. and Wucherer, M. Patient doses in Interventional Radiology, BIR-CEC meeting, London, December 1993.

Vañó, E.; Fernández, J.M.; Guibelalde, E.; Gallego, J.J. y Lezana, A. An evaluation on the radiation protection status in Vascular Interventional Radiology (In Spanish), IX National Congress of Medical Physics, Tenerife, September 1993.

Velasco, A. and Vañó, E. Radiation Protection in Interventional Radiology, Cardiovascular and Interventional Radiological Society of Europe, CIRSE 92 Annual Meeting, Barcelona, September 1992.

Head of project 5 : Dr. Neofotistou

II. Objectives for the reporting period

1. A survey of type and frequency of Interventional Radiology (IR) procedures performed in Hellas. Patients' age and sex distribution.
2. Dosimetry of patient and staff during IR procedures.
3. Quality Control of the radiodiagnostic equipment used for IR.

III. Progress achieved

The principal goals of the research work are

1. Survey of type and frequency of Interventional Radiology procedures in Hellas Patients' age and sex distribution.

Interventional radiology combines imaging with minimally invasive therapy. The latter generally requires prolonged fluoroscopy time and a series of radiographic images.

An extensive database on the number and type of Interventional Radiology (IR) procedures performed in Hellas during 1990 - 1993 showed considerable increases in all type of procedures (Table I) As it can be seen in Table I, during 1992-93 Percutaneous Transluminal Cardiac Angioplasties (PTCA) have increased by almost 30%, Endoscopic Retrograde CholangioPangreatography (ERCP) by 27% whereas the number of angioplasties in peripheral arteries (PTA) has almost doubled. Moreover, during 1990-93 IR centres have increased from 18 to 29 (centres performing biopsies and orthopaedics not included) whereas the number of physicians increases by about 20% per year. IR procedures in neuroradiology (embolisation, revascularisation head-neck and spine - vertebral canal) and in urology have been recently introduced. In 1993, the most frequent interventions performed were in cardiology with 160 PTCAs and 340 pacemakers per 1 million inhabitants

The sex and age distribution of the patients undergoing all kinds of IR procedures show that males constitute 78% whereas 56% of them aged 41-60 years (Fig.1) For the patients undergoing PTCA the percentages are 90% and 54 % respectively.

Table I. Type and frequency of IR procedures in Hellas

	1990	1991	1992	1993
Angiology	57	100	217	366
Cardiology	2823	3505	4213	5090
Neurology	24	26	46	92
Gastroenterology	900	1050	1500	1940
Urology	23	57	125	210
Orthopaedics	2600	3200	3600	4000
Biopsies & drainages	1600	1900	2500	3100
Stents	-	14	20	66

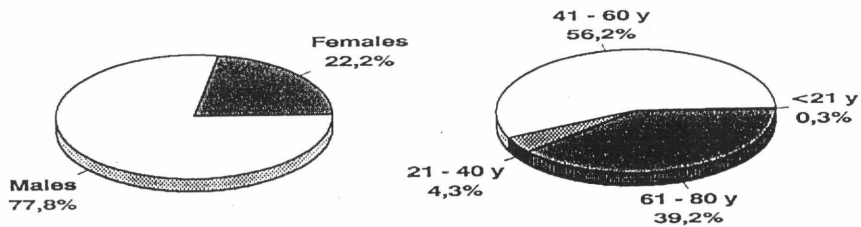


Fig.1. Patients' age and sex distribution

2. Patient dosimetry

2.1 Haemodynamic unit

Since IR procedures in cardiology constitute ca. 35% of the total (PTCAs, insertion of cardiac pacemakers, radiofrequency catheter ablation), emphasis was directed to haemodynamic units. Radiation doses to patients and personnel in actual medical practice were measured in 7 public hospitals in Athens. A flat transmission ionisation chamber was used to determine the energy imparted to the patient since this type of ionisation chamber does not hamper the procedure and its value discounts adequately well for beam quality, fluence and field size. The dose area product (DAP) meter was calibrated in terms of Gy.cm² on every angiographic suite to be measured.

Data concerning IR technique consisted of tube potentials during fluoroscopy and/or cine, image intensifier sizes / projections used, fluoroscopy time and length of film taken, cine frame rate used as well as the way contrast agent was injected (manual or automatic). Patients' dose related characteristics were also recorded (i.e height, weight). An attempt to note the severity of the case was made.

The mean value and standard deviation of DAP, fluoroscopy time and cine film length measured for average-sized patients during PTCA, single-chamber pacemaker insertion, catheter ablation and diagnostic coronary angiography (CAD) are given in the following Table (Table II).

Table II.

	DAP Gy.cm ²	Fluoroscopy time min	Cine Film Length m	No. of cases
CAD	72 ± 5	4.6 ± 1.2	26 ± 6	178
PTCA(+CAD)	93 ± 40	11.5 ± 6	22 ± 12	122
ABLATION	116 ± 78	42 ± 34	-	20
PACEMAKER	32 ± 12	5.2 ± 3.4	-	50

Although CAD is a diagnostic procedure, it was included in the measurements because of the reason that a cardiologist first performs a diagnostic coronary angiography. In case a vessel is found occluded, the patient returns after a period of time in order to have a PTCA when second CAD is performed to re-assess the condition of the vessel. Therefore, the DAP readings measured include the exposures due to PTCA and CAD.

The data collected were subsequently analysed for the 24 cardiologists measured (Fig. 2).

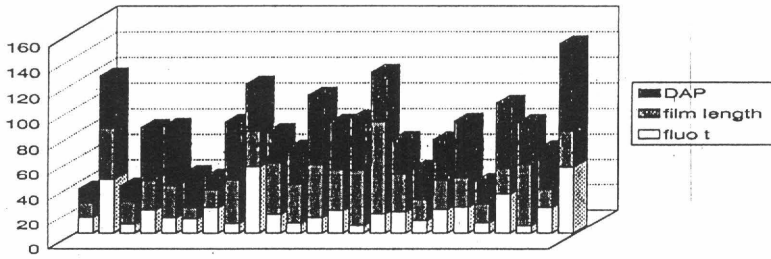


Fig.2 DAP, fluoroscopic time and cine film length per cardiologist

The spread of values noted among physicians is due to variations in examination techniques, physician's skill as well as the severity of the particular case.

As far as the PTCA technique followed is concerned, in all hospitals fluoroscopy was performed with undercouch tubes(total filtration 2.8-3.2 mm Al, 80 kVp). In most cases filming was done at the lowest available frame rate (12.5 fr/s for the digital and 25 fr/s for the conventional units) with the exception of one hospital which used 50 fr/s. The operating dose rates at the entrance of image intensifier in fluoroscopic mode (170 mm mode) varied from 0.35 to 0.85 $\mu\text{Gy/s}$ (variation by a factor of 1.4) whereas the exposure per frame ranged from 0.18 to 0.34 μGy (variation by a factor of 1.9). Four hospitals were equipped with digital units whereas in 3 hospitals contrast agent was injected by a remote control system. The most frequently used projection during fluoroscopy are that of LAO (42.8%) and RAO(35.6%).

Earlier investigators have suggested that systematic registration of fluoroscopy time and length of film taken can effectively assess patient dose. However, our results so far gave no statistically valid equation between DAP reading and the sum of fluoroscopy time and film length.(The linear regression equation derived could apply only to 33 % of the sample). This can be explained by the different technical parameters used (different II sizes, various field sizes etc.) during the procedure.

2.1.2 PACEMAKERS

During the last 3 years a 15% annual increment in the number of the pacemakers inserted is recorded (Table I). The mean values of DAP and fluoroscopy time an experienced cardiologist uses for the insertion of a single-chamber pacemaker are given in Table II. For the insertion of a dual-chamber pacemaker fluoroscopic time is increased by about 20-30%. In case of a trainee the respective fluoroscopic time is 23.5 ± 4.5 .

2.1.3 RADIOFREQUENCY CATHETER ABLATION

Two centres in Hellas offer radiofrequency cardiac catheter ablation and 3 consultants perform about 90 procedures per year. A wide range of values has been noted in the 20 cases assessed(range 5.3-130.0 min) with their mean value and standard deviation given in Table II. Since fluoroscopy time is the longest than in any other IR procedure in cardiology, it should be advisable that the DAP value of each patient is registered in its file in order to estimate possible future problems caused by exposure to radiation .

2.2 ANGIOPLASTIES

Few angioplasties have been measured in "401 Airforce" general military hospital in Athens . The mean fluoroscopy time and number of frames used are given in the following table.

Table III. Frames and fluoroscopic time per intervention

Type of intervention	No. of frames	Fluoroscopy time (min)	No. of cases
PTA (leg)	50	41,7 ± 28	21
liver embolisation	150	47,5 ± 30	8
kidney embolisation	100	28,5 ± 24	5

2.3 GASTROENTEROLOGY (ERCP)

In 1993, twelve centres operated by eighteen gastroenterologists performed about 1600 ERCPs. The mean value and standard deviation for DAP and fluoroscopy time measured during 34 ERCPs in Athens General Hospital are 92 ± 20 mGycm² and 2 ± 0.5 min respectively. In all cases the procedure is aided by a flexible video endoscope which significantly reduces radiation exposure to the patient.

2.4 BIOPSIES

In 1993, about 3100 biopsies(55% liver, 20% kidney, 17% lung and 8% bones) have been performed . The localisation technique used is ultrasound scanner (50%), a computerised tomography (CT)scanner (34%), conventional x-ray system (15%) and MRI (1%). The technique used during 126 biopsies in the CT scanner of Athens General are given in Table IV.

Table IV. Biopsies' technique

Type of biopsy	Technical parameters used	Scanogram performed	Mean No. of slices
kidney	120 kV, 480 mAs	Y	11.3
liver	120 kV, 480 mAs	Y	11.1
lung	120 kV, 208 mAs	Y	18.5

For Philips Tomoscan LX , the average scan dose measured at 0° at the periphery of a 32 cm diam. phantom(120 kV, 150 mA, 1.9 s) equals $3 R \pm 28\%$. The scanogram dose is negligible.

3. Personnel dosimetry performing PTCA

Quantification of personnel exposure is of interest for risk assessment, check of compliance with regulatory dose limits and optimisation of the procedures. The term effective dose is used in order to relate the risk associated with non-uniform exposure to that associated with an equivalent uniform whole-body dose.

The study group consisted of 24 cardiologists performing 92 PTCA's in 7 institutions. The TLD badges used for trunk measurements consisted of an Alnor holder with four elements, two LiF:Mg,Ti. and two CaF₂:Dy chips by Harshaw. A single 3.18mm x 3.18 x 0.89 mm LiF:Mg,Ti. was inserted in a plastic ring for finger dosimetry and a similar one in a protective thin capsule for eye dosimetry. Since TL materials are not capable of measuring low doses in the relevant energy range, radiation doses have been determined by intergrating over 7-10 examinations. All the first hand cardiologists in one hospital shared three TL - dosimeters which were placed outside the lead apron at waist level, on the left hand and at eye level. The dosimeter at waist level was in all cases within the most intense part of the scattered beam. Although the catheterisation team consisted of a cardiologist, an assistant cardiologist, a sterile nurse and a cardiovascular technologist, only the cardiologist was measured since he/she is the one closest to patient's couch. Finally, the protective measures taken in each hospital were noted.

Table V. Personnel doses performing PTCA

Hospital	Eye dose μGy/ exam	Trunk dose μGy/ exam	Finger dose μGy/ exam	Effective dose μSv/exam
“ High staff dose ”	178-200	160-164	191-240	23
“Normal staff dose“	16-45	18-39	38-72	4,6

The effective dose of a physician protected by a lead apron of known thickness was estimated from the reading of the unattenuated gonad dose at 90 kV and lead apron of 0,5 mm Pb equivalent .

As one can see in Table V personnel doses varied because of differences in patient doses and means of shielding used. Although it is difficult to compare results from different personnel radiation studies our measurements could be grouped in 2 categories. In 5 hospitals physicians receive an effective dose of 4.6 μSv per procedure whereas in 2 hospitals the effective dose was five times greater. On further investigation of the techniques followed, this was found because in one hospital cardiologists worked considerably closer to the patient without a lead screen present whereas in the second hospital high frame rate and longer film length was used. Advice on good working practices (frame rate reduction, proper and consistent use of the protective measures available, use of a remotely controlled contrast injection pump etc.) reduced effective doses in the “high staff dose” hospitals by almost 200%.

In 1993, 48 cardiologists performed 1600 PTCA's, their workload varying from 15 to 120 procedures per year. As the PTCA rate is expected to grow worldwide at about 12 % per year, the workload per cardiologist is expected to be increased. Therefore, in the future the radiation exposure of cardiologists should be monitored more carefully in order to assure that workload limits are not exceeded.

4. Quality Control of IR diagnostic equipment

In an angiographic unit, in addition to the measurements described analytically in the protocol for “ The QC of conventional X-ray units “ of the Hellenic Medical Physicists' Association, the cine/spot film was also assessed. In particular the performance of the beam limiting device, exposure rate at the entrance of image intensifier for all the available exposure rates, high and low contrast resolution on the monitor and film and function of automatic exposure control device was checked.

Results on QC of 26 angiographic units (12 conventional and 14 digital) showed that the parameters which were related with image quality were in almost all cases within tolerance limits . However, the parameters concerning patient dose were not as satisfactory The most commonly encountered problems were those of patient entrance skin exposure exceeding in normal mode 5 cGy/min (15%), beam-misalignment (17%) and beam limiting devices not operating properly (18 %) Moreover, 60% of the darkrooms caused high film fogging. Our results demonstrate that although physicians are very much interested in diagnostic image quality in order to make the right diagnosis, their knowledge on radiation protection and equipment performance needs to be improved. Physicians should acquire specific knowledge on the function of x-ray equipment they use and the associated radiation dose rates for each mode of operation.

5. Radiation protection training

A survey carried out on the radiation protection training received by physicians using fluoroscopy showed that only radiologists have appropriate credentials and training Since the awareness of the adverse effects of x-ray radiation will be an important stimulus for the implementation of the ALARA principle, the organisation of physicians' training courses in aspects of ionising radiation is essential

As it can be seen in Fig. 3 , 12 % of physicians never wear their personal dosimeter whereas 30 % of them do never use their protective glasses

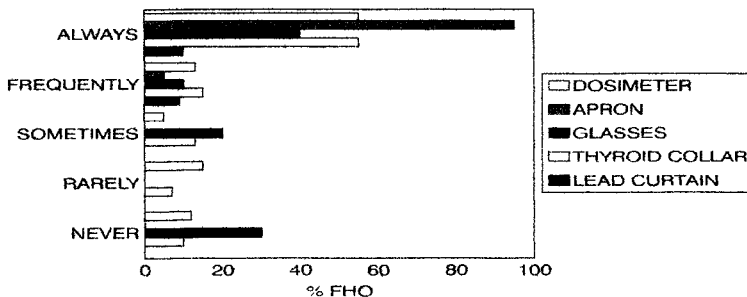


Fig 3 Protective measures taken by the physicians performing IR procedures

Therefore, the Hellenic Ministry of Health and Social Welfare as well as the respective scientific societies have been formally notified about the necessity of organising training courses on aspects of radiation protection

Summary

1. A database on the number and type of IR procedures performed in Hellas during 1990 - 1993 showed considerable increases in the sum total of IR procedures, IR centres and number of physicians. In 1993, the most frequent interventions performed were in cardiology with 160 PTCA's and 340 pacemakers per 1 million inhabitants, PTCA's comprising 35% of the total IR procedures For biopsies-drainages, non ionising imaging techniques was used in 51% of the cases Males constituted 78% of the sample whereas 56% of them aged 41-60 years.

2. Radiation doses to patient and staff in actual medical practice were taken in 7 public hospitals in Athens .Dose area product, fluoroscopy time and cine film length were recorded during PTCA, pacemaker insertion ,catheter ablation,diagnostic coronary angiography and ERCP. The considerable spread of values noted is due to the different examination protocols used,severity of the case, physician's skill and variations in the performance of equipment. In all hospitals undercouch tubes were used and with the exception of one hospital filming was done at the lowest available frame rate . The operating dose rates at the entrance of image intensifier in fluoroscopic mode (170 mm mode) varied from 0.35 to 0.85 $\mu\text{Gy/s}$ whereas the exposure per frame ranged from 0.18 to 0.34 μGy . Physicians' effective dose -protected by a lead apron of known thickness - was estimated from the reading of the unattenuated gonad dose measured with TL-dosimeter. In 5 hospitals physicians received an effective dose of 4.65 $\mu\text{Sv/procedure}$ whereas in 2 hospitals effective dose was 23 $\mu\text{Sv/procedure}$. A questionnaire on the radiation protection training received by physicians using fluoroscopy showed that only radiologists have appropriate credentials and training.

3. Twenty nine X-ray units were checked (58% digital units) according to the protocol of the Hellenic Medical Physicists' Association. The results showed that the parameters related with image quality were in almost all cases within tolerance limits whereas those concerning patient dose were not as satisfactory.Results were presented at the meeting "Radiation Protection in Interventional Radiology" organised by BIR and CEC (London, December 1993) and at 3 Hellenic Congresses held in Athens during 1993-94.

**Final Report
1992 - 1994**

Contract: FI3PCT920013b Duration: 1.9.92 to 30.6.95

Sector C23

Title: Evaluation and management of post-accident situations. Project 1: Data base and decision-aiding techniques.

- | | | |
|----|--------------|---------------------------------------|
| 1) | Després | CEA - FAR |
| 2) | Alonso | Univ. Madrid Politéc. Fundacion Gral. |
| 3) | French | Univ. Leeds |
| 4) | Vanderpooten | Univ. Paris IX |

I. Summary of Project Global Objectives and Achievements

Following an accident with radioactive discharges affecting people and the environment, radiological consequences must be assessed and countermeasures must be proposed. These two points rely heavily on availability and quality of data, imply efficient computer codes and need establishing managerial procedures. The project deals with data acquisition and organization and decision aiding techniques for the selection of appropriate countermeasures. The project is divided in two sections :

a/ The EUROGRID data base

Assessment of doses due to an accidental discharge of radionuclides needs the knowledge of the environment, in terms of populations, livestock and agricultural productions. In order to provide dose assessment codes with such data, European countries are covered with a grid, area of each being 10 000 km². For each mesh of this grid, the following parameters are given :

- population
- land use
- annual agricultural and milk productions
- livestock.

Due to the fact that the gradient of concentrations can be very important in certain meteorological situations, the spatial resolution of this grid is not adequate to calculate the impact of the discharge in the near field of a plant. For this reason each mesh is divided in 100 equal parts and the same parameters are given for each small mesh.

Living habits also influence the doses received after an accidental release, via the inhalation and the external exposure pathways : time spent indoor/outdoor and the nature of building materials have been studied. It clearly appears that at a given place the fraction of time spent indoor strongly vary during the year, and it has not been envisaged to elaborate a data base including the temporal dimension. On the other hand, mean annual values does not dramatically differ from one country to another.

Nature of building material and type of housing is not available in all countries. For Spain and Portugal, the fraction of collective and individual habitations, and their age (old or recent) is given in the data base. For other countries, such data are not available.

The conception of the grid has been done some fifteen years ago and a first data base had been realized at the European Community level. The objectives of the actual contract were .

- to update the former data base on the basis of recent agricultural survey and census;
- to extend the former data base to Nordic Countries and to countries bordering the EC ;
- to introduce other parameters (quantities of collected milk, livestock)

This data base has been realized with close concertation with teams in charge of the development of the RODOS programme.

Grid and data are also available on a format allowing the visualisation on maps, using geographical information systems, as MAPINFO.

a/ The DACFOOD software

Decisions concerning the need to implement countermeasures in case of an accidental discharge of radioactive pollutants, and the selection of the most appropriate action, need a careful examination of several criteria, that can be classified according to two classes :

- the « objective criteria » are those which can be more or less easily quantified. In this category, we have to consider health parameters (doses) and economic parameters (costs of countermeasures) ;
- the more « subjective criteria » as public acceptance.

The relative weight of these criteria depends on the nature of the decision that is needed : during the urgent phase of an accident, doses are of fundamental interest, but as the time after release increases, the management of contaminated foodstuffs needs to be considered and in this case economic and psycho-sociological considerations are of major importance.

Because these two sets of criteria call for different technics and competences, works have been organized according to this classification : IPSN was in charge to provide a decision-aiding tool limited to the consideration of dosimetric and economical parameters and contributions of the Paris-Dauphine University and Leeds University were oriented to the multicriteria analysis, exploring several methods, to deal with the more «subjective criteria ». The final aim of the project was to achieve a global decision-aiding tool including the two parameter categories.

The IPSN has produced a software (DACFOOD) allowing a cost-effectiveness analysis of strategies that can be undertaken in case of foodstuff contamination (a strategy being defined as a set of elementary countermeasures). A scenario has been developed, in order to test the robustness of the system, to verify the consistency of the analysis, and to provide the other contractors with a case study. This scenario has emphasized the need for further work concerning economical data. This software is written in C and can be used independently of acceptance considerations.

A large part of the work conducted by Leeds University was devoted to the comparison of multicriteria analysis methods. During the course of the projet, several kinds of difficulties have been encountered : in particular, the application of outranking methods to the evaluation of countermeasures leads to combinatorial problems, so that the comparison with multi-attribute utility methods cannot be done. The large number of strategies has lead to the development by the Leeds University of a coarse expert system to filter unfeasible strategies. This part of the

contract had been closely turned to the RODOS programme, in which the expert system has been implemented. Leeds University had also produced a report dealing with the global evaluation of the uncertainties, taken into account each module of the code.

In a real case, the number of strategies increases dramatically with the number of groups of population, the number of foodstuffs and of elementary countermeasures. To limit the number of combinations, a multiobjective interactive procedure for supporting the selection of countermeasures has been studied by the Paris-Dauphine University, to define an optimized solution according to « hard constraints » (total amount of concerned foodstuffs, processing capacities,...) and « soft constraints » (maximal acceptable cost, minimal reduction dose required,...). These constraints can be modified by the user during the decision process. This procedure has been tested on a scenario provided by the IPSN.

Difficulties encountered have demonstrated the need for further works in different fields. For this reason, it had not been possible to carry out the final objective of the contract (the elaboration of a software dealing both with dosimetric and economic aspects and with public acceptance).

Head of project 1: Dr. Després

II. Objectives for the reporting period

a/ The EUROGRID data base

The objective during the reporting period was first to merge the data collected and organized by the Univesitat Politecnica Madrid and IPSN, and to second transmit them to the NRPB for implementation in the RODOS programme. These data are available as ASCII files (the requested format for RODOS), but are also available on a format usable for a graphical software, as MAPINFO.

b/ The DACFOOD software

The IPSN task in that field was to provide a decision support system in the case of contaminated foodstuffs following an accidental release of radionuclides, limited to the consideration of economical and dosimetric parameters. After calculating the potential impact of the release due to the ingestion pathway, the system elaborates several strategies (a strategy being defined as a set of elementary countermeasures), estimates the effectiveness (in terms of dose reduction) and the cost of each, and suggests a classification based on the cost effectiveness ratio.

III. Progress achieved including publications

a/ The EUROGRID data base

The objective of the EUROGRID data base is to provide the authorities in charge of risk assessment and management with basic data allowing the calculation of individual and collective doses due an to accidental discharge of radioactive pollutants

Western Europ and Nordic countries are covered by a grid, the meshes of wich having the same area : 10 000 km². For each mesh, the informations concern :

- population
- land use
- annual agricultural and milk production
- livestock.

In order to improve the precision, especially near a discharge site, each mesh is divided in 100 small meshes, the area of each one being 100 km². The same informations are given for small and large meshes.

data sources

populations

For each country of concern, data have been obtained from the national statistics services, as a list of municipalities and the population in each. These data have been coupled with informations issued from national geographical services, that are geographical coordinates of the municipalities. Doing that way, the amount of data for each country is sufficiently large to provide a very good representation of the population density, even in the small meshes. The number of municipalities, for each country, and the reference year are given in the table A1 below.

	number of municipalities	reference year
Luxemburg	118	1989
Italy	8098	1989
Netherlands	672	1989
France	36567	1991
Spain*	8000	1991
Portugal*	243	1991
Belgium	580	1990
Switzerland	2907	1990
Ireland	703	1986
United-Kingdom	**	1991
Germany	**	1987
Denmark	1484	1989
Greece	**	1991
Sweden	284	1991
Norway	440	1992
Finland	455	1993
Austria	2404	1990
Hungary	1027	1991
Slovakia	**	1991

* work carried by the Universidad Politecnica Madrid

** results given in the final form by the authorities. This data is unknown

Table A1 : basic data for the constitution of the population data base

The other parameters

It is not possible to obtain the same level of detail with the other parameters than with the populations data, for two main reasons :

- The agricultural survey does not exists in all countries at the municipality level. When these data exists, a large number of informations is omitted, in order to protect the confidentiality. More precisely, when the number of producers for a given product is less than three in a municipality, the produced quantity for the product is not given ;
- Quantities given in the EUROGRID data base are always associated to a reference year. At the municipality level, these productions can dramatically change from one year to another and then it is necessary to use data corresponding to a higher administrative level in order to guarantee that the validity of informations will persist over time. This last point has been verified by studying the statistics for some productions during 10 years in France and in Belgium. Results of this study are given in the table A2 below. For these reasons, the basic data are issued from regional survey, as communicated by national statistics services or as published in the EUROSTAT documents.

	mean value	maximum value	minimum value	standard deviation	selected value
cereal production in Belgium from 1980 to 1991 (1000 tons)	353.1	390.1	315.1	19.1	315.1
cereal production in France from 1981 to 1992 (1000 tons)	9441	9723	9060	232	9342
oleaginous production in Belgium from 1981 to 1991 (1000 tons)	4.2	7.4	2.4	1.5	5.5
number of pigs in Belgium from 1977 to 1990 (1000 heads)	5477	6440	4935	559	6426
number of pigs in France from 1977 to 1990 (1000 heads)	11472	12275	10764	472	11518

table A2 : temporal variation of some parameters at the nation level

Table A3 below gives the list of agricultural items which exist in the EUROGRID data base. For each of these items and each country, tables A4 to A6 give the reference year. The selection of this reference year results from a compromise between the completeness and the age of the data.

items	Code
Number of dairy cow	01
Number of other cow	02
Total number of cattle	03
Production of cow's milk	08
Production of wheat	10
Production of barley	12
Production of cereals	13
Production of oleaginous	15
Production of sugar beetroot	16
Area of green fodder	17
Production of potato	20
Area of grassland	25
Area of permanent crops	26
Area of wheat	30
Area of barley	32
Area of cereal	33
Area of oleaginous	35
Area of sugar beetroot	36
Area of potato	40
Area of forest	50
Area of arable land	51
Agricultural area using	55
Total agricultural area	56
Number of piglet (weight under 20 kg)	60
Number of piglet (weight between 20 and 50 kg)	61
Number of piglet (weight over 50 kg)	62
Total number of pig	63
Total number of sheep	64

table A3 : list of items

COUNTRY	08	10	12	13	15	16	17	20
Germany	92	91	91	91	91	91	91	91
France	92	92	92	92	92	92	92	92
Italy	92	89	89	89	89	90	89	89
Netherlands	92	92	92	92	92	92	91	92
Belgium	92	90	90	90	90	90	91	90
Luxembourg	92	90	90	90	90	90	90	90
England	92	91	91	90	85	90	88	91
Ireland	92	90	90	90	90	89	88	89
Denmark	92	91	91	91	90	91	91	91
Greece	86	91	91	91	91	91	90	91
Spain	93	91	91	91	91	91	90	91
Portugal	92	88	88	86	89	88	87	88
Austria	94	94	94	94	94	94		94

table A4 : reference year for milk and agricultural productions

COUNTRY	25	26	30	32	33	35	36	40	50	51	55	56
Germany	91	91	91	91	91	91	91	91	89	91	91	89
France	92	92	92	92	92	92	92	92	92	92	92	92
Italy	89	88	89	89	89	89	88	89	88	88	88	88
Netherlands	91	91	92	92	92	92	92	92	85	91	91	91
Belgium	91	91	91	91	91	91	91	91	91	91	91	91
Luxembourg	90	89	90	90	90	90	90	90	90	89	89	90
England	88	88	91	91	91	91	89	91	89	88	88	89
Ireland	88	88	90	90	90	90	90	89	90	88	88	90
Denmark	91	91	91	91	91	90	91	91	91	91	91	91
Greece	87	91	91	91	91	91	91	91	84	91	91	90
Spain	90	90	91	91	91	91	91	91	90	90	90	90
Portugal	87	87	88	88	90	89	87	88	88	88	88	89
Austria	90		90	90	90	90	90	90	90			

table A5 : reference year for land use

COUNTRY	01	02	03	60	61	62	63	64
Germany	90	92	92	90	90	90	90	90
France	89	89	92	88	88	88	88	88
Italy	91	91	91	91	91	91	91	91
Netherlands	92	92	92	92	92	92	92	92
Belgium	90	90	90	90	90	90	90	90
Luxembourg	89	89	89	89	89	89	89	89
England	92	92	92	92	92	92	92	92
Ireland	89	89	91	89	89	89	89	89
Denmark	90	90	90	90	90	90	90	90
Greece	90	90	90	90	90	90	90	90
Spain	89	89	89	89	89	89	89	89
Portugal	91	91	91	91	91	91	91	91
Austria	94						93	93

table A6 : reference year for livestock

A subroutine allows to calculate the contribution of each region in each large mesh (in term of surface). Then, the annual production are weighted in order to give the production from each large mesh. To assess land use and agricultural productions at the small meshes level, it has been assumed a uniform distribution inside large meshes, excepted when large meshes are crossed by a frontier or a coast. In this case, the number of small meshes covered by sea or by a foreign country has been graphically determined.

b/ The DACFOOD software

The DACFOOD software is devoted to the evaluation of countermeasures that can be envisaged after the radioactive contamination of agricultural productions. The aim of this software is to provide the decision makers with a cost effectiveness analysis of the different strategies.

Input data

Before running the code, the user must characterize the environment by defining areas (as much as necessary) in which products are uniformly contaminated. For these areas, the user introduces the number of inhabitants (adults, children and infants), the nature and the amount of contaminated products and the contamination level of these products, radionuclide by radionuclide. This means that measurements of the foodchain contamination are available. Then the input data are the contaminations of the foodstuffs, as measured, but the software can also be used with the ground contamination as an input data. In this case, the model use transfer factors which depend on the growing state of the plant.

Doses due to external exposure and to inhalation are not calculated in the software, but they can be introduced by the user in order to estimate the relative contribution of the ingestion pathway.

The user must also decide if he wants to take into account interventions levels. The CEC intervention levels are suggested as default values, but the user can introduce any other level.

Resident data

Two kinds of data are included in the software :

- data that cannot be modified by the user : transfer factors between soil and agricultural production, dose factors (sievert per becquerel ingested), effectiveness of countermeasures, CEC intervention levels, ICRP recommendations, radioactive half-lives (19 radionuclides are available). When the number of inhabitants, the agricultural production or the livestock in the vicinity of the release are unknown, the user can call a data base, issued from the EUROGRID data base, and which gives these parameters around 53 European nuclear sites.
- default values that can be changed during a working session and which are automatically restored after the session : consumption rates for the three age classes and for each category of foodstuff, cost of countermeasures (per unit of weight) By default, the model considers that the annual consumption is equally issued from all the areas defined, but the user can specify that all the consumed products come from a given area.

Output data

The programme calculates individual and collective effective doses and thyroid doses due to each radionuclide, for each contaminated foodstuff and for each group of population defined, in the case where no countermeasure is implemented. It gives a diagnostic on the acceptability of concentrations in foodstuffs (considering intervention levels when this option has been selected), and on the opportunity to implement countermeasures (with respect to ICRP recommendations on the averted doses). When intervention levels are considered, the software calculates the duration of the ban. Finally, the user can define some strategies (by exemple to decontaminate milk from an area and to destroy green vegetables produced in an other area, or to transform milk to butter in an area and to delay slaughtering in an other one,...) or run a subroutine which creates automatically all the possible strategies. In this last case, rules can be implemented to limit the number of strategies, as an exemple a rule to eliminate strategies leading to a resulting dose higher than intervention levels. The final output is a list of the strategies created, the cost and effectiveness of each.

Dose calculation

Foodstuffs are grouped in six categories : milk, leafy vegetables, root vegetables, cereals, fruits and meat. Integrated ingested activity is calculated according to the following assumption .

milk

It is known that concentrations in milk increase during the three first days following the deposition of radionuclides, and then decrease according to an exponential law. Dates of the deposition and of the measurements are given as input data. As a consequence, concentrations in milk can be calculated at any time, and also the integrated activity during the first year.

other foodstuffs

Concentrations in foodstuffs at the time of harvest (or slaughtering) depend on the delay between deposition and harvest, and on the delay between harvest and consumption. Then, the concentrations are calculated using transfer factors that are function of the growing stage at the deposition time. There is no continuous function to calculate these transfer factors as a function of time, but discrete values are tabulated. To illustrate this method, transfer factors for caesium in leafy vegetables are given in table B1 below :

Deposition date as a function of the growing stages *	Transfer factors (Bq.kg ⁻¹ per Bq m ⁻²)
1) deposition on the soil	10 ⁻³
2) after the raising of the seeds (approximatively 1 week later)	10 ⁻²
3) after the full grown of the plant (approximatively 1 to 2 weeks later)	10 ⁻¹
4) by the time of harvest	0 2

* : total duration of stages : one month

table B1 : Caesium transfer factors to leafy vegetables

Countermeasures

A list of 14 elementary countermeasures (with their cost and effectiveness) is available in the software ; however the user may add (and modify the characteristics of) any other countermeasure. The countermeasures are as follows :

- milk : decontamination, transformation to butter or to cheese, transformation to cream or to skimmed milk
- vegetables : washing, peeling, storage (300 days)
- cereals : milling, storage (400 days)
- meat : feeding with uncontaminated feed, storage (20 days or 700 days)

The cost of a countermeasure is defined either by :

- a fixed component, as cost for decontaminating an installation devoted to the treatment or the storage of contaminated products (exemple : cost to decontaminate a dairy) ;
- a component proportionnal to the quantity, as storage of wastes, transport of products, substitution, etc...

The main difficulty not solved yet, deals with economical aspects, namely in two cases :

- It is difficult to estimate the global cost of the transformation of a product (milk to butter) when countermeasure leads to an increase in the value of the product (when the value of the transformed product is higher than the value of the initial product) ;
- it is also difficult to suggest any countermeasure (destruction excepted) when there is globally an overproduction and when large amounts of the product are stored.

Besides, the contamination modify the economical parameters, so that the cost of a product (and then the cost of a countermeasure) will be modified by the accident : consumers can reject the global production of an area or refuse transformed products...Their is at that time no way to deal with these questions.

The DACFOOD software run on a PC computer equipped with a 80386 microprocessor. It is written in C for Windows, and a run time version is available on request. Both the software and the user's guide are available in French and in English.

Head of project 2: Prof. Alonso

II. Objectives for the reporting period

- Collection of data from Spain and Portugal for the updating of the EUROGRID database, based on the most recent surveys available in national statistics offices. The data are referred to land use, agricultural production, demographic information and housing characteristics.
- Preparation and execution of adequate procedures and programmes for the distribution of the collected data in the European Grid, both in the large (10 000 km²) and in the fine (100 km²) meshes.
- Documentation of the procedures followed for the processing of the data.

III. Progress achieved including publications

In the first part of the reporting period (September '92 - August '93), the most substantial part of the data sets about land use, cultivated areas, agricultural production, livestock and demographics (including number of employees by economic branches) were gathered. In the first and also in the second period (September '93 - May '94) several procedures and programs were developed in order to process these data. The objective was to aggregate them in the categories considered in EUROGRID and to distribute them in the two levels of the European grid. The period from June '94 to May '95 was dedicated to the collection and treatment of data about housing and buildings.

SPAIN

The following sources were used:

- the results of the Agricultural and Livestock Census performed in 1989, were acquired as a magnetic tape from the *Instituto Nacional de Estadística*. The file, with

almost 500,000 records, contains detailed information of land use, cultivated areas and number of heads of livestock for the approximately 8,000 municipalities of peninsular Spain and the Balearic Islands.

- the Agricultural and Livestock Yearbook (1989) published by the *Ministerio de Agricultura, Pesca y Alimentación*, which provided the amount of crops and yields of production of milk.
- the production of dairy products, provided by the *FENIL*, a national association of producers.
- a file with the geographic coordinates and total area of the municipalities, acquired from the *Instituto Geográfico Nacional*.
- the population census of 1991 and the report "*Renta Nacional de España y su distribución provincial*" published by the Bank of Bilbao-Vizcaya, which contains the number of employments classified by economic branches in each province (NUTS III).
- data about buildings and housing, provided by the *Instituto Nacional de Estadística* in the level of aggregation of provinces, from a Census performed in 1991.

Land use and cultivated areas in the cells of Spain were assigned according to the fractions of the total area given in the Agricultural Census for the municipality located in the cell. Cells not having a municipality lying inside its boundaries were assigned to the largest of the closer municipalities. Cells having more than one municipality were assigned to the largest of them.

The production of the different crops considered is calculated using the cultivated areas. Two average yields (one for irrigated and one for non-irrigated lands), corresponding to the province of the municipality assigned to the cell, were calculated based on the provincial productions.

The number of heads of livestock appearing in the Census for each municipality was assigned to the cell where the municipality lies according to its coordinates. The amount of milk and dairy products were assigned to the same cells than the animals that produce the milk, according to the total provincial production and the numbers of heads in the cell.

The population of each municipality was assigned also to the cell where the municipality lies. Number of employments in each activity branch were distributed according to the provincial figures and the population in each cell.

Buildings were grouped in three classes: single family houses, non-individual familiar houses and rest of buildings, and each class splitted in "old" (finished before 1960) and "new" (finished after 1960). Only provincial data were available, and the distribution in the cells of the grid was made according to the population of each cell.

PORTUGAL

The data obtained were:

- the results of the General Agricultural and Livestock Census (1989) for the 66 agricultural zones in which the peninsular Portugal is divided, including land use, cultivated areas and livestock.
- the amounts of agricultural produce in every agricultural zone, extracted from the Agricultural Yearbook for 1989 published by the *Instituto Nacional de Estatística*.
- the distribution of employment in regions (NUTS II) and branches of activity.
- data about housing corresponding to the Census of 1991 for the more than 200 councils, acquired from the *Instituto Nacional de Estatística*, as well as an update of the population figures.

No information about the geographical location of the agricultural zones and the councils was available in an easy-to-read fashion, and consequently it had to be looked up by visual inspection on the maps. Each cell was assigned to an agricultural zone, and the councils, which show in some zones a remarkable level of geographical disaggregation, were associated to with one or two cells. Also an usable area (not corresponding to the sea or to Spain) was assigned to each cell.

The fractions of the total area of the agricultural zone corresponding to the different land uses and cultures were applied to the usable area of the cells assigned to that zone. The areas calculated were also used to estimate the amounts of crop produced in each cell by means of an average yield for each zone.

The number of heads of livestock and the amount of milk and dairy products were distributed in the cells of a given agricultural zone according to the usable area of the cells.

The population of a council was allocated to the associated cell(s). The number of employments in the different branches, available only for regions, was distributed proportionally to the population of the cells.

The data about buildings from Portugal come from an enquiry about housing, and for this reason buildings without any use for habitation are excluded. In a similar way to the Spanish case, the buildings were classified in individual houses, buildings mainly for housing with 2-4 dwellings and rest of the buildings. The splitting between "old" and "modern" buildings was made with the same criterion than for the Spanish buildings.

Publications:

All the programmes and procedures used for the previously mentioned tasks are documented in the following reports:

- Jiménez F., Gallego E. *Distribution of Portuguese Data in the European Grid*. CTN-44/94, Madrid, 1994.
- Jiménez F., Martín J.E., Gallego E. *Distribution of Spanish Data in the European Grid*. CTN-44/94, Madrid, 1994.
- Jiménez F., Gallego E. *Distribution of Data about Buildings from Spain and Portugal in the European Grid*. CTN-31/95, Madrid, 1995.

Head of Project 3: Prof. French

II. Objectives for the reporting period

The original application had the following aims.

- 1) Input on the use of multi-attribute value/utility methods for comparison with the outranking methods used by Professor Roy. The research would focus particularly on exploring the perspective offered by the methods. It is suggested that decision makers should be offered as wide a range of informative perspectives as possible on their problems so that they can appreciate their choices more clearly.
- 2) The development of the decision conferencing approach to use in these circumstances. Note the term *decision conference* is used more generally here than it has been elsewhere, where it has been confined to the use of multi-attribute value methods. Here the term is used to cover any group meeting at which decision aiding techniques are used to help structure and inform decision making. We would attempt to trial the approach with groups of decision makers – or, at least, groups from the radiation protection community who understand the issues well enough to act as proxies for the decision makers.
- 3) At Leeds we have developed an approach to sensitivity analysis which applies to any decision aid for problems with a finite number of alternatives. We can experiment with this approach in the context of decisions in post accident situations, where more than ever there will be a need to test the robustness of decisions.”

Originally the research contract was scheduled to complete at the end of May 1994: however, a supplementary contract, awarded in 1993, extended the period to the end of June 1995. In applying for the extension, Leeds proposed the following.

The work would build upon the methodological understanding currently acquired and being acquired on multi-criteria decision aiding in the context of decision making after a radiation accident. In particular, it will focus on decisions relating to long term countermeasures and the methodology and procedures for providing understanding to senior government officials and politicians.

In the event of a major incident, decision making over the first few days will be supported by systems such as RODOS. By and large, decisions will be greatly constrained by pre-existing guidelines and reference levels. Moreover, decision making in the first few days will take place at a local level. However, after a few days it will be necessary to involve more senior decision makers and to decide policy on long term countermeasures. There will be a need to ‘bring them up to speed’ and to ensure that they take full responsibility from a position of clear understanding. Methodology for enabling this has been partially trialled by the Nordic Co-operation Group¹

III. Progress achieved including publications

Direction of Research and Development

During the course of the project, the work at Leeds moved much closer to the needs of the RODOS system and away from the original objectives. This occurred for a number of reasons.

- Combinatorial problems encountered in applying outranking methods to the evaluation of countermeasures rendered the approach intractable. Hence the comparison with multi-attribute utility methods fell by default.

¹ See S. French, O. Walmod-Larsen and K Sinkko (1993) ‘Decision Conferencing on countermeasures after a large nuclear accident: report of an exercise by the BER-3 group of the NKS BER Programme’ RISØ-R-676(EN) RISØ National Laboratory, Roskilde, Denmark..

- Staffing problems at CEA, our co-ordinator within the European consortium, resulted in only one scenario being developed for analysis.
- It became clear from work elsewhere within the RODOS project that, while decision conferencing and the associated modelling for long-term countermeasures still needs further investigation and development, there is a pressing need to consider decision analytic support for decisions on precautionary countermeasures when there is a threat of an accident.

Achievements

Multi-attribute evaluation methods

A conceptual description of the use of multi-attribute methods during all phases of an accident has been written (French, 1996). This draws upon earlier work in the International Chernobyl project and the Nordic Co-operation Group as well as developing an exemplar analysis for the evaluation of food countermeasures in a scenario developed during the current project by CEA. This exemplar analysis was undertaken using the PC-based resource allocation software EQUITY.

However, although the EQUITY algorithm would probably scale to deal with a full sized problem, it is difficult to modify it to treat some of the constraints that are implicit in the evaluation of countermeasures. Thus the approach proposed is to use a *coarse expert system* to filter out strategies which are clear infeasible in a number of senses: e.g. radiologically, practically, and politically. These would then be evaluated using conventional multi-attribute value and utility methods and finally a more detailed expert system might be used to explain the recommendations to decision makers. This proposal has been written into the conceptual framework for uncertainty handling and data assimilation within RODOS (French, Ranyard and Smith, 1995) and forms an entirely coherent package with the other proposals.

Constraint management coarse expert system

The issue of identifying which packages of countermeasures satisfy feasibility and other constraints together with the certain combinatorial problems are being overcome for multi-attribute value techniques through the use of constraint management logic programming. The coarse expert system is being developed using these techniques to filter out clearly infeasible packages before evaluation takes place. These methods have been prototyped to check computational feasibility (Cunningham, 1995) and will be further developed and implemented in for future versions of the RODOS system.

The HERESY software

A simple additive multi-attribute evaluation module (HERESY) has been written to form part of the ESY module in RODOS. This allows visual interactive sensitivity analysis of a comparison of countermeasure strategies. HERESY is ready to be fully integrated into the RODOS system in its current form; however, it has been written in a highly modular form and can be configured to fit into RODOS in a number of ways, thus supporting decision making in all phases of an accident.

Multi-attribute modelling for precautionary measures in the event of a threat of an accident.

Since late 1994, Leeds has been working with KfK, the University of Mannheim, SCK/CEN, NRPB and CEPN to trial RODOS for decisions on early countermeasures

with groups of emergency planning officers. This work is funded under CEC contracts SUB94-F15-028 and SUB94-F15-045. The purpose is to identify what attributes are important to decision makers and hence to specify any of the outputs of CSY submodules and the displays from ESY and HERESY in particular. Although this work is still continuing, it is clear from two exercises in Germany that decision support for the case when there is a threat of an accident is very difficult. The problems involve many factors, but particularly the issue of equity of treatment of different population groups. On the basis of this information we have, within the context of the research reported under surveyed the literature, found little help there and developed a preliminary form of analysis based upon event conditional multi-attribute modelling (French, Halls and Ranyard. 1995; French Harrison and Ranyard, 1995).

Publications

In Refereed Journals and Proceedings

S. French (1996) "Multi-attribute decision analysis in the event of a nuclear accident." *Journal of Multi-Criteria Decision Analysis* 5 (in press)

Technical Reports

S. French, E. Halls and D.C. Ranyard (1995) "Equity and MCDA in the Event of a Nuclear Accident". RODOS(B)-RP(95)03

S. French, M.T. Harrison and D.C.Ranyard (1995) "Event conditional attribute modelling in decision making on a threatening nuclear accident." School of Computer Studies, University of Leeds. RODOS(B)-RP(95)04

S. French, D. Ranyard and J.Q. Smith (1995) "Uncertainty in RODOS." Research Report 95.10, School of Computer Studies, University of Leeds. Available by connecting to WWW at file://agora.leeds.ac.uk/scs/doc/reports/1995 or by anonymous ftp of the file scs/doc/reports/1995/95_10.ps.Z from agora.leeds.ac.uk. RODOS(B)-RP(94)05

S. French, N. Papamichail, D.C. Ranyard and J.Q. Smith (1995) "Design of a decision support system for use in the event of a radiation accident" Submitted to *Annals of Operations Research*. RODOS(B)-RP(95)05

Conference and Seminar Presentations

[Note: attendance at conference was not claimed as an expense against the contract]

S. French, E. Halls and D.C. Ranyard (1995) "Equity and MCDA in the Event of a Nuclear Accident" Contributed paper at the XIIth International Conferenc on MCDM at Hagen, June 1995.

Seminars on aspects of decision support for nuclear emergencies have been given at:

- Operational Research Society Local Group (Leeds, May, 1995)
- Bradford University(Department of Computer Science, ????)
- Nottingham University (Department of Mathematics, Nov. 1993)
- Technical University of Delft (Department of Mathematics and Infomatics, April, 1994)

Dissertations and Student Reports

[Note: no student received financial support from this contract.]

J. Cunningham (1995) "A prototype expert system for decision analysis"

E. Halls (1994) "Equity, public risk and collective effective dose"

M.T. Harrison (1995) "Modelling uncertainty in a potential nuclear accident"

All dissertations available at the University of Leeds.

Head of project 4: Dr. Vanderpooten

II. Objectives for the reporting period

The objective of our work was to develop a methodology for selecting medium-term countermeasures after a nuclear accident. In order to illustrate the proposed methodology, we focused on the specific problem of contaminated foodstuffs.

The procedure has been designed with the following objectives in mind :

- it must be able to handle strategies of countermeasures which are combinations of elementary countermeasures,
- it must take into account multiple criteria, some of which being qualitative and quite difficult to evaluate (e.g. public acceptability),
- it should favour cooperation between various stakeholders by allowing to explore all possible interesting strategies in an interactive way.

III. Progress achieved including publications

The results we obtained are summarized in the following report which is submitted for publication.

A multiobjective interactive procedure for selecting medium-term countermeasures after nuclear accidents

P. Perny D. Vanderpooten

LAMSADE - Université Paris-Dauphine
Place du Maréchal de Lattre de Tassigny
75775 Paris Cedex 16 - France

1 Introduction

The purpose of this work is to design a methodology for supporting the selection of countermeasures in the case of nuclear accidents. In this context, it is important to distinguish between short term pre or post-accidental decisions on the one hand, and medium or long term post-accidental decisions on the other hand.

The first type of decisions, concerning countermeasures such as evacuation or sheltering of the populations, is characterized by a high degree of *uncertainty* due to the fact that the real impacts of the accident are either unknown or known quite partially. These decisions, which must be made in *emergency*, are often of the yes/no type and in a limited number. The only objective to be considered is to ensure the best possible level of safety for the populations. Some interesting concepts, involving the idea of achieving a balance between risk and equity, have been developed for handling such decisions (see, e.g., [Kee80, FHR95]). The tools for supporting these decisions must be relatively simple because of the time pressure and the limited knowledge of the situation.

The second type of decisions, concerning countermeasures such as decontamination of farm produce or relocation of activities, is characterized by a rather good knowledge of the situation. The time devoted to decision making is also much larger. As a consequence, the decisions can be defined more precisely, in accordance with the situation at hand. This involves that much more alternatives can and must be taken into account. Moreover, if safety remains the main objective, other viewpoints, like the cost of the countermeasures and their public acceptability, are becoming important. Therefore, the tools for supporting such decisions must be able to handle explicitly multiple criteria and, in many cases, large number of alternatives.

We consider here the second type of decisions (medium or long term post-accidental decisions) for which we suggest resorting to multiple criteria interactive procedures (see, e.g., [Van89, VV89]). In order to illustrate the proposed approach, we have been focusing on a well-specified problem: the elaboration of a strategy for decontaminating foodstuffs. We show that using a multiple criteria interactive procedure allows to explore quite easily a large variety of solutions. By incorporating in the proposed procedure several types of dialogues (on the criterion values, but also on the decision variables), the decision makers can test and improve different kinds of solutions.

First, we define the decision problem by introducing an illustrative example and presenting the specificities of the problem (section 2), our model based on multiobjective linear programming is introduced (section 3). A Decision Support System is then proposed which provides various modes of interaction for generating, examining and improving strategies of countermeasures (section 4).

2 Definition of the decision problem

2.1 An illustrative example

We consider here a fictitious scenario of a nuclear accident. This scenario has been proposed by A. Despres (CEA/IPSN)

The release, consisting of ^{131}I and ^{137}Cs , is supposed to be instantaneous. The region around the release site is divided in three areas in which concentrations in foodstuffs are supposed to be homogeneous. The accident is located in area 1 and affects with a decreasing impact area 2 and area 3

Three types of contaminated foodstuffs are considered (Milk, Meat, Vegetables). In each area, the contaminated quantities of each product are given in table 1.

Foodstuffs	Area 1	Area 2	Area 3
Milk	6.85	31.5	145.2
Meat	350	1750	4250
Vegetables	22.5	75	150

Table 1. Contaminated quantities (in tons)

The problem is to determine a suitable combination of elementary countermeasures in order to limit the possibilities of contaminated foodstuffs ingestion, for the population living around the nuclear plant. The elementary countermeasures envisaged here are presented in table 2

Foodstuffs	Countermeasures	
	Name	Description
Milk	None	No Action
	Decont.	Decontamination by addition of a preservative
	Butter	Transformation to butter
Meat	None	No Action
	Decont.	Decontamination by treating animals' feed
Vegetables	None	No Action
	Destr.	Destruction
	Preserv.	Preservation until radioactive decay

Table 2. Elementary countermeasures

In order to appreciate the level of contamination, experts in radiation protection examine the collective dose defined as the sum of the individual doses over a population. In this scenario, three types of population are distinguished, infants, children and adults. Countermeasures are evaluated by examining averted collective doses. Averted collective dose is defined as the difference between initial effective dose and expected residual dose after application of a given countermeasure. Averted collective doses, expressed in ManSv, are computed by the DACFOOD system ([Des83]). The computations not only include doses received by ingestion of contaminated foodstuffs, but also doses due to inhalation or external exposure during the first year after the accident. Notice that a countermeasure taken in a specific area possibly affects the other areas. Such cross effects are also taken into account in computations. The averted collective doses are provided by DACFOOD for each countermeasure and each area. These doses are computed for the quantities recorded in table 1 and listed in tables (3, 4, 5)

Unit costs expressed in Ecus/ton are given in table 6 for each countermeasure in each area

AREA 1

Foodstuffs	Counter-measures	Averted dose		
		<i>Infant</i>	<i>Child</i>	<i>Adult</i>
Milk	None	0	0	0
	Decont	0	400	11
	Butter	0	630	36
Meat	None	0	0	0
	Decont.	0.1	30	39
Vegetables	None	0	0	0
	Destr.	0	80	6
	Preserv	0	40	1

Table 3. Averted collective doses in Area 1 (ManSv)

AREA 2

Foodstuffs	Counter-measures	Averted dose		
		<i>Infant</i>	<i>Child</i>	<i>Adult</i>
Milk	None	0	0	0
	Decont	0	260	58
	Butter	0	880	58
Meat	None	0	0	0
	Decont.	0.1	20	48
Vegetables	None	0	0	0
	Destr.	0	110	11
	Preserv.	0	95	1

Table 4: Averted collective doses in Area 2 (ManSv)

AREA 3

Foodstuffs	Counter-measures	Averted dose		
		<i>Infant</i>	<i>Child</i>	<i>Adult</i>
Milk	None	0	0	0
	Decont.	0	700	38
	Butter	0	810	38
Meat	None	0	0	0
	Decont	0	10	8
Vegetables	None	0	0	0
	Destr.	0	380	26
	Preserv	0	190	11

Table 5: Averted collective doses in Area 3 (ManSv)

Foodstuffs	Counter- measures	Unit costs		
		Area 1	Area 2	Area 3
Milk	None	0	0	0
	Decont	100	100	100
	Butter	150	150	150
Meat	None	0	0	0
	Decont	15	15	15
Vegetables	None	0	0	0
	Destr.	267	267	300
	Preserv.	440	440	500

Table 6. Unit costs of countermeasures (Ecus/t)

2.2 Some important specificities of the problem

A strategy is a complex entity: Considering an accident, different areas with homogeneous levels of concentration are defined around the release site. For each kind of food, various countermeasures can be adopted in each area. Moreover, for a specific food in a specific area, different countermeasures can be mixed (e.g. in area 2, we may decide to destroy 20% of the milk production, decontaminate 35% of this production and do nothing for the remaining 45%). Therefore, a strategy is defined as a rather complex combination of elementary countermeasures.

The set of possible strategies is extremely large: Since any strategy results from a combination of elementary countermeasures, the space of solutions appears to be very large. Reducing this complexity by considering a priori a limited sample of strategies would have a severe impact on the quality of the final decision. Therefore, preserving the possibility of investigating a variety of possible solutions is a crucial issue in this problem.

Different types of constraints must be considered: The selection of strategies is actually limited by different types of restrictions. Some of these restrictions cannot be violated and are necessary to characterize the set of feasible solutions (*hard constraints*). The others, optional and revisable, allow the user to explore some particular types of solutions (*soft constraints*).

The selection process involves several criteria and stakeholders: The criteria which have been considered are related to costs, averted doses, public acceptability. It is worth noting that, within such a framework, the set of criteria reflects conflicting objectives. The problem is to find a compromise solution satisfying the various stakeholders who may have different value systems (health authorities, radiation protection experts, farmers, political actors, ...).

3 The model: a multiobjective linear programming problem

3.1 Decision variables

A strategy of countermeasures is defined by indicating for each area, which countermeasures are applied to each product (food). Formally, a strategy can thus be represented by the following variables:

- x_{ijk} : amount of product i processed by countermeasure j within area k (expressed in tons).

3.2 Criteria

The criteria we are considering are related to averted doses, cost and public acceptability. The outputs provided by the Dacfood software allow to define the following quantities:

- d_{ijklm} : averted dose per unit for population l (infants, children, adults), located in area m , after treating product i by countermeasure j in area k (expressed in ManSv/t). These quantities are easily derived from the data recorded in tables 1, 3, 4 and 5.
- c_{ijk} : processing cost for one unit of product i treated by countermeasure j within area k (expressed in Ecus/t).

The public acceptability refers to the psychological impact of countermeasures on the population concerned with the accident. This important dimension is clearly independent of financial and efficiency aspects and must be taken into account. For instance, some drastic countermeasures (destruction, slaughtering, . . .) considered because of their potential efficiency may be rejected by populations. In the same way, the "doing nothing" decision should not be accepted in spite of its financial appeal. However, this dimension is clearly extremely difficult to define. Moreover, the acceptability may widely vary according to the specific situation (gravity of the accident, location, . . .). Hence, we suggest defining the acceptabilities, by consulting the various experts, only when the decision is to be made. We recommend the use of a qualitative scale of acceptability. Thus, for each countermeasure and possibly for each area, we suggest choosing a level of acceptability in the range [-10, 10] using the following reference points:

- 10 : possibility of strong opposition
- 5 : possibility of weak opposition
- 0 : no real opposition is expected
- 5 : agreement is expected
- 10 : strong agreement seems possible

Therefore, the following values must be defined.

- a_{ijk} : public acceptability of countermeasure j to treat product i within area k . (notice, that, in many cases, it is not necessary to distinguish the acceptability for each area. In such cases, only the values a_{ij} , which represent the acceptability of countermeasure j to treat product i , must be defined. Then, for each area k , we have $a_{ijk} = a_{ij}$).

Considering the above values, the following objective functions are thus defined to represent the criteria:

- Minimize the total processing cost:

$$\min z_1 = \sum_i \sum_j \sum_k c_{ijk} x_{ijk}$$

- Maximize the averted dose for each type of population l .

$$\max z_l = \sum_i \sum_j \sum_k \left(\sum_m d_{ijklm} \right) x_{ijk} \quad (l = 2, 3, 4)$$

with $l = 2$ for infants, $l = 3$ for children, $l = 4$ for adults

- Maximize the average acceptability:

$$\max z_5 = \frac{\sum_i \sum_j \sum_k a_{ijk} x_{ijk}}{\sum_i \sum_j \sum_k x_{ijk}}$$

Notice that the $\sum_i \sum_j \sum_k x_{ijk}$ quantity represents the total amount of contaminated food-stuff to be processed and is thus a constant

3.3 Constraints

Two main types of constraints can be defined to precise the problem:

- **Hard constraints**

Such constraints are used to characterize the basic structure of the problem and to define the irrevocable restrictions.

- consistency constraints

For any product i and any area k , the total amount of processed food cannot exceed the amount of contaminated food:

$$\sum_j x_{ijk} \leq q_{ik} \quad \forall i, \forall k$$

where q_{ik} is the amount of product i to be treated in area k

- limited processing capacities

$$\sum_i \sum_k x_{ijk} \leq p_j \quad \forall j$$

where p_j is the maximal quantity which can be processed by countermeasure j .

Notice that such constraints can also be treated as soft constraints.

- non-negativity constraints

$$x_{ijk} \geq 0 \quad \forall i, \forall j, \forall k$$

- **Soft constraints**

Such constraints may be used to define additional requirements. This is particularly useful when, considering a given strategy, the decision maker wishes to improve it in some respects. Two types of soft constraints may be distinguished.

- constraints on criterion values, e.g.:

- * a maximal acceptable cost
- * a minimal reduction of doses
- * a maximal doses acceptable for the population of infants
- * .

- constraints on decision variables, e.g.:

- * minimal quantities to be processed in each area
- * a uniform repartition of interventions
- * ...

3.4 The model: a framework for exploring efficient strategies

A main advantage of the above model is that it allows to characterize all possible strategies. Because of the multiplicity of conflicting criteria, no solution can be derived which simultaneously optimizes all criteria. The model should then be considered as a framework for exploring feasible strategies. Among all these strategies, we are only generating *efficient* or *non-dominated* strategies (a strategy a is *efficient* if and only if there is no feasible strategy b which is at least as good as a on all criteria and strictly better than a on at least one criterion).

In order to generate such efficient strategies, we optimize a *scalarizing function* which aggregates the various criteria. The selection of an appropriate scalarizing function s is made considering the following requirements:

- s must generate efficient solutions only.
- all efficient solutions may be generated by s

In our case, we selected the following scalarizing function derived from the augmented Tchebychev norm.

$$s(z, \bar{z}) = \max_{r=1, \dots, 5} \{\lambda_r(z_r - \bar{z}_r)\} - \sum_{r=1}^5 \lambda_r z_r$$

where \bar{z} is a reference point representing aspiration levels to be reached on the criteria and n is the number of criteria

Minimizing s over the set of feasible solutions amounts to projecting \bar{z} on the efficient frontier. In other words, such an optimization allows to determine the efficient strategy which is "closest" to a given reference point (feasible or not)

The main advantage of such a function is that it allows to integrate different types of dialogue modes as shown in the next section. This provides an effective and flexible way of exploring the interesting efficient strategies.

4 A flexible Decision Support System for exploring strategies

The above model is the basis of our decision support system. Knowing the parameters characterizing a real post accidental situation, a compromise solution can be found by solving our multiobjective linear program. However, it is extremely important to allow the users to explore different type of solutions, to revise some constraints, to try to improve a given solution, .. This is why we are proposing an interactive procedure which incorporates several types of dialogues.

Let us present the main possibilities of this interactive procedure:

- using the *Spreadsheet Mode* allows the user to test interactively any strategy (what-if analyses) He/she can either create a strategy by indicating which countermeasure should be taken in each area or modify a current strategy. The feasibility of the strategy is tested and its evaluation is given for all criteria. Notice that such strategies suggested by a user are not necessarily efficient. Using the *Optimization mode* (see below) could then allow to improve the current strategy by finding a new one which is better on all criteria.
- using the *Optimization Mode* allows to find an efficient solution realising a compromise between the different conflicting criteria which have been considered. Thus the user is provided with a feasible strategy and its evaluations. The search of an appropriate solution may involve different type of techniques. The different types of search available are:
 - The *Restricted Search* allows the users to specify some requirements in order to restrict the search to a specific region of interest. Such restrictions may be applied on the criterion values (by specifying minimal requirements on these values) but also on the structure of the strategy (by specifying constraints on some decision variables or combinations of decision variables). Let us remark that, in some cases, the set of feasible solutions may become empty because constraints are too demanding. However, the users are allowed to revise these constraints at any time
 - The *Focusing Search* allows the users to specify aspiration levels, that is to say desirable values specified on all or some of the criteria and representing a prototype of the strategy one is looking for. Then, the search is focusing in the neighbourhood of the prototype entered by the user, and generates the closest feasible efficient strategy.
 - The *Partial Search*, where the procedure determines an efficient complement to a partial strategy proposed by a user (already entered variables are considered as fixed values and an optimisation is performed using the free variables)

From a computational point of view, the generation of a new strategy is obtained by solving a linear program. This can be done quite quickly (in a few seconds) using any standard linear programming code. These computational aspects are extremely important since quick response times allow to explore a large variety of solutions. This is particularly relevant in a context where several users, with various value systems, must cooperate in order to define a strategy.

5 An illustrative use of the Decision Support System

A prototype of the proposed procedure has been implemented on Excel using the solver option. We show the possibilities of the procedure using the example introduced in § 2.1.

Prior to the use of the procedure, it is necessary to evaluate the acceptabilities of the elementary countermeasures. As indicated in § 3.2, these acceptabilities may widely vary according to the specificities of the accident. Therefore, the evaluation should be performed by experts just before making the decision. Using the qualitative scale proposed in § 3.2, we suppose that the following acceptabilities have been defined:

Foodstuffs	Counter-measures	Acceptability		
		Area 1	Area 2	Area 3
Milk	None	-5	-5	-5
	Decont.	8	8	8
	Butter	5	5	5
Meat	None	-5	-5	-5
	Decont.	3	3	3
Vegetables	None	-5	-5	-5
	Destr.	3	3	3
	Preserv.	0	0	0

Table 7. Acceptabilities of elementary countermeasures

We present now a series of outputs from Excel which illustrate the different types of exploration. The corresponding tables and figures are gathered in the Appendix and are referred to as table A.x and figure A.x.

We simulate here a situation where stakeholders and experts would try and explore the set of all possible strategies by emphasizing a variety of aspects related to the criterion values and the structure of the strategies.

In order to get a general impression about the different types of available strategies, it is interesting to optimize separately each criterion and present the corresponding strategies (see tables A.1-5). This information is presented in a synthetic form using a pay-off matrix (see table A.6). This matrix illustrates the typical ranges of variation on each criterion and the possible trade-offs between criteria. Observing the criterion values located on the diagonal of the pay-off matrix is also quite instructive since these values represent the best possible values one can obtain on each criterion; for this reason, the fictitious point whose coordinates correspond with these values is called *ideal point*.

Let us introduce now some illustrative examples of explorations performed using either the *spreadsheet mode* or the *optimization mode*.

We consider the following intuitive 'all or nothing' strategy that can be obtained after a first analysis or by playing with the *spreadsheet mode* (see table 8).

The quantities to be treated in strategy *S* are given in table A.7, with the multicriteria evaluation of this strategy. Let us use the *optimization mode* to check whether there exists a more

Foodstuffs	Acceptability				
	Area 1		Area 2		Area 3
Milk	Transf	Butter	Transf	Butter	Decontamination
Meat	Decontamination		None		None
Vegetables	Destruction		Destruction		Destruction

Table 8: Strategy S , a combination of elementary countermeasures

interesting strategy in the neighbourhood of S . Using the focusing search, the point representing strategy S is projected on the efficient frontier and we get the improved solution S' presented in table A.8. Figures A.1 and A.2 provide some Excel graphical displays allowing to compare the two strategies. It is worth noting that S' dominates S and thus is objectively better. This clearly shows the power of our procedure which allows any feasible mixed strategy to be explored.

Let us present now, a simplified example of interactive exploration of the set of feasible strategies using the *optimisation mode*.

In order to get a first compromise solution Z_0 , the ideal point is projected on the efficient frontier; this is obtained by minimizing the scalarizing function s , taking the ideal point as a reference point (see § 3.4). Thus, we get the initial strategy given in table A.9. This strategy is an excellent compromise between the various conflicting objectives. The cost is rather interesting (71213 Ecus), the public acceptability is average and the efficiency expressed in averted doses is significant (0.2 (Infants), 1774 (Children), 196 (Adults)). However, the structure of the solution is not well balanced. Indeed, no countermeasure is taken for vegetables. Suppose that some stakeholders or experts would like to test strategies involving countermeasures for vegetables. It is then easy to add a constraint stipulating for instance that 50% of the total quantity of vegetables must be treated. Optimizing the scalarizing function s , taking this additional constraint into account, leads to a new solution Z_1 given in table A.10.

Solution Z_1 is clearly preferable to Z_0 even if the cost is superior. However, suppose that, for technical reasons, an upper bound limiting the capacity of meat decontamination has been evaluated by experts and temporarily set to 3000 tons. After inserting this constraint in the model, the Excel solver leads to solution Z_2 given in table A.11. This strategy satisfies the two additional constraints without significant alterations of the initial solution Z_0 . A quick comparison of the cost distribution by product is possible for the 3 solutions Z_0 , Z_1 and Z_2 using the graphical functionalities of Excel as shown in figures A.3-5.

Suppose now we are looking for a strategy which emphasizes the decontamination aspects, imposing that collective doses must be decreased below the 300 MSv threshold. These constraints are easily representable by specifying minimal requirements on doses criteria. For example, considering the additional constraints $z_3 \geq 2600$ and $z_4 \geq 260$, a new optimization using the *restricted search* leads to solution Z_3 given in table A.12.

The main weakness of solution Z_3 is its expensive cost. Is there still a good solution if we do not accept to pay more than 100000 Ecus? Unfortunately, if we add this constraint to the previous ones, the *restricted search* indicates that the set of feasible solutions is empty. The set of constraints is too demanding. However, a restricted focusing search is able to point out an interesting solution. Let us relax the doses constraints while keeping the financial constraint of 100000 Ecus. Then we define aspiration levels considering Z_3 as a reference point of desirable values, except for the cost which must be inferior. The new optimization leads to solution Z_4 given in table A.13.

Finally, in order to appreciate the sensitivity of the solution, some experts ask for another exploration, strengthening doses and acceptability requirements while weakening other constraints. Let us assume for instance that only 10% of the quantity of vegetables must be treated and that the maximal capacity of meat decontamination is 5000 tons. While keeping the cost constraint

to 100000 Ecus, we would like averted doses to be close to 0.2, 2500 and 250 for infants, children and adults respectively (aspiration levels). Moreover, we want the public acceptability to be non-negative ($z_5 \geq 0$). A last optimization integrating both restricted, focusing and partial search leads to the Z_5 solution given in table A.14.

6 Conclusion

We investigated the selection of medium or long term countermeasures after a nuclear accident in the specific case of foodstuffs decontamination. Such countermeasures are actually strategies combining several elementary countermeasures. The set of possible strategies is thus extremely large. Moreover, the selection process involves multiple criteria and various stakeholders with different value systems.

We presented an interactive procedure based on a linear multiobjective model. The advantage of such a model is that it preserves the variety of strategies by allowing mixes of elementary countermeasures.

A prototype of this procedure has been implemented using the Excel spreadsheet and solver. This Decision Support System has been tested on a scenario proposed by IPSN, using the results of Dacfood. The experiments with this scenario have shown the flexibility of our approach to investigate the most satisfactory strategies. The combination of the spreadsheet and optimization modes provides indeed an interesting variety of man-machine interactions.

We illustrated the use of this prototype on a scenario provided by IPSN. In particular, we tested the different possibilities of our procedure and showed that:

- It is interesting to give an idea of the variety of solutions by presenting the extreme solutions (those which optimize separately each criterion). These solutions, gathered in the pay-off matrix, illustrate the typical ranges of variation on each criterion and the possible trade-offs between criteria.
- The possibility of improving a strategy partially or totally defined by users is a simple and powerful option. Moreover, the use of this option clearly showed that solutions should not be restricted to 'all or nothing' strategies which are in most cases dominated by 'mixed' strategies.
- The possibility of reacting on some criterion values so as to find an improved solution is classical in multiple criteria interactive procedures. It is one of the main dialogue modes in this procedure which allows to express aspiration levels and/or restrictions on the criterion values.
- An original and important feature of the procedure is that interaction is also supported for the decision variables. This allows to express reactions and suggest modifications in terms of the components (elementary countermeasures) of a given strategy.
- Different types of graphical displays provide the user with a synthetic description of each strategy and allow to evaluate quickly each strategy on all important aspects.
- Response times are critical in any interactive procedure. Since the underlying model is a linear programming model, new solutions can be determined extremely quickly (in a few seconds).

Such a flexible procedure allows an easy exploration of the efficient strategies. Cooperation between the different stakeholders is thus favoured by giving each of them the possibility of reacting and modifying the solution according to their own viewpoint.

In conclusion, we demonstrated the interest and feasibility of our methodology for the specific problem of food decontamination. This methodology can be easily extended by taking into

account additional criteria (e.g. related to averted doses for critical organs). More generally, it can be used in contexts involving combinations of countermeasures to be evaluated on multiple criteria, which is typically the case in the elaboration of medium or long term strategies of countermeasures. The prototype we designed worked quite satisfactorily on the simplified scenario that we considered. However, it would be necessary to develop a specific software, including a standard linear programming routine, in order to obtain a fully operational decision support system.

References

- [Des83] A. Despres. Dacfood, guide de référence. Note CERP 93/01. IPSN, 1983.
- [FHR95] S. French, E. Halls, and D. Ranyard. Equity and MCDA in the event of a nuclear accident. Paper presented in the XIIIth International Conference on Multiple Criteria Decision Making, Hagen, June, 1995.
- [Kee80] R. Keeney. Equity and public risk. *Operations Research*, 28:527-534, 1980.
- [Van89] D. Vanderpooten. The interactive approach in MCDA: a technical framework and some basic conceptions. *Mathematical and Computer Modelling*, 12(10/11):1213-1220, 1989.
- [VV89] D. Vanderpooten and Ph. Vincke. Description and analysis of some representative interactive multicriteria procedures. *Mathematical and Computer Modelling*, 12(10/11):1221-1238, 1989.

Appendix

S*1: Solution minimizing the cost

COUNTERMEASURES

		Area 1	Area 2	Area 3
Milk	None	6.85	31.50	145.20
	Decontamination	0.00	0.00	0.00
	Transf. Butter	0.00	0.00	0.00
Meat	None	350.00	1750.00	4250.00
	Decontamination	0.00	0.00	0.00
Vegetables	None	22.50	75.00	150.00
	Destruction	0.00	0.00	0.00
	Preservation	0.00	0.00	0.00

CRITERIA

		Residual doses
Cost	0	
Averted dose (infants)	0.0	2.6
Averted dose (children)	0.0	2870.0
Averted dose (adults)	0.0	546.0
Public acceptability	-5	

Table 1

S*2: Solution maximizing the averted dose (infants)

COUNTERMEASURES

		Area 1	Area 2	Area 3
Milk	None	6.85	31.50	145.20
	Decontamination	0.00	0.00	0.00
	Transf. Butter	0.00	0.00	0.00
Meat	None	0.00	0.00	4250.00
	Decontamination	350.00	1750.00	0.00
Vegetables	None	22.50	0.00	0.00
	Destruction	0.00	0.00	0.00
	Preservation	0.00	75.00	150.00

CRITERIA

		Residual doses
Cost	139500	
Averted dose (infants)	0.2	2.4
Averted dose (children)	335.0	2535.0
Averted dose (adults)	99.0	447.0
Public acceptability	-2	

Table 2

S*3: Solution maximizing the averted dose (children)

COUNTERMEASURES

		Area 1	Area 2	Area 3
Milk	None	0 00	0 00	0 00
	Decontamination	0 00	0 00	0 00
	Transf. Butter	6 85	31 50	145 20
Meat	None	0 00	0 00	4250 00
	Decontamination	350 00	1750 00	0 00
Vegetables	None	0 00	47 73	0 00
	Destruction	22 50	27 27	150 00
	Preservation	0 00	0 00	0 00

CRITERIA

		Residual doses
Cost	117322	
Averted dose (infants)	0 2	2 4
Averted dose (children)	2870 0	0 0
Averted dose (adults)	255 0	291 0
Public acceptability	.2	

Table 3

S*4: Solution maximizing the averted dose (adults)

COUNTERMEASURES

		Area 1	Area 2	Area 3
Milk	None	0.00	0.00	0.00
	Decontamination	0.00	0.00	145.20
	Transf. Butter	6 85	31.50	0.00
Meat	None	0 00	0 00	0 00
	Decontamination	350 00	1750 00	4250 00
Vegetables	None	0 00	0 00	0 00
	Destruction	22 50	75 00	150 00
	Preservation	0 00	0 00	0 00

CRITERIA

		Residual doses
Cost	186555	
Averted dose (infants)	0.2	2.4
Averted dose (children)	2840 0	30 0
Averted dose (adults)	270 0	276 0
Public acceptability	3	

Table 4

S*5: Solution maximizing the average acceptability

COUNTERMEASURES

		Area 1	Area 2	Area 3
Milk	None	0 00	0 00	0 00
	Decontamination	6 85	31 50	145 20
	Transf. Buffer	0 00	0 00	0 00
Meat	None	0 00	0 00	0 00
	Decontamination	350.00	1750 00	4250 00
Vegetables	None	0 00	0 00	0 00
	Destruction	22 50	75 00	150.00
	Preservation	0 00	0 00	0 00

CRITERIA

		Residual doses
Cost	184638	
Averted dose (infants)	0 2	2 4
Averted dose (children)	1990.0	880 0
Averted dose (adults)	245 0	301 0
Public acceptability	3	

Table 5

Payoff matrix:

	<i>Costs</i>	<i>Averted doses</i>			<i>Accept.</i>
		<i>Infants</i>	<i>Children</i>	<i>Adults</i>	
S*1	0	0	0 0	0.0	-5
S*2	139500	0.2	335 0	99.0	-2
S*3	117322	0 2	2870.0	255.0	-2
S*4	186555	0.2	2840.0	270.0	3
S*5	184638	0.2	1990 0	245 0	3

Table 6

Evaluation of a good intuitive all or nothing strategy S

COUNTERMEASURES

		Area 1	Area 2	Area 3
Milk	None	0 00	0 00	0 00
	Decontamination	0 00	0 00	145.20
	Transf. Butter	6 85	31 50	0 00
Meat	None	0.00	1750 00	4250.00
	Decontamination	350 00	0 00	0 00
Vegetables	None	0.00	0 00	0 00
	Destruction	22.50	75 00	150 00
	Preservation	0.00	0 00	0 00

CRITERIA

		Residual doses
Cost	96555	
Averted dose (infants)	0 1	2 5
Averted dose (children)	2810.0	60.0
Averted dose (adults)	214.0	332 0
Public acceptability	-4	

Table 7

Improved strategy S* obtained from S using the focusing approach

COUNTERMEASURES

		Area 1	Area 2	Area 3
Milk	None	0.00	0 00	0.00
	Decontamination	0 00	0 00	145 20
	Transf. Butter	6.85	31 50	104.22
Meat	None	0.00	0 00	2460.87
	Decontamination	350 00	1750.00	1789 13
Vegetables	None	22.50	75 00	150.00
	Destruction	0.00	0 00	0 00
	Preservation	0.00	0.00	0 00

CRITERIA

		Residual doses	Aspiration levels
Cost	94242		96555
Averted dose (infants)	0.2	2.4	0.1
Averted dose (children)	2845 6	24 4	2810
Averted dose (adults)	249.6	296.4	214
Public acceptability	0		-4

Table 8

Comparative radial representation of strategies S and S*

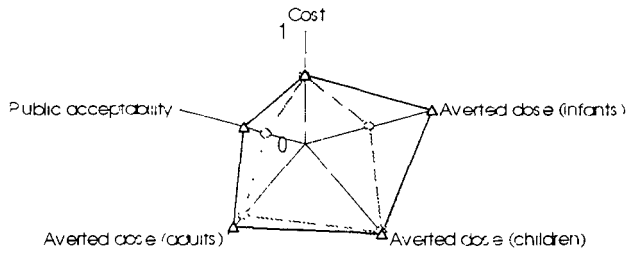


Figure 1

Profiles of strategies S and S*

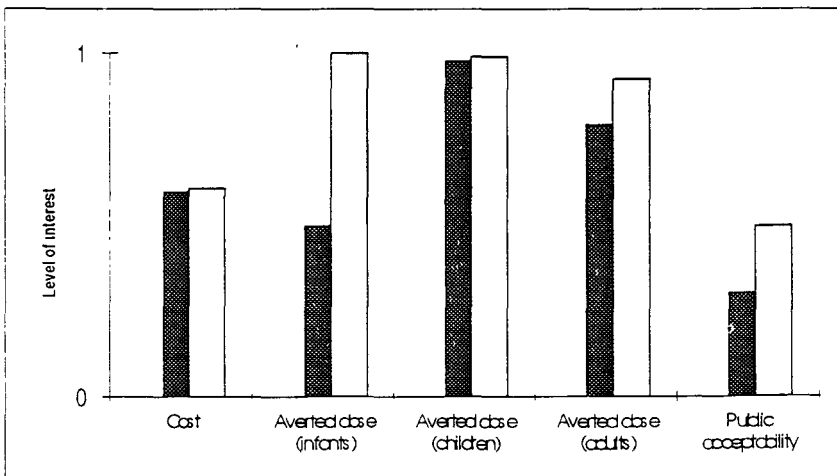


Figure 2

Initial solution Z0

COUNTERMEASURES

		Area 1	Area 2	Area 3
Milk	None	0.00	0.00	101.68
	Decontamination	0.00	0.00	43.52
	Transf. Butter	6.85	31.50	0.00
Meat	None	0.00	0.00	2276.11
	Decontamination	350.00	1750.00	1973.89
Vegetables	None	22.50	75.00	150.00
	Destruction	0.00	0.00	0.00
	Preservation	0.00	0.00	0.00

CRITERIA

		Residual doses
Cost	71213	
Averted dose (infants)	0.2	2.4
Averted dose (children)	1774.4	1095.6
Averted dose (adults)	196.1	349.9
Public acceptability	0	

Table 9

Solution Z1

COUNTERMEASURES

		Area 1	Area 2	Area 3
Milk	None	0.00	11.33	145.20
	Decontamination	0.00	0.00	0.00
	Transf. Butter	6.85	20.17	0.00
Meat	None	0.00	0.00	2956.51
	Decontamination	350.00	1750.00	1293.49
Vegetables	None	0.00	0.00	123.75
	Destruction	22.50	75.00	26.25
	Preservation	0.00	0.00	0.00

CRITERIA

		Residual doses
Cost	88862	
Averted dose (infants)	0.2	2.4
Averted dose (children)	1502.9	1367.1
Averted dose (adults)	184.1	361.9
Public acceptability	-1	

Table 10

Cost distribution associated with solution Z0
(before integrating the constraint on repartition)

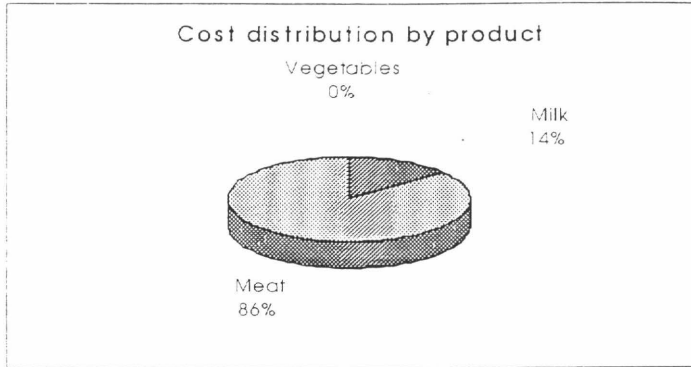


Figure 3

Cost distribution associated with solution Z1
(taking account of the constraint on repartition)

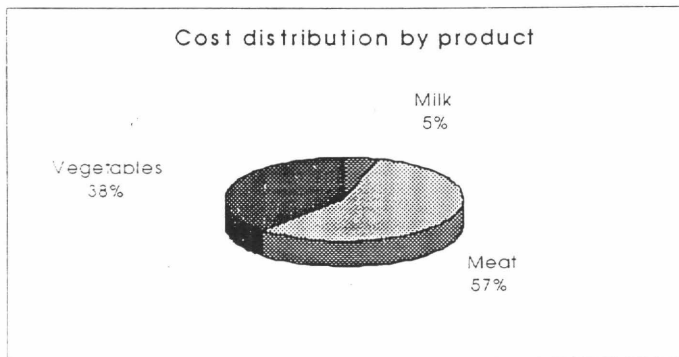


Figure 4

Cost distribution associated with solution Z2
(taking account of the constraint on capacity of meat decontamination)

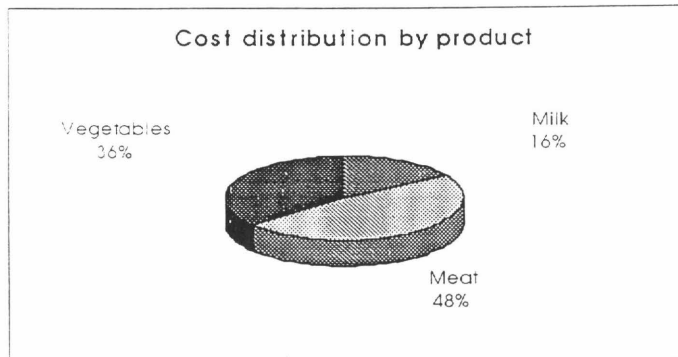


Figure 5

Solution Z2

COUNTERMEASURES

		Area 1	Area 2	Area 3
Milk	None	0.00	0.00	33.53
	Decontamination	6.85	31.50	111.67
	Transf. Butter	0.00	0.00	0.00
Meat	None	0.00	0.00	3350.00
	Decontamination	350.00	1750.00	900.00
Vegetables	None	0.00	0.00	123.75
	Destruction	22.50	75.00	26.25
	Preservation	0.00	0.00	0.00

CRITERIA

		Residual doses
Cost	93910	
Averted dose (infants)	0.2	2.4
Averted dose (children)	1507.0	1363.0
Averted dose (adults)	208.5	337.5
Public acceptability	-1	

Table 11

Solution Z3

COUNTERMEASURES

		Area 1	Area 2	Area 3
Milk	None	0.00	0.00	0.00
	Decontamination	0.00	10.67	145.20
	Transf. Butter	6.85	20.83	0.00
Meat	None	0.00	0.00	4250.00
	Decontamination	350.00	1750.00	0.00
Vegetables	None	0.00	13.64	0.00
	Destruction	22.50	61.36	150.00
	Preservation	0.00	0.00	0.00

CRITERIA

		Residual doses
Cost	118631	
Averted dose (infants)	0.2	2.4
Averted dose (children)	2600.0	270.0
Averted dose (adults)	260.0	286.0
Public acceptability	-2	

Table 12

Solution Z4

COUNTERMEASURES

		Area 1	Area 2	Area 3
Milk	None	0.00	0.00	0.00
	Decontamination	0.00	10.45	145.20
	Transf. Butter	6.85	21.05	0.00
Meat	None	0.00	0.00	4250.00
	Decontamination	350.00	1750.00	0.00
Vegetables	None	0.00	75.00	14.39
	Destruction	22.50	0.00	135.61
	Preservation	0.00	0.00	0.00

CRITERIA

	Residual doses	Aspiration levels
Cost	97941	90000
Averted dose (infants)	0.2	0.2
Averted dose (children)	2477.8	2600
Averted dose (adults)	248.5	260
Public acceptability	-2	-2

Table 13

Solution Z5

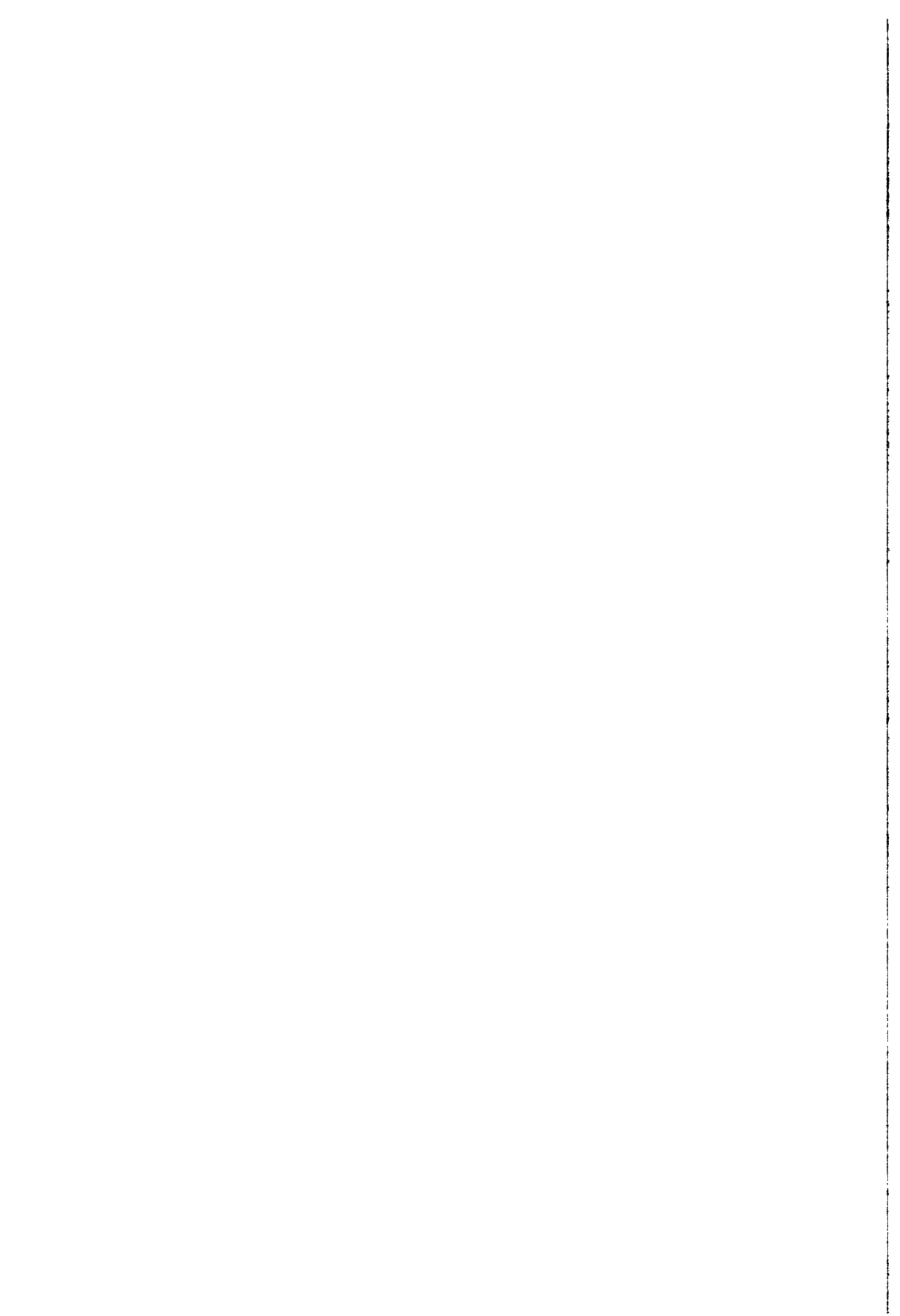
COUNTERMEASURES

		Area 1	Area 2	Area 3
Milk	None	0.00	0.00	7.68
	Decontamination	0.00	22.25	137.52
	Transf. Butter	6.85	9.25	0.00
Meat	None	0.00	0.00	1350.00
	Decontamination	350.00	1750.00	2900.00
Vegetables	None	0.00	72.75	150.00
	Destruction	22.50	2.25	0.00
	Preservation	0.00	0.00	0.00

CRITERIA

	Residual doses	Aspiration levels
Cost	100000	80000
Averted dose (infants)	0.2	0.2
Averted dose (children)	1875.1	2500
Averted dose (adults)	228.8	250
Public acceptability	1	3

Table 14



**Final Report
1992-1995**

Contract: FI3P-CT930068

Duration : 1.1. 93 to 30.6.95

Sector: C23

Title: Assessment and management of post accidental situations. Radiation detriment, risk perception and risk communication.

- | | | |
|----|---------|---------|
| 1) | Brenot | CEA-FAR |
| 2) | Joussen | IFS |
| 3) | Sjöberg | CFR |

Dr. J. Brenot is the coordinator of the contract.

I. Summary of Project. Global objectives.

Risk perception and communication studies are essential for responsible risk management in that they provide : a) a basis for assessing the likely response of the public to advice and information on radiation protection; b) a route to appraising the effectiveness/efficiency of radiation protection; c) criteria and guidelines for coping with problems of risk attenuation and risk amplification.

The research proposed has two main objectives : (1) to undertake research in order to improve the understanding of risk perception in relation to radiation detriment; and (2) to evaluate current approaches in risk communication, and propose appropriate strategies for radiation risk communication in the European Union (EU).

2. Development of the research.

Four tasks were developed :

Task 1. Review of risk perception studies

Task 2. Review of evaluation techniques for risk communication programmes

Task 3. Assessing organisational factors influencing social learning in radiation protection

Task 4. Identification of strategies for coping with risk amplification and attenuation problems

Three groups of researchers were involved : CEA-FAR (IPSN, FRANCE), Head of project : Dr. BRENOT ; IFS (RWTH-AACHEN, GERMANY), Head of project : Dr. JOUSSEN ; and CFR (CFR-STOCKHOLM), Head of Project : Pr. SJÖBERG who intervened as external assistance with two subcontracts, one signed in 1993 and the other in 1995. The first subcontract dealt with the Cultural Theory of risk : general presentation and critical review of the studies which have been made to see the interest of cultural profiles in understanding public risk perceptions. The second subcontract covered two topics, one is the description of four radiation risk situations (indoor radon, X-rays, food irradiation and radioactive waste) in Sweden and the other is an investigation of politicians' and public risk perceptions.

Working meetings were held in Paris 13 September 1993, Aachen 28 April 1994, Stockholm 10 May 1994, Paris 2 December 1994, and in Aachen 26 June 1995.

The state of the project in 1994 was presented to the Commission of European Communities DGXII at a Paris meeting held on October 25, 1994.

Research methods

Analysis and synthesis of concepts, approaches, and differentiation factors in risk perception constitute Task 1. IPSN and CFR were particularly involved in evaluating the validity of Cultural Theory when IFS developed the concept of social representation. Tasks 2, 3 and 4 deal with risk communication. On one side, IFS designed communication strategies in relation with the social representations they had defined in Task 1. On the other side, IPSN and CFR used a more conventional approach to risk communication, that is successively considering the involved parties (transmitters, receivers), their goals, the content of the exchange, and the exchange process.

For the study of risk communication, four situations involving radiation were chosen, namely indoor radon exposure, X-ray diagnostic, consumption of irradiated food, and radioactive waste management. The domains concerned correspond to very different contexts, natural exposure (with indoor radon), daily life (with medical diagnostic and food consumption), and the industrial and energy context (with waste). It has been judged that comparison between these situations in the various countries would be an interesting subject to work out.

The three groups had their own methodologies to get opinion data. IFS Aachen was more qualitative with in depth interviews and the work in focus groups, IPSN and CFR more quantitative designed large surveys in France and Sweden respectively. They analysed also the four situations in their respective countries and in some other countries too when they considered it useful for the research. Respective contributions of the three groups of scientists appear in table 1.

3. Progress achieved in risk perception

Studies in risk perception which constitute Task 1 can be conducted in various ways.

One possibility is to describe the universe of risks. The emphasis on risks means comparison of risk situations, and construction of « cognitive maps » or typologies in which situations similar with respect to perceptions are grouped. Slovic defended this approach, the so-called psychometric approach, when he selected relevant dimensions to characterize the risks and derived a cognitive map by statistical methods.

The second possibility is to focus on the people. This means that one has to search for individual characteristics which could be helpful to explain opinions given by people about risk situations. Characteristics can be either the most common ones (e.g., demographics, experience and skills, personality, occupation) or more specific factors of social and cultural nature. CFR and IPSN used this approach when investigating the interest of Cultural Theory which proposes four worldviews, hierarchy - egalitarianism - individualism and fatalism, to account for those cultural factors. The main results from CFR and IPSN studies are quite similar : the worldviews so defined do not carry out very new elements to explain risk perception. Indeed their corresponding scales show low correlations with various aspects of risk

perception (personal risk, general risk, safety demand, truthness). There is one exception for egalitarianism which correlates with personal risk. Two conclusions can be drawn. First, the cultural scales in the questionnaire used are too simple to account for the richness and complexity of culture. Second, work is needed to clarify the meaning and the content of culture, and also to precise what to keep of the content before any other tentative to relate risk perceptions to cultural factors is made.

Table 1 : work contributions of the three groups

	CEA-FAR IPSN	IFS RWTH-AACHEN	CFR Center for Risk Research
Risk perception Task 1			
Concepts-models	Synthesis		
Psychometric approach			Swedish teachers analysis of responses
Cultural theory	General population survey 1993 analysis		* High achieving students reanalysis of responses * Swedish teachers analysis of responses * Brazilians teachers reanalysis of responses * General population survey 1994 analysis * US church organisation survey 1995 analysis
Social representations Representation types		Methodology * Experts interviews in Germany, Netherlands, Belgium * Experts survey and analysis * Focus groups analysis	
Group patterns			Politicians survey 1995 analysis
Risk communication Tasks 2, 3, 4.			
Evaluation of RC programmes	* Radon (US, UK, France) * Waste France	Low level radioactive waste in Belgium	For Sweden radon X-rays food irradiation radioactive waste
Strategies	For France radon X-rays food irradiation radioactive waste	For D, NL, B radon X-rays food irradiation radioactive waste	For Sweden radon X-rays food irradiation radioactive waste

The third possibility is to favour the interaction between the individual and the risk situation, that is to study the process of opinion formation about one particular risk (in this research : radon exposure, X-ray diagnostic, food irradiation and radioactive

waste). IFS chose this possibility when developing the concept of social representation. Based on discussions in focus groups (in Germany, The Netherlands and Belgium), IFS identified six different representations which formed the background of risk evaluation by focus group members. The representations correspond to specific argumentation patterns used when considering a particular situation. They are as follows : traditional indifferent, individual distant, rational economic, intellectual civic, environmental apprehensive and progressive modern. The IFS study shows, that (i) an individual has not only one representation for all the situations he evaluates, but he takes one or an other depending on the situation, and (ii) the social image of a situation within a society may be derived from individual's representations, see table 2.

4. Progress achieved in risk communication

As mentioned previously, CFR and IPSN studied in a conventional manner risk communication practices for each of the four radiation situations. IFS did differently and proposed for each situation a policy in accordance with its social representation, as illustrated in table 2. Communication policies are six, (1) neutral information - general education, (2) context information - local emphasis, (3) comparing information - involving decision, (4) feedback information - set up dialogue, (5) contrast information - achieving discourses, and (6) no information - shift strategy.

Concerning the indoor radon issue, people knowledge about radon effects are very different from one country to another, at a high level when extensive information campaigns were held, at a low level otherwise. Individuals concerned with indoor radon are very few and one can say that almost all individuals show apathy and low motivation to improve their homes by reducing radon concentrations. Public health authorities by their policy of large information expected that people spontaneously would change their living environment. It failed. It seems now that a possible way, less ambitious, would be authorities regulating the more extreme cases and giving the reasons why to those concerned.

For X-ray diagnostic there are no large differences in perception between countries. The risk is not taken into account by people and risk control is let to the physicians. Communication with the public stands at a very low level and it consists in giving neutral information for general education purpose. Major communication efforts are directed towards medical and dental practitioners to make them aware of dosimetric data and quality insurance necessity.

Regarding food irradiation, the technology and the sale of irradiated food are not allowed in many countries (for instance Sweden and Germany) although scientific evidence of negative effects on health is missing. This fact makes the difference between countries. People living in countries where food irradiation has been banned have a better knowledge of the practice due to the controversial debates which took place at the ban period. In other countries where the practice is authorized, as France, very few people know what it is.

The waste issue constitutes in all countries a major problem for which information has no real influence upon individuals' opinions and behaviours. Analysing risk communication in case-studies of the past, or discussing with experts in focus groups led to similar views. People are always very interested and they have an

« intellectual civic » representation of the issue. As a consequence, individuals behave as citizens who demand communication at its highest level, which means participating to decisions.

Table 2 : social representations and risk communication strategies
for indoor radon, X-rays, food irradiation and radioactive waste
in Germany, Belgium and The Netherlands (IFS study)

↗ = high → = medium ↘ = low ● = nothing

social representation	technology / process / product												risk communication strategy
	radon			x-ray			nucl. waste			food irradiat.			
	D	B	NL	D	B	NL	D	B	NL	D	B	NL	
traditional indifferent	→	↗	↗	↘	↘	↗	↘	↗	→	↘	→	↗	① neutral information general education
individual distant	→	↘	→	↘	→	●	●	●	●	↘	↘	↘	② context information local emphasis
rational economic	↘	↘	●	↗	→	↘	●	→	→	→	↗	↘	③ comparing information involving decisions
intellectual civic	↘	→	↘	↘	↘	→	↗	→	→	↗	↘	↘	④ contrast information achieving discourse
environmental apprehensive	●	●	●	●	●	●	↘	●	●	●	●	●	⑤ [no information] shift strategy
progressive modern	●	●	●	↘	●	●	↘	●	●	●	●	●	⑥ feed-back information set up dialogue
	↓↓↓↓↓↓↓↓			↓↓↓↓↓↓↓↓			↓↓↓↓↓↓↓↓			↓↓↓↓↓↓↓↓			recommended risk communication strategy related to a particular social image
	social image of technology in society			social image of technology in society			social image of technology in society			social image of technology in society			

5. Conclusion

The research was presented at 5 meetings and is developed in 22 publications and reports. Significant progress have been made on the interest of Cultural Theory to explain risk perceptions, and in the use of social representations to describe the « individual-risk » interaction. The study of the radiation risk situations retained allowed to point out interesting differences between countries as for perceptions and communication policies. There is clearly a need for studies in these fields based on a cross-cultural approach.

Head of project 1: Dr. J. BRENOT

II. Objectives for the reporting period

Review of risk perception studies

Concepts have to be clarified and the approaches to risk perception must be described. In general risk issues are harshly debated in the public and they can be better understood when embedding them in the context of other social debates. So the question is : are there approaches which account for political preferences and cultural factors, and how interesting are they to explain risk perceptions?

Risk communication : approaches and programmes

It is needed a clear understanding of the various individual coping strategies which range from apathy, no worry, avoidance, information seeking, changes in life style, inter alia. How they occur and when, is a necessary information for the development of better risk communication programmes. These points can be addressed when studying particular radiation risk situations.

III. Progress achieved

III.1 Progress achieved in risk perception

Review of risk perception studies (1, 5, 8)

The risk concept, the various approaches which aim at describing the perception phenomenon (psychometric, interactionist, and cultural), the dimensions of perception and their use to characterize the various hazards have been developed in three papers (1, 5, 8).

The psychometric approach, proposed by Slovic and colleagues, associates the dimensions of the risk situation with the individual's characteristics. Dimensions may be quantitative indicators (such as probabilities, economic consequences, etc.) and/or qualitative scales (the viewpoints which are considered as important with respect to people perception, such as unknown, familiar, equitable, etc.). Individual characteristics cover personality traits, demographics, physiology, but also knowledge relative to the situation and skills. Within this approach, a typology of the risk situations can be elaborated based on the above dimensions, see for instance the well known « cognitive » map of risks which has been published by Slovic. Individual opinions and behaviours relative to risks are implied by how individuals score the risks on the dimensions.

In the interactionist approach, perceptions of an individual result not only from the personal assessment of the risks but also from how risks are perceived by the other individuals. Thus the perception phenomenon is clearly a dynamic process. Indeed a major source of change in individual's perceptions lies in the fact that the individual is influenced when other individuals are changing their own views.

The cultural approach supports a even more extreme position. People in society share diverse views on the world and the social organization. Such worldviews are orienting dispositions which guide people to respond in complex situations. Concerning the risk domain, four worldviews have been proposed by Douglas, Wildavsky and Dake in the Eighties to explain why people select some risk situations to deal with and neglect others, and how they endorse some common beliefs about risks. The worldviews define the structure of social relations as first an orientation towards the group or privileging the individual, and second a more or less strong support to social norms and rules. The four views so deduced are individualism, hierarchism, fatalism, and egalitarianism which allow four groups of people to be defined. A research action has been pursued by IPSN on those cultural profiles.

Interest of Cultural Theory (2, 3, 6, 7, 10)

Social and cultural factors are recognized to play a role in people's risk perceptions. The cultural profiles offered an interesting alternative to account for such factors which are not always easy to resume with usual individual characteristics. According to the theory, the four basic profiles would be associated with particular perceptions of the risk situations. The research on Cultural Theory validity and interest used the questionnaire designed by K.Dake for his thesis (UCLA, Berkeley 1990).

A translation in French of the 20 items of the questionnaire was tested with students in February 1993 (2) and then introduced in the IPSN May 1993 national survey on perception of risk and safety in France (3). All the results concern a French national representative sample (1022 adults, age 18 and over) and are given in a report (6). Main results were presented on May 1995 at the SRA Conference in Stuttgart (7) and in Oslo on October 1995 (10).

Four scales were used to score a subset of 20 hazardous situations : risk to you and your family (personal risk), residual risk (general risk), safety demand, trust in risk information. Relationships between the scales and the four cultural profiles have been studied. The main results for the French context are the following. The Dake's questionnaire has a satisfactory internal validity. On one hand, the four cultural profiles, hierarchism, egalitarianism, fatalism and individualism show high correlations with political position as expected but also with more usual individual characteristics as age, gender, income, education level. On the other hand, for the hazardous situations considered (mostly industrial and technological) relations with the risk perceived are not as high as expected. Only the egalitarians express a high level of personal risk for most of the situations, and the three other groups show no particular response patterns. Similar results have been obtained in Sweden by L. Sjöberg. So the French and Swedish results do not support Dake's assertions. At this step Cultural Theory, as operationalised in the Dake's questionnaire, does not carry out new elements to explain risk perceptions. One reason lies in the questionnaire which is presumably too simple. The second reason lies in the richness and complexity of the concept of culture which needs to be clarified before any other tentative is made to relate risk perceptions to cultural factors.

III.2 Progress achieved in risk communication

Risk communication approaches (4)

Present French practices in communicating industrial risk and radiation risks have been presented at the Risk Communication Conference held in Stockholm, 9-10 May 1994. Risk communication around chemical plants is driven by the Seveso Directive, and its regulatory basis is European. Local and regional communication around nuclear installations has a French regulatory basis. However in both cases, actual practice is less communication than information giving, and rather one-way process than mutual exchange. Two radiation risk situations were detailed at the Conference, radioactive waste and nuclear power. In the case of waste the communication problem to deal with differs from low level to high level waste. Low level waste rise local awareness and concern small communities. High level waste constitute a society issue not solved yet, and involve national debate and political decisions. In this later case, not only technical information is needed but also a two-way communication enlarging the risk debate up to a social choice. Regarding nuclear power a distinction between power plants and energy is useful. For power plants which are now part of the French landscape and daily life, information is given at the local community level and concerns plant news (energy and economic performances, incident reporting, emergency preparedness). For nuclear energy, information is given at the national level and the risks associated with the technology are generally not included in the message.

The four radiation risk situations (5, 9, 11)

Indoor radon exposure (9)

Radon represents an every day exposure affecting all the individuals who normally should be concerned with. In fact public opinion surveys show that the radon risk is more or less well known, by a majority in the US and UK and by a minority in France ; moreover it is not always perceived as a threat to health. Communication campaigns have been launched to increase people awareness to radon. Actions of the Environmental Protection Agency in the US were extensive and used all the communication channels available (booklets, newspapers, TV, meetings, etc.). A more common communication, rather information, was made in the UK (guides and brochures). In France actions are few. In all countries actions are under the responsibility of public authorities which consider radon as a public health problem and inform home owners about the radon risk. However people in general show apathy and a very low motivation to improve their homes by reducing the radon concentration indoor without any monetary incentives from authorities. Indeed indoor radon mitigation remains in most countries (including France) a home owner's decision, and up to now authorities have not defined when and how such an action should be compulsory. The radon risk situation is a case for which information can be successful, i.e. memorized (see the US experience), but fails to improve the situation, i.e. lower the radon levels. A possible way for improving the situation is the setting of new regulatory requirements on housing by public health authorities which simultaneously would have to inform the public on the reasons of such regulations.

X-ray diagnostic (5)

Concerning people opinions on X-ray diagnostic no specific survey has been conducted in France. All the data obtained come from large questionnaires where X-ray diagnostic was one among many other risky situations. Such questionnaires have been proposed to national representative samples of the French population since 1986. Very few people consider X-ray examinations dangerous (percentages are comprised between 11% and 23%) even if they are 40% on the average to think that the truth about associated risks is not said.

A tentative was made at the end of the Seventies by SCPRI (the French Service in charge of radiological protection) to make the general public aware of their medical and dental diagnostic doses. It took the form of an individual card presented by the patient to his physician who had to fill the card at each examination. No experience feedback has ever been published.

To reduce doses from X-ray diagnostic efforts are now directed towards physician's practice rather than patient's behaviour. Implementation of ALARA methodology in hospitals and clinics is in progress.

Food irradiation

Irradiating foodstuffs is permitted in France and several large installations are operating. Debates about the possible risks of the practice do not reach people and they appear only in scientific magazines with large public audience (Science et Vie, Science et Avenir, etc.). Few data exist on people knowledge and risk perceptions. The use of irradiation for food preserving is not known in general. In a recent French representative survey, people who feel personally endangered by the practice are 29%, 26% do not know precisely, and they are 41% to think no [Report SEGR/LSEES 95/03 January 1995]. To conclude one can say that food irradiation is not a French issue.

Radioactive waste (5)

The French situation for radioactive waste is the following. The first low-level waste site near La Hague is full and the procedure to close it is going on. The second low-level waste site of Soulaing was opened in 1992 and its operating period is estimated to 30 years. The national agency ANDRA in charge of waste management takes funds from operators. High level waste siting has not been solved and only the search of one or two underground laboratories for testing is in progress. This phase was under ANDRA responsibility up to 1990. However increasing opposition from local communities cited as possible choices stopped the process during one year. Since then it is managed at the National Assembly level by French deputies who redefined the whole siting procedure.

Anyway the waste issue is a key point for nuclear energy policy. It is also perceived as an important society problem by a very large majority of people, as underlined by the results of the many surveys performed in France since 1976. Consistently people have considered radioactive waste as one among the most important environmental worries. The feeling of danger to them and relatives due to waste is always high but, however less than the residual risk they perceive at the society level. Fully aware of

the social dimension of this issue, they express a strong demand for safety. Always radioactive waste rank at the top of the demand scale (more than 80% think safety measures extremely urgent) as for water pollution and chemical waste, when lower levels of demand are associated with situations like tobacco, alcohol, road traffic accidents. The ranking clearly does not depend on the number of deaths which could arise in the risk situations studied. An other logic is at work there which emphasizes social control rather than an individual control. It must be noticed also the very low trust in authorities responsible of the management of radioactive waste.

Is the radioactive waste situation very different from those of other wastes, as chemical or industrial ones, especially with respect to site acceptability ? Not really. The siting issue for any type of waste is difficult to solve in France as in all other developed countries. There are no solutions based on the technical arguments of public authorities. The policy is now to involve concerned communities in a global formalised negotiation process driven at the highest political level, which means the participation of elected bodies, interest groups and of the operator which is in most countries a national agency. Health and social considerations enter in the process, but economic incentives as well. Anyway the negotiation is completely site and social context dependent. Experience has shown that lessons gained from the analysis of success or failure at one site do hardly transpose to an other site and social context.

References

- (1) BRENOT J. "Perception of risks from radiation and other sources". Paper for the Nuclear Safety Division IAEA. February 1994., Note SEGR/LSEES 94/18.
- (2) BAUZADAT Ph. Perception des risques. A la recherche des facteurs socio-culturels. Mémoire de stage. Université Paris V René Descartes, Septembre 1993.
- (3) BONNEFOUS S., BRENOT J. Perception des risques et de la sécurité : résultats du sondage de Mai 1993. Note SEGR/LSEES 93/20, Juin 1993.
- (4) BRENOT J. Information and Communication on Risks. Practices and Trends in France. Risk Communication Conference, Center for Risk Research, Stockholm, 9-10 May 1994.
- (5) BONNEFOUS S., BRENOT J., HUBERT Ph. Perception des risques nucléaires et information. IAEA "International Conference on Radiation and Society : Comprehending Radiation Risk", Paris, 24-28 October 1994.
- (6) BRENOT J., BONNEFOUS S. Approche socio-culturelle de la perception des risques. Note SEGR/LSEES n° 95/17, 1995.
- (7) BRENOT J., BONNEFOUS S. Interest of Cultural Theory in Perceived Risk Analysis. A French Experience. SRA Conference 'Risk Analysis and Management in a Global Economy', May 21-25 1995, Stuttgart, Germany.
- (8) BRENOT J., BONNEFOUS S., HUBERT PH. Perception des risques nucléaires. Note SEGR/LSEES n°93/30, Soumis à la revue Radioprotection, 1995.

(9) POMMIER S. Communication sur le risque radon. Bilan des actions menées aux États-Unis, Royaume Uni et France. Note SEGR/LSEES n° 95/61, 1995.

(10) BRENOT J., BONNEFOUS S. Relationship between Cultural Profiles and Risk Perceptions. International Seminar (Workshop) on Radiation Risk, Risk Perception, and Social Constructions. Oslo 19-20 October 1995.

(11) BRENOT J., HESSLER A., JOUSSEN W., SJÖBERG L. Perception of Radiation Risk from a Cross Cultural Perspective. IRPA9 1996 International Congress on Radiation Protection, April 14-19 1996, Vienna, Austria.

Head of project 2 : Dr. W. JOUSSEN

The research was conducted by :

Dr. W. Jousen

B-Plan Büro für sozialwissenschaftliche Analysen und Planungen

Postfach 1245, D-52232 Eschweiler

Tel. 49 2403889160 Fax. 49 2403889170

Dr. A. Hessler.

RWTH AACHEN University of Technology Aachen

Institute für Soziologie (IFS), Director Prof.Dr. Karl Heinz Hörning

D - 52056 Aachen, Karman Forum

Tel. 49 241806096 Fax. 49 2418888160 hessler @rwth-aachen.de

The research was developed around the key concept of social representations and is titled :

Effective Communication of Radiation Risks. Social Representations and Local Contexts in Risk Perception and Risk Communication.

Three reports have been issued : the executive summary for the Final Report, a detailed version of this summary, and a large volume integrating all methodological issues and results.

The executive summary for the Final Report follows. The main points are :

- Problem description and objectives of the study
- Key results
- Problem background and introduction
- Fields of investigation
- Theoretical and methodological framework
- Inventory of risk debates and risk communication strategies : radiation risks and risk communication in Germany, the Netherlands and Belgium
- Results : the role of social representations in risk perception and the importance of local contexts in risk communication efforts
- Discussion
- Conclusion of the results
- Case study of a failed risk communication program : the low level radioactive waste repository in Belgium
- Evaluation of risk communication strategies
- Putting a different focus : communication, social representations and local contexts .

EXECUTIVE SUMMARY

Problem Description and Objectives of the Study

Though modern societies have achieved high levels of welfare and effective ways of policy making, uneasiness is growing about possible risks related to new technologies. For the general public expert based decision making sometimes lack in transparency and often appear more driven by political interests than rational expertise. Information on risks is provided by different stakeholders and frequently contradicts in evaluating hazards or in giving recommendations. As a consequence risk communication (rc) programs intend to get into a more rational dialogue between experts and laypersons and to provide information on risky activities, products or processes; however many programs did not succeed the way it was expected. The objective of this study was (i) to evaluate and categorize rc approaches and (ii) to develop strategies in order to improve the efficiency of such programs.

Key Results

The presented study investigates rc efforts in the fields nuclear waste, x-rays, radon and food irradiation. Based on a comparative study (NL, B, D) we describe the complex interaction of perceived information and the local, cultural and social context where this information will be related to. In contrary to traditional approaches the findings underline the importance of the social representations a particular technology or hazard is embedded in. Our study shows, that (i) one person may link different social representations to the same risks (i.e. ionizing radiation in different contexts) and (ii) the social image of a technology within one society may be derived from individuals' social representations. As a consequence we propose that effective rc efforts have to a. identify first the dominating social representations of a particular technology within groups or society and then b. develop a strategy that fits into the communication requirements of the social image that belongs to a particular technology.

Problem Background & Introduction

As outlined above the task of this study was to investigate and to evaluate risk-communication strategies. In order to do so we chose the field of ionizing radiation. A review of literature in the nuclear field has shown us a big quantity of studies dealing mainly with problems of risk-perception and risk-communication. Research has developed a broad array of explanations why people often behave "irrational" in their actions and decisions and how communication strategies have to address to specific needs of particular groups in order to fulfill certain communication requirements. According to several scientists, lacking success in subsequent rc strategies could be explained e.g. by the fact that radiation is stigmatized; additionally nuclear experts' estimations on risks seem false after the accidents of TMI and Chernobyl thus inducing a sharp decline in confidence people carried towards any scientific expertise in this field.

Taking into account these results we designed our study in a different manner. We wanted to show that the stigma argument for instance does not work in the case of x-raying or radon, and also we wanted to make clear that the often stressed gap between experts' estimations and laypersons is not the crucial problem to overcome. We however tried to understand in a better way why people often use different argumentation patterns when estimating the riskiness of a certain product or process. As a consequence we used the concept of social representations. Our hypotheses was that people use different patterns of argumentation when evaluating the risks

and benefits of particular technologies. During the following pages our study will be presented. First we will outline the four fields of technology our study has focused on, followed by the methodological framework. Our results stress the importance of social representations while the last part of this paper takes up these results for the development of more effective risk communication programs.

Fields of Investigation: Radon, Nuclear Waste, X-rays, Food Irradiation

The presented study focuses on 4 fields of radiation, namely radon, nuclear waste, X-rays and food irradiation. In all of the 4 fields people suffer risks from radiation, however these risks are embedded in different social contexts and stem from different sources. Radon is "natural" whereas the other types stem from use of radiation for certain purposes, e.g. energy production, medical diagnostics and food preservation. People are affected by food irradiation in their everyday-life, whereas other risks are related to special groups or belong to particular actions, like visiting a doctor's office. Risks from food irradiation are not related to any harmful radiation but to possible chemical side effects that were originated during the process of irradiation. However people perceive those risk in the context of "radioactive contamination of food" and associate with this new process of preservation an invention of food industry to increase profits while accepting increased risk for the consumer. In contrast to this "negative" image people have in mind when speaking from the food-industry, the doctor's practice is hardly subject to suspicious misuse of technologies. People have big trust in their doctors believing often in everything those recommend for treatment and such ignoring any possible hazards.

Theoretical and Methodological Framework

Our sociological analysis of risk-communication in advanced industrialized societies which in research design and methodology concentrates on "social representations" and "social networks" will not follow the established traces of psychological risk-communication research. Thus for our study we worked out the below described research design to uncover the effects of different "social representations" and "social networks" in risk assessment and their impact on risk communication processes. We put the focus on risk debates in the public in Germany, the Netherlands and Belgium for selected fields where ionizing radiation is employed or in its natural form may generate dangers. The empirical part consisted in three different approaches:

1 literature & document analysis

We hereby digged into the scientific debates and discourses of the four investigated areas, uncovering ambiguities and uncertainties in the expert community and trying to understand the specific risks related to each field radon / nuclear waste / x-rays / food irradiation

2 expert interviews

The expert interviews were carried out in two parts

- a. face to face interviews with experts in D, NL and B
- b. mailing questionnaires to app. 40 experts

The personal expert interviews stood at the beginning of the project in order get access to the problematique of the specific field the expert represents. Since these experts are in general at the "core" of the discussions they could provide us with informations on social networks and scientific debates on the topic. The main advantage of those face-to-face interviews was a. to get a comprehensive picture on the ongoing controversies and b. to receive "insider information"

that allowed us to look behind many statements of other experts in this field.

The mailing of questionnaires provided us with further data and extended our database for our purpose to evaluate the risk-perception among the expert community. 44 questions were asked, some answers allowed multiple choice, others required short comments. The questionnaires will be attached to the complete volume of this report. The achieved results are presented in the next part on social representations. Inquired experts came from science, governmental organizations, various institutions and policy makers.

3 focus groups

We organized focus group sessions that formed the third and most powerful part of our empirical work. Since this methodological tool was a very useful instrument for our purpose, we will shortly describe the main aspects. As described above, our analysis from the beginning was not limited to the field of nuclear waste as a major field of public and scientific discussion about recent risky technologies, because we wanted to compare risk perception, risk awareness and risk assessment in different fields of ionizing radiation and to find out reasons for different perceptions and assessments. So we selected x-ray, food irradiation, radon and nuclear waste as an adequate scope of the fields where the use or the existence of ionizing radiation is affiliated with risks. Analysis of concepts and risk evaluations there should provide us with reliable answers to our defined research questions. We assumed that despite the fact that all four fields deal with ionizing radiation there existed different "social representations" and "social network" relations, which affect the public awareness and concern about radiation and intervene in risk communication processes. So our basic interests in this part of our study were to

- identify "social representations" in the public with regard to the particular fields,
- identify typical "social networks" to which these "social representations" in the four selected fields are related to,
- analyze attitude formation processes in "natural settings" in the selected fields.

In accordance with our theoretical research frame we developed empirical definitions of our units of analysis "social representations" and "social networks". Our empirical definition of "social representation" for analytical purposes distinguishes between the following 3 dimensions:

- a) information, i.e. an individual's knowledge about and experiences with the particular object,
- b) relation, i.e. an individual's representation/image of the object itself and of the relation between the individual and the object, and
- c) evaluation, i.e. an individual's attitude and assessment of the object.

"Social networks" here were empirically defined as communication systems, an individual's information, relation and evaluation of an object refers to.

Based on our assumptions about the differences of "social representations" and their relation to specific "social networks" in and also between societies our inquiry was outlined as an empirical intra- and intersocial analysis. For this purpose we decided to analyze risk perception and risk assessment of lay-persons in the selected four fields in Germany, the Netherlands and Belgium.

Inventory of Risk Debates and Risk Communication Strategies: Radiation Risks and Risk Communication in Germany, the Netherlands and Belgium

The intention of this part is not to present a detailed and retrospective description of risk debates and risk communication with regard to the utilization and existence of ionizing radiation in Germany, the Netherlands and Belgium in the last 25 years. With the rise of new social

movements the discussion and criticizing at its starting point mainly centered around the use of nuclear power. Since then an enormous number of studies has been published portraying social base and mobilization, dynamics, impacts on society and many other important aspects. So reality here needs not to be reproduced. On the other hand social science analysis in this context still puts focus mainly - and for a long time practically only - on one topic: nuclear energy and since the 80th to the related problem of nuclear waste. Thus far social science went behind nationwide public debates on risks of modern technology. According with this "limited" focus the analysis of risk communication - approaches, success and failure - up to now pretty much concentrated on nuclear energy and nuclear waste nearly without exception and therefore lacks knowledge in other spheres.

Contrary to this and in part with even little or none attention from social sciences new topics emerged on the public agenda, not as spectacular as nuclear energy and waste, not forming new social movements, but obviously with high everyday impacts what makes them interesting topics of popular magazines and books published since the end of the 80th. These new technology risk debates, not yet accompanied by a "new" social movement, but nevertheless very much attracting parts of public interest, emerged on technologies and developments especially in the field of medicine and food. These discussions differ in content and dynamics from the nuclear energy debate: Whereas technology conflicts since the end of the 60th in industrialized countries originated in large scale state-sponsored technological projects, now since a long time existing technologies as is x-rays experience a reevaluation by parts of the public, but especially by parts of experts. So one central characteristics of the new technology risk debates is their "small-scale"-dimension; a second one is their - in a narrow sense of the term - nonpolitical quality i.e. their at first glance missing link to classical and new technology debates since the late 60th. Furthermore these risk debates are not mediated by citizen's initiatives, new organizations and parties but constituting a direct "confrontation" between "producers" and "consumers", and as is for example in the field of medicine between "applicants" (doctors) and "clients" (patients). A third important difference to "old" technological conflicts is their in comparison to others "unusual" origin: was it at the end of the 60th "lay-persons" concern about possible ecological, political and social impacts of some and later on nearly all large-scale technologies and the established bureaucratic and technocratic way of their implementation, now most of the debated small-scale technologies in first instance underlay a critical reevaluation of experts itself. Subject of such new risk debates besides others are "everyday-technologies" employing ionizing radiation (for example x-rays and food irradiation). Additionally in some European countries the radioactive gas radon has reached interest of parts of the scientific community and the public, stressing the importance of protection against risks of natural radiation. Our study examines risk debates in the NL, B and Germany over the past 25 years and aims at lining out the cultural differences such debates were embedded in; however since this summary is limited in its extend more detailed information will be provided with the complete volume of this study.

Results: The Role of Social Representations in Risk Perception and the Importance of Local Contexts in Risk Communication Efforts

Based on the results of our focus group discussions in Germany, the Netherlands and Belgium and the expert interviews we identified 6 different "social representations" of modern technology in general which guided people's interests and activities and formed the background of risk evaluation of particular technologies in modern society. The representations manifest within specific argumentation patterns. In order to understand this concept it is important to make clear that these patterns do not go along with persons (e.g. the "rational expert") but will belong

to the argumentation set of each individual. The social representation links a specific argumentation pattern with a particular technology that is embedded in a specific social context and the socio-cultural experiences of the individual. We formed the following 6 idealtypic argumentation patterns, these patterns derive from the representations that an individual attaches to a specific technology or risk:

- *traditional indifferent*
- *individual distant*
- *rational economic*
- *intellectual civic*
- *environmental apprehensive*
- *progressive modern*

Discussion

We do not want to discuss the results of the focus groups in detail in this short summary, however we would like to stress the strongest deviations that may give us some insight into cultural differences and different social representations.

- comparing the 4 fields over the three countries, argumentation patterns in NL, B and D are similar only for radon
- In the NL people seem less informed and concerned about the risks of x-raying and food irradiation since for both fields they often argue with the *traditional indifferent* pattern
- the *environmental apprehensive* and *progressive modern* pattern only could be detected in Germany, indicating a polarization of argumentation into extrem positions
- Germany has very high levels in the use of the *intellectual civic* pattern for nuclear waste and food irradiation, which shows that these two technologies are strongly associated with a political dimension, including the suspicion of other interests guiding decision making
- the *rational economic* pattern in Germany is highly used for x-rays and never for nuclear waste. This implies that people evaluate the risks in the medical sector in economic terms while for nuclear waste a cost-benefit ratio is neglected.

With the exception of the patterns "progressive modern" and "environmental apprehensive" all of these representations of modern technology could be found in the focus groups in the three studied countries. That the types "progressive modern" and "environmental apprehensive" only appeared in one focus group discussion in Germany together with other results of the German group discussion signalizes that apart from the other countries the evaluation of the technology impacts on modern life here provoked more basic and in part contradictory considerations. So in Germany technology seems to be an issue which plays a major role in favored or denied concepts of actual and future ways of living and thus is a more political issue embedded in entire social and political "theories" whereas in the Netherlands and Belgium dominated a "pragmatic", i.e. a practical approach with shortterm cost- and benefit evaluations for the individual. In accordance with this result in Germany we found less representations of the type "traditional indifferent" and "individual distant" as in both other countries, in which these SR-types were nearly identical in number of appearance. In the Belgium focus groups in general assesment of modern technology in contrast with especially Germany and with less difference to the Netherlands showed to be guided by economic considerations as the distribution of the SR-type "rational economic" in our group discussions profed. Most often German citizens in their

evaluations - and this also stresses the political dimension of this topic there - had a representation which we summarized under the heading of "intellectual civic" expressing the relation between the individual and his socio-political environment in which the "question of technology" is embedded in.

Conclusions of the Results

The achieved results of our study offer some explanations for failing risk communication programs in the past. As pointed out in an earlier part of this report the main problem of communication risks is tied to the decision problem, particularly in individual contexts or in policy-making contexts. Research in different fields has shown with what kind of problems individuals are confronted when they try to rank, prioritize and evaluate information in order to make a "good decision". Using approaches from these areas mainly psychological approaches were able to demonstrate how a person collects and ranks information, how somebody evaluates choices and subsequently how decisions are made. According to the investigation of decision making processes, two objectives were involved: the "descriptive" part aimed at the construction of models that accurately simulated the behavior of the decision maker; the "normative" part of such research was to construct models which would tell the decision maker how he or she should choose the class of the decisions for which the model is appropriate. Monitoring decisions and estimations on risks, it easily became clear for the scientists that a misfit exists between laypersons' decision-making and the normative models. Subsequently theories like regret- or prospect theory helped to explain such behavior where for instance expected utility approaches failed; however controversies increased on the riskiness of particular activities, technologies or products and in most cases the experts' estimations on risk-benefit ratios were significantly different from the laypersons'. In consequence, according to scientists working in this field one of the main tasks in order to overcome these conflicts on risks in society was to bridge the gap between laypersons and experts. Since experts applied scientific - mostly mathematical or statistical - methods for their estimations, their opinion was considered as "rational", whereas the laypersons seemed to make up their mind more intuitively. The classic idea of risk communication strategies is tied to the identified gap between experts' opinions about riskiness and laypersons' perceptions of risks. From this standpoint, action should take place the higher the divergent estimations between the groups are. In order to do so, action means providing information to the supposedly less-informed laypersons. Once these people have achieved this knowledge (statistical death-rates, probability-outcome ratios) it is assumed their behavior will change towards the desired intentions of the risk-communicator, is to say people act in a more 'rational' way. Our study has shown that this "educational model" does not always work out. It can be a successful approach when the particular social representation attached to this field requires this kind of strategy. An investigation of a failed RC approach we investigated for our purpose in Belgium underlines this hypothesis.

Case Study of a Failed RC Program: Low-Level-Radiative-Waste (LLRW) Repository

A part of our study discusses the local conflicts in the planning of a nuclear waste repository in Belgium and investigates reasons for its failure using the previously outlined findings of our study. The analysis is based on interviews with representatives of involved local and regional authorities, document and content analysis. The case of the Belgium village A. gives an example of the structure and dynamics of risk communication and conflict in the field of nuclear waste disposal with a risk communication strategy at its beginning which could be called "establish-

ment dialog" because of the limited scope of involved actors. Furthermore risk communication here was organized along an established political rationality with a formal decision making process in its center. Due to this the target "population" of risk communication in all differentiated phases were local official political bodies which according to a formal political logic seemed to be symbolized in one single person (mayor). This strategy, based on a reductionist perspective on local political decision making processes, neglects the variety of different interests, social representations and network relations in a community, even a very small one. Different from decision making processes on a national level party and other affiliations in the local sphere proved to be of less importance; local political processes more than others are structured by individuals with multiple network relations; and the local sphere apart from others gives rise to a specific type of personal control of politicians and decision makers which in some cases might produce a higher dependency of actual modes in those parts of the population identified as local opinion leaders. So risk communication as performed by ONDRAF in the case of the village A. paradoxically initiated processes at a local level but ignored basic conditions of such communication at that level. In this case an intended local communication approach was conducted according to a formal and non-local rationality ignoring the particularities and dynamics of political and communication processes there.

The results of our previously described investigation on risk communication about nuclear waste, social representations and social networks on one hand stresses the importance of the local level for effective risk communication because the discussions in our focus groups in all countries in general demonstrated decreased affectedness of participants by national politics and affairs and an upgraded interest in local processes and problems due to a obviously widespread frustration about the possibilities of control and participation. So the local sphere is seen as a field which to a higher degree allows individual participation and control, even if participants in our focus group mentioned the necessity of a reconstruction even of local decision making processes with the aim of an upgraded citizen's participation.

Furthermore in our focus group discussions we found a different relation between lay-persons and experts: If lay-persons identified experts being integrated in a local social system, trust and credibility were influenced by the assumption of an effective control in the local system preventing experts from "non-scientific", "non-objective" statements and engagements.

So risk communication in the case of plant LLRW disposals in Belgium as described in our case study started at the right level but employed a strategy which denied essential structural modifications of politics and communication processes about risks in modern "risk societies" in general and specific conditions at the local level.

Evaluation of Risk Communication Strategies

Risk communication takes places in different contexts and may be originated by different parties for different purposes. In its educating origin risk communication aims at reducing risky activities and avoiding "bad" decisions when dealing with risky situations. Upon this background "good" and efficient risk communication processes may be achieved when they:

- reach the goals (whatever those may be) envisioned by the group that induced the communication process
- fulfill the communication need as identified by the decision maker, the communicator and the person who is at risk
- identify well the target groups the program has to address to

- may place the risk successfully in the context of other risks
- involve all the interested parties and stakeholder groups
- maintain open for learning and changes that fit with new emerging needs

However risk communication must be evaluated in order to understand why some campaigns failed and others succeeded. Evaluation studies may provide new information about the risk problem and offer insight into other management options for dealing with a particular problem that cannot be solved in the communication context. It is also possible to imagine some sort of cost-benefit analysis for the organizations that fund such projects or campaigns. On-going monitoring may induce mid-course corrections in the rc-program and increase effectivity. Successful evaluation may lead to higher accountability of risk managers to policymakers and the affected public, implementing more trust and credibility.

In general studies on the evaluation of rc-programs should focus on the content of communication, the process and structure a programme is embedded in, and the effectivity of the outcome. Problems may occur when evaluating such programs since the outcome may result from other variables than the program itself, changes in behavior as a consequence of any program may change back after some time after the program stops, another aspect is related to non-intended consequences of rc-strategies (e.g. panicking).

We assume that in the past many risk communication strategies were only tailored for certain purposes and certain groups within a society, using primarily the model of transmitting rational information. Lacking success was followed by increasing research that tried to explain the reasons for such failure. The results of our research show, that risk communication programs have to be tied to the particular social representations people have in mind when arguing about risks and benefits of a technology. As a consequence we identified the following rc-approaches:

With regard to the 6 idealtypes of social representations of technology we have developed 6 corresponding communication approaches for risk communication. Each approach consists of basic arguments and methods that are particularly related to the communication requirements of a social representation. In practice, these approaches will always be used in a combination that fits the social image of a particular technology, product or process in society. However we will first present the 6 "classic" types that we labeled:

neutral information ● *general education*

context information ● *local emphasis*

comparing information ● *involving decisions*

feed-back information ● *set up dialogue*

contrast information ● *achieving discourse*

[no information] ● *shift strategy*

neutral information ● *general education*

The basic concept of this communication strategy is to inform. It presumes that people just do not have the necessary information in order to act or decide more rational in a certain context. "Neutral information" does not mean that the information in itself must be neutral but assumes that in general information will be perceived as neutral since people do not suspect political or other interests that may be linked to such sort of information. This type of strategy may stress the expert-frame the information is based upon and should imply a strong recommendation approach. The frame of the whole program may have a centralized organization structure, for example information sheets provided by some state department of ministry.

context information ● *local emphasis*

A strategy based on context information provides general information but aims at connecting this to the particular "lebenswelt" of the people who receive the information. "lebenswelt" in this context means the specific local and social environment a person's action is embedded in. Therefore issued information must have a local and social bias and has to follow channels that allow communicator and information to reach a person in "its world". This for instance may be reached by engaging and involving local gatekeepers, agencies, or local media. As a consequence information should be provided in a form that will enable people to link such information with their "lebenswelt". It also has to stress the "you can change it" attitude in order to break up traditional habits and to motivate people to do something for their world. Recommendations are expert-based and underline personal engagement.

comparing information ● *involving decisions*

A strategy based on comparing information presupposes the capability and the willingness of the receiver to compare heterogeneous information that may even include aspects of uncertainty. Information is mainly provided by experts from different fields and the information should be accompanied by quantitative data. Economic cost-benefit analysis is an efficient method in order to demonstrate the risks and benefits of certain action and to recommend decisions.

feed-back information ● *set up dialogue*

Feed-back information strategies are an adequate tool for information-seekers. This strategy is similar to the comparing information approach, however the receiver is interested in getting into dialogue with the information provider and to discuss issues and decisions. Strategies that aim to fulfill the feed-back aspect should underscore the active part of the receiver of information and make available information through multiple channels by multiple providers.

contrast information ● *achieving discourse*

A risk communication strategy that is based on contrast information might be the most challenging strategy since it requires flexibility and transparency in its approach. This strategy aims at setting up a discourse network where interested parties may present their arguments and opinions. A possible forum for such kind of discourse may be a workshop, the media, meetings or information events. This approach does take into account that people have very different opinions of a particular technology/ product /process and acknowledges different "rationalities" for assessment and evaluation. A strategy that is based on contrast information runs the risk that people may be even more confused about possible risks and benefits but it addresses to the variety of priorities and expectations that may be related to certain decisions. It is based on the active role of the information seeker and the intellectual disposition to deal with the complexity of a problem. This approach underlines the political aspects of technological decision-making processes and discusses the goals of the participants, its objective is to include the receiver into the discussions and decisions.

[no information] ● *shift strategy*

With regard to the social representation that manifests in the "environmental apprehensive" pattern the political and ideological impact is so strong that risk-communication strategies do not seem to be the adequate tool in order to achieve the communicator's goals. Consequently other risk-management strategies have to be employed.

Putting a Different Focus: Communication, Social Representations and Local Contexts

This study has shown, that response to risks is mediated by social influences, transmitted by a

social network that may consist of friends, neighbors, or a specific scientific community. In many cases, risk perceptions form afterwards, as part of the ex post facto rationale for one's own behavior. In the past, risk communication was intended to change the perceptions of risks for the target groups and to improve their decision-making capabilities.

We however claim that just the communication about risks does not necessarily change decision-making structures even when perception may change. People may get a lot of information on a particular subject and they may even know the figures and risks, however they may still decide in a certain manner since they belong to specific networks of ideologies, implicit assumptions, heuristics and values. Therefore we argue that effective risk communication has to focus more on the decision part and not so much on the perception part. Decisions occur within particular social settings. In consequence, rc strategies have to address these specific settings in order to achieve their goals. We have shown that these settings can be reached by using the concept of social representations. Social representations guide the argumentation patterns people apply when they evaluate the risks and benefits of any particular technology or activity.

Using the above mentioned results on risk perception and communication in the field of ionizing radiation we have aimed at demonstrating why the traditional approaches failed and how more effective programs may be developed. It makes few sense to develop e.g. a campaign on the risks of ionizing radiation since people perceive this topic in different social contexts, subsequently attaching different evaluations. It also makes no sense to use the same rc strategy for nuclear waste and radon. Our results show, that when evaluating the risks related to nuclear waste people argument with complete different patterns than in the radon case.

Our argumentation leads to the conclusion that an efficient, successful rc-strategy has to address to this particular social image. In consequence a "good" radon rc-program should 1. inform in a general context, since there is still just a deficit in information, but 2. also imply context information, is to say the program should be put into effect through particular local channels (gatekeeper, local media...). A *comparing information* rc-strategy is not so effective for the case of radon, because the *rational economic* pattern is low in this image. Neither the program should be framed with a highly political context within a *contrast information* strategy since people hardly use the *intellectual civic* pattern in order to evaluate the risks of radon.

On the other hand a risk communication strategy for x-rays in Germany should mainly put emphasis on cost-benefit aspects. People mainly argue with the *rational economic* pattern and compare benefits of x-raying with possible risks.

Interestingly the social image of nuclear waste in pretty volatile, not indicating any rational economic pattern for Germany but extremely high *intellectual civic* and even the *environmental apprehensive* and *progressive modern* pattern. This means that successful strategies must push contrasting information and be able to set up a broad discourse environment. People however who argue with the *environmental apprehensive* pattern cannot be reached by any rc-program, consequently other rc-management strategies have to be employed (e.g. mediation or participation programs). For the NL and B the social image for nuclear waste is different to the German one. People there more often use a rational economic argument. As a consequence rc-strategies should focus on these issues by using comparing information and get people involved into the decision making. As demonstrated our results offer a new tool for risk communicators to effectively tailor strategies for their purposes. Following this argumentation the set up of a rc-program has to a. first identify in a pretest study the dominating social representations and social networks a technology and a person are embedded in, and then b. to develop a sophisticated strategy that fits to the particular social image of a technology within society.

Publications

Hessler, A.G. / Hörning, K.H. (1996): Röntgen und Radon: Zur öffentlichen Wahrnehmung von Strahlungsrisiken, in: RWTH Themen (published 1. quarter 1996)

Hessler A.G. / Joußen, W. (1995) Röntgen, Radon, Radioaktivität: Kulturelle Hintergründe von Angst und Vertrauen in öffentlichen Risikodebatten (in print)

Hessler, A.G. (1995) Experten und Öffentlichkeit in Frankreich und Deutschland: Risikodiskurse und Entscheidungsprozesse im Ländervergleich, in: IFS publications 1-2, Institut für Soziologie der RWTH Aachen, Kármán Forum.

Hessler, A.G. (1995) Risky Decision Makers? Some Comments on Experts´ s Work & Responsibilities in Post Modern Societies (working paper)

Hessler, A.G. (1995): Angst um die Umwelt? Ein Streifzug durch die Geschichte der Risikopolitik, in: Joußen, W. / Hessler, A.G. (Hg.): Umwelt und Gesellschaft. Eine Einführung in die sozialwissenschaftliche Umweltforschung, Berlin: Akademie Verlag

Hessler A.G. / Joußen, W. (1994): The Mis-Perception of Risk-Perception, in: Risk Debates, 1,1.

Joußen, W. (1994): Präventiver Umweltschutz und die Steuerung des Umweltverhaltens, in: Umwelt und Gesellschaft. Materialien zur sozialwissenschaftlichen Umweltforschung, 1,1.

Joußen, W. (1995): Risk Debates and Risk Communication Strategies in Germany, the Netherlands and Belgium (working paper)

Joußen, W. (1995): Umweltkampagnen als Instrument zur Steuerung des Umweltverhaltens, in: Joußen, W. / Hessler, A.G. (Hg.): Umwelt und Gesellschaft. Eine Einführung in die sozialwissenschaftliche Umweltforschung, Berlin: Akademie Verlag

Joußen, W. / Hessler, A.G. (1994): Risk Communication, "Social Representations"and "Social Networks" - A Research Approach, in: Risk Debates, 1,2.

Head of project 3 : Prof. L. SJÖBERG

The research was conducted at the Center for Risk Research (CFR), Stockholm School of Economics, Sweden.

II. Objectives for the reporting period

Three topics were developed in the project, the first two dealt with risk perception aspects and the last one was oriented towards risk management and communication. The first topic was to evaluate the interest of Cultural Theory in explaining risk perceptions. A general presentation has been made. Opinion surveys have been designed to study the links between cultural dimensions and risk perceptions, and their results have been discussed and criticized. The second topic dealt with mutual perceptions. Those of politicians have been compared to those of people in the domain of risks. The third topic was the description of four radiation risk situations (indoor radon, X-rays, food irradiation and radioactive waste) in Sweden.

Because of the late signature of Association Agreements between Sweden and the European Union, it was not possible for the Center to apply as a formal contractor. Its intervention in the project took the form of an external assistance provided to IPSN. A first subcontract signed in 1993 dealt with the first topic of Cultural Theory : general presentation, Swedish results analysis and critical review of the studies. A second subcontract signed in 1995 covered the last two topics with respectively two studies, one investigating politicians and public risk perceptions and the other describing the four radiation risk situations in Sweden.

Three reports have been written, referenced (1) (2) and (3). Each topic is developed in a particular report.

The contribution of the Center for Risk Research is important and justifies a separate scientific document included in the Final Report.

III. Progress achieved

III.1 Progress achieved in risk perception

Concerning the risk target (1)

First a clear distinction has to be made between personal and general risk. This distinction lies on the affected target, risk to you and your family or risk to people in general. Indeed there are many risky situations for which perceived risk differs strongly as to level and rank order. When distinction between those targets is not specified, individuals understand the situation considered as affecting people in general and not themselves.

Role of education and knowledge factors : from experts to lay people (1)

For a specific situation (as food irradiation or radioactive waste), there are large differences in perceived risk when surveying particular groups of individuals, such as experts, more or less specialized scientists, and lay public. When the scientists are

not particularly involved in the domain concerned, their opinions do not really differ from those expressed by lay people, or in other words, they have no general tendency to judge the situation differently from the public. This means that general education is not enough to explain the differences observed in perceived risk.

About personality characteristics (1)

Personality characteristics (as anxiety) are often mentioned to play an important role. In fact they do not achieve in general noticeable contribution to perceived risk. More explanatory power can be obtained by introducing dimensions such as general risk sensitivity, trust in risk management and principally in operators, experts, authorities who are in charge of the situation.

Interest of Cultural Theory (1)

Nevertheless an important part of the variability remains unexplained and dimensions accounting for culture, social norms and ideology have been proposed to fill the gap. This approach is the basis of the so-called Cultural Theory of risk which was promoted by anthropologist Mary Douglas and developed by social scientists Thompson, Wildavsky and Dake. In accordance with the theory, four distinct patterns of social relations exist which are : hierarchical, egalitarian, individualistic and fatalist. In the society each individual recognizes himself in one pattern and has the corresponding world views ; also, his opinions towards risks are culturally biased and those bias are precisely at the source of the differences observed in perceived risk.

As for any theory, Cultural Theory must be validated by empirical evidence. Quantitative investigations began when K. Dake designed a questionnaire with four scales in order to capture the four distinct patterns. Since then many studies were performed which used the Dake's questionnaire or parts of it, to test Cultural Theory validity. A presentation of their main results is made in the report (1). It emphasizes the low correlations between the cultural scales and the perceived risk level, and more generally the weak explanatory power of these scales.

On its own, the Center for Risk Research developed an extensive empirical work to test the Theory. Several populations were surveyed : high achieving students (145 persons), teachers in Sweden (94) and in Brazil (102), general public in Sweden (775), and Fresno (141). In the survey of Swedish teachers the goal was not only to test Cultural Theory but also to compare it with the Psychometric approach. Once again, it has been observed in the results that correlations between perceived risk and the four scales were low. Moreover for the Swedish teachers the analysis showed that : a) the psychometric approach accounted for a moderate, but important, share of the variance of perceived risk ; b) adding the cultural scales to the psychometric dimensions gave virtually no improvement in explained variance.

All these results are challenging the assertions made initially which presented Cultural Theory as a promising approach for explaining risk perceptions. Some of the reasons of this disappointing constatation could be : 1) the use of large population samples now instead of small convenience samples in the beginnings; 2) the Dake's questionnaire is too specific of the United States, i.z. item formulation and pertinence cannot be generalized to other countries ; 3) culture is a too complex

concept to be operationalised with a small set of items, or in other words, the questionnaire is quite incomplete ; 4) and more likely, cultural factors are not the major factors in risk perception.

Group differences in risk perception : politicians versus public in Sweden (2)

Previous research on group differences has been mostly concerned with experts, 'elite' groups, teachers, and administrators. Few studies are devoted to politicians' perceptions. A recent study in Finland by Hämäläinen (1991) compared politicians' and experts' opinions with regard to energy options.

In the Swedish study, initiated in 1995, local active politicians specialized in risk and environment questions were interviewed and their opinions have been compared with those of the public. Special emphasis is put on how the two groups view each others' risk perceptions, and how these beliefs are related to a demand for risk mitigation.

A random sample, N = 1100, of the Swedish population in the ages 18-74 was approached with a mailed questionnaire in May 1995. At the same time, all members and their deputies of the Health and Environment Boards (HEBs) of 27 municipalities received the same questionnaire. There were 15-20 persons in each municipality. The 27 municipalities were selected on the following basis : the four largest cities (Stockholm, Göteborg, Malmö and Uppsala) ; a few interesting communities where siting a radioactive waste repository is contemplated (Malä, Storuman) ; a wide sample covering Sweden geographically and in terms of the size of the community.

The questionnaire covered many topics : perceived general risk for 26 hazards, judgements of 18 technologies, Fishbein-type scaling of 5 radiation technologies, judgements of future standard of living and environmental situation, positions on the present Swedish nuclear power and on radioactive waste, competence of and trust in agencies and experts with regard to radioactive waste, psychometric dimension of radioactive waste accidents, and demand of risk mitigation. In particular, for each hazard in the list of 26, the respondent had : a) to give the level of risk perceived ; b) to estimate the level of risk perceived by the other people living in the municipality ; c) to estimate the level of risk perceived by politicians.

The questionnaires were mailed. The response rate was 49% in the public and 63% for politicians. The public sample was reasonably representative. Politicians are dominated by highly educated males, clearly different from the distribution of the sample for the public. Of course, politicians were not homogeneous ; they differed greatly and they are more polarized than the public.

Two main findings emerged from this comparative study : the two groups had very similar risk perception, and the desired risk reduction assessed by politicians was more strongly accounted for by their beliefs about people risk perception than their own risk perception. The fact that politicians in HEB boards really do not differ much from the public makes them different from experts in that respect. At the same time, they had somewhat higher trust in politicians in general, and they saw themselves as more knowledgeable than the public. The question arises if national politicians are different from those who are HEB board members. No answer can be made because there are no data (at least published) on risk perception of members of the

parliament. The politicians in HEBs were more polarized and also more interested in economic aspects of technology than people did.

III.2 Progress achieved in radiation risk communication : the case studies (3)

The four radiation risk situations, exposure to indoor radon - X Rays diagnostic - food irradiation and radioactive waste, have been studied in the Swedish context. A common presentation was used for each situation : the risk to health, authorities' actions, people opinions, experts' views, and recommendations with regard to risk communication.

Indoor radon exposure

Today the Swedish legislation has established two limits for the indoor concentration of radon in air. The first limit is 400 Bq.m⁻³ in homes built before 1981 and the second limit is 200 Bq.m⁻³ in houses built since that date. These limits are similar to the international limits. If the radon concentration is higher than these limits, the exposure is classified as a danger to health. Local authorities are obliged to undertake measures to reduce the concentration in such buildings. The Swedish policy for reduction of radon levels places the central responsibility on the local authorities which should also inform the local population about this risk and how mitigation can be made. Radon exposure can be reduced by installation of a ventilation system and/or tightening the house foundations. These actions are not cost free and since June 1988 the house owner has the possibility to get an allowance for radon mitigation. There are also radon loans that the owner can benefit from.

The Swedish policy goals for radon reduction are the following : 1) a first step would be to monitor at least 80 % of the homes with radon levels above 200 Bq.m⁻³ and to mitigate them. The costs of the project will be around 2. 5 billions SEK ; 2) the radon levels should in future come down 25 Bq.m⁻³ which should be the general mean level of indoor radon for all the Swedish homes. Other proposition to reduce the radon health risk is to increase the allowance from 15 000 SEK to 20 000 SEK. At this time many local authorities are in late for the monitoring of homes in their regions. Monitoring should in general be cost-free and should be done by the local authorities on inhabitant's demand. Usually the reason for the low monitoring rate is limited budget and poor economy. Only 1/3 of the local authorities have schedules. The general public should get more precise information about the radon risk and the local authorities should continuously update that information with new scientific data. Some elementary education about radon should be given at school and there is a great need for researchers with special training in the radon field. The general conclusion is that the local authorities must increase their mapping and work harder to inform the local population about the radon hazard.

With respect to radon risk, people seem to be quite indifferent to the issue at least in regard to their homes. People feel that the risk is low. In comparison with other risks, health risk related to indoor radon is always rated lower than the average risk. In general the difference between personal and general risk is large, which explains why the risk negligence can occur. In Sweden the concern for indoor radon has diminished with time. It was high during the 1970's when the radon risk was

associated with the blue concrete used in construction during the period 1960 - 1970, which implied that there was somebody to blame.

The experts' view is to consider indoor radon as the largest radiation problem in Sweden today and this view is supporting all the recommendations made by the public institutions.

The underestimation of the radon risk by the public is the major conclusion. Possible explanations are : radon is a natural gas, and nature is seen as benevolent and friendly ; the gas cannot be sensed, so the risk is forgotten ; the possible effect, i.z. lung cancer, takes a long time to develop ; the exposure - effect relationship is uncertain, particularly for low exposures ; people think also that their homes are under their own control, so the risk is voluntary taken ; the risk is equitable in some sense, indeed everybody is exposed. Moreover information is lacking about how to test and mitigate. As an ego-related risk, i.z. a risk closely related to self conceptions, the radon tends to be denied and consequently people are reluctant to have their homes monitored and to consider risk mitigation.

The real problem is to increase people consciousness. The Swedish government has tried for many years to do so and the resources spent have been quite significant in terms of communication campaigns. People perceptions seem not to have been greatly affected by the information from the different authorities and very few individuals have taken radon mitigation actions. The situation reveals a confrontation between the policy maker's desire to protect public health on the basis of what the experts know is best, and the freedom of homeowners in their choices. Two evaluations of the radon risk are opposing. For policy makers, the seriousness of the risk is judged by an expected number of cancers in the population due to radon exposure. For each homeowner, there is one possible cancer due to radon which is only one characteristic among the many others associated with his home. Then the government cannot force people into a risk reducing behavior, and the very difficult task remains to induce an attitude change in Swedes which leads them to look for reduction of the indoor radon level.

X-ray diagnostic

In Sweden the regulation in the field of X-rays is done by legislation with the purpose of protecting the employees. Much work has also been done to reduce the patient dose.

Concerning people opinions on X-rays no specific survey has been conducted in Sweden. X-rays are not seen as possible health threat by the general public and the trust in medical personnel is high. Recent articles in the Swedish press insisting upon the risk of cancer associated with X-ray examinations do not seem to have affected the perceived risk.

Experts in the medical radiation area are either those working in governmental institutions or those using the X-ray equipment for medical purposes. At the present time no survey had been conducted to study these experts' opinions. It must be noted that the risk communication process concerns experts only, and more precisely the process is one-way because radiation experts in institutions give the risk information to the medical personnel.

The government has avoided to directly inform the Swedes about the risks of X-ray diagnostic. Most of the governmental actions have been aimed at the medical profession with the intention to reduce the patient dose without alarming the public. This way to achieve risk reduction can be seen as more effective than if the government had tried to increase the awareness of people. In this case X-ray radiation is a market-based risk which means that bearing on the risk generator has been considered as the most efficient alternative.

Food irradiation

Irradiation is a method for food preservation. It reduces the microbial contamination, removes bacterias and avoids germination. The process does not contaminate the food. No toxic effects have been found when the irradiation dose is delivered by an appropriate protocol. An intensive discussion about food irradiation took place in Sweden during the 1970's. It led to prohibit irradiated food. Now it is not possible to irradiate food in Sweden nor to import irradiated foodstuffs.

The general opinion in Sweden with respect to irradiated food is strongly negative. The most common misconceptions are : the food becomes radioactive and unsafe ; the food changes in terms of smell and taste ; nutrients are less. The public opposition has played a central role in authorities' decisions. It led to protective regulations, the main objective being the reduction of public perceived risk.

Experts in this field are working in majority in the National Food Administration. They judge the risk rather small. No particular survey has been made to study the opinions of these experts.

The present situation in Sweden is not very satisfactory. Food irradiation has been prohibited without scientific arguments. The decision was based upon a weak principle of precaution and influenced by the strongly negative attitude of the public. Looking back, it could be argued that the decision to forbid was premature.

Radioactive waste

For the high level radioactive waste, the problem is to find a final repository in Sweden. The process is a lengthy one. The agency in charge of waste management SKB has begun preliminary studies in different regions (Storuman, Malä, and Östhammar). After these studies SKB must have at least two locations candidate for the final repository site, and to end the local population must take part in a referendum before any final decision.

Regarding radioactive waste, public attitudes are affected by how people perceive nuclear power risks and if they feel that the responsible authorities can be trusted. In most cases the local public is strongly opposed to any possible siting of a repository in their community. Many public opinion surveys have been made in Sweden. Respondents did not consider themselves very well informed. For them science was incomplete and experts often disagreed on the issues. People associated radioactive waste risks with the probability of large disasters, non reversible effects, as well as injuries to vegetation and animal life, and to future generations. They thought that waste risks stood for a large share of all nuclear power risks. The waste

issue was judged as important. The data analysis showed that the perceived risk of radioactive waste can be explained by four dimensions : the attitude to nuclear power, a general risk sensitivity, risk aspects, and risk of background radiation. The respondents stated also that they were unlikely to vote in favor of siting in their region. The opinion was that the facility would have negative health effects, give the region a bad reputation, and that the economic impacts of the facility would not be large. In parallel, the Swedes were convinced that the management of their nuclear waste was their own problem.

Experts in radioactive waste come from nuclear institutions and universities. They have been surveyed in 1994. They tended to evaluate the waste risks as very small. For them the disposal problem is solved. Their opinions were at the opposite of those expressed by lay people. They thought that the issue was of very small importance in relation with the general public opinion.

The radioactive waste issue is a popular topic in Sweden because the site of a final repository must be found. For this reason the SKB agency is interested in public opinions. SKB informs the public with booklets and articles. Up to now information campaigns conducted by SKB did not affect people opinions, and risks from radioactive waste are always rated very high. The solution for going ahead in the siting problem seems to be in introducing the concerned citizens in the decision making process rather than just launching one - way information packets.

References

- (1) SJÖBERG L. (1995) Explaining Risk Perception : an Empirical and Quantitative Evaluation of Cultural Theory. Center for Risk Research, Stockholm, Report n°22, August 1994.
- (2) SJÖBERG L. (1995) Risk Perception by Politicians and the Public. Center for Risk Research, Stockholm, August 1995.
- (3) BERNSTRÖM M.L. (1995) Radiation, Risk Perception and Risk Communication. Center for Risk Research, Stockholm, August 1995.

**Final Report
1992 - 1994**

Contract: F13PCT920023

Duration 1.9.1992 to 30.6.1995

Sector C 24

Title: CEC/USNRC joint project on uncertainty analysis of probabilistic accident consequence codes

1)	Goossens	University Delft
2)	Haywood	NRPB
3)	Ehrhardt	KfK
4)	Boardman	UKAEA
5)	Roelofsen	ECN
6)	Hofer	GRS

I. Summary of Project Global Objectives and Achievements

The objectives of the proposed joint project were to further develop and apply expert judgement elicitation techniques in estimating the uncertainties associated with the predictions of probabilistic accident consequence assessment (ACA) codes, and to investigate the use of the results of these studies as input to uncertainty analyses of such codes.

Within the project the following contributions will be made.

- (i) To further develop methodological backgrounds and implementational aspects of expert judgement elicitation techniques to be applied in the joint project (TUD contribution).
- (ii) To further develop mathematical techniques for handling modelling uncertainty (TUD contribution).
- (iii) To perform modifications and extensions of the System for Uncertainty and Sensitivity Analysis (SUSA), that emerge from methodological improvements, for instance from (ii), as well as from the practical applications of the system to results from the COSYMA and possibly MACCS codes (GRS contribution).
- (iv) To provide the necessary detailed information on the relevant parameters and models, in order to:
 - (a) assist in the selection of appropriate experts in specific subject areas of consequence assessment (NRPB-KfK-UKAEA-ECN contributions),
 - (b) provide experts both in the general area of accident consequence assessments, and in particular modelling aspects, who will interact with and advise the chosen experts in other fields (NRPB-KfK-UKAEA-ECN contributions),
 - (c) consider the implications of the results of the expert elicitation with regard to an uncertainty analysis of the COSYMA code (NRPB-KfK contributions)

Achievements

Both the Commission of the European Communities (CEC) and the United States Nuclear Regulatory Commission (USNRC) have expressed their concerns with respect to the expected consequences in cases accidental releases of radionuclides might occur, in various ways. Both commissions have issued ACA codes (COSYMA by the CEC, MACCS by the USNRC), which enable users to make estimates of the risks presented by nuclear installations based on postulated frequencies and magnitudes of potential accidents.

Knowledge of the uncertainty associated with these risk estimates plays a crucial role in the effective allocation of resources to be put in risk reduction measures. In the absence of such estimates, suboptimal priorities might be assigned to particular topics. Fairly comprehensive assessments of the uncertainties regarding the code risk estimates have already been made. These uncertainty assessments were performed by feeding in probability distributions of the relevant parameters to both models.

These uncertainty assessments were largely done by the code developers as opposed to experts in

These uncertainty assessments were largely done by the code developers as opposed to experts in each of the many different scientific disciplines which feature within an ACA code. The formal use of expert judgement has the potential to circumvent these criticisms. Although the use of expert judgement is common in the resolution of complex problems, it is most often used informally and rarely made explicit. The formal use of expert judgement elicitation and evaluation was used extensively in both Europe (by Delft University of Technology) and the US (NUREG-1150 study by Sandia National Laboratories).

These ACA codes consist of several modules, with numerous input parameters of which a relatively small number will determine the uncertainties of the code output. These key input parameters are selected based on previous sensitivity analyses of the ACA codes or modules. The important phenomenological areas for which the key parameter uncertainties are assessed with expert judgement are:

- * atmospheric dispersion and deposition
- * behaviour of deposited materials and the calculation of its related doses
- * foodchain models
- * internal dosimetry
- * early or deterministic health effects, and
- * late or somatic health effects

The current joint project is undertaken with the aim of quantifying the uncertainty on key parameters in these areas.

For example, parameters on which uncertainties are required for atmospheric dispersion and deposition are:

1. achieving a library of uncertainty distributions over **model quantities** such as concentrations in the plume, standard deviation of lateral plume spread, dry deposition velocities and fractions washed out by rain, and
2. achieving a library of uncertainty distributions over **model parameters** such as the power law coefficients of lateral and vertical plume spread and the wash out coefficient parameters, which are the parameters used in both accident consequence codes.

The area of atmospheric dispersion and deposition (2 expert panels with 8 experts each = 16 experts) was the first subject of the study. Teams from the EC and USNRC were able to successfully work together to develop a unified process for the development of uncertainty distributions on consequence code input parameters. Furthermore, in this project, formal expert judgement elicitation has proven to be a valuable vehicle to synthesise the best available information by a most qualified group.

Three more panels of experts were elicited thereafter:

- * foodchain processes, consisting of two separate expert panels:
 - ** on soil/plant transfer and processes (7 experts), and
 - ** on animal transfer and behaviour (9 experts)
- * the behaviour of deposited material and related doses (one panel of 10 experts).

Three additional expert panels were started (each will have approximately 10 to 12 experts = circa 36 experts in total):

- * deterministic or early health effects
- * internal dosimetry
- * late or somatic health effects.

The expert judgement methodology applied in this project is a combination of methods from previous US and EC studies. The NUREG-1150 method and methods developed in Europe at Delft University of Technology.

The formal use of expert judgement elicitation and evaluation follows a procedure set out in a protocol consisting of the following steps.

- * definition of problem area:
The definition of the problem area requires a solid explanation of using experts' subjective assessments in favour of empirical data. Lack of data, or lack of specification of environmental or operational characteristics supports the use of expert judgements. Within the present study the ACA modules form the frame for the identification phase.
- * prioritization of code input variables or target variables:
The target variables over which uncertainty distributions are required need be identified for each subject area. A two step procedure is followed. First, all parameters of the subject's submodel of the ACA code must be selected. Importance is driven by the potential importance of the parameter's distribution to an overall uncertainty analysis. Second, out of this gross list only those parameters are subjected to formal elicitation for which no uncertainty distributions can be obtained alternatively
- * definition of elicitation variables or query variables in terms of observable quantities:
Elicitation variables are defined such that values of observable or potentially observable quantities are asked for. This rule follows from the fact that subjective probability represents uncertainty with regard to potential observations. A probability is in itself not observable Hence the elicitation questions were phrased as "what is the value of quantity X", and not as "what is the probability of quantity X". The experts were asked to provide subjective assessments in the form of three quantile points in the cumulative probability density function: the 5 percent quantile, the 50 percent quantile or median, and the 95 percent quantile These three datapoints encompass the experts' uncertainty assessments on the query variables.
- * definition of case structures:
The case structures document provides the frame for one panel of experts specifying all issues to take into consideration for the expert judgement exercise. It contains: information on the subject area; the objectives of the study; the choice of experts and the elicitation process, the processing of the experts' assessments; a detailed description of the scope of the panel; an overview of the ACA code and the related code module calculations; an overview of the physical, chemical or biological phenomena with respect to the subject area; and what the experts are to consider in their uncertainty assessments and which aspects they do not need to consider. The Annex of the case structures document contains all elicitation questions for the subject area panel.
- * definition of training and seed variables (empirical control variables):
Expert judgement exercises are performed for achieving rational consensus on unknown variables. Rational consensus is driven by a number of principles, including:
 - * scrutability/accountability: all data, including experts' names and assessments, and all processing tools are open to peer review and results must be reproducible by competent reviewers
 - * fairness: experts are not pre-judged
 - * neutrality. methods of elicitation and processing must not bias results
 - * empirical control: quantitative assessments are subjected to empirical controls.
 One method applied in some expert panels is the method of performance control by asking experts to assess performance control variables or seed variables. Seed variables are variables whose values are known or will be known to the analyst within the frame of the expertise, but are not known to the experts Generally, seed variables come from experiments which are not known to the experts in the panel, mainly being unpublished data. For the expert training session comparable variables are used with known realisations.
- * identification and selection of experts:
The term "expert" is used in this context to designate a person whose present or past field of expertise contains the subject in question, or who is regarded by others as being one of the more knowledgeable about the subject. Potential experts were identified and were requested to send in a CV (curriculum vitae) on the subject area. Formal criteria were developed for the expert

nomination and experts were selected by nomination committees (both EC and US-committees).

* dry run exercise

A dry run exercise aims at finding out whether the case structures document and annexed elicitation questions are unambiguously outlined and whether they capture all relevant information and questions for the experts' assessments.

* expert training session:

Experts are requested to provide assessments in terms of three quantile points of the uncertainty distributions over the query variables. Most experts are, in their daily life, less familiar with these concepts, and are not familiar with stating their degree of belief in terms of quantile points. For that reason a training session is organised consisting of probabilistic training sessions and explanations of the case structures and elicitation questions. In general, a training session lasts two days, whereby there is ample time for discussions. After the training session the experts have about 6 to 9 weeks to prepare their assessments and rationales.

* expert elicitation sessions:

With each expert an individual elicitation session is arranged. In this session the expert, a normative and a substantive analyst are present. The normative analyst is a project staff member who is experienced with subjective probabilities and has experience in expert elicitations. The substantive analyst is a project staff member who has experience in the field of interest and who has preferably contributed to the case structures document. The duration of an elicitation session should not exceed four hours.

* processing of experts assessments:

For each query variable, all expert assessments are combined using linear pooling combination schemes. The combined uncertainty distributions (in the form of three quantile points) are weighted sums of the individual experts' distributions. These schemes are termed "decision makers". Two major schemes are explored in the study:

* equal weight decision maker, whereby each expert's contribution is equally weighted

* item weight decision maker, whereby each expert's contribution is determined by the expert's performance on the seed variables questions.

* post-processing analysis.

Post-processing denotes the transformation of the query variables (the model quantities) into code input variables (the model parameters). As the query variables are (potentially) observable quantities and the model parameters may be model artefacts, this transformation procedure is subjected to mathematical analysis applying additional computer codes. For the full uncertainty analysis of the COSYMA code the distributions over model parameters will be used eventually

* documentation:

The main results are and will be published in joint reports between the EC and USNRC as EUR/NUREG-reports and in additional EUR-reports. Contributions to conferences and special events were also provided.

Head of project 1: Dr. Goossens

II. Objectives for reporting period

Within the joint project the chosen expert judgement technique is a combination of the techniques previously developed at TUD and applied in the CEC pilot study on dispersion and deposition (report 91-81 by Roger Cooke, TUDelft for the EC), and the methods previously used by the U.S. Nuclear Regulatory Commission (published under NUREG-1150).

The objectives for the TUD contribution were

- 1 To further develop methodological backgrounds and implementational aspects of expert judgement elicitation techniques to be applied in the joint project.
- 2 To further develop mathematical techniques for handling modelling uncertainty

Ad 1 Under objective 1 TUD was responsible for the contents and organisation of all eight expert panels:

- * atmospheric dispersion and deposition (2 panels)
- * behaviour of deposited materials and the calculation of its related doses (1 panel)
- * foodchain models (2 panels)
- * internal dosimetry (1 panel)
- * early or deterministic health effects (1 panel), and
- * late or somatic health effects (1 panel).

Ad 2 Under objective 2 TUD was responsible for the development of post-processing techniques and for techniques to elicit and process correlations among the assessed variables distributions

III. Progress achieved including publications

1. Expert judgement elicitations

As outlined in the summary section (section I) the expert judgement procedure follows a protocol containing 12 steps, for which TUD was responsible.

The results of the Atmospheric dispersion and deposition panels were finalised in reports EUR 15855 and EUR 15856. In the joint CEC/USNRC effort a programmatic decision was made by USNRC to assign all experts equal weight, i.e. all experts on each respective panel were treated as equally credible. These results are reported in the joint Main Report and Appendices [EUR-15855]. The decision of the CEC on the weighting scheme will be made at the stage of performing the full uncertainty analysis [which is outside the contents of this contract].

For the elicitations in total 16 experts were carefully selected based on the following nomination criteria: reputation and experimental evidence in the field of interest, number and quality of publications, familiarity with uncertainty concepts; diversity in background awards; balance of views, interest in the project, and availability for the project.

For the dispersion panel the following experts were selected:

1. Dr P Cagnetti, *ENEA, Italy*
2. Dr H van Dop, *University of Utrecht, the Netherlands*
3. Dr. F. Gifford, *Consultant, USA*
4. Dr. P Gudiksen, *Lawrence Livermore National Laboratories, USA*
5. Dr S Hanna, *Sigma Research Corporation, USA*
6. Dr. J Kretzschmar, *VITO, Belgium*
7. Dr. K. Nester, *Kernforschungszentrum Karlsruhe, Germany*
8. Dr S Rao, *NOAA/ERL/Air Resources Laboratory, USA*

For the deposition panel the following experts were selected:

1. Dr. J. Brockman, *Sandia National Laboratories, USA*
2. Dr. S. Friedlander, *University of California at Los Angeles, USA*
3. Dr. J. Garland, *AEA Technology, United Kingdom*
4. Dr. J. Pacyna, *Norwegian Institute for Air Research, Norway*
5. Dr. J. Roed, *Risø National Laboratory, Denmark*
6. Dr. R. Scorer, *Imperial College London, United Kingdom*
7. Dr. G. Sehmel, *Battelle, USA*
8. Dr. S. Twomey, *Consultant, USA.*

The aggregated elicited uncertainty distributions on dispersion and deposition represent state-of-the-art knowledge in these areas. These distributions concern physically measurable quantities, conditional on the case structures provided to the experts (non-complex terrains). They were developed by the experts based on a variety of information sources. For dry deposition the distributions capture uncertainty on dry deposition velocities of particles of different sizes, iodine and methyl iodide over different surfaces. For wet deposition the distributions capture the uncertainty on the fraction of particles, iodine and methyl iodide removed by rain. The dispersion distributions capture uncertainty on several downwind distances for four weather conditions over plume centerline concentrations, plume spread, and off-centerline concentration ratios. The distributions were all processed into distributions on the required code input parameters: dry deposition velocities, washout coefficient constants and dispersion power law coefficients.

It was also recognised that applying different techniques and performance based expert judgement techniques would enhance the value of the study. An additional report [EUR-15856] is being published to complement the Main Report by providing additional and more detailed information on

1. the performance based expert judgement results compared to the equal weighting results, and
2. the techniques developed at Delft University of Technology for processing the code input variables' uncertainty distributions.

Performance assessment via seed variables (i.e. variables whose true values are known post hoc) resembling the variables of interest are believed to play an important role in building rational consensus when applying expert judgement. With regard to experts' response to performance measures, the experience in the current study supports experience in previous expert judgement studies in which these measures were employed: experts appreciate a more objective approach to the problems of assessing uncertainty.

The results of the performance based expert judgements for the dispersion panel show a slightly better performance than the equal weighting results. For the deposition panel the calibration scores of both methods are quite uneven. The dry deposition results are not robust against the choice of experts, although the performance based results show markedly better performance with respect to calibration and information.

Although the post-processing PARFUM methods developed by Delft University of Technology only capture modelling uncertainty due to plume growth, and do not capture modelling uncertainty due to non-gaussian cross wind and vertical profiles, they reproduce the experts' assessments best. The PARFUM methods were decided to best represent post-processing results.

The results of the two Foodchain panels and the Deposited materials and related doses panel will soon be published. For all three panels 26 experts were selected. The selection criteria were the same as for the previous panels. For these three panels the following experts were selected

For the panel on deposited materials and related doses:

1. Dr. M. Balonov, *Institute of Radiation Hygiene, Russia*
2. Dr. A. Bouville, *National Cancer Institute, USA*
3. Mrs. J. Brown, *National Radiological Protection Board, U.K.*
4. Dr. M.J. Crick, *International Atomic Energy Agency, Austria*

- 5 Dr E Gallego, *Polytechnical University of Madrid, Spain*
- 6 Dr P. Jacob, *Institute for Radiation Protection, GSF, Germany*
7. Dr. O. Karlberg, *Swedish Radiation Protection Institute, Sweden*
8. Prof.Dr. I. Likhtarev, *Ukraine Scientific Center for Radiation Medicine, Ukraine*
9. Dr. K. Miller, *Environmental Measurements Laboratory, USA*
- 10 Dr. J. Roed, *Risø National Laboratory, Denmark*

For the foodchain panels the diversity of interest was large and it was recognised that not all experts had the same broad view on the whole field.

For the panel on animal transfer and behaviour the following experts were selected:

1. Dr. P.J. Coughtrey, *LC Mouchelle & Partners, U.K.*
- 2 Dr F Daburon, *Laboratory of Applied Radiobiology, CEA/IPSN, France*
3. Dr. O. Hoffman, *Senes, Oak Ridge, USA*
4. Mrs.Dr. B.J. Howard, *Institute of Terrestrial Ecology, Merlewood Research Station, U.K.*
- 5 Prof Dr. J. Pearce, *Food and Agricultural Chemistry Research Division, Department of Agriculture for Northern Ireland, U.K.*
- 6 Dr P. Strand, *National Institute of Radiation Hygiene, Norway*
- 7 Dr. C.M. Vandecasteele, *Radiation Protection Department, CEN/SCK, Belgium*
8. Mrs Dr G Voigt, *Institute for Radiation Protection, GSF, Germany*
9. Prof. G.M Ward, *Colorado State University, USA*

For the panel on soil/plant transfer and processes the following experts were selected:

1. Dr. L. Anspaugh, *Lawrence Livermore National Laboratories, USA*
- 2 Dr. M.J. Frissel, *IUR (International Union of Radioecologists), the Netherlands*
- 3 Dr. J.A. Garland, *AEA Technology, National Environmental Technology Centre, U.K.*
- 4 Ir. R. Kirchmann, *University of Liège, Radio-Ecology / Department of Botany, Belgium*
- 5 Dr. G. Pröhl, *Institute for Radiation Protection, GSF, Germany*
- 6 Dr G Shaw, *Centre for Analytical Research in the Environment, Imperial College of Science Technology and Medicine, U.K.*
- 7 Prof. W Whicker, *Colorado State University, USA.*

The aggregated elicited uncertainty distributions on the foodchain and the external doses represent state-of-the-art knowledge in these areas. These distributions concern physically measurable quantities, conditional on the case structures provided to the experts. They were developed by the experts based on a variety of information sources.

For the foodchain panels the following areas were covered, over which the experts provided uncertainty assessments:

- soil migration and root uptake into plants
- interception, retention and translocation in plants
- resuspension onto plants

- transfer from feedstuffs to milk and meat
- retention in the gut of animals
- biological half-life in meat of animals
- animal diets.

For the area of deposited materials and related doses uncertainty assessments were provided for the external doses to individuals, indoors and outdoors, from activity deposited on the ground and other surfaces in urban and rural areas. The experts also provided assessments on population behaviour. The remaining three panels on Early or deterministic health effects, Internal dosimetry and Late or somatic health effects has commenced and will soon be published. For all three panels about 36 experts will be selected. The selection criteria will be the same as for the previous panels.

On April 12, 1994 a Seminar on Expert judgement: Its elicitation and use was organised by TUD for EC program managers in Brussels. Approximately thirty people were present which has led to a useful information exchange on the applications of expert judgement techniques in other areas than accident consequence assessment codes.

2. Mathematical techniques for post-processing and handling correlations

When subjective probability is recalled to its original meaning, it can only be used to measure an individual's degree of belief regarding outcomes of possible observations. Consequently, in this joint effort experts are only asked about physically observable quantities with which they are familiar. Variables which are physically observable and for which the expert has to provide information will be called query variables. Code parameters whose uncertainty must be quantified in order to perform the uncertainty analysis are called target variables. Target variables may be query variables, but it can also arise that target variables are unsuitable as query variables, since they do not correspond to measurements which the experts can estimate

Two examples from the joint project illustrate the distinction between query variables and target variables

Example 1:

The lateral plume spread σ_y is modelled in the codes as a power law

$$\sigma_y(x) = A_y x^{B_y}$$

where x represents the distance from the source and A_y and B_y are the target variables for the code. Experts have little feeling for the behaviour of A_y and B_y , indeed the physical dimension of A_y must be [meters]^{1-B_y}. For this reason it was decided to elicit the experts over σ_y as this is a quantity which is measured repeatedly and with which the experts are familiar. Asking for the lateral plumespread means that the uncertainty analyst has to develop a method for determining a distribution on the code parameters A_y and B_y .

Example 2.

The migration of radioactive material through various depths of soil is modelled using a so-called box model, see Figure 1.1.

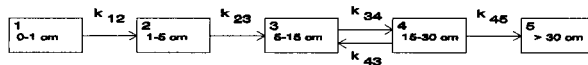


Figure 1: Box-model for soil-migration

The target variables for the code are transfer coefficients k_{ij} , which represent the proportion of material moved from box i to box j in a small time interval. Based on Figure 1.1, a set of first order differential equations can be constructed which, with the appropriate initial conditions, fully specifies the movement of the material between the boxes. The aim is to derive a distribution on all transfer coefficients. Transfer coefficients cannot be measured directly and therefore cannot be query variables. In this case the query variables were on times T_i when half of the mass of the deposited material has past beyond box i . From this information a distribution on the transfer coefficients has to be determined.

The determination of a distribution on the various target variables (A_y, B_y or transfer coefficients), given information on query variables (σ_y or T_i) is called post processing. Below we will discuss post processing techniques which were used and which will be used during the course of the joint effort.

PARFUM

The computer program PARFUM (PARAMeter Fitting for Uncertain Models) can be used for the first example. PARFUM determines a joint distribution on (A_y, B_y). In this section we will briefly describe the technique on which the program is based.

PARFUM determines an optimal distribution over the parameters (A,B) in the equation

$$X = A + B*Y$$

given the quantiles for X at various values of Y, and given an initial search grid. In the case of the first example we can take the log-transform of the powerlaw function in order to obtain the form which can be handled by PARFUM

$$\ln(\sigma_y) = \ln(A_y) + B_y \ln(x)$$

The technique involves the following steps:

- Determine a uniform search grid G of possible values for $\ln(A_y)$ and B_y .
- For each i , determine a distribution P_i on G which is minimally informative relative to the uniform measure on G under the following constraint: the 5%, 50% and 95% quantiles of $A_y x_i^{B_y}$ agree with the input quantiles for $\sigma_y(x_i)$.
- Determine a distribution P on G which is minimally informative with respect to P_1, \dots, P_n . In other words, P solves

$$P = \operatorname{argmin} \sum_{i=1}^n I(P_i, P)$$

where $I(P_i, P)$ denotes the relative information of P_i with respect to P. It can be shown that P is just the average of the P_i ,

$$P = \frac{1}{n} \sum_{i=1}^n P_i$$

The most important step is the first in which the initial search grid G is chosen. If G is large enough, then the final distribution P is insensitive to the choice of G. How large is large enough depends on the number of quantiles elicited and the number of downwind distances elicited

UNICORN

The overall aim is to determine a joint uncertainty distribution over (A_y, A_z, B_y, B_z) , where A_z and B_z are the target variables of the power law for the vertical dispersion. With the use of the simulation program UNICORN this can be done.

UNICORN (UNCertainty analysis with CORrelations) is a computer code for analyzing the uncertainty of output parameters given the uncertainty of input parameters and a model description. The model description specifies an explicit relation between the output parameters and input parameters. Monte Carlo simulation is used to calculate the uncertainty distributions of the output parameters as a function of the uncertainty distribution of the input parameters. UNICORN allows the user to incorporate dependence between the uncertainty distributions of the output parameters

Post-Processing Method developed for foodchain.

From the start of the second phase of the joint effort, in which foodchain and deposited material were treated, it was recognized that new post processing techniques had to be developed. The second example given above shows a problem which was encountered. As also mentioned above, a joint distribution on the transfer coefficients k_j is required, but these coefficients are not measurable. Instead it was decided to elicit the expert on times T_i when half of the mass of the deposited material has past beyond box i . The movement of the material between the boxes can be described by a set of first order differential equations. Based on the solution of the set and the information T_i provided by the expert, a joint distribution on the transfer coefficients will be determined

This technique is still under investigation

Dependencies

For the foodchain and deposited material phase it was regarded that the uncertainty distribution of many input parameters were likely to be correlated. For this reason a simple but effective technique was developed.

Experts were asked to state their conditional probabilities on certain questions. The questions followed a structure such that the positive definiteness of the covariance matrix would be guaranteed. On the bases of this information and a choice of a certain type of joint distribution, a rank correlation coefficients can be determined.

In estimating the conditional probabilities the expert we asked to consider the following experiment.

Conditional probabilities experiment

We consider univariate uncertain quantities X and Y with nice and smooth distributions. The marginal distributions of X and Y are assumed known (or already assessed). We consider an experiment for assessing the (rank) correlation between X and Y.

In every possible world, X and Y realize specific values. The (rank) correlation is a way of summarizing how the realized values of X and Y appear together.

If X and Y are positively (rank) correlated, then, roughly, large values of X appear together with large values of Y, and small values of X appear together with small values of Y.

If X and Y are negatively correlated then the reverse holds: large values of X appear together with small values of Y, etc.

Imagine now that many realizations are examined, and that the values for X and Y in each realization are recorded on a slip of paper and the paper slips are deposited in a large urn. We will draw, say, 1000 slips of paper from this urn (without replacement). We now discard all slips for which the X value is less than the median X value. We now have roughly 500 slips of paper, since the probability of X being less than its median is (by definition) 1/2. Suppose we have exactly 500 slips left on which X is greater than its median value. We now ask: on how many of these slips will Y be greater than the median Y value?

If the answer is "250", then the probability is 1/2 that Y is bigger than its median, given that X is bigger than its median. This would be the case if X and Y were independent. If the answer is "more than 250", then there is a tendency for large X's and large Y's to appear together, and this would be the case if X and Y were positively rank correlated. If the answer is "less than 250" then there is a tendency for large X's and small Y's to appear together, and this would be the case if X and Y were negatively correlated.

The expert is asked to describe his/her feeling for correlation by a number N between 0 and 500. This number is substituted into the following equation

$$P(Y > \text{median} \mid X > \text{median}) = \frac{N}{500}$$

An appropriate joint distribution will then be selected which

- has the assessed marginal distributions
- satisfies the above equation
- has minimal information among all distributions satisfying the above.

Example: Deposited Material

The following conditional probability

- $\text{Pr}(\text{GDR of Zr-95 10 days after depo. above its median value} \mid \text{GDR of Zr-95 immediately after depo. above its median value})$

should be read as follows.

Given that the median value of the Gamma Dose Rate (GDR) of Zr-95 immediately after deposition is above its median value, what would the probability be that for the same experiment the Gamma Dose Rate (GDR) of Zr-95 10 days after deposition is also above its median value

Publications

Harper FT, Goossens LHJ e.a.

Project Plan for Joint CEC/USNRC Model Probability Elicitation, for i.o v. CEC DG XII/Brussels, CEC DG XI/Luxembourg and USNRC/Washington, DC, USA, Sandia National Laboratories, Albuquerque, NM, USA/TU Delft, Safety Science Group, December 1992

Goossens LHJ, Harper FT, Cooke RM, Hora SC, Kelly GN and Glynn JC

Uncertainty analysis of probabilistic accident consequence codes for the nuclear industries - A joint CEC/USNRC expert judgement study, Invited contribution (paper) to the International Conference on Mathematical Models and Supercomputing in Nuclear Applications, 19-23 April 1993, Karlsruhe, Germany, 5 p

Harper FT, Goossens LHJ, Cooke RM, Hora SC, Miller LA, Päsler-Sauer J, Lui C and Kelly GN

Summary of uncertainty analysis of dispersion and deposition modules of the MACCS and COSYMA consequence codes – A joint USNRC/CEC study, Paper presented at PSAM-II Conference, San Diego, Ca/USA, 20-25 March 1994, Vol 1, session 009

Goossens LHJ, Cooke RM and Harper FT

The CEC/USNRC joint study on uncertainty of probabilistic accident consequence codes - Atmospheric dispersion and deposition, Lectures presented at Seminar on "Expert Judgement: its Elicitation and Use", CEC, Brussels/B, 12 April 1994

Goossens LHJ

Results of uncertainty analysis of dispersion and deposition in nuclear accident consequence codes - A joint CEC/USNRC expert judgment study, Proceedings of the First COSYMA Users Group Meeting, KEMA, Arnhem (NL), 25-26 April 1994, Report 40666-NUC 94-5819, pp.56-61

Goossens LHJ

Formal use of expert judgment techniques for quantitative assessments of unknown variables, Paper presented at 2nd Seminar Major Industrial Hazards Model Evaluation, Le Chateau, Cadarache (F), 19 May 1994

Harper FT, Goossens LHJ, Cooke RM, Helton JC, Hora SC, Jones JA, Kraan B, Lui C, McKay MD, Miller LA, Päsler-Sauer J and Young ML

Joint USNRC/CEC consequence uncertainty study: Summary of objectives, approach, applications, and results for the dispersion and deposition uncertainty assessment, NUREG/CR-6244, EUR 15855, SAND94-1453, Washington DC/USA, June 1994

Cooke RM, Goossens LHJ and Kraan B

Methods for CEC/USNRC Accident consequence uncertainty analysis of dispersion and deposition - Performance based aggregating of expert judgments and PARFUM method for capturing modeling uncertainty, EUR 15856, Luxembourg, June 1994

Harper FT, Goossens LHJ, Cooke RM, Hora SC, Young ML, Päsler-Sauer J, Miller LM, Kraan B, Lui C, McKay MD, Helton JC and Jones JA

Joint USNRC/CEC uncertainty study: Dispersion and deposition panels, In: Procedures and computer codes for level-3 probabilistic safety assessment, proceedings of a technical Committee Meeting, Organized by the International Atomic Energy Agency, Vienna, 21-25 November, 1994, IAEA, Vienna, Austria, 1995

Goossens LHJ, Cooke RM, Kraan BCP, Harper FT, Young M, Miller LA, Hora SC, Päsler-Sauer J
Uncertainty analysis of nuclear accident consequence codes: A formal expert judgement approach, Abstract and poster presented at Annual Meeting of the Society for Risk Analysis (Europe) on Risk Analysis and Management in a Global Economy, May 21 - 25, 1995, Forum Ludwigsburg, near Stuttgart, D, Abstracts book, p.453 (to be published in Proceedings)

Goossens LHJ, Cooke RM, Kraan B, Brown J, Jones JA, Boardman J, Harper FT, Young ML and Hora SC

Results of the ongoing probabilistic uncertainty analysis study on COSYMA (and MACCS) for deposited materials and related doses and the food chain models - A joint EC/USNRC expert judgement study, Paper presented at the 2nd COSYMA Users' Group Meeting, Budapest - Hungary, 19-21 June 1995 (to be published in Proceedings)

Head of project 2: Miss Haywood

II. Objectives for reporting period

The main objectives were:

1. to assist in preparing and obtaining results from the atmospheric dispersion and deposition panels (in support of FZK)
2. to assist in preparing and obtaining results from the two foodchain panels (with support from FZK)
3. to assist in preparing and obtaining results from the behaviour of deposited material and related doses panel (in support of UKAEA)
4. to assist in preparing and obtaining results from the internal dosimetry panel as leading institute
5. to assist in preparing and obtaining results from the late or somatic health effects panel.

III. Progress achieved including publications

1. Atmospheric dispersion and deposition panels

NRPB had a supporting role in the work for this panel. NRPB assisted in preparing the case structure document and the final report for the atmospheric dispersion and deposition panels. The results from these panels and their analysis are published ⁽¹⁾.

2. Foodchain Panels

NRPB has taken the lead in the work on determining uncertainties associated with foodchain parameters in ACA codes.

ACA codes produce a number of endpoints which relate to contamination of the foodchain and the subsequent ingestion of contaminated foodstuffs. These endpoints include the individual and collective doses arising from ingestion of radioactivity, the health effects arising in the affected population as a result of these doses, and the effect of food countermeasures imposed to reduce ingestion doses. To calculate these endpoints, ACA codes require input from a terrestrial foodchain model. The foodchain currently linked with the COSYMA code to produce the required input is the NRPB's FARMLAND model⁽²⁾. For the MACCS code a similar foodchain model called COMIDA exists.

The input to the ACA code from the terrestrial foodchain model is in the form of instantaneous and integrated activities in a number of foods as a function of time after deposition, for a number of single radionuclides. The units of this input are Bq/kg (inventory) and Bq y/kg (integral). FARMLAND requires a considerable input of basic foodchain data, to produce the inventories and integrals required as input by COSYMA. This includes the interception factor for pasture grass, the root uptake concentration factors for all radionuclides of interest, and transfer factors from animal feed to animal products.

The main transfer mechanisms in both foodchain models are: migration of radionuclides in soil, root absorption into plants from soil, surface contamination of plants and subsequent translocation, the transfer to animals and metabolism in the animal.

There are two stages at which uncertainty ranges on foodchain input parameters can be considered. These are:

- i) on the basic input data to the foodchain model
- ii) on the input to the ACA code (which is the output of the foodchain model)

The parameters for which expert opinion has been elicited in this study have been chosen to be the input parameters to the foodchain model rather than the activity concentrations in food which are the input to the ACA code. The reasons for this are that correlations in the input to the foodchain model and within the model are an important part of the study and can not be included if only the output of the model is considered. Also, the relevant expertise for eliciting foodchain model output parameters is limited and would probably be restricted to the code developers and to other model developers only, the great expertise in underlying foodchain transfer mechanisms would not be utilised.

It is therefore the uncertainty on the parameters describing the transfer processes within the foodchain, and the influence of these uncertainties on the predictions of the ACA system, that have been considered. The ranges on the activity concentrations in food are being produced during the analysis, rather than as the basic input to the study, as has been the case in other areas of the project.

The diversity of the subject of foodchain transfer together with the large number of interactions between soil, plants and animals and hence processes which require understanding and modelling led to the subdivision of foodchain experts into two panels. One panel considered issues relating to the uncertainties in estimating the transfer through soil and plant systems. The other panel considered transfer into and through animals.

NRPB assisted TUD in the selection of experts for these two panels.

A case structure document has been written for the two panels which described in detail the background to the elicitation questions, including the use of the elicitation variables within foodchain models and the underlying modelling assumptions where these were necessary to clarify the questions asked

These questions covered the following transfer processes:

Soil and Plant Expert Panel

- soil migration
- fixation in soil
- root uptake
- interception of deposited material by crops
- weathering from plant surfaces
- resuspension
- concentration in grain at harvest
- concentration in root vegetables at harvest
- important dependencies between parameters

A schematic representation of the principal mechanisms for the transfer of radionuclides in plants covered by the questions is given in Figure 2 1 The compartment marked 'soil' represents the model for soil migration and radionuclide fixation.

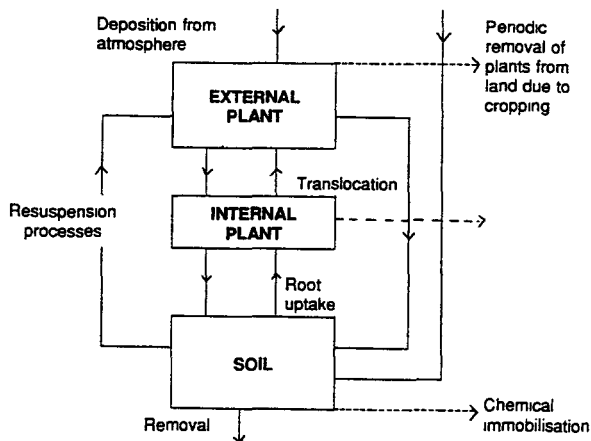


Figure 2 1 Schematic representation of the principal mechanisms for the transfer of radionuclides in plants

Questions were asked for a generic soil type and for a sandy and a highly organic soil and for a range of crops. Where parameters could be dependent on climate the experts were asked to specify whether they believed there would be differences between Europe and the USA. The elements strontium, caesium and iodine were considered.

Animal Expert Panel

- animal consumption rates
- availability of ingested feed
- transfer to meat
- transfer to milk
- transfer to eggs
- biological retention in animals
- important dependencies between parameters

A schematic representation of the principal mechanisms for the transfer of radionuclides in animals covered by the questions is given in Figure 2.2. Ingestion is the most important route of intake by the animal; inhalation is, in general, not important and it has not been included in the elicitation questions for the elements considered in this study. However, it may be significant for those radionuclides whose transfer across the gut is small.

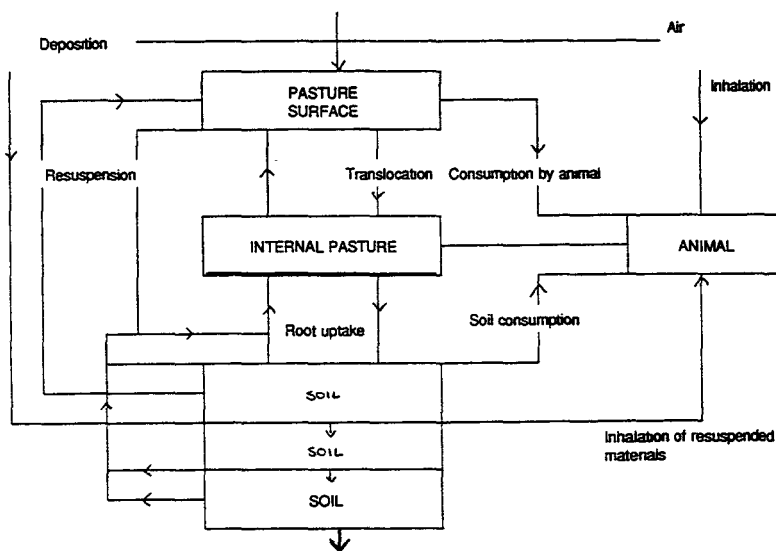


Figure 2.2 Schematic representation of the principal mechanisms for the transfer of radionuclides in animals

Questions were asked for cows, beef cattle, pigs, sheep, goats and chickens, where appropriate. For consumption rates the experts were asked to specify whether they believed there would be differences between Europe and the USA. The elements strontium, caesium and iodine were considered.

A dry run of the elicitation questions and case structure was held at NRPB in December 1994. A training meeting for the European experts on the two panels was held at NRPB in January 1995 in conjunction with the panel considering deposited material and associated doses. In collaboration with colleagues in the US involved with the project a training meeting was held in Albuquerque, New Mexico for the US experts on the two panels (April 1995).

Some important general conditions were identified during the development of the case structure and the training of experts which had an impact on the scope of the foodchain parameter questions. These were:

- 1 the results of the analysis will be used to make estimates of the uncertainty associated with the collective dose from ingestion and the consequences of banning food that are representative of the majority of reactors within Europe and the US. Inevitably, given the diversity of siting land for reactors within Europe and the US, the results can not be universally applicable. In the study the regions of interest were restricted to those typical of warm temperate climates, for example North-Western Europe and North-Eastern/South Eastern USA. Mediterranean countries, arid areas of the USA and areas subject to arctic conditions were not included. The estimates of uncertainty made by the experts were required to be applicable to the main agricultural production areas in these regions. Areas such as semi-natural environments were only considered in so far as they contribute to the food production for the regions of interest in the study
2. the quantity used in the models is the best estimate of the value for the various parameters. In this context, the quantity required is the uncertainty on the average value for the region described. For example, this means that where a parameter refers to the behaviour of radioactivity in animals, the ranges given must describe the uncertainty on that quantity averaged over a group or groups of animals in the region of interest, rather than the variability between animals in these groups.
- 3 the experts were required to produce values for the generic case, for example, a generic soil type. In some cases more detailed information was requested, such as a parameter value as a function of soil type.

Elicitation for the European experts on the two panels were held in February and March 1995 and were carried out by TUD and NRPB.

3. Deposited materials and related doses panel

NRPB had a supporting role in the work for this panel. NRPB assisted in the preparation of the case structure document and the final report which will be published in due course.

4. Internal Dosimetry Panel

NRPB is the leading institute in the work on determining uncertainties associated with internal dosimetry parameters in ACA codes.

Joint meetings for the Internal Dosimetry and Health Effects panels were held at NRPB in February, May and August. Letters to potential experts were sent out in July. A draft case structure and elicitation questions had been prepared and were discussed at the meeting in August. A further meeting will be held in October at NRPB to finalise the choice of experts and agree the case structure document. A dry run exercise is planned for late October and an expert training session for early December.

Questions on internal dosimetry address uncertainties in the biokinetic parameters used in the models. While COSYMA and other ACA codes include doses from a comprehensive list of radionuclides, uncertainty analysis will be undertaken for the most important radionuclides with some consideration of application to other radionuclides. Thus, uncertainties in parameters relating to dose coefficients will be considered for inhalation and ingestion of Sr, I, Cs, and Pu and inhalation of Ru, Ce, Sb, Te. Consideration of uncertainties in doses from Sr will be extended to make comparisons with the other alkaline earth elements Ba and Ra and to isotopes of U for which the same biokinetic model is used. Similarly, Pu will be compared with the other actinides, Am and Cm. Doses to infants and children will be considered as well as doses to adults.

For inhalation, the parameters addressed will include particle deposition in different regions of the respiratory tract, movement of particles out of the respiratory tract to the gut and dissolution and transfer to blood. For ingestion, movement between regions and absorption to blood will be considered. The distribution of radionuclides from blood to body tissues, their retention in body tissues and excretion in urine and faeces will be considered separately for individual elements or groups of

elements. Factors generally not taken into account will include the location of sensitive cells within tissues, and tissue mass and geometric considerations.

5.Late or somatic health effects panel

NRPB is been the leading institute in the work on determining uncertainties associated with late or somatic health effects parameters in ACA codes.

Work has advanced on the assessment of uncertainties in late health effects. Several meetings were held involving the coordinator and NRPB staff to discuss the development of the case structure and the setting up of a panel for the elicitation of uncertainties. A comprehensive list of over 80 potential experts in Europe was compiled and these persons were contacted by the coordinator. Names of some potential experts in the USA were passed to NRC for them to contact. As with the early health effects and internal dosimetry panels, experts from both Europe and the USA will participate. The nomination of experts will take place in October 1995.

The case structure focuses on cancer, in view of the paucity of data on the risks of hereditary disease. The aim is to elicit uncertainties in the risks of various types of cancer, taking account of extrapolation to low doses and low dose rates, as well as the projection of risks over a lifetime and across populations with different baseline rates. Variations in risk by sex and age at exposure are also addressed. Since the experts' responses are likely to rely on common data or assumptions, correlations between their replies to different questions will be quantified for use in post-processing.

The training meeting for European and US experts in the late health effects panel, as well as the other health effects panels mentioned earlier, will be held in the USA on 11-13 December 1995. Elicitation of the experts' assessments will commence the following month.

6. References

1. Harper FT, Goossens LHJ, Cooke RM, Helton JC, Hora SC, Jones JA, Kraan B, Lui C, McKay MD, Miller LA, Päsler-Sauer J and Young ML
Joint USNRC/CEC consequence uncertainty study: Summary of objectives, approach, applications, and results for the dispersion and deposition uncertainty assessment, NUREG/CR-6244, EUR 15855, SAND94-1453, Washington DC/USA, June 1994
2. Brown, J and Simmonds, J R, **FARMLAND: a dynamic model for the transfer of radionuclides through terrestrial foodchains**, NRPB-R273, London HMSO, 1995.

Publications:

Harper FT, Goossens LHJ, Cooke RM, Helton JC, Hora SC, Jones JA, Kraan B, Lui C, McKay MD, Miller LA, Päsler-Sauer J and Young ML

Joint USNRC/CEC consequence uncertainty study: Summary of objectives, approach, applications, and results for the dispersion and deposition uncertainty assessment, NUREG/CR-6244, EUR 15855, SAND94-1453, Washington DC/USA, June 1994

Harper FT, Goossens LHJ, Cooke RM, Hora SC, Young ML, Päsler-Sauer J, Miller LM, Kraan B, Lui C, McKay MD, Helton JC and Jones JA

Joint USNRC/CEC uncertainty study: Dispersion and deposition panels, In: Procedures and computer codes for level-3 probabilistic safety assessment, proceedings of a technical Committee Meeting, Organized by the International Atomic Energy Agency, Vienna, 21-25 November, 1994, IAEA, Vienna, Austria, 1995

Goossens LHJ, Cooke RM, Kraan B, Brown J, Jones JA, Boardman J, Harper FT, Young ML and Hora SC

Results of the ongoing probabilistic uncertainty analysis study on COSYMA (and MACCS) for deposited materials and related doses and the food chain models - A joint EC/USNRC expert judgement study, Paper presented at the 2nd COSYMA Users' Group Meeting, Budapest - Hungary, 19-21 June 1995 (to be published in Proceedings)

Goossens LHJ, Cooke RM, Kraan B, Brown J, Jones JA, Boardman J, Harper FT, Young ML and Hora SC

Results of the ongoing probabilistic uncertainty analysis study on COSYMA (and MACCS) for deposited materials and related doses and the food chain models - A joint EC/USNRC expert judgement study, Paper presented at the 2nd COSYMA Users' Group Meeting, Budapest - Hungary, 19-21 June 1995 (to be published in Proceedings)

Head of project 3: Dr. Ehrhardt

II. Objectives for reporting period

The FZK objectives were

1. to assist in preparing and obtaining results from the atmospheric dispersion and deposition panels as leading consequence institute
2. to assist in preparing and obtaining results from the two foodchain panels as back-up consequence institute (in support of NRPB)
3. to assist in preparing and obtaining results from the early or deterministic health effects panel as back-up consequence institute (in support of ECN).

III. Progress achieved including publications

1. Atmospheric dispersion and deposition panels

FZK has been the leading consequence institute in the work on determining uncertainties associated with atmospheric dispersion and deposition parameters in ACA codes. The results are published in EUR 15855.

Experts were asked to provide distributions over variables within the context of a set of initial and boundary conditions. Each set of initial and boundary conditions for an individual question was termed a case. The ensemble of all cases for the elicitation variable is termed the case structure. The primary consideration in the development of elicitation variables, and case structures was the importance of designing elicitation questions that were not dependent on specific analytical models.

It was the responsibility of the probability elicitation team to develop elicitation variables that were physically measurable parameters. The physically measurable constraint (as opposed to eliciting on a fitted exponent having no interpretation in terms of the physics of the problem) was imposed so that there will be no ambiguity when presenting the definition of the elicitation variables. If the experts assess poorly defined variables, the potential for incompatible assessments is high. Also, assessments on physically measurable parameters are not inherently dependent on any given theoretical model and therefore may be developed from a combination of relevant information sources.

Code input parameters are not always physically measurable parameters. In the case of dispersion, the important code input parameters are mathematical constructs that define the spread of the plume in the Gaussian model. In the MACCS and COSYMA dispersion models, the horizontal spread (σ_y) and vertical spread (σ_z) parameters are modelled using the power law: The code input parameters which define the spread of the plume are the A_y , B_y , A_z , B_z terms of the power law. They are assigned values in MACCS and COSYMA depending on the atmospheric stability class. Because A_y , B_y , A_z , B_z are not physically measurable parameters, it was necessary to elicit distributions on physically measurable parameters from which could be derived distributions on A_y , B_y , A_z , B_z .

The following elicitation variables were subsequently chosen for the dispersion case structures:

- (A) The normalized concentration measured at a collector located at the centerline (x_c/Q)
- (B) The concentration relative to the centerline concentration at a specified crosswind location y (x_y/x_c).
- (C) The concentration relative to the centerline concentration at a vertical distance, z and at the centerline, $y=0$ (x_z/x_c).
- (D) The standard deviation associated with the cross wind concentration (σ_x) as would be measured by a line of collectors at specified distance from the source
- (E) The total area [km²] covered by 90% of the time-integrated concentration in the ring-shaped distance region between r_1 and r_2 (r_1 and r_2 are in the far field).

The elicited distributions obtained for the σ_y and x_c/Q parameters provide enough information to enable the development of distributions over the code input parameters using a mathematical processing method that was partially developed during the CEC pilot study. Project staff chose to elicit distributions for the x_1/x_c and x_2/x_c parameters so that distributions for A_y , B_y , A_z , B_z could also be developed using an alternative, more general mathematical processing methodology.

The code input parameter for dry deposition is the dry deposition velocity, v_d , which is defined as the ratio of the rate of deposition of radioactivity to the ground to the air concentration at ground level. The dry deposition velocity is a physically measurable parameter and was therefore chosen as the elicitation variable for the dry deposition questions.

Distributions were elicited on the dry deposition velocity for four surface types, aerosols of six particle sizes, elemental iodine, and methyl iodide. As with dispersion, the important code input parameters for wet deposition are mathematical constructs, not physically measurable parameters. The important code input parameters for wet deposition are those that define the removal coefficient for wet deposition dependent on the rain intensity. The code input parameters for wet deposition are wet deposition power law coefficients. It was therefore necessary to define a physically measurable elicitation variable from which could be developed uncertainty distributions for the power law coefficients.

The fraction of material removed by wet deposition was chosen as the elicitation variable for wet deposition. Uncertainty distributions were elicited for the fraction of material removed by wet deposition for aerosols (four particle sizes), elemental iodine, and methyl iodide. In addition to questions relating to the elicitation variables, questions were presented to the experts for which experimental answers were known. These variables, known as seed variables, are used to measure performance in encoding scientific belief into probabilistic distributions. These questions were used to provide feedback during the probabilistic training exercise and to form the basis for measuring performance of the elicitation variables.

It was impossible for the experts to provide information over the complete variable space needed to perform a comprehensive consequence uncertainty study. It was therefore necessary to design a case structure that would cover the variable space so that the project could interpolate and extrapolate to all areas necessary to perform consequence uncertainty studies. For the dispersion questions, the case structure consisted of many permutations of downwind distances and the synoptic weather conditions at the source. For the deposition questions, the case structure consisted of many permutations of different surface types, particle sizes, chemical types, rain intensities (for wet deposition), and rain duration (for wet deposition).

The initial iteration of the case structure design for dispersion and deposition resulted in a very large number of cases (in principle an infinite number of situations can be described). 700 dispersion cases, 150 dry deposition cases, and 40 wet deposition cases. It would be impossible to expect the experts to provide distributions for this enormous number of cases. After several iterations, a condensed version of the case structure evolved and was tested in dry run elicitations. The dry run elicitation was performed using two dispersion experts and one deposition expert from Sandia National Laboratories (SNL). After the final iteration on the case structure, the dispersion experts were asked to assess 101 questions. The deposition experts were asked to assess 106 questions (70 on dry deposition and 36 on wet deposition). The project staff believed that sufficient information would be obtained from these questions to allow valid interpolation and extrapolation for coverage of the variable space.

For each elicitation variable, experts were asked to provide three percentile values, 5th, 50th, and 95th, from the cumulative distribution functions, with assessments of the absolute upper and lower bounds optional. These distributions were elicited for various specified atmospheric conditions (case structures). Each of the variables elicited can be explained in terms of realizations from a single event. The variables were elicited for various meteorological conditions at the plume axis height, h . The wind direction is defined as the x -direction. The crosswind direction, y , is perpendicular to the plume centerline direction and parallel to the grade. The vertical height above ground is z . The plume centerline direction is defined as the average transport direction of the plume. The sampling time for each designated downwind, crosswind, and vertical distance is specified. The sampling time is

designated as one hour. Exceptions to the one-hour sampling time were made in a few cases for the seed variables. The release duration of the plume was equal to or exceeded the sampling time in all cases.

Table 3.1. Example Case Structure

Meteorological Condition	Temperature Lapse Rate	Standard Deviation of wind direction at 10 m averaged over 10 min	Average Wind Speed	Surface Roughness
1	-2.0 K/100m	25°	2 m/s	comb. of urban and rural
2	-1.6 K/100m	15°	4 m/s	comb. of urban and rural
3	-1.0 K/100m	10°	6 m/s	comb. of urban and rural
4	2.5 K/100m	2.5°	3 m/s	comb. of urban and rural

Table 3.1 Case structures for the dispersion cases (for clarification the pasquill-Gifford stability class is mentioned at each meteorological condition)

Table 3.1 shows the four generic meteorological conditions that were assessed by the experts. The meteorological conditions prior to the event and during the entire event are constant for elicitation purposes. Conditions were specified at the release point which is $x_0 = 0$, $y_0 = 0$ and $z_0 = 10$ m

Several initial conditions were not specified. The experts were instructed to include any unspecified effects in their uncertainty distributions. For example, the terrain surrounding the release site is specified as simple terrain; however, the uncertainty distribution should include the effects of both flat terrain and gently rolling hills. The experts were instructed not to include the effects of complex terrain. Crosswind broadening of the concentration distribution because of plume meander during the sampling time is another uncertainty that should be included, as well as anything else the expert considered important to include in the uncertainty distribution. Additionally, all experts were asked to specify any assumptions regarding mixing layer height made during their elicitations.

Data were also elicited to assess uncertainty in long term dispersion. A few questions in the following form were asked: What are the 0th, 5th, 50th, 95th, and 100th percentile values for the length of the arc or sum of the arcs crossed by 90% of the material at 80 km, 200 km, and 1000 km downwind of the release? The information elicited for long term dispersion was acquired only for the purpose of developing uncertainty distributions for long term dispersion data. The long term dispersion data will be processed by the consequence analysts performing the uncertainty study. This information was not processed beyond the elicitation exercise in this study.

In the case structures for dry deposition four surface types were considered: (1) urban, (2) meadow, (3) forest, and (4) human skin. The urban surface type consists of buildings and concrete. The meadow surface type includes bare soil, freshly cut grass, pasture, and crops such as harvestable corn. The forest surface type includes any kind of tree, including deciduous and evergreen varieties. Human skin refers to skin that would be exposed to a passing plume. The particulate forms for which data were elicited were: aerosol, elemental iodine, and methyl iodide (for the purposes of the elicitation, iodine is assumed not to deposit on aerosols). The sampled particle sizes for the aerosol cases were specified within the following series: 0.1 μ , 0.3 μ , 1.0 μ , 3.0 μ , and 10.0 μ . Particle sizes are associated to spherical particles of unit density (1 gram/cm³).

The only initial condition specified for dry deposition was the average wind speed. The experts were instructed to include any effects not specified in their uncertainty distributions. For example, humidity, ambient air temperature, chemical reactions, other meteorological conditions, vapor-to-particle conversion, and variations within surface type were considered as unknowns, as well as any other effects the expert considered important.

In the case structures for wet deposition the elicitation variable for wet deposition, the fraction of material removed from the plume, is the total fraction removed during the entire time period specified. The rain intensity was specified in two ways in the case structure:

1. the average rain intensity during 1 hour in which it does not necessarily rain continuously during the hour, and
2. the rain intensity during 10 minutes in which it rains continuously during the 10-minute period. The particulate forms elicited were aerosol, elemental iodine, and methyl iodide. The sampled particle sizes for the aerosol cases were specified within the following series: 0.1 μ , 0.3 μ , 1.0 μ , and 10.0 μ ; particle sizes are associated with spherical particles of unit density (1 gram/cm³). The average rain intensities for the one hour cases were defined as the following amounts of precipitation recorded over one hour: 0.3 mm, including drizzle, rain and showers; 2.0 mm, including rain and showers. The average rain intensities for the ten minute cases were defined as the following amounts of precipitation recorded over ten minutes: 0.05 mm, drizzle, 0.33 mm, rain; 1.67 mm, a shower.

Several initial conditions were not specified. The experts were instructed to include any effects not specified in their uncertainty distributions. For example, chemical reactions, electrostatic effects, vertical profiles and rain rate are considered as unknowns, as well as any other effects the expert considers important. The rain is assumed to be consistent over the entire area.

Several dispersion experts relied on GPMs as the central basis for their elicitations, but they relied on non-Gaussian considerations to develop the requested information on the broader uncertainty distribution. There was more variability among experts for the stable case than for the non-stable case. However, the width of the uncertainty distributions (95th/5th percentile ratios) provided by the experts for the two cases look very similar. The same trend is observed for the elicited crosswind dispersion assessments (σ_y). There is more variability in the stable median values than in the non-stable median values, but the variability in the width of the uncertainty distributions for the two cases is about the same.

The experts seem to agree more closely in their median assessments for the near field, but diverge somewhat as the plume moves downwind. There is more variability among the experts in the widths of the uncertainty distributions, as reflected in the 95th/5th percentile ratios, than in the median assessments.

The variability among responses for the dry deposition was greater for the dry deposition questions than for the dispersion questions. Generally, the deposition experts relied heavily on experimental evidence and used several analytical models to fill the gaps left by the experimental evidence. The results show that most experts, except for the 10 μ particle size, established relatively low medians for aerosol deposition velocities. One expert, however, placed his median deposition velocity much higher. The results show some order of magnitude differences between the width of the uncertainty distributions assessed by the experts.

The highest variability for the dry deposition velocities of elemental iodine is for deposition onto skin. Deposition on skin is not usually considered by deposition experts, and there is an absence of measurements of deposition to skin for the aerosols of interest. The results show an order of magnitude differences in the width of the uncertainty distributions provided by the experts for the dry deposition velocity of elemental iodine.

As with the dry deposition responses, the variability among the wet deposition responses was greater than for the dispersion responses. The results show order of magnitude differences among the experts in both the median assessments and the width of the uncertainty distribution for the fraction of aerosols removed by rainfall. The results also show less than an order of magnitude variability among experts in the fraction of elemental iodine removed, except for one expert. It shows less than an order of magnitude variability in the width of the uncertainty distributions, again with the exception of one expert.

The 50th percentiles from the aggregated experts' distributions appear consistent with the individual assessments. The plots for the 95th/5th ratios show that aggregation of the distributions may result in aggregated distributions which have a wider uncertainty band than any of the individual elicited distributions. The results represent the potential uncertainty in crosswind plume growth, which is substantial.

The 50th percentile aggregated values for the dry deposition velocities appear to be consistent with the individual elicited distributions. As with the dispersion results, the ratios of the 5th and 95th percentile values for the aggregated distributions indicate that the width of the uncertainty distribution is typically greater for the aggregated distributions than for the individual elicited distributions.

As with the dispersion and dry deposition results, the ratios of the 5th and 95th percentile values for wet deposition indicate that the widths of the aggregated distribution are typically greater than for the individual elicited distributions. The central measures for the aggregated wet deposition distributions appear consistent with the individual distributions.

2. Foodchain panels

FZK had a supporting role as a consequence institute in the work for these panels. The results from these panels and their analysis will be published in due course.

3. Early or deterministic health effects

FZK has a supporting role as a consequence institute in the work for this panel. The results from this panel and its analysis will be published in due course.

Publications:

Harper FT, Goossens LHJ, Cooke RM, Hora SC, Miller LA, Päsler-Sauer J, Lui C and Kelly GN

Summary of uncertainty analysis of dispersion and deposition modules of the MACCS and COSYMA consequence codes -- A joint USNRC/CEC study, Paper presented at PSAM-II Conference, San Diego, Ca/USA, 20-25 March 1994, Vol 1, session 009

Harper FT, Goossens LHJ, Cooke RM, Helton JC, Hora SC, Jones JA, Kraan B, Lui C, McKay MD, Miller LA, Pasler-Sauer J and Young ML

Joint USNRC/CEC consequence uncertainty study: Summary of objectives, approach, applications, and results for the dispersion and deposition uncertainty assessment, NUREG/CR-6244, EUR 15855, SAND94-1453, Washington DC/USA, June 1994

Harper FT, Goossens LHJ, Cooke RM, Hora SC, Young ML, Päsler-Sauer J, Miller LM, Kraan B, Lui C, McKay MD, Helton JC and Jones JA

Joint USNRC/CEC uncertainty study: Dispersion and deposition panels, In: Procedures and computer codes for level-3 probabilistic safety assessment, proceedings of a technical Committee Meeting, Organized by the International Atomic Energy Agency, Vienna, 21-25 November, 1994, IAEA, Vienna, Austria, 1995

Goossens LHJ, Cooke RM, Kraan BCP, Harper FT, Young M, Miller LA, Hora SC, Pasler-Sauer J

Uncertainty analysis of nuclear accident consequence codes: A formal expert judgement approach, Abstract and poster presented at Annual Meeting of the Society for Risk Analysis (Europe) on Risk Analysis and Management in a Global Economy, May 21 - 25, 1995, Forum Ludwigsburg, near Stuttgart, D, Abstracts book, p.453 (to be published in Proceedings)

Head of project 4: Miss Boardman

II. Objectives for reporting period

The UKAEA objectives were

1. to assist in preparing and obtaining results from the behaviour of deposited material and related doses panel as leading consequence institute
2. to assist in preparing and obtaining results from the internal dosimetry panel as back-up consequence institute (in support of NRPB).

III. Progress achieved including publications

1. Deposited materials and related doses panel

UKAEA have been involved in the overall project specification, participating in numerous discussions with the EC and USNRC. During the reporting period they have developed the scope and content of the expert panel considering the behaviour of deposited material and related doses. This culminated in the production of a case structure document, some of the details of which are presented below.

UKAEA played an integral role in the selection of ten experts in the subject areas of interest, who represented the breadth of knowledge available within Europe and the USA. UKAEA developed a series of elicitation questions to pose to these experts, covering the subject area, and focusing on particular observable quantities. Having developed the "question set", UKAEA (in conjunction with TUD), performed a dry run of the elicitation session with two of the chosen experts. This allowed them to provide feedback and enabled an update of the case structure document and question set to be carried out prior to a training meeting for the whole expert panel. This meeting was held in the UK in January of 1995 and UKAEA assisted in the presentation of the case structure and ran two discussion sessions on the subject area.

The elicitation questions, handed out at the EC training meeting, were left with the experts for several weeks prior to the performance of an elicitation session. UKAEA and TUD performed eight elicitation sessions with the European experts during February and March of 1995. These were carried out, where possible, at the experts' own institute. The US experts were elicited separately during a training meeting held in Albuquerque in April 1995. During these sessions the subject area and in particular the elicitation questions were discussed in more detail, removing any possible ambiguities. The experts have since provided TUD and UKAEA with a full description of the approach they have taken to answer the questions (in the "rationale" document) and a complete set of answers to the elicitation questions. The results of this study will be published in a joint EC/USNRC report early next year.

As already mentioned, this panel has been convened to consider the issues relating to the uncertainties in estimating the external doses to individuals, indoors and outdoors, from activity deposited on the ground and other surfaces in urban and rural areas. This was the main focus of the panel and the questions posed were related to various aspects of this modelling area.

In order to estimate the total dose to individuals indoors, however, it is important to know the amount of activity penetrating the building, via normal air exchanges for example, and even the amount of activity deposited on internal surfaces. Hence, some of the questions were related directly to the penetration factors in particular in order to help assess the uncertainties associated with the calculation of inhalation dose, as well as external dose, to people indoors.

The external dose models in COSYMA and MACCS are designed to predict the doses to individuals in the population from radioactive material deposited onto the ground. Although the majority of any population live/work in urban and suburban areas, these models take as their baseline the doses predicted for individuals outdoors in a "rural" environment. These doses are then translated, using simple scaling factors, to predict doses to those individuals in urban/suburban areas exhibiting various

patterns of behaviour - for example, spending a certain percentage of their time in cars, cellars or houses of low/med/high shielding. The doses thus predicted are input to health risk models to calculate the overall detriment to the population and they are often used to assess the necessity to enforce particular mitigating actions in order to reduce the doses received by the population in the long term. These may be measures involving movement of the population or options to decontaminate the land surrounding the accident site

Any complexity in the external dose calculations within ACA codes therefore exists in predicting the initial dose to individuals outdoors in a rural environment (denoted the "rural" model), where the behaviour of the radionuclides in undisturbed soil, and energy-dependent attenuation and build-up of radiation is considered as a function of time following initial deposition. These rural outdoor models do not, however, take account of the variation in the retention and weathering properties of those surfaces which are more common to the urban or suburban environments.

The results of these outdoor dose models are commonly known as "dose conversion factors" (DCFs) and they relate the initial deposited activity on the ground (Bq/m^2) to the Dose (Sv) as a function of time following initial deposition. These DCFs are generally pre-calculated and held in data libraries which are accessed during normal running of the code, e.g., COSYMA or MACCS.

Consequence codes predict, for particular meteorological scenarios, the dispersion and deposition of activity during plume travel. The amount of material deposited depends on the outcome of two processes, dry and wet deposition. The dry deposition mechanism is driven by the dry deposition velocity for a particular nuclide or nuclide group. Usually one value is defined for all locations around the release point, thus ignoring any effects of varying surface type. The overall activity deposited by dry mechanisms is usually assumed to be typical of a uniform surface similar to that of undisturbed grassland. Wet deposition is driven by the rainfall occurring during plume travel, modelled using a washout coefficient taking material uniformly from the passing plume. The deposited activity (both wet and dry) is scaled using the DCFs from the data library in order to predict the external dose to individuals outdoors in an average (RURAL) environment. The dose indoors is predicted by reducing the outdoor dose using an average location or shielding factor, representative of an average dwelling in Western Europe and the US. The total dose to a group of individuals takes account of the fraction of time on average that each individual spends outdoors and indoors.

For the inhalation dose delivered to individuals indoors, a reduction in the time integrated air concentration indoors relative to that outdoors is calculated using a scaling or penetration factor typical of an average dwelling in Western Europe or the US.

Therefore, the input variables to these consequence codes which drive the dose models under consideration are of the following form:

- (1) Dose Conversion Factors (Sv per Bq/m^2 deposited on the ground), which translate deposited activity to the individual dose outdoors in a rural environment as a function of time;
- (2) Shielding or Location Factors, representing the necessary reduction in rural, outdoor dose that would be necessary to approximate the dose to individuals indoors in an average dwelling;
- (3) Penetration Factors, which represent the ratio of the time integrated air concentration indoors in an average dwelling to that outdoors in a rural environment.

As already mentioned above, the values in (1) are derived using dose models which are incorporated into other programs external to the main consequence code.

The uncertainties in the above and other related quantities are the "problems" that the expert panel needed to address. The questions were formulated so that likely ranges and median values could be derived for each of the above quantities, together with asking for more generic information which may be of use for future studies.

2. Internal dosimetry

UKAEA has a supporting role as a consequence institute in the work for this panel. The results from this panel and its analysis will be published in due course.

Publications.

Goossens LHJ, Cooke RM, Kraan B, Brown J, Jones JA, Boardman J, Harper FT, Young ML and Hora SC

Results of the ongoing probabilistic uncertainty analysis study on COSYMA (and MACCS) for deposited materials and related doses and the food chain models - A joint EC/USNRC expert judgement study. Paper presented at the 2nd COSYMA Users' Group Meeting, Budapest - Hungary, 19-21 June 1995 (to be published in Proceedings)

Head of project 5: Dr. Roelofsen

II. Objectives for reporting period

The ECN objectives were

1. to assist in preparing and obtaining results from the behaviour of deposited material and related doses panel as back-up consequence institute (in support of UKAEA)
2. to assist in preparing and obtaining results from the early or deterministic health effects panel as leading consequence institute
3. to assist in preparing and obtaining results from the late or somatic health effects panel as back-up consequence institute (in support of NRPB).

III. Progress achieved including publications

1. Deposited materials and related doses panel

NRPB had a supporting role as a consequence institute in the work for this panel. NRPB assisted in the preparation of the case structure document and the final report which will be published in due course

2. Deterministic or early health effects

The Netherlands' Energy Research Foundation (ECN) supports the assessment of uncertainty in the modelling of the relation between the dose a person could receive due to an accident and the probability that this exposure would cause deterministic health effects. The major part of the work will be carried out in the period between June 1995 and March 1996.

The model implemented in MACCS and COSYMA uses a Weibull function and a threshold to calculate the probability of a deterministic health effect. Given a dose history the codes will determine the parameters in the Weibull function the shape parameter and the D_{50} dose (which may be dose rate dependent). The objective of this part of the project is to quantify the statistical distribution of the model parameters needed to perform this calculation. To obtain this result an international team of experts will be contracted.

As this part of the project started only recently, the method of elicitation is currently being developed in close cooperation of ECN and the US NRC. The following approach is considered the experts will be asked to estimate the probability of deterministic health effects, given a dose history that could be expected following a nuclear accident. These dose histories are either calculated using one of the codes, or are based on experiments. The experts will only be asked to assess quantities that can be hypothetically measured or observed. This avoids ambiguity in variable definitions and, more importantly, the elicited quantities are not tied to any particular model and thus have a wider potential application.

It may be too difficult to process the model parameter values from the results the experts will provide. TUD is currently investigating this. If necessary dose histories will be included that provide a direct way to calculate the model parameter values from the results provided by the experts. However, this type of dose histories will not occur during a nuclear accident.

The case structure document, describing the elicitation questions, is under preparation.

3. Late or somatic health effects

ECN has a supporting role as a consequence institute in the work for this panel. The results from this panel and its analysis will be published in due course.

Publications:

None

Head of project 6: Dr. Hofer

II. Objectives for reporting period

The GRS objectives were

- 1 to assist in establishing the link between SUSANA and the relevant modules of COSYMA
- 2 to perform uncertainty analyses on the COSYMA module for atmospheric dispersion and deposition with the uncertainty distributions derived from these two panels
- 3 to perform modifications and extensions of SUSANA that emerge from the actual application of the system to results from the COSYMA code.

III. Progress achieved including publications

A preliminary uncertainty and sensitivity analysis was performed of COSYMA applications for 12 cases selected from the case structure chosen for expert judgement elicitation. The analysis was restricted to those potentially important uncertain parameters that were identified by the panels dealing with the subject areas "atmospheric dispersion and deposition". Only subsets of seven (deposition cases without rain), respectively ten (deposition cases with rain) uncertain parameters were involved per case. The subjective probability distributions and state of knowledge dependence quantifications were those obtained directly from the experts or derived through post-processing by TUD, after aggregation by using equal weights.

COSYMA was run a 100 times per case. The respective set of 100 alternative vectors of parameter values was selected via simple random sampling. Analysis results are illustrated by three typical output figures for each output quantity and case.

The first typical output figure shows the selected output quantity for the 100 model runs, as function of the distance from the source, where appropriate. A (90%, 97.5%) statistical tolerance interval is delimited by the second lowest and the third largest output values. It says, that one can be at least 97.5% confident that at least 90% of the combined influence of all quantified uncertainties are between those two values. This uncertainty statement does account for the possible influence of the sampling error that is due to the fact that a sample of only size 100 was used. The sensitivity measure selected is Spearman's sample rank regression coefficient.

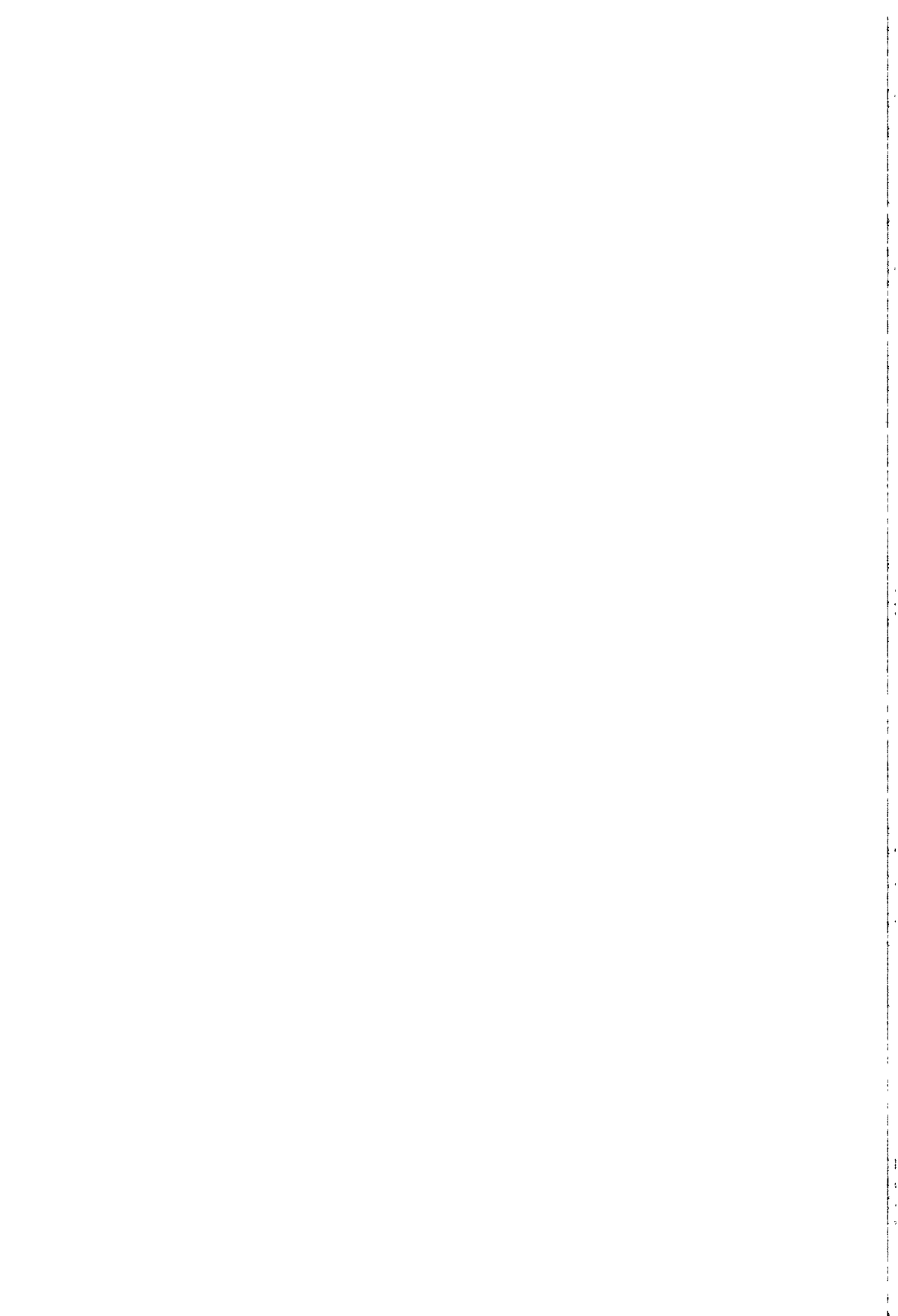
The second typical output figure shows these coefficients, as a function of the distance from the source where appropriate, for each of the uncertain parameters involved in the selected case. The figure indicated where the main contributions to the spread of the output values come from and whether parameter and output quantity tend to move in the same or in opposite direction. Finally, the sample value R^2 of the corresponding coefficient of determination is either provided as a single value or as a function of the distance from the source in a separate typical output figure.

The analysis required only a minor change to SUSANA. The number of quantiles that may be specified for an uncertain parameter had to be increased from 30 to 100.

The results will be published in due time.

Publications.

None.



**Final Report
1992-1994**

Contract: FI3PCT920036 Duration: 1.9.92 to 30.6.95

Sector: C24

Title: Development of a comprehensive decision support system for nuclear emergencies in Europe following an accidental release to atmosphere.

1)	Ehrhardt	KfK
2)	Gland	EDF
3)	Müller	GSF
4)	French	Univ. Leeds
5)	Sohier	CEN/SCK Mol
6)	Haywood	NRPB
7)	Bleasdale	Nuclear Electric
8)	Zelanzy	IEA.CCC
9)	Kanyar	OSSKI
10)	Zelasny	Cyfronet
11)	Mateescu	IFIN
12)	Stubna	NPPRI

1. Project summary (FZK)

1.1 Objectives of the RODOS project

The need for and importance of a coherent and consistent response of the off-site emergency management to any nuclear accident that might in future affect Europe were amply demonstrated during and following the Chernobyl accident; differences in the countermeasures then taken by national authorities contributed greatly to a loss of public confidence. Computerised systems which provide the emergency management with fast and reliable predictions and evaluations of the radiological impact of accidents can greatly assist quick and well founded decisions about the imposition of emergency actions and countermeasures. To minimise the parallel development of many different systems, which may provide information of different kinds and quality, coordinated R&D activities are required to harmonise the methods, models and databases used in such systems.

The development of RODOS, a *Real-time On-line DecisiOn* Support system for off-site emergency management, which would be comprehensive and capable of finding broad application across Europe, was included as a major item within the Radiation Protection Research Action of the European Commission's 3rd Framework Programme in late 1990. The main objectives of the RODOS project are to provide the methodological basis, develop models and data bases and install the hardware and software framework of a system which offers comprehensive decision support from the very early stages of an accident up to many years after the release and from the vicinity of the site to far distant areas unperturbed by national boundaries. In this way it will be possible to provide estimates, analyses, and prognoses of accident consequences, protective actions and countermeasures which are consistent throughout all accident phases and distance ranges. In particular, all relevant environmental data, including radiological and meteorological information and readings, are to be processed, by means of models and mathematical procedures, into understandable, interpretable pictures of the current and predicted future radiological situation. Simulation models for protective actions and countermeasures are designed to permit

- the estimation of the extension in both time and space;
- the estimation of dose and health effects, with quantification of advantages and disadvantages in terms of (averted) radiation doses or (averted) health injuries;
- the quantification of the costs for society and the economy.

It will be possible to evaluate alternative combinations of countermeasures and protective actions in term of feasibility in the given situation, and to support judgements by the decision makers of the public acceptability of the actions, and of the socio-psychological and political implications. This will be achieved through the appropriate use of rule-based expert systems, weights, preference functions and other decision analytic methods. The application of these techniques will result in a ranked order of options together with an explanation of those rules and weights which predominantly have led to the

evaluation. This ranking and supporting explanation will be offered to decision makers for them to take a final decision in the light of the understanding they have achieved. Naturally the decision makers will make this choice in the context of all the predictions and geographic plots presented to them by other modules within RODOS .

With these objectives being achieved, a decision support system will be delivered which provides benefits and functions unavailable elsewhere. These include /A1/:

- better use of resources allocated within the European Union to improve off-site emergency management, inter alia, minimising unnecessary duplication;
- models, methods and data bases drawn from the best available at national and international levels;
- comprehensive decision support will be provided (e. g. at all levels of information processing for each relevant countermeasure at all times and distances from a release);
- novel and enhanced technical features (e. g. assimilation of monitoring data and model predictions, integrated treatment of uncertainties);
- a seamless transition between all distance ranges and temporal phases of an accident offering continuity in providing public information and decision support;
- a design for operational use at local, regional, national and supra-national levels and for training and exercises at these levels;
- a modular design to facilitate long term development and adaptation to user requirements and local/regional conditions;
- a stand-alone interactive training tool for use, inter alia, by those responsible for making decisions on off-site emergency management and their technical advisers at local, regional, national and supra-national levels;
- a more general interactive training and educational tool for radiation protection, nuclear safety and emergency planning personnel with professional interest in or responsibility for off-site emergency management;
- a software framework for developing decision support systems for the management of non-nuclear emergencies with potential off-site consequences.

1.2 Contractual and management arrangements

During the 3rd Framework Programme, the RODOS project has been divided into four individual sub-projects, each with its own contractors and co-ordinator:

- Co-ordination of atmospheric dispersion activities for the real-time decision support system under development at FZK¹ (FI3P-CT92-0044):
 RISØ National Laboratory, DK (coordinator)
 Agenzia Nazionale per la Protezione Del'Ambiente (ANPA), I
 Gesellschaft für Anlagen- und Reaktorsicherheit (GRS), D
 National Centre for Scientific Research "Demokritos" (NCSR), GR
 Swedish Meteorological and Hydrological Institute (SMHI), S
 Danish Meteorological Institute (DMI), DK
 Imperial College Centre for Environmental Technology (ICCET), UK
 Central Research Institute for Physics (CRIP), HU

- Development of a comprehensive decision support system for nuclear emergencies in Europe following an accidental release to atmosphere (FI3P-CT92-0036 incl. the PECO contractors under Suppl. 1 and Suppl. 3)
 Forschungszentrum Karlsruhe GmbH (FZK), D (coordinator)
 Electricite de France (EdF), F
 GSF-Forschungszentrum für Umwelt und Gesundheit GmbH, D
 School of Computer Studies, University of Leeds (UoL), UK
 National Radiological Protection Board (NRPB), UK
 Nuclear Electric, Plc, (NE), UK
 Studiecentrum voor Kernenergie/Centre d'Etude de l'Energie Nucleaire (SCK/CEN), B
 Institute of Atomic Energy (IAE), PL
 Institute for Physics and Nuclear Engineering, Laboratory for Environmental Radioactivity (IFIN-LAB), RO
 National Research Institute for Radiobiology and Radiohygiene (NRIRR), H
 Nuclear Power Plants Research Institute (NPPI), SR

- Evaluation and management of post-accident situations (FI3P-CT92-0013b)
 CEA/CEN de Fontenay-aux-Roses, F (coordinator)
 School of Computer Studies, University of Leeds, UK
 Universidad Polotecnica de Madrid, E
 Universite Paris Dauphine, F

- The Joint Study Project 1 of the EC/CIS Collaborative Agreement for International Collaboration on the Consequences of the Chernobyl Accident (COSU-CT94-0087)
 Forschungszentrum Karlsruhe GmbH (FZK), D (EU coordinator)
 National Radiological Protection Board (NRPB), UK
 N. V. KEMA, NL
 Studiecentrum voor Kernenergie/Centre d'Etude de l'Energie Nucleaire (SCK/CEN), B
 Scientific Production Association TYPHOON, Russia (CIS coordinator)
 Institute of Control Science Problems (ICSP), Russia

1 Kernforschungszentrum Karlsruhe (KfK) has changed the name to Forschungszentrum Karlsruhe (FZK)

Russian Institute of Agricultural Radiology (RIAR), Russia
Institute of Mathematical Machines and Systems, Cybernetics Centre (IMMS CC),
Ukraine
Ukrainian Institute of Agricultural Radiology (UIAR), Ukraine
Institute of Power Engineering problems (IPEP), Belarus
Belorussian Institute of Agricultural Radiology (BIAR), Belarus
Committee for Hydrometeorology (HYDROMET), Belarus

The work performed within the first and the last two contracts is described in the corresponding Final Reports. This report refers to the results achieved by the institutes involved in the second RODOS contract .

The management and co-ordination of the working programme is organised on three levels of interaction: the RODOS Management Group (RMG), nine working groups on special topics (WGs) and contractors' meetings.

The RODOS Management Group has been established by the Commission's Services to assist them in the management and overall co-ordination of the second phase of the RODOS project (1992-1995). The RMG comprises the following members: J. Ehrhardt (Forschungszentrum Karlsruhe, D), G. Fraser, (European Commission DGXI-A-1, L), S. French (University of Leeds, UK), G. N. Kelly (European Commission DGXII-F-6, B), T. Mikkelsen (RISØ National Laboratory, DK) and V. S. Shershakov (SPA TYPHOON, Russia). The RMG is responsible for monitoring and reviewing progress; approving the work schedule; approving procedures for documentation, quality assurance, uncertainties, etc; resolving issues referred to it by RODOS Working Groups or individual contractors; and setting priorities for the next phases of the RODOS project. The minutes of the RMG meetings are distributed to all contractors.

Nine working groups have been established within the reporting period:

WG1 on system development and quality assurance
WG2 on meteorology and atmospheric dispersion
WG3 on countermeasures and consequences
WG4 on hydrological modelling
WG5 on source term estimation, data assimilation and uncertainties
WG6 on evaluation techniques
WG7 on training and exercises
WG8 on international data exchange
WG9 RODOS users group

In general, the membership of the WGs are drawn from different contracts and change with time, according to the scientific expertise required for the problems under discussion and the interaction with other areas. The WGs organise themselves with one contractor taking the lead in preparing meetings, agendas and minutes. The main aims of the WGs are to co-ordinate work in a specific R&D area of the RODOS project, to prepare detailed working programmes, to specify milestones and deliverables within the overall timescale of the project, and to identify problems and issues which need broader discus-

sion. The results of the WG meetings are reported to the RMG via the responsible coordinators.

Since the RODOS project began, five full contractors' meetings were held:

Neuherberg, D, 5 to 6 July 1990
Athens, GR, 26 to 27 September 1991
Karlsruhe, D, 9 to 10 June 92
Interlaken, CH, 20 to 24 June 1994
Budapest, H, 20 to 24 September 1995.

The main objectives of these meetings have been:

- to present to the community of all involved in the RODOS project the progress achieved by the contractors individually or in co-operation with others,
- to support and enhance the co-operation between the institutes involved in the RODOS project, in particular to establish collaborative links between Western and Eastern European countries including the CIS Republics,
- to communicate the next project milestones and time phases and to focus the contractors' attention to the deliverable items at the corresponding points in time.

Information of common interest has been exchanged through the RODOS Newsletters, of which 5 issues were prepared by the Forschungszentrum Karlsruhe. A register of RODOS documents is kept by Forschungszentrum Karlsruhe with support of RISØ National Laboratory. Each document has a unique code, distinguishing between minutes of meetings, technical notes or draft reports for internal exchange, and publications (see also Annex).

1.3 Achievements

On the basis of a design study prepared by FZK in 1990 and its following updates expanded and modified with ideas and contributions of all the contractors, broad agreement was achieved on the objectives, overall structure and content of RODOS. As all partners considered it highly beneficial to develop the hardware and software components as soon as possible based on the features outlined in the design study, FZK laid down the structure of a detailed software framework and its internal logic. Open and lively debates on this issue led to a commonly accepted design, which was realised as prototype Version PRTY 1.0 of RODOS in 1992 /A2/.

The RODOS software framework has been developed as a transportable modular structured software package to run with a UNIX operation system and X-Windows user interface with OSF/MOTIF extensions. The data management is based on SQL standard. At present, it is implemented mainly on workstations HP 9000 models 755 and 735. The modular structure of the RODOS system and the Client-Server principle applied for

modul intercommunication facilitates the integration of application software components developed by the project partners.

The current version RODOS- PRTY 1.3 comprises the following components, which are described in more detail in the various Sections of Chapter 3:

- the operating system OSY for overall system control, data management and user interface (FZK)
- the geographical information system RoGIS (FZK, SPA TYPHOON)
- a meteorological model chain, consisting of
 - the meteorological preprocessor PAD (ANPA)
 - the mass-consistent wind field models MCF (GRS) and LINCOM (RISØ)
 - the Lagrangian puff-model RIMPUFF (RISØ) and, alternatively,
 - the simplified Gaussian puff code ATSTEP (FZK)
- the module DOSBAU for calculating potential early doses and dose segments (FZK)
- the module ECOAMOR for dose calculations via early and late exposure pathways, in particular foodchains (GSF)
- the module EMERSIM for simulating early emergency actions and corresponding dose calculations (FZK)
- the module FRODO for simulating intermediate and late countermeasures and corresponding dose calculations (NRPB)
- the modules HEALTH and ECONOM for calculating deterministic and stochastic health effects and economic consequences (FZK).

Not yet integrated but available as stand-alone programs are

- the module RETRACE for calculating run-off processes after deposition of radionuclides (SPA TYPHOON)
- the one- and two- dimensional modules RIVTOX and COASTOX for describing the behaviour of radionuclides in rivers (IMMS CC)
- the module LAKECO for calculating the behaviour of radionuclides in lakes including biota (KEMA)
- the module EVSIM for simulating the temporal and spatial movement of people on the existing traffic network in case of evacuation (FZK)
- the module STOP for identifying the best-suited routes in case of evacuation (IMMS CC)
- the multi-attribute decision analysis software tools HERESY (UoL) and M-Crit (ICSP, SPA TYPHOON)

In addition to that, methodological investigations have been performed and the corresponding documents have been prepared on

- selection of a model chain for near range atmospheric dispersion (RISØ)
- selection of a model chain for intermediate and far range atmospheric dispersion (RISØ)
- treatment of uncertainties in RODOS (UoL)
- data assimilation (UoL, SCK/CEN)
- guidelines of documentation on RODOS (FZK)

Finally, the "Computer-based training course on off-site emergency response to nuclear accidents" has been developed by FZK, NE, SCK/CEN and EdF. It will be held first at FZK on 22 to 26 April 1996 (see Chapter 4).

The functionality of the current version PRTY 1.3 of RODOS is still limited to the early and intermediate stages of an accident in the distance range of a few tens of kilometres. It has been, or is in the process of being, implemented in partner institutes in Belarus, Germany, Greece, Hungary, Poland, Romania, Russia, the Slovak Republic and the Ukraine by the RODOS team of FZK; institutes in Portugal, Spain, Finland and Czech Republic have requested the system and discussions are proceeding with institutes in other European countries. Further development of the system and its component parts is now proceeding in parallel in many institutes.

Those institutes in Eastern and Western Europe, which run the current version of RODOS already or will do so in the near future, are directly or indirectly responsible for emergency management in their countries. It is their expressed objective that RODOS will become an integrated part of the national emergency management arrangements and thus will be widely used. In addition, the work on the realisation of a European wide network for the exchange of radiological information has started with the main partners of this proposal and the current RODOS users. In this way, the RODOS system will facilitate communication and exchange of information and promote a more coherent and harmonised emergency response within Europe to any future nuclear accident.

2. Concept, structure and development status of the RODOS system (FZK)

2.1 Basic features

Decisions of the emergency management are required from the very early stages of an accident up to many years after the release of radioactive material. Therefore, a key feature of the RODOS system is its real-time and on-line operation coupled to existing meteorological and radiological monitoring networks. For aiding decisions on early emergency actions in the near field, such as sheltering, evacuation and distribution of stable iodine tablets, cycle times of 10 min are realised. Decisions on countermeasures in the later phases of an accident (i.e. after the passage of the plume and/or in the far field), such as relocation, decontamination or agricultural countermeasures, are less urgent, so that longer computing times are not a constraint.

Two modes of operation are provided by the RODOS system: an automatic and an interactive one. In the early emergency situation, a pure dialogue system is inadequate, as - because of stress and psychological pressure - it could be subject to user mistakes and thus create confusion and nervousness. Therefore, RODOS offers the possibility of automatically presenting all information relevant for decision making. The interaction with the system is limited to a minimum of user input necessary to actualise data and to adapt models to reality. In parallel to the automatic mode and in particular at later stages of the accident, when very quick decisions are no longer necessary, the interactive modes is possible with a dialogue oriented communication between the user and the system.

RODOS is designed as a comprehensive system incorporating models and data bases for assessing, presenting and evaluating the accident consequences in the near, intermediate and far distance ranges under due consideration of the mitigating effect of countermeasure actions. Its flexible coding allows to cope with differing site and source term characteristics, differing amounts and quality of monitoring data, and differing national regulations and emergency plans. To facilitate its application over the whole of Europe, the software has been developed as a transportable package; in particular its software framework supports the integration of application software externally developed by many of the contractors. The modular structure of RODOS allows an easy exchange of models and data, and thus facilitates the adaptation of the system to the local/regional and national conditions. Finally RODOS offers a variety of access tools to cope with the different capabilities, knowledge and aims of the future users.

If connected to on-line meteorological and radiological monitoring networks, the RODOS system provides decision support on various stages of information processing which conveniently can be categorised into four distinct levels. The functions performed at any given level include those specified together with those applying at all lower levels.

Level 0: Acquisition and checking of radiological data and their presentation, directly or with minimal analysis, to decision makers, along with geographical and demographic information.

Level 1: Diagnosis and prognosis of the current and future radiological situation (i.e. the distribution over space and time in the absence of countermeasures) based upon monitoring data, meteorological data and models, incl. source term estimation.

Level 2: Simulation of potential countermeasures (e.g. sheltering, evacuation, issue of iodine tablets, relocation, decontamination and food-bans), in particular, determination of their feasibility and quantification of their benefits and disadvantages.

Level 3: Evaluation and ranking of alternative countermeasure strategies by balancing their respective benefits and disadvantages (e.g. costs, averted dose, stress reduction, social and political acceptability) taking account of societal preferences as perceived by decision makers.

Plant data as well as off-site radiological measurement and monitoring data, such as air concentrations, ground contamination and gamma dose rates, allow comparisons between measurements and model predictions. With the help of data assimilation techniques presently under development for level 1 and 2 applications, such as backfitting procedures and statistical forecasting, possibly combined with knowledge bases (expert) systems and components of fuzzy set theory (see Section 3.1.3), the model results and the observed data will be optimally used to achieve a consistent and realistic picture of the environmental contamination and to estimate the source term.

In connection with the development of data assimilation techniques, the quantification of the uncertainties in the predictions of the RODOS system are considered to be a key element of an advanced decision support system (see Section 3.4). Methodological investigations have already been performed on how to assess and propagate uncertainty estimates through the various modules of the RODOS system. The implementation of these techniques will be a main objective of the next Framework Programme.

The flexibility of RODOS described above will allow the system to be used not only in actual accidents, but also as a powerful tool for education and training of personnel involved in the decision making process and in preparing and exercising emergency plans.

2.2 Conceptual structure and development status

In the light of the objectives, requirements and potential applications, the conceptual design of RODOS is as follows (Fig. 1). RODOS is made up of three subsystems, the analysing subsystem (ASY), the countermeasure subsystem (CSY), and the evaluating subsystem (ESY). The modules building these subsystems, together with the database and the user interface, are controlled by the operating subsystem (OSY), which is supported by the supervising subsystem (SSY).

Each of the subsystems consists of a variety of modules developed for processing data and calculating endpoints belonging to the corresponding level of information processing. The modules are fed with data stored in four different data bases comprising real-

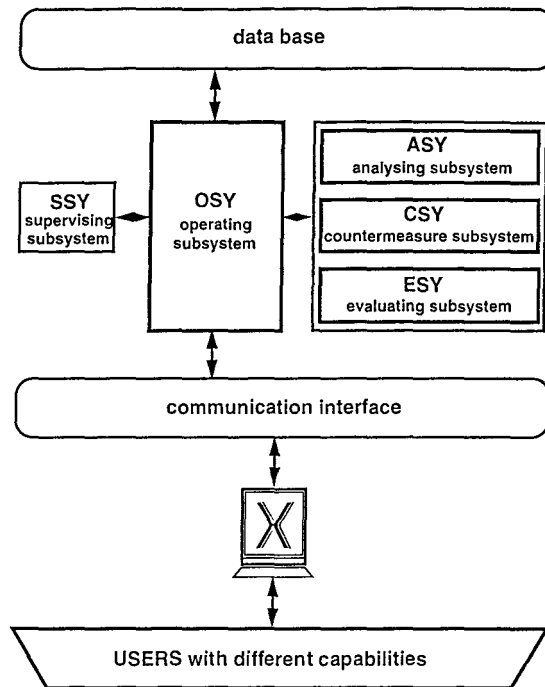


Fig. 1: Overall structure of RODOS

time data with information coming from regional or national radiological and meteorological data networks, geographical data defining the environmental conditions, program data with results obtained and processed within the system, and facts and rules reflecting feasibility aspects and subjective arguments.

The content of the subsystems and the data bases will change with the application of RODOS in relation to a nuclear accident. The temporality of the decisions greatly influences both what information is available and how information is aggregated and integrated. At the different points in time different modules have to be chained together, at least one from each of the subsystems mentioned above, to produce the required output. For example, after the passage of the plume, meteorological forecasts are no longer necessary for the region considered, or after evacuation models for simulating sheltering or relocation in the same area are not needed. The Supervising Subsystem (SSY) will manipulate the components of RODOS in order to respond to user requests.

Characteristics and the current state of development of the subsystems are described in the following sections. For simplicity and better understanding, the structure of the subsystems ASY, CSY and ESY distinguishes between different program packages, which

again consist of individual modules corresponding to the modular design of the whole system.

2.2.1 The operating subsystem OSY

The interconnection of all program modules, the input, transfer and exchange of data, the display of results, and the control of the interactive and automatic modes of operation of the system are all controlled by OSY. The main tasks of OSY are the control of system operation, data management, and the exchange of information among various modules as well as the interaction with users in distributed computer systems. The flexibility of the whole system is defined by OSY, and is independent of the development of program modules. OSY has been designed and developed following the Client-Server Model and coded in the language C as a transportable package to run with a UNIX operation system and X-Windows user interface with OSF/MOTIF extensions. The data management is based on the SQL standard. At present, OSY is implemented on workstations HP 9000, models 755 and 735.

The dialogue between RODOS and a user may be organised in two modes. In the *automatic mode* the system automatically presents all information which is relevant to decision making and quantifiable in accordance with the current state of knowledge in the real cycle time (e.g., 10 minutes in the early phase of an accident). For this purpose, all the data entered into the system in the preceding cycle (either on-line or by the user) are taken into account. Interaction with the system is limited to a minimum of user input necessary to characterise the current situation and adapt models and data.

In parallel to the automatic mode, RODOS can be run optionally in the *interactive mode* with a dialogue oriented menu-driven communication between the user and the system. In particular in later phases of an accident, when longer-term protective actions and countermeasures must be considered and no quick decisions are necessary, this mode of operation becomes more important. Editors specially developed for this purpose allow specific modules to be called, different sequences of modules to be executed, input data and parameter values to be changed, and the output and representation of results to be varied. The Supervising Subsystem SSY supports the user by generating a suitable flow-chart, by which subsystems and modules can be called and which is based on the inherent logic of the spatial and temporal sequence of physical processes and protective actions and countermeasures.

2.2.2 The analysing subsystem ASY

Task Description

The main aim of the analysing subsystem ASY is the continuously updated estimation of the present and future environmental distributions of activity concentrations and derived doses/dose rates in the absence of countermeasures. This comprises assessing the source term, calculating the transport of radionuclides released into the atmosphere and their deposition, and considering the subsequent behaviour of radionuclides in the various environmental compartments, both terrestrial and hydrological. These results have

to be presented on maps with geographical information of the area of interest as grid specific or isolines of concentrations or doses together with monitoring/measurement data.

Sequence of Calculations

The basic conceptual software structure of ASY is described in the following for air and ground contamination and for the food chains.

(a) Source Term Program Package

Fig. 2 illustrates the task which is to supply the system with all information about the release of radionuclides. As long as the radioactive material is still inside the plant, estimates of release parameters, such as time, amount, duration and nuclide composition, are mainly based on expert judgements. During this period, the system uses standard source terms, which are derived from probabilistic safety analyses (PSA) of corresponding

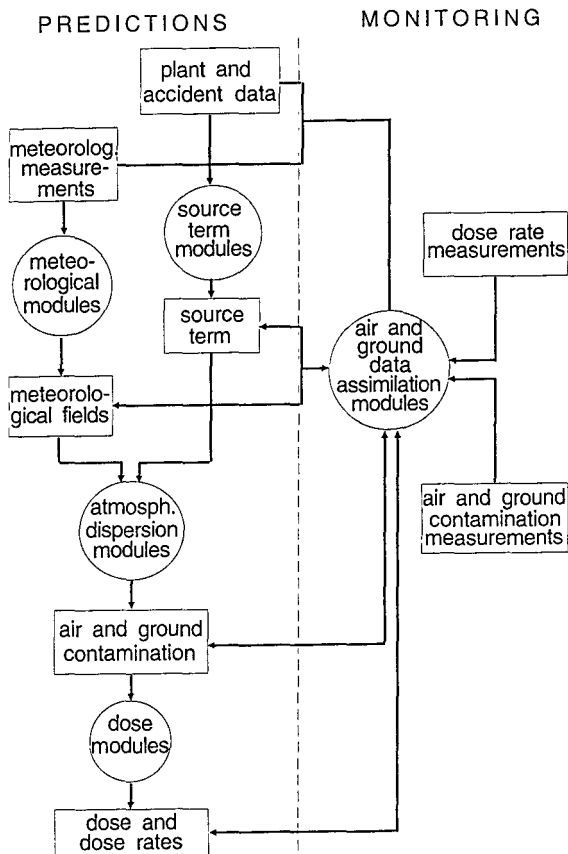


Fig. 2: Basic structure of ASY, air and ground contamination

plants, or a source term derived from radiological measurements inside the plant and other plant data. Optionally the user can generate his own release data by direct input. With the begin of the release, monitoring data will become available from measurements inside or at the plant. They can be directly used for the determination of the source term. Source term reconstructions from further monitoring measurements outside the plant will be supplied by the air and ground data assimilation program package.

(b) Meteorological Program Package

The task is to provide diagnoses of the present weather and analysis of the meteorological situation on the local and intermediate scale out to distances ranging between 20 to 50 km from the power plant. For the accident consequences assessment at further distances and for prognosis purposes, sequences of hourly updated present and forecast winds, turbulence and precipitation fields are on-line provided from National Weather Services or from the European Centre in Reading (ECMWF-UK). Such European-scale high-resolution Limited Area models (LAM's) presently operate on the European scale producing up to more than 36 hour forecasts with a spatial resolution now becoming less than 50 km by 50 km (see Fig. 3).

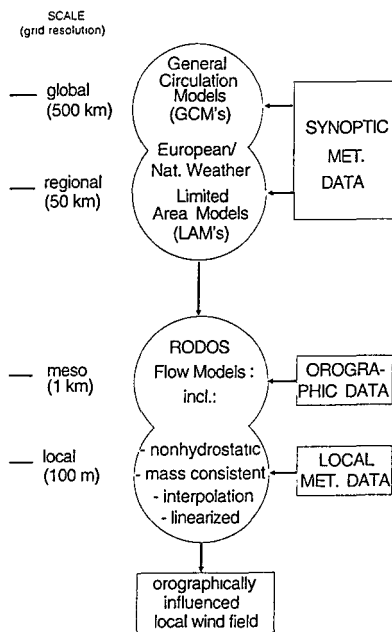


Fig. 3: Chain of meteorological flow models

National scale meteorological models (typical 20 km x 20 km grid) are in use in various European countries. They allow the coupling of non-hydrostatic flow models with a finer grid resolution of 500 m x 500 m. The results of such model chains are hourly updated forecasts for the next 24 hours of 3-dimensional meteorological fields. The problem of analysis and forecast of precipitation patterns will partially be solved by coupling of national rain radar system data to the meteorological models.

For use in real-time and early phase applications of RODOS the two diagnostic flow models MCF (mass consistent flow model) and LINCOM (non-hydrostatic flow model) have been selected. Meteorological preprocessors, such as PAD, are necessary to convert the meteorological data in the format required by the flow and dispersion models. For planning and post-accident assessments, ADREA-FLOW (non-hydrostatic flow model) and HIRLAM (3D-forecast model), have been identified as candidates for difficult topographic terrain and forecasts on regional scale, respectively /A3, A4/.

(c) Atmospheric Dispersion Program Package

The task of the atmospheric dispersion program package is to link the source term with the meteorological fields in order to obtain activity concentrations in air and on ground surface at the locations of interest. The cloud gamma doses in the vicinity of the plant are calculated in this program unit. Models for calculating atmospheric dispersion and deposition have been selected due to the availability of data, the complexity of the meteorological situation, the topographic structure, the distance range from the source, for which results are needed, and the computing times required. There is a variety of models available or under development and the simpler ones are based on Gaussian dispersion, such as straight-line models or plume/puff trajectory models. Lagrange particle models and Eulerian grid models are more sophisticated and are potentially applicable to more complex situations but require more input data and larger computing times. A universal real-time on-line system should have access to a hierarchy of models together with selection criteria, which allow the assignment of the model appropriately adapted to the actual meteorological and environmental situation. A problem which remains to be solved is the assessment of gamma dose rates from a plume whose temporal and spatial distribution of activity concentrations cannot be described by Gaussian atmospheric dispersion models. Quick and reliable integration algorithms are required for use close to a site, where the semi-infinite cloud approximation is not valid. In this case more sophisticated models may be used to calculate the gamma dose-rate contributions from the individual nuclides and from various parts of the radioactive plume.

For operational use in real-time and early phase applications of RODOS, the simplified Gaussian puff model ATSTEP and the puff code RIMPUFF have been implemented (see Sect. 3.1.2). For complex orographic terrain, the Lagrangian particle model ADREA-DIFF is suitable in connection with the ADREA-FLOW model /A3, A4/. Both ATSTEP and RIMPUFF have their own gamma dose rate modules; the one for RIMPUFF has been developed by CRIP.

(d) Air and Ground Data Assimilation Program Package

The task is to provide a consistent picture of the spatial and temporal distributions of activity concentrations and dose rates together with an improved estimation of the source term and other data by the combined evaluation of both monitoring data and model predictions. From the start of the release, monitoring data become available from gamma dose-rate meters and other survey facilities but nuclide specific data in air and on ground surface will come later. All these data are to be used to derive the most important release characteristics for reconstructing the source term and dispersion/deposition data.

(e) Foodchain Transport Program Package

The task is to calculate specific activities of radionuclides in foodstuffs and to transfer them to the dose module. The deposition of radionuclides to and interception by vegetation and soil are estimated taking into account the season of the year. Time-dependent specific activities in feed - and foodstuffs are calculated taking into account processes such as the translocation of activity in the vegetation, migration of activity through the soil, uptake of activity from the soil by plant roots, etc., and assumptions about agricultural practices. The specific activities in foodstuffs are input data for the dose module. RODOS contains the ECOAMOR (see Section 3.2.3) module system which incorporates a dynamic foodchain transport module based on the radioecological model ECOSYS-87 /A5/.

Measured specific activities for elements of the foodchain are compared in the next module.

(f) Food-chain Data Assimilation Program Package

This is illustrated in Fig. 4 and the task, which is similar to (c), is to compare measured specific activities in environmental media with the respective calculated data to provide a consistent picture of the spatial and temporal contamination patterns in the various foodstuffs (see Section 3.2.3). Corresponding mathematical procedures are under development by GSF.

(g) Dose Rate and Dose Estimation Program Package

The task is to perform dose calculations from activity concentrations in air, activity depositions onto the ground and specific activities in foodstuffs. Exposure pathways which lead to an immediate irradiation of the affected persons are external irradiation from the passing cloud, from contaminated rural and urban surfaces, and radionuclides deposited on skin and clothes, and internal irradiation after inhalation of radioactive material directly from the cloud or after resuspension from ground surfaces. More indirect exposure pathways are the external exposure from radionuclides deposited onto the ground and the internal irradiation after ingestion of contaminated foodstuffs. From time-dependent activity concentrations in foodstuffs given by the foodchain module together with age dependent consumption rates and assumptions about food-distribution, the re-

sulting ingestion doses for individuals and in the population can be estimated . The corresponding computer models build the ECOAMOR module system integrated in RODOS.

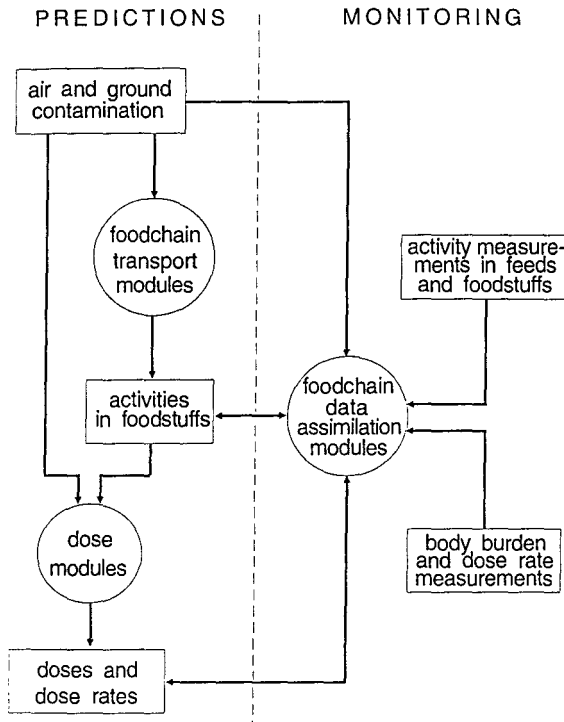


Fig. 4: Basic structure of ASY, food contamination and dose assessment

2.2.3 The countermeasure system CSY

Task Description

The countermeasures required after an accident are in general combinations of a variety of single actions, such as sheltering, evacuation, distribution of stable iodine tablets, relocation, decontamination and banning of foodstuffs. The selection of the best-suited combination is a very complex undertaking and a large number of influences will determine the decisions, such as radiological, economic, ecological, socio-psychological and political consequences. The main task of the countermeasure subsystem CSY is to quantify the benefits and disadvantages of various countermeasure combinations, such as individual/collective doses (averted), health effects and economic costs, areas and number of people affected, together with the technical and personnel aids required. To achieve these results, mathematical models simulating the spatial and temporal patterns of

emergency actions under the actual environmental and economic conditions have been and are being developed by the RODOS contractors.

Sequence of Calculations

The quantification of the benefits and drawbacks of countermeasures requires mathematical models which allow the simulation of time and distance dependent actions. Fig.5 shows the principle structure for analysing the effectiveness and implications of the various countermeasures strategies. The sequence of calculations can be separated into two parts:

- (a) Description and quantification of the consequences of countermeasures already adopted or presently in progress (actual situation). These are a prerequisite to get reliable predictions about the usefulness of further actions.
- (b) Description and quantification of the consequences of supplementary countermeasure actions potentially leading to a further reduction of the radioactive exposure of people or the recovery of contaminated areas (future scenarios).

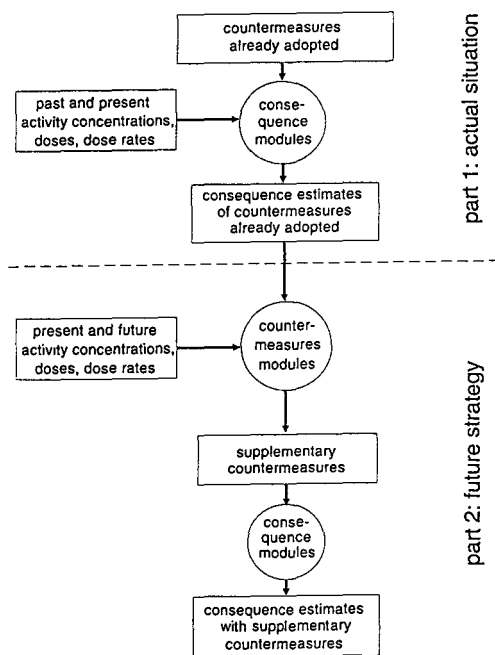


Fig. 5: Basic structure of CSY

Both parts contain models and procedures to simulate single actions and to provide information about their spatial and temporal dependencies allowing for dose reductions of the actions to be calculated. By comparison with the doses which would be received in the case of no action, the net benefit of each single action and the complete countermeasure strategy can be obtained. Various kinds of action consequences are assessed to give a list of consequences for each countermeasure strategy presented on an action-consequence matrix which consists of only one or a few columns or a large number of countermeasure strategies, respectively.

RODOS contains the EMERSIM software for simulating early emergency actions (see Section 3.2.1) and the FRODO module package (see Section 3.2.2), which considers long-term countermeasures, such as relocation, decontamination and food-bans. The EVSIM module (see Section 3.2.1), which builds part of EMERSIM, models the evacuation of the population from areas in the close vicinity of nuclear power plants on the existing road network.

Consequence Program Packages

Six principle types of consequences occur when single or multiple courses of actions are introduced:

- (a) radiation doses to individuals and the public,
- (b) radiation induced health effects,
- (c) areas and number of people affected by countermeasures,
- (d) health effects caused by the countermeasures actions,
- (e) monetary costs quantifying the economic impact of countermeasures and health effects,
- (f) socio-psychological and political implications.

Accident consequence models have been and are being developed for quantifying comprehensively the spectrum of consequences belonging to types (a), (b), (c) and (e). They are implemented in the RODOS module systems EMERSIM, FRODO, HEALTH and ECONOM (see Section 3.2.4). No methods exist for (f) and more information is needed for (d).

2.2.4 The evaluating subsystem ESY

Task Description

Whenever there is an option of two or more actions or action combinations, a choice has to be made. Evaluation techniques may support this task of the decision maker by proposing those courses of actions, which are practicable under the actual or future conditions, and which are ranked by balancing of benefits and effort. Practicability comprises three factors

- (a) consistency with the aims and rules of emergency planning
- (b) consideration of the environmental situation and the behaviour of the population
- (c) availability of technical and administrative support.

If more than one option remains after the selection procedure, a decision problem exists and this can be decided on subjective arguments based on the decision makers opinions. Preferences and judgements can be derived from interviews supported by formal information elicitation procedures.

The evaluating subsystem ESY is being developed mainly to evaluate alternative countermeasure strategies under the aspects of feasibility in a given situation, public acceptance of the actions, socio-psychological and political implementations, and subjective arguments reflecting the judgements of the decision maker. These parameters can be taken into account in ESY using mathematical formulations as rules, weights, and preference functions. The application of these rules results in a ranked order of options together with those rules and preference functions which, above all, have led to this evaluation. This ranking order can be great help to a decision maker in taking a final decision. At present, both multi-attribute decision analysis techniques and expert systems are being studied as potential methodological tools in the evaluation of combinations of alternative actions. The present conceptual structure of ESY is shown in Fig. 6 (see also Section 3.3).

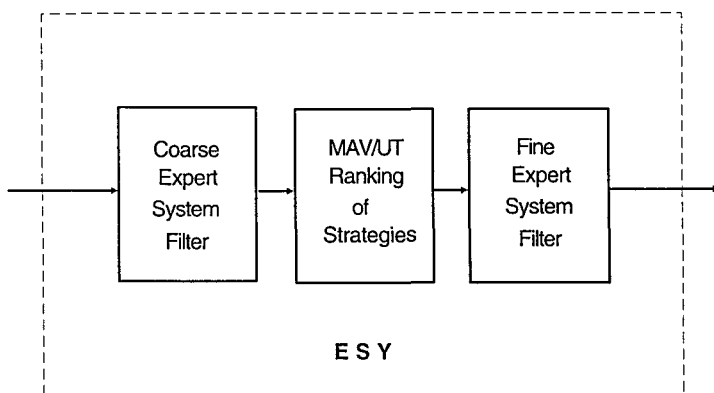


Fig. 6: The conceptual structure of ESY

Sequence of calculations

First, a very simple expert system will be used to discard strategies which are incompatible with the principles of radiological protection, which do not give continuity of treatment, or which fail very coarse practicability rules. The remaining strategies will be passed to a multi-attribute value ranking module, which will identify the top 10 or 20 ranked strategies. The operator will be able to use interactive sensitivity analyses, such as that in the software packages HERESY and M-CRIT, to confirm that these strategies are worth careful consideration. These strategies would then be passed to an expert system

with a much finer and more sophisticated system or rules, each of which could be applied to each of the candidate strategies. The small number of strategies would allow a full set of explanations to be developed, which would give a critique of each of the strategies. Thus the output of RODOS will be a short list of strategies, each of which satisfies the constraints implied by intervention levels, practicability, etc. together with a detailed commentary on each strategy explaining its strength and weaknesses.

2.2.5 The hydrological model chain

The evaluation of the radiological and environmental consequences of the Chernobyl accident demonstrated the significant contribution of contaminated water bodies /A6/. To complete the RODOS methodology and system, a hydrological model chain has been developed, which covers all the relevant processes such as the direct inflow into rivers, the migration and the run-off of radionuclides from watersheds, the transport of radionuclides in large river systems including the exchange with sediments and the behaviour of radionuclides in lakes. The corresponding run-off model RETRACE (SPA TY-PHOON), the river models RIVTOX and COASTOX (IMMS CC) and the lake model LAKECO (KEMA) have been coupled, implemented in RODOS and adapted to the Rhine river system and the lake IJsselmeer, NL /A7/. Other rivers can be readily implemented in RODOS using the same model chain subject to gathering appropriate data.

3. Content and functions of RODOS

3.1 Diagnosis and prognosis of the radiological situation

3.1.1 Source term estimation (NPRRI)

In the event of a nuclear accident resulting in the dispersion of radioactive materials into environment, the effective implementation of measures for the protection of the public will be largely dependent upon the adequacy of advance preparation, including the preparation of environmental monitoring programs and source terms evaluation. In predicting the consequences of accidents, a source term, or a range of source terms, is usually the starting point of the assessment. The brief overview of the overall status of the environmental monitoring network manned by NPP Bohunice and a method for the source term determination during an accident based on a on-line data measured by the environmental monitoring system are presented.

Environmental monitoring system

NPP Bohunice have set up computer based monitoring system for the permanent surveillance of radioactivity of the environment at distances up to 30 km. During accidents this system will provide valuable information on the status of plant and radioactivity in environment.

The main purpose of the environmental monitoring system is to follow continuously chosen values in the surrounding of NPP Bohunice and to display measured data. The parameters, which are available in a on-line mode, are summarised in Table 1. The typical integration time of the on-line data is 5 minutes.

The environmental monitoring network is divided to the three groups:

- 1) the two rings of "fence monitors" at the NPP territory:
 - a) a ring EBO-V1 consists of 24 measure points with 3 stable measure points,
 - b) a ring EBO-V2 consists of 24 measure points with 2 stable measure points;
- 2) a ring consists of 15 stable measure points at the vicinal villages at distances up to 6km;
- 3) 4 measure stable points in significant agglomerations with the greatest concentration of people (Trnava, Hlohovec, Piestany, Vrbove). Details of the geographical positions of the monitors are given in /B1-5/.

The data from the environmental monitoring system are transmitted, and cumulated and stored at the central station situated at the Laboratory of environmental radioactivity control in Trnava.

There are two data transmission points: (a) the retransmission station which cover radio communication between the central station and the inferior stations, and (b) the retrans-

mission station, situated at the local meteorological station, for the transmission of the meteorological data to the central computing system in the central station. The actual local meteorological data such as wind speed and wind direction, stability class and precipitation are also available every 5 minutes.

Type	parameter
release rate	noble gases (stack) gamma dose rate (stack) I131 activity (stack) activity concentration (aerosols, stack) air flow temperature activity concentration (liquid effluent) water flow activity concentration (cooling water)
site specific meteorology	wind direction wind velocity air temperature precipitation atmospheric pressure stability category
environmental situation	gamma dose rate activity concentration of air (aerosol and iodine)

Tab. 1 Parameters of on-line monitoring of the NPP Bohunice environmental monitoring network.

Methodology for interpretation of measured dose rates

For the estimation of the source term the gamma dose rates from the first ring ("fence monitors") are used. The 24 values of the gamma-dose rate from the first ring EBO-V1 are measured with a pair of collimated detectors of type DC-4D-84/N and DC-4D-84/V which cover demanded measure range. The first ring EBO-V2 has also 24 gamma-dose rate measuring points. A detailed description is given in /B4/.

"Sensitive curves" - gamma dose rates [Gy/s] for a 1 Bq/s release in dependence of the distance from the plume axis for each detector from this ring were precalculated with a gaussian-puff dispersion model.

The total gamma dose rate in air from a monoenergetic point source in Gy s⁻¹ can be written

$$\dot{D}(x,y) = \frac{1.6 \times 10^{-13} Q_0}{2\pi^{3/2} u} \sum_i f_i E_i (\mu_{en}/\rho) I_T(E_i) \quad (1)$$

where Q_0 is the release rate in Bq s⁻¹, f_i is the fraction of photons of initial energy E_i emitted per disintegration, E_i is the initial energy of the photon in MeV and the constant $1.6 \cdot 10^{-13}$ has the unit kgGy per MeV. In terms of the reference system given in Fig. 7 the general equation for I_T can be written

$$I_T(E) = \frac{1}{2^{3/2} \sigma} \int_{-x}^{\infty} \int_0^{\infty} \frac{B_{en}(\mu r) \exp(-\mu r)}{m r} \times \left[\exp\left(-\frac{(m-r)^2}{2\sigma^2}\right) - \exp\left(-\frac{(m+r)^2}{2\sigma^2}\right) \right] d\xi dr \quad (2)$$

where $m = (\zeta^2 + y^2 + h^2)^{1/2}$, $\sigma = (\sigma_y + \sigma_z)^{1/2}$ is used for the solution of the problem of correcting for a nonisotropic cloud, $B_{en}(\mu r) = 1 + A\mu r \exp(B\mu r)$ is the Berger form of the buildup factor.

Real data which characterise the location of measurement points, source of release (dimensions of a reactor building, sensible heat) and meteorological conditions (wind direction, wind speed, stability class) were taken into account for the calculation of gamma dose rates for a 1 Bq/s release for given measurement points. Selected "sensitive curves" for the fence monitors of ring EBO V1 are shown as an example on Fig. 8 /B4/.

The ratio between measured dose rates and predicted dose rates gives the set of source terms Q_i [Bq/s] where i is number of detectors where measured values are beyond the background level. This data set has a limited number of Q_i with unknown distribution. Thus, it is important to know the uncertainties that are associated with the source term estimation. Standard analytical methods for uncertainty estimation are not generally applicable since the distribution of partial source terms are not easily transferred to a Gaussian shape. The bootstrap resampling procedure was selected as an alternative method to determine the mean value of Q and confidence limits, since it does not depend on the form of the underlying distribution function. The method is based on the random generating of independent random samples with range i from the empirical function.

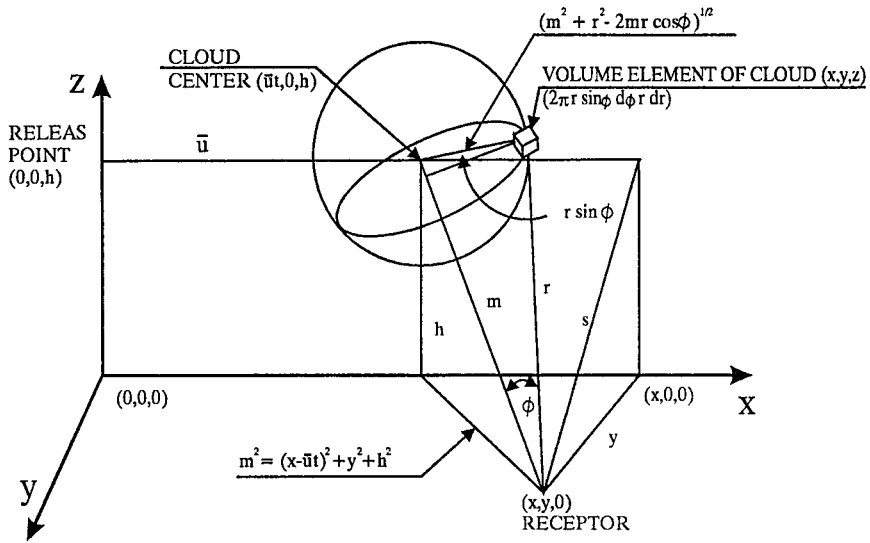


Fig. 7: Coordinate system for cloud gamma-dose calculations

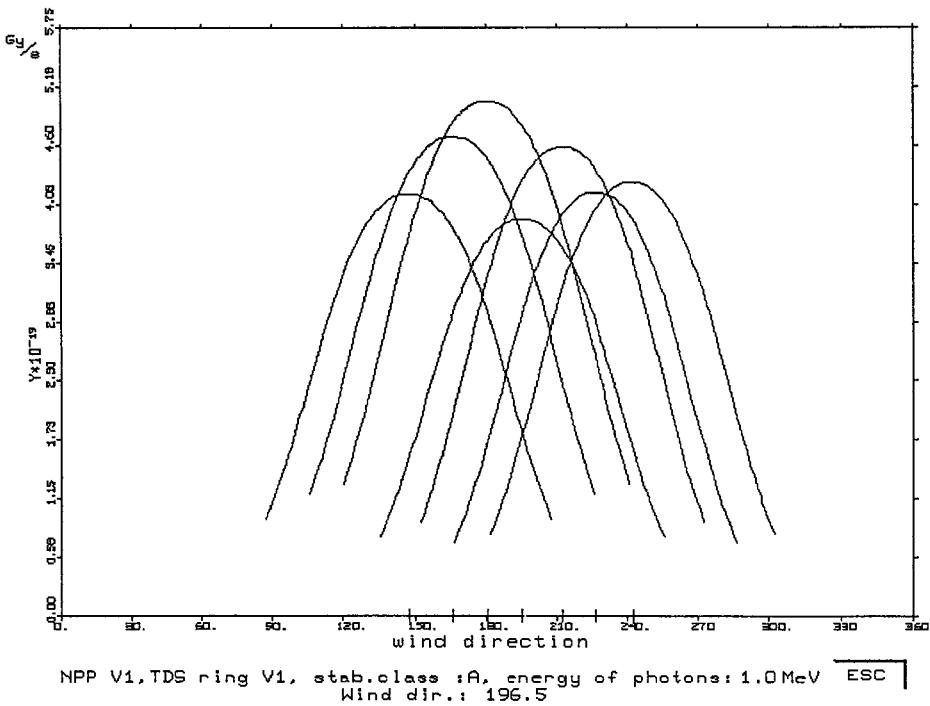


Fig. 8: Selected "sensitive curves" of the ring EBO-V1 in chosen wind direction

The nonparametric percentile method and the bias-corrected percentile method were used for the calculation of the confidence intervals. The fractional bias (FB) which estimates how much the mean over the predictions differs from the mean over the observations was used for the comparison of the empirical and predicted values. Estimates for FB and 95% confidence intervals were computed by two different resampling procedures: bootstrap method and jackknife method. The applied statistical methods are described in more details in /B4, B5/.

Program modules for on-line source term estimation and their implementation to the Bohunice NPP TDS software

The TDS PC net consists of two nets which are connected by telephone modems and internal telephone lines. The first PC net is the base control PC system under QNX operating system. The second PC net is working under Novell operating system. These nets are connected by the QNX-DOS interface and are used for the supporting and interpretation of the values from the teledosimetric system.

The following programs were developed for the estimation of the source term based on gamma dose rates from first ring:

CHARDET	calculation of sensitive curves for 1 Bq/s release in dependence of the distance from the plume axis and construction of special functions for the approximation of these curves,
TDSMDATA	transfer the current measured data of dose rates and meteorological data from the TDS under QNX to DOS; data preparation for the next calculations,
SOURCE	the main program for the estimation of the source term included following main sets of subroutines:
S_READ	reading of input data, calculation of source terms Q_i , storing of data,
EST_Q	estimation of source term Q by Bootstrap resampling method and confidence intervals estimation,
CHECK	calculation of dose rates with estimated source Q in measured points with dose rates over background for comparison of measured and calculated dose rates,
S_SCREEN	the set of subroutines which form an interactive mode for working with program,
S_GRAPH	graphical presentation of results,
TIME	time procedures.

The system chart for the SOURCE code is given in Fig. 9. A detailed description of the computation flow is given in /B4/.

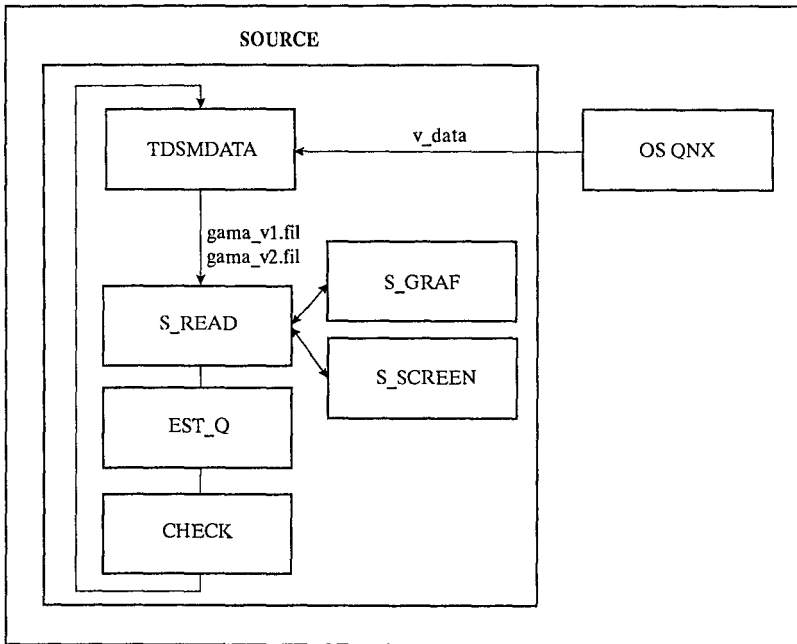


Fig. 9: System chart for the SOURCE code

The program SOURCE was developed as a prototype under DOS and was written in FORTRAN. The SVS FORTRAN 77 compiler was used. Some of procedures were written in C language (TDSMDATA, WIN). All statistical procedures are collected at EST_Q. For the estimation of the source term by bootstrap the procedure CALC_SOURCE is used. CONFID_B, CONFID, MONTE are procedures for the calculation of confidence intervals, BIASES, VYPOCET, STATIST, CONFID_J are procedures for the comparison of predicted and measured dose rates by fractional biases and calculation of the confidence intervals of fractional biases. The following statistical programs were used:

- GEN1 generator of random numbers from the interval (0,1) (multiplicative method),
- GENN1 generator of random numbers from normal distribution with parameters $N(\mu, \sigma)$,
- NORM generator of numbers with normal distribution from the interval (a,b),
- ROVDST generator of numbers with uniform distribution from the interval (a,b),
- DNORM calculation of distribution function of normal distribution,

- DFIN calculation of critical values of normal distribution,
- STUD calculation of critical values of Student's distribution with N degrees of freedom,
- MONTE calculation of confidence intervals: symmetrical interval, percentile interval, bias-corrected percentile interval. This procedure assign the using of following algorithms:
- PPDN calculation of quantiles of normal distribution,
- ALNORM calculation of distribution function of normal distribution.

Data collection is repeated every 5 minutes. In each interval a new calculation of the source term is performed.

Program SOURCE written in FORTRAN requests continuous work and connection with main system under OS QNX, it means this program would have required the next computer for work. Due to the technical and economical reasons this program was rewritten to C 86 language (C language under OS QNX) and in this form was implemented to the main control system TDS under OS QNX. This solution of problem has following advantages:

- 1) initialisation part of program BKG is done automatically during the configuration of TDS system at the beginning,
- 2) the main part of the software COMPUTE will be incorporated in the base control software, it means at the moment when all data from the detectors are available the calculation of source term will be done,
- 3) interpretation software RTARC will have data about source term immediately after the end of the data completion cycle,
- 4) a visualisation of source term data will be a part of the visualisation of the instantaneous TDS state.

Interface program connecting on-line source term estimation with RTARC computer code

Output data files from SOURCE program package with information about source term and meteorological situation are used as the input data files for program package RTARC, (Real Time Accident Release Consequence) which works under MS-DOS.

The source term estimated by the methodology described above is an integral value. An isotopic composition of release is unknown during an accident and can be assumed only on the base of computational analysis. The results obtained on the base of sampling, e.g. PASS, are useful but these results are available much more later as the data of dose rates from on-line teledosimetric system. Therefore, the precalculated characteristics of isotopic composition of release are needed for dose projection. Totally 54 sequences of the accidents and 46 corresponding isotopic compositions were evaluated for VVER 440/213 reactors for LOCA and containment by-pass releases. The information are collected and

performed as an event tree for source term evaluation. A detailed description is given in /B4/.

The real-time on-line decision support software for off-site emergency management of the computer based part of environmental monitoring system provides models for atmospheric dispersion and deposition to predict the spatial and temporal distribution of activity up to distances of 40 km, taking into account the site specific meteorological conditions prevailing during the release and the subsequent time of travel of the plume, and models for dose and consequence assessment taking into account the countermeasures involved to mitigate the effects of the accident. For dose assessment the major exposure pathways are considered, i.e. external dose from the plume and from material deposited on the ground, and internal irradiation from activity taken into the body by inhalation. The countermeasures which may be considered in calculation are sheltering, evacuation and the issue of stable iodine tablets. The final step of an accident consequence assessment is to evaluate the incidence of early health effects based on irradiation of the red bone marrow.

Summary

A methodology and computer code for interpretation of environmental data, i.e. source term assessment, from on-line teledosimetric network was developed. The method is based on the conversion of measured dose rates to the source term, i.e. airborne radioactivity release rate, taking into account real meteorological data and location of the measure points. Due to an unknown distribution of the measured dose rates the bootstrap method for the estimation of the mean value of source term Q and confidence interval of Q was selected. The program module for on-line calculation of Q was developed and implemented to the environmental monitoring system manned by the Nuclear Power Plant Bohunice, Slovakia. The interface program connecting on-line source term estimation program module with computer code for radioactivity dispersion and dose calculation **RTARC (Real Time Accident Release Consequence)** was developed.

3.1.2 Meteorology and Atmospheric Dispersion in RODOS (FZK)

Meteorology and atmospheric dispersion are essential parts of the Analysing Subsystem ASY of RODOS. The main purpose of ASY is the assessment of present and future distributions of activity concentrations and environmental doses and dose rates, irrespective of any protective actions or countermeasures taken. The present software structure of ASY is shown in Fig.10. ASY can work both with actual data (real-time mode) and with forecast data (prognostic mode); depending on the mode of operation, different meteorological data and source term data are entered. In the former case, these are on-line data from nuclear reactor remote monitoring networks and other measurement networks, while in the latter case the data are forecasts of meteorological fields and source term predictions.

Meteorological data are processed in the modules PAD, MCF, and LINCOM. The preprocessor program PAD was developed by the Agenzia Nazionale per la Protezione Del`Ambiente (ANPA) /C1/ and made available for implementation in RODOS. It is the

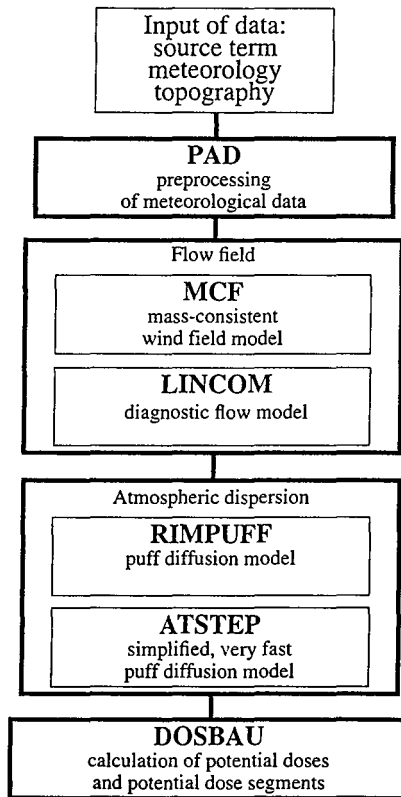


Fig. 10: Sequence of modules in ASY

link between the measured meteorological data entering the system from individual stations and the modules describing the wind field and dispersion. These modules require prepared data indicating the condition of the atmospheric boundary layer. PAD computes these boundary layer data from the measured meteorological data.

The mass-consistent wind field model MCF was made available for implementation in RODOS by the Gesellschaft für Anlagen- und Reaktorsicherheit (GRS) /C2/. It allows a spatial wind vector field free from divergences to be set up over the area covering the computation grid. For this design to be achieved, the boundary layer and wind profile data are required which are calculated in the meteorological preprocessor program PAD. In addition, the topography of the base area is entered; as a consequence, the influence of mountain structures on the wind vector field is taken into account.

The module MCF can be used in the real-time on-line mode to integrate local measured wind data from nuclear reactor remote monitoring stations and other stations into the wind field. In the prognostic mode, large wind fields taken from the weather forecast (e. g. with a resolution of 14 km from the German weather service) can be used as input data in MCF to produce a wind field with higher resolution in the computation area of RODOS.

The flow model LINCOM is a non-hydrostatic diagnostic model /C4/ based on the solution of linearised continuity and momentum equations with a first order spectral turbulent diffusion closure. As an example it processes a single layer of 100x100 grid points in less than 10 seconds on a 486 PC. Its truncated physics of course restricts its application over severe non-uniform terrain, but considerable realism in the flow fields is achieved by use of assimilation techniques to match results to measured tower or forecast winds. LINCOM can be used in a similar way as MCF.

Atmospheric dispersion and deposition as well as nuclide specific activity concentration and gamma radiation fields are calculated in the modules RIMPUFF and ATSTEP.

RIMPUFF is a fast and operational puff diffusion code /C4/ that is suitable for real-time simulation of puff and plume dispersion during time and space changing meteorology. Also optimised for fast response on a PC this model is provided with a puff splitting feature to deal with plume bifurcation and flow divergence due to channeling, slope flow and inversion effects in non-uniform terrain /C5/. RIMPUFF includes fast subroutines for the calculation of gamma doses from airborne and deposited radioactive isotopes, released to the atmosphere from a nuclear power plant. These subroutines have been developed in cooperation with CRIP, Budapest. For real-time applications, RIMPUFF can be driven by wind data from a combination of:

- 1) A permanent network of meteorological towers,
- 2) The flow models LINCOM and/or MCF (or similar), and
- 3) Numerical Weather Forecast data.

The puff or plume diffusion process in RIMPUFF is controlled by the local turbulence levels, either provided directly from on-site measurements, or provided via PAD preprocessor calculations /C1/. RIMPUFF is further equipped with plume rise formulas, inversion and ground level reflection capabilities, gamma dose algorithms and wet/dry depletion.

ATSTEP developed by FZK /C6/ is a very fast, but simplified Gaussian puff diffusion code with lower spatial and temporal resolution than in RIMPUFF. It has all important features of a short range, non-stationary atmospheric dispersion code for radioactive releases. ATSTEP is the dispersion module integrated first into the RODOS system. Its future purpose is the application as a fast dispersion code for emergency training and exercises aided by RODOS.

In the ATSTEP code the atmospheric release and dispersion are modelled by a time series of non- spherical, long puffs shaped similar to Gaussian plume segments, i. e. even for a release duration of several hours only a small number of puffs is needed. Therefore, the computer time needed for a 12 hours real time prognosis of the dispersion and radiological situation with a release duration of several hours is only 3 minutes on a workstation. Each new release step (of either 10 or 30 minutes duration) corresponds to the emission of another long puff. During dispersion all puffs travel along their own trajectories according to the time series of wind or wind field input data. The growth of the puffs by turbulent diffusion is modelled by using sigma parameters depending on Pasquill Gifford diffusion category, roughness length, and effective release height. If the release contains heat energy thermal rising of the puffs is considered. Further on dry and wet deposition and the corresponding cloud depletion is modelled for different deposition groups. The near ground nuclide specific gamma radiation field of each puff is calculated by using line source, cloud correction factor, and gamma submersion methods. In the computation the puffs are represented as fields of air concentration data on an orthogonal coordinate grid with the dimension of 41 x 41 points. In the same way time integrated concentration fields, contaminations, and gamma radiation fields are represented. During a dispersion calculation ATSTEP is operated in a time step loop. After each time step all concentration and radiation field data are available for the graphical presentation on the screen.

The data of a prognosis of a radiological situation calculated in ASY are transferred to the CSY subsystem not in the form of time series of nuclide specific concentration and radiation fields but in the form of "potential dose histories" on the whole computation grid. In a PROGNOSE run of ASY the module DOSBAU calculates the potential dose histories in the form of series of half hour dose segments. These series of dose segments contain all information about the temporal development of doses on the whole computation grid during a release and dispersion time interval of several hours. The dose histories are specific for the pathways cloud radiation, ground radiation, and inhalation, and for the organs lung, bone marrow, thyroid, uterus, and effective. Dose integration times are 1, 7, 14, and 30 days, 0.5, 1, and 50 years. In CSY the dose segments allow for the computation of any special dose desired with and without simulated time dependent countermeasures.

3.1.3. Data assimilation - part 1 : contribution from SCK/CEN

Introduction

RODOS is a decision support system with primary objective to assist decision makers (DM) to define interventions during radiological emergencies. Therefore, the actual as well as the prognosed radiological situation must be assessed as reliable and as soon as possible.

Four phases can be discerned during a nuclear emergency.

- The pre-release phase : based on available on-site data (e.g. analysis accidental sequence, plant-status, expert judgment) anticipative counter-measures (CM) will possibly be taken. An uncertainty of several orders of magnitude concerning the potential release is to be expected rendering the optimisation of the intervention difficult.
- The release and immediate post-release phase (called release-phase). This is the most critical phase for the DM as severe effects can be expected in the near-range (i.e. deterministic effects, high individual doses), the time constraints will be very tight and the available information will be scarce and conflicting. However intervention (early CM) which is not optimised can lead to unacceptable consequences (radiological,socio-economical,...).
- The longer-term post-release phase. This is a much more comfortable situation for the DM: as no urgent CM have to be taken, enough time will be available to obtain a comprehensive picture based on measurements, thus allowing the required optimisation.

Objectives

Once the release starts the DM wants to know how it compares to the previously forecasted release. Next he wants to know the potential doses to the environment. Three situations can occur:

- Near-range doses remain well below early intervention levels (IL). This situation is easily recognised and no intervention is needed.
- Near-range doses are well above early IL's. This situation is again easily recognised and the emergency plans must be deployed to their full extent.
- Near-range doses are comparable to IL's. This situation is more difficult to recognise and requires an optimisation.

The objective is to develop a module in ASY to reconstruct the source term (ST) during the release phase with an uncertainty within one order of magnitude. This will allow to obtain an overall picture and to assist the DM in his task (by means of CSY,ESY). The ST and its components have been defined in /D1/.

Methodology and achievements

The base of the methodology has been given in /D2/. Basic requirements for the methodology is given in /D1/. Monitoring data (MD) expected to become available in the near range during the early phase will be assimilated in a data-base.

For any observed "contamination field" CF_0 (i.e. monitoring of certain type, e.g. air concentrations) the associated calculated (predicted) contamination field CF_P can be obtained in the following way :

$$CF_P(x,y;t) = Q(t) \cdot f(x,y,z;t;\{p_i\})$$

where :

Q is the source term

f is the transfer function based on a physical model

{ p_i } are the input and model parameters

The methodology developed consists of a set of rules that have to be activated depending on the particular accidental situation : that is the type, amount and time-space distribution of MD, the meteorological conditions and the initial knowledge of the accident. Basically two types of rules can be defined :

1) Absolute rules to be applied on data of the same type measured during the same time interval to calculate the magnitude of (a part of) the ST.

2) Relative rules which allow to combine and relate to each other different data types measured during different time intervals to acquire a more detailed knowledge (e.g. nuclide composition) of the ST. The different monitoring types which can reasonably be assumed to be at least partially available are mentioned in /D1/.

Up to now, most of the work have been directed towards ST reconstruction algorithms for use of MD of a single type under time-invariant conditions (i.e. air concentrations during tracer experiments conditions). Tracer experiments (near-range simple topography) have been used to check the methods.

Fuzzy logic

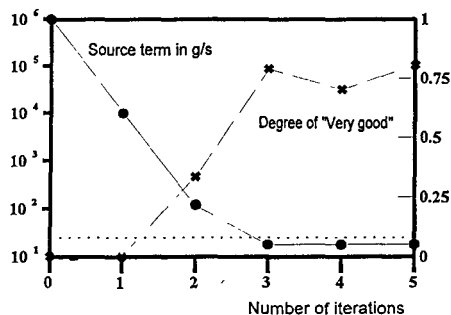
An increasing number of optimisation systems use fuzzy logic instead of numerical optimisation techniques. Fuzzy logic is appropriate to translate a qualitative judgment into a degree of membership to a given group. A logic has been developed to derive a degree of "possibility" or "necessity" to conclusions, based on the combination of several fuzzy information /D3/.

A PC-module based on fuzzy logic has been developed to reconstruct the ST, to adjust the winddirection and, if enough MD are available, to estimate the release height. First, for each observation O a prediction P is calculated using a simple Gaussian model with initial best estimate input parameters. Depending on its value of P/O , five degrees of membership (corresponding to the membership functions very good, good, neutral, bad, very bad) can be associated to each monitoring point /D4/ giving an idea of the

misprediction. The optimisation is based on the application of three operators which change the spatial distribution of P/O's. The three operators are :

- The ST-operator which changes ST-value. E.g. an overprediction in the ST tends to overestimate the predictions with the same value for all monitoring points.
- The DD-operator which changes the winddirection. E.g. a misprediction in the winddirection tends to overestimate the predictions at one side of the (mispredicted) advection direction and to underestimate the predictions at the other side.
- The Heff-operator which changes the plume height. E.g. an overprediction of Heff tends to underestimate the predictions more strongly at short distance than at longer distances. This operator can only be applied if enough MD in function of distance is available, which is not trivial during the release phase.

These operators are applied in a two step procedure. First the system aims to obtain a situation where the largest number of ratios P/O lies in the set "very good". Then a global optimisation is performed on the membership function "Very Good" for all points together. The method was checked against tracer experiments for simple terrain and gave a ST within a factor of 3 in most cases /D5/. The figure below shows, in function of the number of iterations, the behaviour of the calculated source term (for which an arbitrary input value was used) together with the membership function "Very good". The exact source term is given by the dashed line. The example is taken from a tracer experiment realised in Karlsruhe in September 1977 . The advantage of the method is its speed, its main disadvantage is the arbitrary way to define membership functions which makes it non-trivial to use it in conditions deviating from those used in tracer experiments. Therefore a more universal method to be applied under less restricted conditions has been sought.



Least Square Method

The least-square methodology discussed here can be regarded as a spin-off of the JSP-1 research programme /D6/. It is based upon the assumption that the modelled quantities (e.g. air concentrations) satisfy the relation: $L_i(Q, P) = Q L_i(P)$, where i is a given point, Q is the source term and P represents the different parameters such as release height, wind speed, atmospheric stability, etc. Thus, it is possible to define a so-called objective

function F such that $F = \sum (Q L_i - Z_i)^2$, where Z_i are observable quantities. The determination of the source term using the least-square method is equivalent to minimise the sum of residuals, i.e. minimise F . When one minimises F , $Q = \sum L_i Z_i / \sum L_i^2$. This is the expression that enables one to relate the source term with model predictions obtained using a default value of Q and field observations. As it will be seen below the accuracy of this procedure depends, to a large extent, on the method used to determine model predictions at the exact location where the observations took place.

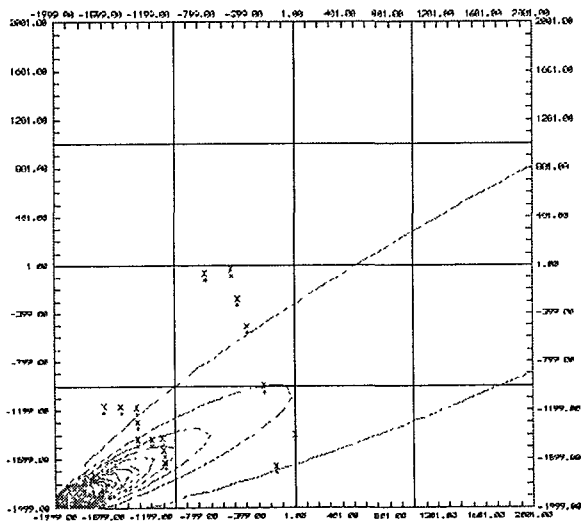
A variation to this approach is the normalisation of F to the sum of the squares of the observations, which confines all possible values of F between 0 and 1, allowing a better interpretation of the results.

The above approach was tested using the segmented-puff dispersion-deposition model ATSTEP, which is currently included in ASY, and that has the advantage of being user friendly, requires a reduced number of input parameters namely, the release height, wind speed, wind direction, atmospheric stability and the source term. The set of observations corresponds to data from tracer experiments carried out in the location of Mol, Belgium.

The first step in the source term reconstruction procedure was the calculation of model estimates under the meteorological conditions observed during the tracer experiments. The release height was known and the emission rate was set to 1 g s^{-1} . At this stage, the default value of the emission rate does not matter very much since the quantity resulting from the minimization of F will determine the exact value of Q for which model predictions and field observations are in agreement. The second step, which perhaps is the most crucial in the whole approach, is the determination of model values at the location where an observation took place. This was done by interpolation using the four grid points with known concentrations that surround the point under consideration. This step is repeated until there is one model estimate for each observation point. Once this is achieved, the determination of Q and F is straight forward. The table below lists the values for the real source term, the calculated one, its standard deviation, the value of the objective function F , as well as the grid size used in the calculations. The idea here is to explain why the agreement predicted-observed is not always as desired, and also to establish the grounds for further developments and improvements.

Mol Tracer Experiments			
	Mol1	Mol2	Mol3
Q _{real}	3.33	3.20	4.20
Q _{calc}	4.09	1.62	0.72
std.dev	0.09	0.03	0.11
F	0.16	0.01	0.18
Grid Size (m)	200	200	400

It can be seen in this table that in the first case the reconstructed source term is in good agreement with the real one, while in the second and third case the calculated source term lies between a factor of two (still acceptable) to six. There are a number of possible causes that produce such a large discrepancy. First, in some cases (see figure below) a significant number of observations were performed away from the plume's center line, which implies that those measurements are prone to large errors. Secondly, the presence of strong concentration gradients implies that in a few hundred meters concentrations can vary by up several orders of magnitude, and this can also be a source of error when measurements are carried out not taking this into account. Third, the accuracy of the above mentioned method relies on the fact that one should have as many observations under the plume's axis as possible. Last but not least, the method of determining model values at specific coordinate points is crucial, in particular when due to the spread of the observation field one is forced to choose a gross grid resolution. Thus, interpolating using a very spaced grid in areas with strong concentrations gradients has proven to produce undesired results (see results for Mol3). It would be necessary that further improvements of this method should include the ability of ATSTEP to calculate estimates at individual points.



Relative position of the observation points (X) with respect to the plume for Mol3

An alternative methodology has been developed in order to account for effects like those shown in the figure above, i.e. measurements carried out away from the plume's center line, or in case when abrupt and unaccounted changes of wind direction occur, or

when there is a displacement between the observed and modelled concentration fields. This method consists of introducing a number of randomly generated transformations such as rotation and translation. All these transformations act on the space containing the observations. This was chosen due to the constraints imposed by computing time. It is faster to perform a transformation on 30 points than on 1681 points, which is the total number of grid points in ATSTEP. Once the observations points have been altered, new modelled values are calculated and then fitted using the approach discussed above. The best solution is basically the one that is achieved when the objective function F has a small value and the magnitude of the transformation introduced is small.

This procedure produced an even better result for Mol1, being the calculated source term 3.25 instead of 4.09 and F was 0.08 instead of 0.16. For Mol2 and Mol3 this approach did not yield significant improvements, which could be due to an interpolation problem as mentioned above. It is worthy to mention that the above results were obtained after performing 100,000 random transformations, which took about 4 min on a 486 33 MHz CPU.

The third stage in this research, still under development, consists of using decision making support software to assist in the selection of the best solution. In other words, the user can establish his preferences a priori and let the system determine which of the results satisfy the above condition, i.e., best fit with small transformation of the observation plane.

As far as uncertainty is concerned, two approaches are still under consideration. One determines the relative error of the reconstructed source term as a function of F (objective function), however it was seen that the magnitude of the transformations often seems more adequate to represent the overall uncertainty, since the measure of uncertainty and F are correlated. The second approach has been proposed by /D7/ and is based upon the quantiles of the F -distribution, which seems more advantageous because it not only gives an idea about uncertainty but also establishes the confidence limits of the source term reconstruction, which is of interest for further error propagation assessments.

Single point method

Above mentioned methods can only work given minimal requirements on MD. A simple method, in case some profiles are available on arcs transversal to the winddirection, is to take the measurement with maximal value and to simply inverse the model to estimate the ST, holding the other input parameters to their best estimate. Checked against tracer experiments it gives mostly acceptable results. Its major advantage is that it eliminates the wind direction which is a major source of uncertainty and it is realistic to obtain MD fulfilling these requirements.

Lessons learned and future developments

Several algorithms can be used with reasonable results for the real-time ST estimation for not too complex situations under conditions similar to tracer experiments. Elaborated methodologies (fuzzy logic, least square, ...) require an extensive set of simultaneous

measurements, which is not trivial to obtain during the release phase. Therefore also more simple methods (e.g. single point) should be used, in function of available data /D8/.

The most important reason for difficulties during the optimisation are:

- Disagreement in location and shape between observed and calculated contamination fields. This can partially be circumvented (single-point method, least square method + transformations).
- Complex meteorological conditions (e.g. plume in stable layer, unstable situation at ground level, windshear, ...) . This is more difficult to circumvent and not trivial to recognise.

In principle, some of the methodologies can cope with an unknown plume height. This can however lead to absurd results during the optimisation. It is strongly desirable to have an idea about the plume height (accident analysis, air-borne measurements).

A meaningful optimisation during the release phase is only possible in case of an adapted monitoring strategy /D8/ : locate the areas of maximum contamination and monitor them. It is advised to develop real-time monitoring guidelines for RODOS.

The quantification and propagation of uncertainty in real-time conditions is still under study and development.

3.1.3 Data assimilation - part 2: contribution from UoL

Overview

The University of Leeds in cooperation with the University of Warwick have developed a version of RIMPUFF Gaussian puff atmospheric dispersion model, coded in C++, which integrates directly into both the RODOS system and the RODOS kernel and which:

- allows for the assimilation of instantaneous and integrated concentration monitoring data;
- provides an estimate of and uncertainty bounds on release height;
- reports means and variances of predicted concentration at given sites;
- estimates the source term with allowance for autoregression;
- make allowances for modelling error.

This version of RIMPUFF is implemented upon HP and SGI workstations.

The algorithm is fast enough for 'real-time' use and only exhibits linear time complexity as the volume of data and number of puffs increase. In achieving this we have developed Bayesian forecasting methodology by extending the theory and algorithms for dynamic junction trees, which underpin the belief net formulations of Bayesian models: see /E1/, /E2/, /E3/, /E9/, /E10/, /E11/.

The SGI version of the software has been validated (without data assimilation) in bench-testing at RISØ in the Spring of 1995.

A version of the software has also been developed which is underpinned by a fully relational data model implemented within an INGRES database. This version runs upon SUN sparcstations.

The puff model and associated uncertainty has been visualised using 3-d colour graphics. Animations of plume spread are provided on SGI workstations. However, the software used is not licensed for HP workstations and the software should be thought of a demonstrator.

Other simpler static plots have been developed to show the fit of the model to data at detector sites, and also to enable 'management by exception'. These have not been fully integrated into the RIMPUFF module nor the full RODOS system.

Introduction to the methodology

An ASY module for an early phase of an accident needs to address the following questions:

What is the likely spread of contamination?

How can this prediction be updated in the light of monitoring data?

What are the uncertainties in the predictions?

A simple and flexible statistical model was built in order to address all three questions, using Bayesian dynamic linear model (DLM) forecasting methodology. This model was integrated into the RIMPUFF atmospheric dispersion model. RIMPUFF is a mesoscale dispersion model in which the continuous release of these airborne contaminants is approximated by a sequence of puffs that are released at regular time intervals and then diffuse and disperse independently. Being a puff model, RIMPUFF is simple to work with and has several advantages. For example, the uneven pattern of accidental releases can be tackled successfully by associating different masses under puffs. The different characteristics of the wind field at puff locations can be represented by merely allocating different parameters to each puff dispersal. Hence, the RIMPUFF model was chosen to be combined with a DLM methodology in order to form the ASY module.

The puffs are indexed such that puff i is released at time $t = i$. Assume that the mass under puff i is q_i . The vector of puff masses approximates the release profile of the source term. Standard priors are used on the shape of the time profile - in statistical terms, time series - of the release. Such priors can model uncertainty about the mass release and its duration. If some engineering activity that will lead to a sudden change in the scale of the release is known, it is possible to intercede in the model and capture that. Away from times when sudden changes in the release are expected, 'smoothness' is encoded in the release profile through the covariances between the q_i . Parameterising on masses under puffs has two significant results. First, the time averaged or instantaneous concentrations at monitoring sites are linear functions of q_t . Second, Kalman filtering - a technique of performing Bayesian updating in linear models without needing to invert large covariance matrices - and other linear techniques to assimilate monitoring data can be used. In this case, normality is assumed for simplicity, but the methods generalise in a straightforward way to assimilate non-normal data: see for example /F10/. Running this DLM leads to estimates of the source term profile and predictions of the contamination spread. However, this model presents some omissions which need to be addressed directly. It clearly does not consider either uncertainty on release height or uncertainty on wind field.

The solution to the above problems is to run mixed models. Uncertainty on release height is dealt with by running models at different release heights for each source term. Probabilities are allocated to each model depending on how likely these models are to run at the real release height. The probabilities and the heights are chosen in such a way that gives a three point approximation to the prior on the release height (e.g. obtained by expert judgement from site engineers). Then, the distribution on the release height of each model is updated in the light of monitoring data by applying Bayesian methods. This results in giving most weight to the most likely model.

The uncertainty on the wind field is dealt with in a similar way. The wind field is non-uniform and reflects local topography. The wind field model can be rotated by a few degrees on the wind direction at the source. Three models - associated with the same source term - run at different wind directions are considered with different probabilities to approximate the uncertainty in the wind direction. The probabilities and the directions are chosen to give a three point approximation to the prior on the wind direction at the source (obtained again by expert judgement from local meteorologists or staff on site). In the above examples nine models run for the different combinations of the release height and the wind direction. The number of the models which run is not a constraint of the methodology.

The model as described so far estimates and provides distributions for: source term, release height and wind direction at the source. But what about:

possibility of plume splitting (to branch around hills)

puffs implying below ground spread (if using spherical puffs)

local wind effects

shearing?

The RIMPUFF model allows puffs to pentify. When a puff's diameter reaches a certain value, it pentifies in the horizontal plane. To model the possibility that the original puff was drifting away from its predicted trajectory, a random component associated with the distribution of mass between the siblings is introduced.

Although the above model would theoretically meet the requirements of an asy module within RODOS, it had several deficiencies. The first problem was its speed. An ASY module has to process the incoming data as quickly as possible and produce usable results within a limited time. The second problem was that the methods described were not easy to generalise for non-Gaussian processes. Thirdly, the emissions themselves would not form a non-trivial stochastic process. Another method, which would incorporate such a stochastic process simply and in a way which preserved efficiency, was required. In order to overcome the above difficulties the fragmenting puff model was restructured and belief networks and dynamic junction trees were introduced.

A belief network is a graphical representation of a problem domain consisting of the statistical variables discerned in the domain and their probabilistic interrelationships. The relationships between the statistical variables are quantified by means of 'local' probabilities together defining a total probability function on the variables. A belief network comprises of two parts: a qualitative representation of the problem domain and an associated quantitative representation.

The present problem domain was represented as a belief network in the following way. Puffs are related either as neighbouring source puffs or parent/child puffs. A collection of related puffs is represented by a clique. Each clique becomes a single node in a junc-

tion tree which is the qualitative representation of the belief network of our problem domain. The nodes in the junction tree contain a local distribution. An arc between two cliques represents their shared puff. Information arrives at a given node and is then propagated to the other nodes via the arcs (i.e. the shared puffs). Each pair of adjacent cliques in the tree shares a common puff, the separator. This implies that the joint distribution over the masses in all the puffs factorises into a very simple form that allows extremely efficient updating algorithms to be developed. Algorithms were developed from standard Bayesian updating algorithms for the case, as here, in which the trees themselves evolve dynamically /E3/. The modified methodology has been defined, explored and illustrated within the RIMPUFF model. However, it is much more generally applicable and allows the quick absorption of information on a junction tree of cliques.

Initial simulations have shown that the algorithm is fast enough to provide forecasts within the requirements of the RODOS decision support system. Indeed, the computational times of the algorithm are of the same order, although longer, as those for the algorithm without any updating for monitoring data. The algorithm seems to behave sensibly in the manner it assimilates data. Currently, it is being tested on data sets derived from tracer experiments. Not only is this a fairer test in absolute terms but also other data assimilation algorithms developed by other groups within the RODOS project and elsewhere are also being tested on the same data.

The algorithm was tested on simulated data sets derived from the Lundtoft Nord tracer experiment. It fitted data which had been simulated from the results of the experiment. However, a more rigorous test was needed. For this purpose, the Siesta data was used. The Siesta data comes from a real experiment, held on November the 30th 1985. It lasted approximately 6 hours and observation data was supplied for the last hour. Having this data as input the program found the scale of the release satisfactorily. The program does not delimit the start of the release, but this might be expected since the nature of the input data - integrated air concentrations taken over a single hour is probably not sufficient to identify this.

3.2 Simulation of countermeasures and quantification of consequences

3.2.1 Early emergency actions (FZK)

The simulation of the effect of early emergency actions on individual doses and the assessment of other radiological and economic consequences without and with these actions is the main objective of the program group EMERSIM, HEALTH and ECONOM in the Countermeasure Subsystem CSY. The emergency actions considered in EMERSIM are:

- Sheltering,
- Evacuation,
- Administration of iodine tablets.

These actions are typically limited to areas within a circle of a few ten kilometres around a nuclear power plant (NPP), and to time intervals from a few hours before the beginning of the release to several hours after the cloud of released nuclides has left the near range. In a given accident situation the areas with emergency actions are defined by a number of dose intervention levels. Whether, where and when the actions really can be carried out is a question of the time left in comparison to the time needed for them, and of the availability of technical and personal support. This question has to be answered by the decision maker. EMERSIM allows the decision maker for choosing different temporal and spatial patterns of countermeasure combinations and quantifies the resulting doses.

Computation grid

All calculations of doses and consequences are carried out on the same coordinate grid as it is used in the ASY Subsystem for calculating the concentration and radiation fields. It is an orthogonal 41 x 41 cells grid. Typical cell size for near range problems is 1 x 1 km² or 2 x 2 km², corresponding to a grid extension of 41 x 41 km² or 82 x 82 km². All quantities on the grid are assigned to the cells; for area specific quantities (like population) the number contained in the cell is assigned, for location specific quantities (like dose) the average or central point value is assigned.

Modelling of emergency actions and dose calculation in EMERSIM

For the calculation of doses with protective actions a scenario has to be defined. On the one hand it consists of a prognosis of the radiological situation including its temporal development from the beginning of the release (ASY PROGNOSE), and - on the other hand - of an action scenario during the prognosis time interval. As mentioned above, in the module DOSBAU the temporal development of the radiological situation is archived in the form of potential dose histories in each grid cell during a PROGNOSE run in ASY. A dose history is a time sequence of half hour dose segments in the prognosis time interval. All histories begin with the start of the release which is identical with the beginning of the prognosis. The definition of an action scenario includes the action areas and the action time intervals. In the interactive version of EMERSIM action areas can be defined indirectly by starting from dose intervention levels which can be edited by the user, or directly by graphical input of these areas in the form of sectors and zones around the NPP or of arbitrary shape. Finally the action areas are sets of grid cells marked with action

specific tags. The tags for sheltering and evacuation are 0, 1, 2, and 3: 0 for no action, 1 for sheltering, 2 and 3 for evacuation with lower and upper intervention level. The tags for administration of iodine tablets are 0 and 1: 0 for no action, 1 for administration. The action time intervals define when a certain action begins and ends in relation to the beginning of the prognosis time interval. The action times are user input to EMERSIM. Furtheron the user can select action components of the action scenario and switch them on or off. With given potential dose histories, action areas, and action time intervals the dose field calculations under consideration of emergency actions can be carried out (a dose field is an array of dose values for all grid cells). For this purpose in each grid cell with the action tag 0 the potential dose segments are summed up. The cells with an action tag 1, 2, or 3 are treated in a different way: the potential dose segments are summed up only at times before the action has started. During or after the action the value of each dose segment is modified by a specific factor or function modelling the effect of actions on dose. Then all cell dose segments are added to get the cell dose. In the upper part of Fig.11 examples of time series of potential dose segments are shown, in the lower part the corresponding time series modified by different actions are shown. The time intervals of the actions are given in the middle:

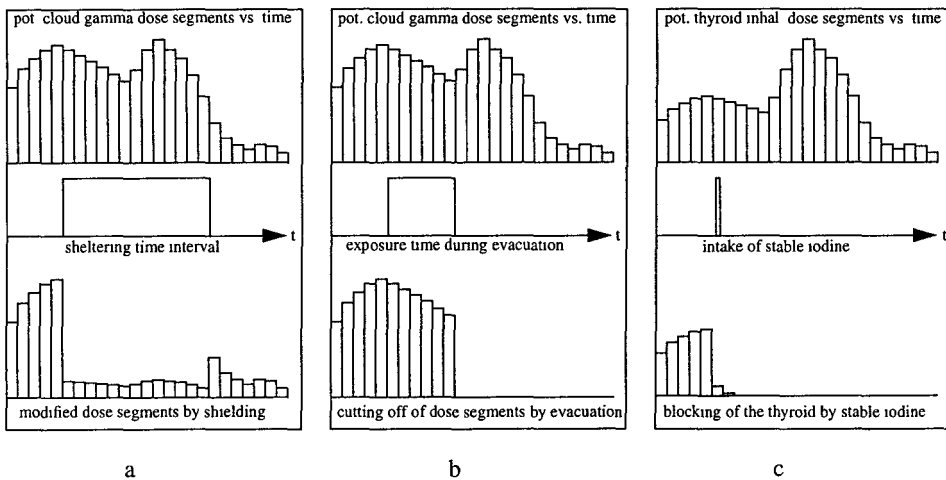


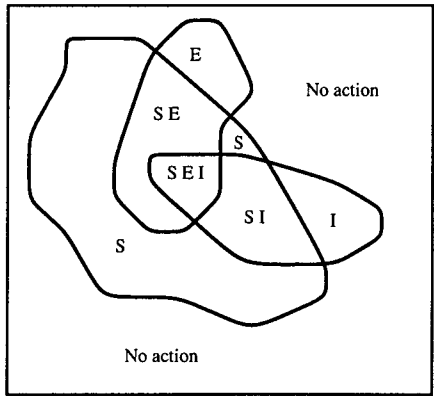
Fig. 11: Modelling of the effect of protective actions on doses
a) Sheltering, b) Evacuation, c) Administration of stable iodine tablets

In Fig. 11a the effect of sheltering against external gamma radiation is shown. The dose reduction during sheltering is simulated in EMERSIM by using building type specific shielding factors for external cloud and ground gamma radiation. The shielding factors are defined as average values for each grid cell and are derived from the building types in that cell. In Fig. 11 b the effect of an evacuation on dose is shown. In the present version of EMERSIM the simplifying assumption is made that before the start of and during the evacuation people get the potential dose of their home location. After the exposure

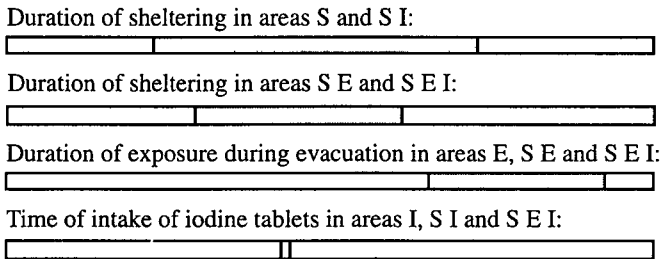
no additional dose is added (dose cut off). In a future version of EMERSIM a more realistic modelling of exposure during the evacuation will be possible by using the results of the evacuation simulation module EVSIM described below. In Fig.11 c the effect of the administration of iodine tablets is shown. The blocking of the thyroid amounts 100% a short time after the intake. The time dependence of the reduction factor is modelled by an exponential function.

Patterns of action scenarios

In the interactive mode of EMERSIM the user can define several overlapping action areas, starting times, and durations. Fig. 12 gives an example. The capital letters denote the action tags of the areas: Sheltering, Evacuation, intake of stable Iodine, the combination SEI means that sheltering, evacuation, and intake of stable iodine take place in the area tagged with it. "No action" denotes areas without emergency actions with normal living conditions:



a) action areas: S = area with sheltering, E = area with evacuation, I = area with iodine tablets intake.



b) action timings

Fig. 12: Example action areas and timings

The starting times and durations of the actions can be chosen independently in different areas as follows: the sheltering time intervals in S and SI areas are equal; the sheltering

time interval in areas with additional E tag (SE and SEI areas) may be completely different. The evacuation starting time is independent of the sheltering times and is the same for all E areas. An evacuation starting before the end of sheltering terminates sheltering. The intake of stable iodine is assumed to occur synchronously in all I tag areas. It is not carried out in E areas if evacuation starts before the time of iodine intake.

Dose results of EMERSIM

Each dose is estimated for 7 different integration times: 24 h, 7 d, 14 d, 30 d, 0.5 y, 1 y, 50 y (except the external cloud gamma dose). The doses are calculated separately for the 3 exposure pathways cloudshine, groundshine, inhalation, and as the sum of all three pathways. All doses are fields defined on the 41 x 41 cells grid. The organ doses calculated are: lung dose, bone marrow dose, thyroid dose, uterus dose and effective dose.

Program structure of EMERSIM

The program structure of EMERSIM is shown in Fig. 13. together with the modules HEALTH and ECONOM (see Section 3.2.4).

EMERSIM starts with the INPUT module, where geographic and demographic data of the region of the NPP are read in from files. Furtheron the prognosis data calculated before with ASY, i.e. the potential dose segments, are loaded from the data bank.

The first dose calculations are carried out in the module NOACDOS. In this module fields of individual doses are calculated under the conditions of "no action", i. e. no protective actions are assumed. Two cases are distinguished: "open air" doses equal to potential individual organ doses, and doses under "normal living" conditions, where shielding factors for external gamma radiation are applied.

In the health effects module HEALTH the numbers of people with deterministic and stochastic somatic health effects are estimated. This is done both for "open air" and for "normal living" conditions.

In the module ECONOM the monetary costs of medical treatment and the productivity losses to society are quantified both for "open air" and for "normal living" conditions. In the interactive mode the user can define her/his action scenario in ACTIONS by putting in emergency action dose intervention levels, a list of actions to be simulated, and starting times and durations. AREAS then determines the areas with grid cells in which the doses exceeded the intervention levels. Once these areas are determined the user can modify them graphically on the screen. Now the action scenario is fully defined and the dose calculation under consideration of the actions is performed in the module ACDOS. At this point the information about the movement of people during an evacuation which is provided by the module EVSIM will enter into ACDOS and allow a more realistic dose calculation. Again in the health effects module HEALTH the numbers of people with deterministic and stochastic somatic health effects are estimated from the doses with protective actions, and finally, in the module ECONOM the monetary costs are assessed (see also Sec. 3.2.4).

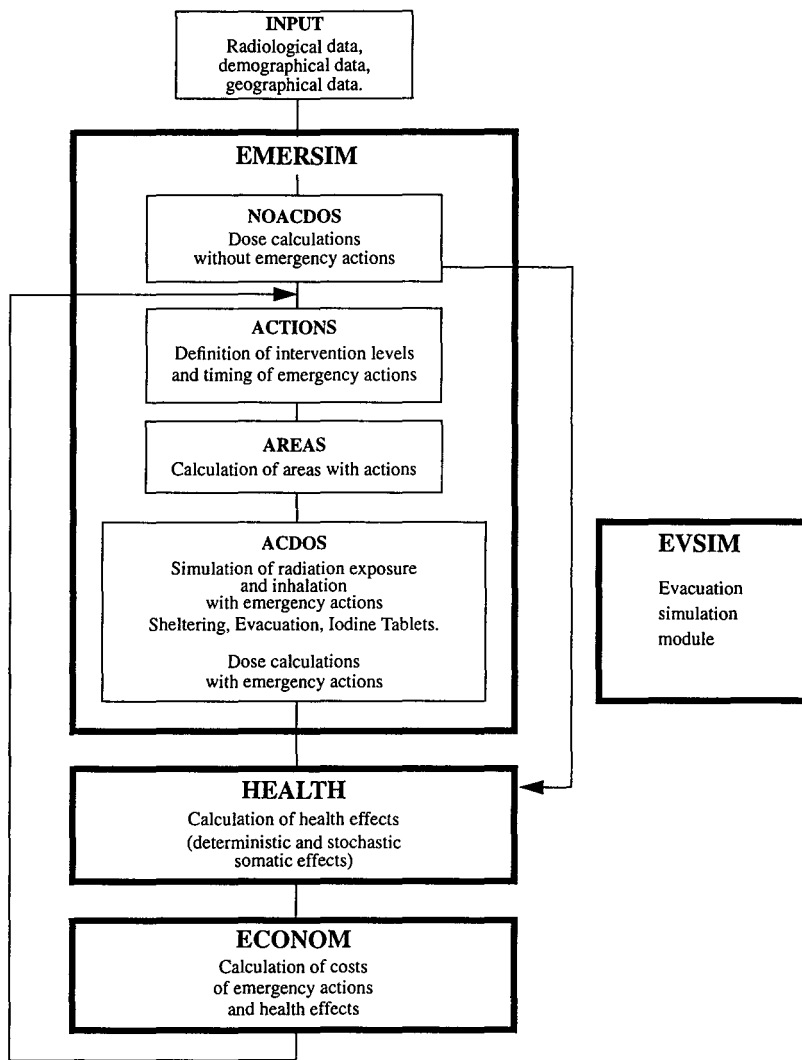


Fig. 13: Sequence of modules for calculating radiological and economic consequences

Model description of the module EVSIM

The task of the evacuation simulation module EVSIM /C7/ is, to estimate the time evolution of the spatial population distribution in the early countermeasure phase. It is not sufficient for EVSIM only to compute the driving times of the individuals since the individual doses depend on the time evolution of the radionuclide distribution and the time evolution of the spatial population distribution in the area of interest. Therefore both the topology and the geometry of the traffic net have to be considered in the model. Because of the need of a very fast evacuation simulation the traffic net in EVSIM is

modelled on a grid. The time evolution of the population distribution is calculated using constant timesteps. In the present version of EVSIM the length of a grid element is 1 kilometer and a timestep of a typical run is one minute of evacuation time. To improve the model efficiency, EVSIM uses the concept of representatives. All individuals which have the same history in the model world will be simulated by one representative in EVSIM. The computed spatial population distributions for every timestep are output data from EVSIM which will be used by other RODOS modules (e.g. to estimate the doses of the individuals arriving at emergency stations). Very important program units of the EVSIM code are the User Interface and the Analysing Module.

User Interface

The objects of evacuation decisions are communities (villages, cities, districts of cities, ...). The time schedule of the evacuations of the communities in the evacuation zone is very important for the success in dose reduction. Therefore an evacuation scenario in EVSIM defines which communities will be evacuated at which time. In EVSIM the user can use predefined scenarios or define by means of the User Interface scenarios completely by himself. Furthermore it is possible to adapt the simulation data to the actual situation using the User Interface (e.g. setting traffic blocks)

Analysing Tool

The analysing module evaluates the efficiency of the simulated evacuation. It presents

- Simulation data which describe in summary the evacuation process simulated by EVSIM
- Driving time distributions
- Dose distributions computed during an EVSIM run

Furthermore it calculates so called "countermeasure indices", which are indicators for the efficiency of the evacuation decisions.

Simulation Data

The summary information comprises the following data:

- Starting time of the whole evacuation
- Duration of the evacuation
- Number of evacuated persons
- Number of persons per private car
- Mean transport performance in persons per hour
- Mean transport performance in cars per hour
- Mean individual driving time in minutes
- Collective driving times
- Quality measure indices for the evacuation process

Driving Times and Countermeasure Indices

The analysing module builds the driving time distributions for communities and for the complete evacuated population from the simulation data. The distributions are presented as data files and as diagrams. The following diagrams are available:

- Driving Times: Absolute Frequency Distribution
- Driving Times: Normalised Frequency Distribution
- Driving Times: Cumulative Absolute Frequency Distribution
- Driving Times: Cumulative Normalized Frequency Distribution
- Countermeasure Quality Index 0 presents the inverse mean personal driving time in $(\text{hour})^{-1}$ for every evacuated community and the whole evacuation zone.
- Countermeasure Quality Index 1 presents the inverse collective driving time in $(\text{hour})^{-1}$ for every evacuated community and the whole evacuation zone.

Individual Doses

Furthermore the user can specify during an EVSIM-run that EVSIM uses dose field data from the EMERSIM module of RODOS for computing individual doses in the evacuation zone. In this case the analysis module of EVSIM calculates a set of histograms for each combination of organs (lungs, bone marrow, thyroid gland, uterus and effective body), exposure pathways integration times (8.5 hours, 1 day, 7 days, 14days, 30 days, 182 days, 1 year and 50 years). A set of histograms consists of the following distributions and moments of distributions:

- Absolute Dose Frequency Distribution
- Normalised Dose Frequency Distribution
- Cumulative Absolute Dose Frequency Distribution
- Cumulative Normalised Dose Frequency Distribution
- Mean Dose presents the mean dose the evacuated individuals got for every evacuated community and the whole evacuation zone.
- Collective Dose presents the sum dose of all evacuated individuals for every evacuated community and the whole evacuation zone.

3.2.2 Late countermeasures (NRPB)

3.2.2.1 Introduction

Models to assess the consequences of the following late countermeasures have been developed by the National Radiological Protection Board, UK:

- temporary and permanent relocation
- decontamination of urban and agricultural land
- agricultural countermeasures applied to land and foodstuffs

These models have been included in a module, FRODO (**F**ood, **Re**l**O**cation and **D**econtamination **O**ptions), which has been implemented within the RODOS system.

Relocation, decontamination and agricultural countermeasures are countermeasures applicable in the intermediate and later phases following an accident. The exposure pathways of importance in these phases are: external exposure from deposited activity, inhalation of resuspended material, and ingestion of contaminated food. Relocation is intended to protect against the first two. It is unlikely to be implemented to protect people against ingestion of food, since this can be more readily achieved by placing restrictions on the consumption of food and the implementation of agricultural countermeasures. The decontamination of buildings or land in the vicinity of buildings is intended to reduce external exposure from deposited activity and inhalation of resuspended material whereas the decontamination of agricultural land is intended to reduce ingestion doses from contaminated food.

The FRODO module includes models for the three countermeasure options described above. The options can be considered individually or the impact of each of the different options on the others can be evaluated to varying extents. The effect of decontamination on the extent and duration of relocation and the need for and duration of food restrictions is evaluated for a number of endpoints including the additional dose saving. Relocation is linked to agricultural countermeasures in so far as endpoints are calculated to provide information on the potential agricultural areas and amounts of food produced and banned in relocation areas. This enables the evaluation of the use of this land and possible agricultural countermeasures that may be considered to make the area agriculturally productive to be made.

The modelling of the countermeasure options, the structure of FRODO and its implementation within RODOS, and the databases developed in support of the models are described below.

3.2.2.2 Modelling

Relocation

Within FRODO endpoints related to the imposition of relocation in the presence or absence of land decontamination are evaluated. Two types of relocation are considered, temporary and permanent. These are defined, as follows:

Permanent relocation

The removal of people from an area with no expectation of their return, however, the land may be released at a later stage and resettled by different individuals.

Temporary relocation

The removal of people from an area for an extended but limited period of time.

The model uses criteria for the imposition and relaxation of relocation in the form of dose levels. The doses compared to the relocation dose criteria are the sum of the doses from external irradiation from deposited activity and the inhalation of resuspended material. The dose quantity compared with the relocation criteria is effective dose; this is in line with current recommendations. The first stage in the model is to decide whether and if so what type of relocation is implemented at each spatial grid point, and the duration of land interdiction. This is done by comparing doses against relocation criteria. If the dose at a location is less than the criterion for the imposition of relocation then no relocation occurs. If the dose is greater than the criterion for the imposition of relocation, the duration of land interdiction is determined by comparing doses with the criteria for the relaxation of relocation. If the predicted duration of relocation is greater than the "maximum temporary relocation duration" then permanent relocation occurs. If the predicted relocation duration is less than the "maximum temporary relocation duration" then temporary relocation occurs. Figure 14 illustrates the modelling of permanent relocation of the population and the possible resettlement of the area.

It is important to have some indication of the extent of the potential overlap between evacuation and relocation. Although this is not modelled in detail in the current version of RODOS, the numbers of people who are both evacuated and relocated are evaluated within FRODO.

The endpoints evaluated relate to the areas of land interdicted, the time periods over which this occurs, the numbers of people relocated, the doses saved as a result of relocation, the doses received by those temporarily relocated following their return, and the doses received by individuals resettling in an area following the lifting of land interdiction after the permanent relocation of the original population. More details of the modelling and the endpoints evaluated are provided in /F1/.

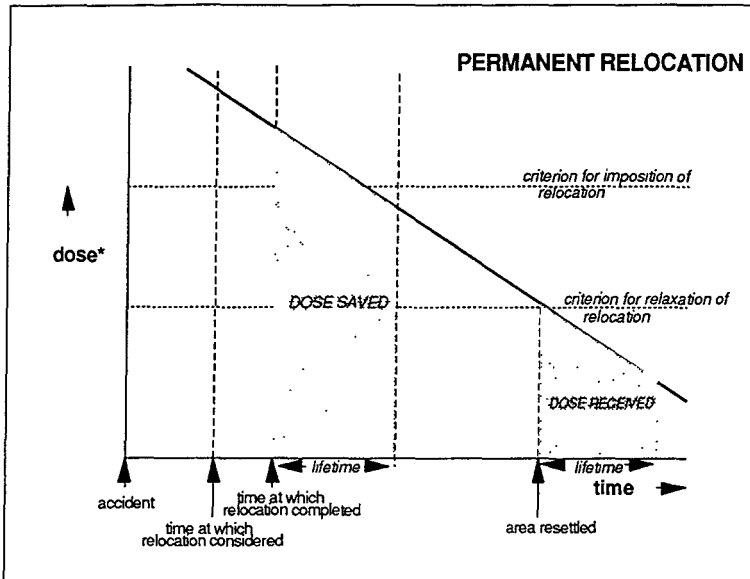


Fig. 14: Modelling of permanent relocation

Decontamination

Decontamination as a countermeasure is considered as a means to prevent or reduce the extent of relocation and as a countermeasure in its own right both to reduce doses due to external exposure from deposited material and to reduce ingestion doses.

The impact of decontamination is modelled using a dose reduction factor which is defined as the fraction that the dose received before decontamination is reduced by, for a given decontamination technique. This factor is used to modify all doses following decontamination. The reduction in individual dose achieved by decontamination depends upon a number of factors including: the decontamination technique employed; the nature of the area of land; the time following deposition that decontamination is carried out; the time following decontamination and the habits of the individual. A robust approach has been taken to the estimation of dose reduction factors in the current version of FRODO and no account is taken of the time dependence in dose reduction following decontamination and the different behaviour of individuals. A database of dose reduction factors has been developed in support of the modelling, this is described in section 3.2.2.5.

The impact of decontamination on relocation can be evaluated for decontamination occurring either before or after relocation is implemented. Figure 15 illustrates the calculation of the dose saved by temporary relocation and decontamination.

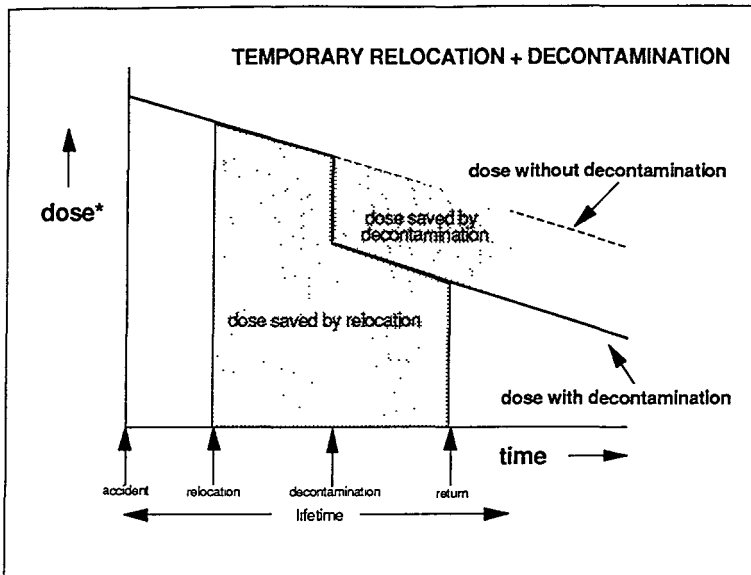


Fig. 15: Doses saved by decontaminating after temporary relocation

The decontamination of agricultural land is included in so far as its impact on the need for or reduction in food restrictions is evaluated. Decontamination of agricultural land by ploughing and soil removal is considered and the effectiveness of the techniques is assessed in terms of the reduction in activity concentrations found in food following decontamination. A database addressing the effectiveness of decontamination in reducing activity concentrations in crops has been developed in support of the model, this is described in section 3.2.2.5. In the current version of FRODO decontamination of agricultural land is not considered in conjunction with any other agricultural countermeasures.

Decontamination can be considered as a countermeasure on its own. The endpoints calculated are the doses saved by decontamination, the doses received following decontamination and the area of land decontaminated. More details of the modelling of decontamination are provided in /F1/.

Agricultural Countermeasures

Within FRODO endpoints related to the imposition of countermeasures on food are evaluated. The agricultural countermeasures considered are:

- banning and disposal

- food storage
- food processing
- supplementing animal feedstuffs with uncontaminated, lesser contaminated or different feedstuffs
- use of sorbents in animal feeds, or boli
- changes in crop variety and species grown
- amelioration of land
- change in land use.

The foodstuffs that each countermeasure can be applied to are given in Table 2. The effects of relocation and decontamination of agricultural land on the imposition of food restrictions are also considered, as described above.

The approach taken to modelling agricultural countermeasure is outlined in Figure 16. The aim of the module is to determine if there is a problem and, if there is, to evaluate the effectiveness of a number of countermeasure options to determine if the need for food restrictions can be avoided, or, if not, how the duration of the restrictions can be reduced. The criteria for banning the consumption of food are defined in terms of the activity concentrations in foods. As a default the European Commission maximum permitted levels in food are used although the user of the system can change the criteria. The activity concentrations in foods are compared with the criteria as a function of time, nuclide and spatial grid point to determine if a ban is required. If a ban is not required for any of the foods then no further agricultural countermeasures are considered. If food bans are implemented a number of countermeasure options are considered for each food. In the current version of RODOS, agricultural countermeasures are not combined other than with a food ban. If restrictions on food are still required following the implementation of a countermeasure option, the user of the system will be informed of this requirement and the length of the restriction that would still be required to reduce activity concentrations below the criteria for banning.

A brief description of the countermeasure options included is given below. In all cases where the timing of the implementation of an option or the duration of a given husbandry or farming practice is included this can be changed by the user of the system to look at a range of possible scenarios. A robust approach is taken in the modelling of the countermeasure options some of which become very complex if the full flexibility of user choice is implemented. This approach is consistent with the aim of the module which is to provide information to enable an assessment of possible courses of action for removing the need for or mitigating food bans.

The banning of foods is linked with disposal and the stopping of food production depending on the duration of the ban.

Agricultural Countermeasure	Foodstuffs/Feedstuffs
Banning and disposal	33 foods (see reference 1)
Food storage	33 foods (see reference 1) Note: Assumed to be stored in processed form.
Food processing	Cow's milk, summer wheat, winter wheat Note: For other foods processing implicitly implies storage (see above).
Supplementing animal feedstuffs with uncontaminated, lesser contaminated or different feedstuffs	Cow's milk, beef (cow and bull), sheep milk, goat's milk, lamb, pork chicken, eggs
Use of sorbents in animal feeds, or boli	Cow's milk, beef (cow and bull), sheep milk, goat's milk, lamb, pork
Amelioration	Foodstuffs: Spring wheat, winter wheat, rye, oats, potatoes, leafy vegetables, root vegetables, fruit Feedstuffs: Grass/hay, maize, winter barley, winter wheat
Changes in crop variety and species	Leafy vegetables, root vegetables, winter wheat, spring wheat, potatoes, fruit
Change in land use	Not applicable. Note: Assumption is that land cannot be used for food production.

Table 2: Foodstuffs considered for each agricultural countermeasure

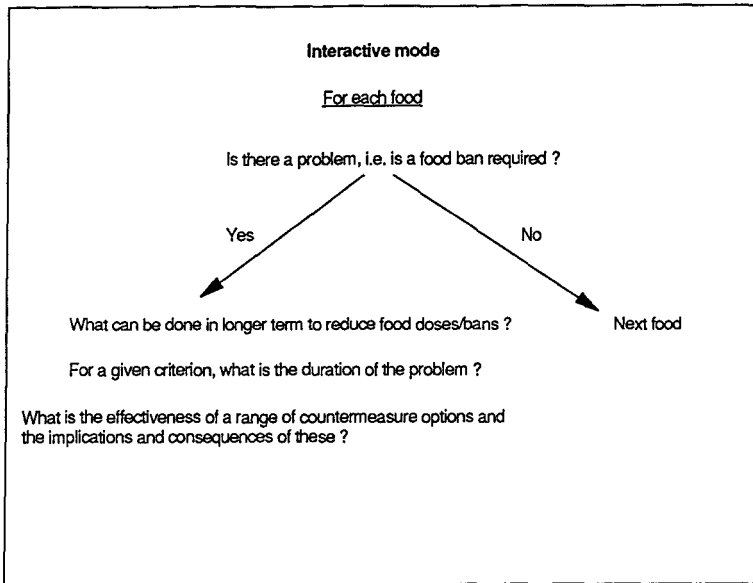


Fig. 16: Approach to modelling agricultural countermeasures

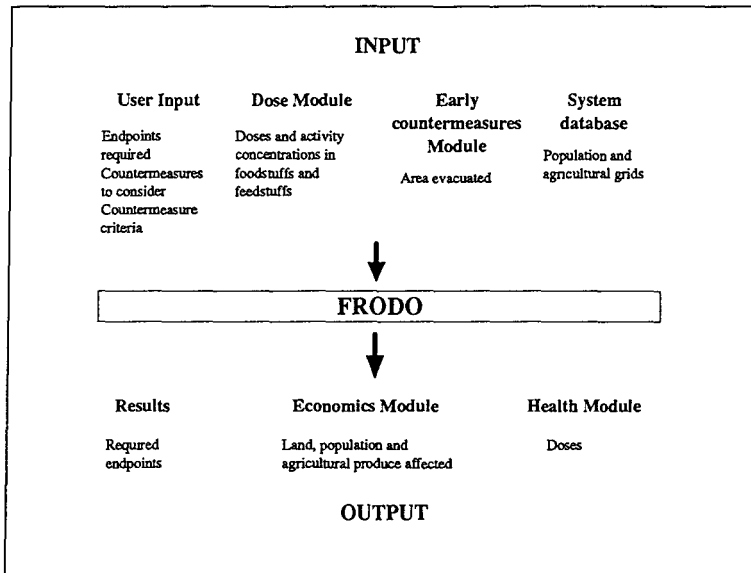


Fig. 17: FRODO Interfaces

Food processing and the storage of food are closely linked. The processing of fresh foods, eg milk, into a form that can be stored is considered only if a ban would not be required on the processed product. Storage is considered with or without processing for all foods. It is, however, only considered for a limited period of time to limit storage to lengths of time that are practicable in terms of the 'shelf life' of processed or fresh foods and so that in practice storage is only considered when the release comprises short-lived radionuclides. The removal of animals from contaminated feed is modelled. The effect of the time at which the animals are removed from contaminated feed and the duration 'clean' feed is given for can be evaluated. In addition a reduction in the amount of contaminated feed given can be considered.

Sorbents can be added to animal feedstuffs or directly to the animals gut in the form of boli. The effectiveness of the sorbent is modelled by reducing all activity concentrations in the animal by a factor for the period over which the sorbents are administered or, in the case of boli, for the period of efficacy in the gut.

The countermeasure of substituting different feedstuffs into animal diets is considered. The activity concentrations in the "new" diet are determined and the revised activity concentrations in the animal are calculated.

The treatment of soils to improve their quality, for example, the addition of fertilisers, and the subsequent reduction or otherwise of the uptake of radionuclides by plants is considered. This countermeasure is not considered until a minimum of 1 year after the accident in the current version of RODOS. Data for a range of techniques are utilised and are represented as a factor by which the activity concentrations in crops are reduced. The effect of repeated applications can be considered.

The change of the crop variety or crop species grown is included as a countermeasure. The assumption is made that this option would only be considered if the crop could not be grown on the land over a chosen time and that by growing another crop the activity concentrations could be reduced to below the criteria for banning.

The change of land use from agricultural production to forestry is considered. The criteria for this option is that the land can not produce food at activity concentrations below the banning criteria for a chosen period of time. In this case the land will be written off for food production.

A database of information on the effectiveness of the agricultural countermeasures has been compiled in support of the modelling, this is described in detail in section 3.2.2.5.

A wide range of endpoints are calculated. These include the individual and collective doses received following the implementation of agricultural countermeasures and the doses saved by implementing the countermeasure. The extent and duration of food restrictions are evaluated and additional information on the impact of the agricultural countermeasures is also calculated, for example, the numbers of animals affected, quantities of materials such as fertilisers and uncontaminated feedstuffs for animals required in order to estimate the economic cost of the countermeasures.

More details of the modelling and the endpoints evaluated are provided in /F1/.

3.2.2.3 FRODO structure

FRODO comprises a control submodule and submodules for relocation, decontamination and agricultural countermeasures. The purpose of the control submodule is to call the relevant subroutines within each of the other three submodules to perform the calculations which will produce the endpoints requested by the user. Each submodule consists of a set of subroutines, thus ensuring a flexible system for implementation within RODOS. More information on the detailed structure of the module is provided in /F1, F 2/

The input data required by FRODO and the output produced are described in general terms below. The data required and results generated for any particular run will depend upon the detailed requirements of the user. More information on input data requirements and output produced is given in /F1/. The FRODO module inputs and outputs are also presented in Figure 17.

Input

Input is required from the user defining the countermeasures to be considered and the implementation criteria to use. The user can also define the endpoints the module will calculate.

The primary data inputs to FRODO are: activity concentrations in foods and animal feed-stuffs as a function of location, nuclide and time; doses without countermeasures from external irradiation from activity deposited on the ground, inhalation of resuspended activity, and ingestion of contaminated foodstuffs, as a function of location, nuclide, time and age group. These data are generated by the dose module ECOAMOR /F3, F4/ (see Section 3.2.3). In addition, databases on the effectiveness of decontamination and agricultural countermeasures in reducing doses and activity concentrations in foods, and gridded information on agricultural production and population sizes are required. If the user requires as an endpoint the number of people relocated following earlier evacuation then the area evacuated is required as input from the early countermeasures module (see Section 3.2.1).

Output

FRODO produces direct output which can be viewed by the user in the framework of the RODOS graphical user interface. FRODO also calculates endpoints which are used by further modules. Doses with countermeasures are required as input to the module which determines numbers of health effects (see Section 3.2.4). Numbers of people, areas of land, quantities of food banned and other factors which relate to the implementation of agricultural countermeasures, such as the quantity of sorbents required if this countermeasure is considered, are evaluated for input to the economics module of RODOS (see Section 3.2.4)

Interfaces

The exact form of the FRODO input and output interfaces with other RODOS modules were discussed and agreed with the developers of associated modules following various meetings. The interfaces are defined in /F1, F 2/.

3.2.2.4 Implementation of FRODO within RODOS

Several visits were made to FZK to assist in the implementation of various versions of FRODO within the RODOS system. These visits allowed problems to be identified and the links with the system to be refined. The final version of FRODO produced under this contract was successfully implemented in RODOS in summer 1995.

3.2.2.5 Databases

Agricultural countermeasures

A database of information on the effectiveness of the agricultural countermeasures has been compiled. FRODO utilises data provided by the foodchain model, ECOSYS, within the module ECOAMOR and a database of effectiveness factors. In addition supporting data are required to provide input for the economic costing of the countermeasure options.

The data in the database are largely based on a compilation of information from the Ukraine, Belarus and Russia on the effectiveness of agricultural countermeasures carried out following the Chernobyl accident. The work was carried out under the EC/CIS collaborative Joint Study Project (JSP1). Two reports have been written which contain the compiled data and supporting information/F5, F6/. Where data are available from the West these have been included either as supplementary data or to provide additional information. The database contains robust, representative data that can be applied to relatively large areas and potentially over long periods of time. More detailed databases will enable the effect of local conditions to be taken into account and will provide data to enable problems on a local scale to be evaluated, eg on the level of advising local farming communities, as well as considering problems on a larger scale when more information on factors such as soil type are available. A more detailed database will be included in RODOS in the future.

A comprehensive database for use in RODOS should include information for a number of radionuclides. However, data available in the aftermath of the Chernobyl accident are predominantly for radiocaesium and a limited amount of data are available for strontium. The database reflects this situation.

As stated above the database uses data predominantly for the CIS. These data will not necessarily be applicable to the West where agricultural systems are very different. In particular, the fertility of the soil is, in general, much higher in the West. Cautions in the use of data are given in /F7/ for the various countermeasures considered, where appropriate.

The database is described in more detail in /F7/.

Decontamination

Decontamination dose reduction factors have been determined using the EXPURT urban dose model/F8/ developed for evaluating external doses from deposited material in urban areas. The effectiveness of a range of decontamination techniques which are feasible have been considered using current sources of data/F9, F10/. The dose reductions calculated for use in FRODO are based on the reduction in the dose integrated to 50 years. The techniques considered in the database are those that have been shown to be effective in reducing external doses, namely: grass cutting and collection, ploughing or rotovating or digging, removing soil to a depth of 5 cm, fire hosing metallised surfaces, vacuum sweeping metallised surfaces and planing metallised surfaces. As a default the combined strategy of grass cutting and either fire hosing or vacuum sweeping metallised surfaces has been considered. The time of implementation of decontamination has been chosen to be that when the optimum decontamination can be achieved for the particular surface, consistent with the decontamination factor chosen for the evaluation of dose reductions.

The effectiveness of decontamination in reducing activity concentrations in crops is determined from a review of available data, primarily from the states of the former Soviet Union and Europe following the Chernobyl accident/F5, F6/ and the use of a dynamic foodchain model, FARMLAND/F11/. A robust approach is taken consistent with the compilation of data from the former Soviet Union /F5, F6/ such that a single reduction factor is used for all crops following the decontamination of agricultural land.

The database is described in more detail in /F7/.

3.2.3 Dose Assessments (GSF)

3.2.3.1 General overview

For the assessment of human radiation exposure within the analysing system (ASY) of RODOS, the module ECOAMOR (ECOSYS ASY Modules for RODOS) /G1/ has been developed. It is based on the dynamic radioecological model ECOSYS-87 /G2/ and the ECOSYS application EURALERT-89 /G3, G4/.

ECOAMOR considers all exposure pathways which might be of importance during and after passage of the radioactive plume:

- external exposure from radionuclides in the plume,
- external exposure from radionuclides deposited on the ground, and on skin and clothes of people,
- internal exposure due to inhalation of radionuclides during passage of the plume as well as afterwards from resuspended soil particles, and
- internal exposure due to ingestion of contaminated foodstuffs.

In the assessment of doses in RODOS, most of the calculational effort is spent in the simulation of the transfer of radionuclides through the foodchain in order to estimate activity concentrations in foodstuffs.

The ECOAMOR module can be used in a very flexible way within the RODOS system. In the automatic mode, it calculates all data which are needed for the subsequent estimation of countermeasures, and it provides a lot of "standard" information about the radiological situation to the user. In the interactive mode of RODOS, ECOAMOR can be used to answer special requests from the user concerning specific exposure pathways, radionuclides, grid points etc. within short time.

Some submodules of ECOAMOR are being used also by the long term countermeasure module FRODO for assessment of doses with countermeasures applied. Figure 18 shows schematically the data flow and structure of the ECOAMOR and FRODO modules within RODOS.

3.2.3.2 Input to the food chain and dose modules

Principal event specific input data for modelling the food chain transfer and dose assessment in ECOAMOR are

- the time-integrated activity concentration in air, and
- the activity deposited during precipitation for the nuclides and locations (grid points) considered,
- the amount of rainfall at these locations,
- the date of deposition, and
- the time dependent activity concentrations in drinking water, animal feeding water and fish in the aftermath of the deposition.

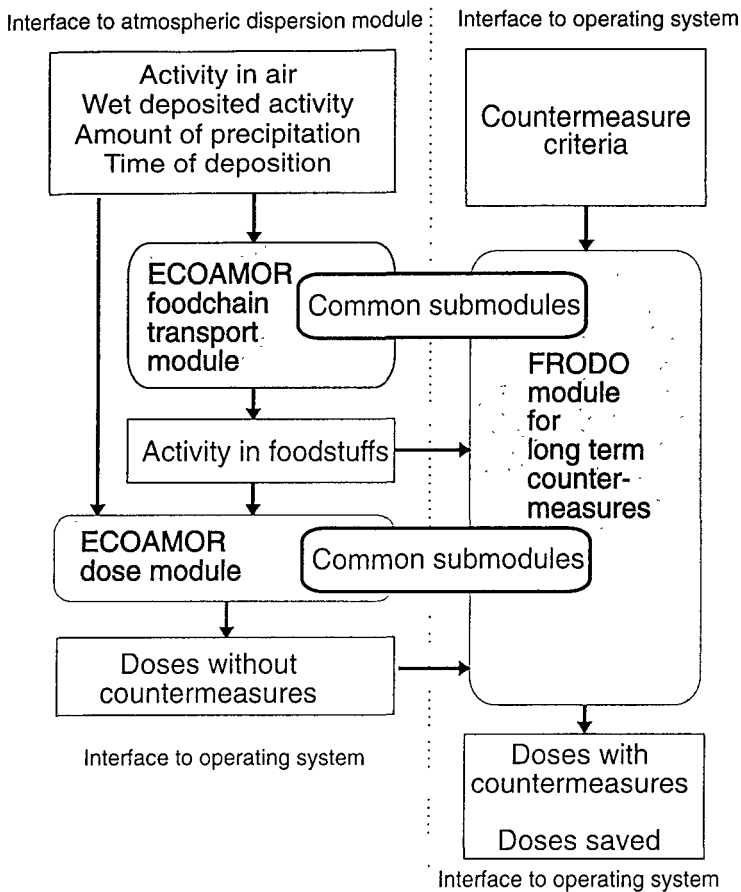


Fig. 18: Data flow in the food chain transfer and dose module ECOAMOR and the long term countemeasure module FRODO within the RODOS system

Moreover, data on population and foodstuff production at the locations of the calculation grid have to be provided by the RODOS data bank if collective doses are to be estimated. In addition to these data, ECOAMOR requires many model parameters characterising transfer processes in the radioecological scenario. Many of these parameters depend on the radioecological (e.g. climatical or agricultural) characteristics of the region considered which vary to a wide extend over different parts of Europe. Therefore, the modules are designed to facilitate the adaptation to different radioecological regions, and they allow to apply different site-specific data sets among the calculation grid points.

3.2.3.3 Methods of food chain transfer modelling and dose assessment

Food chain transfer

Assessment of the activity in foodstuffs after deposition of activity from the atmosphere onto agricultural production areas is performed in five main steps (Fig. 19), i.e. calculation of

- activity deposition onto plant canopies and onto ground,
- time dependent activities in edible parts of the plants (raw products),
- time dependent activities in feedstuffs, taking into account processing and storage,
- time dependent activities in animal products, and
- time dependent activities in foodstuffs, taking into account processing, storage and culinary preparation of vegetable and animal foodstuffs.

For dose assessment after radioactive contamination of water, direct consumption of drinking water and fish, as well as feeding of contaminated water to domestic animals with subsequent transfer to animal products is taken into account.

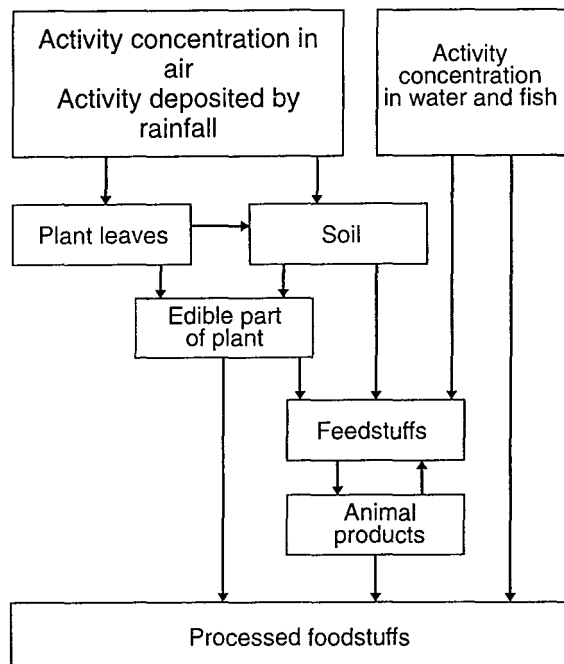


Figure 19: Calculation steps in the assessment of foodstuff contamination

Presently, the products considered include 31 food products (20 plants or plant products and 11 animal products), 22 feedstuffs (17 based on plants, 4 based on animal products, and feeding water), and 35 processed foodstuffs (see Table 3). This relatively large num-

ber of products results on the one hand from the diversification of plant species which is necessary to properly reflect radioecological reality: thus, e.g. 6 species of cereals are distinguished, including winter and spring wheat and barley, since they are affected quite differently by depositions in springtime or early summer. For pasture, both intensive and extensive agricultural management (i.e. fertilisation) is assessed; the latter is an attempt to take care of the radioecological behaviour in certain regions to be found in the uplands of Northern Europe, in parts of the Alps and in Eastern Europe. On the other hand, the model includes also foodstuffs with small average consumption but of possibly high importance to critical groups, as e.g. sheep or goat's milk or meat from animals living in natural environments (roe deer).

Type of product	Individual products considered	Remarks
Plant Products	Summer wheat Winter wheat Rye	Whole grain, flour, and bran can be considered individually for these cereals
	Oats Potatoes Leafy vegetables Root vegetables Fruit vegetables Fruit Berries	
Milk Products	Cow's milk Condensed milk Cream Butter Cheese Goats milk Sheep milk	Cheese from rennet and from acid coagulation can be considered individually
Meat and other animal products	Beef Veal Pork Lamb Roe deer Chicken	Beef from cows and from bulls can be considered individually
Beverages	Drinking water Beer	

Table 1: Foodstuffs considered in the food chain and dose assessment module

For an adequate modelling of the foodchain transfer, the dynamics of the different transfer processes - e.g. the seasonality in the growing cycles of plants, the feeding practices of domestic animals and human dietary habits - are considered, since equilibrium in the model compartments is not reached for a long time. Any day of the year can be used as time of deposition, which results in a pronounced season dependency of the radiological consequences. As an example, Fig. 20 shows the lifetime ingestion dose of an adult as function of the time of the year, when the deposition occurs. The module is flexible to simulate temporally limited changes in the feeding regimes of animals as well as in the

human food consumption habits in response to environmental radioactive contamination.

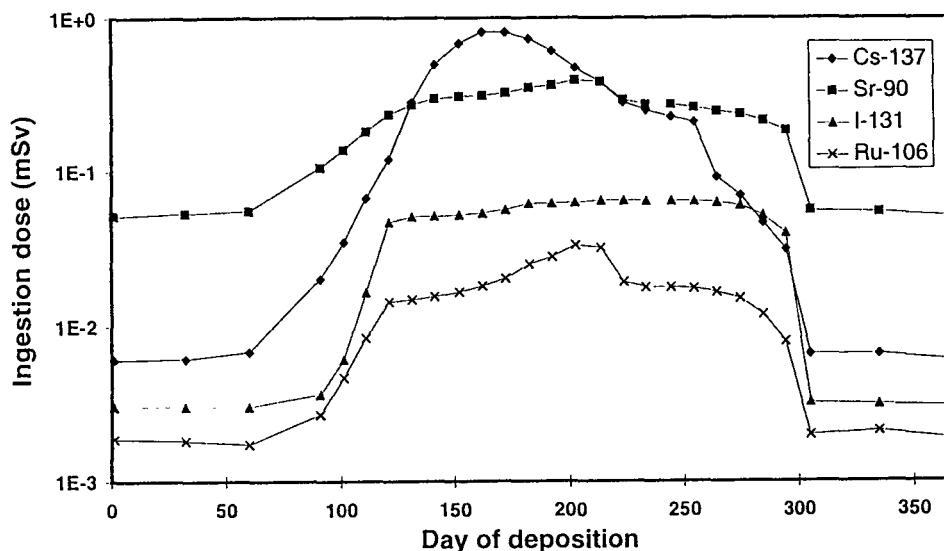


Figure 20: Dependency of lifetime ingestion dose of a 20 year old (at time of deposition) person on the time of deposition. A time-integrated activity concentration in air of $106 \text{ Bq} \cdot \text{s}/\text{m}^3$ and dry deposition only has been assumed for each radionuclide and time of deposition.

The model considers dry and wet deposition of radionuclides separately. Dry deposition to the plant canopies is calculated using a deposition velocity depending on the nuclide considered, the plant type and the seasonal stage of development (expressed by the leaf area index) of the plant canopy. Wet deposition is calculated by taking into account that only a certain fraction of the wet deposited activity remains on the plant leaves. This interception fraction depends on the leaf area index, the total amount of rainfall and the ability of the radionuclide to be fixed on the leaves. For the calculation of root uptake the total deposition onto vegetated soil is estimated.

Direct contamination of the leaves by dry and wet deposition as well as activity transfer from the soil, by root uptake and resuspension, cause the contamination of plant products. For totally consumed plants like grass and leafy vegetables, the time dependence of the contamination is controlled by the activity loss due to growth dilution and weathering effects. For partly eaten plants like potatoes and cereals, the translocation from the leaves to the edible part and the direct deposition onto these edible parts are taken into account. Root uptake is estimated using transfer factors between soil and plant, and considering decreasing availability of radionuclides due to migration into deep soil, and fixation in the soil of the root zone layers for arable and pasture land.

The contamination of animal products results from the activity intake of the animals and the kinetics of the radionuclides within the animals. The activity intake is calculated from the activity in feedstuffs and the season and age dependent feeding rates. Soil eating is included by applying an additional soil-plant transfer factor. Animal feeding water contaminated by radionuclides can be an additional source of activity intake by the animals. The radionuclide transfer from fodder into the animal product is calculated by an equilibrium transfer factor and one or two exponentials describing the biological excretion.

The contamination of animals' feedstuffs and human foodstuffs is calculated from the activity in the raw plant or animal products by applying processing factors describing the activity enrichment or dilution during processing and culinary preparation. For example, the fractionation in milling products due to the enrichment of minerals in the outer layers of grain is considered. Furthermore, radioactive decay during the processing and storage period is taken into account.

Ingestion dose

In the dose module, the ingestion doses are calculated from the activities in foodstuffs, age and possibly season dependent intake rates, and age dependent dose factors. Default mean values for foodstuff consumption are used but also those for critical groups can be applied. For the simulation of temporary changes in the dietary habits during and after an accident correctional factors can be applied. Age dependent doses per unit intake based on the models of ICRP 30 are used.

The collective dose from ingestion is estimated using the contamination and the amount of foodstuffs produced in the considered area, irrespective of where they are consumed. For the estimation of the collective dose saved by certain countermeasures, this is regarded to be an appropriate assumption.

Inhalation dose

Inhalation doses are calculated using age dependent breathing rates and dose factors; reduction factors due to the lower indoor activity concentrations may be taken into account. Short term inhalation from the passing plume as well as long-term inhalation of resuspended material is considered. Age dependent doses per unit intake based on the models of ICRP 30 are used.

For a rough estimation of the collective dose from inhalation (as well as from external exposure) the individual dose for adults and the number of inhabitants at the grid areas is used, without considering the actual age distribution of the population.

External exposure

The assessment of external exposure from radionuclides in the plume is done by two different approaches: at locations sufficiently far away from the emission source it is based on the time-integrated activity concentration in air assuming a semi-infinite homogeneous cloud. For locations in the vicinity of the emission source this approximation by a

semi-infinite homogeneous cloud is not justified; here integration over the plume is performed in the atmospheric dispersion module of RODOS and the kerma in air is passed to the dose module which estimates the organ doses and/or effective dose from it. Shielding effects due to staying at different types of location outside and inside houses are considered. Mean data for a population is used as a default, but data for critical groups as e.g. agricultural workers can also be applied.

The external exposure from nuclides deposited on the ground is calculated on the basis of the total deposited activity onto vegetated soil. Dose reductions from nuclide migration into deeper soil layers and by the shielding of houses are considered, as well as the influence of variable deposition patterns at different urban environments.

As an additional pathway of external exposure, irradiation from radionuclides deposited onto skin and clothes is considered. For all external exposure pathways, age dependent dose conversion factors are used which are based on Monte Carlo calculations using human phantoms /G5, G6/.

3.2.3.4 Output of the food chain and dose modules

Results for direct presentation to the user

ECOAMOR is designed to produce a wide range of output data the user may be interested in. For a number of presently up to 400 locations, the following output can be calculated:

- nuclide-specific activity concentrations in feed and foodstuffs,
- nuclide-specific individual doses from external exposure (from cloud, ground, skin and cloth contamination), inhalation, and the sum of all exposure pathways,
- nuclide- and foodstuff-specific individual doses from ingestion,
- doses due to ingestion for groups of nuclides (e.g. all Iodine isotopes) and groups of foodstuffs (e.g. milk and milk products),
- all doses can be estimated for 5 age groups (1 year infants, 5, 10 and 15 year old children, and adults 20 years old at time of deposition) and 22 organs (including effective dose)
- rough estimation of collective doses for all exposure pathways.

The activity concentrations in feed and foodstuffs, and the doses from ingestion can be given with a detailed time resolution of up to 158 time steps within 70 years after deposition. For external exposure from deposited radionuclides and inhalation of resuspended radionuclides a time resolution of 49 time steps within 70 years after deposition is used. Short term doses due to external exposure from the ground, external exposure from the cloud, inhalation and the sum of these exposure pathways can be assessed with a time resolution as given by the atmospheric dispersion calculations.

Different ways of presenting the results to the user can be chosen (e.g. time series, maps, frequency distributions).

Interface to the long-term countermeasures module

As a basis for the assessment of necessity and effect of countermeasures, the following information is transferred from the ECOAMOR module to the long-term countermeasure module FRODO:

- Specific activities in feed and foodstuffs,
- individual and collective doses from ingestion,
- long-term external exposure from radionuclides deposited on the ground,
- long-term inhalation doses from resuspended radionuclides.

3.2.4 Health effects and economic consequences (FZK)

In the HEALTH part of RODOS, the numbers of people with deterministic and stochastic somatic effects are estimated. Up to version RODOS-PRTY 2.0 HEALTH is still an integral part of the module EMERSIM; the implementation as a module on its own will be realised in the next version.

Input to the health effects models are the organ dose fields calculated in the modules NOACDOS and ACDOS of EMERSIM (see Section 3.2.1) From these dose fields, fields of individual risks are calculated. The numbers of people are calculated from the individual risk fields and the population data.

3.2.4.1 Deterministic effects

The version RODOS-PRTY 2.0 covers the following fatal and non-fatal deterministic health effects:

Fatal effects

- Haemotopoetic syndrome after irradiation of the red bone marrow.
- Pulmonary syndrome after irradiation of the lungs.
- Pre- and neonatal death after irradiation in utero.

Non-fatal effects

- Hypothyroidism from the internal irradiation of the thyroid following the inhalation of radioactive iodine.
- Mental retardation after irradiation in utero.

The risk of suffering from early effects is modelled using a "hazard function" approach, in which the doses which cause health effects in 50% of the exposed population are expressed as a function of dose rate /C8/.

The model in RODOS follows that described in /C9/, the parameter values used are taken from the version 93/1 of the probabilistic consequence assessment code COSYMA /C10/ and are based on extensive studies of the effects of radiation in both humans and animals /C8, C11/.

When calculating the total individual risk of an early health effect an allowance is made for irradiation of more than one organ. The risks of death from each organ are combined in a way which prevents the overall risk exceeding unity.

Output of HEALTH are the individual risk fields and the numbers of people affected for the different effects considered and the sum. It should be noted, that the input individual dose fields and the output individual risk fields refer to representative adult mem-

bers of the population. For estimating the collective effects, it is assumed that the population consists entirely of adults.

3.2.4.2 Stochastic somatic health effects

In RODOS/RESY the overall number of fatal cancers in the affected population is calculated, but breakdown of different cancer types is made.

To obtain this number, the simplified approach is used to multiply an average risk coefficient per unit effective dose for exhibiting a fatal cancer in an exposed representative population by the total collective dose in this population. In RODOS, a nominal fatality probability coefficient of $5 \cdot 10^{-2} \text{ Sv}^{-1}$ is used, which is given in ICRP-60 /C12/ and applies to low doses at all dose rates and to high doses and low dose rates. The total collective effective dose is obtained by multiplication of the individual effective dose fields calculated in ACDOS or NOACDOS with the number of individual with the corresponding doses. The dose fields refer to representative adult individuals in the population, and in calculating the collective effects, it is assumed that the population consists entirely of adults.

3.2.4.3 The economic module ECONOM

In the ECONOM module various off-site consequences of the accident are assessed in the form of monetary costs; this procedure allows different effects to be expressed in the same terms and thus to make these effects comparable.

In the present version of the ECONOM module radiation-induced health effects and the consequences resulting from early evacuation of people are transferred into economic costs. The cost categories calculated in connection with health effects are: medical treatment costs and losses-to-society costs due to illness or premature death of people concerned. The cost categories calculated in connection with evacuation are: transport and accommodation costs due to the movement of people, and loss-of-income costs and costs of lost capital services due to the non-use of production facilities in the evacuated area.

Necessary input data to the ECONOM module are, on the one hand, population data and, if available, data describing the economic structure of the areas affected in terms of the number of employees in different economic sectors, and, on the other hand, specific unit cost data for the various costs categories. Data describing the impact of the accident consequences are the number of different health effects, and the number of people and the area affected by evacuation.

The modelling of the present ECONOM module is based on the corresponding economic module of the program package COSYMA for probabilistic assessments of accident consequences /C13, C14/.

3.3 Evaluation of countermeasure scenarios (UoL)

Much of the work reported here was carried out in conjunction with work undertaken under contract F13P-CT92-0013b. In particular, the HERESY software was written under that contract, as were prototypes of the coarse expert system.

Overview

The main task facing ESY modules is the evaluation of different countermeasure strategies such as issue of iodine tablets, sheltering, evacuation, food bans, decontamination measures and changes in the agriculture. Issues that should be considered during the evaluation stage are the practicability and cost of a countermeasure in the actual situation, public acceptability and behaviour, socio-psychological and political implications, and subjective preferences over the consequences of an action that decision makers may have. The ESY has as input the costs and benefits of possible countermeasures which were identified and quantified by the CSY subsystem. Rules, weights and preference functions are encoded in the esy and applied to a list of alternative countermeasures to provide a ranked short list to decision makers. Both the ASY and the CSY will use several models throughout the accident depending on the time, the location and the actual situation. However, the ESY may be based upon the same software module with different attribute trees and with the preference weights changing over time.

The subsystem will operate in interactive mode through graphical interfaces to communicate with a variety of decision makers who may possess: qualitatively different skills and perspectives such as scientists, medical personnel, engineers, emergency planners, government officials and senior politicians. It will present the countermeasures in a ranked short list together with those rules and preferences that determined the order of the list. Intuitive justifications for choices and underlying uncertainties inherent in the predictions will also be provided. The ESY will assist users in modifying rules, weights and preferences and other model parameters as well as indicating the consequences of each change. Thus, the user can verify and correct the existing model whereas the ESY explains and refines its proposed short list. The ESY will also operate in reporting mode in order to generate reports which will give a detailed commentary on each proposed countermeasure strategy, explaining its strengths and weaknesses. The above facilities will support the decision makers to lead up to a final choice.

The ESY will be split into 3 further subsystems:

A coarse expert system filter which rejects any strategies that are logically infeasible or do not satisfy some given constraints.

A multi-attribute utility theory (MAUT) ranking module which takes the remaining list of strategies as input. It ranks the strategies for their relative effectiveness according to previously elicited utility attributes and preference weights from the decision makers. It may be necessary to revise and re-evaluate these preference weights in any given situation before a particular decision is taken.

A fine expert system filter which takes the top 10-15 strategies and produces a management summary report detailing the costs and benefits of each.

The coarse expert system filter

Typically the region around a nuclear plant is notionally divided into small subregions for emergency planning purposes. A countermeasure strategy applies to a region and generally specifies different protective measures for each subregion depending on its level of contamination. It should be noted that the subregions will be defined after considering the particular geographic and demographic features of the region. For instance, a part only of a block of flats would never be evacuated because some arbitrarily drawn planning line divided it between two subregions.

Suppose that the number of subregions is N and the number of possible actions such as evacuation, sheltering and issue of iodine tablets is k . Then, the number of possible strategies is N^k : the number of strategies to be ranked grows combinatorially. However, some constraints can reduce the number of alternative strategies considerably. They concern the feasibility of countermeasure strategies relating to national and international guidance on radiation protection, the practicability and the continuity of treatment that a strategy should exhibit.

The coarse expert system will discard strategies that do not satisfy these constraints. Thus, it will reduce the number of alternatives to be evaluated in manageable numbers. Infeasible strategies such as the issue of iodine tablets in an area which has been already evacuated should not be considered at later stages. Capacity constraints concern the number of available resources and equipment for decontamination measures like the transformation of contaminated milk to butter. For instance, factories that produce butter in a contaminated area may not be sufficient. This makes the countermeasure of converting all the milk to butter infeasible.

National and intervention guidance in the form of intervention levels result in additional constraints. The guidance is typically given in terms of upper and lower levels. A countermeasure is not advised if the contamination is below the lower level and expected if it is above the upper level. Between the two levels the decision is left to the discretion of the emergency managers. However, if the contamination in an area is above the upper level then only the countermeasures that can reduce the amount of contamination to a level below the upper one should be accepted. The remaining countermeasures should be rejected. Another complicating factor is the fact that different national intervention levels may exist. It has also been suggested that political pressures are such that it may be expected to adopt the countermeasures as soon as the lower level is exceeded.

The strategies must exhibit a continuity of treatment. For instance, the public would not understand nor accept the evacuation of only part of a village. A more specific example might occur in the areas adjacent to the plant. Suppose the meteorological conditions are such that the plume rises steeply in the vicinity of the plant and does not contaminate the areas close to the plant. However, some distance away the radiation exceeds the upper permissible level. Then a plausible strategy might suggest sheltering near the

plant and evacuation far away. Nevertheless the public are unlikely to understand or to accept this advice. Any strategy would be acceptable only if the same treatment such as evacuation was applied to the region extending from the plant until far enough downwind where the expected dose was sufficiently small to be negligible.

Countermeasure strategies should provide equitable treatment of different population groups. However, when risk is involved the evaluation of different strategies is not straightforward. This is because reasonable approaches may have unreasonable effects. Suppose that there are two villages near a nuclear plant which have similar demographic and economic characteristics. An accidental release is expected to take place either in 1 or 3 hours time. Both villages will be put in risk from equal collective doses. There are enough buses to evacuate only one of the villages within one hour. If the accident occurs in three hours time, buses can come back to evacuate the other village. However, both strategies which evacuate only one of the villages should not be accepted because they do not treat equally all the villagers. Decisions makers would prefer another strategy which would evacuate half the population in each village despite the fact that it averts no more collective dose than the previous ones.

The MAV/UT ranking module

After discarding strategies in the coarse expert system filter, the remaining strategies will be passed to a multi-attribute value ranking module. This module will identify the top 10 or 20 ranking strategies. The operator will be able to use interactive sensitivity analysis to confirm that these strategies are worthy of careful consideration.

A prototype of the MAV ranking module, Heresy, has been written at Leeds (under contract F13P-CT92-0013b). The screen is divided into three areas. At the top the attribute hierarchy is shown. In the middle a histogram shows the overall scores (values) of the top ten strategies. At the bottom, a histogram shows the current weights w_i on the attributes. Not all w_i need to be shown at the same time. There may be cognitive advantages in concentrating attention on particular branches within the attribute hierarchy. All bars on the histogram are labelled appropriately.

The user selects a weight with a mouse by clicking on the appropriate bar in the bottom histogram. Then, she increases or decreases the weight either by the keyboard or by pulling with a mouse. As the weight is changed, the middle histogram changes accordingly. When either a change in the ranking of the top strategies occurs or one strategy drops out of the top ten and another one enters, the histogram would rearrange itself. The machine also beeps and informs the user of the change in a text window. This means that the user can identify the sensitivity of the ranking to the default weights in the model.

The computational speed of the prototype confirms that the identification of the top 50 ranking strategies of about 10000 countermeasure strategies and associated sensitivity analysis can be performed in a matter of seconds on a Silicon Graphics Indigo R3000. This machine is less powerful than the Hewlet Packard workstation planned as the support machine for RODOS.

At present, Heresy evaluates alternatives by using a multi-attribute value (MAV) function. This does not explicitly allow for risk attitude. However, a modification which would enable the use of exponential multi-attribute utility (MAU) functions is needed. This is because exponential MAU functions capture gross effects from risk aversion and are simple to elicit, explain and work with, even though they may require considerable computation. Thus, Heresy's interface can be modified to have a further window in which a single risk attitude parameter can be varied and the effect investigated.

The fine expert system filter

The MAV/UT ranking module identifies the top strategies and confirms that they are worthy of careful consideration. These strategies will then be passed on to a fine expert system filter. This is a much finer and more sophisticated system of rules which can be applied to each of the candidate strategies. The small number of strategies allows a full set of explanations to be developed, which give a critique of each strategy. This system will be prototyped and implemented in the next round of development.

Support for software development methodologies

Some work has begun on quality issues in the design and development of RODOS. Most software development technologies which seek to ensure quality in the resulting software have been designed for tightly knit development teams. The RODOS consortia are distributed widely over Europe and come from a variety of organisations. Many developers come from a research not an engineering background and are relatively untrained in quality software engineering. We have begun to look at these issues in some detail and are looking to develop some simple tools which will help the RODOS contractors build a more quality assured system /E4/.

In addition, some work has been undertaken on temporal databases /E13/. This has informed thinking about the software architecture of RODOS and the concept in the temporal control subsystem /E7/.

3.4 Treatment of uncertainties (UoL)

Overview

Leeds/Warwick have co-ordinated a small subgroup of the RODOS contractors to discuss and agree methodologies for assimilating data and handling uncertainty within the system. Building upon the work of this group, a conceptual framework for consistent handling of uncertainty and data assimilation throughout RODOS has been developed /E7, E12/. This framework is to be adopted in future versions of the RODOS system. One essential point is that, because different methodologies for handling uncertainty require different inputs and give different outputs, the choice of methodology cannot be made by the designers of individual submodules without consultation of those writing other interfacing submodules. All submodules must ensure compatibility with those submodules with which they interact. To achieve this, a fully Bayesian decision analytic approach is adopted.

Concerns and Issues

A great deal of uncertainty is inherent in emergency situations which cannot be ignored. Uncertainty handling techniques are being incorporated into RODOS to address the following requirements and issues:

Source term. Uncertainty arises from the incomplete specification of its composition, its time behaviour and its release co-ordinates and effective height.

Radiation monitoring data. These are used to locate the spread of the radiation. Observation errors (human or physical measurement errors) may occur. Local geographic errors and wind patterns result in heterogeneity of the contamination which makes the collected monitoring data less informative.

Weather conditions. Weather forecasting is unreliable. Wind fields, used as an input to the system, are interpolated from meteorological station data which may result in additional errors. Local wind fields, precipitation and stability class can also cause problems.

Expert judgement. Some of the inputs to RODOS such as source term, dispersion characteristics and deposition coefficients are likely to be derived by expert judgement. These estimates involve uncertainty and are subject to calibration and bias effects. Consequently, they have different and less clear characteristics to estimates derived from physical measurements.

Model uncertainty. RODOS is built upon a variety of models. However, models can only be considered as approximations to real world processes. For this reason, they should be tracked and checked.

Implementing countermeasures. The implementation of countermeasures or public compliance may not be satisfactory. Thus, uncertainty is associated with the effectiveness of the proposed countermeasures which is termed as volitional uncertainty.

Attitude to risk. The interplay of equity and risk in the evaluation of different strategies is far from straightforward. Societal attitude to risk involves difficult issues such as that of equity and fairness.

Coherence between modules. RODOS is built upon a client/server architecture which facilitates the exchange of information between modules. The design of conceptual tools to handle and represent uncertainty in one module should consider the needs of the other models. Handling uncertainty within a common framework throughout RODOS is important because it influences the overall quality of the decisions taken.

Feasibility of the methods involved. The methods of handling uncertainty should be verified in order to make sure that they result in a computationally feasible solution. If computational approximations are used they should be assessed.

Communicating uncertainty. Uncertainty should be presented in a number of ways for effective communication with the user. The RODOS system will be used in interactive mode to provide facilities for generating intuitive justifications for choices and for assisting users in modifying model parameters.

Decision makers' value systems. These are their interpretation of the preferences and values of the society which they represent. Such value systems are seldom fully defined. In any particular context, decision makers need to think through and refine their value systems. This need can make them feel uncertainty with regard to their beliefs. This uncertainty though is different from that relating to physical quantities. RODOS will help decision makers resolve any lack of clarity in their understanding of the value systems.

3.5 The Software Framework of RODOS (FZK)

3.5.1 The Modular Design

The RODOS system is based on the Client-Server principle. It is built of modules, which are connected via a Communication Interface. Each of these modules can either be a

- Server, which provides special services to other modules, or a
- Client, which requests services from other modules, or both. Well defined data structures allow the exchange of data between the client and the server.

This modular design is the key feature of the RODOS system. It allows the easy extension of the system by adding new modules for special applications and the flexible control of the calculations. All program control, data management, input and output is done by the appropriate modules of the Operating Subsystem OSY(c.f. Figure 21). The task of the modules of the Analysing, Countermeasure and Evaluation Subsystems is just performing the model calculations for providing the required results.

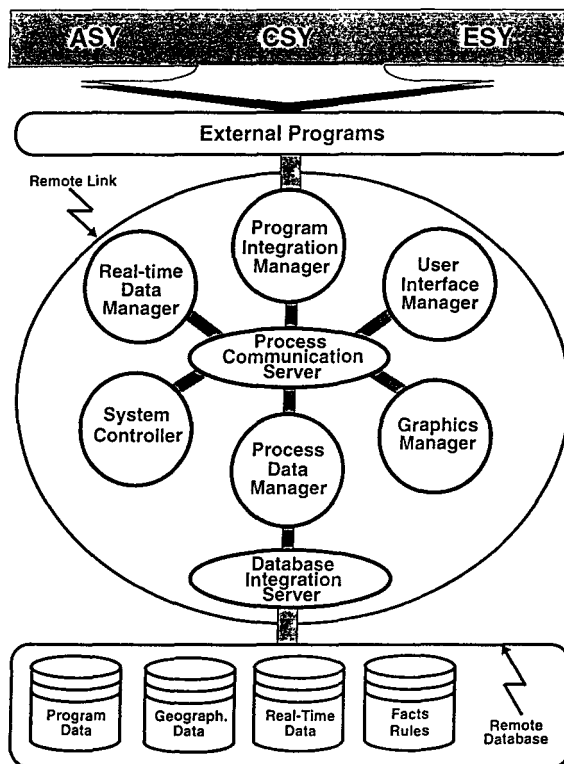


Fig. 21: Modular design of the operating subsystem OSY

The following sections give a brief overview of some of the modules of the Operating Subsystem OSY.

3.5.2 Interactive and Automatic Modes of Operation

Executing an application within the RODOS system requires mainly these steps to be taken:

1. Making available the necessary input data.
2. Executing the program.
3. Visualising the results.

Depending on the systems program, the first item comprises the provision of data for processing in the programs executing the algorithms of the computer models describing radiological events (ASY); the defined types of measures, action criteria, and factors for processing in the programs executing the algorithms for simulation and analysis of protective actions and countermeasures (CSY); the defined facts, rules, evaluation criteria, weights, and preferences for processing in the programs executing the algorithms of the methods for decision making and sensitivity analysis (ESY).

These steps are simultaneously supported by these activities:

- Preparation and generation of the user interface objects for the respective programs (Windows, menus).
- Preparation and generation of the numerical and graphic, respectively, representations of results from the respective programs.
- Management of, and response to, exceptional situations which may be initiated by an interruption caused by a user through the user interface (such as operation of the menu key: stop system), or by an event in measured data processing components via the message transfer in the system (such as a measured value exceeding a set quantity), or by a message from a message sending point through a link (such as reports about traffic congestions in an evacuation area).

In the interactive mode, communication between the user of the system and RODOS passes through a menu interface. Special problems can be formulated for answering by the system; input data and parameter values can be changed, and the output and representation of the results can be varied. Processing units (computer programs) of the system capture, check, transform, select, and represent on the screen the information from various resources. This mode is a straightforward dialogue mode presupposing knowledge both of the way in which the software modules are handled and of the factual contents of all components in the RODOS system. Sessions in the interactive mode take a

long time and are more suitable for calculations and analyses of results and data in the medium and later phases of an emergency situation.

In contrast, relevant information in the early phase of a nuclear accident must be acquired and evaluated quickly and in a manner coordinated in time so that the necessary decisions can be taken.

For this purpose, the automatic mode is implemented in the RODOS system. It is characterised by the cyclic execution by a number of programs whose control sequence is predefined by a processing logic. The processing sequence can be modified by an authorised user via the control interface (query, stop, replace, continue). Cyclic processing is carried out in analogy with the real-time systems of the nuclear power plant remote monitoring system which monitor the operating and environmental status of plants in a quasi-continuous (time-discrete) mode.

Automatic operation comprises these steps, which are carried out automatically:

1. Setting up a configuration list of the computer programs involved.
2. Gathering and preparing the measured data, applying the predefined test criteria to measured data, and providing all the necessary predefined input data.
3. Executing the programs.
4. Preparing the data resulting from these programs.
5. Indicating a subset of these resulting data (the balance of the data will be kept in the background and may be displayed on request).
6. Repeating these steps at predefined time intervals.

3.5.3 Selected Modules of the Operating System

The Message Interface and Communication Server

The draft software is based on the communication and cooperation of a set of autonomous program units designed to offer a variety of services.

The OSY programs together with the external programs constitute a set of cooperating processes jointly executing the operations necessary to achieve the desired endpoints. From the point of view of the client-server model (the standard model for network applications), one process offers services (the server process) which are used by other processes (client process). The processes communicate with each other via the Communication Server by exchanging messages. The Communication Server has the functions of establishing the connections of a communication channel with the respective process through the local network, receiving messages from that process, and transmitting mes-

sages to it. In other words, the Communication Server acts as a central mediator of all messages for the processes involved in the system (see Fig. 22).

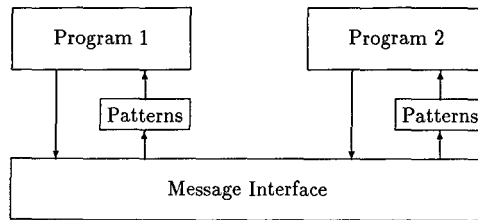


Fig. 22: Message interface of the RODOS System

The type and structure of a message is defined in the RODOS system uniformly. The messages contain fields which define the type, sender and recipient of the message. Three types of messages are considered by the Communication Server:

- Requests are send to other modules to ask for special services.
- Notification is send back by the recipient if the request was successfully completed.
- Failures are send back if some error occurred during the service.
- On startup, each module sends a message to the Communication Server, telling it the message patterns which should be send to this module.

Accordingly, all processes offering any services have a standardised program structure. Each program is made up of a communication segment, control flow segment, and local service segment. The communication segment uses the OSY message protocol and specifies the entire communication by way of the functions made available by the Communication Server. This is to say that the services rendered by other processes can be used if they are specified precisely in a message, and if the message is dispatched to the Communication Server.

Dialogue System

The dialogue system manages the user interface, monitors the subsystems, and controls the entire sequence of events in the RODOS/RESY system. Operationally, it is made up of the Resource Manager, System Controller, and Graphics System.

The Resource Manager supports these functions:

- It makes available the graphic user interface.

- It indicates standard information, such as the systems time, cycle time, process status, events, etc.
- It provides access to program interfaces, such as start, stop, hold, graphics, etc.
- It activates transfer operations, such as editors, data transfer lists, representations of results, etc.

The System Controller has these functions:

- Multiple (cyclic) or once-only sequencing control of the program groups.
- Management of memory access to program groups and programs.
- Initialisation of the OSY environment.
- Functional checks of the OSY processes.
- Functional checks of the active program groups.
- Coordination of tasks.
- Assignment of tasks to memory segments.
- Treatment of all global events.

The Graphics System

The Graphics System must handle all graphics output from various modules of the system. A special graphics program for each module could not be the solution to this problem. It is better to have a universal graphics program, which can handle a large set of graphical output using a well defined data exchange format.

As an additional feature, it should be possible to use part of the Graphics System to create a graphical user interface for programs outside of the RODOS system.

The main design aspects of the Graphics System are:

- Handling of graphics output from various external programs.
- Providing the main functionality of graphics programs, e.g zooming, scrolling, modification of graphics objects.
- Modular design to cope with different applications.
- Access to the functionality via a graphical user interface and a message interface.
- Providing functions to build graphical user interfaces for stand-alone programs.

The requirements for the Graphics System of RODOS led to a modular design. It is divided into three parts:

Graphics Interface Toolbox is a set of functions, which allow the construction of graphics programs and user interfaces.

Graphics Server is a special graphics program designed for the needs of the RODOS system.

Graphics Manager is the interface between the the Graphics Server and the RODOS system (mainly the Database Manager).

Each of the above parts uses the features of the previous parts. Graphics Server and Graphics Manager are independant programs, which communicate via a message interface. The user can select its configuration or create a new one using the above parts. Using this modular design, the Graphics System fits different requirements.

The Graphics Interface Toolbox

contains all functions needed to create a graphics user interface. This user interface can handle graphics output as well as menus to control program execution.

The Graphics Server

is a graphics program and user interface. It handles the graphics output, such as displaying results on geographical maps, histograms or function plots. A user interface gives the user the possibility to interact with the Graphics Server (e.g. zoom the output, modify graphics objects).

The basic features of the Graphics Server are:

- A graphical user interface allows the user to control the Graphics Server.
- A message interface is used to parse messages from external programs.
- The picture is handled as a set of graphics objects, which are collected in layers.
- The user can zoom and scroll the picture. Objects can be selected.
- Basic drawing capabilities for the input and modification of graphics data are available.
- A well defined interface is used to send graphics data from different applications to the Graphics Server.

In a complex system - e.g. RODOS - more than one Graphics Server can be run. This allows users to work with the graphics data from the external programs in RODOS on different screens.

The Graphics Manager

acts as an interface between external programs and the Graphics Server. The main task are

- Transformation of graphics requests from external programs to commands for the Graphics Server.
- Handling of graphics data from several external programs.
- Control of several Graphics Servers in the system.
- Transformation of graphics data to the data interface of the Graphics Server.

There exist several instances of the Graphics Manager. They are customised to

- handle the communication with the Database Manager of RODOS or
- select graphics output directly from the shared memory of external programs.

Both programs - the Graphics Server and the Graphics Manager - can be connected to other programs via the Message Server of RODOS . These programs which use the capabilities of the RODOS message server can access the functionality of the Graphics System or the Graphics Manager by sending requests to these programs.

The Database Manager

A basic feature of the RODOS system is the centralised management of data by a Database Manager. It has to cope with different kinds of information, such as

- program parameters,
- geographical and statistical data,
- on-line measurement data,
- forecast weather data,
- result data from external programs.

The data have to be kept in some databases, send to the programs on request and archived after calculations.

The Data Manager serves for the logical and physical data transfer among all RODOS processes. They cooperate closely with each other. Data transfer comprises these functions:-

- Archiving in the database of the data from memory segments.
- Loading the data from the database in a memory segment.
- Copying the data between memory segments.

The Data Manager analyses the incoming message, selects the appropriate record structure from the database tables, determines the memory address, and passes the information to the File Manager.

The File Manager, acting as an interface with the database, executes these functions:

- Management of the stored data in the database.
- Execution of access operations to the database.
- Execution of selection operations from the database.

The editor offers a Window-oriented user interface supporting users in the definition and description of input and output data.

In accordance with the use of different OSY data structures, the user interface is equipped with various menu and editing sectors and, as a consequence, can be operated easily and in a function-oriented way.

3.5.4 Integration of new Modules and Model Chains

The modular structure of the RODOS system and the Client-Server principle allows the integration of new modules in the system. Because the program control, data management, user input and graphical output is entirely handled by the Operating Subsystem OSY, the model developer can concentrate on the contents of his model. A further advantage of the use of RODOS to develop a new model is the possibility to test it in connection with other - already verified - modules of the model chain.

Adding new modules to the RODOS system is done in several steps:

- Define the services which are provided by the new module (e.g. calculation of organ doses).
- Enter information needed for the program flow into the database (e.g. input data needed by the module, data produced by the module). This will allow the System Controller and the Supervising Subsystem to integrate the module into the program flow.
- Define the input and output data structures of the module.
- Enter the above definitions into the program database of RODOS. This is needed by the Database Manager for the exchange of data.
- Code the module, using a template for the message interface.
- Test the module in the RODOS system.

The integration of already existing stand-alone programs into the RODOS system is done in a similar way. Normally, such a program defines a whole model chain. It is therefore split into its modules, which are integrated into RODOS as described below.

- Define the modules of the program and their interaction.
- For each module, perform the above steps for their integration.
- Enter the model chain into the database. This is done by defining the starting point and each calculation step based on the data flow of the model chain (e.g. start with meteorological data, calculate activity concentrations, calculate potential doses)

3.5.5 The Databases of RODOS

Systems like RODOS have to manage, process and evaluate a large amount of data of different kinds and quantity, such as geographical, meteorological, radiological and eco-

conomic data, messages, criteria, statistics, and expert knowledge (facts, rules, preferences). They may be stored in different data bases and computers with their own data structures and formats. In addition, the concept of developing RODOS distinguishes a stepwise progress with versions of improving functionality and for applications with differing complexity. Therefore, it is impossible to realise from the beginning a data bank for all applications and data-specific aspects.

This led to the concept of a distributed data base allowing for a decentralised data management and the parallel execution of multiple task operations. A corresponding Database Interface Manager program transforms the different data formats in the format of the RODOS operating system and converts the system queries by means of the embedded SQL-interface, and thus increase the flexibility and efficiency of data access.

The data base of RODOS is designed as a distributed data base, which comprises special data bases for geographical information, real-time on-line monitoring data, program data and decision supporting rules (see Figure 23).

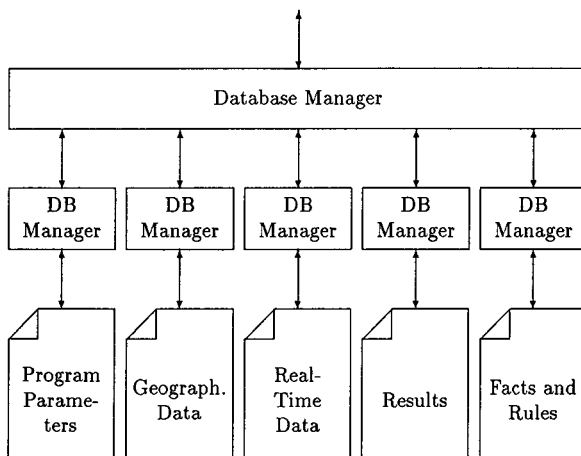


Fig. 23: Structure of the RODOS distributed data base

The program data base contains parameters and results of the application software implemented in RODOS . The real-time database will comprise all kinds of environmental monitoring data and measurements. The information in the rules database consists of expert judgment, facts, rules and preferences required for both evaluating alternative countermeasure combinations and controlling the user interaction and program flow in RODOS .

Each of the data bases of the RODOS system will be a stand-alone data base system, which has its own interface. A Database Interface Manager will give the programs of the RODOS system access to the data stored in these data bases with a unique interface format. The Interface Manager Program will convert the requests from the programs into a request to the appropriate data base. It will enable multiple clients to access multiple da-

tabase servers. The Database Interface Manager will also facilitate access to external databases, such as the REM data bank of the ECURIE system maintained by JRC Ispra.

Program Data

Program data is a term characterising the data of an external program which are both processed internally and used outside the program (e.g., for transfer to another external program, for representation and visualisation, for storing the data in the OSY database), and are also processed externally and used within the program (e.g., for accepting data from some other external program, for influencing a program run from the outside). An external program can claim the OSY services for the data defined in the program if, at the same time, they are defined and assigned by OSY means. In that case, these data are known outside the program in the system and are considered global data.

The OSY system provides a working environment which manages and executes the communication between the programs and supplies data to the programs. It follows from the concept of the program architecture that, in addition to messages, there are local data objects which are processed by functional units of a program. The local data, or parts of the local data of a program, are characterised as program data if programs are supplied by the OSY system. The program data are organised in data blocks made up of a set of arranged data objects. This memory arrangement reflects the definition structure of global data and, hence, the local data definition in a program.

For transfers of the data for the respective submodule of a program, a logical memory image is construed in the database of OSY, which represents an unequivocal access structure of the working memory of the associated program.

To supply global data to programs, these activities must be carried out:

- Modelling data structures with respect to data availability in the RODOS system.
- Modelling data structures with respect to data use in the RODOS system.

The Real-Time Database and On-Line Connections

Main purpose of the Real Time Data Base is the collection, preprocessing and storage of real time data coming from on-line measurements. Its main tasks are

- handle the connection to the networks,
- preprocess the incoming data (handling various data formats),
- validation and quality assurance of the data,
- storage and retrieval of data,
- backup of the data.

A preprocessor, which is located on a separate computer will handle the communication with the network. It will parse the incoming messages, do some preprocessing and validation on the data and transfer it to the Real-Time Database of the RODOS system. This preprocessor can be adapted to various networks and communication protocols.

RODOS will be coupled to on-line information networks. Figure 24 gives an example of such a connection in Germany with the nuclear reactor remote monitoring systems (KFÜ) of a German federal state and the integrated measurement system IMIS of the Federal Republic of Germany. The data will be delivered in 10 min (KFÜ) or 3 hours (IMIS) intervals via ISDN. The proposed data structure for this transfer is the ASCII-message structure of the IMIS system.

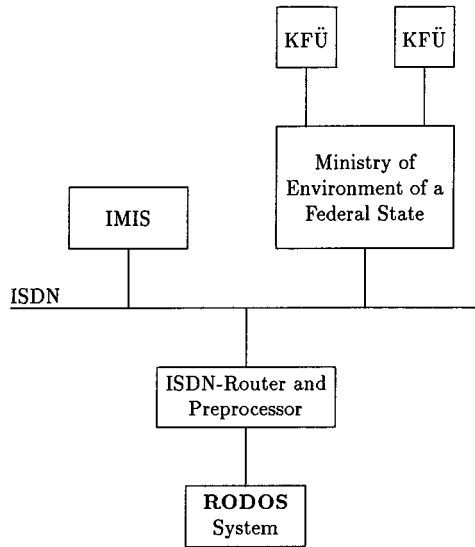


Fig. 24: Example on-line connection of the RODOS System

3.4.5.2 The Geographical Database RoGIS

The **Geographical Information System RoGIS** builds a system for

- handling various geographical and statistical information,
- storing environmental and radiological data,
- organising the access and interchange of data with other environmental data bases.

These features will make RoGIS to an interface between the external programs of the RODOS system and the geographical and statistical information stored as well as to external data bases.

RoGIS is designed as a stand alone program package, which includes all necessary tools for organising the data base and for handling various sets of data. Its structure allows an easy integration of different kinds of data structures. As a part of the RoGIS system, an interface package will give external programs access to the data stored in RoGIS .

Another possible configuration of the RoGIS data base is the integration into the RODOS data base. In this case, the access to the data sets of RoGIS is controlled by the data base

of RODOS . The close connection between the RODOS system and the RoGIS data base will help to install RoGIS at various sites. Main advantage of this will be the possibility of exchanging geographical and environmental data in an easy way, especially to allow radiological forecasts across boundaries.

Although there exist several so called geographical information systems with various applications, the RODOS developers have decided to create such a system of their own. This decision is a consequence of the main aim of the RODOS system, to be a transportable package running on various hardware platforms. The main advantage of RoGIS will be that it is adapted to the needs of RODOS with functionalities not provided by commercial systems . It will be available to other RODOS contractors with no licensing problems and no charge.

The Contents of the Geographical Database RoGIS

The geographical information system RoGIS is designed to hold various sets of information. Main feature of the record structure used in RoGIS is the ability to cope with different data structures. RoGIS is an open data base system, which means, that new hierarchical class structures to describe the information can be defined. Some of them are described here.

The Class **Administrative Data** and its subclasses hold statistical data for Administrative Objects (e.g. countries, cities). Geometrical objects linked to these Administrative Objects define the political and administrative border.

The Class **Nuclear Installation** and its subclasses are used to store information about different types of nuclear installations. Until now there is only one defined subclass for Nuclear Installation - Nuclear Power Plant (NPP). Geometrical object linked to these NPP objects are points which define the geographical coordinates for the object.

3.5.6 The RODOS prototype version PRTY2.0

In 1995, the prototype version PRTY2.0 of RODOS was finished. This version implements most of the features described in the previous sections. The Operating System OSY of the prototype version PRTY2.0 contains the following modules:

System Controller

Message Interface based on the UNIX Socket mechanism.

Graphics System consisting of the Graphics Server and the Graphics Manager.

Database Manager for program parameters and results.

Real-Time Database

Geographical Information System RoGIS

The Operating System OSY contains tools for integrating of new external programs and for defining of new model chains. It supports the interactive and automatic mode.

The software of the Operating System OSY has been developed on Workstations Hewlett Packard 9000/7xx. It uses the programming language C, the X11 Windows Release 5 and OSF/Motif 1.2 user interfaces and the Allbase/SQL database management system.

4. Application of RODOS in training courses on radiation protection (NE, EdF, SCK/CEN, FZK)

4.1 Overview

From the outset, the use of the RODOS system as a didactic tool for training and education in radiological protection and emergency response has been one of the objectives of the RODOS project. To investigate, plan and organize such RODOS applications, in autumn 1992 the Working Group (WG) "Training" was constituted with the following participants:

- Electricité de France (EdF), F: O. Marchand and S. Renier;
- Forschungszentrum Karlsruhe (FZK), Fortbildungszentrum für Technik und Umwelt (FTU), D: K. Burkart;
- Forschungszentrum Karlsruhe (FZK), Institut für Neutronenphysik und Reaktortechnik (INR), D: C. Steinhauer;
- Nuclear Electric (NE), UK: B. Bleasdale (until January 1994) and R.Fox (from February 1994);
- Studiecetrum voor Kernenergie / Centre d'Etude de l'Energie Nucleaire (SCK/CEN), B: A. Sohier.

The activities of the WG "Training" were co-ordinated by FZK/INR.

EdF, NE and SCK/CEN already were involved in courses where in principle RODOS could be utilized; they provided a respective compilation [RODOS(B)-TN(93)01, RODOS(B)-TN(93)02, RODOS(B)-TN(93)03], which was reviewed by the WG during the 1st meeting of the group in September 1992. This review showed that it would be rather difficult to modify or extend the examined courses in order to allow for the inclusion of RODOS. As a consequence, it was decided to design a new course with the intention to convey principles of radiation protection and off-site emergency response as well as to demonstrate the functionality and applicability of the RODOS system.

Following this decision, the general objectives for the envisaged course were laid down. Three basic objectives were identified:

- The transfer of knowledge should be selective and praxis oriented rather than broad and unspecific.
- The participants should actively exercise as much as possible by themselves rather than listening passively to frontal presentations.
- A demonstration of the role and usefulness of RODOS as a decision aiding and training tool should be intervoven with the course.

The target group should consist of individuals with a basic knowledge of radiation protection who wish to develop and/or improve their skills and competence in the area of off-site emergency response to nuclear accidents. The lecturers should be specialists in the respective teaching areas which have background knowledge about decision making and emergency management.

Utilizing the experience especially of FZK/FTU and NE in a systematic approach to training, it was decided to design the course in a modular training package structure, specifying for each package the learning aims and the information that shall be transmitted in lectures and exercises in form of a syllabus. Eight modules were identified, and the main responsibility for the sections was split between the organizations in the following way:

1. Basis of intervention (FZK/FTU)
2. The on-line decision support system RODOS and its role in off-site emergency management (FZK/INR)
3. Source terms and accident scenarios (EdF)
4. Atmospheric dispersion and deposition (SCK/CEN; in co-operation with EdF)
5. Exposure pathways and doses without countermeasures (FZK/INR)
6. Countermeasures and their benefits and disadvantages (NE)
7. Monitoring strategies (SCK/CEN; in co-operation with EdF)
8. Decision support techniques and uncertainties (FZK)

In 5 meetings of the WG between 1993 and April 1995, the learning aims and the scientific content of the lectures were defined (see Section 2.3) and the corresponding syllabus worked out. Finally, potential lecturers were identified and contacted.

With respect to the practical sessions it was decided that the participants shall address the topics covered in the lectures and collect and consolidate experience through the evaluation of a variety of accident scenarios, using RODOS as a tool to provide the technical input for the problems considered. RODOS will be operated by experienced course staff, so that the course participants do not require computer skills. Until June 1995, EdF, NE and SCK/CEN provided some potential accident scenarios, and a fragmentary draft of an exercise syllabus was produced by the group. The detailed preparation of the practical sessions, and in particular the definition and preparation of accident scenarios, will be carried out by FZK/INR and the RODOS team in the 2nd half of 1995 / beginning of 1996.

The course was given the name "Computer-Based Training Course on OFF-SITE EMERGENCY RESPONSE TO NUCLEAR ACCIDENTS". Because of the need for access to computer equipment and course staff, it was decided that the first course should best take place at FZK/FTU. FZK/FTU is responsible for the course logistics and technical organization. An

application was made by FZK to include it in the European Radiation Protection Education and Training (ERPET) activity of the European Commission, which was granted by then end of 1994. The course is summarized below; further detail are given in the Technical Report of the Working Group.

4.2 Topics addressed

The course is concerned with the estimation and evaluation of the off- site radiological situation following a nuclear accident and how this can be managed through the timely and effective introduction of countermeasures. Particular attention is given to accidents in LWRs involving the release of radioactive material to the atmosphere, although the principles addressed are applicable to all types of accident. The course focuses on the early phase of an accident and the emergency actions of sheltering, evacuation, distribution of stable iodine, and food- and feedstuff contamination.

Apart from the assessment of the radiological situation in the different stages of the accident, particular emphasis will be given to the problems involved in the judgement of the situation and of the radiological, economic and other consequences of intervention. The course will not address topics such as legal bases for emergency planning, emergency management structures and procedures, and responsibilities for decision making, as these topics are largely country specific or even different within a federal state.

It is assumed that all quantities relevant for the discussions, which can be available (source term, air- or ground concentrations, radiation doses), are in fact available, either directly from measurements or from model predictions. In particular, the assessment of the source term is not addressed in detail. The course does not intend to train the participants in manual skills for the assessment of the radiological situation under various circumstances of missing information. This is thought to be an item to be covered in national courses for the corresponding personnel.

4.3 Practical sessions

The two special features of the course are the use of the real time on- line decision support system RODOS to complement both presentations and discussions, and the ample time foreseen for practical sessions. Such sessions will accompany the course modules concerned with atmospheric dispersion and deposition, exposure pathways/potential doses, and protective actions.

Illustrative scenarios (source terms, maps, weather sequences) will be pre-defined to cover a representative range of possible accident situations and typical consequences. The scenarios will be introduced in the lectures and used throughout the course in the lectures as well as in the exercises. Also provided will be a set of predefined problems which act as a starting point and focus for discussions. The participants can vary relevant parameters of the scenarios, make own observations about the influence on the accident consequences and discuss the possible implications on decisions about actions. A special "easy to use" interface will allow an uncomplicated and fast realisation of the selected options with RODOS.

Before each practical session, an introduction is given to the respective models in RODOS, the corresponding data input and the available output. During the sessions, the actual operation of the system will be carried out by a person familiar with RODOS. The maximum number of participants that can reasonably work with one unit "terminal + operator" is about five. Given the hardware (two workstations with the possibility to operate three terminals on each) and skilled RODOS personnel available at FZK in 1995, maximally six working groups can be formed, which consist of up to five participants, one operator and one terminal, which allows a maximum number of 30 participants.

4.4 Course plan

1st day

LECTURE: Basis of intervention (Dr. K. Burkart, FZK/FTU, D). Topics:

Summary of dose concepts; summary of health effects due to exposure;

protective actions: classes, aims, features and bases of decision making; principles of intervention; introduction to optimisation; bases of decision making.

Discussions and exercises

LECTURE: RODOS and its role in off-site emergency management (Dr. J. Ehrhardt, FZK/INR, D). Topics: Overview of the RODOS project; overview of the RODOS system; RODOS in off-site emergency management.

Introduction to the practical sessions

DEMONSTRATION: RODOS - Main Windows and Geographical Information (RODOS team, FZK/INR).

2nd day

LECTURE: Source terms (Mr. D. Manesse, Commissariat a l'Energie Atomique, F). Topics: Source term characteristics relevant for radiological consequences; Illustration of the different source terms for a PWR; Importance of the availability of data defining the source term in the decision making process regarding the methods of assessment and their uncertainties; Accident Scenarios used in the course.

LECTURE: Atmospheric dispersion and deposition (Dr.T. Mikkelsen, RISØ. National Laboratory, DK). Topics: Basic phenomena in the lower atmosphere; overview of models for different scales; atmospheric dispersion / deposition and contamination patterns.

LECTURE: RODOS - Source terms and atmospheric dispersion and deposition (RODOS team).

PRACTICAL SESSION: Source terms and atmospheric dispersion and deposition.

3rd day

LECTURE: Exposure pathways and doses without countermeasures (Dr. H. Müller, GSF-Forschungszentrum für Umwelt und Gesundheit, D). Topics: Overview of exposure pathways; details of each exposure pathway (Calculation of doses, characteristic features of pathway; uncertainties); doses from natural background.

LECTURE: Countermeasures and their benefits and disadvantages (Mrs. M. Morrey, National Radiological Protection Board, UK). Topics: Total dose and dose averted; intervention levels; details of countermeasures (effect on exposure pathways, factors influencing the dose reduction, required resources, benefits, disadvantages); impact of conditions on determining intervention levels; impact of non-tangible effects on countermeasures.

LECTURE: RODOS - Exposure pathways and countermeasures (RODOS team).

PRACTICAL SESSION: Exposure pathways.

4th day

PRACTICAL SESSION: Countermeasures

LECTURE: Monitoring strategies (Dr. W. Weiss, Bundesamt für Strahlenschutz, D). Topics: Role of monitoring during the three time phases; objectives and strategies to meet the objectives during the release phase, including the technical link between monitoring and required data; overview of monitoring philosophy and implementation in European countries; principles and problems of source term estimation; considerations about uncertainty.

EXERCISE

5th day

Discussion of exercise

LECTURE: Decision support techniques and uncertainties (Prof. S. French, University of Leeds, UK).

Filling out of course evaluation forms

4.5 Outlook

Dependent on the response to the course, it may be repeated not only at FZK, but also in other institutions within the EC, Central and Eastern European countries and CIS republics, eventually in other languages than English. When the full RODOS system will be available, the course could be extended to cover in detail the longer-term countermeasures relocation and food bans and their optimisation.

Besides this special training course for technical advisors of the emergency management, the future planning foresees the development of courses for the training of RODOS users and the preparation of exercises for emergency management staff.

5. Implementation of RODOS in Central and Eastern Europe

5.1 Implementation of RODOS in Poland (IAE)

5.1.1 Project definition, main goals and realisers

The NDSS-NE/RODOS Project has been defined and initiated by the NDSS-NE/RODOS Research Team in the Institute of Atomic Energy (IAE), Otwock-Swierk for the National Atomic Energy Agency (NAEA). Its main goal - as already reported during 4-th RODOS Contractors Meeting in Interlaken and in the Special Warsaw RODOS Seminar, 17 - 18 November 1994 - is to develop and implement the National Decision Support System for Nuclear Emergency Action after a nuclear accident in Europe (NDSS-NE).

This system is to be compatible with the RODOS system and worked out in close relation and cooperation with the institutes involved in the RODOS project. The Polish project is sponsored by the State Committee for Research, the National Atomic Energy Agency and the European Commission within the Programme "Cooperation in Science and Technology with the Central and European Countries" (PECO).

The project is to be seen not only as a research and development activity but also as an implementation and integration programme oriented to work out hardware and communication structures together with their technical realisations as well as with development of country specific software modules and databases. To secure the realisation of its goals the Project Task Force has had to be defined and created consisting of many cooperating institutions and scientists as well as technical staff. Those institutions and staff shall be in the future considered as a Technical Support Organization of the Project and shall back up the National Nuclear Emergency Center, which is to be developed and maintained by the National Atomic Energy Agency and other governmental institutions responsible for the emergency handling in the country. The creation of National Nuclear Emergency Center and its Technical Support Organization is in fact the main goal of the ongoing organisational and development efforts.

NDSS-NE/RODOS Project is worked out by the NDSS-NE/RODOS Task Force, constituted by the NDSS-NE/RODOS Research Team at the IAE and by many research and development groups located at various research institutions in Poland and abroad. The list of those institutions, where such groups were created or are under the process of creation looks as follows:

- Institute of Meteorology and Water Management (IMWM) responsible in the country for all services connected with weather parameters and forecasting,
- Central Hydrometeorological Bureau of Air Polish Forces (CHB), responsible for meteorological services for aviation purposes,
- Warsaw Technical University, Institute of Environment Engineering, engaged in development of national scale weather forecasting model and problems connected with industrial pollution,
- Mission Research Corporation (MRC) *ASTER Division, and Colorado State University (CSU), Fort Collins, USA engaged in regional weather forecasting system and at-

mospheric dispersion of toxic pollution (for example for Kennedy Space Center in Florida),

- Warsaw University, Institute of Geophysics, specializing in microphysics of atmosphere and precipitation problems,
- Central Laboratory for Radiological Protection (CLRP), engaged mainly in radiological monitoring data collection and dose assessment,
- Topographic Service, General Staff of Polish Army (TSPA), responsible for providing digital maps of various scales and information levels,
- Institute of Geodesy and Cartography (IGC), engaged in photogrammetry and remote sensing activities,
- State Inspectorate for Environmental Protection (SIEP), involved in the development of the Integrated Information System "Environment" for ecosystem studies.

Talks and discussions with other institutions about their participation in the project are going on or are planned to be arranged in the next future. Delineated programme requires efforts of many specialized institutions, planned and implemented in close cooperation and under careful coordination. The main actors of the NDSS-NE/RODOS Task Force and their contribution to the Project were presented during the Special RODOS Seminar, held in Warsaw 17-18 November, 1994.

The global goals set out in the Project require many man-years of efforts and shall be reviewed and reformulated according to the progress achieved and needs met in the process of realisation of the project. Experience and tools developed and tested during the activity of the Project can be applied not only in case of nuclear emergency but also in the case of other emergencies connected with industrial as well as natural accidents and hazards, particularly those which affect larger territories and whose limitations or liquidations require using of distributed resources and careful planning and coordination. The basic requirements is here connected with the gathering of specific data in real-time, characteristic for the nature of accidents and hazards.

On 17-18 November 1995, IAE organised a Special RODOS Seminar in Warsaw. The objectives of this special seminar were:

- to present the background to, and overall objectives of, the RODOS Project to relevant decision makers and their technical staff in Poland and other Central and East European Countries (especially Baltic countries). Particular consideration was given to the development and practical implementation of RODOS as an aid to off-site emergency management in the event of any future accident in Europe and its potential use in National Emergency Centres,
- to enable Polish institutes (i.e. members of the NDSS-NE/RODOS Task Force) to inform representatives of the RODOS Management Group and other participants of the range of activities being carried out in Poland on off-site emergency response. This will facilitate future interaction between the Polish programme, the RODOS project and related developments in other East European countries,

- to discuss collaboration, at both technical and administrative levels, between the East European institutes involved in the RODOS project, in particular with a view to minimising the administrative burden on the overall project coordinator, FZK, and to make best use of the technical resources available within the project.

More than 70 representatives of Polish research and governmental institutions, contractors of the RODOS project from the countries of EU and Central and Eastern Europe took part in the seminar. The RODOS Management Group (RMG) was represented by Dr.G.N.Kelly from the European Commission and Dr. J. Ehrhardt, FZK. The Proceedings of the Special Warsaw RODOS Seminar, published by IAE, contain full material of the meeting.

5.1.2 The basic concepts and directions of the Polish approach

The fundamental assumption of the Polish Project is that the RODOS system shall constitute the software framework of the NDSS-NE. The RODOS Project shall provide the majority of required computational moduli applicable for nuclear emergencies in Europe, ranging from the vicinity of the release and early phases up to far distant areas and later stages of the accident. Transforming RODOS into NDSS-NE, which will operate in real time and on-line coupled with meteorological and radiological monitoring networks requires the modification of the current version of the RODOS software and/or extension according to the national needs, priorities, available computer capacities and organisational constraints. In particular there must be a sound relation between the available databases for radiological and meteorological information and the software of NDSS-NE. The question where data are located, where they are needed, when and how fast they can be sent, should be accounted for in the functional structure of the system and its communication capabilities.

The structure of the system should then account for existence of specialised centers, such as IMWM with responsibilities relative to meteorological fields diagnoses, world numerical forecasting distribution and regional forecasting services, CLRP dealing with measured monitoring data collection, their consistency revision and maintenance of central bases of such data, planned National Emergency Office embedded in NAEA, where projections of radiological situations and feasibility of countermeasures will be examined to work out ranked list of rational decisions and SIEP, where a dedicated integrated computer system "Environment" is being developed, with data banks of accumulated information for ecosystem studies and other centers dealing with land use, demography, health and environmental long term monitoring data.

The structure of the system must also take into account the existence and operation of research reactors MARIA and EVA in Otwock-Swierk, where the Local Swierk Emergency Center must constitute a subsystem of the future National Nuclear Emergency Center with all the organisational and communication requirements.

The fact that the actual version RODOS-PRTY 2.0 is still focussed on near range dispersion and evaluation calculations allows relatively fast and reliable implementation of those moduli for the Local Swierk Emergency Center applications.

Therefore for ensuring high operational performance of NDSS-NE and effective use of resources and technical capabilities of all cooperating institutions and the emergency center organisation and responsibility structure the system should be both distributed and functionally integrated, it means:

- operational system of NDSS-NE should account for a network of the NDSS-NE software kernels implemented along with a dedicated moduli in specialised centers, with the software kernel providing basic function of communication, process and data management and graphic user interface,
- adequate tasks scheduling among the centers of the network should be designed to avoid intercenter transmissions of huge amount of data produced during the intermediate steps of the analysis phase,
- it should be possible to access all the needed resources, which are located on different machines of the network, under different data base systems,
- an appropriate data transfer between computers should be reliable and fast enough,
- individual modules can be executed and maintained on different machines under the supervision of teams of dedicated specialists.

These goals shall be realised by the Heterogeneous Distributed Computer Environment (HEDICE) described in the paper presented at the Special Warsaw RODOS Seminar. The HEDICE allows to constitute an appropriate infrastructure for NDSS-NE, accounting for already existing and further planned development of:

- radiological monitoring and data collection system,
- specialised centers and their services (eg. for weather forecasting and pollutant dispersion predictions),
- bilateral and international cooperation on radiological data exchange.

The structure of HEDICE is an extension of the prototype RODOS version, which at present can work on a single HP workstation. A first attempt to implement RODOS in a heterogeneous-type environment will take place at the Institute of Atomic Energy on a coupled HP and Convex machines environment. Basic elements of this configuration are:

- Convex C3210 (50 Mflops), 7.2 GB disks capacities,
- HP 735 (40 Mflops), 4 GB disks capacities, both connected to LAN (standard Ethernet, allowing data transfer with the 10 Mbits/sec speed).

Finally the software of the distributed NDSS-NE will be developed for a computer network configuration with Convex C3210 and HP-735 computers located at IAE, Cray EL-98 at the Warsaw University, providing services for IMWM, Dec-workstations at CLRP and other RISC workstations of SIEP, all connected to Metropolitan Area Network of Warsaw (WARMAN) based on the ATM technology, allowing the data transfer with the speed of 155 Mbits/sec (see Fig. 25).

Some of the quoted computers may be meantime upgraded or substituted by clusters of workstations or mainframes with enhanced capabilities for parallel processing.

The notion of distributed computer environment and its implementation and testing constitutes interesting contribution to the RODOS project development and should simplify and assist in its practical implementation not only in Polish conditions. Elaborated concepts and implementation experience may be a basis of exchange and cooperation with other countries.

5.1.3 RODOS software experience, comments and development

Using funds from the PECO contract a HP-735 workstation was bought by IAE. Shortly before the Special Warsaw RODOS Seminar the RODOS-PRTY 1.2 version was installed.

Contribution to testing RODOS-PRTY 1.2

The following tests have been carried out by IAE:

a) for distributed computer environment:

- portability for Convex C3210 mainframe, concerning mainly interprocess communication mechanisms, particularly shared memory facilities, and X-Windows/OSF Motif graphics,
- transfer speed based on standard Ethernet line between Convex C3210, HP-735 and Silicon Graphics computers using Internet domain socket facility

b) for operation of RODOS system:

- using editors for integration of external programs,
- simulation of real-time mode of operation,
- graphic user interface,
- visualisation of results

All the results of these tests as well as comments aiming at improving the current RODOS version were delivered to developers of the generic software (Forschungszentrum Karlsruhe).

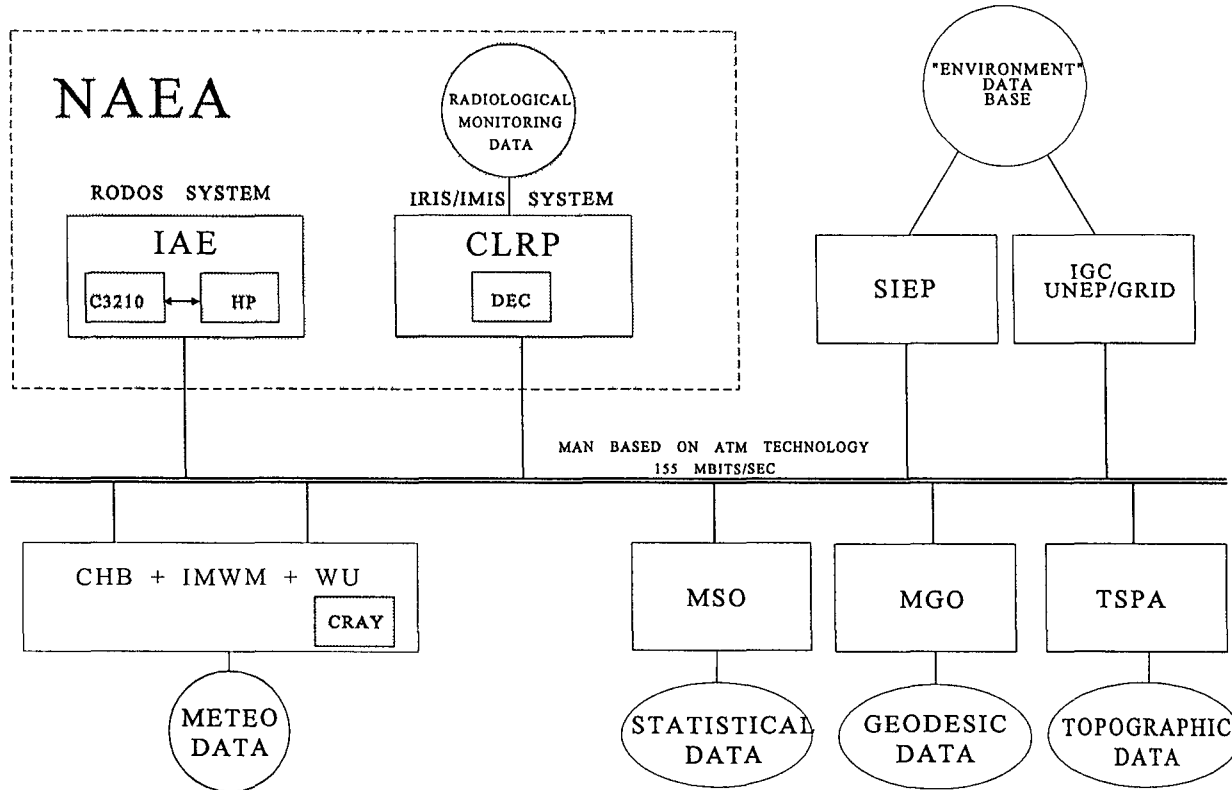


Fig. 25: Computer and data bases environment

Development of Heterogeneous Distributed Computer Environment (HEDICE) - a basic tool for National Decision Support System for Nuclear Emergencies.

The structure of HEDICE has been designed. The main features of HEDICE are the following:

- a heterogeneous distributed data base manager allowing for such operations like to find, retrieve and update on different types of database management systems (Oracle, Ingres, Informix etc.),
- process initialisation and execution on both local and remote hosts (machines) by process manager of the NDSS-NE kernel residing in each node of the network,
- client-server architecture, but in such a way that the same machines can play both roles depending on needs.

The HEDICE can be also treated as a set of nodes (machines) representing autonomous computer systems embedded into the whole environment. Each node provides some specific services of well defined type, like collecting some data, or performing some actions. However, the configuration of the system can be dynamically changed. In such a way HEDICE constitutes a tool for "open distributed computing". This allows also for full integration of emergency data management and RODOS system, that is for interoperability of different elements of the whole system. Two tasks (or nodes) are interoperable if they can interact to execute tasks jointly. This is more than interconnectivity, which means only exchanging messages (for example data) between nodes or tasks.

The HEDICE is based on object oriented approach and message passing concept. The full usage of object orientation technology, that is encapsulation, abstraction and polymorphism leads to flexible and intelligent tool, which will be able to operate in different circumstances during dynamically changing situations. The well-defined interfaces, hiding internal operations will clarify all the available actions for any element of the system.

The implementation of HEDICE will be partially based on freely distributed software, such like: Parallel Virtual Machine (PVM), developed at the University of Tennessee, Oak Ridge Laboratory and Emory University, TCL and TK (tool command language and graphic user interface toolkit) developed at the Sun Microsystems Laboratories by Dr. John Ousterhout and well known GNU software (C/C++ language). The PVM library is the wide used package for parallel computation in heterogeneous computer environment and stands de facto as a standard tool for such calculations. Similarly like RODOS, PVM is based on message passing concept, hence it allows for quite easy integration with generic RODOS software.

All the above mentioned packages are available for almost every hardware platform working under UNIX operating system. This allows for unified approach in integration of basic radiological and meteorological systems in Poland with the RODOS system. The packages have been installed on Convex C3210 and HP-735 computers at IAE. Several tests have been carried out concerning mainly cooperation of these computers. Currently

the packages are being tested on other hardware platforms i.e. Silicon Graphics, Sun, Cray and PC under LINUX system.

5.1.4 Radiological Monitoring Aspects

At present the radiological monitoring system is under reconstruction. A software for collecting monitored radiological data and transmitting them to NAEA has been developed and is being tested. Documentation and installation procedures will follow. Integration of emergency data management and decision support systems will be based on described previously HEDICE tools. A part of the monitoring stations will be probably operated under ARGOS-NT system developed at the Danish Emergency Management Agency (an appropriate agreement between Danish and Polish governments is to be signed). The ultimate goal of all efforts is to approach gradually the technical standards and organizational structures of the system IMIS implementation in Germany. The CLRP is cooperating in this subject with the Institute of Atmospheric Radioactivity, Freiburg. However, at any rate HEDICE will still constitute the basic tool for integration of the used systems.

5.1.5 Meteorological Aspects

The fundamental change in the scope and the role of DSS in nuclear emergency handling lies in the possibility of simulating the radionuclides transport across the continent after the accidental release in nuclear power plant anywhere in Europe. This transport heavily depends on the hydrometeorological conditions during and after the accident. Having a possibility to calculate the deposition and resulting doses one can select and plan the possible emergency actions, taking into account the benefit to costs considerations.

This approach is fundamentally different to the approach based solely on the radiological monitoring data, which are collected simply too late for the purposes of realistic mitigation of the accident consequences. This is the reason why meteorological data are so fundamental for the success of DSS.

- A. It has been decided to add a node to the existing METPAK communication system, for rendering the world and national observational data to the NDSS-NE/RODOS system. Within the METPAK network main forecasting offices are connected with the speed of transmission 19.2Kb/s and others with 9.6 Kb/s. Communication between the node for NDSS-NE/RODOS located at IAE or NAEA and IMWM will be based on dedicated line or satellite VSAT system provided by Telbank, one of the main telecommunication institutions in Poland. Up to the time of the commencing the routine communication links the archive set of meteorological data has been created and delivered to be used as a basis for exercises and initialization purposes.
- B. Another agreement with CHB has been reached to use all the military and civilian data from aerodroms and special hydrometeorological stations used for aviation purposes. Those data are complementary to the data obtained from IMWM. The agreement will allow also to use the mobile stations in emergency situations to get meteorological data from requested points on Poland territory.

- C. As reported on the Warsaw Special RODOS Seminar a common project of the IMWM and IAE on the application a unified model from the Meteorological Office at Bracknell for numerical weather forecasting purposes has been started. The model has been installed on the Cray EL-98 of the Warsaw University with the assistance of Bracknell specialists and should deliver in next future routinely twice a day forecasting data covering the territory of Poland. It is being assumed that the Bracknell model shall be used for stand-by purposes, allowing to start necessary assimilation and initialisation preprocessing for emergency calculation of numerical forecasts connected with the atmosphere dispersion simulations of the NDSS-NE/RODOS system. The necessary data shall be transmitted to the NDSS-NE/RODOS system.
- D. The RAMS model from MRC *ASTER and CSU shall constitute the basis for downscaling and special emergency mode operations for local weather predictions. The RAMS package has been installed on Convex C3210 computer of the IAE and a team of specialists has been created to run it for emergency purposes and for preparing the exercises which shall be carried out routinely to keep staff of the future National Emergency Center prepared for the emergency actions. The RAMS package shall use the data from the Bracknell model (an appropriate interface has been developed) and observational data from public, military, mobile and Doppler radar stations. It will be run on a cluster of machines consisting of Convex C3210 mainframe and HP735 workstation using freely distributed PVM software supported by NCAR and AVS packages for graphics and visualisation..

This approach will in particular concern enhancement of capabilities of uniform approach to the mesoscale and local weather forecasting (downscaling of 12-24 hours time period and large area weather forecasting provided by regional meteorological centers, to the purpose of an emergency situation development tracking). The regional atmospheric system RAMS of CSU and ASTER with its grid nesting features, objective analysis and initialisation, and physical phenomena capability simulation seems to be a tool particularly suitable for achieving that goal, however current testing suggests, that a computer platform of 250-350 Mflops performance will be required to ensure by RAMS an operational support of the NDSS-NE. A relatively low cost solution would be an implementation of a parallelized version of RAMS in a heterogeneous cluster of workstations and/or mainframes. For this purpose the PVM software can be used.

- E. Since the potential nuclear power plants accidents may happen relatively far from Polish territory the NDSS-NE/RODOS Research Team decided to pursue in cooperation with MRC *ASTER and CSU the development of HYPACT code for long distance transport of radionuclides, taking advantage of hybrid Lagrangean and Eulerian characteristics of the code.
- F. The system RAMS-HYPACT shall be loosely coupled with the existing RODOS system to take advantage of the dose assesment capabilities of the RODOS system. Necessary interface shall be elaborated by the NDSS-NE/RODOS Task Force, as the basic

software contribution to the RODOS system in the field of for transport of radionuclides.

- G. Under appropriate licence certificates the meteorological preprocessor PAD from the ANPA (Italy), ADREA code from the NSCR Demokritos (Greece) and RIMPUFF/LINCOM program from the RISØ National Laboratory (Denmark) have been acquired. An appropriate interface between RIMPUFF/LINCOM and Polish meteo data available in the RADMET system (based on radio) has been developed.

5.1.6 Topographic aspects

Transport of radionuclides depends not only on meteorological conditions, distributed over the relevant territory but also on orography, land use with canopy distribution and others data which must be stored together with numerical maps and terrain reliefs in the form of multilevel geographical databases.

After detailed studies the following specific results have been achieved:

- A. According to the presentation on the Warsaw RODOS Seminar TSPA has delivered the 1:1000000 scale numerical map of Poland. Its use depends on delivery of RoGIS package, which is under development at Forschungszentrum, Karlsruhe. This is the very first step in securing the basic content of the topographic data base of NDSS-NE/RODOS System.
- B. Digital Terrain Elevation Data for the grid 1km x 1km is now under preparation by TSPA and will be delivered to IAE by the end of this year. These data should become operational together with the digital map quoted above under the item A after the delivery of RoGIS package.
- C. The new partner of NDSS-NE/RODOS Task Force is the Institute of Geodesy and Cartography. It has elaborated in cooperation with CORINE Project of European Union the 1:100000 scale maps of Poland devoted to land use. The whole territory of Poland will be available at the end of this year. A contract with IGC is under negotiation and is to be signed soon.

The CORINE project seems to be a very good source of digital maps for the RODOS project as it was from the very beginning devoted to environmental studies.

In June 1991, at the European Conference of Dobris Castle, the European Ministers of the Environment stressed the need to improve environmental information and monitoring systems in Europe. They asked for the production of a report describing the state of the environment in Europe, which among other things should become a basis for the effective implementation of environmental policies and strategies. They welcomed the European Commission's proposal to provide information and assistance for the application of the CORINE methodology in other countries as a first step towards the integration of environment information systems throughout Europe.

Three CORINE inventories are applied in six of the CEECs (Bulgaria, the Czech Republic, Hungary, Poland, Slovakia and Romania): CORINE Land Cover, Corinair and CORINE Biotopes.

The project of CORINE Land Cover maps the land cover at the scale 1:100 000 and stores the data in a geographical information system (GIS) in accordance with a nomenclature of 44 items, such as dense urban areas, crop land, grassland, forests, bogs, etc. The methodology involves satellite imagery, together with thematic maps and field observations.

Here also, the status of implementation is different from one country to the other. The main hurdle for starting the projects was the availability of topographic (military) maps; this difficulty has been solved.

The project is well ahead and is expected to be concluded by the end of 1995 for Poland, Hungary, the Czech Republic and Slovakia, and in mid-1996 for Romania and Bulgaria.

The expert team which assumes the technical follow-up and uniformity of the data in the project, stated that the quality achieved in the work is high.

Other initiatives were taken in the frame of this project.

A small expert working group is defining now a CORINE nomenclature and methodology for a more precise cartographic scale 1:50 000, since a demand has been often expressed by local or regional authorities for more detailed land cover information.

A study of land cover changes by means of retrospective imagery will start directly after implementation of the land cover databases.

- D. There is a national programme of creating a digital map of Poland in the scale 1:50000. The programme is being sponsored also by the National Energy Agency. These maps, which are to be available about 1999, should become a part of the NDSS-NE/RODOS system as the final solution of the topographic aspect of the Polish Project. The solutions presented under items A, B and C are considered as preliminary or temporary solution to enable the implementation of NDSS-NE/RODOS system, to study relevant technical problems and prepare qualified staff.

5.1.7 Implementation the for Local Swierk Emergency Centre

Two research reactors are located in Swierk: MARIA and EVA. Both are or were exploited by the Institute of Atomic Energy.

Reactor MARIA:

Water-berilium reactor, high fuel enrichment 80%, power 30 MW, square lattice. The reactor started operation in 1974 and after the Chernobyl accident was under reconstruction to improve safety features and is still operating.

Reactor EVA:

Water reactor, fuel enrichment 30%, power 8 MW, hexagonal lattice. The reactor started operation in 1956 and closing procedure begun in the spring of 1995.

Existing elements of RODOS system have been applied to give the foundation for the Local Swierk Emergency Centre Decision Support System of the type foreseen by the RODOS system. The decision has been undertaken to use the existing version of RODOS to establish the local DSS for emergency handling, as an element of the national project:

To implement it the following steps have been undertaken:

- A. Local observational meteorological data and local radiological data are delivered on-line to feed the ATSTEP programme on HP 735 workstation.
- B. Programmes RIMPUFF and LINCOM have been tested using both local data and data obtained from the Central Hydrometeorological Bureau.
- C. Source term for reactor MARIA accidents has been implemented and tested on ATSTEP programme taking into account the exploitation data from the Reactor Operating Console.
- D. Topographic, digitalized maps of detailed scale for the Local Swierk Emergency Center are under preparation and will be ready by the end of this year.

5.1.8 Conclusions

The global goals set out for the project could not be achieved within the reported period. Therefore work on the topics listed above in Sec. 5.1.1 will be continued in the next years with priorities determined by the availability of software and material provided by the system developers of FZK and cooperating institutions. The emphasis will be put on implementation and testing in shortest possible time period a pilot version of NDSS-NE, whose basic constituents will be distributed configuration of the RODOS kernels, national radiological monitoring data system and communication to IMWM. The high priority will be also given to completing the set of digitalized maps of Poland and country specific countermeasures evaluation. The existing capabilities of the RODOS system will be extensively used for achieving till the end of 1996 an operational pilot version of a local decision support system for the nuclear centre at Swierk, along the lines set out in Germany for the RODOS/RESY application.

5.2 Implementation of RODOS in Hungary (NRIRR)

5.2.1 Objectives

According to the initiation of the Hungarian Atomic Energy Commission in relation to the environmental radiation, a country-wide information network should be established and it has to include

- the early warning system operated by the Hungarian Army and Civil Defence,
- the laboratory type monitoring networks and
- the local systems around the main nuclear facilities.

A closer co-operation is to be promoted for both accident and normal situations in a number of important areas. These include the monitoring programme as a whole, together with data analysis, dose assessments, decision making procedures, international co-operations, to provide information for the Authorities, specialists and the public.

The information network is to be supplied with real-time data collection, telemetric data transmission and resources of hardware and software for data processing both for normal and accidental situations. The software tool of RODOS is planned for off-site decision support. For the effective use of the decision support system the on-line access of the meteorological data provided by the Hungarian Meteorological Service and national data bases of population distributions, consumption habits etc. have to be established.

5.2.2 Achievements

The early warning system with 50 field stations equipped with dose rate proportional counters and meteorological sensors for determination the temperatures, the air pressure, the wind direction and speed and the humidity. Each station is equipped with a PC-computer and the data are transmitted automatically to the national center of the Civil Defence. The stations are mainly placed at the meteorological stations and Civil Defence posts, within the country. The Nuclear Emergency Information Centre has already installed a home made software to simulate the radionuclide dispersion in the air for accidental cases.

The responsibility of the data collection, processing of laboratory type of data, the regularly information and the decision-making with respect to the radiation impact of the population are addressed to the institutes of Ministry of Welfare, mainly to the National Research Institute for Radiobiology and Radiohygiene (NRIRR).

To establish the Information Centre of the Nationwide Environmental Radiation Monitoring System (NERMS) the NRIRR has already installed the facilities of

- SUN SPARCserver-20 workstation with UNIX operation system, C+, C++ , FORTRAN and PASCAL compilers
- INGRES data management software
- three local stations each one with PC-server, Novell Netware and PC- workstations.

The structure of the information system of the NERMS is outlined in Figure 26. The central facilities including the license for INGRES are ready to extend the number of the local stations up to 30. Due to the restricted financial resources the extension is delayed and at the beginning of the next year 10 stations are planned to start. The work is supported by the IAEA as well.

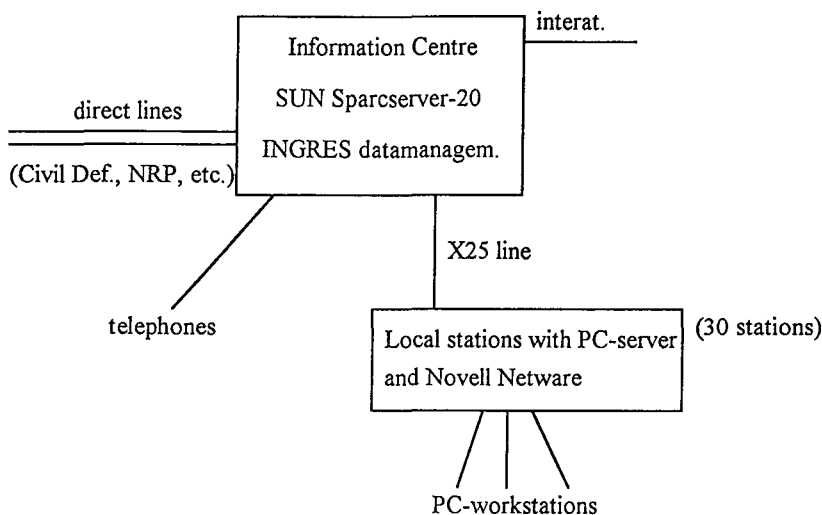


Fig. 27: Structure of the NERMS information system

The user software for the on-line and remote collection and processing of laboratory type of data has been developed in INGRES and tested. The main functions of the software are the followings:

- data collection from the local stations installed in the radiological laboratories,
- selection of data for special purpose, mainly for verifying the data and export the files to an input of statistical etc. packages,
- provide simple results and outputs like main statistics, time series, scatter plots and maps.

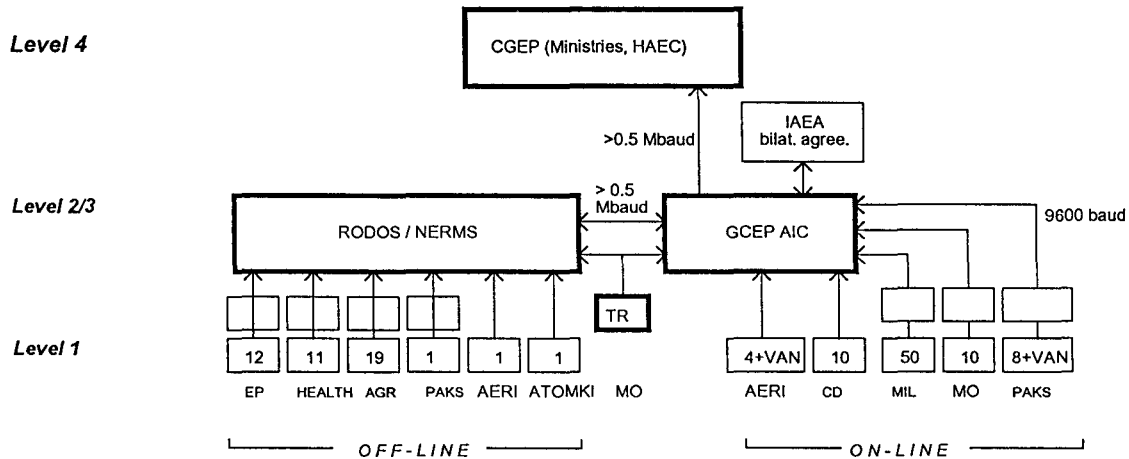
The software is ready to collect data types of

- dose, dose rates both for indoor and outdoor, even for caves etc.
- radionuclide concentration of environmental samples (terrestrial, river etc. ones)
- radionuclide releases from nuclear installations
- radionuclide contents of whole bodies both for animals and man, including organs.

The radionuclides might be natural (like Rn-222) and artificial ones. Plans are to connect the information centres of the early warning system (managed by the Civil Defence), of the Meteorological Service and of the NERMS ones. The dedicated lines are already installed but the proper software for communications are not yet bought. The structure of the planned - and partly already in operation - network is given in Figure 27.

The RODOS System is to be implemented in the Information Centre of the NERMS, by the NRIRR. Therefore the institute has already begun collection of non-nuclear data, mainly consumption habits of the Hungarian population (nearly from 20 thousands inhabitants) to be used for site-specific and more effective management of the software.

The first plan was to install the RODOS to the SUN SPARCserver-20 workstation used for monitoring date management. The latest version is to be installed on an extra computer, probable an HP-725 type one. The financial costs are to be covered by the support of the EC in frame of the contract underlying this Final Report.



RODOS: Real Time On Line Decision Support System
 NERMS: National Environmental Radiation Monitoring System
 GCEP: Governmental Commission for Nuclear Emergency Prep.
 AIC: Accidental Information Centre
 HAEO: Hungarian Atomic Energy
 EP: laboratories of Ministry of Environmental Protection and Regional Policy
 HEALTH: laboratories of Ministry of Health and Welfare
 AGR: laboratories of Ministry of Agriculture

ATOMKI: Nuclear Research Institute (Debrecen)
 AERI: Atomic Energy Research Institute (Budapest)
 TR: Trajectory Model
 PAKS: Nuclear Power Plant (Paks)
 MO: Meteorological Office
 MIL: Military Service
 CD: Civil Defence

Fig. 28: System concept for a nationwide Hungarian Monitoring Information System with four logical levels of data collection (Level 1), data processing (Level 2), data evaluation (Level 3) and decision making (Level 4)

5.3 Implementation of RODOS in Romania (IFIN-LAB)

5.3.1. Project summary

5.3.1.1. Objectives of the RODOS project for IFIN-LAB

The main objectives of IFIN-LAB within the framework of RODOS project during the contract period were:

- a) the establishment, with the FZK's approval and help, of the optimum sized hardware/software (H/S) computing configuration necessary both for transfer from FZK to IFIN-LAB and further development in Romania of the RODOS software system and, consequently, the price negotiation, purchase, installation and operation of the chosen H/S computing configuration;
- b) the training at FZK on RODOS structure and operation of some IFIN-LAB's researchers and engineers;
- c) the transfer from FZK and installation at IFIN-LAB of the actual version of RODOS;
- d) the realisation at IFIN-LAB of an experimental basis interfaceable to the RODOS H/S configuration for the realisation of on-line and real-time features;
- e) the planning and organisation the IFIN-LAB's R&D RODOS activities so that according to our feasibility prospects they match the RODOS project schedule in the next Framework Programme until mid of 1999.

5.3.1.2 Achievements of the IFIN-LAB

The main achievements of IFIN-LAB within the framework of RODOS project during the contract period are as follows:

- a) the acquisition of a Hewlett Packard (HP) workstation 735 under UNIX operating system; this HP H/S configuration has been put into operation and now is working at IFIN-LAB inside of a specially arranged room;
- b) three researchers from IFIN-LAB have been trained on the RODOS structure and operation (June 1995) at FZK; a lecture on the RODOS project and system has been given by the RODOS project coordinator (Dr.J.Ehrhardt) within the IFIN seminar framework in Bucharest-Magurele;
- c) the installation, under countersigned written RODOS agreement conditions, dated 13 July, 1995, of the software of RODOS prototype 1.3 by the FZK's RODOS team;
- d) the construction at the IFIN-LAB site of a 60m height meteorological and radiological surveying tower (MRST) equipped with appropriate detectors and sensors and designing the interface with the RODOS H/S configuration;

- e) the developing of domestic research activities in the field of accident consequences assessment (ACA), as potential contributions of IFIN-LAB to the RODOS system; we started also preliminary studies for CANDU reactor source-term evaluation as a future module to be included in RODOS, keeping in mind that the Romanian NPP is based upon this kind of power reactor;
- f) the connection of RODOS to E-mail and preparedness for long distance communication of data and information by using phone digital equipment installation.

5.3.2 Diagnosis and prognosis of the radiological situation

A physical data bank has been created for gamma and beta emission of the fission product radionuclides. It stores the gamma energies and intensities for 62 radionuclides with decay schemes of different degrees of complexity; these data have been obtained by a proper method of simulation of the radionuclide decay and coding of each radionuclide decay scheme. The data for the beta decay of the radionuclides of interest in nuclear accident and nuclear medicine have been processed to obtain a beta spectra library for use in the radionuclide identification and for precise interpretation of the dosimetric measurements. In this view a computer program has been elaborated which stores up-dated data in the field. The computation of the mean energy of the beta spectra and of the shape of the spectra of 42 radionuclides is made based on the characteristic data. The formulas used in computation are those proposed and checked by the US National Bureau of Standard Computational Laboratory, according to the atomic number of radionuclide, forbidden laws about spin and parity and of the type of the beta spectrum (simple or compound ones). (The results of the (proposed) adopted model are described in "Computer simulation of beta ray spectra for some isotopes of interest in accidental releases" in press, Romanian Journal of Physics, authors: D.Vamanu, G.Ochiana et all.).

5.3.3 Source term estimation

During this year a CANDU power reactor-based NPP, located at Cernavoda city, near Danube large river, will be put into operation. Because, for the time being, this kind of NPP is proper only for Romania and due to its relatively big releases of tritium into the atmosphere (even in normal operation), it requires a particular approach for its source-term evaluation; the IFIN-LAB started already studies and data gathering activities for a CANDU reactor source term evaluation module, as a future component of RODOS.

Bearing this in mind, during the last years, some of our research works were dedicated to studies concerning tritium:

- determination of a method for evaluation of low concentration of atmospheric HTO, by trapping the water vaporous on solid absorbent (molecular sieves, Drierita, silica gel), followed by vacuum extraction of water and liquid scintillation measurement of this water;
- determination of a method for HT/HTO evaluation, by trapping the HTO on solid absorbent, oxidation of HT to HTO on Pd-molecular sieves and adsorbing of water;

- assessment of operational release limits for CANDU NPP, taking in consideration the last recommendations of ICRP and AIEA for maximum admissible dose (1 mSv/year for population);
- uncertainty and sensitivity analysis for the environmental tritium code UFOTRI;
- analysis of transfer parameters for routine release of HTO;
- study of the deposition of atmospheric tritium on soil covered with snow;
- the validation of model prediction for tritium in the international program BIO-MOVS;
- assessment of operational release for CANDU-600 nuclear generating station in Cernavoda, Romania.

5.3.4 Application software

ACA modules for estimating doses, health effects and intervention zones from field measurements of relevant data on environmental contamination following an accidental release to atmosphere has been elaborated during the reported period at the IFIN-LAB.

A comprehensive and non-contradictory integration of data given by field measurements of radioactive release with generic data given by numerical modelling and simulation is an important exigence among reference terms in the realisation of automatic decision support systems for nuclear emergencies. The problem presents a number of scientific and technical aspects regarding the methodologies, measurement systems and techniques, data acquisition systems, telemetry systems methods and systems of data processing, etc., used. The approach used in this work takes into account the last mentioned domain, data processing given by the measurement in the field of environmental contamination (air and soil) in order to obtain information about the spatial distribution of doses, expected health effects and the recommended intervention zones.

To solve these problems a computer code was written which it is based on the assumption that in a reasonable scenario, in nuclear emergency, two types of field measurements are available:

- a) fix points - environmental measurement stations of the surveillance and monitoring network;
- b) aleatory points-in field measurements performed by mobile teams.

To solve these problems many interpolation techniques are available and were programmed for each specific spatial distribution of the field measurements. The computer code, FIELD of 2,367 MBytes, consists of 81 files, 7 executable files and 74 GIS data base files. The validation of the code confirms the quality of the solutions with smooth interpolations, absolute precise in the measurement points (fix or mobile) if a convenient density of measurement is provided. (D.Vamanu, Internal Report, 1994).

5.3.5 Dose assessments

A fast and easy to use method has been elaborated at IFIN- LAB for the computation of irradiation doses in case of human exposure due to post-accident irradiation. In order to restrict to acceptable levels the radiation risks to people, the quantity recommended by ICRU for control and limitation of doses to people is considered in the effective dose equivalent (EDE). A computer program has been elaborated for the evaluation of:

1. external doses (total body) due to the ground deposition;
2. external doses due to water and/or air immersion;
3. internal irradiation in case of inhalation of radionuclides and due to the consumption of contaminated food.

Total doses to be considered are the sum of the dose equivalents for the three mentioned exposure pathways. The main assumptions of the proposed model are:

- a) the concentration levels of radionuclides in air, water and on the ground are known and,
- b) the radioactive content of the food is given as a function of the ground deposition.

Accounting for the type of the release which occurs, the computer programme stores the nuclear data of the radionuclides; the input data are the measured or calculated values of the radionuclide concentrations for each pathway. In case of evaluation of internal irradiation due to the consumption of contaminated food an average individual daily dietary is assumed and it is supposed that the main contribution is given by Cs-137, Cs-134, Sr-90, I-131, I-132 + Te-132 radioisotopes. The total value for EDE is to be compared with dose levels for the introduction of sheltering and evacuation (stored in the computer program too) as recommended by international agencies. A detailed description of the proposed method is given in: "Computational model for human irradiation in post-accidental evaluations" in press, Romanian Journal of Physics, authors: G.Ochiana, D.Vamanu.

5.3.6 Organisational and functional status and perspectives

To underline IFIN-LAB's potential for RODOS project implementation in Romania, a comprehensive study has been elaborated which comprises: basic requirements, regulations and governmental authorities involved in nuclear accident, RODOS system's structure, objectives and requirements, quality assurance and control matters, feasibility potential and demands (including scientific, technical, logistical and financial aspects), the necessary R&D activities to be developed by IFIN-LAB from 1994 until the mid of the 1999 year and their scheduling, etc. (IFA Internal Report, September 1994). On the other hand the IFIN-LAB RODOS R&D group is at present enlarged with young graduates both in mathematical theory of the expert systems, physics of the atmosphere, computer science, nuclear instrumentation and nuclear physics.

For a better definition of the research tasks and responsibilities three subgroups within the IFIN-LAB RODOS group have been settled as follows:

- 1) the first one will be permanently responsible for RODOS-HP configuration maintenance and operation; this subgroup will also work as a human interface between the RODOS system and both the other Romanian participants in the RODOS project and the Romanian end-users of the RODOS system;
- 2) the second subgroup will develop new software modules for the three subsystems (ASY, CSY and ESY) of the RODOS system; this subgroup will also be responsible for the adding new software modules coming from the RODOS community;
- 3) the third subgroup will be responsible for both communications and interfacing the RODOS system with our national RMS networks.

All works related to the RODOS system will be done by IFIN- LAB following QA/QC procedures as stated in the Quality Assurance Manual of our Institute; if necessary, special QA/QC procedures will be elaborated in due time.

A domestic long lasting (from 1994 to 1999) R&D contract has been approved by the Ministry of Research and Technology for the RODOS Project; in accordance with this contract, IFIN-LAB will benefit from April 1994 up to June 1999 of the necessary funds, expressed in Romanian currency which will, mainly cover the expenditures with salaries of the research workers during this period, consummables and internal collaborations.

The buildings of the Institute of Atomic Physics are endowed with all necessary facilities required by the current R&D activities in the nuclear domain; all the three subgroups involved in the RODOS Project have their own working spaces and recently additional rooms have been assigned in close connection and above the Command Room of the Public Authority Headquarters for installation and operation of the RODOS HP configuration.

6. References

6.1 References and publications of FZK belonging to Sections 1, 2

- /A1/ Kelly, G.N., Ehrhardt, J.
RODOS - a comprehensive decision support system for off-site emergency management
Proceedings of the "Fifth Topical Meeting. on Emergency Preparedness and Response", Savannah, Ga., 18 - 21 April 1995, pp 8 - 11
- /A2/ Ehrhardt, J., Päsler-Sauer, J., Schüle, O., Benz, G., Rafat, M., Richter, J.
Development of RODOS, a comprehensive decision support system for nuclear emergencies in Europe - an overview
Radiation Protection Dosimetry, Vol 50, Nos 2 - 4, pp 195 - 203 (1993)
- /A3/ Päsler-Sauer, J., Schichtel, T., Mikkelsen, T., Thykier-Nielsen, S.
Meteorology and atmospheric dispersion, simulation of emergency actions and consequence assessment in RODOS
Proceedings for Oslo Conference on International Aspects of Emergency Management and Environmental Technology, 18 - 21 June 1995, Oslo, pp 197 - 204 (1995)
- /A4/ Mikkelsen, T. (ed.)
Final report of contract FI3P-CT92-0044 (Coordination of atmospheric dispersion activities for the real-time decision support system under development at FZK)
RISØ National Laboratory, September 1995
- /A5/ Müller, H., Pröhl, G.
ECOSYS-87: A Dynamic Model for Assessing Radiological Consequences of Nuclear Accidents
Health Physics 64, pp 232 - 252 (1993)
- /A6/ Bulgakov, A., et al.
Prognosis of Sr-90 and Cs-137 behaviour in soil-water system after the Chernoby accident
Ecology and geophysics aspects of nuclear accident, Moscow, Hydrometeorological Publishing House, pp. 21 - 42, 1992
- /A7/ Raskob, W., Heling, R., Popov, A., Tkalich, P.
The modelling concept for the radioactive contamination of waterbodies in RODOS, the decision support system for nuclear emergencies in Europe
Proceeding of the "International Seminar on Freshwater and Estuarine Radioecology, Lisbon, 21 - 25 March 1994

6.2 References and publications of NPRRI belonging to Section 3.1.1

- /B1/ Stubna M.
RODOS Programme in Slovakia
4th RODOS Contractors Meeting, Interlaken, June 20-24, 1994.
- /B2/ Stubna M., Duranova T.
Design Basis for TDS : Uncertainty and Sensitivity Analysis
4th RODOS Contractors Meeting, Interlaken, June 20-24, 1994
- /B3/ Stubna M., Duranova T., Bohunova J.
NPP Bohunice environmental monitoring network and source term determination during an accident
Special Warsaw RODOS Seminar, Warsaw, November 17-18, 1994
- /B4/ Bohunova J., Duranova T., Kusovska Z., Stubna M.
The determination of the source term and population protection measures on base of the on-line measurements of a first ring
TDS EBO Report VUJE (NPPRI) 172/94, November 1994
- /B5/ Stubna M., Duranova T., Bohunova J., Kostial J.
NPP Bohunice environmental monitoring network and source term determination during an accident
Fifth Topical Meeting On Emergency Preparedness And Response, Savannah, Ga, April 18-21, 1995

6.3 References and publications of FZK belonging to Sections 3.1.2, 3.2.1, 3.2.4, 3.5

- /C1/ Mikkelsen, T. and Desiato, F.
Atmospheric Dispersion Models and Pre-processing of Meteorological Data for Real-time Application.
Proceedings of the Third International Workshop on Real-time Computing of the Environmental Consequences of an Accidental Release to the Atmosphere from a Nuclear Installation, Schloss Elmau, Bavaria, October 25-30 1992. Journal of Radiation Protection Dosimetry Vol 50 Nos 2-4, pp 205- 218(1993).
- /C2/ Martens, R.; Maßmeyer, K.
Untersuchungen zur Verifizierung von komplexen Modellen zur Beschreibung des Schadstofftransports in der Atmosphäre,
Report GRS-A-1844, Gesellschaft für Anlagen- und Reaktorsicherheit, Köln.
- /C3/ Santabarbara, J.S.; Mikkelsen, T.; Kamada, R.; Lai, G.; Sempreviva, A.M.
LINCOM Wind Flow Model, RISØ-Rreport(EN), 37 pp.
Available on request from: Department of Meteorology and Wind Energy, RISØ National Laboratory, P.O. Box 49, DK-4000 Roskilde, Denmark.

- /C4/ Mikkelsen, T.
Atmospheric dispersion models for real-time application in the decision support system being developed within the European Commission.
Olesen, H.R. and T. Mikkelsen (Eds.) 1992: Proceedings of the workshop "Objectives for Next Generation of Practical Short-Range Atmospheric Dispersion Models", RISØ, Denmark, May 6-8 Danish Center for Atmospheric Research (DCAR), P.O. BOX 358, DK-4000 Roskilde. pp 109-130.
- /C5/ Thykier-Nielsen, S.; Mikkelsen, T.; Moreno, J.
Experimental evaluation of a pcbased real-time dispersion modeling system for accidental releases in complex terrain.
Proceedings from 20th International Technical Meeting on Air Pollution Modelling and its Application, Valencia, Spain, November 29 - December 3., 1993.
- /C6/ Päsler-Sauer, J.
Evaluation of Early Countermeasures and Consequences In RODOS/ RESY.
Proceedings of the Third International Workshop on Real-time Computing of the Environmental Consequences of an Accidental Release to the Atmosphere from a Nuclear Installation, Schloss Elmau, Bavaria, October 25-30 1992. Journal of Radiation Protection Dosimetry Vol 50 Nos 2-4, pp 219- 226(1993).
- /C7/ Benz, G., Ehrhardt, J. Faude, D., Fischer, F., Päsler-Sauer, J., Rafat, M., Schichtel, t., Schüle, O., Steinhauer, C.
Contents and functions of Pilot Version I of RODOS/RESY
Report KfK 5259
- /C8/ Evans, J.S., Möller, D.W., Cooper, D.W.
Health effects models for nuclear power plant accident consequences analysis
NUREG/CR-4214 (1985), Rev. 1 (1990)
- /C9/ COSYMA: A new programme package for accident consequence assessments
Joint report by Forschungszentrum Karlsruhe GmbH and National Radiological Protection Board
Brussels, Report EUR 13028 (1991)
- /C10/ COSYMA: User guide
Compiled by I. Hasemann and J.A. Jones
Brussels and Karlsruhe, Report EUR 13045/KfK-4331B (1991)
- /C11/ Stather, J.W. et al.
Health effects models developed from the 1988 UNSCEAR report
Chilton, NRPB-R226 (1988), (London, HMSO)
- /C12/ Annals of the ICRP
1990 recommendations of the International Commission on Radiological Protection, ICRP publication 60, Vol 21 No 1-3 (1991)

/C13/ Faude, D.

COSYMA: Modelling of economic consequences
Report KfK 4336 (1992)

/C14/ Faude, D., Meyer, D.

Extension of the COSYMA-ECONOMICS module cost calculations based on different economic sectors
Report KfK 5442 (1994)

6.4 References and publications of SCK/CEN belonging to Section 3.1.3, part 1

/D1/ Sohier,A.,

Data assimilation during the early phase of an accidental release.
RODOS(B)-RP(94)04.

/D2/ Sohier,A., Van Camp,M., Ruan,D., Govaerts,P.,

Methods for Radiological Assessment in the Near-Field During the Early Phase of an Accidental Release, Using an Incomplete Data Base,
Radiat. Prot. Dosim. 50 (2-4) (1993).

/D3/ Zadeh,L.A.,

Fuzzy Sets,
Inf. Control, 8, 338 (1965).

/D4/ Van Camp,M., Ruan,D., Sohier,A., Govaerts,P.,

The use of fuzzy set theory to reduce uncertainties on the source term and the wind direction in decision aiding systems.
Proc. Joint International Conference on Mathematical Methods and Supercomputing in Nuclear Applications, vol. 1, KfK, Karlsruhe, 1993.

/D5/ Van Camp,M., Van de Walle,B., Ruan,D.,

Reduction of Uncertainties in Nuclear Emergency Decision Aiding Systems,
SCK*CEN Internal Report, October 1993

/D6/ Golubenkov,A., Borodin,R., Sohier,A., Rojas-Palma,C.,

Data Assimilation and Source Term Estimation,
JSP1-report, to be published.

/D7/ Semenov, B.L., Arutyunjan,R.V., Gorshkov,V.E., Tarasov,V.I., Tkalya,E.V.,

A recovery procedure of the radioactive release source term,
Annual Meeting of Nuclear Technology, Nürnberg, May 16-18, 1995, Germany.

/D8/ Sohier,A., Rojas-Palma,C.,

Monitoring Requirements during the Early Phase of an Accident,
NEA-Workshop on Emergency Data Management, 12-14 September 1995, Zürich, Switzerland.

6.5 References and publications of UoL belonging to Sections 3.1.3, part 2, 3.3, 3.4

- /E1/ S. French and J.Q. Smith (1993) "Using monitoring data to update atmospheric dispersion models with an application to the RIMPUFF model." *Radiation Protection Dosimetry* **50**,
- /E2/ J.Q. Smith and S. French (1993) "Bayesian updating of atmospheric dispersion models for use after an accidental release of radiation" *The Statistician* **42**, 501-511.
- /E3/ J.Q. Smith, S. French and D.C. Ranyard (1994) "An efficient graphical algorithm for updating estimates of the dispersal of gaseous waste after an accidental release". In A. Gammerman (ed) *Probabilistic Reasoning and Bayesian Belief Networks*. Alfred Waller, Henley-on-Thames. 125-144
- /E4/ S. French and D.C. Ranyard (1994) "Quality assurance within RODOS" RODOS(B)-TN(94)01, School of Computer Studies, University of Leeds.
- /E5/ S. French, D.C. Ranyard and J.Q. Smith (1993) "Models, data and expert judgement in decision support systems"
- /E6/ S. French, D.C. Ranyard and J.Q. Smith (1994) "Design of a decision support system for use in the event of a radiation accident"
- /E7/ S. French, D. Ranyard and J.Q. Smith (1995) "Uncertainty in RODOS." Research Report 95.10, School of Computer Studies, University of Leeds. Available by connecting to WWW at file: //agora.leeds.ac.uk/scs/doc /reports/1995 or by anonymous ftp from agora.leeds.ac.uk of the file scs/doc/reports/1995/95_10.ps.Z. RODOS(b)-rp(94)05
- /E8/ S. French, N. Papamichail, D.C. Ranyard and J.Q. Smith (1995) "Design of a decision support system for use in the event of a radiation accident" Submitted to *Annals of Operations Research*. RODOS(b)-rp(95)05
- /E9/ A.S. Gargoum and J.Q. Smith (1994) "Approximation schemes for efficient probability propagation in evolving high dimensional Gaussian Processes." *Research Report* **266**, Department of Statistics, University of Warwick.
- /E10/ A.S. Gargoum and J.Q. Smith (1995a) "Bayesian models for emission profiles of toxic gases" *Research Report* **274**, Department of Statistics, University of Warwick.
- /E11/ A.S. Gargoum and J.Q. Smith (1995b) "Dynamic generalised linear junction trees." *Research Report* **278**, Department of Statistics, University of Warwick.
- /E12/ D.C. Ranyard (1994) "Building uncertainty handling into decision support systems for emergency response." School of Computer Studies, University of Leeds.

/E13/ L. Valet and S.A. Roberts (1994) "Identifying the requirement for history of time-varying objects during an object oriented analysis." School of Computer Studies, University of Leeds

Conference and Seminar Presentations

S. French (1995) "MCDA Problem Formulation of the Decision Making in the Event of a Nuclear Accident" Invited paper at IIASA Workshop on Problem Formulation in Decision Support. Sept. 1995.

S. French, D.C. Ranyard and J.Q. Smith (1993) "Decision support for nuclear emergencies." Paper presented at OR35, Operational Research Society Conference, York, September 1993

S. French, D.C. Ranyard and J.Q. Smith (1993) "Models, data and expert judgement in decision support systems" Institute of Nuclear Engineers Conference, Glasgow, Sept. 1993.

S. French, D.C. Ranyard and J.Q. Smith (1994) "Design of a decision support system for use in the event of a radiation accident" Poster session paper presented at Bayesian Statistics 5, Alicante, June 1994.

S. French and J.Q. Smith (1992) "Using monitoring data to update atmospheric dispersion models with an application to the RIMPUFF model." Third International Workshop on Decision Making Support for Off-site Emergency Management. Schloss Elmau, Barvaria, October, 1992.

D.C. Ranyard (1994) "Building uncertainty handling into decision support systems for emergency response." Paper presented at EURO XIII/OR36, Operational Research Society Conference, Strathclyde, July, 1994.

D.C. Ranyard (1995) "Data Assimilation and Uncertainty Handling for Atmospheric Dispersal Forecasting" Paper presented at the Fifth Topical Meeting on Emergency Preparedness and Response, American Nuclear Society, Savannah, Georgia, April, 1995.

J.Q. Smith (1994) "Bayesian models forecasting emissions of toxic gas in a complex environment." Classification Society Conference, Malvern, May 1994.

J.Q. Smith (1995) "Dynamic belief networks and their approximation" Conference on Highly Structured Stochastic Systems, Luminy, France, June 1995.

J.Q. Smith, S. French and D.C. Ranyard (1994) "An efficient graphical algorithm for updating estimates of the dispersal of gaseous waste after an accidental release". Unicom Seminar on Adaptive Computing, Brunel University, Jan 1994.

Seminars on aspects of RODOS have been given at:

- Royal Statistical Society Local Group (Newcastle, Nov. 1993)

- Midlands Probability Seminar (University of Warwick, Sept. 1994)
- Operational Research Society Local Group (Leeds, May, 1995)
- Birmingham University (Department of Statistics, March 1993)
- Bradford University (Department of Computer Science, ????)
- Nottingham University (Department of Mathematics, Nov. 1993)
- Edinburgh University (Department of Mathematics, Dec. 1993)
- Technical University of Delft (Department of Mathematics and Infomatics, April, 1994)
- York University (Department of Mathematics, Nov. 1994)

Dissertations and Student Reports

N.b. No student received financial support from the project.

L. Chien-Sheng (1993) "Development of the Object-Oriented RIMPUFF System"

J. Cunningham (1995) "A prototype expert system for decision analysis"

N. Papamichail (1994) "The Development of a Relational Database for the Object-Oriented RIMPUFF System"

J.E. Thackray (1994) "X Window Interface to RIMPUFF"

6.6 References and publications of NRPB belonging to Section 3.2.2

- /F1/ Functional specification of the late countermeasures module FRODO, version 1. RODOS(B)-TN(93)07, March 1994. Revised version, September 1995.
- /F2/ Technical specification of the late countermeasures module FRODO, version 1, RODOS(B)-TN(95)02, September 1995.
- /F3/ Friedland, W, Müller, H, Pröhl, G, Brown, J, McColl, N P, Jones, J A, and Haywood, S. Modules for foodchain transport, dose assessment and long-term countermeasures in RODOS, the European decision support system. Radiation Protection Dosimetry, 50, 227-234 (1993).
- /F4/ Müller, H and Pröhl, G. ECOSYS-87: A dynamic model for assessing radiological consequences of nuclear accidents. Health Phys. 64, 232-252 (1993).

- /F5/ Brown, J, Wilkins, B T et al.
Compilation of data from the Ukraine, Russia and Belarus on the effectiveness of agricultural countermeasures for use in the RODOS system.
NRPB-M518, Chilton, 1994.
- /F6/ Brown J, et al.
A comparison of data from the Ukraine, Russia, and Belarus on the effectiveness of agricultural countermeasures.
NRPB-M597, Chilton (1995).
- /F7/ Databases associated with the late countermeasures module FRODO,
RODOS(B)-TN(95)03, September 1995.
- /F8/ Crick, M J and Brown, J.
EXPURT - Exposure from urban radionuclide transfer. A model for evaluating exposure from radioactive material deposited in the urban environment.
NRPB-R235 (1990), (London, HMSO).
- /F9/ J Lehto (ed).
Cleanup of large radioactive-contaminated areas and disposal of generated waste, Final report of the KAN2 Project.
TemaNord 1994:567, 1994.
- /F10/ Brown, J, Haywood, S M and Roed, J.
The effectiveness and cost of decontamination in urban areas, IN Proc: International Seminar on Intervention Levels and Countermeasures for Nuclear Accidents, Cadarache, October 1991.
EUR 14469, European Commission 1992.
- /F11/ Brown, J and Simmonds, J R.
FARMLAND: A dynamic model for the transfer of radionuclides through terrestrial foodchains.
NRPB-R273, 1995 (London, HMSO).
- /F12/ Brown, J, Smith, K R, Mansfield P, Smith J, and Muller H.
The modelling of exposure pathways and relocation, decontamination and agricultural countermeasures in the European RODOS system.
In Proceedings of the Oslo Conference on International Aspects of Emergency Management and Environmental Technology, Oslo, June 1995 (Ed K H Drager). Oslo (1995).

6.7 References and publications of GSF belonging to Section 3.2.3

- /G1/ Friedland, W., Müller, H., Pröhl, G., Brown, J., McColl, N. P., Jones, J. A., Haywood, S.:
Modules for foodchain transport, dose assessment and long-term countermeasures in RODOS, the European decision support system
Radiation Protection Dosimetry, 50, 227-234 (1993)
- /G2/ Müller, H. and Pröhl, G.:
ECOSYS-87: A dynamic model for assessing radiological consequences of nuclear accidents
Health Phys. 64, 232-252 (1993)
- /G3/ Catsaros, N., Parmentier, N., Robeau, D., Caracciolo, R., Desiato, F., Masone, M., Müller, H., Paretzke, H. G., Pröhl, G. et al.:
Methods for real-time dose assessment
Proc. Seminar on Methods and Codes for Assessing the Off-site Consequences of Nuclear Accidents, Athens, 7-11 May, 1990, European Commission Brussels, EUR-13013, 1992
- /G4/ Müller, H., Friedland, W., Pröhl, G. and Paretzke, H. G.:
EURALERT-89 Users Guide
GSF-Forschungszentrum, Neuherberg, Germany, GSF-Report 30/90 (1990)
- /G5/ Jacob, P., Rosenbaum, H., Petoussi, N. and Zankl, M.:
Calculation of organ doses from environmental gamma rays using human phantoms and Monte Carlo methods, Part II: Radionuclides distributed in the air or deposited on the ground
GSF-Forschungszentrum, Neuherberg, GSF-Report 12/90 (1990)
- /G6/ Henrichs, K., Eiberweiser, C., Paretzke, H. G.:
Dosisfaktoren für die Kontamination der Haut und der Kleidung
GSF-Forschungszentrum, Neuherberg, Germany, GSF-Report 7/85 (1985)

6.8 References and publications of IAE belonging to Section 5.1

- Borysiewicz M., Furtek A., Potemski S., Stankiewicz R., Wojciechowicz H., Zelazny R.,
National Decision Support System for Nuclear Emergency - Baselines for the Technical
Project of the System and Feasibility of the Project,
Report of National Atomic Energy Agency Contract No 10/SP/93, Dec. 1993, 750 pp
- Borysiewicz M., Furtek A., Potemski S., Stankiewicz R., Wojciechowicz H., Zelazny R.
National Decision Support System for Nuclear Emergency compatible with RODOS, IAE
Ann. Rep. 1993
- Borysiewicz M., Stankiewicz Modelling of Pollution Dispersion in Atmosphere
IAE Report IAE 8/A 1994

Potemski S., Wojciechowicz H.

RODOS (Real Time On-line Decision Support System for Nuclear Emergencies in Europe) implementation on a coupled HP and Convex computers

Proc. ECUC'94 European Convex Users Conference, Cracow, pp.389-395, 1994

Niewodniczański J.

Nuclear Emergency system, basic concepts, organisation and operation,

Proc. of Special Warsaw RODOS Seminar, Warsaw, Nov. 1994, pp. 142-151

IAE Special Issue, 1995

Paluszyński W., Borysiewicz M.,

National Environmental Information System for Poland,

Proc. of Special Warsaw RODOS Seminar, Warsaw, Nov. 1994, pp. 115-141

IAE Special Issue, 1995

Klejnowski R.

Basic meteorological data concerning Poland and their input to the national decision support system in case of nuclear emergency (NDSS-NE/RODOS)

Proc. of Special Warsaw RODOS Seminar, Warsaw, Nov. 1994, pp. 182-189

IAE Special Issue, 1995

Jakubiak B.,

Numerical weather forecast for nuclear emergency - basic concept and development directions

Proc. of Special Warsaw RODOS Seminar, Warsaw, Nov. 1994, pp. 190-202

IAE Special Issue, 1995

Uliasz M.,

Application of coupled mesoscale meteorological and lagrangian particle dispersion models to regional transport and emergency situations

Proc. of Special Warsaw RODOS Seminar, Warsaw, Nov. 1994, pp. 203-213

IAE Special Issue, 1995

Krajewski P.,

Computer model for the transfer of radionuclides in human ecosystem

Proc. of Special Warsaw RODOS Seminar, Warsaw, Nov. 1994, pp. 214-223

IAE Special Issue, 1995

Bednarek. H, Przybyliński P.,

Geographic Information System concepts to be applied in National Decision Support System in Case of Nuclear Emergency,

Proc. of Special Warsaw RODOS Seminar, Warsaw, Nov. 1994, pp. 224-235

IAE Special Issue, 1995

Potemski S.,
Computer Environment for National Decision Support System in Case of Nuclear Emergency Based on RODOS system in Poland,
Proc. of Special Warsaw RODOS Seminar, Warsaw, Nov. 1994, pp. 236-247
IAE Special Issue, 1995

Borysiewicz M., Potemski S.
Heterogeneous Distributed Computer Environment for National Decision Support System for Nuclear Emergencies
Proc. of Fifth Topical Meeting on Emergency Preparedness and Response, Savannah USA, ANS pp. 366-370, 1995

Borysiewicz M., Potemski S.
Integration of emergency data management and decision support systems
to appear in Proc. of the NEA Workshop on Emergency Data Management, Zurich, Switzerland 1995

6.9 References and publications of NRIRR belonging to Section 5.2

- [1] B. Kanyar, N. Fulop
Modelling the variation of the radioactive contamination of the terrestrial food-chains due to the seasonality and measures.
Proc. of the Austrian-Italian-Hungarian Radiation Protection Symposium. Obergurgl, Austria, 1993, Vol. 2, pp. 331-335.
- [2] A. Kerekes, N. Fulop, B. Kanyar
Dose rate and dose calculation in case of time dependent intake of radionuclides.
Proc. of the Austrian-Italian-Hungarian Radiation Protection Symposium. Obergurgl, Austria, 1993, Vol. 2, pp. 249-252.
- [3] B. Kanyar
Implementation of the RODOS into the joint information system of the environmental radiation monitoring networks in Hungary.
RODOS-meeting in Interlaken, Germany, 20-24 June 1994.
Compilation volume.
- [4] B. Kanyar and N. Fulop
RODOS as a part of the information network of the environmental radiation monitoring system in Hungary.
Proc. RODOS-seminar in Warshaw, 16-19. Nov., 1994.
- [5] B. Kanyar, N. Fulop
Modelling the effects of the countermeasures to the radioactive contamination of foods.
Proc. 1st Internat. Confer in Food Physics, J. of Food Physics Suppl., 1994, Hungary.

- [6] B. Kanyar, M. Ivo, S. Tarjan and L.B. Sztanyik
Information System of the Environmental Radiation Monitoring Networks in Hungary.
Proc. Harmonisation of East-West Radioactive Pollutant Measurement, Standardisation of Techniques Considerations of Socio-Economic Factors. Budapest, August 1994.
- [7] B. Kanyar, N. Fulop, N. Glavatszkih and A. Nemeth
The laboratory type data input and processing subsystem of the country-wide environmental radiation monitoring system in Hungary.
Proc. of the Regional IRPA, 4-8. Sept. Portoroz, Slovenia, 1995 (to be appeared)

6.10 References and publications of IFIN-LAB belonging to Section 5.3

"Computer simulation of beta ray spectra for some isotopes of interest in accidental releases" in press, Romanian Journal of Physics, authors: D.Vamanu, G.Ochiana et al.).

Gheorghe A.V., Vamanu D.

"ETH-RISK: Concept and Prototype Software in Nuclear Emergency Planning, Preparedness and Management"

Polyprojekt "Risiko und Sicherheit technischer Systeme" ETH- Zurich, Polyprojekt-Bericht, 1994

Paunescu N. et al

"Method to Determine Low Levels of HTO in Air"

Rom. Journ. Phys. 40 (3), 1995

Paunescu N. et al

"Method to determine low levels of HTO in air"

Reports in Physics, 1994

Galeriu D.

"Transfer Parameters for Routine Release of HTO"

AECL Report, 11052, COG-4-76, 1994

Galeriu D.

"Dispersion of treated water in snow pack"

submitted to Journ. Environm. Radioactivity, 1995 3.1.3. 3.2.

Galeriu D., Davis P., Raskob W.

"Uncertainty and sensitivity analysis for the environmental tritium code UFOTRI"

5-th Topical Meeting on Tritium Technology in Fission, Fusion and Isotope Applications, Italy, May 1995

Davis P., Galeriu D.

"Evolution of HTO concentrations in soil, vegetation and air during an experimental chronic HT release"

5-th Topical Meeting on Tritium Technology in Fission, Fusion and Isotope Applications, Italy, May 1995

Ochiana G. et al

"Computer Simulations of Beta Ray Spectra for Some Isotopes of Interest in Accidental Releases"

Romanian Reports in Physics 1994

"Computational model for human irradiation in post-accidental evaluations" in press, Romanian Journal of Physics, authors: G.Ochiana, D.Vamanu.

Galeriu D., Trivedi. A

"Dose contribution from metabolized organically bound tritium after tritiated water intake"

Annual Health Physics Society Conference San Francisco, SUA, 26-30.06 1994

Trivedi A., Galeriu D.

"Tritium in urine from chronically exposed workers"

Annual Health Physics Society Conference San Francisco, SUA, 26-30.06 1994

Trivedi A., Richardson R.B., Galeriu D.

"Dose from organically bound tritium after acute tritiated water intake in humans"

5-th Topical Meeting on Tritium Technology in Fission, Fusion and Isotope Applications, Italy, May 1995

Galeriu D. et al

"Tritium in people living near a heavy water reactor research facility: dosimetric implication"

Joint Annual Meeting of The Health Physics Society and The American Association of Physicists in Medicine, Boston, Massachusetts, SUA, 1995

Trivedi A., Galeriu D., Takeda H.

"Interpretation of tritium retention and excretion data for dose calculations"

Joint Annual Meeting of The Health Physics Society and The American Association of Physicists in Medicine, Boston, Massachusetts, SUA, 1995

Mocanu N., Galeriu D., Margineanu R., Paunescu N.

"¹³⁷-Cs Soil-to-Plant Transfer in the Field Conditions after the Chernobyl Nuclear Accident"

Journal of Radioanalytical and Nuclear Chemistry, Vol 178, No.2, 1994 3.2.4.

Ochiana G. et al

"Computational Model for Human Irradiation in Post-Accidental Evaluations"

Romanian Reports in Physics, 1994

Mocanu N., Galeriu D., et al

"Cs-137 Soil to Plant Transfer in Field Conditions after Chernobyl Nuclear Accident"

Journ.of Radioanalyt. Chem., Vol. 178 No.2, 1994

Margineanu R. et al

"Chernobyl Cs Migration in Two Forest Soil" Rom.Journ.Phys., 1995 (in press)

RODOS-Documentation

The registration numbers are to be interpreted according to the following coding:

RODOS(P)-DC(93)n

with

(P) subproject to which the document belongs (at present A, B, C, D).

DC Document-type; three different types are distinguished

MN minutes of meetings

TN technical notes

RP reports, papers

(93) year

n consecutive number, starting each year with 01.

RODOS(B)-MN(93)01

final: 8 March 1993 RODOS coordination meeting on the further development of ASY, CSY and ESY modules - Minutes of the contractors' meeting held at Kernforschingszentrum Karlsruhe, 10 -12 February 1993

RODOS(B)-MN(93)02

final: 29 March 1993 Minutes of the RODOS Coordination Meeting on System Hardware and Software Structures, KfK, 18 February 1993

RODOS(B)-MN(93)03

final: 29 March 1993 Minutes of the RODOS coordination meeting on meteorology and atmospherical dispersion, KfK, 24-25 February 1993

RODOS(B)-MN(93)04

final: 13 April 1993 Minutes of the 1st RODOS coordination meeting with CYFRO-NET, KfK, 11 and 12 March 1993

RODOS(B)-MN(93)05

final: 30 April 1993 Minutes of the 2nd contractors meeting, Electricité de France, Paris 6 and 7 April 1993

RODOS(B)-MN(93)06

draft: 22 Nov. 1993 Minutes of the 3rd contractors meeting on RODOS subtask "Training" SCK/CEN Mol, November 15 and 15 1993

RODOS(B)-MN(93)07

Minutes of the RODOS Meeting on dose and Countermeasure Models at kfK, 16 -17 December 1993

RODOS(B)-MN(94)01
 final: 13 January 1994 Minutes of the 2-nd RODOS coordination meeting with IAE Swierk, Poland, KfK, January 12-13,1994

RODOS(B)-MN(94)02 RODOS Uncertainty meeting 2nd/3rd February 1994, Leeds University

RODOS(B)-MN(94)03
 Draft: 10 April Minutes of the 4th contractors meeting on RODOS subtask "Training", NE Barnwood, 29 - 30 March 1994

RODOS(B)-MN(94)04
 draft: 4 July 1994 Briefing on WG5 meeting in Interlaken, June 20 - 24 1994, C. Steinhauer

RODOS(B)-MN(95)01
 Draft: 7 April 1995 Minutes of the WG5 meeting in Karlsruhe, March 28-30,1995, C. Steinhauer

RODOS(B)-TN(93)01 RODOS Subtask "Training": Potential implementation of RODOS in the MOL Training Courses, 26.11.1992/SCK/CEN

RODOS(B)-TN(93)02 RODOS Subtask "Training": Collection of materail dealing with 3 training courses held at EdF, 27.1.93

RODOS(B)-TN(93)03 RODOS Subtask "Training": Proposed RODOS Training Module Suite, 10.3.93, Nuclear Electric

RODOS(B)-TN(93)04 RODOS Phase 2: FRODO-Relocation Endpoints, 19.4.1993, NRPB

RODOS(B)-TN(93)05 Concepts for the Graphics System in Prototype Version 2 of the RODOS System, 11.5.93, KfK

RODOS(B)-TN(93)06 Endpoints of the Calculations in the Foodchain Transport Module and the Dose Module, August 1993, GSF

RODOS(B)-TN(93)07 The RODOS System Phase 2
 Functional Specification of the Late Countermeasure Module FRODO, September 1993, NRPB

RODOS(B)-TN(93)08 Structure of the RODOS System - Documentation
 December 1993, KfK

RODOS(B)-TN(94)01
 Draft 14/4/94 Quality Assurance in RODOS
 Simon French, Dave Ranyard

- RODOS(B)-TN(94)02
 draft: April 1994 The RODOS System Phase 2
 Definition of Shared Common Blocks for the Late Countermeasures Module FRODO/Version 1
 Justin Smith and Phil Mansfield
- RODOS(B)-TN(94)03
 draft: June 1994 Quality Assurance for RODOS
 S. Vade
- RODOS(B)-TN(94)04
 draft: 4 July 1994 Computer Based Training Course on Off-site Emergency Response to Nuclear Accidents, C. Steinhauer
- RODOS(B)-TN(94)05
 final: 7 July 1994 Agenda, list of participants and collection of material presented at the 4th RODOS contractors meeting, Interlaken
- RODOS(B)-TN(94)06
 draft: 29. Sept. 1994 Interfaces between ECOAMOR and OSY concerning aquatic pathways
 H. Müller, GSF
- RODOS(B)-TN(94)07
 draft: December 8 1994 The RODOS System Phase 2: Documentation of the Foodchain and dose module ECOAMOR, Part V: Model Description, GSF
- RODOS(B)-TN(95)01
 final Proceedings of the Special Warsaw RODOS Seminar
 Institut of Atomic Energy, Poland
- RODOS(B)-RP(93)01 Progress Report FI3P-CT92-0036, August 1993
- RODOS(B)-RP(93)02
 final: April 1993 Models, Data and Expert Judgement in Decision Support Systems
- RODOS(B)-RP(94)01
 draft: January 1994 Multi-Attribute Decision Analysis after a Nuclear Accident
 Simon FRENCH
- RODOS(B)-RP(94)02
 final The real-time on-line decision support system RODOS for off-site emergency management
 G. Benz, J. Ehrhardt et al.
- RODOS(B)-RP(94)03
 final: October 1994 Progress Report
 Cooperation in Science and Technology with Central and Eastern

- RODOS(B)-RP(94)04
final: December 1994 Data Assimilation During the Early Phase of an Accidental Release
SCK/CEN Mol
- RODOS(B)-RP(94)05
final: December 1994 Uncertainty in RODOS
S. French, D. Ranyard, J. Smith
- RODOS(B)-RP(94)06 The Modelling Concept for the Radioactive Contamination of Waterbodies in RODOS, the Decision Support System for Nuclear Emergencies in Europe
Proceedings of the "International Seminar on Freshwater and Estuarine Radioecology, Lisbon, March 1995
W. Raskob, R. Heling, A. Popov, P. Tklich
- RODOS(B)-RP(95)01
final RODOS Database Adapter
Gang Xie, M. Rafat
- RODOS(B)-RP(95)02
final Studie zur integrierten Datenverwaltung für RODOS
Abramowicz, Koschel, Wendelgaß, Rafat
- RODOS(B)-RP(95)03
final: May 1995 Equity and MCDA in the event of a Nuclear Accident
S. French, E. Halls, D. Ranyard
- RODOS(B)-RP(95)04 Event conditional attribute modelling in decision making on a threatening nuclear accident
S. French, M.T. Harrison, D. Ranyard
- RODOS(B)-RP(95)05 Design of a decision support system for use in the event of a radiation accident
S. French, N. Papamichail, D. Ranyard, J. Smith
- RODOS(B)-RP(95)06 RODOS- a comprehensive decision support system for off-site emergency management
G.N. Kelly, J. Ehrhardt
Proceedings of the "Fifth Topical Meeting on Emergency Preparedness and Response, April 1995, pp. 8 - 11

- RODOS(B)-RP(95)07 The modelling of exposure pathways and relocation, decontamination and agricultural countermeasures in the European RODOS system
J. Brown, K. Smith, P. Mansfield, J. Smith, H. Müller
Proceeding for Oslo Conference on "International Aspects of Emergency Management and Environmental Technology, June 1995,pp 207-213
- RODOS(B)-RP(95)08 Meteorology and Atmospheric Dispersion, Simulation of Emergency Actions and Consequence Assessment in RODOS
J. Päsler-Sauer, T. Schichtel, T. Mikkelsen, S. Thykier-Nielsen
Proceeding for Oslo Conference on "International Aspects of Emergency Management and Environmental Technology, June 1995,pp 197-204
- RODOS(B)-RP(95)09 RODOS, a Real-Time On-line Decision Support System for Nuclear Emergency Management in Europe
J. Ehrhardt, F. Fischer, I. Hasemann, A. Lorenz, J. Päsler-Sauer, O. Schüle, T. Schichtel, C. Steinhauer, M. Rafat, G. Benz
Proceeding for Oslo Conference on "International Aspects of Emergency Management and Environmental Technology, June 1995,pp 188-194

Final Report

Contract FI3P-CT92-0038

Duration 1.9.1992 - 30.6.1995

Sector C24

Title **Deposition of artificial radionuclides, their subsequent relocation in the environment and implications for radiation exposure**

- | | | |
|----|----------------|------------------------------|
| 1. | J. Tschiersch | GSF, D |
| 2. | J. Roed | RISØ, DK |
| 3. | A.J.H. Goddard | ICSTM, UK |
| 4. | J. Brown | NRPB, UK |
| 5. | K. Rybáček | Inst. of Nuclear Physics, CZ |
| 6. | I. Navarcik | Inst. of Radioecology, SK |
| 7. | P. Zombori | KFKI, H |

Summary

In order to improve, where necessary, parameterizations used in estimating the intensity and spatial distribution of deposited activity and the total impact of such deposits in assessments of the consequences of accidental releases of radionuclides, several experimental studies were performed.

With the aim of improving the characterisation of the wet deposition process of radionuclides by appropriate parameters field studies have been undertaken at GSF. In addition to the measurement of the particle size distribution special emphasis was given to the simultaneous determination of the size distribution of the rain drops. A new developed rain drop spectrometer (pluvio-spectrometer) was used for that purpose. It was found that the scavenging process is strongly influenced by the rain drop size distribution. In the case of large fractions of large drops the dependence of the scavenging process even on the particle size distribution gets small, whereas in the case of a dominating large fraction of small droplets a stronger dependence on the particle size is measured. A comparison with values calculated in accident consequence codes showed that in general at lower precipitation intensities the scavenging efficiency is underestimated, but at higher intensities it tends to be overestimated. It is proposed to develop a parameterization based on particle and rain drop size distribution rather than on rain intensity only.

Deposition by fog proved to be a very efficient path for deposition. Especially for large and hygroscopic aerosol particles high deposition velocities have been measured.

The process of aerosol deposition on indoor surfaces has implications for human exposure to particulate contaminants of both outdoor and indoor origin. Indoor deposition rates have been determined by monitoring the decay of tracer aerosol in three Danish and one British house by Risø and Imperial College. Monodisperse aerosol from 0.5 to 6.5 μm in size were labelled with dysprosium and released in the houses. Sequential air samples were analysed by neutron activation. The results were consistent with increasing deposition velocities for increasing particle size and increasing degree of furnishing. An empirical formula was found by a power regression of the deposition velocity, v_d , as a function of the aerodynamic diameter of the particles, d_p : $v_d = 1.23 \times 10^{-4} \times (d_p \text{ in } \mu\text{m})^{0.65} \text{ ms}^{-1}$. Using this formula dose reduction factors were calculated as a function of particle size.

It has long been recognised that a relationship exists between the occurrence of some adverse health effects and the dermal deposition of airborne contaminants. In order to extend the database for aerosol deposition velocities to skin, and also to hair and clothing, comprehensive measurements were carried out by Imperial College and Risø in close collaboration. It was found that deposition velocities to skin are at least one order of magnitude higher than to internal building surfaces. Considerable variability exists in the values measured, partially attributable to differences in the voluntary test persons. It is suggested that the deposition velocity of aerosol particles of micrometer dimensions to skin are in the order of 10^{-2} m/s. Tests with heated and unheated aluminium cylinders indicate that the measured deposition velocity was higher to the heated surface. This finding demonstrates that body heat may be responsible for a significant proportion of the differences between the deposition velocity values observed to human and inert subjects. The volunteers differ in their arm-hair growth. More aerosol particles were deposited on a hairy arm than on a non-hairy arm, indicating the strong influence of the surface roughness on aerosol deposition velocities. Hair deposition has not been seen to differ significantly from skin deposition; however, a satisfactory protocol for determining hair surface is still under

development. A subject which must also be considered when assessing radiological risk due to aerosol deposition on the body is the efficiency of removal of the deposited material through active decontamination procedures. The removal efficiency for silica particles was found to be higher by washing than by wiping. The mean decontamination efficiency was about 52%.

After caesium depositions from the atmosphere to the ground, fields with undisturbed caesium depth distributions are a major source for the external exposure of the population. Two methods for the determination of the gamma dose rate in air due to caesium distributions in soil have been applied by GSF, Risø, INP Prague and IR Košice. The first method is soil sampling and laboratory measurements, the second method is the peak-to-valley evaluation of *in situ* gamma-ray spectra, a method that has been developed in the framework of this project. From the obtained results, gamma dose rates in air due to caesium in the soil have been calculated. These data have been analytically approximated to allow an easy use of the results in external dose assessment models. The new analytical approximations were compared to former approximations on the base of measurement results from Southern Bavaria after the Chernobyl accident and from the New York area after the atmospheric weapons test fallout. The new approach gives a better approximation to the measured data at medium and long time period after deposition.

Weathering of radioactive substances in urban areas were studied and calculation of location factors in urban dry deposition scenarios were performed by Risø and GSF. The time series of measurements of weathering on urban surfaces in the town of Gävle (Sweden) now spans over almost a decade and has provided a reference against which existing models can be validated. Weathering measurements were also made in other parts of Europe (Bavaria and Russia) and the results were found to agree very well. The weathering effect on radiocaesium on paved surfaces in Bavaria since the Chernobyl accident has been followed all the way from the early phase. Location factors were calculated for various dry deposition scenarios in houses of different shielding effect, partly based on experimental data, and it was established that indoor deposition may have great influence. Other calculations based on *in situ* gamma spectrometry in Bavarian environments (mainly wet deposition) gave location factors which were comparable with those found by the first approach for a medium shielding house.

The behaviour of long-lived radionuclides in the atmosphere: their concentration in ground level air, wet and dry deposition and resuspension, was studied. A considerable amount of experimental data based on two larger-scale nuclear accidents (Chernobyl and Goiania) was collected during the contract period and substantial contributions were provided by Risø, GSF and the PECO partners (INP Prague, IR Košice and AERI Budapest).

All contributors provided data on ^{137}Cs activity concentration in ground level air both for the case of a local contamination (GSF for Goiania) and for global contamination (PECO participants and Risø for the Chernobyl accident). Data are available for atmospheric ^{90}Sr from the IR. The concentration of ^7Be in the air was measured by IR, INP, AERI and Risø for comparison with ^{137}Cs data.

The overall trend for airborne ^{137}Cs concentration of Chernobyl origin is slightly decreasing with time in Central Eastern Europe. The same trend was found for the ^{137}Cs data on the Goiania local contamination accident site. Seasonal variation was observed, atmospheric ^{137}Cs being higher in the winter time than during the summer. In contrast, cosmogenic ^7Be was found to vary in a different way, having higher values in the summer and minima during winter. Seasonal changes in ^{137}Cs data seem to be strongly related with the rainfall rate in the Goiania experiment. A somewhat different seasonality was found for ^{90}Sr , with maxima in winter and summer and minima in spring and autumn.

Regular measurement of airborne ^{137}Cs on the long term is a good basis to derive the resuspension factor K as a function of time. A value of 10^{-9} m^{-1} in recent years (a level slowly decreasing from about $2 \times 10^{-8} \text{ m}^{-1}$ in 1986) was found to be typical in Prague. This value (K around $2 \times 10^{-9} \text{ m}^{-1}$) and trend was also confirmed on a similar surface contamination area (5.4 kBq/m^2) in Budapest and in Risø (K around 10^{-9} since 1991). The experimental data (also in the order of $10^{-9} - 10^{-8} \text{ m}^{-1}$) measured in Goiania show that the resuspension and deposition of ^{137}Cs is a local phenomenon which is, however, somewhat dependent on the extent of the primary deposition. These experimental values were compared with the K parameters used by the codes COSYMA and RODOS.

The dominance of water solubility of ^{137}Cs , observed by INP in the early-phase, air samples later changed towards an higher proportion of the insoluble fraction. This is explained by the penetration of the soluble fraction towards deeper soil layers making the soluble fraction less available for resuspension. Recently IR found that there is a seasonal variation in solubility of airborne ^{137}Cs . The prevailing form is water-soluble in the winter months, acid-soluble in the summer period and insoluble in the end of spring and start of summer. ^{90}Sr is mostly insoluble in the summer while acid-soluble form is dominant for the other seasons.

The two radionuclides observed, ^{137}Cs and ^7Be , showed a different deposition pattern. ^{137}Cs had high dry deposition velocities and showed little or no correlation with precipitation. The high deposition velocities, from 0.02 to 1 ms^{-1} , correspond to the sedimentation velocity of rather large particles, 24 to $173 \text{ }\mu\text{m}$. Estimating the size of resuspended particles in Goiania also showed that a significant fraction of the activity was present in large particles, $d_p > 15 \text{ }\mu\text{m}$. For ^7Be dry deposition velocities were found to be much smaller, around $5 \times 10^{-4} \text{ ms}^{-1}$, and a strong dependence on precipitation was observed. In summary, ^7Be showed a deposition pattern similar to that of a long-range transported radionuclide.

Concerning models used in the assessment of the consequences of accidental releases of radioactivity only little thought had been given to the behaviour of radioactive fallout deposited in an urban environment prior to the Chernobyl accident. Later the need has emerged for contingency strategies which enable the consequences of radioactive contamination of large urban areas to be identified and dealt with as early as possible following contamination. The URGENT (URban Gamma Exposure Normative Tool) and the PARATI (Program for the Assessment of RAdiological consequences in a Town and of Intervention after a radioactive contamination) models have been developed by Risø and GSF in order to facilitate the decision-making in such cases. Experimental data is used for URGENT to describe the system of retention/migration loss processes which might occur on outdoor surfaces in a radioactivity contaminated urban environment. The resulting gamma doses can then be calculated for four different urban or suburban environments using dose conversion factors. The model is restricted to cover the behaviour of the single most important radionuclide concerning external dose from urban contamination - namely ^{137}Cs . Further, a semi-empirical model has been introduced to estimate the relative importance of radiocaesium deposition on internal surfaces of buildings. Also described is a different model for radiological assessments in urban areas, PARATI, which has been developed for similar purposes. The basic functions of the PARATI code are to estimate the radiation exposures for different groups of people as a function of time after an accident with the indication of the fractional contributions to this exposure from each pathway, and to indicate the feasible countermeasures and their relative effectiveness regarding reduction of doses.

An important objective of the programme has been to review and consider the results from the experimental research with a view to their future incorporation into models. First the current models are discussed by NRPB which are used for describing deposition and relocation of material in urban and rural areas for the estimation of doses and risks used in the COSYMA code for probabilistic risk

assessment and in the RODOS code for real time emergency response. Then the available data from the experimental research carried out under this programme and the current status of research in this area are also reviewed in the context of the current models. The contractors, as a whole, have reviewed the adequacy of the current models for their given purpose and how the data from this experimental research programme could be used to improve or support the current modelling approach. This review and recommendations for changes in the models are described. As a consequence of the review some parameters used in COSYMA have been revised and recommendations are given where future research is needed to investigate in more detail first findings in identified sensitive areas.

Introduction

The research programme „Deposition of artificial radionuclides, their subsequent relocation in the environment and implications for radiation exposure“ was initiated in 1992 by the Commission of the European Communities under the Contract FI3P-CT92-0038. The main objective of the programme was to improve, where necessary, the models and their parametrizations used in estimating the intensity and spatial distribution of deposited radionuclides and the total impact of such deposits in assessments of the accidental releases of radioactivity. For that purpose several experimental studies to specific relevant problems were performed and models were developed. The results of the experimental programmes were reviewed and considered for incorporation into nuclear accident consequences assessment codes. The direct link between experimental studies, model development and the improvement of accident consequences assessment codes was one of the main features of the project.

Participants of the project were GSF-Forschungszentrum für Umwelt und Gesundheit, Germany (Coordinator), Risø National Laboratory, Denmark, National Radiological Protection Board, United Kingdom and Imperial College of Science, Technology and Medicine, United Kingdom. In 1993 the PECO-partner Institute of Radiation Dosimetry, Czech Academy of Sciences, Czech Republic, joined the programme (Supplementary Agreement CIPD-CT92-5057). Finally in 1994 the PECO-partners KFKI Atomic Energy Research Institute, Hungary and Institute of Radioecology, Slovak Academy of Sciences, Slovak Republic participated in the project (Supplementary Agreement CIPD-CT93-0432).

In chapter 1-6 of the report the experimental achievements in the research fields of aerosol deposition by rain and fog, indoor deposition and indoor inhalation dose, aerosol deposition on skin, hair and clothing, radionuclide distribution in soil and related dose rate, weathering of ¹³⁷Cs and location factors, and resuspension of deposited material are presented. In chapter 7 new models for the assessment of the radiological impact especially for inhabited areas are discussed. Finally in chapter 8 a review is made of the reported achievements in this contract in regard to improvement of the accident consequence assessment codes in use. The chapters summarise the progress of research in a certain area of radioecology by all the participants of the project (EU and PECO), demonstrating the co-ordinated character of the project on a high level of collaboration. Therefore each chapter is an independent (but cross-linked) contribution with different authors of all participating organisations working in this area. The author list is printed in the beginning of each chapter.

Notwithstanding the progress achieved in this research project, there are future needs of research in experimental radioecology. In the individual contributions crucial points for further efforts are identified and, where appropriate, recommendations are given for future research strategies. It is the general opinion in the co-ordinated project that the established links between all participants, EU and PECO, experimentalists and modelers, should be maintained for a future successful co-operation.

1. Deposition of atmospheric aerosol by rain and fog

Jochen Tschiersch, Frank Trautner and Gerhard Frank
GSF-Forschungszentrum für Umwelt und Gesundheit
Institut für Strahlenschutz
85758 Oberschleißheim
Germany

With the aim of improving the assessment of the consequences of accidental releases of radionuclides experimental investigations have been undertaken to study the influence of various weather conditions on the deposition process. In particular, weather situations which can lead to high depositions, such as intense rain or fog, are considered. Adequate parameters for the description of the deposition process are proposed for use in models dealing with deposition.

1.1 Below-cloud aerosol scavenging

In previous studies on below-cloud aerosol scavenging a large scatter in experimental results and discrepancies with theory were found (e.g. Volken and Schuhmann, 1993). Especially at low precipitation intensities, larger washout coefficients than expected were measured (Frank and Tschiersch, 1992). It appears that not all parameters determining the scavenging process were measured and used for its description.

The below-cloud aerosol scavenging process is dependent not only on the particle size but also on the size of the rain drops. At two rain events with the same precipitation intensity but different rain drop size (drizzle and persistent rain) a significantly higher scavenging coefficient for the drizzle was found. This was observed in field experiments with monodisperse tracer aerosol (Frank and Tschiersch, 1992). The construction of a new rain drop spectrometer, the pluviospectrometer (Frank et al. 1994), made it possible to quantify the rain drop size distribution of the rainfall during the scavenging measurements.

In field experiments the scavenging coefficient $\Lambda(d)$ was determined by the measurement of the decrease of the airborne particle concentration $n(d)$ during rainfall. Assuming constant atmospheric conditions $n(d)$ decreases due to particle scavenging according equation (1.1):

$$n(d,t) = n_0(d) \cdot \exp(-\Lambda(d) \cdot t) , \quad (1.1)$$

with $n_0(d)$: initial particle concentration, $t = 0$,
 d : aerodynamic particle diameter,
 t : time.

The scavenging coefficient $\Lambda(d)$ can be calculated from the measured $n(d,t)$ at two different times $t = t_1$ and $t = t_2$ before and after precipitation by

$$\Lambda(d) = \ln [n(d,t_1) / n(d,t_2)] / (t_2 - t_1) . \quad (1.2)$$

The size-fractionated particle number concentration $n(d)$ is measured with an Aerodynamic Particle Sizer (APS 3300, TSI Inc.). The device was efficiency calibrated down to a particle size of $0.6 \mu\text{m}$ diameter (Karg et al., 1991). The measuring period ($t_2 - t_1$) was 10 - 20 minutes during which the atmospheric conditions for washout remained stable (which was controlled by monitoring the relevant meteorological parameters) and the particle number in the size range $0.6 - 30 \mu\text{m}$ was large enough to measure statistically significant number differences. The corresponding rain rates have been measured with an ombrometer, the rain drop size distribution with the pluviospectrometer.

In Figs. 1.1 - 1.3 the determined washout coefficients are given for different rain rates. The figures also include the calculated values for the washout coefficients Λ as used in the accident consequence code COSYMA (Panitz and Jones, 1991) according to equation (1.3):

$$\Lambda = a \cdot (I / I_0)^b, \quad (1.3)$$

with a, b: see Table 1.1 last row

$I_0 = 1 \text{ mm/h}$

I : rain rate in mm/h.

At lower rain rates (e.g. lower than 3 mm/h) in general the experimentally determined scavenging coefficient is larger than the value calculated in COSYMA, at higher intensities (e.g. higher than 10 mm/h) it is smaller. At the particle size of about $1 \mu\text{m}$ often a minimum of the scavenging coefficient is observed. This minimum, however, can not be observed at high precipitation intensities (Fig. 1.3).

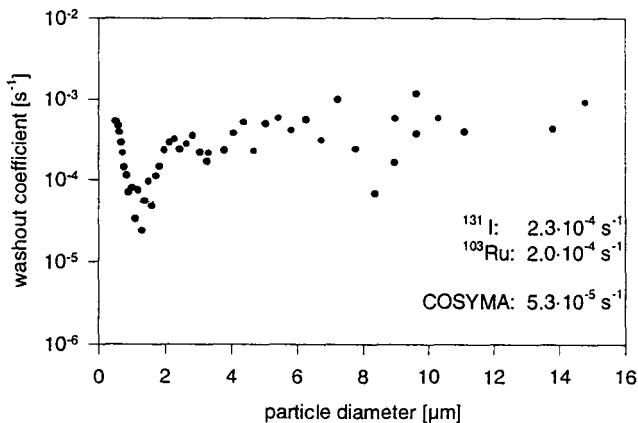


Fig. 1.1 Particle size dependent washout coefficients for a rainfall event with a rain rate of $I = 0.6 \text{ mm/h}$. The corresponding washout coefficient due to the calculations in COSYMA is indicated by the dashed line.

Because of the dependence of the washout coefficient Λ on the particle size, the experimentally determined Λ was calculated for different size distributions. According to measurements after the Chernobyl reactor accident (Tschiersch and Georgi, 1987) two different particle size distributions could be observed : an aged aerosol with an AMAD of about 0.85 μm ($\sigma = 2.0$) for ^{103}Ru and ^{137}Cs and a newer, locally formed aerosol with an activity median aerodynamic diameter (AMAD) of about 0.45 ($\sigma = 2.4$) for ^{131}I . The washout coefficients for aerosols with these size distributions are compared in Fig. 1.6 with values calculated after COSYMA. Fig. 1.6 also includes the fits of the experimental data to a function according to equation (1.3). The resulting coefficients are indicated in Table 1.1.

Table 1.1 Coefficients in equation (1.3) resulting from fits of the experimental data and corresponding values used in COSYMA.

coefficients in equation (1.3)	^{131}I	^{103}Ru	COSYMA
a	$2.8 \cdot 10^{-4}$	$2.6 \cdot 10^{-4}$	$8 \cdot 10^{-5}$
b	0.16	0.17	0.8

The experimentally observed dependence of the scavenging coefficient on the precipitation intensity has a less steep slope than would be expected from COSYMA. Again at lower intensities the scavenging coefficient is underestimated by the model. The same finding was recently made with a different approach, where the scavenging of a fluorescent tracer aerosol by precipitation was examined (Frank and Tschiersch, 1992).

The integral aerosol washout coefficient of a special precipitation event is a very complex quantity which depends on the size distribution of the aerosol as well as on the size distribution of the rains drops and, in second order, on additional environmental parameters. A description of this quantity by means of only a one-parametric relation like in equation (1.2) cannot be satisfactory. Assuming the raindrop size distribution to be an exponential decreasing function, the aerosol size distribution to be a log-normal distribution and neglecting additional parameters, a 4-parametric approach is adequate to characterise the aerosol washout behaviour of a precipitation event. This fact may explain the discrepancies which can be found when comparing the results of different authors.

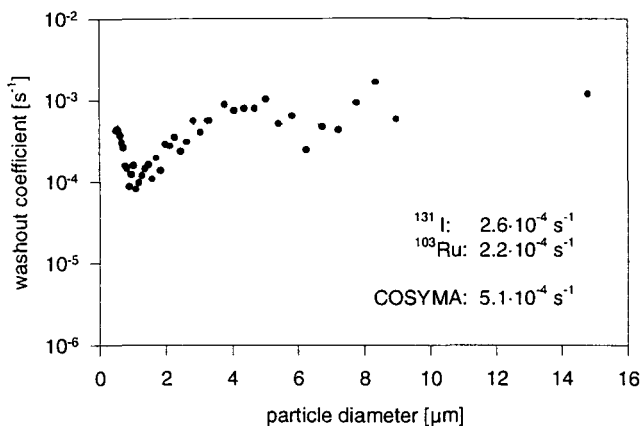


Fig. 1.2 Particle size dependent washout coefficients for a rainfall event with a rain rate of $I = 10 \text{ mm/h}$. The corresponding washout coefficient due to the calculations in COSYMA is indicated by the dashed line.

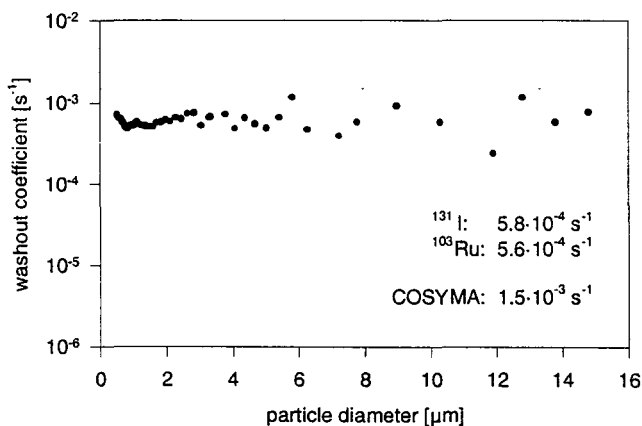


Fig. 1.3 Particle size dependent washout coefficients for a thunderstorm event with a rain rate of $I = 40 \text{ mm/h}$. The corresponding washout coefficient due to the calculations in COSYMA is indicated by the dashed line.

Comparisons of several precipitation events have shown that the washout coefficient is strongly dependent on the size distribution of the rain drops. Large fractions of large drops cause a behaviour where the sensitivity of the particle size dependence is lower, while precipitation events with a large portion of small droplets show a stronger dependence on the aerosol particle size. In Fig. 1.4 a rain drop size distribution with a large portion of small droplets is shown, the corresponding scavenging coefficients are given in Fig. 1.1. Fig. 1.5 shows a heavy shower with a large proportion of large drops; the corresponding scavenging coefficients are given in Fig. 1.3. In this case an uniform distribution with particle size is found.

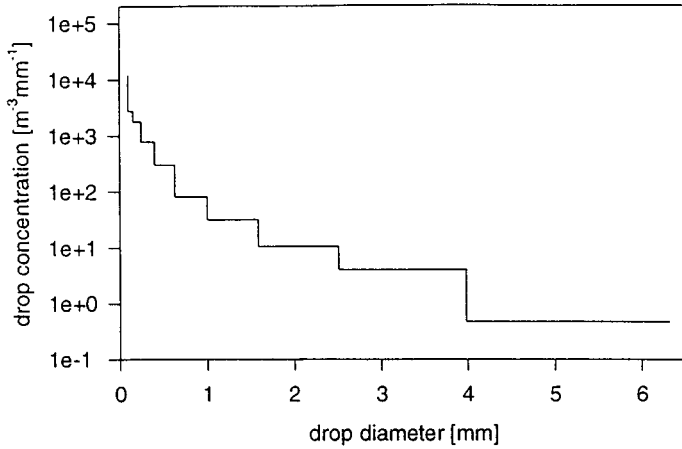


Fig. 1.4 Rain drop size distribution during a rainfall with a rain rate of $I = 0.6$ mm/h. The corresponding scavenging coefficients are given in Fig. 1.1.

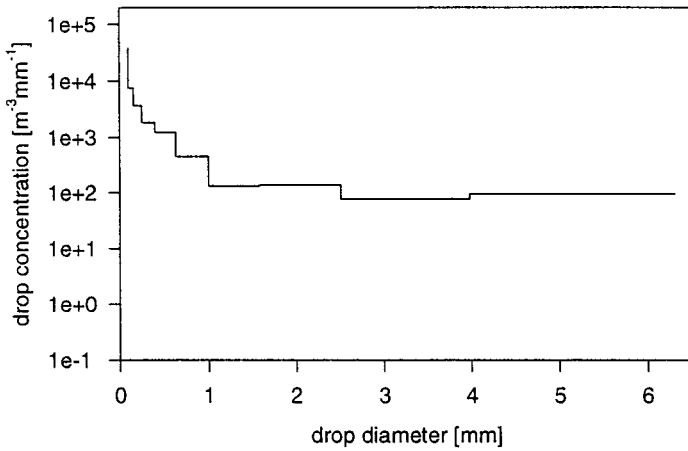


Fig. 1.5 Rain drop size distribution during a thunderstorm with a rain rate of $I = 40$ mm/h. The corresponding scavenging coefficients are given in Fig. 1.3.

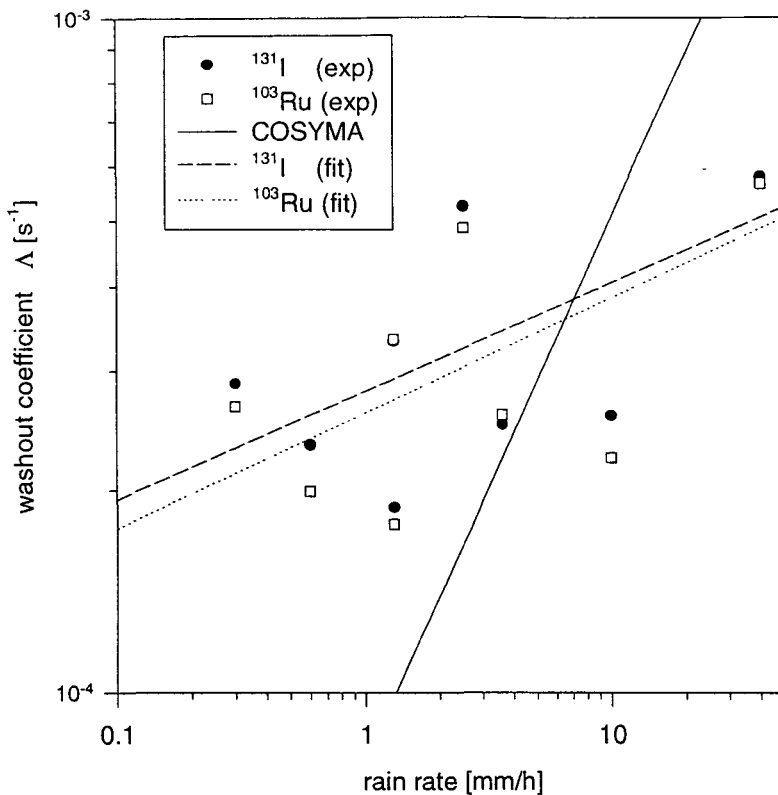


Fig. 1.6 Integral washout coefficients of several precipitation events calculated for two different aerosol size distributions (newly formed = ^{131}I , aged = ^{103}Ru) and curve used in COSYMA.

1.2 Deposition by fog

During the formation of fog, aerosol particles grow due to condensation of water vapour on the particles. Particles in the submicron and micron range can grow by condensation and coagulation to droplets in the size range 10 - 100 μm . The deposition velocity of these expanded particles is larger than for the original particles: sedimentation and impaction on obstacles like plants are more effective.

The deposition process of aerosol by fog water has been studied by field measurements with different devices. Shortly before the fog events, size fractionated aerosol samples were collected on polypropylene foils using an eight stage Berner impactor. Sampling times were between 2 and 4 hours. The liquid water content (mass of water per volume air [g/m^3]) of the fog air is assumed to be an important parameter for the deposition process. It was measured by an optical device (PVM, Gerber Scientific).

Deposited fog water and rime ice has been collected on a polyethylene surface of 0.25 m^2 diameter which is opened in the evening shortly before the fog event and closed in the early

morning. Fog water deposited on a natural surface (a grass surface of 0.42 m² was used) is registered by a balance lysimeter consisting mainly of a very sensitive balance (Mettler Inc.) which allows a weight resolution of 1 g. The change of weight of the grass during fog events corresponds to the deposition of fog water.

Aerosol samples are analysed for their elemental content using PIXE (Particle Induced X-ray Emission). Water samples are analysed for their elemental composition by ICP-AES (Inductively Coupled Plasma-Atomic Emission Spectrometry) and AAS (Atomic Absorption Spectrometry) after acidification of the samples. For sensitivity of the measuring methods see Tschiersch et al. (1989). Anions SO₄²⁻, NO₃⁻ and Cl⁻ are analysed by IC (Ion Chromatography), NH₄⁺ and pH value are analysed using electrodes.

Measurements during radiation fog events in autumn and winter show that the mass of water deposited to grass surface depends on the liquid water content of the air (Trautner et al., 1991). Assuming that the aerosol particles are the only source of the elements in the fog water, element specific deposition velocities V_d can be calculated by

$$V_d = c_{aq} \cdot f_{aq} / c_{air} \quad (1.4)$$

with c_{aq} : element concentration in fog water [µg/ml]
 f_{aq} : flux of fog water [ml/m²s]
 c_{air} : element concentration in airborne particles [µg/m³].

Mean deposition velocities for the elements Fe, Zn, Pb, S and K range from 1 · 10⁻³ to 4 · 10⁻³ m/s (see Table 1.2). The related aerosol has mass median diameters (MMD) in the range 0.2 to 1 µm (see Fig. 1.7). Ca is found in aerosol with a MMD in the range 1 to 3 µm and has a mean deposition velocity of 2 · 10⁻² m/s. The flux of fog water to the grass surface (short grass with length of less than 5 cm) was in the range 0.5 to 15 ml·m⁻²·h⁻¹.

Table 1.2 Deposition velocities for particle bound substances deposited with fogwater during eleven fog events.

distribution parameter	deposition velocity [m / s]					
	Fe	Zn	Pb	S	K	Ca
mean	0.0027	0.0022	0.001	0.0017	0.0043	0.018
maximum	0.0063	0.012	0.0052	0.0075	0.024	0.029
minimum	0.0005	0.00003	0.0002	0.0003	0.0004	0.0044

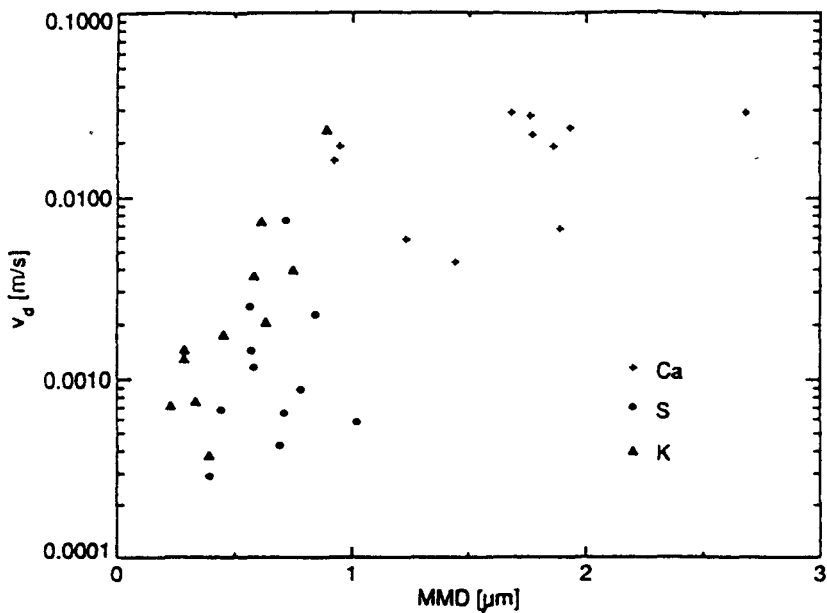


Fig.1.7 Deposition velocities V_d of different elements during fog nights in dependence of the mass median diameter (MMD) of the related aerosol particles.

1.3 Further needs of research

Concerning below cloud scavenging the rain drop size distribution seems to be very important for the deposition process. This finding is supported by another study (Bächmann et al., 1995) in which element concentrations in size-classified rain drops had been determined. There is the need to test several parametrisations for the rain drop size distribution with regard to the scavenging process. This will allow the inclusion of drop size distributions in more sophisticated models. For this purpose the experimental data base must be enlarged to make possible a generalisation of the results. There are hints that during precipitation the aerosol size distribution is changing due to hygroscopic growth (Volken and Schuhmann, 1993). To study this effect, which might explain differences between scavenging theory and experiment, the relative humidity must be tested as an additional parameter and the particle range under consideration should be enlarged to sizes smaller than 0.1 μm .

Deposition by fog is mainly dependent on the size of the finally formed fog droplets. To improve the evidence of the measurements, the fog water samples should be taken size-classified. A sampler which can collect size-fractionated airborne droplets was recently constructed.

1.4 References

Bächmann, K., I. Haag and K. Steigerwald (1995). Determination of transition metals in size-classified rain samples by atomic absorption spectrometry. *Atmospheric Environment*, Vol. 29, 175-177.

Frank, G., T. Härtl and J. Tschiersch (1994). The pluviometer: classification of falling hydrometeors via digital image processing. *Atmospheric Research*, 34, 367-378.

Frank, G. and J. Tschiersch (1992). Parametrisation of below cloud scavenging at low precipitation intensities by using a fluorescent tracer method. *J. Aerosol Sci.*, Vol. 23, S885-S888.

Karg, E., S.K. Dua and J. Tschiersch (1991). Experimental counting efficiency of the TSI aerodynamic particle sizer in the submicron range, *J. Aerosol Sci.*, Vol. 22, S351-354.

Panitz, H.J. and J.A. Jones (1991). The modelling of atmospheric dispersion and deposition in COSYMA. In: *Proceedings of the seminar on methods and codes for assessing the off-site consequences of nuclear accidents* (Eds. G.N. Kelly and F. Luyckx). CEC-Report EUR 13013 EN.

Trautner, F., G. Frank and J. Tschiersch (1991). Deposition of particle bound substances by fog and dew. *J. Aerosol Sci.*, Vol. 22, S529-S532.

Tschiersch, J. and Georgi, B. (1987). Chernobyl Fallout Size Distribution in Urban Areas. *J. Aerosol Sci.*, Vol. 18, 689-692.

Tschiersch, J., B. Hietel and P. Schramel (1989). Wet deposition of aerosol: test of the method. *J. Aerosol Sci.*, Vol.20, 1181-1184.

Volken, M. and T. Schuhmann (1993). A critical review of below-cloud aerosol scavenging results on Mt. Rigi. *Water, Air, and Soil Pollution*, 68, 15-28.

2. Indoor deposition measurements and implications for indoor inhalation dose

Christian Lange and Jørn Roed
Risø National Laboratory, MIL-114
4000 Roskilde
Denmark

Miriam A. Byrne and Antony J. H. Goddard
Imperial College of Science, Technology and Medicine
London SW7 2BX
United Kingdom

Abstract

The process of aerosol deposition on indoor surfaces has implications for human exposure to particulate contaminants of both outdoor and indoor origin. Indoor deposition rates have been determined by monitoring the decay of tracer aerosol in three Danish and one British house. Monodisperse aerosol from 0.5 to 6.5 μm in size were labelled with dysprosium and released in the houses. Sequential air samples were analysed by neutron activation. The results were consistent with increasing deposition velocities for increasing particle size and increasing degree of furnishing. An empirical formula was found by a power regression of the deposition velocity, v_d , as a function of the aerodynamic diameter of the particles, d_p : $v_d = 1.23 \times 10^{-4} \times (d_p \text{ in } \mu\text{m})^{0.65} \text{ ms}^{-1}$ ($r = 0.96$). Using this formula dose reduction factors were calculated as a function of particle size.

2.1 Introduction

When an accident occurs that involves releases to the atmosphere of toxic materials the first action of the civil defence authorities is to urge people to go indoors and close the windows and doors. It is assumed that the house will offer some protection against the inhalation of airborne gases and particles.

A review of measurements of Indoor/Outdoor concentration of airborne pollutants reveals that most substances of outdoor origin have a lower concentration in indoor air. Alzona et al. (1979) investigated I/O ratios for airborne metals using X-ray fluorescence. The mean I/O value ranged from 0.1 to 0.42 depending on the element. Filtration by the building envelope, indoor deposition and resuspension were the parameters considered in the modelling of the results. Filtration by the building envelope was considered to be of minor importance since experiments performed with windows open, where filtration should be close to zero, still yielded a 50% reduction of indoor concentration levels. Experiments where pumps were moved out of the test room and filters were changed with a minimum of human presence did not show any difference from earlier experiments and from this they concluded that resuspension due to human and mechanical activity probably was of minor importance for the

I/O ratio. Cohen and Cohen (1979) measured I/O ratios at 20 sites in Pittsburgh using X-ray fluorescence of Ca, Fe, Zn, Pb and Br. From measurements in the literature of the typical size distributions of each element they divided the result into a sub-micron and supra micron set. For the sub-micron particles their best estimate was a dose reduction factor, DRF, of 0.5 and for larger particles they found a DRF of 0.25. The conclusions of this review are that the DRF or I/O ratios generally lie between 0.2 and 0.5 with the largest reductions for coarse particles.

To establish a platform for discussion, it is useful to establish an equation describing the problem and to identify the parameters of interest. This requires a definition of the mechanisms determining indoor concentration of pollutants of outdoor origin and their interaction. First it will be useful to define a term that describe our objective, namely a measure of the reduction in inhalation dose achievable by sheltering indoors. Since inhalation dose is directly proportional to air concentration (for a given particle size) the dose reduction factor, DRF, can be defined theoretically as the ratio between the indoor pollutant concentration, C_i , and the outdoor pollutant concentration, C_o , integrated from the start of the cloud passage, t_0 , to infinity:

$$DRF = \frac{\int_{t_0}^{\infty} C_i dt}{\int_{t_0}^{\infty} C_o dt} \quad (2.1)$$

Considering the house to be a single box with an air exchange with an infinite outdoor volume a simple differential equation can be derived by equating the change in indoor concentration per unit time with the difference between the production (ingression from the outside) and loss of particles (indoor deposition). This equation can be solved analytically and the solution shows this equation is that the time integrated DRF equals the equilibrium ratio for constant outdoor pollutant concentration:

$$DRF = \frac{\int_{t_0}^{\infty} C_i(t) dt}{\int_{t_0}^{\infty} C_o(t) dt} = f \frac{\lambda_r}{\lambda_r + \lambda_d} \quad (2.2)$$

where f is the fraction of particles in outdoor air penetrating the building envelope, λ_r is the air exchange rate and λ_d is the deposition constant. This is a general result for all shapes of passing clouds, as emphasized by Roed et al. (1991), when it is assumed that λ_r and λ_d are constant. The air exchange rate, λ_r , may change if the weather conditions change, but in all circumstances the value used in modeling will be an average value, which again will give an average value for the dose reduction factor. The deposition constant, λ_d , will vary with the particle size, but for each size class and type of pollutant the expression will be valid. Some authors, e.g. Engelmann (1992), have given a more optimistic expression for the DRF by including a term describing ventilation of the house right after the passage of an rectangular cloud and thus reducing or removing the contribution to dose from the 'tail' after passage. From equation (2.2) three parameters of importance can be identified: the air exchange rate, λ_r , the filter factor of the building envelope, f , and the deposition constant, λ_d .

Indoor deposition is the least well known parameter determining the indoor inhalation dose. Very little information exists on the deposition of particles larger than 0.5 μm in houses. In order to improve our understanding of the mechanisms governing the indoor-outdoor air activity ratio Imperial College and Risø National Laboratory have developed a technique to measure the deposition in houses for different particle sizes.

2.2 Experimental technique

During a previous CEC research contract Imperial College and Risø National Laboratory developed a technique where silica particles were labelled with dysprosium and used as tracers for indoor deposition experiments. The idea was to disperse the particles in a real house and measure the decrease in tracer concentration by taking consecutive air filter samples. During the experiment, the air-exchange rate was to be measured and the deposition constant, λ_d was then to be found by subtracting the air exchange rate, λ_r , from the decay constant, λ_c :

$$\lambda_d = \lambda_c - \lambda_r \quad (2.3)$$

The air-exchange rate was measured by releasing SF₆ gas into the test room and monitoring the decrease in concentration by gas chromatography. The absolute decrease with time of both the tracer gas and the particle concentration is proportional to the concentration and the decay will thus follow an exponential curve if the experimental conditions are constant during the test. Both these decay constants are found by linear regression. For all the four houses studied the deposition velocity, v_d , has been calculated using the geometric surface, S, to volume, V, ratio. That is, no contribution from the surface of furniture, etc. has been included in the surface area of the furnished rooms. Such measurements would be difficult to make in an objective and reproducible way.

$$v_d = \frac{(\lambda_c - \lambda_r)V}{S} \quad (2.4)$$

The deposition constant, λ_d , is found by subtracting the air exchange rate, λ_r , from the decay constant, λ_c . The average deposition velocity is found by multiplication with the volume to surface ratio, V/S, as shown in equation (2.4). The calculation of a v_d makes it possible to compare the results from different houses. For instance, the average ceiling height in Risø Huse 27, the Danish house where the first measurements were made, was half a meter higher than in the other test houses and this will give a different deposition constant, but the average v_d should be similar to that found in other houses. Furthermore, the average v_d can be used to estimate deposition constants in rooms with different S/V ratios than those used for the experiments.

2.2.1 The particles

During the research two types of particles have been used. Monodisperse silica particles labelled with dysprosium bought in 4 nominal sizes and a nebulization of a indium-acetyl-acetate powder in alcohol. The five-particle sizes used are summarized in Table 2.1.

Table 2.1 Review of particles used in the house experiments. The APS diameter is the median volume aerodynamic diameter. The Geometric Standard Deviation, GSD, is for a log-normal fit to the distribution. The last column gives the number of particles you need in one sample to achieve one gamma-emission per second after irradiation for 10 minutes by a thermal flux of $37 \times 10^{15} \text{ Nm}^{-2}\text{s}^{-1}$.

Nominal size	AD diameter	GSD	Volume of one Particle	Gram tracer per particle	Number of particles
[μm]	[μm]	[]	[μm^3]	[10^{-15}g]	for 1 g.e.s^{-1}
-	0.48	1.60	0.058	13.3	209
1	2.5	1.48	8.18	40.9	47
3	3	1.20	14.14	70.7	27
5	4.5	1.07	33.51	167.6	11
10	5.5	1.18	87.11	435.6	4.4

2.2.2 Summary of experimental technique

- Particles labelled with rare-earth elements are released in the test room.
- SF_6 tracer gas is released in the test room with all doors and windows closed.
- After the release 10 to 12 air samples are made each of 10 minutes duration. Each filter paper is handle with a forceps and sealed in separate bags immediately after use. The volume of air sucked through each filter is measured with a gas meter.
- The decay of the SF_6 tracer gas is monitored using gas chromatography. After the test the air exchange rate is worked out by a linear regression of the logarithm of the tracer concentration and the measurement time.
- The air samples are neutron activated and the activity content in each filter is determined by gamma spectrometry. The activity per volume of air is found by dividing with volume of air in the individual samples and the decay constant is found by linear regression.
- The deposition constant is found by subtracting the air exchange rate from the decay constant. The average deposition velocity is found by multiplying the deposition constant with the volume to surface ratio of the room.

2.3 Results and discussion

The method used have proven to give reasonable results as reported by Roed et al. (1991). The decay curves for the first four experiments have been shown in Figure 2.1. As can be seen from the figure all four tests had very straight decay curves ($r > 0.999$ in all cases) and the results were consistent with increasing deposition velocity for increasing particle size and degree of furnishing. Indoor deposition rates have been measured in one house during a previous CEC contract and in three new houses during this contract. Results and a detailed description of the individual experiments have been given by Roed et al. (1991), Byrne (1995) and Lange (1995). Despite the differences between the test conditions in the various houses, the results are in good agreement. Table 2.2 shows the average results for furnished and unfurnished rooms. As tests only were made with furniture in the room during the Jersey experiment there is actually only 'unfurnished' results from three houses. In all experiments, the deposition velocity was highest in the furnished houses. In Table 2.2 the deposition can also be seen to increase with particle size as predicted by deposition theory for supra-micron particles, but the actual deposition velocities exceeds those predicted by the theories that only includes gravitational settling by a factor of 2 to 5 as can be seen in Table 2.3. When the results were compared with the measurements of indoor deposition presented in Roed & Cannell (1987). In Table 2 good agreement was observed. For Be-7 which is associated with particles in the size range of 0.5 to 1.0 μm , Lange (1994), an average deposition velocity of $0.71 \times 10^{-4} \text{ ms}^{-1}$ was found. The indium particles had a AMAD of 0.5 to 0.7 μm , which is close to that of Be-7, and the deposition velocity has been found to be $0.61 \times 10^{-4} \text{ ms}^{-1}$ for unfurnished rooms and $0.82 \times 10^{-4} \text{ ms}^{-1}$ for a furnished room on average. Roed and Cannell found a v_d of 3.1 to $3.9 \times 10^{-4} \text{ ms}^{-1}$ for Ce-144. This corresponds to the v_d of 4 or 5.5 μm particles in Table 4.9 and this would be reasonable size for cerium as it belongs to refractory group of release products as described in Rulik et al. (1987).

Table 2.2 Measurements of indoor Deposition Velocities in four houses. The first two columns show size and geometric standard deviation, GSD, of the test aerosol. The last two columns gives the average deposition to all surfaces measured in three different test houses. The numbers in the parentheses give the number of tests for each condition.

Size	GSD	Avg. v_d Unfurnished	Avg. v_d Furnished
[μm]	[]	[10^{-4} ms^{-1}]	[10^{-4} ms^{-1}]
0.5	1.60	$0.61 \pm 0.08(2)$	$0.82 \pm 0.08(6)$
2	1.48	$1.13 \pm 0.16(5)$	$1.36 \pm 0.50(5)$
3	1.20	$1.33 \pm 0.37(2)$	2.25(1)
4	1.07	$2.42 \pm 0.17(5)$	$3.11 \pm 0.6(5)$
5.5	1.18	$3.03 \pm 0.04(2)$	3.24(1)

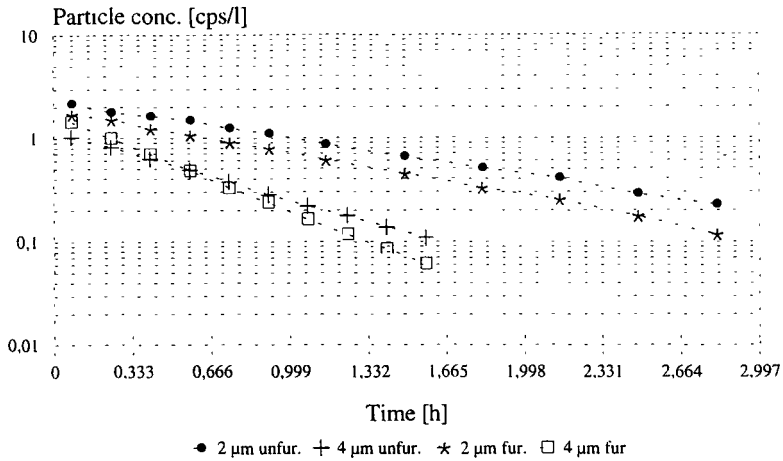


Figure 2.1 First results obtained with the tracer particles as reported by Roed et al. (1991). The decay curves were steeper for the larger particles and when furniture was present in the room. This deposition pattern together with the straight decay curves implied that the experimental technique used produced reliable and useful results.

Table 2.3 Review of experimental results and theoretical values of average indoor deposition velocities. The second and third column gives the values obtained by the I/O impactor experiment in Ferslev reported in Lange (1995). The column termed silica particles have been obtained by using the empirical formula given by equation (2.5). The 'Nazaroff & Cass' and 'Sehmel' column was obtained by reading the figures in the respective papers. The last column gives the theoretical sedimentation velocity for a particle of the given size.

Size	Be-7 Natural air-ex.	Be-7 Forced air-ex.	Silica particles	Nazaroff & Cass(1989)	Sehmel (1973)	v_g Reist(1984)
[μm]	[10^{-4}ms^{-1}]	[10^{-4}ms^{-1}]	[10^{-4}ms^{-1}]	[10^{-4}ms^{-1}]	[10^{-4}ms^{-1}]	[10^{-4}ms^{-1}]
0.35	0.19	0.17	-	0.04-0.07	0.08-0.25	0.05
0.71	0.17	1.33	0.98	0.06-0.09	0.3-0.4	0.19
1.4	0.13	2.66	1.53	0.2	1.0-1.5	0.66
2.8	0.67	3.88	2.40	0.6	3-10	2.48
5.5	-	-	3.03	2.2	15-100	9.29

In Table 2.3 the experimental results obtained from the Be-7 experiments and from the indoor deposition measurements using artificial tracers are compared with the theoretical results obtained by Nazaroff & Cass (1989) and the wind tunnel results of Sehmel (1973). In general the theoretical predictions of Nazaroff & Cass are similar to the deposition velocities measured in the unoccupied houses with Be-7 as a tracer and a natural air exchange. The deposition velocities measured with artificial tracers were about 4 times larger than these values in the size range from 0.5 to 2.8 μm . This increase in deposition velocity must be attributed to the presence of scientists, pumps and other equipment in the test room created an increased air motion and additional surface for deposition. When a forced air-exchange was applied the deposition velocities increased both in Vellerup and Ferslev and again it must be attributed to the increased air motion.

2.3.1 Empirical models for indoor deposition

Two data sets were selected where the correlation coefficients were better than 0.95 for the tracer aerosol decay curves. Twelve results from unfurnished houses and fifteen results from furnished houses were chosen. Experiments where small mixing fans were operated during the test have been included in these data sets. A power regression and a linear regression have been made for the two data sets, expressing the deposition velocity as a function of the particle size. Average deposition velocity was chosen rather than the deposition constant in order to take the different surface to volume ratios of the test rooms into account. Equation (2.5) shows the power regression expressions found for the furnished rooms. The correlation coefficient is given in the parentheses:

$$v_d = 1.23(d_p)^{0.65}, \quad (r = 0.96) \quad (2.5)$$

where v_d is the average deposition velocity to all surfaces and d_p is the particle diameter. In both the unfurnished and the furnished rooms the power regression had the best correlation coefficient, i.e. 0.96 compared to 0.90 and 0.95. The deposition velocity was found to increase with the 0.71 and the 0.65 power of d_p . This clearly is not in line with the theoretical predictions of Nazaroff and Cass (1989) that for particles larger than 1 μm the deposition velocity should increase according to the square of the diameter of a particle. Also the deposition velocities found were much greater than those predicted by the theories presented by Nazaroff and Cass. However, the magnitude of the v_d 's measured in this work are in good agreement with the experimental results by Schneider et al. (1994). They found that the deposition velocity increased linearly with the particle size in the particle size range investigated. Since the formulae presented in equations (2.3) to (2.5) are purely empirical, it must be emphasised that they are not valid outside the particle size range investigated, i.e. 0.5 to 5.5 μm .

2.3.2 A simple model for the protective value of a house.

Engelmann (1992) made an important point when he noted that estimates of the protection offered by buildings in case accidents involving releases to the atmosphere should be realistic and not conservative if an optimum emergency response is to be achieved. When the civil defence authorities need to decide between evacuation or sheltering they need to have a realistic picture of the consequences in order to make the correct decision. Present models of the effect of sheltering during releases of radioactive materials to the atmosphere consist of a single factor giving a common dose reduction factor, DRF, for all nuclides. A value of 0.5 is currently used in probabilistic accident consequence assessment codes, Brown (1989) (except noble gases for which DRF = 1.0, i.e. no reduction in inhalation due to indoor residence). In order to provide a more realistic model that takes into account properties of the released

material the empirical formula for indoor deposition is used together with equation (2.2) to calculate dose reduction factors. Equation (2.6) shows the derived formula:

$$DRF = \frac{\lambda_r(U_{wind}, \Delta T)}{S/V - 1.23(d_p)^{0.65} + \lambda_r(U_{wind}, \Delta T)} \quad (2.6)$$

where the deposition constant, λ_d , is found by multiplying the average deposition velocity with an average S/V ratio for the buildings in question. In the review by Engelmann (1992) surface to volume ratios were summarised for a number of different buildings: 1.74 m^{-1} for apartment buildings/houses, 1.3 m^{-1} for office buildings and 0.66 m^{-1} for industrial buildings. These values do not include contributions from furniture and equipment in the room. The average S/V of the test rooms was 1.69 m^{-1} and a value of 1.7 m^{-1} has been used in the model calculations shown in Figure 2.2.

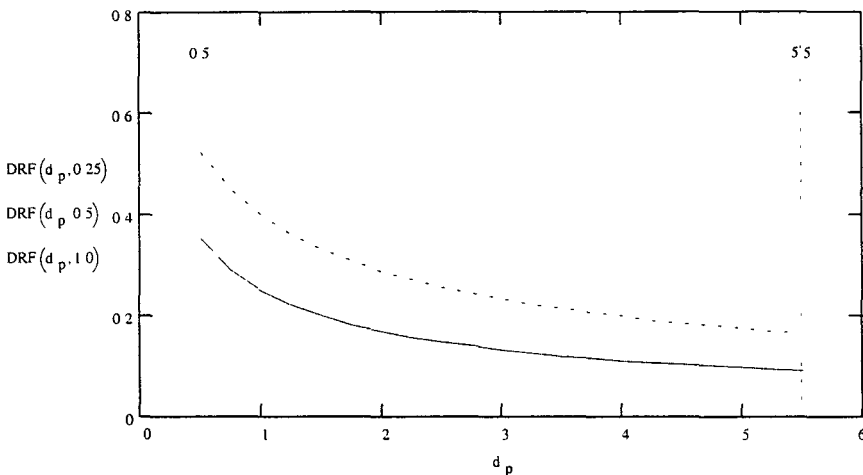


Figure 2.2 DRF's as function of the particle size in μm and the air-exchange rate. The number after ' d_p ' in the left margin of the figure is the air-exchange rate for that line style. A surface to volume ratio of 1.7 m^{-1} have been used corresponding to a medium sized living room. The vertical lines indicate the valid particle size range, i.e. 0.5 to 5.5 μm .

The air-exchange rate can be expressed as a function of the weather conditions, outdoor temperature and wind speed. The temperature difference over the building envelope can be expressed as the difference between the outdoor temperature and the indoor temperature, typically about $21 \text{ }^\circ\text{C}$. The air-exchange rate was determined as a function of these parameters for a typical Danish houses by Kvisgaard et al. (1988). In Figure 2.2 the DRF is plotted as a function of particle size for three different values of the air-exchange rate. An assumed surface to volume ratio of 1.7 m^{-1} was used in these calculations. It can be seen that the DRF decreases significantly with particle size. The three values for the air-exchange rate used (0.25 , 0.5 and 1.0 h^{-1}) represents a low, medium and high value and the DRF varies between 0.1 and 0.7 or factor of seven depending on the particle size for these air-exchange rates. These relatively large variations in DRF clearly justifies a more detailed model for the DRF.

In 1986 the reactor unit no. 4 at the Chernobyl nuclear power plant blew up and the biggest release to the atmosphere of radioactive material from a nuclear power plant occurred. Some information was obtained on the size distribution of the released nuclides, especially in western

Europe, partly to investigate isotope specific DRFs that could be assumed for the release products and partly to suggest DRFs that might apply in future situations. With the equation derived here for the protective effect of houses protection factors were calculated for the three main groups of Chernobyl aerosol for a house with $\lambda_r = 0.5 \text{ h}^{-1}$:

- Particulate iodine: The AMAD of particulate iodine was about $d_p = 0.5 \text{ }\mu\text{m}$ (e.g. Tschiersch and Georgi (1987)) and from this a DRF of 0.5 is obtained.
- The volatile group: Cs-137 had an aerodynamic diameter of $d_p = 1.0 \text{ }\mu\text{m}$ can be assumed (e.g. Jost et al. (1986)), and that leads to a DRF of 0.4.
- The refractory group: For this group that includes the fuel fragments an AMAD of $4 \text{ }\mu\text{m}$ at some distances from the point of release can be assumed (e.g. Rulik et al. (1989)) leading to a DRF of 0.2. Closer to the plant much larger particles was present and the DRF would be even smaller.

Current accident models assume a uniform DRF of 0.5 for indoor residence. The results presented here suggest that an isotope-specific DRF would be justified with lower DRFs for the refractory group. Particle size measurements closer to the accident site plant would probably have recorded an even larger AMAD for this group and subsequently an even better DRF. The variation in the DRF depends on the activity size distribution of the isotope, and that is dependent on the properties of the corresponding chemical element.

2.3.4 Temporal variations of the Indoor / Outdoor ratio.

Several authors, as discussed in the introduction, believed that increased ventilation after passage of a cloud of radioactive particles is an important part of the potential DRF. To examine this view the differential equation for the one-box house model has been solved numerically for a non-rectangular cloud passage. As the effect of ventilation will be greatest for particles with a lower deposition velocity (they remain airborne longer) a deposition constant of $\lambda_d = 0.4$ (corresponding to the minimum deposition velocity observed for a $0.5 \text{ }\mu\text{m}$ particle, app. $0.6 \times 10^{-5} \text{ ms}^{-1}$) was assumed in the calculations. The cloud passage has been described by a stepwise linear function (the dotted line in Figures 2.3). For 100 minutes the outdoor concentration was assumed to increase linearly to a pollutant concentration of 100 in arbitrary units, it then stayed constant for 100 minutes and then it declined linearly for 100 minutes. A solution has been calculated for two values of λ_r : 0.4 h^{-1} corresponding to the average for Danish houses and 0.8 h^{-1} , which is a suitable value for a British houses. The equilibrium ratio between indoor and outdoor concentration is shown by the broken line and the indoor concentration is shown by the solid line in Figures 2.3.

By comparing the indoor and outdoor concentrations shown in figure 2.3 it can be seen that there will be a significant time delay from the start of the decline of the outdoor concentration until the indoor concentration is actually higher than the outdoor concentration. The exact time for this will under all circumstances be impossible to detect in case of an accident as it will differ from house to house. From a practical point of view the earliest time for advising the public to open doors and windows must be when the outdoor concentration approaches zero. If it is assumed that the persons under shelter breathe clean air from this moment a reduction in the inhalation dose of 19 % will be achieved. This value is for nearly optimal conditions: a slowly depositing particle in a reasonably well sealed house, for a cloud passage of short duration and without including a time delay from the cloud passage and until confirmed noticed

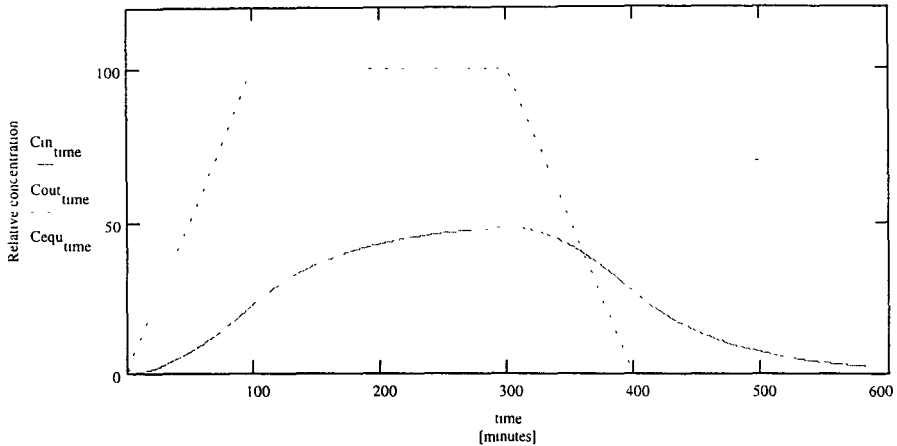


Figure 2.3 Non-rectangular cloud passage and equilibrium ratio for $\lambda_r = 0.4 \text{ h}^{-1}$. The outdoor concentration, C_{out} , is given by the dashed line. The equilibrium concentration, C_{equ} , is given by the semi dashed line and the indoor concentration, C_{in} , is given by the solid line.

can broadcast to people in a specific area. If the air-exchange rate is increased to 0.8 h^{-1} a reduction of only 10 % will be obtained. In all these calculations it has been assumed that the indoor pollutant concentration could be reduced immediately by opening door and windows but even in this case the air exchange might be rather slow especially in weather with little or no wind and the achieved reduction will be lower. For cloud passages of longer duration, for larger particles with a higher deposition velocity and for more leaky houses the reduction due to ventilation after the cloud passage becomes negligible.

Such uncertain possibilities for dose reduction do not justify the incorporation of ventilation after cloud passage as an inherent part of the Dose Reduction Factor, but of course the civil defence authorities should keep the positive effect in mind in case of an accident and encourage ventilation after a toxic release has passed an inhabited area, especially if the release involves slowly depositing gases.

2.4 References

- Alzona, J.; Cohen, B.L.; Rudolph, H.; Jow, H.N. and J.O. Frohlinger, Indoor-outdoor relationships for airborne particulate matter of outdoor origin, Atmospheric Environment, Vol. 13, pp. 55-60, 1979.
- Brown, J., Sheltering in the event of an accident. Atom 389, pp. 17-19, 1989.
- Byrne, M. An experimental study of the deposition of aerosol on indoor surfaces, Ph.D. dissertation, Imperial College, London, 1995.
- Cohen, A.F. and B.L. Cohen, Infiltration of Particulate Matter into Buildings, SAND79-2079, NUREG/CR-1151, (1979).

- Engelmann, R.J. Sheltering effectiveness against plutonium provided by buildings. *Atmospheric Environment*. Vol. 26A, No. 11, pp. 2037-2044, 1992.
- Jost, D.T.; Gaggeler, H.W.; Baltensperger, U.; Zinder, B. and P. Haller, Chernobyl fallout in size-fractionated aerosol, *Nature*, Vol. 324, pp. 22-23, 1986.
- Lange, C., Size distribution of atmospheric particles containing Beryllium-7. *Journal of Aerosol Science*, Vol. 25, S1, pp. 55-56, 1994.
- Lange, C., Indoor deposition and The protective effect of houses against airborne pollution, *Risø-R-780(EN)*, 1995.
- Nazaroff, W.W. and G.R. Cass, Mathematical Modelling of Indoor Aerosol Dynamics, *Environmental Science and Technology*, Vol. 23, No. 2, 1989.
- Rasmussen, N.C. et al. Reactor Safety Study - WASH 1400. U.S. Nuclear Regulatory Commission, Washington, D.C. 1975.
- Reineking, A.; Becker, K.H.; Porstendörfer J. and A. Wicke, Air Activity Concentrations and Particle Size Distributions of the Chernobyl Aerosol, *Radiation Protection Dosimetry*, Vol. 19, No. 3, pp. 159 - 163, 1987.
- Reist, P.C., *Introduction to Aerosol Science*, Macmillan Publishing Company, New York, 1984.
- Roed, J. & R.J. Cannell. Relationship between Indoor and Outdoor aerosol concentration following the Chernobyl accident. *Radiation Protection Dosimetry*, Vol. 21, No. 1/3, pp. 107-110, 1987.
- Roed, J.; Goddard, A.J.H.; MacCurtain, J.; Byrne, M. & C. Lange. Reduction of Dose from Radioactive Matter ingressed in Buildings. *Cadarache*, 1991.
- Rulik, P.; Bucina, I. and I. Malatova, Aerosol Particle Size Distribution in Dependence on the Type of Radionuclide after the Chernobyl Accident end in the NPP effluents, *Proceedings of the XVth Regional Congress of IRPA on the Radioecology of Natural and Artificial Radionuclides*. Sweden, FS-89-48T, 1013-4506, 1989.
- Schneider, T.; Bohgard, M. and A. Gudmundsson, A semiempirical model for particle deposition onto facial skin and eyes. Role of air currents and electrical fields, *Journal of Aerosol Science*, Vol. 25, 3, pp. 583-593, 1994.
- Tschiersch, J. and B. Georgi, Chernobyl Fallout Size Distribution in Urban Areas, *J. of Aerosol Science*, Vol. 18, No. 6, pp. 689-692, 1987.



3. Aerosol deposition on skin, hair and clothing

Miriam A. Byrne and Antony J. H. Goddard
Imperial College of Science, Technology and Medicine
London SW7 2BX
United Kingdom

Christian Lange and Jørn Roed
Risø National Laboratory, MIL-114
4000 Roskilde
Denmark

3.1 Introduction

It has long been recognised that a relationship exists between the occurrence of some adverse health effects and the dermal deposition of airborne contaminants; in the radiological context, Jones (1990) has shown that the predicted number of early deaths arising due to radiation doses from deposited aerosol material is sensitive to the value used for the aerosol deposition velocity to skin. In the derivation of emergency reference levels for countermeasure introduction following accidental atmospheric releases of radioactivity, a deposition velocity value, for 1 mm particles to skin, of 10^{-3} ms^{-1} was used by Linsley et al. (1986); this value was inferred from a limited experimental database. In order to extend the database for aerosol deposition velocities to skin, and also to hair and clothing, comprehensive measurements were carried out during the contract period by Risø and Imperial College, with the research groups from the two institutions working in close collaboration. The following sections of this chapter describe experimental design considerations, test procedures adopted and results obtained.

3.2 Experimental Methodology

3.2.1 Selection of test subjects

A preliminary measurement, carried out during a series of deposition velocity measurements to indoor surfaces conducted at Ferslev, Denmark (described in Chapter 2 of this report and also in Lange (1993)), which involved the analysis of a skin wipe from one of the experimentalists, indicated that the deposition velocity to human body surfaces is at least an order of magnitude higher than that to internal building surfaces. A review of the limited number of earlier measurements indicates some of the factors which might contribute to this enhancement. The earliest recorded measurements are those of Asset & Pury (1954), who studied the deposition of $6.5 \mu\text{m}$ particles, on volunteers' arms (hairy and non-hairy) in a wind tunnel at two windspeeds: 2.2 m/s and 0.88 m/s; increasing windspeed and body hair growth were both observed to enhance aerosol deposition velocity. A value of 10^{-3} m/s for the deposition velocity of 1 mm particles to skin can be inferred from these measurements, which were hindered by a low detection sensitivity for the tracer aerosol used. A later series of measurements, carried out by Parker et al (1990), did not aim to determine actual deposition

velocity values, but simply the effect of body heat on local aerosol concentration; the measurements were carried out using an aerosol of mass median diameter $0.5 \mu\text{m}$ and an anthropomorphic phantom which was periodically heated. The application of heat to the phantom was seen to increase the aerosol concentration flux towards the surface. More recent measurements have involved the use of phantoms which are also anthropomorphic but are non-heated; aerosol deposition measurements on the eyes of an unheated phantom, by direct surface sampling and aerosol concentration monitoring, were made by Gudmundsson et al (1992) using particles in the aerodynamic size range $2\text{-}32 \mu\text{m}$ in a wind tunnel. Measurements were made with the phantom at various orientations with respect to the wind direction and for various degrees of turbulence. Values in the range 10^{-4} - $2.7 \times 10^{-3} \text{ms}^{-1}$ to the eyes of the phantom were reported. Additional aerosol deposition velocity values, in the range 6×10^{-4} - $9.8 \times 10^{-3} \text{ms}^{-1}$, to the forehead of the same phantom, are presented by Schneider et al (1994).

In summary, the early results indicate that human factors (for example, body temperature and hairiness) are important influences on aerosol deposition but that environmental factors may also contribute. It was decided that a comprehensive series of aerosol deposition velocity measurements should be carried out using human volunteers; it was considered that the use of phantoms would not be representative since the human body has complex surface characteristics (notably heat, roughness, electrostatic nature, and humidity) and also exhibits breathing and animation. Although the use of a limited number of volunteers may not completely span the extensive range of human body surface characteristics which exist, analysis of even a small population would identify those human characteristics which have the greatest influence and therefore merit the greatest attention. In addition, the effect of environmental conditions on aerosol deposition velocity to the body may be assessed by the use of a small population sample.

3.2.2 Selection of test aerosol

Neutron activatable tracer-labelled aerosol has been extensively used by Risø and Imperial College in experiments designed to measure indoor aerosol deposition velocities; the particle labelling techniques, experimental procedures and results have been discussed in Chapter 2 of this report (and Byrne et al, 1992). These tracers are particularly suitable for aerosol deposition velocity measurements to the human body; they can be detected, when deposited on surfaces, with a very high sensitivity, which means that aerosol concentrations below the occupational exposure limits for inhalation can be used. Neither silica or indium are toxidermic substances at the low concentrations used and no adverse health effects are expected should dermal penetration occur via skin pores and hair follicles. In addition, neither silica or indium are water soluble, so that percutaneous absorption is unlikely.

The four aerosols available for this work are described in Table 3.1. The size distributions of these aerosols span a large proportion of the range relevant to accidental radioactive emissions; the aerodynamic median diameter of Chernobyl-associated aerosol was $0.5 \mu\text{m}$ for particulate iodine (Tschiersch & Georgi, 1987), $1.0 \mu\text{m}$ for the volatile elements (Jost et al, 1986) and $4.0 \mu\text{m}$ for the refractory elements (Rulik et al, 1989).

Table 3.1 Description of the four aerosol size distributions used.

Particle size (MMAD*)	σ_{g+}	Tracer label	Aerosol generation method
0.5 μm	1.36	¹¹³ In	Nebulisation/inertial separation
2.5 μm	1.50	¹⁶⁴ Dy	Dispersion of labelled silica
4.5 μm	1.10	¹⁶⁴ Dy	Dispersion of labelled silica
5.4 μm	1.30	¹⁶⁴ Dy	Dispersion of labelled silica

* MMAD= mass mean aerodynamic diameter; σ_{g+} =geometric standard deviation

3.2.3 Aerosol mass balance tests

V_d , the aerosol deposition velocity to an individual surface, can be expressed as follows:

$$V_d = F/X \quad (3.1)$$

where F is the ratio of the mass flux to the surface per unit area per unit time and X is the mean aerosol concentration some distance from that surface, where the aerosol is well-mixed. The maintenance of an aerosol concentration which does not deviate significantly from the mean value involves the use of extensive recirculation ducting and results in considerable expense due to aerosol particle losses. For this reason, the aerosol deposition velocity measurements reported here are made following a single aerosol injection event, after which the aerosol concentration decays exponentially; the high detection sensitivity afforded by the use of neutron-activatable aerosol allows experimental durations to be minimised, so that large aerosol concentration gradients are avoided.

Measurements at Risø and Imperial College have shown that the average deposition velocity to all the surfaces of a room, calculated by analysis of sequential air samples, is comparable to the value obtained by direct sampling of selected surfaces, extrapolated over the whole area. In order to make aerosol mass balance checks which have greater relevance to deposition on the human body, rigorous experiments were carried out in the Imperial College test chamber to ensure that the aerosol particle mass deposited on a body suspended in the centre of the chamber could be estimated by calculating the difference between the mass removed from the air (from air sample analysis) and the mass deposited on the internal chamber surfaces (measured by direct surface sampling). As shown in Byrne et al (1995), agreement within a factor of two was found between the measured and estimated values. This technique, successfully applied to the case of an inanimate object with uniform surface characteristics, could, in principle, be applied to estimate, in a non-invasive way, the global aerosol deposition velocity to an entire human body. In practice, however, risk assessment calculations related to humans require deposition velocity data for more specific regions of the body, for example, the areas likely to be uncovered by clothing, i.e. the hands and face, so that invasive analysis of small samples is more appropriate.

3.3 Experimental Configuration

A typical experiment, designed to measure aerosol deposition velocities to human body surfaces, proceeds as follows: a human volunteer is seated in the centre of the test room, with at least one lower forearm exposed; the other forearm, if not bare, is covered with a piece of smooth fabric (in some of the UK tests, rough fabric samples were also used). A pulse of tracer gas is injected into the room and a small fan is used to aid mixing until a detector registers the same gas concentration at all the individual sampling points. The aerosol generator is then activated and a period of aerosol dispersal (typically of 2-3 minutes duration) follows, during which small fans are used to aid mixing. Sequential air filter samples, each of approximately ten minutes duration, are collected at the centre of the room by the human volunteer, who otherwise remains stationary (while engaging in some light activity, such as reading, or using a computer). The experimental duration is in the range 0.3 - 1.5 hours. Air velocity fluctuations, relative humidity and temperature in the room are recorded automatically throughout the experimental period. At the end of this period, the volunteer leaves the room and some, or all, of the following samples are collected:

- * wipe samples from the face
- * wipe samples from the bare forearm(s)
- * fabric samples (smooth and/or rough) from the covered forearm
- * hair samples

The wipes, hair samples and fabric samples are then analysed for tracer aerosol particle content by neutron activation analysis.

Five series of tests have been carried out in this work; Table 3.2 summaries the investigations.

Table 3.2 A summary of the experimental configurations used.

Series Number	Enclosure Type	Number of Volunteers	Samples Collected
1	Room in UK test house	1	skin wipes (face&arms) rough & smooth clothing hair samples
2	Room in Danish house	1	skin wipes (face &arms) smooth clothing hair samples
3	UK room-sized test chamber	1	skin wipes (face & arms) smooth clothing
4	Danish office	2	skin wipes (face & arms)
5	Danish office	2	skin wipes (arms)

3.4 Experimental Results

Table 3.3 shows representative values for deposition velocities to skin, obtained in the five test series. Comparing these values with those in Chapter 2, it can be seen that deposition velocities to skin are at least an order of magnitude higher than to internal building surfaces.

Table 3.3 Aerosol deposition velocity data for skin surfaces. Each value is derived from during only one measurement period (with several consecutive wipes of the sample area), unless a bold superscript indicates otherwise. The percentage uncertainties associated with each value are shown in parentheses.

Surface	Aerosol deposition velocity* (10^{-4} ms $^{-1}$)			
	0.5 μ m	2.5 μ m	4.5 μ m	5.4 μ m
Series 1				
Arm	----	13.1 (3%)	37.6 (2%)	463 (2%)
Face	---	11.0 (2%)	43.0 (3%)	213 (2%)
Series 2				
Arm	2.07 ⁵ (32%)	16.7 ² (22%)	16.22 ² (25%)	39.45
Face	2.61 ⁵ (40%)	19.41 ² (21%)	21.17	60.16
Series 3				
Arm	15.0 (22%)	17.2 (11%)	29.0 (35%)	62.2 (13%)
Face	20.4 (23%)	20.2 (33%)	15.7 (46%)	124 (80%)
Series 4				
Arm (1)	13.47 (8%)	81.6 (18%)	—	—
Arm (2)	8.19 (14%)	63.5 (21%)	—	—
Face (1)	5.92 (14%)	66.1 (21%)	—	—
Face (2)	7.25 (14%)	33.3 (44%)	—	—
Series 5				
Arm (1) ^{**}	4.1 ³ (64%)	94.8 ³ (55%)	—	—
Arm (2) ^{**}	16.6 ³ (54%)	167.0 ³ (51%)	—	—

* : 100% tracer recovery assumed

** : each value represents an average of samples from several locations on the arm; in parentheses s.d. on the averaged values is given

Considerable variability exists in the values shown in Table 3.3, partially attributable to differences in volunteer characteristics and also, notably, to the absence of a standardised skin wiping protocol. The procedure used in the measurements to date has involved making consecutive wipes (up to five) on the test area; water was used as a wetting agent by Imperial College, while Risø used ethanol. It was assumed that tracer recovery by this process should be unity. However, subsequent to the aerosol deposition velocity measurements, tests carried out on in-vitro skin at Imperial College have shown that 5 consecutive skin wipes results in a recovery of 15-40% of the 4.5 µm tracer aerosol particles, indicating that the deposition velocities values presented in Table 3.3 may be up to six times higher. These wiping efficiency assessments were carried out using water; no such tests have yet been carried out using ethanol but since the solubility of silica in ethanol is similar to its solubility in water (i.e. close to zero in both cases), the recovery efficiency may not be significantly different. Bearing these considerations in mind, it is suggested that the deposition velocity of aerosol particles of micrometre dimensions to skin may be of the order of 10^{-2} m/s and that the values shown in Table 3.3 should be regarded as lower bounds.

In addition to the overall conclusion that deposition velocities to skin are appreciably higher than to inert surfaces, several observations can be made by analysing the results of the individual test series, as discussed below.

(1) As indicated in Table 3.2, deposition velocities to hair and clothing were determined in test series 1-3. Figure 3.1 shows the measured deposition velocities to various body surfaces, determined in Series 1(Imperial College). It can be seen that higher deposition velocities were observed to the bare skin of the volunteer's forearm than to the forearm covered with fabric and that this difference was reduced when rough fabric was used. This phenomenon was also observed in the Imperial College test chamber measurements (Series 3) but not in any of the Danish tests, highlighting the necessity for urgent standardisation of skin wiping protocols.

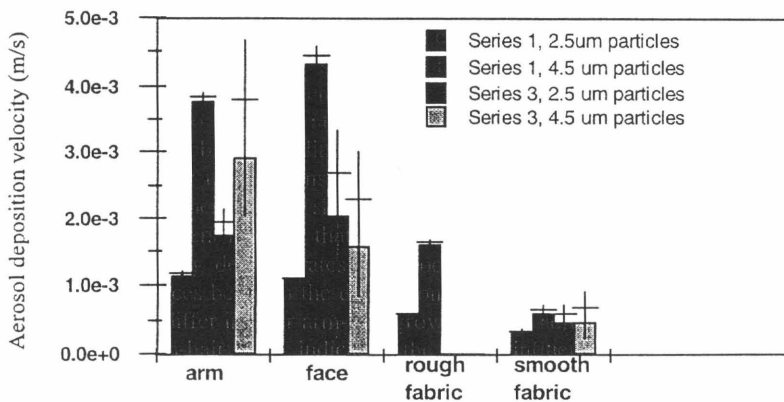


Figure 3.1 Measured aerosol deposition velocity values to skin and fabric surfaces.

(2) As already indicated, it is likely that a combination of human factors contribute to the large aerosol deposition velocity values to human body surfaces shown in Table 3.3. In an attempt to estimate the magnitude of the effect on aerosol deposition of one isolated factor- the temperature difference between a human body and its surroundings- an aluminium cylinder, of comparable dimensions to the torso of a human volunteer was incorporated in both series of tests carried out by Imperial College (Series 1 & 3). In Series 1, the cylinder was unheated and in Series 3, the cylinder was heated to body temperature. In both cases, filter papers, placed on the top and side of the cylinder during the aerosol deposition period, were collected for analysis. Table 3.4 compares the measured deposition velocity to the volunteer's arm (normalised to unity) with the deposition velocity to the heated and unheated cylinder surfaces, for 2.5 μm particles. The results indicate that the measured deposition velocity was higher to the heated surface; this is in agreement with the observation of Parker et al (1990) that the aerosol concentration (analogous to deposition velocity) close to a heated phantom was higher than close to an unheated phantom. It should be noted that the relative magnitudes of the values for the cylinder and the skin are biased by differences in tracer recovery efficiencies (the skin was sampled with non-unity efficiency by wiping, whereas filter paper samples were collected directly from the cylinder surface); it is the *difference* between the values for the heated and unheated cylinder cases, relative to skin, which is of particular interest. It can be seen that body heat may be responsible for a significant proportion of the difference between the deposition velocity values observed to human and inert subjects.

Table 3.4 Comparative deposition velocities, for two aerosol particle size distributions, to the arm of a volunteer and to heated and unheated aluminium cylinders; the deposition velocity to the arm is given the value unity.

Arm	Cylinder top (heated)	Cylinder top (unheated)	
1	0.53	0.23	[0.5 μm particles]
1	0.71	0.16	[2.5 μm particles]

(3) The later tests carried out by Risø (Series 4 and 5) are particularly informative since, in all cases, two volunteers were involved who were subjected to identical environmental conditions and sampling procedures. Figure 3.2 shows the measured deposition velocity to the arms of the two volunteers, from one test in Series 5. Considerably higher values were observed for volunteer 2, who had prolific arm-hair growth, compared with volunteer 1 who had minimal arm-hair growth, indicating the strong influence of surface roughness on aerosol deposition velocities. This observation is in agreement with the early measurements of Asset & Pury (1954), who observed that, at a wind-speed of 2.2 m/s, nine times more aerosol was deposited on a hairy arm than on a non-hairy arm.

(4) The implications of aerosol deposition on the hair of the head also merit consideration in radiological risk assessment since (a) the significant roughness of the hair surface is likely to enhance aerosol deposition and (b) the proportion of body surface area covered by head hair may, in many cases, be considerable. Some semi-anecdotal evidence of high deposition velocities to hair exists; Mackie et al (1994) observed, by gamma tomography of hospital staff

members who became contaminated during administration of Tc-labelled aerosol to patients, that the greatest surface contamination was on the hair. In the tests carried out by Imperial College & Risø under the current contract, hair deposition has not been seen to differ significantly from skin deposition; however, a satisfactory protocol for determining hair surface area is still under development. In the Imperial College measurements, deposition velocities were calculated on the basis of the area of a small hair sample; the Risø measurements (where a complete haircut was performed), based on the area of the entire head of hair, yielded deposition velocity values which differed from deposition velocity values to skin by no more than a factor of two.

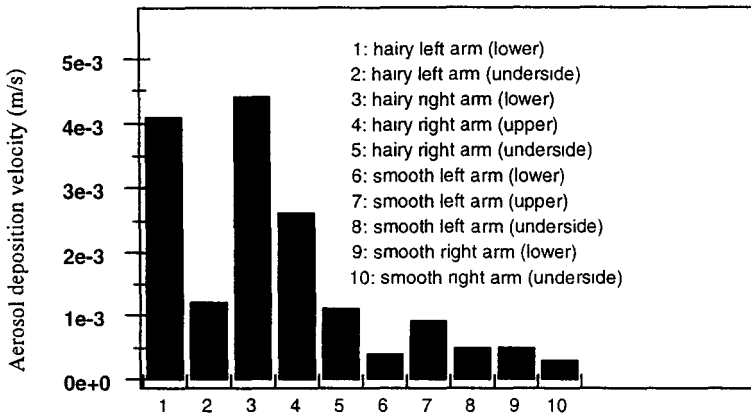


Figure 3.2 Measured deposition velocities of 0.5 μm aerosol particles to the arms of two volunteers- one hairy and one smooth.

(5) A subject which must also be considered when assessing radiological risk due to aerosol deposition on the body is the efficiency of removal of the deposited material through active decontamination procedures. Decontamination data for body surfaces is extremely limited. The wipe efficiency tests carried out under this contract by Imperial College indicate that wiping, within minutes of the end of a 2 hour contamination period, is not a fully efficient means of removal of particulate contaminants from the skin. A small number of tests of the efficiency of removal of tracer particles from hair have been carried out at Imperial College, by comparing hair samples collected before and after normal washing of the head. A summary of the decontamination data is presented in Table 3.5.

Based on the limited data available (and making the assumption that decontamination of hair occurs in the same way as decontamination of skin), the removal efficiency for silica particles by washing is higher than by wiping; this seems reasonable if it is considered that the act of wiping may drive particles into crevices/ pores in the skin structure. The difference in removal efficiency of 0.5 μm indium particles and larger silica particles from hair is thought to be attributable more to the difference in solubility and surface characteristics of the two species than to the difference in particle size. The mean decontamination efficiency, based on the data in Table 3.5, is 52% (s.d. = 28%).

Table 3.5 A summary of the decontamination data generated in this work.

Contaminant	Decontamination procedure	% Removal efficiency
5.4 μm silica particles	water soaked wipes (5 consecutive) -on skin	28+/- 13 (8)
5.4 μm , 2.5 μm silica particles	washing (water, no detergent) -of hair	64 +/- 14 (2)
0.5 μm indium particles	washing (water, no detergent) -of hair	15

3.5 Recommendations for Future Research

The results of the work reported in this chapter indicate that aerosol deposition velocities to human body surfaces are appreciably greater than to inert surfaces, adding further weight to the suggestion of Jones (1990) that skin deposition is an important dose pathway. It is clear from the measurements performed that human factors contribute to these elevated values; earlier work suggests that environmental factors also contribute. In order to provide the ability to make realistic assessments of which population sectors are most at risk from aerosol deposition on body surfaces in the aftermath of nuclear accidents, it is recommended that the work reported here is continued in the following key areas:

(1) Measurements have been reported which illustrate, by use of phantoms, the influence of body heat on aerosol deposition, relative to other human factors (such as charge, humidity, hairiness, breathing, movement). Further tests of this type could be designed to examine other human factors in isolation which would provide elucidation of the results of volunteer studies.

(2) It has been shown by Imperial College that skin wiping has a large associated variability in tracer recovery efficiency. Since accurate aerosol deposition velocity data can only be obtained using a skin sampling technique which has a consistent, quantifiable tracer recovery efficiency, work is underway to standardise skin sampling procedures (some of the variables are the number of wipes used, the wetting agent used and the pressure applied in wiping). In addition, the tracer recovery efficiency of other skin sampling techniques is under investigation.

(3) The measurements reported have been carried out at low air-flow rates and air turbulence levels which are characteristic of the indoor (domestic and occupational) environment. In order to extend the relevance of these data to other sectors of the population, the measurements should be extended, by use of volunteers and phantoms in wind tunnels, to consider conditions which are representative of the outdoor environment. It is expected that some enhancement of aerosol deposition velocities to human body surfaces may occur under outdoor environmental conditions; the early measurements of Asset & Pury (1954) showed that, by varying the wind-tunnel air-speed from 0.88 m/s to 2.2 m/s, the aerosol deposition velocity to the arm of a volunteer could be increased by a factor of five.

(4) Preliminary measurements on decontamination efficiency of hair and skin have been reported. To increase the relevance of these data, measurements spanning a greater range of

decontamination procedures are desirable; in addition, the database should be extended to consider the decontamination of clothing, covering both normal fabrics and those worn in the occupational environment. A non-invasive system for fluorescent aerosol detection has been recently developed at Imperial College so that the rate of body surface decontamination due to normal human activity (i.e. in the absence of active cleaning procedures) can be addressed.

To supplement the data generated in this work, a thorough search of the literature should be conducted to obtain relevant information from accounts of radioactive aerosol spillages, and subsequent worker decontamination procedures, in the industrial context.

3.6 References

- Asset, G., D. Pury, Deposition of wind-borne particles on human skin. Archives of Industrial Hygiene and Occupational Medicine, 9, No.4, 273-283, 1954.
- Byrne, M.A., Lange C., Goddard A.J.H., J. Roed, Indoor aerosol deposition studies using neutron activatable tracers. Journal of Aerosol Science 23, Suppl. 1, S543-S546, 1992.
- Byrne, M.A., Goddard, A.J.H., Lange, C., J. Roed, Stable tracer aerosol deposition measurements in a test chamber. Journal of Aerosol Science, 26, No.4, 645-653, 1995.
- Gudmussion, A., Schneider, T., Petersen, O.H., Vinzents, P.S., Bohgard, M., K.R. Akselsson, Determination of particle deposition velocity onto the human eye. Journal of Aerosol Science, 23 Suppl. 1, S563-S566, 1992.
- Jones, J.A., The importance of deposition to skin in accident consequence assessments. EUR 13013, 1990.
- Jost, D.T., Gaggeler, H.W., Baltensperger, U., Zinder B., P. Haller, Chernobyl fallout in size-fractionated aerosol. Nature, 324, 22-23, 1986.
- Lange, C., Roed, J., Byrne, M.A., A.J.H. Goddard, Indoor aerosol deposition studies using rare-earth tagged particles. Journal of Aerosol Science, 25, Suppl. 1, S571-S572, 1994.
- Linsley, G.R., Crick, M.J., Simmonds, J.R., S.M. Haywood, Derived emergency reference levels for the introduction of countermeasures in the early stages of emergencies involving release of radioactive materials in the atmosphere. NRPB Report DL10, 1986.
- Mackie, A., Hart, G.C., Ibbett, D.A., R.J.S. Whitehead, Airborne radioactive contamination following aerosol ventilation studies. Nuclear Medicine Communications, 15, 161-167, 1994.
- Rulik, P., Bucina, I., I. Malatova, Aerosol particle size distributions in dependence on the type of radionuclide after the Chernobyl accident and in the NPP effluents. Proceedings of the XVth Regional Congress of IRPA, FS-89-48T, 1013-4506, 1989.
- Schneider, T., Bohgard, M., A. Gudmundsson, A semi-empirical model for particle deposition onto the facial skin and eyes. Role of air currents and electric fields. Journal of Aerosol Science, 25, No.3, 583-594, 1994.
- Tschiersch, J., B. Georgi, Chernobyl fallout size distribution in urban areas. Journal of Aerosol Science, 18, No. 6, 689-692, 1987.

4. Radionuclide distributions in undisturbed soil and related gamma dose rates in air

P. Jacob, R. Meckbach, U. Hillmann
GSF Forschungszentrum für Umwelt und Gesundheit, Institut für Strahlenschutz
85764 Oberschleißheim
Germany

K.G. Andersson, J. Roed
Risø National Laboratory
4000 Roskilde
Denmark

S. Palágyi, J. Palágyi
Institute of Nuclear Physics, Academy of Sciences of Czech Republic
18086 Prague 8
Czech Republic

A. Mitro
Institute of Radioecology, j.s.c.
04061 Kosice
Slovak Republic

After caesium depositions from the atmosphere to the ground, fields with undisturbed caesium depth distributions are a major source for the external exposure of the population (Jacob and Meckbach, 1987). Possible countermeasures such as ploughing or the removal of the upper soil layer are not considered here. Two methods for the determination of the gamma dose rate in air due to caesium distributions in soil have been applied in the current project. The first method is soil sampling and laboratory measurements, the second method is the peak-to-valley evaluation of *in situ* gamma-ray spectra, a method that has been developed in the framework of this project. From the obtained results, gamma dose rates in air due to caesium in the soil have been calculated. These data have been analytically approximated to allow an easy use of the results in external dose assessment models.

4.1 Caesium and strontium migration in column experiments

The distributions of ^{137}Cs and ^{85}Sr in undisturbed agricultural soils have been studied during their irrigation with atmospheric precipitation in dependence on time under laboratory conditions for about one year. The influence of grass cover and zeolite on the migration has been investigated.

In the experiments soil samples, mostly of chernozem and brown soil type (with 2.1-2.9% of organic matter), were taken from 4 localities in the environment of the Dukovany Nuclear Power Plant (NPP) and from 4 localities in the vicinity of the Bohunice NPP. The size of the undisturbed soil cylinders were 9 cm in diameter and 20 cm in height. The samples were put into columns made of 1 l polyethylene bottles cutting their bottoms off and placed upside

down. The soil profiles were contaminated on their surface with aqueous solutions of $^{137}\text{CsCl}$ and $^{85}\text{SrCl}_2$. The zeolite was applied on the surface of the soil profiles in the amount of 5 g/sample. Then the irrigation of soil cylinders were started and repeated successively in weekly intervals with the collected wet fallout in the amount corresponding to the long term average of atmospheric precipitation. After the elapsed time of observation, the cylinders were cut into discs of 0.5 or 1.0 cm thickness and counted by Ge(Li) gamma spectrometry.

The migration rate decreased with time for both radionuclides. The ratio of Cs:Sr migration rates is around 2 for the corresponding soil samples and their rates have reached values of 1.4-8.1 cm/year, according to the type of soils and their agrochemical properties. The migration rates of ^{137}Cs in soils with grass cover are between 1.2-2.1 cm/year and those of ^{85}Sr 2.3-3.1 cm/year. The corresponding values for soils with applied zeolite are between 1.0-3.5 cm/year and 1.8-4.3 cm/year, respectively.

From the results obtained it follows that the majority of radiocaesium is retained in the 1 cm layer of soil: after 5 months about 94% and after 12 months 78%. Radiostrontium has a greater tendency to move along the vertical soil profile and after 5 months about 50% and 12 months 31% remains only in 1 cm layer. The presence of the grass cover, in accordance with the reported migration rates, causes an increase of the retention of mainly ^{85}Sr : after 5 months of about 66% and after 12 months 40%. The application of zeolite is effective in retardation of radiostrontium for a relatively shorter time: 5 months around 72% and 12 months 40%, but after about 5 months it causes a certain remobilization of ^{137}Cs and its retention decreases in comparison with untreated soils: 5 months around 92% and 12 months 60%.

The values of the migration rate constant in the 0.5 cm layer are higher than in the 1.0 cm layer for each radionuclide in all soil profiles. The migration rate constants of ^{137}Cs for 0.5 cm layers of soils are between $1.2-2.3 \times 10^{-3} \text{ d}^{-1}$ and for ^{85}Sr lie between $6.3-12.2 \times 10^{-3} \text{ d}^{-1}$. The migration rates in 1.0 cm layers are between $0.3-2.0 \times 10^{-3} \text{ d}^{-1}$ for 5 months and $0.4-3.2 \times 10^{-3} \text{ d}^{-1}$ for 12 months observation of radiocaesium and $3.5-8.7 \times 10^{-3} \text{ d}^{-1}$ for 5 months and $2.5-4.1 \times 10^{-3} \text{ d}^{-1}$ for 12 months observation of radiostrontium migration. In average, the ratio of the respective values for ^{137}Cs to the values for ^{85}Sr are 4.9 in 0.5 cm layers and 7.0 or 2.8 in 1.0 cm layers of soil profiles. These last two numbers also indicate the decrease of the difference in radiostrontium and radiocaesium rate constants in the first and in the second 0.5 cm soil layers. In accordance with the tendency of migration rates, the migration rate constants are also negatively influenced by the presence of the grass cover in the case of ^{85}Sr , whereas it has no influence on the rate constants for ^{137}Cs . The application of zeolite has similar effect as the presence of the grass cover, but it is limited to several months only.

The migration rate constants can be implemented in relations used to evaluate the extent of resuspension of radionuclides from ground surface following their deposition.

4.2 Measurements of caesium distributions by soil sampling

RISØ has measured depth distributions at Gävle in Sweden during summer 1994. Figure 4.1 shows the dependence of the soil density $\rho(z)$ from the depth z in the ground for five sites. The density changes from about 0.4 g cm^{-3} at the uppermost surface layer to about 1.5 g cm^{-3} at a depth of 12 cm. Due to this considerable change of the soil density with depth, for a determination of gamma dose rates in air it is not sufficient to know the caesium activity distribution as a function of depth. For this purpose the mass per unit area $\zeta(\text{g} \cdot \text{cm}^{-2})$ above a given source element (Rybacek et al. 1992, ICRU 1995)

$$\zeta = \int_0^z \rho(z') \cdot dz', \quad (4.1)$$

has to be known.

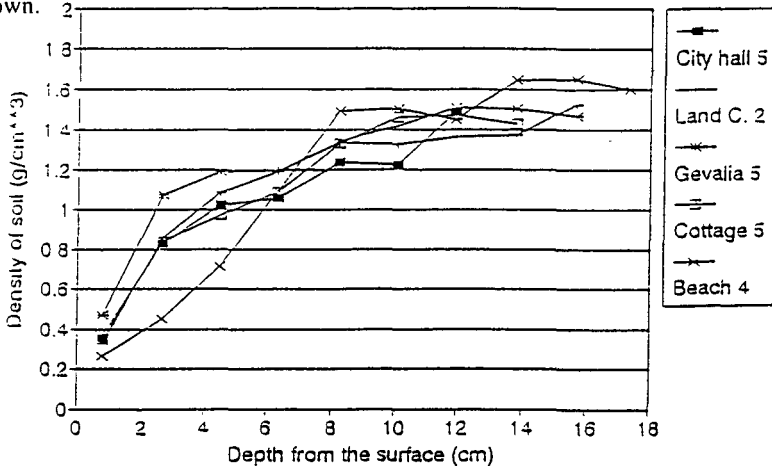


Figure 4.1 Density of the soil as a function of the depth in the ground at five sites in Gävle, Sweden. The figures behind the names of the sites indicate the number of depth profiles that have been taken at the corresponding site.

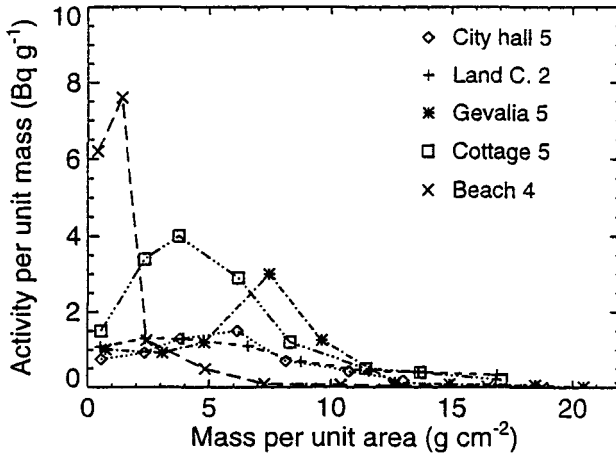


Figure 4.2 Cs-137 activity distributions in soil in June 1994 at five sites in Gävle, Sweden. The figures behind the names of the sites indicate the number of profile samples that have been taken at the corresponding site.

The caesium distributions in soil obtained by RISØ in Gävle, Sweden, in September 1994 are shown in Fig. 4.2. The position of the maximum caesium activity per unit mass varies between 3 cm for the beach to 6 cm for the sites Gevalia and City Hall. These depths correspond to soil masses per unit area of $1.5 \text{ g} \cdot \text{cm}^{-2}$. The caesium activity per unit mass in the uppermost sampling layer was smaller by a factor of 1.2 to 3 than in the sampling layer with the maximum caesium activity per unit mass.

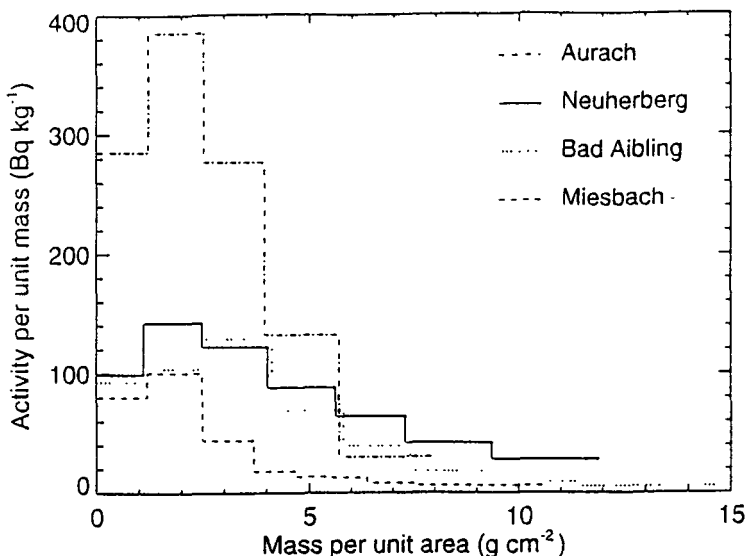


Figure 4.3 Cs-134 activity distributions in September/October 1990 at four sites in Southern Bavaria.

GSF analysed caesium distributions in soil at four sites in Southern Bavaria (Jacob et al. 1994). To avoid disturbances by atomic weapons tests fallout, Cs-134 distributions were studied. At each of the sites at least five profiles each with a cross section of 18 cm² were measured, averaged distributions are shown in Fig. 4.3. The position of the maximum caesium activity per unit area varied between depths corresponding to 1.5 g cm⁻² and 3 g cm⁻². The caesium activity per unit mass in the uppermost sampling layer was smaller by a factor of 1.2 to 1.4 than in the sampling layer with the maximum caesium activity per unit mass. In the framework of the project ECP5 "The behaviour of radionuclides in natural and semi-natural environments" caesium distributions in soil were measured in July 1993 at ten sites in Southern Bavaria (Hillmann et al., 1995). As in the previous study the atomic weapons tests fallout was separated from the Chernobyl deposit. For the caesium deposited after Chernobyl maximum activities per unit mass were found in the range of 1.9 g cm⁻² to 4.4 g cm⁻².

The three studies give consistent results, showing how the maximum activity per unit area migrates from its initial location at the surface to deeper layers.

4.3 Analytical approximation of caesium distributions in soil

Soil sampling is an appropriate method to determine caesium distributions in soil and related gamma dose rates in air (Jacob et al. 1994). However, the method is time consuming and many profiles need to be known for deriving a reliable model of external exposures, since the migration depends on the characteristics of the deposit (physico-chemical form and weather conditions during deposition) and of the site (soil properties and meteorological conditions) and since the time dependence of the process also has to be studied. Alternative methods that

* Project supported by the EC under the contract COSU-C593-0043

allow the determination the gamma dose rate in air due to the deposited caesium in a less labour-intensive way have been developed.

The first method is to measure the activity per unit area at a site once and then to perform a time series of *in situ* gamma-ray spectrometry at the site. Assuming an exponential shape of the caesium distribution in the soil, effective exponential distributions of the caesium in the soil may be derived from the measurements. This method has been shown give good results as long as the caesium distributions in the soil do not deviate too much from the exponential shape (Jacob et al. 1994). For sites in Southern Bavaria the systematic error of the method was less than 10% for the first five years after deposition.

The second method is based on an improved evaluation of *in situ* gamma-ray spectra and does not need any soil sampling (Rybacek et al. 1992). Again, an exponential shape of the caesium distribution in soil is assumed. The activity per unit area and the relaxation mass per unit area are determined from the fluences in air of 662 keV gamma rays and of 32 keV X-rays.

Both methods are based on an assumption of an exponential shape of the caesium distribution in soil that has been shown in section 4.1 to be not valid for longer times after the deposition at sites in Middle and Northern Europe. Different distributions have been studied to approximate the dependence of the caesium activity per unit mass $A_m(\zeta)$ on the soil mass per unit area above the activity. Figure 4.4 shows for two examples that the Lorentz distribution

$$A_m(\zeta) = \frac{A_1}{(\zeta - A_2)^2 + A_3^2} \quad (4.2)$$

approximates the measured caesium distributions per unit mass well. The activity per unit mass in the upper most sampling layer, in the layer with the maximum activity, and in the tail at larger depths is well reproduced.

Cs-134 distributions in soil measured in the period 1990 to 1993 in Southern Bavaria have been approximated by the Lorentz distribution (Hillmann and Jacob 1995). Figure 4.5 shows that the soil mass per unit area A_2 above the maximum activity per unit mass is correlated with the width A_3 of the distribution. The best fit of the correlation in the form

$$A_3 = a \cdot A_2 \quad (4.3)$$

is obtained for $a=1.75$, and most of the obtained parameter pairs fall in the range for a of 1.25 to 2.25. Figure 4.5 shows, how the depth of the maximum activity per unit mass and the width of the caesium distribution in soil grow with time.

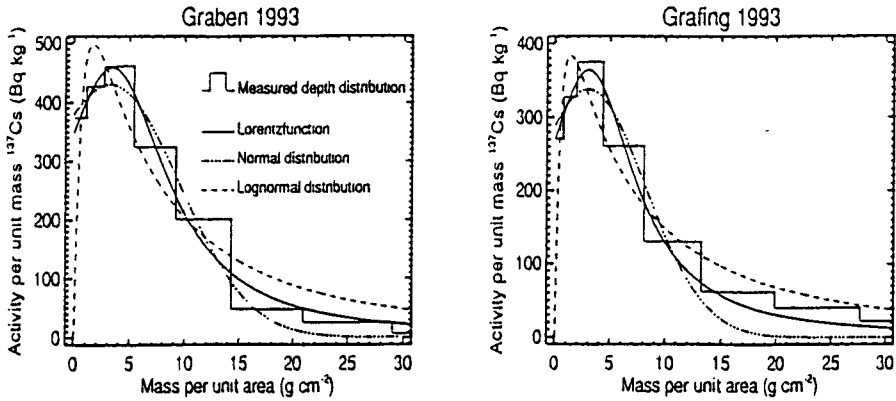


Figure 4.4 Measured and approximated caesium distributions in soil from Southern Bavaria. The activity per unit mass is plotted without the fraction of nuclear weapons tests.

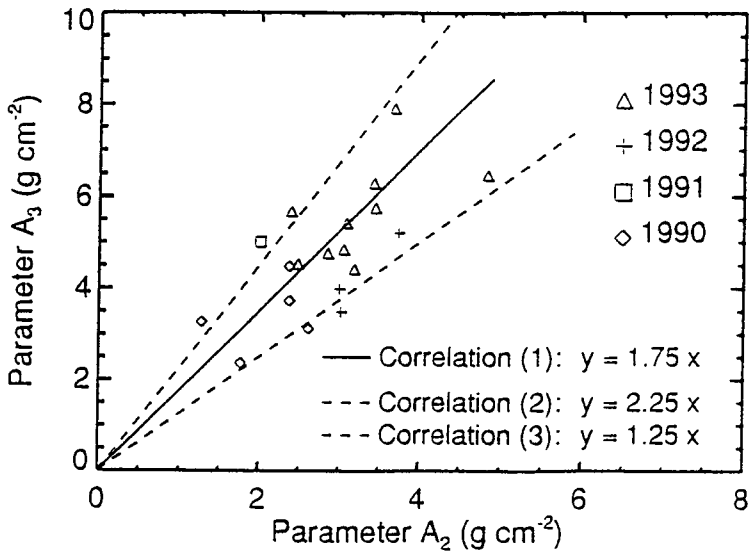


Figure 4.5 Parameters A₂ plotted versus A₃ for all investigated and approximated Cs-134 distributions in soil in Southern Bavaria in the period 1990-1993.

4.4 *In situ* determination of caesium distributions in soil

Recently a new method has been proposed for determining caesium distribution in soil from *in situ* gamma ray spectra (Zombori et al. 1992). The method is called the peak-to-valley method and is based on the count rates in a peak area and in a valley area of the measured spectrum as exemplified in Fig. 4.6. It uses the fact that the ratio between these two count rates (after subtraction of background counts) depends on the attenuation of the radiation in the soil. In the framework of the current project the Lorentz approximations and the parameter correlations described in section 4.3 have been used to develop this idea to a powerful method for *in situ* determinations of caesium distributions in soil (Hillmann and Jacob 1995). For this purpose the spectral photon fluence in air at a height of 1 m above ground due to caesium in the soil has been calculated by Monte Carlo simulations. Results were obtained for Lorentz distributions with the parameter A_2 in the range of 0 to $8 \text{ g} \cdot \text{cm}^{-2}$ and the parameter A_3 in the range of 0 to $15 \text{ g} \cdot \text{cm}^{-2}$. Calculated response functions of the used detector (Meckbach et al., 1995) were applied to obtain theoretical peak-to-valley ratios for caesium with Lorentz distributions in the soil (Fig. 4.7).

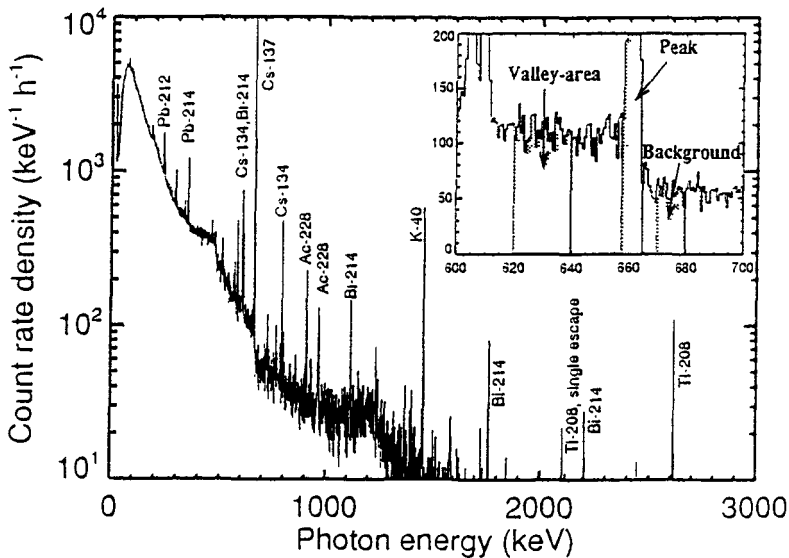


Figure 4.6 Measured impulse-height-distributions from Bad Reichenhall, Southern Bavaria. The upper right box shows the area from 600 keV to 700 keV in more detail. The counting areas of background, peak and valleys are marked.

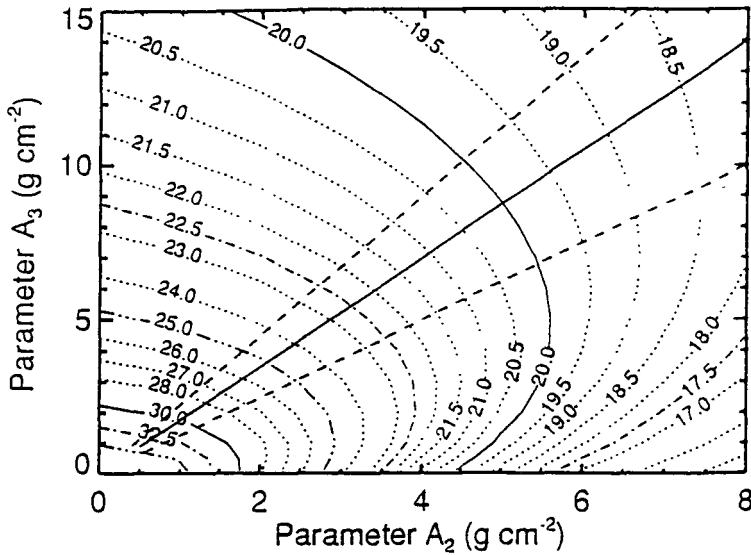


Figure 4.7 Peak-to-valley ratios calculated by simulating the photon transport in the air-over-soil geometry and the response function of the used high purity germanium detector. The isolines represent Lorentz distributions with the same peak-to-valley ratio, the straight lines the parameter correlation shown in Figure 4.5.

Measured valleys and background counts were corrected for disturbing lines and the higher contribution of the 796 keV line of Cs-134 and the 1461 keV line of K-40 to the valley counts, compared to the background counts. Then, the measured peak-to-valley ratios determined an isoline as shown in Fig. 4.7. Using the correlation shown in Fig. 4.5 the parameter pair (A_2 , A_3) of an effective Lorentz distribution was determined. Finally, the parameter A_1 was determined from the peak count rate, using tables for fluence rates of unscattered photons in air due to caesium with Lorentz distributions in soil (Jacob et al., 1995). The activity per unit area A_a was calculated according to an integration of the Lorentz distribution over the soil mass per unit area:

$$A_a = \frac{A_1}{A_3} \left(\frac{\pi}{2} + \arctan \frac{A_2}{A_3} \right) \quad (4.4)$$

Results are compared in Table 4.1 with the results of soil sampling in 1993. In general, the agreement is within 20%. Exceptions are the site 'Gigliberg', where the activity per unit area is considered to be below the range of applicability of the method and the site 'Bad Aibling' with a deviation of 27%. Table 4.1 shows also the robustness of the method against changes of the assumed correlations of the parameters A_2 and A_3 . This indicates that the method can be expected to be also applicable if the caesium distributions in the soil deviates from the assumed Lorentz shape.

Table 4.2 shows that the gamma dose rate in air derived by the peak-to-valley method also agrees with the results from soil sampling within 20%, again with the exception of the site with a low activity per unit area (Gigliberg), and a further site 'Grafring' with a deviation of 23%.

Table 4.1 Activity per unit area derived from *in situ* measurements and soil sampling. The columns 1, 2 and 3 of *in situ* refer to the different parameter correlations from Figure 4.5. The columns 2 and 3 contain the deviation in % of the result in column 1 (kBq·m⁻²), when using correlation 2 or 3 instead of 1 from Figure 4.5.

Measuring site	Activity per unit area (kBq m ⁻²)			
	Soil Sampling	In situ		
		1	2(%)	3(%)
Bad Aibling	16.4 ± 0.8	12.9 ± 4.6	+3	- 4
Engl. Garten	13.2 ± 0.7	15.2 ± 3.5	+5	-3
Giglberg	11.1 ± 0.6	7.7 ± 2.9	+3	-4
Graben	52.2 ± 2.6	55.6 ± 8.9	+5	-5
Grafring	42.6 ± 2.1	46.3 ± 7.8	+5	-5
Neuherberg	16.7 ± 0.8	17.3 ± 3.8	+3	-4
Pullach	27.8 ± 1.4	28.4 ± 5.4	+5	-5
Reichenhall	41.4 ± 2.1	49.3 ± 9.4	+5	-5
Simsee	16.4 ± 0.8	16.2 ± 4.2	+5	-5

Table 4.2 Kerma rate in air one metre above the ground derived from *in situ* measurements and soil sampling, using the data table from Jacob et al. (1995).

Measuring site	Attenuation		Kerma rate in air (nGy·h ⁻¹)	
	Sampling	In situ	Sampling	In situ
Bad Aibling	0.28	0.35	11.3	11.3
Engl. Garten	0.29	0.31	10.1	12.0
Giglberg	0.34	0.39	11.1	7.5
Graben	0.30	0.31	38.7	43.2
Grafring	0.28	0.31	29.6	36.4
Neuherberg	0.34	0.36	14.2	15.7
Pullach	0.31	0.33	21.3	23.0
Reichenhall	0.32	0.31	33.4	39.1
Simsee	0.28	0.33	11.7	13.4

4.5 Gamma dose rates in air

The results for the attenuation of the gamma dose rate in air $r(t)$, defined by the ratio of the gamma dose rate in air determined and the gamma dose rate in air due to a plane source on a smooth surface with the same activity per unit area, have been analytically approximated (Jacob et al. 1994) in the form

$$r(t) = p_1 \cdot \exp(-p_2 \cdot t) + p_3 \cdot \exp(-p_4 \cdot t). \quad (4.5)$$

Three types of approximations have been performed. First results obtained for the Chernobyl deposit were approximated. It turned out that the parameters were strongly correlated and the asymptotic standard deviations of the constants in the exponents were larger than their best estimates. Therefore, in a second approximation p_4 was set equal to zero, and the results are given in Table 4.3.

Whereas the migration behaviour of caesium deposited after the reactor accident of Chernobyl has been observed for 6 years, the fallout from atomic weapon test has been studied over much longer periods of time. Miller et al. (1990) published some results on the migration of caesium deposited in the New York area after the atmospheric nuclear weapons test (see Fig. 4.8). As in Southern Bavaria, the annual precipitation was in the range of 1000-1500 mm. Also, in both cases the caesium was attached to natural aerosols before it was deposited and not to fuel particles, as may have been partly the case in the Ukraine and Russia. Only one of the measurement sites in the study of Miller et al. involved a very sandy soil. It is not included in the following discussion due to its exceptional behaviour. For the other sites there was no obvious deviation of the characteristics from the measurement sites in Southern Bavaria. Therefore, the two data sets were combined into one data set. Table 4.3 gives the results of the four-parameter fit of these data with the function given in Eq. (4.5).

To predict gamma dose rates for periods longer than the observation period of 24 years, this function should be used with caution: it has been observed that the caesium is fixed to the soil matrix in processes lasting at least several years (Schimmack and Bunzl, 1992). Therefore, it can be expected that the four-parameter approximation will underestimate the gamma dose rates for times longer than 30 years of deposition. For long-time applications in radiation protection, the three-parameter approximation of the data set is recommended, results of which are given in Table 4.3. The numerical results for the attenuation obtained by this fit are similar to the results of the fit to the data from the first 5.5 years after deposition.

Table 4.3 Parameters of analytical approximations (Eq. 4.5) of results on the attenuation of gamma dose rates in air due to surface roughness and migration into the soil. The uncertainty bounds indicate the asymptotic standard deviations according to the fit procedure.

Region/time after deposition	p_1	$p_2(a^{-1})$	p_3	$p_4(a^{-1})$
Southern Bavaria/up to 5.5 years	0.34 ± 0.03	0.55 ± 0.14	0.34 ± 0.03	0.0*
Southern Bavaria/up to 5.5 years	0.31 ± 0.04	0.61 ± 0.18	0.37 ± 0.04	0.015 ± 0.008
including USA/24 years	0.38 ± 0.03	0.38 ± 0.07	0.28 ± 0.03	0.0*

*Value set equal to zero (see text)

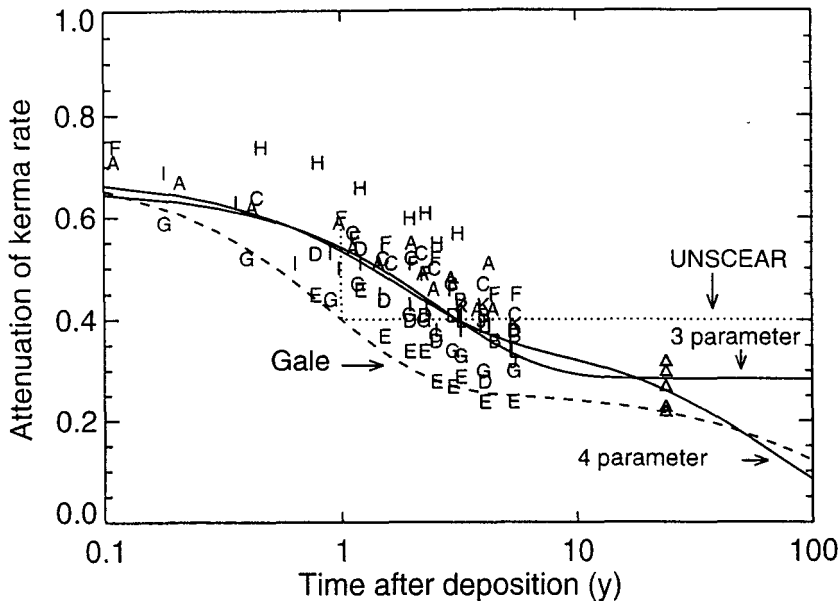


Figure 4.8 Analytical approximation for the attenuation of the kerma rate in air due to surface roughness and migration into the soil as derived from caesium data from Southern Bavaria after Chernobyl (*capital letters*,) and from the New York area (*triangles*) after atmospheric weapons test fallout (Miller et al. 1990) The solid line indicated by '4 parameter' is the analytical approximation of the shown data according to Eq. (4.5), for the one indicated by '3 parameter' p_4 was set equal to zero. The broken line is the analytical approximation of Gale et al. (1964); the *dotted line* the UNSCEAR model (1988).

The analytical approximations are shown in Fig. 4.8 together with the measurement results. Gale et al. (1964) derived a function for the attenuation factor of the gamma dose rate in air, which has been used in many applications. Since the experiments were performed for wet deposition, the function was normalised in Fig. 4.8 to have a value for the time of deposition comparable to the measured values. Then the function of Gale et al. underestimates the gamma dose rates compared with the measurement results. On the other hand, the function of Gale et al. provides a good approximation for the data from southern Bavaria and the United States for times later than 2 months after deposition if an initial attenuation factor of the order of 0.8 - 0.9 is assumed for the surface roughness and the initial migration. The UNSCEAR model (1988) approximates the values from Southern Bavaria but gives higher gamma dose rates for longer times after deposition than the measurements from the New York area.

The results given above apply to caesium that has been predominantly attached to the natural aerosol and was predominantly deposited with precipitation. After the reactor accident of Chernobyl the caesium was observed to migrate considerably slower into the soil at close distances (<100 km) of the reactor and to show an intermediate behaviour at intermediate distances up to 1000 km (Balonov et al. 1995, Jacob et al. 1994, Konopler et al. 1992).

4.6 References

- Gale H.J., Humphreys D.L.O., Fisher E.M.R. (1964) Weathering of Caesium-137 in soil. *Nature* **4916**, 257-261.
- Hillmann U., Jacob P. (1995) Determination of soil contamination by *in situ* gamma-ray spectrometry. In preparation.
- Hillmann U., Schimmack W., Jacob P., Bunzl K. (1995) A new model for describing Cs-137 distributions in soil. In preparation.
- ICRU (1995) Gamma-ray spectrometry in the environment. ICRU Report 53. International Commission on Radiation Units and Measurements, Bethesda, MA, USA.
- Jacob P., Meckbach R. (1987) Shielding factors and external dose evaluation. *Radiat. Prot. Dosim.* **21**, 79-85.
- Jacob P., Meckbach R., Paretzke H.G., Likhtarev I., Los I., Kovgan L., Komarikov I. (1994) Attenuation effects on the kerma rates in air after caesium depositions on grasslands. *Radiat. Environ. Biophys.* **33**, 251-267.
- Jacob P., Saito K., Rosenbaum H. (1995) Photon fluences and kerma rates in air due to radioactive sources distributed in soil (in preparation).
- Konoplev A.V., Bulgakov A.A., Popov V.E., Bobovnikova Ts.I. (1992) Behaviour of long-lived Chernobyl radionuclides in a soil-water system. *Analyst.* **117**, 1041-1047.
- Meckbach R., Fehrenbacher G., Jacob P., Paretzke, H.G. (1995) Unfolding of the reponse of a Ge detector used for *in situ* spectrometry. In preparation.
- Miller K.M., Kuiper J.L., Helfer I.K. (1990) ¹³⁷Cs fallout depth distributions in forest versus field sites: implication for external gamma dose rates. *J. Environ. Radioactivity* **12**, 23-47.
- Rybacek K., Jacob P., Meckbach R. (1992) *In situ* determination of deposited radionuclide activities: Improved method using derived depth distributions from the measured photon spectra. *Health Phys.* **62**, 519-428.
- Schimmack W., Bunzl K. (1992) Migration of radiocaesium in two forest soils as obtained from field and column investigations. *Sci. Total Environ.* **116**, 97-107.
- United Nations Scientific Committee on the Effects of Atomic Radiation (1988) Sources, effects and risks of ionising radiation. 1988 Report to the General Assembly, United Nations, New York.
- Zombori P., Andrási A., Németh I. (1992) A new method for the detection of radionuclide distribution in the soil by *in situ* gamma-ray spectrometry. Report KFKI-1992-20/K, Institute for Atomic Energy Research, Budapest.

5. Weathering of ^{137}Cs on various surfaces in inhabited areas and calculated location factors

Kasper G. Andersson and Jørn Roed
Risø National Laboratory, MIL-114
4000 Roskilde
Denmark

Peter Jacob and Reinhard Meckbach
GSF-Institut für Strahlenschutz
85758 Oberschleißheim
Germany

Introduction

This section reports the achievements of the research project FI3P-CT92-0038 on the topics of weathering of radioactive substances in urban areas and calculation of location factors in urban dry deposition scenarios and the state of the art on the topics. The measurements of weathering on urban surfaces in the town of Gävle in Sweden were continued. This time series of data now spans over almost a decade and has provided a reference against which existing models (see Chapter 7) can be validated. Weathering measurements were also made in other parts of Europe (Bavaria and Russia) and the results were found to be in line with the Gävle experience. The weathering effect on radiocaesium on paved surfaces in Bavaria since the Chernobyl accident has been followed all the way from the early phase. Location factors were calculated for various dry deposition scenarios in houses of different shielding effect, partly based on experimental data and it was established that indoor deposition may have great influence. Other calculations based on in situ gamma spectrometry in Bavarian environments (mainly wet deposition) gave location factors which were comparable with those found by the first approach for a medium shielding house.

5.1 Measurements of weathering in Gävle

Through the years that have passed since the Chernobyl accident occurred in 1986, the weathering effects on deposited radiocaesium on different types of surface in urban, suburban and industrial areas, including areas of soil (these are treated separately in Chapter 4) have been followed in the Gävle area of Sweden. Shortly after the Chernobyl accident, a radioactive cloud passed over Gävle city when heavy rain caused deposition of high levels of contamination in and around the city. As a result of this, Gävle is probably the most heavily contaminated urban centre outside the former USSR. The radiocaesium levels were sufficiently high to permit the use of germanium detector gamma spectrometry for in situ measurements.

In situ measurements with lead colimated/shielded germanium detectors were conducted in the centre of Gävle, in a light industrial area about 1 km east of the town centre and in a

suburban/rural area about 13 km to the north-east of the town centre. The radiocaesium levels were measured on various kinds of urban surface such as walls, pavements, walkways, roads and grassed areas. In order to investigate the changes in the contamination levels with time on these surfaces, exact the same measurement points were used in the successive measurement campaigns.

Although the first campaign was made in 1987, a comparison with the measurements of Karlberg and Sundblad (1986) in the same area in May-October of 1986 made it possible to approximately relate the measured results to the initial radiocaesium deposition in the area. Six measurement campaigns were conducted in the Gävle area in the period 1987-1994.

Table 5.1 shows the levels measured on impervious surfaces in Gävle, Sweden in 1987, 1988, 1990, 1991, 1993 and 1994. The evaluation of accuracy was based on the assumption that the most important factors governing this were the uncertainty on the calibration of the detector and the uncertainties associated with the observation of random events. From repeated calibration sessions this factor was estimated to about 3 %. As can be seen, the total standard deviations on the measurements were found to range from 6 % to 33 %, which is sufficiently small to record significant ^{137}Cs changes on the surfaces.

The ^{137}Cs levels on grassed areas are the highest (46-78 kBq/m²), and the levels on the other surfaces are now only a few percent or less of those measured on grassed areas.

As can be seen from the table, very little, if any decrease in the levels of radiocaesium contamination on walls of buildings was identifiable 8 years after the deposition. In one case, the level has actually increased at one point. This change is, however, not highly significant, but may have been caused by a wash-down of radioactive substances from the upper parts of the wall. Anyway, the measurement at this site the following year showed the expected decrease. Although it is difficult to distinguish between the weathering rates on the walls in Gävle previous efforts have shown that radiocaesium is retained most effectively by micaceous construction materials, especially those that have been fired at comparatively low temperatures, where the small openings in the mica structure are intact. A yellow brick wall on the fire station has a very low contamination level compared with the other walls because it was exposed to only dry deposition as the structure of the building prevents the wall from contamination with precipitation.

In contrast to the situation on walls, the levels of radiocaesium on asphalt surfaces have now decreased so much that less than 10 % of what was measured in 1988 is left. A comparison with the results of Karlberg and Sundblad shows that this means that less than 2 percent of the initially deposited radiocaesium is now left on the road. These levels are now generally below the detection limit. This ties in with the results of laboratory investigations, which have shown that only a very little fraction of a caesium contamination is associated with the bitumen fraction of the asphalt. A large fraction of the caesium has been found to be associated with the more mobile street-dust, which usually contains micaceous substances weathered off various surfaces.

As for the concrete paved surfaces, the remaining 10 % of the initially deposited radiocaesium seems very firmly fixed. No significant decrease has been recorded over the latest 3 years. The weathering on horizontal hard surfaces was generally found to be faster in the more heavily trafficated spots.

The field observations on pavings in Gävle (measurements DK) are presented in Figure 5.1 together with the results of Karlberg and Sundblad (measurements S) in the same area and the

results of measurements in Germany (Roed and Jacob, 1990). The radiocaesium concentration is given relative to the initial deposition in the area. Also shown is the result of computer simulations with the URGENT model.

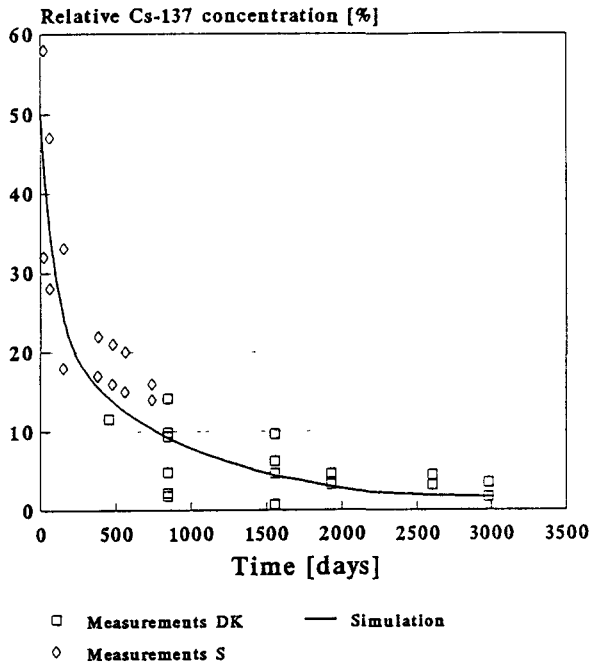


Figure 5.1 Weathering of Chernobyl ^{137}Cs on pavings. Concentrations relative to initial deposition, given as a function of time.

Clay roof tiles which were contaminated due to the Chernobyl accident and exposed to the wind and weather in Gävle for four years were collected and brought to Risø, where the contamination level at this stage was assessed. The tiles were subsequently exposed to Danish weather after having been placed on a specially constructed scaffold. A decrease in the radiocaesium contamination level of between 28 and 35 % was recorded over the following 19 months period, in addition to radioactive decay of the caesium.

This is in reasonably good agreement with the results of measurements on different types of roof which were contaminated by Chernobyl fallout at Risø (Figure 5.2). The clay tiles, which were fired at comparatively low temperatures (600-700°C) where the micaceous structure is intact, were found to be the most effective in retaining the contamination, while the smooth silicon-treated eternite roofs retained the least. The measurements are shown together with estimates based on a semi-empirical model (Roed, 1988).

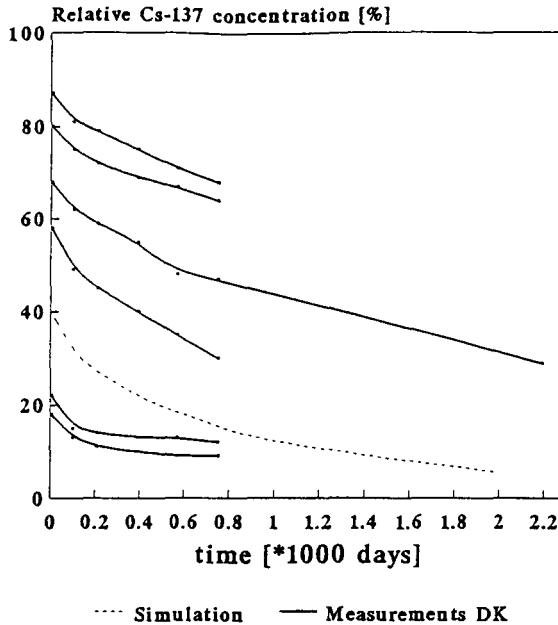


Figure 5.2. Weathering of Chernobyl ¹³⁷Cs on various roofs contaminated in Denmark. Concentrations relative to initial deposition, given as a function of time.

The capacity of clay tiles to intercept and retain radiocaesium was investigated in a laboratory experiment (Andersson, 1992). As rainwater always contains alkali metals, including caesium, it might be expected that where tiles had been exposed to the weather for many years any sites showing a high selectivity for caesium could have been saturated with caesium during those years of exposure. However, the experiment showed that common Redland clay tiles have a caesium acid site capacity of 35 µg/cm². According to published data on the typical level of caesium in rainwater this means that the amount of time that would have to pass just to fill up these acid sites in the tile, on which fixation is reversible, could be as much as 50,000 years (Andersson, 1992).

The Gävle experience can be summarized in Table 5.2, which gives the ranges of caesium contamination found immediately after the Chernobyl accident, 2 years later and 4 years later. Bearing in mind the more specific conditions and factors that may locally influence the situation, this table can be used as an indicator of the expected weathering effects in housing environments.

Table 5.2 Relative distributions of wet deposited ¹³⁷Cs retained on urban surfaces in Gävle, Sweden.

Urban surface	Relative ¹³⁷ Cs conc. immediately after deposition	Relative ¹³⁷ Cs conc. after 2 years	Relative ¹³⁷ Cs conc. after 8 years
roofs	0.3 - 0.9	0.1 - 0.7	-
walls	0.01 - 0.03	0.01 - 0.03	0.005 - 0.02
pavements, roads	0.4 - 0.8	0.01 - 0.2	0.003 - 0.02
grassed areas	1	1	1

5.2 Measurements of weathering in the former Soviet Union

Weathering effects were also investigated in situ in areas of the former Soviet Union. In the town of Pripjat, less than 4 km away from the Chernobyl power plant, high levels of radioactive contamination were recorded compared with other investigated areas, although this area received a dry deposited contamination. In other, more remote Ukrainian towns and villages where measurements were made, such as Poleskoie, Vladimirovka and Varovice as well as the Russian towns Yalovka and Novozybkov, more than 100 km away from the power plant, deposition of Chernobyl debris occurred with rain.

Measurements made in Pripjat in the summer of 1993 with shielded germanium detectors showed that the contamination level on sandstone walls was in the range of 199-350 kBq/m² (a comparison with the levels in the soil shows that the decrease since 1986 must have been very small), compared with 0.9-28 kBq/m² in the more remote towns. On the 'impervious' horizontal surfaces, such as roads and pavements, the caesium contamination level was found to be of the order of 30-350 kBq/m² in Pripjat, with the highest levels on concrete pavements and the lowest on asphalt. From the contamination level and distribution of radiocaesium in soil areas it was possible to estimate the caesium contamination level on pavings in the area shortly after the accident to about 1.5 MBq/m². This means that a much larger fraction remains on the paved surfaces in Pripjat than in Gävle. However, there has been very little traffic in Pripjat since the Chernobyl accident. If the weathering processes in the two towns had been the same, the remaining fractions in Pripjat would probably have been the smallest at this stage. Anyway, it was easier to remove caesium in Pripjat by forced decontamination trials than in other more remote towns. The reason for this is believed to be that the contamination in Pripjat took place with large (insoluble) core fragment particles.

5.3 Measurements of weathering in Southern Bavaria.

After the Chernobyl accident in-situ gamma spectrometric measurements have been performed in Munich and in smaller towns in Southern Bavaria. At the measurement sites about two thirds of the total contamination was deposited by rain. For grassland, the attenuation of the radiation from ¹³¹I, ¹⁰³Ru, ¹³⁴Cs and ¹⁴⁰Ba due to the migration of the radionuclides in the ground and due to the surface roughness was found to be similar. However, large variations between the retention of the various elements on smooth surfaces have been observed. Figure 5.3 shows the weathering effect on caesium on asphalt, concrete and cobble stone paved surfaces in Southern Bavaria. The results are in line with what has been found in other areas of Europe and very clearly show that where street areas are subjected to ordinary traffic by far the major part of a radiocaesium contamination is rapidly weathered off (within the first year). The cobble stone pavements apparently retain somewhat more than do the asphalt and concrete pavements. A likely explanation for this is that weathered-off radioactive material is accumulated in the space between the individual cobble stones.

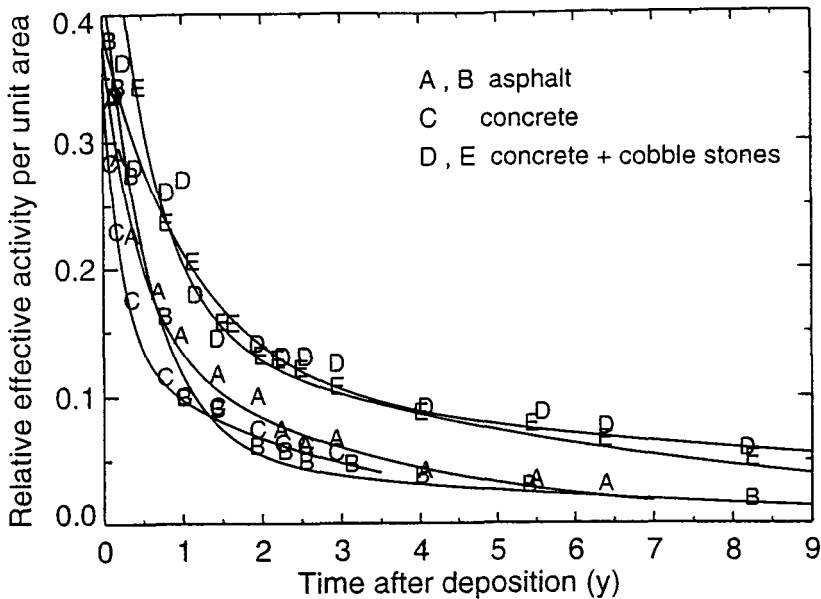


Figure 5.3 Effective ^{137}Cs activities per unit area divided by the activity deposited per unit area by a wet deposition on a nearby lawn.

5.4 Location factor calculations for ^{137}Cs and ^{131}I for urban dry deposition scenarios.

The numbers presented below for the location factor (defined as the ratio of the effective dose rate received indoors to that received outdoors following a uniform deposit of radiopollutants) were calculated for typical dry deposition scenarios. The dose rates inside and outside buildings due to an outdoor deposition have been calculated using the URGENT computer code (see Chapter 7) for dynamic dose modelling in urban areas. The dose rate contributions due to deposition of radionuclides on indoor surfaces were estimated using a semi-empirical modelling method which is also described in detail in Chapter 7.

The calculations were based on the following assumptions: The relative deposition figures for ^{131}I and ^{137}Cs were assumed to be as given by Roed (1990). The dose rates from outdoor deposition were calculated exactly as shown in Chapter 7, whereas the dose rate from indoor deposition was calculated with the following parameters: $\lambda_d = 0.8 \text{ h}^{-1}$, $\lambda_r = 0.4 \text{ h}^{-1}$, $f = 1.0$, which are considered to be realistic. The deposited iodine was assumed to be in particulate form. The indoor deposition of iodine was calculated from the same formula that was used to calculate indoor deposition of caesium, only for iodine it was assumed that the deposition velocity to clipped grass was $22 \times 10^{-4} \text{ m/s}$ as stated by Roed (1990). The indoor deposition velocity of particulate iodine was taken from Roed and Cannell (1987).

In accordance with the assumptions of Chapter 7, the doses from indoor deposition were calculated at a position 1 m above the ground at the centre of a room with a ground area of 4 m by 4 m and a height of 3 m. The dose contributions from scattered radiation and

deposition on indoor surfaces of neighbouring rooms were not included in the calculations. It was assumed that the average indoor contamination level decreases to 85 % after 1 year and to 70 % in 10 years. These reductions almost follow the reduction of the dose from a lawn due to downward migration of radiocaesium. The indoor dose relations between ^{137}Cs and ^{131}I (no shielding) were found from Lauridsen (1982). The outdoor environments are the same as those described in Chapter 7 (excluding the environment with terrace houses).

The four tables shown below compare the calculated location factors with and without indoor deposition. Calculations were made for ^{131}I immediately after dry deposition and for ^{137}Cs at time 0, 1 year and 10 years following dry deposition.

As can be seen, the influence of indoor deposition on the location factor in dry deposition scenarios can be great. Indeed, in areas of buildings with good shielding effect, this contribution will dominate. The relationship between the location factors for ^{137}Cs with and without indoor deposition does not appear to change significantly with time.

Table 5.3 Location factors at time = 0, relating to a dry deposition of I-131, assuming that no indoor deposition occurs and assuming that an indoor deposition occurs.

Location factor	Without indoor dep.	With indoor dep.
Low shielding building	0.58	0.64
Medium shielding building	0.10	0.16
High shielding building	0.023	0.091

Table 5.4 Location factors at time = 0, relating to a dry deposition of Cs-137, assuming that no indoor deposition occurs and assuming that an indoor deposition occurs.

Location factor	Without indoor dep.	With indoor dep.
Low shielding building	0.62	0.68
Medium shielding building	0.14	0.19
High shielding building	0.031	0.097

Table 5.5 Location factors at time = 1 year, relating to a dry deposition of Cs-137, assuming that no indoor deposition occurs and assuming that an indoor deposition occurs.

Location factor	Without indoor dep.	With indoor dep.
Low shielding building	0.57	0.64
Medium shielding building	0.12	0.17
High shielding building	0.028	0.093

Table 5.6 Location factors at time = 10 years, relating to a dry deposition of Cs-137, assuming that no indoor deposition occurs and assuming that an indoor deposition occurs.

Location factor	Without indoor dep.	With indoor dep.
Low shielding building	0.51	0.59
Medium shielding building	0.091	0.14
High shielding building	0.019	0.083

In situ gamma-ray spectrometry was also performed at various locations in three one-family houses and one multistorey building in Bavaria. The results were normalized to the unscattered photon fluences over close areas of open grasslands. The results in Table 5.7 show how the attenuation of the unscattered radiation depends on the photon energy. In the attic of the one-family house Munich-H, the 365 keV radiation is reduced by more than a factor of 3 more than the 1596 keV radiation. This is a combined effect of the better shielding for the low energy radiation of iodine and of the relatively low retention of iodine on roofs. In the administration building the 662 keV radiation was attenuated by a factor of four more than in the one-family houses. This difference is relatively small because the detector was placed in the administration building not too far from large windows that reach from the ceiling to the floor.

Table 5.7 Unscattered photon fluences at various indoor locations relative to unscattered photon fluences over an open area of grassland. Uncertainties of the given value (expressed in terms of one standard deviation) are not greater than 15 %, for the values in parantheses less than 20 %.

House/type/site/ date of measu- rement	radionuclide/ photon energy	location		
One-family house Munich H 30 May 1986		Ground floor	First floor	Attic
	¹³¹ I/365 keV	(0.050)	-	0.11
	¹⁰³ Ru/497 keV	(0.053)	(0.034)	0.13
	¹³⁷ Cs/662 keV	(0.068)	0.057	0.23
	¹³⁴ Cs/796 keV	(0.066)	0.052	0.22
	¹⁴⁰ La/1596 keV	-	-	0.33
Admn. Building Neuherberg, 11 June 1986		First floor	Second floor	Fourth floor
	¹³⁷ Cs/662 keV	0.015	0.015	(0.014)
One-family house Munich J 23 June 1986		Ground floor	Ground floor	First floor
	¹³⁷ Cs/662 keV	0.060	0.051	0.044
One-family house Grafing 4 July 1986		Ground floor	First floor	Attic
	¹⁰³ Ru/497 keV	0.048	0.034	0.032
	¹³⁷ Cs/662 keV	0.057	0.046	0.066
	¹³⁴ Cs/796 keV	0.062	0.044	0.067

Extensive Monte-Carlo calculations have been performed to simulate the photon transport in urban environments. Among the studied locations there were some which were comparable to those, for which gamma ray spectra were measured. The calculated build-up factors and the location measured unscattered photon fluences were used to assess the location factors. The results in Table 5.8 confirm Monte-Carlo calculations for wet depositions (Meckbach et al., 1988).

A comparison with Tables 5.3-5.6 shows that the location factor data for the Bavarian houses are similar to those calculated for medium shielding buildings.

Table 5.8 Location factors for various indoor locations. The results were obtained from in situ gamma-ray spectrometry and calculated buildup factors.

House/type/site/ date of measu- rement	radionuclide/ photon energy	location		
One-family house Munich H 30 May 1986	$^{131}\text{I}/365\text{ keV}$ $^{103}\text{Ru}/497\text{ keV}$ $^{137}\text{Cs}/662\text{ keV}$ $^{134}\text{Cs}/796\text{ keV}$ $^{140}\text{La}/1596\text{ keV}$	Ground floor (0.08) (0.08) 0.11 0.11 -	First floor - (0.06) 0.10 0.10 -	Attic 0.11 0.18 0.32 0.31 0.45
Admin. Building Neuherberg 11 June 1986	$^{137}\text{Cs}/662\text{ keV}$	First floor 0.02	Second floor 0.02	Fourth floor (0.02)
One-family house Munich J 23 June 1986	$^{137}\text{Cs}/662\text{ keV}$	Ground floor 0.09	Ground floor 0.08	First floor 0.07
One-family house Grafing 4 July 1986	$^{103}\text{Ru}/497\text{ keV}$ $^{137}\text{Cs}/662\text{ keV}$ $^{134}\text{Cs}/796\text{ keV}$	Ground floor 0.06 0.08 0.06	First floor 0.06 0.08 0.08	Attic 0.03 0.08 0.08

References

Andersson, K.G., Contamination and Decontamination of Urban Areas. Ph.D. thesis 1991, Risø National Laboratory/Technical University of Denmark (1992).

Karlberg, O. and Sundblad, B., A Study of Weathering Effects on Deposited Activity in the Studsvik and Gävle Area, Studsvik Technical Note NP 86/78 (1986).

Lauridsen, B., Table of Exposure Rate Constants and Dose Equivalent Rate Constants, Risø-M-2322 (1982).

Meckbach, R., Jacob, P., Paretzke, H.G., Gamma Exposures due to Radionuclides Deposited in Urban Environments, part 1: Kerma Rates from Contaminated Urban Surfaces, Rad. Prot. Dos. vol.25, no.3, pp. 167-179 (1988).

Roed, J., Modelling of Run-off and Weathering Processes, presented at the MARIA workshop at Kernforschungszentrum Karlsruhe (1988).

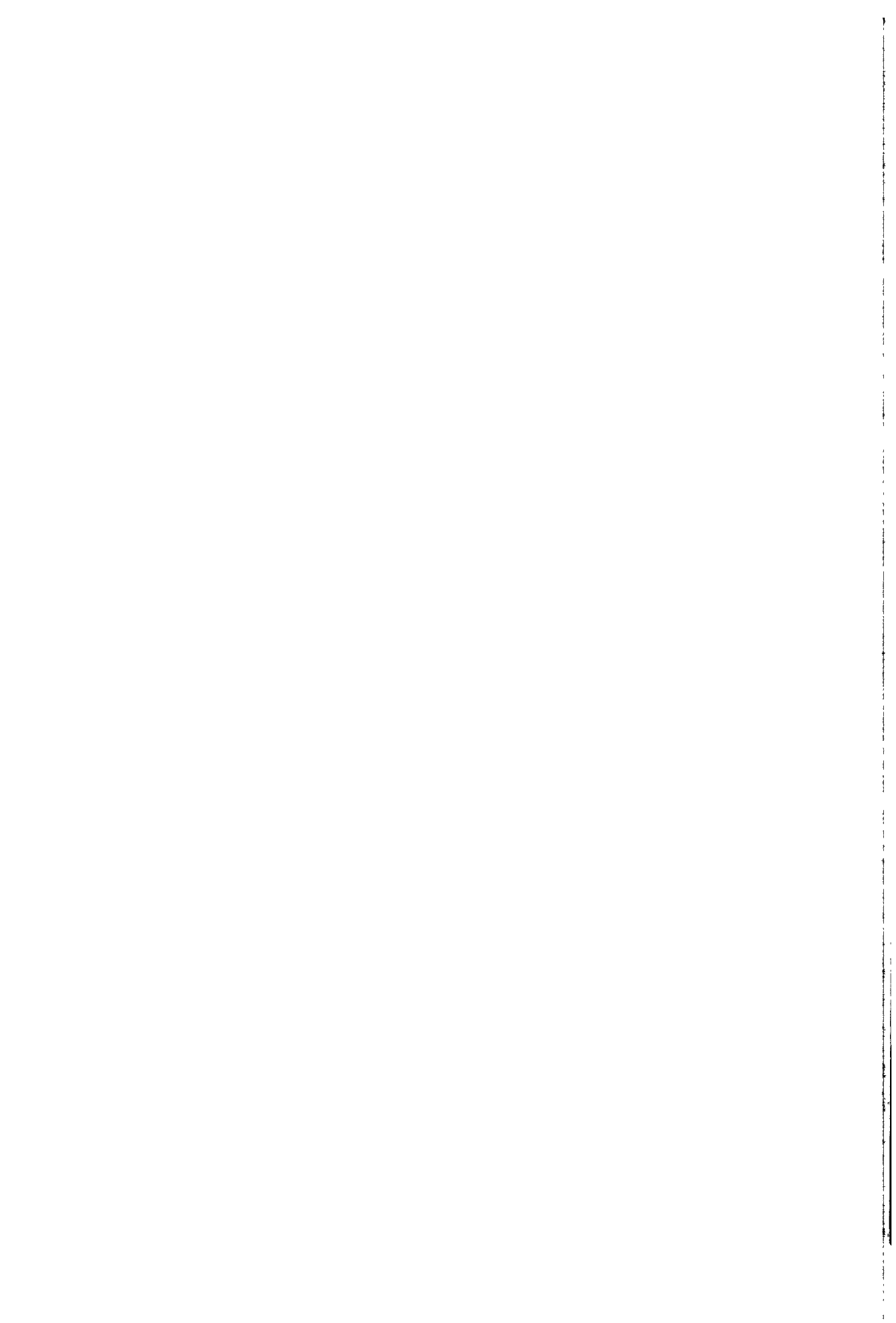
Roed, J., Deposition and Removal of Radioactive Substances in an Urban Area, Nordic Liaison Committee for Atomic Energy (1990).

Roed, J. and Cannell, R.J., Relationship Between Indoor and Outdoor Aerosol Concentration Following the Chernobyl Accident, Rad. Prot. Dos. vol. 21, no. 1/3, pp. 107-110 (1987).

Roed, J. and Jacob, P., Deposition on Urban Surfaces and Subsequent Weathering, in proc. from Seminar on Methods and Codes for Assessing the Off-site Consequences of Nuclear Accidents, Athens (1990).

Table 5.1 ¹³⁷Cs levels measured in Gavle, Sweden in 1987, 1988, 1990, 1991, 1993 and 1994

ID	Place	Nature	Material	Code	¹³⁷ Cs levels measured in Gavle (kBq/m ²)					
					1987	1988	1990	1991	1993	1994
J	City hall	wall	plaster	southeast	-	0.78 ± 11%	-	-	-	0.53 ± 12%
Q	City hall	wall	plaster	southwest	-	0.55 ± 16%	-	-	-	0.21 ± 27%
M	City hall	pavement	flagstone	edge	-	6.75 ± 6%	-	-	-	-
O	City hall	pavement	flagstone	middle	-	9.71 ± 6%	4.26 ± 7%	3.13 ± 8%	3.10 ± 9%	-
P	City hall	pavement	flagstone	west	-	6.40 ± 6%	3.15 ± 7%	2.17 ± 8%	2.12 ± 9%	2.12 ± 6%
Y	City hall	pavement	flagstone	unshielded	-	-	(7.68cps)	(4.24cps)	(4.99cps)	(4.06cps ± 1%)
OM	City hall	pavement	flagstone	unshielded, edge	-	-	-	(2.97cps)	-	-
R	City hall	road	asphalt		-	1.49 ± 9%	0.44 ± 17%	-	-	-
A	Gevalia	wall	red brick	south, washing	1.93 ± 9%	1.65 ± 9%	-	-	-	-
E	Gevalia	wall	red brick	north, washing	-	3.93 ± 7%	-	1.85 ± 7%	2.13 ± 15%	1.89 ± 7%
D	Fire station	wall	yellow brick	north, dry dep	0.25	0.42 ± 15%	-	-	-	0.14 ± 36%
F	Transformer substation	wall	yellow brick	south, washing	-	1.06 ± 11%	-	0.80 ± 10%	0.76 ± 10%	-
C	Magasin St	wall	plaster	north, washing	0.99	-	-	0.98	-	-
S	General Food	wall	plaster	east	-	1.14 ± 10%	-	-	-	0.59 ± 12%
U	Fire station	pavement	asphalt+flagstone		-	-	3.21	2.38	-	-
AA	Fire station	pavement	asphalt+flagstone	unshielded	-	-	-	(3.23cps)	-	(2.34cps ± 2%)
B	Gevalia	car park	asphalt	washing	3.17	3.28 ± 7%	-	-	-	-
G	Gevalia	cross-roads	asphalt		-	1.19 ± 9%	-	-	-	-
V	Fire station	road	asphalt		-	-	0.50 ± 15%	-	-	-
X	Fire station	road	asphalt	unshielded	-	-	(2.30cps)	(1.78cps)	-	-



6. Resuspension of deposited material

Christian Lange and Jørn Roed,
Risø National Laboratory, MIL-114
4000 Roskilde
Denmark

Peter Zombori and István Fehér
KFKI Atomic Energy Research Institute
1525 Budapest
Hungary

Herwig G. Paretzke and Jochen Tschiersch
GSF-Institut für Strahlenschutz, Neuherberg
85758 Oberschleißheim
Germany.

Karel Rybáček and Milan Tomášek
Institute of Nuclear Physics
18086 Prague 8
Czech Republic

Igor Navarcík, Vladimír Jansta, Ivan Datelinka and Andrea Cipáková
Institute of Radioecology, j.s.c
04061 Košice
Slovak Republic

Introduction

One of the major topics studied within the framework of the co-ordinated research project contract FI3P-CT92-0038 is the behaviour of long-lived radio-nuclides in the atmosphere: their concentration in ground level air, wet and dry deposition and resuspension. A considerable amount of experimental data based on two larger-scale nuclear accidents (Chernobyl and Goiania) was collected during the contract period and substantial contributions were provided by the original CEC-member institutions as well as by the PECO partners. The new experimental data can be used as a basis for the revision of model parameters applied by some widely used nuclear accident consequence analysis and simulation codes.

6.1 Summary

Contributions to the topic of the outdoor atmospheric radionuclide concentration and resuspension arrived from GSF (Neuherberg), Risø National Laboratory and the PECO partners (INP Prague, IR Košice and AERI Budapest). The individual research projects are described in the subsequent sections of this chapter. The main results of the studies can be summarised as follows:

1. Radio-nuclides of interest

All contributors provided data on ^{137}Cs activity concentration in ground level air both for the case of a local contamination (GSF for Goiania) and for global contamination (PECO participants and Risø for the Chernobyl accident). Data are available for atmospheric ^{90}Sr from the IR. The concentration of ^7Be in the air was measured by IR, INP, AERI and Risø for comparison with ^{137}Cs data.

2. Temporal variation

The overall trend for airborne ^{137}Cs concentration of Chernobyl origin is slightly decreasing with time in Central Eastern Europe, as it is clearly shown from data of INP and AERI. The same trend was found for the ^{137}Cs data by the GSF on the Goiania local contamination accident site. Seasonal variation was observed by all the PECO participants, atmospheric ^{137}Cs being higher in the winter time than during the summer. In contrast, cosmogenic ^7Be was found to vary in a different way, having higher values in the summer and minima during winter, in agreement with the former observations of many investigators. Seasonal changes in ^{137}Cs data seem to be strongly related with the rainfall rate in the Goiania experiment. A somewhat different seasonality was found for ^{90}Sr by the IR, with maxima in winter and summer and minima in spring and autumn.

3. Resuspension factor (K)

The most directly applicable parameter for the late-phase post-accident situation (and thus the joining point to the modellers) is the resuspension factor K. The regular measurement of airborne ^{137}Cs on the long term is a good basis to derive K values as a function of time. A value of 10^{-9} m^{-1} in recent years (a level slowly decreasing from about $2 \cdot 10^{-8} \text{ m}^{-1}$ in 1986) was found by INP to be typical for K in Prague. This value (K around $2 \cdot 10^{-9} \text{ m}^{-1}$) and trend was also confirmed by AERI on a similar surface contamination area (5.4 kBq/m^2) of Budapest and by Risø (K around 10^{-9} since 1991). The experimental data (also in the order of $10^{-9} - 10^{-8} \text{ m}^{-1}$) measured by GSF in Goiania show that the resuspension and deposition of ^{137}Cs is a local phenomenon which is, however, somewhat dependent on the extent of the primary deposition.

These experimental values were compared with the K parameters used by the codes COSYMA and RODOS. In the long term both codes provide the same value for resuspension (10^{-9} m^{-1} 5-10 years after primary deposition) in good agreement with the experimental values. The data of AERI show, however, that the 1993 version of COSYMA tends to overestimate this effect shortly after the contamination event while RODOS predictions are within a factor of 2 of the measurements. The experimental data obtained within the framework of the project may lead to the revision of the resuspension expression constants in COSYMA (see Chapter 8).

4. Speciation and chemical fractions

The dominance of water solubility of ^{137}Cs observed by INP in the early-phase air samples later changed towards an higher proportion of the insoluble fraction. This is explained by the penetration of the soluble fraction towards deeper soil layers making the soluble fraction less available for resuspension.

Recently IR found that there is a seasonal variation in solubility of airborne ^{137}Cs . The prevailing form is water-soluble in the winter months, acid-soluble in the summer period and insoluble in the end of spring and start of summer. ^{90}Sr is mostly insoluble in the summer while acid-soluble form is dominant for the other seasons.

5. Deposition

The two radio-nuclides observed, ^{137}Cs and ^7Be , showed a different deposition pattern. ^{137}Cs had high dry deposition velocities and showed little (INP) or no (Risø) correlation with precipitation. The high deposition velocities, from 0.02 to 1 ms^{-1} , correspond to the sedimentation velocity of rather large particles, 24 to 173 μm . Sizing of resuspended particles (by GSF in Goiania) also showed that a significant fraction of the activity was present in large particles, $d_p > 15 \mu\text{m}$.

For ^7Be dry deposition velocities was found to be much smaller, around $5 \times 10^{-4} \text{ms}^{-1}$, and a strong dependence with precipitation was observed. In summary, ^7Be showed a deposition pattern similar to that of a long-range transported radio-nuclides.

6.2 ^{137}Cs in ground level air of Budapest

The radioactive aerosol concentration in the atmosphere of Budapest has been continuously measured since the arrival of the first clouds carrying the pollutants from Chernobyl, Feher (1988). The method of measurements and results obtained by the analysis of the temporal variation of ground level air concentration of radioaerosols are presented in this report.

Air samples were taken with a high volume sampling device: a pump sucking air through a combined filter system with an average flow rate of 60 m^3/h . The filter cartridge contained a plastic fiber pre-filter for aerosol sampling and a cartridge of 1.5 l activated charcoal for detection of gaseous ^{131}I components. Daily (1400 m^3) samples were taken for two weeks after the accident, then sampling frequency was switched back to the weekly sampling (10 000 m^3) of normal monitoring practice. Filters were measured without chemical preparation by Ge-gamma spectrometry (with a typical 0.1 Bq detection limit for ^{137}Cs in aerosol filters).

A rapid exponential clearance of atmospheric ^{137}Cs concentration was observed with a 'half life' of 5.7 days in the period of 15-50 days after the accident. The long term variation is characterized by a two-component exponential decrease with fluctuations and anomalous peaks in the winter times (see Fig. 6.1). The first component (with a 'half life' of 95 days is dominant in the period of 50-200 days while a slow diminishing of the ^{137}Cs concentration (with a 'half life' of about 1500 days) can be observed after 200 days. For comparison with the ^{137}Cs contamination, the atmospheric concentration of the cosmogenic radionuclide ^7Be was also measured, as shown in Fig. 6.1.

6.2.1 Discussion

The origin of ^{137}Cs in the ground level air of Budapest in the last days of April 1986 is well known and its behaviour in the first weeks was governed by the inflow of the contaminated air masses. After two weeks the extinction of the reactor fire and construction of the sarcophagus prevented further massive emission and the concentration of both radionuclides in ground level air decreased rapidly, mainly due to dilution and gravitational deposition with a one week-'half life' exponential clearance.

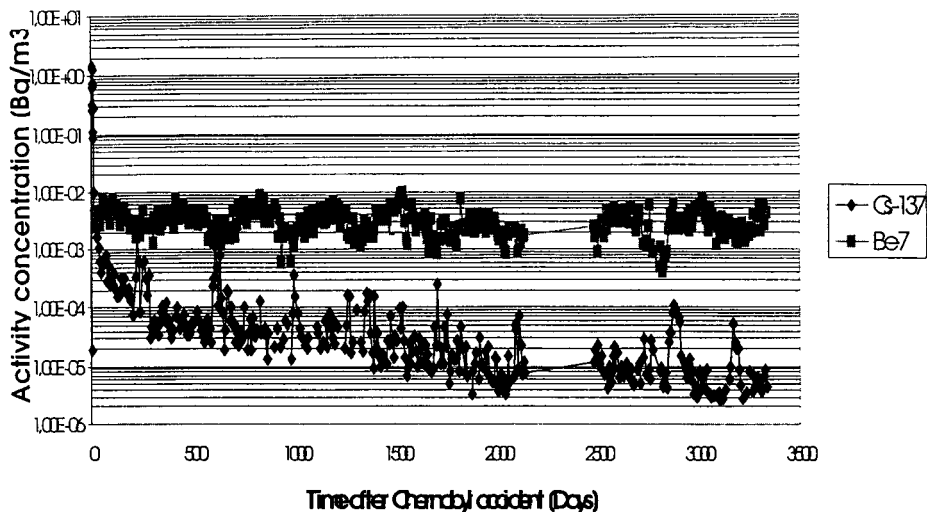


Figure 6.1 Long term variation of ^{137}Cs and ^7Be radionuclides in the ground level air of Budapest in function of time after the accident.

About 50 days after the accident an equilibrium was reached and the concentration of ^{137}Cs (the only significant radionuclide remaining by that time) was by then determined by the resuspension of deposited contamination. This process shows a basically two-component exponential decrease. The first (faster) component can be the result of the higher initial mobility of the surface contamination in the first months which was substantially diminished by the gradual fixation of the deposited radionuclides by the end of the first vegetation season. After this period the concentration of airborne radiocaesium decreases slowly with time, with some fluctuations especially during winters. This slow decrease is due to the migration of ^{137}Cs into the deeper layers of the soil.

The 'baseline' value of the resuspension factor K - the ratio of the air concentration to the deposition (5400 Bq/m^2 for Budapest) - can be expressed by the following function:

$$K = 1.04 \cdot 10^{-7} \exp\left(\frac{-\ln 2 \cdot t}{95}\right) + 6.5 \cdot 10^{-9} \exp\left(\frac{-\ln 2 \cdot t}{1500}\right) \quad (6.1)$$

where t is the time in days, elapsed since the primary clearance of the atmosphere (about 50 days after the accident).

Comparing the time dependence of resuspension factor K for ^{137}Cs with published data, IAEA(1992) - as shown in Fig. 6.2 - it can be seen that our results are close to the range given for the experimental values in Europe (though in the higher region) but they differ considerably from the predictions of prominent modellers.

The anomalous winter peaks, however, cannot be explained by the usual resuspension from the ground. These elevated concentrations (by one order of magnitude or more) were observed even when the soil was covered by snow. Excluding the possibility of stratospheric input

(which is contradicted by the contra-variation with the ^7Be concentration) trees and bushes uncovered by snow were identified as potential sources for resuspension in the local environment. In a study 100 - 1000 Bq/tree of ^{137}Cs was measured in the bark of medium size trees which results in an elevated airborne radiocaesium contamination in the winter when stronger winds can enhance detachment of aerosol-bound radionuclides from the outer skirt of the plants.

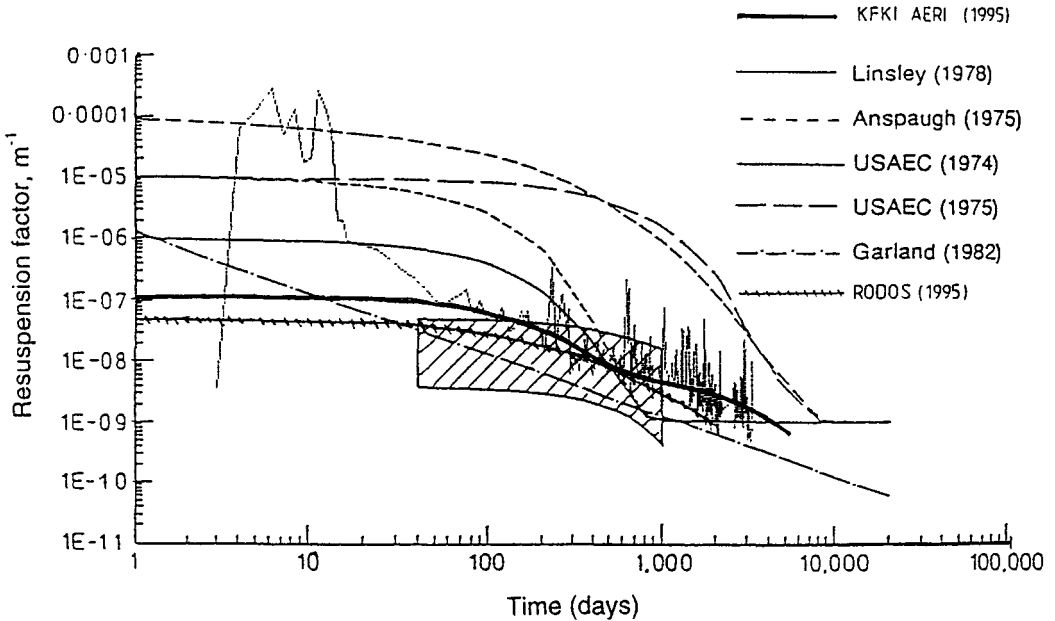


Figure 6.2 Resuspension factors (K) for radiocaesium measured in Europe (hatched area) compared with models. The model relationships are:

$$\text{KFKI AERI (1995)} \quad K = 1.04 \cdot 10^{-7} \exp(-0.0073 \cdot t) + 6.5 \cdot 10^{-9} \exp(-0.00046 \cdot t) ;$$

$$\text{Linsley (1978)} \quad K = 10^{-6} \exp(-0.01 \cdot t) + 10^{-9} ;$$

$$\text{Anspaugh (1975)} \quad K = 10^{-4} \exp(-0.15 \cdot t^{0.5}) + 10^{-9} ;$$

$$\text{USAEC (1974)} \quad K = 10^{-5} \exp(-0.0139 \cdot t) + 10^{-9} ;$$

$$\text{USAEC (1975)} \quad K = 10^{-5} \exp(-0.00185 \cdot t) + 10^{-9} ;$$

$$\text{Garland (1982)} \quad K = 1.2 \cdot 10^{-6} \cdot t^{-1} ;$$

$$\text{RODOS (1995)} \quad K = 5.0 \cdot 10^{-8} \exp(-0.003 \cdot t) + 10^{-9} ;$$

where t is time after deposition in days and K is in m^{-1} .

6.3 ^{137}Cs in the atmosphere of Prague

Through the years the locality of Prague has accumulated a ^{137}Cs contamination of about 5.2 kBq/m^2 from nuclear bomb tests and some 5.4 kBq/m^2 from the Chernobyl accident. The Institute of Radiation Dosimetry started to collect data on ^{137}Cs atmospheric radioactivity after the Chernobyl accident as a part of the resuspension monitoring network and since 1993 its programme became a part of this CEC Programme.

Aerosols have been collected on a 0.25 m^2 plane fibre filter at an air-flow rate of $150 \text{ m}^3/\text{h}$. The sampling period was mostly 14 days. Exposed filters were compressed into cylindrical shape and measured by gamma-spectrometry.

Combined dry and wet fallout has been sampled by a basin collector having 0.20 m^2 of collecting area covered by a constant level of water. At the end of the sampling period the deposition sample was filtered to separate the undissolved fraction and the filtrate water was evaporated to 0.45 l volume. Since July 1993 we stopped adding 0.1 N chloride acid to the water in the basin (which was recommended to prevent the fallout from hydrolysis and adsorption of ^{137}Cs on the basin surface). Subsequently, the filters were compressed to a cylindrical shape and the water was sealed in Marinelli beakers and then measured by gamma-spectrometry.

The sampling devices were located on the terrace of the institute's building (A) and since the winter of 1993-94 a second basin (B) was placed on the ground some 20 meters away from the institute.

6.3.1 Results

Results from 1993-1994 fit well with the trend observed since 1989. The long-term trend of radio-caesium aerosol concentration in the ground layer atmosphere (Fig. 6.3) shows a steady decline with a half-life of about 2 years. It may be explained by a decreasing resuspension with the resuspension factor of the order of magnitude of $1 \cdot 10^{-9} \text{ m}^{-1}$ or by the diminishing reservoir of available ^{137}Cs in the upper soil layer.

Garland and Pomeroy(1994) examined the dependence of the resuspension factor with the total deposition. In Fig. 6.4 the value for Prague ($K = 2.10^{-8} \text{ m}^{-1}$ and a total deposition of 5.4 kBq/m^2) can be seen together with the results from Garland and Pomeroy (1994). The resuspension factor for Prague seems to be slightly higher than a mean value corresponding to the local mixed deposition.

Fig. 6.5 shows a time sequence of the total ^{137}Cs fallout activity in both location A and B. The mean concentration in A is a factor of 1.5 higher for ^7Be and a factor 3 higher for ^{137}Cs compared to B, which indicates a strong locality dependence of the deposition of resuspended ^{137}Cs . The data on the mixed deposition and the activity concentration in the air were also used to calculate the deposition velocity of ^{137}Cs and ^7Be . The derived deposition velocities seems to be fairly constant for both ^{137}Cs and ^7Be since 1989. We examined the dependence of v_d on the precipitation intensity for ^{137}Cs and ^7Be (Fig. 6.6). There is a positive correlation for both radio-nuclides with precipitation, the slope for ^{137}Cs , however, is less steep than that for ^7Be . One of the possible explanations is that suspended ^7Be is more soluble than ^{137}Cs , another is that ^{137}Cs unlike ^7Be is spread mostly in the ground layer air.

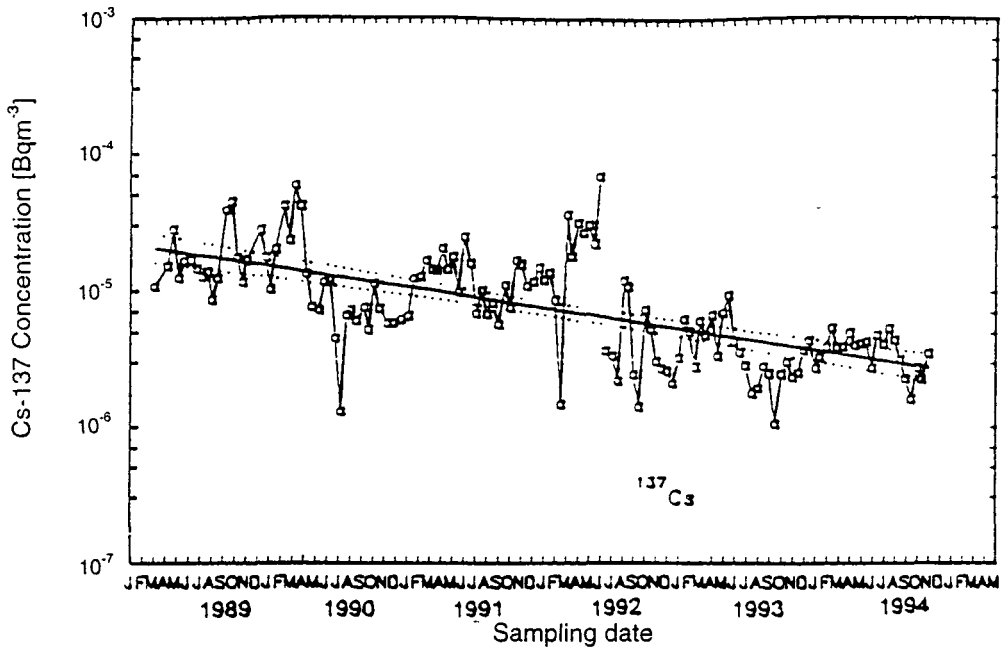


Figure 6.3 ^{137}Cs activity concentrations in Prague air from 1989 to 1994.

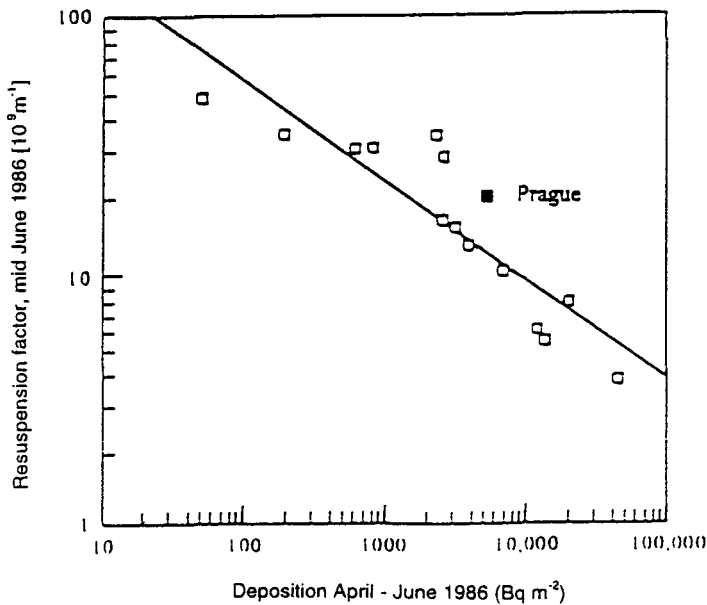


Figure 6.4 The variation of the apparent resuspension factor at a selection of European sites. The Prague value is plotted on a figure adapted from Garland and Pomeroy (1994).

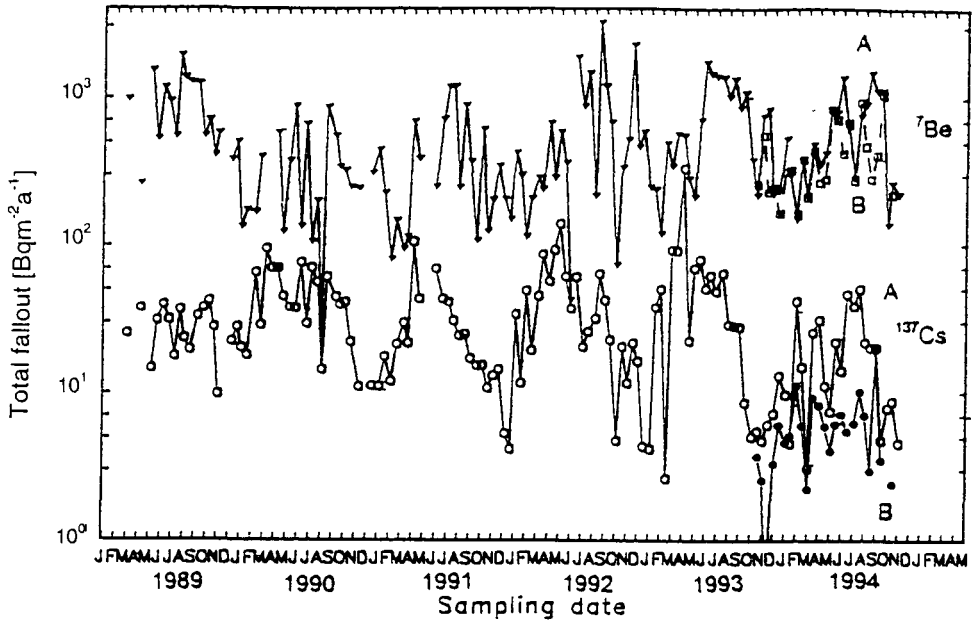


Figure 6.5 Mixed wet and dry deposition in Prague collected in two wet surface basins (A, B).

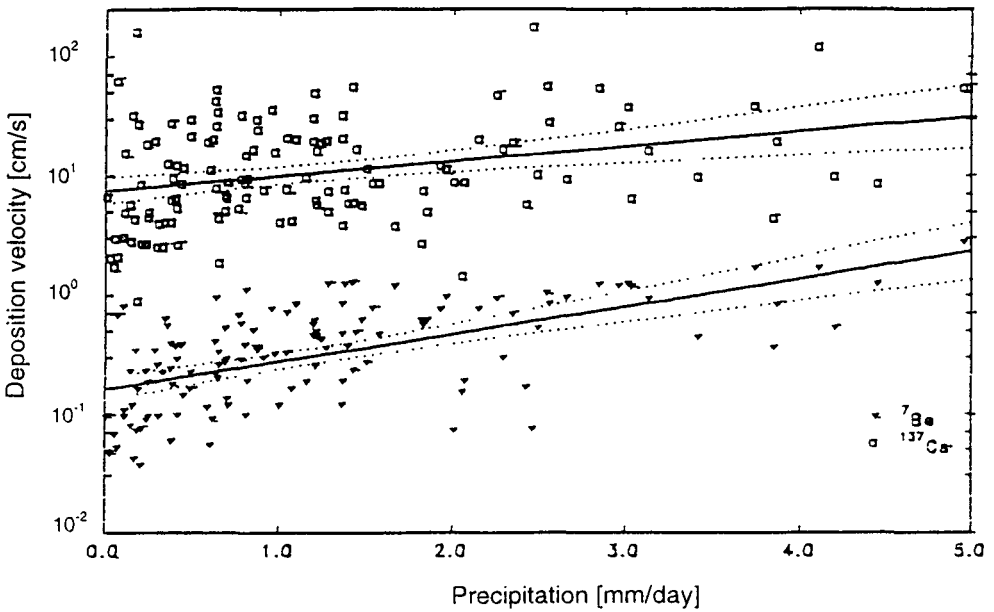


Figure 6.6 Apparent deposition velocity as a function of precipitation.

Solubility of the fallout ^{137}Cs and ^7Be in collector basin water was examined. Until the sampling procedure was changed by stopping the addition of 0.1 N HCl to the basin, the ratio of dissolved and undissolved fractions remained almost constant: about 70% undissolved ^{137}Cs and 5% undissolved ^7Be . Since this change occurred the undissolved fractions increased up to about 90% for ^{137}Cs (Fig. 6.7) and to about 30% for ^7Be . We further examined the influence of acidity on ^{137}Cs and ^7Be fallout solubility. It can be concluded from Fig. 6.7. and Fig. 6.8 that ^{137}Cs solubility is dependent on the acidity if pH is below 3. For ^7Be , the upper limit of dependence on the water acidity seems to reach at least pH=5 and thus it can be observed under natural conditions. However, under various natural conditions, e.g. acid rain, decaying vegetation in the upper soil layer etc., when low values of pH can be reached, the effect on ^{137}Cs solubility and thus its mobility and penetration in the depth should be taken into account.

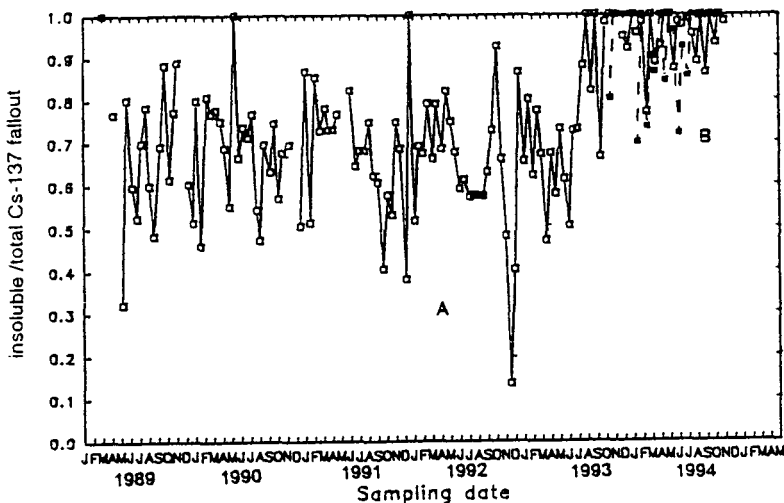


Figure 6.7 Insoluble/total ^{137}Cs collected in the two wet basins.

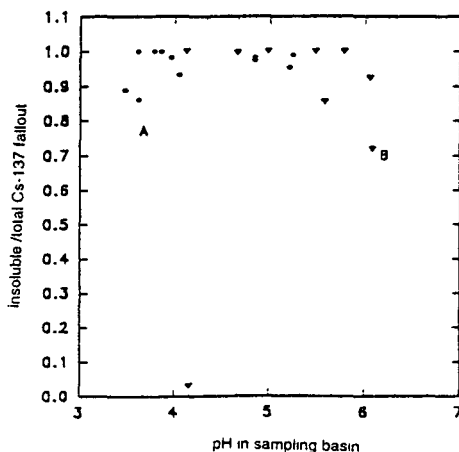


Figure 6.8 Insoluble ^{137}Cs fraction as a function of pH in the two basins.

6.4 Chemical fraction of radioactive caesium in atmospheric aerosol in Prague after the Chernobyl accident

Physico-chemical forms of radiocaesium released into the atmosphere during the nuclear power plant accident in Chernobyl can significantly influence its behaviour, above all resuspension and transport to other compartments of the natural environment, including the pedosphere and hydrosphere.

Hilton et al.(1992) analyzed ^{137}Cs forms in atmospheric aerosol collected in May 1986 in Oxfordshire (UK), and found marked differences compared to results of the analysis of samples collected in 1959 containing ^{137}Cs from nuclear weapon tests. The most distinct difference was in the water-soluble ^{137}Cs fraction amounting to 72% in the Chernobyl samples as compared to only 8% in the stored samples. On the other hand, Bobovnikova et al.(1992) found in the analysis of fallout material collected at a distance of 18 km from the Chernobyl NPP during the period of the accident 26 April - 3 May 1986 that for ^{137}Cs the insoluble form was dominant. The proportion of water-soluble radiocaesium was about 9% on average and during the studied period it ranged from 2.6 to 19%. Jansta (1988) found from the analysis of the fallout material collected in Košice (Slovak Republic) in the period 28 April - 21 May 1986 that the soluble fraction was less than 10% of the total ^{137}Cs activity in the fallout.

On the basis of these different results we decided to analyze the forms of radiocaesium on filter samples made in Prague during the period after the Chernobyl accident, Wilhelmová et al.(1989). The aim of this analysis was to verify the hypothesis that the physico-chemical forms of radiocaesium in the deposits following the accident depends on the transport conditions, including the distance of the sampling locations from Chernobyl.

A sequential extraction analysis was applied to four aerosol filters (marked A - D) made in the period of initial contamination after the Chernobyl accident. The set was then completed with an air filter sample E, which was exposed after the initial release had passed. For analysis, only a half of each filter was used, the initial area of the filter is 0.25 m². The parameters for the five filter samples are summarized in Table 6.1.

Table 6.1 Dates, volume and activities of analysed samples collected on FPP-1.5 Petrianova (USSR) filters.

Sample mark	A	B	C	D	E
beginning of exp*	30.4.86	1.5.86	4.5.86	6.5.86	12.5.86
end of exp*	1.5.86	2.5.86	5.5.86	7.5.86	19.5.86
sample volume**/m ³ /	3456	3382	3324	3314	22429
^{137}Cs activity***/kBq/	25.2	1.86	3.06	1.25	0.037

*6.15 GMT

**the volume recalculated to 1/2 of initially exposed filters

*** corrected to 30 April 1986

The procedure used for sequential analysis was based on the method proposed by Tessier et al.(1989) for the study of soils and modified for the analysis of aerosol filters as described by Hilton et al.(1992). Only leaching with warm hydrofluoric acid (HF) was not used. Solutions

were prepared from chemicals pure for analysis and distilled water. Their concentrations, temperature at the start of leaching and application period are given in Table 6.2. Leaching was carried out in 250 ml polyethylene bottles placed in a laboratory shaking machine during the application period. After leaching had finished, the solution was centrifuged at 3000 rpm and poured off or filtered. Each solution was applied in two doses of 200 ml, the second part was used for rinsing the analyzed sample. Only in the last step, after leaching the mixture of H₂O₂ and HNO₃, a solution of ammonium acetate was used for rinsing. Both fractions were poured together into a Marinelli beaker and distilled water was added up to a volume of 450 ml. The ¹³⁷Cs activity in the analyzed filters, solutions and in the undissolved residue was determined by gamma-spectroscopy using a GeLi detector.

Table 6.2 Solutions and conditions of a sequential analysis

Step	Extractant	Application time /h/	Temperature /°C/
1	distilled water	65	ambient
2	1M MgCl ₂ (pH 7)	1	ambient
3	1M NH ₄ Cl	1	ambient
4	1M NaOAc (pH 5)	1	ambient
5	0.04M NH ₂ OH.HCl in 25% HOAc	1	96
6	0.1M HCl	1	ambient
7.a	3 vol. 0.02M HNO ₃ + 5 vol. 30% H ₂ O ₂	2	60
7.b	3.2M NH ₄ OAc in 20% HNO ₃	wash out	ambient

6.4.1 Results

The results of the sequential analysis of ¹³⁷Cs forms in the samples of atmospheric aerosol collected in Prague in the period of direct contamination after the Chernobyl accident are summarized in Table 6.3 and illustrated in Fig. 6.9. For comparison are also given the results of the analysis of a sample from a later period E and the results adopted from Hilton et al.(1992) concerning atmospheric aerosol collected at Oxfordshire (UK) in May, 1986. Also mentioned are the fractions of ¹³⁷Cs activity dissolved in the individual steps, standardized to total activity in the solutions and the undissolved residue.

From the results it is obvious that the dominant fraction was the water-soluble radiocaesium, ranging from 40 to 49%. The higher value in the case of sample C was most likely caused by the presence of turbidity which could not be removed by filtration. The determined fraction is however substantially lower than the results given by Hilton et al.(1992), who found 72% of soluble ¹³⁷Cs. The second most important fraction was formed by undissolved residues. Here the fraction of ¹³⁷Cs ranged from 2 to 26%, gradually decreasing with time after the accident. Another significant portion was found after leaching with MgCl₂ solution, i.e. in the fraction subject to ion exchange. This portion ranged from 14 to 25% and did not seem to depend on time after the release. The percentage of ¹³⁷Cs in this fraction also differs significantly from the results published by Hilton et al.(1992). The use of acid leaching and omitting steps 4 and 5 in the case of samples A and C resulted in the shift of the respective caesium fractions. They were separated only in the 7th step after application of H₂O and ammonium acetate in HNO₃.

The results of analysis for sample E showed an increase in the radiocesium content of the undissolved residue and a decrease of the water-soluble fraction. This was as expected when resuspended material becomes the main contamination source of ground atmosphere layers after the initial release has passed. In resuspension insoluble caesium fractions are prevailing, because they stay in the surface without penetrating into deeper soil layers. In addition to this, the increase with time of the insoluble ^{137}Cs fraction will be influenced by the interaction of soluble radiocesium fractions with soil complexes which results in the firm binding of radiocesium with soil particles and its immobilization in the surface soil, Palágyi and Palágyiova (1994).

From the results presented it can be concluded that the physico-chemical forms of radiocesium in the atmospheric aerosol and deposits after the Chernobyl accident (as well as size distribution of contaminant particles) depends on the distance and the conditions of the transport from the contamination source to the sample location. This change of form could explain the observed differences in the penetration of ^{137}Cs into the soil and the variations of the resuspension factor for different European locations reported by Garland and Pomeroy (1994).

Table 6.3 Results of a sequential extraction analysis of radio-caesium in atmospheric aerosol samples (portion of the total activity in %)

Step	Extractant	A	B	C	D	E	UK**
1	H ₂ O	43	44	49*	40	30	72
2	MgCl ₂	14	21	16	26	16	0,5
3	NH ₄ Cl	3	4	4	7	3	15
4	NaOAc+HOAc	N	2	N	6	1	3
5	NH ₂ OH.HCl+HOAc	N	2	N	8	2	2
6	HCl	2	N	3	N	N	N
7	H ₂ O ₂ + HNO ₃	12	2	13	11	6	2,5
8	Residue	26	25	15	2	43	5

*non-filtrable turbidity

**taken from Hilton et al. (1992)

N the solution was not applied

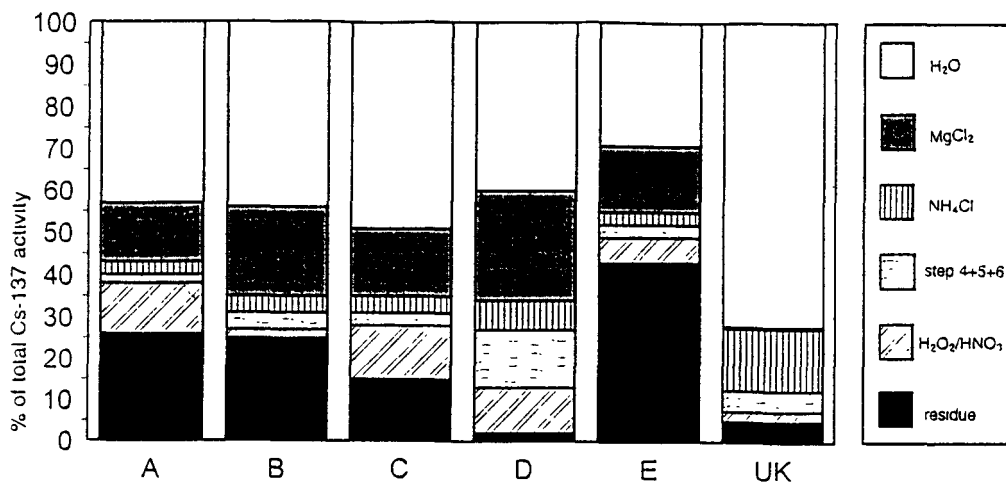


Figure 6.9 Chemical fraction of ¹³⁷Cs in air samples collected in Prague following the Chernobyl accident compared with results from the UK by Hilton et al. (1992).

6.5 Speciation of deposited artificial radionuclides

Atmospheric aerosols are, through deposition, the basic source of food chain contamination by artificial radio-nuclides after an accident as well as during normal conditions. Water and acid soluble forms in aerosols, together with soluble and pseudo-colloidal forms in the resulting deposits are very important parameters from this point of view.

Atmospheric precipitation and dry deposition were sampled monthly in Košice - Horný Bankov. A stainless steel sampling funnel with an area of 4 m² (2 m x 2 m), situated on the roof of our monitoring station was used. Samples were collected and stored in polyethylene cans until analysed. The analysis sequence consisted of filtration with membrane filters (8 μm followed by 0.45 μm pores) and subsequent columns of cation exchanger, anion exchanger and activated charcoal. The individual segments of this line were then dried, transferred into Petri dishes and counted gamma-spectrometrically. ⁹⁰Sr was determined radio-chemically.

For the measurements of airborne radionuclide concentrations an air-sampler with an air flow of 20 - 200 m³/h was used with nitro-cellulose microfibre filters with an area of 0,34 m². Navarcík and Jansta (1989). The collected filters were gamma-spectrometrically analysed. Furthermore, extracts with water and 2 M HNO₃ were made, evaporated and counted. Radiochemical determination of ⁹⁰Sr was then made, Jansta (1988).

6.5.1 Results

The total activity in atmospheric aerosols and the ratio of water-soluble, available (acid-soluble) and insoluble forms of radio-nuclides in the aerosols are presented in Fig. 6.10-6.12. ¹³⁷Cs activity in aerosols shows seasonal variation: maximum at the end of the autumn, during the winter and at the start of the spring and minimum during the summer, except July 1994, are characteristic. The water-soluble form is prevailing in the winter months, the acid-soluble in the summer months and the insoluble form at the end of the spring and in the start of the summer. For the winter months the contribution of the insoluble forms is negligible. The total activity of

^{90}Sr in aerosols has maximal values in winter and summer periods, a spring maximum is absent. Acid-soluble form is dominant. The insoluble form is prevailing in the summer period. The total activity of cosmogenic ^7Be in aerosols has a maximum in the spring and summer months, due to the so called European summer monsoon, that can occur from April to June or August. The acid soluble form is the least represented fraction. The predominance of the water-soluble and the insoluble forms can not be described seasonally. In the spring and summer months insoluble forms are prevailing (except June 1994). In the autumn and winter months the contribution of water soluble forms prevails.

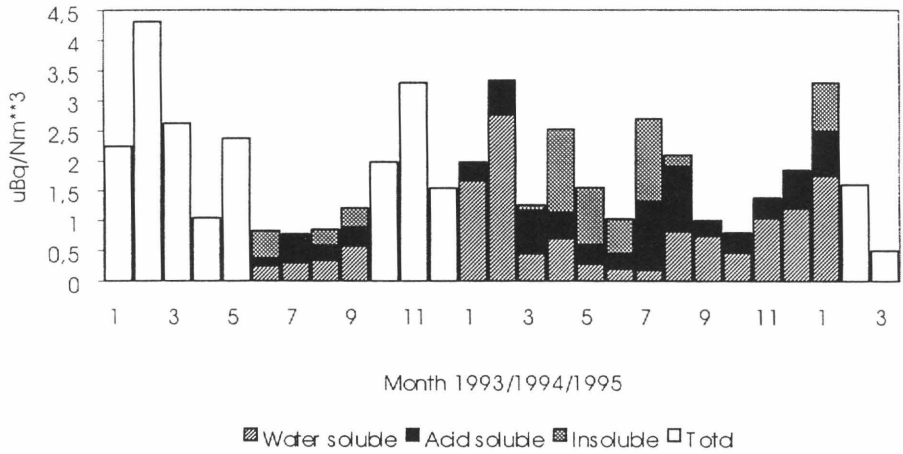


Figure 6.10 ^{137}Cs activity concentration in atmospheric aerosol sampled at Horny Bankov.

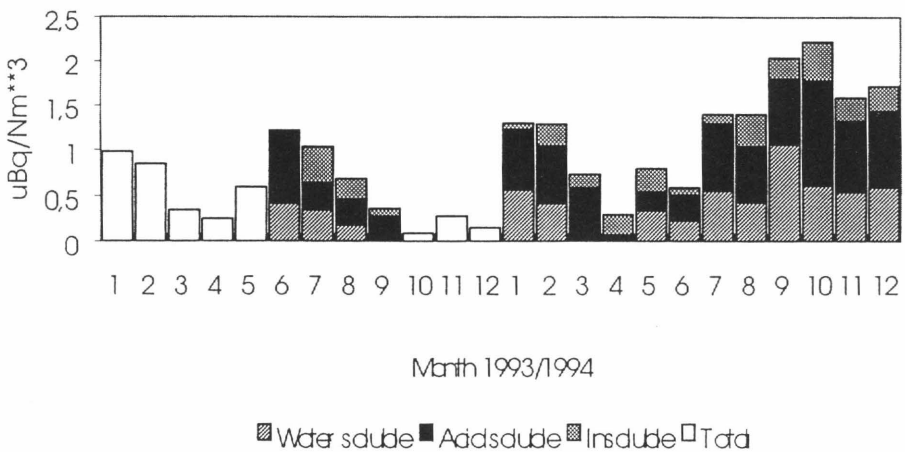


Figure 6.11 ^{90}Sr activity concentration in atmospheric aerosol sampled at Horny Bankov.

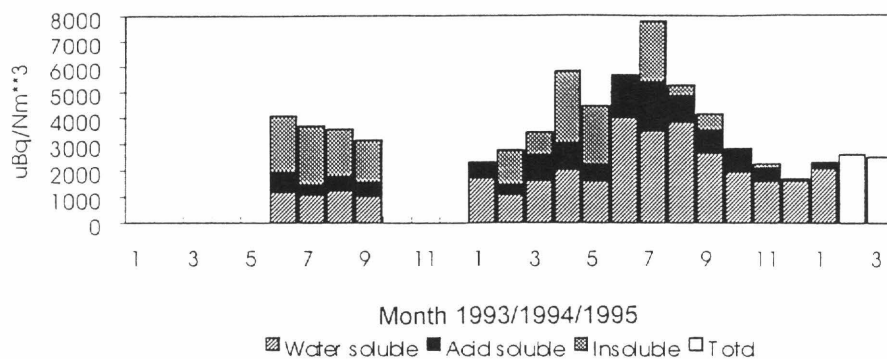


Figure 6.12 ⁷Be activity concentration in atmospheric aerosol sampled at Horny Bankov.

The results of total activities and speciation of radionuclide forms in mixed wet and dry deposition are presented in Fig. 6.13 - 6.15.

The total ¹³⁷Cs activities in dry and wet deposition are characterised by a conspicuous spring maximum (mainly in May) and a minimum in the autumn and winter. The particulate forms are dominant and their fraction is maximal in the spring. The soluble forms that were separated by cation exchange are prevailing, having the highest representation in the spring and summer. The contribution from other forms is minimal.

The total activity of ⁹⁰Sr in dry and wet depositions has a spring maximum, that can continue into the summer period. The soluble forms separated by cation exchange and the particulate forms are the dominant extractions. A significant fraction separated on active charcoal, probably representing pseudo-colloids, is an interesting finding. It is impossible to unambiguously determine seasonality of mutual forms ratio.

The total activity of cosmogenic ⁷Be in dry and wet deposits has a seasonal maximum in the spring and summer months and a minimum in the winter. The cationic form is dominant, the insoluble particulate fractions is also significant. The forms separated by anion exchange and active charcoal are not characteristic. The seasonality of the forms ratio can not be unambiguously determined.

In June and July 1994 sampling of aerosols and depositions was modified to obtain samples for dry and wet periods separately. Activities of ¹³⁷Cs and ⁹⁰Sr in aerosols and deposits were in majority of cases below the detection limit. Results indicate that the capacities of our samplers at present concentrations of ¹³⁷Cs and ⁹⁰Sr activities are not sufficient for this type of sampling.

For a more detailed characterisation of the seasonal variations of radionuclide forms in aerosols and in the deposits it is necessary to monitor them for several years.

A correlation analysis between individual parameters was carried out for each of the observed radio-nuclides in the air samples and in the deposits. The total activity of ¹³⁷Cs and ⁷Be in the mixed deposits, as well as particulate form and water-soluble form, significantly correlate with the precipitation, indicating the importance of precipitation for the transfer of airborne activity to the ground. The most significant correlations were determined for cosmogenic ⁷Be. This is

due to the different physico-chemical characteristics of ^7Be compared to ^{137}Cs and ^{90}Sr . ^7Be originates in the high layers of the atmosphere and during transport the chemical reactions of ^7Be with the components of the atmosphere are probably finished and they only slightly influence the deposition process of the ground-level ^7Be .

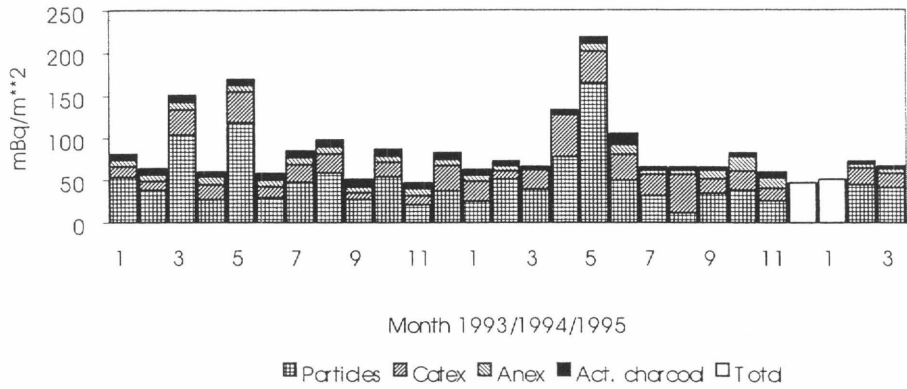


Figure 6.13 ^{137}Cs in total deposition (wet and dry) sampled at Horny Bankov.

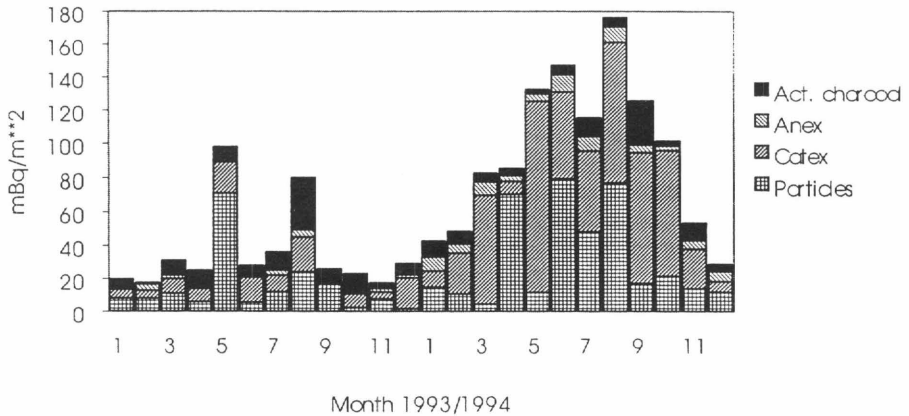


Figure 6.14 ^{90}Sr in total deposition sampled at Horny Bankov.

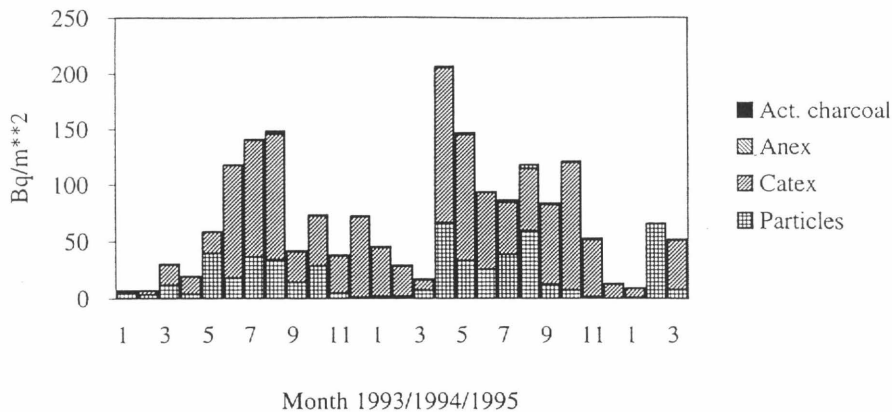


Figure 6.15 ⁷Be in total deposition sampled at Horny Bankov.

6.5.2 Discussion

The study of artificial radionuclide transport from source to man through the food chain is one of the most important tasks of our research activity. The result has to be the preparation of a dynamic mathematical model of transport for planning of medium and long term countermeasures.

The contamination of plants happens in two ways:

1. direct contamination of above ground plant parts (mainly leaves and pine-needles)
2. uptake through root system of soil deposits.

A part of the deposited activity of directly contaminated plant surfaces (mainly leaves) will be removed by rainwater or by washing of the harvested plant. The removable portion is high in the beginning, but decreases with time due to the transport of radio-nuclides into the plant tissue. The water soluble forms especially will be transported, but also the particulate forms with dimensions smaller than the pore size can be absorbed. The influencing on the solubility by the plant enzymes is minimal in this case. The uptake through the roots from soil takes place through the binding of the dissolved ionised forms by the plants transport enzymes. The water soluble as well as the particulate forms with dimensions smaller than the soil capillaries are transported from the soil surface to the roots. The particulate forms may be dissolved by micro-biological action and by action of the plant enzymes. All these forms of each radionuclide have individual transfer velocity constants between each food chain compartment. The effort to verify the calculation models for food chains brought us to the actual selection of the described speciations. Unfortunately, the models used at present do not enable the application of individual velocity constants.

The total activities of radio-nuclides as well as the speciation ratios in the air samples have a seasonal variability. There are at least two possible explanations for this:

1. The seasonality of the total activities is determined by the laws of long distance transport of contaminants as well as by the magnitude of resuspension in the neighbourhood of the locality. The speciation ratio variability depends on the physic-chemical characteristics of the radio-nuclides and the local aerosols as well as on the type and the intensity of the photochemical reactions between them.
2. The activity peaks could be related to the pollination of plants, mainly trees.

Seasonality in the mixed deposition is present too, but the total deposited activities are strongly influenced by precipitations (rain, fog, snow). The speciation of the deposits needs not to be similar to the speciation of the airborne activity. The differences are probably caused by chemical reactions during the deposition processes and by the differences of aerosols from various heights and places of origin.

The correlations between the radio-nuclides are determined by the physico-chemical characteristics of the radio-nuclides, the character of the source of the radioactive contaminants and by the affinity of the airborne radio-nuclides to the components for the local aerosols and the deposition mechanism.

6.6 Resuspension studies in Goiania, Brazil

GSF have participated in the study of resuspension after the Goiania accident in Brazil and a full description of the achievements is given by Pires de Rio et al. (1994). The contamination was caused by an accidental opening of a ^{137}Cs teletherapy source, which led to the contamination of about 1 km^2 with app. 50 TBq ^{137}Cs . From the evaluation of the environmental measurement the following conclusions can be derived:

- The activity concentrations in air and deposition rates of resuspended ^{137}Cs in Goiania, two years after the primary contamination, show a very slow long-term decrease with time but a significant seasonality (see Fig. 6.16 and Fig. 6.17).
- The results indicate that the resuspension and deposition of ^{137}Cs is a local phenomenon and resuspension factors of the order of 10^{-8} to 10^{-9} m^{-1} were derived for this scenario.
- No significant correlation between the air activity and its deposition rate was found and a wide range of elevated values for the deposition velocities was observed. The results confirm that in an urban area rather complex processes determine resuspension.
- Average nominal dry deposition velocities of about $5\text{-}6 \text{ cm s}^{-1}$ were found. The usual assumption of a deposition velocity of 0.1 cm s^{-1} for measured air activity concentrations would underestimate the actual deposition rates by a factor of approximately 50-60.
- Andersen impactor measurements indicate that about 30 to 60 % of the total aerosol mass in air might result from aerosol particles above $15 \mu\text{m}$ diameter; these are not collected by the EPA-type air samplers.
- No significant spreading of ^{137}Cs throughout the city occurred during this study from the initially contaminated area by resuspension and air transport. This is to be expected from these measurements since most activity is associated with large particles with high deposition velocities.
- In addition, the contribution of resuspension and soil adhesion to the contamination of leafy vegetables was studied. The contributions of soil splash were found to account for 70-90 % of the contamination of lettuce and for 50-60 % for green cole. The results call attention to the possibly important contribution of the soil splash to radionuclide uptake by plants which have edible parts near the surface and low root uptake transfer factors.

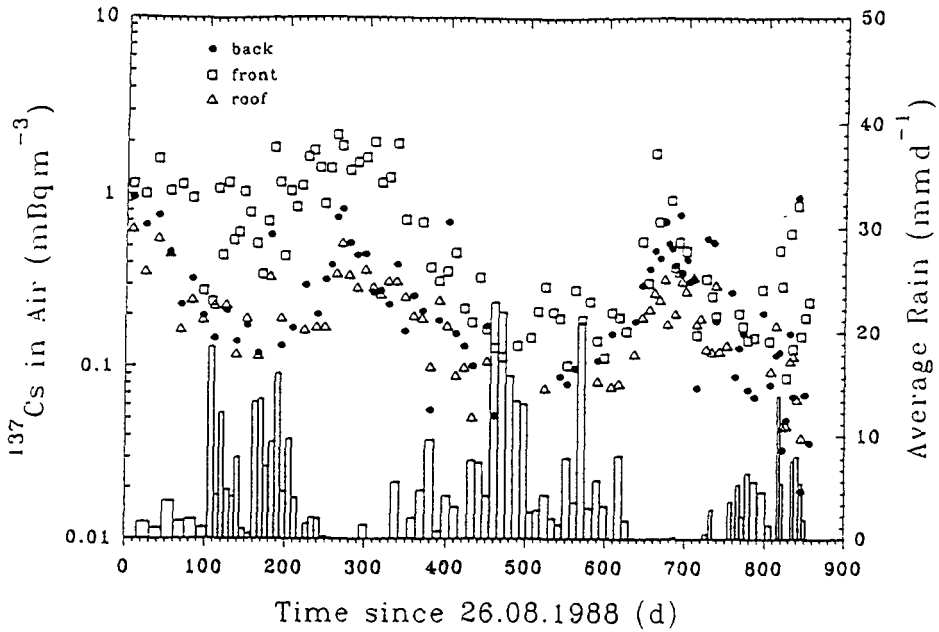


Figure 6.16 ^{137}Cs activity concentrations in air as function of time after the start of the measurements by an EPA-type sampler and average rainfall during the sampling period ("back": backyard at 1 m height, "front": frontyard at 1 m and "roof": backyard at 3 m height.).

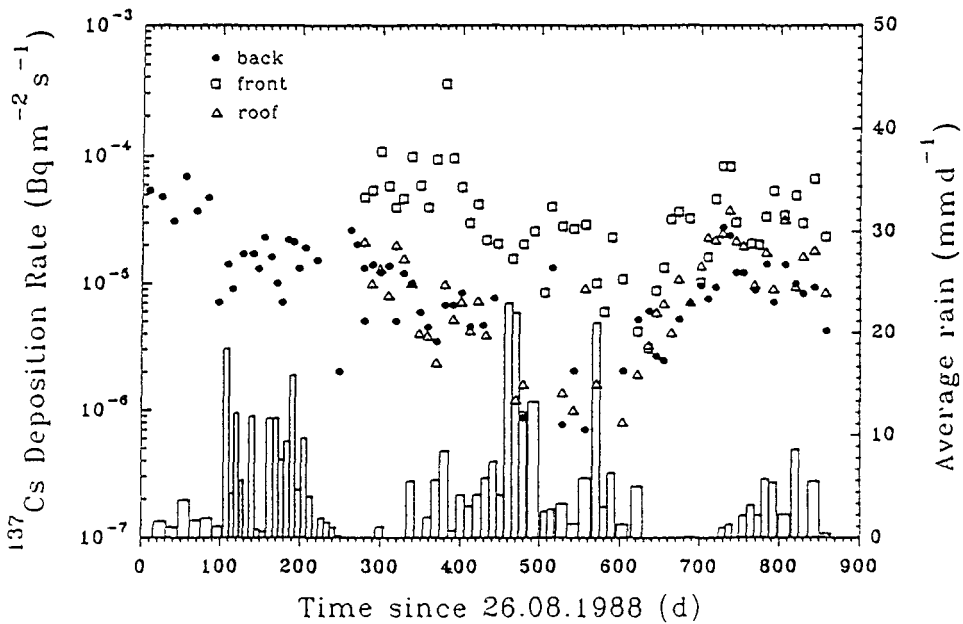


Figure 6.17 ^{137}Cs deposition rate as function of time after the start of the measurements by an EPA-type sampler and average rainfall during the sampling period ("back" backyard at 1 m height, "front": frontyard at 1 m height and "roof": backyard at 3 m height.).

6.7 Radionuclide resuspension and mixed deposition at different heights

The radionuclide content in the atmosphere have been monitored for more than 30 years at Risø National Laboratory. After the initial release from the Chernobyl accident had settled the ^{137}Cs content in the atmosphere and the derived resuspension factor have shown a two component decrease similar to that observed by the other partners. Results are summarised in Aarkrog et al.(1992). The two exponential expressions had a half-live of 157 days with an initial value of 55×10^{-9} and 2410 days with an initial value of 6.7×10^{-9} .

As a part of the study of the behaviour of radio-nuclides undertaken under this research contract two rain collectors were constructed in one and three meters height above ground in order to enable the study of the height dependence of resuspension for ^{137}Cs . Each collector had a surface area of 10 m^2 and they were situated app. 15 meters apart. The nearest major source for resuspension was a highway 200 meters away with a medium traffic load (app. 10,000 cars a day). The site was shielded against the wind by trees, bushes and buildings in the vicinity.

The rainwater was sampled on a monthly basis, filtered and ion-exchanged. After emptying the rainwater tank the surface of the collectors was cleaned with 1 % HNO_3 acid and rinsed with water. The wash-off and the filter-mass from the ion-exchangers was dried, incinerated and mixed with the ion-exchange material. The sample was then analysed by gamma-spectroscopy for Cs-137 and Be-7. From the speciations made by IR we can see that nearly all the activity is present in the particulate and ion-exchanged (water soluble) fractions and that no significant activity is lost by not using active charcoal for a final filtering.

Activity levels in air is determined by gamma analysis of weekly $300,000 \text{ m}^3$ air samples using glass-fibre and cellulose filters. Typical ^{137}Cs levels range from 0.5 to $2 \mu\text{Bqm}^{-3}$ and ^7Be have a typical activity concentration around $2500 \mu\text{Bqm}^{-3}$. The average resuspension factor for ^{137}Cs during the three and a half year of measurements was $1.01 \times 10^{-9} \pm 0.51 \times 10^{-9}$.

The correlation between the amount of ^{137}Cs deposited on the two collectors, the air activity concentrations and the precipitation have been examined. From Table 6.4 it can be seen that the mixed deposition have little or no correlation with precipitation with correlation coefficients of 0.024 and 0.109. This can also be seen on Figure 6.18. The collector at 1 meters height also had a low correlation with the air concentration ($r=0.012$), whereas the mixed deposition in 3 meters height had a reasonable correlation ($r=0.556$), Figure 6.19, with the air activity. Looking at a time series of the measurements it can be seen that in the 17 months of the experiment the low rain collector had increased levels of ^{137}Cs compared to the high rain collector that did not correlate either to the air concentration or to the measurements from the high collector. At this time the surface of the low rain collector was changed from glass-fibre to stainless steel. After this change the measurements at the low rain collector have started to show better correlation with the air concentration and the measurements at the high collector. It is our belief that the remnant of ^{137}Cs from the first shower over Risø after the Chernobyl accident still was present in the relatively rough surface of the glass-fibre. Taking the average deposition velocity, 0.018 ms^{-1} , observed for ^{137}Cs as a sedimentation velocity, it corresponds to a mean particle size of $24 \mu\text{m}$. In summary, the observed deposition pattern for ^{137}Cs corresponds with a thin layer close to the ground with relatively large resuspended particles.

Table 6.4 Correlation factors between mixed deposition and air concentration of ^{137}Cs and precipitation. The last column of the table refers to the last 19 months where the low rain collector had a stainless steel surface.

Species	Correlation with precipitation	Correlation with ^{137}Cs in air	Correlation with ^{137}Cs in air - last 19 months
^{137}Cs 1 meter	0.024	0.012	0.319
^{137}Cs 3 meter	0.109	0.556	0.795

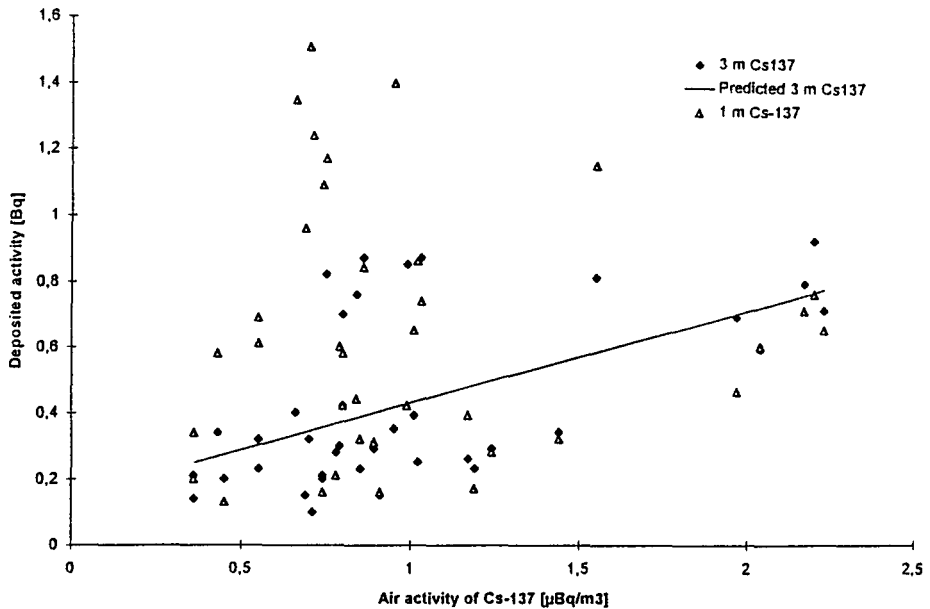


Figure 6.18 Mixed deposition of ^{137}Cs as function of air concentration at 3 m height.

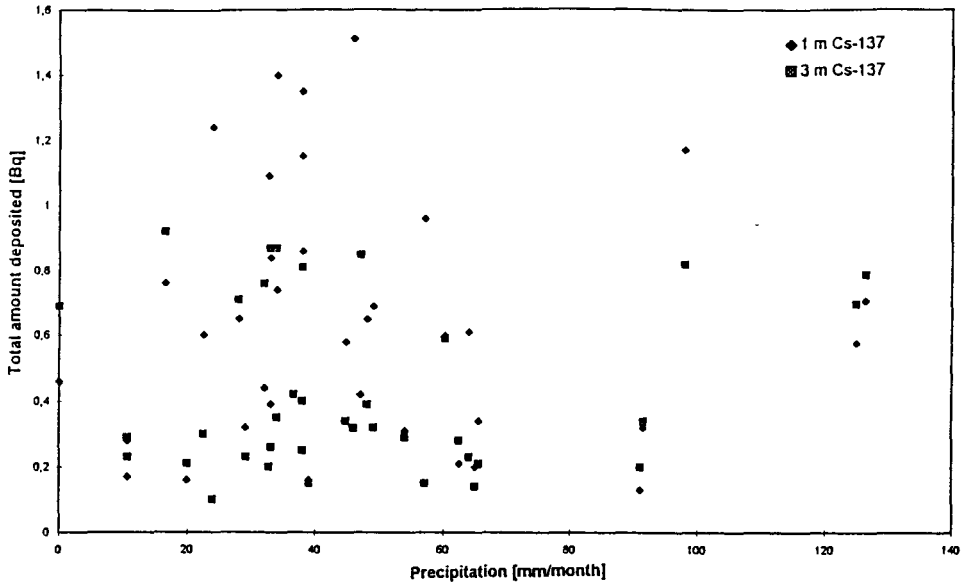


Figure 6.19 Mixed deposition as function of precipitation for ^{137}Cs .

The ^7Be measurements at the two heights were almost identical. The average activity collected was 596 Bq at 1 meters height and 631 Bq at 3 meters height. The correlation between the mixed deposition and the air activities was small ($r=0.26$, see Table 6.5), but a good correlation was found between the mixed deposition and the precipitation ($r=0.68$ and $r=0.59$). By dividing the total deposition with the average air concentration during the month and the sampling time a deposition velocity was derived. The deposition velocity correlated very well with the precipitation ($r=0.76$ for the combined 1 & 3 meters measurements, Figure 6.20). From the slope of the regression and some assumptions on average rainfall intensities wash out coefficients can be obtained. The good correlation between ^7Be deposition and precipitation is in good agreement with the knowledge that ^7Be labelled particles are present in increasing concentrations up through the atmosphere and thus subject to scavenging over a much wider range than ^{137}Cs labelled particles.

Table 6.5 Correlation factors for the ^7Be measurements.

Species	Correlated against:	Correlation coefficient	Slope $\text{ms}^{-1}/\text{mm rain}$	Y-axis intercept ms^{-1}
^7Be 1 m	precipitation	0.68		
^7Be 3 m	precipitation	0.59		
v_d 1 m	precipitation	0.73	0.000234 ± 0.000039	0.0012 ± 0.0016
v_d 3 m	precipitation	0.74	0.000212 ± 0.000037	0.0016 ± 0.0015
v_d 1 & 3 m	precipitation	0.76	0.000224 ± 0.000024	0.0014 ± 0.0010
^7Be 3 m	air conc.	0.26		

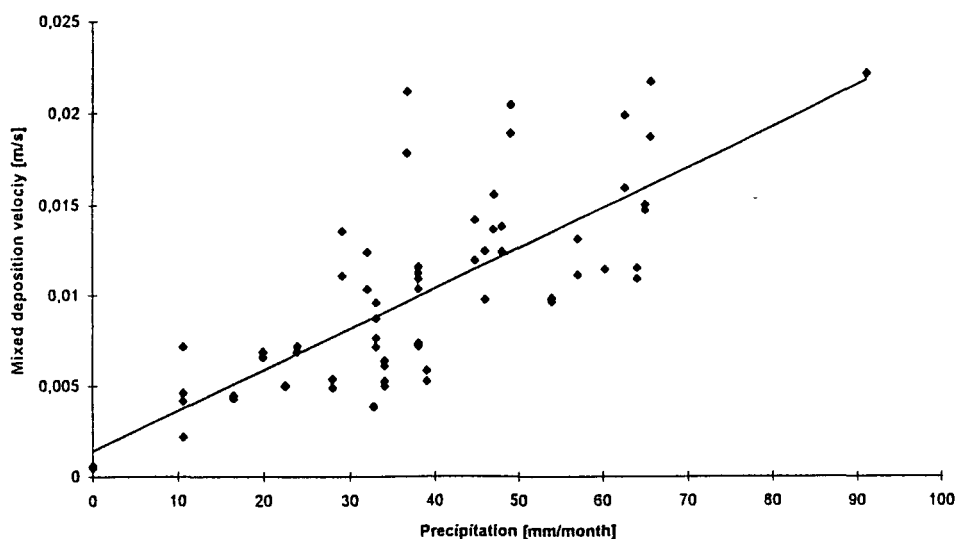


Figure 6.20 Mixed deposition velocity as function of precipitation for ^7Be .

The y-axis intercept corresponds to the dry deposition velocity for ^7Be . The activity size distribution measurements of ^{137}Cs after Chernobyl, Tschiersch and Georgi (1987), and ^7Be , Lange (1994) are almost identical. In one sampling month there was no precipitation and the deposition velocity here was $5.2 \pm 0.6 \times 10^{-4} \text{ ms}^{-1}$. This corresponds well with the deposition velocities found for ^{137}Cs on smooth surfaces after Chernobyl and it supports the assumption that ^7Be results are similar to those for other long-range transported materials.

6.8 References

Aarkrog, A.; Bøtter-Jensen, L.; Qing Jiang, C.; Dahlgaard, H.; Hansen, H.; Holm, E.; Lauridsen, B.; Nielsen, S.P.; Strandberg, M. and J. Søgaard-Hansen, Environmental Radioactivity in Denmark in 1990 and 1991, Risø-R-621(EN), 1992.

Bobovnikova C.I., Machonko K.P., Siverina A.A., Rabotna F.A., Gutareva V.P., Volokitin A.A.: Physico-chemical forms of radionuclides in the fallout after the NPP accident at Chernobyl and their transport in soils. (In Russian.) Atomnaya Energiya 71, no. 5, pp. 449 - 454, 1991.

Feher, I.; Experience in Hungary on the radiological consequences of the Chernobyl accident. Environmental International, Vol. 14, Pergamon Press, 1988

Garland J.A., Pomeroy I.R.: Resuspension of fall-out material following the Chernobyl accident. J. Aerosol. Sci., Vol. 25, pp.793-806, 1994.

Jansta V.: Separation of species of radionuclides from precipitation and fallout samples. J. of Radioanal. Nucl. Chemistry, Vol. 121, pp. 295 - 306, 1988.

Jansta, V., Navarcík, I., Datelínka, I., Cipáková, A.: Speciation at deposition of artificial radionuclides, *Journal of Radioecology*, Vol. 2, pp. 3-11, 1994.

Hilton J., Cembray R.S., Green N.: Chemical fractionation of radioactive caesium in airborne particles containing bomb fallout, Chernobyl fallout and atmospheric material from the Sellafield site. *J. Environ. Radioactivity*, Vol. 15, pp. 103 - 111, 1992.

Lange, C., Size distribution of atmospheric particles containing Beryllium-7, *Journal of Aerosol Science*, Vol. 25, S1, pp. 55-56, 1994.

Modelling of resuspension, seasonality and losses during food processing. First report of the VAMP Terrestrial Working Group. IAEA-TECDOC-647, 1992

Navarcík, I., Jansta, V.: System of atmosphere radioactivity monitoring, Symp. INTERECOCONTROL, INCHEBA, Bratislava, June 27-29, 1989

Palágyi, Š., Palágyiová, J.: Migration of radionuclides in undamaged vertical soil profiles. (In Czech.) Report of Radiation Dosimetry Department of the Institute of Nuclear Physics of the Academy of Sciences 396/94, Prague 1994.

Pires do Rio, M.A., Amaral, E.C.S., Paretzke, H.G.: The resuspension and redeposition of ¹³⁷Cs in an urban area: The experience after the Goiania accident. *J. Aerosol Sci.*, Vol. 25, 821-831, 1994.

Tessier, A., Campbell, P.G.C., Bisson, M.: Sequential extraction procedure for the speciation of particulate trace metals. *Analytical Chem.*, Vol. 51 (7), pp. 844 - 851, 1979.

Tschiersch, J. and B. Georgi, Chernobyl Fallout Size Distribution in Urban Areas, *J. of Aerosol Science*, Vol. 18, No. 6, pp. 689-692, 1987.

Wilhelmová, L., Tomášek, M., Rybáček, K.: Evaluation of air radioactivity in Prague after the Chernobyl accident. *Isotopenpraxis*, Vol. 35, pp. 124 - 126, 1989.

7. Modelling of the radiological impact of a deposit of artificial radionuclides in inhabited areas

Kasper G. Andersson and Jørn Roed
Risø National Laboratory, MIL-114
4000 Roskilde
Denmark

Herwig G. Paretzke and Jochen Tschiersch
GSF-Institut für Strahlenschutz
85758 Oberschleißheim
Germany

Introduction

Prior to the Chernobyl accident in 1986 very little thought had been given to the behaviour of radioactive fallout deposited in an urban environment or indeed as to how the contaminated area might be cleaned. The reason for this may be the erroneous assumption that the consequences of credible accidents would be relatively short-term and restricted to rural areas. As a result of the Chernobyl accident a need has emerged for contingency strategies which enable the consequences of radioactive contamination of large urban areas to be identified and dealt with as early as possible following contamination. The URGENT (URban Gamma Exposure Normative Tool) model has been developed in order to facilitate the decision-making in such cases. The aim of this work is to use experimental data to describe the system of retention/migration loss processes which might occur on outdoor surfaces in a radioactively contaminated urban environment. The resulting gamma doses can then be calculated for four different urban or suburban environments using the dose conversion factors presented by Meckbach et al. (1988). The model is restricted to cover the behaviour of the single most important radionuclide concerning external dose from urban contamination - namely ^{137}Cs . Further, a semi-empirical model has been introduced to estimate the relative importance of radiocaesium deposition on internal surfaces of buildings. Also described is a different model for radiological assessments in urban areas, PARATI, which has been developed for similar purposes. The basic functions of the PARATI code are to estimate the radiation exposures for different groups of people as a function of time after an accident with the indication of the fractional contributions to this exposure from each pathway, and to indicate the feasible countermeasures and their relative effectiveness regarding reduction of doses. The two models of which results are presented in this chapter are not the only urban dose models that have been developed in the EU. Also the URBAPAT model developed by CIEMAT in Spain and the EXPURT model developed by NRPB in UK, from which results were presented as early as 1987, were developed for similar purposes.

7.1 Methods for calculation of doses from outdoor sources

This section describes the methods and assumptions made in the development of the URGENT and PARATI codes as well as the background for the semi-empirical model developed for calculations of relative dose rate from radionuclides deposited on internal walls of buildings.

7.1.1 The URGENT model

The model URGENT runs on a personal computer and is mainly based on the linear compartment model theory. Thus, the transfer rate for radioactive matter following deposition on a given type of surface, m , can be written as:

$$\frac{dX_m}{dt} = \sum_{n=1}^P S_{nm} X_n - \left(\sum_{n=1}^P S_{mn} \right) X_m - L_m X_m + F_m$$

in which X_m and X_n represent the radioactive matter in compartments m and n , respectively, at a time t . S_{nm} is the transfer coefficient from compartment n to m . L_m is the transfer coefficient for flow of radioactivity out of the system, etc. (for instance, loss by radioactive decay), while F_m is the initial input to compartment m .

The flow diagram (Fig. 7.1) shows the principle of the migration model with its assumptions. The dotted lines indicate that the processes taking place are discrete events. The term 'impermeable surfaces' means all horizontal surfaces that are not easily penetrated by water, such as asphalt and concrete.

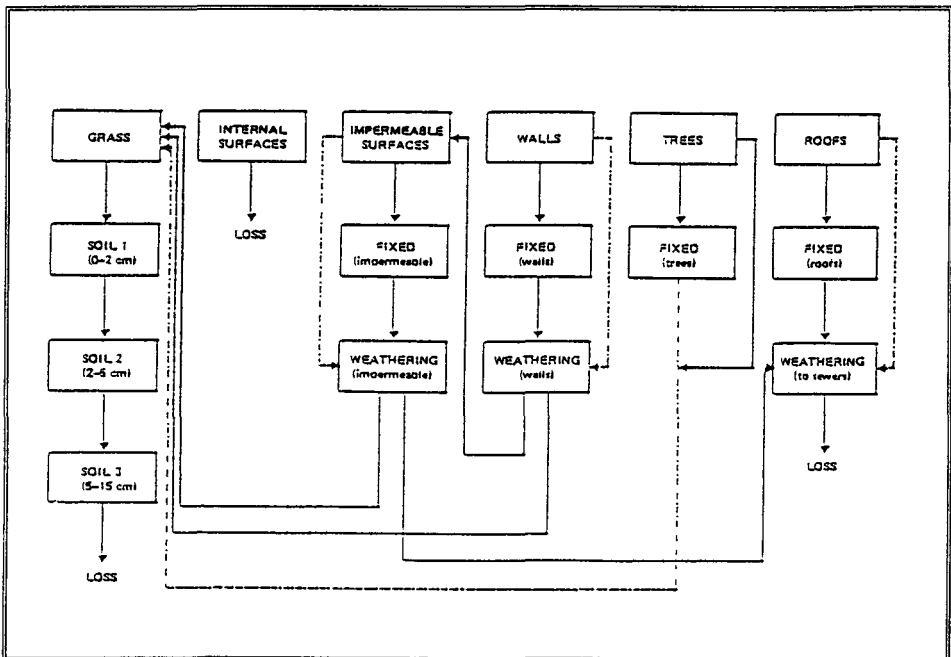


Figure 7.1 URGENT contamination flow chart.

For those 'hard' surfaces on which weathering processes are likely to cause a migration of caesium contamination from one type of surface to another (paved horizontal surfaces, walls and roofs), the migration / retention is accommodated by splitting the radioactive matter into three 'pools'. These represent three different states at which radioactive substances may be found on the particular surface. The first is the mobile phase representing part of the initially dry deposited material. The second state is the more strongly bound phase. Weathering processes will however mobilize the material in this state, and it is here that the third state arises, representing the remobilized material. It is suggested that the mobile fraction is so loosely bound to the surface that a heavy rain shower giving at least 3 mm of rain within a few hours (depending on the time of year, porosity, etc. (Roed, 1988 a)) can displace the entire content of this compartment (Ritchie et al., 1976). This, though, is likely to be important only in cases where heavy rain falls shortly after contamination.

For the activity deposited on trees the model structure is different. Based on published data, it is difficult to evaluate the effect of heavy rain or other weathering processes on the activity deposited on the trees. However, a slow transfer of activity from the trees to the grass due to the effects of wind and rain is taken into account in the model. A large fraction of the fixed activity will be removed from deciduous trees by leaf fall in the first autumn. It is assumed that all the leaves fall on a grassed area during the month of October and that a variable fraction is left on the ground to moulder.

The subdivision of the soil into three different depth compartments allows a simulation of removal of layers of top soil, or normal or deep ploughing. It also permits shielding calculations. In principle, it is possible in this model to simulate any decontamination procedure at any time following deposition by removing a part of the radioactivity in a number of compartments.

The input parameters in URGENT are, where possible, based on experimental results. These parameters are clearly connected with considerable uncertainties since they represent a mean value of a number of results of independent measurements obtained under different conditions and on different materials, all of which fall within the same model category.

The transfer coefficient for fixation of radionuclides dry deposited on walls, 'wall > wfix', like that for impermeable horizontal surfaces (imps), roof material and trees has been set to 0.23 days^{-1} , corresponding to the assumption that 90 % of the material would be 'fixed' within 10 days if no radioactive matter were removed by weathering processes. At present, little information is available on the subject and the parameterisation in URGENT has been based on coarse experiments by Sandalls et al. (1986), Warming (1982), and experiments carried out at Risø (Andersson, 1991).

The velocity with which radiocaesium is typically removed by weathering processes varies widely depending on the surface type, mode of deposition and weathering conditions. The weathering processes on 'hard' surfaces were modelled by two component functions:

	Fraction	Half-life	Fraction*	Half-life
Roofs :	0.5	$1.5 \times 10^3 \text{ d}$	0.5	$3.4 \times 10^2 \text{ d}$
Imperm.:	0.5	$6.9 \times 10^2 \text{ d}$	0.5	$6.9 \times 10^1 \text{ d}$
Walls :	0.8	$6.9 \times 10^3 \text{ d}$	0.2	$6.9 \times 10^1 \text{ d}$

The weathering process on roofs was modelled according to the recommendations of Roed (1988 b), with slight modifications based on later measurements made at Risø. The weathering coefficients for impermeable horizontal surfaces were based on analytical expressions by Jacob et al. (1987), while the coefficients for walls were based more loosely on Risø measurements in Gävle, Sweden (campaigns in 1987, 1988, 1990, 1991, 1993 and 1994) and the findings of Sandalls et al. (1986).

The behaviour of ^{137}Cs deposited on a grass cover has been modelled on the grounds of recommendations from Krieger & Burman (1969). It is advisable to adjust the relationship between the fraction initially deposited on the ground and that deposited on the rougher grassed surface in the light of the assumed wet/dry deposition relationship. The migration of ^{137}Cs in soil has been modelled according to Andersson & Roed (1994). For dose calculations, the shielding factors for caesium in the different soil layers have been based on the work of Jacob & Paretzke (1986).

Where possible, the standard deviations on the input parameters have been based on the variations in the individual experiments which led to the parameterisation.

7.1.2 The PARATI model

PARATI (Program for the Assessment of Radiological Consequences in a Town and of Intervention after a Radioactive Contamination) is a dynamic exposure model for the assessment of doses to individuals of the public resulting from a radioactive contamination in urban and semi-urban environments. This model was designed to fulfill two fundamental tasks that arise after such a contamination, that are (1) the estimation of the radiation exposures for different groups of people as a function of time afterwards with the indication of the fractional contributions to this exposure from each pathway, and (2) the indication of feasible countermeasures and their relative effectiveness regarding the reduction of doses. It is focused on the assessment of the medium and long term consequences of an accident, and therefore essentially has its starting point when the material is already in the environment during and after the passage of a radioactive cloud.

The structure of the PARATI model is in some features similar to that of the URGENT model. For instance, the weathering processes in both models essentially follow single or double exponential functions. On the permeable surfaces, such as soil, the weathering of caesium is assumed to be mainly due to the migration towards deeper layers by rainfall. This movement results also in a decrease of the exposure rate above non-stabilized surfaces due to increasing 'self-shielding'. This was observed by a large set of in situ gamma spectrometry measurements performed after the Chernobyl accident. This data could also be approximated by a double exponential equation for the time-dependency of the measured kerma rates for external irradiation over several surfaces (Jacob et al. 1990). The parameters for this approximation (Jacob et al. 1990) were used in PARATI for the simulation of the time dependent behaviour of kerma rates due to material deposited on urban environments.

The material lost by weathering is considered in the PARATI model, but its transfer to any other compartment is not simulated since weathering is usually a very slow process for most common urban construction materials and it is therefore assumed that the activity transported is small.

Assuming that the activity fraction retained on a surface after weathering for a time t can be described by $Y_{\text{sur}}(t) = a e^{-bt} + c e^{-dt}$, the transfer parameters shown in Table 7.1 were used in the PARATI model.

A comparison with the parameters of the URGENT model shows that a larger fraction is assumed to be rapidly weathered off roofs in the PARATI model, but the half-lives of the slowly removed fraction are similar. The PARATI half-lives of the weathering processes on streets are longer than those of the URGENT model, and the difference between the half-lives of the two fractions for weathering on walls is smaller in PARATI.

Table 7.1. Parameters describing the exponential time dependence of the weathering from urban surfaces.

Surface	a	b (y ⁻¹)	c	d(y ⁻¹)
Clay tile roof	0.7	6	0.3	0.1
Eternite roof	0.8	13	0.2	0.2
Neighbour walls	0.7	0.7	0.3	0.1
Windows	1	8	0	1
Paved streets	0.7	0.7	0.3	0.1
Cracked streets	0.4	0.6	0.6	0.1
Unpaved streets	0.5	0.4	0.5	0.1
Trees	0.9	18	0.1	3.2
Sand	0.5	0.5	0.5	0.1
Soil, lawn	0.5	0.4	0.5	0.1
Internal surfaces	0.9	36	0.1	0.7

In PARATI the external air of each urban 'environment' is considered to be contaminated just through resuspension of the surface of local soils, according to the following equation:

$$C_{air}(t) = K(S) A_{soil}(0-1,t), \quad \text{where}$$

$C_{air}(t)$ = activity concentration in air (Bq/m³)

$A_{soil}(0-1,t)$ = activity within the 1 cm top layer of soil (Bq/m²)

$K(S)$ = resuspension factor, during season class s (wet or dry) (m⁻¹).

The values for $K(S)$ used in PARATI are $5E-8$ m⁻¹ and $5E-9$ m⁻¹ for the dry and wet seasons, respectively, and were estimated from literature data (Garland and Pattenden 1990) after the Chernobyl accident and from field studies (Amaral et al. 1991) after the Goiânia accident.

Also indoor contamination, contamination of skin and clothes as well as contamination of food products are considered in the PARATI model, but not in the URGENT model. As in the URGENT model, the assessment of kerma rates in the PARATI model is based on the work of Meckbach et al. (1988). Modifications have been made to these parameters to fit urban environments typically found in tropical areas of South America for calculations concerning the Goiânia accident.

Both models can be used to estimate the effect of different countermeasures applied at different times following the deposition.

7.2 Method for calculation of dose from indoor sources

From the assumption of a constant aerosol concentration outside a building, and the knowledge of the rate coefficient of ventilation (the fraction, termed λ_r , of air exchanged per unit time), the rate coefficient of deposition (the fraction termed λ_d of aerosols in the building deposited per unit time), the filtering factor f (the fraction of aerosols entering the building which is not retained in cracks and fissures of the building structure), the relationship between the equilibrium indoor aerosol concentration (C_i) and the outdoor aerosol concentration (C_o) can be calculated as:

$$C_i / C_o = f \lambda_r / (\lambda_r + \lambda_d).$$

If the average local indoor deposition velocity ($v_d = \lambda_d V/A$, where V is the indoor volume and A is the indoor surface area), and V_{dg} (the average deposition velocity on a grassed outdoor surface) are also known, a relationship can be established between the average deposited contaminant concentration on indoor surfaces (D_i) and the deposited contaminant concentration on a smooth, cut lawn (the common reference surface for outdoor contamination) here termed D_o :

$$D_i / D_o = (V_d / V_{dg}) f \lambda_r / (\lambda_r + \lambda_d).$$

Field investigations by Roed (1990) showed the caesium aerosol to have a typical deposition velocity of $4.3 \cdot 10^{-4}$ m/s on cut grass surfaces (V_{dg}). A representative value of the relationship V/A for a furnished room is 0.5 m. Following the Chernobyl accident, a series of experiments (Roed and Cannell, 1987) were made in which the typical values of λ_r , λ_d and f were determined for the Chernobyl ^{137}Cs aerosol in a furnished Danish house. These values were used in the calculations of the mean indoor deposition (kBq/m^2) that form the basis for the calculations of doses received from indoor relative to outdoor deposited ^{137}Cs .

7.3 Calculation results

The following doses from external surfaces in urban environments (Table 7.2) accumulated over 1 and 10 years following a wet or dry deposition on the 26th of April were calculated with the URGENT model assuming a deposition on grass of 1 MBq/m^2 ^{137}Cs . The relative deposition on other outdoor urban surfaces was assumed to be as given by Roed et al. (1990). It was further considered that the average person living in one of the four urban environments, for which dose conversion factors are available, spends 85 % of the time at indoor locations, equally distributed between the different residential floors, 10% of the time in the garden and 5 % on the streets.

As can be seen, in the examined environments, the location averaged dose contribution from grassed areas is dominant (65 % - 95 % of the total first year dose and 83 % - 95 % of the total ten years dose from outdoor surfaces). However, it would be dangerous to make decisions based only on location averaged figures, as dose contributions to people living on specific floors of tall buildings may be very different. For instance, the first year dose contribution from contamination on roofs to people living on top floors of multistorey buildings is dominant according to these calculations. Later, the relative importance of roofs will decrease due to weathering.

In order to verify the dynamics of the model, results of URGENT simulations have been compared to experimental data from different parts of Europe. A reasonable agreement was found for all surfaces. Examples are given in Figures 1 and 2 of chapter 4.

Table 7.2. URGENT calculations. External location averaged doses (mGy) from different contaminated outdoor surfaces accumulated over 1 and 10 years following a wet or dry deposition on 26. April of 1 MBq/m^2 ^{137}Cs in four different environments described by Meckbach et al. (1988). Contamination on indoor surfaces is not included here.

Wet dep. 1 y	ROOFS	WALLS	ROADS	TREES	GRASS
Prefabricated	0.72	0.034	-	0.098	8.20
Semidetached	0.39	0.010	-	0.026	3.13
Terrace-house	0.15	0.008	0.320	0.022	1.89
Multistorey	0.006	0.008	0.434	0.011	1.34

Wet dep. 10 y	ROOFS	WALLS	ROADS	TREES	GRASS
Prefabricated	2.58	0.250	-	0.133	55.6
Semidetached	1.39	0.076	-	0.036	22.3
Terrace-house	0.54	0.061	0.822	0.031	13.1
Multistorey	0.022	0.057	1.119	0.015	9.55

Dry dep. 1 y	ROOFS	WALLS	ROADS	TREES	GRASS
Prefabricated	1.79	0.34	-	2.93	9.01
Semidetached	1.16	0.13	-	0.79	3.53
Terrace-house	0.37	0.08	0.26	0.68	2.04
Multistorey	0.015	0.07	0.37	0.34	1.45

Dry dep. 10 y	ROOFS	WALLS	ROADS	TREES	GRASS
Prefabricated	6.41	2.48	-	3.98	68.7
Semidetached	3.44	0.76	-	1.08	27.4
Terrace-house	1.34	0.61	0.75	0.93	14.9
Multistorey	0.054	0.57	1.11	0.46	10.9

Figure 7.2 shows an example of kerma rates calculated with the PARATI model for the outdoor and indoor 'locations' of different types of urban constructions after a dry deposition of 1000 Bq/m^2 on a smooth lawn surface and the main surfaces contributing to this rate. Here the exposure rate is larger outdoors than for 'indoor' locations; the relative contribution of a surface to the total kerma rate is a function of time. The house LS is characterized by a low shielding construction material such as wood; shortly after a dry deposition a major contribution to the kerma rate comes from many trees around the house. Afterwards the contribution of trees decreases and their relative importance is almost negligible after the first two years. For the outdoor 'locations', the soil is usually the main contributor. This effect dominates the total location weighted kerma rate, as shown by the URGENT model calculations. For the indoor 'location' of house LS (one-storey low-shielding building), initially the trees are the main contributors to the kerma rate, followed by the roof and soil. After the first one or two months, this order is inverted, and the external soil becomes the main contributor up to 70 years. This is expected since the dry deposition on trees is very high, and the construction material of this house does not provide enough shielding for the externally deposited material.

The data for the HSR (high shielding multistorey house) are for average locations of a multi-storey building facing a park area. The external soil is the main contributor to the exposure at indoor and outdoor 'locations'. Neighbouring buildings have a significant contribution to the exposure at outdoor 'locations' while internal surfaces show some decreasing relative importance with time for the indoor exposure. House WS1FS is built in high shielding material such as bricks. The outdoor location shows a behaviour similar to that of the low shielding house LS since they have similar configurations. For the indoor effect of the higher shielding against the exposure from the activity deposited on outdoor trees and the ground surfaces can be seen. The kerma rates at the 'locations' are also a function of the kind of deposition as this leads to different patterns of deposition on the 'surfaces'. The kerma rates for the indoor and outdoor locations of this well shielded one floor house with garden are also given for a wet deposition of 1000 Bq/m² on a smooth grass surface with a low rainfall rate. As compared to the data for dry deposition, there is a lower initial contribution from the trees (due to a smaller relative amount retained of deposited material) than from the soil, showing that location factors are also a function of the kind of deposition. A direct comparison of the results obtained by the PARATI and URGENT models is difficult to make, since completely different environments were simulated.

Using the method outlined in section 7.2, the calculated mean indoor depositions are given in Table 7.3 for a variety of what are considered to be realistic values of f , λ_d and λ_r concerning aerosols of the Chernobyl ¹³⁷Cs size.

Table 7.3 Calculated mean indoor deposition (kBq/m²) under different circumstances relating to an outdoor deposition on grass of 1 MBq/m².

$f = 0.4$	$\lambda_d = 0.36 \text{ h}^{-1}$	$\lambda_d = 0.60 \text{ h}^{-1}$	$\lambda_d = 1 \text{ h}^{-1}$
$\lambda_r = 0.3 \text{ h}^{-1}$	21	26	30
$\lambda_r = 0.4 \text{ h}^{-1}$	24	30	37
$\lambda_r = 0.6 \text{ h}^{-1}$	29	39	48
$f = 0.6$	$\lambda_d = 0.36 \text{ h}^{-1}$	$\lambda_d = 0.60 \text{ h}^{-1}$	$\lambda_d = 1 \text{ h}^{-1}$
$\lambda_r = 0.3 \text{ h}^{-1}$	32	39	45
$\lambda_r = 0.4 \text{ h}^{-1}$	36	45	56
$\lambda_r = 0.6 \text{ h}^{-1}$	44	58	72
$f = 1.0$	$\lambda_d = 0.36 \text{ h}^{-1}$	$\lambda_d = 0.60 \text{ h}^{-1}$	$\lambda_d = 1 \text{ h}^{-1}$
$\lambda_r = 0.3 \text{ h}^{-1}$	53	65	75
$\lambda_r = 0.4 \text{ h}^{-1}$	60	75	93
$\lambda_r = 0.6 \text{ h}^{-1}$	73	97	120

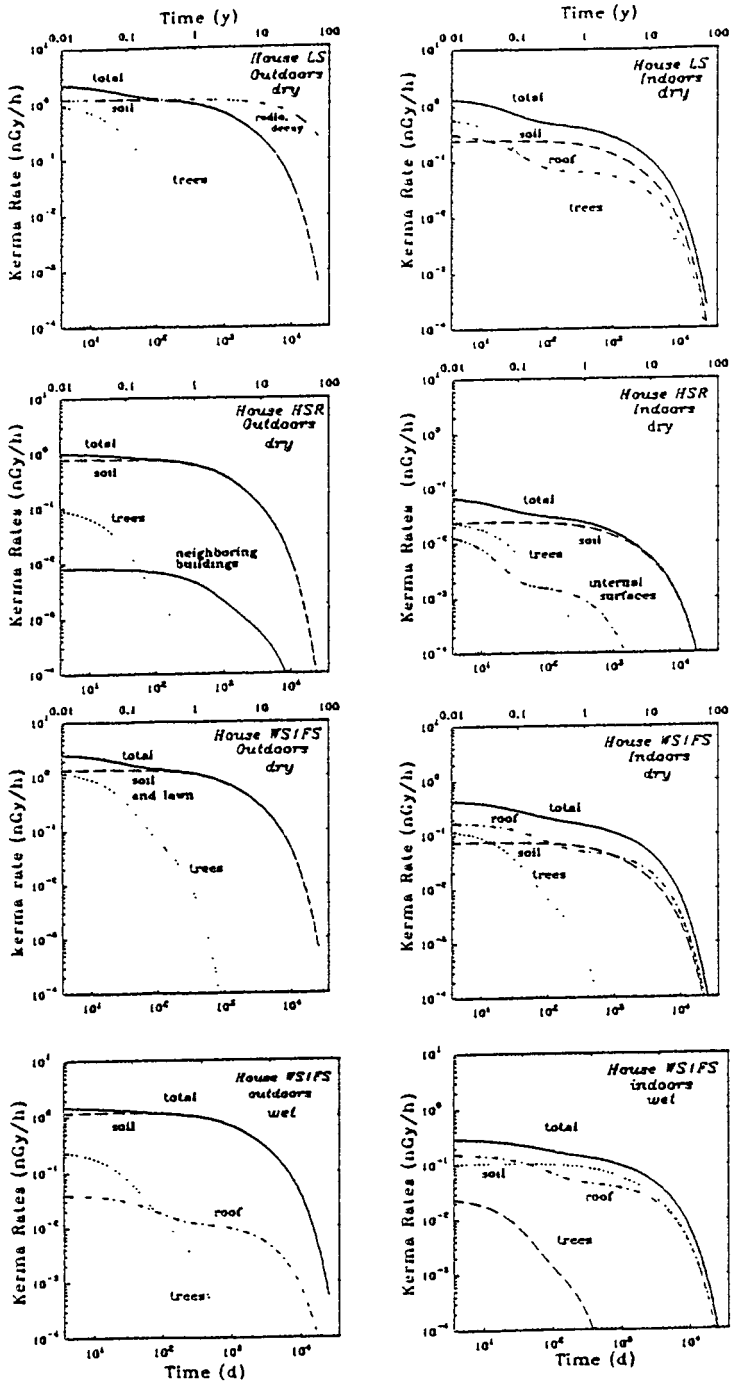


Figure 7.2 PARATI calculations. Contributions to kerma rates as a function of time at different 'locations' in three houses after a dry or wet deposition of 1000 Bq/m² on a lawn. For comparison a curve is added in the left upper panel indicating the time dependency of dose rate due to radioactive decay only.

The corresponding dose estimates for indoor surfaces were made equivalent to a target position 1 m above the ground in a room with height 3 m and in the centre of a ground area of 4 m by 4 m. The dose contribution from scattered radiation and deposition on internal surfaces of neighbouring rooms was not included. It was stipulated in the dynamic calculations that the caesium level on the floor decreases with a half-life of 1 month due to vacuuming, and that the effective half-life on walls, furniture and ceiling is 5 years, as these surfaces are usually only rarely treated.

Recent experiments carried out by Lange (1995) using porous silica particles of various monodisperse size distributions ranging from 0.7 to 20 microns and labelled with neutron activatable tracers have shown that the deposition velocity to the floor approximately equals the sum of the deposition velocities to the four walls and the ceiling (Table 7.4). This distribution pattern was applied in the dose modelling.

Table 7.4 Mean deposition velocities (10^{-4} m/s) of monodisperse 0.7 micron particles collected on hard pressed Whatman 542 filters on surfaces of different orientation in a room.

Ceiling	Wall (N)	Wall (S)	Wall (E)	Wall (W)	Floor
0.189	0.235	0.230	0.117	0.249	1.581

Table 7.5 Estimated received doses the first year following contamination (mGy), equivalent to a target position 1m above ground in a room with height 3 m and in the centre of a 4m by 4m ground area assuming the above mean indoor concentrations and that 50 % of the total amount of caesium is deposited on the floor, while the rest is equally distributed on the walls and ceiling.

$f = 0.4$	$\lambda_d = 0.36 \text{ h}^{-1}$	$\lambda_d = 0.60 \text{ h}^{-1}$	$\lambda_d = 1 \text{ h}^{-1}$
$\lambda_r = 0.3 \text{ h}^{-1}$	0.19	0.23	0.27
$\lambda_r = 0.4 \text{ h}^{-1}$	0.22	0.27	0.33
$\lambda_r = 0.6 \text{ h}^{-1}$	0.26	0.35	0.4
$f = 0.6$	$\lambda_d = 0.36 \text{ h}^{-1}$	$\lambda_d = 0.60 \text{ h}^{-1}$	$\lambda_d = 1 \text{ h}^{-1}$
$\lambda_r = 0.3 \text{ h}^{-1}$	0.29	0.35	0.41
$\lambda_r = 0.4 \text{ h}^{-1}$	0.32	0.40	0.51
$\lambda_r = 0.6 \text{ h}^{-1}$	0.39	0.53	0.65
$f = 1.0$	$\lambda_d = 0.36 \text{ h}^{-1}$	$\lambda_d = 0.60 \text{ h}^{-1}$	$\lambda_d = 1 \text{ h}^{-1}$
$\lambda_r = 0.3 \text{ h}^{-1}$	0.48	0.59	0.68
$\lambda_r = 0.4 \text{ h}^{-1}$	0.54	0.68	0.84
$\lambda_r = 0.6 \text{ h}^{-1}$	0.66	0.88	1.08

As can be seen, the first year doses from deposition on internal surfaces of buildings may be rather large compared with those from the outdoor surfaces. In buildings with a high ventilation rate, a

high deposition rate, and a low degree of filtration of caesium aerosols passing through the building, the first year dose from indoor surfaces may in certain cases be almost as much as that from outdoor surfaces.

7.4 References

Amaral, E.C.S., Vianna, M.E.C., Godoy, J.M., Rochedo, E.R.R., Campos, M.J., Pires do Rio, M.A., Oliveira, J.P., Pereira, J.C.A., Reis W.G., Distribution of Cs-137 in soils due to the Goiania accident and decisions for remedial action during the recovery phase, *Health Physics* 60, pp. 91- 98, 1991.

Andersson, K.G., Contamination and Decontamination of Urban Areas, Ph.D. Thesis. Risø National Laboratory & Technical University of Denmark, 1991.

Andersson, K.G. and Roed, J., The Behaviour of Chernobyl ^{137}Cs , ^{134}Cs and ^{106}Ru in Undisturbed Soil: Implications for External Radiation, *J. Environ. Radioactivity* 22, pp. 183-196, 1994.

Fehlberg, E., Klassische Runge-Kutta-Formeln Fünfter und Siebenter Ordnung mit Schrittweiten-Kontrolle, *Computing* 4, pp. 93-106, 1969.

Garland, J.A. and Pattenden, N.J., Resuspension following Chernobyl, in *Proceedings of the Seminar on Methods and Codes for Assessing the Off-Site Consequences of Nuclear Accidents*, Report EUR 13013, pp. 451-470, 1990.

Jacob, P. and Paretzke, H.G., Gamma Ray Exposure from Contaminated Soil, *Nuclear Sci. and Eng.* 93, pp. 248-261, 1986.

Jacob, P., Meckbach, R. and Müller, H.M., Reduction of External Exposure from Deposited Chernobyl Activity by Run-off, Weathering, Street Cleaning and Migration in the Soil, *Rad. Prot. Dos.*, vol. 21, No.1/3, pp. 51-57, 1987.

Jacob, P., Meckbach, R., Müller, H.M. and Meimberg, K., Abnahme der abgelagerten künstlichen Radioaktivität in städtischer Umgebung, *GSF-Bericht* 17/90, 1990.

Kanyar, B. and Nielsen, S.P., Users Guide for the Program TAMDYN, Risø report M-2741, 1988.

Karlberg, O., Weathering and Migration of Chernobyl Fallout in Sweden, Studsvik Report NP 216 EA, Sweden, 1988.

Krieger, H.L. and Burmann, F.J., Effective Half-times of Sr-85 and Cs-134 for a Contaminated Pasture, *Health Physics* 17, pp.811-824, 1969.

Lange, C., Indoor Deposition and the Protective Effect of Houses against Airborne Pollution, PhD Thesis, Risø-R-780 (En), ISBN 87-550-2024-0, 1995.

Meckbach, R., Jacob, P. and Paretzke, H.G., Gamma Exposures due to Radionuclides Deposited in Urban Environments. Part 1: Kerma Rates from Contaminated Urban Surfaces, *Rad. Prot. Dos.* vol 25, No.3, pp. 167-179, 1988.

Ritchie, L.T., Effects of Rainstorms and Run-off in Consequences of Nuclear Accidents, SAND 76-0429, Sandia Laboratories, Albuquerque, New Mexico, USA, 1976.

Roed, J., The Distribution on Trees of Dry Deposited Material from the Chernobyl Accident, presented at the Joint CEC/OECD (NEA) workshop 'Recent Advances in Reactor Accident Consequence Assessment, Rome, Italy, January, 1988-a.

Roed, J., Modelling of Run-off and Weathering Processes, presented at the MARIA workshop at Kernforschungszentrum, Karlsruhe, October, 1988-b.

Roed, J., Deposition and Removal of Radioactive Substances in an Urban Area. Nordic Liaison Committee for Atomic Energy, 1990.

Roed, J., Andersson, K.G. and Sandalls, J., Reclamation of Nuclear Contaminated Urban Areas, presented at the BIOMOVS Symposium and Workshop on the Validity of Environmental Transfer Models, Stockholm, 8-12 Oct., 1990.

Roed, J. and Cannell, R.J., Relationship Between Indoor and Outdoor Aerosol Concentration Following the Chernobyl Accident, Rad. Prot. Dos. vol. 21, No. 1/3, pp. 107-110, 1987.

Roed, J. and Jacob, P., Deposition on Urban Surfaces and Subsequent Weathering, in proceedings from the Seminar on Methods and Codes for Assessing the Off-site Consequences of Nuclear Accidents, Athens, May, 1990.

Sandalls, F.J., Stewart, S.P. and Wilkins, B.T., Natural and Forced Decontamination of Urban Surfaces Contaminated with Radiocaesium, Assessing Off-site radiological consequences of nuclear accidents, Proc. CEC workshop Luxembourg, April 1985, Rep. EUR-10397, CEC, 1986.

Warming, L., Weathering and Decontamination of Radioactivity Deposited on Asphalted Surfaces, Risø-M-2273, 1982

8. Review of current external dose models and recent experimental research on the deposition and subsequent relocation of artificial radionuclides

Joanne Brown and J. Arthur Jones
National Radiological Protection Board
Chilton, Didcot, Oxon OX11 0RQ
United Kingdom

Miriam A. Byrne and Antony J. H. Goddard
Imperial College of Science, Technology and Medicine
London SW7 2BX
United Kingdom

Peter Jacob and Jochen Tschiersch
GSF-Forschungszentrum für Umwelt und Gesundheit
85758 Oberschleißheim
Germany

Christian Lange, Jørn Roed and Kasper G. Andersson
Risø National Laboratory, MIL-114
4000 Roskilde
Denmark

Peter Zombori and István Fehér
KFKI Atomic Energy Research Institute
1525 Budapest
Hungary

8.1 Introduction

As stated in earlier chapters of this report, an objective of the project has been to review and consider the results from the experimental research with a view to their future incorporation into models. Many simplifying assumptions have had to be made in models in the past due to the lack of data on the behaviour of radionuclides in urban and rural areas. However, much of the experimental data available since the Chernobyl accident through research and measurement programmes has not been utilised in the models. This chapter describes the current models used for describing deposition and relocation of material in urban and rural areas for the estimation of doses and risks used in the COSYMA code for probabilistic risk assessment and in the RODOS code for real time emergency response. The available data from the experimental research carried out under this programme and the current status of research in this area are also reviewed in the context of the current models.

An important part of the review has been to obtain agreement with the other contractors within the programme, about the ways in which exposure from deposited material is included and modelled in doses assessments, and in particular in the COSYMA and RODOS programs. The contractors, as a whole, have reviewed the adequacy of the current models for their given purpose and how the data

from this experimental research programme could be used to improve or support the current modelling approach. This review and recommendations for changes in the models are described in this chapter.

8.2 Required complexity of models

Accident consequence assessment (ACA) codes use relatively simple models to describe the processes by which material released in accidents travels through the environment and irradiates people. More complex models exist, or could be developed. In making decisions on whether the models currently used are adequate a number of questions should be addressed regarding the advantages and disadvantages of using complex versus simple models:

1. The reliability of complex models. Simple models tend to use parameters for which values can be specified reasonably easily. Complex models describe more detailed aspects of the situation considered, and may use parameters for which a value cannot easily be obtained. Complex models are often derived for particular conditions, and may not work well in other conditions.
2. Complex models are able to describe the differences between doses in different situations. For example, models like EXPURT (Crick and Brown 1990), and URGENT (Andersson 1994) can describe the variations in deposited γ dose for different types of buildings in the area. In order to use these models in a more general application, some averaging over the range of conditions considered is required.
3. Complex models can require considerably more computer resources (CP time or disk storage) than simple ones. The use of these resources may not be warranted if the effect being considered does not make a major contribution to the quantity being calculated.

8.3 Existing models for the deposited γ dose in rural and urban areas

Simple methods for calculating the external γ dose from deposited activity ignore the differences between doses in rural and urban areas.

The simplest model assumes that the deposited material is present on an infinite, uniform, smooth, horizontal surface, and that the deposition density is constant over the area from which γ rays can reach the point at which the dose is being calculated. Changes in dose rate in this model reflect only the radioactive decay of the deposited nuclides and the ingrowth of daughter products. Some models combine this with a modification factor, typically about 0.7, to allow for the non-uniformity of the surface, and shielding by roughness elements and irregularities on the surface. This type of model was used in some early accident consequence assessment (ACA) codes. It gives a reasonable representation of the dose and dose rates in rural areas for the first few months after deposition.

This type of model can be extended by considering the migration of the deposited material into the soil over the period following deposition. The dose is then calculated allowing for attenuation by layers of soil above the radioactive material. This type of model is strictly only applicable for the dose in rural areas. However, it can be used with suitable location factors for calculating doses in other areas. The NRPB model DOSE-MARC (Hill et al 1988) is of this type. This type of model has been widely used in creating data files for use in accident consequence assessment codes.

GSF has developed a model which is similar to the ones described above. In this model the radioactive material is assumed to be at a particular constant depth of 5 mm below the soil surface (Jacob et al 1990). A corrective factor is subsequently applied for the shielding obtained due to migration of radionuclides into deeper soil layers (Jacob et al 1992).

In recent years urban dose models have been developed to more accurately reflect the physical movement of material within the urban area, for example, the weathering of material from urban surfaces, in order to provide more realistic estimates of doses to people living in urban areas. These models can also take into account the behaviour of groups of the population in terms of their indoor and outdoor occupancy. The more realistic modelling of the urban environment not only improves the prediction of doses to exposed individuals but also enables the effect of decontamination in urban areas to be studied in detail. The models available are compartmental in nature with different compartments representing different surfaces in the urban environment. Transfer between these compartments enables the physical movement of radioactivity within the urban area, eg. the weathering of material from building surfaces onto roads and soil to be represented. Some of these models have also been developed to model the different processes that are important following deposition under wet and dry conditions. Models of this type include EXPURT, developed at NRPB (Crick and Brown 1990), URGENT developed at Risø (Andersson 1994) and URPAT developed at UPM (Martin et al, 1992). The EXPURT model is used to determine external gamma doses in urban areas for use in COSYMA as discussed in Section 8.4.2. In these urban external dose models the relative deposition onto the surfaces in an urban area: roofs, external walls, paved surfaces, soil, internal surfaces and trees, are modelled. The fraction of material deposited that is initially retained on each surface is dependent on whether deposition is under dry or wet conditions. Weathering from each surface and the redistribution of material within the urban environment with time are modelled. Doses are calculated to the population as a function of time, taking into account the level of urbanisation, building types and where people spend their time.

8.4 Models used in COSYMA and RODOS

This section describes the models used in COSYMA and in RODOS, and gives the default values for some of the parameters adopted. However, it should be noted that RODOS is at a prototype stage of its development, and the values given here may change before the final system is completed. In both codes, the user can easily modify the values of any of the parameters involved.

8.4.1 Deposition

Dry deposition includes all processes which deposit material to the ground in the absence of precipitation. The deposition rate depends on the air concentration near the ground. It is calculated using the deposition velocity, which is the ratio of deposition rate per unit area to air concentration per unit volume. The value of deposition velocity depends on the physical and chemical form of the depositing material, and the nature and orientation of the underlying surface. In common with most ACA and real time codes, COSYMA and RODOS distinguish between the deposition velocities of noble gases (which are assumed not to deposit), aerosols and iodine, with a further distinction between iodine in elemental form, as organic iodides or attached to aerosols. The deposition velocity of aerosols depends on the aerosol size. ACA codes often assume that the deposition velocity for 1 μm particles is 10^{-3} m s^{-1} . This value is appropriate for deposition to grass; a value roughly an order of magnitude lower would be appropriate for most urban surfaces. The default values used in COSYMA and RODOS, which can be changed by the user, are given in Table 8.1.

Wet deposition includes all processes whereby precipitation deposits material to the ground. It thus includes deposition by rain and snow. Removal caused by rain falling through a cloud of dispersing material is known as washout, while removal caused by processes occurring in the rain cloud is known as rainout. Fog can also increase the deposition rate of material (see chapter 1 and section 8.5.1.2).

Most assessment codes only consider washout. The deposition rate is generally modelled using the washout coefficient, which is the fraction of material in the plume which is removed by rain in unit time. ACA and real time codes assume that material is retained within the atmospheric boundary layer, below the base of any rain clouds, and so do not distinguish between washout and rainout. ACA and real time models generally allow for the variation of washout coefficient with rainfall rate.

COSYMA and RODOS allow for the variation of washout coefficient with rainfall rate using a formula

$$\Lambda = a R^b \quad (1)$$

where Λ is expressed in units of s^{-1} , and R is the rainfall rate in $mm\ h^{-1}$. This model is intended for use when the available meteorological data include the rainfall rate for each hour of interest. The default values of a and b used in RODOS and COSYMA are given in Table 8.1.

Table 8.1 Default deposition parameters in COSYMA and RODOS.

	Deposition velocity ($m\ s^{-1}$)	Washout coefficient parameters	
		a	b
Noble gas	0.0	0.0	0.0
Aerosol	$1.0\ 10^{-3}$	$8.0\ 10^{-5}$	0.8
Elemental iodine	$1.0\ 10^{-2}$	$8.0\ 10^{-5}$	0.6
Organic iodine	$5.0\ 10^{-4}$	$8.0\ 10^{-7}$	0.8

COSYMA and PC COSYMA include doses from material deposited on skin and clothes. The amount of material deposited is calculated by multiplying the dry deposition to ground by a factor which depends on the physical and chemical form of the depositing radionuclides. The default value is 1.0 for all forms.

8.4.2 Data libraries for deposited γ dose

8.4.2.1 COSYMA

The data library used in the mainframe and PC versions of COSYMA contains deposited γ doses for the radionuclides Cs-134, Cs-137, I-131, Te-132, Ba-140, Ru-103 and Ru-106 calculated using the EXPURT model. These are the most important radionuclides contributing to deposited γ dose for typical fission reactor source terms (Charles et al 1983). Deposited γ doses for all other radionuclides considered in COSYMA for fission reactors were calculated using the NRPB program DOSE-MARC (Hill et al 1988). Additional deposited γ doses have been included for radionuclides of potential importance for fusion reactor releases using the GSF deposited γ dose model (Haywood et al 1995).

The EXPURT values are for an 'average' environment (actually a type of urban environment calculated by weighting a range of urban and rural environments based on population density in the UK) and average UK weather conditions. The DOSE-MARC data library (Hill et al 1988) values are for deposited γ doses over a large undisturbed soil surface.

The outdoor doses predicted by the DOSE-MARC model show very similar time-dependence, for nuclides other than Cs-137, to the outdoor doses predicted by EXPURT for the radionuclides that contribute significantly to external γ doses. Data are not available on the behaviour of other long-lived radionuclides in urban environments and it was considered that the inclusion of these in the EXPURT model could not be justified due to the uncertainty of their behaviour. It is therefore considered reasonable to approximate the outdoor doses produced by EXPURT with those obtained using the DOSE-MARC model for the radionuclides not considered in the EXPURT model. The difference due to mixing the two models is less than 20%.

The difference in the protection offered in one outdoor location to that implicit in the data library can also be represented using location factors in the estimation of outdoor external doses. Urban dose models have been used to study the difference between doses in various outdoor locations and recommendations on location factors to use for different situations have been given (Jacob and Meckbach, 1990, Brown and Jones, 1994). Similarly location factors can be used to reflect the difference between doses following deposition under wet and dry conditions compared to a data library representing average weather conditions or deposition under dry conditions only.

8.4.2.2 RODOS

The data library used in RODOS is derived from the GSF model (Jacob et al 1990, Jacob et al, 1992). The downward migration in soil that is assumed is based on measurements of the external exposure from caesium deposited on the ground after the Chernobyl accident. These are regarded as representative for average weather conditions. For other elements, equivalent data are not available and the data for caesium are applied to all elements. However, as the long-term exposure is dominated by caesium isotopes this assumption is reasonable.

The corrective function used for shielding due to migration of radionuclides into deeper soil layers is:

$$S = a_1 e^{-\lambda_1 t} + a_2 e^{-\lambda_2 t}$$

where

λ are migration rates ($\lambda_1 = 1.01 \cdot 10^{-3} \text{ d}^{-1}$, $\lambda_2 = 0.0 \text{ d}^{-1}$)

a_1, a_2 = contribution fractions of the migration rates ($a_1 = 0.6$, $a_2 = 0.5$).

8.4.2.3 Further developments to deposited γ dose data libraries

Further improvements to models for deposited γ dose are, within the present structure of COSYMA and RODOS, restricted to the production of a single data library. This single data library represents the average of the dose in urban and rural areas for use in general assessments as described above. Any data library produced could be used with appropriate location factors for applications in which effects in a specific sub-group of the population are being calculated. More detailed modelling, in which for example differences in the dose per unit deposit in rural and urban conditions are considered, and which therefore requires the use of more than one data library would require very extensive changes to COSYMA. Similar remarks are appropriate for other probabilistic consequence codes and RODOS.

8.4.3 Shielding of groups of the population

8.4.3.1 COSYMA

Late health effects are calculated assuming that the dose response relationship is linear. Therefore, it is adequate to calculate an average dose to the population, averaging over the periods when people are outdoors and indoors, using a location factor weighted for outdoor and indoor occupancy. This procedure is used in both the mainframe and PC versions of COSYMA when calculating late health effects.

Early health effects are calculated using non-linear dose response relationships, and so differences between doses to different groups of the population become more important. These are calculated in different ways, with varying levels of complexity, in accident consequence codes. Some codes, such as PC COSYMA, only consider a single population group, as for late effects. Others calculate the doses and risks to two groups, one indoors and the other outdoors in the time before countermeasures are taken. The mainframe version of COSYMA considers the doses to several groups of the population who are assumed to be either outdoors or in buildings with different shielding properties. The user must specify the fraction of the population in each of the groups considered. These fractions are assumed to apply at each grid point used in the calculation.

In assessment codes shielding is described using location factors which describe the differences between the doses in the situation in which they are to be calculated and those considered in the data libraries of deposited γ dose per unit deposition used in the code. The flexibility of the models to take into account the shielding offered by different buildings, levels of urbanisation and populations with different habits within a particular urban or rural environment depends on the assessment code.

Values of location factors can be chosen to reflect the behaviour of the population during the period over which they are exposed, and values can be specified for the period before countermeasures are taken, during sheltering or while in cars being evacuated, and for normal behaviour outside the countermeasures area or after return from evacuation or relocation.

The most recent work for shielding against external irradiation has been carried out by Meckbach and Jacob (1988). Location factors for different levels of urbanisation have also been estimated using EXPURT (Brown and Jones, 1994) and location factors for use in ACA codes have been reviewed by Brown and Jones (1993).

From these sources, location factors for general use and for ACA codes have been derived. The default values for external gamma dose location factors are given in Table 8.2. Location factors for Cs-137 and I-131 have also been calculated with the URGENT model utilising experimental data on

weathering and indoor deposition (see chapter 5). The estimated location factors are comparable to the default values in COSYMA for low and medium shielded buildings. However, the location factors calculated for high shielded buildings including the doses from material deposited indoors are higher by up to a factor of 10 than those used in COSYMA. This location factor is higher than other values reported in the literature. It is not recommended that the current default values in COSYMA are changed on the basis of this work. However, for the calculation of early health effects in situations where a large fraction of the population is in high shielded buildings, the use of a higher location factor should be considered. A default location factor for inhalation dose reduction indoors of 0.5 is used. Advice is given to the user of COSYMA on the possible variation in location factors across Europe due to differences in ventilation rates of buildings. This is discussed further in section 8.5.1.3.

Table 8.2 Default location factors for external gamma doses in COSYMA.

Environment	Ratio of indoor dose to outdoor dose
DEFAULT:	0.04
UK weighted average environment	
Rural	0.2
Residential	0.1
City	0.02
Building type or position	Ratio of indoor dose to outdoor dose
Low shielding ¹	0.5
Medium shielding ¹	0.1
High shielding ¹	0.01
Cellars with windows	0.02
Cellars without windows	$5 \cdot 10^{-4}$
Cars	0.7

Note: 1. A low shielded building is representative of a mobile home, caravan or lightly constructed building; a medium shielded building is representative of a typical residential house; and a high shielded building is representative of a multistoried building, ie, office block or flats.

8.4.3.2 RODOS

RODOS uses location factors for different types of houses together with information on the type of house at each location at which doses are to be calculated. These take account of the fraction of time that the population is indoors at each location. The values used, for external γ irradiation, are given in Table 8.3.

Table 8.3 Default location factors for external deposited gamma doses in RODOS.

Building type	Location factor
Multifamily dwellings, big and thick buildings	0.01
Stone construction single family dwellings and agricultural buildings.	0.1
Wood and stone construction single family dwellings.	0.5

8.4.4 Resuspension

Resuspension is included in both the mainframe and PC versions of COSYMA and in RODOS, by means of a resuspension factor which is the ratio of the resuspended air concentration to the total amount of material deposited. The resuspension factor R is obtained from the formula

$$R = a e^{-bt} + c$$

where t is the time after deposition. a, b and c are constants which can be changed by the user. Both COSYMA and RODOS use the same formula for the resuspension factor and the default values for the 1993 version of COSYMA and RODOS are shown in Table 8.4. As a result of this contract, the values used in COSYMA have been revised, and the 1995 version of COSYMA will use the same values as shown in the table for RODOS.

Table 8.4 Default resuspension coefficients used in COSYMA and RODOS.

Parameter	COSYMA 93/1 value	RODOS value
a	$1.0 \cdot 10^{-5} \text{ m}^{-1}$	$5.0 \cdot 10^{-8} \text{ m}^{-1}$
b	$1.62 \cdot 10^{-7} \text{ s}^{-1}$	$3.5 \cdot 10^{-8} \text{ s}^{-1}$
c	$1.0 \cdot 10^{-9} \text{ m}^{-1}$	$1.0 \cdot 10^{-9} \text{ m}^{-1}$

8.4.5 Decontamination

COSYMA and PC COSYMA allow for the consideration of decontamination in determining when people can return from evacuation or relocation. COSYMA only considers return from evacuation or relocation at a discrete series of times, and allows the user to specify a decontamination factor for each of these periods. The factor represents the amount by which the dose rate is reduced by the decontamination process, rather than the fraction of material which can be removed from a particular surface. COSYMA assumes that this factor applies to the dose and dose rate equally at all times after decontamination.

The approach in RODOS is similar to that used in COSYMA. The model can use a number of factors representing the reduction in dose that will be achieved following a range of decontamination techniques; these are applied to the external γ dose data libraries. No account is

taken of the time dependence in dose reduction following decontamination and the different behaviour of individuals. The dose reduction factors have been determined using EXPURT.

The use of an urban dose model such as EXPURT enables decontamination factors to be applied at any particular time to a particular surface and the temporal and spatial changes in the distribution of activity between the surfaces of the urban environment can be studied. These models have also been developed to model the different processes that are important in urban areas following deposition under wet and dry conditions. The difference in efficiency of a decontamination technique following contamination of the surface under wet or dry weather conditions can, therefore, be incorporated into the models where necessary.

Several reviews of data on decontamination have been carried out (Roed 1990, IAEA 1989, Robinson et al 1990, Brown et al 1992) with emphasis, where possible, on data that are applicable for small particle sizes appropriate for nuclear reactor accidents. The most comprehensive data available are from measurement and experimental programmes following the Chernobyl accident and these data have been compiled and provide a comprehensive synthesis of all the field measurements (Brown et al 1992, Sinnaeve 1991). The effectiveness of a range of feasible decontamination techniques applied at different times following deposition have been considered using these sources of data and are included in RODOS.

8.5 Review of sub-process modelling in light of current data and research under this contract

8.5.1 Deposition

8.5.1.1 Parameterisation of dry deposition

Dry deposition rates are generally calculated using the deposition velocity, which is the ratio of the deposition rate per unit area to the air concentration per unit volume. Deposition rates to surfaces such as grass depend on the amount of grass growing on the surface, and so the value which should be assigned to deposition velocity depends on the grass density. Roed (1987) has shown that variation in the density of grass can be a significant contributor to the variation of deposition velocity between different locations. He observed deposition velocities for a caesium aerosol ranging between $1.8 \cdot 10^{-4}$ and $8.8 \cdot 10^{-4} \text{ m s}^{-1}$. Roed has also considered a quantity which he calls the bulk deposition; this is the deposition rate per unit area divided by the amount of grass growing in a unit area, and has units of $\text{m}^3 \text{ s}^{-1} \text{ kg}^{-1}$. Roed observed that this quantity varied between 7.9 and $21 \cdot 10^{-4} \text{ m}^3 \text{ s}^{-1} \text{ kg}^{-1}$ for the same set of conditions. He also observed that for iodine the bulk deposition varied much less than the deposition velocity for the same conditions.

The use of a bulk deposition parameter rather than the deposition velocity to grass in codes like COSYMA and RODOS would not reduce the uncertainty on the deposition predictions as a value would be needed for the amount of grass per unit area which, as discussed above, is highly variable.

However, it would be useful in the event of an accident, when model predictions are compared with monitoring data. Here an allowance for the actual amount of grass per unit area could be made, and one source of uncertainty could be reduced in the fitting procedure.

8.5.1.2 Effect of fog on dry deposition

During fog, aerosol particles could attach to the water droplets present in the atmosphere. They would then deposit at a rate characteristic of particles with the size of the water droplets, rather than

that of the original aerosol. This suggests that the deposition velocity of particulate material should increase in foggy weather.

GSF (see chapter 1) has carried out measurements of the deposition velocity of six elements (Fe, Zn, Pb, S, Ca and K) in foggy conditions to a polyethylene surface. The measured deposition velocities, particularly that for Ca, are higher than would be expected under non-foggy conditions.

Underwood (1988,1993) has considered the effects on consequence predictions of the increased deposition velocity expected in foggy conditions. He showed that, in some situations, the changes in the predicted consequences caused by including fog could be important, and that they would not be modelled by the other types of atmospheric conditions normally considered in probabilistic consequence assessments. Underwood considered increases in deposition velocity which were similar to the ones measured by GSF.

The GSF experiment has only considered the increase in the deposition velocity to a single, horizontal surface. This information could be used if the deposited γ dose library was derived from a simple model which did not distinguish the contributions made by material deposited on different surfaces in urban areas. Further information, on the deposition velocities to typical urban surfaces, including walls, would be needed before models such as EXPURT or URGENT could be applied to calculate the external γ dose from material deposited in urban areas during foggy conditions.

The increase in deposition velocity is only one aspect which needs to be considered before the effects of fog can be modelled in accident consequence codes. Atmospheric dispersion in foggy conditions may be different from that in other conditions. Part of this difference might be reflected in the atmospheric stability category, which may be incorrectly given in the meteorological data files used, depending on how they were derived. The changes in particle size caused by the incorporation of material into fog droplets could also affect the inhalation dose.

The meteorological data used with current ACA codes do not identify the occurrence of fog. Therefore, better data would be required if this is to be included in PRA codes. As the increase in deposition velocity depends on the amount of water in the atmosphere, the data would need to include this parameter.

It can be concluded that the dispersion and deposition of radioactive material in foggy conditions should be considered further and the state of the modelling in this area has not progressed sufficiently to enable the overall importance of considering fog in ACA codes and real-time systems and the degree of modelling complexity required to be assessed.

8.5.1.3 Indoor deposition and air concentrations

Imperial College and Risø have developed a model for the ratio of air concentration indoors to that outdoors, in terms of the air exchange rate of the building and the indoor deposition velocity. This model utilises data from three series of house experiments carried out by Imperial College and Risø where the average deposition velocity to indoor surfaces in furnished and unfurnished rooms has been measured (Byrne et al 1995). Details of the measurements and the model are given in chapter 2.

This model could be used to calculate the reduction in inhalation dose obtained by remaining indoors. Some predicted reduction factors are given in Table 8.5.

There is only limited information on the air exchange rates of houses in Europe, based on surveys of a small number of houses in several countries. The data suggest that the ventilation rates vary between about 0.2 and 0.7 air changes per hour, with a representative value of about 0.4 air

changes per hour. This implies a ratio of indoor to outdoor air concentration of 0.5 for iodine vapour, 0.4 for 1 μm particles and 0.2 for 4 μm particles. Further details can be found in Chapter 2.

Table 8.5 Ratios of indoor to outdoor air concentrations.

Air exchange rate (h^{-1})	Protection factor	
	2 μm particles	4 μm particles
0.2	0.2	0.12
1.0	0.54	0.39
2.0	0.7	0.57

COSYMA and RODOS use a single location factor for all radionuclides to represent the reduction in inhalation dose due to indoor occupancy. This approach is adequate for use in ACA codes and RODOS providing appropriate location factors are used for the situation being considered. For general assessments it is recommended that the current default value of 0.5 is used which is appropriate for iodine vapour and 1 μm particles. This is supported by the information above. For certain situations, eg. for countries where the ventilation rates differ greatly from about 0.4 h^{-1} , alternative values may be more appropriate (see Chapter 2).

8.5.1.4 Deposition to skin and clothes

There is very little information available on the deposition velocity to skin and the residence time of deposited material on the skin. NRPB has shown that deposition to skin could be an important contributor to early death following a large accidental release from a nuclear reactor, depending on the value assigned to deposition velocity to skin (Jones 1990).

Imperial College and Risø have undertaken some measurements of deposition to skin and hair in a variety of test rooms for a range of particle sizes. The results are described in chapter 3 of this report. The results suggest that the deposition velocity to skin is about an order of magnitude greater than that observed for grass and a few observations have yielded even higher values.

In further work, currently at a preliminary stage, Imperial College (Byrne, 1995) has determined the deposition velocities with and without a fan running in the chamber. The fan increased the turbulence levels in the chamber, so that the deposition velocities would reflect, to some extent, the turbulence levels outdoors which are greater than those indoors. This work is currently only at a preliminary stage, but the results suggest that the deposition velocity was greater when the fan was running than when it was not.

Prior to this project there was very little information available on deposition velocities to skin. The work carried out under the project has provided information which shows that the deposition velocity to skin is larger than to other surfaces. The deposition velocities found here, without the fan running, are a factor of 10 higher than the highest values considered by Jones (Jones 1990). This suggests that skin deposition could be the most important pathway for early deaths from large reactor accidents.

This study has demonstrated the need for further work in this area. The experiments described here suggest that the deposition velocity to skin could be an order of magnitude greater than the default value used in COSYMA. Work is also needed to determine the natural removal rate of material deposited on skin, and the likely effect of decontaminating skin.

8 5.1.5 The need to consider deposition to trees in ACA codes

The amount of material deposited on a tree by dry deposition processes can be much larger than that deposited on the area of ground covered by the tree, and so trees could be a major source of external irradiation for people who are outdoors. They would also increase the dose to people indoors for two reasons. First, the extra amount of material deposited will increase the dose in all locations and, second, trees may be of a similar height as the windows in some houses, and so there may be less shielding between the γ source and the target locations in houses. Calculations by Jacob suggest that the dose from material deposited on trees could equal that from material deposited on all other surfaces for a person outdoors.

The data library used with COSYMA makes no allowance for material deposited on trees, shrubs, garden walls or fences. Investigations with EXPURT show that material deposited on soil in dry conditions contributes 75% or more of the dose to a person outdoors and some tens of percent of the dose to people indoors, depending on the shielding properties of the houses. The total amount of material dry deposited on features such as trees, shrubs and fences in gardens could be similar to that deposited on the lawn and the soil (ie. to that considered in COSYMA). Therefore, the total activity in the surrounding area could be increased by almost a factor of 2. It would therefore increase the dose to people indoors by some tens of percent, and to people outdoors by no more than a factor of 2. However, there is some variation in these factors reflecting the variation in the types of urban areas and in many areas trees etc will produce an increase in dose which is less than these figures suggest. The amount of material deposited on trees and shrubs clearly depends on the time of year. The deposition on deciduous trees during the times when they do not have leaves may be small compared to the direct deposition on soil, and so the increase in doses caused by including trees in the model will be considerably less than the factors suggested here for at least half of the year.

Deposition on trees in wet conditions will not increase the total amount of material deposited in an urban area, as all the activity contained in the rain water is deposited somewhere. Considering trees would merely affect where within the area the material is deposited. There is therefore little effect on dose if the material is deposited in wet conditions, which occur in much of Europe for about 10% of the time.

Some consequences of an accident will be more sensitive than others to changes in the modelling of deposited γ dose. The most sensitive endpoints are those where the response increases more than linearly with the dose, and so early health effects are more sensitive than late health effects. Endpoints relating to countermeasures are also likely to be sensitive to changes in the modelling of deposited γ dose.

There is a further point for consideration when examining the likely sensitivity of late health effects. These are calculated from the collective dose in the whole of the exposed population. If the amount of material deposited in the region near the site is increased because of deposition to trees, then less material is carried in the plume to affect people at larger distances from the site. For some applications, ACA codes follow the dispersing material to distances which are sufficiently large that essentially all of the released material has been deposited. To some extent, the collective dose per unit deposit is independent of where the material is deposited, and so the change in the predicted collective dose would be less than the change in the dose per unit deposition.

The inclusion of the contribution of trees to deposited γ dose should be considered for inclusion in the data libraries of ACA codes. However, it can not be concluded that on average that the doses will be significantly underestimated by the omission of this exposure source for the reasons outlined above.

8.5.1.6 Wet deposition

As described in chapter 1, GSF (Frank and Tschiersch 1992) has carried out measurements of the washout coefficient of particulate material. At rainfall rates below about 3 mm/h the values determined here are larger than the COSYMA values, while they are lower than the COSYMA values at rainfall rates above about 10 mm/h.

The values used in COSYMA and RODOS are based on extensive earlier research. The values found by GSF are rather different from those used in COSYMA and RODOS and provide an additional data set to the extensive database of information. The value for the scavenging coefficient in COSYMA and RODOS do not require changing in light of this additional data.

Comparisons of several precipitation events have shown that the washout coefficient is strongly dependent on the drops size distribution of the rain. Large fractions of large drops cause a behaviour where the sensitivity of the particle size dependence is lower, while precipitation events with a large portion of small droplets show a stronger dependence on the aerosol particle size.

The aerosol washout coefficient of a specific precipitation event depends on the size distribution of the aerosol as well as on the size distribution of the rains drops and, in second order, on additional environmental parameters. A description of this quantity by means of only a one-parametric relation as in equation (8.1) cannot be satisfactory. Assuming the raindrop size distribution to be an exponential decreasing function, the aerosol size distribution to be a log-normal distribution and neglecting additional parameters, a 4-parametric approach is adequate to characterise the aerosol washout behaviour of a precipitation event. This may explain the discrepancies which are found when comparing the results of different authors.

COSYMA uses historic data on atmospheric conditions provided by national weather services. The rain droplet size distribution is not routinely measured, and so at present this improved parameterisation could not be incorporated into COSYMA. Similarly, RODOS would use information on rainfall rate at the time of an accident provided by weather services. The improved parameterisation could not be used unless information on the droplet size is provided.

8.5.2 Resuspension

Within this project, resuspension has been studied by GSF at Goiânia and by KFKI AERI at a site in Hungary (see chapter 6). Outside this project, the VAMP Terrestrial Working Group (VAMP 1992) has reviewed information available from measurements made after the Chernobyl accident.

KFKI AERI has derived an expression for the resuspension factor from measurements made in Hungary following Chernobyl. This expression gives values for the resuspension factor which are within the range of the measurements made across Europe following the Chernobyl accident (VAMP 1992) after about 200 days and slightly higher than the range at earlier times. A comparison of the data from Hungary with the other data for Europe and a number of model predictions is given in Figure 6.2.

The resuspension values used in RODOS are consistent with the available measured data from Europe following the Chernobyl accident and the data from KFKI AERI. The expression proposed for resuspension by KFKI AERI gives values within a factor of 2 of those obtained from the

formula used in RODOS for the period up to about 10 years after deposition. The values for the first year following deposition are substantially lower than those used in the 1993 version of COSYMA.

Following the review of available data and models for resuspension it is proposed that the simple model used in the codes is adequate. The resuspension coefficients used in the version of COSYMA to be issued in 1995 have been revised as a result of this contract, to be the same as those used by RODOS.

8.5.3 Weathering

8.5.3.1 Soil Migration

As described in Section 8.3 the effect of migration in the soil is modelled in ACA codes. A comparison of model predictions shows that there is reasonable consensus on the γ dose rate above a soil surface for several years after deposition but subsequently there is a large variation in the predictions reflecting uncertainty in the migration in soil into the future (VAMP, 1994).

The effect of surface roughness and migration of caesium into soil on the gamma dose-rate in air over grassland has been observed by Jacob et al (1992) over a 6 year period following the Chernobyl accident in Bavaria and the Ukraine. An analytical approximation for the attenuation of kerma rate in air due to surface roughness and migration into the soil derived from these data is discussed in Chapter 4.

Under this project, measurements have been made at several sites on the distribution of Cs-137 with depth in soil. These measurements, which are discussed in Chapter 4, provide valuable additional information on the time-dependence of Cs migration in soil.

The models used for soil migration in ACA codes, both as simple rural models and as part of more complex urban dose models show a great variation in predicted external doses at long times following deposition. The assumptions on soil migration over a few tens of years are very important for estimating the dose from caesium-137 over this timescale. There is a lack of data on soil migration for predicting external doses over long timescales. Given that this is not going to improve until the Chernobyl deposit has been followed up over many years a consistent approach to modelling soil migration and caesium external doses over tens of years following deposition is needed.

8.5.3.2 Weathering from urban surfaces

Measurements have been made on the retention of caesium on surfaces in urban areas, namely roofs, walls and paved surfaces following the Chernobyl accident in 1986. A series of measurements in Gavle, Sweden have been reported under this project (Chapter 5) and elsewhere (Karlberg, 1987) and measurements have also been made in Munich (Jacob and Meckback, 1987) and at Risø (Andersson, 1991, Roed 1987, Roed and Andersson 1993). Experimental measurements were also made on urban surfaces at Risø and in the UK before the Chernobyl accident (Warming, 1982, 1984, Wilkins 1987).

The urban dose models which have been developed simulate the weathering of material from urban surfaces. The weathering models used for the different urban surfaces have been partially validated under the International Modelling Validation Exercise, VAMP (VAMP TecDoc 3) using some of the data described in Chapter 5. The continuing adequacy of the models should be reviewed as more data becomes available on the long term behaviour of radionuclides, in particular caesium, on urban surfaces.

8.6 Recommendations for further work

This chapter has described the implications of work undertaken in this project and other recent studies for accident consequence and real time assessment models. Two main areas where further work is required have been identified.

The first is the deposition of material to, and removal from, skin. Studies have shown that this could be an important contributor to the overall risk of early health effects following large accidents.

The results from Imperial College and Risø work under this project suggest that the deposition velocity to skin could be an order of magnitude or more higher than the values currently used in accident consequence codes.

The second is the variation of external dose from deposited material over a period of years. There is a reasonable consensus between the predictions of external dose models at times within a few years after deposition, but their predictions increasingly diverge at longer times. Work has been undertaken at GSF in this project to measure dose rates from material deposited after the Chernobyl accident. This work should be continued so that models for the behaviour of deposited activity over some tens of years can be derived.

8.7 References

- Andersson, K G, URGENT - A model for prediction of exposure from radiocaesium deposited in urban areas. Presented at Workshop on Dose Reconstruction, Bad Honnef, June 1994.
- Andersson, K G, Contamination and decontamination of urban areas. Ph. D Thesis 1991, Risø National Laboratory / Technical University of Denmark.
- Brown J, Haywood S M and Roed J. The effectiveness and cost of decontamination in urban areas. In Proc International Seminar on Intervention Levels and Countermeasures for Nuclear Accidents. Cadarache Oct 1991 EUR-14469 (1992)
- Brown J and Jones J A. Location factors for modification of external radiation doses. Radiol Prot Bull 144 10-13 (1993)
- Brown J and Jones J A, Incorporation of the results of the EXPURT external dose model into the ACA system COSYMA, Chilton, NPRB M-510, (1994).
- Byrne, M A, Goddard, A J H, Lange, C and Roed, J. Stable tracer aerosol deposition measurements in a test chamber. J. Aerosol Sci. 26, 645-653 (1995).
- Byrne, M A, personal communication, (1995).
- Charles D, Hallam J and Kelly G N. Contributions of nuclides and exposure pathways to the radiological consequences of degraded core accidents postulated for the Sizewell PWR. Chilton, NRPB-M100 (1983)
- Crick, M J and Brown, J, EXPURT: A model for evaluating exposure from radioactive material deposited in the urban environment, NRPB-R235, London HMSO, 1990.
- Frank G and Tschiersch J. Parameterisation of below cloud scavenging at low precipitation intensities by using a fluorescent tracer method. J Aerosol Science, 23 suppl 1 S885 - S888, (1992)

Haywood, S M, Brown, J et al, Databases for activities in foodstuffs, for external exposure from the ground and for dose per unit intake, for fusion radionuclides for input to the COSYMA ACA system, Chilton, NRPB M-??? (in preparation).

Hill M D, Simmonds J R and Jones J A. The NRPB methodology for assessing the radiological consequences of accidental releases of radionuclides to atmosphere - MARC-1. Chilton NRPB-R224 (London HMSO) (1988)

IAEA. Cleanup of large areas contaminated as a result of a nuclear accident. Technical Report Series no 300 (1989)

IAEA, Modelling of resuspension, seasonality and losses during food processing. First report of the VAMP Terrestrial Working Group, Vienna, IAEA-TECDOC-647 (1992)

IAEA, Modelling of weathering and decontamination, third report of the VAMP Urban Working Group, IAEA-TECDOC (in preparation).

Jacob, P, Meckbach, R and Miller, H M, Reduction of external exposures from deposited radioactivity by run-off, weathering, street cleaning and migration in the soil. Rad. Prot. Dos. 21 (1-3) 51 (1987).

Jacob P, Rosenbaum H, Petoussi N and Zankl M. Calculation of organ doses from environmental gamma rays using human phantoms and Monte Carlo methods. Part II: Radionuclides distributed in the air or deposited on the ground. GSF-Bericht 12/90 (1990)

Jacob P, Meckbach R, Paretzke H G, Likhtariov I, Los I, Kovgan L and Komarikov I. Dose rates in air after cesium depositions on grassland. Submitted to Health Physics (1992)

Jones J A. The importance of deposition to skin in accident consequence assessments. IN Proc Seminar on methods and codes for assessing the off-site consequences of nuclear accidents, Athens May 1990, EUR-13013 (1991)

Karlberg, O. Weathering and migration of Chernobyl fallout in Sweden, Rad. Prot. Dos. 21 (1-3) 75 (1987).

Martin J E, Gallego e and Alonso A. URBAPAT: Modeleado de la irradiación externa y de la eficacia de las medidas de protección en entornos urbanos contaminados radioactivamente. Cátedra de Tecnología Nuclear, Madrid, Report CTN 82/92 (1992)

Meckbach R and Jacob P. Gamma exposures due to radionuclides deposited in urban environments. Part II: Location factors for different deposition patterns. Radiat Prot Dosim 25 (3) 181 (1988)

Robinson C A, Haywood S M and Brown J. The cost-effectiveness of various decontamination procedures. In Proc Seminar on methods and codes for assessing the off-site consequences of nuclear accidents, May 1990. EUR-13013 (1990)

Roed, J, Run-off from roof material following the Chernobyl accident. Rad. Prot. Dos. 21 (1-3) 59 (1987).

Roed, J, Dry deposition in rural and urban areas in Denmark, Rad. Prot. Dos 21 (1-3), p33-36, 1987.

Roed J. The distribution on trees of dry deposited material from the Chernobyl accident. Proc Joint CEC/NEA Workshop on Recent Advances in Reactor Accident Consequence Assessment, Rome 1988. EUR 11408 (1988)

Roed J. Deposition and removal of radioactive substances in an urban area. Final report of the NKA Project AKTU-245 (1990)

Roed, J and Andersson, K G, Using In situ Gamma-ray spectrometry to guide clean-up of radioactive contaminated urban areas. Presented at 15th Mendeleev Congress in Minsk, May 1993.

Sinnaeve, J and Olast, M (eds), Improvement of practical countermeasures: the urban environment, Post-Chernobyl Action, CEC, EUR 12555, Luxembourg, 1991.

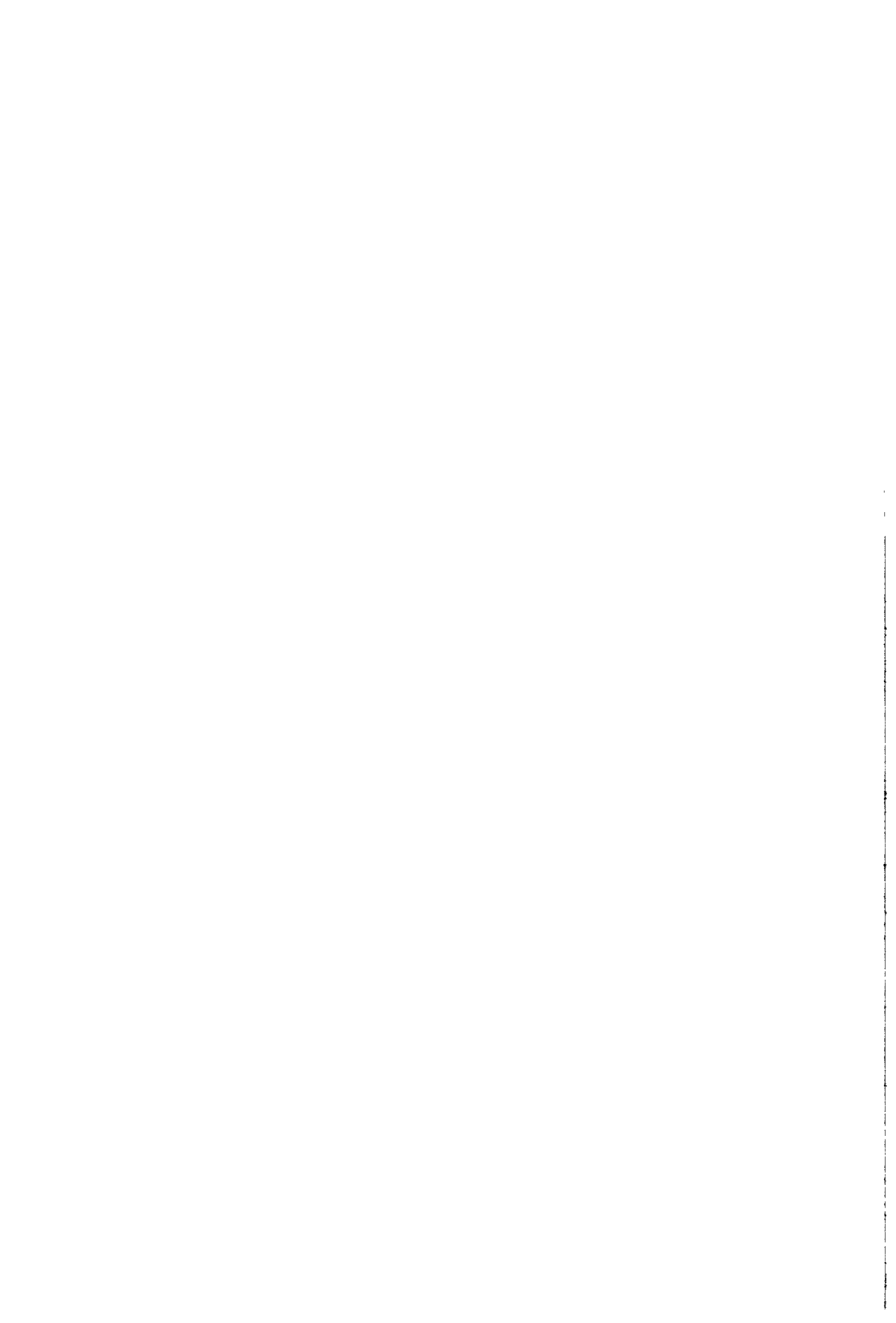
Underwood B Y, Deposition in foggy conditions. SRD R 487 (1988)

Underwood B Y. Modelling fog in probabilistic consequence assessment SRD R 595 (1993)

Warming, L, Weathering and decontamination of radioactivity deposited on asphalt surfaces. Risø-M-2273 (Risø National Laboratory, DK-4000 Roskilde, Denmark) (1982).

Warming, L, Weathering and decontamination of radioactivity deposited on concrete surfaces. Risø-M-2473 (Risø National Laboratory, DK-4000 Roskilde, Denmark) (1984).

Wilkins, B T, Retention behaviour of radiocaesium by common building materials under natural outdoor conditions. Rad. Prot. Dos. 21 (1-3) 51 (1987).



**Final Report
1992-1994**

Contract: FI3PCT920044 Duration: 1.9.92 to 30.6.95

Sector: C24

Title: Coordination of atmospheric dispersion activities for the real-time decision support system under development at KFK.

1)	Mikkelsen	Lab. Risø
2)	ApSimon	IMPCOL
4)	Desiato	ENEA
5)	Rasmussen	DMI
6)	Thykier-Nielsen	Lab. Risø
7)	Bartzis	NCSR "Demokritos"
8)	Massmeyer	GRS
9)	Deme	HAS.RIAE (PECO partner)

I. Summary of Project Global Objectives and Achievement

I. 1 Global Objectives:

*This projects task has been to coordinate activities among the **RODOS Atmospheric Dispersion sub-group A** participants (1) - (9), with the overall objective of developing and integrating an atmospheric transport and dispersion module for the joint European **Real-time On-line DecisiOn Support system RODOS** headed by FZK (formerly KfK), Germany.*

The projects final goal is the establishment of a fully operational, system-integrated atmospheric transport module for the RODOS system by year 2000, capable of consistent now- and forecasting of radioactive airborne spread over all types of terrain and on all scales of interest, including in particular complex terrain and the different scales of operation, such as the local, the national and the European scale.

For the reporting contracting period (1.9.92 to 30.6.95), the main achievements and tasks is summarized under **I.2 Achievements** below.

Reference to enclosed individual progress report provided by partner No. x is indicated by (x).

Extensive documentation has been prepared, cf. point 7. below: RODOS(A) DOCUMENTATION PROFILE.

Extensive lists of publications are furthermore included in the individual partners progress reports (1)- (9).

Copies of the listed RODOS A documents can be obtained on request from the coordinator.

I. 2 RODOS Atmospheric Dispersion Achievements: (1.9.92 to 30.6.95):

1. ATMOSPHERIC DISPERSION MODEL CHAIN:

Task: Establishment of a comprehensive and consistent atmospheric dispersion module (covering all scales)

1.1 Integrated near-range atmospheric dispersion model chain

Task: Near range flow and dispersion model chain, incl. met-preprocessors

A new and comprehensive real-time flow and dispersion model chain has been established in order to complement the existing RODOS near-range (0-20 km) dispersion model ADSTEP (a segmented Gaussian plume model), consisting of the following codes and modules (the number in parenthesis refer to the partner(s) providing code and documentation):

PAD - a meteorological preprocessor provided by ENE (4),
MCF- a hilly terrain mass consistent wind model provided by GRS (8)
LINCOM- an extremely fast "wind over hilly terrain" wind model (1)
RIMPUFF- a real-time atmospheric dispersion puff model by Risø (6),
including a new gamma dose module (Version R.3.0) (9).

1.1.1 Preparation of modules

Task: Coordination of model structure and data flow in codes for integration in RODOS-ASY

The near-range model chain (1.1) has been internally integrated with respect to data flow and file transfer, and has been tested as a stand alone system on PC platforms. (Ref.: RODOS(A)-TN(95)4; RODOS(A)-TN(95)3).

Availability status: all near-range modules (in Fortran code) is available to RODOS partners.

1.1.2 System integration under RODOS

Task: UNIX system integration in RODOS-ASY: "Kernel" system-integration of the atmospheric dispersion sub-module within the RODOS-UNIX environment, beginning with the near-range atmospheric model chain.

Lead responsibility for the specific RODOS system integration of the model chain (to reside within the UNIX system sub-module RODOS ASY) was transferred from FZK to Risø in May 1995. A system-specific RODOS-ASY modular integration of the RIMPUFF code is progressing and is expected to be completed by end 1995.

1.2 Stand-alone model system for complex terrain

Task: DEMOKRITOS (7) provides a "stand-alone" near-range model system for severe complex terrain. Output data integration with RODOS ASY.

1.2.1 Near-range Complex terrain-stand alone DEMOKRITOS system: Complex terrain models from the DEMOKRITOS system (ADREA, DELTA and DIPCOT) have been prepared for RODOS system integration (7).

1.3 Long-range model system

Task: Specification of a long-range modelling capability for RODOS:

Suitable models for Meso (National scale) and Long (European scale) range dose assessments have been identified: (3DRAW (U.K.); MATCH (S); DERMA (DK) and DREAM (DK).

The Swedish MATCH model have been selected for (stand-alone) integration during the 4. EU frame work program, where it will be adapted for long range applications including backfitting procedures in connection with on-line data transfer of numerical weather data to RODOS .

A coupling of the near-range model outputs to long range model inputs has been established and tested, see (1).

2. METEOROLOGICAL DATA

Task: The RODOS atmospheric dispersion subgroup has been concerned with incorporation of on-line numerical weather forecast data in the model chain

2.1 Local (on-site) weather stations

Task: To integrate local wind and stability data from (on-site) weather stations

This feature has been tested used extensively during the simulation of field experiments, but a need for a more general pre-preprocessor for such data of various quality has emerged, and will result in a proposal for study contract during the 4. Frame Work Program (EU).

2.2 On-line access to forecast data available at national weather services

Task: Establishment of a data protocol/interface to European scale Numerical Weather Forecast (NWF) data.

2.2.1 On-line data transfer from a numerical weather forecast (NWF) center

Task: Provision for on-line data transfer to serve the RODOS model chains on both local and long range

Experience has been gained with on-line data transfer from numerical weather forecast (NWF) centers: The operational weather forecast center at DMI have provided additional weather data for the period Sep 8. - 21. '93. Further, DMI is now daily transferring forecast data to the Danish Nuclear Emergency Center.

DMI and Risø has furthermore assessed data transfer requirements for an operational RODOS center supplied by on-line numerical weather information on the European scale. The concept is found suitable for real-time on-line connection. Ref. (1) and (5).

3. EXPERIMENTAL

Task: To provide RODOS with full-scale diffusion data sets of high temporal and spatial resolution suitable for evaluation of real-time dispersion modes on all scales. Also to provide real-time diffusion data suitable for training and education including accident simulations.

Extensive experimental evaluation have been undertaken by comparing the near range model results with data from atmospheric diffusion experiments, both regarding the near range models themselves and also by using the model chain to transfer dispersion to the long-range modules, ref. (1).

3.1 The near-range "MADONA" experiments

Task: Provision of detailed evaluation experimental data from dispersion experiments

Real-time experimental data of high spatial and temporal detail has been obtained during the 1992 MADONA experiments, see (1). All measured data is set available via CD-ROM media and the data sets have been prepared for uncertainty and training acquaintance in connection with the near range atmospheric dispersion model chain, see (1).

3.2 Graphical training facility using the MADONA CD-ROM data base

Task: Provision of graphical training facilities for atmospheric dispersion

The Risø group has been involved in the provision of a Meteorological Graphical User-Interface for the MADONA data base.

This activity involved coordination and integration of computer codes and experimentally obtained dispersion data (MADONA), with special consideration on quality assured and user-friendliness with codes and data bases, establishment of interactive menus and interactive graphical systems, see (1) and (6).

3.3 Evaluation experiments long range (ETEX)

Task: To provide real-time dispersion data on the National/European scale and to compare and select suitable long range models for RODOS.

Several partners (1), (5) (6) including Swedish associates (SMHI) have participated in the ETEX long-range experiments (October 1994).

Also a atmospheric dispersion modelling "functional" exercise was held at Risø in June '95 for evaluation of the Nordic countries different long range models-based on the ETEX-1 data set, see (1).

4. DATA ASSIMILATION AND BACKFITTING ACTIVITIES

Task: Make provision for the use of data assimilation and back-fitting techniques in order to integrate on-line radiological measurements and for post-accidental source term determination. In particular to prepare the model chains (both near range and long range) for "on the fly" backfitting and data assimilation methods.

The group has obtained experience with both backfitting and with data assimilation via different projects during the reporting period:

4.1 Data assimilation with RIMPUFF - Version UoL

A version of RIMPUFF has been developed by RODOS partner UoL that accommodates data assimilation to real-time radiological observations based on Bayesian statistical methods.

4.2 Source determination

A version of RIMPUFF was used by Russian JSP-1 partners at SPA-TYPHOON, Obninsk for source term determination during the Tomsk -7 accident, see (1) for references.

5. UNCERTAINTY MEASURES.

Task: To assess, and even more important, to communicate uncertainties associated with atmospheric dispersion prediction - on the different scales, times, topographies, forecasting periods etc.

5.1 Presentation of uncertainty in long-range particle models

In connection with the long-range particle model 3DRAW, partner (2) has demonstrated the use of color-coding the graphical displays of particle positions in the 3DRAW model according to uncertainty.

5.2 Effects of orography(2)

Partner (2) has also estimated the enhancements in wet-deposition introduced by underlying orography

6. QUALITY ASSURANCE AND VERSION CONTROL OF CODE

Task: To maintain quality assurance and version control of codes and data flow in the atmospheric model chains

5.1 First RIMPUFF benchmark (ref RODOS DOC)

A first RIMPUFF workshop on "Quality Assurance and Version Control" was held at Risø in January 1995., see (1) and (6). Version control of RODOS software reside by code authors to the extent possible.

5.2 Automated software and code control

Partners from IMPCOL have initiated an automatic procedure for quality assuring of RODOS codes, see (2).

7. RODOS(A) DOCUMENTATION

Extensive documentation has been prepared, cf. 1) RODOS(A) included below, and 2) references included by individual partners in the included progress reports by partners (1)- (9).

Minutes of meetings:

RODOS(A)-MN(93)1

final version 12. March 1993.

Subgroup meeting: Coordinator/DMI (sent to DMI, KfK, Typhoon)

RODOS(A)-MN(93)2

final version 1. July 1993.

Subgroup meeting: Coordinator/GRS

RODOS(A)-MN(93)3

final version 16. August 1993.

Subgroup meeting: Coordinator/PSI

RODOS(A)-MN(93)4

final version 21. December 1993.

Subgroup meeting: Coordinator/SMHI

RODOS(A)-MN(94)1

final version 13. Feb. 1994.

Subgroup meeting: Coordinator/GRS

RODOS(A)-MN(94)2

final version 4. March 1994.

Subgroup meeting: Coordinator/IAE-Poland

RODOS(A)-MN(94)3

final version 22. December 1994.

Subgroup meeting: Coordinator/KfK/GRS/AERI/GEO-Switzerland

Technical notes:

RODOS(A)-TN(93)1

draft 1. Sep. 1993.

List of regional scale forecast data requirements from National Weather Services, by Torben Mikkelsen, Risø.

RODOS(A)-TN(93)2

final version 22. April 1993.

On methods to calculate the divergence of a flow within MCF, by Klaus Massmeyer, GRS Köln.

RODOS(A)-TN(93)3

final version. Sep. 1. 1993.

Nordic NKS-BER1 Exercise June 21. 1993
Figures and fax-messages distributed between participating Nordic Institutes, by Alix Rasmussen (DMI)

RODOS(A)-TN(93)4

final version 22. September 1993.

Description of NORVIEW, the presentation standard for operational nuclear accident dispersion models.
Mika Salonoja and Ilkka Valkama, Finnish Meteorological Institute, Helsinki.

RODOS(A)-TN(94)1

final version 18. March 1994.

A Strategy Note on Integration of Medium and Long-Range Dispersion Models in RODOS - Data transfer requirements.
Torben Mikkelsen, Risø National Laboratory, Denmark

RODOS(A)-TN(94)2**final version 6. May 1994.**Liste der globalen Parameter im Modell MCF.
K. Massmeyer, GRS**RODOS(A)-TN(94)3****draft 1. Sep. 1994.**HIRLAM-RIMPUFF data format,
Jens Havskov Sørensen, DMI**RODOS(A)-TN(94)4****draft 8.Sep. 1994.**Specification of Input Parameters for the
RODOS version of RIMPUFF,
Søren Thykier-Nielsen, Risø**RODOS(A)-TN(94)5****draft 17. Nov. 1994.**Kurzbeschreibung des deutsch-französischen
Modell für die atmosphärische Ausbreitung in
Unfallsituationen, Reinhard. Martens, Klaus
Massmeyer, Klaus Nester and Horst Schnadt.**RODOS(A)-TN(94)6****draft 12. Dec. 1994.**Specifications for RIMPUFF Benchmark
Søren Thykier-Nielsen, Risø**RODOS(A)-TN(95)1****Final version 8. May 1995**First International Benchmark for RIMPUFF:
Questionnaires and description of model versions;
Risø, February 2-3 1995.
Søren Thykier-Nielsen and Torben Mikkelsen**RODOS(A)-TN(95)2****Final version 8. May 1995.**First RIMPUFF Version Control and Benchmark
Test: Collection of Papers and Overheads
Presented during the 1. International RIMPUFF
Benchmark held at Risø, February 2-3 1995.
Søren Thykier-Nielsen and Torben Mikkelsen**RODOS(A)-TN(95)3****Draft version 30. Sep. 1995.**RODOS SYSTEM: ANALYZING SUB-
SYSTEM ASY:
Atmospheric Dispersion Module RIMPUFF
Version R3.0 USER'S GUIDE.
Søren Thykier-Nielsen, Sándor Deme and
Torben Mikkelsen**RODOS(A)-TN(95)4****Draft version 30. Sep. 1995.**The RODOSNear-range Atmospheric Dispersion
Model Chain PAD/MCF/LINCOM/RIM-
PUFF/ADSTEP: Specification of Data Structure
and Data flow Requirements by Torben
Mikkelsen and Søren Thykier-Nielsen.

Reports, papers:**RODOS(A)-RP(93)1****final version: 3. Feb. 1993.**Langner, J., C Persson and L. Robertson (1993):
The Chernobyl accident: A case study of
dispersion of ¹³⁷Cs using high resolution
meteorological data. SMHI report 8 pp + 7
figures.**RODOS(A)-RP(93)2****final version: 8. March 1993.**The DMI Operational HIRLAM Forecasting
System. 8pp.**RODOS(A)-RP(93)3****final version: 22. March 1993.**Massmeyer, K. et al.: Regional flow fields in
Northrhine Westfalia - a case study comparing
flow models of different complexity. In: Air
Poll. and its Application VIII (Plenum press),
8pp.**RODOS(A)-RP(93)4****final version: 4. April 1993.**Desiato, F.: A long-range dispersion model
evaluation study with Chernobyl data.
Atmospheric Environment, Vol. 26A, No. 15,
pp2805-2840.**RODOS(A)-RP(93)5****final version: August 1. 1993.**Mikkelsen, T. RODOS: A comprehensive
decision support system for nuclear emergencies
in Europe. ENVIRONews, Vol. 1., No. 3 June-
July 1993 pp. 14-17.**RODOS(A)-RP(93)6****final version: February 1. 1993.**Bartzis, J.G.: ADREA-1 : A Three-Dimensional
Finite Volume Transport Code for Mesoscale
Atmospheric Transport (Part I: The model
description, 73 pp; Part II: Code structure and
users manual, 14pp + Appendix A-E).**RODOS(A)-RP(93)7****final version: May 1. 1993.**Thykier-Nielsen, S. S. Deme and E. Láng:
Calculation Method for Gamma-Dose Rates
from Spherical Puffs. Risø-R-692(EN), 26pp.,
May 1993. Available on request from Risø
Library, Risø National Laboratory, P.O.Box 49,
400-Roskilde, Denmark.**RODOS(A)-RP(93)8****final version: December 31. 1993.**Thykier Nielsen, S., T. Mikkelsen and J. M.
Santabàrbara: Experimental Evaluation and a

PC-Based Real Time Dispersion Modelling System For Accidental Releases in Complex Terrain. In: Proceedings from the : 20th ITM on Air Pollution Modelling and Its Applications, Valencia, Spain , December 1993. 8 pp. Plenum, NY (in press).

RODOS(A)-RP(94)1

final version: March 30. 1994.

ERCOFTAC workshop on: Database for evaluating numerical simulation of dispersion behind buildings: Full scale studies of building effects on plume dispersion from an elevated non-buoyant continuous release.

Hans. E. Jørgensen, Torben Mikkelsen, Per Løfstrøm, Erik Lyck Hans Erbrink and Rudy Scholten.

RODOS(A)-RP(94)2

final version: 1. aug. 1994

Short-term Prediction of Local Wind Conditions. Lars Landberg and Simon Watson (Boundary-Layer Meteorology 70: 171-195, 1994)

RODOS(A)-RP(94)3

final version: 20. August 1994.

Calculation of Atmospheric Boundary Layer Height based on DMI-HIRLAM.

Jens Havskov Sørensen, Alix Rasmussen and Henrik Svensmark.

RODOS(A)-RP(94)4

final version: 22. September 1994.

Atmospheric Dispersion at a Nuclear Power plant Building:

- a tracer experimental evaluation.

R.D.A Scholten, J.J. Erbrink, A. van Melle, H.E. Jørgensen, T. Mikkelsen, E. Lyck, P. Løfstrøm and T. Ellermann. Joint KEMA/RISØ/NERI Report 158 pp.

RODOS(A)-RP(94)5

draft: October 6. 1994.

Report from the NKS (Nordic Nuclear Safety Research) Program 1990-1993:

Medium- to long-range atmospheric "real-time" transportation and dispersion models in use in the Nordic Countries. Editor Ulf Tveten.

RODOS(A)-RP(94)6

final version: 31. October 1994.

Analysis and Prognosis of Radiation Exposure Following the Accident at the Siberian Chemical Combine Toms-7.

S.M. Vakulovski, V.M. Shershakov, R.V. Borodin, O.I. Vozzhennikov, Ya.I. Gaziev, V.S. Kosykh, K.P. Makhon'ko, and V.B. Chumichev. Risø-R-report No.750 (EN), 47 pp.

RODOS(A)-RP(94)7

final version: 31. Oktober 1994.

Vinddiagnosmodell bygget kring LINCOM. (In Swedish).

Jan Burman (FOA report- D--94-00025-4.5--SE), 27pp.

RODOS(A)-RP(94)8

final version: 31. June 1995.

Calculation Method for Gamma Dose Rates from Gaussian Puffs.

Søren Thykier-Nielsen, Sandor Deme and Edit Láng. Risø-Report No. 775, 22 pp.

RODOS(A)-RP(94)9

final version: 1. December 1994.

MADONA: Diffusion Measurements of Smoke Plumes and of Smoke Puffs.

Torben Mikkelsen, Hans E. Jørgensen, Kenneth Nyrén and Jürgen Streicher, 4pp.

RODOS(A)-RP(94)10

final version: 1. December 1994.

MADONA: On-site Real-time Turbulence Measurements

Torben Mikkelsen and Hans E. Jørgensen, 4pp.

RODOS(A)-RP(94)11

final version: 1. December 1994.

MADONA: Real-time Diffusion Model Simulations

Søren Thykier-Nielsen, Torben Mikkelsen, Josep Moreno Santabarbara, David Ride, Tim Higgs, and Harald Weber, 4pp.

RODOS(A)-RP(94)12

final version: 1. December 1994.

Using a Combination of Two Models in Tracer Simulation.

(Risø's RIMPUFF and NERI's long-range Eulerian transport model - the Chernobyl accident). Jørgen Brandt, Torben Mikkelsen, Søren Thykier-Nielsen and Zahari Zlatev, 22 pp.

RODOS(A)- RP(95)1

final version: 1. May 1995

The High Resolution Data Set from Trial MADONA (Meteorology and Dispersion over Non-Uniform Areas) CD-ROM VERSION 2.0.

D.J. Ride, T. Higgs, C. Biltoft, J.H. Byers, R.M. Cionco, C.G. Collins, A.R.T. Hin, C.D. Jones, P.E. Johansson, H.E. Jørgensen, W. aufm Kampe, J.F. Kimber, T. Mikkelsen, M. Nordstrand, K. Nyrén, H. van Raden, R. Robson, J. M. Santabarbara, R. Sterkenberg, J.M. Streicher, H. Weber.

Head of Project 1: Dr. Mikkelsen

II. Objectives for the reporting period

As coordinator for the Subgroup-A activities (Atmospheric Dispersion), this partners contribution for the reporting period (1.9.92 to 30.6. 1995) has mainly been:

- Model selection, model evaluation and model integration of a near-range (0-20 km) atmospheric dispersion model chain in the RODOS-system.
- Provision of real-time atmospheric diffusion data obtained from full-scale atmospheric dispersion experiments and undertake their subsequent integration in an RODOS compatible framework, in order to enable RODOS users to obtain system acquaintance and hands-on training experience based on realistic real-time dispersion scenarios.
- Model selection and interfacing of a long-range atmospheric dispersion chain for now and forecasting spread to longer (national and European) scales. In this respect, to enable on-line system access to weather stations and to forecast data available at national and international weather services.

III. Progress achieved including publications

Progress reported by partner No. 1 can be subdivided into the following three main groups:

1. The near and long range model chains

Under this heading, the first task of this partner has been concerned with the interfacing and system integration of the local scale (0 - 20 km) atmospheric model chain consisting of: 1) preprocessor PAD, 2) flow models LINCOM and MCF, and 3) dispersion model RIMPUFF, previously selected for the RODOS decision support system.

A second task has been concerned with the selection and incorporating of models for the long range atmospheric transport module, which can calculate both now- and forecasts of trajectories and radioactive airborne spread on National and European scales.

A third activity has been concerned about interfacing the system to 1) local (on-site) weather stations and 2) on-line data available at the national weather services.

2. Experimental evaluation and training module

A second category of activities, relating to experimental evaluation of both the near-range and the long-range atmospheric flow and dispersion models have been undertaken, based on data from controlled tracer experiments obtained with high temporal and spatial resolution measurements of puff and plume spread including wind fields.

Also the provision of a computer-based real-time training and visualization software package "MAD-MOVIE" have been developed and is available in a RODOS-compatible UNIX version based on full-scale experimental data from the MADONA experiments.

3. Rimpuff code improvements and implementation

A third activity has been to improve, interface and system integrate the RIMPUFF code,

including quality assurance and quality control, hereunder benchmark testing and version control within the Subgroup A participants. This activity has involved close collaboration with FZK regarding model modifications and model improvements in order to meet the system specifications, quality assurance and control laid out for the RODOS system. A specific report regarding this activity is given by partner No. 6, see enclosed.

[1] THE RODOS ATMOSPHERIC DISPERSION MODEL CHAIN

1.1 Near-range atmospheric model chain, evaluation

Model chain development and model evaluation (based on RODOS models PAD/LINCOM/MCF/RIMPUFF) and intercomparison with experimental data from the GUARDO, BOREX, MADONA and BORSSELE is mainly reported by partner No. 6. Some more specific topics regarding data transfer and long range modeling are however included below.

Refs.: Thykier-Nielsen et al (1995a) and Thykier-Nielsen et al (1995b).

1.2 Near range model chain: RIMPUFF Benchmark test and version control

Specifications for a RIMPUFF Benchmark and general quality assurance study were initiated by RODOS partners from UoL (Leeds- UK) and were send out to relevant RIMPUFF users in December 1994.

The specifications included a call for a first International Benchmark test of RIMPUFF, including also a questionnaires and description of model versions.

A workshop meeting was subsequent held at Risø during the days of February 2-3 1995.

Results: A general strategy for future version control and regular bench marking of similar software was set up and has been reported in the RODOS newsletter. In short the conclusion was: 1) Quality control of code(s) is a common issue among all users, 2) Version control should remain by the original model developers.

A collection of papers and overheads presented during the "1. International RIMPUFF Benchmark" is available from Risø.

Refs.: RODOS document files: RODOS(A)-TN(94)6; RODOS(A)-TN(95); RODOS(A)-TN(95)2

1.3 Integration of on-line Numerical Weather Forecast Data in RODOS

In order to establish and test an on-line coupling of the RODOS to a NWF weather forecast center, it was decided to establish 3 test reference data sets data for distribution to participants.

The Danish Meteorological Institute (partner No. 5) have subsequently provided numerical

weather forecast data from their European scale HIRLAM model covering the entire of Europe, including a large part of Russia and the Atlantic Ocean.

Numerical weather data were "logged" on mass storage devised at DMI during the following period: May 17. - 23. '93; July 8. - 21. '93 and Sep 8. - 21. '93 , and were subsequently distributed to RODOS subgroup-A partner No. 7: DEMOKRITOS.

A strategy note on integration of medium and long range dispersion models in RODOS, including data transfer requirements, was provided by Mikkelsen (1994). It contains experience from the 1993 Ignalina-to-Scandinavia sub-scale (1000 km). The report also describes the data requirements for on-line transfer of numerical weather forecast data required for driving RODOS near and long range dispersion models:

ANALYSES	DKV-HIRLAM	Mega byte
00 UTC	0,+3,+6,...,+36 HRS	13*6Mbyte ¹⁾ =78 Mbyte
06 UTC	0, +3, +6 HRS	3*6Mbyte=18 Mbyte
12 UTC	0, +3, +6, ..., +36 HRS	13*6Mbyte=78 Mbyte
18 UTC	0,+3,+6 HRS	3*6Mbyte=18 Mbyte

¹⁾ Each time step contains approximately 6 Megabyte fully compressed data including all levels and all variables.

Table 1.1 *Data transfer requirements for a RODOS on-line connection to the DK-HIRLAM Europe scale model: DKV_HIRLAM (Version November 1995): Table 1 shows the data transfer requirements based on +3 HRS time steps and including all the models 31 vertical layers between ground and up to 20 km, based on a 23 km by 23 km horizontal resolution and including all of the weather models primary variables (horizontal winds, temperature, specific humidity) and several surface-related variables such as topography, roughness, shear-stresses, heat fluxes, pressure, soil temperature and wetness, precipitation and more.*

Forecast Met-data transfer time estimates:

Peak load on data transfer will occur twice a day at: 00 UTC and 12 UTC. Then ~78 Mega bytes will have to be transferred. Example of data transfer via a single-line 64 kbit/sec dedicated ISDN line:

$$Transfer\ time = \frac{78 \cdot 10^6 \cdot 8}{64 \cdot 10^3 \cdot 3600} Hrs = \frac{1 \cdot 10^3}{4 \cdot 10^3} Hrs = 2.7 Hrs$$

Some possible reduction factors can later be introduced by, eg.:

- a) Reducing the number of vertical layers (by 1/2) and reducing the horizontal area (by 2/3 say), cuts the data transfer time down to ~ 1 hr.

- b) The use of multiple ISDN lines: reduction by factor of 2,4,..are possible.
(For instance, with 4 dedicated parallel lines, which is indeed feasible today, the transfer time reduces to ~ 1/4 Hr.)

A draft report on automatic provision of input data to near-range models LINCOM and RIMPUFF based on forecast data provided by HIRLAM is being prepared by DMI.

Ref.: Mikkelsen (1994). See also progress report by partner No. 5 (DMI).

1.4 The TOMSK-7 accident (Dose reconstruction)

Risø has assisted FZK by publishing a report in English on the "Analysis and prognosis of radiation exposure following the accident at the Siberian chemical combine Tomsk-7". The study, made by SPA-TYPHOON, Obninsk, Russia, demonstrated the use of RIMPUFF as a suitable tool for dose reconstruction and post-accident source strength determination.

Ref.: Vakulovski et al. (1994).

1.5 New near-range wind flow model LINCOM -T

A new version of the RIMPUFF wind model LINCOM has been developed so that the model now responds to thermal effects such as slope and valley breeze winds. This work has been done in collaboration with Ph. D student Josep Moreno Santabàrbara, ITEMA, Barcelona.

By specifying a prescribed mean temperature field, the previous neutral LINCOM code has been extended so it now responds to (to 1. order) thermal stratification effects, such as daytime up-valley convection and nighttime cold-air drainage flows.

The new code has been evaluated with wind measurements from the MADONA experiments.

Refs.: Moreno et al. (1994) and Santabàrbara et al. (1995)

[2] EXPERIMENTAL ACTIVITIES: DATA FOR MODEL EVALUATION

2.1 General Objective:

To providing detailed experimental diffusion data suitable for real-time modeling based on atmospheric diffusion experiments for various ranges and sites, ranges, atmospheric stabilities, source types and release scenarios. This activity implies integration of real-time full-scale diffusion measurements in the RODOS system for training purposes based on the Risø mini-LIDAR systems for remote sensing of smoke plumes.

Establishment of an RODOS-integrated training and hands-on database involving data from full scale based international experiments: GUARDO (E); BOREX (DK); MADONA (UK) and BORSSELE (NL).

Refs.: Mikkelsen and Werner (1994)

2.2 A full-scale building wake diffusion experiment from the nuclear power plant Borssele in Holland Sep. 1993.

A full-scale combined tracer-gas and tracer-smoke diffusion experiment was conducted from a Dutch nuclear power plant "Borssele" near Vlissingen in Holland during Sep. '93, with the purpose to study the influence of nearby building effects on the near-range atmospheric dispersion characteristics.

Smoke and tracer gas was released from top of the generator building and from the containment's ventilation chimney. Both Lidar and tracer-gas techniques were used to measure the resulting downwind, building-wake influenced, dispersion pattern.

Our measurements show that building effects have tremendous effect on the on-site and near-range dispersion characteristics and model parameterization of building wake effects have been modified accordingly in the RIMPUFF code.

A detailed data report, jointly produced by KEMA (NL) and NERI and Risø (DK) is available. Refs: Jørgensen et al. (1994) and Scholten et al. (1994).

2.3 Visualization program for graphical presentation of model and experimental data.

Real-time handling and inter-comparison of large amounts of vector fields (video-animation) resulting from real-time model and measurements have been eased by the construction of several (both PC and UNIX based) menu driven visualization programs suitable for presentation of RODOS atmospheric dispersion model results and corresponding experimental data.

The program "S" provides an easy-to-use and user-friendly training facility within the RODOS system. Demonstrations based on "S" were presented during the Schloss Elmau workshop, cf. Jørgensen et al. (1993) and Thykier-Nielsen et al. (1993).

The programs "MADMOVIE" and "PLOSIG" presents real-time experimental data from the

near-range MADONA diffusion experiments, and runs on both PC and UNIX platforms. An example of the interactive menu driven utility program PLOSIG is shown below. The program displays experimental data together with various plume and puff spread parameterizations in the same graph. The RODOS user can with PLOSIG easily get acquainted by the different data sets and the different stability parameterizations, further the user can easily see the difference from selecting different plume and puff parameterization schemes, some based on simple Pasquill-Gifford-Turner parameterization schemes, others based on more advanced similarity theory.

Ref.: Jørgensen et al. (1993) and Thykier-Nielsen et al. (1993).

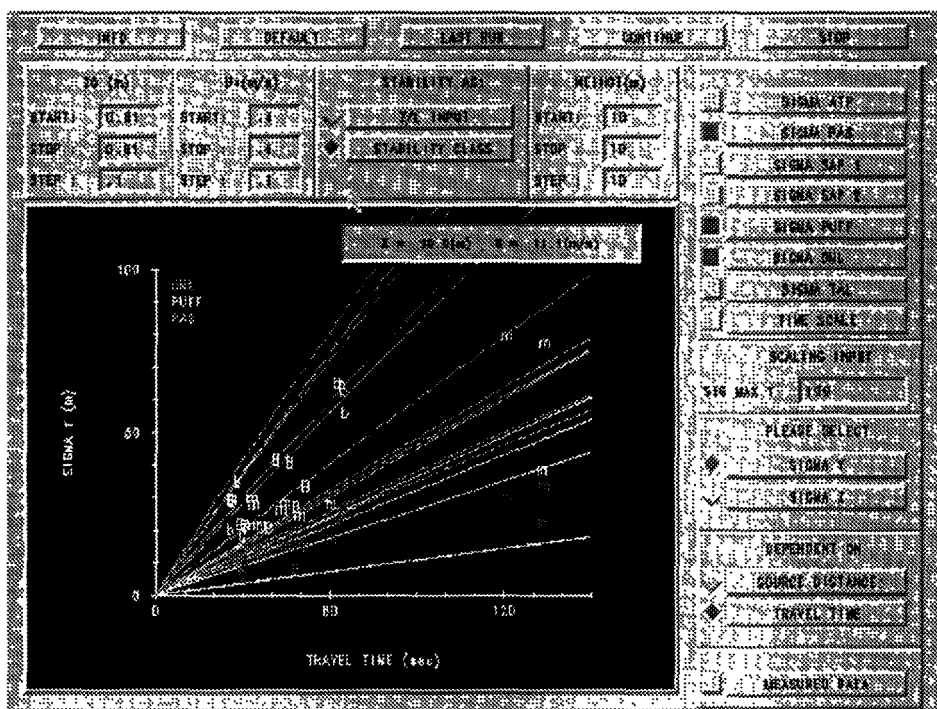


Figure 1: The PLOSIG menu-driven "model vs. data" display interface: acknowledgements to colleagues H. Weber and W. aufm Kampe at the German Military Geophysical Office, GMGO, Traben-Trarbach for integrating both dispersion curves and MADONA data in the presentation software MADMOVIE and PLOSIG. Refs.: Cionco et al. (1995) and Ride et al. (1995).

2.4 The MADONA experiments

Objectives

Provision of real-time LIDAR-measurements of smoke plumes and corresponding micro-meteorological model input data for integration on a MADONA flow and diffusion CD-ROM data base for distribution among RODOS members including "easy to use" interactive visualization software.

The experiments:

A comprehensive field trial named "MADONA" for "Meteorology and Diffusion Over Non-uniform Areas" took place at the CBDE's test site near Porton Down in the UK during Sep. 1992.

In a joint venture with participation from US Army, CBDE UK, DLR, Germany, Risø Denmark, FOA4 Sweden and TNO Holland, detailed and high resolution atmospheric dispersion measurements were obtained over moderately rolling terrain on the 2-4 km scale, supported by detailed micro-meteorological mean and turbulence measurements in order to characterize the atmospheric flow and stability.

Both ground and elevated puffs, tracer gas and ground level continuous smoke were released and measured by several Lidar systems, including Risø's and DLR's mini-Lidar systems. With the Porton Down area being characterized by rolling and non-uniform terrain, extensive meteorological instrumentations (14 ten-meter high met towers, in addition to 2 on-line sonic anemometers) were recording around the clock. Interesting non-stationary dispersion scenarios was here encountered during transition zones and best visualized by the "S" real-time graphics display program, the above described tool for fast sequential presentations (movie) of 2-D fields of scalars (concentrations) and vectors (winds).

MADONA results and outcome:

Extensive data reduction and preparation of this data set has meanwhile been undertaken by the MADONA field trial participants. In order that the MADONA trials to be included in the RODOS training data base, the entire comprehensive experimental data base has been released, first as a beta-version on a CD-ROM Database Version 1.01 (June 1994) and later Version 2.0 (February 1995). Work is continuing into the 3. FWP to further update the cd-rom with more data and graphical display programs. The programs and corresponding data base are available in both PC and UNIX based graphical display and presentation programs for visualization purposes. The experiment is suited for training and exercises within the RODOS framework.

Refs.: Cionco et al. (1995), Ride et al. (1995), Jørgensen et al. (1995), Mikkelsen and Jørgensen (1995) and Mikkelsen et al. (1995), and Thykier-Nielsen et al (1995).

2.5 Progress with the Risø LIDAR system-based real-time dispersion measurement techniques:

An important corner stone for experimental evaluation of the real-time near-range atmospheric model chain have been the existence of high-resolution real-time plume spread data obtained via Lidar measurements during various diffusion trials.

The Risø mini-lidar has been central to all the real-time measurement campaigns conducted during this project. By today, the Risø LIDAR technique is fully operational and lidar-measurements of plume spread have been fully justified by comparison of data simultaneously conducted calibrated gas-tracer experimental techniques (using SF₆). Inter-comparison of lidar data with tracer diffusion data has here finally justified the use of LIDAR technique as an accurate qualitative measurement method for determination of plume spread, cf. Jørgensen and Mikkelsen (1993) and Jørgensen et al. (1995).

New LIDAR for improved range and temporal resolution:

Risø has lately (during the years 1994-1995) finalized the construction and testing of a new 2. generation mini-LIDAR system suitable for two-dimensional plume scanning and diffusion measurements over longer ranges. This new LIDAR was first set in operation during the BOREX '95 experiments, where it operated successfully at high repetition frequencies (55 Hz) and on longer ranges than previously, - out to several kilometers downwind from the source point.

LIDAR-II is improved with respect to LIDAR-I with respect to the following features: It has improved detector systems and a new computerized data acquisition system for fast data transfer and control (up to 55 Hz repetition frequency). Also a new telescope has been purchased, and a new fast repetition pulsed Nd:YAG laser (55 Hz - 10 mJ pr shot) build by Big Sky lasers. Inc. Montana, USA has been integrated successfully.

The BOREX '94 and '95 experiments:

Two comprehensive field experiments, BOREX' 94 and BOREX' 95 have been conducted during the reporting period.

Both ground level and elevated release diffusion experiments have been conducted over flat terrain during field trials, using joint smoke and tracer released from the ground or from a 25 meter high meteorological tower over flat terrain near the town of Borris in Western Jutland (DK).

A grand total of more than ~ 60 daytime and 10 night time reference experiments was obtained during intensive two-week campaign in June and July 1994 and 1995.

LIDAR-measured plume statistics have subsequently been obtained at various downwind measurement points out to several kilometers from the source point. The experiments were also accompanied by simultaneous conducted tracer-gas diffusion experiments (SF₆) provided by Danish colleagues from the Danish "EPA" (NERI) institute in order to determine the mean-value and for inter-calibration purposes. Results analyzed to date (so far only from the BOREX'94 field trials) have shown surprisingly good agreement with mean concentration profiles of the lidar systems as compared to tracer-gas determined concentrations. Vertical cross-section scans, supported by only a few ground based SF₆-reference measurements, have in this way been

demonstrated as a possible venue for determination of both horizontal and vertical plume spread in a single experiment.

As with the MADONA experiment, also the BOREX data sets are planned to be issued on CD-ROM media for integration in the interactive RODOS data base for training and uncertainty studies.

Refs: Jørgensen and Mikkelsen (1993) and Jørgensen et al. (1995).

2.6 Nordic Long-range Model Intercomparison and Validation Exercise based on ETEX-1

Also a long-range (European scale) dispersion model evaluation, that included RODOS candidate long-range model chain wind (DERMA by DMI) and dispersion (MATCH by SMHI) has been undertaken during 1995. Both models use HIRLAM data.

Incidentally, both RODOS models participated in the joint European long range model evaluations study named ETEX, where long-range tracer technique is used to monitor a simulated accidental releases on the European scale.

The tracer gas Perflourcarbon, released in Rennes in France on Oct. 23 was measured with particular high accuracy and hourly resolution by Danish colleagues at the co-located NERI institute as it passed over Risø on October 25 1995.

A Nordic dispersion and trajectory model intercomparison and validation exercise were held at Risø June 6-7 1995 with participation of Nordic modelers before the results of the NERI measurements, and before the official ETEX results were disseminated to the participants.

The purpose was to perform a realistic accident exercise on the Nordic scale, where later actual measurements would be available.

Table 2: Summary of long-range exercise results from the Risø intercomparison:

ETEX-1: DATA (Measured by NERI)	DMI DERMA	SMHI MATCH
Arrival time at Risø: +44 Hrs	44 Hrs	45 Hrs
Duration: 20 Hrs	20 Hrs	24 Hrs
Conc. Max.: 1.08 ng ¹	0.6 ng	1ng

¹ The measured maximum concentration at Risø was 12 times above the background concentration of PFC.

Results

It is seen that both RODOS long range candidates perform surprisingly well in the Risø-exercise. Preliminary results released from the official ETEX "Real time Long Range Dispersion Model Evaluation" study, prepared for the ETEX modelers Meeting in Prague October 1995, seems to confirm this good simulation ability of the RODOS models, also when evaluation is made on the entire ETEX-1 sampling station network. Both models seem to be top performing in both intercomparison tests.

Ref.: Tveten and Mikkelsen (1995).

New Publications during the reporting period (1.9.92 to 30.6. 1995):

1993:

Jørgensen, H.E. and T. Mikkelsen (1993). Lidar measurements of plume statistics, *Boundary-Layer-Meteorology*, Vol 62, pp. 361-378.

Jørgensen, H.E. (1993). Studies of concentration fluctuations in the atmospheric surface layer Ph.D - thesis, 118 pp., Available on request from: Dep. of Meteorology and Wind Energy, Risø National Laboratory, P.O. Box 49, DK-4000 Roskilde, Denmark.

Jørgensen, H.E., J.M. Santabarbara and T. Mikkelsen (1993). A real-time uncertainty-knowledge and training data base. *Radiation Protection Dosimetry* Vol. 50, Nos 2-4, pp 289-294

Mikkelsen, T. and F. Desiato (1993). Atmospheric dispersion models and pre-processing of meteorological data for real-time application. *Radiation Protection Dosimetry* Vol 50, Nos. 2-4, pp 205-218.

Thykyer-Nielsen, S., J.M. Santabarbara and T. Mikkelsen (1993). Dispersion scenarios over complex terrain *Radiation Protection Dosimetry*, Vol. 50, Nos 2-4, pp 249-255.

1994:

Jørgensen, H.E., T. Mikkelsen, P. Løfstrøm, E. Lyck, H. Erbrink and R. Scholten (1994). Full-scale Studies of Building Effects on Plume Dispersion from an Elevated Non-buoyant Continuous Release ERCOFTAC Workshop on Databases for evaluating Numerical Simulations of Dispersion behind Buildings, Cambridge, March 30, 1994.

Mikkelsen, T. (1994). A Strategy Note on Integration of Medium and Long-Range Dispersion Models in RODOS. RODOS document file RODOS(A)-TN(94)1. Available on request from: Dep. of Meteorology and Wind Energy, Risø National Laboratory, P.O. Box 49, DK-4000 Roskilde, Denmark

Mikkelsen, T. (1994). RODOS - a comprehensive decision support system for nuclear emergencies in Europe. Nordic Seminar on Preparedness Against Nuclear Emergencies, Oslo, Norway, May 4.-6, Sundvollen, Norway Unpublished, abstract available from: Information Service Department, P.O. Box 49, Risø National Laboratory, DK-4000 Roskilde, Denmark.

Mikkelsen, T. and C. Werner (1994). Validation, - training and uncertainty study experiments for real-time atmospheric dispersion models. In: *Progress Report, Radiation Protection Programme 1990-91, Final report, Vol 2. European Commission, Luxembourg, EUR-15295, pp 1871-1883.*

Moreno, J., A.M. Sempreviva, T. Mikkelsen, G. Lai and R. Kamada (1994) A spectral diagnostic model for wind flow simulation. extension to thermal forcing. In proceedings of the: Second International Conference on Air Pollution, 27-29 September 1994, Barcelona, Spain. Eds. J.M. Baldasano, C.A. Brebbia, H. Power and P. Zanetti, Computational Mechanics Publications, Southhamton, U.K., Vol II, pp 51-58.

Scholten, R.D.A., J.J. Erbrink, A. van Melle, H.E. Jørgensen, T. Mikkelsen, E. Lyck, P. Løfstrøm and T. Ellermann (1994). Atmospheric dispersion at a nuclear Power Plant building - a tracer experiment and model evaluation. A KEMA, RISØ and NERI joint report No 40357-KES/MLU-93-3226, 159 pp

Vakulovski, S.M., Shershakov, R.V. Bolodin, O.I. Vozzhennikov, Ya.I. Gaziev, V.S. Kysykh, P.P. Makhon'ko, and V.B. Chumichev (1994). Analysis and prognosis of radiation exposure following the accident at the Siberian chemical combine Tomsk-7. Risø-R-750(EN), 46 pp.

1995:

Brandt, J., T. Mikkelsen, S. Thykier-Nielsen and Z. Zlatev (1995). Using a combination of two models in tracer simulations. Accepted for publication in: *J. Math. Comp. Modelling*, 20pp.

Brandt, J. T. Ellermann, E. Lyck, T. Mikkelsen, S. Thykier-Nielsen and Z. Zlatev (1995). Validation of a combination of two models for long-range tracer simulations. 12 pp,

Cionco R.M., W. aufm Kampe, C. Biltoft, J.H. Byers, C.G. Collins, T.J. Higgs, A.R.T. Hin, P.-E. Johansson, C.D. Jones, H.E. Jørgensen, J.F. Kimber, T. Mikkelsen, K. Nyren, D.J. Ride, R. Robson, J.M. Santabarbara, J. Streicher, S. Thykier-Nielsen, H. van Raden, H. Weber (1995): An overview of MADONA: A multi-national field study of high-resolution meteorology and diffusion over complex. In: Proceedings of the 11th Symposium on Boundary Layers and Turbulence, Charlotte, N.C., USA, March 1995, pp. 306-311 (Submitted to: *Bulletin of the American Meteorological Society*).

Erhardt, J. and T. Mikkelsen (1995) The RODOS system: atmospheric dispersion module and meteorological data. Proceedings of the Special Warsaw RODOS Seminar, Warsaw, Poland, November 1994, pp 93-102.

Jørgensen, H.E., T. Mikkelsen, D. J. Ride, T. Higgs, C. J., W. aufm Kampe, H. Weber, K. Nyrén and P.E. Johansson (1995): MADONA. Concentration fluctuation analysis. In: Proceedings of the 11th Symposium on Boundary Layers and Turbulence, Charlotte, N.C., USA, March 1995, pp 306-311.

Jørgensen, H.E., T. Mikkelsen, J. Streicher, H. Herrmann, C. Werner and E. Lyck (1995) Lidar Calibration Experiments. Submitted to: *Applied Physics B*, September 1995

Mikkelsen, T. and H.E. Jørgensen (1995) MADONA: On-site real-time turbulence measurements. In: Proceedings of the 11th Symposium on Boundary Layers and Turbulence, Charlotte, N.C., USA, March 1995, pp. 445-448

Mikkelsen, T., H.E. Jørgensen, K. Nyrén and J. Streicher (1995). MADONA: Diffusion measurements of smoke plumes and of smoke puffs. In: Proceedings of the 11th Symposium on Boundary Layers and Turbulence, Charlotte, N.C., USA, March 1995, pp 319-322.

Mikkelsen, T (1995) RODOS, a comprehensive decision support system for nuclear emergencies in Europe. EUROSAP Newsletter No. 24, pp.19-20.

Santabarbara, J.M., J. Calbo, J.F. Harnández, T. Mikkelsen and J.M. Baldasano (1995) Wind Flow over Complex Terrain: A Comparison of three State-of the Art Models and Full-Scale Observations. To be presented at the 21. International Technical Meeting on Air Pollution Modelling and Its Application, Baltimore, USA, 6-10 November, 1995.

Päsler-Sauer, J., T. Schichtel, T. Mikkelsen, and S. Thykier Nielsen (1995). Meteorology and atmospheric dispersion, simulation of emergency actions and consequence assessment in RODOS. Proceedings of Oslo Conference on International Aspects of Emergency Management and Environmental Technology, Oslo, Norway, June 19.-22., 1995, 195-204

Ride, D.J., W. aufm Kampe, C. Biltoft, J.H. Byers, Cionco R.M., C.G. Collins, T.J. Higgs, A.R.T. Hin, P.-E. Johansson, C.D. Jones, H.E. Jørgensen, J.F. Kimber, T. Mikkelsen, K. Nyren, R. Robson, J.M. Santabarbara, J. Streicher, S. Thykier-Nielsen, H. van Raden, H. Weber (1995): MADONA, the high-resolution data set from trial MADONA (Meteorology and Dispersion over NON-uniform Areas). Version 2. Available from: CBDE-Porton Down, Salisbury, England, 1 CD ROM.

Thykier-Nielsen, S, T. Mikkelsen, J.M. Santabarbara, D.J. Ride, T. Higgs and H. Weber (1995 a) MADONA: Real-time diffusion model simulations. In: Proceedings of the 11th Symposium on Boundary Layers and Turbulence, Charlotte, N.C., USA, March 1995, pp. 327-330

Thykier-Nielsen, S, T. Mikkelsen, J.M. Santabarbara (1995 b) Experimental evaluation of a PC based real-time

dispersion modelling system for accidental releases in complex terrain. In: Air pollution Modelling and Its Application, X. Proceedings of the 20th International Technical Meeting on Air Pollution Modelling and its Application, Valencia, Spain, 20 Nov.- 3. Dec 1993. Eds. S E Gryning and M Mullan, Plenum Press, New York, 1994, pp 383-394.

Tveten, U. and T. Mikkelsen (Eds) (1995). Report of the Nordic dispersion-/trajectory model comparison with the ETEX-1 fullscale experiment. NKS/ECO-4 intercomparison/validation exercise held at Risø, Denmark, 6-7 June 1995. Risø-R-847 (EN), ISBN 87-550-2118-2. Available on request from: Information Service Department, Risø National Laboratory, P.O. Box 49, DK-4000 Roskilde, Denmark.

Head of project 2: Dr ApSimon

1.) Objectives for the reporting period

Title: Real time modelling of atmospheric dispersion on trans-European scale

3DRAW is a computer program that models atmospheric dispersion and deposition over continental scale distances following a nuclear accident. The aims during this reporting period have been:

- i) To improve the physics of 3DRAW, so as to realistically model the wet deposition of radioactive material.
- ii) To improve the usefulness of the model when used in an emergency situation as a part of the RODOS system. A method for indicating the level of confidence or uncertainty in the model predictions of contaminated areas has been developed.
- iii) To prepare the 3DRAW software for incorporation in the RODOS system. Quality assurance of the code was initiated. The results of this work could be useful to other contractors in further stages of the RODOS project.

2.) Progress achieved including publications

A. Introduction

When a nuclear accident occurs at a specific site, authorities in other countries up to thousands of kilometres from the release will have many concerns. These will include: will the radioactive material reach their territory, if so, when? will it give rise to significant contamination? There will be a need to reassure the public, and to also ascertain where citizens abroad could be at risk. At longer distances from the source serious contamination is most likely to occur if the radioactive cloud encounters rain or snow, and particles or soluble gases are deposited.

The 3DRAW model was developed to utilise information from weather prediction models to forecast the atmospheric transport and associated deposition of radioactive material. The model simulates the release as an assembly of particles, each of which is independently advected. The evolution of the wind-fields is simulated, as is the random displacement associated with smaller, sub-grid scale eddies. The user of 3DRAW can specify the amount of constituent radionuclides to be carried by each particle. These quantities are depleted according to the probability of deposition. This depends on the nature of the radionuclide, weather conditions and underlying surface. Both dry deposition from surface air, and wet deposition in precipitation are modelled. The first is important for radionuclides such as I131

B. Treatment of wet deposition

The treatment of wet deposition has been made more sophisticated, and has been tested, in this current contract period. Two types of wet deposition have been distinguished: frontal systems and convective precipitation. The first leads to widespread deposition subject to significant enhancement over land at higher altitudes by the feeder-seeder mechanism; the second is likely to be more patchy and give rise to isolated hot spots of contamination. For both types of deposition, modern weather radar can be useful in locating likely areas of contamination, provided the position of the radioactive material is known. Allowance for orographic enhancement in frontal precipitation can also be indicated when used with a GIS system incorporating altitude of the terrain.

Distinguishing the two types of precipitation is important because of the different spatial characteristics of the precipitation. The treatment of wet deposition in convective systems has also been made more realistic by replacing the original "wash-out" model with a system which, allows upward venting of the material. This mechanism helps to explain how material was detected at distant locations after the Chernobyl accident after transport at higher levels in the atmosphere.

Modelling wet deposition in frontal systems is more difficult because of their complex three dimensional nature. In such systems there is an overturning of air. Typically warm air from southern regions forms a broad stream of air that rises above colder air to the north. Strong wind gradients often divide air masses, and are also found in the vortex structure of low pressure systems. It is difficult to identify the frontal surfaces between the air masses precisely from weather forecasting data. This means that the trajectories of material within and following passage through frontal systems is very uncertain.

In such situations it would be valuable to identify the source region from which air is most likely to feed into the frontal system, and whether this air is contaminated. This means reversing the usual approach in 3DRAW. In effect, this asks the question "from where has the air in a frontal system come?" An alternative version of 3DRAW has therefore been developed. This begins with a regular array of particles which surrounds a frontal system, and follows the particle's trajectories forwards in time. This simple technique can indicate which air is forecast to pass through a frontal system within the next 24 hours.

C. Combining model results and measurements

In the above situation measurement and modelling are complementary. The prediction of particle trajectories, as discussed below, becomes increasingly uncertain as travel time increases. If measurements are available, they can improve modelling. In the case of a frontal system, radiological measurements taken in regions where air will most likely enter the frontal system can be useful.

To revise predictions, 3DRAW has an option to begin modelling particles from a prescribed set of points that corresponds to observed measurement locations. If we are modelling 24 hours after a release, it is quite likely that measurements and model results will not agree. In this case the original release can be replaced by a set of new particles representing the observed cloud, and a new forecast prepared. Care has to be taken in areas where measurements are sparse or absent, for example over the sea, or at higher altitudes. In this way measurements can be used to revise and improve forecasts over longer travel times and distances from the original release.

D. Confidence limits and uncertainties

A key problem when interpreting model is the uncertainty attached to these predictions and the confidence which can be placed in them. The 3DRAW model has been extended to include “stray” parameters which indicate the uncertainty in position of each particle. Each particle keeps track of two additional quantities that indicate the root mean square deviation attributed to uncertainty in its position. These can be used to define a radius of positional uncertainty round each particle. The spatial distribution of the cloud can then be displayed with the assembly of particles coloured according to this radius of uncertainty. When measurements are subsequently superimposed this will help to indicate whether the two are consistent, and identify those areas where further data would be valuable.

The calculation of the stray parameters reflects the fact that a spatial displacement has a greater effect when wind gradients are large, so that a small difference in position can imply a big difference in the advecting wind. In these circumstances errors in the position of particles grow very quickly, whereas where windfields are more uniform, trajectories are more predictable. The root mean square values in positional co-ordinates, the stray parameters, are thus defined such that

$$dS_x/dt = k \cdot S_x \cdot \delta U/\delta x$$

$$dS_y/dt = k \cdot S_y \cdot \delta V/\delta x$$

where U and V are the horizontal components of the wind (usually along lines of constant latitude and longitude respectively), and k is a constant such that the initial values of S match local scale spread of a Gaussian puff or plume close to the source.

It is evident that the stray parameters grow exponentially with time at rates determined by the wind gradients. As might be expected particles often move with relatively slow growth of the stray parameters for some time until they move into a region with strong wind gradients such as a depression, when their uncertainty in position rapidly grows. Confidence in particle positions depends on the stray parameters remaining small. Typically the radius of positional uncertainty deduced from the stray parameters grows to 200 or more kilometres within a day (compared with the grid used in the model for the calculation of concentrations the order of 100 km). This emphasises the importance of being able to revise model predictions from observations of the movement of a the radioactive material.

Uncertainty in Particle Position

24 hours after release

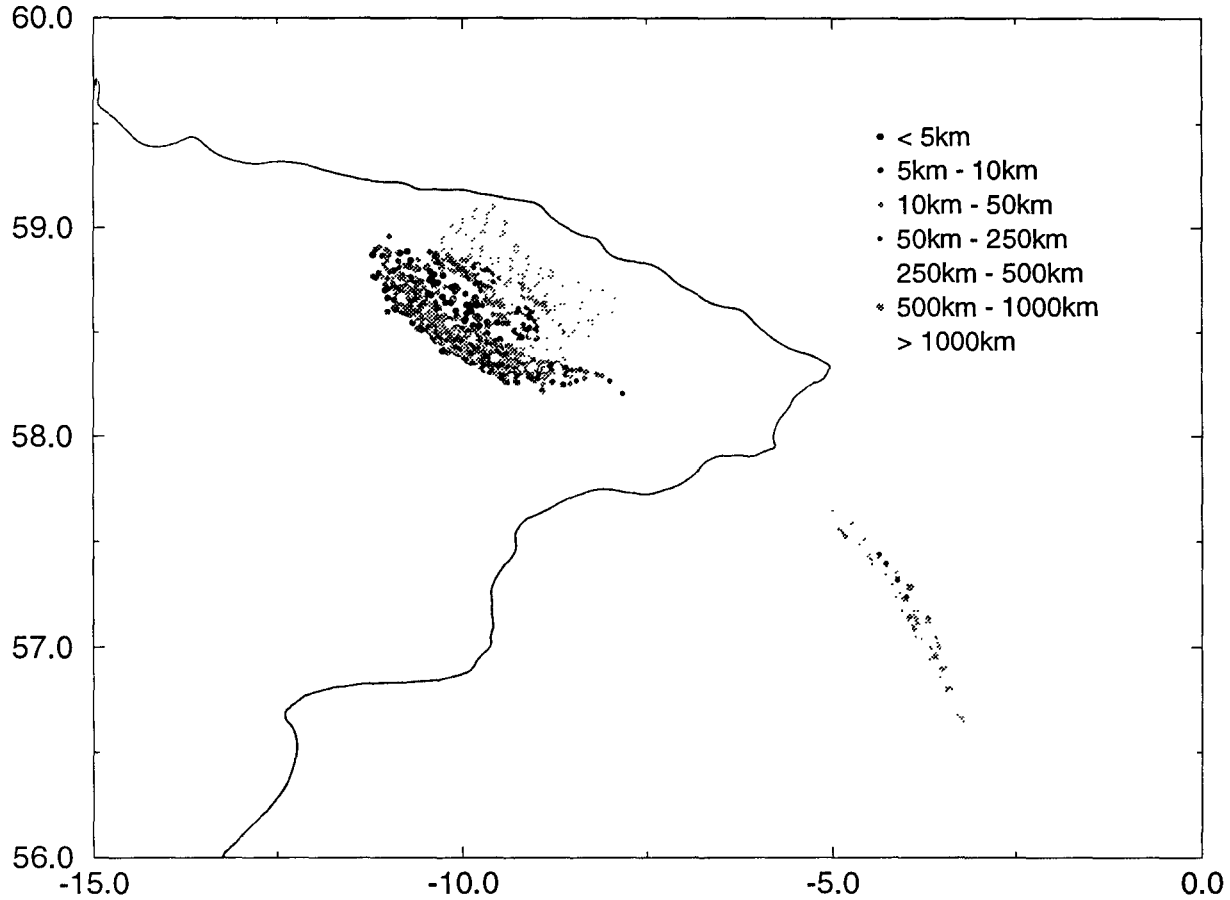


Figure 1 illustrates the radii of uncertainty attached to a limited sample of particles tracked for 24 hours after a release. This is much clearer when colour coding is employed, and used in conjunction with a GIS system.

E. Software quality assurance

1. Introduction

The primary focus of the past year's work has been quality assurance of the 3DRAW software. The model was developed in the way that much scientific software is written: scientists who are capable programmers, but not computing specialists, writing an initial program and then improving the model bit by bit. The mainframe computer that the first 3DRAW program ran on would today be considered obsolete. This computer's memory limitations meant that complex programming 'tricks' were needed to process the massive data sets that the model requires. These factors suggested that it might be useful to focus on quality assurance of the software before integrating the program with the RODOS system. The main objectives have been to assess and, where necessary, improve the quality of the 3DRAW software.

Quality assurance has been identified as a major goal for the next phase of the RODOS project. Many of the software modules within the RODOS system have been developed in similar circumstances to 3DRAW; it is likely that the experience gained in this activity could well be applicable to other software in the RODOS project.

2. Assessment of software quality

The quality of the 3DRAW software was assessed in two ways: A comprehensive manual inspection was first performed, which was then supplemented by measuring a limited number of program metrics. The structure of the RODOS system, which embeds modelling programs within a graphical user interface (GUI), meant that it was inappropriate to consider the quality of the current user interface. The three *quality attributes* that this project has focused on are: correctness, reliability, and maintainability.

a) Software Inspection

The 3DRAW software was manually inspected using published standards of "good coding practice". There are four distinct areas which were examined: the code within each module, the interface between modules, the data structure, and the operating system level. The observations made in each area will be described in turn:

Intra-module Level

Within individual subroutines the program was well structured. There were a few problems with the robustness of the code. These were largely due to the use of standard Fortran 77. Many of the safety related features of Fortran were only standardised in the ANSI Fortran 90 standard. These robustness problems were later addressed.

Inter-module Level

Modularity is a measure of how well a program is decomposed into discrete functions. By maximising *cohesion*, the degree to which subroutines perform only one function, and minimising *coupling*, the degree to which routines share data, we can maximise the maintainability and testability of software. Many of the subroutines within 3DRAW were found to have low cohesion. Reworking software that has modularity problems is very time-consuming, as it involves rewriting whole subroutines and cannot be automated to any significant degree. The problems that were observed with coupling suggested that testing individual modules would be very difficult.

Data Level

Scientific software is typically more algorithm-oriented than data-oriented, whilst business applications are typically the converse. 3DRAW is atypical as it has a relatively complex data flow for its size. The program's data had been decomposed in a fragmented manner, which made it difficult to understand the data flow within the program. This was in part due to deficits in earlier standards of the Fortran language, which have been overcome in the Fortran 90 standard. In view of the risk of introducing error, the data structures have largely been left untouched.

System Level

The maintainability of software is also affected by factors external to the program proper. These include program documentation (structure charts, call graphs), on-line test data, regression test scripts, and revision control, etc. There were no systems in place to attend to these concerns. This was identified as a pressing concern for the quality improvement phase of the project.

In summary, manual inspection of the software showed good low-level quality accompanied by increasing concerns as a higher level view was taken.

b) Software Metrics

A software tool was used to analyse the complexity of the code. This indicated individual subroutines which were likely to cause future problems.

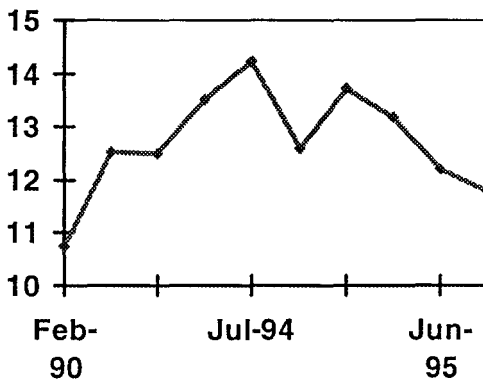
The quality assessment phase of the project identified those parts of 3DRAW which would most benefit from quality improvement work. These concerns were addressed by restructuring, testing & repairing, and documenting the 3DRAW system. These activities will be described in turn.

3.Improvement of software quality

a)Restructuring

There were a minority of subroutines whose structure was extremely difficult to understand. These routines were rewritten; in some instances this rewriting uncovered bugs which had been unknown. The program was reformatted as a whole using software restructuring tools which ensured a consistent style. The figures shows how the complexity of 3DRAW, as measured by McCabes' V(g) statistic, reduced once restructuring began. The second peak in the graph shows the increase in complexity caused by adding the particle uncertainty function already described.

Complexity vs time



Before the restructuring was performed, a system for revision control was started. This meant that changes to the source code were automatically recorded. It enables programmers to retrieve any given version of the software.

b)Testing and Repair

A variety of testing methods were applied to 3DRAW. Those testing methods that involve directly executing the program are described as dynamic approaches. Those methods which involved inspecting the source code, by hand or computer are known as static approaches.

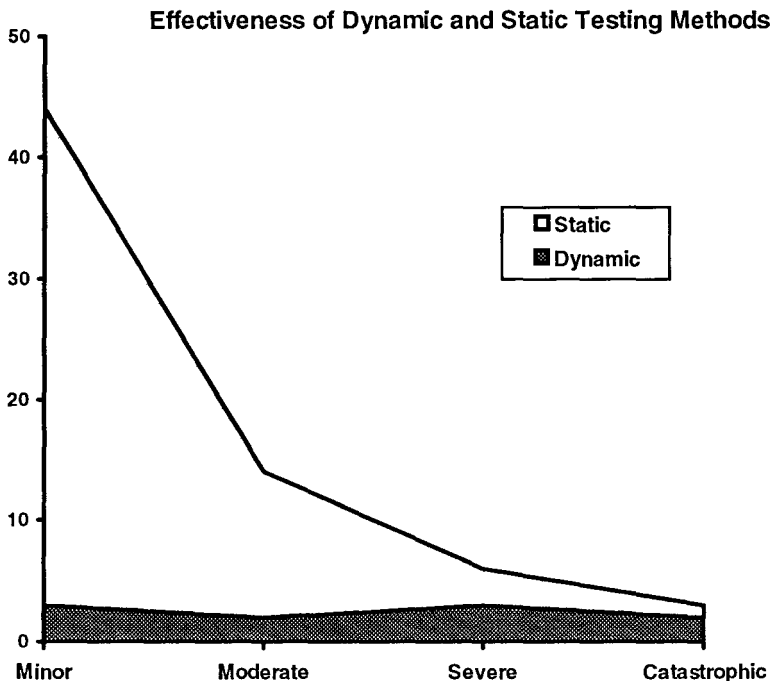
(i)Dynamic testing

New subroutines were unit tested using traditional “black box” methods. This process was extremely time consuming, because of the strong coupling identified in the quality assessment phase. A set of regression tests were developed, so as to ensure that any changes to the program do not introduce new bugs. The process of developing these tests identified a couple of severe bugs within the code. These tests were implemented using simple Unix I/O redirection. Their effectiveness could be increased by using automated test driver software.

The 3DRAW program was tested on three different hardware platforms using different compilers: Sun, Hewlett Packard, and Linux on a Pentium.

(ii)Static testing

A wide range of static test tools were used to identify errors in the 3DRAW code. These tools picked up a greater number of minor errors than dynamic testing. Many of the errors were portability issues, where code written with a forgiving compiler could be broken by a newer compiler. It was noted that each of the eight static test tools identified errors which no other tool found. This suggests that software engineers working on RODOS need to have a large set of software tools, if they are to produce software of known high quality.



c) Documenting

(i) Source code

The internal documentation of the 3DRAW source code was enhanced systematically over the course of the project. This was largely an automated procedure. Unix shell scripts were written to read the program's symbol table, so as to determine which variables are used by or modified by each subroutine, and this information was added to the administrative comment block that preceded each subroutine. This input/output information is often the most important information a programmer needs to know when modifying or debugging a program.

Subroutine call charts, cross reference tables of variables and common blocks were also produced. These allow the structure of the software to be more clearly shown.

(ii) Data files

3DRAW uses a number of ASCII data files. The format of these files was documented.

(iii) Defect Monitoring

It is extremely difficult to directly measure how correct a program is. One useful source of information is the defect history of the program - how many bugs have been found? how many have been fixed? how serious? etc. A simple defect database was created and any faults or failures found in the program were logged in this database. This record proved to be useful in evaluating the performance of the different testing approaches used.

4. Discussion

The quality assurance work produced two distinct benefits. The first is a demonstrated improvement in the quality of the 3DRAW software. The second, possibly more important benefit is a better understanding of the specific quality deficits that this software has. The main areas of concern were modularity of the code, procedures for configuration management and testing, and portability of the code.

The RODOS project, as a whole, is challenged by issues which are unusual in large scale software development projects. These features include:

- software written by non-computing specialists
- a lack of independent testing
- geographical separation of developers

In addition, the nature of the application that RODOS addresses, mathematical modelling, is one in which software errors will be intrinsically difficult to recognise. When programmers develop applications such as word processors, or transaction control, errors tend to be much more visible. It is important that future work on quality assurance within RODOS be tailored so as to address these characteristics of the project.

F. Conclusion

As a result of this work, it is now considered that 3DRAW is now far more suitable for integration into the RODOS system. We also believe that the problems encountered are likely to be common to other models prepared for RODOS. Accordingly we believe that quality assessment and improvement by the methods described above could be valuable on a wider scale in the final stages of the RODOS project.

A paper is in preparation on the uncertainty analysis now incorporated in 3DRAW for submission to Atmospheric Environment. It is also intended that the work undertaken on quality assurance will provide at least two papers in journals dedicated to software engineering.

II Objectives for the reporting period

The objective of the activity is in the context of providing and assisting the implementation of usable modules into the Analysing Subsystem (ASY) of RODOS. ANPA is involved in the development and application of software modules for pre-processing the meteorological data in order to provide the atmospheric dispersion models with the necessary input in real-time. Within the framework of this general objective, the following partial objectives have been pursued:

- to develop and to test routines for pre-processing meteorological data;
- to design a scheme for the automated selection of primary meteorological data and the activation of alternative pre-processing routines for real-time dispersion modeling;
- to transfer suitable software pre-processing modules to the Analysing Subsystem (ASY) of RODOS;
- to validate methods for estimating crucial parameters, such as mixing height in convective conditions, by comparing model estimates with experimental data sets.

III Progress achieved

In order to provide the real-time dispersion models of RODOS with the input parameters based on different types of meteorological data, a set of pre-processing routines have been developed, based on the most widely used and documented methods. The list of parameters includes Monin-Obukhov length, friction velocity, sensible heat flux, mixing height, wind speed profile, turbulence parameters (Mikkelsen and Desiato, 1993).

For the purpose of applying and testing the routines through a quick and user-friendly interface, a pre-processing package (PAD: Pre-processor for atmospheric dispersion models) has been implemented on a RISC DEC Station ALPHA 3000 in ULTRIX and OSF MOTIF environment. For each parameter the input can be edited through guided masks and the output can be displayed in the form of tables or time diagrams.

A scheme for linking the meteorological pre-processor with the on-line meteorological data-base and the atmospheric dispersion models included into a centralized emergency response system such as RODOS, has been designed. The scheme actually corresponds to the presently operational one within the ARIES system at the Italian Environmental Protection Agency (ANPA) (Desiato and Bider, 1994). The automatic preprocessing is perhaps the most complex and delicate module of the real-time dispersion evaluation. In this phase, accuracy and reliability requirements for estimation of the parameters, and need for a reduced execution time, must be considered. In addition, flexibility with respect to the available primary information in different situations must be maintained. For long-range dispersion, preprocessing mainly consists of proper selection in space and time of the analyzed and/or forecasted meteorological fields and of topography and roughness data. For the short and medium range models the procedure is more complex. Some data, like wind speed and direction needed by the wind field model, may be selected, in space and time, from the on-line data-base. Other parameters, which are not measured by standard meteorological instrumentation, are derived through a decision-tree procedure which relies on a pre-defined table of spatial and temporal representativeness of the meteorological observations.

A few pre-processing routines have been transferred and integrated into the prototype version of RODOS, which relies on a pre-defined set of meteorological data. The method used and the complete list of input and output parameters for each pre-processing module are documented at the beginning of each corresponding software routine.

The pre-processing capabilities have been extended to the preparation of turbulence parameters needed by three-dimensional dispersion models. In particular, several routines for deriving the scaling parameters and the vertical profiles of wind fluctuation components and of Lagrangian time scales have been incorporated into the ARCO (Atmospheric Release in COmplex terrain) and APOLLO (Atmospheric POLlutant LOng range dispersion) models. ARCO is a three-dimensional Lagrangian particle model for short/medium range dispersion in complex topography areas, and is suitable to be coupled with a diagnostic mass-consistent wind field model. It has been tested against the tracer data collected during the TRANSALP 1989 experimental campaign (Anfossi et al., 1994; ferrero et al., 1995), carried out by several european institutions within the framework of the EUROTRAC-TRACT project. APOLLO is a long-range Lagrangian particle model which is operationally coupled with the ECMWF meteorological fields in the ARIES-I system, to provide real-time estimate of the transport and diffusion of accidental releases. APOLLO has been successfully tested in ATMES and is one of the models involved in the real-time ETEX experiment.

Some pre-processing routines have been included into a recent long-term regulatory dispersion code developed at ANPA (AMETISTA, Desiato and Inghilesi, 1993). This provided the opportunity to test and validate pre-processing algorithms against experimental data sets collected during the two extensive and well-documented campaigns carried out at Copenhagen and Kincaid. As regards the Copenhagen data set, the results show that the model performance is quite satisfactory in predicting the crosswind integrated concentration, i.e. in modeling the vertical diffusion, while the horizontal plume spread is overestimated. The standard parametrization of the horizontal wind standard deviation and Lagrangian time scale may account for a conspicuous part of the inaccuracy in the prediction of maximum concentration (Desiato and Inghilesi, 1994). As regards the Kincaid data set, the attention has been focused on standard deviation of both horizontal and vertical wind components, and on the diurnal evolution of mixing height. Some results are shown in figs. 1-3. The statistical performance of the convective mixing height algorithm, based on the Gryning-Batchvarova scheme, is quite similar to that based on the HPDM model, which was extensively validated against the Kincaid data set by S. Hanna. A detailed analysis of the results of both the pre-processor and the dispersion modules will be addressed in the near future.

References

Anfossi D., Desiato F., Tinarelli G., Brusasca G., Ferrero E. and Sacchetti D., 1994, TRANSALP 1989 experimental campaign - Part II: simulation of a tracer experiment with Lagrangian particle models, submitted to Atmospheric Environment.

Ferrero E., Desiato F., Brusasca G., Anfossi D., Tinarelli G., Morselli M.G., Finardi S., Sacchetti D., 1995, Intercomparison of 3-D flow and particle models with TRANSALP 1989 meteorological and tracer data, to be presented at the 21th NATO/CCMS Int. Techn. Meeting on Air Pollution Modelling and its Application, Baltimora, USA.

Desiato F. and Inghilesi R., 1993, AMETISTA: a model for the evaluation of long-term atmospheric pollution caused by stack emissions, ENEA/DISP ISSN/0393-3016, Rome.

Desiato F. and Inghilesi R., 1994, Air Pollution II, V. 1, J.M. Baldasano, C.A. Brebbia, H. Power and P. Zannetti Editors, Computational Mechanics Publications, Southampton Boston.

Desiato F. and Bider M., 1994, ARIES-I: a computer system for real-time modelling of atmospheric dispersion at different space and time scales, Environmental Software 9, 201-212.

Mikkelsen T. and Desiato F., 1993, Atmospheric dispersion models and pre-processing of meteorological data for real-time application, Radiation Protection Dosimetry, 50, 2-4, 205-216, Nucl. Techn. Publ.

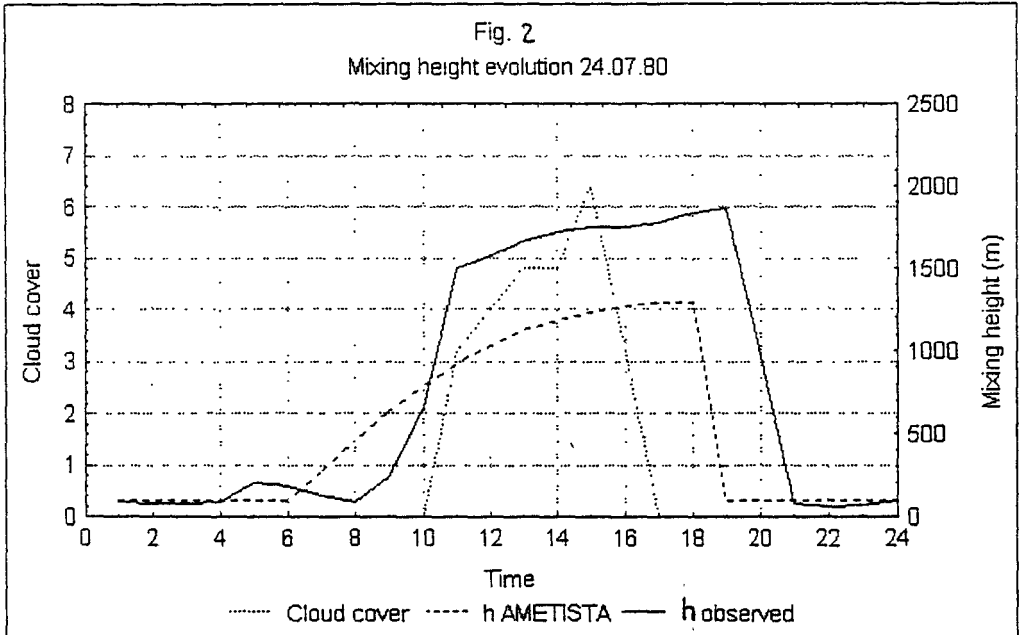
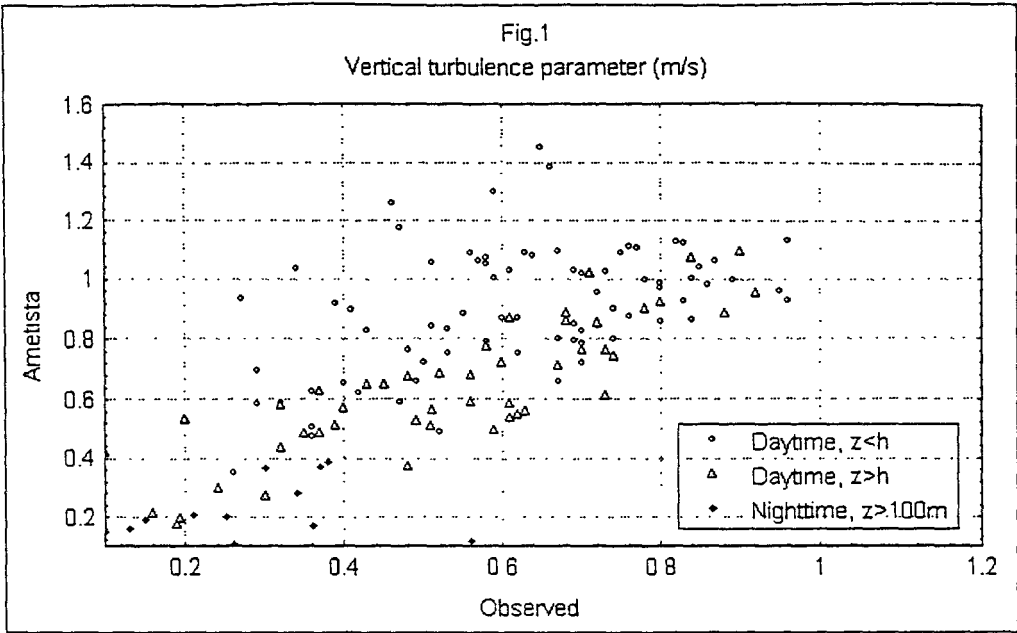
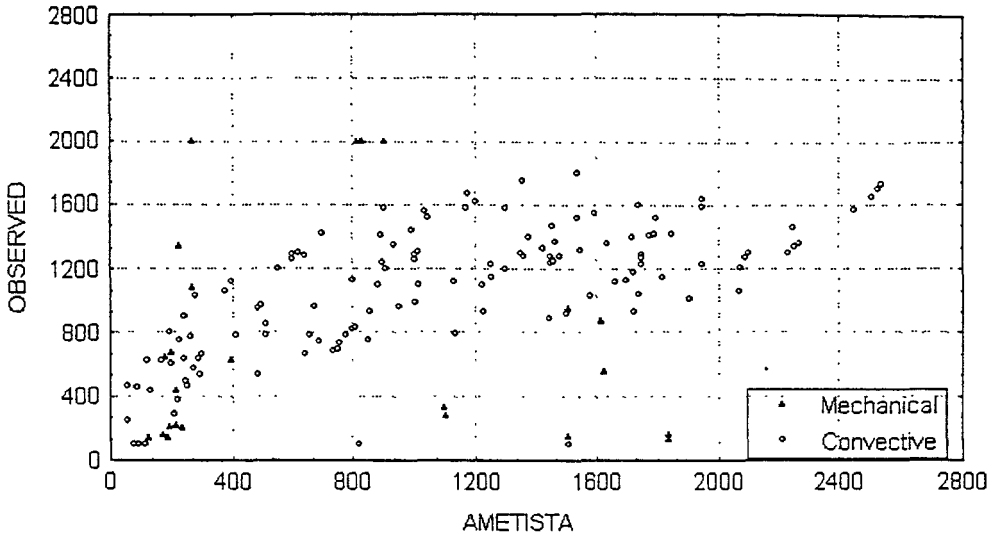


Fig. 3
Mixig height h (m) scatter diagram



RODOS A partner Danish Meteorological Institute (DMI)

Project 5: **A. Rasmussen**
 J. Havskov Sørensen

I. Objectives for the reporting period June 1994 -- June 1995

In general, to assist and provide forecast and analysed data from the Danish version of the numerical weather-prediction model HIRLAM as input to the atmospheric dispersion models in RODOS for case studies.

In particular to:

- Provide RODOS with validated DMI-HIRLAM boundary-layer parameters advantageous for atmospheric dispersion models.
- Provide RODOS with DMI-HIRLAM data for the ETEX (European Tracer EXperiment) periods for post-analysis.
- Improve the parametrisations of the atmospheric boundary layer in DMI-HIRLAM.
- Investigate fast file-transfer methods of large quantities of data.

III. Progress achieved

DMI-HIRLAM data for RODOS

The interface to the operational database at DMI, containing the output from the DMI-HIRLAM models, has been improved. This interface is capable of extracting data, relevant for the RODOS project, for a given geographical sub-area.

The height of the atmospheric boundary layer, which is of great importance in dispersion models, is not calculated in the present HIRLAM system. It may, however, be derived from the output of HIRLAM by a method proposed by Troen and Mahrt [1]. The method, which is based on a calculation of a bulk Richardson number, shows promising results verified against radiosonde data.

Two DMI-HIRLAM data sets have been provided for RODOS covering the ETEX periods:

DKV-HIRLAM data for a period of four days following each of the two ETEX releases (from October 23, 12 UTC to October 27, 12 UTC, and from November 14, 12 UTC to November 18, 12 UTC) were extracted for an area approximately 44--64° N and 4° W--25° E. Analysed data are from 00 and 12 UTC, while the forecast data come in 3-hour intervals up to +36 hours. Data from the 10 lowest model levels were extracted thus covering approximately the lower 2.5 km of the atmosphere. The following parameters were extracted: height above ground, wind speed and direction, precipitation, atmospheric boundary-layer height and orography.

DMI-HIRLAM

Presently, the DMI-HIRLAM model utilises 31 vertical layers, and DMI-HIRLAM is run operationally in two versions: GRV with a horizontal resolution of about 46 km and forecast length 48 hours is covering all of Europe, including a large part of Russia and the northern part of the Atlantic Ocean. DKV has a higher horizontal resolution of about 23 km and a forecast length of 36 hours but does not cover the southern part of the EU. By the end of 1995, DMI has planned to buy a new super computer replacing the present Convex 3880. This enables improved versions of DMI-HIRLAM. Thus, the future version of DKV-HIRLAM will cover all of EU.

An improved mixing-length parametrisation within HIRLAM, as well as a non-local vertical diffusion scheme, are presently studied [2, 3, 4]. There are strong indications that these new parametrisations will imply significant improvements of the boundary-layer parameters.

ETEX

DMI participated in ETEX, which is organised by WMO, IAEA and EU. The objective of ETEX is to conduct a long-range atmospheric tracer experiment (up to some 2,000 km), to test the capability of real-time forecasts for atmospheric dispersion on this scale, and to assemble a database of environmental measurements of the tracer and the source terms allowing evaluation of long-range transport models. Air samples were taken by a network of nearly 200 sampling stations located mainly at WMO synoptic stations covering a large part of Europe. DMI participated with 11 such air sampling stations.

Also on the modelling side, DMI participated in ETEX. The atmospheric long-range transport model DERMA (Danish Emergency Response Model for the Atmosphere), which is developed at DMI, was utilised for this purpose.

For the periods following the two ETEX releases, DMI delivered real-time HIRLAM data to Dr. Nathan Dinar, Dept. for Applied Mathematics, Israel Institute for Biological Research (IIBR), enabling him and co-workers to participate in ETEX using their atmospheric long-range transport model LORA.

RIMPUFF benchmark

DMI has taken part in a benchmark of the RIMPUFF atmospheric dispersion model. The benchmark was arranged by the Risø National Laboratory. The purpose was to compare different implementations of the code with respect to output and execution time using the same input parameters. In total, the benchmark was run on ten different platforms (PCs and workstations). DMI contributed with five work stations (Sun Sparc IPX, Sun Sparc 10, SGI Indy, SGI Indigo and SGI Challenge).

ARGOS-NT

A formal agreement between the Danish Emergency Management Agency and DMI has been signed concerning the ARGOS-NT system, which is developed by the Danish

Emergency Management Agency. This system, which has many similarities with RODOS, yet it is much simpler, has recently become operational. ARGOS-NT enables forecasts of dose patterns in case of radioactive releases from nuclear power plants nearer than 300 km from Denmark. The dispersion calculations are performed by the RIMPUFF model [5] based on DKV-HIRLAM data. These data are transferred from DMI in real time to the Danish Emergency Management Agency twice a day immediately after completion of the DKV-HIRLAM runs.

References

- [1] I. Troen and L. Mahrt, A simple model of the atmospheric boundary layer; sensitivity to surface evaporation, *Boundary-Layer Meteorol.*, 1984, 15, 129--148
- [2] Gollvik, B. Bringfelt, V. Perov and A.A.M. Holtslag, Experiments with nonlocal vertical diffusion in HIRLAM. HIRLAM Technical Report 18 (1995) Oslo (1994)
- [3] N. Woetmann Nielsen and B. Hansen Sass, A new mixing length parameterization in HIRLAM. HIRLAM 3 Workshop in Physical Parameterization Oslo (1994)
- [4] A.A.M. Holtslag and B.A. Boville, Local versus nonlocal boundary-layer diffusion in a global climate model. *Journal of Climate* 6 (1993) 1825--1842 Oslo (1994)
- [5] S. Thykier-Nielsen, T. Mikkelsen, S.E. Larsen, I. Troen, A.F. de Baas, R. Kamada, C. Skupniewicz, and G. Schacher, in *Air Pollution Modeling and Its Application VII, A Model for Accidental Releases in Complex Terrain*. Ed. H. van Dop (Plenum Publ. Corp., 1989) 65--76

Head of Project 6: Dr. Søren Thykier-Nielsen

II Objectives for the reporting period

Implementation of a new version of RIMPUFF in RODOS, including the following enhancements:

- a. Gamma-dose module for asymmetrical puffs (AERI, Budapest, Hungary)
- b. LINCOM (neutral version) including the fitting procedure
- c. Evaluation of the LINCOM and RIMPUFF models, with special emphasis on complex terrain.
- d. Enhancement of RIMPUFF such that the model can handle 3 D windfields. This work will be based on the RIMPUFF version already developed by GRS, Köln.
- e. Consolidation of the interface between RIMPUFF and RODOS.
- f. Optimization of the code concerning speed, data-management etc.
- g. Training system for users: Creation of a "Movie" system for display of temporal and spatial variations in meteorological data and in calculated concentration fields

Implementation and testing of new models for plume rise, building wake and dry deposition in RIMPUFF. Development and testing of the coupling to regional scale models in the emergency preparedness system. Testing and further development of the user-friendly interactive version of RIMPUFF, based on the ARGOS-NT system. Model evaluation.

III Progress achieved including publications

III.1 Introduction

During the contract period high priority has been given to the interfacing of RIMPUFF with the RODOS system. Work has concentrated on topics that are important concerning the local scale atmospheric dispersion modeling in the emergency response system. An interface between RIMPUFF and the regional scale wind prognosis model HIRLAM has been created in close cooperation with DMI. Emphasis has also been placed on visualization of model results and other aspects of user training.

A new structure for the dispersion modeling system (preprocessors, flow and dispersion models) has been elaborated. This involves redesigning of interfaces between modules and a new structure for input and output from the system.

Further a considerable effort has been spent within the areas of model development and evaluation. Emphasis has been placed on identifying and improving the areas where the RIMPUFF / LINCOM model complex needs improvements in the context of the real-time emergency response system.

III.2 Interfacing with RODOS

The implementation of RIMPUFF in RODOS includes the items given below:

- a. Rewriting RIMPUFF such that a "shell" program, e.g., RODOS can:
 1. Start RIMPUFF and let it run for one time-step and then use the output from RIMPUFF for processing by other modules in the system.
 2. Continue running RIMPUFF for the next time-step based on a new set of meteorological data. The status of RIMPUFF: puff positions, concentrations etc. are preserved from time-step to time-step.
 3. Restart RIMPUFF for a new source.
- c. Further enhancements of RIMPUFF include:
 1. The ability to calculate doses/concentrations for multiple isotopes in each time-step, i.e., each puff may contain a mixture of isotopes.
 2. For each time-step the following is calculated for each grid-point for all isotopes released:
 - a. Instantaneous value of air-concentration
 - b. Instantaneous value of gamma-dose from airborne activity
 - c. Integrated air-concentration
 - d. Integrated total deposition on the ground
 - e. Integrated wet deposition on the ground
 - f. Integrated gamma-dose from airborne activity
 3. Modules for calculation of gamma doses from airborne (and deposited) activity has been included. These modules have been created by AERI, Budapest, Hungary.

All communication between the operating system in RODOS and the atmospheric dispersion module should take place through SHARED COMMON statements. Therefore a special version of RIMPUFF has been created and transferred to FZK. This version is without write and read statements. Further the updated modules for calculations of gamma-doses are included in this version.

RIMPUFF has been coupled to the MCF mass consistent flow model and the PAD pre-processor. Stand-alone tests of this program system have been made both on a PC and on an HP workstation. Preliminary tests of the coupling of this dispersion modeling system to RODOS have been made.

III.3 Gamma dose modeling

In cooperation with AERI, Budapest, development of fast subroutines for the calculation of gamma doses from airborne and deposited radioactive isotopes, released to the atmosphere from a nuclear power plant. The first versions of these subroutines have been included in the version of RIMPUFF coupled to RODOS. The gamma dose modules have been tested for typical releases of radioactivity. A new version, which can calculate gamma-doses from

asymmetrical puffs has been tested and is ready for inclusion in RODOS.

III.4 Flow modeling

For complex terrain fluid-equation based wind field calculations are normally based on a single upwind and terrain unperturbed observation. However, for neutral conditions, a procedure has been set up to calculate a wind field, which gives the best fit to a network of simultaneous observations at multiple stations. This fitting procedure has been implemented in RIMPUFF.

III.5 Similarity Approach and Other Model Enhancements

A new option for the calculation of sigma-y and sigma-z according to similarity approach has been added to RIMPUFF. The theory is based on a time dependent sigma calculation from Hanna and Strimaitis (1990):

$$\sigma_y(t) = \sigma_v * \frac{t}{\sqrt{1 + \frac{t}{2 t_{L_v}}}}$$

$$\sigma_z(t) = \sigma_w * \frac{t}{\sqrt{1 + \frac{t}{2 t_{L_w}}}}$$

Where:

t diffusion time

σ_v standard deviation of turbulent velocity (lateral)

σ_w standard deviation of turbulent velocity (vertical)

t_{L_v} , t_{L_w} Lagrange time scales (lateral and vertical)

The time derivation of $\sigma_y(t)$ may be used to calculate the increment of $\sigma_y(t + \delta t)$ according to:

$$\sigma_y(t + \delta t) = \sigma_y(t) + \delta t * \frac{d\sigma_y(t)}{dt}$$

This has been introduced in RIMPUFF as a new option for stability specifications. The necessary vertical profiles of σ_v , σ_w , $t_{L,v}$ and $t_{L,w}$ may be parametrized by functions depending upon boundary layer parameters to be found e.g. in Hanna (Nieuwstad, van Dop, 1984).

A bufferzone for the puffs has been introduced. This means, that the contributions from a given puff to dose and concentrations within the grid are taken into account when the puff center is within a certain distance from the grid border. This distance is typically equal to $2 \cdot \sigma_{\text{puff}}$ for the puff in question.

The pentafurcation concept has been changed: A specific puff may only pentafy n times, where n typically is equal to 3. This should give a more realistic dispersion modeling in the situations where pentafurcation takes place. Further the number of puffs in the grid is drastically reduced, thus also the calculating times.

Modeling of chemical reactions involving the materials released to the atmosphere will be included in RIMPUFF. A preliminary version of RIMPUFF, which can consider simple chemical processes is now available.

III.6 Dry deposition modeling

In assessing the environmental consequences of accidental releases to the atmosphere, estimating the activity deposited on ground surfaces usually plays an important role. One exception is for noble gases, though. Deposition can be separated into dry and wet deposition, of which only the former is dealt with here. Dry deposition rates are different for gases and particles, and both are highly controlled by the surface, so different materials have different deposition to different surfaces. In RIMPUFF dry deposition is modeled using the so-called source depletion model, where dry deposition for a given material is characterized by a deposition velocity, which is specified as a function of atmospheric stability and wind speed (Thykier-Nielsen, and Larsen, (1982)). The new version of the model takes the surface type in to account. This is done in characterizing each type of surface (urban, rural, forest and water) by its surface resistance, which primarily depends on surface roughness and friction velocity (for a given material) (Hummelshøj (1994), Jensen (1981) and Roed (1990)).

To illustrate the significance of taking into account the surface type in the assessment of consequences of radioactivity releases, deposition following a 1 hour release from the Swedish Barsebäck reactor has been calculated (Hoe et al. (1994)). The calculations of integrated ground concentrations have been made with 2 types of dry deposition models:

- a. No dependence on deposition from surface roughness i.e., the roughness in the entire area is the same = rural areas.
- b. The area is classified in roughness classes as described earlier.

The results for a Cs137 release at the height 95 m show that there is a significant change of the deposition pattern, when the roughness variation is allowed for. Deposition and thus gamma doses in the urban area close to the coast are reduced by a factor of 2 - 3. Deposition over the urban area close to the city is increased about 20 - 50% while there are only small changes in the amount deposited at

longer distances. For higher release heights and/or isotopes with lower deposition rate the influence of surface type is less significant and vice versa.

III.7 Pre-processing of input data

Pre-processing of meteorological data for dispersion models has been studied in cooperation with ENEA (*Project no. 7*). The implementations in RIMPUFF of these pre-processing subroutines are being consolidated.

III.8 New structure for atmospheric dispersion module

All models in the system will be compiled for a maximum domain size. This domain size is used within the diffusion model (RIMPUFF) and also in all pre-processor models (windflow models MCF, LINCOM .. or simple met preprocessor models). These parameters should have the same names in all models and should be included using an INCLUDE FILE.

A setup file is available for all models containing specific model related input data. e.g. MCF needs an over-relaxation factor or RIMPUFF needs to know whether pentafurcation should be used etc..

A special project directory is created and contains all the data (Including the setup files).

A general setup file for the project contains information used by all models within the system. => project.sup

A set of files is available giving the meteorological input data. The names of the files are the date/time group of the time of measurement with an extension met e.g. Measurements for 9. August 1995 at 12:13

=> 199508091213.met

Measurements for 9. August 1995 at 12:19

=> 199508091219.met

Measurements for 9. August 1995 at 12:29

=> 199508091229.met

These files should all have the same structure allowing a wide span of possible meteorological input data. => YYYYMMDDhhmm.met

The simplest pre-processor model will read in this data and should produce new data files (unformatted data files which will be used than following models. This pre-processor model (PREPRO) has a setup file respectively containing information of

- what kind of time interpolation scheme should be used
- what kind of horizontal interpolation scheme should be used
- what kind of vertical interpolation scheme should be used
- what should be as stability

This program will produce output files for the times and mz layers defined in project.sup

=> 199508091200.pre
=> 199508091215.pre
=> 199508091230.pre

More sophisticated model (MCF, LINCOM ...) can read these data files and produce new output files. With new extensions like YYYYMMDDhhmm.mcf or YYYYMMDDhhmm.lin

RIMPUFF will be able to read all these data files and use them as met input. The output files produced will be in the same format using date/time group plus extension e.g.

YYYYMMDDhhmm.con
YYYYMMDDhhmm.dos

An input file for RIMPUFF containing the source data has is specified in similar way.

III.9 Visualization of model results

New computer programs displaying time series of calculated and measured dispersion data has been developed. The program called S, designed as a tool for time-series representation of a large number of data fields. Several kinds of data (vectors, scalars etc.) can be analyzed. The program is applied in the analysis of the 1990 Guardo and the 1992 MADONA trials.

The program, MADMOVIES, developed by Amt für Wehrgeophysik, is specially designed for analysis of the MADONA experiment. However the program may easily be applied for other experiments.

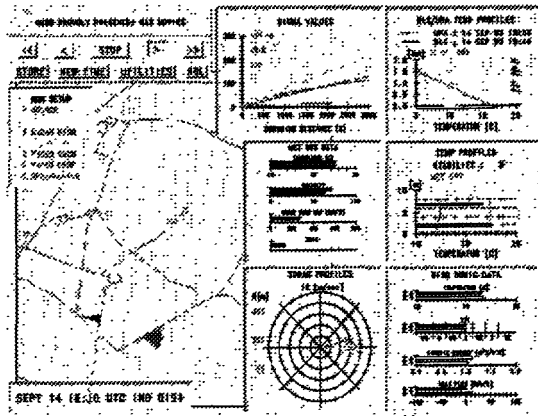


Figure 1 Screen layout for the MADMOVIES program for visualization of experimental measurements and simulations.

In cooperation with the Danish Emergency Management Agency, a version of RIMPUFF is being created for running under the WINDOWS-NT operating system (Hoe et al. (1994)). This new system

includes simple menu-driven information displays, showing results, and drawing attention to important features or anomalies. In this project substantial effort is assigned to methods of assessing and interpretation of the model results, and to their communication with the user through user friendly graphics and display systems. The first version of this system will be available by the end of 1994.

III.10 Model evaluation

A series of 15 full-scale dispersion experiments from the 1990 Guardo trials, carried out over complex terrain in Northern Spain are being analyzed. Actual wind and turbulence measurements taken during the experiment are used as input data for a series of simulations made with Risø's combined flow and diffusion model (LINCOM/RIMPUFF). Considerable effort is devoted to the testing of the improved features for taking into account wind shear and plume rise in RIMPUFF. In collaboration with project no. 8, the wind field "fitting" procedure described in paragraph IV.4 has been tested in simulations of 2 of the Guardo experiments.

An experimental evaluation of flow field and dispersion modeling has been performed, using data from the complex terrain SIESTA experiment (SF6 International Experiment in STagnant Air). Two alternative flow-field calculation methods were evaluated as "drivers" for the dispersion model RIMPUFF: One is the diagnostic mean-flow model LINCOM based on (linearized) Navier-Stokes equations, the second is based on simple interpolation method using tower data (objective wind analysis).

SIESTA was performed by several European groups in November 1985. Measurements were taken of advection, turbulence and dispersion during neutral and convective weak-wind situations over complex terrain of the Jura ridge and the hilly prealpine region. Dispersion characteristics were determined by use of SF6-tracer gas released from the met-tower of the Gösgen nuclear power station at 6 meters height.

Three of the SIESTA experiments were simulated, using RIMPUFF/LINCOM. In one of the experiments, wind direction and turbulence condition changed strongly with time. The comparison between measured and calculated values were quantified by the determination of Chi square, relative Chi square, correlation coefficient and mean error factor. In an orographically influenced dispersion scenario, like SIESTA, potential of improvements by use of high-resolution mean flow model LINCOM was found. Further possible improvements of the simulations using multi-level precalculated flow fields are being investigated.

In September 1992 the 3-week lasting MADONA (Meteorology And Diffusion Over Non-uniform Area) trials took place at Porton Down, UK. Here both ground and elevated puffs, tracer gas and ground level continuous smoke were released and measured by several Lidar systems. With the Porton Down area being characterized by rolling and non-uniform terrain, extensive meteorological measurements were recorded around the clock. Evaluation of this experiment has started using RIMPUFF and LINCOM.

A system has been created for transferring regional scale flow and precipitation field data from the HIRLAM flow model to RODOS contractors. This system has been tested in a project concerning the assessment of the possible consequences in Denmark from radioactivity releases from nuclear power

plants in the Baltic countries. In the period from May 1. , 1993 to September 30. , 1993, trajectories were calculated every 3 hour by the Danish Meteorological Institute. Only in the period from September 8., at 00 hrs UTC until September 21., at 21 hrs UTC it was possible to transport substantial amounts of radioactive material from Lithuania to Denmark. For this period 3 hourly wind and precipitation fields from HIRLAM have been transferred from the Danish Meteorological Institute to Risø. These fields were on-line converted to a format suitable for use in connection with RIM-PUFF. Results show that an accidental release of radioactivity in this period could give measurable radiation doses to the Danish population.

Cs137: Accumulated Deposition [Bq/m2], 12 days after release start

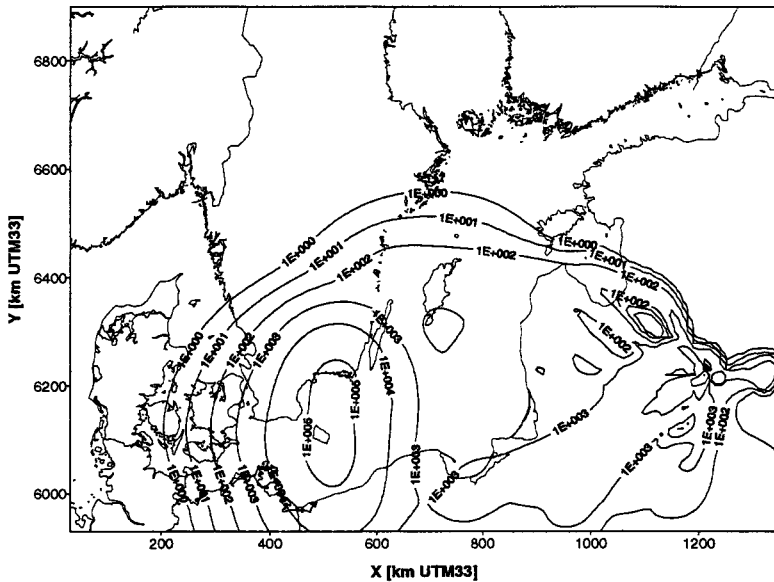


Figure 2. Deposition pattern from a fictive release from the Nuclear Power Ignalina in Lithuania. Calculated 12 days after release start, with RIM-PUFF/HIRLAM

III.11 References

- Jensen, N. O. (1981). A Micrometeorological Perspective on Deposition. Health Physics, Vol. 40. pp. 887-891.
- Roed, J. (1990). Final Report of the NKA Project AKTU-245: Deposition and Removal of Radioactive Substances in an Urban Area. Nordic Liaison Committee for Atomic Energy.
- Hummelshøj, P. (1994). Dry Deposition of Particles and Gases. Risø National Laboratory. Risø-R-658(EN).
- Nieuwstadt, F.T.M. and Van Dop, H. (Ed.) (1984). Atmospheric Turbulence and Air Pollution Modelling. Dordrecht (Holland): D.Reidel Publ.
- Weber, H. and aufm Kampe W. (1992). Das programmsystem "HEARTS" (Hazard Estimation after Accidental Release of Toxic Substances), Annalen der Meteorologie 27, Deutsche Meteorologen-Tagung 1992, Selbstverlag des Deutschen Wetterdienstes, ISSN 0072-4122, Offenbach am Main, Germany.
- Weber, H., aufm Kampe W. and Cionco R. M. (1995). Visualization of the MADONA data base and use of selected sequences in a wind flow and diffusion simulation system. Proceedings of the Eleventh AMS Symposium on Boundary Layers and Turbulence, Charlotte, NC, U.S.A., March 27-31, 1995. Published by the American Meteorological Society, Boston, MA, pp 440-442.

III.12 Publications

- Thykier-Nielsen S., Mikkelsen T, and Herrnberger V.(1991), Real-time wind- and dispersion simulation of tracer experiments conducted over complex terrain during weak and neutral flow conditions, Proceedings of the OECD/NEADB Specialists' Meeting on Advanced Modelling and Computer Codes for Calculating Local Scale and Meso-Scale Atmospheric Dispersion of Radionuclides and their Applications (AD-LMS'91), 6 - 8 March 1991, OECD NEA Data Bank, Saclay.

- Thykier-Nielsen S. and Mikkelsen T. (1992), Fitting of Pre-calculated Wind Fields - A short Guide, 30 pp., Risø National Laboratory, DK-4000 Roskilde, Denmark.
- Santabarbara, J.M. (1992): S. User & Reference Manual. Interim Risø report, October 1992. Available on request from: Department of Meteorology and Wind Energy, Risø National Laboratory, P.O. Box 49, DK-4000 Roskilde, Denmark.
- Jørgensen, H.E., J.M. Santabarbara and T. Mikkelsen (1993). A real-time uncertainty-knowledge and training data base. In: Proceedings of the 3. International Workshop on Real-time Computing of the Environmental Consequences of an Accidental Release to the Atmosphere from a Nuclear Installation. Schloss Elmau, Bavaria, Oct 25-30, 1992. Accepted for publication in: Radiation Protection Dosimetry, 1993.
- Mikkelsen, T. and F. Desiato, (1993). Atmospheric dispersion models and pre-processing of meteorological data for real-time application. In: Proceedings of the 3. International Workshop on Real-time Computing of the Environmental Consequences of an Accidental Release to the Atmosphere from a Nuclear Installation. Schloss Elmau, Bavaria, Oct 25-30, 1992. Accepted for publication in: Radiation Protection Dosimetry, 1993.
- Thykier-Nielsen, S., Moreno, J. and Mikkelsen, T.(1993), A real-time dispersion scenario over complex terrain. In: Proceedings of the 3. International Workshop on Real-time Computing of the Environmental Consequences of an Accidental Release to the Atmosphere from a Nuclear Installation. Schloss Elmau, Bavaria, Oct 25-30, 1992. Accepted for publication in: Radiation Protection Dosimetry, Nov. 1993.
- Thykier-Nielsen, S. and Mikkelsen T. (1993). **RIMPUFF USER'S GUIDE** (Version 33 - PC version). Available on request from: Department of Meteorology and Wind Energy, Risø National Laboratory, P.O. BOX 49, DK 4000 Roskilde.
- Thykier-Nielsen, S. (1993). PLUCON5 - Users Guide. Department of Meteorology and Wind Energy. Risø National Laboratory.
- Thykier-Nielsen, S., Mikkelsen T. and Moreno, J. (1993), Experimental evaluation of a pc-based real-time dispersion modeling system for accidental releases in complex terrain. Proceedings from 20th International Technical Meeting on Air Pollution Modelling and its Application, Valencia, Spain, November 29 - December 3., 1993.
- Thykier-Nielsen, S., Deme, S. and Láng, E. (1993). Calculation method for gamma-dose rates from spherical puffs. Risø National Laboratory, Risø-R-692 (EN), July 1993.
- Thykier-Nielsen, S. (1994). Consequence Calculations for Large Scale Releases of Radioactivity using RIMPUFF and a Numerical Weather Forecast Model. Proceedings from COSYMA User Group meeting, April 25. to 26., at KEMA, Arnhem, the Netherlands. KEMA rapport nr. 40666-NUC 94-5819, editor: J. van der Steen, October 1994.
- Hoe, S., Thykier-Nielsen, S. and Steffensen, L. B. (1994): ARGOS-NT: A computer based emergency management system. Proceedings from the International Workshop on Scientific Bases for

Decision Making After a Radioactive Contamination of an Urban Environment, August 29 - September 2, 1994. Rio de Janeiro and Goiânia, Brazil.

- Brandt, J., Mikkelsen T., Thykier-Nielsen, S. and Zlatev, Z. (1994). Using a Combination of Two Models in Tracer Simulations. National Environmental Research Institute and Risø National Laboratory, Denmark.

- Päsler-Sauer, J., Schictel T., Mikkelsen, T. and Thykier-Nielsen, S. (1995). Meteorology and Atmospheric Dispersion, Simulation of Emergency Actions and Consequence Assessment in RODOS. In: International Aspects of Emergency Management and Environmental Technology. Proceedings for the Oslo Conference. Royal Christiania Hotel, Oslo, Norway, June 18-21, 1995. (A/S Quasar Consultants, Oslo, 1995). p. 195-204.

- Hoe, S., Thykier-Nielsen, S. and Steffensen, L. B. (1995).: ARGOS-NT: A Nuclear emergency management system. Proceedings from Fifth Topical Meeting on Emergency Preparedness and Response, April 18. to 21., Savannah , Georgia, U.S.A.

- Martens R. (1995).: Changes in the Fortran sources supplied by Søren Thykier-Nielsen (03.07 95) in order to implement a Sigma-calculation according to similarity approach. Internal memo from GRS, Köln, Germany.

II. Objectives for the reporting period

The work has been continued on the following objectives:

- a. Integration of the Demokritos Transport System Modules into RODOS System.
- b. Module Evaluation and Uncertainties.
- c. Model Development on Run-off and radioactivity accumulation area on terrains of high complexity.

III. Progress achieved including publications

A. Module Integration

The major effort has been given towards the accomplishment of this objective. More specifically, the weather pre-processor FILMAKER has been upgraded to include the effect of both sensible heat flux and net radiation together with cloud cover index on the evaluation of stability and mixing layer height. The inputted meteorological parameters can come from any organized output such as HIRLAM-ECWMF or any randomly located set of weather stations. The x-y spacing can be in polar or UTM coordinates and the vertical one in meters (ASL or AGL), sigma-theta and pressure.

The DELTA/GAIA topography simulator, FILMAKER weather preprocessor and DIPCOT puff Langrangian dispersion module provide an almost complete (ADREA-I (diagnostic) for wind speed correction) set of codes needed for only dispersion problem analysis. These three programs have been fully integrated into RODOS system. This way data input/output can be transferred from DATA BASE to SHARED MEMORY and vice versa using RODOS provided tools. Furthermore GSY subsystem is utilized for any topography and concentration graphical representation. Demonstration will be given in PSAM III (5).

The above well tuned RODOS-DEMOKRITOS system was used in the case of ALPS passive tracer experiment with results in a well expected range (1,2).

B. Module Evaluation and Uncertainties

The systematic effort on prediction comparison with well document field data has been continued. The case selected was TRANSALP Experiment, a tracer release in South Switzerland with direction towards the main Alpine range. The dispersion main features and concentration have been well reproduced by the model (1,2).

Further effort have been given on quantification of uncertainties using statistical methodology. The bootstrap resembling method has been utilised in order for the concentration uncertainty to be estimated. The proposed method utilises only a smaller initial sample to propagate the uncertainty to other locations away from the source where measurements are not available just yet. As new data come in the former uncertainty estimation is amended accordingly (6).

Additionally, is the framework of the "4th Workshop on Harmonisation within Atmospheric Dispersion Modelling for Regulatory Purposes". Demokritos has undertaken the initiative to organise a benchmark exercise a complex Terrain Dispersion Modelling with more than 20 participants from USA and Canada with the aim to quantify the uncertainties on dispersion (7).

C. Run-off and Radiation, Accumulation Areas

The DELTA/HYDRO model has been further developed which simulates overland flow networks on watersheds of complex topography. The model utilises the simulation of the topography performed by the DELTA/GAIA model by means of adjacent triangular surfaces of known geometrical and physical properties. The overland water flow follows the direction of the deepest slope on each individual triangular ground surface. Water accumulation areas are also determined on the simulated complex topography, which are areas of locally minimal altitude.

The DELTA/HUMUS model has been developed, which simulates the water infiltration in unsaturated soils. The model solves the 1- D water moisture and heat transport equations for a variety of unsaturated soil types and an ensemble of initial and boundary conditions. The equations solved are complied by the intermediary of a water content-dependent soil thermal conductivity (4).

IV. References

1. Varvayanni, M., Graziani, G., Bartzis J.G. (1995), Numerical Simulation of Mesoscale Flows over Highly Complex Terrain, presented in "XX General Assembly, on Transformation, Transport and Turbulent Diffusion of Pollutants over Complex Terrain, Hamburg, Germany, 3-7 April 1995".
2. Bartzis, J.G., Varvayanni, M., Graziani, G., Davakis, S., Deligiannis, P., Catsaros, N. (1995), The TRANSALP Experimental Tracer Release and Transport Simulation, proceedings of the International conference "Air Pollution 95", 26-29 Sept. 1995, Porto Carras, Greece.
3. Statistical evaluation of dispersion uncertainty using air quality models, Journal of Atmospheric Environment (to be submitted).
4. Catsaros, N., Varvayanni, M., Mita, K., Bartzis, J.G., (1995), Moisture and Heat Transfer in Unsaturated Soils, DEMO-Report /95.
5. Deligiannis, P. and Bartzis, J.G., RODOS Application on Complex Terrain Dispersion problem using Demokritos TRANsport for Complex Terrain code system. ESREL'96, PSAM-III, International Conference on Probabilistic Safety Assessment and Management, Crete, Greece, June 24-28, 1996 (accepted).
6. Deligiannis, P. and Bartzis, J.G., Statistical evaluation of dispersion uncertainty using air quality models. 4th International Conference Air Pollution '96, Toulouse France, 28-30 August, 1996, (submitted).
7. Bartzis, J.G., Deligiannis, P., Davakis, S., Konte P. 4th Workshop on Harmonization within Atmospheric Dispersion Modeling for Regulatory Purposes, Oostende, Belgium, 6-9 May, 1996.

Head of project 8: Prof. Dr. Maßmeyer/Dr. Martens

II. Objectives for the reporting period

GRS contributes to the atmospheric dispersion activities within the real time decision support system RODOS in the context of providing a mass consistent flow model MCF and to assist in the implementation including the link between the meteorological preprocessor PAD and the dispersion model RIMPUFF.

The updated and streamlined PC-based versions of MCF and RIMPUFF have to be implemented in the RODOS prototype version at the Research Centre Karlsruhe (FZK). The model link PAD - MCF - RIMPUFF has to be refined and tested.

A users manual of the updated version of MCF has to be prepared.

III. Progress achieved including publications

GRS has given assistance in system integration of the modules PAD, MCF/LINCOM and RIMPUFF into the RODOS prototype version under UNIX. This work comprised the following working steps:

1. Harmonization of the parametrizations of the atmospheric boundary layer within the different modules of RODOS

The parametrizations for the stability dependent vertical profiles of

- wind speed,
- standard deviations of wind speed components and
- Lagrangean time scales

used in the modules PAD, MCF/LINCOM and RIMPUFF have been harmonized. As a first approximation the corresponding equations from the meteorological preprocessor PAD have been implemented in MCF and RIMPUFF. The selected parametrization scheme can easily be replaced by another ones. Possible other parametrizations may be taken from the Danish OML-system /OLE 92/ or the UK Atmospheric Dispersion System /CAR 92/, respectively.

2. New option for the calculation of dispersion parameters in RIMPUFF

A new option for the calculation of the dispersion parameters has been implemented in the RIMPUFF-Version of RODOS. With this option the dispersion parameters σ_y and σ_z may be calculated on the basis of similarity scaling instead of Pasquill stability categories. This modification is based on the following equations /HAN 90/:

$$\sigma_y = \frac{\sigma_v t}{\sqrt{1+0.5 \cdot \frac{t}{T_{Lv}}}}, \quad \sigma_z = \frac{\sigma_w t}{\sqrt{1+0.5 \cdot \frac{t}{T_{Lw}}}}$$

t travel time

$\sigma_{v,w}$ standard deviations of lateral and vertical wind speed components

$T_{Lv,w}$ Lagrangean time scales (lateral and vertical)

The parametrizations for $\sigma_{v,w}$ and $T_{Lv,w}$ have been taken as defined according to no. 1.

3. Participation in the first RIMPUFF Version Control and Benchmark Test

The GRS as a frequent user of RIMPUFF has participated in discussions about version control of the atmospheric dispersion model chain in RODOS. In a first step Risoe has organized a RIMPUFF benchmark test which has been carried out in spring 1995. Based on a common benchmark input data set GRS has joined the benchmark calculations. Risoe National Laboratory has evaluated the results of the participants considering the accuracy of calculated concentrations, CPU time and memory requirements. Further information may be drawn from the RODOS Newsletter 1-95 /ROD 95/.

4. Completion of the users manual of the actual version of MCF.

Literature

/OLE 92/ Olesen, H. R., P. Lofstroem, R. Berkowitz, A. B. Jensen:

An improved Dispersion model for regulatory use - The OML model

in: H. van Dop, G. Kallos (eds.), Air Pollution Modeling and Its Application IX,

Plenum Press, New York, 1992, pp. 29 - 38 (Nato Committee on the Challenges of Modern Society, Vol. 17)

- /CAR 92/ Carruthers, D. J., R. J. Holroyd, J. C. R. Hunt et al.:
UK Atmospheric Dispersion System
in: H. van Dop, G. Kallos (eds.), Air Pollution Modeling and Its Application IX,
Plenum Press, New York, 1992, pp. 15 - 28 (Nato Committee on the Challenges
of Modern Society, Vol. 17)
- /HAN 90/ S. R. Hanna, D. G. Strimaitis:
Rugged Terrain Effects on Diffusion
Chapter 6 in: Atmospheric Processes over Complex Terrain (ed. W. Blumen),
Meteorological Monographs, Vol. 23, No. 45, June 1990,
American Meteorological Society, Boston
- /MIK 95/ Mikkelsen, T.:
First RIMPUFF Version Control and Benchmark Test Held at Risoe
pp. 3 - 4, in: RODOS Newsletter (ed. J. Ehrhardt), No. 1-95,
Forschungszentrum Karlsruhe (FZK/INR), 1995

Head of project 9: Dr. S. Deme

II. Objectives for the reporting period

1. Development of a dose calculation method for Gaussian puffs

1.1 A preliminary comparison of the initial and the simplified (spherical) new gamma dose model

1.2 Elaboration of the full (real) dose model and calculation of database for reasonable range of puff's parameters

2. Study of parameter dependence of dose rates from asymmetrical puffs

3. Application of a simplified calculation procedure for accidental atmospheric releases from a nuclear reactor

III. Progress achieved including publications

1. Development of a dose calculation method for Gaussian puffs

The mesoscale dispersion model RIMPUFF (Thykier-Nielsen and Mikkelsen, 1987) is a fast and operational computer code suitable for real-time simulation of releases of environmentally hazardous materials and gases to the atmosphere. Suitable as a real-time model for emergency preparedness, it has recently been selected for inclusion in the CEC RODOS, real-time decision support system under development at KfK.

RIMPUFF includes models for calculating external gamma doses from airborne as well as deposited radioactivity. In order to improve these, very simple, models KFKI AERI and Risø has started a joint project supported by the CEC. Results were summarized in two Risø reports, one for spherical approximation (1993) and the other for real (asymmetric) puffs (1995).

1.1 A preliminary comparison of the initial and the simplified (spherical) new gamma dose model

The initial gamma dose model used in RIMPUFF was based on the semiinfinite cloud model with correction factors given in (Slade, 1968). In fig. 1 the Slade's values, i.e. the ratio of the dose rate to centreline infinite dose rate are reproduced (continuous line) for several σ values and y distances (given in σ units). For comparison our preliminary results for spherical puffs are also shown (dotted line). For small relative y (given in σ units) and large σ values the differences between the results of two models are insignificant, but for other cases they can reach a factor of 5 and in some combinations even more. Differences between two sets of calculations are mainly due to the fact that Slade's calculations refer to a cylindrical plume instead of spherical puffs. For asymmetric puffs the differences to Slade's values may be much more significant.

1.2 Elaboration of the full (real) dose model and calculation of database for reasonable range of puff's parameters

The method for calculation of gamma dose rates from Gaussian puff model is based on the solution of the equation below:

$$d(Q, E_\gamma, \sigma_y, \sigma_z, H, R_{xy}) = 2K\sigma_{en}E_\gamma \int_{x=-\infty}^{\infty} \int_{y=0}^{\infty} \int_{z=-\infty}^{\infty} \frac{B(\mu r)}{4\pi r^2} e^{-\mu r} X(x, y, z) dx dy dz \quad [\text{Gy/s}]$$

where

- Q activity in one puff [Bq] (1 photon/disintegration)
- E_γ energy of gamma radiation [MeV]
- σ_y crosswind puff dispersion parameter [m] ($\sigma_x = \sigma_y$)
- σ_z vertical puff dispersion parameter [m]
- H height of the puff centre [m]
- R_{xy} distance of the puff centre base point ($x=y=0, z=-H$) from the receptor point [m]
- K constant, $1.6 \cdot 10^{-13}$ [Gy/s/MeV/kg]
- σ_{en} energy absorption coefficient for air [m²/kg]
- B build up factor
- μ linear attenuation factor for air [m⁻¹]
- r distance of the volume $dx dy dz$ from the receptor located at the distance R_{xy} from the puff centre base point
- $X(x, y, z)$ the concentration in point x, y, z [Bq/m³] (puff centre $x=y=z=0$) given by equation

$$X(x, y, z) = \frac{Q}{(2\pi)^{3/2} \sigma_y^2 \sigma_z} \exp\left(-\frac{x^2}{2\sigma_y^2}\right) \exp\left(-\frac{y^2}{2\sigma_y^2}\right) \exp\left(-\frac{z^2}{2\sigma_z^2}\right)$$

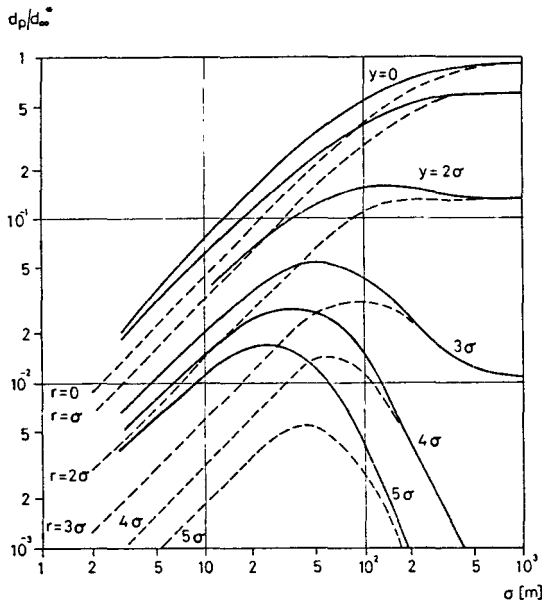


Figure 1. Ratio of gamma dose rates to puff centre dose rate for several distances as function of σ values. Continuous line - after (Slade, 1968), dotted line - recent calculations for spherical puffs.

The above equation was solved for different sets of parameters (E_γ , σ_y , σ_z , H , R_{xy}) by numeric volume integral method. The steps in the numerical integration were specified as follows: $\Delta x = \Delta y = \sigma_y/10$ and $\Delta z = \sigma_z/10$ up to $\pm 5\sigma_y$ and $\pm 5\sigma_z$, except around the receptor point where integration steps of $\sigma_y/40$ and $\sigma_z/40$ were used for a volume of $\pm \sigma_y$ and $\pm \sigma_z$.

Geometric arrangement for these calculations is illustrated in fig. 2. It is assumed that the ground surface is totally reflecting for airborne concentration. Due to symmetry both the semiinfinite (with reflection) and the infinite (without ground reflection) dose models give the same gamma-dose rate at ground level.

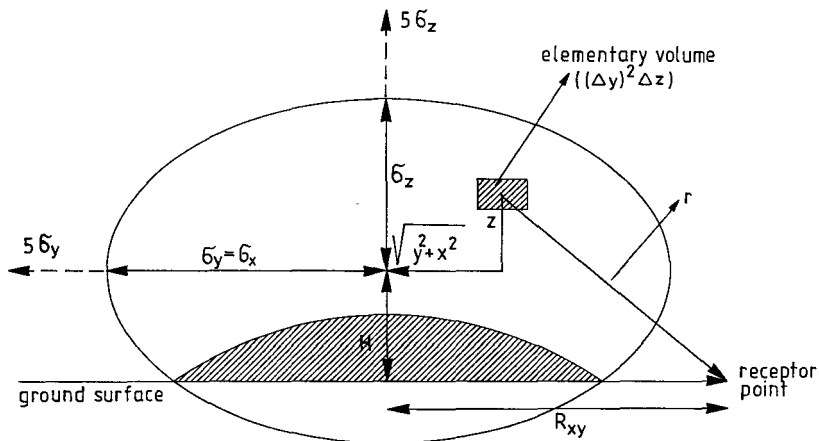


Figure 2. Geometric arrangement of calculations

By this calculational method a database containing the dose rates due to 1 MeV/s energy release by the puff was calculated using the following set of numerical data:

- Q 1 Bq MeV/ E_γ where E_γ is given in MeV (for the present case Q is equal to 5; 2; 1 and 0.5 Bq, respectively)
- E_γ 0.2; 0.5; 1 and 2 MeV
- B Capo polynomials from (Hedemann-Jensen, 1980)
- σ_y range from 10 - to 2000 m (8 values)
- σ_z given as a function of σ_y for a range of σ_y/σ_z , ie. the asymmetry factor, from 0.4 to 40 (11 values)
- H range from 10 to 500 m (8 values)
- R_{xy} up to a distance where the dose rate decreases below 1% of dose rate at $R_{xy}=0$ (number of values between 8 and 32)
- σ_{en} data by Storm 1967 reproduced in (Lauridsen, 1982)
- μ for air data interpolated from (Thykier-Nielsen, 1978). The numerical values are:

0.2 MeV - $1.60 \cdot 10^{-2} \text{ m}^{-1}$	0.5 MeV - $1.14 \cdot 10^{-2} \text{ m}^{-1}$
1.0 MeV - $8.30 \cdot 10^{-3} \text{ m}^{-1}$	2.0 MeV - $5.70 \cdot 10^{-3} \text{ m}^{-1}$

A database for radionuclides specified by RODOS requirements was also created using the photon energies and yields for isotopes as given in (Lauridsen, 1982). This isotope library

contains the energy release rate for unit activity in 4 energy groups. These energy groups were taken around the nominal photon energies as follows:

Group	E nominal [MeV]	Energy range [MeV]
1	0.2	≤ 0.35
2	0.5	$> 0.35 \dots 0.75$
3	1.0	$> 0.75 \dots 1.5$
4	2.0	> 1.5

Using the isotope library and the dose rate values precalculated for the set of parameters mentioned above the dose module within the RIMPUFF works in the following way.

For a puff with actual values of σ_y , σ_y/σ_z , H and R_{xy} (the latter related to the grid point of interest) an interpolation is made within the precalculated database in each energy group. Then the dose rate for an isotope is simply the sum of the 4 interpolated values multiplied by the energy released in the energy group in 1 s. The latter quantity is calculated on the basis of the precalculated isotope library and the actual inventory of the puff for the isotope specified.

The stand alone gamma dose programme module developed by E. Lång (AERI) was integrated into RIMPUFF by S. Thykier-Nielsen (Risø).

Range of Parameters Used for Calculation of Gamma Doses from Asymmetrical Puffs

Besides the photon energy dependence of doses there are 4 independent parameters in dose estimation: the puff's centre height (H), the distance from the puff's base point R_{xy} , the horizontal dispersion parameter (σ_y) and the asymmetry factor (σ_y/σ_z).

For these parameters, calculations are made for the ranges described below. A height interval of $10 \leq H \leq 500$ m has been chosen (divided in 8 points). For R_{xy} the distance is increased so that the dose rate is less than 1% of the maximum, i.e. the dose rate for $R_{xy}=0$ m. This results in a varying number of points (between 8 and 40) for the different cases.

It is more complicated to determine the possible ranges of σ_y and of the asymmetry factor. If the height-dependent dispersion parameters of the Karlsruhe/Jülich system are used, a range of $13 \leq \sigma_y \leq 67000$ and $0.07 \leq \sigma_y/\sigma_z \leq 100$ can be found in a distance range from the source within 100 and 20 000 m. The extremely high values of σ_y/σ_z occur in stable categories and at large distances. It should be noted, that the Karlsruhe/Jülich dispersion parameters refer to a 1 hour averaging time. If the meteorological parameters are to be updated every 10 minutes as it is the intention for RODOS for short distances, much lower σ_y values should be used in stable categories. This would result in much lower maximum values of σ_y/σ_z .

Moreover, based on investigations on the applicability of the infinite cloud model, it was proved that when σ_y is of the order 2000 m the infinite cloud model can be applied for any values of R_{xy} and H . This is illustrated in fig. 3. Therefore the maximum value of σ_y used for numeric integration method was set to 2000 m.

For the upper limit of the vertical dispersion parameter (σ_z) used in dose calculation by numeric calculation method the followings must be considered. In the case of inversion conditions the vertical Gaussian distribution of concentration is gradually distorted due to multiple reflections between the ground and the inversion lid resulting in homogeneous distribution from distances where $\sigma_z = H_{inv}$ i.e. the height of inversion lid. This reflection was not taken into account in the present dose model as it would result in a 6th parameter (H_{inv}) which exact value is rarely known in real dispersion situations. Therefore the semiinfinite dose model using ground surface concentrations calculated by RIMPUFF is applicable from the distance where $\sigma_z = H_{inv}$.

Using the assumptions made above (i.e. $\sigma_y \leq 2000$ m, $\sigma_z \leq H_{inv}$) a smaller range for the asymmetry factor can be estimated. In the present dose model a range from 0.4 to 40 is applied for asymmetry factor. If the actual value of a parameter is outside the range covered by calculations either the semiinfinite model is used (in cases of $\sigma_y > 2000$ m, $\sigma_z > H_{inv}$, $R_{xy} > R_{xy,max}$) or the actual value is set equal to the minimum or maximum value of the range of interest.

A similar approach was applied for the build up factor for larger distances than the validity ranges. Using the Capo-polynomials for $E_\gamma > 0.2$ MeV and the Risø values for $E_\gamma = 0.2$ MeV the validity range of build up factors is determined as follows:

$$\begin{aligned} 0 \leq \mu r \leq 20 & \quad \text{for } E_\gamma > 0.2 \text{ MeV} \\ 0 \leq \mu r \leq 7 & \quad \text{for } E_\gamma = 0.2 \text{ MeV} \end{aligned}$$

Using the numeric integration method for large σ -s and/or large distances an elementary volume may be much further from the receptor point than the build up polynomials could be applied. Therefore the calculation program uses the last acceptable value for B outside the range of approximation.

To test the correctness of the used build up factors, the numerical integral and semiinfinite model have been compared for the case of uniformly distributed activity. It has been found that both methods gives the same results with a systematic error less than 5%. As in this case the calculated by numerical integral dose rate values reach their saturation value inside validity range this control can serve only for checking the build up factors inside the validity range and not for extrapolated values.

2 Parameter Dependence of Dose Rates from Asymmetrical Puffs

If, as a first approximation, the energy dependence is neglected, the new parameters compared to the case of spherical puffs are the horizontal distance and the asymmetry factor. In fig. 4 the dose rate on the ground surface just below the puff's centre is shown as a function of the asymmetry factor. The volume of the puff determined by $\sigma_{eff} = (\sigma_y^2 \sigma_z)^{1/3}$ is kept constant, just its shape is changing. For small puffs it was shown that the shape of the puff actually does not affect the values of dose rate if the puff's distance from the ground is large enough compared to σ_{eff} . For large puffs (fig. 4) the situation is the opposite. The farther the puff is from the ground the more significant dependence of dose rates on the asymmetry factor can

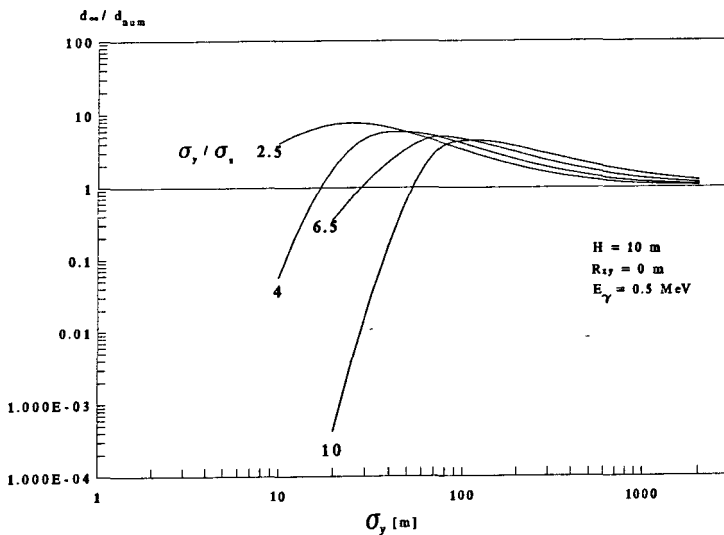


Figure 3. The ratio of dose rates calculated by the semiinfinite and numerical integration methods as a function of σ_y for different values of σ_y/σ_z

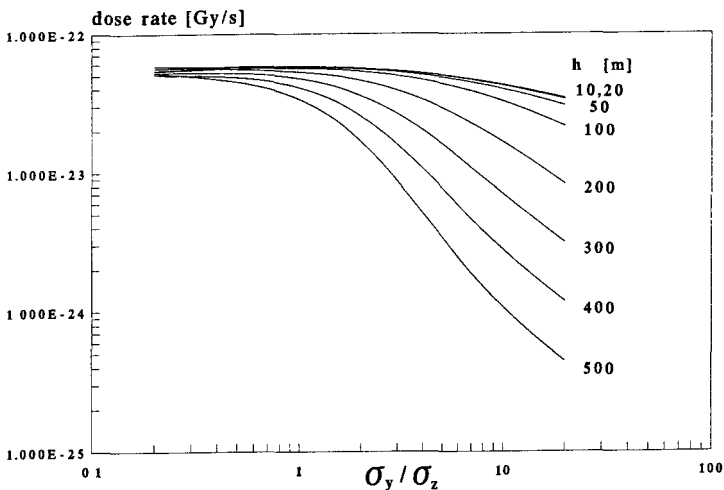


Figure 4. Dose rate as a function of asymmetry factor for different puff heights ($\sigma_{eff} = 500$ m, $E_\gamma = 0.5$ MeV)

be realized. Fig. 5 illustrates the dose rate as a function of distance from the puff's centre in the x-y plane. The second independent variable is the asymmetry factor. The height of the puff from the ground is 10 m here. For large puffs as in fig. 5 in the further away from the release point the larger differences in dose rates arise due to the puff's shape. In the case of small

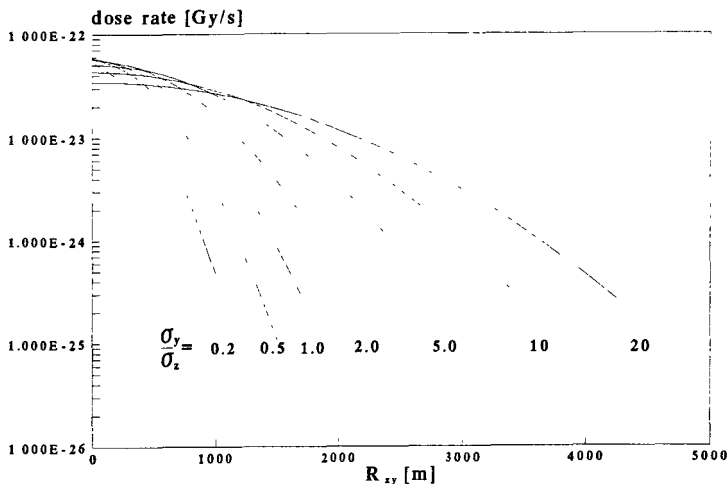


Figure 5. Dose rate as a function of horizontal distance from the puff's centre in the case of different asymmetry factors ($\sigma_{eff} = 500$ m, $E_\gamma = 0.5$ MeV)

puffs an opposite tendency was experienced. The asymmetry factor affects the dose rate significantly only at small distances from the puff's centre (i.e. up to several σ_{eff}).

3. Application of a Simplified Calculation Procedure for Accidental Atmospheric Releases from a Nuclear Reactor

Because of limitations on computer time for real-time calculations it is important to have a fast procedure for calculation of gamma dose rates from Gaussian puffs. As the computing time is proportional to the number of gamma energy groups it is reasonable to decrease the number of groups, provided the additional computation error does not increase significantly. Therefore the use of a single energy group has been investigated for estimating the total cloudshine dose due to a reactor accident.

In order to select one energy group the mean photon energy of radionuclides released to the atmosphere was calculated. A limited set of the most important radionuclides was selected according to the default data in COSYMA and RODOS programs. Shut down inventories were taken from (COSYMA, 1990) and - in some cases - from (Kelly, 1982).

Values of "time before release", "duration of release" and the "fraction of core inventory released to environment" were taken from (Kelly, 1982) for three accident release categories, namely UK1A, UK5A and UK11. A constant rate of emission was assumed during the time of release. The original core inventory after shut-down was corrected for decay and daughter element production.

The time dependence of the mean photon energy was calculated for short-term and long-term releases. In the case of short-term releases (UK1A, UK5A) the mean energy is between 0.7 -0.8 MeV with slight decrease in time, while for long-term releases (fig. 6) it decreases from ~0.8 to ~0.2 MeV. For comparison, the mean energy calculated for a long-term release of the Paks Nuclear Power Plant (Hungary) is also shown.

The order of magnitude of the errors made in the dose calculations by using a mean photon energy instead of the individual energies was also investigated based on our preliminary database for spherical puffs.

Figure 7 shows that near the puff centre where the dose rates are high there is good agreement between the results of the two calculation methods. Here the use of the mean energy results in an overestimation of 6-8% compared to the real dose rates. At larger distances from the puff centre the use of the mean energy leads to underestimation of the dose rates. Though this error may be an order of magnitude or even more, note that the dose rates are very low in such distances relative to the maximum value.

The agreement in centreline doses (instead of dose rates) calculated by the mean and the individual photon energies is even better. The total dose originating from a puff that passes over a receptor point leads to a difference less than 6-7% between the doses calculated by the two methods mentioned above. This does not apply to points far away from the puff's centreline. In such cases the use of the mean energy leads to underestimation of the relatively low doses.

As it was stated in the beginning of this paragraph the mean photon energy of radionuclides released to the atmosphere is varying between 0.2 to 0.8 Mev with time including both short- and long-term releases. As a last step for investigation of the applicability of simplified method the energy dependence of dose

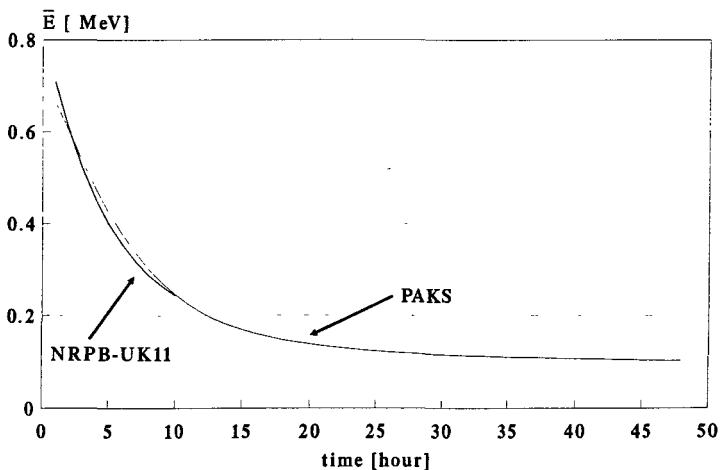


Figure 6. Mean photon energy of radionuclides due to long-term accidental releases

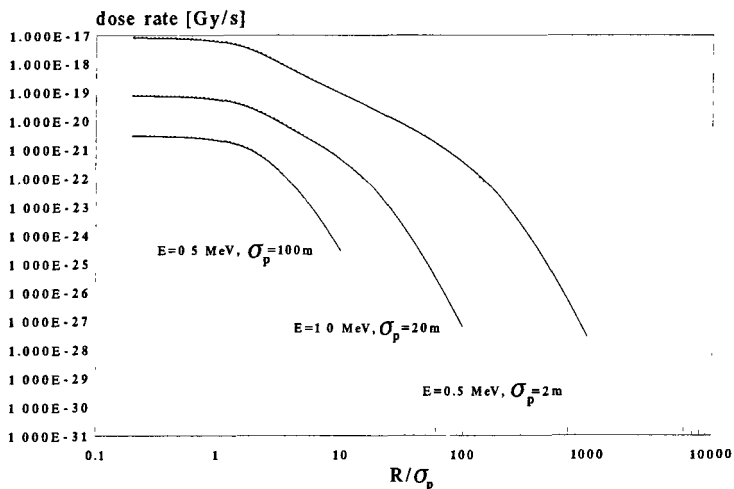


Figure 7. Dose rates calculated by the mean (dotted line) and the actual photon energies

calculations was examined. Instead of time varying mean photon energy a nominal medium energy (0.5 MeV) was taken. Dose rates were compared to those calculated by the lower and upper limits of the actual mean photon energies, i.e. 0.2 and 0.8 MeV respectively (fig. 8). Near the puff's centre the use of nominal energy leads to underestimation or overestimation of dose rates compared to 0.2 and 0.8 MeV. The size of these differences does

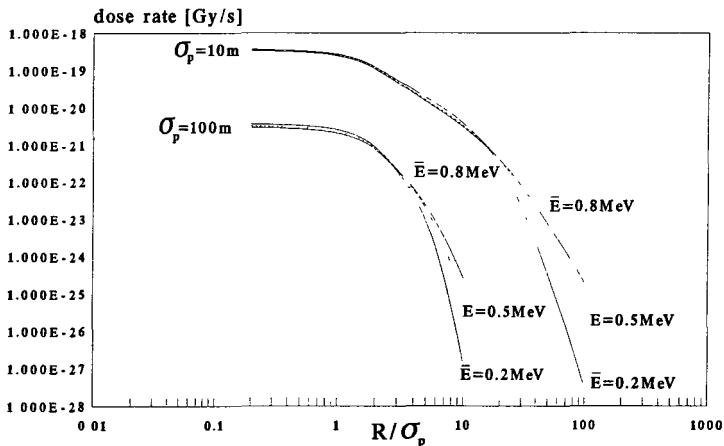


Figure 8. Energy dependence of dose rate (range of 0.2 - 0.8 MeV)

not exceed \pm 5-15%. Further from the puff's centre, i.e. at relatively low dose rates the sign of the differences is the opposite and they are one order of magnitude. These calculation tests resulted in differences of \pm 4-10% when applying them for doses instead of dose rates.

It can be concluded from these investigations that the use of the mean photon energy (moreover the use of a nominal medium photon energy, i.e. 0.5 MeV for the examined types of accidental releases) is an acceptable approximation for estimating the total cloudshine dose due to a reactor accident. This simplified method is applicable with really good results for places where the doses are high.

Conclusions

The method described will significantly improve the procedure for calculation of the gamma radiation doses from puffs. The tabulated dose rate values can be used for fast real-time calculations in case of an accident.

A simplified method has been given for early phase of atmospheric releases in case of a reactor accident.

References

COSYMA - A New Programme Package for Accident Consequences Assessment. Report EUR 13028 EN. (Brussels: CEC) (1990)

Hedemann-Jensen, P. and Thykier-Nielsen, S. (1980): Recommendations on Dose Build up Factors Used in Models for Calculating Gamma Doses from a Plume, Risø-M-2204

Kelly, G.N. and Clarke, R.H. (1982): An Assessment of the Radiological Consequences of Releases from Degraded Core Accidents for the Sizewell PWR. NRPB-R137

Lauridsen, B. (1982): Table of Exposure Rate Constants and Dose Equivalent Rate Constants. Risø-M-2322

Mikkelsen, T., Larsen, S.E. and Thykier-Nielsen, S. (1984): Description of the Risø Puff Diffusion Model, Nuclear Technology, Vol. 67, pp. 56-65

Slade, D.H. (editor) (1968): Meteorology and Atomic Energy, TID-24190.

Thykier-Nielsen, S. (1978): Comparison of Nordic Dose Models, Risø-M-1972, p. 180.

Publications

Thykier-Nielsen, S., Deme, S. and Láng, E. (1993): Calculation Method for Gamma-Dose Rates from Spherical Puffs. Risø-R-692(EN)

Thykier-Nielsen, S., Deme, S. and Láng, E. (1995): Calculation Method for Gamma-Dose Rates from Gaussian Puffs. Risø-R-775(EN)



**Final Report
1992 - 1995**

Contract: FI3PCT920057 **Duration:** 1.9.92 to 30.6.95 **Sector:** C24

Title: Methodology for evaluating the radiological consequences of radioactive effluent released in accidents - the MARIA project.

1)	Jones	NRPB	National Radiological Protection Board, UK
2)	Ehrhardt	FZK	Forschungszentrum Karlsruhe GmbH, Germany
3)	Alonso	UPM	Univ. Politéc. Madrid, Spain
4)	Van der Steen	KEMA N.V.	Netherlands
5)	Iordanov	BAS	Bulgarian Academy of Sciences, Bulgaria
6)	Koblinger	KFKI-AERI	Atomic Energy Research Institute, Hungary

I Summary of Project Global Objectives and Achievements

The overall objectives of the project are:

- i) The maintenance support and development of the COSYMA system. This includes modelling and data improvements to the system and updating of the supporting documentation, and continual adaptation of the system to the needs of users.
- ii) The further development of a PC version of the COSYMA system, to allow non-expert users to undertake ACA studies without access to large computer resources. A feature of this system is an interactive interface. The PC system, like the mainframe system, is available to organisations inside and outside the EU through the CEC.
- iii) Participation of the COSYMA system in the CEC/NEA ACA code intercomparison exercise, and documentation of the results. The formation and running of a user group.
- iv) Further work on the development of techniques for assessing the economic impact, including impact beyond the areas affected by countermeasures, the incorporation into the COSYMA system of an alternative economics model, and site-specific features of economics modelling.

The principal achievements during the period of the contract have been:

- i) the release of version 93/1 and the finalisation of version 95/1 of COSYMA,
- ii) the release of the first version of PC COSYMA, and the preparation of the second version for release in 1995,
- iii) the coordination of the COSYMA User Group, and the organisation of its first and second meetings,
- iv) an additional economics module for COSYMA, incorporating the MECA2 model and a new model for the analysis of the effects of a nuclear accident on the economic variables of the directly affected and surrounding areas.

Head of project 1: Dr Jones

II Objectives for the reporting period

- i) To assist FZK in the maintenance, support and development of the COSYMA system, primarily in the area of data improvements and updates to the system and the supporting documentation, and to release the system as appropriate.
- ii) To take the lead, with assistance from FZK in the further development of the PC version of the COSYMA system, to release the system as appropriate, and to support users of the system,
- iii) To undertake a review, with assistance from the other participants in the project, of the current position of probabilistic ACA modelling and codes, with a view to identifying the needs and priorities for future research.

III Progress achieved including publications

The NRPB work is described in sections 2, 3, 5 and 6 of this report.

Head of project 2: Dr Ehrhardt

II Objectives for the reporting period

- i) To take the lead, with assistance from NRPB, in the further development of COSYMA, primarily in the refinement of models, updating of data sets and making the system more user-friendly, to release the system as appropriate, and to support users of the system.
- ii) To assist NRPB in the further development of the PC version of COSYMA, primarily in the refinement of models and the addition of new features.
- iii) To take part in the International Intercomparison Exercise on accident consequence models, and in particular to assist KEMA in understanding the reasons for differences between the predictions obtained by COSYMA users.

III Progress achieved including publications

The FZK work is described in sections 2, 3, 4 and 6 of this report.

Head of project 3: Prof Alonso

II Objectives for the reporting period

- i) Conclusion of the participation with MECA2 (Model for Economic Consequence Assessment) in the CEC/NEA(OECD) PCA code Benchmark exercise.
- ii) Incorporation of MECA2 into COSYMA as an additional economics module.
- iii) Review, evaluation and selection of new methods for assessing the direct and indirect economic impact of nuclear accidents.
- iv) Application of the selected methodology to deterministic calculations using data from specific nuclear sites.
- v) Incorporation of the new model into the COSYMA system, thus allowing to use it for probabilistic calculations of the direct and indirect economic consequences of nuclear accidents.

III Progress achieved including publications

The UPM work is described in sections 4 and 6 of this report.

Head of project 4: Mr J van der Steen

II Objectives for the reporting period

- i) To coordinate the activities of the COSYMA Users Group according to its terms of reference;
- ii) To identify and evaluate weaknesses in COSYMA and PC COSYMA, as identified by the users in their applications of the code, and to advise in the maintenance and further development of the COSYMA system;
- iii) To assist in a review of the current position of PCA codes and models, with respect to the needs and priorities for future research.

III Progress achieved including publications

The KEMA work is described in sections 5, 6 and 7 of this report.

Head of project 5: Dr I Iordanov

II Objectives of the reporting period

To carry out a probabilistic risk analysis for the Kozloduy nuclear power plant in Bulgaria. The project is intended to analyse the transport of radionuclides through the environment and to assess the public health consequences of severe accidents. The calculation of the source term is also to be carried out.

III Progress achieved including publications.

The BAS work is described in section 8 of this report.

Head of project 6: Dr L Koblinger

II Objectives for the reporting period

To supply specific Hungarian data (population, agricultural production, land use and meteorological) for use in the COSYMA data libraries. The data to be supplied in the required format were:

- 1 Population data: as input for the GRIDS program, the population data for Hungary on a gridded system with a grid size of 100 km², sorted from south to north and west to east.
- 2 Agricultural and land use data: for milk, milk products, beef, cow's liver, sheep meat, sheep liver, grain, green vegetables, root vegetables and crop areas, in the same grid resolution used for population data.
- 3 Meteorological data: site-specific data for Paks nuclear power plant giving for each hour for one year the measured wind speed and direction, the stability category, rain fall rate and mixing layer depth.

III Progress achieved including publications

The KFKI-AERI work is described in sections 2 and 3 of this report.

1 INTRODUCTION

The MARIA project was initiated more than 10 years ago, to develop expertise within the European Union (EU) in accident consequence assessment (ACA). During this period, the European Commission (EC) has supported considerable work on the development of models for use in ACA. The first version of COSYMA (Code system from MARIA), a code for calculating the off-site consequences of accidental releases, was developed under an earlier stage of the MARIA contract. The work undertaken during the reporting period has mainly been concerned with six areas related to the modelling of the off-site consequences of accidental releases of radioactive material to atmosphere, namely:

- 1 the further development and maintenance of COSYMA, an accident consequence assessment code for use on large mainframe computers originally written in an earlier phase of the MARIA contract,
- 2 the development and maintenance of a PC version of COSYMA which is intended for people who do not need the full features of the mainframe version,
- 3 the development of methods for modelling the economic impact of accidents, and their incorporation in the mainframe and PC versions of COSYMA,
- 4 a review on the current state of COSYMA, and the needs for further research and development into aspects of the modelling used in COSYMA,
- 5 the use of COSYMA in an international comparison of the predictions of accident consequence assessment programs,
- 6 the creation and organisation of a COSYMA user group at which people can discuss their needs and applications of the mainframe and PC versions of COSYMA.

During this reporting period, 4 organisations from within the EU have been involved in the MARIA contract. The scope and content of the research carried out by the four EU partners and KFKI-AERI was such that close cooperation and interaction between the partners was essential for the effective conduct of the work. Consequently, this progress report describes the work undertaken under the contract by these five organisations as a coherent whole on a subject by subject basis, rather than describing the work of each organisation separately.

The work of the Bulgarian Academy of Sciences (BAS), which was concerned with a probabilistic consequence assessment for a Bulgarian power plant, was largely self-contained and is, therefore, reported separately. In undertaking this task, BAS collaborated with the National Centre for Scientific Research (Democritos) (NCSR) in Greece, whose participation was supported by a separate study contract from the Commission.

The main achievements under the contract are summarised below. They are described in more detail in the later sections of this report. The summaries also identify which partners were involved in the various pieces of work.

Mainframe COSYMA Two further updates of the mainframe version of COSYMA have been prepared. One was released in 1993, the second will be released towards the end of 1995. This work has been mainly carried out by FZK and NRPB, and is described in chapter 2 of this report.

PC COSYMA The first version of PC COSYMA was released at the same time as the 1993 version of mainframe COSYMA. A second version is being finalised for release in 1995. This

work has mainly been carried out by NRPB and FZK. This work is described in chapter 3 of this report.

KFKI-AERI has provided data libraries for distribution with the forthcoming mainframe and PC versions of COSYMA, as indicated in chapters 2 and 3 of this report.

Economic modelling New models for modelling the economic consequences of accidents have been developed by the Polytechnic University of Madrid and FZK, and incorporated into the mainframe version of COSYMA. This work is described in chapter 4 of this report.

Research needs A review of the needs for further research and development into aspects of the modelling used in COSYMA has also been carried out. This was carried out mainly by NRPB and KEMA, but has drawn heavily on discussions during meetings of the COSYMA User Group. The review is presented in chapter 5 of this report.

International code comparison The mainframe version of COSYMA was included in an international intercomparison of ACA codes. This work was undertaken mainly by FZK and NRPB, and is described in section 6.1. Alongside this, other users of COSYMA carried out their own intercomparison exercise. This was co-ordinated by KEMA with assistance from FZK and UPM (for the economics endpoints) in understanding the differences between the various predictions. This work is described in section 6.2.

COSYMA User Group The COSYMA User Group was formed as a result of the international code comparison, and has had two meetings subsequently. KEMA provides the secretariat for the group, and all other contractors have taken an active role in the group's work. As noted above, discussions in the user group have fed into the review of modelling and research needs. This part of the work is described in chapter 7.

Consequence assessment for Bulgarian power plant BAS has carried out a probabilistic consequence assessment for a Bulgarian power plant. This is described in chapter 8.

2 MAINFRAME COSYMA

The program package COSYMA jointly developed by FZK and NRPB was released in September 1993 in its mainframe version 93/1. Some 30 institutions in the EU and in other countries were provided copies of the program package for implementation on their computer together with the updated documentation. In the meantime the further improved version 95/1 has been completed and is ready for distribution.

Within the reporting period, some refinements of models and updated data sets have been incorporated in COSYMA together with an improvement of user-friendliness and flexibility. The most significant modifications are described in this section. The improvements of models and data files have also been introduced in the PC version of COSYMA. Mainframe COSYMA 93/1 corresponds to PC COSYMA 1.0 and version 95/1 is compatible with PC version 2.0.

2.1 *Further development of models*

2.1.1 **Health effects model**

The 'Health Effects Model' developed in the US builds the basis for the modelling of deterministic effects in COSYMA as in other accident consequence assessment codes¹. The COSYMA versions released before 93/1, however, neglected the dependence on the dose-rate of the D50-value (ie the dose at which half of the irradiated population experiences the health effect considered). For most of the deterministic health effects the radiation doses accumulated at low dose-rates over longer time periods are less effective than those resulting from short term exposure at high dose-rates; therefore, the individual risks have been overestimated by this simplification.

In consultation with NRPB, those dose-rate dependencies have been considered in the 93/1 version of COSYMA which are quantified in the 'Health Effects Model', ie for the haematopoietic syndrome, the pulmonary syndrome and for lung function impairment. Finally, the model has been updated again in version 95/1 taking into account dose-rate dependencies for all deterministic health effects, based on a review carried out at NRPB² of the USNRC reports. The model currently implemented in COSYMA is described in detail in reference 3.

For each of the deterministic health effects considered in COSYMA, a certain number i of time periods is distinguished, within which the dose $D(i)$ accumulates; the value $D50(i)$ is assigned to each of these time intervals. It is calculated by the formula

$$D50(i) = D_0 / DR(i) + D_\infty$$

with

$$DR(i) = D(i) / T(i) \text{ average dose-rate in the time interval } T(i)$$

and

$$D_0, D_\infty \text{ model parameters.}$$

This model predicts that there is some risk of early health effects for very small doses, which is unreasonable. Therefore the individual risks are assumed to be zero below a user-defined threshold value.

Another modification has been made in the model for deterministic health effects. The model now allows for different RBE-values for high and low LET irradiation for the different early health effects.

The following default values for the deterministic health effects model have been taken from the NRPB review² and can be changed by the user:

TABLE 2.1 Default values for the health effects model for deterministic effects

Health effect	D _∞ (Gy)	D ₀ (Gy ² /h)	RBE for α irradiation
Lung function impairment	5.0	15.0	7.0
Hypothyroidism	60.0	30.0	0.0
Cataracts	3.0	0.01	0.0
Mental retardation	1.5	0.0	20.0
Effects on skin	20.0	5.0	0.0
Pulmonary syndrome	10.0	30.0	7.0
Haematopoietic syndrome	4.5	0.105	2.0
Gastrointestinal syndrome	35.0	0.0	0.0
Pre/neonatal death	1.5	0.0	20.0
Death from skin burns	20.0	5.0	0.0

2.1.2 Model for effectiveness of iodine tablets in reducing thyroid dose

A model has been incorporated in version 95/1 and PC version 2.0 of COSYMA to describe the effectiveness of iodine tablets taken at a certain time after the inhalation of the radioactive iodine in reducing the thyroid dose. The effectiveness depends on the difference between the times at which the iodine tablets are taken and the radioactive iodine is inhaled. All material is assumed to be inhaled at the time at which the plume first arrives at the location considered.

The thyroid dose from inhaled iodine allowing for the effect of iodine tablets is calculated as the dose without tablets multiplied by a factor F determined according to the following formula suggested by NRPB⁽⁴⁾

$$F = 1 - \exp (-\ln 2 (t + 0.25) / 4)$$

where t is the time in hours between inhaling radioactive iodine and taking the tablets, and is positive if the inhalation occurs before the tablets are taken. The formula assumes that inhaled iodine is instantly transferred to the blood, and that the half-life for uptake by the thyroid is 4 hours. The 0.25 hours represent the delay time for incorporated iodine to reach the blood stream. If the tablets are taken 0.25 hours or more before the arrival of the plume, then the thyroid dose from iodine is assumed to be zero.

The user can specify the times (relative to the start of the release) at which iodine tablets are taken; these times can be different in the two areas considered in COSYMA for iodine tablets. In the geometric area the tablets will presumably be distributed more rapidly than in the dose

based area. Default values for these times are 2 and 4 hours. These represent the times which might be taken for emergency staff to distribute the tablets after the accident.

The effectiveness of iodine tablets is also considered in the calculation of the effective dose and effective dose equivalent, respectively.

2.1.3 Resuspension model

In the framework of an EC contract on reviewing models for describing the behaviour of radioactive material after deposition, NRPB investigated the implications of the experimental work of other organisations on the modelling in COSYMA (see also Section 5 of this progress report)⁵. As a result, new default parameter values for the resuspension coefficients were agreed and have been incorporated in COSYMA (see Table 2.2). The resuspension factor $r(t)$ is defined as the ratio of the resuspended air concentration to the total amount of material deposited where t is the time after deposition; it is obtained from the formula

$$r(t) = r_0 \exp(-\lambda_r t) + r_e$$

With the updated parameter values FZK calculated new activity-risk coefficients⁵ for the resuspension pathway for use in the mainframe version of COSYMA to calculate late health effects.

TABLE 2.2 Default resuspension coefficients used in COSYMA

Parameter	COSYMA 93/1	COSYMA 95/1
r_0	$1.0 * 1.E-5 \text{ m}^{-1}$	$5.0 * 1.E-8 \text{ m}^{-1}$
λ_r	$1.62 * 1.E-7 \text{ s}^{-1}$	$3.5 * 1.E-8 \text{ s}^{-1}$
r_e	$1.0 * 1.E-9 \text{ m}^{-1}$	$1.0 * 1.E-9 \text{ m}^{-1}$

2.1.4 Economics model

In order to take into account regional or local economic peculiarities of a nuclear site for the calculation of loss-of-income costs in the case of evacuation or relocation, the ECONOMICS module was extended by a site-specific option. In this case, the calculation is based on the number of employees in different economic sectors (instead of the number of people) in the evacuation or relocation area together with the respective GDP-per-employee value. The model builds the basis of version 93/2 (which was only distributed on request) and is also incorporated in version 95/1; it requires very detailed economic data and is therefore not included in PC COSYMA. A more detailed description is given in Section 4 of this progress report and in reference 6.

2.1.5 Additional options and endpoints

Recommendations and comments given by the International COSYMA Users Group established in 1993 (see also Section 7 of this progress report) on missing options and endpoints have been included in the code as far as reasonable and feasible. The definition of countermeasure areas

was extended to allow for a geometrically defined sheltering area, to initiate the distribution of iodine tablets on a dose criterion and to restrict the dose based countermeasure areas to a certain distance.

In the standard applications of COSYMA, consequences within the whole population or integrated over a whole distance band are assessed. However, it can be of interest to evaluate individual results (eg activity concentrations, individual doses and risks, the probability to impose a countermeasure) at a particular point specified by angle and distance from the site. A corresponding option has been incorporated in COSYMA which allows for calculating such results. However, to get the same statistical accuracy, overall and point specific results should not be calculated with the same meteorological conditions. For the point specific evaluation, weather samples have to be selected in such a way, that the point of interest is affected. The program METSAM for selecting sets of weather sequences has been modified to cope with both types of endpoints.

Evaluation programs have been included to provide statistical information on the intervention doses for countermeasures and to calculate and evaluate individual and collective doses averted. For the individual dose results, the breakdown by single nuclides can now be obtained not only for each exposure pathway separately, but also for the total dose.

2.1.6 Increase of flexibility and user-friendliness

Some months after the distribution of version 91/1 of the program package COSYMA a questionnaire was drawn up by FZK and sent out to all users asking for problems in COSYMA applications and proposals for future improvements. The evaluation of the answers is documented in the report on the COSYMA Users Intercomparison Exercise⁷. The comments given by the users on how to increase the flexibility and user-friendliness are considered in versions 93/1 and 95/1 as far as reasonable and feasible. Some examples are: variable number of nuclide groups specified for the source term and simplified input for these groups, possibility to calculate within the same run deterministic health effects and individual doses integrated over a specified short time period; options to specify a cut-off distance for assessing early consequences and to apply an average shielding factor for determining early consequences without considering countermeasures; simplification of the user-input for the timing of early countermeasures and the calculation of individual doses integrated over a specified time period; printout of information on the intervention doses for emergency actions; option to include a printout of the input file in the control output; improvement of printout from the evaluation programs.

2.2 Further development of data files

2.2.1 Inclusion of activation products from fusion reactors

The application of COSYMA for assessments within fusion reactor studies required the extension of its nuclide list. To that purpose, the nuclide data base of COSYMA has been extended from 145 radionuclides in version 93/1 to 197 in version 95/1. The list of nuclides which can be considered in the newest versions of COSYMA is given in Table 2.3.

The dose conversion factors and foodchain data for the activation products have been provided by NRPB and GSF for internal exposure pathways (inhalation, ingestion) and GSF for external exposure from material in the cloud, or deposited on the ground or on skin and clothing, under a separate CEC-contract⁸. They were transferred to FZK for implementation into the code. With the new dosimetry and food chain data FZK calculated new activity-risk coefficients⁵ for use in the mainframe version of COSYMA to calculate late health effects.

2.2.2 Data sets of dose conversion factors

External doses from material deposited on the ground are calculated by multiplying the activity concentration on ground surface by a dose conversion factor giving the dose per unit material deposited. A revised data set containing these values at a series of times for each of a large number of nuclides, including the contribution from daughter products formed after deposition, is provided for COSYMA version 93/1. The new dose conversion factors are appropriate for people staying outdoors and were derived by NRPB using two models. The values for the nuclides which make the most important contributions to deposited dose from typical accidental releases (Ru-103, Ru-106, I-131, Te-132, Cs-134, Cs-137 and Ba-140) were calculated using the NRPB model EXPURT⁹. This model considers the amounts of material deposited on different surfaces in residential areas, the movement of material between these surfaces into the soil column, and the dose from material deposited on the different surfaces. The doses for all other nuclides were calculated using a simpler model which assumes that the dose in the area where people live can be represented by that over an open field; they also allow for material to move into the soil column.

The 93/1 data base has been extended to consider also activation products. The dose conversion factors provided by GSF for these nuclides have been included by FZK to form the 95/1 data file.

The dose conversion factors for the fusion nuclides for external irradiation from material in the cloud and from contamination of skin have been taken from the data originally provided by GSF and added to the 93/1 data base.

The dose per unit intake libraries (inhalation and ingestion) in version 93/1 and PC version 1.0 are based on the dosimetric models described in ICRP publication 30. New data libraries have been prepared by NRPB and implemented by FZK for version 95/1 and PC version 2.0, respectively. They are based on the new ICRP respiratory tract model and the biokinetics models described in ICRP publications 56, 67 and 69, and in the revised International Basic Safety Standards¹⁰.

A limited comparison of values undertaken by NRPB for a series of nuclides showed that the ingestion doses from the 95/1 libraries tend to be smaller than those from the 93/1 libraries. The 95/1 inhalation doses for class Y material also tend to be smaller than the 93/1 doses. However, for other lung classes the doses for some nuclides are smaller than the 93/1 values but are larger for other nuclides.

Whenever the dosimetry files have changed, new data sets of activity-risk-coefficients have been calculated by FZK and implemented for use in the mainframe version of COSYMA.

2.2.3 Data sets of foodchain data

The activity-in-food default files version IG-91/AX were replaced by the updated version IG-93/AX, in which apparent errors present in the old data were removed and some assumptions about the agricultural practices and parameter values were revised following a comprehensive review of the FARMLAND model at NRPB. As before, the data were calculated with the dynamic foodchain transport model FARMLAND and provided by NRPB. The implementation of the data into the code was done by FZK. The data libraries are intended for general application in central and northern Europe and use assumptions on the agricultural practice and parameter values agreed by NRPB and GSF as part of a separate CEC contract.

For the 95/1 version of COSYMA some minor errors in the previous data affecting longer-lived nuclides in milk, beef and lamb were recognised and have been removed. Additionally, the IG-95/AX data base includes foodchain data for activation products. However, these data are only available for a release in July. For a release in January, the corresponding data sets have been generated using the July-data for the affected nuclides.

Data libraries have also been provided by GSF using the ECOSYS model, and incorporated into the system. These give concentrations for nuclides from both fission and fusion reactor accidents, for both summer and winter conditions.

With the new food chain data, new data sets of activity-risk-coefficients for the ingestion pathway have been calculated by FZK for use within the mainframe version of COSYMA.

2.2.4 Gridded data for human population and agricultural production

CEA collected gridded data for human population and agricultural production under a separate CEC-contract. The data available were transferred to NRPB and FZK in the European grid format country by country together with a program to combine the countries and to transfer the data into the mainframe COSYMA grid format. However, data have not been received for all European countries. Population data have been delivered for Belgium, Denmark, Finland, France, Germany, Hungary, Ireland, Italy, Luxembourg, the Netherlands, Portugal, Slovakia, Spain, Switzerland, Sweden and UK in the European grid format. Data for Greece and Slovenia have been sent directly to NRPB/FZK in different formats and have been incorporated by FZK in the COSYMA data base. Data for agricultural production could only be obtained from Hungary and UK. The missing new data lead to the task to fill these gaps with the values from the old gridded data base. This was done by FZK for the population data and for the agricultural production data by NRPB.

2.3 References for section 2

- 1 International Comparison Exercise on Probabilistic Accident Assessment Codes - Overview Report, Paris, OECD and CEC, 1994
- 2 Edwards A A. Private Communication
- 3 Ehrhardt J, Hasemann I, Matzerath-Boccaccini C, Steinhauer C, and Raicevic J. COSYMA: Health effects models. Karlsruhe, Report FZK-5567, 1995

- 4 Kovari M D, Effect of delay time on effectiveness of stable iodine prophylaxis after intake of radio-iodine. *J Radiol Prot* 14 131-136 (1994)
- 5 Tschiersch J (editor) Deposition of radionuclides. their subsequent relocation in the environment and resulting implications. Final report on contract F13P-CT92-0038 EUR report, To be published
- 6 Faude D and Meyer D. Extension of the COSYMA-ECONOMICS module: cost calculation based on different economic sectors. Karlsruhe, Report KfK-5442, 1994
- 7 van Wonderen E, van der Steen J and Hasemann I. COSYMA: Users Intercomparison Exercise CEC, Report EUR-15108, 1993
- 8 Haywood S M, Brown J, Jones J A, Fayers C, Smith J G, Pröhl G, Bleher M, Jacob P and Müller H. Databases for activities in foodstuffs for external exposure from the ground and for dose per unit intake for fusion radionuclides for the COSYMA ACA system. TO be published.
- 9 Crick M J and Brown J. EXPURT: a model for evaluating exposure from radioactive material deposited in the urban environment. Chilton NRPB-R235 (1990)
- 10 FAO, IAEA, ILO, OECD/NEA, PAHO, WHO. International basic safety standards for protection against ionizing radiation and for the safety of radiation sources. Interim edition. Vienna, IAEA Safety Series 115-I, (1994)

TABLE 2.3 List of nuclides which can be considered in COSYMA

No. nuclide name	No. nuclide name	No. nuclide name	No. nuclide name
1 Be-7	51 Sr-90	101 Te-127m	151 Eu-156
2 Be-10	52 Sr-91	102 Te-127	152 Hf-175
3 Na-22	53 Sr-92	103 Te-129m	153 Hf-181
4 Na-24	54 Sr-93	104 Te-129	154 Hf-182
5 Si-32	55 Y-90m	105 Te-131m	155 Ta-179
6 P-32	56 Y-90	106 Te-131	156 Ta-182m
7 P-33	57 Y-91m	107 Te-132	157 Ta-182
8 Ar-41	58 Y-91	108 Te-133m	158 Ta-183
9 Sc-44m	59 Y-92	109 Te-133	159 W -181
10 Sc-44	60 Y-93	110 Te-134	160 W -183m
11 Sc-46	61 Zr-89	111 I -125	161 W -185
12 Sc-47	62 Zr-93	112 I -129	162 W -187
13 Sc-48	63 Zr-95	113 I -130	163 Re-184m
14 V-48	64 Zr-97	114 I -131	164 Re-184
15 V-49	65 Nb-91m	115 I -132	165 Re-186m
16 Cr-51	66 Nb-92m	116 I -133	166 Re-186
17 Mn-52m	67 Nb-92	117 I -134	167 Re-188m
18 Mn-52	68 Nb-93m	118 I -135	168 Re-188
19 Mn-53	69 Nb-94m	119 Xe-131m	169 Hg-197m
20 Mn-54	70 Nb-94	120 Xe-133m	170 Hg-197
21 Mn-56	71 Nb-95m	121 Xe-133	171 Hg-203
22 Fe-52	72 Nb-95	122 Xe-135m	172 Po-208
23 Fe-55	73 Nb-97	123 Xe-135	173 Po-210
24 Fe-59	74 Mo-93	124 Xe-138	174 Ra-226
25 Fe-60	75 Mo-99	125 Cs-134m	175 U -234
26 Co-56	76 Mo-101	126 Cs-134	176 U -235
27 Co-57	77 Tc-95m	127 Cs-135	177 U -238
28 Co-58m	78 Tc-95	128 Cs-136	178 Np-237
29 Co-58	79 Tc-96	129 Cs-137	179 Np-238
30 Co-60m	80 Tc-99m	130 Cs-138	180 Np-239
31 Co-60	81 Tc-99	131 Ba-139	181 Pu-236
32 Co-61	82 Tc-101	132 Ba-140	182 Pu-238
33 Ni-59	83 Ru-103	133 La-140	183 Pu-239
34 Ni-63	84 Ru-105	134 La-141	184 Pu-240
35 Ni-65	85 Ru-106	135 La-142	185 Pu-241
36 Cu-62	86 Rh-103m	136 Ce-141	186 Pu-242
37 Cu-64	87 Rh-105	137 Ce-143	187 Am-241
38 Cu-66	88 Ag-108m	138 Ce-144	188 Am-242m
39 Zn-65	89 Ag-110m	139 Pr-143	189 Am-242
40 Zn-69m	90 Ag-110	140 Pr-145	190 Am-243
41 Se-75	91 Ag-111	141 Nd-147	191 Cm-242
42 Kr-83m	92 Sb-124	142 Pm-147	192 Cm-243
43 Kr-85m	93 Sb-125	143 Pm-148m	193 Cm-244
44 Kr-85	94 Sb-126	144 Pm-148	194 Cm-245
45 Kr-87	95 Sb-127	145 Pm-149	195 Cm-246
46 Kr-88	96 Sb-128L	146 Pm-151	196 Cm-247
47 Rb-86	97 Sb-129	147 Eu-152m	197 Cm-248
48 Rb-88	98 Sb-130L	148 Eu-152	
49 Rb-89	99 Sb-131	149 Eu-154	
50 Sr-89	100 Te-125m	150 Eu-155	

3 PC COSYMA

The program package COSYMA for use on a mainframe was released in 1990¹. In 1993, a PC version 1.0 of this package with user-friendly input and results interfaces was developed by NRPB and FZK^{2,3}. It was released and distributed by NRPB in 1993, at the same time as the mainframe version 93/1. Both packages contained the same underlying models. However, the PC version included some simplifications, particularly to the way in which risks of early health effects are calculated for groups of people in positions with different shielding factors. Over one hundred copies have been distributed to organisations in 37 countries throughout the world.

A revised and extended version of the PC system has been developed at FZK and NRPB and has been released in late 1995^{4,5}, to accompany the release of a revised mainframe version 95/1. Version 2 contains improvements both in the models used and in the range of endpoints available. The overall presentation and user-friendliness of the system have been improved using the experience gained from using version 1 and comments received from many other organisations who have used the system. The first version of PC COSYMA was released and developed during the first part of the period covered by this contract report. However, the report concentrates on the modifications made for the second version of the system.

The majority of the improvements to the models and data bases in this reporting period apply to both the mainframe and PC packages. The mainframe package has been described earlier in this report. This section on the PC package describes work undertaken specifically on the PC package with reference to the mainframe package where appropriate.

3.1 *Further development of models*

3.1.1 **Early health effects model**

PC COSYMA includes all the early health effects which are considered in the mainframe version. Version 1 contained only dose-rate dependent D50-values for pulmonary and haematopoietic syndromes and for lung function impairment. The models have been extended to include similar dose-rate dependent values for all early health effects. The D50-values for each organ comprise two parts representing high and low dose rate components and the user may change these parameters for all organs. The models also allow for a different RBE for high and low LET irradiation. The user may not change these values. The time periods over which the dose rate is calculated may not be changed in the PC version by the user. The default parameter values are the same as those used in the mainframe version of COSYMA, and are given in section 2.1.1.

The user may set a threshold value of individual risk below which all risks are assumed zero. The default is 0.01.

3.1.2 **Model for effectiveness of iodine tablets in reducing thyroid dose**

The model for calculating the effectiveness of iodine tablets in reducing the thyroid dose from inhaled and resuspended activity has been revised to allow for the variation of effectiveness of this countermeasure with the time the tablets are taken relative to the time when the inhalation of radioactive iodine occurs⁸, see section 2.1.2. Two areas for the distribution of iodine tablets

may be modelled; an area where distribution is automatic in a geometrically defined area and an area based on potential thyroid dose. The user specifies the time in each of these areas following the accident when the tablets are taken. Both areas may be defined together with the geometric area taking precedence.

3.1.3 Economics model

Version 2 includes an economics model for calculating the costs of countermeasures and health effects, based on the mainframe economics model version 93/1⁶ which is also included as an option in the mainframe version 95/1. The results are presented in terms of the costs of moving people, ie evacuation, relocation and the costs of any decontamination methods, the costs of food bans, the total costs of countermeasures, early and late health effects combining cancers and hereditary effects and the total costs.

Two 'default' sets of input parameters are supplied, for Germany⁶ and for the UK⁷. The user may choose either of these as a baseline and then may convert these values and further modify them for use in his own country and currency by making suitable changes to currency conversion factors and inflationary factors. The effects of economic depreciation may also be considered.

Costs of moving people are defined in terms of transport costs, food and accommodation costs, loss of income costs and loss of capital services costs, eg housing, land and consumer durables, through depreciation once recovery recommences.

Food bans may be costed in terms of the amount of food which must be thrown away per year in terms of litres of milk, numbers of livestock or areas of crops.

Health effects may be modelled using one of two approaches. The human capital approach assigns a cost for each health effect based on cost of treatment, loss of income during illness or treatment and, where the effect is fatal, the loss of income as a result of premature death. The subjective approach quantifies the cost of each health effect by representing an individual's aversion to that type of effect. This reflects either the amount of money an individual would accept in order to compensate for an increase in risk of suffering a particular effect, or the amount he or she would pay in order to reduce this risk by a given amount.

3.1.4 Ingestion model

The only ingestion doses considered by version 1 of PC COSYMA were the collective doses which were calculated from the agricultural production assuming that all food produced is consumed somewhere. No calculation of individual ingestion doses or radius dependent doses was therefore possible. Version 2 allows the calculation of radius-dependent individual doses and risks assuming that all food is produced at the point of consumption. The doses are calculated for adults only. The user of the system is able to specify the consumption rate, which need not be the same as that used when calculating food doses for comparison with intervention levels, if food bans on the basis of dose are being used. Ingestion doses used in calculating collective doses and health effects continue to be obtained using data on the agricultural production grids, with the assumption that all food produced is consumed somewhere.

The data base of food concentrations as a function of time produced by the NRPB model FARMLAND has been extended to include a pork concentrations. The FARMLAND model has also produced new concentrations for the fusion nuclides. Work at GSF has also provided an extended file of food concentrations from the ECOSYS model. The differences in the two models has meant that the ingestion calculations must be kept separate for each model. The user must choose whether to use the FARMLAND or ECOSYS models when choosing ingestion. The package then produces agricultural production data appropriate for the list of foods included in each of the models, see table 3.1.

TABLE 3.1 Foods included in the FARMLAND and ECOSYS models

FARMLAND	ECOSYS
Milk	Milk
Cows meat	Beef
Cows liver	Pork
Pork	Grain
Sheep meat	Potatoes
Sheep liver	Leafy vegetables
Green vegetables	Non-leafy vegetables
Root vegetables	Root vegetables
Potatoes	
Grain	

3.1.5 Additional countermeasures

Food bans

Version 2 gives the user the option of defining food bans on the basis of potential ingestion dose as well as on activity concentrations in food. For bans on the basis of activity concentrations, the user may set intervention levels for initiating and withdrawing bans in each of the element groups strontium, iodine, α -emitters and other long-lived elements for 'milk and cream' and for other foods. The definition of long-lived elements is those with a half-life greater than 10 days. This parameter may not be changed in the PC version.

For bans on the basis of dose, the user may set dose intervention levels for each of the foods and for a particular age group. Different levels may be set for the effective dose and for the thyroid dose. The user may specify consumption rates for each food.

Sheltering

Version 1 allowed the user to reduce the risks of early health effects by sheltering on the basis of a dose level. Version 2 allows there to be an additional geometric area within which sheltering is the only countermeasure against the risk of early effects. The user defines a distance to specify this circular area.

The option to shelter in a pre-defined radius to reduce the risks of long term effects has been removed.

Resettlement and decontamination

The dose integration time over which doses are integrated to determine whether people can return from relocation may be set by the user in version 2. The default values are 1 year for all pathways included in the determination of relocation. The dose reduction factors which are applied to the doses for determining resettlement in the case of decontamination may be set for each time period defined by the user. This allows the modelling of time varying decontamination techniques.

3.1.6 Calculations at a specific point

Standard applications of PC COSYMA calculate consequences in the population as a whole. Version 2 has incorporated the changes in the mainframe package which allow the calculation of probability distributions of consequences at a point. For calculations at a specified point, no averaging of results over sectors is performed. No calculations of consequences in the population are allowed in the same run. The user defines the point of interest by specifying a direction and a distance. The program calculates results at this distance and to within 2.5 degrees of the point, by defining a suitable polar grid around the site of the accident.

3.2 Further development of data files

3.2.1 Gridded data

Revised population and agricultural data for the whole of Europe are included. These have been supplied by CEA and by users of the system for their own countries. Gridded data for animal numbers and crop areas are now included to allow the calculation of the economic impact of accidents on the agricultural practices in a region. A pork grid has been derived in order to obtain collective ingestion doses from pork. The grids are based on the same basic data used with the mainframe version, and described in section 2.2.4 of this report. However, a grid size of 100 km² is used for PC COSYMA, while the mainframe version uses a grid size of 25 km².

The latitudes for the available data have been extended to include the region 34.7° to 68.4° N. The option for the user to include his own gridded data in the near range close to the site has been extended to include agricultural production as well as population. The user must provide a single file containing near range data for population and then as many of the agricultural grids as he has data available.

Version 1 gave some confusion concerning the definition of the near range grid. The previously labelled '1 km' grids were unhelpful as the extent in kilometres of the near range grid varies considerably between the lower and upper latitudes in order to maintain each grid at a constant area of 1 km². The term near range data, the referencing of the grids as having grid elements with areas of 100 km² and 1 km² and a fuller description in the user guide as to how to calculate the extent of the near range grid for a chosen site-latitude has made this valuable option clearer.

3.2.2 Radionuclides and dose libraries

A complete revision of the dosimetry files for inhalation and ingestion based on ICRP 60 and including the new respiratory tract model has been made. The number of radionuclides has been increased from 145 to 197 to include those for fusion reactors. PC COSYMA considers the same list of nuclides used with the mainframe version, and given in table 2.3. The number of nuclides considered in one run of the system has been increased from 50 to 60 with an increase in the number of hourly release phases from 3 to 6. The user may now define for himself the release fraction group to which each element belongs.

The default reactor inventory remains that of a PWR. An inventory for a VVER reactor has been supplied by KFKI Budapest and may be loaded into the system by the user.

3.2.3 Hourly meteorological data

As well as a data file containing 1 year of hourly weather conditions for a site in Western Europe, KFKI Budapest have supplied similar data which may be more appropriate for a more central European site. Suitable starting times for running the meteorological sampling program are supplied with both these data.

3.3 Additional Endpoints

For probabilistic runs, the probability distributions have been extended to include air and ground concentrations and short and long term doses and risks. CCDFs of all quantities are presented at two distances specified by the user. Percentiles are presented as a function of distance.

Short and long term doses are presented as a function of nuclide contribution to total dose as well as a function of pathway. For deterministic calculations, doses and risks can be presented at every grid point to obtain a far more thorough picture of the effects of the accident in space. Long term individual doses and risks include the contribution from ingestion and indicate the contribution of each route of exposure. The presentation of short-term effective dose is now possible. The user may choose between effective dose (ICRP 60) or effective dose equivalent (ICRP 26) in the calculations of all dose quantities, be it for individual doses with or without countermeasures or for doses used for initiating countermeasures. The same choice is used throughout.

Economic costs are presented for early and late health effects and for countermeasures, with a percentage contribution for each separate countermeasure.

3.4 The PC package

All parts of the calculation processes, ie the input of parameter values, the generation of site-specific gridded data, the main calculations and the viewing and storing of results, are driven from a single screen, where the user selects between the input interface, the calculations and the results interface.

3.4.1 The Input Interface

The input interface has been revised to include the parameters required for the user to access the revised data libraries and models described above. The co-ordinates of the site, the inclusion of site-specific data for population distribution including higher resolution near-range data and the division of the region into sectors and distance bands are all now contained within the input interface. The user may retrieve the specification of a previous site when defining a new site. Near-range site-specific agricultural data may now be included together with a local population. Longitudes for the near-range grid are now specified in degrees.

In the section on meteorological sampling, the user may now provide a text file of starting times and probabilities. The season of the year should also be supplied in the case of runs including the ingestion pathway to allow the correct food chain data library to be accessed.

For calculations at a specified point, the options for setting up the met. sampling input parameters are reduced. The user must define the total number of sequences to be run. The program then drives the met. sampling program such that all but three of the wind directions chosen cross the point of interest.

A large fraction of the computing time in probabilistic runs is taken in generating the normalised air concentrations as a function of space and time. The option of using a previous file of normalised air concentrations is available to the user. This reduces the computation time, but similarly forbids the user from making changes to the spatial distribution used and the definition of some of the release parameters.

In the source term section, the user may retrieve and edit a previous inventory and release parameters independently of any other previous parameters. This may be useful when looking at the effects of different releases on a defined countermeasures scenario. The total activity released may be scaled by a specified amount. This affects the total inventory for each nuclide.

Parameter values and results for each run may be saved to a unique sub-directory specified by the user. This allows the user to store on the PC parameter values and sets of results for 30 runs at a time, if suitable disk space is available. Edit fields of parameter values now allow insertion, deletion and overwriting of characters. Menus are clearer to understand; titles are shown in yellow and options which are not allowed are 'hidden' from user selection.

3.4.2 The Results Interface

The results interface has been enlarged to accommodate all the additional endpoints described above. Endpoints may be presented as tables or in a graphical presentation of either graphs, pie-charts or a pictorial representation of countermeasures at each grid point. The options for saving

all or a selected part of the results for report presentation have been increased. The menu selection is improved by means of a better structuring of the endpoints available to the user. There are similar options for early and late parts of each endpoint.

The main improvement to the results interface is in the split screen presentation of tables with an accompanying graphical display, as illustrated in Figure 3.1. The screen includes pull-down menus allowing the user to re-display the data in a different way, change titles and labels and in the saving and retrieving of previous and current results. The tabular or graphical presentations can be expanded to fill the whole of the screen. The system determines the appropriate presentation for each endpoint.

The results interface now has two modes of operation, interactive or automatic. The interactive mode is the default and allows the user to view all the results for each of the endpoints selected in any order. The automatic mode has been designed to present an overview of the more common endpoints of the system. These are saved automatically by the system and then may be viewed in turn by the user. The user is given only the choice of presentation in the form of tables or graphs. In both modes, selected results are saved to a file and may easily be retrieved later without having to repeat the decision tree of various menus in order to reach the desired endpoint.

The results interface also contains a number of other new features. Printer drivers are directly linked to the system to allow either direct screen printing or for the user to save data from a screen for later printing. The user may choose from a library of printers and the system saves this choice for use in later runs. An ASCII text file of an entire table or selected columns may be produced. All results screens may be saved to a file and recalled later, so giving the user the ability to present at a later time a subset of all the results calculated.

Separate from the results interface is a single ASCII text file produced by the calculation programs which contains all the results calculated by the system in a format similar to the output from the mainframe version.

3.5 Training courses

Three training courses on the use of PC COSYMA have been held during this period. The first, held in the UK in 1993, was organised by NRPB. The second, held in Kiev Ukraine in 1994, was organised by the Institute of Mathematical Machines and Systems of the Cybernetics Centre. The third, held in Madrid Spain in 1995, was organised by CIEMAT. In all cases, the courses included lectures on the models and assumptions in the system, demonstrations of the system and practical sessions in which the students could use the system. The lectures and demonstrations were given by staff from NRPB and FZK. The courses have been attended by more than 100 people from 26 countries. The first and second courses were concerned with the use of version 1 of PC COSYMA, while the third course dealt with a prototype of version 2.

3.6 Applications of mainframe and PC COSYMA

The mainframe and PC versions of COSYMA have been used by a number of organisations other than NRPB and FZK, the code developers, outside the MARIA project. This section briefly mentions some of these applications to show the ways in which the systems are being used.

FZK has performed studies to quantify the dependence of the areas affected by evacuation and relocation on the amount of radioactive material released⁹. The lower reference levels of the German regulations were used for the intervention criteria. The results show that in general the area affected is proportional to the source term. If the source term includes a release of 100% of the noble gas inventory, the affected areas remain constant for releases with less than about 1% of the remainder of the reactor inventory. The investigations also showed that ground level releases with 100% of the noble gas inventory and up to 1% of the iodine, caesium and tellurium inventory lead in 95% of all weather situations to affected areas which are covered by the existing German planning zones. Using these results, the German Reactor Safety Commission concluded that the emergency planning zones do not need to be extended as the frequency of releases larger than the ones considered have been reduced as far as is possible.

FZK has investigated¹⁰ the new generation of PWRs under discussion in Europe. The study showed that significant off-site emergency measures, such as evacuation or relocation, would not be required for a future 1400 MWe PWR even following a severe core melt if it had a double containment with the annulus vented through an appropriate emergency standby filter. A set of parameters for accident conditions have been elaborated under which the lower reference levels for evacuation will not be exceeded.

A third FZK study¹¹ was part of the licensing procedure for upgrading the BER II swimming pool reactor from 5 to 10 MW with HEU or LEU fuel elements. The consequences of an airplane crash were considered. The radiological consequences for the different types of fuel were found to show no significant differences.

COSYMA has been used in the Netherlands as part of the safety assessments for its two nuclear power stations^{12,13} and for the research reactor at Delft Technical University¹⁴. COSYMA has been used to investigate the consequences of an airplane crash onto the research reactor at Rossendorf, Germany, and the resulting doses compared with the intervention levels for countermeasures¹⁵. PC COSYMA has been used to investigate the consequences of a postulated loss-of-coolant accident with core melt at the Democritus research reactor in Greece¹⁶.

COSYMA has also been used in a study to investigate the dependence of accident consequence assessments for nuclear power plants on the different environmental characteristics between Korea and Germany¹⁷. For this study, data libraries appropriate for Korean conditions, such as food chains, had to be prepared.

PC COSYMA was used by the Institute of Radiation Hygiene in Russia to reconstruct external doses following the Chernobyl accident¹⁸. External doses from deposited material calculated with PC COSYMA were compared with observed values. Good agreement between the observations and predictions was obtained.

KFKI-AERI¹⁹ has used PC COSYMA to calculate consequences of hypothetical accidents at the Paks nuclear power plant in Hungary, as a step in emergency planning. Consequences were calculated assuming that countermeasures would or would not be implemented, and so the effect of implementing countermeasures could be seen.

IPSN²⁰ has used COSYMA to determine whether or not the health effects following an accident could be detected by an epidemiological study. The study showed that the statistical power of an epidemiological study would depend on the dose cut-off considered.

References for section 3

- 1 COSYMA A new program package for accident consequence assessment, FZK and NRPB, EUR Report 13028, (1990)
- 2 Jones, J.A, Mansfield, P.A., Haywood, S.M., Nisbet, A.F., Hasemann, I., Steinhauer, C. and Ehrhardt, J., PC COSYMA: An Accident Consequence Assessment Package for use on a PC, EUR Report 14916, CEC (1993)
- 3 PC COSYMA Version 1 User Guide, NRPB and FZK, EUR 14917, NRPB-SR259, (1993)
- 4 Jones, J.A, Mansfield, P.A., Haywood, S.M., Hasemann, I., Steinhauer, C., Ehrhardt, J. and Faude, D., PC COSYMA: An Accident Consequence Assessment Package for use on a PC, EUR Report 16239, EC (1995)
- 5 PC COSYMA Version 2 User Guide, NRPB and FZK, EUR 16240, (1995)
- 6 Faude, D., COSYMA Modelling of Economic Consequences, KfK Report 4336, (1992)
- 7 Haywood, S.M. and Robinson, C.A., COCO-1: Model for Assessing the Cost of Offsite Consequences of Accidental Releases of Radioactivity, NRPB-R243 (1991)
- 8 Kovari, M., Effect of delay time on effectiveness of stable iodine prophylaxis after intake of radio-iodine, J. Radiol. Prot. 14, 131-136 (1994)
- 9 Ehrhardt J and Qu J. Neue Ergebnisse von Studien mit dem Programmsystem COSYMA und ihre Relevanz für den Strahlenschutz. SSK-Band 25: Notfallschutz und Vorsorgemaßnahmen bei kerntechnischen Unfällen. p 120-144 Gustav Fischer Verlag, Stuttgart, ISBN 3-437-11520-0 (1993)
- 10 Keßler G, Kuczera B and Ehrhardt J. On the confinement of the radiological source term during beyond design basis events in future pressurised water reactors. Nuclear Technology. To be published.
- 11 Böhnert R, Rödder P, Ehrhardt J, Axmann A and Buchholz H. Differences in the radiological effects of a major accident using HEU or LEU fuel elements at the BER II. Proc of the 16th International Meeting on Reduced Enrichment for Research and Test Reactors, 3-7 Oct 1993, Oarai, Ibaraki, Japan.
- 12 Environmental Impact Report, Modification nuclear power plant Borssele. KEMA report 53388-KET, (1993)
- 13 Environmental Impact Report, Modifications nuclear power plant Dodewaard, GKN report 94-008/GKN/R (1994)
- 14 Wonderen E van. Consequence analysis of the design base accident for the higher education reactor in Delft. KEMA report 40288-NUC 93-5775 (1993)

- 15 Franke E. Berechnung radiologischer Auswirkungen potentiell schwerer Unfälle auf dem Forschungsstandort Rossendorf mit dem Programm COSYMA. Report VKTA-14 (1994)
- 16 Synodinou. Risk evaluation of a research reactor in a large population centre. Presented at the COSYMA User Group Meeting, Arnhem, April 1994.
- 17 Kim B-W and Han M-H. A comparative accident consequence assessment for a Korean and a German nuclear power plant. Presented at a Technical Committee meeting on Guidelines on Probabilistic Consequence Assessment, Vienna, IAEA, Nov 1992.
- 18 Danilova I O, Golikov V Yu, Balonov M I. Attempt of use of program COSYMA for reconstruction of external doses in Bryansk region after the Chernobyl accident. Presented at the 2nd COSYMA user group meeting, Budapest, 1995
- 19 Comparing the environmental consequences of hypothetical accidents at VVER installations of Hungary. L Sagi and L Koblinger. Presented at the 2nd COSYMA user group meeting, Budapest, 1995
- 20 Mansoux H, Verger P, Thomassin A. Use of COSYMA in design of epidemiological plan. Presented at the 2nd COSYMA user group meeting, Budapest, 1995

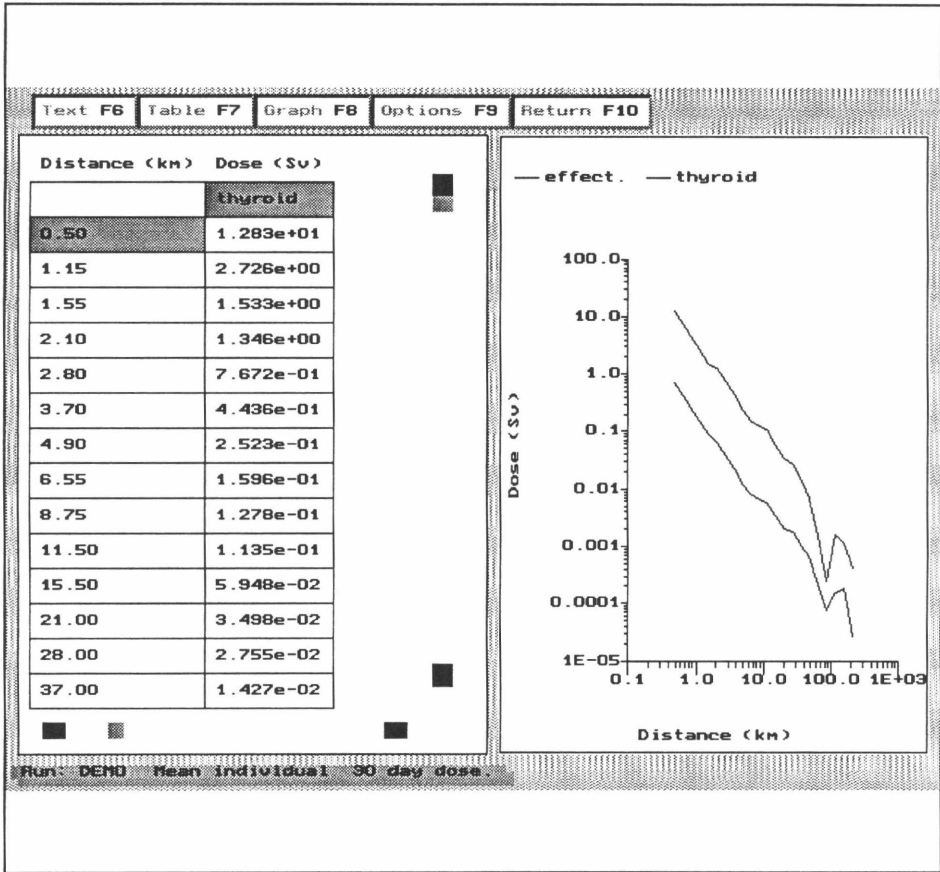


FIGURE 3.1 An example of the presentation of results in tabular and graphical form

4 ECONOMICS MODELLING

The modelling of the economic consequences of accidental releases of radioactive material to the atmosphere is one of the main endpoints of several ACA codes. However, as it was observed in the conclusions of the last CEC/NEA Benchmark Exercise, this is the least mature area of PCA modelling, with a need identified of research on the potential importance of indirect costs that were not modelled in any of the existing PCA codes. For that reason, one of the main topics in the project has been economics modelling.

Two participant institutions have put significant efforts in this field: FZK and UPM. The first with the development of an extended ECONOMICS module of COSYMA, and the second with a study of new methods and the coupling of new economics models to COSYMA as an option. The result is a varied set of optional models that can be used with COSYMA, depending on the objectives of a particular study and on the availability of data. A detailed comparison of the modelling characteristics in each case is available in the Proceedings of the last COSYMA User's Group Meeting(1). An overall description of the research and results obtained is presented in the following sub-sections.

4.1 *Extension of the COSYMA-ECONOMICS module*

FZK has developed an extension of the ECONOMICS module of COSYMA in order to take into account more regional or local economic peculiarities around a nuclear site. This is more important with respect to the "movement of people" countermeasures, for which the dominant cost categories are "loss-of-income costs" and "costs of lost capital services". In the original version of the ECONOMICS module these costs are calculated on the basis of the total number of people moved -together with the respective unit cost values *per capita*.

In the extended version, the calculation of loss-of-income costs and costs of lost capital services is based on the number of employees in different economic sectors (instead of the total number of people) in the evacuation or relocation area; the corresponding unit cost values have to be provided in this case on a *per-employee* basis, distributed in up to 18 economic sectors.

Comparative calculations have shown that the advantage of the new procedure is evident for small areas of evacuation or relocation, or if only one single weather sequence is considered. On the other hand, the larger the affected areas become, the more the local peculiarities of the economic situation tend to approach the nation-wide average. Therefore, the extended version has been implemented only for the near-range versions of COSYMA, ie NE (evacuation) and NL (relocation). It has not been regarded as reasonable to extend the FL version because in that case large relocation areas would be considered by definition.

4.2 *Incorporation of MECA2 in COSYMA*

MECA2 (Model for Economic Consequence Assessment)¹ is a computer model for the probabilistic assessment of the off-site economic risk derived from nuclear reactor accidents. Its development by the UPM started in 1987 in the framework of the MARIA-2 project. The first versions were coupled to the U.S. ACA code MACCS²; linked to it, MECA2 participated in the CEC/NEA PCA code Benchmark exercise.

A comparison was needed between the MECA2 model and the COCO-1 model³ which is the model implemented in the ECONOMICS module of COSYMA. The easiest way of undertaking this comparison was to implement the MECA2 model into COSYMA, as an alternative economics model. Together with the Benchmark results, in which no large differences in results were observed, this complements previous theoretical comparisons.

MECA2 has been coupled to COSYMA as a post-processor independent module. No modifications in the main COSYMA system have been made. The MECA2 program can now read the information in the databases used by COSYMA: population, land-water distribution, economic regions, crops and livestock products distribution. This simplifies the preparation of data files, and the program can be run with no additional data sets, only with the user input file containing the needed information.

The description of the accident and weather sequences that should be analysed by the model is transferred from COSYMA through the corresponding intermediate results files containing the sample of weather sequences, the flags for the kind and duration of the countermeasures in each element of the calculation grid, and the number of health effects estimated by COSYMA.

Economic estimates made for each weather sequence are stored and processed producing CCDF curves and percentiles for a large number of related consequences (not only costs, but also amounts of persons, areas or produce affected by countermeasures).

The main differences between COCO-1, the "normal" ECONOMICS model in COSYMA, and MECA2 come from: (1) the cost of interdicting and abandoning areas in case of a relocation of the population, with different categories of property and depreciation rates considered; (2) the cost of food banning, which is based in the amounts of different products lost in the first year, and in the GDP per employee for the subsequent years; (3) the cost of health effects, which uses a valuation of direct medical care costs plus subjective compensation costs.

The tests performed have include an intercomparison of results for three hypothetical scenarios, based on two real Spanish nuclear sites. The calculations were made using generic source terms, taken from the specialised literature, and merging meteorological data measured at different sites so that the conditional probabilities obtained are not representative at all of the site atmospheric conditions. The only truly representative data for the sites were the economic-relevant data, such as the distributions of the population, agricultural and livestock products, crop areas, and more specific data like the Gross Value Added at factor cost by economic sectors. It is important to note that the results obtained are thus only valid for economic modelling intercomparison purposes, and they do not represent the risk or the consequences associated with any real site.

The main characteristics of the three cases studied are summarised in Table 4.1, and the mean values obtained for each of the runs are included in Table 4.2. In these calculations, the same weather sequences and patterns of countermeasures calculated by COSYMA are used by MECA2 to assess their economic impact. The first important conclusion is that there are no big differences in the predicted consequences due to the differences in the economics models used. However, some trends can be observed, and are probably amplified by the site characteristics. In general, for the relocation of people MECA2 predicts higher values than ECONOM, probably due to the differences in modelling the costs of interdiction.

MECA2 can calculate decontamination costs using a more complete data base on decontamination techniques and costs for different types of surfaces than that used by COCO-1. However, for this case, it was limited to only one type and technique, as done in COSYMA. MECA2 predicts a slightly lower cost than COCO-1. Food bans are always a very important item, and the differences in the models and categories of costs considered in both models result in opposite behaviour depending on the scenario; this may reflect the greater detail considered in MECA2. Finally, for health effects MECA2 normally results in smaller costs, at least for stochastic effects.

Looking to the probability distributions, Figure 4.1 shows the CCFD curves produced by both models for the Zorita scenario A. It can be seen that relocation and health effect costs seem very similar for the two codes. MECA2 relocation costs are always higher and health effect costs smaller, and the most significant differences are attributable to food ban costs. Figure 4.2 displays the curves for Vandellós scenario B, in which again relocation and health effect cost curves are very close. However, the curves for food ban costs are difference, but the higher values are now given by MECA2.

The results for food bans costs are strongly influenced by the assumed countermeasures; basically a complete disposal of crops in the first year, and withdrawal of land in the following years if food contamination would be above permissible levels. Therefore, the modelling of alternative countermeasures for food is considered as a priority before trying to improve cost assessment for food countermeasures in PCA codes.

4.3 Development of new methods for the study of direct and indirect economic impact

One of the objectives of the research was to evaluate the economic impacts of the accidents on both the area directly affected, and the areas which have economic relations with the area directly affected. In agreement with other authors^{4,5} the Input-Output methodology has been considered the most appropriate for the study of such effects, and a simple Input-Output model has been developed, tested and incorporated in the MECA code, thus allowing to run it in connection with COSYMA. Before that incorporation, two different scenarios were analysed by a separate economist team of the Economics Department at ETSII-UPM. Their conclusions were very useful for the final development of the model.

The Input-Output economic analysis is based on the transactions existing between all the economic sectors. The model used is a "demand model" (*demand driven*), which considers that the variations in demand will influence the output level and the amount of productive factors employed. Their basic structure is described from the Input-Output table characteristics.

	S_1	S_2	...	S_n	DF_i	O_i
S_1	X_{11}	X_{12}	...	X_{1n}	DF_1	O_1
S_2	X_{21}	X_{22}	...	X_{2n}	DF_2	O_2
...	X_{ij}
S_n	X_{n1}	X_{n2}	...	X_{nn}	DF_n	O_n
F_j	F_1	F_n	...	F_n		
I_j	I_1	I_2	...	I_n		

Where:

- S_i - Economic Sectors.
- DF_i - Final demand of each sector: private and public consumption, investment, stock variations and exports.
- F_j - Payments to the productive factors of each sector: GVA at factors cost, indirect taxes, subsidies to companies and imports.
- O_i - Output or total production of each sector.
- I_j - Input of each sector.
- X_{ij} - The production sold by sector i to j

The technical coefficients are defined as: $a_{ij} = X_{ij} / I_j$

And expressed as matrices, since for the same economic sector ($i=j$) the input is equal to the output ($I_i = O_j$), it can be expressed as $\{DF_i\} = \{I-A\} \cdot \{I_j\}$, where $\{DF_i\}$ is the array column of final demand, I is the unit matrix, A is the technical coefficient matrix, and I_j is the array column of total outputs (=inputs). The matrix $\{I-A\}$ is usually known as Leontieff's matrix, and inverting it, the variations in Inputs could be expressed as a function of the variations in the final demand $\{\Delta I_j\} = \{I-A\}^{-1} \cdot \{\Delta DF_i\}$.

Therefore, the model can be used to evaluate the impact on the total production of an economic system, in case of variations in their final demand. Countermeasures implemented in a given area will directly affect the demand of that area, and also that of the surrounding regions. The basic assumptions implicit in the model are as follows:

- As the Input-Output tables are not normally available at regional level, the technical coefficients will be taken as identical to those at the national level. The implication of this assumption is that the technology and efficiency are the same as at national level. Thus a single I-O table is needed for use in the model, and it is adapted to the region studied taking into account the GVA of the region and its population.
- Different Input-Output tables are built for the affected area and for the surrounding areas, so that the effect of the time evolution and the nature of the impact of the accident could be considered (eg some zones will be relocated for a longer time than other). The

distribution of GVA by economic sectors in the affected and non-affected areas is used to adapt the I-O table to the peculiarities of each, and to estimate economic flux between both areas, that will be stopped in case of a population relocation.

- In case of population relocation, the full final demand of the affected areas will be lost, thus inducing an Output loss. For the surrounding regions, a loss will come from the loss-of-demand normally associated with the relocated area (no exports can be made during the relocation period to the affected area); but also positive effects can be estimated from the consideration that private consumption of the relocated population is transferred to the non-relocated areas, thus originating an increase in their final demand, and an output increase at the end.

The MECA2 plus the new model has been renamed as MECA3, and it can use the new model as an option, or the previous MECA2 model. A reference guide has been prepared for the users, and some test cases have been analysed, based on the same scenarios described above. The basic results are presented in Table 4.3. For the Vandellós scenarios, since an I-O table is available for Catalonia, it was used as a test to compare with the results using the national I-O table of Spain. No significant differences were observed, thus indicating that, probably, for many sites within a given country, the non-availability of specific I-O tables is not a serious limitation for the kind of exercise that ACA represents.

Probably, the most interesting conclusion is that positive effects in the areas non-directly impacted by the countermeasures can largely overcome the negative effects in the same regions. This can be only partially true since, as the deterministic studies performed have shown, for peculiar sites like Vandellós that have a very important tourism sector, if that sector would be paralysed it could represent as much as $4.16 \cdot 10^5$ MPTA. This is true even for relatively small releases, since these effects are more of psycho-sociological nature, and are not amenable to be included in a PCA model. Needless to say that such effects, of course, would also not be strongly affected by the criteria followed to implement countermeasures, but more by the public attitude shown by the authorities with respect to the affected populations.

4.4 References for chapter 4

- 1 Gallego E., "MECA2. Model for Economic Consequence Assessment, Version 2. Reference Guide". Report CTN-43/92. Cátedra de Tecnología Nuclear, UPM (1994).
- 2 Jow, H-N., Sprung, J.L., Rollstin, J.A., Ritchie, L.T. and Chanin, D.I., "MELCOR Accident Consequence Code System (MACCS). Model Description". U.S. NRC Report NUREG/CR-4691, (SAND86-1562), Vol.2. Sandia National Laboratories (1990).
- 3 Haywood S.M., Robinson C.A., Heady C., *COCO-1: Model for Assessing the Cost of Offsite Consequences of Accidental Release of Radioactivity*. Report NRPB-R243. National Radiological Protection Board (1991).
- 4 Assouline M., *Evaluation des conséquences socio-économiques d'une évacuation de population en cas d'accident grave d'origine industrielle*, CEA-IPSN, Département de la Protection Sanitaire, (1984).
- 5 Cartwright, J.V., Beemiller, R.M., and Gustly, R.D. *Regional input-output modelling system (RIMS-II); estimation, evaluation and application of a disaggregated regional impact model*. Washington, Department of Commerce (1981).

TABLE 4.1 Main characteristics of three hypothetical scenarios.

- Scenario A: Zorita site (Guadalajara).
N.P.P. Westinghouse PWR - 1 Loop. 160 Mw_{th}, 510 Mw_e.
- Scenarios B & C: Vandellós site (Tarragona).
N.P.P. Westinghouse PWR - 3 Loop. 2775 Mw_{th}, 992 Mw_e.
- End of equilibrium cycle inventories for 60 radionuclides.
- Source terms representative of LOCA with core fusion and late overpressure containment failure (A & B) or explosive early containment failure (C).

Source term characteristics							
	A) CLUSTER 27 Zion (NUREG-1150)		B) RZ2 Zion (NUREG/CR-6094)		C) CLUSTER 11 Zion (NUREG-1150)		
			A	B	C		
Start of release (from reactor scram)			7.90 h	12 h	2.4 h		
Release duration			1.82 h	3 h	5 h		
Warning time (from reactor scram)			5.75 h	5 h	0.4 h		
Thermal power in the release			2.5E+5 w	-	5.0E+6 w		
Height of the release			10 m	10 m	10		
TOTAL RELEASE FRACTIONS BY RADIONUCLIDE GROUPS							
	Kr Xe	I	Cs Rb	Te	Sr Ba	Ru	La Ce
A	9.3E-1	8.0E-2	9.7E-3	5.3E-3	5.0E-4	3.4E-6	7.0E-5
B	1.0	3.0E-2	6.0E-6	7.0E-6	1.0E-6	2.0E-8	1.0E-7
C	9.2E-1	1.8E-1	7.0E-2	3.4E-1	1.2E-1	4.0E-2	5.0E-2

Countermeasures criteria:

- Short-term emergency actions (evacuation, sheltering, iodine prophylaxis) according to Spanish regulations.
- Population relocation criterion: 10 mSv effective dose in 30 days.
Resettlement: 50 mSv in 365 days.
- Food ban criterion: 5 mSv in 1 year (COSYMA default values).

**TABLE 4.2 Mean values of economic consequences for three hypothetical scenarios
Zorita scenario A**

Economic cost (MPTA)	COSYMA 93/1		ECA2	
Relocation of population	5.01 10 ²	3.2%	7.66 10 ²	9.8%
Decontamination	8.40 10 ⁰	0%	5.45 10 ⁰	0.1%
Food Bans	1.14 10 ⁴	72.2%	3.74 10 ³	48.1%
Early Health Effects	0.0	0%	0.0	0%
Late Health Effects	3.89 10 ³	24.6%	3.27 10 ³	42%
Total Costs	1.58 10 ⁴	100%	7.78 10 ³	100%

Vandellós scenario B

Economic cost (MPTA)	COSYMA 93/1		MECA2	
Relocation of population	1.38 10 ²	10.1%	2.02 10 ²	3.8%
Decontamination	0.0	0%	0.0	0%
Food Bans	6.94 10 ²	51%	4.72 10 ³	89.5%
Early Health Effects	0.0	0%	0.0	0%
Late Health Effects	5.29 10 ²	38.9%	3.51 10 ²	6.7%
Total Costs	1.36 10 ³	100%	5.27 10 ³	100%

Vandellós scenario C

Economic cost (MPTA)	COSYMA 93/1		ECA2	
Relocation of population	6.80 10 ⁴	33.8%	1.00 10 ⁵	43.2%
Decontamination	6.42 10 ³	3.2%	1.05 10 ³	0.5%
Food Bans	7.05 10 ⁴	35.1%	9.50 10 ⁴	41.1%
Early Health Effects	8.77 10 ⁰	0%	9.32 10 ⁰	0%
Late Health Effects	5.61 10 ⁴	27.9%	3.53 10 ⁴	15.2%
Total Costs	2.01 10 ⁵	100%	2.31 10 ⁵	100%

TABLE 4.3 Mean economic impact in the areas affected and non affected by the countermeasures for the three scenarios.

Zorita scenario A

Economic Impact (MPTA, 1989)	Total
Areas directly affected	8.30 10 ²
Areas non-affected, Loss of Input	1.48 10 ²
Areas non-affected, Increase of Input	4.78 10 ²

Vandellós scenario B

Economic Impact (MPTA, 1989)	Total (Spain I-O Table)	Total (Catalonia I-O Table)
Areas directly affected	2.44 10 ²	2.91 10 ²
Areas non-affected, Loss of Input	6.66 10 ¹	7.15 10 ¹
Areas non-affected, Increase of Input	1.14 10 ²	1.27 10 ²

Vandellós scenario C

Economic Impact (MPTA, 1989)	Total (Spain I-O Table)	Total (Catalonia I-O Table)
Areas directly affected	9.81 10 ⁴	1.19 10 ⁵
Areas non-affected, Loss of Input	8.86 10 ³	9.02 10 ³
Areas non-affected, Increase of Input	5.15 10 ⁴	5.73 10 ⁴

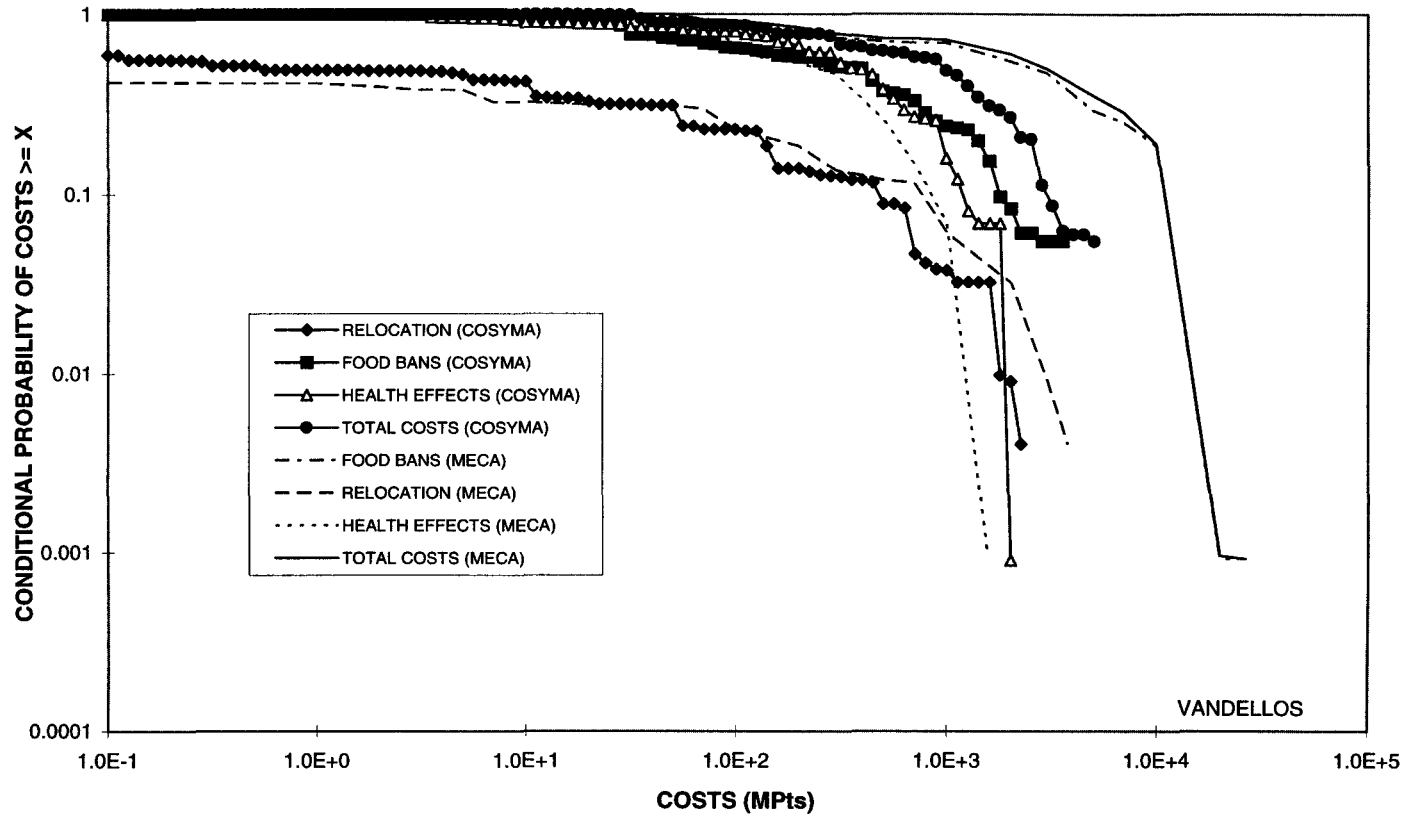


FIGURE 4.1 CCFD comparison between MECA2 and COSYMA for Zorita scenario A

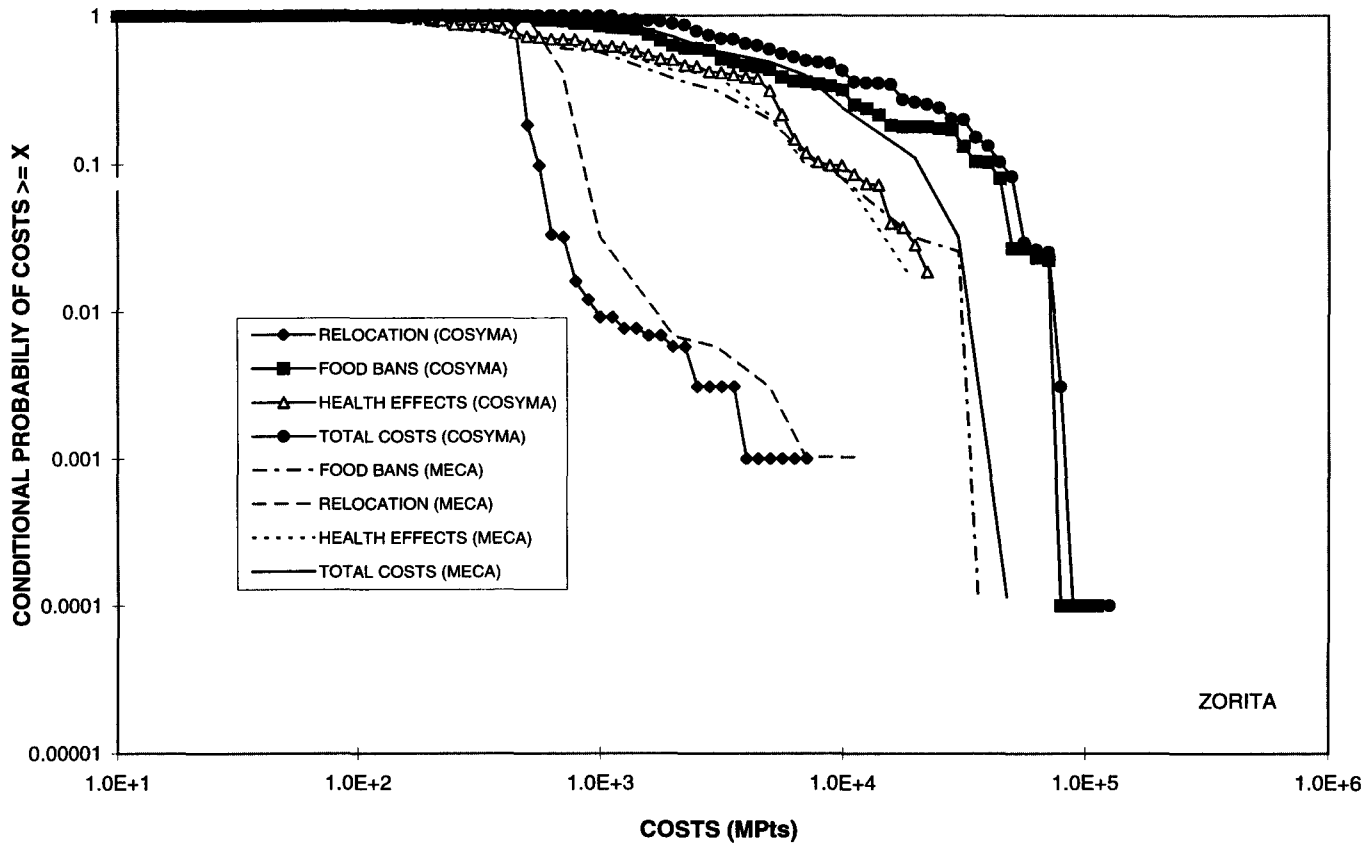


FIGURE 4.2 CCFD comparison between MECA2 and COSYMA for Vandellós scenario B

5 RESEARCH NEEDS FOR ACA PROGRAMS

COSYMA was developed under the EC MARIA project, which was initiated over 10 years ago and is now coming to an end. During this period the MARIA project has supported considerable work on the development of models for use in ACA codes, as well as the development of the mainframe and PC versions of COSYMA. The end of this project provides an opportunity to look at the current status of accident consequence modelling in general, and to comment on whether there are some areas where COSYMA might be further developed. A number of recent initiatives have related to the needs for further development of ACA programs. This section reviews these, and comments on them from the point of view of the needs for further development of the mainframe and PC versions of COSYMA. The section also compares and contrasts the major ACA codes available at present.

Throughout this section the term "COSYMA" refers to both the mainframe and the PC versions of the system. Where comments refer only to the mainframe or PC version, then this is specifically identified.

5.1 *Projects relating to ACA research needs*

There are several current or recent initiatives which relate to research needs for ACA codes, which are discussed in this chapter, namely

- the EC contract on behaviour of deposited material
- IAEA meeting, November 1994, on "Procedures and computer codes for level-3 probabilistic safety assessment"
- a meeting at NRPB, December 1994, to discuss the adequacy of the models in COSYMA and RODOS,
- the current EC contract on uncertainty analysis
- discussions at COSYMA user group meetings, where needs for further versions of COSYMA have been considered
- general research work not specifically related to MARIA or COSYMA.

5.2 *EC contract on behaviour of deposited material*

This contract¹ mainly involves experimental work into the behaviour of material after deposition in urban areas, though other areas such as deposition to skin, indoor air concentrations and washout have also been considered. The contractors are GSF, Germany; Riso National Laboratory, Denmark; Imperial College, UK; NRPB, UK; KFKI Atomic Energy Research Institute, Hungary; Institute of Radiation Dosimetry, Czech Republic and Institute of Radioecology, Slovak Republic. The main areas of interest are external γ dose from deposited activity and location factors, skin deposition, resuspension, indoor air concentration and indoor deposition. NRPB's involvement is to get agreement between modellers and experimenters on the adequacy of the current models and the parameter values used.

In the short term this could lead to new parameter values within the existing models. The default COSYMA values for the resuspension factor have changed as a result of this contract. New information has been provided for the deposition velocity to skin suggesting an increase of an order of magnitude in the deposition velocity generally used in consequence modelling. Further

information has been provided on location factors for external irradiation and for inhalation, which supports the values currently used in COSYMA. The contract has provided data which could form the basis of a review or revision of models for deposited γ dose, and particularly the penetration of material into soil, in the longer term. Unfortunately it has not yet been possible to examine these data as part of either this contract or the MARIA contract.

5.3 IAEA meeting

IAEA held a meeting on "Procedures and computer codes for level-3 probabilistic safety assessment codes" in November 1994². One of the aims was to identify needs of ACA programs. To some extent the needs depend on the specific code being considered, as the various codes include some different features. The meeting identified the following needs:-

- 1 Development of documents which provide guidance for the selection of appropriate values for code input parameters. The documents should comment on the application of the codes to extreme events such as earthquakes and floods, and to scenarios for which the codes were not specifically designed, such as long duration releases.
- 2 Incorporation of the capability for uncertainty analysis into ACA codes, and the completion of full generic (ie not site specific) uncertainty analyses.
- 3 The extension of ACA codes to consider long range atmospheric dispersion.
- 4 The extension of ACA codes to short range, and particularly to the calculation of on-site consequences - this was raised particularly in the context of sites in USA, which can be several tens of km across.
- 5 The use of averted dose to initiate countermeasures. Countermeasures are currently assumed to be implemented on the basis of the projected dose to individuals.
- 6 Incorporation of site-specific terrain modelling features. In particular, that code developers should investigate the feasibility of developing and implementing "simplified" complex terrain dispersion models.
- 7 The adequacy of currently available codes which model direct aquatic releases for probabilistic use. The need to extend codes for atmospheric releases to consider fresh water pathways.
- 8 The ability to handle non-reactor facilities, particularly areas such as expanded lists of radionuclides, dispersion following fires or explosions, source terms with high steam content and UF_6 dispersion.
- 9 The ability to handle different particle sizes.

The current generation of ACA codes is based to a large extent on the US code CRAC, developed in the 1970's. The models and data libraries have been updated, but the code structure is largely unchanged since then. It is reasonable to suggest that, if a new code were to be designed today, it would differ in many ways from the existing codes. In particular, the current generation of codes applies average values to many quantities and so do not model the full variation of doses and risks in the exposed population. A new code could use, for example, different values of deposition velocities for different grid elements depending on the underlying surface at each element. The meeting also suggested that sensitivity studies should be carried out to determine whether more detailed modelling is required for

- variation of deposition velocity with underlying surface
- age dependent risk factors and age dependent dosimetry

- deposited γ dose rates depending on the underlying surface (rural or urban)
- food chain concentrations for different regions or for different types of soil
- groups of people with different shielding factors.

The implications for COSYMA of these are as follows:-

1 Documentation

We believe that there is a considerable amount of information on the applicability of both mainframe and PC COSYMA, including descriptions of the models involved and guidance on the choice of parameter values. However, the material is spread among a number of publications (eg the user guides, reports on the systems, conference proceedings) and there would be some benefit in either drawing it together or compiling a list of available references.

At present there is no information on the adequacy of any ACA code for releases caused by earthquakes or floods. One of the aims of the COSYMA User Group is to provide a forum where people can discuss possible applications of the system, and any changes which may be needed if COSYMA is to be used for "unusual" applications. This could lead to such information becoming available in the future.

2 Uncertainty analyses

Uncertainty analyses require many runs of the computer codes with non-standard values of the parameters. The main feature of codes which makes this difficult is the inability to change the parameter values, either because they are obtained from data libraries or because they are "hard-wired" into the code. The use of data libraries cannot be avoided, as ACA codes require more "standard" values than can be provided in any other way. However, the mainframe COSYMA user guide includes a detailed description of the libraries, so that anyone wishing to replace them with their own libraries could do so. COSYMA provides default values for the many input parameters required. However, the user of the mainframe version can change the value for essentially all of the parameters through the input file. PC COSYMA enables the user to change a large number of the parameters, but is not intended for users who wish to alter data libraries.

A second feature of uncertainty or sensitivity analyses is the need to undertake many runs of only part of the whole system. The structure of mainframe COSYMA is such that the calculation can be started at any of the modules, using values for the quantities calculated in earlier modules from a previous run of the system. This means that sensitivity and uncertainty analyses of parts of the code can be undertaken without having to run the whole system each time.

A separate EC project is undertaking an uncertainty analysis of COSYMA. This is considered later in this chapter³.

3 Long range dispersion models

The mainframe version of COSYMA includes a separate module intended for use when calculating consequences at long distances from the source, and based on a trajectory model of dispersion which is applicable at long range. This is particularly useful when calculating

consequences within a region some distance from the site, rather than when calculating consequences in a large region including the site.

4 Short range dispersion modelling

No ACA code includes a dispersion model which is appropriate for releases from groups of buildings - in fact there is no simple dispersion model currently available for this situation which could be built into an ACA code. All codes therefore have only limited applicability to those situations where the only consequences of interest arise within a very short distance of typical nuclear sites. The modular structure of COSYMA is such that a short range model could easily be inserted in place of the standard model, were one to be available. Alternatively, results from such a model (or an experimental investigation) could be used with COSYMA by writing a file in the form produced by the dispersion module and starting the calculating after the dispersion step.

5 Dose averted

At present, no ACA code can initiate countermeasures on the basis of the dose averted. The COSYMA user group has established a sub-group to examine this problem, and plans are underway to incorporate some features of this in a future release of COSYMA. As many international organisations, include the EC, have recommended that countermeasures be initiated on the basis of dose averted, it is important that COSYMA should be extended to consider this.

6 Site-specific terrain modelling

The response to point 4 above covers this.

7 Aquatic releases and fresh-water pathways

At the IAEA meeting, it was indicated that for nuclear installations located at the shore of large lakes, accidents with direct releases to the surface water might contribute considerably to the total frequency of accidental releases. Also, as has been shown after the Chernobyl accident, in certain countries the indirect contamination of fresh-water systems by deposition of material released to the atmosphere can lead to substantial consequences, both for doses to certain population groups and particularly for the economic implications due to the long duration of the contamination in such ecosystems. The inclusion of models to assess, in a probabilistic way, the consequences contamination of fresh-water systems, either by direct liquid releases or following deposition from the atmosphere, seems therefore to be important.

8 Non-reactor facilities

The adequacy of current ACA codes for several aspects of modelling accidents at non-reactor facilities can be considered.

The nuclides likely to be released from such facilities may not be the same as those released in reactor accidents. The COSYMA data libraries include data for 197 nuclides. This list means that the system is applicable to most types of release provided that the released material is not heavier than air, or does not undergo chemical transformations which affect its dispersion or

deposition properties during the period in which it is dispersing. The libraries do not include tritium, but mainframe COSYMA includes a separate program (UFOTRI) for application to tritium releases. The ability to calculate the consequences of tritium releases using simple extensions to the normal dispersion model should be investigated to determine whether PC COSYMA could be easily extended to consider tritium.

The material released in accidents at some types of facility may be such that the standard dispersion models are not applicable. For example, accidents at enrichment facilities would release UF₆, which is converted to fluorine gas and uranium oxide during plume passage. These disperse in a different way to the original UF₆ effluent as the uranium oxide could be in the form of large particles and fluorine is less dense than air. Accidents at some facilities could involve releases with a high steam content. The steam would condense to water in the air, and could lead to much higher deposition than predicted by the dispersion models normally used in ACA codes.

The applicability of COSYMA to such releases should be carefully considered in any particular situation. Documents describing the ways in which COSYMA has been applied to such facilities are required. These could identify the problems encountered, and the way in which COSYMA was used to solve them. The COSYMA User Group is a possible forum for compiling a list of such applications.

9 Different particle sizes

The COSYMA data libraries are appropriate for an aerosol of 1 µm AMAD. COSYMA could be applied to different particle sizes by simply replacing the libraries, provided that the release could be described by a single particle size distribution, and that this distribution did not change during dispersion as a result of preferential deposition of the larger particles. This would be appropriate for a filtered release, where the aerosol size will be determined by the size range which can pass through the filter. Other cases would require modification to the coding.

This aspect may be less important than some other features considered in this section as, up to now, there has been little information available about the size distribution of the released aerosol.

Sensitivity studies

The modelling of the full variation of risk within the population is probably of more importance in real time codes than in ACA codes. However, it is a topic which has not been considered, and such sensitivity studies should be undertaken.

Mainframe COSYMA makes a limited allowance for some of these factors. The calculation of the numbers of late health effects includes considering age dependent doses and risks. However, it assumes that the same age distribution of the population for each grid location at which doses and risks are calculated. It also considers groups of people with different shielding factors when calculating the numbers of early health effects. Again, however, the fraction of the population with the different shielding factors is the same at each location. It also has a limited capacity to represent the variation of deposition velocity with underlying surface.

5.4 Model adequacy meeting

This was attended by the MARIA contractors and the EU contractors for the "deposition" contract. The original intention was to provide a means for pursuing NRPB's contractual commitments under these contracts, by allowing a discussion of the future needs for COSYMA and the implications of the experimental work under the "deposition contract". However, the objectives were extended to include the adequacy of the models in COSYMA and RODOS (a decision support system for use in real time following an accident⁴), and ways of maintaining those codes as "state of the art". A number of actions were placed, some requiring documents to be prepared for discussion at the deposition contractors meeting, and others for discussion at the COSYMA user group meeting.

The notes for discussion at the deposition contractors meeting were on:

- the time variation of the location factor for deposited γ dose in urban areas, including the effects of trees on the location factor, and the problems of averaging.
- the problems of using lawns as the reference surface for urban doses.
- the spatial and temporal variation of the location factor for air concentration in buildings, and to recommend the best average value for use in Europe.
- on deposition to and removal from skin, giving a current best value for the deposition velocity.
- note on the importance of including the dose to skin in COSYMA. The only component of dose to skin currently considered in COSYMA is the β dose from material on skin.
- the time variation of external exposure from deposited material on undisturbed land over Europe, and the best way of modelling this.
- the adequacy of the current parameter values for washout coefficient, in the light of the high values measured by GSF.

The conclusions from these notes have been incorporated into the final report for the deposition contract. That report concludes that further work is required in two main areas, namely the rates at which material is deposited to and removed from skin, and the improvement of models for calculating the external γ dose from deposited activity at times more than a few years after the deposition.

One note (on the implications of considering food countermeasures other than bans) was to be prepared for discussion at the COSYMA user group meeting. This note concluded that some actions could be included in COSYMA using modifying factors with the current data libraries while others may require the insertion of a limited food chain model within COSYMA. It also suggested that the countermeasures routine would require substantial changes to reflect the combination of different actions and the criteria with which they would be implemented.

The meeting suggested that the COSYMA user group should

- give advice on how to undertake site specific calculations in the near range, and to give guidance on the use of COSYMA in non-standard situations.
- to consider the need to include models for contamination of fresh water, considering both the doses and the economic implications of the contamination.
- consider the use of COSYMA for nuclear installations other than reactors.

- consider the need for, and the ways of, translating the PC COSYMA screens and user guide into other European languages.

The first three points here are similar to points raised at the IAEA meeting, discussed in the previous section. These points were discussed at the COSYMA User group meeting, as described in section 7 of this report.

5.5 *Uncertainty analysis contract*

This contract³ can be considered in two stages. In the first, the distributions of parameter values are being obtained using formal processes for eliciting expert opinion. In the second, a full uncertainty analysis of COSYMA will be undertaken.

The project could affect research needs in two ways. It will identify those parameters where the uncertainty makes a major contribution to the overall model uncertainty, and so indicate areas where research may be needed. It may also indicate areas where the current models are not consistent with experts' opinions, and where the models could be improved on the basis of current knowledge.

It is important that this project should continue.

5.6 *Other general research*

There is a project at Imperial College to do further work on deposition to and removal from skin. As noted above, it is important that work in this area should continue.

The VAMP project^{5,6} may provide validation of parts of the external dose models, and may lead to a continual review of model adequacy. This project has identified the long term predictions of soil migration as an area where there is considerable diversity between models. As noted above, this is an important area in which further work is required.

The JSPs and ECPs provide additional data for databases, particularly long term measurements and information on population habits⁷. Some of this information may only be appropriate for the CIS. It is important that the results of these studies should be evaluated to determine whether they can be used to improve models and data bases in COSYMA.

5.7 *The maintenance of data libraries*

COSYMA includes a large number of data libraries, for example gridded data files covering the population and agricultural production distributions over Europe, the various dosimetric files and files of the concentrations of nuclides in food for unit deposit. The need to extend the dosimetric and food chain files to include additional nuclides has been discussed above. There is a further need to ensure that the information for those nuclides currently included in the libraries is updated as and when research elsewhere enables improvements in the current values.

COSYMA requires information on the distributions of population and agricultural production in distance bands and sectors around the site of the release. This information is derived from gridded data covering the whole of Europe. For the countries of the European Union, the data

are derived from work carried out by CEA under contract to the Commission, and have a resolution of 100 km². Data for other countries have been derived from atlases and national statistics on agricultural production, and so are on a much coarser grid. The data used with even the 1995 version of COSYMA is old, particularly for the agricultural production distributions. There is a need to ensure that these distributions are updated for countries of western Europe, and that the resolution is improved for countries of eastern Europe.

5.8 Summary of recommendations

This chapter has commented on a number of recent initiatives to determine research needs for ACA codes, and several areas where further work is required have been identified. The main areas where work is required are summarised below.

- 1 The current exercise leading to an uncertainty analysis of the whole of COSYMA should be completed. This may also lead to the identification of further research needs when important contributions to the overall uncertainty are identified.
- 2 It is important that COSYMA should be extended to consider dose averted as the basis for initiating countermeasures.
- 3 Further experimental work to determine the rates at which material is deposited to, and removed from, skin should be undertaken. The importance of this pathway for ACA codes should then be reviewed.
- 4 Information is becoming available on the external γ dose from material deposited about 10 years ago from the Chernobyl accident. The experimental work in this area should continue. The possible revision of the models in COSYMA, to take account of the new data, should be considered.
- 5 COSYMA can be used for calculating the consequences of accidents at non-reactor facilities, though the user must be aware of the problems which might arise in this type of application. The writing of guidance documents for the application of COSYMA is important.
- 6 It is important that data libraries should be kept up to date, and that the number of nuclides included in the libraries should be extended where possible.
- 7 Work should be undertaken to investigate the adequacy of models for calculating doses from freshwater pathways, following either releases directly to water bodies or contamination of water bodies from releases to atmosphere.

5.9 References for section 7

- 1 Tschiersch J (Co-ordinator) Deposition of radionuclides, their subsequent relocation in the environment and resulting implications. Final report on contract FI3P-CT92-0038. To be published.
- 2 International Atomic Energy Agency. Proceedings of a Technical Committee Meeting on "Procedures and computer codes for level-3 probabilistic safety assessment", November 21-25 1994. IAEA, Vienna, J4-TC-835.2 (1995)
- 3 Goossens L H J et al, Results of the ongoing probabilistic uncertainty analysis study on COSYMA (and MACCS) for deposited materials and related doses - a joint EC/USNRC expert judgement study. Presented at the COSYMA user group meeting, Budapest June 1995, and to appear in the proceedings

- 4 Ehrhardt J et al. Development of RODOS, a comprehensive decision support system for nuclear emergencies in Europe - an overview. Rad Prot Dos. 50 (2-4) 195-203 (1993)
- 5 International Atomic Energy Agency. Modelling of resuspension, seasonality and losses during food processing. First report of the VAMP Terrestrial Working Group. IAEA-TECDOC-647 (1992)
- 6 International Atomic Energy Agency. Modelling the deposition of airborne radionuclides into the urban environment. First report of the VAMP urban working group. IAEA-TECDOC-760 (1994)
- 7 Kelly G N and Cecille L. CEC/CIS joint programme on the consequences of the Chernobyl accident. IN Assessing the radiological impact of past nuclear activities and events. IAEA-TECDOC-755 (1994)

6 CEC/OECD-NEA BENCHMARK

6.1 *The International Code Intercomparison Exercise*

The International Code Intercomparison Exercise on probabilistic accident consequence assessment codes initiated by CEC and OECD-NEA in 1991 was completed during the reporting period. After the pilot study and several revisions of the task specifications in the preceding contract period, NRPB and FZK agreed suitable input values and FZK carried out the required runs for the Benchmark tasks C1 to C10 until the beginning of the MARIA IV contract using COSYMA version 92/1. This version contained some modifications concerning the evaluation of results especially for the Benchmark exercise and the new health effects model of 93/1. It was only for internal use and was not distributed generally.

During an expert group meeting in Brussels in November 1992 the results predicted by the six participating codes were discussed and analysed and a document interpreting the differences was prepared. This draft report was presented at the 4th ad-hoc group meeting in Paris in January 1993 and intensively commented upon. Based on these discussions, SRD provided the Overview¹ and the Technical Report² in a draft version which was the subject of the final meeting in Madrid in April 1993. A final draft version was then sent out to the members of CRPPH and CSNI for comments. In 1994 both reports were published by CEC and OECD-NEA.

6.2 *The International COSYMA Users Intercomparison Exercise*

In the framework of this International Code Intercomparison Exercise, an internal intercomparison was also performed of predictions made by different users of COSYMA. In total ten organisations took part in the exercise, which was coordinated by KEMA. Some of the organisations combined their efforts and produced jointly a set of predictions as shown in Table 6.1. This resulted in seven sets of calculations and results. To reach the objectives of this exercise it was not necessary to repeat the tasks already calculated in an earlier phase of the Intercomparison Exercise. Thus, slight differences in the specifications and the use of the COSYMA version 91/1 led to a second set of results delivered by FZK/NRPB for this special exercise. Section 6.2.1 of this report summarises the specifications of the COSYMA intercomparison exercise.

TABLE 6.1 List of participants in the COSYMA intercomparison exercise

Belgium	SCK/CEN, Mol, jointly with Tractebel, Brussels (S-T)
France	IPSN/CEA, Fontenay-aux-Roses (CEA)
Germany	GRS, Köln (GRS)
Germany / UK	FZK, Karlsruhe, jointly with NRPB, Chilton (K-N)
The Netherlands	KEMA, Arnhem (KEM)
The Netherlands	ECN, Petten (ECN)
Spain	CSN, Madrid, jointly with UPM, Madrid (C-U)

In general, the results of the participants are in good agreement, but as expected there is a spread in the various results due to differences in assumptions and interpretations of the specification of the scenarios. It was possible to investigate and explain differences by studying their sources in specifically designed exercises and tests carried out by KEMA. A document giving a very

detailed analysis of the differences in the results was drafted by KEMA and FZK. After discussions with the COSYMA participants about this report in Madrid, the final version was published by CEC³. The most interesting results of the analysis are outlined in Section 6.2.2 of this report. An overview is also given in reference 4.

The exercise has provided a valuable international forum for discussion on the use of COSYMA and on various approaches to ACA model and code development. This has increased the awareness of the applicability of these methods and will support the process of international harmonisation. As COSYMA was released only shortly before the start of the exercise many of the users were unfamiliar with the code. Therefore, the outcome of the intercomparison exercise was also a test on the ease of use of the code. The exercise gave feedback to the owner and developers of the code and has given advice on future improvements. As a result, an international COSYMA users group has been established with having yearly meetings coordinated by KEMA. The activities of this group are described in detail in Section 7 of this progress report.

6.2.1 Tasks, endpoints and objectives

The internal COSYMA intercomparison exercise made use of the framework of the code intercomparison exercise using basically the same specifications. Given the need to explain observed differences between the various participants, a large number of calculations could in principle be performed. It was decided however that, to reach the objectives of the COSYMA intercomparison, it was not necessary to perform calculations for all the cases used in the code intercomparison. Therefore, predictions were only made for four of the seven cases (ie C1, C2, C3 and C5; see Table 6.2) used in the code intercomparison exercise. To minimise differences in atmospheric dispersion modelling caused by the sampling of the meteorological data base which could obscure underlying differences in the results, the participants in the COSYMA intercomparison used a fixed set of weather sequences provided by NRPB for all near range endpoints.

Additional to these cases, the COSYMA users performed two extra exercises provided by FZK and NRPB. Case C11 was designed to study specifically the implementation of countermeasure strategies by the users and to give confidence to the users by demonstrating that they could use the very complex countermeasure module in the system. In case C12 all input parameters were fixed except for the meteorological sampling scheme; this exercise was intended to investigate the effects of different sets of weather sequences on the predicted consequences. To give a clearer explanation of the differences observed in the results, further calculations and specifically designed studies were carried out by KEMA.

TABLE 6.2 Cases for which calculations have been made

C1	a single phase release at 10 m height, without thermal energy, with countermeasures, fixed meteorological sampling scheme
C2	as C1 but with a long duration release
C3	as C1 but with no countermeasures
C5	a two phase release with thermal energy, rest as C1
C11	as C1 but with extended countermeasures
C12	as C1 with fixed input parameters, but calculated with participant's own meteorological sampling scheme

A large number of quantities, termed endpoints, reflecting different aspects of the consequences of accidental releases can be calculated by probabilistic accident consequence assessment codes like COSYMA. The endpoints considered in this exercise included:

- total collective dose
- air and ground concentrations at 1 and 30 km due North
- individual doses at 1 and 30 km due North
- number of early and late health effects
- individual risk of health effects as a function of distance from the release point
- effects of countermeasures, i.e. numbers of people and areas of land evacuated and relocated, their time integrals and the amounts of food banned
- economic costs of countermeasures and health effects

The following specific objectives of the COSYMA users intercomparison were established for the study:

- to investigate and explain differences in the predictions produced by the different users
- to study the sources of these differences by performing specifically designed tests
- to serve as a forum for exchange of experiences in using the COSYMA code
- to give feedback to the owner and the developers on weaknesses in the code and in the user guide and to give advice on future improvements

6.2.2 Presentation of results

(a) *Atmospheric dispersion endpoints*

Accident consequence assessment (ACA) models must be run for a large number of sequences of atmospheric conditions representing the range of conditions which might occur at a site. A calculation with a selected set of starting times should produce the same probability distribution of results for an endpoint of interest as would be obtained from a calculation in which all possible starting times are considered. Therefore when designing the sampling scheme the type of application has to be taken into account.

Normally, probabilistic ACA codes calculate probability distributions of consequences for a distance band or an area up to a certain distance. The standard sampling schemes for the trajectory model included in COSYMA for atmospheric dispersion are designed for this type of application. Non-standard applications, such as results at a specified point, would require a modified sampling strategy (see Section 2.1.6). However, in the intercomparison exercise the same meteorological sampling scheme was used for both the calculations at specific locations and the other tasks leading to a too low statistical accuracy of the predictions at a specific location as only few of the chosen weather sequences affect the point of interest because of changing wind directions.

Therefore, the results predicted by the participants for this type of endpoint show a wide spread when using their own sampling scheme (case C12). As an example Figure 1 shows the CCFDs of ground concentrations of Cs-137 at 1 km due North with the expectation value differing by up to a factor of 6. A further study was carried out to investigate the effect of different random samples drawn from the same sampling scheme. As Figure 2 shows, the spread is even larger,

with more than an order of magnitude difference between the expectation values predicted of the five runs of COSYMA. However, when using these different random samples for endpoints calculated in the whole distance band, the results predicted are close together as can be seen in Figure 3.

The predicted probability distributions of ground concentrations of Cs-137 at a point 30 km due North of the site are shown in Figure 4 for the base case C1. Although these results were calculated using the same set of weather sequences, there is an increasing difference at lower concentrations, with about a factor of 4 difference in the probability that the plume will pass over the point of interest. The results agree well at the higher concentrations. In these calculations the participants used grids which extended to different outermost distances. The maximum distance used affects the predicted concentration distribution because of the number of "returning plumes" it allows. As the amount of material in a returning plume is orders of magnitude lower than during the first passage, no differences can be seen in the high concentration values.

One of the calculations specified in the exercise was a release at a uniform rate over a period of 24 hours. COSYMA models a long release as a series of release phases lasting one hour. The participants made their own compromise between the desire to model this release in detail and the limits of computational requirements (both disk storage space and processor time) when considering a large number of phases. To investigate the influence of the subdivision of the release into phases on the results, a special phase test study was carried out varying the number of release phases between 1 and 24. It can be stated that when more phases are used the area affected increases and the maximal concentration values decrease.

(b) Early near range doses

When considering countermeasures another aspect has to be taken into account in subdividing the release into several phases. The timing of the phases relative to the early countermeasure scenario has to be chosen carefully. Modelling only very few phases can lead to a considerable over- or underestimation of the amount of material released before people shelter or evacuate. Additionally, the consideration of radioactive decay of short-living radionuclides may not be adequate when combining many hours of the release to a single release phase.

In the specification for the intercomparison exercise shielding factors defining the ratio of the dose indoors to that outdoors were set out. Further it was stated that for the population behaviour outside the area where emergency actions were taken, normal living conditions should be applied. This was specified as people spending 90% of their time indoors and the rest of the time outdoors. As COSYMA does not allow the use of time-dependent shielding factors, the participants modelled this specification in two different ways. Some assumed that 10% of people were outdoors and 90% indoors continuously. The other participants calculated doses for a single group of people with time-averaged shielding factors. These different assumptions can be seen in the results for the acute bone marrow dose at 30 km due North presented in Figure 5.

(c) Early health effects and risks

There is assumed to be a threshold dose, below which the risks of early health effects are zero and above which the risk rises rapidly. The calculation of the number of early deaths was

found to be sensitive to the dose calculation applying different shielding factors to represent the difference between doses indoors and outdoors and the fraction of the time people spend indoors. The predicted results of the participants shown in Figure 6 for the number of early deaths considering countermeasures clearly reflect the different assumptions made because of the assumed non-linear variation of risk with dose. Modelling a population group staying outdoors continuously leads to doses exceeding the threshold dose more often than using average shielding factors for all people.

A further threshold test was carried out to examine the sensitivity of the predicted number of early health effects to the assumed shielding factors adopted. The results presented in Figure 7 show the number of early deaths using different shielding factors varying by no more than a factor of 3. The spread in the predicted number of early deaths, however, is seen to vary by more than an order of magnitude. The doses leading to early death are clearly very close to the threshold for these effects. To investigate the sensitivity for effects where the doses are further from the threshold, the predicted number of hypothyroidisms was also examined in the same test. The results shown in Figure 8 confirm the reduced sensitivity on the shielding factor modelling for this effect.

6.2.3 Conclusions

In general, the results show that the predictions of the participants are in good agreement. Thus, implementation and use of the code did not give rise to serious problems. The specific objectives of the COSYMA users intercomparison exercise have been met to a large extent. In particular:

- By providing the participants with a range of problems, the exercise has been a fairly rigorous test of both the users and COSYMA. This has considerably enhanced the quality assurance aspects of the code and its use.
- Differences in the predictions produced by the users could be investigated and explained. Sources of these differences were studied by performing specifically designed tests.
- The exercise has provided a valuable international forum for discussion on the use of COSYMA in particular and on various approaches to PCA model and code development in general.
- An international COSYMA users group has been established, with the purpose of reinforcing the feedback between users and code developers and of providing a forum for the exchange of experiences between users.
- The exercise has given feedback to the owner and the developers on weaknesses in the code and in the user guide and has given advice on future improvements.

6.3 References for section 6

- 1 International Comparison Exercise on Probabilistic Accident Assessment Codes - Overview Report Paris, OECD and CEC, 1994
- 2 International Comparison Exercise on Probabilistic Accident Assessment Codes - Technical Report Brussels, CEC, Report EUR-15109, 1993
- 3 E. van Wonderen, J. van der Steen, I. Hasemann. COSYMA: Users Intercomparison Exercise. CEC, Report EUR-15108, 1993

- 4 J. van der Steen, E. van Wonderen, I. Hasemann. COSYMA: Users Intercomparison Exercise. Proceedings of the technical committee meeting "Procedures and computer codes for level-3 probabilistic safety assessment" organized by OECD, Vienna, 1995

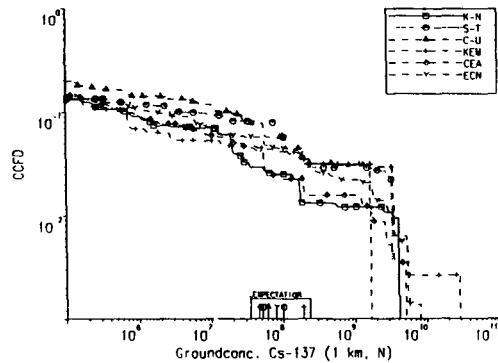


FIGURE 1 CCFDs of ground concentrations of Cs-137, 1 m due North; user's own meteorological sampling scheme (case C12)

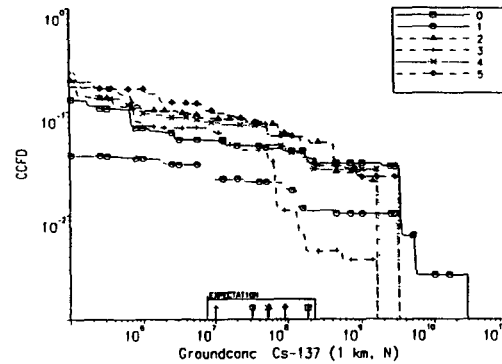


FIGURE 2 CCFDs of ground concentrations of Cs-137, 1 km due North; different samples from same meteorological sampling scheme (special test for case C12)

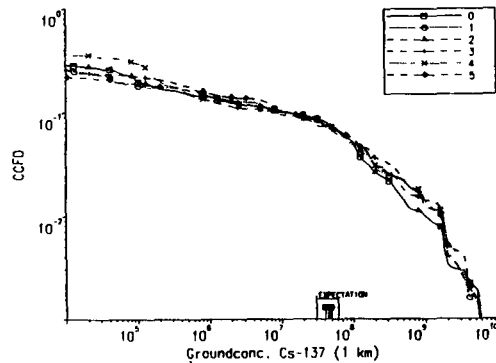


FIGURE 3 CCFDs of ground concentrations of Cs-137, 1 km, in the whole distance band; different samples from same met. sampling scheme (special test for case C12)

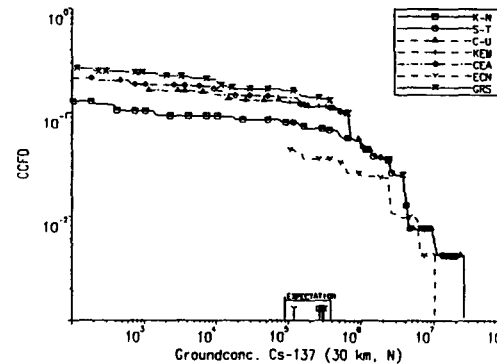


FIGURE 4 CCFDs of ground concentrations of Cs-137, 30 km due North (case 1)

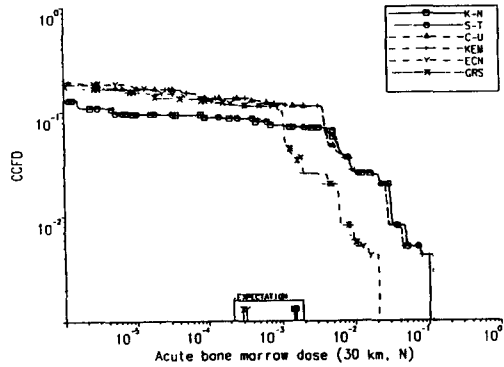


FIGURE 5 CCFDs of acute individual bone marrow dose, 30 km due North (case 1)

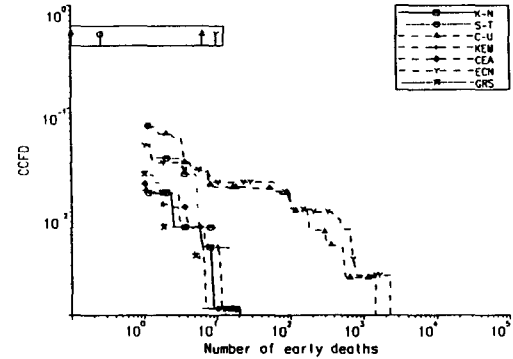


FIGURE 6 CCFDs of number of early deaths (case C1)

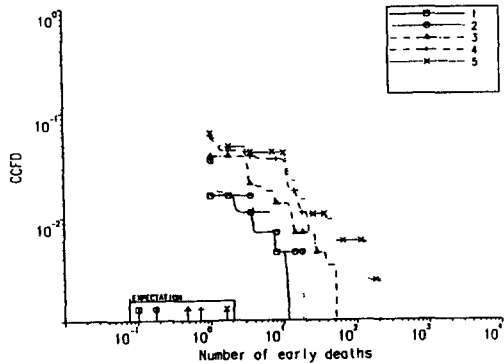


FIGURE 7 CCFDs of number of early deaths; application of different shielding factors (special test for case C1)

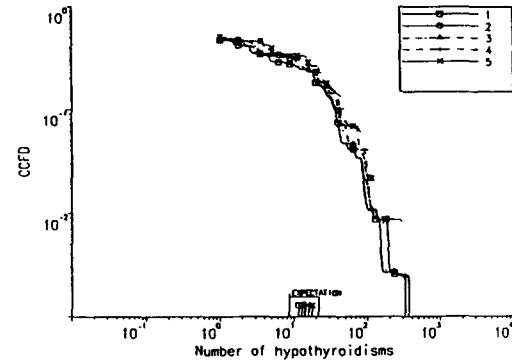


FIGURE 8 CCFDs of number of hypothyroidisms; application of different shielding factors (special test for case C1)

7 COSYMA Users GROUP

7.1 *Establishment of the COSYMA Users Group*

The COSYMA Users Intercomparison Exercise, organized in the framework of the CEC/OECD-NEA International Code Intercomparison Exercise (see Section 6), provided COSYMA users with a regular forum for discussion on the use of the code. This contributed to the quality assurance of the code and provided feedback between code users and code developers in those areas where improvements could be made both in the COSYMA code and its User Guide. At the final meeting of the International Code Intercomparison Exercise there was a broad agreement that there would be considerable value in continuing the exchange between COSYMA users and between users and developers, given the wide distribution of the code.

The most effective way of achieving this was through the establishment of a COSYMA Users Group. The need for such a group was further enhanced by the release of PC COSYMA, and its consequential use by even a larger number of institutes. After the successful ending of the COSYMA Users Intercomparison Exercise, it was therefore decided to establish a users group both for COSYMA and PC COSYMA users. KEMA was asked to coordinate its activities, according to the Terms of Reference of the Group.

7.2 *Terms of Reference*

The Terms of Reference of the COSYMA Users Group have been specified as follows:

The International COSYMA Users Group has been established to provide a forum for the exchange of experiences of the users of the COSYMA code and the PC COSYMA code. The aim of the Group is to reinforce the feedback between users, owner and developers of the code in order to enhance the quality assurance aspects of the code and its use.

The COSYMA Users Group will:

- stimulate the communication between owner, developers and users of the code;
- produce a COSYMA newsletter with official announcements, comments and problems identified by users;
- serve as a reference point for questions;
- keep record of all COSYMA related matters;
- organize a yearly meeting of users to discuss and inform about applications, difficulties encountered, missing options or functions, etc.;
- discuss new developments in probabilistic accident consequence assessment;
- promote harmonization of PSA level 3 methods and codes;
- suggest R&D work on modelling improvements, data base generation or methodological investigations.

7.3 *Coordination of the COSYMA Users Group activities*

7.3.1 Mail Box

One of the coordinative tasks is to serve as a mail box for those having questions about the code or its applications. During the reporting period several questions have reached the coordinator,

mainly about problems related to running the code. Most of the questions could be answered by the coordinator. In a few cases, FZK was consulted for answering the questions.

7.3.2 COSYMA Newsletters

Several issues of the COSYMA Newsletter have been produced and sent to users of both COSYMA and PC COSYMA and other interested persons. The newsletters hold articles on improvements and new developments in the latest releases of COSYMA and PC COSYMA, news on the COSYMA Users Group Meetings, applications of the code, and other relevant information on PSA codes in general and COSYMA in particular. The number of articles sent to the editor is continuously increasing, indicating that users find their way to communicate by means of the Newsletter. A list of Newsletter issues is given in section 9. At the end of the reporting period, the mailing list runs to more than 230 addresses.

7.3.3 COSYMA Users Group Meetings

The first COSYMA Users Group Meeting was held at KEMA, Arnhem, The Netherlands, on 25-26 April 1994. The meeting was attended by 25 participants from 12 countries, reflecting the wide spread of COSYMA and PC COSYMA even outside the European Union. During the meeting 14 papers were presented, divided in two sessions on system related issues and on applications. The papers concerned both the COSYMA code and the PC COSYMA code.

In the session on system related issues, presentations were given by the code developers FZK and NRPB on improvements that are to be implemented in the mainframe COSYMA version 95/1 and PC COSYMA version 2. The improvements in COSYMA refer to improved iodine prophylaxis, health effects and economics models, extended and updated data libraries, modified meteorological sampling programs and new endpoints. Details are given in section 2. Also the new version of PC COSYMA will be considerably improved with new endpoints, new and modified models, revised data libraries, improved interfaces and increased dimensions, as is reported in section 3.

With respect to the economics model, a presentation was given on the integration of MECA2 in the COSYMA code. Further presentations in the system related session were related to uncertainty and sensitivity analysis and on the dose-early health effect relationship and the dose and risk presentation in COSYMA.

In the applications session presentations were given on the use of COSYMA and PC-COSYMA for various purposes in different countries.

Ample time was taken for discussion, and several issues have been mentioned for future work of the Users Group. The most important are:

- to document special applications of the code by the coordinator in order to provide future assistance for related applications
- to consider the establishment of a subgroup on evaluation programs for non-standard results
- to consider the establishment of a subgroup on the implementation of the 'averted dose' concept in countermeasure strategies
- to advise on the interface between PSA level 2 results and PSA level 3 input
- to advise on an intermediate model for local and regional foodstuff production and consumption

- to encourage the extension of the population data on the 10x10 km grid used in COSYMA.

The proceedings of that meeting have been published by KEMA and the reference is included in section 9.

As a result of the meeting, the two subgroups mentioned above have been established. The subgroup on evaluation programs for non-standard results is chaired by ECN, The Netherlands, and the subgroup on the implementation of the 'averted dose' concept in countermeasure strategies is chaired by SCK/CEN, Belgium.

The second COSYMA Users Group Meeting was held at the end of the MARIA project, on 19-21 June 1995 in Budapest, Hungary. This country was chosen to facilitate the attendance of East European COSYMA and PC COSYMA users, and it proved to be very successful: 39 participants, among which many East Europeans, attended the meeting. 14 presentations were given. The presentations gave rise to keen discussions, underlining the usefulness of the meeting. The chairmen of the subgroups were asked to prepare a first meeting of their subgroup during the second COSYMA Users Group Meeting. At these subgroup meetings the work program for the coming year was discussed, and reports of the discussions were presented during the final plenary meeting of the COSYMA Users Group. The proceedings of the second COSYMA Users Group Meeting are now under preparation.

In the subgroup on evaluation programs for non-standard results many problems have been discussed, mostly tabled by new and unexperienced users. Specifically from this subgroup meeting, it became very clear that bringing together experienced and unexperienced users to discuss the problems encountered in applying the code is very important in order to enhance the quality of the applications of the code.

In the subgroup on the implementation of the 'averted dose' concept in countermeasure strategies, it was recognized that this concept has been adopted by international organizations as the basis for the promulgation of countermeasures. At the same time, it was also recognized that implementing this concept in the COSYMA code has a major impact on the structure of the code. It was decided that some participants of this subgroup, i.e. FZK, KEMA, NRPB and SCK/CEN, will identify the possibilities and problems of the implementation and will make a proposal for such work.

At the first International MACCS Users Group Meeting, held at Brookhaven National Laboratory from 8 to 10 November 1994, an interaction between the MACCS and COSYMA Users Groups was considered positive, and a first proposal was to interchange newsletters. This has led to sending the COSYMA Newsletter to the MACCS users. As a result some MACCS users attended the second COSYMA Users Group Meeting. During the meeting, it was discussed whether other forms of interaction could be performed, and it was decided that a presentation of the outcomes of the COSYMA Users Group Meeting at the next MACCS Users Group Meeting, and vice versa, would be an effective way of information for both groups.

7.3.4 Identification of problem areas and advice for future maintenance

In the general discussion at the second COSYMA Users Group Meeting, several issues have been mentioned for future work of the Users Group. The most important are:

- There is a need for dose evaluations for different time periods, with starting times other than zero. This can only be done by complex calculations and should be simplified.
- The proposed exclusion of pork as one of the foodstuffs in the ingestion pathway in the 95/1 version of COSYMA was considered to be questionable, as in many countries pork is a major component of the food. As a result of this it was decided by FZK and NRPB that pork should be incorporated in the 95/1 version. The release of this version is expected in October 1995.
- Meteorological sampling is, as has been shown by NRPB, very critical for some endpoints. There still is a need for guidance in this topic, specifically for new and unexperienced users.
- Wind shear and methods of establishing stability classes may have a considerable effect on the dispersion of radionuclides on short distances, and thus on the number of early health effects. It should be clarified if these are important factors in standard calculations; they might however be in specific applications, such as deterministic calculations.
- Specific guidance is needed in the field of uncertainty analysis. The results of the EC/USNRC project on uncertainty analysis should be taken into account for use in COSYMA when they are available.
- There is also a need for guidance on the use of long range dispersion models, in connection with meteorological sampling methods.
- Deposition in urban areas needs specific modelling of certain phenomena, like external gamma dose in combination with location factors, skin deposition, resuspension, indoor air concentrations and indoor deposition. These phenomena may also have a significant effect on certain endpoints, as has been shown by NRPB.
- There is a need for calculating the effective dose in the module NE of COSYMA, as in certain countries short term effective doses including the effects of countermeasures have to be calculated as an endpoint.
- There is a need for an intermediate model for local and regional foodstuff production and consumption.
- There is a need for countermeasures other than food bans in the ingestion pathway. Such countermeasures could include for instance remedial actions to decrease the concentration of radionuclides in food.
- There is a tendency to use PSA level 3 codes for on site consequence calculations. However, this needs specific modelling of dispersion on the short range, in particular sophisticated building wake effect models.
- The extension of population and agricultural data on the European grid used in COSYMA to middle and east European countries has been discussed. Such data bases should be made available by these countries for incorporation in the data base of COSYMA.
- The inclusion of models to assess the consequences of contamination of fresh water, with respect to doses and to the economic implications of such contaminations, seems to be important. This is specifically relevant for the long term, as has been shown after the Chernobyl accident in certain countries.
- There is also a need for specific models and data bases to be applied in areas, such as for instance the Arctic, that are different from northwest Europe. Such models and data bases might have been developed in the framework of other research projects, like the IAEA coordinated research programme VAMP or in the BIOMOVs project, organized by the IUR. If so, they may be available for incorporation in COSYMA.
- There is a need for translation of the English versions of COSYMA and, specifically, PC COSYMA into different languages. However, it is felt that this is in principle the responsibility of the user.

Several of these items are also discussed in section 5 of this report. In fact, a presentation on modelling needs for accident consequence assessment codes has been presented by NRPB on the meeting. The conclusions were discussed in the Users Group and there was a general agreement that the paper covered all the main topics in this area.

8 RISK ANALYSIS FOR THE KOZLODUY NUCLEAR POWER PLANT, BULGARIA

A calculation of the risks posed to the Bulgarian population by a number of hypothetical accidents at the Kozloduy nuclear power plant has been carried out. The release fractions of the different elements in the reactor core were provided as part of a separate study. This study included the calculation of the reactor inventory, and the consequences in the population of the assumed releases. The study was carried out using the MACCS computer code.

8.1 *Inventory calculation*

The ORIGEN 2.1 code system was used to evaluate the radionuclide composition of the "Kozloduy" nuclear power plant core. ORIGEN2.1 is a versatile computer code and represents a revision and update of the original ORIGIN computer code, which was developed at the Oak Ridge National Laboratory (ORNL). Included in ORIGEN2.1 are provisions for incorporating data generated by more sophisticated reactor physics codes, free-format input, and a highly flexible and controllable output; with these features, ORIGEN2.1 has the capability for simulating a wide variety of fuel cycle flow sheets. The code incorporates updates of the reactor models, cross sections, fission products yields, decay data and decay photon data and includes additional libraries for standard and extended-burnup calculations. ORIGEN2.1 uses a matrix exponential method to solve a large system of coupled, linear, first-order ordinary differential equations with constant coefficients. The output is capable of displaying great detail concerning the contribution of each individual nuclide to the overall totals for each engineering unit (characteristic). The nuclides contained in the ORIGEN2.1 data bases have been divided into three segments: 130 actinides, 830 fission products, and 720 activation products (a total of 1700 nuclides). These segments are formed by aggregating the 1300 unique nuclides (300 stable) in the data base since some nuclides appear in more than one segment. The calculations of nuclide compositions and characteristics of nuclear fuel for VEER-440 and VEER-1000 main regimes were performed. The relative error in calculating decay heat of VEER-440 and VEER-1000 is 0.96% and 3.29% respectively, and for nuclide composition of the core is 8.89% for VEER-440 and 8.04% for VEER-1000. Such type of calculations have been performed for the first time for the "Kozloduy" nuclear power plant.

The calculations allowed for the operating regime of the reactor, in which fuel is irradiated for about one year before the reactor is shut down for some days for re-fuelling. One third of the reactor fuel is replaced at each refuelling stage. The inventory used in the calculations allows for parts of the fuel to have remained in the reactor for different periods.

The Kozloduy plant consists of two reactors, the VVER-440 and VVER-1000 reactors. Calculations were performed for both reactors. Characteristics that are calculated are the total radionuclide composition of reactor fuel, total fuel cladding composition and total structural materials composition of the reactor core. Results include light nuclides (such as Fe, Zr and other activation structural materials), actinides and daughters (such as U, Pu, Cf, etc), and fission products (such as Zn, Xe etc).

The calculated inventories have been provided to NCSR, Greece, who are also undertaking calculations of consequences of accidents at Kozloduy to the Greek population.

8.2 Preparation of input data

To estimate the potential impact of Kozloduy five characteristic major nuclear accidents classified as level 7 accidents on the International Nuclear Event Scale and involving significant releases of radionuclide materials into the environment are postulated to occur. Scenario A is based on a core meltdown followed by a steam explosion from contact of molten fuel with the residual water in the reactor vessel. Scenario B is associated with the failure of core cooling systems and core melting concurrent with the failure of containment spray and heat removal systems. Scenario C involves an overpressure failure of the containment heat removal. Scenario D involves failure of the core cooling system and the containment spray injection system after a loss of coolant accident, together with a concurrent failure of the containment system to properly isolate. Finally Scenario E is based on a release corresponding to the V-sequence (by-pass) in the NUREG-1150 Study. This accident sequence involves interfacing system LOCA, check valves that separate the low-pressure emergency core cooling system from the high-pressure primary system fail, the pathway for release bypasses the protection normally provided by the containment building, so the retention capabilities of the reactor coolant system and of the safeguards building are particularly important. This sequence potentially involves a large fission product release to the atmosphere. The selection of accident scenarios and the related radionuclide release data have been evaluated commonly. The release characteristics and the fractions of the radioactive substances of the core inventory released into the environment are presented in Table 1.

Probabilistic accident consequence calculations also require information on the atmospheric conditions over a period of one or more years at a meteorological station near the site. There is an automatic meteorological station situated close to the Kozloduy nuclear power plant. Data from this station for the year 1994 were obtained. Special computer programs were written to transfer the data into the form required by the MACCS computer code.

Data is also required for the distribution of population around the plant. Data from the 1992 Bulgarian census were used to give the required information in terms of the numbers of people living at certain distances and directions from the site.

8.3 Summary of calculated consequences

The consequences that would result for the population of Bulgaria from the postulated accident scenarios, would be due to the both early and chronic exposure. The health effects considered in this study include cancer fatalities and other long term injuries. Doses to various organs of an individual of certain distances from the reactor site, and the corresponding collective doses were also calculated. Some of the results are presented in Table 2 for the Bulgarian population. The results of the analysis have been calculated under very conservative assumptions, such as a constant northern wind, and the occurrence of very severe accident scenarios.

Under these assumptions, the magnitude of the corresponding consequences implies the need to adopt countermeasures. Some countries have numerical criteria to judge whether the risks posed by nuclear reactors are acceptable. There are no such criteria in Bulgaria, and so countermeasures were not considered in this study. This report presents the beginning of the scientific activities related to PSA level 2 and 3 in our country. Further work in this area will be undertaken in future, and this will include a consideration of the effects of countermeasures in reducing the doses.

9 PUBLICATIONS

Publications from NRPB

P Mansfield, J A Jones, S M Haywood, I Hasemann, C Steinhauer and J Ehrhardt. PC COSYMA: A PC version of the probabilistic accident consequence code COSYMA. Poster presentation at the Third International Workshop on Real-time Computing of the Environmental Consequences of an Accidental Release to Atmosphere from a Nuclear Installation, Schloss Elmau, Bavaria, Oct 1992

Jones J A, Mansfield P A, Haywood S M, Nisbet A F, Hasemann I, Steinhauer C, and Ehrhardt J. PC COSYMA: an accident consequence assessment package for use on a PC. Brussels, EUR-14916 (1993)

NRPB and KfK. User guide for the PC version of COSYMA. Brussels, EUR-14917 (1993)

Mansfield P, Jones J A, Haywood S M, Hasemann I and Ehrhardt J. PC COSYMA: A PC system for the probabilistic assessment of consequences from accidental releases of radioactive material. Presented at International Conference on Modelling and Simulation for the Nuclear Industry, Glasgow, Sept 1993

Brown J and Jones J A. Incorporation of the results of the EXPURT external dose model into the accident consequence analysis system COSYMA. NRPB-M510 (1994)

Jones J A, Mansfield P A and Hasemann I. COSYMA, a mainframe and PC program package for accident consequence assessments. Presented at the IAEA Technical Committee Meeting on Procedures and Codes Computer for Level-3 PSA, Vienna, Nov 1994 (1994)

J A Jones and J van der Steen. Research needs for ACA programs. Presented at the COSYMA user group meeting, Budapest June 1995, and to appear in the proceedings

J A Jones. Meteorological sampling in COSYMA. Presented at the COSYMA user group meeting, Budapest June 1995, and to appear in the proceedings

J A Jones and P A Mansfield. Effects of new ICRP dosimetric models in predicted consequences. Presented at the COSYMA user group meeting, Budapest June 1995, and to appear in the proceedings

J Brown and J A Jones. Incorporating food countermeasures other than bans into COSYMA. Presented at the COSYMA user group meeting, Budapest June 1995, and to appear in the proceedings

P A Mansfield, J A Jones and I Hasemann. PC COSYMA 2. Presented at the COSYMA user group meeting, Budapest June 1995, and to appear in the proceedings

Publications from FZK

E. van Wonderen, J. van der Steen, I. Hasemann COSYMA: Users Intercomparison Exercise CEC, Report EUR-15108, 1993

J.A. Jones, P.A. Mansfield, S.M. Haywood, A.F. Nisbet, I. Hasemann, C. Steinhauer, J. Ehrhardt PC COSYMA: An Accident Consequence Assessment Package For Use on a PC CEC, Report EUR-14916, 1993

NRPB and KfK PC COSYMA Version 1.0 - User Guide CEC, Report EUR-14917, 1993

International Comparison Exercise on Probabilistic Accident Assessment Codes - Overview Report Paris, OECD and CEC, 1994

International Comparison Exercise on Probabilistic Accident Assessment Codes - Technical Report Brussels, CEC, Report EUR-15109, 1993

I. Hasemann, J. Ehrhardt COSYMA: Dose models and countermeasures for external exposure and inhalation Karlsruhe, Report KfK-4333, 1994

D. Faude, D. Meyer Extension of the COSYMA-ECONOMICS module: cost calculation based on different economic sectors Karlsruhe, Report KfK-5442, 1994

J. Ehrhardt, I. Hasemann, C. Matzerath-Boccaccini, C. Steinhauer, J. Raicevic COSYMA: Health effects models Karlsruhe, Report FZK-5567, 1995

J. van der Steen, E. van Wonderen, I. Hasemann COSYMA: Users Intercomparison Exercise Proceedings of the technical committee meeting "Procedures and computer codes for level-3 probabilistic safety assessment" organized by OECD, Vienna, 1995

Publicatons from UPM

Faude D., Meyer D., Extension of the COSYMA-ECONOMICS Module Cost Calculations Based on Different Economic Sectors., KfK Report KfK 5442, Kernforschungszentrum Karlsruhe, (1994).

Gallego E., "MECA2. Model for Economic Consequence Assessment, Version 2. Reference Guide". Report CTN-43/92. Cátedra de Tecnología Nuclear, UPM (1994).

Gallego E., Integration of MECA2 (Model for Economic Consequence Assessment) in the COSYMA System. In Proc. First COSYMA User's Group Meeting, Arnhem, April 1994.

Gallego E., Alternative Models for the Evaluation of Economic Consequences in COSYMA. In Proc. Second COSYMA User's Group Meeting, Budapest, June 1995.

Hidalgo A., Gallego E., Muñoz A., Modelo del Impacto Económico Externo de los Accidentes Nucleares, In Proc. XX Annual Meeting of the Spanish Nuclear Society, Córdoba, October 1994.

Hidalgo A., Gallego E., Muñoz A., Modelo del Impacto Económico Externo de los Accidentes Nucleares, submitted for publication in Información Comercial Española. Revista de Economía.

Hidalgo A., Gallego E., Muñoz A., Pavón J., Evaluación del Impacto Económico Externo de los Accidentes Nucleares, Report CTN-88/94. ETSII-UPM (1994, first version, enlarged 1995).

Gallego E., MECA3. Model for Economic Consequence Assessment, Version 3. Reference Guide. Report CTN-50/95. Cátedra de Tecnología Nuclear, UPM (1995).

Publications from KEMA

E.L.M.J. van Wonderen, J. van der Steen and I. Hasemann; COSYMA: Users Intercomparison Exercise; EUR report nr 15108 EN, 1994.

J. van der Steen (ed); COSYMA Newsletter 93/1, September 1993.

J. van der Steen (ed); COSYMA Newsletter 94/1, January 1994.

J. van der Steen (ed); COSYMA Newsletter 94/2, April 1994.

J. van der Steen (ed); COSYMA Newsletter 94/3, September 1994.

J. van der Steen (ed); COSYMA Newsletter 95/1, February 1995.

J. van der Steen (ed); COSYMA Newsletter 95/2, May 1995.

J. van der Steen (ed); Proceedings of the first COSYMA Users Group Meeting, 25-26 April 1994, Arnhem, The Netherlands; KEMA report 40666-NUC 94-5819, 1994.

Publications from BAS

Iordanov I D and Hristov Y Ch. Integrated computer codes for nuclear power plant severe accident analysis, Proceedings of the Technical Committee Meeting "Bulgarian Nuclear Energy", Kozloduy, 1994

Hristov Y Ch and Iordanov I D. Analyses of nuclide compositions and characteristics of nuclear fuel for VVER type reactors. Proceedings of the National Scientific Forum, Varna, 1995

Hristov Y Ch and Iordanov I D. Calculations of inventory of real core for VVER-440 and VVER-1000 reactors. Proceedings of the National Scientific Forum, Varna, 1995

Publications from KFKI-AERI

Sági L and Koblinger L. Comparing the environmental consequences of hypothetical accidents at VVER installations of Hungary. Presented at the COSYMA user group meeting, Budapest 1995, and to appear in the proceedings.

Koblinger L and Sági L. Calculations for the VVER-type reactor at the Paks NPP (Hungary) with the COSYMA and MACCS codes. Presented at the COSYMA user group meeting, Budapest 1995, and to appear in the proceedings.

Final Report **1992 - 1994**

Contract: FI3PCT930073 **Duration:** 1.1.93 to 30.6.95

Title: Analysis and modelling of the migration of radionuclides deposited in catchment basins of fresh water systems

- | | | |
|----|---------------|---------------------|
| 1) | Monte | ENEA |
| 2) | Van der Steen | KEMA N.V. |
| 3) | Boardman | UKAEA |
| 4) | Kozhoukharov | BAS |
| 5) | Bergström | Studsvik Eco&Safety |

I. Summary of Project Global Objectives and Achievements

The main aim of the present project was the development of models describing the migration, via rivers and run-off and wash-off waters, of radionuclides deposited in drainage areas. The turn-over of radionuclides in fresh water systems has been deeply studied during past decades and, following those studies, a variety of efforts were attempted to model the behaviour of radionuclide in catchments. The behaviour of radionuclides of Chernobyl origin in the aquatic environment gave the opportunity of testing the validity of the methods and approaches adopted by the existing models to predict the migration of radionuclides in water bodies. Therefore, the present project has been mainly focused on the identification of the phenomenological behaviours that are poorly predicted by the traditional models, on the development of new approaches to improve the reliability of predictions and on the search of objective methodologies to evaluate the model performances. The research was based on methodological approaches that can be very useful in lightning the role and the importance of modelling in environmental sciences and in the management of environmental contamination. The present project was based on a preliminary scientific literature survey and on the analysis of the characteristics of the existing models developed to predict the migration of radionuclide in catchments of fresh water bodies. This step gave the opportunity of getting a profound outline of the state-of-the-art of the modelling for assessing radionuclide migration through catchments. The need of an objective evaluation of the reliability of models stimulated the search of new techniques of model validation. The evaluation of the performances of a model may be carried out by the direct comparison of the model output with independent experimental data set. This straightforward approach was adopted by the most important and valuable post-Chernobyl international validation exercises (VAMP and BIOMOV5). Nevertheless, the "model output - experimental data" comparisons may show some degrees of subjectivity. Indeed the personal judgement of the scientist, that carries out the validation, may play an important role when evaluating the model performances. A different technique of model validation was adopted in occasion of the present programme. The analysis of the performances of a model was carried out by comparing the mathematical form of the experimental

radionuclide transfer functions (TF) (Transfer Function = the observed amount of radionuclide flowing per unit time from upstream drainage basin to a water body following a single-pulse deposition of radioactive substance) evaluated for various rivers in Europe contaminated after the Chernobyl accident, with the "Green functions" (GF) (Green Function = the radionuclide flow per unit time from catchment to water body calculated by the model as result of a single-pulse input deposition) characterising some of the most common models. The GF of a model, being a characteristic of the model strictly related to the model structure, ultimately summarises all the model properties. If the structure of experimental TF is different from the structure of the model GF, the model does not account for important phenomena and processes that strongly influence the behaviour of the analysed system. This method of validation, being based on the comparison of two mathematical structures, is objective, independent on the personal judgement of the researcher and may suggest what aspects of the migration processes are reliably predicted by the model and what need a better understanding and modelling. Generally TFs are the sum of some time-dependent exponential components due to both the radionuclide physical decay and the removal environmental effects. The analysis showed that two main components (a short-term and a long term-component) may be detected over a period of some years after the accident. The order of magnitude of the effective decay constant of the short-term component is 10^{-7} s^{-1} (radionuclides ^{137}Cs , ^{90}Sr and ^{103}Ru). The geometric mean of the long term effective decay constant, calculated for some European rivers, is $1.5 \times 10^{-8} \text{ s}^{-1}$ (^{137}Cs) and $4.9 \times 10^{-9} \text{ s}^{-1}$ (^{90}Sr). Moreover, the analysis of TFs showed that the radionuclide migration flux from catchment (Bq s^{-1}) is not ever linear as function of the water flux through the catchment ($\text{m}^3 \text{ s}^{-1}$). This occurrence was verified for ^{90}Sr dissolved in water and for particulate ^{137}Cs . In case of this last radionuclide this non linearity effect may be easily explained. Indeed the amount of ^{137}Cs transported in particulate form depends on the content of eroded particles in water, content that increases with the water flux. The comparison of TF and GF showed that: a) models based on the traditional concept of k_d (the radionuclide partition coefficient between the soil in catchment and water) do not explain the higher value of the experimental long-term effective-decay constant for ^{137}Cs compared with ^{90}Sr ; b) models not accounting for the time behaviour of the distribution of flowing water through the various horizontal layers of a catchment do not explain the nonlinear dependence of dissolved ^{90}Sr migration flux from catchment as a function of the water flux. The results of the "TF-GF" comparison are reported in details in the description of project 1. In the same description it was demonstrated that, accounting some nonreversible effects that may reduce the availability to the migration of radionuclide in catchment (such as the nonreversible interaction of dissolved radionuclide with soil particles and the removal of radionuclide in particulate form due to the depletion of eroded particles from catchment) and the effects of water saturation in different horizontal soil layers, it is possible to give reason of a) and b). The analysis of the existing models clearly showed the importance of k_d and, more generally, of the mechanisms of interaction of radionuclide with soil in drainage areas. In project 2, following a critical analysis of literature models, an application of a model to predict the radionuclide migration in catchments of river Rhine and lake Hillesjön was carried out

evaluating, by means of simple formulas, the role of erosion and the correlation of k_d with some chemical characteristics of the soil in catchment.

The above discussion clearly throws light on the need of ameliorating traditional modelling approaches. The attempt of improving these modelling techniques was based on the analysis of the general aims and characteristics of the modelling process to search for new strategies that make models reliable and usable for practical purposes. Generally speaking, models may be subdivided in two categories: "empirical models" and "conceptual models". A pure "empirical model", that is often called "black box" model, is an algorithm relating outputs to inputs without any reference to the occurring phenomena and their relationships. These models show an obvious disadvantage: in most cases, they are characterised by sets of parameters having "site-specific" values. As consequence it is almost impossible to use them to make predictions in circumstances different from those of the model calibration. A pure "conceptual model" is based on the knowledge of the fundamental processes responsible for the behaviour of the considered system and on the quantitative evaluation of the correlation among the involved processes. Conceptual models are extremely important tools for understanding the dynamic and the behaviour of a system. The structure of a conceptual model for predicting the migration of radionuclide in catchment, generally, includes three sub-models: a hydrological model predicting the movement of water in catchment, a model of erosion predicting the transport of eroded particles and a radionuclide migration model based on the quantitative analysis of the radionuclide interaction with water, rocks and transported particles in the catchment. Examples of conceptual models and relevant codes, developed on the occasion of the present research, are reported in description of project 3 and project 4. These models give a very clear idea of the relative importance of the various phenomena related to the movement of water in catchment and to the consequent radionuclide migration from drainage areas to water bodies. They represent the logical frame system of the migration processes and their quantitative relationships. A disadvantage of the conceptual models is their complexity and, consequently, the large amount of parameters and of input functions they need. These last, indeed, can be, in some cases, not available or difficult to obtain. Moreover, the possibility of predicting the migration, in the course of the time, of radionuclides in catchment using this sort of models may be, in some circumstances, illusive; indeed, on principles, a pure "conceptual model" needs the exact knowledge of the rainfall rates over the catchment to calculate the various components of the water fluxes. As the prediction of rainfall is extremely uncertain, the usefulness of these models may be vain when they are used as "predicting tool" to forecast, in the short time, the behaviour of radionuclides in drainage areas. On the other hand, if the conceptual model is used to make predictions of the time average values of radionuclide fluxes, it is possible to use, as model parameters and input functions, the mean values (for instance on a seasonal or monthly basis) of rainfall and of the other hydrological characteristics. Such strategy allows one to simplify the structure of the hydrological sub-model without diminishing the reliability of the model applied to the specific circumstances.

The above considerations suggested to explore further modelling approaches based on the development of "collective" (or "aggregate") models that show characteristics intermediate between the "pure empirical" and "pure conceptual" models. "Collective models" are based on the idea that some complex

environmental processes, that strongly interact one with the other, may lead to stable and somewhat predictable behaviour. If such circumstance occurs, it is possible to develop simple, reliable model of the analysed system that may be successfully used to predict the behaviour of contaminant substances in the environment. During the present research this approach was deeply analysed to test its validity and to evaluate the possibility of developing such kind of models. An example of model based on "collective" parameters is reported in details in description of project 1. Basically this model may be useful to predict the approximate, average behaviour of a contaminant substance in a catchment. As it is simple and easy to use, it may represent, for practical applications, an effective tool to predict the migration of the contamination in drainage areas.

On the other hand, it is quite obvious that simplification process must stop at some stage. Indeed, "oversimplified models" may not predict the migration of the toxic substances in the environment with a sufficient accuracy. One of the questions that arises is the following: what is the simplest model that can explain the experimental behaviour of a complex system? This question may have a unique answer, indeed the simplest model whose Green Function reflects the structure of the experimental Transfer Function is the "minimal model" to predict the analysed processes. As said before, such kinds of collective models are characterised by simple structure and, consequently, by a little number of parameters that must show some peculiar characteristics to make the model useful and usable in practical circumstances. Two characteristics are of great importance. Firstly the calculations or the experimental evaluations of the model parameters must be straight and easy. The second desirable characteristic is that the values of such parameters are "stable" (they do not vary too much from site to site or when changing the environmental conditions of a site) or must be strongly related to specific characteristics of the environment (there must be high correlation between the parameter values and specific environmental conditions that are easy to identify and characterise and are approximately constant on time and on space). The parameter stability can allow one to use the model as a generic tool to predict the migration of radionuclide through catchment basins when site specific values of the parameters are not available. The minimal model described in part 1 of this report, besides being an example of application of the above principles, presents some parameters that are "stable" for practical applications aimed to estimate the approximate time behaviour of the radionuclide fluxes from catchment to water bodies. Of course minimal model must satisfy an extremely important requisite. It must be logically "coherent" with complex models describing in details the behaviour of radionuclide in catchments. The "coherence" is satisfied when the "minimal model" may be derived by the "complex model" by means of mathematical simplification based on clear and reasonable hypotheses (or, using a standard general method, showing that the GFs of the models have the same structure). The present research had also the aim of identifying the most important processes that must be modelled to develop "minimal" reliable models predicting the behaviour of radionuclide migrating in catchment of fresh water systems. Some peculiar behaviours of radionuclide in complex catchments were identified. Among them the most important are the effects due to the presence in a catchment of compartments that accumulate radionuclides and release those on the long run. These compartments are bog areas in the catchment, glaciers and perennial snows in catchment partially or completely located in high mountain regions, bottom

sediments and lakes showing long mean water retention times. These important aspects of the radionuclide behaviour in catchment are described in more details in project 5.

The present project gave the opportunity of developing a set of models of various complexities that can be applied to a variety of environmental scenarios with goals ranging from research applications to environment management.

Head of project 1: Dr. Monte

II. Objectives for the reporting period

During the reporting period the following actions were completed:

- Collection of radionuclide concentration data in a variety of Italian fresh water systems to evaluate the most important characteristics of the time behaviour of the radionuclides in the aquatic environment and to identify and measure the parameters that control the relevant phenomena (migration rates to sediments, residence times, transfer rate from catchment to water bodies, etc.);
- Development of a conceptual model (new version of model MARTE) to analyse and explain, on a rational basis, the most important phenomena relevant to the migration of radionuclide through catchments;
- Development of the simplest generic model for predicting the time behaviour of ^{137}Cs and ^{90}Sr migration from catchment to water bodies.

III. Progress achieved including publications

In the past years a variety of models were developed for predicting the migration of radionuclide in catchments. These models are based on the quantitative evaluation of the most important processes accounting for the transport of radionuclides in drainage areas. A model is characterized by the so called "Green Function" (GF) that is here defined as the amount of radionuclide, calculated by means of the model, flowing per unit time from catchment to water body following a single pulse deposition. From the experimental point of view, the radionuclide migration process is characterised by the so called transfer function (TF), which is the measured amount of radionuclide flowing per unit time from an upstream drainage basin to a water body following a single pulse deposition of a radioactive material. As stated in the summary, the comparison of the GF of a model with the experimental TFs is useful to evaluate the model performances. It allows one to understand what aspects of the migration processes are adequately modelled and what improvements need to ameliorate the quality of model predictions. The "GF-TF" comparison is an objective method to validate models. The first aim of this study was to determine the essential features of models, developed to predict the behaviour of the radionuclide in catchments, by analyzing their GFs and comparing these with the experimental TFs "catchment to water body" evaluated after the Chernobyl accident using water contamination data collected by some European Laboratories. During the present project the GFs of various models were evaluated by means of analytical calculations. The results were reported in detail in the scientific literature (Monte, to be published). In the present report we will summarise the results of the analysis of two models (Korhonen, 1990; Joshi & Shukla, 1991) accounting for the most important processes affecting radionuclide migration in catchments. In general, these models consider important aspects of the migration processes. They show interesting, fundamental approaches that are used by almost all the other models aimed to predict the migration of radionuclides in catchments. The model developed by Korhonen shows a high level of complexity. Soil in the drainage

area is subdivided in layers of various thicknesses. The migration of radionuclides from one layer to the other is evaluated accounting for the water balance. The model hypothesises constant rates of water infiltration from one layer to the other. As a consequence the water content of each layer is supposed to be constant with time. The last layer is a sink compartment. Only the first layer contributes to the runoff. As the Korhonen's model is based on the subdivision of soil in 5 layers, the last one being a sink compartment, the model GF ($\Gamma_r(t)$) (dissolved radionuclide) is composed of four exponential terms:

$$\Gamma_r(t) = \sum_{i=1}^4 A_i e^{-(\lambda_i + \lambda)t} \quad (1)$$

where λ is the radioactive decay constant, $\lambda_i + \lambda$ the effective time decay constants due to environmental effects an A_i are dimensionless constants accounting for the relative weight of each exponential component. Supposing that the thicknesses of the various layers are, respectively, 1 cm, 4 cm, 10 cm and 15 cm (data used by Korhonen) we get:

$$\lambda_1 = \frac{3.333 \cdot 10^{-6}}{R}; \lambda_2 = \frac{6.564 \cdot 10^{-7}}{R}; \lambda_3 = \frac{2.299 \cdot 10^{-7}}{R}; \lambda_4 = \frac{2.448 \cdot 10^{-8}}{R} \quad \text{s}^{-1} \quad (2)$$

Using $R = 3000$ (a value obtained supposing the density of soil equal to 1 kg dm^{-3} and $k_d = 3000 \text{ dm}^3 \text{ kg}^{-1}$ (Korhonen 1990)), the values of the eigenvalues are:

$$\lambda_1 = 1.1 \cdot 10^{-9}; \lambda_2 = 2.2 \cdot 10^{-10}; \lambda_3 = 7.7 \cdot 10^{-11}; \lambda_4 = 8.2 \cdot 10^{-12} \quad \text{s}^{-1} \quad (3)$$

The model developed by Joshi & Shukla (1991) is mainly focused on the role of the "soil-water" partition coefficient (k_d). The GF of the model may be calculated by the model equations. Define $V_{wi}(t)$ as the rate of rainfall (m s^{-1}), $V_{si}(t)$ as the water penetration depth (m), λ as the radioactive decay constant and k_{di} as the dimensionless partition coefficient ($k_{di} = \rho k_d$, $\rho = \text{soil density expressed as } \text{kg m}^{-3}$, $k_d = \text{soil-water partition coefficient expressed as } \text{m}^3 \text{ kg}^{-1}$). The structure of the model GF depends on the time behaviour of $V_{si}(t)$ and $V_{wi}(t)$. Joshi and Shukla (1991) hypothesise that the ratio $V_{si}(t)/V_{wi}(t) = \xi$ is constant with time. The dissolved radionuclide flux (GF) is

$$\Gamma_r(t) = \frac{1}{\xi k_{di}} I_i(0) e^{-\left(\lambda + \frac{1}{\xi k_{di}}\right)t} \quad (4)$$

where $I_i(0)$ is the radionuclide inventory in the watershed at initial time. The TF for some rivers in Europe were evaluated (Monte, 1995a), following the Chernobyl accident, using the results of measurements carried out by some European laboratories (Kaniviets & Voitcekhovich, 1992; VAMP Aquatic Working Group, Status Report, 1992; Queirazza & Martinotti, 1987). The experimental dissolved radionuclide flux in the examined rivers, which collect running water from large catchments, may be fitted by the following function

$$\Phi_T(t) = \varepsilon D (\mu_1 \Phi(t)^{\alpha_1} A_1 e^{-(\lambda_1 + \lambda)t} + \mu_2 \Phi(t)^{\alpha_2} A_2 e^{-(\lambda_2 + \lambda)t}) \quad (5A)$$

$$A_1 + A_2 = 1 \quad (5B)$$

$$\mu_1 = \Phi(0)^{1-\alpha_1} \quad (5C)$$

$$\mu_2 = \Phi(0)^{1-\alpha_2} \quad (5D)$$

The list of symbol used in equations 5A-5D are reported in Table 1. Evaluations of the parameters of the above equations are summarised in table 2. The available experimental data did not allow to evaluate α_1 with accuracy. As a consequence the data-fit were carried out using $\alpha_1=1$.

It is now possible to focus on the comparison of TFs and model GFs. The models are based on the role of k_d on dissolved radionuclide migration. The Korhonen (1990) model predicts 4 exponential components due to the runoff of water in soils. Using a soil-water ^{137}Cs partition coefficient of $3 \text{ m}^3\text{kg}^{-1}$ and, consequently, $R=3000$, the shortest component of the GF, that corresponds to the highest eigenvalue of the model equations, shows an effective decay constant of $1.1 \cdot 10^{-9} \text{ s}^{-1}$. This means that the model is not able to simulate the value of the effective-decay constant of the TF short-term component which is of the order of 10^{-7} s^{-1} (see Table 2). Using constant thickness layers ($h_1=h_2=h_3=h_4$), it is possible to derive a general expression for λ_1 : $\lambda_1 = 5 \cdot 10^{-8} / (R h_1) \text{ s}^{-1}$. To get a value of λ_1 of the order of 10^{-7} s^{-1} we must use $h_1 \approx 0.17 \cdot 10^{-3} \text{ m}$. As consequence, the short component of the experimental TF may be simulated, using Korhonen (1990) model, supposing that the runoff takes part in a very thin soil layer of, approximately, two tenths of millimetre. As this result does not seem realistic, we must conclude that the short term component of experimental TF can not be explained exclusively by the water run-off in the upper soil layer. Other processes, such as the vegetation wash-off, may be responsible of the TF short term.

Both Joshi & Shukla (1991) and Korhonen (1990) models are based on the correlation of the effective decay constants with the k_d . The models account for this correlation by means of an inverse function: as k_d increases the effective decay constant decreases [see equations (2) and (4)]. This seems in contrast to the experimental observations. Indeed (see Table 2) the experimental long term effective decay constant for ^{90}Sr , a radionuclide characterised by a low value of k_d , is lower than the corresponding parameters for ^{137}Cs (high k_d radionuclide).

When α_2 (or α_1), in equation 5A, is different from 1, the concentration of dissolved radionuclide in water, that may be calculated as the ratio $\Phi_T(t)/\Phi(t)$, depends on the water flux. This non linearity effect, that is significant for the long term component of ^{90}Sr (see Table 2), is not explicitly accounted by the analysed models. The high value of the ^{137}Cs experimental effective long term decay constant may be related to some non-reversible processes, such as the radionuclide interaction with soil particles in the catchment, that are responsible of the decrease, with time, of radionuclide availability to migration. Possible explanations of the non linearity effect are the different contributions of dissolved radionuclide from soil layers of different depth, the effect of water saturation of soil layers and the effect of sediment in watercourse beds. Indeed the upper part of the soil is heavily contaminated and contributes considerably to the contamination carried by the running waters. Due to the saturation effects of the

soil layers (see for instance Vardavas 1988) the amount of radionuclide transported by running water rises with the water flux. Indeed, as the water flux in catchments increases, the water saturation of the beneath soil layers implies that a larger amount of the water flux interacts with the more contaminated upper soil layer. When the running waters reach watercourses, the interaction with the bottom contaminated sediments involves a modification of the levels of radionuclide concentration in water. For instance, if the run-off waters show levels of contamination higher than the watercourse, bottom sediments will partially remove the exceeding amount of radionuclide. This effect is more conspicuous for ^{137}Cs (large k_d value) than for ^{90}Sr (low k_d value).

The experimentally calculated TFs refer to systems composed of a catchment and of a watercourse collecting waters from the catchment itself, whereas the analysed models do not ever account for the effects of watercourse on the "catchment to water body" migration process. The MARTE (Model for Assessing Radionuclide Transport in aquatic Environment) model, was developed to predict the dissolved radionuclide concentration in a watercourse collecting water from a catchment. The model is based on important phenomena that may explain some of the peculiar behaviour of dissolved radionuclide in catchment-river system which are not properly predicted by the other models analyzed here. The model comprises two sub-models: a) sub-model A to predict the radionuclide migration in catchment; b) sub-model B to predict the radionuclide behavior in a watercourse collecting water from the catchment modelled by A.

Sub-model A, whose structure is reported in figure 1, considers the catchment vertical profile divided in three horizontal layers. This choice seems appropriate to predict the radionuclide migration over a period of few years. The equations used to describe the migration of radionuclides in these layers are based on the following processes:

a) processes relevant to radionuclide behaviour:

- interception of deposited radionuclide;
- radioactive decay;
- removal of radionuclide due to the wash-off water;
- migration of radionuclide from the first layer to the second layer as consequence of water infiltration.

b) processes relevant to water flow:

- horizontal movement of water through the layer;
- water saturation effects in the layer;
- contribution of the layer to water run-off;
- water infiltration from the first layer to the second layer.

The equations of the model are reported in details in Monte (to be published). For reasons of brevity they are not showed here. All the non-reversible process implying a reduction of the radionuclide availability to migration in catchment, such as the non reversible interaction of radionuclide with soil and sediment particles (see for instance Comans & Hockley, 1992) and the removal of radionuclide in attached phases as consequence of the migration of eroded particles in the catchment, are summarised as a first order process. The above phenomena play an important role for caesium but are relatively non significant for strontium.

Sub-model A is linked with sub-model B, described in detail elsewhere (Monte 1993, Monte 1995b), simulating the migration of radionuclide in watercourses.

The structure of sub-model B is reported in figure 2. The model is based on the following processes:

- the input to watercourse of radionuclide from catchment basin;
- the direct deposition of radionuclide onto the water surface;
- the flow of radionuclides in dissolved form;
- the flow of radionuclides attached to the suspended particulate;
- the migration of radionuclide from the upper sediment "interface layer" to the bottom sediment;
- the radioactive decay;
- the removal of radionuclides by sedimentation;
- the migration of radionuclides from bottom sediment to the "interface layer".
- the migration of radionuclides to deep sediment;
- the radionuclide migration to deep sediment as result of the upward movement, due to the sedimentation, of the interface and bottom sediment layers.

The water fluxes, in the various soil layers, are considered input functions and are empirically related to the total water flux in the catchment.

The model was solved using Ithink™ Software running on a Mac Intosh IICI computer. Although, the model explains the characteristic behaviour of radionuclides (such as ^{137}Cs and ^{90}Sr) in catchments, however, it may be impractical due to its complexity. It is possible to develop a semi-empirical, two-box "minimal model" of the considered radionuclides in catchment characterised by a GF whose structure corresponds to the mathematical form of TFs. Let F and S, respectively, the radionuclide deposit (Bq m^{-2}), available for migrating, in the fast and in the slow "radionuclide storage" compartments of catchment. F may be considered as the amount of radionuclide in the vegetation cover and, in general, in all "fast" compartments of the catchment; S is the radionuclide stored in the upper soil layer.

F and S are solutions of the following equations (see Table 1 - list of symbol):

$$\frac{dF}{dt} = -(\lambda_1 + \lambda)F + A_1 D(t)$$

$$\frac{dS}{dt} = -(\lambda_2 + \lambda)S + A_2 D(t)$$

The radionuclide flux from the catchment (Bq s^{-1}) is:

$$\Phi_r = \varepsilon \Phi(t) \left\{ F + \left[\frac{\Phi(t)}{\Phi(0)} \right]^{\alpha_2 - 1} S \right\}$$

Simple calculations show that the Green function of the model corresponds to the mathematical form of the experimental transfer function (5A-5D). The model may be applied in practical circumstances to get an approximate evaluation of the migration of radionuclide from a catchment. In case of ^{90}Sr ε may be supposed, at least, one order of magnitude greater than the corresponding value for Cs.

REFERENCES

Comans R.N. J. & Hockley D.E. Kinetics of cesium sorption on illite. *Geochimica et Cosmochimica Acta* Vol. 56: 1157-1164; 1992

Hilton J., Livens F.R., Spezzano P. & Leonard D.R.P. Retention of radioactive caesium by different soils in the catchment of a small lake. *The Science of the Total Environment*, 129: 253-266; 1993

Joshi S.R. & Shukla B.S. The role of water/soil distribution coefficient in the watershed transport of environmental radionuclides. *Earth and Planetary Science Letters*, 105: 314-318; 1991

Kaniviets, V.V. & Voitcekhovich, O. V. (1992). Scientific report: Radioecology of water systems in zone of consequences of Chernobyl accident. Report of Ministry of Chernobyl Affairs of Ukraine. Contract Number 1/92 (in Russian).

Korhonen R. Modeling transfer of ^{137}Cs fallout in a large Finnish watercourse. *Health Physics* 59 : 443-454; 1990.

Monte, L. A predictive model for the behaviour of radionuclides in lake systems. *Health Phys.* 65:288-294; 1993.

Monte, L. Evaluation of Radionuclide Transfer Functions from Drainage Basins of Fresh Water Systems. *J. Environ. Radioactivity* 26: 71-82; 1995a

Monte, L. A simple Formula to Predict Approximate Initial Contamination of Lake Water Following a Pulse Deposition of Radionuclide. *Health Phys.* 68:397-400; 1995b

Monte, L. Analysis of Models Assessing the Radionuclide Migration from Catchments to Water Bodies. *Health Phys.* (to be published)

Queirazza, G. & Martinotti, W. - Radioattività nell'acqua del Po: tratto mediano e delta. (Radioactivity in water of river Po: median tract and delta) *Acqua Aria* 7: 819-830; 1987

Sundblad B., Bergström U., Sverker E. Long term transfer of fallout nuclides from the terrestrial to the aquatic environment. In: Moberg, L., ed. *The Chernobyl fallout in Sweden. Results from a research program on environmental radiology.* Stockholm, The Swedish Radiation Protection Institute 207:238; 1991

VAMP - VALIDATION of Model Predictions (IAEA). Status report produced at Aquatic Working Group meeting, 2-5 March 1992 Vienna, Austria

Vardavas I. M. A simple water balance daily rainfall-runoff model with application to the tropical Magela Creek Catchment. *Ecological Modelling*, 42: 245-264; 1998.

Table 1-List of symbols

A_1, A_2	= relative weight of short and long term components of transfer function (pure numbers); condition $A_1 + A_2 = 1$;
D	= radionuclide deposition on catchment (Bq m^{-2});
$D(t)$	= radionuclide deposition rate on catchment ($\text{Bq m}^{-2} \text{ s}^{-1}$);
t	= time (s);
α_1, α_2	= exponents of water flux to account non-linearity effects;
$\Gamma_r(t)$	= Model Green function (Bq s^{-1});
ε	= transfer coefficient deposition->water (m^{-1});
$\Phi(t)$	= water flux ($\text{m}^3 \text{ s}^{-1}$);
$\Phi_r(t)$	= Transfer Function (Bq s^{-1});
$\lambda_1 + \lambda$	= effective time decay constant due to environmental effects (short term component) (s^{-1});
$\lambda_2 + \lambda$	= effective time decay constant due to environmental effects (long term component) (s^{-1});
λ	= radioactive decay constant;
μ_1, μ_2	= normalisation factor introduced to assure that units of measurements are consistent.

Table 2 - Review of measured values of TF parameters.

River	radionuclide	ϵ (m^{-1}) (order of magnitude)	A_2 (dimen- sionless)	α_2 (dimen- sionless)	standard deviation of α_2	$\lambda_1+\lambda$ (s^{-1})	standard deviation of $\lambda_1+\lambda$	$\lambda_2+\lambda$ (s^{-1})	standard deviation of $\lambda_2+\lambda$	reference
Po (a)	^{137}Cs	$10^{-3} - 10^{-2}$				2.3×10^{-7}	5.5×10^{-8}			Monte (1995)
Rhine (a)	^{137}Cs	$10^{-2} - 10^{-1}$	0.052	0.53	0.3	6.5×10^{-7}	1.3×10^{-7}	2.7×10^{-8}	0.6×10^{-8}	Monte (1995)
Prypiat (a)	^{137}Cs	$10^{-2} - 10^{-1}$	0.035	1.08	0.06	5.2×10^{-7}	6.5×10^{-7}	1.8×10^{-8}	0.7×10^{-9}	Monte (1995)
Dnieper (a)	^{137}Cs	$10^{-2} - 10^{-1}$	0.028	0.86	0.06	8.8×10^{-7}	1.1×10^{-7}	1.1×10^{-8}	0.7×10^{-9}	Monte (1995)
Teterev (a)	^{137}Cs			0.96	0.15			8.2×10^{-9}	$2. \times 10^{-9}$	Monte (1995)
Uzh (a)	^{137}Cs			1.02	0.1			1.5×10^{-8}	1.8×10^{-9}	Monte (1995)
Inlets of Devoke Water ^(b)	^{137}Cs			1.0-1.3				1.2×10^{-8}		Hilton et al. (1993)
Inlets of lakes Hillesjön and Salgsjön ^(b)	^{137}Cs					$.6 \times 10^{-7}$ - 1.5×10^{-7}		$7. \times 10^{-9}$ - $2. \times 10^{-8}$		Sundblad et al. (1991)
Po (a)	^{131}I					1.1×10^{-6}	6.5×10^{-8}			Monte (1995)
Po (a)	^{103}Ru					4.7×10^{-7}	4.0×10^{-8}			Monte (1995)
Prypiat (a)	^{90}Sr		0.048	1.41	0.08	9.0×10^{-7}	1.1×10^{-7}	4.9×10^{-9}	0.9×10^{-9}	Monte (1995)
Dnieper (a)	^{90}Sr		0.166	1.4	0.08	5.2×10^{-7}	1.5×10^{-7}	5.5×10^{-9}	0.9×10^{-9}	Monte (1995)
Teterev (a)	^{90}Sr			1.12	0.14			3.6×10^{-9}	2.1×10^{-9}	Monte (1995)
Uzh (a)	^{90}Sr			1.31	0.09			5.9×10^{-9}	1.8×10^{-9}	Monte (1995)

(a) dissolved radionuclide

(b) total ^{137}Cs (particulate+dissolved)

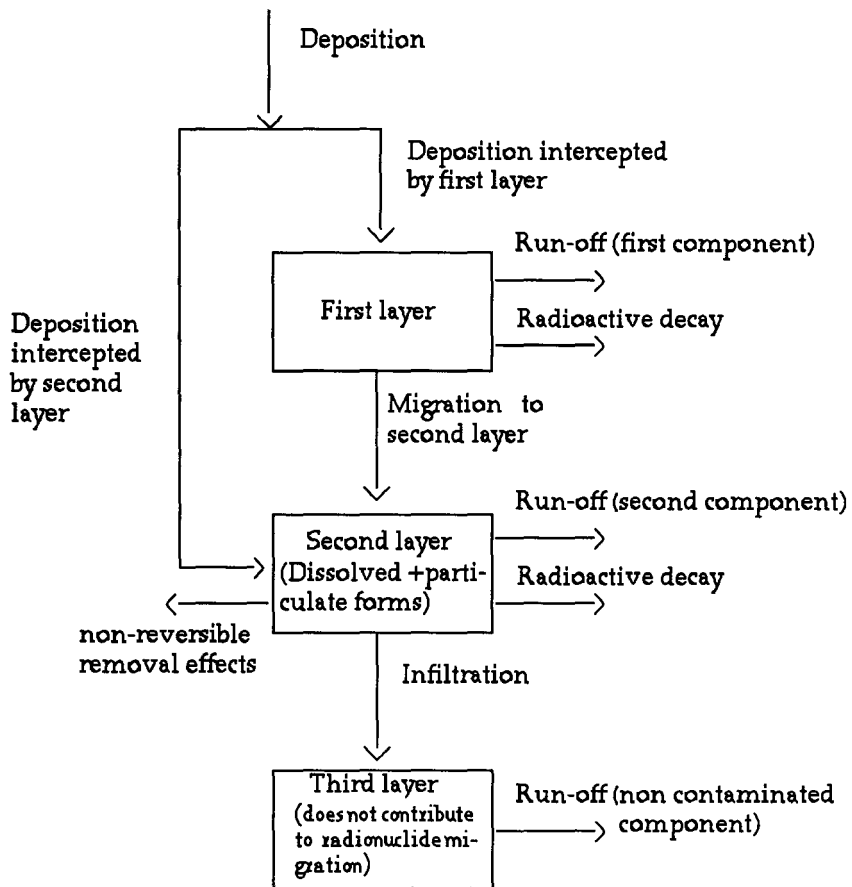


Figure 1

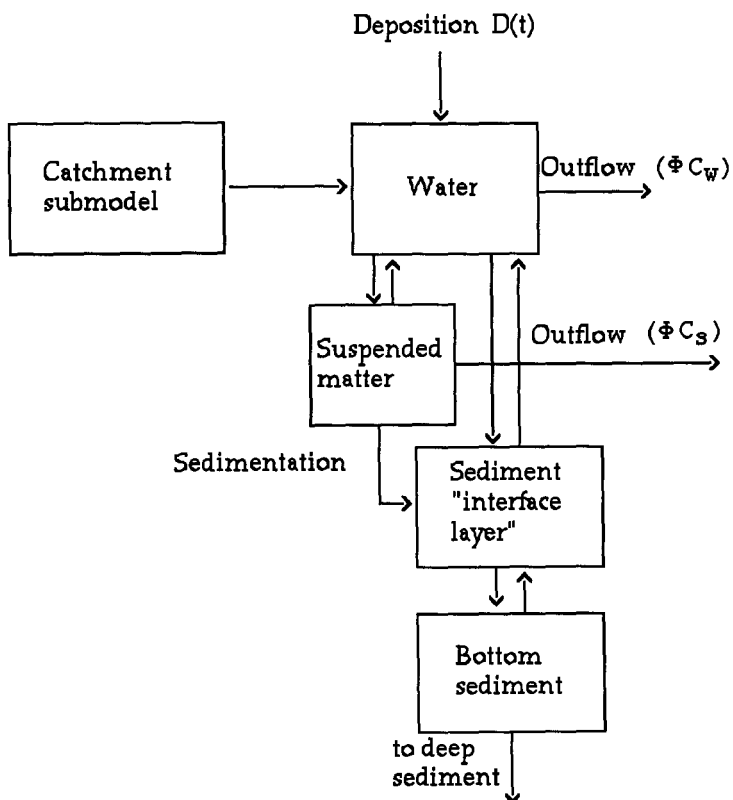


Figure 2

Head of Project 2: Dr. J. Van der Steen

Author: R. Heling

Department of Radiation Protection, Business Unit Nuclear, KEMA NV, P.O. Box 9035, 600 ET Arnhem, The Netherlands

II Objectives for the reporting period

The study, during the reporting period, can be subdivided into two phases. These are in order of execution:

1. data collection for the case study Rhine Catchment and lake Hillesjön:

1a. collection and evaluation of hydrological data which is of importance for the evaluation of the behaviour of radionuclides in the Rhine Catchment.

1b. collection of data concerning radionuclides in the Rhine River and its tributaries.

1c. collection of general data such as maps supplying information on land use, relief, and soil composition.

1d. collection and evaluation of chemical and geochemical data concerning the Rhine catchment area.

2. Studying the differences in amounts of transported radionuclides in the subcatchments of the Rhine River by combining the various types of collected data and application of a suitable process description (see also point 1). Estimation of the values of the dominant parameters of the model by means of an empirically based submodel or by the determination of parameter values by tuning the model on the two different catchment systems.

III Progress achieved including publications

INTRODUCTION

In 1993, seven years after the accident with the nuclear power plant in Chernobyl, enhanced levels of radiocaesium are measured in rivers in Russia and Ukraine. Also in aquatic systems far away from Chernobyl activity concentrations have not reached the pre-Chernobyl levels yet. At present the Rhine River continues transporting radiocaesium to the lake IJsselmeer. This secondary load is mainly due to leaching from the catchment area. Because of the long-term transfer for ^{137}Cs , besides radionuclides which adsorb less persistently to sediments or soil, the assessment of this transfer is under investigation. The objective of this project is to describe the transfer of radionuclides adequately, by means of data analysis in combination with a literature search and model development. This will lead to an enhanced system of simple models predicting the leaching rates of radionuclides from any possible catchment area. Explaining the differences in leaching rates of various types of river catchments and the identification of the dominating parameters are the most important aims of this study. This study is performed within the framework of the Nuclear Safety Fission Project. Its aim is among others to gain a better insight in the varying behaviour of radionuclides in catchment systems in Europe. Hydrological, geochemical, and terrestrial information is collected and analyzed in order to provide parameter values for the application in an enhanced model. This report gives an overview of the progress in the previous project years.

THE MODEL DESCRIPTION

In this section the description of the simple catchment model emphasizes on the mathematical descriptions of the processes reported in literature. A model approach from literature is selected, and additionally scientifically based processes are implemented in the model. The parameters of this enhanced model are subsequently based on field data, instead of generic literature values.

Generally, the first pulse of radionuclides can be modelled by a combination of river and runoff models. The complexity of these models can vary from very simple, using a transfer rate for the complete catchment (Joshi & Sukhla, 1991; McDougall et al, 1991; Korhonen, 1991) to very complex runoff models (Braun & Renner, 1992; Chiew et al 1993; Popov, 1993) with a high resolution. However, most of these models calculate the pulse of radionuclides in a catchment system in the short period after an accidental release.

To determine the transport of radionuclides in the mid- and long-term, the pulse of radionuclides into a lake after the Chernobyl accident and the more constant leaching from the catchment is evaluated (Mundschenk, 1992). Two different approaches to describe the long term behaviour of radionuclides can be distinguished: the first approach is a description of the transfer of radionuclides at the river inlet of lake systems by means of a so-called exponential transfer function. The second approach is the application of a simple box-type runoff-model describing the leakage of radionuclides.

Monte (Monte, 1994) evaluated the pulse into several lake ecosystems by means of a transfer function giving insight in the long term behaviour for different types of catchments. The transfer function, is applied on various catchments in Europe (Po, Pripjat, Dnieper, Teterev), resulting in exponential coefficients of approximately the same value for the long-term transfer in large watercourses. The transfer function $\phi(t)$ is generally expressed as the sum of time-dependant exponential terms (equation 1).

$$\Phi(t) = \sum_i k_i e^{-(\lambda_i + \lambda_r)t} \quad (1)$$

λ_l being the leaching rate (s^{-1}), λ_r the decay rate (s^{-1}), and k_i is a combination of parameters dependent on the initial deposition and the water flow.

Another approach has been worked out by McDougall (McDougall et al, 1991). She applied a simple linear equation to describe the transfer from the catchment to the lake. This approach was successfully applied on the relatively small lake ecosystems Windermere and Esthwaite in Cumbria England. By coincidence very heavy rainfall caused there relatively high contaminations after the

Chernobyl accident. In this model it is assumed that caesium enters the catchment by polluted rainfall at the first day, followed by two types of "loss" of ^{137}Cs : immediate loss due to runoff at the day of deposition and a long term runoff transport of the accumulated ^{137}Cs in the period afterwards. It is assumed, that the rapid runoff of radionuclides is caused mainly by nuclides dissolved in water, while the slow catchment loss is particulate, that is attached to soil particles. The change in concentration of radionuclides in the catchment is described by the following equation:

$$\frac{d[\text{Cs}]}{dt} = N * C_r * R * (1 - L_r) - (L_a + k) * C_c \quad (2)$$

where C_r is the concentration of caesium in rainfall (Bq l^{-1}), R is the average daily rainfall (mm d^{-1}), L_r is the portion of freshly deposited caesium lost (removed from the catchment) in immediate runoff, L_a is the proportion of accumulated caesium lost in long-term runoff (d^{-1}), C_c is the concentration of available caesium in the catchment (Bq m^{-2}), and N the duration of contaminated rainfall (d).

This approach implies, since there is no time-dependant term for the description of the short-term runoff, that the dissolved portion of caesium leaves the catchment immediately at the moment of the deposition in the same time step equal to the duration of the rainfall. This is the reason why this term is called "immediate runoff". It's a hypothetical assumption without any further proof, whether this process does actually takes place in reality in such a manner. The second term is a slow process, assuming a constant leaching of caesium accumulated during the rainfall period. In fact the $(1 - L_r)$ fraction becomes accumulated in the catchment and is leaking from the catchment to the lake in the period afterwards.

The flow $\phi(t)$ after the initial flush of radionuclides into the lake can be derived, solving the differential equation:

$$\Phi_i(t) = A L_a * (C_{c,0} * e^{-(k+L_a)t}) \quad (3)$$

Joshi (Joshi & Suhkla, 1991) proposed another model, supposing that the fluvial removal (removal by rivers) of radionuclides F_{ir} ($\text{Bq m}^{-2} \text{ s}^{-1}$) is proportional to the total radionuclide inventory of the watershed I_r ,

$$F_{ir} = K_i I_r \quad (4)$$

After multiplying this with the size of the catchment, the total transfer $\phi(t)$ (Bq s^{-1}) is obtained:

$$\Phi(t) = A * k_i I_r \quad (5)$$

k_i in equation (5) is the removal constant, and is defined as:

$$k_i = \frac{V_{wi}(t)}{V_{si}(t)K_{di}} \quad (6)$$

$V_{wi}(t)$ is the rate of annual volume of rainfall (cm/yr), V_{si} the water penetration depth (cm), λ the radioactive decay coefficient and K_{di} is the dimensionless distribution coefficient. This coefficient can also be written as $\rho \cdot K_d$ (K_d is the distribution coefficient between dissolved and adsorbed radionuclides in $m^3 kg^{-1}$ in the soil and ρ is the density of the top layer of the soil in $kg m^{-3}$). $1/k_i$ can be considered as the residence time of a certain radionuclide in the catchment.

The inventory of the catchment is calculated by the following equation:

$$\frac{dI_i}{dt} = F_i(t) - I_i(t) \left(\lambda + \frac{V_{wi}(t)}{V_{si}(t)K_{di}} \right) \quad (7)$$

where F_i is the time-dependent radionuclide deposition on the watershed ($Bq m^{-2} s^{-1}$).

The time-dependant behaviour of V_{si} and V_{wi} makes the transfer very complex. Joshi however assumed the ratio between those two variables (β) to be constant. Furthermore it is assumed that these parameters are nuclide-independent. After substitution of $\beta = V_{si}/V_{wi}$, and solving the equation for the long term, neglecting the initial behaviour of the pulse, the following equation for the flux $\phi(t)$ ($Bq m^{-2} d^{-2}$) from the catchment to the river or lake ecosystem is finally obtained using equation (2) and the solution of equation (6):

$$\Phi_i(t) = \frac{A}{\beta K_{di}} * I_0 * e^{-\left(\lambda + \frac{1}{\beta K_{di}}\right)t} \quad (8)$$

Another approach is followed by Korhonen (1990). In comparison with the aforementioned models Korhonen's model (Korhonen, 1990) shows a high level of complexity, using 5 layers of soil, and transfer of radionuclides in both the vertical and horizontal direction. However this approach is not discussed here, as these parameters are based on mathematically driven transfers rate without physical meaning. Other complex models like the runoff models summarized by Chiew (Chiew et al, 1993) and by Braun (Braun & Renner, 1992) mainly predict runoff dynamics. These models should be applied only for the transfer of radionuclides by short term runoff transporting dissolved radionuclides. Popov (Popov et al, 1993) took the downward migration and the time-dependent interaction with sediments into account in describing the release of radionuclides from the catchment. This model RETRACE also included the change in the distribution coefficient in the course of time due to the leaching of fuel particles and irreversible fixation processes. As stated above these models are, due to their complexity not convenient for the application on larger

catchment areas for long term predictions.

Model considerations

The model of Joshi and McDougall are both based on the same basic principle describing the release of radionuclides. The outflow from the area is considered proportional with the amount of radionuclides deposited on the area and therefore described by a linear equation. The difference between the two models is mainly found in the description of the initial contamination and the effective release of the radionuclides from the systems in the long term.

Both models have some parameters with a high uncertainty. Although in Joshi's model the leakage seems to be related to field parameters (the leakage is inversely proportional with both the distribution coefficient K_d of the soil and the ratio between the amount of rainfall and the penetration depth) the model accuracy and the predictive power is not higher than for the approach of McDougall. This is because the distribution coefficient in the soil (K_d), which governs the residence time of radionuclides in the catchment, is not known in many cases due to a lack of field data.

However this could be solved for a great part by assessing the K_d based on soil properties. The properties concern e.g. the grain size distribution, the capability of the soil to exchange cations (CEC), and the concentration of competitive ions like potassium and ammonium, which are in some cases known environmental parameters (ISSS; Comans, 1994). A first attempt to relate these parameters is the empirical derived relationship between the CEC, the potassium and ammonium concentration at the one hand and the K_d at the other hand. If the CEC is known, equation (9) can be applied to estimate the distribution coefficient. In the case no information is available, 100 - 200 $\mu\text{eq/g}$ can be selected as a default parameter.

$$K_d = \frac{1.5\% \cdot \text{CEC}}{M_k + 5M_{\text{NH}_4}} \quad (9)$$

K_d is the distribution coefficient ($\text{m}^3 \text{kg}^{-1}$), CEC is the cation exchange capacity ($\mu\text{eq g}^{-1}$), M_k the molarity of potassium ions (mM), M_{NH_4} the molarity of ammonium ions (mM).

The second parameter, the ratio between rainfall and penetration depth is more difficult to assess, partly because this ratio is a function of time. Indeed because of this Joshi encountered a lack of input data to test the model properly on large catchment systems. So the presence of measurable physical parameters in the equations seems is not necessarily an improvement in all cases in comparison to the application of rates, as new uncertainties might be introduced.

Since both models are hard to validate, the leaching parameters have to be assessed by means of parameter fitting on several catchment systems. In order to find these leakage rates, one could conclude that the approach brought forth by Monte is to a certain extent an useful tool to obtain insight in the overall leaching rates. Assuming linear behaviour of the system, the use of environment specific parameters can be tested in two ways. The first way is to adapt Joshi's approach of describing the leaching by a linear process and to compare the leaching parameters calculated by Monte's approach by recalculating the environmental parameters of the equations of Joshi. These calculated values can be validated with measurement data of field parameters or with the outcomes of simple empirical models describing these field parameters. The second way is to reject Joshi's approach and to find some non-linear empirical relationship between the leaching parameters and the collected data sets. This method, however, finding dimensionless numbers with parameters which influence the transfer requires even more parameter information for a great number of catchments.

To identify the different behaviour of the various types of catchments in this study, the first approach has been applied on subcatchments of the Rhine River, and on lake Hillesjön in Sweden.

A drawback of this approach is the fact, that the transfer of radionuclides in the catchment is caused by the transfer of radionuclides attached to particles, since erosion removes a part of the top layer of the soil. Therefore the equation for the leaching rate k_l can then be extended to take into account the removal of radionuclides due to the transport of particles. The leaching rate equation can then be described as follows:

$$k_l = \frac{1}{\beta K_{dl}} + \frac{E_c}{\beta * V_w}$$

where K_{dl} is the dimensionless distribution coefficient, and E_c the erosion rate in cm/yr.

A disadvantage of the extension of the leaching rate parameter is the introduction of new uncertainties in the prediction of the long term transfer of radionuclides. On the other hand an advantage is that the K_{dl} is more related to the real K_d as used in radiological studies. This makes the substitution of the K_d by means of a K_{dl} submodel more reliable. So in the study the sets with measurement data are used to derive possible values for the E_c and rainwater penetration depth V_s (see equation (6)).

PARAMETERS

According to the simple approach of Joshi's model a small number of parameters are required to describe the transfer of radionuclides from a catchment. A summary of the parameters and their default values, giving the best results, are listed in table 1.

Table 1. Parameters of the Model. ND = no default value or range: site specific parameter.

Value	Units	Defintion	
V_s	0.1	cm	Water penetration depth
V_w	75	cm/yr	Yearly rainfall rate
E_c	0.08	cm/yr	Erosion rate
A	ND	km ²	Surface of (sub)catchment
D	ND	kBq/m ²	Deposition on catchment
K_{dl}	calculated	m ² /kg	Soil-water distribution
K^+	10	mg/l	Potassium content soil
NH ₄	0	mg/l	Ammonium content in soil
F_n	0.5-0.9	-	Available fraction radionuclides for runoff transport

The water penetration depth V_s is based on the calibration and fixed for most of the subcatchments on 0.1 cm, except for the mountainous area, for which 0.05 cm is used. The question arises, whether these values are representative for run-off in large catchments or not. A combination of laboratory measurements (Bulgakov, 1991) and field observation shows that for the flood plains in the Chernobyl area, the runoff mainly transports nuclides from the upper 2-3 mm. The rainfall rate is fixed on 75 mm yearly for the distinct subcatchments of the Rhine River and for lake Hillesjön.

The erosion rate is simply based on the assumption, that a certain part of the toplayer of the soil, in which radiocaesium is fixed, is transported by runoff. A value of 80% has been found, based on the validation test itself. It is obvious that the erosion of particle associated caesium is governing the total leaching rate.

The surface area A was based on the division into subcatchments according to maps issued by the Rhine Commission (KHR/CHR, 1989). The deposition D is derived from deposition maps issued after the Chernobyl accident.

Although a wide range of different soil types are present, the information available from literature (ISSS) on soil properties is not detailed enough, to determine the various K_d values for each soil type with acceptable uncertainty. In general the potassium levels in soil is relatively high since the catchment of the Rhine River is eutrophic. Above a concentration of 1-2 mg/l potassium in the soil, the predicted distribution coefficient K_d is less sensitive for the potassium levels. The calculated K_d is 8.3 m³/kg. Validation of the K_d submodel for each subcatchment of the river Rhine could not be performed, since in literature the required K_d measurements for the various types of soils indicated on the soil maps are not available. So the adopted approach has been the selection of one value for K_d , representative for the entire catchment. This simplification can be omitted, when more detailed information about soil properties becomes available. An alternative approach is the calculation of K_d on the basis of a rough classification into 3 - 5 soil types.

The for runoff transport available fraction radiocaesium, which can be regarded as the fraction of the catchment area in direct contact with the adjacent water bodies, is very difficult to assess. The value is assumed to range between 0.5 - 0.9. Values at the lower bound of this range can be expected in low land area, while in mountainous areas the available fraction is increasing up to 1. However model results in agreement with the observations for lake Hillesjön, were only achieved assuming an available fraction of only 1 - 2 percent of the total deposited radiocaesium.

MODEL VALIDATION: RESULTS AND DISCUSSION

Joshi's model has been applied on both the catchment of the Dutch Lake IJsselmeer, and the Swedish lake Hillesjön. The lakes differ considerably in hydrological, and climatological properties. Lake IJsselmeer's catchment has an area of 183,000 km², while the catchment of Hillesjön has an area of 19 km².

The Rhine Catchment covers the centre of Europe, namely the main part of Germany, and the Netherlands half of Switzerland, Luxembourg, and the North-Eastern part of France. The terrain varies from mountain areas in the Swiss part, to flat land area with flood plains in the northern part (the Netherlands). The altitude varies between 3000 m (with snow-covered summits with a height of 4000 m or more in Switzerland), to 6.5 m below sea level in the western part of the Netherlands. Soil types in the catchment varies from areas with glaciers in Switzerland, via Luvisols, and Cambisols in the southern and middle part of Germany, Fluvisols in and around the river bed, Podzols, and in some areas e.g. in the eastern part of the Netherlands (ISSS; CHR, 1970), Luvisols. The water discharge in the main tributaries of the Rhine River varies from 200-300 m³ s⁻¹ in the smaller subcatchments and in the Swiss part of the catchment, up to about 2200 m³ s⁻¹ at the border between the Netherlands and Germany in the main river.

The largest subcatchments around the tributaries are (in order of size): the River Mosel area (20,700 km²), the River Main area (19,600 km²), the River Aare catchment (17,800 km²) and the River Neckar area (14,000 km²). The main branch can be subdivided into smaller areas. The largest areas are the Dutch part of the Rhine Catchment with an area of 23,000 km² (the major part of the country), and the area around the city Bonn, with a size of 10,000 km² (CHR, 1970; ISSS; CHR, 1989).

In this study calculations on the ^{137}Cs transport have been performed to obtain the transport in the first 4 years after the initial deposition. The hydrological behaviour, important for the description of the transfer of each subcatchment, can be represented by discharge rates at the endpoint of each tributary. These sites are located before the junction with the main river where some 95% of the water budget of the subcatchment is passing.

Data were taken from an extensive database from time-dependent data on discharge rates, suspended matter and radiological data supplied by the National Institute of Public Health and Environmental Protection in the Netherlands, the German *Bundesanstalt für Gewässerkunde* and the Swiss *Landeshydrologie und -geologie*. Special software packages (in Fortran-language) have been developed to handle these extensive data sets. Not for all endpoints of the tributaries, discharges rates and radionuclide measurements were available. In these cases the model was applied without the possibility of comparing the outcomes with radiounuclide budgets.

Model calculations of the transfer of radiocaesium in a number of tributaries compared with the calculated quarterly loads of radiocaesium are presented in figure 1. This figure shows the calculation of the transport of ^{137}Cs through the Rhine River respectively near the city Basel (165.1 km from Lake Constance), near Garstadt located at the River Main (324.8 km from the junction with the Rhine River), near the city of Koblenz at the River Mosel, near the junction with the Rhine, and near Lobith (862.1 km from Lake Constance), where the Rhine River enters the Netherlands. Missing values (md) in the figures are due to differences in resolution, sample frequency and/or length of the timeseries in the available measured data.

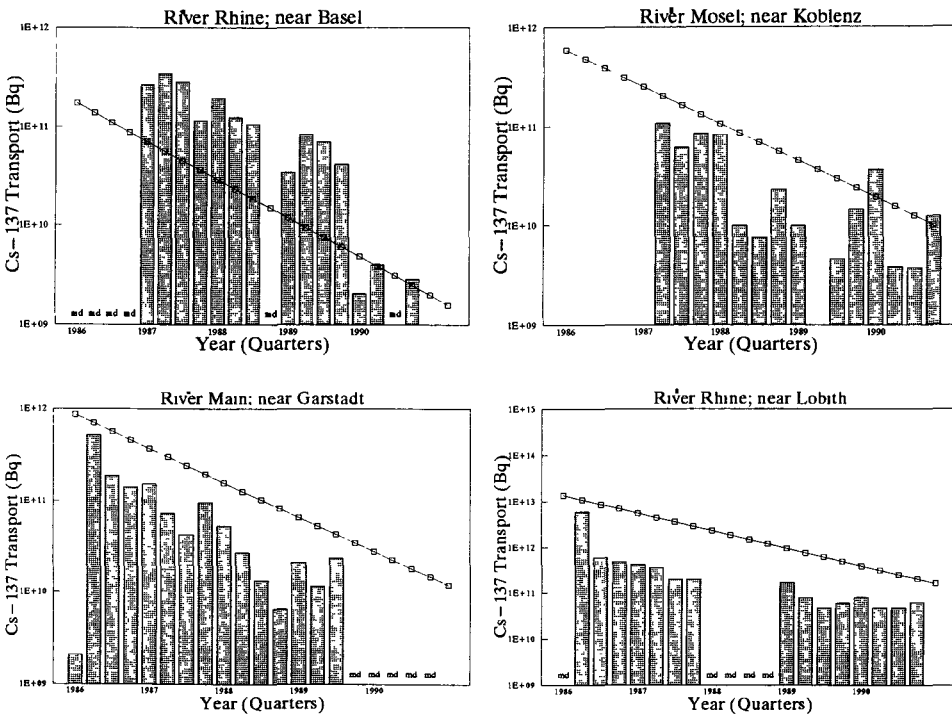


Fig. 1 Validation results of the application of Josh's model on 4 locations in the catchment of the Rhine River. Top left: River near Basel. Top right: River Mosel near Koblenz. Bottom left: River Main, near Gardstadt. Bottom right, Rhine River near Lobith. md = missing data.

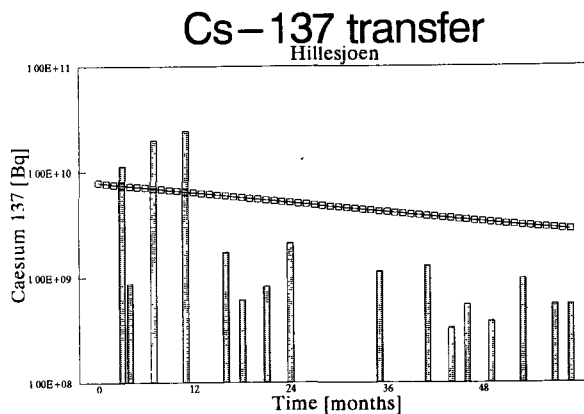


Fig. 2 Validation results of the application of Joshi's model on lake Hillesjön. Comparison model results (line) with measurements (bars).

The effective long term leaching rate calculated by Monte (Monte, 1994) for the total Rhine River is $2.7 \cdot 10^{-8} \text{ s}^{-1}$ (0.85 per year). The model predictions supplied an effective decay of radiocaesium on annual basis ranging between 0.85 and 0.89 over the various subcatchments. Mundschenk (Mundschenk, 1992) derived the gradient of the time-dependent behaviour of radiocaesium and found for both the mainstream and the tributaries of the Rhine River a value of 0.32 per year. The difference between this gradient and the value found by Monte (Monte, 1992) is caused by the fact, that Monte calculated this gradient from the period directly three quarter of year after the initial pulse, while Mundschenk selected the period 1.5 year after the initial pulse in May 1986. It must be stated, that the input parameters β and K_d not only determine the leaching rate, but also the initial value of the flux of radionuclides. Both values have to fit with the measurements which limits the possibility of tuning the model. For Hillesjön the gradient was 0.2 on yearly basis.

The value for β , the ratio between the penetration depth V_s , and the rainfall rate V_{wi} , is $1.3 \cdot 10^{-3} \text{ year}$, for the subcatchments of the Rhine River, except for the mountainous areas, i.e. upper Rhine area including the river Aare. The value obtained for β for these upstream areas is $6.7 \cdot 10^{-4} \text{ year}$. These values are in agreement with the estimated value in Joshi's studies (Joshi & Shukla, 1991) for ^{137}Cs in different watersheds. For the Hillesjön catchment a value of β of $1.3 \cdot 10^{-3} \text{ year}$ is appropriate to obtain sufficient results. In this case similar values for the penetration depth of water and for the yearly rainfall rate are applied. The erosion rate however is fixed on 20% of the penetration depth. Higher fractions give worse model results.

The K_d values for ^{137}Cs reported in Joshi's study are one to two orders of magnitude higher, than calculated in this study. Since the residence time τ of the radionuclide is proportional to the dimensionless distribution factor K_d , the residence time or the effective half life of ^{137}Cs for the Rhine catchment appeared to be lower in this study than estimated in Joshi's study for various catchments in the world. For lake Hillesjön the potassium in the soil is fixed on 0.5 mg/l to achieve reasonable results. Measurements of the CEC and the potassium concentration in the soil around the lake could support this assumption. The most extreme deviation from the Rhine River modelling was the for runoff available fraction, in the case of Hillesjön good results were obtained by selecting 2% of the deposited amount of radionuclides. In comparison with the Rhine River this is a small fraction, but in perfect in agreement with the fraction of peat bog areas in the catchment of this lake.

The problem is in fact the determination of the erosion rate E_c . Physical models can be applied to determine these rates. Joshi suggests to determine these rates by using the knowledge of the behaviour of two different radionuclides in a catchments. This is often, however, difficult to obtain. Good model results were achieved by selecting an annual removal by erosion of 50% - 80% of the penetration depth of the rainwater.

Summarizing the outcomes of the model tests and calibration it can be concluded that in the case of the application of the extended Joshi's approach, a great number of parameters are required (such as the penetration depth of water, and erosion rate, and the for runoff available fraction). Furthermore it is concluded that the layer in which runoff transport takes place, is relatively small, only a few millimetres. It is not clear at present, whether this result indicates that this value is without physical meaning, or represents the overall behaviour of runoff in large catchments, taking into account that a large variation in properties in the catchment are summarized in one single value.

It can be concluded from this model validation study, using a limited number of input data, that Joshi's approach is an useful tool to predict the long-term behaviour. The extension to the use of the real K_d by introducing the erosion of soil and the K_d submodel can improve the model reliability. Large catchments can be treated by this approach, taking into consideration that the meaning of some of the parameters may deviate from the real physical meaning. Fixed values for parameters such as penetration depth as a result of the validation, can be introduced. The difference in parameter selection between a large catchment such as the Rhine River catchment, and small areas such as lake Hillesjön appeared to be the difference in ratio erosion rate and penetration depth. However, more data is required, and more catchments studied to substantiate this conclusion. More data are required in terms of soil properties, erosion rates etc, to evaluate which part of the catchment plays dominant role in the transfer. Additional large and complex catchment models should supply input data for this common approach.

A remarkable fact however, arising from this study is that the subcatchment of the Rhine River, although varying in size, relief, and radiocaesium inventory can be modelled by selecting the same or similar input parameters. This might indicate that large catchments systems behave similarly in terms of leaching of radionuclides, and deviates from small lake catchments. Also the fact that the transfer of radionuclides in various European catchments appeared to vary only one or two orders of magnitude underline this statement (Monte, 1994).

CONCLUSIONS AND RECOMMENDATIONS

- In the literature only non-calibrated models are found to describe and analyze the transfer of radionuclides from terrestrial areas to aquatic systems. The present models which are present are based on linear equations with simplified approaches in terms of hydrological loads containing input parameters which are to some extent related with field data.
- Assuming linearity in the leakage of radionuclides from the catchment, the transfer of radionuclides can be derived by means of transfer functions using measurement data collected from the Rhine River. These empirically derived leaching rates are used to calculate the site specific parameters. These calculated values can be compared with real field data. In the case these predictions are in accordance with the field data, Joshi's box-model approach can be considered as valid and valuable tool to assess the long term leaching of radionuclides from a large catchment area.
- The submodel introduced in Joshi's model increases the predictive and descriptive power of this model by providing one of the dominant parameters of the box-model like the distribution of radionuclides between the dissolved and particulate phase. Since no validation data is available, the outcomes of this submodel were applied to obtain the fit of the box-model on measurement data of the Rhine River Catchment and Hillesjön. Joshi's extended model can be a reliable tool, if some of the input parameters are fixed on values resulting from the validation tests. Whether or

not the obtained input parameters can easily be applied on other large catchments is not certain, but also not unlikely, since large catchments generally show similar behaviour in terms of leaching of radionuclides.

LITERATURE

International Society of Soil Science (ISSS); Soil Map Middle Europe 1: 1 000 000 with Explanatory Text. ISSS-AISS-IBG

Mundschenk, H. (1992) On long term effects of the accident of the Nuclear Power Plant in Chernobyl in the German Federal Waterways. Deutsche Gewässerkundliche Mitteilungen 36, 1992.

Chiew, F.H.S. Stewardson, M.J., McMahon, T.A., (1993) Comparison of six rainfall-runoff modelling approaches. Journal of Hydrology, 147 pp 1-36

Braun, L.N., Renner, C.B. Application of a conceptual runoff model in different physiographic regions of Switzerland. (1993) Hydrological Sciences - Journal des Sciences Hydrologiques, 37 3 6/1992

Bulgakov, A.A., Konoplev, A.V., Popov, Y.E., Shercherbak. (1991) Removal of long-lived radionuclides from the soil by surface run-off near the Chernobyl Nuclear Power Station. Soviet Soil Science, v23, n1.

Joshi, S.R., Shukla, B.S. (1991) The role of water/soil distribution coefficient in the watershed transport of environmental radionuclides. Earth and planetary Science Letters, 105 (1991) 314-318

McDougall, S, Hilton, J., Jenkins, A. (1991) A Dynamic Model of Caesium Transport in Lakes and their Catchments. Wat. Res. Vol 24 no.4 pp437-445

internationale Kommission für die Hydrologie des Rheingebietes/ Commission international de l'Hydrologie du bassin du Rhin (CHR/KHR) (1989) Verzeichnis der für internationalen Organisationen wichtigen Meßstellen im Rheingebiet/Tableau de stations de mesure important pour les organismes internationaux dans le bassin du Rhin. Lelystad, the Netherlands

Internationale Kommission für die Hydrologie des Rheingebietes/ Commission international de l'Hydrologie du bassin du Rhin (CHR/KHR) (1971). Le Basin du Rhin/Das Rheingebiet.

Monte, L., (1994). Evaluation of Radionuclide Transfer Functions from Drainage Bassins of Fresh Water Systems. J. Environ. Radioactivity 24.

1 INTRODUCTION

The activities of AEA Technology (formerly SRD), within the freshwater collaborative project were three-fold :

- (i) To perform a review of freshwater catchment modelling techniques
- (ii) To produce a generic model for the prediction of the transport of radionuclides through freshwater environments. This model was to draw on the conclusions of the catchment modelling review and was also to cover transportation through river and lake systems. The model was also to be developed into a software code called OTTER.
- (iii) To use the OTTER software code to perform validation exercises on the models.

The produced code, OTTER, was also used to perform an initial assessment of the relative importance of the freshwater pathway in radiological risk assessment.

2 REVIEW OF FRESHWATER CATCHMENT MODELLING

Various approaches to freshwater catchment modelling have been reviewed during the lifetime of the project. Some of the conclusions from this review process are summarised here. Several models have been considered in detail, covering a range of possible approaches. The conclusions of the modelling review subsequently fed into the AEA Technology freshwater environment model, OTTER, which is described below.

Broadly speaking the models can be distinguished by the extent to which they are "conceptual" (sometimes referred to as process or white-box models) or "empirical". In a purely "empirical" model, outputs are related to inputs without reference to any physical consideration of the system. By contrast, "conceptual" models use information and concepts that are related to those environmental characteristics and processes considered by the modeller to be responsible for the behaviour of the system. The latter group of models can be ranked further from the "functional" to the "mechanistic", according to the level to which the modeller simplifies the system. Empirical models are popular with field researchers, providing ready tools to characterise catchment response under observation. Their disadvantages are that they have often been developed to simulate specific catchment characteristics and conditions and are not readily applicable to other situations. Conceptual models, however, are developed by consideration of the catchment processes that may affect the removal of deposited radionuclides from the drainage area. The earliest modelling was performed using systems based on well established hydrology models. These models, often called capacity models, differ from other conceptual models in that they define changes (rather than rates of change) in amounts of contaminant and water content, and usually use capacity factors (rather than rate coefficients), such as volumetric water content and field capacity. In more recent years a class of functional process models known as compartment models have become popular. In fact, most of the models presented at the international BIOSpheric MOdel Validation Study (BIOMOVs) were of this type. The basic assumption is a simple one, in that all regions of the contaminated environment are represented by

"compartments" in which radionuclides are assumed to be homogeneously distributed over the minimum timescale of interest. Transfer coefficients between compartments are often derived by simple consideration of the processes involved, with input parameters averaged over the minimum timeframe of the model. In parallel with the development of compartment models more sophisticated models with greater predictive ability are being developed that can distinguish in more detail the effects that different weather patterns, catchment topology, vegetation and soil type, etc, may have on catchment response. Three of these models have been considered:

- RIVTOX, developed by the Ukrainian academy of science as part of the RODOS system (Real-time on-line decision support system for off-site emergency management following a nuclear accident);
- PRIMA-LO, a detailed generic catchment and lake model developed by CIEMAT-IMA in Spain and recently applied to Esthwaite Water in the UK Lake District; and
- SHETRAN-UK, a research tool based on the state of the art SHE (European Hydrological System) model.

Simple empirical models are difficult to justify when used generically, particularly where model parameters have been estimated using limited catchment specific data sets. More complex systems take account of the physical and chemical processes involved but they are traditionally data intensive and the particular environment to be modelled may not always support such large data input. The overall conclusions are, not surprisingly, that any model developer should select the type and complexity of model which would best fit the purpose, since a more complex system is not necessarily most appropriate in all cases.

3 THE OTTER MODEL AND SOFTWARE CODE

Based on the above review, the AEA Technology freshwater pathways software model, OTTER, was first developed and then, following further modelling reviews, refined to produce version 2.03 of the OTTER software code. The details of the OTTER version 2.03 modelling scheme and a description of the features and facilities of the code are given in depth in [1]. A summary of the models is, however, provide below.

The OTTER code consists of three main modules - a lake module, a river module and a catchment slope module and developments to the OTTER system during the reporting period have principally targeted on the catchment module.

The fast, surface runoff, component of the new OTTER catchment model is physically based and was developed with the aim of parameterizing the catchment area in terms of readily available data. For OTTER the only physical data required for each catchment area are the length, gradient and area of the catchment slope and the soil and vegetation cover types (categorized into broad classes); each catchment can be considered to consist of up to three connected slopes and this data must be supplied for each slope. The modelling of the height and velocity of the runoff water is developed from [2] with all transient characteristics of the flow neglected as insignificant over the timescales of interest. It is further assumed that the

flow is 'forced' by excess rain. The flow of soil particles associated with over-land flow of runoff water is modelled via the Peter-Meyer formula [3] with the partition of radionuclides between the aqueous and absorbed phases modelled by K_d 's.

In the present model, the slope is represented by a set of closed packed cylinders of constant radius which flow down the catchment slope. The surface profile, although rather approximate, is intended to represent: the undulations on a slope; the fact that at small flows only a small fraction of the slope area is covered by flowing water and; the fact that at small heights the texture of the soil surface dramatically increases the hydraulic radius of the flow.

The OTTER modelling of the groundwater transport of radionuclides follows [4] and is implemented with the assumption that deposited activity is instantaneously available to groundwater transport.

The river modelling implemented into OTTER was originally a simple bulk flow model, but this has now been expanded to consider both advection and diffusion terms. Conceptually, the river is formulated as a series of sections termed meshes, or nodes. Temporal water quality variation occurs along the river as the water is transported out of one mesh and into another. Sources of activity to the river considered in OTTER come from inflow from catchment areas, lakes and other rivers. Activity is considered lost from the river via the following mechanisms : drinking water extraction; sedimentation (resuspension is also considered); biological uptake and; radioactive decay.

Within OTTER, lakes are modelled by both physical compartments (*eg* epilimnion, lake bed, *etc*) and biological compartments (*eg* benthos, plants, fish, *etc*) with the pollutant entering the epilimnion and then migrating through the other compartments. Uptake of the pollutant by fish is considered, as is extraction of both fish and drinking water for human consumption. OTTER models stratification and the seasonal effects on biological activity such as ingestion rates of fish. Sedimentation and resuspension are also modelled.

Other features the OTTER software include the implementation of a more sophisticated, keyword driven, user interface and the modelling of radioactive decay. The module interfaces of OTTER have also been improved and now allow the modelling of complex freshwater environments involving any number of inter-connecting rivers, lakes and catchment slopes in singles runs of the code.

4 VALIDATION OF OTTER

Following the development of OTTER, the code was subject to a series of 'validation' exercises. One of the main difficulties in performing such an exercise was the procurement of relevant experimental data. The best data sets found were for Esthwaite Water and Windermere North Basin in Cumbria, UK, for Plynlimon in North Wales and for Par Pond in the USA. Full details of the results and conclusions of the validation exercise are presented in [5], but some details are now summarised.

For the Cumbrian lakes, measurements of post-Chernobyl activity levels of (mainly) Cs137 and Cs 134 in and around the lakes were used for the exercise. The OTTER system was used to model these lakes and their associated catchment areas and rivers and the calculated levels of activity in various compartments of the lakes (*eg* epilimnion, hypolimnion, large

fish etc) over time were then compared with the experimental data.

The OTTER simulations performed for the exercise demonstrated remarkable agreement with the experimental data. To illustrate this two sample figures are represented below :

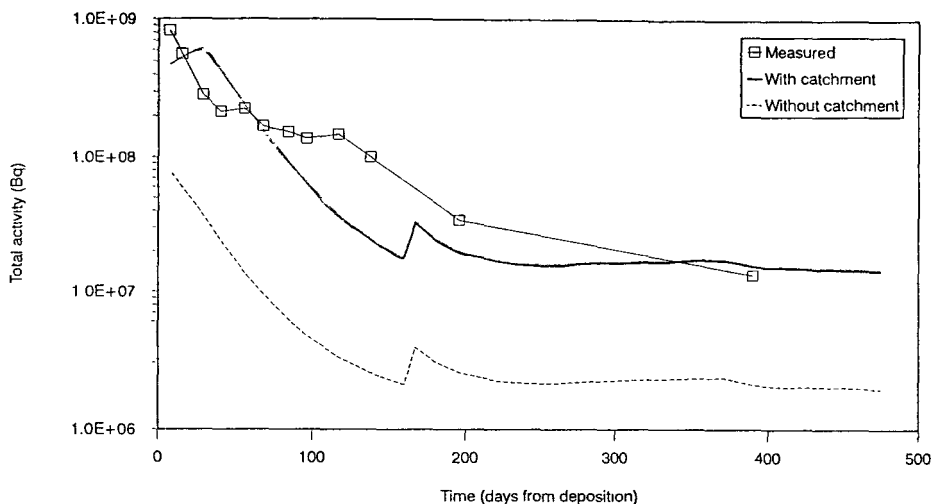


Figure 1 Cs 137 Activity in Esthwaite Epilimnion

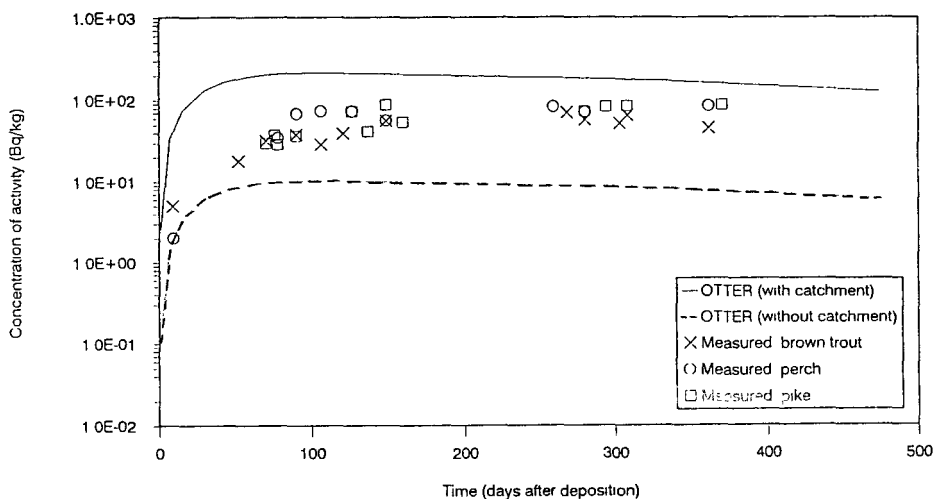


Figure 2 Cs137 Activity in Windermere Big Fish

Figure 1 shows the activity in the Esthwaite epilimnion against time and compares the OTTER simulation results with the experimental data. In this figure two OTTER simulations are presented, one for which the contribution from the catchment areas is ignored (*ie* only the activity deposited directly onto the lake is considered), and one for which all catchment contributions are accounted for. This thus illustrates the role of the catchment contribution to activity levels in surface water bodies. Figure 2 shows the comparison between the

OTTER simulation (with catchment area contributions) and actual data for activity levels in big lake fish against time. Both figures demonstrate the close agreement between OTTER and the actual data.

Whilst, due to the uncertainties in many of the model parameters - not least the K_d values, generally such good fits as those demonstrated above cannot be guaranteed *a priori*, the OTTER model may be considered 'validated' for typical UK freshwater environments.

Figure 3 presents validation data for the Par Pond semi-natural reactor cooling reservoir for the Savannah River plant, South Carolina, USA. Quantities of Cs-137 were released into the pond between 1954 and 1964. OTTER's predictions of water concentrations and compared with experimental data in Figure 3 and again show a reasonably good fit.

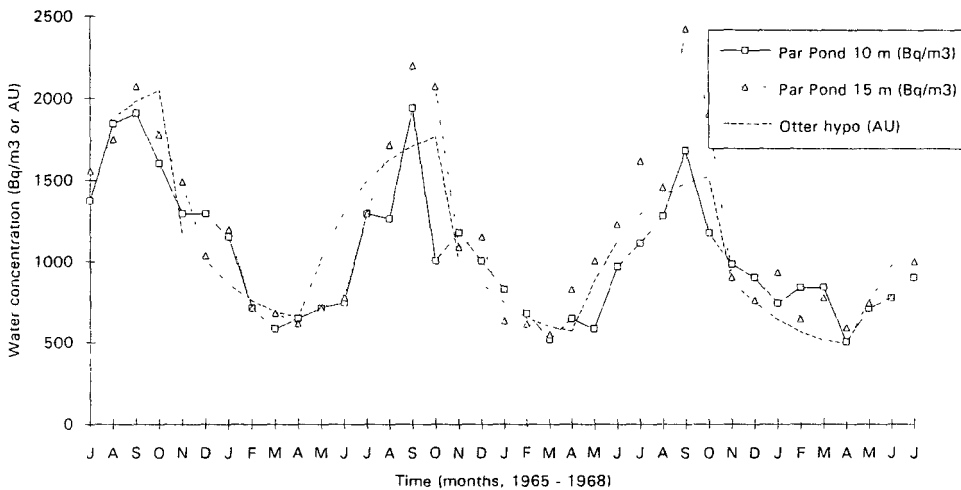


Figure 3 Water Concentrations in Par Pond Between 1965 and 1968

Figure 3 also demonstrates the seasonal effects of resuspension. Annual cycling in lakes of naturally-occurring elements, such as iron and manganese, is well established. This is usually explained in terms of the cycle of oxia/anoxia in the bed. The lake water dissolves oxygen from the atmosphere through its surface, and while the lake is well-mixed, this oxygen is carried down to the bed. The chemistry of the oxidic bed is such that iron and other elements become bound up in bed sediments. After the lake stratifies, however, oxygen cannot be transported into the hypolimnion and bed, where biotic activity continues to consume oxygen until the lower parts of the lake become anoxic. The chemical changes this produces, including the production of NH_4^+ , cause the iron to resuspend.

In the case of artificially introduced pollutants, the OTTER model implies that it is possible that annual cycling may occur in seasonally stratified lakes simply through the dynamics of the lake, without them becoming anoxic. Consider a simple model lake, in which the only processes for transporting activity are throughflow of uncontaminated water, and re-equilibration to or from the bed, and suppose the bed constitutes a large potential source. While the lake is unstratified, concentrations throughout the lake water will decrease due to activity being flushed out by throughflow. While the lake is stratified, the concentration in

the epilimnion decreases further due to throughflow; meanwhile the concentration in the hypolimnion increases, due to resuspension from the bed. When turnover occurs, the epilimnion concentration rises again and the hypolimnion concentration drops. In this way, cycling may be driven by throughflow removing activity and resuspension replacing it. Note that this mechanism only applies to added pollutants: naturally occurring elements such as iron would have reached equilibrium with the throughflow water and the bed. Also, in a real lake, and in OTTER, there are several other processes moving activity between the various compartments, which will cause (possibly large) perturbations to this simplified behaviour.

Thus, there are two possible mechanisms for producing annual cycling of radionuclides in (real and simulated) lakes, which may interact to produce very complex behaviour.

5 RELATIVE IMPORTANCE OF THE FRESHWATER PATHWAY

The relative importance of the freshwater pathways in radiological risk assessment has also been studied. This exercise was performed by comparison of the individual and collective doses from ingestion of freshwater fish and drinking water, estimated by scoping calculations from activity levels calculated by OTTER, with the doses from various other pathways calculated by the radiological risk assessment code CONDOR [6] for several release scenarios. The dose conversion factors used for the estimation of doses from the ingested activity in freshwater fish and drinking water were consistent with those used in CONDOR and the ingestion rates for fish and water were based on 'typical' values for critical groups whose freshwater fish and drinking water is supplied from the contaminated water body.

This assessment of the importance of the freshwater pathway was performed as an initial investigation. The scope of the assessment was limited and thus its conclusions must be considered in this context. However, the estimated doses arising from the ingestion of contaminated freshwater fish and drinking water suggest that the pathway may be of more significance than previously considered. However, considerably more work needs to be performed in this area, before the importance of the pathway can be comprehensively assessed.

References

1. JJ Hancox, J MacKenzie, MJ Peirce and SJ Stansby, "OTTER Version 2.03: A Transport Model for Radionuclides Deposited within the Freshwater Environment", CS/16401807/ZJ829/001, 1995.
2. Zheleznyak, M.J., "*Documentation and User Manual for RIVOX*", (CEC) Cybernetics Centre, Ukrainian Academy of Science, Kiev-Karlsruhe, 1993.
3. Agüero, A. and García-Olivares, A., "*The Model PRYMO-LO for the Transfer of Cs137 in Watershed Scenarios*", CEIMAT-IMA, Madrid, Spain.
4. US Nuclear regulatory Commission, "*A Collection of Mathematical Models for Dispersion in Surface Water and Groundwater*", NUREG-0868, 1982.
5. MJ Peirce and J MacKenzie, "OTTER version 2.03: A Validation Study", AEA/CS/16401807/ZJ829/002, 1995.
6. "*CONDOR 1 : A Probabilistic Consequence Assessment Code Applicable to Releases of Radionuclides to the Atmosphere*", AEA Consultancy Services, Nuclear Electric and National Radiological Protection Board joint report, SRD R598, TD/ETB/REP/7021, NRPB-R258, 1993.

Subcontract: ERBCIPDCT930416 (to the EU Contract FI3PCT930073)
Duration: 1.7.94 to 30.6.95

Title: Regional Numerical Modelling of Radionuclide Migration
in Aquifers of Catchment Basins

Head of the subcontract: D.Kozhoukharov-Geological Institute,Bulgarian Academy of Sciences

Authors: N.Troshanov -Geological Institute, Bulgarian Academy of Sciences
K. Petrov -Geological Institute, Bulgarian Academy of Sciences

Objectives for the reporting period

The main goal of the considered subproject was the software development for regional modelling of dissolved radionuclide migration in aquifer systems in the framework of particular catchment basin on the base of previously developed deterministic mathematical model. The generic numerical model and its implementation take into account the hydraulic interconnection between both surface and ground water as well as the interaction between them in cases of radionuclide contamination of unconfined aquifers (in both unsaturated and saturated zones) induced by radiological polluted surface water. Applying the software, the evaluation of 3D unsteady-state aquifer reaction induced by different kinds of surface radionuclide impacts on a regional (or local) scale is possible. The software can be used in groundwater pollution prediction either from radioactive or non-radioactive substances and, in this way, it is able to support decision-making process in areas of water resources management and safety assessment.

Description of the developed model

Introduction

There are two main objectives of groundwater management that should be achieved

- Sustainable use of groundwater formed within the boundaries of any catchment basin.
- Effective groundwater protection from different sources of pollution (including radioactive pollution).

In order to reach the above mentioned objectives it is necessary:

- to identify the spatial boundaries of ground-water bodies of interest;
- to identify the hydrodynamic and migration parameters of the host groundwater system in regional scale;
- to know the regime of operating exploitation equipment as well as rainfall intensity and artificial recharge data in the region;
- to know groundwater level and contaminant distribution in groundwater body and the same for the existing surface-water bodies in framework of the catchment basin of interest

When these data are available they can be used for the prediction of different quantity and quality processes in ground water bodies. Usually, the tool of such prediction is the regional groundwater numerical modelling with an appropriate software implementation. Development of such a model for radionuclide migration was a main goal of this study.

Groundwater fills in the void spaces of many different geological formations which can be distributed in the framework of any catchment basin whatever their type, origin or age. When a layer of rock or sediments (or series of such layers) is sufficiently porous to store water and permeable enough to transmit water in quantities that can be economically exploited this geological body is considered as an *aquifer* (Chilton, 1992).

Two zones are usually distinguished in aquifers occurring below ground surface: an *unsaturated zone* that contains water in form of moisture, and a *saturated zone* where water is

in saturated conditions. In the first zone the pressure of water is less than atmospheric, and in the second zone the pressure of water is greater than atmospheric with the exception of the pressure on the groundwater table (the boundary between the both zones) where it is equal to atmospheric. The low boundary of these aquifers is commonly semipervious or impervious stratum (respectively, aquitard or aquiclude).

This structure of aquifer refers to so called *unconfined* (or *phreatic*) *aquifers* in which groundwater possesses a free surface open to the atmosphere. These aquifers are the most vulnerable of the processes of pollution. That is why only the unconfined aquifers in catchment basins are subject of this study.

The governing process in mass (activity) transport in groundwater systems is the hydrodynamic dispersion. It includes two processes: *convective diffusion* (mechanical dispersion) and *molecular diffusion*. Convective diffusion depends on both the water flow and the pore system through which flow takes place whereas molecular diffusion results from variations of radionuclide concentration (activity) within the liquid phase. Although the two processes occur simultaneously, molecular diffusion alone can take place in the absence of water movement. Convective diffusion is the main process of contaminant migration in aquifers. The greater the flow velocity in the aquifer (i.e., permeability or hydraulic gradient of the aquifer is greater), the greater the role convective migration plays in the hydrodynamic dispersion.

The characteristics of the developed model are shown on Table 1.

Table 1. Characteristics of the developed model.

<i>Model Name</i>	<i>System</i>	<i>Flow</i>	<i>Solute Transport Processes</i>	<i>Method</i>
FERMI (Finite Element Radionuclide Migration), version 1.0	Anisotropic, hetero- geneous, water-table (unconfined) porous aquifer (saturated + unsaturated zone) with/without hydraulic contact with surface fresh-water bodies	Three- dimensional, transient (unsteady- state)	Convection, dispersion, diffusion, adsorption, radioactive decay	Finite element

Partial differential equations of water movement and radionuclide migration governing the FERMI model

The FERMI software program for the prediction of radionuclide migration is based on a transient (unsteady-state) mathematical model taking into account the processes of water movement and mass transport of the radionuclide of interest in both the unsaturated and saturated zones of the unconfined aquifer.

The governing three-dimensional transient partial differential equation of water movement in unsaturated-saturated conditions can be written in its generic expression as follows (modified from Neuman, 1973 and Marino, 1981):

$$\frac{\partial}{\partial x_i} (K_r K_{ii}^s \frac{\partial \psi}{\partial x_i}) + \frac{\partial}{\partial x_3} K_r K_{33}^s + S = (\xi + \beta S_s) \frac{\partial \psi}{\partial t}, \quad i = 1, 2, 3 \quad (1)$$

where:

- x_i ($i=1,2,3$) - Cartesian co-ordinates (x_3 - vertical one, positive upward), L;
- ψ - pressure head, L;
- K_r - relative hydraulic conductivity ($K_r = K^u/K^s$, where K^u - unsaturated hydraulic conductivity, LT^{-1}), dimensionless;
- K_{ii}^s ($i=1,2,3$) - principal components of the saturated hydraulic conductivity tensor, LT^{-1} ;

$\xi = \partial\theta/\partial\psi$ - specific moisture capacity, L^{-1} ;

θ - volumetric water content, dimensionless;

$\beta = \theta/\phi$ - ($\beta = 0$ in the unsaturated zone and $\beta = 1$ in the saturated zone), dimensionless;

ϕ - porosity, dimensionless;

S - source (positive) or sink (negative) term (e.g., a source can be the intensity of infiltration or artificial recharge and a sink can be the intensity of evaporation or artificial discharge), LT^{-1} ;

S_s - specific storage (in the unsaturated zone S_s can be disregarded), L^{-1} ;

t - time, T .

In equation (1) as well as in the following equations the indicial notation $i=1,2,3$ stands for summation.

Since hysteresis will not be taken into account, K_r and ψ are single-valued functions of θ (Fig. 1)

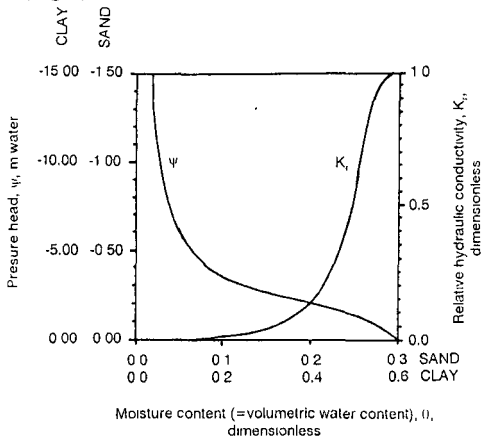


Figure 1. Variation of ψ and K_r with moisture content in unsaturated zone for two soils (from Neuman, 1973)

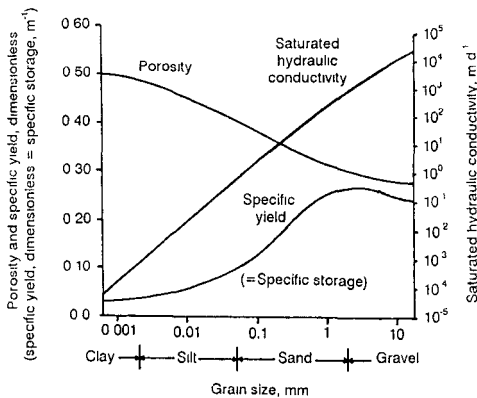


Figure 2. Porosity, specific yield (=specific storage) and saturated hydraulic conductivity of granular materials (Chilton, 1992, modified from Davis & De Wiest, 1966).

From Darcy's law, the components of the average pore-water velocity, v_i , can be written as follows:

$$v_i = \frac{q_i}{\theta} = - \frac{K_r K_{r,ii}^s}{\theta} \frac{\partial h}{\partial x_i}, \quad i=1,2,3 \quad (2)$$

where q_i (LT^{-1}) is the Darcy flux tensor and $h=\psi+z$ (L) is hydraulic head.

The initial and boundary conditions for the solution of (1) are:

$$\psi(x_i, 0) = \Psi_0(x_i), \quad \psi(x_i, t) = \Psi(x_i, t) \quad \text{on } \Gamma_1 \quad (3), (4)$$

$$K_r(K_{ii}^s \frac{\partial \psi}{\partial x_i} + K_{33}^s) \mathbf{n} = -V(x_i, t), \quad i=1,2,3, \quad \text{on } \Gamma_2 \quad (5)$$

where Ψ_0 - known function of x_i (L); Ψ , V - prescribed functions of x_i and t (LT^{-1}), \mathbf{n} - unit outer normal vector on the boundary of the region, dimensionless, and $\Gamma = \Gamma_1 + \Gamma_2$ - total boundary of the flow region (aquifer).

Equation (3) denotes the initial distribution of the pressure head, and equation (4) shows the prescribed pressure heads at each point along the boundary. Equation (5) describes the prescribed normal flux at each point along the boundary.

The rainfall (irrigation) infiltration through the ground surface into the unsaturated zone is prescribed with appropriate boundary conditions. The type and values of these boundary conditions depend on intensity of the rainfall (irrigation), degree of the soil saturation and their relation with respect to the value of ψ on the ground surface.

The governing partial differential equation describing mass (activity) transport of the dissolved radionuclides in a saturated or partially-saturated porous medium can be written in three dimensions (modified from Bear, 1972, and Marino, 1981)

$$\frac{\partial}{\partial x_i} (\theta D_{ij} \frac{\partial C}{\partial x_j}) - q_i \frac{\partial C}{\partial x_i} + S \bar{C} = [\theta + (1+\theta)(1-\phi)\rho_s k_d] (\frac{\partial C}{\partial t} + \lambda C) \quad (6)$$

where:

- x_i, x_j ($i, j=1,2,3$) - Cartesian co-ordinates, L;
- C - radionuclide concentration (activity) of water in porous medium, ML^{-3} or AL^{-3} ;
- \bar{C} - radionuclide concentration (activity) of a source or sink fluid, ML^{-3} or AL^{-3} ;
- D_{ij} - hydrodynamic dispersion tensor ($i, j=1,2,3$), $L^2 T^{-1}$;
- ρ_s - specific gravity (density of soil without any pores, $\phi=0$), ML^{-3} ;
- λ - radioactive decay constant of radionuclide of interest, T^{-1} ;
- k_d - distribution coefficient ($k_d = F/C$, where F - concentration (activity) of radionuclide in the sorbed phase), $L^3 M^{-1}$;
- $(1+\theta)(1-\phi)\rho_s = \rho$ - bulk density of porous medium, ML^{-3} .

The values of specific gravity, ρ_s , and porosity, ϕ , are constant parameters of a certain type of soil, and θ is variable in time, i.e., the considered mathematical model is able to account time variability of bulk density, ρ , at any time step. The values of θ (as initial values), as well as those of mean grain size of the soil, d_{50} , are basic input data for estimation of the other input model parameters according to relationships presented in Figures 1 and 2. These relationships were tabulated in the FERMI numerical code.

The initial and boundary conditions for the solution of equation (6) are as follows

$$C(x_i, 0) = C_0(x_i), \quad C(x_i, t) = C'(x_i, t) \quad \text{on } \Gamma_3 \quad (7), (8)$$

$$\theta D_{ij} \frac{\partial C}{\partial x_j} = 0, \quad i, j=1,2,3 \quad \text{on } \Gamma_4 \quad (9)$$

$$(\theta D_{ij} \frac{\partial C}{\partial x_j} + q_i C) \mathbf{n} = q_i C'', \quad i, j=1,2,3 \quad \text{on } \Gamma_5 \quad (10)$$

where:

- C_0 - initial prescribed radionuclide concentration (activity), ML^{-3} or BqL^{-3} ;
- C' - prescribed radionuclide concentration (activity) on the boundary, ML^{-3} or AL^{-3} ;

C' - prescribed radionuclide concentration (activity) of influx water, ML^{-3} or AL^{-3} ,
 $\Gamma = \Gamma_3 + \Gamma_4 + \Gamma_5$ - total boundary of the aquifer.

Since hydrodynamic dispersion includes both convective and molecular diffusion the coefficient of hydrodynamic dispersion D can be expressed as:

$$D = D' + D'' \quad (11)$$

where:

D' - coefficient of convective diffusion, L^2T^{-1} ;

D'' - coefficient of molecular diffusion, L^2T^{-1}

Usually, in permeable geological media (aquifers) the contribution of D'' to hydrodynamic dispersion can be disregarded because of $D' \gg D''$. Therefore, it will be assumed that $D = D'$.

Using the assumption for isotropy the porous medium with respect to dispersion (Bear, 1972):

$$D_{ij} = \alpha_T v \delta_{ij} + (\alpha_L - \alpha_T) v_i v_j / v \quad (12)$$

where:

D_{ij} ($i, j = 1, 2, 3$) - principal components of the hydrodynamic dispersion coefficients, L^2T^{-1} ,

α_L - longitudinal dispersivity of the porous medium (in the direction of flow), L ,

α_T - transverse dispersivity of the porous medium (normal to the direction of flow), L ,

v_i, v_j , - components of the seepage velocity, LT^{-1} ;

v - magnitude of the velocity, LT^{-1} ;

δ_{ij} - Kronecker delta, dimensionless.

Using the finite-element discretization scheme the finite-element formulation and integration over time were carried out.

Short description of the FERMI numerical code

Version 7.0 of Borland Pascal computer language was used in developing of the FERMI computer code. The hardware tool was IBM compatible PC with Pentium/60 MHz processor and 16 MB RAM.

The main characteristics of the original FERMI numerical code are

- Module structure allowing changing to each input parameter and boundary condition(s) at any time step.
- Direct memory access through the addresses of the memory elements.
- Memory management according to the finite-element discretisation, respectively to the number of the finite-element nodes and elements.
- Successive Over-Relaxation (SOR) method for solving of the obtained linear systems of equations
- Compact storage of the elements of the stiffness matrix avoiding of zero operations during the solving of the linear system of equations.
- An opportunity to solve problems with a great number of finite-element discretisation nodes: about 2500 nodes per 1 MB of PC RAM for 3D-problems and 6000 nodes per 1 MB of PC RAM for 2D-problems.
- Solving of 2D- and 3D-problems.
- Regular finite-element mesh in the horizontal directions and non-regular finite-element mesh in the vertical direction.

Schematic structural presentation of the FERMI numerical computer code is shown on Figure 3.

The input model characteristics are as follows:

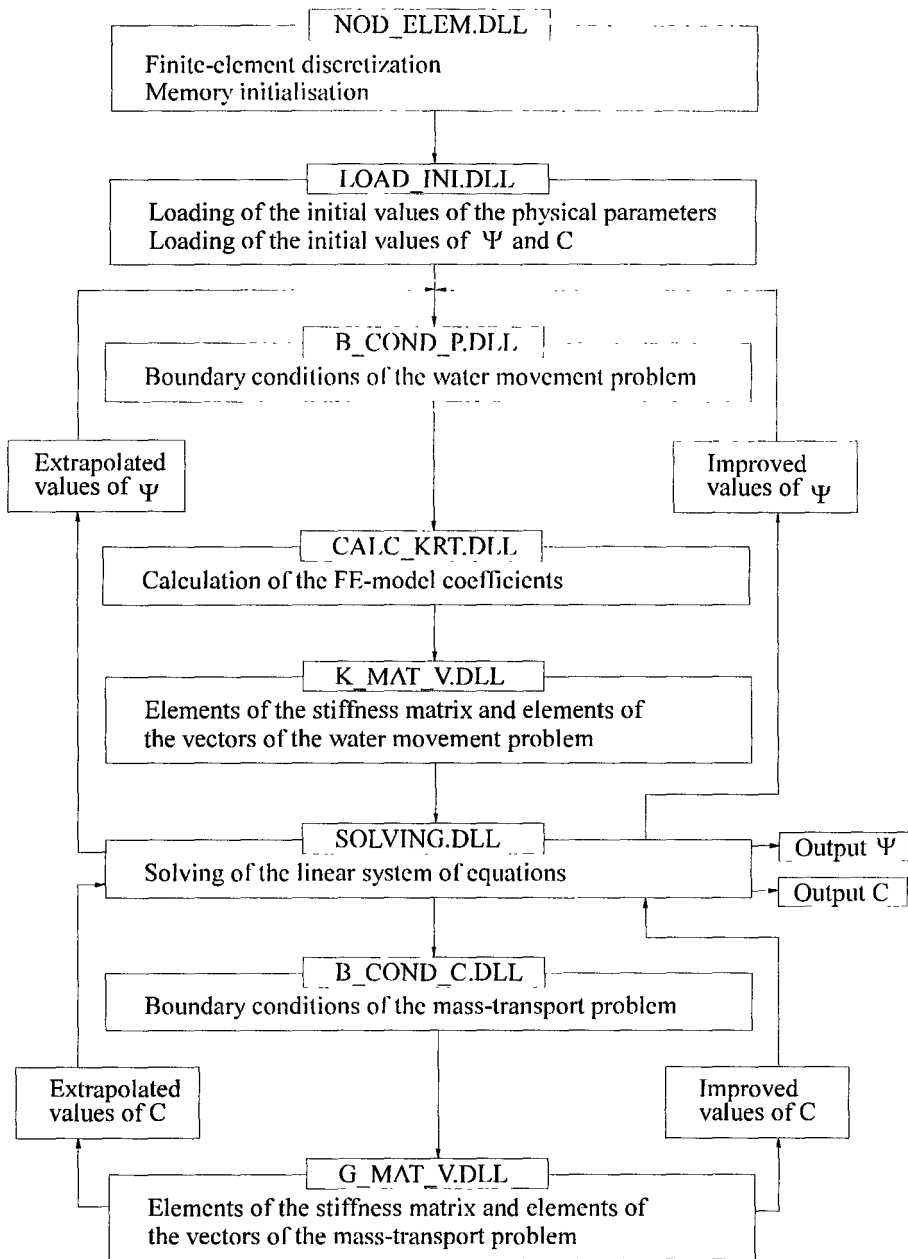


Figure 3. Schematic presentation of the FERMI computer code structure.

- *Water flow:* $K_r, K^s, \theta, \phi, S_s, S, \psi$ (initial values, i.e., $\Psi_0(x,y,z)$), $\Psi(x,y,z,t)$, $V(x,y,z,t)$, intensity of rainfall (irrigation) I .
- *Mass transport:* $\alpha_L, \alpha_T, \rho_s, \lambda, k_d, C$ (initial values), \bar{C}, C', C'' .

In case of lack of available data for some input model characteristics (including ρ_s) the FERMI model has the capability to prescribe these data on the base of relationships shown on Figures 1 and 2.

Two types of result are output from the model: a) numerical all data of ψ and C of the appropriate model nodes are presented with their numerical values, and b) graphic. 3D solutions for pressure head, ψ , and contaminant (radioactive or not) concentration (activity), C , at different moments of time, presented on 2D cross-sections with different orientation

Analysis of the FERMI model results

Verification of the computer code

The finite-element computer code was tested versus the analytical solution for two-dimensional convection-dispersion. The governing partial differential equation in saturated zone of the unconfined aquifer is as follows (Fried, 1975):

$$\alpha_L u \frac{\partial^2 C}{\partial x^2} + \alpha_T u \frac{\partial^2 C}{\partial y^2} - u \frac{\partial C}{\partial x} = \frac{\partial C}{\partial t} \quad (13)$$

When the source of pollution has a unit intensity at the moment $t=0$ the obtained analytical solution is as follows:

$$C(x,y,t) = \frac{1}{4\pi ut(\alpha_L \alpha_T)^{1/2}} \exp\left[-\frac{(x-ut)^2}{4\alpha_L ut} - \frac{y^2}{4\alpha_T ut}\right] \quad (14)$$

where:

u - velocity of the water movement;

α_L, α_T - longitudinal and transverse dispersivity of the porous medium.

The comparison between both model and analytical solution results is shown on Figure 4 for the case where $u = 5.5, \alpha_L = 20, \alpha_T = 5, x=10, y=0$ presented as dimensionless values

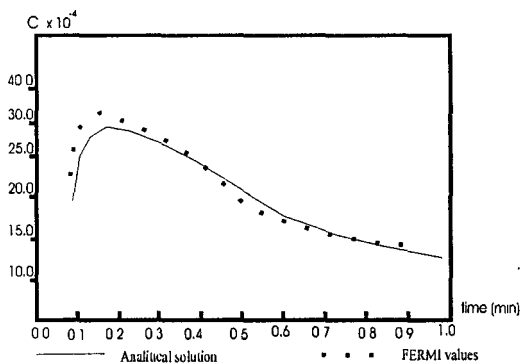


Figure 4. Comparison between the results of the FERMI model and the analytical solution of Fried (1975).

Sensitivity analysis

In order to estimate the influence of the main model parameters on the predicted contaminant distribution the theory of Sorek and Bear (1990) is applied

The solution domain is subdivided into zones with different constant values of flow and mass-transport parameters as saturated hydraulic conductivity, K^s , specific storage, S_s , porosity, ϕ , distribution coefficient, k_d , longitudinal and transverse dispersivity of the porous medium, α_L and α_T , etc. According to Sorek and Bear (1990) jumps in the values of the coefficients may take place across the boundary between the zones. The aim is to determine how sensitive are the hydraulic head, ψ , and the contaminant concentration, C , at same point P to changes in each of the parameters and boundary conditions at point P' .

Our sensitivity test example considers 3D region which is 18.3 m high, 30.5 m long and 12.2 m wide. The finite-element network contains 1440 elements and 385 nodes. It is divided into three zones disposed between parallel plains ($z=0$ m; $z=6.1$ m, $z=12.2$ m, and $z=18.3$ m). All the applied initial and boundary conditions are designed to give a nearly uniform pressure head gradient along the x -axis extending from the left to the right side of the region.

Let to be assumed that the solutions for hydraulic head, $\psi(P,t)$, and concentration $C(P,t)$ are obtained with prescribed values of the coefficients (C_{ln}^0 ; $C=K, S_s, \phi, k_d, \rho_s, \lambda$) in each zone where:

n - number of zone ($n=1+3$);

l - number of coefficient ($l=1+6$).

Now we change the coefficient (l) in zone (n) and keep the values of all others ($LN-1$) coefficients unchanged. Then we obtain solutions for pressure head, ψ , and concentration, C . In Sorek and Bear (1990) the sensitivity U_{pn}^l is defined as:

$$U_{pn}^l = \frac{\Delta\psi_{pl}}{\Delta C_{ln} / C_{ln}^0} \quad (15)$$

where: $\Delta C_{ln} = C_{ln} - C_{ln}^0$
 $\Delta\psi_{pl} = \psi_{pl} - \psi_{pl}^0$

$\Delta\psi_{pl}$ and ΔC_{ln} are the values at point P after the changing the coefficient C_{ln}

In our test example each coefficient of interest was changed with 25% in comparison with its initial value. The results for sensitivity of the model are shown on Table 2.

Table 2. Results obtained in the model sensitivity analysis.

Model coefficient	$\Delta\psi$ - Sensitivity, m	ΔC - Sensitivity, 10^{-3} kg.m ⁻³
S_s - specific storage	0.092	0.040
K - hydraulic conductivity	0.0896	0.230
ϕ - porosity	-	0.244
k_d - distribution coefficient	-	0.148
ρ_s - specific gravity	-	0.148
λ - decay constant	-	0.380

The sensitivity results obtained show that the model solution for the concentration is the most sensitive with respect to porosity, ϕ , among the parameters characterising the porous medium (λ is a characteristic of the radionuclide).

Uncertainty analysis

The model prediction uncertainty is estimated by the variance of the state variables (hydraulic head and concentration), computed by the model. First-order uncertainty analysis of the model FE equations (Mckinney, Loucks, 1990) was applied to calculate the FERMI model prediction variance.

Let $Y(u)$ is a vector of the system state variables [Ψ, C], which depends on u a vector of the system parameters [$S_s, K, \phi, k_d, \rho_s, \lambda$]. If u^* is a vector which components are some

nominal values of the parameters, the vector \mathbf{Y} of the system state variables can be approximated by a first-order Taylor series expanded about \mathbf{u}^* .

$$\mathbf{Y}(\mathbf{u}) = \mathbf{Y}(\mathbf{u}^*) + \frac{\partial \mathbf{Y}}{\partial \mathbf{u}} (\mathbf{u} - \mathbf{u}^*) \quad (16)$$

where $\frac{\partial \mathbf{Y}}{\partial \mathbf{u}}$ is a sensitivity matrix of derivatives of the state variables with respect to the parameters.

Using the equation (19) one can obtain first-order approximations of the mean and covariance of \mathbf{Y} , considering the model parameters like stochastic variables.

The first-order approximations of the mean and covariance of the state variables are

$$\mathbf{Y}^* = E\{\mathbf{Y}(\mathbf{u})\} \approx \mathbf{Y}(\mathbf{u}^*) \quad (17)$$

$$E\{[\mathbf{Y} - \mathbf{Y}^*][\mathbf{Y} - \mathbf{Y}^*]'\} \approx -\mathbf{P}_u \frac{\partial \mathbf{Y}}{\partial \mathbf{u}} \quad (18)$$

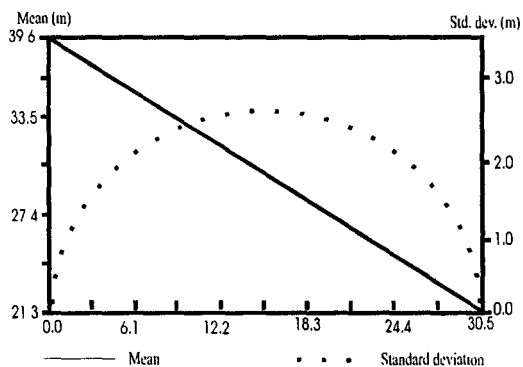


Figure 5. Mean head and head standard deviation.

$\text{m}^3 \cdot \text{kg}^{-1}$, $\lambda = 0 \text{ min}^{-1}$, $\rho_s = 2.7 \times 10^3 \text{ kg} \cdot \text{m}^{-3}$. A point source of contaminant ($5 \times 10^{-3} \text{ kg} \cdot \text{m}^{-3}$) is located on the aquifer centerline at $x=9.15 \text{ m}$ and constant concentration of $0 \text{ kg} \cdot \text{m}^{-3}$ is maintained on the left and right boundaries.

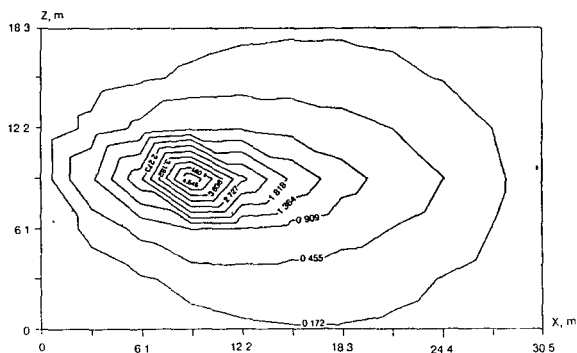


Figure 6. First-order mean concentration (in $10^{-3} \text{ kg} \cdot \text{m}^{-3}$).

The first-order uncertainty analysis method was applied to an example and the mean and standard deviation of head and concentration was approximated. The 3D FE-mesh is the same as in the verification example. The hydraulic conductivity was assumed to be a stochastic variable with log-normal distribution. The boundary conditions are constant head on the left ($h=39.6 \text{ m}$) and right ($h=21.3 \text{ m}$) and they are applied to give a uniform head gradient along the x-coordinate axis in an saturated part of the aquifer. The other simulation parameters are $S_s=0$, $\phi=1$, $k_d=0$

Figure 5 shows the head mean and standard deviation along the centerline of the test body ($y=6.1 \text{ m}$, $z=9.15 \text{ m}$). As expected, the mean head is linear, its values are from 39.6 m on the left to 21.3 m on the right boundary and its gradient is uniform. The standard deviation is 0 m on the boundaries with a fixed head and reaches maximal value of 2.6 m in the center. These results are in good agreement with stochastic simulation results of McLaughlin and Wood (1988a,b)

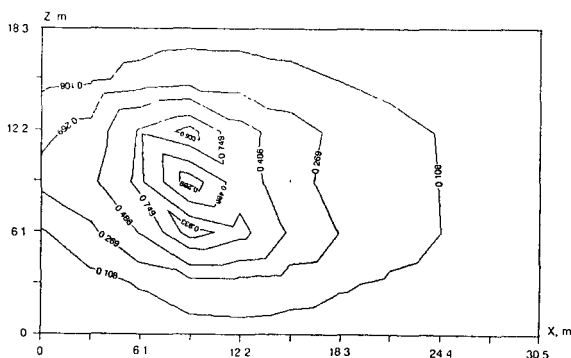


Figure 7. First-order concentration standard deviation (in $10^{-3} \text{ kg.m}^{-3}$).

Figure 6 shows the first-order mean concentration for the vertical plane cross-section $y=6 \text{ m}$ and Figure 7 shows the first-order concentration standard deviation contours for the solution at the same vertical plane. The standard deviation values are proportional to the values of the concentration gradient, as expected from the FE-theory and these results are identical with these of McKinney and Loucks (1990). Consequently, the FE-mesh density should be greater in areas

where the greatest gradients of the solution function can be expected.

Erosion process and radionuclide migration through the catchment

Some radionuclides with high values of k_d (for example, Cs^{137}) are strongly adsorbed by clay particles in the surface horizons of the soil and resist leaching through the soil profile. Thus, the further movement by natural chemical means is limited. Hence, a physical surface process such as erosion could be the most important reason of radionuclide movement on the ground surface from the place of its initial deposition to freshwater bodies. This movement leads to decreasing of radionuclide concentration (activity) on the ground surface at the fallout place. Consequently, erosion in a given catchment must be considered as an input parameter in the radionuclide migration evaluation. This means that the magnitude of the radionuclide migration depends on the factors governing the erosion process: catchment slope length, slope gradient, rainfall intensity, mean velocity and depth of the surface (overland) flow, bed shear stress and its critical value, size of the sediments and their specific mass.

The influence of the erosion on the radionuclide migration could be input in the FERMI model using the source term of the mass (activity) transport equation in form of appropriate boundary conditions.

References

1. Bear, J. 1972. *Dynamics of Fluids in Porous Media* - American Elsevier, New York, N.Y., 764 pp.
2. Chilton, J. 1992. Groundwater, in D. Chapman [ed.], *Water Quality Assessments*, Chapter 8, UNESCO, WHO, UNEP, Chapman & Hall, University Press, Cambridge, 371-466.
3. Davis, S.N., R.J.M. DeWiest. 1966. *Hydrogeology*. - John Wiley & Sons, Inc., New York.
4. Fried, J.J. 1975. *Groundwater Pollution (Theory, Methodology, Modelling and Practical Rules)*. - Elsevier Scientific Publishing Company, Amsterdam-Oxford-New York.
5. Marino, M.A. 1981. Analysis of the transient movement of water and solutes in stream-aquifer systems - *J. Hydrol.*, 49, 1-17.
6. McKinney, D.C., D.P. Loucks. 1990. Uncertainty Analysis Methods in Groundwater Modeling, in Gambolati, G. (ed.), *Computational Methods in Subsurface Hydrology*. Proceedings of the Eighth International Conference on Computational Methods in Water Resources, held in Venice, Italy, June 11-15, 1990. - Computational Mechanics Publications, Southampton Boston, 455-462.
7. McLaughlin, D., E.F. Wood. 1988a. A distributed parameter approach for evaluating the accuracy of groundwater model predictions. 1. Theory. - *Water Resources Research*, vol. 24, No. 7, 1037-1047.
8. McLaughlin, D., E.F. Wood. 1988b. A distributed parameter approach for evaluating the accuracy of groundwater model predictions. 2. Application to groundwater flow. - *Water Resources Research*, vol. 24, No. 7, 1048-1060.
9. Neuman, S.P. 1973. Saturated - unsaturated seepage by finite elements. - *J. Hydraul. Div., Proc. Am. Soc. Civ. Eng.*, 99, 2233-2250.
10. Sorek, S., J. Bear. 1990. Sensitivity Analysis with Parameter Estimation in a Heterogeneous Aquifer with Abrupt Parameter Changes Theory, in Gambolati, G. (ed.), *Computational Methods in Subsurface Hydrology*. Proceedings of the Eighth International Conference on Computational Methods in Water Resources, held in Venice, Italy, June 11-15, 1990. - Computational Mechanics Publications, Southampton Boston, 455-462.

1 Introduction

The aim of the project is analysis and modelling of the long-term migration of radionuclides deposited in catchment basins of freshwater systems. There are a lot of processes like water retention time, seasonality, sedimentation, size and properties of catchment area, morphometry of the lake, trophic status of the lake, physical and chemical qualities of water and catchment which affect the distribution of Cs-137 deposited onto aquatic ecosystems.

The contributions from Studsvik Eco & Safety AB have been, analysis of data concerning composition of catchment area (size of bog area) and leakage to the lake of Cs-137, literature review of Cs-137 in lake sediments, sampling of sediment from lake Hillesjön to determine the distribution and speciation of Cs-137 within the profiles. Chemical fractionation technique (Broberg, to be published) has been used to assess the bioavailability of Cs-137. Furthermore, the impact of bioturbation and the leakage of Cs-137 from sediment to water was experimentally studied. Finally a generic model of Cs-137 turn-over in lakes has been designed.

The major pool of Cs-137 deposited onto lakes will be refound in the sediments. After this initial load the processes of maintaining increased levels of Cs-137 in water is either due to leakages from the contaminated drainage areas or transfer from the contaminated sediments back to water. These main processes are physically and chemically due to several phenomena in combination with the prevailing environmental conditions. The main purpose of these above mentioned subjects is to identify important phenomena in order to improve the long-term modelling of radionuclides in fresh-water system, emphasised on lakes.

2 Leakage from catchment area

To clarify the importance of properties of the drainage areas for leakage of Cs-137 to surface water correlations were carried out between the percentual of bog areas in the drainage and the annual inflow rates observed. The analysis showed a strong relation between these parameters, see Figure 1. Other Swedish studies have confirmed that bog areas constitute the main source from the drainage areas. (Nyhlen, 1994). This is also valid for great drainage areas in Finland (Saxén, 1994). It is well-known that Cs-137 is strongly bound to clay particles and if the transport occurs in such particulate form it should be expected to be relatively quickly transferred to the sediments. The presence of bogs in the catchments implies a higher content of humic substances in the inflow which in its turn retain Cs-137 in the water and thereby available for uptake in the aquatic feed chains. On the other hand a high fraction of clays in the catchments causes a high sorption on the suspended particles and an effective settling to the bottoms.

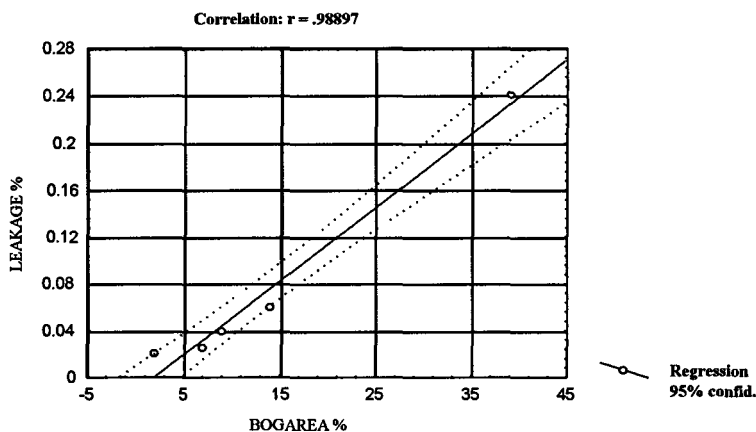


Figure 1

Regression analysis of the correlation between bog area and leakage from catchment in Lake Hillesjön, Lake Sälgsjön, Lake Ekholmssjön, Lake Siggeforasjön and Lake Flatsjön 1990.

Also an English study carried out for Devoke lake, (Hilton et al, 1993) has showed this secondary load of Cs-137 suggested to be in particulate form caused by soil erosion.

These current leakages have occurred by surface water runoff, erosion etc and not by inflow of ground water. In a longer time perspective also this transfer may contribute as has been shown by Bergman et al, 1993 for a boreal forest ecosystem. Thereby an increase of rates were shown about 10 years after the bomb fallout.

The inflow of leaking Cs-137 from catchment varies seasonally, it is known that not only the volume of water increase during spring flood, but also concentration of Cs-137 in the water (Bergman et al 1993, Spezzano et al 1993). The quantitatively most important transfer occurs then during spring, but in autumn with heavy rain and decomposition, the inflow of Cs-137 in plant material is significant (Hongve et al, 1994).

Some budgetcalculations were earlier carried out for Lake Hillesjön showing an accumulated total loss during 1986 to 1991 of Cs-137 to 8 % of the deposited amounts in the catchments area (Sundblad *et al* 1991).

3 Cs-137 in sediments

As earlier mentioned the major pool of Cs-137 is within the sediments. Several sitespecific studies in Finland, Great Britain and Sweden have been compared.

In some lakes the accumulation of Cs-137 increases, the area specific concentrations exceed the deposition of Cs-137 (Ilus et al, 1993, Kansaaneen et al, 1991, Malmgren & Jansson, 1991). However there are also lakes showing mean specific radioactivity similar to deposited amounts of Cs-137 (Broberg & Andersson, 1991, Meili et al, 1991). In some Scottish lakes, the inventory of Cs-137 in the sediments has also increased significantly during a 5 year period since the Chernobyl accident. But it has not exceeded the estimated atmospheric fallout inventory. These lakes appear to have a fairly constant sediment accumulation rate (Appelby et al, 1993).

The geographical location of the lake seems to affect the accumulation of Cs-137 within the aquatic system, with higher accumulation in lakes situated at higher latitudes (Figure 2). However another important factor is the size of the catchment area. Lake Öreträsk, which shows the highest normalised inventory of Cs-137 (Figure 2) has also the greatest catchment area.

In lake Eastwaite and Round Lake of Galloway in United Kingdom the normalised sediment content of Cs-137 is much less than in the Nordic lakes.

This may show a tendency for a lower transport of Cs-137 to the sediments in lakes situated further south. On the other hand the chemical composition of the fallout may play an important role in combination with soil-type in the areas.

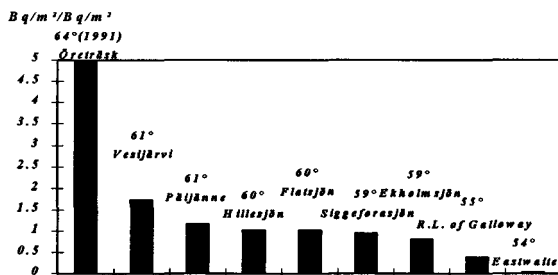


Figure 2

Comparison of the mean normalised Cs-137 inventory and longitude in lakes 1989, all lakes except Lake Eastwaite and Round Lake of Galloway are situated in northern Scandinavia.

The further fate of Cs-137 within the sediments are due to several processes driven by the annual cycle and the chemical composition of the sediments. The following can easily be classified, bioaccumulation, trophic transfer, migration of organisms between contaminated and uncontaminated areas, biodegradation, bioturbation and mechanistic influence. Observations from the Swedish lake Hillesjön has confirmed the latter as a major transport of Cs-137 from the sediments back to water. Budget calculations based upon concentrations of Cs-137 in inlet and outlet water are shown in Figure 3. Concerning chemical conditions, one parameter of importance is the concentration of NH_4 in the sediments. In water with anoxic sediments, peaks have been observed during cold periods in contrast to the summer season when NH_4 is used by plants (Kaminski, 1995) Another parameter is the organic content of the sediments which shows a positive correlation to the amounts (Hongve et al, 1994). Clay-content is also important due to big affinity caesium has to clay-particles.

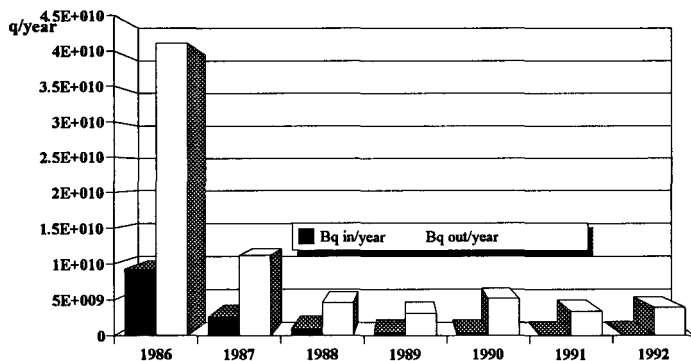


Figure 3

The total amount Cs-137 in Bq/year, arriving and leaving through inlet and outlet water, in lake Hillesjön, showing a net loss.

4 Experimental studies in lake Hillesjön

The experimental studies undertaken emphasised the following purposes, redistribution and chemical form of Cs-137 within the sediments and the effect of bioturbation in fresh-water sediments.

4.1 Distribution and chemical fractionation of Cs-137

Sediment cores were sampled, with a Limnos corer, at three different sites, Figure 4 (two cores at each site) in lake Hillesjön. The sediment was sliced into two centimetre slices, down to a depth of 28 cm for measurements of the radioactivity. These samples were also used for chemical fractionation, according to the schedule of (Broberg to be published).

4.2 Bioturbation

From the sampling site in Lake Hillesjön 10 sediment cores were collected with a Kajac-corer. The sediment was preserved in Plexiglas cores and frozen to kill all living animals. Five of the sediment cores were incubated, with mixed Chironomid larvae, of the families *Chironominae* and *Tanyptodidae*, in varying 5, 10, 30, 50 and 100. The Chironomids were collected in Lake Trobbofjärden. The other five cores were incubated without larvae.

4.3 Results

4.3.1 Distribution with depth of Cs-137

Cs-137 is maintained in relatively high concentrations in the upper layers of the sediment. It also appears to be a significant redistribution of the Cs-137 within the lake. There is a focusing effect

towards the outlet (Figures 4 and 5). There are clear peak values in the profiles, which could be attributed to the year of deposition.

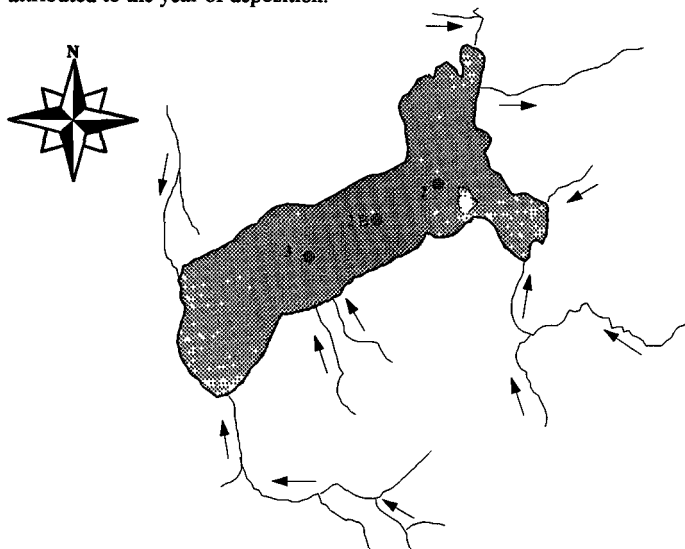


Figure 4
The sample stations in Lake Hillesjön, inlets and outlets.

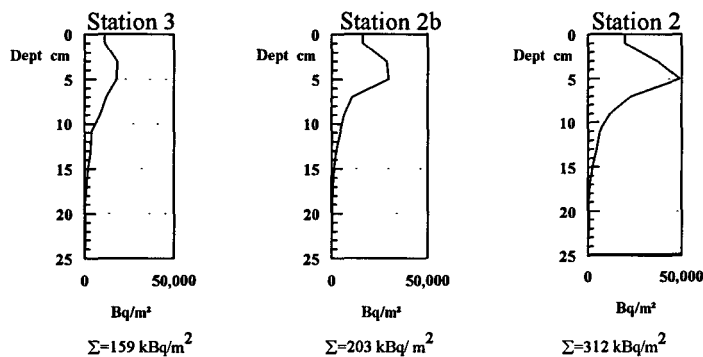


Figure 5
Area specific activity of Cs-137 at the sample stations in Lake Hillesjön in September 1993.

4.3.2 Bioturbation

There was a significant loss of Cs-137 in all cores, however the two controls show a smaller loss of Cs-137, 1.65 ± 0.83 kBq per m² and day, than cores with larvae. The maximum loss of Cs-137 is in core no. 1 with 400 larvae/m, where the loss was 3.93 ± 0 kBq per m² and day, (Figure 6). There is a correlation between loss rates and number of animals.

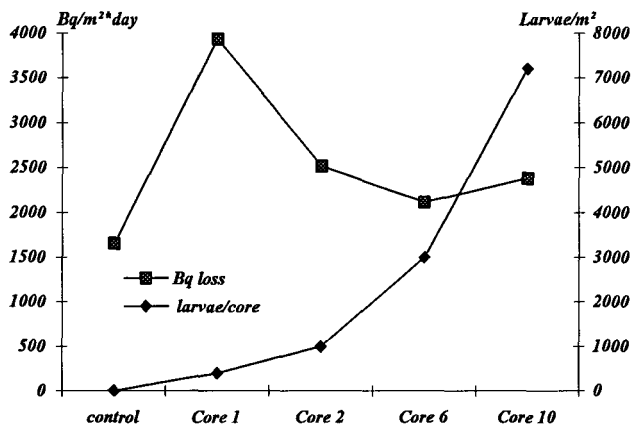


Figure 6
Sediment cores from station no. 3 with number of larvae and loss of in kBq/ m² and day.

5 A generic dynamic model of Cs-137 turn over in lakes

A generic model was designed with the aim to develop a model which treated secondary load of Cs-137 to the water body from the sediment and drainage area, more specifically than earlier models (Nordlinder et al, 1995), see Figure 7. The development of the model was based upon observation data from four lakes: Lake Hillesjön and Lake Sälgsjön in the high deposition area north of town Gävle and Lake Ankarvattnet and Lake Storsjouten in the northern part of Sweden in the mountain area. The model was then executed and evaluated for other lakes without any further modifications than changes of volumes, depths and water retention times.

The model is based on compartment theory with generations of parameter values from prescribed distributions by Latin-hyper cube samplings. Activi in the code system, BIOPATH (Bergström et al, 1982) was used for solving the differential equations and the PRISM-system for the sensitivity analysis (Gardner et al, 1983).

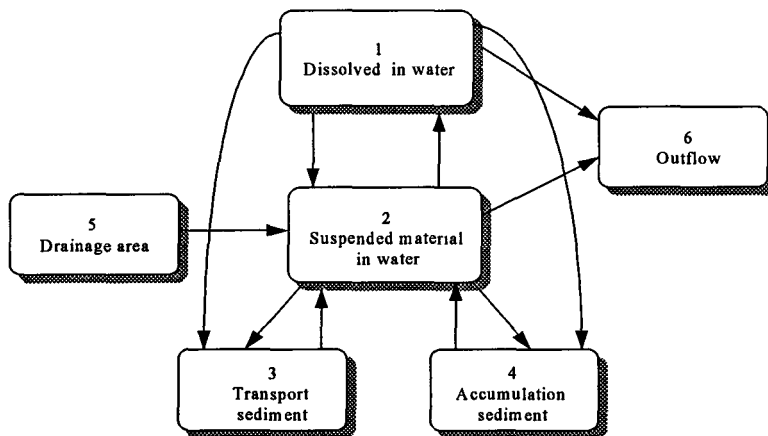


Figure 7
Structure of a generic compartment model for the turn over of Cs-137 in a lake. The arrows indicate the resulting flows of Cs-137 within the system.

5.1 Transport of Cs-137 within the system

The model is based upon easily measured environmental parameters. The time unit used in this model is 1 month. The outflow from the drainage area is correlated to amount of bog areas. The leakage from drainage area has been set to 2 % yearly of the total deposited on the bog and other wet areas. A monthly variation of the resulting transfer coefficients has been assumed due to the spring flood (Spezzano *et al* 1994). Leakage from woodlands and open ground is assumed to be negligible compared to the leakage from bog areas. Data from Gideå, Sweden (Ittler *et al*, to be published) reveals no reduction in Cs-137 contents when deposited in forests ecosystem.

Long-term leakage from contaminated groundwater and diffusion may occur, but will not affect the result during the studied period of time.

5.2 Results

Results for the concentrations of Cs-137 in water and in sediment for lake Hillesjön are presented in Figures 8 and 9, respectively. The calculated values are averages of the entire lake while the observed values corresponds to sampling at different locations.

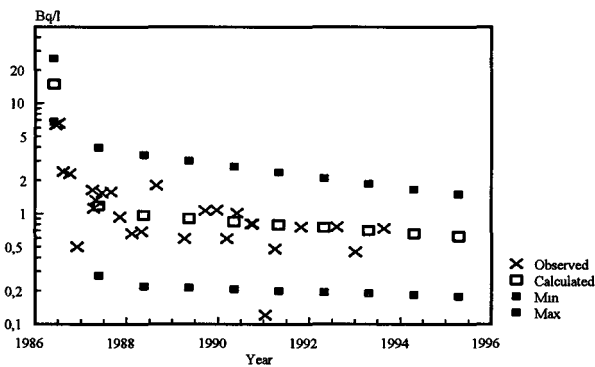


Figure 8

Lake Hillesjön; Observed (*) and calculated (□) concentrations of Cs-137 in water (Bq/l), the results are shown as interval of 95 % confidence (-).

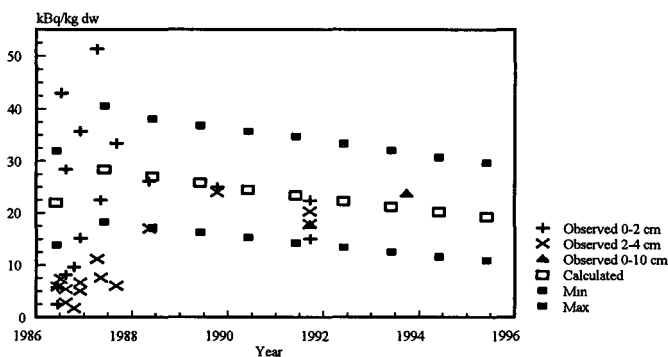


Figure 9

Lake Hillesjön; Observed (x=0-2 cm, ▲=2-4 cm and ■=0-10 cm) and calculated (□) concentrations of Cs-137 in sediment (Bq/kg dw), the results are shown as interval of 95 % confidence (-).

In Figures 10 and 11, results from evaluation of the model for a subarctic lake is presented. The calculated values are average of the entire lake, while the observed are sampled at different places in the lake.

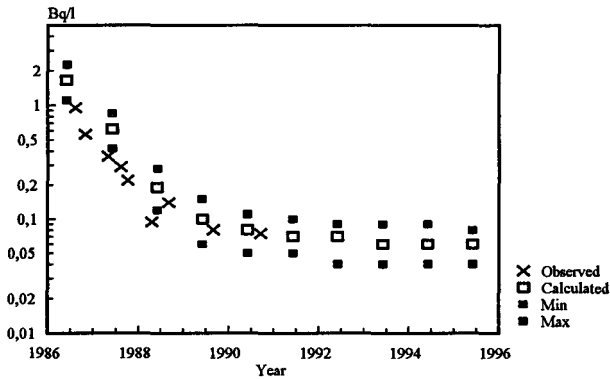


Figure 10

Lake Björkvatten observed (*) and calculated (□) concentrations of Cs-137 in water (Bq/l), the results are shown as interval of 95 % confidence (-).

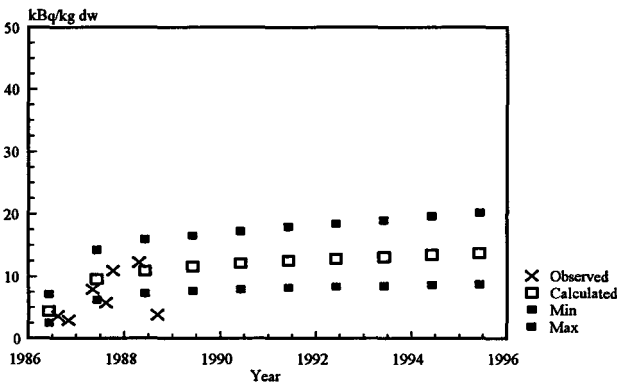


Figure 11

Lake Björkvatten observed (*) and calculated (□) concentrations of Cs-137 in sediment (Bq/kg dw), the results are shown as interval of 95 % confidence (-).

6 Discussion

It could be worthwhile to point out one potential source of uncertainty in analysing the long-term behaviour of Cs-137 in lakes ecosystem, the inhomogeneity and great variability of observations of Cs-137-levels within sediments. Also the deposition is variable and may vary even locally with a factor of ten. There is also continuous transport in the sediments from lower areas to deeper situated ones.

However it is without doubt a loss of Cs-137 within the shallow lake Hillesjön in contrast to two other lakes, lake Heimdalsvattnet in Norway and lake Sarisjärvi in Finland. In Heimdalsvattnet and Sarisjärvi 45 % of the Cs-137 in inflowing water phase was retained within the lake, while in lake Hillesjön 10 times as much Cs-137 flowed out than flowed in during the period of observation (Björnstad et al,

1995). This is also illustrated in Figure 3. These results stress the question of which processes dominating the Cs-137 accumulation in different lakes.

In lake Hillesjön samples of the groundwater have not been taken regularly in later years and would be an interesting future project, to determine if it is a possible source.

Seasonal cycling of Cs-137 in the water column within the lake has also been observed. This is explained by flux to the water due to microbial decomposition of organic matter, which persists throughout the whole year, whereas there is a back flux of Cs-137 from the water into organic matter restricted to summer (Kaminski, 1994).

To be able to see variation in the concentration of Cs-137, in inlet and outlet water concentration and corresponding volumes, more frequent water samples of the surface water should be taken. If there is a variation it is possible that it could have been missed in previous water samples which were taken once a month.

Lake Hillesjön is a eutrophic lake and macrophytes cover a major part of the lake. This means that parts of the sediment will be anoxic, during periods of intense decomposition. Particle bound Cs-137 is known to be mobilised from anoxic sediments, by ion exchange with NH_4^+ , which reaches high concentrations during anoxic conditions (Comans, 1989). Potassium is used in plant metabolism and certain transport mechanisms exist. Cs-137 has a lot of qualities in common with potassium, Cs-137 could be taken up by the plants instead of potassium (Fernandez et al, 1994, Sokolik and Yurin 1994, Bergman et al, 1993). The resulting pool of Cs-137 in the macrophytes varies seasonally, growing plants have a greater demand of potassium and in autumn-winter the plant material is broken down.

This could affect the Cs-137 content in samples. Therefore samples should be taken, at the same sample stations, at different times of the year. It would also be interesting to take samples, for Cs-137 analysis, from the different macrophytes inhabiting the lake, during different seasons. A thorough inventory of the mass and volume of the macrophytes would also be useful, making Cs-137 budget calculations of the lake. Investigations in other lakes (Broberg & Andersson 1991), not eutrophic, showed that the content of Cs-137 in macrophytes was 1990 only about 0,1 % of total Cs-137 content, while 99 % remained in the sediment.

In a German lake, Lake Vorse, 3-5 %, of the total Cs-137 amount in water, was found in the biogenic calcite formations covering the water plants in the lake (Kaminski, 1994).

Chironomids have been shown to increase the release of ammonia, phosphate, lithium, silicate, copper and manganese from lake sediment to the water (Matisoff, 1985, Krantzberg & Stokes 1985). Through their burrowing activities and pumping of water, Chironomids and other zoobenthos increase the redox potential of the sediment. Through their respiratory movements they increase the contact between pore water with higher concentration of dissolved substances and overlaying water with lower concentrations. This speeds up the diffusion rate and may also affect the overlaying water turbidity (Petr, 1977). Some species of Chironomids eat sediment and thereby, they increase the mineralisation rate (Graneli, 1979).

In this experiment sediment cores from the same sample station were used, despite that, there was a great variability in Cs-137 content which made any results very uncertain.

The release of phosphorus and organic nitrogen from lake sediments has been shown to increase linearly up to Chironomid densities of 1100 - 2200/m and decrease with higher densities (Fukuhara, 1987). This could be the explanation for the decreasing loss of Cs-137 with increasing densities in the experiment.

The model designed based upon compartment theory seems to be able to make reliable prognoses for Cs-137, levels in water. Basically the same approach has been adopted in international evaluation or validation studies such as BIOMOVS and VAMP. The conclusions coincide concerning water and for these latter also fish. However for sediments there is one major problem with the current methodology as it assumes a homogenous mixing within the compartment, obviously so is not the case for sediments. The error propagation method used improves considerably the possibilities to identify major reasons to uncertainties in the results. The calculations showed inflow from drainage areas as important for the long term concentration of Cs-137 in water for deep lakes and for those having a considerable fraction of bog areas in their drainage areas. For shallow lakes resuspension due to wind and wave actions keep up the concentrations of Cs-137 in water.

7 Conclusions

In order to make prognoses of accidental releases to fresh water system care must be taken of secondary inputs like leakages from drainage areas and resuspension from the sediments. One controlling property in drainage areas is the fraction of wet areas. Another important parameter is the amount of clays which effectively will bind Cs-137 and cause a build up in the sediments. The inflow is most effective during springs but in highly situated lakes organic bound Cs-137 will be effectively carried to the lake during heavy autumns rains and degradation.

Sediments are the major pool for Cs-137 in lakes ecosystem. As a rough estimate the inventories in sediments coincide with the deposited amounts for the Chernobyl fallout. There are deviations from this generic rule especially for subarctic lakes with big drainage areas, which were snow and ice covered during the fallout.

Sediments in deep lakes accumulate continuously Cs-137 while shallow lakes have a net loss due to resuspension from the bottom-

Chemical analyses show that the major part of Cs-137 is in particulate form, followed by carbonates. The experimental study confirms a transport though minor by chironomids back to water from Cs-137 deposited.

The designed model seems to be possible for use in predicting levels of Cs-137 in water and sediment. However, it is awkward to evaluate it for a longer period of time and several locations.

7 References

APPLEBY, P G, RICHARDSSON, N and SMITH, J T

The use of radionuclide records from Chernobyl and weapons test fallout for assessing the reliability of Pb²¹⁰ in dating very recent sediments. *Verh Internat Verein Limnol* 25, pp 266-269, September 1993.

BERGMAN, R

The distribution of radioactive caesium in boreal forest ecosystem. *Nordic radioecology, The transfer of radionuclides through Nordic ecosystem to man*, edit by H Dahlgard, Elsevier Science 1994.

BERGMAN, R, NYLÉN, T, NELIN, P and PALO, T

Cesium-137 in boreal forest ecosystem. Aspects on the long term behaviour FOA, Sweden 1993 (report C 40284-4.3).

BERGSTRÖM, U, EDLUND, O, EVANS, S and RÖJDER, B

BIOPATH - A computer code for calculation of the turnover of nuclides in the biosphere and the resulting doses to man. *Studsvik Energiteknik AB, Sweden 1982 (STUDSVIK/NW-82/261)*.

BJÖRNSTAD, H E, BRITAIN, J E, SAXÉN, R and SUNDBLAD, B

The characterization of radiocaesium transport and retention in Nordic lakes. In: *Nordic radioecology, The transfer of radionuclides through Nordic ecosystem to man*, edit by H Dahlgard, Elsevier Science 1994.

BONETT, P J P and APPLEBY, P G

Rates of removal of sediment associated radiocaesium from the plyndimon experimental catchment, Porvys, UK. *Environmental pollution* 83(194 327-334).

BROBERG, A and ANDERSSON, E

Distribution and circulation of Cs-137 in lake ecosystem. In: *The Chernobyl fallout in Sweden: results from a research program on environmental radioecology*, Ed L Moberg Swedish radiation protection institute, Sweden 1991 (SSI 151-175).

BROBERG, A

The distribution and characterization of radiocaesium in lake sediments. In: *Nordic radioecology, The transfer of radionuclides through Nordic ecosystem to man*, edit by H Dahlgard, Elsevier Science 1994.

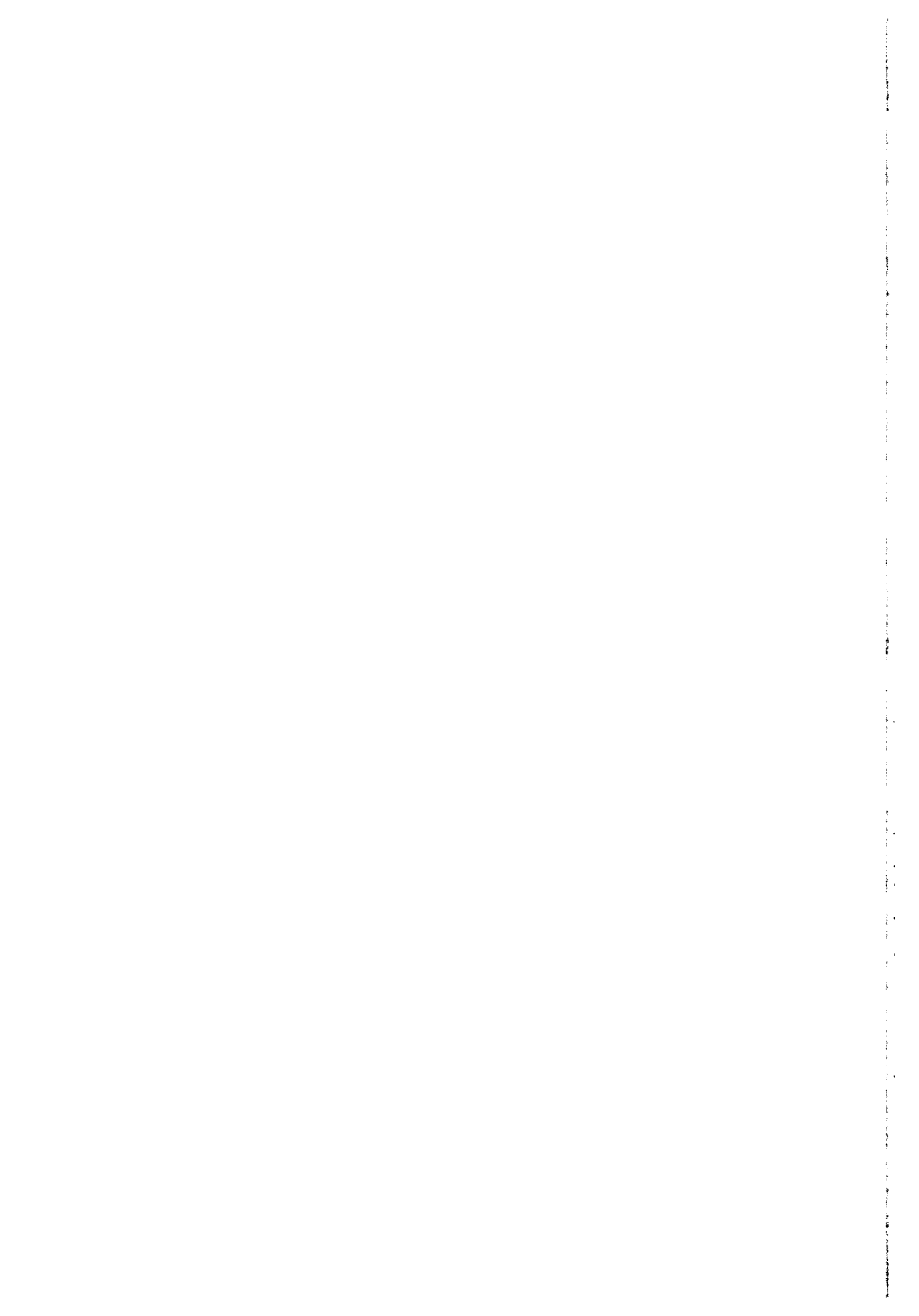
COMANS, R N J, MIDDELBURG, J J, ZONDERHUIS, J, WOITTEZ, J R W, De LARGE, G J, DAS, H A and Van der WEIJDEN, C H Mobilization of radiocaesium in pore water of lake sediments. *Nature* vol 339, No. 6223, pp 367-369, 1st June 1989.

FERNÁNDEZ, J A, HEREDIA, A M, GARCHIA-SÁNCHEZ, M J, GIL, J A, VAS CARREIRO, M C and DIEZ DE LOS RIOS, A Mechanisms of Radio Cesium uptake and accumulation in *Riccia Fluitans*; to be published.

FUKUHARA, H and SAKAMOTO, M

Enhancement of inorganic nitrogen and phosphate release from lake sediment by tubificid worms and Chironomid larvae. 1987, *OIKOS* 48:331-320.

- GARDNER, R H, RÖJDER, B and BERGSTRÖM, U
PRISMER - A systematic method for determining the effect of parameter uncertainties on model predictions. Studsvik Energiteknik AB, Sweden 1982 (STUDSVIK/NW-85/555).
- HAMMAR, J, NOTTER, M and NEUMANN, G
Caesium in Arctic char lakes - Effects of the Chernobyl accident. Information from institute of freshwater research of the Swedish national board of fisheries, 3 (Swedish with English summary)1991
- HILON, J, LIVENS, F R, SPEZZANO, P and LEONARDO, D R P
Retention of radioactive caesium by different soils in the catchment of a small lake.
The Science of Total Environment, 129 p 253-266
- ILUS, E, PUHAKAINEN, M and SAXÉN, R
Gamma-emitting radionuclides in the bottom sediments of some Finnish lakes. Finnish centre for radiation and nuclear safety, Finland 1993 (STUK report A112).
- KAMINSKI, S, RICHTER, T, WALSER, M, LINDNER, G and SCHINK, B
Microbially mediated redissolution of Cesium radionuclides from the sediment of a shallow eutrophic Lake, to be published.
- KANSAANEN, P H, JAAKKOLA, T, KULMALA, S and SUUTARINEN, R
Sedimentation and distribution of gamma emitting radionuclides in bottom sediments of southern lake Päijänne, Finland , after the Chernobyl accident. Hydrobiologia 222:121-140. 1991.
- KRANZBERG, G and STOKES, P M
Benthic macro invertebrates modify copper and zinc partitioning in freshwater-sediment.
Micro cosmos, Can J Fish, Aquat, Sci Vol. 142, pp 1465-1473, 1985.
- MALMGREN, L and JANSSON, M
Contamination of freshwater and estuarine environment in northern Sweden by Cs-137 from Chernobyl accident. In: Det sjette Nordiske Radioøkologi Seminar. Torshavn, 14-18 June 1992.
- MATISOTT, G, FISHER, B J and MATIS, S
Effects of benthic macro invertebrates on the exchange of solutes between sediments and freshwater.
Hydrobiologia 122, 19-33, 1985.
- MEILL, M, RUDBECK, A, BREWER, A and HOWARD, J
Cs-137 in Swedish forest lake sediments, 2 and 3 years after Chernobyl. In: The radioecology of natural and artificial radionuclides, Ed. W Feldt. Verlag TÜV Rheinland GmbH, Köln, Germany. 306-311, 1989.
- NORDLINDER, S, BERGSTRÖM, U, HAMMAR, J and NOTTER, M
Modelling turnover of Cs-137 in Two Subarctic Salmonid Ecosystem Nordic J Freshwater Res (1993):68, p 21 - 33
- NORDLINDER, S, BERGSTRÖM, U and AQUILONIUS, K
A generic dynamic model of Cs-137 turnover in Nordic lakes. To be published
- PETR, T
Bioturbation and exchange of chemicals in the mud water interface, Interactions between sediments and freshwater Golterman, H L ed, Dr W Junk: The Hague p 216-226, 1977.
- SOKOLIK, A I and YURIN, V M
Basic mechanisms of Cs-137 and Sr-90 transport through the plasma lenna of freshwater algae cells. To be published
- SPEZZANO, P, BORTOLUZZI, S, GIACOMELI, R and MASSIRONI, L
Seasonal variations of Cs-137 activities in the Dora Baltea river (Northwest Italy) after the Chernobyl accident.
J Environ . Radioactivity 21 000-000. 1993.
- SUNDBLAD, B, EVANS, S and BERGSTRÖM, U
The turnover of Chernobyl fallout within two catchment areas - Hillesjön and Sälgsjön - in the Gävle area, Sweden.STUDSVIK AB, Sweden 1989 (STUDSVIK/NP-89/51).
- SUNDBLAD, B
Radioecological observations during 1986 - 1991 within the catchments of lake Hillesjön and Sälgsjön - A data report.STUDSVIK AB, Sweden 1991 (STUDSVIK/NS-91/89).
- SUNDBLAD, B, BERGSTRÖM, U and EVANS, S
Long term transfer of fallout nuclides from the terrestrial to the aquatic environment. Evaluation of ecological models. In: The Chernobyl fallout in Sweden : Results from a research program on environmental radioecology, Ed. L Moberg. Swedish Radiation Protection Institute, Sweden 1991 (SSI, 207-238).



Final Report

Contract:

FI3P-CT930077

Sector: C24

Title: Multifractal Analysis and Simulation of Chernobyl Radioactive Fallout in Europe

- | | | |
|----|-----------|-----------------------------|
| 1) | Ratti | University of Pavia (Italy) |
| 2) | Schertzer | CNRM (France) |

1. Project summary description

The complexity of the post-Chernobyl ^{137}Cs cumulative soil deposition distribution, involving the presence of "hot spots", is due to the nonlinear meteorological mechanisms mainly responsible of the radioactive fallout phenomenon at all space-time scales.

In fact, geophysical fields show abundant evidence of nonlinear variability resulting from strong nonlinear interactions between different scales, different structures, and different fields. This variability involves a large range of scales (from 10000 Km to a few meters in space and from at least several years to less then a few seconds in time), and shows that the dynamics involved in the phenomena is mainly characterized by turbulent features. This aspect introduce nontrivial difficulties for risk assessment and monitoring, since the human risk depends primarily on local doses.

A non-standard approach to nonlinearity in geophysics has been first elaborated by Schertzer and Lovejoy in 1987 and is based on scale invariance. This is a fundamental symmetry property of the nonlinear dynamical equations (e.g. Navier Stokes). The simplest way of understanding how geophysical variability occurs over a very large range of scales, is to suppose that the same type of elementary process acts at each relevant scale. In the past ten years, the fundamental role of the space-time scaling in determining the intermittency in geophysical processes has become widely recognised: new scale invariant multifractal models provide valuable hints on how to cast order in disorder.

It is worth pointing out that the theoretical predictions of universal multifractals have been well verified in both wind tunnel and atmospheric turbulence experiments. Furthermore, a fundamental new feature is that different intensity levels (e.g., in our case, the radioactive concentrations in space and time), corresponds to different orders of statistical moments and may have different limits of predictability: in fact, in these systems, error propagation is a scaling phenomenon, and scaling exponents are fundamental.

Given the above considerations, in this Project we carry out the analysis of several variables (fields) related to the presence of the post-Chernobyl radioactive pollution in the environment exploiting both a fractal and a multifractal approach.

In particular, we focus our attention on the ^{137}Cs cumulative soil deposition in some European Countries, including the most polluted sites nearest to the Chernobyl nuclear plant, where the highest concentrations of radioactivity and the strongest fluctuations are found: to get an idea of the magnitude of the variability, we may mention data from a village close to the Chernobyl nuclear plant, showing soil radioactive concentrations ranging from ≈ 100 to 200000 Bq/m^2 . Also, we analyse the rainfall data for about three weeks after the accident and study the turbulent features of the wind and temperature fields in a multifractal framework. Finally, we devise original fractal and multifractal techniques to estimate the radioactive concentration even in locations where no measurements are available and provide an overall description of the pollutant distribution over regions as large as a whole Country.

1.1. Mono- and multifractal analysis of radioactive fallout and rainfall

The meteorological phenomena involved in the Chernobyl fallout feature high time-space variability, as much as the radioactivity released in the environment. Multifractals might

significantly improve the knowledge of its time-space evolution and provide parameters whose meanings and values are directly related to the statistical properties of each data set: in fact multifractals provide a coherent theoretical framework and a powerful operative tool to analyse and characterize each of the available data sets.

The (multi)fractal analysis of Chernobyl radioactive fallout involves first an a priori analysis of the available data (both of meteorological and radioactive nature), since the selection of reliable measurements/networks and some quality assurance is needed in order to provide certified and consistent samples as a starting point. We also have to mention the difficulties we had to face in order to access data of former Soviet Union and to digitise them starting from a simple "paper format".

An advantage of using multifractal analysis techniques is that they can characterise the detailed structure of the pollutant distribution over the entire range of scales, from the strictly local concentration up to the largest spatial average. It is then possible to get a deeper insight into the "violent" fluctuating behaviour of the pollutant distribution at all scales: the strong fluctuations are not regarded as anomalous and discarded, on the contrary they are kept as an essential feature of the phenomenon itself.

The fractal dimension represents a measure of the sparseness of a set of points and it may provide an useful tool for choosing an "optimal" configuration of (e.g.) a monitoring network. Nevertheless, the presence of "holes" is often intrinsic to real networks (as it is the case of Chernobyl fallout data base over Europe analyzed in this Project), in the sense that it is not always possible to increase the number, or to change the positions, of the monitoring stations in order to get a uniform "space filling" sampling. Hence, even if the phenomena are independent of the networks used to measure their evolution and features, the typically fractal nature of a network may significantly alter the inferred statistical properties of a phenomenon measured on it: clearly, the larger the fractal dimension, the smaller the loss of information. In other words, the value of the fractal dimension provides a quantitative measure of the sampling efficiency of a given network.

Unfortunately, strong fluctuations (e.g. the "hot spots") are usually concentrated on very sparse regions. Then, due to the Intersection Theorem for fractal sets, it might be possible that they are not sampled by using a fractal network, spoiling any further risk assessment analysis. In other words, the dimensional resolution of real networks rarely allows to detect all the components of the investigated phenomenon: often, the sparsest (and hence most intense) regions of natural processes might be missed in the "gaps" of the networks. This fact implies that special techniques are needed in order to properly take into account the "influence" of the network, and this can be done in terms of multifractals considering, e.g., the density of the network stations as a multifractal measure.

Our primary goal is to provide a multifractal characterisation of ^{137}Cs cumulative soil deposition in some European Countries, along with the analysis of the corresponding rainfall intensity during the whole critical phase of the nuclear accident (about three weeks). Then we test whether such fields are the result of complex nonlinear, but scale invariant, processes. The justification for applying multifractal analysis to the pollution is that, over the relevant space-time scales, all of the turbulent mechanisms involved are expected (and, in fact, it has already been verified in geophysics) to be cascade processes operating over wide ranges of scales, and it is now known that such mechanisms generally lead to multifractal fields.

One may then proceed to estimate the multifractal features of the ^{137}Cs radioactive fallout along with the calculation of the influences and the effects of the corresponding networks. At the same time, a similar study needs to be performed over the available meteorological data. Clearly, this step allows to identify the processes generating the fallout in terms of the relevant multifractal parameters, over several ranges of scale, both in space and in time.

An important issue concerns the extreme behaviour of a multifractal field (e.g. the "hot spots" of radioactive fallout), which is obtained considering the analogue of first and second order phase transitions, leading to appearance of a (non classical) Self-Organised Criticality. The multifractal approach allows to identify the hyperbolic (intermittent) behaviour of a system, a property related to the presence of Self-Organised Criticality and leading to the appearance of the "hot spots".

Since the radioactivity of the Chernobyl cloud is transported by aerosols, which are advected by atmospheric dynamics, it is also of interest to study the influence of atmospheric turbulence on the dispersion of the pollutant and we perform such analysis in a scale invariant

multifractal framework. First, we study atmospheric turbulence using rainfall, temperature and wind velocity turbulent data. Then, given the experimental fact that the Chernobyl cloud is a (chemically active) passive scalar, we analyse passive scalar atmospheric turbulence. Finally, we present a possible approach to turbulence dispersion in a Lagrangian framework: in fact, there is a strong connection between multifractal Eulerian (spatial) and Lagrangian (temporal) viewpoints, due to the ergodic property of turbulence. The merging of multifractal techniques for turbulent diffusion with the Lagrangian formulation gives relevant clues in describing the Chernobyl cloud dispersion.

As it is well evident, the above tasks have to face several formidable difficulties, both practical and theoretical. Given the strongly inhomogeneous nature of the phenomena under investigation, no standard mathematics can be exploited; this difficulty may be overcome relying on the theoretical framework of multifractals, exploiting some general properties of random variables related to (violent) multifractal fields.

1.2. Multifractal forecasting, interpolation and predictability

In this Project we outline several possible approaches to the problem of multifractal forecasting, interpolation and predictability. As far as we know, these represent the very first attempts to exploit the mathematics of multifractals in the area of stochastic estimate.

As a practical application, we also devise an empirical procedure to estimate the ^{137}Cs cumulative soil deposition in a few European Countries, even in sites where no measurements are available. In order to accomplish this task we study, first, the monofractal and multifractal behaviour of the radioactivity measured in the environment and, second, making use of only such empirical information, we devise a multifractal model describing the overall distribution of radioactive pollutant. The model is based on the Fractal Sum of Pulses theory. The basic idea is to consider the value of a certain quantity (e.g. radioactive pollution), in a given region at a given time, as the sum of primary pulses, whose intensity, time duration and geometrical spread are random variables properly distributed and generated according to a precise strategy. Depending on the choice of such probability distributions, we may reproduce some physical features of the phenomenon under investigation, such as the presence of “hot spots”. Most of all, this task is carried out starting out only from the information about the position and the radioactive concentration measured by the available monitoring stations.

As a result, the comparison with the available data is always empirically fairly good. The “hot spots” are almost always correctly reproduced and the model estimates the radioactive concentration even in locations not sampled by the networks. Also, some tests performed neglecting a fraction of the input data have shown that the quality of the outputs is not significantly affected by this lack of input information, indicating a fairly good “stability” of the model.

1.3. Conclusions

The results presented yield the following considerations and preliminary conclusions.

First of all, data may contain much more information than initially expected. Moreover, data need some preliminary quality assurance, since the selection of reliable samples is indeed fundamental in order to provide certified and consistent measurements as a starting point. Unfortunately, due to the difficulty in accessing the data, we were not in position of doing the same for Eastern data. However, in general, the data bases collecting pollution measurements are often statistically poor: only a limited amount of data is available to estimate the relevant parameters of interest here and the data themselves need to be checked with great accuracy to avoid misuse of information.

Then, we outlined the mathematics of fractals and multifractals, presenting both the theoretical framework and the practical analysis techniques; these are then used to investigate the available data. The geometrical monofractal analysis of the sampling networks (both for radioactivity and rainfall) in four Countries (i.e., Austria, Czechoslovakia, Northern Italy and Western Germany) shows their fractal nature over a relevant range of scales; such a study confirms the sparseness and the inhomogeneity of the monitoring structure, and provides a measure of the amount of information (almost surely) “lost” in the gaps of such networks.

The study of the data statistics in the same four Countries shows the presence of a Self Organised Criticality (hyperbolic) behaviour; as a consequence, strong fluctuations (i.e. the “hot spots” found in the available data) are expected even at a theoretical level. Also, the

problem of the divergence of moments may affect the analysis, indicating the necessity of a multifractal characterisation of the phenomenon. In fact, the results strongly support the multifractal nature of the phenomena investigated; even more, the underlying multifractal dynamics may be classified as an "unconditionally hard" multifractal process. The same considerations apply also in the case of the radioactive concentration data collected in the region surrounding the Chernobyl nuclear plant.

Overall, using universal multifractals we achieved two main results. On the one hand, the statistical characterisation of the phenomenon is obtained simply by means of easily-implementable procedures. On the other hand, we gain a deeper insight into the intermittent behaviour of the data distribution at all scales: the wild fluctuations are not regarded as anomalous and discarded, on the contrary they are kept as an essential feature of the phenomenon. The former conclusion has mainly implications for generating fast computer codes (e.g., in case of environmental pollution accidents due to radioactive release). Moreover, there might be further important theoretical and practical consequences in environmental sciences: in fact, we provided a relatively simple way to study the statistics of sparse data, preserving their intrinsic features such as intermittency (i.e. no "a priori" regularity or smoothness hypotheses are required as in conventional objective analyses), and we investigated the phenomenon at all scales, from the strictly local concentration up to the largest spatial average.

Finally, we feel important to stress that the estimates of the multifractal parameters allows to generate stochastic simulations. For the purpose of the analysis, as an offspring of the present Contract, a special software (named "Multifractalia") performing the multifractal analysis of 1D and 2D data has been provided and it is freely available together with the Final Report. Clearly, exploiting such a parametrization and the mathematics of multifractals it might be possible in the near future to create statistical procedures able to estimate the intensity of a field (e.g. radioactive pollution) even in the "gaps" of a (multi)fractal network, possibly exploiting the knowledge of other fields (such as rainfall, wind, ...). The original techniques outlined represent a first contribution to the ongoing researches concerning the estimate of multifractal fields and may have wide and fruitful applications in many areas of environmental sciences and risk assessment, since natural phenomena are often sampled over sparse networks.

In conclusion, we believe that the work done in this Project not only demonstrates the relevance of multifractal notions and techniques to assess and monitor radioactive fallout, but also supports the feasibility of the corresponding routine techniques. By means of the free software provided together with the Final Report, in spite of the underlined difficulties, one may already proceed to analyse and forecast experimental data as outlined above.

1- Specific objectives of the reporting period

The analysis of the available data of ^{137}Cs cumulative soil deposition and rainfall in a few European Countries after the Chernobyl accident requires, first, some “quality assurance” operation, since the selection of reliable measurements and networks is needed in order to provide certified and consistent samples as a starting point. Once these preliminary analyses are done, the estimate of fractal and multifractal features of both radioactive concentration and rainfall is sought, along with the calculation of the influences of the network structure. This step allows to classify the (turbulent) stochastic processes generating the radioactive fallout and the rainfall fields in terms of multifractal parameters. Finally, new recovering techniques working for highly variable multifractal fields might be applied in order to estimate the overall distribution of pollutant, even in those sites where no data are available.

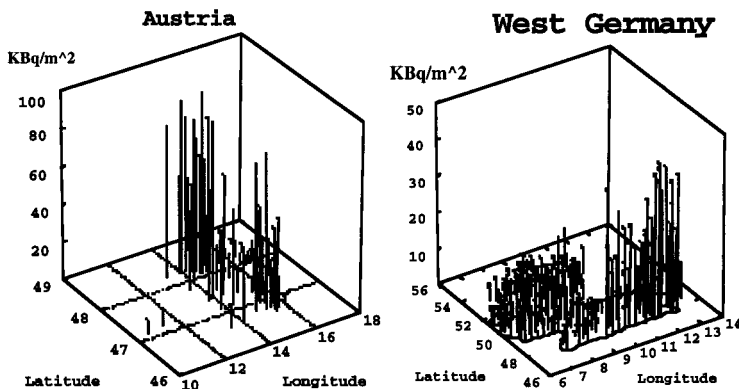
2- Progresses made and results obtained

The available data of ^{137}Cs cumulative soil deposition come from the REM (Radioactivity Environmental Monitoring) data bank, containing some thousand radiological measurements of several kinds collected after the Chernobyl accident by different Laboratories, Universities and Private Institutions in all Europe. For the purposes of the present Project, only four Countries are selected, making up a contiguous spatial region where radioactive fallout are significantly sampled: i.e., Austria (AU), Czechoslovakia (CZ), Northern Italy (NI), and Western Germany (WG).

The analysis of the data base raises several questions. In fact, a few data are discarded since indicating meaningless geographical or radioactive concentration information. Also, the sampling date changes from measurement to measurement, ranging from a few days up to 2-3 years after the accident, introducing a temporal inhomogeneity. A rather empirical formula exploiting the exponential radioactive decay law may overcome such a problem:

$$N(t_2) = N(t_1) e^{-\frac{t_2-t_1}{\tau}} \quad (1)$$

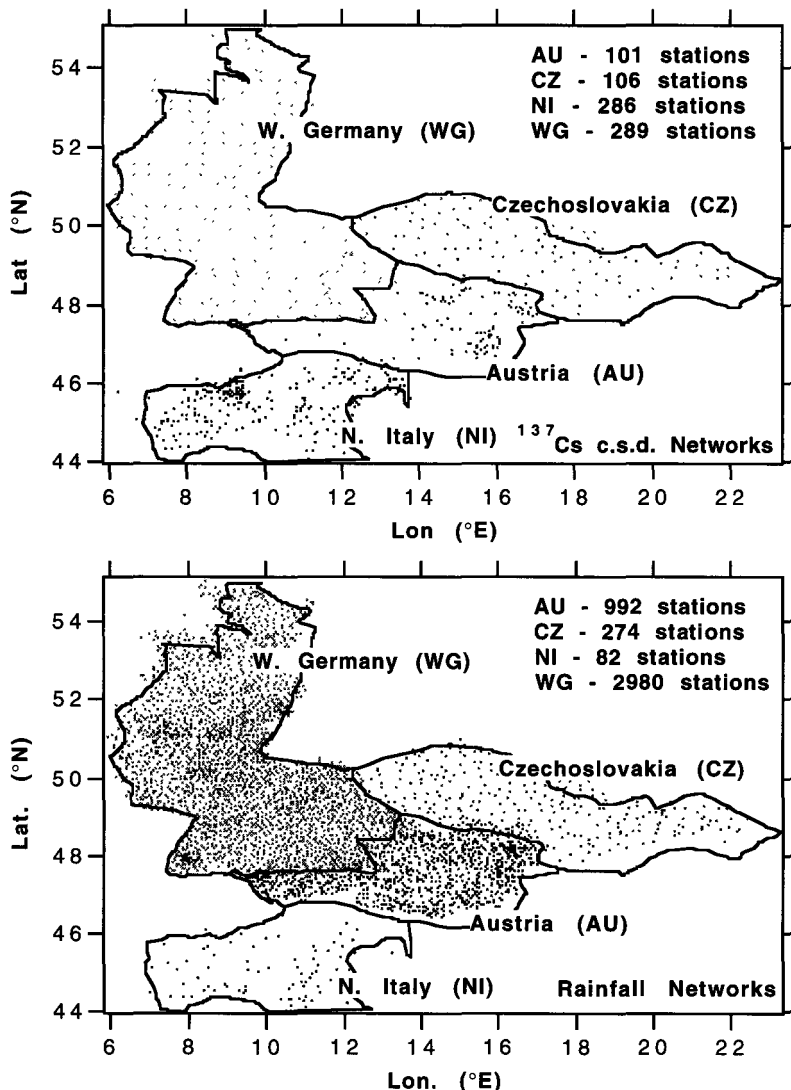
where $N(t)$ is the amount of radioactivity at time t , and τ is the mean life time of the nuclide considered. From a physical point of view, considering dates about a couple of weeks after the accident, the relation (1) provides a reliable first order approximation of the value $N(t_2)$. A sketch of the radioactivity data in Austria and, respectively, Western Germany is shown in Figs. 1: the “hot spot” regions are well evident.



Figs. 1. The available data of ^{137}Cs c.s.d. in Austria and Western Germany.

The rainfall data were provided by the Joint Research Centre of Ispra (Italy) and contain daily rainfall samples collected in 28 European and Mediterranean Countries, starting April 25th, 1986, and ending May 16th, 1986. As in the case of fallout, quite a few "suspicious" measurements are discarded and the same four Countries of interest are selected.

In Figs. 2 we present the sampling networks of ¹³⁷Cs cumulative soil deposition and, respectively, rainfall in the four Countries of interest. In Tab. I we report the ranges of radioactive concentration and rainfall in the same Countries.



Figs. 2. (Top) The ¹³⁷Cs cumulative soil deposition networks of Austria, Czechoslovakia, Northern Italy, and Western Germany. (Bottom) The corresponding rainfall networks.

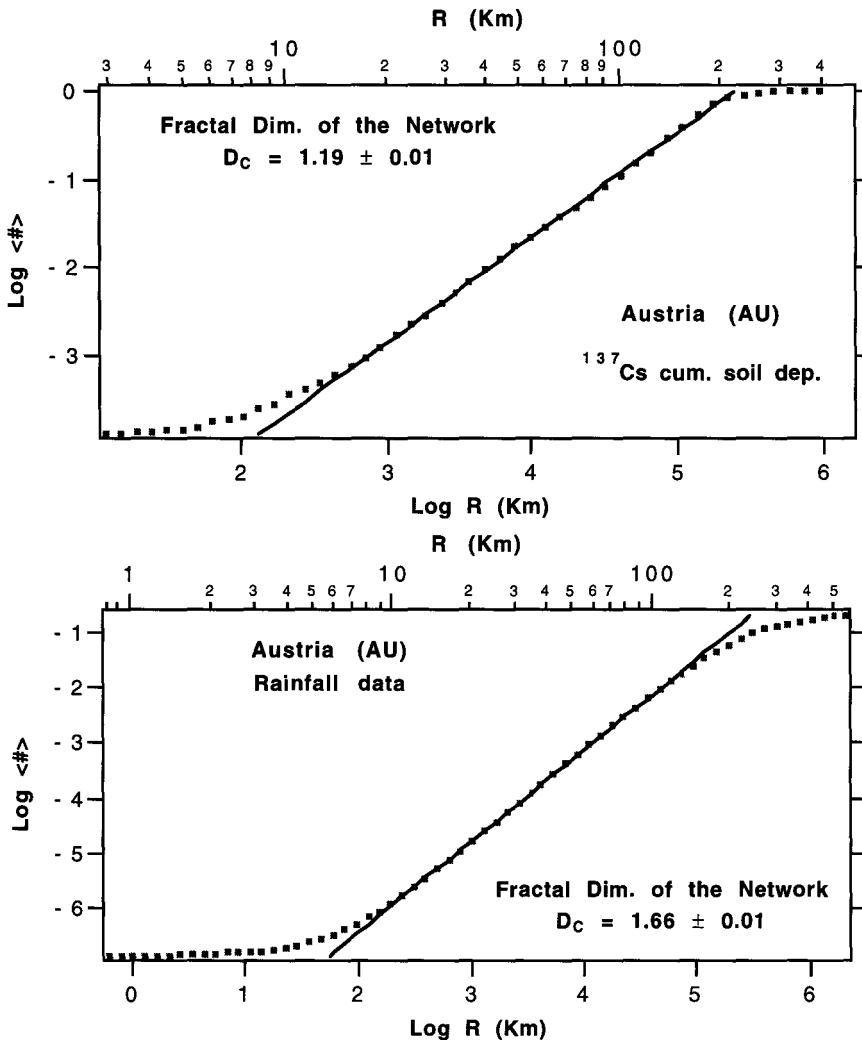
Comparing Figs. 2 it is evident that the rainfall networks are less "sparse" than the ones used to measure radioactivity; practically, this means that in the latter case a relevant portion of information about radioactive concentration is missed in the largest and more frequent gaps of the monitoring networks. The sampling efficiency of a given network can be quantified by

calculating its fractal dimension D_F : the larger the fractal dimension, the smaller the loss of information (this result is also clearly stated by the Intersection Theorem for fractal sets).

	Austria	Czechoslovakia	N. Italy	W. Germany
^{137}Cs c.s.d. (KBq/m ²)	≈ 0.7 - 580	≈ 0.2 - 20	≈ 10 ⁻³ - 500	≈ 0.5 - 50
Rainfall (mm/day)	≈ 0 - 80	≈ 0 - 40	≈ 0 - 70	≈ 0 - 70

Tab. I. Estimate of the data range of ^{137}Cs cumulative soil deposition and rainfall in a few European Countries.

In Figs. 3 we show the estimate of the fractal (correlation) dimension of ^{137}Cs cumulative soil deposition and, respectively, rainfall networks in Austria: the slope of the fit gives the value of D_F . In Tab. II we report the estimates of D_F in the four Countries of interest.



Figs. 3. Calculation of the fractal (correlation) dimension D_C of ^{137}Cs cumulative soil deposition network (Top) and rainfall network (Bottom) in the case of Austria.

Country	N - ^{137}Cs	D_F - ^{137}Cs	N - Rainfall	D_F - Rainfall
Austria	101	1.19±0.01	992	1.66±0.01
Czechoslovakia	106	1.47±0.01	274	1.56±0.01
Northern Italy	286	1.25±0.01	82	1.32±0.01
Western Germany	289	1.59±0.01	2980	1.76±0.01

Tab. II. The fractal features of both the radioactivity and the rainfall networks in a few European Countries. Here N is the number of available data and D_F is the fractal dimension.

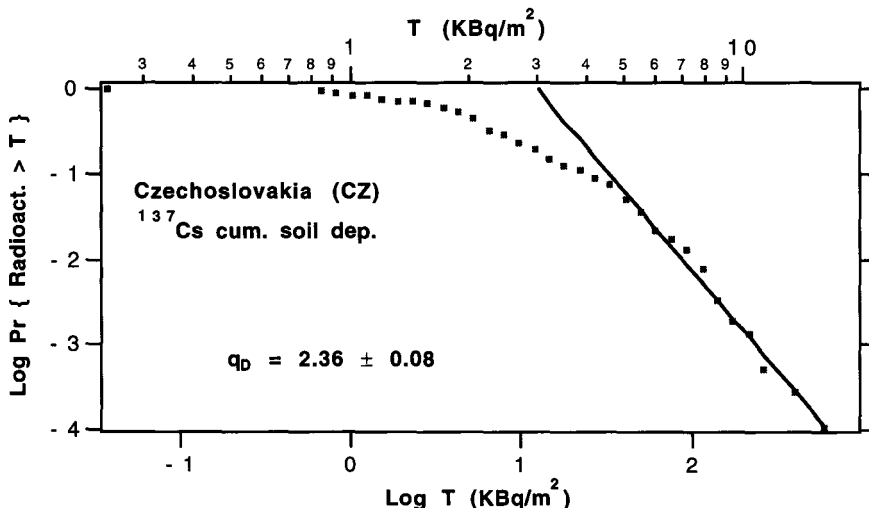
From a practical point of view, the fact that the fractal dimension is well defined and always less than two (the dimension of the plane), means that the network is not space-filling, i.e. "holes" occur at all scales. It is also interesting to note that, as expected, the networks of radioactive concentration are sparser (and hence less "efficient") than the rainfall ones, as it is "qualitatively" evident at a simple visual inspection (see Figs. 2 and 3). In Figs.

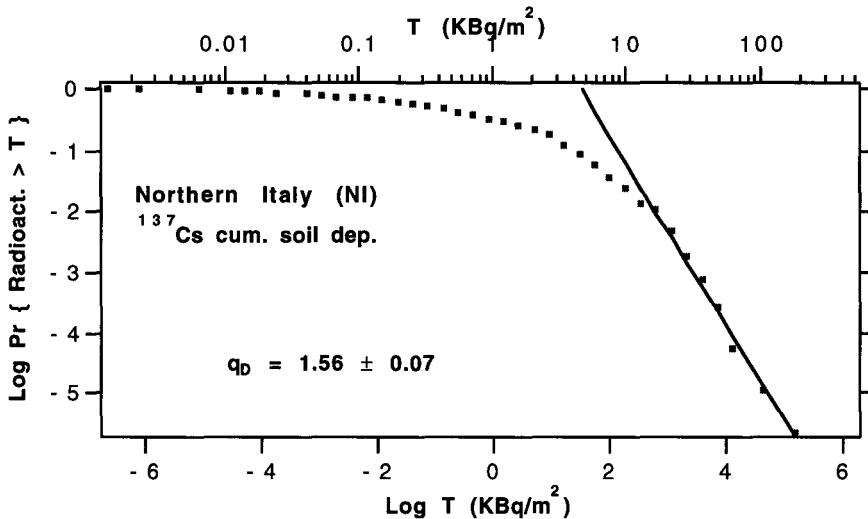
Due to the (possible) extreme variability of the in situ data, the actual measurements of a phenomenon are sometimes averaged over the scale of the detecting network. Nevertheless (e.g. in the case of radioactive pollution), the physical effects may often depend on the strictly local intensity of the phenomenon itself. Indeed, areas of high concentrations ("hot spots") invisible to the detecting network may nonetheless be significant from a health perspective. The advantage of using multifractals is that they can characterise the detailed structure of the pollutant distribution over the entire range of scales, from the strictly local concentration up to the largest spatial average. In fact, multifractality is usually associated with the presence of large random fluctuations of the intensity of a phenomenon (a non classical Self Organised Criticality). A way to model such a behaviour is to consider hyperbolic laws of the type:

$$\Pr\{X \geq s\} \approx s^{-q_D} \quad (s \gg 1) \Leftrightarrow \langle X^q \rangle = \infty \quad \text{for } q \geq q_D \quad (q_D > 1) \quad (2)$$

Divergence of moments of order higher than q_D (the critical order of divergence) corresponds to a "hyperbolic" (algebraic) fall-off of the probability distribution: strong events still receive a not-negligible probability, as opposed to the Gaussian case. An important clarification on the extreme behaviour of a multifractal field is described by the critical order of moment q_D , which may objectively discriminate the "hot spots" from the background radiation.

In Figs. 4 we show the estimate of the critical order of divergence q_D for the ^{137}Cs cumulative soil deposition data in, respectively, Czechoslovakia and Northern Italy: the slope of the fit gives the value of q_D .





Figs. 4. Calculation of the critical order of divergence q_D for the ^{137}Cs cumulative soil deposition data in the case of Czechoslovakia (Top) and Northern Italy (Bottom).

In Tab. III we report the estimated values of q_D for the ^{137}Cs cumulative soil deposition data collected in the four Countries of interest. The relatively low values of q_D might indicate the divergence of the low order statistical moments of the stochastic process “generating” the observed distribution of radioactivity; this corresponds to a hyperbolic behaviour and justify, even at a theoretical level, the presence of wild singularities (e.g. “hot spots”).

The statistical analysis of a phenomenon can be carried out once its probabilistic structure is known. The probability density of the multifractal field ε_λ (at resolution λ) is:

$$\text{Pr}\{\varepsilon_\lambda \geq \lambda^\gamma\} \propto \lambda^{-c(\gamma)} \quad (3)$$

where $c(\gamma)$ is the codimension function describing both the “sparseness” of the field intensities and the probability of given events. Roughly, $c(\gamma)$ is a measure of the fraction of the probability space “occupied” by singularities of order equal or greater than γ . Thus, eq. (3) relates the intensity of the field ε_λ to its probability of occurrence through the codimension function. The corresponding law for the statistical moments is:

$$\langle \varepsilon_\lambda^q \rangle \approx \lambda^{\gamma \max\{q\gamma - c(\gamma)\}} = \lambda^{K(q)} \quad (4)$$

where $K(q)$ is the q^{th} -moment scaling function. It is interesting to note that $c(\gamma)$ and $K(q)$ form a Legendre transformation pair.

Considering the class of Universal Multifractals, corresponding to “basins of attraction” of probability laws, the functions $c(\gamma)$ and $K(q)$ take well defined parametric forms:

$$\begin{cases} c(\gamma - H) = C_1 \left(\frac{\gamma}{C_1 \alpha'} + \frac{1}{\alpha} \right)^{\alpha'} & \text{for } \alpha \neq 1 \\ c(\gamma - H) = C_1 e^{\frac{\gamma}{C_1} - 1} & \text{for } \alpha = 1 \end{cases} \quad (5a)$$

$$\begin{cases} K(q) - qH = \frac{C_1 \alpha'}{\alpha} (q^\alpha - q) & \text{for } \alpha \neq 1 \\ K(q) - qH = C_1 q \text{ Log}(q) & \text{for } \alpha = 1 \end{cases} \quad (5b)$$

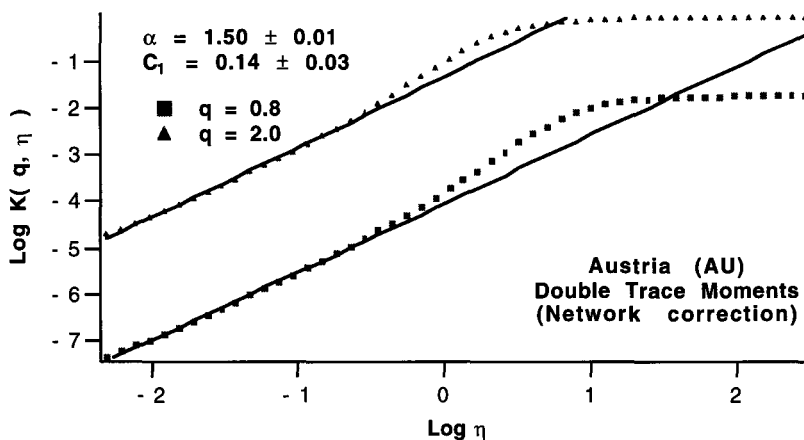
where $\frac{1}{\alpha} + \frac{1}{\alpha'} = 1$, $0 \leq \alpha \leq 2$ and $q > 0$ for $\alpha \neq 2$. The meaning of the three parameters H , C_1 and α is the following: H describes the deviation from conservation of the flux: $\langle \varepsilon_\lambda \rangle \approx \lambda^{-H}$ ($H=0$ for conservative fields); C_1 is the mean inhomogeneity as it is the codimension of the mean singularity: $C_1 = c(C_1 - H)$; in the case of conservative fluxes ($H=0$) it is also the order of the mean singularity (and simultaneously the fixed point of $c(\gamma)$); α represents the degree of multifractality (the Lévy index of the generator of the stochastic process), which increases with the range of singularities.

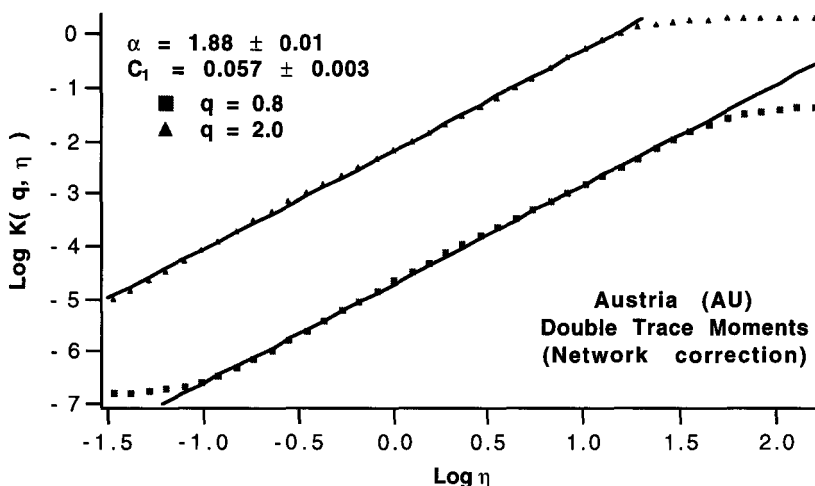
Depending upon the value of the Lévy index α , we may distinguish between different types of multifractals: for $1 \leq \alpha \leq 2$ we have unconditionally hard multifractals, i.e. the corresponding multifractal process will show divergence of moments (also called hard behaviour) above a (critical) order q_D given by the solution of the equation $K(q) = D(q-1)$, where D is the dimension of the observing space; for $\alpha < 1$ we have conditionally soft/hard multifractals (for large enough but finite values of the dimension D all of the moments converge, i.e. $q_D = \infty$). Thus, the parameters H , C_1 and α are sufficient to describe the statistics of a (universal) multifractal field.

Our aim is to describe the statistics of ^{137}Cs cumulative soil deposition and rainfall in terms of multifractals, i.e. to test the hypothesis their distribution is the result of complex nonlinear, but scale invariant, processes. The justification for applying multifractal analysis to the pollution is that "a priori", over the relevant length scales, all of the turbulent mechanisms involved are expected to be cascade processes operating over wide ranges of scales, and it is now known that such mechanisms generally lead to multifractal fields.

Several techniques exist to estimate the multifractal parameters H , C_1 and α (e.g., the Double Trace Moments technique); however, the "sparse" (fractal) nature of the monitoring networks may spoil such calculations when dealing with experimental data. A possible way to overcome the problem is to consider the density of the monitoring stations as a multifractal measure; then, by properly combining the scaling functions $K(q)$ of both the data and the network, it is possible to remove the influence of the network itself. Thus, the multifractal parameters can be objectively estimated, independently of the structure of the network.

In Tab. III we report the values of α and C_1 for, respectively, the ^{137}Cs cumulative soil deposition and the rainfall data collected in the four Countries of interest. The statistical characterisation in terms of such multifractal parameters is consistent: in fact, the scaling of the relevant quantities is fairly well present in all cases and, therefore, the estimate of both α and C_1 is straightforward. In Figs. 5 we show the calculation of α and C_1 in Austria, both for the fallout and the rainfall data: the slope of the fits give the value of α , while C_1 is found by means of the intercept.





Figs. 5. Estimate of α and C_1 for, respectively, the ^{137}Cs cumulative soil deposition data (Top) and the rainfall data (Bottom) collected in Austria.

^{137}Cs c.s.d.	Austria	Czechoslovakia	N. Italy	W. Germany
q_D	4.12 ± 0.89	2.36 ± 0.08	1.56 ± 0.07	1.60 ± 0.04
α	1.50 ± 0.01	1.96 ± 0.01	1.97 ± 0.01	1.50 ± 0.02
C_1	0.14 ± 0.03	0.07 ± 0.01	0.25 ± 0.02	0.21 ± 0.11
Rainfall	Austria	Czechoslovakia	N. Italy	W. Germany
q_D	6.14 ± 0.26	2.40 ± 0.06	3.84 ± 0.15	4.23 ± 0.07
α	1.88 ± 0.01	1.90 ± 0.03	1.90 ± 0.03	1.90 ± 0.03
C_1	0.057 ± 0.003	0.082 ± 0.009	0.052 ± 0.001	0.057 ± 0.002

Tab. III. Estimate of the multifractal features of ^{137}Cs cumulative soil deposition and rainfall in a few European Countries. Here q_D is the order of divergence of moments, α and C_1 are the multifractal parameters calculated by taking into account the effects of the networks.

As a general comment, we see that the “correcting” procedure allows to get rid of the presence of the (qualitatively and quantitatively) different networks, providing an objective investigation of the “true” phenomenon. Both the radioactive concentration and the rainfall intensity show clear multifractal features (see Tab. III). Given the fact that $\alpha > 1$ in all cases, we may classify the phenomena as “unconditionally hard” multifractal process, corresponding to a class of extremely wild phenomena. From a physically point of view it is worth noting that, eventually, we find a well defined, Country-independent, multifractal parametrization, depending on the date to which the measurements are renormalised (i.e., May 1st for Austria and Western Germany, May 17th for Czechoslovakia and Northern Italy). Also, the constancy of the values of α in the case of rainfall is striking.

As a practical application, we devise an empirical procedure able to estimate the ^{137}Cs cumulative soil deposition in a few European Countries, even in sites where no measurements are available. In order to accomplish this task, we first calculate the (multi)fractal behaviour of the radioactivity measured in the environment. This step first requires the calculation of both the multifractal spectrum of the radioactive concentration (i.e. the values of the fractal dimensions corresponding to stations measuring increasing levels of pollution - see Fig. 6) and the critical order of divergence of moments q_D (see Figs. 4 and Tab. III).

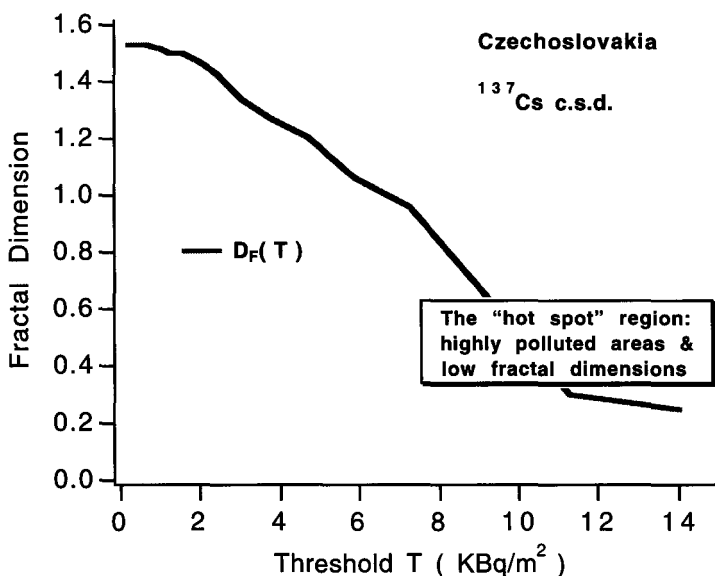


Fig. 6. The multifractal spectrum of ^{137}Cs cumulative soil deposition in Czechoslovakia.

Then, making use of only such an empirical information, we devise a procedure based on the Fractal Sum of Pulses theory: the basic idea is to consider the value of a certain quantity (e.g. radioactive pollution), in a given region at a given time, as the sum of primary pulses, whose intensity, time duration and geometrical spread are random variables properly distributed and generated according to a precise strategy. Depending on the choice of such probability distributions, we may reproduce some physical features of the phenomenon under investigation, such as the “hot spots”.

In Figs. 7 we show the estimated concentration of ^{137}Cs cumulative soil deposition in Austria and Western Germany; these pictures should be compared with Figs. 1. As a result, the comparison with the available data is always fairly good. The “hot spots” are almost always correctly reproduced and the model is able to estimate the radioactive concentration even in locations not sampled by the networks.

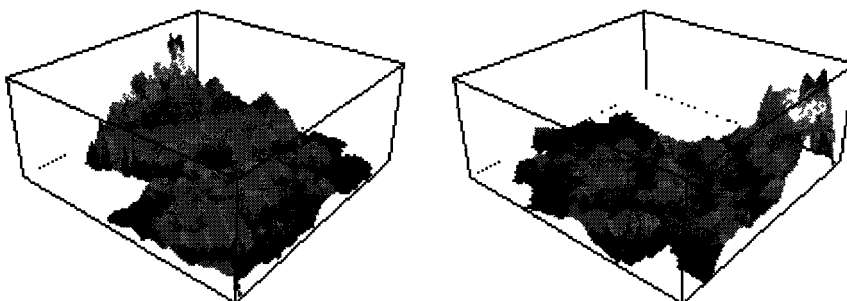


Fig. 7. Estimated concentration of ^{137}Cs cumulative soil deposition in Austria (Left) and Western Germany (Right). The ranges of the values are reported in Tab. I.

Also, as a further verification, we performed some tests neglecting a fraction of the input data: this reduces the amount of starting available information and may be representative of practical critical situations when only a few data are provided. As a result, the quality of the outputs is not too much affected, indicating a fairly good “stability” of the model.

3- List of Publications

- Ranzi, R., R.Rosso, G.Salvadori, B.Bacchi, D.Schertzer, and S.Lovejoy, Investigating Multifractal Features of a Stochastic Model of Rainfall Field in the Space-Time Domain, Ann. Geophys., part II, supp. II to vol. 11, C305, 1993.
- Ratti, S.P., G.Salvadori, G.Belli, and E.Quinto, A Monofractal Model of Air Radioactive Pollution, Proc. Conv. Naz. AIRP "Modellistica dei Sistemi Complessi e Radioprotezione", Taormina, 13-15 Ottobre, 1993.
- Quinto, E., G.Salvadori, S.P.Ratti, G.Belli, E.Quinto, G.Graziani, and M.DeCort, From Monofractal to Multifractal Models of Radioactive Pollution, presented at AIH93, Obergurgl, Austria, 1993.
- Salvadori, G., D.Schertzer, S.Lovejoy, S.P.Ratti, and G.Belli, Multifractal Objective Analysis of Sparse Fields, Ann. Geophys., part II, supp. II to vol. 11, C310, 1993.
- Salvadori, G., A Multifractal Technique for Estimating the Statistics of Sparse in situ Measurements, presented at HYDROFRACTALS'93, Ischia, 1993.
- Salvadori, G., S.P.Ratti, G.Belli and E. Quinto, Multifractal Estimating Techniques: Theory and Applications to Environmental Pollution Data, presented at NVAG3, Cargèse (Corsica), 1993.
- Ratti, S.P., G.Salvadori, G.Belli, G.Graziani, E.Quinto, e S.P.Ratti, Modelli Frattali per la Simulazione dell'Inquinamento da Radionuclidi in Aria e al Suolo dopo Chernobyl, presented at LXXXIX Congr. Naz. della Società Italiana di Fisica, Udine, 1993.
- Salvadori, G., Multifrattali Stocastici: Teoria e Applicazioni, Tesi di Dottorato di Ricerca, Biblioteca Nazionale di Roma, Diss. 93/1316; Biblioteca Nazionale di Firenze, TDR.1993.1278; 1993.
- Salvadori, G., S.P.Ratti, G.Belli, E.Quinto, and F.Missineo, First Application of Multifractal Objective Analysis in Natural Hazards, Ann. Geophys., part II, supp. II to vol. 12, C495, 1994.
- Belli, G., G.Salvadori, S.P.Ratti, S.Lovejoy, and D.Schertzer, Multifractal Objective Analysis of Seveso Ground Pollution, Toxicological and Environmental Chemistry, **43**, 63, 1994.
- Belli, G., G.Salvadori, S.P.Ratti, F.Missineo, E.Giroletti, I.Kobal, e J.Vaupotic, Analisi Multifrattale della Distribuzione di ²²²Rn "Indoor" in Slovenia, Proc. 3^o Conv. Naz. ARIA '94, Roma, 26-28 Ottobre, 1994.
- Ratti, S.P., G.Salvadori, G.Belli, e E.Quinto, Frattali e Radioprotezione: l'Esperienza di Chernobyl, presented at Sc. Sup. di Radioprot. "C. Polvani", Villa Olmo (Como), 6 Settembre, 1994.
- Salvadori, G., S.P.Ratti, G.Belli, E.Quinto, G.Graziani, and M. de Cort, Fractal Modelling of Chernobyl's Radioactive Fallout in Europe , Proc. Seminar on Fractals in Geosciences and Remote Sensing, Ispra (Italy), 14-15 Aprile, 1994, Eds. G.G.Wilkinson et al., Report EUR 16092 EN, Vol. 1, 237, 1994.
- Ratti, S.P., G.Salvadori and G.Belli, Multifractal Characterization of Environmental Pollution from Small to Large Scales, presented at Third SIAM Conference on "Mathematical and Computational Issues in the Geosciences", S. Antonio (Texas, USA), February 8-10, 1995.
- Salvadori, G., S.P.Ratti, G.Belli, F.I.Kobal, and J.Vaupotic, The Spatial distribution of ²²²Rn "Indoor" in Slovene as a stochastic multifractals process, Proc. IRPA Regional Symposium on "Radiation Protection in Neighbouring Countries in Central Europe - 1995", Portoroz (Slovene), 4-8 Settembre, 1995.
- Salvadori, G., S.P.Ratti, G.Belli, and E.Quinto, A fractal view of Chernobyl radioactive fallout in Northern Italy and Europe, Proc. IRPA Regional Symposium on "Radiation Protection in Neighbouring Countries in Central Europe - 1995", Portoroz (Slovene), 4-8 Settembre, 1995.
- Ratti, S.P., G.Salvadori and G.Belli, The Chernobyl Radioactive Fallout (I): Empirical Time Evolution in Italy and France, 1995. Salvadori, G., S.P.Ratti, G.Belli, and E.Quinto, The Chernobyl Radioactive Fallout (II): Cross-estimate of the Empirical Parameters, 1995. Salvadori, G., S.P.Ratti, G.Belli, and E.Quinto, Modelling the Chernobyl Fallout in Northern Italy and in Europe: a Fractal Approach, 1995. (all submitted to Health Phys.).
- Schertzer, D., Y.Chigirinskaya, S.Lovejoy, S.P.Ratti, G.Salvadori, and G.Belli, Multifractal Analysis of Chernobyl Fallout: Self-organized Criticality and "Hot Spots", Proc. Mathematics and Computations, Reactor Physics, and Environmental Analyses, Portland (Oregon), April 30 - May 4, 1995, American Nuclear Society Publ., Illinois, 743, 1995.
- Ratti, S.P., G.Belli, and G.Salvadori, Risk Analysis and Assessment in Environmental Sciences: use of Statistical Methods to handle the Information, Toxic. Environm. Chem., 1995 (acc.).
- Salvadori, G., S.P.Ratti, G.Belli, e E.Quinto, Frattali e Radioprotezione: l'Esperienza di Chernobyl, La Radiologia Medica, 1995 (acc.).
- Software Production:** a special software (named "Multifractalia") performing the multifractal analysis of 1D and 2D data has been devised and is freely distributed together with the Final Report; it includes an *Instruction Manual* and runs both on the standard Macintosh and on the new RISC PowerMac.

1- Specific objectives of the reporting period

The problem of time evolution and prediction of geophysical fields may be properly faced exploiting fractals and multifractals, which provide a global theoretical framework describing the dynamical relations among several factors, by considering scaling interactions between different fields. Experimental evidence of the highly variable and multifractal nature of the Chernobyl fallout is provided, along with the multifractal characterization of some related atmospheric fields such as rainfall, wind and temperature. Specific techniques can be devised in order to simulate (in space as well as in time) the radioactive concentration and to give predicting schemes/algorithms feasible for the practical purposes of radioprotection and risk assessment. In particular it could be possible to exploit the properties of multifractal processes in order to create/improve stochastic predicting models.

2- Progresses made and results obtained

Geophysical fields show abundant evidence of nonlinear variability resulting from strong nonlinear interactions between different scales, different structures, and different fields. This variability is quite extreme and is occasionally associated with catastrophic natural events. Another fundamental characteristic of such variability is the very large range of scales involved, which often extends from 10000 Km to a few meters in space and from at least several years to less than a few seconds in time, featuring a turbulent dynamics.

Such an extreme variability implies highly complex distribution of fallout (e.g. the “hot spots”) creating nontrivial difficulties for risk assessment and monitoring, since the risks depend primarily on local doses. To get an idea of the magnitude of the variability, consider data from a single village close to Chernobyl, where the soil radioactive concentration ranges from ≈ 100 to 200000 Bq/m². It is then of primary interest to investigate first the multifractal structure and properties of those violent fields involved in the process of dispersing the Chernobyl radioactivity in the environment (namely, rainfall, wind and temperature), as well as the features of the fallout in the most polluted sites closest to the nuclear plant.

Actually, two digitised data bases were created respectively for short range and medium range fallout using, as primary sources, the booklets published (in Russian) by the ex-Soviet Hydromet Office (Moscow, Obninsk or Minks) from 1989 to 1992. Indeed, Hydromet was in charge of centralising all isotopes analyses of soil tests provided by more than 31 different Organisations of former Soviet Union, in order to constitute a free access data bank. Unfortunately, we did not get any confirmation of such an access to digitised data; rather, we already had difficulties to get information on publications of data.

The data were published as booklets of records of ¹³⁷Cs (and ⁹⁰Sr) cumulative soil deposition collected in Russia, Belarus and Ukraine after the Chernobyl accident. For each site, the minimum, mean and maximum values are given. Unfortunately, the geographical coordinates (e.g., Longitude and Latitude) of the sampling locations are never provided and the sampling frequency was not regular. For each town the number of measurement ranges from one to a few hundreds, but the precise location of each specific site is not given. The publication (Hydromet, Moscow) of June 1989 only displays the average value of radioactive concentration in a given town.

Booklets published by the Hydromet Office (Obninsk) on March and July 1989, containing data collected until such year, were the major sources for the generation of the two following data bases used in the present Project:

- HO1: short range fallout (≈ 100 Km radius around Chernobyl); data consist of ¹³⁷Cs soil deposition (minimum, mean and maximum values) measured in 1986, collected in 148 towns in Ukraine; the number of measurements per town varies from 1 to 150;
- HO2: medium range fallout (≈ 300 Km radius around Chernobyl); data consist of ¹³⁷Cs soil deposition measurements made in Russia, Belarus and Ukraine; mean values of radioactive concentration have been obtained by regularly remapping the sparse measurements on a 128×128 grid (one pixel corresponds to an area of $\approx 5 \times 5$ Km).

In Fig. 1 we show the network of the 148 towns in Ukraine where ^{137}Cs soil deposition has been collected; geographical coordinates are not present in the original data and are not displayed (however, for sake of reference, the distance of the farthest site from Chernobyl is of the order of ≈ 100 Km). The values range from ≈ 9 to $\approx 6 \cdot 10^5$ KBq/m^2 and the “hot spot” corresponding to Chernobyl represents an “outlier” which is a fingerprint of multifractality.

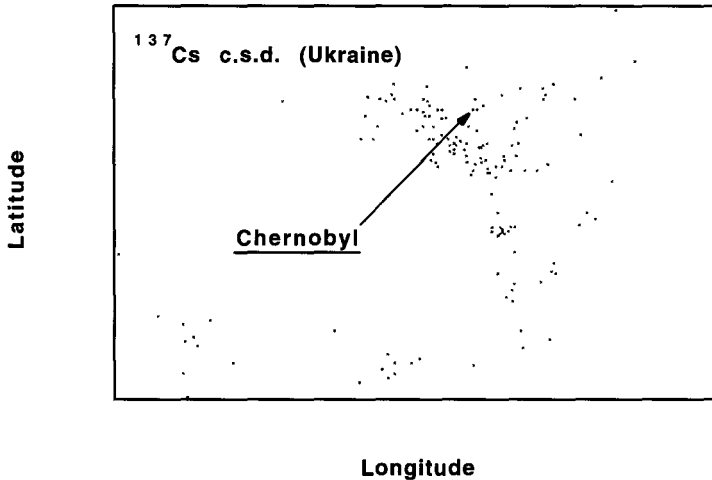


Fig. 1. Map of the 148 towns in Ukraine where samples of ^{137}Cs soil deposition have been collected; the distance of the farthest site from Chernobyl is ≈ 100 Km.

The analysis of the measurements is carried out by first estimating the codimension function by means of the PDMS technique; an (asymptotic) linear regression on $c(\gamma)$ allows to calculate the parameter q_D ; the results are summarised in Tab. I. Finally, we calculate the multifractal parameters α and C_1 by means of the DTM technique; the results are summarised in Tab. II.

	HO1			HO2
	min. conc.	mean conc.	max. conc.	
q_D	≈ 1.60	≈ 1.56	≈ 1.26	≈ 2.67

Tab. I. Calculation of q_D in the cases of the ^{137}Cs cumulative soil deposition data.

Data set	α	C_1
HO1 (without Chernobyl “hot spot”)	≈ 1.6	≈ 0.2
HO2 (without Chernobyl “hot spot”)	≈ 1.6	≈ 0.4
HO2 (with Chernobyl “hot spot”)	≈ 2.0	≈ 0.1

Tab. II. Estimates of the parameters α and C_1 of the ^{137}Cs cumulative soil deposition data.

The calculation of the codimension function for the data set HO2 is shown in Fig. 2; the empirical estimate is fairly good, given the large amount of data (≈ 16000). The slope of the (asymptotic) linear regression allows to calculate the parameter q_D (≈ 2.67). As for the case of the fallout in Western Europe, the relatively low values of q_D might indicate the divergence of the low order statistical moments of the stochastic process “generating” the observed distribution of radioactivity.

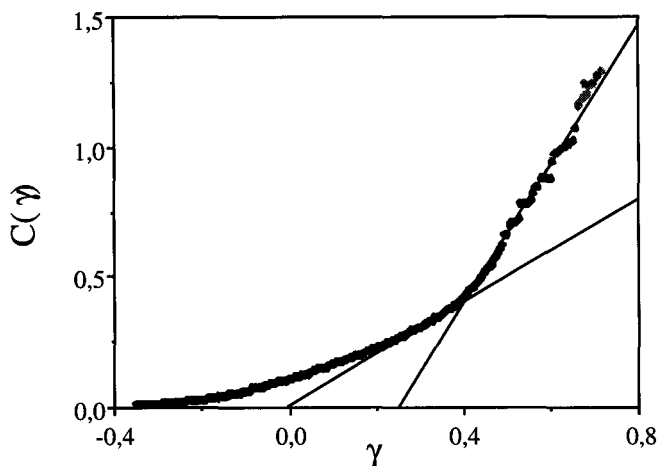


Fig. 2. The codimension function $c(\gamma)$ for the measured concentration of ^{137}Cs cumulative soil deposition in Russia, Belarus and Ukraine.

In Fig. 3 we show the estimate of the multifractal parameters α and C_1 by means of the DTM technique (with correction of the effects of the networks) for the data set HO1, where the Chernobyl source has been (temporarily) removed. The scaling is fairly good, yielding a value of $\alpha \approx 1.6$ and $C_1 \approx 0.2$. The results of the DTM technique for the data set HO2, both excluding the Chernobyl source and including it, indicate that the scaling is fairly good. In the first case we estimate $\alpha \approx 1.6$ and $C_1 \approx 0.4$, consistent with those calculated for the data set HO1 excluding the Chernobyl source; on the contrary, including the Chernobyl source yields $\alpha \approx 2$ and $C_1 \approx 0.1$. Given the fact that $\alpha > 1$ in all cases, we may classify the phenomenon as an “unconditionally hard” multifractal process.

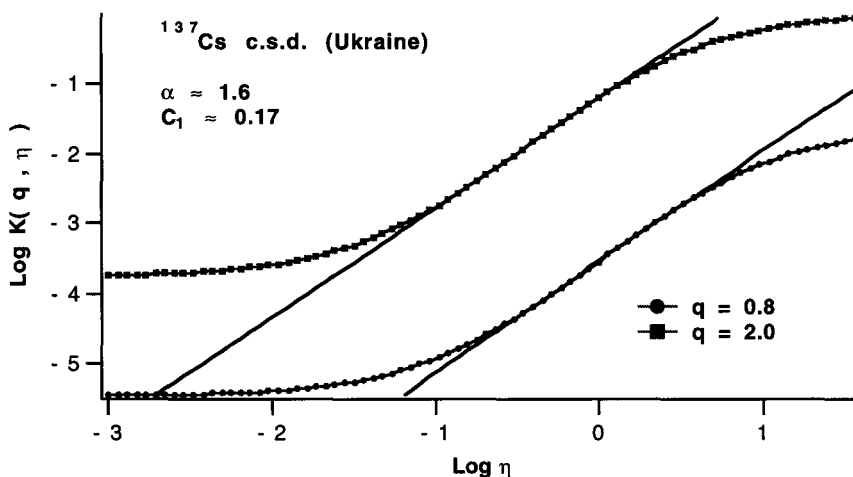


Fig. 3. Estimate of α and C_1 for the ^{137}Cs cumulative soil deposition data in Ukraine (data set HO1 but excluding the Chernobyl source) with correction of the effects of the networks.

As a general comment, the above analyses show the clear multifractal nature of the ^{137}Cs cumulative soil deposition due to the Chernobyl accident, considering both short-, medium-, and long-range fallout. Such an experimental result is indeed new and relevant, and may provide the empirical starting point for exploiting some multifractal interpolating techniques.

The radioactivity of the Chernobyl cloud is transported by aerosols, which are advected by atmospheric dynamics. It is then of primary interest to study the influence of atmospheric turbulence on the dispersion of the Chernobyl cloud. In order to characterise atmospheric turbulence and rain statistical properties, we analysed various types of turbulent velocity, passive scalars and rain data bases.

The main features of the available wind velocity data are described in Tab. III; reported are: the type of data and anemometer, the sampling frequency (in Hz), the sampling location, the altitude (only for the atmospheric data) and the estimates of the parameters α and C_1 . All the measurements are recorded in time at a fixed location (see Fig. 4 for a sketch of the data, showing their extreme variability at all scales), except the ones collected on the South China Sea (aircraft data). The important point is the constancy of the results for atmospheric data. In Fig. 5 we show the power spectrum of the wind velocity measurements in the atmosphere: as it is evident, there is scaling over a wide range of scales. In Fig. 6 we also show the empirical structure function scaling exponent compared to Kolmogorov trivial scaling (line $q/3$). The concavity of the curve is an indication of multifractality.

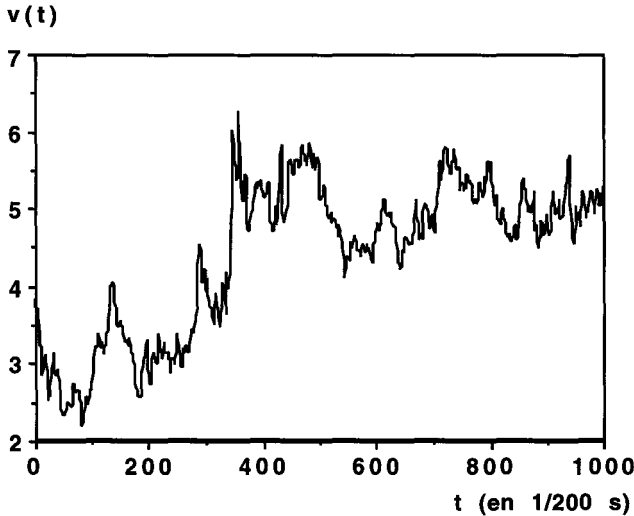


Fig. 4. A sketch of the available atmospheric wind velocity data.

Data Type	Anemom.	Freq. (Hz)	Source	Altit. (m)	α	C_1
Wind tunnel (1)	Hot wire	10000	Modane		1.30 ± 0.1	0.25 ± 0.05
Ground (2)	Hot wire	2000	Montreal	3	1.50 ± 0.05	0.25 ± 0.05
Ground (3)	Sonic	200	Paris	20	1.45 ± 0.1	0.29 ± 0.1
Ground (4)	Sonic	10	Bordeaux	25	1.45 ± 0.1	0.24 ± 0.1
Aircraft (5)	Sonic	8	China	50 - 5000	1.40 ± 0.1	0.30 ± 0.1

Tab. III. Main features of the wind velocity measurements.

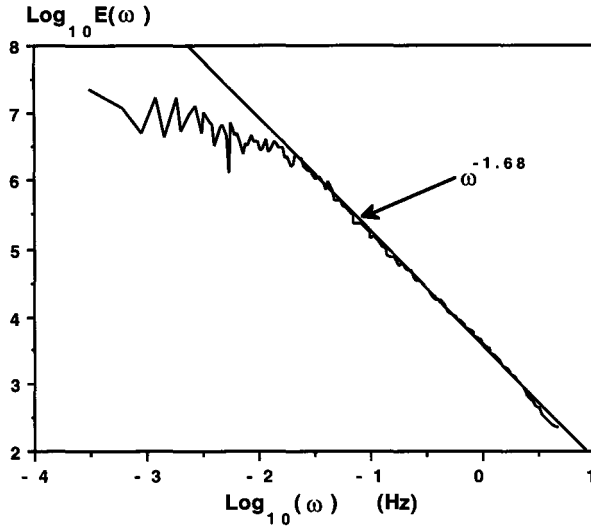


Fig. 5. The power spectrum of the wind velocity measurements in the atmosphere.

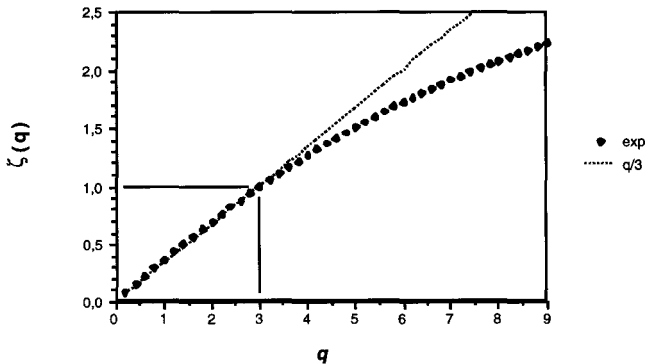


Fig. 6. The empirical structure function scaling exponent .

The temperature in a turbulent fluid can be considered as a passive scalar advected by turbulence; in Fig. 7 we present a sketch of the data, showing their extreme variability at all scales. In Fig. 8 we show the (scaling) power spectrum of the temperature fluctuations. The main features of the available data are described in Tab. IV: shown are the type of data and anemometer, the sampling frequency (in Hz), the sampling location and the altitude.

Data Type	Anemometer	Frequency (Hz)	Source	Altitude (m)
Ground (1)	Cold wire	5	Montreal	10
Ground	Sonic	10	Bordeaux	25
Aircraft (2)	Sonic	8	China	50 - 5000

Tab. IV. Main features of the atmospheric turbulent temperature measurements.

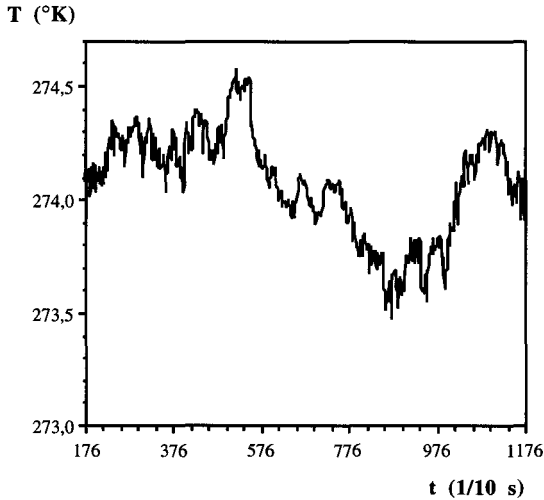


Fig. 7. A sketch of the available atmospheric turbulent temperature data.

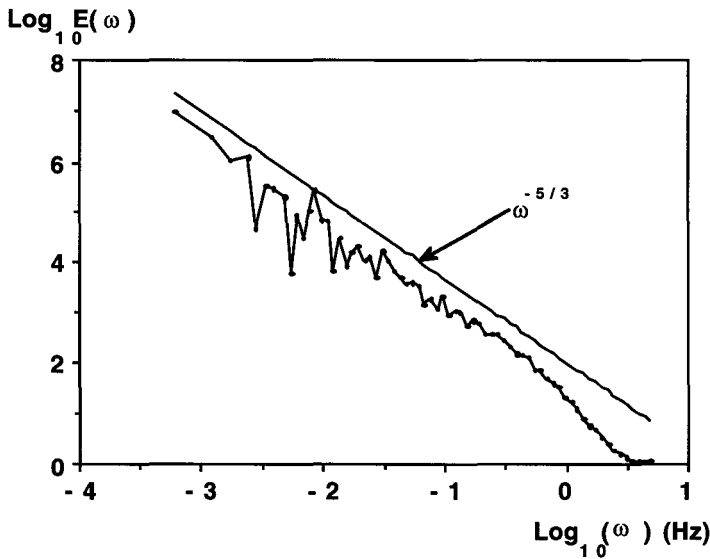


Fig. 8. The power spectrum of the temperature fluctuations.

The application of the DTM technique to estimate the multifractal parameters α and C_1 of the available atmospheric turbulent temperature data gives good results, since the scaling is well respected; for these data, $\alpha \approx 1.2$ and $C_1 \approx 0.15$.

The rain rate data are recorded every 12 hours at Nîmes (France) between 1949 and 1992 (more than forty years of sampling). As an example, in Fig. 9 we present a sketch of the data, showing their extreme intermittency: indeed, the mean rain rate is of about 1.1 mm, but quite a few maxima exceed the value of 100 mm in 12h. The application of the DTM technique to estimate the multifractal parameters gives good results, since the scaling is well respected; for these data the parameter α is ≈ 0.45 .

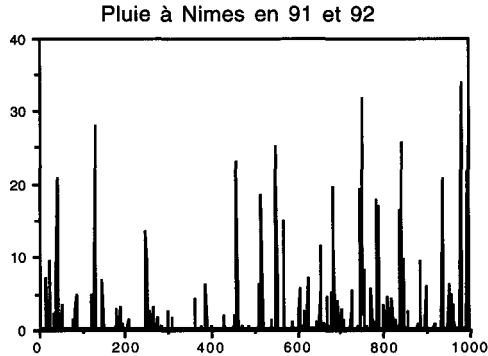


Fig. 9. A sketch of the available 12h-resolution rain rate data at Nîmes (France) during the period 1991 and 1992. The vertical scale (rain rate) is in mm.

For both the theoretical and empirical reasons already outlined, it has become increasingly urgent to investigate the predictability properties of multifractal process. In particular, we examine a simple class of stochastic multifractals (i.e. the lognormal multifractals, where $\alpha=2$) which are high (eventually infinite) dimensional and show well defined (multi)scaling properties. These are the simplest case of an important class of stable, attractive scaling dynamics, associated with “universal multifractals”. The theoretical predictions of universal multifractals have been well verified in both wind tunnel and atmospheric turbulence. A method of predicting these fields as well as a theoretical characterisation of the limits to the predictability has thus become increasingly important and fundamental.

In most applications, the use of multifractal analysis/simulation concerns mainly geophysical fields described in a space domain (either 1, 2 or 3 dimensional), at a given time; the hypothesis that such a field has time invariance (i.e. stationarity) allows us to claim that the statistical properties of this field are independent of the time of the observation. In that sense, different “snapshots” of the same system at different times simply correspond to different realisations of that given system.

Though we do not depart from the assumption that the system is stationary, the extension of the normal space (3-dimensional space) to a space-time domain (4-dimensional space) gives us the opportunity to introduce dynamics for stationary multifractal fields. These dynamics are understood as scaling symmetries involving the field at different locations in space-time. Thus, correlation functions (e.g., the correlation spectrum or higher order moments) can measure the influence of the state of the field at a given time and place over its state at another location in space-time. Earlier works on that issue showed that simulations of time-evolving clouds subject to turbulent dynamics may give interesting results.

Many similarities exist between statistical properties involving a multifractal field either in the “normal” 3D space or in the “extended” 4D space. However, the time coordinate has causality properties, i.e. past influences the future but future does not influence past. This primordial feature can be introduced in the multifractal framework, by modifying the transformation that cast a multifractal field into a Gaussian or Lévy noise.

Multifractal simulation can be viewed as the numerical construction of realisations of multifractal fields, controlled by the usual α , C_1 and H parameters. Starting from the so called sub-generator $\gamma(\vec{x}, t)$, a white noise field (Gaussian noise for $\alpha=2$, Lévy noise for $\alpha<2$), we introduce the scaling properties by performing a convolution of this field with Green functions exhibiting scaling properties. The field so obtained, called the generator $\Gamma(\vec{x}, t)$, is then exponentiated to finally give the multifractal field in space-time $\varepsilon(\vec{x}, t)$. Thus, there exists a global transformation $\Omega[\]$ that generates a multifractal field starting from a white noise field: $\varepsilon(\vec{x}, t) = \Omega[\gamma(\vec{x}, t)]$.

When considering the time coordinate, we have to face the problem of causality. The transformation $\Omega[\]$ is thus expected to respect the causality. In order to construct a causal

transformation, we first have to understand how such a transformation is performed. This convolution is calculated, in the isotropic “normal” 3D space case, in a volume between two balls of radius λ^{-1} and 1, where λ corresponds to the resolution and 1 is the integral (maximum) scale (thus $\lambda = \ell^{-1}$, where ℓ is the scale of observation). We then simply have

$$\Gamma_{\lambda}(\bar{x}) = \int_{|\bar{y}|=\lambda^{-1}}^{|\bar{y}|=1} d\bar{y} G(\bar{x} - \bar{y}) \gamma(\bar{y}) \text{ where } G(\bar{x} - \bar{y}) \text{ is a Green function exhibiting proper scaling. Finally,}$$

$$\text{considering the extended 4D space, we similarly obtain } \Gamma_{\lambda}(\bar{x}, t) = \int_{|\bar{y}|=\lambda^{-1}}^{|\bar{y}|=1} \int_{|\tau|=\lambda^{-1}}^{|\tau|=1} d\tau G_{\text{causal}}(\bar{x} - \bar{y}, t - \tau) \gamma(\bar{y}, \tau).$$

Technically, when performing simulations, two approaches are possible, yielding to similar results; the causality can be introduced either at the level of the Green function or by truncating the volume of integration. The first approach is the most satisfactory, leading to an interesting interpretation of the dynamics at the very level of the singularities of the field (see below). Moreover, the definition of the Green function in Fourier space allows a faster numerical treatment (the convolution being performed on an isotropic, not truncated, volume), and enables us to work directly in the Fourier space, where the convolution becomes a simple multiplication. In the “normal” 3D case, this function is $\hat{G}(\bar{k}) = \|\bar{k}\|^{-\alpha'}$, where d is the

dimension of the space (d=3 normally) and α' is such that $\frac{1}{\alpha} + \frac{1}{\alpha'} = 1$.

It can be shown that we can generalise this Green function to obtain a causal Green function (considering the time coordinate); defining $\hat{G}_{\rightarrow}(\bar{k}, \omega)$ as the causal Green function corresponding to $\hat{G}(\bar{k}, \omega)$, we simply have: $\hat{G}_{\rightarrow}(\bar{k}, \omega) = \hat{G}(\bar{k}, \omega) * \hat{H}(\omega)$, where the convolution is performed only on the ω variable, and $\hat{H}(\omega)$ is the Fourier transform of the Heaviside function $H(t)$: $\hat{H}(\omega) = \frac{1}{2} \delta(\omega) + \frac{1}{2\pi} \text{p.v.} \frac{1}{\omega}$ (p.v. stands for the Cauchy principal value). A straightforward calculation gives us, replacing $\hat{G}(\bar{k}, \omega)$ by the traditional Green function defined in the 4D space, $\hat{G}_{\rightarrow}(\bar{k}, \omega) = \frac{\|\bar{k}\|^{1-\alpha'}}{\|\bar{k}\| - i\omega}$. In the special case where d=2 (t and only one space coordinate x) and $\alpha=2$ (Gaussian case), such a convolution can be written as $(\partial_t + |\bar{k}|) \hat{\Gamma}(\bar{k}, t) = \hat{\gamma}(\bar{k}, t)$ which is the equivalent of a diffusion equation; the generator is thus the result of some kind of diffusion of the source term represented by the sub-generator. In the general case, this equation of diffusion becomes $(\partial_t + \|\bar{k}\|) \|\bar{k}\|^{-1+\alpha'} \hat{\Gamma}(\bar{k}, t) = \hat{\gamma}(\bar{k}, t)$.

This interpretation in terms of diffusion gives a better and more understandable picture of the mechanism involved with these dynamics; the singularities of the generator are thus causally diffused on a larger and larger domain as time increases, the size of this domain growing as a power law of time. Note that this equation of diffusion is only definable when the resolution λ is kept finite; when λ tends to infinity, we have to face the problems of divergence for the generator, which makes this interpretation irrelevant.

In the context of prediction, the transformation $\Omega[\]$ is remarkable, in the sense that its inverse allows to keep all the information represented by the measurements (the multifractal field $\varepsilon(\bar{x}, t)$) and to work on a representation of the field (which exhibits non-vanishing correlation theoretically extending in all scales) for which the correlation in space-time is minimised. We now see that, in order to interpolate a given multifractal field localised in a closed volume in space-time, we have to perform the inverse transformation $\Omega^{-1}[\]$ on $\varepsilon(\bar{x}, t)$, and then extend the obtained white noise field to a larger domain containing the point (\bar{x}_0, t_0) that we want to interpolate from the known (measured) field. Transforming with $\Omega[\]$ this extended field finally gives the interpolated multifractal field.

These methods enable us to create a possible realisation of the field in a given volume, given the knowledge of this field on a separated domain. The only information concerning the part of the sub-generator that we create is the nature of this field (a white noise), its Lévy index α and the parameter C_1 that holds all the information about the covariance of the noise.

If, instead of a realisation of this process, we take this part of the sub-generator equals to the mean of the noise (which is equal to zero), we clearly obtain the "best" realisation, i.e. the most probable one. The best predictor is thus defined by a null white noise for the extended domain.

Physical systems ruled by non-linear dynamics (like most of the geophysical processes such as turbulent flows, responsible in the atmosphere for the transport of passive scalars like water concentration) are intrinsically subject to a loss of memory of their past states; as time increases, a perturbed system will quickly diverge from the non-perturbed system. After some time, the initial information (saying that the two systems were almost identical) is completely lost, and their features are as different as the ones of two fields that would be initially completely uncorrelated. Thus, when one wants to model such a system, and then predict the future evolution of a given realisation, one will face the problem of the limit of predictability of such system (actually of the model, which should take into account the non-linearity of the dynamics, and thus exhibit this limit of predictability, which can differ from the one of the actual system).

In order to study the limit of predictability of our model, we construct two sub-generators $\gamma_1(\bar{x}, t)$ and $\gamma_2(\bar{x}, t)$, exactly equal for $t < t_0$, and completely uncorrelated for $t > t_0$. We can then observe the difference of the two multifractal fields $\varepsilon_1(\bar{x}, t) = \Omega[\gamma_1(\bar{x}, t)]$ and $\varepsilon_2(\bar{x}, t) = \Omega[\gamma_2(\bar{x}, t)]$. We expect that the loss of information, initially confined at small scale, tends to reach larger scales as time increases, and eventually spoils all the scale up to the integral scale, when the two systems have completely forgotten their common past.

A simple calculation shows that the statistical quantity $W_{(k_1, k_2, t)} = \langle \hat{\varepsilon}_1(k_1, t) \hat{\varepsilon}_2(k_2, t) \rangle$ is a good candidate to observe the decorrelation developing from small scales to large scales as time increases. Indeed, we may obtain that $W_{(k_1, k_2, t)} = \delta_{(k_1+k_2)} k_1^{-1+\beta} \theta_{(k_c(t) - k_1)}$, where β is a small correction ($\beta = K(2)$), $\theta_{(k)}$ corresponds to some kind of cut-off around the first mode $k = 0$, and $k_c(t)$ is the cut-off wave number characterising the largest scale being spoiled at time t (thus $k_c(t) = k_{\max}$ for $t < t_0$, and $\partial_t k_c(t) < 0$ for $t > t_0$).

These results can be linked with those obtained using the "best" predictor in prediction methods. As observed earlier, the large structures (structures at large scales) tends in average to be more persistent than the smaller ones. When comparing two fields originally completely correlated, we in fact observe that small structures first undergo significant distortions due to larger scales, this process being roughly interpreted (in a statistical sense) as the destruction and replacement of these structures by new ones (different for the two fields), causing the decorrelation to grow strongly at these scales; then, larger structures are replaced as well, and so on, this process resulting in this scaling law linking spatial scale and structure life time/predictability time $\tau_l \sim \ell$.

This phenomenology can be deduced in a straightforward manner when considering turbulent flows. In this case the system is no more isotropic in space/time but anisotropic, and simple dimensional arguments (following the phenomenology introduced by Kolmogorov) show that $\tau_l \sim \ell^{2/3}$.

3- List of Publications

- Ladoy, Ph., F.Schmitt, D.Schertzer, and S.Lovejoy, Variabilité temporelle multifractale des observations pluviométriques à Nîmes, *C. R. Acad. Sci. Paris*, 317, série II, 775, 1993.
- Lovejoy, S., D.Schertzer, P.Silas, Y.Tessier, and D.Lavallée, The unified scaling model of the atmospheric dynamics and systematic analysis of scale invariance in cloud radiances, *Annales Geophysicae*, 11, 119, 1993.
- Pecknold, S., S.Lovejoy, D.Schertzer, C.Hooge, and J.F.Malouin, The simulation of universal multifractals, In, *Cellular Automata*, Eds. Perdanf and Lejeune, World Scientific, 228, 1993
- Schertzer, D., and S.Lovejoy, Scaling and Multifractal Processes, *Lecture Notes* prepared for NVAG3, Cargèse, Corsica, Sept. 10-17, 1993.

- Schmitt, F., D.Schertzer, S.Lovejoy, Y.Brunet, Estimation of universal multifractal indices for atmospheric turbulent velocity fields, Fractals, **1**, 568, 1993.
- Tessier, Y., S.Lovejoy, and D.Schertzer, Universal Multifractals: Theory and Observations for Rain and Clouds, J. Appl. Meteo., **32**, n. 2, 223, 1993.
- Schmitt, F., D.Schertzer, S.Lovejoy, Y.Brunet, Empirical study of multifractal phase transitions in atmospheric turbulence, Nonlinear Processes in Geophysics, **1**, 95, 1994.
- Belli, G., G.Salvadori, S.P.Ratti, S.Lovejoy, and D.Schertzer, Multifractal Objective Analysis of Seveso Ground Pollution, Toxicological and Environmental Chemistry, **43**, 63, 1994.
- Tessier, Y., S.Lovejoy, and D.Schertzer, Multifractal Analysis and Simulation of the Global Meteorological Network, J. Appl. Meteo., **33**, n. 12, 1572, 1994.
- Chigirinskaya, Y., About two digitized data bases of Chernobyl fallout (short range and medium range), LMD Internal Report, CNRS, Paris, 1994.
- Chigirinskaya, Y., D.Schertzer, and S.Lovejoy, Multifractal analysis of tropical turbulence; part I: self organized structures and typhoon generation, Nonlinear Processes in Geophysics, **1**, 105, 1994.
- Lazarev, A., D.Schertzer, and S.Lovejoy, Multifractal analysis of tropical turbulence; part II: vertical scaling and the unified scaling of atmospheric dynamics, Nonlinear Processes in Geophysics, **1**, 115, 1994.
- Schertzer, D., Y.Chigirinskaya, S.Lovejoy, S.P.Ratti, G.Salvadori, and G.Belli, Multifractal Analysis of Chernobyl Fallout: Self-organized Criticality and "Hot Spots", Proc. Mathematics and Computations, Reactor Physics, and Environmental Analyses, Portland (Oregon), April 30 - May 4, 1995, American Nuclear Society Publ., Illinois, 743, 1995.

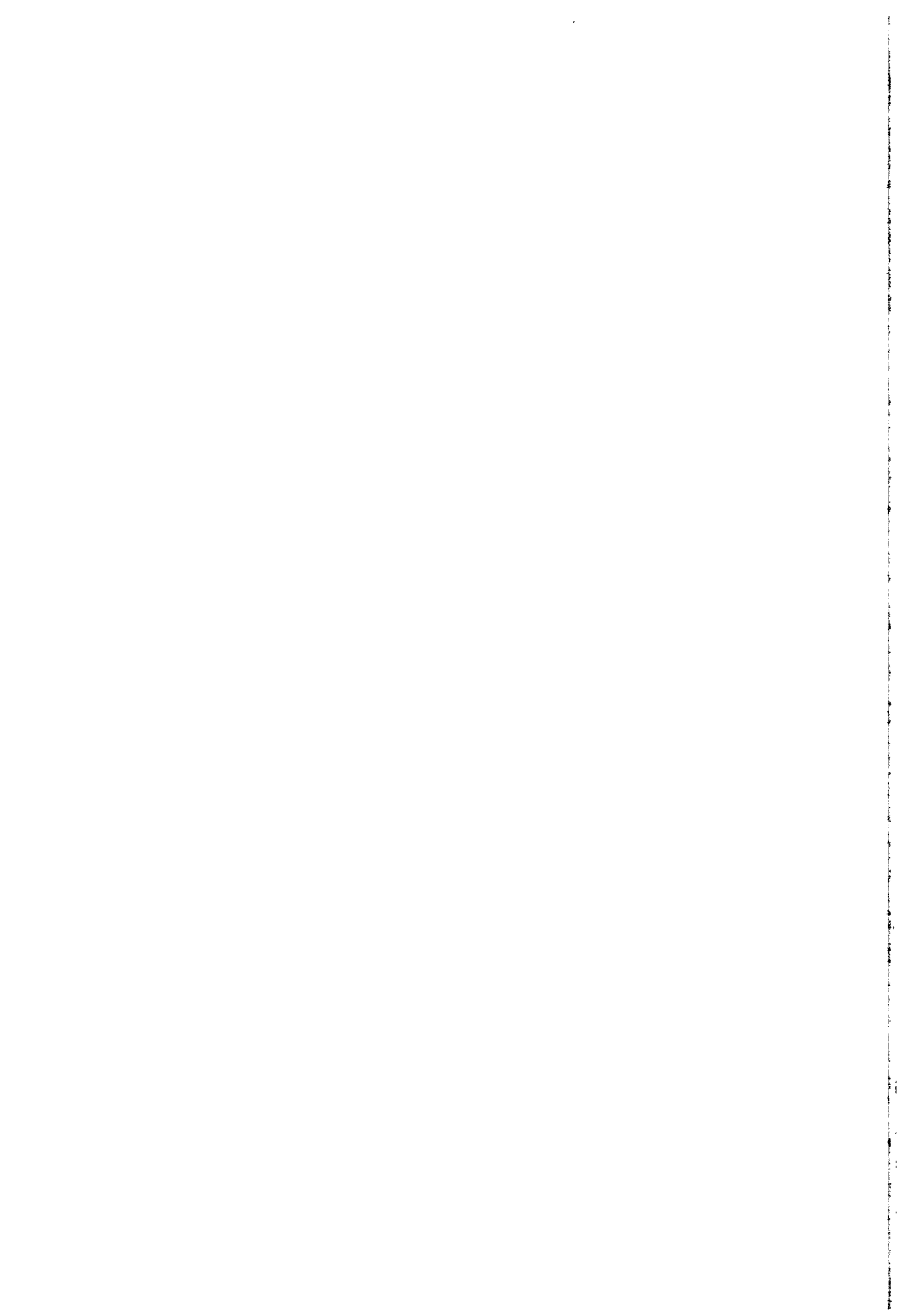


IV

KOORDINIERUNGSTÄTIGKEIT

COORDINATION ACTIVITIES

ACTIVITES DE COORDINATION

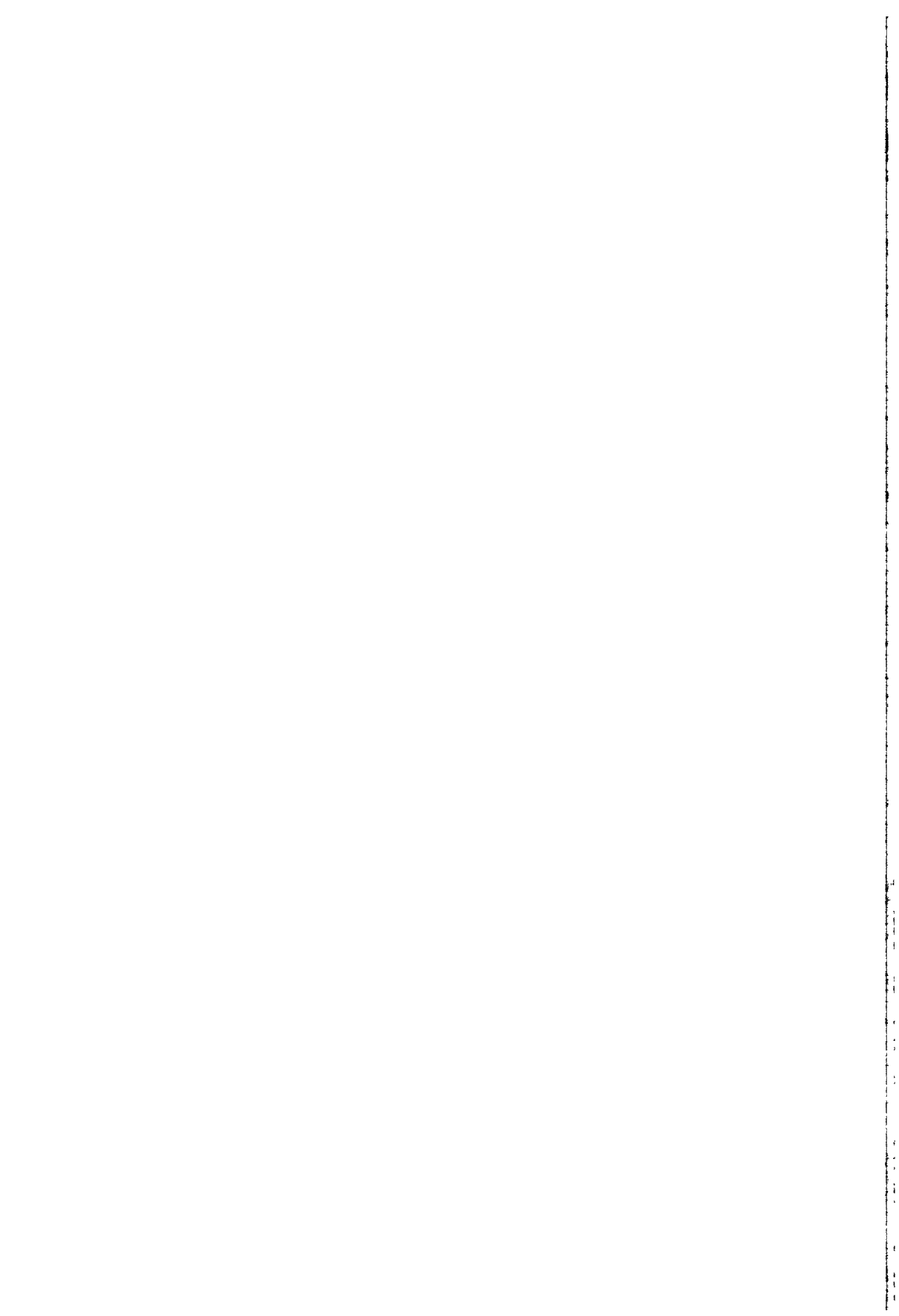


IV. Coordination

Study Group meetings, Workshops, Seminars and Symposia have proved to be a most effective means of coordination because they are naturally adapted to scientific work and easily accepted by scientists. These meetings, focusing on the evaluation of particular subjects areas of the Radiation Protection Actions are attended by research workers involved in the contract programme, as well as scientists from non-participating laboratories or organizations and by scientific staff members of the Commission.

On the following pages the various meetings held in the period from December 1992 to June 1995 are listed:

- A: Meetings of Study Groups, where scientists involved in the contract programme, independent experts and Staff Members of the Commission discuss specific subject areas of the programme. (Page 4429)
- B: Meetings organized, coorganized or cosponsored by the European Commission on special subject areas of interest for radiation protection and where contacts among scientists from a wider range of disciplines and countries might be established. (Page 4445)
- C: Meetings of experts appointed for the purpose of coordinating and stimulating efforts toward practical measures of radiation protection as foreseen in Chapter III of the EURATOM Treaty or convened by the Commission for special tasks. (Page 4457)



A

Meetings of Study Groups

Study Group on Thyroid cancer in children living near Chernobyl

Brussels (B), 21 - 22 December 1992

Panel Members from 12 countries and the EC

Principal subjects:

- Follow-up of the Panel mission to Minsk, Belarus;
- Finalize the Consensus Opinion on childhood thyroid cancer in Belarus;
- Semi-finalize the CEC report on Post-Chernobyl Thyroid Cancer in Children: a CEC Thyroid Expert Panel Report;
- Development of experimental collaboration projects on thyroid cancer.

Study Group on Uncertainty Analysis of Accident Consequence Codes (CEC/US NRC Project)

Chilton (UK), 21 - 22 January 1993

13 participants from 3 countries and the EC

Principal subjects:

- Expert judgement elicitation
- Uncertainty analysis
- Application of methodology to health effects, environmental transfer, urban pathways and metabolic models

Study Group on CEC/NEA Intercomparison of Probabilistic Accident Consequence Assessment Codes: meetings of Project Management (PMG) and ad-hoc Groups (AHG)

Paris (F), 26 - 29 January 1993

39 participants from 15 countries, OECD/NEA and the EC

Principal subjects:

- Intercomparison of probabilistic accident consequence codes
- COSYMA and MACCS users' groups
- Review of results of intercomparison
- Preparation of overview and technical reports

Study Group on Uncertainty Analysis of Accident Consequence Codes (CEC/US NRC Project)

Albuquerque (USA), 8 - 10 February 1993
12 participants from 3 countries and the EC

Principal subjects:

- Expert judgement
- Case studies for elicitation of experts in atmospheric dispersion and deposition
- Pre- and post-processors for uncertainty analysis

Study Group on marine radioecology, including problems around the Arctic Sea

Madrid (E), 28 February - 2 March 1993
10 participants from 7 countries and the EC

Principal subjects:

- Discussion of the progress made by the different participants
- Plans of works of the initial group and of the newly added institutes
- Presentation by the Norwegian and Swedish scientists regarding the situation in the Arctic zone

Study Group on Decision Support Systems for Off-site Emergency Management (JSP1)

Obninsk (Russia), 2 - 4 March 1993
26 participants from 6 countries and the EC

Principal subjects:

- RODOS decision support system
- Off-site emergency management
- Data bases of early environmental measurements
- Transfer of hardware/software configuration

Study Group of RODOS Management Group

Karlsruhe (D), 17 March 1993
6 participants from 4 countries and the EC

Principal subjects:

- Establishment of RODOS Project Management Group
- Quality assurance of software products
- Documentation
- RODOS newsletter
- Integration of other projects and PECO contractors

Study Group on the Behaviour in Forests and Semi-Natural Ecosystems

Thessaloniki (GR), 23 - 25 March 1993
10 participants from 6 countries and the EC

Principal subjects:

- Presentation and evaluation of a joint intercomparison experiment called the "Uppsala project".
- Presentation and discussion of the ongoing research in the different groups.
- Discussion of the replies received upon a questionnaire concerning opinion of the members of the group on the future of the research on the semi-natural environment and its contribution to the dose to man now and on the long-term.
- Discussion about interactions which could be stimulated among related but different projects.

Study Group on What's new and what's needed in radiation effects research

Bad Honnef (D), 29 March - 1 April 1993
45 contractors from 12 countries, M. Frazier (US DOE) and the EC

Principal subjects:

- To bring physicists, radiation chemists, researchers working in molecular and cellular radiobiology and in animal research together, as well as epidemiologists.
- The necessity for multidisciplinary approach in research aimed at understanding the mechanisms of radiation induced changes in animals and humans.
- To identify what is new and what is needed in radiation effects research for the forthcoming framework programme.
- Draft a report of the meeting to be published by the Commission.

Study Group on Data Analysis in Quality Control and Radiation Protection of the Patient in Diagnostic Radiology and Nuclear Medicine

Brussels (B), 18 April 1993
8 participants from 5 countries and the EC

Principal subjects:

- Preparation of the Workshop on subject area
- Selection of abstracts of proffered papers
- Subject areas and scope of invited papers

Study Group on Optimisation of Radiation Protection of the Patient

Brussels (B), 19 - 21 April 1993

37 participants from 13 countries and the EC

Principal subjects:

- Presentation of ongoing research work of contracts with the CEC
- Establishment of cooperation plans
- Establishment of subjects for specific study groups
- Role and responsibility of contract coordinator
- 1994-1998 research priorities

Study Group on CEC/NEA Intercomparison of Probabilistic Accident Consequence Assessment Codes: meeting of programme management group (PMG) and ad-hoc group (AHG)

Madrid (E), 27 - 29 April 1993

50 participants from 15 countries, OECD and the EC

Principal subjects:

- Probabilistic accident consequence codes
- Intercomparison of code predictions for postulated accidental releases from thermal reactors
- Quality assurance of codes
- Users groups for the codes COSYMA and MACCS

Study group on Uncertainty Analysis of Accident Consequence Codes: Elicitation of Experts in the Areas of Atmospheric Dispersion and Deposition (CEC/US NRC Project).

Albuquerque (USA), 24 - 27 May 1993

28 participants from 6 countries and the EC

Principal subjects:

- Uncertainty analysis of accident consequence codes
- Expert judgement
- Elicitation of experts in atmospheric dispersion
- Elicitation of experts in deposition

Study Group - Programme Committee on the International Symposium on Remediation and Restoration of Radioactive-contaminated Sites in Europe

Antwerp (B), 22 June 1993

10 participants from 8 countries and the EC

Principal subjects:

- Inventory of contaminated sites in Europe
- Criteria for remediation and restoration
- Techniques for restoration
- Selection of papers and arrangements for symposium

Study group - 5th meeting of the IAEA/CEC CRP on "Validation of Models for Radionuclide Transfer in the Terrestrial, Urban and Aquatic Environments (VAMP)"

Vienna (A), 5 - 9 July 1993

75 participants from 27 countries, IAEA and the EC

Principal subjects:

- Model validation and performance
- Environmental impact assessments
- Terrestrial environment models
- Aquatic environment models
- Urban environment models
- Multiple pathways models

Study Group - Establishment of the scope and content of JSP5 pathways and dose and JSP6 cartography.

Moscow (Russia), 30 August - 3 September 1993

26 participants from 5 countries and the EC

Principal subjects:

- Pathway analysis and dose estimation for contaminated areas around Chernobyl
- Development of reliable models for dose estimation and their validation
- European atlas of radioactive contamination and external dose from the Chernobyl accident
- Atlas of other levels of radiation or contamination from natural or other sources (eg, weapons fallout)

Study Group on Resuspension and Contamination of Surfaces (ECP1)

Kiev, Ukraine, 22 - 24 September 1993
14 participants from 8 countries and the EC

Principal subjects:

- Wind driven and technogenic resuspension
- Transfer of deposited contamination by resuspension
- Resuspension during grass and forest fires
- Distribution of particle sizes in resuspended material
- Public and occupational health impact of resuspension

Study group of RODOS Management Group

Karlsruhe (D), 28 - 29 September 1993
5 participants from 4 countries and the EC

Principal subjects:

- Decision support system for off-site emergency management (RODOS)
- Atmospheric dispersion, foodchain, hydrological and countermeasures modelling
- Collaborative programme with the CIS
- Documentation of system and software

Study Group - JSP2 on Evaluation of strategies and intervention levels for mitigation of the consequences of the Chernobyl accident

Paris (F), 21 - 22 October 1993
37 participants from 8 countries and the EC

Principal subjects:

- Conceptual basis of intervention policy
- Social and psychological impacts of countermeasures
- Decision support system to evaluate countermeasures' strategies
- Dose distributions in settlements contaminated from the Chernobyl accident
- Historical portrayal of countermeasures taken following the Chernobyl accident

Study Group - Elicitation of judgements of decision makers involved in emergency management.

Mol (B), 16 November 1993
7 participants from 4 countries and the EC

Principal subjects:

- Decision support system for off-site emergency management (RODOS)
- Elicitation of preferences of emergency management decision makers
- Training courses with RODOS

Study Group - JSP on Integration of decision support systems in JSP1 and JSP2 and interface with data bases in JSP6

Karlsruhe (D), 24 November 1993
4 participants from 2 countries and the EC

Principal subjects:

- Decision support systems for emergency management (RODOS):
- Long term countermeasures
- Mitigation of accident consequences
- Software and hardware for the DSS

Study Group - on The implementation of the RODOS Decision Support System for off-site emergency management in Ukraine and Belarus.

Kiev (Ukraine) and Minsk (Belarus), 6 - 10 December 1993
26 participants from 3 countries and the EC

Principal subjects:

- Decision support system for off-site emergency response
- Mitigation of Chernobyl consequences
- Meteorological and radiation monitoring

Study Group on Dosimetry in Mammography

London (UK), 9 December 1993
5 participants from 4 countries and the EC

Principal subjects:

- Preparation of the European Protocol on Dosimetry in Mammography
- Evaluation of existing national and regional protocols

Study Group - Studies related to the expression of detriment associated with radiation exposure

Didcot (UK), 20 - 21 December 1993
6 participants from 2 countries and the EC

Principal subjects:

- Health effects models
- Expression of radiation detriment
- Development of Windows software package, ASQRAD
- Peer review of ASQRAD and training course on its use

Study Group on Treatment of Accident Victims

Commissariat à l'Énergie Atomique (CEA)

Paris (F), 31 January - 1 February 1994

25 scientists: partners of the contract, clinicians and the EC

Principal subjects:

- The general goals are to standardize methodology; to be able to purify and to characterize the phenotype and the genotype of the stem cells, to investigate the possibilities of cord blood transplantation; to have more coordination in different labs for the research work on the immune system.
- The main questions to be answered are:
 - What is the best treatment for acute radiation syndrome;
 - How, when and in which combination to use growth factors, which ones are effective, or more effective.
- New ideas are:
 1. Purification, Identification and quantification of stem cells of different sources.
 2. Growth Factors.
 3. Engraftment.
 4. Biological Indicators.

Study Group on Development of Quality Criteria for CT

Brussels (B), 8 - 9 February 1994

10 participants from 5 countries and the EC

Principal subjects:

- Elaboration of technical, physical and clinical parameters for performance quality and dose reduction in CT

Study Group on Quality Criteria Development in Adult Radiology

Brussels (B), 10 - 11 February 1994

8 participants from 4 countries and the EC

Principal subjects:

- Evaluation of European wide trials on Quality Criteria for Diagnostic Radiographic Images
- Improvement of the existing working document XII/173/90 on the same subject

Study group on EUROSIL-RESSAC

Cadarache (Fr) Date, 28 February - 2 March 1994

13 participants from UK, BE, ES, Fr, DE, Gr and the EC

Principal subjects:

- Discussion of the results of the performance testing of the lysimeters set up in the RESSAC building
- Adaptation of the experimental planning further to the results obtained in the test phase.

Study Group - JSP1 on "Decision Support Systems for Off-site Emergency Management"

Obninsk (Russia), 2 - 4 March 1994

26 participants from 6 countries and the EC

Principal subjects:

- RODOS decision support system
- Off-site emergency management
- Data bases of early environmental measurements
- Transfer of hardware/software configuration

Study Group - 3rd Meeting of RODOS Management Group

Roskilde (DK), 22 - 23 March 1994

6 participants from 4 countries and the EC

Principal subjects:

- RODOS decision support system for off-site emergency response
- Atmospheric dispersion and analytic techniques
- Consequences and countermeasures
- Quality assurance and documentation

Study Group on Dosimetry in Mammography

Rijswijk (NL), 24 - 25 March 1994

10 participants from 6 countries and the EC

Principal subjects:

- Draft Protocol on Dosimetry in Mammography to be adapted to the requirements of quality control measures in diagnostic radiology

Study Group on Interventional Radiology

Nürnberg (D), 19 - 20 April 1994
7 participants from 5 countries and the EC

Principal subjects:

- Intercomparison of dose measurement methods
- Analysis of acquired data

Study Group on Quality Criteria Development in Adult Radiology

Brussels (B), 19 - 21 June 1994
8 participants from 4 countries and the EC

Principal subjects:

- Revision and extension of the Working Document XII/173/90 on Quality Criteria for Diagnostic Radiographic Images

Study Group - RODOS/JSP1 Contractors Meeting

Interlaken (CH), 20 - 24 June 1994
60 participants from 16 countries and the EC

Principal subjects:

- RODOS decision support system for off-site emergency management
- Atmospheric dispersion at near and far ranges
- Modelling of countermeasures
- Data assimilation and uncertainty
- Environmental transfer
- Training courses

Study Group on Recent Developments in Radiation Cytology

Horta, Faial (P), 16 - 19 July 1994
18 participants from the European Union and the EC

Principal Subjects:

- Basic aspects of Radiation Induced Chromosomal Aberrations
- Applied aspects of radiation induced Chromosomal Aberrations
- Automated detection of chromosomal aberrations by flow cytometry and image analysis.

Study Group on Dosimetry in Mammography

Stockholm (S), 17 - 18 July 1994

5 participants from 4 countries

Principal subjects:

- Draft protocol to be presented in view of its use by medical staff, technicians and physicists

Study Group - CEC/NRPB Association contract on "Reduction of Risk of Late Effects from Incorporated Radionuclides"

CEA, Paris, 15 September 1994

15 participants, partners of the contract and the EC

Principal subjects:

- Discussion of the work already completed, to present the work in progress and to review the contractual commitments until June 1995, i.e., the end of the contract.
- For the period beyond June 1995, the chemical and biochemical considerations underlying successful decorporation therapy and the future strategy for decorporation research in Europe was discussed.

Study Group - JSP5 on Pathways of exposure and dose assessment

St. Petersburg (Russia), 21 - 23 September 1994

40 participants from 7 countries and the EC

Principal subjects:

- Assessment and modelling of doses in settlements affected by the Chernobyl accident
- Pathways of exposure and dose distributions
- Integration of model predictions and measurements (eg, TLD, whole body monitoring, levels in food and environmental media, etc) for dose assessment
- Stochastic modelling of exposures in population with particular attention on the more exposed groups

Study group on the COSU ECP5 The behaviour of radionuclides in natural and seminatural ecosystems

Ascot (UK) Date, 27 - 29 September 1994

14 participants from UK, Ukr, BL, RU, It, BE, DE, EIR and the EC

Principal subjects:

- Elaboration of the workplan for the forthcoming field campaign
- Discussion of the approach to be followed to evaluate the results obtained.
- Discussion of the conceptualisation of the model, in which the data are to be incorporated, and the evaluation of the operative parameters which determine the dynamics of seminatural ecosystems.

Study group - Contamination of fresh water ecosystems

Antwerp (BE) Date, 14 October 1994

13 participants from UK, It, BE, ES, PT, NL and the EC

Principal subjects:

- Discussion of the results obtained regarding the role of physico-chemical and biological parameters on the residence of radionuclides in freshwater systems in Western-Europe.
- Discussion of the results obtained in the Chernobyl catchment to the Dnieper in Ukraine.
- Evaluation of data and integration of the work of the groups in a dynamic model. Assessment of the usefulness of the modelling exercise for environmental management of catchments.

Study Group - IAEA/CEC Coordinated Research Programme on the Validation of Models for Predicting Radionuclide Transfer in Terrestrial, Urban and Aquatic Environments (VAMP)

Vienna (A), 31 October - 4 November 1994

110 participants from 27 countries and the EC

Principal subjects:

- Model validation and performance
- Environmental impact assessments
- Terrestrial environment models
- Aquatic environment models
- Urban environment models
- Multiple pathways models

Study Group on Dosimetry in Mammography

Brussels (B), 5 - 7 November 1994

9 participants from 5 countries and the EC

Principal subjects:

- Finalisation of the European Protocol on Dosimetry in Mammography (see Report EUR 16263)

Study Group - on Adequacy of environmental modelling in the accident consequence code, COSYMA

Chilton (UK), 12 - 13 December 1994

13 participants from 7 countries and the EC

Principal subjects:

- Environmental models in COSYMA, particularly those describing the behaviour of radionuclides deposited in an urban environment
- Deposition of radionuclides on skin
- Shielding factors and migration in soil
- Model validation and uncertainty
- Parameterisation of models

Study Group - 5th Meeting of the RODOS Management Group

Chilton (UK), 14 December 1994

5 participants from 3 countries and the EC

Principal subjects:

- Progress reports on the major sub-projects
- Software development and documentation
- Promotional material on RODOS
- Quality assurance and project management
- Progress with installation of prototype in Eastern Europe

Study group COSU ECP9 on the transfer of radionuclides to animals, their comparative importance under different agricultural systems and elaboration of appropriate countermeasures.

Oslo (NO), Date: 16 - 20 December 1994

18 participants from N, UK, UKR, BL, I, E, S, GR and the EC

Principal subjects:

- Discussion of the results of the comparison of doses received from collective farms with those received at private farms.
- Discussion of the influence of traditional habits and dietary intake on the dose.
- Discussion of the role of seminatural ecosystems on the persistence and ecological half-life of the deposited radionuclides.
- Discussion of the relation between the energy flow through farm systems and the dose received.

Study Group - EC/USNRC Uncertainty Study of ACA codes: expert panels on food chain transfer and external doses from deposited material

Chilton (UK), 9 - 11 January 1995

30 participants from 12 countries and the EC

Principal subjects:

- Uncertainty analysis
- Probabilistic accident consequence assessment
- Expert judgement elicitation
- Transfer of radionuclides through food chains
- External exposure from deposited radionuclides

Study Group on Development of Quality Criteria in CT

Brussels (B), 18 - 19 January 1995

10 participants from 5 countries and the EC

Principal subjects:

- Elaboration of the lists of quality criteria for the most common types of CT examinations: chest, head, spine, osseous trauma, abdomen

Study Group - EC/USNRC on Uncertainty Analysis of Accident Consequence Codes: Project Planning Meeting

Albuquerque (USA), 4 - 7 April 1995
20 participants from 3 countries and the EC

Principal subjects:

- Probabilistic accident consequence codes
- Uncertainty analysis
- Elicitation of expert judgements
- External exposure in urban areas
- Transfer of radioactive material through foodchains
- Panels on health effects and internal dosimetry

Study Group - EC/USNRC Uncertainty Study of Accident Consequences Codes - case structures for internal dosimetry and health effects modules

Chilton (UK), 18 - 19 May 1995
7 participants from 2 countries and the EC

Principal subjects:

- Probabilistic accident consequence codes
- Uncertainty analysis
- Expert judgement elicitation
- Internal dosimetry models
- Late and early health effects models

International Symposium on the Natural Radiation Environment

Organised by the Clarkson University (U.S.), the U.S Department of Energy, the U.S. Environmental Protection Agency, the Atomic Energy Control Board (Canada), Health Canada and the European Commission.

Montréal 5 - 9 June 1995

264 participants

Principal subjects:

- Measurement techniques and metrology
- Radionuclides in the earth, atmosphere, marine and other aquatic systems
- Transfer pathways and radionuclide migration in the biosphere
- Surveys, their methodology and population exposure
- Epidemiological, animal and dosimetry studies of natural radiation
- Cellular and molecular mechanisms of radiation-induced carcinogenesis particularly for chronic exposure at low exposure rates
- Technologically enhanced levels of radiation exposure
- Remedial actions for reducing exposure
- National and international control policies and recommendations for the protection of the general public and workers

B

Meetings Organized or Coorganized by the EC

EURADOS Working Group 11

Organised by the EC

Luxembourg (L), 22 - 23 March 1993

15 participants from 8 countries and the EC

Principal subject:

- Radiation exposure of civil aircrew.

Seminar: Molecular Mechanisms in Radiation induced Mutagenesis and Carcinogenesis

Co-organised with US DOE Office of Health and Environmental Research and Dutch Institute for Public Health and Environment

Doorwerth (NL), 19 - 22 April 1993

75 international scientists from 15 countries and the EC

Principal Subjects:

- DNA Repair and Mutation
- Induced Instability, Cytotoxicity, Mutation
- Recombination and Mutagenesis
- Molecular Analysis of Mutations
- High LET Induced Mutations
- Hereditary Mutations
- Mechanisms in Solid Tumours
- Mechanisms in Leukaemia/Lymphoma
- Modelling Oncogenesis

4th European Seminar on Radiation Protection Optimisation

Organised by the EC

Luxembourg (L), 20 - 22 April 1993

187 participants from 29 countries, OECD and the EC

Principal subjects:

- Optimisation in occupational exposure
- Optimisation in radioactive effluents
- Optimisation in complex situations
- Optimisation in regulation

Workshop on Individual Monitoring of Ionizing Radiation: The Impact of Recent ICRP and ICRU Publications

Co-organised by the EC, the European Radiation Dosimetry Group (EURADOS), the Paul Scherrer Institut (CH) and the US DOE (US).

Villigen (CH), 5 - 7 May 1993

120 participants from Member States, Switzerland, Sweden, USA, Canada, Japan, Russia, Poland, Czechoslovakia, Hungary and the EC

Principal subjects:

- Aspects of ICRP 60 and ICRU 47 of relevance to individual monitoring
- Radiation quantities: their interrelationship
- Significance of angular and energy distributions of the radiation field
- Required accuracy and dose thresholds
- Performance requirements and tests
- Quality control and quality assurance

International Intercomparison of criticality accident dosimetry systems

Co-organised with CEA (F)

Valduc (F), 7 - 18 June 1993

53 participants from 15 countries and the EC

Principal subjects:

- Calibration of accident dosimetry systems.
- Irradiation of dosimeters in a reactor under simulated criticality accident situation.
- Assessment and evaluation of measurements.

Workshop on Dynamic Processes in Radioecology

Co-organised with GSF (D)

Bad Honnef (D) 21 - 24 June 1993

39 participants from EC countries

Principal subjects:

- General aspects of radioecology
- Deposition, interception and resuspension
- Soil-plant transfer
- Plant-animal transfer
- Aquatic ecosystems
- Natural and semi-natural ecosystems
- Urban environment
- Countermeasures

Workshop on Indoor Radon Remedial Action. The Scientific Basis and the Practical Implications

Co-organised with the Ente per le Nuove Tecnologie, l'Energia e l'Ambiente; the Istituto Superiore di Sanita; the International Centre for Theoretical Physics; the International Centre for Theoretical and Applied Ecology; the United States Department of Energy and the United States Environmental Protection Agency.

Roma (I), 27 June - 2 July 1993

212 participants from 32 countries and the EC

Principal subjects:

- Mitigation Measures - General Aspects
- Mitigation Measures - Practical Approaches
- Health Effects - Biological Studies
- Health Effects - Physical Factors
- Radon Sources - Ingress Studies
- Radon Sources - Mapping and Geology
- Radon Sources - Methods Measurements
- Policy Matters - Surveys and Outcomes
- Policy Matters - Risks and strategies

ECURIE - M.S. Representatives

Organised by the EC

Luxembourg (L), 5 - 7 July 1993

36 participants from 12 countries and the EC

Principal subjects:

- Preparation of ECURIE Users Guide
- Review of exercises and future programme
- Software

4th L.H. Gray Workshop on Microbeam Probes of Cellular Radiation Response

Co-organised with the L H Gray Trust (UK)

Northwood (UK), 8 - 10 July 1993

40 scientists from 12 countries (Europe, Japan and USA) and the EC

Principal Topics:

- Rationale for microbeams: protection level studies
- Rationale for microbeams: Mechanistic studies
- Rationale for microbeams: Targeted therapy
- Particle microbeam approaches
- X- ray microprobes
- Collimation, Detection and Imaging
- Biological experiments using microbeam, probes and single cell assays

EURADOS Working Group 11

Organised by the EC
Prévessin (F), 27 July 1993
5 participants from 4 countries and the EC

Principal subject:

- Radiation exposure of civil aircrew.

Workshop on Intakes of Radionuclides; Detection, Assessment and Limitation of Occupational Exposure

Co-organised by the EC, US DOE, NRPB and IPSN.
Bath (UK), 13 - 17 September 1993
120 scientists from 18 countries and the EC

Principal subjects:

- To review existing information on the different physico-chemical and biokinetic characteristics of radioactive material encountered at the workplace.
- To develop approaches for a better definition of site-and material-specific Annual Limits of Intake (ALIs), their range of application and the methods available for demonstrating compliance with dose limits.
- The proceedings of the meeting will be published as a special issue of the journal Radiation Protection Dosimetry.

International Symposium on Molecular Mechanisms of Radiation and Chemical Carcinogen Induced Cell Transformation

Co-organised with US DOE Office for Health and Environmental Research
Mackinac Island, Michigan (USA), 19 - 23 September 1993
70 scientists working in cell transformation from 15 countries and the EC

Principal Subjects:

- Human and Animal Cell transformation systems
- Overview of Cell Transformation Systems
- Mechanisms of Radiation-Induced Cell Transformation and Modulation Factors
- Radiation-Induced Cell Transformation
- Role of Gene Expression in Cell Transformation
- Gene Expression of Cell Senescence and Acquisition of an Infinite Lifespan

Workshop on Data analysis in quality control and radiation protection of the patient in Radiodiagnostic Radiology and Nuclear Medicine

Co-organised with the Unitá Sanitaria Locale N°7, Udine (I) and co-sponsored by the WHO Grado (I), 29 September - 1 October 1993

145 participants from 12 European and non-European countries and the EC

Principal subjects:

- Evaluation of a decade of research and the existence of the Council Directive concerning radiation protection of the patient.
- Prospectives and priorities in the subject area.

International Workshop on Childhood Cancer Clusters and Radiation

Moor Row, Cumbria (UK), 4 - 7 October 1993

50 international scientists and the EC

Principal Subjects:

- Childhood Leukaemia Clusters
- Inherited Predisposition and Susceptibility
- Infectious Agents, Population Influx and Cancer
- Cancer Clusters around Nuclear Installations
- The Seascale Leukaemia Cluster
- Statistical Analysis of Cancer Clusters
- Transgenerational Carcinogenesis
- Molecular Indicators of the Cancer Process
- Scientific Evidence and the Law

International Symposium on Remediation and Restoration of Radioactive Contaminated Sites in Europe

Co-organised with SCK/CEN Mol (B) and the State Committee of the Russian Federation on Chernobyl Affairs

Antwerp (B), 11 - 15 October 1993

196 participants from 27 countries, IAEA and the EC

Principal subjects:

- Inventory of radioactive contaminated restoration of sites
- Conceptual basis of and criteria for remediation
- Case studies for restored sites
- Methodologies for environmental risk assessment

Presentation of the Manual on Radiation and Radiation Protection

Luxembourg (L), 16 November 1993
75 participants from 14 countries and the EC

Principal subject:

- Presentation of a Manual on Radiation and Radiation Protection for primary and secondary schools.

Eurados Working Group 11

Luxembourg (L), 31 January - 1 February 1994
16 participants from 9 countries and the EC.

Principal subject:

- Radiation exposure of civil aircrew.

Workshop - Early exchange of information in the event of a radiological emergency (ECURIE). (Exercices Working Group)

Luxembourg (L), 8-9 February 1994 (Exercices Working Group).
12 Participants from 8 countries and the EC.

Principal subject:

- Evolution of ECURIE exercises, implementation of new communication systems.

Seminar on freshwater and estuarine radioecology

Lisbon (P) Date, 21 - 25 March 1994
95 Participants from 19 countries and the EC

Principal subjects:

- Chemical and physical processes of radionuclide transport in lakes, rivers and their catchment areas
- Uptake and release of radionuclides by aquatic organisms and their transport through the food chain
- The scientific basis for radiological assessments and countermeasures in an aquatic environment.

International Seminar "Health effects of internally deposited radionuclides: emphasis on radium and thorium"

Co-organised with the US Department of Energy (DOE) and the German Cancer Research Centre, Heidelberg (DKFZ)

Heidelberg, Germany, 18 - 21 April 1994

80 scientists from Europe, US, and Japan and the EC

Principal subjects:

- After the opening of the Seminar a memorial lecture for C. Mays was given on "Dosimetry".
- The Seminar included seven sessions: Dosimetry; Biokinetics and analytics; Epidemiology - surveys of major studies; Epidemiology - special problems; Animal studies in comparison with the human situation; Mechanisms of internal radiation carcinogenesis; and Molecular biology investigations and genetic background. There was an invited lecture on "The use of Epidemiological and Experimental Data in Assessing the Risks from Internally Incorporated Radionuclides" and a closing lecture on "Risk Estimates for High LET α -Irradiation of Skeletal Tissues" followed by General Conclusions and Future Needs.
- There were 75 proffered papers, of whom 7 were invited speakers. Five young scientist awards were given.

Workshop - European Atlas of Radioactive Contamination and External Exposures Resulting from the Chernobyl Accident.

Brussels (B), 19 - 22 April 1994

30 participants from 22 countries and the EC

Principal subject:

- Inventory of available contamination data; discuss the opportunity of printing an Atlas of Caesium contamination after the Chernobyl accident.

Seminar "The radiological exposure of the population of the European Community from radioactivity in the mediterranean sea - MARINA-MED.

Rome (I), 17 - 19 May 1994

60 participants from 15 countries and the EC.

Principal subject:

- The seminar analysed and discussed the results of the "Marina-Med" project, reviewed other work relevant to this subject and provided a forum for an exchange of views on the evaluation of the overall radiological situation in the Mediterranean Sea.

Workshop on Dose Reconstruction

Co-organised with GSF Forschungszentrum für Umwelt und Gesundheit, IAEA, the German Association of Radiation Research (GAST).

Bad Honnef (D), 6 - 9 June 1994

60 scientists from 12 countries (including Belarus, Russia and Ukraine) and the EC

Principal subjects:

- Purposes of dose reconstruction
- Physical and biological methods of retrospective dosimetry
- Available data and methods applied during the initial phase of the Chernobyl accident
- Methods for individual dose reconstruction
- Environmental measurements and retrospective environmental dosimetry
- Internal exposures
- Groups of populations exposed after the Chernobyl accident

Workshop on "The Integration of social and ethical values in radiological risk-management"

Mons (B), 12 - 14 June 1994

18 participants from 7 countries and the EC

Principal subjects:

- Integration of social and ethical issues in risk management
- Willingness to pay
- Economic theory and risk perception
- Determination of risk preferences

Eurados Working Group 11

Luxembourg (L), 30 June - 1 July 1994

5 participants from 4 countries and the EC.

Principal subject:

- Summary report of the groups activities

Cooperative Research Programme on Radiation Protection in Diagnostic Radiology

Co-organised by the EC and the IAEA

Vienna (A), 11 - 12 July 1994

8 participants from 4 countries, IAEA and the EC

Principal subjects:

- Elaboration of a research project on radiation protection requirements and measures in diagnostic radiology in Asia
- Concept of a training manual for radiation protection and quality assurance in diagnostic radiology, nuclear medicine and radiation therapy

Workshop - Early exchange of information in the event of a radiological emergency (ECURIE).

Luxembourg (L), 19 - 21 July 1994

30 participants from 13 countries and the EC

Principal subject:

- Discuss changes proposed by the Experts Group convened in February; evaluation of the last level 3 Exercise (08.06.94).

Eurados Working Group 11

Strasbourg (F), 5 - 7 September 1994

15 experts from 8 countries and the EC

Principal subject:

- Radiation exposure of civil aircrew

Workshop: Sensitivity and Predisposition to Radiation Induced Cancer

San Miniato (I), 6 - 11 September 1994

45 Contractors working on radiation effects research and the EC

Principal Subjects:

- Radiation Cytogenetics: New Developments
- Radiation Damage and its Consequences
- DNA Repair: Looking to the Future
- Cell Cycle Control: Effects and Consequences
- Radiation Carcinogenesis in Animals: Looking to the Future
- Senescence and Carcinogenesis

Workshop on Advances in Radiation Measurements: Applications and Research Needs in Health Physics and Dosimetry

Co-organised with EURADOS, Atomic Energy of Canada Limited (AECL), Candu Owners Group (COG)

Chalk River (Canada), 3 - 6 October 1994

85 participants from 18 countries and the EC

Principal subjects:

- Advanced particle detection techniques
- Dosimetry and spectrometry methods for radiation protection
- Active dosimeters and spectrometers in radiation protection practice
- Detector and electronic technology for active devices
- Particle interaction in tissue, cellular and sub-cellular targets
- Basic data and processes in gas and semi-conductor detectors.

International Seminar on RODOS - a decision support system for off-site emergency management

Warsaw (Poland), 17 - 18 November 1994

70 participants from 13 countries and the EC

Principal subjects:

- RODOS decision support system for emergency management
- Implementation of RODOS in Eastern Europe
- Major Polish activities on off-site emergency response
- Interfacing of IMIS and RODOS
- RODOS Users' Group

Workshop - Early exchange of information in the event of a radiological emergency (ECURIE).

Luxembourg (L), 19 - 20 December 1994 (exercice working group)

27 participants from 16 countries and the EC

Principal subject:

- Discussion on the evolution proposed exercises and communication means

Intercomparison and calibration of in-vivo monitoring systems in Europe

Luxembourg (L), 3 - 4 May 1995
35 participants from 16 countries and the EC

Principal subjects:

- The meeting was held in order to:
- prepare the scientific content of the programme
- establish the timetable
- discuss the execution of the programme
- create a working group to evaluate and analyse the results of the programme

Centenary of the Discovery of the X-Rays: Academic Ceremony for the Opening of the Centenary Festivities

Co-organised by 3 EC services and the Belgian Society for Radiology
Brussels (B), 22 - 23 June 1995
200 participants from 4 countries and the EC

Principal subjects:

- Scientific, medical and historical overviews on achievements relating to the discovery of the X-ray

Tenth International Congress of Radiation Research

Co-organised by the EC
Würzburg, Germany, 28 August - 1 September 1995
1500 Radiation Research Scientists and the EC

Principal subjects:

- The programme was very large including all fields of radiation research
- A symposium was organised by the Radiation Protection Research Programme on the "Epidemiology of radiation-induced cancer" with 4 speakers. The first speaker G.R. Howe, presented an overview on "leukaemia in irradiated populations"; the next speaker T. Abelin gave a very interesting talk on thyroid cancer near Chernobyl; B. Boecker gave a general overview on cancer and internal emitters and talked about the Ra-226 dial painters, persons injected with contrast medium Thorotrast, persons treated with Ra-224 for ankylosing spondylitis and about uranium miners inhaling radon progeny while mining. The last speaker E. Cardis discussed the cancer risk following low dose, protracted exposures in nuclear industry workers.

International Workshop - RODOS: decision support system of off-site emergency management of nuclear accidents

Budapest, 18 - 22 September 1995

74 participants from 21 countries and the EC

Principal subjects:

- Off-site emergency preparedness
- Decision support systems for off-site emergency management
- Data assimilation and uncertainty
- Transfer of radioactive material through the environment
- Countermeasures

C

Meetings of Experts

Article 31 Working Group on Relocation

Chilton (UK), 7 - 8 January 1993
6 participants from 3 countries and the EC

Principal subjects:

- Criteria for relocation
- Generic guidance on intervention levels

ECURIE - Experts

Brussels (B), 24 February 1993
14 participants from 12 countries and the EC

Principal subject:

- preparation of annual full-scale exercise, 1993

ECURIE - Experts

Luxembourg (L), 5 - 7 April 1993
14 participants from 12 countries and the EC

Principal subject:

- examination of results of annual full-scale exercise, 1993

Third meeting of the Advisory Committee established by Article 19 of Council Directive 92/3/EURATOM on the supervision and control of shipments of radioactive waste between Member States and into and out of the Community.

Luxembourg (L), 15 - 16 April 1993
18 participants from 10 countries and the EC

Principal subject:

- Standard documents referred to in the Directive.

Fourth meeting of the Advisory Committee established by Article 19 of Council Directive 92/3/EURATOM on the supervision and control of shipments of radioactive waste between Member States and into and out of the Community.

Luxembourg (L), 3 May 1993
14 participants from 10 countries and the EC

Principal subject:

- Standard documents referred to in the Directive.

Group of experts referred to in Article 31 of the Euratom Treaty

Luxembourg (L), 22 June 1993
25 participants from 11 countries and the EC

Principal subjects:

- Revision of the basic safety standards.
- Radiation risks and radiation protection of civil aircrew.
- Industrial gammagraphy.
- Manual on radiation protection for transport workers.

Qualified experts in radiation protection.

Luxembourg (L), 20 July 1993
14 participants from 11 countries and the EC

Principal subject:

- Community harmonisation of qualification criterias.

Art. 31 Working Group on Recycling

Brussels (B), 9 November 1993
10 participants from 6 countries and the EC

Principal subject:

- Recycling of materials from the dismantling of nuclear installations.

Advisory Committee established by Article 19 of Council Directive 92/3/EURATOM on the supervision and control of shipments of radioactive waste between Member States and into and out of the Community.

Luxembourg (L), 23 November 1993.

19 participants from 12 countries and the EC.

Principal subjects:

- Criteria for the export of radioactive waste to third countries.
- Report on the implementation of Directive 92/3/EURATOM.

Management and dosimetry in relation to the Directive on outside workers.

Luxembourg (L), 24 November 1993.

16 participants from 10 countries and the EC.

Principal subject:

- Operational protection of outside workers.

Art. 31 Working Group on Recycling

Luxembourg (L), 22 - 23 February 1994

7 participants from 6 countries and the EC

Principal subject:

- Recycling of materials from the dismantling of nuclear installations.

Assistance in the event of a nuclear accident or a radiological emergency

Luxembourg (L), 16 March 1994

21 participants from 8 countries and the EC.

Principal subject:

- Achieve a programme for the co-ordinating work within the E.U. in the field of material assistance and emergency arrangements.

Technical criteria for radiodiagnostic equipment

Luxembourg (L), 30 March 1994

16 Participants from 10 countries and the EC

Principal subjects:

- Quality control of the technical aspects of mammograph screening.
- Technical criteria in the field of pediatrics.

Ad Hoc Committee set up to establish a list of Products excluded from Council Regulation (EEC) No. 737/90 of 22 March 1990.

Luxembourg (L), 10 May 1994.

16 participants from 9 countries and the EC.

Principal subject:

- Review of the list of products excluded from the Council Regulation.

Art. 31 Working group on "Recycling".

Luxembourg (L), 18-19 May 1994

9 participants from 6 countries and the EC.

Principal subject:

- Recycling of materials from the dismantling of nuclear installations.

Group of experts referred to in Article 31 of the EURATOM Treaty.

Luxembourg (L), 10 June 1994.

26 participants from 11 countries and the EC.

Principal subjects:

- Revision of the Basic Safety Standards Directive
- Commission activities on the Convention on nuclear safety.
- Revision of the "Patient" Directive
- Dose constraints.

Advisory Committee established by Article 19 of Council Directive 92/3/EURATOM on the supervision and control of shipments of radioactive waste between Member States and into and out of the Community.

Luxembourg (L), 20 June 1994.

24 participants from 12 countries and the EC.

Principal subject:

- Consideration of the draft summary report to be submitted from the Commission to the Parliament.

Ad Hoc Committee set up to establish a list of Products excluded from Council Regulation (EEC) No. 737/90 of 22 March 1990.

Luxembourg (L), 11 July 1994.

19 participants from 11 countries and the EC.

Principal subject:

- Review of the list of products excluded from the Council Regulation

Group of experts referred to in Article 37 of the EURATOM Treaty.

Luxembourg (L), 15 - 16 September 1994.

34 participants from 17 countries and the EC.

Principal subject:

- Evaluation of the General Data relating to the plans for the disposal of radioactive waste from the CHOOZ B NPP.

Art. 31 Working group on "Recycling".

Luxembourg (L), 21 September 1994.

18 participants from 10 countries and the EC

Principal subject:

- Recycling of materials from the dismantling of nuclear installations

Working group "Revision of the Patient Directive".

Brussels (B), 22 - 23 September 1994

9 participants from 10 countries and the EC.

Principal subject:

- Revision of Council Directive 84/466/EURATOM laying down basic measures for the radiation protection of persons undergoing medical examination or treatment.

Art. 31 Working Group on "Dose constraints".

Paris (F), 28 - 29 September 1994.

6 participants from 4 countries and the EC.

Principal subject:

- Establishment of guidelines on the application of the concept of dose constraints introduced in the revision of the basic safety standard directive.

Group of experts referred to in Article 37 of the EURATOM Treaty.

Luxembourg (L), 29 September 1994.
18 participants from 10 countries and the EC.

Principal subject:

- Evaluation of the General Data relating to the plans for the disposal of radioactive waste from the CHOOZ B NPP.

Working group "Revision of the Patient Directive".

Bruxelles (B), 31 October 1994.
10 participants from 9 countries and the EC.

Principal subject:

- Revision of Council Directive 84/466/EURATOM laying down basic measures for the radiation protection of persons undergoing medical examination or treatment.

Art. 31 Working Group on "Dose constraints".

Brussels (B), 15 November 1994.
9 participants from 6 countries and the EC.

Principal subject:

- Establishment of guidelines on the application of the concept of dose constraints introduced in the revision of the Basic Safety Standards Directive.

Art. 31 Working group on "Natural Radiation".

Luxembourg (L), 22 - 23 November 1994.
9 participants from 7 countries and the EC.

Principal subjects:

- Conventional conversion of exposure to effective dose
- Action levels in workplaces
- Identification of workplaces where radon exposure requires attention.

Radiation Protection in Nuclear Power Plants

Luxembourg (L), 10 - 11 December 1994
20 participants from 7 countries and the EC.

Principal subjects:

- Analysis of data on collective doses
- Presentation of experiences in radiation protection in different countries.

Group of experts referred to in Article 31 of the EURATOM Treaty.

Luxembourg (L), 12 - 13 December 1994.
25 participants from 15 countries and the EC.

Principal subjects:

- Revision of the Basic Safety Standards Directive.
- Information of different working groups
- Revision of the "Patient Directive".

Assistance in the Event of a Nuclear Accident or a Radiological Emergency.

Luxembourg (L), 17 January 1995.
26 participants from 13 countries and the EC.

Principal subject:

- Finalization of the "Radiological Emergency Operational Manual"

Radiation Protection in Nuclear Power Plants.

Luxembourg (L), 9 - 10 March 1995.
15 participants from 6 countries and the EC.

Principal subjects:

- Presentation of analysis and statistics on collective doses.
- Presentation of experiences in radiation protection in different countries.

Working group "Revision of the Patient Directive".

Brussels (B) 16 - 17 March 1995.

10 participants from 9 countries and the EC.

Principal subject:

- Revision of Council Directive 84/466/EURATOM laying down basic measures for the radiation protection of persons undergoing medical examination or treatment.

Management and dosimetry in relation to the Directive on outside workers.

Luxembourg (L) 29 March 1995.

19 participants from 11 countries and the EC.

Principal subject:

- Operational protection of outside workers.

Art. 31 Working group on "Natural Radiation".

Brussels (B), 6 April 1995.

10 participants from 7 countries and the EC.

Principal subject:

- Discussion about Natural Radiation Sources at the Workplace to provide guidance on the implementation of Title VII of the proposed Basic Safety Standards Directive.

Group of experts referred to in Articles 35 and 36 of the EURATOM Treaty.

Luxembourg (L), 20 - 21 April 1995.

29 participants from 14 countries and the EC.

Principal subjects:

- Publication of Community-wide environmental radioactivity data.
- Categories of data to be transmitted by Member States
- Mode of transmission to the REM data base.

Art. 31 Working Group on the application of art. 13 of the Basic Safety Standards Directive.

Brussels (B), 27 April 1995.

5 participants from 4 countries and the EC.

Principal subject:

- Application of art. 13 of the Basic Safety Standards Directive.

Group of experts referred to in Article 31 of the EURATOM Treaty.

Luxembourg (L), 31 May 1995.

32 participants from 15 countries and the EC.

Principal subjects:

- Workprogramme of the group for the current mandate
- Directive on medical exposures



V

ERPET

**EUROPÄISCHE AUS- UND FORTBILDUNG
AUF DEM GEBIET DES STRAHLENSCHUTZES**

EUROPEAN RADIATION PROTECTION EDUCATION AND TRAINING

**ENSEIGNEMENT ET FORMATION EUROPEENS
EN RADIOPROTECTION**

V. ERPET - European Radiation Protection Education and Training - Activities Period: December 1992 - June 1995

The EC is promoting education and training activities in radiation protection in order to maintain and extend Community expertise in radiation protection, in particular in view of the forthcoming developments in the Community. These education and training activities are in compliance with Article 33 of the EURATOM Treaty and were emphasised by the Council Directives concerning the Radiation Protection Research Action of the reporting period (O.J. L336/42, 7.12.91).

Education and training activities are organised by the Commission's services in charge of Radiation Protection: DG XI, DG XII and, where appropriate, the service for EURO Courses of the JRC-ISPRA, together with competent institutions in the Member States, existing cooperative groups or other groups created for this purpose.

The education and training activities involve:

- Organisation of training courses;
- Development and provision of information and training packages;
- Exchange of scientists and promotion of participation in scientific conferences.

On the following pages, training courses and other ERPET activities organised in the period from December 1992 to June 1995 are listed. The courses provided coordinated, up-to-date programmes on key problems in radiation protection, for which a consistent Community approach is crucial. Some of these courses were repeated after evaluation and updating in order to ensure that a larger number of interested persons become familiarised with the most advanced knowledge in radiation protection.

ERPET EC Course on Current Techniques in Radiation Mutagenesis

Leiden (NL), 4 December 1992

11 students from EU countries

Principal subjects:

- Molecular analysis of mutants;
- Gene specific repair;
- Premature chromosome condensation;
- In situ hybridisation.

Training Course on Quality Assurance and Radiation Protection in Diagnostic Radiology

Jointly organised by the EC, Unitá Sanitaria Locale N° 7, Udine (I) and IRS Ltd. Liverpool (UK), course held in English and Spanish.

Udine (I), 31 May - 4 June 1993

65 participants from all regions of Italy

Purpose: To provide up-to-date operational aspects and measures of radiation protection practice in diagnostic radiology.

Principal subjects:

- Background information to operational and legislative framework for radiation protection of the patient as well as the staff
- Quality assurance in diagnostic radiology: quality requirements with regard to radiographic images and patient dose
- Quality control programmes: organisation, implementation, measurements
- Role of technical developments, practical demonstrations.

Target groups:

All those actively involved in the day-to-day practice of diagnostic radiology, as well as those responsible for education and training of radiographers and radiological technicians.

4th ERPET Training Course on Off-Site Emergency Planning and Response for Nuclear Accidents

Jointly organised by CEN/SCK Mol (B) and the EC
Mol (B), 21 - 25 June 1993
57 participants from 23 countries

Principal subjects:

- Principles of intervention planning, organisation and decision making with respect to off-site intervention in the case of an accidental release of radioactive material to the environment
- Consequences of accidental releases
- Exposure pathways and health effects
- Agricultural countermeasures
- Environmental monitoring
- Emergency exercises

Target groups:

Professionals involved in emergency planning.

Training Course on the use of the PC version of the Probabilistic Accident Consequence Code COSYMA

Jointly organised by KfK Karlsruhe (D), the NRPB, Chilton (UK) and the EC
Wallingford, Oxfordshire (UK), 28 June - 2 July 1993
37 participants from 20 countries

Purpose: Training in the use of PC COSYMA

Principal subjects:

- Training course on PC COSYMA
- Probabilistic accident consequence models
- Atmospheric dispersion and deposition
- Transfer to the terrestrial environment
- Health effects
- Use of software and preparation of input data for code

Target groups:

Those professionally involved with risk assessment in nuclear safety.

Second Summer School on Radiecology

Jointly organised by IUR, Hungarian National Research Institute for Radiobiology and Radiohygiene and the EC

Budapest (H), 26 July - 7 August 1993

25 participants from 11 countries and the EC

Purpose: To fulfil the needs of qualified graduates in environmental radioactivity in the following fields:

- Basic principles applied to radiecology.
- Radionuclides transfer in terrestrial ecosystems, in aquatic ecosystems, in food chains and modelling.
- Ecological effects of radiation and its consequences.
- Dose limits and legislation.
- Accident situations and emergency procedures en relation to dose assessment and remedial actions.
- Application of radiological knowledge to waste management problems.

Target group:

Young scientists working at research centres, universities and government bodies, as well as in private industry involved in radioecology.

Training Course on the use of Decision Aiding Software for Optimising Radiological Protection

Jointly organised by the University of Leeds (UK), TNO, Rijswijk (NL) and the EC

Leeds (UK), 6 - 8 September 1993

13 participants from 4 countries

Purpose: Training in the use of more complex optimisation programmes

Principal subjects:

- Setting of Multi-Attribute Value Theory
- Multi-Attribute Value Analysis
- Understanding Sensitivity Analysis
- Structuring Attribute Trees
- MAVT Exercises
- Uncertainty modelling

Target groups:

Those professionally involved with optimisation of radiological protection in nuclear safety and waste management

First ERPET Advanced Training MSc. Course in Radiation Biology

Jointly organised by the University of London, The Medical College of Saint Bartholomew's Hospital, London (UK) and the EC

London (UK), 4 October 1993 - 16 September 1994

7 participants from 5 countries

Purpose: to stimulate young scientists to specialise in Radiation Biology

Principal subjects:

- Basic course:

- radiation physics and chemistry
- radiation effects on cells and tissues
- late effects
- radiation genetics and in utero effects
- radiation protection
- statistics and scientific reporting

- Advanced course: specific fields of importance for radiation protection measures:

- free radicals in biology
- microdosimetry and biological dosimetry
- molecular genetics and repair
- experimental radiation carcinogenesis
- epidemiology of radiation induced cancer
- radiation biology related to diagnostic radiology, nuclear medicine and therapy
- radioecology

Target groups: students or young postgraduates in physics, chemistry, biology, medicine who wish to specialise in radiation biology

5th ERPET Training Course on Off-Site Emergency Planning and Response for Nuclear Accidents

Jointly organised by the Greek Atomic Energy Commission, Athens (GR), CEN/SCK Mol (B) and the EC
Chalkida (GR), 25 - 29 October 1993

25 participants from 4 countries

Purpose: Training in off-site emergency planning and response to nuclear accidents.

Principal Subjects:

- On-site emergency planning at Kozloduy plant
- Off-site emergency planning in Bulgaria
- Greek nuclear emergency plan and environmental monitoring
- Assessment of off-site consequences and real-time consequence assessment
- Consequences of accidental releases
- Exposure pathways and health effects
- Principles of intervention
- Agricultural countermeasures
- Environmental monitoring
- Emergency response exercises

Target groups:

Those involved in contingency planning e.g. civil protection and environmental protection officers, persons responsible for the management of radiation protection or emergency planning at nuclear facilities.

ERPET Training Course on Diagnostic and Treatment of Radiation Victims

Jointly organised by INSTN (F), NRPB (UK), BfS (D) and the EC

Saclay (F), 15 - 19 November 1993

23 participants from 14 countries

Purpose: To harmonise the actions to be taken in diagnosis and treatment in case there is an accident.

Principal subjects:

- The need for well defined protocols and guidelines for overexposed and for skin;
- How to recognize reversible, irreversible damage to the stem-cell compartment and to determine the limits of the use of haemopoietic growth factors to stimulate haemopoiesis;
- Development of a quantitative model to predict the outcome as the basis for the therapeutic measures;
- To answer the question as to what type of therapeutic intervention should be done and whether stem cell transplantation is a good solution and when.

Target groups: There were 23 students from 13 different countries. Mostly medical doctors working in radiation protection, occupational medicine, nuclear medicine.

2nd ERPET Training Course on Dosimetry in Diagnostic Radiology

Jointly organised by ICTP (I), PTB (D) and the EC

Trieste (I), 14 - 18 March 1994

27 participants from 11 countries

Purpose: Dose reduction measures

Principal subjects:

- Basic physical principles
- Radiological instrumentation
- Dose measurement techniques
- Quality assurance
- Practical exercises

Target groups: Medical physicists, radiologists, technicians, representatives of national radiation protection supervisory bodies from the EU and Eastern Europe

ERPET Training Course on Medical Physics in Diagnostic Radiology

Jointly organised by EFOMP, SFPH and the EC

Nancy (F), 19 - 25 June 1994

43 participants from 14 countries, including Eastern Europe

Purpose: To present the training required (as stated by EFOMP) for a medical physicist who wishes to become a qualified expert in Radiophysics related to Diagnostic Radiology

Principal subjects:

- Framework for radiation protection
- Quality assurance programmes
- Quality control of radiological equipment
- Dose measurements and risk assessment
- Patient and staff protection

Target groups: Medical physicists working in the application of ionising radiation in medicine

2nd ERPET Advanced Training MSc Course in Radiation Biology

Jointly organised by the University of London, The Medical College of Saint Bartholomew's Hospital, London (UK) and the EC

London (UK), 2 October 1994 - 14 September 1995

7 participants from 6 countries

Purpose: to stimulate young scientists to specialise in Radiation Biology

Principal subjects:

- Basic course:

- radiation physics and chemistry
- radiation effects on cells and tissues
- late effects
- radiation genetics and in utero effects
- radiation protection
- statistics and scientific reporting

- Advanced course: specific fields of importance for radiation protection measures:

- free radicals in biology
- microdosimetry and biological dosimetry
- molecular genetics and repair
- experimental radiation carcinogenesis
- epidemiology of radiation induced cancer
- radiation biology related to diagnostic radiology, nuclear medicine and therapy
- radioecology

Target groups: students or young postgraduates in physics, chemistry, biology, medicine who wish to specialise in radiation biology

ERPET Training Course on Dose Assessment from Intakes of Radionuclides

Jointly organised by EURADOS, IPSN (F) and the EC in collaboration with AEA and NRPB Cadarache (F), 18 - 22 April 1994

40 participants from throughout Europe

Purpose: Dissemination of knowledge and techniques for the assessment of doses from incorporated radionuclides using the most recent models through lectures and practical exercises.

Principal subjects:

- Intake routes and biokinetics of radionuclides: Occupational exposure and environmental releases.
- ICRP models for lung
- Air sampling and bioassay techniques

- In-vivo monitoring techniques
- Approaches to internal dosimetry in various countries
- Hands on practical exercises using hand-held calculators and PCs

Target groups: Health physicists and scientists involved in assessment of doses resulting from intakes in radionuclides.

2nd ERPET Training Course on The Use of the PC Version of the Probabilistic Accident Consequence Code COSYMA

Jointly organised by KFK (D), NRPB (UK), State Committee for Chernobyl (CIS) and the EC

Kiev (CIS), 16 - 20 May 1994

50 participants from 7 eastern and central european countries

Purpose: Training in the use of PC COSYMA

Principal subjects:

- Probabilistic accident consequence codes
- PC software package
- Dispersion, meteorology, food chain transfer, dosimetry, health effects models
- Countermeasures and economic costs
- Application of PC COSYMA in risk studies and for emergency planning

ERPET Training Course - 4th Training Course on Off-Site Emergency Planning and Response for Nuclear Accidents

Jointly organised by SCK/CEN and the EC
Mol, (B), 27 June - 1 July 1994
53 participants from 20 countries and the EC

Purpose: Training in off-site emergency planning and response to nuclear accidents

Principal subjects:

- Off-site emergency planning
- Consequences of accidental releases
- Exposure pathways and health effects
- Principles of intervention
- Agricultural countermeasures
- Environmental monitoring
- Emergency exercises

Target groups: Professionals involved in emergency planning

ERPET Training Course on Application of Modern Methods in Radiation Measurements and Dosimetry

Jointly organised by EURADOS, GSF (D), IARR and the EC
Neuherberg (Munich) (D), 11 - 16 September 1994
36 participants from throughout Europe

Purpose: Dissemination of knowledge and expertise in applying advanced detector and electronics technology in dosimetry through lectures and practical exercises.

Principal subjects:

- Radiation detectors
- Specification of radiation quality
- Dosimetric concepts and quantities in radiation protection
- In-situ spectrometry
- Dosimetry using EPR (Electro Paramagnetic Resonance)
- Calibration techniques
- Low energy X-ray detector
- Individual dosimetry in neutron fields
- Radon detection and activity measurements

Target groups: Young scientists working in radiation protection or radiation research

5th ERPET Training Course on Off-site Emergency Planning for & Response to Nuclear Accidents

Jointly organised by the University of Prague (CS), CEN/SCK (B) and the EC Prague (CS), 10 - 14 October 1994
25 participants from Eastern and Central European countries

Purpose: Provide a comprehensive understanding of all aspects of today's emergency planning and response

Principal subjects:

- Experience of past accidents
- Potential accident scenarios
- Transfer to the environment
- Exposure pathways
- Health aspects
- Accident consequences
- Remedial actions
- Intervention criteria
- Emergency planning reference accidents
- Real-time assessments
- Environmental monitoring
- Decision aiding techniques
- Information of the public
- Organisation of emergency plans
- Emergency response exercises

Target groups: Those involved in contingency planning, e.g. civil protection and environmental protection officers, persons responsible for the management of radiation protection or emergency planning at nuclear facilities.

4th ERPET Training Course on Optimisation of Radiological Protection in the Design and Operation of Nuclear Facilities

Jointly organised by the Kernforschungszentrum Karlsruhe (D), CEPN (F), NRPB (UK) and the EC.

Karlsruhe (D), 7 - 11 November 1994

29 participants from 6 countries

Purpose: Present tools and structures that can help to implement the concept of optimisation at the practical level

Principal subjects:

- ALARA principles and procedure
- Quantification of factors
- Dose calculations and modelling, measurement systems
- Past experience analysis
- Experience of work management in different countries
- Case studies

Target groups: Plant designers, system planners, maintenance operation planners, operation managers, engineers and health physicists

ERPET Training Course on Clinical Optimisation and Radiation Protection in Digital Radiography

Jointly organised by the University of Heidelberg-Mannheim (D), the EAR and the EC

Trier (D), 22 - 25 February 1995

32 participants from 12 countries

Purpose: To present theory of and practical work with digital imagery methods and strategies for optimisation of the clinical use and of radiation protection.

Principal subjects:

- Specific aspects of optimisation and radiation protection in digital radiography and computed tomography
- Impact of postprocessing
- Radiation protection measures

Target groups: Medical and auxiliary staff, who start to use digital imaging procedures

ERPET Training Course on PC COSYMA - a probabilistic accident consequence assessment code

Jointly organised by CIEMAT, NRPB, FZK and the EC
Madrid (E), 20 - 24 March 1995
26 participants from 11 countries and the EC

Purpose: Training in the use of PC COSYMA

Principal subjects:

- Probabilistic accident consequence codes
- PC software package
- Dispersion, meteorology, food chain transfer, dosimetry, health effects models
- Countermeasures and economic costs
- Application of PC COSYMA in risk studies and for emergency planning

Target groups: Those professionally involved with assessing the radiological risk from nuclear installations

2nd ERPET Training Course on Radiation Protection of the Patient

Jointly organised by BfS (D), NRPB (UK), INSTN (F) and the EC
Berlin (D), 8 - 12 May 1995
30 participants from 16 countries (including 12 from 6 Central European countries)

Purpose: To provide theory of and practical work with radiation protection measures in medicine

Principal subjects:

- Basic concepts and principles of radiation protection in diagnostic radiology, nuclear medicine and radiation therapy
- European protocol and projects in the field
- Demonstration

Target groups: All those working in alliance with medical staff in hospitals, universities, research institutes and health authorities

ERPET Training Course on ASQRAD - Software for Studying the Detriment Associated with Radiation Exposure

Jointly organised by NRPB (UK), CEPN (F) and the EC
Chilton, Oxfordshire (UK), 5 - 7 June 1995
19 participants from 7 countries

Purpose: Training in the use of ASQRAD

Principal subjects:

- epidemiological data
- health effects models
- uncertainties in risk estimates
- description of software
- demonstrations of and exercises using software

Target groups: Professionals with an interest in the estimation of detriment and its use.

ERPET Training course on Geographical Information Systems in Radioecology, an introductory training course

Jointly organised by the Institute of Terrestrial Ecology, Merlewood and the EC
Grange-over-Sands (UK), 13 - 20 June 1995
22 participants from 12 countries

Purpose: Over the past 25 years Geographical Information Systems (GIS) have developed to provide powerful tools for the manipulation, analysis and presentation of spatial data, to be used for environmental assessments. Since environmental management and restoration has become a key chapter in radioecology it has obvious requirements for the application of GIS in different areas and at different scales.

Main topics: Definition of the basic elements in GIS, identification of the potential for application in radioecology, introduction of the theoretical aspects of GIS, introduction to Geostatistical analysis, introduction and guidance in 'hands on' use of systems, practical introduction in field mapping, remote sensing and Geographical Positioning Systems (GPS), questions of application of GIS for radioecology.

Target groups: experienced radioecologists confronted with the processing of large amounts of spatial data, experienced GIS users confronted with problems of radioecology and environmental management

ERPET Training Course - Offsite Emergency Planning and Response to Nuclear Accidents

Jointly organised by SCK/CEN and the EC

Mol (B), 26 - 30 June 1995

39 participants from 19 countries

Purpose: Training in off-site emergency planning and response to nuclear accidents

Principal subjects:

- Off-site emergency planning
- Consequences of accidental releases
- Exposure pathways and health effects
- Principles of intervention
- Agricultural countermeasures
- Environmental monitoring
- Emergency exercises

Target groups: Professionals involved in emergency planning and response

ERPET Training course - Radon Indoor Risk and Remedial Actions

Jointly organised by SSI and the EC

Stockholm (S), 10 - 15 September 1995

37 participants from 20 countries

Purpose: Dissemination of knowledge and expertise in the radon field, scientific basis and practical methods of monitoring and mitigation.

Principal subjects:

- Origin of radon
- Properties and behaviour of radon and decay products
- Concentrations and radioactive aerosol size distribution
- Models for radon transport
- Detectors uncertainties, quality requirements, calibration
- Radon exhalation measurements
- Radiation influence on cells and organs
- Animals exposed to radon
- Lung dosimetry modelling for short-lived radon progeny
- Surveys of radon in dwellings
- Radon epidemiology
- Radon risk mapping and geological aspects
- Radon mitigation methods
- Radon guidelines, recommendations and limits

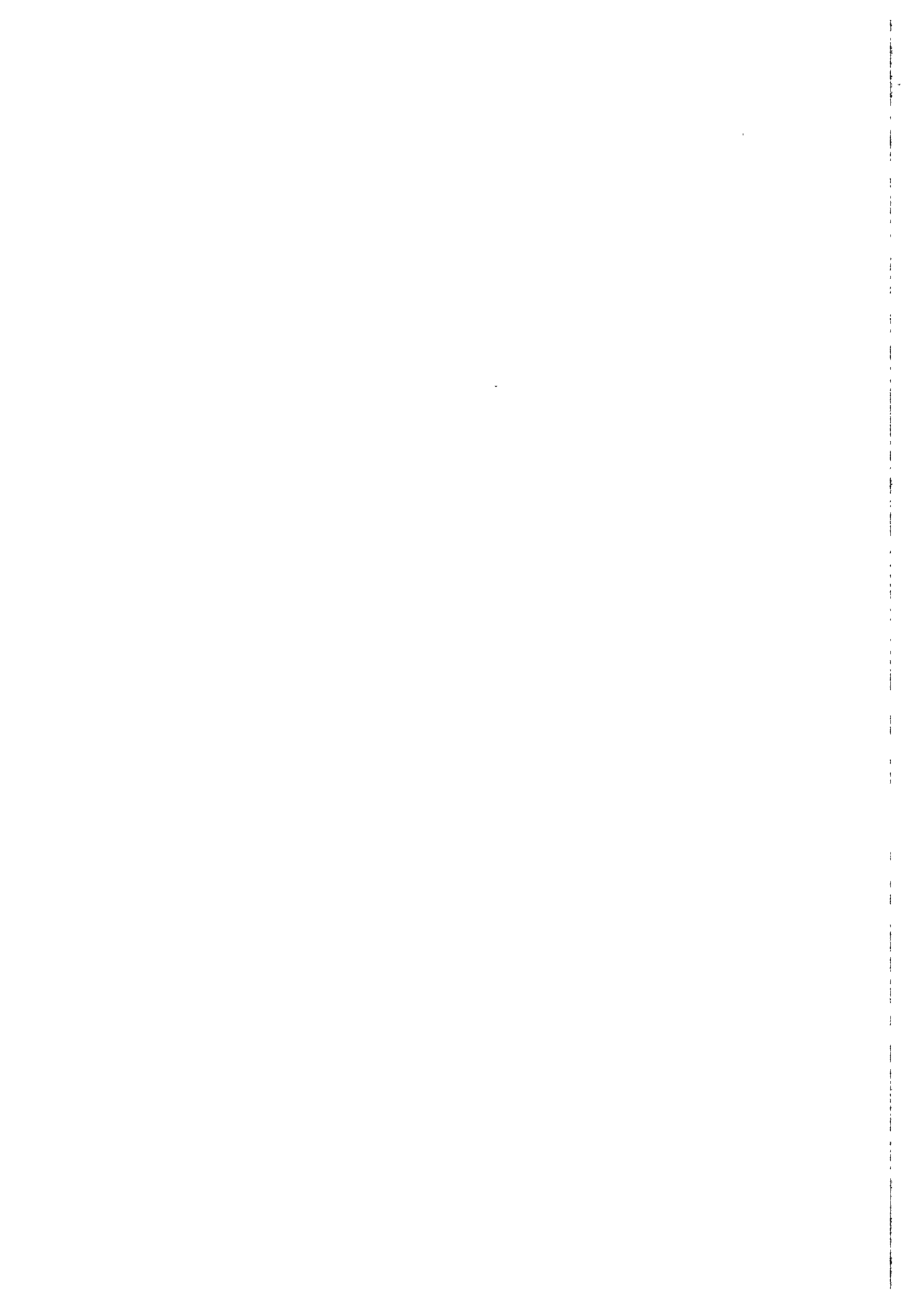
Target groups: Young scientists who are involved with scientific work about the problem of indoor exposure to radon and persons responsible for the general management of the radon problem.

VI

**AUSWAHL EINIGER AUF VERANLASSUNG DER KOMMISSION
ERSCHIENENER VERÖFFENTLICHUNGEN**

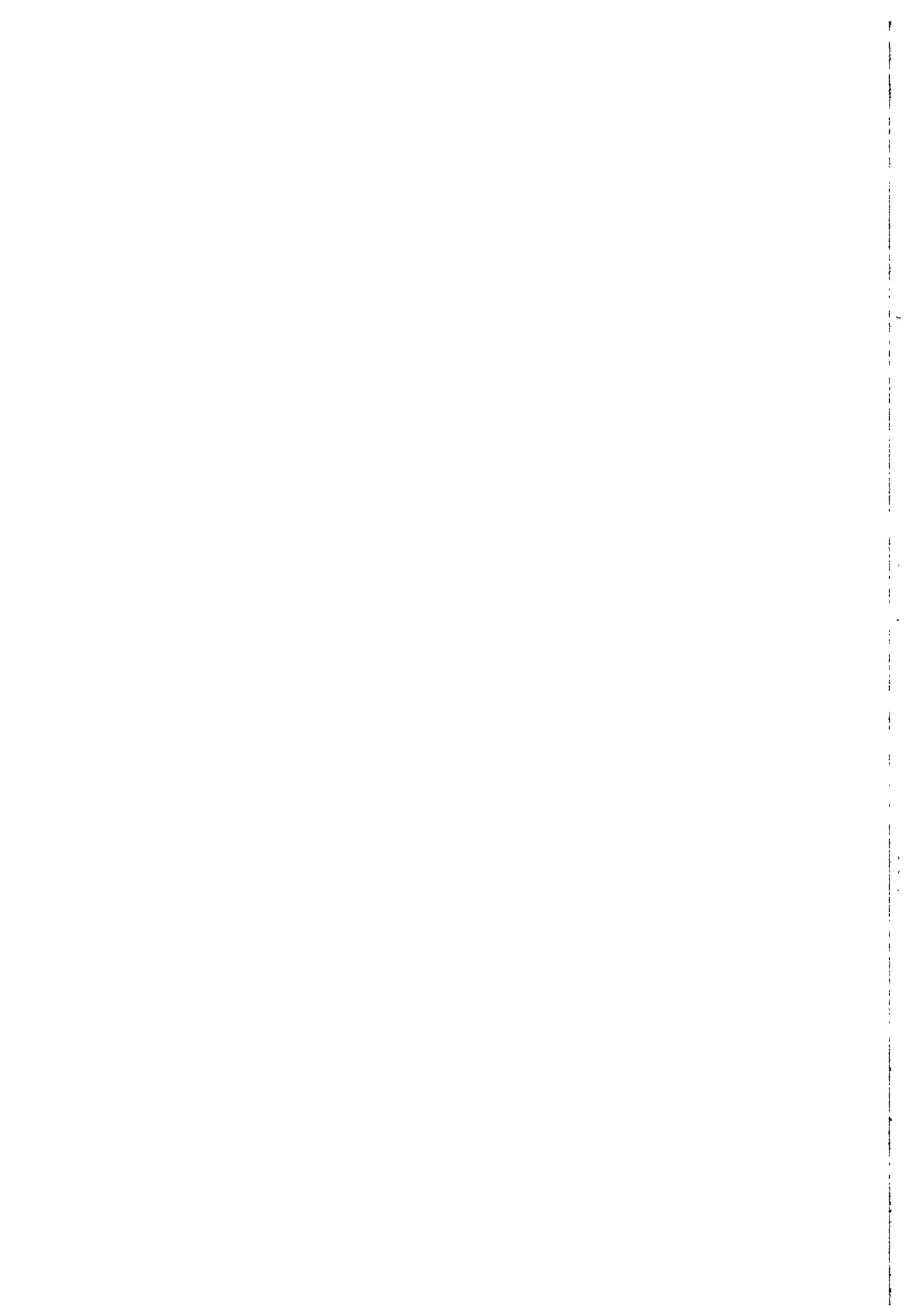
**SELECTION OF PUBLICATIONS ISSUED ON THE INITIATIVE
OF THE COMMISSION**

**CHOIX DE PUBLICATIONS EDITEES SUR L'INITIATIVE
DE LA COMMISSION**



VI. Publications, Period: December 1992 - June 1995

The scientific research results of the Commission's Radiation Protection Actions are presented in articles published in scientific journals. References to these are given in the corresponding Final Reports. In certain cases the Commission initiated surveys of detailed results of specific activities in the field of radiation protection and published them as monographs and reports with software (Page 4497), and proceedings (Page 4489). Short descriptions of those publications, published or prepared in the period from December 1992 to June 1995, are given on the following pages.



PROCEEDINGS

What's New and What's Needed in Radiation Effects Research

Proceedings of the second Bad Honnef contractors meeting held in Bad Honnef (D)
Bad Honnef (D), 29 March - 1 April 1993

The meeting brought physicists, radiation chemists, researchers working in molecular and cellular radiobiology and in animal research together, as well as epidemiologists. The necessity for multidisciplinary approach in research aimed at understanding the mechanisms of radiation induced changes in animals and humans is a major point of the report. It also identifies what is new and what is needed in radiation effects research for the fourth framework programme.

To be ordered through:

The Commission of the European Communities
Radiation Protection Research - DG XII.F.6
Rue de la Loi 200
B-1049 Brussels

Radiation protection optimization "Achievements and Opportunities"

Proceedings of the Fourth European Scientific Seminar
Luxembourg (LU), 20 to 22 April 1993.

Edited by DG XI-C-1, Radiation Protection, Luxembourg.

The system of radiation protection within the Community is based on the provisions of Council Directive 80/836/EURATOM, which apply to all activities involving a hazard arising from ionizing radiation and lay down the basic safety standards for the health protection of the general public and workers against the dangers of ionizing radiation.

The Commission organized, on 20 - 22 April 1993, in Luxembourg the fourth scientific seminar on the optimization principle (ALARA) which is a key element of the above mentioned Council Directive.

The seminar analysed progress made since the third optimization seminar in 1988 on the practical implementation of the optimization principle and focused in particular on its application to 'practices'. It was attended by about 150 participants from the 12 Member States, other European countries, the United States, Canada and India.

The report contains the 23 original contributions presented, the four review papers issued in advance of the conference, and an overview of each session containing the conclusions reached.

Report EUR 15234 EN, 1994, 455 pages
Radiation Protection series No. 63.

To be ordered through :

Office for Official Publications of the European Communities
L - 2985 LUXEMBOURG

Price: 53 ECU

Individual Monitoring of Ionising Radiation

Proceedings of the Workshop on Individual Monitoring of Ionising Radiation: The Impact of recent ICRP and ICRU Publications, jointly organised by the European Radiation Dosimetry Group (EURADOS), the Paul Scherrer Institut (PSI) the United States Department of Energy and the European Commission
Villigen (Switzerland), 5 - 7 May 1993

Edited by H.G. Menzel, T.O. Marshall, C. Wernli and M.N. Varma

The Workshop was part of a continuous effort by the EC to ensure that achievements in radiation protection research are transferred efficiently into practical applications in operational protection. In fact, the Workshop attracted scientists and officials from the research, operational and regulatory areas, and provided a forum for intensive exchange of information and discussions.

The Workshop addressed most aspects relevant to individual monitoring, including the system of radiation dose quantities and their interrelationship, type testing and calibration of personal dosimeters, required accuracy and dose thresholds, performance requirements and tests, record keeping and regulatory aspects, quality control and quality assurance and new detector developments. A considerable part of the discussion focused on perceived shortcomings or inconsistencies of the ICRP and ICRU recommendations, in particular on the fact that the quality factor - LET relationship used for the operational quantities and the radiation weighting factor used for risk limiting quantities were not congruent for neutrons, and that the new operational quantities were not in all cases conservative with regard to the new limiting quantities. Nevertheless, it was concluded that the immediate implications of the ICRP and ICRU recommendations appeared to have been assimilated and that most remaining specific problems can be solved. There was consensus that within Europe the harmonisation of standards required greater emphasis to be placed on performance testing and quality assurance.

The proceedings provide a comprehensive account of the presentations of the Workshop. Of particular value for practical purposes are the data and quantitative information with regard to the new recommendations.

Published by Nuclear Technology Publishing in
Radiation Protection Dosimetry Vol. 54, Nos. 3-4
EUR 15394 EN, 1994, 220 pages
ISBN 1 870965 299

To be ordered through:
Nuclear Technology Publishing
P.O. Box No. 7
GB - Ashford, Kent TN23 1YW

Price: 45 UKL

Indoor Radon Remedial Action

Proceedings of a workshop on Indoor Radon Remedial Action jointly organised by United States Department of Energy, United States Environmental Protection Agency, Ente per le Nuove Tecnologie l'Energia e l'Ambiente, Istituto Superiore di Sanita, International Centre for Theoretical Physics, International Centre for theoretical and Applied Ecology, and the European Commission.

Rimini (Italy), 27 June - 2 July 1993

Edited by G. Campos-Venuti, A. Janssens, M. Olast, S. piermattei, J. Sinnaeve and L. Tommasino.

In view of the recommendation of the European Communities of 21 February 1990, on the protection of the public against indoor exposure to radon (Official Journal of the European Communities N° L80, pp 26-28, 27.03.90) and because of the increasing awareness of the significance of indoor exposure to radon by the population and by decision-makers, there is a pressing need for more information on mitigation techniques.

The primary objective of the workshop was to present and discuss the different actions developed to reduce the radon hazards in both domestic and occupational buildings. The accent was on the technical description of remedial measures, their feasibility as a function of the different building characteristics, their long-term performance and on cost-effectiveness analysis.

The workshop, however, as planned, went beyond radon mitigation aspects and other topics such as radon ingress and modelling, health effects and new measurement techniques were also included.

Published by Nuclear Technology Publishing in

Radiation Protection Dosimetry Vol. 56, Nos 1-4

EUR 16005 EN 1994

386 pages

ISBN 1 870965 30 2

To be ordered through:

Nuclear Technology Publishing

P.O. Box 7

GB - Ashford Kent TN23 1YW

Proceedings of a Workshop on Data Analysis in Quality Control and Radiation Protection in Diagnostic Radiology and Nuclear Medicine

Jointly organised by the Unità Sanitaria Locale n°7, Udine, and the European Commission, and co-sponsored by the WHO

Grado (I), 29 September - 1 October 1993

Edited by G.Contento, B.Wall, H.Schibilla and D.Teunen

The Workshop was conceived as a forum for the evaluation of ten years of efforts in Quality Assurance in the diagnostic use of ionising radiation and radionuclides.

The proceedings contain about 100 papers involving some 300 research workers contributing to approach the list of detailed objectives of the Workshop, such as:

- evaluation of overviews, trends and evolution, of intercomparisons of dose reduction concepts, methods and practices,
- definition of means, ways, procedures of optimisation in the field of radiation protection, as well on the clinical, the equipment, the organisational as on the training side,
- analysis of the relationship cost-risk-benefit,
- perspectives of transfer of know-how to the user.

A series of open questions brought forward by these objectives were partly answered through the papers and posters, reproduced in these Proceedings. The main topics of interest in this Workshop were:

- Guidance,
- European and multinational trends and activities,
- Image quality,
- Computer applications, subdivided into knowledge based systems, and models and tools,
- Quality control, subdivided into instruments and methods, and surveys,
- Radiation protection of the patient, subdivided into dose evaluation methods, dose reduction, and surveys.

The discussions are summarised in the penultimate chapter, followed by conclusions which emphasise the consensus that a multidisciplinary approach is needed in order to lay down explicit links between the medical and radiation protection requirements.

Published by Nuclear Technology Publishing in Radiation Protection Dosimetry, Vol.57, nos 1-4,

Report EUR 15257, EN, 1995, 512 pages

ISBN 1 870965 37X

To be ordered through:

Nuclear Technology Publishing

P.O.Box 7

GB - Ashford TN23 1YW, Kent

Price: 90 UKL

Remediation and Restoration of radioactive contaminated sites in Europe.

Proceedings of an international symposium organized by the European Commission, State Committee of the Russian Federation on Chernobyl Affairs and the SCK-CEN, Nuclear Research Centre Mol (Belgium)
Antwerp (B), 11 - 15 October 1993.

Edited by DG XI-C-1, Radiation Protection, Luxembourg

During the last five decades, large scale nuclear facilities, both for civil and defence purposes, were developed and extensive use was made in industry of radioactive and fissile materials. Some of these facilities have meanwhile ceased to operate and have been decommissioned. The sites on which these industrial complexes were located remain in general under various degrees of surveillance. Dismantling actions need to be assessed in the light of site restoration through decontamination of building, materials and soils, aiming at uncontrolled future use.

Site restoration may also be required following environmental contamination caused by accidents or by inappropriate disposal of large amounts of liquid and solid wastes. The amounts involved and the lack of precautions may have resulted in the contamination of rivers and soils at levels that are cause of concern. The standard of performance for the operation of nuclear facilities has considerably improved over the past decades. The relics of past practices however remain and may require intervention to mitigate the consequences for human health. In the long term, restoration of these sites may be required.

Site restoration will therefore become an increasingly important issue. The conceptual framework needs to be clarified, criteria need to be defined, suitable techniques must be explored. This symposium is the first to be entirely devoted to this topic and thus focussed on the identification of the major contaminated sites, in Europe and in the Asean part of the former U.S.S.R., and to assess their environmental impact.

The initiative for this symposium was also taken in the light of the increasing awareness of important site contamination problems in the former U.S.S.R. The remarkable openness on the existence of such problems in the present republics of the CIS has culminated in the contribution of a number of keynote papers from these countries. They provide us not only with new relevant information on the situation in Chernobyl and the South Urals, but also on the impact of nuclear weapons testing and of waste dumping practices.

Doc. XI - 5027/94, 504 Pages - Radiation Protection series No. 74.

To be ordered through :
European Commission - Radiation Protection Division
Mr. H. LELLIG
Bât. Wagner - Bureau C 336
Rue Alcide de Gasperi
L - 2920 LUXEMBOURG

Price: free of charge

The radiological exposure of the population of the European Community to radioactivity in the Mediterranean Sea – Marina-Med project

Proceedings of a seminar held in Rome at the European Nuclear Energy Agency headquarters Rome (I), 17 to 19 May 1994.

Edited by DG XI-C-1, Radiation Protection, Luxembourg

The seminar analysed and discussed the results of the Marina-Med project, reviewed other work relevant to this subject and provided a forum for an exchange of views on the evaluation of the overall radiological situation in the Mediterranean Sea.

The report contains the four Marina-Med working group reports, the 27 original contributions presented and the conclusions reached.

Report EUR 15564 EN, 662 pages

ISBN 92-826-8398-2

Radiation Protection series No. 70.

To be ordered through:

Office for Official Publications of the European Communities

L - 2985 LUXEMBOURG

Price: ECU 66

Advances in Radiation Measurements

Proceedings of a Workshop on Advances in Radiation Measurements: Applications and Research Needs in Health Physics and Dosimetry, jointly organised by AECL (Atomic Energy of Canada Limited), Candu Owners Group, European Radiation Dosimetry Group (EURADOS) and the European Commission
Chalk River (Canada), 3 - 6 October 1994

Edited by A.J. Waker, P. Pihet and H.G. Menzel

In recent times advances have been made in the understanding of the physics and chemistry of radiation interaction in gases and solids and, in the same period, new knowledge of radiation effects at the molecular and cellular level has been acquired. New knowledge brings in its wake new possibilities and new challenges. It was therefore considered timely that a multidisciplinary workshop should be organised to help Health Physicists and Dosimetrists in their task of developing the most appropriate instruments and methods for improving the quantitative assessment of radiation exposure and the associated health risks.

The objectives of the Workshop specified by the Programme Committee were framed within the context of three questions: Where is current research and development able to take us in solving radiation monitoring problems; how can physical measurements be made relevant to what is happening in the biological sciences; and how can advantage be taken of advanced particle detection techniques developed in other areas of science such as astronomy and high energy physics?

The interdisciplinary nature of the workshop led to a scientifically stimulating and invigorating experience. It confirmed that, with care, an interdisciplinary meeting is a good method of facilitating progress at a time when new knowledge is being accumulated faster than it can be digested and incorporated into the general conceptual framework of radiation protection.

Published by Nuclear Technology Publishing in

Radiation Protection Dosimetry Vol. 61, Nos. 1-3
EUR 16177 EN 1995, 291 pages
ISBN 1 870965 33 7

To be ordered through:

Nuclear Technology Publishing
P.O. Box No. 7
GB - Ashford Kent TN23 1YW

Price: 75 UKL

MONOGRAPHS AND REPORTS WITH SOFTWARE

International Chernobyl Project - Input from the Commission of the European Communities to the Evaluation of the Relocation Policy adopted by the former Soviet Union

Report prepared by J. Lochard and T. Schneider, CEPN (F) (Part A) and S. French, University of Leeds (UK) (Part B) under contract nos. BI7-0060-GB and 90-ET-027 for the Commission of the European Communities

Edited by: G.N. Kelly and F. Luykx

An International Advisory Committee was convened by IAEA at the request of the Government of the former USSR, to assess the concept used to enable the population to live safely in areas affected by radioactive contamination following the Chernobyl accident. The Commission was represented in the International Advisory Committee and this report summarises the major technical inputs it made to the evaluation. In particular an analysis was made of the costs and effectiveness of the existing and alternative policies to ensure safe living conditions and a series of Decision Conferences were held to identify the major factors that were influencing policy decisions in this area.

Report EUR 14543 EN, 1992, 151 pages

To be ordered through:

Office for Official Publications of the European Communities
Boîte Postale 1003
L-2985 Luxembourg

Price: 15 ECU

European Guidelines for Quality Assurance in Mammography Screening

Report prepared by: A. Kirkpatrick, S. Törnberg, M.A.O. Thijssen, in collaboration with the EC Study Group on Quality Control in Mammography

Edited by C.J.M. de Wolf

This report outlines the requirements of a Quality Assurance programme with regard to a number of aspects of the mammographic screening system. It does not attempt to define the guidelines for treatment. The report gives detailed guidance for the medical diagnostic and technical aspects of the screening test itself. The document is merged from two documents: the general Quality Assurance guidelines which have been provided by the EC "Europe against Cancer" Programme, and the European Protocol for the Quality Control of the Technical Aspects of Mammography Screening which has been prepared within the framework of the EC Radiation Protection Actions.

With regard to the quality of mammography screening, three aspects are of prime importance: medical performance, organisation and the imaging process.

The Guidelines deal with these three aspects and incorporate the present state of knowledge on systematic breast cancer screening. They are applicable to all breast screening units and mammography equipment within all medical services. The European Protocol for the Quality Control of the Technical Aspects of Mammography Screening includes 12 sample data sheets for quality control reporting.

The list of references indicates nearly all existing quality control guidance available at local, regional and national level.

These Guidelines are available in the following languages: English (original), Danish, French, German, Greek, Italian, Portuguese and Spanish.

Published by the Commission of the European Communities in the Medicine and Health series.

EUR 14821 EN, 1993, 86 pages.
ISBN 92-826-5644-6

To be ordered through
Office for Official Publications of the European Communities
Rue Mercier, 2
L-2985 Luxembourg

Price: 7,50 ECU

PC COSYMA, Version 1.0: Users Guide and Software

Report and software prepared by NRPB (UK) and FZK (D) for the European Commission

Report and software package EUR 14917 EN, 1993, 420 pages

A personal computer version of the probabilistic accident consequence code, COSYMA, has been developed for assessing the risk presented by nuclear installations. The software package is available to interested users subject to entering into an Agreement on conditions of use with the European Commission. The Users Guide accompanying the software contains detailed guidance on the use of the software.

To be ordered through:

European Commission
DG XII/F/6
Dr G N Kelly
Rue de la Loi 200
B-1049 Bruxelles
Belgium

Price: 400 UKL

Thyroid Cancer in Children living near Chernobyl

Expert Panel report on the consequences of the Chernobyl accident

Edited by D. Williams, A. Pinchera, A. Karaoglou, K.H. Chadwick

In January 1992, under the Radiation Protection Research Action, a Panel of experts was set up to evaluate the current situation concerning reported increased incidence of thyroid cancer in children living near Chernobyl at the time of the nuclear reactor accident on 26 April 1986.

The report written by this Panel documents their findings with respect to the occurrence of childhood thyroid cancer in Belarus and the Northern Ukraine. The Panel arrives to a consensus opinion and makes strong recommendations for urgent technical and humanitarian assistance and research cooperation.

Published by: The Commission of the European Communities - Radiation Protection Research and Training Programme

Report EUR 15248 EN, 1993, 108 pages
ISBN 92-826-5515-6

To be ordered through:

Office for Official Publications of the European Communities
Boîte Postale 1003
L-2985 Luxembourg

Price: 13,50 ECU

Development of a general guideline for the radiological optimisation of the restoration of former nuclear sites.

Report prepared by Th. Zeevaert and P. Govaerts, SCK-CEN, Mol (B) for the European Commission

A methodology was developed for assessing dose impacts to man in normal evolution and accidental scenarios for various restoration approaches.

Distinction is made between primary sources (independent sources present at the time of abandonment of the nuclear activities) and secondary sources (formed or fed by others through the transplantation of radionuclides). The modelling steps comprise:

- the evolution of primary sources with time;
- the transport of radionuclides subsequent to their release, giving rise to secondary sources;
- the influence of barriers against release and transport, etc.;
- the dose impact assessments following various exposure pathways.

This dose assessment approach is illustrated by a simple example with a typical primary source (a contaminated soil layer) feeding a typical secondary source (a groundwater well) with the transport between the sources being counteracted by a vertical barrier.

Radiation Protection Series No. 59 EN, 1993, 77 pages.

To be ordered through:

European Commission
Radiation Protection Division
Mr. Herbert LELLIG
Centre Wagner C 336
Rue Alcide de Gasperi
L-2920 Luxembourg

Price: free of charge

Principles and methods for establishing concentrations and quantities (exemption values) below which reporting is not required in the European Directive.

Report prepared by M. Harvey, S. Mobbs, J. Cooper, A.M. Chapuis, A. Sugier, T. Schneider, J. Lochard and A. Janssens.

The Community Basic Safety Standards for the health protection of the general public and workers against the dangers of ionising radiation incorporate values of activities not to be exceeded so that the requirements for reporting and obtaining prior authorisation of activities involving a hazard arising from ionising radiation need not be applied (Article 4 of Council Directive 80/386). For this purpose all relevant nuclides have been classified in four groups, according to their relative toxicity. Also radioactive substances of a concentration less than 100 Bq/g are exempted from this requirement, this limit being increased to 500 Bq/g for solid natural radioactive substances. These exemptions, while allowing competent authorities in Member States to disregard a multitude of trivial practices, have so far not given rise to any situations where the health of the general public or of workers were put at risk. However, the opportunity of a major revision of the Basic Safety Standards, to bring these in line with the latest recommendations of the ICRP (Publication 60), was taken to introduce a more transparent and consistent methodology for establishing exemption levels on a nuclide-specific basis.

Radiation Protection Series No. 65 EN, 1993, 94 pages.

To be ordered through:

European Commission
Radiation Protection Division
Mr. Herbert LELLIG
Centre Wagner C 336
Rue Alcide de Gasperi
L-2920 Luxembourg

Price: free of charge

Radiological Protection Principles for relocation and return of people in the event of accidental releases of radioactive material.

Recommendations of the group of experts set up under the terms of Article 31 of the Euratom Treaty.

The report sets out the principles for intervention and elaborates upon their application to the relocation of people after and accidental release of radioactive material. Because of the diversity of circumstances that might be encountered following an accident, there are limits to the degree to which detailed planning for relocation can be made in advance or, indeed, would be sensible. The guidance given here has, therefore, been kept deliberately simple and is intended to be broadly applicable. Of necessity it will need to be refined in the light of the particular circumstances of an accident.

The guidance is intended to form a basic framework for decision making within which other factors and considerations can be integrated. Indeed, social and political factors which go beyond the scope of this guidance will need to be taken into account in the event of an accident, and decisions will ultimately be taken at political level.

Radiation Protection Series No. 64, 1993, 42 pages.

To be ordered through:

European Commission
Radiation Protection Division
Mr. Herbert LELLIG
Centre Wagner C 336
Rue Alcide de Gasperi
L-2920 Luxembourg

Price: free of charge

PC COSYMA: an Accident Consequence Assessment Package for Use on a PC

Report prepared by J.A. Jones, P.A. Mansfield, S.M. Haywood, A.F. Nisbet, NRPB (UK) and I. Hasemann, C. Steinhauer, J Ehrhardt, FZK (D) for the European Commission

The report describes the main technical content and basis of the probabilistic accident consequence code, PC COSYMA, that has been developed for use on a Personal Computer. The essential features of the models (eg, dispersion of radioactive material in the atmosphere, deposition, transfer through the environment, exposure of people, used in the code are described. Inputs required by the code are specified together with the main quantities estimated (eg, radiation doses, health effects in the exposed population, effects on agricultural production, countermeasures, economic impact, etc).

Report EUR 14916 EN, 1994, 63 pages
ISBN 92-826-7441-X

To be ordered through:

Office for Official Publications of the European Communities
Rue de Mercier, 2
L-2985 Luxembourg

Price: 10 ECU

COSYMA: Users Intercomparison Exercise

Report prepared by E. van Wonderen, J. van der Steen, KEMA (NL) and I. Hasemann, FZK (D) for the European Commission

The report describes an intercomparison of the predictions of the radiological consequences of postulated accidental releases made by different users of the probabilistic accident consequence code, COSYMA. Reasons for differences in the predictions were identified and have led to the development of improved guidance for users and also to model refinements which better satisfied user needs.

Report EUR 15108 EN, 1994, 239 pages
ISBN 92-826-7369-3

To be ordered through:

Office for Official Publications of the European Communities
Rue de Mercier, 2
L-2985 Luxembourg

Price: 25 ECU

Probabilistic Accident Consequence Assessment Codes: Second International Comparison - Technical Report

Report prepared by W. Nixon et al, SRD (UK), S. Acharya, USDOE, U. Bäverstam, SRPI (SW), J. Ehrhardt et al, FZK (D), E. Gallego Diaz, UPM (ES), J. Glynn, USNRC, T. Homma et al, JAERI (J), J.A. Jones et al, NRPB (UK), G.N. Kelly, EC, L. Neymotin, BNL (US), J. van der Steen, KEMA (NL), C. Viktorsson, OECD, and S. Vuori et al, VTT (SF) for the European Commission and the OECD Nuclear Energy Agency.

This report sets out the detailed technical results of a second international intercomparison of probabilistic accident consequence codes which are used to assess the radiological risk presented by nuclear installations. The intercomparison was jointly organised by the European Commission and the OECD Nuclear Energy Agency. The report is intended for specialists in this area. It identifies major differences between the predictions of the various codes and their origins.

Report EUR 15109 EN, 1994, 338 pages
ISBN 92-826-4114-7

To be ordered through:

Office for Official Publications of the European Communities
Rue de Mercier, 2
L-2985 Luxembourg

Price: 40 ECU

Probabilistic Accident Consequence Assessment Codes: Second International Comparison - Overview Report

Report prepared by an ad hoc Group on the EC/NEA Intercomparison Exercise on Probabilistic Accident Consequence Assessment Codes for the European Commission and the OECD Nuclear Energy Agency.

This report summarises the main results of a second international intercomparison of probabilistic accident consequence codes which are used to assess the radiological risk presented by nuclear installations. The intercomparison was jointly organised by the European Commission and the OECD Nuclear Energy Agency. The report is not intended for specialists in this area but for those who may use the results from such assessments as an input into decisions on safety and risk management. Conclusions are reached on the current state of adequacy of probabilistic accident consequence codes and recommendations made on where improvements would be warranted.

Report EUR 15237 EN, 1994, 104 pages
ISBN 92-64-14101-4

To be ordered through:
OECD Publications
2 rue André-Pascal
75775 PARIS CEDEX 16
France

Molecular Mechanisms in Radiation Mutagenesis and Carcinogenesis

Edited by: K.H. Chadwick (CEC, Brussels), R. Cox (NRPB, Chilton), H.P. Leenhouts (RIVM, Bilthoven), J. Thacker (MRC-RU, Chilton)

The principal aim of the seminar was to explore the molecular mechanisms of ionizing radiation induced mutagenesis and carcinogenesis using data derived from cellular and whole animal studies. Molecular studies are already yielding much information on the nature of mutations induced at a number of loci in cultured somatic rodent and human cells. It is now possible to begin to address questions on the relative mutational sensitivity of different genes and DNA sequences, on the relationship between DNA repair and mutagenesis, and on the predominant forms of mutation in somatic and germ cells. Such studies provide not only for specific comment on the nature of the heritable risk in man following radiation exposure, but, at the mechanistic level, have important implications for radiation carcinogenesis. It has become increasingly clear that specific gene mutations in somatic tissues underlie the induction of neoplasia. What is less certain is the extent to which these genes act as targets for radiation and how well we can model such cancer-inducing mutations at the molecular level in whole animal and cellular systems.

This book presents the proceedings of the International Seminar together with a report of the formal discussion. The book should be of interest to all scientists working on the effects of radiation in the field of radiation protection and radiation therapy, and especially to those using molecular biological techniques. The book could also be useful to scientists working on the molecular and cytological aspects of carcinogenesis.

EUR 15294 EN, 1994, 320 pages
ISBN 92-826-7321-9

To be ordered through:

Office of Official Publications of the European Commission
Rue de Mercier 2
L-2985 Luxembourg

Price: 36,50 ECU

Environmental Radioactivity in the European Community: 1987 - 1990

Edited by DG XI-C-1, Radiation Protection, Luxembourg

Quarterly average values of radioactivity levels in airborne particulates, surface water, drinking water, milk and mixed diet are reported for the twelve countries of the European Union (sparse and dense network), and for some sampling locations outside the European Union (sparse network), for the years 1987 - 1990.

Report EUR 15699 EN, 156 pages
Radiation Protection series No. 80

To be ordered through:
Office for Official Publications of the European Communities
L-2985 LUXEMBOURG

Intakes of Radionuclides - Detection, Assessment and Limitation of Occupational Exposure

Edited by: J.W. Stather (NRPB, Chilton) & A. Karaoglou (CEC Brussels)

There is increasing evidence that the control of occupational exposure to radionuclides should be defined for specific situations in the workplace. This Workshop reviewed the problem of occupational exposure to radionuclides and the implications of the new ICRP recommendations; it considered information on the physico-chemical and biokinetic characteristics of radioactive material encountered at the workplace with the aim of developing approaches for a better definition of site and material-specific ALIs, their range of application and the methods available for demonstrating compliance with dose limits. The Workshop also covered the problem of assessing radiation doses from bioassay or whole body monitoring data, the move to physiologically based dosimetric models and recent developments in the treatment of accidental intakes of radionuclides.

Published by Nuclear technology Publishing in Radiation Protection Dosimetry

EUR 15714 EN, 1994, 360 pages
ISBN 1 870965 28 0

To be ordered through:

Nuclear technology Publishing
P.O. Box No.7
Ashford, Kent TN23 1YW England

Probabilistic Accident Consequence Uncertainty Analysis: Dispersion and Deposition
Uncertainty Assessment

Report prepared by F.T. Harper et al, Sandia NL (US), S.C. Hora, Univ Hawaii (US), C.H. Liu, USNRC, M.D. McKay, Los Alamos NL (US), J.C. Helton, ASU (US), L. Goossens et al, TUD (NL), J. Päsler-Sauer, FZK (D), J.A. Jones, NRPB (UK) for the European Commission and the United States Nuclear Regulatory Commission.

The European Commission and the United States Nuclear Regulatory Commission are co-sponsoring a joint study to estimate the uncertainties associated with predictions of probabilistic accident consequence codes, in particular COSYMA and MACCS which have found widespread use in Europe and the US, respectively. Formal expert elicitation is being used in assessing the uncertainties in each of the main modules of the code prior to undertaking a complete uncertainty assessment. This report is concerned with the assessment of uncertainties in two modules of the code, namely the dispersion and deposition of radioactive material in the atmosphere. The uncertainty judgements expressed by the experts are documented together with how these have been processed for subsequent use within the two consequence codes. The uncertainty distributions derived on dispersion in the atmosphere and on deposition by dry and wet processes also have a wider use beyond their immediate application to assess uncertainties in probabilistic accident consequence codes. Subsequent reports in this series will address uncertainties in other code modules, ie, food chain transfer, external doses from deposited material, internal dosimetry, deterministic health effects and stochastic health effects.

Report NUREG/CR-6244
EUR 15855 EN
SAND94-1453, 1994, 3 vols, 460 pages

To be ordered through:
The NRC Public Document Room
2120 L Street, NW., Lower Level
Washington DC 20555-0001
USA

or:

European Commission
DG XII/F/6
Dr G N Kelly
Rue de la Loi 200
B-1049 Bruxelles
Belgium

Price: free of charge

Methods for EC/USNRC Accident Consequence Uncertainty Analysis of Dispersion and Deposition

Report prepared by R.M. Cooke, L.H.J. Goossens and B.C.P. Kraan, Delft University of Technology (NL) for the European Commission

The report provides a detailed description of the methods used in a joint study between the European Commission and the United States Nuclear Regulatory Commission to assess the uncertainty associated with the predictions of probabilistic accident consequence codes used to assess the risk from nuclear installations. Formal elicitation of expert judgement is used as the basis for estimating uncertainties and the methods were applied to two of the physical processes modelled in the consequence codes, namely the dispersion and deposition of released radioactive material in the atmosphere. Particular consideration is given to the relative merits of using equal or performance based weighting of the experts when evaluating their respective judgements.

Report EUR 15856 EN, 1995, 209 pages
ISBN 92-827-0388-6

To be ordered through:

European Commission
DG XII/F/6
Dr G N Kelly
Rue de la Loi 200
B-1049 Bruxelles
Belgium

Price: free of charge

Health effects of internally deposited radionuclides: emphasis on radium and thorium

Edited by: G. van Kaick (DKFZ, Heidelberg), A. Karaoglou (CEC Brussels) & A.M. Kellerer (GSF, Neuherberg)

The motivation for this Seminar arose from the scientific challenge caused primarily by on-going epidemiological cohort studies evaluating the late effects of human beings in three continents. During the six-year interval between the last meeting and this Seminar new molecular biological techniques for the investigation of cancers have developed so that the Seminar offered a timely opportunity to review the current state of knowledge of the induction of cancer in humans by internally deposited radionuclides. Moreover, the topics considered at this meeting were broadened to radionuclides other than Radium and Thorium, such as Polonium, Plutonium, Americium, and Strontium. The use of epidemiological data for radiation protection requirements is dependent on a knowledge of the accumulated dose to the target cells. There is a large uncertainty in the identification of the target cells, the distribution in and elimination of the radionuclides from the body and therefore the dose to the target cells. Therefore, biophysical measurements, calculations, and animal experiments are crucial for the understanding of the human data. Bearing this in mind more emphasis was given at this Seminar to creating a bridge between epidemiology, molecular biology, cancer genetics and low-dose effects.

The meeting revealed that in the human studies the pathohistological results of neoplastic diseases need to be revised critically. A standardisation of the histological and epidemiological evaluation of the data is absolutely necessary for pooling of the data of the different studies in the near future. For example in Europe the data of 4000 to 5000 Thorotrast patients could be pooled and analysed, thus providing a strong and reliable statistic power of the results.

EUR 15877 EN, 1995, 442 pages
ISBN 981-02-2015-4

To be ordered through:

World Scientific Publishing Co. Pte. Ltd.
P.O. Box 128
Farrer Road, Singapore 9128

Deposition of Radionuclides, their Subsequent Relocation in the Environment and Resulting Implications

Report prepared by J. Tschiersch et al, GSF (D), J. Røed et al, Risø (DK), A. Goddard , ICSTM (UK), J. Brown et al, NRPB (UK), K. Rybáček et al, Inst of Nuclear Physics (CZ), I. Navarčík et al, Inst of Radioecology (SK) and P. Zombori et al, KFKI (H) for the European Commission.

The report provides a summary of the results of a major research programme concerned with the deposition of artificial radionuclides, particularly in urban environments, their subsequent transfer and the implications for radiation exposure. Results of the experimental research are given, in particular those dealing with aerosol deposition by rain and fog: indoor deposition and exposure from inhalation indoors: aerosol deposition on skin, hair and clothing: distribution of deposited radionuclides in soil and resulting exposures: weathering of caesium-137 from various urban surfaces and the variation of dose rate depending on habits and location: and the resuspension of deposited material. These findings have been used to develop improved models for assessing the radiological impact of deposited radionuclides in inhabited areas. The model improvements are described and recommendations are made on where future research should be directed to further enhance model reliability.

Report EUR 16604 EN, 1995, 111 pages
ISBN 92-827-4903-7

To be ordered through:

European Commission
DG XII/F/6
Dr G N Kelly
Rue de la Loi 200
B-1049 Bruxelles
Belgium

Price: free of charge

PC COSYMA (Version 2): an Accident Consequence Assessment Package for Use on a PC

Report prepared by J.A. Jones, P.A. Mansfield, S.M. Haywood, A.F. Nisbet, NRPB (UK) and I. Hasemann, C. Steinhauer, J Ehrhardt, D. Faude, FZK (D) for the European Commission

The report describes the main technical content and basis of Version 2 of the probabilistic accident consequence code, PC COSYMA, that has been developed for use on a Personal Computer. The essential features of the models (eg, dispersion of radioactive material in the atmosphere, deposition, transfer through the environment, exposure of people, used in the code are described. Inputs required by the code are specified together with the main quantities estimated (eg, radiation doses, health effects in the exposed population, effects on agricultural production, countermeasures, economic impact, etc). This report updates EUR 14916 which was concerned with the Version 1 of the code.

Report EUR 16239 EN, 1995, 63 pages

To be ordered through:

Office for Official Publications
of the European Communities
Rue de Mercier, 2
L-2985 Luxembourg

Price: free of charge

PC COSYMA, Version 2.0: Users Guide and Software

Report and software prepared by NRPB (UK) and FZK (D) for the European Commission

Report EUR 16240 EN, 1995, 440 pages
ISBN 92-87- 4480-9

A second version of PC COSYMA, a probabilistic accident consequence code for use on a personal computer, has been released. The code is used for assessing the risk presented by nuclear installations and the second version contains a number of improvements, in particular in the user interface, the presentation of graphical output and more comprehensive treatment of deterministic assessments. The software package is available to interested users subject to entering into an Agreement on conditions of use with the European Commission. The Users Guide accompanying the software contains detailed guidance on the use of the software.

To be ordered through:

European Commission
DG XII/F/6
Dr G N Kelly
Rue de la Loi 200
B-1049 Bruxelles
Belgium

Price: 400 UKL

ASQRAD: Assessment System for the Quantification of Radiation Detriment

Report and software prepared by CEPN (F) and NRPB (UK) for the European Commission

ASQRAD (Assessment System for the Quantification of Radiation Detriment) is a PC based computer code developed for the purposes of evaluating the detriment from radiation exposure. The code, which runs under Windows, enables estimates to be made of the radiation risks to different population groups taking account, inter alia, of age and sex. It provides a basis for assessing the effects of different modelling assumptions and for determining the significance of various factors in estimating detriment. The package contains the software and a detailed Users Guide. The latter describes the basis modelling assumptions and provides detailed guidance on the use of the software.

Report EUR 16644 EN, 1995, 180 pages
ISBN 92-827-5085-X

To be obtained through:
CEPN
BP No 48
F-92263 Fontenay-aux-Roses
France

Price: 300 ECU

Technical recommendations for monitoring individuals occupationally exposed to external radiation

Edited by DG XI-C-1, Radiation Protection, Luxembourg

These technical recommendations for the monitoring of workers and other persons exposed to external ionizing radiation are providing technical guidance in view of practical applications of dosimetric concepts. The document gives information on the general principles for monitoring individuals as well as requirements for personal dose meters such as type and performance testing. Also covered are aspects of dose record-keeping systems and administrative problems.

Report EUR 14852 EN, 86 pages
ISBN 92-826-7364-2
Radiation Protection series No. 73

To be ordered through:
Office for Official Publications of the European Communities
L - 2985 LUXEMBOURG

Price: 11,50 ECU

Methodology for assessing the radiological consequences of routine releases of radionuclides to the environment

Edited by DG XI-C-1, Radiation Protection, Luxembourg

Assessing the radiological consequences of radioactive releases to the environment involves estimating radiation exposures to both individuals and to population groups. A comprehensive methodology, CREAM (Consequences of releases to the environment: assessment methodology), has been developed for evaluating the radiological consequences of discharges of radioactive effluents during normal operations. This work was carried out under contract to the European Commission with the National Radiological Protection Board (NRPB) coordinating the work of other institutions in the European Community. CREAM revises and updates a previous methodology published in 1979. Although primarily developed for application in Western Europe, a generalized approach has been adopted so that models and methods are appropriate for wider use. Default values are given for many parameters and have been used to determine illustrative results. The models adopted in the methodology are those considered appropriate for routine releases; the limitations of the models are discussed in this report.

The methodology consists of a series of interlinked models which describe the transfer of radionuclides through the various sectors of the environment, the pathways by which people may be exposed to radiation and the resulting health detriment. Radioactive effluents may be discharged to both the atmospheric and aquatic environment and models are provided for both situations. Some radionuclides, due to relatively long radioactive half-lives and their behaviour in the environment, may come globally dispersed and act as long-term sources of exposure to large populations: appropriate models are included.

The radiological consequences of routine releases of radionuclides are determined using the framework of the system of radiological protection recommended by the International Commission on Radiological Protection (ICRP). The most recent recommendations of the ICRP, issued in Publication 60, have been taken into account in developing this methodology: effective doses have been evaluated and the revised risk factor has been adopted. The methodology, CREAM, is intended to find application in evaluating individual and collective doses together with health detriment primarily from routine discharges of radioactive effluents to the environment.

Report EUR 15760 EN, 351 pages

ISBN 92-826-9059-8

Radiation Protection series No. 72.

To be ordered through:

Office for Official Publications of the European Communities

L-2985 LUXEMBOURG

Price: 40 ECU

Study on consumer products containing radioactive substances in the EU Member States

Edited by DG XI-C-1, Radiation Protection, Luxembourg

This study is based on chapter III of Euratom Treaty and highlights the practical application of Title II (Articles 2, 3, 4 and 5) of the basic safety standards Directive (Council Directive 80/836/Euratom, of July 1980).

The report first describes the different types of consumer products in which radioactive substances are intentionally incorporated as well as products with high natural radioactivity.

The second part of the report gives an overview on the legislative and regulatory situation within the EU Member States in view of prior reporting and authorization. The report also gives information on the situation of the non EU Member States, Sweden and Switzerland.

Report EUR 15846 EN, 112 pages

ISBN 92-826-9000-8

Radiation Protection series No. 76

To be ordered through:

Office for Official Publications of the European Communities

L - 2985 LUXEMBOURG

Price: 13,50 ECU

Radioactive effluents from nuclear power stations and nuclear fuel reprocessing plants in the European Community, 1977-86

Part 1: Discharge data 1977-86

Part 2: Radiological aspects

Edited by DG XI-C-1, Radiation Protection, Luxembourg

The report covers operational nuclear power stations of capacity greater than 50 MWe and nuclear fuel reprocessing plants in the European Community. Data on radioactive gaseous and liquid effluent discharges from these installations are given in Part 1 of the report for the decade 1977 to 1986, expressed both in absolute terms (GBq/y) and normalized to net electricity production from the fuel (GBq/GWh).

The collective exposure of the EC population from each year's discharges in 1977 to 1986 has been calculated and is presented in Part 2. Detailed results including radionuclide and pathway breakdowns of the collective exposure are given for discharges in 1977 to 1986. Maximum individual doses are also presented for discharges from selected sites in 1977 and 1986. Overall the results of this study show a reduction in the collective exposure of the EC population from discharges in 1986 when compared with discharges in 1977. The main reason for this reduction is a decline in the levels of liquid releases from the reprocessing plant at Sellafield.

Report EUR 15928 EN, 164 pages

ISBN 92-826-8924-7

Radiation Protection series No. 77

To be ordered through:

Office for Official Publications of the European Communities

L - 2985 LUXEMBOURG

Price: 18,50 ECU

European Guidelines on Quality Criteria for Diagnostic Radiographic Images

Edited by J. Carmichael, C. Maccia, B.M. Moores, J.W. Oestmann, H. Schibilla, F.E. Stieve, D. Teunen, R. Van Tiggelen, B. Wall

The European initiative on the establishment of Quality Criteria for Diagnostic Radiographic Images was promoted to develop a comprehensive quality and safety culture throughout the European Union with regard to the medical use of ionising radiation.

The Quality Criteria have been elaborated in a common effort by radiologists, radiographers, physicists, radiation protection experts, health authorities and professional national and international organisations. They were first set up for conventional radiography of adult patients. It has been recognised that the quality criteria must be specifically adapted to paediatric radiology (see Report EUR 16261).

The applicability of the Quality Criteria for adult radiology has been checked in European wide trials, involving some hundred radiological departments and about 3000 radiographic images and dose measurements. The results have been discussed at workshops, by working parties and by dedicated study groups; advice and comments have been collected from professional associations, individual experts and health care authorities. **The conclusions have been integrated into the present Document and provided elements for the improvement of the lists of Quality Criteria.**

The European Guidelines on Quality Criteria for Diagnostic Radiographic Images contains four chapters: the first one concerns the updated lists of the Quality Criteria for six conventional examinations: Chest, Skull, Pelvis, Lumbar Spine, Urinary Tract and Breast. It defines Diagnostic Requirements for a normal, basic radiograph, specifying anatomical image criteria and important image details; it indicates criteria for the radiation dose to the patient and gives an example for good radiographic technique by which the Diagnostic Requirements and the dose criteria can be achieved. The second chapter summarises the analysis of the findings of the European wide Trials and explains the updating of the Quality Criteria, as listed in Chapter 1. The third chapter outlines a procedure for implementing and auditing the Quality Criteria. A model questionnaire and scoring tables for the six examinations, which were elaborated during the evaluation of the Trials, have been reproduced and could become tools for self-education and performance checking. The fourth chapter presents all those to whom the Commission's services wish to express their sincere thanks for their cooperation and creative criticism, from which the Commission's Radiation Protection Actions drew its encouragement to concentrate on the development of this Quality Criteria concept.

The Guidelines will be available in nine official languages of the European Union.

EUR 16260 EN, approx. 80 pages, *in press*

To be published by:
Office for Official Publications of the European Commission
Rue Mercier 2
L - 2985 Luxembourg

European Guidelines on Quality Criteria for Diagnostic Radiographic Images in Paediatrics

Edited by M. Kohn, B.M. Moores, H. Schibilla, K. Schneider, H. St. Stender, F.E. Stieve, D. Teunen, B. Wall

The Quality Criteria for paediatric radiology have been elaborated in a common effort by a European Group of paediatric radiologists (the Lake Starnberg Group), together with radiographers, physicists, radiation protection experts, health authorities and professional national and international organisations.

The applicability of the Quality Criteria has been checked in European wide Trials involving about 160 paediatric X-ray departments in 14 Member States and other European countries, and roughly 1600 radiographic films and dose measurements.

The results have been discussed at Workshops, by working parties and dedicated study groups, as well as by independent experts all over the world. The conclusions have been integrated in the present Guidelines and provided elements for the improvement of the lists of Quality Criteria.

The European Guidelines on Quality Criteria for Diagnostic Radiographic images in Paediatrics contain four chapters:

The first chapter concerns the updated lists of the Quality Criteria for conventional paediatric examinations of chest, skull, pelvis, segmental and full spine, abdomen and urinary tract for different projections and, where necessary, specific criteria for newborns. This first chapter defines Diagnostic Requirements for a normal, basic radiograph, specifying anatomical Image Criteria; indicates Criteria for the Radiation Dose to the Patient, as far as available, and gives an Example for Good Radiographic Technique by which the Diagnostic Requirements and the dose criteria can be achieved. The second chapter summarises the analysis of the findings of the European wide Trials and explains the updating of the Quality Criteria as listed in Chapter 1. The third chapter outlines a procedure for implementing and auditing the Quality Criteria; a model of the scoring tables and adapted questionnaires that have been developed during the evaluation of the Trials are reproduced and can become tools for self-learning and performance checking. The fourth chapter presents all those to whom the European Commission's services wish to express their sincere thanks for co-operation and creative criticism, which encouraged the EC's Radiation Protection Actions to concentrate on the development of this Quality Criteria concept.

The European Guidelines will be available in 9 official languages of the European Union.

EUR 16261 EN, approx. 80 pages, *in press*

To be published by:
Office for Official Publications of the European Commission
Rue Mercier 2
L - 2985 Luxembourg

Working Document on Quality Criteria for Computed Tomography

Report prepared by: G. Bongartz, K. Geleijns, S.J. Golding, K.A. Jessen, A.G. Jurik, M. Leonardi, W. Panzer, H. Schibilla, P. Shrimpton, D. Teunen, G. Tosi

Computed tomography (CT) revolutionized X-ray imaging by providing high quality images which reproduced differentiated transverse cross sectional slices of the body. The remarkable potential of the imaging modality has been realised by rapid technological developments that have allowed a continuing expansion of CT practice. As a result, numbers of examinations are ever increasing, involving relatively high levels of patient dose. CT has therefore not only made a substantial impact on patient care, but also on patient and population exposure from medical X-rays. Today, it accounts for approximately 20% of the resultant collective dose from Diagnostic Radiology in some countries of the European Union (EU).

CT successfully reduces the influence of non-useful scattered X-rays, which are a problem in conventional tomographic techniques. However, the complexity and the variability of scanner settings in comparison with conventional radiology may adversely affect the levels of image quality. There is, therefore, a need to establish quality criteria for CT which will provide the required clinical information in its optimum form, while facilitating reduction of patient exposure. The quality criteria concept, as developed for conventional X-ray examinations of adult and paediatric patients by the European Commission's (EC) research actions, has proved to be an efficient means for optimising the use of ionising radiation in medical imaging procedures. The purpose of such quality criteria for CT should therefore be to provide an operational framework for radiation protection initiatives, which links the desired image quality for a CT examination to the technical parameters necessary to produce this quality with reasonable patient dose.

This Working Document presents guidance based on the definition and introduction of quality criteria for diagnostic images and equipment performance, as well as for dose to the patient. It is intended to give advice on day-to-day practice consistent with implementation of the Council Directive laying down basic measures for the radiation protection of persons undergoing medical examination or treatment. The Working Document will be available in EN, FR and D.

EUR 16262 EN, approx. 50 pages, *in press*

To be published by:
Office for Official Publications
of the European Commission
Rue Mercier 2
L - 2985 Luxembourg

European Protocol on Dosimetry in Mammography

Report prepared by J. Zoetelief, M. Fitzgerald, W. Leitz, M. Säbel; D.R. Dance, M. Gambaccini, J.T.M. Jansen, C. Maccia, B.M. Moores, H. Schibilla, M.A.O. Thijssen

Mammography as a radiological technique for breast cancer detection is receiving particular attention by several programmes and initiatives of the Commission of the European Communities. Special efforts for its optimization are supported by the programmes "Europe against Cancer" and "Regulatory Aspects and Research Actions in Radiation Protection", as well as by "VALUE" which is the specific programme for the dissemination and utilization of scientific and technological research results.

Various actions were taken in the 1990-1994 period:

- strategies for optimizing of the functioning of mammography screening centres were developed, giving rise to the definition of reference centres for guidance in quality assurance and quality control;
- the concept of quality criteria was set up, dealing with image criteria, image details, parameters of good radiographic techniques and criteria for radiation dose to the patient, including reference dose values;
- trials were carried out in nearly all European countries on the practical application of the quality criteria;
- workshops were organised for the discussion of more standardized quality control tools and methods, for specifying the requirements of test phantoms for mammography and for assessing the perspectives of digitization in mammography.

For the effective implementation of the conclusions of these actions, the "European Guidelines for Quality Assurance in Mammography Screening" were published, including a European Protocol for the Quality Control of the Technical Aspects of Mammography Screening (Report EUR 14821 1993).

During the elaboration of these European Guidelines it became evident that dose measurement is a crucial part and requires specific definitions and guidance for a standardized approach. Thus the present protocol specifies some of the most practicable methods and levels of possible accuracy of dose measurements in mammography. It should allow for comparability and evaluation of dose data that will be acquired from now on, whilst at the same time increasing the awareness of the need for periodical quality control and radiation protection measures.

The European Protocol will be available in EN, FR and D.

EUR 16263 EN, approx. 60 pages, *in press*

To be published by:
Office for Official Publications
of the European Commission
Rue Mercier 2
L - 2985 Luxembourg

The 1991 Trial on Quality Criteria for Diagnostic Radiographic Images: Detailed Results and Findings

Edited by C. Maccia, B.M. Moores, B. Wall

The report presents and analyses the results of the EC Trial on Quality Criteria for Diagnostic Radiographic Images, carried out in 1991 in 83 radiological departments in 16 European countries. More than 2000 radiographs have been collected and were evaluated by the field radiologists as well as by a panel of independent radiologists and medical physicists with regard to the list of quality criteria established by the EC Radiation Protection Research Action. The doses to the patient had been assessed from TLD measurements for all the radiographs.

After a brief review of the methodology, the first part of the report describes the scope of the Trial in terms of overall participation by country and by type of examination: Chest, Lumbar Spine and Breast.

In the second part, a more detailed analysis of the results gathered for each type of examination is presented. Three aspects are considered separately: technical parameters used in carrying out examinations, entrance surface doses received by the patients, and both field and independent radiologists' ranking of the radiographs in relation to the Quality Criteria listings.

In the third part of the report an attempt is made to explore the potential of the Quality Criteria concept as a tool for optimisation of radiation protection of the patient.

EUR 16635 EN, approx. 160 pages, *in press*

To be published by:
Office for Official Publications
of the European Commission
Rue Mercier 2
L - 2985 Luxembourg

Radiation and Radiation Protection – A course for primary and secondary schools

Edited by DG XI-C-1, Radiation Protection, Luxembourg

Radioactivity, ionizing radiation and non-ionizing radiation are fairly complex and abstract subjects, in particular for younger and less advanced pupils. Moreover, the pupils for whom this coursebook is intended constitute a remarkable heterogeneous group in which cognitive abilities may vary considerably. It has also been necessary to take account of the fact that this course will be used in different educational systems within the European Community. Therefore it was sometimes necessary to simplify scientific and technical concepts throughout this course.

In preparing the course, the option of a "spiral curriculum" was chosen. This means that items recur in a gradually more complex form.

The selected material is divided into five age levels. The first three levels are designed for use in primary education while the last two levels are aimed at secondary education. Each level can be thought as a self-contained unit, although the teacher is free to use material from previous or subsequent levels. The course may therefore be regarded as a source of reference material with which the teacher can construct his own lessons.

In the first three levels emphasis is put on relating radiation to pupils' personal and everyday experiences and observations. Pupils are made aware of the risks and benefits of ionizing and non-ionizing radiation.

In the final two levels, a more detailed examination is made of the subject from both the technical and social points of view, the aim being to enable pupils to develop an informed and balanced view of radiation.

Radiation Protection series No. 67

Available in EN, FR, DE, NL, ES; other languages are in preparation.

To be ordered through:

Office for Official Publications of the European Communities

L - 2985 LUXEMBOURG

Price: 30 ECU

Radiation Protection for the transport of radioactive substances

Edited by DG XI-C-1, Radiation Protection, Luxembourg

The work of DG XI in the field of radiation protection is governed by the Euratom Treaty. This treaty, and the directives made under it, stress the importance of keeping both workers and the general public informed. The aim is to produce balanced information: people should be aware of the potential dangers of ionizing radiation, but also appreciate that it can be used safely.

With this aim in view the Commission has undertaken a range of activities, including the organisation of several seminars on information and training in radiation and radiation protection. It was as a result of discussions at these seminars that the Commission decided to draw up training material for workers involved in the transport of radioactive substances in order to provide them with clear, scientifically valid and objective information in the form of a manual.

The first draft of the manual was developed by the Commission with the assistance of a consultant, Mr. R.M. Guest, lecturer at Suffolk College (UK) and specialist in radiation protection, and in close collaboration with experts in the field of the transport of radioactive materials.

It was then tested by a restricted group of transport workers and found to be very useful. Thereafter, it was presented to the Standing Working Group on the safe Transport and Radioactive Materials and the group of scientific experts established under Art. 31 of the EURATOM Treaty. Reactions were generally favourable, but a number of suggestions were made and the document was thoroughly revised in the light of the valuable remarks received.

The final product represents, therefore, the fruit of a considerable joint effort throughout the Community.

Radiation Protection series No. 68; 159 ppages
Available in EN, FR, DE, NL; other languages in preparation.

To be ordered through:
Office for Official Publications of the European Communities
L - 2985 LUXEMBOURG

Price: 40 ECU

Present status of practical aspects of individual dosimetry

Part I: EU Member States

Part II: East European Countries

Edited by DG XI-C-1, Radiation Protection, Luxembourg

This document describes the radiation protection legislation of the EU Member States and the administrative and regulatory measures taken in order to comply with the requirements of the Directive on basic safety standards. It provides an overview of practical aspects of personal radiation dosimetry, which is the most important instrument to assure adequate radiation monitoring and consequently radiation protection of workers. The document is updated to the situation within the Member States up to the end of 1993.

The second volume describes the radiation protection legislation in East European countries. It provides an overview of the respective national legislations, administrative measures and regulatory steps in relation to personal radiation dosimetry as far as the transitory situation in these countries allow this. It provides the best possible overview on individual radiation monitoring aspects for occupationally exposed workers. The document is updated to the situation up to the end of 1992.

Radiation Protection series No. 78

Part I: ISBN 92-827-0174-3, 126 pages

Part II: ISBN 92-827-0175-1, 79 pages

Parts I and II: ISBN 92-827-0173-5

To be ordered through:

Office for Official Publications of the European Communities

L - 2985 LUXEMBOURG

Price:

Part I: 13 ECU

Part II: 10 ECU

Part I and II: 19,50 ECU

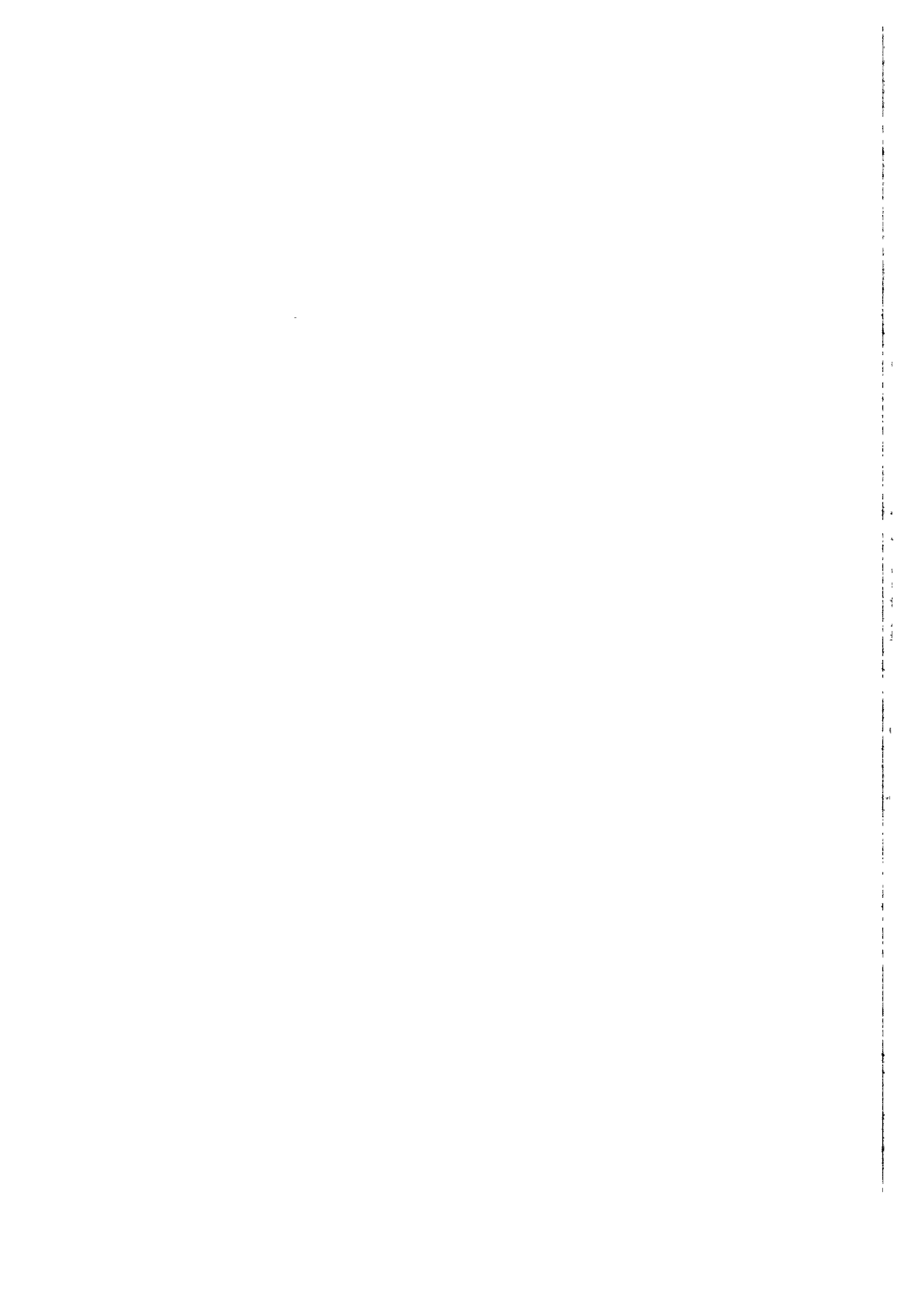


VII

LISTE DES ACRONYME UND ABKÜRZUNGEN

LIST OF ACRONYMS AND ABBREVIATIONS

LISTE DES ACRONYMES ET DES ABBREVIATIONS



AECB	Atomic Energy Control Board, Ottawa (Canada)
AECL	Atomic Energy of Canada Limited (Canada)
AFPPE	Association Française du Personnel Paramédical d'Electrocardiologie, Paris (F)
AIRM	Associazione Italiana di Radioprotezione Medica (I)
AIRP	Associazione Italiana di Protezione contro le Radiazioni (I)
ALARA	As Low As Reasonably Achievable
BfS	Bundesamt für Strahlenschutz, Salzgitter (D)
CAATS/INSERM	Centre d'évaluation pour l'Assurance de qualité des Applications Technologiques dans le domaine de la Santé/Institut National de la Santé et de la Recherche Médicale, Bourg-la-Reine (F)
CEA	Commissariat à l'Energie Atomique, Fontenay-aux-Roses (F)
CEC	Commission of the European Communities, Brussels (B)
CEDHYS	Centre de Développement des Etudes et Applications en Hygiène et Sécurité, Paris (F)
CEN/SCK	Centre d'Energie Nucléaire/Studie Centrum voor Kernenergie, Mol (B)
CEPN	Centre d'étude sur l'Evaluation de la Protection dans le domaine Nucléaire, Fontenay-aux-Roses (F)
CIEMAT	Centro de Investigaciones Energéticas, Medioambientales y Tecnológicas, Madrid (E)
CIR	Centre International de Radiopathologie, Fontenay-aux-Roses (F)
CNEN	Comitato Nazionale per la Ricerca e per lo Sviluppo dell'Energia Nucleare e delle Energie Alternative, Rome (I)
COSYMA	Code System Maria
CRSA	Centro Regionale per la Sperimentazione Agraria per il Friuli-Venezia-Giulia, Udine (I)
CT	Computed Tomography
EAR	European Association of Radiology
EBMT	European Bone Marrow Transplant Group
EC	European Commission
ECP(I)	Experimental Collaboration Project (No.)
EURIE	Early Exchange of Information in the Event of Radiological Emergency
EFOMP	European Federation of Organisations of Medical Physics, York (UK)
ENEA/DISP	Comitato Nazionale per la Ricerca e per lo Sviluppo dell'Energia Nucleare e delle Energie Alternative, Direzione Sicurezza Nucleare e Protezione Sanitaria, Rome (I)
ENEL	Ente Nazionale per l'Energia Elettrica, Roma (I)
ERPET	European Radiation Protection Education and Training EC DG XI/C/1, Luxembourg (L) & DG XII/F/6, Brussels (B)
EULEP	European Late Effects Project Group
EURADOS/CENDOS	European Radiation Dosimetry Group/Collection and Evaluation of Neutron Dosimetry Data
EUROMET	European Metrology
DG	Directorate General of the EC
GSF	Gesellschaft für Strahlen- und Umweltforschung, Neuherberg (D)
IAEA	International Atomic Energy Agency (A)
IARC	International Agency for Research on Cancer, Lyon (F)
IARR	International Association for Radiation Research
ICRP	International Commission on Radiological Protection
ICRU	International Commission on Radiation Units and Measurements
ICSTM	Imperial College of Techn. and Medicine Science, London (UK)
ICTP	International Centre for Theoretical Physics, Trieste (I)
IFE	Institute of Freshwater Ecology, Ambleside (UK)
INTECHMER-CNAM	Institut National des Techniques de la Mer - Conservatoire National des Arts et Métiers-Cherbourg (F)
INSTN	Institut National des Sciences et Techniques Nucléaires, Saclay (F)

IPSN	Institut de Protection et de Sûreté Nucléaire, Fontenay-aux-Roses(F)
IOMP	International Organisation of Medical Physicists
IRS	Integrated Radiological Services Ltd, Liverpool (UK)
ISH	Institut für Strahlenhygiene/Bundesamt für Strahlenschutz, Salzgitter/Neuherberg (D)
ITE	Institute of Terrestrial Ecology, Grange-over-Sands (UK)
ITRI	Inhalation Toxicology Research Institute, Albuquerque, NM (USA)
ITRI/TNO	Instituut voor Toegepaste Radiobiologie en Immunologie, TNO Rijswijk (NL)
IUR	International Union of Radioecologists
JRC	Joint Research Center of the EC at ISPRA
JSP()	Joint Study Project (No.)
KFA	Forschungsanlage, Jülich (D)
KfK	Kernforschungszentrum Karlsruhe (D)
KUL	Katholieke Universiteit Leuven (B)
LNETH	Laboratorio Nacional de Engenharia e Tecnologia Industrial, Lisboa (P)
MAFF	Ministry of Agriculture, Food and Fisheries, Lowestoft (UK)
MARIA	Methods for Assessing the Radiological Impact of Accidents
MLURI	McAulay Land Use Research Institute, Edinburgh (UK)
NEB	Nuclear Energy Board of Ireland, Dublin (IRL)
NIRP	National Institute of Radiation Protection, Stockholm (S)
NCSR	Democritos, National Centre for Scientific Research, Athens (GR)
NRPB	National Radiological Protection Board, Chilton (UK)
NPP	Nuclear Power Plant, Vattenfalls (S)
OECD/NEA	Organisation for Economic Cooperation and Development/Nuclear Energy Agency
ORNL	Oak Ridge National Laboratory, Knoxville, Tennessee (USA)
PTB	Physikalisch-Technische Bundesanstalt, Braunschweig (D)
RADE-AID	Radiological Accident Decision Aiding System
RBE	Relative Biological Effectiveness
REM	Radioactivity Environmental Monitoring
RERF	Radiation Effects Research Foundation, Hiroshima (Japan)
RIVM	Rijks Instituut voor Volksgezondheid en Milieu, Bilthoven (NL)
SCRPI	Service Central pour la Protection contre les Rayonnements Ionisants, Le Vésinet (F)
SEPR	Sociedad Española de Protección Radiológica (E)
SFEN	Société Française d'Énergie Nucléaire, Paris (F)
SFPH	Société Française des Physiciens d'Hôpital (F)
SFRP	Sociedad Española de Protección Radiológica (E)
SRD	Safety and Reliability Directorate, Warrington (UK)
SSI	Statens Strålskyddsinstitut (S)
SUAS	Swedish University of Agricultural Sciences, Umea (S)
TEPC	Tissue-Equivalent Proportional Counter
TNO	Nederlandse Organisatie voor Toegepast Natuurwetenschappelijk Onderzoek, Rijswijk (NL)
UKAEA	United Kingdom Atomic Energy Authority, Harwell (UK)
ULB	Université Libre de Bruxelles, Brussels (B)
US DOE	US Department of Energy, Washington DC (USA)
US EPA	US Environmental Protection Agency
US NCI	US National Cancer Institute, Bethesda (USA)
US NRC	US Nuclear Regulatory Commission
US NIES	US National Institute of Environmental Sciences
USL	Unità Sanitaria Locale, N° 7, Udine (I)
WHO	World Health Organisation

VIII

VERZEICHNIS DER FORSCHUNGSGRUPPENLEITER

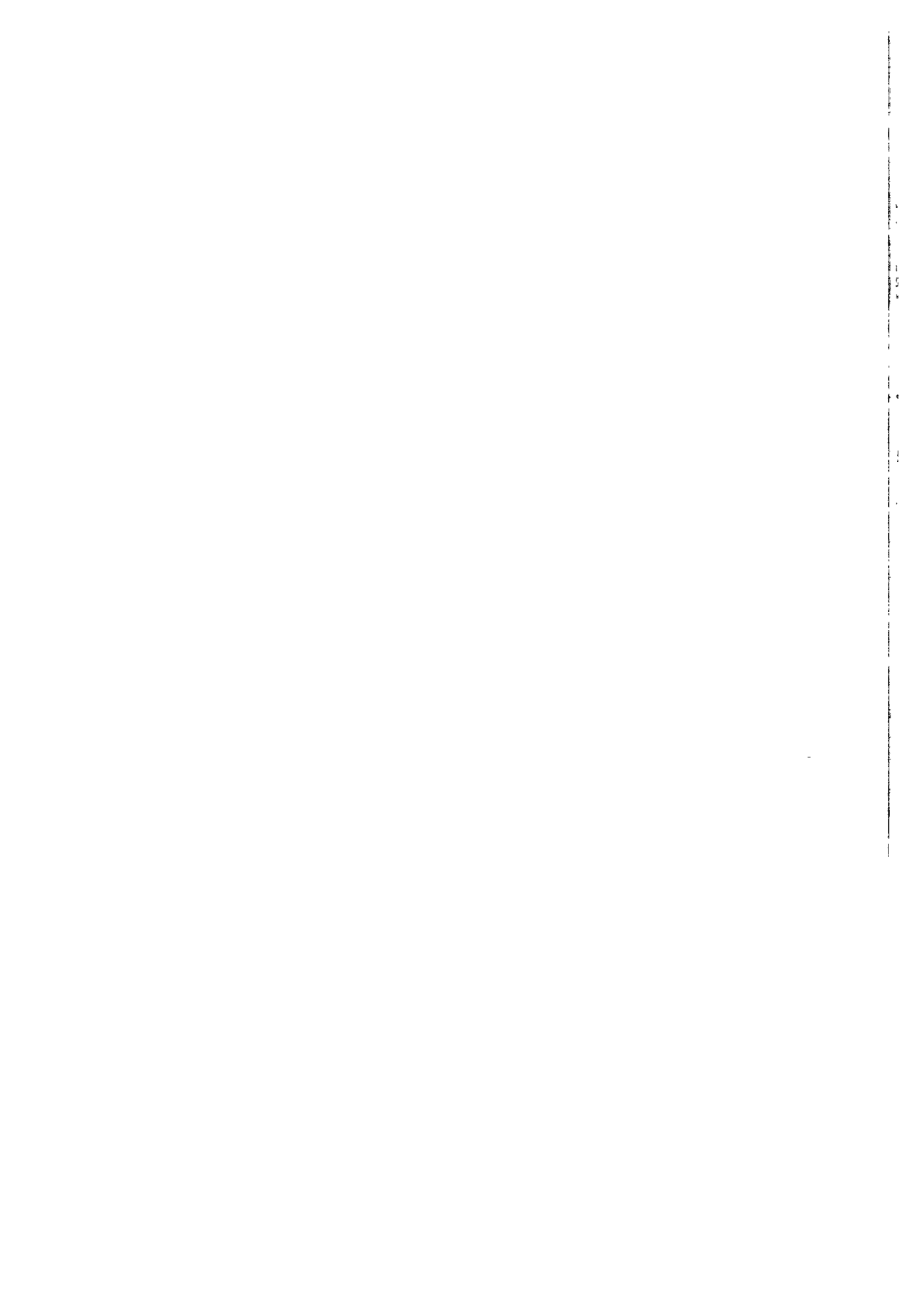
LIST OF RESEARCH GROUP LEADERS

INDEX DES CHEFS DE GROUPE DE RECHERCHE



RESEARCH GROUP LEADERS

Allisy A.	17	Madden J.	3149
Aten J.A.	2221	Magdelenat H.	2595
Bailey M.R.	703	Maisin J.	1687
Bailiff I.	55	Malone J.F.	3587
Belot Y.	1059	Masse R.	2651
Brenot J.	3903	McAulay I.R.	283
Bunnenberg C.	1169	McGarry A.	1481
Bøtter-Jensen L.	219	Mikkelsen T.	4215
Cancio D.	1617	Miles J.	3059
Cardis E.	3519	Mill A.J.	2097
Cherubini R.	2155	Minski M.J.	1327
Chmelevsky D.	3463	Mitchell P.I.	905
Christensen P.	339	Monte L.	4347
Cigna A.	795	Mothersill C.	2307
Clark M.J.	123	Muirhead C.R.	3239, 3341
Colautti P.	1769	Natarajan A.T.	1927
Colle C.	1647	Nosske D.	651
Davelaar J.	2061	Olivieri G.	2029
Després A.	3863	Paretzke H.G.	1705
Dietze G.	25	Parkin D.	3331
Dreicer M.	3209	Parry J.M.	1879
Edwards A.	2265	Poffijn A.	3293
Ehrhardt J.	3963	Porstendörfer J.	2911
Favor J.	2423	Ratti S.P.	4401
Fliedner T.M.	2535	Reyners H.	2753
Foulquier L.	1533	Roth P.	605
Fritsch P.	2477	Sabroux J.C.	3009
Goossens L.	3933	Sankaranarayanan K.	2379
Harrison J.D.	2795	Schmidt T.	3829
Hilton J.	813	Ségur P.	467
Howard B.J.	1237	Smith H.	3537
Höfler H.	2503	Smith T.	3749
Janowski M.	1913	Stradling G.N.	2607
Jessen K.A.	3643	Tates A.D.	2355
Jones A.	4281	Tschiersch J.	4099
Kellerer A.M.	435	Van der Eb A.J.	1969
Klein H.	161	van Kaick G.	3261
Lamy F.	2709	Van Loon R.E.	3681
Lefaire C.	3545	Vanmarcke H.	2869
Lembrechts J.F.M.	991, 1085	Vareille J.C.	533
Lohman P.H.M.	1819	Wall B.	3787
Maccia C.	3713	Wirth E.	1359





The Community Research and Development Information Service

Your European R&D Information Source

CORDIS represents a central source of information crucial for any organisation - be it industry, small and medium-sized enterprises, research organisations or universities - wishing to participate in the exploitation of research results, participate in EU funded science and technology programmes and/or seek partnerships.

CORDIS makes information available to the public through a collection of databases. The databases cover research programmes and projects from their preparatory stages through to their execution and final publication of results. A daily news service provides up-to-date information on EU research activities including calls for proposals, events, publications and tenders as well as progress and results of research and development programmes. A partner search facility allows users to register their own details on the database as well as search for potential partners. Other databases cover Commission documents, contact information and relevant publications as well as acronyms and abbreviations.

By becoming a user of CORDIS you have the possibility to:

- Identify opportunities to manufacture and market new products
- Identify partnerships for research and development
- Identify major players in research projects
- Review research completed and in progress in areas of your interest

The databases - nine in total - are accessible on-line free of charge. As a user-friendly aid for on-line searching, Watch-CORDIS, a Windows-based interface, is available on request. The databases are also available on a CD-ROM. The current databases are:

News (English, German and French version) - Results -
Partners - Projects - Programmes - Publications -
Acronyms - Comdocuments - Contacts

CORDIS on World Wide Web

The CORDIS service was extended in September 1994 to include the CORDIS World Wide Web (WWW) server on Internet. This service provides information on CORDIS and the CORDIS databases, various software products, which can be downloaded (including the above mentioned Watch-CORDIS) and the possibility of downloading full text documents including the work programmes and information packages for all the research programmes in the Fourth Framework and calls for proposals.

The CORDIS WWW service can be accessed on the Internet using browser software (e.g. Netscape) and the address is: <http://www.cordis.lu/>

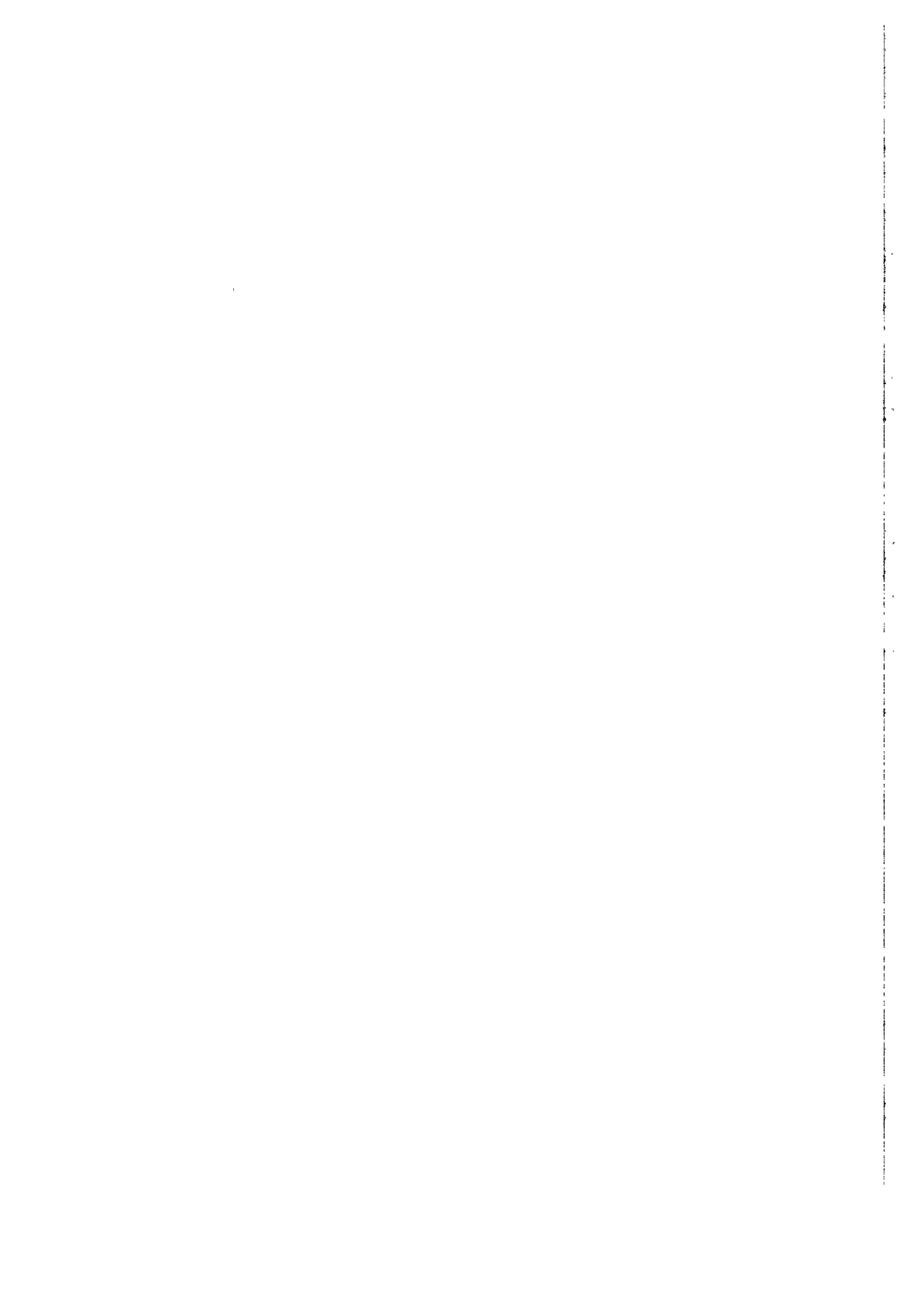
The CORDIS News database can be accessed through the WWW.

Contact details for further Information

If you would like further information on the CORDIS services, publications and products, please contact the CORDIS Help Desk :

CORDIS Customer Service
B.P. 2373
L-1023 Luxembourg

Telephone: +352-401162-240
Fax: +352-401162-248
E-mail: helpdesk@cordis.lu
WWW: <http://www.cordis.lu/>



Europäische Kommission
European Commission
Commission européenne

EUR 16769

Nuclear fission safety programme 1992-94
Radiation protection research action
(Volume 3)

Luxembourg: Office des publications officielles des Communautés européennes

1997 — XXIV, 2877-4547 pp., num. tab., fig. — 16.2 x 22.9 cm

ISBN (Volume 1) 92-827-7983-1
ISBN (Volume 2) 92-827-7984-X
ISBN (Volume 3) 92-827-7985-8
ISBN (Volumes 1, 2 and 3) 92-827-7982-3

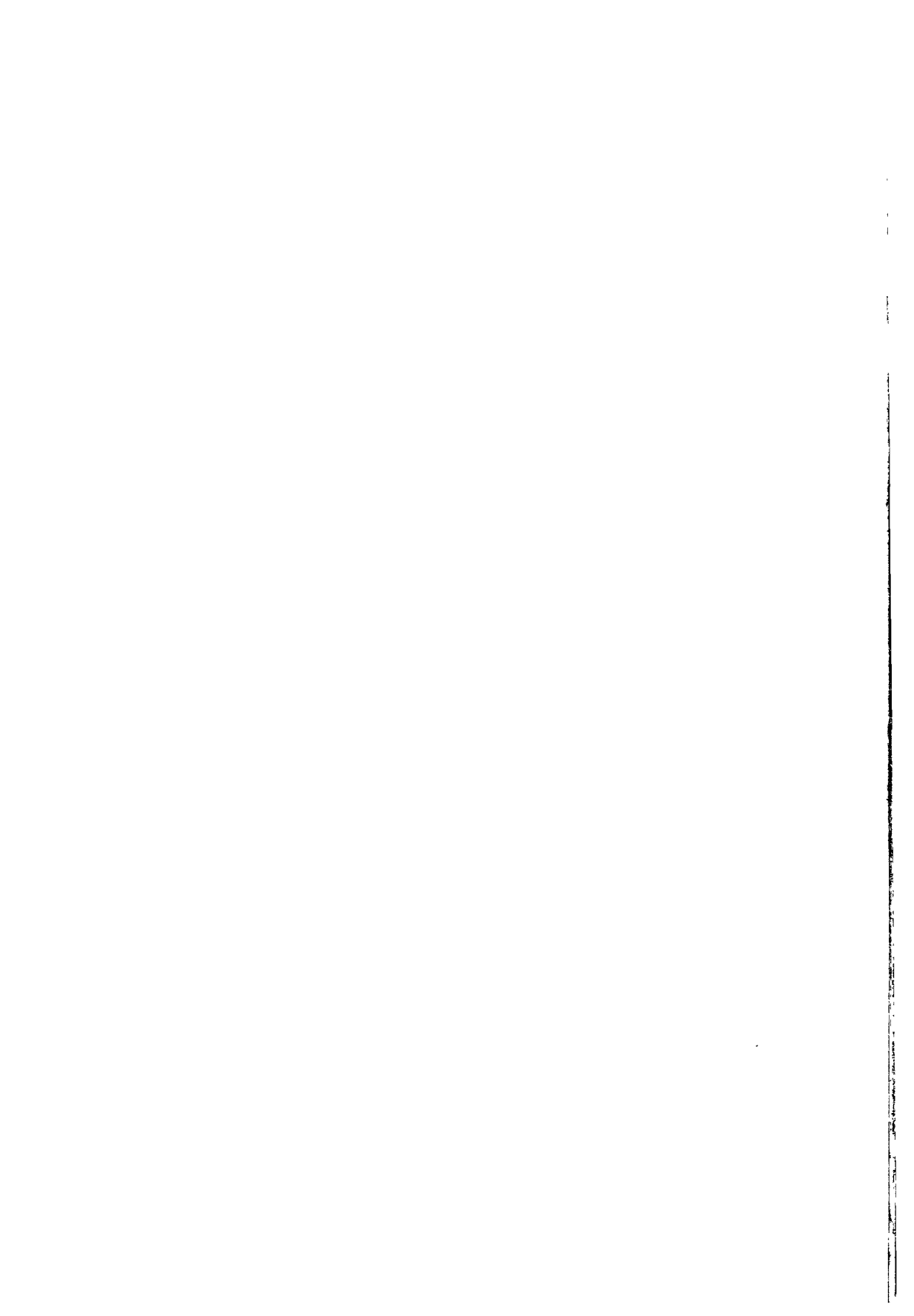
Preis in Luxemburg (ohne MwSt.):
Price (excluding VAT) in Luxembourg: ECU 194 (Volumes 1, 2 and 3)
Prix au Luxembourg (TVA exclue):

The final report of the 1992-94 period of the radiation protection programme outlines the research work carried out during the whole contractual period under all contracts between the European Commission and research groups in the Member States. More than 450 scientists collaborated on this programme. Results of more than 500 projects are reported. They are grouped into three sectors:

1. Human exposure to radiation and radioactivity, which includes:
 - 1.1. Measurement of radiation dose and its interpretation
 - 1.2. Transfer and behaviour of radionuclides in the environment
2. Consequences of radiation exposure to Man; assessment, prevention and treatment, which includes:
 - 2.1. Stochastic effects of radiation
 - 2.2. Non-stochastic effects of radiation
 - 2.3. Radiation effects on the developing organism
3. Risks and management of exposure, which includes:
 - 3.1. Assessment of human exposure and risks
 - 3.2. Optimization and management of radiation protection

Within the framework programme, the aim of this scientific research is to improve the conditions of life with respect to work and protection of man and his environment and to assure safe production of energy, i.e.:

- (i) to improve methods necessary to protect workers and the population by updating the scientific basis for appropriate standards;
- (ii) to prevent and counteract harmful effects of radiation;
- (iii) to assess radiation risks and provide methods to cope with the consequences of radiation accidents.



Venta • Salg • Verkauf • Πωλήσεις • Sales • Vente • Vendita • Verkoop • Venda • Myynti • Försäljning

BELGIQUE/BELGIE

Montieur belge/Belgisch Staatsblad
Rue de Louvain 40-42/Leuvenseweg 40-42
B-1000 Bruxelles/Brussel
Tel (32-2) 552 22 11
Fax (32-2) 511 01 84

Jean De Lannoy
Avenue du Roi 202/Koningslaan 202
B-1060 Bruxelles/Brussel
Tel (32-2) 538 51 69
Fax (32-2) 538 08 41
E-mail jean.de.lannoy@infoboard.be
URL http://www.jean-de.lannoy.be

Librairie européenne/Europese Boekhandel
Rue de la Loi 244/Wetstraat 244
B-1040 Bruxelles/Brussel
Tel (32-2) 295 26 39
Fax (32-2) 735 08 60

DANMARK

J. H. Schultz Information A/S
Herstedvang 10-12
DK-2620 Albertslund
Tel (45) 43 63 23 00
Fax (45) 43 63 19 69
E-mail schultz@schultz.dk
URL http://www.schultz.dk

DEUTSCHLAND

Bundesanzeiger Verlag
Breite Straße 78-80
Postfach 10 05 34
D-50667 Köln
Tel (49-221) 20 29-0
Fax (49-221) 20 92 98
E-mail vertrieb@bundesanzeiger.de
URL http://www.bundesanzeiger.de

ΕΛΛΑΔΑ/GREECE

G. C. Eleftheroudakis SA
International Bookstore
Panepistimiou 17
GR-10564 Athina
Tel (30-1) 331 41 801/2/3
Fax (30-1) 333 98 21
E-mail elebooks@netor.gr

ESPAÑA

Mundi Prensa Libros, SA
Castello, 37
E-28001 Madrid
Tel (34-1) 431 33 99
Fax (34-1) 575 39 98
E-mail libreria@mundiprensa.es
URL http://www.mundiprensa.es

Boletín Oficial del Estado

Trafalgar, 27
E-28010 Madrid
Tel (34-1) 538 21 11 (Libros)/
384 17 15 (Suscripciones)
Fax (34-1) 538 21 11 (Libros)/
384 17 14 (Suscripciones)
E-mail webmaster@boe.es
URL http://www.boe.es

FRANCE

Journal officiel
Service des publications des CE
26, rue Desaix
F-75727 Paris Cedex 15
Tel (33) 140 58 77 01/31
Fax (33) 140 58 77 00

IRELAND

Government Supplies Agency
Publications Section
4-5 Harcourt Road
Dublin 2
Tel (353-1) 661 31 11
Fax (353-1) 475 27 60

ITALIA

Licosa SpA
Via Duca di Calabria, 1/1
Casella postale 552
I-50125 Firenze
Tel (39-55) 64 54 15
Fax (39-55) 64 12 57
E-mail licosa@fiboc.it
URL http://www.fiboc.it/licosa

LUXEMBOURG

Messageries du livre S.A.R.L.
5, rue Raiffeisen
L-2411 Luxembourg
Tel (352) 40 10 20
Fax (352) 49 06 61
E-mail mdl@pt.lu

Abonnements

Messageries Paul Kraus
11, rue Christophe Plantin
L-2339 Luxembourg
Tel (352) 49 98 88-9
Fax (352) 49 98 88-444
E-mail mpx@pt.lu
URL http://www.mpx.lu

NETERLAND

SDU Servicecentrum Uitgevers
Externe Fondsen
Postbus 20014
2500 EA Den Haag
Tel (31-70) 378 98 80
Tel (31-70) 378 97 83
E-mail sdu@edu.nl
URL http://www.sdu.nl

ÖSTERREICH

**Manz'sche Verlags- und
Universitätsbuchhandlung GmbH**
Siebenbrunnengasse 21
Postfach 1
A-1050 Wien
Tel (43-1) 53 16 13 34/40
Fax (43-1) 53 16 13 39
E-mail auslieferung@manz.co.at
URL http://www.austria.eu.net/81/manz

PORTUGAL

Imprensa Nacional-Casa da Moeda, EP
Rua Marquês de Sá da Bandeira, 16 A
P-1050 Lisboa Codex
Tel (351-1) 353 03 99
Fax (351-1) 353 02 94, 384 01 32

Distribuidora de Livros Bertrand Ld.º

Rua das Terras dos Vales, 4/A
Apartado 60037
P-2701 Amadora Codex
Tel (351-1) 465 90 50, 495 87 87
Fax (351-1) 496 02 55

SUOMI/FINLAND

**Aktioidenmyyjä/Akademiska
Bokhandeln**
Pohjoisesplanadi 39/
Norra esplanaden 39
PL/PB 128
FIN-00101 Helsinki/Helsingfors
P/fn (358-9) 121 41
F/fax (358-9) 121 44 35
E-mail aktioiden@stockmann.maine.fi
URL http://booknet.cultnet.fi/aka/index.htm

SVERIGE

BTJ AB
Traktorvägen 11
S-221 82 Lund
Tfn (46-46) 18 00 00
Fax (46-46) 30 79 47
E-post btjeu-pub@btj.se
URL http://www.btj.se/media/au

UNITED KINGDOM

**The Stationery Office Ltd
International Sales Agency**
51 Nine Elms Lane
London SW8 5DR
Tel (44-171) 873 90 90
Fax (44-171) 873 84 63
E-mail jill.speed@theso.co.uk
URL http://www.the-stationery-office.co.uk

ISLAND

Bokabud Larusar Blondal
Skólavörðung, 2
IS-101 Reykjavík
Tel (354) 551 56 50
Fax (354) 552 55 60

NORGE

NIC Info A/S
Osterjovøien 18
Boks 6512 Etterstad
N-0606 Oslo
Tel (47-22) 97 45 00
Fax (47-22) 97 45 45

SCHWEIZ/SUISSE/SVIZZERA

OSEC
Stamphenbachstraße 85
CH-8035 Zurich
Tel (41-1) 365 53 15
Tel (41-1) 365 54 11
E-mail ulembacher@osec.ch
URL http://www.osec.ch

BÁLJARÍA

Europress-Euromedia Ltd
59, Bld Vitoshka
BG-1000 Sofia
Tel (359-2) 980 37 66
Fax (359-2) 980 42 30

ČESKA REPUBLIKA

NIS CR — prodejná
Konviktská 5
CZ-113 57 Praha 1
Tel (420-2) 24 22 94 33, 24 23 09 07
Fax (420-2) 24 22 94 33
E-mail nkposp@dec.nis.cz
URL http://www.nis.cz

CYPRUS

Cyprus Chamber of Commerce & Industry
Gnva-Digeni 38 & Delligiorgi 3
Mail orders
PO Box 1455
CY-1509 Nicosia
Tel (357-2) 44 95 00, 46 23 12
Fax (357-2) 36 10 44
E-mail cy1691_eric_cyprus@vans.infonet.com

MAGYARORSZAG

Euro Info Service
Europa Haz
Margitsziget
PO Box 475
H-1386 Budapest 62
Tel (36-1) 111 60 61, 111 62 16
Fax (36-1) 302 50 35
E-mail euroinfo@mail.matax.hu
URL http://www.euroinfo.hu/index.htm

MALTA

Miller Distributors Ltd
Malta International Airport
PO Box 25
LQA 05 Malta
Tel (356) 86 44 88
Fax (356) 67 67 99

POLSKA

Arts Polonia
Krakowskie Przedmiescie 7
Skř pocztowa 1001
PL-00-950 Warszawa
Tel (48-22) 826 12 01
Fax (48-22) 826 62 40, 826 53 34, 826 86 73
E-mail ars_pot@bevy.hsn.com.pl

ROMANIA

EUROMEDIA
Str. G-ral Berthelot Nr 41
RO-70749 Bucuresti
Tel (40-1) 210 44 01, 614 06 64
Fax (40-1) 210 44 01, 312 96 46

SLOVAKIA

**Slovak Centre of Scientific and Technical
Information**
Námestie slobody 19
SK-81223 Bratislava 1
Tel (421-7) 531 83 64
Fax (421-7) 531 83 64
E-mail europ@btb1.stk.stuba.sk

SLOVENIA

Gospodarski Vestnik
Založniška skupina d d
Dunajska cesta 5
SLO-1000 Ljubljana
Tel (386) 611 33 03 54
Fax (386) 611 33 31 23
E-mail belic@gvestnik.si
URL http://www.gvestnik.si

TÜRKIYE

Dünya İntofel AS
İstiklal Cad No 469
TR-80050 Tunel-Istanbul
Tel (90-212) 251 91 98
Fax (90-212) 251 91 97

AUSTRALIA

Hunter Publications
PO Box 404
3187 Abbotsford, Victoria
Tel (61-3) 94 17 53 61
Fax (61-3) 94 17 51 54

CANADA

Subscriptions only/Uniquement abonnements
Renouf Publishing Co Ltd
5369 Chemin Canotek Road Unit 1
K1J 9J3 Ottawa, Ontario
Tel (1-613) 745 26 65
Fax (1-613) 745 76 60
E-mail renouf@fox.nsn.ca
URL http://www.renoufbooks.com

EGYPT

The Middle East Observer
41, Sherif Street
Cairo
Tel (20-2) 393 97 32
Fax (20-2) 393 97 32

HRVATSKA

Mediatrade Ltd
Pavla Hrtza 1
HR-10000 Zagreb
Tel (385-1) 43 03 92
Fax (385-1) 43 03 92

INDIA

EBIC India
3rd Floor, Y B Chavan Centre
Gen J Bhosale Marg
400 021 Mumbai
Tel (91-22) 282 60 64
Fax (91-22) 285 45 64
E-mail ebic@gasbri01.vsnl.net.in

ISRAËL

ROY International
17, Shimon Hatarass Street
PO Box 13056
61130 Tel Aviv
Tel (972-3) 546 14 23
Fax (972-3) 546 14 42
E-mail roy@netvision.net.il
Sub-agent for the Palestinian Authority

Index Information Services

PO Box 19502
Jerusalem
Tel (972-2) 627 16 34
Fax (972-2) 627 12 19

JAPAN

PSI-Japan
Asahi Sanbancho Plaza #206
7-1 Sanbancho, Chiyoda-ku
Tokyo 102
Tel (81-3) 32 34 69 21
Fax (81-3) 32 34 69 15
E-mail psijapan@jcom.com
URL http://www.psi-japan.com

MALAYSIA

EBIC Malaysia
Level 7, Wisma Hong Leong
18 Jalan Perak
50450 Kuala Lumpur
Tel (60-3) 262 62 98
Fax (60-3) 262 61 98
E-mail ebic-kl@net.my

PHILIPPINES

EBIC Philippines
19th Floor, PS Bank Tower Sen
Gil J Puyat Ave cor Tindalo St
Makati City
Metro Manila
Tel (63-2) 759 66 80
Fax (63-2) 759 66 90
E-mail epcocom@globe.com.ph

RUSSIA

COEC
60-Ishya Otkryavaya Av 9
117312 Moscow
Tel (70-95) 135 52 27
Fax (70-95) 135 52 27

SOUTH AFRICA

Safto
5th Floor Export House,
CNR Maude & West Streets
PO Box 782 706
2146 Sandton
Tel (27-11) 883 37 37
Fax (27-11) 883 65 69

SOUTH KOREA

Kyowa Book Company
1 F1, Phyang Hwa Bldg
411-2 Hap Jeong Dong, Mapo Ku
121-220 Seoul
Tel (82-2) 322 67 80/1
Fax (82-2) 322 67 82
E-mail kyowa2@knet.co.kr

THAILANDE

EBIC Thailand
Vanessa Building 8th Floor
29 So Chulom
Ploenchit
10330 Bangkok
Tel (66) 655 06 27
Fax (66-2) 655 06 28
E-mail ebicth@ksc15.th.com

UNITED STATES OF AMERICA

Bernan Associates
4611-F Assembly Drive
MD20706 Lanham
Tel (800) 274 44 47 (toll free telephone)
Fax (800) 865 34 50 (toll free fax)
E-mail query@bernan.com
URL http://www.bernan.com

**ANDERE LANDER/OTHER COUNTRIES/
AUTRES PAYS**

Bitte wenden Sie sich an ein Büro Ihrer
Wahl / Please contact the sales office of
your choice / Veuillez vous adresser au
bureau de vente de votre choix

NOTICE TO THE READER

Information on European Commission publications in the areas of research and innovation can be obtained from:

◆ **CORDIS, the Community R&D Information Service**

For more information, contact:

CORDIS Customer Service, BP 2373, L-1023 Luxembourg

Tel. (352) 40 11 62-240, Fax (352) 40 11 62-248, e-mail: helpdesk@cordis.lu

or visit the website at <http://www.cordis.lu/>

◆ **euro abstracts**

The European Commission's periodical on research publications, issued every two months. For a subscription (1 year: ECU 65) please write to the sales office in your country.

Preis in Luxemburg (ohne MwSt.):

Price (excluding VAT) in Luxembourg: ECU 194 (Volumes 1, 2 and 3)

Prix au Luxembourg (TVA exclue):



AMT FÜR AMTLICHE VERÖFFENTLICHUNGEN
DER EUROPÄISCHEN GEMEINSCHAFTEN

OFFICE FOR OFFICIAL PUBLICATIONS
OF THE EUROPEAN COMMUNITIES

OFFICE DES PUBLICATIONS OFFICIELLES
DES COMMUNAUTÉS EUROPÉENNES

L-2985 Luxembourg

ISBN 92-827-7985-8



9 789282 779859
